Scientific and Technical Aerospace Reports

STAR

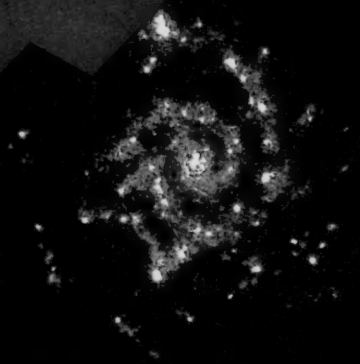

An Abstract Journal

NASA

Volume 33, Number 3
March 1995
N95-13610 to N95-15918

The NASA STI Office ... in Profile

Since its founding, NASA has been dedicated to the advancement of aeronautics and space science. The NASA Scientific and Technical Information (STI) Office plays a key part in helping NASA maintain this important role.

The NASA STI Office provides access to the NASA STI Database, the largest collection of aeronautical and space science STI in the world. The Office is also NASA's institutional mechanism for disseminating the results of its research and development activities.

Specialized services that help round out the Office's diverse offerings include creating custom thesauri, translating material to or from 34 foreign languages, building customized databases, organizing and publishing research results ... even providing videos.

For more information about the NASA STI Office, you can:

- **Phone** the NASA Access Help Desk at (301) 621-0390
- **Fax** your question to the NASA Access Help Desk at (301) 621-0134
- **E-mail** your question via the **Internet** to help@sti.nasa.gov
- **Write** to:

NASA Access Help Desk
NASA Center for AeroSpace Information
800 Elkridge Landing Road
Linthicum Heights, MD 21090-2934

Scientific and Technical Aerospace Reports

Scientific and Technical Aerospace Reports (STAR), is published each month as a major product of the NASA Scientific and Technical Information (STI) Office.

Inside this issue you will find:

- **Front Matter** containing a typical citation and abstract sample explaining the standard format, including codes for ordering reports
- **An Abstract Section** containing citations and abstracts of reports and publications that provide comprehensive coverage of worldwide aerospace-related topics including aeronautics and space science technology. *STAR* lists published and publicly available reports entered into the NASA STI Database during the four weeks preceding publication of this issue. These citations and abstracts are listed by subject categories.
- **An Index Section**
  - Subject
  - Personal author
  - Corporate source
  - Contract number
  - Report number
- **An Appendix** containing a guide for ordering cited reports, registering with the NASA STI Office, and using the available products and services. Additionally, price schedules, phone numbers, and addresses are included in this information packed section.

NASA also sponsors the companion journal, *NASA Open Volumes on Aerospace (NOVA)*, which lists abstracts of the open literature on aerospace subjects available worldwide. *NOVA* is for internal NASA use only, available from the NASA Center for AeroSpace Information (CASI).

Entries found in *STAR* are available through the NASA online retrieval service, RECON, and through DIALOG as the Aerospace Database.

The NASA STI Office gathers information through national and international agreements and exchanges and makes this information available to the NASA community and to the public in many forms through various outlets.

For additional information on the NASA STI Office, call the NASA Access Help Desk at (301) 621-0390, or write to:

NASA Center for AeroSpace Information
800 Elkridge Landing Road
Linthicum Heights, Maryland 21090-2934

US ISSN 0036-8741

This publication was prepared by the NASA Center for AeroSpace Information,
800 Elkridge Landing Road, Linthicum Heights, MD 21090-2934, (301) 621-0390.

Volume 33 Number 3 / March 1995

TABLE OF CONTENTS

AERONAUTICS For related information see also *Astronautics.*

01 AERONAUTICS (GENERAL) **391**

02 AERODYNAMICS **392**
Includes aerodynamics of bodies, combinations, wings, rotors, and control surfaces; and internal flow in ducts and turbomachinery. For related information see also *34 Fluid Mechanics and Heat Transfer.*

03 AIR TRANSPORTATION AND SAFETY **405**
Includes passenger and cargo air transport operations; and aircraft accidents. For related information see also *16 Space Transportation* and *85 Urban Technology and Transportation.*

04 AIRCRAFT COMMUNICATIONS AND NAVIGATION ..... **N.A.**
Includes digital and voice communication with aircraft; air navigation systems (satellite and ground based); and air traffic control. For related information see also *17 Space Communications, Spacecraft Communications, Command and Tracking* and *32 Communications and Radar.*

05 AIRCRAFT DESIGN, TESTING AND PERFORMANCE **408**
Includes aircraft simulation technology. For related information see also *18 Spacecraft Design, Testing and Performance* and *39 Structural Mechanics.* For land transportation vehicles see *85 Urban Technology and Transportation.*

06 AIRCRAFT INSTRUMENTATION **410**
Includes cockpit and cabin display devices; and flight instruments. For related information see also *19 Spacecraft Instrumentation* and *35 Instrumentation and Photography.*

07 AIRCRAFT PROPULSION AND POWER **411**
Includes prime propulsion systems and systems components, e.g., gas turbine engines and compressors; and onboard auxiliary power plants for aircraft. For related information see also *20 Spacecraft Propulsion and Power, 28 Propellants and Fuels,* and *44 Energy Production and Conversion.*

08 AIRCRAFT STABILITY AND CONTROL **412**
Includes aircraft handling qualities; piloting; flight controls; and autopilots. For related information see also *05 Aircraft Design, Testing and Performance.*

09 RESEARCH AND SUPPORT FACILITIES (AIR) **412**
Includes airports, hangars and runways; aircraft repair and overhaul facilities; wind tunnels; shock tubes; and aircraft engine test stands. For related information see also *14 Ground Support Systems and Facilities (Space).*

ASTRONAUTICS For related information see also *Aeronautics.*

12 ASTRONAUTICS (GENERAL) **413**
For extraterrestrial exploration see *91 Lunar and Planetary Exploration.*

13 ASTRODYNAMICS ..... **N.A.**
Includes powered and free-flight trajectories; and orbital and launching dynamics.

14 GROUND SUPPORT SYSTEMS AND FACILITIES (SPACE) **418**
Includes launch complexes, research and production facilities; ground support equipment, e.g., mobile transporters; and simulators. For related information see also *09 Research and Support Facilities (Air).*

15 LAUNCH VEHICLES AND SPACE VEHICLES **419**
Includes boosters; operating problems of launch/space vehicle systems; and reusable vehicles. For related information see also *20 Spacecraft Propulsion and Power.*

16 SPACE TRANSPORTATION **419**
Includes passenger and cargo space transportation, e.g., shuttle operations; and space rescue techniques. For related information see also *03 Air Transportation and Safety* and *18 Spacecraft Design, Testing and Performance.* For space suits see *54 Man/System Technology and Life Support.*

17 SPACE COMMUNICATIONS, SPACECRAFT COMMUNICATIONS, COMMAND AND TRACKING ..... **N.A.**
Includes telemetry; space communications networks; astronavigation and guidance; and radio blackout. For related information see also *04 Aircraft Communications and Navigation* and *32 Communications and Radar.*

N.A.—No abstracts were assigned to this category for this issue.

18 SPACECRAFT DESIGN, TESTING AND PERFORMANCE **420**
Includes satellites; space platforms; space stations; spacecraft systems and components such as thermal and environmental controls; and attitude controls. For life support systems see *54 Man/System Technology and Life Support.* For related information see also *05 Aircraft Design, Testing and Performance, 39 Structural Mechanics,* and *16 Space Transportation.*

19 SPACECRAFT INSTRUMENTATION **429**
For related information see also *06 Aircraft Instrumentation* and *35 Instrumentation and Photography.*

20 SPACECRAFT PROPULSION AND POWER **429**
Includes main propulsion systems and components, e.g., rocket engines; and spacecraft auxiliary power sources. For related information see also *07 Aircraft Propulsion and Power, 28 Propellants and Fuels, 44 Energy Production and Conversion,* and *15 Launch Vehicles and Space Vehicles.*

CHEMISTRY AND MATERIALS

23 CHEMISTRY AND MATERIALS (GENERAL) **431**

24 COMPOSITE MATERIALS **432**
Includes physical, chemical, and mechanical properties of laminates and other composite materials. For ceramic materials see *27 Nonmetallic Materials.*

25 INORGANIC AND PHYSICAL CHEMISTRY **437**
Includes chemical analysis, e.g., chromatography; combustion theory; electrochemistry; and photochemistry. For related information see also *77 Thermodynamics and Statistical Physics.*

26 METALLIC MATERIALS **444**
Includes physical, chemical, and mechanical properties of metals, e.g., corrosion; and metallurgy.

27 NONMETALLIC MATERIALS **448**
Includes physical, chemical, and mechanical properties of plastics, elastomers, lubricants, polymers, textiles, adhesives, and ceramic materials. For composite materials see *24 Composite Materials.*

28 PROPELLANTS AND FUELS **457**
Includes rocket propellants, igniters and oxidizers; their storage and handling procedures; and aircraft fuels. For related information see also *07 Aircraft Propulsion and Power, 20 Spacecraft Propulsion and Power,* and *44 Energy Production and Conversion.*

29 MATERIALS PROCESSING **457**
Includes space-based development of products and processes for commercial application. For biological materials see *55 Space Biology:*

ENGINEERING For related information see also *Physics.*

31 ENGINEERING (GENERAL) **459**
Includes vacuum technology; control engineering; display engineering; cryogenics; and fire prevention.

32 COMMUNICATIONS AND RADAR **460**
Includes radar; land and global communications; communications theory; and optical communications. For related information see also *04 Aircraft Communications and Navigation* and *17 Space Communications, Spacecraft Communications, Command and Tracking.* For search and rescue see *03 Air Transportation and Safety,* and *16 Space Transportation.*

33 ELECTRONICS AND ELECTRICAL ENGINEERING **471**
Includes test equipment and maintainability; components, e.g., tunnel diodes and transistors; microminiaturization; and integrated circuitry. For related information see also *60 Computer Operations and Hardware* and *76 Solid-State Physics.*

34 FLUID MECHANICS AND HEAT TRANSFER **478**
Includes boundary layers; hydrodynamics; fluidics; mass transfer and ablation cooling. For related information see also *02 Aerodynamics* and *77 Thermodynamics and Statistical Physics.*

35 INSTRUMENTATION AND PHOTOGRAPHY **496**
Includes remote sensors; measuring instruments and gauges; detectors; cameras and photographic supplies; and holography. For aerial photography see *43 Earth Resources and Remote Sensing.* For related information see also *06 Aircraft Instrumentation* and *19 Spacecraft Instrumentation.*

36 LASERS AND MASERS **498**
Includes parametric amplifiers. For related information see also *76 Solid-State Physics.*

37 MECHANICAL ENGINEERING **500**
Includes auxiliary systems (nonpower); machine elements and processes; and mechanical equipment.

38 QUALITY ASSURANCE AND RELIABILITY **505**
Includes product sampling procedures and techniques; and quality control.

39 STRUCTURAL MECHANICS **505**
Includes structural element design and weight analysis; fatigue; and thermal stress. For applications see *05 Aircraft Design, Testing and Performance* and *18 Spacecraft Design, Testing and Performance.*

GEOSCIENCES For related information see also *Space Sciences.*

42 GEOSCIENCES (GENERAL) ..... **N.A.**

43 EARTH RESOURCES AND REMOTE SENSING **514**
Includes remote sensing of earth resources by aircraft and spacecraft; photogrammetry; and aerial photography. For instrumentation see *35 Instrumentation and Photography.*

44 ENERGY PRODUCTION AND CONVERSION **517**
Includes specific energy conversion systems, e.g., fuel cells; global sources of energy; geophysical conversion; and windpower. For related information see also *07 Aircraft Propulsion and Power, 20 Spacecraft Propulsion and Power,* and *28 Propellants and Fuels.*

45 ENVIRONMENT POLLUTION **521**
Includes atmospheric, noise, thermal, and water pollution.

46 GEOPHYSICS **525**
Includes aeronomy; upper and lower atmosphere studies; ionospheric and magnetospheric physics; and geomagnetism. For space radiation see *93 Space Radiation.*

47 METEOROLOGY AND CLIMATOLOGY **532**
Includes weather forecasting and modification.

48 OCEANOGRAPHY **535**
Includes biological, dynamic, and physical oceanography; and marine resources. For related information see also *43 Earth Resources and Remote Sensing.*

LIFE SCIENCES

51 LIFE SCIENCES (GENERAL) **537**

52 AEROSPACE MEDICINE **539**
Includes physiological factors; biological effects of radiation; and effects of weightlessness on man and animals.

53 BEHAVIORAL SCIENCES **551**
Includes psychological factors; individual and group behavior; crew training and evaluation; and psychiatric research.

54 MAN/SYSTEM TECHNOLOGY AND LIFE SUPPORT **554**
Includes human engineering; biotechnology; and space suits and protective clothing. For related information see also *16 Space Transportation.*

55 SPACE BIOLOGY ..... **N.A.**
Includes exobiology; planetary biology; and extraterrestrial life.

MATHEMATICAL AND COMPUTER SCIENCES

59 MATHEMATICAL AND COMPUTER SCIENCES (GENERAL) **564**

60 COMPUTER OPERATIONS AND HARDWARE **566**
Includes hardware for computer graphics, firmware, and data processing. For components see *33 Electronics and Electrical Engineering.*

61 COMPUTER PROGRAMMING AND SOFTWARE **567**
Includes computer programs, routines, algorithms, and specific applications, e.g., CAD/CAM.

62 COMPUTER SYSTEMS **577**
Includes computer networks and special application computer systems.

63 CYBERNETICS **580**
Includes feedback and control theory, artificial intelligence, robotics and expert systems. For related information see also *54 Man/System Technology and Life Support.*

64 NUMERICAL ANALYSIS **584**
Includes iteration, difference equations, and numerical approximation.

65 STATISTICS AND PROBABILITY **588**
Includes data sampling and smoothing; Monte Carlo method; and stochastic processes.

66 SYSTEMS ANALYSIS ..... **N.A.**
Includes mathematical modeling; network analysis; and operations research.

67 THEORETICAL MATHEMATICS **589**
Includes topology and number theory.

PHYSICS For related information see also *Engineering.*

70 PHYSICS (GENERAL) **589**
For precision time and time interval (PTTI) see *35 Instrumentation and Photography*; for geophysics, astrophysics or solar physics see *46 Geophysics, 90 Astrophysics*, or *92 Solar Physics.*

71 ACOUSTICS **590**
Includes sound generation, transmission, and attenuation. For noise pollution see *45 Environment Pollution.*

72 ATOMIC AND MOLECULAR PHYSICS **592**
Includes atomic structure, electron properties, and molecular spectra.

73 NUCLEAR AND HIGH-ENERGY PHYSICS **599**
Includes elementary and nuclear particles; and reactor theory. For space radiation see *93 Space Radiation.*

74 OPTICS **601**
Includes light phenomena and optical devices. For lasers see *36 Lasers and Masers.*

75 PLASMA PHYSICS **616**
Includes magnetohydrodynamics and plasma fusion. For ionospheric plasmas see *46 Geophysics.* For space plasmas see *90 Astrophysics.*

76 SOLID-STATE PHYSICS **619**
Includes superconductivity. For related information see also *33 Electronics and Electrical Engineering* and *36 Lasers and Masers.*

77 THERMODYNAMICS AND STATISTICAL PHYSICS **627**
Includes quantum mechanics; theoretical physics; and Bose and Fermi statistics. For related information see also *25 Inorganic and Physical Chemistry* and *34 Fluid Mechanics and Heat Transfer.*

SOCIAL SCIENCES

80 SOCIAL SCIENCES (GENERAL) **629**
Includes educational matters.

81 ADMINISTRATION AND MANAGEMENT **630**
Includes management planning and research.

82 DOCUMENTATION AND INFORMATION SCIENCE **630**
Includes information management; information storage and retrieval technology; technical writing; graphic arts; and micrography. For computer documentation see *61 Computer Programming and Software.*

83 ECONOMICS AND COST ANALYSIS ..... **N.A.**
Includes cost effectiveness studies.

84 LAW, POLITICAL SCIENCE AND SPACE POLICY ..... **N.A.**
Includes NASA appropriation hearings; aviation law; space law and policy; international law; international cooperation; and patent policy.

85 URBAN TECHNOLOGY AND TRANSPORTATION **634**
Includes applications of space technology to urban problems; technology transfer; technology assessment; and surface and mass transportation. For related information see *03 Air Transportation and Safety, 16 Space Transportation,* and *44 Energy Production and Conversion.*

SPACE SCIENCES For related information see also *Geosciences.*

88 SPACE SCIENCES (GENERAL) **634**

89 ASTRONOMY **636**
Includes radio, gamma-ray, and infrared astronomy; and astrometry.

90 ASTROPHYSICS **642**
Includes cosmology; celestial mechanics; space plasmas; and interstellar and interplanetary gases and dust. For related information see also *75 Plasma Physics.*

91 LUNAR AND PLANETARY EXPLORATION **644**
Includes planetology; and manned and unmanned flights. For spacecraft design or space stations see *18 Spacecraft Design, Testing and Performance.*

92 SOLAR PHYSICS **646**
Includes solar activity, solar flares, solar radiation and sunspots. For related information see also *93 Space Radiation.*

93 SPACE RADIATION **646**
Includes cosmic radiation; and inner and outer earth's radiation belts. For biological effects of radiation see *52 Aerospace Medicine.* For theory see *73 Nuclear and High-Energy Physics.*

GENERAL

Includes aeronautical, astronautical, and space science related histories, biographies, and pertinent reports too broad for categorization; histories or broad overviews of NASA programs.

99 GENERAL **647**

SUBJECT INDEX **I-1**

PERSONAL AUTHOR INDEX **I-115**

CORPORATE SOURCE INDEX **I-129**

CONTRACT NUMBER INDEX **I-147**

REPORT NUMBER INDEX **I-151**

APPENDIX **A-1**

TYPICAL CITATION AND ABSTRACT

NASA SPONSORED — ON MICROFICHE

ACCESSION NUMBER → **N95-10148*#** National Aeronautics and Space Administration. Lewis Research Center, Cleveland, OH. ← CORPORATE SOURCE

TITLE → **EFFECTS OF A FORWARD-SWEPT FRONT ROTOR ON THE FLOWFIELD OF A COUNTERROTATION PROPELLER**

AUTHORS → M. Nallasamy (NYMA, Inc., Brook Park, OH.) and Gary G. Podboy Aug. 1994 19 p Presented at the 30th Joint Propulsion Conference, Indianapolis, IN, 27-29 Jun. 1994; sponsored by AIAA, ASME, SAE, and ASEE ← PUBLICATION DATE

CONTRACT OR GRANT → (Contract NAS3-27186; RTOP 538-03-11)

REPORT NUMBERS → (NASA-TM-106671; E-8994; NAS 1.15:106671; AIAA Paper 94-2694) Avail: CASI HC A03/MF A01; 6 functional color pages ← AVAILABILITY SOURCE AND PRICE CODE

The effects of a forward-swept front rotor on the flowfield of a counterrotation model propeller at takeoff conditions at zero degree angle of attack are studied by solving the unsteady three-dimensional Euler equations. The configuration considered is an uneven blade count counterrotation model with twelve forward-swept blades on the fore rotor and ten aft-swept blades on the aft rotor. The flowfield is compared with that of a reference aft-swept counterrotation geometry and Laser Doppler Velocimeter (LDV) measurements. At the operating conditions considered, the forward-swept blade experiences a higher tip loading and produces a stronger tip vortex compared to the aft-swept blade, consistent with the LDV and acoustic measurements. Neither the solution nor the LDV data indicated the formation of a leading edge vortex. The predicted radial distribution of the circumferentially averaged axial velocity at the measurement station agreed very closely with LDV data, while crossflow velocities showed poor agreement. The discrepancy between prediction and LDV data of tangential and radial velocities is due in part to the insufficient mesh resolution in the region between the rotors and in the tip region to track the tip vortex. The vortex is diffused by the time it arrives at the measurement station. The uneven blade count configuration requires the solution to be carried out for six blade passages of the fore rotor and five passages of the aft rotor, thus making grid refinement prohibitive.

Author

VOLUME 33 NUMBER 3 / March 1995

Scientific and Technical Aerospace Reports

A Monthly Publication of the National Aeronautics and Space Administration

01 AERONAUTICS (GENERAL)

N95-13642*# National Aeronautics and Space Administration. Ames Research Center, Moffett Field, CA.

MODIFICATION OF THE AMES 40- BY 80-FOOT WIND TUNNEL FOR COMPONENT ACOUSTIC TESTING FOR THE SECOND GENERATION SUPERSONIC TRANSPORT

F. H. Schmitz, J. R. Allmen, and P. T. Soderman Oct. 1994 41 p
(RTOP 505-38-13)
(NASA-TM-108850; A-94143; NAS 1.15:108850) Avail: CASI HC A03/MF A01

The development of a large-scale anechoic test facility where large models of engine/airframe/high-lift systems can be tested for both improved noise reduction and minimum performance degradation is described. The facility development is part of the effort to investigate economically viable methods of reducing second generation high speed civil transport noise during takeoff and climb-out that is now under way in the United States. This new capability will be achieved through acoustic modifications of NASA's second largest subsonic wind tunnel: the 40-by 80-Foot Wind Tunnel at the NASA Ames Research Center. Three major items are addressed in the design of this large anechoic and quiet wind tunnel: a new deep (42 inch (107 cm)) test section liner, expansion of the wind tunnel drive operating envelope at low rpm to reduce background noise, and other promising methods of improving signal-to-noise levels of inflow microphones. Current testing plans supporting the U.S. high speed civil transport program are also outlined. Author

N95-13662*# National Aeronautics and Space Administration. Ames Research Center, Moffett Field, CA.

USER'S GUIDE FOR ENSAERO: A MULTIDISCIPLINARY PROGRAM FOR FLUID/STRUCTURAL/CONTROL INTERACTION STUDIES OF AIRCRAFT (RELEASE 1)

Guru P. Guruswamy Oct. 1994 47 p
(RTOP 509-10-11)
(NASA-TM-108853; A-94148; NAS 1.15:108853) Avail: CASI HC A03/MF A01

Strong interactions can occur between the flow about an aerospace vehicle and its structural components resulting in several important aeroelastic phenomena. These aeroelastic phenomena can significantly influence the performance of the vehicle. At present, closed-form solutions are available for aeroelastic computations when flows are in either the linear subsonic or supersonic range. However, for aeroelasticity involving complex nonlinear flows with shock waves, vortices, flow separations, and aerodynamic heating, computational methods are still under development. These complex aeroelastic interactions can be dangerous and limit the performance of aircraft. Examples of these detrimental effects are aircraft with highly swept wings experiencing vortex-induced aeroelastic oscillations, transonic regime at which the flutter speed is low, aerothermoelastic loads that play a critical role in the design of high-speed vehicles, and flow separations that often lead to buffeting with undesirable structural oscillations. The simulation of these complex aeroelastic phenomena requires an integrated analysis of fluids and structures. This report presents a summary of the development, applications, and procedures to use the multidisciplinary computer code ENSAERO. This code is based on the Euler/Navier-Stokes flow equations and modal/finite-element structural equations. Author

N95-13891*# National Aeronautics and Space Administration. Ames Research Center, Moffett Field, CA.

DYNAMICS OF THE MCDONNELL-DOUGLAS LARGE SCALE DYNAMIC RIG AND DYNAMIC CALIBRATION OF THE ROTOR BALANCE

Khanh Nguyen and Benton Lau Oct. 1994 28 p
(RTOP 505-59-36)
(NASA-TM-108855; A-94007; NAS 1.15:108855) Avail: CASI HC A03/MF A01

A shake test was performed on the Large Scale Dynamic Rig in the 40- by 80-Foot Wind Tunnel in support of the McDonnell Douglas Advanced Rotor Technology (MDART) Test Program. The shake test identifies the hub modes and the dynamic calibration matrix of the rotor balance. For hub mode identification, three configurations were tested: wind tunnel scale unlocked with dampers engaged and disengaged, and wind tunnel scale locked. Test data were analyzed with a multi-degree-of-freedom time domain algorithm to identify the modal properties of the hub modes. The damping of the low frequency hub modes (ground resonance modes) increases significantly with the wind tunnel dampers engaged. For dynamic calibration of the rotor balance, the shake test was performed only with the wind tunnel dampers engaged. The dynamic calibration matrix, computed from the shake test data using a least squares error method, is used to correct the five-per-rev vibratory balance readings. The corrections are large for the side force, moderate for the axial force and inplane hub moments, and small for the normal force. Author

N95-14144# Air Force Inst. of Tech., Wright-Patterson AFB, OH. School of Engineering.

DAMAGE TOLERANT REPAIR TECHNIQUES FOR PRESSURIZED AIRCRAFT FUSELAGES M.S. Thesis

Robert S. Fredell 1994 280 p
(AD-A281982; AFIT/CI/CIA-94-095) Avail: CASI HC A13/MF A03

Concerns over the safety of the continued use of aging transport aircraft have been voiced in the industry. A key component in the structural integrity of aging aircraft is the damage tolerance of fuselage structural repairs. The investigation focuses on the analysis and testing of contemporary repair methods and develops two improvements. The first technique, known as soft patching, is appropriate for damage tolerant riveted repairs to incidental fuselage damage. Soft patching involves the use of high strength, moderate elastic modulus GLARE 3 fiber metal laminate patches. They extend the fatigue life of riveted repairs to monolithic aluminum fuselages while reducing life cycle costs. The second technique involves bonded crack patching of intact fatigue cracks in fuselage skins. An easy to use analysis program is presented along with analytical and test results of a low cost, high performance patch material known as GLARE 2. The findings demonstrate that GLARE 2 can replace the expensive boron/epoxy composites used in fuselage crack patching applications. DTIC

N95-14419*# National Aeronautics and Space Administration. Ames Research Center, Moffett Field, CA.

HIGHER HARMONIC CONTROL ANALYSIS FOR VIBRATION REDUCTION OF HELICOPTER ROTOR SYSTEMS

Khanh Q. Nguyen Oct. 1994 138 p
(RTOP 505-61-51)
(NASA-TM-103855; A-91113; NAS 1.15:103855) Avail: CASI HC A07/MF A02

An advanced higher harmonic control (HHC) analysis has been developed and applied to investigate its effect on vibration reduction levels, blade and control system fatigue loads, rotor performance, and power

requirements of servo-actuators. The analysis is based on a finite element method in space and time. A nonlinear time domain unsteady aerodynamic model, based on the indicial response formulation, is used to calculate the airloads. The rotor induced inflow is computed using a free wake model. The vehicle trim controls and blade steady responses are solved as one coupled solution using a modified Newton method. A linear frequency-domain quasi-steady transfer matrix is used to relate the harmonics of the vibratory hub loads to the harmonics of the HHC inputs. Optimal HHC is calculated from the minimization of the vibratory hub loads expressed in term of a quadratic performance index. Predicted vibratory hub shears are correlated with wind tunnel data. The fixed-gain HHC controller suppresses completely the vibratory hub shears for most of steady or quasi-steady flight conditions. HHC actuator amplitudes and power increase significantly at high forward speeds (above 100 knots). Due to the applied HHC, the blade torsional stresses and control loads are increased substantially. For flight conditions where the blades are stalled considerably, the HHC input-output model is quite nonlinear. For such cases, the adaptive-gain controller is effective in suppressing vibratory hub loads, even though HHC may actually increase stall areas on the rotor disk. The fixed-gain controller performs poorly for such flight conditions. Comparison study of different rotor systems indicates that a soft-inplane hingeless rotor requires less actuator power at high speeds (above 130 knots) than an articulated rotor, and a stiff-inplane hingeless rotor generally requires more actuator power than an articulated or a soft-inplane hingeless rotor. Parametric studies for a hingeless rotor operating in a transition flight regime and for an articulated rotor operating at the level-flight boundary (high speed and high thrust conditions) indicate that blade parameters including flap, lag, torsion stiffness distributions, linear pretwist, chordwise offset of center-of-mass from elastic axis and chordwise offset of elastic axis from aerodynamic center can be selected to minimize the actuator power requirements for HHC. Author

N95-14921*# National Aeronautics and Space Administration. Ames Research Center, Moffett Field, CA.

AIR-BREATHING AEROSPACE PLANE DEVELOPMENT ESSENTIAL: HYPERSONIC PROPULSION FLIGHT TESTS

Unmeel B. Mehta Nov. 1994 16 p Presented at the Second European Symposium on Aerothermodynamics for Space Vehicles, ESTEC, Noordwijk (The Netherlands), 21-23 Nov. 1994

(RTOP 505-59-53)

(NASA-TM-108857; A-95017; NAS 1.15:108857) Avail: CASI HC A03/MF A01

Hypersonic air-breathing propulsion utilizing scramjets can fundamentally change transatmospheric accelerators for low earth-to-orbit and return transportation. The value and limitations of ground tests, of flight tests, and of computations are presented, and scramjet development requirements are discussed. It is proposed that near full-scale hypersonic propulsion flight tests are essential for developing a prototype hypersonic propulsion system and for developing computational-design technology so that it can be used for designing this system. In order to determine how these objectives should be achieved, some lessons learned from past programs are presented. A conceptual two-stage-to-orbit (TSTO) prototype/experimental aerospace plane is recommended as a means of providing access-to-space and for conducting flight tests. A road map for achieving these objectives is also presented. Author

N95-15331# Sytronics, Inc., Dayton, OH.

MORE SUPPORTABLE T-38A ENHANCEMENT STUDY Final Report, Dec. 1993 - Jun. 1994

William T. Kilpatrick 20 Jun. 1994 312 p

(Contract F33657-93-C-2440)

(AD-A283671; DOC-0710-001) Avail: CASI HC A14/MF A03

The purpose of the More Supportable T-38A Enhancement Study was to investigate methods of improving T-38A fleet readiness and reduce operational support costs. A comparative and functional analysis approach was utilized to identify specific T-38A aircraft design and system support deficiencies that could be improved through a redesign effort or maintenance procedural changes. Several aircraft components were identified and targeted as potential redesign candidates. These T-38A components are also common to the F-5 and improvements to these components will enhance both T-38 and F-5 supportability. DTIC

N95-15550* National Aeronautics and Space Administration, Washington, DC.

AERONAUTICAL ENGINEERING: A CONTINUING BIBLIOGRAPHY WITH INDEXES (SUPPLEMENT 310)

Nov. 1994 29 p

(NASA-SP-7037(310); NAS 1.21:7037(310)) Avail: CASI HC A03

This bibliography lists 29 reports, articles, and other documents introduced into the NASA scientific and technical information system in Nov. 1994. Subject coverage includes: engineering and theoretical aspects of design, construction,evaluation testing, operation, and performance of aircraft (including aircraft engines) and associated components, equipment and systems. It also includes research and development in aerodynamics, aeronautics, and ground support equipment for aeronautical vehicles. Author

N95-14477*# Monash Univ., Clayton (Australia). Dept. of Mechanical Engineering.

DEVELOPMENT OF A COMPOSITE REPAIR AND THE ASSOCIATED INSPECTION INTERVALS FOR THE F-111C STIFFENER RUNOUT REGION

R. Jones, L. Molent, J. Paul, T. Saunders, and W. K. Chiu *In* NASA. Langley Research Center, FAA/NASA International Symposium on Advanced Structural Integrity Methods for Airframe Durability and Damage Tolerance Sep. 1994 p 339-350 (For primary document see N95-14453 03-39) Avail: CASI HC A03/MF A04

02 AERODYNAMICS

Includes aerodynamics of bodies, combinations, wings, rotors, and control surfaces; and internal flow in ducts and turbomachinery.

For related information see also *34 Fluid Mechanics and Heat Transfer.*

N95-13701*# Old Dominion Univ., Norfolk, VA. Dept. of Mechanical Engineering.

AERODYNAMIC SHAPE OPTIMIZATION OF A HSCT TYPE CONFIGURATION WITH IMPROVED SURFACE DEFINITION Progress Report, 1 May 1993 - 30 Jun. 1994

Almuttil M. Thomas and Surendra N. Tiwari Oct. 1994 32 p

(Contract NCC1-68)

(NASA-CR-197011; NAS 1.26:197011) Avail: CASI HC A03/MF A01

Two distinct parametrization procedures of generating free-form surfaces to represent aerospace vehicles are presented. The first procedure is the representation using spline functions such as nonuniform rational b-splines (NURBS) and the second is a novel (geometrical) parametrization using solutions to a suitably chosen partial differential equation. The main idea is to develop a surface which is more versatile and can be used in an optimization process. Unstructured volume grid is generated by an advancing front algorithm and solutions obtained using an Euler solver. Grid sensitivity with respect to surface design parameters and aerodynamic sensitivity coefficients based on potential flow is obtained using an automatic differentiator precompiler software tool. Aerodynamic shape optimization of a complete aircraft with twenty four design variables is performed. High speed civil transport aircraft (HSCT) configurations are targeted to demonstrate the process. Author

N95-13817*# National Aeronautics and Space Administration. Lewis Research Center, Cleveland, OH.

AN ADAPTIVELY-REFINED, CARTESIAN, CELL-BASED SCHEME FOR THE EULER AND NAVIER-STOKES EQUATIONS Ph.D. Thesis - Michigan Univ.

William John Coirier Oct. 1994 249 p

(RTOP 505-62-52)

(NASA-TM-106754; E-9174; NAS 1.15:106754) Avail: CASI HC A11/MF A03

A Cartesian, cell-based scheme for solving the Euler and Navier-Stokes equations in two dimensions is developed and tested. Grids about geometrically complicated bodies are generated automatically, by recursive subdivision of a single Cartesian cell encompassing the entire flow domain. Where the resulting cells intersect bodies, polygonal 'cut' cells are created. The geometry of the cut cells is computed using polygon-clipping algorithms.

The grid is stored in a binary-tree data structure which provides a natural means of obtaining cell-to-cell connectivity and of carrying out solution-adaptive refinement. The Euler and Navier-Stokes equations are solved on the resulting grids using a finite-volume formulation. The convective terms are upwinded, with a limited linear reconstruction of the primitive variables used to provide input states to an approximate Riemann solver for computing the fluxes between neighboring cells. A multi-stage time-stepping scheme is used to reach a steady-state solution. Validation of the Euler solver with benchmark numerical and exact solutions is presented. An assessment of the accuracy of the approach is made by uniform and adaptive grid refinements for a steady, transonic, exact solution to the Euler equations. The error of the approach is directly compared to a structured solver formulation. A non smooth flow is also assessed for grid convergence, comparing uniform and adaptively refined results. Several formulations of the viscous terms are assessed analytically, both for accuracy and positivity. The two best formulations are used to compute adaptively refined solutions of the Navier-Stokes equations. These solutions are compared to each other, to experimental results and/or theory for a series of low and moderate Reynolds numbers flow fields. The most suitable viscous discretization is demonstrated for geometrically-complicated internal flows. For flows at high Reynolds numbers, both an altered grid-generation procedure and a different formulation of the viscous terms are shown to be necessary. A hybrid Cartesian/body-fitted grid generation approach is demonstrated. In addition, a grid-generation procedure based on body-aligned cell cutting coupled with a viscous stensil-construction procedure based on quadratic programming is presented. Author

N95-14103# Advisory Group for Aerospace Research and Development, Neuilly-Sur-Seine (France). Fluid Dynamics Panel.

SCALE EFFECTS ON AIRCRAFT AND WEAPON AERODYNAMICS [LES EFFETS D'ECHELLE ET L'AERODYNAMIQUE DES AERONEFS ET DES SYSTEMES D'ARMES]

A. Barry Haines (Aircraft Research Association Ltd., Bedford, England.) and A. D. Young Jul. 1994 247 p

(AGARD-AG-323; ISBN-92-835-0754-1) Copyright Avail: CASI HC A11/MF A03

The present state of knowledge on scale effects at high lift and low speeds, at transonic speeds, and on aircraft drag are presented. In addition, scale effects in various important specific scale-sensitive areas such as forebody vortex flows, the flow in and near open cavities, the flow into an air intake, the flow over propellers, and on ice accretion simulation testing are discussed. The emphasis is on scale effects that have been observed in flight-tunnel comparisons for specific aircraft. It is concluded that much has been learned about scale effects; however, precise prediction can still be difficult. Twenty recommendations for further research are mentioned. This AGARDograph has been produced at the request of the Fluid Dynamics Panel of AGARD. Author

N95-14182* National Aeronautics and Space Administration. Marshall Space Flight Center, Huntsville, AL.

PARACHUTE HAVING IMPROVED VENT LINE STACKING Patent

John E. Hengel 1 Nov. 1994 7 p Filed 29 Mar. 1993 Supersedes N94-11021 (32 - 1, p 14)

(NASA-Case-MFS-28508-1; US-Patent-5,360,187; US-Patent-Appl-SN-037877; US-Patent-Class-244-145; US-Patent-Class-244-142; Int-Patent-Class-B64D-17/02) Avail: US Patent and Trademark Office

A parachute having an improved vent line stacking wherein the parachute is provided with a canopy having a central vent opening and a vent band secured to the canopy around the periphery of the vent opening, with a plurality of vent lines each lying on a diameter of the vent opening and having its ends secured to the vent band on opposite sides of the vent opening is described. The vent lines are sewed to the vent band in an order such that the end of a first vent line is sewed to the vent band at a starting point with the end of a second vent band then being sewed to the vent band adjacent to and counterclockwise from the first band. A third vent band is sewed to the vent band adjacent to and clockwise from the first band, with a fourth vent band being sewed to the vent band adjacent to and counterclockwise from the second vent band. It can be seen that, if the vent lines are numbered in the order of being sewed to the vent band, the odd numbered vent lines will run consecutively in a clockwise direction and the even numbered lines will run consecutively in a counterclockwise direction from the starting point. With this order of assembly, each and every vent line will be separated from adjacent vent lines by no more than one vent line in the center of the vent opening where the vent lines cross. Author (revised)

N95-14197# Advisory Group for Aerospace Research and Development, Neuilly-Sur-Seine (France). Fluid Dynamics Panel.

QUALITY ASSESSMENT FOR WIND TUNNEL TESTING [L'APPRECIATION DE LA QUALITE POUR LES ESSAIS EN SOUFFLERIE]

Jul. 1994 92 p

(AGARD-AR-304; ISBN-92-835-0753-3) Copyright Avail: CASI HC A05/MF A01

The wind tunnel continues to be the main instrument for providing experimental aerodynamic data to the aerospace industry and the aerodynamic researcher for the purpose of load and performance evaluation of theoretical results. In both cases, it is imperative that the user has confidence in the quality of the results, which means that he must have information of what accuracy to attach to the data. This report describes a practical approach for assessing the uncertainty of experimental measurements. Although it concentrates on aerodynamic references data, the approach presented can be used to report data and associated uncertainties for any other condition. The methodology described is designed to facilitate communications and to encourage professional and practical analyses of complex problems. The most recent accepted technical concepts have been included in the methodology. This report presents the results of a study by Working Group 15 of the AGARD Fluid Dynamics Panel. Author

N95-14229*# National Aeronautics and Space Administration. Hugh L. Dryden Flight Research Center, Edwards, CA.

FOURTH HIGH ALPHA CONFERENCE, VOLUME 1

Jul. 1994 212 p Conference held at Edwards, CA, 12-14 Jul. 1994 (RTOP 505-68-30)

(NASA-CP-10143-Vol-1; H-2007-Vol-1; NAS 1.55:10143-Vol-1) Avail: CASI HC A10/MF A03

The goal of the Fourth High Alpha Conference was to focus on the flight validation of high angle-of-attack technologies and provide an in-depth review of the latest high angle-of-attack activities. Areas that were covered include: high angle-of-attack aerodynamics, propulsion and inlet dynamics, thrust vectoring, control laws and handling qualities, tactical utility, and forebody controls. For individual titles, see N95-14230 through N95-14238.

N95-14230*# National Aeronautics and Space Administration. Langley Research Center, Hampton, VA.

HIGH ALPHA TECHNOLOGY PROGRAM (HATP) GROUND TEST TO FLIGHT COMPARISONS Status Report

R. M. Hall, D. W. Banks, David F. Fisher, F. Ghaffari, D. G. Murri, J. C. Ross, and Wendy R. Lanser *In* NASA. Dryden Flight Research Center, Fourth High Alpha Conference, Volume 1 Jul. 1994 25 p (For primary document see N95-14229 03-02)

Avail: CASI HC A03/MF A03

This status paper reviews the experimental ground test program of the High Alpha Technology Program (HATP). The reasons for conducting this ground test program had their origins during the 1970's when several difficulties were experienced during the development programs of both the F-18 and F-16. A careful assessment of ground test to flight correlations appeared to be important for reestablishing a high degree of confidence in our ground test methodology. The current paper will then focus on one aspect of the HATP program that is intended to improve the correlation between ground test and flight, high-alpha gritting. The importance of this work arises from the sensitivity of configurations with smooth-sided forebodies to Reynolds number. After giving examples of the effects of Reynolds number, the paper will highlight efforts at forebody gritting. Finally, the paper will conclude by summarizing the charter of the HATP Experimental Aerodynamics Working Group and future experimental testing plans. Author

N95-14231*# National Aeronautics and Space Administration. Hugh L. Dryden Flight Research Center, Edwards, CA.

FLIGHT AND FULL-SCALE WIND-TUNNEL COMPARISON OF PRESSURE DISTRIBUTIONS FROM AN F-18 AIRCRAFT AT HIGH ANGLES OF ATTACK

David F. Fisher and Wendy R. Lanser *In its* Fourth High Alpha Conference, Volume 1 20 p(SEE N95-14229 03-02) Jul. 1994 (For primary document see N95-14229 03-02)

Avail: CASI HC A03/MF A03

Pressure distributions were obtained at nearly identical fuselage stations and wing chord butt lines in flight on the F-18 HARV at NASA Dryden Flight Research Center and in the NASA Ames Research Center's 80 by 120 ft wind tunnel on a full-scale F/A-18 aircraft. The static pressures were measured at the identical five stations on the forebody, three stations on the left and right leading-edge extensions, and three spanwise stations on the wing. Comparisons of the flight and wind-tunnel pressure distributions were made at alpha = 30 deg, 45 deg, and 60 deg/59 deg. In general, very good agreement was found. Minor differences were noted at the forebody at alpha = 45 deg and 60 deg in the magnitude of the vortex footprints and a Mach number effect was noted at the leading-edge extension at alpha = 30 deg. The inboard leading edge flap data from the wind tunnel at alpha = 59 deg showed a suction peak that did not appear in the flight data. This was the result of a vortex from the corner of the leading edge flap whose path was altered by the lack of an engine simulation in the wind tunnel. Author

N95-14232*# National Aeronautics and Space Administration. Ames Research Center, Moffett Field, CA.

NUMERICAL SIMULATION OF THE FLOW ABOUT AN F-18 AIRCRAFT IN THE HIGH-ALPHA REGIME

Scott M. Murman (MCAT Inst., Moffett Field, CA.) and Yehia M. Rizk *In* NASA. Dryden Flight Research Center, Fourth High Alpha Conference, Volume 1 Jul. 1994 33 p (For primary document see N95-14229 03-02)

Avail: CASI HC A03/MF A03

The current research is aimed at developing and extending numerical methods to accurately predict the high Reynolds number flow about the NASA F-18 HARV at large angles of attack. The resulting codes are validated by comparison of the numerical results with in-flight aerodynamic measurements and flow visualization obtained on the HARV. Further, computations have been used to provide an analysis and numerical optimization of a pneumatic slot blowing concept, and a mechanical strake concept, for use as potential forebody flow control devices in improving high-alpha maneuverability. Author

N95-14233*# Analytical Services and Materials, Inc., Hampton, VA.

HYBRID STRUCTURED/UNSTRUCTURED GRID COMPUTATIONS FOR THE F/A-18 AT HIGH ANGLE OF ATTACK

Robert T. Biedron and David L. Whitaker *In* NASA. Dryden Flight Research Center, Fourth High Alpha Conference, Volume 1 Jul. 1994 17 p (For primary document see N95-14229 03-02)

Avail: CASI HC A03/MF A03

At high angles of attack, vortical flows play a crucial role in the maintenance of lift for fighter aircraft. However, under certain conditions, the vortical flow can have an adverse effect on the aircraft. On the F/A-18 the LEX vortex can impinge on the tail; at high angles of attack the unsteady flow from vortex bursting can cause structural fatigue on the vertical tails. At high angles of attack, the flow field can be quite complex, and a computational analysis challenging. A full configuration analysis with viscous structured grids can be computationally expensive and the task of generating the requisite grids can be quite difficult. To mitigate these difficulties and provide a medium-fidelity analysis tool, a hybrid structured/unstructured approach was adopted for this work. In this analysis, the formation and roll-up of the LEX vortex is computed with a structured Navier-Stokes solver, and the resulting vortex propagated downstream with an unstructured Euler solver. Author

N95-14234*# National Aeronautics and Space Administration. Langley Research Center, Hampton, VA.

COMPARISON OF X-31 FLIGHT, WIND-TUNNEL, AND WATER-TUNNEL YAWING MOMENT ASYMMETRIES AT HIGH ANGLES OF ATTACK

Brent R. Cobleigh (Planning Research Corp., Edwards, CA.), Mark A. Croom, and B. F. Tamrat *In* NASA. Dryden Flight Research Center, Fourth High Alpha Conference, Volume 1 Jul. 1994 p 21 (For primary document see N95-14229 03-02)

Avail: CASI HC A03/MF A03

The X-31 aircraft are being used in the enhanced fighter maneuverability (EFM) research program, which is jointly funded by the (U.S.) Advanced Research Projects Agency (ARPA) and Germany's Federal Ministry of Defense (FMOD). The flight test portion of the program, which involves two aircraft, is being conducted by an International Test Organization (ITO) comprising the National Aeronautics and Space Administration (NASA), the U.S. Navy, the U.S. Air Force, Rockwell International, and Deutsche Aerospace (DASA). The goals of the flight program are to demonstrate EFM technologies, investigate close-in-combat exchange ratios, develop design requirements, build a database for application to future fighter aircraft, and develop and validate low-cost prototype concepts. For longitudinal control the X-31 uses canards, symmetrical movement of the trailing-edge flaps, and pitch deflection of the thrust vectoring system. The trim, inertial coupling, and engine gyroscopic coupling compensation tasks are performed primarily by the trailing-edge flaps. For lateral-directional control the aircraft uses differential deflection of the trailing-edge flaps for roll coordination and a conventional rudder combined with the thrust vectoring system to provide yaw control. The rudder is only effective up to about 40 deg angle of attack (alpha), after which the thrust vectoring becomes the primary yaw control effector. Both the leading-edge flaps and the inlet lip are scheduled with the angle of attack to provide best performance. Author

N95-14235*# Deutsche Forschungs- und Versuchsanstalt fuer Luft- und Raumfahrt, Brunswick (Germany). Inst. of Flight Mechanics.

PARAMETER IDENTIFICATION FOR X-31A AT HIGH ANGLES OF ATTACK

S. Weiss, D. Rohlf, and Ermin Plaetschke *In* NASA. Dryden Flight Research Center, Fourth High Alpha Conference, Volume 1 Jul. 1994 12 p (For primary document see N95-14229 03-02)

Avail: CASI HC A03/MF A03

The U.S./German experimental aircraft X-31A was designed and constructed to demonstrate enhanced fighter maneuverability. Post-stall maneuvering is enabled by applying new technologies such as high angle of attack aerodynamics and flight control system integrated thrust vectoring. Two demonstrator aircraft have been built by the main contractors, Rockwell International and Deutsche Aerospace (formerly MBB). Flight testing started in October 1990 and before the end of 1992 both aircraft had accomplished a significant number of flights covering the entire AoA regime from about -5 to 70 deg. Throughout the envelope expansion, DLR Institute of Flight Mechanics conducted parameter identification (PID) to determine the aerodynamic parameters of the aircraft from flight test data and to compare the results to the predictions from the aerodynamic dataset (ADS). The application of system identification to high AoA / post-stall flight data raises some major problems, which are discussed in this paper. Results from both longitudinal and lateral-directional motion will be presented. Author

N95-14236*# Bihrle Applied Research, Inc., Jericho, NY.

VALIDATION OF THE NASA DRYDEN X-31 SIMULATION AND EVALUATION OF MECHANIZATION TECHNIQUES

Edward Dickes, Jacob Kay, and John Ralston *In* NASA. Dryden Flight Research Center, Fourth High Alpha Conference, Volume 1 Jul. 1994 23 p (For primary document see N95-14229 03-02)

Avail: CASI HC A03/MF A03

This paper shall discuss the evaluation of the original Dryden X-31 aerodynamic math model, processes involved in the justification and creation of the modified data base, and comparison time history results of the model response with flight test. Author

N95-14237*# National Aeronautics and Space Administration. Ames Research Center, Moffett Field, CA.

FREE-TO-ROLL TESTS OF X-31 AND F-18 SUBSCALE MODELS WITH CORRELATION TO FLIGHT TEST RESULTS

David L. Williams, II (Notre Dame Univ., IN.), Robert C. Nelson (Notre Dame Univ., IN.), and David F. Fisher *In* NASA. Dryden Flight Research Center, Fourth High Alpha Conference, Volume 1 Jul. 1994 28 p (For primary document see N95-14229 03-02)

Avail: CASI HC A03/MF A03

This presentation will concentrate on a series of low-speed wind tunnel tests conducted on a 2.5 percent subscale F-18 model and a 2 percent subscale X-31 model. The model's control surfaces were unaugmented; and for the most part, were deflected at a constant angle throughout the tests. The tests consisted mostly of free-to-roll experiments conducted with the use of an air-bearing, surface pressure measurements, off-surface flow visualization, and force-balance tests. Where possible the results of the subscale tests have been compared to flight test data, or to other wind tunnel data taken at higher Reynolds numbers. Author

N95-14238*# Eidetics Aircraft, Inc., Torrance, CA.
STATIC AND DYNAMIC FORCE/MOMENT MEASUREMENTS IN THE EIDETICS WATER TUNNEL
Carlos J. Suarez and Gerald N. Malcolm *In* NASA. Dryden Flight Research Center, Fourth High Alpha Conference, Volume 1 Jul. 1994 24 p (For primary document see N95-14229 03-02)
(Contract NAS2-13571)
Avail: CASI HC A03/MF A03

Water tunnels have been utilized in one form or another to explore fluid mechanics and aerodynamics phenomena since the days of Leonardo da Vinci. Water tunnel testing is attractive because of the relatively low cost and quick turn-around time to perform flow visualization experiments and evaluate the results. The principal limitation of a water tunnel is that the low flow speed, which provides for detailed visualization, also results in very small hydrodynamic (aerodynamic) forces on the model, which, in the past, have proven to be difficult to measure accurately. However, the advent of semi-conductor strain gage technology and devices associated with data acquisition such as low-noise amplifiers, electronic filters, and digital recording have made accurate measurements of very low strain levels feasible. The principal objective of this research effort was to develop a multi-component strain gage balance to measure forces and moments on models tested in flow visualization water tunnels. A balance was designed that allows measuring normal and side forces, and pitching, yawing and rolling moments (no axial force). The balance mounts internally in the model and is used in a manner typical of wind tunnel balances. The key differences between a water tunnel balance and a wind tunnel balance are the requirement for very high sensitivity since the loads are very low (typical normal force is 0.2 lbs), the need for water proofing the gage elements, and the small size required to fit into typical water tunnel models. Author

N95-14239*# National Aeronautics and Space Administration. Hugh L. Dryden Flight Research Center, Edwards, CA.
FOURTH HIGH ALPHA CONFERENCE, VOLUME 2
Jul. 1994 235 p Conference held at Edwards, CA, 12-14 Jul. 1994
(RTOP-505-68-30)
(NASA-CP-10143-Vol-2; H-2007-Vol-2; NAS 1.55:10143-Vol-2) Avail: CASI HC A11/MF A03

The goal of the Fourth High Alpha Conference, held at the NASA Dryden Flight Research Center on July 12-14, 1994, was to focus on the flight validation of high angle of attack technologies and provide an in-depth review of the latest high angle of attack activities. Areas that were covered include high angle of attack aerodynamics, propulsion and inlet dynamics, thrust vectoring, control laws and handling qualities, and tactical utility. For individual titles, see N95-14240 through N95-14250.

N95-14240*# National Aeronautics and Space Administration. Hugh L. Dryden Flight Research Center, Edwards, CA.
F-18 HIGH ALPHA RESEARCH VEHICLE: LESSONS LEARNED
Albion H. Bowers, Victoria A. Regenie, and Bradley C. Flick *In its* Fourth High Alpha Conference, Volume 2 15 p(SEE N95-14239 03-02) Jul. 1994 (For primary document see N95-14239 03-02)
Avail: CASI HC A03/MF A03

The F-18 High Alpha Research Vehicle has proven to be a useful research tool with many unique capabilities. Many of these capabilities are to assist in characterizing flight at high angles of attack, while some provide significant research in their own right. Of these, the thrust vectoring system, the unique ability to rapidly reprogram flight controls, the reprogrammable mission computer, and a reprogrammable onboard excitation system have allowed an increased utility and versatility of the research being conducted. Because of this multifaceted approach to research in the high angle of attack regime, the capabilities of the F-18 High Alpha Research Vehicle were designed to cover as many high alpha technology bases as the program would allow. These areas include aerodynamics, controls, handling qualities, and propulsion. Derived from text

N95-14241*# National Aeronautics and Space Administration. Hugh L. Dryden Flight Research Center, Edwards, CA.
DESIGN AND DEVELOPMENT OF AN F/A-18 INLET DISTORTION RAKE: A COST AND TIME SAVING SOLUTION
Andrew J. Yuhas, Ronald J. Ray, Richard R. Burley, William G. Steenken, Leon Lechtenberg, and Don Thornton *In its* Fourth High Alpha Conference, Volume 2 17 p(SEE N95-14239 03-02) Jul. 1994 (For primary document see N95-14239 03-02)
Avail: CASI HC A03/MF A03

An innovative inlet total-pressure distortion measurement rake has been designed and developed for the F/A-18 A/B/C/D aircraft inlet. The design was conceived by NASA and General Electric Aircraft Engines (Evendale, Ohio). This rake has been flight qualified and flown in the F-18 High Alpha Research Vehicle (HARV) at NASA Dryden Flight Research Center. The rake's eight-legged, one-piece wagon wheel design was developed at a reduced cost and offers reduced installation time compared with traditional designs. The rake features 40 dual measurement ports for both low- and high-frequency pressure measurements with the high-frequency transducer mounted at the port. The high-frequency transducer offers direct absolute pressure measurements from low frequency to the highest frequency of interest, thereby allowing the rake to be used during highly dynamic aircraft maneuvers. Outstanding structural characteristics are inherent to the design through its construction and use of lightweight materials.
Derived from text

N95-14242*# Naval Air Warfare Center, Patuxent River, MD. Aircraft Div.
X-31 POST-STALL ENVELOPE EXPANSION AND TACTICAL UTILITY TESTING
Dave Canter *In* NASA. Dryden Flight Research Center, Fourth High Alpha Conference, Volume 2 Jul. 1994 19 p (For primary document see N95-14239 03-02)
Avail: CASI HC A03/MF A03

Technical and nontechnical lessons learned from the X-31 aircraft program are described in this viewgraph presentation. The tactical utility of high angle of attack flight and thrust vector control is discussed. CASI

N95-14243*# Deutsche Aerospace A.G., Munich (Germany).
X-31 QUASI-TAILLESS FLIGHT DEMONSTRATION
Peter Huber and Harvey G. Schellenger *In* NASA. Dryden Flight Research Center, Fourth High Alpha Conference, Volume 2 Jul. 1994 14 p (For primary document see N95-14239 03-02)
Avail: CASI HC A03/MF A03

The primary objective of the quasi-tailless flight demonstration is to demonstrate the feasibility of using thrust vectoring for directional control of an unstable aircraft. By using this low-cost, low-risk approach it is possible to get information about required thrust vector control power and deflection rates from an inflight experiment as well as insight in low-power thrust vectoring issues. The quasi-tailless flight demonstration series with the X-31 began in March 1994. The demonstration flight condition was Mach 1.2 at 37,500 feet. A series of basic flying quality maneuvers, doublets, bank to bank rolls, and wind-up-turns have been performed with a simulated 100% vertical tail reduction. Flight test and supporting simulation demonstrated that the quasi-tailless approach is effective in representing the reduced stability of tailless configurations. The flights also demonstrated that thrust vectoring could be effectively used to stabilize a directionally unstable configuration and provide control power for maneuver coordination. Derived from text

N95-14244*# National Aeronautics and Space Administration. Hugh L. Dryden Flight Research Center, Edwards, CA.
X-31 HIGH ANGLE OF ATTACK CONTROL SYSTEM PERFORMANCE
Peter Huber (Deutsche Aerospace A.G., Munich, Germany.) and Patricia Seamount *In its* Fourth High Alpha Conference, Volume 2 19 p(SEE N95-14239 03-02) Jul. 1994 (For primary document see N95-14239 03-02)
Avail: CASI HC A03/MF A03

The design goals for the X-31 flight control system were: (1) level 1

handling qualities during post-stall maneuvering (30 to 70 degrees angle-of-attack); (2) thrust vectoring to enhance performance across the flight envelope; and (3) adequate pitch-down authority at high angle-of-attack. Additional performance goals are discussed. A description of the flight control system is presented, highlighting flight control system features in the pitch and roll axes and X-31 thrust vectoring characteristics. The high angle-of-attack envelope clearance approach will be described, including a brief explanation of analysis techniques and tools. Also, problems encountered during envelope expansion will be discussed. This presentation emphasizes control system solutions to problems encountered in envelope expansion. An essentially 'care free' envelope was cleared for the close-in-combat demonstrator phase. High angle-of-attack flying qualities maneuvers are currently being flown and evaluated. These results are compared with pilot opinions expressed during the close-in-combat program and with results obtained from the F-18 HARV for identical maneuvers. The status and preliminary results of these tests are discussed.

Derived from text

N95-14245*# Lockheed Corp., Fort Worth, TX.

FLIGHT TEST RESULTS OF THE F-16 AIRCRAFT MODIFIED WITH THE AXISYMMETRIC VECTORING EXHAUST NOZZLE

Paul D. Anna and David S. Kidman *In* NASA. Dryden Flight Research Center, Fourth High Alpha Conference, Volume 2 Jul. 1994 15 p (For primary document see N95-14239 03-02)

Avail: CASI HC A03/MF A03

The results of the envelope expansion phase of the F-16 Multi-Axis Thrust Vectoring (MATV) program are presented in viewgraph format. The objectives and test approach are presented followed by results of testing with the initial control law configuration. The revised flight control laws are discussed followed by test results with the revised control laws. Additional testing added to the program, nose chines, parameter identification maneuvers, and the extended range angle of attack cones are briefly discussed.

Derived from text

N95-14246*# National Aeronautics and Space Administration. Langley Research Center, Hampton, VA.

FLIGHT VALIDATION OF GROUND-BASED ASSESSMENT FOR CONTROL POWER REQUIREMENTS AT HIGH ANGLES OF ATTACK

Marilyn E. Ogburn, Holly M. Ross, John V. Foster, Joseph W. Pahle, Charles A. Sternberg, Ricardo Traven, James B. Lackey, and Troy D. Abbott *In* NASA. Dryden Flight Research Center, Fourth High Alpha Conference, Volume 2 Jul. 1994 20 p (For primary document see N95-14239 03-02)

Avail: CASI HC A03/MF A03

A review is presented in viewgraph format of an ongoing NASA/U.S. Navy study to determine control power requirements at high angles of attack for the next generation high-performance aircraft. This paper focuses on recent flight test activities using the NASA High Alpha Research Vehicle (HARV), which are intended to validate results of previous ground-based simulation studies. The purpose of this study is discussed, and the overall program structure, approach, and objectives are described. Results from two areas of investigation are presented: (1) nose-down control power requirements and (2) lateral-directional control power requirements. Selected results which illustrate issues and challenges that are being addressed in the study are discussed including test methodology, comparisons between simulation and flight, and general lessons learned. Derived from text

N95-14247*# National Aeronautics and Space Administration. Langley Research Center, Hampton, VA.

HIGH ANGLE OF ATTACK FLYING QUALITIES CRITERIA FOR LONGITUDINAL RATE COMMAND SYSTEMS

David J. Wilson (McDonnell-Douglas Aerospace, Saint Louis, MO.), Kevin D. Citurs (McDonnell-Douglas Aerospace, Saint Louis, MO.), and John B. Davidson *In* NASA. Dryden Flight Research Center, Fourth High Alpha Conference, Volume 2 Jul. 1994 14 p (For primary document see N95-14239 03-02)

Avail: CASI HC A03/MF A03

This study was designed to investigate flying qualities requirements of alternate pitch command systems for fighter aircraft at high angle of attack. Flying qualities design guidelines have already been developed for angle of attack command systems at 30, 45, and 60 degrees angle of attack, so this research fills a similar need for rate command systems. Flying qualities tasks that require post-stall maneuvering were tested during piloted simulations in the McDonnell Douglas Aerospace Manned Air Combat Simulation facility. A generic fighter aircraft model was used to test angle of attack rate and pitch rate command systems for longitudinal gross acquisition and tracking tasks at high angle of attack. A wide range of longitudinal dynamic variations were tested at 30, 45, and 60 degrees angle of attack. Pilot comments, Cooper-Harper ratings, and pilot induced oscillation ratings were taken from five pilots from NASA, USN, CAF, and McDonnell Douglas Aerospace. This data was used to form longitudinal design guidelines for rate command systems at high angle of attack. These criteria provide control law design guidance for fighter aircraft at high angle of attack, low speed flight conditions. Additional time history analyses were conducted using the longitudinal gross acquisition data to look at potential agility measures of merit and correlate agility usage to flying qualities boundaries. This paper presents an overview of this research.

Author (revised)

N95-14248*# Lockheed Corp., Fort Worth, TX.

VISTA/F-16 MULTI-AXIS THRUST VECTORING (MATV) CONTROL LAW DESIGN AND EVALUATION

W. D. Zwerneman and B. G. Eller *In* NASA. Dryden Flight Research Center, Fourth High Alpha Conference, Volume 2 Jul. 1994 19 p (For primary document see N95-14239 03-02)

Avail: CASI HC A03/MF A03

For the Multi-Axis Thrust Vectoring (MATV) program, a new control law was developed using multi-axis thrust vectoring to augment the aircraft's aerodynamic control power to provide maneuverability above the normal F-16 angle of attack limit. The control law architecture was developed using Lockheed Fort Worth's offline and piloted simulation capabilities. The final flight control laws were used in flight test to demonstrate tactical benefits gained by using thrust vectoring in air-to-air combat. Differences between the simulator aerodynamics data base and the actual aircraft aerodynamics led to significantly different lateral-directional flying qualities during the flight test program than those identified during piloted simulation. A 'dial-a-gain' flight test control law update was performed in the middle of the flight test program. This approach allowed for inflight optimization of the aircraft's flying qualities. While this approach is not preferred over updating the simulator aerodynamic data base and then updating the control laws, the final selected gain set did provide adequate lateral-directional flying qualities over the MATV flight envelope. The resulting handling qualities and the departure resistance of the aircraft allowed the 422nd—squadron pilots to focus entirely on evaluating the aircraft's tactical utility.

Derived from text

N95-14249*# National Aeronautics and Space Administration. Hugh L. Dryden Flight Research Center, Edwards, CA.

MULTI-APPLICATION CONTROLS: ROBUST NONLINEAR MULTIVARIABLE AEROSPACE CONTROLS APPLICATIONS

Dale F. Enns (Honeywell, Inc., Minneapolis, MN.), Daniel J. Bugajski (Honeywell, Inc., Minneapolis, MN.), John Carter, and Bob Antoniewicz *In its* Fourth High Alpha Conference, Volume 2 26 p(SEE N95-14239 03-02) Jul. 1994 (For primary document see N95-14239 03-02)

Avail: CASI HC A03/MF A03

This viewgraph presentation describes the general methodology used to apply Honywell's Multi-Application Control (MACH) and the specific application to the F-18 High Angle-of-Attack Research Vehicle (HARV) including piloted simulation handling qualities evaluation. The general steps include insertion of modeling data for geometry and mass properties, aerodynamics, propulsion data and assumptions, requirements and specifications, e.g. definition of control variables, handling qualities, stability margins and statements for bandwidth, control power, priorities, position and rate limits. The specific steps include choice of independent variables for least squares fits to aerodynamic and propulsion data, modifications to the management of the controls with regard to integrator windup and actuation limiting and priorities, e.g. pitch priority over roll, and command limiting to prevent departures and/or undesirable inertial coupling or inability to recover to a stable trim condition. The HARV control problem is characterized by significant nonlinearities and multivariable interactions in the low speed, high angle-of-attack, high angular rate flight regime. Systematic approaches to the control of vehicle motions modeled with coupled nonlinear equations of motion have been developed. This paper will discuss the dynamic inversion approach which explicity accounts for

nonlinearities in the control design. Multiple control effectors (including aerodynamic control surfaces and thrust vectoring control) and sensors are used to control the motions of the vehicles in several degrees-of-freedom. Several maneuvers will be used to illustrate performance of MACH in the high angle-of-attack flight regime. Analytical methods for assessing the robust performance of the multivariable control system in the presence of math modeling uncertainty, disturbances, and commands have reached a high level of maturity. The structured singular value (mu) frequency response methodology is presented as a method for analyzing robust performance and the mu-synthesis method will be presented as a method for synthesizing a robust control system. The paper concludes with the author's expectations regarding future applications of robust nonlinear multivariable controls.

Author (revised)

N95-14250*# Eidetics Aircraft, Inc., Torrance, CA.

COMBAT AGILITY MANAGEMENT SYSTEM (CAMS)

Andrew Skow and William Porada *In* NASA. Dryden Flight Research Center, Fourth High Alpha Conference, Volume 2 Jul. 1994 19 p (For primary document see N95-14239 03-02)

Avail: CASI HC A03/MF A03

The proper management of energy becomes a complex task in fighter aircraft which have high angle of attack (AOA) capability. Maneuvers at high AOA are accompanied by high bleed rates (velocity decrease), a characteristic that is usually undesirable in a typical combat arena. Eidetics has developed under NASA SBIR Phase 1 and NAVAIR SBIR Phase 2 contracts a system which allows a pilot to more easily and effectively manage the trade-off of energy (airspeed or altitude) for turn rate while not imposing hard limits on the high AOA nose pointing capability that can be so important in certain air combat maneuver situations. This has been accomplished by incorporating a two-stage angle of attack limiter into the flight control laws. The first stage sets a limit on AOA to achieve a limit on the maximum bleed rate (selectable) by limiting AOA to values which are dependent on the aircraft attitude and dynamic pressure (or flight path, velocity, and altitude). The second stage sets an AOA limit near the AOA for C(sub l max). One of the principal benefits of such a system is that it enables a low-experience pilot to become much more proficient at managing his energy. The Phase 2 simulation work is complete, and an exploratory flight test on the F-18 HARV is planned for the Fall of 1994 to demonstrate/validate the concept. Derived from text

N95-14251*# National Aeronautics and Space Administration. Hugh L. Dryden Flight Research Center, Edwards, CA.

FOURTH HIGH ALPHA CONFERENCE, VOLUME 3

Jul. 1994 191 p Conference held at Edwards, CA, 12-14 Jul. 1994 (RTOP-505-68-30)

(NASA-CP-10143-Vol-3; H-2007-Vol-3; NAS 1.55:10143-Vol-3) Avail: CASI HC A09/MF A02

Thie goal of this conference was to focus on the flight validation of high-angle-of-attack technologies and provide an in-depth review of the latest high-angle-of-attack activities. Areas covered include: (1) high-angle-of-attack aerodynamics; (2) propulsion and inlet dynamics; (3) thrust vectoring; (4) control laws and handling qualities; (5) tactical utility; and (6) forebody controls. For individual titles, see N95-14252 through N95-14259.

N95-14252*# Naval Air Warfare Center, Patuxent River, MD.

NAVY AND THE HARV: HIGH ANGLE OF ATTACK TACTICAL UTILITY ISSUES

Charles A. Sternberg, Ricardo Traven, and James B. Lackey *In* NASA. Dryden Flight Research Center, Fourth High Alpha Conference, Volume 3 Jul. 1994 19 p (For primary document see N95-14251 03-02)

Avail: CASI HC A03/MF A02

This presentation will highlight results from the latest Navy evaluation of the HARV (March 1994) and focus primarily on the impressions from a piloting standpoint of the tactical utility of thrust vectoring. Issue to be addressed will be mission suitability of high AOA flight, visual and motion feedback cues associated with operating at high AOA, and the adaptability of a pilot to effectively use the increased control power provided by the thrust vectoring system. Derived from text

N95-14253*# National Aeronautics and Space Administration. Ames Research Center, Moffett Field, CA.

COMPUTATIONAL ANALYSIS OF FOREBODY TANGENTIAL SLOT BLOWING

Ken Gee (MCAT Inst., Moffett Field, CA.), Roxana M. Agosta-Greenman, Yehia M. Rizk, Lewis B. Schiff, and Russell M. Cummings *In* NASA. Dryden Flight Research Center, Fourth High Alpha Conference, Volume 3 Jul. 1994 22 p (For primary document see N95-14251 03-02)

Avail: CASI HC A03/MF A02

An overview of the computational effort to analyze forebody tangential slot blowing is presented. Tangential slot blowing generates side force and yawing moment which may be used to control an aircraft flying at high-angle-of-attack. Two different geometries are used in the analysis: (1) The High Alpha Research Vehicle; and (2) a generic chined forebody. Computations using the isolated F/A-18 forebody are obtained at full-scale wind tunnel test conditions for direct comparison with available experimental data. The effects of over- and under-blowing on force and moment production are analyzed. Time-accurate solutions using the isolated forebody are obtained to study the force onset timelag of tangential slot blowing. Computations using the generic chined forebody are obtained at experimental wind tunnel conditions, and the results compared with available experimental data. This computational analysis compliments the experimental results and provides a detailed understanding of the effects of tangential slot blowing on the flow field about simple and complex geometries.

Derived from text

N95-14254*# Eidetics Aircraft, Inc., Torrance, CA.

F/A-18 AND F-16 FOREBODY VORTEX CONTROL, STATIC AND ROTARY-BALANCE RESULTS

Brian Kramer and Brooke Smith *In* NASA. Dryden Flight Research Center, Fourth High Alpha Conference, Volume 3 Jul. 1994 22 p (For primary document see N95-14251 03-02)

Avail: CASI HC A03/MF A02

The results from research on forebody vortex control on both the F/A-18 and the F-16 aircraft will be shown. Several methods of forebody vortex control, including mechanical and pneumatic schemes, will be discussed. The wind tunnel data includes both static and rotary balance data for forebody vortex control. Time lags between activation or deactivation of the pneumatic control and when the aircraft experiences the resultant forces are also discussed. The static (non-rotating) forces and pressures are then compared to similar configurations tested in the NASA Langley and DTRC Wind Tunnel, the NASA Ames 80'x120' Wind Tunnel, and in flight on the High Angle of Attack Research Vehicle (HARV).

Derived from text

N95-14255*# National Aeronautics and Space Administration. Ames Research Center, Moffett Field, CA.

COMPARISON OF FULL-SCALE, SMALL-SCALE, AND CFD RESULTS FOR F/A-18 FOREBODY SLOT BLOWING

Wendy R. Lanser, Larry A. Meyn, and Kevin D. James *In* NASA. Dryden Flight Research Center, Fourth High Alpha Conference, Volume 3 Jul. 1994 19 p (For primary document see N95-14251 03-02)

Avail: CASI HC A03/MF A02

It has been shown experimentally that forebody flow control devices provide a significant increase in yaw control for fighter aircraft at high angle-of-attack. This study presents comparisons of the various experimental and computational results for tangential slot blowing on the F/A-18 configuration. Experimental results are from the full-scale and 6 percent-scale model test and computational solutions are from both isolated forebody and and full aircraft configurations. The emphasis is on identifying trends in the variation of yawing moment with blowing-slot exit conditions. None of the traditional parameters (mass flow ratio, blowing momentum coefficient, velocity ratio) succeeded in collapsing all of the results into a common curve. Several factors may effect the agreement between the 6 percent- and full-scale results including Reynolds number effects, sensitivity of boundary layer transition from laminar to turbulent flow, and poor geometric fidelity, particularly of the blowing slot. The disagreement between the full-scale and computed yawing moments may be due to a mismatch in the slot exit conditions for the same mass flow ratio or aircraft configuration modeling. The general behavior of slot blowing on the 6 percent-scale and computational models is correct, but neither matches the full-scale results.

Author

N95-14256*# McDonnell-Douglas Research Labs., Saint Louis, MO.
LOW-ENERGY PNEUMATIC CONTROL OF FOREBODY VORTICES
Frederick W. Roos *In* NASA. Dryden Flight Research Center, Fourth High Alpha Conference, Volume 3 Jul. 1994 16 p (For primary document see N95-14251 03-02)
Avail: CASI HC A03/MF A02

This research will be exploring the prospect of employing bluntness, known to suppress the tendency toward asymmetry on slender forebodies, jointly with pneumatic manipulation as a system of forebody asymmetry control. The influences of jet location and direction, blowing rate, relative noise bluntness, angle of attack, and state of flow separation feeding the vortices (laminar vs. turbulent) will be evaluated. Derived from text

N95-14257*# National Aeronautics and Space Administration. Langley Research Center, Hampton, VA.
PREPARATIONS FOR FLIGHT RESEARCH TO EVALUATE ACTUATED FOREBODY STRAKES ON THE F-18 HIGH-ALPHA RESEARCH VEHICLE
Daniel G. Murri, Gautam H. Shah, and Daniel J. DiCarlo *In* NASA. Dryden Flight Research Center, Fourth High Alpha Conference, Volume 3 Jul. 1994 20 p (For primary document see N95-14251 03-02)
Avail: CASI HC A03/MF A02

As part of the NASA High-Angle-of-Attack Technology Program (HATP), flight tests are currently being conducted with a multi-axis thrust vectoring system applied to the NASA F-18 High Alpha Research Vehicle (HARV). A follow-on series of flight tests with the NASA F-18 HARV will be focusing on the application of actuated forebody strake controls. These controls are designed to provide increased levels of yaw control at high angles of attack where conventional aerodynamic controls become ineffective. The series of flight tests are collectively referred to as the Actuated Nose Strakes for Enhanced Rolling (ANSER) Flight Experiment. The development of actuated forebody strake controls for the F-18 HARV is discussed and a summary of the ground tests conducted in support of the flight experiment is provided. A summary of the preparations for the flight tests is also provided. Derived from text

N95-14258*# McDonnell-Douglas Corp., Saint Louis, MO.
INTEGRATION OF A MECHANICAL FOREBODY VORTEX CONTROL SYSTEM INTO THE F-15
Richard E. Boalbey, Kevin D. Citurs, Wayne L. Ely, Stephen P. Harbaugh, William B. Hollingsworth, and Ronald L. Phillips *In* NASA. Dryden Flight Research Center, Fourth High Alpha Conference, Volume 3 Jul. 1994 20 p (For primary document see N95-14251 03-02)
Avail: CASI HC A03/MF A02

The goal of the F-15 Forebody Vortex Control (FVC) program is to develop a production FVC system for the F-15. The system may consist of either a mechanically actuated device such as the strakes developed for the HARV program, or a pneumatic device such as the port blowing system being tested on the X-29. Both types of systems are being evaluated under this program. Background information on the F-15 and a description and overview of forebody vortex controls (FVC) will be presented.
Derived from text

N95-14259*# Wright Lab., Wright-Patterson AFB, OH.
FLIGHT EVALUATION OF PNEUMATIC FOREBODY VORTEX CONTROL IN POST-STALL FLIGHT
Lawrence A. Walchli *In* NASA. Dryden Flight Research Center, Fourth High Alpha Conference, Volume 3 Jul. 1994 24 p (For primary document see N95-14251 03-02)
Avail: CASI HC A03/MF A02

The following topics are discussed: (1) X-29 description; Vortex Flow Control (VFC) technology description; (3) X-29 VFC wind tunnel results (forebody only); (4) X-29 VFC wind tunnel results (full configuration yawing moment); (5) X-29 VFC wind tunnel results (full configuration C(sub n) with sideslip); (6) X-29VFC wind tunnel results (full configuration pitching moment); (7) VFC optimized nozzle details; (8) X-29 forebody nozzle configuration; (9) X-29 VFC system stored gas schematic; (10) X-29 VFC system stored gas installation; (11) VFC effectiveness at zero sideslip; (12) VFC effectiveness at 35 AOA with sideslip; (13) 'VFC Roll' at 40 AOA; (14) Effects of VFC on wing rock; (15) Integrated controls C(sub n) prediction; (16) Proposed F-15 with lateral control laws with active VFC; (17) Simulated F-15 roll performance with active VFC; (18) Simulated F-15 spin recovery with active VFC; (19) Test team restructuring; (20) testbed selection; (21) Simulation for risk reduction; (22) Benefits of high pressure system; and (23) Advanced weapon system integration. Derived from text

N95-14264# Advisory Group for Aerospace Research and Development, Neuilly-Sur-Seine (France). Fluid Dynamics Panel.
COMPUTATIONAL AERODYNAMICS BASED ON THE EULER EQUATIONS [L'AERODYNAMIQUE NUMERIQUE A PARTIR DES EQUATIONS D'EULER]
J. W. Slooff, ed. (National Aerospace Lab., Amsterdam, Netherlands.) and W. Schmidt, ed. (Deutsche Aerospace A.G., Munich, Germany.) Sep. 1994 250 p Original contains color illustrations
(AGARD-AG-325; ISBN-92-836-1005-9) Copyright Avail: CASI HC A11/MF A03

A survey of the state of the art of Computational Aerodynamics based on the Euler Equations is presented. For the major Euler Codes that are currently in use in the NATO countries, numerical schemes, algorithms, grid generation, physical and numerical aspects, as well as a wide range of applications are included. Background material required for understanding the physics modelled by the Euler Equations is also presented. Areas of application concentrate on numerical simulation of external flows about aerospace vehicles. Internal flows and turbomachinery applications are not extensively treated but touched upon where considered appropriate.
Author

N95-14297*# National Aeronautics and Space Administration. Lewis Research Center, Cleveland, OH.
A CARTESIAN, CELL-BASED APPROACH FOR ADAPTIVELY-REFINED SOLUTIONS OF THE EULER AND NAVIER-STOKES EQUATIONS
William J. Coirier and Kenneth G. Powell Nov. 1994 16 p Presented at the 33rd Aerospace Sciences Meeting and Exhibit, Reno, NV, 9-12 Jan. 1995; sponsored by AIAA
(RTOP 505-62-52)
(NASA-TM-106786; E-9241; NAS 1.15:106786; AIAA Paper 95-0566)
Copyright Avail: CASI HC A03/MF A01

A Cartesian, cell-based approach for adaptively-refined solutions of the Euler and Navier-Stokes equations in two dimensions is developed and tested. Grids about geometrically complicated bodies are generated automatically, by recursive subdivision of a single Cartesian cell encompassing the entire flow domain. Where the resulting cells intersect bodies, N-sided 'cut' cells are created using polygon-clipping algorithms. The grid is stored in a binary-tree structure which provides a natural means of obtaining cell-to-cell connectivity and of carrying out solution-adaptive mesh refinement. The Euler and Navier-Stokes equations are solved on the resulting grids using a finite-volume formulation. The convective terms are upwinded: a gradient-limited, linear reconstruction of the primitive variables is performed, providing input states to an approximate Riemann solver for computing the fluxes between neighboring cells. The more robust of a series of viscous flux functions is used to provide the viscous fluxes at the cell interfaces. Adaptively-refined solutions of the Navier-Stokes equations using the Cartesian, cell-based approach are obtained and compared to theory, experiment, and other accepted computational results for a series of low and moderate Reynolds number flows. Author

N95-14418*# National Aeronautics and Space Administration. Lewis Research Center, Cleveland, OH.
AXIS SWITCHING AND SPREADING OF AN ASYMMETRIC JET: ROLE OF VORTICITY DYNAMICS
K. B. M. Q. Zaman Nov. 1994 18 p Presented at the 33rd Aerospace Sciences Meeting and Exhibit, Reno, NV, 9-12 Jan. 1995; sponsored by AIAA
(RTOP 505-62-52)
(NASA-TM-106385; E-9230; NAS 1.15:106385; AIAA Paper 95-0889)
Copyright Avail: CASI HC A03/MF A01

The effects of vortex generators and periodic excitation on vorticity dynamics and the phenomenon of axis switching in a free asymmetric jet are studied experimentally. Most of the data reported are for a 3:1 rectangular jet at a Reynolds number of 450,000 and a Mach number of 0.31. The vortex generators are in the form of 'delta tabs', triangular shaped protrusions into the flow, placed at the nozzle exit. With suitable placement of the tabs, axis switching could be either stopped or augmented. Two mechanisms

are identified governing the phenomenon. One, as described by previous researchers and referred to here as the omega(sub theta)-induced dynamics, is due to difference in induced velocities for different segments of a rolled up azimuthal vortical structure. The other, omega(sub x)-induced dynamics, is due to the induced velocities of streamwise vortex pairs in the flow. Both dynamics can be active in a natural asymmetric jet; the tendency for axis switching caused by the omega(sub theta)-induced dynamics may be, depending on the streamwise vorticity distribution, either resisted or enhanced by the omega(sub x)-induced dynamics. While this simple framework qualitatively explains the various observations made on axis switching, mechanisms actually in play may be much more complex. The two dynamics are not independent as the flow field is replete with both azimuthal and streamwise vortical structures which continually interact. Phase averaged flow field data for a periodically forced case, over a volume of the flow field, are presented and discussed in an effort to gain insight into the dynamics of these vortical structures. Author

N95-14445# Advisory Group for Aerospace Research and Development, Neuilly-Sur-Seine (France). Fluid Dynamics Panel.

MISSILE AERODYNAMICS [L'AERODYNAMIQUE DES MISSILES]

Jun. 1994 341 p Special course held in Rhode-Saint-Genese, Belgium, 6-10 Jun. 1994 and in Ankara, Turkey, 13-17 Jun. 1994; sponsored by AGARD and VKI

(AGARD-R-804; ISBN-92-835-0752-5) Copyright Avail: CASI HC A15/MF A03

Lecture notes for the AGARD Fluid Dynamics Panel (FDP) Special Course on 'Missile Aerodynamics' have been assembled in this report. The aim and scope of this course was to present the current state of the art on specific topics of tactical missile aerodynamics. Specifically, topics and methods covered include: Aeromechanical Design of Modern Missiles, Semi-empirical Predictive Tools, Lateral Jet Control, High Angle of Attack Aerodynamics, Analysis and Modelling of Missile Infrared Radiation, Navier-Stokes Computations for Complete Missile Configurations, and Navier-Stokes and Euler Computations for Supersonic Air Intakes. The material assembled in this report was prepared under the combined sponsorship of the AGARD Fluid Dynamics Panel, the Consultant and Exchange Program of AGARD, and the von Karman Institute (VKI) for Fluid Dynamics. For individual titles, see N95-14446 through N95-14452.

N95-14446# Deutsche Aerospace A.G., Munich (Germany). Missile Systems Div.

AEROMECHANICAL DESIGN OF MODERN MISSILES

P. Hennig and P. G. Lacau *In* AGARD, Missile Aerodynamics Jun. 1994 76 p (For primary document see N95-14445 03-02)

Copyright Avail: CASI HC A05/MF A03

The changes in the political and strategic situation in the world, especially in Europe, result in new kinds of military scenarios and in different approaches to well-known scenarios. In combination with technological advances and with new mathematical and physical solutions for system component design and for improvements in system performance this leads to a request for advanced and new types of missiles with corresponding design goals and criteria. From such more general demands associated with the overall system design new requirements for the aerodynamical and aeromechanical design goals can be derived in correspondence. Advanced experimental and theoretical tools support the project aerodynamicist in coping with these new problems. Examples for the demands for new missile types and for the new system requirements are given. The most important aeromechanical work packages in the design procedure of modern missiles are identified and methods to get solutions sufficient for qualitative answers in early project phases are presented. Author

N95-14447# Naval Surface Warfare Center, Dahlgren, VA. Weapons Systems Dept.

ENGINEERING CODES FOR AEROPREDICTION: STATE-OF-THE-ART AND NEW METHODS

Frank G. Moore *In* AGARD, Missile Aerodynamics Jun. 1994 82 p (For primary document see N95-14445 03-02)

Copyright Avail: CASI HC A05/MF A03

This paper discusses the pros and cons of numerical, semiempirical, and empirical aeroprediction codes. It then summarizes many of the more popular approximate analytical methods used in state-of-the-art (SOTA) semiempirical aeroprediction codes. It also summarizes some recent new nonlinear semiempirical methods that allow more accurate calculation of static aerodynamics on complete missile configurations to higher angles of attack. Results of static aerodynamic calculations on complete missile configurations compared to wind tunnel data are shown for several configurations at various flight conditions. Calculations show the new nonlinear methods being far superior to some of the former linear technology when used at angles of attack greater than about 15 degrees. Author

N95-14448# Office National d'Etudes et de Recherches Aerospatiales, Paris (France).

LATERAL JET CONTROL FOR TACTICAL MISSILES **c08**

P. Champigny and R. G. Lacau *In* AGARD, Missile Aerodynamics Jun. 1994 57 p (For primary document see N95-14445 03-02)

Copyright Avail: CASI HC A04/MF A03

The aim of this paper is to give a survey of lateral jets as control system of tactical missiles. The paper is divided into four parts. The first part gives a brief analysis of new control requirements pertaining to tactical missiles, presents the advantages of lateral jet control, and describes two types of applications for missiles designed and developed by Aerospatiale-Missiles. The first example relates to the ground/surface-to-air missile ASTER which has antimissile capability; the second example concerns the antitank missile ERYX. The second part presents in detail the phenomenological aspects of lateral jets and the influence of various flow parameters and missile geometry on control system performance. The third part describes some wind-tunnel testing problems. The fourth and last part is dedicated to computation for valuation and understanding of the aerodynamic interactions. Derived from text

N95-14449# Grumman Aerospace Corp., Bethpage, NY.

MISSILE INFRARED RADIATION ANALYSIS **c74**

Michel Engelhardt *In* AGARD, Missile Aerodynamics Jun. 1994 27 p (For primary document see N95-14445 03-02)

Copyright Avail: CASI HC A03/MF A03

Modern trends in electro-optical/infrared (E-O/IR) technology for use in missile detection is presented as part of the NATO Advisory Group for Aerospace Research and Development (AGARD) special course on 'Missile Aerodynamics.' The course focuses on the operations of E-O/IR systems. The functions of the components of an E-O/IR system are summarized along with the missile source, background, contrast, and IR detection range equation. Author

N95-14450# Office National d'Etudes et de Recherches Aerospatiales, Paris (France).

HIGH ANGLE OF ATTACK AERODYNAMICS

P. Champigny *In* AGARD, Missile Aerodynamics Jun. 1994 19 p (For primary document see N95-14445 03-02)

Copyright Avail: CASI HC A03/MF A03

The demand for continually increased performance of missiles and aircraft leads to considering flight at very high angles of attack where control is very difficult. This is mainly due to the shedding of asymmetric vortices from the forebody, producing side forces even at zero sideslip. The purpose of this paper is not to make a review of missile aerodynamics at high angle of attack, but to focus on an understanding of the phenomena which give rise to asymmetric vortices, from an experimental as well as a theoretical point of view. Author

N95-14451# Army Research Lab., Aberdeen Proving Ground, MD. Propulsion and Flight Div.

NAVIER-STOKES PREDICTIONS OF MISSILE AERODYNAMICS

Paul Weinacht and Jubaraj Sahu *In* AGARD, Missile Aerodynamics Jun. 1994 48 p (For primary document see N95-14445 03-02)

Copyright Avail: CASI HC A03/MF A03

This paper discusses the application of Navier-Stokes computational methods to the prediction of the aerodynamics of missile configurations. The governing equations, turbulence models, and numerical approaches used to solve these equations are briefly described. The paper focuses mainly on aerodynamic coefficient prediction. Static and dynamic aerodynamic derivative prediction methods and applications are presented for axisymmetric and finned bodies and comparisons are made with experimental data. Results of validation studies are also presented for the purpose of demonstrating the accuracy as well as potential shortcomings

of these techniques. The paper also discusses the application of Navier-Stokes methods in the prediction of base flow. Application of these techniques to unpowered, base bleed, and powered configurations is shown. Author

N95-14452# Aerospatiale, Verrieres-L-Buisson (France).
COMPUTATION OF SUPERSONIC AIR-INTAKES
R. G. Lacau, P. Garnero, and F. Gaible *In* AGARD, Missile Aerodynamics Jun. 1994 21 p (For primary document see N95-14445 03-02)
Copyright Avail: CASI HC A03/MF A03

The aim of this paper is to present how some CFD tools can be used to compute external and internal flowfields involved in the design of supersonic air-intakes. These tools help the designer to better understand flow phenomena, to determine favorable intake locations, and to predict air-intake performances such as pressure recovery and mass flow ratio. As supersonic intakes are mainly used on ramjet missiles, we limit this paper to ramjet air-intakes. After a brief overview of the existing types of air-intakes, we describe the way their performances are quantified. Then we present the CFD tools used to evaluate air-intake characteristics. Finally, selected applications of these tools demonstrate how a comprehensive study of air-intake may be achieved through CFD. Both external and internal flowfield computations are presented, which allows predictions of air-intake performances. Derived from text

N95-14612*# MCAT Inst., San Jose, CA.
NUMERICAL SIMULATION OF THE SOFIA FLOWFIELD Annual Report
Stephen P. Klotz Jul. 1994 75 p Original contains color illustrations
(Contract NCC2-636)
(NASA-CR-197025; NAS 1.26:197025) Avail: CASI HC A04/MF A01; 1 functional color page

This report provides a concise summary of the contribution of computational fluid dynamics (CFD) to the SOFIA (Stratospheric Observatory for Infrared Astronomy) project at NASA Ames and presents results obtained from closed- and open-cavity SOFIA simulations. The aircraft platform is a Boeing 747SP and these are the first SOFIA simulations run with the aircraft empennage included in the geometry database. In the open-cavity run the telescope is mounted behind the wings. Results suggest that the cavity markedly influences the mean pressure distribution on empennage surfaces and that 110-140 decibel (db) sound pressure levels are typical in the cavity and on the horizontal and vertical stabilizers. A strong source of sound was found to exist on the rim of the open telescope cavity. The presence of this source suggests that additional design work needs to be performed in order to minimize the sound emanating from that location. A fluid dynamic analysis of the engine plumes is also contained in this report. The analysis was part of an effort to quantify the degradation of telescope performance resulting from the proximity of the port engine exhaust plumes to the open telescope bay. Author

N95-14613*# MCAT Inst., San Jose, CA.
CONTROL OF UNSTEADY SEPARATED FLOW ASSOCIATED WITH THE DYNAMIC STALL OF AIRFOILS Annual Report
M. C. Wilder 31 Jul. 1994 69 p Original contains color illustrations
(Contract NCC2-637)
(NASA-CR-197024; NAS 1.26:197024; MCAT-94-20) Avail: CASI HC A04/MF A01; 1 functional color page

A unique active flow-control device is proposed for the control of unsteady separated flow associated with the dynamic stall of airfoils. The device is an adaptive-geometry leading-edge which will allow controlled, dynamic modification of the leading-edge profile of an airfoil while the airfoil is executing an angle-of-attack pitch-up maneuver. A carbon-fiber composite skin has been bench tested, and a wind tunnel model is under construction. A baseline parameter study of compressible dynamic stall was performed for flow over an NACA 0012 airfoil. Parameters included Mach number, pitch rate, pitch history, and boundary layer tripping. Dynamic stall data were recorded via point-diffraction interferometry and the interferograms were analyzed with in-house developed image processing software. A new high-speed phase-locked photographic image recording system was developed for real-time documentation of dynamic stall. Author

N95-14614*# MCAT Inst., San Jose, CA.
NUMERICAL SIMULATION OF THE FLOW ABOUT THE F-18 HARV AT HIGH ANGLE OF ATTACK Annual Report
Scott M. Murman Aug. 1994 7 p Original contains color illustrations
(Contract NCC2-729)
(NASA-CR-197023; NAS 1.26:197023; MCAT-94-11) Avail: CASI HC A02/MF A01; 2 functional color pages

As part of NASA's High Alpha Technology Program, research has been aimed at developing and extending numerical methods to accurately predict the high Reynolds number flow about the NASA F-18 High Alpha Research Vehicle (HARV) at large angles of attack. The HARV aircraft is equipped with a bidirectional thrust vectoring unit which enables stable, controlled flight through 70 deg angle of attack. Currently, high-fidelity numerical solutions for the flow about the HARV have been obtained at alpha = 30 deg, and validated against flight-test data. It is planned to simulate the flow about the HARV through alpha = 60 deg, and obtain solutions of the same quality as those at the lower angles of attack. This report presents the status of work aimed at extending the HARV computations to the extreme angle of attack range. Derived from text

N95-14656 California Inst. of Tech., Pasadena, CA. Graduate Aeronautical Labs.
INTERACTION OF CHEMISTRY, TURBULENCE, AND SHOCK WAVES IN HYPERVELOCITY FLOW Annual Technical Report, 15 May 1993 - 14 May 1994
G. V. Candler, P. E. Dimotakis, H. G. Hornung, A. Leonard, and D. I. Meiron May 1994 67 p Limited Reproducibility: More than 20% of this document may be affected by microfiche quality
(Contract F49620-93-1-0338)
(AD-A282941; GALCIT-FM-94-2; AFOSR-94-0448) Avail: CASI HC A04

Significant progress was made during the first year of an interdisciplinary experimental, numerical and theoretical program to extend the state of knowledge and understanding of the effects of chemical reactions in hypervelocity flows. The program addressed the key problems in aerothermochemistry that arise from interactions between the three strongly nonlinear effects: compressibility; vorticity; and chemistry. Important new results included: (1) Experimental data on the effect of enthalpy on transition in hypervelocity flow (first visualization of high-enthalpy turbulent boundary layer structure); (2) New data on hypervelocity flow over spheres, confirming computations and new theory; (3) Progress on methods of parallel computation of shock-vortex interaction and new computations of three-dimensional leeward reacting flow; (4) Development and tests of a greatly improved low-cost, thermocouple heat transfer gauge; (5) Upgrade of the supersonic shear-layer facility to all-hyperbolic operation and exploration of this regime with a new Rayleigh scattering method; (6) Test of the validity of vibration-dissociation coupling models from shock tunnel data; (7) Successful application of new parallelized algorithm of the extended Schwinger multi-channel method to computation of electron-molecule collision cross-sections; and (8) Prediction and realization of a new non-intrusive diagnostic method, laser-induced thermal acoustics, for accurate measurement of sound speed and bulk viscosity. DTIC

N95-14803*# Georgia Inst. of Tech., Atlanta, GA. School of Aerospace Engineering.
NUMERICAL STUDY OF THE EFFECTS OF ICING ON VISCOUS FLOW OVER WINGS Final Report
L. N. Sankar Oct. 1994 156 p
(Grant NAG3-768)
(NASA-CR-197102; NAS 1.26:197102) Avail: CASI HC A08/MF A02

An improved hybrid method for computing unsteady compressible viscous flows is presented. This method divides the computational domain into two zones. In the outer zone, the unsteady full-potential equation (FPE) is solved. In the inner zone, the Navier-Stokes equations are solved using a diagonal form of an alternating-direction implicit (ADI) approximate factorization procedure. The two zones are tightly coupled so that steady and unsteady flows may be efficiently solved. Characteristic-based viscous/inviscid interface boundary conditions are employed to avoid spurious reflections at that interface. The resulting CPU times are less than 60 percent of that required for a full-blown Navier-Stokes analysis for steady flow applications and about 60 percent of the Navier-Stokes CPU times for unsteady flows in non-vector processing machines. Applications of the method are presented for a rectangular NACA 0012 wing in low subsonic steady flow at moderate and high angles of attack, and for an F-5 wing in steady and unsteady subsonic and transonic flows. Steady surface pressures are in very good agreement with experimental data and

are essentially identical to Navier-Stokes predictions. Density contours show that shocks cross the viscous/inviscid interface smoothly, so that the accuracy of full Navier-Stokes equations can be retained with a significant savings in computational time. Author

N95-14878*# National Aeronautics and Space Administration. Langley Research Center, Hampton, VA.
HIGH-SPEED RESEARCH: 1994 SONIC BOOM WORKSHOP: ATMOSPHERIC PROPAGATION AND ACCEPTABILITY STUDIES
David A. McCurdy, ed. Oct. 1994 222 p The 3rd workshop was held in Hampton, VA, 1-3 Jun. 1994
(RTOP 537-03-21-03)
(NASA-CP-3279; L-17434; NAS 1.55:3279) Avail: CASI HC A10/MF A03

The workshop proceedings include papers on atmospheric propagation and acceptability studies. Papers discussing atmospheric effects on the sonic boom waveform addressed several issues. It has long been assumed that the effects of molecular relaxation are adequately accounted for by assuming that a steady state balance between absorption and nonlinear wave steepening exists. It was shown that the unsteadiness induced by the nonuniform atmosphere precludes attaining this steady state. Further, it was shown that the random atmosphere acts as a filter, effectively filtering out high frequency components of the distorted waveform. Several different propagation models were compared, and an analysis of the sonic boom at the edge of the primary carpet established that the levels there are bounded. Finally, a discussion of the levels of the sonic boom below the sea surface was presented. For individual titles, see N95-14879 through N95-14892.

N95-14879*# National Aeronautics and Space Administration. Langley Research Center, Hampton, VA.
AN OPTICAL TECHNIQUE FOR EXAMINING AIRCRAFT SHOCK WAVE STRUCTURES IN FLIGHT **c35**
Leonard M. Weinstein *In its* High-Speed Research: 1994 Sonic Boom Workshop: Atmospheric Propagation and Acceptability Studies Oct. 1994 p 1-17 (For primary document see N95-14878 03-02)
Avail: CASI HC A03/MF A03

The detailed properties of sonic booms have to be better understood before commercial, next generation, supersonic and hypersonic aircraft can be properly developed. Experimental tests and measurements are needed to help sort the physical details of the flows at realistic test conditions. Some of these tests can be made in wind tunnels, but the need for full flight conditions simulation, the problem of tunnel wall interference, and the short distance the shocks can be examined from the aircraft, limit the usefulness of wind tunnel tests. Previous measurement techniques for examining the flow field of aircraft in flight have included pressure measurements on the aircraft, ground based pressure measurements, and flow field measurements made with chase aircraft. Obtaining data with chase planes is a slow and difficult process, and is limited in how close it can be obtained to the test aircraft. A need clearly existed for a better technique to examine the shock structure from the plane to large distances from the plane. A new technique has been recently developed to obtain schlieren photographs of aircraft in flight (SAF). Preliminary results have been obtained, and the technique holds promise as a tool to study the shape and approximate strength of the shock wave structure around the test aircraft, and examine shock wave details all the way from the aircraft to near the ground. The current paper describes this approach, and gives some preliminary test results. Author

N95-14880*# Texas Univ., Austin, TX. Dept. of Mechanical Engineering.
EFFECT OF STRATIFICATION AND GEOMETRICAL SPREADING ON SONIC BOOM RISE TIME
Robin O. Cleveland, Mark F. Hamilton, and David T. Blackstock *In* NASA. Langley Research Center, High-Speed Research: 1994 Sonic Boom Workshop: Atmospheric Propagation and Acceptability Studies Oct. 1994 p 19-38 (For primary document see N95-14878 03-02)
Avail: CASI HC A03/MF A03

The purpose of our investigation is to determine the effect of unsteadiness (not associated with turbulence) on rise time. The unsteadiness considered here is due to (1) geometrical spreading, (2) stratification, which includes variation in density, temperature, and relative humidity, and (3) N shaped waveform. A very general Burgers equation, which includes all these effects, is the propagation model for our study. The equation is solved by a new computational algorithm in which all the calculations are done in the time domain. The present paper is a progress report in which some of the factors contributing to unsteadiness are studied, namely geometrical spreading and variation in relative humidity. The work of Pierce and Kang, which motivated our study, is first reviewed. We proceed with a discussion of the Burgers equation model and the algorithm for solving the equation. Some comparison tests to establish the validity of the algorithm are presented. The algorithm is then used to determine the distance required for a steady-state shock, on encountering an abrupt change in relative humidity, to reach a new steady state based on the new humidity. It is found that the transition distance for plane shocks of amplitude 70 Pa is about 4 km when the change in relative humidity is 10 percent. Shocks of amplitude 140 Pa require less distance. The effect of spherical and cylindrical spreading is also considered. We demonstrate that a spreading shock wave never reaches steady state and that its rise time will be less than the equivalent steady state shock. Finally we show that an N wave has a slightly shorter rise time than a step shock of the same amplitude.
Author

N95-14881*# Science Applications International Corp., Austin, TX.
AN EVALUATION OF RISE TIME CHARACTERIZATION AND PREDICTION METHODS
Leick D. Robinson *In* NASA. Langley Research Center, High-Speed Research: 1994 Sonic Boom Workshop: Atmospheric Propagation and Acceptability Studies Oct. 1994 p 39-45 (For primary document see N95-14878 03-02)
Avail: CASI HC A02/MF A03

One common method of extrapolating sonic boom waveforms from aircraft to ground is to calculate the nonlinear distortion, and then add a rise time to each shock by a simple empirical rule. One common rule is the '3 over P' rule which calculates the rise time in milliseconds as three divided by the shock amplitude in psf. This rule was compared with the results of ZEPHYRUS, a comprehensive algorithm which calculates sonic boom propagation and extrapolation with the combined effects of nonlinearity, attenuation, dispersion, geometric spreading, and refraction in a stratified atmosphere. It is shown there that the simple empirical rule considerably overestimates the rise time estimate. In addition, the empirical rule does not account for variations in the rise time due to humidity variation or propagation history. It is also demonstrated that the rise time is only an approximate indicator of perceived loudness. Three waveforms with identical characteristics (shock placement, amplitude, and rise time), but with different shock shapes, are shown to give different calculated loudness. This paper is based in part on work performed at the Applied Research Laboratories, the University of Texas at Austin, and supported by NASA Langley.
Author

N95-14882*# Virginia Polytechnic Inst. and State Univ., Blacksburg, VA.
FINE STRUCTURE OF TRANSIENT WAVES IN A RANDOM MEDIUM: THE CORRELATION AND SPECTRAL DENSITY FUNCTIONS **c71**
Alan R. Wenzel *In* NASA. Langley Research Center, High-Speed Research: 1994 Sonic Boom Workshop: Atmospheric Propagation and Acceptability Studies Oct. 1994 p 47-59 (For primary document see N95-14878 03-02)
Avail: CASI HC A03/MF A03

This is essentially a progress report on a theoretical investigation of the propagation of transient waves in a random medium. The emphasis in this study is on applications to sonic-boom propagation, particularly as regards the effect of atmospheric turbulence on the sonic-boom waveform. The analysis is general, however, and is applicable to other types of waves besides sonic-boom waves. The phenomenon of primary concern in this investigation is the fine structure of the wave. A figure is used to illustrate what is meant by finestructure. Author

N95-14883*# Centre National de la Recherche Scientifique, Ecully (France). Lab. de Mecanique des Fluides et Acoustique.
NUMERICAL MODEL FOR THE WEAKLY NONLINEAR PROPAGATION OF SOUND THROUGH TURBULENCE **c71**
Bart Lipkens and Philippe Blanc-Benon *In* NASA. Langley Research Center, High-Speed Research: 1994 Sonic Boom Workshop: Atmospheric Propagation and Acceptability Studies Oct. 1994 p 61-80 (For

primary document see N95-14878 03-02)
Avail: CASI HC A03/MF A03

When finite amplitude (or intense) sound, such as a sonic boom, propagates through a turbulent atmosphere, the propagation is strongly affected by the turbulence. The interaction between sound and turbulence has mostly been studied as a linear phenomenon, i.e., the nonlinear behavior of the intense sound has been neglected. It has been shown that turbulence has an effect on the perceived loudness of sonic booms, mainly by changing its peak pressure and rise time. Peak pressure and rise time are important factors that determine the loudness of the sonic boom when heard outdoors. However, the interaction between turbulence and nonlinear effects has mostly not been included in propagation studies of sonic booms. It is therefore important to investigate the influence of acoustical nonlinearity on the interaction of intense sound with turbulence. Author

N95-14884*# Rensselaer Polytechnic Inst., Troy, NY. Dept. of Mechanical Engineering.

SONIC BOOM INTERACTION WITH TURBULENCE

Zvi Rusak and Thomas E. Giddings *In* NASA. Langley Research Center, High-Speed Research: 1994 Sonic Boom Workshop: Atmospheric Propagation and Acceptability Studies Oct. 1994 p 81-97 (For primary document see N95-14878 03-02)
(Grants NAG1-1362; NGT-S1113)
Avail: CASI HC A03/MF A03

A recently developed transonic small-disturbance model is used to analyze the interactions of random disturbances with a weak shock. The model equation has an extended form of the classic small-disturbance equation for unsteady transonic aerodynamics. It shows that diffraction effects, nonlinear steepening effects, focusing and caustic effects and random induced vorticity fluctuations interact simultaneously to determine the development of the shock wave in space and time and the pressure field behind it. A finite-difference algorithm to solve the mixed-type elliptic hyperbolic flows around the shock wave is presented. Numerical calculations of shock wave interactions with various deterministic vorticity and temperature disturbances result in complicate shock wave structures and describe peaked as well as rounded pressure signatures behind the shock front, as were recorded in experiments of sonic booms running through atmospheric turbulence. Author

N95-14885*# Boston Univ., MA. Dept. of Aerospace and Mechanical Engineering.

ATMOSPHERIC PROPAGATION AT LARGER LATERAL DISTANCES FROM THE FLIGHT TRACK **c71**

Allan D. Pierce *In* NASA. Langley Research Center, High-Speed Research: 1994 Sonic Boom Workshop: Atmospheric Propagation and Acceptability Studies Oct. 1994 p 99-122 Sponsored in part by Air Force Systems Command, Wright-Patterson AFB, OH (For primary document see N95-14878 03-02)
Avail: CASI HC A03/MF A03

Sonic booms received on the ground tend to be restricted to a region of finite lateral extent below the flight track. This occurs because of refraction and because the effective speed of sound, even with winds taken into account, decreases with altitude in the lower atmosphere. Not all rays proceeding initially downwards from the flight track within an allowable range of initial directions will reach the ground. The restricted region which can be reached by rays impacting the ground is known as the primary carpet. However, weak rumbles are heard in the nominal shadow zone beyond the edge of this carpet. A full wave theory is necessary for explaining waveforms in that region, and the present paper gives a matched asymptotic expansion technique for a suitable approximate full wave theory that involves a relatively small number of parameters. The outer solution is derived from the structure of the system of rays that impact near the corridor edge; the inner solution involves a solution of the parabolic equation and results in the special functions encountered in the diffraction of sound over the tops of hills. Author

N95-14886*# Mississippi Univ., University, MS. Dept. of Physics and Astronomy.

ATMOSPHERIC EFFECTS ON THE RISETIME AND WAVESHAPE OF SONIC BOOMS **c71**

Richard Raspet, Henry E. Bass, and Patrice Boulanger *In* NASA. Langley Research Center, High-Speed Research: 1994 Sonic Boom Workshop: Atmospheric Propagation and Acceptability Studies Oct. 1994 p 123-136 (For primary document see N95-14878 03-02)
Avail: CASI HC A03/MF A03

Accurate prediction of human response to sonic booms from proposed HSCT aircraft depends on a knowledge of the waveshape and risetime of the boom at the ground. In previous work, we have developed a numerical technique to predict the combined effects of molecular absorption and finite wave distortion on the sonic boom as it propagates from the aircraft to the top of the turbulent boundary layer. We have more recently developed a scattering center based model to calculate the effects of turbulence on the sonic boom waveform as it propagates through this boundary layer. Calculations have been performed using single scales of turbulence and compared to measurements at Edwards AFB in the late 1960's. A model of the atmosphere involving two scales each for convective and mechanical turbulence has been developed and fit to meteorological data collected during JAPE 2. Scattering calculations employing this model underpredict the number of unperturbed waveforms. In order to develop a more realistic model of the atmosphere, the JAPE 2 meteorological data has been fit to a von Karman spectrum. Results of scattering using this multi-scale model will be presented. The combination of finite wave effects with turbulent scattering predictions includes the principal effects of the atmosphere on the sonic boom from the HSCT. Author

N95-14887*# Pennsylvania State Univ., University Park, PA.

THE EFFECT OF AIRCRAFT SPEED ON THE PENETRATION OF SONIC BOOM NOISE INTO A FLAT OCEAN **c71**

Victor W. Sparrow *In* NASA. Langley Research Center, High-Speed Research: 1994 Sonic Boom Workshop: Atmospheric Propagation and Acceptability Studies Oct. 1994 p 137-156 (For primary document see N95-14878 03-02)
Avail: CASI HC A03/MF A03

As U.S. aircraft manufacturers now have focused their HSCT efforts on overwater supersonic flight, a great deal more must be known about sonic booms propagating overwater and interacting with the ocean. For example, it is thought that atmospheric turbulence effects are often much less severe over water than over land. Another important aspect of the overwater flight problems is the penetration of the sonic boom noise into the ocean, where there could be an environmental impact on sea life. This talk will present a brief review on the penetration of sonic boom noise into a large body of water with a flat surface. It has been determined recently that faster supersonic speeds imply greater penetration of sonic boom noise into the ocean. The new theory is derived from the original Sawyers paper and from the knowledge that for level flight a boom's duration is proportional to the quantity M/(M(exp 2)-1)(exp 3/8) where M is the Mach number. It is found that for depths of 10 m or less, the peak SPL varies less than 6 dB over a wide range of M. For greater depths, 100 m for example, increased Mach numbers may increase the SPL by 15 dB or more. Author

N95-14888*# National Aeronautics and Space Administration. Hugh L. Dryden Flight Research Center, Edwards, CA.

SIMPLE ATMOSPHERIC PERTURBATION MODELS FOR SONIC-BOOM-SIGNATURE DISTORTION STUDIES **c71**

L. J. Ehernberger, Morton G. Wurtele, and Robert D. Sharman *In* NASA. Langley Research Center, High-Speed Research: 1994 Sonic Boom Workshop: Atmospheric Propagation and Acceptability Studies Oct. 1994 p 157-169 (For primary document see N95-14878 03-02)
Avail: CASI HC A03/MF A03

Sonic-boom propagation from flight level to ground is influenced by wind and speed-of-sound variations resulting from temperature changes in both the mean atmospheric structure and small-scale perturbations. Meteorological behavior generally produces complex combinations of atmospheric perturbations in the form of turbulence, wind shears, up- and down-drafts and various wave behaviors. Differences between the speed of sound at the ground and at flight level will influence the threshold flight Mach number for which the sonic boom first reaches the ground as well as the width of the resulting sonic-boom carpet. Mean atmospheric temperature and wind structure as a function of altitude vary with location and time of year. These average properties of the atmosphere are well-documented and have been used in many sonic-boom propagation assessments. In contrast, smaller scale atmospheric perturbations are also known to modulate the shape and amplitude of sonic-boom signatures

reaching the ground, but specific perturbation models have not been established for evaluating their effects on sonic-boom propagation. The purpose of this paper is to present simple examples of atmospheric vertical temperature gradients, wind shears, and wave motions that can guide preliminary assessments of nonturbulent atmospheric perturbation effects on sonic-boom propagation to the ground. The use of simple discrete atmospheric perturbation structures can facilitate the interpretation of the resulting sonic-boom propagation anomalies as well as intercomparisons among varied flight conditions and propagation models. Author

N95-14889*# Wyle Labs., Inc., Arlington, VA.
USAF SINGLE-EVENT SONIC BOOM PREDICTION MODEL: PCBoom3 **c71**
Kenneth J. Plotkin, Micah Downing, and Juliet A. Page *In* NASA. Langley Research Center, High-Speed Research: 1994 Sonic Boom Workshop: Atmospheric Propagation and Acceptability Studies Oct. 1994 p 171-184 (For primary document see N95-14878 03-02)
Avail: CASI HC A03/MF A03

The Air Force has developed PCBoom3, a general-purpose, single-event sonic boom prediction model. The model operates on an IBM PC or compatible, under DOS or Windows. It is accessed via an integrated environment which controls building of input cases, running boom calculations, displaying contours and signatures, and managing all associated data. The primary boom calculation is via a variation of FOBOOM, the focus-boom extension of Thomas's program. Aircraft input is either via a user-provided F-function, or simple N-wave F-functions tabulated for about 20 current aircraft. A fast boom calculation, based on Plotkin's SBORT algorithms, is included for simple N-wave F-functions in a windless atmosphere and flight altitudes up to 60,000 feet. After a run is complete, the user can access an index identifying significant events (focal zones, beginning of footprint, etc.), then plot boom amplitude contours and signatures or spectra at any point in the footprint. The primary uses of this program are expected to be operational planning and boom incident investigation. However, because of the commonality between FOBOOM and the MDBOOM program currently being used for low boom configuration design, this program is of interest to the HSCT community, especially as supersonic route planning activity increases. The Air Force recently conducted a flight test program to evaluate the focal zone capabilities of PCBoom3. Initial results of that program validate the prediction of focal zone geometry, amplitudes, and waveforms. Author

N95-14890*# BBN Systems and Technologies Corp., Canoga Park, CA.
DERIVING A DOSAGE-RESPONSE RELATIONSHIP FOR COMMUNITY RESPONSE TO HIGH-ENERGY IMPULSIVE NOISE **c45**
Sanford Fidell and Karl S. Pearsons *In* NASA. Langley Research Center, High-Speed Research: 1994 Sonic Boom Workshop: Atmospheric Propagation and Acceptability Studies Oct. 1994 p 185-192 (For primary document see N95-14878 03-02)
Avail: CASI HC A02/MF A03

The inability to systematically predict community response to exposure to sonic booms (and other high energy impulsive sounds) is a major impediment to credible analyses of the environmental effects of supersonic flight operations. Efforts to assess community response to high energy impulsive sounds are limited in at least two important ways. First, a paucity of appropriate empirical data makes it difficult to infer a dosage-response relationship by means similar to those used in the case of general transportation noise. Second, it is unclear how well the 'equal energy hypothesis' (the notion that duration, number, and level of individual events are directly interchangeable determinants of annoyance) applies to some forms of impulsive noise exposure. Some of the issues currently under consideration by a CHABA working group addressing these problems are discussed. These include means for applying information gained in controlled exposure studies about different rates of growth of annoyance with impulsive and non-impulsive sound exposure levels, and strategies for developing a dosage-response relationship in a data-poor area. Author

N95-14891*# National Aeronautics and Space Administration. Langley Research Center, Hampton, VA.
AN IN-HOME STUDY OF SUBJECTIVE RESPONSE TO SIMULATED SONIC BOOMS **c53**
David A. McCurdy, Sherilyn A. Brown, and R. David Hilliard *In its* High-Speed Research: 1994 Sonic Boom Workshop: Atmospheric Propagation and Acceptability Studies Oct. 1994 p 193-208 (For primary document see N95-14878 03-02)
Avail: CASI HC A03/MF A03

The proposed development of a second-generation supersonic commercial transport has resulted in increased research efforts to provide an environmentally acceptable aircraft. One of the environmental issues is the impact of sonic booms on people. Aircraft designers are attempting to design the transport to produce sonic boom signatures that will have minimum impact on the public. Current supersonic commercial aircraft produce an 'N-wave' sonic boom pressure signature that is considered unacceptable by the public. This has resulted in first-generation supersonic transports being banned from flying supersonically over land in the United States, a severe economic constraint. By tailoring aircraft volume and lift distributions, designers hope to produce sonic boom signatures having specific shapes other than 'N-wave' that may be more acceptable to the public and could possibly permit overland supersonic flight. As part of the effort to develop a second-generation supersonic commercial transport, Langley Research Center is conducting research to study people's subjective response to sonic booms. As part of that research, a system was developed for performing studies of the subjective response of people to the occurrence of simulated sonic booms in their homes. The In-Home Noise Generation/Response System (IHONORS) provides a degree of situational realism not available in the laboratory and a degree of control over the noise exposure not found in community surveys. The computer-controlled audio system generates the simulated sonic booms, measures the noise levels, and records the subjects' rating and can be placed and operated in individuals' homes for extended periods of time. The system was used to conduct an in-home study of subjective response to simulated sonic booms. The primary objective of the study was to determine the effect on annoyance of the number of sonic boom occurrences in a realistic environment.
Author

N95-14892*# Fields (James M.), Silver Spring, MD.
RESIDENTS' REACTIONS TO LONG-TERM SONIC BOOM EXPOSURE: PRELIMINARY RESULTS **c53**
James M. Fields, Carey Moulton, Robert M. Baumgartner, and Jeff Thomas *In* NASA. Langley Research Center, High-Speed Research: 1994 Sonic Boom Workshop: Atmospheric Propagation and Acceptability Studies Oct. 1994 p 209-217 (For primary document see N95-14878 03-02)
Avail: CASI HC A02/MF A03

This presentation is about residents' reactions to sonic booms in a long-term sonic boom exposure environment. Although two phases of the data collection have been completed, the analysis of the data has only begun. The results are thus preliminary. The list of four authors reflects the complex multi-disciplinary character of any field study such as this one. Carey Moulton is responsible for Wyle Laboratories' acoustical data collection effort. Robert Baumgartner and Jeff Thomas of HBRS, a social science research firm, are responsible for social survey field work and data processing. The study is supported by the NASA Langley Research Center. The study has several objectives. The preliminary data addresses two of the primary objectives. The first objective is to describe the reactions to sonic booms of people who are living where sonic booms are a routine, recurring feature of the acoustical environment. The second objective is to compare these residents' reactions to the reactions of residents who hear conventional aircraft noise around airports. Here is an overview of the presentation. This study will first be placed in the context of previous community survey research on sonic booms. Next the noise measurement program will be briefly described and part of a social survey interview will be presented. Finally data will be presented on the residents' reactions and these reactions will be compared with reactions to conventional aircraft. Twelve community studies of residents' reactions to sonic booms were conducted in the United States and Europe in the 1960's and early 1970's. None of the 12 studies combined three essential ingredients that are found in the present study. Residents' long-term responses are related to a measured noise environment. Sonic booms are a permanent feature of the residential environment. The respondents' do not live on a military base. The present study is important because it provides the first dose/response relationship for sonic booms that could be expected to apply to residents in civilian residential areas. Author

N95-15319# Naval Postgraduate School, Monterey, CA.
LOW-SPEED WIND TUNNEL TESTING OF THE NPS AND NASA AMES MACH 6 OPTIMIZED WAVERIDER M.S. Thesis
Mark E. Cedrun 16 Jun. 1994 106 p
(AD-A283585) Avail: CASI HC A06/MF A02

Low-speed wind tunnel tests were conducted to determine the subsonic aerodynamic characteristics of an optimized supersonic (Mach 6) conical-flow waverider designed for a deck-launched intercept mission. These tests are part of the continuing waverider research being conducted by the Naval Postgraduate School and the NASA Ames Research Center. The tests consisted of performing Alpha and Beta sweeps, at different dynamic pressures, with a 15 inch aluminum waverider model in the NPS low-speed wind tunnel. Force and moment data were then collected using a six-degree-of-freedom sting balance. Coefficients of lift, drag and pitch were calculated from the data and compared to theory and existing waverider subsonic aerodynamic performance data. Flow visualization using tufts was also done. The results of the experiments show that waverider exhibits high lift characteristics at positive angles of attack. The design also compares favorably with both subsonic thin airfoil theory and the results of the delta wing and subsonic waverider analysis done by Vanhoy. However, flow visualization showed that vortex bursting occurred at a dynamic pressure of 12.11bf at +/-15 degrees angle of attack. Based upon the data collected in this analysis, the development of an actual waverider aircraft using the NPS/NASA Ames waverider design as a baseline is a plausible endeavor. DTIC

N95-15465 Wright Lab., Wright-Patterson AFB, OH.
PRESSURE MEASUREMENTS ON AN F/A-18 TWIN VERTICAL TAIL IN BUFFETING FLOW. VOLUME 2: STEADY AND UNSTEADY RMS PRESSURE DATA Final Report
Chris Pettit, Dansen Brown, Michael Banford, and Ed Pendleton 1 Aug. 1994 383 p Limited Reproducibility: More than 20% of this document may be affected by microfiche quality
(AD-A281581; WL-TM-94-3065-Vol-2) Avail: CASI HC A17

Buffeting pressure measurements were made on the vertical tail surface of a full scale F/A-18 aircraft model in the National Full Scale Aerodynamics Complex at NASA Ames Research Center. Test variables included aircraft angle-of-attack, aircraft sideslip angle, and dynamic pressure. Accelerometers were used to obtain vertical tail accelerations. Pressure transducers were mounted on the starboard vertical tail. Steady and unsteady pressures were obtained. Unsteady pressure data were reduced to PSD and CSD forms. Both steady and unsteady RMS pressure coefficients are also presented. Volume 1 contains the general description of the model, the test program, and highlights of the reduced data. Volume 2 contains steady and unsteady RMS data. Volume 3 contains unsteady PSD results. Volume 4 contains unsteady CSD results. DTIC

N95-15570# Sandia National Labs., Albuquerque, NM.
A THREE-DIMENSIONAL FAST SOLVER FOR ARBITRARY VORTON DISTRIBUTIONS
J. H. Strickland and R. S. Baty May 1994 63 p
(Contract DE-AC04-94AL-85000)
(DE94-012581; SAND-93-1641) Avail: CASI HC A04/MF A01

A method which is capable of an efficient calculation of the three-dimensional flow field produced by a large system of vortons (discretized regions of vorticity) is presented in this report. The system of vortons can, in turn, be used to model body surfaces, container boundaries, free-surfaces, plumes, jets, and wakes in unsteady three-dimensional flow fields. This method takes advantage of multipole and local series expansions which enables one to make calculations for interactions between groups of vortons which are in well-separated spatial domains rather than having to consider interactions between every pair of vortons. In this work, series expansions for the vector potential of the vorton system are obtained. From such expansions, the three components of velocity can be obtained explicitly. A Fortran computer code FAST3D has been written to calculate the vector potential and the velocity components at selected points in the flow field. In this code, the evaluation points do not have to coincide with the location of the vortons themselves. Test cases have been run to benchmark the truncation errors and CPU time savings associated with the method. Non-dimensional truncation errors for the magnitudes of the vector potential and velocity fields are on the order of 10(exp -4)and 10(exp -3) respectively. Single precision accuracy produces errors in these quantities of up to 10(exp -5). For less than 1,000 to 2,000 vortons in the field, there is virtually no CPU time savings with the fast solver. For 100,000 vortons in the flow, the fast solver obtains solutions in 1% to 10% of the time required for the direct solution technique depending upon the configuration. DOE

N95-15762*# California Polytechnic State Univ., San Luis Obispo, CA. Dept. of Aeronautical Engineering.
NUMERICAL DESIGN OF ADVANCED MULTI-ELEMENT AIRFOILS Final Report
Donovan L. Mathias and Russell M. Cummings Oct. 1994 105 p
(Contract NCC2-813)
(NASA-CR-197135; NAS 1.26:197135) Avail: CASI HC A06/MF A02

The current study extends the application of computational fluid dynamics to three-dimensional high-lift systems. Structured, overset grids are used in conjunction with an incompressible Navier-Stokes flow solver to investigate flow over a two-element high-lift configuration. The computations were run in a fully turbulent mode using the one-equation Baldwin-Barth turbulence model. The geometry consisted of an unswept wing which spanned a wind tunnel test section. Flows over full and half-span Fowler flap configurations were computed. Grid resolution issues were investigated in two dimensional studies of the flapped airfoil. Results of the full-span flap wing agreed well with experimental data and verified the method. Flow over the wing with the half-span was computed to investigate the details of the flow at the free edge of the flap. The results illustrated changes in flow streamlines, separation locations, and surface pressures due to the vortex shed from the flap edge. Author

N95-15852*# NYMA, Inc., Brook Park, OH. Engineering Services Div.
RESONANT INTERACTION OF A LINEAR ARRAY OF SUPERSONIC RECTANGULAR JETS: AN EXPERIMENTAL STUDY Final Report
Ganesh Raman and Ray Taghavi Cleveland, OH NASA Nov. 1994 25 p Presented at the 33rd Aerospace Sciences Meeting and Exhibit, 9-12 Jan. 1994; sponsored by the AIAA
(Contract NAS3-27186; RTOP 537-02-22)
(NASA-CR-195398; E-9128; NAS 1.26:195398) Copyright Avail: CASI HC A03/MF A01

This paper examines a supersonic multi jet interaction problem that we believe is likely to be important for mixing enhancement and noise reduction in supersonic mixer-ejector nozzles. We demonstrate that it is possible to synchronize the screech instability of four rectangular jets by precisely adjusting the inter jet spacing. Our experimental data agrees with a theory that assumes that the phase-locking of adjacent jets occurs through a coupling at the jet lip. Although the synchronization does not change the frequency of the screech tone, its amplitude is augmented by 10 dB. The synchronized multi jets exhibit higher spreading than the unsynchronized jets, with the single jet spreading the least. We compare the nearfield noise of the four jets with synchronized screech to the noise of the sum of four jets operated individually. Our noise measurements reveal that the more rapid mixing of the synchronized multi jets causes the peak jet noise source to move up stream and to radiate noise at larger angles to the flow direction. Based on our results, we believe that screech synchronization is advantageous for noise reduction internal to a mixer-ejector nozzle, since the noise can now be suppressed by a shorter acoustically lined ejector. Author

N95-15853*# National Aeronautics and Space Administration. Lewis Research Center, Cleveland, OH.
AN APPROACH FOR DYNAMIC GRIDS
John W. Slater, Meng-Sing Liou, and Richard G. Hindman Nov. 1994 11 p Presented at the 32nd Aerospace Sciences Meeting and Exhibit, Reno, NV, 10-13 Jan. 1994; sponsored by the AIAA
(Grant NGT-50441; RTOP 505-62-52)
(NASA-TM-106774; E-9124-1; NAS 1.15:106774; AIAA Paper 94-0319)
Avail: CASI HC A03/MF A01

An approach is presented for the generation of two-dimensional, structured, dynamic grids. The grid motion may be due to the motion of the boundaries of the computational domain or to the adaptation of the grid to the transient, physical solution. A time-dependent grid is computed through the time integration of the grid speeds which are computed from a system of grid speed equations. The grid speed equations are derived from the time-differentiation of the grid equations so as to ensure that the

dynamic grid maintains the desired qualities of the static grid. The grid equations are the Euler-Lagrange equations derived from a variational statement for the grid. The dynamic grid method is demonstrated for a model problem involving boundary motion, an inviscid flow in a converging-diverging nozzle during startup, and a viscous flow over a flat plate with an impinging shock wave. It is shown that the approach is more accurate for transient flows than an approach in which the grid speeds are computed using a finite difference with respect to time of the grid. However, the approach requires significantly more computational effort.
Author

N95-15912*# Toledo Univ., OH.
ENHANCED CAPABILITIES AND UPDATED USERS MANUAL FOR AXIAL-FLOW TURBINE PRELIMINARY SIZING CODE TURBAN Final Report
Arthur J. Glassman Nov. 1994 18 p
(Grant NAG3-1165; RTOP 505-69-50)
(NASA-CR-195405; E-9252; NAS 1.26:195405) Avail: CASI HC A03/MF A01

Several modifications have been made to the axial-flow turbine preliminary sizing code TURBAN. Turbine cooling has been added to the analysis. New alternative input options allow direct specification of stage reaction, stage work factor, and stage work split. The Reynolds number loss dependency was modified and an internal calculation of air viscosity was added. A complete description of input and output along with sample cases are included. Author

N95-13719*# National Aeronautics and Space Administration. Ames Research Center, Moffett Field, CA.
VUV SHOCK LAYER RADIATION IN AN ARC-JET WIND TUNNEL EXPERIMENT
Roger A. Craig (MCAT Inst., Moffett Field, CA.), Giuseppe Palumbo (Eloret Corp., Santa Clara, CA.), and Armando Carrasco *In* MCAT Inst., Planetary Entry Experiments Jul. 1994 27 p (For primary document see N95-13717 03-91)
(Contract NCC2-653)
Avail: CASI HC A03/MF A02

N95-13720*# National Aeronautics and Space Administration. Ames Research Center, Moffett Field, CA.
MEASURED AND CALCULATED SPECTRAL RADIATION FROM A BLUNT BODY SHOCK LAYER IN AN ARC-JET WIND TUNNEL
Dikran S. Babikian (Eloret Corp., Palo Alto, CA.), Giuseppe Palumbo (Eloret Corp., Palo Alto, CA.), Roger A. Craig (MCAT Inst., Moffett Field, CA.), Chul Park, Grant Palmer, and Surendra P. Sharma *In* MCAT Inst., Planetary Entry Experiments Jul. 1994 11 p Presented at the 32d Aerospace Sciences Meeting, Reno, NV, 10-13 Jan. 1994; sponsored by AIAA (For primary document see N95-13717 03-91)
(Contract NCC2-653)
(AIAA Paper 94-0086) Avail: CASI HC A03/MF A02

N95-14646# Kossel (Horst), Shrewsbury, MA.
ACTIVATED BUOYANCY PROPULSION = PARADOX POWER (TM)
Horst Kossel *In* Huntsville Association of Technical Societies, TABES 1994: 10th Annual Technical and Business Exhibition and Symposium 1994 7 p (For primary document see N95-14633 03-12)
(TABES Paper 94-619) Avail: CASI HC A02/MF A04

N95-14894# Pennsylvania State Univ., University Park, PA. Dept. of Aerospace Engineering.
WAKE TURBULENCE
Barnes W. McCormick *In* AGARD, Flight in an Adverse Environment Nov. 1994 15 p (For primary document see N95-14893 03-03)
Copyright Avail: CASI HC A03/MF A02

03 AIR TRANSPORTATION AND SAFETY

Includes passenger and cargo air transport operations; and aircraft accidents.

For related information see also *16 Space Transportation* and *85 Urban Technology and Transportation.*

N95-14179# National Inst. of Standards and Technology, Gaithersburg, MD. Building and Fire Research Lab.
RISK ANALYSIS FOR THE FIRE SAFETY OF AIRLINE PASSENGERS
R. L. Smith Jun. 1994 40 p
(Contract DTFA03-92-Z-00018)
(PB94-194065; NISTIR-5441) Avail: CASI HC A03/MF A01

The purpose of this report is to describe the National Institute of Standards and Technology's work to date relating to the general methodology being developed for the project Risk Analysis for the Fire Safety of Airline Passengers and the software being used to facilitate this methodology. The approach selected involved the use of influence diagrams. Therefore, a brief discussion of influence diagrams is given. The status of their application to the water mist system for passenger planes is given and the overall approach to carrying out the project is described. An example is included that shows how the process works, but the case is fictional, not intended to be realistic. NTIS

N95-14199# Advisory Group for Aerospace Research and Development, Neuilly-Sur-Seine (France). Flight Mechanics Panel.
THE PRINCIPLES OF FLIGHT TEST ASSESSMENT OF FLIGHT-SAFETY-CRITICAL SYSTEMS IN HELICOPTERS [LES PRINCIPES DE L'EVALUATION, DANS LE CADRE DES ESSAIS EN VOL, DES SYSTEMES INDISPENSABLES A LA SECURITE DE VOL DES HELICOPTERES]
J. D. L. Gregory Aug. 1994 29 p Flight Test Techniques Series
(AGARD-AG-300-Vol-12; ISBN-92-836-1001-6) Copyright Avail: CASI HC A03/MF A01

Modern helicopters usually incorporate many engineering systems (including pilot-aiding systems such as autostabilizers and flight directors) which are essential to the safe and effective use of the helicopter. Where the helicopter can be endangered by failure of a system (or of one of its units), that system is termed flight-safety-critical. In general, the use of those systems should not incur a higher probability of hazard to the helicopter than that considered acceptable from considerations of structural or mechanical failure. In assessing the suitability of a helicopter for its intended mission(s), it has become increasingly important to consider the effects of the various systems provided. In particular, assessments of the implications of systems performance and failures derived from calculation and ground test should be validated by flight tests. This paper seeks to establish the general principles applicable to the testing in flight of any flight-safety-critical system, with emphasis on certification rather than system development. It does not deal with the testing of particular systems, but it is hoped that readers will find the principles described readily applicable to specific cases. This document has been sponsored by the Flight Mechanics Panel of AGARD. Author (revised)

N95-14350# Federal Aviation Administration, Atlantic City, NJ.
PROCEEDINGS OF THE FAA INSPECTION PROGRAM AREA REVIEW Final Report
Christopher Smith Jul. 1994 922 p Review held in Ames, IA, 5-7 Apr. 1994
(AD-A283849; DOT/FAA/CT-94/64) Avail: CASI HC A99/MF A10

This publication is a compendium of the Proceedings, of the FAA Inspection Program Are Review Presentations given at the Center for Aviation Systems Reliability held at Iowa State University at Ames, Iowa on April 5-7, 1994. DTIC

N95-14421# Naval Research Lab., Washington, DC.
FLIGHTLINE AIRCRAFT FIRE INCIDENTS AND SUPPRESSION AGENT EFFECTS: FIELD INQUIRIES AND INCIDENT ANALYSIS Final Report, Sep. 1992 - Apr. 1993
J. T. Leonard, E. K. Budnick, E. R. Rosenbaum, D. J. Perrault, and E. D. Hayes Apr. 1994 121 p
(AD-A284027; WL-TR-93-3519) Avail: CASI HC A06/MF A02

Air Force flightline fire incidents are characterized by a bimodal

distribution; small fires constitute 95% of the database and are considered sensitive to both effectiveness and collateral damage potential of the extinguishing agent. Large fires are relatively infrequent and are less sensitive to collateral damage. The Air Force also experiences approximately 600 'unreported' agent discharges each year. The agent most frequently used for small and unreported incidents is Halon 1211. A relatively low loss rate of $12.2 K per incident is attributable to minimal collateral damage associated with the use of Halon 1211. The high frequency of these incidents indicates that conversion to a potentially contaminating agent such as a dry chemical can have a significant adverse impact on aircraft 'out of service' and repair costs. The annual costs associated with engine repairs due to collateral damage could be as high as $40.5 M. This assumes an annual frequency of 162 incidents involving contamination of aircraft. DTIC

N95-14611*# National Aeronautics and Space Administration. Ames Research Center, Moffett Field, CA.

CTAS DATA ANALYSIS PROGRAM

Frank Neuman, Heinz Erzberger, and Michael S. Schueller 4 Oct. 1994 53 p

(RTOP 505-64-13)

(NASA-TM-108842; A-94121; NAS 1.15:108842) Avail: CASI HC A04/MF A01

The analysis program (AN) is specifically designed to produce graphic and tabular information to aid in the design and checkout of the Center TRACON Automation System (CTAS). To best reveal CTAS operation and possible problems, data are plotted in many different ways both in detail and summary form. AN has been designed to analyze both radar surveillance data and output data from CTAS. AN has been extensively used to debug and refine CTAS. It is also being used in the field to monitor and assess CTAS performance. AN is continuously refined to keep up with changing needs. The present version of AN grew out of analysis of Denver Center data. However, the AN software has been written to be adaptable to any other facility Center or TRACON. Presently, one can select Denver Stapleton, Denver International, Dallas/Fort Worth International Airport, and Dallas Love Field. Author

N95-14893# Advisory Group for Aerospace Research and Development, Neuilly-Sur-Seine (France). Flight Vehicle Integration Panel.

FLIGHT IN AN ADVERSE ENVIRONMENT [LE VOL EN ENVIRONNEMENT HOSTILE]

Nov. 1994 161 p Lecture series held in Brunswick, Germany, 7-8 Nov. 1994, in Lisbon, Portugal, 10-11 Nov. 1994, and in Atlantic City, NJ, 15-16 Nov. 1994

(AGARD-LS-197; ISBN-92-836-1006-7) Copyright Avail: CASI HC A08/MF A02

The environment in which an airplane must operate is a major cause of aircraft accidents. This lecture series focuses on specific aspects of the environment, both natural and man-made, which are the major contributors to these accidents as follows: (1) wake turbulence and the generation of trailing vortex systems; (2) the results of an extensive flight test program concerning winter storms off the east coast of Canada including effect on aircraft operations; (3) electromagnetic effects including electrical discharge properties, in-flight test program, in-flight lightning models and lightning simulation techniques; (4) response of an aircraft to wind shear and methods of detection and quantifying this natural hazard; (5) heavy rain effects on aircraft systems performances in the light of full scale and model tests; (6) measurements of atmospheric turbulence, treatment of aircraft response to random turbulence and discrete gusts. For individual titles, see N95-14894 through N95-14900.

N95-14894# Pennsylvania State Univ., University Park, PA. Dept. of Aerospace Engineering.

WAKE TURBULENCE **c02**

Barnes W. McCormick *In* AGARD, Flight in an Adverse Environment Nov. 1994 15 p (For primary document see N95-14893 03-03)

Copyright Avail: CASI HC A03/MF A02

Wake turbulence is a misnomer. Turbulence implies a random process whereas the term 'wake turbulence' refers to the hazard posed to smaller airplanes by the ordered, rotational flow in the trailing vortex systems behind larger airplanes. This lecture begins by examining the relationship of aircraft size, geometry and operating conditions to the strength of an aircraft's trailing vortex system. Next, the velocity field initially induced close behind the generating airplane by its trailing vortex system is defined. This is followed by a discussion of the various ways in which a vortex system can dissipate and the many factors which affect the dissipation. In particular, the effects of atmospheric turbulence, ground proximity and vortex bursting on the ensuing behavior of the vortex system are considered. The paper continues with a study of the dynamics of an aircraft encountering the wake of a larger airplane. The degree to which an aircraft is threatened by a given vortex system of known characteristics is analyzed and the hazard posed by a given vortex system to a following aircraft quantified. Finally, the paper concludes with recommendations on possible ways to alleviate the safety and operational problems associated with wake turbulence. Author

N95-14895# Institute for Aerospace Research, Ottawa (Ontario). Flight Research Lab.

WINTER STORMS RESEARCH IN CANADA **c47**

J. Ian MacPherson and George A. Isaac *In* AGARD, Flight in an Adverse Environment Nov. 1994 21 p Sponsored by Federal Panel on Energy Research and Development; Atmospheric Environment Service; National Research Council of Canada; National Search and Rescue Secretariat, Dept. of National Defence; Boeing Commercial Airplane Co.; and Airbus Industrie (For primary document see N95-14893 03-03)

Copyright Avail: CASI HC A03/MF A02

Canada has undertaken long-term research program to study winter storms in coastal regions, with the objectives of improving their forecast and understanding their embedded mesoscale features, rapid intensification, and microphysical conditions associated with aircraft icing. In cooperation with the Atmospheric Environment Service of Environment Canada (AES), the National Research Council (NRC) Twin Otter and Convair 580 aircraft have been instrumented to measure the motion and thermal structure of the atmosphere and the microphysics of cloud and precipitation. The aircraft have been flown in two Atlantic Storms projects in conditions that pilots usually attempt to avoid. Examples of the hazardous conditions encountered in these research flights are presented in this paper, along with supporting air motion and microphysics data recorded aboard the aircraft. Incidents of airframe icing, turbulence, strong winds and wind shear serve as an introduction to the more detailed treatment of these subjects by subsequent lecturers. Other related subjects covered include research reduced visibility and on-ground icing of aircraft. Information is presented on recent developments in instrumentation for the early recognition and warning of hazardous flight conditions. The paper concludes with a look to the future for coping with winter storms in Canada, including planned research field programs. Author

N95-14896# Office National d'Etudes et de Recherches Aerospatiales, Paris (France). Dept. of Physics.

ESD AND LIGHTNING INTERACTIONS ON AIRCRAFT

Jean Louis Boulay *In* AGARD, Flight in an Adverse Environment Nov. 1994 19 p (For primary document see N95-14893 03-03)

Copyright Avail: CASI HC A03/MF A02

Under certain adverse conditions, particularly inside or in the vicinity of clouds, aircraft may be affected by two different electric phenomena: electrostatic discharges and lightning discharges. When electrostatic charges accumulate on an aircraft structure, electric discharges occur. These discharges generate RF interference that severely impairs the operation of onboard radio navigation and communication equipment. Sometimes energetic discharges have direct effects on structural components like radomes, windshields and canopies. Lightning discharges may have a very powerful and dangerous effects on an aircraft in flight. The electromagnetic coupling of any repetitive current pulses through the airframe can upset or deteriorate airborne equipment; and under certain circumstances, lightning flashes may also cause serious direct damage to structural components. Author

N95-14897*# National Aeronautics and Space Administration. Lewis Research Center, Cleveland, OH.

ICING: ACCRETION, DETECTION, PROTECTION

John J. Reinmann *In* AGARD, Flight in an Adverse Environment Nov. 1994 27 p (For primary document see N95-14893 03-03)

Copyright Avail: CASI HC A03/MF A02

The global aircraft industry and its regulatory agencies are currently involved in three major icing efforts: ground icing; advanced technologies

for in-flight icing; and tailplane icing. These three major icing topics correspondingly support the three major segments of any aircraft flight profile: takeoff; cruise and hold; and approach and land. This lecture addressess these three topics in the same sequence as they appear in flight, starting with ground deicing, followed by advanced technologies for in-flight ice protection, and ending with tailplane icing. Derived from text

N95-14898# Woodfield (Alan A.), Bedford (England).
WIND SHEAR AND ITS EFFECTS ON AIRCRAFT
Alan A. Woodfield *In* AGARD, Flight in an Adverse Environment Nov. 1994 31 p (For primary document see N95-14893 03-03)
Copyright Avail: CASI HC A03/MF A02

Wind shear has been responsible for several major accidents and many incidents during landing and take off. In aviation terms, wind changes that cause flight path deviations (wind shear) are mainly those occurring over distances between about 150 and 3000m, i.e. approximately 3 to 40 sec. at approach speeds. General characteristics of many forms of wind shear are described together with measured data on the probability of meeting headwind shears of different magnitudes. This is followed by analysis of the basic response of aircraft to both horizontal wind changes and downdrafts, and discussion of aircraft sensitivity to wind shear. Several recorded examples of wind shear in both normal operational and accident scenarios are presented. The relevance of different ways of quantifying wind shear severity is examined, including a calculation of height loss that can be used when a wind shear is fully defined, and the 'F' factor, which is used with reactive wind shear measuring systems. Some insight into the probabilities of false or missed warnings with each system is derived using the measured probability data. A brief outline is given of the relevant characteristics of different wind shear prediction and detection systems. The lecture concludes with a study of the ways in which pilots can be trained and assisted to survive most wind shear encounters and, hopefully, avoid those which could be catastrophic. It is concluded that, given appropriate training and aircraft systems, it is possible to survive encounters with nearly all those wind shears that caused fatal accidents in previous years. New predictive detection systems offer the possibility to warn an aircraft before it attempts to penetrate those extremely rare wind shears that are beyond its performance capability. Author

N95-14899*# National Aeronautics and Space Administration. Langley Research Center, Hampton, VA.
HEAVY RAIN EFFECTS
R. Earl Dunham, Jr. *In* AGARD, Flight in an Adverse Environment Nov. 1994 17 p (For primary document see N95-14893 03-03)
Copyright Avail: CASI HC A03/MF A02

This paper summarizes the current state of knowledge of the effect of heavy rain on airplane performance. Although the effects of heavy rain on airplane systems and engines are generally known, only recently has the potential aerodynamic effect of heavy rain been recognized. In 1977 the United States Federal Aviation Administration (FAA) conducted a study of 25 aircraft accidents and incidents which occurred between 1964 and 1976 in which low-altitude wind shear could have been a contributing factor. Of the 25 cases (23 approach or landing and 2 take-off) in the study, ten cases had occurred in a rain environment, and in five cases these were classified as intense or heavy rain encounters. These results led to the reconsideration of high-intensity, short-duration rainfall as a potential weather-related aircraft safety hazard, particularly in the take-off and/or approach phases of flight. Author

N95-14900# Technische Univ., Brunswick (Germany). Inst. of Flight Guidance and Control.
TURBULENCE: ENGINEERING MODELS, AIRCRAFT RESPONSE c08
Manfred Swolinsky *In* AGARD, Flight in an Adverse Environment Nov. 1994 20 p (For primary document see N95-14893 03-03)
Copyright Avail: CASI HC A03/MF A02

This paper covers problems of flight in a turbulent atmosphere. A realistic simulation of aircraft behavior in turbulent air requires different engineering models. On one hand, this means a mathematical description of random turbulence or short scale gusts. For simple problems, a computation of the turbulence velocity vector only at the trajectory of the aircraft is sufficient. In cases of detailed investigations, the generation of a 3-dimensional spatial turbulence field is necessary. Additional real time requirements imply special approaches, such as the realization of a matrix wind model. On the other hand the description of the interaction between turbulence or short scale gusts and aircraft may require complex aerodynamic models especially if the gust scale and the aircraft scale are in the same order of magnitude. The presented multi point or lifting surface models consider the wind vector at several points along the wing span under real time constraints. Based on simulation results and flight test data, the dynamic aircraft response is discussed. Single gust effects are demonstrated by examples of cross flights through the updraft of a powerplant cooling tower. Author

N95-14916# National Transportation Safety Board, Washington, DC.
AIRCRAFT ACCIDENT REPORT: OVERSPEED AND LOSS OF POWER ON BOTH ENGINES DURING DESCENT AND POWER-OFF EMERGENCY, LANDING SIMMONS AIRLINES, INC., d/b/a, AMERICAN EAGLE FLIGHT 3641, N349SB FALSE RIVER AIR PARK, NEW ROADS, LOUSIANA, 1 FEBRUARY 1994
27 Sep. 1994 80 p
(NTSB/AAR-94/06; PB94-910408) Avail: CASI HC A05/MF A01

This report explains the emergency landing of American Eagle flight 3641, a Saab 340B airplane, at False River Air Park, New Roads, Louisiana, on February 1, 1994. The safety issues in the report focused on the safety hazards involved with the inflight operation of propellers in the beta mode in airplanes for which such operation is prohibited. The Safety Board reiterated Safety Recommendation A-94-62, which is intended to prevent the in-flight beta operation unless the airplane is certified for such use. Author

N95-15066# National Transportation Safety Board, Washington, DC.
ANNUAL REVIEW OF AIRCRAFT ACCIDENT DATA: US AIR CARRIER OPERATIONS, CALENDAR YEAR 1992
15 Sep. 1994 72 p
(NTSB/ARC-94/02; PB95-100319) Avail: CASI HC A04/MF A01

This publication presents the record of aviation accidents involving revenue operations of U.S. Air Carriers including Commuter Air Carriers and On Demand Air Taxis for calendar year 1992. The report is divided into three major sections according to the federal regulations under which the flight was conducted - 14 CFR 121, Scheduled 14 CFR 135, or Nonscheduled 14 CFR 135. In each section of the report tables are presented to describe the losses and characteristics of 1992 accidents to enable comparison with prior years. Author

N95-15439 Midwest Research Inst., Kansas City, MO.
DEVELOPMENT OF ANTI-ICING TECHNOLOGY
R. R. Blackburn, E. J. McGrane, C. C. Chappelow, D. W. Harwood, and E. J. Fleege Apr. 1994 497 p See also PB253268, PB271250, PB88-233705 and PB88-233713 Prepared in cooperation with Minnesota Dept. of Transportation, Duluth, MN
(Contract DOT-SHRP-H-208A)
(PB94-195369; SHRP-H-385; ISBN-0-309-05761-2) Copyright Avail: Issuing Activity

Scandinavian and other European countries have shown that applying a chemical freezing-point depressant on a highway pavement prior to, or very quickly after, the start of frozen participation minimizes the formation of an ice-pavement bond. Nine state highway agencies conducted anti-icing experiments when possible during the 1991-92 and 1992-93 winters. These tests were used to develop a better understanding of both the conditions under which anti-icing will be effective and how to conduct anti-icing efficiently to ensure the greatest success. Prewetted salt and liquid chemicals were used during the anti-icing experiments. The project also involved evaluating specialized equipment for applying controlled quantities of solid, prewetted or liquid chemicals at minimum application rates required for effective anti-icing treatment. NTIS

04 AIRCRAFT COMMUNICATIONS AND NAVIGATION

Includes digital and voice communication with aircraft; air navigation systems (satellite and ground based); and air traffic control.

For related information see also *17 Space Communications, Spacecraft Communications, Command and Tracking* and *Communications and Radar.*

No abstracts in this category.

05 AIRCRAFT DESIGN, TESTING AND PERFORMANCE

Includes aircraft simulation technology.

For related information see also *18 Spacecraft Design, Testing and Performance* and *39 Structural Mechanics.*For land transportation vehicles see *85 Urban Technology and Transportation.*

N95-13703*# Universities Space Research Association, Columbia, MD.
VIPER
L. E. Paul Gilbert, Cassie Berry, Dana Lamborn, Jack Murphy, and Chris OKelly 8 Dec. 1993 19 p
(Contract NASw-4435)
(NASA-CR-197191; NAS 1.26:197191; F93-2B-0R15) Avail: CASI HC A03/MF A01

A Viper aircraft was redesigned with a new airfoil and engine to verify if improvements can be made to the baseline configuration. The two major redesigning processes were: replacing the baseline aircraft's NACA 652-415 airfoil with an NLF 0414 Natural Laminar Flow airfoil, and the baseline aircraft's Lycoming 0-235 engine with a Teledyne Continental GR-36 rotary combustion engine. As a result of these changes: (1) the Viper aircraft becomes smaller in most respects (gross weight, wing platform area, and horizontal tail area); (2) overall drag of the aircraft decreased (due to reduction in area and the reduced drug of the new airfoil); (3) cruise velocity, the maximum rate of climb at sea level, and takeoff distance (but not landing distance) decreased; and (4) cost increased. Although the overall drag decreased, the performance remained about the same due to the reduced horsepower available from the Teledyne Continental engine. CASI

N95-13981 Federal Aviation Administration, Kansas City, MO. Aircraft Certification Service.
FATIGUE EVALUATION OF EMPENNAGE, FORWARD WING, AND WINGLETS/TIP FINS ON PART 23 AIRPLANES Final Technical Report
15 Feb. 1994 64 p Limited Reproducibility: More than 20% of this document may be affected by microfiche quality
(PB94-196813; FAA/ACE-100-01) Avail: Issuing Activity (National Technical Information Service (NTIS))

This report provides technical guidance for complying with the fatigue evaluation requirements of Part 23 (small and commuter category airplanes) of the Federal Aviation Regulations, Section 23.572, pertaining to empennage, forward wing, and winglets/tip fins. Detailed procedures are described for developing empennage repeated loads using published airplane center-of-gravity normal acceleration spectra in conjunction with basic airplane data. An alternate approach that eliminates calculating applied loads uses empirically derived stress equations from measured flight strain survey data, coupled with the airplane center-of-gravity normal acceleration spectra and proposed airplane usage data. NTIS

N95-14102# Advisory Group for Aerospace Research and Development, Neuilly-Sur-Seine (France). Flight Mechanics Panel.
IDENTIFICATION OF DYNAMIC SYSTEMS. VOLUME 3: APPLICATIONS TO AIRCRAFT. PART 2: NONLINEAR ANALYSIS AND MANOEUVRE DESIGN [L'IDENTIFICATION DES SYSTEMES DYNAMIQUES: APPLICATIONS AUX AERONEFS. TITRE 2: L'ANALYSE NON-LINEAIRE ET LA CONCEPTION DE LA MANOEUVRE]
J. A. Mulder (Technische Univ., Delft, Netherlands.), J. K. Sridhar (Technische Univ., Delft, Netherlands.), and J. H. Breeman (National Aerospace Lab., Amsterdam, Netherlands.) May 1994 213 p Flight Test Techniques Series
(AGARD-AG-300-Vol-3-Pt-2; ISBN-92-835-0748-7) Copyright Avail: CASI HC A10/MF A03

This AGARDograph is a sequel to the previous AGARDographs published in the AGARD Flight Test Techniques Series, Volume 2 on 'Identification of Dynamic Systems' and Volume 3 on 'Identification of Dynamic Systems - Applications to Aircraft - Part 1: The Output Error Approach' both written by R.E. Maine and K.W. Iliff. The intention of the present document is to cover some of those areas which were either absent or only briefly mentioned in those volumes. These areas are Flight Path Reconstruction, Nonlinear Model Identification, Optimal Input Design and Flight Test Instrumentation. The present approach to identification is rather different from that presented in the earlier AGARDographs in the sense that the identification problem is decomposed into a state estimation and a parameter identification part. This approach is referred to as the Two-Step Method (TSM), although one will find other names like Estimation Before Modelling (EBM) in the literature. It will be shown in the present AGARDograph that this approach has significant practical advantages over methods which no attempt is made to decompose the joint parameter-state estimation problem. The two-step method is generally applicable to flight vehicles such as fixed wing aircraft and rotorcraft which are equipped with state of the art inertial reference systems. The theoretical developments in the present AGARDograph will be illustrated with examples of a flight test program with the De Havilland DHC-2 Beaver aircraft, the experimental aircraft of the Delft University of Technology which has been used for almost two decades to test new ideas in the science of aircraft parameter identification. Author

N95-14205# Naval Air Warfare Center, Patuxent River, MD. Aircraft Div.
ADD A DIMENSION TO YOUR ANALYSIS OF THE HELICOPTER LOW AIRSPEED ENVIRONMENT
Herman Kolwey 1994 30 p
(AD-A283982) Avail: CASI HC A03/MF A01

We have long strived to better define the low airspeed relative wind limits of the helicopter and also to define the helicopter performance in a 3-dimensional (3-D) format. These concepts were first presented in an AHS paper in 1977 also published as NAVAIRTESTCEN Technical Memorandum TM 77-2 RW of 29 April 1977. Recent analysis of the low airspeed environment for purposes of defining deficiencies and evaluating an Unanticipated Right Yaw (URY) or Loss of Tail Rotor Effectiveness (LTE) problem have developed a new method of reducing and presenting critical azimuth test data. A new method of reducing test data was presented to the Society of Flight Test Engineers in a 1992 paper and involved the automatic handling of test data along with including the oscillatory component of the trim point. In our opinion, presentation formats were more logical than the classical methods of presentation of critical azimuth data, but they were still presented in a 2-dimensional (2-D) format. Dispersion data on the plot gave indications of the third dimension of workload as has been presented by the Army in their reports, but still on a 2-D plot. The location of interference effects could be determined by looking at six or seven 2-D plots of the type presented in the prior paper. DTIC

N95-14306# Loral Systems, Inc., Orlando, FL. Adst Program Office.
ADVANCED DISTRIBUTED SIMULATION TECHNOLOGY ADVANCED ROTARY WING AIRCRAFT. STUDY COMPARING APPROACHES TO MODELING THE ARWA MAIN ROTOR
Roger Branson 18 Mar. 1994 19 p
(Contract N61339-91-D-0001)
(AD-A280824; ADST/TR-94-003280) Avail: CASI HC A03/MF A01

The Advanced Distributed Simulation Technology (ADST) Advanced Rotary Wing Aircraft (ARWA) study comparing approaches to modeling the ARWA main rotor provides details of technical approaches for both a blade element model and a rotor disk model to simulate the flying qualities of the ARWA simulation system. A background of aeromodeling and discussion of the technical and cost merits for both approaches is provided. DTIC

N95-14604*# National Aeronautics and Space Administration. Lewis Research Center, Cleveland, OH.
GRAPHICAL USER INTERFACE FOR THE NASA FLOPS AIRCRAFT PERFORMANCE AND SIZING CODE

Thomas M. Lavelle and Brian P. Curlett Oct. 1994 39 p
(RTOP 505-69-50)
(NASA-TM-106649; E-8957; NAS 1.15:106649) Avail: CASI HC A03/MF A01

XFLOPS is an X-Windows/Motif graphical user interface for the aircraft performance and sizing code FLOPS. This new interface simplifies entering data and analyzing results, thereby reducing analysis time and errors. Data entry is simpler because input windows are used for each of the FLOPS namelists. These windows contain fields to input the variable's values along with help information describing the variable's function. Analyzing results is simpler because output data are displayed rapidly. This is accomplished in two ways. First, because the output file has been indexed, users can view particular sections with the click of a mouse button. Second, because menu picks have been created, users can plot engine and aircraft performance data. In addition, XFLOPS has a built-in help system and complete on-line documentation for FLOPS. Author

N95-14794*# Rockwell International Corp., Downey, CA. Space Systems Div.
REQUIREMENTS REPORT FOR SSTO VERTICAL TAKE-OFF AND HORIZONTAL LANDING VEHICLE
H. S. Greenberg 4 Nov. 1994 156 p
(Contracts NCC1-193; NCC2-9003; NCC8-39)
(NASA-CR-197029; NAS 1.26:197029; SSD94D0217B) Avail: CASI HC A08/MF A02

This document describes the detailed design requirements and design criteria to support Structures/TPS Technology development for SSTO winged vehicle configurations that use vertical take-off and horizontal landing and delivers 25,000 lb payloads to a 220 nm circular orbit at an inclination of 51.6 degrees or 40,000 lb payloads to a 150 nm circular orbit at a 28.5 degree inclination. Derived from text

N95-14840# Joint Technical Coordinating Group for Aircraft Survivability, Wright-Patterson AFB, OH.
BIBLIOGRAPHY OF JOINT AIRCRAFT SURVIVABILITY REPORTS AND RELATED DOCUMENTS Final Report, 1975 - 1994
James A. Buckner Jul. 1994 130 p
(AD-A282795; JTCG/AS-94-D-004) Avail: CASI HC A07/MF A02

A JTCD/AS bibliography publication of Joint Aircraft Survivability reports and other related documents are enclosed. Subgroup titles are as follows: (1) Susceptibility reduction documentation; (2) Vulnerability reduction documentation; (3) Survivability methodology documentation; (4) Administrative and group projects documentation; (5) Aircraft battle damage repair documentation; and (6) Aircraft survivability projects (those not JTCG/AS funded). Documents are indexed by report number and title. CASI

N95-14849# Naval Postgraduate School, Monterey, CA.
ARTIFICIAL NEURAL NETWORK MODELING OF DAMAGED AIRCRAFT M.S. Thesis
Clifford A. Brunger Mar. 1994 109 p
(AD-A283227) Avail: CASI HC A06/MF A02

Aircraft design and control techniques rely on the proper modeling of the aircraft's equations of motion. Many of the variables used in these equations are aerodynamic coefficients which are obtained from scale models in wind tunnel tests. In order to model damaged aircraft, every aerodynamic coefficient must be determined for every possible damage mechanism in every flight condition. Designing a controller for a damaged aircraft is particularly burdensome because knowledge of the effect of each damage mechanism on the model is required before the controller can be designed. Also, a monitoring system must be employed to decide when and how much damage has occurred in order to reconfigure the controller. Recent advances in artificial intelligence have made parallel distributed processors (artificial neural networks) feasible. Modeled on the human brain, the artificial neural network's strength lies in its ability to generalize from a given model. This thesis examines the robustness of the artificial neural network as a model for damaged aircraft. DTIC

N95-14852*# National Aeronautics and Space Administration. Langley Research Center, Hampton, VA.
SPATIAL AWARENESS COMPARISONS BETWEEN LARGE-SCREEN, INTEGRATED PICTORIAL DISPLAYS AND CONVENTIONAL EFIS DISPLAYS DURING SIMULATED LANDING APPROACHES
Russell V. Parrish, Anthony M. Busquets, Steven P. Williams, and Dean E. Nold Oct. 1994 25 p Prepared in cooperation with Army Communications-Electronics Command, Fort Monmouth, NJ
(RTOP 505-64-53-03; DA Proj. 1L1-62211-A-47-A)
(NASA-TP-3467; L-17356; NAS 1.60:3467; CECOM-TR-94-E-1) Avail: CASI HC A03/MF A01

An extensive simulation study was performed to determine and compare the spatial awareness of commercial airline pilots on simulated landing approaches using conventional flight displays with their awareness using advanced pictorial 'pathway in the sky' displays. Sixteen commercial airline pilots repeatedly made simulated complex microwave landing system approaches to closely spaced parallel runways with an extremely short final segment. Scenarios involving conflicting traffic situation assessments and recoveries from flight path offset conditions were used to assess spatial awareness (own ship position relative the the desired flight route, the runway, and other traffic) with the various display formats. The situation assessment tools are presented, as well as the experimental designs and the results. The results demonstrate that the integrated pictorial displays substantially increase spatial awareness over conventional electronic flight information systems display formats. Author

N95-14909*# Mississippi State Univ., State College, MS. Computational Fluid Dynamics Lab.
PROPULSION/AIRFRAME INTERFERENCE FOR DUCTED PROPFAN ENGINES WITH GROUND EFFECT Final Report, Mar. 1993 - Feb. 1995
Abdollah Arabshahi and Ramesh Pankajakshan 11 Nov. 1994 17 p Prepared in cooperation with NSF, Washington, DC
(Grant NAG1-226)
(NASA-CR-197110; NAS 1.26:197110) Avail: CASI HC A03/MF A01

The advanced propfan propulsion systems design of the next-generation subsonic transport aircraft has been of interest to many airline companies in the past several years. This is due to the studies which indicate that an efficient ducted propfan engine technology offers a significant reduction in aircraft fuel consumption. However, because of the geometric complexity of the configuration, one challenge is the integration of the ducted propfan engine with the airframe so that aerodynamic interference effects frequently encountered near the nacelle can be minimized, or perhaps, optimized. To understand this interaction phenomenon better, it is desirable to have a reliable and efficient computational tool that can predict propeller effects on the flowfield around complex configurations. Derived from text

N95-15451 RAND Corp., Santa Monica, CA.
THE F-16 MULTINATIONAL STAGED IMPROVEMENT PROGRAM: A CASE STUDY OF RISK ASSESSMENT AND RISK MANAGEMENT
Frank Camm 1993 123 p Limited Reproducibility: More than 20% of this document may be affected by microfiche quality
(Contract F49620-91-C-0003)
(AD-A281706; RAND/N-3619-AF) Avail: CASI HC A06

The F-16 Multinational Staged Improvement Program (MSIP) is the development program that the F-16 program has used to move beyond the F-16A/B. Its primary product has been the F-16C/D, an aircraft whose design evolves over time as new technological capabilities become available or attractive to incorporate in its design. MSIP is the program that F-16C/D developers have used to introduce these capabilities over time. The prime contractor for the F-16, General Dynamics, and the F-16 System Program Office (SPO) formally initiated the program in 1980. This study examines MSIP, giving special attention to means of assessing and managing the risks associated with system development. It is one of seven case studies conducted by RAND for the Air Force to examine the Air Force's management of risk in development programs during the 1980's. DTIC

N95-15742*# Universities Space Research Association, Columbia, MD.
THE ALUMINUM FALCON: A LOW COST MODERN COMMERCIAL TRANSPORT
Mark Bryant, Estela Hernandez, Gregory King, Alex Choua Lor, Jana Musser, Deanne Trigs, and Susan Yee 6 Jun. 1994 109 p

(Contract NASw-4435)
(NASA-CR-197180; NAS 1.26:197180) Avail: CASI HC A06/MF A02

The American Institute of Aeronautics and Astronautics (AIAA) released a Request For Proposal (RFP) in the form of an undergraduate design competition for a 153 passenger jet transport with a range of 3,000 nautical miles. The primary requirement for this aircraft was low cost, both in acquisition and operation, with a technology availability date of the year 2000. This report presents the Non-Solo Design Group's response to the RFP, the Aluminum Falcon (AF-1). Non-Solo's approach to development was to take the best elements of seven individual preliminary designs, then combine and refine them. The resulting aircraft meets or exceeds all requirements of both the RFP and the Federal Aviation Administration (FAA). Highlights include a revolutionary wing planform, known as an M-wing, which offers many advantages over a conventional aft swept wing. For example, the M-wing lessens the travel in the aircraft center of gravity caused by fuel being stored in the wing. It also reduces the amount of torque imposed on the center wing box because more of the lifting load acts near the fuselage joint, rather than behind it. In essence, the M-wing offers the best of both worlds: using a forward swept wing root places the aerodynamic center of the wing further forward and allows the landing gear to be placed without the use of a yahudi. At the same time, with the outboard section swept backward the tip retains an amount of aeroelastic dampening that is lost on a completely forward swept wing. The result is a wing which has many advantages of a straight, unswept wings without the severe compressibility effects at high Mach numbers. Other highlights include judicious use of composites, giving recognition to the importance of weight and its effect on aircraft cost and performance, and an advanced passenger entertainment system which can be used as a source of revenue for the airlines. This aircraft meets the low-cost doctrine with an acquisition cost of $29 million and a direct operating cost of 3.5 cents per seat mile. The AF-1 incorporates new ideas with existing technology to result in an aircraft that will retain market viability well into the next century. Author

N95-15815# Army Test and Evaluation Command, Aberdeen Proving Ground, MD.
TEST OPERATION PROCEDURE (TOP): VIBRATION TESTING OF HELICOPTER EQUIPMENT Final Report
26 Aug. 1994 42 p
(AD-A284433; TOP-7-3-531) Avail: CASI HC A03/MF A01

This TOP provides guidelines and procedures for helicopter vibration calibration and measurements. Guides are provided for vibration frequencies and magnitudes to be expected. Procedures are developed for transducer selection and placement, instrumentation system design, and data collection. Emphasis is placed on use of piezoelectric accelerometers for vibration measurement and tape recorders for data storage. Step-by-step procedures are provided for accelerometer sensitivity measurement and calibration, instrumentation system adjustments and calibrations, and data collection and handling. DTIC

N95-15821 Technische Hochschule, Aachen (Germany). Inst. fuer Mechanik.
PREDICTION OF ROTOR-BLADE DEFORMATIONS DUE TO UNSTEADY AIRLOADS Interim Report No. 1, May 1994 - Jun. 1995
J. Ballmann and S. Schlechtriem 31 Jul. 1994 9 p Limited Reproducibility: More than 20% of this document may be affected by microfiche quality
(Contract N68171-94-C-9068)
(AD-A284467; R/D-7213-AN-01) Avail: Issuing Activity (Defense Technical Information Center (DTIC))

SOFIA, a computer code for aeroelastic computations, was applied to predict the rotor blade deformations due to unsteady airloads caused by blade-vortex interaction (BVI) and to investigate appropriate control movements to minimize vibration and noise. The computation of the unsteady, compressible, inviscid flow about rotor-blades uses an Euler CFD code, while a quasi one-dimensional structural solver is used to compute the deformation of the rotor blades. DTIC

N95-14469*# Rockwell International Corp., El Segundo, CA.
EXTRACTING A REPRESENTATIVE LOADING SPECTRUM FROM RECORDED FLIGHT DATA
Anthony G. Denyer *In* NASA. Langley Research Center, FAA/NASA International Symposium on Advanced Structural Integrity Methods for Airframe Durability and Damage Tolerance Sep. 1994 p 225-240 (For primary document see N95-14453 03-39)
Avail: CASI HC A03/MF A04

N95-14481*# Aeronautical Systems Div., Wright-Patterson AFB, OH.
CHALLENGES FOR THE AIRCRAFT STRUCTURAL INTEGRITY PROGRAM
John W. Lincoln *In* NASA. Langley Research Center, FAA/NASA International Symposium on Advanced Structural Integrity Methods for Airframe Durability and Damage Tolerance Sep. 1994 p 409-423 (For primary document see N95-14453 03-39)
Avail: CASI HC A03/MF A04

N95-14486*# Academy of Sciences (USSR), Moscow (USSR). Central Aerohydrodynamic Inst.
ADVANCED METHOD AND PROCESSING TECHNOLOGY FOR COMPLICATED SHAPE AIRFRAME PART FORMING
P. V. Miodushevsky and G. A. Rajevskaya *In* NASA. Langley Research Center, FAA/NASA International Symposium on Advanced Structural Integrity Methods for Airframe Durability and Damage Tolerance Sep. 1994 p 497-503 (For primary document see N95-14453 03-39)
Avail: CASI HC A02/MF A04

06 AIRCRAFT INSTRUMENTATION

Includes cockpit and cabin display devices; and flight instruments.

For related information see also *19 Spacecraft Instrumentation* and *35 Instrumentation and Photography.*

N95-13984 Thomson-CSF, Paris (France).
TECHNICAL REVUE THOMSON-CSF, VOLUME 26, NO. 1, MARCH 1994. FLAT PANELS FOR VISUALISATION [ECRANS PLATS POUR VISUALISATION. REVUE TECHNIQUE, VOLUME 26, NO. 1, MARS 1994. ECRANS PLATS POUR VISUALISATION]
Mar. 1994 270 p In ENGLISH and FRENCH
(PB94-197969) Avail: Issuing Activity (National Technical Information Service (NTIS))

The following topics are discussed: (1) Visualization displays towards flat panels; (2) An introduction to liquid crystal displays; (3) Active matrix liquid crystal displays: Principles and technology; (4) Low temperature polysilicon TFT's for active matrix LCD's; (5) Liquid crystal polymer composites for display applications; (6) Flat screen plasma displays; (7) Matrix displays for avionics; (8) LCD rear projection: The emerging technology for the large size TV consumer market; (9) Polarized illumination liquid crystal projector; and (10) Flat panel displays used in ruggedized data terminals. NTIS

N95-14175# Starmark Corp., Arlington, VA.
CIVIL USE OF NIGHT VISION DEVICES: EVALUATION PILOT'S GUIDE, PART 2 Final Report
David L. Green Jul. 1994 31 p Prepared for Science Applications International Corp., Arlington, VA
(DOT/FAA/RD-94/19; Rept-91RR-44-Pt-2) Avail: CASI HC A03/MF A01

This document was developed to aid in the evaluation of the use of night vision goggles (NVG's) by civil helicopter pilots. This report was used to prepare pilots to participate in the flight test program. The principal task was to determine if there are any unresolved safety issues that would preclude pilot use of NVG's during helicopter operations under Federal Aviation Regulations Parts 91 or 135. Certainly NVG's can enable a pilot to 'see better' at night and to accomplish certain flight objectives. However, the question is, is safety degraded during any phase of the flight operation if pilots use these devices. Even if the use of NVG's dramatically improves operational effectiveness, current safety margins must be maintained or improved during all phases of flight. This report is one of three documents that were developed for evaluating the use of night vision goggles (NVG's) by EMS helicopter pilots. The other two reports are: (1) FAA/RD-94/18, Civil Use of Night Vision Devices - Evaluation Pilot's Guide, Part I; and (2) FAA/RD-94/20, Assessment of Night Vision Goggle Workload - Flight Test Engineer's Guide. Author

N95-14518* National Aeronautics and Space Administration. Ames Research Center, Moffett Field, CA.
AIRCRAFT MANEUVER ENVELOPE WARNING SYSTEM Patent
Courtland C. Bivens, inventor (to NASA), Joel M. Rosado, inventor (to NASA), and Burnett Lee, inventor (to NASA) 25 Oct. 1994 9 p Filed 16 Mar. 1993
(NASA-Case-ARC-11953-1; US-Patent-5,359,326; US-Patent-Appl-SN-032067; US-Patent-Class-340-971; US-Patent-Class-340-945; US-Patent-Class-340-978; Int-Patent-Class-G01C-21/00) Avail: US Patent and Trademark Office

A maneuver envelope warning system for an aircraft having operating limits, operating condition sensors and an indicator driver. The indicator driver has a plurality of visual indicators. The indicator driver determines a relationship between sensed operating conditions and the operating limits; such as, a ratio therebetween. The indicator driver illuminates a number of the indicators in proportion to the determined relationship. The position of the indicators illuminated represents to a pilot in an easily ascertainable manner whether the operational conditions are approaching operational limits of the aircraft, and the degree to which operational conditions lie within or exceed operational limits. Author

N95-14799*# Rockwell International Corp., Downey, CA. Space Systems Div.
STRATEGIC AVIONICS TECHNOLOGY DEFINITION STUDIES, POWER VOTER REDUNDANCY MANAGEMENT. POWER VOTER APPLICATIONS IN NEW VEHICLE ARCHITECTURES Final Report
Mel Weiss, J. A. McKinney, and K. L. Cureton 31 Oct. 1994 24 p
(Contract NAS9-18880)
(NASA-CR-197049; NAS 1.26:197049; SSD94D0343) Avail: CASI HC A03/MF A01

The power voter hybrid module (PVHM) is a power switch that is resettable in flight or on the ground. If an overcurrent situation arises, the PVHM detects it and shuts the load off. By simply recycling the vote off back to on, the PVHM can now be ready to reactivate the load. This feature, other discussed features, and its low power dissipation make the PVHM an excellent candidate to replace current drivers and relay drivers presently within most systems. The front end of the PVHM is a 3 of 5 voter. However, it can easily be tailored to meet the requirements of present and future systems. Derived from text

N95-15392 Naval Surface Warfare Center, Dahlgren, VA.
ELECTROMAGNETIC REVERBERATION CHARACTERISTICS OF A LARGE TRANSPORT AIRCRAFT Final Report
Michael O. Hatfield, Gustav J. Freyer, D. M. Johnson, and Charles L. Farthing Jul. 1994 95 p Limited Reproducibility: More than 20% of this document may be affected by microfiche quality
(AD-A282923; NSWCDD/TR-93/339) Avail: CASI HC A05

A demonstration test to investigate the reverberation characteristics of the avionics bay and cockpit of a typical commercial aircraft was conducted on a decommissioned Boeing 707-720B aircraft. The aircraft, located at the Aerospace Maintenance and Regeneration Center, Davis Monthan Air Force Base, Arizona, had a significant fraction of its electronics equipment remaining in the avionics bay and cockpit and the passenger compartment was essentially intact. A simulated avionics box was placed in an equipment rack and a trace on an internal circuit board was monitored. The simulated avionics box was also tested in the Naval Surface Warfare Center, Dahlgren Division (NSWCDD) mode stirred chamber (MSC). The avionics bay and cockpit were internally excited from 100 MHz to 18 GHz using a pair of horn and wire antennas placed in several locations. Aluminum foil tuners, each 2 x 2 ft, were located in the avionics bay and the cockpit. The internal electromagnetic environment was measured by a horn and a wire antenna placed successively in several locations in the avionics bay and cockpit. Limited measurements of the local ambient environment, both external to the aircraft and within the aircraft, were obtained for the FM band (88 to 108 MHz) and the VHF/UHF bands (100 MHz to 1 GHz). Cavity losses were characterized by comparing the received power to the input power. The cavity loss for the avionics bay was about 15 dB greater than the loss in the NSWCDD MSC. The loss for the cockpit was about 12 dB greater than the NSWCDD MSC. The observed stirring ratios (ratio of maximum received signal to minimum received signal at a particular frequency as the tuner rotates) were generally less than 10 dB up to about 800 MHz. DTIC

07 AIRCRAFT PROPULSION AND POWER

Includes prime propulsion systems and systems components, e.g., gas turbine engines and compressors; and onboard auxilliary power plants for aircraft.

For related information see also *20 Spacecraft Propulsion and Power, 28 Propellants and Fuels,* and *44 Energy Production and Conversion.*

N95-15329# Naval Postgraduate School, Monterey, CA.
COMBUSTION EFFICIENCY IN A DUAL-INLET SIDE-DUMP RAMJET COMBUSTOR M.S. Thesis
Martin W. Deppe Jun. 1994 50 p
(AD-A283564) Avail: CASI HC A03/MF A01

A dual, axially-in-line, side-dump, liquid-fueled ramjet combustor was designed and tested with varying fuel-air ratios, atomizer types, and air distributions between the two inlets. Particle size distributions produced by the atomizers were measured at the inlet duct plane. When operated in a contra-flow direction, all of the atomizers produced excellent atomization with a Sauter mean diameter less than 14 microns. The dual, in-line inlets provided improved flammability limits and combustion efficiencies at lean fuel-air ratios when compared to single side-dump performance. Direct injection of approximately 20 percent of the fuel flow into the dome region was found to provide improved lean flammability limits for the single side-dump, but was not required with the dual inlets. The fuel distribution in the inlet duct required for good flammability limits and combustion efficiency was opposite to that required to prevent pressure oscillations, indicating that a dump plane aero-grid will often be necessary. A dump angle of 45 deg resulted in lower than desired combustion efficiencies, apparently due to poor mixing with the air from the aft inlet. DTIC

N95-15683# Purdue Univ., West Lafayette, IN. Research Foundation.
GAS TURBINE PREDIFFUSER-COMBUSTOR PERFORMANCE DURING OPERATION WITH AIR-WATER MIXTURE Interim Report, 10 May 1992 - 20 Aug. 1993
P. Laing and S. N. B. Murthy Aug. 1994 139 p
(Grant FAA-92-G-002)
(DOT/FAA/CT-93/52; M/FAA/002-93-1) Avail: CASI HC A07/MF A02

In a continuing effort to establish performance changes due to water ingestion into an aircraft gas turbine engine and possible design improvements, an experimental investigation was performed with a model gas turbine prediffuser-combustor sector utilizing a number of mixture and flow conditions in a tunnel operating with a two-phase, air-liquid film-droplet mixture. For given entry conditions into the prediffuser (which can be related to the exit conditions of the core compressor in a bypass engine, and, therefore, also to ingestion conditions at the engine face) the two main issues are (1) the amount of water entering the primary zone of the combustor, and (2) the local reduction in temperature, flame-water interactions, and the vitiation caused by the vaporizing of water. Flow visualization and estimates of water flow and droplet size in the primary zone have been undertaken under cold flow conditions. The amount of water entering the primary zone has been found to be a complex function of (1) the air-water mixture conditions at entry to the prediffuser, and (2) the effects of gravity on the flowfield for given geometry of the prediffuser-combustor, and the flow split between the primary and the coolant streams in the combustor. Combustion tests have been carried out to establish the effects on performance, occurrence of flameout, and recoverability of combustor exit temperature by enhancement of one or both of the fuel equivalence ratio and the oxygen content of air. It was tentatively concluded that the observed effects of the presence of water are a result of the interactive effects of heat transfer to water, vitiation by water vapor on combustion, and the total heat release in the primary zone. the latter being the dominant factor in stabilizing the flame with a large increase in combustor exit temperature, as found in the tests with the addition of both fuel and oxygen to a given burning mixture. Author

N95-14645# Spectra Research Systems, Inc., Huntsville, AL.
A GRAPHICAL USER INTERFACE FOR DESIGN AND ANALYSIS OF AIR BREATHING PROPULSION SYSTEMS
Charles P. DePlachett and Richard K. Steinberg *In* Huntsville Association of Technical Societies, TABES 1994: 10th Annual Technical and Business

Exhibition and Symposium 1994 7 p Sponsored by Army Missile Command (For primary document see N95-14633 03-12)
(TABES Paper 94-616) Avail: CASI HC A02/MF A04

08 AIRCRAFT STABILITY AND CONTROL

Includes aircraft handling qualities; piloting; flight controls; and autopilots.

For related information see also *05 Aircraft Design, Testing and Performance.*

N95-14343 Carnegie-Mellon Univ., Pittsburgh, PA. Dept. of Computer Science.
COMPUTING QUANTITATIVE CHARACTERISTICS OF FINITE-STATE REAL-TIME SYSTEMS
S. Campos, E. Clarke, W. Marrero, and M. Minea 4 May 1994 23 p Limited Reproducibility: More than 20% of this document may be affected by microfiche quality
(Contract MDA972-90-C-0035)
(AD-A282839; CMU-CS-94-147) Avail: CASI HC A03

Current methods for verifying real-time systems are essentially decision procedures that establish whether the system model satisfies a given specification. We present a general method for computing quantitative information about finite-state real-time systems. We have developed algorithms that compute exact bounds on the delay between two specified events and on the number of occurrences of an event in any given interval. This technique allows us to determine performance measures such as schedulability, response time, and system load. Our algorithms produce more detailed information than traditional methods. This information leads to a better understanding of system behavior, in addition to determining its correctness. We also show that our technique can be extended to a more general representation of real-time systems, namely, timed transition graphs. The algorithms presented in this paper have been incorporated into the SMV model checker and used to verify a model of an aircraft control system. The results obtained demonstrate that our method can be successfully applied in the verification of real-time system designs DTIC

N95-14815# Technische Univ., Delft (Netherlands). Faculty of Aerospace Engineering.
A SIMULINK ENVIRONMENT FOR FLIGHT DYNAMICS AND CONTROL ANALYSIS: APPLICATION TO THE DHC-2 BEAVER. PART 1: IMPLEMENTATION OF A MODEL LIBRARY IN SIMULINK. PART 2: NONLINEAR ANALYSIS OF THE BEAVER AUTOPILOT (Diskette Supplement) M.S. Thesis
Marc O. Rauw Sep. 1993 265 p Diskette supplement: 3.5-inch DSDD
(NONP-NASA-Suppl-DK-94-28027) Avail: CASI SET A19 (HC,DK)

The design of advanced Automatic Aircraft Control Systems (AACS's) can be improved upon considerably if the designer can access all models and tools required for control system design and analysis through a graphical user interface, from within one software environment. This MSc-thesis presents the first step in the development of such an environment, which is currently being done at the Section for Stability and Control of Delft University of Technology, Faculty of Aerospace Engineering. The environment is implemented within the commercially available software package MATLAB/SIMULINK. The report consists of two parts. Part 1 gives a detailed description of the AACS design environment. The heart of this environment is formed by the SIMULINK implementation of a nonlinear aircraft model in block-diagram format. The model has been worked out for the old laboratory aircraft of the Faculty, the DeHavilland DHC-2 'Beaver', but due to its modular structure, it can easily be adapted for other aircraft. Part 1 also describes MATLAB programs which can be applied for finding steady-state trimmed-flight conditions and for linearization of the aircraft model, and it shows how the built-in simulation routines of SIMULINK have been used for open-loop analysis of the aircraft dynamics. Apart from the implementation of the models and tools, a thorough treatment of the theoretical backgrounds is presented. Part 2 of this report presents a part of an autopilot design process for the 'Beaver' aircraft, which clearly demonstrates the power and flexibility of the AACS design environment from part 1. Evaluations of all longitudinal and lateral control laws by means of nonlinear simulations are treated in detail. A floppy disk containing all relevant MATLAB programs and SIMULINK models is provided as a supplement. Author (revised)

N95-14448# Office National d'Etudes et de Recherches Aerospatiales, Paris (France).
LATERAL JET CONTROL FOR TACTICAL MISSILES
P. Champigny and R. G. Lacau *In* AGARD, Missile Aerodynamics Jun. 1994 57 p (For primary document see N95-14445 03-02)
Copyright Avail: CASI HC A04/MF A03

N95-14900# Technische Univ., Brunswick (Germany). Inst. of Flight Guidance and Control.
TURBULENCE: ENGINEERING MODELS, AIRCRAFT RESPONSE
Manfred Swolinsky *In* AGARD, Flight in an Adverse Environment Nov. 1994 20 p (For primary document see N95-14893 03-03)
Copyright Avail: CASI HC A03/MF A02

09 RESEARCH AND SUPPORT FACILITIES (AIR)

Includes airports, hangars and runways; aircraft repair and overhaul facilities; wind tunnels; shock tubes; and aircraft engine test stands.

For related information see also *14 Ground Support Systems and Facilities (Space).*

N95-13687# Wright Lab., Wright-Patterson AFB, OH.
DEVELOPMENTS IN LASER-BASED DIAGNOSTICS FOR WIND TUNNELS IN THE AEROMECHANICS DIVISION: 1987-1992 Final Report, Jan. 1987 - Dec. 1992
Linda G. Smith, Mark S. Maurice, Charles Tyler, John D. Schmisseur, and George L. Seibert May 1994 107 p
(AF Proj. 2404)
(AD-A283011; WL-TR-94-3054) Avail: CASI HC A06/MF A02

The Aero-Diagnostics Research Section of the Aeromechanics Division develops and advances laser-based diagnostic techniques for use in a variety of subsonic through hypersonic wind tunnel facilities. These include laser velocimetry, laser induced fluorescence, Rayleigh scattering, phase shift holographic interferometry, and chemiluminescence. The purpose of this report is to bring the reader up to date on the status of these and other techniques under development in the Aeromechanics Division at the Wright Laboratory. DTIC

N95-14415* National Aeronautics and Space Administration. Langley Research Center, Hampton, VA.
AIRPLANE TAKEOFF AND LANDING PERFORMANCE MONITORING SYSTEM Patent
David B. Middleton, inventor (to NASA), Raghavachari Srivatsan, inventor (to NASA), and Lee H. Person, Jr., inventor (to NASA) 4 Oct. 1994 28 p Filed 6 Apr. 1993 Continuation of abandoned US-Patent-Appl-SN-755248, filed 5 Sep. 1991 which is a continuation-in-part of US-Patent-Appl-SN-192562, filed 11 May 1988 which is a continuation-in-part of US-Patent-Appl-SN-082766, filed 6 Aug. 1987
(NASA-Case-LAR-14745-2-SB; US-Patent-5,353,022;
US-Patent-Appl-SN-045337; US-Patent-Appl-SN-755248;
US-Patent-Appl-SN-192562; US-Patent-Appl-SN-082766;
US-Patent-Class-340-959; US-Patent-Class-73-178T;
US-Patent-Class-364-427; Int-Patent-Class-G08B-21/00) Avail: US Patent and Trademark Office

The invention is a real-time takeoff and landing performance monitoring system for an aircraft which provides a pilot with graphic and metric information to assist in decisions related to achieving rotation speed (VR) within the safe zone of a runway, or stopping the aircraft on the runway after landing or take-off abort. The system processes information in two segments: a pretakeoff segment and a real-time segment. One-time inputs of ambient conditions and airplane configuration information are used in the pretakeoff segment to generate scheduled performance data. The real-time segment uses the scheduled performance data, runway length data and transducer measured parameters to monitor the performance of the airplane throughout the takeoff roll. Airplane acceleration and engine-performance anomalies are detected and annunciated. A novel and important feature of this segment is that it updates the estimated runway rolling friction coefficient. Airplane performance predictions also reflect

changes in head wind occurring as the takeoff roll progresses. The system provides a head-down display and a head-up display. The head-up display is projected onto a partially reflective transparent surface through which the pilot views the runway. By comparing the present performance of the airplane with a continually predicted nominal performance based upon given conditions, performance deficiencies are detected by the system and conveyed to pilot in form of both elemental information and integrated information. Official Gazette of the U.S. Patent and Trademark Office

N95-14513# Pacific Southwest Forest and Range Experiment Station, Berkeley, CA.
TILTING WIND TUNNEL FOR FIRE BEHAVIOR STUDIES Final Report
D. R. Weise Apr. 1994 6 p
(PB94-204625; FSRN-PSW-417) Avail: CASI HC A02/MF A01

The combined effects of wind velocity and slope on wildland fire behavior can be studied in the laboratory using a tilting wind tunnel. The tilting wind tunnel requires a commercially available fan to induce wind and can be positioned to simulate heading and backing fires spreading up and down slope. The tunnel is portable and can be disassembled for transport using a full-size pickup truck. Vertical velocity profiles indicate that the average turbulence level is about 15 percent of mean wind velocity. NTIS

N95-15328# Systems Control Technology, Inc., Arlington, VA.
VERTICAL FLIGHT TERMINAL OPERATIONAL PROCEDURES. A SUMMARY OF FAA RESEARCH AND DEVELOPMENT Final Report
Raymond H. Matthews Jul. 1994 53 p
(Contract DTFA01-87-C-00014)
(AD-A283550; SCT-92-RR-9; DOT/FAA/RD-94/24) Avail: CASI HC A04/MF A01

Common-carrier operations by helicopters are becoming increasingly routine. Prospects for their future utilization are promising as the variety of uses continues to grow and public acceptance expands. The Federal Aviation Administration (FAA) and industry are working to more fully integrate vertical flight vehicles in to the National Airspace System (NAS). Rotorcraft, including tiltrotor, tiltwing, and helicopters, are unique and each offers potential benefits that may provide relief to the delay problems being experienced throughout the NAS. Before these advantages can be fully exploited, a myriad of untested areas must be explored through research and development (R and D) activities to prove their viability. One important area is safety in terminal area operations. Safety includes such diversified subjects as approach and departure procedures, one-engine-inoperative (OEI) operations, loss of engine during critical flight phases, and landing site qualifications and capabilities. Pilot qualification, training of pilots and ground service personnel, precision approach glideslope angles, obstruction avoidance, etc., are also important safety concerns. Some of these topics have been addressed, others are currently under investigation, while others are still in the planning stages. DTIC

12 ASTRONAUTICS (GENERAL)

For extraterrestrial exploration see *91 Lunar and Planetary Exploration.*

N95-13825# ISRO Satellite Centre, Peenya, Bangalore (India).
JOURNAL OF SPACECRAFT TECHNOLOGY, VOLUME 4, NO. 2, JULY 1994
Jul. 1994 90 p
(ISSN 0971-1600)
Avail: CASI HC A05/MF A01

A series of papers on the in-depth coverage of technology related to Indian communication and other satellites is presented. The lead article presents an overview of satellite communications technology and related applications. The other articles cover such topics as remote programming for on-board attitude and orbit control computers; star trackers; computer aided design of spaceborne equipment; modeling of spatial distribution of space debris; an algorithm for spacecraft rendezvous and docking; simulated availability for communication satellite constellations; and the design of a test rig for a solar array deployment mechanism calibration system. For individual titles, see N95-13826 through N95-13833.

N95-13826# Indian Space Research Organization, Ahmedabad. Space Application Centre.
SATELLITE COMMUNICATION TECHNOLOGY AND APPLICATIONS, 1995-2010 c32
N. Pant *In* ISRO Satellite Centre, Journal of Spacecraft Technology, Volume 4, No. 2, July 1994 Jul. 1994 p 1-28 (For primary document see N95-13825 03-12)
Avail: CASI HC A03/MF A01

This article attempts to give an overview of the past, present and possible future trends in the area of satellite communication technology. Projections have been made for India's future communications requirements and thrust areas have been identified, focussing on the Indian scenario, where more efforts need to be put in. Author

N95-13827# ISRO Satellite Centre, Peenya, Bangalore (India). Control Systems Group.
REMOTE PROGRAMMING IN INSAT-2A/2B ON-BOARD ATTITUDE AND ORBIT CONTROL COMPUTER (AOCC) c61
M. Mahendra Nayak, R. S. Manjunatha, V. K. Agrawal, and N. K. Malik *In its* Journal of Spacecraft Technology, Volume 4, No. 2, July 1994 Jul. 1994 p 29-35 (For primary document see N95-13825 03-12)
Avail: CASI HC A02/MF A01

Remote programming is a feature incorporated in INSAT-2A/2B Attitude and Orbit Control Computer (AOCC) to provide a means of modifying on-board AOCC algorithms; gains and control flow in case of some unforeseen failures. Even though fault tolerant features like Fault Detection and Isolation Logic (FDI), Safe Mode and Long Pulse Detection Logic (LPD) have been provided in the AOCC, some unforeseen events can cause a problem leading to mission failure. A simple remote programming feature has been incorporated in the AOCC without much overhead or hardware/software. Even though this feature has not been extensively used, the facilities provided for Remote Programming have been used in the mission in monitoring certain parameters which are otherwise not telemetered. During the ground testing the Remote Programming procedures have been used effectively to study the effect of change in gain and increase in cycle time. Remote Programming in INSAT-2A/2B On-board Attitude & Orbit Control computer (AOCC) can be modified for various changes in control flow as well as controller selection. Author

N95-13828# Indian Space Research Organization, Bangalore. Lab. for Electro-Optics Systems
STAR SENSOR FOR INDIAN REMOTE SENSING SATELLITE (IRS 1C) c89
Philip Thomas, Goparaju Nagendra Rao, G. Pratap, V. Koteswara Rao, and Y. K. Jain *In* ISRO Satellite Centre, Journal of Spacecraft Technology, Volume 4, No . 2, July 1994 Jul. 1994 p 36-42 (For primary document see N95-13825 03-12)
Avail: CASI HC A02/MF A01

A microprocessor-based star sensor system using an array Charge Coupled Device (CCD) as detector has been developed for the attitude determination of Indian Remote Sensing Satellites IRS 1C & 1D. A pair of sensors with Field of View (FOV) of 8 deg x 6 deg, mounted in skewed configuration in the 3-axis stabilized satellite platform, capable of detecting stars up to 5.0 visual magnitude (Mv) can give an attitude determination accuracy of better than 0.01 deg. Author

N95-13829# Indian Space Research Organization, Trivandrum. Precision Fabrication and Assembly Facility.
COMPUTER AIDED TECHNIQUES FOR THE REALISATION OF THE DIAPHRAGM OF THE PSM FOR THE IRS-1C c61
D. Sam Dayala Dev and N. Sivasubramanian *In* ISRO Satellite Centre, Journal of Spacecraft Technology, Volume 4, No . 2, July 1994 Jul. 1994 p 43-51 (For primary document see N95-13825 03-12)
Avail: CASI HC A02/MF A01

The Indian Remote Sensing satellite IRS- 1C is configured with a Payload Steering Mechanism (PSM) to orient its Panchromatic Camera System, which has a resolution of 10 meters for remote sensing applications. The PSM is designed with a linear force-deflection behavior, axially compliant member, namely, the diaphragm, to protect its sensitive, high-precision ball bearings. The design optimization of this diaphragm was carried out using CAD techniques to obtain a low axial stiffness of 20 Kg/mm and a very high radial stiffness of more than 10,000 Kg/mm, with a non-linear behavior

within 5 percent of its range of load. The various shape options for the diaphragm were designed and analyzed using Finite Element methods in a CAD workstation. The optimized corrugated configuration was fed back to the common CAD database. CAN techniques were adopted to realize the hardware in the CNC Schaublin 130 lathe using the same database with suitable CAM interface software. Optimized machining methods and toolings were chosen to achieve the designed tolerances of the component. Computer Aided Inspection (CAI) methods were followed to measure the designed parameters of the diaphragm using a 3 Coordinate CNC based measuring machine. The measured values were fed back to the CAD system and compared with the original profile. Also, from the measured values, the behavior of the realized diaphragm was predicted. The two diaphragms realized were tested for their load-deflection characteristics. The results were compared with the designed value and are well within the scope of the specification. This has proved that the non-linear behavior of the corrugated diaphragm is within 5 percent when compared to a value of 170 percent in the case of a flat diaphragm over its operating range. The above optimization has been achieved using extensive Computer Aided techniques without realizing multiple prototypes as followed conventionally. This paper explains in detail the design, optimization and manufacturing methods in realizing the corrugated diaphragm for the PSM application. Author

N95-13830# Indian Space Research Organization, Bangalore. Flight Dynamics Div.

MODELLING THE LOW EARTH SPACE DEBRIS ENVIRONMENT c18

A. S. Ganeshan, S. C. Rathnakara, and Subir Banerjee *In* ISRO Satellite Centre, Journal of Spacecraft Technology, Volume 4, No . 2, July 1994 Jul. 1994 p 52-59 (For primary document see N95-13825 03-12)
Avail: CASI HC A02/MF A01

On-orbit fragmentation events in space, of which more than a hundred have occurred, have created trackable debris exceeding 7000 objects. Untrackable debris by far outnumber this count, constituting orders of magnitude more in number of un-monitored debris which calls for concerted effort to evolve appropriate and affordable strategies to minimize the impact of space debris on future space missions. The spatial density of debris is quite pronounced in the IRS altitude band of 800-1000 Km. This altitude band has a small orbit decay rate and hence the debris have protracted life time in these orbits. To assess the possible risk to active spacecraft in this band, a catalog for Low Earth Orbits (LEO), containing debris characteristics such as velocity, mass, size and their individual orbital information is required. However, the non-availability of such data even in the trackable regime readily engenders the necessity for mathematically modelling the trackable debris, characterizing the debris with its mass, size and orbital information. Such a model, which yields itself to extension to the untrackable region, has been developed here. It is shown how this model compares with experimental findings and how it is an improvement over the other existing models for space debris characterization. Author

N95-13831# ISRO Satellite Centre, Peenya, Bangalore (India). Control Systems Group.

A VISION BASED ATTITUDE AND POSITION ESTIMATION ALGORITHM FOR RENDEZVOUS AND DOCKING c18

R. Mukundan, R. V. Raghu Narayanan, and N. K. Philip *In its* Journal of Spacecraft Technology, Volume 4, No. 2, July 1994 Jul. 1994 p 60-67 (For primary document see N95-13825 03-12)
Avail: CASI HC A02/MF A01

This paper presents an algorithm for estimating the attitude and position parameters of an object from its image using point correspondence information. The attitude of the object is defined in terms of quarternion elements and is related to the measured image coordinates of three feature points through a system of non-linear equations. A closed-form solution of this system is derived for the direct estimation of the quarternion parameters as well as the position vector components. The algorithm finds application in the development of computer vision-based autonomous guidance schemes for the final approach phase of a rendezvous and docking mission. Author

N95-13832# ISRO Satellite Centre, Peenya, Bangalore (India).

A SIMULATION ALGORITHM FOR AVAILABILITY COMPUTATION OF A COMMUNICATION SATELLITE CONSTELLATION c32

P. S. Rajeshwari, V. N. Purohit, N. Ramani, and R. D. Gambhir *In its* Journal of Spacecraft Technology, Volume 4, No. 2, July 1994 Jul. 1994 p 68-77 (For primary document see N95-13825 03-12)
Avail: CASI HC A02/MF A01

This paper provides an algorithm to compute the availability of constellation of satellites. The computation of availability of a constellation of satellites is different from a system which has a main element and its corresponding redundant element/elements. This is basically because the constellation as a total system has many main elements and the constellation (with only the main elements) characteristics itself will help in providing redundancy to some users while it may not be present for other users. The degree of redundancy also varies among the users and with time. This will have a greater impact on its service availability. Also, the failure of a satellite need not affect all the users. The duration of the time for which a dip in availability is seen may vary in accordance with the replenishment strategy or the replenishment time adopted. These factors tend to make the mathematical modelling of the system more complex and impractical. Hence, even for a single constellation makes it volluminous since it consists of availability figures for various users, for different durations and for various combinations of the sharing philosophy, replenishment strategy, reliability of individual satellite, launch vehicles considered, etc. The algorithm validation is run on a sample basis and results are demonstrated. Author

N95-13833# ISRO Satellite Centre, Peenya, Bangalore (India). Quality Assurance Div.

DEPLOYMENT MECHANISM CALIBRATION SYSTEM c37

P. R. Marur and S. G. Raghavan *In its* Journal of Spacecraft Technology, Volume 4, No. 2, July 1994 Jul. 1994 p 78-83 (For primary document see N95-13825 03-12)
Avail: CASI HC A02/MF A01

A torque measurement system is designed for the characterization of the deployment mechanism at various stages of its assembly. It is a total drive and measurement apparatus that can be used both under ambient and thermo-vacuum conditions. The system has been used for the characterization of IRS-1B and INSAT-2A solar panel deployment mechanisms. The salient features of the system and the test results are presented. Author

N95-14290# Naval Postgraduate School, Monterey, CA.

SPACE EXPERIMENTS ABOARD ROCKETS: SPEAR 3 M.S. Thesis

James H. Morris Mar. 1994 90 p
(AD-A280778) Avail: CASI HC A05/MF A01

The SPEAR 3 experiment was conducted in an effort to better understand and compensate for the effects of satellite charging, at levels up to kV. This experiment was designed as a lower-ionosphere test to both record vehicle charging and the effect of neutral-gas grounding systems. Prelaunch tests were conducted at the NASA-Plum Brook facility; launch took place at the NASA-Wallops facility. Electrostatic analyzer data provided a record of the rocket body potential, and indications of ion production, or energy-angle scattering within the plasma sheath. Plasma wave information was extracted from floating probe data and skin current probe data. Both provided sampling to resolve signals up to 10 kHz; the skin current probe also provided burst-mode sampling up to 500 MHz. There were no obvious signals in the 0-10 kHz data, other than a diffuse, low-frequency noise. The burst-mode data, acquired at the initiation of each 5-second charging sequence, showed a strong signal at around 100 kHz. This roughly corresponds to the lower-hybrid resonance frequency. It is possible that LHR waves are responsible for energy-angle scattering of the ion flux accelerated to the charged rocket body. DTIC

N95-14633# Huntsville Association of Technical Societies, AL.

TABES 1994: 10TH ANNUAL TECHNICAL AND BUSINESS EXHIBITION AND SYMPOSIUM

1994 391 p Symposium held in Huntsville, AL, 10-11 May 1994
Avail: CASI HC A17/MF A04

A compilation of papers submitted at the Tenth Annual Business Exhibition and Symposium sponsored by the Huntsville Association of Technical Societies in the following areas: government/industry relations; technology utilization; space commercialization; intelligent manufacturing systems; environmentally sound manufacturing; optical systems; hypervelocity impact test facilities; international trade and cooperation; rocket engine propellants; computer systems design; buoyancy propulsion; computerized

simulation; functional specifications for a global emergency observation and warning system; spacecraft docking; and project management. For individual titles, see N95-14634 through N95-14653.

N95-14634*# National Aeronautics and Space Administration, Washington, DC.
SPACE SCIENCE IN THE 1990'S AND BEYOND
Wesley T. Huntress, Jr., Mary E. Kicza, and T. Jens Feeley *In* Huntsville Association of Technical Societies, TABES 1994: 10th Annual Technical and Business Exhibition and Symposium 1994 7 p (For primary document see N95-14633 03-12)
(TABES Paper 94-204) Avail: CASI HC A02/MF A04

NASA's Office of Space Sciences is changing its approach to our missions, both current and future. Budget realities are necessitating that we change the way we do business and the way we look at our role in the Federal Government. These challenges are being met by a new and innovative approach that focuses on achieving a balanced world-class space science program that requires far less resources while providing an enhanced role for technology and education as integral components of our Research and Development (R&D) programs. Author

N95-14635# Wheeling Coll., WV. National Technology Transfer Center.
HELPING SMALL COMPANIES COMMERCIALIZE PUBLIC-SECTOR TECHNOLOGY c85
Lee W. Rivers *In* Huntsville Association of Technical Societies, TABES 1994: 10th Annual Technical and Business Exhibition and Symposium 1994 8 p (For primary document see N95-14633 03-12)
(TABES Paper 94-407) Avail: CASI HC A02/MF A04

The federal government spends about $70 billion annually on research and development (R&D) - about half the R&D done in the United States. Access to federal technology is freer and more fair now that legislation encourages the federal laboratories to cooperate with the private sector. Commonality of the access process is spreading across the agencies. One problem that remains is that small and medium-sized, and sometimes even large-sized companies do not know where to start looking for assistance or technologies. The National Technology Transfer Center is the hub of a one-stop, accessible national network that has removed much of the difficulty from the initial approach. Derived from text

N95-14636*# National Aeronautics and Space Administration. Marshall Space Flight Center, Huntsville, AL.
ENVIRONMENTALLY SOUND MANUFACTURING c20
Larry A. Caddy, Ross Bowman, and Rex A. Richards *In* Huntsville Association of Technical Societies, TABES 1994: 10th Annual Technical and Business Exhibition and Symposium 1994 7 p (For primary document see N95-14633 03-12)
(TABES Paper 94-502) Avail: CASI HC A02/MF A04

The NASA/Thiokol/industry team has developed and started implementation of an environmentally sound manufacturing plan for the continued production of solid rocket motors. They have worked with other industry representatives and the U.S. Environmental Protection Agency to prepare a comprehensive plan to eliminate all ozone depleting chemicals from manufacturing processes and to reduce the use of other hazardous materials used to produce the space shuttle reusable solid rocket motors. The team used a classical approach for problem solving combined with a creative synthesis of new approaches to attack this problem. As our ability to gather data on the state of the Earth's environmental health increases, environmentally sound manufacturing must become an integral part of the business decision making process. Author (revised)

N95-14637# Vanderbilt Univ., Nashville, TN. Center for Intelligent Systems.
INTELLIGENT MANUFACTURING SYSTEMS STATE OF THE ART c81
Gautam Biswas, Kazuhiko Kawamura, and Ashraf Saad *In* Huntsville Association of Technical Societies, TABES 1994: 10th Annual Technical and Business Exhibition and Symposium 1994 7 p (For primary document see N95-14633 03-12)
(TABES Paper 94-503) Avail: CASI HC A02/MF A04

This paper discusses intelligent manufacturing and its impact on mass customization and environmentally conscious manufacturing. Knowledge systems and the explicit modeling of product and process knowledge are crucial to developing this technology. With the globalization of markets, the international IMS project seems to be a key to the success of the intelligent manufacturing enterprise. Author

N95-14638# Army Strategic Defense Command, Huntsville, AL. Technology Integration and Matrix Management Office.
AERO-OPTICS SYSTEM INTEGRATION c74
Troy A. Street *In* Huntsville Association of Technical Societies, TABES 1994: 10th Annual Technical and Business Exhibition and Symposium 1994 4 p Sponsored by Secretary of the Army (For primary document see N95-14633 03-12)
(TABES Paper 94-604) Avail: CASI HC A01/MF A04

A Delphi study has been conducted in the field of aero-optics research and development. The study includes the system components of aerodynamics, optical materials, optical analytics, optical seekers, and aero-optical integration of the system components into an aero-optical system. The Delphi forecast data is divided into short, medium, and long range periods for planning purposes. The study results are applicable to the stated planning periods for endoatmospheric interceptors with full range infrared guidance systems. Author

N95-14639*# Auburn Univ., AL. Space Power Inst.
HYPERVELOCITY IMPACT TEST FACILITY: A GUN FOR HIRE
Calvin R. Johnson, M. F. Rose, D. C. Hill, S. Best, T. Chaloupka, G. Crawford, M. Crumpler, and B. Stephens *In* Huntsville Association of Technical Societies, TABES 1994: 10th Annual Technical and Business Exhibition and Symposium 1994 7 p (For primary document see N95-14633 03-12)
(Contract NAG1-1329; DNA001-90-C-0127)
(TABES Paper 94-605) Avail: CASI HC A02/MF A04

An affordable technique has been developed to duplicate the types of impacts observed on spacecraft, including the Shuttle, by use of a certified Hypervelocity Impact Facility (HIF) which propels particulates using capacitor driven electric gun techniques. The fully operational facility provides a flux of particles in the 10-100 micron diameter range with a velocity distribution covering the space debris and interplanetary dust particle environment. HIF measurements of particle size, composition, impact angle and velocity distribution indicate that such parameters can be controlled in a specified, tailored test designed for or by the user. Unique diagnostics enable researchers to fully describe the impact for evaluating the 'targets' under full power or load. Users regularly evaluate space hardware, including solar cells, coatings, and materials, exposing selected portions of space-qualified items to a wide range of impact events and environmental conditions. Benefits include corroboration of data obtained from impact events, flight simulation of designs, accelerated aging of systems, and development of manufacturing techniques. Author (revised)

N95-14640# Itall Corp., Meridianville, AL.
DESIGN IN HUNTSVILLE, MANUFACTURE IN ESTONIA, SELL IN EUROPE c81
Ilmar Luik *In* Huntsville Association of Technical Societies, TABES 1994: 10th Annual Technical and Business Exhibition and Symposium 1994 4 p (For primary document see N95-14633 03-12)
(TABES Paper 94-607) Avail: CASI HC A01/MF A04

Collapse of the Soviet Union made it possible for the Republic of Estonia to regain its independence and pre-World War 2 gold reserves which are being used to create a most business friendly environment next to the highest cost European countries. In the past two years, over 4,000 western enterprises have opened subsidiaries in Estonia to take advantage of its enterprise tax structure, hard currency, good banking system, low inflation, freedom to repatriate 100 percent of profits at any time in any currency, stable U.S. friendly government, membership in the European Union, good infrastructure, well educated population, low production costs, and in the near future, associate membership in NATO permitting Estonian firms to bid on NATO and some U.S. military contracts. Opening a subsidiary in Estonia for the purpose of developing commercial products solves cost production cost problems and adds the advantage of duty free access to the European Community. Author (revised)

N95-14641# Loral AeroSys, Seabrook, MD.
EFFICIENT MISSION CONTROL FOR THE 48-SATELLITE GLOBALSTAR CONSTELLATION c18

Dan Smith *In* Huntsville Association of Technical Societies, TABES 1994: 10th Annual Technical and Business Exhibition and Symposium 1994 6 p (For primary document see N95-14633 03-12)
(TABES Paper 94-609) Avail: CASI HC A02/MF A04

Globalstar will use 48 satellites to create a world-wide mobile communications system. As a large, long-term commercial system Globalstar provides an opportunity to explore innovative solutions for highly efficient satellite command and control. Design and operational concepts being developed are unencumbered by existing physical and organizational infrastructures. This paper discusses the Globalstar system and challenges and presents early engineering concepts, system design decisions, and operations concepts which address the combined needs and concerns of satellite, ground system, and operational teams. Author (revised)

N95-14642# ENSR Consulting and Engineering, Florence, AL.
RECYCLED PLASTIC: A CLEAN AND LOW COST ROCKET FUEL c28
Kenneth W. Schulze *In* Huntsville Association of Technical Societies, TABES 1994: 10th Annual Technical and Business Exhibition and Symposium 1994 8 p (For primary document see N95-14633 03-12)
(TABES Paper 94-610) Avail: CASI HC A02/MF A04

Recycled polyethylene plastic as a hybrid rocket fuel takes advantage of a low cost and readily available resource and eliminates toxic exhaust emissions for a cleaner combustion fuel. Solid rocket motors produce extremely harmful exhaust compounds of hydrochloric acid, nitrogen dioxide, and metal oxide particles. The manufacturing and operations of solid rocket motors represents a substantial safety hazard with both fuel and oxidizer held in a polymer binder with solid particle composite. The solid fuel in a hybrid rocket motor is inert since the oxidizer (liquid or gas) is separate from the fuel until initiation of combustion. Combustion is controlled by the oxidizer flow rate and has the capability of start, stop and restart. The safety and simplicity was demonstrated by multiple test firings which were conducted with relative ease and without risk of explosive failures. Hybrid rocket technology, and polyethylene plastic fuel, has potential application for low cost sounding rockets, gas generators, or as a clean burn heat source. Author

N95-14643*# National Aeronautics and Space Administration. Marshall Space Flight Center, Huntsville, AL.
A NASA/INDUSTRY/UNIVERSITY PARTNERSHIP FOR DEVELOPMENT OF DUAL-USE VIBRATION ISOLATION TECHNOLOGY
Michael L. Tinker *In* Huntsville Association of Technical Societies, TABES 1994: 10th Annual Technical and Business Exhibition and Symposium 1994 7 p (For primary document see N95-14633 03-12)
(TABES Paper 94-613) Avail: CASI HC A02/MF A04

A partnership is described that was formed as a result of a NASA university grant for the study of wire rope vibration isolation systems. Vibration isolators of this type are currently used in the Space Shuttle Orbiter and engine test facility, and have potential application in the international space station and other space vehicles. Wire rope isolators were considered for use on the Hubble Space Telescope and the military has used wire rope technology extensively. The desire of the wire rope industry to expand sales in commercial markets coupled with results of the prior NASA funded study, led to the formation of a partnership including NASA, the university involved in the research grant, and a small company that designs wire rope systems. Goals include the development of improved mathematical models and a designers handbook to facilitate the use of the new modeling tools. Author (revised)

N95-14644# ENSR Consulting and Engineering, Florence, AL.
COMPREHENSIVE FACILITY DECOMMISSIONING THROUGH THE USE OF INNOVATIVE TECHNOLOGY TO REDUCE COST, SCHEDULE, AND ENVIRONMENTAL LIABILITY c81
Scott S. Huismann, Michael S. Astin, and Terrance M. Fleet *In* Huntsville Association of Technical Societies, TABES 1994: 10th Annual Technical and Business Exhibition and Symposium 1994 7 p (For primary document see N95-14633 03-12)
(TABES Paper 94-615) Avail: CASI HC A02/MF A04

This paper describes the use of a comprehensive approach to decommissioning activities at a manufacturing and testing facility which saves time and money while reducing environmental liability. Before demolition, the facility consisted of six connected buildings. A detailed facility characterization to identify contaminated areas was completed prior to facility decommissioning. Remediation activities were scheduled to coincide with facility demolition, and specialized subcontractors performed such tasks as asbestos and lead paint abatement, soil bioremediation, underground storage tank and clarifier removal, and facility destruction and recycling. The project timetable was reduced by using several crews simultaneously to conduct recycling, demolition, and remediation. Costs were offset by selling remaining equipment, scrap metals, overhead lights and fixtures, and a premanufactured steel building. On-site recycling and remediation were used wherever possible to reduce cost and associated hauling liabilities. Author (revised)

N95-14645# Spectra Research Systems, Inc., Huntsville, AL.
A GRAPHICAL USER INTERFACE FOR DESIGN AND ANALYSIS OF AIR BREATHING PROPULSION SYSTEMS c07
Charles P. DePlachett and Richard K. Steinberg *In* Huntsville Association of Technical Societies, TABES 1994: 10th Annual Technical and Business Exhibition and Symposium 1994 7 p Sponsored by Army Missile Command (For primary document see N95-14633 03-12)
(TABES Paper 94-616) Avail: CASI HC A02/MF A04

Existing air breathing propulsion engine analysis software requires extensive training to use. Therefore, a need exists for a user friendly computer simulation which is capable of analyzing air breathing propulsion cycles quickly and efficiently. Human factors studies have been performed for real-time interactive computer displays for DOD systems. The technologies resulting from these real-time display designs are being used to produce an optimal graphical user interface (GUI) which will provide a means for interactive design and/or modification of air breathing propulsion systems. Author

N95-14646# Kossel (Horst), Shrewsbury, MA.
ACTIVATED BUOYANCY PROPULSION = PARADOX POWER (TM) c02
Horst Kossel *In* Huntsville Association of Technical Societies, TABES 1994: 10th Annual Technical and Business Exhibition and Symposium 1994 7 p (For primary document see N95-14633 03-12)
(TABES Paper 94-619) Avail: CASI HC A02/MF A04

The PARADOX POWER(tm) concept recognizes molecular activity/heat of all fluids as an unlimited source of clean kinetic energy, accessible to do 'work' within the lower atmosphere and open water. By expending minimal energy to selectively subtract from the molecular impulse (pressure) on a surface of a macroscopic body, acceleration is provided by momentum transfer to the normal (opposite) surface, directly by ambient pressure. Energy from a separate source is used to increase the parallel velocity of microscopic size particles, within the invisible Attached Ionized Boundary Layer (U.S. Pat. Appl. No. 106,867). Controllable, super efficient vehicle operation results, doubling microscopic oscillation velocity increases the atmospheric propulsive force four times; deceleration functions similarly. Molecular oscillation by rapidly reversing alternating current, causing an imbalance, provides clean, quiet, controlled 'buoyancy' propulsion. Author

N95-14647# Unisys Corp., Houston, TX. Space Systems Div.
APPLYING CASE TECHNOLOGY TO THE SOFTWARE MAINTENANCE LIFE CYCLE c61
Linda Barker, Daryl Cain, and Michael Bishop *In* Huntsville Association of Technical Societies, TABES 1994: 10th Annual Technical and Business Exhibition and Symposium 1994 7 p (For primary document see N95-14633 03-12)
(TABES Paper 94-620) Avail: CASI HC A02/MF A04

A large number of the software systems in use today are 'legacy systems' which were originally developed using the obsolete methods and technology of the past. The importance of these systems in facilitating the performance of enterprise processes dictates that they must be transitioned to new state-of-the practice methods and technology in order to reduce maintenance costs. However, budget restrictions, especially in the areas of defense and space, preclude the option of redeveloping them from the beginning. The only way to sustain these systems in the future is to reengineer them in such a way that they can take advantage of current methods and technology and still leverage original system components as much as possible. This paper describes how CASE technology is being applied on a NASA contract in order to address the task of reverse engineering, the initial phase in the software reengineering life cycle.
Author

N95-14648*# National Aeronautics and Space Administration. Marshall Space Flight Center, Huntsville, AL.

SPACE SHUTTLE MAIN ENGINE TURBOPUMP BEARING ASSESSMENT PROGRAM

Barbara Spiegel Breithaupt *In* Huntsville Association of Technical Societies, TABES 1994: 10th Annual Technical and Business Exhibition and Symposium 1994 7 p (For primary document see N95-14633 03-12)
(TABES Paper 94-621) Avail: CASI HC A02/MF A04

This paper documents the work done on the bearing assessment program over the past two and a half years. The objective of the program is to develop a nondestructive evaluation system for the space shuttle main engine high pressure oxidizer turbopumps which would be used to detect anomalies in installed bearings without component disassembly. Databases of various signatures are obtained by slowly turning the pump shafts before and after an engine firing. These signatures are then analyzed and compared to the original signatures to more accurately predict bearing wear. Author

N95-14649*# National Aeronautics and Space Administration. Marshall Space Flight Center, Huntsville, AL.

THE GLOBAL EMERGENCY OBSERVATION AND WARNING SYSTEM

Angelia P. Bukley and John A. Mulqueen *In* Huntsville Association of Technical Societies, TABES 1994: 10th Annual Technical and Business Exhibition and Symposium 1994 5 p (For primary document see N95-14633 03-12)
(TABES Paper 94-622) Avail: CASI HC A01/MF A04

Based on an extensive characterization of natural hazards, and an evaluation of their impacts on humanity, a set of functional technical requirements for a global warning and relief system was developed. Since no technological breakthroughs are required to implement a global system capable of performing the functions required to provide sufficient information for prevention, preparedness, warning, and relief from natural disaster effects, a system is proposed which would combine the elements of remote sensing, data processing, information distribution, and communications support on a global scale for disaster mitigation. Derived from text

N95-14650# Nichols Research Corp., Huntsville, AL. Tactical Systems Integration Div.

PRODUCT LIFE CYCLE DATA BASE, ANALYSIS AND SIMULATION INTEGRATION METHODOLOGY **c82**

Catherine Farless, Van Brewer, and Jim McCullough *In* Huntsville Association of Technical Societies, TABES 1994: 10th Annual Technical and Business Exhibition and Symposium 1994 7 p (For primary document see N95-14633 03-12)
(TABES Paper 94-626) Avail: CASI HC A02/MF A04

The reduction of development and manufacturing costs is a goal for commercial and government systems. Early attempts to achieve this have focused on manufacturing and logistics. To address the entire life-cycle of a product, significant problems are encountered with integration of product data bases, design drawings, analysis tools, and analysis results. Tools for this task must be adaptable to changing requirements and technology. Special purpose software rarely meets this criterion and development costs are uneconomical. As a result, a tool set based on integration of commercially available software is being developed. The Integrated Product Life Cycle Analysis and Simulation Environment (IPLCase) consists of a database management system, a wide range of product specific life-cycle management tools, and built in configuration and access control. IPLCase supports concurrent engineering from concept development through production and distribution with 3-D visualization and object manipulation and is tailored to the product to ensure successful product development and production. Author (revised)

N95-14651*# Alabama Univ., Huntsville, AL. Dept. of Computer Science.

NEURAL NETWORKS: ALTERNATIVES TO CONVENTIONAL TECHNIQUES FOR AUTOMATIC DOCKING

Bradley L. Vinz *In* Huntsville Association of Technical Societies, TABES 1994: 10th Annual Technical and Business Exhibition and Symposium 1994 7 p (For primary document see N95-14633 03-12)
(Grant NGT-50679)
(TABES Paper 94-627) Avail: CASI HC A02/MF A04

Automatic docking of orbiting spacecraft is a crucial operation involving the identification of vehicle orientation as well as complex approach dynamics. The chaser spacecraft must be able to recognize the target spacecraft within a scene and achieve accurate closing maneuvers. In a video-based system, a target scene must be captured and transformed into a pattern of pixels. Successful recognition lies in the interpretation of this pattern. Due to their powerful pattern recognition capabilities, artificial neural networks offer a potential role in interpretation and automatic docking processes. Neural networks can reduce the computational time required by existing image processing and control software. In addition, neural networks are capable of recognizing and adapting to changes in their dynamic environment, enabling enhanced performance, redundancy, and fault tolerance. Most neural networks are robust to failure, capable of continued operation with a slight degradation in performance after minor failures. This paper discusses the particular automatic docking tasks neural networks can perform as viable alternatives to conventional techniques. Author (revised)

N95-14652# Rockwell International Corp., Huntsville, AL. Rocketdyne Div.

AUTOMATED TEST ENVIRONMENT FOR A REAL-TIME CONTROL SYSTEM **c63**

Ronald O. Hall *In* Huntsville Association of Technical Societies, TABES 1994: 10th Annual Technical and Business Exhibition and Symposium 1994 5 p (For primary document see N95-14633 03-12)
(TABES Paper 94-631) Avail: CASI HC A01/MF A04

An automated environment with hardware-in-the-loop has been developed by Rocketdyne Huntsville for test of a real-time control system. The target system of application is the man-rated real-time system which controls the Space Shuttle Main Engines (SSME). The primary use of the environment is software verification and validation, but it is also useful for evaluation and analysis of SSME avionics hardware and mathematical engine models. It provides a test bed for the integration of software and hardware. The principles and skills upon which it operates may be applied to other target systems, such as those requiring hardware-in-the-loop simulation and control system development. Potential applications are in problem domains demanding highly reliable software systems requiring testing to formal requirements and verifying successful transition to/from off-nominal system states. Author

N95-14653*# National Aeronautics and Space Administration. Marshall Space Flight Center, Huntsville, AL.

BUILDING COMPLEX SIMULATIONS RAPIDLY USING MATRIX(x): THE SPACE STATION REDESIGN

C. K. Carrington *In* Huntsville Association of Technical Societies, TABES 1994: 10th Annual Technical and Business Exhibition and Symposium 1994 7 p (For primary document see N95-14633 03-12)
(TABES Paper 94-632) Avail: CASI HC A02/MF A04

MSFC's quick response to the Space Station redesign effort last year required the development of a computer simulation to model the attitude and station-keeping dynamics of a complex body with rotating solar arrays in orbit around the Earth. The simulation was written using a rapid-prototyping graphical simulation and design tool called MATRIX(x) and provided the capability to quickly remodel complex configuration changes by icon manipulation using a mouse. The simulation determines time-dependent inertia properties, and models forces and torques from gravity-gradient, solar radiation, and aerodynamic disturbances. Surface models are easily built from a selection of beams, plates, tetrahedrons, and cylinders. An optimization scheme was written to determine the torque equilibrium attitudes that balance gravity-gradient and aerodynamic torques over an orbit, and propellant-usage estimates were determined. The simulation has been adapted to model the attitude dynamics for small spacecraft. Author

N95-14582*# National Aeronautics and Space Administration. Lewis Research Center, Cleveland, OH.

THE PATH TO AN EXPERIMENT IN SPACE (FROM CONCEPT TO FLIGHT)

Jack A. Salzman *In its* Second Microgravity Fluid Physics Conference Aug. 1994 p 409-418 (For primary document see N95-14522 03-34)
Avail: CASI HC A02/MF A04; 2 functional color pages

13 ASTRODYNAMICS

Includes powered and free-flight trajectories; and orbital and launching dynamics.

N95-14282*# Texas Univ., Austin, TX. Center for Space Research.
PRECISION ORBIT DETERMINATION OF ALTIMETRIC SATELLITES
C. K. Shum, John C. Ries, and Byron D. Tapley *In* NASA. Goddard Space Flight Center, Satellite Laser Ranging in the 1990s: Report of the 1994 Belmont Workshop Nov. 1994 p 65-70 (For primary document see N95-14274 03-46)
Avail: CASI HC A02/MF A02

14 GROUND SUPPORT SYSTEMS AND FACILITIES (SPACE)

Includes launch complexes, research and production facilities; ground support equipment, e.g., mobile transporters; and simulators.

For related information see also *09 Research and Support Facilities (Air).*

N95-13890*# Lockheed Engineering and Sciences Co., Hampton, VA.
RESULTS OF DEMONSTRATION TEST FOR RECEIVING AND PROCESSING OF FLIGHT DATA FROM THE SPACE TRANSPORTATION SYSTEM
James W. Russell Sep. 1994 19 p
(Contract NAS1-19000; RTOP 237-01-02-01)
(NASA-CR-194986; NAS 1.26:194986) Avail: CASI HC A03/MF A01

This report presents the methodology used for receiving, processing, and analyzing flight data from the Space Transportation System at NASA Langley Research Center (LaRC) on a near real time basis. The task was performed in October 1993 during the STS-58 mission using data from the Orbital Acceleration Research Experiment (OARE). The transmitting and receiving of OARE data on a near real time basis at LaRC were highly successful. The time to receive and record the data from the payload tape recorder required 20 to 30 minutes. Payload tape recorder data were downlinked at intervals of 4 to 6 hours rather than continuously. The quality check of the data at LaRC required 2 minutes. Four to 5 minutes of time was required to obtain preliminary acceleration levels of the Orbiter that are within 1 micro-g of the absolute accelerations This demonstration has shown that, with operational modifications LaRC has the capability to serve as a User Operation Center for receiving and processing flight data from the Space Shuttle and Space Station. Author

N95-15357# Sandia National Labs., Albuquerque, NM.
GOUGE INITIATION IN HIGH-VELOCITY ROCKET SLED TESTING
R. D. M. Tachau, T. G. Trucano, and C. H. Yew 1994 24 p Presented at the 1994 Hypervelocity Impact Symposium, Santa Fe, NM, 16-20 Oct. 1994
(Contract DE-AC04-94AL-85000)
(DE94-014288; SAND-94-1333C; CONF-9410131-3) Avail: CASI HC A03/MF A01

A model is presented which describes the formation of surface damage 'gouging' on the rails that guide rocket sleds. An unbalanced sled can randomly cause a very shallow-angle, oblique impact between the sled shoe and the rail. This damage phenomenon has also been observed in high-velocity guns where the projectile is analogous to the moving sled shoe and the gun barrel is analogous to the stationary rail. At sufficiently high velocity, the oblique impact will produce a thin hot layer of soft material on the contact surfaces. Under the action of a normal moving load, the soft layer lends itself to an anti-symmetric deformation and the formation of a 'hump' in front of the moving load. A gouge is formed when this hump is overrun by the sled shoe. The phenomenon is simulated numerically using the CTH strong shock physics code, and the results are in good agreement with experimental observation. DOE

N95-14070*# National Aeronautics and Space Administration. Goddard Space Flight Center, Greenbelt, MD.
CLEAN ASSEMBLY AND INTEGRATION TECHNIQUES FOR THE HUBBLE SPACE TELESCOPE HIGH FIDELITY MECHANICAL SIMULATOR
David W. Hughes (Swales and Associates, Beltsville, MD.) and Randy J. Hedgeland *In its* Eighteenth Space Simulation Conference: Space Mission Success Through Testing Nov. 1994 p 99-111 (For primary document see N95-14062 03-18)
Avail: CASI HC A03/MF A04

N95-14079*# Canadian Space Agency, Ottawa (Ontario).
DAVID FLORIDA LABORATORY THERMAL VACUUM DATA PROCESSING SYSTEM
Elie Choueiry *In* NASA. Goddard Space Flight Center, Eighteenth Space Simulation Conference: Space Mission Success Through Testing Nov. 1994 p 223-230 (For primary document see N95-14062 03-18)
Avail: CASI HC A02/MF A04

N95-14085*# Space Systems/Loral, Palo Alto, CA.
REFURBISHMENT OF A 39 FOOT THERMAL VACUUM CHAMBER
Arthur A. Edwards *In* NASA. Goddard Space Flight Center, Eighteenth Space Simulation Conference: Space Mission Success Through Testing Nov. 1994 p 271-297 (For primary document see N95-14062 03-18)
Avail: CASI HC A03/MF A04

N95-14086*# European Space Agency. European Space Research and Technology Center, ESTEC, Noordwijk (Netherlands).
HYDRA, A NEW TOOL FOR MECHANICAL TESTING
P. W. Brinkmann *In* NASA. Goddard Space Flight Center, Eighteenth Space Simulation Conference: Space Mission Success Through Testing Nov. 1994 p 299-312 (For primary document see N95-14062 03-18)
Avail: CASI HC A03/MF A04

N95-14094*# TRW, Inc., Redondo Beach, CA. Space and Electronics Group.
ALPHA LAMP INTEGRATION FACILITY
Richard Oshiro, Dennis Sowers, Joe Gargiulo, and Mark McGahey *In* NASA. Goddard Space Flight Center, Eighteenth Space Simulation Conference: Space Mission Success Through Testing Nov. 1994 p 411-425 (For primary document see N95-14062 03-18)
(Contract SDIO84-C-0003)
Avail: CASI HC A03/MF A04

N95-14095*# Kassel Univ. (Germany). Control Engineering and System Theory Group.
SIMULATION OF A SPATIAL, SERVO-HYDRAULIC TEST FACILITY FOR SPACE STRUCTURES
K.-D. Leimbach and H. Hahn *In* NASA. Goddard Space Flight Center, Eighteenth Space Simulation Conference: Space Mission Success Through Testing Nov. 1994 p 427-439 (For primary document see N95-14062 03-18)
Avail: CASI HC A03/MF A04

N95-14097*# Calspan Corp., Arnold AFS, TN. Engineering Development Center.
THE AEDC AEROSPACE CHAMBER 7V: AN ADVANCED TEST CAPABILITY FOR INFRARED SURVEILLANCE AND SEEKER SENSORS
W. R. Simpson *In* NASA. Goddard Space Flight Center, Eighteenth Space Simulation Conference: Space Mission Success Through Testing Nov. 1994 p 451-465 (For primary document see N95-14062 03-18)
Avail: CASI HC A03/MF A04

N95-14098*# Nauchno-Issledovatelskii Inst. Grafit, Moscow (Russia).
NEW POTENTIALS OF NIICHIMMASH'S THERMAL VACUUM FACILITIES Abstract Only
N. A. Afanassiev, A. A. Makarov, and V. L. Galjaev *In* NASA. Goddard Space Flight Center, Eighteenth Space Simulation Conference: Space Mission Success Through Testing Nov. 1994 p 467 (For primary document see N95-14062 03-18)
Avail: CASI HC A01/MF A04

N95-14621*# Jet Propulsion Lab., California Inst. of Tech., Pasadena, CA.
THE LONG-TERM FORECAST OF STATION VIEW PERIODS
M. W. Lo *In its* The Telecommunications and Data Acquisition Report 15 Aug. 1994 p 1-13 (For primary document see N95-14620 03-32)
(RTOP 310-10-63-50)
Avail: CASI HC A03/MF A02

N95-14631*# Jet Propulsion Lab., California Inst. of Tech., Pasadena, CA.
THE NETWORK OPERATIONS CONTROL CENTER UPGRADE TASK: LESSONS LEARNED
J. S. Sherif (California State Univ., Fullerton, CA.), T.-L. Tran, and S. Lee *In its* The Telecommunications and Data Acquisition Report 15 Aug. 1994 p 160-168 (For primary document see N95-14620 03-32)
(RTOP 314-30-43-09-01)
Avail: CASI HC A02/MF A02

N95-14632*# Jet Propulsion Lab., California Inst. of Tech., Pasadena, CA.
LOW-EARTH-ORBITER RESOURCE ALLOCATION AND CAPACITY PLANNING FOR THE DSN USING LEO4CAST
G. Fox and C. Borden *In its* The Telecommunications and Data Acquisition Report 15 Aug. 1994 p 169-178 (For primary document see N95-14620 03-32)
(RTOP 315-90-71-10-08)
Avail: CASI HC A03/MF A02

N95-15146*# Baylor Coll. of Medicine, Houston, TX. Dept. of Physical Medicine.
THE CARDIOVASCULAR RESPONSE TO THE AGS
David Cardus and Wesley G. McTaggart *In* International Union of Physiological Sciences, The Physiologist, Volume 36, Number 1, Supplement Feb. 1993 3 p (For primary document see N95-15089 03-52)
(Grant NAGw-1691)
Avail: CASI HC A01/MF A02

15 LAUNCH VEHICLES AND SPACE VEHICLES

Includes boosters; operating problems of launch/space vehicle systems; and reusable vehicles.

For related information see also *20 Spacecraft Propulsion and Power.*

N95-13700* National Aeronautics and Space Administration. Goddard Space Flight Center, Greenbelt, MD.
DELTA, AMERICA'S SPACE AMBASSADOR (Videotape)
Oct. 1994 Videotape: 24 min. playing time
(NASA-TM-110046; NONP-NASA-VT-94-29868) Avail: CASI VHS A01/BETA A22

This video presentation features the major satellites launched by the Delta rocket in a celebration of this dependable launch vehicle's past. GSFC

N95-13893*# National Aeronautics and Space Administration. Lewis Research Center, Cleveland, OH.
NASA LERC'S ACOUSTIC FILL EFFECT TEST PROGRAM AND RESULTS
William O. Hughes, Mark E. McNelis, and Jerome E. Manning Oct. 1994 22 p Presented at the 65th Shock and Vibration Symposium, San Diego, CA, 31 Oct. - 3 Nov. 1994; sponsored by SAVIAC
(Contract NAS3-25972)
(NASA-TM-106688; E-9044; NAS 1.15:106688) Avail: CASI HC A03/MF A01

NASA Lewis Research Center, in conjunction with General Dynamics Space Systems Division, has performed a test program to investigate the acoustic fill effect for an unblanketed payload fairing for a variety of payload simulators. This paper will discuss this test program and fill factor test data, and make comparisons with theoretical predictions. This paper will also address the NASA acoustic fill effect standard which was verified from the test data analysis. Author

16 SPACE TRANSPORTATION

Includes passenger and cargo space transportation, e.g., shuttle operations; and space rescue techniques.

For related information see also *03 Air Transportation and Safety* and *18 Spacecraft Design, Testing and Performance.* For space suits see *54 Man/System Technology and Life Support.*

N95-15447# Naval Postgraduate School, Monterey, CA.
COLD FLOW SIMULATION OF THE ALTERNATE TURBOPUMP DEVELOPMENT TURBINE OF THE SPACE SHUTTLE MAIN ENGINE HIGH PRESSURE FUEL TURBOPUMP M.S. Thesis
Richard J. Rutkowski Mar. 1994 85 p
(AD-A281676) Avail: CASI HC A05/MF A01

Completion of the installation at the Naval Postgraduate School of a cold-flow test facility for the turbine of the Space Shuttle Main Engine High Pressure Fuel Turbopump is reported. The article to be tested is the first stage of the Alternate Turbopump Development model designed and manufactured by Pratt & Whitney. The purpose of the facility is to enable the development of non-intrusive flow measurements and comparison of those measurements with numerical simulations. Flow field characteristics of the turbine stator were predicted using a three-dimensional viscous flow code. A sensitivity study was conducted to determine the effect of inlet profile to flow field solution. Recommendations are made for future use of the test facility and validation of the numerical simulation scheme. DTIC

N95-15552*# Boeing Aerospace and Electronics Co., Seattle, WA.
SPACE TRANSFER VEHICLE CONCEPTS AND REQUIREMENTS STUDY. VOLUME 3: PROGRAM COST ESTIMATES. BOOK 2: WBS AND DICTIONARY Final Report, Aug. 1989 - Apr. 1991
A. F. Peffley 1 Apr. 1991 86 p Original contains color illustrations
(Contract NAS8-37855)
(NASA-CR-192447; NAS 1.26:192447; D180-32040-3-Vol-3-Bk-2) Avail: CASI HC A05/MF A01; 1 functional color page

This document describes the products and services to be developed, tested, produced, and operated for the Space Transfer Vehicle (STV) Program. The Work Breakdown Structure (WBS) and WBS Dictionary are program management tools used to catalog, account by task, and summarize work packages of a space system program. The products or services to be delivered or accomplished during the STV C/D phase are the primary focus of this work breakdown structure document. Author

N95-15900 National Aeronautics and Space Administration. Lyndon B. Johnson Space Center, Houston, TX.
STS-66 POST FLIGHT PRESENTATION (Videotape)
1994 Videotape: 40 min. 30 sec. playing time, in color, with sound
(NASA-TM-110077; NONP-NASA-VT-94-33203) Avail: CASI VHS A02/BETA A22

This video contains mission footage selected by the STS-66 crew of pre-launch, launch, onboard activities and experiments, ATLAS-3, CRISTA/SPAS, SSBUV/A, ESCAPE II, Earth views, and landing. Crew members provide descriptive voice-over narration of the scenes. JSC

N95-14089*# National Aeronautics and Space Administration. Ames Research Center, Moffett Field, CA.
SIMULATION OF SHUTTLE LAUNCH G FORCES AND ACOUSTIC LOADS USING THE NASA AMES RESEARCH CENTER 20G CENTRIFUGE
T. L. Shaw, J. M. Corliss, D. P. Gundo, G. M. Mulenburg, G. A. Breit, and J. B. Griffith *In* NASA. Goddard Space Flight Center, Eighteenth Space Simulation Conference: Space Mission Success Through Testing Nov. 1994 p 349-371 (For primary document see N95-14062 03-18)
Avail: CASI HC A03/MF A04

N95-14474*# Rockwell International Corp., Downey, CA. Space Systems Div.
SPACE SHUTTLE FATIGUE LOADS SPECTRA FOR PRELAUNCH AND LIFTOFF LOADS
Judith Goldish and Raphael Ortasse *In* NASA. Langley Research Center, FAA/NASA International Symposium on Advanced Structural Integrity Methods for Airframe Durability and Damage Tolerance Sep. 1994

p 289-306 (For primary document see N95-14453 03-39)
(Contract NAS9-18500)
Avail: CASI HC A03/MF A04

17 SPACE COMM., SPACECRAFT COMM., COMMAND & TRACKING

Includes telemetry; space communications networks; astronavigation and guidance; and radio blackout.

For related information see also *04 Aircraft Communications and Navigation* and *32 Communications and Radar.*

N95-14162*# Fairchild Space Co., Germantown, MD. Communications, Data Handling, and Power Systems.
EVOLUTIONARY TELEMETRY AND COMMAND PROCESSOR (TCP) ARCHITECTURE
John R. Schneider *In* Research Inst. for Computing and Information Systems, RICIS Symposium 1992: Mission and Safety Critical Systems Research and Applications 30 Oct. 1992 20 p (For primary document see N95-14156 03-61)
Avail: CASI HC A03/MF A03

18 SPACECRAFT DESIGN, TESTING AND PERFORMANCE

Includes satellites; space platforms; space stations; spacecraft systems and components such as thermal and environmental controls; and attitude controls.

For life support systems see *54 Man/System Technology and Life Support.* For related information see also *05 Aircraft Design, Testing and Performance, 39 Structural Mechanics,* and *16 Space Transportation.*

N95-13728*# National Aeronautics and Space Administration. Lewis Research Center, Cleveland, OH.
DESIGN FOR RELIABILITY: NASA RELIABILITY PREFERRED PRACTICES FOR DESIGN AND TEST
Vincent R. Lalli Oct. 1994 27 p Presented at the Reliability and Maintainability Symposium, Anaheim, CA, 24-27 Jan. 1994; cosponsored by ASQC, IIE, IEEE, SOLE, IES, AIAA, SSS, and SRE
(RTOP 323-44-19)
(NASA-TM-106313; E-8053; NAS 1.15:106313) Avail: CASI HC A03/MF A01

This tutorial summarizes reliability experience from both NASA and industry and reflects engineering practices that support current and future civil space programs. These practices were collected from various NASA field centers and were reviewed by a committee of senior technical representatives from the participating centers (members are listed at the end). The material for this tutorial was taken from the publication issued by the NASA Reliability and Maintainability Steering Committee (NASA Reliability Preferred Practices for Design and Test. NASA TM-4322, 1991). Reliability must be an integral part of the systems engineering process. Although both disciplines must be weighed equally with other technical and programmatic demands, the application of sound reliability principles will be the key to the effectiveness and affordability of America's space program. Our space programs have shown that reliability efforts must focus on the design characteristics that affect the frequency of failure. Herein, we emphasize that these identified design characteristics must be controlled by applying conservative engineering principles. Author

N95-13729*# National Aeronautics and Space Administration. Langley Research Center, Hampton, VA.
THREE-AXIS STABILIZATION OF SPACECRAFT USING PARAMETER-INDEPENDENT NONLINEAR QUATERNION FEEDBACK
Suresh M. Joshi and Atul G. Kelkar Sep. 1994 10 p
(RTOP 233-01-01-05)
(NASA-TM-109150; NAS 1.15:109150) Avail: CASI HC A02/MF A01

This paper considers the problem of rigid spacecraft. A nonlinear control law which uses the feedback of the unit quaternion and the measured angular velocities is proposed and is shown to provide global asymptotic stability. The control law does not require the knowledge of the system parameters, and is therefore robust to modeling errors. The significance of the control law is that it can be used for large-angle maneuvers with guaranteed stability. Author

N95-14062*# National Aeronautics and Space Administration. Goddard Space Flight Center, Greenbelt, MD.
EIGHTEENTH SPACE SIMULATION CONFERENCE: SPACE MISSION SUCCESS THROUGH TESTING
Joseph L. Stecher, III, comp. Washington Nov. 1994 455 p Conference held in Baltimore, MD, 31 Oct. - 3 Nov. 1994; sponsored by AIAA, American Society for Testing and Materials and Canadian Space Agency
(RTOP 750-00-00)
(NASA-CP-3280; Rept-94B00132; NAS 1.55:3280) Avail: CASI HC A20/MF A04

The Institute of Environmental Sciences' Eighteenth Space Simulation Conference, 'Space Mission Success Through Testing' provided participants with a forum to acquire and exchange information on the state-of-the-art in space simulation, test technology, atomic oxygen, program/system testing, dynamics testing, contamination, and materials. The papers presented at this conference and the resulting discussions carried out the conference theme 'Space Mission Success Through Testing.' For individual titles, see N95-14063 through N95-14099.

N95-14063*# Dayton Univ. Research Inst., OH.
EVALUATION OF REFORMULATED THERMAL CONTROL COATINGS IN A SIMULATED SPACE ENVIRONMENT. PART 1: YB-71 **c27**
Clifford A. Cerbus and Patrick S. Carlin *In* NASA. Goddard Space Flight Center, Eighteenth Space Simulation Conference: Space Mission Success Through Testing Nov. 1994 p 1-23 (For primary document see N95-14062 03-18)
Avail: CASI HC A03/MF A04

The Air Force Space and Missile Systems Center and Wright Laboratory Materials Directorate (WL/ML) have sponsored and effort to effort to reformulate and qualify Illinois Institute of Technology Research Institute (IITRI) spacecraft thermal control coatings. S13G/LO-1, Z93, and YB-71 coatings were reformulated because the potassium silicate binder, Sylvania PS-7, used in the coatings is no longer manufactured. Coatings utilizing the binder's replacement candidate, Kasil 2130, manufactured by The Philadelphia Quartz (PQ) Corporation, Baltimore, Maryland, and undergoing testing at the Materials Directorate's Space Combined Effects Primary Test and Research Equipment (SCEPTRE) Facility operated by the University of Dayton Research Institute (UDRI). The simulated space environment consists of combined ultraviolet (UV) and electron exposure with in site specimen reflectance measurements. A brief description of the effort at IITRI, results and discussion from testing the reformulated YB-71 coating in SCEPTRE, and plans for further testing of reformulated Z93 and S13G/LO-1 are presented. Author

N95-14064*# Lockheed Missiles and Space Co., Sunnyvale, CA. Space Systems Div.
PREDICTION OF PARTICULATE CONTAMINATION ON APERTURE WINDOW **c74**
Aleck L. Lee and Michael C. Fong *In* NASA. Goddard Space Flight Center, Eighteenth Space Simulation Conference: Space Mission Success Through Testing Nov. 1994 p 25-35 (For primary document see N95-14062 03-18)
Avail: CASI HC A03/MF A04

This paper presents an analysis to predict the effects of light scattering by surface particles on the sensor window of a missile during ascent flight. The particulate contaminant distribution on the window is calculated by tallying the number of particles in a set of size ranges. The particulate contamination at the end of the mission is predicted by adding the contributions from the events of ground and flight operations. The surface particle redistributions caused by vibroacoustically induced surface acceleration was found to contribute the most of the particulate surface contamination. The analytical surface obscuration calculation with a set of particle counts was compared to the results of image analyzer measurement. The analytical results, which were calculated with a given function of particle shape depending on the size, were more conservative than the measurement. A scattering calculation using a verified BSDF model showed

that the scattering was less than 0.001 at 20 off the direction of the incident light in the mid IR wavelength when the surfaces were at Level 300 initially. Author

N95-14065*# Nauchno-Issledovatelskii Inst. Grafit, Moscow (Russia).
EXPERIMENTAL STUDY OF SOLAR SIMULATOR MIRROR CRYOCONTAMINATION Abstract Only **c74**
V. L. Galjaev, A. A. Makarov, and N. A. Afanassiev *In* NASA. Goddard Space Flight Center, Eighteenth Space Simulation Conference: Space Mission Success Through Testing Nov. 1994 p 37 (For primary document see N95-14062 03-18)
Avail: CASI HC A01/MF A04

The background and tasks formulation of the study of Solar Simulator collimation mirror cryocontamination in Large Thermal Vacuum Facility are outlined, research methods and experiment procedures are described, experimental relationships obtained are analyzed and practical recommendations are given. The accepted procedure of thermal vacuum tests as a rule defines the sequence of operations for verifying the spacecraft under test without taking into account measures for preventing Solar Simulator collimation mirror contamination and degradation. On the other hand, evacuation procedures is defined for conditions of achieving the required vacuum in the shortest possible time with using the available evacuation equipment at a regime close to the optimum one. Similarly, cryopanel cooling down cyclogram and test object preparation process are not analyzed from the viewpoint of ways of reducing environmental detrimental effects on thermal vacuum facility contamination-sensitive systems. Solar Simulator mirror contamination and its reflective characteristics change results in degradation of solar flux parameters and reduction of simulator continuous operation time. Methods of consideration of optical effects due to mirror surface contamination are actually missing. The effects themselves are not quite understood and data cited in literature as a rule, were obtained under conditions different from real thermal vacuum facility and therefore should be subjected to additional experimental verification. Only in the last few years contamination effect on optical surfaces degradation has been considered with using empirical relations. Mirror reflective properties degradation leads to the increase of Solar Simulator errors. This ultimately has an adverse effect on S/C ground development, schedule and cost of thermal vacuum tests. Besides, the mirror maintenance in operable state becomes more expensive. The present paper is dedicated to the study of Solar Simulator collimation mirror contamination and to the search of ways for improving the mirror design and thermal vacuum test procedure. On the basis of tests performed, recommendations are devised on reducing chamber inner-optical surfaces cryocontamination and degradation. Author

N95-14066*# Lockheed Missiles and Space Co., Sunnyvale, CA.
ASTM E 1559 METHOD FOR MEASURING MATERIAL OUTGASSING/DEPOSITION KINETICS HAS APPLICATIONS TO AEROSPACE, ELECTRONICS, AND SEMICONDUCTOR INDUSTRIES **c27**
J. W. Garrett, A. P. M. Glassford, and J. M. Steakley *In* NASA. Goddard Space Flight Center, Eighteenth Space Simulation Conference: Space Mission Success Through Testing Nov. 1994 p 39-56 (For primary document see N95-14062 03-18)
Avail: CASI HC A03/MF A04

The American Society for Testing and Materials has published a new standard test method for characterizing time and temperature-dependence of material outgassing kinetics and the deposition kinetics of outgassed species on surfaces at various temperatures. This new ASTM standard, E 1559(1), uses the quartz crystal microbalance (QCM) collection measurement approach. The test method was originally developed under a program sponsored by the United States Air Force Materials Laboratory (AFML) to create a standard test method for obtaining outgassing and deposition kinetics data for spacecraft materials. Standardization by ASTM recognizes that the method has applications beyond aerospace. In particular, the method will provide data of use to the electronics, semiconductor, and high vacuum industries. In ASTM E 1559 the material sample is held in vacuum in a temperature-controlled effusion cell, while its outgassing flux impinges on several QCM's which view the orifice of the effusion cell. Sample isothermal total mass loss (TML) is measured as a function of time from the mass collected on one of the QCM's which is cooled by liquid nitrogen, and the view factor from this QCM to the cell. The amount of outgassed volatile condensable material (VCM) on surfaces at higher temperatures is measured as a function of time during the isothermal outgassing test by controlling the temperatures of the remaining QCM's to selected values. The VCM on surfaces at temperatures in between those of the collector QCM's is determined at the end of the isothermal test by heating the QCM's at a controlled rate and measuring the mass loss from the end of the QCM's as a function of time and temperature. This reevaporation of the deposit collected on the QCM's is referred to as QCM thermogravimetric analysis. Isothermal outgassing and deposition rates can be determined by differentiating the isothermal TML and VCM data, respectively, while the evaporation rates of the species can be obtained as a function of temperature by differentiating the QCM thermogravimetric analysis data. Author

N95-14067*# Soreq Research Establishment, Israel Atomic Energy Commission, Yavneh (Israel).
SELF CONTAMINATION EFFECTS IN THE TAUVEX UV TELESCOPE: GROUND TESTING AND COMPUTER SIMULATION **c27**
Y. Lifshitz, Y. Noter, E. Grossman, L. Genkin, M. Murat, N. Saar, and A. Blasberger *In* NASA. Goddard Space Flight Center, Eighteenth Space Simulation Conference: Space Mission Success Through Testing Nov. 1994 p 57-73 Sponsored by ISA; Ministry of Science; and Ministry of Absorption (For primary document see N95-14062 03-18)
Avail: CASI HC A03/MF A04

The contamination effects due to outgassing from construction materials of the TAUVEX (Tel Aviv University UV Telescope) were evaluated using a combination of ground testing and computer simulations. Tests were performed from the material level of the system level including: (1) High sensitivity CVCM(10(exp -3 percent) measurements of critical materials. (2) Optical degradation measurements of samples specially contaminated by outgassing products at different contamination levels. (3) FTIR studies of chemical composition of outgassed products on above samples. (4) High resolution AFM studies of surface morphology of contaminated surfaces. The expected degradation of TAUVEX performance in mission was evaluated applying a computer simulation code using input parameters determined experimentally in the above tests. The results have served as guidelines for the proper selection of materials, cleanliness requirements, determination of the thermal conditions of the system and bakeout processes. Author

N95-14068*# National Aeronautics and Space Administration. Goddard Space Flight Center, Greenbelt, MD.
HUBBLE SPACE TELESCOPE SERVICING MISSION SCIENTIFIC INSTRUMENT PROTECTIVE ENCLOSURE DESIGN REQUIREMENTS AND CONTAMINATION CONTROLS **c74**
Patricia A. Hansen (Swales and Associates, Beltsville, MD.), David W. Hughes (Swales and Associates, Beltsville, MD.), Randy J. Hedgeland, Craig J. Chivatero, Robert J. Studer, and Peter J. Kostos *In its* Eighteenth Space Simulation Conference: Space Mission Success Through Testing Nov. 1994 p 75-85 (For primary document see N95-14062 03-18)
Avail: CASI HC A03/MF A04

The Scientific Instrument Protective Enclosures were designed for the Hubble Space Telescope Servicing Missions to provide a beginning environment to a Scientific Instrument during ground and on orbit activities. The Scientific Instruments required very stringent surface cleanliness and molecular outgassing levels to maintain ultraviolet performance. Data from the First Servicing Mission verified that both the Scientific Instruments and Scientific Instrument Protective Enclosures met surface cleanliness level requirements during ground and on-orbit activities. Author

N95-14069*# McDonnell-Douglas Space Systems Co., Rockville, MD.
USING A TEMPERATURE-CONTROLLED QUARTZ CRYSTAL MICROBALANCE IN A SPACE EQUIPMENT CLEANROOM TO MONITOR MOLECULAR CONTAMINATION **c35**
William J. Mitchell *In* NASA. Goddard Space Flight Center, Eighteenth Space Simulation Conference: Space Mission Success Through Testing Nov. 1994 p 87-97 (For primary document see N95-14062 03-18)
Avail: CASI HC A03/MF A04

There is a need for continuous monitoring for molecular contamination in clean rooms where spaceflight equipment is assembled, integrated, and tested to insure that contamination budgets are met. The TQCM (temperature-controlled quartz crystal microbalance) can be used to provide both a real time warning and a cumulative measurement of molecular

contamination. It has advantages over the other measurement methods such as witness mirrors, NVR (non-volatile residue) plates, and gas analyzers. A comparison of the TQCM sensitivity and ease of operations is made with the other methods. The surface acoustic wave microbalance (SAW), a newly developed instrument similar to TQCM, is considered in the comparison. An example is provided of TQCM use at Goddard Space Flight Center when the Wide Field Planetary Camera 2(WFPC-2) and the Corrective Optics Space Telescope Axial Replacement (COSTAR) were undergoing integrated testing prior to their installation in the Hubble Space Telescope on its first servicing mission. Areas for further investigation are presented. Author

N95-14070*# National Aeronautics and Space Administration. Goddard Space Flight Center, Greenbelt, MD.

CLEAN ASSEMBLY AND INTEGRATION TECHNIQUES FOR THE HUBBLE SPACE TELESCOPE HIGH FIDELITY MECHANICAL SIMULATOR **c14**

David W. Hughes (Swales and Associates, Beltsville, MD.) and Randy J. Hedgeland *In its* Eighteenth Space Simulation Conference: Space Mission Success Through Testing Nov. 1994 p 99-111 (For primary document see N95-14062 03-18)

Avail: CASI HC A03/MF A04

A mechanical simulator of the Hubble Space Telescope (HST) Aft Shroud was built to perform verification testing of the Servicing Mission Scientific Instruments (SI's) and to provide a facility for astronaut training. All assembly, integration, and test activities occurred under the guidance of a contamination control plan, and all work was reviewed by a contamination engineer prior to implementation. An integrated approach was followed in which materials selection, manufacturing, assembly, subsystem integration, and end product use were considered and controlled to ensure that the use of the High Fidelity Mechanical Simulator (HFMS) as a verification tool would not contaminate mission critical hardware. Surfaces were cleaned throughout manufacturing, assembly, and integration, and reverification was performed following major activities. Direct surface sampling was the preferred method of verification, but access and material constraints led to the use of indirect methods as well. Although surface geometries and coatings often made contamination verification difficult, final contamination sampling and monitoring demonstrated the ability to maintain a class M5.5 environment with surface levels less than 400B inside the HFMS. Author

N95-14071*# Physical Sciences, Inc., Andover, MA.

LABORATORY SIMULATION OF LOW EARTH ORBIT (LEO) ATOMIC OXYGEN EFFECTS **c25**

George E. Caledonia, Robert H. Krech, and David B. Oakes *In* NASA. Goddard Space Flight Center, Eighteenth Space Simulation Conference: Space Mission Success Through Testing Nov. 1994 p 113-120 Sponsored by NASA. Johnson Space Center and DNA (For primary document see N95-14062 03-18)

Avail: CASI HC A02/MF A04

A pulsed fast oxygen atom source has been used extensively over the last 7 years to investigate the effects of ambient oxygen atoms impacting materials placed in low Earth orbit. In this period, we irradiated well over 2000 material samples with 8 km/s oxygen atoms generated in our source. Typical irradiance level is 3 x 10(exp 20) O atoms/sq cm although some materials have been irradiated to fluence levels as high as 6 x 10(exp 21) O atoms/sq cm. The operating principles and characteristics of our source are reviewed along with diagnostic and handling procedures appropriate to material testing. Representative data is presented on the velocity dependence of oxygen atom erosion rates (the PSI source provides oxygen atoms tunable over the velocity range of 5 to 12 km/s) as well as the dependence on material temperature. Specific examples of non-linear oxidative effects related to surface contamination and test duration are also be provided. Author (revised)

N95-14072*# Phillips Lab., Edwards AFB, CA.

A FACILITY TO PRODUCE AN ENERGETIC, GROUND STATE ATOMIC OXYGEN BEAM FOR THE SIMULATION OF THE LOW-EARTH ORBIT ENVIRONMENT **c72**

Andrew D. Ketsdever, David P. Weaver, and E. P. Muntz *In* NASA. Goddard Space Flight Center, Eighteenth Space Simulation Conference: Space Mission Success Through Testing Nov. 1994 p 121-138 Prepared in cooperation with University of Southern California, Los Angeles, CA (For primary document see N95-14062 03-18)

Avail: CASI HC A03/MF A04

Because of the continuing commitment to activity in low-Earth orbit (LEO), a facility is under development to produce energetic atmospheric species, particularly atomic oxygen, with energies ranging from 5 to 80 eV. This relatively high flux facility incorporates an ion engine to produce the corresponding specie ion which is charge exchanged to produce a neutral atomic beam. Ion fluxes of around 10(exp 15) sec(exp -1) with energies of 20-70 eV have been achieved. A geometrically augmented inertially tethered charge exchanger (GAITCE) was designed to provide a large column depth of charge exchange gas while reducing the gas load to the low pressure portion of the atomic beam facility. This is accomplished using opposed containment jets which act as collisional barriers to the escape of the dense gas region formed between the jets. Leak rate gains to the pumping system on the order of 10 were achieved for moderate jet mass flows. This system provides an attractive means for the charge exchange of atomic ions with a variety of gases to produce energetic atomic beams. Author

N95-14073*# Soreq Research Establishment, Israel Atomic Energy Commission, Yavneh (Israel).

ATOMIC OXYGEN (ATOX) SIMULATION OF TEFLON FEP AND KAPTON H SURFACES USING A HIGH INTENSITY, LOW ENERGY, MASS SELECTED, ION BEAM FACILITY **c72**

R. Vered, E. Grossman, G. D. Lempert, and Y. Lifshitz *In* NASA. Goddard Space Flight Center, Eighteenth Space Simulation Conference: Space Mission Success Through Testing Nov. 1994 p 139-156 Sponsored by Israel Space Agency; Ministry of Science; and Ministry of Absorption (For primary document see N95-14062 03-18)

Avail: CASI HC A03/MF A04

A high intensity (greater than 10(exp 15) ions/sq cm) low energy (down to 5 eV) mass selected ion beam (MSIB) facility was used to study the effects of ATOX on two polymers commonly used for space applications (Kapton H and Teflon FEP). The polymers were exposed to O(+) and Ne(+) fluences on 10(exp 15) - 10(exp 19) ions/sq cm, using 30eV ions. A variety of analytical methods were used to analyze the eroded surfaces including: (1) atomic force microscopy (AFM) for morphology measurements; (2) total mass loss measurements using a microbalance; (3) surface chemical composition using x-ray photoelectron spectroscopy (XPS), and (4) residual gas analysis (RGA) of the released gases during bombardment. The relative significance of the collisional and chemical degradation processes was evaluated by comparing the effects of Ne(+) and O(+) bombardment. For 30 eV ions it was found that the Kapton is eroded via chemical mechanisms while Teflon FEP is eroded via collisional mechanisms. AFM analysis was found very powerful in revealing the evolution of the damage from its initial atomic scale (roughness of approx. 1 nm) to its final microscopic scale (roughness greater than 1 micron). Both the surface morphology and the average roughness of the bombarded surfaces (averaged over 1 micron x 1 micron images by the system's computer) were determined for each sample. For 30 eV a non linear increase of the Kapton roughness with the O(+) fluence was discovered (a slow increase rate for fluences phi less than 5 x 10(exp 17) O(+)/sq cm, and a rapid increase rate for phi greater than 5 x 10(exp 17) O(+)/sq cm). Comparative studies on the same materials exposed to RF and DC oxygen plasmas indicate that the specific details of the erosion depend on the simulation facility emphasizing the advantages of the ion beam facility. Author

N95-14074*# National Aeronautics and Space Administration. Langley Research Center, Hampton, VA.

THE EFFECT OF LOW EARTH ORBIT EXPOSURE ON SOME EXPERIMENTAL FLUORINE AND SILICON-CONTAINING POLYMERS **c27**

John W. Connell, Philip R. Young, Carol G. Kalil, Alice C. Chang, and Emilie J. Siochi *In* NASA. Goddard Space Flight Center, Eighteenth Space Simulation Conference: Space Mission Success Through Testing Nov. 1994 p 157-175 (For primary document see N95-14062 03-18)

Avail: CASI HC A03/MF A04

Several experimental fluorine and silicon-containing polymers in film form were exposed to low Earth orbit (LEO) on a Space Shuttle flight experiment (STS-46, Evaluation of Oxygen Interaction with Materials, EOIM-3). The environmental parameters of primary concern were atomic

oxygen (AO) and ultraviolet (UV) radiation. The materials were exposed to 2.3 plus or minus 0.1 x 10(exp 20) oxygen atoms/sq cm and 30.6 UV sun hours during the flight. In some cases, the samples were exposed at ambient, 120 C and 200 C. The effects of exposure on these materials were assessed utilizing a variety of characterization techniques including optical, scanning electron (SEM) and scanning tunneling (STM) microscopy, UV-visible (UV-VIS) transmission, diffuse reflectance infrared (DR-FTIR), x-ray photoelectron (XPS) spectroscopy, and in a few cases, gel permeation chromatography (GPC). In addition, weight losses of the films, presumably due to AO erosion, were measured. The fluorine-containing polymers exhibited significant AO erosion and exposed films were diffuse or 'frosted' in appearance and consequently displayed dramatic reductions in optical transmission. The silicon-containing films exhibited minimum AO erosion and the optical transmission of exposed films was essentially unchanged. The silicon near the exposed surface in the films was converted to silicate/silicon oxide upon AO exposure which subsequently provided protection for the underlying material. The silicon-containing epoxies are potentially useful as AO resistant coatings and matrix resins as they are readily processed into carbon fiber reinforced composites and cured via electron radiation. Author

N95-14075*# Enhanced Technologies, Houston, TX.
A SIMULATION FACILITY FOR TESTING SPACE STATION ASSEMBLY PROCEDURES
Ankur R. Hajare, Daniel T. Wick, and Nagy M. Shehad *In* NASA. Goddard Space Flight Center, Eighteenth Space Simulation Conference: Space Mission Success Through Testing Nov. 1994 p 177-186 (For primary document see N95-14062 03-18)
Avail: CASI HC A02/MF A04

NASA plans to construct the Space Station Freedom (SSF) in one of the most hazardous environments known to mankind - space. It is of the utmost importance that the procedures to assemble and operate the SSF in orbit are both safe and effective. This paper describes a facility designed to test the integration of the telerobotic systems and to test assembly procedures using a real-world robotic arm grappling space hardware in a simulated microgravity environment. Author

N95-14076*# Able Engineering Co., Inc., Goleta, CA.
MARTIAN ENVIRONMENTAL SIMULATION FOR A DEPLOYABLE LATTICE MAST **c91**
Robert M. Warden *In* NASA. Goddard Space Flight Center, Eighteenth Space Simulation Conference: Space Mission Success Through Testing Nov. 1994 p 187-193 (For primary document see N95-14062 03-18)
Avail: CASI HC A02/MF A04

The Mars Pathfinder mission (formerly Mars Environmental Survey or MESUR) is scheduled for launch in December 1996 and is designed to place a small lander on the surface of Mars. After impact, the lander unfolds to expose its solar panels and release a miniature rover. Also on board is the Imager for Mars Pathfinder (IMP) binocular camera which is elevated by a deployable mast to obtain a panoramic view of the landing area. The design of this deployable mast is based on similar designs which have a long and successful flight history. In the past when this type of self-deployable mast has been used, a rate limiter has been incorporated to control the speed of deployment. In this application, to reduce weight and complexity, it was proposed to eliminate the rate limiter so that the mast would deploy without restraint. Preliminary tests showed that this type of deployment was possible especially if the deployed length was relatively short, as in this application. Compounding the problem, however, was the requirement to deploy the mast at an angle of up to 30 degrees from vertical. The deployment process was difficult to completely analyze due to the effects of gravitational and inertial loads on the mast and camera during rapid extension. Testing in a realistic manner was imperative to verify the system performance. A deployment test was therefore performed to determine the maximum tilt angle at which the mast could reliably extend and support the camera on Mars. The testing of the deployable mast requires partial gravity compensation to simulate the smaller force of Martian gravity. During the test, mass properties were maintained while weight properties were reduced. This paper describes the testing of a deployable mast in a simulated Martian environment as well as the results of the tests. Author

N95-14077*# Alenia Spazio S.p.A., Turin (Italy).
SPACE SIMULATION TECHNIQUES AND FACILITIES FOR SAX STM TEST CAMPAIGN
Pietro Giordano, Giacomo Raimondo, and Piero Messidoro *In* NASA. Goddard Space Flight Center, Eighteenth Space Simulation Conference: Space Mission Success Through Testing Nov. 1994 p 195-209 (For primary document see N95-14062 03-18)
Avail: CASI HC A03/MF A04

SAX is a satellite for X-Ray astronomy. It is a major element of the overall basic Science Program of the Italian Space Agency (ASI) and is being developed with the contribution of the Netherlands Agency for Aerospace Programs (NIVR). The scientific objectives of SAX are to carry out systematic and comprehensive observations of celestial X-Ray sources over the 0.1 - 300 KeV energy range with special emphasis on spectral and timing measurements. The satellite will also monitor the X-Ray sky to investigate long-term source variability and to permit localization and study of X-Ray transients. Alenia Spazio is developing the satellite that is intended for launch in the second half of 1995 in a low, near-equatorial Earth orbit. At system level a Structural Thermal Model (STM) has been conceived to verify the environmental requirements by validating the mechanical and thermal analytical models and qualifying satellite structure and thermal control. In particular, the following tests have been carried out in Alenia Spazio, CEA/CESTA and ESTEC facilities: Modal Survey, Centrifuge, Acoustic, Sinusoidal/Random Vibration and Thermal Balance. The paper, after a short introduction of the SAX satellite, summarizes the environmental qualification program performed on the SAX STM. It presents test objectives, methodologies and relevant test configurations. Peculiar aspects of the test campaign are highlighted. Problems encountered and solutions adopted in performing the tests are described as well. Furthermore, test results are presented and assessed. Author

N95-14078*# Mitre Corp., Greenbelt, MD.
ENVIRONMENTAL TESTING TO PREVENT ON-ORBIT TDRS FAILURES
Robert M. Cutler *In* NASA. Goddard Space Flight Center, Eighteenth Space Simulation Conference: Space Mission Success Through Testing Nov. 1994 p 211-221 (For primary document see N95-14062 03-18)
(Contract NAS5-32607)
Avail: CASI HC A03/MF A04

Can improved environmental testing prevent on-orbit component failures such as those experienced in the Tracking and Data Relay Satellite (TDRS) constellation? TDRS communications have been available to user spacecraft continuously for over 11 years, during which the five TDRS's placed in orbit have demonstrated their redundancies and robustness by surviving 26 component failures. Nevertheless, additional environmental testing prior to launch could prevent the occurrence of some types of failures, and could help to maintain communication services. Specific testing challenges involve traveling wave tube assemblies (TWTA's) whose lives may decrease with on-off cycling, and heaters that are subject to thermal cycles. The development of test conditions and procedures should account for known thermal variations. Testing may also have the potential to prevent failures in which components such as diplexers have had their lives dramatically shortened because of particle migration in a weightless environment. Reliability modeling could be used to select additional components that could benefit from special testing, but experience shows that this approach has serious limitations. Through knowledge of on-orbit experience, and with advances in testing, communication satellite programs might avoid the occurrence of some types of failures, and extend future spacecraft longevity beyond the current TDRS design life of ten years. However, determining which components to test, and how must testing to do, remain problematical. Author

N95-14079*# Canadian Space Agency, Ottawa (Ontario).
DAVID FLORIDA LABORATORY THERMAL VACUUM DATA PROCESSING SYSTEM **c14**
Elie Choueiry *In* NASA. Goddard Space Flight Center, Eighteenth Space Simulation Conference: Space Mission Success Through Testing Nov. 1994 p 223-230 (For primary document see N95-14062 03-18)
Avail: CASI HC A02/MF A04

During 1991, the Space Simulation Facility conducted a survey to assess the requirements and analyze the merits for purchasing a new thermal vacuum data processing system for its facilities. A new, integrated, cost effective PC-based system was purchased which uses commercial

off-the-shelf software for operation and control. This system can be easily reconfigured and allows its users to access a local area network. In addition, it provides superior performance compared to that of the former system which used an outdated mini-computer and peripheral hardware. This paper provides essential background on the old data processing system's features, capabilities, and the performance criteria that drove the genesis of its successor. This paper concludes with a detailed discussion of the thermal vacuum data processing system's components, features, and its important role in supporting our space-simulation environment and our capabilities for spacecraft testing. The new system was tested during the ANIK E spacecraft test, and was fully operational in November 1991. Author (revised)

N95-14080*# Spar Aerospace Ltd., Sainte-Anne-de-Bellevue (Quebec).
THERMAL BALANCE TESTING OF MSAT 2 SPACECRAFT Abstract Only
Serge Samson and Elie Choueiry *In* NASA. Goddard Space Flight Center, Eighteenth Space Simulation Conference: Space Mission Success Through Testing Nov. 1994 p 231 (For primary document see N95-14062 03-18)
Avail: CASI HC A01/MF A04

The present work reports on the recently completed infrared thermal balance/thermal vacuum testing of a MSAT satellite, the first satellite to provide mobile communications service for all of continental North America. MSAT is a two spacecraft program, using a three-axis stabilized Hughes HS-601 series Bus as the vehicle for the Canadian designed Payload. The thermal tests which were performed at the Canadian Space Agency's David Florida Laboratory in Ottawa, Canada, lasted approximately 35 days. The infrared (IR) heating rig was designed to provide radiant heat inputs into seven spacecraft zones during Thermal Vacuum (TV) testing. The TV test was divided into multiple phases. It began with a thermal balance cold phase, followed by a thermal cold cycle and a hot balance phase, complemented by a thermal hot cycle to finish with a thermal cycle with continuous monitoring of the Bus and Payload. The spacecraft's external heat fluxes were provided by IR lamp sources. To ensure flux uniformity, highly reflective baffles and IR East and West faces; the Earth facing (Nadir); and the inside of the thrust cylinder. The aft-end panel heat fluxes were provided by a heated LN2 shroud. The radiation flux intensity on the spacecraft zones from the various rig elements was measured using Monitored Background Radiometers (MBR's) and compared with direct calculations and with pretest predictions. The temperature measurement system was based on Uniform Temperature References (UTR's) located inside the chamber such that all feedthroughs were copper-copper. This system was devised to achieve a temperature measurement accuracy of plus/minus 0.5 C for over 850 thermocouples used in the test. A PC-(QNX-based) based real-time data acquisition system was utilized to provide continuous monitoring of all channels based on a 30-second time scan. In addition, the data acquisition system was able to retrieve telemetry stream from the Satellite Test Equipments (STE) station for real-time data manipulation. Preliminary results showed the test to be successful from both the thermal balance side and the electrical testing side. Author

N95-14081*# Jet Propulsion Lab., California Inst. of Tech., Pasadena, CA.
THE REALUMINIZING OF THE 7-METER-DIAMETER SOLAR SIMULATOR COLLIMATING MIRROR **c27**
E. W. Noller *In* NASA. Goddard Space Flight Center, Eighteenth Space Simulation Conference: Space Mission Success Through Testing Nov. 1994 p 233-239 (For primary document see N95-14062 03-18)
Avail: CASI HC A02/MF A04

This paper describes the modification of a three-electron-beam (EB) gun system for vacuum depositing a highly reflective aluminum coating on a 7.01-m (23-ft) -diam nickel-plated aluminum collimating mirror. The mirror is part of the JPL 7.62-m space simulator that was recently modernized with a new high vacuum pumping system, solar lamp power supplies, solar optic lens system, and refurbished collimating mirror. The 7.01-m 12,700-kg (14-ton) spherical collimating mirror was removed from this facility for replating with 381 micron (0.015 in.) of electroless nickel and polished to a specular finish for realuminizing. The space chamber served as the vacuum coating vessel for the realuminizing coating process. The mirror is the primary reflector for the solar simulation system and the aluminized reflective surface is its most critical performance element. The uniformity of thickness and high reflectivity of the coating in visible and near-ultraviolet (UV) light governs the accuracy of the beam for solar testing. The uniformity of the thin-film thickness also controls the durability of the mirror over time. The mirror was polished to a 64-percent reflectivity with a uniformity of 1.5 percent. The performance goal for the aluminizing was 89 percent with +/- 0.5-percent variation over the mirror. Author

N95-14082*# Spar Aerospace Ltd., Sainte-Anne-de-Bellevue (Quebec).
THERMAL BALANCE TESTING OF THE MSAT SPACECRAFT
Serge Samson, Elie Choueiry, and Kenneth Pang *In* NASA. Goddard Space Flight Center, Eighteenth Space Simulation Conference: Space Mission Success Through Testing Nov. 1994 p 241-254 (For primary document see N95-14062 03-18)
Avail: CASI HC A03/MF A04

This paper reports on the recently completed thermal balance/thermal vacuum testing of an MSAT satellite, the first satellite to provide mobile communications service for all of continental North America. MSAT is a two-spacecraft program, using a three-axis-stabilized HUGHES HS-601 series bus as the vehicle for the Canadian-designed payload. The thermal tests performed at the Canadian Space Agency's David Florida Laboratory in Ottawa, Canada, lasted approximately 32 days. Author

N95-14083*# Naval Research Lab., Washington, DC. Center for Space Technology.
THERMAL DESIGN VERIFICATION TESTING OF THE CLEMENTINE SPACECRAFT: QUICK, CHEAP, AND USEFUL Abstract Only
Jeong H. Kim and Nelson L. Hyman *In* NASA. Goddard Space Flight Center, Eighteenth Space Simulation Conference: Space Mission Success Through Testing Nov. 1994 p 255 (For primary document see N95-14062 03-18)
Avail: CASI HC A01/MF A04

At this writing, Clementine had successfully fulfilled its moon-mapping mission; at this reading it will have also, with continued good fortune, taken a close look at the asteroid Geographos. The thermal design that made all this possible was indeed formidable in many respects, with very high ratios of requirements-to-available resources and performance-to-cost and mass. There was no question that a test verification of this quite unique and complex design was essential, but it had to be squeezed into an unyielding schedule and executed with bare-bones cost and manpower. After describing the thermal control subsystem's features, we report all the drama, close-calls, and cost-cutting, how objectives were achieved under severe handicap but (thankfully) with little management and documentation interference. Topics include the newly refurbished chamber (ready just in time), the reality level of the engineering model, using the analytical thermal model, the manner of environment simulation, the hand-scratched film heaters, functioning of all three types of heat pipes (but not all heat pipes), and the BMDO sensors' checkout through the chamber window. Test results revealed some surprises and much valuable data, resulting in thermal model and flight hardware refinements. We conclude with the level of correlation between predictions and both test temperatures and flight telemetry. Author

N95-14084*# National Inst. of Standards and Technology, Gaithersburg, MD.
PARTIAL PRESSURE ANALYSIS IN SPACE TESTING **c35**
Charles R. Tilford *In* NASA. Goddard Space Flight Center, Eighteenth Space Simulation Conference: Space Mission Success Through Testing Nov. 1994 p 257-269 Sponsored by JHU (For primary document see N95-14062 03-18)
Avail: CASI HC A03/MF A04

For vacuum-system or test-article analysis it is often desirable to know the species and partial pressures of the vacuum gases. Residual gas or Partial Pressure Analyzers (PPA's) are commonly used for this purpose. These are mass spectrometer-type instruments, most commonly employing quadrupole filters. These instruments can be extremely useful, but they should be used with caution. Depending on the instrument design, calibration procedures, and conditions of use, measurements made with these instruments can be accurate to within a few percent, or in error by two or more orders of magnitude. Significant sources of error can include relative gas sensitivities that differ from handbook values by an order of magnitude, changes in sensitivity with pressure by as much as two orders of magnitude, changes in sensitivity with time after exposure to chemically active gases, and the dependence of the sensitivity for one gas on the pressures of

other gases. However, for most instruments, these errors can be greatly reduced with proper operating procedures and conditions of use. In this paper, data are presented illustrating performance characteristics for different instruments and gases, operating parameters are recommended to minimize some errors, and calibrations procedures are described that can detect and/or correct other errors. Author

N95-14085*# Space Systems/Loral, Palo Alto, CA.
REFURBISHMENT OF A 39 FOOT THERMAL VACUUM CHAMBER c14
Arthur A. Edwards *In* NASA. Goddard Space Flight Center, Eighteenth Space Simulation Conference: Space Mission Success Through Testing Nov. 1994 p 271-297 (For primary document see N95-14062 03-18)
Avail: CASI HC A03/MF A04

The 39' thermal vacuum chamber at Space Systems/Loral has been used to test numerous spacecraft including those of the GOES, Intelsat, Insat, Superbird, N-Star, NATO and other programs. Ten years ago, the aluminum LN2 shroud experienced serious fatigue failures in the field welded jumper tubing, effectively shutting down the chamber for vacuum testing. The problem was repaired at the time, but new failures began to reappear a few months ago and are now occurring at a rate that suggests that the shroud may again become inoperable. Consequently, Space Systems/Loral is spending in excess of $6 million to replace the shroud and the existing LN2 equipment with a new, state of the art cryogenic system. In May, 1994, a contract was awarded to remove the existing shroud and LN2 pumping system and replace it with a gravity fed shroud and distribution system. Included in the contract are eight skid mounted gaseous nitrogen pumping systems capable of controlling shroud zone temperatures between +150 C and -180 C. The project is scheduled to be completed in April 1995. Author (revised)

N95-14086*# European Space Agency. European Space Research and Technology Center, ESTEC, Noordwijk (Netherlands).
HYDRA, A NEW TOOL FOR MECHANICAL TESTING c14
P. W. Brinkmann *In* NASA. Goddard Space Flight Center, Eighteenth Space Simulation Conference: Space Mission Success Through Testing Nov. 1994 p 299-312 (For primary document see N95-14062 03-18)
Avail: CASI HC A03/MF A04

The introduction outlines the verification concept for programs of the European Space Agency (ESA). The role of the Agency in coordinating the activities of major European space test centers is summarized. Major test facilities of the environmental test center at ESTEC, the Space Research and Technology Center of ESA, are shown and their specific characteristics are highlighted with special emphasis on the 6-degree-of-freedom (6-DOF) hydraulic shaker. The specified performance characteristics for sine and transient tests are presented. Results of single-axis hardware tests and 6-DOF computer simulations are included. Efforts employed to protect payloads against accidental damage in case of malfunctions of the facility are listed. Finally the operational advantages of the facility, as well as the possible use of the HYDRA control system design for future applications are indicated. Author

N95-14087*# Kinetic Research Corp., Annapolis, MD.
SYSTEM LEVEL MECHANICAL TESTING OF THE CLEMENTINE SPACECRAFT
James Haughton, Joseph Hauser, William Raynor, and Peter Lynn *In* NASA. Goddard Space Flight Center, Eighteenth Space Simulation Conference: Space Mission Success Through Testing Nov. 1994 p 313-331 (For primary document see N95-14062 03-18)
Avail: CASI HC A03/MF A04

This paper discusses the system level structural testing that was performed to qualify the Clementine Spacecraft for flight. These tests included spin balance, combined acoustic and axial random vibration, lateral random vibration, quasi-static loads, pyrotechnic shock, modal survey and on-orbit jitter simulation. Some innovative aspects of this effort were: the simultaneously combined acoustic and random vibration test; the mass loaded interface modal survey test; and the techniques used to assess how operating on board mechanisms and thrusters affect sensor vision. Author

N95-14088*# Kentucky Univ., Lexington, KY. Dept. of Mechanical Engineering.
EVALUATION OF SENSOR PLACEMENT ALGORITHMS FOR ON-ORBIT IDENTIFICATION OF SPACE PLATFORMS
Robin S. Glassburn and Suzanne Weaver Smith *In* NASA. Goddard Space Flight Center, Eighteenth Space Simulation Conference: Space Mission Success Through Testing Nov. 1994 p 333-348 Sponsored by NASA. Kennedy Space Center (For primary document see N95-14062 03-18)
Avail: CASI HC A03/MF A04

Anticipating the construction of the international space station, on-orbit modal identification of space platforms through optimally placed accelerometers is an area of recent activity. Unwanted vibrations in the platform could affect the results of experiments which are planned. Therefore, it is important that sensors (accelerometers) be strategically placed to identify the amount and extent of these unwanted vibrations, and to validate the mathematical models used to predict the loads and dynamic response. Due to cost, installation, and data management issues, only a limited number of sensors will be available for placement. This work evaluates and compares four representative sensor placement algorithms for modal identification. Most of the sensor placement work to date has employed only numerical simulations for comparison. This work uses experimental data from a fully-instrumented truss structure which was one of a series of structures designed for research in dynamic scale model ground testing of large space structures at NASA Langley Research Center. Results from this comparison show that for this cantilevered structure, the algorithm based on Guyan reduction is rated slightly better than that based on Effective Independence. Author

N95-14089*# National Aeronautics and Space Administration. Ames Research Center, Moffett Field, CA.
SIMULATION OF SHUTTLE LAUNCH G FORCES AND ACOUSTIC LOADS USING THE NASA AMES RESEARCH CENTER 20G CENTRIFUGE c16
T. L. Shaw, J. M. Corliss, D. P. Gundo, G. M. Mulenburg, G. A. Breit, and J. B. Griffith *In* NASA. Goddard Space Flight Center, Eighteenth Space Simulation Conference: Space Mission Success Through Testing Nov. 1994 p 349-371 (For primary document see N95-14062 03-18)
Avail: CASI HC A03/MF A04

The high cost and long times required to develop research packages for space flight can often be offset by using ground test techniques. This paper describes a space shuttle launch and reentry simulating using the NASA Ames Research Center's 20G centrifuge facility. The combined G-forces and acoustic environment during shuttle launch and landing were simulated to evaluate the effect on a payload of laboratory rates. The launch G force and acoustic profiles are matched to actual shuttle launch data to produce the required G-forces and acoustic spectrum in the centrifuge test cab where the rats were caged on a free-swinging platform. For reentry, only G force is simulated as the aero-acoustic noise is insignificant compared to that during launch. The shuttle G-force profiles of launch and landing are achieved by programming the centrifuge drive computer to continuously adjust centrifuge rotational speed to obtain the correct launch and landing G forces. The shuttle launch acoustic environment is simulated using a high-power, low-frequency audio system. Accelerometer data from STS-56 and microphone data from STS-1 through STS-5 are used as baselines for the simulations. This paper provides a description of the test setup and the results of the simulation with recommendations for follow-on simulations. Author

N95-14090*# National Aeronautics and Space Administration. Ames Research Center, Moffett Field, CA.
DEVELOPMENT OF LIFE SCIENCES EQUIPMENT FOR MICROGRAVITY AND HYPERGRAVITY SIMULATION c51
G. M. Mulenburg, J. Evans, M. Vasques, D. P. Gundo, J. B. Griffith, J. Harper, and T. Skundberg *In* NASA. Goddard Space Flight Center, Eighteenth Space Simulation Conference: Space Mission Success Through Testing Nov. 1994 p 373-386 (For primary document see N95-14062 03-18)
Avail: CASI HC A03/MF A04

The mission of the Life Science Division at the NASA Ames Research Center is to investigate the effects of gravity on living systems in the spectrum from cells to humans. The range of these investigations is from

microgravity, as experienced in space, to Earth's gravity, and hypergravity. Exposure to microgravity causes many physiological changes in humans and other mammals including a headward shift of body fluids, atrophy of muscles - especially the large muscles of the legs - and changes in bone and mineral metabolism. The high cost and limited opportunity for research experiments in space create a need to perform ground based simulation experiments on Earth. Models that simulate microgravity are used to help identify and quantify these changes, to investigate the mechanisms causing these changes and, in some cases, to develop countermeasures. Author

N95-14091*# National Aeronautics and Space Administration. Ames Research Center, Moffett Field, CA.

UNIQUE LIFE SCIENCES RESEARCH FACILITIES AT NASA AMES RESEARCH CENTER **c51**

G. M. Mulenburg, M. Vasques, W. F. Caldwell, and J. Tucker *In* NASA. Goddard Space Flight Center, Eighteenth Space Simulation Conference: Space Mission Success Through Testing Nov. 1994 p 387-400 (For primary document see N95-14062 03-18)

Avail: CASI HC A03/MF A04

The Life Science Division at NASA's Ames Research Center has a suite of specialized facilities that enable scientists to study the effects of gravity on living systems. This paper describes some of these facilities and their use in research. Seven centrifuges, each with its own unique abilities, allow testing of a variety of parameters on test subjects ranging from single cells through hardware to humans. The Vestibular Research Facility allows the study of both centrifugation and linear acceleration on animals and humans. The Biocomputation Center uses computers for 3D reconstruction of physiological systems, and interactive research tools for virtual reality modeling. Psycophysiological, cardiovascular, exercise physiology, and biomechanical studies are conducted in the 12 bed Human Research Facility and samples are analyzed in the certified Central Clinical Laboratory and other laboratories at Ames. Human bedrest, water immersion and lower body negative pressure equipment are also available to study physiological changes associated with weightlessness. These and other weightlessness models are used in specialized laboratories for the study of basic physiological mechanisms, metabolism and cell biology. Visual-motor performance, perception, and adaptation are studied using ground-based models as well as short term weightlessness experiments (parabolic flights). The unique combination of Life Science research facilities, laboratories, and equipment at Ames Research Center are described in detail in relation to their research contributions. Author

N95-14092*# Kaman Sciences Corp., Alexandria, VA.

INVESTIGATING AND IMPLEMENTING ENHANCEMENTS TO THE SIMULATION OF SHORT-TERM COLLISION HAZARDS

Jeffrey S. Huth, Dawne E. LeKang, and Darren S. McKnight *In* NASA. Goddard Space Flight Center, Eighteenth Space Simulation Conference: Space Mission Success Through Testing Nov. 1994 p 401-408 (For primary document see N95-14062 03-18)

Avail: CASI HC A02/MF A04

A software tool, the Relative Collision Matrix (RCM), has been developed to provide a quick-look representation of the shortterm collision hazard to space systems from a fragmentation event in Earth orbit. The software performs multiple fragmentation simulations of space objects to quantify the probability of collision for a satellite or a constellation of satellites nearby. Previously, the results were displayed in a color matrix format which showed the relative hazard of each constellation. The RCM can be used for scientific research and operational assessments even though it was designed for test and evaluation applications. Because of its successful use as an analytical tool, the capabilities of RCM are being extended by enhancing the orbital hazard analysis routines, developing ballistic trajectory hazard analysis routines, and expanding the breakup modeling. Improvements are also being made to the RCM's usability and presentation quality by developing a graphical user interface and by providing graphical animated and nonanimated output. Author

N95-14093*# Kaman Sciences Corp., Alexandria, VA.

APPLICATIONS OF A FAST AND EFFICIENT METHOD FOR SIMULATING ORBITAL MISSION SAFETY Abstract Only

Jeffrey Huth, Darren McKnight, Zachari Khutorovsky, and Sergei Kamensky *In* NASA. Goddard Space Flight Center, Eighteenth Space Simulation Conference: Space Mission Success Through Testing Nov. 1994 p 409 (For primary document see N95-14062 03-18)

Avail: CASI HC A01/MF A04

A fast and efficient method for simulating potential interactions between space objects is presented. The specialized hazard analysis simulation is run at the Russian Space Surveillance Center. It simulates the motion of objects in space and determines close encounters between these objects. First, ephemerides are predicted for all space objects over the time interval of concern. Second, using the predicted ephemerides, pairs of satellites that would likely collide are grouped together. Throughout the process, the pairs initially chosen are refined until all pairs of satellites are found which come within a certain miss distance of each other. In addition to the miss distance, other characteristics of the encounter including angle of incidence, relative velocity, type of approaching object, and probability of collision come out of the simulation. There are many potential applications of this simulation and its results to missing planning and mission safety. Artificial objects can be introduced to the simulation to examine potential encounters between the new objects and current objects for mission design applications. The simulation can be run many times to create data for statistical analysis of encounter parameters. These as well as many other potential applications are presented and discussed. Author

N95-14094*# TRW, Inc., Redondo Beach, CA. Space and Electronics Group.

ALPHA LAMP INTEGRATION FACILITY **c14**

Richard Oshiro, Dennis Sowers, Joe Gargiulo, and Mark McGahey *In* NASA. Goddard Space Flight Center, Eighteenth Space Simulation Conference: Space Mission Success Through Testing Nov. 1994 p 411-425 (For primary document see N95-14062 03-18)

(Contract SDIO84-C-0003)

Avail: CASI HC A03/MF A04

This paper describes the activity recently completed to meet the simulated space environment requirements for the ground-based testing of an integrated Space Based Laser (SBL) system experiment. The need to maintain optical alignment in the challenging dynamic environment of the pressure recovery system required to simulate space dominated the design requirements. A robust system design was established which minimized the total program costs, most notably by reducing the cost of integrating the components of the experiment. The components of the experiment are integrated on an optical bench in a clean area adjacent to the vacuum chamber and moved on air bearings into the chamber for testing. Author

N95-14095*# Kassel Univ. (Germany). Control Engineering and System Theory Group.

SIMULATION OF A SPATIAL, SERVO-HYDRAULIC TEST FACILITY FOR SPACE STRUCTURES **c14**

K.-D. Leimbach and H. Hahn *In* NASA. Goddard Space Flight Center, Eighteenth Space Simulation Conference: Space Mission Success Through Testing Nov. 1994 p 427-439 (For primary document see N95-14062 03-18)

Avail: CASI HC A03/MF A04

In this paper different control concepts for servo-hydraulic test facilities are derived using exact linearization techniques. Based on different linear and nonlinear models of the test table and the actuator dynamics several nonlinear controllers of different complexity are derived. The closed loop system performance of the controlled servo-hydraulic test facility is tested in various computer simulations using both, standard test signals and large test signals as system inputs. The simulation results turn out, that in case of standard input signals the test facility controller must include a linear test table mechanics model and a nonlinear servo-hydraulic actuator model. Additional simulations demonstrate the robustness of the control concept selected for standard test signals with respect to variations of plant parameters. Author

N95-14096*# Industrieanlagen-Betriebsgesellschaft m.b.H., Ottobrunn (Germany).

THERMOACOUSTIC ENVIRONMENTS TO SIMULATE REENTRY CONDITIONS

Gerhard Bayerdoerfer *In* NASA. Goddard Space Flight Center, Eighteenth Space Simulation Conference: Space Mission Success Through Testing Nov. 1994 p 441-450 Sponsored by BMFT (For primary document

see N95-14062 03-18)
Avail: CASI HC A02/MF A04

Aerothermal environments as encountered during the reentry of spaceplanes or during the cruise of hypersonic aircrafts represent complex loading conditions for the external structures of those vehicles. In order to shield against the aerodynamic heating a special Thermal Protection System (TPS) is required which is designed as a light weight structure to reduce the weight penalty. TPS is therefore vulnerable to vibroacoustic fatigue caused by the pressure fluctuations of the environment. Because of the complex interactions between the loading forces and the resulting structural response which make an analytical treatment difficult and in order to provide means for fatigue testing IABG has designed and built a thermoacoustic facility which recently became operational. The facility is capable to produce surface temperatures up to 1.300 C at sound pressure levels up to 160 dB. This paper describes the design of the facility, some operational test work it also deals with problems associated with the facility instrumentation. Author

N95-14097*# Calspan Corp., Arnold AFS, TN. Engineering Development Center.
THE AEDC AEROSPACE CHAMBER 7V: AN ADVANCED TEST CAPABILITY FOR INFRARED SURVEILLANCE AND SEEKER SENSORS c14

W. R. Simpson *In* NASA. Goddard Space Flight Center, Eighteenth Space Simulation Conference: Space Mission Success Through Testing Nov. 1994 p 451-465 (For primary document see N95-14062 03-18)
Avail: CASI HC A03/MF A04

An advanced sensor test capability is now operational at the Air Force Arnold Engineering Development Center (AEDC) for calibration and performance characterization of infrared sensors. This facility, known as the 7V, is part of a broad range of test capabilities under development at AEDC to provide complete ground test support to the sensor community for large-aperture surveillance sensors and kinetic kill interceptors. The 7V is a state-of-the-art cryo/vacuum facility providing calibration and mission simulation against space backgrounds. Key features of the facility include high-fidelity scene simulation with precision track accuracy and in-situ target monitoring, diffraction limited optical system, NIST traceable broadband and spectral radiometric calibration, outstanding jitter control, environmental systems for 20 K, high-vacuum, low-background simulation, and an advanced data acquisition system. Author

N95-14098*# Nauchno-Issledovatelskii Inst. Grafit, Moscow (Russia).
NEW POTENTIALS OF NIICHIMMASH'S THERMAL VACUUM FACILITIES Abstract Only c14

N. A. Afanassiev, A. A. Makarov, and V. L. Galjaev *In* NASA. Goddard Space Flight Center, Eighteenth Space Simulation Conference: Space Mission Success Through Testing Nov. 1994 p 467 (For primary document see N95-14062 03-18)
Avail: CASI HC A01/MF A04

The potentialities of existing test facilities as to simulating space environment governing factors for spacecraft successful development thermal vacuum testing are analyzed, ways of modernizing existing test facilities and specific proposals on their redesign are considered. The problem of spacecraft (S/C) ground development in simulated external environments, the solution of which started more than 30 years ago, has not lost its urgency today. Stringent requirements on S/C active lifetime under space conditions, module large dimensions, great number of extension elements and complicated mode of their interaction in long mission do not allow S/C designers to abandon ground tests. S/C thermal modes development is a combination of calculations, thermal vacuum tests and actions on improving S/C design and its thermal control system. Traditionally, tests are carried out by stages from component and end unit level verifications to complex tests of modules and S/C as a whole. In our opinion, sufficient correctness of calculated models and experience gained in organizations designing space systems allow to reduce cost and time of autonomous tests. Unfortunately, this is not true for complex (integrated) thermal vacuum tests. More than that, their recent programs include tasks of verifying other (than thermal control system) systems if S/C for operation under space simulated conditions. The outlined circumstances are the main reason for critical review of the potentialities of the existing test base, and of NIICHIMMASH's two large thermal vacuum chambers, first of all. The reasons for and ways of enlargement of these facilities potentially are analyzed and the results attained are described. Author

N95-14099*# National Aeronautics and Space Administration. Ames Research Center, Moffett Field, CA.
FROM ANTARCTICA TO SPACE: USE OF TELEPRESENCE AND VIRTUAL REALITY IN CONTROL OF REMOTE VEHICLES Abstract Only c63

Carol Stoker, Butler P. Hine, III, Michael Sims, Daryl Rasmussen, Phil Hontalas, Terrence W. Fong, Jay Steele, Don Barch, Dale Andersen, and Eric Miles et al *In* NASA. Goddard Space Flight Center, Eighteenth Space Simulation Conference: Space Mission Success Through Testing Nov. 1994 p 471 (For primary document see N95-14062 03-18)
Avail: CASI HC A01/MF A04

In the Fall of 1993, NASA Ames deployed a modified Phantom S2 Remotely-Operated underwater Vehicle (ROV) into an ice-covered sea environment near McMurdo Science Station, Antarctica. This deployment was part of the antarctic Space Analog Program, a joint program between NASA and the National Science Foundation to demonstrate technologies relevant for space exploration in realistic field setting in the Antarctic. The goal of the mission was to operationally test the use of telepresence and virtual reality technology in the operator interface to a remote vehicle, while performing a benthic ecology study. The vehicle was operated both locally, from above a dive hole in the ice through which it was launched, and remotely over a satellite communications link from a control room at NASA's Ames Research Center. Local control of the vehicle was accomplished using the standard Phantom control box containing joysticks and switches, with the operator viewing stereo video camera images on a stereo display monitor. Remote control of the vehicle over the satellite link was accomplished using the Virtual Environment Vehicle Interface (VEVI) control software developed at NASA Ames. The remote operator interface included either a stereo display monitor similar to that used locally or a stereo head-mounted head-tracked display. The compressed video signal from the vehicle was transmitted to NASA Ames over a 768 Kbps satellite channel. Another channel was used to provide a bi-directional Internet link to the vehicle control computer through which the command and telemetry signals traveled, along with a bi-directional telephone service. In addition to the live stereo video from the satellite link, the operator could view a computer-generated graphic representation of the underwater terrain, modeled from the vehicle's sensors. The virtual environment contained an animate graphic model of the vehicle which reflected the state of the actual vehicle, along with ancillary information such as the vehicle track, science markers, and locations of video snapshots. The actual vehicle was driven either from within the virtual environment or through a telepresence interface. All vehicle functions could be controlled remotely over the satellite link. Author

N95-14420# Arnold Engineering Development Center, Arnold AFS, TN.
OPTICAL ANALYSIS METHODS FOR MATERIAL FILMS CONDENSED ON CRYOGENIC SURFACES OF SPACECRAFT Final Report, Mar. - Sep. 1993

K. F. Palmer (Westminster Coll., Fulton, MO.), M. Z. Williams (Westminster Coll., Fulton, MO.), B. A. Budde (Westminster Coll., Fulton, MO.), and W. T. Bertrand (Calspan Corp., Arnold AFS, TN.) Aug. 1994 53 p
(AF Proj. 0107)
(AD-A284014; AEDC-TR-94-3) Avail: CASI HC A04/MF A01

Exhaust gases from rocket motors and outgassing products of spacecraft materials can migrate, in a space environment, to other surfaces of the spacecraft and affect their functions. Cryogenically cooled optical systems are particularly vulnerable to these contaminants as are thermal control surfaces and solar cells. One of the goals of the contamination program at AEDC (Arnold Encineering Development Center) is to predict the optical effects of contaminant layers on optical systems from laboratory measurements of the optical indices, n and k, of contaminant materials. Because the cloud of contaminant molecules, which eventually form a condensate, contain a mixture of molecular species, researchers are seeking ways to predict the optical properties of films composed of constituents using the known properties of each constituent. In this report, the authors examine the physics which describe the optical properties of thin films composed of mixtures of constituents. Examples of the analysis methods are presented for thin films composed of mixtures using AEDC data on

20K thin films of simple molecules and 80K films condensed from the outgassing products of selected spacecraft materials. DTIC

N95-14510*# National Aeronautics and Space Administration. Goddard Space Flight Center, Greenbelt, MD.
SATELLITE SITUATION REPORT, VOLUME 33, NUMBER 2
30 Jun. 1993 90 p
(NASA-TM-109965; NAS 1.15:109965) Avail: CASI HC A05/MF A01

This report consists of data computed at United States Space Command, GFSC, or provided by satellite owners. A space objects box score table is presented with data under the following headings: source/organization, objects in orbit, and decayed objects. The objects in orbit and decayed objects' headings have payload, debris, and total as subheadings. The bulk of the document is objects in orbit tables with data under the following headings: international designation, name, catalog number, source, launch date, period minutes, inclination, apogee (km), perigee (km) and notes. Author

N95-14521*# Minnesota Univ., Minneapolis, MN.
ACCESS TO SPACE Final Report
1 Jul. 1994 137 p
(Contract NASw-4435)
(NASA-CR-197153; NAS 1.26:197153) Avail: CASI HC A07/MF A02

The goal of this conceptual design was to devise a reusable, commercially viable, single-stage-to-orbit vehicle. The vehicle has the ability to deliver a 9100 kg (20,000 lb) payload to a low earth orbit of 433 km to 933 km (250 n.mi. - 450 n.mi.). The SSTO vehicle is 51 meters in length and has a gross takeoff mass of 680,400 kg (1,500,000 lb). The vehicle incorporates three RD-701 engines for the main propulsion system and two RL-10 engines for the orbital maneuvering system. The vehicle is designed for a three day stay on orbit with two crew members. Author

N95-14599# Phillips Lab., Hanscom AFB, MA.
PRE-FLIGHT POLAR CODE PREDICTIONS FOR THE CHAWS SPACE FLIGHT EXPERIMENT
David L. Cooke, John Talbot, and Graeme Shaw 31 Jan. 1994 18 p
(AD-A280951; AD-E201983; PL-TR-94-2056; ERP-1147) Avail: CASI HC A03/MF A01

The POLAR code is a 3D plasma simulation which has been used to design and predict the behavior of the Charge Hazards and Wake Studies (CHAWS) space flight experiment. The most recent results from the POLAR code are presented here prior to the launch of the Space Shuttle Discovery. CHAWS will measure the current-voltage (IV) characteristics of a high voltage probe mounted on the wake side of the Wake Shield Facility (WSF) free flyer. POLAR results indicate that ion currents to the negatively biased probe will be near 'zero' only for potentials less than 30 to 300 V in magnitude. As the potential increases to the CHAWS limit of -5 kV, the ion current will quickly rise to levels comparable to that which the probe would collect if orbiting unshielded. Author (DTIC)

N95-14664# Sandia National Labs., Albuquerque, NM.
NUMERICAL SOLUTION OF TWO-DIMENSIONAL ABLATION PROBLEMS USING THE FINITE CONTROL VOLUME METHOD WITH UNSTRUCTURED GRIDS
R. E. Hogan, B. F. Blackwell, and R. J. Cochran 1994 10 p Presented at the 6th AIAA/ASME Thermophysics and Heat Transfer Conference, Colorado Springs, CO, 20-23 Jun. 1994
(Contract DE-AC04-94AL-85000)
(DE94-015012; SAND-94-1644C; AIAA Paper 94-2085; CONF-940625-8)
Avail: CASI HC A02/MF A01

This paper presents the solution of two-dimensional axisymmetric ablation problems with unstructured grids. The energy equation is formulated and solved using the Finite Control Volume Method. The exterior shape of the ablating body is determined from a surface energy balance with the interior mesh displaced in response to the surface ablation as if the body was a linear elastic solid. Boundary condition matrices are formulated for both heat of ablation and generalized thermochemical ablation boundary conditions. Computed recession rates are compared to an analytical solution to demonstrate the accuracy and convergence of this approach. Additionally, the practical application of this approach to the ablation of a reentry vehicle nose tip is presented. DOE

N95-14850 Naval Postgraduate School, Monterey, CA.
EVALUATION OF ENERGY-SINK STABILITY CRITERIA FOR DUAL-SPIN SPACECRAFT M.S. Thesis
Vincent M. Ortiz Jun. 1994 152 p Limited Reproducibility: More than 20% of this document may be affected by microfiche quality
(AD-A283228) Avail: Issuing Activity (Defense Technical Information Center (DTIC))

The nutational stability of a dual-spin, quasi-rigid, axisymmetric spacecraft containing a driven rotor is analyzed. The purpose is to examine a revised energy-sink stability theory that properly accounts for the energy contribution of the motor. An inconsistency in the development disproves the existing energy-sink theory's assumption that the motor of the system contributes exactly enough energy to offset the frictional losses between the rotor and the platform. Using the concept of core energy, the revised stability criteria for a dual-spin, quasi-rigid, axisymmetric spacecraft containing a driven rotor is derived. An expression for nutation angle as a function of core energy over time is then determined. Numerical simulations are used to verify the revised energy-sink stability theory. The dual-spin, quasi-rigid, axisymmetric system presented by D. L. Mingori was chosen for the simulation. Equations for angular momentum and total energy were necessary to validate the numerical simulation and confirm aspects of the revised energy-sink stability theory. These equations are derived from the first principles of dynamics and are included in the analysis. An explicit relationship for core energy as a function of time does not exist. Various models postulating core energy are presented and analyzed. The numerical simulations of the computed nutation angles as a function of the postulated core energy compare well with the actual nutation angles of the system to confirm the revised energy-sink stability criteria. DTIC

N95-14951 Keo Consultants, Brookline, MA.
SPACE DEBRIS DETECTION AND ANALYSIS
Robert H. Eather and Ronald Siewert 28 Feb. 1994 19 p Limited Reproducibility: More than 20% of this document may be affected by microfiche quality
(Contract F19628-92-C-0070)
(AD-A282012; PL-TR-94-2067; AD-E202063; SR-1) Avail: Issuing Activity (Defense Technical Information Center (DTIC))

A 16 telescope with an image-intensified CCD camera has been deployed for testing for space debris detection. Sensitivity calibrations will take place after the ODERACS mission deploys calibration spheres from the Space Shuttle. An image analysis facility has been set up at Phillips Laboratory, and appropriate software has been written for image digitization and analysis. Various algorithms to extract low-level debris signatures from the night-sky background have been investigated. A model has been developed for debris population prediction from a known starting population distribution. DTIC

N95-13830# Indian Space Research Organization, Bangalore. Flight Dynamics Div.
MODELLING THE LOW EARTH SPACE DEBRIS ENVIRONMENT
A. S. Ganeshan, S. C. Rathnakara, and Subir Banerjee *In* ISRO Satellite Centre, Journal of Spacecraft Technology, Volume 4, No . 2, July 1994 Jul. 1994 p 52-59 (For primary document see N95-13825 03-12)
Avail: CASI HC A02/MF A01

N95-13831# ISRO Satellite Centre, Peenya, Bangalore (India). Control Systems Group.
A VISION BASED ATTITUDE AND POSITION ESTIMATION ALGORITHM FOR RENDEZVOUS AND DOCKING
R. Mukundan, R. V. Raghu Narayanan, and N. K. Philip *In its* Journal of Spacecraft Technology, Volume 4, No. 2, July 1994 Jul. 1994 p 60-67 (For primary document see N95-13825 03-12)
Avail: CASI HC A02/MF A01

N95-14210*# National Aeronautics and Space Administration. Marshall Space Flight Center, Huntsville, AL.
BASIC FEATURES OF THE STS/SPACELAB VIBRATION ENVIRONMENT
Charles R. Baugher and N. Ramachandran *In its* Joint Launch + One Year Science Review of USML-1 and USMP-1 with the Microgravity Measurement Group May 1994 p 45-64 (For primary document see

N95-14207 03-88)
Avail: CASI HC A03/MF A04

N95-14641# Loral AeroSys, Seabrook, MD.
EFFICIENT MISSION CONTROL FOR THE 48-SATELLITE GLOBALSTAR CONSTELLATION
Dan Smith *In* Huntsville Association of Technical Societies, TABES 1994: 10th Annual Technical and Business Exhibition and Symposium 1994 6 p (For primary document see N95-14633 03-12)
(TABES Paper 94-609) Avail: CASI HC A02/MF A04

19 SPACECRAFT INSTRUMENTATION

For related information see also *06 Aircraft Instrumentation* and *35 Instrumentation and Photography.*

N95-14106*# Virginia Polytechnic Inst. and State Univ., Blacksburg, VA. Dept. of Mechanical Engineering.
EXPERIMENTAL DESIGN FOR THE EVALUATION OF HIGH-T(SUB c) SUPERCONDUCTIVE THERMAL BRIDGES IN A SENSOR SATELLITE Annual Report
Elaine P. Scott and Kasey M. Lee 10 Oct. 1994 104 p Original contains color illustrations
(Grant NAG1-1500)
(NASA-CR-197003; NAS 1.26:197003) Avail: CASI HC A06/MF A02; 5 functional color pages

Infrared sensor satellites, which consist of cryogenic infrared sensor detectors, electrical instrumentation, and data acquisition systems, are used to monitor the conditions of the earth's upper atmosphere in order to evaluate its present and future changes. Currently, the electrical connections (instrumentation), which act as thermal bridges between the cryogenic infrared sensor and the significantly warmer data acquisition unit of the sensor satellite system, constitute a significant portion of the heat load on the cryogen. As a part of extending the mission life of the sensor satellite system, the researchers at the National Aeronautics and Space Administration's Langley Research Center (NASA-LaRC) are evaluating the effectiveness of replacing the currently used manganin wires with high-temperature superconductive (HTS) materials as the electrical connections (thermal bridges). In conjunction with the study being conducted at NASA-LaRC, the proposed research is to design a space experiment to determine the thermal savings on a cryogenic subsystem when manganin leads are replaced by HTS leads printed onto a substrate with a low thermal conductivity, and to determine the thermal conductivities of HTS materials. The experiment is designed to compare manganin wires with two different types of superconductors on substrates by determining the heat loss by the thermal bridges and providing temperature measurements for the estimation of thermal conductivity. A conductive mathematical model has been developed and used as a key tool in the design process and subsequent analysis. Author (revised)

N95-15824*# Alabama Univ., Huntsville, AL. Center for Space Plasma and Aeronomic Research.
MASS ANALYSIS ADDITION TO THE DIFFERENTIAL ION FLUX PROBE (DIFP) STUDY Final Report
K. H. Wright, Jr. and Richard Jolley 25 Oct. 1994 34 p
(Contract NAS8-38609)
(NASA-CR-196531; NAS 1.26:196531) Avail: CASI HC A03/MF A01

The objective of this study is to develop a technique to measure the characteristics of space plasmas under highly disturbed conditions; e.g., non-Maxwellian plasmas with strong drifting populations and plasmas contaminated by spacecraft outgassing. The approach, conducted in conjunction with current MSFC activities, is to extend the capabilities of the Differential Ion Flux Probe (DIFP) to include a high throughput mass measurement that does not require either high voltage or contamination sensitive devices such as channeltron electron multipliers or microchannel plates. This will significantly reduce the complexity and expense of instrument fabrication, testing, and integration of flight hardware compared to classical mass analyzers. The feasibility of the enhanced DIFP has been verified by using breadboard test models in a controlled plasma environment. The ability to manipulate particles through the instrument regardless of incident angle, energy, or ionic component has been amply demonstrated. The energy analysis mode is differential and leads directly to a time-of-flight mass measurement. With the new design, the DIFP will separate multiple ion streams and analyze each stream independently for ion flux intensity, velocity (including direction of motion), mass, and temperature (or energy distribution). In particular, such an instrument will be invaluable on follow-on electrodynamic TSS missions and, possibly, for environmental monitoring on the space station. Author (revised)

N95-13718*# MCAT Inst., Moffett Field, CA.
SCIENCE OBJECTIVES AND PERFORMANCE OF A RADIOMETER AND WINDOW DESIGN FOR ATMOSPHERIC ENTRY EXPERIMENTS
Roger A. Craig, William C. Davy, and Ellis E. Whiting *In its* Planetary Entry Experiments Jul. 1994 41 p (For primary document see N95-13717 03-91)
Avail: CASI HC A03/MF A02

N95-14584*# National Aeronautics and Space Administration. Lewis Research Center, Cleveland, OH.
CONCEPTUAL DESIGN OF THE SPACE STATION FLUIDS MODULE
Dennis W. Rohn, Daniel P. Morilak, Jennifer L. Rhatigan, and Todd T. Peterson *In its* Second Microgravity Fluid Physics Conference Aug. 1994 p 429-448 (For primary document see N95-14522 03-34)
Avail: CASI HC A03/MF A04; 2 functional color pages

20 SPACECRAFT PROPULSION AND POWER

Includes main propulsion systems and components, e.g., rocket engines; and spacecraft auxilliary power sources.

For related information see also *07 Aircraft Propulsion and Power, 28 Propellants and Fuels, 44 Energy Production and Conversion,* and *15 Launch Vehicles and Space Vehicles.*

N95-13668*# National Aeronautics and Space Administration. Lewis Research Center, Cleveland, OH.
FAST TRACK NTR SYSTEMS ASSESSMENT FOR NASA'S FIRST LUNAR OUTPOST SCENARIO
Stanley K. Borowski and Stephen W. Alexander Oct. 1994 28 p Presented at the 28th Joint Propulsion and Exhibit, Nashville, TN, 6-8 Jul. 1994; cosponsored by AIAA, SAE, ASME and ASEE
(RTOP 232-01-06)
(NASA-TM-106748; E-9164; NAS 1.15:106748; AIAA Paper 92-3812)
Avail: CASI HC A03/MF A01

Integrated systems and mission study results are presented which quantify the rationale and benefits for developing and using nuclear thermal rocket (NTR) technology for returning humans to the moon in the early 2000's. At present, the Exploration Program Office (ExPO) is considering chemical propulsion for its 'First Lunar Outpost' (FLO) mission, and NTR propulsion for the more demanding Mars missions to follow. The use of an NTR-based lunar transfer stage, capable of evolving to Mars mission applications, could result in an accelerated schedule, reduced cost approach to moon/Mars exploration. Lunar mission applications would also provide valuable operational experience and serve as a 'proving ground' for NTR engine and stage technologies. In terms of performance benefits, studies indicate that an expendable NTR stage powered by two 50 klbf engines can deliver approximately 96 metric tons (t) to trans-lunar injection (TLI) conditions for an initial mass in low earth orbit (IMLEO) of approximately 199 t compared to 250 t for a cryogenic chemical TLI stage. The NTR stage liquid hydrogen (LH2) tank has a 10 m diameter, 14.8 m length, and 68 t LH2 capacity. The NTR utilizes a 'graphite' fuel form consisting of coated UC2 particles in a graphite substrate, and has a specific impulse capability of approximately 870 s, and an engine thrust-to-weight ratio of approximately 4.8. The NTR stage and its piloted FLO lander has a total length of approximately 38 m and can be launched by a single Saturn V-derived heavy lift launch vehicle (HLLV) in the 200 to 250 t-class range. The paper summarizes NASA's First Lunar Outpost scenario, describes characteristics for representative engine/stage configurations, and examines the impact on engine selection and vehicle design resulting from a consideration of alternative NTR fuel forms and lunar mission profiles.
Author

N95-13697*# Space Exploration Association, Cedarville, OH.
HIGH PERFORMANCE ARCJET ENGINES Final Report
Elliot B. Kennel, Alexey Nikolayevich Ivanov, and Yuri Vyacheslavovich Nikolayev Oct. 1994 76 p
(Contract NAS3-27023; RTOP 140-20-0A)
(NASA-CR-195397; E-9199; NAS 1.26:195397) Avail: CASI HC A04/MF A01

This effort sought to exploit advanced single crystal tungsten-tantalum alloy material for fabrication of a high strength, high temperature arcjet anode. The use of this material is expected to result in improved strength, temperature resistance, and lifetime compared to state of the art polycrystalline alloys. In addition, the use of high electrical and thermal conductivity carbon-carbon composites was considered, and is believed to be a feasible approach. Highly conductive carbon-carbon composite anode capability represents enabling technology for rotating-arc designs derived from the Russian Scientific Research Institute of Thermal Processes (NIITP) because of high heat fluxes at the anode surface. However, for US designs the anode heat flux is much smaller, and thus the benefits are not as great as in the case of NIITP-derived designs. Still, it does appear that the tensile properties of carbon-carbon can be even better than those of single crystal tungsten alloys, especially when nearly-single-crystal fibers such as vapor grown carbon fiber (VGCF) are used. Composites fabricated from such materials must be coated with a refractory carbide coating in order to ensure compatibility with high temperature hydrogen. Fabrication of tungsten alloy single crystals in the sizes required for fabrication of an arcjet anode has been shown to be feasible. Test data indicate that the material can be expected to be at least the equal of W-Re-HfC polycrystalline alloy in terms of its tensile properties, and possibly superior. We are also informed by our colleagues at Scientific Production Association Luch (NP0 Luch) that it is possible to use Russian technology to fabricate polycrystalline W-Re-HfC or other high strength alloys if desired. This is important because existing engines must rely on previously accumulated stocks of these materials, and a fabrication capability for future requirements is not assured. Author

N95-14173*# National Aeronautics and Space Administration. Lewis Research Center, Cleveland, OH.
SELECTION OF SOLAR SIMULATOR FOR SOLAR DYNAMIC GROUND TEST
Carol M. Tolbert Aug. 1994 8 p Presented at the 29th Intersociety Energy Conversion Engineering Conference, Monterey, CA, 7-12 Aug. 1994; sponsored by SAE, ACS, AIAA, ASME, IEEE, and AIChE
(RTOP 233-03-0B)
(NASA-TM-106608; E-8889; NAS 1.15:106608) Avail: CASI HC A02/MF A01

The 2 kWe Solar Dynamic (SD) Ground Test Demonstration (GTD) experiment will be conducted in 1995 at NASA Lewis Research Center (LeRC). This solar dynamic power system test will be conducted in a simulated space environment and will require an artificial sun. To address the solar simulator requirements for the GTD, Arnold Engineering Development Center (AEDC) was hired under contract to review and visit four existing solar simulator facilities. The four facilities included, AEDC's Mark 1 Chamber, NASA-JSC Chamber A, AEDC's 12V Chamber, and NASA-JPL Space Simulator Chamber. Two design concepts were considered following several months of evaluating existing solar simulator facilities throughout the United States. To satisfy system requirements for the SD GTD experiment the solar simulator needs to provide a uniform light flux to the SD concentrator, provide the light within a subtense angle of one degree, and provide an intensity of one solar constant (1.37 kW/sq m) at airmass zero. Most solar simulators are designed for supplying heat loads to spacecraft where a cone angle as large as 3 degrees is acceptable. It was also concluded that a solar simulator, such like these considered in the AEDC study, would require major facility modifications for NASA LeRC and result in significant impacts to the program. The advanced solar simulator concept developed by NASA LeRC will meet the system requirements for the SD GTD experiment Since SD GTD solar simulator requirements could not be addressed by existing simulator, an advanced concept was considered. Author

N95-14174*# National Aeronautics and Space Administration. Lewis Research Center, Cleveland, OH.
ALKALI METAL RANKINE CYCLE BOILER TECHNOLOGY CHALLENGES AND SOME POTENTIAL SOLUTIONS FOR SPACE NUCLEAR POWER AND PROPULSION APPLICATIONS
James R. Stone Jul. 1994 22 p
(RTOP 584-04-21)
(NASA-TM-106593; E-8863; NAS 1.15:106593) Avail: CASI HC A03/MF A01

Alkali metal boilers are of interest for application to future space Rankine cycle power conversion systems. Significant progress on such boilers was accomplished in the 1960's and early 1970's, but development was not continued to operational systems since NASA's plans for future space missions were drastically curtailed in the early 1970's. In particular, piloted Mars missions were indefinitely deferred. With the announcement of the Space Exploration Initiative (SEI) in July 1989 by President Bush, interest was rekindled in challenging space missions and, consequently in space nuclear power and propulsion. Nuclear electric propulsion (NEP) and nuclear thermal propulsion (NTP) were proposed for interplanetary space vehicles, particularly for Mars missions. The potassium Rankine power conversion cycle became of interest to provide electric power for NEP vehicles and for 'dual-mode' NTP vehicles, where the same reactor could be used directly for propulsion and (with an additional coolant loop) for power. Although the boiler is not a major contributor to system mass, it is of critical importance because of its interaction with the rest of the power conversion system; it can cause problems for other components such as excess liquid droplets entering the turbine, thereby reducing its life, or more critically, it can drive instabilities-some severe enough to cause system failure. Funding for the SEI and its associated technology program from 1990 to 1993 was not sufficient to support significant new work on Rankine cycle boilers for space applications. In Fiscal Year 1994, funding for these challenging missions and technologies has again been curtailed, and planning for the future is very uncertain. The purpose of this paper is to review the technologies developed in the 1960's and 1970's in the light of the recent SEI applications. In this way, future Rankine cycle boiler programs may be conducted most efficiently. This report is aimed at evaluating alkali metal boiler technology for space Rankine cycle systems. Research is summarized on the problems of flow stability, liquid carryover, pressure drop and heat transfer, and on potential solutions developed, primarily those developed by the NASA Lewis Research Center in the 1960's and early 1970's. Author

N95-14301*# National Aeronautics and Space Administration. Lewis Research Center, Cleveland, OH.
DEVELOPMENT STATUS OF THE NASA 30-cm ION THRUSTER AND POWER PROCESSOR
James S. Sovey, Thomas W. Haag, John A. Hamley, Maris A. Mantenieks, Michael J. Patterson, Luis R. Pinero, Vincent K. Rawlin, Michael T. Kussmaul, David H. Manzella, and Roger M. Myers et al Sep. 1994 10 p Presented at the 29th Intersociety Energy Conversion Engineering Conference, Monterey, CA, 7-12 Aug. 1994; cosponsored by IEEE, ACS, AIAA, ANS, ASME, and SAE
(Contracts NAS3-27186; NAS3-25776; RTOP 232-02-02)
(NASA-TM-106740; E-9147; NAS 1.15:106740; AIAA Paper 94-3981)
Avail: CASI HC A02/MF A01

Xenon ion propulsion systems are being developed by NASA Lewis Research Center and the Jet Propulsion Laboratory to provide flight qualification and validation for planetary and earth-orbital missions. In the ground-test element of this program, light-weight (less than 7 kg), 30 cm diameter ion thrusters have been fabricated, and preliminary design verification tests have been conducted. At 2.3 kW, the thrust, specific impulse, and efficiency were 91 mN, 3300 s, and 0.65, respectively. An engineering model thruster is now undergoing a 2000 h wear-test. A breadboard power processor is being developed to operate from an 80 V to 120 V power bus with inverter switching frequencies of 50 kHz. The power processor design is a pathfinder and uses only three power supplies. The projected specific mass of a flight unit is about 5 kg/kW with an efficiency of 0.92 at the full-power of 2.5 kW. Preliminary integration tests of the neutralizer power supply and the ion thruster have been completed. Fabrication and test of the discharge and beam/accelerator power stages are underway. Author

N95-14669*# Science Applications International Corp., Torrance, CA.
ENGINE SYSTEM ASSESSMENT STUDY USING MARTIAN PROPELLANTS Final Report
Dennis Pelaccio, Mark Jacobs, Christine Scheil, and John Collins Jun. 1992 338 p
(Contract NAS3-25809; RTOP 506-42-72)
(NASA-CR-189188; NAS 1.26:189188; E-0265-079) Avail: CASI HC A15/MF A03

A top-level feasibility study was conducted that identified and characterized promising chemical propulsion system designs which use two or more of the following propellant combinations: LOX/H2, LOX/CH4, and LOX/CO. The engine systems examined emphasized the usage of common subsystem/component hardware where possible. In support of this study, numerous mission scenarios were characterized that used various combinations of Earth, lunar, and Mars propellants to establish engine system requirements to assess the promising engine system design concept examined, and to determine overall exploration leverage of such systems compared to state-of-the-art cryogenic (LOX/H2) propulsion systems. Initially in the study, critical propulsion system technologies were assessed. Candidate expander and gas generator cycle LOX/H2/CO, LOX/H2/CH4, and LOX/CO/CH4 engine system designs were parametrically evaluated. From this evaluation baseline, tripropellant Mars Transfer Vehicle (MTV) LOX cooled and bipropellant Lunar Excursion Vehicle (LEV) and Mars Excursion Vehicle (MEV) engine systems were identified. Representative tankage designs for a MTV were also investigated. Re-evaluation of the missions using the baseline engine design showed that in general the slightly lower performance, smaller, lower weight gas generator cycle-based engines required less overall mission Mars and in situ propellant production (ISPP) infrastructure support compared to the larger, heavier, higher performing expander cycle engine systems. Author

N95-15058*# Science Applications International Corp., San Diego, CA.
REUSABLE ROCKET ENGINE TURBOPUMP HEALTH MANAGEMENT SYSTEM Final Report
Pamela Surko Oct. 1994 91 p
(Contract NAS3-25882; RTOP 584-03-11)
(NASA-CR-195388; E-9153; NAS 1.26:195388) Avail: CASI HC A05/MF A01

A health monitoring expert system software architecture has been developed to support condition-based health monitoring of rocket engines. Its first application is in the diagnosis decisions relating to the health of the high pressure oxidizer turbopump (HPOTP) of Space Shuttle Main Engine (SSME). The post test diagnostic system runs off-line, using as input the data recorded from hundreds of sensors, each running typically at rates of 25, 50, or .1 Hz. The system is invoked after a test has been completed, and produces an analysis and an organized graphical presentation of the data with important effects highlighted. The overall expert system architecture has been developed and documented so that expert modules analyzing other line replaceable units may easily be added. The architecture emphasizes modularity, reusability, and open system interfaces so that it may be used to analyze other engines as well. Author

N95-15609*# National Aeronautics and Space Administration. Marshall Space Flight Center, Huntsville, AL.
VEHICLE HEALTH MANAGEMENT USING ADAPTIVE TECHNIQUES Final Report
J. H. Kim and R. Kissel Nov. 1994 45 p
(NASA-TM-108472; NAS 1.15:108472) Avail: CASI HC A03/MF A01

Automated engine diagnostics using cognitive computing methodologies are investigated. Space shuttle main engine vibrational data is used to test the algorithms. Author

N95-15682*# National Aeronautics and Space Administration. Lewis Research Center, Cleveland, OH.
THE RATIONALE/BENEFITS OF NUCLEAR THERMAL ROCKET PROPULSION FOR NASA'S LUNAR SPACE TRANSPORTATION SYSTEM
Stanley K. Borowski Sep. 1994 21 p Presented at the 27th Joint Propulsion Conference, Sacramento, CA, 24-26 Jun. 1991; cosponsored by AIAA, SAE, ASME, and ASEE
(RTOP 232-01-06)
(NASA-TM-106739; E-9142; NAS 1.15:106739; AIAA Paper 91-2052)
Avail: CASI HC A03/MF A01

The solid core nuclear thermal rocket (NTR) represents the next major evolutionary step in propulsion technology. With its attractive operating characteristics, which include high specific impulse (approximately 850-1000 s) and engine thrust-to-weight (approximately 4-20), the NTR can form the basis for an efficient lunar space transportation system (LTS) capable of supporting both piloted and cargo missions. Studies conducted at the NASA Lewis Research Center indicate that an NTR-based LTS could transport a fully-fueled, cargo-laden, lunar excursion vehicle to the Moon, and return it to low Earth orbit (LEO) after mission completion, for less initial mass in LEO than an aerobraked chemical system of the type studied by NASA during its '90-Day Study.' The all-propulsive NTR-powered LTS would also be 'fully reusable' and would have a 'return payload' mass fraction of approximately 23 percent--twice that of the 'partially reusable' aerobraked chemical system. Two NTR technology options are examined--one derived from the graphite-moderated reactor concept developed by NASA and the AEC under the Rover/NERVA (Nuclear Engine for Rocket Vehicle Application) programs, and a second concept, the Particle Bed Reactor (PBR). The paper also summarizes NASA's lunar outpost scenario, compares relative performance provided by different LTS concepts, and discusses important operational issues (e.g., reusability, engine 'end-of life' disposal, etc.) associated with using this important propulsion technology. Author

N95-15769*# National Aeronautics and Space Administration. Lewis Research Center, Cleveland, OH.
ENVIRONMENTAL DURABILITY ISSUES FOR SOLAR POWER SYSTEMS IN LOW EARTH ORBIT
Kim K. deGroh, Bruce A. Banks, and Daniela C. Smith Nov. 1994 14 p Presented at the 1995 International Solar Energy Conference, Lahaina, HI, 19-24 Mar. 1995; sponsored by ASME, JSME and JSES
(RTOP 233-01-OE)
(NASA-TM-106775; E-9226; NAS 1.15:106775) Avail: CASI HC A03/MF A01

Space solar power systems for use in the low Earth orbit (LEO) environment experience a variety of harsh environmental conditions. Materials used for solar power generation in LEO need to be durable to environmental threats such as atomic oxygen, ultraviolet (UV) radiation, thermal cycling, and micrometeoroid and debris impact. Another threat to LEO solar power performance is due to contamination from other spacecraft components. This paper gives an overview of these LEO environmental issues as they relate to space solar power system materials. Issues addressed include atomic oxygen erosion of organic materials, atomic oxygen undercutting of protective coatings, UV darkening of ceramics, UV embrittlement of Teflon, effects of thermal cycling on organic composites, and contamination due to silicone and organic materials. Specific examples of samples from the Long Duration Exposure Facility (LDEF) and materials returned from the first servicing mission of the Hubble Space Telescope (HST) are presented. Issues concerning ground laboratory facilities which simulate the LEO environment are discussed along with ground-to-space correlation issues. Author

N95-14636*# National Aeronautics and Space Administration. Marshall Space Flight Center, Huntsville, AL.
ENVIRONMENTALLY SOUND MANUFACTURING
Larry A. Caddy, Ross Bowman, and Rex A. Richards *In* Huntsville Association of Technical Societies, TABES 1994: 10th Annual Technical and Business Exhibition and Symposium 1994 7 p (For primary document see N95-14633 03-12)
(TABES Paper 94-502) Avail: CASI HC A02/MF A04

23 CHEMISTRY AND MATERIALS (GENERAL)

N95-13631*# National Aeronautics and Space Administration. Lewis Research Center, Cleveland, OH.
A NEW TRIBOLOGICAL TEST FOR CANDIDATE BRUSH SEAL MATERIALS EVALUATION Final Report
James A. Fellenstein (Ohio Aerospace Inst., Cleveland, OH.) and Christopher

DellaCorte Oct. 1994 20 p Prepared for the Society of Tribologists and Lubrication Engineers, Chicago, IL, 15-20 May 1995
(Contract RTOP 778-34-28; DE-AI01-91CE-50306)
(NASA-TM-106753; E-9139; NAS 1.15:106753; DOE/NASA/50306-6)
Avail: CASI HC A03/MF A01

A new tribological test for candidate brush seal materials evaluation has been developed. The sliding contact between the brush seal wires and their mating counterface journal is simulated by testing a small tuft of wire against the outside diameter of a high speed rotating shaft. The test configuration is similar to a standard block on ring geometry. The new tester provides the capability to measure both the friction and wear of candidate wire and counterface materials under controlled loading conditions in the gram to kilogram range. A wide test condition latitude of speeds (1 to 27 m/s), temperatures (25 to 700 C), and loads (0.5 to 10 N) enables the simulation of many of the important tribological parameters found in turbine engine brush seals. This paper describes the new test rig and specimen configuration and presents initial data for candidate seal materials comparing tuft test results and wear surface morphology to field tested seal components. Author

N95-14603*# Boeing Defense and Space Group, Seattle, WA.
RESULTS OF THE EXAMINATION OF LDEF POLYURETHANE THERMAL CONTROL COATINGS Technical Report, Oct. 1989 - Aug. 1993
Johnny L. Golden Hampton, VA NASA Jul. 1994 160 p Original contains color illustrations
(Contracts NAS1-18224; NAS1-19247; RTOP 506-43-61-02; RTOP 233-03-02-04)
(NASA-CR-4617; NAS 1.26:4617) Avail: CASI HC A08/MF A02; 17 functional color pages

This report summarizes the condition of polyurethane thermal control coatings subjected to 69 months of low earth orbit (LEO) exposure on the Long Duration Exposure Facility (LDEF) mission. Specimens representing all environmental aspects obtainable by LDEF were analyzed. Widely varying changes in the thermo-optical and mechanical properties of these materials were observed, depending on atomic oxygen and ultraviolet radiation fluences. High atomic oxygen fluences, regardless of ultraviolet radiation exposure levels, resulted in near original optical properties for these coatings but with a degradation in their mechanical condition. A trend in solar absorptance increase with ultraviolet radiation fluence was observed. Contamination, though observed, exhibited minimal effects. Author

N95-14920*# National Aeronautics and Space Administration. Langley Research Center, Hampton, VA.
THE CHARACTERIZATION OF WIDESPREAD FATIGUE DAMAGE IN FUSELAGE STRUCTURE
Robert S. Piascik, Scott A. Willard, and Matthew Miller Sep. 1994 16 p
(RTOP 538-02-10-01)
(NASA-TM-109142; NAS 1.15:109142) Avail: CASI HC A03/MF A01

The characteristics of widespread fatigue damage (WSFD) in fuselage riveted structure were established by detailed nondestructive and destructive examinations of fatigue damage contained in a full size fuselage test article. The objectives of this were to establish an experimental data base for validating emerging WSFD analytical prediction methodology and to identify first order effects that contribute to fatigue crack initiation and growth. Detailed examinations were performed on a test panel containing four bays of a riveted lap splice joint. The panel was removed from a full scale fuselage test article after receiving 60,000 full pressurization cycles. The results of in situ examinations document the progression of fuselage skin fatigue crack growth through crack linkup. Detailed tear down examinations and fractography of the lap splice joint region revealed fatigue crack initiation sites, crack morphology, and crack linkup geometry. From this large data base, distributions of crack size and locations are presented and discussions of operative damage mechanisms are offered. Author

24 COMPOSITE MATERIALS

Includes physical, chemical, and mechanical properties of laminates and other composite materials.

For ceramic materials see *27 Nonmetallic Materials.*

N95-13641*# National Aeronautics and Space Administration. Lewis Research Center, Cleveland, OH.
MONITORING FIBER STRESS DURING CURING OF SINGLE FIBER GLASS- AND GRAPHITE-EPOXY COMPOSITES
Madhu S. Madhukar (Tennessee Univ., Knoxville, TN.), Ranga P. Kosuri (Tennessee Univ., Knoxville, TN.), and Kenneth J. Bowles Nov. 1994 11 p
(RTOP 505-63-12)
(NASA-TM-4568; E-8522; NAS 1.15:4568) Avail: CASI HC A03/MF A01

The difference in thermal expansion characteristics of epoxy matrices and graphite fibers can produce significant residual stresses in the fibers during curing of composite materials. Tests on single fiber glass-epoxy and graphite-epoxy composite specimens were conducted in which the glass and graphite fibers were preloaded in tension, and the epoxy matrix was cast around the fibers. The fiber tension was monitored while the matrix was placed around the fiber and subjected to the temperature-time curing cycle. Two mechanisms responsible for producing stress in embedded fibers were identified as matrix thermal expansion and contraction and matrix cure shrinkage. A simple analysis based on the change in fiber tension during the curing cycle was conducted to estimate the produced stresses. Experimental results on single fiber glass- and graphite-epoxy composites show that the fiber was subjected to significant tensile stresses when the temperature was raised from the first to the second dwell period. When initial fiber pretension is about 60 percent of the fiber failure load, these curing-induced stresses can cause tensile fracture of the embedded fiber. Author

N95-13643# Oak Ridge National Lab., TN.
PROCESSING OF THERMOSET PREPREG LAMINATE VIA EXPOSURE TO MICROWAVE RADIATION
F. L. Paulauskas and T. T. Meek 1994 10 p Presented at the Spring Meeting of the Materials Research Society, San Francisco, CA, 4-8 Apr. 1994
(Contract DE-AC05-84OR-21400)
(DE94-013268; CONF-940411-29) Avail: CASI HC A02/MF A01

Studies of microwave-assisted curing of neat resins (epoxy) and unidirectional glass and carbon fiber laminates have shown that a substantial reduction in the curing time was obtained. This may be explained by the penetration of microwave energy directly and throughout the laminate with enhancement of the kinetics of the chemical reaction. Results of this work indicate that the microwave assisted curing of glass fiber laminates also shows a substantial reduction of the required curing time. Microwave radiation of 2.45 GHz has been demonstrated to be an acceptable method to cure unidirectional carbon fiber laminates. Also, effective curing of crossply (0/90) laminates through this method was observed when proper rotation of the parts accompanied the curing process. This is in accordance with previous work. Multidirectional carbon fiber/epoxy laminates demonstrate a lack of coupling during the curing process. A direct curing of these laminates was not possible by microwave radiation with the experimental approach used, in agreement with previous work. Nevertheless, a moderate reduction in the curing time of these thin laminates was observed due to hybrid curing. DOE

N95-13646*# National Aeronautics and Space Administration. Lyndon B. Johnson Space Center, Houston, TX.
CRATERING AND PENETRATION EXPERIMENTS IN TEFLON TARGETS AT VELOCITIES FROM 1 TO 7 km/s
Friedrich Horz, Mark Cintala, Ronald P. Bernhard, Frank Cardenas, William Davidson, Gerald Haynes, Thomas H. See, Jerry Winkler, and Jeffrey Knight Jul. 1994 198 p Original contains color illustrations
(NASA-TM-104797; S-771; NAS 1.15:104797) Avail: CASI HC A09/MF A03; 60 functional color pages

Approximately 20 sq m of protective thermal blankets, largely composed of Teflon, were retrieved from the Long Duration Exposure Facility after the spacecraft spent approximately 5.7 years in space. Examination of

these blankets revealed that they contained thousands of hypervelocity impact features ranging from micron-sized craters to penetration holes several millimeters in diameter. We conducted impact experiments to reproduce such features and to understand the relationships between projectile size and the resulting crater or penetration hole diameter over a wide range of impact velocities. Such relationships are needed to derive the size and mass frequency distribution and flux of natural and man-made particles in low-earth orbit. Powder propellant and light-gas guns were used to launch soda-lime glass spheres into pure Teflon targets at velocities ranging from 1 to 7 km/s. Target thickness varied over more than three orders of magnitude from finite halfspace targets to very thin films. Cratering and penetration of massive Teflon targets is dominated by brittle failure and the development of extensive spall zones at the target's front and, if penetrated, the target's rear side. Mass removal by spallation at the back side of Teflon targets may be so severe that the absolute penetration hole diameter can become larger than that of a standard crater. The crater diameter in infinite halfspace Teflon targets increases, at otherwise constant impact conditions, with encounter velocity by a factor of V (exp 0.44). In contrast, the penetration hole size in very thin foils is essentially unaffected by impact velocity. Penetrations at target thicknesses intermediate to these extremes will scale with variable exponents of V. Our experimental matrix is sufficiently systematic and complete, up to 7 km/s, to make reasonable recommendations for velocity-scaling of Teflon craters and penetrations. We specifically suggest that cratering behavior and associated equations apply to all impacts in which the shock-pulse duration of the projectile is shorter than that assigned a unique projectile size, provided an impact velocity is known or assumed. This calibration seems superior to the traditional ballistic-limit approach. Author (revised)

N95-13655# Missouri Univ., Rolla, MO. Dept. of Chemistry.
DYNAMICS OF THE INTERFACE IN A MODEL COMPOSITE SYSTEM Technical Report, 1 Jan. 1993 - 7 Jul. 1994
Frank D. Blum 7 Jul. 1994 11 p
(Contract N00014-91-J-1274)
(AD-A281910; UMR-FDB-40) Avail: CASI HC A03/MF A01

A review of recent experiments on the dynamics of aminofunctional silane coupling agents is given. Of special emphasis are two coupling agents, aminopropylsilane (APS) and aminobutylsilane (ABS), which were deuterated in gamma-position. These two coupling agents have similar chemical behavior, but different dynamics. Deuterium NMR studies reveal that the APS moves slower on the silica surface than ABS. The mobility of the interfacial ABS was also found to be significantly slowed when it was overcoated with a polymerized layer of bismaleimide to form a composite. When the composite was treated with water, the interfacial mobility of the ABS increased. The flexural strength of the APS treated composite was the highest compared to ABS-treated and bulk glass in an epoxy-glass composite. DTIC

N95-13682 Argonne National Lab., IL.
EFFECTS OF IN SITU FIBER STRENGTH CHARACTERISTICS ON MECHANICAL PROPERTIES OF SiC(f)/SiC COMPOSITES
D. Singh, J. P. Singh, and M. J. Wheeler Jun. 1994 11 p Presented at the 96th Annual Meeting of the American Ceramic Society, Indianapolis, IN, 24-28 Apr. 1994 Limited Reproducibility: More than 20% of this document may be affected by microfiche quality
(Contract W-31-109-eng-38)
(DE94-013965; ANL/ET/CP-81654; CONF-940416-13) Avail: CASI HC A03

Nicalon-fiber-reinforced silicon carbide (SiC) matrix composites were tested in flexure at room and elevated temperatures. The measured strength of composites decreased slightly from a room temperature value of 400 MPa to 380 MPa at 1200 C. However, at 1300 C strength decreased significantly to 290 Mpa. The rapid decrease in strength over 1300 C is believed to be due to degradation in strength of the reinforcing fibers. In situ fiber strength and fiber pullout distribution in fractured composites were estimated by fractographic techniques. Correlations were made between the measured strengths of composites to the in situ fiber strength characteristics to explain the mechanical properties of composites at room and elevated temperatures. DOE

N95-13836*# National Aeronautics and Space Administration. Langley Research Center, Hampton, VA.
IMPROVED COMPOSITE MATERIAL AND METHOD FOR PRODUCTION OF IMPROVED COMPOSITE MATERIAL Patent Application
Gary L. Farley, inventor (to NASA) (Army Aerostructures Directorate, Hampton, VA.) 24 Jun. 1994 15 p
(NASA-Case-LAR-14892-1; NAS 1.71:LAR-14892-1;
US-Patent-Appl-SN-265361) Avail: CASI HC A03/MF A01

A laminated composite material with improved interlaminar strength and damage tolerance having short rods distributed evenly throughout the composite material perpendicular to the laminae is introduced. Each rod is shorter than the thickness of the finished laminate, but several times as long as the thickness of each lamina. The laminate is made by inserting short rods in layers of prepreg material, and then stacking and curing prepreg material with rods inserted therethrough. NASA

N95-13993 Los Alamos National Lab., NM.
ANALYSIS OF NEUTRON DIFFRACTION PEAK BROADENING CAUSED BY INTERNAL STRESSES IN COMPOSITE MATERIALS
R. I. Todd (Oxford Univ., Oxford, England.), C. Borsa (Oxford Univ., Oxford, England.), B. Derby (Oxford Univ., Oxford, England.), and M. A. M. Bourke 1994 20 p Presented at the Workshop on Neutron Scattering Data Analysis, Isis, England, Apr. 1994 Limited Reproducibility: More than 20% of this document may be affected by microfiche quality
(Contract W-7405-eng-36)
(DE94-014453; LA-UR-94-1891; CONF-9404181-1) Avail: CASI HC A03

Neutron diffraction is an essential tool in the study of internal stresses in composite materials. In most work only the peak shifts caused by the related elastic strains are considered, but other valuable information exists in the form of peak shape changes. The conditions under which the pure diffraction profile of the composite (i.e. the profile when all sources of broadening not caused by the residual stresses are removed) represents the probability distribution of the peak shifts corresponding to the strains are examined. It is shown that in these conditions the pure diffraction profile has no attributes of particle size broadening (and vice versa), thereby providing a test for the validity of results interpreted in this way. The experimental derivation of measured strain distributions in Al2O3/SiCp composites using neutron diffraction is described. No apparent particle size broadening was detected, demonstrating the validity of the results, which also satisfied other tests for consistency. DOE

N95-14148# National Defence Research Establishment, Stockholm (Sweden). Dept. of Weapon Systems, Effects and Protection.
NEW ARMOUR MATERIALS: METAL MATRIX COMPOSITES
S. J. Savage Feb. 1994 23 p
(ISSN 0347-3694)
(PB94-189131; FOA-C-20961-2.4) Avail: CASI HC A03/MF A01

The ballistic properties of metal matrix composites are reviewed and discussed. All the data located treats aluminum-base composites reinforced with silicon carbide, boron carbide or aluminum oxide particles. Most of these materials have not been optimized for use as ballistic protection, but nonetheless show improvements in ballistic efficiencies of up to three times, compared to the unreinforced alloy. Metal matrix composites offer enhanced protection against both small caliber and large caliber projectiles and shaped charges. Protection equal to a reference aluminum oxide armor has been demonstrated, with the advantage of multiple hit capacity. The present state of knowledge concerning the ballistic performance of metal composites is rudimentary, although preliminary attempts to model the penetration process seem promising, and offer the possibility to simulate the performance of alternative metal composites. Wider use of metal composites as ballistic protection may be expected in the near future. NTIS

N95-14298*# National Aeronautics and Space Administration. Lewis Research Center, Cleveland, OH.
EFFECTS OF THERMAL CYCLING ON THERMAL EXPANSION AND MECHANICAL PROPERTIES OF SiC FIBER-REINFORCED REACTION-BONDED Si3N4 COMPOSITES
R. T. Bhatt and A. R. Palczer Oct. 1994 21 p Presented at the 16th Annual Conference on Composites and Advanced Ceramics, Cocoa Beach, FL, 7-10 Jan. 1992, sponsored by the American Ceramic Society Prepared in cooperation with Army Research Lab., Cleveland, OH

(RTOP 501-01-10; DA Proj. 1L1-62211-A-47-A)
(NASA-TM-106665; E-8983; NAS 1.15:10665; ARL-MR-156) Avail: CASI HC A03/MF A01

Thermal expansion curves for SiC fiber-reinforced reaction-bonded Si3N4 matrix composites (SiC/RBSN) and unreinforced RBSN were measured from 25 to 1400 C in nitrogen and in oxygen. The effects of fiber/matrix bonding and cycling on the thermal expansion curves and room-temperature tensile properties of unidirectional composites were determined. The measured thermal expansion curves were compared with those predicted from composite theory. Predicted thermal expansion curves parallel to the fiber direction for both bonding cases were similar to that of the weakly bonded composites, but those normal to the fiber direction for both bonding cases resulted in no net dimensional changes at room temperature, and no loss in tensile properties from the as-fabricated condition. In contrast, thermal cycling in oxygen for both composites caused volume expansion primarily due to internal oxidation of RBSN. Cyclic oxidation affected the mechanical properties of the weakly bonded SiC/RBSN composites the most, resulting in loss of strain capability beyond matrix fracture and catastrophic, brittle fracture. Increased bonding between the SiC fiber and RBSN matrix due to oxidation of the carbon-rich fiber surface coating and an altered residual stress pattern in the composite due to internal oxidation of the matrix are the main reasons for the poor mechanical performance of these composites. Author

N95-14348# Massachusetts Inst. of Tech., Cambridge. Dept. of Ocean Engineering.
BOLTED JOINT STUDIES IN GRP M.S. Thesis
David M. Fox May 1994 124 p
(Contract N00123-89-G-0580)
(AD-A283843) Avail: CASI HC A06/MF A02

Glass-reinforced polymeric (GRP) materials offer certain advantages to the designer of Naval ships. A large strength-to-weight ratio, coupled with electromagnetic transparency and (possibly engineered) sound-dampening properties, render GRP materials as attractive materials for ship decks and deckhouse skins. Unfortunately, these materials, which use a thermosetting resin as a matrix material, cannot be welded as steel can. Thus, if a large structure is to be built of GRP, the inevitable joints must be either adhesively bounded or mechanically fastened. These joining techniques are frequently combined in joints which must support large loads. Because of this, an understanding of the mechanical behavior of joints in GRP is important. DTIC

N95-14360# California Univ., San Diego, La Jolla, CA. Dept. of Applied Mechanics and Engineering Sciences.
CENTER FOR ADVANCED MATERIALS OF HIGH QUALITY DYNAMIC PERFORMANCE (FELLOWSHIPS) Final Technical Report, 1 Sep. 1986 - 31 Aug. 1993
Siavouche Nemat-Nasser 28 Feb. 1994 16 p
(Contract DAAL03-86-G-0196)
(AD-A281377; ARO-24619.1-MS-UIF) Avail: CASI HC A03/MF A01

Under the designation of this fellowship grant, seven URI fellows were supported in the pursuit of their Masters Degrees and Ph.D.'s. This final report identifies the degrees conferred, placement of the fellows, and brief description of research. These research topics have been reviewed during the ARO panel annual reviews and their status and progress have been reported in the yearly technical reports which were distributed during the ARO URI site visits. DTIC

N95-14366 Virginia Univ., Charlottesville, VA. Dept. of Chemistry.
BORON ATOM MATRIX CHEMISTRY Annual Report, 1 Jun. 1993 - 31 May 1994
Lester Andrews 31 May 1994 2 p Limited Reproducibility: More than 20% of this document may be affected by microfiche quality
(Contract F49620-93-1-0331)
(AD-A282840; AFOSR-94-0452TR) Avail: CASI HC A01

Research has been done with pulsed-laser evaporated B, Be and Mg atoms and molecular hydrogen to explore the reactivities of these metals with He and to investigate infrared spectra of the product molecules in solid argon. The major products in the B/H2 system were BH, (H2)(BH), BH3, (H2)(BH3) and B2H6. It is clear that molecular hydrogen is complexed to BH and BH3 in these experiments DTIC

N95-14387# California Univ., Berkeley. Lawrence Berkeley Lab, CA.
AEM AND HREM EVALUATION OF CARBON NANOSTRUCTURES IN SILICA AEROGELS
X. Y. Song, W. Cao, and A. J. Hunt Apr. 1994 6 p Presented at the Spring Meeting of the Materials Research Society, San Francisco, CA, 4-8 Apr. 1994
(Contract DE-AC03-76SF-00098)
(DE94-014913; LBL-35626; CONF-940411-41) Avail: CASI HC A02/MF A01

Nanostructured carbon has been deposited in silica aerogels by chemical vapor infiltration using acetylene or ferrocene at moderate temperatures. Using analytical electron microscopy and high-resolution electron microscopy, we have observed various carbon rings and nanotubes in the silica aerogel-based carbon composite. Both X-ray microanalysis and nano-probe diffraction techniques have been used to confirm the presence of those carbon nanostructures. Morphologies and structural properties of the carbon nanotubes and rings have also been examined in detail. DOE

N95-14409# Aeronautical Research Labs., Melbourne (Australia).
RESIDUAL STRENGTH OF COMPOSITES WITH MULTIPLE IMPACT DAMAGE
J. J. Paul, S. C. Galea, and R. Jones Mar. 1994 27 p
(AD-A284230; ARL-RR-13; DODA-AR-008-383) Avail: CASI HC A03/MF A01

In recent years the issue of damage interaction, with particular emphasis on multi-site damage, has been of concern to the aircraft industry. Whilst most attention focused on fuselage lap joints, related problems occur in composite structures which are subjected to multiple impact damage. This paper reveals that, for the cases of multiple impact damage in composite structures investigated, little interaction between damaged regions was observed. Thus a simple repair methodology, previously developed for single impact damaged structures, was applied. This methodology was verified via a coupon test program and an experimental evaluation of two damaged F/A-18 horizontal stabilators. DTIC

N95-14411# Boeing Defense and Space Group, Seattle, WA.
THE ADVANCED DEVELOPMENT OF X-RAY COMPUTED TOMOGRAPHY APPLICATIONS Final Report, Jul. 1988 - Feb. 1994
Richard H. Bossi and Benjamin W. Knutson 15 Mar. 1994 43 p
(Contract F33615-88-C-5404; AF Proj. 3153)
(AD-A284211; WL-TR-93-4016) Avail: CASI HC A03/MF A01

The application of X-ray computed tomography (CT) for aircraft and aerospace structure and ancillary equipment has been investigated in the Advanced Development of X-Ray Computed Tomography Applications demonstration (CTAD) program sponsored by the NDE Branch of the Materials Directorate at the Air Force Wright Laboratory (WL). X-ray CT offers a new inspection capability for aircraft hardware that provides quantitative information on material density/constituents and dimensions. This capability has economic value as an engineering tool for improving the evaluation and control of materials and processes used in aircraft/aerospace structures. The CTAD effort has investigated a wide variety of application areas for CT. These include electronics, closed systems, castings, composites, and advanced materials and processes. Applications of CT in these areas include: configuration control, anomaly detection, dimensional measurements and material uniformity. By using the actual dimensional characteristics of features and anomalies in a component, and the material characteristics, such as density and elemental composition, that are derivable from the CT data, engineers can perform a variety of analyses to arrive at quantitative measurements that are of economical value to improving the overall product cycle from development to deployment. Until specifications requiring CT are implemented, CT will be employed primarily as a supplement to other NDE (nondestructive evaluation) methodologies for engineering evaluations such as product development/material characterization measurements, failure analysis and engineering problem solving, noninvasive micrography and geometry acquisition. DTIC

N95-14800*# Rockwell International Corp., Downey, CA. Space Systems Div.
MILESTONE 4: THRUST STRUCTURE CONCEPTS AND IHM SCREENING GRAPHITE COMPOSITE PRIMARY STRUCTURE (GCPS)
H. S. Greenberg 4 Nov. 1994 31 p

(Contract NCC1-193)
(NASA-CR-197053; NAS 1.26:197053; SSD94D0328) Avail: CASI HC A03/MF A01

The first part of the task was to select up to three promising thrust structure constructions and to select materials for screening tests. Part of the nondestructive evaluation and inspection (NDE/I) and integrated health management (IHM) task is to acquire and develop NDE/I sensor technologies and to integrate those sensors into the full scale test articles which will be produced under the TA2 program. Review of the anticipated fault modes and the available sensor technology data indicates that three sensor technologies should be assessed for the in-situ monitoring of the composite primary structure elements. These are: ultrasonics (dry contact), acoustic emissions, and fiber optics (embedded or attached). In fact, a combination of sensor technologies will be needed to detect and evaluate the fault modes; not only do sensor technology have specific capabilities and applicability, but the three Gr/Ep primary structures being demonstrated under the TA2 effort have differing requirements based on their respective failure modes and designs. Derived from text

N95-14801*# Rockwell International Corp., Downey, CA. Space Systems Div.

MILESTONE 4: TEST PLAN FOR REUSABLE HYDROGEN COMPOSITE TANK SYSTEM (RHCTS). TASK 3: COMPOSITE TANK MATERIALS

H. S. Greenberg 4 Nov. 1994 61 p
(Contract NCC8-39)
(NASA-CR-197036; NAS 1.26:197036; SD94D0329) Avail: CASI HC A04/MF A01

This document is the detailed test plan for the series of tests enumerated in the preceding section. The purpose of this plan is to present the test objectives, test parameters and procedures, expected performance and data analysis plans, criteria for success, test schedules, and related safety provisions and to describe the test articles, test instrumentation, and test facility requirements. Initial testing will be performed to screen four composite materials for suitability for SSTO LH2 tank loads and environmental conditions. The laminates for this testing will be fabricated by fiber placement, which is the manufacturing approach identified as baseline for the tank wall. Even though hand layup will be involved in fabricating many of the internal structural members of the tank, no hand-layup laminates will be evaluated in the screening or subsequent characterization testing. This decision is based on the understanding that mechanical properties measured for hand-layup material should be at least equivalent to properties measured for fiber-placed material, so that the latter should provide no less than a conservative approximation of the former. A single material will be downselected from these screening tests. This material will be subsequently characterized for impact-damage tolerance and durability under conditions of mechanical and thermal cycling, and to establish a preliminary design database to support ongoing analysis. Next, testing will be performed on critical structural elements fabricated from the selected material. Finally, the 8-foot diameter tank article, containing the critical structural features of the full-scale tank, will be fabricated by fiber placement and tested to verify its structural integrity and LH2 containment. Derived from text

N95-14865*# Virginia Polytechnic Inst. and State Univ., Blacksburg, VA. Dept. of Engineering Science and Mechanics.

INNOVATIVE DESIGN OF COMPOSITE STRUCTURES: DESIGN, MANUFACTURING, AND TESTING OF PLATES UTILIZING CURVILINEAR FIBER TRAJECTORIES Final Report, 15 Aug. 1988 - 31 Dec. 1993

M. W. Hyer, R. J. Rust, and W. A. Waters, Jr. Nov. 1994 23 p
Presented at the 10th DOD/NASA/FAA Conference on Fibrous Composites in Structural Design, Apr. 1994
(Grant NAG1-901)
(NASA-CR-197045; NAS 1.26:197045; VPI-E-94-08) Avail: CASI HC A03/MF A01

As a means of improving structural design, the concept of fabricating flat plates containing holes by incorporating curvilinear fiber trajectories to transmit loads around the hole is studied. In the present discussion this concept is viewed from a structural level, where access holes, windows, doors, and other openings are of significant size. This is opposed to holes sized for mechanical fasteners. Instead of cutting the important load-bearing fibers at the hole edge, as a conventional straightline design does, the curvilinear design preserves the load-bearing fibers by orienting them in smooth trajectories around the holes, their loading not ending abruptly at the hole edge. Though the concept of curvilinear fiber trajectories has been studied before, attempts to manufacture and test such plates have been limited. This report describes a cooperative effort between Cincinnati Milacron Inc., NASA Langley Research Center, and Virginia Polytechnic Institute and State University to design, manufacture, and test plates using the curvilinear fiber trajectory concept. The paper discusses details of the plate design, details of the manufacturing, and a summary of results from testing the plates with inplane compressive buckling loads and tensile loads. Comparisons between the curvilinear and conventional straightline fiber designs based on measurements and observation are made. Failure modes, failure loads, strains, deflections, and other key responses are compared. Author

N95-14913*# National Aeronautics and Space Administration. Marshall Space Flight Center, Huntsville, AL.

BUCKLING OF COMPOSITE BEAMS (CDDF) Final Report

P. Thompson Washington Oct. 1994 51 p
(Proj. 91-20)
(NASA-TP-3512; M-765; NAS 1.60:3512) Avail: CASI HC A04/MF A01

Presented are the results of an investigation of the twisting/warping deformation occurring in open-section composite beams. A series of C and L channels were manufactured using both hand layup and the innovative 'hot-drape forming' techniques. A transverse tip load was applied at the free end of the cantilevered open-section beams. The test setup allowed the tip load to be applied at various locations along the plane of and at the beam's shear center. Charts are included in this report depicting various angles of ply layups, loads applied, and load application points. A major verification resulting from this study is that the shear center of an open section composite beam can be altered, if not completely controlled, through laminate layup. Also, it was observed that the choice of the material system does not have an effect on the amount of deformation, as expected, and the material affects the location of an unsymmetric open section composite beam's true shear center. The results from this study have provided a foundation for further investigation into the apparent shifting of the shear center location in open-section composite beams.
Author (revised)

N95-15417 Illinois Univ., Champaign, IL.

COMPOSITES WITH IMPROVED COMPRESSIVE PROPERTIES Final Report

James Economy 30 Jun. 1994 5 p Limited Reproducibility: More than 20% of this document may be affected by microfiche quality
(Contract N00014-91-J-1044)
(AD-A283411) Avail: Issuing Activity (Defense Technical Information Center (DTIC))

A two year program was initiated on October 1, 1990 to pursue new approaches on improving the compressive properties of polymer based composites. This included work directed at new kinds of reinforcing agents, improved matrices and on the fiber matrix interface. A number of significant breakthroughs were achieved as a result of this study. In the case of the polymer matrix studies sufficient progress was made to justify additional funding and time extensions. DTIC

N95-15427# Army Cold Regions Research and Engineering Lab., Hanover, NH.

EFFECT OF MATRIX STIFFNESS ON WAVY FIBER BEHAVIOR IN SINGLE-CARBON-FIBER-EPOXY COMPOSITES

Madhu S. Madhukar and Piyush K. Dutta Apr. 1994 17 p
(AD-A280970; CRREL-SR-94-10) Avail: CASI HC A03/MF A01

This research identifies the mechanisms responsible for lowering the tensile strength of unidirectional polymer matrix composites at low temperatures. Since the stiffness of polymer matrices increases and toughness decreases when the temperature is lowered, the effect of low temperature was simulated by changing the matrix stiffness and toughness. Composite specimens containing a single carbon fiber embedded in an epoxy matrix were cast. The fibers were cast in curved geometries, and the specimens were loaded in tension. The fiber and interfacial failure processes were observed under polarized and unpolarized light through an optical microscope. Increasing the tensile load on the single fiber-epoxy specimens broke the embedded fiber into small fragments, whose lengths were smaller in the regions where the fiber was lying parallel to the

loading axis. A significant fiber/matrix interfacial debonding, observed near the broken fiber ends in all specimens, was much more pronounced when the fiber was to the loading axis. Transverse tensile stresses at the interface caused this interfacial debonding. Specimens with higher matrix stiffness had long matrix cracks at the broken fiber ends, which were perpendicular to the fiber axis. These matrix cracks tend to propagate perpendicular to the fiber axis, increasing the composite's cold sensitivity. The major conclusions are as follows: (1) When fibers are wavy, they are not loaded to their full capacity because of premature interfacial debonding started by the interfacial shear stresses and the transverse tensile stresses. The transverse tensile stresses at the interface are not present in the straight fiber specimens. (2) At higher stiffness and lower toughness values, the matrix cracks emanating at the broken fiber ends make the composite weaker. DTIC

N95-15441 Southern Research Inst., Birmingham, AL.
MECHANICAL BEHAVIOR OF HIGH TEMPERATURE COMPOSITES Final Report
Terry R. Barnett and H. S. Starrett Apr. 1994 59 p Limited Reproducibility: More than 20% of this document may be affected by microfiche quality
(Contract F33615-88-C-5055)
(AD-A281582; WL-TR-94-4060) Avail: Issuing Activity (Defense Technical Information Center (DTIC))

The objective of this program is to develop an understanding of ceramic composites and oxidation-protected carbon-carbon composites, and to provide guidance for future material development of composites by the evaluation and characterization of these materials from 25 C to 2200 C in inert and oxidizing environments. DTIC

N95-15443 North Carolina State Univ., Raleigh, NC.
DEFORMATION, STRENGTH, AND FAILURE MODES OF LAMINATED CONVENTIONAL AND HYBRID POLYMER-MATRIX COMPOSITES LOADED IN THE THICKNESS DIRECTION Final Report, 15 Jul. 1985 - 28 Feb. 1991
A. A. Fahmy Jun. 1994 51 p Limited Reproducibility: More than 20% of this document may be affected by microfiche quality
(Contract DAAG29-85-K-0195)
(AD-A281587; ARO-22339.3-MS) Avail: CASI HC A04

Thickness properties of laminated composites have not been as thoroughly investigated as in plane properties. Previous work by this investigator indicated that these properties, both elastic and strength, differ significantly from the transverse properties of unidirectional composites of the same materials system although the thickness direction is transverse to each play in the laminate. In this investigation the thickness properties of both single system, and hybrid laminates are studied; namely, graphite-epoxy, kevlar-epoxy, glass-epoxy, graphite-epoxy/ kevlar-epoxy, and graphite-epoxy/ glass-epoxy. However, knowledge of the in-plane properties of the laminates was also obtained since this was essential for the analysis and are also reported. Failure modes of the hybrid composites are characterized and discussed. DTIC

N95-15573# Los Alamos National Lab., NM.
COMPUTATIONAL MODELING OF FIBER-REINFORCED COMPOSITES
F. L. Addessio and J. B. Aidun 1994 5 p Presented at the World Congress on Computational and Applied Mathematics, Atlanta, GA, 11-15 Jul. 1994
(Contract W-7405-eng-36)
(DE94-012914; LA-UR-94-1520; CONF-940719-3) Avail: CASI HC A01/MF A01

A homogenization technique for simulating the dynamic response of metal-matrix composites has been implemented into EPIC, a three-dimensional, finite-element computer program. The technique includes a micromechanical model for the elastic-plastic response of the constituents. New additions to the constitutive description were a nonlinear mean stress-volumetric strain relation, a rate-form flow stress model, and four micromechanical failure modes. Preliminary simulations of Taylor impact tests gave satisfactory results; the composite anisotropy was well represented and the damage effects were qualitatively correct. The calculations were slowed by less than 20% using the micromechanical homogenization model explicitly. Computing speed should be recovered substantially for matrix yield models like viscoplasticity that permit direct calculation of the plastic strain. The metal plasticity model requires solving for the microvariables twice each time step. The present approach can be extended to epoxy or ceramic composites by inclusion of appropriate constitutive relations. DOE

N95-15763*# National Aeronautics and Space Administration. Marshall Space Flight Center, Huntsville, AL.
BASIC MECHANICS OF LAMINATED COMPOSITE PLATES
Alan T. Nettles Washington Oct. 1994 103 p
(NASA-RP-1351; M-764; NAS 1.61:1351) Avail: CASI HC A06/MF A02

The mechanics of laminated composite materials is presented in a clear manner with only essential derivations included. The constitutive equations in all of their forms are developed and then summarized in a separate section. The effects of hygrothermal effects are included. The prediction of the engineering constants for a laminate are derived. Strength of laminated composites is not covered. Author

N95-15873 Naval Postgraduate School, Monterey, CA.
THREE-DIMENSIONAL EFFECTS OF CRACK CLOSURE IN LAMINATED COMPOSITE PLATES SUBJECTED TO BENDING LOADS M.S. Thesis
Mehmet Baskaya Jun. 1994 46 p Limited Reproducibility: More than 20% of this document may be affected by microfiche quality
(AD-A283342) Avail: CASI HC A03

Fracture is one of the dominant failure modes in structures subjected to external loads. Stress and deformation fields around the crack tip are important to understand the crack propagation and arrest. For a plate with a through-the-thickness crack and subjected to a bending load, there is crack closure on the compression side of the crack face. The present study investigates effects of crack closure on the stress and deformation fields on the tension side of the crack face. A three-dimensional finite element analysis is performed for laminated composite plates using both the line and surface crack closure models. For a composite whose longitudinal elastic modulus is much greater than the transverse modulus, line and surface closure models result in higher stresses near the crack tip in comparison to the no-closure solution. Hence, no-closure solutions are nonconservative for the composite. Transverse shear is the major cause for the nonconservative solution. DTIC

N95-15911*# NYMA, Inc., Brook Park, OH. Engineering Services Div.
CHARACTERIZATION OF DAMAGE PROGRESSION IN SCS-6/TIMETAL 21S (0)4 UNDER THERMOMECHANICAL FATIGUE LOADINGS
Michael G. Castelli Cleveland, OH NASA Nov. 1994 21 p Presented at the Symposium on Life Prediction Methodology for Titanium Matrix Composites, Hilton Head, SC, 22-24 Mar. 1994; sponsored by American Society for Testing and Materials
(Contract NAS3-27186; RTOP 763-22-41)
(NASA-CR-195399; E-9221; NAS 1.26:195399) Avail: CASI HC A03/MF A01

A detailed experimental investigation was performed at a single maximum cyclic stress (sigma max) level to physically characterize the progression of thermomechanical fatigue (IW) damage in continuously reinforced (0 deg) SCS-6/Timetal 21S, a titanium matrix composite. In-phase (IP) and out of-phase (OP) loadings were investigated at sigma max = 1000 MPa with a temperature cycle from 150 to 6500 C. Damage progression, in terms of macroscopic property degradation, was experimentally quantified through an advanced TMF test methodology which incorporates explicit measurements of the isothermal static moduli at the TMF temperature extremes and the coefficient of thermal expansion (CTE) as functions of the TMF cycles. Detailed characterization of the physical damage progression at the microstructural level was performed by interrupting multiple TMF tests at various stages of mechanical property degradation and analyzing the microstructure through extensive destructive metallography. Further, the extent of damage was also quantified through residual static strength measurements. Results indicated that damage initiation occurred very early in cyclic life (N less than 0.1Nf) for both the IP and OP TMF loadings. IP TMF damage was found to be dominated by fiber breakage with a physical damage progression in the microstructure which was difficult to quantify. OP TMF loadings produced matrix cracking exclusively associated with surface initiations. Here, damage progression was easily distinguished in terms of both the number of cracks and their relative inward progressions toward the outer fiber rows with increased cycling. The point at which the leading cracks reached the outer fiber rows (when localized fiber/matrix

de-bonding and matrix crack bridging occurred) appeared to be reflected in the macroscopic property degradation curves. Author

25 INORGANIC AND PHYSICAL CHEMISTRY

Includes chemical analysis, e.g., chromatography; combustion theory; electrochemistry; and photochemistry.

For related information see also *77 Thermodynamics and Statistical Physics.*.

N95-13652 Toronto Univ. (Ontario). Inst. for Aerospace Studies.
HYDROGEN TRANSPORT AND TRAPPING IN GRAPHITE
S. Chiu and A. A. Haasz Jul. 1994 27 p CFFTP-G-9316 Sponsored by Natural Sciences and Engineering Research Council of Canada, Canadian Fusion Fuels Technology Project, and Ontario Center for Materials Research
(ISSN 0082-5255)
(UTIAS-347) Copyright Avail: Issuing Activity

Graphite is extensively being used in present-day fusion devices and has been selected as the reference material for plasma-facing components in the International Thermonuclear Experimental Reactor, ITER. There has been a growing appreciation for the role of plasma surface interactions and the effects of the resulting impurity production and hydrogen fuel loss due to wall erosion and hydrogen trapping. In many cases it has become clear that the observed characteristics of the discharge are determined more by the plasma-surface interactions than by plasma physics. Molecule formation upon interaction of graphite with hydrogen ions has been of special interest because of recent experimental evidence indicating a possible subsurface molecule formation mechanism leading to hydrogen reemission. This report attempts to examine the phenomena of hydrogen transport and trapping in graphite, in particular with regard to molecule formation at the end of ion range. HD molecule emission during sequential and simultaneous H+/D+ irradiations of graphite indicates that hydrogen diffuses as atoms in the implantation zone. On the other hand, methane molecules are found to be formed locally at the end of ion range, on inner surfaces that are either inherent in graphite or are created during ion bombardment. Methane molecules formed during ion irradiation at 800 K appear to be partially broken up by the incoming ions as they diffuse to the front surface. The extent of breakup was found to be dependent on energy, flux, and fluence of the incident beam. Thermal release of H+/D+ implanted in graphite shows that both hydrogen and methane molecules are formed locally at the end of the ion range in the absence of ion irradiation. The difference between the thermal desorption and reemission results indicates that atom diffusion in the implantation layer is an ion-induced effect. A model, consistent with the observed experimental observations, is proposed for hydrogen transport and molecule formation in graphite. Author (revised)

N95-14141# California Univ., San Diego, La Jolla, CA. Dept. of Chemistry.
ELECTRODEPOSITION OF CONDUCTORS AND SEMICONDUCTORS WITH CONTROLLED STOICHIOMETRIES AND MORPHOLOGIES Interim Report
Michael J. Sailor, Robert D. Herrick, II, and Audrey S. Kaplan 21 Jun. 1994 3 p
(Contract N00014-92-J-1810)
(AD-A280743; TR-8-ONR) Avail: CASI HC A01/MF A01

In an attempt to electrodeposit carbon from CCl4 in nonaqueous solvents, we observed growth of several unusual morphologies. Fibers with diameters on the order of 0.1-5 microns were synthesized by cathodic galvanostatic electrodeposition from nonaqueous solvents (CH3CN or CH2Cl2) and an electrolyte containing CCl4 and tetrabutylammonium salts. The fibrous morphology forms without the help of a structural template. Production of fibers can be observed on Ni, Fe, or Cu substrates, with the morphology being very dependent on current density, CCl4 concentration, and electrode surface preparation. The materials apparently consist of carbon or a carbon nitride compound. The aspect ratio of the fibers ranges from about 2:1 to greater than 100:1, depending upon deposition conditions. Growth of the unusual morphology is presumed to be driven by directional covalent bonding in a graphitic material, analogous to buckminsterfullerene-derived nanotubes. DTIC

N95-14268*# Old Dominion Univ., Norfolk, VA. Dept. of Mechanical Engineering.
NUMERICAL SIMULATION OF SHOCK-INDUCED COMBUSTION PAST BLUNT BODIES USING SHOCK-FITTING TECHNIQUE Progress Report, period ending 30 Jun. 1994
J. K. Ahuja, D. J. Singh, and S. N. Tiwari Aug. 1994 54 p
(Grants NAG1-423; NAG1-363)
(NASA-CR-197013; NAS 1.26:197013; ODURF-144029) Avail: CASI HC A04/MF A01

Two-dimensional axisymmetric, reacting viscous flow over blunt projectiles is computed to study shock-induced combustion at Mach 5.11 and Mach 6.46 in hydrogen-air mixture. A finite-difference, shock-fitting method is used to solve the complete set of Navier-Stokes and species conservation equations. In this approach, the bow shock represents a boundary of the computational domain and is treated as a discontinuity across which Rankine-Hugoniot conditions are applied. All interior details of the flow such as compression waves, reaction front, and the wall boundary layer are captured automatically in the solution. Since shock-fitting approach reduces the amount of artificial dissipation, all the intricate details of the flow are captured much more clearly than has been possible with the shock-capturing approach. This has allowed an improved understanding of the physics of shock-induced combustion over blunt projectiles and the numerical results can now be explained more readily with one-dimensional wave-interaction model than before. Author

N95-14307# Sandia National Labs., Albuquerque, NM.
DETERMINATION OF THE SHEAR MODULUS IN SELF-ASSEMBLED MONOLAYERS USING QUARTZ RESONATORS
T. W. Schneider, S. J. Martin, and G. C. Frye 1994 7 p Presented at the 186th Meeting of the Electrochemical Society, Miami, FL, 9-14 Oct. 1994
(Contract DE-AC04-94AL-85000)
(DE94-013449; SAND-94-1309C; CONF-941063-4) Avail: CASI HC A02/MF A01

This work examined self-assembled monolayers (SAM's) of n-alkane thiols using quartz resonators to determine the shear storage and loss moduli. Network analyzer measurements of electrical admittance at fundamental and corresponding harmonic values are fit to an equivalent circuit model. Shear modulus depends on frequency; the modulus values are three orders of magnitude lower than expected for a liquid or elastomeric polymer, more like those of a dense gas or supercritical fluid. A density of around 0.45 g/cm(exp 3) is calculated for a dodecane thiol SAM; this is roughly half of the bulk density. In conclusion, quartz resonators can be used to inertially deform SAM's. DOE

N95-14312# Sandia National Labs., Albuquerque, NM.
MICROCONTAMINATION DETECTION USING HEAVY ION BACKSCATTERING SPECTROMETRY
J. A. Knapp, J. C. Banks, and A. C. Diebold 1994 9 p Presented at the Microcontamination 1994, San Jose, CA, 5-6 Oct. 1994
(Contract DE-AC04-94AL-85000)
(DE94-014182; SAND-94-1619C; CONF-9410132-1) Avail: CASI HC A02/MF A01

Heavy Ion Backscattering Spectrometry (HIBS) is a new ion beam analysis tool using heavy, low-energy ions in backscattering mode which can detect very low levels of surface contamination. By taking advantage of the greatly increased scattering cross-section for such ion beams and eliminating unwanted substrate scattering with a thin carbon foil, our research system has achieved a sensitivity ranging from approximately 5 x 10(exp 10) atoms/cm(exp 2) for Fe to approximately 1 x 10(exp 9) atoms/cm(exp 2) for Au on Si, without preconcentration. A stand-alone HIBS prototype now under construction in collaboration with SEMATECH is expected to achieve detection limits of approximately 5 x 10(exp 9) atoms/cm(exp 2) for Fe and approximately 1 x 10(exp 8) atoms/cm(exp 2) for Au on Si, again without preconcentration. Since HIBS is standardless and has no matrix effects, it will be useful not only as a standalone tool, but also for benchmarking standards for other tools. This conference is testimony to the importance of controlling contamination in microelectronics manufacturing. By the turn of the century, very large scale integrated circuit processing is expected to require contamination levels well below 1 x 10(exp 9) atoms/cm(exp 2) in both starting materials and introduced by processing. One of the most sensitive of existing general-purpose tools is

Total reflection X-Ray Fluorescence (TXRF), which can detect approximately 1 x 10(exp 10) atoms/cm(exp 2) levels of some elements such as Fe and Cu, but for many elements it is limited to 1 x 10(exp 12) atoms/cm(exp 2) or worse. TXRF can achieve a sensitivity of 10(exp 8) atoms/cm(exp 2) through the use of synchrotron radiation or via pre-concentration using Vapor Phase Decomposition. HIBS provides an ion beam analysis capability with the potential for providing similar sensitivity at medium Z and higher sensitivity at larger Z, all without pre-concentration or matrix effects. DOE

N95-14371# Brookhaven National Lab., Upton, NY.
PRACTICAL ASPECTS OF CORROSION FUNDAMENTALS
H. S. Isaacs 1994 11 p Presented at the 185th Electrochemical Society Meeting, San Francisco, CA, 22-27 May 1994
(Contract DE-AC02-76CH-00016)
(DE94-015842; BNL-49792; CONF-940529-18) Avail: CASI HC A03/MF A01

Aspects important in corrosion have been introduced. They are: (1) 'Pourbaix Diagrams' which consider thermodynamic stability of metals as a function of electrical potential and water pH; (2) the anodic interfacial reaction rates which depend on potential and accumulation of reaction products; (3) the prediction of polarization curves based on the kinetics and thermodynamics; and (4) localized corrosion models, as this form of corrosion is a major cause of corrosion failures. DOE

N95-14372# National Inst. of Standards and Technology, Boulder, CO. Thermophysics Div.
THERMOPHYSICAL PROPERTIES OF HCFC ALTERNATIVES
W. M. Haynes Jul. 1994 6 p
(Contract DE-FG02-91CE-23810)
(DE94-016646; DOE/CE-23810/42A) Avail: CASI HC A02/MF A01

Numerous fluids and fluid mixtures have been identified as promising alternatives to the HCFC refrigerants, but, for many of them, reliable thermodynamic data do not exist. Reliable thermodynamic properties data and models are needed to predict the performance of the new refrigerants in heating and cooling equipment and to design and optimize equipment to be reliable and energy efficient. The objective of this project is to measure, with high accuracy, selected thermodynamic properties data for two pure refrigerants and nine refrigerant blends; these data will be used to fit equations of state and other property models which can be used in equipment design. The new data will fill in gaps in the existing data and resolve problems and differences that exist in and between existing data sets. Most of the studied fluids and blends are potential replacements for HCFC-22 and/or R502; in addition, one pure fluid and one blend are potential replacements for CFC-13 in low temperature refrigeration applications. DOE

N95-14375# Oak Ridge National Lab., TN.
ASSESSING POST-FIRE COMBUSTION OF POLYURETHANE
W. R. Williams and J. C. Anderson 1994 10 p Presented at the DOE Defense Programs Packaging Workshop, Knoxville, TN, 16-19 May 1994
(Contract DE-AC05-84OR-21400)
(DE94-011461; CONF-9405109-6) Avail: CASI HC A02/MF A01

In defining hypothetical accident condition thermal test requirements, 10 CFR 71.73(c)(3) states that 'any combustion of materials of construction must be allowed to proceed until it terminates naturally.' Two examples of extended burning of packages following the regulatory fire are documented. This paper addresses extended burning after cessation of the 30-min, 1475 F regulatory fire from an analytical perspective with specific application to a package containing polyurethane insulation. Issues include identifying conditions under which materials of construction burn, estimating burn rate, and establishing criteria for cessation of burning. These data and criteria are then applied to determine package temperature profiles using a finite element model. Development of the illustrative problem demonstrates a number of difficulties that are faced when using analytical models to simulate hypothetical thermal accident conditions. DOE

N95-14386# State Univ. of New York, Buffalo, NY. Dept. of Chemistry.
DETERMINATION OF SOLVATION KINETICS IN SUPERCRITICAL FLUIDS
F. V. Bright 1994 5 p
(Contract DE-FG02-90ER-14143)
(DE94-016491; DOE/ER-14143/3) Avail: CASI HC A01/MF A01

This project is directed on determining effects of supercritical fluids on salvation and chemical reactions. Sub-projects are: understanding the effects of neat and entrainer-modified supercritical fluids on solute-fluid interactions; determining the influence of supercritical fluids on energetics and dynamics of solute conformation; and probing effects of continuous phase density on internal dynamics of reverse micelles formed in supercritical fluids. In order to follow these fast molecular-level processes, modern picosecond in-situ optical spectroscopy is being used. To date this work has: helped define how 'diffusion controlled' reactions proceed in supercritical fluids; determined how and on what time scale entrainers preferentially solvate solutes in the near-critical region; shown that the conformation (i.e., reactivity) of flexible solutes can be altered easily with fluid density; shown how lateral diffusion within reverse micelles (formed in supercritical alkanes) is affected by the continuous phase density; and begun to probe how the conformation of polymers can be controlled with supercritical fluids. This is leading to a better molecular-level understanding of the chemistry of supercritical fluids. DOE

N95-14388# Louisiana State Univ., Baton Rouge, LA. Dept. of Chemical Engineering.
ACTIVITY OF Ga, In AND Cu MODIFIED MFI ZEOLITES FOR AMINE REACTIONS
V. Kanazirev and G. L. Price 1994 8 p Presented at the 10th International Zeolite Conference, Garmish-Partenkirchen, Germany, 17-22 Jul. 1994
(Contract DE-FG05-92ER-14291)
(DE94-016532; CONF-940744-5) Avail: CASI HC A02/MF A01

High densities of Ga, In and Cu cations (Me/Al=1) in MFI zeolites have been obtained via thermal treatment of mechanical mixtures of metal oxides with H-MFI resulting in solid state ion-exchange. Ga and In require an H2 reducing agent during thermal treatment while Cu requires only an absence of O2 and undergoes autoreduction during thermal treatment. Using both thermal analysis with MS detection and catalytic testing in a gradientless batch recirculating reactor, the modified catalysts have been shown to be highly reactive towards amines. The desorption features of 1-propanamine with cation containing MFI generally differ from those of pure HMFI zeolite. Propanenitrile, C2-C6 alkenes and aromatics appear in the decomposition products. Catalytic experiments have revealed that Ga, In, and Cu zeolitic cations promote dehydrogenation and condensation reactions of propanamine to different extents. Such behavior probably results from Lewis acid interactions of the zeolite cation with the amine. DOE

N95-14391# Sandia National Labs., Albuquerque, NM.
MODELING TURBULENT FLAME PROPAGATION
W. T. Ashurst 1994 27 p Presented at the 25th Combustion Symposium, Irvine, CA, 1 Aug. 1994
(Contract DE-AC04-76DR-00789)
(DE94-016618; SAND-94-8701C; CONF-940838-7) Avail: CASI HC A03/MF A01

Laser diagnostics and flow simulation techniques are now providing information that if available fifty years ago, would have allowed Damkoehler to show how turbulence generates flame area. In the absence of this information, many turbulent flame speed models have been created, most based on Kolmogorov concepts which ignore the turbulence vortical structure, Over the last twenty years, the vorticity structure in mixing layers and jets has been shown to determine the entrainment and mixing behavior and these effects need to be duplicated by combustion models. Turbulence simulations reveal the intense vorticity structure as filaments and simulations of passive flamelet propagation show how this vorticity creates flame area and defines the shape of the expected chemical reaction surface. Understanding how volume expansion interacts with flow structure should improve experimental methods for determining turbulent flame speed. Since the last decade has given us such powerful new tools to create and see turbulent combustion microscopic behavior, it seems that a solution of turbulent combustion within the next decade would not be surprising in the hindsight of 2004. DOE

N95-14392# Rice Univ., Houston, TX.
INFRARED ABSORPTION SPECTROSCOPY AND CHEMICAL KINETICS OF FREE RADICALS
R. F. Curl and G. P. Glass 1994 13 p

(Contract DE-FG05-85ER-13439)
(DE94-016642; DOE/ER-13439/T4) Avail: CASI HC A03/MF A01

Rate of reaction of ketenyl radical with O2 at room temperature was determined as 6.5(6) x 10(exp -13) cm(exp 3) molecules(exp -1) s(exp -1) and an upper bound of 1 x 10(exp -13) cm(exp 3) molecule(exp -1) s(exp -1) was estimated for the reaction rate of acetylene with ketenyl. The high resolution spectrum of the nu(sub 1) acetylenic CH stretch of propargy1 radical (HCCCH2) near 3322 cm(exp -1) has obtained and analyzed. Nuclear spin weights demonstrate that the CH2 hydrogen atoms are in the carbon atom plane. We have attempted to measure the propargyl recombination rate constant at 296 K; however, the observed rate constant of (1.2 +/- 0.2) x 10(exp -10) cc-molecule(exp -1) s(exp -1) may be affected by other reactions. The CH stretch fundamental, nu(sub 1), of HCCN has been observed, assigned, and analyzed. Analysis of the hot bands associated with bending shows thatHCCN is a quasilinear molecule with a very floppy potential function for the HCC bending angle. The barrier to linearity is estimated to be about 100 cm(exp -1). Rate of the reaction between C2H and H2 has been measured at 295-855 K. The rate constant exhibited a non-Arrhenius form well represented by k = (9.44 +/- 0.50) x 10(exp -14)T(sup 0.9)exp(-1003 +/- 40/T)cm(exp 3)molecule(exp -1)s(exp -1). The reaction between atomic oxygen and the amidogen radical, NH2 has been studied at 295 K; the room temperature rate constant was measured as (6.5 +/- 1.3) x 10(exp -1) s(exp -1). The minor channel leading to NH + OH was observed but accounted for at most about 8% of the NH2 reacting. The rate constant for the reaction NH+O was determined from fitting the NH time profile to be 6.6 +/- 10(exp -11) cm(exp 3) molecule(exp -1) s(exp -1). DOE

N95-14435# Massachusetts Inst. of Tech., Cambridge. Dept. of Chemical Engineering.
CONVERSION OF LIGHT HYDROCARBON GASES IN METAL CARBIDES FOR PRODUCTION OF LIQUID FUELS AND CHEMICALS Quarterly Technical Report, 1 Oct. - 31 Dec. 1993
A. F. Diaz, A. J. Modestino, J. B. Howard, J. W. Tester, and W. A. Peters Feb. 1994 7 p
(Contract DE-AC22-92PC-92111)
(DE94-013933; DOE/PC-92111/5; FE-MIT-92111-5) Avail: CASI HC A02/MF A01

The plasma gun was redesigned, after accidental burn-out in the previous period, to eliminate any possible arcing pathways outside of the inter-electrode region. A stable Argon arc discharge was obtained during the first test-firing of the completely rebuilt gun. The system flow capacity was determined to be about 3 cfm at ambient conditions. Procurement and installation of process and safety monitoring devices and of components of the sample collection system are in progress. The gas-quenched and water-cooled sample collection probe is fully assembled and is ready for installation. Shakedown-testing of the thermal plasma reactor has also commenced. Debottlenecking work on the gas and cooling water lines was performed to relieve excessive pressure drop through both gas and cooling water systems. For the next period, the shakedown testing will proceed first with the determination of the maximum power levels at which the plasma reactor can be operated at each gas flowrate, with Argon as the plasma-forming gas. The next step will be to complete the assembly of the sample collection system and to check out the entire system to determine other process constraints first without firing and then with firing, still utilizing Argon as plasma gas. Preliminary temperature profile measurements in the cooling chamber will be taken using thermocouples to map out a safe penetration length of the sample collection probe into the chamber. Once the shakedown-testing is completed, the Miller powder feeder will be procured on a trial basis and preliminary scoping runs with methane and CaO and with methane and MgO will be performed. DOE

N95-14663# Pacific Northwest Lab., Richland, WA.
FLUID DYNAMIC EFFECTS ON PRECISION CLEANING WITH SUPERCRITICAL FLUIDS
M. R. Phelps, M. O. Hogan, and L. J. Silva Jun. 1994 10 p Presented at the Joint Army, Navy, NASA, Air Force Environmentally Benign Cleaning and Degreasing Technical Workshop, Indian Head, MD, 14-15 Jun. 1994
(Contract DE-AC06-76RL-01830)
(DE94-015001; PNL-SA-24365; CONF-9406181-3) Avail: CASI HC A02/MF A01

Pacific Northwest Laboratory staff have assembled a small supercritical fluids parts cleaning test stand to characterize how system dynamics affect the efficacy of precision cleaning with supercritical carbon dioxide. A soiled stainless steel coupon, loaded into a 'Berty' autoclave, was used to investigate how changes in system turbulence and solvent temperature influenced the removal of test dopants. A pulsed laser beam through a fiber optic was used to investigate real-time contaminant removal. Test data show that cleaning efficiency is a function of system agitation, solvent density, and temperature. These data also show that high levels of cleaning efficiency can generally be achieved with high levels of system agitation at relatively low solvent densities and temperatures. Agitation levels, temperatures, and densities needed for optimal cleaning are largely contaminant dependent. Using proper system conditions, the levels of cleanliness achieved with supercritical carbon dioxide compare favorably with conventional precision cleaning methods. Additional research is currently being conducted to generalize the relationship between cleaning performance and parameters such as contaminant solubilities, mass transfer rates, and solvent agitation. These correlations can be used to optimize cleaning performance, system design, and time and energy consumption for particular parts cleaning applications. DOE

N95-14838# Brown Univ., Providence, RI. Div. of Engineering.
BEHAVIOR OF CHARRING MATERIALS IN SIMULATED FIRE ENVIRONMENTS Final Report, 1990 - 1992
E. M. Suuberg, I. Milosavljevic, and W. D. Lilly Jun. 1994 625 p Prepared for National Inst. of Standards and Technology, Gaithersburg, MD
(Grant NIST-60NANB0D1042)
(PB94-196045; NIST/GCR-94/645) Avail: CASI HC A99/MF A06

The focus of this study was the behavior of thick charring solids in fire situations. Clearly one of the most important parameters governing the fire phenomenon is the rate of release of combustible volatiles into the gas phase, in which they actually burn. Over the years, fire researchers have learned how to model the processes in the gas phase, so that the rate of heat feedback to the solid surface can be reasonably well predicted. Likewise, there exists the ability to model the heat transfer processes at the solid surface and within the solid itself. This study was concerned with the possibility that the inability to come to complete closure on the charring polymer fire problem might derive from difficulties in applying laboratory scale kinetics to actual fire conditions. Specifically, we were concerned about how well small scale laboratory experiments used to derive the kinetics of pyrolysis could be used to predict the behavior of charring solids in fire situations. NTIS

N95-14867*# Auburn Univ., AL. Space Power Inst.
[X-RAY PHOTOELECTRON SPECTROSCOPY (XPS), RUTHERFORD BACK SCATTERING (RBS) STUDIES] Final Report
W. C. Neely, M. J. Bozak, and J. R. Williams 16 Dec. 1993 41 p
(Contract NAS8-39131)
(NASA-CR-196536; NAS 1.26:196536) Avail: CASI HC A03/MF A01

X-ray photoelectron spectroscopy (XPS), Rutherford Back Scattering (RBS) studies of each of sample received were completed. Since low angle X-ray could not be performed because of instrumentation problems, Auger spectrometry was employed instead. The results of these measurements for each of the samples is discussed in turn. Author (revised)

N95-14903*# Cleveland State Univ., OH. Dept. of Electrical Engineering.
ELECTRICAL CHARACTERIZATION OF 6H CRYSTALLINE SILICON CARBIDE M.S. Thesis Final Report
Stephen E. Lempner Sep. 1994 109 p
(Contract NCC3-121)
(NASA-CR-197047; NAS 1.26:197047) Avail: CASI HC A06/MF A02

Crystalline silicon carbide (SiC) substrates and epilayers, undoped as well as n- and p-doped, have been electrically characterized by performing Hall effect and resistivity measurements (van der Pauw) over the temperature range of approximately 85 K to 650 K (200 K to 500 K for p-type sample). By fitting the measured temperature dependent carrier concentration data to the single activation energy theoretical model: (1) the activation energy for the nitrogen donor ranged from 0.078 eV to 0.101 eV for a doping concentration range of 10(exp 17) cm(exp -3) to 10(exp 18) cm(exp -3) and (2) the activation energy for the aluminum acceptor was 0.252 eV for

a doping concentration of 4.6 x 10(exp 18) cm(exp -3). By fitting the measured temperature dependent carrier concentration data to the double activation energy level theoretical model for the nitrogen donor: (1) the activation energy for the hexagonal site was 0.056 eV and 0.093 eV corresponding to doping concentrations of 3.33 x 10 (exp 17) cm(exp -3) and 1.6 x 10(exp 18) cm(exp -3) and (2) the activation energy for the cubic site was 0.113 and 0.126 eV corresponding to doping concentrations of 4.2 x 10(exp 17) cm(exp -3) and 5.4 x 10(exp 18) cm(exp -3). Author

N95-14958# Physical Sciences, Inc., Andover, MA.
ULTRASENSITIVE INFRARED CHEMILUMINESCENCE DETECTION Final Report, Sep. 1988 - Sep. 1993
W. T. Rawlins, M. E. Fraser, K. W. Holtzclaw, W. J. Marinelli, and H. C. Murphy Oct. 1993 353 p
(Contract F19628-88-C-0173)
(AD-A283531; PSI-1059/TR-1277; PL-TR-93-2266) Avail: CASI HC A16/MF A03

This document is the Final Report for a 5-year project dedicated to investigations of chemical processes related to the excitation of infrared chemiluminescent radiation in the upper atmosphere. The effort has included experimental measurements of molecular infrared fluorescence, from 2 to 25 micrometers, excited by energetic chemical reactions involving upper atmospheric and aurorally excited species. Observed IR radiators include electronically excited molecular nitrogen, vibrationally excited N20, and rovibrationally excited CO(v,J) and NO(v,J). Additional experimental measurements in a discharge-flow reactor quantified the kinetics and spectroscopy of energetic IR precursor species including metastable electronic states of molecular oxygen, molecular nitrogen, and atomic nitrogen. Results from the experimental measurements were included in a critical review of nitric oxide kinetics, and were applied to predictive modeling of nitric oxide excitation in the auroral upper atmosphere. DTIC

N95-15056*# National Aeronautics and Space Administration. Lewis Research Center, Cleveland, OH.
LSENS: A GENERAL CHEMICAL KINETICS AND SENSITIVITY ANALYSIS CODE FOR HOMOGENEOUS GAS-PHASE REACTIONS. PART 1: THEORY AND NUMERICAL SOLUTION PROCEDURES
Krishnan Radhakrishnan (NYMA, Inc., Brook Park, OH.) Jan. 1994 371 p
(RTOP 505-62-52)
(NASA-RP-1328-Pt-1; E-5140-1-Pt-1; NAS 1.61:1328-Pt-1) Avail: CASI HC A16/MF A03

LSENS, the Lewis General Chemical Kinetics and Sensitivity Analysis Code, has been developed for solving complex, homogeneous, gas-phase chemical kinetics problems and contains sensitivity analysis for a variety of problems, including nonisothermal situations. This report is part 1 of a series of three reference publications that describe LENS, provide a detailed guide to its usage, and present many example problems. Part 1 derives the governing equations and describes the numerical solution procedures for the types of problems that can be solved. The accuracy and efficiency of LSENS are examined by means of various test problems, and comparisons with other methods and codes are presented. LSENS is a flexible, convenient, accurate, and efficient solver for chemical reaction problems such as static system; steady, one-dimensional, inviscid flow; reaction behind incident shock wave, including boundary layer correction; and perfectly stirred (highly backmixed) reactor. In addition, the chemical equilibrium state can be computed for the following assigned states: temperature and pressure, enthalpy and pressure, temperature and volume, and internal energy and volume. For static problems the code computes the sensitivity coefficients of the dependent variables and their temporal derivatives with respect to the initial values of the dependent variables and/or the three rate coefficient parameters of the chemical reactions. Author

N95-15057*# National Aeronautics and Space Administration. Lewis Research Center, Cleveland, OH.
LSENS: A GENERAL CHEMICAL KINETICS AND SENSITIVITY ANALYSIS CODE FOR HOMOGENEOUS GAS-PHASE REACTIONS. PART 3: ILLUSTRATIVE TEST PROBLEMS
David A. Bittker and Krishnan Radhakrishnan Mar. 1994 150 p
(RTOP 505-62-52)
(NASA-RP-1330-Pt-3; E-5140-3-Pt-3; NAS 1.61:1330-Pt-3) Avail: CASI HC A07/MF A02

LSENS, the Lewis General Chemical Kinetics and Sensitivity Analysis Code, has been developed for solving complex, homogeneous, gas-phase chemical kinetics problems and contains sensitivity analysis for a variety of problems, including nonisothermal situations. This report is part 3 of a series of three reference publications that describe LSENS, provide a detailed guide to its usage, and present many example problems. Part 3 explains the kinetics and kinetics-plus-sensitivity analysis problems supplied with LSENS and presents sample results. These problems illustrate the various capabilities of, and reaction models that can be solved by, the code and may provide a convenient starting point for the user to construct the problem data file required to execute LSENS. LSENS is a flexible, convenient, accurate, and efficient solver for chemical reaction problems such as static system; steady, one-dimensional, inviscid flow; reaction behind incident shock wave, including boundary layer correction; and perfectly stirred (highly backmixed) reactor. In addition, the chemical equilibrium state can be computed for the following assigned states: temperature and pressure, enthalpy and pressure, temperature and volume, and internal energy and volume. For static problems the code computes the sensitivity coefficients of the dependent variables and their temporal derivatives with respect to the initial values of the dependent variables and/or the three rate coefficient parameters of the chemical reactions. Author (revised)

N95-15291# Rust Coll., Holly Springs, MS.
SIMULATION OF COAL AND CHAR NITROGEN REACTIONS IN COMBUSTION
S. K. Kumpaty Oct. 1993 52 p
(Contract DE-FG22-92MT-92022)
(DE94-013941; DOE/MT-92022/1) Avail: CASI HC A04/MF A01

The observed rate of increase of N2O (0.18 percent to 0.26 percent annually) is a matter of increasing concern both because N2O is a greenhouse gas and has a major and unfavorable influence on the ozone layer (Weiss, 1981). The combustion contribution to the overall nitrous oxide budget is difficult to assess; yet the emission of N2O from fluidized bed combustion (FBC) has been identified in the past few years as significant. It was concluded in the European workshop, 1988 that the emission level from a coal-fired fluidized bed boiler is 50-200 ppM but it is only 1-20 ppm in boilers equipped with other types of combustion devices. For this reason it is worthwhile to investigate the emissions from FBC more thoroughly. Gaseous fuels (Miller and Bowman, 1989), but the N2O emissions under fluidized bed conditions is poorly understood. In fluidized bed combustion, N2O can arise from homogeneous gas phase reactions involving amines and cyano species (Hiltunen et al, 1991) or it can be formed from heterogeneous reactions (eg. char oxidation). Removal of N2O can be brought about by gas phase reactions or by catalytic or non-catalytic heterogeneous reduction on char/limestone. This work was carried out with an objective of enhancing the fundamental understanding of coal and char nitrogen reaction pathways in fluidized bed combustion environment. The formation and destruction of HCN and N2O under variety of influential parameters were investigated. This simulation contained a nonisothermal single particle combustion in a preheated reactor and a gas phase reaction are designed to stimulate the nitrogen chemistry in a circulating fluidized bed. The LSODE differential equation solver used for single particle combustion and the CHEMKIN package, developed by Sandia National Laboratories, was applied for gas phase reactions. This computational work was done as an exploratory research program under the solicitation of the DOE fossil energy utilization. DOE

N95-15297# Los Alamos National Lab., NM.
SPECTROPHOTOMETRIC DETERMINATION OF PLUTONIUM-239 BASED ON THE SPECTRUM OF PLUTONIUM 3 CHLORIDE
D. J. Temer and L. F. Walker Jul. 1994 13 p
(Contract W-7405-eng-36)
(DE94-015172; LA-12765) Avail: CASI HC A03/MF A01

This report describes a spectrophotometric method for determining plutonium-239 (Pu-239) based on the spectrum of Pu(III) chloride. The authors used the sealed-reflux technique for the dissolution of plutonium oxide with hydrochloric acid (HCl) and small amounts of nitric and hydrofluoric acids. To complex the fluoride, they added zirconium, and to reduce plutonium to Pu(III), they added ascorbic acid. They then adjusted the solution to a concentration of 2 M HCl and measured the absorbances at five wavelengths of the Pu(III) chloride spectrum. This spectrophotometric

determination can also be applied to samples of plutonium metal dissolved in HCl. DOE

N95-15303* National Aeronautics and Space Administration. Lewis Research Center, Cleveland, OH.
GRAPHITE FLUORIDE FROM IODINE INTERCALATED GRAPHITIZED CARBON Patent
Ching-Cheh Hung, inventor (to NASA) 15 Feb. 1994 6 p Filed 15 May 1992 Supersedes 92N34206 (30 - 24, p 4153)
(NASA-Case-LEW-15360-1; US-Patent-5,286,471;
US-Patent-Appl-SN-884097; US-Patent-Class-423-448;
US-Patent-Class-423-460; Int-Patent-Class-C01B-31/04) Avail: US Patent and Trademark Office

Graphite fluoride is produced from graphitized carbon. A bromine iodine mixture reacts with graphitized carbon to produce iodine intercalated graphitized carbon that is then exposed to fluorine.
Official Gazette of the U.S. Patent and Trademark Office

N95-15345 Georgia Inst. of Tech., Atlanta, GA. School of Chemical Engineering.
HIGH TEMPERATURE MEMBRANES FOR H2S AND SO2 SEPARATIONS
J. Winnick 1994 29 p Limited Reproducibility: More than 20% of this document may be affected by microfiche quality
(Contract DE-FG22-90PC-90293)
(DE94-017125; DOE/PC-90293/T13) Avail: CASI HC A03

High temperature membrane separation techniques have been applied to gas mixtures involved in coal utilization. For coal gasification, H2S has been removed from the syn-gas stream, split into hydrogen which enriches the syn-gas, and sulfur which can be condensed from an inert gas sweep stream. For coal combustion, SO2 has been separated from the flue gas, with concentrated SO3 produced as a by-product. Both processes appear economically viable but each requires fundamental improvements: both the H2S and SO2 cells require more efficient membranes and the H2S cell needs a more efficient anode. Membranes will be fabricated by either hot-pressing, impregnation of sintered bodies, or tape casting. Research conducted during the present quarter is highlighted, with an emphasis on progress toward these goals. DOE

N95-15346 South Carolina Univ., Columbia, SC. Dept. of Chemistry.
THE TRANSFORMATION OF ORGANIC AMINES BY TRANSITION METAL CLUSTER COMPOUNDS
R. D. Adams Jan. 1994 20 p Limited Reproducibility: More than 20% of this document may be affected by microfiche quality
(Contract DE-FG09-84ER-13296)
(DE94-017151; DOE/ER-13296/10) Avail: CASI HC A03

In the recent year, the authors extended investigations into insertion reactions by investigating the insertion of dicarboxylate acetylene into the metal-metal bond of Re2(CO)9(NCMe). Secondly, the authors considered the ring opening reactions of the cyclic thioethers: tetrahydrothiophene and thiacyclohexane when complexed to Os3(CO)10(NCMe)2. In a third effort, various osmium complexes of cyclobutynes were synthesized and the subsequent reactivity probed. Finally, energy storage (via absorption of UV-visible photons) in osmium cluster compounds was investigated. DOE

N95-15347 Georgia Univ., Athens. Research Foundation.
THEORETICAL STUDIES OF HYDROCARBON COMBUSTION CHEMISTRY
H. F. Schaefer, III 1994 7 p Limited Reproducibility: More than 20% of this document may be affected by microfiche quality
(Contract DE-FG09-87ER-13811)
(DE94-017155; DOE/ER-13811/6) Avail: CASI HC A02

The author reports here the results of DZP CISD calculations for methylcarbene. Geometry, symmetry, and vibrational modes for the radical are reported for both the singlet and the triplet state. Future work will focus on the ethyl radical-oxygen interaction relevant to hydrocarbon combustion. DOE

N95-15352# Kentucky Univ., Lexington, KY. Dept. of Mechanical Engineering.
UPWARD FLAME SPREAD ALONG THE VERTICAL CORNER WALLS (OCTOBER 1993) Final Report
C. Qian, H. Ishida, and K. Saito Oct. 1993 46 p See also PB89-214787
(Grant NIST-60NANB2D1295)
(PB94-206299; NIST/GCR-94/648) Avail: CASI HC A03/MF A01

Flame spread behavior and the pyrolysis region spread characteristics along vertical corner walls were studied in detail with an automated infrared imaging temperature measurement technique (IR technique). The technique was recently developed for the measurement of transient pyrolysis temperature on both charring and non-charring materials. Temporal isotherms on PMMA samples were successfully obtained, from which the progress rate of the pyrolysis front was automatically deduced. It was found that the pyrolysis front shape was always M-shaped, i.e., no spread along the corner, and the maximum spread is in a few centimeters away from the corner. Understanding of the mechanism of the M-shape formation is important in developing a prediction model of the spread rate. Four possible mechanisms were identified and flame displacement effects are found to be the principal mechanism. Transient total heat flux distributions above the M-shape pyrolysis peak for a spreading fire were measured. Using these values, it was shown that the upward spread rate is predictable from simple, one-dimensional, thermal model. NTIS

N95-15353# Pennsylvania State Univ., University Park, PA. Dept. of Mechanical Engineering.
TURBULENT UPWARD FLAME SPREAD ON A VERTICAL WALL UNDER EXTERNAL RADIATION Annual Report, 30 Sep. 1991 - 15 Jan. 1993
A. K. Kulkarni, E. Brehob, S. Manohar, and R. Nair Feb. 1994 93 p See also PB92-112531
(Grant NIST-60NANB8D0849)
(PB94-207388; NIST/GCR-94/638) Avail: CASI HC A05/MF A01

The overall objective is to understand the upward flame spread phenomenon under simulated surrounding fire conditions by establishing a data base for upward flame spread under external radiation, developing a mathematical model, measuring the relevant basic material properties needed, and checking the validity of the model by comparing its results with data. Emphasis is placed on studying and predicting the behavior of practical wall materials used in building and vehicle interiors, and textiles. In the past year, the authors measured flame spread on several different materials under a range of external radiant fluxes of up to 15 kW/sq m. A model for describing the upward flame spread process was developed and numerical results were compared with data. The model needed input of certain properties, such as the burning rate characteristics and surface radiation properties. A series of supporting studies were undertaken which provided the needed input properties to the model and other useful material property data. NTIS

N95-15354# National Inst. of Standards and Technology, Gaithersburg, MD. Building and Fire Research Lab.
COMPARISON OF WALL-FIRE BEHAVIOR WITH AND WITHOUT A CEILING
H. E. Mitler and K. D. Steckler Nov. 1993 34 p See also PB85-133973
(PB94-207404; NISTIR-5380) Avail: CASI HC A03/MF A01

This paper demonstrates that the effects of the ceiling on the progress of a wall fire are quite significant, and that a project to quantify and model the effects of a ceiling on the progress of a wall fire is indeed justified. Experimental results from the open literature are used for this purpose, as well as previously unpublished experimental results obtained at NIST. The wall-fire SPREAD and the room-fire model FIRST are used seriatim to show that part of this effect can be calculated now. NTIS

N95-15370# National Inst. of Standards and Technology, Gaithersburg, MD.
OPTICALLY DRIVEN SURFACE REACTIONS: LASER PROBES OF SURFACE DYNAMICS
R. R. Cavanagh and D. S. King 1994 4 p
(Contract DE-AI05-84ER-13150)
(DE94-015311; DOE/ER-13150/T5) Avail: CASI HC A01/MF A01

The author's study of the dynamics of photodesorption of NO from Si(111) 7x7 under conditions of low NO coverage has been completed. The final results are discussed herein. In addition, studies of the

photodecomposition of MoCO6 absorbed on Si(111) have been initiated. Preliminary results and future studies are outlined. DOE

N95-15375# Sandia National Labs., Albuquerque, NM.
EFFECTS OF TWO-PHASE FLOW ON THE DEFLAGRATION OF POROUS ENERGETIC MATERIALS
S. B. Margolis (Sandia National Labs., Livermore, CA.) and F. A. Williams (California Univ., San Diego, La Jolla, CA.) Jul. 1994 33 p
(Contract DE-AC04-94AL-85000)
(DE94-015353; SAND-94-8649) Avail: CASI HC A03/MF A01

Theoretical analyses are developed for the multi-phase deflagration of porous energetic solids, such as degraded nitramine propellants, that experience significant gas flow in the solid preheat region and are characterized by the presence of exothermic reactions in a bubbling melt layer at their surfaces. Relative motion between the gas and condensed phases is taken into account in both regions, and expressions for the mass burning rate and other quantities of interest, such as temperature and volume-fraction profiles, are derived by activation-energy asymptotics. The model extends recent work by allowing for gas flow in the unburned solid, and by incorporating pressure effects through the gas-phase equation of state. As a consequence, it is demonstrated how most aspects of the deflagration wave, including its structure, propagation speed and final temperature, depend on the local pressure in the two-phase regions. DOE

N95-15386# Xavier Univ. of Louisiana, New Orleans, LA. Dept. of Physics/Engineering.
INVESTIGATION OF SYNGAS INTERACTION IN ALCOHOL SYNTHESIS CATALYSTS
10 Feb. 1994 7 p
(Contract DE-FG22-93MT-93010)
(DE94-013939; DOE/MT-93010/1) Avail: CASI HC A02/MF A01

The project establishes the necessary experiment and laboratory facilities at Xavier University. This phase of the work has taken a considerable amount of time, due to the limited laboratory space and the involved administrative policies and procedures in procuring the necessary chemicals, glassware, and auxiliary supplies. Though there still remain some minor problems with space, the laboratory is now equipped for preparation of catalysts. During this period, the authors focused their attention toward analyzing the magnetic nature of extensively used trimetallic catalyst system Cu-Co-Cr for the production of higher alcohols. The authors decided to investigate the effect of method of preparation and intermetallic ratio on the magnetic behavior of the system. DOE

N95-15387# Los Alamos National Lab., NM.
PROTOTYPE EXPLOSIVES-DETECTION SYSTEM BASED ON NUCLEAR-RESONANCE ABSORPTION IN NITROGEN
R. E. Morgado, G. Arnone, C. C. Cappiello, S. D. Gardner, C. L. Hollas, L. E. Ussery, J. M. White, J. D. Zahrt, and R. A. Krauss Jun. 1994 13 p
(Contract W-7405-eng-36)
(DE94-015069; LA-12776-MS) Avail: CASI HC A03/MF A01

A prototype explosives-detection system (EDS) that was developed for experimental evaluation of a nuclear-resonance absorption technique is described. The major subsystems are a proton accelerator and beam transport, high-temperature proton target, an airline-luggage tomographic inspection station, and an image-processing/detection-alarm subsystem. The detection system performance, based on a limited experimental test, is reported. DOE

N95-15408 Lawrence Livermore National Lab., Livermore, CA.
CORE-LEVEL SPECTROSCOPY OF THIN OXIDES AND OXYNITRIDES
F. J. Himpsel (International Business Machines Corp., Yorktown Heights, NY.), H. Akatsu (International Business Machines Corp., Yorktown Heights, NY.), and J. A. Carlisle 19 Jul. 1994 10 p Presented at the 185th Electrochemical Society Meeting, San Francisco, CA, 22-27 May 1994 Limited Reproducibility: More than 20% of this document may be affected by microfiche quality
(Contract W-7405-eng-48)
(DE94-016598; UCRL-JC-117504; CONF-940529-20) Avail: CASI HC A02

Several spectroscopic methods are discussed that use core levels, such as photoelectron spectroscopy and absorption spectroscopy with photoelectron or fluorescence detection. Measurements are presented on the desorption of a chemical oxide and the growth of oxynitrides with N20 on Si(100). The stoichiometry is found to change strongly with thickness, from a nitrogen-terminated Si surface to a nearly-pure oxide in the outer region of 40--60 (Angstrom) films. Using a third generation synchrotron beam line a sensitivity of better than a tenth of a monolayer is achieved by a simple photocurrent measurement. DOE

N95-15436# EG and G Energy Measurements, Inc., Idaho Falls, ID.
A THEORETICAL STUDY OF 30 TO 50 ANGSTROM NOBLE GAS HEAVY ION LITHOGRAPHY
C. B. Nelson and H. Makowitz Feb. 1994 11 p
(Contract DE-AC07-76ID-01570)
(DE94-015262; EGG-MS-11063) Avail: CASI HC A03/MF A01

The feasibility of using heavy noble gas ions to etch 30 to 50 (Angstrom) wide lines in polymethylmethacrylate (PMMA) on a silicon substrate was investigated. The TRIM91 computer code was used to model point sources of neon, argon, xenon, krypton, or uranium ions penetrating a two-dimensional geometry consisting of a 50 (Angstrom) layer of PMMA over a 50 (Angstrom) layer of silicon. For ions with a kinetic energy less than 500 e, the energy deposition is so confined that the proximity effect is virtually nonexistent. These and other considerations indicate that heavy noble gas ions may be ideal for etching angstrom-level features in this geometry. DOE

N95-15512*# National Aeronautics and Space Administration. Lewis Research Center, Cleveland, OH.
LSENS, A GENERAL CHEMICAL KINETICS AND SENSITIVITY ANALYSIS CODE FOR HOMOGENEOUS GAS-PHASE REACTIONS. 2: CODE DESCRIPTION AND USAGE
Krishnan Radhakrishnan (NYMA, Inc., Brook Park, OH.) and David A. Bittker Feb. 1994 153 p
(RTOP 505-62-52)
(NASA-RP-1329; E-5140-2; NAS 1.61:1329) Avail: CASI HC A08/MF A02

LSENS, the Lewis General Chemical Kinetics Analysis Code, has been developed for solving complex, homogeneous, gas-phase chemical kinetics problems and contains sensitivity analysis for a variety of problems, including nonisothermal situations. This report is part 2 of a series of three reference publications that describe LSENS, provide a detailed guide to its usage, and present many example problems. Part 2 describes the code, how to modify it, and its usage, including preparation of the problem data file required to execute LSENS. Code usage is illustrated by several example problems, which further explain preparation of the problem data file and show how to obtain desired accuracy in the computed results. LSENS is a flexible, convenient, accurate, and efficient solver for chemical reaction problems such as static system; steady, one-dimensional, inviscid flow; reaction behind incident shock wave, including boundary layer correction; and perfectly stirred (highly backmixed) reactor. In addition, the chemical equilibrium state can be computed for the following assigned states: temperature and pressure, enthalpy and pressure, temperature and volume, and internal energy and volume. For static problems the code computes the sensitivity coefficients of the dependent variables and their temporal derivatives with respect to the initial values of the dependent variables and/or the three rate coefficient parameters of the chemical reactions. Part 1 (NASA RP-1328) derives the governing equations describes the numerical solution procedures for the types of problems that can be solved by ISENS. Part 3 (NASA RP-1330) explains the kinetics and kinetics-plus-sensitivity-analysis problems supplied with LSENS and presents sample results. Author

N95-15541 Wisconsin Univ., Madison, WI. Dept. of Physics.
SOLID TARGET BORONIZATION OF THE MST REVERSED-FIELD PINCH DURING PULSED DISCHARGE CLEANING
D. J. DenHartog and R. D. Kendrick Jun. 1994 14 p Presented at the 11th International Conference on Plasma Surface Interactions in Controlled Fusion Devices, Mito, Japan, 23-27 May 1994 Limited Reproducibility: More than 20% of this document may be affected by microfiche quality
(Contract DE-FG02-85ER-53198)
(DE94-015535; DOE/ER-53198/242; CONF-940580-7) Avail: CASI HC A03

concept of measuring the conductivity directly using a second vertical derivative of H(sub z). Conductivity profiles interpreted from field data using this technique reproduced accurately the electrical logs for a test site near Devine, Texas. It was found in this study that the inversion techniques are more stable when the first vertical derivative of H(sub z) is used rather than H(sub z) itself. Using data from a salt water injection experiment at the Richmond Field test site in Berkeley it was also found that these robust layer inversions were successful in identifying the preferential flow direction of the injected brine to four boreholes surrounding the injection well. DOE

N95-15871# Technische Univ., Delft (Netherlands).
SELECTIVE RF PULSES IN NMR AND THEIR EFFECT ON COUPLED AND UNCOUPLED SPIN SYSTEMS Ph.D. Thesis
J. Slotboom 4 Oct. 1993 194 p
(PB94-195526; ISBN-90-6275-907-6) Copyright Avail: CASI HC A09/MF A03

This thesis describes various aspects of the usage of shaped RF-pulses for volume selection and spectral editing. Contents: Introduction--The History of Magnetic Resonance in a Nutshell, and The Usage of RF Pulses in Contemporary MRS and MRI; Theoretical and Practical Aspects of Localized NMR Spectroscopy; The Effects of RF Pulse Shape Discretization on the Spatially Selective Performance; Design of Frequency-Selective RF Pulses by Optimizing a Small Number of Pulse Parameters; A Single-Shot Localization Pulse Sequence Suited for Coils with Inhomogeneous RF Fields Using Adiabatic Slice-Selective RF Pulses; The Bloch Equations for an AB System and the Design of Spin State Selective RF Pulses for Coupled Spin Systems; The Effects of Frequency Selective RF Pulses on J Coupled Spin-1/2 Systems; A Quantitative (1)H MRS in vivo Study of the Effects of L-Ornithine-L-Aspartate on the Development of Mild Encephalopathy Using a Single Shot Localization Technique Based on SAR Reduced Adiabatic 2(pi) Pulses. NTIS

N95-13826# Indian Space Research Organization, Ahmedabad. Space Application Centre.
SATELLITE COMMUNICATION TECHNOLOGY AND APPLICATIONS, 1995-2010
N. Pant *In* ISRO Satellite Centre, Journal of Spacecraft Technology, Volume 4, No. 2, July 1994 Jul. 1994 p 1-28 (For primary document see N95-13825 03-12)
Avail: CASI HC A03/MF A01

N95-13832# ISRO Satellite Centre, Peenya, Bangalore (India).
A SIMULATION ALGORITHM FOR AVAILABILITY COMPUTATION OF A COMMUNICATION SATELLITE CONSTELLATION
P. S. Rajeshwari, V. N. Purohit, N. Ramani, and R. D. Gambhir *In its* Journal of Spacecraft Technology, Volume 4, No. 2, July 1994 Jul. 1994 p 68-77 (For primary document see N95-13825 03-12)
Avail: CASI HC A02/MF A01

N95-13900*# Tianjin Univ. (China). Dept. of Physics.
HIGH-ORDER SQUEEZING OF THE QUANTUM ELECTROMAGNETIC FIELD AND THE GENERALIZED UNCERTAINTY RELATIONS IN TWO-MODE SQUEEZED STATES
Xi-Zeng Li and Bao-Xia Su *In* NASA. Goddard Space Flight Center, Third International Workshop on Squeezed States and Uncertainty Relations May 1994 p 33-37 Sponsored by National Natural Science Foundation of China (For primary document see N95-13896 03-74)
Avail: CASI HC A01/MF A06

N95-13921*# Seoul National Univ. (Republic of Korea). Dept. of Physics.
A METHOD OF MEASURING THE AMPLITUDE-MODULATED VACUUM FIELD NEAR A CONDUCTING MIRROR
Sun-Hyun Youn, Jai-Hyung Lee, and Joon-Sung Chang *In* NASA. Goddard Space Flight Center, Third International Workshop on Squeezed States and Uncertainty Relations May 1994 p 195-202 (For primary document see N95-13896 03-74)
Avail: CASI HC A02/MF A06

N95-13922*# Universidad Nacional Autonoma de Mexico, Mexico City. Centro de Instrumentos.
HOW TO CHARACTERIZE THE NONLINEAR AMPLIFIER?
Dmitri Kouznetsov Kallistratova (Academy of Sciences, USSR, Moscow, USSR.) and Carlos Flores Cotera *In* NASA. Goddard Space Flight Center, Third International Workshop on Squeezed States and Uncertainty Relations May 1994 p 203-206 Sponsored in part by Comitet Nacional de Ciencia y Technologia (For primary document see N95-13896 03-74)
Avail: CASI HC A01/MF A06

N95-14283*# Hughes STX, Inc., Greenbelt, MD.
RADAR ALTIMETER CALIBRATION USING SLR
Steven M. Klosko *In* NASA. Goddard Space Flight Center, Satellite Laser Ranging in the 1990s: Report of the 1994 Belmont Workshop Nov. 1994 p 71-76 (For primary document see N95-14274 03-46)
Avail: CASI HC A02/MF A02

N95-14285*# Maryland Univ., College Park, MD.
SLR TRACKING OF GPS-35
Erricos C. Pavlis *In* NASA. Goddard Space Flight Center, Satellite Laser Ranging in the 1990s: Report of the 1994 Belmont Workshop Nov. 1994 p 81-84 (For primary document see N95-14274 03-46)
Avail: CASI HC A01/MF A02

N95-14286*# Texas Univ., Austin, TX. Center for Space Research.
SYNERGISM OF SLR AND GPS
Bob E. Schutz *In* NASA. Goddard Space Flight Center, Satellite Laser Ranging in the 1990s: Report of the 1994 Belmont Workshop Nov. 1994 p 85-86 (For primary document see N95-14274 03-46)
Avail: CASI HC A01/MF A02

N95-14288*# National Aeronautics and Space Administration. Goddard Space Flight Center, Greenbelt, MD.
SLR 2000
John J. Degnan *In its* Satellite Laser Ranging in the 1990s: Report of the 1994 Belmont Workshop Nov. 1994 p 101-106 (For primary document see N95-14274 03-46)
Avail: CASI HC A02/MF A02

N95-14289*# National Aeronautics and Space Administration. Goddard Space Flight Center, Greenbelt, MD.
A STRAWMAN SLR PROGRAM PLAN FOR THE 1990S
John J. Degnan *In its* Satellite Laser Ranging in the 1990s: Report of the 1994 Belmont Workshop Nov. 1994 p 107-114 (For primary document see N95-14274 03-46)
Avail: CASI HC A02/MF A02

33 ELECTRONICS AND ELECTRICAL ENGINEERING

Includes test equipment and maintainability; components, e.g., tunnel diodes and transistors; microminiaturization; and integrated circuitry.

For related information see also *60 Computer Operations and Hardware* and *76 Solid-State Physics.*

N95-13684# Argonne National Lab., IL.
MATERIALS AND MECHANISMS OF HIGH TEMPERATURE LITHIUM SULFIDE BATTERIES
T. D. Kaun, M. C. Hash, G. L. Henriksen, A. N. Jansen, and D. R. Vissers May 1994 26 p Presented at the 2nd Chilean Lithium Symposium, Santiago, Chile, 24-27 May 1994
(Contract W-31-109-eng-38)
(DE94-012634; ANL/CMT/CP-82954; CONF-9405130-3) Avail: CASI HC A03/MF A01

New materials have encouraged development of bipolar Li-Al/FeS2 batteries for electric vehicle (EV) applications. Current technology employs a two-phase Li-alloy negative electrode low-melting, LiCl-rich LiCl-LiBr-KBr molten salt electrolyte, and either an FeS or an upper-plateau (UP) FeS2 positive electrode. These components are assembled in a sealed bipolar

battery configuration. Use of the two-phase Li-alloy (alpha + beta Li-Al and Li5Al5Fe2) negative electrode provides in situ overcharge tolerance that renders the bipolar design viable. Employing LiCl-rich LiCl-LiBr-KBr electrolyte in 'electrolyte-starved' cells achieves low-burdened cells that possess low area-specific impedance, comparable to that of flooded cells using LiCl-LiBr-KBr eutectic electrolyte. The combination of dense UP FeS2 electrodes and low-melting electrolyte produces a stable and reversible couple, achieving over 1000 cycle life in flooded cells, with high power capabilities. In addition, a family of stable sulfide ceramic/sealant materials was developed that produce high-strength bonds between a variety of metals and ceramics, which renders lithium/iron suffide bipolar stacks practical. Bipolar Li-Al/FeS2 cells and four-cell stacks using these seals are being built and tested in the 13 cm diameter size for EV applications. To date, Li-Al/FeS2 cells have attained 400 W/kg power at 80% DOD and 180 Wh/kg energy at the 30 W/kg rate. When cell performance characteristics are used to model full-scale EV and hybrid vehicle (HV) batteries, they are projected to meet or exceed the performance requirements for a large variety of EV and HV applications. Efficient production and application of Li-alloys and Li-salt electrolyte are critical to approaching battery cost objectives. DOE

N95-13685# CryoPower Associates, Los Alamos, NM.
HIGH TEMPERATURE SUPERCONDUCTORS WITH IMPROVED CURRENT DENSITIES Final Report, 1 Jul. 1991 - 30 Jun. 1993
H. L. Laquer 15 Jun. 1994 13 p
(Contract F49620-91-C-0065)
(AD-A282996; AFOSR-94-0467TR) Avail: CASI HC A02/MF A01

We have developed a novel technique for processing bulk high temperature superconductors and other ceramics under precisely controlled conditions of pressure, temperature, atmospheric composition, and strain rate. We achieve essentially uni-axial deformation of a pre-compacted disc inside a bellows-like capsule with massive end plates or 'anvils'. The capsule is located inside a Hot Isostatic Press (HIP), but has an independent gas supply. This makes it possible to maintain a specified gaseous atmosphere within the capsule and exert considerable forces on its contents via the anvils, simply by manipulating the two gas pressures. We call the process Differential Pressure HIP Forging, or DPHF, and are filing a patent application on the modifications to the, otherwise, conventional apparatus. DPHF opens a new regime for processing sensitive materials at elevated pressures and temperatures. DTIC

N95-13824* National Aeronautics and Space Administration. Pasadena Office, CA.
THIN COMPOSITE SOLID ELECTROLYTE FILM FOR LITHIUM BATTERIES Patent
Emmanuel Peled, inventor (to NASA), Ganesan Nagasubramanian, inventor (to NASA), Gerald Halpert, inventor (to NASA), and Alan I. Attia, inventor (to NASA) 1 Nov. 1994 9 p Filed 20 Aug. 1993 Supersedes N94-17325 (32 - 3, p 1014)
(Contract NAS7-918)
(NASA-Case-NPO-18694-1-CU; US-Patent-5,360,686;
US-Patent-Appl-SN-112483; US-Patent-Class-429-191;
US-Patent-Class-429-192; Int-Patent-Class-H01M-6/18) Avail: US Patent and Trademark Office

A composite solid electrolyte film for a lithium battery comprising a dispersion of small reinforcing particles such as alumina in a binder rein such as polyethylene oxide is presented. The particles are coated with a compatible lithium salt such as lithium iodide and the alumina particles preferably have a size below 0.5 microns.
Official Gazette of the U.S. Patent and Trademark Office

N95-13975# Sandia National Labs., Albuquerque, NM.
ASSEMBLY FEASIBILITY AND RELIABILITY STUDIES OF SURFACE MOUNT CIRCUIT BOARDS MANUFACTURED WITH LEAD-FREE SOLDERS
P. T. Vianco, I. Artaki, A. M. Jackson, and J. H. Sampala 1994 23 p Presented at the Surface Mount International Meeting, San Jose, CA, 28 Aug. - 1 Sep. 1994
(Contract DE-AC04-94AL-85000)
(DE94-013783; SAND-94-0140C; CONF-9408109-2) Avail: CASI HC A03/MF A01

Manufacturing feasibility and reliability evaluations were performed on circuit board test vehicles assembled with the lead-free solders 96.5Sn-3.5Ag (T(sub eut) = 221 C) and 58Bi-42Sn (T(sub eut) = 138 C). Manufacturability was assessed by defect analysis of the test vehicles. The reliability evaluation was performed by thermal cycling selected test vehicles for 1000, 2500, and 5000 cycles (0-100 C and 30 min cycles); the quantitative and qualitative metrics were solder joint strength and joint microstructure, respectively. Both lead-free solders demonstrated adequate assembly performance. A slightly reduced degree of spreading (wetting) was the predominant defect which was largely attributed to nonoptimized paste components. Fatigue damage in the form of grain boundary and/or phase boundary sliding resulted from thermal cycling of the 96.5Sn-3.5Ag and 58Bi-42Sn solder joints. The damage was distributed primarily in the solder located between the lead or termination and the pad. The absence of well developed cracks allowed the joints to maintain structural integrity, even when fatigue damage was appreciable. DOE

N95-13983 Technische Univ., Delft (Netherlands).
AUTOMATED HIERARCHICAL TESTABLE DESIGN OF DIGITAL CIRCUITS Ph.D. Thesis
M. Kraak 23 Mar. 1993 150 p Limited Reproducibility: More than 20% of this document may be affected by microfiche quality
(PB94-197936) Avail: CASI HC A07

The thesis gives an overview of approaches dealing with the selection of test strategies and methods for digital circuits and the incorporation of test in designs. A review is provided of existing testability analyzers. A new way to analyze testability at three hierarchical levels of abstraction is presented. It is shown how this approach is contained in an expert system rule-base called TRI Stage Testability Analysis (TRISTAN). The paper then deals with testability synthesis. It is shown that a new synthesis method had to be devised to be able to hierarchically select test strategies and methods. The testability synthesizer is also contained in a rule-base, called Intelligent Synthesis of Testable Designs (ISOLDE). TRISTAN and ISOLDE are parts of an expert system called WAGNER. The knowledge processor for WAGNER is covered, presenting its knowledge representation scheme, knowledge acquisition and inference mechanism. Results of experiments done with WAGNER on board and chip level designs are given. Conclusive remarks provide an outlook to continued research. NTIS

N95-14112*# National Aeronautics and Space Administration. Langley Research Center, Hampton, VA.
TACTILE DISPLAY DEVICE USING AN ELECTRORHEOLOGICAL FLUID Patent Application
H. Douglas Garner, inventor (to NASA) 4 Aug. 1994 17 p
(NASA-Case-LAR-14860-1; NAS 1.71:LAR-14860-1;
US-Patent-Appl-SN-286031) Avail: CASI HC A03/MF A01

A tactile display device utilizes an electrorheological fluid to activate a plurality of tactile dots. A voltage is selectively produced uniformly across an electrorheological fluid flowing between a common ground electrode and a plurality of conductive dot electrodes, thereby producing an increase in the fluid's viscosity to the extent that fluid flow between the two electrodes is restricted. The flow restriction produces a build-up of electrorheological fluid in a corresponding dot actuator chamber. The resulting pressure increase in the chamber displaces an elastic diaphragm fixed to a display surface to form a lump which can be perceived by the reader as one dot in a Braille character cell. A flow regulation system provides a continually pressurized flow system and provides for free flow of the electrorheological fluid through the plurality of dot actuator chambers when they are not activated. The device is adaptable to printed circuit techniques and can simultaneously display tactile dots representative of a full page of Braille characters stored on a medium such as a tape cassette or to display tactile dots representative of non-Braille data appearing on a computer monitor or contained on another data storage medium. In an alternate embodiment, the elastic diaphragm drives a plurality of spring-loaded pins provided with positive stops to maintain consistent displacements of the pins in both their actuated and nonactuated positions. NASA

N95-14149# Technische Univ., Delft (Netherlands).
FISH METHOD: INTERACTION BETWEEN AC-MACHINES AND SWITCHING POWER CONVERTERS Ph.D. Thesis
A. Veltman 25 Jan. 1994 245 p
(PB94-191210; ISBN-90-9006763-9) Avail: CASI HC A11/MF A03

When studying the complex interaction between AC-machines and

converters, proper simulation models are necessary. This thesis is devoted to a new viewpoint on this complex matter: the Fish Method. Based on a seemingly reckless simplification of the machine model, the fish method provides a simple approximate mathematical description between switching pattern and stator current in terms of flux. A coordinate transformation of the stator flux orbit renders a graph that can be seen as a unique switching pattern's signature: the flux-fish. The transformed current orbit of almost the same shape is called the current-fish. Some size-related flux-fish characteristics are incorporated into a generally applicable quality criterion, independent of machine parameters, enabling straightforward switching pattern comparison. The performance of any switching converter that operates at a fixed frequency output can be evaluated in a graphical and numerical way by means of transforming the terminal voltages into a flux fish. At a single glance, the graphical flux fish shows a lot of information to the trained eye. NTIS

N95-14261# Lawrence Livermore National Lab., Livermore, CA.
DESIGN OF RELIABLE HIGH VOLTAGE AVALANCHE TRANSISTOR PULSERS
E. S. Fulkerson and R. Booth Jun. 1994 8 p Presented at the 21st International Power Modulator Symposium, Costa Mesa, CA, 28-30 Jun. 1994
(Contract W-7405-eng-48)
(DE94-015323; UCRL-JC-116309; CONF-940678-5) Avail: CASI HC A02/MF A01

Avalanche transistor based pulsers were developed for use as pockel cell drivers and for impulse radar work. The output voltages range from 1 to 8kV, with rise times of 100 to 200 picoseconds and repetition rates in excess of 1kHz. Several of these units have been in service for over a year with no failures. The design of these units is discussed in detail, including circuit design, component selection, diagnostics, and the all important physical layout. DOE

N95-14294* National Aeronautics and Space Administration. Langley Research Center, Hampton, VA.
INDUCTION HEATING COUPLER Patent
Robert L. Fox, inventor (to NASA), Carl E. Copeland, inventor (to NASA), Robert J. Swaim, inventor (to NASA), Robert H. Coultrip, inventor (to NASA), David F. Johnston, inventor (to NASA), W. Morris Phillips, inventor (to NASA), Samuel D. Johnson, inventor (to NASA), James R. Dinkins, inventor (to NASA), and John D. Buckley, inventor (to NASA) 27 Sep. 1994 14 p Filed 12 May 1993
(NASA-Case-LAR-14278-1; US-Patent-5,350,902;
US-Patent-Appl-SN-060940; US-Patent-Class-219-633;
US-Patent-Class-219-659; US-Patent-Class-219-670;
US-Patent-Class-219-635; US-Patent-Class-156-380.2;
Int-Patent-Class-H05B-6/14) Avail: US Patent and Trademark Office

An induction heating device includes a handle having a hollow interior and two opposite ends, a wrist connected to one end of the handle, a U-shaped pole piece having two spaced apart ends, a tank circuit including an induction coil wrapped around the pole piece and a capacitor connected to the induction coil, a head connected to the wrist and including a housing for receiving the U-shaped pole piece, the two spaced apart ends of the pole piece extending outwardely beyond the housing, and a power source connected to the tank circuit. When the tank circuit is energized and a susceptor is placed in juxtaposition to the ends of the U-shaped pole piece, the susceptor is heated by induction heating due to magnetic flux passing between the two ends of the pole piece.
Official Gazette of the U.S. Patent and Trademark Office

N95-14302*# National Aeronautics and Space Administration. Lewis Research Center, Cleveland, OH.
ADVANCED SOLAR CELLS FOR SATELLITE POWER SYSTEMS
Dennis J. Flood and Irving Weinberg Nov. 1994 11 p
(RTOP 233-01-0A)
(NASA-TM-106777; E-9229; NAS 1.15:106777) Avail: CASI HC A03/MF A01

The multiple natures of today's space missions with regard to operational lifetime, orbital environment, cost and size of spacecraft, to name just a few, present such a broad range of performance requirements to be met by the solar array that no single design can suffice to meet them all. The result is a demand for development of specialized solar cell types that help to optimize overall satellite performance within a specified cost range for any given space mission. Historically, space solar array performance has been optimized for a given mission by tailoring the features of silicon solar cells to account for the orbital environment and average operating conditions expected during the mission. It has become necessary to turn to entirely new photovoltaic materials and device designs to meet the requirements of future missions, both in the near and far term. This paper will outline some of the mission drivers and resulting performance requirements that must be met by advanced solar cells, and provide an overview of some of the advanced cell technologies under development to meet them. The discussion will include high efficiency, radiation hard single junction cells; monolithic and mechanically stacked multiple bandgap cells; and thin film cells. Author

N95-14308# Sandia National Labs., Albuquerque, NM.
RESONATOR RESPONSE TO NON-NEWTONIAN FLUIDS
S. J. Martin, T. W. Schneider, G. C. Frye, R. W. Cernosek, and S. D. Senturia 1994 11 p Presented at the 186th Meeting of the Electrochemical Society, Miami, FL, 9-14 Oct. 1994
(Contract DE-AC04-94AL-85000)
(DE94-013450; SAND-94-1308C; CONF-941063-3) Avail: CASI HC A03/MF A01

The thickness-shear mode (TSM) resonator typically consists of a thin disk of AT-cut quartz with circular electrodes patterned on both sides. An RF voltage applied between these electrodes excites a shear mode mechanical resonance when the excitation frequency matches the crystal resonant frequency. When the TSM resonator is operated in contact with a liquid, the shear motion of the surface generates motion in the contacting liquid. The liquid velocity field, v(sub x)(y), can be determined by solving the one-dimensional Navier-Stokes equation. Newtonian fluids cause an equal increase in resonator motional resistance and reactance, R(sub 2)(sup (N) = X(sub 2)(sup (N), with the response depending only on the liquid density-viscosity product (rho(eta)). Non-Newtonian fluids, as illustrated by the simple example of a Maxwell fluid, can cause unequal increases in motional resistance and reactance. For the Maxwell fluid, R(sub 2)(sup (M) greater than X(sub 2)(sup (M), with relaxation time tau proportional to the difference between R(sub 2)(sup (M) and X(sub 2)(sup (M). Early results indicate that a TSM resonator can be used to extract properties of non-Newtonian fluids. DOE

N95-14310# Sandia National Labs., Albuquerque, NM.
QUARTZ RESONATOR STATE-OF-CHARGE MONITOR FOR LEAD-ACID BATTERIES
R. W. Cernosek, S. J. Martin, K. O. Wessendorf, and A. N. Rumpf 1994 6 p Presented at the 186th Meeting of the Electrochemical Society, Miami, FL, 9-14 Oct. 1994
(Contract DE-AC05-84OR-21400)
(DE94-013823; SAND-94-1244C; CONF-941063-5) Avail: CASI HC A02/MF A01

We have demonstrated that a thickness shear mode quartz resonator can be used as a real-time, in situ monitor of the state-of-charge of lead-acid batteries. The resonator is sensitive to changes in the density and viscosity of the sulfuric acid electrolyte. Both of these liquid parameters vary monotonically with the battery state-of-charge. This new monitor is more precise than sampling hydrometers, and since it is compatible with the corrosive electrolyte environment, it can be used for in situ monitoring. A TSM resonator consists of gold electrodes deposited on opposite surfaces of a thin AT-cut quartz crystal. When an RF voltage is applied to the electrodes, a shear strain is introduced in the piezoelectric quartz and mechanical resonance occurs between the surfaces. A liquid in contact with one of the quartz surfaces is viscously entrained, which perturbs the resonant frequency and resonance magnitude. If the surface is smooth, the changes in both frequency and magnitude are proportional to (rho(eta))(exp (1/2)), where rho is the liquid density and eta is the viscosity. DOE

N95-14314# Sandia National Labs., Albuquerque, NM.
I(SUB DDQ) TESTING FOR ULTIMATE LOW POWER DESIGN VERIFICATION AND DEFECT DETECTION
C. F. Hawkins (New Mexico Univ., Albuquerque, NM.), F. W. Hewlett, and J. M. Soden 1994 3 p Presented at the Symposium on Low-Power Electronics, San Diego, CA, 10-12 Oct. 1994

(Contract DE-AC04-94AL-85000)
(DE94-014281; SAND-94-1316C; CONF-941087-1) Avail: CASI HC A01/MF A01

I(sub DDQ) testing is mandatory to ensure that low power CMOS IC's meet their design intent. I(sub DDQ) testing is both a design verifier for low quiescent current and a sensitive production test for defects. Quiescent power reduction is particularly important for products such as cardiac pacemakers, laptop computers, and cellular telephones. DOE

N95-14315# Sandia National Labs., Albuquerque, NM.
CUT-OFF-MESA ISOLATED RIB OPTICAL WAVEGUIDE FOR 3-5 HETEROSTRUCTURE PICs
G. A. Vawter and R. E. Smith 1994 3 p Presented at the Annual Conference of the Optical Society of America and Exhibit, Boston, MA, 30 Oct. - 4 Nov. 1994
(Contract DE-AC04-94AL-85000)
(DE94-014661; SAND-94-1503C; CONF-941006-1) Avail: CASI HC A01/MF A01

A new waveguide is designed using a cut-off slab waveguide for fabrication of single-mode rib optical waveguides with mesa isolation. These waveguides are easy to fabricate and offer crosstalk performance perhaps better than BH waveguides. DOE

N95-14319# Sandia National Labs., Albuquerque, NM.
A COMPACT HIGH VOLTAGE PULSE GENERATOR
G. J. Rohwein and S. R. Babcock 1994 3 p Presented at the 21st International Power Modulator Symposium, Costa Mesa, CA, 27-30 Jul. 1994
(Contract DE-AC04-94AL-85000)
(DE94-015282; SAND-94-1782C; CONF-9407102-1) Avail: CASI HC A01/MF A01

A compact, easily transportable, pulse generator has been developed for a variety of applications that require a pulse duration in the range of 1 mu sec., voltages from 150 to 300 KV and current levels from 2,000 to 3,000 amps. The generator has a simple cylindrical configuration and modular construction to facilitate assembly and service. The generator may be operated single-pulse or repetitively at pulse repetition rates to 50 Hz in a burst mode. DOE

N95-14355# Illinois Univ., Urbana, IL. Coordinated Science Lab.
A GATE LEVEL SIMULATOR FOR ALPHA-PARTICLE-INDUCED TRANSIENT FAULTS
Hungse Cha 22 Aug. 1994 110 p
(Contract N00014-90-J-1270)
(AD-A283871; UILU-ENG-94-2228; CRHC-94-13) Avail: CASI HC A06/MF A02

Mixed analog and digital mode simulators have been available for accurate alpha-particle-induced transient fault simulation. However, they are not fast enough to simulate a large number of transient faults on a relatively large circuit in a reasonable amount of time. This thesis describes a fast transient fault simulator which can evaluate the effects of alpha-particle hits or single event upsets (SEU's) in CMOS standard cell based synchronous sequential VLSI circuits. The speed comes from approximating the initial analog effects with gate level models, as well as using an improved transient fault simulation algorithm in a hierarchy of simulators. The simulator is shown to be between four to five orders of magnitude faster than a very accurate circuit simulator at the expense of some accuracy and some limitations on the types of circuits simulatable. Using this simulator, benchmark circuits have been tested for their behavior under alpha-particle injections. The experiment show that the one bit flip model is not a good model for injecting faults in highly fault tolerant systems. The experiments also show that at the pin level, no simple model exists which can mimic the behavior of the circuit hit with the alpha particle. The simulator's usefulness is also shown in the development of a transient pulse tolerant D flip-flop (DFF). The tool is used to demonstrate the tradeoff between transient pulse tolerance and latch performance. DTIC

N95-14359# Massachusetts Inst. of Tech., Cambridge.
DAMAGE ANALYSIS OF INTERNAL FAULTS IN FLUX CONCENTRATING PERMANENT MAGNET MOTORS M.S. Thesis
Francis R. Colberg Jun. 1994 139 p
(Contract N00123-89-G-0380)
(AD-A283883) Avail: CASI HC A07/MF A02

It is the purpose of the proposed research to develop a digital computer simulation model to study the effects of an internal fault in a large permanent magnet ac synchronous motor. Permanent magnet motors are being considered as an alternative for ships with electric propulsion systems. In an electric propulsion system a large motor will be directly connected to a propulsion shaft. A windmilling shaft will continue to turn the rotor of the propulsion motor after the motor has been disconnected from its electrical power supply source. Following an internal electrical fault in a propulsion motor, it is expected that the motor will be disconnected from its electrical supply source. With the ship operation at or near rated speed following a casualty to the propulsion plant, the ship will coast down to a stop or until the crew takes action to stop the ship. A windmilling permanent magnet motor will generate a large enough internal voltage to continue to support large fault currents. This research will focus on the fault transient and the motor behavior during the time that the propulsion shaft is windmilling. Shorting the motor terminals will be considered as a means of reducing the power input into the fault. DTIC

N95-14401# National Inst. of Standards and Technology, Gaithersburg, MD. Semiconductor Electronics Div.
SEMICONDUCTOR MEASUREMENT TECHNOLOGY: IMPROVED CHARACTERIZATION AND EVALUATION MEASURMENTS FOR HgCdTe DETECTOR MATERIALS, PROCESSES, AND DEVICES USED ON THE GOES AND TIROS SATELLITES
David G. Seiler, Jeremiah R. Lowney, W. Robert Thurber, Joseph J. Kopanski, and George G. Harman Washington GPO Apr. 1994 188 p
(PB94-188810; NIST/SP-400-94) Avail: CASI HC A09/MF A02; SOD HC

An extensive study was carried out to improve the characterization and evaluation methods used for HgCdTe (mercury cadmium telluride) photoconductive infrared detectors used in GOES and TIROS satellites. High-field magnetotransport techniques were used to determine the electrical properties of the detector accumulation layers, which partially control their detectivities. Assessments were made of the quality of the bonding and packaging used in detector fabrication, and a list of recommended practices was produced. The applicability of scanning capacitance microscopy and test structures to detector-array evaluation is discussed, and finally recommendations are made for standardized detector calibration. The results of this work have provided new and more refined measurement methods that can be adapted by the detector manufacturers to improve performance and yield. NTIS

N95-14402# National Inst. of Standards and Technology, Gaithersburg, MD. Semiconductor Electronics Div.
ELECTRONICS AND ELECTRICAL ENGINEERING LABORATORY TECHNICAL PROGRESS BULLETIN COVERING LABORATORY PROGRAMS, JANUARY TO MARCH 1994 WITH 1994/1995 EEEL EVENTS CALENDAR
J. M. Rohrbaugh, comp. Jun. 1994 50 p
(PB94-193810; NISTIR-5434) Avail: CASI HC A03/MF A01

This is the forty-sixth issue of a quarterly publication providing information on the technical work of the National Institute of Standards and Technology, Electronics and Electrical Engineering Laboratory (EEEL). This issue of the EEEL Technical Progress Bulletin covers the first quarter of calendar year 1994. Abstracts are provided by technical area for both published papers and papers approved by NIST for publication. Major subject headings include the following: fundamental electrical measurements; semiconductor microelectronics; signal acquisition; processing and transmission; electrical systems; electromagnetic interference; and video technology. NTIS

N95-14425# International Business Machines Corp., San Jose, CA.
SCREENING OF CHARGED ELECTRODES IN AQUEOUS ELECTROLYTES
Michael R. Philpott and James N. Glosli 29 Aug. 1994 12 p
(Contract N00014-92-C-0173)
(AD-A284065; TR-10) Avail: CASI HC A03/MF A01

Molecular dynamics simulations are used to demonstrate for the first time that systems about 4 nm thick containing 1200 to 1600 water molecules and NaCl at 1M to 3M concentrations exhibit the main components of electric double layers at charged metal surfaces. In particular for the system

chosen there are regions clearly identifiable as a bulk electrolyte zone, a diffuse layer that screens the charge on the electrode and a layer of oriented water localized next to the electrode. The width of the diffuse layer increases with decrease in salt concentration from 0.2 nm at 3 M to 0.5 nm at 1 M. All the calculations are based on the simple point charge model (SPCE) water model and the immersed electrode approximation.

DTIC

N95-14444# National Science Foundation, Washington, DC.

PROCEEDINGS OF THE 3RD INTERNATIONAL WORKSHOP ON COMPUTATIONAL ELECTRONICS

20 May 1994 344 p Workshop held in Portland, OR, 18-20 May 1994

(AD-A284214) Avail: CASI HC A15/MF A03

A unique study of several previously reported computer simulations which solve the Boltzmann Transport Equation (BTE) for electrons in silicon has been completed. A total of 47 individuals representing 19 laboratories in 6 countries participated in this comparison, with a total of 21 data sets contributed. Most of the simulations are based on the Monte Carlo particle technique, and have been used here to calculate a set of transport characteristics for intrinsic silicon at room temperature with a homogeneous electric field. From a global perspective the results vary widely, but they provide for the first time a quantitative comparison of many silicon transport models. If we group the data sets according to their bandstructure models and compare groups to one another the separate effects of bandstructure and phonon scattering rates can be seen. In the group of full-band models we observe a striking and unexpected agreement between 4 of the data sets, and the possible significance of this observation will be discussed.

DTIC

N95-14516* National Aeronautics and Space Administration. Lewis Research Center, Cleveland, OH.

PULSED MODE CATHODE Patent

Roger M. Myers, inventor (to NASA) and Vinvent K. Rawlin, inventor (to NASA) 25 Oct. 1994 5 p Filed 25 Jun. 1993

(NASA-Case-LEW-15753-1; US-Patent-5,357,747;

US-Patent-Appl-SN-081893; US-Patent-Class-60-203.1;

US-Patent-Class-313-341; US-Patent-Class-313-346R;

US-Patent-Class-313-346DC; US-Patent-Class-315-111.81;

Int-Patent-Class-H01J-1/14; Int-Patent-Class-H01J-1/15) Avail: US Patent and Trademark Office

A cathode in an MPD thruster has an internal heater and utilizes low work function material. The cathode is preheated to operating temperature, and then the thruster is fired by discharging a capacitor bank in a pulse forming network.

Author

N95-14606# Argonne National Lab., IL. Energy Technology Div.

PROGRESS IN DEVELOPMENT OF TAPES AND MAGNETS MADE FROM BI-2223 SUPERCONDUCTORS

U. Balachandran, A. N. Iyer, P. Haldar, J. G. Hoehn, Jr., and L. R. Motowidlo May 1994 19 p Presented at the 4th International Conference and Exhibition of the World Congress on Superconductivity, Orlando, FL, 27 Jun. - 1 Jul. 1994

(Contract W-31-109-eng-38)

(DE94-015067; ANL/ET/CP-82348; CONF-940627-3) Avail: CASI HC A03/MF A01

Long lengths of (Bi,Pb)2Sr2Ca2Cu3O(x) tapes made by powder-in-tube processing have been wound into coils. The performance of these coils has been measured at temperatures of 4.2 to 77 K. Microstructures have been examined by X-ray diffraction and electron microscopy and have been related to superconducting properties. A summary of recent results and an overview of future goals are presented.

DOE

N95-14851*# Old Dominion Univ., Norfolk, VA. Dept. of Aerospace Engineering.

MODELLING OF EDDY CURRENTS RELATED TO LARGE ANGLE MAGNETIC SUSPENSION TEST FIXTURE Final Progress Report, 1 Nov. 1993 - 31 Oct. 1994

Colin P. Britcher and Lucas E. Foster Nov. 1994 34 p

(Grant NAG1-1056)

(NASA-CR-197028; NAS 1.26:197028) Avail: CASI HC A03/MF A01

This report presents a preliminary analysis of the mathematical modelling of eddy current effects in a large-gap magnetic suspension system. It is shown that eddy currents can significantly affect the dynamic behavior and control of these systems, but are amenable to measurement and modelling. A theoretical framework is presented, together with a comparison of computed and experimental data related to the Large Angle Magnetic Suspension Test Fixture at NASA Langley Research Center.

Author

N95-14866*# Auburn Univ., AL. Dept. of Electrical Engineering.

DESIGN OF POWER ELECTRONICS FOR TVC AND EMA SYSTEMS Final Report

R. Mark Nelms, J. Brett Bell, and Michael T. Shepherd 7 Nov. 1994 41 p

(Contract NAS8-39131)

(NASA-CR-197067; NAS 1.26:197067) Avail: CASI HC A03/MF A01

The EMA systems proposed for future space transportation applications are high power systems operating at voltages up to 270 Vdc and at current levels on the order of hundreds of amperes. The position of the actuator is controlled by modulating the flow of energy from the source to an electric motor with an inverter. Hard-switching of the semiconductor devices in the inverter results in considerable device switching stresses and losses and in the generation of substantial amounts of EMI. Both of these can be reduced by employing zero-voltage-switching (ZVS) techniques in the inverter. This project has focused on the development of a ZVS inverter for the Marshall Space Center EMA prototypes, which utilize brushless dc motors to convert electrical energy to mechanical energy. An inverter which permitted zero-voltage switching and a quasi-PWM operation was selected for study and implementation. A waveshaping circuit is added to the front of a standard three-phase inverter to achieve the desired switching properties. This circuit causes the input voltage of the three-phase inverter to ring to zero where it is clamped for a short period of time. During this zero-voltage period, any of the semiconductor switches in the three-phase inverter are switched on or off at zero voltage resulting in a reduction in switching losses and EMI. The operation of this waveshaping circuit and its interaction with the three-phase inverter are described. The different circuit modes were analyzed using equivalent circuits. Based on this analysis, design relationships were developed for calculating component values for the circuit elements in the waveshaping circuit. Waveforms of various voltages and currents in the waveshaping circuit were plotted and used to determine the ratings of the semiconductors in the waveshaping circuit. The implementation of this inverter are described. Block diagrams for the overall control system and the waveshaping circuit control are presented and discussed. The current control scheme employed in the controller is also described.

Author

N95-15302# Fermi National Accelerator Lab., Batavia, IL.

A HIGH SPEED, WIDE DYNAMIC RANGE DIGITIZER CIRCUIT FOR PHOTOMULTIPLIER TUBES

R. J. Yarema, G. W. Foster, K. Knickerbocker, M. Sarraj, R. Tschirhart, J. Whitmore, T. Zimmerman, and M. Lindgren Jun. 1994 5 p Presented at the 6th Pisa Meeting on Advanced Detectors, Elba, Italy, 22-28 May 1994

(Contract DE-AC02-76CH-03000)

(DE94-015187; FNAL-TM-1895; CONF-9405168-3) Avail: CASI HC A01/MF A01

High energy physics experiments running at high interaction rates frequently require long record lengths for determining a level 1 trigger. The easiest way to provide a long event record is by digital means. In applications requiring wide dynamic range, however, digitization of an analog signal to obtain the digital record has been impossible due to lack of high speed, wide range FADC's. One such application is the readout of thousands of photomultiplier tubes in fixed target and colliding beam experiment calorimeters. A circuit has been designed for digitizing PMT signals over a wide dynamic range (17-18 bits) with 8 bits of resolution at rates up to 53 MHz. Output from the circuit is in a floating point format with a 4 bit exponent and an 8 bit mantissa. The heart of the circuit is a full custom integrated circuit called the QIE (Charge Integrator and Encoder). The design of the QIE and associated circuitry reported here permits operation over a 17 bit dynamic range. Tests of the circuit with a PMT input and a pulsed laser have provided respectable results with little off line correction. Performance of the circuit for demanding applications can be significantly enhanced with additional off line correction. Circuit design, packaging issues, and test results of a multirange device are presented for the first time.

DOE

N95-15325# Naval Postgraduate School, Monterey, CA.
THEORY AND IMPLEMENTATION OF A VLSI STRAY INSENSITIVE SWITCHED CAPACITOR COMPOSITE OPERATIONAL AMPLIFIER M.S. Thesis
Raphael Anestis Jun. 1994 188 p
(AD-A283536) Avail: CASI HC A09/MF A02

In this research, improved analog circuits are implemented using VLSI technology by combining the properties of switched capacitors and composite amplifiers. This combined design solves some of the problems of the single operational amplifier (OA) such as finite dc gain, limited bandwidth and lower slew rate, as well as enhancing the overall network passive and active sensitivities. For the first time, a theoretical analysis was conducted in a newly-defined discrete transform domain. The analysis was used to justify the circuits that were first designed in the continuous domain and also debug the initial attempts that were made to build an analog chip. The switched capacitor design is implemented using both the toggle switched inverter and the modified open floating resistor techniques. The composite OA is implemented using the C20A-1 design out of all the CNOA-i possibilities. The two alternatives, together with two single CMOS OA's that were added for comparison reasons, are produced on a single analog/digital microchip. The digital part includes the two-phase non-overlapping clock and programmable switches. It is isolated from the analog part using a low-noise design technique. Sufficient simulations were made to anticipate results in positive and negative finite gain configurations, and also to evaluate the two different techniques. Finally, neural networks applications of the chip are suggested evoking thoughts for the advantages of this promising technique. DTIC

N95-15327# SRI International Corp., Menlo Park, CA.
FIELD-EMITTER ARRAYS FOR RF VACUUM MICROELECTRONICS Final Report, 19 Aug. 1991 - 30 Jul. 1994
C. A. Spindt 19 Aug. 1994 81 p
(Contract MDA972-91-C-0029; ARPA Order 8162)
(AD-A283549) Avail: CASI HC A05/MF A01

SRI International has completed a program to develop field-emitter arrays for vacuum microelectronics. We have met the first-phase program goals of 5 mA total emission, with a current density of 5 A/sq cm for at least 2 hours and demonstrated modulation of the emission current at a frequency of 1 GHz. Principal efforts involved the development of a process for forming emitter cones in small diameter apertures and with improved aspect ratios to reduce stress accumulation on film, modification of reactive ion etching chemistry to eliminate sulfur contamination of the cathode, investigation of galvanic etching resulting from a deionized-water rinse, and methods of fabricating emitters arrays with increased geometric field-enhancement factors and higher packing densities. Final efforts involved the application of small-hole lithography to low-capacitance cathode geometry, and investigation of emitter-array performance by conducting Muller microscopic imaging, Auger spectroscopy, and emission microscope measurements. DTIC

N95-15356# Sandia National Labs., Albuquerque, NM.
AUTOMATED CLEANING OF ELECTRONIC COMPONENTS
W. Drotning, L. Meirans, W. Wapman, Y. Hwang, L. Koenig, and B. Petterson 1994 6 p Presented at the 5th World Conference on Robotics Research, Cambridge, MA, 27-29 Sep. 1994
(Contracts DE-AC04-94AL-85000; DE-AC04-76DP-00789)
(DE94-014122; SAND-93-2018C; CONF-9409163-1) Avail: CASI HC A02/MF A01

Environmental and operator safety concerns are leading to the elimination of trichloroethylene and chlorofluorocarbon solvents in cleaning processes that remove rosin flux, organic and inorganic contamination, and particulates from electronic components. Present processes depend heavily on these solvents for manual spray cleaning of small components and subassemblies. Use of alternative solvent systems can lead to longer processing times and reduced quality. Automated spray cleaning can improve the quality of the cleaning process, thus enabling the productive use of environmentally conscious materials, while minimizing personnel exposure to hazardous materials. We describe the development of a prototype robotic system for cleaning electronic components in a spray cleaning workcell. An important feature of the prototype system is the capability to generate the robot paths and motions automatically from the CAD models of the part to be cleaned, and to embed cleaning process knowledge into the automatically programmed operations. DOE

N95-15397 Wisconsin Univ., Milwaukee, WI. Dept. of Physics.
ULTRASONIC CHARACTERIZATION OF HIGH T(c) AND OTHER UNCONVENTIONAL SUPERCONDUCTORS Summary Report, 1 Oct. 1993 - 31 May 1994
Moises Levy 31 May 1994 8 p Limited Reproducibility: More than 20% of this document may be affected by microfiche quality
(Contract N00014-91-J-1211)
(AD-A282835) Avail: CASI HC A02

Ultrasonic techniques have been used to characterize properties of high T(sub c) and other unconventional superconductors. Attenuation and velocity measurements with shear waves have been performed on a sintered sample of HgBa2CuO4 and single crystal and melt textured samples of YBCO as a function of magnetic field. Anomalous behavior is observed which may be due to the fact that sound waves are sensitive to the total number of flux lines sampled, regardless of their orientation. A pontoon technique was used to launch surface acoustic waves SAW through a single crystal platelet of YBCO. A relative maximum in attenuation is observed at around 90 K which may be associated with a relaxation process. Measurements on a SAW reflective array compressor made of superconducting YBCO appear to indicate that the YBCO reflecting chevrons are more effective in reflecting the SAW in the normal state than in the superconducting state. The insertion loss of a SAW delay line made with YBCO interdigital electrodes decreased when the electrodes became superconducting. A theoretical model has been developed to quantitatively explain these results. DTIC

N95-15399 Westinghouse Electric Corp., Baltimore, MD. Electronic Systems Support Div.
FERROELECTRIC OXIDE MEMORY FET (FEMFET) DEVELOPMENT Final Technical Report, Jun. 1992 - May 1994
Donald R. Lampe, H. Buhay, M. H. Francombe, D. A. Adams, and J. W. Dzimianski May 1994 176 p Limited Reproducibility: More than 20% of this document may be affected by microfiche quality
(Contract N00014-90-C-0159; DARPA Order 7503)
(AD-A283203) Avail: Issuing Activity (Defense Technical Information Center (DTIC))

This Final Technical Report covers the integration of oxide ferroelectric thin films (e.g. bismuth titanate = Bi4Ti3Ol2 = BTO or lead zirconate titanate = PZT) into the gate dielectric of a metal-insulator-silicon field effect transistor (MISFET), capable of functioning in a non-volatile, non-destructive readout (NDRO) ferroelectric random access memory (FERRAM). Also provided is a detailed description of the test vehicles implemented for the study of fabrication process integration and optimization and the resultant properties of ferroelectric/(semiconductor) memory FET (FEMFET) and related structures. The Interim Report covering the first phase of this contract described an investigation of UHV-deposited ferroelectric fluoride (BaMgF4 = BMF) films as gate insulators; however, BMF transistor structures exhibited rather poor reproducibility, and electrical instability manifested as poor retention capability. Results of the second phase of this program are presented in this report, which focuses on exploration of oxide ferroelectric films for the FEMFET gate dielectric. There is growing evidence that layers of ferroelectric oxides, when suitably processed may possess switching and stability properties that are far superior to those attainable with BMF layers. DTIC

N95-15410# Sandia National Labs., Albuquerque, NM.
THE EFFECTS OF SPATIAL LOCATION OF DEFECT STATES ON THE SWITCHING CHARACTERISTICS OF AMORPHOUS AND POLYCRYSTALLINE SILICON THIN FILM TRANSISTORS: A NUMERICAL SIMULATION USING AMPS 2-D
J. Smith, S. Fonash, and A. Kalkan 1994 4 p Presented at the 1994 International Display Research Conference, Monterey, CA, 10-13 Oct. 1994 Sponsored in part by ONR, EPRI and ARPA
(Contract DE-AC04-94AL-85000)
(DE94-013437; SAND-94-1381C; CONF-9410116-1) Avail: CASI HC A01/MF A01

We demonstrate a two-dimensional device simulator for MOSFET structures that incorporates models for defect distributions and show

predicted effects on device switching performance for various spatial distributions of defects in amorphous and polycrystalline silicon. DOE

N95-15454 Virginia Univ., Charlottesville, VA. School of Engineering and Applied Science.
INTERNATIONAL SEMICONDUCTOR DEVICE RESEARCH SYMPOSIUM (ISDRS-93) Final Report, 1 Jul. 1993 - 30 Jun. 1994
Michael Shur Apr. 1994 8 p Limited Reproducibility: More than 20% of this document may be affected by microfiche quality
(Contract DAAH04-93-G-0384)
(AD-A281715; UVA/525025/EE94/101) Avail: Issuing Activity (Defense Technical Information Center (DTIC))

The goal of this second biannual international meeting was to provide a congenial forum for the exchange of information and new ideas for researchers from university, industry and government laboratories in the field of semiconductor devices and device physics. To this end, we have an unusually short period between the submission of papers and the conference, a speedy publication of the proceedings, poster sessions, panel discussions, and a wide dissemination of the conference proceedings. Our other goal is to make this conference truly international. To achieve this, the symposium has sub-committees in Asia, Europe and the former Soviet Union. This conference is organized in cooperation with the IEEE MTT Society, the European Physical Society, the United States National Committee of URSI and the Russian Physical Society. Generous financial support has been provided by the Army Research Office, the Office of Naval Research, the NASA Ames Research Center and the Soros International Science Foundation. Papers cover a broad range of topics, including novel and ultrasmall devices, photonics and optoelectronics, heterostructure and cryogenic devices, wide band gap semiconductors, thin film transistors, MOSFET technology and devices, carrier transport phenomena, materials and device characterization, simulation and modeling. It is hoped that such a broad range of topics will foster a cross-fertilization of the different fields related to semiconductor materials and devices. DTIC

N95-15456 North Carolina Univ., Chapel Hill, NC. Dept. of Chemistry.
CHEMICALLY MODIFIED ELECTRODES BY NUCLEOPHILIC SUBSTITUTION OF CHLOROSILYLATED PLATINUM OXIDE SURFACES Interim Report, May 1993 - Jun. 1994
Chun-Hsien Chen, James H. Hutchison, Timothy A. Postlethwaite, John N. Richardson, and R. W. Murray 1 Jul. 1994 22 p Limited Reproducibility: More than 20% of this document may be affected by microfiche quality
(Contract N00014-90-J-1230)
(AD-A281567; TR-58) Avail: Issuing Activity (Defense Technical Information Center (DTIC))

Chlorosilylated platinum oxide electrode surfaces can be generated by reaction of SiCl4 vapor with an electrochemically prepared monolayer of platinum oxide. A variety of nucleophilic agents (such as alcohols, amines, thiols, and Grignard reagents) can be used to displace chloride and thereby functionalize the metal surface. Electroactive surfaces prepared with ferrocene methanol as the nucleophile show that derivatization by small molecules can achieve coverages on the order of a full monolayer. Surfaces modified with long-chain alkyl groups efficiently block electrode reactions of redox probes dissolved in the contacting solution, but other electrochemical (double layer capacitance and surface coverage) and contact angle measurements suggest that these molecule films are not highly ordered, self-assembled monolayers. DTIC

N95-15459 Arizona Univ., Tucson, AZ. Optical Sciences Center.
ASYMMETRIC COUPLED QUANTUM WELLS FOR HIGH SPEED OPTICAL MODULATORS AT COMMUNICATION WAVELENGTHS Final Report, Jan. 1993 - Jan. 1994
B. P. McGinnis, Sergey Ten, N. Peyghamberian, Mark F. Krol, and Michael J. Hayduk Jun. 1994 20 p Limited Reproducibility: More than 20% of this document may be affected by microfiche quality
(Contract F30602-93-C-0005)
(AD-A281572; RL-TR-94-69) Avail: Issuing Activity (Defense Technical Information Center (DTIC))

A novel design for electro-optic modulators operating at wavelengths compatible with fiber-based optical interconnects and networks is presented. This design uses InGaAs/InAlAs asymmetric coupled quantum wells (ACQWS) to enhance the electro-optic effect within the material and results in a low power modulator capable of high-speed operation. A device was fabricated which shows real charge transfer between the ACQW's. This device shows that without modulation doping and real charge transfer the quantum confined stark effect in InGaAs/InAlAs is insufficient to provide strong modulation at low drive voltages. Standard pump-probe techniques were also used to study the dynamics of charge transfer between the wells. Picosecond recovery times were exhibited by these devices and were found to be independent of the barrier width. DTIC

N95-15460 Syracuse Univ., NY. Office of Sponsored Programs.
HIGH-EFFICIENCY ELECTRO-OPTIC GRATING ON PLZT CERAMIC WAFER FOR OPTICAL SWITCHING Final Report, Mar. 1992 - Jun. 1993
Q. W. Song Apr. 1994 27 p Limited Reproducibility: More than 20% of this document may be affected by microfiche quality
(Contract F30602-93-C-0036)
(AD-A281573; A2-1852; RL-TR-94-68) Avail: Issuing Activity (Defense Technical Information Center (DTIC))

A high diffraction efficiency electro-optic phase grating is fabricated by depositing transparent interdigital electrodes on a PLZT ceramic wafer. The underlying principle is the electrical field induced periodic change in refractive index of the wafer. The diffraction efficiency is controlled by an applied DC voltage. The zero-order light is completely shut off when the first-order diffraction reaches its maximum, with a voltage of 140V. The preliminary analysis and experimental results are provided. This device can be used as a voltage-controlled switch in optical interconnects. DTIC

N95-15544# Sandia National Labs., Albuquerque, NM.
HIGH GAIN GaAs SWITCHES FOR IMPULSE SOURCES: MEASUREMENT OF THE SPEED OF CURRENT FILAMENTS
G. M. Loubriel, F. J. Zutavern, M. W. OMaliey, R. R. Gallegos, W. D. Helgeson, H. P. Hjalmarson, A. G. Baca, and T. A. Plut 1994 4 p Presented at the 21st International Power Modulator Symposium, Costa Mesa, CA, 28-30 Jun. 1994
(Contract DE-AC04-94AL-85000)
(DE94-015281; SAND-93-2243C; CONF-940678-4) Avail: CASI HC A01/MF A01

A high peak power impulse pulser that is controlled with high gain, optically triggered GaAs Photoconductive Semiconductor Switches (PCSS) has been constructed and tested. The system has a short 50 ohm line that is charged to 100 kV and discharged through the switch when the switch is triggered with as little as 90 nJ of laser energy. The authors have demonstrated that the GaAs switches can be used to produce either a monocycle or a monopulse with a period of total duration of about 3 ns. For the monopulse, the voltage switched was above 100 kV, producing a peak power of about 48 MW to the 30 ohm load at a burst repetition rate of 1 kHz. The laser that is used is a small laser diode array whose output is delivered through a fiber to the switch. The current in the system has rise times of 430 ps and a pulse width of 1.4 ns when two laser diode arrays are used to trigger the switch. The small trigger energy and switch jitter are due to a high gain switching mechanism in GaAs. This experiment also shows a relationship between the rise time of the voltage across the switch and the required trigger energy and switch jitter. The time evolution of the current filaments in an optically triggered, high gain GaAs switch was studied by recording the infrared photoluminescence from the filaments. When the system is triggered with two laser diode arrays that are activated within 1 ns of each other, two current filaments are observed. By delaying one laser with respect to the other, the evolution of the filament was recorded in a time resolved fashion. The filament that is triggered first crosses the switch, the voltage drops and the other filament ceases to grow. By varying the delay between the trigger lasers, the tip velocity is measured to be up to 5.9 +/- 1 x 10(exp 9) cm/s. DOE

N95-15587*# National Aeronautics and Space Administration. Lewis Research Center, Cleveland, OH.
SURFACE PASSIVATION FOR 3-5 SEMICONDUCTOR PROCESSING: STABLE GALLIUM SULPHIDE FILMS BY MOCVD
Andrew N. MacInnes (Gallia, Inc., Weston, MA.), Phillip P. Jenkins (Sverdrup Technology, Inc., Cleveland, OH.), Michael B. Power (Gallia, Inc., Weston, MA.), Soon Kang (Case Western Reserve Univ., Cleveland, OH.), Andrew R. Barron (Harvard Univ., Cambridge, MA.), Aloysius F. Hepp, and Massood Tabib-Azar Nov. 1994 11 p Presented at the Spring Meeting, San

Francisco, CA, 12-16 Apr. 1993; sponsored by the Materials Research Society
(RTOP 233-01-0A)
(NASA-TM-106761; E-9201; NAS 1.15:106761) Avail: CASI HC A03/MF A01

Gallium sulphide (GaS) has been deposited on GaAs to form stable, insulating, passivating layers. Spectrally resolved photoluminescence and surface recombination velocity measurements indicate that the GaS itself can contribute a significant fraction of the photoluminescence in GaS/GaAs structures. Determination of surface recombination velocity by photoluminescence is therefore difficult. By using C-V analysis of metal-insulator-semiconductor structures, passivation of the GaAs with GaS films is quantified. Author

N95-15611# Helsinki Univ. of Technology, Espoo (Finland). Circuit Theory Lab.
NEW FIVE-STANDARD CALIBRATION PROCEDURES FOR NETWORK ANALYZERS AND WAFER PROBES
K. Silvonen Mar. 1994 21 p
(PB94-197662; ISBN-951-22-1989-1) Avail: CASI HC A03/MF A01

New calibration procedures using five two-port standards are developed for network analyzer, test fixture and wafer prober environments. The theory and calibration equations for a 16-term error model are shown. Based on numerical simulations, it is pointed out that five two-port calibration measurements are needed to exactly calibrate the 16 parameter error model. Possible combinations of calibration standards are studied. The nonsingular and the singular combinations are listed in Tables. The limitations of the Super-TSD algorithm are defined for the first time. NTIS

N95-15613 Raytheon Co., Lexington, MA. Research Div.
RF VACUUM MICROELECTRONICS Final Report, 1 Jul. 1993 - 30 Jun. 1994
Alan Palevsky 29 Jul. 1994 52 p Limited Reproducibility: More than 20% of this document may be affected by microfiche quality
(Contract MDA972-91-C-0032)
(AD-A283123; Ray/RD/S-5005) Avail: Issuing Activity (Defense Technical Information Center (DTIC))

The results of the 12 month option portion of the research and development project on high frequency Field Emission Array (FEA) cathodes is presented. Details of structure capacitance and triode operation are discussed in detail. The results did not meet the program goals and the reasons for the lack of success relative to these goals and the outlook for this technology for use at microwave frequencies are presented DTIC

N95-15628# Naval Postgraduate School, Monterey, CA.
A SIMPLE ANALYTICAL MODEL FOR DENSE WDM/OOK SYSTEMS M.S. Thesis
Tso-Chuan Chou Jun. 1994 68 p
(AD-A283229) Avail: CASI HC A04/MF A01

The closed form expression for the bit error probability of dense WDM systems employing an external OOK modulator was derived. This model is based upon a close approximation of the optical Fabry-Perot filter in the receiver as a single-pole RC filter for the signals that are bandlimited to a frequency band approximately equal to one sixtieth of the Fabry-Perot filter's free spectral range. This model can handle bit rates up to 2.5 Gb/s for a free spectral range of 3800 GHz and up to 5 Gb/s when the power penalty is 1 db or less. DTIC

N95-15669* National Aeronautics and Space Administration. Lewis Research Center, Cleveland, OH.
METHOD OF LOCATING GROUND FAULTS Patent
Richard L. Patterson, inventor (to NASA), Allen H. Rose, inventor (to NASA), and Ronald C. Cull, inventor (to NASA) 15 Nov. 1994 7 p Filed 21 Jan. 1993 Supersedes N94-15706 (32 - 3, p 1009)
(NASA-Case-LEW-15407-1; US-Patent-5,365,175;
US-Patent-Appl-SN-006413; US-Patent-Class-324-501;
US-Patent-Class-324-509; US-Patent-Class-324-512;
US-Patent-Class-324-539; US-Patent-Class-324-96;
Int-Patent-Class-G01R-31/08) Avail: US Patent and Trademark Office

The present invention discloses a method of detecting and locating current imbalances such as ground faults in multiwire systems using the Faraday effect. As an example, for 2-wire or 3-wire (1 ground wire) electrical systems, light is transmitted along an optical path which is exposed to magnetic fields produced by currents flowing in the hot and neutral wires. The rotations produced by these two magnetic fields cancel each other, therefore light on the optical path does not read the effect of either. However, when a ground fault occurs, the optical path is exposed to a net Faraday effect rotation due to the current imbalance thereby exposing the ground fault. Author

N95-15681* National Aeronautics and Space Administration. Goddard Space Flight Center, Greenbelt, MD.
PROGRAMMABLE HIGH VOLTAGE POWER SUPPLY WITH REGULATION CONFINED TO THE HIGH VOLTAGE SECTION Patent
Karen D. Castell, inventor (to NASA) and Arthur P. Ruitberg, inventor (to NASA) 8 Nov. 1994 14 p Filed 1 Apr. 1994
(NASA-Case-GSC-13289-1; US-Patent-5,363,288;
US-Patent-Appl-SN-041373; US-Patent-Class-363-21;
Int-Patent-Class-H02M-3/335) Avail: US Patent and Trademark Office

A high voltage power supply in a dc-dc converter configuration includes a pre-regulator which filters and regulates the dc input and drives an oscillator which applies, in turn, a low voltage ac signal to the low side of a step-up high voltage transformer. The high voltage side of the transformer drives a voltage multiplier which provides a stepped up dc voltage to an output filter. The output voltage is sensed by a feedback network which then controls a regulator. Both the input and output of the regulator are on the high voltage side, avoiding isolation problems. The regulator furnishes a portion of the drive to the voltage multiplier, avoiding having a regulator in series with the load with its attendant, relatively high power losses. This power supply is highly regulated, has low power consumption, a low parts count and may be manufactured at low cost. The power supply has a programmability feature that allows for the selection of a large range of output voltages. Author

N95-14577*# National Aeronautics and Space Administration. Marshall Space Flight Center, Huntsville, AL.
ROLE OF DIELECTRIC CONSTANT IN ELECTROHYDRODYNAMICS OF CONDUCTING FLUIDS
Percy H. Rhodes, Robert S. Snyder, and Glyn O. Roberts *In* NASA. Lewis Research Center, Second Microgravity Fluid Physics Conference Aug. 1994 p 369-374 (For primary document see N95-14522 03-34)
Avail: CASI HC A02/MF A04; 2 functional color pages

34 FLUID MECHANICS AND HEAT TRANSFER

Includes boundary layers; hydrodynamics; fluidics; mass transfer; and ablation cooling.

For related information see also *02 Aerodynamics* and *77 Thermodynamics and Statistical Physics.*

N95-13653*# National Aeronautics and Space Administration. Lewis Research Center, Cleveland, OH.
THE FLOW INDUCED BY THE COALESCENCE OF TWO INITIALLY STATIONARY DROPS
M. R. Nobari (Michigan Univ., Ann Arbor, MI.) and G. Tryggvason Oct. 1994 27 p
(Contract NCC3-233; NAG3-1317)
(NASA-TM-106752; ICOMP-94-24; E-9168; NAS 1.15:106752) Avail: CASI HC A03/MF A01

The coalescence of two initially stationary drops of different size is investigated by solving the unsteady, axisymmetric Navier-Stokes equations numerically, using a Front-Tracking/Finite Difference method. Initially, the drops are put next to each other and the film between them ruptured. Due to surface tension forces, the drops coalesce rapidly and the fluid from the small drop is injected into the larger one. For low nondimensional viscosity, or Ohnesorge number, little mixing takes place and the small drop fluid forms a blob near the point where the drops touched initially. For low Ohnesorge number, on the other hand, the small drop forms a jet that penetrates far into the large drop. The penetration depth also depends on the size of the drops and shows that for a given fluid of sufficiently low viscosity, there is a maximum penetration depth for intermediate size ratios. Author

N95-13664*# Arizona State Univ., Tempe, AZ. Dept. of Mechanical and Aerospace Engineering.

EXPERIMENTS TO VERIFY NONPARALLEL STABILITY THEORY AT VIRGINIA POLYTECHNIC INSTITUTE AND STATE UNIVERSITY, BLACKSBURG, VIRGINIA Final Report

William S. Saric 19 Dec. 1988 17 p

(Grant NsG-1608)

(NASA-CR-196993; NAS 1.26:196993) Avail: CASI HC A03/MF A01

The effects of normal mass injection and suction on boundary-layer stability and transition are studied on a flat plate. Titanium panels, in which 0.063 mm diameter holes were drilled on 0.635 mm centers, are inserted in the plate. Suction level and distribution are variable. Disturbances are introduced by means of a vibrating ribbon and measurements of both mean- and disturbance-flow velocities are made with a hot wire. Disturbance amplitudes are measured as a function of Reynolds number, frequency, and suction characteristics, and are compared with the previous results obtained over a Dynapore surface. Transition measurements under natural and forced conditions are also made. The stabilizing effects of suction are documented. It is also shown that very high local flow rates through the suction holes (which approach a hole Reynolds number of 300) do not destabilize the flow. On the other hand, weak blowing lowers the transition Reynolds number, but is found not to cause serious problems. Author

N95-13665*# National Aeronautics and Space Administration. Lewis Research Center, Cleveland, OH.

COMPUTATIONAL ANALYSIS IN SUPPORT OF THE SSTO FLOWPATH TEST

Beverly S. Duncan (NYMA, Inc., Brook Park, OH.) and Charles J. Trefny Oct. 1994 24 p

(Contract NAS3-27186; RTOP 505-70-59)

(NASA-TM-106757; E-9179; NAS 1.15:106757) Avail: CASI HC A03/MF A01

A synergistic approach of combining computational methods and experimental measurements is used in the analysis of a hypersonic inlet. There are four major focal points within this study which examine the boundary layer growth on a compression ramp upstream of the cowl lip of a scramjet inlet. Initially, the boundary layer growth on the NASP Concept Demonstrator Engine (CDE) is examined. The follow-up study determines the optimum diverter height required by the SSTO Flowpath test to best duplicate the CDE results. These flow field computations are then compared to the experimental measurements and the mass average Mach number is determined for this inlet. Author

N95-13679 Argonne National Lab., IL.

IMPULSIVE RESPONSE OF NONUNIFORM DENSITY LIQUID IN A LATERALLY EXCITED TANK

Y. Tang and Y. W. Chang Apr. 1994 22 p Limited Reproducibility: More than 20% of this document may be affected by microfiche quality

(Contract W-31-109-eng-38)

(DE94-013722; ANL/RE-94/1) Avail: CASI HC A03

A study on the impulsive component of the dynamic response of a liquid of nonuniform density in a tank undergoing lateral base excitations is presented. The system considered is a circular cylindrical tank containing an incompressible and inviscid liquid whose density increases with the liquid depth. The density distribution along the depth can be of any arbitrary continuous or discontinuous function. In the analysis, the liquid field is divided into n layers. The thickness of the liquid layers can be different, but the density of each liquid layer is considered to be uniform and is equal to the value of the original liquid density at the mid-height of that layer. The problem is solved by the eigenfunction expansion in conjunction with the transfer matrix technique. The effect of the nonuniform liquid density on the impulsive component of the dynamic response is illustrated in a numerical example in which the linear and cosine distributions of the liquid density are assumed. The response quantities examined include the impulsive pressure, base shear, and moments. The results are presented in tabular and graphical forms. It is found that the impulsive pressure distribution along the tank wall is not sensitive to the detailed distribution function of the density, and the base shear and moments for the nonuniform liquid can be estimated by assuming an equivalent uniform liquid density that preserves the total liquid weight. The effect of tank flexibility is assessed by a simple approach in which the response quantities for flexible tanks are evaluated by simplified equations. DOE

N95-13892*# National Aeronautics and Space Administration. Hugh L. Dryden Flight Research Facility, Edwards, CA.

NUMERICAL MODELING OF A CRYOGENIC FLUID WITHIN A FUEL TANK

Donald S. Greer Washington Oct. 1994 15 p Presented at the Second Thermal Structures Conference, Charlottesville, VA, 18-21 Oct. 1994

(RTOP 505-70-63)

(NASA-TM-4651; H-2029; NAS 1.15:4651) Copyright Avail: CASI HC A03/MF A01

The computational method developed to study the cryogenic fluid characteristics inside a fuel tank in a hypersonic aircraft is presented. The model simulates a rapid draining of the tank by modeling the ullage vapor and the cryogenic liquid with a moving interface. A mathematical transformation was developed and applied to the Navier-Stokes equations to account for the moving interface. The formulation of the numerical method is a transient hybrid explicit-implicit technique where the pressure term in the momentum equations is approximated to first order in time by combining the continuity equation with an ideal equation of state. Author

N95-14104*# Alabama Univ., Huntsville, AL. Dept. of Mechanical and Aerospace Engineering.

NUMERICAL STUDIES OF THE SURFACE TENSION EFFECT OF CRYOGENIC LIQUID HELIUM Annual Report, period ending 30 Sep. 1994

R. J. Hung Oct. 1994 62 p

(Grant NAG8-938)

(NASA-CR-197014; NAS 1.26:197014) Avail: CASI HC A04/MF A01

The generalized mathematical formulation of sloshing dynamics for partially filled liquid of cryogenic superfluid helium II in dewar containers driven by both the gravity gradient and jitter accelerations applicable to scientific spacecraft which is eligible to carry out spinning motion and/or slew motion for the purpose of performing scientific observation during the normal spacecraft operation is investigated. An example is given with Gravity Probe-B (GP-B) spacecraft which is responsible for the sloshing dynamics. The jitter accelerations include slew motion, spinning motion, atmospheric drag on the spacecraft, spacecraft attitude motions arising from machinery vibrations, thruster firing, pointing control of spacecraft, crew motion, etc. Explicit mathematical expressions to cover these forces acting on the spacecraft fluid systems are derived. The numerical computation of sloshing dynamics has been based on the non-inertia frame spacecraft bound coordinate, and solve time-dependent, three-dimensional formulations of partial differential equations subject to initial and boundary conditions. The explicit mathematical expressions of boundary conditions to cover capillary force effect on the liquid vapor interface in microgravity environments are also derived. The formulations of fluid moment and angular moment fluctuations in fluid profiles induced by the sloshing dynamics, together with fluid stress and moment fluctuations exerted on the spacecraft dewar containers, have been derived. Author

N95-14127# Advisory Group for Aerospace Research and Development, Neuilly-Sur-Seine (France). Propulsion and Energetics Panel.

TURBOMACHINERY DESIGN USING CFD [LA CONCEPTION DES TURBOMACHINES PAR L'AERODYNAMIQUE NUMERIQUE]

May 1994 251 p Lecture series held in OH, 24-25 May 1994, in Ankara, Turkey, 6-7 Jun. 1994, and in Munich, Germany, 9-10 Jun. 1994 Original contains color illustrations

(AGARD-LS-195; ISBN-92-835-0749-5) Copyright Avail: CASI HC A12/MF A03

Computational Fluid Dynamics (CFD) has become a major design tool for designers of turbomachinery. The progress in this area is fast, and the use of 3-D methods is becoming increasingly applicable to the design process. This Lecture Series will include: (1) Computational methods for preliminary design and geometry definitions; (2) Methods for computing through-flows, blade-to-blade flows and geometry generation; (3) Optimization strategies; (4) Designing in three dimensions; (5) Code validation, mesh influence on solution accuracy; (6) Turbulence and transition modelling; (7) Comparison of time averaged flow solvers and 3-D unsteady CFD codes; (8) Industrial use of CFD and the points of view of the designers. For individual titles, see N95-14128 through N95-14136.

N95-14128# Sulzer Innotec A.G., Winterthur (Switzerland). Fluid Dynamics Lab.

COMPUTATIONAL METHODS FOR PRELIMINARY DESIGN AND GEOMETRY DEFINITION IN TURBOMACHINERY **c37**

M. V. Casey *In* AGARD, Turbomachinery Design Using CFD May 1994 22 p (For primary document see N95-14127 03-34)

Copyright Avail: CASI HC A03/MF A03

A review of the turbomachinery preliminary design process is given with particular emphasis on axial and radial compressors. The review covers the selection of machine type, mean-line analysis and correlations, stagestacking calculations and the use of design charts and optimization techniques to find optimum values for design parameters. A comparison is made between the most successful correlations for endwall losses in axial compressors to highlight the different approaches that are possible. The preliminary design process provides an initial definition of the skeletal geometry of the blading and the annulus of the turbomachine. Turbomachinery design systems are then based on design by analysis, whereby the blading is assessed using CFD codes and is iteratively refined. A numerically based parametric blade geometry definition system makes the use of CFD considerably more effective. Examples of modern turbomachinery geometry definition methods involving Bezier surfaces and B-splines are described. Author

N95-14129# General Electric Co., Cincinnati, OH. Aircraft Engines Div.

ELEMENTS OF A MODERN TURBOMACHINERY DESIGN SYSTEM **c37**

Ian K. Jennions *In* AGARD, Turbomachinery Design Using CFD May 1994 22 p (For primary document see N95-14127 03-34)

Copyright Avail: CASI HC A03/MF A03

The aerodynamic design system at GE Aircraft Engines (GEAE) consists of many parts: throughflow, secondary flow, geometry generators, blade-to-blade and fully three-dimensional (3D) analysis. This paper describes each of these elements and discusses optimization and computer architecture issues. Emphasis is placed on those areas in which the company is thought to have special capability. Author

N95-14130# Cambridge Univ., Cambridge (England). Dept. of Engineering.

DESIGNING IN THREE DIMENSIONS **c37**

J. D. Denton *In* AGARD, Turbomachinery Design Using CFD May 1994 14 p (For primary document see N95-14127 03-34)

Copyright Avail: CASI HC A03/MF A03

This lecture advocates the direct use of three-dimensional flow calculations for turbomachinery design. The limitations of the usual quasi-three dimensional approach are discussed and it is shown that fully 3D calculations overcome the modelling limitations inherent in them. Fully 3D calculations also avoid the need to iterate between throughflow and blade to blade calculations. This leads to fewer routine operations (e.g. data transfers) being needed during the design process and hence more efficient use of the designer's time. With a flexible geometrical package, able to generate blade sections and transfer their geometry directly to a 3D data set, changes of stage geometry can be made in minutes. An outline of such a package is given. Modern 3D calculation methods, Ref(11), enable complete stage solutions. with adequate accuracy for design purposes, to be obtained in the order of I hour on a workstation. Hence several design iterations per day can be easily be performed for a single stage of a machine. An example used to design a very high pressure ratio (3:1) axial fan is given and discussed. Author (revised)

N95-14131# Vrije Univ., Brussels (Belgium). Dept. of Fluid Mechanics.

CFD METHODOLOGY AND VALIDATION FOR TURBOMACHINERY FLOWS

Ch. Hirsch *In* AGARD, Turbomachinery Design Using CFD May 1994 44 p (For primary document see N95-14127 03-34)

Copyright Avail: CASI HC A03/MF A03

The essential problem today, in the application of 3D Navier-Stokes simulations to the design and analysis of turbomachinery components, is the validation of the numerical approximation and of the physical models, in particular the turbulence modelling. Although most of the complex 3D flow phenomena occurring in turbomachinery bladings can be captured with relatively coarse meshes, many detailed flow features are dependent on mesh size, on the turbulence and transition models. A brief review of the present state of the art of CFD methodology is given with emphasis on quality and accuracy of numerical approximations related to viscous flow computations. Considerations related to the mesh influence on solution accuracy are stressed. The basic problems of turbulence and transition modelling are discussed next, with a short summary of the main turbulence models and their applications to representative turbomachinery flows. Validations of present turbulence models indicate that none of the available turbulence models is able to predict all the detailed flow behavior in complex flow interactions. In order to identify the phenomena that can be captured on coarser meshes a detailed understanding of the complex 3D flow in compressor and turbines is necessary. Examples of global validations for different flow configurations, representative of compressor and turbine aerodynamics are presented, including secondary and tip clearance flows. Author

N95-14132# Pratt and Whitney Aircraft, East Hartford, CT.

UNSTEADY FLOWS IN TURBINES: IMPACT ON DESIGN PROCEDURE

O. P. Sharma, R. H. Ni, and S. Tanrikut *In* AGARD, Turbomachinery Design Using CFD May 1994 27 p Original contains color illustrations (For primary document see N95-14127 03-34)

Copyright Avail: CASI HC A03/MF A03

The impact of recent research activities in unsteady flows and flow simulation methods used in the turbine design process are outlined. Results from a number of experimental investigations are described to quantify the effect of unsteadiness on the time-averaged flows in turbines. Results from numerical simulations, obtained by using 3-D unsteady Computational Fluid Dynamics (CFD) codes, are also shown to indicate that some of the unsteady flow features can be fairly accurately predicted. An overall discussion is presented to distinguish flow parameters that can be modeled with existing steady CFD codes, from those that require unsteady codes. Author

N95-14133# Sulzer Innotec A.G., Winterthur (Switzerland). Fluid Dynamics Lab.

THE INDUSTRIAL USE OF CFD IN THE DESIGN OF TURBOMACHINERY

M. V. Casey *In* AGARD, Turbomachinery Design Using CFD May 1994 24 p (For primary document see N95-14127 03-34)

Copyright Avail: CASI HC A03/MF A03

The numerical simulation of the internal flowfield now plays a major role in all turbomachinery aerodynamic designs, from aero-engines to hydraulic turbines and pumps. With the help of CFD codes an experienced designer is able to produce more adventurous, better engineered and more clearly understood designs more rapidly at lower cost. This paper reviews the use of CFD as an engineering tool in modern turbomachinery design from the standpoint of a turbomachinery designer. Particular attention is given to the current limitations with regard to performance prediction. The necessary engineering criteria used by turbomachinery designers to overcome these limitations and to assess the weak points of their designs using CFD flowfield computations are discussed. Examples of the application of these general aerodynamic design criteria to most classes of turbomachines using a variety of different CFD codes are given. Author

N95-14134# Societe Nationale d'Etude et de Construction de Moteurs d'Aviation, Moissy-Cramayel (France). Div. Recherches et Etudes Avancees.

NEW METHODS, NEW METHODOLOGY: ADVANCED CFD IN THE SNECMA TURBOMACHINERY DESIGN PROCESS

Christophe Vuillez and Bertrand Petot *In* AGARD, Turbomachinery Design Using CFD May 1994 26 p Original contains color illustrations (For primary document see N95-14127 03-34)

Copyright Avail: CASI HC A03/MF A03

CFD tools represent a significant source of improvements in the design process of turbomachinery components, leading to higher performances, cost and cycle savings as well as lower associated risks. Such methods are the backbone of compressor and turbine design methodologies at Snecma. In the 80's, the use of 3D Euler solvers was a key factor in designing fan blades with very high performance level. Counter rotating high speed propellers designed with this methodology reached measured performances very close to their ambitious objective from the first test series. In the late 80's and the beginning of the 90's, new, more powerful methods were rapidly developed and are now commonly used in the design process: a quasi-3D, compressible, transonic inverse method; quasi-3D and

3D Navier-Stokes solvers; 3D unsteady Euler solvers. As an example, several hundred 3D Navier-Stokes computations are run yearly for the design of low and high pressure compressor and turbine blades. In addition to their modelling capabilities, the efficient use of such methods in the design process comes from their close integration in the global methodology and from an adequate exploitation environment. Their validation, their calibration, and the correlations between different levels of modelling are of critical importance to an actual improvement in design know-how. The integration of different methods in the design process is described. Several examples of application illustrate their practical utilization. Comparisons between computational results and test results show their capabilities as well as their present limitations. The prospects linked to new developments currently under way are discussed. Author

N95-14135# General Electric Co., Cincinnati, OH. Aircraft Engines Div.
THE ROLE OF CFD IN THE DESIGN PROCESS
Ian K. Jennions *In* AGARD, Turbomachinery Design Using CFD May 1994 34 p (For primary document see N95-14127 03-34)
Copyright Avail: CASI HC A03/MF A03

Over the last decade the role played by CFD codes in turbomachinery design has changed remarkably. While convergence/stability or even the existence of unique solutions was discussed fervently ten years ago, CFD codes now form a valuable part of an overall integrated design system and have caused us to re-think much of what we do. The geometric and physical complexities addressed have also evolved, as have the number of software houses competing with in-house developers to provide solutions to daily design problems. This paper reviews how GE Aircraft Engines (GEAE) uses CFD in the turbomachinery design process and examines many of the issues faced in successful code implementation. Author

N95-14136# Technische Univ., Munich (Germany).
AERO DESIGN OF TURBOMACHINERY COMPONENTS: CFD IN COMPLEX SYSTEMS
Klaus Broichhausen *In* AGARD, Turbomachinery Design Using CFD May 1994 23 p (For primary document see N95-14127 03-34)
Copyright Avail: CASI HC A03/MF A03

The importance of CFD in the design of turbocomponents is no longer a matter of discussion. Since the fundamental publications of Wu and the first successful attempts to determine the potential 2D flow in blade rows the position of computational fluid dynamics in the design of jet-engine turbocomponents has increased continuously. This mainly has been driven by the two factors 'time' and 'cost'. As a result the design engineer of today can rely on a mature set of numerical approaches for the aerodynamic optimization of turbomachines. This design system is structured differently in the specific companies. Generally, however, an inverse correlation between the complexity of the problem and the complexity of the numerical approach can be observed: The most complex problems rely on relatively simple codes with a big portion of empiricism and vice versa. An overview of the design problems and the application of computational methods is given. Author

N95-14201# Advisory Group for Aerospace Research and Development, Neuilly-Sur-Seine (France). Fluid Dynamics Panel.
A SELECTION OF EXPERIMENTAL TEST CASES FOR THE VALIDATION OF CFD CODES, VOLUME 1 [RECUEIL DE CAS D'ESSAI EXPERIMENTAUX POUR LA VALIDATION DES CODES DE L'AERODYNAMIQUE NUMERIQUE]
Aug. 1994 152 p
(AGARD-AR-303-Vol-1; ISBN-92-836-1002-4) Copyright Avail: CASI HC A08/MF A02

This report presents the results of a study by Working Group 14 of the AGARD Fluid Dynamics Panel. This group was formed to establish an accessible, detailed experimental data base for the validation of Computational Fluid Dynamics (CFD) codes. The thirty nine test cases that are documented cover the subsonic, transonic, and supersonic flow regimes and five classes of geometries. Included in the five classes of geometries are: two dimensional airfoils; three dimensional wings, designed for predominantly attached flow conditions; slender bodies, typical of missile type configurations; delta wings, characterized by a conical type of vortex flow; and complex configurations, either in a geometrical sense or because of complicated flow interactions. The report is presented in two volumes. Volume 1 provides a review of the theoretical and experimental requirements, a general introduction and summary of the test cases, and recommendations for the future. Volume 2 contains detailed information on the test cases. The relevant data of all test cases has been compiled on floppy disks, which can be obtained through National Centers. Author

N95-14269*# Old Dominion Univ., Norfolk, VA. Dept. of Mechanical Engineering.
RADIATIVE INTERACTIONS IN MULTI-DIMENSIONAL CHEMICALLY REACTING FLOWS USING MONTE CARLO SIMULATIONS Final Report, Aug. 1991 - Jul. 1994
Jiwen Liu and Surendra N. Tiwari Oct. 1994 172 p
(Grants NAG1-423; NAG1-363)
(NASA-CR-197012; NAS 1.26:197012; ODURF-144029) Avail: CASI HC A08/MF A02

The Monte Carlo method (MCM) is applied to analyze radiative heat transfer in nongray gases. The nongray model employed is based on the statistical narrow band model with an exponential-tailed inverse intensity distribution. The amount and transfer of the emitted radiative energy in a finite volume element within a medium are considered in an exact manner. The spectral correlation between transmittances of two different segments of the same path in a medium makes the statistical relationship different from the conventional relationship, which only provides the non-correlated results for nongray methods is discussed. Validation of the Monte Carlo formulations is conducted by comparing results of this method of other solutions. In order to further establish the validity of the MCM, a relatively simple problem of radiative interactions in laminar parallel plate flows is considered. One-dimensional correlated Monte Carlo formulations are applied to investigate radiative heat transfer. The nongray Monte Carlo solutions are also obtained for the same problem and they also essentially match the available analytical solutions. the exact correlated and non-correlated Monte Carlo formulations are very complicated for multi-dimensional systems. However, by introducing the assumption of an infinitesimal volume element, the approximate correlated and non-correlated formulations are obtained which are much simpler than the exact formulations. Consideration of different problems and comparison of different solutions reveal that the approximate and exact correlated solutions agree very well, and so do the approximate and exact non-correlated solutions. However, the two non-correlated solutions have no physical meaning because they significantly differ from the correlated solutions. An accurate prediction of radiative heat transfer in any nongray and multi-dimensional system is possible by using the approximate correlated formulations. Radiative interactions are investigated in chemically reacting compressible flows of premixed hydrogen and air in an expanding nozzle. The governing equations are based on the fully elliptic Navier-Stokes equations. Chemical reaction mechanisms were described by a finite rate chemistry model. The correlated Monte Carlo method developed earlier was employed to simulate multi-dimensional radiative heat transfer. Results obtained demonstrate that radiative effects on the flowfield are minimal but radiative effects on the wall heat transfer are significant. Extensive parametric studies are conducted to investigate the effects of equivalence ratio, wall temperature, inlet flow temperature, and nozzle size on the radiative and conductive wall fluxes. Author

N95-14273*# National Aeronautics and Space Administration. Ames Research Center, Moffett Field, CA.
EDDY VISCOSITY TRANSPORT EQUATIONS AND THEIR RELATION TO THE k-EPSILON MODEL
F. R. Menter Nov. 1994 22 p
(RTOP 505-59-59)
(NASA-TM-108854; A-95006; NAS 1.15:108854) Avail: CASI HC A03/MF A01

A formalism will be presented that allows the transformation of two-equation eddy viscosity turbulence models into one-equation models. The transformation is based on an assumption that is widely accepted over a large range of boundary layer flows and that has been shown to actually improve predictions when incorporated into two-equation models of turbulence. Based on that assumption, a new model will be tested in great detail against a previously introduced one-equation model and against its parent two-equation model. Author

N95-14295*# NYMA, Inc., Brook Park, OH. Engineering Services Div.
UPDATE TO THE NASA LEWIS ICE ACCRETION CODE LEWICE Final Report

William B. Wright Cleveland, OH NASA Oct. 1994 50 p See also N90-20943
(Contract NAS3-27186; RTOP 505-68-10)
(NASA-CR-195387; E-9150; NAS 1.26:195387) Avail: CASI HC A03/MF A01

This report is intended as an update to NASA CR-185129 'User's Manual for the NASA Lewis Ice Accretion Prediction Code (LEWICE).' It describes modifications and improvements made to this code as well as changes to the input and output files, interactive input, and graphics output. The comparison of this code to experimental data is shown to have improved as a result of these modifications. Author

N95-14299*# National Aeronautics and Space Administration. Lewis Research Center, Cleveland, OH.
HYPERSONIC ENGINE LEADING EDGE EXPERIMENTS IN A HIGH HEAT FLUX, SUPERSONIC FLOW ENVIRONMENT
Herbert J. Gladden and Matthew E. Melis Oct. 1994 13 p Presented at the Winter Annual Meeting, Chicago, IL, 6-11 Nov. 1994; sponsored by the ASME Original contains color illustrations
(RTOP 505-62-52)
(NASA-TM-106742; E-9152; NAS 1.15:106742) Avail: CASI HC A03/MF A01; 2 functional color pages

A major concern in advancing the state-of-the-art technologies for hypersonic vehicles is the development of an aeropropulsion system capable of withstanding the sustained high thermal loads expected during hypersonic flight. Three aerothermal load related concerns are the boundary layer transition from laminar to turbulent flow, articulating panel seals in high temperature environments, and strut (or cowl) leading edges with shock-on-shock interactions. A multidisciplinary approach is required to address these technical concerns. A hydrogen/oxygen rocket engine heat source has been developed at the NASA Lewis Research Center as one element in a series of facilities at national laboratories designed to experimentally evaluate the heat transfer and structural response of the strut (or cowl) leading edge. A recent experimental program conducted in this facility is discussed and related to cooling technology capability. The specific objective of the experiment discussed is to evaluate the erosion and oxidation characteristics of a coating on a cowl leading edge (or strut leading edge) in a supersonic, high heat flux environment. Heat transfer analyses of a similar leading edge concept cooled with gaseous hydrogen is included to demonstrate the complexity of the problem resulting from plastic deformation of the structures. Macro-photographic data from a coated leading edge model show progressive degradation over several thermal cycles at aerothermal conditions representative of high Mach number flight. Author

N95-14351# Air Force Inst. of Tech., Wright-Patterson AFB, OH.
EFFECT OF SURFACE ROUGHNESS ON LOCAL FILM COOLING EFFECTIVENESS AND HEAT TRANSFER COEFFICIENTS Ph.D. Thesis
Douglas N. Barlow Aug. 1994 297 p
(AD-A283854; AFIT/CI/CIA-94-033D) Avail: CASI HC A13/MF A03

In high temperature gas turbine engines, the life cycle of the hot section is extremely dependent on accurate design prediction of component temperature distribution. Particular attention must be paid to the film cooling performance of the first stage turbine stator vanes where the highest heat loads are encountered. Recent investigations have determined during operation the smooth surface of high pressure turbine vanes become rough due to corrosion, oxidation and particulate impact. A transient experimental method has been developed to obtain both local heat transfer and cooling effectiveness information downstream of a row of film cooling holes on a rough flat plate. This investigation provides information on the effects of roughness on film cooling heat transfer for a Reynolds number and dimensionless boundary layer momentum thickness which match conditions applicable to the pressure side of the first stage turbine vane of the Pratt and Whitney F-100-PW229 engine. Data for film cooling on rough surfaces are extremely limited in the literature. However, comparison with the available data is made. DTIC

N95-14407# National Inst. of Standards and Technology, Gaithersburg, MD. Building and Fire Research Lab.
SINGLE-PHASE HEAT TRANSFER AND PRESSURE DROP CHARACTERISTICS OF AN INTEGRAL-SPINE-FIN WITHIN AN ANNULUS
M. A. Kedzierski and M. S. Kim Jun. 1994 37 p Sponsored by DOE
(PB94-194073; NISTIR-5454) Avail: CASI HC A03/MF A01

The laminar, single phase heat transfer and friction characteristics of an integral-spine-fin pipe within an annulus are presented. The heat transfer coefficient was determined using a modified version of the Wilson Plot method. The test fluid was pumped through the annulus of a straight, 3 m test section. Three fluids were investigated: (1) tap water, (2) 34% ethylene glycol/water mixture, and (3) 40% ethylene glycol/water mixture. These fluids produced a significant variation in the Prandtl number so that its exponential dependence could be determined. The annulus-Reynolds numbers were varied from 100 to 1400 to obtain the Reynolds number exponent. An empirical correlation for the Nusselt number was developed which accounts for the development of the thermal boundary layer. An empirical correlation for the friction factor is also presented. It is demonstrated that the spines enhance the heat transfer through additional surface area and fluid mixing. NTIS

N95-14522*# National Aeronautics and Space Administration. Lewis Research Center, Cleveland, OH.
SECOND MICROGRAVITY FLUID PHYSICS CONFERENCE
Aug. 1994 455 p Conference held in Cleveland, OH, 21-23 Jun. 1994 Original contains color illustrations
(RTOP 962-24-00)
(NASA-CP-3276; E-9046; NAS 1.55:3276) Avail: CASI HC A20/MF A04; 2 functional color pages

The conference's purpose was to inform the fluid physics community of research opportunities in reduced-gravity fluid physics, present the status of the existing and planned reduced gravity fluid physics research programs, and inform participants of the upcoming NASA Research Announcement in this area. The plenary sessions provided an overview of the Microgravity Fluid Physics Program information on NASA's ground-based and space-based flight research facilities. An international forum offered participants an opportunity to hear from French, German, and Russian speakers about the microgravity research programs in their respective countries. Two keynote speakers provided broad technical overviews on multiphase flow and complex fluids research. Presenters briefed their peers on the scientific results of their ground-based and flight research. Fifty-eight of the sixty-two technical papers are included here. For individual titles, see N95-14523 through N95-14584.

N95-14523*# Northwestern Univ., Evanston, IL. Dept. of Chemical Engineering.
FUTURE DIRECTIONS IN TWO-PHASE FLOW AND HEAT TRANSFER IN SPACE
S. George Bankoff *In* NASA. Lewis Research Center, Second Microgravity Fluid Physics Conference Aug. 1994 p 3-11 (For primary document see N95-14522 03-34)
Avail: CASI HC A02/MF A04; 2 functional color pages

Some areas of opportunity for future research in microgravity two-phase flow and heat transfer are pointed out. These satisfy the dual requirements of relevance to current and future needs, and scientific/engineering interest. Author

N95-14524*# California Univ., Los Angeles, CA. Dept. of Mechanical, Aerospace and Nuclear Engineering.
STABILIZATION OF THERMOCAPILLARY CONVECTION BY MEANS OF NONPLANAR FLOW OSCILLATIONS
Robert E. Kelly and Arthur Or *In* NASA. Lewis Research Center, Second Microgravity Fluid Physics Conference Aug. 1994 p 15-20 (For primary document see N95-14522 03-34)
Avail: CASI HC A02/MF A04; 2 functional color pages

Nonplanar flow oscillations have been shown to be effective in stabilizing buoyancy-induced Rayleigh-Benard convection. The present study was initiated to see if thermocapillary convection of the Marangoni type might also be stabilized by the same means. When surface deflection can be ignored, significant stabilization occurs. However, when the operating parameters are such that surface deflection is nonnegligible, destabilization can occur, in contrast to Rayleigh-Benard convection. Mechanisms for both stabilization and destabilization are discussed. Author

N95-14525*# Georgia Inst. of Tech., Atlanta, GA. School of Mechanical Engineering.

CONTROL OF OSCILLATORY THERMOCAPILLARY CONVECTION IN MICROGRAVITY

G. Paul Neitzel *In* NASA. Lewis Research Center, Second Microgravity Fluid Physica Conference Aug. 1994 p 21-26 (For primary document see N95-14522 03-34)

Avail: CASI HC A02/MF A04; 2 functional color pages

Laboratory and numerical experiments are underway to generate, and subsequently suppress, oscillatory thermocapillary convection in thin layer of silicone oil. The laboratory experiments have succeeded in characterizing the flow state in a limited range of Bond number-Marangoni number space of interest, identifying states of: (1) steady, unicellular, thermocapillary convection; (2) steady, multicellular, thermocapillary convection; and (3) oscillatory thermocapillary convection. Comparisons between experimental results and stability computations for a related basic state will be made. Author

N95-14526*# Rutgers Univ., Piscataway, NJ. Dept. of Mechanical and Aerospace Engineering.

OSCILLATORY THERMOCAPILLARY CONVECTION

Michael R. Mundrane and Abdelfattah Zebib *In* NASA. Lewis Research Center, Second Microgravity Fluid Physics Conference Aug. 1994 p 27-32 (For primary document see N95-14522 03-34)

(Grant NAG3-1453)

Avail: CASI HC A02/MF A04; 2 functional color pages

We study thermocapillary and buoyant thermocapillary convection in rectangular cavities with aspect ratio A = 4 and Pr = 0.015. Two separate problems are considered. The first is combined buoyant thermocapillary convection with a nondeforming interface. We establish neutral curves for transition to oscillatory convection in the Re-Gr plane. It is shown that while pure buoyant convection exhibits oscillatory behavior for Gr is greater than Gr(sub cr) (where Gr(sub cr) is defined for the pure buoyant problem), pure thermocapillary convection is steady within the range of parameters tested. In the second problem, we consider the influence of surface deformation on the pure thermocapillary problem. For the range of parameters considered, thermocapillary convection remained steady. Author

N95-14527*# Texas Univ., Austin, TX. Dept. of Physics.

ONSET OF HEXAGONS IN SURFACE-TENSION-DRIVEN BENARD CONVECTION

Michael F. Schatz, Stephen J. VanHook, John B. Swift, William D. McCormick, and Harry L. Swinney *In* NASA. Lewis Research Center, Second Microgravity Fluid Physics Conference Aug. 1994 p 33-38 (For primary document see N95-14522 03-34)

(Grant NAG3-1382)

Avail: CASI HC A02/MF A04; 2 functional color pages

High resolution laboratory experiments with large aspect ratio are being conducted for thin fluid layers heated from below and bounded from above by a free surface. The fluid depths are chosen sufficiently small (less than 0.06 cm) so that surface tension is the dominant driving mechanisms; the Rayleigh number is less than 5 for the results reported here. Shadowgraph visualization reveals that the primary instability leading to hexagons is slightly hysteretic (approximately 1 percent). Preliminary measurements of the convection amplitude using infrared imaging are also presented. Author

N95-14528*# Arizona Univ., Phoenix, AZ. Dept. of Aerospace and Mechanical Engineering.

EXPERIMENTAL INVESTIGATION OF THE MARANGONI EFFECT ON THE STABILITY OF A DOUBLE-DIFFUSIVE LAYER

Josef Tanny and Chuan F. Chen *In* NASA. Lewis Research Center, Second Microgravity Fluid Physics Conference Aug. 1994 p 39-44 (For primary document see N95-14522 03-34)

(Grant NAG3-1386)

Avail: CASI HC A02/MF A04; 2 functional color pages

Stability experiments were carried out in 4-cm-thick, salt-stratified fluid layer by heating from below and cooling from above. The bottom boundary was rigid while the top was either free or rigid. The initial solute Rayleigh number varied from 2.5 x 10(exp 6) to 4.6 x 10(exp 7). For the rigid-free case, at initial solute Rayleigh numbers R(sub s) greater than 5.4 x 10(exp 6), thermal Marangoni instabilities were observed to onset along the free surface at a relatively low thermal Rayleigh number, R(sub t). The convection was very weak, and it had almost no effect on the concentration and temperature distributions. Double-diffusive instabilities along the top free surface were observed to onset at a higher R(sub t), with much stronger convection causing changes in the concentration and temperature distributions near the top. At a yet higher R(sub t), double-diffusive convection was observed to onset along the bottom boundary. Fluid motion in the layer then evolved into fully developed thermal convection of a homogeneous fluid without any further increase in the imposed Delta T. For layers with R(sub s) less than 5.4 x 10(exp 6), Marangoni and double-diffusive instabilities onset simultaneously along the free surface first, while double-diffusive instabilities along the bottom wall onset at a higher R(sub t). Author

N95-14529*# Wisconsin Univ., Madison, WI. Dept. of Materials Science and Engineering.

THERMOCAPILLARY CONVECTION IN FLOATING ZONES UNDER SIMULATED REDUCED-GRAVITY CONDITIONS

Y. Tao, B. Xiong, and Sindo Kou *In* NASA. Lewis Research Center, Second Microgravity Fluid Physics Conference Aug. 1994 p 45-50 (For primary document see N95-14522 03-34)

Avail: CASI HC A02/MF A04; 2 functional color pages

The present study demonstrated that calculated thermocapillary convection in a non-cylindrical floating zone can now be compared with measured one, by considering the lens effect of the floating zone. Flow visualization and computer simulation of thermocapillary convection in a silicone oil zone and a molten zone in an NaNO3 rod were conducted. The calculated results agree very well with the measured ones, including the free surface shapes, the solid/melt interface shapes and the velocity fields. Author

N95-14530*# Georgia Inst. of Tech., Atlanta, GA. School of Mechanical Engineering.

THE BEHAVIOR OF UNSTEADY THERMOCAPILLARY FLOWS

David R. Vrane and Marc K. Smith *In* NASA. Lewis Research Center, Second Microgravity Fluid Physics Conference Aug. 1994 p 51-56 (For primary document see N95-14522 03-34)

(Grant NAG3-1455)

Avail: CASI HC A02/MF A04; 2 functional color pages

The thermocapillary-driven flow of a liquid in a shallow slot provides a simple model to explore the effects of free-surface deflection and end walls on the stability of the flow. Such an investigation may be useful in understanding the complex flow seen in processes such as the float-zone refining of single crystals. A linear stability analysis of the viscously-dominated slot flow indicates stable basic states to both tow- and three-dimensional infinitesimal disturbances for capillary numbers below 43.3. Above this capillary number steady solutions do not exist. We also discuss current work involving the development of an inertially-dominated slot-flow model using singular perturbation methods. If these flows are unstable, inertial effects would be the only possible cause of the instability. Author

N95-14531*# National Aeronautics and Space Administration. Lewis Research Center, Cleveland, OH.

OSCILLATORY/CHAOTIC THERMOCAPILLARY FLOW INDUCED BY RADIANT HEATING

Kwang-Chung Hsieh, Robert L. Thompson, David VanZandt, Kenneth DeWitt, and Jon Nash *In its* Second Microgravity Fluid Physics Conference Aug. 1994 p 57-63 (For primary document see N95-14522 03-34)

Avail: CASI HC A02/MF A04; 2 functional color pages

The objective of this paper is to conduct ground-based experiments to measure the onset conditions of oscillatory Marangoni flow in laser-heated silicone oil in a cylindrical container. For a single fluid, experimental data are presented using the aspect ratio and the dynamic Bond number. It is found that for a fixed aspect ratio, there seems to be an asymptotic limit of the dynamic Bond number beyond which no onset of flow oscillation could occur. Experimental results also suggested that there could be a lower limit of the aspect ratio below which there is no onset of oscillatory flow. Author

N95-14532*# Colorado Univ., Boulder, CO. Dept. of Aerospace Engineering Sciences.

MULTILAYER FLUID DYNAMICS OF IMMISCIBLE LIQUIDS

Jean N. Koster *In* NASA. Lewis Research Center, Second Microgravity Fluid Physics Conference Aug. 1994 p 65-71 (For primary document see N95-14522 03-34)
(Contracts NCC3-210; NAG3-1094; NGT-51179; NATO-CRG-921122; NSF CTS-89-06846; NSF CTS-91-14775; NSF GER-92-55698; GIT Proj. E-25-X77-S1)
Avail: CASI HC A02/MF A04; 2 functional color pages

A comprehensive analytical, numerical and experimental study of convective flow in multilayer immiscible liquids has been performed. Studies include transparent high Prandtl number of liquid as well as opaque low Prandtl metallic melts. A new radioscopic flow visualization has been developed for the latter studies. Author

N95-14533*# Alabama Univ., Huntsville, AL. Center for Microgravity and Materials Research.
DYNAMICS AND STATICS OF NONAXISYMMETRIC AND SYMMETRIC LIQUID BRIDGES
J. Iwan D. Alexander, Andrew H. Resnick, William F. Kaukler, and Yiqiang Zhang *In* NASA. Lewis Research Center, Second Microgravity Fluid Physics Conference Aug. 1994 p 75-82 (For primary document see N95-14522 03-34)
(Grant NAG8-1384)
Avail: CASI HC A02/MF A04; 2 functional color pages

This program of theoretical and experimental ground-based research focuses on the understanding of the dynamics and stability limits of nonaxisymmetric and symmetric liquid bridges. There are three basic objectives: First, to determine the stability limits of nonaxisymmetric liquid bridges held between non-coaxial parallel disks, Second, to examine the dynamics of nonaxisymmetric bridges and nonaxisymmetric oscillations of initially axisymmetric bridges. The third objective is to experimentally investigate the vibration sensitivity of liquid bridges under terrestrial and low gravity conditions. Some of these experiments will require a low gravity environment and the ground-based research will culminate in a definitive flight experiment. Author

N95-14534*# California Univ., Berkeley. Lawrence Berkeley Lab, CA. Dept. of Mathematics.
EQUILIBRIUM FLUID INTERFACE BEHAVIOR UNDER LOW- AND ZERO-GRAVITY CONDITIONS
Paul Concus and Robert Finn *In* NASA. Lewis Research Center, Second Microgravity Fluid Physics Conference Aug. 1994 p 83-88 (For primary document see N95-14522 03-34)
(Contracts NCC3-329; DE-AC03-76SF-00098; NSF DMS-89-02831)
Avail: CASI HC A02/MF A04; 2 functional color pages

We describe here some of our recent mathematical work, which forms a basis for the Interface Configuration Experiment scheduled for USML-2. The work relates to the design of apparatus that exploits microgravity conditions for accurate determination of contact angle. The underlying motivation for the procedures rests on a discontinuous dependence of the capillary free surface interface S on the contact angle gamma, in a cylindrical capillary tube whose section (base) omega contains a protruding corner with opening angle 2 alpha. Specifically, in a gravity-free environment, omega can be chosen so that, for all sufficiently large fluid volume, the height of S is uniquely determined as a (single-valued) function mu(x,y) entirely covering the base; the height mu is bounded over omega uniformly in gamma throughout the range absolute value of (gamma -(pion/2)) less than or equal to alpha, while for absolute value of (gamma - (pion/2)) greater than alpha fluid will necessarily move to the corner and uncover the base, rising to infinity (or falling to negative infinity) at the vertex, regardless of volume. We mention here only that procedures based on the phenomenon promise excellent accuracy when gamma is close pion/2 but may be subject to experimental error when gamma is close to zero (orpion), as the 'singular' part of the domain over which the fluid accumulates (or disappears) when a critical angle gamma theta is crossed then becomes very small and may be difficult to observe. We ignore the trivial case gamma is equal to pion/2 (planar free surface), to simplify the discussion. Author

N95-14535*# Clarkson Univ., Potsdam, NY. Dept. of Mechanical and Aeronautical Engineering.
THE BREAKUP OF A LIQUID JET AT MICROGRAVITY
Sung P. Lin and Andrew Honohan *In* NASA. Lewis Research Center, Second Microgravity Fluid Physics Conference Aug. 1994 p 89-94 (For primary document see N95-14522 03-34)
(Contract NAG3-1402; DAAL03-89-K-0179)
Avail: CASI HC A02/MF A04; 2 functional color pages

The parameter ranges in which a viscous liquid jet emanating into a viscous gas will breakup in three different modes are calculated. The three modes of jet breakup are: Rayleigh mode of capillary pinching, Taylor mode of atomization, and the absolute instability mode. The apparatus designed for elucidating these three different modes of instability is described. Some preliminary results of the ongoing ground based experiments will be reported. Author

N95-14536*# Carnegie-Mellon Univ., Pittsburgh, PA. Dept. of Physics.
MICROSCALE HYDRODYNAMICS NEAR MOVING CONTACT LINES
Stephen Garoff, Q. Chen, Enrique Rame, and K. R. Willson *In* NASA. Lewis Research Center, Second Microgravity Fluid Physics Conference Aug. 1994 p 95-99 (For primary document see N95-14522 03-34)
Avail: CASI HC A01/MF A04; 2 functional color pages

The hydrodynamics governing the fluid motions on a microscopic scale near moving contact lines are different from those governing motion far from the contact line. We explore these unique hydrodynamics by detailed measurement of the shape of a fluid meniscus very close to a moving contact line. The validity of present models of the hydrodynamics near moving contact lines as well as the dynamic wetting characteristics of a family of polymer liquids are discussed. Author

N95-14537*# Colorado Univ., Boulder, CO. Dept. of Chemical Engineering.
PHASE SEGREGATION DUE TO SIMULTANEOUS MIGRATION AND COALESCENCE
Robert H. Davis, Hua Wang, and Debra Hawker *In* NASA. Lewis Research Center, Second Microgravity Fluid Physics Conference Aug. 1994 p 101-106 (For primary document see N95-14522 03-34)
(Grant NAG3-1389)
Avail: CASI HC A02/MF A04; 2 functional color pages

Ground-based modeling and experiments have been performed on the interaction and coalescence of drops leading to macroscopic phase separation. The focus has been on gravity-induced motion, with research also initiated on thermocapillary motion of drops. The drop size distribution initially shifts toward larger drops with time due to coalescence, and then a back towards smaller drops due to the larger preferentially settling out. As a consequence, the phase separation rate initially increases with time and then decreases. Author

N95-14538*# Cornell Univ., Ithaca, NY. School of Chemical Engineering.
INFLUENCE OF FLOW ON INTERFACE SHAPE STABILITY IN LOW GRAVITY
Paul H. Steen *In* NASA. Lewis Research Center, Second Microgravity Fluid Physics Conference Aug. 1994 p 107-112 (For primary document see N95-14522 03-34)
Avail: CASI HC A02/MF A04; 2 functional color pages

The objectives are to: (1) Understand the influence in low gravity of flow on interface shape. For example, document and control the influence of axial flow on the Plateau-Rayleigh instability of a liquid bridge; and (2) Extend the ground-based density-matching technique of low gravity simulation to situations with flow; that is, develop Plateau chamber experiments for which flow can be controlled. Containerless containment of liquid by surface tension has broad importance in low gravity. For space vehicles, the behavior of liquid/gas interfaces is crucial to successful liquid management systems. In microgravity science, free interfaces are exploited in various applications. Examples include float-zone crystal growth, phase separation near the critical point of liquid mixtures (spinoidal decomposition) and quenching of miscibility gap molten metal alloys. In some cases, it is desired to stabilize the capillary instability while in others it is desired to induce capillary breakup. In all cases, understanding the stability of interface shape in the presence of liquid motion is central. Author

N95-14539*# City Coll. of the City Univ. of New York, NY. Dept. of Physics.
WETTING AND SPREADING AT THE MOLECULAR SCALE
Joel Koplik and Jayanth R. Banavar *In* NASA. Lewis Research Center,

Second Microgravity Fluid Physics Conference Aug. 1994 p 113-118 (For primary document see N95-14522 03-34)
Avail: CASI HC A02/MF A04; 2 functional color pages

We have studied the microscopic aspects of the spreading of liquid drops on a solid surface by molecular dynamics simulations of coexisting three-phase Lennard-Jones systems of liquid, vapor and solid. We consider both spherically symmetric atoms and chain-like molecules, and a range of interaction strengths. As the attraction between liquid and solid increases we observed a smooth transition in spreading regimes, from partial to complete to terraced wetting. In the terraced case, where distinct monomolecular layers spread with different velocities, the layers are ordered but not solid, with qualitative behavior resembling recent experimental findings, but with interesting differences in the spreading rate. Author

N95-14540*# Florida State Univ., Tallahassee, FL. Supercomputer Computations Research Inst.

STOCHASTIC MODEL OF THE RESIDUAL ACCELERATION ENVIRONMENT IN MICROGRAVITY **c29**

Jorge Vinals *In* NASA. Lewis Research Center, Second Microgravity Fluid Physics Conference Aug. 1994 p 119-124 (For primary document see N95-14522 03-34)
(Contract NAG3-1284; DE-FC05-85ER-25000)
Avail: CASI HC A02/MF A04; 2 functional color pages

We describe a theoretical investigation of the effects that stochastic residual accelerations (g-jitter) onboard spacecraft can have on experiments conducted in a microgravity environment. We first introduce a stochastic model of the residual acceleration field, and develop a numerical algorithm to solve the equations governing fluid flow that allow for a stochastic body force. We next summarize our studies of two generic situations: stochastic parametric resonance and the onset of convective flow induced by a fluctuating acceleration field. Author

N95-14541*# Jet Propulsion Lab., California Inst. of Tech., Pasadena, CA.

NONLINEAR DYNAMICS OF DROPS AND BUBBLES AND CHAOTIC PHENOMENA

Eugene H. Trinh, L. G. Leal, Z. C. Feng, and R. G. Holt *In* NASA. Lewis Research Center, Second Microgravity Fluid Physics Conference Aug. 1994 p 127-133 (For primary document see N95-14522 03-34)
Avail: CASI HC A02/MF A04; 2 functional color pages

Nonlinear phenomena associated with the dynamics of free drops and bubbles are investigated analytically, numerically and experimentally. Although newly developed levitation and measurement techniques have been implemented, the full experimental validation of theoretical predictions has been hindered by interfering artifacts associated with levitation in the Earth gravitational field. The low gravity environment of orbital space flight has been shown to provide a more quiescent environment which can be utilized to better match the idealized theoretical conditions. The research effort described in this paper is a closely coupled collaboration between predictive and guiding theoretical activities and a unique experimental program involving the ultrasonic and electrostatic levitation of single droplets and bubbles. The goal is to develop and to validate methods based on nonlinear dynamics for the understanding of the large amplitude oscillatory response of single drops and bubbles to both isotropic and asymmetric pressure stimuli. The first specific area on interest has been the resonant coupling between volume and shape oscillatory modes isolated gas or vapor bubbles in a liquid host. The result of multiple time-scale asymptotic treatment, combined with domain perturbation and bifurcation methods, has been the prediction of resonant and near-resonant coupling between volume and shape modes leading to stable as well as chaotic oscillations. Experimental investigations of the large amplitude shape oscillation modes of centimeter-size single bubbles trapped in water at 1 G and under reduced hydrostatic pressure, have suggested the possibility of a low gravity experiment to study the direct coupling between these low frequency shape modes and the volume pulsation, sound-radiating mode. The second subject of interest has involved numerical modeling, using the boundary integral method, of the large amplitude shape oscillations of charged and uncharged drops in the presence of a static or time-varying electric field. Theoretically predicted non linearity in the resonant frequency of the fundamental quadrupole mode has been verified by the accompanying experimental studies. Additional phenomena such as hysteresis in the frequency response of ultrasoncially levitated droplets in the presence of a time varying electric field, and mode coupling in the oscillations of ultrasonically modulated droplets, have also been uncovered. One of the results of this ground-based research has been the identification and characterization of phenomena strictly associated with the influence of the gravitational field. This has also allowed us to identify the specific requirements for potential microgravity investigations yielding new information not obtainable on Earth. Author

N95-14542*# Michigan Univ., Ann Arbor, MI. Dept. of Mechanical Engineering.

COMPUTATIONS OF DROP COLLISION AND COALESCENCE

Gretar Tryggvason, Damir Juric, Mohammed H. R. Nobari, and Selman Nas *In* NASA. Lewis Research Center, Second Microgravity Fluid Physics Conference Aug. 1994 p 135-140 (For primary document see N95-14522 03-34)
(Grants NAG3-1317; NGT-51070)
Avail: CASI HC A02/MF A04; 2 functional color pages

Computations of drops collision and coalescence are presented. The computations are made possible by a recently developed finite difference/front tracking technique that allows direct solutions of the Navier-Stokes equations for a multi-fluid system with complex, unsteady internal boundaries. This method has been used to examine the boundaries between the various collision modes for drops of equal size and two examples, one of a 'reflective' collision and another of a 'grazing' collision is shown. From drops of unequal size, coalescence can result in considerable mixing between the fluid from the small and the large drop. This problem is discussed and one example showed. In many cases it is necessary to account also for heat transfer along with the fluid mechanics. We show two preliminary results where we are using extensions of the method to simulate such a problem. One example shows pattern formation among many drops moving due to thermal migration, the other shows unstable evolution of a solidification front. Author

N95-14543*# National Aeronautics and Space Administration. Lewis Research Center, Cleveland, OH.

A REALISTIC MODEL OF EVAPORATION FOR A LIQUID DROPLET

An-Ti Chai and V. S. Arpaci *In its* Second Microgravity Fluid Physics Conference Aug. 1994 p 141-147 (For primary document see N95-14522 03-34)
Avail: CASI HC A02/MF A04; 2 functional color pages

An intuitive delineation along with dimensional considerations and experimental evidences are presented to show that in a general case, the evaporation of a liquid droplet undergoes three regimes through the process. Initially, the heat transfer inside the evaporating droplets is conduction controlled; then, in the second stage, convective heat transfer may take over; finally, the convections subside, and the process returns to conduction controlled mode. Author

N95-14544*# Virginia Univ., Charlottesville, VA. Dept. of Mechanical, Aerospace, and Nuclear Engineering.

THERMOCAPILLARY MOTION OF DEFORMABLE DROPS

Hossein Haj-Hariri, Qingping Shi, and Ali Borhan *In* NASA. Lewis Research Center, Second Microgravity Fluid Physics Conference Aug. 1994 p 149-154 (For primary document see N95-14522 03-34)
(Grant NAG3-1390)
Avail: CASI HC A02/MF A04; 2 functional color pages

The thermocapillary motion of initially spherical drops/bubbles driven by a constant temperature gradient in an unbounded liquid medium is simulated numerically. Effects of convection of momentum and energy, as well as shape deformations, are addressed. The method used is based on interface tracking on a base cartesian grid, and uses a smeared color or indicator function for the determination of the surface topology. Quad-tree adaptive refinement of the cartesian grid is implemented to enhance the fidelity of the surface tracking. It is shown that convection of energy results in a slowing of the drop, as the isotherms get wrapped around the front of the drop. Shape deformation resulting from inertial effects affect the migration velocity. The physical results obtained are in agreement with the existing literature. Furthermore, remarks are made on the sensitivity of the calculated solutions to the smearing of the fluid properties. Analysis and simulations show that the migration velocity depends very strongly on the smearing of the interfacial force whereas it is rather insensitive to the smearing of other properties, hence the adaptive grid. Author

N95-14545*# California Univ., Los Angeles, CA. Dept. of Mechanical Engineering.

GROUND BASED STUDIES OF THERMOCAPILLARY FLOWS IN LEVITATED DROPS

Satwindar Singh Sadhal and Eugene H. Trinh *In* NASA. Lewis Research Center, Second Microgravity Fluid Physics Conference Aug. 1994 p 155-160 (For primary document see N95-14522 03-34)

Avail: CASI HC A02/MF A04; 2 functional color pages

Analytical studies along with ground-based experiments are presently being carried out in connection with thermocapillary phenomena associated with drops and bubbles in a containerless environment. The effort here focuses on the thermal and the fluid phenomena associated with the local heating of acoustically levitated drops, both at 1-g and at low-g. In particular, the Marangoni effect on drops under conditions of local spot-heating and other types of heating are being studied. With the experiments conducted to date, fairly stable acoustic levitation of drops has been achieved and successful flow visualization by light scattering from smoke particles has been carried out. The results include situations with and without heating. As a preliminary qualitative interpretation of these experimental results, we consider the external flow pattern as a superposition of three discrete circulation cells operating on different spatial scales. The observations of the flow fields also indicate the existence of a steady state torque induced by the streaming flows. The theoretical studies have been concentrated on the analysis of streaming flows in a gaseous medium with the presence of a spherical particle undergoing periodic heating. A matched asymptotic analysis was carried out for small parameters derived from approximations in the high frequency range. The heating frequency being 'in tune' with the acoustic frequency results in a nonzero time-averaged thermal field. This leads to a steady heat flow across the equatorial plane of the sphere. Author

N95-14546*# National Aeronautics and Space Administration. Lewis Research Center, Cleveland, OH.

THERMOCAPILLARY MIGRATION AND INTERACTIONS OF BUBBLES AND DROPS

R. Shankar Subramanian (Clarkson Univ., Potsdam, NY.) and R. Balasubramaniam *In its* Second Microgravity Fluid Physics Conference Aug. 1994 p 161-166 (For primary document see N95-14522 03-34) (Grants NAG3-1122; NAG3-1470)

Avail: CASI HC A02/MF A04; 2 functional color pages

Results from ground-based theoretical and experimental research on the motion of bubbles and drops in a temperature gradient are described and a brief account is given of plans for a flight experiment scheduled in 1994. Author

N95-14547*# General Atomics Technologies Corp., San Diego, CA.

UNIFORM HYDROGEN FUEL LAYERS FOR INERTIAL FUSION TARGETS BY MICROGRAVITY **c29**

P. B. Parks and Robert L. Fagaly *In* NASA. Lewis Research Center, Second Microgravity Fluid Physics Conference Aug. 1994 p 167-172 (For primary document see N95-14522 03-34)

Avail: CASI HC A02/MF A04; 2 functional color pages

A critical concern in the fabrication of targets for inertial confinement fusion (ICF) is ensuring that the hydrogenic (D(sub 2) or DT) fuel layer maintains spherical symmetry. Solid layered targets have structural integrity, but lack the needed surface smoothness. Liquid targets are inherently smooth, but suffer from gravitationally induced sagging. One method to reduce the effective gravitational field environment is freefall insertion into the target chamber. Another method to counterbalance field gravitational force is to use an applied magnetic field combined with a gradient field to induce a magnetic dipole force on the liquid fuel layer. Based on time dependent calculations of the dynamics of the liquid fuel layer in microgravity environments, we show that it may be possible to produce a liquid layered ICF target that satisfies both smoothness and symmetry requirements. Author

N95-14548*# National Inst. of Standards and Technology, Gaithersburg, MD.

CONVECTION AND MORPHOLOGICAL STABILITY DURING DIRECTIONAL SOLIDIFICATION **c26**

Sam R. Coriell, A. A. Chernov, Bruce T. Murray, and G. B. McFadden *In* NASA. Lewis Research Center, Second Microgravity Fluid Physics Conference Aug. 1994 p 175-180 (For primary document see N95-14522 03-34)

Avail: CASI HC A02/MF A04; 2 functional color pages

For growth of a vicinal face at constant velocity, the effect of anisotropic interface kinetics on morphological stability is calculated for a binary alloy. The dependence of the interface kinetic coefficient on crystallographic orientation is based on the motion and density of steps. Anisotropic kinetics give rise to traveling waves along the crystal-melt interface, and can lead to a significant enhancement of morphological stability. The stability enhancement increases as the orientation approaches a singular orientation and as the solidification velocity increases. Shear flows interact with the traveling waves and, depending on the direction of the flow, may either stabilize or destabilize the interface. Specific calculations are carried out for germanium-silicon alloys. Author

N95-14549*# Northwestern Univ., Evanston, IL. Dept. of Engineering Sciences and Applied Mathematics.

SHEAR STABILIZATION OF SOLIDIFICATION FRONTS **c26**

Stephen H. Davis and T. P. Schulze *In* NASA. Lewis Research Center, Second Microgravity Fluid Physics Conference Aug. 1994 p 181-186 (For primary document see N95-14522 03-34)

Avail: CASI HC A02/MF A04; 2 functional color pages

A linear-stability analysis is performed on the interface formed during the directional solidification of a dilute binary alloy in the presence of a time-periodic flow. In general, the flow is generated by the elliptical motion of the crystal parallel to the interface. The presence of the flow can either stabilize or destabilize the system relative to the case without flow with the result depending on the frequency and amplitude of the oscillations as well as the properties of the material. In the particular, we find that the morphological instability present in the absence of flow can be entirely suppressed with respect to disturbances of the same frequency as the oscillation. Author

N95-14550*# Ohio State Univ., Columbus.

CRYSTAL GROWTH AND FLUID MECHANICS PROBLEMS IN DIRECTIONAL SOLIDIFICATION **c76**

Saleh Tanveer, Gregory R. Baker, and Michael R. Foster *In* NASA. Lewis Research Center, Second Microgravity Fluid Physics Conference Aug. 1994 p 187-192 (For primary document see N95-14522 03-34)

Avail: CASI HC A02/MF A04; 2 functional color pages

Broadly speaking, our efforts have been concentrated in two aspects of directional solidification: (A) a more complete theoretical understanding of convection effects in a Bridgman apparatus; and (B) a clear understanding of scalings of various features of dendritic crystal growth in the sensitive limit of small capillary effects. For studies that fall within class A, the principal objectives are as follows: (A1) Derive analytical formulas for segregation, interfacial shape and fluid velocities in mathematically amenable asymptotic limits. (A2) Numerically verify and extend asymptotic results to other ranges of parameter space with a view to a broader physical understanding of the general trends. With respect to studies that fall within class B, the principal objectives include answering the following questions about dendritic crystal growth: (B1) Are there unsteady dendrite solutions in 2-D to the completely nonlinear time evolving equations in the small surface tension limit with only a locally steady tip region with well defined tip radius and velocity? Is anisotropy in surface tension necessary for the existence of such solutions as it is for a true steady state needle crystal? How does the size of such a local region depend on capillary effects, anisotropy and undercooling? (B2) How do the different control parameters affect the nonlinear amplification of tip noise and dendritic side branch coarsening? Derived from text

N95-14551*# Institute of Theoretical Astronomy, Cambridge (England). Dept. of Applied Mathematics and Theoretical Physics.

INTERACTIONS BETWEEN SOLIDIFICATION AND COMPOSITIONAL CONVECTION IN MUSHY LAYERS **c26**

M. Grae Worster *In* NASA. Lewis Research Center, Second Microgravity Fluid Physics Conference Aug. 1994 p 193-198 (For primary document see N95-14522 03-34)

Avail: CASI HC A02/MF A04; 2 functional color pages

Mushy layers are ubiquitous during the solidification of alloys. They are regions of mixed phase wherein solid crystals are bathed in the melt from which they grew. The matrix of crystals forms a porous medium

through which the melt can flow, driven either by external forces or by its own buoyancy in a gravitational field. Buoyancy-driven convection of the melt depends both on temperature gradients, which are necessary for solidification, and on compositional gradients, which are generated as certain components of the alloy are preferentially incorporated in the solid phase and the remaining components are expelled into the melt. In fully liquid regions, the combined action of temperature and concentration on the density of the liquid can cause various forms of double-diffusive convection. However, in the interior of mushy regions the temperature and concentration are thermodynamically coupled so only single-diffusive convection can occur. Typically, the effect of composition on the buoyancy of the melt is much greater than the effect of temperature, and thus convection in mushy layers in driven primarily by the computational gradients within them. The rising interstitial liquid is relatively dilute, having come from colder regions of the mushy layer, where the liquidus concentration is lower, and can dissolve the crystal matrix through which it flows. This is the fundamental process by which chimneys are formed. It is a nonlinear process that requires the convective velocities to be sufficiently large, so fully fledged chimneys (narrow channels) might be avoided by means that weaken the flow. Better still would be to prevent convection altogether, since even weak convection will cause lateral, compositional inhomogeneities in castings. This report outlines three studies that examine the onset of convection within mushy layers. Author

N95-14552*# Wooster Coll., OH. Physics Dept.

TURBIDITY OF A BINARY FLUID MIXTURE: DETERMINING ETA

Donald T. Jacobs *In* NASA. Lewis Research Center, Second Microgravity Fluid Physics Conference Aug. 1994 p 201-206 (For primary document see N95-14522 03-34)

Avail: CASI HC A02/MF A04; 2 functional color pages

A ground based (1-g) experiment is in progress that will measure the turbidity of a density-matched, binary fluid mixture extremely close to the critical point. By covering the range of reduced temperatures t is equivalent to (T-T(sub c))/T(sub c) from 10(exp -8) to 10(exp -2), the turbidity measurements will allow the critical exponent eta to be determined. No experiment has determined a value of the critical exponent eta, yet its value is significant to theorists in critical phenomena. Interpreting the turbidity correctly is important if future NASA flight experiments use turbidity as an indirect measurement of relative temperature in shuttle experiments on critical phenomena in fluids. Author

N95-14553*# Pittsburgh Univ., Pittsburgh, PA. Dept. of Physics and Astronomy.

A COARSE GRAINED APPROACH TO THERMOCAPILLARITY EFFECTS IN BINARY SYSTEMS

Jorge Llambias, Aritomo Shinozaki, and David Jasnow *In* NASA. Lewis Research Center, Second Microgravity Fluid Physics Conference Aug. 1994 p 207-212 (For primary document see N95-14522 03-34)

(Grant NAG3-1403)

Avail: CASI HC A02/MF A04; 2 functional color pages

An coarse-grained approach to thermocapillarity effects in binary fluid systems is discussed along with example numerical results. Author

N95-14554*# Lockheed Missiles and Space Co., Palo Alto, CA. Research Lab.

HELIUM 2 SLOSH IN LOW GRAVITY

Graham O. Ross *In* NASA. Lewis Research Center, Second Microgravity Fluid Physics Conference Aug. 1994 p 213-218 (For primary document see N95-14522 03-34)

(Contract NASw-4803)

Avail: CASI HC A02/MF A04; 2 functional color pages

This paper describes the status and plans for the work being performed under NASA NRA contract NASW-4803 so that members of the Microgravity Fluid Dynamics Discipline Working Group are aware of this program. The contract is a cross-disciplinary research program and is administered under the Low Temperature Microgravity Research Program at the Jet Propulsion Laboratory. The purpose of the project is to perform low-gravity verification experiments on the slosh behavior of He II to use in the development of a CFD model that incorporates the two-fluid physics of He II. The two-fluid code predicts a different fluid motion response in low-gravity environment from that predicted by a single-fluid model, while the 1g response is identical for the both types of model. Author

N95-14555*# Levy (Salomon), Inc., Campbell, CA.

STUDY OF TWO-PHASE FLOW AND HEAT TRANSFER IN REDUCED GRAVITIES

Davood Abdollahian and Fred Barez *In* NASA. Lewis Research Center, Second Microgravity Fluid Physics Conference Aug. 1994 p 221-226 (For primary document see N95-14522 03-34)

Avail: CASI HC A02/MF A04; 2 functional color pages

Design of the two-phase systems which are anticipated to be utilized in future spacecraft thermal management systems requires a knowledge of two-phase flow and heat transfer parameters in reduced gravities. A program has been initiated by NASA to design a two-phase test loop and perform a series of experiments to generate the data for the Critical Heat Flux (CHF) and onset of instability under reduced gravities. In addition to low gravity airplane trajectory testing, the experimental program consists of a set of laboratory tests with vertical upflow and downflow configurations. Modularity is considered in the design of this experiment and the test loop in instrumented to provide data for two-phase pressure drop and flow regime behavior. Since the program is in the final stages of the design and construction task, this article is intended to discuss the phenomena, design approach, and the description of the test loop. Author

N95-14556*# National Aeronautics and Space Administration. Lewis Research Center, Cleveland, OH.

CHARACTERIZATION OF ANNULAR TWO-PHASE GAS-LIQUID FLOWS IN MICROGRAVITY

W. Scott Bousman (Houston Univ., TX.) and John B. McQuillen *In its* Second Microgravity Fluid Physics Conference Aug. 1994 p 227-232 (For primary document see N95-14522 03-34)

(Grant NAG3-510)

Avail: CASI HC A02/MF A04; 2 functional color pages

A series of two-phase gas-liquid flow experiments were developed to study annular flows in microgravity using the NASA Lewis Learjet. A test section was built to measure the liquid film thickness around the perimeter of the tube permitting the three dimensional nature of the gas-liquid interface to be observed. A second test section was used to measure the film thickness, pressure drop and wall shear stress in annular microgravity two-phase flows. Three liquids were studied to determine the effects of liquid viscosity and surface tension. The result of this study provide insight into the wave characteristics, pressure drop and droplet entrainment in microgravity annular flows. Author

N95-14557*# Rensselaer Polytechnic Inst., Troy, NY. Center for Multiphase Research.

ANALYSIS OF PHASE DISTRIBUTION PHENOMENA IN MICROGRAVITY ENVIRONMENTS **c29**

Richard Lahey, Jr. and Fabian Bonetto *In* NASA. Lewis Research Center, Second Microgravity Fluid Physics Conference Aug. 1994 p 233-240 (For primary document see N95-14522 03-34)

Avail: CASI HC A02/MF A04; 2 functional color pages

In the past one of NASA's primary emphasis has been on identifying single and multiphase flow experiments which can produce new discoveries that are not possible except in a microgravity environment. While such experiments are obviously of great scientific interest, they do not necessarily provide NASA with the ability to use multiphase processes for power production and/or utilization in space. The purpose of the research presented in this paper is to demonstrate the ability of multidimensional two-fluid models for bubbly two-phase flow to accurately predict lateral phase distribution phenomena in microgravity environments. If successful, this research should provide NASA with mechanistically-based analytical methods which can be used for multiphase space design and evaluation, and should be the basis for future shuttle experiments for model verification. Author

N95-14558*# Wisconsin Univ., Milwaukee, WI. Dept. of Mechanical Engineering.

EXPERIMENTAL AND THEORETICAL STUDIES OF REWETTING OF UNHEATED/HEATED GROOVED PLATES

Shih H. Chan *In* NASA. Lewis Research Center, Second Microgravity Fluid Physics Conference Aug. 1994 p 241-246 (For primary document see N95-14522 03-34)

(Grant NAG3-1381)

Avail: CASI HC A02/MF A04; 2 functional color pages

Theoretical experimental investigations of the rewetting characteristics

of thin liquid films over unheated and heated grooved plates were performed. Studied factors which affected the rewetting characteristics of the plate were mass flow rate of the rewetting liquid on the plate, the orientation of the plate (face up, face down or inclined) and smooth/groove surface conditions. The initial plate temperature was also varied, with experiments being performed between room temperature and 150 C. It was found that the rewetting velocity increased with the initial plate temperature. But when the temperature was increased further above the Leidenfrost temperature (liquid front temperature), the rewetting velocity decreases with the initial plate temperature. Hydrodynamically controlled and conductively controlled rewetting models were presented to explain and to predict the rewetting characteristics in these two distinct regions. Also found was a higher rewetting velocity when the grooved plate was placed in the face up orientation than in the face down orientation. Author

N95-14559*# Dayton Univ., OH. Dept. of Mechanical and Aerospace Engineering.

EFFECTS OF THERMOCAPILLARITY ON AN EVAPORATING EXTENDED MENISCUS IN MICROGRAVITY

Kevin P. Hallinan and Q. He *In* NASA. Lewis Research Center, Second Microgravity Fluid Physics Conference Aug. 1994 p 247-252 (For primary document see N95-14522 03-34)

(Grant NAG3-1391)

Avail: CASI HC A02/MF A04; 2 functional color pages

An analytical investigation of the effects of thermocapillarity on the flow field within and heat transfer from the extended meniscus region of a heated meniscus which is re-supplied by capillarity is presented. Microgravity conditions are considered. The analysis shows that even for extremely small temperature differences between the wall and the vapor (less than 1 mK) thermocapillary stresses at the liquid-vapor interface due to a non-uniform interfacial temperature drastically alters the flow field. At the same time, these stresses were shown to have only a slight effect on the heat transfer from the extended meniscus but increasing with an increasing temperature difference. Additionally, thermocapillary effects were shown to be sensitive to pore size. A criterion was established from a scaling analysis identifying the conditions necessary for thermocapillarity to affect the operation of capillary-pumped heat transport devices in microgravity. A critical Marangoni number and corresponding critical temperature difference between wall and vapor were identified. Author

N95-14560*# Rensselaer Polytechnic Inst., Troy, NY. Dept. of Chemical Engineering.

INTERFACIAL FORCE FIELD CHARACTERIZATION OF A CONSTRAINED VAPOR BUBBLE THERMOSYPHON USING IAI

Sunando DasGupta, Joel L. Plawsky, and Peter C. Wayner, Jr. *In* NASA. Lewis Research Center, Second Microgravity Fluid Physics Conference Aug. 1994 p 253-258 (For primary document see N95-14522 03-34)

(Grant NAG3-1399)

Avail: CASI HC A02/MF A04; 2 functional color pages

The isothermal profiles of the extended meniscus in a quartz cuvette were measured in a gravitational field using IAI (image analyzing interferometer) which is based on computer enhanced video microscopy of the naturally occurring interference fringes. The experimental results for heptane and pentane menisci were analyzed using the extended Young-Laplace Equation. These isothermal results characterized the interfacial force field in-situ at the start of the heat transfer experiments by quantifying the dispersion constant for the specific liquid-solid system. The experimentally obtained values of the disjoining pressures and the dispersion constants are compared to the subsequent non-isothermal experiments because one of the major variables in the heat sink capability of the CVBT is the dispersion constant. In all previous studies of micro heat pipes the value of the dispersion constant has been 'guesstimated'. The major advantages of the current glass cell is the ability to view the extended meniscus at all times. Experimentally, we find that the extended Young-Laplace Equation is an excellent model for for the force field at the solid-liquid vapor interfaces. Author

N95-14561*# Washington State Univ., Pullman, WA. Dept. of Mechanical and Materials Engineering.

BUBBLE DYNAMICS, TWO-PHASE FLOW, AND BOILING HEAT TRANSFER IN A MICROGRAVITY ENVIRONMENT

Jacob N. Chung *In* NASA. Lewis Research Center, Second Microgravity Fluid Physics Conference Aug. 1994 p 259-264 (For primary document see N95-14522 03-34)

Avail: CASI HC A02/MF A04; 2 functional color pages

The two-phase bubbly flow and boiling heat transfer in microgravity represents a substantial challenge to scientists and engineers and yet there is an urgent need to seek fundamental understanding in this area for future spacecraft design and space missions. At Washington State University, we have successfully designed, built and tested a 2.1 second drop tower with an innovation airbag deceleration system. Microgravity boiling experiments performed in our 0.6 second Drop Tower produced data flow visualizations that agree with published results and also provide some new understanding concerning flow boiling and microgravity bubble behavior. On the analytical and numerical work, the edge effects of finite divergent electrode plates on the forces experienced by bubbles were investigated. Boiling in a concentric cylinder microgravity and an electric field was numerically predicted. We also completed a feasibility study for microgravity boiling in an acoustic field. Author

N95-14562*# Michigan Univ., Ann Arbor, MI. Mechanical Engineering.

POOL AND FLOW BOILING IN VARIABLE AND MICROGRAVITY c29

Herman Merte, Jr. *In* NASA. Lewis Research Center, Second Microgravity Fluid Physics Conference Aug. 1994 p 265-272 (For primary document see N95-14522 03-34)

Avail: CASI HC A02/MF A04; 2 functional color pages

As is well known, boiling is an effective mode of heat transfer in that high heat flux levels are possible with relatively small temperature differences. Its optimal application requires that the process be adequately understood. A measure of the understanding of any physical event lies in the ability to predict its behavior in terms of the relevant parameters. Despite many years of research the predictability of boiling is currently possible only for quite specialized circumstances, e.g., the critical heat flux and film boiling for the pool boiling case, and then only with special geometries. Variable gravity down to microgravity provides the opportunity to test this understanding, but possibly more important, by changing the dimensional and time scales involved permits more detailed observations of elements involved in the boiling process, and perhaps discloses phenomena heretofore unknown. The focus here is on nucleate boiling although, as will be demonstrated below, under but certain circumstances in microgravity it can take place concurrently with the dryout process. In the presence of earth gravity or forced convection effects, the latter process is usually referred to as film boiling. However, no vapor film as such forms with pool boiling in microgravity, only dryout. Initial results are presented here for pool boiling in microgravity, and were made possible at such an early date by the availability of the Get-Away-Specials (GAS). Also presented here are some results of ground testing of a flow loop for the study of low velocity boiling, eventually to take place also in microgravity. In the interim, variable buoyancy normal to the heater surface is achieved by rotation of the entire loop relative to earth gravity. Of course, this is at the expense of varying the buoyancy parallel to the heater surface. Two questions which must be resolved early in the study of flow boiling in microgravity are (1) the lower limits of liquid flow velocity where buoyancy effects become significant to the boiling process (2) the effect of lower liquid flow velocities on the Critical Heat Flux when buoyancy is removed. Results of initial efforts in these directions are presented, albeit restricted currently to the ever present earth gravity. Author

N95-14563*# Carnegie-Mellon Univ., Pittsburgh, PA.

TRANSPORT PHENOMENA IN STRATIFIED MULTI-FLUID FLO W IN THE PRESENCE AND ABSENCE OF GRAVITY

Norman Chigier, Min Xu, David Squarer, and Nasser Rashidnia *In* NASA. Lewis Research Center, Second Microgravity Fluid Physics Conference Aug. 1994 p 273-278 (For primary document see N95-14522 03-34)

Avail: CASI HC A02/MF A04; 2 functional color pages

An experiment is being conducted to study the effects of buoyancy on planar stratified flows. A wind tunnel has been designed and constructed to generate planar flows with separate heating for the top and bottom planar air jets emerging from slot nozzles separated by an insulating splitter plate. The objective is to generate planar jet flows with well defined and well controlled velocity and temperature profiles. Magnitudes of velocity and temperature will be varied separately in each flow for both laminar and turbulent flow conditions. Both stably and unstably stratified flows will

be studied by changing the temperature distributions in each air stream. This paper reports on the design of the apparatus and initial measurements of velocity and turbulence made by laser Doppler velocimetry. Author

N95-14564*# National Aeronautics and Space Administration. Langley Research Center, Hampton, VA.
PARTICLE EXPERIMENTS IN THERMAL AND VELOCITY GRADIENTS
Ivan O. Clark and Edward J. Johnson *In* NASA. Lewis Research Center, Second Microgravity Fluid Physics Conference Aug. 1994 p 279-284 (For primary document see N95-14522 03-34)
Avail: CASI HC A02/MF A04; 2 functional color pages

The physical scales of velocity, length, time, thermal gradient magnitude likely to be involved in gas-solid multiphase flight experiments are assessed for 1-100 micron particles. Author

N95-14565*# Missouri Univ., Columbia, MO. Particulate Systems Research Center.
CROSS-EFFECTS IN MICROGRAVITY FLOWS **c29**
Sudarshan K. Loyalka *In* NASA. Lewis Research Center, Second Microgravity Fluid Physics Conference Aug. 1994 p 285-289 (For primary document see N95-14522 03-34)
Avail: CASI HC A01/MF A04; 2 functional color pages

In microgravity materials growth (i.e., crystal growth via vapor deposition) experiments, it is of interest ot understand and control the flows that arise from the molecular rather than the mere continuum nature of the gases and the vapors. The project research is a theoretical and experimental investigation of the flow of gas/vapor mixtures in realistic geometries and environments, as well as the application of new fundamental understandings to simulating flows in the ampoules. Towards this goal, the research tasks are: to obtain a theoretical description of the flow by solving appropriate kinetics equations; to verify the results by acquiring experimental data in a diffusion cell; and to explore applications of the results above to simulations of flows in the ampoules. The paper provides a description of the cross-phenomena and the progress realized to-date by the project personnel. Author

N95-14566*# Notre Dame Univ., IN. Dept. of Chemical Engineering.
TWO-LAYER VISCOUS INSTABILITY IN A ROTATING COUETTE DEVICE
Christopher Gallagher, Tom Kropnewicki, David T. Leighton, and Mark j. McCready *In* NASA. Lewis Research Center, Second Microgravity Fluid Physics Conference Aug. 1994 p 291-296 (For primary document see N95-14522 03-34)
(Grant NAG3-1398)
Avail: CASI HC A02/MF A04; 2 functional color pages

A novel experiment to study the interfacial shear instability between two liquids is described. Density-matched immiscible liquids are confined between concentric cylinders such that the interface is parallel to the cylinder walls. Interfacial waves that develop because of viscosity differences between the shearing fluids are studied as a function of rotation rate and depth ratio using optical techniques. Conditions neutral stability and the most unstable wavenumber agree reasonably well with predictions from linear stability analysis of the Navier-Stokes equations. Illumination using laser sheets allows precise measurement of the interface shape. Future experiments will verify the correctness of weakly nonlinear theories that describe energy transfer and saturation of wave growth by nonlinear effects. Measurements of solitary wave shapes, that occur far above neutral stability, will be compared to similar measurements for systems that have gravity as an important force to determine how gravity effects large disturbances. These results will be used to interpret slug and annular flow data that have been obtained in other mu g studies. Author

N95-14567*# Creare, Inc., Hanover, NH.
AN APPLICATION OF MINISCALE EXPERIMENTS ON EARTH TO REFINE MICROGRAVITY ANALYSIS OF ADIABATIC MULTIPHASE FLOW IN SPACE **c29**
Paul H. Rothe, Christine Martin, and Julie Downing *In* NASA. Lewis Research Center, Second Microgravity Fluid Physics Conference Aug. 1994 p 297-302 (For primary document see N95-14522 03-34)
Avail: CASI HC A02/MF A04; 2 functional color pages

Adiabatic two-phase flow is of interest to the design of multiphase fluid and thermal management systems for spacecraft. This paper presents original data and unifies existing data for capillary tubes as a step toward assessing existing multiphase flow analysis and engineering software. Comparisons of theory with these data once again confirm the broad accuracy of the theory. Due to the simplicity and low cost of the capillary tube experiments, which were performed on earth, we were able to closely examine for the first time a flow situation that had not previously been examined appreciably by aircraft tests. This is the situation of a slug flow at high quality, near transition to annular flow. Our comparison of software calculations with these data revealed overprediction of pipeline pressure drop by up to a factor of three. In turn, this finding motivated a reexamination of the existing theory, and then development of a new analytical and is in far better agreement with the data. This sequence of discovery illustrates the role of inexpensive miniscale modeling on earth to anticipate microgravity behavior in space and to complete and help define needs for aircraft tests. Author

N95-14568*# California Univ., Los Angeles, CA. Dept. of Physics.
MICROGRAVITY FOAM STRUCTURE AND RHEOLOGY **c29**
Douglas J. Durian and Anthony D. Gopal *In* NASA. Lewis Research Center, Second Microgravity Fluid Physics Conference Aug. 1994 p 305-310 (For primary document see N95-14522 03-34)
Avail: CASI HC A02/MF A04; 2 functional color pages

Our long-range objective is to establish the fundamental interrelationship between the microscopic structure and dynamics of foams and their macroscopic stability and rheology. Foam structure and dynamics are to be measured directly and noninvasively through the use and development of novel multiple light scattering techniques such as diffusing-wave spectroscopy (DWS). Foam rheology is to be measured in a custom rheometer which allows simultaneous optical access for multiple light drainage of liquid from in between gas bubbles as the liquid:gas volume fraction in increased towards the rigidity-loss transition. Author

N95-14569*# Harvard Univ., Cambridge, MA. Div. of Applied Sciences.
THE EXTENSIONAL RHEOLOGY OF NON-NEWTONIAN MATERIALS
Stephen H. Spiegelberg, Samuel Gaudet, and Gareth H. McKinley *In* NASA. Lewis Research Center, Second Microgravity Fluid Physics Conference Aug. 1994 p 311-317 (For primary document see N95-14522 03-34)
Avail: CASI HC A02/MF A04; 2 functional color pages

It has been proposed to measure the extensional viscosity function of a non-Newtonian polymer solution in a reduced gravity environment as part of the Advanced Fluid Module. In ground-based extensional measurements, the no-sip boundary condition at solid-fluid interfaces always result in appreciable shear gradients in the test fluid; however the removal of gravitational body forces permits controlled extensional deformation of containerless test samples and the first unambiguous measurements of this kind. Imperative to successful implementation of this experiment is the generation and subsequent deformation of a stable cylindrical column of test fluid. A study of the generation and deformation of liquid bridges demonstrates that Newtonian liquid bridges undergo capillary breakup as anticipated when stretched beyond a critical aspect ratio; non-Newtonian liquid bridges, however, are stabilized by the strain-hardening phenomenon exhibited by these materials. Numerical simulations of Newtonian breakup are compared with experimental results, and show that previous ground-based attempts at measuring the extensional viscosity of Newtonian fluids are of limited accuracy. Author

N95-14570*# Pittsburgh Univ., Pittsburgh, PA. Dept. of Physics and Astronomy.
NUCLEATION AND CHIRAL SYMMETRY BREAKING UNDER CONTROLLED HYDRODYNAMIC FLOWS
Xiao-Lun Wu, Brian Martin, and Arnold Tharrington *In* NASA. Lewis Research Center, Second Microgravity Fluid Physics Conference Aug. 1994 p 319-324 (For primary document see N95-14522 03-34)
Avail: CASI HC A02/MF A04; 2 functional color pages

The effects of hydrodynamic convection on nucleation and broken chiral symmetry have been investigated for a simple inorganic molecule, sodium chlorate ($NaClO_3$). Our experiment suggests that the symmetry breaking is a result of hydrodynamic amplification of rare nucleation events. The effect is more pronounced when the primary nucleation occurs on the solute-vapor interface, where mixing in the surface sublayer becomes important. The

transition from the achiral to the chiral states appears to be smooth as the hydrodynamic parameters, such as flow rate, are varied. Author

N95-14571*# Iowa Univ., Iowa City, IA.
PLASMA DUST CRYSTALLIZATION **c75**
John Goree, H. Thomas, and G. Morfill *In* NASA. Lewis Research Center, Second Microgravity Fluid Physics Conference Aug. 1994 p 325-330 (For primary document see N95-14522 03-34)
(Grant NAG8-292)
Avail: CASI HC A02/MF A04; 2 functional color pages

In a ground-based definition study, a concept for a new type of microgravity experiment is developed. We formed a new state of matter: a crystalline lattice structure of charged micron-size spheres, suspended in a charge-neutral plasma. The plasma is formed by a low-pressure radio-frequency argon discharge. Solid microspheres are introduced, and they gain a negative electric charge. They are cooled by molecular drag on the ambient neutral gas. They are detected by laser light scattering and video photography. Laboratory experiments have demonstrated that a two-dimensional nonquantum lattice forms through the Coulomb interaction of these spheres. Microgravity is thought to be required to observe a three-dimensional structure. Author

N95-14572*# National Aeronautics and Space Administration. Lewis Research Center, Cleveland, OH.
FLOCCULATION AND AGGREGATION IN A MICROGRAVITY ENVIRONMENT (FAME) **c29**
Rafat R. Ansari, Harbans S. Dhadwal, and Kwang I. Suh *In its* Second Microgravity Fluid Physics Conference Aug. 1994 p 333-339 (For primary document see N95-14522 03-34)
Avail: CASI HC A02/MF A04; 2 functional color pages

An experiment to study flocculation phenomena in the constrained microgravity environment of a space shuttle or space station is described. The small size and light weight experiment easily fits in a Spacelab Glovebox. Using an integrated fiber optic dynamic light scattering (DLS) system we obtain high precision particle size measurements from dispersions of colloidal particles within seconds, needs no onboard optical alignment, no index matching fluid, and offers sample mixing and shear melting capabilities to study aggregation (flocculation and coagulation) phenomena under both quiescent and controlled agitation conditions. The experimental system can easily be adapted for other microgravity experiments requiring the use of DLS. Preliminary results of ground-based study are reported. Author

N95-14573*# Princeton Univ., NJ. Dept. of Physics.
DYNAMICS OF HARD SPHERE COLLOIDAL DISPERSIONS
J. X. Zhu, Paul M. Chaikin, S.-E. Phan, and W. B. Russel *In* NASA. Lewis Research Center, Second Microgravity Fluid Physics Conference Aug. 1994 p 341-345 Original contains color illustrations (For primary document see N95-14522 03-34)
(Grant NAG3-1158)
Avail: CASI HC A01/MF A04; 2 functional color pages

Our objective is to perform on homogeneous, fully equilibrated dispersions the full set of experiments characterizing the transition from fluid to solid and the properties of the crystalline and glassy solid. These include measurements quantifying the nucleation and growth of crystallites, the structure of the initial fluid and the fully crystalline solid, and Brownian motion of particles within the crystal, and the elasticity of the crystal and the glass. Experiments are being built and tested for ideal microgravity environment. Here we describe the ground based effort, which exploits a fluidized bed to create a homogeneous, steady dispersion for the studies. The differences between the microgravity environment and the fluidized bed is gauged by the Peclet number Pe, which measures the rate of convection/sedimentation relative to Brownian motion. We have designed our experiment to accomplish three types of measurements on hard sphere suspensions in a fluidized bed: the static scattering intensity as a function of angle to determine the structure factor, the temporal autocorrelation function at all scattering angles to probe the dynamics, and the amplitude of the response to an oscillatory forcing to deduce the low frequency viscoelasticity. Thus the scattering instrument and the colloidal dispersion were chosen such as that the important features of each physical property lie within the detectable range for each measurement. Derived from text

N95-14574*# Massachusetts Inst. of Tech., Cambridge. Dept. of Chemical Engineering.
MEASUREMENT OF RESISTANCE TO SOLUTE TRANSPORT ACROSS SURFACTANT-LADEN INTERFACES USING A FLUORESCENCE RECOVERY AFTER PHOTOBLEACHING (FRAP) TECHNIQUE
Edward P. Browne, Thierry Nivaggioli, and T. Alan Hatton *In* NASA. Lewis Research Center, Second Microgravity Fluid Physics Conference Aug. 1994 p 347-352 Original contains color illustrations (For primary document see N95-14522 03-34)
Avail: CASI HC A02/MF A04; 2 functional color pages

A noninvasive fluorescence recovery after photobleaching (FRAP) technique is under development to measure interfacial transport in two phase systems without disturbing the interface. The concentration profiles of a probe solute are measured in both sides of the interface by argon-ion laser, and the system relaxation is then monitored by a microscope-mounted CCD camera. Author

N95-14575*# Princeton Univ., NJ. Dept. of Physics.
NEW TECHNIQUES FOR DIFFUSING-WAVE SPECTROSCOPY **c25**
T. G. Mason, Hu Gang, A. H. Krall, and David A. Weitz *In* NASA. Lewis Research Center, Second Microgravity Fluid Physics Conference Aug. 1994 p 353-360 (For primary document see N95-14522 03-34)
Avail: CASI HC A02/MF A04; 2 functional color pages

We present two new types of measurements that can be made with diffusing-wave spectroscopy (DWS), a form of dynamic light scattering that applies in limit of strong multiple scattering. The first application is to measure the frequency-dependent linear viscoelastic moduli of complex fluids using light scattering. This is accomplished by measuring the mean square displacement of probe particles using DWS. Their response to thermal fluctuations is determined by the fluctuation-dissipation relation, and is controlled by the response of the surrounding complex fluid. This response can be described in terms of a memory function, which is directly related to the complex elastic modulus of the system. Thus by measuring the mean square displacement, we are able to determine the frequency dependent modulus. The second application is the measurement of shape fluctuations of scattering particles. This is achieved by generalizing the theory for DWS to incorporate the effects if amplitude fluctuations in the scattering intensity of the particles. We apply this new method to study the thermally induced fluctuations in the shape of spherical emulsion droplets whose geometry is controlled by surface tension. Author

N95-14576*# Arizona Univ., Tucson, AZ. Dept. of Chemical Engineering.
ELECTROHYDRODYNAMIC DEFORMATION AND INTERACTION OF A PAIR OF EMULSION DROPS
James C. Baygents *In* NASA. Lewis Research Center, Second Microgravity Fluid Physics Conference Aug. 1994 p 363-368 (For primary document see N95-14522 03-34)
Avail: CASI HC A02/MF A04; 2 functional color pages

The response of a pair of emulsion drops to the imposition of a uniform electric field is examined. The case studied is that of equal-sized drops whose line of centers is parallel to the axis of the applied field. A new boundary integral solution to the governing equations of the leaky dielectric model is developed; the formulation accounts for the electrostatic and hydrodynamic interactions between the drops, as well as their deformations. Numerical calculations show that, after an initial transient during which the drops primarily deform, the pair drift slowly together due to their electrostatic interactions. Author

N95-14577*# National Aeronautics and Space Administration. Marshall Space Flight Center, Huntsville, AL.
ROLE OF DIELECTRIC CONSTANT IN ELECTROHYDRODYNAMICS OF CONDUCTING FLUIDS **c33**
Percy H. Rhodes, Robert S. Snyder, and Glyn O. Roberts *In* NASA. Lewis Research Center, Second Microgravity Fluid Physics Conference Aug. 1994 p 369-374 (For primary document see N95-14522 03-34)
Avail: CASI HC A02/MF A04; 2 functional color pages

Electrohydrodynamic sample distortion during continuous flow electrophoresis is an experiment to be conducted during the second International Microgravity Laboratory (IML-2) in July 1994. The specific objective of this experiment is the distortion caused by the difference in dielectric constant between the sample and surrounding buffer. Although

the role of sample conductivity in electrohydrodynamic has been the subject of both flight and ground experiments, the separate role of dielectric constant, independent of sample conductivity, has not been measured. This paper describes some of the laboratory research and model development that will support the flight experiment on IML-2. Author

N95-14578*# Colorado Univ., Boulder, CO. Dept. of Chemical Engineering.

ELECTROPHORETIC INTERACTIONS AND AGGREGATION OF COLLOIDAL BIOLOGICAL PARTICLES **c25**

Robert H. Davis, Scott C. Nichols, Michael Loewenberg, and Paul Todd *In* NASA. Lewis Research Center, Second Microgravity Fluid Physics Conference Aug. 1994 p 379-384 (For primary document see N95-14522 03-34)

(Grant NAG8-945)

Avail: CASI HC A02/MF A04; 2 functional color pages

The separation of cells or particles from solution has traditionally been accomplished with centrifuges or by sedimentation; however, many particles have specific densities close to unity, making buoyancy-driven motion slow or negligible, but most cells and particles carry surface charges, making them ideal for electrophoretic separation. Both buoyancy-driven and electrophoretic separation may be influenced by hydrodynamic interactions and aggregation of neighboring particles. Aggregation by electrophoresis was analyzed for two non-Brownian particles with different zeta potentials and thin double layers migrating through a viscous fluid. The results indicate that the initial rate of electrophoretically-driven aggregation may exceed that of buoyancy-driven aggregation, even under conditions in which buoyancy-driven relative motion of noninteracting particles is dominant. Author

N95-14579*# Delaware Univ., Newark, DE. Dept. of Chemical Engineering.

SURFACTANT-BASED CRITICAL PHENOMENA IN MICROGRAVITY **c29**

Eric W. Kaler and Michael E. Paulaitis *In* NASA. Lewis Research Center, Second Microgravity Fluid Physics Conference Aug. 1994 p 387-392 (For primary document see N95-14522 03-34)

(Grant NSF DMR-91-22444)

Avail: CASI HC A02/MF A04; 2 functional color pages

The objective of this research project is to characterize by experiment and theoretically both the kinetics of phase separation and the metastable structures produced during phase separation in a microgravity environment. The particular systems we are currently studying are mixtures of water, nonionic surfactants, and compressible supercritical fluids at temperatures and pressures where the coexisting liquid phases have equal densities (isopycnic phases). In this report, we describe experiments to locate equilibrium isopycnic phases and to determine the 'local' phase behavior and critical phenomena at nearby conditions of temperature, pressure, and composition. In addition, we report the results of preliminary small angle neutron scattering (SANS) experiments to characterize microstructures that exist in these mixtures at different fluid densities. Author

N95-14580*# Case Western Reserve Univ., Cleveland, OH. Dept. of Mechanical and Aerospace Engineering.

GRAVITY-DEPENDENT TRANSPORT IN INDUSTRIAL PROCESSES **c29**

Simon Ostrach and Yasuhiro Kamotani *In* NASA. Lewis Research Center, Second Microgravity Fluid Physics Conference Aug. 1994 p 393-400 (For primary document see N95-14522 03-34)

Avail: CASI HC A02/MF A04; 2 functional color pages

Gravity-dependent transport phenomena in various industrial processes are investigated in order to address a broader range of microgravity phenomena and to develop new applications of microgravity. A number of important topics are identified and analyzed in detail. The present article describes results on coating flow, zeolite growth, and rotating electrochemical system. Author (revised)

N95-14581*# Carnegie-Mellon Univ., Pittsburgh, PA. Dept. of Chemical Engineering.

ELECTROKINETIC TRANSPORT OF HETEROGENEOUS PARTICLES IN SUSPENSION **c25**

D. Velegol, Stephen Garoff, and John L. Anderson *In* NASA. Lewis Research Center, Second Microgravity Fluid Physics Conference Aug. 1994 p 401-405 (For primary document see N95-14522 03-34)

(Grant NAG8-964)

Avail: CASI HC A01/MF A04; 2 functional color pages

The Smoluchowski equation for electrophoresis predicts that the electrophoretic velocity of a particle is proportional to its zeta potential but not its size, shape, or orientation. Furthermore, the equation predicts that the rotation rate is identically zero. The Smoluchowski equation fails for heterogeneous particles (i.e., those with nonuniform zeta potentials). Recent theories and experiments show that particles with a dipole moment of zeta potential rotate into alignment with an externally applied electric field. For doublets (particles composed of two spheres) the rotation rate depends on (1) whether the spheres are rigidly rocked or freely rotating, and (2) the gap distance between the spheres. The relative configuration of two coagulated spheres is determined by the colloidal forces of the system. The goal of our research is to use measurements of electrophoretic rotation to determine the gap between two spheres of a colloidal doublet and also to determine whether or not the doublet is rigid. Author

N95-14582*# National Aeronautics and Space Administration. Lewis Research Center, Cleveland, OH.

THE PATH TO AN EXPERIMENT IN SPACE (FROM CONCEPT TO FLIGHT) **c12**

Jack A. Salzman *In its* Second Microgravity Fluid Physics Conference Aug. 1994 p 409-418 (For primary document see N95-14522 03-34)

Avail: CASI HC A02/MF A04; 2 functional color pages

The following are discussed in this viewgraph presentation on developing flight experiments for NASA's Microgravity Science and Applications Program: time from flight PI selection to launch; key flight experiment phases and schedule drivers; microgravity experiment definition/development process; definition and engineering development phase; ground-based reduced gravity research facilities; project organization; responsibilities and duties of principle investigator/co-investigators, project scientist, and project manager; the science requirements document; flight development phase; experiment cost and schedule; and keys to experiment success. CASI

N95-14583*# National Aeronautics and Space Administration. Lewis Research Center, Cleveland, OH.

FLUIDS FLIGHT HARDWARE

Nancy Shaw *In its* Second Microgravity Fluid Physics Conference Aug. 1994 p 419-427 (For primary document see N95-14522 03-34)

Avail: CASI HC A02/MF A04; 2 functional color pages

The following are discussed in this viewgraph presentation: Glovebox-2 investigations, study of oscillatory thermocapillary flows and validate physical models on the second U.S. Microgravity Laboratory Mission (USML-2), pool boiling experiment, critical fluid viscosity measurement experiment, Hitchhiker-G typical structural configuration, ZENO-critical fluid light scattering experiment, isothermal dendritic growth experiment, microgravity acceleration environment support, and the space acceleration measurement system (SAMS). CASI

N95-14584*# National Aeronautics and Space Administration. Lewis Research Center, Cleveland, OH.

CONCEPTUAL DESIGN OF THE SPACE STATION FLUIDS MODULE **c19**

Dennis W. Rohn, Daniel P. Morilak, Jennifer L. Rhatigan, and Todd T. Peterson *In its* Second Microgravity Fluid Physics Conference Aug. 1994 p 429-448 (For primary document see N95-14522 03-34)

Avail: CASI HC A03/MF A04; 2 functional color pages

The purpose of this paper is to describe the conceptual design of the Fluids Module for the International Space Station Alpha (ISSA). This module is part of the Space Station Fluids/Combustion Facility (SS FCF) under development at the NASA Lewis Research Center. The Fluids/Combustion Facility is one of several science facilities which are being developed to support microgravity science investigations in the US Laboratory Module of the ISSA. The SS FCF will support a multitude of fluids and combustion science investigations over the lifetime of the ISSA and return state-of-the-art science data in a timely and efficient manner to the scientific communities. This will be accomplished through modularization of hardware, with planned, periodic upgrades; modularization of like scientific investigations that make use of common facility functions; and use of orbital replacement units (ORU's) for incorporation of new technology and new functionality. Portions of the SS FCF are scheduled to become operational on-orbit in 1999. The

Fluids Module is presently scheduled for launch to orbit and integration with the Fluids/Combustion Facility in 2001. The objectives of this paper are to describe the history of the Fluids Module concept, the types of fluids science investigations which will be accommodated by the module, the hardware design heritage, the hardware concept, and the hardware breadboarding efforts currently underway. Derived from text

N95-14605# Stanford Univ., CA. Dept. of Mathematics.
MATHEMATICAL PROBLEMS OF NONLINEAR WAVE PROPAGATION AND OF WAVES IN HETEROGENEOUS MEDIA Final Report, 1 Nov. 1990 - 31 Oct. 1993
Joseph Keller 31 Oct. 1993 5 p
(Grant AF-AFOSR-0061-91)
(AD-A282217; AFOSR-94-0328TR) Avail: CASI HC A01/MF A01

This document contains a brief outline of research findings, and manuscripts published or submitted for publication. Some of the findings are on the following subject areas: non-reflecting boundary conditions to elastic waves, finite element method for domains with corners, motion of slender jets and thin sheets taking account of surface tension, singularities of semilinear waves, stability of rotating shear flows in shallow water by asymptotic method, tri-stable reaction diffusion equations, and semilinear heat equation. CASI

N95-14607*# National Aeronautics and Space Administration. Lewis Research Center, Cleveland, OH.
A MODIFIED MIXING LENGTH TURBULENCE MODEL FOR ZERO AND ADVERSE PRESSURE GRADIENTS M.S. Thesis - Akron Univ., 1993
Julianne M. Conley and B. P. Leonard Nov. 1994 23 p Presented at the 30th Joint Propulsion Conference, Indianapolis, IN, 27-29 Jun. 1994; cosponsored by AIAA, ASME, SAE, and ASEE See also N94-32947
(RTOP 505-62-52)
(NASA-TM-106772; E-9220; NAS 1.15:106772) Avail: CASI HC A03/MF A01

The modified mixing length (MML) turbulence model was installed in the Proteus Navier-Stokes code, then modified to make it applicable to a wider range of flows typical of aerospace propulsion applications. The modifications are based on experimental data for three flat-plate flows having zero, mild adverse, and strong adverse pressure gradients. Three transonic diffuser test cases were run with the new version of the model in order to evaluate its performance. All results are compared with experimental data and show improvements over calculations made using the Baldwin-Lomax turbulence model, the standard algebraic model in Proteus. Author

N95-14658 Naval Postgraduate School, Monterey, CA. Dept. of Mechanical Engineering.
SPECTRAL ANALYSIS OF VORTEX/FREE-SURFACE INTERACTION M.S. Thesis
Glenn D. Hofert Jun. 1994 73 p Limited Reproducibility: More than 20% of this document may be affected by microfiche quality
(AD-A283210) Avail: CASI HC A04

The unsteady flow phenomena resulting from the interaction of vorticity with a free surface has been investigated through the use of a three-color Laser Doppler-Velocimeter. The vorticity field was provided by a single tip vortex generated by an airfoil, placed in the test section of a recirculating water tunnel at a suitable angle of attack. All of the statistical quantities of flow such as turbulence and Reynolds stresses and in particular the spectrum of the fluctuations have been measured and analyzed. The results have shown that the free surface redistributes part or all of the normal turbulent kinetic energy into streamwise and spanwise components. Furthermore, the energy spectra have also shown that there exists an energy gradient on the free surface, on either side of the vertical passing through the original vortex. It is believed that the scars observed on the free surface are a consequence of the matching of the Bragg wave length with the wave length of the surface signatures within a particular spectrum. DTIC

N95-14869*# Foster-Miller Associates, Inc., Waltham, MA.
LUNAR BASE HEAT PUMP Final Report, 1 Apr. - 15 Jun. 1994
Jeffrey H. Goldman, R. Tetreault, D. Fischbach, and D. Walker Oct. 1994 64 p
(Contract NAS9-18819; RTOP 921-43-00-1A)
(NASA-CR-188356; NAS-8819-FM-9614-856; NAS 1.26:188356) Avail: CASI HC A04/MF A01

A heat pump is a device which elevates the temperature of a heat flow by a means of an energy input. By doing this, the heat pump can cause heat to transfer faster from a warm region to a cool region, or it can cause heat to flow from a cool region to a warmer region. The second case is the one which finds vast commercial applications such as air conditioning, heating, and refrigeration. Aerospace applications of heat pumps include both cases. The NASA Johnson Space Center is currently developing a Life Support Systems Integration Facility (LSSIF, previously SIRF) to provide system-level integration, operational test experience, and performance data that will enable NASA to develop flight-certified hardware for future planetary missions. A high lift heat pump is a significant part of the TCS hardware development associated with the LSSIF. The high lift heat pump program discussed here is being performed in three phases. In Phase 1, the objective is to develop heat pump concepts for a lunar base, a lunar lander, and for a ground development unit for the SIRF. In Phase 2, the design of the SIRF ground test unit is being performed, including identification and evaluation of safety and reliability issues. In Phase 3, the SIRF unit will be manufactured, tested, and delivered to the NASA Johnson Space Center. Author

N95-14912*# Lockheed Engineering and Sciences Co., Hampton, VA.
AN APPROXIMATE RIEMANN SOLVER FOR THERMAL AND CHEMICAL NONEQUILIBRIUM FLOWS
Ramadas K. Prabhu Oct. 1994 18 p
(Contract NAS1-19000; RTOP 232-01-04-06)
(NASA-CR-195003; NAS 1.26:195003) Avail: CASI HC A03/MF A01

Among the many methods available for the determination of inviscid fluxes across a surface of discontinuity, the flux-difference-splitting technique that employs Roe-averaged variables has been used extensively by the CFD community because of its simplicity and its ability to capture shocks exactly. This method, originally developed for perfect gas flows, has since been extended to equilibrium as well as nonequilibrium flows. Determination of the Roe-averaged variables for the case of a perfect gas flow is a simple task; however, for thermal and chemical nonequilibrium flows, some of the variables are not uniquely defined. Methods available in the literature to determine these variables seem to lack sound bases. The present paper describes a simple, yet accurate, method to determine all the variables for nonequilibrium flows in the Roe-average state. The basis for this method is the requirement that the Roe-averaged variables form a consistent set of thermodynamic variables. The present method satisfies the requirement that the square of the speed of sound be positive. Author

N95-14932*# Lehigh Univ., Bethlehem, PA. Dept. of Mechanical Engineering and Mechanics.
EMBEDDED FUNCTION METHODS FOR COMPRESSIBLE HIGH SPEED TURBULENT FLOW Final Report
J. D. A. Walker Sep. 1994 5 p
(Grant NAG1-832)
(NASA-CR-196936; NAS 1.26:196936) Avail: CASI HC A01/MF A01

This is the final report on the work performed on the grant 'Embedded Function Methods for Compressible High Speed Turbulent Flow' carried out at Lehigh University during the contract period from September, 1987, to October of 1991. Work has continued at Lehigh on this project on an unfunded basis to the present. The original proposed work had two separate thrusts which were associated with developing embedded function methods in order to obviate the need to expend computational resources on turbulent wall layers in Navier Stokes and boundary-layer calculations. Previous work on the incompressible problem had indicated that this could be done successfully for two-dimensional and three-dimensional incompressible flows. The central objective here was to extend the basic approach to the high speed compressible problem. Derived from text

N95-15315# Technische Univ., Delft (Netherlands).
ROBUST MULTIGRID METHODS FOR THE STEADY AND UNSTEADY INCOMPRESSIBLE NAVIER-STOKES EQUATIONS IN GENERAL COORDINATES Ph.D. Thesis
C. W. Oosterlee 14 Sep. 1993 158 p
(PB94-195534) Avail: CASI HC A08/MF A02

Two important aspects of the work in this thesis are the following. First, investigation of the accuracy of the discretization of the incompressible

Navier-Stokes equations in general domains with a finite volume method. Second, the search for robust fast multigrid solution methods to solve the resulting systems of discretized equations. The authors chose to use the standard nonlinear multigrid method to solve the steady incompressible Navier-Stokes equations. This algorithm is presented for the stationary equations in general coordinates in Chapter 4, where several smoothing methods are investigated for robustness. In Chapter 5 three robust multigrid methods to solve the unsteady incompressible Navier-Stokes equations for arbitrarily shaped domains are compared. These algorithms for unsteady equations possess more or less the same sequential complexity, while they differ in efficiency on parallel computers. Here, the efficiency on one processor of a vector machine is compared to see whether the algorithms are also efficient on these machines. NTIS

N95-15332# MSB Systems, Inc., Norwalk, CT.
LEAK DETECTION BY ACOUSTIC EMISSION MONITORING. PHASE 1: FEASIBILITY STUDY Final Report, Aug. 1987 - Mar. 1988
Bernard Lichtenstein and A. A. Winder 26 May 1994 56 p
(Contract F08635-87-C-0366)
(AD-A283775; MSB-228; AL/EQ-TR-1994-0031) Avail: CASI HC A04/MF A01

This investigation was conducted to determine the feasibility of detecting leaks from underground storage tanks or pipelines using acoustic emissions. An extensive technical literature review established that distinguishable acoustic emission signals will be generated when a storage tank is subjected to deformation stresses. A parametric analysis was performed which indicated that leak rates less than 0.1 gallons per hour can be detected for leak sizes less than 1/32 inch with 99% probability if the transient signals were sensed with an array of accelerometers (cemented to the tank or via acoustic waveguides), each having a sensitivity greater than 250 mv/g over a frequency range of 0.1 to 4000 Hz, and processed in a multi-channel Fourier spectrum analyzer with automatic threshold detection. An acoustic transient or energy release processor could conceivably detect the onset of the leak at the moment of fracture of the tank wall. The primary limitations to realizing reliable and robust acoustic emission monitoring of underground fluid leaks are the various masking noise sources prevalent at Air Force bases, which are attributed to aircraft, motor traffic, pump station operation, and ground tremors. DTIC

N95-15351# Sandia National Labs., Albuquerque, NM.
A PROPOSED FRAMEWORK FOR COMPUTATIONAL FLUID DYNAMICS CODE CALIBRATION AND VALIDATION
W. L. Oberkampf 1993 12 p Presented at the 18th AIAA and Astronautics Aerospace Ground Test Conference, Colorado Springs, CO, 20-23 Jun. 1994
(Contract DE-AC04-94AL-85000)
(DE94-015799; SAND-93-2525C; CONF-9406188-3) Avail: CASI HC A03/MF A01

The paper reviews the terminology and methodology that have been introduced during the last several years for building confidence in the predictions from Computational Fluid Dynamics (CFD) codes. Code validation terminology developed for nuclear reactor analyses and aerospace applications is reviewed and evaluated. Currently used terminology such as 'calibrated code', 'validated code', and a 'validation experiment' is discussed along with the shortcomings and criticisms of these terms. A new framework is proposed for building confidence in CFD code predictions that overcomes some of the difficulties of past procedures and delineates the causes of uncertainty in CFD predictions. Building on previous work, new definitions of code verification and calibration are proposed. These definitions provide more specific requirements for the knowledge level of the flow physics involved and the solution accuracy of the given partial differential equations. As part of the proposed framework, categories are also proposed for flow physics research, flow modeling research, and the application of numerical predictions. The contributions of physical experiments, analytical solutions, and other numerical solutions are discussed, showing that each should be designed to achieve a distinctively separate purpose in building confidence in accuracy of CFD predictions. A number of examples are given for each approach to suggest methods for obtaining the highest value for CFD code quality assurance. DOE

N95-15390 Virginia Polytechnic Inst. and State Univ., Blacksburg, VA. Interdisciplinary Center for Applied Mathematics.
COMPUTATIONAL METHODS FOR PDE'S IN FLOW CONTROL, SUPERCONDUCTIVITY, FLUID FLOWS AND OTHER APPLICATIONS Final Technical Report, 1 Dec. 1992 - 28 Feb. 1994
Max D. Gunzburger 30 Apr. 1994 27 p Limited Reproducibility: More than 20% of this document may be affected by microfiche quality
(Contract F49620-93-1-0061)
(AD-A282912; AFOSR-94-0429TR) Avail: CASI HC A03

We give an overview of the research carried out under grant sponsorship and then give details concerning four of the problems we have worked on and for which we have obtained significant results. These are: least-squares finite element methods for incompressible, viscous flows; analysis of a shape control problem for the Navier-Stokes equations; finite dimensional approximation of a class of nonlinear optimal control problems; and feedback control of Karman vortex shedding. We then give lists of papers prepared and personnel supported under grant sponsorship. DTIC

N95-15530# Lawrence Livermore National Lab., Livermore, CA.
COMPARISON OF DIFFERENT STATISTICAL MODELS OF TURBULENCE BY SIMILARITY METHODS
C. Cherfils and A. K. Harrison May 1994 9 p Presented at the 1994 ASME Fluids Engineering Summer Meeting, Lake Tahoe, NV, 19-23 Jun. 1994
(Contract W-7405-eng-48)
(DE94-015326; UCRL-JC-117404; CONF-940659-9) Avail: CASI HC A02/MF A01

The process of implosion by inertial confinement is perturbed by hydrodynamic instabilities such as Rayleigh-Taylor, Richtmyer-Meshkov and Kelvin-Helmholtz instabilities. They may generate turbulent flow, causing the mixing of constituents and the degradation of the symmetry of the implosion. The authors extend Barenblatt's study (1983) of a one-equation turbulence model to a variety of two-equation models. They consider the problem of the propagation of incompressible turbulence generated by an instantaneous plane source, for which the evolution of the turbulence is determined completely by diffusive and dissipative processes. It is then possible to find for each model a self-similar solution asymptotic to the exact flow. The authors then compare the self-similar temporal and spatial behavior of several two-equation models, including the dependence on model coefficients. They also observe the predicted self-similar behavior and evaluate similarity exponents by numerical solution of the model equations. The combined analytic and numerical approach not only elucidates the analysis but also assists in the validation of the turbulence modeling codes. Some of this analysis has previously been carried out by one of the authors on two turbulence models (Cherfils, 1993), and related work has been reported by Neuvazhaev et al. (1991). DOE

N95-15571# Brookhaven National Lab., Upton, NY.
DYNAMIC RESPONSE OF RIGID TANKS WITH INHOMOGENEOUS LIQUIDS
P. Shivakumar, A. Veletsos, and K. Bandyopadhyay Apr. 1994 51 p
(Contract DE-AC02-76CH-00016)
(DE94-012619; BNL-52420) Avail: CASI HC A04/MF A01

A study of the free vibrational characteristics and of the response to horizontal ground shaking of a rigid cylindrical tank containing an inviscid liquid with a continuous vertical variation in density is presented. The response quantities examined include the vertical sloshing motions of the liquid at its free-surface, and the impulsive and convective components of the hydrodynamic wall pressures and associated tank forces. The equations of motion for the system are formulated for an arbitrary variation in liquid density but the solutions presented are for a density that increases exponentially from top to bottom. Comprehensive numerical data are included which elucidate the underlying response mechanisms and the effects and relative importance of the various parameters involved. The solution for the continuous density variation considered herein is also compared with a previously reported solution in which the liquid was modeled as a multi-layered, discrete system. DOE

N95-15604*# Lockheed Engineering and Sciences Co., Hampton, VA.
LAMINAR AND TURBULENT FLOW COMPUTATIONS OF TYPE 4 SHOCK-SHOCK INTERFERENCE AEROTHERMAL LOADS USING UNSTRUCTURED GRIDS

Gururaja R. Vemaganti Oct. 1994 58 p
(Contract NAS1-19000; RTOP 232-01-04-06)
(NASA-CR-195008; NAS 1.26:195008) Avail: CASI HC A04/MF A01

This report presents computations for the Type 4 shock-shock interference flow under laminar and turbulent conditions using unstructured grids. Mesh adaptation was accomplished by remeshing, refinement, and mesh movement. Two two-equation turbulence models were used to analyze turbulent flows. The mean flow governing equations and the turbulence governing equations are solved in a coupled manner. The solution algorithm and the details pertaining to its implementation on unstructured grids are described. Computations were performed at two different freestream Reynolds numbers at a freestream Mach number of 11. Effects of the variation in the impinging shock location are studied. The comparison of the results in terms of wall heat flux and wall pressure distributions is presented. Author

N95-15605*# Old Dominion Univ., Norfolk, VA. Dept. of Mechanical Engineering.
INVESTIGATION OF RAMP INJECTORS FOR SUPERSONIC MIXING ENHANCEMENT Final Report, 8 Dec. 1992 - 15 Aug. 1994
Y. Haimovitch, E. Gartenberg, and A. S. Roberts, Jr. Hampton, VA NASA Nov. 1994 244 p
(Contract NAS1-19858; RTOP 505-70-62-12)
(NASA-CR-4634; NAS 1.26:4634) Avail: CASI HC A11/MF A03

A comparative study of wall mounted swept ramp injectors fitted with injector nozzles of different shape has been conducted in a constant area duct to explore mixing enhancement techniques for scramjet combustors. Six different injector nozzle inserts, all having equal exit and throat areas, were tested to explore the interaction between the preconditioned fuel jet and the vortical flowfield produced by the ramp: circular nozzle (baseline), nozzle with three downstream facing steps, nozzle with four vortex generators, elliptical nozzle, tapered-slot nozzle, and trapezoidal nozzle. The main flow was air at Mach 2, and the fuel was simulated by air injected at Mach 1.63 or by helium injected at Mach 1.7. Pressure and temperature surveys, combined with Mie and Rayleigh scattering visualization, were used to investigate the flow field. The experiments were compared with three dimensional Navier-Stokes computations. The results indicate that the mixing process is dominated by the streamwise vorticity generated by the ramp, the injectors' inner geometry having a minor effect. It was also found that the injectant/air mixing in the far-field is nearly independent of the injector geometry, molecular weight of the injectant, and the initial convective Mach number. Author

N95-15760# State Univ. of New York, Buffalo, NY. Lab. for Ceramic and Reaction Engineering.
MODELING, SIMULATION AND ENGINEERING SCALE-UP PROCEDURES FOR DESIGN OF CVD REACTORS Final Report
Vladimir Hlavacek 1993 6 p
(Contract N00014-89-J-3203)
(AD-A284919) Avail: CASI HC A02/MF A01

The research program, initiated in 1989 by the Laboratory for Ceramic and Reaction Engineering (LCRE), was aimed towards the development of generic processes for growing thick films deposited by CVD techniques. The application of thick-film technology includes the manufacturing of optical windows and ceramic plates, fabrication of optical domes and refractory crucibles, production of refractory metal tubes, ceramic fibers, etc. The objective of this research was to understand the complex phenomena which could occur in a CVD system, including problems of reactive fluid flow, instability of the deposition process at the interphase fluid-solid, stability of the nucleation process on the solid surface, and generation and development of stresses due to thermal gradients and growth-induced mechanisms. New ways of increasing the rate of deposition were also contemplated. Scale-up of CVD reactors for the applications previously mentioned, has not received much attention in the literature. LCRE has since been working on such Chemical Engineering procedures as the gathering and measuring of necessary data, and a priori simulation of laboratory bench-scale units and scale-up to pilot-plant size. DTIC

N95-15861# Northwestern Univ., Evanston, IL. Dept. of Engineering Sciences and Applied Mathematics.
INTERACTING FRONTS IN A MODEL FOR BINARY-MIXTURE CONVECTION
H. Riecke and H. Herrero 1994 9 p Presented at the 12th Symposium on Energy Engineering Sciences, Argonne, IL, 27-29 Apr. 1994
(Contract DE-FG02-92ER-14303)
(DE94-013595; DOE/ER-14303/3; CONF-9404137-3) Avail: CASI HC A02/MF A01

Motivated by the observation of localized traveling-wave states ('pulses') in convection in binary liquid mixtures, the interaction of fronts is investigated in a real Ginzburg-Landau equation which is coupled to a large-scale field. In that system the Ginzburg-Landau equation describes the traveling-wave amplitude and the large-scale field corresponds to a concentration mode which arises due to the slowness of mass diffusion. For single fronts the large-scale field can lead to a hysteretic transition between slow and fast fronts. Its contribution to the interaction between fronts can be attractive as well as repulsive and depends strongly on their direction of propagation. Based on this mechanism alone, pairs of fronts in binary-mixture convection are expected to form stable pulses if they travel backward, i.e. opposite to the linear group velocity. For positive velocities the interaction becomes attractive and destabilizes the pulses. This is in qualitative agreement with recent experimental results. This new localization mechanism does not require any dispersion in contrast to that operating in the complex Ginzburg-Landau equation. DOE

N95-15867# California Univ., Berkeley. Lawrence Berkeley Lab, CA.
TWO METHODS FOR THE STUDY OF VORTEX PATCH EVOLUTION ON LOCALLY REFINED GRIDS Ph.D. Thesis
M. L. Minion May 1994 121 p
(Contract DE-AC03-76SF-00098)
(DE94-014965; LBL-35719) Avail: CASI HC A06/MF A02

Two numerical methods for the solution of the two-dimensional Euler equations for incompressible flow on locally refined grids are presented. The first is a second order projection method adapted from the method of Bell, Colella, and Glaz. The second method is based on the vorticity-stream function form of the Euler equations and is designed to be free-stream preserving and conservative. Second order accuracy of both methods in time and space is established, and they are shown to agree on problems with a localized vorticity distribution. The filamentation of a perturbed patch of circular vorticity and the merger of two smooth vortex patches are studied. It is speculated that for nearly stable patches of vorticity, an arbitrarily small amount of viscosity is sufficient to effectively eliminate vortex filaments from the evolving patch and that the filamentation process affects the evolution of such patches very little. Solutions of the vortex merger problem show that filamentation is responsible for the creation of large gradients in the vorticity which, in the presence of an arbitrarily small viscosity, will lead to vortex merger. It is speculated that a small viscosity in this problem does not substantially affect the transition of the flow to a statistical equilibrium solution. The main contributions of this thesis concern the formulation and implementation of a projection for refined grids. A careful analysis of the adjointness relation between gradient and divergence operators for a refined grid MAC projection is presented, and a uniformly accurate, approximately stable projection is developed. An efficient multigrid method which exactly solves the projection is developed, and a method for casting certain approximate projections as MAC projections on refined grids is presented. DOE

N95-15868# California Univ., Berkeley. Lawrence Berkeley Lab, CA.
PHASE TRANSITIONS AND CONNECTIVITY IN THREE-DIMENSIONAL VORTEX EQUILIBRIA
J. H. Akao May 1994 201 p
(Contract DE-AC03-76SF-00098)
(DE94-014967; LBL-35630) Avail: CASI HC A10/MF A03

The statistical mechanics of collections of closed self avoiding vortex loops on a lattice are studied. The system is related to the vortex form of the three dimensional XY model and to lattice vortex equilibrium models of turbulence. The system exhibits vortex connectivity and screening effects, and models in vorticity variables the superfluid transition. The equilibrium states of the system are simulated by a grand canonical Monte Carlo method. A set of geometric transformations for self-avoiding loops is developed. The numerical method employs histogram sampling techniques and utilizes a modification to the Metropolis flow which enhances efficiency. Results are given for a region in the temperature-chemical potential plane, where the chemical potential is related to the vortex fugacity. A line of second order transitions is identified at low temperature. The transition is

shown to be a percolation threshold at which connected vortex loops of infinite size appear in the system. The nature of the transition supports the assumption that the lambda transition in bulk superfluid helium is driven by vortices. An asymptotic analysis is performed for the energy and entropy scaling of the system as functions of the system size and the lattice spacing. These estimates indicate that the infinite temperature line is a phase boundary between small scale fractal vortices and large scale smooth vortices. A suggestion is made that quantum vortices have uniform structure on the scale of the lattice spacing and lie in the positive temperature regime, while classical vortices have uniform structure on the scale of the domain and lie in the negative temperature regime. DOE

N95-15898*# National Aeronautics and Space Administration. Langley Research Center, Hampton, VA.

WIND-TUNNEL BLOCKAGE AND ACTUATION SYSTEMS TEST OF A TWO-DIMENSIONAL SCRAMJET INLET UNSTART MODEL AT MACH 6

Scott D. Holland Nov. 1994 38 p See also videotape supplement L-0194-41

(RTOP 763-23-35-08)

(NASA-TM-109152; NAS 1.15:109152) Avail: CASI HC A03/MF A01

The present study examines the wind-tunnel blockage and actuation systems effectiveness in starting and forcibly unstarting a two-dimensional scramjet inlet in the NASA Langley 20-Inch Mach 6 Tunnel. The intent of the overall test program is to study (both experimentally and computationally) the dynamics of the inlet unstart; however, prior to the design and fabrication of an expensive, instrumented wind-tunnel model, it was deemed necessary first to examine potential wind-tunnel blockage issues related to model sizing and to examine the adequacy of the actuation systems in accomplishing the start and unstart. The model is equipped with both a moveable cowl and aft plug. Windows in the inlet sidewalls allow limited optical access to the internal shock structure; schlieren video was used to identify inlet start and unstart. A chronology of each actuation sequence is provided in tabular form along with still frames from the schlieren video. A pitot probe monitored the freestream conditions throughout the start/unstart process to determine if there was a blockage effect due to the model start or unstart. Because the purpose of this report is to make the phase I (blockage and actuation systems) data rapidly available to the community, the data is presented largely without analysis of the internal shock interactions or the unstart process. This series of tests indicated that the model was appropriately sized for this facility and identified operability limits required first to allow the inlet to start and second to force the unstart. Author

N95-15899* National Aeronautics and Space Administration. Langley Research Center, Hampton, VA.

TWO-DIMENSIONAL SCRAMJET INLET UNSTART MODEL: WIND-TUNNEL BLOCKAGE AND ACTUATION SYSTEMS TEST (Videotape Supplement)

Scott D. Holland Nov. 1994 See also NASA-TM-109152 Videotape supplement: 10 min. 52 sec. playing time, in color, in VHS and Beta formats

(RTOP 763-23-35-08)

(NASA-TM-109984; NONP-NASA-Suppl-VT-94-32020) Avail: CASI VHS A02/BETA A22

This supplement to NASA TM 109152 shows the Schlieren video (10 min. 52 sec., color, Beta and VHS) of the external flow field and a portion of the internal flow field of a two-dimensional scramjet inlet model in the NASA Langley 20-Inch Mach 6 Tunnel. The intent of the overall test program is to study (both experimentally and computationally) the dynamics of the inlet unstart; this (phase I) effort examines potential wind-tunnel blockage issues related to model sizing and the adequacy of the actuation systems in accomplishing the start and unstart. The model is equipped with both a moveable cowl and aft plug. Windows in the inlet sidewalls allow limited optical access to the internal shock structure. In the video, flow is from right to left, and the inlet is oriented inverted with respect to flight, i.e., with the cowl on top. The plug motion is obvious because the plug is visible in the aft window. The cowl motion, however, is not as obvious because the cowl is hidden from view by the inlet sidewall. The end of the cowl actuator arm, however, becomes visible above the inlet sidewalls between the windows when the cowl is up (see figure 1b of the primary document). The model is injected into the tunnel and observed though several actuation sequences with two plug configurations over a range of unit freestream Reynolds number at a nominal freestream Mach number of 6. The framing rate and shutter speed of the camera were too slow to fully capture the dynamics of the unstart but did prove sufficient to identify inlet start and unstart. This series of tests indicated that the model was appropriately sized for this facility and identified operability limits required first to allow the inlet to start and second to force the unstart. Author

N95-15908*# National Aeronautics and Space Administration. Lewis Research Center, Cleveland, OH.

ON THE BEHAVIOR OF THREE-DIMENSIONAL WAVE PACKETS IN VISCOUSLY SPREADING MIXING LAYERS

Thomas F. Balsa Nov. 1994 49 p Prepared in cooperation with Arizona Univ., Tucson, AZ

(RTOP 505-90-5K)

(NASA-TM-106770; ICOMP-94-26; E-9218; NAS 1.15:106770) Avail: CASI HC A03/MF A01

We consider analytically the evolution of a three-dimensional wave packet generated by an impulsive source in a mixing layer. The base flow is assumed to be spreading due to viscous diffusion. The analysis is restricted to small disturbances (linearized theory). A suitable high-frequency ansatz is used to describe the packet; the key elements of this description are a complex phase and a wave action density. It is found that the product of this density and an infinitesimal material volume convecting at the local group velocity is not conserved: there is a continuous interaction between the base flow and the wave action. This interaction is determined by suitable mode-weighted averages of the second and fourth derivatives of the base-flow velocity profile. Although there is some tendency for the dominant wave number in the packet to shift from the most unstable value toward the neutral value, this shift is quite moderate. In practice, wave packets do not become locally neutral in a diverging base flow (as do instability modes), therefore, they are expected to grow more suddenly than pure instability modes and do not develop critical layers. The group velocity is complex; the full significance of this is realized by analytically continuing the equations for the phase and wave action into a complex domain. The implications of this analytic continuation are discussed vis-a-vis the secondary instabilities of the packet: very small scale perturbations on the phase can grow very rapidly initially, but saturate later because most of the energy in these perturbations is convected away by the group velocity. This remark, as well as the one regarding critical layers, has consequences for the nonlinear theories. Author

N95-15917*# Institute for Computer Applications in Science and Engineering, Hampton, VA.

ON THE EVOLUTION OF CENTRIFUGAL INSTABILITIES WITHIN CURVED INCOMPRESSIBLE MIXING LAYERS Final Report

S. R. Otto (Birmingham Univ., England.), T. L. Jackson, and F. Q. Hu Hampton, VA NASA Oct. 1994 31 p Submitted for publication

(Contract NAS1-19480; RTOP 505-90-52-01)

(NASA-CR-194991; NAS 1.26:194991; ICASE-94-83) Avail: CASI HC A03/MF A01

It is known that certain configurations which possess curvature are prone to a class of instabilities which their 'flat' counterparts will not support. The main thrust of the study of these centrifugal instabilities has concentrated on curved solid boundaries and their effect on the fluid motion. In this article attention is shifted towards a fluid-fluid interface observed within a curved incompressible mixing layer. Experimental evidence is available to support the conjecture that this situation may be subjected to centrifugal instabilities. The evolution of modes with wavelengths comparable with the layer's thickness is considered and the high Taylor/Gortler number regime is also discussed which characterizes the ultimate fate of the modes. Author

35 INSTRUMENTATION AND PHOTOGRAPHY

Includes remote sensors; measuring instruments and gages; detectors; cameras and photographic supplies; and holography.

For aerial photography see *43 Earth Resources and Remote Sensing*. For related information see also *06 Aircraft Instrumentation*, and *19 Spacecraft Instrumentation*.

N95-13669# Lawrence Livermore National Lab., Livermore, CA.
ENERGY AND TECHNOLOGY REVIEW, APRIL 1994
W. J. Quirk, ed., J. Canada, ed., L. deVore, ed., K. Gleason, ed., R. D Kirvel, ed., L. McElroy, ed., and H. Kroopnick, ed. Apr. 1994 21 p
(Contract W-7405-eng-48)
(DE94-012133; UCRL-52000-94-4) Avail: CASI HC A03/MF A01

The Lawrence Livermore National Laboratory was established in 1952 to do research on nuclear weapons and magnetic fusion energy. Since then, other major programs have been added, including technology transfer, laser science, biology and biotechnology, environmental research and remediation, arms control and nonproliferation, advanced defense technology, and applied energy technology. These programs in turn require research in basic scientific disciplines including chemistry and materials science, computing science and technology, engineering, and physics. This review highlights two R&D 100 award winning research topics: (1) The world's fastest digitizer which captures 30 ps transient electrical events, and (2) the MACHO camera system which fully exploits the power of large format digital imagers and integrates into one package the taking and analysis of images at a prodigious rate and the storage and archiving of extensive amounts of data. DOE

N95-13837*# National Aeronautics and Space Administration. Langley Research Center, Hampton, VA.
SURFACE ACOUSTIC WAVE OXYGEN PRESSURE SENSOR Patent Application
Donald M. Oglesby, inventor (to NASA) (Old Dominion Univ., Virginia Beach, VA.), Billy T. Upchurch, inventor (to NASA), and Bradley D. Leighty, inventor (to NASA) 2 Apr. 1994 14 p
(NASA-Case-LAR-15266-1-CU; NAS 1.71:LAR-15266-1-CU; US-Patent-Appl-SN-238040) Avail: CASI HC A03/MF A01

A transducer for the measurement of absolute gas-state oxygen pressure from pressures of less than 100 Pa to atmospheric pressure (1.01 x 10(exp 5) Pa) is based on a standard surface acoustic wave (SAW) device. The piezoelectric material of the SAW device is coated with a compound which will selectively and reversibly bind oxygen. When oxygen is bound by the coating, the mass of the coating increases by an amount equal to the mass of the bound oxygen. Such an increase in the mass of the coating causes a corresponding decrease in the resonant frequency of the SAW device. NASA

N95-14146# Sandia National Labs., Albuquerque, NM.
CALIBRATION AND CHARACTERIZATION OF WIDE RANGE HYDROGEN SENSORS
S. L. Miller, K. L. Hughes, J. L. Rodriguez, and P. J. McWhorter 1994 9 p Presented at the 1994 Conference on Advanced Earth-to-Orbit Propulsion Technology, Huntsville, AL, 17-19 May 1994
(Contract DE-AC04-94AL-85000)
(DE94-013765; SAND-94-0721C; CONF-9405178-1) Avail: CASI HC A02/MF A01

Crucial to the successful implementation of hydrogen sensing devices is the basic ability to quantitatively relate hydrogen concentration to the time-dependent electrical signals originating from the sensing structures, i.e. the sensor must be calibrated. A simple technique is developed for calibrating the resistor sensing structure for time-varying thermal environments and hydrogen concentrations in excess of approximately 1%. A procedure to achieve equilibrium calibration of the transistor for hydrogen concentrations less than approximately 1% is also presented. The rate limiting mechanisms governing the time-dependent response of the transistor are investigated. The evolution of hydrogen out of the transistor structure is shown to be thermally activated, and has been accurately modeled for a wide range of time-dependent thermal environments. DOE

N95-14180* National Aeronautics and Space Administration. Lyndon B. Johnson Space Center, Houston, TX.
ACCELERATION RECORDER AND PLAYBACK MODULE Patent
Richard J. Bozeman, Jr., inventor (to NASA) 1 Nov. 1994 7 p Filed 3 Sep. 1992 Supersedes N93-17077 (31 - 5, p 1169)
(NASA-Case-MSC-22008-1; US-Patent-5,359,896; US-Patent-Appl-SN-940420; US-Patent-Class-73-590; US-Patent-Class-73-593; Int-Patent-Class-G06F-15/74) Avail: US Patent and Trademark Office

The present invention is directed to methods and apparatus relating to an accelerometer electrical signal recorder and playback module. The recorder module may be manufactured in lightweight configuration and includes analog memory components to store data. Signal conditioning circuitry is incorporated into the module so that signals may be connected directly from the accelerometer to the recorder module. A battery pack may be included for powering both the module and the accelerometer. Timing circuitry is included to control the time duration within which data is recorded or played back so as to avoid overloading the analog memory components. Multiple accelerometer signal recordings may be taken simultaneously without analog to digital circuits, multiplexing circuitry or software to compensate for the effects of multiplexing the signals.
Official Gazette of the U.S. Patent and Trademark Office

N95-14414* National Aeronautics and Space Administration. Langley Research Center, Hampton, VA.
ACTIVE THERMAL ISOLATION FOR TEMPERATURE RESPONSIVE SENSORS Patent
Scott D. Martinson, inventor (to NASA), David L. Gray, inventor (to NASA), Debra L. Carraway, inventor (to NASA), and Daniel C. Reda, inventor (to NASA) 27 Sep. 1994 9 p Filed 18 Jan. 1994 Division of US-Patent-Appl-SN-820431, filed 2 Jan. 1992
(NASA-Case-LAR-14612-2; US-Patent-5,349,851; US-Patent-Appl-SN-181938; US-Patent-Appl-SN-820431; US-Patent-Class-73-147; US-Patent-Class-73-204.18; Int-Patent-Class-G01F-1/68; Int-Patent-Class-G01M-9/00) Avail: US Patent and Trademark Office

A temperature responsive sensor is located in the airflow over the specified surface of a body and is maintained at a constant temperature. An active thermal isolator is located between this temperature responsive sensor and the specified surface of the body. The temperature of this isolator is controlled to reduce conductive heat flow from the temperature responsive sensor to the body. This temperature control includes: (1) operating the isolator at the same temperature as the constant temperature of the sensor and (2) establishing a fixed boundary temperature which is either less than or equal to or slightly greater than the sensor constant temperature. Official Gazette of the U.S. Patent and Trademark Office

N95-14839 Helsinki Univ. of Technology, Otaniemi (Finland). Dept. of Technical Physics.
ECCENTRICITY OF THE ELECTRON BEAM IN A GYROTRON CAVITY
O. Dumbrajs 1994 9 p Limited Reproducibility: More than 20% of this document may be affected by microfiche quality
(PB94-197639; TKK-F-C162) Avail: CASI HC A02

Dependence of the coupling of the electron beam and RF field in a gyrotron cavity on eccentricity of the electron beam is studied. NTIS

N95-14841# Department of the Navy, Washington, DC.
TORSIONAL SHEAR WAVE TRANSDUCER Patent
Alan K. Walden, inventor (to Navy) and Thomas R. Howarth, inventor (to Navy) 14 Jun. 1994 10 p Filed 6 Apr. 1993
(AD-D016347; US-Patent-5,321,333; US-Patent-Appl-SN-43641; US-Patent-Class-310-333) Avail: US Patent and Trademark Office

A low frequency torsional transducer for the generation and/or reception of shear waves in a substantially solid medium. The transducer includes a spool like radiating structure to which are fixedly attached spaced piezoelectric elements. The elements undergo shear movement upon being electrically excited or upon receiving shear waves. This shear movement causes the opposite ends of the radiating structure to move torsionally. The torsional movement causes radiation of shear waves which can be detected by a sensor and used to determine the degree of support for shear wave propagation in the media. DTIC

N95-15334 Microsensor Systems, Inc., Springfield, VA.
SURFACE ACOUSTIC WAVE (SAW) MICROSENSORS TO MONITOR MULTI-COMPONENT VAPOR CHALLENGES TO ADSORBENTS AND ADSORBENT-BASED AIR FILTRATION SYSTEMS Final Report, May 1990 - May 1991
N. L. Jarvis Jul. 1994 30 p Limited Reproducibility: More than 20% of this document may be affected by microfiche quality
(Contract DAAA15-90-C-1028)
(AD-A284222; ERDEC-CR-133) Avail: CASI HC A03

The current effort was done to assess the utility of surface acoustic wave (SAW) detectors for analyzing multicomponent gaseous mixtures in real time. Tasks included surveying currently available SAW detector capability, selecting several candidate SAW coating materials, fabricating vapor monitors, and testing for sensitivity and selectivity. An assessment of possible SAW designs for real-time analysis of multicomponent mixtures is attempted. DTIC

N95-15413# Helsinki Univ. of Technology, Espoo (Finland). Circuit Theory Lab.
ACCELEROMETER MODEL IN APLAC
T. Veijola Feb. 1994 58 p
(PB94-197647; ISBN-951-22-1988-3) Avail: CASI HC A04/MF A01

A model of a silicon capacitive accelerometer is presented. An electric equivalent circuit is used to model the mechanical and electrical properties of the acceleration sensor. The mechanical properties include the squeezed-film effect in the small air gaps and the electrostatic force equations. The model has been implemented in the general purpose circuit simulator tool APLAC. The accelerometer model is available in all basic analysis modes including DC, AC, transient and steady state analyses. Several examples demonstrating the model usage are presented. NTIS

N95-15580# Fermi National Accelerator Lab., Batavia, IL.
FLUORESCENT COMPOUNDS FOR PLASTIC SCINTILLATION APPLICATIONS
A. Pla-Dalmau and A. D. Bross Apr. 1994 12 p Presented at the Spring Meeting of the Materials Research Society, San Francisco, CA, 4-8 Apr. 1994
(Contract DE-AC02-76CH-03000)
(DE94-013235; FNAL/C-94/100; CONF-940411-25) Avail: CASI HC A03/MF A01

Several 2-(2'-hydroxyphenyl) -benzothiazole, -benzoxazole, and -benzimidazole derivatives have been prepared. Transmittance, fluorescence, light yield, and decay time characteristics of these compounds have been studied in a polystyrene matrix and evaluated for use in plastic scintillation detectors. Radiation damage studies utilizing a C-60 source have also been performed. DOE

N95-15728*# Cincinnati Univ., OH. Dept. of Aerospace Engineering and Engineering Mechanics.
ASSESSMENT OF CTAS ETA PREDICTION CAPABILITIES Annual Report
Michael A. Bolender 1 Nov. 1994 42 p
(Contract NCC2-669)
(NASA-CR-197224; NAS 1.26:197224) Avail: CASI HC A03/MF A01

This report summarizes the work done to date in assessing the trajectory fidelity and estimated time of arrival (ETA) prediction capability of the NASA Ames Center TRACON Automation System (CTAS) software. The CTAS software suite is a series of computer programs designed to aid air traffic controllers in their tasks of safely scheduling the landing sequence of approaching aircraft. in particular, this report concerns the accuracy of the available measurements (e.g., position, altitude, etc.) that are input to the software, as well as the accuracy of the final data that is made available to the air traffic controllers. Derived from text

N95-15785*# Cincinnati Univ., OH. Dept. of Aerospace Engineering and Engineering Mechanics.
GROUNDSPEED FILTERING FOR CTAS
Gary L. Slater 11 Nov. 1994 16 p
(Contract NCC2-669)
(NASA-CR-197223; NAS 1.26:197223) Avail: CASI HC A03/MF A01

Ground speed is one of the radar observables which is obtained along with position and heading from NASA Ames Center radar. Within the Center TRACON Automation System (CTAS), groundspeed is converted into airspeed using the wind speeds which CTAS obtains from the NOAA weather grid. This airspeed is then used in the trajectory synthesis logic which computes the trajectory for each individual aircraft. The time history of the typical radar groundspeed data is generally quite noisy, with high frequency variations on the order of five knots, and occasional 'outliers' which can be significantly different from the probable true speed. To try to smooth out these speeds and make the ETA estimate less erratic, filtering of the ground speed is done within CTAS. In its base form, the CTAS filter is a 'moving average' filter which averages the last ten radar values. In addition, there is separate logic to detect and correct for 'outliers', and acceleration logic which limits the groundspeed change in adjacent time samples. As will be shown, these additional modifications do cause significant changes in the actual groundspeed filter output. The conclusion is that the current ground speed filter logic is unable to track accurately the speed variations observed on many aircraft. The Kalman filter logic however, appears to be an improvement to the current algorithm used to smooth ground speed variations, while being simpler and more efficient to implement. Additional logic which can test for true 'outliers' can easily be added by looking at the difference in the a priori and post priori Kalman estimates, and not updating if the difference in these quantities is too large.
Derived from text

N95-15799 Department of the Navy, Washington, DC.
TRANSDUCERS AND METHODS FOR MAKING SAME Patent
Manfred Kahn, inventor (to Navy) and Chulho Kim, inventor (to Navy) 28 Jun. 1994 10 p Filed 9 Jun. 1993
(AD-D016349; US-Patent-5,325,011; US-Patent-Appl-SN-076135;
US-Patent-Class-310-358) Avail: US Patent and Trademark Office

Elongated electrically nonconducting transducer preforms are made from a stiff resin. The preforms have grooves in their upper and lower surfaces. Transducer elements may be formed from stacked preforms whereby grooves in their upper and lower surfaces form compartments between adjoining stacked preforms. PZT rods are disposed in the grooves disposed on the upper surface of each stacked preform, and a soft resin surrounds the rods and fills the compartment. The method for making the transducer assembly includes the steps of loading by gravity the rods into the upper grooves of the preforms; stacking the loaded preforms so that upper grooves in the lower preform communicate with lower grooves in the upper preform, thus forming cavities; flowing a soft resin around the rods; and curing the soft resin. DTIC

N95-15915* National Aeronautics and Space Administration. Lewis Research Center, Cleveland, OH.
APPARATUS FOR PERFORMING HIGH-TEMPERATURE FIBER PUSH-OUT TESTING Patent
Jeffrey I. Eldridge, inventor (to NASA) and Ben T. Ebihara, inventor (to NASA) 8 Nov. 1994 7 p Filed 21 Dec. 1992
(NASA-Case-LEW-15470-1; US-Patent-5,361,641;
US-Patent-Appl-SN-968087; US-Patent-Class-73-842;
Int-Patent-Class-G01N-3/42) Avail: US Patent and Trademark Office

The apparatus disclosed in the present invention measures the force at which a fiber resist the motion of an indenter driven at constant speed. This apparatus conducts these test in a vacuum of about 10(exp -6) tort and at temperatures up to 1100 C. Temperature and vacuum environment are maintained while controlling indenter motion, sample position, and providing magnified visual inspection during the test. Author

N95-14069*# McDonnell-Douglas Space Systems Co., Rockville, MD.
USING A TEMPERATURE-CONTROLLED QUARTZ CRYSTAL MICROBALANCE IN A SPACE EQUIPMENT CLEANROOM TO MONITOR MOLECULAR CONTAMINATION
William J. Mitchell *In* NASA. Goddard Space Flight Center, Eighteenth Space Simulation Conference: Space Mission Success Through Testing Nov. 1994 p 87-97 (For primary document see N95-14062 03-18)
Avail: CASI HC A03/MF A04

N95-14084*# National Inst. of Standards and Technology, Gaithersburg, MD.
PARTIAL PRESSURE ANALYSIS IN SPACE TESTING
Charles R. Tilford *In* NASA. Goddard Space Flight Center, Eighteenth Space Simulation Conference: Space Mission Success Through Testing

Nov. 1994 p 257-269 Sponsored by JHU (For primary document see N95-14062 03-18)
Avail: CASI HC A03/MF A04

N95-14679*# Texas Univ., Austin, TX. Electrical Engineering Research Lab.
PHOTOGRAMMETRIC MOBILE SATELLITE SERVICE PREDICTION
Riza Akturan and Wolfhard J. Vogel *In* JPL, Proceedings of the Eighteenth NASA Propagation Experimenters Meeting (NAPEX 18) and the Advanced Communications Technology Satellite (ACTS) Propagation Studies Miniworkshop 1 Aug. 1994 p 159-163 Sponsored in part by Loral Aerospace Corp. and Motorola, Inc. (For primary document see N95-14670 03-32)
Avail: CASI HC A01/MF A04; 4 functional color pages

N95-14683*# Oklahoma Univ., Norman, OK.
RADIOMETER CALIBRATION PROCEDURE AND BEACON ATTENUATION ESTIMATION REFERENCE LEVEL
Robert K. Crane *In* JPL, Proceedings of the Eighteenth NASA Propagation Experimenters Meeting (NAPEX 18) and the Advanced Communications Technology Satellite (ACTS) Propagation Studies Miniworkshop 1 Aug. 1994 p 273-286 (For primary document see N95-14670 03-32)
Avail: CASI HC A03/MF A04; 4 functional color pages

N95-14879*# National Aeronautics and Space Administration. Langley Research Center, Hampton, VA.
AN OPTICAL TECHNIQUE FOR EXAMINING AIRCRAFT SHOCK WAVE STRUCTURES IN FLIGHT
Leonard M. Weinstein *In its* High-Speed Research: 1994 Sonic Boom Workshop: Atmospheric Propagation and Acceptability Studies Oct. 1994 p 1-17 (For primary document see N95-14878 03-02)
Avail: CASI HC A03/MF A03

36 LASERS AND MASERS

Includes parametric amplifiers.
For related information see also *76 Solid-State Physics*.

N95-13629* National Aeronautics and Space Administration. Pasadena Office, CA.
BURST-BY-BURST LASER FREQUENCY MONITOR Patent
Carlos Esproles, inventor (to NASA) 6 Sep. 1994 5 p Filed 1 Feb. 1993 Supersedes N93-28132 (31 - 10, p 3048)
(Contract NAS7-918)
(NASA-Case-NPO-18596-1-CU; US-Patent-5,345,168; US-Patent-Appl-SN-023252; US-Patent-Class-324-76.48; US-Patent-Class-324-76.62; US-Patent-Class-377-42; Int-Patent-Class-G01R-23/02) Avail: US Patent and Trademark Office

The invention is a system for real-time frequency monitoring and display of an RF burst where the burst frequency is analyzed and displayed on a burst-by-burst basis in order to allow for frequency control. Although the invention was made for monitoring the laser frequency of a LIDAR system, it has other applications where realtime monitoring is required. The novelty of the invention resides in the use of a counter that is reset at the beginning of each unit time of monitoring and then gated for a unit of time. The invention also has an LED bar graph for displaying the measure of frequency at the end of each unit time in either a bar length mode or a moving dot mode. In the latter mode, the operator makes necessary adjustments to maintain the dot at the center of the bar graph.
Official Gazette of the U.S. Patent and Trademark Office

N95-13695 Stanford Univ., CA.
ADVANCED LASER SOURCE RESEARCH Annual Report, 1 Oct. 1993 - 30 Sep. 1994
Richard N. Zare, Stephen E. Harris, and Arthur L. Schawlow Jul. 1994 57 p Limited Reproducibility: More than 20% of this document may be affected by microfiche quality
(Contract N00014-91-J-1023)
(AD-A283110) Avail: Issuing Activity (Defense Technical Information Center (DTIC))

We now have a laser system which allows us to observe electromagnetically induced transparency in regions never before accessible. Briefly, the system produces two wavelengths (406 nm and 283 nm), each with a frequency stability of several MHz and with energy of several mJ. Using this system, we are now able to observe an increase in transparency of over a factor of 10,000 in an exponent. We also observe optical group velocities as slow as c/100. We are beginning the observation and study of large signal effects. The other important area of work this year has been the identification of the normal modes of electromagnetically induced transparency. These modes follow from the basic properties of this effect, wherein the electromagnetic field creates population-trapped atoms and where population-trapped atoms produce matched pulses. DTIC

N95-13994# Los Alamos National Lab., NM.
REVIEW OF DRIVE SYMMETRY MEASUREMENT AND CONTROL EXPERIMENTS ON THE NOVA LASER SYSTEM
J. M. Mack, A. A. Hauer, and N. D. Delamater et al 1994 10 p Presented at the 11th Topical Meeting on the Technology of Fusion Energy, New Orleans, LA, 19-24 Jun. 1994
(Contract W-7405-eng-36)
(DE94-014455; LA-UR-94-1887; CONF-940630-22) Avail: CASI HC A02/MF A01

Symmetric radiation drive is required for achieving ignition in laboratory experiments. Over the last two years, concerted series of drive symmetry experiments have been performed on the Nova laser system. The goals of this work were to develop measurements techniques and to apply them to symmetry variation and control experiments. The emphasis in this initial work has been on time integrated measurements (integrated over the laser drive pulse). The authors have also begun work on methods for time resolved measurements. Most of their work used the symmetry signature impressed on the compressed core of a capsule imploded in a hohlraum (cylindrical canister) environment. X-ray imaging of this core provides a mapping that can be compared with theoretical modeling and related to a specific amount of drive asymmetry. This method is indirect and they have taken great care in understanding the formation of the symmetry signature and in its comparison with simulations. A review of drive symmetry measurement and control experiments is presented, including data from time integrated and time resolved measurements; these measurements are also compared to modeling. Under carefully controlled conditions results from symmetry measurements (and from other auxiliary measurements) are reproducible, and indicate that aspects of implosions symmetry can be controlled. DOE

N95-14291# Naval Postgraduate School, Monterey, CA.
SIMULATIONS OF THE HIGH AVERAGE POWER SELENE FREE ELECTRON LASER PROTOTYPE M.S. Thesis
Dennis D. Quick Jun. 1994 63 p
(AD-A280780) Avail: CASI HC A04/MF A01

Free electron laser (FEL) technology continues to advance, providing alternative solutions to existing and potential problems. The capabilities of an FEL with respect to tunability, power, and efficiency make it an attractive choice when moving into new laser utilization fields. The initial design parameters, for any new system, offer a good base to begin system simulation tests in an effort to determine the best possible design. This is a study of the Novosibirsk design which is a prototype for the proposed Space Laser Energy (SELENE) FEL. The design uses a three-section, low-power optical klystron followed by a single-pass, high-power radiator. This system is inherently sensitive to electron beam quality, but affords flexibility in achieving the final design. The performance of the system is studied using the initial parameters. An FEL, configured as a simple, two section optical klystron is studied to determine the basic operating characteristics of a high current FEL klystron. DTIC

N95-14318# Lawrence Livermore National Lab., Livermore, CA.
DOUBLE IONIZATION IN GASES DRIVEN BY OPTICAL FIELD IONIZATION USING ULTRASHORT LASER PULSES
P. R. Bolton and D. N. Fittinghoff Jun. 1994 5 p Presented at the Optical Society of America Conference on High Field Interactions, St. Malo, France, 21-25 Aug. 1994
(Contract W-7405-eng-48)
(DE94-015137; UCRL-JC-117523; CONF-9408121-1) Avail: CASI HC A01/MF A01

Rapid optical field ionization (OFI) for atoms and ions is distinguished

using ultra-short laser pulses focused to peak fields comparable to Coulomb binding values. This nonperturbative field description facilitates understanding of standard sequential ionization and distinguishes the double (or two-electron ejection) ionization process. Following our discovery of double optical field ionization in He(+2) at 614 nm we have extended experiments to include helium, neon and argon at an 800 nm wavelength with varying ellipticity. We compare double ionization data with predictions from the semi-classical model by Corkum. New experimental results at 800 nm use 130 femtosecond laser pulses focused to intensities of order 10(exp 16) W/cm in the extraction region of a 1 meter time-of-flight spectrometer. Gas pressures ranged from 10(exp -8) to 10(exp -5) torr. DOE

N95-14364# California Univ., Santa Barbara, CA. Dept. of Electrical and Computer Engineering.

IN SITU GROWN QUANTUM-WIRE LASERS Final Report, 15 May 1991 - 14 Jan. 1994

L. A. Coldren, A. C. Gossard, J. H. English, D. Mui, and S. W. Corzine 7 Apr. 1994 37 p

(Contract DAAL03-91-G-0134)

(AD-A281381; ECE-TR-94-09; ARO-28922.14-EL-SDI) Avail: CASI HC A03/MF A01

This program concentrated on developing techniques to better understand and fabricate quantum-confined structures. The goal was to create the enabling technology for more efficient semiconductor lasers and integrated optoelectronic circuits. Over the contract period, significant advances occurred in the development of quantum-confined lasers, UHV in-situ processing technology, and the underlying theory for quantum-confined laser structures. The quantum-confined laser work included both quantum-wire laser and vertical-cavity laser development. This latter effort also required substantial improvements in the MBE growth technology. Much of this technology is now ready for transfer to industry. In fact, a number of joint projects with industry are underway, as a result of this program. DTIC

N95-14427# Lawrence Livermore National Lab., Livermore, CA.

HIGH POWER DIODE PUMPED SOLID STATE LASER DEVELOPMENT AT LAWRENCE LIVERMORE NATIONAL LABORATORY

R. Solarz, G. Albrecht, and L. Hackel et al Mar. 1994 9 p Presented at the 8th High Temperature Materials Conference, Vienna, Austria, 5-8 May 1994

(Contract W-7405-eng-48)

(DE94-015899; UCRL-JC-116823; CONF-940554-1) Avail: CASI HC A02/MF A01

The authors' recent developments in high powered diode pumped solid state lasers at Lawrence Livermore National Laboratory are presented. Over the past year the authors have made continued improvements to semiconductor pump array technology which includes the development of higher average power and lower cost pump modules. They report the performance of high power AlGaAs, InGaAs, and AlGaInP arrays. They also report on improvement to the integrated micro-optics designs in conjunction with lensing duct technology which gives rise to very high performance end pumping designs for solid state lasers which have major advantages which they detail. Substantial progress on beam quality improvements to near the diffraction limit at very high power have also been made and will be reported. They also will discuss recent experiments on high power non-linear materials for q-switches, harmonic converters, and parametric oscillators. Advances in diode pumped devices at LLNL which include tunable Cr:LiSrAlF6, mid-IR Er:YAG, holmium based lasers and other developments will also be outlined. Concepts for delivering up to 30 kilowatts of average power from a DPSSL oscillator will be described. DOE

N95-14515* National Aeronautics and Space Administration. Goddard Space Flight Center, Greenbelt, MD.

LASER RETROREFLECTOR ARRAY HAVING CAT-EYE RETROREFLECTORS Patent

Peter O. Minott, inventor (to NASA) 18 Oct. 1994 5 p Filed 22 Sep. 1992

(NASA-Case-GSC-13264-1; US-Patent-5,357,371;

US-Patent-Appl-SN-949199; US-Patent-Class-359-534;

US-Patent-Class-359-546; US-Patent-Class-359-731;

Int-Patent-Class-G02B-5/126) Avail: US Patent and Trademark Office

A laser retroreflector array is provided having an array of cat-eye retroreflectors each with an image forming objective through which the laser beam passes and a partial mirror at the focal plane of the image forming objective. By using the cat-eye retroreflectors to reflect the laser beam, the field of view can be angularly limited so that only one retroreflector in the array at a time reflects the laser beam. Author

N95-14519* National Aeronautics and Space Administration. Langley Research Center, Hampton, VA.

METHOD AND APPARATUS FOR DETECTION AND CONTROL OF PRELASING IN A Q-SWITCHED LASER Patent

George E. Lockard, inventor (to NASA) 11 Oct. 1994 10 p Filed 3 Dec. 1992 Supersedes N93-19373 (31 - 6, p 1542)

(NASA-Case-LAR-14790-1; US-Patent-5,355,383;

US-Patent-Appl-SN-988082; US-Patent-Class-372-38;

US-Paternt-Class-372-10; US-Patent-Class-372-12;

Int-Patent-Class-H01S-3/00) Avail: US Patent and Trademark Office

The present invention detects prelasing in a Q-switch laser and terminates laser operation upon such detection. A detector senses the presence of light beyond a Q-switch and generates an appropriate electrical signal. A comparison stage circuit compares this detector signal with an established threshold value indicative of prelasing and generates a trigger signal if this detector signal exceeds this threshold value. A control stage circuit receives both this trigger value and a sampled Q-switch signal indicative of an opening of the Q-switch. The control stage circuit terminates operation of the laser if the trigger signal from the comparison stage is received while the sampled Q-switch signal is being received to avoid the effects of prelasing. Appropriate delays and timing sequences are established.

Official Gazette of the U.S. Patent and Trademark Office

N95-14668*# National Aeronautics and Space Administration. Ames Research Center, Moffett Field, CA.

MULTI-VELOCITY COMPONENT LDV Patent Application

Dennis A. Johnson, inventor (to NASA) 21 Nov. 1994 19 p

(NASA-Case-ARC-11925-1; NAS 1.71:ARC-11925-1;

US-Patent-Appl-SN-727263) Avail: CASI HC A03/MF A01

A laser doppler velocimeter uses frequency shifting of a laser beam to provide signal information for each velocity component. A composite electrical signal generated by a light detector is digitized and a processor produces a discrete Fourier transform based on the digitized electrical signal. The transform includes two peak frequencies corresponding to the two velocity components. Ames Research Center, Mail Code 200-11A, Moffett Field, California, 94035. Approved NASA forms for application for nonexclusive or exclusive license are available from the above address.

Author

N95-14901*# Johns Hopkins Univ., Baltimore, MD. Dept. of Electrical and Computer Engineering.

RECEIVER DESIGN, PERFORMANCE ANALYSIS, AND EVALUATION FOR SPACE-BORNE LASER ALTIMETERS AND SPACE-TO-SPACE LASER RANGING SYSTEMS Interim Progress Report, 15 Apr. - 15 Oct. 1994

Frederic M. Davidson, Xiaoli Sun, and Christopher T. Field Oct. 1994 56 p

(Grant NAG5-2232)

(NASA-CR-197050; NAS 1.26:197050) Avail: CASI HC A04/MF A01

This interim report consists of two reports: 'Space Radiation Effects on Si APDs for GLAS' and 'Computer Simulation of Avalanche Photodiode and Preamplifier Output for Laser Altimeters.' The former contains a detailed description of our proton radiation test of Si APD's performed at the Brookhaven National Laboratory. The latter documents the computer program subroutines which were written for the upgrade of NASA's GLAS simulator. Author

N95-15388# Technische Univ., Delft (Netherlands).

LASER ABLATION AND DEPOSITION OF ALLOYS Ph.D. Thesis

R. P. vanIngen 12 Oct. 1993 148 p Prepared in cooperation with Philips Gloeilampenfabrieken N.V., Eindhoven, Netherlands Sponsorsored by Stichting voor Fundamenteel Onderzoek der Materie

(PB94-191384) Avail: CASI HC A07/MF A02

This thesis concerns (1) the physics of laser ablation and (2) the materials science of thin films grown by Laser ablation deposition (LAD).

The basic ablation mechanisms play an important role in determining the properties of thin films grown by LAD. Laser ablation and deposition mechanisms can roughly be separated into three categories: category 1 involves the mechanisms associated with the interaction between laser pulses and a target, category 2 involves the mechanisms associated with the interaction between laser pulses and ablated species and the interactions among the latter, and category 3 involves the mechanisms associated with the interaction between ablated species and a substrate (and the target).
NTIS

N95-15391 Phillips Lab., Kirtland AFB, NM.
DEPARTMENT OF DEFENSE HIGH POWER LASER PROGRAM GUIDANCE Final Report
Clifford H. Muller 6 Jun. 1994 23 p Limited Reproducibility: More than 20% of this document may be affected by microfiche quality
(AD-A282915) Avail: CASI HC A02/MF A01

The DoD investment of nominally $200 million per year is focused on four high power laser (HPL) concepts: Space-Based Laser (SBL), a Ballistic Missile Defense Organization effort that addresses boost-phase intercept for Theater Missile Defense and National Missile Defense; Airborne Laser (ABL), an Air Force effort that addresses boost-phase intercept for Theater Missile Defense; Ground-Based Laser (GBL), an Air Force effort addressing space control; and Anti-Ship Missile Defense (ASMD), a Navy effort addressing ship-based defense. Each organization is also supporting technology development with the goal of achieving less expensive, brighter, and lighter high power laser systems. These activities represent the building blocks of the DoD program to exploit the compelling characteristics of the high power laser. Even though DoD's HPL program are focused and moderately strong, additional emphasis in a few technical areas could help reduce risk in these programs. In addition, a number of options are available for continuing to use the High-Energy Laser System Test Facility (HELSTF) at White Sands Missile Range. This report provides a brief overview and guidance for the five efforts which comprise the DoD HPL program (SBL, ABL, GBL, ASMD, HELSTF). DTIC

N95-15395 Houston Univ., TX. Dept. of Physics.
LASER SPECTROSCOPY OF COMBUSTION INTERMEDIATES IN A SUPERSONIC JET EXPANSION Final Report, 30 Apr. 1990 - 31 Mar. 1994
Prabhakar Misra Mar. 1994 52 p Limited Reproducibility: More than 20% of this document may be affected by microfiche quality
(Contract F33615-90-C-2038)
(AD-A283201; WL-TR-94-2034) Avail: CASI HC A04

A detailed analysis of the laser-induced fluorescence spectra of jet-cooled alkoxy, alkylthio and aromatic radicals has helped to characterize these radicals spectroscopically. All three groups of radicals are involved in the chemistry of organic fuel combustion. A clearer knowledge about the spectroscopy of these chemical intermediates is necessary for improved understanding of the free-radical controlled reaction steps occurring in combustion processes. DTIC

N95-13903*# Academy of Sciences of the Armenian SSR, Erivan. Inst. for Physical Research.
SPECTRAL, NOISE AND CORRELATION PROPERTIES OF INTENSE SQUEEZED LIGHT GENERATED BY A COUPLING IN TWO LASER FIELDS
Gagik Yu. Kryuchkyan and Karen V. Kheruntsyan *In* NASA. Goddard Space Flight Center, Third International Workshop on Squeezed States and Uncertainty Relations May 1994 p 51-64 (For primary document see N95-13896 03-74)
Avail: CASI HC A03/MF A06

N95-13925*# Academy of Sciences (USSR), Moscow (USSR). Physics Inst.
MODES IN LIGHT WAVE PROPAGATING IN SEMICONDUCTOR LASER
Margarita A. Manko *In* NASA. Goddard Space Flight Center, Third International Workshop on Squeezed States and Uncertainty Relations May 1994 p 219-224 (For primary document see N95-13896 03-74)
Avail: CASI HC A02/MF A06

N95-14287*# Smithsonian Astrophysical Observatory, Cambridge, MA.
SATELLITE LASER RANGING OPERATIONS
Michael R. Pearlman *In* NASA. Goddard Space Flight Center, Satellite Laser Ranging in the 1990s: Report of the 1994 Belmont Workshop Nov. 1994 p 89-99 (For primary document see N95-14274 03-46)
Avail: CASI HC A03/MF A02

37 MECHANICAL ENGINEERING

Includes auxiliary systems (nonpower); machine elements and processes; and mechanical equipment.

N95-13645# Westinghouse Savannah River Co., Aiken, SC.
WELDING IRRADIATED STAINLESS STEEL
W. R. Kanne, Jr., G. T. Chandler, D. Z. Nelson, and E. A. Franco-Ferreira 1993 20 p Presented at the 17th Symposium on Effects of Radiation on Materials, Sun Valley, ID, 20-23 Jun. 1994
(Contract DE-AC09-89SR-18035)
(DE94-013661; WSRC-MS-93-619; CONF-940657-1) Avail: CASI HC A03/MF A01

Conventional welding processes produced severe underbead cracking in irradiated stainless steel containing 1 to 33 appm helium from n,a reactions. A shallow penetration overlay technique was successfully demonstrated for welding irradiated stainless steel. The technique was applied to irradiated 304 stainless steel that contained 10 appm helium. Surface cracking, present in conventional welds made on the same steel at the same and lower helium concentrations, was eliminated. Underbead cracking was minimal compared to conventional welding methods. However, cracking in the irradiated material was greater than in tritium charged and aged material at the same helium concentrations. The overlay technique provides a potential method for repair or modification of irradiated reactor materials. DOE

N95-13654* National Aeronautics and Space Administration. Marshall Space Flight Center, Huntsville, AL.
WELDING NOZZLE POSITION MANIPULATOR Patent
Jeffrey L. Gilbert, inventor (to NASA) (Rockwell International Corp., Canoga Park, CA.) and David A. Gutow, inventor (to NASA) (Rockwell International Corp., Canoga Park, CA.) 1 Nov. 1994 6 p Filed 31 Aug. 1993 Supersedes N94-15882 (32 - 3, p 1047)
(NASA-Case-MFS-29837-1; US-Patent-5,360,157;
US-Patent-Appl-SN-114043; US-Patent-Class-228-45;
US-Patent-Class-228-02; Int-Patent-Class-B23K-37/02) Avail: US Patent and Trademark Office

The present invention is directed to a welding nozzle position manipulator. The manipulator consists of an angle support to which the remaining components of the device are attached either directly or indirectly. A pair of pivotal connections attach a weld nozzle holding link to the angle support and provide a two axis freedom of movement of the holding link with respect to the support angle. The manipulator is actuated by a pair of adjusting screws angularly mounted to the angle support. These screws contact a pair of tapered friction surfaces formed on the upper portion of the welding nozzle holding link. A spring positioned between the upper portions of the support angle and the holding link provides a constant bias engagement between the friction surfaces of the holding link and the adjustment screws, so as to firmly hold the link in position and to eliminate any free play in the adjustment mechanism. The angular relationships between the adjustment screws, the angle support and the tapered friction surfaces of the weld nozzle holding link provide a geometric arrangement which permits precision adjustment of the holding link with respect to the angle support and also provides a solid holding link mount which is resistant to movement from outside forces.
Official Gazette of the U.S. Patent and Trademark Office

N95-13819* National Aeronautics and Space Administration. Marshall Space Flight Center, Huntsville, AL.
HYBRID BEARINGS FOR TURBOPUMPS AND THE LIKE Patent
John F. Justak, inventor (to NASA) (Pratt and Whitney Aircraft, West Palm Beach, FL.) and Gregg R. Owens, inventor (to NASA) (Pratt and Whitney Aircraft, West Palm Beach, FL.) 20 Sep. 1994 5 p Filed 27 Jan. 1993 Supersedes N93-28326 (31 - 10, p 3052)
(NASA-Case-MFS-28491-1; US-Patent-5,348,401;

US-Patent-Appl-SN-010030; US-Patent-Class-384-101;
Int-Patent-Class-F16C-21/00) Avail: US Patent and Trademark Office

In rocket engines power is usually obtained by burning fuel and oxidizer which are mixed, pressurized, and directed to a combustion chamber by means of turbopumps. Roller bearings are generally used in these turbopumps, but because of bearing demands hydrostatic bearings were proposed. The use of such bearings is quite feasible because during flight hydrostatic lubrication can reduce roller bearing wear. A disadvantage of such proposals is that during startup, acceleration, and shutdown high pressure fluids are not available for hydrostatic bearings. The fluid lubrication film is not always present in bearings of turbopumps. During these periods a second bearing is required to carry the load. This requirement suggests the use of hybrid bearings in rocket engine turbopumps. Such duplex bearings were provided, but when their inner races are keyed to the shaft or journal two of them are required. And such duplex bearings do not wear evenly. A hybrid hydrostatic-rolling element bearing was provided wherein the rolling element bearing is locked on the stationary housing rather than on the rotating journal.

Official Gazette of the U.S. Patent and Trademark Office

N95-14005# Oak Ridge National Lab., TN.
EXPERIMENTAL IMPLEMENTATION OF A ROBUST DAMPED-OSCILLATION CONTROL ALGORITHM ON A FULL-SIZED, TWO-DEGREE-OF-FREEDOM, AC INDUCTION MOTOR-DRIVEN CRANE
R. L. Kress, J. F. Jansen, and M. W. Noakes 1994 9 p Presented at the 5th International Symposium on Robotics and Manufacturing, Maui, HI, 14-18 Aug. 1994
(Contract DE-AC05-84OR-21400)
(DE94-012113; CONF-940859-19) Avail: CASI HC A02/MF A01

When suspended payloads are moved with an overhead crane, pendulum like oscillations are naturally introduced. This presents a problem any time a crane is used, especially when expensive and/or delicate objects are moved, when moving in a cluttered and/or hazardous environment, and when objects are to be placed in tight locations. Damped-oscillation control algorithms have been demonstrated over the past several years for laboratory-scale robotic systems on dc motor-driven overhead cranes. Most overhead cranes presently in use in industry are driven by ac induction motors; consequently, Oak Ridge National Laboratory has implemented damped-oscillation crane control on one of its existing facility ac induction motor-driven overhead cranes. The purpose of this test was to determine feasibility, to work out control and interfacing specifications, and to establish the capability of newly available ac motor control hardware with respect to use in damped-oscillation-controlled systems. Flux vector inverter drives are used to investigate their acceptability for damped-oscillation crane control. The purpose of this paper is to describe the experimental implementation of a control algorithm on a full-sized, two-degree-of-freedom, industrial crane; describe the experimental evaluation of the controller including robustness to payload length changes; explain the results of experiments designed to determine the hardware required for implementation of the control algorithms; and to provide a theoretical description of the controller. DOE

N95-14150 Technische Univ., Delft (Netherlands).
DEXTROUS GRIPPING IN A HAZARDOUS ENVIRONMENT Ph.D. Thesis
W. Jongkind 7 Jun. 1993 234 p Limited Reproducibility: More than 20% of this document may be affected by microfiche quality
(PB94-191244; ISBN-90-9005806-0) Avail: Issuing Activity (National Technical Information Service (NTIS))

The main aims of the research were to propose a framework based on mechanics and system theory for designing a practical gripper and its control system, able to operate in the hazardous nuclear environment, and to combine theoretical and heuristic guidelines for integrating multiple aspects of gripper design in one synthetic design procedure. The objective is to arrive at a proposal for a practical realizable prototype of the gripper able to operate in the hazardous environment. The research has resulted in the following new aspects: a framework for designing a gripper which is based on tasks to be performed, the environment and design criteria; a proposal for the realization of the gripper with a high degree of dexterity whereby the dexterity is further enhanced by an active palm; a radiation resistant gripper since no radiation sensitive, active electronic components are located in the gripper; a mixed position-force gripper control algorithm based on the gripper functioning as a closed kinematic system; and a control algorithm able to keep grasping forces at a desired value in the presence of varying external exerted forces. NTIS

N95-14183*# National Aeronautics and Space Administration. Langley Research Center, Hampton, VA.
BASE PASSIVE POROSITY FOR DRAG REDUCTION Patent Application
Steven X. S. Bauer, inventor (to NASA) and Richard M. Wood, inventor (to NASA) 19 Oct. 1994 13 p
(NASA-Case-LAR-15246-1; NAS 1.71:LAR-15246-1;
US-Patent-Appl-SN-327061) Avail: CASI HC A03/MF A01

A device for controlling drag on a ground vehicle is presented. The device consists of a porous skin mounted on the trailing surface of the ground vehicle. The porous skin may be separated from the vehicle surface by a distance of at least two times the boundary layer formed on the surface. Alternately, the trailing surface of the ground vehicle may be porous. The device minimizes the strength of the separation in the base and wake regions of the ground vehicle, thus reducing drag. NASA

N95-14186*# National Aeronautics and Space Administration. Langley Research Center, Hampton, VA.
ADJUSTABLE REED FOR WEAVING NET-SHAPED TAILORED FABRICS Patent Application
Gary L. Farley, inventor (to NASA) (Army Vehicle Structures Lab., Hampton, VA.) 10 Jun. 1994 19 p
(NASA-Case-LAR-15072-1; NAS 1.71:LAR-15072-1;
US-Patent-Appl-SN-260162) Avail: CASI HC A03/MF A01

The invention is an apparatus and method for forming woven fabrics through the use of an adjustable reed. The adjustable reed has multiple groups of reed wires that guide the warp yarns. The groups of reed wires move on reed rails parallel to the warp direction. In addition, rail expanders permit the space between the reed wires to be modified and telescoping rods attached to the rail sliders can be turned to permit the reed wires to be skewed to alter the fill yarn angle. These adjustments to the reed permit simultaneous variation of fill yarn angles and fabric widths and allow these variations to be made during fabrication, without the need to halt production. NASA

N95-14336# Naval Postgraduate School, Monterey, CA.
THE STABLE AND PRECISE MOTION CONTROL FOR AN AUTONOMOUS MOBILE ROBOT M.S. Thesis
Ten-Min Lee Mar. 1994 93 p
(AD-A283776) Avail: CASI HC A05/MF A01

The major problem addressed by this research is how to develop a motion control algorithm for stable and precise control of the motion of an autonomous mobile robot. The approach taken was to clearly define the robot's motion descriptions and to design a high-level, machine independent robot control language called MML (Mode-based Mobile robot Language). The results are that the robot can implement line to line, line to circle, circle to circle path tracking or the combinations of these. Based on the motion control algorithm which was developed in this thesis, the robot is able to use external sensors to execute complicated missions such as obstacle avoidance (sonar is used in this thesis work). DTIC

N95-14347# Massachusetts Inst. of Tech., Cambridge. Dept. of Ocean Engineering.
DIRECT OBSERVATION OF OIL CONSUMPTION MECHANISMS IN A PRODUCTION SPARK IGNITION ENGINE USING FLUORESCENCE TECHNIQUES M.S. Thesis
Roderick M. Lusted May 1994 193 p
(Contract N00123-89-G-0580)
(AD-A283842) Avail: CASI HC A09/MF A03

The oil consumption characteristics of a four cylinder, normally aspirated spark-ignition engine were investigated for different piston ring end-gap configurations. A radiotracer was used to perform direct measurement of the oil consumption while Laser-induced Fluorescence (LIF) was used to perform the oil film thickness measurements for consumption predictions using the 'Puddle Theory of Oil Consumption,' which relates oil consumption to second land film thickness and reverse flow through top ring gap. The consumption data was evaluated to determine the impact of top ring end-gap azimuthal location on oil consumption. The film thickness data was used to evaluate the extent to which the oil Puddle Theory predicts variations

seen in the actual oil consumption. A tritium radiotracer oil consumption measurement system with an accuracy of 94.6 percent was designed and constructed. This was used to perform direct measurements of the test engine oil consumption in two different test matrices. The first evaluated a piston ring configuration with the rings free to rotate. The second evaluated configurations with the top ring and second piston rings pinned to fix the azimuthal location of the end-gap; the azimuth of the top ring was varied. In the second test matrix, the oil film thickness on the piston's second land was measured, and predictions were made on the basis of that measurement. DTIC

N95-14517* National Aeronautics and Space Administration. Goddard Space Flight Center, Greenbelt, MD.

FLEX-GEAR POWER TRANSMISSION SYSTEM FOR TRANSMITTING EMF BETWEEN SUN AND RING GEARS Patent

John M. Vranish, inventor (to NASA) 25 Oct. 1994 7 p Filed 25 Jan. 1993

(NASA-Case-GSC-13540-1; US-Patent-5,358,460; US-Patent-Appl-SN-008424; US-Patent-Class-475-344; US-Patent-Class-475-149; US-Patent-Class-475-345; US-Patent-Class-74-411; Int-Patent-Class-F16H-57/00) Avail: US Patent and Trademark Office

A plurality of flexible cylindrical members, termed flex-gears and having gear tooth type perimeters are located in an annular space between two concentric rotating gear members, one an inner gear member and the other an outer ring gear member, both of which have mutually facing toothed surfaces which engage the flex-gears. The flex-gears rotate and orbit around the annular space as planetary gears when the inner and outer gear members rotate with respect to one another. Pairs of these elements located in two mutually parallel planes and separated by insulators provide two electrical conductor paths across which an electrical signal source, AC or DC, can be connected and coupled to an electrical device. Alternatively, one set of elements including outer gears segmented into mutually insulated semicircles and inner gears segmented into mutually insulated quadrants can be used. Author

N95-14666*# National Aeronautics and Space Administration. Marshall Space Flight Center, Huntsville, AL.

DUAL-LATCHING SOLENOID-ACTUATED VALVE ASSEMBLY Patent Application

Myron J. Brudnicki, inventor (to NASA) (Allied-Signal Corp., Morristown, NJ.) and Jeff Yang, inventor (to NASA) (YS Controls.) 24 Aug. 1994 13 p

(NASA-Case-MFS-28714-1; NAS 1.71:MFS-28714-1; US-Patent-Appl-SN-296551) Avail: CASI HC A03/MF A01

A tube-type shutoff valve is electrically positioned to its open or closed position by a concentric electromagnetic solenoid. The valve is dual latching in that the armature of the solenoid maintains the sliding tube of the valve in an open or closed position by means of permanent magnets which are effective when current is not supplied to the solenoid. The valve may also be actuated manually. Author

N95-14797*# Texas A&M Univ., College Station, TX. Dept. of Mechanical Engineering.

DESIGN REVIEW AND ANALYSIS FOR A PRATT AND WHITNEY FLUID-FILM BEARING AND SEAL TESTING RIG Final Report

Dara W. Childs 3 Nov. 1994 34 p

(Grant NAG8-294)

(NASA-CR-197035; NAS 1.26:197035) Avail: CASI HC A03/MF A01

A design review has been completed for a Pratt and Whitney (P&W)-designed fluid-film bearing and annular-seal test rig to be manufactured and installed at George C. Marshall Space Flight Center (MSFC). Issues covered in this study include: (1) the capacity requirements of the drive unit; (2) the capacity and configuration of the static loading system; (3) the capacity and configuration of the dynamic excitation system; (4) the capacity, configuration, and rotordynamic stability of a test bearing, support bearings, and shaft; and (5) the characteristics and configuration of the measurement transducers and data channels. Author (revised)

N95-14904*# Auburn Univ., AL. Dept. of Civil Engineering.

EXPERIMENTAL ANALYSIS OF THREAD MOVEMENT IN BOLTED CONNECTIONS DUE TO VIBRATIONS Final Report

G. Ed Ramey and Robert C. Jenkins Aug. 1994 176 p

(Contract NAS8-39131)

(NASA-CR-197065; NAS 1.26:197065) Avail: CASI HC A09/MF A02

The objective of this study was to identify the main design parameters contributing to loosening of bolts due to vibration and to identify their relative importance and degree of contribution to bolt loosening. Vibration testing was conducted on a shaketable with a controlled-random input in the dynamic testing laboratory of the Structural Test Division of MSFC. Test specimens which contained one test bolt were vibrated for a fixed amount of time and percentage of pre-load loss was measured. Each specimen tested implemented some combination of eleven design parameters as dictated by the design of experiment methodology employed. The eleven design parameters were: bolt size (diameter), lubrication on bolt, hole tolerance, initial pre-load, nut locking device, grip length, thread pitch, lubrication between mating materials, class of fit, joint configuration and mass of configuration. These parameters were chosen for this experiment because they are believed to be the design parameters having the greatest impact on bolt loosening. Two values of each design parameter were used and each combination of parameters tested was subjected to two different directions of vibration and two different g-levels of vibration. One replication was made for each test to gain some indication of experimental error and repeatability and to give some degree of statistical credibility to the data, resulting in a total of 96 tests being performed. The results of the investigation indicated that nut locking devices, joint configuration, fastener size, and mass of configuration were significant in bolt loosening due to vibration. The results of this test can be utilized to further research the complex problem of bolt loosening due to vibration. Author (revised)

N95-14907*# Old Dominion Univ., Norfolk, VA.

ANNULAR SUSPENSION AND POINTING SYSTEM (ASPS) MAGNETIC ROTARY JOINT

W. E. Smith, W. Quach, and W. Thomas 1993 108 p Prepared in cooperation with USRA, Columbia, MD

(Contract NASw-4435)

(NASA-CR-197197; NAS 1.26:197197) Avail: CASI HC A06/MF A02

The Annular Suspension and Pointing System (ASPS) is a prototype of flight hardware for a high-accuracy space payload pointing mount. The long term project objective is to perform modifications and implement improvements to the existing ASPS in hopes of recommission. Also, new applications will be investigated for this technology. This report will focus on the first aspect of this overall goal, to establish operation of a single bearing station. Presented is an overview of the system history and bearing operation followed by the processes, results, and status of the single bearing study. Author

N95-14910*# Martin Marietta Corp., Denver, CO. Payloads Sensors and Instruments.

SAMPLE ACQUISITION AND INSTRUMENT DEPLOYMENT (SAID) Annual Technical Report, Oct. 1993 - Nov. 1994

Robert C. Boyd 21 Nov. 1994 28 p Original contains color illustrations

(Contract NASw-4818)

(NASA-CR-197104; NAS 1.26:197104; MCR-94-1328) Avail: CASI HC A03/MF A01; 1 functional color page

This report details the interim progress for contract NASW-4818, Sample Acquisition and Instrument Deployment (SAID), a robotic system for deploying science instruments and acquiring samples for analysis. The system is a conventional four degree of freedom manipulator 2 meters in length. A baseline design has been achieved through analysis and trade studies. The design considers environmental operating conditions on the surface of Mars, as well as volume constraints on proposed Mars landers. Control issues have also been studied, and simulations of joint and tip movements have been performed. A passively braked shape memory actuator with the ability to measure load has been developed. The wrist also contains a mechanism which locks the lid output to the bucket so that objects can be grasped and released for instrument deployment. The wrist actuator has been tested for operational power and mechanical functionality at Mars environmental conditions. The torque which the actuator can produce has been measured. Also, testing in Mars analogous soils has been performed. Author

N95-14923*# Syracuse Univ., NY. Dept. of Mechanical, Aerospace and Manufacturing Engineering.

LINEAR AND NONLINEAR DYNAMIC ANALYSIS OF REDUNDANT LOAD PATH BEARINGLESS ROTOR SYSTEMS

V. R. Murthy and Louis A. Shultz Oct. 1994 126 p
(Grant NAG2-306)
(NASA-CR-197220; NAS 1.26:197220) Avail: CASI HC A07/MF A02

The goal of this research is to develop the transfer matrix method to treat nonlinear autonomous boundary value problems with multiple branches. The application is the complete nonlinear aeroelastic analysis of multiple-branched rotor blades. Once the development is complete, it can be incorporated into the existing transfer matrix analyses. There are several difficulties to be overcome in reaching this objective. The conventional transfer matrix method is limited in that it is applicable only to linear branch chain-like structures, but consideration of multiple branch modeling is important for bearingless rotors. Also, hingeless and bearingless rotor blade dynamic characteristics (particularly their aeroelasticity problems) are inherently nonlinear. The nonlinear equations of motion and the multiple-branched boundary value problem are treated together using a direct transfer matrix method. First, the formulation is applied to a nonlinear single-branch blade to validate the nonlinear portion of the formulation. The nonlinear system of equations is iteratively solved using a form of Newton-Raphson iteration scheme developed for differential equations of continuous systems. The formulation is then applied to determine the nonlinear steady state trim and aeroelastic stability of a rotor blade in hover with two branches at the root. A comprehensive computer program is developed and is used to obtain numerical results for the (1) free vibration, (2) nonlinearly deformed steady state, (3) free vibration about the nonlinearly deformed steady state, and (4) aeroelastic stability tasks. The numerical results obtained by the present method agree with results from other methods. Derived from text

N95-15294 Massa Products Corp., Hingham, MA.

LEGGED VEHICLE FOR UNDERWATER MOBILE OPERATIONS Progress Report

Jim Jalbert and Joseph Ayers 5 Jul. 1994 12 p Limited Reproducibility: More than 20% of this document may be affected by microfiche quality
(Contract N00014-94-C-0078)
(AD-A282891) Avail: Issuing Activity (Defense Technical Information Center (DTIC))

This report summarizes technical information gained from an investigation into utilizing SMA actuators as muscle components for the biologically based lobster system to be developed under this project. In order for the SMA actuators to be of value in controlling leg motion of the lobster they must be able to contract and relax in a controlled manner much like muscles. SMA wires made of Nitinol do contract when heated and relax when cooled. The heating mechanism in this application is directly related to current density passed through the wire. If a large number of cycles are required, as in our application, the contraction should be limited to about 3 percent. This can provide a cycle life of millions provided that proper protection from overstressing, overstraining, and overheating are designed into the system. SMA contraction time can be quite fast (0.1 seconds or less) depending on the current pulse amplitude and width. SMA wires are very strong relative to their size. A 4 percent contraction can exert stresses of 25,000 psi. Control of each actuator requires that current pulses of proper amplitude and duration be applied at the correct times in order to not overheat the wires. Proper control of SMA wires for this application will require sensory feedback. DTIC

N95-15305* National Aeronautics and Space Administration. Marshall Space Flight Center, Huntsville, AL.

SADDLE CLAMP ASSEMBLY Patent

Charles R. Belrose, inventor (to NASA) 25 Jan. 1994 6 p Filed 17 Nov. 1992 Supersedes 93N17057 (31 - 5, p 1178)
(NASA-Case-MFS-28701-1; US-Patent-5,281,042;
US-Patent-Appl-SN-977468; US-Patent-Class-403-234;
US-Patent-Class-403-21; US-Patent-Class-403-12;
US-Patent-Class-248-74.4; Int-Patent-Class-F16L-3/10) Avail: US Patent and Trademark Office

A saddle clamp assembly is presented. The assembly is comprised of a hollow cylindrical body centered about a longitudinal axis and being diametrically split into semicircular top and bottom sections. Each section has a pair of connection flanges, at opposite ends, that project radially outward. A pair of bolts are retained on the top section flanges and are threadable into nuts retained on the bottom section flanges. A base member is anchored to a central underside portion of the bottom clamp body section and has a pair of connection tabs positioned beneath the bottom clamp body section connection flanges on opposite sides of the clamp axis. A pair of bolts are retained on the base member connection tabs and are threadable into a pair of nuts retainable on a support structure. The connection tab and connection flanges on each side of the clamp body are axially offset in a manner permitting downward installation/removable tool access to the lower bolts past the connection flanges. An elongated retention tether is used to connect the top clamp body section to the balance of the clamp assembly. This prevents loss of the top clamp body section when it is removed from the bottom clamp body section. Official Gazette of the U.S. Patent and Trademark Office

N95-15306* National Aeronautics and Space Administration. Lyndon B. Johnson Space Center, Houston, TX.

LANDING GEAR ENERGY ABSORPTION SYSTEM Patent

Christopher P. Hansen, inventor (to NASA) 22 Nov. 1994 7 p Filed 1 Dec. 1993 Supersedes N94-29448 (32 - 8, p 3300)
(NASA-Case-MSC-22277-1; US-Patent-5,366,181;
US-Patent-Appl-SN-159606; US-Patent-Class-244-104R;
US-Patent-Class-244-100R; US-Patent-Class-188-381;
Int-Patent-Class-B64C-25/58) Avail: US Patent and Trademark Office

A landing pad system is described for absorbing horizontal and vertical impact forces upon engagement with a landing surface where circumferentially arranged landing struts respectively have a clevis which receives a slidable rod member and where the upper portion of a slidable rod member is coupled to the clevis by friction washers which are force fit onto the rod member to provide for controlled constant force energy absorption when the rod member moves relative to the clevis. The lower end of the friction rod is pivotally attached by a ball and socket to a support plate where the support plate is arranged to slide in a transverse direction relative to a housing which contains an energy absorption material for absorbing energy in a transverse direction.
Official Gazette of the U.S. Patent and Trademark Office

N95-15601* National Aeronautics and Space Administration. Langley Research Center, Hampton, VA.

SMALL UHV COMPATIBLE HYPERTHERMAL OXYGEN ATOM GENERATOR Patent

Ronald A. Outlaw, inventor (to NASA) and Mark R. Davison, inventor (to NASA) 22 Nov. 1994 15 p Filed 2 Jul. 1993
(NASA-Cas-LAR-14674-1; US-Patent-5,367,161; US-Patent-Appl-SN-088963; US-Patent-Class-250-251; Int-Patent-Class-H05H-3/00) Avail: US Patent and Trademark Office

A high purity, hyperthermal, continuous beam atomic oxygen source capable of retrofitting to existing UHV systems has been developed. The instrument complements a general system capability, while its small size and simplicity of design permits tailoring the instrument for most experimental geometries. The flux level presently available is near 1 x 10 (exp 14) cm(exp -2)s(exp -1)(3P) but may be extended toward the theoretical limit of 3x10(exp 15 cm(exp -2)s(exp -1). The energy distribution of the emitted neutrals shows that the mean kinetic energy is about the same as observed for the ions or about 4 eV. The energy of the oxygen atoms may be substantially reduced for other applications by collision with a temperature controlled, non-reactive surface (with a concomitant spread in the energy distribution). Author

N95-15670* National Aeronautics and Space Administration. Marshall Space Flight Center, Huntsville, AL.

PLASMA ARC WELDING TORCH HAVING MEANS FOR VORTEXING PLASMA GAS EXITING THE WELDING TORCH Patent

Daniel J. Rybicki, inventor (to NASA) (Martin Marietta Space Systems, Inc., Huntsville, AL.) and William F. McGee, inventor (to NASA) (Martin Marietta Space Systems, Inc., Huntsville, AL.) 8 Nov. 1994 6 p Filed 29 Nov. 1993 Supersedes N94-29351 (32 - 8, p 3298)
(NASA-Case-MFS-28828-1; US-Patent-5,362,938;
US-Patent-Appl-SN-158327; US-Patent-Class-219-121.51;
US-Patent-Class-219-121.49; US-Patent-Class-219-121.45;

US-Patent-Class-219-121.48; US-Patent-Class-313-231.51;
Int-Patent-Class-B23K-9/00; Int-Patent-Class-B23K-10/00) Avail: US Patent and Trademark Office

A plasma arc welding torch is described wherein a plasma gas is directed through the body of the welding torch and out of the body across the tip of the welding electrode disposed at the forward end of the body. The plasma gas is provided with a vortexing motion prior to exiting the body by a vortex motion imparting member which is mounted in an orifice housing member and carried in the forward portion of the torch body. The orifice housing member is provided with an orifice of an predetermined diameter through which the electric arc and the plasma gas exits. Author

N95-15747# Southwest Research Inst., San Antonio, TX. Belvoir Fuels and Lubricants Research Facility.

WEAR MECHANISM EVALUATION AND MEASUREMENT IN FUEL-LUBRICATED COMPONENTS Interim Report

Paul I. Lacey Sep. 1994 144 p
(Contracts DAAK70-87-C-0043; DAAK70-92-C-0059)
(AD-A284870; BFLRF-286) Avail: CASI HC A07/MF A02

Previous studies have demonstrated that the durability of some fuel injection systems on compression-ignition engines will be adversely affected by fuels of sufficiently low lubricity. However, no widely accepted lubricity measure is available; indeed, the wear mechanisms present have not been conclusively defined. The results of the present study indicate that oxidative corrosion is the predominant mechanism with very highly processed fuels, resulting in catastrophic wear and rapid failure. A laboratory test procedure directed toward the oxidative wear mechanism was evaluated and a number of modifications suggested. Two closely related laboratory wear test procedures that rely on the transition from mild boundary lubricated wear to adhesive scuffing were also developed. The resulting procedures allow the fuels to be either ranked using a continuous scale or separated using a simple pass/fail criteria. All the procedures are sensitive to the addition of trace quantities of lubricity additives and show directional correlation with refinery severity, as measured by sulfur and aromatic content. As a result, the tests produced excellent correlation with full-scale equipment tests performed at a number of locations, as well as the criteria necessary for oxidative corrosion. However, the scuffing load tests show greatly increased separation between good and unacceptable fluids compared to the oxidative corrosion tests. Evaluation of commercially available fuels indicates that fuel lubricity is decreasing and that very poor lubricity fuels are occasionally observed. DTIC

N95-15914* National Aeronautics and Space Administration. Lewis Research Center, Cleveland, OH.

SERVICE EQUIPMENT FOR USE IN HOSTILE ENVIRONMENTS Patent

James L. Dolce, inventor (to NASA) and Andrew L. Gordon, inventor (to NASA) 22 Nov. 1994 10 p Filed 26 Jul. 1993 Supersedes N93-31314 (31 - 12, p 3734) Division of US-Patent-Appl-SN-889572, filed 28 May 1992
(NASA-Case-LEW-14906-2-SB; US-Patent-5,366,384;
US-Patent-Appl-SN-104951; US-Patent-Appl-SN-889572;
US-Patent-Class-439-372; US-Patent-Class-439-196;
US-Patent-Class-439-374; Int-Patent-Class-H01R-13/639;
Int-Patent-Class-B25B-5/00) Avail: US Patent and Trademark Office

Service equipment for use in hostile environments includes a detachable service unit secured to a stationary service unit. The detachable service unit includes a housing with an exterior plate, a power control interface for connection to an exterior power source, locating pins located in said exterior plate, an electrical connector in the exterior plate electrically coupled to said power control interface, and a pair of clamping receptacles formed in the exterior plate and located on adjacent opposite edges of the exterior plate. The stationary unit includes an electrical connector for connection to the electrical connector of the detachable service unit, a clamping apparatus for clamping and unclamping the detachable service unit from the stationary unit, a base clamp assembly for mounting the clamping apparatus onto the stationary unit, and locating pin holes for receiving the locating pins and aligning the detachable service unit onto the stationary unit. The detachable service unit and stationary unit have mating scalloped faces which aid in alignment and provide a mechanism for heat dissipation. Author

N95-13833# ISRO Satellite Centre, Peenya, Bangalore (India). Quality Assurance Div.

DEPLOYMENT MECHANISM CALIBRATION SYSTEM

P. R. Marur and S. G. Raghavan *In its* Journal of Spacecraft Technology, Volume 4, No. 2, July 1994 Jul. 1994 p 78-83 (For primary document see N95-13825 03-12)
Avail: CASI HC A02/MF A01

N95-14023*# Naval Ocean Systems Center, Kailua, HI. Marine Sciences and Technology Dept.

TELEROBOTIC REMOTE PRESENCE: ACHIEVEMENTS AND CHALLENGES Abstract Only

Walter A. Aviles *In* NASA. Ames Research Center, Human Machine Interfaces for Teleoperators and Virtual Environments Jun. 1991 p 31 (For primary document see N95-14013 03-54)
Avail: CASI HC A01/MF A02

N95-14026*# Woods Hole Oceanographic Inst., MA. Deep Submergence Lab.

TELEROBOTICS IN THE DEEP OCEAN Abstract Only

Hagen Schempf and Dana R. Yoerger *In* NASA. Ames Research Center, Human Machine Interfaces for Teleoperators and Virtual Environments Jun. 1991 p 36 (For primary document see N95-14013 03-54)
Avail: CASI HC A01/MF A02

N95-14027*# Washington Univ., Seattle, WA. Dept. of Electrical Engineering.

MODELS OF REMOTE MANIPULATION IN SPACE

Blake Hannaford *In* NASA. Ames Research Center, Human Machine Interfaces for Teleoperators and Virtual Environments Jun. 1991 p 37-40 (For primary document see N95-14013 03-54)
Avail: CASI HC A01/MF A02

N95-14128# Sulzer Innotec A.G., Winterthur (Switzerland). Fluid Dynamics Lab.

COMPUTATIONAL METHODS FOR PRELIMINARY DESIGN AND GEOMETRY DEFINITION IN TURBOMACHINERY

M. V. Casey *In* AGARD, Turbomachinery Design Using CFD May 1994 22 p (For primary document see N95-14127 03-34)
Copyright Avail: CASI HC A03/MF A03

N95-14129# General Electric Co., Cincinnati, OH. Aircraft Engines Div.

ELEMENTS OF A MODERN TURBOMACHINERY DESIGN SYSTEM

Ian K. Jennions *In* AGARD, Turbomachinery Design Using CFD May 1994 22 p (For primary document see N95-14127 03-34)
Copyright Avail: CASI HC A03/MF A03

N95-14130# Cambridge Univ., Cambridge (England). Dept. of Engineering.

DESIGNING IN THREE DIMENSIONS

J. D. Denton *In* AGARD, Turbomachinery Design Using CFD May 1994 14 p (For primary document see N95-14127 03-34)
Copyright Avail: CASI HC A03/MF A03

N95-14947# Alcatel Espace, Toulouse (France).

MISSION, TECHNOLOGIES AND DESIGN OF PLANETARY MOBILE VEHICLE

Michel Hayard *In* AGARD, Advanced Guidance and Control Aspects in Robotics Jun. 1994 7 p (For primary document see N95-14942 03-63)
Copyright Avail: CASI HC A02/MF A03

N95-14948# Bateman (Peter J.), Camberly (England).

GUIDANCE AND CONTROL FOR UNMANNED GROUND VEHICLES

Peter J. Bateman *In* AGARD, Advanced Guidance and Control Aspects in Robotics Jun. 1994 33 p (For primary document see N95-14942 03-63)
Copyright Avail: CASI HC A03/MF A03

38 QUALITY ASSURANCE AND RELIABILITY

Includes product sampling procedures and techniques; and quality control.

N95-13835*# National Aeronautics and Space Administration. Langley Research Center, Hampton, VA.
RADIOGRAPHIC MOIRE Patent Application
Eric Irvine Madaras, inventor (to NASA) 31 May 1994 12 p
(NASA-Case-LAR-15104-1; NAS 1.71:LAR-15104-1;
US-Patent-Appl-SN-251434) Avail: CASI HC A03/MF A01

A method for the x-ray inspection of materials making use of the Moire effect is described. The Moire effect results when two patterns are superimposed; a third pattern is produced. Any change in either of the first two patterns creates a change in the third. Moire inspection is common with visible light. This invention allows the technique to be extended to locations inaccessible to visual inspection. A first pattern of high radio contrast material is attached to or included in the sample. X-rays are projected through the sample. A second pattern is imposed at the observation point, either before or after the formation of the x-ray image. The two patterns interact to create a third, Moire, pattern. As the material is stressed the Moire pattern changes, the degree of change indicating the degree of stress. NASA

N95-13840*# Vitro Corp., Silver Spring, MD.
ENGINEERING, TECHNICAL, AND MANAGEMENT SUPPORT SERVICES Final Summary Report, 22 Feb. 1988 - 10 Feb. 1994
10 Feb. 1994 95 p
(Contract NASw-4311)
(NASA-CR-196977; NAS 1.26:196977) Avail: CASI HC A05/MF A01

This report summarizes by task the engineering, technical, and management support services provided by Vitro Corporation to NASA Headquarters Office of Safety, Reliability, Maintainability, and Quality Assurance (now called Office of Safety and Mission Assurance (OSMA)) (Code Q) under Contract Number NASW-4311 from the period February 10, 1994. Each task summary includes significant Vitro accomplishments, conclusions, and recommendations for future efforts in each of the divisions within OSMA. Derived from text

N95-13886*# University of Central Florida, Orlando, FL. Dept. of Mechanical and Aerospace Engineering.
NONDESTRUCTIVE ANALYSIS AND DEVELOPMENT Final Report, Jan. 1990 - Dec. 1992
Faissal A. Moslehy Aug. 1993 113 p Original contains color illustrations
(Grant NAG10-0058)
(NASA-CR-196987; NAS 1.26:196987) Avail: CASI HC A06/MF A02; 9 functional color pages

This final report summarizes the achievements of project #4 of the NASA/UCF Cooperative Agreement from January 1990 to December 1992. The objectives of this project are to review NASA's NDE program at Kennedy Space Center (KSC) and recommend means for enhancing the present testing capabilities through the use of improved or new technologies. During the period of the project, extensive development of a reliable nondestructive, non-contact vibration technique to determine and quantify the bond condition of the thermal protection system (TPS) tiles of the Space Shuttle Orbiter was undertaken. Experimental modal analysis (EMA) is used as a non-destructive technique for the evaluation of Space Shuttle thermal protection system (TPS) tile bond integrity. Finite element (FE) models for tile systems were developed and were used to generate their vibration characteristics (i.e. natural frequencies and mode shapes). Various TPS tile assembly configurations as well as different bond conditions were analyzed. Results of finite element analyses demonstrated a drop in natural frequencies and a change in mode shapes which correlate with both size and location of disbond. Results of experimental testing of tile panels correlated with FE results and demonstrated the feasibility of EMA as a viable technique for tile bond verification. Finally, testing performed on the Space Shuttle Columbia using a laser doppler velocimeter demonstrated the application of EMA, when combined with FE modeling, as a non-contact, non-destructive bond evaluation technique. Author

N95-15584*# Vanderbilt Univ., Nashville, TN. Dept. of Mechanical Engineering.
MECHANICAL SYSTEM RELIABILITY FOR LONG LIFE SPACE SYSTEMS Final Report
Michael T. Kowal Nov. 1994 115 p
(Grant NAG3-1352)
(NASA-CR-197215; NAS 1.26:197215) Avail: CASI HC A06/MF A02

The creation of a compendium of mechanical limit states was undertaken in order to provide a reference base for the application of first-order reliability methods to mechanical systems in the context of the development of a system level design methodology. The compendium was conceived as a reference source specific to the problem of developing the noted design methodology, and not an exhaustive or exclusive compilation of mechanical limit states. The compendium is not intended to be a handbook of mechanical limit states for general use. The compendium provides a diverse set of limit-state relationships for use in demonstrating the application of probabilistic reliability methods to mechanical systems. The compendium is to be used in the reliability analysis of moderately complex mechanical systems. Derived from text

N95-15777# Los Alamos National Lab., NM.
SELECTION OF NON-DESTRUCTIVE ASSAY METHODS: NEUTRON COUNTING OR CALORIMETRIC ASSAY?
T. L. Cremers and J. R. Wachter 1994 8 p Presented at the Institute of Nuclear Materials Management Annual Meeting, Naples, FL, 17-20 Jul. 1994
(Contract W-7405-eng-36)
(DE94-016211; LA-UR-94-2377; CONF-940748-39) Avail: CASI HC A02/MF A01

The transition of DOE facilities from production to D&D has lead to more measurements of product, waste, scrap, and other less attractive materials. Some of these materials are difficult to analyze by either neutron counting or calorimetric assay. To determine the most efficacious analysis method, variety of materials, impure salts and hydrofluorination residues have been assayed by both calorimetric assay and neutron counting. New data will be presented together with a review of published data. The precision and accuracy of these measurements are compared to chemistry values and are reported. The contribution of the gamma ray isotopic determination measurement to the overall error of the calorimetric assay or neutron assay is examined and discussed. Other factors affecting selection of the most appropriate non-destructive assay method are listed and considered. DOE

N95-14475*# Northwestern Univ., Evanston, IL. School of Engineering and Applied Science.
FATIGUE RELIABILITY METHOD WITH IN-SERVICE INSPECTIONS
H. H. Harkness, M. Fleming, B. Moran, and T. Belytschko *In* NASA. Langley Research Center, FAA/NASA International Symposium on Advanced Structural Integrity Methods for Airframe Durability and Damage Tolerance Sep. 1994 p 307-326 Sponsored in part by National Inst. for Standards and Technology and FAA (For primary document see N95-14453 03-39) Avail: CASI HC A03/MF A04

39 STRUCTURAL MECHANICS

Includes structural element design and weight analysis; fatigue; and thermal stress.

For applications see *05 Aircraft Design, Testing and Performance* and *18 Spacecraft Design, Testing and Performance.*

N95-13839*# Virginia Polytechnic Inst. and State Univ., Blacksburg, VA. Dept. of Engineering Science and Mechanics.
THE BUCKLING RESPONSE OF SYMMETRICALLY LAMINATED COMPOSITE PLATES HAVING A TRAPEZOIDAL PLANFORM AREA M.S. Thesis Interim Report No. 98, Aug. 1990 - May 1994
H. D. Radloff, II, M. W. Hyer, and M. P. Nemeth Aug. 1994 185 p
(Grant NAG1-343)
(NASA-CR-196975; NAS 1.26:196975; CCMS-94-10; VPI-E-94-07) Avail: CASI HC A09/MF A02

The focus of this work is the buckling response of symmetrically laminated composite plates having a planform area in the shape of an

isosceles trapezoid. The loading is assumed to be inplane and applied perpendicular to the parallel ends of the plate. The tapered edges of the plate are assumed to have simply supported boundary conditions, while the parallel ends are assumed to have either simply supported or clamped boundary conditions. A semi-analytic closed-form solution based on energy principles and the Trefftz stability criterion is derived and solutions are obtained using the Rayleigh-Ritz method. Intrinsic in this solution is a simplified prebuckling analysis which approximates the inplane force resultant distributions by the forms Nx=P/W(x) and Ny=Nxy=0, where P is the applied load and W(x) is the plate width which, for the trapezoidal planform, varies linearly with the lengthwise coordinate x. The out-of-plane displacement is approximated by a double trigonometric series. This analysis is posed in terms of four nondimensional parameters representing orthotropic and anisotropic material properties, and two nondimensional parameters representing geometric properties. For comparison purposes, a number of specific plate geometry, ply orientation, and stacking sequence combinations are investigated using the general purpose finite element code ABAQUS. Comparison of buckling coefficients calculated using the semi-analytical model and the finite element model show agreement within 5 percent, in general, and within 15 percent for the worst cases. In order to verify both the finite element and semi-analytical analyses, buckling loads are measured for graphite/epoxy plates having a wide range of plate geometries and stacking sequences. Test fixtures, instrumentation system, and experimental technique are described. Experimental results for the buckling load, the buckled mode shape, and the prebuckling plate stiffness are presented and show good agreement with the analytical results regarding the buckling load and the prebuckling plate stiffness. However, the experimental results show that for some cases the analysis underpredicts the number of halfwaves in the buckled mode shape. In the context of the definitions of taper ratio and aspect ratio used in this study, it is concluded that the buckling load always increases as taper ratio increases for a given aspect ratio for plates having simply supported boundary conditions on the parallel ends. There are combinations of plate geometry and ply stackling sequences, however, that reverse this trend for plates having clamped boundary conditions on the parallel ends such that an increase in the taper ratio causes a decrease in the buckling load. The clamped boundary conditions on the parallel ends of the plate are shown to increase the buckling load compared to simply supported boundary conditions. Also, anisotropy (the D16 and D26 terms) is shown to decrease the buckling load and skew the buckled mode shape for both the simply supported and clamped boundary conditions. Author

N95-14138*# National Aeronautics and Space Administration. Langley Research Center, Hampton, VA.

JOINT FOR A VARIABLE GEOMETRY TRUSS AND METHOD OF CONSTRUCTING SAME Patent Application

Garnett C. Horner, inventor (to NASA) 14 Oct. 1994 18 p

(NASA-Case-LAR-15136-1; NAS 1.71:LAR-15136-1; US-Patent-Appl-SN-325723) Avail: CASI HC A03/MF A01

A joint and a method of constructing a joint for a variable geometry truss having a variable number of planes of variable length battens connected together in a triangular configuration, each plane being connected by six fixed length longerons in a Stewart platform configuration, are presented. The variable length battens allow the orientation of one end plane of the variable geometry truss to be changed to the other end plane in a controlled manner by selectively adjusting the lengths of the variable length battens. A main pivot joint pivotally connects two battens about a pivotal axis. A universal joint is pivotally connected to the main joint such that the pivotal axis of the universal joint is coextensive with the pivotal axis at the main joint. Two longerons are pivotally connected to the universal joint. Each longeron is thereby provided with three intersecting axes of rotation. Each longeron may include a revolute joint, allowing rotation about the longitudinal axis of the longeron. NASA

N95-14198# Advisory Group for Aerospace Research and Development, Neuilly-Sur-Seine (France). Structures and Materials Panel.

HIGH TEMPERATURE CYCLIC BEHAVIOUR OF AEROSPACE MATERIALS: ROOM TEMPERATURE VALIDATION TESTS OF Ti-6Al-4V [LE COMPORTEMENT CYCLIQUE HAUTE TEMPERATURE DES MATERIAUX AEROSPATIAUX: LES ESSAIS DE VALIDATION DU TI-6AL-4V]

C. Wilkinson (Defence Research Agency, Farnborough, Hampshire, England.) and C. R. Gostelow (Defence Research Agency, Farnborough, Hampshire, England.) Jun. 1994 37 p

(AGARD-AR-328; ISBN-92-835-0716-9) Copyright Avail: CASI HC A03/MF A01

Materials specification and distribution of Ti-6Al-4V specimens are presented along with the collated data from those participants that have supplied test results. Crack propagation and strain control low cycle fatigue data are discussed, along with a number of points of clarification regarding test technique. This report, sponsored by the Structures and Materials Panel of AGARD, contains all relevant information on the validation exercise conducted by participants of Working Group 26. Author

N95-14270*# Old Dominion Univ., Norfolk, VA. Dept. of Aerospace Engineering.

THERMAL STRUCTURE ANALYSES FOR CSM TESTBED (COMET) Final Report, 16 May 1992 - 15 Aug. 1994

David Y. Xue and Chuh Mei Oct. 1994 65 p

(Grant NAG1-1431)

(NASA-CR-196998; NAS 1.26:196998; ODURF-124453) Avail: CASI HC A04/MF A01

This document is the final report for the project entitled 'Thermal Structure Analyses for CSM Testbed (COMET),' for the period of May 16, 1992 - August 15, 1994. The project was focused on the investigation and development of finite element analysis capability of the computational structural mechanics (CSM) testbed (COMET) software system in the field of thermal structural responses. The stages of this project consisted of investigating present capabilities, developing new functions, analysis demonstrations, and research topics. The appendices of this report list the detailed documents of major accomplishments and demonstration runstreams for future references. Derived from text

N95-14320# General Electric Co., Schenectady, NY. Atomic Power Lab.

ANALYSIS OF WELDING-INDUCED RESIDUAL STRESSES WITH THE ADINA SYSTEM

W. W. Wilkening and J. L. Snow Dec. 1993 20 p Presented at the 9th Nonlinear Finite Element Analysis and ADINA Conference, Boston, MA, 23-25 Jun. 1993

(Contract DE-AC12-76SN-00052)

(DE94-015359; KAPL-4782; CONF-9306354-1) Avail: CASI HC A03/MF A01

Welding-induced residual stresses analysis procedure (WIRSAP), based on ADINA system of nonlinear finite element software, is described and results of several WIRSAP analyses are discussed. Several 2D axisymmetric WIRSAP analyses were performed for pipe girth welds and for several multi-pass girth-like welds attaching small nozzles to large, thick-walled pressure vessels. The analytical methodology follows closely Rybicki et al, enhanced by several specialized modeling techniques available in ADINA. The element birth option is used to simulate the addition of weld metal, and the mixed pressure/displacement element formulation is used, in conjunction with temperature-dependent bi-linear plasticity material model. Some of the welds analyzed involve backing rings, which were subsequently 'machined off' via use of the element death option. The auto-time-stepping algorithm and matrix update iteration scheme are used in structural solutions. WIRSAP involves, a pass-by-pass analysis of uncoupled thermal and structural problems, but some analyses have been performed with an 'enveloping' technique for grouping several weld passes together. The analyses are all 2D, but most are large problems and pose challenge to software and hardware. Operations are performed on a network of Silicon Graphics workstations, and ADINA and ADINA-T are executed on a 64 MW, eight-processor CRAY YIMP. Nominally 50 solution steps are utilized for each weld pass and weld joints involving as many as 31 individual weld passes analyzed on a pass-by-pass basis. Results from several WIRSAP analyses are discussed, and potential use of WIRSAP in a hypothetic attachment weld design optimization study is illustrated. DOE

N95-14356# Missouri Univ., Columbia, MO.

[THE EFFECT OF MICROSTRESSES ON FATIGUE CRACK PROPAGATION IN STEEL] Annual Report, 1 Jul. 1993 - 30 Jun. 1994

R. A. Winholtz 19 Aug. 1994 11 p

(Contract N00014-93-1-1049)

(AD-A283872; Rept-1) Avail: CASI HC A03/MF A01

The first goal of this project is to determine the effects of plastically

induced microstresses on fatigue crack propagation in steel. To accomplish this specimens and heat treatment have been designed, the specimens have been deformed to introduce different microstress states, and the microstresses measured using neutron diffraction. Neutron measurements of the stresses in the cementite phase were successful and confirm that only microstresses are produced by the plastic deformation. Initial results from the neutron measurements of the microstresses indicate that there is some asymmetry in the magnitude of the stresses introduced by tensile and compressive deformations. This effect is probably due to preexisting thermal residual microstresses between the phases. Fatigue crack propagation tests are now being performed. DTIC

N95-14417*# Colorado State Univ., Fort Collins, CO. Dept. of Civil Engineering.

DISCRETE-LAYER PIEZOELECTRIC PLATE AND SHELL MODELS FOR ACTIVE TIP-CLEARANCE CONTROL Final Report

P. R. Heyliger, G. Ramirez, and K. C. Pei Oct. 1994 170 p
(Grant NAG3-1520; RTOP 505-63-5B)
(NASA-CR-195383; E-9133; NAS 1.26:195383) Avail: CASI HC A08/MF A02

The objectives of this work were to develop computational tools for the analysis of active-sensory composite structures with added or embedded piezoelectric layers. The targeted application for this class of smart composite laminates and the analytical development is the accomplishment of active tip-clearance control in turbomachinery components. Two distinct theories and analytical models were developed and explored under this contract: (1) a discrete-layer plate theory and corresponding computational models, and (2) a three dimensional general discrete-layer element generated in curvilinear coordinates for modeling laminated composite piezoelectric shells. Both models were developed from the complete electromechanical constitutive relations of piezoelectric materials, and incorporate both displacements and potentials as state variables. This report describes the development and results of these models. The discrete-layer theories imply that the displacement field and electrostatic potential through-the-thickness of the laminate are described over an individual layer rather than as a smeared function over the thickness of the entire plate or shell thickness. This is especially crucial for composites with embedded piezoelectric layers, as the actuating and sensing elements within these layers are poorly represented by effective or smeared properties. Linear Lagrange interpolation polynomials were used to describe the through-thickness laminate behavior. Both analytic and finite element approximations were used in the plane or surface of the structure. In this context, theoretical developments are presented for the discrete-layer plate theory, the discrete-layer shell theory, and the formulation of an exact solution for simply-supported piezoelectric plates. Finally, evaluations and results from a number of separate examples are presented for the static and dynamic analysis of the plate geometry. Comparisons between the different approaches are provided when possible, and initial conclusions regarding the accuracy and limitations of these models are given. Author

N95-14453*# National Aeronautics and Space Administration. Langley Research Center, Hampton, VA.

FAA/NASA INTERNATIONAL SYMPOSIUM ON ADVANCED STRUCTURAL INTEGRITY METHODS FOR AIRFRAME DURABILITY AND DAMAGE TOLERANCE

Charles E. Harris, ed. Sep. 1994 506 p Symposium held in Hampton, VA, 4-6 May 1994 Sponsored by NASA, Washington and FAA
(RTOP 538-02-10-01)
(NASA-CP-3274-Pt-1; L-17432-Pt-1; NAS 1.55:3274-Pt-1) Avail: CASI HC A22/MF A04

International technical experts in durability and damage tolerance of metallic airframe structures were assembled to present and discuss recent research findings and the development of advanced design and analysis methods, structural concepts, and advanced materials. The symposium focused on the dissemination of new knowledge and the peer-review of progress on the development of advanced methodologies. Papers were presented on: structural concepts for enhanced durability, damage tolerance, and maintainability; new metallic alloys and processing technology; fatigue crack initiation and small crack effects; fatigue crack growth models; fracture mechanics failure, criteria for ductile materials; structural mechanics methodology for residual strength and life prediction; development of flight load spectra for design and testing; and advanced approaches to resist corrosion and environmentally assisted fatigue. For individual titles, see N95-14454 through N95-14486.

N95-14454*# Engineering Software Research and Development, Inc., Saint Louis, MO.

ELASTIC-PLASTIC MODELS FOR MULTI-SITE DAMAGE

Ricardo L. Actis and Barna A. Szabo *In* NASA. Langley Research Center, FAA/NASA International Symposium on Advanced Structural Integrity Methods for Airframe Durability and Damage Tolerance Sep. 1994 p 1-16 (For primary document see N95-14453 03-39)
(Grant NAG9-622)
Avail: CASI HC A03/MF A04

This paper presents recent developments in advanced analysis methods for the computation of stress site damage. The method of solution is based on the p-version of the finite element method. Its implementation was designed to permit extraction of linear stress intensity factors using a superconvergent extraction method (known as the contour integral method) and evaluation of the J-integral following an elastic-plastic analysis. Coarse meshes are adequate for obtaining accurate results supported by p-convergence data. The elastic-plastic analysis is based on the deformation theory of plasticity and the von Mises yield criterion. The model problem consists of an aluminum plate with six equally spaced holes and a crack emanating from each hole. The cracks are of different sizes. The panel is subjected to a remote tensile load. Experimental results are available for the panel. The plasticity analysis provided the same limit load as the experimentally determined load. The results of elastic-plastic analysis were compared with the results of linear elastic analysis in an effort to evaluate how plastic zone sizes influence the crack growth rates. The onset of net-section yielding was determined also. The results show that crack growth rate is accelerated by the presence of adjacent damage, and the critical crack size is shorter when the effects of plasticity are taken into consideration. This work also addresses the effects of alternative stress-strain laws: The elastic-ideally-plastic material model is compared against the Ramberg-Osgood model. Author

N95-14455*# United Technologies Research Center, East Hartford, CT.

SMALL CRACK TEST PROGRAM FOR HELICOPTER MATERIALS

Bal Annigeri and George Schneider *In* NASA. Langley Research Center, FAA/NASA International Symposium on Advanced Structural Integrity Methods for Airframe Durability and Damage Tolerance Sep. 1994 p 17-32 (For primary document see N95-14453 03-39)
(Contract F09603-89-G-0096)
Avail: CASI HC A03/MF A04

Crack propagation tests were conducted to determine crack growth behavior in five helicopter materials for surface cracks between 0.005 to 0.020 inches in depth. Constant amplitude tests were conducted at stress ratios R equals 0.1 and 0.5, and emphasis was placed on near threshold data (i.e., 10-8 to 10-6 inches/cycle). Spectrum tests were conducted using a helicopter spectrum. The test specimen was an unnotched tension specimen, and cracks were initiated from a small EDM notch. An optical/video system was used to monitor crack growth. The material for the test specimens was obtained from helicopter part forgings. Testing was conducted at stresses below yield to reflect actual stresses in helicopter parts. Author

N95-14456*# Purdue Univ., West Lafayette, IN. School of Aeronautics and Astronautics.

BENDING EFFECTS OF UNSYMMETRIC ADHESIVELY BONDED COMPOSITE REPAIRS ON CRACKED ALUMINUM PANELS

Cory Arendt and C. T. Sun *In* NASA. Langley Research Center, FAA/NASA International Symposium on Advanced Structural Integrity Methods for Airframe Durability and Damage Tolerance Sep. 1994 p 33-48 (For primary document see N95-14453 03-39)
(AF Proj. 1397)
Avail: CASI HC A03/MF A04

The bending effects of unsymmetrically bonded composite repairs on cracked aluminum panels were quantified using a plate linear finite element model. Stress intensity factors and strain energy release rates were obtained from the model twice, once with out-of-plane displacement suppressed and another time without these restrictions. Several configurations were examined, crack growth stability was identified, and the effect of a debond

was considered. The maximum stress intensity factor was also analyzed. Previous work by other authors was found to underpredict the bending effect. Author

N95-14457*# Textron Specialty Materials, Lowell, MA.
EVALUATION OF BONDED BORON/EPOXY DOUBLERS FOR COMMERCIAL AIRCRAFT ALUMINUM STRUCTURES
Bruce Belason, Paul Rutherford, Matthew Miller, and Shreeram Raj *In* NASA. Langley Research Center, FAA/NASA International Symposium on Advanced Structural Integrity Methods for Airframe Durability and Damage Tolerance Sep. 1994 p 49-60 (For primary document see N95-14453 03-39)
Avail: CASI HC A03/MF A04

An 18 month laboratory test and stress analysis program was conducted to evaluate bonded boron/epoxy doublers for repairing cracks on aluminum aircraft structures. The objective was to obtain a core body of substantiating data which will support approval for use on commercial transports of a technology that is being widely used by the military. The data showed that the doublers had excellent performance. Author

N95-14458*# Federal Aviation Administration, Cambridge, MA. National Transportation Systems Center.
INSPECTING FOR WIDESPREAD FATIGUE DAMAGE: IS PARTIAL DEBONDING THE KEY?
John Brewer *In* NASA. Langley Research Center, FAA/NASA International Symposium on Advanced Structural Integrity Methods for Airframe Durability and Damage Tolerance Sep. 1994 p 61-70 (For primary document see N95-14453 03-39)
Avail: CASI HC A02/MF A04

Experimental and analytical results indicate that cracks can initiate, grow, and coalesce more rapidly in fuselage lap joints that have experienced partial or complete debonding. Computational analysis in this paper shows that stress concentrations and stress intensity factors at the rivet holes are far less severe when the bond is intact. Debonding hastens the initiation of widespread fatigue cracks and significantly increases crack growth rate. Thus, debonded regions serve as 'breeding grounds' for widespread fatigue damage. Therefore, the effectiveness of lap joint inspection programs may be enhanced if detailed inspections are focused on areas in which debonding has been detected. Author

N95-14459*# Aluminum Co. of America, Alcoa Center, PA. Product Design and Mechanics Div.
MICROSTRUCTURALLY BASED MODEL OF FATIGUE INITIATION AND GROWTH
J. R. Brockenbrough, A. J. Hinkle, P. E. Magnusen, and R. J. Bucci *In* NASA. Langley Research Center, FAA/NASA International Symposium on Advanced Structural Integrity Methods for Airframe Durability and Damage Tolerance Sep. 1994 p 71-84 Sponsored in part by ONR (For primary document see N95-14453 03-39)
Avail: CASI HC A03/MF A04

A model to calculate fatigue life is developed based on the assumption that fatigue life is entirely composed of crack growth from an initial microstructural inhomogeneity. Specifically, growth is considered to start from either an ellipsoidal void, a cracked particle, or a debonded particle. The capability of predicting fatigue life from material microstructure is based on linear elastic fracture mechanics principles, the sizes of the crack-initiating microstructural inhomogeneities, and an initiation parameter that is proportional to the cyclic plastic zone size. A key aspect of this modeling approach is that it is linked with a general purpose probability program to analyze the effect of the distribution of controlling microstructural features within the material. This enables prediction of fatigue stress versus life curves for various specimen geometries using distributional statistics obtained from characterizations of the microstructure. Results are compared to experimental fatigue data from an aluminum alloy. Author

N95-14460*# FractuResearch, Inc., Galena, OH.
TESTING AND ANALYSIS OF FLAT AND CURVED PANELS WITH MULTIPLE CRACKS
David Broek, David Y. Jeong, and Douglas Thomson *In* NASA. Langley Research Center, FAA/NASA International Symposium on Advanced Structural Integrity Methods for Airframe Durability and Damage Tolerance Sep. 1994 p 85-98 (For primary document see N95-14453 03-39)
Avail: CASI HC A03/MF A04

An experimental and analytical investigation of multiple cracking in various types of test specimens is described in this paper. The testing phase is comprised of a flat unstiffened panel series and curved stiffened and unstiffened panel series. The test specimens contained various configurations for initial damage. Static loading was applied to these specimens until ultimate failure, while loads and crack propagation were recorded. This data provides the basis for developing and validating methodologies for predicting linkup of multiple cracks, progression to failure, and overall residual strength. The results from twelve flat coupon and ten full scale curved panel tests are presented. In addition, an engineering analysis procedure was developed to predict multiple crack linkup. Reasonable agreement was found between predictions and actual test results for linkup and residual strength for both flat and curved panels. The results indicate that an engineering analysis approach has the potential to quantitatively assess the effect of multiple cracks in the arrest capability of an aircraft fuselage structure. Author

N95-14461*# Israel Aircraft Industries Ltd., Tashan (Israel). Engineering Center.
PROBABILISTIC INSPECTION STRATEGIES FOR MINIMIZING SERVICE FAILURES
Abraham Brot *In* NASA. Langley Research Center, FAA/NASA International Symposium on Advanced Structural Integrity Methods for Airframe Durability and Damage Tolerance Sep. 1994 p 99-109 (For primary document see N95-14453 03-39)
Avail: CASI HC A03/MF A04

The INSIM computer program is described which simulates the 'limited fatigue life' environment in which aircraft structures generally operate. The use of INSIM to develop inspection strategies which aim to minimize service failures is demonstrated. Damage-tolerance methodology, inspection thresholds and customized inspections are simulated using the probability of failure as the driving parameter. Author

N95-14462*# Battelle Memorial Inst., Columbus, OH.
NONLINEAR FRACTURE MECHANICS-BASED ANALYSIS OF THIN WALL CYLINDERS
Frederick W. Brust, Brian N. Leis, and Thomas P. Forte *In* NASA. Langley Research Center, FAA/NASA International Symposium on Advanced Structural Integrity Methods for Airframe Durability and Damage Tolerance Sep. 1994 p 111-126 (For primary document see N95-14453 03-39)
Avail: CASI HC A03/MF A04

This paper presents a simple analysis technique to predict the crack initiation, growth, and rupture of large-radius, R, to thickness, t, ratio (thin wall) cylinders. The method is formulated to deal both with stable tearing as well as fatigue mechanisms in applications to both surface and through-wall axial cracks, including interacting surface cracks. The method can also account for time-dependent effects. Validation of the model is provided by comparisons of predictions to more than forty full scale experiments of thin wall cylinders pressurized to failure. Author

N95-14463*# Purdue Univ., West Lafayette, IN. School of Aeronautics and Astronautics.
FATIGUE ANALYSIS OF MULTIPLE SITE DAMAGE AT A ROW OF HOLES IN A WIDE PANEL
Kimberley Buhler, Alten F. Grandt, Jr., and E. J. Moukawsher *In* NASA. Langley Research Center, FAA/NASA International Symposium on Advanced Structural Integrity Methods for Airframe Durability and Damage Tolerance Sep. 1994 p 127-143 (For primary document see N95-14453 03-39)
Avail: CASI HC A03/MF A04

This paper is concerned with predicting the fatigue life of unstiffened panels which contain multiple site damage (MSD). The initial damage consists of through-the-thickness cracks emanating from a row of holes in the center of a finite width panel. A fracture mechanics analysis has been developed to predict the growth, interaction, and coalescence of the various cracks which propagate in the panel. A strain-life analysis incorporating Neuber's rule for notches, and Miner's rule for cumulative damage, is also employed to predict crack initiation for holes without initial cracking. This analysis is compared with the results of a series of fatigue tests on 2024-T3 aluminum panels, and is shown to do an excellent job of predicting the influence of MSD on the fatigue life of nine inch wide specimens.

Having established confidence in the ability to analyze the influence of MSD on fatigue life, a parametric study is conducted to examine the influence of various MSD scenarios in an unstiffened panel. The numerical study considered 135 cases in all, with the parametric variables being the applied cyclic stress level, the lead crack geometry, and the number and location of MSD cracks. The numerical analysis provides details for the manner in which lead cracks and MSD cracks grow and coalesce leading to final failure. The results indicate that MSD located adjacent to lead cracks is the most damaging configuration, while for cases without lead cracks, MSD clusters which are not separated by uncracked holes are most damaging. Author

N95-14464*# Defence Research Agency, Farnborough, Hampshire (England).

A METHOD OF CALCULATING THE SAFE FATIGUE LIFE OF COMPACT, HIGHLY-STRESSED COMPONENTS

Arthur W. Cardick and Vera J. Pike *In* NASA. Langley Research Center, FAA/NASA International Symposium on Advanced Structural Integrity Methods for Airframe Durability and Damage Tolerance Sep. 1994 p 145-156 (For primary document see N95-14453 03-39)

Avail: CASI HC A03/MF A04

This paper describes a method which has been developed for estimating the safe fatigue life of compact, highly-stressed and inaccessible components for aeroplanes and helicopters of the Royal Air Force. It is explained why the Design Requirements for British Military Aircraft do not favor the use of a damage-tolerance approach in these circumstances. Author

N95-14465*# Lehigh Univ., Bethlehem, PA. Dept. of Mechanical Engineering and Mechanics.

CORROSION AND CORROSION FATIGUE OF AIRFRAME ALUMINUM ALLOYS **c26**

G. S. Chen, M. Gao, D. G. Harlow, and R. P. Wei *In* NASA. Langley Research Center, FAA/NASA International Symposium on Advanced Structural Integrity Methods for Airframe Durability and Damage Tolerance Sep. 1994 p 157-173 (For primary document see N95-14453 03-39)

(Grant FAA-92-G-0006)

Avail: CASI HC A03/MF A04

Localized corrosion and corrosion fatigue crack nucleation and growth are recognized as degradation mechanisms that effect the durability and integrity of commercial transport aircraft. Mechanically based understanding is needed to aid the development of effective methodologies for assessing durability and integrity of airframe components. As a part of the methodology development, experiments on pitting corrosion, and on corrosion fatigue crack nucleation and early growth from these pits were conducted. Pitting was found to be associated with constituent particles in the alloys and pit growth often involved coalescence of individual particle-nucleated pits, both laterally and in depth. Fatigue cracks typically nucleated from one of the larger pits that formed by a cluster of particles. The size of pit at which fatigue crack nucleates is a function of stress level and fatigue loading frequency. The experimental results are summarized, and their implications on service performance and life prediction are discussed. Author

N95-14466*# Stevens Inst. of Tech., Hoboken, NJ. Dept. of Mechanical Engineering.

COMPUTATIONAL PREDICTIVE METHODS FOR FRACTURE AND FATIGUE

J. Cordes, A. T. Chang, N. Nelson, and Y. Kim *In* NASA. Langley Research Center, FAA/NASA International Symposium on Advanced Structural Integrity Methods for Airframe Durability and Damage Tolerance Sep. 1994 p 175-192 (For primary document see N95-14453 03-39)

Avail: CASI HC A03/MF A04

The damage-tolerant design philosophy as used by aircraft industries enables aircraft components and aircraft structures to operate safely with minor damage, small cracks, and flaws. Maintenance and inspection procedures insure that damages developed during service remain below design values. When damage is found, repairs or design modifications are implemented and flight is resumed. Design and redesign guidelines, such as military specifications MIL-A-83444, have successfully reduced the incidence of damage and cracks. However, fatigue cracks continue to appear in aircraft well before the design life has expired. The F16 airplane, for instance, developed small cracks in the engine mount, wing support, bulk heads, the fuselage upper skin, the fuel shelf joints, and along the upper wings. Some cracks were found after 600 hours of the 8000 hour design service life and design modifications were required. Tests on the F16 plane showed that the design loading conditions were close to the predicted loading conditions. Improvements to analytic methods for predicting fatigue crack growth adjacent to holes, when multiple damage sites are present, and in corrosive environments would result in more cost-effective designs, fewer repairs, and fewer redesigns. The overall objective of the research described in this paper is to develop, verify, and extend the computational efficiency of analysis procedures necessary for damage tolerant design. This paper describes an elastic/plastic fracture method and an associated fatigue analysis method for damage tolerant design. Both methods are unique in that material parameters such as fracture toughness, R-curve data, and fatigue constants are not required. The methods are implemented with a general-purpose finite element package. Several proof-of-concept examples are given. With further development, the methods could be extended for analysis of multi-site damage, creep-fatigue, and corrosion fatigue problems. Author

N95-14467*# National Aeronautics and Space Administration. Langley Research Center, Hampton, VA.

INFLUENCE OF CRACK HISTORY ON THE STABLE TEARING BEHAVIOR OF A THIN-SHEET MATERIAL WITH MULTIPLE CRACKS

D. S. Dawicke (Analytical Services and Materials, Inc., Hampton, VA.), J. C. Newman, Jr., M. A. Sutton, and B. E. Amstutz *In its* FAA/NASA International Symposium on Advanced Structural Integrity Methods for Airframe Durability and Damage Tolerance Sep. 1994 p 193-212 (For primary document see N95-14453 03-39)

Avail: CASI HC A03/MF A04

Fracture tests were conducted on 2.3mm thick, 305mm wide sheets of 2024-T3 aluminum alloy with from one to five collinear cracks. The cracks were introduced (crack history) into the specimens by three methods: saw cutting, fatigue precracking at a low stress range, and fatigue precracking at a high stress range. For the single crack tests, the initial crack history influenced the stress required for the onset of stable crack growth and the first 10mm of crack growth. The effect on failure stress was about 4 percent or less. For the multiple crack tests, the initial crack history was shown to cause differences of more than 20 percent in the link-up stress and 13 percent in failure stress. An elastic-plastic finite element analysis employing the CTOA fracture criterion was used to predict the fracture behavior of the single and multiple crack tests. The numerical predictions were within 7 percent of the observed link-up and failure stress in all the tests. Author

N95-14468*# Rutgers Univ., Piscataway, NJ. Federal Aviation Administration for Computational Modeling of Aircraft Structures.

STUDY OF MULTIPLE CRACKS IN AIRPLANE FUSELAGE BY MICROMECHANICS AND COMPLEX VARIABLES

Mitsunori Denda and Y. F. Dong *In* NASA. Langley Research Center, FAA/NASA International Symposium on Advanced Structural Integrity Methods for Airframe Durability and Damage Tolerance Sep. 1994 p 213-223 (For primary document see N95-14453 03-39)

Avail: CASI HC A03/MF A04

Innovative numerical techniques for two dimensional elastic and elastic-plastic multiple crack problems are presented using micromechanics concepts and complex variables. The simplicity and the accuracy of the proposed method will enable us to carry out the multiple-site fatigue crack propagation analyses for airplane fuselage by incorporating such features as the curvilinear crack path, plastic deformation, coalescence of cracks, etc. Author

N95-14469*# Rockwell International Corp., El Segundo, CA.

EXTRACTING A REPRESENTATIVE LOADING SPECTRUM FROM RECORDED FLIGHT DATA **c05**

Anthony G. Denyer *In* NASA. Langley Research Center, FAA/NASA International Symposium on Advanced Structural Integrity Methods for Airframe Durability and Damage Tolerance Sep. 1994 p 225-240 (For primary document see N95-14453 03-39)

Avail: CASI HC A03/MF A04

One of the more important ingredients when computing the life of a structure is the loading environment. This paper describes the development of an aircraft loading spectrum that closely matches the service experience, thus allowing a more accurate assessment of the structural life. The paper

outlines the flight loads data collection system, the procedures developed to compile and interpret the service records and the techniques used to define a spectrum suitable for structural life analysis. The areas where the procedures were tailored to suit the special situation of the USAF B-1B bomber are also discussed. the results of the methodology verification, achieved by comparing the generated spectra with the results of strain gage monitoring during service operations, are also presented. Author

N95-14470*# Utah Univ., Salt Lake City, UT. Quality and Integrity Design Engineering Center.

THE ROLE OF FRETTING CORROSION AND FRETTING FATIGUE IN AIRCRAFT RIVET HOLE CRACKING Status Report

Charles B. Elliott, III, Mark Moesser, and David W. Hoeppner *In* NASA. Langley Research Center, FAA/NASA International Symposium on Advanced Structural Integrity Methods for Airframe Durability and Damage Tolerance Sep. 1994 p 241-246 (For primary document see N95-14453 03-39)
(Grants FAA-92-G-0004; FAA-93-G-0068)
Avail: CASI HC A02/MF A04

Personnel in the Quality and Integrity Design Engineering Center (QIDEC) at the University of Utah are working under a two year grant from the FAA to better understand the role of fretting corrosion and fretting fatigue in aircraft rivet hole cracking. The current program follows a one year grant program which was completed in 1993. This paper provides a status report on the results of these grant programs. Recent effort has been focused on developing basic fretting fatigue models which consider variation in the coefficient of friction with time and location within the fretting interface. This is a very important characteristic of the QIDEC model because coefficient of friction varies significantly during the fretting fatigue process. Copies of QIDEC documents discussed in this paper can be obtained by contacting the authors. Author

N95-14471*# Alberta Univ., Edmonton. Dept. of Mechanical Engineering.

INITIATION AND PROPAGATION OF SMALL CORNER CRACKS

Ferdnand Ellyin, Daniel Kujawski, and David F. Craig *In* NASA. Langley Research Center, FAA/NASA International Symposium on Advanced Structural Integrity Methods for Airframe Durability and Damage Tolerance Sep. 1994 p 247-258 Sponsored by Natural Sciences and Engineering Research Council (For primary document see N95-14453 03-39)
Avail: CASI HC A03/MF A04

The behaviour of small corner cracks, inclined or perpendicular to loading direction, is presented. There are two aspects to this investigation: initiation of small cracks and monitoring their subsequent growth. An initial pre-cracking procedure under cyclic compression is adopted to minimize the residual damage at the tip of the growing and self-arresting crack under cyclic compression. A final fatigue specimen, cut from the larger pre-cracked specimen, has two corner flaws. The opening load of corner flaw is monitored using a novel strain gauge approach. The behaviour of small corner cracks is described in terms of growth rate relative to the size of the crack and its shape. Author

N95-14472*# Northwestern Univ., Evanston, IL. Center for Quality Engineering and Failure Prevention.

STATISTICAL INVESTIGATION OF FATIGUE CRACK INITIATION AND GROWTH AROUND CHAMFERED RIVET HOLES IN ALCLAD 2024 T3 AS AFFECTED BY CORROSION

M. I. Fadragas, M. E. Fine, and B. Moran *In* NASA. Langley Research Center, FAA/NASA International Symposium on Advanced Structural Integrity Methods for Airframe Durability and Damage Tolerance Sep. 1994 p 259-275 Sponsored by FAA (For primary document see N95-14453 03-39)
Avail: CASI HC A03/MF A04

In panel specimens with rivet holes cracks initiate in the blunted knife edge of the chamfered rivet hole and propagate inward as well as along the hole. The fatigue lifetime to dominant crack information was defined as the number of cycles, N500 micrometer, to formation of a 500 micrometer long crack. Statistical data on N500 micrometer and on crack propagation after N500 micrometer were obtained for a large number of uncorroded specimens and specimens corroded in an ASTM B 117 salt spray. Considerable variation in N500 micrometer and crack propagation behavior was observed from specimen to specimen of the same nominal geometry with chamfered rivet holes increased the probability for both early formation and later formation of a propagating 500 micrometer fatigue crack. The growth of fatigue cracks after 500 micrometer size was little affected by prior salt spray. Author

N95-14473*# National Aeronautics and Space Administration. Lyndon B. Johnson Space Center, Houston, TX.

DEVELOPMENT OF THE NASA/FLAGRO COMPUTER PROGRAM FOR ANALYSIS OF AIRFRAME STRUCTURES

R. G. Forman, V. Shivakumar, and J. C. Newman, Jr. *In* NASA. Langley Research Center, FAA/NASA International Symposium on Advanced Structural Integrity Methods for Airframe Durability and Damage Tolerance Sep. 1994 p 277-288 (For primary document see N95-14453 03-39)
Avail: CASI HC A03/MF A04

The NASA/FLAGRO (NASGRO) computer program was developed for fracture control analysis of space hardware and is currently the standard computer code in NASA, the U.S. Air Force, and the European Agency (ESA) for this purpose. The significant attributes of the NASGRO program are the numerous crack case solutions, the large materials file, the improved growth rate equation based on crack closure theory, and the user-friendly promptive input features. In support of the National Aging Aircraft Research Program (NAARP); NASGRO is being further developed to provide advanced state-of-the-art capability for damage tolerance and crack growth analysis of aircraft structural problems, including mechanical systems and engines. The project currently involves a cooperative development effort by NASA, FAA, and ESA. The primary tasks underway are the incorporation of advanced methodology for crack growth rate retardation resulting from spectrum loading and improved analysis for determining crack instability. Also, the current weight function solutions in NASGRO or nonlinear stress gradient problems are being extended to more crack cases, and the 2-d boundary integral routine for stress analysis and stress-intensity factor solutions is being extended to 3-d problems. Lastly, effort is underway to enhance the program to operate on personal computers and work stations in a Windows environment. Because of the increasing and already wide usage of NASGRO, the code offers an excellent mechanism for technology transfer for new fatigue and fracture mechanics capabilities developed within NAARP. Author

N95-14474*# Rockwell International Corp., Downey, CA. Space Systems Div.

SPACE SHUTTLE FATIGUE LOADS SPECTRA FOR PRELAUNCH AND LIFTOFF LOADS **c16**

Judith Goldish and Raphael Ortasse *In* NASA. Langley Research Center, FAA/NASA International Symposium on Advanced Structural Integrity Methods for Airframe Durability and Damage Tolerance Sep. 1994 p 289-306 (For primary document see N95-14453 03-39)
(Contract NAS9-18500)
Avail: CASI HC A03/MF A04

Fatigue loads spectra for the prelaunch and liftoff flight segments of the Space Shuttle were developed. A variety o methods were used to determine the distributions of several important parameters, such as time of exposure on the launch, pad, month of launch, and wind speed. Also, some lessons learned that would be applicable to development of fatigue loads spectra for other reusable space vehicles are presented. Author

N95-14475*# Northwestern Univ., Evanston, IL. School of Engineering and Applied Science.

FATIGUE RELIABILITY METHOD WITH IN-SERVICE INSPECTIONS **c38**

H. H. Harkness, M. Fleming, B. Moran, and T. Belytschko *In* NASA. Langley Research Center, FAA/NASA International Symposium on Advanced Structural Integrity Methods for Airframe Durability and Damage Tolerance Sep. 1994 p 307-326 Sponsored in part by National Inst. for Standards and Technology and FAA (For primary document see N95-14453 03-39)
Avail: CASI HC A03/MF A04

The first reliability method (FORM) has traditionally been applied in a fatigue reliability setting to one inspection interval at a time, so that the random distribution of crack lengths must be recharacterized following each inspection. The FORM presented here allow each analysis to span several inspection periods without explicit characterization of the crack length distribution upon each inspection. The method thereby preserves the attractive feature of FORM in that relatively few realizations in the random variable space need to be considered. Examples are given which show

that the present methodology gives estimates which are in good agreement with Monte Carlo simulations and is efficient even for complex components. Author

N95-14476*# Federal Aviation Administration, Cambridge, MA. Research and Special Programs Administration.
NONLINEAR BULGING FACTOR BASED ON R-CURVE DATA
David Y. Jeong and Pin Tong *In* NASA. Langley Research Center, FAA/NASA International Symposium on Advanced Structural Integrity Methods for Airframe Durability and Damage Tolerance Sep. 1994 p 327-338 (For primary document see N95-14453 03-39)
Avail: CASI HC A03/MF A04

In this paper, a nonlinear bulging factor is derived using a strain energy approach combined with dimensional analysis. The functional form of the bulging factor contains an empirical constant that is determined using R-curve data from unstiffened flat and curved panel tests. The determination of this empirical constant is based on the assumption that the R-curve is the same for both flat and curved panels. Author

N95-14477*# Monash Univ., Clayton (Australia). Dept. of Mechanical Engineering.
DEVELOPMENT OF A COMPOSITE REPAIR AND THE ASSOCIATED INSPECTION INTERVALS FOR THE F-111C STIFFENER RUNOUT REGION **c01**
R. Jones, L. Molent, J. Paul, T. Saunders, and W. K. Chiu *In* NASA. Langley Research Center, FAA/NASA International Symposium on Advanced Structural Integrity Methods for Airframe Durability and Damage Tolerance Sep. 1994 p 339-350 (For primary document see N95-14453 03-39)
Avail: CASI HC A03/MF A04

This paper presents an overview of the structural aspects of the design and development of a local reinforcement designed to lower the stresses in a region of the F-111C wing fitting which is prone to cracking. The stress analysis, with particular emphasis on the use of a unified constitutive model for the cyclic inelastic response of the structure, representative specimen testing, thermal analysis and full scale static testing of this design are summarized. Author

N95-14478*# National Aerospace Lab., Amsterdam (Netherlands).
RECENT ADVANCES IN THE MODELLING OF CRACK GROWTH UNDER FATIGUE LOADING CONDITIONS
A. U. deKoning, H. J. tenHoeve, and T. K. Henriksen *In* NASA. Langley Research Center, FAA/NASA International Symposium on Advanced Structural Integrity Methods for Airframe Durability and Damage Tolerance Sep. 1994 p 351-374 (For primary document see N95-14453 03-39)
(Contracts NIVR-1823; NIVR-9691)
Avail: CASI HC A03/MF A04

Fatigue crack growth associated with cyclic (secondary) plastic flow near a crack front is modelled using an incremental formulation. A new description of threshold behaviour under small load cycles is included. Quasi-static crack extension under high load excursions is described using an incremental formulation of the R-(crack growth resistance)- curve concept. The integration of the equations is discussed. For constant amplitude load cycles the results will be compared with existing crack growth laws. It will be shown that the model also properly describes interaction effects of fatigue crack growth and quasi-static crack extension. To evaluate the more general applicability the model is included in the NASGRO computer code for damage tolerance analysis. For this purpose the NASGRO program was provided with the CORPUS and the STRIP-YIELD models for computation of the crack opening load levels. The implementation is discussed and recent results of the verification are presented. Author

N95-14479*# Washington Univ., Seattle, WA. Dept. of Mechanical Engineering.
AXIAL CRACK PROPAGATION AND ARREST IN PRESSURIZED FUSELAGE
M. Kosai, A. Shimamoto, C.-T. Yu, S. I. Walker, A. S. Kobayashi, and P. Tan *In* NASA. Langley Research Center, FAA/NASA International Symposium on Advanced Structural Integrity Methods for Airframe Durability and Damage Tolerance Sep. 1994 p 375-392 (For primary document see N95-14453 03-39)
(Grant FAA-92-G-0005)
Avail: CASI HC A03/MF A04

The crack arrest capability of a tear strap in a pressurized precracked fuselage was studied through instrumented axial rupture tests of small scale models of an idealized fuselage. Upon pressurization, rapid crack propagation initiated at an axial through crack along the stringer and immediately kinked due to the mixed modes 1 and 2 state caused by the one-sided opening of the crack flap. The diagonally running crack further turned at the tear straps. Dynamic finite element analysis of the rupturing cylinder showed that the crack kinked and also ran straight in the presence of a mixed mode state according to a modified two-parameter crack kinking criterion. Author

N95-14480*# Georgia Inst. of Tech., Atlanta, GA. School of Mechanical Engineering.
FRACTURE MECHANICS VALIDITY LIMITS
Dennis M. Lambert and Hugo A. Ernst *In* NASA. Langley Research Center, FAA/NASA International Symposium on Advanced Structural Integrity Methods for Airframe Durability and Damage Tolerance Sep. 1994 p 393-407 (For primary document see N95-14453 03-39)
Avail: CASI HC A03/MF A04

Fracture behavior is characteristics of a dramatic loss of strength compared to elastic deformation behavior. Fracture parameters have been developed and exhibit a range within which each is valid for predicting growth. Each is limited by the assumptions made in its development: all are defined within a specific context. For example, the stress intensity parameters, K, and the crack driving force, G, are derived using an assumption of linear elasticity. To use K or G, the zone of plasticity must be small as compared to the physical dimensions of the object being loaded. This insures an elastic response, and in this context, K and G will work well. Rice's J-integral has been used beyond the limits imposed on K and G. J requires an assumption of nonlinear elasticity, which is not characteristic of real material behavior, but is thought to be a reasonable approximation if unloading is kept to a minimum. As well, the constraint cannot change dramatically (typically, the crack extension is limited to ten-percent of the initial remaining ligament length). Rice, et al investigated the properties required of J-type parameters, J(sub x), and showed that the time rate, dJ(sub x)/dt, must not be a function of the crack extension rate, da/dt. Ernst devised the modified-J parameter, J(sub M), that meets this criterion. J(sub M) correlates fracture data to much higher crack growth than does J. Ultimately, a limit of the validity of J(sub M) is anticipated, and this has been estimated to be at a crack extension of about 40-percent of the initial remaining ligament length. None of the various parameters can be expected to describe fracture in an environment of gross plasticity, in which case the process is better described by deformation parameters, e.g., stress and strain. In the current study, various schemes to identify the onset of the plasticity-dominated behavior, i.e., the end of fracture mechanics validity, are presented. Each validity limit parameter is developed in detail, and then data is presented and the various schemes for establishing a limit of the validity are compared. The selected limiting parameter is applied to a set of fracture data showing the improvement of correlation gained. Author (revised)

N95-14481*# Aeronautical Systems Div., Wright-Patterson AFB, OH.
CHALLENGES FOR THE AIRCRAFT STRUCTURAL INTEGRITY PROGRAM **c05**
John W. Lincoln *In* NASA. Langley Research Center, FAA/NASA International Symposium on Advanced Structural Integrity Methods for Airframe Durability and Damage Tolerance Sep. 1994 p 409-423 (For primary document see N95-14453 03-39)
Avail: CASI HC A03/MF A04

Thirty-six years ago the United States Air Force established the USAF Aircraft Structural Integrity Program (ASIP) because flight safety had been degraded by fatigue failures of operational aircraft. This initial program evolved, but has been stable since the issuance of MIL-STD-1530A in 1975. Today, the program faces new challenges because of a need to maintain aircraft longer in an environment of reduced funding levels. Also, there is increased pressure to reduce cost of the acquisition of new aircraft. It is the purpose of this paper to discuss the challenges for the ASIP and identify the changes in the program that will meet these challenges in the future. Author

N95-14482*# Utah Univ., Salt Lake City, UT.
THE EFFECTS OF PITTING ON FATIGUE CRACK NUCLEATION IN 7075-T6 ALUMINUM ALLOY **c26**
Li Ma and David W. Hoeppner *In* NASA. Langley Research Center, FAA/NASA International Symposium on Advanced Structural Integrity Methods for Airframe Durability and Damage Tolerance Sep. 1994 p 425-440 Sponsored by Boeing Commercial Airplane Co. (For primary document see N95-14453 03-39)
Avail: CASI HC A03/MF A04

A high-strength aluminum alloy, 7075-T6, was studied to quantitatively evaluate chemical pitting effects of its corrosion fatigue life. The study focused on pit nucleation, pit growth, and fatigue crack nucleation. Pitting corrosion fatigue experiments were conducted in 3.5 percent NaCl aqueous solution under constant amplitude sinusoidal loading at two frequencies, 5 and 20 Hz. Smooth and unnotched specimens were used in this investigation. A video recording system was developed to allow in situ observation of the surface changes of the specimens during testing. The results indicated that pitting corrosion considerably reduces the fatigue strength by accelerating fatigue crack nucleation. A metallographic examination was conducted on the specimens to evaluate the nature of corrosion pits. First, the actual shapes of the corrosion pits were evaluated by cross-sectioning the pits. Secondly, the relation between corrosion pits and microstructure was also investigated. Finally, the possibility of another corrosion mechanism that might be involved in pitting was explored in this investigation. The fractography of the tested specimens showed that corner corrosion pits were responsible for fatigue crack nucleation in the material due to the associated stress concentration. The pits exhibited variance of morphology. Fatigue life for the experimental conditions appeared to be strongly dependent on pitting kinetics and the crack nucleation stage. Author

N95-14483*# Virginia Univ., Charlottesville, VA. Center for Electrochemical Science and Engineering.
MODELING TIME-DEPENDENT CORROSION FATIGUE CRACK PROPAGATION IN 7000 SERIES ALUMINUM ALLOYS **c26**
Mark E. Mason and Richard P. Gangloff *In* NASA. Langley Research Center, FAA/NASA International Symposium on Advanced Structural Integrity Methods for Airframe Durability and Damage Tolerance Sep. 1994 p 441-462 (For primary document see N95-14453 03-39)
(Grant NAG1-745)
Avail: CASI HC A03/MF A04

Stress corrosion cracking and corrosion fatigue experiments were conducted with the susceptible S-L orientation of AA7075-T651, immersed in acidified and inhibited NaCl solution, to provide a basis for incorporating environmental effects into fatigue crack propagation life prediction codes such as NASA FLAGRO. This environment enhances da/dN by five to ten-fold compared to fatigue in moist air. Time-based crack growth rates from quasi-static load experiments are an order of magnitude too small for accurate linear superposition prediction of da/dN for loading frequencies above 0.001 Hz. Alternate methods of establishing da/dt, based on rising-load or ripple-load-enhanced crack tip strain rate, do not increase da/dt and do not improve linear superposition. Corrosion fatigue is characterized by two regimes of frequency dependence; da/dN is proportional to f(exp -1) below 0.001 Hz and to F(exp 0) to F(exp -0.1) for higher frequencies. Da/dN increases mildly both with increasing hold-time at K(sub max) and with increasing rise-time for a range of loading waveforms. The mild time-dependence is due to cycle-time-dependent corrosion fatigue growth. This behavior is identical for S-L nd L-T crack orientations. The frequency response of environmental fatigue in several 7000 series alloys is variable and depends on undefined compositional or microstructural variables. Speculative explanations are based on the effect of Mg on occluded crack chemistry and embritting hydrogen uptake, or on variable hydrogen diffusion in the crack tip process zone. Cracking in the 7075/NaCl system is adequately described for life prediction by linear superposition for prolonged load-cycle periods, and by a time-dependent upper bound relationship between da/dN and delta K for moderate loading times.
Author

N95-14484*# Southwest Research Inst., San Antonio, TX.
ANALYSIS OF SMALL CRACK BEHAVIOR FOR AIRFRAME APPLICATIONS
R. C. McClung, K. S. Chan, S. J. Hudak, Jr., and D. L. Davidson *In* NASA. Langley Research Center, FAA/NASA International Symposium on Advanced Structural Integrity Methods for Airframe Durability and Damage Tolerance Sep. 1994 p 463-479 Sponsored in part by AFOSR; AFWAL; ARO; and ONR (For primary document see N95-14453 03-39)
Avail: CASI HC A03/MF A04

The small fatigue crack problem is critically reviewed from the perspective of airframe applications. Different types of small cracks-microstructural, mechanical, and chemical-are carefully defined and relevant mechanisms identified. Appropriate analysis techniques, including both rigorous scientific and practical engineering treatments, are briefly described. Important materials data issues are addressed, including increased scatter in small crack data and recommended small crack test methods. Key problems requiring further study are highlighted. Author

N95-14485*# Boeing Co., Seattle, WA.
FULL-SCALE TESTING AND ANALYSIS OF FUSELAGE STRUCTURE
M. Miller, M. L. Gruber, K. E. Wilkins, and R. E. Worden *In* NASA. Langley Research Center, FAA/NASA International Symposium on Advanced Structural Integrity Methods for Airframe Durability and Damage Tolerance Sep. 1994 p 481-496 (For primary document see N95-14453 03-39)
Avail: CASI HC A03/MF A04

This paper presents recent results from a program in the Boeing Commercial Airplane Group to study the behavior of cracks in fuselage structures. The goal of this program is to improve methods for analyzing crack growth and residual strength in pressurized fuselages, thus improving new airplane designs and optimizing the required structural inspections for current models. The program consists of full-scale experimental testing of pressurized fuselage panels in both wide-body and narrow-body fixtures and finite element analyses to predict the results. The finite element analyses are geometrically nonlinear with material and fastener nonlinearity included on a case-by-case basis. The analysis results are compared with the strain gage, crack growth, and residual strength data from the experimental program. Most of the studies reported in this paper concern the behavior of single or multiple cracks in the lap joints of narrow-body airplanes (such as 727 and 737 commercial jets). The phenomenon where the crack trajectory is curved creating a 'flap' and resulting in a controlled decompression is discussed. Author

N95-14486*# Academy of Sciences (USSR), Moscow (USSR). Central Aerohydrodynamic Inst.
ADVANCED METHOD AND PROCESSING TECHNOLOGY FOR COMPLICATED SHAPE AIRFRAME PART FORMING **c05**
P. V. Miodushevsky and G. A. Rajevskaya *In* NASA. Langley Research Center, FAA/NASA International Symposium on Advanced Structural Integrity Methods for Airframe Durability and Damage Tolerance Sep. 1994 p 497-503 (For primary document see N95-14453 03-39)
Avail: CASI HC A02/MF A04

Slow deformation modes of forming give considerably higher residual fatigue life of the airframe part. It has experimentally proven that fatigue life of complicated shape integral airframe panels made of high strength aluminum alloys is significantly increased after creep deformation process. To implement the slow deformation mode forming methods, universal automated equipment was developed. Multichannel forming systems provide high accuracy of airframe part shape eliminating residual stresses and spring effect. Forming process multizone control technology was developed and experimentally proved that static/fatigue properties of formed airframe parts are increased. Author

N95-14617*# National Aeronautics and Space Administration. Ames Research Center, Moffett Field, CA.
EXPERIMENTAL/ANALYTICAL APPROACH TO UNDERSTANDING MISTUNING IN A TRANSONIC WIND TUNNEL COMPRESSOR
Teri Kaiser, Reed S. Hansen, Nhan Nguyen, Roy W. Hampton, Doug Muzzio, Mladen K. Chargin, Roy Guist, Ken Hamm, and Len Walker Jun. 1994 16 p
(NASA-TM-108833; A-94104; NAS 1.15:108833) Avail: CASI HC A03/MF A01

This paper will briefly set forth some of the basic tenets of mistuned rotating bladed-disk assemblies. The experience with an existing three stage compressor in a transonic wind tunnel will be documented. The manner in which the theoretical properties manifest themselves in this non-ideal compressor will be described. A description of mistuning behaviors that can and cannot be accurately substantiated will be discussed. Author

N95-14922*# Eloret Corp., Palo Alto, CA.
DEVELOPMENT AND APPLICATION OF STRUCTURAL DYNAMICS ANALYSIS CAPABILITIES Final Technical Report, 1 Feb. 1988 - 30 Sep. 1994
Klaus W. Heinemann and Shig Hozaki 15 Nov. 1994 240 p
(Contract NCC2-518)
(NASA-CR-197229; NAS 1.26:197229) Avail: CASI HC A11/MF A03

Extensive research activities were performed in the area of multidisciplinary modeling and simulation of aerospace vehicles that are relevant to NASA Dryden Flight Research Facility. The efforts involved theoretical development, computer coding, and debugging of the STARS code. New solution procedures were developed in such areas as structures, CFD, and graphics, among others. Furthermore, systems-oriented codes were developed for rendering the code truly multidisciplinary and rather automated in nature. Also, work was performed in pre- and post-processing of engineering analysis data. Author

N95-15055*# National Aeronautics and Space Administration. Marshall Space Flight Center, Huntsville, AL.
AN INELASTIC ANALYSIS OF A WELDED ALUMINUM JOINT
R. E. Vaughan Sep. 1994 81 p Original contains color illustrations
(NASA-TP-3508; M-760; NAS 1.60:3508) Avail: CASI HC A05/MF A01; 5 functional color pages

Butt-weld joints are most commonly designed into pressure vessels which then become as reliable as the weakest increment in the weld chain. In practice, weld material properties are determined from tensile test specimen and provided to the stress analyst in the form of a stress versus strain diagram. Variations in properties through the thickness of the weld and along the width of the weld have been suspect but not explored because of inaccessibility and cost. The purpose of this study is to investigate analytical and computational methods used for analysis of welds. The weld specimens are analyzed using classical elastic and plastic theory to provide a basis for modeling the inelastic properties in a finite-element solution. The results of the analysis are compared to experimental data to determine the weld behavior and the accuracy of prediction methods. The weld considered in this study is a multiple-pass aluminum 2219-T87 butt weld with thickness of 1.40 in. The weld specimen is modeled using the finite-element code ABAQUS. The finite-element model is used to produce the stress-strain behavior in the elastic and plastic regimes and to determine Poisson's ratio in the plastic region. The value of Poisson's ratio in the plastic regime is then compared to experimental data. The results of the comparisons are used to explain multipass weld behavior and to make recommendations concerning the analysis and testing of welds. Author

N95-15348 Selskapet for Industriell og Teknisk Forskning, Trondheim (Norway).
OBSERVATION OF MICROCRACK DEVELOPMENT IN CONCRETE BY USE OF TV-HOLOGRAPHY AND DEFORMATION PHASE GRADIENT CALCULATION
E. Vikhagen, E. A. Hansen, J. E. Barkenaes, and S. Smeplass 21 Dec. 1993 12 p See also PB92-203165 Prepared in cooperation with Technical Univ. of Norway, Trondheim
(PB94-207990; STF19-A93015) Avail: Issuing Activity (National Technical Information Service (NTIS))

A phase shifting TV-holography technique with digital image processing is used to observe the development of microcracks in high strength concrete. With this sensitive technique surface cracks of width ranging down to 0.1 micrometer are detected. Microcracking is observed during an ordinary fracture energy test on notched beams. Any special surface treatment of the specimen is not required. To detect surface areas with local inhomogeneous deformations indicating cracks, the deformation phase gradients are calculated and displayed. This procedure improves the interpretation with respect to crack detection in two ways. It displays the discontinuities with better resolution than in the fringe pattern and, at the same time, it removes disturbing speckles reflecting irrelevant continuous deformations. The distinct identification of microcracks provides accurate surveillance of the development of the fracture process zone. It is confirmed that the fracture process zone is dominated by a main crack, that crack branching occur, that major aggregates arrest propagating cracks and that there is a preference for interfacial cracks. NTIS

N95-15429 Technische Univ., Delft (Netherlands). Faculty of Aerospace Engineering.
STATIC STRENGTH OF RIVETED JOINTS IN FIBRE METAL LAMINATES Ph.D. Thesis
W. J. Slagter 25 Apr. 1994 186 p Limited Reproducibility: More than 20% of this document may be affected by microfiche quality
(PB94-201472; ISBN-90-9007089-3) Copyright Avail: Issuing Activity (National Technical Information Service (NTIS))

The ultimate strength of riveted joints utilizing fiber metal laminates (FML), a composite of aluminum alloy and glass or aramid prepreg layers, is investigated both analytically and experimentally. A structural analysis of the static strength of the joints, the failure modes including delamination, the effects of residual stress, and the application of a computer program to the design of joints are described. CASI

N95-15547 Wright Lab., Wright-Patterson AFB, OH.
LARGE AMPLITUDE NONLINEAR RESPONSE OF FLAT ALUMINUM, AND CARBON FIBER PLASTIC BEAMS AND PLATES Interim Report, 1 Oct. 1992 - 1 Sep. 1993
Howard F. Wolfe and Cynthia A. Shroyer Jun. 1994 92 p Limited Reproducibility: More than 20% of this document may be affected by microfiche quality
(AF Proj. 2401)
(AD-A282440; WL-TM-94-3077) Avail: Issuing Activity (Defense Technical Information Center (DTIC))

This progress report presents the results of a continuing study to improve the understanding of nonlinear dynamic behavior of aerospace structures subjected to high levels of excitation. Tests were continued with a clamped-clamped (C-C) aluminum beam. A summary of the results is presented. Tests were conducted with a C-C carbon fiber reinforced plastic (CFRP) beam and a pinned-pinned (P-P) aluminum beam. A summary of these results is also presented. Flat plate tests began with an aluminum plate. The shapes of the total, axial, and bending strain power spectral densities for the C-C aluminum and the CFRP beams were quite similar. Both showed a small frequency increase and slight peak broadening as the levels of excitation increased. The nonlinear displacement shapes for the two cases were also quite similar. Further analysis is needed for the P-P aluminum beam case. Finally, a method of estimating the RMS stress for the multimodal response of a panel is presented. DTIC

N95-15620 Army Research Lab., Watertown, MA. Materials Directorate.
TENSILE CREEP STRAIN AND ACTIVATION ENERGY Final Report
Albert A. Warnas Jul. 1994 15 p Limited Reproducibility: More than 20% of this document may be affected by microfiche quality
(AD-A283264; ARL-TR-455) Avail: CASI HC A03

In a set of PMMA creep curves, at several temperatures under the same dead load, any constant tensile creep strain e will intercept a set of time-temperature points. In PMMA we can relate such a set of time-temperature points to an equivalent set of relaxation time-temperature points associated with a constant activation energy delta H obtained with the Arrhenius equation. Then delta H is proportional to e over their common intercepted set of time-temperature points. DTIC

N95-15621 Army Research Lab., Watertown, MA. Materials Directorate.
LOADING-STRAIN EQUIVALENCE BETWEEN THERMOMECHANICAL, CREEP, AND TENSILE TESTS: HIGH DENSITY POLYETHYLENE Final Report
Albert A. Warnas Jul. 1994 61 p Limited Reproducibility: More than 20% of this document may be affected by microfiche quality
(AD-A283265; ARL-TR-456) Avail: CASI HC A04

The initiation of any mechanical test, performed on a specimen of any material, requires first that the specimen be loaded. Any loading of a specimen causing it to deform may affect the test it initiates. The creep test (CT) is a dead-load test while the engineering tensile test (TT) is a pure loading test (load versus strain at constant crosshead-speed from its initiation to the yield point). In the CT, the specimen requires dead-load loading (DLL) at some DLL initial-crosshead-speed (HS) after which it creep-strains with time under a constant dead-load. In the literature, however, there is a neglect for loading (for example, neglecting to specify loading rates) in the CT. The assumption, in many cases, is that loading plays a minor role in creep-strain initiation so that loading effects can be precinded from regarding the remainder of the CT. This paper attempts to show that

the loading parameters are very important for the initiation of the CT in plastics and that the loading mode has a bearing not only on the CT but also on the thermomechanical test (TMT). DTIC

N95-15802 Illinois Univ., Urbana, IL. Dept. of Civil Engineering.
SIZE AND DEFORMATION LIMITS TO MAINTAIN CONSTRAINT IN K(SUB Ic) AND J(SUB c) TESTING OF BEND SPECIMENS Technical Report, 1 Jan. - 31 Dec. 1993
Kyle C. Koppenhoefer, Robert H. Dodds, Jr., and Mark T. Kirk Jan. 1994 26 p Limited Reproducibility: More than 20% of this document may be affected by microfiche quality
(Contracts N61533-90-K-0059; N00167-92-K-0038)
(AD-A284363; UILU-ENG-94-2002; SRS-586; CARDIVNSWC-TR-61-CR-94/01) Avail: CASI HC A03

The ASTM Standard Test Method for Plane-Strain Fracture Toughness of Metallic Materials (E399-83) restricts test specimen dimensions to insure the measurement of highly constrained fracture toughness values (K sub Ic). These requirements insure small-scale yielding conditions at fracture, and thereby the validity of linear elastic fracture mechanics. When these conditions are satisfied, the diameter of the plastic zone is nearly twenty five times smaller than all specimen dimensions. The need for this degree of plastic zone confinement, set by the factor 2.5 in a, b, B greater than or equal to 2.5 (K sub q/sigma sub ys)(exp 2) was based on K sub Ic data for many different alloys. These data show that all specimens satisfying the size requirements of E399 produce highly constrained fracture toughness values. However, the required multiplier ranges from 1.0 for certain steel alloys to 2.5 for titanium alloy 6-6-2 in the aged condition. To maintain a standard test method applicable to all materials, the more restrictive 2.5 value has been retained by ASTM Committee E08. Recently, Dodds and Anderson have proposed a less restrictive size requirement for cleavage fracture toughness measured in terms of the J-integral (J sub c). Dodds and Anderson performed finite element analyses to calculate the ratio of J in the finite-sized specimen (J sub SE(B)) to J under small-scale yielding (J sub SSY) needed to produce equivalent stresses ahead of both crack tips, and thereby equivalent conditions for cleavage fracture. DTIC

N95-15803 Naval Surface Warfare Center, Bethesda, MD. Survivability Structures and Materials Directorate.
EFFECTS OF TENSILE LOADING ON UPPER SHELF FRACTURE TOUGHNESS
J. A. Joyce and R. E. Link Jun. 1994 125 p Limited Reproducibility: More than 20% of this document may be affected by microfiche quality
(AD-A284364; CARDIVNSWC-SSM-61-93/23) Avail: CASI HC A06

The objective of this work is to develop some upper shelf, elastic-plastic experimental results to attempt to investigate the applicability of the Q and T stress parameters to the correlation of upper shelf initiation toughness and J resistance curves. The first objective was to obtain upper shelf J resistance curves, J sub Ic, and tearing resistance, T sub mat, results for a range of applied constraint. The J-Q and J-T stress loci were developed and compared with the expectations of previous analyses. Constraint was varied by changing the crack length and also by changing the mode of loading from bending to predominantly tensile. The principle conclusions of this work are that J sub Ic does not appear to be dependent on T stress or Q while the material tearing resistance is dependent on T stress and Q, with the tearing modulus increasing as constraint decreases. DTIC

N95-15805 Naval Postgraduate School, Monterey, CA. Dept. of Mathematics.
ANALYTICAL TRIPPING LOADS FOR STIFFENED PLATES Technical Report, Oct. - Dec. 1993
D. A. Danielson Dec. 1993 18 p Limited Reproducibility: More than 20% of this document may be affected by microfiche quality
(AD-A284368; NPS-MA-94-006) Avail: CASI HC A03

The buckling behavior of a rectangular plate, with parallel thin-walled stiffeners attached to one side, subjected to a combination of axial compression, lateral pressure, and bending moment is discussed. The plate is modeled by the Von Karman plate equations and the stiffeners by a nonlinear beam theory recently derived. An analytical solution is obtained for the buckling load corresponding to a torsional tripping mode of the stiffeners. The effects of various boundary conditions, imperfections, and residual stress are included. DTIC

N95-15913*# Rockwell International Corp., Downey, CA. Space Systems Div.
MILESTONE 5 TEST REPORT. TASK 5, SUBTASK 5.2: TILE TO FOAM STRENGTH TESTS
H. S. Greenberg 2 Dec. 1994 33 p Prepared in cooperation with Hercules, Inc., Wilmington, DE
(Contract NCC8-39)
(NASA-CR-197241; NAS 1.26:197241; SSD94D0298) Avail: CASI HC A03/MF A01

This report summarizes work that has been performed to date on the strength of a cryotank insulation system using Rohacell foam and TUFI-coated AETB-12 ceramic tiles directly bonded to a simulated graphite-epoxy tank wall. Testing utilized a custom specimen design which consists of a long tensile specimen with eccentric loading to induce curvature similar to the curvature expected due to 'pillowing' of the tank when pressurized. A finite element model was constructed to predict the specific element strains in the test article, and to assist with design of the test specimen to meet the specific goals of curvature and laminate strain. The results indicate that the heat treated 3.25-pcf density Rohacell foam does not provide sufficient strength for the induced stresses due to curvature and stress concentration at the RTV bondline to the TUFI tile. The test was repeated using higher density non-heat treated Rohacell foam (6.9 pcf) without foam failure. The finite element model was shown to predict specimen behavior, and validation of the model was successful. It is pertinent to mention that the analyses described herein accurately predicted the failure of the heat treated foams and based on this analysis method it is expected that the untreated 3.25 pcf Rohacell foam will be successful.
Author

42 GEOSCIENCES (GENERAL)

No abstracts in this category.

43 EARTH RESOURCES AND REMOTE SENSING

Includes remote sensing of earth resources by aircraft and spacecraft; photogrammetry; and aerial photography.
For instrumentation see *35 Instrumentation and Photography.*

N95-13639*# AI Signal Research, Inc., Huntsville, AL.
DEVELOP ADVANCED NONLINEAR SIGNAL ANALYSIS TOPOGRAPHICAL MAPPING SYSTEM Technical Progress Report
Jen-Yi Jong Sep. 1993 20 p
(Contract NAS8-39393)
(NASA-CR-194414; NAS 1.26:194414; AISR-TR-4002-93-09) Avail: CASI HC A03/MF A01

This study will provide timely assessment of SSME component operational status, identify probable causes of malfunction, and indicate feasible engineering solutions. The final result of this program will yield an advanced nonlinear signal analysis topographical mapping system (ATMS) of nonlinear and nonstationary spectral analysis software package integrated with the Compressed SSME TOPO Data Base (CSTDB) on the same platform. This system will allow NASA engineers to retrieve any unique defect signatures and trends associated with different failure modes and anomalous phenomena over the entire SSME test history across turbopump families.
Derived from text

N95-13693 Naval Postgraduate School, Monterey, CA.
REMOTE SENSING, PROCESSING AND TRANSMISSION OF DATA FOR AN UNMANNED AERIAL VEHICLE M.S. Thesis
Donald B. Howard Jun. 1994 97 p Limited Reproducibility: More than 20% of this document may be affected by microfiche quality
(AD-A283104) Avail: Issuing Activity (Defense Technical Information Center (DTIC))

This thesis chronicles the development of a proof-of-concept, stand-alone,

Unattended Ground Sensor (UGS) that can be used to sense and process signals associated with the motion of large vehicles, troops, or aircraft. The results of this signal processing are then transmitted to an Unmanned Aerial Vehicle (UAV). The UGS uses acoustic and seismic sensors to provide data to a Digital Signal Processing (DSP) computer. Digital signal processing algorithms can be independently developed in the C programming language and linked with the software developed for this project. DTIC

N95-13704*# Aerojet-General Corp., Azusa, CA.
EARTH OBSERVING SYSTEM (EOS)/ADVANCED MICROWAVE SOUNDING UNIT-A (AMSU-A): CALIBRATION MANAGEMENT PLAN Final Report
Sep. 1994 69 p
(Contract NAS5-32314; RTOP 422-00-00)
(NASA-CR-189376; NAS 1.26:189376; Aerojet-10356) Avail: CASI HC A04/MF A01

This is the Calibration Management Plan for the Earth Observing System/Advanced Microwave Sounding Unit-A (AMSU-A). The plan defines calibration requirements, calibration equipment, and calibration methods for the AMSU-A, a 15 channel passive microwave radiometer that will be used for measuring global atmospheric temperature profiles from the EOS polar orbiting observatory. The AMSU-A system will also provide data to verify and augment that of the Atmospheric Infrared Sounder.
Author (revised)

N95-13885*# Aerojet-General Corp., Azusa, CA.
EARTH OBSERVING SYSTEM (EOS)/ADVANCED MICROWAVE SOUNDING UNIT-A (AMSU-A) SOFTWARE ASSURANCE PLAN Final Report, 1-28 Feb. 1994
Robert Schwantje and Claude Smith Aug. 1994 51 p
(Contract NAS5-32314)
(NASA-CR-196059; NAS 1.26:196059; CRDL-309; Rept-10428A) Avail: CASI HC A04/MF A01

This document defines the responsibilities of Software Quality Assurance (SOA) for the development of the flight software installed in EOS/AMSU-A instruments, and the ground support software used in the test and integration of the EOS/AMSU-A instruments. Author

N95-14125# Forest Service, New Orleans, LA. Southern Forest Experiment Station.
FOREST COVER FROM LANDSAT THEMATIC MAPPER DATA FOR USE IN THE CATAHOULA RANGER DISTRICT GEOGRAPHIC INFORMATION SYSTEM
D. L. Evans Apr. 1994 17 p
(PB94-203056; FSGTR-SO-99) Avail: CASI HC A03/MF A01

A forest cover classification of the Kisatchie National Forest, Catahoula Ranger District, was performed with Landsat Thematic Mapper data. Data base retrievals and map products from this analysis demonstrated the use of Landsat for forest management decisions. NTIS

N95-14313# Sandia National Labs., Albuquerque, NM.
INTERFEROMETRIC SYNTHETIC APERTURE RADAR TERRAIN ELEVATION MAPPING FROM MULTIPLE OBSERVATIONS
D. C. Ghiglia and D. E. Wahl 1994 5 p Presented at the Institute of Electrical and Electronics Engineers (IEEE) Digital Signal Processing Workshop, Yosemite, CA, 3-5 Oct. 1994
(Contract DE-AC04-94AL-85000)
(DE94-014185; SAND-94-0624C; CONF-941090-2) Avail: CASI HC A01/MF A01

All prior interferometric SAR imaging experiments to date dealt with pairwise processing. Simultaneous image collections from two antenna systems or two-pass single antenna collections are processed as interferometric pairs to extract corresponding pixel by pixel phase differences which encode terrain elevation height. The phase differences are wrapped values which must be unwrapped and scaled to yield terrain height. We propose two major classes of techniques that hold promise for robust multibaseline (multiple pair) interferometric SAR terrain elevation mapping. The first builds on the capability of a recently published method for robust weighted and unweighted least-squares phase unwrapping, while the second attacks the problem directly in a maximum likelihood (ML) formulation. We will provide several examples (actual and simulated SAR imagery) that illustrate the advantages and disadvantages of each method. DOE

N95-14358# Army Construction Engineering Research Lab., Champaign, IL.
A MULTISCALE RANDOM FIELD MODEL FOR BAYESIAN IMAGE SEGMENTATION Final Report
Michael Shapiro, Charles Bouman, and Calvin F. Bagley Jun. 1994 53 p
(DA Proj. 4A1-62720-A-896)
(AD-A283875; CERL-TR-EC-94/21) Avail: CASI HC A04/MF A01

The Army's Land Condition Trend Analysis (LCTA) program collects both space-based remotely-sensed data and ground-level data for natural resource inventory and evaluation. Coupling remotely sensed digital data with traditional ecological ground data could help Army land managers inventory and monitor natural resources. This study used LCTA data sets to test image segmentation algorithms that may be used to interpret remotely sensed digital data. Many approaches to Bayesian image segmentation have used maximum a posteriori (MAP) estimation in conjunction with Markov random fields (MRF). This study developed a new approach to Bayesian image segmentation that replaces the MRF model with a novel multiscale random field (MSRF), and replaces the MAP estimator with a sequential MAP (SMAP) estimator derived from a novel estimation criteria. Together, the proposed estimator and model result in a noniterative segmentation algorithm that can be computed in time proportional to MN, where M is the number of classes and N is the number of pixels. Results show that the SMAP algorithm improves classification accuracy when applied to the segmentation of multispectral remotely sensed images with ground-truthed data, especially with the introduction of mixed signatures to represent the spectral information about the classes. DTIC

N95-14793 Fish and Wildlife Service, Onalaska, WI. Environmental Management Technical Center.
DEVELOPMENT OF A SYSTEMIC LAND COVER/LAND USE DATABASE FOR THE UPPER MISSISSIPPI RIVER SYSTEM DERIVED FROM LANDSAT THEMATIC MAPPER SATELLITE DATA. LONG TERM RESOURCE MONITORING PROGRAM
M. S. Laustrup and C. D. Lowenberg May 1994 89 p Limited Reproducibility: More than 20% of this document may be affected by microfiche quality
(PB94-186889; LTRMP-94-T001) Avail: CASI HC A05

Procedures were developed for using 1989 Landsat Thematic Mapper data to map land cover/land use for the Upper Mississippi River System (UMRS). The procedures include: image mosaicking, projection, atmospheric correction, floodplain extraction, classification, editing, quality assurance, and distribution. The mapping classes include: water, aquatic vegetation, grasses, forbs, woody terrestrial, agriculture, urban/developed, and sand. Acreage summaries are provided for the 35 navigation pools as well as the open river reaches. Classification error was assessed and confidence limits were generated for each of the seven Landsat scenes required to map the UMRS. The database provides resource managers throughout the UMRS with access to site-specific land cover/land use information. In addition, these data will be used to verify the adequacy of LTRMP sampling designs and to evaluate the spatial distribution of habitats throughout the system which includes 1,137,035 hectares (2,809,575 acres). Author

N95-15546 RAND Corp., Santa Monica, CA.
US SPACE-BASED REMOTE SENSING: CHALLENGES AND PROSPECTS
Dana J. Johnson, Max Nelson, and Robert J. Lempert 1993 69 p Limited Reproducibility: More than 20% of this document may be affected by microfiche quality
(AD-A282439; RAND/N-3589-AF/A/OSD) Avail: Issuing Activity (Defense Technical Information Center (DTIC))

U.S. space-based remote sensing programs and activities are facing a number of critical junctures in the coming decade. The U.S. government will have some critical decisions about its own requirements for exploiting remote sensing capabilities for environmental, meteorological, and national security uses, balanced against limited and decreasing budgets for those activities. Furthermore, there are ongoing debates within the Administration, in the Congress, and by the American public over the extent of the role government should play in fostering the commercial remote sensing sector. The explosion in geographical information system technologies for enhancing raw remote sensing data is also encouraging the development of a commercial market. These trends and others, such as expanding international

capabilities, have combined to produce a dynamic remote sensing arena, an arena requiring a balanced approach to resource allocation and long-range planning. This note presents a survey of remote sensing policy issues for the 1990s, with the purpose of assisting in the development of a future space-related RAND research agenda. DTIC

N95-15727*# Old Dominion Univ., Norfolk, VA. Dept. of Engineering Technology.

INVESTIGATION OF ALLAN VARIANCE FOR DETERMINING NOISE SPECTRAL FORMS WITH APPLICATION TO MICROWAVE RADIOMETRY Final Report

William D. Stanley Nov. 1994 66 p

(Contract NAS1-19858; RTOP 233-01-03-22)

(NASA-CR-194985; NAS 1.26:194985) Avail: CASI HC A04/MF A01

An investigation of the Allan variance method as a possible means for characterizing fluctuations in radiometric noise diodes has been performed. The goal is to separate fluctuation components into white noise, flicker noise, and random-walk noise. The primary means is by discrete-time processing, and the study focused primarily on the digital processes involved. Noise satisfying the requirements was generated by direct convolution, fast Fourier transformation (FFT) processing in the time domain, and FFT processing in the frequency domain. Some of the numerous results obtained are presented along with the programs used in the study. Author

N95-15791# Politecnico di Milano, Milan (Italy). Dipt. di Ingegneria Idraulica, Ambientale e del Rilevamento.

INTERNATIONAL GEOID SERVICE BULLETIN NO. 1

Apr. 1993 110 p Sponsored by Ist. Nazionale di Geofisica

(Bull-1) Avail: CASI HC A06/MF A02

This is the initial bulletin of the International Geoid Service (IGeS) which was recently established in Italy as part of the International Association of Geodesy. The Bulletin contains articles on: the structure and activities of the IGeS; a questionnaire on the importance of the Geoid in Canada; a project to determine the geoid and sea surface topography in the Mediteranean Sea; a description of the organization and activities of the Bureau Gravimetrique International; the European Geoid project; validation of global digital height models for Italy; and a strategy for numerical analysis of geoid models. For individual titles, see N95-15792 through N95-15798.

N95-15792# Politecnico di Milano, Milan (Italy). Dipt. di Ingegneria Idraulica, Ambientale d del Rilevamento.

INTRODUCING THE INTERNATIONAL GEOID SERVICE

Fernando Sanso and F. Migliaccio *In its* International Geoid Service Bulletin No. 1 Apr. 1993 p 2-5 (For primary document see N95-15791 03-43)

Avail: CASI HC A01/MF A02

As announced in the circular letter issued in June 1992 by Bulletin Geodesique, the International Geoid Service (IGeS) was established in the summer of 1992, and became operational in September 1993. The proposal for the new service dates back to 1988, when the International Geoid Commission (IGC) was created by the International Association of Geodesy (IAC) Section 3. The President of IGC proposed the IGeS as the operational group of IGC 'working for the benefit of the international scientific community without any commercial interest'. The IGeS will concentrate on: collecting and testing geopotential global models and the relative software; collecting and documenting preprocessing software; issuing an annual bulletin providing information on the service; starting a first course of the International School for Technical Training for geoid computations; participating in international research projects related to the determination of the geoid.

Author (revised)

N95-15793# Energy, Mines and Resources Canada, Ottawa (Ontario). Geodetic Survey Div.

GEODETIC SURVEY OF CANADA: RESULTS ON A GEOID QUESTIONNAIRE

Andre Mainville *In* Politecnico di Milano, International Geoid Service Bulletin No. 1 Apr. 1993 p 14-28 (For primary document see N95-15791 03-43)

Avail: CASI HC A03/MF A02

As proposed by the Canadian advisory committee on geoid matters, a questionnaire on the importance of the geoid was prepared by the Geodetic Survey of Canada with the committee's collaboration, and sent to 965 of its users in November 1989. The purpose of the questionnaire was to determine the needs for geoid information in Canada and to evaluate the direction the geoid research and development is taking. Some highlights of the results are as follows. Out of 965 questionnaires, 125 have been returned. As seen from the 109 responses to question no. 12 (From whom would you like to obtain geoid data: Federal Gov't, Provincial Gov't, Private Industry or other), it is very clear that the Canadian community expects the federal government to show leadership in geoid matters. Fifty-four percent of the respondents favor receiving geoid information from the federal government only. An additional 22 percent favor receiving geoid information from federal and provincial sources. As seen from the 109 responses to question 13 (How important is it to you that reliable geoid values be readily available? Not very important, Important or Very important.), the availability of reliable geoid values is considered 'very important' by 31 percent and 'important' by an additional 38 percent of the responders. The paper summarizes the questionnaire results. The respondents have clarified the products required to satisfy their geoid needs. According to 68 percent of the respondents, ongoing geoid solution refinement is required until a plus or minus 1 cm precise geoid is obtained. Author

N95-15794# Politecnico di Milano, Milan (Italy).

THE GEOMED PROJECT

M. A. Brovelli *In its* International Geoid Service Bulletin No. 1 Apr. 1993 p 31-43 (For primary document see N95-15791 03-43)

Avail: CASI HC A03/MF A02

Since the International Geoid Service (IGeS) is new, we decided that, in the trial stage, we would concentrate our efforts on international projects. One of them is the Geomed (GEoid in the MEDiterranean sea), which is a project supported by the European Economic Community aimed at studying the problem of determining the geoid and the sea surface topography in closed seas with particular regard for the Mediterranean. The geoid, or better some equipotential surface of the gravity field suitably fitting the physical surface of the Mediterranean is determined as the basic surface in Geodesy to which orthometric heights are referred. Author (revised)

N95-15795# Bureau Gravimetrique International, Toulouse (France).

THE BUREAU GRAVIMETRIQUE INTERNATIONAL

G. Balmino *In* Politecnico di Milano, International Geoid Service Bulletin No. 1 Apr. 1993 p 44-59 (For primary document see N95-15791 03-43)

Avail: CASI HC A03/MF A02

In geodesy, gravity values play a great part in the modelling of the Earth gravity field, which is of permanent use for the computation of precise satellite orbits. It is also an essential information for the determination of the geoid, and for the determination of the ocean mean surface used for the study of the global circulation. In geophysics, the interpretation of the gravity field anomalies allows to study density variations in the lithosphere or the mantle, with applications in oil and mineral prospecting. The Bureau Gravimetrique Internatinal (BGI) is one of the offices of the Federation of Astronomical and Geophysical Services which operate under the auspices of the International Council of Scientific Unions and the United Nations Educational, Scientific and Cultural Organization. This paper describes the organizational structure and activities of the BGI. Author (revised)

N95-15796# Technische Univ., Hanover (Germany). Inst. fuer Erdmessung.

THE EUROPEAN GEOID PROJECT

Heiner Denker and Wolfgang Torge *In* Politecnico di Milano, International Geoid Service Bulletin No. 1 Apr. 1993 p 60-74 (For primary document see N95-15791 03-43)

Avail: CASI HC A03/MF A02

Regional geoid with respect to quasigeod determinations are now required with an accuracy of plus or minus 1 to 10 cm over distances from 100 to some 1000 km to meet the demands of geodesy, geophysics, oceanography and engineering. Especially the combination of Global Positioning System (GPS) height date with classical leveling is one of the primary drivers for precise geoid computations. Thus, the International Geoid Commission decided to establish a subcommission for Europe to support the derivation of a new geoid model for Europe, one significantly improved in spatial resolution and accuracy as compared with presently available models. The Institut fur Erdmessung (IfE), University of Hannover, serves as a computing center in this project. In this report, we first review some

of the more important geoid (quasigeoid) calculations performed for Europe from the 1950's to 1980's. We then discuss the possibilities for improved geoid determinations and give a summary of the work performed since 1990. This discussion includes the most recent quasigeoid calculation performed in 1991, as well as some of the more recent developments of the European Geoid Project with respect to data collection and evaluation. It should be noted that in all our computations we deal with the quasigeoid because this has the advantage that only gravity field data observed at the earth's surface and in the exterior of the earth enter into the calculations, and no assumptions about the gravity field in the earth's interior have to be made. A subsequent transformation to the geoid introducing a density model can easily be performed. Author (revised)

N95-15797# Graz Univ. (Austria). Inst. of Mathematical Geodesy and Geoinformatics.

VALIDATION OF THE GLOBAL DIGITAL HEIGHT MODEL ETOPO5U REFERRING TO THE ITALIAN MODEL (ITALIAN DEM)

E. Hoeck and H. Scharler *In* Politecnico di Milano, International Geoid Service Bulletin No. 1 Apr. 1993 p 75-92 (For primary document see N95-15791 03-43)

Avail: CASI HC A03/MF A02

The existing set of high resolution local digital terrain models gives the possibility to combine this detailed information available with a global 5' x 5' model to get a proper reference topography in the Mediterranean area. Within the merging process the global model is validated referred to the local one in the sub-area common to both. In particular the validation and merging steps are presented in the case of one local data set. Author

N95-15798# Reggio Calabria Univ., Reggio Calabria, Reggio Calabria (Italy). Ist. Ing. Civile ed Energetica.

A STRATEGY FOR GEOID REPAIRING

R. Barzaghi and M. A. Brovelli *In* Politecnico di Milano, International Geoid Service Bulletin No. 1 Apr. 1993 p 93-105 (For primary document see N95-15791 03-43)

Avail: CASI HC A03/MF A02

The presence of undetected outliers in database introduces errors in the derived estimates. If, in an 'a posteriori' processing, a small number of outliers is found, the problem of correcting properly the estimates arises. Particularly, in geodetic applications, gravity outliers can affect geoid estimates. In this paper, we try to define a procedure to repair the distortions in geoid estimates caused by a small number of outliers in the gravity database without recomputing the solution globally. Numerical tests have been carried out to analyze the practical application of the devised method. Author

N95-15848*# Massachusetts Univ., Amherst, MA. Microwave Remote Sensing Lab.

VALIDATION OF ERS-1 ENVIRONMENTAL DATA PRODUCTS Final Report, 1 Nov. 1991 - 28 Feb. 1992

Mark A. Goodberlet, Calvin T. Swift, and John C. Wilkerson 10 Nov. 1994 43 p

(Grant NAGw-2581)

(NASA-CR-197111; NAS 1.26:197111) Avail: CASI HC A03/MF A01

Evaluation of the launch-version algorithms used by the European Space Agency (ESA) to derive wind field and ocean wave estimates from measurements of sensors aboard the European Remote Sensing satellite, ERS-1, has been accomplished through comparison of the derived parameters with coincident measurements made by 24 open ocean buoys maintained by the National Oceanic and Atmospheric Administration). During the period from November 1, 1991 through February 28, 1992, data bases with 577 and 485 pairs of coincident sensor/buoy wind and wave measurements were collected for the Active Microwave Instrument (AMI) and Radar Altimeter (RA) respectively. Based on these data, algorithm retrieval accuracy is estimated to be plus or minus 4 m/s for AMI wind speed, plus or minus 3 m/s for RA wind speed and plus or minus 0.6 m for RA wave height. After removing 180 degree ambiguity errors, the AMI wind direction retrieval accuracy was estimated at plus or minus 28 degrees. All of the ERS-1 wind and wave retrievals are relatively unbiased. These results should be viewed as interim since improved algorithms are under development. As final versions are implemented, additional assessments should be conducted to complete the validation. Author

N95-15851*# Aerojet-General Corp., Azusa, CA.

EARTH OBSERVING SYSTEM (EOS)/ADVANCED MICROWAVE SOUNDING UNIT-A (AMSU-A) WORST-CASE ANALYSIS: ANTENNA BEAM POINTING Final Report

Wayne Ely 20 Nov. 1994 11 p

(Contract NAS5-32314)

(NASA-CR-197218; NAS 1.26:197218; Aerojet-10357) Avail: CASI HC A03/MF A01

This report presents a worst-case analysis of the EOS/AMSU-A (Earth Observing System/Advanced Microwave Sounding Unit-A) Antenna beam-pointing accuracy. There are three sources of beam pointing error. These are mechanical tolerances in the manufacture and assembly of the parts, allowable axial displacement of the reflector relative to the motor shaft, and on-orbit thermal distortions. For the worst-case analysis, each will be assumed to act independently and thus each contribution is additive. Derived from text

N95-15916*# EMR-Photoelectric, Princeton, NJ.

FIRST YEAR PIDDP REPORT ON GAMMA-RAY AND X-RAY SPECTROSCOPY: X-RAY REMOTE SENSING AND IN SITU SPECTROSCOPY FOR PLANETARY EXPLORATION MISSIONS AND GAMMA-RAY REMOTE SENSING AND IN SITU SPECTROSCOPY FOR PLANETARY EXPLORATION MISSIONS

M. Mahdavi, K. L. Giboni, S. Vajda, J. S. Schweitzer, and J. A. Truax 25 Aug. 1994 141 p

(Contract NAS5-32486; RTOP 691-00-00)

(NASA-CR-189374; NAS 1.26:189374) Avail: CASI HC A07/MF A02

Detectors that will be used for planetary missions must have their responses calibrated in a reproducible manner. In addition, it is important to characterize a detector system at uneven portions of its life cycle, for example after exposure to different amounts of radiation. A calibration and response characterization facility has been constructed at Schlumberger-Doll Research for all types of gamma- and x-ray detectors that may be used for planetary measurement. This facility is currently being tested. Initial use is expected for the MARS 94 detectors. The facility will then also be available for calibrating other detectors as well as arrays of detectors such as the NEAR detector with its central NaI(Tl) crystal surrounded with a large BGO crystal. Cadmium telluride detectors are investigated for applications in space explorations. These detectors show an energy resolution of 5 keV for the 122 keV 57Co line. Earlier reported polarization effects are not observed. The detectors can be used at temperatures up to 100 C, although with reduced energy resolution. The thickness of standard detectors is limited to 2 mm. These detectors become fully efficient at bias voltages above 200 V. Initial results for a 1 cm thick detector show that the quality of the material is inferior to the thinner standard detectors and hole trapping affects the pulse height. A detailed characterization of the detector is in progress. Prototypes of photomultipliers based on a Channel Electron Multiplier (CEM) are being built to study their performance. Such photomultipliers promise better timing characteristics and a higher dynamic range while being more compact and of lower in weight. Author

N95-14275*# National Aeronautics and Space Administration. Goddard Space Flight Center, Greenbelt, MD.

SCIENTIFIC ANALYSIS OF SATELLITE RANGING DATA

David E. Smith *In its* Satellite Laser Ranging in the 1990s: Report of the 1994 Belmont Workshop Nov. 1994 p 15-25 (For primary document see N95-14274 03-46)

Avail: CASI HC A03/MF A02

44 ENERGY PRODUCTION AND CONVERSION

Includes specific energy conversion systems, e.g., fuel cells; global sources of energy; geophysical conversion; and windpower.

For related information see also *07 Aircraft Propulsion and Power, 20 Spacecraft Propulsion and Power,* and *28 Propellants and Fuels.*

N95-14002# Pacific Northwest Lab., Richland, WA.

SYNTHESIS, PROCESSING AND PROPERTIES OF MATERIALS FOR SOFCs

J. L. Bates, T. A. Armstrong, J. J. Kingsley, and L. R. Pederson Mar.

1994 17 p Presented at the Materials Science Issues Related to High-Temperature Fuel Cells Conference, La Jolla, CA, 24 Mar. 1994
(Contract DE-AC06-76RL-01830)
(DE94-014491; PNL-SA-23936; CONF-9403136-1) Avail: CASI HC A03/MF A01

The synthesis and processing methods of complex oxide materials can significantly influence use in solid oxide fuel cells (SOFC's). This paper discusses (1) effects of powder synthesis and conditioning on fabrication, i.e., sintering, where close, reproducible control of composition and structure are required, and (2) influences on electrical, mechanical, structural and electrochemical properties that can influence SOFC performance. Examples are given for chromites, manganites and related oxides used as interconnections and electrodes in SOFC's. Materials, from source to incorporation into the fuel cell and generator, are a major issue in the development of solid oxide fuel cells (SOFC's). An integral part of this is the synthesis from chemicals and other virgin materials, generally as an oxide or metal powder, which can become a SOFC component. In some instances, such as with electrochemical vapor deposition, the component is formed directly from the chemicals. The synthesized materials are then conditioned and processes prior to fabrication into the fuel cell component, either separately or in conjunction with other material components. DOE

N95-14143 Fuel Cell Engineering Corp., Danbury, CT.
MCFC PRODUCT DEVELOPMENT TEST
18 Jan. 1994 17 p Limited Reproducibility: More than 20% of this document may be affected by microfiche quality
(Contract DE-FC21-92MC-29237)
(DE94-014334; DOE/MC-29237/3798) Avail: CASI HC A03

The project is for the design, construction, and testing of a 2 MW carbonate fuel cell power plant in the City of Santa Clara, California. The report is divided into sections which describe the progress in various program activities. Section 2.0 provides an overview of the program, including the project objectives, site location, and schedule. Section 3.0 describes the project progress in the areas of stack module design, balance of plant process and mechanical design, stack fabrication, and balance of plant procurement. DOE

N95-14191# National Renewable Energy Lab., Golden, CO.
WIND-ELECTRIC ICE MAKING FOR VILLAGES IN THE DEVELOPING WORLD
H. Davis (Bergey Windpower Co., Inc., Norman, OK.), S. Drouilhet, L. Flowers, M. Bergey, and M. Brandemuehl Jul. 1994 13 p Presented at the American Wind Energy Association Annual Conference and Exhibition, Minneapolis, MN, 9-13 May 1994
(Contract DE-AC36-83CH-10093)
(DE94-011854; NREL/TP-441-7044; CONF-940548-6) Avail: CASI HC A03/MF A01

For many villages in the developing world, renewable energy sources are the most economical means of providing power. There is a significant need for ice to preserve fish and produce for shipment to market. Since fishing villages are near coastlines with fairly reliable wind resources, wind-powered ice machines would capitalize on a good match between ice demand and energy supply. To date little work has been done on the use of wind turbines for ice making applications. This paper presents the results of wind-electric ice making research project conducted by the University of Colorado, the National Renewable Energy Laboratory and Bergey Windpower Co. Several potential problems related to intermittent and variable frequency operation were determined prior to testing. Initial tests were conducted using a dynamometer to evaluate the significance of these potential problems under simulated conditions and to define basic performance expectations for ice makers in the 1.2 tons/day size range. Field testing will be completed soon to determine long-term performance of one ice maker. DOE

N95-14194# National Renewable Energy Lab., Golden, CO.
GROWTH MECHANISMS AND CHARACTERIZATION OF HYDROGENATED AMORPHOUS-SILICON-ALLOY FILMS Final Report, 15 Feb. 1991 - 14 Apr. 1994
A. Gallagher, D. Tanenbaum, A. Laracuente, and P. Kalra Jul. 1994 23 p Prepared for National Inst. of Standards and Technology, Boulder CO
(Contract DE-AC36-83CH-10093)
(DE94-011842; NREL/TP-411-6864) Avail: CASI HC A03/MF A01

This report describes work performed to better understand the atomic-scale structure of glow-discharge-produced a-Si:H, a-Ge:H, and a-Si:Ge:H films; its effect on film quality; and its dependence on deposition discharge conditions. Hydrogenated a-Si films are from a silane RF discharge onto atomically flat crystal Si and GaAs substrates. The substrates are then transferred in a scanning tunneling microscope, where the atomic-scale surface morphology is measured. The films were deposited using device-quality deposition conditions; IR absorption, sigma(L), and sigma(D) indicate high-quality intrinsic films. From the thickness dependence of the surface morphology, we determined that the films initially conform smoothly to an atomically flat Si or GaAs substrate, but as the thickness increases the roughness steadily increases to approximately 10% of the length of the scanned region. The surface of 100-400-nm-thick films is highly inhomogeneous, with steep hills and canyons in some areas and large atomically smooth regions in others. These unexpectedly large surface irregularities indicate severe and often connected void structures in the growing film, as well as relatively limited-range surface diffusion of the incorporating SiH3 radicals. On the other hand, large atomically flat surface were occasionally found, indicating the possibility of growing a homogeneous and compact amorphous film if appropriate growth conditions could be discovered. DOE

N95-14326# Department of Energy, Washington, DC. Office of Energy Markets and End Use.
ENERGY REVIEW Annual Report, 1993
14 Jul. 1994 404 p
(DE94-015828; DOE/EIA-0384(93)) Avail: CASI HC A18/MF A04

This twelfth edition of the Annual Energy Review (AER) presents the Energy Information Administration's historical energy statistics. For most series, statistics are given for every year from 1949 through 1993. Because coverage spans four and a half decades, the statistics in this report are well-suited to long-term trend analyses. The AER is comprehensive. It covers all major energy activities, including consumption, production, trade, stocks, and prices, for all major energy commodities, including fossil fuels and electricity. The AER also presents Energy Information Administration (EIA) statistics on some renewable energy sources. EIA estimates that its consumption series include about half of the renewable energy used in the United States. For a more complete discussion of EIA's renewables data, see p. xix, 'Introducing Expanded Coverage of Renewable Energy Data Into the Historical Consumption Series'. Copies of the 1993 edition of the Annual Energy Review may be obtained by using the order form in the back of this publication. Most of the data in the 1993 edition also are available on personal computer diskette. For more information about the diskettes, see the back of this publication. In addition, the data are available as part of the National Economic, Social, and Environmental Data Bank on a CD-ROM. DOE

N95-14341# Hi-Z Technology, Inc., La Jolla, CA.
PRELIMINARY DESIGN OF A MINIATURE THERMOELECTRIC GENERATOR Final Report
John C. Bass 8 Apr. 1994 75 p
(Contract DAAK70-93-C-0062)
(AD-A283834; HZ-08084-1) Avail: CASI HC A04/MF A01

The U.S. Marine Corps has need for power sources in the 500 Watt area. These sources should be highly reliable, small, lightweight, signal suppressed, and be able to use liquid fuels, preferably Diesel, as the energy source. The desire to burn Diesel stems from the Armed Services desire to use Diesel as their main fuel source. Other fuels such as gasoline create a logistic problem and therefore, is to be avoided if at all possible. There are currently no known power supplies of this type commercially available on the open market. The Diesel motor generator sets that are available have higher power outputs and typically have a rather low mean-time before failure (MTBF). Earlier contact with Army personnel indicate that the MTBF of small portable Diesel motor/generator sets were about 175 hours. Similar experience has been reported by the U.S. Coast Guard in both their Major Aids to Navigation, Major ATON, and their Weather Data Buoys. DTIC

N95-14393# Oak Ridge National Lab., TN.
THE INTEGRATION OF RENEWABLE ENERGY SOURCES INTO ELECTRIC POWER DISTRIBUTION SYSTEMS. VOLUME 1: NATIONAL ASSESSMENT
P. R. Barnes, J. W. VanDyke, F. M. Tesche, and H. W. Zaininger Jun. 1994 84 p
(Contract DE-AC05-84OR-21400)
(DE94-015935; ORNL-6775-Vol-1) Avail: CASI HC A05/MF A01

Renewable energy technologies such as photovoltaic, solar thermal electricity, and wind turbine power are environmentally beneficial sources of electric power generation. The integration of renewable energy sources into electric power distribution systems can provide additional economic benefits because of a reduction in the losses associated with transmission and distribution lines. Benefits associated with the deferment of transmission and distribution investment may also be possible for cases where there is a high correlation between peak circuit load and renewable energy electric generation, such as photovoltaic systems in the Southwest. Case studies were conducted with actual power distribution system data for seven electric utilities with the participation of those utilities. Integrating renewable energy systems into electric power distribution systems increased the value of the benefits by about 20 to 55% above central station benefits in the national regional assessment. In the case studies presented in Vol. 2, the range was larger: from a few percent to near 80% for a case where costly investments were deferred. In general, additional savings of at least 10 to 20% can be expected by integrating at the distribution level. Wind energy systems were found to be economical in good wind resource regions, whereas photovoltaic systems costs are presently a factor of 2.5 too expensive under the most favorable conditions. DOE

N95-14430# National Renewable Energy Lab., Golden, CO.
ROLE OF POINT DEFECTS AND DEFECT COMPLEXES IN SILICON DEVICE PROCESSING: BOOK OF ABSTRACTS
Jun. 1994 96 p Workshop held in Beaver Creek, CO, 27-29 Jun. 1994
(Contract DE-AC36-83CH-10093)
(DE94-011828; NREL/CP-413-7033; CONF-9406203) Avail: CASI HC A05/MF A01

The 41 abstracts are arranged into 6 sessions: impurities and defects in commercial substrates: their sources, effects on material yield, and material quality; new approaches to cell processing; impurity gettering in silicon: limits and manufacturability of impurity gettering and in silicon solar cells; impurity/defect passivation; new concepts in silicon growth: improved initial quality and thin films; and silicon solar cell design opportunities. DOE

N95-14432# National Renewable Energy Lab., Golden, CO.
ROLE OF POLYCRYSTALLINITY IN CdTe AND CuInSe2 PHOTOVOLTAIC CELLS Final Report, 1 Apr. 1990 - 30 Nov. 1993
J. R. Sites (Colorado State Univ., Fort Collins, CO.) Jul. 1994 58 p
(Contract DE-AC36-83CH-10093)
(DE94-011849; NREL/TP-451-7047) Avail: CASI HC A04/MF A01

The report describes the exploration of several aspects of the role of polycrystallinity in the operation of CdTe, CuInSe2, and Cu(In,Ga)Se2 solar cells. The work included the refinement of several analytical techniques, the documentation and understanding of time-dependent voltage effects, the analysis of a large number of individual cells, and significant progress toward developing a viable current-voltage model. This work was integral to the doctoral training of four students and was greatly assisted by several active collaborations within the polycrystalline thin-film solar cell community. DOE

N95-14433# National Renewable Energy Lab., Golden, CO.
THE NATIONAL WIND TECHNOLOGY CENTER
R. W. Thresher, S. M. Hock, R. R. Loose, and J. B. Cadogon Jul. 1994 13 p Presented at the American Wind Energy Association Annual Conference and Exhibition, Minneapolis, MN, 9-13 May 1994
(Contract DE-AC36-83CH-10093)
(DE94-011853; NREL/TP-440-6628; CONF-940548-5) Avail: CASI HC A03/MF A01

Wind energy research began at the Rocky Flats test site in 1976 when Rockwell International subcontracted with the Energy Research and Development Administration (ERDA). The Rocky Flats Plant was competitively selected from a number of ERDA facilities primarily because it experienced high instantaneous winds and provided a large, clear land area. By 1977, several small wind turbines were in place. During the facility's peak of operation, in 1979-1980, researchers were testing as many as 23 small wind turbines of various configurations, including commercially available machines and prototype turbines developed under subcontract to Rocky Flats. Facilities also included 8-kW, 40-kW, and 225-kW dynamometers; a variable-speed test bed; a wind/hybrid test facility; a controlled velocity test facility (in Pueblo, Colorado); a modal test facility, and a multimegawatt switchgear facility. The main laboratory building was dedicated in July 1981 and was operated by the Rocky Flats Plant until 1984, when the Solar Energy Research Institute (SERI) and Rocky Flats wind energy programs were merged and transferred to SERI. SERI and now the National Renewable Energy Laboratory (NREL) continued to conduct wind turbine system component tests after 1987, when most program personnel were moved to the Denver West Office Park in Golden and site ownership was transferred back to Rocky Flats. The Combined Experiment test bed was installed and began operation in 1988, and the NREL structural test facility began operation in 1990. In 1993, the site's operation was officially transferred to the DOE Golden Field Office that oversees NREL. This move was in anticipation of NREL's renovation and reoccupation of the facility in 1994. DOE

N95-14802*# Auburn Univ., AL. Space Power Inst.
SUMMARY OF SOLAR CELL DATA FROM THE LONG DURATION EXPOSURE FACILITY (LDEF) Final Report, 21 Jul. 1993 - 19 Aug. 1994
David C. Hill and M. Frank Rose 21 Oct. 1994 61 p
(Contract NAS8-39131)
(NASA-CR-197069; NAS 1.26:197069) Avail: CASI HC A04/MF A01

The Long Duration Exposure Facility (LDEF) was composed of many separate experiments, some of which contained solar cells. These solar cells were distributed at various positions on the LDEF and, therefore, were exposed to the space environment with an orientational dependence. This report will address the space environmental effects on solar cells and solar cell assemblies (SCA's), including electrical interconnects and associated insulation blankets where flown in conjunction with solar cells. Derived from text

N95-14853*# Auburn Univ., AL. Space Power Inst.
ANALYSIS OF SPACE ENVIRONMENT DAMAGE TO SOLAR CELL ASSEMBLIES FROM LDEF EXPERIMENT A0171-GSFC TEST PLATE Final Report, 21 Jul. 1993 - 19 Aug. 1994
David C. Hill and M. Frank Rose 2 Sep. 1994 91 p
(Contract NAS8-39131)
(NASA-CR-197066; NAS 1.26:197066) Avail: CASI HC A05/MF A01

The space environment in earth orbit has been extensively studied and documented. The most serious factors influencing electrical systems (including solar arrays) are the local radiation environment, thermal cycling effects, local plasma density, neutral particle density, spacecraft surfaces outgassing/effuent products, and the meteroid and debris flux. The radiation environment (proton, electron, and photon), fueled primarily by the sun but also by other stellar sources, encountered by spacecraft in earth orbit is complex and depends upon such factors as orbital altitude, inclination, and current solar activity levels, and can result in exposures which vary over several orders of magnitude per orbit. The effects of these particles and electromagnetic radiation can cause major changes in the properties of insulators and semiconductors by ionization, atomic displacements or local changes due to chemical reactions. The severity of a radiation-induced change under multi-factor stressing depends on the total dose, intensity, particle species, impingement angle, presence of shielding, mechanical stress, local induced environment, temperature, and the presence of system-generated electromagnetic fields. Author

N95-15290# National Renewable Energy Lab., Golden, CO.
WIND/HYBRID POWER SYSTEM TEST FACILITIES IN THE UNITED STATES AND CANADA
H. J. Green, R. N. Clark, C. Brothers, and Bernard Saulnier May 1994 12 p Presented at the American Wind Energy Association Annual Conference and Exhibition, Minneapolis, MN, 9-13 May 1994
(Contract DE-AC02-83CH-10093)
(DE94-006930; NREL/TP-441-6626; CONF-940548-2) Avail: CASI HC A03/MF A01

By 1995, there will be four facilities available for testing of wind/hybrid

power systems in the United States and Canada. This paper describes the mission, approach, capabilities, and status of activity at each of these facilities. These facilities have in common a focus on power systems for remote, off-grid locations that include wind energy. At the same time, these facilities have diverse, yet complimentary, missions that range from research to technology development to testing. The first facility is the test facility at the Institut de Recherche d'Hydro-Quebec (IREQ), Hydro-Quebec's research institute near Montreal, Canada. This facility, not currently in operation, was used for initial experiments demonstrating the dynamic stability of a high penetration, no-storage wind/diesel (HPNSWD) concept. The second facility is located at the Atlantic Wind Test Site (AWTS) on Prince Edward Island, Canada, where testing of the HPNSWD concept developed by Hydro-Quebec is currently underway. The third is the Hybrid Power Test Facility planned for the National Wind Technology Center at the National Renewable Energy Laboratory (NREL) in Golden, Colorado, which will focus on testing commercially available hybrid power systems. The fourth is the U.S. Department of Agriculture (USDA) Conservation and Production Research Laboratory in Bushland, Texas, where a test laboratory is being developed to study wind-energy penetration and control strategies for wind/hybrid systems. The authors recognize that this summary of test facilities is not all inclusive; for example, at least one U.S. industrial facility is currently testing a hybrid power system. Our intent, though, is to describe four facilities owned by nonprofit or governmental institutions in North America that are or will be available for ongoing development of wind/hybrid power systems. DOE

N95-15355# Harvard Univ., Cambridge, MA.
OPTIMIZATION OF TRANSPARENT AND REFLECTING ELECTRODES FOR AMORPHOUS-SILICON SOLAR CELLS
R. G. Gordon, J. Hu, D. Lacks, J. Musher, J. Thornton, and H. Liang Jul. 1994 63 p Prepared in cooperation with National Renewable Energy Lab, Golden, CO
(Contract DE-AC36-83CH-10093)
(DE94-011841; NREL/TP-411-6856) Avail: CASI HC A04/MF A01

Fluorine-doped zinc oxide was shown to have the lowest absorption loss of any of the known transparent conductors. An apparatus was constructed to deposit textured, transparent, conductive, fluorine-doped zinc oxide layers with uniform thickness over a 10 cm by 10 cm area, using inexpensive, high-productivity atmospheric pressure chemical vapor deposition. Amorphous silicon solar cells grown on these textured films show very high peak quantum efficiencies (over 90 percent). However, a significant contact resistance develops at the interface between the amorphous silicon and the zinc oxide. Transparent, conductive gallium-doped zinc oxide films were grown by APCVD at a low enough temperature (260 C) to be deposited on amorphous silicon as a final conductive back contact to solar cells. A quantum-mechanical theory of bonding was developed and applied to some metal oxides; it forms a basis for understanding TCO structures and the stability of their interfaces with silicon. DOE

N95-15376# New Energy and Industrial Technology Development Organization, Tokyo (Japan).
DEVELOPMENT OF THE FUEL CELL POWER GENERATION TECHNOLOGY, 2
Feb. 1994 503 p In JAPANESE
(DE94-780614; ETDE/JP-MF-94780614) Avail: CASI HC A22/MF A04

NEDO arranged results of the research on the development of the fuel cell power generation technology during fiscal 1981 to 1987. During 1981 to 1983, research and development were made on a dispersed generation type fuel cell power generation system using phosphoric acid fuel cells (low temperature/pressure type) and a thermal power plant substitution type fuel cell power generation system (high temperature/pressure type). During 1984 to 1986, in addition to the above, research was made on a total system of phosphoric acid fuel cells, trial operation of a molten carbonate fuel cell power plant (matrix electrolyte method, paste electrolyte method) and a total system. In 1987, as to molten carbonate fuel cells, researches were made on stacks and a peripheral system, support, and a total system. As a comprehensive technology development of phosphoric acid fuel cells, researches were made on a fuel cell power generation system for isolated island use and a fuel cell power generation system for business use. DOE

N95-15377# New Energy and Industrial Technology Development Organization, Tokyo (Japan).
DEVELOPMENT OF THE FUEL CELL POWER GENERATION TECHNOLOGY, 1
Feb. 1994 508 p In JAPANESE
(DE94-780648; ETDE/JP-MF-94780648) Avail: CASI HC A22/MF A04

NEDO arranged results of the research on the development of the fuel cell power generation technology during fiscal 1988 to 1992. In 1988, as a comprehensive research on phosphoric acid fuel cells, research and development were made on an isolated island use fuel cell power generation system and a business use fuel cell power generation system. As a research on a molten carbonate fuel cell power generation system, studies were made on stacks, a peripheral system, support, and a total system. In 1989, in addition to the above, research and development were made on elementary technology and a power generation system of solid electrolyte fuel cells. In 1990, conducted were a comprehensive study of phosphoric acid fuel cells and a study of the high efficiency turbine/compressor and system. Afterward, phosphoric acid fuel cell 1000 kW power generation facilities were dismantled and removed. In 1991 and 1992, research and development were continued on the molten carbonate fuel cell power generation system and solid electrolyte fuel cells. DOE

N95-15405# National Renewable Energy Lab., Golden, CO.
DEVELOPMENT OF LARGE-AREA MONOLITHICALLY INTEGRATED SILICON-FILM(TM) PHOTOVOLTAIC MODULES
J. A. Rand (Astropower, Inc., Newark, DE.), J. E. Cotter (Astropower, Inc., Newark, DE.), A. E. Ingram (Astropower, Inc., Newark, DE.), T. R. Ruffins (Astropower, Inc., Newark, DE.), C. J. Thomas (Astropower, Inc., Newark, DE.), R. B. Hall (Astropower, Inc., Newark, DE.), and A. M. Barnett (Astropower, Inc., Newark, DE.) Jun. 1994 19 p
(Contract DE-AC36-83CH-10093)
(DE94-011830; NREL/TP-413-6853) Avail: CASI HC A03/MF A01

This report describes work performed under a program to develop Silicon-Film(trademark) Product III into a low-cost, stable solar cell for large-scale terrestrial power applications. The Product III structure is a thin polycrystalline layer of silicon on a durable, insulating, ceramic substrate. The insulating substrate allows the silicon layer to be isolated and metallized to form a monolithically interconnected array of solar cells. High efficiency is achievable with the use of light trapping and a passivated back surface. The long-term goal for the product is a 1200-square cm, 18 percent efficient solar module. This report discusses material quality improvements due to the use of new metallurgical barrier technologies. The barrier is essential in preventing impurity interaction between the silicon film and the low-cost substrate. Also, a new filament-based fabric substrate material was investigated. Efficiencies greater than 10 percent were achieved on 1.0-square cm devices made on these substrates. We also demonstrated the monolithic fabrication sequence by the fabrication of a prototype array using the device processing sequences developed during Phase 11 of this program. DOE

N95-15406# National Renewable Energy Lab., Golden, CO.
SMALL-ANGLE X-RAY SCATTERING STUDIES OF MICROVOIDS IN AMORPHOUS-SILICON-BASED SEMICONDUCTORS
D. L. Williamson (Colorado School of Mines, Golden, CO.), S. J. Jone (Colorado School of Mines, Golden, CO.), and Y. Chen (Colorado School of Mines, Golden, CO.) Jul. 1994 41 p
(Contract DE-AC36-83CH-10093)
(DE94-011840; NREL/TP-411-6855) Avail: CASI HC A03/MF A01

This report describes work performed to provide new details of the microstructure for the size scale from about 1 nm to 30 nm in high-quality hydrogenated amorphous-silicon and related alloys prepared by current state-of-the-art deposition methods as well as by new and emerging deposition technologies. The purpose of this work is to help determine the role of microvoids and other density fluctuations in controlling the opto-electronic and photovoltaic properties. The approach involved collaboration with several groups that supplied relevant systematic sets of samples and the associated opto-electronic/photovoltaic data to help address particular issues. The small-angle X-ray scattering (SAXS) technique, as developed during this project, was able to provide microstructural information with a high degree of sensitivity not available from other methods. It is particularly sensitive to microvoids or H-rich microdomains and to the presence of oriented microstructures. The latter is readily associated with

columnar-type growth and can even be observed in premature stages not detectable by transmission electron microscopy. Flotation density measurements provided important complementary data. Systematic correlations demonstrated that material with more SAXS-detected microstructure has to-electronic and photovoltaic properties and increased degradation under light soaking. New results related to alloy randomness emerged from our ability to measure the diffuse scattering component of the SAXS. DOE

N95-15407# National Renewable Energy Lab., Golden, CO.
ALTERNATIVE FABRICATION TECHNIQUES FOR HIGH-EFFICIENCY CuInSe2 AND CuInSe2-ALLOY FILMS AND CELLS
A. Rockett (Illinois Univ., Urbana, IL.), L. C. Yang (Illinois Univ., Urbana, IL.), G. Kenshole (Illinois Univ., Urbana, IL.), E. Banda (Illinois Univ., Urbana, IL.), and A. Feen (Illinois Univ., Urbana, IL.) Jul. 1994 25 p
(Contract DE-AC36-83CH-10093)
(DE94-011846; NREL/TP-451-6862) Avail: CASI HC A03/MF A01

Work performed during the course of this subcontract has led to improved CuInSe2 (CIS) processing techniques and materials resulting in improved solar cell performance (up to 10 percent active area efficiency) based on a thick conductive evaporated CdS window layer and an indium-tin-oxide transparent conductor. Modeling of the device performance has indicated that an optimal CdS thickness should exist if pinholes occur in the CIS layer (for example, due to adhesion failures) leading to shunts between the CdS and the back contact. Pinholes in the CIS layer have been dramatically reduced by the use of a Cu-Mo two-phase back contact metallization resulting from significant increases in adhesion between the CIS and the back contact. Controlled leaching of the Cu from the back contact apparently contributes to this improvement without degradation of the solar cells. Finally, CIS has been grown epitaxially on GaAs. Preliminary results suggest explanations for the morphology and defect structures of polycrystalline layers used in devices as well as indicating the general mechanism for growth of CIS by vapor phase methods. DOE

N95-15420# Sandia National Labs., Albuquerque, NM.
MONITORING SOLAR-THERMAL SYSTEMS: AN OUTLINE OF METHODS AND PROCEDURES
A. Rosenthal (New Mexico State Univ., Las Cruces, NM.) Apr. 1994 44 p
(Contract DE-AC04-94AL-85000)
(DE94-015599; SAND-94-0007) Avail: CASI HC A03/MF A01

This manual discusses the technical issues associated with monitoring solar-thermal systems. It discusses some successful monitoring programs that have been implemented in the past. It gives the rationale for selecting a program of monitoring and gives guidelines for the design of new programs. In this report, solar thermal monitoring systems are classified into three levels. For each level, the report discusses the kinds of information obtained by monitoring, the effort needed to support the monitoring program, the hardware required, and the costs involved. Ultimately, all monitoring programs share one common requirement: the collection of accurate data that characterize some aspect or aspects of the system under study. This report addresses most of the issues involved with monitoring solar thermal systems. It does not address such topics as design fundamentals of thermal systems or the relative merits of the many different technologies employed for collection of solar energy. DOE

N95-15863# Golden Photon, Inc., Golden, CO.
MODULE PROCESS OPTIMIZATION AND DEVICE EFFICIENCY IMPROVEMENT FOR STABLE, LOW-COST, LARGE-AREA, CADMIUM TELLURIDE-BASED PHOTOVOLTAIC MODULE PRODUCTION
S. P. Albright and S. X. Johnson Jun. 1994 34 p Prepared for Midwest Research Inst., Golden, CO
(Contract DE-AC36-83CH-10093)
(DE94-011817; NREL/TP-413-6633) Avail: CASI HC A03/MF A01

This report describes work performed under a three-phase subcontract. The objectives of the program include (1) achievement of active-area efficiencies of greater than 14% on small cells; (2) achievement of aperture-area efficiencies of greater than 13% on 0.09-sq m (1 sq ft) modules; (3) achievement of aperture-area efficiencies of greater than 12.5% on 0.37-sq m (4 sq ft) modules; and achievement of greater than 20-year module life (based on life testing extrapolations) with no greater than 10% efficiency degradation. The results obtained and described herein include the following: (1) efficiencies of 12.7% were achieved on small-area devices; (2) 0.09-sq m(1 sq ft) modules achieved greater than 8% aperture-area efficiency, but work for further efficiency improvement was redirected toward the 0.37-sq m(4 sq ft) modules; (3) 0.37-sq m (4 sq ft) modules achieved 26.5-W output, which calculates to 8.0% aperture-area efficiency; (4) consistent prototype production was focused on and substantially achieved within Phase 2; (5) life testing at the National Renewable Energy Laboratory showed no inherent stability problems with the CdTe technology, and the accuracy of module measurement was satisfactorily resolved; and (6) a 'cradle-to-cradle' recycling program was begun based upon the philosophy that the establishment of such mechanisms will be required to ensure maximum recapture and recycling of all manufacturing waste materials and/or modules returned from the field. DOE

45 ENVIRONMENT POLLUTION

Includes atmospheric, noise, thermal, and water pollution.

N95-14121# Environmental Protection Agency, Cincinnati, OH. Center for Environmental Research Information.
EMERGING TECHNOLOGY SUMMARY: DESTRUCTION OF ORGANIC CONTAMINANTS IN AIR USING ADVANCED ULTRAVIOLET FLASHLAMPS
Jul. 1993 9 p See also PB93-205383
(PB94-194479; EPA/540/SR-93/516) Avail: CASI HC A02/MF A01

The summary describes a new process for photooxidization of volatile organic compounds (VOC's) in air using an advanced ultraviolet (UV) source, and a pulsed xenon flashlamp. The flashlamps have greater output at 200 to 250 nm than medium-pressure mercury lamps at the same power and, therefore, cause much more rapid direct photolysis of VOC's. The observation of quantum yields greater than unity indicate the involvement of chain reactions for trichloroethene (TCE), perchloroethene (PCE), 1,1-dichloroethylene (DCE), CHCl3, and CH2Cl2. TCE was examined more closely because of its widespread occurrence and very high destruction rate. NTIS

N95-14122# National Oceanic and Atmospheric Administration, Research Triangle Park, NC. Atmospheric Sciences Modeling Div.
COMPUTATIONAL MODELING ISSUES IN NEXT GENERATION AIR QUALITY MODELS
D. W. Byun, D. Hwang, C. J. Coats, M. T. Odman, and R. L. Dennis 1994 5 p See also PB94-139540 and PB94-158623
(PB94-197449; EPA/600/A-94/148) Avail: CASI HC A01/MF A01

The U.S. Environmental Protection Agency's Atmospheric Research and Exposure Assessment Laboratory is leading a major effort to advance urban/regional multipollutant air quality modeling through development of a third-generation modeling system, Models-3. The Models-3 system is being developed within a high-performance computing technology framework to take advantage of developments in science and the computer and communication fields. The authors discuss several issues with Models-3 prototype examples. One area of important work is assessing the trade-off between speed and accuracy, either through development of new algorithms or optimizing existing ones to the computer architecture. The authors provide examples of such work on characterization of numerical algorithms. A second issue is how best to optimize codes for high performance architectures. Finally, the authors compare sensitivity estimation methods such as an automatic differentiation of the air quality model and a simple brute-force sensitivity analysis. NTIS

N95-14123# ManTech Environmental Technology, Inc., Research Triangle Park, NC.
STUDY OF INTERFERENCES IN OZONE UV AND CHEMILUMINESCENCE MONITORS
E. E. Hudgens, T. E. Kleindienst, F. F. McElroy, and W. M. Ollison 1994 12 p Presented at the AREAL/AWMA Symposium on Toxic Air Pollutants, 3 May 1994
(Contract EPA-68-D0-0106)
(PB94-197456; EPA/600/A-94/149) Avail: CASI HC A03/MF A01

A study was conducted to examine interferences and other measurement anomalies in chemiluminescence and ultraviolet ozone monitors. Previous results had shown that there was a positive deviation in the

chemiluminescence monitors and no direct interference with ultraviolet monitors due to the presence of water at noncondensing concentrations. The present study continues this effort, examining both potential positive and negative effects of moisture and other interferences on these monitors. Aromatic compounds and their oxidation products could potentially show a positive interference with ultraviolet monitors, and test measurements were made with aromatics such as toluene, benzaldehyde, and nitrotoluene to determine their possible retention in the ozone scrubber and their absorption in the cell as a function of the humidity. A detailed examination of the scrubbers used in ultraviolet ozone monitors has also been undertaken. Ozone scrubbers that have shown anomalous behavior in the field have been studied in various reduced-efficacy modes under controlled laboratory conditions. Longer term tests of unused scrubbers for possible ozone breakthrough under exposure to various simulated field conditions were initiated. NTIS

N95-14124# Environmental Protection Agency, Washington, DC. Environmental Monitoring and Assessment Program.

EMAP INFORMATION MANAGEMENT STRATEGIC PLAN, 1993-1997

R. F. Shepanek Mar. 1994 127 p See also PB94-136256

(PB94-176823; EPA/620/R-94-017) Avail: CASI HC A07/MF A02

The Information Management Strategic Plan for the Environmental Monitoring and Assessment Program (EMAP) describes how EMAP information will be managed from field sampling through the delivery of products to the user. This plan cuts across the entire EMAP program and explains the process for developing an information management infrastructure which will enable EMAP to achieve its long-term objectives. The plan provides a strategy for meeting hardware, software, documentation support, and system designs that will meet EMAP Resource and Coordinating Group requirements. Users of EMAP data and information are discussed in the plan as well as the process and technology with which they can access EMAP data and other data sources. Author (NTIS)

N95-14187# Argonne National Lab., IL.

REMOTE SENSING STRATEGY AT THE FIRST ATMOSPHERIC RADIATION MEASUREMENT FIELD SITE

M. L. Wesely and J. W. Griffin 1994 4 p Presented at the 3rd International Symposium on Tropospheric Profiling: Needs and Technologies, Hamburg, Germany, 30 Aug. - 2 Sep. 1994

(Contracts W-31-109-eng-38; DE-AC06-76RL-01830)

(DE94-015091; ANL/ER/CP-83276; CONF-9408118-1) Avail: CASI HC A01/MF A01

The Atmospheric Radiation Measurement (ARM) Program was initiated in 1990 by the US Department of Energy to improve climate model simulations of radiative energy transport and cloud formation, maintenance, and dissipation. ARM stresses the modeling of phenomena occurring at subgrid scales in general circulation models (GCMs). Measurements to support the modeling research will be made at three primary locations. The central facility, the primary location at the Southern Great Plains (SGP) site for study of radiative transfer, uses ground-based remote sensing instrumentation to observe radiation and the atmospheric properties that affect it. Remote sensing instruments and balloon-borne sounding systems installed at several boundary facilities on the perimeter of the overall Cloud and Radiation Testbed (CART) site evaluate vertical profiles of wind, temperature, and humidity. These observations are needed to run single-column models derived from GCMs for a single grid square with an area equivalent to the overall CART area. Observations of local meteorological conditions, air-surface exchange, and solar and infrared radiation at up to 23 extended facilities scattered throughout the CART site provide the surface boundary information needed in the single-column models. Finally, auxiliary facilities at the central facility and at a few locations within 10 km of the central facility will contain whole-sky imaging systems to map cloud characteristics. The purpose of this presentation is to describe the strategy used to obtain remote sensing instrumentation for continuous operation at the central facility. DOE

N95-14195# Pacific Northwest Lab., Richland, WA.

THREE NEURAL NETWORK BASED SENSOR SYSTEMS FOR ENVIRONMENTAL MONITORING

P. E. Keller, R. T. Kouzes, and L. J. Kangas May 1994 6 p Presented at the Electro International Conference, Boston, MA, 10-12 May 1994

(Contracts DE-AC06-76RL-01830; DE-FG06-89ER-75522)

(DE94-014557; PNL-SA-24175; CONF-9405197-1) Avail: CASI HC A02/MF A01

Compact, portable systems capable of quickly identifying contaminants in the field are of great importance when monitoring the environment. One of the missions of the Pacific Northwest Laboratory is to examine and develop new technologies for environmental restoration and waste management at the Hanford Site. In this paper, three prototype sensing systems are discussed. These prototypes are composed of sensing elements, data acquisition system, computer, and neural network implemented in software, and are capable of automatically identifying contaminants. The first system employs an array of tin-oxide gas sensors and is used to identify chemical vapors. The second system employs an array of optical sensors and is used to identify the composition of chemical dyes in liquids. The third system contains a portable gamma-ray spectrometer and is used to identify radioactive isotopes. In these systems, the neural network is used to identify the composition of the sensed contaminant. With a neural network, the intense computation takes place during the training process. Once the network is trained, operation consists of propagating the data through the network. Since the computation involved during operation consists of vector-matrix multiplication and application of look-up tables unknown samples can be rapidly identified in the field. DOE

N95-14317# Lawrence Livermore National Lab., Livermore, CA.

DDI, THE DATA AND DIMENSIONS INTERFACE

C. L. Anderson, R. Drach, and D. N. Williams Apr. 1994 8 p Presented at the Visualization 1994, Washington, DC, 17-21 Oct. 1994

(Contract W-7405-eng-48)

(DE94-014750; UCRL-JC-116238; CONF-941085-4) Avail: CASI HC A02/MF A01

The Data and Dimensions Interface (DDI) addresses a significant problem in the visualization of large datasets: extracting only the relevant data and providing it to a chosen destination in the required form without significant effort. Many different research communities have developed formats for storing and retrieving scientific data and its associated information. These formats, while similar in their intent, are not intercompatible. Lack of support for these formats in commercial visualization systems has been an impediment to their use. Data file size may also cause problems; while sometimes generated on supercomputers, these files are often visualized on smaller machines. DDI was developed as a collaboration between the Program for Climate Model Diagnosis and Intercomparison (PCMDI) and the National Energy Research Supercomputer Center (NERSC), both of Lawrence Livermore National Laboratory (LLNL). DDI was inspired by the PCMDI Graphics Package, as well as NCSA Collage. DOE

N95-14337# Naval Postgraduate School, Monterey, CA.

OXIDES OF NITROGEN: THEIR FORMATION AND CONTROL IN STATIONARY SOURCES M.S. Thesis

Sonja P. Pedrozo 24 Apr. 1994 65 p

(Contract N00123-91-G-0566)

(AD-A283780) Avail: CASI HC A04/MF A01

Over the last fifty years, a major concern of environmentalists, health care providers, national governments, and international organizations has been the unhealthy and destructive effects of air pollution. In this regard, much attention has been given to a primary pollutant of air - oxides of nitrogen (NO(x)). The two most important oxides of nitrogen with respect to pollution are nitric oxide (NO) and nitrogen dioxide (NO2). In the atmosphere, elevated concentrations of these gases contribute to the greenhouse effect and ozone depletion. In addition, they foster the formation of acid rain and photochemical smog. Lastly, not only do NO(x) contribute directly to these atmospheric reactions, but they also participate in the production of secondary pollutants which have similar effects. DTIC

N95-14344# Harvard Coll. Observatory, Cambridge, MA.

MEASUREMENTS OF ULTRAVIOLET ABSORPTION CROSS SECTIONS OF NO2 AT VARIOUS PRESSURES AND TEMPERATURES Status Report

W. H. Parkinson and Kouichi Yoshino 1994 9 p

(Contract N00014-93-1-G037)

(AD-A283835) Avail: CASI HC A02/MF A01

An account is given of progress towards the measurements of absolute, ultra violet cross sections of NO2 during the ten-month period

10/1/93-7/31/94. The accomplishments include: (1) construction of an absorption cell; (2) construction of vacuum system; (3) the assembly of an optical system including focusing of a 6.65 m spectrograph; (4) obtaining high resolution photographic spectra of NO2 in absorption; and (5) the first measurements of cross sections of NO2 at 295 K. The high resolution absorption spectrum of NO2 has been obtained from National Research Council of Canada. The high resolution cross sections of NO2 at 295 K have been measured photoelectrically in the wavelength region 390-452 nm. No pressure dependency has been observed. The absolute cross section scale agrees with published values, but there are large wavelength shifts in earlier works. DTIC

N95-14403# Environmental Protection Agency, Research Triangle Park, NC. Air and Energy Engineering Research Lab.

FUZZY LOGIC MOTOR CONTROL FOR POLLUTION PREVENTION AND IMPROVED ENERGY EFFICIENCY Report, Oct. 1992 - Aug. 1993

Ronald J. Spiegel, P. J. Chappell, M. A. Maxwell, J. G. Cleland, and B. K. Bose Oct. 1993 13 p Presented at the Conference on Environmental Commerce, Chattanooga, TN, 17-20 Oct. 1993

(Grant EPA-R-818282-02)

(PB94-190865; EPA/600/A-94/118) Avail: CASI HC A03/MF A01

The paper discusses an EPA program investigating fuzzy logic motor control for improved pollution prevention and energy efficiency. Initial computer simulation and laboratory results have demonstrated that fuzzy logic energy optimizers can consistently improve motor operational efficiency over conventional adjustable-speed drive (ASD) operation. This is significant in terms of both potential U.S. pollution prevention and energy savings possibilities. The addition of a fuzzy logic energy optimizer microchip to an ASD is minimal in terms of cost because low-power microchips are very cheap when manufactured in volume. Thus, the energy savings and enhanced motor operation and lifespan should be regarded as almost free because the cost payback is potentially so short. NTIS

N95-15361# Lawrence Livermore National Lab., Livermore, CA.

INTEGRATED SCIENCE MODEL FOR ASSESSMENT OF CLIMATE CHANGE

A. K. Jain, D. J. Wuebbles, and H. S. Kheshgi Apr. 1994 19 p Presented at the Annual Meeting and Exhibition of the Air and Waste Management Association, Cincinnati, OH, 19-24 Jun. 1994

(Contract W-7405-eng-48)

(DE94-016363; UCRL-JC-116526-Rev-1; CONF-940632-10-Rev-1) Avail: CASI HC A03/MF A01

Past measurements show that greenhouse gas concentrations, many of which are affected by human related activities, are increasing in the atmosphere. There is wide consensus that this increase influences related activities, are increasing the earth's energy balance and concern that this will cause significant change in climate. Many different policies could be adopted in response to the prospects of greenhouse warming. Models are used by policy markers to analyze the range of possible policy options developed as a response to concerns about climate change. A fully integrated assessment model that spans the many aspects of climate change, including economics, energy options, effects of climate, and impacts of climate change, would be a useful tool. With this goal in mind, the science modules which estimate the effect of emissions of greenhouse gasses on global temperature and sea level are being developed. This is a report of the current characteristics and performance of an Integrated Science Model which consists of coupled modules for carbon cycle, atmospheric chemistry of other trace gases, radiative forcing by greenhouse gases, energy balance model for global temperature, and a model for sea level response. DOE

N95-15363# Pacific Northwest Lab., Richland, WA.

CLIMATOLOGICAL DATA SUMMARY 1993 WITH HISTORICAL DATA

D. J. Hoitink and K. W. Burk Jun. 1994 504 p

(Contract DE-AC06-76RL-01830)

(DE94-016624; PNL-9809) Avail: CASI HC A22/MF A04

This document presents the climatological data summary for calendar year 1993. It presents updated historical climatologies for temperature, wind, precipitation, and other miscellaneous meteorological parameters from the Hanford Meteorology Station (HMS) and Hanford Meteorological Monitoring Network. It also presents climatological normal and extreme values of temperature and precipitation for the HMS. Previous documents have included climatological data collected at the old Hanford Townsite, located approximately 10 miles east-northeast of the present HMS. The records for these two different sites have been frequently interchanged as if representing the same location. With the exception of Section 2.0, the remainder of this document uses data only from the HMS, with a period of record beginning December 7, 1944. DOE

N95-15364# Lawrence Livermore National Lab., Livermore, CA.

POINT BASED HYDRODYNAMICS APPLIED TO SHALLOW WATER EQUATIONS

P. Eltgroth May 1994 9 p

(Contract W-7405-eng-48)

(DE94-016629; UCRL-ID-117420) Avail: CASI HC A02/MF A01

Smoothed Particle Hydrodynamics (SPH) has proven useful for many problems of scientific interest. This report is concerned with a generalization to the SPH method which may be of value for problems such as climate modeling. The main objective of the work is to carry out the new formulation, called Point Interactive Physics and to compare results for PIP and standard finite difference techniques on a simple test problem. The basic SPH approach describes a system using a set of points. These points are not associated with a grid or mesh, as in most approaches. The individual points are each assigned a mass and move with the material velocity. Thus the original SPH method is Lagrangian. Properties of the system are expressed as sums over the sample points using a weighting function called a kernel function. For most problems, tile weighting function extends over a relatively short range, called the smoothing length. The Point Interacting Physics (PIP) approach also samples information at a set of points, and then uses kernel functions to infer physical properties everywhere. The points are not assigned fixed values of mass and they are allowed to undergo arbitrary physically reasonable motion. In this report, results will be presented for fixed points arranged irregularly over a spherical surface. Thus, this version of PIP will be applied in an Eulerian fashion. The basic reason for the Eulerian treatment is enhanced efficiency arising from the fixed geometric relationships among the points. After a brief description of the SPH and PIP methods, the PIP formulation will be compared to a normal finite difference approach for a simple shallow water advection test problem. It appears that accurate simulations can be accomplished, but that computational speed is comparable to that observed for other techniques. DOE

N95-15382# Research Triangle Inst., Research Triangle Park, NC.

TEST METHOD FOR THE MEASUREMENT OF METHANOL EMISSIONS FROM STATIONARY SOURCES

B. A. Pate, M. R. Peterson, R. K. M. Jayanty, and M. Jayanty May 1994 74 p See also PB93-222230

(Contract EPA-68-D1-0009)

(PB94-170297; EPA/600/R-94/080) Avail: CASI HC A04/MF A01

Methanol was designated under Title 3 of the Clean Air Act Amendments of 1990 as a pollutant to be regulated. A test method has been developed for the measurement of methanol emissions from stationary sources. The methanol sampling train (MST) consists of a glass-lined heated probe, two condensate knock-out traps, and three sorbent cartridges packed with Anasorb 747. The Anasorb samples were desorbed with a 1:1 mixture of carbon disulfide and N,N-dimethylformamide. All samples were analyzed by gas chromatography with flame ionization detection. Following laboratory testing, field tests of the MST and the National Council of the Paper Industry for Air and Stream Improvement (NCASI) sampling method for methanol were conducted at two pulp and paper mills. In accordance with EPA Method 301, two pairs of trains were run in parallel for six runs, collecting a total of 24 samples by each method. During each run, half of the trains were spiked with a known amount of methanol. The sampling location at the first test was an inlet vent to a softwood bleach plant scrubber where the methanol concentration was about 30 ppm. A second field test was conducted at the vent of a black liquor oxidation tank where the methanol concentration was about 350 ppm. Samples were shown to be stable for at least two weeks after collection. NTIS

N95-15389# Rijksinstituut voor Volksgezondheid en Milieuhygieene, Bilthoven (Netherlands).

FIELD INTERCOMPARISON WITH FIVE AUTOMATIC AMMONIA MONITORS

M. G. Mennen, B. G. vanElzakker, J. vanHellemond, G. P. Wyers, and R.

P. Otjes Jan. 1993 31 p Sponsored by Directorate-General for Environmental Protection
(PB94-192879; RIVM-223107002) Avail: CASI HC A03/MF A01

A field intercomparison with automatic ammonia monitors was held in Bilthoven, The Netherlands, for a period of two weeks. Six instruments were continuously and simultaneously operated to measure the ammonia concentration in ambient air. During the intercomparison these instruments were studied with respect to their performance and potential suitability as a monitor for the National Air Quality Monitoring Network (NAQMN) of the Netherlands. The instruments were a continuous-flow denuder, two thermodenuders, a commercial Differential Optical Absorption Spectrometry (DOAS) system of OPSIS, a photoacoustic monitor, and a (non-automatic) Annular Denuder System, used as a reference. With the latter method ammonium concentrations were also measured. NTIS

N95-15432# Pacific Northwest Lab., Richland, WA.
DEVELOPMENT AND ANALYSIS OF HIGH-ENERGY CORONA PROCESS FOR AIR PURIFICATION
W. O. Heath, S. E. Barlow, T. M. Bergsman, D. L. Lessor, T. M. Orlando, A. J. Peurrung, and R. R. Shah Jun. 1994 6 p Presented at the 1st International Conference on Advanced Oxidation Technologies for Water and Air Remediation, London, Ontario, 25-30 Jun. 1994
(Contract DE-AC06-76RL-01830)
(DE94-015207; PNL-SA-24432; CONF-9406143-1) Avail: CASI HC A02/MF A01

This paper gives an overview of the High-Energy Corona (HEC) technology being developed for treating air and other gas streams, summarizes results of an initial field test of the HEC process and follow-up laboratory experiments, and outlines the progress and approach toward better understanding of the underlying physical and chemical mechanisms to guide further development. The High-Energy Corona process uses high-voltage ac fields developed in a packed bed of dielectric pellets to form a nonequilibrium plasma in the void spaces between the pellets. The pellets refract the electric fields, creating extremely high field strengths capable of initiating electron-impact ionization of the air (and contaminants). The present-generation HEC device is a coaxial cylinder with an inner metal electrode, an outer tube made of glass, and dielectric pellets filling the annular gap. A metal foil or screen in contact with the outside surface of the tube serves as the ground electrode. The inner electrode is connected to a high-volume (25 to 30 kV) ac power supply operated at a fixed frequency of 60 Hz. The glass tube serves as the reaction vessel and as a dielectric barrier to inhibit direct charge transfer between electrodes. The gas to be treated is simply pulled through the packed bed where reactant species are produced and subsequent chemical reactions occur. Thus, far, the HEC process has been effective in destroying trichloroethylene, perchloroethylene, carbon tetrachloride, benzene, and heptane in the gas phase and naphthalene in the liquid phase. Further tests are planned with other compounds. DOE

N95-15455# EG and G Energy Measurements, Inc., Idaho Falls, ID.
RESULTS OF TSP METALS MONITORING AT MCMURDO STATION, ANTARCTICA
R. M. Lugar Apr. 1994 22 p
(Contract DE-AC07-76ID-01570)
(DE94-015264; EGG-CIET-11270) Avail: CASI HC A03/MF A01

This report presents the results of ambient air monitoring of metals in total suspended particulate (TSP) matter performed during the 1992-1993 austral summer at McMurdo Station, Antarctica. Seven samples of TSP were collected from three different locations and analyzed for arsenic, beryllium, cadmium, chromium, lead, nickel, and mercury. Critical-flow high-volume air samplers with a sample flow rate of approximately 1.1 cu m/minute were used to collect the particulate matter on quartz fiber filters for subsequent laboratory analysis. Sampling site selection, sampling procedures, and quality assurance procedures used were consistent with US Environmental Protection Agency guidance for local ambient air quality networks. The data indicate that McMurdo operations have a measurable impact on the qualitative toxic metals composition of suspended particulate matter in the ambient air; however a definitive quantitative impact could not be concluded. The levels measured are well below the US National Ambient Air Quality Standards and American Conference of Governmental Industrial Hygienists worker exposure levels. Lead was the most prevalent of the seven toxic metals and was detected in all samples at concentrations ranging from 1.4 ng/cu m to 38 ng/cu m. Data on the concentration of eleven other metal species are presented. Most notable was the relatively high abundance of titanium and copper, which were detectable at levels up to 2,100 ng/cu m and 230 ng/cu m, respectively. DOE

N95-15575# Sandia National Labs., Albuquerque, NM.
LARGE SCALE OBSCURATION AND RELATED CLIMATE EFFECTS OPEN LITERATURE BIBLIOGRAPHY
N. A. Russell, J. Geitgey, Y. K. Behl, and B. D. Zak May 1994 64 p
(Contract DE-AC04-94AL-85000)
(DE94-012992; SAND-92-2244) Avail: CASI HC A04/MF A01

Large scale obscuration and related climate effects of nuclear detonations first became a matter of concern in connection with the so-called 'Nuclear Winter Controversy' in the early 1980's. Since then, the world has changed. Nevertheless, concern remains about the atmospheric effects of nuclear detonations, but the source of concern has shifted. Now it focuses less on global, and more on regional effects and their resulting impacts on the performance of electro-optical and other defense-related systems. This bibliography reflects the modified interest. DOE

N95-15623 Boston Coll., Chestnut Hill, MA.
CHEMICAL KINETICS AND ATMOSPHERIC MODIFICATION Final Report, 31 Aug. 1989 - 31 Dec. 1993
David L. McFadden 1 May 1994 36 p Limited Reproducibility: More than 20% of this document may be affected by microfiche quality
(Contract F19628-89-K-0043)
(AD-A283304; PL-TR-94-2164; AD-E202153) Avail: CASI HC A03

Electron attachment rate constants were obtained and negative ion product analysis was performed over the temperature between 300 and 1200 degrees range for a series of seventeen halomethane molecules that undergo dissociative electron attachment. The reactant molecules include CH3Cl, CF2H2, CH3F, CF2HCl, CHFCl2, CH2Br2, CCl2H2, and CCl3H. Positive activation energies were observed for most of the reactions. The results of molecular structure calculations for both the neutral and anionic species suggest that the magnitude of the rate constants and of the temperature coefficients for dissociative electron attachment in these systems can be understood in terms of the geometrical reorganization associated with negative ion formation. DTIC

N95-15779# Lawrence Livermore National Lab., Livermore, CA.
PROGRESS REPORT ON TERRESTRIAL MODEL DEVELOPMENT (TERRA AND HABITAT): RESEARCH IN SUPPORT OF THE CERES EARTH SYSTEM MODELING PROJECT
J. R. Kercher, M. C. Axelrod, J. S. Amthor, and J. Q. Chambers May 1994 25 p
(Contract W-7405-eng-48)
(DE94-016362; UCRL-ID-116677) Avail: CASI HC A03/MF A01

Although there is only a developing understanding of the many processes affecting and coupling the atmosphere, oceans, and land systems of the earth, we are embarked on an effort to construct a prototype model (CERES) of the full Earth system. As part of this effort, we have proposed to the EPA to construct an Earth System Framework for the CERES model that supports flexible, modular development, coupling, and replacement of Earth System submodel components. This project has two specific areas of study. These areas are (1) the terrestrial contribution to the biogeochemical cycling and (2) the interactions of climate and the land ecosystems. The objectives of these two areas of study are: development of a globally distributed model of terrestrial ecosystem productivity, linking model to the submodels, using coupled system to explore biogeochemical cycles, exploration of greenhouse effect, development of models of surface, and the study of the dynamics of climate change and vegetation response. DOE

N95-15814 University of Western Washington, Bellingham, WA. Inst. of Environmental Toxicology and Chemistry.
DEVELOPMENT OF TECHNIQUES FOR THE EVALUATION OF TOXICANT IMPACTS TO MULTISPECIES SYSTEMS Final Report, 1 Jun. 1991 - 31 May 1994
Wayne G. Landis 31 May 1994 949 p Limited Reproducibility: More than 20% of this document may be affected by microfiche quality
(Grant AF-AFOSR-0291-91)

(AD-A284426; AFOSR-94-0524TR) Avail: Issuing Activity (Defense Technical Information Center (DTIC))

New methods of data analysis were applied to the analysis of multispecies toxicity tests using three complex toxicants. The water soluble fraction of the turbine fuels Jet-A, JP-4, and JP-8 have been examined as stressors for two microcosm protocols, the standardized aquatic microcosm (SAM) and the mixed flask culture (MFC). The SAM is a 3 L system inoculated with standard cultures of algae, zooplankton, bacteria, and protozoa. In contrast, the MFC is 1 L and is inoculated with a complex mixture of organisms derived from a natural source. Analysis of the organism counts and physical data were conducted using conventional and newly derived multivariate nonmetric clustering methods and computer visualization techniques. Several fundamental discoveries regarding the impacts of toxicants on ecological systems were made. The first is that recovery of an ecosystem in the sense that it returns to the original or reference state is not a property of these systems. In fact, it is unlikely that recovery is a property of other larger ecological systems. In our experiments the various treatment groups incorporated the information as to toxicant concentration that was expressed after periods of so-called recovery. The differentiation of the treatment groups occurred even after the elimination of the toxicant from the test system. Another fundamental discovery is that multispecies toxicity tests are not repeatable, although within one experiment the replicates of a treatment group are replicable. In other words, initial conditions are important. The outcome of this research may lead to a new viewpoint in describing the impacts of toxicants on complex ecological systems. This viewpoint is described as the community conditioning hypothesis. DTIC

N95-15847*# Denver Univ., Denver, CO. Dept. of Engineering.
COUNTING CONDENSATION IN THE ANTARCTIC OZONE MISSION Final Technical Report, 1 Apr. 1987 - 31 Dec. 1993
James Charles Wilson Nov. 1994 62 p Original contains color illustrations
(Grants NAG2-458; NAG2-31)
(NASA-CR-197113; NAS 1.26:197113) Avail: CASI HC A04/MF A01; 1 functional color page

The work done on this grant primarily concerns the measurement of aerosol in the stratosphere from NASA ER-2 aircraft in studies of stratospheric ozone depletion in the northern and southern hemispheres. The ER-2 Condensation Nucleus Counter (CNC) measures the number concentration of particles in the diameter range of approximately 0.01 to 1 micron. The Passive Cavity Aerosol Spectrometer measures size distributions in the 0.17 to 3 micron diameter range. This instrument was upgraded during this grant period to a Focused Cavity Aerosol Spectrometer (FCAS). This upgrade permitted the instrument to measure particles as small as 0.05 micron in diameter. The inlet for the PCAS and FCAS was modified and characterized under this grant so that the modifications to the aerosol due to anisokinetic sampling and heating upon sampling and in transport to the measurement location were accounted for in the data analysis. These measurements permitted observations of particle production in the southern hemisphere winter polar vortex and observation of the impact of denitrification on the number concentration of the aerosol in the denitrified air. In the northern polar vortex, the measurements provided a characterization of the sulfate aerosol. Following the eruption of Mount Pinatubo in 1991, the measurements permitted an accurate characterization of the sulfate aerosol enhancements resulting from the eruption. This led to studies of the impact of heterogeneous chemistry on the partitioning of the partitioning of the reactive nitrogen species and the partitioning of the chlorine reservoir. Author (revised)

N95-15864# Brookhaven National Lab., Upton, NY.
DEVELOPMENT AND TESTING OF A HIGH-RESOLUTION MODEL FOR TROPOSPHERIC SULFATE DRIVEN BY OBSERVATION-DERIVED METEOROLOGY
C. M. Benkovitz May 1994 287 p
(Contract DE-AC02-76CH-00016)
(DE94-014910; BNL-60535) Avail: CASI HC A13/MF A03

A high-resolution three-dimensional Eulerian transport and transformation model has been developed to simulate concentrations of tropospheric sulfate for specific times and locations; it was applied over the North Atlantic and adjacent continental regions during October and November, 1986. The model represents emissions of anthropogenic SO2 and sulfate and of biogenic sulfur species, horizontal and vertical transport, gas-phase oxidation of SO2 and dimethylsulfide, aqueous-phase oxidation of SO2, and wet and dry deposition of SO2, sulfate, and methanesulfonic acid (MSA). The meteorological driver is the 6-hour output from the forecast model of the European Centre for Medium-Range Weather Forecasts. Calculated sulfate concentrations and column burdens, examined in detail for October 15 and October 22 at 6Z, are related to existing weather patterns. These results exhibit rich temporal and spatial structure; the characteristic (1/e) temporal autocorrelation time for the sulfate column burdens over the central North Atlantic averages 20 hours; 95% of the values were 25 hours or less. The characteristic distance of spatial autocorrelation over this region depends on direction and averages 1,600 km; with 10(sup th) percentile value of 400 km and 90(sup th) percentile value of 1,700 km. Daily average model sulfate concentrations at the lowest vertical accurately represent the spatial variability, temporal episodicity, and absolute magnitudes of surface concentrations measured by monitoring stations in Europe, Canada and Barbados. DOE

N95-15870# Technische Univ., Delft (Netherlands).
PROCESS DEVELOPMENT OF THERMAL HYDRODECHLORINATION Ph.D. Thesis
A. J. B. tenKate 4 Oct. 1993 254 p Sponsored by Ministerie van Volkshuisvesting, Ruimtelijke Ordening en Milieubeheer, The Hague, Netherlands
(PB94-195518; ISBN-90-6275-911-4) Copyright Avail: CASI HC A12/MF A03

The properties that make chlorinated compounds so attractive during their economic lifetime are closely related to, if not similar to, the properties causing the environmental problems. A very promising method for proper chlorinated waste treatment is thermal hydrodechlorination. This process turns chlorinated waste into HCl, that might be recycled, and into organics which can used as a fuel. The objective of the study underlying this thesis is scaling up thermal hydrodechlorination to a waste destruction process at industrial scale. To get answers to the unknown two installations have been raised: a mini pilot plant, and a bench scale installation. NTIS

N95-14890*# BBN Systems and Technologies Corp., Canoga Park, CA.
DERIVING A DOSAGE-RESPONSE RELATIONSHIP FOR COMMUNITY RESPONSE TO HIGH-ENERGY IMPULSIVE NOISE
Sanford Fidell and Karl S. Pearsons *In* NASA. Langley Research Center, High-Speed Research: 1994 Sonic Boom Workshop: Atmospheric Propagation and Acceptability Studies Oct. 1994 p 185-192 (For primary document see N95-14878 03-02)
Avail: CASI HC A02/MF A03

46 GEOPHYSICS

Includes aeronomy; upper and lower atmosphere studies; ionospheric and magnetospheric physics; and geomagnetism.

For space radiation see *93 Space Radiation.*

N95-13627*# Smithsonian Astrophysical Observatory, Cambridge, MA.
MEASUREMENT AND INTERPRETATION OF CRUSTAL DEFORMATION RATES ASSOCIATED WITH POSTGLACIAL REBOUND Semiannual Status Report No. 5, 14 Mar. - 15 Sep. 1994
James L. Davis Oct. 1994 56 p
(Grants NAG5-1930; NAG5-538; NSF EAR-91-05502)
(NASA-CR-196440; NAS 1.26:196440) Avail: CASI HC A04/MF A01

Analysis of Global Positioning System (GPS) data from two sites separated by horizontal distance of only approximately 2.2 m yielded phase residuals exhibiting a systematic elevation angle dependence. One of the two GPS antennas was mounted on an approximately 1 m high concrete pillar, and the other was mounted on a standard wooden tripod. We performed elevation angle cutoff tests with these data, and established that the vertical coordinate of site position was sensitive to the minimum elevation angle (elevation cutoff) of the data analyzed. For example, the vertical coordinate of site position changed by 9.7 plus or minus 0.8 mm when the minimum elevation angle was increased from 10 to 25. We performed simulations based on a simple (ray tracing) multipath model with a single horizontal reflector, and demonstrated that the elevation angle cutoff test results and the pattern of the residual versus elevation angle could be qualitatively reproduced if the reflector were located 0.1-0.2 m

beneath the antenna phase center. We therefore, hypothesized that the source of the elevation-angle-dependent error were multipath reflections and scattering and that the horizontal surface of the pillar, located a distance of approximately 0.2 m beneath the antenna phase center, was the primary reflector. We tested this hypothesis by placing microwave absorbing material between the antenna and the pillar in a number of configurations and analyzed the changes in apparent position of the antenna. The results indicate that (1) the horizontal surface of the pillar is indeed the main reflector, (2) both the concrete and the metal plate embedded in the pillar are significant reflectors, and (3) the reflection can be reduced to a great degree by the use of microwave absorbing materials. These results have significant implications for the accuracy of global GPS geodetic tracking networks which use pillar-antenna configuration identical or similar to the one used here (at the Westford WFRD GPS site). Author

N95-13818*# SRI International Corp., Menlo Park, CA.
STUDY OF AURORAL DYNAMICS WITH COMBINED SPACECRAFT AND INCOHERENT SCATTER RADAR DATA Final Report
Jeffrey P. Thayer, Odile delaBeaujardiere, and Jurgen Watermann Sep. 1994 33 p Original contains color illustrations
(Contract NASw-4063; SRI Proj. 2781)
(NASA-CR-196974; NAS 1.26:196974) Avail: CASI HC A03/MF A01; 1 functional color page

The objectives of this project were to study the coupling between the ionosphere and the magnetosphere, and to understand how this coupling was affected by changes in the solar wind. The data used consisted of satellite measurements coordinated with Sondrestrom incoherent scatter radar observations. We focused our efforts on the study of temporal and spatial changes in the dayside auroral precipitation and electric field. Author

N95-13974 National Oceanic and Atmospheric Administration, Boulder, CO. Aeronomy Lab.
ANALYSIS OF DEEP CONVECTIVE CLOUDS AND THEIR ASSOCIATION WITH NON-MIGRATING ATMOSPHERIC DIURNAL TIDES IN THE TROPICAL TROPOSPHERE
C. R. Williams May 1994 204 p Limited Reproducibility: More than 20% of this document may be affected by microfiche quality
(PB94-187457; NOAA-TM-ERL-AL-13) Avail: CASI HC A10

The diurnal oscillating tropospheric winds measured by 50 MHz wind profilers located in the tropical Pacific are compared with the tidal winds produced form an f-plane equivalent gravity wave tidal model forced by water vapor solar radiation absorption. The differences between observations and model can not be explained using classical tidal theory with migrating tidal forcing functions. Therefore, the global distribution of latent heat released by diurnal oscillating deep convective clouds is investigated as a possible forcing of the non-migrating atmospheric diurnal tides in the tropical troposphere. The inclusion of non-migrating tidal forcing from the global distribution of latent heat released by deep convective clouds can explain some of the differences between the observed diurnal winds across the Pacific as well as discrepancies between observations and current tidal models. NTIS

N95-13995# Los Alamos National Lab., NM.
AN OBSERVATIONAL TEST OF MAGNETOSPHERIC FIELD MODELS AT GEOSYNCHRONOUS ORBIT
M. F. Thomsen, L. A. Weiss, D. J. McComas, M. B. Moldwin, and G. D. Reeves 1994 5 p Presented at the 8th International Symposium on Solar Terrestrial Physics, Sendai, Japan, 6-10 Jun. 1994
(Contract W-7405-eng-36)
(DE94-014462; LA-UR-94-2130; CONF-9406192-1) Avail: CASI HC A01/MF A01

The configuration of the geomagnetic field is an indicator of the response of the magnetosphere to the solar wind input. A number of empirical magnetospheric field models are currently in use which estimate the magnetic field direction and magnitude at any point within the magnetosphere under a variety of conditions. Here, the global nature of the Tsyganenko 89 magnetospheric magnetic field model is tested by comparison of the model-predicted field orientations with the field orientations derived simultaneously at two different locations in geosynchronous orbit from the axis of symmetry of the plasma electron distribution function (30 eV - 40 keV). The results for the particular time interval studied are inconclusive because the Tsyganenko 89 model does not describe the field at one of the satellites well enough, but the procedure itself appears promising. DOE

N95-14267*# Purdue Univ., West Lafayette, IN. Dept. of Earth and Atmospheric Sciences.
TOWARDS DEVELOPING AN ANALYTICAL PROCEDURE OF DEFINING THE EQUATORIAL ELECTROJET FOR CORRECTING SATELLITE MAGNETIC ANOMALY DATA Final Report, 1 Jul. 1989 - 31 Oct. 1991
Dhananjay Ravat and William J. Hinze Nov. 1991 45 p
(Grant NAGw-1819)
(NASA-CR-193621; NAS 1.26:193621) Avail: CASI HC A03/MF A01

Analysis of the total magnetic intensity MAGSAT data has identified and characterized the variability of ionospheric current effects as reflected in the geomagnetic field as a function of longitude, elevation, and time (daily as well as monthly variations). This analysis verifies previous observations in POGO data and provides important boundary conditions for theoretical studies of ionospheric currents. Furthermore, the observations have led to a procedure to remove these temporal perturbations from lithospheric MAGSAT magnetic anomaly data based on 'along-the-dip-latitude' averages from dawn and dusk data sets grouped according to longitudes, time (months), and elevation. Using this method, high-resolution lithospheric magnetic anomaly maps have been prepared of the earth over a plus or minus 50 deg latitude band. These maps have proven useful in the study of the structures, nature, and processes of the lithosphere. Author (revised)

N95-14274*# National Aeronautics and Space Administration. Goddard Space Flight Center, Greenbelt, MD.
SATELLITE LASER RANGING IN THE 1990S: REPORT OF THE 1994 BELMONT WORKSHOP
John J. Degnan, ed. Washington Nov. 1994 110 p Workshop held in Elkridge, MD, 1-2 Feb. 1994
(RTOP 920-00-00)
(NASA-CP-3283; Rept-95B00003; NAS 1.55:3283) Avail: CASI HC A06/MF A02

An international network of 43 stations in 30 countries routinely collects satellite ranging data which is used to study the solid Earth and its interactions with the oceans, atmosphere, and Moon. Data products include centimeter accuracy site positions on a global scale, tectonic plate motions, regional crustal deformation, long wavelength gravity field and geoid, polar motion, and variations in the Earth's spin rate. By calibrating and providing precise orbits for spaceborne microwave altimeters, satellite laser ranging also enables global measurement of sea and ice surface topography, mean sea level, global ocean circulation, and short wavelength gravity fields and marine geoids. It provides tests of general relativity and a means or subnanosecond time transfer. This workshop was convened to define future roles and directions in satellite laser ranging. For individual titles, see N95-14275 through N95-14289.

N95-14275*# National Aeronautics and Space Administration. Goddard Space Flight Center, Greenbelt, MD.
SCIENTIFIC ANALYSIS OF SATELLITE RANGING DATA **c43**
David E. Smith *In its* Satellite Laser Ranging in the 1990s: Report of the 1994 Belmont Workshop Nov. 1994 p 15-25 (For primary document see N95-14274 03-46)
Avail: CASI HC A03/MF A02

A network of satellite laser ranging (SLR) tracking systems with continuously improving accuracies is challenging the modelling capabilities of analysts worldwide. Various data analysis techniques have yielded many advances in the development of orbit, instrument and Earth models. The direct measurement of the distance to the satellite provided by the laser ranges has given us a simple metric which links the results obtained by diverse approaches. Different groups have used SLR data, often in combination with observations from other space geodetic techniques, to improve models of the static geopotential, the solid Earth, ocean tides, and atmospheric drag models for low Earth satellites. Radiation pressure models and other non-conservative forces for satellite orbits above the atmosphere have been developed to exploit the full accuracy of the latest SLR instruments. SLR is the baseline tracking system for the altimeter missions TOPEX/Poseidon, and ERS-1 and will play an important role in providing the reference frame for locating the geocentric position of the

ocean surface, in providing an unchanging range standard for altimeter calibration, and for improving the geoid models to separate gravitational from ocean circulation signals seen in the sea surface. However, even with the many improvements in the models used to support the orbital analysis of laser observations, there remain systematic effects which limit the full exploitation of SLR accuracy today. Author (revised)

N95-14276*# National Aeronautics and Space Administration. Goddard Space Flight Center, Greenbelt, MD.

GLOBAL REFERENCE FRAME: INTERCOMPARISON OF RESULTS (SLR, VLBI AND GPS)

Chopo Ma, Michael M. Watkins, and M. Heflin *In its* Satellite Laser Ranging in the 1990s: Report of the 1994 Belmont Workshop Nov. 1994 p 27-31 (For primary document see N95-14274 03-46)

Avail: CASI HC A01/MF A02

The terrestrial reference frame (TRF) is realized by a set of positions and velocities derived from a combination of the three space geodetic techniques, SLR, VLBI and GPS. The standard International TRF is constructed by the International Earth Rotation Service in such a way that it is stable with time and the addition of new data. An adopted model for overall plate motion, NUVEL-1 NNR, defines the conceptual reference frame in which all the plates are moving. In addition to the measurements made between reference points within the space geodetic instruments, it is essential to have accurate, documented eccentricity measurements from the instrument reference points to ground monuments. Proper local surveys between the set of ground monuments at a site are also critical for the use of the space geodetic results. Eccentricities and local surveys are, in fact, the most common and vexing sources of error in the use of the TRF for such activities as collocation and intercomparison. Author (revised)

N95-14277*# National Aeronautics and Space Administration. Goddard Space Flight Center, Greenbelt, MD.

MEASURING TEMPORAL GRAVITATIONAL VARIATIONS USING SLR DATA

Robert S. Nerem *In its* Satellite Laser Ranging in the 1990s: Report of the 1994 Belmont Workshop Nov. 1994 p 33-38 (For primary document see N95-14274 03-46)

Avail: CASI HC A02/MF A02

Redistribution of mass within the Earth system changes its gravitational field, and thus changes the orbits of Earth satellites. While these variations are small, Satellite Laser Ranging (SLR) to precise geodetic satellites such as Lageos-1, Lageos-2, Starlette, Ajisai, and Stella can detect these changes at their broadest spatial scales (currently greater than 10,000 km). The satellites sense only the combined variation in the solid Earth-ocean-atmosphere system; however, modeling of these different components has led to detection of long-wavelength variations in the distribution of atmospheric mass, changes in the amplitudes of atmospheric and oceanic tides, and secular variations caused by the post-glacial adjustment of the Earth's crust. The unambiguous detection of ocean mass redistribution by SLR has not been verified due largely to inadequacies in current ocean models. Great progress has been made in recent years in the determination of luni-solar tides and the braking they induce in the Earth-Moon-Sun system (leading to secular changes in the length-to-day and lengthening of the lunar orbit period) using a wide variety of techniques including ocean tide gauges, satellite altimetry, Lunar Laser Ranging, and near-Earth satellite orbit modeling. Recent investigations of the more complex and less predictable non-tidal temporal variations in the gravity field have generally proceeded along two fronts: 1) the determination of long-wavelength variations in the gravity field through the changing perturbations seen in the orbits of near-Earth satellites, and 2) the prediction of temporal variations in gravity using geophysical, atmospheric, and oceanic models. A convergence of these efforts is sought to better understand the source of observed changes in the Earth's gravitational field. Author

N95-14278*# Hughes STX, Inc., Greenbelt, MD.

GLOBAL AND REGIONAL KINEMATICS FROM SLR STATIONS

Peter J. Dunn *In* NASA. Goddard Space Flight Center, Satellite Laser Ranging in the 1990s: Report of the 1994 Belmont Workshop Nov. 1994 p 39-46 (For primary document see N95-14274 03-46)

Avail: CASI HC A02/MF A02

The stations of the Global Laser Tracking Network have significantly contributed to the measurement of plate kinematics. The expanding network of progressively improved instruments clearly demonstrates the systems' centimeter positioning accuracy. Several satellite laser ranging (SLR) analysis groups have adopted techniques to distill geodynamic information from the Lageos-1 satellite observations using orbital arc lengths from an hour to a decade. SLR observations now provide the scale for the International Terrestrial Reference System and help to define the Earth's polar motion in this system. Agreement between positions separately determined with SLR, VLBI and GPS systems has been established at the level of a few centimeters in position and a few millimeters per year in horizontal velocity. Derived from text

N95-14279*# Massachusetts Inst. of Tech., Cambridge.

GLOBAL AND REGIONAL KINEMATICS WITH GPS

Robert W. King *In* NASA. Goddard Space Flight Center, Satellite Laser Ranging in the 1990s: Report of the 1994 Belmont Workshop Nov. 1994 p 47-54 (For primary document see N95-14274 03-46)

Avail: CASI HC A02/MF A02

The inherent precision of the doubly differenced phase measurement and the low cost of instrumentation made GPS the space geodetic technique of choice for regional surveys as soon as the constellation reached acceptable geometry in the area of interest: 1985 in western North America, the early 1990's in most of the world. Instrument and site-related errors for horizontal positioning are usually less than 3 mm, so that the dominant source of error is uncertainty in the reference frame defined by the satellites orbits and the tracking stations used to determine them. Prior to about 1992, when the tracking network for most experiments was globally sparse, the number of fiducial sites or the level at which they could be tied to an SLR or VLBI reference frame usually, set the accuracy limit. Recently, with a global network of over 30 stations, the limit is set more often by deficiencies in models for non-gravitational forces acting on the satellites. For regional networks in the northern hemisphere, reference frame errors are currently about 3 parts per billion (ppb) in horizontal position, allowing centimeter-level accuracies over intercontinental distances and less than 1 mm for a 100 km baseline. The accuracy of GPS measurements for monitoring height variations is generally 2-3 times worse than for horizontal motions. As for VLBI, the primary source of error is unmodeled fluctuations in atmospheric water vapor, but both reference frame uncertainties and some instrument errors are more serious for vertical than horizontal measurements. Under good conditions, daily repeatabilities at the level of 10 mm rms were achieved. This paper will summarize the current accuracy of GPS measurements and their implication for the use of SLR to study regional kinematics. Author (revised)

N95-14280*# National Aeronautics and Space Administration. Goddard Space Flight Center, Greenbelt, MD.

GLOBAL AND REGIONAL KINEMATICS WITH VLBI

Chopo Ma *In its* Satellite Laser Ranging in the 1990s: Report of the 1994 Belmont Workshop Nov. 1994 p 55-59 (For primary document see N95-14274 03-46)

Avail: CASI HC A01/MF A02

Since a VLBI station cannot operate in isolation and since simultaneous operation of the entire VLBI network is impractical, it is necessary to design observing programs with periodic observing sessions using networks of 3-7 stations that, when treated together, will have the necessary interstation data and network overlaps to determine the desired rates of change. Thus, there has been a mix of global, intercontinental, transcontinental, and regional networks to make measurements ranging from plate motions to deformation over a few hundred km. Over time, even networks focusing on regional deformation using mobile VLBI included large stations removed by several thousand km to increase sensitivity, determine EOP more accurately, and provide better ties to the terrestrial reference frame (TRF). Analysis products have also evolved, beginning with baseline components, and then to full three-dimensional site velocities in a global TRF. Author (revised)

N95-14281*# Texas Univ., Austin, TX. Center for Space Research.

EARTH ORIENTATION PARAMETERS

Richard J. Eanes *In* NASA. Goddard Space Flight Center, Satellite Laser Ranging in the 1990s: Report of the 1994 Belmont Workshop Nov. 1994 p 61-63 (For primary document see N95-14274 03-46)

Avail: CASI HC A01/MF A02

Since the beginning of regular space geodetic measurements, Satellite

Laser Ranging (SLR) has routinely provided polar motion and length of day solutions. At the present time, Global Positioning Systems (GPS) regularly produces daily polar motion solutions with 0.4 mas accuracy, equivalent to the routine 1-day VLBI experiments and SLR solutions using 3 days of Lageos-1 data. This rapid progress of the GPS technique forces a review of any resource allocations for VLBI and SLR measurements of Earth orientation. Derived from text

N95-14282*# Texas Univ., Austin, TX. Center for Space Research.
PRECISION ORBIT DETERMINATION OF ALTIMETRIC SATELLITES **c13**

C. K. Shum, John C. Ries, and Byron D. Tapley *In* NASA. Goddard Space Flight Center, Satellite Laser Ranging in the 1990s: Report of the 1994 Belmont Workshop Nov. 1994 p 65-70 (For primary document see N95-14274 03-46)
Avail: CASI HC A02/MF A02

The ability to determine accurate global sea level variations is important to both detection and understanding of changes in climate patterns. Sea level variability occurs over a wide spectrum of temporal and spatial scales, and precise global measurements are only recently possible with the advent of spaceborne satellite radar altimetry missions. One of the inherent requirements for accurate determination of absolute sea surface topography is that the altimetric satellite orbits be computed with sub-decimeter accuracy within a well defined terrestrial reference frame. SLR tracking in support of precision orbit determination of altimetric satellites is significant. Recent examples are the use of SLR as the primary tracking systems for TOPEX/Poseidon and for ERS-1 precision orbit determination. The current radial orbit accuracy for TOPEX/Poseidon is estimated to be around 3-4 cm, with geographically correlated orbit errors around 2 cm. The significance of the SLR tracking system is its ability to allow altimetric satellites to obtain absolute sea level measurements and thereby provide a link to other altimetry measurement systems for long-term sea level studies. SLR tracking allows the production of precise orbits which are well centered in an accurate terrestrial reference frame. With proper calibration of the radar altimeter, these precise orbits, along with the altimeter measurements, provide long term absolute sea level measurements. The U.S. Navy's Geosat mission is equipped with only Doppler beacons and lacks laser retroreflectors. However, its orbits, and even the Geosat orbits computed using the available full 40-station Tranet tracking network, yield orbits with significant north-south shifts with respect to the IERS terrestrial reference frame. The resulting Geosat sea surface topography will be tilted accordingly, making interpretation of long-term sea level variability studies difficult. Author (revised)

N95-14283*# Hughes STX, Inc., Greenbelt, MD.
RADAR ALTIMETER CALIBRATION USING SLR **c32**

Steven M. Klosko *In* NASA. Goddard Space Flight Center, Satellite Laser Ranging in the 1990s: Report of the 1994 Belmont Workshop Nov. 1994 p 71-76 (For primary document see N95-14274 03-46)
Avail: CASI HC A02/MF A02

Clearly a calibration of the TOPEX altimeter (and future TOPEX-class altimeters) which is more accurate and better prepared to meet the demands of global sea level trend monitoring is warranted. TOPEX/Posideon (T/P) is in its second year of data acquisition. If it survives or surpasses the two to five year projected baseline, an unprecedented opportunity for monitoring global sea level trends at mm/y levels will have been lost due to insufficient accuracy in its altimeter calibration. It is therefore paramount to revisit the design of the T/P calibration experiment and implement a more direct approach which better utilizes the accuracy of SLR to perform this needed bias assessment. Author (revised)

N95-14284*# Texas Univ., Austin, TX. Center for Space Research.
THE ROLE OF SLR AND LLR IN RELATIVITY **c77**

John C. Ries *In* NASA. Goddard Space Flight Center, Satellite Laser Ranging in the 1990s: Report of the 1994 Belmont Workshop Nov. 1994 p 77-79 (For primary document see N95-14274 03-46)
Avail: CASI HC A01/MF A02

While General Relativity has been adopted as the standard theory of relativity, there are alternative theories, with important implications for gravitational physics, which can only be discounted with tests of sufficient accuracy. In addition to its contributions to lunar and solar system dynamics, Lunar Laser Ranging, in combination with other solar system data continues to refine some important limits. Satellite laser ranging tracking of geodetic satellites can provide similar tests, but the accuracy is usually limited by gravitational and nongravitational perturbations. Derived from text

N95-14285*# Maryland Univ., College Park, MD.
SLR TRACKING OF GPS-35 **c32**

Erricos C. Pavlis *In* NASA. Goddard Space Flight Center, Satellite Laser Ranging in the 1990s: Report of the 1994 Belmont Workshop Nov. 1994 p 81-84 (For primary document see N95-14274 03-46)
Avail: CASI HC A01/MF A02

An experiment was designed to launch a corner cube retroreflector array on one of the Global Positioning Satellites (GPS). The launch on Aug. 31, 1993 ushered in the era of SLR tracking of GPS spacecraft. Once the space operations group finished the check-out procedures for the new satellite, the agreed upon SLR sites were allowed to track it. The first site to acquire GPS-35 was the Russian system at Maidanak and closely after the MLRS system at McDonald Observatory, Texas. The laser tracking network is currently tracking the GPS spacecraft known as GPS-35 or PRN 5 with great success. From the NASA side there are five stations that contribute data regularly and nearly as many from the international partners. Upcoming modifications to the ground receivers will allow for a further increase in the tracking capabilities of several additional sites and add some desperately needed southern hemisphere tracking. We are analyzing the data and are comparing SLR-derived orbits to those determined on the basis of GPS radiometric data. Author (revised)

N95-14286*# Texas Univ., Austin, TX. Center for Space Research.
SYNERGISM OF SLR AND GPS **c32**

Bob E. Schutz *In* NASA. Goddard Space Flight Center, Satellite Laser Ranging in the 1990s: Report of the 1994 Belmont Workshop Nov. 1994 p 85-86 (For primary document see N95-14274 03-46)
Avail: CASI HC A01/MF A02

The launch of GPS-35 (RPN 5) with a laser retroreflector has provided an opportunity to compare SLR-determined orbits of a GPS satellite with those determined by GPS receivers operated with the transmitted radio signals on the L(sub 1) and L(sub 2) frequencies. Operational considerations of the SLR and hardware design have influenced the amount and quality of SLR data collected on this satellite. As of February 1, 1994, all of the collected SLR data have been collected from northern hemisphere stations. Adequate southern hemisphere coverage is required to fully compare the results obtained from L(sub 1)/L(sub 2) and from SLR. Author

N95-14287*# Smithsonian Astrophysical Observatory, Cambridge, MA.
SATELLITE LASER RANGING OPERATIONS **c36**

Michael R. Pearlman *In* NASA. Goddard Space Flight Center, Satellite Laser Ranging in the 1990s: Report of the 1994 Belmont Workshop Nov. 1994 p 89-99 (For primary document see N95-14274 03-46)
Avail: CASI HC A03/MF A02

Satellite Laser Ranging (SLR) is currently providing precision orbit determination for measurements of: 1) Ocean surface topography from satellite borne radar altimetry, 2) Spatial and temporal variations of the gravity field, 3) Earth and ocean tides, 4) Plate tectonic and regional deformation, 5) Post-glacial uplift and subsidence, 6) Variations in the Earth's center-of-mass, and 7) Variations in Earth rotation. SLR also supports specialized programs in time transfer and classical geodetic positioning, and will soon provide precision ranging to support experiments in relativity. Author

N95-14288*# National Aeronautics and Space Administration. Goddard Space Flight Center, Greenbelt, MD.
SLR 2000 **c32**

John J. Degnan *In its* Satellite Laser Ranging in the 1990s: Report of the 1994 Belmont Workshop Nov. 1994 p 101-106 (For primary document see N95-14274 03-46)
Avail: CASI HC A02/MF A02

SLR 2000 is a concept for a totally automated subcentimeter SLR system presently being studied at GSFC. If funding permits, a prototype would be installed and tested at the Goddard Geophysical and Astronomical Observatory (GCAO) in FY98 and a small number of automated stations would be fielded by the year 2000. Unlike present systems, the 'SLR 2000' system is being designed to: 1) operate autonomously without the need for onsite operators; 2) present no hazards (i.e., optical, electrical,

and/or chemical) to personnel in the vicinity or to overflying aircraft; and 3) have a mean time between failures (MTBF) of at least three months. It is assumed that the systems are located at 'friendly' sites where some level of security is provided and where certain low level service functions (e.g. commercial power, communications, heat pump service cleaning, etc.) are available or can be contracted for locally on an as-needed basis. The main system consists of two parts - an optical head and electronics rack. The optical head contains the laser transmitter and power supply, transmit/receive switch, optical telescope, tracking angle sensor (intensified CCD camera), detector and power supply, two angular encoders, azimuth and elevation motors, and a protective dome. The optical head mounts directly to the top of a concrete pier which contains the geodetic monument and forms part of the environmental housing for the hardware and servicing personnel. It is equipped with electronic levels for leveling the mount and monitoring its stability. Author

N95-14289*# National Aeronautics and Space Administration. Goddard Space Flight Center, Greenbelt, MD.
A STRAWMAN SLR PROGRAM PLAN FOR THE 1990S c32
John J. Degnan *In its* Satellite Laser Ranging in the 1990s: Report of the 1994 Belmont Workshop Nov. 1994 p 107-114 (For primary document see N95-14274 03-46)
Avail: CASI HC A02/MF A02

A series of programmatic and technical goals for the satellite laser ranging (SLR) network are presented. They are: (1) standardize the performance of the global SLR network; (2) improve the geographic distribution of stations; (3) reduce costs of field operations and data processing; (4) expand the 24 hour temporal coverage to better serve the growing constellation of satellites; (5) improve absolute range accuracy to 2 mm at key stations; (6) improve satellite force, radiative propagation, and station motion models and investigate alternative geodetic analysis techniques; (7) support technical intercomparison and the Terrestrial Reference Frame through global collocations; (8) investigate potential synergisms between GPS and SLR. Derived from text

N95-14404 Environmental Protection Agency, Research Triangle Park, NC. Atmospheric Research and Exposure Assessment Lab.
PC-BASED MIE SCATTERING PROGRAM FOR THEORETICAL INVESTIGATIONS OF THE OPTICAL PROPERTIES OF ATMOSPHERIC AEROSOLS AS A FUNCTION OF COMPOSITION AND RELATIVE HUMIDITY
William E. Wilson and Parker C. Reist 1994 10 p Repr. from Atmosheric Environment (England, Elsevier Science Ltd.), v. 28, no. 5, 1994 p 803-809
(PB94-192739; EPA/600/J-94/306) Copyright Avail: Issuing Activity (National Technical Information Service (NTIS))

Over the past decade there has been interest in exploring possible relationships between atmospheric visibility (extinction of light) and the chemical form of aerosols in the atmosphere. A user-friendly, menu-driven program for the personal computer (AT 286 with math coprocessor or higher) has been developed which both calculates the equilibrium composition of the atmospheric aerosol of specified compositions (including particle-bound water as a function of relative humidity) and also applies optical parameters from these end-products to estimating scattering and extinction. Presented here is a description of such a program, with a discussion of the assumptions and approaches implicit in it. The program appears to give results which are similar to results reported by others. NTIS

N95-14428# Pacific Northwest Lab., Richland, WA.
AN EXPERIMENTAL AND NUMERICAL STUDY OF THE MODIFICATIONS OF MIXED-LAYER STRUCTURE BY INHOMOGENEOUS SURFACE FLUXES AND SECONDARY CIRCULATIONS
S. Zhong and J. C. Doran Jul. 1994 5 p Presented at the 6th Conference on Mesoscale Processes, Portland, OR, 18-22 Jul. 1994
(Contract DE-AC06-76RL-01830)
(DE94-015945; PNL-SA-23559; CONF-940769-6) Avail: CASI HC A01/MF A01

The problem of scale interactions in the planetary boundary layer (PBL), i.e., how forcing mechanisms of differing spatial and temporal scales affect the properties of the PBL, has been a subject of considerable interest for some time. One aspect of this problem that has received increasing attention in recent years is the representation in mesoscale and general circulation models of the effects of subgrid-scale inhomogeneities in surface properties. Differences in sensible and latent heat fluxes between adjacent areas can result in secondary circulations, modifications to the boundary layer structure, and the transport of heat and moisture from one area to another. Despite their potential included on local PBL properties, such effects can not be resolved by numerical models whose scale is too coarse; thus, suitable parameterizations that account for these phenomena are needed. In this paper the authors present some results of wind and temperature measurements over an area with significant variations in surface fluxes on scales of O(10 km). They then use fine resolution numerical simulations to show how synoptic, topographical, and thermal forcing combine to affect the properties of the PBL in the region. Specifically, they consider the relative importance of topography and land-use differences on the generation of secondary circulations and on the depth of the mixed layer, and they show how these effects are modified by synoptic wind fields. Implications for coarser resolution models are also discussed. DOE

N95-14434# Los Alamos National Lab., NM. CST Div.
THE 226RA AND 231PA SYSTEMATICS OF AXIAL, MORB, CRUSTAL RESIDENCE AGES, AND MAGMA CHAMBER CHARACTERISTICS AT 9 TO 10 DEGREE N EAST PACIFIC RISE
S. J. Goldstein, M. T. Murrell, M. R. Perfit, R. Batiza, and D. J. Fornari 1994 4 p Presented at the VM Goldschmidt Conference, Edinburgh, England, 29 Aug. - 2 Sep. 1994
(Contract W-7405-eng-36)
(DE94-013084; LA-UR-94-1668; CONF-9408102-1) Avail: CASI HC A01/MF A01

Mass spectrometric measurements of (230)Th-(226)Ra and (235)U-(231)Pa disequilibria for axial basalts are used to determine crustal residence ages for MORB magma and investigate the temporal and spatial characteristics of axial magma chambers (AMC) at 9-10 degrees N East Pacific Rise (EPR). Relative crustal residence ages can be calculated from variations in (226)Ra/(230)Th and (231)Pa/(235)U activity ratios for axial lavas, if (1) mantle sources and melting are uniform, and mantle transfer times are constant or rapid for axial N-MORB, and (2) (231)Pa/(235)U and (226)Ra/(230)Th in the melt are unaffected by shallow level fractional crystallization. Uniform Th, Sr, and Nd isotopic systematics and incompatible element ratios for N-MORB along the 9-10 degrees N segment indicate that mantle sources and transfer times are similar. In addition, estimated bulk solid/melt partition coefficients for U, Th, and Pa are small, hence effects of fractional crystallization on (231)Pa/(235)U ratios for the melt are expected to be negligible. However, fractional crystallization of plagioclase in the AMC would lower (226)Ra/(230)Th ratios in the melt and produce a positive bias in (226)Ra crustal residence ages for fractionated lavas. DOE

N95-14436# Lawrence Livermore National Lab., Livermore, CA.
LITHOLOGICAL AND RHEOLOGICAL CONSTRAINTS ON FAULT RUPTURE SCENARIOS FOR GROUND MOTION HAZARD PREDICTION
L. Hutchings and W. Foxall 18 Apr. 1994 4 p Presented at the International Union of Theoretical and Applied Mechanics Symposium on Mechanics Problems in Geodynamics, Beijing, China, 5-9 Sep. 1994
(Contract W-7405-eng-48)
(DE94-014742; UCRL-JC-116437; CONF-9409167-1) Avail: CASI HC A01/MF A01

This paper tests an approach to predict the range of ground motion hazard at specific sites generated by earthquakes on specific faults. The approach is based upon structural, lithological and rheological descriptions of the fault zones, development of fault rupture scenarios, and computation of synthetic seismograms using empirical Green's functions. Faults are placed within a regional geomechanical model. The approach is based upon three hypothesis: (1) An exact solution of the representation relation that utilizes empirical Green's functions enables very accurate computation of ground motions generated by a given rupture; (2) a general description of the rupture is sufficient; and (3) the structural, lithological and theological characteristics of a fault can be used to constrain, in advance, possible future rupture histories. Ground motion hazard here refers to three-component, full wave train descriptions of displacement, velocity, and acceleration over the frequency band 0.01 to 25 Hz. Corollaries to these hypotheses are that the range of possible fault rupture histories is narrow

enough to functionally constrain the range of strong ground motion predictions, and that a discreet set of rupture histories is sufficient to span the infinite combinations possible from a given range of rupture parameters. DOE

N95-14598# Lamont-Doherty Geological Observatory, Palisades, NY.
SATELLITE IMAGERY AND TOPOGRAPHIC DATA IN VERIFICATION Final Report, 17 Apr. 1989 - 30 Jun. 1992
David Simpson and Arthur Lerner-Lam 28 Sep. 1993 127 p
(Contract F19628-89-K-0007)
(AD-A280950; PL-TR-93-2211; AD-E201980) Avail: CASI HC A07/MF A02

Analysis procedures, hardware platforms, and software systems for the analysis of digital topographic data, satellite images, and generic time series have been developed. These have been implemented in a distributed processing environment on commonly available platforms and are available over Internet. Our imaging analysis methodologies have been applied to the southern border regions of the former Soviet Union. This area contains some of the most interesting tectonics on the planet and until recently has been relatively inaccessible to modern field programs. We demonstrate how views of available digital data sets can be combined to yield new insight and overviews of tectonic setting. A spatial- and time-domain deconvolution methodology based on inverse theory, which offers the advantage of adaptation to noisy data and incorporation of scientific constraints, has been developed. It is applied to the problem of singular deconvolution of noisy time series as an example. DTIC

N95-14836 New Energy and Industrial Technology Development Organization, Tokyo (Japan).
SURVEY OF THE 1991 GEOTHERMAL EXPLORATION PROMOTION
Mar. 1993 358 p Limited Reproducibility: More than 20% of this document may be affected by microfiche quality
(DE94-780690; ETDE/JP-MF-94780690) Avail: Issuing Activity (Department of Energy (DOE))

The paper reports development of a geothermal reservoir evaluation method. This method includes development of a simulator, a model field survey and simulation. Simulators to be developed are a geothermal reservoir simulator (SING) and a geothermal well two-phase flow simulator (WENG). The following are conducted for SING-III: improvement/problem analysis of the simulator, exercise analysis of the tracer analytical function, arrangement of the graphic output feature. As to WENG, simulator development is made based on a modeling of the fluid including NaCl. A model field survey based on the development of this method is made. In the Mori area, made is a geothermal reservoir concept model which well reproduces the natural condition. From the simulation conducted using this model, it is confirmed that the pressure history is well reproduced. In the Oguni area, a geothermal reservoir concept model is also made and used for simulation. The simulation confirms that the natural condition is well reproduced and that the obtained pressure interference data agree with the measured data. DOE

N95-14855*# Denver Univ., Denver, CO. Dept. of Engineering.
CONDENSATION NUCLEI MEASUREMENT IN THE STRATOSPHERE FOR THE NASA ACE PROGRAM Final Report, 1 Feb. 1980 - 31 Jan. 1987
James Charles Wilson 3 Nov. 1994 14 p
(Grant NAG2-31)
(NASA-CR-197031; NAS 1.26:197031) Avail: CASI HC A03/MF A01

A condensation nucleus counter which operated at stratospheric pressures was developed, designed, and constructed. It was calibrated in the laboratory. Its response as a function of particle size and concentration was reported. This was the first time that the response of such an instrument was verified in the laboratory. An inlet was constructed which provided near isokinetic sampling. The resulting instrument, the U-2 CNC, was deployed on NASA U-2 aircraft in the study of the climatic effects of aerosol. These studies occurred in March, April, May, July, November, and December of 1992 and in April, May, June, and December of 1983. The U-2 CNC was used in the study of the aerosol cloud resulting from the eruption of El Chichon. It permitted the observation of new particle formation in the stratosphere. Derived from text

N95-14862# Army Cold Regions Research and Engineering Lab., Hanover, NH.
DEPENDENCE OF SEGREGATION POTENTIAL ON THE THERMAL AND HYDRAULIC CONDITIONS PREDICTED BY MODEL M1
Yoshisuke Nakano Apr. 1994 17 p
(AD-A280969; CRREL-94-4) Avail: CASI HC A03/MF A01

The segregation potential (SP) model is semiempirical in nature. An accurate mathematical model is needed that provides the functional dependence of SP on pertinent variables specifying given thermal and hydraulic conditions in terms of well-defined functions (or parameters) describing the properties of a given soil. In response to such a need a mathematical model called M(sub 1) was introduced and efforts have been made to validate M(sub 1) with empirical findings and experimental data. We show that the functional dependence of SP on pertinent variables predicted by M(sub 1) is consistent with empirical findings that were used to build the SP model. Author (DTIC)

N95-14956# Texas Univ., Austin, TX. Dept. of Geological Sciences.
ENERGY FLUX AND HYDROGEOLOGY OF THERMAL ANOMALIES IN THE GULF OF MEXICO BASIN: SOUTH TEXAS EXAMPLE Progress Report, 1 Sep. 1993 - 28 Feb. 1994
J. M. Sharp, Jr. Mar. 1994 12 p
(Contract DE-FG05-92ER-14278)
(DE94-015122; DOE/ER-14278/T2) Avail: CASI HC A03/MF A01

This report covers the period from 1 September 1993 through 28 February 1994. The last Technical Progress Report was submitted in September 1993. In this period, we have focused our efforts on the following activities: (1) Finalizing collection of radiogenic heat production data; (2) Evaluating petrographic controls on thermal conductivity; (3) Modeling one-dimensional heat conduction with sources; (4) Completing base geologic cross-section; (5) Acquiring pressure data to augment data base; (6) Putting map and well data into digital format for analysis; (7) Analyzing salinity, temperate and fluid potential data for propensity of free convection; (8) Finalizing preliminary investigation into depressurization of reservoirs; (9) Preparing presentations for AAPG meeting in Denver; (10) Presenting results at the Geological Society of America Meeting in Boston (October 1993); (11) Collaborating with project members of the DOE funded Global Basins Research Network who are working on a project in the Eugene Island Block, offshore Louisiana; and (12) Collaborating with others working on research in the Gulf of Mexico Basin in our Department and with CSIRO scientists in Adelaide, Australia. DOE

N95-15295# Eclectic, Inc., Oak Ridge, TN.
LEAK DETECTION BY ACOUSTIC EMISSIONS MONITORING: AN EXPERIMENTAL INVESTIGATION OF THE ACOUSTIC PROPERTIES OF LEAKS AND THE ATTENUATION CHARACTERISTICS OF SOIL
James F. Kilpatrick and Patrick A. March 27 May 1994 96 p
(Contract F08635-87-C-0377)
(AD-A283250; AL/EQ-TR-1994-0032) Avail: CASI HC A05/MF A01

This study experimentally explored the conditions, equipment, and methodology necessary for the acoustic detection of small leaks of jet fuel (JP4) from underground storage tank (UST) systems. The study indicates that acoustic leak detection of very small leaks is feasible. In general, significant JP4 fuel leaks which occur across a 5 PSI (pounds per square inch) or greater pressure drop are acoustically active and can be detected with proper sensors and proper placement of sensors. The primary source of leak noise is turbulent flow through the leak orifice. At lower pressures, the leak flow becomes laminar, and the leak becomes virtually silent. With direct transducer contact on the pipe or tank wall and sufficient system pressure, leaks smaller than 0.1 GPH (gallons per hour) can be detected. Larger leaks can be detected through short distances in soil. However, sand, which is the most commonly used fill material for UST systems, provides significant acoustic attenuation. Consequently, waveguides must be used when monitoring distances exceeding about 1 foot of travel through sand. Sand acts to reduce background noise levels, providing an ideal environment for acoustic leak detection using sensors mounted directly on the pipe or tank wall. DTIC

N95-15401# Photometrics, Inc., Woburn, MA.
RESEARCH ON CHARACTERIZATION OF THE UPPER ATMOSPHERE USING LIDAR Final Report, 10 Aug. 1990 - 28 Feb. 1994
Michael Burka 28 Mar. 1994 16 p

(Contract F19628-90-C-0175)
(AD-A283241; PL-TR-94-2136; AD-E202069) Avail: CASI HC A03/MF A01

A three year effort to characterize the upper atmosphere using sodium fluorescence and Rayleigh lidar techniques and progress in the development of sodium fluorescence lidar is described. The range of the PL/GPIM fixed base and mobile lidar systems through development of combined analog/photon counting techniques, development of Raman lidar channels, improvement of background rejection and injection locking of transmitter lasers has been extended. The applicability of lidar to measure changes in the density of excited nitrogen in the lower atmosphere was investigated. This reseach was conducted in Massachusetts, Alaska and Hawaii on high altitude density and temperature characteristics and on the aerosol layer produced by the Mt. Pinatubo volcano. The reliability, performance and overall productivity of the lidar systems has been improved. DTIC

N95-15411# Sandia National Labs., Albuquerque, NM.
MEASUREMENTS OF UPPER TROPOSPHERIC MOISTURE WITH A RAMAN LIDAR
S. E. Bisson, J. E. M. Goldsmith, and A. D. DelGenio 1994 4 p Presented at the 17th International Laser Radar Conference, Sendai (Japan), 25-29 Jul. 1994
(Contract DE-AC04-94AL-85000)
(DE94-015748; SAND-94-8716C; CONF-9407106-1) Avail: CASI HC A01/MF A01

We describe water vapor profile measurements made with the Sandia Raman lidar. The goal of this study is to determine the effect of convection on the upper tropospheric moisture budget. At present, considerable controversy exists over the nature of the vertical redistribution of water vapor in a changing climate, and particularly the distribution of water vapor in the upper troposphere. Although upper tropospheric moisture concentrations are several orders of magnitude lower than those near the surface, upper tropospheric moisture exerts an important influence on climate. On a per-molecule basis, greenhouse absorption due to water vapor is about one hundred times more effective at high altitudes than at low altitudes. Several one-dimensional radiative convective models have been used to demonstrate the importance of upper tropospheric moisture on climate. What these models show is that for a given fractional increase in water vapor at a given altitude the response or change in surface temperature is qualitatively the same. Understanding upper tropospheric moistening processes are therefore of prime importance in addressing the water vapor feedback question. The goal of this study is to determine the upper tropospheric moisture budget associated with convective events, and in particular to extend process models to higher altitudes than have been achieved previously. DOE

N95-15428# Army Cold Regions Research and Engineering Lab., Hanover, NH.
TRAVELING WAVE SOLUTIONS TO THE PROBLEM OF QUASI-STEADY FREEZING OF SOILS
Yoshisuke Nakano Mar. 1994 25 p
(AD-A280971; CRREL-94-3) Avail: CASI HC A03/MF A01

The results of mathematical and experimental studies clearly show that the model M(sub 1) accurately describes the properties of a frozen fringe when the steady growth of an ice layer occurs. The steady growth of ice-rich frozen soil is studied by using M(sub 1). Deriving a traveling wave solution to the problem, we have found that the condition of steady growth of ice-rich frozen soil is uniquely determined by a set of two physical variables, such as alpha(sub 0) and alpha(sub 1) used earlier, under given hydraulic conditions and over-burden pressures and that the traveling wave solution converges to the solution to the problem of a steadily growing ice layer when the velocity of the 0 C isotherm relative to the unfrozen part of the soil vanishes. Author (DTIC)

N95-15586*# Massachusetts Inst. of Tech., Cambridge. Research Lab. of Electronics.
HIGH-SPATIAL-RESOLUTION PASSIVE MICROWAVE SOUNDING SYSTEMS Final Report, 1 Feb. 1980 - 14 Mar. 1994
D. H. Staelin and P. W. Rosenkranz 1 Nov. 1994 23 p
(Grant NAG5-10)
(NASA-CR-197131; NAS 1.26:197131; MIT-OSP-89029) Avail: CASI HC A03/MF A01

The principal contributions of this combined theoretical and experimental effort were to advance and demonstrate new and more accurate techniques for sounding atmospheric temperature, humidity, and precipitation profiles at millimeter wavelengths, and to improve the scientific basis for such soundings. Some of these techniques are being incorporated in both research and operational systems. Specific results include: (1) development of the MIT Microwave Temperature Sounder (MTS), a 118-GHz eight-channel imaging spectrometer plus a switched-frequency spectrometer near 53 GHz, for use on the NASA ER-2 high-altitude aircraft, (2) conduct of ER-2 MTS missions in multiple seasons and locations in combination with other instruments, mapping with unprecedented approximately 2-km lateral resolution atmospheric temperature and precipitation profiles, atmospheric transmittances (at both zenith and nadir), frontal systems, and hurricanes, (3) ground based 118-GHz 3-D spectral images of wavelike structure within clouds passing overhead, (4) development and analysis of approaches to ground- and space-based 5-mm wavelength sounding of the upper stratosphere and mesosphere, which supported the planning of improvements to operational weather satellites, (5) development of improved multidimensional and adaptive retrieval methods for atmospheric temperature and humidity profiles, (6) development of combined nonlinear and statistical retrieval techniques for 183-GHz humidity profile retrievals, (7) development of nonlinear statistical retrieval techniques for precipitation cell-top altitudes, and (8) numerical analyses of the impact of remote sensing data on the accuracy of numerical weather predictions; a 68-km gridded model was used to study the spectral properties of error growth. Author

N95-15684*# North Carolina State Univ., Raleigh, NC. Dept. of Marine, Earth, and Atmospheric Sciences.
MESO-BETA SCALE NUMERICAL SIMULATION STUDIES OF TERRAIN-INDUCED JET STREAK MASS/MOMENTUM PERTURBATIONS Annual Report, Nov. 1994
Yuh-Lang Lin and Michael L. Kaplan Nov. 1994 30 p
(Grant NAG5-1790)
(NASA-CR-197226; NAS 1.26:197226) Avail: CASI HC A03/MF A01

An in-depth analysis of observed gravity waves and their relationship to precipitation bands over the Montana mesonetwork during the 1981 CCOPE case study indicates that there were two episodes of coherent internal gravity waves. One of the fundamental unanswered questions from this research, however, concerns the dynamical processes which generated the observed waves, all of which originated from the region encompassing the borders of Montana, Idaho, and Wyoming. While geostrophic adjustment, shearing instability, and terrain where all implicated separately or in concert as possible wave generation mechanisms, the lack of upper-air data within the wave genesis region made it difficult to rigorously define the genesis processes from observations alone. In this report we employ a mesoscale numerical model to help diagnose the intricate early wave generation mechanisms during the first observed wave episode. Author (revised)

N95-15745*# National Aeronautics and Space Administration. Goddard Space Flight Center, Greenbelt, MD.
TECHNICAL REPORT SERIES ON GLOBAL MODELING AND DATA ASSIMILATION. VOLUME 3: AN EFFICIENT THERMAL INFRARED RADIATION PARAMETERIZATION FOR USE IN GENERAL CIRCULATION MODELS
Max J. Suarez, ed. and Ming-Dah Chou Nov. 1994 93 p
(Contract NAS5-32332; RTOP 910-00-00)
(NASA-TM-104606-Vol-3; Rept-95B00011-Vol-3; NAS 1.15:104606-Vol-3) Avail: CASI HC A05/MF A01

A detailed description of a parameterization for thermal infrared radiative transfer designed specifically for use in global climate models is presented. The parameterization includes the effects of the main absorbers of terrestrial radiation: water vapor, carbon dioxide, and ozone. While being computationally efficient, the schemes compute very accurately the clear-sky fluxes and cooling rates from the Earth's surface to 0.01 mb. This combination of accuracy and speed makes the parameterization suitable for both tropospheric and middle atmospheric modeling applications. Since no transmittances are precomputed the atmospheric layers and the vertical distribution of the absorbers may be freely specified. The scheme can also account for any vertical distribution of fractional cloudiness with arbitrary optical thickness. These features make the parameterization very flexible and extremely well suited for use in climate modeling studies. In addition, the numerics and the FORTRAN implementation have been carefully

designed to conserve both memory and computer time. This code should be particularly attractive to those contemplating long-term climate simulations, wishing to model the middle atmosphere, or planning to use a large number of levels in the vertical. Author

47 METEOROLOGY AND CLIMATOLOGY

Includes weather forecasting and modification.

N95-13725*# Cincinnati Univ., OH. Dept. of Aerospace Engineering and Engineering Mechanics.

ATMOSPHERIC AND WIND MODELING FOR ATC Final Report

Gary L. Slater Nov. 1990 48 p

(Grant NAG2-175)

(NASA-CR-196786; NAS 1.26:196786) Avail: CASI HC A03/MF A01

The section on atmospheric modeling covers the following topics: the standard atmosphere, atmospheric variations, atmosphere requirements for ATC, and implementation of a software model for Center/Tracon Advisory System (CTAS). The section on wind modeling covers the following topics: wind data -- NOAA profiler system; wind profile estimation; incorporation of various data types into filtering scheme; spatial and temporal variation; and software implementation into CTAS. The appendices contain Matlab codes for atmospheric routines and for wind estimation. CASI

N95-14117# National Severe Storms Forecast Center, Kansas City, MO.

VERIFICATION OF SEVERE LOCAL STORMS FORECASTS ISSUED BY THE NATIONAL SEVERE STORMS FORECAST CENTER: 1993

R. W. Anthony Jun. 1994 20 p See also PB93-216844

(PB94-195898; NOAA-TM-NWS-NSSFC-38) Avail: CASI HC A03/MF A01

The Severe Local Storms (SELS) Unit of the National Severe Storms Forecast Center routinely issues convective outlooks and severe local storm watches to delineate areas that are favorable for development of severe local storms. During 1993 the SELS Unit issued 957 severe local storm watches. Of these, 350 were tornado watches. There were 13,986 severe local storm events during 1993. Of these, 1173 were tornadoes. In terms of the total number of events, this was the most active season on record. Author (NTIS)

N95-14118# Miami Univ., FL. Cooperative Inst. for Marine and Atmospheric Studies.

STATISTICAL ASPECTS OF THE PRECIPITATION REGIMES AT MIAMI INTERNATIONAL AIRPORT (MIA) AND PALM BEACH INTERNATIONAL AIRPORT (PBI): 1961-1990

S. L. Rosenthal May 1994 40 p

(PB94-194289; NOAA-TM-ERL-AOML-80) Avail: CASI HC A03/MF A01

Low-frequency components of the time series of mean annual precipitation for 1961-1990 at Miami International Airport (MIA) and Palm Beach International Airport (PBI) are closely in phase. The data show a decadal-scale variation with relatively high precipitation in the 1960's and 1980's and relatively low precipitation in the 1970's. This fluctuation is concomitant with a statistically significant decadal-scale fluctuation in tropical weather system frequency. MIA precipitation is systematically related to tropical weather system frequency on monthly and seasonal time scales but not so precisely that one can conclude a cause and effect relationship exists. Spectral analysis showed well marked peaks in the MIA and PBI spectra (computed from annual precipitation totals) at a period of 15 years. Co-spectral calculations indicated that the covariance of the MIA and PBI annual precipitation totals was primarily the result of fluctuations with periods of 10 years or more. The time series of annual rainfall totals at both stations, when smoothed with five-year running means, showed maxima in the decade of the 1960's. Analyses of year-month cross sections showed that these maxima were the result of anomalously high rainfall in June and September-October during the later half of that decade. NTIS

N95-14120# Florida Sea Grant Coll., Gainesville, FL.

FLORIDA HURRICANES AND TROPICAL STORMS 1871-1993: AN HISTORICAL SURVEY

F Doehring, I. W. Duedall, and J. M. Williams Jun. 1994 135 p See also PB85-246163 and PB93-174993 Prepared in cooperation with Florida Inst. of Tech., Melbourne, FL

(Contract NA-36RG-0070)

(PB94-198017; TP-71; ISBN-0-912747-08-0) Avail: CASI HC A07/MF A02

The book presents, by historical periods, a summary of the hurricanes and tropical storms that struck Florida's more than 1200-mile long coastline during the 122 years from 1871 through 1993. The author's primary goal in preparing this book was to update the historical work as it pertains to Florida, to consolidate and standardize the technical terms published at the beginning of each hurricane season on hurricane tracking maps, and to introduce the following new material pertaining to Florida: (1) a detailed historical discussion, (2) a chronological listing of all Florida hurricanes, (3) 13 plates of hurricane and tropical storm tracks grouped into 10-year increments, and (4) a table showing the number of tropical storms and hurricanes by 10-year increments. The book is written in a nontechnical level for the general reader who is interested in knowing when and where hurricanes affected Florida and the magnitude of damage inflicted by the storms. NTIS

N95-14265*# Colorado Univ., Boulder, CO. Dept. of Astrophysical, Planetary and Atmospheric Sciences.

GLOBAL SURFACE-BASED CLOUD OBSERVATION FOR ISCCP Final Report, 18 Mar. 1989 - 30 Jun. 1994

18 Oct. 1994 100 p

(Grant NAG1-998)

(NASA-CR-196990; NAS 1.26:196990) Avail: CASI HC A05/MF A02

Visual observations of cloud cover are hindered at night due to inadequate illumination of the clouds. This usually leads to an underestimation of the average cloud cover at night, especially for the amounts of middle and high clouds, in climatologies on surface observations. The diurnal cycles of cloud amounts, if based on all the surface observations, are therefore in error, but they can be obtained more accurately if the nighttime observations are screened to select those made under sufficient moonlight. Ten years of nighttime weather observations from the northern hemisphere in December were classified according to the illuminance of moonlight or twilight on the cloud tops, and a threshold level of illuminance was determined, above which the clouds are apparently detected adequately. This threshold corresponds to light from a full moon at an elevation angle of 6 degrees or from a partial moon at higher elevation, or twilight from the sun less than 9 degrees below the horizon. It permits the use of about 38% of the observations made with the sun below the horizon. The computed diurnal cycles of total cloud cover are altered considerably when this moonlight criterion is imposed. Maximum cloud cover over much of the ocean is now found to be at night or in the morning, whereas computations obtained without benefit of the moonlight criterion, as in our published atlases, showed the time of maximum to be noon or early afternoon in many regions. Cloud cover is greater at night than during the day over the open oceans far from the continents, particularly in summer. However, near noon maxima are still evident in the coastal regions, so that the global annual average oceanic cloud cover is still slightly greater during the day than at night, by 0.3%. Over land, where daytime maxima are still obtained but with reduced amplitude, average cloud cover is 3.3% greater during the daytime. The diurnal cycles of total cloud cover we obtain are compared with those of ISCCP for a few regions; they are generally in better agreement if the moonlight criterion is imposed on the surface observations. Using the moonlight criterion, we have analyzed ten years (1982-1991) of surface weather observations over land and ocean, worldwide, for total cloud cover and for the frequency of occurrence of clear sky, fog and precipitation The global average cloud cover (average of day and night) is about 2% higher if we impose the moonlight criterion than if we use all observations. The difference is greater in winter than in summer, because of the fewer hours of darkness in the summer. The amplitude of the annual cycle of total cloud cover over the Arctic Ocean and at the South Pole is diminished by a few percent when the moonlight criterion is imposed. The average cloud cover for 1982-1991 is found to be 55% for northern hemisphere land, 53% for southern hemisphere land, 66% for northern hemisphere ocean, and 70% for southern hemisphere ocean, giving a global average of 64%. The global average for daytime is 64.6% for nighttime 63.3%. Author

N95-14271*# Alabama Univ., Huntsville, AL. Dept. of Chemistry.

PRODUCE DOCUMENTS AND MEDIA INFORMATION Final Report, 1 Dec. 1993 - 1 Jun. 1994

Melanie A. Alzmann and G.A. Miller 1 Jun. 1994 33 p
(Contract NAS8-38609)
(NASA-CR-196521; NAS 1.26:196521; UAH-5-33407) Avail: CASI HC A03/MF A01

Lightning network data and information were collected from the United States, Germany, France, Brazil, China, and Australia for the compilation of a global lightning data base. Publications were written, edited, and produced to describe lightning detection from space. They included descriptions of the Optical Transient Detector and the Lightning Imaging Sensor. Travel to New Mexico and Wallops Flight Facility in Virginia were conducted to collect both lightning network information and to help define the tasks of lightning detection studies by high altitude aircraft and satellite instrumentation. Derived from text

N95-14340# Army Research Lab., White Sands Missle Range, NM.
DETERMINATION OF THE SIMILARITY THEORY SCALING PARAMETERS FROM THE VERTICAL GRADIENTS Final Report
Frank V. Hansen, Henry Rachele, and Arnold Tunick Jun. 1994 34 p
(AD-A283833; ARL-TR-286) Avail: CASI HC A03/MF A01

Dynamic similarity of flows theory as applied to the surface boundary layer of the atmosphere must be treated as an interwoven quardrapartite function of trivariant orthoginal turbulent motion, the thermal structure and associated vertical gradients, evaporation at the interface, and vertical transport of water vapor with respect to the specific humidity as a function of height. Physical studies of the surface layer are typically conducted with respect to the buoyant heat flux and the momentum flux. Buoyancy is associated with the sensible and latent heat fluxes. The key parameters for establishing the vertical fluxes are the scaling velocity, scaling temperature, and scaling humidity. An interpretation of the similarity theory developed from the basis of the mean value theorem of calculus allows evaluation of the scaling parameters, without utilizing the mathematically complex diabatic influence functions, but directly from the vertical gradients of wind, temperature, and specific humidity. DTIC

N95-14410# National Weather Service, Silver Spring, MD. Techniques Development Lab.
AFOS TERMINAL AERODROME FORECAST ENCODING
J. F. Wantz Jun. 1994 15 p See also PB89-101240
(PB94-203247; NOAA-NWS-TDL-CP-94-3) Avail: CASI HC A03/MF A01

Most WSFO's prepare Terminal Forecasts (FT's) for domestic aviation and Terminal Aerodrome Forecasts (TAF's) for international flights. Because much of the information contained in FT's is also contained in TAF's, the forecaster must issue two forecasts for the same location and weather elements. To assist WSFO's in preparing TAF's, this application program, TAFENC, has been written to format a guidance TAF from an FT. The program also promotes consistency between FT's and the TAF's, as well as eliminating the necessity of writing two separate forecasts. It accomodates the revised TAF format (NWS 1993). It should be stressed that the product created by TAFENC is a guidance product and not the official forecast because of assumptions that the program must make. NTIS

N95-14423# Naval Postgraduate School, Monterey, CA.
SHORT TERM TELECONNECTIONS ASSOCIATED WITH WESTERN PACIFIC TROPICAL CYCLONES M.S. Thesis
Cory A. Springer Jun. 1994 151 p
(AD-A284032) Avail: CASI HC A08/MF A02

The short term teleconnections arising from an individual tropical cyclone in the western Pacific were examined using a global operational data assimilation system and forecast model. In the data assimilation, the tropical cyclone was modified using a tropical cyclone bogusing procedure that either maintained the storm in, or eliminated the storm from, the model's initial conditions. These different initial conditions were used as the initial fields for several 20 day runs of the forecast model. These runs were used to simulate the global atmosphere with and without the tropical cyclone. The differences between these simulations were used to infer the global teleconnection response to the tropical cyclone. This response was dominated by a strong, quasi-stationary Rossby wave train that extended from east Asia across the North Pacific into North America. This wave train was initiated when an anticyclonic circulation formed near Japan as the tropical cyclone approached the east Asian jet. The anticyclone formation was primarily the result of the absolute vorticity advection by the divergent wind and vortex stretching (i.e., the Rossby wave source) associated with the tropical cyclone. The wave response continued to develop after this wave source, and the tropical cyclone itself, dissipated. This development was clearly seen in the growth and eastward propagation of Rossby wave energy across the midlatitude North Pacific and North America. The growth tended to be greater near areas of potential barotropic instability along the North Pacific jet, while the propagation tended to occur parallel to the jet. DTIC

N95-14848 City Coll. of the City Univ. of New York, NY. Dept. of Earth and Atmospheric Sciences.
MODERN METHODS IN METEOROLOGICAL AND OCEANOGRAPHIC DATA ACQUISITION AND ANALYSES Technical Report, 1 Mar. 1993 - 28 Feb. 1994
Ward Hindman 25 Jul. 1994 7 p Limited Reproducibility: More than 20% of this document may be affected by microfiche quality
(Contract N00014-93-1-0486)
(AD-A283038) Avail: CASI HC A02

The first objective is to educate and train students to collect and analyze meteorological and oceanographic data using the new weather station computer system. The second objective is to keep the systems networking and computation capabilities up-to-date by procuring system upgrades. The third objective is to teach students scientific programming. DTIC

N95-14952 Air Force Inst. of Tech., Wright-Patterson AFB, OH.
WATER VAPOR AND TEMPERATURE INVERSIONS NEAR THE 0 C LEVEL OVER THE TROPICAL WESTERN PACIFIC M.S. Thesis
Kenneth A. Hart 1994 112 p Limited Reproducibility: More than 20% of this document may be affected by microfiche quality
(AD-A282023; AFIT/CI/CIA-94-032) Avail: CASI HC A06

During the Intensive Observation Period (IOP), several periods of water vapor and temperature inversions near the 0 C level were observed. Satellite and radiosonde data from TOGA COARE are used to document the large-scale conditions and thermodynamic and kinematic structures present during three extended periods in which moisture and temperature inversions near the freezing level were very pronounced. Observations from each case are synthesized into schematics which represent typical structures of the inversion phenomena. Frequency distributions of the inversion phenomena along with climatological humidity and temperature profiles are calculated for the four-month IOP. DTIC

N95-15323# Oceanweather, Inc., Cos Cob, CT.
UPGRADE OF TROPICAL CYCLONE SURFACE WIND FIELD MODEL Final Report
Vincent J. Cardone, Andrew T. Cox, J. A. Greenwood, and Edward F. Thompson Jul. 1994 103 p
(Contract DACW39-93-C-0022)
(AD-A283530; CERC-MP-94-14) Avail: CASI HC A06/MF A02

The U.S. Army Corps of Engineers (CE) tropical cyclone surface wind field model has been a very useful tool in ocean response modeling for more than a decade. Recently, its limitations were assessed in light of present knowledge and technology. Model limitations were identified and evaluated in terms of their perceived importance to ocean response modeling and the level of effort required to develop improved solutions. The limitations are summarized in this report. Two aspects of the CE model were targeted for improvement. This report describes the improvements developed for the upgraded model. First, the model was upgraded to include more computationally intensive options which give improved resolution and areal coverage. Up to seven nested grids are now available, compared to only five nests in the standard model. In a typical application, this upgrade can be used to achieve 2-km resolution around the eye (as compared to 5-km resolution often used in the standard model) and an expanded total coverage area. The second upgrade allows a more general specification of the axisymmetric pressure profile. This upgrade can be used to create wind fields with maxima at two different radii or with a broad maximum extending over a range of radii. It also provides more flexibility in fitting the shape of single peaked wind profiles. The upgraded model is demonstrated with historical hurricanes. The five-nest and seven-nest models are applied to Hurricane Camille. The fully upgraded model, with seven nests and general pressure specification, is applied to Hurricane Gilbert. This hurricane was chosen because it is well-documented by Black and Willoughby (1992)

and it evolved into some nontraditional storm structures. The upgraded model was more effective than the standard CE model in simulating the storm. Author (DTIC)

N95-15383# National Oceanic and Atmospheric Administration, Silver Spring, MD. Atmospheric Sciences Modeling Div.
OVERVIEW OF PAMS METEOROLOGICAL MONITORING REQUIREMENTS
G. H. Crescenti 1994 10 p See also PB92-122795 Sponsored by EPA
(PB94-176658; EPA/600/A-94/099) Avail: CASI HC A02/MF A01

The Photochemical Assessment Monitoring Station (PAMS) requires the incorporation of surface and upper air meteorological instrumentation. The platform for the surface instrumentation is a 10 m tower. The variables to be collected include horizontal wind speed, horizontal wind direction, air temperature, relative humidity, solar radiation, and barometric pressure. Upper air data may be acquired using a variety of platforms which include aircraft, tall towers, tethered and expendable radiosondes, and ground-based remote profilers. The variables to be collected include profiles of horizontal wind speed and direction, vertical wind speed, and air temperature. In addition, the mixing layer height should be determined from the upper air data. This paper summarizes the meteorological sensor requirements for PAMS which are not specifically addressed in the Code of Federal Regulations (40 CFR Part 58). NTIS

N95-15402 Hughes STX, Inc., Lexington, MA.
INTRODUCTION TO HEFeS (HIERARCHICAL ENVIRONMENTAL FEATURE SIMULATOR)
Albert R. Boehm 21 Jan. 1994 18 p Limited Reproducibility: More than 20% of this document may be affected by microfiche quality
(Contract F19628-93-C-0051)
(AD-A283244; PL-TR-94-2013; AD-E202112; SR-2) Avail: Issuing Activity (Defense Technical Information Center (DTIC))

This report discusses a Hierarchical Environmental Feature Simulation (HEFeS) which is an object-oriented representation of the natural environment based on kinematics, climatology, and intricate detail produced from space/time structure functions. HEFeS is a compact storage and fast retrieval of all required environmental attributes at any required resolution within any specified space/time window. DTIC

N95-15614# Atmospheric and Environmental Research, Inc., Cambridge, MA.
SUPPORT OF ENVIRONMENTAL REQUIREMENTS FOR CLOUD ANALYSIS AND ARCHIVE (SERCAA): ALGORITHM DESCRIPTIONS
G. B. Gustafson, R. G. Isaacs, R. P. DEntremont, J. M. Sparrow, and T. M. Hamill 28 Mar. 1994 108 p
(Contract F19628-92-C-0149)
(AD-A283240; PL-TR-94-2114; AD-E202068; SR-2) Avail: CASI HC A06/MF A02

This report describes the SERCAA multiplatform, multisensor, multispectral cloud product analysis algorithms. These algorithms incorporate high-resolution sensor data from multiple military and civilian satellites, polar and geostationary, into a real-time cloud analysis model and apply multispectral cloud analysis techniques that improve the detection and specification of clouds, especially cirrus and low clouds. The SERCAA algorithms consist of a number of processes involved in integrating cloud analyses from multiple satellite platforms into a single cloud analysis product. The steps required to process the raw sensor data, collected from each of the satellite platforms, into each of the individual cloud analysis products include total cloud algorithms for DMSP, AVHRR, and geostationary platforms, cloud layer and type algorithms, and an analysis integration algorithm. The SERCAA data products for the CDFS II baseline include: total cloud cover fraction, number of cloud layers (up to four floating layers), cloud layer coverage fraction, cloud type, cloud height, and analysis confidence level. DTIC

N95-15618# Air Force Inst. of Tech., Wright-Patterson AFB, OH.
NOWCASTING CONVECTIVE STORM EVOLUTION IN EAST-CENTRAL FLORIDA USING SATELLITE AND DOPPLER RADAR DATA M.S. Thesis
Marvin H. Treu 1994 183 p
(AD-A283260; AFIT/CI-94-109) Avail: CASI HC A09/MF A02

The relationship between infrared cloud top temperatures from the Geostationary Operational Environmental Satellite's (GOES) Visible and Infrared Spin Scan Radiometer (VISSR) and radar reflectivity returns from NCAR's CP-4 C-band Doppler radar is examined for nine thunderstorm cells over east central Florida. The cell data are from three case study days during the summer 1991 Convective and Precipitation/Electrification (CaPE) Experiment. Rapid scan satellite data available during the selected case study days provide a high frequency of image times (delta t = 5-15 min.) for better temporal resolution in the data comparisons. A method was developed to graphically combine GOES visible and infrared images with universal format Doppler radar reflectivity and velocity scans for display on a PC workstation. Previous studies, personal forecasting experience, and the present study illustrate a need to combine meteorological data sources in order to improve operational nowcasting capabilities. DTIC

N95-15627 Air Force Inst. of Tech., Wright-Patterson AFB, OH.
THE SEASONAL CYCLE DEPENDENCE OF TEMPERATURE FLUCTUATIONS IN THE ATMOSPHERE M.S. Thesis
Bridget F. Tobin Aug. 1994 61 p Limited Reproducibility: More than 20% of this document may be affected by microfiche quality
(AD-A283220; AFIT/CI/CIA-94-103) Avail: CASI HC A04

The correlation statistics of meteorological fields have been of interest in weather forecasting for many years and are also of interest in climate studies. A better understanding of the seasonal variation of correlation statistics can be used to determine how the seasonal cycle of temperature fluctuations should be simulated in noise-forced energy balance models. It is shown that the length scale does have a seasonal dependence and will have to be handled through the seasonal modulation of other coefficients in noise-forced energy balance models. The temperature field variance and spatial correlation fluctuations exhibit seasonality with fluctuation amplitudes larger in the winter hemisphere and over land masses. Another factor contributing to seasonal differences is the larger solar heating gradient in the winter. DTIC

N95-15666# Colorado State Univ., Fort Collins, CO. Dept. of Atmospheric Science.
JUNE TO SEPTEMBER RAINFALL IN THE AFRICAN SAHEL: VERIFICATION OF OUR 1994 FORECASTS AND AN EXTENDED RANGE FORECAST FOR 1995, 3
C. W. Landsea, P. W. Mielke, Jr., K. J. Berry, and W. M. Gray 1 Dec. 1994 5 p
(TR-521) Avail: CASI HC A01/MF A01

Observations show that changes are occurring in African Sahel rainfall. During 1994 rainfall was substantially higher than it has been in recent years. We forecast that Sahelian rainfall in 1995 will continue this upward trend. We project rainfall amounts somewhat above the 1950-1991 average. This should enhance the probability of an active 1995 hurricane season. Author

N95-15749# Massachusetts Inst. of Tech., Cambridge. Lincoln Lab.
TDWR SCAN STRATEGY IMPLEMENTATION
Daniel P. Hynek 2 Sep. 1994 19 p
(Contracts DTFA01-93-Z-02012; F19628-90-C-0002)
(AD-A284877; ATC-222) Avail: CASI HC A03/MF A01

The Terminal Doppler Weather Radars (TDWR's) installed at major airports around the country are intended to enhance the safety of air travel by the detection and timely warning of hazardous wind shear conditions in the airport terminal area. To meet these objectives, scan strategies to efficiently cover the protected airspace were developed after extensive testing at several sites with different meteorological environments. Since the topology and geometry differ at each TDWR location, special considerations were necessary to define the specific scan sequences for each site. This report describes the criteria used to establish these scan sequences, including the determination of the lowest practicable elevation angle for each site - the 'surface scan,' which is used to detect microburst surface outflows, and other special scans such as the 'MTS scan,' which is used to illuminate the remote Moving Target Simulator (MTS). DTIC

N95-15771# Georgia Inst. of Tech., Atlanta, GA.
METEOROLOGICAL INVESTIGATION OF OZONE ANOMALIES DURING THE ARCTIC BOUNDARY LAYER EXPERIMENT (ABLE 3A) Ph.D.

Thesis
David A. Smarsh Aug. 1994 247 p Sponsored by AFIT
(AD-A284494; AFIT-CI/CIA94-034D) Avail: CASI HC A11/MF A03

Partial contents include the following: The Arctic Boundary Layer Experiment (ABLE 3A); and Methods of analysis: Isentropic Trajectory; Total Ozone Mapping Spectrometer (TOMS); Parcel-Time Series; Station-Time Series; Cross-Sections; Tropopause Vertical Velocity; Isentropic Potential Vorticity (IPV); Constant Pressure Charts; and Skew-T.

Author (DTIC)

N95-15819# North Carolina Univ., Raleigh, NC. Dept. of Marine Earth and Atmospheric Sciences.
THE OPERATIONAL FORECASTING/NOWCASTING OF PRECIPITATION TYPE IN THE SOUTHEASTERN UNITED STATES TYPE OF PRECIPITATION: DESCRIPTIVE AND OBJECTIVE GUIDANCE M.S. Thesis
Craig A. Souza 1994 129 p Sponsored by AFIT
(AD-A284456; AFIT-CI/CIA94-126) Avail: CASI HC A07/MF A02

Frozen and freezing precipitation are hazardous to modern society. Even small amounts of frozen or freezing precipitation can significantly affect the public in the southeastern United States (SEUS). Improved forecasts of and specificity of precipitation type are critical to public and private sector responses to wintry precipitation. A significant percentage of frozen or freezing precipitation cases in this region are associated with shallow polar airmasses (i.e. cold air damming (CAD) situations) and occur as a mix of wintry precipitation. CAD episodes are not routinely portrayed accurately by current operational numerical weather prediction models. Hence, right or wrong, there can be a lack of confidence in the model output statistics (MOS) generated from these models. As a supplement to the MOS, a type of precipitation: descriptive and objective guidance (TOP DOG) approach consisting of regression equations (conditional probability) and nomograms is developed regionally and for individual stations in the SEUS. Due to the frequency of mixed precipitation events in the SEUS, emphasis is directed towards specifying a variety of precipitation subtypes (e.g., mixed liquid but nonaccumulating frozen, all snow versus mixed accumulating frozen). Six hour precipitation type guidance is derived directly from climatological (1973-1991) upper air sounding and surface data. TOP DOG uses logistical regression, more representative of the phenomena than linear regression used previously. DTIC

N95-14895# Institute for Aerospace Research, Ottawa (Ontario). Flight Research Lab.
WINTER STORMS RESEARCH IN CANADA
J. Ian MacPherson and George A. Isaac *In* AGARD, Flight in an Adverse Environment Nov. 1994 21 p Sponsored by Federal Panel on Energy Research and Development; Atmospheric Environment Service; National Research Council of Canada; National Search and Rescue Secretariat, Dept. of National Defence; Boeing Commercial Airplane Co.; and Airbus Industrie (For primary document see N95-14893 03-03)
Copyright Avail: CASI HC A03/MF A02

48 OCEANOGRAPHY

Includes biological, dynamic, and physical oceanography; and marine resources.

For related information see also *43 Earth Resources and Remote Sensing.*

N95-14204# Oregon State Univ., Corvallis, OR. Dept. of Civil Engineering.
A WORKSHOP ON NEW DIRECTIONS IN EXTREMAL STOCHASTIC ANALYSIS OF NONLINEAR OCEAN SYSTEMS Final Report
Solomon C. Yim 30 Oct. 1993 3 p Workshop was held on 7-8 Jul. 1993
(Contract N00014-93-1-0480)
(AD-A283969) Avail: CASI HC A01/MF A01

The objective of the workshop was to facilitate the advancement of the state of knowledge for the evaluation of the response of nonlinear ocean systems to stochastic excitation, with emphasis on response characteristics of significance for reliability analysis. The workshop would provide a forum for: (1) ONR supported researchers under the new program on 'Reliability of Nonlinear Ocean Structures Under Stochastic Excitation' (the reliability program) and experienced Navy personnel to hold discussions and exchange ideas on Naval needs to date and new research directions; and (2) the coordination of research efforts among physics, mathematical sciences, and engineering researchers under the program to achieve cross-field synergistic effects. Author

N95-14335# Woods Hole Oceanographic Inst., MA.
REAL TIME SYSTEM FOR PRACTICAL ACOUSTIC MONITORING OF GLOBAL OCEAN TEMPERATURE, VOLUME 3 Quarterly Progress Report No. 5, 1 Apr. - 30 Jun. 1994
John L. Spiesberger, Daniel E. Frye, and John M. Kenny 30 Jun. 1994 206 p
(Contract MDA972-93-1-0004)
(AD-A283774) Avail: CASI HC A10/MF A03

Work continues on all GAMOT Tasks as described in ARPA Grant No: MDA972-93-1-004. (1) Task A. Task A work remains on schedule and we have completed the following work: We are writing a new eigenray finder for use in identifying the paths which sound take from sources to the surface suspended acoustic receivers; A theoretical investigation has been conducted which has found that it is possible that ray theory can be extended to acoustic frequencies below 100 Hz; A new parabolic approximation to the acoustic wave equation has been developed. Unlike all previous parabolic approximations, the new approximation predicts delays of acoustic pulses with little error; The acoustic multipaths from the Kaneohe source have been identified at one SOSUS station using a ray tracing algorithm called ZRAY. This was a breakthrough since this is the furthest, 4000 km, that ray theory has been successfully used to understand acoustic propagation in the ocean; (2) Task B. Task B tasks and deliverables are on schedule. We have completed writing of a manuscript detailing the travel time anomaly estimates using a reduced gravity model of the northeast Pacific. We have designed an acoustic tomography assimilation method for a similar model but with spatially variable density. The plan for monitoring the Pacific Ocean for long term change is contained in the Task B section; (3) Task C. Fabrication of ten operational SSAR's is continuing. Two units are being prepared for a test cruise at the AUTEC Range in August and two units are being prepared for testing in the Pacific in November. No significant delays or problems ahve been encountered; and (4) Task D. The 70 Hz source proposal was submitted to ARPA on April 19, 1994. No action has yet been taken on the proposal. DTIC

N95-14352# Army Engineer Waterways Experiment Station, Vicksburg, MS.
ADCIRC: AN ADVANCED THREE-DIMENSIONAL CIRCULATION MODEL FOR SHELVES, COASTS, AND ESTUARIES. REPORT 4: HURRICANE STORM SURGE MODELING USING LARGE DOMAINS
C. A. Blain, J. J. Westerink, and R. A. Luettich, Jr. Aug. 1994 69 p
(AD-A283868; WES/TR/DRP-92-6) Avail: CASI HC A04/MF A01

This report investigates the use of large domains in modeling hurricane storm surge. The hydrodynamic model used in this study is the ADCJIRC-2DDI code, which is based on a two-dimensional, depth-integrated, finite element formulation. Hurricane wind stress and pressure forcing from Hurricane Kate are produced by the HURWIN code, a vertically averaged planetary boundary layer wind model. Storm surge predictions are conducted over three computational domains, which have varying sizes. The smallest domain covers the continental shelf, another domain includes the Gulf of Mexico, and the final domain is quite large and extends into the deep ocean. Domains over the continental shelf and the Gulf of Mexico are shown to be inadequate for modeling hurricane storm surge. On the contrary, a large domain, which includes the Western North Atlantic Ocean, the Caribbean Sea, and the Gulf of Mexico, is optimal for use with storm surge models. The influence of an inverted barometer condition applied at the open boundary is examined for each computational domain. DTIC

N95-14906*# Florida Univ., Gainesville, FL.
DESIGN OF COMPONENTS FOR THE NASA OCEAN PROJECT
Jenna Wright, ed., James Clift, Bryan Dumais, Shannon Gardner, Juan Carlos Hernandez, Laura Nolan, Mia Park, Don Peoples, Elizabeth Phillips, and Mark Tillman et al Dec. 1993 84 p Prepared in cooperation with Universities Space Research Association, Columbia, MD
(Contract NASw-4435)
(NASA-CR-197207; NAS 1.26:197207) Avail: CASI HC A05/MF A01

The goal of the Fall 1993 semester of the EGM 4000 class was to design, fabricate, and test components for the 'Ocean CELSS Experimental Analog NASA' Project (OCEAN Project) and to aid in the future development of NASA's Controlled Ecological Life Support System (CELSS). The OCEAN project's specific aims are to place a human, Mr. Dennis Chamberland from NASA's Life Science Division of Research, into an underwater habitat off the shore of Key Largo, FL for three months. During his stay, he will monitor the hydroponic growth of food crops and evaluate the conditions necessary to have a successful harvest of edible food. The specific designs chosen to contribute to the OCEAN project by the EGM 4000 class are in the areas of hydroponic habitat monitoring, human health monitoring, and production of blue/green algae. The hydroponic monitoring system focused on monitoring the environment of the plants. This included the continuous sensing of the atmospheric and hydroponic nutrient solution temperatures. Methods for monitoring the continuous flow of the hydroponic nutrient solution across the plants and the continuous supply of power for these sensing devices were also incorporated into the design system. The human health monitoring system concentrated on continuously monitoring various concerns of the occupant in the underwater living habitat of the OCEAN project. These concerns included monitoring the enclosed environment for dangerous levels of carbon monoxide and smoke, high temperatures from fire, and the ceasing of the continuous airflow into the habitat. The blue/green algae project emphasized both the production and harvest of a future source of food. This project did not interact with any part of the OCEAN project. Rather, it was used to show the possibility of growing this kind of algae as a supplemental food source inside a controlled ecological life support system. Author

N95-15324 Naval Postgraduate School, Monterey, CA. Dept. of Oceanography.

TIDAL DYNAMICS AND MIXING OVER STEEP TOPOGRAPHY Ph.D. Thesis

Emanuel F. Coelho Jun. 1994 221 p Limited Reproducibility: More than 20% of this document may be affected by microfiche quality

(AD-A283535) Avail: CASI HC A10

Coastal currents and water column stratification frequently are determined by local phenomena that interact to produce complex dynamics. A process study was designed to assess the role of tides over a coastal shelf break as a local source of internal waves spatially-inhomogeneous, baroclinic residual currents, and internal mixing. The temporal evolution of three dimensional stratification and currents were characterized within a 4Kmx4Km box close to the mouth of Monterey Canyon, California. Strong, baroclinic, unidirectional, spatially inhomogeneous jet-like currents were observed with 24 hour periods, together with the occurrence of semidiurnal thermocline oscillations and vertically mixed layers. The linear theory of Baines predicts the existence of significant tidally forced internal waves in the area, with an interfacial mode at the thermocline decoupled from the internal waves propagating in the weaker stratification below. A ray tracing method is developed to study the nonlinear propagation of these tidally forced internal waves by considering wave advection and straining by the topographically controlled barotropic tidal flow while neglecting internal wave-wave interactions. It is found that nonlinear interaction of tidally forced internal waves with the topographically controlled barotropic tidal flow is a mechanism capable of forcing residual currents and internal wave shear instabilities that are capable of creating internal mixed layers similar to those observed at the mouth of Monterey Canyon. DTIC

N95-15330# Naval Command, Control and Ocean Surveillance Center, San Diego, CA. RDT and E Div.

DATA PROCESSING ROUTINES FOR THE SIPPICAN MK-12 XBT SYSTEM Final Report

Alvan Fisher, Jr. Apr. 1994 18 p

(AD-A283570) Avail: CASI HC A03/MF A01

This experimental software program is designed to assist the user to smooth, edit, and output expendable bathythermograph (XBT) data in BATHY message format. The MS-DOS routines described in this document should be compatible with most IBM-compatible personal computers. Author (DTIC)

N95-15425# Texas A&M Univ., College Station, TX. Dept. of Oceanography.

OPTICAL VARIABILITY IN THE EQUATORIAL AND SOUTHEAST PACIFIC

Wilford D. Gardner and Mary J. Richardson Aug. 1994 3 p

(Contract N00014-89-J-1478)

(AD-A283894) Avail: CASI HC A01/MF A01

The ultimate goal of this research is to obtain global coverage of the three-dimensional spatial distribution of beam attenuation. These data will be combined with hydrographic data and available satellite data to identify the physical and biogeochemical processes responsible for the observed optical distributions. These interpretations will help to divide the oceans into biohydrographic provinces to which different algorithms can be applied to extrapolate from satellite signals to estimate values of various oceanic parameters. DTIC

N95-15440# Massachusetts Inst. of Tech., Cambridge. Lab. for Water Resources and Hydrodynamics.

CALCULATION OF MOVABLE BED FRICTION FACTORS Final Report

Palitha N. Wikramanayake and Ole S. Madsen Aug. 1994 154 p

(AD-A283529; WES/CR/DRP-94-5) Avail: CASI HC A08/MF A02

When wind-generated waves propagate from the deep ocean onto the continental shelf, they begin to feel the effects of the bottom. These bottom effects are accounted for as bottom friction, which arises due to the no-slip flow condition on the bottom. This condition gives rise to a bottom shear stress and a thin boundary layer where significant energy dissipation can take place. The goal of this study was to develop a simple, physically realistic method to predict the friction factor over a movable sand bed under field conditions. Since reliable field measurements are available only for ripple geometry, laboratory data were used to derive the friction factor. Laboratory experiments are outlined in this report along with a brief description of the methods involved in the model derivation. The model is formulated in two stages, deriving predictive relations for the ripple geometry of a given wave condition, and developing a relationship among flow, ripple geometry, and the resulting friction factor. The relation between ripple geometry and roughness and the relationship between the friction factor and the wave, sediment, and fluid parameters are analyzed. Finally, simple relationships for the prediction of the roughness of a movable bed under regular and irregular waves are proposed and numerical examples illustrating use of the relationships are given. DTIC

N95-15452 Coastal Engineering Research Center, Vicksburg, MS.

SELECTING WAVE GAUGE SITES FOR MONITORING HARBOR OSCILLATIONS: A CASE STUDY FOR KAHULUI HARBOR, HAWAII Final Report

Michele Okihiro, R. T. Guza, and W. C. OReilly May 1994 35 p Limited Reproducibility: More than 20% of this document may be affected by microfiche quality

(AD-A281707; CERC-MP-94-10) Avail: Issuing Activity (Defense Technical Information Center (DTIC))

Wave measurements are required to observe and ultimately predict the response of the ocean to dynamic loading. While remote sensing techniques may eventually provide continuous spatial definition of wave energy for large regions, current engineering practice relies on point measurements from wave gauges. The U.S. Army Corps of Engineers' Field Wave Gaging Program (FWGP) operates a nationwide network of wave gauges and serves as the Corps' central, access point for all U.S. wave data. The program also supports a variety of activities to enhance the quality and efficiency of wave data collection, processing, and distribution. This is the third in a series of FWGP reports describing, through case studies, the process of selecting sites for wave gauges. DTIC

N95-15626 Naval Postgraduate School, Monterey, CA.

AN ANALYSIS OF EDDY RESOLVING GLOBAL OCEAN MODELS IN THE SOUTHERN OCEAN M.S. Thesis

Rosemarie OCarroll Mar. 1994 134 p Limited Reproducibility: More than 20% of this document may be affected by microfiche quality

(AD-A283211) Avail: CASI HC A07

Comparisons between the two model runs, a half degree resolution and a quarter degree resolution of the Semtner-Chervin eddy-resolving global ocean model, and the Hydrographic Atlas of the Southern Ocean observations are conducted by analyzing horizontal and vertical sections.

The quarter degree model, employing a Mercator grid, was interpolated forward from the half degree model initialization. For the last three years of the model run time, the resolution was improved to 0.25 deg on average and ECMWF winds were used. Also, no deep restoring in the last three years is introduced into the model. Another difference between the half degree model and the quarter degree model is that in the latter, the bathymetry is unsmoothed, so that not only is the resolution finer, the topography is more realistic. The model is shown to produce very realistic circulation and temperature and salinity distributions. Volume transport and meridional volume and heat transports are also calculated. The quarter degree model shows marked improvement over the half degree model although both models have salinities to the south and near the surface which are higher than those observed. This could be due to errors in surface flux parameterizations. DTIC

N95-15751*# Mississippi State Univ., Bay Saint Louis, MS. Center for Air Sea Technology.

DESIGN DOCUMENT FOR THE SURFACE CURRENTS DATA BASE (SCDB) MANAGEMENT SYSTEM (SCDBMS), VERSION 1.0

Ramesh Krisnnamagaru, Cheryl Cesario, M. S. Foster, and Vishnumohan Das Aug. 1994 42 p

(Contract NAS13-330)

(NASA-CR-197019; NAS 1.26:197019; AD-A284894; CAST-TN-8-94)

Avail: CASI HC A03/MF A01

The Surface Currents Database Management System (SCDBMS) provides access to the Surface Currents Data Base (SCDB) which is maintained by the Naval Oceanographic Office (NAVOCEANO). The SCDBMS incorporates database technology in providing seamless access to surface current data. The SCDBMS is an interactive software application with a graphical user interface (GUI) that supports user control of SCDBMS functional capabilities. The purpose of this document is to define and describe the structural framework and logistical design of the software components/units which are integrated into the major computer software configuration item (CSCI) identified as the SCDBMS, Version 1.0. The preliminary design is based on functional specifications and requirements identified in the governing Statement of Work prepared by the Naval Oceanographic Office (NAVOCEANO) and distributed as a request for proposal by the National Aeronautics and Space Administration (NASA). DTIC

N95-15753*# Mississippi State Univ., Bay Saint Louis, MS. Center for Air Sea Technology.

USERS MANUAL FOR THE SURFACE CURRENTS DATA BASE (SCDB) MANAGEMENT SYSTEM (SCDBMS), VERSION 1.0

Ramesh Krisnnamagaru, Cheryl Cesario, M. S. Foster, and Valentine Anantharaj Aug. 1994 41 p

(Contract NAS13-330)

(NASA-CR-197021; NAS 1.26:197021; AD-A284895; CAST-TN-7-94)

Avail: CASI HC A03/MF A01

The SCDBMS provides access to the Surface Current Data Base (SCDB) which is maintained by the Naval Oceanographic Office (NAVOCEANO). The SCDBMS incorporates relational database technology in providing seamless access to surface current observational data. The SCDBMS is an interactive software application. A graphical user interface (GUI) supports user access to its functional capabilities. The SCDBMS operates exclusively on surface current observation data. Each observation is composed of a location (latitude and longitude), a date (month, year, day), a classification code, a source code, the current speed (in knots) and direction (in degrees from which the current is flowing). Header information is neither necessary nor included in surface current observations data files. The import/export data files are written in ASCII format (SCDB ADMIN). Within the database, surface current data is stored using the generic latitude/longitude/time (LLT) data structure of the Navy Environmental Operational Nowcast Systems (NEONS). DTIC

51 LIFE SCIENCES (GENERAL)

N95-13638*# Louisville Univ., KY. Dept. of Microbiology and Immunology Sciences.

COSMOS 2229 IMMUNOLOGY STUDY (EXPERIMENT K-8-07) Final Report

Gerald Sonnenfeld Nov. 1993 49 p

(Grant NAG2-707)

(NASA-CR-196984; NAS 1.26:196984) Avail: CASI HC A03/MF A01

The purpose of the current study was to further validate use of the rhesus monkey as a model for humans in future space flight testing. The areas of immunological importance examined in the Cosmos 2229 flight were represented by two sets of studies. The first set of studies determined the effect of space flight on the ability of bone marrow cells to respond to granulocyte/monocyte colony stimulating factor (GM-CSF). GM-CSF is an important regulator in the differentiation of bone marrow cells of both monocyte/macrophage and granulocyte lineages and any change in the ability of these cells to respond to GM-CSF can result in altered immune function. A second set of studies determined space flight effects on the expression of cell surface markers on both spleen and bone marrow cells. Immune cell markers included in this study were those for T-cell, B-cell, natural killer cell, and interleukin-2 populations. Variations from a normal cell population percentage, as represented by these markers, can be correlated with alterations in immunological function. Cells were stained with fluorescein-labelled antibodies directed against the appropriate antigens, and then analyzed using a flow cytometer. Derived from text

N95-13702*# Young (Laurence R.), Rumney, NH.

LIFE SCIENCES CENTRIFUGE FACILITY REVIEW Final Report

Laurence R. Young 13 Sep. 1994 7 p

(NASA Order H-22785-D)

(NASA-CR-196849; NAS 1.26:196849; DCN 1-4-EA-00896) Avail: CASI HC A02/MF A01

The Centrifuge Facility Project at ARC was reviewed by a code U team to determine appropriateness adequacy for the ISSA. This report represents the findings of one consultant to this team and concentrates on scientific and technical risks. This report supports continuation of the project to the next phase of development. Author (revised)

N95-13990 Technische Univ., Delft (Netherlands).

ANALYSIS OF ELECTRON MICROSCOPE IMAGES: 3-D LOCALIZATION OF IMMUNO-MARKERS Ph.D. Thesis

J. P. P. Starink 6 Apr. 1993 137 p Limited Reproducibility: More than 20% of this document may be affected by microfiche quality

(PB94-197977; ISBN-90-9005917-2) Avail: CASI HC A07

Biologists have used microscopes for a long time to study cells. For that purpose, there are two groups of microscopes: (1) the light microscopes (LM); and (2) the electron microscopes (EM). Nowadays interest is shifting towards processing of 3-D information, for example to reveal structures within the cell or to elucidate cellular processes. To localize the proteins associated with the structures and processes under investigation, antibodies are used. A detectable marker is coupled to the antibodies. For LM this is a fluorescent group, and for EM an electron dense particle, such as colloidal gold. In this thesis the authors have focused on the analysis of EM images of immunogold labelled proteins. In this thesis the authors have investigated the question whether the gold particles can be localized in three dimensions using two tilted recordings with the aid of image processing techniques. User assistance is preferably needed only in actions in which no quantitative data is generated or altered. The problem can be divided into four steps: (1) Localization of the gold particles in the stereo pair images; (2) Solving the misalignment between the stereo pair images; (3) Finding the corresponding particles in both images; and (4) Depth recovery of the particles. NTIS

N95-14796*# California Univ., La Jolla, CA. School of Medicine.

ADAPTATION OF SKELETAL MUSCLE TO SPACEFLIGHT: COSMOS RHESUS PROJECT. COSMOS 2044 AND 2229 Final Report

Sue Bodine-Fowler 3 Oct. 1994 19 p

(Grant NAG2-653)

(NASA-CR-197041; NAS 1.26:197041) Avail: CASI HC A03/MF A01

The proposed experiments were designed to determine the effects of the absence of weight support on hindlimb muscles of the monkey: an ankle flexor (tibialis anterior, TA), two ankle extensors (medial gastrocnemius, MG and soleus, SOL), and a knee extensor (vastus lateralis, VL). These effects were assessed by examining the biochemical and morphological properties of muscle fibers obtained from biopsies in young Rhesus monkeys (3-4 Kg). Biopsies taken from ground base experiments were analyzed to determine: (1) the effects of chair restraint at 1 G on muscle properties and (2) the growth rate of flexor and extensor muscles in the Rhesus. In addition, two sets of biopsies were taken from monkeys which were in the flight pool and the four monkeys that flew on the Cosmos 2044 and 2229 biosatellite missions. Based on data collected in rats it is generally assumed that extensors atrophy to a greater extent than flexors in response to spaceflight or hindlimb suspension. Consequently, the finding that fibers in the TA (a fast flexor) of the flight monkeys atrophied, whereas fibers in the Sol (a predominantly slow extensor) and MG (a fast extensor) grew after a 14-day spaceflight (Cosmos 2044) and 12-day spaceflight (Cosmos 2229) was unexpected. In Cosmos 2044, the TA in both flight monkeys had a 21 percent decrease in fiber size, whereas the Sol and MG both had a 79 percent increase in fiber size. In Cosmos 2229, the TA in both flight monkeys showed significant atrophy, whereas the Sol and MG showed slight growth in one monkey (906) and slight atrophy in the other monkey (151). Derived from text

N95-14090*# National Aeronautics and Space Administration. Ames Research Center, Moffett Field, CA.
DEVELOPMENT OF LIFE SCIENCES EQUIPMENT FOR MICROGRAVITY AND HYPERGRAVITY SIMULATION
G. M. Mulenburg, J. Evans, M. Vasques, D. P. Gundo, J. B. Griffith, J. Harper, and T. Skundberg *In* NASA. Goddard Space Flight Center, Eighteenth Space Simulation Conference: Space Mission Success Through Testing Nov. 1994 p 373-386 (For primary document see N95-14062 03-18)
Avail: CASI HC A03/MF A04

N95-14091*# National Aeronautics and Space Administration. Ames Research Center, Moffett Field, CA.
UNIQUE LIFE SCIENCES RESEARCH FACILITIES AT NASA AMES RESEARCH CENTER
G. M. Mulenburg, M. Vasques, W. F. Caldwell, and J. Tucker *In* NASA. Goddard Space Flight Center, Eighteenth Space Simulation Conference: Space Mission Success Through Testing Nov. 1994 p 387-400 (For primary document see N95-14062 03-18)
Avail: CASI HC A03/MF A04

N95-14227*# Colorado Univ., Boulder, CO. BioServ Space Technologies.
COMMERCIAL INVESTIGATION RESULTS FOR THE GENERIC BIOPROCESSING APPARATUS FLOWN ON UNITED STATES MICROGRAVITY LABORATORY-1
Louis S. Stodieck, M. C. Robinson, and M. W. Luttges *In* NASA. Marshall Space Flight Center, Joint Launch + One Year Science Review of USML-1 and USMP-1 with the Microgravity Measurement Group May 1994 p 473-507 (For primary document see N95-14207 03-88)
Avail: CASI HC A03/MF A04

N95-15094*# Aerospace Medical Research Labs., Brooks AFB, TX. Lab. for Aerospace Cardiovascular Research.
TRANSESOPHAGEAL ECHOCARDIOGRAPHIC EVALUATION OF BABOONS DURING MICROGRAVITY INDUCED BY PARABOLIC FLIGHT
Marina N. Vernalis, Ricky D. Latham, John W. Fanton, and F. Andrew Geffney *In* International Union of Physiological Sciences, The Physiologist, Volume 36, Number 1, Supplement Feb. 1993 2 p (For primary document see N95-15089 03-52)
(NASA Order A-2401-D; AF Proj. 2312)
Avail: CASI HC A01/MF A02

N95-15098# CERB, Baugy (France).
TWENTY FOUR HOURS HEAD-DOWN TILT DECREASES ARTERIAL BAROREFLEX FUNCTION IN CONSCIOUS RAT
E. Martel, P. Champeroux, P. Lacolley, J. L. Cuche, and M. E. Safar *In* International Union of Physiological Sciences, The Physiologist, Volume 36, Number 1, Supplement Feb. 1993 2 p (For primary document see N95-15089 03-52)
Avail: CASI HC A01/MF A02

N95-15099# Northwestern Polytechnical Univ., Xian (China). Lab. of Applied and Systems Physiology.
CARDIOVASCULAR DECONDITIONING EFFECTS OF LONG-TERM SIMULATED WEIGHTLESSNESS IN RATS
Li-Fan Zhang, Jie Chen, Zhao-Ping Ding, and Jin Ma *In* International Union of Physiological Sciences, The Physiologist, Volume 36, Number 1, Supplement Feb. 1993 2 p (For primary document see N95-15089 03-52)
(Contract NNSF-39170795)
Avail: CASI HC A01/MF A02

N95-15101# Institute of Biomedical Problems, Moscow (USSR).
CHANGING GRAVITY LEVEL AND THE DEVELOPMENT OF ANIMALS
Lyubov V. Serova *In* International Union of Physiological Sciences, The Physiologist, Volume 36, Number 1, Supplement Feb. 1993 3 p (For primary document see N95-15089 03-52)
Avail: CASI HC A01/MF A02

N95-15102# Texas Univ. Health Science Center, Houston, TX. Dept. of Orthodontics.
TERATOGENIC EFFECTS OF DELTA g: THE CONCEPT OF ALLOMETRIC GROWTH
P. Jackie Duke, Dina Montufar-Solis, and Elizabeth Daane *In* International Union of Physiological Sciences, The Physiologist, Volume 36, Number 1, Supplement Feb. 1993 4 p (For primary document see N95-15089 03-52)
Avail: CASI HC A01/MF A02

N95-15103# Harvard Medical School, Boston, MA. Dept. of Otolaryngology and Communication Disorders.
ARE OTOCONIA DYNAMIC IN BIRDS AND MAMMALS?
Kenneth G. Pote *In* International Union of Physiological Sciences, The Physiologist, Volume 36, Number 1, Supplement Feb. 1993 4 p (For primary document see N95-15089 03-52)
Avail: CASI HC A01/MF A02

N95-15104*# Purdue Univ., West Lafayette, IN. Dept. of Anatomy.
THE AVIAN EMBRYO RESPONDING TO MICROGRAVITY OF SPACE FLIGHT
Ronald L. Hullinger *In* International Union of Physiological Sciences, The Physiologist, Volume 36, Number 1, Supplement Feb. 1993 4 p Sponsored by NASA, Washington; Kentucky Fried Chicken, Inc.; and Gore (D. R.) Trust (For primary document see N95-15089 03-52)
Avail: CASI HC A01/MF A02

N95-15106# Slovak Academy of Sciences, Bratislava (Czechoslovakia). Inst. of Animal Biochemistry.
BEHAVIOUR OF NEWLY HATCHED AND ADULT JAPANESE QUAIL AND THE FEASIBILITY OF ADAPTATION TO WEIGHTLESSNESS
L. Kostal, B. Bilcik, M. Jurani, K. Boda, E. Ja. Sepelev, T. S. Gurjeva, V. Sabo, I. Solcova, and J. Sykora *In* International Union of Physiological Sciences, The Physiologist, Volume 36, Number 1, Supplement Feb. 1993 3 p (For primary document see N95-15089 03-52)
Avail: CASI HC A01/MF A02

N95-15113# Louisville Univ., KY. Dept. of Microbiology and Immunology.
SPACE FLIGHT AND HUMORAL AND CELLULAR IMMUNITY OF ANIMALS
Gerald Sonnenfeld and Edwin S. Miller *In* International Union of Physiological Sciences, The Physiologist, Volume 36, Number 1, Supplement Feb. 1993 3 p (For primary document see N95-15089 03-52)
(Contract NCC2-213; NAG9-181; NAG9-234; NAG2-614; NAG2-624; NAG2-707)
Avail: CASI HC A01/MF A02

N95-15115# Florida Inst. of Tech., Melbourne, FL. Dept. of Biological Sciences.
DEVELOPMENT OF THE CHICK'S AUDITORY OSSICLE, THE COLUMELLA
Glenn M. Cohen and Walter Hersing *In* International Union of Physiological Sciences, The Physiologist, Volume 36, Number 1, Supplement Feb. 1993 2 p (For primary document see N95-15089 03-52)
(Grant NIH-RR-09032-1)
Avail: CASI HC A01/MF A02

N95-15116# Florida Inst. of Tech., Melbourne, FL. Dept. of Biological Sciences.
NEURONAL TYPES IN THE CHICKEN'S STATOACOUSTIC GANGLION
Glenn M. Cohen and John E. Love *In* International Union of Physiological Sciences. The Physiologist, Volume 36, Number 1, Supplement Feb. 1993 2 p Sponsored by Space Research Inst. (For primary document see N95-15089 03-52)
Avail: CASI HC A01/MF A02

N95-15117# Florida Inst. of Tech., Melbourne, FL. Dept. of Biological Sciences.
STRUCTURE OF AVIAN TECTORIAL, OTOLITHIC AND CUPULAR MEMBRANES
Glenn M. Cohen *In* International Union of Physiological Sciences, The Physiologist, Volume 36, Number 1, Supplement Feb. 1993 2 p Sponsored by Deafness Research Foundation (For primary document see N95-15089 03-52)
Avail: CASI HC A01/MF A02

N95-15118# Fujita Health Univ., Toyohashi (Japan). School of Health Sciences.
POSTURAL CONTROL OF FISH RELATED TO GRAVITY INPUT
Akira Takabayashi, Satoru Watanabe, and Sadaharu Takagi *In* International Union of Physiological Sciences, The Physiologist, Volume 36, Number 1, Supplement Feb. 1993 2 p (For primary document see N95-15089 03-52)
Avail: CASI HC A01/MF A02

N95-15119# Osaka Univ., Toyonaka (Japan). Div. of Neuromuscular Skills.
FUNCTIONAL PARTICIPATION OF THE VALVULA CEREBELLI ON THE GOLDFISH DORSAL LIGHT RESPONSE
Dai Yanagihara, Satoru Watanabe, and Sadaharu Takagi *In* International Union of Physiological Sciences, The Physiologist, Volume 36, Number 1, Supplement Feb. 1993 2 p (For primary document see N95-15089 03-52)
Avail: CASI HC A01/MF A02

N95-15132# Centre National de la Recherche Scientifique, Paris (France). Lab. de Neurobiologie des Regulations.
ALTERATIONS OF BODY TEMPERATURE, FEEDING, DRINKING AND SLEEP-WAKE CIRCADIAN RHYTHMS IN RHESUS MONKEY DURING A 19 DAY SPACELAB FLIGHT SIMULATION
Victor H. Demaria-Pesce and Emmanuel Balzamo *In* International Union of Physiological Sciences, The Physiologist, Volume 36, Number 1, Supplement Feb. 1993 2 p (For primary document see N95-15089 03-52)
(Grants CNES-90/0313; CNES-90/0295)
Avail: CASI HC A01/MF A02

N95-15133*# California Univ., Davis, CA. Section of Animal Physiology.
THE REGULATION OF RAT ACTIVITY FOLLOWING EXPOSURE TO HYPERDYNAMIC FIELDS
Charles A. Fuller, Linda M. Ishihama, and Dean M. Murakami *In* International Union of Physiological Sciences, The Physiologist, Volume 36, Number 1, Supplement Feb. 1993 2 p (For primary document see N95-15089 03-52)
(Grant NAGw-2195)
Avail: CASI HC A01/MF A02

N95-15135*# National Aeronautics and Space Administration. Ames Research Center, Moffett Field, CA.
NEW FINDINGS REGARDING LIGHT INTENSITY AND ITS EFFECTS AS A ZEITGEBER IN THE SPRAGUE-DAWLEY RAT
A. C. Tischler, C. M. Winget, D. C. Holley, C. W. Deroshia, J. Gott, G. Mele, and P. X. Callahan *In* International Union of Physiological Sciences, The Physiologist, Volume 36, Number 1, Supplement Feb. 1993 2 p Prepared in cooperation with San Jose State Univ., CA (For primary document see N95-15089 03-52)
(Contract NCC2-593)
Avail: CASI HC A01/MF A02

N95-15141# University Medical School of Debrecen, Debrecen (Hungary). Inst. of Pathophysiology.
EFFECT OF SHORT- AND LONG-TERM SPACEFLIGHT ON THE CONTRACTILE PROPERTIES OF RAT SKELETAL MUSCLES WITH DIFFERENT FUNCTIONS
M. Rapcsak, V. S. Oganov, T. Szilagyi, and A. Szoor *In* International Union of Physiological Sciences, The Physiologist, Volume 36, Number 1, Supplement Feb. 1993 4 p Prepared in cooperation with Institute of Biomedical Problems, Moscow, USSR (For primary document see N95-15089 03-52)
Avail: CASI HC A01/MF A02

N95-15142# Jikei Univ., Tokyo (Japan). First Dept. of Anatomy.
INFLUENCE TO ORGANS BY TEN WEEKS TAIL SUSPENSION
Kazuo Kosugi, Masayuki Nakaya, Shuji Takeuchi, and Hiroshi Yamashita *In* International Union of Physiological Sciences, The Physiologist, Volume 36, Number 1, Supplement Feb. 1993 2 p (For primary document see N95-15089 03-52)
Avail: CASI HC A01/MF A02

N95-15143# Jikei Univ., Tokyo (Japan). Space Medicine Lab.
RELATIONSHIP BETWEEN HIND-LIMB MUSCLE ATROPHY AND SERUM ENZYMES IN TAIL SUSPENDED RATS
Masayuki Nakaya, Kazuo Kosugi, and Shuji Takeuchi *In* International Union of Physiological Sciences, The Physiologist, Volume 36, Number 1, Supplement Feb. 1993 2 p (For primary document see N95-15089 03-52)
Avail: CASI HC A01/MF A02

N95-15144# Slovak Academy of Sciences, Bratislava (Czechoslovakia). Inst. of Animal Biochemistry and Genetics.
ACTIVITY OF ORNITHINE DECARBOXYLASE IN MUSCLE OF JAPANESE QUAIL IN HYPERGRAVITY CONDITIONS
Marian Jurani, Koloman Boda, Jan Jankela, Erika Juraniova, and Vladimir Sabo *In* International Union of Physiological Sciences, The Physiologist, Volume 36, Number 1, Supplement Feb. 1993 2 p (For primary document see N95-15089 03-52)
Avail: CASI HC A01/MF A02

N95-15148# Centre d'Enseignement et de Recherches de Medecine Aeronautique, Bretigny (France). Div. Histophysiologie.
ENHANCEMENT OF INSULIN RECEPTOR MEDIATED ENDOCYTOSIS IN CULTURED OSTEOBLASTIC CELLS UNDER HYPERGRAVITY
A. Malouvier, X. Holy, E. Zerath, P. J. Marie, and D. A. Schmitt *In* International Union of Physiological Sciences, The Physiologist, Volume 36, Number 1, Supplement Feb. 1993 2 p (For primary document see N95-15089 03-52)
Avail: CASI HC A01/MF A02

52 AEROSPACE MEDICINE

Includes physiological factors; biological effects of radiation; and effects of weightlessness on man and animals.

N95-13661*# National Aeronautics and Space Administration. Ames Research Center, Moffett Field, CA.
THE EFFECTS OF AUTOGENIC-FEEDBACK TRAINING ON MOTION SICKNESS SEVERITY AND HEART RATE VARIABILITY IN ASTRONAUTS

William B. Toscano (California Univ., Los Angeles, CA.) and Patricia S. Cowings Oct. 1994 138 p
(Contract NCC2-115; RTOP 199-70-12-14)
(NASA-TM-108840; A-94116; NAS 1.15:108840) Avail: CASI HC A07/MF A02

Space motion sickness (SMS) affects 50 percent of all people during early days of spaceflight. This study describes the results of two Shuttle flight experiments in which autogenic-feedback training (AFT), a physiological conditioning method, was tested as a treatment for this disorder. Of the six who were designated as flight subjects (two women and four men), three were given treatment and three served as controls (i.e., no AFT). Treatment subjects were given 6 hours of preflight AFT. Preflight results showed that AFT produced a significant increase in tolerance to rotating chair motion sickness tests. Further, this increased tolerance was associated with changes in specific physiological responses and reports of reduced malaise. Flight results showed that two of the three control subjects experienced repeated vomiting on the first mission day, while one subject experienced only moderate malaise. Of the three treatment subjects, one experienced mild discomfort, one moderate discomfort, and one severe motion sickness. Only the three control subjects took medication for symptom suppression. Measures of cardiac function reflective of vagal control were shown to be affected especially strongly on the first day of space flight. AFT given for control of heart rate, respiration, and other autonomic activity influenced both the vagal control measures and SMS. These data suggest that AFT may be an effective treatment for space motion sickness; however, this cannot be demonstrated conclusively with the small number of subjects described. Author

N95-13971 Edgerton, Germeshausen and Grier, Inc., Albuquerque, NM.
BLAST OVERPRESSURE STUDIES WITH ANIMALS AND MAN Final Report, 21 Jun. 1988 - 30 Sep. 1993
Daniel L. Johnson, John T. Yelverton, William Hicks, and Roy Doyal 15 Nov. 1993 75 p Limited Reproducibility: More than 20% of this document may be affected by microfiche quality
(Contract DAMD17-88-C-8141; DA Proj. 3M1-62787-A-878)
(AD-A280435) Avail: CASI HC A04

Anesthetized sheep were exposed to a reverberant wave environment like that produced from firing an anti-tank weapon from a room. The simulation was accomplished by detonating a C4 explosive outside a chamber of 18.2 m(exp 3) volume. The blast wave traveled into the chamber through a 20 cm I.D. tube and was reflected off the back wall and subsequently throughout the chamber. The resulting waveform very closely approximated that generated by a Carl-Gustav anti-tank weapon fired form a chamber. A series of 1 shot; 3 shot, 2.5 min. apart; or 12 shot, 2.5 min. apart exposures were used. The results indicate that multiple shots have a strong additive effect, decreasing the subthreshold levels. The subthreshold for a single blast is estimated to be below a smoothed peak of 31 kPa (approximately 65 kPa unsmoothed). The subthreshold for 3 exposures is estimated to be below 21.5 kPa (approximately 46 kPa unsmoothed). The subthreshold for 12 exposures was not found. DTIC

N95-14142# Michigan Univ., Ann Arbor, MI. Div. of Research Development and Administration.
EPIC COMPUTATIONAL MODELS OF PSYCHOLOGICAL REFRACTORY-PERIOD EFFECTS IN HUMAN MULTIPLE-TASK PERFORMANCE
David E. Meyer and David E. Kieras 1 Jun. 1994 56 p
(Contract N00014-92-J-1173)
(AD-A280924; TR-94/ONR-EPIC-2) Avail: CASI HC A04/MF A01

Perceptual-motor and cognitive processes whereby people perform multiple concurrent tasks have been studied through an overlapping-tasks procedure. During this procedure, two successive choice-region tasks are performed with a variable interval (stimulus onset asynchrony, or SOA) between the beginning of the first and second tasks. Subjects' reaction times (RTs) for Task 2 are typically greater after very short SOA's. The RT increase, called the psychological refractory-period (PRP) effect, reveals basic characteristics of multiple-task performance. In the present report, quantitative computational models are formulated to explain and predict the PRP effect together with other related phenomena on the basis of the EPIC information-processing architecture, a theoretical framework for precisely modeling human performance under representative single-task and multiple-task conditions (Kieras & Meyer, 1994, Tech. Report TR-94/ONR-EPIC-1). Computer simulations with these models suggest that the PRP effect may stem from subjects' task strategies and limitations on their peripheral perceptual-motor resources, rather than from a cognitive decision or response-selection 'bottleneck.' The goodness-of-fit between simulated and empirical data documents the EPIC architecture's utility for understanding and characterizing human multiple-task performance. DTIC

N95-14145# Air Force Inst. of Tech., Wright-Patterson AFB, OH.
MONITORING AUDIOMETRY IN HEARING CONSERVATION PROGRAMS Ph.D. Thesis
Thereas Y. Schulz 1994 195 p
(AD-A282024; AFIT/CI/CIA-94-006D) Avail: CASI HC A09/MF A03

An issue of crucial importance to any hearing conservation program is the criteria for determining significant threshold shift (STS), that is, the cut point for positive (abnormal) versus negative (normal) findings for an audiometric test. A second issue of importance is the follow-up process that most efficiently confirms that STS. The goal of an appropriate STS criteria is to identify individuals early in the process of noise-induced hearing loss before serious hearing loss occurs, but to avoid falsely identifying normal variability as noise-induced hearing loss. Data from the US Air Force Hearing Conservation Data Registry were used to evaluate these issues. DTIC

N95-14176# Federal Aviation Administration, Oklahoma City, OK. Civil Aeromedical Inst.
THE APPLICABILITY OF COMMERCIAL GLARE TEST DEVICES IN THE AEROMEDICAL CERTIFICATION OF PILOT APPLICANTS Final Report
Van B. Nakagawara, Ronald W. Montgomery, and Kathryn J. Wood Aug. 1994 20 p
(DOT/FAA/AM-94/15) Avail: CASI HC A03/MF A01

In his FY-92/93 Annual Program Guidance and Current Policy Statement, the Federal Air Surgeon requested continued investigation of new testing modalities, such as glare vision testing, as to their relevance to medical certification. Glare sensitivity is a normal age-related physiological change depriving the human visual system of vital information. An instrument that can effectively detect and measure visual performance loss from glare in a clinical environment would be a valuable tool for an Aviation Medical Examiner evaluating pilot applicants. This study evaluated several commercially available glare tests using factors of measured visual performance loss and relevant clinical features. Sixteen subjects (32 eyes) with normal ocular health were tested with a Brightness Acuity Tester (BAT), Penlight Test, MCT 8000, and a Miller-Nadler Glare Tester to determine each instrument's ability to detect visual acuity changes under simulated glare conditions. In addition, individual glare testers were subjectively rated by examining personnel as to clinical features important for use in an aeromedical screening, such as cost, training and space requirements, ease of operation and scoring, etc. Our results suggest that the BAT by Mentor O&O Inc., presented preferred test sensitivity and clinical features for use in screening glare disability. The other procedures either demonstrated an inability to detect visual acuity changes under simulated glare conditions or exhibited undesirable clinical features for use in aeromedical glare screening. These data may be used in evaluating future glare testers. Guidelines are provided for incorporating glare testing into the aeromedical certification process. Additional research is planned to identify specific glare problems in the aviation environment. Author

N95-14177# Federal Aviation Administration, Oklahoma City, OK. Civil Aeromedical Inst.
UNREPORTED MEDICATIONS USED IN INCAPACITATING MEDICAL CONDITIONS FOUND IN FATAL CIVIL AVIATION ACCIDENTS Final Report
Dennis V. Canfield, Jo Flemig, Jerry Hordinsky, and Stephen Veronneau Aug. 1994 8 p
(DOT/FAA/AM-94/14) Avail: CASI HC A02/MF A01

One of the major concerns in aviation medicine is sudden incapacitation of the pilot resulting in a fatal accident. The Office of Aviation Medicine (OAM) for the Federal Aviation Administration (FAA) is charged with the medical certification of pilots. All pilots are required by OAM to receive a medical examination by a qualified AME before they can receive medical certification. The pilots must complete a Medical Certification Form listing all of their medical conditions and medications. The Civil Aeromedical Institute's (CAMI) Toxicology and Accident Research Laboratory analyzes

all fatal aviation accidents that occur in the United States. This paper reports the cases where drugs used in the treatment of incapacitating illnesses were found along with the frequency with which these drugs and illnesses had been reported on the pilots' medical examinations. Specimens were collected by pathologists near the accident and placed in evidence containers provided by CAMI. These samples were refrigerated and shipped by overnight air. Upon receipt the specimens were inventoried and accessioned for the analysis of drugs, alcohol, carbon monoxide, and cyanide. All data collected by the laboratory were electronically entered into a computer for future analysis. We identified those cardiovascular, neurological, and psychiatric drugs most likely to be associated with the treatment of potentially incapacitating illness. Pilots using drugs for neurological and psychiatric conditions would normally not receive their medical certification. A full review of the complete accident file was conducted in several of the cases reported in this research. The Toxicology and Accident Research Laboratory received specimens from 2192 pilots for postmortem toxicology analysis between 1987 to 1992. Drugs used in the treatment of potentially incapacitating medical conditions were found in 48 of the cases received during this time. Most of the pilots did not report these drugs and medical conditions to their AME and the FAA. Drugs used in the treatment of cardiovascular diseases were found in 13 cases. Neurological medications were found in 7 of the cases. Medications used in the treatment of psychiatric conditions were found in 28 of the cases. In most of the cases reported, the drugs or illnesses found would have caused OAM to reject certification of the pilot. These pilots might not have died in the accident if they had notified their AME and the FAA of the drugs and medical conditions found. Some of the pilots who are deceitful in completing their medical certification forms are not identified and do receive medical certification. The information in this report will provide useful information to Aviation Medical Examiners regarding cases in which pilots did not report potentially incapacitating illnesses and the drugs used in the treatment of these illnesses. Author

N95-14184*# National Aeronautics and Space Administration. Langley Research Center, Hampton, VA.

PASSIVE FETAL HEART RATE MONITORING APPARATUS AND METHOD WITH ENHANCED FETAL HEART BEAT DISCRIMINATION Patent Application

Stephen A. Zahorian, inventor (to NASA) (Old Dominion Univ., Norfolk, VA.), David L. Livingston, inventor (to NASA) (Old Dominion Univ., Norfolk, VA.), and Robert A. Pretlow, III, inventor (to NASA) (Lockheed Engineering and Sciences Co., Hampton, VA.) 13 Oct. 1994 26 p

(NASA-Case-LAR-15129-1; NAS 1.71:LAR-15129-1; US-Patent-Appl-SN-323943) Avail: CASI HC A03/MF A01

An apparatus for acquiring signals emitted by a fetus, identifying fetal heart beats and determining a fetal heart rate is presented. Multiple sensor signals are outputted by a passive fetal heart rate monitoring sensor. Multiple parallel nonlinear filters filter these multiple sensor signals to identify fetal heart beats in the signal data. A processor determines a fetal heart rate based on these identified fetal heart beats. The processor includes the use of a figure of merit weighting of heart rate estimates based on the identified heart beats from each filter for each signal. The fetal heart rate thus determined is outputted to a display, storage, or communications channel. A method for enhanced fetal heart beat discrimination includes acquiring signals from a fetus, identifying fetal heart beats from the signals by multiple parallel nonlinear filtering, and determining a fetal heart rate based on the identified fetal heart beats. A figure of merit operation in this method provides for weighting a plurality of fetal heart rate estimates based on the identified fetal heart beats and selecting the highest ranking fetal heart rate estimate. NASA

N95-14394# Walter Reed Army Medical Center, Washington, DC.

MEDICAL RESEARCH PUBLICATIONS: A BIBLIOGRAPHY OF WALTER REED ARMY MEDICAL CENTER STAFF, 1986-1992, VOLUME 2 Final Report, 1 Jan. 1986 - 31 Dec. 1992

Judith O. Hartman and Hoyt W. Galloway Oct. 1993 528 p Supersedes AD-A238568

(PB94-177797; AD-A279317) Avail: CASI HC A23/MF A04

Medical Research Publications is Volume 2 of a staff bibliography produced by the Medical Library Service for the Walter Reed Army Medical Center (WRAMC). This second bibliography is cumulative (containing all citations from volume 1) and includes published monographs from January 1, 1986 to December 31, 1992. During those seven years WRAMC authors published 2,032 journal articles, journal letters, book chapters, and complete books. The bibliography does not list publications from authors assigned exclusively to WRAIR, AFIP, or any other tenant activities. All citation lists submitted to the Medical Library were authenticated by reprints, on-line database printouts, or original monographs. Citations listed in the bibliography include journal articles and letters, books, and book chapters. Abstracts, presentations, 'in press,' or 'submitted for review' listings submitted to the library were excluded. Medical files from MEDLARS and Dialog online systems were comprehensively searched to provide most of the items contained in the bibliography. NTIS

N95-14408# New York Univ. Medical Center, New York, NY.

MEASUREMENT AND REGULATION OF CENTRAL NORADRENERGIC RECEPTORS Annual Report, 1 Dec. 1992 - 30 Nov. 1993

Eric A. Stone, Guoying Bing, and Yi Zhang 30 Nov. 1993 8 p

(Contract F49620-92-J-0084; AF Proj. 2312)

(AD-A284219; AFOSR-94-0505TR) Avail: CASI HC A02/MF A01

In the past year we have continued our investigation of the relationship between central catecholaminergic systems and the effects of stress. We have completed or made progress in three studies of the role of the noradrenergic system in biochemical and behavioral effects of stress and one study of the role of the dopaminergic system in these behavioral effects. The first noradrenergic study concerned the mechanism of a biochemical response to stress which is believed to play a role in long term stress adaptation, the activation of the immediate early gene, c-fos, in the brain. On the basis of previous data we had hypothesized that the noradrenergic system is involved in the activation of this gene in the brain by stress. In the past year we confirmed this hypothesis by showing that the c-fos mRNA and protein responses to stresses could be reduced by treatment with the beta blocker, propranolol, and enhanced by the norepinephrine (NE) reuptake inhibitor, desmethylimipramine (DMI). These findings have supported a role of the noradrenergic system in adaptational phenomena. The second and third studies concerned the role of noradrenergic processes in two behavioral effects of stress, increased anxiety and motor impairment. In the study on stress-induced anxiety, we found that blockade of beta receptors with propranolol potentiates the stimulatory effect of stress on anxiety in two tests of the latter, passive avoidance and defensive withdrawal. DTIC

N95-14424# Naval Aerospace Medical Research Lab., Pensacola, FL.

NAVAL AEROSPACE MEDICAL RESEARCH LABORATORY. 1993 COMMAND HISTORY Final Report, Jan. - Dec. 1993

R. E. Gadolin, comp. and K. S. Mayer, comp. Apr. 1994 144 p

(AD-A284038) Avail: CASI HC A07/MF A02

This publication is a compilation of significant events that occurred at the Naval Aerospace Medical Research Laboratory during 1993. DTIC

N95-15089# International Union of Physiological Sciences. Commission on Gravitational Physiology.

THE PHYSIOLOGIST, VOLUME 36, NUMBER 1, SUPPLEMENT

Hilding Bjurstedt, ed. (Karolinska Inst., Stockholm, Sweden.) Bethesda, MD American Physiological Society Feb. 1993 181 p The 14th Annual Meeting of the International Union of Physiological Sciences was held in Berlin, Germany, 29 Sep. - 2 Oct. 1992; sponsored by International Society for Gravitational Physiology

Avail: CASI HC A09/MF A02

The special environments under study encompass, in addition to normal gravity, those created by the microgravity of space flight, and the high G-loadings encountered in high performance aircraft. These environments expose human subjects to extreme variations in gravitational forces ranging from zero to as much as nine times normal or more. The problems originating from these in part artificial but very real environments all center around the largely unknown role of gravity in the physiological equation. Topics covered in the papers presented include: current concepts in gravitational physiology, cardiovascular systems, gravitational effects on embryogenesis and development in animals, gravity and the immune system, vestibular systems, operational requirements in preventing G-induced loss of consciousness in high performance aircraft, cercadian rhythms, bone and muscles, metabolism, and hypergravity. For individual titles, see N95-15090 through N95-15150.

N95-15090# Danish Aerospace Medical Center of Research, Copenhagen (Denmark). National Univ. Hospital.

GRAVITATIONAL STRESS AND REGULATION OF NEUROENDOCRINE ELEMENTS AND FLUID VOLUME IN HUMANS

Peter Norsk *In* International Union of Physiological Sciences, The Physiologist, Volume 36, Number 1, Supplement Feb. 1993 4 p (For primary document see N95-15089 03-52)

Avail: CASI HC A01/MF A02

A change in gravitational stress on the human body has a profound influence upon renal fluid and sodium handling. As an example, human subjects immersed in water to the neck exhibit a 5 to 10 fold increase in renal sodium and water excretion compared to a corresponding upright seated control. Changing the direction of gravitational stress also induces a profound change in renal fluid and sodium excretion in humans. Weightlessness in orbital space flight, where the gravitational stress upon the human body is totally abolished, should also theoretically induce an augmented increase in renal fluid and sodium excretion. This is however, not clear as of today. It is known from results of the Skylab flights that astronauts immediately lose several kilograms of body mass upon entering the weightlessness environment. This paper presents recent laboratory results on the relationship between on the one hand cardiovascular baroreflexes and endocrine elements and on the other endocrine mediators and renal function during changes in gravitational stress. Author (revised)

N95-15091# Institute of Biomedical Problems, Moscow (USSR).

NEUROHUMORAL REACTIONS TO LONG-TERM VESTIBULAR STIMULATION IN MAN

Igor A. Nichiporuk, Alexander N. Rapotkov, Oleg I. Orlov, and Anatoly I. Grigoriev *In* International Union of Physiological Sciences, The Physiologist, Volume 36, Number 1, Supplement Feb. 1993 4 p (For primary document see N95-15089 03-52)

Avail: CASI HC A01/MF A02

Neuroendocrine metabolism regulation during vestibular stimulation studies in man are wide-spread in gravitational physiology and space medicine in the recent past. As a rule, these investigations are associated with vestibular stimulation for only several minutes or dozens of minutes in length. Practically, there are no modern research studies of neuroendocrine reactions to labyrinth stimulation extending over several hours or even several days. Such prolonged stimuli are especially interesting with reference to critical periods of motion sickness susceptibility in the acute period of adaptation to microgravity during space flight. Author (revised)

N95-15092# Mainz Univ. (Germany). Aerospace Medicine Group.

WILL MAN NEED THE VESTIBULAR SYSTEM IN GENERATIONS TO COME?

Joachim Wetzig *In* International Union of Physiological Sciences, The Physiologist, Volume 36, Number 1, Supplement Feb. 1993 4 p (For primary document see N95-15089 03-52)

(Grant DARA-10-QV-9050)

Avail: CASI HC A01/MF A02

Some people are of the opinion, that man's evolution reached a plateau when he became self-aware. Thus the argument goes, he was enabled to reflect on what happened to him and what he did to his environment. Subsequent to that, man would think ahead to the consequences of his actions and thereby actively shape his future to ensure optimal survival of his species. And this state of course no longer could be called evolution in the classical sense. Need one comment on the vanity of the hope for such a state? Let us assume then, that the evolution of man has not ended, but will continue and that man has barely a clue, yet, as to the direction it may lead. Author

N95-15093# Academy of Sciences (USSR), Moscow (USSR). Aviation and Space Medicine Service.

PSYCHOPHYSIOLOGICAL ASPECTS OF INCREASING RESISTANCE TO SPACE MOTION SICKNESS

E. S. Berezhnov, O. A. Vorobjev, and E. V. Lapaev *In* International Union of Physiological Sciences, The Physiologist, Volume 36, Number 1, Supplement Feb. 1993 3 p (For primary document see N95-15089 03-52)

Avail: CASI HC A01/MF A02

One of the problems of the adaptation period to microgravity is space motion sickness which negatively influences the well-being and performance of crewmembers in the initial and highly crucial phase of orbital flight. Among the measures available for decreasing space motion sickness, preflight training is very important. In this study, the efficiency of application of various combinations of vestibular-visual impacts are investigated. Author (revised)

N95-15094*# Aerospace Medical Research Labs., Brooks AFB, TX. Lab. for Aerospace Cardiovascular Research.

TRANSESOPHAGEAL ECHOCARDIOGRAPHIC EVALUATION OF BABOONS DURING MICROGRAVITY INDUCED BY PARABOLIC FLIGHT **c51**

Marina N. Vernalis, Ricky D. Latham, John W. Fanton, and F. Andrew Geffney *In* International Union of Physiological Sciences, The Physiologist, Volume 36, Number 1, Supplement Feb. 1993 2 p (For primary document see N95-15089 03-52)

(NASA Order A-2401-D; AF Proj. 2312)

Avail: CASI HC A01/MF A02

Transthoracic echocardiography (TTE) is a feasible method to noninvasively examine cardiac anatomy during parabolic flight. However, transducer placement on the chest wall is very difficult to maintain during transition to microgravity. In addition, TTE requires the use of low frequency transponders which limit resolution. Transesophical echocardiography (TEE) is an established imaging technique which obtains echocardiographic information from the esophagus. It is a safe procedure and provides higher quality images of cardiac structure than obtained with TTE. This study is designed to determine whether TEE was feasible to perform during parabolic flight and to determine whether acute central volume responses occur in acute transition to zero gravity by direct visualization of the cardiac chambers. Derived from text

N95-15095*# Aerospace Medical Research Labs., Brooks AFB, TX. Lab. for Aerospace Cardiovascular Research.

CIRCULATORY FILLING PRESSURES DURING TRANSIENT MICROGRAVITY INDUCED BY PARABOLIC FLIGHT

Ricky D. Latham, John W. Fanton, C. D. White, Mariana N. Vernalis, R. P. Crisman, and S. C. Koenig *In* International Union of Physiological Sciences, The Physiologist, Volume 36, Number 1, Supplement Feb. 1993 2 p (For primary document see N95-15089 03-52)

(NASA Order A-2401-D; AF Proj. 2312)

Avail: CASI HC A01/MF A02

Theoretical concepts hold that blood in the gravity dependent portion of the body would relocate to more cephalad compartments under microgravity. The result is an increase in blood volume in the thoraic and cardiac chambers. However, experimental data has been somewhat contradictory and nonconclusive. Early studies of peripheral venous pressure and estimates of central venous pressure (CVP) from these data did not show an increase in CVP under microgravity. However, CVP recorded in human volunteers during a parabolic flight revealed an increase in CVP during the microgravity state. On the STS 40 shuttle mission, a payload specialist wore a fluid line that recorded CVP during the first few hours of orbital insertion. These data revealed decreased CVP. When this CVP catheter was tested during parabolic flight in four subjects, two had increased CVP recordings and two had decreased CVP measurements. In 1991, our laboratory performed parabolic flight studies in several chronic-instrumented baboons. It was again noted that centrally recorded right atrial pressure varied with exposure to microgravity, some animals having an increase, and others a decrease. Author (revised)

N95-15096# Keimyung Univ., Taegu (Republic of Korea). Dept. of Physiology.

HEMODYNAMIC RESPONSES TO PASSIVE BODY TILTS

E. U. Chae and Y. S. Suh *In* International Union of Physiological Sciences, The Physiologist, Volume 36, Number 1, Supplement Feb. 1993 2 p (For primary document see N95-15089 03-52)

Avail: CASI HC A01/MF A02

To investigate the relationship between the effects of gravity and hemodynamic response to body tilt in the early steady-state, twelve healthy young adult males were passively tilted from the supine control position to the 15 degree, 30 degree, and 60 degree head-up position, and then to the minus 15 degree and minus 30 degree head-down position. Cardiac output, stroke volume, acceleration index of the heart, thoracic fluid volume, blood pressure, heart rate, total peripheral vascular resistance, and ECG

were measured. The changes of hemodynamic parameters except in blood pressure, were linearly related to the sine of the tilt angle regardless of the subjects being in the head-up or head-down position. Author (revised)

N95-15097# Tokyo Univ. (Japan). Dept. of Health Administration.
CARDIOVASCULAR RESPONSE TO COLD PRESSOR AND LBNP TESTS BEFORE AND AFTER 20-DAY-BEDREST
Yuichiro Haruna, Kiyoshi Kawakubo, Yoji Suzuki, and Atsuaki Gunji *In* International Union of Physiological Sciences, The Physiologist, Volume 36, Number 1, Supplement Feb. 1993 2 p (For primary document see N95-15089 03-52)
Avail: CASI HC A01/MF A02

Orthostatic hypotension after weightlessness has been suggested mainly because of the blood volume reduction, and decrease in stroke volume and cardiac output as its consequence. However, since bedrest is characterized as removal of orthostasis and exercise, which are major physiological stressors to the autonomic nervous system in normal daily life of humans, it may be possible that general autonomic activity itself would be deconditioned in the central nervous system after bedrest. Thus we hypothosized that 20-day bedrest may modify the cardiovascular responses to a cold pressor test which has been used to evaluate the autonomic response and which might be independent of blood volume changes. It was also hypothesized that if there were any changes in the response to the cold pressor test, they may be related to the changes of responses to a lower body negative pressure test. Author

N95-15098# CERB, Baugy (France).
TWENTY FOUR HOURS HEAD-DOWN TILT DECREASES ARTERIAL BAROREFLEX FUNCTION IN CONSCIOUS RAT **c51**
E. Martel, P. Champeroux, P. Lacolley, J. L. Cuche, and M. E. Safar *In* International Union of Physiological Sciences, The Physiologist, Volume 36, Number 1, Supplement Feb. 1993 2 p (For primary document see N95-15089 03-52)
Avail: CASI HC A01/MF A02

In humans, zero gravity induces a cardiovascular deconditioning. The transfer of blood from the periphery to the thoracic compartment, occurring immediately at the beginning of the exposure to microgravity seems to be involved in this phenomenon. Some studies have shown that microgravity induces an impairment of the baroreflex sensitivity in humans, but its involvement in the cardiovascular deconditioning is not completely understood. The aim of this study was to determine the modification of the artrial baroreflex using a model of simulated weightlessness in conscious rats during the exposure to microgravity. Results suggest that the alteration of the baroreflex functions, especially the impairment of its sympathetic component activity, may be involved in the orthostatic hypotension observed after weightlessness. Author (revised)

N95-15099# Northwestern Polytechnical Univ., Xian (China). Lab. of Applied and Systems Physiology.
CARDIOVASCULAR DECONDITIONING EFFECTS OF LONG-TERM SIMULATED WEIGHTLESSNESS IN RATS **c51**
Li-Fan Zhang, Jie Chen, Zhao-Ping Ding, and Jin Ma *In* International Union of Physiological Sciences, The Physiologist, Volume 36, Number 1, Supplement Feb. 1993 2 p (For primary document see N95-15089 03-52)
(Contract NNSF-39170795)
Avail: CASI HC A01/MF A02

We investigated the cardiovascular deconditioning effect of long-term simulated weightlessness to elucidate its mechanisms. Our research goal was established for the following three reasons. First, even after several decades of extensive research, there still exist significant gaps in our knowledge concerning microgravity induced cardiovascular effect. Second, in order to guarantee the health and safety of astronauts in future prolonged missions, it is important to understand the cardiovascular adaptation to long-term weightlessness. Third, the reported ultrastructural degenerative changes in myocardium of rats flown on the Cosmos 1887 bio-satellite has raised concerns about whether long-term space flight may lead to myocardial degeneration. In this paper, we focus primarily on findings from our recent work on the cardiovascular deconditioning effect of 90-/120-day tail suspension and changes in baroreflex responsiveness and in contractility and ultrastructure of the heart in rats. Author (revised)

N95-15100# California Univ., Davis, CA. Section of Animal Physiology.
SOME GENETIC ASPECTS OF ADAPTATION TO HYPERDYNAMIC ENVIRONMENTS
Arthur H. Smith *In* International Union of Physiological Sciences, The Physiologist, Volume 36, Number 1, Supplement Feb. 1993 3 p (For primary document see N95-15089 03-52)
Avail: CASI HC A01/MF A02

Reports by many investigators have described a wide variety of biological changes in man and animals exposed to gravitational fields, some of these having a beneficial effect, but others are detrimental. These changes are considered to result from the alteration in the gravitational field since (a) they appear when the field is changed, (b) the degree of change tends to be proportional to the change in acceleration strength, and (c) these changes disappear, and at varying rates, when the gravitational field is returned to normal gravity. However, little information has been developed concerning the reception and transduction of the gravitational stimulus, or its lack, to produce these biological changes. Author

N95-15101# Institute of Biomedical Problems, Moscow (USSR).
CHANGING GRAVITY LEVEL AND THE DEVELOPMENT OF ANIMALS **c51**
Lyubov V. Serova *In* International Union of Physiological Sciences, The Physiologist, Volume 36, Number 1, Supplement Feb. 1993 3 p (For primary document see N95-15089 03-52)
Avail: CASI HC A01/MF A02

Space biology has accumulated a great body of information concerning the influence of microgravity upon objects of varying levels of biological organization; from microorganisms to higher animals and humans. However, the choice of biological objects was in most cases random, and there has been no attempt at a comparative biological analysis of the results obtained. A similar situation is found in hypergravity research where responses in various animal classes are compared mainly with respect to differences in body masses rather than in the level of biological organization. Author

N95-15102# Texas Univ. Health Science Center, Houston, TX. Dept. of Orthodontics.
TERATOGENIC EFFECTS OF DELTA g: THE CONCEPT OF ALLOMETRIC GROWTH **c51**
P. Jackie Duke, Dina Montufar-Solis, and Elizabeth Daane *In* International Union of Physiological Sciences, The Physiologist, Volume 36, Number 1, Supplement Feb. 1993 4 p (For primary document see N95-15089 03-52)
Avail: CASI HC A01/MF A02

Changes in fetal bone growth have been noted both in excess and microgravity. This paper examines the relationship between the length of the ossified area of the tibia of fetuses developing under excess gravity with fetal mass at 1 gravity and fetal weight at the gravity force level of exposure. Derived from text

N95-15103# Harvard Medical School, Boston, MA. Dept. of Otolaryngology and Communication Disorders.
ARE OTOCONIA DYNAMIC IN BIRDS AND MAMMALS? **c51**
Kenneth G. Pote *In* International Union of Physiological Sciences, The Physiologist, Volume 36, Number 1, Supplement Feb. 1993 4 p (For primary document see N95-15089 03-52)
Avail: CASI HC A01/MF A02

The sensory detectors within the inner ears of vertebrates have a variety of morphologies built on a common theme: a sensory hair cell with an accessory, extracellular structure to increase the sensitivity to the end-organ's specific modality. These accessory structures are the tectorial membrane in the cochlea, the cristae in the apullae, and the otoconial membrane in the masculae. They enhance respectively, the detection of sound, of angular acceleration, and of linear acceleration by the underlying hair cell-containing sensory epithelium. Little is known about these extracellular structures in terms of their protein composition, their regulation of the expression of these proteins, or whether the proteins and minerals are turned over. This paper discusses experiments which have attempted to address the question of the dynamics of the otoconial protein and mineral phases in relation to their sensitivity to changes in gravitational forces. Author

N95-15104*# Purdue Univ., West Lafayette, IN. Dept. of Anatomy.
THE AVIAN EMBRYO RESPONDING TO MICROGRAVITY OF SPACE FLIGHT **c51**
Ronald L. Hullinger *In* International Union of Physiological Sciences, The Physiologist, Volume 36, Number 1, Supplement Feb. 1993 4 p Sponsored by NASA, Washington; Kentucky Fried Chicken, Inc.; and Gore (D. R.) Trust (For primary document see N95-15089 03-52)
Avail: CASI HC A01/MF A02

Of all the many potential and real microenvironmental influences, only gravity would appear to have remained relatively constant and ubiquitous for developing organisms. Histo- and organogenesis as well as differential growth of the embryo and fetus may have evolved with a constant environmental factor of gravity. Chick embryos of 2-day and 9-day stages of incubation were flown in an incubator on the Space Shuttle during a 9-day mission. Significant differences in embryo response to this microgravity environment were observed. This paper offers an analysis and suggests mechanisms which may contribute to these results. Derived from text

N95-15105*# Nebraska Univ., Lincoln, NE. Neurophysiology Lab.
VESTIBULAR ONTOGENY: MEASURING THE INFLUENCE OF THE DYNAMIC ENVIRONMENT
Timothy A. Jones, Sherri M. DeVries, Linda M. DuBois, and Rick C. Nelson *In* International Union of Physiological Sciences, The Physiologist, Volume 36, Number 1, Supplement Feb. 1993 4 p (For primary document see N95-15089 03-52)
(Grant NAGw-1275)
Avail: CASI HC A01/MF A02

In comparison to other special senses, we are only meagerly informed about the development of vestibular function and the mechanisms that may operate to control or influence the course of vestibular ontogeny. Perhaps one contributing factor to this disparity is the difficulty of evaluating vestibular sense organs directly and noninvasively. The present report describes a recently developed direct noninvasive vestibular function test that can be used to address many basic questions about the developing vestibular system. More particularly, the test can be used to examine the effects of the dynamic environment (e.g. gravitational field and vibration) on vestibular ontogeny. Author

N95-15106# Slovak Academy of Sciences, Bratislava (Czechoslovakia). Inst. of Animal Biochemistry.
BEHAVIOUR OF NEWLY HATCHED AND ADULT JAPANESE QUAIL AND THE FEASIBILITY OF ADAPTATION TO WEIGHTLESSNESS **c51**
L. Kostal, B. Bilcik, M. Jurani, K. Boda, E. Ja. Sepelev, T. S. Gurjeva, V. Sabo, I. Solcova, and J. Sykora *In* International Union of Physiological Sciences, The Physiologist, Volume 36, Number 1, Supplement Feb. 1993 3 p (For primary document see N95-15089 03-52)
Avail: CASI HC A01/MF A02

The aim of cosmic biology is to create conditions necessary for the long-term stay of man on cosmic orbital complexes and planetary stations. Such conditions should be provided by the autonomous closed ecosystem - a simplified model of the terrestrial biogenesis. As an experimental model of the higher heterotrophic link of this ecosystem the Japanese quail was chosen. This paper presents recent knowledge on the behavior of newly hatched and adult quails under conditions of weightlessness. Videorecords made as part of the experiments aboard the MIR orbital station do not meet the criteria of systematic behavioral observation required for qualitative and quantitative behavioral analysis on earth. Nevertheless, the data is highly interesting and original, and was therefore analysed and summarized. Author

N95-15107# Graz Univ. (Austria). Research Group for Volume Regulation and Space Medicine.
COMPARISON OF HEMODYNAMIC AND VOLUME RESPONSES TO DIFFERENT LEVELS OF LOWER BODY SUCTION AND HEAD-UP TILT
Eva Maria Koenig, Gabriele Sauseng-Fellegger, and Helmut Hinghofer-Szalkay *In* International Union of Physiological Sciences, The Physiologist, Volume 36, Number 1, Supplement Feb. 1993 3 p Sponsored by Austrian Ministry for Sciences and Research (For primary document see N95-15089 03-52)
Avail: CASI HC A01/MF A02

Orthostatic challenge such as lower body suction or head-up tilt induce marked shifts of blood from the cardiopulmonar into lower extremity vascular compartments. As a reaction to central hypovolemia, counterregulating mechanisms take place immediately, including central/peripheral circulatory and neurohumoral responses. Compensatory actions are exerted via autonomic reflexes. The sympathetic nervous system increases heart rate and peripheral resistance to adjust the cardiovascular system to the stress. This study investigates two grades of lower body suction and two tilt angles in 12 male subjects. Before, during, and after cardiovascular loading we recorded heart rate, systolic, diastolic, and mean arterial blood pressure. For calculation of blood volume shifts, plasma density, and hematocrit were measured. We addressed the following: if (1) heart rate and blood pressure react similarly to lower body negative pressure and head-up tilt, (2) there is evidence of unloading of high pressure receptors with low levels of orthostatic/circulatory stress, and (3) a correlation between the amount of fluid loss and grade of stimulus intensity can be established. Author (revised)

N95-15108# Amsterdam Univ. (Netherlands). Dept. of Physiology.
BODY POSITION AND VOLUME STATUS AS DETERMINANTS OF CARDIOVASCULAR RESPONSES TO TRANSITION INTO MICROGRAVITY IN PARABOLIC FLIGHT
John M. Karemaker, Wim J. Stok, and Rick D. Latham *In* International Union of Physiological Sciences, The Physiologist, Volume 36, Number 1, Supplement Feb. 1993 2 p Sponsored by Space Research Organization Netherlands Prepared in cooperation with Army Aeromedical Research Lab., Fort Rucker, AL (For primary document see N95-15089 03-52)
Avail: CASI HC A01/MF A02

The present project is part of a larger study involving noninvasive cardiac monitoring by echo-Doppler. We will focus in this report on blood pressure and heart rate changes as observed by noninvasive finger blood pressure measurement. Our test subjects were followed through a number of parabolas while lying supine or sitting upright in a euhydrated condition (experiment 1), later followed by experiment 2 where we induced hypervolemia by having them in the supine legs-up position for at least two hours before the flight. These experiments aimed at unravelling the effects of hydrostatics on baroreceptors and fluid shifts on the venous side. Author

N95-15109# Sheffield Univ. (England).
CARDIOVASCULAR AND METABOLIC RESPONSES TO 6 DEG HEAD-DOWN TILT (HDT) AND 70 DEG HEAD-UP TILT (HUT) FOLLOWING EXERCISE
Erik L. O. Seedhouse *In* International Union of Physiological Sciences, The Physiologist, Volume 36, Number 1, Supplement Feb. 1993 4 p (For primary document see N95-15089 03-52)
Avail: CASI HC A01/MF A02

In the aim of suppressing or minimizing the cardiovascular disadaptation observed when subjects return to normal gravity after exposure to weightlessness, some countermeasures have been applied during space flight. Among these, exercise which leads to a distribution of blood volume similar to that observed in normal gravity, is currently incorporated in all missions. An immediate effect of entry into zero gravity is the removal of the head to foot gravitational force on the cardiovascular system. The purpose of this study was to evaluate and examine the cardiorespiratory, metabolic, and blood pressure response to submaximal exercise in two conditions. Author (revised)

N95-15110# Laboratoire de Medecine Aerospatiale, Bretigny-sur-Orge (France). Centre d'Essais en Vol.
A MATHEMATICAL MODEL OF THE CARDIOVASCULAR RESPONSE TO +Gz ACCELERATION
Francois M. Melchior, R. Srini Srinivasan, Gerard Ossard, and Jean-Michel Clere *In* International Union of Physiological Sciences, The Physiologist, Volume 36, Number 1, Supplement Feb. 1993 2 p (For primary document see N95-15089 03-52)
(Grant DRET-90-1053J)
Avail: CASI HC A01/MF A02

The cardiovascular system is the limiting factor for human tolerance to positive gravity (head to foot) acceleration induced during maneuvers of fighter aircraft. Safe handling of modern fighter aircraft with higher acceleration capabilities requires the use of countermeasures such as a G-suit or breathing at a positive pressure. A better understanding of the mechanisms involved in the cardiovascular response to high gravity force

acceleration would help improve the design and application of protective measures. This paper presents a simple mathematical model of the cardiovascular system which incorporates arterial and cardiopulmonary baroreflexes, left ventricular-peripheral circulation interaction and decreased venous return. This model is capable of reproducing observed overall cardiovascular response to positive gravity acceleration. Author

N95-15111# Bunka Women's Univ. (Japan). Lab. of Physical Education.
EFFECTS OF 20 DAYS BED-REST ON CARDIO-RESPIRATORY FUNCTIONS DURING SUB-MAXIMAL EXERCISE IN YOUNG WOMEN
J. Nagano, S. Torikoshi, K. Yokozawa, K. Itoh, and Y. Suzuki *In* International Union of Physiological Sciences, The Physiologist, Volume 36, Number 1, Supplement Feb. 1993 2 p (For primary document see N95-15089 03-52)
Avail: CASI HC A01/MF A02

The effects of 20 days bed rest on cardiorespiratory functions during the sub-maximal exercise in different body positions was studied. Three young women of 20-23 years of age participated in the study using the sitting, supine and 30 degrees head-down position. Despite the differences in body position, oxygen uptake and heart rate during the sub-maximal exercise increased due to the 20 days of bed rest, and returned to the initial levels 9 weeks after the bed rest period. CASI

N95-15112# Office National d'Etudes et de Recherches Aerospatiales, Paris (France).
MODELING AND NUMERICAL SIMULATION OF THE CEREBRAL BLOOD FLOW UNDER ACCELERATION
D. Gaffie, A. Guillaume, and P. Quandieu *In* International Union of Physiological Sciences, The Physiologist, Volume 36, Number 1, Supplement Feb. 1993 2 p Sponsored by DRET Prepared in cooperation with Centre d'Enseignement et de Recherches de Medecine Aeronautique, Bretigny, France (For primary document see N95-15089 03-52)
Avail: CASI HC A01/MF A02

When fighter aircraft change directions, the pilots are subject to a centrifugal force. This force can be enough to induce pilot loss of consciousness (LOC). The physiological cause of this LOC is brain hypoxia which results from an increase in hydrostatic pressure. Under gradual onset rate of positive gravitational acceleration, the brain hypoxia occurs with visual effects familiar to fighter pilots. They feel a reduction in peripheral vision (grey out), followed by a loss of central vision (black out). The useful time of consciousness can be prolonged by using an anti-G suit. Under rapid onset rates of positive gravitational acceleration, new symptoms of the LOC, characterized by the absence of a grey or black out have been observed. The objective of this study is a better understanding of mechanisms which cause fighter pilot inflight LOC. A physical method has been developed which takes into account the influence of the rate of change in acceleration on the cerebrovascular system. Author (revised)

N95-15113# Louisville Univ., KY. Dept. of Microbiology and Immunology.
SPACE FLIGHT AND HUMORAL AND CELLULAR IMMUNITY OF ANIMALS **c51**
Gerald Sonnenfeld and Edwin S. Miller *In* International Union of Physiological Sciences, The Physiologist, Volume 36, Number 1, Supplement Feb. 1993 3 p (For primary document see N95-15089 03-52)
(Contract NCC2-213; NAG9-181; NAG9-234; NAG2-614; NAG2-624; NAG2-707)
Avail: CASI HC A01/MF A02

The use of animal surrogates for the study of the effects of space flight on immune response is desirable for several reasons. First, animal models are very useful in conditions where the use of human subjects would be difficult. This is certainly true in the space flight environment, where the number of human subjects is small, the human subjects are often too occupied with space flight duties to serve as subjects, and where sampling could be difficult under adverse conditions. Second, because of the intense interest in the immune system, many animal models and reagents already exist that are readily adaptable to space flight studies. Therefore, animal models have been used for many years for space flight studies on immunity. The predominant model used has been the rat, although recently, development of a rhesus monkey model has begun. The focus of this paper will be a description of the results of ground based and space flight animal models to determine the effects of space flight on immune responses. Author

N95-15114*# National Aeronautics and Space Administration. Lyndon B. Johnson Space Center, Houston, TX.
IMMUNE CHANGES IN HUMANS CONCOMITANT WITH SPACE FLIGHTS OF UP TO 10 DAYS DURATION
Gerald R. Taylor *In* International Union of Physiological Sciences, The Physiologist, Volume 36, Number 1, Supplement Feb. 1993 4 p (For primary document see N95-15089 03-52)
Avail: CASI HC A01/MF A02

The time relation of various classes of in-flight human physiological changes is illustrated. Certain problems, such as neurovestibular, fluid, and electrolyte imbalances tend to occur early in a flight, followed by stabilization at some microgravity equilibrium level. Cardiovascular dysfunctions and erythrocyte mass losses appear to follow a similar pattern, although the significant changes occur later in flight. Bone and calcium changes and radiation effects are thought to progressively worsen with time, whereas the time course of immune change is yet to be fully understood. Significant immunologic changes in cosmonauts and astronauts during and after space flight have been documented as have microbiological changes. Thus, space flight can be expected to effect a blunting of the human cellular immune mechanism concomitant with a relative increase in potentially pathogenic microorganisms. This combination would seem to increase the probability of infectious disease events in flight. Derived from text

N95-15115# Florida Inst. of Tech., Melbourne, FL. Dept. of Biological Sciences.
DEVELOPMENT OF THE CHICK'S AUDITORY OSSICLE, THE COLUMELLA **c51**
Glenn M. Cohen and Walter Hersing *In* International Union of Physiological Sciences, The Physiologist, Volume 36, Number 1, Supplement Feb. 1993 2 p (For primary document see N95-15089 03-52)
(Grant NIH-RR-09032-1)
Avail: CASI HC A01/MF A02

The avian middle ear contains a single auditory ossicle that is composed of a bony columella and a cartlaginous extracolumella. The columellar footplate (clipeolus) inserts into the oval window at its proximal end. The extracolumella attaches to the tympanic membrane at its distal end. The present study was undertaken to determine the patterns of growth, chondrification, and ossification of the chick's auditory ossicle before and after hatching. Author

N95-15116# Florida Inst. of Tech., Melbourne, FL. Dept. of Biological Sciences.
NEURONAL TYPES IN THE CHICKEN'S STATOACOUSTIC GANGLION **c51**
Glenn M. Cohen and John E. Love *In* International Union of Physiological Sciences, The Physiologist, Volume 36, Number 1, Supplement Feb. 1993 2 p Sponsored by Space Research Inst. (For primary document see N95-15089 03-52)
Avail: CASI HC A01/MF A02

In the hearing organs of vertebrates, bipolar sensory (afferent) neurons innervate the hair cells (sensory epithelium) by their dendritic (peripheral) processes. In the mammalian cochlea two neuronal types (1 and 2) innervate the inner and outer hair cells, respectively. By comparison, the correspondence between neuronal and hair cell types is uncertain in the avian auditory lagena (cochlea). The objective of the present study was to identify and map the relative distributions neuronal types in the chicken's statoacoustic ganglion (SAG) by means of morphometric analysis and immuno-reactivity to neuron-specific enolase (NSE) and neuro-filament protein 200 kDa (NPF-200). Author

N95-15117# Florida Inst. of Tech., Melbourne, FL. Dept. of Biological Sciences.
STRUCTURE OF AVIAN TECTORIAL, OTOLITHIC AND CUPULAR MEMBRANES **c51**
Glenn M. Cohen *In* International Union of Physiological Sciences, The Physiologist, Volume 36, Number 1, Supplement Feb. 1993 2 p Sponsored by Deafness Research Foundation (For primary document see N95-15089 03-52)
Avail: CASI HC A01/MF A02

Any explanation of cochlear and vestibular micromechanics must include the contributions of the tectorial (TM), otolithic (OM) and cupular (CM) membranes. However, unresolved questions about the microarchitechture of these membranes and the types and number of attachments to their underlying sensory areas have hampered the development of micromechanical modes of transduction. These membranes are notoriously difficult to preserve because they undergo severe shrinkage during fixation and embedding. We have empirically developed fixation procedures that reduce shrinkage, and thereby preserve the microarchitectures. As a result, we can realistically depict the spatial relations and attachments of tectorial, otolithic, and cupular membranes to their respective sensory areas.
Author

N95-15118# Fujita Health Univ., Toyohashi (Japan). School of Health Sciences.
POSTURAL CONTROL OF FISH RELATED TO GRAVITY INPUT c51
Akira Takabayashi, Satoru Watanabe, and Sadaharu Takagi *In* International Union of Physiological Sciences, The Physiologist, Volume 36, Number 1, Supplement Feb. 1993 2 p (For primary document see N95-15089 03-52)
Avail: CASI HC A01/MF A02

The disappearance of gravity input during space flight causes many functional disorders in animal and human postural control systems. On the other hand, it has been shown that these functional deficits are reduced or disappear with time and adaptation to weightlessness. Fish behavior observed during spaceborne experiments suggest that fish might provide a good model for investigating adaptation of sensory motor interaction in microgravity. In this investigation, the behavioral changes of bilaterally labrinthectomized and unilaterally labrinthectomized fish adapted for more than 3 months on the ground postoperatively were used to analyze whether buoyancy was affected by injecting of a contrast medium into the swimming bladder. Author (revised)

N95-15119# Osaka Univ., Toyonaka (Japan). Div. of Neuromuscular Skills.
FUNCTIONAL PARTICIPATION OF THE VALVULA CEREBELLI ON THE GOLDFISH DORSAL LIGHT RESPONSE c51
Dai Yanagihara, Satoru Watanabe, and Sadaharu Takagi *In* International Union of Physiological Sciences, The Physiologist, Volume 36, Number 1, Supplement Feb. 1993 2 p (For primary document see N95-15089 03-52)
Avail: CASI HC A01/MF A02

The vestibular organs of fish are well developed and play an important role in maintaining postural equilibrium. Postural equilibrium in teleost fish also depends on visual information. The dorsal light response (DLR), an innate behavior of teleost fish whereby the back is oriented toward a given light source represents a simple interaction between the visual and vestibular sensory inputs. In order to identify the neural center of the DLR in goldfish, lesion studies of the goldfish brain were conducted. The DLR was not affected by the expiration of the corpus cerebelli, but was entirely abolished after bilateral lesions of the valvula cerebelli, which in goldfish, was separated into the medial and lateral lobes by a longitudinal fissure. In spite of many reported findings, the function and fiber connections of the vavula cerebelli, especially its lateral lobe, are still unknown. Therefore, we examined the afferent connections of the lateral lobe by means of a tracing technique with horseradish perioxidase. Furthermore, we investigated the effects of selective lesions of the medial and lateral valvula cerebelli on DLR. Author (revised)

N95-15120# Udine Univ. (Italy). Dipt. di Scienze e Tecnologie Biomediche.
ON-EARTH EVALUATION OF THE NEUROVESTIBULAR TOLERANCE TO CENTRIFUGE SIMULATED ARTIFICIAL GRAVITY IN HUMANS
G. Antonutto, D. Linnarsson, and P. E. diPrampero *In* International Union of Physiological Sciences, The Physiologist, Volume 36, Number 1, Supplement Feb. 1993 3 p Sponsored by Italian MURST and Swedish National Space Board (For primary document see N95-15089 03-52)
Avail: CASI HC A01/MF A02

Exposure to microgravity, besides affecting the neurovestibular system, causes a general functional decay of several organs and appartuses of the human body, particularly at the level of the circulatory and musculo-skeletel systems. Since it is generally believed that artificial gravity can prevent these adverse effects, means of mimicking the Earth's gravitational field in space have recently become a highly debated topic, particularly in view of long term space flights. The aim of the present study was to investigate whether and to what extent subjects exposed to altered conditions similar to those encountered by astronauts when riding a proposed twin bikes system would be susceptible to acute motion sickness. Author (revised)

N95-15121# Tuebingen Univ. (Germany). Dept. of Neurology.
THE INFLUENCE OF GRAVITY ON VESTIBULAR NYSTAGMUS IN HUMANS
E. Koenig, D. Tweed, M. Fetter, D. Fischer, and H. Misslisch *In* International Union of Physiological Sciences, The Physiologist, Volume 36, Number 1, Supplement Feb. 1993 2 p (For primary document see N95-15089 03-52)
Avail: CASI HC A01/MF A02

Traditionally, the human vestibular system is tested by acceleration and deceleration in a rotating chair, simulating the horizontal semicircular canals. This kind of testing provides no information about the performance of the two pairs of vertical (anterior and posterior) canals and the two pairs of otoliths. Testing the vestibulo-ocular reflex (VOR) in its entirety requires rotations around the 3 axis of the head (yaw, pitch, and roll) as well as rotation where the axis is not aligned with gravity. The data presented here are, to our knowledge, the first measurements of the VOR in normal humans obtained with 3-dimensional high resolution recording techniques.
Author

N95-15122# Universities Space Research Association, Houston, TX.
THE RELATIONSHIP BETWEEN SPACE SICKNESS AND PREFLIGHT DIET
Karl E. Simanonok, Randall L. Kohl, and John B. Charles *In* International Union of Physiological Sciences, The Physiologist, Volume 36, Number 1, Supplement Feb. 1993 2 p (For primary document see N95-15089 03-52)
Avail: CASI HC A01/MF A02

Some preflight variables relating to fluid, electrolyte, and cardiovascular status, and to environmental exposures, have previously been found to have significant relationships to space sickness. The purpose of this study was to determine if diet could be another factor contributing to space sickness, since diet determines so much of physiology and behavior.
Author

N95-15123# Karolinska Inst., Stockholm (Sweden). Dept. of Environmental Physiology.
MANIPULATING THE ARTERIAL PRESSURE TO PREVENT G-LOC
Hilding Bjurstedt *In* International Union of Physiological Sciences, The Physiologist, Volume 36, Number 1, Supplement Feb. 1993 2 p (For primary document see N95-15089 03-52)
Avail: CASI HC A01/MF A02

The procedures that can be used to manipulate the arterial blood pressure at head level are categorized. G-loss of consciousness (G-LOC) is compared with other types of loss of consciousness that may occur in healthy individuals. From a hemodynamic point of view, there are several important differences between the G-LOC of flight and other cardiovascular types of loss of consciousness. In the syncope of motionless standing at normal gravity, in positive pressure breathing, prolonged valsalva maneuvers, in exposure to lower body negative pressure, venous pooling occurs as a primary event. Another type is the classical or 'simple' faint, sometimes called vasodepressor or vasovagal syncope. G-LOC in flight, or on the centrifuge, is distinctly different. Here the anti-G suit largely prevents venous pooling, and cardiac filling is preserved. But the hydrostatic pressure components are so great, that the arterial pressure falls to near zero at head level. This is a direct consequence of the increased effective weight of the blood column between heart and head. Derived from text

N95-15124# Aerospace Medical Research Labs., Brooks AFB, TX.
GUIDELINES FOR A RESEARCH AND DEVELOPMENT (R/D) PROGRAM FOR HIGH SUSTAINED G
Russell R. Burton *In* International Union of Physiological Sciences, The Physiologist, Volume 36, Number 1, Supplement Feb. 1993 4 p (For

primary document see N95-15089 03-52)
Avail: CASI HC A01/MF A02

This article focuses on operational requirements to prevent G-induced loss of consciousness (G-LOC) in high performance aircraft. There are two types of requirements: (a) pre-G-LOC detection devices that monitor physiological changes of the pilot before G-LOC occurs, and (b) the more generic personal G protection systems to increase G tolerance. Recently there have been major advances in G-protection research and development systems that significantly improve G-level and G-duration tolerances. These are: (1) positive pressure breathing systems assisted by chest counterpressure that are activated by an increase in G-levels, (2) An improved anti-G suit that provides uniform pressure of the lower body that includes the operational anti-G suit abdominal bladder, and (3) a combination of the positive pressure breathing systems and the improved G-suit (advanced tactical anti-G suit). Author (revised)

N95-15125# Royal Air Force Inst. of Aviation Medicine, Farnborough (England).
NON-INVASIVE PHYSIOLOGICAL MONITORING RELEVANT TO G-INDUCED LOSS OF CONSCIOUSNESS
David H. Glaister *In* International Union of Physiological Sciences, The Physiologist, Volume 36, Number 1, Supplement Feb. 1993 3 p (For primary document see N95-15089 03-52)
Avail: CASI HC A01/MF A02

The aim of this paper is to look briefly at some of the newer technologies being applied to centrifuge studies and which have the potential to provide much of the data needed to elucidate the mechanisms involved in G-loss of consciousness. Of particular interest are techniques which use near infrared spectroscopy to measure the cerebral oxygen status at the cellular level. All such techniques must, however, be validated against standard methodologies or be shown to give appropriate responses to stressors having well documented effects. Author

N95-15126# Laboratoire de Medecine Aerospatiale, Bretigny-sur-Orge (France). Centre d'Essais en Vol.
PHYSIOLOGICAL CONSIDERATIONS CONCERNING POSITIVE PRESSURE BREATHING (PBG) DURING +Gz
J. M. Clere, G. Ossard, and F. Melchior *In* International Union of Physiological Sciences, The Physiologist, Volume 36, Number 1, Supplement Feb. 1993 4 p (For primary document see N95-15089 03-52)
Avail: CASI HC A01/MF A02

The ability to tolerate high gravity radial acceleration depends primarily on the maintenance of sufficient head level arterial pressure and cerebral blood flow to prevent the occurrence of blackout and G-induced loss of consciousness (G-LOC). Because of the hydrostatic effect on the heart to head blood column during high gravity acceleration, if exposures to higher high gravity levels are to be tolerated, either the column must be shortened or arterial pressure at heart level must be elevated. This paper is an overview of the effect and concomitant side effects of positive pressure breathing (PBG) as a means to increase arterial pressure at the heart and indirectly, at the cerebral level. However, before doing that, it is necessary to summarize the different ways for increasing arterial pressure to obtain tolerance to high gravity loads: (1) reclined seat, (2) anti-G suits, (3) anti-G straining maneuver. Author (revised)

N95-15127# Mayo Clinic, Rochester, MN.
OPERATIONAL REQUIREMENTS FOR AVOIDANCE AND EVENTUAL ELIMINATION OF Gz-INDUCED LOSS OF CONSCIOUSNESS (G-LOC) IN FLIGHT
Earl Wood *In* International Union of Physiological Sciences, The Physiologist, Volume 36, Number 1, Supplement Feb. 1993 4 p Sponsored by Waters Instruments and Clark (David) Co., Inc. (For primary document see N95-15089 03-52)
Avail: CASI HC A01/MF A02

On the basis of the physiology involved in G-induced loss of consciousness (G-LOC) and because of the very high cost in pilot lives and their airplanes due to G-LOC, three operational requirements are described: (1) a noninvasive on-line real-time recording of arterial pulsations at brain level should be a mandatory requirement for every human centrifuge exposure to high G accelerations that carry an appreciable likelihood of loss of vision and/or consciousness. A similar system should be mandatory for every pilot when performing high-G air-to-air or air-to-ground combat maneuvers both in training and in actual combat; (2) a physiological forewarning system based on arterial pulsations at the head level coupled with a last resort automatic airplane recovery system should be installed in all advanced fighter aircraft; (3) A G-LOC avoidance system based on a 9-G or greater activated timer should be installed in all advanced fighter aircraft. Failure of pilot response should then activate a follow-on automatic airplane recovery system. For future operations, an advanced high-G cockpit for flight in the fully horizontal position should be developed.
Derived from text

N95-15128*# National Aeronautics and Space Administration. Ames Research Center, Moffett Field, CA.
REGIONAL CUTANEOUS MICROVASCULAR FLOW RESPONSES DURING GRAVITATIONAL AND LBNP STRESSES
Gregory A. Breit, Donald E. Watenpaugh, Richard E. Ballard, Gita Murthy, and Alan R. Hargens *In* International Union of Physiological Sciences, The Physiologist, Volume 36, Number 1, Supplement Feb. 1993 2 p Sponsored in part by NAS-NRC (For primary document see N95-15089 03-52)
(RTOP 199-14-12-04)
Avail: CASI HC A01/MF A02

Due to the regional variability of local hydrostatic pressures, microvascular flow responses to gravitational stress probably vary along the length of the body. Although these differences in local autoregulation have been observed previously during whole-body tilting, they have not been investigated during application of artificial gravitational stresses, such as lower body negative pressure or high gravity centrifugation. Although these stresses can create equivalent G-levels at the feet, they result in distinct distributions of vascular transmural pressure along the length of the body, and should consequently elicit different magnitudes and distributions of microvascular response. In the present study, the effects of whole-body tilting and lower body negative pressure on the level and distribution of microvascular flows within skin along the length of the body were compared. Author

N95-15129# Universities Space Research Association, Houston, TX.
PHYSIOLOGIC MECHANISMS EFFECTING CIRCULATORY AND BODY FLUID LOSSES IN WEIGHTLESSNESS AS SHOWN BY MATHEMATICAL MODELING
Karl E. Simanonok, R. Srini Srinivasan, and John B. Charles *In* International Union of Physiological Sciences, The Physiologist, Volume 36, Number 1, Supplement Feb. 1993 2 p (For primary document see N95-15089 03-52)
Avail: CASI HC A01/MF A02

The purpose of this study was to examine the mechanisms which could explain the loss of body fluids in weightlessness and how a cardiovascular preadaptation countermeasures previously tested ameliorated body fluid losses. It is assumed that the physiology of head down tilt provides a reasonable accurate analog of weightless exposure. Author

N95-15130# Krug Life Sciences, Inc., Houston, TX.
SIMULATION OF THE FLUID RETENTION EFFECTS OF A VASOPRESSIN ANALOG USING THE GUYTON MODEL OF CIRCULATION
R. Srini Srinvasan, Karl E. Simanonok, S. M. Fortney, and John B. Charles *In* International Union of Physiological Sciences, The Physiologist, Volume 36, Number 1, Supplement Feb. 1993 2 p (For primary document see N95-15089 03-52)
Avail: CASI HC A01/MF A02

Fluid Loading (FL) consisting of water and salt tablets equivalent to 32 oz of isotonic saline is a countermeasure currently in use by NASA to improve the orthostatic tolerance of astronauts during Shuttle reentry. However, the effectiveness of this countermeasure has been observed to decrease with the duration of space flight. Possible ways to improve fluid retention and thus the effectiveness of FL include use of analogs of vasopressin such as lypressin (LVP). This study used a computer simulation approach to analyze the potential benefits on fluid retention with LVP administered before FL. Author

N95-15131# Graz Univ. (Austria). Volume Regulation and Space Medicine Research Group.

TRANSIENT BLOOD/PLASMA DENSITY AND HEMATOCRIT EFFECTS AFTER PASSIVE (SITTING) THERMONEUTRAL WATER IMMERSION IN MEN

Helmut Hinghofer-Szalkay, Eva Marie Koenig, and Hanns-Christian Gunga *In* International Union of Physiological Sciences, The Physiologist, Volume 36, Number 1, Supplement Feb. 1993 3 p Sponsored by Academy of Sciences (For primary document see N95-15089 03-52)

Avail: CASI HC A01/MF A02

At the beginning of and with ceasing of suction exerted upon the lower parts of the body, we have recently discovered transient hemodillution/hemoconcentration effects using high precision so called mechanical oscillator techniques. Since transient effects are useful for biological systems analysis, we questioned if such transients in blood and plasma density also occur with and immediately after water immersion in humans. In this paper, we present evidence that, as with termination of lower body suction, there might be transient hemoconcetration in the first minutes of thermoneutral water immersion in a sitting position in men, but no evidence could be obtained for any counterdirected transient hemodillution when test subjects were passivly brought out (in sitting position) from the water, as was found with starting lower body suction (in supine position). Author (revised)

N95-15132# Centre National de la Recherche Scientifique, Paris (France). Lab. de Neurobiologie des Regulations.

ALTERATIONS OF BODY TEMPERATURE, FEEDING, DRINKING AND SLEEP-WAKE CIRCADIAN RHYTHMS IN RHESUS MONKEY DURING A 19 DAY SPACELAB FLIGHT SIMULATION c51

Victor H. Demaria-Pesce and Emmanuel Balzamo *In* International Union of Physiological Sciences, The Physiologist, Volume 36, Number 1, Supplement Feb. 1993 2 p (For primary document see N95-15089 03-52)

(Grants CNES-90/0313; CNES-90/0295)

Avail: CASI HC A01/MF A02

Previous experiments performed with mammals during spaceflight suggest that microgravity may affect the circadian timekeeping system. However, this system could also be influenced by other factors related to the spaceflight environment, such as the animal compartment. In order to clarify the influence of the spaceflight environment, other than microgravity itself, on the circadian timekeeping system, we evaluated the characteristics of the circadian rhythms of body temperature, food and water intake, and sleep-wake cycles in Rhesus monkeys during the first 19-day flight simulation of this project. Author

N95-15133*# California Univ., Davis, CA. Section of Animal Physiology.

THE REGULATION OF RAT ACTIVITY FOLLOWING EXPOSURE TO HYPERDYNAMIC FIELDS c51

Charles A. Fuller, Linda M. Ishihama, and Dean M. Murakami *In* International Union of Physiological Sciences, The Physiologist, Volume 36, Number 1, Supplement Feb. 1993 2 p (For primary document see N95-15089 03-52)

(Grant NAGw-2195)

Avail: CASI HC A01/MF A02

The microgravity of space flight and the hyperdynamic fields produced via centrifugation have allowed researchers to examine the effect of altered gravitational environments on the regulation of physiological systems. In this study, a high frequency light/dark cycle was provided for 24 hours as an environmental challenge to assess the recovery of homeostatic and circadian components of physiological regulation in rats. For example, the nocturnal rat exhibited a homeostatic increase in body temperature during the dark periods and a decrease during the light periods. In addition, the magnitude of the body temperature response exhibits a time of day variation demonstrating the effect on circadian regulation. Author (revised)

N95-15134# Tokyo Woman's Christian Univ. (Japan). Lab. of Human Physiology.

WATER INTAKE AND URINARY VOLUME DURING 20 DAYS BED-REST IN YOUNG WOMEN

Kikuko Yokozawa, Shigeyo Torikoshi, Junko Nagano, Katsuko Ito, and Yoji Suzuki *In* International Union of Physiological Sciences, The Physiologist, Volume 36, Number 1, Supplement Feb. 1993 2 p (For primary document see N95-15089 03-52)

Avail: CASI HC A01/MF A02

During bed rest in young subjects, the water intake should be depressed because the diuretic is probably accelerated and then total body water and body weight is decreased by the water loss. The present study investigates whether urinary volume is independent of water intake during 20 days of horizontal bed rest in young women. Author (revised)

N95-15135*# National Aeronautics and Space Administration. Ames Research Center, Moffett Field, CA.

NEW FINDINGS REGARDING LIGHT INTENSITY AND ITS EFFECTS AS A ZEITGEBER IN THE SPRAGUE-DAWLEY RAT c51

A. C. Tischler, C. M. Winget, D. C. Holley, C. W. Deroshia, J. Gott, G. Mele, and P. X. Callahan *In* International Union of Physiological Sciences, The Physiologist, Volume 36, Number 1, Supplement Feb. 1993 2 p Prepared in cooperation with San Jose State Univ., CA (For primary document see N95-15089 03-52)

(Contract NCC2-593)

Avail: CASI HC A01/MF A02

In most mammals, the suprachiasmatic nucleus of the anterior hypothalamus has been implicated as the central driving mechanism of circadian rhythmicity. The photic input from the retina, via the retino-hypothalamic tract, and modulation from the pineal gland help regulate the clock. In this study, we investigated the effects of low light intensity on the circadian system of the Sprague-Dawley rat. A series of light intensity experiments were conducted to determine if a light level of 0.1 Lux will maintain entrained circadian rhythms of feeding, drinking, and locomotor activity. Author

N95-15136*# National Aeronautics and Space Administration. Ames Research Center, Moffett Field, CA.

MUSCULOSKELETAL ADAPTATION TO MECHANICAL FORCES ON EARTH AND IN SPACE

Robert Whalen *In* International Union of Physiological Sciences, The Physiologist, Volume 36, Number 1, Supplement Feb. 1993 4 p (For primary document see N95-15089 03-52)

Avail: CASI HC A01/MF A02

A major concern of the US and Russian space programs is the health and safety of astronauts and cosmonauts. One of the areas receiving the most attention has been the effects of long duration space flight on the musculoskeletel system. After three decades of space flight and research, questions continue. Can exercise in space maintain musculoskeletal tissue mass and function in an adult? The objective of this paper is to address this question in a way that hopefully provides a rational basis for quantifying and evaluating the influnence of daily activities on muscle and bone on Earth and in space. Author (revised)

N95-15137# Deutsche Sporthochschule, Cologne (Germany). Physiologisches Inst.

EFFECTS OF MICROGRAVITY ON INTERSTITIAL MUSCLE RECEPTORS AFFECTING HEART RATE AND BLOOD PRESSURE DURING STATIC EXERCISE

D. Essfeld, K. Baum, U. Hoffmann, and J. Stegemann *In* International Union of Physiological Sciences, The Physiologist, Volume 36, Number 1, Supplement Feb. 1993 4 p (For primary document see N95-15089 03-52)

(Contract DARA-50-WB-9113)

Avail: CASI HC A01/MF A02

During space flight large muscle groups, in particular the leg muscles, are subjected to substantial and persisting fluid losses while other reflexogenic areas see only mild, if any, permanent changes. Mechanical, thermal and various chemical changes have been reported to excite group 3 and 4 afferents from the musculature. During the last years we collected some experimental evidence that the already broad range of receptive properties includes a sensitivity to the local state of hydration. These findings indicate that some local, interstitial dehydration sensitivity exists independently of the cause of the extracellular volume reduction. We therefore hypothesized that leg exercise in weightlessness will augment heart rate and blood pressure responses to a similar extent as during local, interstitial dehydration on Earth. Author (revised)

N95-15138# Deutsche Gesellschaft fuer Luft- und Raumfahrt, Cologne (Germany). Inst. for Aerospace Medicine.
ORTHOSTATIC STRESS BY LOWER BODY NEGATIVE PRESSURE AND ITS BODY FLUID DISTRIBUTION KINETICS UNDER MICROGRAVITY
F. J. Baisch *In* International Union of Physiological Sciences, The Physiologist, Volume 36, Number 1, Supplement Feb. 1993 4 p (For primary document see N95-15089 03-52)
Avail: CASI HC A01/MF A02

To support the hypothesis that interstitial fluid loss is one of the components of the 'cardiovascular deconditioning' induced by space flight, a series of three experiments was performed on one subject after 5 days in space: (1) standard thigh cuffs were inflated up to suprasystolic pressure values (CUFF 1) for two minutes; (2) half an hour later a lower body negative pressure test (LBNP) followed with minus 15 mmHg for 5, minus 30 mmHg for 5, and minus 40 mmHg for 15 minutes; (3) twenty minutes after that, the CUFF maneuver was repeated (CUFF 2). Author

N95-15139*# National Aeronautics and Space Administration. Ames Research Center, Moffett Field, CA.
A METHOD FOR CONTINUOUS MONITORING OF THE GROUND REACTION FORCE DURING DAILY ACTIVITY
Robert Whalen, Jason Quintana, and Jeff Emery *In* International Union of Physiological Sciences, The Physiologist, Volume 36, Number 1, Supplement Feb. 1993 2 p (For primary document see N95-15089 03-52)
Avail: CASI HC A01/MF A02

Theoretical models and experimental studies of bone remodeling have identified peak cyclic force levels (or cyclic tissue strain energy density), number of daily loading cycles, and load (strain) rate as possible contributors to bone modeling and remodeling stimulus. To test our theoretical model and further investigate the influence of mechanical forces on bone density, we have focused on the calcaneus as a model site loaded by calcaneal surface tractions which are predominantly determined by the magnitude of the external ground reaction force (GRF). Author

N95-15140*# National Aeronautics and Space Administration. Ames Research Center, Moffett Field, CA.
BONE GEOMETRY, STRUCTURE AND MINERAL DISTRIBUTION USING DUAL ENERGY X RAY ABSORPTIOMETRY (DXA)
Robert Whalen and Tammy Cleek *In* International Union of Physiological Sciences, The Physiologist, Volume 36, Number 1, Supplement Feb. 1993 2 p (For primary document see N95-15089 03-52)
Avail: CASI HC A01/MF A02

Dual energy x-ray absorptiometry (DXA) is currently the most widely used method of analyzing regional and whole body changes in bone mineral content (BMC) and areal (g/sq cm) bone mineral density (BMD). However, BMC and BMD do not provide direct measures of long bone geometry, structure, or strength nor do regional measurements detect localized changes in other regions of the same bone. The capabilities of DXA can be enhanced significantly by special processing of pixel BMC data which yields cross-sectional geometric and structural information. We have extended this method of analysis in order to develop non-uniform structural beam models of long bones. Author

N95-15141# University Medical School of Debrecen, Debrecen (Hungary). Inst. of Pathophysiology.
EFFECT OF SHORT- AND LONG-TERM SPACEFLIGHT ON THE CONTRACTILE PROPERTIES OF RAT SKELETAL MUSCLES WITH DIFFERENT FUNCTIONS c51
M. Rapcsak, V. S. Oganov, T. Szilagyi, and A. Szoor *In* International Union of Physiological Sciences, The Physiologist, Volume 36, Number 1, Supplement Feb. 1993 4 p Prepared in cooperation with Institute of Biomedical Problems, Moscow, USSR (For primary document see N95-15089 03-52)
Avail: CASI HC A01/MF A02

Contractile properties of rat skeletal muscles were investigated in the Cosmos biosatellite experiments. After the end of the space flights the rats were sacrificed and the muscles of both the forelimbs (brachial muscle and the caput medials of the triceps muscle) and the hindlimbs (extensor digitorum longus, soleus and medial gastrocnemius muscles) were excised. The results obtained in the investigation of the animals participating in the space flight were compared to the data of both the vivarium controls and the synchronous controls kept under identical terrestrial conditions.
Author

N95-15142# Jikei Univ., Tokyo (Japan). First Dept. of Anatomy.
INFLUENCE TO ORGANS BY TEN WEEKS TAIL SUSPENSION c51
Kazuo Kosugi, Masayuki Nakaya, Shuji Takeuchi, and Hiroshi Yamashita *In* International Union of Physiological Sciences, The Physiologist, Volume 36, Number 1, Supplement Feb. 1993 2 p (For primary document see N95-15089 03-52)
Avail: CASI HC A01/MF A02

The subject of atrophy has been the focus of interest for morphologists as well as the scientist in space medicine. Muscle atrophy was noted to be influenced by microgravity in space. Using tail suspension techniques, we have studied the influence of gravity on rats. In the present study, we tried to study the influence of long term microgravity, with ten weeks tail suspension. Author (revised)

N95-15143# Jikei Univ., Tokyo (Japan). Space Medicine Lab.
RELATIONSHIP BETWEEN HIND-LIMB MUSCLE ATROPHY AND SERUM ENZYMES IN TAIL SUSPENDED RATS c51
Masayuki Nakaya, Kazuo Kosugi, and Shuji Takeuchi *In* International Union of Physiological Sciences, The Physiologist, Volume 36, Number 1, Supplement Feb. 1993 2 p (For primary document see N95-15089 03-52)
Avail: CASI HC A01/MF A02

Many studies on the effects of gravity have been reported using animals or human beings since gravity influences the biological body in space. Especially suspension techniques for rats have been used as a microgravity simulation. This study is a report on the relation between serum enzymes such as CK and muscle atrophy, caused by tail suspension in rats.
Author

N95-15144# Slovak Academy of Sciences, Bratislava (Czechoslovakia). Inst. of Animal Biochemistry and Genetics.
ACTIVITY OF ORNITHINE DECARBOXYLASE IN MUSCLE OF JAPANESE QUAIL IN HYPERGRAVITY CONDITIONS c51
Marian Jurani, Koloman Boda, Jan Jankela, Erika Juraniova, and Vladimir Sabo *In* International Union of Physiological Sciences, The Physiologist, Volume 36, Number 1, Supplement Feb. 1993 2 p (For primary document see N95-15089 03-52)
Avail: CASI HC A01/MF A02

Ornithine decarboxylase (ODC) is the rate limiting enzyme in the synthesis of polyamines which are generally required for animal cell proliferation. Because of many different stimuli changing the activity of ODC, the effect of hypergravity on muscle ODC activity in Japanese quail was investigated. Adult Japanese quail cockerels were exposed to 2G in the centrifuge permanently for 96 hours. The activity of ODC was determined by radioisotope method in supernatant of homogenized breast and fibular muscles (m. pectoralis minor, m. superficialis fibrularis). The activity of ODC was higher in breast muscle than in the fibular muscle in both control and experimental groups. Exposition of quail to hypergravity evokes approximately two fold increase of ODC activity in both breast and fibular muscles. The results suggest that 96 hours of permanent hypergravitation (2G) caused activation of polyamine synthesis and their involvement in biochemical processes of adaptation to hypergravity. Author

N95-15145# Tokyo Univ. (Japan). Dept. of Health Administration.
20 DAYS BED-REST ON INSULIN ACTION IN RELATION TO BODY FAT IN YOUNG SUBJECTS
Y. Suzuki, K. Kawakubo, Y. Makita, S. Goto, and A. Gunji *In* International Union of Physiological Sciences, The Physiologist, Volume 36, Number 1, Supplement Feb. 1993 2 p (For primary document see N95-15089 03-52)
Avail: CASI HC A01/MF A02

It is well known that daily positive physical activity is able to control body fat and to improve insulin action for intaking glucose in the muscles, especially under administration of nutrition in humans. Conversely, when exposed to prolonged inactive conditions such as bed-rest in spite of control of nutrition, the insulin action may be decreased due to less glucose intake in the muscles and thus insulin secretion may be increased to maintain blood glucose levels. If it is so, the increased insulin should

accelerate intake of neutral fat and lower fatty acid in fat tissues. Further, if the prolonged inactivity decreases plasma epinephrine and norepinepherine secretion, the breakdown of the stored fat should be declined due to declining hormone susceptible lipase secretion, resulting in increases in body fat, which may reflect changes in lipo-proteins and apo-proteins. In the present study, the hypotheses mentioned above were investigated in young students. Author (revised)

N95-15146*# Baylor Coll. of Medicine, Houston, TX. Dept. of Physical Medicine.

THE CARDIOVASCULAR RESPONSE TO THE AGS **c14**

David Cardus and Wesley G. McTaggart *In* International Union of Physiological Sciences, The Physiologist, Volume 36, Number 1, Supplement Feb. 1993 3 p (For primary document see N95-15089 03-52)

(Grant NAGw-1691)

Avail: CASI HC A01/MF A02

This paper reports the preliminary results of experiments on human subjects conducted to study the cardiovascular response to various g-levels and exposure times using an artificial gravity simulator (AGS). The AGS is a short arm centrifuge consisting of a turntable, a traction system, a platform and four beds. Data collection hardware is part of the communication system. The AGS provides a steep acceleration gradient in subjects in the supine position. Author (revised)

N95-15147*# National Aeronautics and Space Administration. Ames Research Center, Moffett Field, CA.

CENTRIFUGES IN GRAVITATIONAL PHYSIOLOGY RESEARCH

Rodney W. Ballard, Phil Davies, and Charles A. Fuller *In* International Union of Physiological Sciences, The Physiologist, Volume 36, Number 1, Supplement Feb. 1993 2 p (For primary document see N95-15089 03-52)

Avail: CASI HC A01/MF A02

Data from space flight and ground based experiments have clearly demonstrated the importance of Earth gravity for normal physiological function in man and animals. Gravitational Physiology is concerned with the role and influence of gravity on physiological systems. Research in this field examines how we perceive and respond to gravity and the mechanisms underlying these responses. Inherent in our search for answers to these questions is the ability to alter gravity, which is not physically possible without leaving Earth. However, useful experimental paradigms have been to modify the perceived force of gravity by changing either the orientation of subjects to the gravity vector (i.e., postural changes) or by applying inertial forces to augment the magnitude of the gravity vector. The later technique has commonly been used by applying centripetal force via centrifugation. Author

N95-15148# Centre d'Enseignement et de Recherches de Medecine Aeronautique, Bretigny (France). Div. Histophysiologie.

ENHANCEMENT OF INSULIN RECEPTOR MEDIATED ENDOCYTOSIS IN CULTURED OSTEOBLASTIC CELLS UNDER HYPERGRAVITY **c51**

A. Malouvier, X. Holy, E. Zerath, P. J. Marie, and D. A. Schmitt *In* International Union of Physiological Sciences, The Physiologist, Volume 36, Number 1, Supplement Feb. 1993 2 p (For primary document see N95-15089 03-52)

Avail: CASI HC A01/MF A02

The effects of space flight on cell physiology have been investigated since the first balloon flights in 1965. Experiments aboard the Space Shuttle and Cosmos biosatellites have shown that cellular activation can be altered when cells are exposed to a space flight. It has been confirmed in vitro, in parabolic flight on lymphocytes and in sounding rockets on cultured epidermal cells. The aim of the present work was to determine through quantitative analysis whether Receptor-Mediated Endocytosis, a ubiquitous mechanism whereby cellular ligands are internalized by the cells after binding to a specific membrane receptor, is sensitive to a continuous 2G exposure. Author (revised)

N95-15149# Liege Univ. (Belgium). Hemoliege.

ISOLATION OF THE PHYSIOLOGICAL REGULATION COMPONENT OF THE ARTERIAL PRESSURE TIME VARIATION AFTER POSTURAL STRESSES BY A MODEL OF THE GRAVITATIONAL AND ARTERIAL KINKING EFFECTS

Thierry F. Pochet, Michel J. Pirotton, and Paul L. Gerard *In* International Union of Physiological Sciences, The Physiologist, Volume 36, Number 1, Supplement Feb. 1993 2 p (For primary document see N95-15089 03-52)

Avail: CASI HC A01/MF A02

The aim of this study is to separate the cardiovascular regulation component of the arterial pressure time course from the pressure evolution that would naturally appear in the network without physiological contribution. This takes into account the natural gravitational fluid dynamics phenomena imposed on the arterial blood. Derived from text

N95-15150# Space Biomedical Research Inst., Houston, TX.

A COMPARISON OF OVERALL MATHEMATICAL MODELS OF THE CARDIOVASCULAR SYSTEM FOR SIMULATING RESPONSE TO ORTHOSTATIC STRESSES

E. H. Karam, R. Srini Srinivasan, and John B. Charles *In* International Union of Physiological Sciences, The Physiologist, Volume 36, Number 1, Supplement Feb. 1993 2 p (For primary document see N95-15089 03-52)

Avail: CASI HC A01/MF A02

Although numerous mathematical models of the cardiovascular system (CVS) have appeared in the literature, only a few of them are models of the entire system with detailed representation of the heart, the vasculture, and the control elements. Like all models of biological systems, these models vary in complexity, and most of them are stimulus specific. In this paper, three mathematical models of CVS are examined in terms of their response to different orthostatic stressess, namely lower body negative pressure, head-up tilt, and blood loss. The short term orthostatic responses of the models are compared to available experimental data. Author

N95-15304* National Aeronautics and Space Administration, Washington, DC.

AEROSPACE MEDICINE AND BIOLOGY: A CONTINUING BIBLIOGRAPHY WITH INDEXES (SUPPLEMENT 395)

Dec. 1994 45 p

(NASA-SP-7011(395); NAS 1.21:7011(395)) Avail: CASI HC A04

This bibliography lists 82 reports, articles and other documents introduced into the NASA Scientific and Technical Information System during Nov. 1992. Subject coverage includes: general life sciences; aerospace medicine (including physiological factors, biological effects of radiation, and effects of weightlessness on man and animals); behavioral sciences (including psychological factors, individual and group behavior, crew training and evaluation, and psychic research); man/system technology and life support (including human engineering, biotechnology, and space suits and protective clothing) and space biology (including exobiology, planetary biology, and extraterrestrial life). Author

N95-15445 Yale Univ., New Haven, CT. School of Medicine.

WORLD REFERENCE CENTER FOR ARBOVIRUSES Final Report, 9 Feb. 1990 - 8 Dec. 1993

Robert E. Shope 7 Jun. 1994 13 p Limited Reproducibility: More than 20% of this document may be affected by microfiche quality

(Contract DAMD17-90-Z-0020)

(AD-A281635) Avail: CASI HC A03

The World Reference Center for Arboviruses characterized Sabia and Guanarito viruses, two new arenaviruses causing hemorrhagic fever in Brazil and Venezuela, respectively. A new genotype of Japanese encephalitis virus was discovered from Indonesia. Classifications of Venezuelan encephalitis and arenaviruses were revised. Outbreaks of arenavirus hemorrhagic fever in Venezuela and Brazil were investigated. Military watchdogs had an antibody to Japanese encephalitis virus. Rapid PCR-based diagnostic techniques for encephalitides were developed. Neutralization tests of sera of army volunteers supported the licensing of the Japanese encephalitis inactivated vaccine. Recombinant vaccinia viruses expressing the prM/E genes were developed as candidate vaccines. Reagents were distributed to laboratories in 24 countries. DTIC

N95-15649*# National Aeronautics and Space Administration. Ames Research Center, Moffett Field, CA.

CREW FACTORS IN FLIGHT OPERATIONS 2: PSYCHOPHYSIOLOGICAL RESPONSES TO SHORT-HAUL AIR TRANSPORT OPERATIONS

Philippa H. Gander (San Jose State Univ., CA.), R. Curtis Graeber, H.

Clayton Foushee, John K. Lauber, and Linda J. Connell Nov. 1994 68 p
(RTOP 505-64-53)
(NASA-TM-108856; A-95012; NAS 1.15:108856) Avail: CASI HC A04/MF A01

Seventy-four pilots were monitored before, during, and after 3- or 4-day commercial short-haul trip patterns. The trips studied averaged 10.6 hr of duty per day with 4.5 hr of flight time and 5.5 flight segments. The mean rest period lasted 12.5 hr and occurred progressively earlier across successive days. On trip nights, subjects took longer to fall asleep, slept less, woke earlier, and reported lighter, poorer sleep with more awakenings than on pretrip nights. During layovers, subjective fatigue and negative affect were higher, and positive affect and activation lower, than during pretrip, in-flight, or posttrip. Pilots consumed more caffeine, alcohol, and snacks on trip days than either pretrip or posttrip. Increases in heart rate over mid-cruise were observed during descent and landing, and were greater for the pilot flying. Heart-rate increases were greater during takeoff and descent under instrument meteorological conditions (IMC) than under visual meteorological conditions (VMC). The following would be expected to reduce fatigue in short-haul operations: regulating duty hours, as well as flight hours; scheduling rest periods to begin at the same time of day, or progressively later, across the days of a trip; and educating pilots about alternatives to alcohol as a means of relaxing before sleep. Author

N95-15757# Naval Academy, Annapolis, MD.
ROBOTIC CONTROL USING MUSCULAR AND NEURAL ELECTRICAL SIGNALS
William M. Gotten, Jr. 19 May 1994 159 p
(AD-A284908; USNA-TSPR-216) Avail: CASI HC A08/MF A02

The human body is capable of producing measurable electrical potentials ranging from the nanovolt to millivolt range. The actions needed to produce these potentials can be as simple as blinking an eye or flexing a muscle. The voltages can even be created within and by the brain, although this process is not well understood at the present time. This design project explores the possibility and practicality of harnessing these potentials into signals that can reliably control a robotic arm. DTIC

N95-15767 Army Aeromedical Research Lab., Fort Rucker, AL.
COLLECTION OF REAL-TIME, MULTICHANNEL EEG DATA FROM HELICOPTER PILOTS IN FLIGHT: A FEASIBILITY STUDY Final Report
John A. Caldwell, James A. Lewis, Stephen R. Darling, Robert M. Dillard, and Parley P. Johnson May 1994 64 p Limited Reproducibility: More than 20% of this document may be affected by microfiche quality
(DA Proj. 3M1-62787-A-879)
(AD-A284396; USAARL-94-26) Avail: Issuing Activity (Defense Technical Information Center (DTIC))

An initial assessment of whether valid electroencephalographic (EEG) data could be collected on helicopter pilots in flight was conducted using 20 volunteers. Each subject provided a brief eyes-open and eyes-closed EEG in the laboratory and then in a helicopter. During helicopter flights, data were monitored and recorded on the ground in real-time via a radio telemetry system. Initial hardware problems resulted in the exclusion of several records, but these problems were resolved toward the end of the study. Analysis of the remaining acceptable EEG records indicated that the typical increase in alpha activity (7.5-13.0 Hz) due to eye closure was clearly observable at every analyzed electrode site regardless of whether the testing occurred in the laboratory or in the helicopter. Further examinations of delta, theta, and beta bands showed that the EEG data were not overly contaminated by artifacts, although it was much more difficult to find 'clean' segments on records collected in the helicopter than in the laboratory. It was concluded that it is possible to record and telemeter useable EEG from the in-flight helicopter environment. Follow-on studies will examine the feasibility of analyzing EEG data collected while the pilot is performing flight-related tasks. DTIC

N95-15810 Army Aeromedical Research Lab., Fort Rucker, AL.
AVIATION EPIDEMIOLOGY DATA REGISTER: GENDER-SPECIFIC ATTRITION FROM THE TRAINED US ARMY AVIATOR COHORT OF 1988 Final Report
Samuel G. Shannon, Kevin T. Mason, and Jennifer P. Harper Jul. 1994 23 p Limited Reproducibility: More than 20% of this document may be affected by microfiche quality
(DA Proj. 301-62787-A-878)
(AD-A284395; USAARL-94-36) Avail: CASI HC A03

Women have been involved in U.S. Army aviation for more than two decades. Little has been written about the integration of women into this traditionally male occupation. One indicator of successful integration of women is their retention rate in aviation service. The aviation Epidemiology Data Register was queried to find out the attrition rate among trained U.S. Army male and female aviators from 1988 to 1992. Results: In the trained aviator cohort of 1988, male aviators were significantly older than female aviators (Mantel-Haenszel chi(exp 2), P less than 0.001), whatever the component of service. The crude attrition rate for all age group was 55.4 percent (11,847 of 21,395) for males, compared to 54.1 percent (265 of 490) for females. Based on male attrition and after controlling for the age difference between male and female aviators, the observed attrition of females (265) exceeded the expected attrition (243) by 22 females (9.1 percent excess attrition). For the age groups 18 to 44 years old there was a significantly higher risk for attrition among female aviators (Mantel-Haenszel or = 1.23, CI(sub 0.95) = 1.025, 1.470). This increased attrition rate was found primarily in the age groups of 18 to 34 years old. The cause for the observed excess attrition of female Army aviators is unknown and requires further study of factors affecting retention in aviation service. DTIC

N95-14223*# National Aeronautics and Space Administration. Lyndon B. Johnson Space Center, Houston, TX.
EXTENDED DURATION ORBITER MEDICAL PROJECT VARIABILITY OF BLOOD PRESSURE AND HEART RATE (STS-50/USML-1)
Janice M. Fritsch-Yelle, John B. Charles, and Sheila W. Boettcher *In* NASA. Marshall Space Flight Center, Joint Launch + One Year Science Review of USML-1 and USMP-1 with the Microgravity Measurement Group May 1994 p 383-389 (For primary document see N95-14207 03-88)
Avail: CASI HC A02/MF A04

N95-14224*# National Aeronautics and Space Administration. Lyndon B. Johnson Space Center, Houston, TX.
EXTENDED DURATION ORBITER MEDICAL PROJECT COUNTERMEASURE TO REDUCE POST SPACE FLIGHT ORTHOSTATIC INTOLERANCE (LBNP) (STS-50/USML-1)
John B. Charles and Sheila W. Boettcher *In* NASA. Marshall Space Flight Center, Joint Launch + One Year Science Review of USML-1 and USMP-1 with the Microgravity Measurement Group May 1994 p 391-407 (For primary document see N95-14207 03-88)
Avail: CASI HC A03/MF A04

53 BEHAVIORAL SCIENCES

Includes psychological factors; individual and group behavior; crew training and evaluation; and psychiatric research.

N95-13715# Civil Aeromedical Inst., Oklahoma City, OK.
AGE 60 RULE. PART 3: CONSOLIDATED DATABASE EXPERIMENTS Final Report
Edwin J. Kay (Lehigh Univ., Bethlehem, PA.), Donald J. Hillman (Lehigh Univ., Bethlehem, PA.), Diane T. Hyland (Lehigh Univ., Bethlehem, PA.), Robert S. Voros (Lehigh Univ., Bethlehem, PA.), Regina M. Harris (Hilton Systems, Inc., Cherry Hill, NJ.), and Jim D. Deimler (Hilton Systems, Inc., Cherry Hill, NJ.) Washington Oct. 1994 97 p
(Contract DTFA02-90-C-90125; FAA Task AM-A-91-HRR-138)
(DOT/FAA/AM-94/22-Pt-3; Rept-8025-3C-Pt-3) Avail: CASI HC A05/MF A02

The purpose of this study was to conduct statistical analysis on historical data to investigate the relationship between pilot age and accident rates. The ultimate long-term aim of the Age 60 Project was to enhance aviation safety by increasing understanding about the relationships among pilot age, experience, and accident rates. The specific aims of the project were: (1) to consolidate the currently separate databases related to pilot certification and aviation accidents and incidents; and (2) to use this consolidated database to statistically examine the relationships that exist among chronological age, accidents, and other factors. Although the study was primarily directed at pilots who fly for FAR Part 121 air carriers who are subject to the Age 60 Rule, additional analyses were conducted for

other categories of pilots to take advantage of additional data available for active pilots beyond the age of 60, and to further examine the influence of confounding factors. Author

N95-14369# Brigham and Women's Hospital, Boston, MA.
DEVELOPING GUIDED SEARCH 3.0. THE NEXT GENERATION OF A MODEL VISUAL SEARCH Annual Report, Jun. 1993 - Jun. 1994
Jeremy M. Wolfe 1 Jul. 1994 7 p
(Grant AF-AFOSR-10407-93)
(AD-A283956; AFOSR-94-0541TR) Avail: CASI HC A02/MF A01

There are numerous situations, from picking fruit to flying a plane, that require an observer to find a target item in a field filled with distracting items. Guided Search (GS) is our model of this visual search process. This project aims to develop the next generation of that model. In the past year, progress has been made in three areas: (1) The GS computer simulation has been improved, notably by equipping it with the ability to learn how to select useful information from the available input channels. (2) Our study of individual differences between subjects indicates that the differences revealed by standard search paradigms are probably mere noise. However, we can modify the usual paradigm by using larger display set sizes. This produces reliable individual differences that can be used to evaluate theories of search. (3) There are many tasks that require search through visually complex technical information. Using electrical diagrams as an example, we have developed techniques to speed search by graphical recoding of diagram information. We do this while preserving the standard structure of the diagrams. Our goal is 'hybrid search' in which human and computer both contribute to the success of the search. DTIC

N95-14600# Washington State Univ., Pullman, WA. Dept. of Psychology.
AUGMENTATION OF RESEARCH ON COGNITIVE CONTROL Annual Technical Report, 1 May 1993 - 30 Apr. 1994
Paul Whitney 7 Jun. 1994 9 p
(Contract F49620-92-J-0243)
(AD-A280956; AFOSR-94-0370TR) Avail: CASI HC A02/MF A01

The influence of individual differences in working memory span (WMS) on comprehension of instructional text was examined. Results from the second year of the AASERT grant showed that readers across the range of WMS paid special attention to thematic statements when they read instructional texts. This was shown through longer reading times of sentences in the initial position of paragraphs. However, if comprehension of specific details was stressed by asking about details after each passage, then high WMS readers increased thematic processing in comparison to reading times obtained when the questions asked about topics and details. Low WMS readers did not increase thematic processing when details were stressed. The increased thematic processing by high WMS readers was associated with better comprehension of both topics and details on a later surprise test of learning. Higher WMS may allow some readers to use integrative strategies not available to other readers. DTIC

N95-14863# Oklahoma Univ. Health Sciences Center, Norman, OK. Center for Alcohol and Drug-Related Studies.
LOW-DOSE ALCOHOL EFFECTS ON HUMAN BEHAVIOR AND PERFORMANCE: A REVIEW OF POST-1984 RESEARCH Final Report
Frank A. Holloway Washington FAA Nov. 1994 49 p
(DOT/FAA/AM-94/24; FAA-AAM-A-HRR-126) Avail: CASI HC A03/MF A01

The purpose of this review was to survey the literature examining alcohol effects on human behavior and performance, especially low alcohol dose effects. Other comprehensive reviews on this topic from 1975 to 1990 found that alcohol could affect all classes of performance, but that the kinds of performance most sensitive to low dose effects depended on: (a) the analysis of skills or abilities (selective attention), (b) the kind of task (divided attention tasks), (c) task characteristics (multiple tasks with high demand and/or complexity), and (d) categories of alcohol effects (negative subjective effects and controlled performance). This review examined 155 empirical studies dating from 1985 to mid-1993, using the alcohol effect schema of Kruger, and reached several general conclusions that were largely in agreement with previous reviews on this topic. First, sensitivity to the subjective intoxicating effects of alcohol was greater than that for all other performance classes and appeared to display a 'threshold' with respect to blood alcohol concentration (BAC), rather than the linear relation evident in performance data. Second, sensitivity to performance impairment in 'controlled' performance and simulator tasks was greater than that for psychophysical functions or 'automatic' performance. Finally, a variety of task, subject, and environmental characteristics or conditions were found to mediate the magnitude and sensitivity to alcohol effects, particularly at lower doses. This review concluded that since alcohol sensitivity can vary from time to time, person to person, and situation to situation, the setting of a 'safe' BAC will always be arbitrary, being based on a low, but non-zero, incidence of effects below that level. Author

N95-14864*# Old Dominion Univ., Norfolk, VA. Dept. of Psychology.
THE ELECTROCORTICAL CORRELATES OF FLUCTUATING STATES OF ATTENTION DURING VIGILANCE TASKS Progress Report, 16 Aug. 1993 - 16 Nov. 1994
Stephen G. Cunningham and Frederick Freeman Nov. 1994 91 p
(Contract NCC1-176)
(NASA-CR-197051; NAS 1.26:197051) Avail: CASI HC A05/MF A01

This study investigated the electrocortical correlates of attention. Sixteen subjects (seven females, nine males) engaged in a forty-minute target detection vigilance task. Task-irrelevant probe tones were presented every 2-4 seconds. While performing the vigilance task, the subjects were asked to press a button if they were daydreaming (i.e. having a task unrelated thought or TUT). Continuous electroencephalograms (EEG's) and event-related potentials (ERP's) were recorded from the subjects during the entire task. The continuous EEG data were analyzed for differences in absolute power throughout the task as well as before and after the subjects indicated that they were daydreaming (TUT response). ERP's elicited by task-irrelevant probe tones were analyzed in the same manner. The results indicated performance decrements as reflected by increased RT to correct detections, and decreased number of hits. Further, as the task progressed, the number of reports of daydreaming increased. The analysis of the EEG data indicated a significant difference in the absolute power of the different frequency bands across periods. The greatest difference was observed at the posterior parietal electrode sites. In addition, when the EEG data was converted into band ratios (beta/alpha and beta/alpha+theta), the pre-TUT conditions were found to be significantly different than the post-TUT conditions in the posterior sites. The ERP components (N1, N2, and P2) were not significantly different before and after a TUT response or across periods. However, the ERP's across periods exhibited amplitudes that were similar to those found in previous studies of vigilance and ERP's. Author

N95-15326# Army Research Inst. for the Behavioral and Social Sciences, Alexandria, VA.
THE EFFECT OF RESPONSE FORMAT ON RELIABILITY ESTIMATES FOR TACIT KNOWLEDGE SCALES Research Note, May - Nov. 1993
Peter J. Legree Jul. 1994 22 p
(AD-A283547; ARI-RN-94-25) Avail: CASI HC A03/MF A01

Most aptitude scales adopt a Forced Choice response format in which answers are scored as either correct or incorrect. Such a scoring procedure is consistent with the nature of the knowledge underlying these aptitude scales because the relevant knowledge domains can usually be used to either support or contradict a specific supposition. Assessing performance with tacit knowledge scales that lack an academic knowledge base often requires the opinions of subject matter experts and responses cannot always be unambiguously scored. Data indicate that an improvement in the reliability of a Tacit Knowledge Scale could be realized by substituting a Likert response format in place of a traditional Forced Choice format; this finding demonstrates the power of the Likert response format to measure individual differences in an uncertain knowledge domain. This research was conducted in support of the development and validation of a Social Intelligence scale. DTIC

N95-15588# Rochester Univ., NY. Dept. of Computer Science.
SUPERVISED LEARNING WITHOUT OUTPUT LABELS
Ramesh R. Sarukkai Nov. 1994 22 p Revised
(Grant NSF IRI-89-03582)
(TR-510-Rev) Avail: CASI HC A03/MF A01

Supervised, neural network learning algorithms have proven very successful at solving a variety of learning problems. However, they suffer from a common problem of requiring explicit output labels. This requirement makes such algorithms implausible as biological models. In this paper it is shown that pattern classification can be achieved, in a multilayered,

feedforward neural network, without requiring explicit output labels, by a process of supervised self-organization. The class projection is achieved by optimizing appropriate within-class uniformity and between-class discernability criteria. The mapping function and the class labels are developed together iteratively using the derived self-organizing back-propagation algorithm. The ability of the self-organizing network to generalize on unseen data is also experimentally evaluated on real data sets, and compares favorably with the traditional labeled supervision with neural networks. However, interesting features emerge out of the proposed self-organizing supervision, which are absent in conventional approaches. The further implications of self-organizing supervision with neural networks are also discussed. Author (revised)

N95-15642# Rochester Univ., NY. Dept. of Computer Science.
FIRST RESULTS WITH INSTANCE-BASED STATE IDENTIFICATION FOR REINFORCEMENT LEARNING
R. Andrew McCallum Apr. 1994 28 p Sponsored by Human Science Frontiers
(Grants NSF IRI-89-03582; NIH-1R24RRO6853)
(TR-502) Avail: CASI HC A03/MF A01

When a reinforcement learning agent's next course of action depends on information that is hidden from the sensors because of problems such as occlusion, restricted range, bounded field of view and limited attention, we say the agent suffers from the hidden state problem. State identification techniques use history information to uncover hidden state. Previous approaches to encoding history include: finite state machines, recurrent neural networks, and genetic programming with indexed memory. A chief disadvantage of all these techniques is their long training time. This report presents instance-based state identification, a new approach to reinforcement learning with state identification that learns with much fewer training steps. Noting that learning with history and learning in continuous spaces both share the property that they begin without knowing the granularity of the state space, the approach applies instance-based (or 'memory-based') learning to history sequences-instead of recording instances in a continuous geometrical space, we record instances in action-perception-reward sequence space. The first implementation of this approach, called Nearest Sequence Memory, learns with an order of magnitude fewer steps than several previous approaches. Author

N95-15768 Aerospace Medical Research Labs., Brooks AFB, TX. Aerospace Medicine Directorate.
VALIDATION OF MMPI SCALES FOR PERSONALITY DISORDERS: A PILOT AND OTHER AVIATOR STUDY Interim Report, May 1991 - Mar. 1993
Raymond E. King, Gary L. Schofield, John C. Patterson, William J. Besich, and William G. Jackson Jul. 1994 16 p Limited Reproducibility: More than 20% of this document may be affected by microfiche quality
(AF Proj. 7755)
(AD-A284397; AL/AO-TR-1994-0030) Avail: Issuing Activity (Defense Technical Information Center (DTIC))

The Minnesota multiphasic personality inventory (MMPI), long a psychometric staple, has not been readily compatible with the third Diagnostic and Statistical Manual of Mental Disorders (DSM-3 and DSM-3-R). Morey, Waugh, and Blashfield rationally/empirically constructed MMPI personality disorder scales to assess these DSM-3 Axis 2 conditions, but adequate outpatient validation remains to be accomplished. The present study, based on 104 male aviators referred to as consultation service, found significant (p less than 0.001) positive correlations in nine of 11 personality disorder scale comparisons between the MMPI and the millon clinical multiaxial inventory (MCMI), a test that attempts to more closely correspond to the criterion of the DSM-3/DSM-3-R. The antisocial and compulsive personality disorder scales failed to significantly correlate. The MMPI personality disorder scales, however, did not significantly identify which subjects had psychiatrically noted maladaptive personality traits. DTIC

N95-15770 State Univ. of New York, Binghamton, NY.
PERCEPTION OF AUDITORY EVENTS: ATTENTIONAL LIMITATIONS Annual Technical Report, 1 Jul. 1993 - 30 Jun. 1994
Richard E. Pastore 26 Jul. 1994 5 p Limited Reproducibility: More than 20% of this document may be affected by microfiche quality
(Contract F49620-93-1-0327)
(AD-A284399; AFOSR-94-0547TR) Avail: Issuing Activity (Defense Technical Information Center (DTIC))

There is strong evidence that objects presented simultaneously in a visual array have their component features initially processed in parallel, then subsequently combined to form the perceived objects. The evidence is in the form of the nature and frequency of perceptual errors and the pattern of reaction times for recognition of presented features and objects. Continuing project research is providing equivalent evidence which demonstrates, for the first time, similar analyses and perceptual processing for auditory events. An important side benefit to the research is the validation of new methods to define the elemental features for the perception of important classes of auditory stimuli. In addition to training future scientists, long-term benefits of the research are (1) in defining important, moderate- and higher-level limits (e.g., beyond masking or sensory acuity) to accurately and rapidly perceiving auditory events (and the sources of the events) under stressful, noisy conditions, and (2) in defining effective strategies for reliably circumventing those newly-identified limits. DTIC

N95-15787# Rochester Univ., NY. Dept. of Computer Science.
VISION, LEARNING, AND DEVELOPMENT
Christopher M. Brown May 1994 46 p Revised
(Grants NSF CDA-88-22724; NSF IRI-92-02816)
(TR-492-Rev) Avail: CASI HC A03/MF A01

It seems to be a common feeling that animals learn to see, and this feeling, together with the reemergence of computer learning paradigms that mimic many forms of human learning, has raised hopes that learning is the key to the computer vision problem. Indeed, it seems clear that nature does not 'program' all our visual capabilities into the genome, and we certainly know that programming a computer with a closed-form solution to the vision problem is a daunting task. The aim of this informal and elementary report (basically a term paper) is to cast doubt on the idea that biological systems learn to see. The complex process of development, beginning at fertilization and ending with a mature individual, could be considered to have genetic ('nature') and learning ('nurture') processes as logical endpoints or opposite poles. This report mostly considers what goes on between those endpoints, and is meant to raise the possibility that some of the least understood processes in biology are responsible for visual capabilities. Author

N95-15816 Institute for Perception RVO-TNO, Soesterberg (Netherlands).
TARGET ACQUISITION: HUMAN OBSERVER PERFORMANCE STUDIES AND TARGAC MODEL VALIDATION Final Report, Sep. 1991 - Nov. 1993
J. M. Valeton and P. Biji Jun. 1994 132 p Limited Reproducibility: More than 20% of this document may be affected by microfiche quality
(Contract DAJA45-91-C-0013)
(AD-A284436; R/D-6720-EN-01) Avail: Issuing Activity (Defense Technical Information Center (DTIC))

Human target acquisition performance was studied using thermal imagery that was collected during the field trial BEST TWO, organized by NATO AC243/Panel4/RSG.15 in 1990. In a number of carefully controlled laboratory experiments, recognition and identification probabilities were measured for a large number of stationary and moving targets at ranges between 1 and 4 km. Target detection was not investigated. The target acquisition model TARGAC was validated by comparing its predictions with observed recognition ranges. For all trials that were used in the observer experiments, TARGAC predictions were calculated on the basis of meteorological, target, background, and time information that was measured in the field. The major conclusion of the observer experiments is that the human acquisition performance depends considerably on factors such as target structure, local terrain structure, and cognitive factors. In TARGAC, these factors are not modeled. For the BEST TWO situation, the model predictions were determined solely by target size and thermal imager resolution limit. DTIC

N95-14891*# National Aeronautics and Space Administration. Langley Research Center, Hampton, VA.
AN IN-HOME STUDY OF SUBJECTIVE RESPONSE TO SIMULATED SONIC BOOMS
David A. McCurdy, Sherilyn A. Brown, and R. David Hilliard *In its* High-Speed Research: 1994 Sonic Boom Workshop: Atmospheric

Propagation and Acceptability Studies Oct. 1994 p 193-208 (For primary document see N95-14878 03-02)
Avail: CASI HC A03/MF A03

N95-14892*# Fields (James M.), Silver Spring, MD.
RESIDENTS' REACTIONS TO LONG-TERM SONIC BOOM EXPOSURE: PRELIMINARY RESULTS
James M. Fields, Carey Moulton, Robert M. Baumgartner, and Jeff Thomas *In* NASA. Langley Research Center, High-Speed Research: 1994 Sonic Boom Workshop: Atmospheric Propagation and Acceptability Studies Oct. 1994 p 209-217 (For primary document see N95-14878 03-02)
Avail: CASI HC A02/MF A03

54 MAN/SYSTEM TECHNOLOGY AND LIFE SUPPORT

Includes human engineering; biotechnology; and space suits and protective clothing.

For related information see also *16 Space Transportation*.

N95-13671# Lawrence Livermore National Lab., Livermore, CA.
DEVELOPMENTS IN GROUND-PENETRATING RADAR AT LLNL
P. D. Sargis May 1994 18 p Presented at the Unexploded Ordnance Detection and Range-Remediation Conference, Golden, CO, 17-19 May 1994
(Contract W-7405-eng-48)
(DE94-012236; UCRL-JC-116074; CONF-9405159-1) Avail: CASI HC A03/MF A01

Lawrence Livermore National Laboratory (LLNL) is developing a side-looking, ground-penetrating impulse radar system that will eventually be mounted on an airborne platform to locate buried minefields. Presently, the radar system is mounted on top of a 60-foot adjustable boom. Several unique as well as commercial antennas having bandwidths in the 200 to 2000 MHz range are being experimented with. Also, LLNL-developed monocycle pulse generators are tailored to be most efficient over this frequency range. A technical description of the system will be presented with details about the video pulser, the wideband antennas, the receiver hardware, and the data acquisition system. The receiver and data acquisition hardware consist of off-the-shelf components. Testing of this system is conducted on a minefield located at the Nevada Test Site (NTS). The minefield contains real and surrogate mines of various sizes placed in natural vegetation. Some areas of the minefield have been cleared for noncluttered studies. In addition, both metal and plastic mines are buried in the minefield. There is room in the NTS minefield for burying additional objects, such as unexploded ordnance, and this is expected to be done in the future. Recent results indicate success in imaging the NTS minefield using the ground-penetrating radar system. The data has been processed using in-house image reconstruction software, and has been registered with the ground truth data. Images showing clearly visible mines, surface reference markers, and ground clutter are presented. DOE

N95-13888*# National Aeronautics and Space Administration, Washington, DC.
SUITED FOR SPACEWALKING: TEACHER'S GUIDE WITH ACTIVITIES FOR PHYSICAL AND LIFE SCIENCE
Gregory L. Vogt (National Aeronautics and Space Administration. Lyndon B. Johnson Space Center, Houston, TX.), Cheryl A. Manning, and Carla B. Rosenberg Aug. 1994 69 p Revised
(NASA-EG-101; NAS 1.19/4:101) Avail: CASI HC A04/MF A01

Space walking has captured the imagination of generations of children and adults since science-fiction authors first placed their characters on the Moon. This publication is an activity guide for teachers interested in using the intense interest many children have in space exploration as a launching point for exciting hands-on learning opportunities. The guide begins with brief discussions of the space environment, the history of space walking, the Space Shuttle spacesuit, and working in space. These are followed by a series of activities that enable children to explore the space environment as well as the science and technology behind the functions of spacesuits. The activities are not rated for specific grade levels because they can be adapted for students of many ages. The chart on curriculum application at the back of the book is designed to help teachers incorporate activities into various subject areas. Derived from text

N95-14013*# National Aeronautics and Space Administration. Ames Research Center, Moffett Field, CA.
HUMAN MACHINE INTERFACES FOR TELEOPERATORS AND VIRTUAL ENVIRONMENTS
Nathaniel I. Durlach, comp., Thomas B. Sheridan, comp., and Stephen R. Ellis, comp. Jun. 1991 169 p Conference held in Santa Barbara, CA, 4-9 Mar. 1990; sponsored by ONR and IBM
(RTOP 506-47-00)
(NASA-CP-10071; A-91035; NAS 1.55:10071) Avail: CASI HC A08/MF A02

In Mar. 1990, a meeting organized around the general theme of teleoperation research into virtual environment display technology was conducted. This is a collection of conference-related fragments that will give a glimpse of the potential of the following fields and how they interplay: sensorimotor performance; human-machine interfaces; teleoperation; virtual environments; performance measurement and evaluation methods; and design principles and predictive models. For individual titles, see N95-14014 through N95-14061.

N95-14014*# Massachusetts Inst. of Tech., Cambridge. Dept. of Brain and Cognitive Sciences.
VISUAL INTERFACES: THE HUMAN PERCEIVER Abstract Only
Richard M. Held *In* NASA. Ames Research Center, Human Machine Interfaces for Teleoperators and Virtual Environments Jun. 1991 p 5-6 (For primary document see N95-14013 03-54)
Avail: CASI HC A01/MF A02

How knowledge of visual perception can be applied to achieve teleoperation and virtual worlds is discussed. Derived from text

N95-14015*# Boston Univ., MA. Dept. of Biomedical Engineering.
AUDITORY INTERFACES: THE HUMAN PERCEIVER Abstract Only
H. Steven Colburn *In* NASA. Ames Research Center, Human Machine Interfaces for Teleoperators and Virtual Environments Jun. 1991 p 7-8 (For primary document see N95-14013 03-54)
Avail: CASI HC A01/MF A02

A brief introduction to the basic auditory abilities of the human perceiver with particular attention toward issues that may be important for the design of auditory interfaces is presented. The importance of appropriate auditory inputs to observers with normal hearing is probably related to the role of hearing as an omnidirectional, early warning system and to its role as the primary vehicle for communication of strong personal feelings. Derived from text

N95-14016*# Massachusetts Inst. of Tech., Cambridge. Sensory Communication Group.
TACTUAL INTERFACES: THE HUMAN PERCEIVER Abstract Only
M. A. Srinivasan *In* NASA. Ames Research Center, Human Machine Interfaces for Teleoperators and Virtual Environments Jun. 1991 p 9-10 (For primary document see N95-14013 03-54)
Avail: CASI HC A01/MF A02

Increasingly complex human-machine interactions, such as in teleoperation or in virtual environments, have necessitated the optimal use of the human tactual channel for information transfer. This need leads to a demand for a basic understanding of how the human tactual system works, so that the tactual interface between the human and the machine can receive the command signals from the human, as well as display the information to the human, in a manner that appears natural to the human. The tactual information consists of two components: (1) contact information which specifies the nature of direct contact with the object; and (2) kinesthetic information which refers to the position and motion of the limbs. This paper is mostly concerned with contact information. Derived from text

N95-14017*# Princeton Univ., NJ. Dept. of Psychology.
THE DISPLAY OF TACTILE INFORMATION Abstract Only
Carl E. Sherrick *In* NASA. Ames Research Center, Human Machine Interfaces for Teleoperators and Virtual Environments Jun. 1991 p 11-12 (For primary document see N95-14013 03-54)
Avail: CASI HC A01/MF A02

There are a number of examples of natural tactile displays that can five us some insights about the solid geometry of touch, and recent experimental work on the subject has extended our thinking considerably. The concern of here is, however, more with synthetic or artificial displays for the production of a virtual environment. Features of synthetic displays that have enjoyed some success in one of the following two enterprises are discussed: the study of the spatio-temporal dimensions of stimuli that afford accurate and rapid processing of environmental information, or the use of displays in the design of sensory aids for disabled persons.

Derived from text

N95-14018*# Nebraska Univ., Omaha, NE. Dept. of Physiology.

NEURAL MECHANISMS OF KINESTHESIA Abstract Only

Francis J. Clark *In* NASA. Ames Research Center, Human Machine Interfaces for Teleoperators and Virtual Environments Jun. 1991 p 13-14 (For primary document see N95-14013 03-54)

Avail: CASI HC A01/MF A02

Our primary interest is in where the signals for position and movement of the limbs originate and how the information is encoded. Humans can independently sense the positions and movements of their limbs in the absence of vision, and their senses are derived from mechanoreceptors located in the limbs. Receptors in muscles, skin and joints are potential sources of position and movement signals, but how (and whether) each of these groups contributes to kinesthesia remains uncertain. Recent evidence indicates that a sense of static-position derives from length receptors in muscle, whereas receptors in the skin, and possibly though not likely the joints, can signal movement of a limb but not its static position. At present, we are examining the consequences of not having a static-position sense at the fingers apart from an inability to detect very slow displacements. Using a more demanding test, we have found no substantial difference in the accuracy of reproducing target positions passively imposed on the MCP joint and the proximal interphalangeal (PIP) joint of the index finger. Our working hypothesis is that subjects normally use movement sense mechanisms to detect displacements, probably because they are faster, but how (or whether) subjects manage to obtain an absolute position reference with only a movement sense available remains unknown and is an issue under investigation. Derived from text

N95-14019*# McGill Univ., Montreal (Quebec). Physical and Occupational Therapy.

ANALYSIS OF THE HUMAN OPERATOR SUBSYSTEMS Abstract Only

Lynette A. Jones and Ian W. Hunter *In* NASA. Ames Research Center, Human Machine Interfaces for Teleoperators and Virtual Environments Jun. 1991 p 15-16 (For primary document see N95-14013 03-54)

Avail: CASI HC A01/MF A02

Except in low-bandwidth systems, knowledge of the human operator transfer function is essential for high-performance telerobotic systems. This information has usually been derived from detailed analyses of tracking performance, in which the human operator is considered as a complete system rather than as a summation of a number of subsystems, each of which influences the operator's output. Studies of one of these subsystems, the limb mechanics system, demonstrate that large parameter variations can occur that can have a profound effect on the stability of force-reflecting telerobot systems. An objective of this research was to decompose the performance of the human operator system in order to establish how the dynamics of each of the elements influence the operator's responses.

Derived from text

N95-14020*# Brandeis Univ., Waltham, MA.

INTERSENSORY COORDINATION Abstract Only

James R. Lackner *In* NASA. Ames Research Center, Human Machine Interfaces for Teleoperators and Virtual Environments Jun. 1991 p 17-18 (For primary document see N95-14013 03-54)

Avail: CASI HC A01/MF A02

The dependence of body orientation and body configuration perception on multiple sources of afferent and efferent information about the spatial configuration of the body and its relationship to the support and force characteristics of the surroundings is discussed. Derived from text

N95-14021*# International Business Machines Corp., Yorktown Heights, NY. Continuous Speech Recognition Group.

WATCH WHAT YOU SAY, YOUR COMPUTER MIGHT BE LISTENING: A REVIEW OF AUTOMATED SPEECH RECOGNITION Abstract Only **c63**

Stephen V. DeGennaro *In* NASA. Ames Research Center, Human Machine Interfaces for Teleoperators and Virtual Environments Jun. 1991 p 19-20 (For primary document see N95-14013 03-54)

Avail: CASI HC A01/MF A02

Spoken language is the most convenient and natural means by which people interact with each other and is, therefore, a promising candidate for human-machine interactions. Speech also offers an additional channel for hands-busy applications, complementing the use of motor output channels for control. Current speech recognition systems vary considerably across a number of important characteristics, including vocabulary size, speaking mode, training requirements for new speakers, robustness to acoustic environments, and accuracy. Algorithmically, these systems range from rule-based techniques through more probabilistic or self-learning approaches such as hidden Markov modeling and neural networks. This tutorial begins with a brief summary of the relevant features of current speech recognition systems and the strengths and weaknesses of the various algorithmic approaches. Derived from text

N95-14022*# California Univ., Berkeley, CA. Telerobotics Unit.

EYE MOVEMENT CONTROL AND TOP-DOWN SCANPATH VISION AS A DESIGN METAPHOR FOR ROBOTIC VISION AND CONTROL **c63**

Lawrence W. Stark *In* NASA. Ames Research Center, Human Machine Interfaces for Teleoperators and Virtual Environments Jun. 1991 p 21-28 (For primary document see N95-14013 03-54)

(Contract NCC2-86)

Avail: CASI HC A02/MF A02

The topics covered include the following: eye movement control; higher level eye movement control and Scanpath Theory; top-down robotic vision; and overall robotic control scheme. CASI

N95-14023*# Naval Ocean Systems Center, Kailua, HI. Marine Sciences and Technology Dept.

TELEROBOTIC REMOTE PRESENCE: ACHIEVEMENTS AND CHALLENGES Abstract Only **c37**

Walter A. Aviles *In* NASA. Ames Research Center, Human Machine Interfaces for Teleoperators and Virtual Environments Jun. 1991 p 31 (For primary document see N95-14013 03-54)

Avail: CASI HC A01/MF A02

The topics discussed include the following: telepresence, telerobotics, teleoperators, man machine systems, robot control, and remote control.

Author (revised)

N95-14024*# Utah Univ., Salt Lake City, UT. Center for Engineering Design.

ISSUES IN THE DESIGN OF HIGH DEXTERITY, FORCE REFLECTIVE TELEOPERATORS

Stephen C. Jacobsen, E. K. Iversen, C. C. Davis, K. B. Biggers, and D. K. Backman *In* NASA. Ames Research Center, Human Machine Interfaces for Teleoperators and Virtual Environments Jun. 1991 p 32-33 (For primary document see N95-14013 03-54)

Avail: CASI HC A01/MF A02

The Center for Engineering and Design at the University of Utah is developing an anthropomorphic, hydraulically actuated, teleoperated arm. The system includes a sixteen degree-of-freedom slave manipulator controlled by a kinematically identical, sixteen degree-of-freedom force-reflective, exoskeletal master. The project has focused on four areas: (1) formulating a realistic set of design objectives which balance, against technical realities, the desire for performance, reliability and economy; (2) understanding control issues; (3) designing and fabricating new subsystems necessary for the construction of a successful machine; and (4) integrating subsystems, through a series of prototype stages, into an operational teleoperation system. Derived from text

N95-14025*# Ministry of International Trade and Industry, Tsukuba (Japan). Biorobotics Div.

TELE-EXISTENCE AND/OR CYBERNETIC INTERFACE STUDIES IN JAPAN

Susumu Tachi *In* NASA. Ames Research Center, Human Machine

Interfaces for Teleoperators and Virtual Environments Jun. 1991 p 34-35 (For primary document see N95-14013 03-54)
Avail: CASI HC A01/MF A02

Tele-existence aims at a natural and efficient remote control of robots by providing the operator with a real time sensation of presence. It is an advaced type of teleoperation system which enables a human operator at the controls to perform remote manipulation tasks dexterously with the feeling that he or she exists in one of the remote anthropomorphic robots in the remote environment, e.g., in a hostile environment such as those of nuclear radiation, high temperature, and deep space. In order to study the use of the tele-existence system in the artificially constructed environment, the visual tele-existence simulator has been designed, a pseudo-real-time binocular solid model robot simulator has been made, and its feasibility has been experimentally evaluated. An anthropomorphic robot mechanism with an arm having seven degrees of freedom has been designed and developed as a slave robot for feasibility experiments of teleoperation using the tele-existence method. An impedance controlled active display mechanism and a head mounted display have also been designed and developed as the display subsystem for the master. The robot's structural dimensions are set very close to those of humans. Derived from text

N95-14026*# Woods Hole Oceanographic Inst., MA. Deep Submergence Lab.
TELEROBOTICS IN THE DEEP OCEAN Abstract Only **c37**
Hagen Schempf and Dana R. Yoerger *In* NASA. Ames Research Center, Human Machine Interfaces for Teleoperators and Virtual Environments Jun. 1991 p 36 (For primary document see N95-14013 03-54)
Avail: CASI HC A01/MF A02

This paper presents experimental results of the control system for the JASON ROV that has been designed for precision survey and other automated applications. The JASON control system emphasizes a form of supervisory control where the human pilot and the automatic system share the control tasks. Results presented include hovering, automatic track following, and several interactive modes. Author (revised)

N95-14027*# Washington Univ., Seattle, WA. Dept. of Electrical Engineering.
MODELS OF REMOTE MANIPULATION IN SPACE **c37**
Blake Hannaford *In* NASA. Ames Research Center, Human Machine Interfaces for Teleoperators and Virtual Environments Jun. 1991 p 37-40 (For primary document see N95-14013 03-54)
Avail: CASI HC A01/MF A02

Robots involved in high value manipulation must be effectively coupled to a human operator either at the work-site or remotely connected via communication links. In order to make use of experimental performance evaluation data, models must be developed. Powerful models of remote manipulation by humans can be used to predict manipulation performance in future systems based on today's laboratory systems. In this paradigm, the models are developed from experimental data, and then used to predict performance in slightly different situations. Second, accurate telemanipulation will allow design of manipulation systems which extend manipulation capability beyond its current bounds. Derived from text

N95-14028*# Systems Technology, Inc., Hawthorne, CA.
SOME CRITERIA FOR TELEOPERATORS AND VIRTUAL ENVIRONMENTS FROM EXPERIENCES WITH VEHICLE/OPERATOR SIMULATION
Henry R. Jex *In* NASA. Ames Research Center, Human Machine Interfaces for Teleoperators and Virtual Environments Jun. 1991 p 42-47 (For primary document see N95-14013 03-54)
Avail: CASI HC A02/MF A02

A review is given of a wide range of simulations in which operator steering control of a vehicle is involved and the dominant-clues, closed-loop bandwidth, measured operator effective time-delay, and ratio of bandwidth-to-inverse delay are summarized. A correlation of kinetosis with dynamic scene field-of-view is shown. The use of moving base simulators to improve the validity of locomotion teleoperations is discussed. some rules-of-thumb for good 'feel-system' simulation, such as for control manipulanda are given. Finally, simulation tests of teleoperators and virtual environments should include three types of measures: system performance, operator (or robot) 'behavior', and mental workload evaluations.
Derived from text

N95-14029*# Center for Engineering Applications, Memphis, TN.
MAN-MACHINE INTERFACES IN HEALTH CARE Abstract Only
Steve Charles and Roy E. Williams *In* NASA. Ames Research Center, Human Machine Interfaces for Teleoperators and Virtual Environments Jun. 1991 p 48-49 (For primary document see N95-14013 03-54)
Avail: CASI HC A01/MF A02

The surgeon, like the pilot, is confronted with an ever increasing volume of voice, data, and image input. Simultaneously, the surgeon must control a rapidly growing number of devices to deliver care to the patient. The broad disciplines of man-machine interface design, systems integration, and teleoperation will play a role in the operating room of the future. The purpose of this communication is to report the incorporation of these design concepts into new surgical and laser delivery systems. A review of each general problem area and the systems under development to solve the problems are presented. Derived from text

N95-14030*# Stanford Univ., CA. Center for Design Research.
TELEROBOTICS IN REHABILITATION: BARRIERS TO A VIRTUAL EXISTENCE
Larry Leifer, Machiel VanDerLoos, and Stefan Michalowski *In* NASA. Ames Research Center, Human Machine Interfaces for Teleoperators and Virtual Environments Jun. 1991 p 50-59 (For primary document see N95-14013 03-54)
Avail: CASI HC A02/MF A02

The topics covered include the following: the need for telerobotics in rehabilitation; barriers to telerobotics technology in rehabilitation and health care; institutional barriers; technical barriers; and a partial view of the future. CASI

N95-14031*# Washington Univ., Seattle, WA. Dept. of Industrial Engineering.
CREATING BETTER VIRTUAL WORLDS
Thomas A. Furness, III *In* NASA. Ames Research Center, Human Machine Interfaces for Teleoperators and Virtual Environments Jun. 1991 p 63-65 (For primary document see N95-14013 03-54)
Avail: CASI HC A01/MF A02

The topics discussed include the following: virtual reality, man machine systems, and human-computer interface. CASI

N95-14032*# Massachusetts Inst. of Tech., Cambridge. Media Lab.
INTERACTING WITH VIRTUAL WORLDS Abstract Only
David Zeltzer *In* NASA. Ames Research Center, Human Machine Interfaces for Teleoperators and Virtual Environments Jun. 1991 p 66 (For primary document see N95-14013 03-54)
Avail: CASI HC A01/MF A02

What tools should we provide the user for defining and interacting with objects and agents in virtual environments at varying levels of complexity? Understanding the appropriate simplifications to make is critical for modeling nontrivial environments and agents with varying levels of autonomy. I describe a set of abstraction mechanisms appropriate for constructing and interacting with virtual worlds, and I discuss how programming, and direct manipulation of guiding techniques, can be used to afford users interactive access to graphical simulations at appropriate levels of abstraction.
Derived from text

N95-14033*# North Carolina Univ., Chapel Hill, NC. Dept. of Computer Science.
VIRTUAL REALITY AT WORK Abstract Only
Frederick P. Brooks, Jr. *In* NASA. Ames Research Center, Human Machine Interfaces for Teleoperators and Virtual Environments Jun. 1991 p 67-68 (For primary document see N95-14013 03-54)
Avail: CASI HC A01/MF A02

The utility of virtual reality computer graphics in telepresence applications is not hard to grasp and promises to be great. When the virtual world is entirely synthetic, as opposed to real but remote, the utility is harder to establish. Vehicle simulators for aircraft, vessels, and motor vehicles are proving their worth every day. Entertainment applications such as Disney World's StarTours are technologically elegant, good fun, and economically viable. Nevertheless, some of us have no real desire to spend our lifework

serving the entertainment craze of our sick culture; we want to see this exciting technology put to work in medicine and science. The topics covered include the following: testing a force display for scientific visualization -- molecular docking; and testing a head-mounted display for scientific and medical visualization. Derived from text

N95-14034*# National Aeronautics and Space Administration. Ames Research Center, Moffett Field, CA.

THE AMES VIRTUAL ENVIRONMENT WORKSTATION: IMPLEMENTATION ISSUES AND REQUIREMENTS

Scott S. Fisher, R. Jacoby, S. Bryson, P. Stone, I. McDowall, M. Bolas, D. Dasaro, Elizabeth M. Wenzel, C. Coler, and D. Kerr *In its* Human Machine Interfaces for Teleoperators and Virtual Environments Jun. 1991 p 70-73 (For primary document see N95-14013 03-54)

Avail: CASI HC A01/MF A02

This presentation describes recent developments in the implementation of a virtual environment workstation in the Aerospace Human Factors Research Division of NASA's Ames Research Center. Introductory discussions are presented on the primary research objectives and applications of the system and on the system's current hardware and software configuration. Principle attention is then focused on unique issues and problems encountered in the workstation's development with emphasis on its ability to meet original design specifications for computational graphics performance and for associated human factors requirements necessary to provide compelling sense of presence and efficient interaction in the virtual environment. Derived from text

N95-14035*# National Aeronautics and Space Administration. Ames Research Center, Moffett Field, CA.

VIRTUAL ACOUSTIC DISPLAYS

Elizabeth M. Wenzel *In its* Human Machine Interfaces for Teleoperators and Virtual Environments Jun. 1991 p 74-77 (For primary document see N95-14013 03-54)

Avail: CASI HC A01/MF A02

A 3D auditory display can potentially enhance information transfer by combining directional and iconic information in a quite naturalistic representation of dynamic objects in the interface. Another aspect of auditory spatial clues is that, in conjunction with other modalities, it can act as a potentiator of information in the display. For example, visual and auditory cues together can reinforce the information content of the display and provide a greater sense of presence or realism in a manner not readily achievable by either modality alone. This phenomenon will be particularly useful in telepresence applications, such as advanced teleconferencing environments, shared electronic workspaces, and monitoring telerobotic activities in remote or hazardous situations. Thus, the combination of direct spatial cues with good principles of iconic design could provide an extremely powerful and information-rich display which is also quite easy to use. An alternative approach, recently developed at ARC, generates externalized, 3D sound cues over headphones in realtime using digital signal processing. Here, the synthesis technique involves the digital generation of stimuli using Head-Related Transfer Functions (HRTF's) measured in the two ear-canals of individual subjects. Other similar approaches include an analog system developed by Loomis, et. al., (1990) and digital systems which make use of transforms derived from normative mannikins and simulations of room acoustics. Such an interface also requires the careful psychophysical evaluation of listener's ability to accurately localize the virtual or synthetic sound sources. From an applied standpoint, measurement of each potential listener's HRTF's may not be possible in practice. For experienced listeners, localization performance was only slightly degraded compared to a subject's inherent ability. Alternatively, even inexperienced listeners may be able to adapt to a particular set of HRTF's as long as they provide adequate cues for localization. In general, these data suggest that most listeners can obtain useful directional information from an auditory display without requiring the use of individually-tailored HRTF's. Derived from text

N95-14036*# National Aeronautics and Space Administration. Ames Research Center, Moffett Field, CA.

VARIETIES OF VIRTUALIZATION

Stephen R. Ellis *In its* Human Machine Interfaces for Teleoperators and Virtual Environments Jun. 1991 p 78-80 Prepared in cooperation with California Univ., Berkeley (For primary document see N95-14013 03-54)

Avail: CASI HC A01/MF A02

Natural environments have a content, i.e., the objects in them; a geometry, i.e., a pattern of rules for positioning and displacing the objects; and a dynamics, i.e., a system of rules describing the effects of forces acting on the objects. Human interaction with most common natural environments has been optimized by centuries of evolution. Virtual environments created through the human-computer interface similarly have a content, geometry, and dynamics, but the arbitrary character of the computer simulation creating them does not insure that human interaction with these virtual environments will be natural. The interaction, indeed, could be supernatural but it also could be impossible. An important determinant of the comprehensibility of a virtual environment is the correspondence between the environmental frames of reference and those associated with the control of environmental objects. The effects of rotation and displacement of control frames of reference with respect to corresponding environmental references differ depending upon whether perceptual judgement or manual tracking performance is measured. The perceptual effects of frame of reference displacement may be analyzed in terms of distortions in the process of virtualizing the synthetic environment space. The effects of frame of reference displacement and rotation have been studied by asking subjects to estimate exocentric direction in a virtual space. Derived from text

N95-14037*# National Aeronautics and Space Administration. Ames Research Center, Moffett Field, CA.

THE EXPLORATION METAPHOR **c91**

Michael W. McGreevy *In its* Human Machine Interfaces for Teleoperators and Virtual Environments Jun. 1991 p 81-82 (For primary document see N95-14013 03-54)

Avail: CASI HC A01/MF A02

NASA's experience in planetary exploration has demonstrated that the desktop workstation is inadequate for many visualization situations. The primary mission displays for the unmanned Surveyor missions to the moon during the mid-1960's, for example, were environmental images assembled on the inside surfaces of spherical shells. Future exploration missions will greatly benefit from advances in digital computer and display technology, but there remain unmet user interface needs. Alternative user interfaces and metaphors are needed for planetary exploration and other interactions with complex spatial environments. These interfaces and metaphors would enable the user to directly explore environments and naturally manipulate objects in those environments. Personal simulators, virtual workstations, and telepresence user interfaces are systems capable of providing this integration of user space and task space. The Exploration Metaphor is a useful concept for guiding the design of user interfaces for virtual environments and telepresence. To apply the Exploration Metaphor is to assert that computing is like exploration, and to support objects, operations, and contexts comparable to those encountered in the exploration of natural environments. The Exploration Metaphor, under development for user interfaces in support of NASA's planetary exploration missions and goals, will also benefit other applications where complex spatial information must be visualized. Visualization methods and systems for planetary exploration are becoming increasingly integrated and interactive as computing technology improves. These advances will benefit from virtual environment and telepresence interface technology. A key development has been the processing of multiple images and other sensor data to create detailed digital models of the planets and moons. Data from images of the Earth, Mars, and Miranda, for example, have been converted into 3D models, and dynamic virtual fly-overs have been computed as demonstrations. Similar processing of lower altitude photography and the use of computer aided design tools promise to produce very detailed models in the future.

Derived from text

N95-14038*# California Univ., Los Angeles, CA.

MEASUREMENT AND MODIFICATION OF THE EEG AND RELATED BEHAVIOR

M. B. Sterman *In* NASA. Ames Research Center, Human Machine Interfaces for Teleoperators and Virtual Environments Jun. 1991 p 83-84 Sponsored in part by Northrop Corp. Prepared in cooperation with Veterans Administration Hospital, Sepulveda, CA. (For primary document see N95-14013 03-54)

Avail: CASI HC A01/MF A02

Electrophysiological changes in the sensorimotor pathways were found to accompany the effect of rhythmic EEG patterns in the sensorimotor

cortex. Additionally, several striking behavioral changes were seen, including in particular an enhancement of sleep and an elevation of seizure threshold to epileptogenic agents. This raised the possibility that human seizure disorders might be influenced therapeutically by similar training. Our objective in human EEG feedback training became not only the facilitation of normal rhythmic patterns, but also the suppression of abnormal activity, thus requiring complex contingencies directed to the normalization of the sensorimotor EEG. To achieve this, a multicomponent frequency analysis was developed to extract and separate normal and abnormal elements of the EEG signal. Each of these elements was transduced to a specific component of a visual display system, and these were combined through logic circuits to present the subject with a symbolic display. Variable criteria provided for the gradual shaping of EEG elements towards the desired normal pattern. Some 50-70% of patients with poorly controlled seizure disorders experienced therapeutic benefits from this approach in our laboratory, and subsequently in many others. A more recent application of this approach to the modification of human brain function in our lab has been directed to the dichotomous problems of task overload and underload in the contemporary aviation environment. At least 70% of all aviation accidents have been attributed to the impact of these kinds of problems on crew performance. The use of EEG in this context has required many technical innovations and the application of the latest advances in EEG signal analysis. Our first goal has been the identification of relevant EEG characteristics. Additionally, we have developed a portable recording and analysis system for application in this context. Findings from laboratory and in-flight studies suggest that we will be able to detect appropriate changes in brain function, and feed this information to on-board computers for modification of mission requirements and/or crew status.

Derived from text

N95-14039*# Ruhr Univ., Bochum (Germany).

THE TELEPRASENZ CONSORTIUM: STRUCTURE AND INTENTIONS

Jens Blauert *In* NASA. Ames Research Center, Human Machine Interfaces for Teleoperators and Virtual Environments Jun. 1991 p 85 (For primary document see N95-14013 03-54)

Avail: CASI HC A01/MF A02

The Teleprasenz-Consortium is an open group of currently 37 scientists of different disciplines who devote a major part of their research activities to the foundations of telepresence technology. Telepresence technology is basically understood as a means to bridge spatial and temporal gaps as well as certain kinds of concealment, inaccessibility and danger of exposure. The activities of the consortium are organized into three main branches: virtual environment, surveillance and control systems, and speech and language technology. A brief summary of the main activities in these areas is given.

Derived from text

N95-14040*# McGill Univ., Montreal (Quebec). Physical and Occupational Therapy.

THE HUMAN OPERATOR TRANSFER FUNCTION: IDENTIFICATION OF THE LIMB MECHANICS SUBSYSTEM

Lynette A. Jones and Ian W. Hunter *In* NASA. Ames Research Center, Human Machine Interfaces for Teleoperators and Virtual Environments Jun. 1991 p 105-106 (For primary document see N95-14013 03-54)

Avail: CASI HC A01/MF A02

The objective of our research is to decompose the performance of the human operator in terms of the subsystems that determine the operator's responses in order to establish how the dynamics of these component subsystems influence the operator's performance. In the present experiment, the dynamic stiffness of the human elbow joint was measured at rest and under different levels of biceps muscle activation; this work forms part of the analysis of the limb mechanics subsystem.

Derived from text

N95-14041*# Massachusetts Inst. of Tech., Cambridge. Sensory Communication Group.

TACTILE DISCRIMINATION AND REPRESENTATIONS OF TEXTURE, SHAPE, AND SOFTNESS Abstract Only

M. A. Srinivasan and R. H. LaMotte *In* NASA. Ames Research Center, Human Machine Interfaces for Teleoperators and Virtual Environments Jun. 1991 p 107 (For primary document see N95-14013 03-54)

Avail: CASI HC A01/MF A02

We present here some of the salient results on the tactual discriminabilities of human subjects obtained through psychophysical experiments, and the associated peripheral neural codes obtained through electrophysiological recordings from monkey single nerve fibers. Humans can detect the presence of a 2 micron high single dot on a smooth glass plate stroked on the skin, based on the responses of Meissner type rapidly adapting fibers (RAs). They can also detect a 0.06 micron high grating on the plate, owing to the response of Pacinian corpuscle fibers. Among all the possible representations of the shapes of objects, the surface curvature distribution seems to be the most relevant for tactile sensing. Slowly adapting fibers respond to both the change and rate of change of curvature of the skin surface at the most sensitive spot in their receptive fields, whereas RAs respond only to the rate of change of curvature. Human discriminability of compliance of objects depends on whether the object has a deformable or rigid surface. When the surface is deformable, the spatial pressure distribution within the contact region is dependent on object compliance, and hence information from cutaneous mechanoreceptors is sufficient for discrimination of subtle differences in compliance. When the surface is rigid, kinesthetic information is necessary for discrimination, and the discriminability is much poorer than that for objects with deformable surfaces.

Author (revised)

N95-14042*# Massachusetts Inst. of Tech., Cambridge. Lab. for Biomechanics and Human Rehabilitation.

A HIGH PERFORMANCE TWO DEGREE-OF-FREEDOM KINESTHETIC INTERFACE

Bernard D. Adelstein and Michael J. Rosen *In* NASA. Ames Research Center, Human Machine Interfaces for Teleoperators and Virtual Environments Jun. 1991 p 108-113 (For primary document see N95-14013 03-54)

Avail: CASI HC A02/MF A02

This summary focuses on the kinesthetic interface of a virtual environment system that was developed at the Newman Laboratory for Biomechanics and Human Rehabilitation at M.I.T. for the study of manual control in both motorically impaired and able-bodied individuals.

Author

N95-14043*# National Aeronautics and Space Administration. Ames Research Center, Moffett Field, CA.

PERCEPTUAL AND PERFORMANCE CONSEQUENCES OF FLIGHT IN VIRTUAL WORLDS Abstract Only

C. Thomas Bennett, Martin Schwirzke, and James S. Tittle *In its* Human Machine Interfaces for Teleoperators and Virtual Environments Jun. 1991 p 114 (For primary document see N95-14013 03-54)

Avail: CASI HC A01/MF A02

There are two primary purposes for head-mounted systems in aeronautical settings. One is for helmet-mounted sights and teleoperated (head-slaved) weapons systems. Bennett, Johnson, Perrone, and Phatak (1988) evaluated head tracking performance during passive and controlled flight. In that study, comparisons were also made of head tracking performance in sterile and relatively complex virtual worlds. That study confirmed the robustness of head tracking performance across a wide variety of visual scenes. A second use of virtual world displays is for aircraft control. Aircraft controllability using head-mounted, panel-mounted, or simulated out-the-window scenes has been systematically examined. Those studies reported the range of rotorcraft flight tasks in which head-mounted virtual worlds provided some advantages. Two studies will be reported that examine the perceptual/performance effects of virtual worlds. The first examines head tracking performance with roll-stabilized versus non-roll stabilized virtual worlds. The purpose of the study was to (1) examine display strategies used in current display systems and (2) study the adaptability of observers to estimated glide slope angles using head-slaved versus head-stabilized imagery. The purpose of this study was to examine the usefulness of wide field-of-regards during final approaches to a runway.

Author (revised)

N95-14044*# Stanford Univ., CA. Dept. of Mechanical Engineering.

A DECADE OF TELEROBOTICS IN REHABILITATION: DEMONSTRATED UTILITY BLOCKED BY THE HIGH COST OF MANIPULATION AND THE COMPLEXITY OF THE USER INTERFACE Abstract Only

Larry Leifer, Stefan Michalowski, and Machiel VanDerLoos *In* NASA. Ames Research Center, Human Machine Interfaces for Teleoperators and Virtual Environments Jun. 1991 p 115 (For primary document see

N95-14013 03-54)
Avail: CASI HC A01/MF A02

The Stanford/VA Interactive Robotics Laboratory set out in 1978 to test the hypothesis that industrial robotics technology could be applied to serve the manipulation needs of severely impaired individuals. Five generations of hardware, three generations of system software, and over 125 experimental subjects later, we believe that genuine utility is achievable. The experience includes development of over 65 task applications using voiced command, joystick control, natural language command and 3D object designation technology. A brief foray into virtual environments, using flight simulator technology, was instructive. If reality and virtuality come for comparable prices, you cannot beat reality. A detailed review of assistive robot anatomy and the performance specifications needed to achieve cost/beneficial utility will be used to support discussion of the future of rehabilitation telerobotics. Poised on the threshold of commercial viability, but constrained by the high cost of technically adequate manipulators, this worthy application domain flounders temporarily. In the long run, it will be the user interface that governs utility. Author

N95-14045*# Edinburgh Univ. (Scotland).
A PHYSICAL CONTROL INTERFACE WITH PROPRIOCEPTIVE FEEDBACK AND MULTIPLE DEGREES OF FREEDOM **c66**
G. H. Creasey, D. Gow, Y. Sloan, and B. Meadows *In* NASA. Ames Research Center, Human Machine Interfaces for Teleoperators and Virtual Environments Jun. 1991 p 116-117 Prepared in cooperation with Princess Margaret Rose Orthopaedic Hospital, Edinburgh, Lothian, Scotland (For primary document see N95-14013 03-54)
Avail: CASI HC A01/MF A02

The use of the drug thalidomide by pregnant mothers in Britain resulted in a variety of deformities including the birth of children having no arms. Such children were provided with powered artificial arms with up to five degrees of freedom simultaneously controlled in real time by shoulder movement. The physiological sense of proprioception was extended from the user into the device, reducing the need for visual feedback and conscious control. With the banning of thalidomide, this technique fell into disuse but it is now being re-examined as a control mechanism for other artificial limbs and it may have other medical applications to allow patients to control formerly paralyzed limbs moved by electrical stimulation. It may also have commercial applications in robotic manipulation or physical interaction with virtual environments. To allow it to be investigated further, the original pneumatic control system has recently been converted to an electrical analogue to allow interfacing to electronic and computer-assisted systems. A harness incorporates force-sensitive resistors and linear potentiomenters for sensing position and force at the interface with the skin, and miniature electric motors and lead screws for feeding back to the user the position of the robotic arm and the forces applied to it. In the present system, control is applied to four degrees of freedom using elevation/depression and protraction/reaction of each shoulder so that each collar bone emulates a joystick. However, both electrical and mechanical components have been built in modular form to allow rapid replication and testing of a variety of force and position control strategies.
Author (revised)

N95-14046*# National Aeronautics and Space Administration. Ames Research Center, Moffett Field, CA.
ROTATIONAL WIND INDICATOR ENHANCES CONTROL OF ROTATED DISPLAYS Abstract Only **c61**
H. A. Cunningham and Misha Pavel *In its* Human Machine Interfaces for Teleoperators and Virtual Environments Jun. 1991 p 118 Sponsored by AFOSR and NAS-NRC Prepared in cooperation with Stanford Univ., CA (For primary document see N95-14013 03-54)
(Contract NCC2-307)
Avail: CASI HC A01/MF A02

Rotation by 108 deg of the spatial mapping between a visual display and a manual input device produces large spatial errors in a discrete aiming task. These errors are not easily corrected by voluntary mental effort, but the central nervous system does adapt gradually to the new mapping. Bernotat (1970) showed that adding true hand position to a 90 deg rotated display improved performance of a compensatory tracking task, but tracking error rose again upon removal of the explicit cue. This suggests that the explicit error signal did not induce changes in the neural mapping, but rather allowed the operator to reduce tracking error using a higher mental strategy. In this report, we describe an explicit visual display enhancement applied to a 108 deg rotated discrete aiming task. A 'wind indicator' corresponding to the effect of the mapping rotation is displayed on the operator-controlled cursor. The human operator is instructed to oppose the virtual force represented by the indicator, as one would do if flying an airplane in a crosswind. This enhancement reduces spatial aiming error in the first 10 minutes of practice by an average of 70 percent when compared to a no enhancement control condition. Moreover, it produces adaptation aftereffect, which is evidence of learning by neural adaptation rather than by mental strategy. Finally, aiming error does not rise upon removal of the explicit cue. Author

N95-14047*# Northrop Corp., Lomita, CA.
OBJECTIVE EVALUATION OF SITUATION AWARENESS FOR DYNAMIC DECISION MAKERS IN TELEOPERATIONS Abstract Only
Mica R. Endsley *In* NASA. Ames Research Center, Human Machine Interfaces for Teleoperators and Virtual Environments Jun. 1991 p 119 (For primary document see N95-14013 03-54)
Avail: CASI HC A01/MF A02

Situation awareness, a current mental mode of the environment, is critical to the ability of operators to perform complex and dynamic tasks. This should be particularly true for teleoperators, who are separated from the situation they need to be aware of. The design of the man-machine interface must be guided by the goal of maintaining and enhancing situation awareness. The objective of this work has been to build a foundation upon which research in the area can proceed. A model of dynamic human decision making which is inclusive of situation awareness will be presented, along with a definition of situation awareness. A method for measuring situation awareness will also be presented as a tool for evaluating design concepts. The Situation Awareness Global Assessment Technique (SAGAT) is an objective measure of situation awareness originally developed for the fighter cockpit environment. The results of SAGAT validation efforts will be presented. Implications of this research for teleoperators and other operators of dynamic systems will be discussed. Author

N95-14048*# Tokyo Univ. (Japan).
DEVELOPMENT OF VISUAL 3D VIRTUAL ENVIRONMENT FOR CONTROL SOFTWARE **c61**
Michitaka Hirose, Takeshi Myoi, Haruo Amari, Kohei Inamura, and Lawrence Stark *In* NASA. Ames Research Center, Human Machine Interfaces for Teleoperators and Virtual Environments Jun. 1991 p 120-124 Prepared in cooperation with Tokyo Electric Power Co., Inc., Japan and California Univ., Berkeley (For primary document see N95-14013 03-54)
Avail: CASI HC A01/MF A02

Virtual environments for software visualization may enable complex programs to be created and maintained. A typical application might be for control of regional electric power systems. As these encompass broader computer networks than ever, construction of such systems becomes very difficult. Conventional text-oriented environments are useful in programming individual processors. However, they are obviously insufficient to program a large and complicated system, that includes large numbers of computers connected to each other; such programming is called 'programming in the large.' As a solution for this problem, the authors are developing a graphic programming environment wherein one can visualize complicated software in virtual 3D world. One of the major features of the environment is the 3D representation of concurrent process. 3D representation is used to supply both network-wide interprocess programming capability (capability for 'programming in the large') and real-time programming capability. The authors' idea is to fuse both the block diagram (which is useful to check relationship among large number of processes or processors) and the time chart (which is useful to check precise timing for synchronization) into a single 3D space. The 3D representation gives us a capability for direct and intuitive planning or understanding of complicated relationship among many concurrent processes. To realize the 3D representation, a technology to enable easy handling of virtual 3D object is a definite necessity. Using a stereo display system and a gesture input device (VPL DataGlove), our prototype of the virtual workstation has been implemented. The workstation can supply the 'sensation' of the virtual 3D space to a programmer. Software for the 3D programming environment is implemented on the workstation. According to preliminary assessments, a 50 percent reduction of programming effort is achieved by using the virtual 3D environment. The

authors expect that the 3D environment has considerable potential in the field of software engineering. Derived from text

N95-14049*# Technion - Israel Inst. of Tech., Haifa (Israel). Dept. of Electrical Engineering.

HUMAN OPERATOR TRACKING PERFORMANCE WITH A VIBROTACTILE DISPLAY Abstract Only

Gideon F. Inbar *In* NASA. Ames Research Center, Human Machine Interfaces for Teleoperators and Virtual Environments Jun. 1991 p 125 (For primary document see N95-14013 03-54)

Avail: CASI HC A01/MF A02

Vibrotactile displays have been designed and used as a sensory aid for the blind. In the present work the same 6 x 24 'Optacon' type vibrotactile display (VTD) was used to characterize human operator (HO) tracking performance in pursuit and compensatory tasks. The VTD was connected via a microprocessor to a one-dimensional joy stick manipulator. Various display schemes were tested on the VDT, and were also compared to visual tracking performance using a specially constructed photo diode matrix display comparable to the VTD. Author

N95-14050*# Cybernet Systems Corp., Ann Arbor, MI.

IMPLEMENTATION ISSUES FOR A COMPACT 6 DEGREE OF FREEDOM FORCE REFLECTING HANDCONTROLLER WITH CUEING OF MODES Abstract Only

Heidi Jacobus, Alan J. Riggs, Charles Jacobus, and Yechiel Weinstein *In* NASA. Ames Research Center, Human Machine Interfaces for Teleoperators and Virtual Environments Jun. 1991 p 126 (For primary document see N95-14013 03-54)

(Contract NAS9-18094)

Avail: CASI HC A01/MF A02

Teleoperated control requires a master human interface device that can provide haptic input and output which reflect the responses of a slave robotic system. The effort reported in this paper addresses the design and prototyping of a six degree-of-freedom (DOF) Cartesian coordinate hand controller for this purpose. The device design recommended is an XYZ stage attached to a three-roll wrist which positions a flight-type handgrip. Six degrees of freedom are transduced and control brushless DC motor servo electronics similar in design to those used in computer controlled robotic manipulators. This general approach supports scaled force, velocity, and position feedback to aid an operator in achieving telepresence. The generality of the device and control system characteristics allow the use of inverse dynamics robotic control methodology to project slave robot system forces and inertias to the operator (in scaled form) and at the same time to reduce the apparent inertia of the robotic handcontroller itself. The current control design, which is not multiple fault tolerant, can be extended to make flight control or space use possible. The proposed handcontroller will have advantages in space-based applications where an operator must control several robot arms in a simultaneous and coordinated fashion. It will also have applications in intravehicular activities (within the Space Station) such as microgravity experiments in metallurgy and biological experiments that require isolation from the astronauts' environment. For ground applications, the handcontroller will be useful in underwater activities where the generality of the proposed handcontroller becomes an asset for operation of many different manipulator types. Also applications will emerge in the Military, Construction, and Maintenance/Manufacturing areas including ordnance handling, mine removal, NBC (Nuclear, Chemical, Biological) operations, control of vehicles, and operating strength and agility enhanced machines. Future avionics applications including advanced helicopter and aircraft control may also become important. Author

N95-14051*# Minnesota Univ., Minneapolis, MN. Dept. of Mechanical Engineering.

ON THE ROLE OF EXCHANGE OF POWER AND INFORMATION SIGNALS IN CONTROL AND STABILITY OF THE HUMAN-ROBOT INTERACTION Abstract Only

H. Kazerooni *In* NASA. Ames Research Center, Human Machine Interfaces for Teleoperators and Virtual Environments Jun. 1991 p 127-128 (For primary document see N95-14013 03-54)

Avail: CASI HC A01/MF A02

A human's ability to perform physical tasks is limited, not only by his intelligence, but by his physical strength. If, in an appropriate environment, a machine's mechanical power is closely integrated with a human arm's mechanical power under the control of the human intellect, the resulting system will be superior to a loosely integrated combination of a human and a fully automated robot. Therefore, we must develop a fundamental solution to the problem of 'extending' human mechanical power. The work presented here defines 'extenders' as a class of robot manipulators worn by humans to increase human mechanical strength, while the wearer's intellect remains the central control system for manipulating the extender. The human, in physical contact with the extender, exchanges power and information signals with the extender. The aim is to determine the fundamental building blocks of an intelligent controller, a controller which allows interaction between humans and a broad class of computer-controlled machines via simultaneous exchange of both power and information signals. The prevalent trend in automation has been to physically separate the human from the machine so the human must always send information signals via an intermediary device (e.g., joystick, pushbutton, light switch). Extenders, however are perfect examples of self-powered machines that are built and controlled for the optimal exchange of power and information signals with humans. The human wearing the extender is in physical contact with the machine, so power transfer is unavoidable and information signals from the human help to control the machine. Commands are transferred to the extender via the contact forces and the EMG signals between the wearer and the extender. The extender augments human motor ability without accepting any explicit commands: it accepts the EMG signals and the contact force between the person's arm and the extender, and the extender 'translates' them into a desired position. In this unique configuration, mechanical power transfer between the human and the extender occurs because the human is pushing against the extender. The extender transfers to the human's hand, in feedback fashion, a scaled-down version of the actual external load which the extender is manipulating. This natural feedback force on the human's hand allows him to 'feel' a modified version of the external forces on the extender. The information signals from the human (e.g., EMG signals) to the computer reflect human cognitive ability, and the power transfer between the human and the machine (e.g., physical interaction) reflects human physical ability. Thus the information transfer to the machine augments cognitive ability, and the power transfer augments motor ability. These two actions are coupled through the human cognitive/motor dynamic behavior. The goal is to derive the control rules for a class of computer-controlled machines that augment human physical and cognitive abilities in certain manipulative tasks. Author

N95-14052*# Artificial Reality Corp., Vernon, CT.

A TWO DIMENSIONAL ARTIFICIAL REALITY Abstract Only

Myron W. Krueger *In* NASA. Ames Research Center, Human Machine Interfaces for Teleoperators and Virtual Environments Jun. 1991 p 129-131 (For primary document see N95-14013 03-54)

Avail: CASI HC A01/MF A02

The current presumption is that it is necessary to don goggles, gloves and a data suit to experience artificial reality. However, there is another technology that offers an alternative or complement to the encumbering techniques associated with NASA. In VIDEOPLACE, your image appears in a 2D graphic world created by a computer. The VIDEOPLACE computer can analyze a person's image in 1/30 second and can detect when an object is touched. Thus, it can generate a graphic or auditory response to an illusory contact. VIDEOPLACE technology exists in two formats: the VIDEODESK and the VIDEOPLACE. In the VIDEODESK environment, the image of your hands can be used to perform the normal mouse functions, such as menuing and drawing. In addition, you have the advantage of multipoint control. For instance, you can use the thumbs and forefingers of each hand as control points for a spline curve. Perhaps most important, the image of your hands can be compressed and transmitted to a colleague over an ISDN voice channel to appear on the remote screen superimposed over identical information. Likewise, the image of your colleague's hands can appear on both screens. The result is that the two of you can use your hands to point to features on your respective screens as you speak, exactly as you would if you were sitting together. In the VIDEOPLACE environment, you can interact with graphic creatures and the images of other people in other locations in a graphic world. Your whole body can be moved, scaled and rotated in real-time without regard to the laws of physics. Thus, VIDEOPLACE can be used to create a fantasy world in which the laws of cause and effect are composed by an artist. Author

N95-14053*# Ruhr Univ., Bochum (Germany).
BINAURAL ROOM SIMULATION Abstract Only **c71**
H. Lehnert, Jens Blauert, and W. Pompetzki *In* NASA. Ames Research Center, Human Machine Interfaces for Teleoperators and Virtual Environments Jun. 1991 p 132-133 (For primary document see N95-14013 03-54)
Avail: CASI HC A01/MF A02

In every-day listening the auditory event perceived by a listener is determined not only by the sound signal that a sound emits but also by a variety of environmental parameters. These parameters are the position, orientation and directional characteristics of the sound source, the listener's position and orientation, the geometrical and acoustical properties of surfaces which affect the sound field and the sound propagation properties of the surrounding fluid. A complete set of these parameters can be called an Acoustic Environment. If the auditory event perceived by a listener is manipulated in such a way that the listener is shifted acoustically into a different acoustic environment without moving himself physically, a Virtual Acoustic Environment has been created. Here, we deal with a special technique to set up nearly arbitrary Virtual Acoustic Environments, the Binaural Room Simulation. The purpose of the Binaural Room Simulation is to compute the binaural impulse response related to a virtual acoustic environment taking into account all parameters mentioned above. One possible way to describe a Virtual Acoustic Environment is the concept of the virtual sound sources. Each of the virtual sources emits a certain signal which is correlated but not necessarily identical with the signal emitted by the direct sound source. If source and receiver are non moving, the acoustic environment becomes a linear time-invariant system. Then, the Binaural Impulse Response from the source to a listener' s eardrums contains all relevant auditory information related to the Virtual Acoustic Environment. Listening into the simulated environment can easily be achieved by convolving the Binaural Impulse Response with dry signals and representing the results via headphones. Author

N95-14054*# California Univ., Santa Barbara, CA. Dept. of Psychology.
ACTIVE LOCALIZATION OF VIRTUAL SOUNDS Abstract Only **c71**
Jack M. Loomis, C. Hebert, and J. G. Cicinelli *In* NASA. Ames Research Center, Human Machine Interfaces for Teleoperators and Virtual Environments Jun. 1991 p 134 (For primary document see N95-14013 03-54)
Avail: CASI HC A01/MF A02

We describe a virtual sound display built around a 12 MHz 80286 microcomputer and special purpose analog hardware. The display implements most of the primary cues for sound localization in the ear-level plane. Static information about direction is conveyed by interaural time differences and, for frequencies above 1800 Hz, by head sound shadow (interaural intensity differences) and pinna sound shadow. Static information about distance is conveyed by variation in sound pressure (first power law) for all frequencies, by additional attenuation in the higher frequencies (simulating atmospheric absorption), and by the proportion of direct to reverberant sound. When the user actively locomotes, the changing angular position of the source occasioned by head rotations provides further information about direction and the changing angular velocity produced by head translations (motion parallax) provides further information about distance. Judging both from informal observations by users and from objective data obtained in an experiment on homing to virtual and real sounds, we conclude that simple displays such as this are effective in creating the perception of external sounds to which subjects can home with accuracy and ease. Author

N95-14055*# EXOS, Inc., Lexington, MA.
HUMAN-MACHINE INTERFACE HARDWARE: THE NEXT DECADE Abstract Only
Elizabeth A. Marcus *In* NASA. Ames Research Center, Human Machine Interfaces for Teleoperators and Virtual Environments Jun. 1991 p 135 (For primary document see N95-14013 03-54)
Avail: CASI HC A01/MF A02

In order to understand where human-machine interface hardware is headed, it is important to understand where we are today, how we got there, and what our goals for the future are. As computers become more capable, faster, and programs become more sophisticated, it becomes apparent that the interface hardware is the key to an exciting future in computing. How can a user interact and control a seemingly limitless array of parameters effectively? Today, the answer is most often a limitless array of controls. The link between these controls and human sensory motor capabilities does not utilize existing human capabilities to their full extent. Interface hardware for teleoperation and virtual environments is now facing a crossroad in design. Therefore, we as developers need to explore how the combination of interface hardware, human capabilities, and user experience can be blended to get the best performance today and in the future. Author

N95-14056*# California Polytechnic State Univ., San Luis Obispo, CA.
COORDINATION OF HUMAN UPPER ARM AND FOREARM MOTION IN RAPID EXTENSIONS Abstract Only
Mahmood Nahvi *In* NASA. Ames Research Center, Human Machine Interfaces for Teleoperators and Virtual Environments Jun. 1991 p 136 (For primary document see N95-14013 03-54)
Avail: CASI HC A01/MF A02

In many movements of the upper limb such as reaching, positioning, and displacing the objects, the hand moves smoothly along a uni-directional planar trajectory with a bell-shaped speed profile. Because of variability of the load, gravitational and velocity interaction forces between its segments, the dynamics of the arm during the motion is very complex. Motion of the upper arm and the forearm are coordinated to produce smooth movements despite such complex dynamics. This coordination constitutes an important organizational feature of arm movement. The present paper describes some experimental results related to the above and interprets their role in producing smooth motion of the hand. Trajectories of the right upper limb in vertical plane and the simultaneous muscles' EMG activities were recorded for extensions of various amplitudes under four loads. The forearm trajectories are smooth with bell-shaped speed profiles. The upper arm trajectories may have bimodal speed profiles and three segments, resembling an inverted 'Z.' Segmentation is sharper for the points near the shoulder joint, and is accentuated by load. As one moves from the central points near the shoulder joint to the peripheral points near the hand, the three segments merge and result in smooth curves with single-peaked speed profiles. The three segments have a coherent time course and can be identified rather accurately and non-ambiguously. The observed trajectories and the EMG patterns reveal an effective coordination strategy which utilizes the structure and the dynamics of the moving arm to produce smooth movement. Author

N95-14057*# Massachusetts Inst. of Tech., Cambridge. Sensory Communication Group.
MANUAL DISCRIMINATION OF FORCE Abstract Only
Xiao-Dong Pang, Hong-Z. Tan, and Nathaniel I. Durlach *In* NASA. Ames Research Center, Human Machine Interfaces for Teleoperators and Virtual Environments Jun. 1991 p 137 (For primary document see N95-14013 03-54)
Avail: CASI HC A01/MF A02

Optimal design of human-machine interfaces for teleoperators and virtual-environment systems which involve the tactual and kinesthetic modalities requires knowledge of the human's resolving power in these modalities. The resolution of the interface should be appropriately matched to that of the human operator. We report some preliminary results on the ability of the human hand to distinguish small differences in force under a variety of conditions. Experiments were conducted on force discrimination with the thumb pushing an interface that exerts a constant force over the pushing distance and the index finger pressing against a fixed support. The dependence of the sensitivity index d' on force increment can be fit by a straight line through the origin and the just-noticeable difference (JND) in force can thus be described by the inverse of the slope of this line. The receiver operating characteristic (ROC) was measured by varying the a priori probabilities of the two alternatives, reference force and reference force plus an increment, in one-interval, two-alternative, forced-choice experiments. When plotted on normal deviate coordinates, the ROC's were roughly straight lines of unit slope, thus supporting the assumption of equal-variance normal distributions and the use of the conventional d' measure. The JND was roughly 6-8 percent for reference force ranging from 2.5 to 10 newtons, pushing distance from 5 to 30 mm, and initial finger-span from 45 to 125 mm. Also, the JND remained the same when the subjects were instructed to change the average speed of pushing from 23 to 153 mm/sec. The pushing was terminated by reaching either a wall or a well, and the JND's were essentially the same in both cases. Author

N95-14058*# Massachusetts Inst. of Tech., Cambridge. Media Lab.
IMPLEMENTATION OF A THREE DEGREE OF FREEDOM, MOTOR/BRAKE HYBRID FORCE OUTPUT DEVICE FOR VIRTUAL ENVIRONMENT CONTROL TASKS
Massimo Russo, Alfred Tadros, Woodie Flowers, and David Zeltzer *In* NASA. Ames Research Center, Human Machine Interfaces for Teleoperators and Virtual Environments Jun. 1991 p 138-142 (For primary document see N95-14013 03-54)
Avail: CASI HC A01/MF A02

The advent of high resolution, physical model based computer graphics has left a gap in the design of input/output technology appropriate for interacting with such complex virtual world models. Since virtual worlds consist of physical models, it is appropriate to output the inherent force information necessary for the simulation to the user. The detailed design, construction, and control of a three degree freedom force output joystick will be presented. A novel kinematic design allows all three axes to be uncoupled, so that the system inertia matrix is diagonal. The two planar axes are actuated through an offset gimbal, and the third through a sleeved cable. To compensate for friction and inertia effects, this transmission is controlled by a force feedforward and a closed force feedback proportional loop. Workspace volume is a cone of 512 cubic inches, and the device bandwidth is maximized at 60 Hz for the two planar and 30 Hz for the third axis. Each axis is controlled by a motor/proportional magnetic particle brake combination fixed to the base. The innovative use of motors and brakes allows objects with high resistive torque requirements to be simulated without the stability and related safety issues involved with high torque, energy storing motors alone. Position, velocity, and applied endpoint force are sensed directly. Different control strategies are discussed and implemented, with an emphasis on how virtual environment force information, generated by the MIT Media Lab Computer Graphics and Animation Group BOLIO system, is transmitted to the device controller. The design constraints for a kinesthetic force feedback device can be summarized as: How can the symbiosis between the sense of presence in the virtual environment be maximized without compromising the interaction task under the constraints of the mechanical device limitations? Research in this field will yield insights to the optimal human sensory feedback mix for a wide spectrum of control and interaction problems. A flexible research tool that is designed as an easily reproducible product prototype has been constructed to explore the variety of possible force interaction. Author

N95-14059*# National Advanced Robotics Research Centre, Salford, Lancashire (England).
HUMAN FACTORS REQUIREMENTS FOR TELEROBOTIC COMMAND AND CONTROL: THE EUROPEAN SPACE AGENCY EXPERIMENTAL PROGRAMME Abstract Only
Robert J. Stone *In* NASA. Ames Research Center, Human Machine Interfaces for Teleoperators and Virtual Environments Jun. 1991 p 143-144 (For primary document see N95-14013 03-54)
Avail: CASI HC A01/MF A02

Space Telerobotics research, performed under contract to the European Space Agency (ESA), concerning the execution of human factors experiments, and ultimately leading to the development of a telerobotics test bed, has been carried out since 1985 by a British Consortium consisting of British Aerospace, the United Kingdom Atomic Energy Authority and, more recently, the UK National Advanced Robotics Research Centre. The principal aim of the first study of the series was to derive preliminary requirements for a teleoperation servicing system, with reference to two mission model scenarios. The first scenario introduced the problem of communications time delays, and their likely effect on the ground-based operator in control of a manipulator system on board an unmanned servicing vehicle in Low Earth Orbit. In the second scenario, the operator was located on the NASA Orbiter aft flight deck, supervising the control of a prototype manipulator in the 'servicing' of an experimental payload in the cargo bay area. Human factors analyses centered on defining the requirements for the teleoperator workstation, such as identifying basic ergonomic requirements for workstation and panel layouts, defining teleoperation strategies, developing alphanumeric and graphic screen formats for the supervision or direct control of the manipulator, and the potential applications of expert system technology. The second study for ESA involved an experimental appraisal of some of the important issues highlighted in the first study, for which relevant human factors data did not exist. Of central importance during the second study was the issue of communications time delays and their effect on the manual control of a teleoperated manipulator from a ground-based command and control station. Author

N95-14060*# National Advanced Robotics Research Centre, Salford, Lancashire (England).
VERDEX: A VIRTUAL ENVIRONMENT DEMONSTRATOR FOR REMOTE DRIVING APPLICATIONS Abstract Only
Robert J. Stone *In* NASA. Ames Research Center, Human Machine Interfaces for Teleoperators and Virtual Environments Jun. 1991 p 145-147 (For primary document see N95-14013 03-54)
Avail: CASI HC A01/MF A02

One of the key areas of the National Advanced Robotics Centre's enabling technologies research program is that of the human system interface, phase 1 of which started in July 1989 and is currently addressing the potential of virtual environments to permit intuitive and natural interactions between a human operator and a remote robotic vehicle. The aim of the first 12 months of this program (to September, 1990) is to develop a virtual human-interface demonstrator for use later as a test bed for human factors experimentation. This presentation will describe the current state of development of the test bed, and will outline some human factors issues and problems for more general discussion. In brief, the virtual telepresence system for remote driving has been designed to take the following form. The human operator will be provided with a helmet-mounted stereo display assembly, facilities for speech recognition and synthesis (using the Marconi Macrospeak system), and a VPL DataGlove Model 2 unit. The vehicle to be used for the purposes of remote driving is a Cybermotion Navmaster K2A system, which will be equipped with a stereo camera and microphone pair, mounted on a motorized high-speed pan-and-tilt head incorporating a closed-loop laser ranging sensor for camera convergence control (currently under contractual development). It will be possible to relay information to and from the vehicle and sensory system via an umbilical or RF link. The aim is to develop an interactive audio-visual display system capable of presenting combined stereo TV pictures and virtual graphics windows, the latter featuring control representations appropriate for vehicle driving and interaction using a graphical 'hand,' slaved to the flex and tracking sensors of the DataGlove and an additional helmet-mounted Polhemus IsoTrack sensor. Developments planned for the virtual environment test bed include transfer of operator control between remote driving and remote manipulation, dexterous end effector integration, virtual force and tactile sensing (also the focus of a current ARRL contract, initially employing a 14-pneumatic bladder glove attachment), and sensor-driven world modeling for total virtual environment generation and operator-assistance in remote scene interrogation. Author

N95-14061*# Florida Univ., Gainesville, FL.
DESTABILIZING EFFECTS OF VISUAL ENVIRONMENT MOTIONS SIMULATING EYE MOVEMENTS OR HEAD MOVEMENTS
Keith D. White, D. Shuman, J. H. Krantz, C. B. Woods, and L. A. Kuntz *In* NASA. Ames Research Center, Human Machine Interfaces for Teleoperators and Virtual Environments Jun. 1991 p 148-155 (For primary document see N95-14013 03-54)
Avail: CASI HC A02/MF A02

In the present paper, we explore effects on the human of exposure to a visual virtual environment which has been enslaved to simulate the human user's head movements or eye movements. Specifically, we have studied the capacity of our experimental subjects to maintain stable spatial orientation in the context of moving their entire visible surroundings by using the parameters of the subjects' natural movements. Our index of the subjects' spatial orientation was the extent of involuntary sways of the body while attempting to stand still, as measured by translations and rotations of the head. We also observed, informally, their symptoms of motion sickness. Author

N95-14263# Advisory Group for Aerospace Research and Development, Neuilly-Sur-Seine (France). Aerospace Medical Panel.
THE MUSCULOSKELETAL AND VESTIBULAR EFFECTS OF LONG TERM REPEATED EXPOSURE TO SUSTAINED HIGH-G [LES EFFETS MUSCULOSQUELETTIQUES ET VESTIBULAIRES DE L'EXPOSITION REPETEE ET PROLONGEE AUX FACTEURS DE CHARGE ELEVES SOUTENS]

May 1994 70 p
(AGARD-AR-317; ISBN-92-835-0745-2) Copyright Avail: CASI HC A04/MF A01

Medical concerns of mechanical loading of biological systems during repeated sustained acceleration exposure of high performance aircraft were expressed during an AGARD conference of 24th-28th April 1989 (AGARD-CP-471) entitled 'Neck Injury in Advanced Military Aircraft Environments'. Biological systems of primary concern were direct effects on the spine causing neurological injury and on the otoliths of the vestibular system causing disorientation related pathologies. In addition, secondary vestibular effects can occur from cervical pathologies. The technical evaluation and overview of that conference expressed concerns that 'large gaps exist in our clinical and biomechanical knowledge of the problems of neck injury in high performance aircraft'. Advisory Report (AR) 317 addresses those concerns with an in-depth review of available pertinent information with recommendations on several courses of action directed towards the spine and vestibular systems. Specific topics covered include: (1) the physical environment of aerial combat maneuvers; (2) anatomy and biomechanics of the spine; (3) G-loading effects on the musculoskeletal system of the spine including risk factors and the prevention of injuries; (4) imaging considerations; (5) high sustained G effects on the vestibular system and methods to test organ dysfunctions; and (6) topical research proposals. Recommendations include: (1) study requirements; (2) aircrew selection training and education; (3) equipment modifications and development; and (4) research requirements. AR 317 contains 215 references.
Author (revised)

N95-14854*# Universities Space Research Association, Columbia, MD.
PROPOSAL FOR AN ASTRONAUT MASS MEASUREMENT DEVICE FOR THE SPACE SHUTTLE
Neil Beyer, Jon Lomme, Holly McCollough, Bradford Price, and Heidi Weber 1 Apr. 1994 50 p
(Contract NASw-4435)
(NASA-CR-197198; NAS 1.26:197198) Avail: CASI HC A03/MF A01

For medical reasons, astronauts in space need to have their mass measured. Currently, this measurement is performed using a mass-spring system. The current system is large, inaccurate, and uncomfortable for the astronauts. NASA is looking for new, different, and preferably better ways to perform this measurement process. After careful analysis our design team decided on a linear acceleration process. Within the process, four possible concept variants are put forth. Among these four variants, one is suggested over the others. The variant suggested is that of a motor-winch system to linearly accelerate the astronaut. From acceleration and force measurements of the process combined Newton's second law, the mass of an astronaut can be calculated.
Author

N95-15309# Mechanical Technology, Inc., Latham, NY.
INTERACTIVE COMPUTER-ENHANCED REMOTE VIEWING SYSTEM (ICERVS): SUBSYSTEM DESIGN REPORT, PHASE 2
D. A. Smith 22 Apr. 1994 246 p
(Contract DE-AC21-92MC-29113)
(DE94-014513; DOE/MC-29113/3766-Phase-2) Avail: CASI HC A11/MF A03

This ICERVS Phase 2 Subsystem Design Report describes the detailed software design of the Phase II Interactive Computer-Enhanced Remote Viewing System (ICERVS). ICERVS is a computer-based system that provides data acquisition, data visualization, data analysis, and model synthesis to support robotic remediation of hazardous environments. Due to the risks associated with hazardous environments, remediation must be conducted remotely using robotic systems, which, in turn, must rely on 3D models of their workspace to support both task and path planning with collision avoidance. Tools such as ICERVS are vital to accomplish remediation tasks in a safe, efficient manner. The 3D models used by robotic systems are based on solid modeling methods, in which objects are represented by enclosing surfaces (polygons, quadric surfaces, patches, etc.) or collections of primitive solids (cubes, cylinders, etc.). In general, these 3D models must be created and/or verified by actual measurements made in the robotics workspace. However, measurement data is empirical in nature, with typical output being a collection of xyz triplets that represent sample points on some surface(s) in the workspace. As such, empirical data cannot be readily analyzed in terms of geometric representations used in robotic workspace models. The primary objective of ICERVS is to provide a reliable description of a workspace based on dimensional measurement data and to convert that description into 3D models that can be used by robotic systems. ICERVS will thus serve as a critical factor to allow robotic remediation tasks to be performed more effectively (faster, safer) and economically than with present systems.
DOE

N95-15449 Naval Research Lab., Washington, DC.
USE OF THE USER ACTION NOTATION AT THE NAVAL RESEARCH LABORATORY HUMAN-COMPUTER INTERACTION LABORATORY
Joe Chase, Deborah Hix, David Tate, and James Templeman 30 Jun. 1994 34 p Limited Reproducibility: More than 20% of this document may be affected by microfiche quality
(AD-A281680; NRL/MR/5530-94-7488) Avail: CASI HC A03

This report describes introduction of researchers in the Information Technology Division of the Naval Research Laboratory (NRL) to the User Action Notation (UAN), a notation developed at Virginia Tech for representing the design of the interaction component of interactive systems. This report also presents use of the UAN in describing a variety of unique, innovative interaction techniques to evaluate the notation for its ability to represent such techniques, and exploration of possibilities for future research and technology transition with the UAN collaboratively between NRL and Virginia Tech.
DTIC

N95-15755# Dayton Univ., OH.
DISTANCE ESTIMATION TRAINING WITH NIGHT VISION GOGGLES: A PRELIMINARY STUDY Interim Report, Aug. - Oct. 1993
Jack D. Reising and Elizabeth L. Martin Aug. 1994 26 p
(Contract F33615-90-C-0005)
(AD-A284900; AL/HR-TR-1994-0090) Avail: CASI HC A03/MF A01

Aircrews have reported significant problems in depth perception and distance estimation with night vision goggles (NVG's). The purposes of this experiment was to develop a methodology for quantifying distance estimation abilities with NVG's and to examine the value of a simple training procedure as a means of reducing errors. Absolute distance estimates were obtained from eight male aviators using Aviators Night Vision Imaging System (ANVIS) AN/AVS-6 NVG's before and after exposure to a set of known distances. The results revealed that distance estimates were linear and significant reductions in errors and variability followed exposure to the training procedure. The results are discussed within the context of previous research. Issues for future research are addressed.
DTIC

N95-15759# Army Research Lab., Aberdeen Proving Ground, MD.
PRELIMINARY ANALYSIS OF ARMY AIRCREW REQUIREMENTS FOR JOINT SURVEILLANCE TARGET ATTACK RADAR SYSTEM (JSTARS): HUMAN PERFORMANCE REQUIREMENTS AND JOB DEMANDS Final Report
Beverly G. Knapp Aug. 1994 45 p
(DA Proj. 1L1-62716-AH-70)
(AD-A284917; ARL-MR-178) Avail: CASI HC A03/MF A01

In response to a request from Training and Doctrine Command (TRADOC) Systems Manager for the Joint Surveillance Target Attack Radar System (JSTARS), the U.S. Army Research Institute Field Office, now the Human Research and Engineering Directorate (HRED) of the U.S. Army Research Laboratory, located at Fort Huachuca, Arizona, conducted an analysis of Army aircrew positions aboard the JSTARS E-8 aircraft. The objective was to determine skills and abilities requirements, task demands, and implications of training and selection. The analytical approach included using the job comparison and analysis tool (JCAT) by experts who had flown on JSTARS in Operation Desert Storm. Data from these analyses indicate a significant cognitive (mental) demand for the three Army aircrew positions, a need for auditory attention ability at a midlevel experience range, and a strong emphasis on oral and written interpersonal communication skills. Findings suggest that these positions must be filled by experience personnel.
DTIC

N95-15850 Institute of Sound and Vibration Research, Southampton (England). Audiology and Human Effects Group.
INDIVIDUAL VARIABILITY IN THE TRANSMISSION OF VERTICAL VIBRATION FROM SEAT TO HEAD
Gurmail S. Paddan and Michael J. Griffin Nov. 1994 51 p Sponsored by UK Ministry of Defence

(ISVR-TR-236) Copyright Avail: Issuing Activity (Inst. of Sound and Vibration Research, Univ. of Southampton, Southampton SO9 5NH, England)

The variability in the transmission of vertical vibration from a seat to the heads of seated subjects is presented. An intra-subject variability study involved 12 repeat measures for 1 male subject. Twelve male subjects participated in an inter-subject variability study. The effects of two sitting postures were investigated: 'back-on' (leaning slightly against the seat backrest) and 'back-off' (a comfortable upright posture with no contact with the seat backrest). Transfer functions (transmissibility and phase) between vertical seat and vertical head motion are presented in graphical and tabular form. The variability is quantified by the median and interquartile ranges. Author

N95-14228*# Wisconsin Univ., Madison, WI. Center for Space Automation and Robotics.

THE ASTROCULTURE (TM)-1 EXPERIMENT ON THE USML-1 MISSION

Theodore Tibbitts, R. J. Bula, and R. C. Morrow *In* NASA. Marshall Space Flight Center, Joint Launch + One Year Science Review of USML-1 and USMP-1 with the Microgravity Measurement Group May 1994 p 509-523 (For primary document see N95-14207 03-88)

Avail: CASI HC A03/MF A04

N95-14949# Massachusetts Inst. of Tech., Cambridge.

HUMAN FACTORS CONSIDERATIONS FOR REMOTE MANIPULATION

Thomas B. Sheridan *In* AGARD, Advanced Guidance and Control Aspects in Robotics Jun. 1994 24 p (For primary document see N95-14942 03-63)

Copyright Avail: CASI HC A03/MF A03

55 SPACE BIOLOGY

Includes exobiology; planetary biology; and extraterrestrial life.

No abstracts in this category.

59 MATHEMATICAL AND COMPUTER SCIENCES (GENERAL)

N95-14585*# National Aeronautics and Space Administration. Goddard Space Flight Center, Greenbelt, MD.

1994 SCIENCE INFORMATION MANAGEMENT AND DATA COMPRESSION WORKSHOP

James C. Tilton, ed. Washington Sep. 1994 106 p Workshop held in Greenbelt, MD, 26-27 Sep. 1994; cosponsored by IEEE

(RTOP 930-00-00)

(NASA-CP-3277; Rept-94B00116; NAS 1.55:3277) Avail: CASI HC A06/MF A02

This document is the proceedings from the 'Science Information Management and Data Compression Workshop,' which was held on September 26-27, 1994, at the NASA Goddard Space Flight Center, Greenbelt, Maryland. The Workshop explored promising computational approaches for handling the collection, ingestion, archival and retrieval of large quantities of data in future Earth and space science missions. It consisted of eleven presentations covering a range of information management and data compression approaches that are being or have been integrated into actual or prototypical Earth or space science data information systems, or that hold promise for such an application. The workshop was organized by James C. Tilton and Robert F. Cromp of the NASA Goddard Space Flight Center. For individual titles, see N95-14586 through N95-14596.

N95-14586*# Wisconsin Univ., Madison, WI. Dept. of Computer Science.

PERFORMANCE OF CUSTOMIZED DCT QUANTIZATION TABLES ON SCIENTIFIC DATA **c62**

Viresh Ratnakar and Miron Livny *In* NASA. Goddard Space Flight Center, 1994 Science Information Management and Data Compression Workshop Sep. 1994 p 1-8 (For primary document see N95-14585 03-59)

(Grants NAGw-3914; NSF IRI-92-24741)

Avail: CASI HC A02/MF A02

We show that it is desirable to use data-specific or customized quantization tables for scaling the spatial frequency coefficients obtained using the Discrete Cosine Transform (DCT). DCT is widely used for image and video compression (MP89, PM93) but applications typically use default quantization matrices. Using actual scientific data gathered from divers sources such as spacecrafts and electron-microscopes, we show that the default compression/quality tradeoffs can be significantly improved upon by using customized tables. We also show that significant improvements are possible for the standard test images Lena and Baboon. This work is part of an effort to develop a practical scheme for optimizing quantization matrices for any given image or video stream, under any given quality or compression constraints. Author

N95-14587*# Glamorgan Univ., Pontypridd, Glamorgan (Wales). Dept. of Mathematics and Computing.

COMPARISON OF TRANSFORM CODING METHODS WITH AN OPTIMAL PREDICTOR FOR THE DATA COMPRESSION OF DIGITAL ELEVATION MODELS **c62**

Michael Lewis *In* NASA. Goddard Space Flight Center, 1994 Science Information Management and Data Compression Workshop Sep. 1994 p 9-26 (For primary document see N95-14585 03-59)

Avail: CASI HC A03/MF A02

Statistical encoding techniques enable the reduction of the number of bits required to encode a set of symbols, and are derived from their probabilities. Huffman encoding is an example of statistical encoding that has been used for error-free data compression. The degree of compression given by Huffman encoding in this application can be improved by the use of prediction methods. These replace the set of elevations by a set of corrections that have a more advantageous probability distribution. In particular, the method of Lagrange Multipliers for minimization of the mean square error has been applied to local geometrical predictors. Using this technique, an 8-point predictor achieved about a 7 percent improvement over an existing simple triangular predictor. Author

N95-14588*# National Aeronautics and Space Administration. Goddard Space Flight Center, Greenbelt, MD.

RADIOMETRIC RESOLUTION ENHANCEMENT BY LOSSY COMPRESSION AS COMPARED TO TRUNCATION FOLLOWED BY LOSSLESS COMPRESSION **c62**

James C. Tilton and Mareboyana Manohar *In its* 1994 Science Information Management and Data Compression Workshop Sep. 1994 p 27-39 (For primary document see N95-14585 03-59)

Avail: CASI HC A03/MF A02

Recent advances in imaging technology make it possible to obtain imagery data of the Earth at high spatial, spectral and radiometric resolutions from Earth orbiting satellites. The rate at which the data is collected from these satellites can far exceed the channel capacity of the data downlink. Reducing the data rate to within the channel capacity can often require painful trade-offs in which certain scientific returns are sacrificed for the sake of others. In this paper we model the radiometric version of this form of lossy compression by dropping a specified number of least significant bits from each data pixel and compressing the remaining bits using an appropriate lossless compression technique. We call this approach 'truncation followed by lossless compression' or TLLC. We compare the TLLC approach with applying a lossy compression technique to the data for reducing the data rate to the channel capacity, and demonstrate that each of three different lossy compression techniques (JPEG/DCT, VQ and Model-Based VQ) give a better effective radiometric resolution than TLLC for a given channel rate. Author

N95-14589*# Georgia Inst. of Tech., Atlanta, GA. School of Electrical Engineering.

BLOCKING REDUCTION OF LANDSAT THEMATIC MAPPER JPEG BROWSE IMAGES USING OPTIMAL PSNR ESTIMATED SPECTRA ADAPTIVE POSTFILTERING Abstract Only **c62**

Irving Linares, Russell M. Mersereau, and Mark J. T. Smith *In* NASA. Goddard Space Flight Center, 1994 Science Information Management and Data Compression Workshop Sep. 1994 p 41 (For primary document see N95-14585 03-59)

Avail: CASI HC A01/MF A02

Two representative sample images of Band 4 of the Landsat Thematic Mapper are compressed with the JPEG algorithm at 8:1, 16:1 and 24:1 Compression Ratios for experimental browsing purposes. We then apply the Optimal PSNR Estimated Spectra Adaptive Postfiltering (ESAP) algorithm to reduce the DCT blocking distortion. ESAP reduces the blocking distortion while preserving most of the image's edge information by adaptively postfiltering the decoded image using the block's spectral information already obtainable from each block's DCT coefficients. The algorithm iteratively applied a one dimensional log-sigmoid weighting function to the separable interpolated local block estimated spectra of the decoded image until it converges to the optimal PSNR with respect to the original using a 2-D steepest ascent search. Convergence is obtained in a few iterations for integer parameters. The optimal logsig parameters are transmitted to the decoder as a negligible byte of overhead data. A unique maxima is guaranteed due to the 2-D asymptotic exponential overshoot shape of the surface generated by the algorithm. ESAP is based on a DFT analysis of the DCT basis functions. It is implemented with pixel-by-pixel spatially adaptive separable FIR postfilters. PSNR objective improvements between 0.4 to 0.8 dB are shown together with their corresponding optimal PSNR adaptive postfiltered images. Author

N95-14590*# MacDonald, Dettwiler and Associates Ltd., Richmond (British Columbia).

SYNTHETIC APERTURE RADAR SIGNAL DATA COMPRESSION USING BLOCK ADAPTIVE QUANTIZATION **c62**

Gopinath Kuduvalli, Melanie Dutkiewicz, and Ian Cumming *In* NASA. Goddard Space Flight Center, 1994 Science Information Management and Data Compression Workshop Sep. 1994 p 43-57 Sponsored by ESA (For primary document see N95-14585 03-59)

Avail: CASI HC A03/MF A02

This paper describes the design and testing of an on-board SAR signal data compression algorithm for ESA's ENVISAT satellite. The Block Adaptive Quantization (BAQ) algorithm was selected, and optimized for the various operational modes of the ASAR instrument. A flexible BAQ scheme was developed which allows a selection of compression ratio/image quality trade-offs. Test results show the high quality of the SAR images processed from the reconstructed signal data, and the feasibility of on-board implementation using a single ASIC. Author

N95-14591*# Nebraska Univ., Lincoln, NE.

COMPRESSION OF REGIONS IN THE GLOBAL ADVANCED VERY HIGH RESOLUTION RADIOMETER 1-km DATA SET **c62**

Barbara L. Kess, Daniel R. Steinwand, and Stephen E. Reichenbach *In* NASA. Goddard Space Flight Center, 1994 Science Information Management and Data Compression Workshop Sep. 1994 p 59-64 Prepared for Hughes STX, Inc., Greenbelt, MD (For primary document see N95-14585 03-59)

(Contract USGS-14-34-92-C-40004)

Avail: CASI HC A02/MF A02

The global advanced very high resolution radiometer (AVHRR) 1-km data set is a 10-band image produced at USGS' EROS Data Center for the study of the world's land surfaces. The image contains masked regions for non-land areas which are identical in each band but vary between data sets. They comprise over 75 percent of this 9.7 gigabyte image. The mask is compressed once and stored separately from the land data which is compressed for each of the 10 bands. The mask is stored in a hierarchical format for multi-resolution decompression of geographic subwindows of the image. The land for each band is compressed by modifying a method that ignores fill values. This multi-spectral region compression efficiently compresses the region data and precludes fill values from interfering with land compression statistics. Results show that the masked regions in a one-byte test image (6.5 Gigabytes) compress to 0.2 percent of the 557,756,146 bytes they occupy in the original image, resulting in a compression ratio of 89.9 percent for the entire image. Author (revised)

N95-14592*# Tokyo Univ. (Japan). Inst. of Industrial Science.

LOSSLESS COMPRESSION OF NOAA-AVHRR SATELLITE DATA **c62**

Seishi Takamura and Mikio Takagi *In* NASA. Goddard Space Flight Center, 1994 Science Information Management and Data Compression Workshop Sep. 1994 p 65-73 (For primary document see N95-14585 03-59)

Avail: CASI HC A02/MF A02

A high-performance lossless compression system for satellite NOAA data is developed. The data is called 'high resolution picture transmission' (HRPT) data, and consists of around 93 percent advanced very high resolution radiometer (AVHRR) multi-channel image data and 7 percent of miscellaneous data. In compressing the image portion, we classify each pixel into 10 different groups and apply a multi-channel prediction and a non-linear error conversion. The entropy coder is an arithmetic coder which is adaptive and regenerates the approximation of the statistical properties of the source as an initial probability table. To compress the non-image part, we used the general compressor (gzip). From experimental results, the original information is compressed down to 25 percent to approx. 40 percent. Author

N95-14593*# National Aeronautics and Space Administration. Goddard Space Flight Center, Greenbelt, MD.

THE DEVELOPMENT OF LOSSLESS DATA COMPRESSION TECHNOLOGY FOR REMOTE SENSING APPLICATIONS **c62**

Pen-Shu Yeh and Warner H. Miller *In its* 1994 Science Information Management and Data Compression Workshop Sep. 1994 p 75-82 (For primary document see N95-14585 03-59)

Avail: CASI HC A02/MF A02

Lossless data compression has been studied for many NASA missions to achieve the benefit of increased science return, reduced onboard memory requirement, station contact time and communication bandwidth. This paper first addresses the requirement for onboard applications and provides rational for the selection of the Rice algorithm among other available techniques. A top-level description of the Rice algorithm will be given, along with some new capabilities already implemented in both software and hardware VLSI forms. The paper then addresses systems issues important for onboard implementation including sensor calibration, error propagation and data packetization. The latter part of the paper provides several case study examples drawn from a broad spectrum of science instruments including the thematic mapper, x-ray telescope, gamma-ray spectrometer, and acousto-optical spectrometer. Author

N95-14594*# New Hampshire Univ., Durham. Complex Systems Research Center.

LANDSAT PATHFINDER TROPICAL FOREST INFORMATION MANAGEMENT SYSTEM **c82**

W. Salas, W. Chomentowski, J. Harville, D. Skole, and K. Vellekamp *In* NASA. Goddard Space Flight Center, 1994 Science Information Management and Data Compression Workshop Sep. 1994 p 83-93 (For primary document see N95-14585 03-59)

Avail: CASI HC A03/MF A02

A Tropical Forest Information Management System—(TFIMS) has been designed to fulfill the needs of HTFIP in such a way that it tracks all aspects of the generation and analysis of the raw satellite data and the derived deforestation dataset. The system is broken down into four components: satellite image selection, processing, data management and archive management. However, as we began to think of how the TFIMS could also be used to make the data readily accessible to all user communities we realized that the initial system was too project oriented and could only be accessed locally. The new system needed development in the areas of data ingest and storage, while at the same time being implemented on a server environment with a network interface accessible via Internet. This paper summarizes the overall design of the existing prototype (version 0) information management system and then presents the design of the new system (version 1). The development of version 1 of the TFIMS is ongoing. There are no current plans for a gradual transition from version 0 to version 1 because the significant changes are in how

the data within the HTFIP will be made accessible to the extended community of scientists, policy makers, educators, and students and not in the functionality of the basic system. Author

N95-14595*# National Aeronautics and Space Administration. Goddard Space Flight Center, Greenbelt, MD.
PLANNING/SCHEDULING TECHNIQUES FOR VQ-BASED IMAGE COMPRESSION **c62**
Nicholas M. Short, Jr., Mareboyana Manohar, and James C. Tilton *In its* 1994 Science Information Management and Data Compression Workshop Sep. 1994 p 95-104 (For primary document see N95-14585 03-59)
Avail: CASI HC A02/MF A02

The enormous size of the data holding and the complexity of the information system resulting from the EOS system pose several challenges to computer scientists, one of which is data archival and dissemination. More than ninety percent of the data holdings of NASA is in the form of images which will be accessed by users across the computer networks. Accessing the image data in its full resolution creates data traffic problems. Image browsing using a lossy compression reduces this data traffic, as well as storage by factor of 30-40. Of the several image compression techniques, VQ is most appropriate for this application since the decompression of the VQ compressed images is a table lookup process which makes minimal additional demands on the user's computational resources. Lossy compression of image data needs expert level knowledge in general and is not straightforward to use. This is especially true in the case of VQ. It involves the selection of appropriate codebooks for a given data set and vector dimensions for each compression ratio, etc. A planning and scheduling system is described for using the VQ compression technique in the data access and ingest of raw satellite data. Author

N95-14596*# Hughes STX, Inc., Greenbelt, MD.
AN OVERVIEW OF THE EOSDIS V0 INFORMATION MANAGEMENT SYSTEM: LESSONS LEARNED FROM THE IMPLEMENTATION OF A DISTRIBUTED DATA SYSTEM Abstract Only **c82**
Patrick M. Ryan *In* NASA. Goddard Space Flight Center, 1994 Science Information Management and Data Compression Workshop Sep. 1994 p 105 (For primary document see N95-14585 03-59)
Avail: CASI HC A01/MF A02

The EOSDIS Version 0 system, released in July, 1994, is a working prototype of a distributed data system. One of the purposes of the V0 project is to take several existing data systems and coordinate them into one system while maintaining the independent nature of the original systems. The project is a learning experience and the lessons are being passed on to the architects of the system which will distribute the data received from the planned EOS satellites. In the V0 system, the data resides on heterogeneous systems across the globe but users are presented with a single, integrated interface. This interface allows users to query the participating data centers based on a wide set of criteria. Because this system is a prototype, we used many novel approaches in trying to connect a diverse group of users with the huge amount of available data. Some of these methods worked and others did not. Now that V0 has been released to the public, we can look back at the design and implementation of the system and also consider some possible future directions for the next generation of EOSDIS. Author

60 COMPUTER OPERATIONS AND HARDWARE

Includes hardware for computer graphics, firmware, and data processing.

For components see *33 Electronics and Electrical Engineering.*

N95-13716*# National Aeronautics and Space Administration. Lewis Research Center, Cleveland, OH.
A PROTOTYPE LISP-BASED SOFT REAL-TIME OBJECT-ORIENTED GRAPHICAL USER INTERFACE FOR CONTROL SYSTEM DEVELOPMENT
Jonathan Litt (Army Research Lab., Cleveland, OH.), Edmond Wong, and Donald L. Simon Oct. 1994 23 p Prepared in cooperation with Army Research Lab., Adelphi, MD
(RTOP 468-01-11; DA Proj. 1L1-61102-AH-45)
(NASA-TM-106743; E-9155; NAS 1.15:106743; ARL-TR-571) Avail: CASI HC A03/MF A01

A prototype Lisp-based soft real-time object-oriented Graphical User Interface for control system development is presented. The Graphical User Interface executes alongside a test system in laboratory conditions to permit observation of the closed loop operation through animation, graphics, and text. Since it must perform interactive graphics while updating the screen in real time, techniques are discussed which allow quick, efficient data processing and animation. Examples from an implementation are included to demonstrate some typical functionalities which allow the user to follow the control system's operation. Author

N95-14107*# Auburn Univ., AL. Dept. of Computer Science and Engineering.
INTEGRATION/EVALUATION OF A HCI PROTOTYPING ENVIRONMENT Final Report, 23 Sep. 1993 - 31 Jul. 1994
Loretta A. Moore 17 Oct. 1994 105 p
(Contract NAS8-39131)
(NASA-CR-196996; NAS 1.26:196996; CSE-94-16) Avail: CASI HC A06/MF A02

Components of a human computer interface (HCI) prototyping environment have been integrated and evaluated. This environment will be valuable in developing and refining HCI standards and evaluating program/project interface development, especially the International Space Station Alpha's on-board displays for payload operations. This environment, which allows for rapid prototyping and evaluation of graphical interfaces, includes four components: (1) a HCI format development tool, (2) a test and evaluation simulator development tool, (3) a dynamic, interactive interface between the HCI prototype and simulator, and (4) an embedded evaluation capability to evaluate the adequacy of a HCI based on a user's performance. The objective of the research was to determine whether or not the functional components could be integrated and could provide the needed functionality for a rapid prototyping environment. Author

N95-14338# Lawrence Livermore National Lab., Livermore, CA.
THE CONSOLE PASSWORD FEATURE FOR DEC WORKSTATIONS
A. L. VanLehn Oct. 1993 16 p
(Contract W-7405-eng-48)
(DE94-015721; UCRL-MA-115604) Avail: CASI HC A03/MF A01

New VAXstations and all DECstations offer a 'hardware' password feature that, when enabled, restricts unauthorized access to your system console terminal when turned on or restarted. VAXstation 3100's shipped after July, 1989 offer this feature. A description of this feature should be part of the Hardware User Guide for your workstation, however, some of the early systems did not document this security enhancement. This document is based on the author's investigation as well as information provided by the Digital Equipment Corporation. DOE

N95-14514*# Christopher Newport Coll., Newport News, VA. Dept. of Physics and Computer Science.
SODR MEMORY CONTROL BUFFER CONTROL ASIC Final Technical Report, 18 May 1992 - 31 Jul. 1994
Robert F. Hodson 2 Nov. 1994 54 p
(Grant NAG1-1439)
(NASA-CR-197001; NAS 1.26:197001) Avail: CASI HC A04/MF A01

The Spacecraft Optical Disk Recorder (SODR) is a state of the art mass storage system for future NASA missions requiring high transmission rates and a large capacity storage system. This report covers the design and development of an SODR memory buffer control applications specific integrated circuit (ASIC). The memory buffer control ASIC has two primary functions: (1) buffering data to prevent loss of data during disk access times, (2) converting data formats from a high performance parallel interface format to a small computer systems interface format. Ten 144 p in, 50 MHz CMOS ASIC's were designed, fabricated and tested to implement the memory buffer control function. CASI

N95-14662# Pacific Northwest Lab., Richland, WA.
LOW LATENCY REMOTE MEMORY ACCESS ON THE INTEL PARAGON
M. Rosing and P. Pierce 20 Jun. 1994 9 p Presented at the Intel Supercomputing Users Group Meeting, San Diego, CA, 25-29 Jun. 1994
(Contract DE-AC06-76RL-01830)

(DE94-014993; PNL-SA-24486; CONF-9406205-1) Avail: CASI HC A02/MF A01

We describe a cooperative project between Pacific Northwest Laboratory and Intel on providing low latency communications on the Intel Paragon. Our interest is in developing modules that are tailored to specific types of communication and are optimized for these cases. The modules described are implemented as simple extensions to the Paragon operating system. The first extension supports remote reads, writes, and accumulates on subsections of matrices. This module is intended to be used where the communication pattern is not known until run time. The second extension is designed to support low latency communication for short messages in a pipelined fashion. Finally, an interface for doing highly structured communication where the patterns of communication are well understood ahead of time is described. This is intended to be used in global communications such as global reduction. DOE

N95-15809 Computer Sciences Corp., Falls Church, VA.
DISTRIBUTED HETEROGENEOUS VISUALIZATION, BOP (BAG-O-POLYGONS) AND BOP VIEW Progress Report, Sep. 1992 - Oct. 1993
Jerry A. Clarke Sep. 1994 23 p Prepared in cooperation with Minnesota Univ., Minneapolis, MN Limited Reproducibility: More than 20% of this document may be affected by microfiche quality
(Contract DAAL03-89-C-0088)
(AD-A284393; ARL-CR-172) Avail: Issuing Activity (Defense Technical Information Center (DTIC))

With the increased use of parallel and super computers in scientific computing, the size of datasets that need to be visualized can easily reach into the gigabyte range. Even by utilizing data reduction techniques such as isosurface generation, scenes containing hundreds of thousands or millions of polygons are common. Standard techniques of data visualization quickly become overwhelmed and too time consuming to be practical. New methods and utilities need to be developed to handle these massive datasets. Bop (Bag-O-Polygons), Bop View, and associated utilities are an attempt to use distributed and parallel techniques to ease the processing of these datasets. Bop is a data format designed for large number of polygons. A library of routines is provided for reading and writing this data to disk files. Additional routines allow this polygonal information to be shared across heterogeneous architectures. Finally, an application called Bop-View is provided to efficiently display the resulting information. DTIC

N95-14159*# Rome Lab., Griffiss AFB, NY.
GENERIC ARCHITECTURES FOR FUTURE FLIGHT SYSTEMS
Richard J. Wood *In* Research Inst. for Computing and Information Systems, RICIS Symposium 1992: Mission and Safety Critical Systems Research and Applications 30 Oct. 1992 16 p (For primary document see N95-14156 03-61)
Avail: CASI HC A03/MF A03

N95-14160*# Rome Lab., Griffiss AFB, NY.
ARCHITECTURE FOR SURVIVABLE SYSTEMS PROCESSING (ASSP). TECHNOLOGY BENEFITS FOR OPEN SYSTEM INTERCONNECTS
Richard J. Wood *In* Research Inst. for Computing and Information Systems, RICIS Symposium 1992: Mission and Safety Critical Systems Research and Applications 30 Oct. 1992 12 p (For primary document see N95-14156 03-61)
Avail: CASI HC A03/MF A03

61 COMPUTER PROGRAMMING AND SOFTWARE

Includes computer programs, routines, alogorithms, and specific applications, e.g., CAD/CAM.

N95-13632*# Aerojet-General Corp., Azusa, CA.
EARTH OBSERVING SYSTEM (EOS) ADVANCED MICROWAVE SOUNDING UNIT-A (AMSU-A) SPARES PROGRAM PLAN Final Report
Weldon Chapman Sep. 1994 15 p
(Contract NAS5-32314; RTOP 422-00-00)
(NASA-CR-189380; Aerojet-10340; NAS 1.26:189380) Avail: CASI HC A03/MF A01

This plan specifies the spare components to be provided for the EOS/AMSU-A instrument and the general spares philosophy for their procurement. It also address key components not recommended for spares, as well as the schedule and method for obtaining the spares. The selected spares list was generated based on component criticality, reliability, repairability, and availability. An alternative spares list is also proposed based on more stringent fiscal constraints. Derived from text

N95-13633*# Aerojet-General Corp., Azusa, CA.
EARTH OBSERVING SYSTEM (EOS)/ADVANCED MICROWAVE SOUNDING UNIT-A (AMSU-A): INSTRUMENT LOGIC DIAGRAMS Final Report
Sep. 1994 21 p
(Contract NAS5-32314; RTOP 422-00-00)
(NASA-CR-189378; NAS 1.26:189378; Aerojet-10448) Avail: CASI HC A03/MF A01

This report contains all of the block diagrams and internal logic diagrams for the Earth Observation System Advanced Microwave Sounding Unit-A (AMSU-A). These diagrams show the signal inputs, outputs, and internal signal flow for the AMSU-A. Derived from text

N95-13635*# Smithsonian Astrophysical Observatory, Cambridge, MA. Advanced X-Ray Astrophysics Facility.
WORK BREAKDOWN STRUCTURE (WBS) AND WBS DICTIONARY
F. Cocuzzo 12 Jan. 1994 26 p Revised
(Contract NAS8-36123)
(NASA-CR-196448; NAS 1.26:196448; SAO-AXAF-DR-94-067-Rev; DRD-MA-784-004-Rev) Avail: CASI HC A03/MF A01

This document is intended to provide the framework for defining all work to be accomplished under the proposed contract for the mission support program as defined by Section J-1 Statement of Work (SOW) of the RFP No.8-1-3-TA-50030 dated 11/2/93. The time period of performance of this contract will be from 3/1/94 through to the end of fiscal 1999. In addition to providing the framework for the integration of the cost, schedule, and manpower planning necessary to accomplish this work it establishes the association among the WBS elements, the SOW, and the Technical Proposal. Derived from text

N95-13651*# Aerojet-General Corp., Azusa, CA.
EARTH OBSERVING SYSTEM (EOS) ADVANCED MICROWAVE SOUNDING UNIT-A (AMSU-A): INSTRUMENTATION INTERFACE CONTROL DOCUMENT
Sep. 1994 54 p
(Contract NAS5-32314; RTOP 422-00-00)
(NASA-CR-189377; NAS 1.26:189377; Aerojet-10506) Avail: CASI HC A04/MF A01

This Interface Control Document (ICD) defines the specific details of the complete accomodation information between the Earth Observing System (EOS) PM Spacecraft and the Advanced Microwave Sounding Unit (AMSU-A)Instrument. This is the first submittal of the ICN: it will be updated periodically throughout the life of the program. The next update is planned prior to Critical Design Review (CDR). Author

N95-13676# Argonne National Lab., IL.
PARADIGMS AND STRATEGIES FOR SCIENTIFIC COMPUTING ON DISTRIBUTED MEMORY CONCURRENT COMPUTERS
I. T. Foster and D. W. Walker 1994 6 p Presented at the High Performance Computing 1994: Grand Challenges in Computer Simulation, La Jolla,CA, 11-15 Apr. 1994
(Contract W-31-109-eng-38)
(DE94-013305; ANL/MCS/CP-82972; CONF-940428-3) Avail: CASI HC A02/MF A01

We examine recent advances in parallel languages and abstractions that have the potential for improving the programmability and maintainability of large-scale, parallel, scientific applications running on high performance architectures and networks. This paper focuses on Fortran M, a set of extensions to Fortran 77 that supports the modular design of message-passing programs. We describe the Fortran M implementation of a particle-in-cell (PIC) plasma simulation application, and discuss issues in

the optimization of the code. The use of two other methodologies for parallelizing the PIC application are considered. The first is based on the shared object abstraction as embodied in the Orca language. The second approach is the Split-C language. In Fortran M, Orca, and Split-C the ability of the programmer to control the granularity of communication is important is designing an efficient implementation. DOE

N95-13699*# Cornell Univ., Ithaca, NY. Dept. of Computer Science.
HYBRID VERIFICATION BY EXPLOITING THE ENVIRONMENT
Limor Fix and Fred B. Schneider Jul. 1994 18 p
(Contracts NAG2-893; N00014-91-J-1219; F49620-94-1-0198; NSF CCR-90-03440; NSF CCR-90-14363)
(NASA-CR-195810; NAS 1.26:195810; AD-A283182; TR-94-1436) Avail: CASI HC A03/MF A01

A method for verifying hybrid systems is given. Such systems involve state components whose values are changed by continuous (physical) processes. The verification method is based on proving that only those executions that satisfy constraints imposed by an environment also satisfy the property of interest. A suitably expressive logic then allows the environment to model state components that are changed by physical processes. DTIC

N95-13889*# Institute for Computer Applications in Science and Engineering, Hampton, VA.
EFFICIENT BULK-LOADING OF GRIDFILES Final Report
Scott T. Leutenegger and David M. Nicol NASA Aug. 1994 26 p Submitted for publication
(Contract NAS1-19480; NAG1-1132; RTOP 505-90-52-01; NSF CCR-92-10372)
(NASA-CR-194974; NAS 1.26:194974; ICASE-94-74) Avail: CASI HC A03/MF A01

This paper considers the problem of bulk-loading large data sets for the gridfile multiattribute indexing technique. We propose a rectilinear partitioning algorithm that heuristically seeks to minimize the size of the gridfile needed to ensure no bucket overflows. Empirical studies on both synthetic data sets and on data sets drawn from computational fluid dynamics applications demonstrate that our algorithm is very efficient, and is able to handle large data sets. In addition, we present an algorithm for bulk-loading data sets too large to fit in main memory. Utilizing a sort of the entire data set it creates a gridfile without incurring any overflows. Author

N95-13894*# National Aeronautics and Space Administration. Lewis Research Center, Cleveland, OH.
GSOSTATS DATABASE: USAF SYNCHRONOUS SATELLITE CATALOG DATA CONVERSION SOFTWARE. USER'S GUIDE AND SOFTWARE MAINTENANCE MANUAL, VERSION 2.1
Paul G. Mallasch (Analex Corp., Brook Park, OH.) and Slavoljub Babic Oct. 1994 54 p
(Contract NAS3-25776; RTOP 235-01-02)
(NASA-TM-106760; E-9195; NAS 1.15:106760) Avail: CASI HC A04/MF A01

The United States Air Force (USAF) provides NASA Lewis Research Center with monthly reports containing the Synchronous Satellite Catalog and the associated Two Line Mean Element Sets. The USAF Synchronous Satellite Catalog supplies satellite orbital parameters collected by an automated monitoring system and provided to Lewis Research Center as text files on magnetic tape. Software was developed to facilitate automated formatting, data normalization, cross-referencing, and error correction of Synchronous Satellite Catalog files before loading into the NASA Geosynchronous Satellite Orbital Statistics Database System (GSOSTATS). This document contains the User's Guide and Software Maintenance Manual with information necessary for installation, initialization, start-up, operation, error recovery, and termination of the software application. It also contains implementation details, modification aids, and software source code adaptations for use in future revisions. Author

N95-13976# Sandia National Labs., Albuquerque, NM.
AN OPTICAL SIMULATION OF SHARED MEMORY
L. A. Goldberg, Y. Matias, and S. Rao 1994 11 p Presented at the Symposium on Parallel Algorithms and Architectures, Cape May, NJ, 27-29 Jun. 1994
(Contract DE-AC05-84OR-21400)
(DE94-013824; SAND-94-0512C; CONF-9406186-1) Avail: CASI HC A03/MF A01

We present a work-optimal randomized algorithm for simulating a shared memory machine (PRAM) on an optical communication parallel computer (OCPC). The OCPC model is motivated by the potential of optical communication for parallel computation. The memory of an OCPC is divided into modules, one module per processor. Each memory module only services a request on a timestep if it receives exactly one memory request. Our algorithm simulates each step of an n lg lg n-processor EREW PRAM on an n-processor OCPC in O(lg lg n) expected delay. The probability that the delay is longer than this is at most n(exp -alpha) for any constant alpha. The best previous simulation, due to Valiant, required Theta(lg n) expected delay. DOE

N95-13977# Argonne National Lab., IL.
A STUDY OF THE INVARIANT SUBSPACE DECOMPOSITION ALGORITHM FOR BANDED SYMMETRIC MATRICES
C. Bischof, X. Sun, A. Tsao, and T. Turnbull 1994 5 p Presented at the 5th SIAM Conference on Applied Linear Algebra, Snowbird, UT, 15-18 Jun. 1994
(Contract W-31-109-eng-38)
(DE94-013872; ANL/MCS/CP-83197; CONF-9406184-1) Avail: CASI HC A01/MF A01

The authors give an overview of the Invariant Subspace Decomposition Algorithm for banded symmetric matrices and describe a sequential implementation of this algorithm. Our implementation uses a specialized routine for performing banded matrix multiplication together with successive band reduction, yielding a sequential algcrithm that is competitive for large problems with the LAPACK QR code in computing all of the eigenvalues and eigenvectors of a dense symmetric matrix. Performance results are given on a variety of machines. DOE

N95-13989# Helsinki Univ. of Technology, Espoo (Finland). Dept. of Computer Science.
PHOENIX USER MANUAL. FIRST VERSION
P. Kuittinen, H. Mallat, and V. Toermaenen 1994 68 p
(PB94-189081; TKO-C66) Avail: CASI HC A04/MF A01

Phoenix is an interactive tool for creating and editing true color bitmap images. Its uses range from recreational and creative use to retouching and editing scanned images. The manual is divided into two sections: the Tutorial and the Reference Guide. The tutorial consists of introducing the program to the new user and demonstrating its use. It first introduces the user interface and then shows the use of the basic and frequently used tools and functions, gradually increasing in complexity. The Reference Guide describes the tools and functions in such a manner that the advanced user can easily seek description of a specific operation from there. It goes through the menubar entries in the order they appear in the program, giving a description of each. It also explains the possible error messages and reasons why they might appear. Installation of the program is described in Appendix A, and Appendix B holds information about specific files called I/O filters. The glossary of technical terms used can be found in Appendix C. NTIS

N95-14010 Argonne National Lab., IL.
A MULTI-LEVEL OBJECT STORE AND ITS APPLICATION TO HEP DATA ANALYSIS
E. May, D. Lifka, D. Malon, R. L. Grossman, X. Qin, D. Valsamis, and W. Xu 1994 4 p Presented at the Meeting on Computing in High-Energy Physics, San Francisco, CA, 21-27 Apr. 1994 Limited Reproducibility: More than 20% of this document may be affected by microfiche quality
(Contract W-31-109-eng-38)
(DE94-014010; ANL-HEP-CP-94-29; CONF-940492-7) Avail: CASI HC A01

We present a design and demonstration of a scientific data manager consisting of a low overhead, high performance object store interfaced to a hierarchical storage system. This was done with the framework of the Mark 1 testbeds of the PASS project. DOE

N95-14152# Technische Univ., Delft (Netherlands).
KNOWLEDGE-BASED COMPUTATIONAL APPROACH TO ARCHITECTURAL PRECEDENT ANALYSIS Ph.D. Thesis

N. Fang 28 Jun. 1993 257 p
(PB94-191269; ISBN-90-5269-133-9) Copyright Avail: CASI HC A12/MF A03

This work is generally concerned with the question 'How can precedent knowledge be used in architectural design computation.' Specifically, the work investigates how plans of architectural precedents could be analyzed so that some characteristics of their spatial organization can be represented and used for generating new designs. In architectural design practice, generating new forms on the basis of precedents is a common approach. Yet, it has not received enough attention in design computation research. The objective of this work is to develop a framework for the use of architectural precedent knowledge that combines both architectural and computational perspectives. NTIS

N95-14153# Technische Univ., Delft (Netherlands).
PARALLEL IMAGE RENDERING ALGORITHM AND ARCHITECTURE BASED ON RAY TRACING AND RADIOSITY SHADING Ph.D. Thesis
L. S. Shen 25 Oct. 1993 222 p
(PB94-191277) Avail: CASI HC A10/MF A03

This dissertation is about the parallelization of an algorithm that has become known as the two-pass radiosity method, for rendering artificial scenes with photo realism on the screen of a workstation. It first provides the background for the radiosity method and ray tracing. It then presents a ray-tracing based two-pass approach that serves as basis for the target algorithm. It then presents the shelling technique. By and large, it is an algorithm that strives to build the visibility orderings for the sets of input patches and rays. It then turns to the resource management problem. It first points out some dynamic behaviors like latencies in memory accesses, communications and synchronizations which make the scheduling problem very difficult to manage and analyze at compile time. This leads to a so-called runtime resource management problem which defers the actual scheduling to some point during program execution. Next, it presents the system configuration of the radiosity engine, and discusses some essential issues such as the memory structure, network design and synchronization mechanism and gives an outline of the functionality of the system. Finally, it quantifies the performance of the radiosity engine by using Monte Carlo simulation, and gives some conclusions. NTIS

N95-14156*# Research Inst. for Computing and Information Systems, Houston, TX.
RICIS SYMPOSIUM 1992: MISSION AND SAFETY CRITICAL SYSTEMS RESEARCH AND APPLICATIONS
30 Oct. 1992 357 p Symposium held in Houston, TX, 28-30 Oct. 1992 (Contract NCC9-16)
(NASA-CR-196963; NAS 1.26:196963) Avail: CASI HC A16/MF A03

This conference deals with computer systems which control systems whose failure to operate correctly could produce the loss of life and or property, mission and safety critical systems. Topics covered are: the work of standards groups, computer systems design and architecture, software reliability, process control systems, knowledge based expert systems, and computer and telecommunication protocols. For individual titles, see N95-14157 through N95-14172.

N95-14157*# Southwest Texas State Univ., San Marcos, TX. Dept. of Computer Science.
EUROPEAN WORKSHOP INDUSTRICAL COMPUTER SCIENCE SYSTEMS APPROACH TO DESIGN FOR SAFETY
Janusz Zalewski *In* Research Inst. for Computing and Information Systems, RICIS Symposium 1992: Mission and Safety Critical Systems Research and Applications 30 Oct. 1992 14 p (For primary document see N95-14156 03-61)
Avail: CASI HC A03/MF A03

This paper presents guidelines on designing systems for safety, developed by the Technical Committee 7 on Reliability and Safety of the European Workshop on Industrial Computer Systems. The focus is on complementing the traditional development process by adding the following four steps: (1) overall safety analysis; (2) analysis of the functional specifications; (3) designing for safety; (4) validation of design. Quantitative assessment of safety is possible by means of a modular questionnaire covering various aspects of the major stages of system development. Author (revised)

N95-14158*# Research Inst. for Computing and Information Systems, Houston, TX.
MISSION: MISSION AND SAFETY CRITICAL SUPPORT ENVIRONMENT. EXECUTIVE OVERVIEW
Charles McKay and Colin Atkinson *In its* RICIS Symposium 1992: Mission and Safety Critical Systems Research and Applications 30 Oct. 1992 6 p Sponsored by NASA, Washington (For primary document see N95-14156 03-61)
Avail: CASI HC A02/MF A03

For mission and safety critical systems it is necessary to: improve definition, evolution and sustenance techniques; lower development and maintenance costs; support safe, timely and affordable system modifications; and support fault tolerance and survivability. The goal of the MISSION project is to lay the foundation for a new generation of integrated systems software providing a unified infrastructure for mission and safety critical applications and systems. This will involve the definition of a common, modular target architecture and a supporting infrastructure. Derived from text

N95-14159*# Rome Lab., Griffiss AFB, NY.
GENERIC ARCHITECTURES FOR FUTURE FLIGHT SYSTEMS c60
Richard J. Wood *In* Research Inst. for Computing and Information Systems, RICIS Symposium 1992: Mission and Safety Critical Systems Research and Applications 30 Oct. 1992 16 p (For primary document see N95-14156 03-61)
Avail: CASI HC A03/MF A03

Generic architecture for future flight systems must be based on open system architectures (OSA). This provides the developer and integrator the flexibility to optimize the hardware and software systems to match diverse and unique applications requirements. When developed properly OSA provides interoperability, commonality, graceful upgradability, survivability and hardware/software transportability to greatly minimize life cycle costs and supportability. Architecture flexibility can be achieved to take advantage of commercial developments by basing these developments on vendor-neutral commercially accepted standards and protocols. Rome Laboratory presently has a program that addresses requirements for OSA. Author

N95-14160*# Rome Lab., Griffiss AFB, NY.
ARCHITECTURE FOR SURVIVABLE SYSTEMS PROCESSING (ASSP). TECHNOLOGY BENEFITS FOR OPEN SYSTEM INTERCONNECTS c60
Richard J. Wood *In* Research Inst. for Computing and Information Systems, RICIS Symposium 1992: Mission and Safety Critical Systems Research and Applications 30 Oct. 1992 12 p (For primary document see N95-14156 03-61)
Avail: CASI HC A03/MF A03

The Architecture for Survivable Systems Processing (ASSP) program is a two phase program whose objective is the derivation, specification, development and validation of an open system architecture capable of supporting advanced processing needs of space, ground, and launch vehicle operations. The output of the first phase is a set of hardware and software standards and specifications defining this architecture at three levels. The second phase will validate these standards and develop the technology necessary to achieve strategic hardness, packaging density, throughput requirements, and interoperability/interchangeability. Derived from text

N95-14161*# Lockheed Engineering and Sciences Co., Houston, TX.
SPACE GENERIC OPEN AVIONICS ARCHITECTURE (SGOAA): OVERVIEW
Richard B. Wray and John R. Stovall *In* Research Inst. for Computing and Information Systems, RICIS Symposium 1992: Mission and Safety Critical Systems Research and Applications 30 Oct. 1992 16 p (For primary document see N95-14156 03-61)
Avail: CASI HC A03/MF A03

A space generic open avionics architecture created for NASA is described. It will serve as the basis for entities in spacecraft core avionics, capable of being tailored by NASA for future space program avionics ranging from small vehicles such as Moon ascent/descent vehicles to large ones such as Mars transfer vehicles or orbiting stations. The standard consists of: (1) a system architecture; (2) a generic processing hardware architecture; (3) a six class architecture interface model; (4) a system services functional subsystem architectural model; and (5) an operations control functional subsystem architectural model. Author (revised)

N95-14162*# Fairchild Space Co., Germantown, MD. Communications, Data Handling, and Power Systems.
EVOLUTIONARY TELEMETRY AND COMMAND PROCESSOR (TCP) ARCHITECTURE **c17**
John R. Schneider *In* Research Inst. for Computing and Information Systems, RICIS Symposium 1992: Mission and Safety Critical Systems Research and Applications 30 Oct. 1992 20 p (For primary document see N95-14156 03-61)
Avail: CASI HC A03/MF A03

A low cost, modular, high performance, and compact Telemetry and Command Processor (TCP) is being built as the foundation of command and data handling subsystems for the next generation of satellites. The TCP product line will support command and telemetry requirements for small to large spacecraft and from low to high rate data transmission. It is compatible with the latest TDRSS, STDN and SGLS transponders and provides CCSDS protocol communications in addition to standard TDM formats. Its high performance computer provides computing resources for hosted flight software. Layered and modular software provides common services using standardized interfaces to applications thereby enhancing software re-use, transportability, and interoperability. The TCP architecture is based on existing standards, distributed networking, distributed and open system computing, and packet technology. The first TCP application is planned for the 94 SDIO SPAS 3 mission. The architecture enhances rapid tailoring of functions thereby reducing costs and schedules developed for individual spacecraft missions. Author (revised)

N95-14163*# Texas A&M Univ., College Station, TX. Dept. of Computer Science.
CAPTIONALS: A COMPUTER AIDED TESTING ENVIRONMENT FOR THE VERIFICATION AND VALIDATION OF COMMUNICATION PROTOCOLS
C. Feng, X. Sun, Y. N. Shen, and Fabrizio Lombardi *In* Research Inst. for Computing and Information Systems, RICIS Symposium 1992: Mission and Safety Critical Systems Research and Applications 30 Oct. 1992 22 p (For primary document see N95-14156 03-61)
Avail: CASI HC A03/MF A03

This paper covers the verification and protocol validation for distributed computer and communication systems using a computer aided testing approach. Validation and verification make up the so-called process of conformance testing. Protocol applications which pass conformance testing are then checked to see whether they can operate together. This is referred to as interoperability testing. A new comprehensive approach to protocol testing is presented which address: (1) modeling for inter-layer representation for compatibility between conformance and interoperability testing; (2) computational improvement to current testing methods by using the proposed model inclusive of formulation of new qualitative and quantitative measures and time-dependent behavior; (3) analysis and evaluation of protocol behavior for interactive testing without extensive simulation. Author (revised)

N95-14164*# Texas A&M Univ., College Station, TX. Dept. of Computer Science.
PERFORMANCE COMPARISON OF TOKEN RING PROTOCOLS FOR HARD-REAL-TIME COMMUNICATION **c62**
Sanjay Kamat and Wei Zhao *In* Research Inst. for Computing and Information Systems, RICIS Symposium 1992: Mission and Safety Critical Systems Research and Applications 30 Oct. 1992 32 p (For primary document see N95-14156 03-61)
Avail: CASI HC A03/MF A03

The ability to guarantee the deadlines of synchronous messages while maintaining a good aggregate throughput is an important consideration in the design of distributed real-time systems. In this paper, we study two token ring protocols, the priority driven protocol and the timed token protocol, for their suitability for hard real-time systems. Both these protocols use a token to control access to the transmission medium. In a priority driven protocol, messages are assigned priorities and the protocol ensures that messages are transmitted in the order of their priorities. Timed token protocols do not provide for priority arbitration but ensure that the maximum access delay for a station is bounded. For both protocols, we first derive the schedulability conditions under which the transmission deadlines of a given set of synchronous messages can be guaranteed. Subsequently, we use these schedulability conditions to quantitatively compare the average case behavior of the protocols. This comparison demonstrates that each of the protocols has its domain of superior performance and neither dominates the other for the entire range of operating conditions. Author

N95-14165*# IBM Federal Systems Div., Houston, TX.
POSIX REAL-TIME EXTENSIONS **c62**
Henry H. Robbins *In* Research Inst. for Computing and Information Systems, RICIS Symposium 1992: Mission and Safety Critical Systems Research and Applications 30 Oct. 1992 31 p (For primary document see N95-14156 03-61)
Avail: CASI HC A03/MF A03

POSIX is an evolving set of operating system interface standards, whose parts are in varying stages of production in a number of standards working groups. This presentation separates the real-time POSIX standards work in process from the rest and provides an overview of the purpose, status, dependencies, content, and project schedule of each. Author

N95-14166*# CAE-Link Corp., Houston, TX. Space Technology Div.
Ada 9X OVERVIEW
David G. Weller *In* Research Inst. for Computing and Information Systems, RICIS Symposium 1992: Mission and Safety Critical Systems Research and Applications 30 Oct. 1992 7 p (For primary document see N95-14156 03-61)
Avail: CASI HC A02/MF A03

The current version of Ada has been an ANSI standard since 1983. In 1988, the Ada Joint Program Office was tasked with reevaluating the language and proposing changes to the standard. Since that time, the world has seen a tremendous explosion in object-oriented languages, as well as other growing fields such as distributed computing and support for very large software systems. The speaker will discuss new features being added to the next version of Ada, currently called Ada 9X, and what transition issues must be considered for current Ada projects.
Author (revised)

N95-14167*# SBS Engineering, Inc., Houston, TX.
CIFO 3.0
Pat Rogers *In* Research Inst. for Computing and Information Systems, RICIS Symposium 1992: Mission and Safety Critical Systems Research and Applications 30 Oct. 1992 15 p (For primary document see N95-14156 03-61)
Avail: CASI HC A03/MF A03

The Ada Runtime Environment Working Group has, since 1985, developed and published the Catalog of Interface Features and Options (CFIO) for Ada runtime environments. These interfaces, expressed in legal Ada, provide 'hooks' into the runtime system to export both functionality and enhanced performance beyond that of 'vanilla' Ada implementations. Such enhancements include high- and low-level scheduling control, asynchronous communications facilities, predictable storage management facilities, and fast interrupt response. CIFO 3.0 represents the latest release, which incorporates the efforts of the European real time community as well as new interfaces and expansions of previous catalog entries. This presentation will give both an overview of the Catalog's contents and an 'insider's' view of the Catalog as a whole. Author

N95-14168*# Texaco, Inc., Houston, TX. Dept. of Information Technology.
INTELLIGENT ALARMING
W. B. Braden *In* Research Inst. for Computing and Information Systems, RICIS Symposium 1992: Mission and Safety Critical Systems Research and Applications 30 Oct. 1992 5 p (For primary document see N95-14156 03-61)
Avail: CASI HC A01/MF A03

This talk discusses the importance of providing a process operator with concise information about a process fault including a root cause diagnosis of the problem, a suggested best action for correcting the fault, and prioritization of the problem set. A decision tree approach is used to illustrate one type of approach for determining the root cause of a problem. Fault detection in several different types of scenarios is addressed, including pump malfunctions and pipeline leaks. The talk stresses the need for a good data rectification strategy and good process models along with a method for presenting the findings to the process operator in a focused and understandable way. A real time expert system is discussed as an

effective tool to help provide operators with this type of information. The use of expert systems in the analysis of actual versus predicted results from neural networks and other types of process models is discussed.
Author

N95-14169*# Gensym Corp., The Woodlands, Tx.
EXPERT SYSTEMS IN THE PROCESS INDUSTRIES
G. M. Stanley *In* Research Inst. for Computing and Information Systems, RICIS Symposium 1992: Mission and Safety Critical Systems Research and Applications 30 Oct. 1992 8 p (For primary document see N95-14156 03-61)
Avail: CASI HC A02/MF A03

This paper gives an overview of industrial applications of real-time knowledge based expert systems (KBES's) in the process industries. After a brief overview of the features of a KBES usefui in process applications, the general roles of KBES's are covered. A particular focus is diagnostic applications, one of the major applications areas. Many applications are seen as an expansion of supervisory control. The lessons learned from numerous online applications are summarized. Author

N95-14170*# Massachusetts Inst. of Tech., Cambridge. Dept. of Chemical Engineering.
FAULT DETECTION AND DIAGNOSIS USING NEURAL NETWORK APPROACHES **c63**
Mark A. Kramer *In* Research Inst. for Computing and Information Systems, RICIS Symposium 1992: Mission and Safety Critical Systems Research and Applications 30 Oct. 1992 31 p (For primary document see N95-14156 03-61)
Avail: CASI HC A03/MF A03

Neural networks can be used to detect and identify abnormalities in real-time process data. Two basic approaches can be used, the first based on training networks using data representing both normal and abnormal modes of process behavior, and the second based on statistical characterization of the normal mode only. Given data representative of process faults, radial basis function networks can effectively identify failures. This approach is often limited by the lack of fault data, but can be facilitated by process simulation. The second approach employs elliptical and radial basis function neural networks and other models to learn the statistical distributions of process observables under normal conditions. Analytical models of failure modes can then be applied in combination with the neural network models to identify faults. Special methods can be applied to compensate for sensor failures, to produce real-time estimation of missing or failed sensors based on the correlations codified in the neural network.
Author

N95-14171*# Virginia Univ., Charlottesville, VA. Dept. of Computer Science.
SOFTWARE DEVELOPMENT FOR SAFETY-CRITICAL MEDICAL APPLICATIONS
John C. Knight *In* Research Inst. for Computing and Information Systems, RICIS Symposium 1992: Mission and Safety Critical Systems Research and Applications 30 Oct. 1992 14 p (For primary document see N95-14156 03-61)
Avail: CASI HC A03/MF A03

There are many computer-based medical applications in which safety and not reliability is the overriding concern. Reduced, altered, or no functionality of such systems is acceptable as long as no harm is done. A precise, formal definition of what software safety means is essential, however, before any attempt can be made to achieve it. Without this definition, it is not possible to determine whether a specific software entity is safe. A set of definitions pertaining to software safety will be presented and a case study involving an experimental medical device will be described. Some new techniques aimed at improving software safety will also be discussed.
Author

N95-14172*# IBM Federal Systems Div., Houston, TX.
FORMAL METHODS TECHNOLOGY TRANSFER: SOME LESSONS LEARNED
David Hamilton *In* Research Inst. for Computing and Information Systems, RICIS Symposium 1992: Mission and Safety Critical Systems Research and Applications 30 Oct. 1992 5 p (For primary document see N95-14156 03-61)
Avail: CASI HC A01/MF A03

IBM has a long history in the application of formal methods to software development and verification. There have been many successes in the development of methods, tools and training to support formal methods. And formal methods have been very successful on several projects. However, the use of formal methods has not been as widespread as hoped. This presentation summarizes several approaches that have been taken to encourage more widespread use of formal methods, and discusses the results so far. The basic problem is one of technology transfer, which is a very difficult problem. It is even more difficult for formal methods. General problems of technology transfer, especially the transfer of formal methods technology, are also discussed. Finally, some prospects for the future are mentioned.
Author

N95-14178# Texas A&M Univ., College Station, TX. Dept. of Electrical Engineering.
HARDWARE IMPLEMENTATION OF A DESKTOP SUPERCOMPUTER FOR HIGH PERFORMANCE IMAGE PROCESSING. COLOR IMAGE PROCESSING USING CELLULAR NEURAL NETWORKS Technical Report, 1 May - 1 Aug. 1994
Jose P. DEGyvez 3 Aug. 1994 42 p
(Contract N00014-94-1-0516)
(AD-A283071; Rept-93-549/2) Avail: CASI HC A03/MF A01

This report presents a software prototype capable of performing image processing applications using Cellular Neural Networks (CNN). The software is based on a CNN multi-layer structure in which each primary color is assigned to a unique layer. This allows an added flexibility as different processing applications can be performed in parallel. To be able to handle a full range of color tones, two novel color mapping schemes were derived. In the proposed schemes the color information is obtained from the cell's state rather than from its output. This modification is necessary because CNN has binary outputs from which only either a fully saturated or a black color can be obtained. Additionally, a post processor capable of performing pixelwise logical operations among color layers was developed to enhance the results obtained from CNN. Examples in the areas of medical image processing, image restoration and weather forecasting are provided to demonstrate the robustness of the software and the vast potential of CNN.
DTIC

N95-14190# Lawrence Livermore National Lab., Livermore, CA.
DEVELOPING MOLECULAR DYNAMICS SIMULATION CODES USING MIXED LANGUAGE PROGRAMMING
T. DeBoni, J. T. Feo, H. Caffey, and F. Hausheer May 1994 13 p Presented at the DIMACS Workshop on the Specification of Parallel Algorithms, Princeton, NJ, 9-11 May 1994
(Contract W-7405-eng-48)
(DE94-015456; UCRL-JC-116641; CONF-9405200-1) Avail: CASI HC A03/MF A01

Problems experienced parallelizing a large-scale scientific application to model systems of discrete particles are described. The approach and tasks undertaken to parallelize this application using two different programming paradigms (imperative and functional) are explained. The objectives of both exercises were to maximize performance, parallelism and portability, and to minimize program development costs. This study reveals an important relationship between conventional and novel parallel programming paradigms, and identifies important attributes that novel paradigms must have to gain wide acceptance.
DOE

N95-14196# Argonne National Lab., IL.
A HIGH PERFORMANCE GRAPHICS ALGORITHM
M. J. North and S. Zhao 1994 6 p Presented at the 2nd Pacific Conference on Computer Graphics and Applications and 4th International Conference on CAD, CAM Technology, Beijing, China, 26-29 Aug. 1994
(Contract W-31-109-eng-38)
(DE94-015033; ANL/DIS/CP-82284; CONF-9408120-1) Avail: CASI HC A02/MF A01

Rendering images of complex collections of general objects in multidimensional space is typically very time consuming. The process of displaying such images is often a linear function of the number objects being considered. This behavior can become unacceptable when the number of objects to be considered is large. This paper describes an algorithm to

address this problem. The graphics algorithm presented here is composed of a storage algorithm and a selection algorithm. Both of these components are described in relation to a specialized tree data structure. The storage algorithm is proven to exhibit O(n log n) average time behavior and the selection algorithm is proven to exhibit O(log n) average time behavior. This paper focuses on two dimensional images but natural extensions of the basic algorithms to higher dimensional spaces are also considered. DOE

N95-14206*# National Aeronautics and Space Administration. Lewis Research Center, Cleveland, OH.

NLEdit: A GENERIC GRAPHICAL USER INTERFACE FOR FORTRAN PROGRAMS

Brian P. Curlett Aug. 1994 25 p

(RTOP 505-69-50)

(NASA-TM-4543; E-8049; NAS 1.15:4543) Avail: CASI HC A03/MF A01

NLEdit is a generic graphical user interface for the preprocessing of Fortran namelist input files. The interface consists of a menu system, a message window, a help system, and data entry forms. A form is generated for each namelist. The form has an input field for each namelist variable along with a one-line description of that variable. Detailed help information, default values, and minimum and maximum allowable values can all be displayed via menu picks. Inputs are processed through a scientific calculator program that allows complex equations to be used instead of simple numeric inputs. A custom user interface is generated simply by entering information about the namelist input variables into an ASCII file. There is no need to learn a new graphics system or programming language. NLEdit can be used as a stand-alone program or as part of a larger graphical user interface. Although NLEdit is intended for files using namelist format, it can be easily modified to handle other file formats. Author

N95-14339# Carnegie-Mellon Univ., Pittsburgh, PA. Software Engineering Inst.

TOWARD DERIVING SOFTWARE ARCHITECTURES FROM QUALITY ATTRIBUTES Final Report

Rick Kazman and Len Bass Aug. 1994 34 p

(Contract F19628-90-C-003)

(AD-A283827; CMU/SEI-94-TR-10; ESC-TR-94-010) Avail: CASI HC A03/MF A01

A method for deriving software architectures from a consideration of the non-functional qualities of the system is presented. The method is based on identifying a set of six 'unit operations' and using those operations to partition the functionality of the system. These unit operations were derived from the literature and from expert practice. The relationship between the unit operations and a set of eight non-functional qualities is explored. Evidence is provided for the validity of the method by using it to derive six well-known architectures from the areas of user interface software and compiler construction. DTIC

N95-14349# Carnegie-Mellon Univ., Pittsburgh, PA. Software Engineering Inst.

BENEFITS OF CMM-BASED SOFTWARE PROCESS IMPROVEMENT: INITIAL RESULTS Final Report

James Herbsleb, Anita Carleton, James Rozum, Jane Siegel, and David Zubrow Aug. 1994 62 p

(Contract F19628-90-C-0003)

(AD-A283848; CMU/SEI-94-TR-13; ESC-TR-94-013) Avail: CASI HC A04/MF A01

Data from 13 organizations were collected and analyzed to obtain information on the results of CMM-based software process improvement efforts. We report the cost and business value of improvement efforts, as well as the yearly improvement in productivity, early defect detection, time to market, and post-release defect reports. Improvement efforts and results in five organizations are reported in more depth in case studies. In addition, technical issues that we confronted as we tried to measure the results of software process improvement are discussed. We end with conclusions about the results of SPI efforts. DTIC

N95-14357# Loral Systems, Inc., Orlando, FL. Advanced Distribution Simulation Technology Program Office.

ADST ARWA VISUAL SYSTEM MODULE SOFTWARE DESIGN DOCUMENT

Robert Anschuetz 28 Feb. 1994 67 p

(Contract N61339-91-D-0001)

(AD-A283874; ADST/WDL/TR-94-00325) Avail: CASI HC A04/MF A01

The ADST ARWA Visual System Module Software Design Document describes the system design of the VSM CSCI. This Software Design Document outlines the structure and composition of the CSCI sub-functions (CSC's and CSU's) and provides a detailed description of each. DTIC

N95-14520*# Rockwell Space Operations Co., Houston, TX.

REUSEABLE OBJECTS SOFTWARE ENVIRONMENT (ROSE): INTRODUCTION TO AIR FORCE SOFTWARE REUSE WORKSHOP

William L. Cottrell 2 Aug. 1994 24 p Workshop held in Scott AFB, IL, 4 Aug. 1994

(Contract NAS9-18000)

(NASA-CR-197017; NAS 1.26:197017) Avail: CASI HC A03/MF A01

The Reusable Objects Software Environment (ROSE) is a common, consistent, consolidated implementation of software functionality using modern object oriented software engineering including designed-in reuse and adaptable requirements. ROSE is designed to minimize abstraction and reduce complexity. A planning model for the reverse engineering of selected objects through object oriented analysis is depicted. Dynamic and functional modeling are used to develop a system design, the object design, the language, and a database management system. The return on investment for a ROSE pilot program and timelines are charted. Derived from text

N95-14615*# Old Dominion Univ., Norfolk, VA. Dept. of Computer Science.

SOFTWARE RELIABILITY STUDIES Final Report, period ending 31 Oct. 1994

Mary Ann Hoppa and Larry W. Wilson Nov. 1994 19 p

(Grant NAG1-750)

(NASA-CR-197027; NAS 1.26:197027) Avail: CASI HC A03/MF A01

There are many software reliability models which try to predict future performance of software based on data generated by the debugging process. Our research has shown that by improving the quality of the data one can greatly improve the predictions. We are working on methodologies which control some of the randomness inherent in the standard data generation processes in order to improve the accuracy of predictions. Our contribution is twofold in that we describe an experimental methodology using a data structure called the debugging graph and apply this methodology to assess the robustness of existing models. The debugging graph is used to analyze the effects of various fault recovery orders on the predictive accuracy of several well-known software reliability algorithms. We found that, along a particular debugging path in the graph, the predictive performance of different models can vary greatly. Similarly, just because a model 'fits' a given path's data well does not guarantee that the model would perform well on a different path. Further we observed bug interactions and noted their potential effects on the predictive process. We saw that not only do different faults fail at different rates, but that those rates can be affected by the particular debugging stage at which the rates are evaluated. Based on our experiment, we conjecture that the accuracy of a reliability prediction is affected by the fault recovery order as well as by fault interaction. Derived from text

N95-14616# Army Armament Research, Development and Engineering Center, Picatinny Arsenal, NJ. Fire Support Armaments Center.

COMPUTER AIDED ENGINEERING (CAE) OVERVIEW

Hegel G. Neira Jun. 1994 20 p

(AD-A280966; ARFSD-TR-93045) Avail: CASI HC A03/MF A01

Computer aided engineering (CAE) refers to a collection of software and hardware tools integrated into a system (a computer) that is providing the circuit designer and circuit troubleshooter with step-by-step assistance during each phase of the design and analysis cycle, as well as during development, documentation, and maintenance. Under the CAE umbrella a number of commonly called 'automated design tools,' which are the software components of CAE, are revolutionizing and transforming engineering environments from the 'hands-on' way of conducting business into a virtual or simulated 'hands-on' mode of operating, and are having a tremendous

impact throughout all engineering disciplines. They have not yet displaced breadboarding and other methods of developing circuit boards but are making their presence known to the point of being totally necessary in the design of certain devices. It is the intention of this report to promote the use of these tools in the government by providing engineering management with an overview of the hardware and software products available for electronic simulation, while covering trends, new technologies, and costs. DTIC

N95-14842 Carnegie-Mellon Univ., Pittsburgh, PA. Robotics Inst.
VARIABLE WINDOW GABOR FILTERS AND THEIR USE IN FOCUS AND CORRESPONDENCE
Yalin Xiong and Steven A. Shafer Mar. 1994 27 p Limited Reproducibility: More than 20% of this document may be affected by microfiche quality
(Contract F33615-90-C-1465; ARPA Order 7597)
(AD-A282837; CMU-RI-TR-94-06) Avail: CASI HC A03

More and more low level vision algorithms are being carried out in the spatial frequency domain, using Gabor filters. There are two basic problems concerned with Gabor filterings we will address in this paper. One is the window size problem, in which we will adopt a set of 2D variable window Gabor filters, and compare its performance with those of fixed window filters. We will show that the variable window scheme is more adaptive to image contents, while fixed window schemes may suffer either large errors or instabilities when image contents are changed. The other problem we will address is the stability of amplitude and phase information resulting from convolving the filters with images. We will extend Fleet's ID phase stability analysis to 2D phase and amplitude stability analysis based upon the assumption of local resemblance of filter outputs to a single sinusoid. Applications on focus quality measurement and 2D correspondence are described, and the results demonstrate improvements of performance by detecting unstable information using the criterion developed. DTIC

N95-14905*# Summitec Corp., Oak Ridge, TN.
HIGH TEMPERATURE CALIBRATION FURNACE SYSTEM USER'S GUIDE Final Report
Feb. 1994 42 p
(Contract NAS8-39351)
(NASA-CR-196526; NAS 1.26:196526) Avail: CASI HC A03/MF A01

The High Temperature Calibration Furnace System (HTCFS) was developed by Summitec Corporation. It is a high precision instrument providing a constant temperature which can be used to calibrate high temperature thermocouples. Incorporating the many recent technological advances from the fields of optical fiber thermometry, material science, computer systems interfacing, and process control, the engineers at Summitec Corporation have been able to create a system that can reach a steady operating temperature of 1700 C. The precision for the system requires the measurement of temperature to be within 1 C in two hours and within 2 C in 24 hours. As documented, the experimental result shows that this system has been able to stay within .5 C in 5 hours. No other systems commercially available have been able to achieve such high temperature precision. This manual provides an overview of the system design, instructions for instrument setup, and operation procedures. Also included are a vendor list and the source codes for the custom-designed software. Derived from text

N95-14917# Federal Aviation Administration, Oklahoma City, OK. Civil Aeromedical Inst.
SUMMARY PROCEEDINGS OF THE JOINT INDUSTRY-FAA CONFERENCE ON THE DEVELOPMENT AND USE OF PC-BASED AVIATION TRAINING DEVICES Final Report
Kevin W. Williams, ed. Nov. 1994 22 p Conference held in Oklahoma City, OK, 16-17 Jun. 1994
(DOT/FAA/AM-94/25) Avail: CASI HC A03/MF A01

This report is a summarization of the proceedings of a joint industry - FAA conference on the development and use of PC-based aviation training devices (PCATDs) that was held June 16-17, 1994 in Oklahoma City, Oklahoma. Attendees to the conference included representatives from the PC development community, various universities conducting aviation training research, and the FAA. The primary purpose of the conference was to provide a forum of open dialog among interested PCATD parties, with the aim of finding common ground or areas of consensus, through which progress can be made in reducing or resolving any differences in viewpoint. Aside from the welcoming addresses by FAA representatives, the conference consisted of volunteered presentations by attendees, followed by open discussion of the points made by the presenter. A variety of topics were discussed and an attempt was made to let points and contentions be explored to the extent the group wished to pursue them. No attempt was made to provide a verbatim reproduction of the content of presentations and discussions. However, a concerted effort was made to capture the essence of each presenter's position, to accurately paraphrase major points, and to include brief summaries of group discussions through the insertion of editor's notes. Author

N95-15151# Rochester Univ., NY. Dept. of Computer Science.
CONTROL OF SELECTIVE PERCEPTION USING BAYES NETS AND DECISION THEORY
Raymond D. Rimey Dec. 1993 153 p
(Contract MDA972-92-J-1012; NSF IRI-89-20771; NSF IRI-89-03582)
(TR-468) Avail: CASI HC A08/MF A02

A selective vision system sequentially collects evidence to support a specified hypothesis about a scene, as long as the additional evidence is worth the effort of obtaining it. Efficiency comes from processing the scene only where necessary, to the level of detail necessary, and with only the necessary operators. Knowledge representation and sequential decision making are central issues for selective vision, which takes advantage of prior knowledge of a domain's abstract and geometrical structure and models for the expected performance and cost of visual operators. The TEA-1 selective vision system uses Bayes nets for representation and benefit-cost analysis for control of visual and non-visual actions. It is the high-level control for an active vision system, enabling purposive behavior, the use of qualitative vision modules, and a pointable multiresolution sensor. TEA-1 demonstrates that Bayes nets and decision theoretic techniques provide a general, reusable framework for constructing computer vision systems that are selective perception systems, and that Bayes nets provide a general framework for representing visual tasks. Control, or decision making, is the most important issue in a selective vision system. TEA-1's decisions about what to do next are based on general hand-crafted 'goodness functions' constructed around the core decision theoretic elements. Several goodness functions for different decisions are presented and evaluated. The TEA-1 system solves a version of the T-world problem, an abstraction of a large set of domains and tasks. Some key factors that affect the success of selective perception are analyzed by examining how each factor affects the overall performance of TEA-1 when solving ensembles of randomly produced, simulated T-world domains and tasks. TEA-1's decision making algorithms are also evaluated in this manner. Experiments in the lab for one specific T-world domain, table settings, are also presented. Author

N95-15311# Pacific Northwest Lab., Richland, WA. Molecular Science Research Center.
HIGH PERFORMANCE COMPUTATIONAL CHEMISTRY: TOWARDS FULLY DISTRIBUTED PARALLEL ALGORITHMS
M. F. Guest, E. Apra, and D. E. Bernholdt 1994 12 p Presented at the 1994 Society for Computer Simulation Multiconference, San Diego, CA, 11-15 Apr. 1994
(Contract DE-AC06-76RL-01830)
(DE94-014561; PNL-SA-24162; CONF-940456-21) Avail: CASI HC A03/MF A01

An account is given of work in progress within the High Performance Computational Chemistry Group (HPCC) at the Pacific Northwest Laboratory (PNL) to develop molecular modeling software applications for massively parallel processors (MPP's). A discussion of the issues in developing scalable parallel algorithms is presented, with a particular focus on the distribution, as opposed to the replication, of key data structures. Replication of large data structures limits the maximum calculation size by imposing a low ratio of processors to memory. Only applications that distribute both data and computation across processors are truly scalable. The use of shared data structures, which may be independently accessed by each process even in a distributed-memory environment, greatly simplifies development and provides a significant performance enhancement. In describing tools to support this programming paradigm, an outline is given of the implementation and performance of a highly efficient and scalable algorithm to perform quadratically convergent, self-consistent field calculations on molecular systems. A brief account is given of the development of corresponding

MPP capabilities in the areas of periodic Hartree Fock, Moeller-Plesset perturbation theory (MP2), density functional theory, and molecular dynamics. Performance figures are presented using both the Intel Touchstone Delta and Kendall Square Research KSR-2 supercomputers. DOE

N95-15335 Navy Computer and Telecommunications Station, Pensacola, FL.
PERFORMANCE INFORMATION MANAGEMENT SYSTEM (PIMS) COMMUNICATION Final Report
Kathryn P. Winter 31 Dec. 1993 9 p Limited Reproducibility: More than 20% of this document may be affected by microfiche quality
(AD-A284851) Avail: CASI HC A02

The objective of this project is to modify and enhance the capabilities of the Mailnet telephonic bulletin board system and create hooks for accessing a performance data base remotely. DTIC

N95-15336 Department of the Navy, Washington, DC.
SLAVE CONTROLLER FOR EFFECTING A BLOCK TRANSFER OF SIXTEEN BIT WORDS BETWEEN A MEMORY AND A DATA TRANSFER BUS Patent
Nelson D. Lau, inventor (to Navy) 7 Jun. 1994 15 p Filed 25 Aug. 1992
(AD-D016463; US-Patent-5,319,767; US-Patent-Appl-SN-937624; US-Patent-Class-395-425) Avail: US Patent and Trademark Office

A slave controller with block transfer capability for transferring data blocks of between one and two hundred fifty six sixteen bit words between a memory and the VERSA MODULE EUROPE bus (VMEbus) is described. The slave controller comprises a programmable array logic device which receives control and address modifier signals from the VMEbus and an address enable signal from a decoding circuit which provides the address enable signal to the programmable array logic device in response to an address strobe signal provided by the VMEbus. The programmable array logic device being responsive to these signals enables the memory for a read or write operation. The programmable array logic device next provides a write pulse to the memory when data is to be written into the memory at addresses provided by a binary counter. When data is to be read from the memory, the programmable array logic device maintains the memory's write enable input at an inactive state and generates an output enable pulse allowing data to be read from the memory at addresses provided by the binary counter. The first address for a block transfer of data is provided by the VMEbus to the counter. DTIC

N95-15384# Sandia National Labs., Albuquerque, NM.
USING Pro/ENGINEER'S (TM) INTERFACE MODULE
J. Schulze Jun. 1994 38 p
(Contract DE-AC04-94AL-85000)
(DE94-013364; SAND-94-1388) Avail: CASI HC A03/MF A01

When the ACCORD Process introduced Pro/ENGINEER to Sandia several years ago, a new process for design/definition was implemented. Prior to ACCORD, engineers and draftsmen worked in the 2-D mode with a program called ANVIL (tm), which had limited capabilities. Although the transition from 2-D modeling to 3-D modeling met with some resistance, most engineers have embraced this new concept with enthusiasm. They are now able to work in the 3-D mode and at increased levels of productivity with appropriate time savings never achieved before. One area that Pro/ENGINEER is noted for that this report will concentrate on is the powerful interface module with its wide selection of transfer file configurations. This allows the engineer to create parts or assemblies and transfer them to many different second party software packages whose vendors can provide the capability for stress analysis, rapid prototypes, virtual reality environments, or many other forms of advanced manufacturing modes of communication. The ACCORD Program has at its core the Pro/ENGINEER program from Parametric Technology Inc. Included in the ACCORD program are several supporting programs from other vendors to make this cooperation between software packages a reality. It is possible to create parts in Pro/ENGINEER, transfer those parts to another package that has the capability to analyze the parts for deficiencies, then optimize those parts, and allow for changes to be made. Also included in this report are other packages closely tied to Pro/ENGINEER, but not necessarily supported under the ACCORD program. Some of these packages allow creation of very impressive video productions, or allow meandering through a virtual reality scenario. All of these new software packages will give a new perspective on performance. This report will show how some of these interfaces work, and how to improve productivity by utilizing the ACCORD program as it is implemented here at Sandia. DOE

N95-15396 Newcastle-upon-Tyne Univ., Newcastle (England). Dept. of Computing Science.
SEQUENTIALLY t-DIAGNOSABLE SYSTEMS
J. Xu Jun. 1994 29 p
(PB94-205093; TRS-481) Copyright Avail: Issuing Activity (National Technical Information Service (NTIS))

In the system-level fault diagnosis area, the fundamental problem of characterizing sequentially t-diagnosable systems in the PMC model has remained open for more than two decades. We resolve this problem by providing a complete characterization of such systems. Our solution to the delicate characterization problem leads to the correct identification of optimal sequentially t-diagnosable D sub(delta,k) systems. An efficient algorithm for sequentially identifying the set of faulty units in a sequentially t-diagnosable D sub(delta,k) system is given along the lines of the proposed characterization, which is linear with respect to the number of tests in the system. NTIS

N95-15418# Fermi National Accelerator Lab., Batavia, IL.
Xwake 1.0: A NEW TOOL FOR WAKEFIELD AND IMPEDANCE CALCULATIONS
T. G. Jurgens, G. W. Saewert, and F. A. Harfoush Jul. 1994 5 p Presented at the 4th European Particle Accelerator Conference, London, England, 27 Jun. - 1 Jul. 1994
(Contract DE-AC02-76CH-03000)
(DE94-015545; FNAL/C-94/191; CONF-940618-20) Avail: CASI HC A01/MF A01

Xwake, a user friendly Finite Difference Time Domain (FDTD) code for wakefield and impedance calculations of rotationally symmetric structures is described. Contrary to the traditional stepped edge or half cell approach used in other codes, Xwake 1.0 incorporates the contour modeling approach allowing it to accurately represent curved boundaries. Other features include a mesh generator that allows for the handling of lossy materials, dielectrics, and ferrites, modeling of regions that are simply or multiply connected and automatic dynamic memory management. Xwake 1.0 is a fully integrated interactive code and is distributed free of charge. Xwake is written in ANSI-C for portability and has been demonstrated to run on several Unix platforms. A graphical user interface (GUI) allows easy access to all the processing modules in the code. The GUI uses the OSF/Motifl.1 widget set and the X11R4 window system. Simulation results emphasizing its capabilities, in particular for a very slowly tapered beam pipe, are presented. DOE

N95-15536# Oak Ridge National Lab., TN.
A MULTIPLE DIVIDE-AND-CONQUER (MDC) ALGORITHM FOR OPTIMAL ALIGNMENTS IN LINEAR SPACE
X. Guan and E. C. Uberbacher Jun. 1994 13 p
(Contract DE-AC05-84OR-21400)
(DE94-015457; ORNL/TM-12764) Avail: CASI HC A03/MF A01

Dynamic programming algorithms are often used to find the similarities of sequences as well as to deliver the actual alignment of two sequences. Two kinds of alignments are used to compare sequences: local alignments and global alignments. The local alignments attempt to locate conserved regions, while the global alignments identify overall relationship between two sequences. While dynamic programming algorithms are relatively time consuming, the space required is often the limiting factor when aligning long sequences. A linear space algorithm for computing maximal common subsequences, proposed by Hirschberg, was applied by Myers and Miller to deliver optimal alignments in linear space. The authors have improved the Myers and Miller algorithm by introducing a multiple divide and conquer technique that reduces the algorithm's running time while maintaining its linear space property. Efficient sequence alignment algorithms have been an active topic in computational biology. DOE

N95-15543# Sandia National Labs., Albuquerque, NM.
SUNMOS FOR THE INTEL PARAGON, A BRIEF USER'S GUIDE
A. B. Maccabe (New Mexico Univ., Albuquerque, NM.), R. Riesen, K. S. McCurley, and S. R. Wheat 1994 7 p Presented at the Intel Supercomputing Users Group Meeting, San Diego, CA, 25-29 Jun. 1994

(Contract DE-AC04-94AL-85000)
(DE94-015277; SAND-94-1583C; CONF-9406205-2) Avail: CASI HC A02/MF A01

SUNMOS is an acronym for Sandia/UNM Operating System. It was originally developed for the nCUBE-2 MIMD supercomputer between January and December of 1991. Between April and August of 1993, SUNMOS was ported to the Intel Paragon. This document provides a quick overview of how to compile and run jobs using the SUNMOS environment on the Paragon. The primary goal of SUNMOS is to provide high performance message passing and process support an example of its capabilities. SUNMOS Release 1.4 occupies approximately 240K of memory on a Paragon node, and is able to send messages at bandwidths of 165 megabytes per second with latencies as low as 42 microseconds using Intel NX calls. By contrast, Release 1.2 of OSF/1 for the Paragon occupies approximately 7 megabytes of memory on a node, has a peak bandwidth of 65 megabytes per second, and latencies as low as 42 microseconds (the communication numbers are reported elsewhere in these proceedings). DOE

N95-15549 Clemson Univ., SC.
POLYHEDRAL APPROACHES FOR SOLVING 0-1 POLYNOMIAL PROGRAMMING PROBLEMS Final Report, 1 Mar. 1990 - 30 Nov. 1993
W. P. Adams Jun. 1994 12 p Limited Reproducibility: More than 20% of this document may be affected by microfiche quality
(Grant AF-AFOSR-0191-90)
(AD-A282448; AFOSR-94-0423TR) Avail: Issuing Activity (Defense Technical Information Center (DTIC))

New algorithms for the solution of quadratic assignment problems and of bilinear programming problems have been devised. Empirical evaluation of these algorithms against other published results have been conducted. DTIC

N95-15597# Rochester Univ., NY. Dept. of Computer Science.
UNAMBIGUOUS COMPUTATION: BOOLEAN HIERARCHIES AN SPARSE TURING-COMPLETE SETS
Lane A. Hemaspaandra and Jorg Rothe 7 Jan. 1994 25 p Sponsored by German Academic Exchange Service; and NAS-NRC
(Grants NSF CCR-89-57604; NSF INT-91-16781; JSPS ENGR-207)
(TR-483) Avail: CASI HC A03/MF A01

This paper studies, for UP, two topics that have been intensely studied for NP: Boolean hierarchies and the consequences of the existence of sparse Turing-complete sets. Unfortunately, as is often the case, the results for NP draw on special properties of NP that do not seem to carry over straightforwardly to UP. Nonetheless, we prove that if UP has sparse Turing-complete sets, then the levels of the unambiguous polynomial hierarchy are simpler than one would otherwise expect: they collapse one level in terms of their location in the promise unambiguous polynomial hierarchy. We obtain related results under the weaker assumption that UP has sparse Turing-hard sets. Regarding Boolean hierarchies over UP, we show that the symmetric difference hierarchy over UP contains exactly the Boolean closure of UP. However, in contrast to the NP case, we show that neither the nested difference hierarchy over UP nor the Hausdorff hierarchy over UP contains the Boolean closure of UP in all relativized worlds. Author

N95-15640# Rochester Univ., NY. Dept. of Computer Science.
i-speech: EXPERIMENTS WITH A SINGLE LEVEL FEEDBACK PARADIGM
Ramesh R. Sarukkai and Dana H. Ballard May 1994 9 p
(Grants NSF IRI-89-03582; NIH-1R24RR06853)
(TR-509) Avail: CASI HC A02/MF A01

Speech of multiple speakers is transformed to speech produced by a single speaker (speech normalization) using cross-coding network. Internal representations for classification are acquired by feeding back the speech (i-speech) produced. Training proceeds by unfolding the network through time, and combining the classification error with the intermediate speaker-normalization errors. Experimental results on multi-speaker syllable recognition tasks with trained and new speakers are discussed. Author

N95-15644# Rochester Univ., NY. Dept. of Computer Science.
TWO HEADS ARE BETTER THAN TWO TAPES
Tao Jiang (McMaster Univ., Hamilton, Ontario.), Joel I. Seiferas, and Paul M. B. Vitanyi 10 Mar. 1994 13 p Presented at the STOC 1994, the 26th Annual ACM Symposium on Theory of Computing Submitted for publication Sponsored by European Union's NeuroCOLT ESPRIT
(Contract NSERC-OGP-0046613; NF-62-376; NFI Proj. ALADDIN)
(TR-493) Avail: CASI HC A03/MF A01

We show that a Turing machine with two single-head one-dimensional tapes cannot recognize the set ((chi)2(chi)' such that chi is a member of the set (0,1)* and chi' is a prefix of chi) in real time, although it can do so with three tapes, two-dimensional tapes, or one two-head tape, or in linear time with just one tape. In particular, this settles the longstanding conjecture that a two-head Turing machine can recognize more languages in real time if its heads are on the same one-dimensional tape than if they are on separate one-dimensional tapes. Author

N95-15645# Rochester Univ., NY. Dept. of Computer Science.
CONNECTIONS AMONG SPACE-BOUNDED AND MULTIHEAD PROBABILISTIC AUTOMATA
Ioan I. Macarie Jan. 1994 15 p
(Grant NSF CDA-88-22724)
(TR-476) Avail: CASI HC A03/MF A01

We show that the heads of multihead unbounded-error or bounded-error or one-sided error probabilistic finite automata are equivalent alternatives to the storage tapes of the corresponding probabilistic Turing machines (Theorem 1). These results parallel the classic ones concerning deterministic and nondeterministic automata. Several important properties of logarithmic-space (nondeterministic and probabilistic) Turing machines follow trivially (Observations 1-3) from the more refined versions that we prove in the setting of multihead finite automata (Theorems 2-4). Author

N95-15721# Rochester Univ., NY. Dept. of Computer Science.
UPWARD SEPARATION FOR FewP AND RELATED CLASSES
Rajesh P. N. Rao, Joerg Rothe, and Osamu Watanabe 22 Feb. 1994 11 p Sponsored by German Academic Exchange Service
(Grants NSF CDA-88-22724; NSF CCR-89-57604; NSF INT-91-16781; JSPS ENGR-207)
(TR-488) Avail: CASI HC A03/MF A01

This paper studies the range of application of the upward separation technique that has been introduced by Hartmanis to relate certain structural properties of polynomial-time complexity classes to their exponential-time analogs and was first applied to NP. Later work revealed the limitations of the technique and identified classes defying upward separation. In particular, it is known that coNP as well as certain promise classes such as BPP, R, and ZPP do not possess upward separation in all relative worlds, and it had been suspected that this was also the case for other promise classes such as UP and FewP. In this paper, we refute this conjecture by proving that, in particular, FewP does display upward separation, thus providing the first upward separation result for a promise class. In fact, this follows from a more general result the proof of which heavily draws on recently discovered tally encoding of sparse sets. As consequences of our main result, we obtain upward separations for various known counting classes. Some applications and open problems are discussed. Author

N95-15783 Unisys Corp., Reston, VA.
MODEL CONTRACTS/AGREEMENTS. COMPREHENSIVE APPROACH TO REUSABLE DEFENSE SOFTWARE (CARDS)
25 Mar. 1994 57 p Limited Reproducibility: More than 20% of this document may be affected by microfiche quality
(Contract F19628-93-C-0130)
(AD-A284403; STARS-VC-B014/001/00) Avail: Issuing Activity (Defense Technical Information Center (DTIC))

The Central Archive for Reusable Defense Software (CARDS) Program, sponsored by the U.S Air Force (ESC/ENS), Hanscom AFB, MA, has been investigating business areas that impact software reuse. An on-going forum, made up of DOD lawyers and contracting officers familiar with software reuse, has been established by the CARDS Program to examine legal issues and concerns related to software reuse. One primary finding from these software reuse legal forums is: risk can be managed by carefully negotiating and drafting agreements. This document provides sample agreements and associated guidelines for implementation by the CARDS Library staff. They are based on the current CARDS Command Center Library's business, operational, and qualification processes and concepts, as well as recommended policy changes. This will allow the CARDS Library staff to interact with its customers (suppliers of components, users of the

reusable components, and interoperating libraries) to help reduce operating risk, meet its operational and technical goals, and meet the needs of its customers. DTIC

N95-15788# Rochester Univ., NY. Dept. of Computer Science.
A PROMISE CLASS AT LEAST AS HARD AS THE POLYNOMIAL HIERARCHY
Joerg Rothe (Friedrich-Schiller Univ., Jena, German D.R..) 14 Jan. 1994 21 p Sponsored by German Academic Exchange Service
(Grant NSF CCR-89-57604)
(TR-484) Avail: CASI HC A03/MF A01

An open problem raised by Toda and Ogiwara is reformulated in the context of promise problems to make precise its very nature, thereby answering it partially, which, by intuition, is due to the promise in the definition of SPP. In particular, it is shown that the polynomial hierarchy is contained in a promise class that naturally corresponds to the class BP dot SPP (even though for this class itself, unfortunately, the original problem remains unsolved). Furthermore, some properties of several related classes defined via operators are studied. Author (revised)

N95-15789# Rochester Univ., NY. Dept. of Computer Science.
DENSITY CONTROL AND ON-LINE LABELING PROBLEMS Ph.D. Thesis
Ju Zhang Dec. 1993 80 p
(TR-481) Avail: CASI HC A05/MF A01

We extend the notion of density to individual points on a discrete distribution. We provide a linear time algorithm to find points with certain density, showing that our definition is computationally efficient. The Hot-Spot Lemma guarantees the existence of 'congestion.' This fact lets us find overall structure on density and enables density control. We will prove an Omega(n log n) lower bound for a List Labeling Problem with a polynomial number of labels, hence we will solve a problem open for over ten years. The lower bound proof is based on an adversary strategy. The adversary will always insert the new item to a 'crowded' point which can be located by maintaining structure based on the Hot-Spot Lemma. When the adversary cannot see the actual labeling, i.e., the adversary is oblivious, we are able to provide a probabilistic adversary which forces an expected Omega (n log n/log n) relabling cost. When we restrict the algorithm to be smooth, which is satisfied by all the known labeling algorithms, a simple adversary strategy which always inserts at one end will give the following lower bounds: (1) when the number of labels is a polynomial in the number of items, the lower bound is Omega(n log n). (2). When the number of labels is linear in the number of items, the lower bound is Omega(n log sq n). (3) When the number of labels is equal to the number of items, the lower bound is Omega(n log (exp 3) n). Author

N95-15806 Unisys Corp., Reston, VA.
SOFTWARE TECHNOLOGY FOR ADAPTABLE, RELIABLE SYSTEMS (STARS)
25 Mar. 1994 77 p Limited Reproducibility: More than 20% of this document may be affected by microfiche quality
(Contract F19628-93-C-0130)
(AD-A284373) Avail: Issuing Activity (Defense Technical Information Center (DTIC))

The Market Study supplies the Central Archive for Reusable Defense Software (CARDS) program with information regarding the current state-of-the-practice of software development and maintenance within the military services. Results of analysis of collected data reflect current practices, as well as identify needs within each military service for establishment of a suitable infrastructure to enable reuse. Full comprehension of the software needs of potential reusers is required before CARDS can address its ultimate goal of facilitating widespread software reuse throughout the DoD. The focus of results has therefore been geared toward facilitating the CARDS process of institutionalizing software reuse within the Department of Defense (DoD) by more finely concentrating our development, technology transfer, and franchising efforts toward satisfaction of identified requirements. DTIC

N95-15817 Pittsburgh Univ., Pittsburgh, PA. Learning Research and Development Center.
ASPM2: PROGRESS TOWARD THE ANALYSIS OF SYMBOLIC PARAMETER MODELS Final Technical Report
Thad A. Polk, Kurt VanLehn, and Dirk Kalp 1 Sep. 1994 28 p Limited Reproducibility: More than 20% of this document may be affected by microfiche quality
(Contract N00014-91-J-1529)
(AD-A284437) Avail: CASI HC A03

Model-fitting, the problem of finding parameter settings that cause a model to fit given data as closely as possible, is a hard but important problem in cognitive science in general, and in cognitive diagnosis in particular. Efficient solutions have been found for certain types of model-fitting problems (e.g., linear and integer programming) that involve specific types of parameters (usually continuous) and models (usually linear). But these techniques usually do not apply to computational cognitive models whose internal workings must be treated as a black box for the purposes of fitting. We present ASPM (Analysis of Symbolic Parameter Models), a suite of computational tools for fitting and analyzing such symbolic parameter models, show how it can be used to fit and analyze computational models with well over 10 billion parameter settings, and describe a few changes in the initial design that will make it even more powerful as well as easier to use. DTIC

N95-15825# Rochester Univ., NY. Dept. of Computer Science.
EFFICIENT ALGORITHMS FOR QUALITATIVE REASONING ABOUT TIME
Alfonso Gerevini (Trento Univ., Povo, Italy.) and Lenhart Schubert Mar. 1994 50 p Presented at the Fourth International Conference on Principles of Knowledge Representation and Reasoning (KR1994), Bonn, Germany, 1994 Submitted for publication Sponsored by Boeing
(Contract F30602-91-C-0010)
(TR-496) Avail: CASI HC A03/MF A01

Reasoning about temporal information is an important task in many areas of artificial intelligence. We address the problem of scalability in temporal reasoning by providing a collection of new algorithms for efficiently managing large sets of qualitative temporal relations. We focus on the class of relations forming the point algebra (PA-relations) and on a major extension to include binary disjunctions of PA-relations (PA-disjunctions). Such disjunctions add a great deal of expressive power, including the ability to stipulate disjointness of temporal intervals, which is important in planning applications. Our representation of time is based on timegraphs, graphs partitioned into a set of chains on which the search is supported by a metagraph data structure. The approach is an extension of the time representation proposed by Schubert, Taugher, and Miller in the context of story comprehension. The algorithms herein enable construction of a timegraph from a given set of PA-relations, querying a timegraph, and efficiently checking the consistency of a timegraph augmented by a set of PA-disjunctions. Experimental results illustrate the efficiency of the proposed approach. Author

N95-15856# Rochester Univ., NY. Dept. of Computer Science.
GENETIC PROGRAMMING WITH ADAPTIVE REPRESENTATIONS
Justinian P. Rosca and Dana H. Ballard Feb. 1994 31 p Sponsored by Human Science Frontiers Program
(Grants NSF IRI-89-03582; NIH-1R24RR06853)
(TR-489) Avail: CASI HC A03/MF A01

Machine learning aims towards the acquisition of knowledge based on either experience from the interaction with the external environment or by analyzing the internal problem-solving traces. Both approaches can be implemented in the Genetic Programming (GP) paradigm. Hillis (1990) proves in an ingenious way how the first approach can work. There have not been any significant tests to prove that GP can take advantage of its own search traces. This paper presents an approach to automatic discovery of functions in GP based on the ideas of discovery of useful building blocks by analyzing the evolution trace, generalizing of blocks to define new functions and finally adapting of the problem representation on-the-fly. Adaptation of the representation determines a hierarchical organization of the extended function set which enables a restructuring of the search space so that solutions can be found more easily. Complexity measures of solution trees are defined for an adaptive representation framework and empirical results are presented. Author

N95-15857# Rochester Univ., NY. Dept. of Computer Science.
SEEING BEHIND OCCLUSIONS
Dana H. Ballard and Rajesh P. N. Rao Feb. 1994 15 p Sponsored

by Human Science Frontiers Program
(Grant NSF CDA-88-22724)
(TR-487) Avail: CASI HC A03/MF A01

The location of objects in images is difficult owing to the view variance of geometric features but can be determined by developing view-insensitive descriptions of the intensities local to image points. View-insensitive descriptions are achieved in this work by describing points in terms of the responses of steerable filters at multiple scales. Owing to the use of multiple scales, the vector for each point is, for all practical purposes, unique, and thus can be easily matched to other instances of the point in other images. We show that this method can be extended to handle the case where the area near a point of interest is partially occluded. The method uses a description of the occluder in the form of a template that can be obtained easily via active vision systems using a method such as disparity filtering. Author

N95-15858# Rochester Univ., NY. Dept. of Computer Science.
P-SELECTIVITY: INTERSECTIONS AND INDICES
Lane A. Hemaspaandra and Zhigen Jiang 3 Jan. 1994 11 p
(Grants NSF CCR-89-57604; NSF INT-91-16781; JSPS ENGR-207)
(TR-482) Avail: CASI HC A03/MF A01

The P-selective sets are those sets for which there is a polynomial-time algorithm that, given any two strings, determines which is 'more likely' to belong to the set: if either of the strings is in the set, the algorithm chooses one that is in the set. We prove that, for each k, the k-ary Boolean connectives under which the P-selective sets are closed are exactly those that are either completely degenerate or almost-completely degenerate. We determine the complexity of the index set of the r.e. P-selective sets -- Sigma(sup 0, sub 3)-complete. Author

N95-15860# Rochester Univ., NY. Dept. of Computer Science.
LEARNING WITH INCOMPLETE SELECTIVE PERCEPTION
R. Andrew McCallum 29 Mar. 1993 46 p Sponsored by Human Science Frontiers Program
(Grants NSF IRI-89-03582; NIH-1R24RRO6853)
(TR-453) Avail: CASI HC A03/MF A01

An agent with selective perception focuses its sensors on those parts of the environment that are relevant to the task at hand. Selective perception is an efficient method of gathering information from the world, but it presents problems for a learning agent when different actions are required in situations for which the selective perception system cannot produce distinguishing outputs. If this happens the agent is said to have incomplete perception, and the agent may be able to use internal state determined by past perceptions and actions in order to choose the correction action. I propose research on learning algorithms that use short-term memory to disambiguate the incomplete perception that arises with selective perception. I present the Utile Distinction Memory algorithm (UDM) that solves the incomplete perception problem using a partially observable Markov decision process to represent the agent's internal state space. A significant feature of the algorithm is that it will build an internal state space proportionate to the task at hand, not as large as would be required to represent all of the perceivable world. A second algorithm, part of work in progress, will keep the advantages of UDM while improving learning speed and the ability to recognize the significance of memories that span multiple time steps. Learning to use memory is difficult and will require a strong bias to learn efficiently. I will investigate 'learning by watching' as a method of providing bias. Two applications I propose to study are: driving a simulated car using vision from the driver's point of view, and setting a table with human cooperation of interference. Using the results of psychophysical experiments, I will compare my algorithm's perceptual actions with the perceptual actions made by human subjects. Author

N95-13827# ISRO Satellite Centre, Peenya, Bangalore (India). Control Systems Group.
REMOTE PROGRAMMING IN INSAT-2A/2B ON-BOARD ATTITUDE AND ORBIT CONTROL COMPUTER (AOCC)
M. Mahendra Nayak, R. S. Manjunatha, V. K. Agrawal, and N. K. Malik *In its* Journal of Spacecraft Technology, Volume 4, No. 2, July 1994 Jul. 1994 p 29-35 (For primary document see N95-13825 03-12)
Avail: CASI HC A02/MF A01

N95-13829# Indian Space Research Organization, Trivandrum. Precision Fabrication and Assembly Facility.
COMPUTER AIDED TECHNIQUES FOR THE REALISATION OF THE DIAPHRAGM OF THE PSM FOR THE IRS-1C
D. Sam Dayala Dev and N. Sivasubramanian *In* ISRO Satellite Centre, Journal of Spacecraft Technology, Volume 4, No . 2, July 1994 Jul. 1994 p 43-51 (For primary document see N95-13825 03-12)
Avail: CASI HC A02/MF A01

N95-14046*# National Aeronautics and Space Administration. Ames Research Center, Moffett Field, CA.
ROTATIONAL WIND INDICATOR ENHANCES CONTROL OF ROTATED DISPLAYS Abstract Only
H. A. Cunningham and Misha Pavel *In its* Human Machine Interfaces for Teleoperators and Virtual Environments Jun. 1991 p 118 Sponsored by AFOSR and NAS-NRC Prepared in cooperation with Stanford Univ., CA (For primary document see N95-14013 03-54)
(Contract NCC2-307)
Avail: CASI HC A01/MF A02

N95-14048*# Tokyo Univ. (Japan).
DEVELOPMENT OF VISUAL 3D VIRTUAL ENVIRONMENT FOR CONTROL SOFTWARE
Michitaka Hirose, Takeshi Myoi, Haruo Amari, Kohei Inamura, and Lawrence Stark *In* NASA. Ames Research Center, Human Machine Interfaces for Teleoperators and Virtual Environments Jun. 1991 p 120-124 Prepared in cooperation with Tokyo Electric Power Co., Inc., Japan and California Univ., Berkeley (For primary document see N95-14013 03-54)
Avail: CASI HC A01/MF A02

N95-14623*# Solomon (G.), Pasadena, CA.
CONVOLUTIONAL ENCODING OF SELF-DUAL BLOCK CODES (2)
G. Solomon and Y. Jin *In* JPL, The Telecommunications and Data Acquisition Report 15 Aug. 1994 p 22-25 (For primary document see N95-14620 03-32)
(RTOP 310-30-71-83-02)
Avail: CASI HC A01/MF A02

N95-14630*# Jet Propulsion Lab., California Inst. of Tech., Pasadena, CA.
A TRAJECTORY PREPROCESSOR FOR ANTENNA POINTING
S. R. Tyler *In its* The Telecommunications and Data Acquisition Report 15 Aug. 1994 p 139-159 (For primary document see N95-14620 03-32)
(RTOP 314-40-42-01-03)
Avail: CASI HC A03/MF A02

N95-14647# Unisys Corp., Houston, TX. Space Systems Div.
APPLYING CASE TECHNOLOGY TO THE SOFTWARE MAINTENANCE LIFE CYCLE
Linda Barker, Daryl Cain, and Michael Bishop *In* Huntsville Association of Technical Societies, TABES 1994: 10th Annual Technical and Business Exhibition and Symposium 1994 7 p (For primary document see N95-14633 03-12)
(TABES Paper 94-620) Avail: CASI HC A02/MF A04

62 COMPUTER SYSTEMS

Includes computer networks and special application computer systems.

N95-13677# Argonne National Lab., IL.
PARALLEL PERFORMANCE OF A SYMMETRIC EIGENSOLVER BASED ON THE INVARIANT SUBSPACE DECOMPOSITION APPROACH
C. Bischof, X. Sun, S. Huss-Lederman, A. Tsao, and T. Turnbull 1994 8 p Presented at the Scalable High Performance Computing Conference, Knoxville, TN, 23 May 1994
(Contract W-31-109-eng-38)
(DE94-013314; ANL/MCS/CP-82959; CONF-9405100-8) Avail: CASI HC A02/MF A01

We discuss work in progress on a complete eigensolver based on the

invariant subspace decomposition algorithm for dense symmetric matrices (SYISDA). We describe a recently developed acceleration technique that substantially reduces the overall work required by this algorithm and review the algorithmic highlights of a distributed-memory implementation of this approach. These include a fast matrix-matrix multiplication algorithm, a new approach to parallel band reduction and tridiagonalization, and a harness for coordinating the divide-and-conquer parallelism in the problem. We present performance results for the dominant kernel, dense matrix multiplication, as well as for the overall SYISDA implementation on the Intel Touchstone Delta and the Intel Paragon. DOE

N95-14116# Argonne National Lab., IL.
NEXUS: AN INTEROPERABILITY LAYER FOR PARALLEL AND DISTRIBUTED COMPUTER SYSTEMS
I. Foster, C. Kesselman, R. Olson, and S. Tuecke 25 Oct. 1994 31 p
(Contract W-31-109-eng-38)
(DE94-015816; ANL/MCS-TM-189) Avail: CASI HC A03/MF A01

Nexus is a set of services that can be used to implement various task-parallel languages, data-parallel languages, and message-passing libraries. Nexus is designed to permit the efficient portable implementation of individual parallel programming systems and the interoperability of programs developed with different tools. Nexus supports lightweight threading and message technology, allowing integration of message passing and threads. Author

N95-14292# Naval Postgraduate School, Monterey, CA.
AN EVALUATION OF B-ISDN FOR THE COMMUNICATION ARCHITECTURE REQUIREMENTS OF DISTRIBUTED INTERACTIVE SIMULATION (DIS) M.S. Thesis
Christopher V. Arias Mar. 1994 68 p
(AD-A280783) Avail: CASI HC A04/MF A01

Distributive Interactive Simulation (DIS) requires a communication architecture to support large scale simulations (100,000 entities). The communication architecture requirements for DIS are now being defined. DIS will require a wide area network that supports high data rates, multicasting, and low latency. DOD can no longer afford unique solutions for the their wide area networking needs and must align their service requirements with the services provided by common carriers. An analysis is presented on how the future Broadband Integrated Services Digital Network (B-ISDN) and its technology standard, Asynchronous Transfer Mode (ATM), could help meet the WAN communication architecture requirements of DIS. The requirements of DIS are presented and mapped into a format compatible with international standards for common carrier services. Quality of Services (QoS) parameter values for DIS information types are estimated and compared to those of B-ISDN. Conclusions reveal that B-ISDN and its underlying technology, ATM, will help meet the DIS WAN communication architecture needs. Also, QoS parameter values for DIS require further definition and specificity to enable DOD to take advantage of the future common carrier services. DOD needs to define its future application requirements that are compatible with common carrier services. DTIC

N95-14380 Argonne National Lab., IL.
AN INFORMAL INTRODUCTION TO PROGRAM TRANSFORMATION AND PARALLEL PROCESSORS
K. W. Hopkins (Southwest Baptist Univ., Bolivar, MO.) 1994 17 p
Limited Reproducibility: More than 20% of this document may be affected by microfiche quality
(Contract W-31-109-eng-38)
(DE94-016343; ANL/MCS/PP-77111) Avail: CASI HC A03

In the summer of 1992, I had the opportunity to participate in a Faculty Research Program at Argonne National Laboratory. I worked under Dr. Jim Boyle on a project transforming code written in pure functional Lisp to Fortran code to run on distributed-memory parallel processors. To perform this project, I had to learn three things: the transformation system, the basics of distributed-memory parallel machines, and the Lisp programming language. Each of these topics in computer science was unfamiliar to me as a mathematician, but I found that they (especially parallel processing) are greatly impacting many fields of mathematics and science. Since most mathematicians have some exposure to computers, but certainly are not computer scientists, I felt it was appropriate to write a paper summarizing my introduction to these areas and how they can fit together. This paper is not meant to be a full explanation of the topics, but an informal introduction for the 'mathematical layman.' I place myself in that category as well as my previous use of computers was as a classroom demonstration tool. DOE

N95-14384# Wisconsin Univ., Madison, WI. Dept. of Computer Sciences.
PERFORMANCE MEASUREMENT AND ANALYSIS TECHNIQUES FOR PARALLEL AND DISTRIBUTED PROGRAMS
B. P. Miller and J. R. Larus 1994 4 p
(Contract DE-FG02-93ER-25176)
(DE94-016429; DOE/ER-25176/1) Avail: CASI HC A01/MF A01

During the first year of our grant, we have made substantial progress on our performance tools research. We have concentrated on our techniques for dynamic program instrumentation and on support of high-level parallel languages and environments. In addition, we have performed an interesting study in a related area, virtual memory scheduling for parallel systems. DOE

N95-14422# Computer Sciences Corp., Falls Church, VA.
PARALLEL ISOSURFACE GENERATOR FOR HUGE DATA SETS Final Report, Jan. - Dec. 1993
Kathy A. Burke Aug. 1994 26 p Prepared in cooperation with Minnesota Univ., Minneapolis, MN
(Contract DAAL03-89-C-0038)
(AD-A284030; ARL-CR-171) Avail: CASI HC A03/MF A01

A parallel C implementation of the marching cubes method is discussed. The input data for the code consists of a variation of the unformatted PLOT3D grid and solution files. PLOT3D files can define an irregularly or regularly spaced mesh and the associated scalars given by v(x,y,z), F(x,y,z), and S(sub n) = F(x,y,z), respectively. The output is a collection of three-sided polygons defining a constant value of F(x,y,z), and a second scalar which will be mapped onto this surface. The output is given in the Bop (Bag-O-Polygons) file format. DTIC

N95-14953 Air Force Inst. of Tech., Wright-Patterson AFB, OH.
ON THE LU FACTORIZATION OF SEQUENCES OF IDENTICALLY STRUCTURED SPARSE MATRICES WITHIN A DISTRIBUTED MEMORY ENVIRONMENT Ph.D. Thesis
Steven M. Hadfield 1994 221 p Limited Reproducibility: More than 20% of this document may be affected by microfiche quality
(AD-A282025; AFIT/CI/CIA-94-005D) Avail: CASI HC A10

This research effort studies the parallel LU factorization of sequences of identically structured sparse matrices using the unsymmetric-pattern, multi-frontal method of Davis and Duff. Computational burden is reduced by using the computational structure (called an assembly directed acyclic graph (DAG)) that results from analysis of the first matrix for the numerical factorization of the subsequent matrices. Execution time is reduced via exploitation of parallelism in the assembly DAG. The theoretical parallelism in the assembly DAG is investigated using both analysis and simulation. Achievable parallelism is evaluated using a simulation model based on the nCUBE 2 distributed memory multiprocessor. Author (revised)

N95-15416 Tennessee Univ., Knoxville, TN. Dept. of Computer Science.
STRUCTURED APPROACHES FOR PROBLEMS OF NETWORK DESIGN AND UTILIZATION Final Technical Report, 1 May 1988 - 30 Apr. 1991
Michael A. Langston 15 Jul. 1994 3 p Limited Reproducibility: More than 20% of this document may be affected by microfiche quality
(Contract N00014-88-K-0343)
(AD-A282925) Avail: CASI HC A01

Basic research has been conducted in the design and analysis of algorithms. Fundamental questions in computer software and systems research have been addressed, concentrating on two particularly promising areas: (1) practical approaches to problems for which only the existence of asymptotically fast algorithms is guaranteed and (2) efficient strategies for parallel computing in realistic, resource-bounded environments. The former is motivated by dramatic recent results in discrete mathematics. The latter is driven by continuing advances in parallel computer architectures. DTIC

N95-15434# EG and G Energy Measurements, Inc., Idaho Falls, ID.
AUTOMATIC TLI RECOGNITION SYSTEM, PART 1

J. K. Partin, G. D. Lassahn, and J. R. Davidson May 1994 59 p
(Contract DE-AC07-76ID-01570)
(DE94-015253; EGG-EE-11298-Pt-1) Avail: CASI HC A04/MF A01

This report describes an automatic target recognition system for fast screening of large amounts of multi-sensor image data, based on low-cost parallel processors. This system uses image data fusion and gives uncertainty estimates. It is relatively low cost, compact, and transportable. The software is easily enhanced to expand the system's capabilities, and the hardware is easily expandable to increase the system's speed. This volume gives a general description of the ATR system. DOE

N95-15442* Illinois Univ., Urbana, IL. Center for Reliable and High-Performance Computing.
CHECKPOINTING AND ROLLBACK RECOVERY IN DISTRIBUTED SHARED MEMORY SYSTEMS
Bob Janssens and W. K. Fuchs Mar. 1994 21 p Limited Reproducibility: More than 20% of this document may be affected by microfiche quality
(Contract NAG1-6131-J-1283; N00014-91-J-1283)
(AD-A281583; NASA-CR-196886; NAS 1.26:196886) Avail: Issuing Activity (Defense Technical Information Center (DTIC))

Checkpointing techniques in parallel systems use dependency tracking and/or message logging to ensure that a system rolls back to a consistent state. Traditional dependency tracking in distributed shared memory systems (DSM) is expensive because of high frequency of communication. In this paper we show that, because of information redundancy, not all message-passing dependences need to be considered to roll back to a consistent state in DSM systems, resulting in reduced dependency tracking overhead and reduced potential for rollback propagation. We develop a model of execution where client processes running an application interact atomically with a set of shared-memory server processes on every access to shared data. We show that under this model, dependences are significantly reduced over the message-passing model. We use results from simulation with multiprocessor address traces to demonstrate the reduction in dependences. DTIC

N95-15450 Naval Research Lab., Washington, DC.
CONNECTION MACHINE SOFTWARE CONVERSION OF THE NAVY TOPS MODEL
Paul B. Anderson and Michael A. Young 5 Jul. 1994 23 p Limited Reproducibility: More than 20% of this document may be affected by microfiche quality
(AD-A281681; NRL/MR/5590-94-7494) Avail: CASI HC A03

The introduction of highly parallel machines with peak performance significantly exceeding the Cray machines has sparked interest in running scientific models on these new architectures. This report describes a software conversion, of the Navy model called TOPS, starting with a Cray Y-MP/8 version in Fortran 77 and ending with a Fortran 90 version for the Connection Machine CM-5. Data mapping, conversion planning, and performance points of view are considered. DTIC

N95-15534# EG and G Energy Measurements, Inc., Idaho Falls, ID.
AUTOMATIC TLI RECOGNITION SYSTEM, PART 2
J. K. Partin, G. D. Lassahn, and J. R. Davidson May 1994 93 p
(Contract DE-AC07-76ID-01570)
(DE94-015393; EGG-EE-11298-Pt-2) Avail: CASI HC A05/MF A01

This report describes an automatic target recognition system for fast screening of large amounts of multi-sensor image data, based on low-cost parallel processors. This system uses image data fusion and gives uncertainty estimates. It is relatively low cost, compact, and transportable. The software is easily enhanced to expand the system's capabilities, and the hardware is easily expandable to increase the system's speed. This volume is a user's manual for an Automatic Target Recognition (ATR) system. This guide is intended to provide enough information and instruction to allow individuals to the system for their own applications. DOE

N95-15581# Fermi National Accelerator Lab., Batavia, IL.
DATA FLOW MANAGER FOR DART
D. Berg, D. Black, D. Slimmer, J. Engelfried, and V. ODell Apr. 1994 5 p Presented at the Meeting on Computing in High-Energy Physics, San Francisco, CA, 21-27 Apr. 1994
(Contract DE-AC02-76CH-03000)
(DE94-013236; FNAL/C-94/104; CONF-940492-5) Avail: CASI HC A01/MF A01

The DART Data Flow Manager (dfm) integrates a buffer manager with a requester/provider model for scheduling work on buffers. Buffer lists, representing built events or other data, are queued by service requesters to service providers. Buffers may be either internal (reside on the local node), or external (located elsewhere, e.g., dual ported memory). Internal buffers are managed locally. Wherever possible, dfm moves only addresses of buffers rather than buffers themselves. DOE

N95-15590# Rochester Univ., NY. Dept. of Computer Science.
THE PROSPECTS FOR ON-LINE HYBRID COHERENCY PROTOCOLS ON BUS-BASED MULTIPROCESSORS
Jack E. Veenstra and Robert J. Fowler Mar. 1994 26 p
(Grant NSF CDA-88-22724)
(TR-490) Avail: CASI HC A03/MF A01

Since data access patterns vary from application to application, neither write-invalidate nor write-update is the better strategy for maintaining cache coherence in all cases. Thus, it may be advantageous to use a hybrid cache coherency protocol that combines the best aspects of each. Although write-invalidate is the dominant approach in commercial multiprocessors, the recent introduction of coalescing write buffers combined with relaxed models of memory consistency can be expected to improve the performance of protocols based on updating. This motivates our reexamination of the relative performance of write-invalidate, write-update, and on-line dynamic hybrid protocols. Using a detailed program-driven simulation of a high-performance bus-based multiprocessor with release-consistent caching, we compare the performance of several variations on the hybrid protocol used in DEC AXP multiprocessors with the performance of several more conventional protocols. The variations on the hybrid protocol are introduced to correct weaknesses that appeared during the study. Though coalescing write buffers offer large performance improvements to the protocols that use update, conventional write-invalidate protocols also benefit. It appears that, although hybrid protocols do not offer any significant advantage over the best choice of pure protocol for a particular program, they may offer good performance over a wider range of applications than any single pure protocol. Author

N95-15616 Brown Univ., Providence, RI. Dept. of Computer Science.
THE PRINCIPLES OF FAULT-TOLERANT AND EFFICIENT PARALLEL COMPUTATION Final Report
Paris O. Kanellakis 15 Jun. 1994 5 p Limited Reproducibility: More than 20% of this document may be affected by microfiche quality
(Contract N00014-91-J-1613)
(AD-A283254) Avail: CASI HC A01

The high-performance potential of parallel and distributed computation can only be realized with significant computation speed-ups from the coordinated action of many processors. A basic problem that has to be addressed, in order to realize this potential, is the unreliability of the resulting (highly complex) systems of many processors. The research of N00014-91-J-1613 'Principles of Fault-Tolerant and Efficient Parallel Computation' has focused, primarily, on the algorithmic principles of fault-tolerant and efficient parallel computing. The desirable combination of reliability and performance is nontrivial since efficiency implies removing redundancy, whereas fault-tolerance requires adding some redundancy to computations. DTIC

N95-15617 Brown Univ., Providence, RI. Dept. of Computer Science.
FAULT-TOLERANCE AND EFFICIENCY IN MASSIVELY PARALLEL ALGORITHMS
Paris O. Kanellakis and Alex A. Shvartsman 1993 29 p Limited Reproducibility: More than 20% of this document may be affected by microfiche quality
(Contract N00014-91-J-1613)
(AD-A283255) Avail: CASI HC A03

Presented is an overview of massively parallel deterministic algorithms which combine high fault-tolerance and efficiency. This desirable combination (called robustness here) is nontrivial, since increasing efficiency implies removing redundancy whereas increasing fault-tolerance requires adding redundancy to computations. A spectrum of algorithmic models for which significant robustness is achievable, from static fault, synchronous computation to dynamic fault, asynchronous computation was studied. In

addition to fail-stop processor models, arbitrarily initialized memory and restricted memory access concurrency were examined and worked with. The deterministic upper bounds for the basic Write-All primitive, the lower bounds on its efficiency, and the identify of somethe key open questions were studied. Also, the robust computing of functions to relations was generalized; this new approach can model approximate computations. We show how to compute approximate Write-All optimally. Finally, the state-of-the-art in a complexity classification, which extends with fault-tolerance the traditional classification of efficient parallel algorithms was synthesized. DTIC

N95-14164*# Texas A&M Univ., College Station, TX. Dept. of Computer Science.
PERFORMANCE COMPARISON OF TOKEN RING PROTOCOLS FOR HARD-REAL-TIME COMMUNICATION
Sanjay Kamat and Wei Zhao *In* Research Inst. for Computing and Information Systems, RICIS Symposium 1992: Mission and Safety Critical Systems Research and Applications 30 Oct. 1992 32 p (For primary document see N95-14156 03-61)
Avail: CASI HC A03/MF A03

N95-14165*# IBM Federal Systems Div., Houston, TX.
POSIX REAL-TIME EXTENSIONS
Henry H. Robbins *In* Research Inst. for Computing and Information Systems, RICIS Symposium 1992: Mission and Safety Critical Systems Research and Applications 30 Oct. 1992 31 p (For primary document see N95-14156 03-61)
Avail: CASI HC A03/MF A03

N95-14586*# Wisconsin Univ., Madison, WI. Dept. of Computer Science.
PERFORMANCE OF CUSTOMIZED DCT QUANTIZATION TABLES ON SCIENTIFIC DATA
Viresh Ratnakar and Miron Livny *In* NASA. Goddard Space Flight Center, 1994 Science Information Management and Data Compression Workshop Sep. 1994 p 1-8 (For primary document see N95-14585 03-59)
(Grants NAGw-3914; NSF IRI-92-24741)
Avail: CASI HC A02/MF A02

N95-14587*# Glamorgan Univ., Pontypridd, Glamorgan (Wales). Dept. of Mathematics and Computing.
COMPARISON OF TRANSFORM CODING METHODS WITH AN OPTIMAL PREDICTOR FOR THE DATA COMPRESSION OF DIGITAL ELEVATION MODELS
Michael Lewis *In* NASA. Goddard Space Flight Center, 1994 Science Information Management and Data Compression Workshop Sep. 1994 p 9-26 (For primary document see N95-14585 03-59)
Avail: CASI HC A03/MF A02

N95-14588*# National Aeronautics and Space Administration. Goddard Space Flight Center, Greenbelt, MD.
RADIOMETRIC RESOLUTION ENHANCEMENT BY LOSSY COMPRESSION AS COMPARED TO TRUNCATION FOLLOWED BY LOSSLESS COMPRESSION
James C. Tilton and Mareboyana Manohar *In its* 1994 Science Information Management and Data Compression Workshop Sep. 1994 p 27-39 (For primary document see N95-14585 03-59)
Avail: CASI HC A03/MF A02

N95-14589*# Georgia Inst. of Tech., Atlanta, GA. School of Electrical Engineering.
BLOCKING REDUCTION OF LANDSAT THEMATIC MAPPER JPEG BROWSE IMAGES USING OPTIMAL PSNR ESTIMATED SPECTRA ADAPTIVE POSTFILTERING Abstract Only
Irving Linares, Russell M. Mersereau, and Mark J. T. Smith *In* NASA. Goddard Space Flight Center, 1994 Science Information Management and Data Compression Workshop Sep. 1994 p 41 (For primary document see N95-14585 03-59)
Avail: CASI HC A01/MF A02

N95-14590*# MacDonald, Dettwiler and Associates Ltd., Richmond (British Columbia).
SYNTHETIC APERTURE RADAR SIGNAL DATA COMPRESSION USING BLOCK ADAPTIVE QUANTIZATION
Gopinath Kuduvalli, Melanie Dutkiewicz, and Ian Cumming *In* NASA. Goddard Space Flight Center, 1994 Science Information Management and Data Compression Workshop Sep. 1994 p 43-57 Sponsored by ESA (For primary document see N95-14585 03-59)
Avail: CASI HC A03/MF A02

N95-14591*# Nebraska Univ., Lincoln, NE.
COMPRESSION OF REGIONS IN THE GLOBAL ADVANCED VERY HIGH RESOLUTION RADIOMETER 1-km DATA SET
Barbara L. Kess, Daniel R. Steinwand, and Stephen E. Reichenbach *In* NASA. Goddard Space Flight Center, 1994 Science Information Management and Data Compression Workshop Sep. 1994 p 59-64 Prepared for Hughes STX, Inc., Greenbelt, MD (For primary document see N95-14585 03-59)
(Contract USGS-14-34-92-C-40004)
Avail: CASI HC A02/MF A02

N95-14592*# Tokyo Univ. (Japan). Inst. of Industrial Science.
LOSSLESS COMPRESSION OF NOAA-AVHRR SATELLITE DATA
Seishi Takamura and Mikio Takagi *In* NASA. Goddard Space Flight Center, 1994 Science Information Management and Data Compression Workshop Sep. 1994 p 65-73 (For primary document see N95-14585 03-59)
Avail: CASI HC A02/MF A02

N95-14593*# National Aeronautics and Space Administration. Goddard Space Flight Center, Greenbelt, MD.
THE DEVELOPMENT OF LOSSLESS DATA COMPRESSION TECHNOLOGY FOR REMOTE SENSING APPLICATIONS
Pen-Shu Yeh and Warner H. Miller *In its* 1994 Science Information Management and Data Compression Workshop Sep. 1994 p 75-82 (For primary document see N95-14585 03-59)
Avail: CASI HC A02/MF A02

N95-14595*# National Aeronautics and Space Administration. Goddard Space Flight Center, Greenbelt, MD.
PLANNING/SCHEDULING TECHNIQUES FOR VQ-BASED IMAGE COMPRESSION
Nicholas M. Short, Jr., Mareboyana Manohar, and James C. Tilton *In its* 1994 Science Information Management and Data Compression Workshop Sep. 1994 p 95-104 (For primary document see N95-14585 03-59)
Avail: CASI HC A02/MF A02

63 CYBERNETICS

Includes feedback and control theory, artificial intelligence, robotics and expert systems.

For related information see also *54 Man/System Technology and Life Support.*

N95-13727*# Texas A&M Univ., College Station, TX. Dept. of Electrical Engineering.
KNOWLEDGE-BASED PROCESSING FOR AIRCRAFT FLIGHT CONTROL
John H. Painter, Emily Glass, Gregory Economides, and Paul Russell Hampton, VA NASA Oct. 1994 97 p
(Grant NAG1-1066; RTOP 505-64-52-01)
(NASA-CR-194976; NAS 1.26:194976) Avail: CASI HC A05/MF A02

This Contractor Report documents research in Intelligent Control using knowledge-based processing in a manner dual to methods found in the classic stochastic decision, estimation, and control discipline. Such knowledge-based control has also been called Declarative, and Hybid. Software architectures were sought, employing the parallelism inherent in modern object-oriented modeling and programming. The viewpoint adopted was that Intelligent Control employs a class of domain-specific software architectures having features common over a broad variety of implementations, such as management of aircraft flight, power distribution,

etc. As much attention was paid to software engineering issues as to artificial intelligence and control issues. This research considered that particular processing methods from the stochastic and knowledge-based worlds are duals, that is, similar in a broad context. They provide architectural design concepts which serve as bridges between the disparate disciplines of decision, estimation, control, and artificial intelligence. This research was applied to the control of a subsonic transport aircraft in the airport terminal area. Author

N95-13895# Galaxy Scientific Corp., Pleasantville, NJ.
ARTIFICIAL INTELLIGENCE WITH APPLICATIONS FOR AIRCRAFT Final Report
L. Harrison, P. Saunders, and J. Janowitz Aug. 1994 374 p
(Contract DTFAO3-89-C-00043)
(DOT/FAA/CT-94/41) Avail: CASI HC A16/MF A03

This report provides an overview of artificial intelligence (AI) technology, one of the more complex applications of digital systems. This report examines AI-based technology, focusing on three fields: neural networks, fuzzy logic, and expert systems. This report provides the reader with the background and a basic understanding of the fundamentals of these fields. Another section examines aspects of the AI development environment, including languages, tools, and AI-based hardware components. Some of the proposed aviation-related applications for both civil and military aircraft, including pilot assistants and diagnostic aids, are surveyed. Additionally, certification issues, including regulations, guidelines, and verification and validation techniques are examined. Human factors issues relating to the use of this technology are identified and reviewed. In addition, the report identifies safety issues and concerns over the use of this technology in airborne systems. Author

N95-14377# Los Alamos National Lab., NM.
AN EFFICIENT NETWORK FOR INTERCONNECTING REMOTE MONITORING INSTRUMENTS AND COMPUTERS
J. K. Halbig, K. E. Gainer, and S. F. Klosterbuer 1994 10 p Presented at the Institute of Nuclear Materials Management Annual Meeting, Naples, FL, 17-20 Jul. 1994
(Contract W-7405-eng-36)
(DE94-016213; LA-UR-94-2531; CONF-940748-67) Avail: CASI HC A02/MF A01

Remote monitoring instrumentation must be connected with computers and other instruments. The cost and intrusiveness of installing cables in new and existing plants presents problems for the facility and the International Atomic Energy Agency (IAEA). The authors have tested a network that could accomplish this interconnection using mass-produced commercial components developed for use in industrial applications. Unlike components in the hardware of most networks, the components -- manufactured and distributed in North America, Europe, and Asia -- lend themselves to small and low-powered applications. The heart of the network is a chip with three microprocessors and proprietary network software contained in Read Only Memory. In addition to all nonuser levels of protocol, the software also contains message authentication capabilities. This chip can be interfaced to a variety of transmission media, for example, RS-485 lines, fiber topic cables, rf waves, and standard ac power lines. The use of power lines as the transmission medium in a facility could significantly reduce cabling costs. DOE

N95-14847 California Univ., Irvine, CA. Dept. of Cognitive Sciences.
VISUAL MOTION PERCEPTION AND VISUAL INFORMATION PROCESSING Final Report, 1 Dec. 1993 - 28 Feb. 1994
George Sperling 28 Feb. 1994 21 p Limited Reproducibility: More than 20% of this document may be affected by microfiche quality
(Contract F49620-94-1-0073)
(AD-A282928; AFOSR-94-0470TR) Avail: Issuing Activity (Defense Technical Information Center (DTIC))

This final progress report summarizes the results of a study that successfully determined the functional architecture of visual motion perception, in the sense of defining the mechanisms involved and the relations between them. It was proved that visual motion is computed by two neural systems: primitive motion-energy extraction (e.g., Reichardt detector) and higher-level feature tracking. A psychophysical pedestal paradigm was used to exclude the feature-tracking process and thereby to obtain pure measures of motion-energy extraction. Motion energy extraction was found to be exclusively monocular, fast (cutoff frequency is 12 Hz) and sensitive (can utilize 0.2 percent contrast), 'bottom-up', and, to operate on both luminance (first-order) and contrast (second-order) motion stimuli. Motion feature tracking was found to operate interocularly as well as monocularly, have a cutoff frequency of 3 Hz, and to be both bottom up (it computes motion from luminance, contrast, depth, motion-motion, flicker and other type of stimuli) and top-down (e.g., attentional states influence what appears to move). The full report is appended. DTIC

N95-14942# Advisory Group for Aerospace Research and Development, Neuilly-Sur-Seine (France). Guidance and Control Panel.
ADVANCED GUIDANCE AND CONTROL ASPECTS IN ROBOTICS [LA PERCEPTION DE L'ENVIRONNEMENT PAR SENSEURS AUTOMATIQUES]
Jun. 1994 227 p Lecture series held in Lisbon, Portugal, 6-7 Jun. 1994, in Athens, Greece, 9-10 Jun. 1994, and in Ontario, 21-22 Jun. 1994
(AGARD-LS-193; ISBN-92-835-0751-7) Copyright Avail: CASI HC A11/MF A03

To ensure the capability of defense, a demand for equipment and systems which can be embraced under the title of 'Robotics' will emerge in the near future. In this context, 'Robotics' represents a specific problem area involving all the guidance and control functions which are associated with achieving goal-oriented autonomous behavior in structured and unstructured environments for mobile and manipulator systems as applied to ground, sea, air, and space operations. Related robotic systems must combine constituent functions such as intelligent decision making, control, manipulation, motion, sensing, and communication. The scope of the special course will cover new developments in the areas of autonomous navigation for planetary and surface systems, and control and operations of remote manipulators. For individual titles, see N95-14943 through N95-14949.

N95-14943*# National Aeronautics and Space Administration, Washington, DC.
ROBOTICS TECHNOLOGY DEVELOPMENTS IN THE UNITED STATES SPACE TELEROBOTICS PROGRAM
David Lavery *In* AGARD, Advanced Guidance and Control Aspects in Robotics Jun. 1994 21 p (For primary document see N95-14942 03-63)
Copyright Avail: CASI HC A03/MF A03

In the same way that the launch of Yuri Gagarin in April 1961 announced the beginning of human space flight, last year's flight of the German ROTEX robot flight experiment is heralding the start of a new era of space robotics. After a gap of twelve years since the introduction of a new capability in space remote manipulation, ROTEX is the first of at least ten new robotic systems and experiments which will fly before the year 2000. As a result of redefining the development approach for space robotic systems, and capitalizing on opportunities associated with the assembly and maintenance of the space station, the space robotics community is preparing a whole new generation of operational robotic capabilities. Expanding on the capabilities of earlier manipulation systems such as the Viking and Surveyor soil scoops, the Russian Lunakhods, and the Shuttle Remote Manipulator System (RMS), these new space robots will augment astronaut on-orbit capabilities and extend virtual human presence to lunar and planetary surfaces. Author

N95-14944# CompEngServ Ltd., Ottawa (Ontario).
MACHINE INTELLIGENCE: THE KEY TO GUIDANCE AND CONTROL IN ROBOTICS
B. Archie Bowen and David G. Bowen *In* AGARD, Advanced Guidance and Control Aspects in Robotics Jun. 1994 43 p (For primary document see N95-14942 03-63)
Copyright Avail: CASI HC A03/MF A03

A robotics system is composed of a hardware platform which provides the stability, mobility, and manual dexterity and a software system which acts to interpret the input sensor data and the mission statement and then to create the required excitation to the hardware. Stated in this rather simplistic way, there seems to be little reason for the vast array of laboratories feverishly working on the creation of fully autonomous robots. The overall task and its components, however, has proven of intricate complexity, with succeeding layers of hidden problems becoming exposed just as a solution appears imminent. This paper is concerned only with the software components of a robotics system, and in particular with that

portion of the system which comes under the general description of intelligent software. It is a 'stand-off' approach derived from a software engineer's point of view. The intent is to review, from a particular and perhaps novel point of view, the various software paradigms and their intrinsic capabilities and functionalities. This review provides the basis for a detailed map of the current capabilities of software paradigms onto the guidance and control problems of intelligent robotics systems. The paper is partitioned into two parts: Machine Intelligence as a Robotics Component, and Expectations and Projections. In the first, a perspective of intelligent software is presented which provides the basis for considering guidance and control problems. In the second part, the utility of this perspective is demonstrated by exploring a generic guidance and control architecture. The paper ends by suggesting some approaches for future directions in developments in this field.
Author

N95-14945# Martin Marietta Corp., Denver, CO. Astronautics Div.
CONTROL OF REMOTELY OPERATED MANIPULATION SYSTEMS
Paul L. Shattuck *In* AGARD, Advanced Guidance and Control Aspects in Robotics Jun. 1994 25 p (For primary document see N95-14942 03-63)
Copyright Avail: CASI HC A03/MF A03

Robotics systems are beginning to emerge as an effective alternative to humans for tasks that are either hazardous or routine and repetitive. Remotely operated manipulation systems have been accepted and widely used for the past ten to twenty years in two terrestrial applications: underwater exploration, servicing, and repair and handling of hazardous materials in the nuclear industry. Technology advances have enabled new, broad space and terrestrial applications for remotely operated manipulation systems. However, in order to promulgate robotic systems further in the terrestrial work place, elements of these systems must have requirements traceable to operations with humans nearby, or manipulation of delicate objects. A representative space-system manipulator will be used to provide an illustrative example of the evolution of remotely operated manipulation systems. The manipulator is initially intended to provide the astronauts a tool to perform routine tasks such as inspection, worksite preparation/teardown, or routine servicing and maintenance, thereby improving the astronauts' efficiency during EVA's. Emphasis is placed on the system-level requirements and design drivers. Technology advances that enable new applications, and impediments to using robotics, will also be discussed. Control techniques and the operator interface developed for this manipulator could be commercially demonstrated in an underwater servicing exercise - providing the link to the remotely operated manipulation system that are the subject of this lecture. Author

N95-14946# Canadian Space Agency, Saint Hubert (Quebec). Space Station Program.
CONTROL AND OPERATION OF SPACE MANIPULATOR SYSTEMS
Cameron P. Trudel, D. G. Hunter, and M. E. Stieber *In* AGARD, Advanced Guidance and Control Aspects in Robotics Jun. 1994 19 p (For primary document see N95-14942 03-63)
Copyright Avail: CASI HC A03/MF A03

As manned space flight passes into its fourth decade, many of the activities in space appear to be almost routine. However, the space environment is exceedingly hostile to humans and necessitates substantial effort and funding to provide an infrastructure to support human life. Increased attention is therefore being directed toward the application of robotics technology to more effectively carry out tasks in space which, up to now, have been carried out by human extravehicular activity (EVA), or which could not be carried out because of human limitations or limitations of available equipment. Manipulator systems are better suited to operation in the external space environment and can augment or replace the human presence. They can also play an important role in the spacecraft intravehicular activity (IVA) to replace some of the human tasks. To date few robots have been developed for space applications; however, as human activity increases in earth orbit and beyond, robotic systems will play an increasingly vital role. Control and operation of space manipulator systems are addressed with emphasis on those designed for the external space environment. Applications of the technology are discussed in the context of the Mobile Servicing System (MSS) being developed for the International Space Station. The Mobile Servicing System incorporates two manipulator systems, the Space Station Remote Manipulator System (SSRMS) and the Special Purpose Dexterous Manipulator (SPDM). The modes of operation and selectable control features are discussed with some of the more advanced features demonstrated by simulation and laboratory test results.
Author

N95-14947# Alcatel Espace, Toulouse (France).
MISSION, TECHNOLOGIES AND DESIGN OF PLANETARY MOBILE VEHICLE **c37**
Michel Hayard *In* AGARD, Advanced Guidance and Control Aspects in Robotics Jun. 1994 7 p (For primary document see N95-14942 03-63)
Copyright Avail: CASI HC A02/MF A03

The French Space Agency (CNES) started a study in late 1992 of an autonomous rover VAP (for Planetary Autonomous Vehicle). The aim of this study was to investigate multimission mobile platform design. The focus was placed on a martian mission for several reasons: (1) there is a very high scientific interest for Mars surface exploration leading to a better understanding of the solar system and Earth evolution; (2) roving on the planet is one mandatory and preliminary step before the conquest of the 'red planet' by manned mission; and (3) it is a necessary complement to fixed networks and sample return, in order to get data relevant to very large areas. The overall system concept including launch, cruise, deboost from Mars orbit, Mars atmosphere entry, and landing is not part of the study but is only kept in mind, as these phases of the mission induce several constraints. The main results of the study are given, showing the two possibilities: a large vehicle of 450 kg as the baseline and a smaller vehicle of 250 kg as an option. The various subsystems are described and the choices justified. The expected performances are summarized.
Author

N95-14948# Bateman (Peter J.), Camberly (England).
GUIDANCE AND CONTROL FOR UNMANNED GROUND VEHICLES **c37**
Peter J. Bateman *In* AGARD, Advanced Guidance and Control Aspects in Robotics Jun. 1994 33 p (For primary document see N95-14942 03-63)
Copyright Avail: CASI HC A03/MF A03

Techniques for the guidance, control, and navigation of unmanned ground vehicles are described in terms of the communication bandwidth requirements for driving and control of a vehicle remote from the human operator. Modes of operation are conveniently classified as conventional teleoperation, supervisory control, and fully autonomous control. The fundamental problem of maintaining a robust non-line-of-sight communications link between the human controller and the remote vehicle is discussed, as this provides the impetus for greater autonomy in the control system and the greatest scope for innovation. While supervisory control still requires the man to be providing the primary navigational intelligence, fully autonomous operation requires that mission navigation is provided solely by on-board machine intelligence. Methods directed at achieving this performance are described using various active and passive sensing of the terrain for route navigation and obstacle detection. Emphasis is given to TV imagery and signal processing techniques for image understanding. Reference is made to the limitations of current microprocessor technology and suitable computer architectures. Some of the more recent control techniques involve the use of neural networks, fuzzy logic, and data fusion and these are discussed in the context of road following and cross country navigation. Examples of autonomous vehicle testbeds operated at various laboratories around the world are given. Author

N95-14949# Massachusetts Inst. of Tech., Cambridge.
HUMAN FACTORS CONSIDERATIONS FOR REMOTE MANIPULATION **c54**
Thomas B. Sheridan *In* AGARD, Advanced Guidance and Control Aspects in Robotics Jun. 1994 24 p (For primary document see N95-14942 03-63)
Copyright Avail: CASI HC A03/MF A03

This paper presents human factors considerations of remote manipulation, sometimes called teleoperation. The paper reviews two broad classes of sensing and display considerations, namely (1) vision and video feedback, and (2) haptic sensing and display, including force and touch feedback from remote manipulators. Next 'telepresence' and virtual environments are discussed in relation to one another. The paper then discusses two broad classes of teleoperator control, namely (1) direct manual control and

(2) supervisory control. Finally the paper considers briefly the subjects of cognition and mental models as they relate to remote manipulation.
Author (revised)

N95-15369# Sandia National Labs., Albuquerque, NM.
DEFINING A CONTROLLER ARCHITECTURE FOR THE LONG-REACH MANIPULATOR
W. E. Ford Jun. 1994 25 p
(Contract DE-AC04-94AL-85000)
(DE94-015165; SAND-94-0514) Avail: CASI HC A03/MF A01

To draft a procurement specification for the Long-Reach Manipulator (LRM), the benefits and limitations of the various robotic control system architectures available need to be determined. This report identifies and describes the advantages and potential disadvantages of using an open control system versus a closed (or proprietary) system, focusing on integration of interfaces for sensors, end effectors, tooling, and operator interfaces. In addition, the various controls methodologies of several recent systems are described. Finally, the reasons behind the recommendation to procure an open control system are discussed. DOE

N95-15398 Maryland Univ., College Park, MD.
VISION-BASED NAVIGATION AND RECOGNITION Technical Report, Apr. 1992 - Mar. 1993
Azriel Rosenfeld Jul. 1994 29 p Limited Reproducibility: More than 20% of this document may be affected by microfiche quality
(Contract DACA76-92-C-0009)
(AD-A282962; TEC-0047) Avail: CASI HC A03

The research summarized in this report deals with many aspects of computer vision as applied to both navigation and object recognition. In particular, this research has concentrated on eight areas: parallel algorithms for vision; diffusion processes and their roles in early vision; invariant properties and their roles in object recognition; recovery of three-dimensional scene properties from single images; recovery of observer motion and scene structure from image sequences; direct motion analysis; visual interception; and vision-based navigation. Specific topics include algorithms for image and graph computations, parallel search and stereo matching; the application of diffusion processes to image morphing and face recognition; projective, affine, and deformation invariants of images; reliability of geometric computations on images of three-dimensional scenes; properties of foliage regarded as a three-dimensional texture; monocular and binocular recovery of motion and structure from feature correspondents in an image sequence; a unified treatment of feature-based and flow-based motion estimation; motion analysis based on global properties of the flow field; vision-based target interception; visibility on terrain; and landmark-based localization DTIC

N95-15403 International Computer Science Inst., Berkeley, CA.
SPATIO-TEMPORAL NEURAL NETWORKS FOR VISION, REASONING AND RAPID DECISION MAKING Annual Productivity Report, 1 Sep. 1993 - 31 Aug. 1994
Lokendra Shastri 31 Aug. 1994 237 p Limited Reproducibility: More than 20% of this document may be affected by microfiche quality
(Contract N00014-93-1-1149)
(AD-A283251) Avail: CASI HC A11

A spatio-temporal system for recognizing handprint digit strings was designed and trained to recognize handprinted ZIP codes. The results of our work on a biologically motivated model of reflexive reasoning were used to implement a pilot system for performing rapid reasoning using very large knowledge bases. The pilot system which runs on a 32 node CM-5, can encode over 300,000 items and respond in less than 500 msec. to queries requiring reasoning up to a depth of eight. DTIC

N95-15461 Massachusetts Univ., Amherst, MA.
AN ARCHITECTURE FOR INTELLIGENT MULTICHIP MODULE RELIABILITY ANALYSIS Final Report, Mar. 1992 - Aug. 1993
Daniel D. Corkill Apr. 1994 46 p Limited Reproducibility: More than 20% of this document may be affected by microfiche quality
(Contract F30602-93-C-0036)
(AD-A281574; FTR-528226; RL-TR-94-71) Avail: Issuing Activity (Defense Technical Information Center (DTIC))

This report describes the development of a computer-based modeling and analysis system called the Intelligent Multichip Module (MCM) Analyzer (IMCMA). IMCMA is a blackboard-based software tool that automatically performs finite-element and knowledge-based analysis of MCM designs to rapidly assess their reliability. In IMCMA, modeling effort and expert-operator requirements have been reduced through: (1) use of high-level representation of devices as the interface between the designer and the analysis tools; (2) capturing the expertise of experienced design analysts in an intelligent assistant for use by less experienced designers. Nine knowledge sources (KS's) were completed that take a high-level device specification through model generation and simplification, finite-element generation, and thermal analysis. These KS's include stand-alone FORTRAN finite-element generation codes that have been integrated into IMCMA by using the generic blackboard framework, GBB. This initial IMCMA prototype quickly produces a thermal analysis when given a high-level MCM design description. DTIC

N95-15548 Maryland Univ., College Park, MD.
ROBUST ROUTING IN DYNAMIC NETWORKS, PART 1 Final Report, Jan. 1990 - Sep. 1993
Ashok K. Agrawala Apr. 1994 442 p Limited Reproducibility: More than 20% of this document may be affected by microfiche quality
(Contract F30602-90-C-0010)
(AD-A282445; RL-TR-94-37-Pt-2) Avail: Issuing Activity (Defense Technical Information Center (DTIC))

The goal of various control schemes used in a network is to assure a continued good performance as the load and other network characteristics change. Many of the flow and congestion control schemes are designed with assumed network dynamics. In order to get a better understanding of the network dynamics a tool was designed that can be used to monitor the detailed end-to-end behavior of a path of Internet for extended periods of time. The transit times and loss characteristics are observed by probe packets that are sent at regular intervals. Traditionally the flow control techniques used in the networks have been designed assuming a stochastic behavior for the load as well as the components of the network. In this research the approach has been to model a network and its connections using deterministic modeling techniques as far as possible, invoking stochastic assumptions only when deterministic assumptions cannot be justified or the lack of information makes it essential. A new version of Maryland Routing Simulator (MaRS) with improved front end has been completed and distributed through FTP. It has been copied by over 250 sites. DTIC

N95-15598* National Aeronautics and Space Administration. Goddard Space Flight Center, Greenbelt, MD.
STEERING CAPACIFLECTOR SENSOR Patent
Del T. Jenstrom, inventor (to NASA) and Robert L. McConnell, inventor (to NASA) 8 Nov. 1994 7 p Filed 23 Nov. 1992 Supersedes 94N15704 (32 - 3, p 1164)
(NASA-Case-GSC-13489-1; US-Patent-5,363,051;
US-Patent-Appl-SN-979987; US-Patent-Class-324-661;
US-Patent-Class-324-688; US-Patent-Class-361-181;
US-Patent-Class-340-870.37; Int-Patent-Class-G01R-27/26;
Int-Patent-Class-G08C-19/10; Int-Patent-Class-H01H-47/12) Avail: US Patent and Trademark Office

A capacitive type proximity sensor having substantial range and sensitivity between a machine and an intruding object in the immediate vicinity of the machine and having a steerable sensing field has an outer electrical conductor on the machine forming one electrode of a sensor capacitor, the other electrode is the object. The outer conductor is a thin sheet of conductive material with a pair (or more) of intermediate electrical conductors located between the outer conductor and the machine. The pair of intermediate electrical conductors are in close proximity to each other and together form a surface having a size substantially larger than the outer conductor to act as a shield for reducing the parasitic capacitance between the outer conductor and the machine and to steer the sensor field. The pair of intermediate conductors are thin sheets of conductive material substantially wider than the first conductor. The outer and pair of intermediate conductors are attached to a surface on the machine in electrical isolation and with no gaps between the conductors and no gap between the surface and the pair of intermediate conductors. The outer and pair of intermediate conductors are also in conformance with each other and the surface of the machine, and the surface of the machine acts as a ground plane. Variable gain voltage follower circuits are used for

coupling, in phase, the instantaneous voltage at the outer electrical conductor to the pair of intermediate electrical conductors and a signal generator is coupled to the outer conductor and is responsive to the capacitance of the sensor capacitor for generating a control signal to the machine.
Official Gazette of the U.S. Patent and Trademark Office

N95-15786# Rochester Univ., NY. Dept. of Computer Science.
THE TEMPORAL REASONING SYSTEMS TimeGraph 1-2
Alfonso Gerevini (Trento Univ., Povo, Italy.), Lenhart Schubert, and Stephanie Schaeffer Apr. 1994 26 p Revised
(TR-494-Rev) Avail: CASI HC A03/MF A01

We describe two domain-independent temporal reasoning systems called TimeGraph 1 and 2 which can be used in AI-applications as tools for efficiently managing large sets of relations in the point algebra, in the interval algebra, and metric information such as absolute times and durations. Our representation of time is based on timegraphs, graphs partitioned into a set of chains on which the search is supported by a metagraph data structure. TimeGraph 1 was originally developed by Taugher, Schubert, and Miller in the context of story comprehension. TimeGraph 2 provides useful extensions, including efficient algorithms for handling inequations, and relations expressing point-interval exclusion and interval disjointness. These extensions make the system much more expressive in the representation of qualitative information and suitable for a large class of applications. Author

N95-15811 Massachusetts Inst. of Tech., Cambridge. Artificial Intelligence Lab.
INTELLIGENCE IN SCIENTIFIC COMPUTING Final Report, 1 Apr. 1989 - 31 Dec. 1993
Hal Abelson and Gerald J. Sussman 31 Dec. 1993 35 p Limited Reproducibility: More than 20% of this document may be affected by microfiche quality
(Contract N00014-89-J-3202)
(AD-A284410) Avail: Issuing Activity (Defense Technical Information Center (DTIC))

Project objectives were to develop new computer representations and reasoning mechanisms that enable intelligent systems to autonomously design, monitor, and understand complicated physical systems, through appropriate mixtures of numerical and symbolic computing. As part of this research we demonstrated novel computational tools that autonomously monitor, understand, and control complex physical systems. These tools understand the models, monitor the execution of the simulations, and formulate qualitative explanations of the results. These tools interact with their human users in symbolic terms, allowing them to specify qualitative goals for measurement and intelligent control applications. DTIC

N95-14021*# International Business Machines Corp., Yorktown Heights, NY. Continuous Speech Recognition Group.
WATCH WHAT YOU SAY, YOUR COMPUTER MIGHT BE LISTENING: A REVIEW OF AUTOMATED SPEECH RECOGNITION Abstract Only
Stephen V. DeGennaro *In* NASA. Ames Research Center, Human Machine Interfaces for Teleoperators and Virtual Environments Jun. 1991 p 19-20 (For primary document see N95-14013 03-54)
Avail: CASI HC A01/MF A02

N95-14022*# California Univ., Berkeley, CA. Telerobotics Unit.
EYE MOVEMENT CONTROL AND TOP-DOWN SCANPATH VISION AS A DESIGN METAPHOR FOR ROBOTIC VISION AND CONTROL
Lawrence W. Stark *In* NASA. Ames Research Center, Human Machine Interfaces for Teleoperators and Virtual Environments Jun. 1991 p 21-28 (For primary document see N95-14013 03-54)
(Contract NCC2-86)
Avail: CASI HC A02/MF A02

N95-14099*# National Aeronautics and Space Administration. Ames Research Center, Moffett Field, CA.
FROM ANTARCTICA TO SPACE: USE OF TELEPRESENCE AND VIRTUAL REALITY IN CONTROL OF REMOTE VEHICLES Abstract Only
Carol Stoker, Butler P. Hine, III, Michael Sims, Daryl Rasmussen, Phil Hontalas, Terrence W. Fong, Jay Steele, Don Barch, Dale Andersen, and Eric Miles et al *In* NASA. Goddard Space Flight Center, Eighteenth Space Simulation Conference: Space Mission Success Through Testing Nov. 1994 p 471 (For primary document see N95-14062 03-18)
Avail: CASI HC A01/MF A04

N95-14170*# Massachusetts Inst. of Tech., Cambridge. Dept. of Chemical Engineering.
FAULT DETECTION AND DIAGNOSIS USING NEURAL NETWORK APPROACHES
Mark A. Kramer *In* Research Inst. for Computing and Information Systems, RICIS Symposium 1992: Mission and Safety Critical Systems Research and Applications 30 Oct. 1992 31 p (For primary document see N95-14156 03-61)
Avail: CASI HC A03/MF A03

N95-14652# Rockwell International Corp., Huntsville, AL. Rocketdyne Div.
AUTOMATED TEST ENVIRONMENT FOR A REAL-TIME CONTROL SYSTEM
Ronald O. Hall *In* Huntsville Association of Technical Societies, TABES 1994: 10th Annual Technical and Business Exhibition and Symposium 1994 5 p (For primary document see N95-14633 03-12)
(TABES Paper 94-631) Avail: CASI HC A01/MF A04

64 NUMERICAL ANALYSIS

Includes iteration, difference equations, and numerical approximation.

N95-13694 Notre Dame Univ., IN. Dept. of Electrical Engineering.
HIGH-SPEED FIXED AND FLOATING POINT IMPLEMENTATION OF DELTA-OPERATOR FORMULATED DISCRETE TIME SYSTEMS Interim Report, 1 Jan. - 30 Jun. 1994
Peter H. Bauer 5 Aug. 1994 27 p Limited Reproducibility: More than 20% of this document may be affected by microfiche quality
(Contract N00014-94-1-0387)
(AD-A283109) Avail: Issuing Activity (Defense Technical Information Center (DTIC))

This report addresses the analysis and design of finite wordlength implementations of linear t.i.v. delta-systems and the development of a 2-D delta-operator state space model. It is shown that in fixed point arithmetic linear t.i.v. systems implementation in delta-operator form do not generally outperform their q-operator counterpart. In fact, delta-operator systems always show unstable limit cycle behavior and convergence to incorrect equilibrium points, independent of the choice of the realization or the sampling time. The coefficient sensitivity for delta-systems is still superior to the shift-operator. In the case of floating point arithmetic, delta-operator implementations perform consistently better than their shift-operator counterparts. Delta-systems show superior quantization noise and sensitivity properties. The zero-convergence problem of the fixed point case does not exist if the mantissa length is chosen sufficiently large. Due to its attractive finite wordlength properties, the concept of delta-operators has been extended to the multi-dimensional case. A 2-D state space model was developed and the notions of reachability and observability gramian and balanced realization have been introduced. The problem of directly checking stability in the delta-domain has also been addressed. Similarly to the 1-D case, the sensitivity and roundoff noise behavior was analyzed DTIC

N95-13980 Newcastle-upon-Tyne Univ., Newcastle (England). Dept. of Computing Science.
2D REGULAR ARRAYS FOR A SPECIAL CLASS OF NON UNIFORM RECURRENCE EQUATIONS
V. N. Aleksandrov and S. Fidanova Dec. 1993 20 p
(PB94-195633; TRS-462) Copyright Avail: Issuing Activity (National Technical Information Service (NTIS))

A special class of non uniform recurrent equations producing data dependency graphs which involve non-constant data dependencies on the input data f(i) is considered in this paper. This class includes for example Dynamic Programming recurrence equations for Knapsack Type Problems. 2D regular arrays for such equations are derived. It is shown that the execution time is m + c on 2D arrays of size m x (f sub max/alpha),

where alpha is the size of the cell memory. In addition it is proved that the mathematical expectation of the execution time on the fixed sized (p x q) regular arrays is ET = 0(m(c + 1)/pq + m + q), i.e. optimal, for the case when f(i) is less than or equal to t less than c and it is measured by ET = O(m(c + 1)(sup 2)/p(sup 2)q + m(c + 1)/pq + m +q) in the case when t = c under the assumption that f(i) are independently drawn from the uniform distribution over (1, 2, ..., t) and p(sup 3)q less than or equal to (t + 1)/2. NTIS

N95-13991 Technische Univ., Delft (Netherlands).
METHODOLOGY FOR THE PARALLEL DIRECT SOLUTION OF FINITE ELEMENT SYSTEMS Ph.D. Thesis
H. X. Lin 12 Oct. 1993 214 p Limited Reproducibility: More than 20% of this document may be affected by microfiche quality
(PB94-198009) Avail: CASI HC A10

The dissertation describes a methodology for the parallel direct solution of finite element (FE) systems. The work was started as part of a project to parallelize the FE software package DIANA for structural analysis. A generalized optimizing domain decomposer is presented which combines the advantages of several known techniques. An efficient storage scheme for sparse matrices is then described. It has a block oriented data structure suited for vector and distributed processing. Ordering techniques are considered for fill-in control and for parallel computation. A performance analysis is done on DIANA's parallel solver PARASOL, and a macro data flow implementation of PARASOL is presented. Finally, concluding remarks and discussions are given regarding the described methodology to parallelize FE computations and future developments. NTIS

N95-14154 Technische Univ., Delft (Netherlands).
DEPENDENT RANDOM VARIABLES IN UNCERTAINTY ANALYSIS Ph.D. Thesis
A. M. H. Meeuwissen 8 Nov. 1993 142 p Limited Reproducibility: More than 20% of this document may be affected by microfiche quality
(PB94-191293; ISBN-90-9006471-0) Copyright Avail: CASI HC A07

The central topic of this Ph.D. thesis is the analysis of mathematical models that contain parameters with unprecisely known values. These parameters are modelled as random variables. The probability distributions of the random variables quantify the uncertainty about the true parameter values. The effect of the parameter uncertainties on the model predictions can be analyzed by means of Monte Carlo simulation. This is also called 'uncertainty analysis'. NTIS

N95-14296*# National Aeronautics and Space Administration. Lewis Research Center, Cleveland, OH.
AN EFFICIENT SPECTRAL METHOD FOR ORDINARY DIFFERENTIAL EQUATIONS WITH RATIONAL FUNCTION COEFFICIENTS
Evangelos A. Coutsias (New Mexico Univ., Albuquerque, NM.), David Torres (New Mexico Univ., Albuquerque, NM.), and Thomas Hagstrom Oct. 1994 29 p
(Contracts NCC3-233; RTOP 505-90-5K; DE-FG03-92ER-25128; NSF DMS-91-08072; NSF DMS-93-04406)
(NASA-TM-106762; E-9205; ICOMP-94-25; NAS 1.15:106762) Avail: CASI HC A03/MF A01

We present some relations that allow the efficient approximate inversion of linear differential operators with rational function coefficients. We employ expansions in terms of a large class of orthogonal polynomial families, including all the classical orthogonal polynomials. These families obey a simple three-term recurrence relation for differentiation, which implies that on an appropriately restricted domain the differentiation operator has a unique banded inverse. The inverse is an integration operator for the family, and it is simply the tridiagonal coefficient matrix for the recurrence. Since in these families convolution operators (i.e. matrix representations of multiplication by a function) are banded for polynomials, we are able to obtain a banded representation for linear differential operators with rational coefficients. This leads to a method of solution of initial or boundary value problems that, besides having an operation count that scales linearly with the order of truncation N, is computationally well conditioned. Among the applications considered is the use of rational maps for the resolution of sharp interior layers. Author

N95-14300*# National Aeronautics and Space Administration. Lewis Research Center, Cleveland, OH.
NONLINEAR ASYMPTOTIC INTEGRATION ALGORITHMS FOR ONE-DIMENSIONAL AUTONOMOUS DISSIPATIVE FIRST-ORDER ODEs
Henry W. Haslach, Jr. (Maryland Univ., College Park, MD.), Alan D. Freed, and Kevin P. Walker Nov. 1994 28 p
(Grant NAG3-1321; RTOP 505-63-5A)
(NASA-TM-106780; E-9233; NAS 1.15:106780) Avail: CASI HC A03/MF A01

Nonlinear asymptotic integrators are applied to one-dimensional, nonlinear, autonomous, dissipative, ordinary differential equations. These integrators, including a one-step explicit, a one-step implicit, and a one- and two-step midpoint algorithm, are designed to follow the asymptotic behavior of a system approaching a steady state. The methods require that the differential equation be written in a particular asymptotic form. This is always possible for a one-dimensional equation with a globally asymptotic steady state. In this case, conditions are obtained to guarantee that the implicit algorithms are well defined. Further conditions are determined for the implicit methods to be contractive. These methods are all first order accurate, while under certain conditions the midpoint algorithms may also become second order accurate. The stability of each method is investigated and an estimate of the local error is provided. Author

N95-14381# Los Alamos National Lab., NM.
VARIABLE METRIC CONJUGATE GRADIENT METHODS
T. Barth and T. Manteuffel 1994 24 p Presented at the International PCG Symposium on Matrix Analysis and Parallel Computing, Yokohama, Japan, 15-16 Mar. 1994
(Contract W-7405-eng-36)
(DE94-014796; LA-UR-94-1602; CONF-9403142-1) Avail: CASI HC A03/MF A01

In this paper we present a framework that includes many well known iterative methods for the solution of nonsymmetric linear systems of equations, Ax = b. Section 2 begins with a brief review of the conjugate gradient method. Next, we describe a broader class of methods, known as projection methods, to which the conjugate gradient (CG) method and most conjugate gradient-like methods belong. The concept of a method having either a fixed or a variable metric is introduced. Methods that have a metric are referred to as either fixed or variable metric methods. Some relationships between projection methods and fixed (variable) metric methods are discussed. The main emphasis of the remainder of this paper is on variable metric methods. In Section 3 we show how the biconjugate gradient (BCG), and the quasi-minimal residual (QMR) methods fit into this framework as variable metric methods. By modifying the underlying Lanczos biorthogonalization process used in the implementation of BCG and QMR, we obtain other variable metric methods. These, we refer to as generalizations of BCG and QMR. DOE

N95-14657 Stanford Univ., CA. Dept. of Computer Science.
WORKSHOP ON ADVANCES IN SCIENTIFIC COMPUTATION AND DIFFERENTIAL EQUATIONS 1993 (SCADE) Final Report, 30 Sep. 1992 - 29 Sep. 1993
Gene H. Golub 18 Jul. 1994 13 p Workshop held in Auckland, New Zealand, 3-8 Jan. 1993 Limited Reproducibility: More than 20% of this document may be affected by microfiche quality
(Contract N00014-92-J-1934)
(AD-A283111) Avail: CASI HC A03

The primary focus of the Scientific Computation and Differential Equations '93 (SCADE) conference was on theoretical numerical analysis, with the Runge-Kutta method receiving the dominant emphasis. Quite a few papers were also concerned with algorithm and software issues; several focused on applications. The vast majority of the talk topics concerned initial value problems, but a few were on the boundary value problems for ordinary differential equations. Although computing is an integral part of the numerical methods of ODE's, Butcher and his colleagues are primarily analyzing the ODE methods. In addition, a list of papers presented at SCADE '93 is attached. Derived from text

N95-14843 General Electric Co., Schenectady, NY.
REPRESENTATION AND RECOGNITION WITH ALGEBRAIC INVARIANTS AND GEOMETRIC CONSTRAINT MODELS Quarterly Report, 1 Sep. - 1 Dec. 1993

Joseph L. Mundy 1 Dec. 1993 9 p Limited Reproducibility: More than 20% of this document may be affected by microfiche quality
(Contract MDA972-91-C-0053; DARPA Order 8228)
(AD-A282926) Avail: CASI HC A02

The theory of invariants of repeated structures has been validated experimentally. This class of object description appears very promising and extends the usefulness of invariants to a broad class of man-made objects. DTIC

N95-15342 Argonne National Lab., IL.
DYNAMICS ON THE ATTRACTOR FOR THE COMPLEX GINZBURG-LANDAU EQUATION
P. Takac (Vanderbilt Univ., Nashville, TN.) 1994 51 p Limited Reproducibility: More than 20% of this document may be affected by microfiche quality
(Contract W-31-109-eng-38)
(DE94-016902; ANL/MCS/PP-75712) Avail: Issuing Activity (Department of Energy (DOE))

We present a numerical study of the large-time asymptotic behavior of solutions to the one-dimensional complex Ginzburg-Landau equation with periodic boundary conditions. Our parameters belong to the Benjamin-Feir unstable region. Our solutions start near a pure-mode rotating wave that is stable under sideband perturbations for the Reynolds number R ranging over an interval (R(sub sub),R(sub sup)). We find sub- and super-critical bifurcations from this stable rotating wave to a stable 2-torus as the parameter R is decreased or increased past the critical value R(sub sub) or R(sub sup). As R greater than R(sub sup) further increases, we observe a variety of dynamical phenomena, such as a local attractor consisting of three unstable manifolds of periodic orbits or 2-tori cyclically connected by manifolds of connection orbits. We compare our numerical simulations to both rigorous mathematical results and experimental observations for binary fluid mixtures. DOE

N95-15412# Institut des Hautes Etudes Scientifiques, Bures-sur-Yvette (France).
CARNOT-CARATHEODORY SPACES SEEN FROM WITHIN
M. Gromov Feb. 1994 234 p
(PB94-195617; IHES/M/94/6) Avail: CASI HC A11/MF A03

Chapter headings are the following: Basic definitions, examples and problems; Horizontal curves and small C-C balls; Hypersurfaces in C-C spaces; Carnot-Caratheodory geometry of contact manifolds; Pfaffian geometry in the internal light; Anisotropic connections. NTIS

N95-15424# Army Topographic Engineering Center, Fort Belvoir, VA.
LINEAR ESTIMATION OF HYPERSPECTRAL MIXED PIXEL COMPONENTS
Edmundo Simental and Elisa Gonzalez Aug. 1994 13 p
(AD-A283893; TEC-R-235) Avail: CASI HC A03/MF A01

This paper presents a method to determine end members along with their relative concentration in a hyperspectral mixed pixel. The method is modeled as a linear combination of the end members reflectance spectra and a library of spectral prototypes. This method was tested with 431-band, laboratory controlled, data sets. Indications are that this method can be extended to field data observations with a small number of end members and that at least some error source can be identified and data and results adjusted accordingly. DTIC

N95-15538# Oak Ridge National Lab., TN.
NUMERICAL SOLUTION OF A TUNNELING EQUATION
C. Y. Wang, M. D. Carter, D. B. Batchelor, and E. F. Jaeger Apr. 1994 22 p
(Contract DE-AC05-84OR-21400)
(DE94-015514; ORNL/TM-12721) Avail: CASI HC A03/MF A01

A numerical method is presented to solve mode conversion equations resulting from the use of radio frequency (RF) waves to heat plasmas. The solutions of the mode conversion equations contain exponentially growing modes, and ordinary numerical techniques give large errors. To avoid the unphysical growing modes, a set of boundary conditions are found, that eliminate the unphysical modes. The mode conversion equations are then solved with the boundary conditions as a standard two-point boundary value problem. A tunneling equation (one of the mode conversion equations without power absorption) is solved as a specific example of this numerical technique although the technique itself is very general and can be easily applied to solve any mode conversion equation. The results from the numerical calculation agree very well with those found from asymptotic analysis. DOE

N95-15589# Rochester Univ., NY. Dept. of Computer Science.
COMPILER OPTIMIZATIONS FOR CACHE LOCALITY AND COHERENCE
Wei Li Apr. 1994 30 p Sponsored by Cornell Theory Center and Hewlett-Packard Corp.
(TR-504) Avail: CASI HC A03/MF A01

Almost every modern processor is designed with a memory hierarchy organized into several levels, each of which is smaller, faster, and more expensive than the the level below. High performance requires the effective use of the cached data, i.e., cache locality. Smart compiler transformations can relieve the programmer from hand-optimizing for specific machine architectures. In a multiprocessor system, data inconsistency may occur between memory and caches. For example, the memory and multiple caches may have inconsistent copies of the same cache block. This introduces the problem of cache coherence. Several cache coherence protocols have been developed to maintain data coherence for multiple processors. Since multiple variables are located in the same block, it may cause the obstacle to high performance. Therefore, in a multiprocessor system, we need to avoid false sharing as well as exploit cache locality. In this paper, we first develop a new data reuse model and an algorithm called height reduction to improve cache locality. The advantage of this algorithm is that it can improve band matrix programs as well as dense matrix programs. It is more accurate and general than the existing techniques on improving cache locality, which were developed to optimize dense matrix programs. Then with the height reduction algorithm, we extend loop tiling to exploit not only intra-tile data locality but also inter-tile data locality. We call the new tiling affinity tiling. Our experiments show that affinity tiling is less sensitive to the choice of the tile size. Finally, we show that the algorithm also helps to eliminate or reduce false sharing in multiprocessor systems. With the height reduction algorithm and affinity tiling, significant performance improvement (speedups from 2.5 to 10) has been observed on HP workstations and KSR1 multiprocessors. Author

N95-15594# Rochester Univ., NY. Dept. of Computer Science.
PSEUDORANDOM GENERATORS AND THE FREQUENCY OF SIMPLICITY
Yenjo Han and Lane A. Hemaspaandra 3 May 1994 15 p
(Grants NSF CCR-89-57604; NSF INT-91-16781; JSPS ENGR-207)
(UR-DCS-TR-94-507) Avail: CASI HC A03/MF A01

Allender showed that if there are dense P languages containing only a finite set of Kolmogorov-simple strings, then all pseudorandom generators are insecure. We extend this by proving that if there are dense P (or even BPP) languages containing only a sparse set of Kolmogorov-simple strings, then all pseudorandom generators are insecure. Author

N95-15595# Rochester Univ., NY. Dept. of Computer Science.
DISCOURSE INTERPRETATION AND THE SCOPE OF OPERATORS Ph.D. Thesis
Massimo Poesio Jun. 1994 154 p
(Contracts N00014-92-J-1512; F30602-91-C-0010; NSF CDA-88-22724)
(TR-518) Avail: CASI HC A08/MF A02

The problem of ambiguity is central to any theory of language interpretation, whether we are interested in language processing in humans or in developing a usable natural language processing system. Psycholinguistic evidence suggests that human subjects are able to choose an interpretation when necessary, and that competing factors are involved in this choice; however, no theory of language interpretation deals satisfactorily with the combinatorial explosion paradox - the fact that no matter how ambiguous natural language sentences are, they are usually interpreted without significant effort. The main idea presented in this dissertation is that the scope preferences observed in the literature are not the result of an independent 'scope disambiguation' module, but of independent interpretation processes such as definite description interpretation or the interpretation of modals. None of these interpretive procedures is especially concerned with 'scope disambiguation,' but the result of these inferences is that relations of contextual dependency such as anaphoric reference or presuppositionality become part of the common

ground; the scope preferences observed in the literature reflect these relations of dependency. The dissertation includes a formal proposal concerning the representation of contextual dependency, and its impact on the semantics of sentence constituents. My theory of ambiguity is based on a distinction between semantic ambiguity, that can be capture implicitly, by means of under specified representations, and perceived ambiguity, that results from the process of discourse interpretation. My model of the common ground can be used to characterize both situations characterized by the presence of semantic ambiguity, and situations characterized by the existence of perceived ambiguity. The reasoning that leads to the establishment of scoping preferences makes use, ! argue, of information that is pragmatic in nature; this calls for a model of discourse interpretation in which the 'common ground' contains such information. In the case of spoken language conversations, the common ground must be a model of the discourse situation of the conversational participants. Author

N95-15596# Rochester Univ., NY. Dept. of Computer Science.
WEIGHTED NP OPTIMIZATION PROBLEMS: LOGICAL DEFINABILITY AND APPROXIMATION PROPERTIES
Marius Zimand Jun. 1994 32 p
(Grant NSF CCR-89-57604)
(TR-516) Avail: CASI HC A03/MF A01

Extending a well known property of polynomially bounded NP optimization problems, we observe that, by attaching weights to tuples over the domain of the input, all NP optimization problems admit a certain logical characterization. We show that any NP optimization problem can be stated as a problem in which the constraint conditions can be expressed by a Pi(sub 2) first-order formula and this is the best possible result. We further analyze the weighted analog of all syntactically defined classes of optimization problems that are known to have good approximation properties: MAX NP, MAX SNP, MAX SNP(pi), MIN F+Pi(sub 1), and MIN F+Pi(sub 2)(1). All these classes continue to have the same approximation properties in the case of positive weights. Using reductions from multiprover interactive systems, we show that if NP is not contained in DTIME(2(exp log(exp O(1)) n)), the approximation properties of the above classes devaluates considerably when negative weights are also allowed (with the exception of MIN F+Pi(sub 1), where only a weaker deterioration could be proven). It follows that the general weighted versions of MAX 2SAT, SET COVER, PRIORITY ORDERING, and of some other closely related natural problems are not approximable in quasipolynomial time within a factor of 2(exp log(exp mu) n) (which depends on the problem), unless NP is contained in DTIME(2(exp log(exp O(1)) n)). Under the same hypothesis, we show that the maximization variant of SET PARTITION is also not superpolylog approximable. A stronger result is proven for the minimization variant of SET PARTITION: if P does not equal NP, then MIN SET PARTITION cannot be approximated in polynomial time within a factor of n(exp O(1)).
Author (revised)

N95-15612 Naval Postgraduate School, Monterey, CA. Dept. of Mathematics.
CONDITIONAL GRAPH COMPLETIONS Technical Report, Oct. - Dec. 1993
Craig W. Rasmussen 1 May 1994 14 p Limited Reproducibility: More than 20% of this document may be affected by microfiche quality
(AD-A282914; NPS-MA-94-005) Avail: CASI HC A03

If G = (V, E) is a simple graph of order p and size q, and if P is a property held by G, we say that G is P-completeable if there is an ordering e(sub 1), e(sub 2),...,e(sub (p,2)-q) of the edges of K(sub p)-G such that G(sub k) = V, E + U(sub i=1), (sup k), e(sub i) has property P for each k = 1,2,...,(p,2)-q. The sequence (G(sub k)) is called a P-completion sequence. If all graphs with property P are P-completeable, we say that P is a completeable property and that the the class II of graphs with property P is a completion class. Of interest are conditional completion classes, i.e., classes for which not all orderings lead to completion sequences. We show that several familiar classes of graphs are conditional completion classes. DTIC

N95-15641# Rochester Univ., NY. Dept. of Computer Science.
ON ACCESSING AND HIDING INFORMATION Ph.D. Thesis
Yenjo Han May 1994 91 p
(Grants NSF CCR-89-57604; NSF INT-91-16781)
Avail: CASI HC A05/MF A01

In computational complexity theory, an oracle is an abstract form of database that a computation with limited resources can consult to get useful information at unit cost per access. Throughout this thesis, we are interested in studying the power of various methods of access to certain types of oracles. In particular, we study three main issues: secure computation in the presence of a powerful eavesdropper, access to oracles of low information content, and filtered access to NP oracles. Author

N95-15643# Rochester Univ., NY. Dept. of Computer Science.
ON POINT-BASED TEMPORAL DISJOINTNESS
Alfonso Gerevini (Trento Univ., Povo, Italy.) and Lenhart Schubert Mar. 1994 19 p Sponsored by CNR and MAIA
(Contract F30602-91-C-0010)
(TR-497) Avail: CASI HC A03/MF A01

We address the problems of determining consistency and of finding a solution for sets of 3-point relations expressing exclusion of a point from an interval, and for sets of 4-point relations expressing interval disjointedness. Availability of these relations is an important requirement for dealing with the sorts of temporal constraints encountered in many AI applications such as plan reasoning. We prove that consistency testing is NP-complete and finding a solution is NP-hard. Author

N95-15732# Rochester Univ., NY. Dept. of Computer Science.
UNIVERSALLY SERIALIZABLE COMPUTATION
Lane A. Hemaspaandra and Mitsunori Ogihara 23 Jun. 1994 20 p
(Grants NSF CCR-89-57604; NSF INT-91-16781; JSPS ENGR-207)
(TR-520) Avail: CASI HC A03/MF A01

Cai and Furst proved that every PSPACE language can be solved via a large number of identical, simple tasks, each of which is provided with the original input, its own unique task number, and at most three bits of output from the previous task. In the Cai-Furst model, the tasks are required to be run in the order specified by the task numbers. To study the extent to which the Cai-Furst PSPACE result is due to this strict scheduling, we remove their ordering restriction, allowing tasks to execute in any serial order. We provide upper bounds on the complexity of the sets thus accepted. Our bounds suggest that Cai and Furst's surprising PSPACE result is due in large part to the fixed order of their task execution. Author

N95-15733# Rochester Univ., NY. Dept. of Computer Science.
THE LAMBDA LOOP TRANSFORMATION TOOLKIT (USER'S REFERENCE MANUAL)
Wei Li and Keshav Pingali May 1994 31 p Sponsored by Cornell Univ. and Hewlett-Packard Co.
(TR-511) Avail: CASI HC A03/MF A01

Loop transformations are becoming critical to exploiting parallelism and data locality in parallelizing and optimizing compilers. This document describes the Lambda loop transformation toolkit, an implementation of the nonsingular matrix transformation theory, which can represent any linear one-to-one transformation. Lambda has a simple interface, and is independent of any compiler intermediate representation. It has been used in parallelizing compilers for multiprocessor machines as well as optimizing compilers for uniprocessor machines. Author

N95-15775# Rochester Univ., NY. Dept. of Computer Science.
GAZE SELECTION FOR VISUAL SEARCH Ph.D. Thesis
Lambert Ernest Wixson May 1994 170 p Sponsored in part by Human Science Frontiers Program
(Grant NSF IRI-89-03582)
(TR-512) Avail: CASI HC A08/MF A02

This dissertation studies the problem of searching for a target object with a visual sensor. In particular, it studies the task of selecting a sequence of viewpoints, viewing directions, and fields of view that efficiently examines the area being searched. This is made difficult by two problems, namely the need for high image resolution and the presence of obstacles that occlude portions of the search area from certain viewpoints. Searches for objects that require high image resolution to be recognizable can potentially require the examination of a large number of images; high resolution requires a narrow field of view, and hence more images are necessary to span a given visual angle. This dissertation considers a method for increasing search efficiency by searching only those subregions that are especially likely to contain the object. Searches that use this method, called indirect searches, repeatedly find a cheaply-locatable 'intermediate' object that

commonly participates in a spatial relationship with the target object, and then look for the target in the restricted region specified by this relationship. A decision-theoretic model of search efficiency is developed. The second problem facing a searcher is that portions of the area being searched are often hidden from view. Multiple viewpoints are therefore often necessary. This dissertation examines the selection of such viewpoints. Traditional viewpoint selection methods involve detailed maps of the scene portions viewed so far. Simpler model-free methods are presented that, though less selective about their viewpoints, find objects without significantly more effort than map-based methods. They suggest that the main requirement for selecting efficient viewpoint sequences is that the searcher possesses a mechanism for ensuring that it systematically traverses the viewpoint space. Such mechanisms can be much simpler than maps. One drawback of model-free methods is that when the object is not present, they can waste more effort before aborting. Suggestions for remedying this are presented. Author (revised)

N95-15854# Rochester Univ., NY. Dept. of Computer Science.
A GENERAL METHOD TO CONSTRUCT ORACLES REALIZING GIVEN RELATIONSHIPS BETWEEN COMPLEXITY CLASSES
Andrei A. Muchnik (Institute of New Technologies, Moscow, USSR.) and Nikolai K. Vereshchagin (Institute of New Technologies, Moscow, USSR.) Apr. 1994 50 p Sponsored by American Mathematical Society; Soviet Union Aid Fund; International Science Foundation; and NAS-NRC
(Grant NSF CCR-89-57604)
(TR-500) Avail: CASI HC A03/MF A01

We present a method to prove oracle results of the following type. Let K(sub 1),..., K(sub 2n) and L(sub 1),..., L(sub 2m) be complexity classes. Our method provides a general framework for constructing an oracle A such that K(sup A, sub 2i-1) does not equal K(sup A, sub 2i) for i = 1,..., n and L(sup A, sub 2j-1) equals L(sup A, sub 2j) for j = 1,..., m. Using that method we prove several results of this kind. The hardest of them is the existence of an oracle A such that P(sup A) does not equal NP(sup A), P(sup A)equals BPP(sup A) and both Co-NP(sup A)-sets and NP(sup A)-sets are P(sup A)-separable. We exhibit also two theorems that cannot be proved by that method. Author

N95-15855# Rochester Univ., NY. Dept. of Computer Science.
LOWER BOUNDS FOR PERCEPTRONS SOLVING SOME SEPARATION PROBLEMS AND ORACLE SEPARATION OF AM FROM PP
Nikolai K. Vereshchagin (Moscow Inst. of New Technologies, Russia.) 29 Apr. 1994 18 p Sponsored by NAS-NRC; Army Map Service; and Cultural Initiative Foundation
(Grant NSF CCR-89-57604)
(TR-498) Avail: CASI HC A03/MF A01

We prove that perceptrons separating Boolean matrices in which each row has a one from matrices in which many rows have no one must have large size or large order. This result partially strengthens one-in-a-box theorem by Minsky and Papert stating that perceptrons of small order cannot decide if each row of given Boolean matrix has a one. As a consequence, we prove that AM intersects co-AM not contained in PP under some oracle. This contrasts the fact that MA is contained in PP under any oracle. Author

N95-13911*# Israel Inst. of Tech., Haifa (Israel). Dept. of Physics.
UNCERTAINTY RELATIONS AS HILBERT SPACE GEOMETRY
Samuel L. Braunstein *In* NASA. Goddard Space Flight Center, Third International Workshop on Squeezed States and Uncertainty Relations May 1994 p 117-122 (For primary document see N95-13896 03-74)
Avail: CASI HC A02/MF A06

N95-13915*# Utrecht State Univ. (Netherlands). Dept. of History and Foundations of Mathematics and Science.
TWO NEW KINDS OF UNCERTAINTY RELATIONS
Jos Uffink *In* NASA. Goddard Space Flight Center, Third International Workshop on Squeezed States and Uncertainty Relations May 1994 p 155-160 (For primary document see N95-13896 03-74)
Avail: CASI HC A02/MF A06

N95-13926*# Moscow Physical-Technical Inst. (Russia).
SQEEZING GENERATED BY A NONLINEAR MASTER EQUATION AND BY AMPLIFYING-DISSIPATIVE HAMILTONIANS
V. V. Dodonov, M. A. Marchiolli, Solomon S. Mizrahi; and M. H. Y. Moussa *In* NASA. Goddard Space Flight Center, Third International Workshop on Squeezed States and Uncertainty Relations May 1994 p 227-238 Sponsored by Fundacao de Amparo a Pesquisa do Estado de Sao Paulo and CNPq (For primary document see N95-13896 03-74)
Avail: CASI HC A03/MF A06

N95-13942*# University of Southern California, Los Angeles, CA. Dept. of Physics.
SCHROEDINGER OPERATORS WITH THE q-LADDER SYMMETRY ALGEBRAS
Sergei Skorik and Vyacheslav Spiridonov *In* NASA. Goddard Space Flight Center, Third International Workshop on Squeezed States and Uncertainty Relations May 1994 p 373-379 Sponsored by Natural Sciences and Engineering Research Council and Fonds FCAR (For primary document see N95-13896 03-74)
Avail: CASI HC A02/MF A06

65 STATISTICS AND PROBABILITY

Includes data sampling and smoothing; Monte Carlo method; and stochastic processes.

N95-14370# California Univ., Los Angeles, CA. Dept. of Mathematics.
NONLINEAR AND STOCHASTIC NUMERICAL METHODS AND THEIR APPLICATIONS Final Report
Russel E. Caflisch 31 Jul. 1994 6 p
(Contract DAAL03-91-G-0162)
(AD-A284863) Avail: CASI HC A02/MF A01

Research under the grant was concentrated on development of innovative numerical methods, in particular methods that are nonlinear and random, which are directly useful for computation in science and engineering. Our research also includes applications to problems in fluid mechanics, material science, transport theory and other fields. DTIC

N95-15400 Air Force Inst. of Tech., Wright-Patterson AFB, OH. School of Engineering.
LARGE-SCALE DATA ENVELOPMENT ANALYSIS MODELS AND RELATED APPLICATIONS Ph.D. Thesis
Matthew L. Durchholz 21 May 1994 142 p Limited Reproducibility: More than 20% of this document may be affected by microfiche quality
(AD-A283214; AFIT/CI-94-026D) Avail: CASI HC A07

This dissertation presents several advances in data envelopment analysis (DEA), a method for assessing the efficiency of decision units through the identification of empirical best-practice frontiers. First, a new hierarchical decomposition approach for solving large-scale problems is described with results of computational testing in both serial and parallel environments, that dramatically reduces the solution time for realistic DEA applications. Second, a new set of models for stratifying and ranking decision units provides important newer insights into relationships among the units than what was possible with traditional frontier analysis. Because of the intensive computational requirements of these models, their practicality builds on the effectiveness of hierarchical process. Finally, a new means of assessing the robustness of a decision-unit's efficiency is given which spans all current models and assists managers in their evaluation of process and organizational improvement options. It is expected that these advances will permit practicioners and researchers to be more expansive and ambitious in their use of this important class of models, and will hopefully encourage new and even more exciting applications of DEA. DTIC

N95-15533# EG and G Energy Measurements, Inc., Idaho Falls, ID.
TESTS OF A HOMOGENEOUS POISSON PROCESS AGAINST CLUSTERING AND OTHER ALTERNATIVES
C. L. Atwood May 1994 28 p
(Contract DE-AC07-76ID-01570)
(DE94-015382; EGG-RAAM-11182) Avail: CASI HC A03/MF A01

This report presents three closely related tests of the hypothesis that data points come from a homogeneous Poisson process. If there is too much observed variation among the log-transformed between-point distances, the hypothesis is rejected. The tests are more powerful than

the standard chi-squared test against the alternative hypothesis of event clustering, but not against the alternative hypothesis of a Poisson process with smoothly varying intensity. DOE

N95-15859# Rochester Univ., NY. Dept. of Computer Science.
SEEKING STRONGER SEPARATIONS: PROBABILITY ONE BALANCED- AND BI-IMMUNITY
Lane A. Hemaspaandra and Marius Zimand 20 Dec. 1993 21 p
(Grant NSF CCR-89-57604)
(TR-480) Avail: CASI HC A03/MF A01

We prove that NP and +(in circle)P are P balanced immune relative to a random oracle. Such a result is unobtainable for NT, as we prove that NT is not P balanced immune (and this result itself relativizes). However, we prove that NT is P bi-immune relative to a random oracle. We note also that UP and coUP differ relative to a random oracle. Author

66 SYSTEMS ANALYSIS

Includes mathematical modeling; network analysis; and operations research.

N95-14045*# Edinburgh Univ. (Scotland).
A PHYSICAL CONTROL INTERFACE WITH PROPRIOCEPTIVE FEEDBACK AND MULTIPLE DEGREES OF FREEDOM
G. H. Creasey, D. Gow, Y. Sloan, and B. Meadows *In* NASA. Ames Research Center, Human Machine Interfaces for Teleoperators and Virtual Environments Jun. 1991 p 116-117 Prepared in cooperation with Princess Margaret Rose Orthopaedic Hospital, Edinburgh, Lothian, Scotland (For primary document see N95-14013 03-54)
Avail: CASI HC A01/MF A02

67 THEORETICAL MATHEMATICS

Includes topology and number theory.

N95-13630 Selskapet for Industriell og Teknisk Forskning, Oslo (Norway). Dept. of Instrumentation.
CHAOTIC TIME SERIES. PART 2: SYSTEM IDENTIFICATION AND PREDICTION
B. Lillekjendlie, D. Kugiumtzis, and N. Christophersen 19 Jan. 1994 29 p See also PB94-206968 Prepared in cooperation with Oslo Univ., Norway
(PB94-207115; STF31-A93046-Pt-2) Avail: Issuing Activity (National Technical Information Service (NTIS))

This paper is the second in a series of two, and describes the current state of the art in modeling and prediction of chaotic time series. Sampled data from deterministic non-linear systems may look stochastic when analyzed with linear methods. However, the deterministic structure may be uncovered and on-linear models constructed that allow improved prediction. We give the background for such methods from a geometrical point of view; and briefly describe the following types of methods: global polynomials, local polynomials, multilayer perceptrons and semi-local methods including radial basis functions. Some illustrative examples from known chaotic systems are presented, emphasizing the increase in prediction error with time. We compare some of the algorithms with respect to prediction accuracy and storage requirements and list applications of these methods to real data from widely different areas. NTIS

N95-13979# Institut des Hautes Etudes Scientifiques, Bures-sur-Yvette (France).
DUALITY THEOREM IN THE MULTIVARIABLE IWASAWA THEORY OF LOCAL FIELDS
W. G. McCallum Feb. 1994 30 p Prepared for National Science Foundation, Arlington, VA
(Grants NSF DMS-90-02095; NSF DMS-93-02976)
(PB94-192325; IHES/M/94/11) Avail: CASI HC A03/MF A01

Let K a finite extension of Q(sub p), K(sub infinity)/K an extension with Galois group G isomorphic Z(sub p)(sup r), and X the Galois group of the maximal abelian p-extension of K(sub infinity). The conjugation action of G on X gives rise to a Lambda-module structure, where Lambda is the Iwasawa algebra of bounded Z(sub p)-valued measures on G. In this paper, the authors define a non-degenerate sesqui-linear pairing a Lambda -modules X (times) X yields Lambda, where Lambda is the algebra of Z(sub p) (1)-valued measures on G (noncanonically isomorphic to Lambda as a Lambda-module). The pairing is obtained from the Hilbert pairing in a very simple way. Specifically, the authors show in Theorem 4.7 that the pairing is perfect when r is greater than 2 and K(sub infinity)/K is quasi-regular when K(sub infinity)/K can be embedded in an extension of K whose Galois group is a free pro-p-group. NTIS

N95-13901*# Florence Univ. (Italy). Dipt. di Fisica.
Q-DERIVATIVES, COHERENT STATES AND SQUEEZING
E. Celeghini (Istituto Nazionale di Fisica Nucleare, Naples, Italy.), S. DeMartino (Salerno Univ., Italy.), S. DeSiena (Salerno Univ., Italy.), M. Rasetti (Politecnico di Torino, Torino, Italy.), and G. Vitiello (Salerno Univ., Italy.) *In* NASA. Goddard Space Flight Center, Third International Workshop on Squeezed States and Uncertainty Relations May 1994 p 39-44 (For primary document see N95-13896 03-74)
Avail: CASI HC A02/MF A06

N95-13935*# Academy of Sciences (USSR), Moscow (USSR). Physical Inst.
THE STOKES LINE WIDTH AND UNCERTAINTY RELATIONS
A. I. Nikishov and V. I. Ritus *In* NASA. Goddard Space Flight Center, Third International Workshop on Squeezed States and Uncertainty Relations May 1994 p 307-314 (For primary document see N95-13896 03-74)
Avail: CASI HC A02/MF A06

70 PHYSICS (GENERAL)

For precision time and time interval (PTTI) see *35 Instrumentation and Photography;* for geophysics, astrophysics or solar physics see *46 Geophysics, 90 Astrophysics,* or *92 Solar Physics.*

N95-13656# Scientific Research Associates, Inc., Glastonbury, CT.
CAPACITANCE CALCULATIONS IN NANOSTRUCTURE DEVICES VIA THE QUANTUM LIOUVILLE EQUATION IN THE COORDINATE REPRESENTATION Final Report, 1 May 1991 - 31 Jan. 1994
Harold L. Grubin and T. R. Govindan 31 May 1994 50 p
(Contract DAAL03-91-C-0035)
(AD-A281936; ARO-28646.4-EL) Avail: CASI HC A03/MF A01

Through the use of numerical methods the quantum Liouville equation in the coordinate representation has been implemented for the study of semiconductor devices with nanoscale feature sizes. This document summarizes work performed under US Army Contract DAAL03-91-C-0035 to evaluate the significance of calculating the capacitance voltage characteristics of quantum structures via the quantum Liouville equation. All studies were to be performed with a user-friendly workstation based algorithm, copies of which have been placed at the U.S. Army Research Laboratory at Fort Monmouth. DTIC

N95-13972# American Association of Physics Teachers, College Park, MD.
THE 24TH INTERNATIONAL PHYSICS OLYMPIAD
18 Jul. 1993 209 p Olympiad held in Williamsburg, VA, 10-18 Jul. 1993
(AD-A280584) Avail: CASI HC A10/MF A03

Contents include the following: listings of committees, grading teams, participating and observing delegations, and sponsors; the Michelson Interferometer; the opening ceremony; social, cultural and scientific events; the closing ceremony; and award winners. The examination and its syllabus are included with histograms of the scores. The International Board is listed along with observers, student participants, and guides. Preliminary mailings are included. CASI

N95-13987# Helsinki Univ. of Technology, Espoo (Finland). Electromagnetics Lab.
POLARIZABILITY PROPERTIES OF BIANISOTROPIC SPHERES WITH NONCOMPLETE MAGNETOELECTRIC DYADICS Report No. 164

A. H. Sihvola Feb. 1994 11 p
(ISSN 0784-848X)
(PB94-189065; ISBN-951-22-2004-0) Avail: CASI HC A03/MF A01

The polarizability expressions for bianisotropic scatterers are often complicated expressions of the material parameters. The communication treats the question how the dyadic inversion operations needed in the expressions can be carried out in a well-behaving way. Also, the particular polarizabilities of biaxial chiral spheres are studied in detail. NTIS

N95-13986# Helsinki Univ. of Technology, Espoo (Finland). Electromagnetics Lab.
STATIC IMAGE THEORY FOR A SPHERE WITH IMPEDANCE SURFACE
I. V. Lindell Mar. 1994 10 p See also PB93-224970
(ISSN 0784-848X)
(PB94-189073; ISBN-951-22-2033-4) Avail: CASI HC A02/MF A01

The static image theory of Kelvin for a conducting sphere and that of Neumann for a material sphere, recently rediscovered, are complemented by a corresponding theory for a sphere with impedance boundary conditions. The image of a point source is seen to consist of a point source and line source consisting of two components obeying simple algebraic laws. The theory is tested by showing that the image for the planar impedance surface, known from previous work, is obtained as a special case. NTIS

N95-14137*# National Aeronautics and Space Administration. Marshall Space Flight Center, Huntsville, AL.
MULTILAYER THIN FILM HALL EFFECT DEVICE Patent Application
Palmer N. Peters, inventor (to NASA) and R. Charles Sisk, inventor (to NASA) 30 Sep. 1994 26 p
(NASA-Case-MFS-28764-1; NAS 1.71:MFS-28764-1;
US-Patent-Appl-SN-317071) Avail: CASI HC A03/MF A01

A Hall effect device and a method of obtaining a magnetic field map of a magnetic body with the Hall effect device are presented. The device comprises: (1) a substrate, (2) a first layer having a first Hall coefficient deposited over the substrate, and (3) a second layer having a second Hall coefficient deposited over the first layer, the first and second layers cooperating to create, in the Hall effect device, a third Hall coefficient different from the first and second Hall coefficients. Creation of the third Hall coefficient by cooperation of the first and second layers allows use of materials for the first and second layers that were previously unavailable for Hall effect devices due to their relatively weak Hall coefficient. NASA

N95-14440# Brookhaven National Lab., Upton, NY. Dept. of Applied Science.
FERROMAGNETIC GRAIN BOUNDARY SIGNATURE IN DIE-UPSET RE-Fe-B MAGNETS
L. Henderson Lewis, Yimei Zhu, and D. O. Welch 1994 14 p Presented at the Acta Metallurgical Meeting on Novel Magnetic Structures and Properties, Santa Fe, NM, 24-25 Jun. 1994
(Contract DE-AC02-76CH-00016)
(DE94-014904; BNL-60437; CONF-9406204-1) Avail: CASI HC A03/MF A01

Previous nanostructural and nanocompositional studies performed on the boundaries of deformed grains in two die-upset rare earth magnets with bulk compositions Nd(13.75)Fe(80.25)B6 and Pr(13.75)Fe(80.25)B6 indicate that the intergranular phase in many grain boundaries is enriched in iron relative to the bulk. Preliminary magnetic data are presented that provide further evidence that this grain boundary phase is indeed iron-rich, and in fact appears to be ferromagnetic. Hysteresis loops were performed at 800 K on die-upset magnets with the above compositions. Each sample showed a clear hysteresis with coercivities between 34 and 40 Oe average remanence 4(pi)M(sub R) of 6.8 G for the Nd-based sample and 10.3 G for the Pr-based sample. The ferromagnetic signals measured at high temperature in these magnets are attributed to the iron-rich grain boundary phase. The implications of this conclusion with respect to coercivity are discussed. DOE

N95-13917*# Baylor Univ., Waco, TX. Dept. of Physics.
THE QUANTUM MEASUREMENT OF TIME
Scott R. Shepard *In* NASA. Goddard Space Flight Center, Third International Workshop on Squeezed States and Uncertainty Relations May 1994 p 167-172 (For primary document see N95-13896 03-74)
Avail: CASI HC A02/MF A06

71 ACOUSTICS

Includes sound generation, transmission and attenuation. For noise pollution see *45 Environmental Pollution.*

N95-13683# Iowa Univ., Iowa City, IA. Dept. of Physics and Astronomy.
THE MEAN ACOUSTIC FIELD IN LAYERED MEDIA WITH ROUGH INTERFACES
David H. Berman 15 Jul. 1994 27 p Sponsored by ONR
(AD-A281960) Avail: CASI HC A03/MF A01

An algorithm is presented for determining the mean acoustic field in a layered medium containing rough interfaces. It is assumed that scattering by the rough interfaces when considered separately and in the absence of sound speed and density variation can be well-approximated. It is also assumed that propagation in layered media with flat interfaces can be well approximated. The present work shows how these results can be combined to yield the mean field in a stack of layers with variable sound speeds and densities which are separated by rough interfaces. DTIC

N95-13985 Metraflu, Ecully (France).
FLOW-RADIATED NOISE. STUDY OF THE PROPAGATIVE SPECTRAL RANGE OF THE WALL PRESSURE FIELD Final Report [BRUIT RAYONNE PAR L'ECOULEMENT. ETUDE DU DOMAINE SPECTRAL PROPAGATIF DU CHAMP DE PRESSION PARIETALE]
E. Benarrous 1994 60 p In FRENCH Sponsored by Direction des Recherches, Etudes et Techniques and Centre de Documentation de l'Armement
(PB94-201290) Avail: Issuing Activity (National Technical Information Service (NTIS))

The complete model of the wall pressure field developed here incorporates many experimentally observed and proven partial similarities, as well as hypotheses to offset experimental gaps in certain frequency ranges and wave numbers. Initial comparisons show good agreement with experimental results across a wide range of frequencies and wave numbers. The main advantages of the model are: non-dependent adjustment constants; the explicit dependence of local, boundary layer scales; the explicit formulation of physical scales that control the similarity of frequencies and levels; incorporation of the whole range of frequencies and wave numbers; complete determination of the spectrum and interspectrum; and calculation of the root mean square. The study's acoustical range model explains the asymptotic behavior of the low-frequency spectrum, by separating incompressible and acoustic factors. This can be used to calculate the share of wall pressure fluctuations migrating in the form of a sound wave, thus providing an essential element in the problem of antenna or SONAR dome set noise and radiated noise. NTIS

N95-14110*# National Aeronautics and Space Administration. Langley Research Center, Hampton, VA.
PIEZOELECTRIC LOUDSPEAKER Patent Application
Curtis Randall Regan, inventor (to NASA), Antony Jalink, Jr., inventor (to NASA), Richard F. Hellbaum, inventor (to NASA), and Wayne W. Rohrbach, inventor (to NASA) 11 Oct. 1994 16 p
(NASA-Case-LAR-15138-1; NAS 1.71:LAR-15138-1;
US-Patent-Appl-SN-326804) Avail: CASI HC A03/MF A01

A piezoelectric loudspeaker suitable for midrange frequencies uses a dome shaped piezoelectric actuator to drive a speaker membrane directly. The dome shaped actuator is made from a reduced and internally biased oxygen wafer, and generates excursion of the apex of the dome in the order of 0.02 - 0.05 inches when a rated drive voltage of 350 V rms is applied between the convex and the concave surfaces of the dome shaped actuator. The load capacity exceeds 10 lbs. The edge of the rim of the dome shaped actuator must be free to rock when the dome height varies to ensure low distortion in the loudspeaker. This is achieved by mounting the rim of the dome shaped actuator on a support surface by prestress only. An exceptionally simple design uses a planar speaker membrane with the center part of one side pressed against the rim of a dome shaped actuator by prestress from a stretched latex surround member. NASA

N95-14396# Scripps Institution of Oceanography, La Jolla, CA. Marine Physical Lab.
WIDEBAND BEAMFORMING FOR A SPARSE NONUNIFORMLY SPACED ARRAY Final Report, 30 Aug. 1992 - 29 Aug. 1993
Jeff Krolik Jan. 1994 7 p
(Contract N00014-89-D-0142)
(AD-A280833; MPL-U-9/94) Avail: CASI HC A02/MF A01

This project concerns the continued development and evaluation of a computationally-efficient wideband adaptive beamformer for a large nonuniformly-spaced sensor array which effectively extends its operation to wavelengths which are considerably smaller than the average interelement spacing. DTIC

N95-14610*# Pratt and Whitney Aircraft, East Hartford, CT.
ULTRA-HIGH BYPASS RATIO JET NOISE Final Report
John K. C. Low Cleveland, OH NASA Oct. 1994 64 p
(Contract NAS3-26618; RTOP 538-03-11)
(NASA-CR-195394; E-9172; NAS 1.26:195394) Avail: CASI HC A04/MF A01

The jet noise from a 1/15 scale model of a Pratt and Whitney Advanced Ducted Propulsor (ADP) was measured in the United Technology Research Center anechoic research tunnel (ART) under a range of operating conditions. Conditions were chosen to match engine operating conditions. Data were obtained at static conditions and at wind tunnel Mach numbers of 0.2, 0.27, and 0.35 to simulate inflight effects on jet noise. Due to a temperature dependence of the secondary nozzle area, the model nozzle secondary to primary area ratio varied from 7.12 at 100 percent thrust to 7.39 at 30 percent thrust. The bypass ratio varied from 10.2 to 11.8 respectively. Comparison of the data with predictions using the current Society of Automotive Engineers (SAE) Jet Noise Prediction Method showed that the current prediction method overpredicted the ADP jet noise by 6 decibels. The data suggest that a simple method of subtracting 6 decibels from the SAE Coaxial Jet Noise Prediction for the merged and secondary flow source components would result in good agreement between predicted and measured levels. The simulated jet noise flight effects with wind tunnel Mach numbers up to 0.35 produced jet noise inflight noise reductions up to 12 decibels. The reductions in jet noise levels were across the entire jet noise spectra, suggesting that the inflight effects affected all source noise components. Author

N95-14618*# National Aeronautics and Space Administration. Lewis Research Center, Cleveland, OH.
NOISE RADIATION BY INSTABILITY WAVES IN COAXIAL JETS
Milo D. Dahl and Philip J. Morris 1994 16 p Presented at the 25th Fluid Dynamics Conference, Colorado Springs, CO, 20-23 Jun. 1994; sponsored by AIAA
(RTOP 505-62-52)
(NASA-TM-106738; E-9141; NAS 1.15:106738; AIAA Paper 94-2190)
Avail: CASI HC A03/MF A01

In this paper predictions are made for the noise radiation from supersonic coaxial jets. The noise in the downstream arc of a supersonic jet is dominated by highly directional radiation from the supersonically convecting large scale structures in the jet mixing layer. Since the mean flow is not described easily in terms of simple analytic functions, a numerical prediction is made for its development. The compressible Reynolds-averaged boundary layer equations in cylindrical polar coordinates are solved. A mixing length turbulence model is used. Empirical correlations are developed the effects of velocity and temperature ratio and Mach number. Both normal and inverted velocity profiles are considered. Comparisons with measurements for both single and coaxial jets show good agreement. The large scale structures are modeled as instability waves. The noise radiation generated by the instability waves is determined by a matching between the inner instability wave solution and the outer acoustic solution. Predictions are made for the differences between the noise radiated by coaxial jets with different operating conditions and a single equivalent jet with the same exit area, thrust, and mass-flow. Author

N95-15059*# National Aeronautics and Space Administration. Lewis Research Center, Cleveland, OH.
THE AEROACOUSTICS OF SUPERSONIC COAXIAL JETS
Milo D. Dahl Nov. 1994 182 p
(RTOP 505-52-52)
(NASA-TM-106782; E-9235; NAS 1.15:106782) Avail: CASI HC A09/MF A02

Instability waves have been established as the dominant source of mixing noise radiating into the downstream arc of a supersonic jet when the waves have phase velocities that are supersonic relative to ambient conditions. Recent theories for supersonic jet noise have used the concepts of growing and decaying linear instability waves for predicting radiated noise. This analysis is extended to the prediction of noise radiation from supersonic coaxial jets. Since the analysis requires a known mean flow and the coaxial jet mean flow is not described easily in terms of analytic functions, a numerical prediction is made for its development. The Reynolds averaged, compressible, boundary layer equations are solved using a mixing length turbulence model. Empirical correlations are developed for the effects of velocity and temperature ratios and Mach number. Both normal and inverted velocity profile coaxial jets are considered. Comparisons with measurements for both single and coaxial jets show good agreement. The results from mean flow and stability calculations are used to predict the noise radiation from coaxial jets with different operating conditions. Comparisons are made between different coaxial jets and a single equivalent jet with the same total thrust, mass flow, and exit area. Results indicate that normal velocity profile jets can have noise reductions compared to the single equivalent jet. No noise reductions are found for inverted velocity profile jets operated at the minimum noise condition compared to the single equivalent jet. However, it is inferred that changes in area ratio may provide noise reduction benefits for inverted velocity profile jets. Author

N95-15320# Naval Undersea Warfare Center, Newport, RI.
THE MODAL DECOMPOSITION OF AN IMPEDANCE TUBE Ph.D. Thesis
Andrew J. Hull 8 Jun. 1994 37 p
(AD-A283591; NUWC-NPt-TR-10675) Avail: CASI HC A03/MF A01

Impedance tubes are commonly used for determining the acoustic impedance of a material. This process is accomplished by placing the material into the end of the tube, where it is subjected to acoustic energy. Additional uses for impedance tubes include the testing and calibration of microphones or instruments at a predetermined location inside the tube through insonification. Impedance tubes usually consist of long ducts, with a speaker mounted at one end or in the duct wall and with the material placed at the other end. Holes are drilled in the tube at various locations to allow pressure measurements with microphones. In the past, a steady-state continuous model was used to predict the response of an impedance tube for pressure excitation at one end and an unknown acoustic impedance at the other end. The work presented here extends the modeling of impedance tubes by developing an eigenvalue-based model of the tube in modal space that can incorporate the transient or steady state response of velocity sources on the spatial domain and the pressure sources at the end of the tube. Experimental verification is included for several different test configurations. Finally, the inverse problem is solved, which allows the determination of acoustic impedance from the eigenvalues of the measured system response. DTIC

N95-15359# Los Alamos National Lab., NM. Safeguards Systems Group.
ACOUSTIC RESONANCE SPECTROSCOPY INTRINSIC SEALS
C. T. Olinger, T. Burr, and D. R. Vnuk 1994 8 p Presented at the Institute of Nuclear Materials Management Annual Meeting, Naples, FL, 17-20 Jul. 1994
(Contract W-7405-eng-36)
(DE94-016207; LA-UR-94-2445; CONF-940748-40) Avail: CASI HC A02/MF A01

We have begun to quantify the ability of acoustic resonance spectroscopy (ARS) to detect the removal and replacement of the lid of a simulated special nuclear materials drum. Conceptually, the acoustic spectrum of a container establishes a baseline fingerprint, which we refer to as an intrinsic seal, for the container. Simply removing and replacing the lid changes some of the resonant frequencies because it is impossible to exactly duplicate all of the stress patterns between the lid and container. Preliminary qualitative results suggested that the ARS intrinsic seal could discriminate between cases where a lid has or has not been removed. The present work is directed at quantifying the utility of the ARS intrinsic seal technique, including the technique's sensitivity to 'nuisance' effects, such as temperature swings, movement of the container, and placement of the transducers.

These early quantitative tests support the potential of the ARS intrinsic seal application, but also reveal a possible sensitivity to nuisance effects that could limit environments or conditions under which the technique is effective. DOE

N95-15448 Naval Postgraduate School, Monterey, CA.
IMPROVING TRANSIENT SIGNAL SYNTHESIS THROUGH NOISE MODELING AND NOISE REMOVAL M.S. Thesis
Kenneth L. Frack, Jr. Mar. 1994 69 p Limited Reproducibility: More than 20% of this document may be affected by microfiche quality
(AD-A281677) Avail: CASI HC A04

This thesis examines signal modeling techniques and their application to ambient ocean noise for purposes of noise removal and for generating realistic synthetic noise to add to synthetically generated transient signals. Higher order statistics of the noise are examined to test for Gaussianity. Stochastic approaches to AR, MA, and ARMA modeling are compared to see which technique yields the best synthetic noise. Results from the modeling process are used to develop a short-time Wiener filter which can be used to condition a real signal for further processing through effective noise removal. DTIC

N95-15453 Texas Univ., Austin, TX. Dept. of Mechanical Engineering.
PROBLEMS IN NONLINEAR ACOUSTICS: SURFACE ACOUSTIC WAVES, DIFFRACTING SOUND BEAMS, AND FLUID-SOLID INTERFACE EFFECTS Annual Summary Report No. 6, 1 Sep. 1993 - 31 May 1994
Mark F. Hamilton 31 May 1994 28 p Limited Reproducibility: More than 20% of this document may be affected by microfiche quality
(Contracts N00014-89-J-1003; N00014-93-J-1135)
(AD-A281714; ASR-6) Avail: Issuing Activity (Defense Technical Information Center (DTIC))

Three subject areas, with emphasis on nonlinear acoustics, are discussed in this annual summary report: (1) Surface Acoustic Waves (evolution equations, generalized model equations for complex space-time dependencies, and nonlinearity coefficients for Rayleigh waves, and model equation for Stoneley waves); (2) Diffracting Sound Beams (modeling of noise and relaxation, measurements of focused beams, and transient solution for radiation from a parabolic antenna); and (3) Fluid-Solid Interface Effects (comparisons of 2-D and 3-D reflection for piston and Gaussian sources). DTIC

N95-14053*# Ruhr Univ., Bochum (Germany).
BINAURAL ROOM SIMULATION Abstract Only
H. Lehnert, Jens Blauert, and W. Pompetzki *In* NASA. Ames Research Center, Human Machine Interfaces for Teleoperators and Virtual Environments Jun. 1991 p 132-133 (For primary document see N95-14013 03-54)
Avail: CASI HC A01/MF A02

N95-14054*# California Univ., Santa Barbara, CA. Dept. of Psychology.
ACTIVE LOCALIZATION OF VIRTUAL SOUNDS Abstract Only
Jack M. Loomis, C. Hebert, and J. G. Cicinelli *In* NASA. Ames Research Center, Human Machine Interfaces for Teleoperators and Virtual Environments Jun. 1991 p 134 (For primary document see N95-14013 03-54)
Avail: CASI HC A01/MF A02

N95-14882*# Virginia Polytechnic Inst. and State Univ., Blacksburg, VA.
FINE STRUCTURE OF TRANSIENT WAVES IN A RANDOM MEDIUM: THE CORRELATION AND SPECTRAL DENSITY FUNCTIONS
Alan R. Wenzel *In* NASA. Langley Research Center, High-Speed Research: 1994 Sonic Boom Workshop: Atmospheric Propagation and Acceptability Studies Oct. 1994 p 47-59 (For primary document see N95-14878 03-02)
Avail: CASI HC A03/MF A03

N95-14883*# Centre National de la Recherche Scientifique, Ecully (France). Lab. de Mecanique des Fluides et Acoustique.
NUMERICAL MODEL FOR THE WEAKLY NONLINEAR PROPAGATION OF SOUND THROUGH TURBULENCE
Bart Lipkens and Philippe Blanc-Benon *In* NASA. Langley Research Center, High-Speed Research: 1994 Sonic Boom Workshop: Atmospheric Propagation and Acceptability Studies Oct. 1994 p 61-80 (For primary document see N95-14878 03-02)
Avail: CASI HC A03/MF A03

N95-14885*# Boston Univ., MA. Dept. of Aerospace and Mechanical Engineering.
ATMOSPHERIC PROPAGATION AT LARGER LATERAL DISTANCES FROM THE FLIGHT TRACK
Allan D. Pierce *In* NASA. Langley Research Center, High-Speed Research: 1994 Sonic Boom Workshop: Atmospheric Propagation and Acceptability Studies Oct. 1994 p 99-122 Sponsored in part by Air Force Systems Command, Wright-Patterson AFB, OH (For primary document see N95-14878 03-02)
Avail: CASI HC A03/MF A03

N95-14886*# Mississippi Univ., University, MS. Dept. of Physics and Astronomy.
ATMOSPHERIC EFFECTS ON THE RISETIME AND WAVESHAPE OF SONIC BOOMS
Richard Raspet, Henry E. Bass, and Patrice Boulanger *In* NASA. Langley Research Center, High-Speed Research: 1994 Sonic Boom Workshop: Atmospheric Propagation and Acceptability Studies Oct. 1994 p 123-136 (For primary document see N95-14878 03-02)
Avail: CASI HC A03/MF A03

N95-14887*# Pennsylvania State Univ., University Park, PA.
THE EFFECT OF AIRCRAFT SPEED ON THE PENETRATION OF SONIC BOOM NOISE INTO A FLAT OCEAN
Victor W. Sparrow *In* NASA. Langley Research Center, High-Speed Research: 1994 Sonic Boom Workshop: Atmospheric Propagation and Acceptability Studies Oct. 1994 p 137-156 (For primary document see N95-14878 03-02)
Avail: CASI HC A03/MF A03

N95-14888*# National Aeronautics and Space Administration. Hugh L. Dryden Flight Research Center, Edwards, CA.
SIMPLE ATMOSPHERIC PERTURBATION MODELS FOR SONIC-BOOM-SIGNATURE DISTORTION STUDIES
L. J. Ehernberger, Morton G. Wurtele, and Robert D. Sharman *In* NASA. Langley Research Center, High-Speed Research: 1994 Sonic Boom Workshop: Atmospheric Propagation and Acceptability Studies Oct. 1994 p 157-169 (For primary document see N95-14878 03-02)
Avail: CASI HC A03/MF A03

N95-14889*# Wyle Labs., Inc., Arlington, VA.
USAF SINGLE-EVENT SONIC BOOM PREDICTION MODEL: PCBoom3
Kenneth J. Plotkin, Micah Downing, and Juliet A. Page *In* NASA. Langley Research Center, High-Speed Research: 1994 Sonic Boom Workshop: Atmospheric Propagation and Acceptability Studies Oct. 1994 p 171-184 (For primary document see N95-14878 03-02)
Avail: CASI HC A03/MF A03

72 ATOMIC AND MOLECULAR PHYSICS

Includes atomic structure, electron properties, and molecular spectra.

N95-13675# Oak Ridge National Lab., TN.
CHARGE STATE DISTRIBUTIONS FROM HIGHLY CHARGED IONS CHANNELED AT A METAL SURFACE
L. Folkerts, F. W. Meyer, and S. Schippers 1994 6 p Presented at the 15th Werner Brandt Workshop on Penetration Phenomena, Gainesville, FL, 10-11 Mar. 1994
(Contract DE-AC05-84OR-21400)
(DE94-012755; CONF-9403123-2) Avail: CASI HC A02/MF A01

The vast majority of the experimental work in the field of multicharged ion-surface interactions, to date, has focused on x-ray and particularly on electron emission. These experiments include measurements of the total electron yield, the emission statistics of the electrons, and, most of all, the electron energy distributions. So far, little attention has been paid to the fate of the multicharged projectile ions after the scattering. To our knowledge,

the only measurement of the charge state distribution of the scattered ions is the pioneering experiment of de Zwart et al., who measured the total yield of scattered 1+, 2+, and 3+ ions as a function of the primary charge state q (q = 1-11) for 20 keV Ne, Ar, and Kr ions after reflection from a polycrystalline tungsten target. Their main finding is the sudden onset of scattered 3+ ions when inner-shell vacancies are present in the primary particles. This suggests that a certain fraction of the inner-shell vacancies survives the entire collision event, and decays via autoionization on the outgoing path. Since the projectiles scattered in the neutral charge state could not be detected in the experiment of de Zwart et al., they were not able to provide absolute charge state fractions. In our present experiment, we focus on the scattered projectiles, measuring both the final charge state and the total scattering angle with a single 2D position sensitive detector (PSD). This method gives us the number of positive, as well as neutral and negative, scattered ions, thus allowing us to extract absolute charge state fractions. Using a well-prepared single Au(110) crystal and a grazing incidence geometry, we were able to observe surface channeling along the zone axes (001) channels. DOE

N95-13678 Argonne National Lab., IL.
INELASTIC NEUTRON SCATTERING AND MOLECULAR DYNAMICS SIMULATIONS OF WATER ADSORBED IN THE MOLECULAR SIEVES AlPO4-11, AlPO4-5, AlPO4-8 AND VPI-5
F. Trouw, L. E. Iton, and M. E. Davis 1994 9 p Presented at the 10th International Zeolite Conference, Garmish-Partenkirchen, Germany, 17-22 Jul. 1994 Limited Reproducibility: More than 20% of this document may be affected by microfiche quality
(Contract W-31-109-eng-38)
(DE94-013337; ANL/IPNS/CP-80966; CONF-940744-3) Avail: Issuing Activity (Department of Energy (DOE))

The properties of adsorbed water in VPI-5 and AlPO4-5 have been investigated using inelastic neutron scattering (INS), in conjunction with molecular dynamics simulations of AlPO4-5, AlPO4-8, and VPI-5. DOE

N95-13680 Fermi National Accelerator Lab., Batavia, IL.
MEASUREMENT OF THE B CROSS SECTION AT CDF VIA B SEMILEPTONIC DECAYS
May 1994 18 p Presented at the 27th International Conference on High Energy Physics, Glasgow, Scotland, 21-27 Jul. 1994 Limited Reproducibility: More than 20% of this document may be affected by microfiche quality
(Contract DE-AC02-76CH-03000)
(DE94-013842; FNAL/C-94/134-E; CONF-940722-2) Avail: CASI HC A03

Using data collected during the 1992-1993 collider run at Fermilab, CDF has reconstructed several hundred charmed mesons (D(sup 0), D(sup +), D(sup *+) and D(sub s)) in association with leptons from B semileptonic decays. We report on a measurement of the cross section of B and B(sub s) mesons as a function of transverse momentum using this sample. The observation of a charmed meson eliminates many systematic uncertainties in the background subtraction inherent in previous measurements from inclusive lepton samples, and allows the backgrounds to be measured from the data. The B meson PT range probed by the lepton + charm technique is 18 GeV and above, and thus these measurements complement similar measurements at lower PT in the fully exclusive channels B yields J/psi K and B yields J/psi K(sup *). Results are compared to other Tevatron measurements and next-to-leading-order QCD predictions. DOE

N95-14000# Los Alamos National Lab., NM.
FINITE BOSON MAPPINGS OF FERMION SYSTEMS
C. W. Johnson and J. N. Ginocchio 1994 13 p Presented at the International Conference on Perspectives for the Interacting Boson Model on the Occasion of its 20th Anniversary, Padua, Italy, 13-17 Jun. 1994
(Contract W-7405-eng-36)
(DE94-014478; LA-UR-94-2100; CONF-940697-1) Avail: CASI HC A03/MF A01

We discuss a general mapping of fermion pairs to bosons that preserves Hermitian conjugation, with an eye towards producing finite and usable boson Hamiltonians that approximate well the low-energy dynamics of a fermion Hamiltonian. DOE

N95-14001# Los Alamos National Lab., NM.
FROM THE SHELL MODEL TO THE INTERACTING BOSON MODEL
J. N. Ginocchio and C. W. Johnson 1994 13 p Presented at the International Symposium on Frontiers of Nuclear Structure Physics, Tokyo, Japan, 2-5 Mar. 1994
(Contract W-7405-eng-36)
(DE94-014486; LA-UR-94-2228; CONF-9403135-1) Avail: CASI HC A03/MF A01

Starting from a general, microscopic fermion-pair-to-boson mapping of a complete fermion space that preserves Hermitian conjugation, we show that the resulting infinite and non-convergent boson Hamilitonian can be factored into a finite (e.g., a 1 + 2-body fermion Hamiltonian is mapped to a 1 + 2-body boson Hamiltonian) image Hamilitonian times the norm operator, and it is the norm operator that is infinite and non-convergent. We then truncate to a collective boson space and we give conditions under which the exact boson images of finite fermion operators are also finite in the truncated basis. DOE

N95-14011 Argonne National Lab., IL.
DIRECT DETECTION OF NEUTRAL METAL ATOMS IN ELECTRON-STIMULATED DESORPTION: Al FROM CH3O/Al(111). VELOCITY DISTRIBUTION AND ABSOLUTE YIELD
J. E. Whitten, C. E. Young, M. J. Pellin, D. M. Gruen, and P. L. Jones 1994 13 p Limited Reproducibility: More than 20% of this document may be affected by microfiche quality
(Contract W-31-109-eng-38)
(DE94-014011; ANL/CHM/PP-73572) Avail: CASI HC A03

Electron-stimulated desorption of neutral aluminum from the system CH3O/Al(111) has been directly monitored via quasiresonant photoionization with 193 nm excimer laser light and confirmed by two-step resonant ionization, utilizing the Al 3D (sup 2)D manifold. Velocity distribution measurements for the neutral Al peak at approximately 800 m/s for 1 keV incident electron energy. An absolute yield of 3.2 x 10(exp -6) Al atoms/electron was determined by comparison with sputtering measurements in the same apparatus. This is the first observation of electron-stimulated metal desorption from adsorbate-covered metallic surfaces. DOE

N95-14155# California Inst. of Tech., Pasadena, CA.
ASSERT-1992. FUNDAMENTAL STUDIES OF A HIGH ENERGY MOLECULAR SYSTEM: SPECTROSCOPY OF BORON IN HYDROGEN CLUSTERS Annual Report No. 1, 1 Jun. 1993 - 31 May 1994
Mitchio Okumura 24 Jun. 1994 3 p
(Contract F49620-93-1-0326)
(AD-A283181; AFOSR-94-0445TR) Avail: CASI HC A01/MF A01

The graduate student and the undergraduates supported by this AASERT award have designed and fabricated a molecular beam spectroscopy apparatus for the study of metal-hydrogen complexes. This instrument is necessary for accomplishing the tasks set out for both the parent award and the AASERT grant. The students have also aided in the design of both a novel cryogenically-cooled laser vaporization source and a second chamber, currently being fabricated, for resonant multiphoton ionization spectroscopy. They have optimized the collection of UV laser-induced fluorescence spectra using a free jet expansion of benzene, and are now beginning their first studies of metal-hydrogen systems with the prototype HEDM system Al.H2. DTIC

N95-14309# Brookhaven National Lab., Upton, NY.
STUDY OF THE LONG TERM STABILITY OF THE EFFECTIVE CONCENTRATION OF IONIZED SPACE CHARGES (N(SUB eff)) OF NEUTRON IRRADIATED SILICON DETECTORS FABRICATED BY VARIOUS THERMAL OXIDATIONS
Z. Li, W. Chen, H. W. Kraner, V. Eremin, and G. Lindstroem Mar. 1994 6 p Presented at the Nuclear Science Symposium: Medical Imaging Conference, Norfolk, VA, 30 Oct. - 5 Nov. 1994
(Contract DE-AC02-76CH-00016)
(DE94-013734; BNL-60294; CONF-941061-4) Avail: CASI HC A02/MF A01

Experimental study of the reverse annealing of the effective concentration of ionized space charges (N(sub eff), also called effective doping or impurity concentration) of neutron irradiated high resistivity silicon detectors fabricated on wafers with various thermal oxides has been conducted at room temperature (RT) and elevated temperature (ET). Various thermal oxidations

with temperatures ranging from 975 C to 1200 C with and without trichlorethane (TCA), which result in different concentrations of oxygen and carbon impurities, have been used. It has been found that, the RT annealing of the N(sub eff) is hindered initially (t less than 42 days after the radiation) for detectors made on the oxide with high carbon concentration, and there was no carbon effect on the long term (t greater than 42 days after the radiation) N(sub eff) reverse annealing. No apparent effect of oxygen on the N(sub eff) stability has been observed at RT. At elevated temperature (80 C), no significant difference in annealing behavior has been found for detectors fabricated on silicon wafers with various thermal oxides. It is apparent that for the initial stages (first and or second) of N(sub eff) reverse annealing, there may be no dependence on the oxygen and carbon concentrations. DOE

N95-14362# Duke Univ., Durham, NC. Dept. of Physics.
INFRARED/SUBMILLIMETER WAVE STUDIES OF MOLECULAR COLLISION KINETICS Final Report, 1 Mar. 1990 - 31 Jan. 1994
David D. Skatrud 16 May 1994 22 p
(Contract DAAL03-89-D-0002)
(AD-A281379; ARO-27888.3-PH) Avail: CASI HC A03/MF A01

Time-resolved, infrared/millimeter wave double resonance (IRMMWDR) techniques have been used to investigate rotational and vibrational state changing collisions in molecules. Studies of several isotopic species of CH3Cl and CH3F have led to a relatively simple model of the collisional energy transfer processes which accounts for an extremely large and diverse set of data. More specifically, about 350 IRMMWDR time-resolved data sets can be well predicted by a model which uses only five parameters for the rotational energy kinetics. Further, these five parameters are related to well known physical parameters. DTIC

N95-14374# California Univ., Berkeley. Lawrence Berkeley Lab, CA.
SEARCHES FOR MASSIVE NEUTRINO EMISSION IN C-14 BETA AND Fe-55 ELECTRON-CAPTURE DECAYS Ph.D. Thesis
F. E. Wietfeldt May 1994 153 p
(Contract DE-AC03-76SF-00098)
(DE94-016863; LBL-35568) Avail: CASI HC A08/MF A02

In 1985 Simpson reported evidence for the emission of a 17 keV mass neutrino in a small fraction of tritium beta decays. An experimental controversy ensued in which a number of both positive and negative results were reported. The beta spectrum of C-14 was collected in a unique C-14-doped planar germanium detector and a distortion was observed that initially confirmed Simpson's result. Further tests linked this distortion to a splitting of the collected charge between the central detector and the surrounding guard ring in a fraction of the events. A second C-14 measurement showed no evidence for emission of a 17 keV mass neutrino. In a related experiment, a high statistics electron-capture internal-bremsstrahlung photon spectrum of Fe-55 was collected with a coaxial germanium detector. A local search for departures from a smooth shape near the endpoint was performed, using a second-derivative technique. An upper limit of 0.65% (95% C.L.) for the mixing of a neutrino in the mass range 5-25 keV was established. The upper limit on the mixing of a 17 keV mass neutrino was 0.14% (95% C.L.). DOE

N95-14383 Lawrence Livermore National Lab., Livermore, CA.
SECOND INTERNATIONAL CONFERENCE ON COMPUTER SIMULATION OF RADIATION EFFECTS IN SOLIDS
T. D. delaRubia and G. H. Gilmer 1994 136 p Presented at the 2d International Conference on Computer Simulation of Radiation Effects, Santa Barbara, CA, 24-29 Jul. 1994 Limited Reproducibility: More than 20% of this document may be affected by microfiche quality
(Contract W-7405-eng-48)
(DE94-016368; CONF-940731-Absts) Avail: CASI HC A07

A total of 102 abstracts are included, arranged under the following headings: interatomic potentials and theoretical methods, displacement cascades and radiation effects in metals, radiation effects in semiconductors, sputtering and surface processes, cluster-solid interactions, highly charged ions and inelastic effects, and posters (A and B). DOE

N95-14385# Lawrence Livermore National Lab., Livermore, CA.
ENDL TYPE FORMATS FOR THE LLNL EVALUATED ATOMIC DATA LIBRARY, EADL, FOR THE EVALUATED ELECTRON DATA LIBRARY, EEDL, AND FOR THE EVALUATED PHOTON DATA LIBRARY, EPDL
S. T. Perkins and D. E. Cullen Jul. 1994 27 p
(Contract W-7405-eng-48)
(DE94-016487; UCRL-ID-117796) Avail: CASI HC A03/MF A01

Over the past five years, Lawrence Livermore National Laboratory has published extensive compilations derived from three of its main atomic data libraries. These are specifically the evaluated atomic relaxation data library, EADL, the evaluated electron interaction data library, EEDL, and the evaluated photon interaction data library, EPDL. All of these libraries span atomic numbers, Z, from 1 to 100. Additionally the particle interaction libraries cover the incident particle energy range from 10 eV to 100 GeV. The purpose of these libraries is to furnish data for particle transport calculations. Thus the files have been released for external distribution in a machine independent characterized format. In a complete coupled electron-photon transport analysis, results from all three of the data files are required. Therefore it is reasonable to discuss the format for all three libraries in the same work; that is the approach taken here. This report is composed of three sections, each section describing one of the libraries. For ease of reading, each section is separate and unique unto itself, including its own table numbers and references. This report will accompany any request for copies of these evaluated data libraries. This report and these three data libraries are available from the data centers at Brookhaven National Laboratory, RSIC (Oak Ridge National Laboratory), OECD/NEA Data Bank (France), and IAEA (Vienna). DOE

N95-14441# Brookhaven National Lab., Upton, NY.
OBSERVATION OF DIFFRACTION EFFECTS IN POSITRON CHANNELING
J. C. Palathingal (Puerto Rico Univ., Mayaguez.), J. P. Peng, K. G. Lynn, X. Y. Wu, and P. J. Schultz 1994 5 p Presented at the 10th International Conference on Positron Annihilation, Beijing, China, 23-29 May 1994
(Contract DE-AC02-76CH-00016)
(DE94-014909; BNL-60538; CONF-9405170-6) Avail: CASI HC A01/MF A01

An experimental investigation of positron channeling was made with a high-angular resolution apparatus, employing positrons of kinetic energy 1 MeV, derived from the Brookhaven National Laboratory Dynamitron. The pattern of transmission through a Si(100) single crystal of thickness 0.245 mu m was investigated for a number of major planes. The authors have observed for the first time, in excellent detail, the fine structure of the channeling pattern expected to arise from the particle diffraction effects, theoretically explainable in terms of the quantum-mechanical many-beam calculations. DOE

N95-14660# Washington Univ., Seattle, WA. Inst. for Nuclear Theory.
HADRONIZATION OF QCD AND EFFECTIVE INTERACTIONS
M. R. Frank 1994 16 p Presented at the 14th International Conference on Few Body Problems in Physics, Williamsburg, VA, 26-31 May 1994
(Contract DE-FG06-90ER-40561)
(DE94-014975; DOE/ER-40561/147; CONF-9405132-6) Avail: CASI HC A03/MF A01

An introductory treatment of hadronization through functional integral calculus and bifocal Bose fields is given. Emphasis is placed on the utility of this approach for providing a connection between QCD and effective hadronic field theories. The hadronic interactions obtained by this method are nonlocal due to the QCD substructure, yet, in the presence of an electromagnetic field, maintain the electromagnetic gauge invariance manifest at the quark level. A local chiral model which is structurally consistent with chiral perturbation theory is obtained through a derivative expansion of the nonlocalities with determined, finite coefficients. Tree-level calculations of the pion form factor and pi pi(-) scattering, which illustrate the dual constituent-quark-chiral-model nature of this approach, are presented. DOE

N95-14661# Fermi National Accelerator Lab., Batavia, IL.
RECENT QCD RESULTS FROM THE TEVATRON (-p)p COLLIDER AT THE SQUARE ROOT OF s = 1.8 TeV
Jaehoon Yu (Rochester Univ., NY.) Jun. 1994 30 p Presented at the INS Symposium, Tokyo, Japan, 8-10 Mar. 1994
(Contract DE-AC02-76CH-03000)
(DE94-014986; FNAL/C-94-167; CONF-9403122-2) Avail: CASI HC A03/MF A01

Recent results of QCD studies from the CDF and D0 experiments at the Tevatron (-p)p collider at Fermilab are presented. The inclusive jet cross section, the internal structure of jets, di-jet angular distributions, di-jet triple differential cross sections, and properties of multi-jet final states are studied and compared with NLO QCD predictions. The comparisons show good agreement between theoretical predictions and the experimental data in general. Some systematic disagreement between LO predictions and the data are observed in di-jet triple differential cross sections. Results of a rapidity gap study are also presented together with an upper limit on the gap fraction. In addition, the inclusive photon cross section and the di-photon cross sections are presented and compared with NLO QCD predictions. DOE

N95-14950 Massachusetts Univ., Lowell, MA. Center for Atmospheric Research.

THE ATOM-ATOM POTENTIAL IN PRESSURE-BROADENED LINE WIDTH CALCULATIONS FOR XY2-AB: NEW EXPRESSIONS IN THE II(R), II(L), AND I(R) REPRESENTATIONS

R. R. Gamache and S. P. Neshyba Aug. 1993 50 p Limited Reproducibility: More than 20% of this document may be affected by microfiche quality

(Contract F19628-92-K-0018)

(AD-A282011; PL-TR-93-2170; SR-1) Avail: Issuing Activity (Defense Technical Information Center (DTIC))

With the help of symbolic manipulations in FORTRAN and MATHEMATICA, we have computerized the procedure for obtaining atom-atom intermolecular potentials from the two-center expansion. We have calculated the atom-atom potential for an XY2 molecule (C2 sub v symmetry) and a linear, AB molecule with the XY2 molecule positioned in the molecule-fixed axes at three different orientations (representations) labeled I sup R, II sup R, and II sup L. We have found that the previous development of the atom-atom potential in the II sup R representation is incorrect, leading to a mixed formulation with electrostatic terms in the I sup R and atom-atom terms in the III sup L representation. Broadening-coefficient calculations presented there show that when the correct potential is used anomalous oscillations in the Ka''=1 transitions for O3 broadened by N2 disappear. Further investigation has shown that the variations can be associated with particular quantum symmetries. Improved agreement with the experimental measurements is observed. DTIC

N95-15301# Fermi National Accelerator Lab., Batavia, IL.

PRODUCTION PROPERTIES OF Z BOSONS WITH JETS IN 1.8 TeV (ANTI p)p COLLISIONS

May 1994 14 p Presented at the 27th International Conference on High Energy Physics, Glasgow, England, 21-27 Jul. 1994

(Contract DE-AC02-76CH-03000)

(DE94-015184; FNAL/C-94/154-E; CONF-940722-13) Avail: CASI HC A03/MF A01

The authors have measured the production of Z bosons from 1.8 TeV (anti p)p collisions using 19.3 pb(exp -1) of integrated luminosity collected by the CDF during the 1992-93 Tevatron run. The production properties of the hadronic jets associated with the Z bosons are compared to leading-order QCD calculations using the VECBOS Monte Carlo program. For a subsample of events, B jets are identified using CDF's silicon tracker, and the rates compared to those expected from events with generic QCD jets. DOE

N95-15310# Pacific Northwest Lab., Richland, WA.

BETA DECAY DATA FOR NEUTRON-RICH LI-CI NUCLIDES

P. L. Reeder, Y. Kim, W. K. Hensley, H. S. Miley, R. A. Warner, D. J. Vieira, J. M. Wouters, Z. Y. Zhou, and H. L. Seifert May 1994 4 p Presented at the International Conference on Nuclear Data for Science and Technology, Gatlinburg, TN, 9-13 May 1994

(Contract DE-AC06-76RL-01830)

(DE94-014556; PNL-SA-23097; CONF-940507-23) Avail: CASI HC A01/MF A01

We have used the Time-of-Flight Isochronous (TOFI) spectrometer at the LAMPF accelerator to systematically measure the half-life t(sub 1/2), delayed neutron emission probability P(sub n), beta-delayed multi-neutron emission, average energy of delayed neutron spectra, and beta-delayed alpha emission for a large number of neutron-rich isotopes for all Z values between Li and Cl. The TOFI spectrometer measures the A, Z, and Q of each neutron-rich ion and determines the decay properties by means of a delayed coincidence between each ion and subsequent decay products. DOE

N95-15318# Stanford Univ., CA. Center for Integrated Systems.

LOW ENERGY ELECTRON AND ATOM ELASTIC SCATTERING CROSS SECTIONS FROM 0.1 TO 30 keV

R. Browning, T. Z. Li, B. Chui, Jun Ye, and R. F. Pease 1994 17 p

(Contract N00014-92-J-1996)

(AD-A283584) Avail: CASI HC A03/MF A01

Empirical forms for electron/atom scattering cross sections predict backscattering factors that compare well with those calculated using tabulated Mott data from 0.1 to 30keV. The form of the empirical total cross section is similar to the screened Rutherford cross section. The fit to the tabulated differential Mott cross sections is decomposed into two parts, one part being of the same mathematical for as the screened Rutherford cross section and the second part being an isotropic distribution. The ratio of the total cross sections between the screened Rutherford part of the differential scattering cross section and the isotropic part of the distribution, is fitted to give the same ratio of forward to backscattered currents as the tabulated Mott differential cross sections. The three equations, one for the total elastic cross section and two equations describing the differential cross section, one for the Rutherford screening parameter and one for the ratio of total cross section give backscattering results covering all the major trends with energy and atomic number compared to the backscattering coefficients calculated using tabulated Mott cross sections. Author (DTIC)

N95-15350 Selskapet for Industriell og Teknisk Forskning, Trondheim (Norway). Div. of Industrial Mathematics.

COMPUTATIONAL CHEMISTRY PACKAGES ON THE CRAY Y-MP IN TRONDHEIM

X. Li 9 Mar. 1994 29 p

(PB94-208246; STF10-A94002) Avail: Issuing Activity (National Technical Information Service (NTIS))

The report gives a general description of the computational chemistry packages installed on CRAY. The main principles followed by the calculations, the main features of each program, and the performance on CRAY have been discussed. For macromolecular modeling and dynamics simulation programs, the authors have looked at the AMBER 4.0, CHARMm 22, DISCOVER, GROMOS 87, and X-PLOR packages. (DISCOVER and X-PLOR are however not installed on CRAY currently). For quantum chemistry computational programs, the CRYSTAL 92, GAMESS, and GAUSSIAN 92 packages have been discussed in the report. NTIS

N95-15362# Argonne National Lab., IL.

MACROTURBULENCE IN SUPERCONDUCTORS

V. K. Vlasko-Vlasov (Academy of Sciences, USSR, Moscow, USSR.), V. I. Nikitenko (Academy of Sciences, USSR, Moscow, USSR.), A. A. Polyanskii (Academy of Sciences, USSR, Moscow, USSR.), G. W. Crabtree, U. Welp, and B. W. Veal Jul. 1994 3 p Presented at the Meeting on Materials and Mechanisms of Superconductivity: High Temperature Superconductors, Grenoble (France), 4-9 Jul. 1994

(Contract W-31-109-eng-38)

(DE94-016371; ANL/MSD/CP-83617; CONF-940701-17) Avail: CASI HC A01/MF A01

Direct magneto-optic observation of coupling of the Abrikosov vortices into macroscopic drops of increased flux density at remagnetization of the YBCO single crystal is presented. Appearance of these flux structures correspond to strong perturbations of the current trajectories and transition from laminar to turbulent current flow. DOE

N95-15372# Pennsylvania State Univ., University Park, PA. Dept. of Physics.

THEORETICAL STUDIES IN ELEMENTARY PARTICLE PHYSICS

J. Collins 1994 11 p

(Contract DE-FG02-90ER-40577)

(DE94-015343; DOE/ER-40577/4) Avail: CASI HC A03/MF A01

This is a report on research conducted at Penn State University under grant number DE-FG02-90ER-40577, from November 1992 to present. The author is a member of the CTEQ collaboration (Coordinated Theoretical and Experimental Project on Quantitative QCD). Some of the work in

CTEQ is described in this report. Topics which the authors work has touched include: polarized hard scattering; hard diffraction; small x and perturbative pomeron physics; gauge-invariant operators; fundamental QCD; heavy quarks; instantons and deep inelastic scattering; non-perturbative corrections to (tau) decay. DOE

N95-15379 Rutherford Appleton Lab., Chilton (England).
INTRODUCTION TO muSR: WHAT, HOW, WHERE
S. F. J. Cox Mar. 1994 19 p
(PB94-192267; RAL-94-033) Avail: Issuing Activity (National Technical Information Service (NTIS))

(mu)SR spectroscopy uses implanted muons to probe the structure and dynamics of matter at the microscopic level. The acronym stands for muon spin rotation, relaxation and resonance, covering the various ways in which the muon spin polarization can evolve following implantation, in response to the local magnetic environment. The definition could now be extended to include muon level crossing resonance ((mu)LCR), which is a double resonance technique informative on local electronic structure. Applications span a wide range of studies in physics, chemistry and materials science. Common features are the sensitivity of the muons' response to magnetic and hyperfine fields and the manner in which the positive muon behaves, in its chemical and elastic interactions with matter, as a lightweight proton. The experiments must be performed at accelerator laboratories where suitable muon beams are available. The beam is stopped in the material of interest, which may be gas, liquid or solid. Muons are short-lived particles, decaying with a lifetime of about 2 microseconds; they provide the classic illustration of parity violation in radioactive decay, and it is this phenomenon which is the basis for the (mu)SR techniques. This Lecture introduces the field by answering some obvious questions (or by indicating, at least, in which subject areas the answers are to be found). Most of the topics are treated in greater depth in subsequent lectures. NTIS

N95-15380 Rutherford Appleton Lab., Chilton (England).
APPROXIMATE NEXT-TO-LEADING ORDER RELATION BETWEEN THE LOW-x F2 SCALING VIOLATIONS AND THE GLUON DENSITY
K. Prytz May 1994 11 p See also PB93-180792
(PB94-192283; RAL-94-036) Avail: Issuing Activity (National Technical Information Service (NTIS))

Due to the large alpha(sub s, sup 2) corrections to the F(sub 2) scaling violations in the kinematical region of HERA, the previously determined approximate leading order relation between the F(sub 2) scaling violations and the gluon distribution at low-x need to be corrected. A new relation is presented in next-to-leading order and found to give reasonable agreement with the exact calculation. NTIS

N95-15381# Argonne National Lab., IL.
THE STRUCTURE OF NEW SYNTHETIC MANGANESE OXIDE OCTAHEDRAL MOLECULAR SIEVES
S. R. Wasserman, K. A. Carrado, S. E. Yuchs, Y. F. Shen, H. Cao, and S. L. Suib 11 Jul. 1994 8 p Presented at the 8th International Conference on X-Ray Absorption Fine Structure, Berlin, Germany, 28 Aug. - 2 Sep. 1994
(Contract W-31-109-eng-38)
(DE94-016348; ANL/CHM/CP-82279; CONF-9408131-1) Avail: CASI HC A02/MF A01

Manganese K-edge X-ray absorption spectra are used to examine the average oxidation state and local structure of new synthetic manganese oxide photocatalysts, including the materials known as octahedral molecular sieves. The structures of these materials are compared to the natural minerals cryptomelane and todorokite. DOE

N95-15437# Sandia National Labs., Albuquerque, NM.
TIME-OF-FLIGHT DETECTOR FOR HEAVY ION BACKSCATTERING SPECTROMETRY
J. A. Knapp, J. C. Banks, and B. L. Doyle Apr. 1994 12 p
(Contract DE-AC04-94AL-85000)
(DE94-015600; SAND-94-0391) Avail: CASI HC A03/MF A01

This report describes the results of a two-year laboratory directed research and development project to explore advanced concepts in Heavy Ion Backscattering Spectrometry (HIBS), undertaken with the goal of extending the sensitivity of this relatively new technique to levels unattainable by any other existing trace element surface analysis. Improvements in sensitivity are required for the application of HIBS to contamination control in the microelectronics industry. Tools with sensitivity approaching 10(exp 8) atoms/sq cm are expected to be essential for enabling advanced IC production by the year 2000. During the project the authors developed a new analysis chamber with channeling goniometer and a prototype time-of-flight detector with a demonstrated sensitivity of approximately 5 x 10(exp 8) atoms/sq cm for Au on Si and approximately 5 x 10(exp 10) for Fe, and sufficient mass resolution to separate contributions from Fe and Cu. DOE

N95-15446 Lehigh Univ., Bethlehem, PA. Dept. of Physics.
EXCIMER EMISSION FROM ALKALI DIATOMIC AND ALKALINE-EARTH-NOBLE GAS MOLECULES
John Huennekens 1 Mar. 1994 7 p Limited Reproducibility: More than 20% of this document may be affected by microfiche quality
(Contract DAAH04-93-G-0063)
(AD-A281662; ARO-30440.4-PH) Avail: CASI HC A02

We have carried out a series of experiments to study collisional and radiative processes in alkali metal and alkaline-earth vapors. Our principal interest has been to understand fundamental atom-atom, atom-molecule, and atom-light interactions in order to model alkali diatomic and alkaline-earth excimer systems for possible laser applications. During this funding period, we have concentrated on collisional excitation transfer, quenching and diffusion processes involving the metastable 6s5d (sup 3)D(sub J) levels of barium. We have also investigated alkali and alkaline-earth vapors as media for observing low threshold nonlinear optical processes. DTIC

N95-15457 California Inst. of Tech., Pasadena, CA.
ELECTRON-MOLECULE COLLISIONS AND UV SIGNATURES IN FLOWFIELDS Final Report, 1 Aug. 1986 - 1 Oct. 1991
Vincent McKoy Jun. 1994 14 p Limited Reproducibility: More than 20% of this document may be affected by microfiche quality
(Contract DAAL03-86-K-0140)
(AD-A281569; ARO-24487.2-EG-SDI) Avail: Issuing Activity (Defense Technical Information Center (DTIC))

The high-performance, cost-effective computing provided by massively parallel computers can be expected to have a significant impact on our ability to simulate complex physical and engineering systems. Such capabilities will strengthen the competitiveness of U.S. defense and commercial industries. However, robust simulations of systems such as flowfields over hardbodies and plumes must increasingly rely on an adequate data base for the fundamental chemical and physical processes occurring in these systems. Much of this data base is either unavailable or experimentally inaccessible. The use of parallel computers in these studies of electron collisions with molecules for modelling of flowfields is an early example of the significant role that scalable high-performance computing can play in meeting such data-base needs for several defense and dual-use applications. With the projected scaling of these machines to much larger numbers of microprocessors and improvements in hardware and algorithms, performance levels well in excess of that achieved on the early versions of the machines used in these studies can be expected. In summary, these machines will certainly have a revolutionary impact on our ability to model complex systems. DTIC

N95-15537# Boston Univ., MA. Dept. of Physics.
RESEARCH ACCOMPLISHMENTS AND FUTURE GOALS IN PARTICLE PHYSICS
Jun. 1994 151 p
(Contract DE-AC02-89ER-40509)
(DE94-015483; DOE/ER-40509/4) Avail: CASI HC A08/MF A02

This proposal presents the research accomplishments and ongoing activities of Boston University researchers in high energy physics. Some changes have been made in the structure of the program from the previous arrangement of tasks. Task B, Accelerator Design Physics, is being submitted as a separate proposal for an independent grant; this will be consistent with the nature of the research and the source of funding. Boston University is active in seven principal areas: (1) Task A: Colliding Beams - physics of e(sup +)e(sup -) and (anti p)p collisions; (2) Task C: MACRO Experiment - search for magnetic monopoles and study of cosmic rays; (3) Task D: Proton Decay - search for nucleon instability and study of neutrino interactions; (4) Tasks E, J, and N: Particle Theory - theoretical high energy particle physics, including two Outstanding Junior Investigator awards;

(5) Task F: Muon G-2 - measurement of the anomalous magnetic moment of the muon; (6) Task K: SSCintcal - calorimetry for the GEM Experiment; (7) Task L: Muon Detectors for the GEM Experiment. The body of the proposal is devoted to detailed discussions of each of the tasks. The total budget request for the program appears in a summary chapter that includes a general budget discussion and individual budget requests and explanations for each of the tasks. DOE

N95-15545# Stanford Linear Accelerator Center, CA.
THE PARTON DISTRIBUTION FUNCTIONS IN THE LIMIT CHI(SUB Bj) APPROACHES 1
D. Mueller May 1994 5 p Presented at the Workshop on Quantum Field Theoretical Aspects of High Energy Physics, Bad Frankenhausen, Germany, 20-24 Sep. 1993
(Contract DE-AC03-76SF-00515)
(DE94-013799; SU-SLAC-PUB-6496; CONF-9309386-2) Avail: CASI HC A01/MF A01

We review both the counting rule and the influence of the evolution in Q(sub 2) for the large chi(sub Bj) behavior of the valence quark distribution functions. Based on a factorization procedure we present a more general perturbative treatment to compute this behavior. A complete analysis is performed in the scalar phi(sup 3) theory for the parton distribution function of the 'meson,' which shows that logarithmical corrections arise from the distribution amplitude and that the reference momentum square Q(sub 0)(sup 2) is fixed by chi(sub Bj). DOE

N95-15572# Michigan Univ., Ann Arbor, MI.
POSITRON STUDIES IN CATALYSIS RESEARCH
1994 8 p
(Contract DE-FG02-90ER-12103)
(DE94-012793; DOE/ER-12103/3) Avail: CASI HC A02/MF A01

During the past eight months, the authors have made progress in several areas relevant to the eventual use of positron techniques in catalysis research. They have come closer to the completion of their positron microscope, and at the same time have performed several studies in their non-microscopic positron spectrometer which should ultimately be applicable to catalysis. The current status of the efforts in each of these areas is summarized in the following sections: Construction of the positron microscope (optical element construction, data collection software, and electronic sub-assemblies); Doppler broadening spectroscopy of metal silicide; Positron lifetime spectroscopy of glassy polymers; and Positron lifetime measurements of pore-sizes in zeolites. DOE

N95-15629# Fermi National Accelerator Lab., Batavia, IL.
ELECTROWEAK BOSON PAIR PRODUCTION AT CDF
Jun. 1994 21 p Presented at the 27th International Conference on High Energy Physics, Glasgow, England, 21-27 Jul. 1994
(Contract DE-AC02-76CH-03000)
(DE94-015183; FNAL/C-94/158-E; CONF-940722-11) Avail: CASI HC A03/MF A01

Preliminary results from CDF on W + (gamma), Z + (gamma) and W(+)W(-), WZ, ZZ boson pair production in (radical)s = 1.8 TeV (anti p)-p collisions from the 1992-93 collider run are presented. Measurements of the production cross section (times) decay branching ratios (sigma) * B(W + (gamma)) and (sigma) * B(Z + (gamma)) have been obtained. The cross section ratios R(W(gamma)/W), R(Z(gamma)/Z), R(W(gamma)/Z(gamma)) and R(W/Z) are discussed. The authors extract direct limits on CP-conserving and CP-violating WW(gamma), WWZ, ZZ(gamma) and Z(gamma)(gamma) anomalous couplings. In the static limit, the direct experimental limits on WW(gamma) and ZZ(gamma) anomalous couplings are related to bounds on the higher-order static (transition) EM moments of the W (Z) bosons. Expectations from the on-going and future Tevatron collider runs are discussed. DOE

N95-15630# Fermi National Accelerator Lab., Batavia, IL.
SEARCH FOR W(PRIME) (YIELDS) e(nu) IN p(ANTI p) COLLISIONS AT (RADICAL)s = 1,800 GeV
Jun. 1994 13 p Presented at the 27th International Conference on High Energy Physics, Glasgow, England, 21-27 Jul. 1994
(Contract DE-AC02-76CH-03000)
(DE94-015188; FNAL/C-94/155-E; CONF-940722-12) Avail: CASI HC A03/MF A01

The authors have searched for new, heavy charged gauge bosons, W(prime). The signature searched for is W(prime) (yields) e(nu), where it is assumed that the neutrino in this decay is stable and non-interacting, thus leaving a momentum imbalance in the detector. They have examined the highest transverse mass electron + missing momentum events from p(anti p) collisions at (radical)s = 1.8 TeV for new Jacobian peaks above the W mass. The data used in the search represent 19.7 pb(sup -1) collected by CDF at the Fermilab Tevatron Collider. The authors establish limits on the W(prime) cross section times branching ratio; assuming standard couplings of the W(prime) to fermions, they establish the limit M(sub W(prime)) greater than 634 GeV/c(sup 2) (95 percent C.L.). DOE

N95-15826# Argonne National Lab., IL.
TECHNOLOGY AND SCIENCE AT AT HIGH-POWER SPALLATION SOURCE: PROCEEDINGS
Jan. 1994 115 p Workshop held in Argonne, IL, 13-16 May 1993
(Contract W-31-109-eng-38)
(DE94-009685; ANL/IPNS/PROC-81937; CONF-9305339) Avail: CASI HC A06/MF A02

These proceedings cover many aspects of the usefulness of spallation neutrons. Nine different areas are considered: surfaces and interfaces, engineering, materials science, polymers and complex fluids, chemistry, structural biology, nuclear engineering and radiation effects, condensed matter physics, and fundamental physics. DOE

N95-15862# Fermi National Accelerator Lab., Batavia, IL.
STUDIES OF QUARKONIA PRODUCTION WITH CDF
V. Papadimitriou Oct. 1993 11 p Presented at the Workshop on Physics at Current Accelerators and the Supercollider, Argonne, IL, 2-5 Jun. 1993
(Contract DE-AC02-76CH-03000)
(DE94-013220; FNAL/C-93/291-E; CONF-9306176-23) Avail: CASI HC A03/MF A01

In the 1988-89 collider run the authors studied the reactions p(anti p) yields J /psi((psi)(2S)) X yields mu(sup +) mu(sup minus) X by using 2.6(+-)0.2 pb(sup minus 1) of data. This allowed them to shed some light on the quarkonia production mechanisms at the Tevatron energy. The production mechanisms of the J/psi's ((psi)(2S)'s) are B decays, direct charmonium production and the recently suggested gluon fragmentation. They have also reconstructed chi(sub c) mesons through the decay chain chi(sub c) yields J/psi(gamma), J/psi yields mu(sup +) mu(sup minus) using the same data set. In the 1992-93 run they have approximately a factor of 5 more J/psi's per pb(sup minus 1) than in the previous run. They show the J/psi mass spectrum from a 12 pb(sup minus 1) sample which represents ca 60% of the 1992-93 data. From the measurement of the average b lifetime with inclusive J/psi's they have indications that the fraction of J/psi's coming from b's is lower than the one they assumed in the previous run. With the new data set they are also reconstructing a respectable sample of chi(sub c) decays. This sample will be used to measure the fraction f(sub chi) and to cross check the fraction f(sub b) measured with the SVX. Since they can now measure the J/psi differential cross section from b's and from chi(sub c)'s, it will be much easier to disentangle the different J/psi production mechanisms. The authors know that several of the 1988-89 CDF b-quark cross section measurements were statistically limited or were derived under certain assumptions; they expect that the analysis of the data set they collected during the 1992-93 run will shed light onto the problem. From (14.3(+-)1.0) pb(sup minus 1) of the 1992-93 data they also reconstructed 104(+-)21 J/(psi)K(sup (+-)) and 26(+-)8 J/(psi)K(sup 0*) events for P(sub T)(sup B) greater than 6.0 GeV/c and P(sub T)(sup B) greater than 9.0 GeV/c respectively. The corresponding b-quark cross sections are given. DOE

N95-15865# California Univ., Berkeley. Lawrence Berkeley Lab, CA.
TOPICS IN THE STRUCTURE OF HADRONIC SYSTEMS Ph.D. Thesis
R. F. Lebed Apr. 1994 124 p
(Contract DE-AC03-76SF-00098)
(DE94-014924; LBL-35371) Avail: CASI HC A06/MF A02

In this dissertation the author examines a variety of different problems in the physics of strongly-bound systems. Each is elucidated by a different standard method of analysis developed to probe the properties of such systems. It begins with an examination of the properties and consequences of the current algebra of weak currents in the limit of heavy quark spin-flavor

symmetry. In particular, the assumptions in the proof of the Ademollo-Gatto theorem in general and for spin-flavor symmetry are examined, and the constraints imposed upon matrix elements by this theorem are exhibited. Then he utilizes the renormalization-group method to create composite fermions in a three-generation electroweak model. Such a model is found to reproduce the same low energy behavior as the top-condensate electroweak model, although in general it may have strong constraints upon its Higgs sector. Next the subtleties in the nonrelativistic quark model that drastically alter the picture of the physical origins of meson electromagnetic and hyperfine mass splittings are uncovered; in particular, the explicit contributions due to (m(sub d)(minus)m(sub u)) and electrostatic potentials may be overwhelmed by other effects. Such novel effects are used to explain the anomalous pattern of mass splittings recently measured in bottom mesons. Finally, the topic of baryon masses in heavy fermion chiral perturbation theory, including both tree-level and loop effects are considered. DOE

N95-15869# Wisconsin Univ., Madison, WI. Dept. of Physics.
NEUTRINO OSCILLATIONS IN NOISY MEDIA
F. N. Loreti and A. B. Balantekin 27 May 1994 32 p
(Contract DE-FG06-90ER-40561)
(DE94-014973; DOE/ER-40561/143) Avail: CASI HC A03/MF A01

The authors develop the Redfield equation for delta-correlated gaussian noise and apply it to the case of two neutrino flavor or spin precession in the presence of a noisy matter density or magnetic field, respectively. The criteria under which physical fluctuations can be well approximated by the delta-correlated gaussian noise for the above cases are examined. Current limits on the possible neutrino magnetic moment and solar magnetic field suggest that a reasonably noisy solar magnetic field would not appreciably affect the solar electron neutrino flux. However, if the solar electron density has fluctuations of a few percent of the local density and a small enough correlation length, the MSW effect is suppressed for a range of parameters. DOE

N95-13898*# Colby Coll., Waterville, ME. Dept. of Physics.
SUPERSYMMETRY AND RADIAL SQUEEZED STATES FOR RYDBERG WAVE PACKETS
Robert Bluhm and V. Alan Kostelecky *In* NASA. Goddard Space Flight Center, Third International Workshop on Squeezed States and Uncertainty Relations May 1994 p 15-25 (For primary document see N95-13896 03-74)
Avail: CASI HC A03/MF A06

N95-13908*# Open Univ., Milton Keynes (England). Faculty of Mathematics.
SIMULTANEOUS TWO COMPONENT SQUEEZING IN GENERALIZED q-COHERENT STATES
Roger J. McDermott and Allan I. Solomon *In* NASA. Goddard Space Flight Center, Third International Workshop on Squeezed States and Uncertainty Relations May 1994 p 93-98 (For primary document see N95-13896 03-74)
Avail: CASI HC A02/MF A06

N95-13909*# Ulm Univ. (Germany). Abteilung fuer Quantenphysik.
PHOTON STATISTICS OF A TWO-MODE SQUEEZED VACUUM
Guenter Schrade, V. M. Akulin, W. P. Schleich, and Vladimir I. Manko *In* NASA. Goddard Space Flight Center, Third International Workshop on Squeezed States and Uncertainty Relations May 1994 p 99-104 (For primary document see N95-13896 03-74)
Avail: CASI HC A02/MF A06

N95-13918*# Instituto Politecnico Nacional, Mexico City. Dept. de Fisica.
MANIPULATION OF QUANTUM EVOLUTION
David Jose Fernandez Cabera and Bogdan Mielnik *In* NASA. Goddard Space Flight Center, Third International Workshop on Squeezed States and Uncertainty Relations May 1994 p 173-178 Sponsored by CONACyT (For primary document see N95-13896 03-74)
Avail: CASI HC A02/MF A06

N95-13920*# Arkansas Univ., Fayetteville, AR. Dept. of Physics.
SQUEEZED LIGHT FROM MULTI-LEVEL CLOSED-CYCLING ATOMIC SYSTEMS
Min Xiao and Yi-Fu Zhu *In* NASA. Goddard Space Flight Center, Third International Workshop on Squeezed States and Uncertainty Relations May 1994 p 189-194 (For primary document see N95-13896 03-74)
Avail: CASI HC A02/MF A06

N95-13932*# Martin Marietta Corp., Moorestown, NJ. Government Electronic Systems.
PARTICLE LOCALIZATION, SPINOR TWO-VALUEDNESS, AND FERMI QUANTIZATION OF TENSOR SYSTEMS
Frank Reifler and Randall Morris *In* NASA. Goddard Space Flight Center, Third International Workshop on Squeezed States and Uncertainty Relations May 1994 p 281-286 (For primary document see N95-13896 03-74)
Avail: CASI HC A02/MF A06

N95-13934*# Tel-Aviv Univ., Ramat-Aviv, Tel-Aviv (Israel). School of Physics and Astronomy.
HOW TO DETECT AN EXCITED ATOM WITHOUT DISTURBING IT OR HOW TO LOCATE A SUPER-MINE WITHOUT EXPLODING IT
Lev Vaidman *In* NASA. Goddard Space Flight Center, Third International Workshop on Squeezed States and Uncertainty Relations May 1994 p 299-305 Sponsored by Basic Research Foundation and and Israel Academy of Sciences and Humanities (For primary document see N95-13896 03-74)
Avail: CASI HC A02/MF A06

N95-13937*# Villanova Univ., PA. Dept. of Physics.
CORRELATED QUADRATURES OF RESONANCE FLUORESCENCE AND THE GENERALIZED UNCERTAINTY RELATION
Henk F. Arnoldus, Thomas F. George, and Rolf W. F. Gross *In* NASA. Goddard Space Flight Center, Third International Workshop on Squeezed States and Uncertainty Relations May 1994 p 321-329 (For primary document see N95-13896 03-74)
(Grant NSF CHE-91-96214)
Avail: CASI HC A02/MF A06

N95-13940*# Liverpool Univ. (England). Dept. of Electrical Engineering and Electronics.
COHERENT STATES ON THE m-SHEETED COMPLEX PLANE AS m-PHOTON STATES
Apostolos Vourdas *In* NASA. Goddard Space Flight Center, Third International Workshop on Squeezed States and Uncertainty Relations May 1994 p 353-364 (For primary document see N95-13896 03-74)
Avail: CASI HC A03/MF A06

N95-13945*# Goettingen Univ. (Germany). Inst. fuer Theoretische Physik.
CAUSALITY PROBLEMS FOR FERMI'S TWO-ATOM SYSTEM
Gerhard C. Hegerfeldt *In* NASA. Goddard Space Flight Center, Third International Workshop on Squeezed States and Uncertainty Relations May 1994 p 393-399 (For primary document see N95-13896 03-74)
Avail: CASI HC A02/MF A06

N95-13955*# Texas A&M Univ., College Station, TX. Dept. of Physics.
QUANTUM NOISE LIMITS TO MATTER-WAVE INTERFEROMETRY
Marlan O. Scully (Max-Planck-Inst. fuer Quantenoptik, Garching, Germany.) and Jonathan P. Dowling (Army Missile Command, Redstone Arsenal, AL.) *In* NASA. Goddard Space Flight Center, Third International Workshop on Squeezed States and Uncertainty Relations May 1994 p 475-484 Sponsored by ONR and NAC-NRC (For primary document see N95-13896 03-74)
Avail: CASI HC A02/MF A06

N95-13961*# Boston Univ., MA. Dept. of Physics.
COMPLEMENTARITY AND PATH DISTINGUISHABILITY: SOME RECENT RESULTS CONCERNING PHOTON PAIRS
Abner Shimony and Gregg Jaeger *In* NASA. Goddard Space Flight Center, Third International Workshop on Squeezed States and Uncertainty Relations May 1994 p 523-533 (For primary document see N95-13896

03-74)
(Grant NSF PHY-90-22345)
Avail: CASI HC A03/MF A06

N95-13963*# Maryland Univ. Baltimore County, Catonsville, MD. Dept. of Physics.
THE PHOTON: EXPERIMENTAL EMPHASIS ON ITS WAVE-PARTICLE DUALITY
Yan-Hua Shih, A. V. Sergienko, Morton H. Rubin, Thomas E. Kiess, and Carroll O. Alley *In* NASA. Goddard Space Flight Center, Third International Workshop on Squeezed States and Uncertainty Relations May 1994 p 545-562 (For primary document see N95-13896 03-74)
(Contract N00014-91-J-1430)
Avail: CASI HC A03/MF A06

N95-13964*# Maryland Univ. Baltimore County, Catonsville, MD. Dept. of Physics.
THE GENERATION OF ENTANGLED STATES FROM INDEPENDENT PARTICLE SOURCES
Morton H. Rubin and Yan-Hua Shih *In* NASA. Goddard Space Flight Center, Third International Workshop on Squeezed States and Uncertainty Relations May 1994 p 563-568 (For primary document see N95-13896 03-74)
(Contract N00014-91-J-1430)
Avail: CASI HC A02/MF A06

N95-13965*# Universidade Federal do Rio de Janeiro (Brazil). Inst. de Fisica.
NONLOCAL EFFECTS ON THE POLARIZATION STATE OF A PHOTON, INDUCED BY DISTANT ABSORBERS
Luis Carlos B. Ryff *In* NASA. Goddard Space Flight Center, Third International Workshop on Squeezed States and Uncertainty Relations May 1994 p 569-573 (For primary document see N95-13896 03-74)
Avail: CASI HC A01/MF A06

N95-14072*# Phillips Lab., Edwards AFB, CA.
A FACILITY TO PRODUCE AN ENERGETIC, GROUND STATE ATOMIC OXYGEN BEAM FOR THE SIMULATION OF THE LOW-EARTH ORBIT ENVIRONMENT
Andrew D. Ketsdever, David P. Weaver, and E. P. Muntz *In* NASA. Goddard Space Flight Center, Eighteenth Space Simulation Conference: Space Mission Success Through Testing Nov. 1994 p 121-138 Prepared in cooperation with University of Southern California, Los Angeles, CA (For primary document see N95-14062 03-18)
Avail: CASI HC A03/MF A04

N95-14073*# Soreq Research Establishment, Israel Atomic Energy Commission, Yavneh (Israel).
ATOMIC OXYGEN (ATOX) SIMULATION OF TEFLON FEP AND KAPTON H SURFACES USING A HIGH INTENSITY, LOW ENERGY, MASS SELECTED, ION BEAM FACILITY
R. Vered, E. Grossman, G. D. Lempert, and Y. Lifshitz *In* NASA. Goddard Space Flight Center, Eighteenth Space Simulation Conference: Space Mission Success Through Testing Nov. 1994 p 139-156 Sponsored by Israel Space Agency; Ministry of Science; and Ministry of Absorption (For primary document see N95-14062 03-18)
Avail: CASI HC A03/MF A04

N95-14624*# Jet Propulsion Lab., California Inst. of Tech., Pasadena, CA.
SPIN GLASSES AND ERROR-CORRECTING CODES
M. L. Belongie *In its* The Telecommunications and Data Acquisition Report 15 Aug. 1994 p 26-36 (For primary document see N95-14620 03-32)
(RTOP 315-91-40-20-36)
Avail: CASI HC A03/MF A02

N95-15839*# National Inst. of Standards and Technology, Boulder, CO. Joint Inst. for Lab. Astrophysics.
INVESTIGATING THE 3.3 MICRON INFRARED FLUORESCENCE FROM NAPHTHALENE FOLLOWING ULTRAVIOLET EXCITATION
Richard M. Williams (Colorado Univ., Boulder, CO.) and Stephen R. Leone *In* NASA Ames Research Center, The Diffuse Interstellar Bands: Contributed Papers May 1994 p 59-64 (For primary document see N95-15827 03-89)
Avail: CASI HC A02/MF A02

N95-15844*# Ecole Normale Superieure, Paris (France). Astrochimie Quantique.
QUANTUM CHEMISTRY AND EXCITED STATES: FIRST INVESTIGATIONS ON PYRENE-LIKE MOLECULES
Olivier Parisel and Y. Ellinger *In* NASA. Ames Research Center, The Diffuse Interstellar Bands: Contributed Papers May 1994 p 91-97 (For primary document see N95-15827 03-89)
Avail: CASI HC A02/MF A02

73 NUCLEAR AND HIGH-ENERGY PHYSICS

Includes elementary and nuclear particles; and reactor theory. For space radiation see *93 Space Radiation.*

N95-15360# Los Alamos National Lab., NM.
DIRECT-CURRENT PROTON-BEAM MEASUREMENTS AT LOS ALAMOS
J. Sherman, R. R. Stevens, J. D. Schneider, and T. Zaugg 1994 8 p Presented at the International Conference on Accelerated-Driven Transmutation Technologies and Applications, Las Vegas, NV, 25-28 Jul. 1994
(Contract W-7405-eng-36)
(DE94-016280; LA-UR-94-2553; CONF-9407103-15) Avail: CASI HC A02/MF A01

Recently, a CW proton accelerator complex was moved from Chalk River Laboratories (CRL) to Los Alamos National Laboratory. This includes a 50-keV dc proton injector with a single-solenoid low-energy beam transport system (LEBT) and a CW 1.25-MeV, 267-MHz radiofrequency quadrupole (RFQ). The move was completed after CRL had achieved 55-mA CW operation at 1.25 MeV using 250-kW klystrode tubes to power the RFQ. These accelerator components are prototypes for the front end of a CW linac required for an accelerator-driven transmutation linac, and they provide early confirmation of some CW accelerator components. The injector (ion source and LEBT) and emittance measuring unit are installed and operational at Los Alamos. The dc microwave ion source has been operated routinely at 50-keV, 75-mA hydrogen-ion current. This ion source has demonstrated very good discharge and H(sub 2) gas efficiencies, and sufficient reliability to complete CW RFQ measurements at CRL. Proton fraction of 75% has been measured with 550-W discharge power. This high proton fraction removes the need for an analyzing magnet. Proton LEBT emittance measurements completed at Los Alamos suggest that improved transmission through the RFQ may be achieved by increasing the solenoid focusing current. Status of the final CW RFQ operation at CRL and the installation of the RFQ at Los Alamos is given. DOE

N95-15367# California Univ., Berkeley. Lawrence Berkeley Lab, CA.
ACCELERATOR AND FUSION RESEARCH DIVISION: 1993 SUMMARY OF ACTIVITIES
J. Chew Apr. 1994 126 p
(Contract DE-AC03-76SF-00098)
(DE94-015157; LBL-35476) Avail: CASI HC A07/MF A02

The Accelerator and Fusion Research Division (AFRD) is not only one of the largest scientific divisions at LBL, but also one of the most diverse. Major efforts include: (1) investigations in both inertial and magnetic fusion energy; (2) operation of the Advanced Light Source, a state-of-the-art synchrotron radiation facility; (3) exploratory investigations of novel radiation sources and colliders; (4) research and development in superconducting magnets for accelerators and other scientific and industrial applications; and (5) ion beam technology development for nuclear physics and for industrial and biomedical applications. Each of these topics is discussed in detail in this book. DOE

N95-15371# Cornell Univ., Ithaca, NY.
INVESTIGATION OF THE COHERENT SYNCHROTRON RADIATION SPECTRUM AS A PROBE OF CHARGE DYNAMICS
A. J. Sievers and M. Tigner 11 Apr. 1994 23 p

(Contract DE-FG02-92ER-40734)
(DE94-015340; DOE/ER-40734/2) Avail: CASI HC A03/MF A01

The authors search for coherent Bremsstrahlung radiation was unsuccessful but during those measurement attempts, they made the first observation of coherent Cherenkov radiation in a solid. (Previous measurements had all been made in gases.) Because of the large index of refraction in solids, Cherenkov radiation is emitted at a large angle with respect to the electron beam while transition radiation is not. The result is that both components of the coherent spectrum can be examined at the same time. While the authors have already shown that coherent transition radiation provides spectral information on the longitudinal form factor of the bunch, the Cherenkov radiation produces spectral information related to the transverse form factor. Complete testing of the prototype grid interferometer has led to a final design for the large aperture low frequency interferometer. Different high sensitivity detectors have been examined. For the highest sensitivity work the cooled Si bolometer detector provides the best match to the interferometer optics. They also propose to test a wideband room temperature integrated receiver in an attempt to examine single bunches with the interferometric technique. The authors have also found that a time resolved approach to the analysis of single bunches can be carried out if a grating with a sinusoidal groove profile can be produced. With the help of a computerized mill, they propose to rule such a grating with mm spacing in aluminum. The advantage to such a design is that intensity for a given wavelength is only diffracted into the first grating order. Since different wavelengths will now appear at different diffraction angles, a mm wave spectrograph can be fabricated. By using a sensitive detector array it should be possible to measure the entire frequency spectrum produced by the coherent radiation from a single bunch without time averaging. DOE

N95-15539# Northwestern Univ., Evanston, IL.
RESEARCH IN HIGH ENERGY PHYSICS Annual Progress Report, 1 Jul. 1993 - 30 Jun. 1994
Jerome Rosen, Martin Block, David Buchholz, Bruno Gobbi, Heidi Schellman, Donald Miller, Eric Braaten, Robert Oakes, and Heidi Schellman Jul. 1994 88 p
(Contract DE-FG02-91ER-40684)
(DE94-015519; DOE/ER-40684/4) Avail: CASI HC A05/MF A01

Progress on Task A centered around data analysis. E835 is now approved. It will extend E760 studies, exploring new charmonium states and featuring an upgraded detector system plus operation at 4--6 times higher luminosity. Results are given on E760 analysis. Task B has 10 papers that have either appeared in print, or have been prepared for publication. They break down into four categories; experimental physics, theoretical physics, and computer computational techniques. They are described here along with an exciting new experimental proposal to use Da(Phi)ne, the (Phi) factory that is being constructed at Frascati National Laboratory. Progress for Task C which includes participating in the D0 project at TeV 1, and the photoproduction experiment, E687, at TeV 2 is given. While Northwestern is not participating in the top quark physics group at D0, they have been involved in the data analysis and the discussions that led to the limits on the top quark mass. Task D comprises the shared services for the Northwestern DOE contract. This includes the maintenance and operation of all computers within the HEP group. The projects supported by Task D during the past year are given. Task E progress was to resolve the apparent conflict between EMC, SMC, and SLAC results on nucleon structure functions and Bjorken sum rules. Task F covered research in hadronic decay of the tau, thermal field theory, plasma effects in astrophysics, and heavy quarkonium. Task G covers E665, a general purpose muon scattering experiment which can detect both the scattered muon and most charged and neutral hadrons produced in the forward region. The Northwest group has collaborated very closely in the past year with the Harvard group on analyses of structure functions and vector meson production in the 1991 data sample. DOE

N95-15582# Fermi National Accelerator Lab., Batavia, IL.
ELECTROWEAK AND b-PHYSICS AT THE TEVATRON COLLIDER
K. Hara (Tsukuba Univ., Ibaraki, Japan.) Apr. 1994 20 p Presented at the INS Symposium, Tokyo, Japan, 8-10 Mar. 1994
(Contract DE-AC02-76CH-03000)
(DE94-013239; FNAL/C-94/088-E; CONF-9403122-1) Avail: CASI HC A03/MF A01

The CDF and D0 experiments have collected integrated luminosities of 21 pb(exp -1) and 16 pb(exp -1), respectively, in the 1992--1993 run (Run Ia) at the Fermilab Tevatron. Preliminary results on electroweak physics are reported from both experiments: the W mass, the leptonic branching ratios Gamma(W yields l(nu)), the total W width, gauge boson couplings, W decay asymmetry and W'/Z' search. Preliminary new results on b physics are presented: B(sup o) - (bar B)(sup o) mixing from D0, and masses and lifetimes of B-mesons from CDF. DOE

N95-15606*# National Aeronautics and Space Administration. Langley Research Center, Hampton, VA.
MULTIPLE-SCATTERING MODEL FOR INCLUSIVE PROTON PRODUCTION IN HEAVY ION COLLISIONS
Francis A. Cucinotta Nov. 1994 20 p
(RTOP 199-45-16-11)
(NASA-TP-3470; L-17387; NAS 1.60:3470) Avail: CASI HC A03/MF A01

A formalism is developed for evaluating the momentum distribution for proton production in nuclear abrasion during heavy ion collisions using the Glauber multiple-scattering series. Several models for the one-body density matrix of nuclei are considered for performing numerical calculations. Calculations for the momentum distribution of protons in abrasion are compared with experimental data for inclusive proton production. Author

N95-15633# Brookhaven National Lab., Upton, NY.
A RELATIVISTIC CASCADE FOR HEAVY ION COLLISIONS
T. J. Schlagel, Y. Pang, and S. H. Kahana Jul. 1994 7 p Presented at the Intersections of Particle and Nuclear Physics, St. Petersburg, FL, 31 May - 6 Jun. 1994
(Contracts DE-AC02-76CH-00016; DE-FG02-93ER-40768)
(DE94-015846; BNL-60633; CONF-940514-5) Avail: CASI HC A02/MF A01

Au on Au collisions at the BNL/AGS (11.6 GeV-A/c) are expected to produce a short-lived state of matter at high baryon density. If the baryons reach sufficiently high density, they may produce a quark-gluon plasma (QGP). The signals from a QGP phase may be difficult to distinguish from those of ordinary hadronic matter. The authors have constructed a relativistic cascade (ARC) for hadrons in an attempt to model the dynamics of ordinary hadronic matter in a heavy ion collision, in the hopes that deviations from the cascade results may indicate new physics. In this contribution the authors discuss the formation of high baryon density matter, and its effect on antiproton production. DOE

N95-15780# Lawrence Livermore National Lab., Livermore, CA.
A COMPARISON OF DRIVER CONCEPTS FOR HEAVY-ION FUSION
W. M. Sharp 28 Apr. 1994 14 p Presented at the 11th International Workshop on Laser Interaction and Related Plasma Phenomena, Monterey, CA, 25-29 Oct. 1993
(Contract W-7405-eng-48)
(DE94-016451; UCRL-JC-114969-Rev-1; CONF-931048-9-Rev-1) Avail: CASI HC A03/MF A01

The indirect-drive targets being considered for inertial fusion require the driver to deposit 5 MJ on a target in less than 10 ns. This requirement can in principle be met by heavy-ion beams with particle masses between 120 and 240 amu, an ion kinetic energy in the range of 6-12 GeV, and a total current in excess of 30 kA. Three strategies for generating beams with these parameters are currently being studied. European laboratories are investigating the use of low-current beams from a radio-frequency accelerator. To obtain the needed current density, these beams would be stacked and accumulated in storage rings and then directed simultaneously at the target. American researchers are developing high-current induction accelerators, and the two principal configurations under consideration are the linear driver and the 'recirculator,' in which ion pulses pass repeatedly through the same accelerator elements. The merits of the three approaches are compared, and key physics uncertainties in each are identified. DOE

N95-13912*# Rochester Univ., NY. Dept. of Physics and Astronomy.
TIME-DEPENDENT DISTINGUISHABILITY: CHOOSING TO BE A WAVE OR A PARTICLE
T. P. Grayson, X.-Y. Zou, D. Branning, J. R. Torgerson, and Leonard Mandel *In* NASA. Goddard Space Flight Center, Third International Workshop on Squeezed States and Uncertainty Relations May 1994

p 123-128 Sponsored by NSF and ONR (For primary document see N95-13896 03-74)
Avail: CASI HC A02/MF A06

N95-13944*# Naples Univ. (Italy). Dipt. di Scienze.
THE THERMAL-WAVE MODEL: A SCHROEDINGER-LIKE EQUATION FOR CHARGED PARTICLE BEAM DYNAMICS
Renato Fedele and G. Miele *In* NASA. Goddard Space Flight Center, Third International Workshop on Squeezed States and Uncertainty Relations May 1994 p 387-392 Prepared in cooperation with Istituto Nazionale di Fisica Nucleare, Naples, Italy (For primary document see N95-13896 03-74)
Avail: CASI HC A02/MF A06

74 OPTICS

Includes light phenomena; and optical devices.
For lasers see *36 Lasers and Masers.*

N95-13644# Brookhaven National Lab., Upton, NY.
SPECIFYING THE SURFACE FINISH OF X RAY MIRRORS
E. L. Church (Army Armament Research, Development and Engineering Center, Picatinny Arsenal, NJ.) and P. Z. Takacs 1993 3 p Presented at the Optical Society of America (OSA) Topical Meeting on Soft X Ray Projection Lithography, Monterey, CA, 10-12 May 1993
(Contract DE-AC02-76CH-00016)
(DE94-013537; BNL-60378; CONF-9305159-10) Avail: CASI HC A01/MF A01

Our measurements of x-ray mirrors at Brookhaven indicate that the power spectral densities of their finish errors have inverse power-law or fractal forms, rather than being flat at low frequencies as is usually assumed. This paper reviews these data and discusses how this apparent divergent behavior leads to finite but unconventional effects in imaging. Results are then used to develop more rational and realistic surface-finish specifications. DOE

N95-13660*# Georgia Inst. of Tech., Atlanta, GA.
INVESTIGATION OF THE EFFECTS OF LONG DURATION SPACE EXPOSURE ON ACTIVE OPTICAL SYSTEM COMPONENTS Final Report
M. D. Blue Hampton, VA NASA Oct. 1994 89 p
(Contract NAS1-14654; RTOP 506-43-61-07)
(NASA-CR-4632; NAS 1.26:4632) Avail: CASI HC A05/MF A01

This experiment was exposed to the space environment for 6 years on the Long Duration Exposure Facility (LDEF). It investigated quantitatively the effects of the long-duration space exposure on the relevant performance parameters of a representative set of electron-optic system components, including lasers, radiation detectors, filters, modulators, windows, and other related components. It evaluated the results and implications of the measurements indicating real or suspected degradation mechanisms. This information will be used to establish guidelines for the selection and use of components for space-based, electro-optic systems. Author

N95-13666*# Sverdrup Technology, Inc., Brook Park, OH.
COMPACT SIMULTANEOUS-BEAM OPTICAL STRAIN MEASUREMENT SYSTEM, PHASE 5 Final Report
Christian T. Lant Cleveland, OH NASA Oct. 1994 10 p
(Contract NAS3-24105; RTOP 584-03-11)
(NASA-CR-195396; E-9197; NAS 1.26:195396) Avail: CASI HC A02/MF A01

Recent advances on the laser speckle strain measurement system under development at NASA Lewis Research Center have resulted in a compact, easy-to-use measurement package having many performance improvements over previous systems. NASA has developed this high performance optical strain measurement system for high temperature material testing applications. The system is based on I. Yamaguchi's two-beam speckle-shift strain measurement theory, and uses a new optical design that allows simultaneous recording of laser speckle patterns. This design greatly improves system response over previous implementations of the two-beam speckle-shift technique. The degree of immunity to transient rigid body motions is no longer dependent on the data transfer rate. The system automatically calculates surface strains at a frequency of about 5 Hz using a high speed digital signal processor in a personal computer. This system is fully automated, and can be operated remotely. This report describes the designs and methods used by the system, and shows low temperature strain test results obtained from small diameter tungsten-rhenium and palladium-chrome wires. Author

N95-13670# Lawrence Livermore National Lab., Livermore, CA.
PROJECT OART: WDM, EDFA'S AND MIXED DATA RATES IN A REAL-WORLD TESTBED
L. Thombley, K. Hugenberg, D. Sweider, and R. Arce May 1994 17 p Presented at the National Fiber Optic Engineers Conference, San Diego, CA, 13-16 Jun. 1994
(Contract W-7405-eng-48)
(DE94-012234; UCRL-JC-117400; CONF-9406169-1) Avail: CASI HC A03/MF A01

Pacific Bell, Lawrence Livermore National Laboratory (LLNL), and the University of California at Berkeley have established a joint fiber testbed located in the San Francisco Bay Area. The fiber to be used in the trial is representative of Pacific Bell's current fiber plant. This ongoing project is a year long collaboration involving the wavelength division multiplexing (WDM) of data and video on a link using erbium doped fiber amplifiers (EDFA). Designated Project OART for Optical Amplifier Reliability Trial, this project will provide the Network Technology District of Pacific Bell a valuable testbed for gathering information and experience with future network designs that will use WDM, EDF's, and the simultaneous transmission of high-speed digital and video information. LLNL's interest in this link is driven by a need to evaluate various future means of interconnecting high performance users with high performance storage and computation sites over remote connections. The OART link will consist of a four channel WDM system on a pair of fibers over a link amplified by two pairs of EDFA's. Three wavelengths will be data communication channels transmitted between LLNL in Livermore and UCB in Berkeley at a distance of 98 km. A fourth channel of video will be carried from a Pacific Bell test facility in Concord on 73 km of fiber to a video lab at LLNL. DOE

N95-13672# Lawrence Livermore National Lab., Livermore, CA.
ADAPTIVE OPTICS AT LICK OBSERVATORY: SYSTEM ARCHITECTURE AND OPERATIONS
J. M. Brase, J. An, and K. Avicola et al Mar. 1994 17 p Presented at the Society of Photo-Optical Instrumentation Engineers (SPIE) Conference, Kona Beach, HI, 13-18 Mar. 1994
(Contract W-7405-eng-48)
(DE94-012387; UCRL-JC-115106; CONF-940391-8) Avail: CASI HC A03/MF A01

We describe an adaptive optics system developed for the 1 meter Nickel and 3 meter Shane telescopes at Lick Observatory. Observing wavelengths are in the visible for the 1 meter telescope and in the near IR on the 3 meter. The adaptive optics system design is based on a 69 actuator continuous surface deformable mirror and a Hartmann wavefront sensor equipped with an intensified CCD framing camera. The system has been tested at the Cassegrain focus of the 1 meter telescope where the subaperture size is 12.5 cm. The wavefront control calculations are performed on a four processor single board computer controlled by a Unix-based system. We describe the optical system and give details of the wavefront control system design. We present predictions of the system performance and initial test results. DOE

N95-13674# Oak Ridge National Lab., TN.
RESOLUTION MEASUREMENT FOR SCANNING ELECTRON MICROSCOPES
J. Bentley, E. A. Kenik, and N. D. Evans 1994 2 p Presented at the 13th International Congress on Electron Microscopy, Paris, France
(Contract DE-AC05-84OR-21400)
(DE94-012747; CONF-940766-5) Avail: CASI HC A01/MF A01

The resolution performance of a scanning electron microscope (SEM) is a primary specification of the instrument. For a high-resolution SEM (HRSEM) equipped with a field emission gun (FEG), image resolutions of less than 2 nm are commonly claimed. Generally, both manufacturers and customers identify image resolution as the single most important performance criterion. It is traditionally determined with specimens such as gold islands on bulk carbon supports, where the minimum apparent separation of two

islands is claimed as the resolution. This procedure is highly subjective since the spacings are not known independently. Dodson and Joy have pointed out the paradox implicit in this approach - that 'the resolution of a given instrument can be verified only after a better instrument is available to characterize the structure spacing.' By analogy to the now standard approach for high-resolution transmission electron microscopes (TEM's), Dodson and Joy investigated the use of Fourier transforms (FT) of high-resolution SEM images for measuring resolution. Problems encountered by Dodson and Joy included obtaining a specimen with structural detail over the required range of spatial frequencies, and practical aspects of performing the FT processing. While we hope and expect that such FT techniques will be developed in the future, we have explored a different route to a less subjective resolution test that was also prompted by TEM experience, and which directly addresses the paradox posed by Dodson and Joy. DOE

N95-13823* National Aeronautics and Space Administration. Pasadena Office, CA.

ABERRATION CORRECTION OF UNSTABLE RESONATORS Patent

Robert J. Lang, inventor (to NASA) 11 Oct. 1994 12 p Filed 22 Feb. 1993 Supersedes N93-28428 (31 - 10, p 3148)

(Contract NAS7-918)

(NASA-Case-NPO-18662-1-CU; US-Patent-5,355,388; US-Patent-Appl-SN-020813; US-Patent-Class-372-99; US-Patent-Class-372-95; Int-Patent-Class-H01S-3/08) Avail: US Patent and Trademark Office

Construction of aspheric reflectors for unstable resonator lasers to provide an arbitrary laser mode inside the resonator to correct aberrations of an output beam by the construction of the shape of an end reflector opposite the output reflector of the resonator cavity, such as aberrations resulting from refraction of a beam exiting the solid of the resonator having an index of refraction greater than 1 or to produce an aberration in the output beam that will precisely compensate for the aberration of an optical train into which the resonator beam is coupled.

Official Gazette of the U.S. Patent and Trademark Office

N95-13841*# Alabama Univ., Huntsville, AL. Center for Applied Optics.

INVESTIGATIONS INTO MIRROR FABRICATION METROLOGY ANALYSIS Final Report No. 4, 1 Jun. 1993 - 31 Aug. 1994

John O. Dimmock Aug. 1994 71 p

(Contract NAS8-38609)

(NASA-CR-196522; NAS 1.26:196522; UAH-5-33359/60) Avail: CASI HC A04/MF A01

This final report describes the work performed under this delivery order from June 1993 through August 1994. The scope of work included three distinct tasks in support of the AXAF-I program. The objective of the first task was to perform investigations of the grinding and polishing characteristics of the zerodur material by fabricating several samples. The second task was to continue the development of the integrated optical performance modeling software for AXAF-I. The purpose of third and final task was to develop and update the database of AXAF technical documents for an easy and rapid access. The MSFC optical and metrology shops were relocated from the B-wing of Building 4487 to Room BC 144 of Building 4466 in the beginning of this contract. This included dismantling, packing, and moving the equipment from its old location, and then reassembling it at the new location. A total of 65 zerodur samples, measuring 1 inch x 2 inches x 6 inches were ground and polished to a surface figure of lambda/10 p-v, and a surface finish of 5A rms were fabricated for coating tests. A number of special purpose tools and metal mirrors were also fabricated to support various AXAF-I development activities. In the metrology area, the ZYGO Mark 4 interferometer was relocated and also upgraded with a faster and more powerful processor. Surface metrology work was also performed on the coating samples and other optics using ZYGO interferometer and WYKO profilometer. A number of new features have been added to the GRAZTRACE program to enhance its analysis and modeling capabilities. A number of new commands have been added to the command mode GRAZTRACE program to provide a better control to the user on the program execution and data manipulation. Some commands and parameter entries have been reorganized for a uniform format. The command mode version of the convolution program CONVOLVE has been developed. An on-line help system and a user's manual have also been developed for the benefit of the users. The database of AXAF technical documents continues to progress. The titles, company name, date, and location of over 390 documents have been entered in this database. This database provides both a data search and retrieval function, and a data adding function. These functions allow a user to quickly search the data files for documents or add new information. A detailed user's guide has also been prepared. This user guide includes a document classification guide, a list of abbreviations, and a list of acronyms, which have been used in compiling this database of AXAF-I technical documents. Author

N95-13896*# National Aeronautics and Space Administration. Goddard Space Flight Center, Greenbelt, MD.

THIRD INTERNATIONAL WORKSHOP ON SQUEEZED STATES AND UNCERTAINTY RELATIONS

D. Han, ed., Y. S. Kim, ed., Morton H. Rubin, ed., Yan-Hua Shih, ed., and Woodford W. Zachary, ed. May 1994 612 p Workshop held in Catonsville, MD, 10-13 Aug. 1993; cosponsored by Academy of Sciences Sponsored by American Physical Society; International Science Foundation; Lab. of Physical Sciences; NSF; and ONR

(Contract NAS5-30376)

(NASA-CP-3270; Rept-94B00074; NAS 1.55:3270) Avail: CASI HC A99/MF A06

The purpose of these workshops is to bring together an international selection of scientists to discuss the latest developments in Squeezed States in various branches of physics, and in the understanding of the foundations of quantum mechanics. At the third workshop, special attention was given to the influence that quantum optics is having on our understanding of quantum measurement theory. The fourth meeting in this series will be held in the People's Republic of China. For individual titles, see N95-13897 through N95-13970.

N95-13897*# Joint Inst. for Nuclear Research, Moscow (USSR). Lab. of Theoretical Physics.

PROPERTIES OF TWO-MODE SQUEEZED NUMBER STATES

Alexei V. Chizhov and B. K. Murzakhmetov *In* NASA. Goddard Space Flight Center, Third International Workshop on Squeezed States and Uncertainty Relations May 1994 p 3-13 (For primary document see N95-13896 03-74)

Avail: CASI HC A03/MF A06

Photon statistics and phase properties of two-mode squeezed number states are studied. It is shown that photon number distribution and Pegg-Barnett phase distribution for such states have similar (N + 1)-peak structure for nonzero value of the difference in the number of photons between modes. Exact analytical formulas for phase distributions based on different phase approaches are derived. The Pegg-Barnett phase distribution and the phase quasiprobability distribution associated with the Wigner function are close to each other, while the phase quasiprobability distribution associated with the Q function carries less phase information. Author

N95-13898*# Colby Coll., Waterville, ME. Dept. of Physics.

SUPERSYMMETRY AND RADIAL SQUEEZED STATES FOR RYDBERG WAVE PACKETS **c72**

Robert Bluhm and V. Alan Kostelecky *In* NASA. Goddard Space Flight Center, Third International Workshop on Squeezed States and Uncertainty Relations May 1994 p 15-25 (For primary document see N95-13896 03-74)

Avail: CASI HC A03/MF A06

Atomic supersymmetry provides an analytical effective-potential model useful for describing certain aspects of Rydberg atoms. Experiments have recently demonstrated the existence of Rydberg wave packets localized in the radial coordinated with p-state angular distribution. This paper shows how atomic supersymmetry can be used to treat radial Rydberg wave packets via a particular analytical type of squeezed state, called a radial squeezed state. Author

N95-13899*# Malaya Univ., Kuala-Lumpur. Dept. of Physics.

EFFECT OF DISPERSION FORCES ON SQUEEZING WITH RYDBERG ATOMS **c27**

S. K. Ng, M. R. Muhamad, and M. R. B. Wahiddin *In* NASA. Goddard Space Flight Center, Third International Workshop on Squeezed States and Uncertainty Relations May 1994 p 27-32 Sponsored by Malaysia

IRPA (For primary document see N95-13896 03-74)
Avail: CASI HC A02/MF A06

We report exact results concerning the effect of dipole-dipole interaction (dispersion forces) on dynamic and steady-state characteristics of squeezing in the emitted fluorescent field from two identical coherently driven two-level atoms. The atomic system is subjected to three different damping baths in particular the normal vacuum, a broad band thermal field and a broad band squeezed vacuum. The atomic model is the Dicke model, hence possible experiments are most likely to agree with theory when performed on systems of Rydberg atoms making microwave transitions. The presence of dipole-dipole interaction can enhance squeezing for realizable values of the various parameters involved. Author

N95-13900*# Tianjin Univ. (China). Dept. of Physics.
HIGH-ORDER SQUEEZING OF THE QUANTUM ELECTROMAGNETIC FIELD AND THE GENERALIZED UNCERTAINTY RELATIONS IN TWO-MODE SQUEEZED STATES **c32**
Xi-Zeng Li and Bao-Xia Su *In* NASA. Goddard Space Flight Center, Third International Workshop on Squeezed States and Uncertainty Relations May 1994 p 33-37 Sponsored by National Natural Science Foundation of China (For primary document see N95-13896 03-74)
Avail: CASI HC A01/MF A06

It is found that two-mode output quantum electromagnetic field in two-mode squeezed states exhibits higher-order squeezing to all even orders. And the generalized uncertainty relations are also presented for the first time. The concept of higher-order squeezing of the single-mode quantum electromagnetic field was first introduced and applied to several processes by Hong and Mandel in 1985. Lately Li Xizeng and Shan Ying have calculated the higher-order squeezing in the process of degenerate four-wave mixing and presented the higher-order uncertainty relations of the fields in single-mode squeezed states. In this paper we generalize the above work to the higher-order squeezing in two-mode squeezed states. The generalized uncertainty relations are also presented for the first time. Author

N95-13901*# Florence Univ. (Italy). Dipt. di Fisica.
Q-DERIVATIVES, COHERENT STATES AND SQUEEZING **c67**
E. Celeghini (Istituto Nazionale di Fisica Nucleare, Naples, Italy.), S. DeMartino (Salerno Univ., Italy.), S. DeSiena (Salerno Univ., Italy.), M. Rasetti (Politecnico di Torino, Torino, Italy.), and G. Vitiello (Salerno Univ., Italy.) *In* NASA. Goddard Space Flight Center, Third International Workshop on Squeezed States and Uncertainty Relations May 1994 p 39-44 (For primary document see N95-13896 03-74)
Avail: CASI HC A02/MF A06

We show that the q-deformation of the Weyl-Heisenberg (q-WH) algebra naturally arises in discretized systems, coherent states, squeezed states and systems with periodic potential on the lattice. We incorporate the q-WH algebra into the theory of (entire) analytical functions, with applications to theta and Bloch functions. Author

N95-13902*# Academia Sinica, Beijing (China). Inst. of Physics.
SUM-FREQUENCY GENERATION FROM PHOTON NUMBER SQUEEZED LIGHT
Ling-An Wu, Cong-Shi Du, Mei-Juan Wu, and Shi-Qun Li *In* NASA. Goddard Space Flight Center, Third International Workshop on Squeezed States and Uncertainty Relations May 1994 p 45-49 Sponsored by National Natural Science Foundation of China (For primary document see N95-13896 03-74)
Avail: CASI HC A01/MF A06

We investigate the quantum fluctuations of the fields produced in sum-frequency (SF) generation from light initially in the photon number squeezed state. It is found that, to the fourth power term, the output SF light is sub-Poissonian whereas the quantum fluctuations of the input beams increase. Quantum anticorrelation also exists in SF generation. Author

N95-13903*# Academy of Sciences of the Armenian SSR, Erivan. Inst. for Physical Research.
SPECTRAL, NOISE AND CORRELATION PROPERTIES OF INTENSE SQUEEZED LIGHT GENERATED BY A COUPLING IN TWO LASER FIELDS **c36**
Gagik Yu. Kryuchkyan and Karen V. Kheruntsyan *In* NASA. Goddard Space Flight Center, Third International Workshop on Squeezed States and Uncertainty Relations May 1994 p 51-64 (For primary document see N95-13896 03-74)
Avail: CASI HC A03/MF A06

Two schemes of four-wave mixing oscillators with nondegenerate pumps are proposed for above-threehold generation of squeezed light with nonzero mean-field amplitudes. Noise and correlation properties and optical spectra of squeezed-light beams generated in these schemes are discussed. Author

N95-13904*# Academy of Sciences (USSR), Moscow (USSR). Physical Inst.
MULTIMODE SQUEEZING, BIPHOTONS AND UNCERTAINTY RELATIONS IN POLARIZATION QUANTUM OPTICS
V. P. Karassiov *In* NASA. Goddard Space Flight Center, Third International Workshop on Squeezed States and Uncertainty Relations May 1994 p 65-76 Sponsored in part by American Physical Society (For primary document see N95-13896 03-74)
Avail: CASI HC A03/MF A06

The concept of squeezing and uncertainty relations are discussed for multimode quantum light with the consideration of polarization. Using the polarization gauge SU(2) invariance of free electromagnetic fields, we separate the polarization and biphoton degrees of freedom from other ones, and consider uncertainty relations characterizing polarization and biphoton observables. As a consequence, we obtain a new classification of states of unpolarized (and partially polarized) light within quantum optics. We also discuss briefly some interrelations of our analysis with experiments connected with solving some fundamental problems of physics. Author

N95-13905*# National Aeronautics and Space Administration. Goddard Space Flight Center, Greenbelt, MD.
A NEW APPROACH TO THE PHOTON LOCALIZATION PROBLEM
D. Han, Y. S. Kim, and Marilyn E. Noz *In its* Third International Workshop on Squeezed States and Uncertainty Relations May 1994 p 77-82 (For primary document see N95-13896 03-74)
Avail: CASI HC A02/MF A06

Since wavelets form a representation of the Poincare group, it is possible to construct a localized superposition of light waves with different frequencies in a Lorentz-covariant manner. This localized wavelet satisfies a Lorentz-invariant uncertainty relation, and also the Lorentz-invariant Parseval's relation. A quantitative analysis is given for the difference between photons and localized waves. It is then shown that this localized entity corresponds to a relativistic photon with a sharply defined momentum in the non-localization limit. Waves are not particles. It is confirmed that the wave-particle duality is subject to the uncertainty principle. Author

N95-13906*# Moscow State Univ. (Russia). Astronomical Inst.
PRODUCTION OF SQUEEZED STATES FOR MACROSCOPIC MECHANICAL OSCILLATOR **c77**
V. V. Kulagin *In* NASA. Goddard Space Flight Center, Third International Workshop on Squeezed States and Uncertainty Relations May 1994 p 83-86 (For primary document see N95-13896 03-74)
Avail: CASI HC A01/MF A06

The possibility of squeezed states generation for macroscopic mechanical oscillator is discussed. It is shown that one can obtain mechanical oscillator in squeezed state via coupling it to electromagnetic oscillator (Fabry-Perot resonator) and pumping this Fabry-Perot resonator with a field in squeezed state. The degradation of squeezing due to mechanical and optical losses is also analyzed. Author

N95-13907*# Universidad Nacional Autonoma de Mexico, Mexico City. Inst. de Ciencias Nucleares.
SQUEEZING IN A 2-D GENERALIZED OSCILLATOR **c77**
Octavio Castanos, Ramon Lopez-Pena, and Vladimir I. Manko *In* NASA. Goddard Space Flight Center, Third International Workshop on Squeezed States and Uncertainty Relations May 1994 p 87-92 Sponsored in part by DGAPA (For primary document see N95-13896 03-74)
Avail: CASI HC A02/MF A06

A two-dimensional generalized oscillator with time-dependent parameters is considered to study the two-mode squeezing phenomena. Specific choices of the parameters are used to determine the dispersion matrix and analytic expressions, in terms of standard hermite polynomials, of the wavefunctions and photon distributions. Author

N95-13908*# Open Univ., Milton Keynes (England). Faculty of Mathematics.
SIMULTANEOUS TWO COMPONENT SQUEEZING IN GENERALIZED q-COHERENT STATES **c72**
Roger J. McDermott and Allan I. Solomon *In* NASA. Goddard Space Flight Center, Third International Workshop on Squeezed States and Uncertainty Relations May 1994 p 93-98 (For primary document see N95-13896 03-74)
Avail: CASI HC A02/MF A06

Using a generalization of the q-commutation relations, we develop a formalism in which it is possible to define generalized q-bosonic operators. This formalism includes both types of the usual q-deformed bosons as special cases. The coherent states of these operators show interesting and novel noise reduction properties including simultaneous squeezing in both field components, unlike the conventional case in which squeezing is permitted in only one component. This also contrasts with the usual quantum group deformation which also only permits one component squeezing.
Author

N95-13909*# Ulm Univ. (Germany). Abteilung fuer Quantenphysik.
PHOTON STATISTICS OF A TWO-MODE SQUEEZED VACUUM **c72**
Guenter Schrade, V. M. Akulin, W. P. Schleich, and Vladimir I. Manko *In* NASA. Goddard Space Flight Center, Third International Workshop on Squeezed States and Uncertainty Relations May 1994 p 99-104 (For primary document see N95-13896 03-74)
Avail: CASI HC A02/MF A06

We investigate the general case of the photon distribution of a two-mode squeezed vacuum and show that the distribution of photons among the two modes depends on four parameters: two squeezing parameters, the relative phase between the two oscillators and their spatial orientation. The distribution of the total number of photons depends only on the two squeezing parameters. We derive analytical expressions and present pictures for both distributions.
Author

N95-13910*# Massachusetts Inst. of Tech., Cambridge. Dept. of Electrical Engineering and Computer Science.
ON THE THEORY OF QUANTUM MEASUREMENT **c77**
Hermann A. Haus and Franz X. Kaertner *In* NASA. Goddard Space Flight Center, Third International Workshop on Squeezed States and Uncertainty Relations May 1994 p 107-115 (For primary document see N95-13896 03-74)
(Contract N00014-92-J-1302)
Avail: CASI HC A02/MF A06

Many so called paradoxes of quantum mechanics are clarified when the measurement equipment is treated as a quantized system. Every measurement involves nonlinear processes. Self consistent formulations of nonlinear quantum optics are relatively simple. Hence optical measurements, such as the quantum nondemolition (QND) measurement of photon number, are particularly well suited for such a treatment. It shows that the so called 'collapse of the wave function' is not needed for the interpretation of the measurement process. Coherence of the density matrix of the signal is progressively reduced with increasing accuracy of the photon number determination. If the QND measurement is incorporated into the double slit experiment, the contrast ratio of the fringes is found to decrease with increasing information on the photon number in one of the two paths.
Author

N95-13911*# Israel Inst. of Tech., Haifa (Israel). Dept. of Physics.
UNCERTAINTY RELATIONS AS HILBERT SPACE GEOMETRY **c64**
Samuel L. Braunstein *In* NASA. Goddard Space Flight Center, Third International Workshop on Squeezed States and Uncertainty Relations May 1994 p 117-122 (For primary document see N95-13896 03-74)
Avail: CASI HC A02/MF A06

Precision measurements involve the accurate determination of parameters through repeated measurements of identically prepared experimental setups. For many parameters there is a 'natural' choice for the quantum observable which is expected to give optimal information; and from this observable one can construct an Heinsenberg uncertainty principle (HUP) bound on the precision attainable for the parameter. However, the classical statistics of multiple sampling directly gives us tools to construct bounds for the precision available for the parameters of interest (even when no obvious natural quantum observable exists, such as for phase, or time); it is found that these direct bounds are more restrictive than those of the HUP. The implication is that the natural quantum observables typically do not encode the optimal information (even for observables such as position, and momentum); we show how this can be understood simply in terms of the Hilbert space geometry. Another striking feature of these bounds to parameter uncertainty is that for a large enough number of repetitions of the measurements all V quantum states are 'minimum uncertainty' states - not just Gaussian wave-packets. Thus, these bounds tell us what precision is achievable as well as merely what is allowed.
Author

N95-13912*# Rochester Univ., NY. Dept. of Physics and Astronomy.
TIME-DEPENDENT DISTINGUISHABILITY: CHOOSING TO BE A WAVE OR A PARTICLE **c73**
T. P. Grayson, X.-Y. Zou, D. Branning, J. R. Torgerson, and Leonard Mandel *In* NASA. Goddard Space Flight Center, Third International Workshop on Squeezed States and Uncertainty Relations May 1994 p 123-128 Sponsored by NSF and ONR (For primary document see N95-13896 03-74)
Avail: CASI HC A02/MF A06

Interference experiments with connected parametric down-converters have demonstrated that the possibility, in principle, of identifying the photon path through the interferometer is sufficient to wipe out all interference, irrespective of whether the identification is actually made. The distinguishability of the photon path can be controlled by a time-dependent shutter, which leaves the choice whether the photon behaves as a wave or as a particle in the experimenter's hands. By contrast, in some more recent experiments involving the addition of a low-Q cavity, each idler photon makes the choice whether the associated signal photon behaves like a wave and exhibits interference, or like a particle.
Author

N95-13913*# Pavia Univ. (Italy). Dipt. di Fisica.
HOMODYNING AND HETERODYNING THE QUANTUM PHASE **c77**
Giacomo M. DAriano, C. Macchiavello, and M. G. A. Paris *In* NASA. Goddard Space Flight Center, Third International Workshop on Squeezed States and Uncertainty Relations May 1994 p 129-147 (For primary document see N95-13896 03-74)
Avail: CASI HC A03/MF A06

The double-homodyne and the heterodyne detection schemes for phase shifts between two synchronous modes of the electromagnetic field are analyzed in the framework of quantum estimation theory. The probability operator-valued measures (POM's) of the detectors are evaluated and compared with the ideal one in the limit of strong local reference oscillator. The present operational approach leads to a reasonable definition of phase measurement, whose sensitivity is actually related to the output r.m.s. noise of the photodetector. We emphasize that the simple-homodyne scheme does not correspond to a proper phase-shift measurements as it is just a zero-point detector. The sensitivity of all detection schemes are optimized at fixed energy with respect to the input state of radiation. It is shown that the optimal sensitivity can be actually achieved using suited squeezed states.
Author

N95-13914*# Technische Univ., Eindhoven (Netherlands). Theoretical Physics Group.
JOINT AND ANGLE-COVARIANT SPIN MEASUREMENTS WITH A QUADRUPOLE MAGNETIC FIELD **c77**
Hans Martens and Willem M. deMuynck *In* NASA. Goddard Space Flight Center, Third International Workshop on Squeezed States and Uncertainty Relations May 1994 p 149-154 Sponsored by Foundation for Philosophical Research and Netherlands Organization for Applied Scientific Research (For primary document see N95-13896 03-74)
Avail: CASI HC A02/MF A06

We study a Stern-Gerlach type setup, with a quadrupole magnetic field, for neutral particles of arbitrary spin. The Hamiltonian is of a form proposed for joint measurements of the incompatible observables. The measurement results are discussed, showing the limitation of such Hamiltonians. Some remarks are made on the relevance of covariance as a criterion for measurement schemes.
Author

N95-13915*# Utrecht State Univ. (Netherlands). Dept. of History and Foundations of Mathematics and Science.
TWO NEW KINDS OF UNCERTAINTY RELATIONS **c64**

Jos Uffink *In* NASA. Goddard Space Flight Center, Third International Workshop on Squeezed States and Uncertainty Relations May 1994 p 155-160 (For primary document see N95-13896 03-74)
Avail: CASI HC A02/MF A06

We review a statistical-geometrical and a generalized entropic approach to the uncertainty principle. Both approaches provide a strengthening and generalization of the standard Heisenberg uncertainty relations, but in different directions. Author

N95-13916*# Humboldt Univ., Berlin (German D.R.). Arbeitsgruppe Nichtklassische Strahlung.
MEASUREMENT OF VERY SMALL PHASE FLUCTUATIONS BY MEANS OF THE OPERATIONAL APPROACH **c77**
Arno Bandilla *In* NASA. Goddard Space Flight Center, Third International Workshop on Squeezed States and Uncertainty Relations May 1994 p 161-165 (For primary document see N95-13896 03-74)
Avail: CASI HC A01/MF A06

Recently Noh, Fourgeres and Mandel (NFM) have improved the operational approach to the quantum phase problem substantially and measured the phase dispersion of coherent light down to very small means photon numbers of the order of 10(exp -2). This has prompted many other investigations and clarified some important questions in relation to what is actually measured. Although their treatment is rather general, we confine ourselves here to the case of a strong local oscillator (LO) and reproduce their measurement scheme. Surprisingly enough, this simultaneous measurement of the sine and the cosine of the phase difference is completely equivalent to an old proposal to measure the phase after strong linear amplification realized experimentally by the Welling group. The reason for this rests on the fact, that in both cases the results are determined by the Q function of the signal. This was shown for amplification in and for the measurement after beam splitting by Lai and Haus. Author

N95-13917*# Baylor Univ., Waco, TX. Dept. of Physics.
THE QUANTUM MEASUREMENT OF TIME **c70**
Scott R. Shepard *In* NASA. Goddard Space Flight Center, Third International Workshop on Squeezed States and Uncertainty Relations May 1994 p 167-172 (For primary document see N95-13896 03-74)
Avail: CASI HC A02/MF A06

Traditionally, in non-relativistic Quantum Mechanics, time is considered to be a parameter, rather than an observable quantity like space. In relativistic Quantum Field Theory, space and time are treated equally by reducing space to also be a parameter. Herein, after a brief review of other measurements, we describe a third possibility, which is to treat time as a directly observable quantity. Author

N95-13918*# Instituto Politecnico Nacional, Mexico City. Dept. de Fisica.
MANIPULATION OF QUANTUM EVOLUTION **c72**
David Jose Fernandez Cabera and Bogdan Mielnik *In* NASA. Goddard Space Flight Center, Third International Workshop on Squeezed States and Uncertainty Relations May 1994 p 173-178 Sponsored by CONACyT (For primary document see N95-13896 03-74)
Avail: CASI HC A02/MF A06

The free evolution of a non-relativistic charged particle is manipulated using time-dependent magnetic fields. It is shown that the application of a programmed sequence of magnetic pulses can invert the free evolution process, forcing an arbitrary wave packet to 'go back in time' to recover its past shape. The possibility of more general operations upon the Schrodinger wave packet is discussed. Author

N95-13919*# Ulm Univ. (Germany). Abteilung fuer Quantenphysik.
QUANTUM STATE ENGINEERING **c77**
Karl Vogel, V. M. Akulin, and W. P. Schleich *In* NASA. Goddard Space Flight Center, Third International Workshop on Squeezed States and Uncertainty Relations May 1994 p 181-188 Sponsored in part by QED Associates (For primary document see N95-13896 03-74)
Avail: CASI HC A02/MF A06

We show how to create an arbitrary field state in a cavity by sending appropriately prepared two-level atoms through the cavity and subsequently detecting them in their ground state. Author

N95-13920*# Arkansas Univ., Fayetteville, AR. Dept. of Physics.
SQUEEZED LIGHT FROM MULTI-LEVEL CLOSED-CYCLING ATOMIC SYSTEMS **c72**
Min Xiao and Yi-Fu Zhu *In* NASA. Goddard Space Flight Center, Third International Workshop on Squeezed States and Uncertainty Relations May 1994 p 189-194 (For primary document see N95-13896 03-74)
Avail: CASI HC A02/MF A06

Amplitude squeezing is calculated for multi-level closed-cycling atomic systems. These systems can last without atomic population inversion in any atomic bases. Maximum squeezing is obtained for the parameters in the region of lasing without inversion. A practical four-level system and an ideal three-level system are presented. The latter system is analyzed in some detail and the mechanism of generating amplitude squeezing is discussed. Author

N95-13921*# Seoul National Univ. (Republic of Korea). Dept. of Physics.
A METHOD OF MEASURING THE AMPLITUDE-MODULATED VACUUM FIELD NEAR A CONDUCTING MIRROR **c32**
Sun-Hyun Youn, Jai-Hyung Lee, and Joon-Sung Chang *In* NASA. Goddard Space Flight Center, Third International Workshop on Squeezed States and Uncertainty Relations May 1994 p 195-202 (For primary document see N95-13896 03-74)
Avail: CASI HC A02/MF A06

Electromagnetic fields of the vacuum mode near a conducting mirror are modified with respect to those in free space, with their amplitudes having a sinusoidal spatial dependence from the mirror. Therefore if we combine this spatially amplitude-modulated vacuum field mode and intense coherent light with a beam splitter, we may detect this fluctuation of the vacuum mode in a homodyne detection scheme. It will give a new method to produce squeezed states of light with a single mirror placed close to an unused port of a beam splitter. We show that the amplitude fluctuation of the combined light can be reduced by a factor of 2 below that of the coherent light. We also discuss the limitations due to the finite line width of the laser and the effective absorption length of the photodiodes. Author

N95-13922*# Universidad Nacional Autonoma de Mexico, Mexico City. Centro de Instrumentos.
HOW TO CHARACTERIZE THE NONLINEAR AMPLIFIER? **c32**
Dmitri Kouznetsov Kallistratova (Academy of Sciences, USSR, Moscow, USSR.) and Carlos Flores Cotera *In* NASA. Goddard Space Flight Center, Third International Workshop on Squeezed States and Uncertainty Relations May 1994 p 203-206 Sponsored in part by Comitet Nacional de Ciencia y Technologia (For primary document see N95-13896 03-74)
Avail: CASI HC A01/MF A06

The conception of the amplification of the coherent field is formulated. The definition of the coefficient of the amplification as the relation between the mean value of the field at the output to the value at the input and the definition of the noise as the difference between the number of photons in the output mode and square of the modulus of the mean value of the output amplitude are considered. Using a simple example it is shown that by these definitions the noise of the nonlinear amplifier may be less than the noise of the ideal linear amplifier of the same amplification coefficient. Proposals to search another definition of basic parameters of the nonlinear amplifiers are discussed. This definition should enable us to formulate the universal fundamental lower limit of the noise which should be valid for linear quantum amplifiers as for nonlinear ones. Author

N95-13923*# Sogang Univ., Seoul (Republic of Korea). Dept. of Physics.
PHASE PROPERTIES OF MULTICOMPONENT SUPERPOSITION STATES IN VARIOUS AMPLIFIERS
Kang-Soo Lee and M. S. Kim *In* NASA. Goddard Space Flight Center, Third International Workshop on Squeezed States and Uncertainty Relations May 1994 p 207-212 Sponsored by Korea Research Foundation (For primary document see N95-13896 03-74)
Avail: CASI HC A02/MF A06

There have been theoretical studies for generation of optical coherent superposition states. Once the superposition state is generated it is natural to ask if it is possible to amplify it without losing the nonclassical properties

of the field state. We consider amplification of the superposition state in various amplifiers such as a sub-Poissonian amplifier, a phase-sensitive amplifier and a classical amplifier. We show the evolution of phase probability distribution functions in the amplifier. Author

N95-13924*# Academy of Sciences (USSR), Moscow (USSR). Physical Inst.

SUB-POISSONIAN LIGHT AND PHOTOCURRENT SHOT-NOISE SUPPRESSION IN CLOSED OPTO-ELECTRONIC LOOP

A. V. Masalov, A. A. Putilin, and Michael V. Vasilyev *In* NASA. Goddard Space Flight Center, Third International Workshop on Squeezed States and Uncertainty Relations May 1994 p 213-218 (For primary document see N95-13896 03-74)

Avail: CASI HC A02/MF A06

We examine experimentally photocurrent noise reduction in the opto-electronic closed loop. Photocurrent noise density 12.5 dB below the shot-noise was observed. So large suppression was not reached in previous experiments and cannot be explained in terms of an ordinary sub-Poissonian light in the loop. We propose the concept of anticorrelation state for the description of light in the loop. Author

N95-13925*# Academy of Sciences (USSR), Moscow (USSR). Physics Inst.

MODES IN LIGHT WAVE PROPAGATING IN SEMICONDUCTOR LASER **c36**

Margarita A. Manko *In* NASA. Goddard Space Flight Center, Third International Workshop on Squeezed States and Uncertainty Relations May 1994 p 219-224 (For primary document see N95-13896 03-74)

Avail: CASI HC A02/MF A06

The study of semiconductor laser based on an analogy of the Schrodinger equation and an equation describing light wave propagation in nonhomogeneous medium is developed. The active region of semiconductor laser is considered as optical waveguide confining the electromagnetic field in the cross-section (x,y) and allowing waveguide propagation along the laser resonator (z). The mode structure is investigated taking into account the transversal and what is the important part of the suggested consideration longitudinal nonhomogeneity of the optical waveguide. It is shown that the Gaussian modes in the case correspond to spatial squeezing and correlation. Spatially squeezed two-mode structure of nonhomogeneous optical waveguide is given explicitly. Distribution of light among the laser discrete modes is presented. Properties of the spatially squeezed two-mode field are described. The analog of Franck-Condon principle for finding the maxima of the distribution function and the analog of Ramsauer effect for control of spatial distribution of laser emission are discussed. Author

N95-13926*# Moscow Physical-Technical Inst. (Russia).

SQEEZING GENERATED BY A NONLINEAR MASTER EQUATION AND BY AMPLIFYING-DISSIPATIVE HAMILTONIANS **c64**

V. V. Dodonov, M. A. Marchiolli, Solomon S. Mizrahi, and M. H. Y. Moussa *In* NASA. Goddard Space Flight Center, Third International Workshop on Squeezed States and Uncertainty Relations May 1994 p 227-238 Sponsored by Fundacao de Amparo a Pesquisa do Estado de Sao Paulo and CNPq (For primary document see N95-13896 03-74)

Avail: CASI HC A03/MF A06

In the first part of this contribution we show that the master equation derived from the generalized version of the nonlinear Doebner-Goldin equation leads to the squeezing of one of the quadratures. In the second part we consider two familiar Hamiltonians, the Bateman- Caldirola-Kanai and the optical parametric oscillator; going back to their classical Lagrangian form we introduce a stochastic force and a dissipative factor. From this new Lagrangian we obtain a modified Hamiltonian that treats adequately the simultaneous amplification and dissipation phenomena, presenting squeezing, too. Author

N95-13927*# European Nuclear Agency, Rome (Italy). Settore Elettroottica e Laser.

PHASE-SPACE ANALYSIS OF CHARGED AND OPTICAL BEAM TRANSPORT: WIGNER ROTATION ANGLE

G. Dattoli and Amalia Torre *In* NASA. Goddard Space Flight Center, Third International Workshop on Squeezed States and Uncertainty Relations May 1994 p 239-249 (For primary document see N95-13896 03-74)

Avail: CASI HC A03/MF A06

The possibility of using the phase space formalism to establish a correspondence between the dynamical behavior of squeezed states and optical or charged beams, propagating through linear systems, has received a great deal of attention during the last years. In this connection, it has been indicated how optical experiments may be conceived to measure the Wigner rotation angle. In this paper we address the topic within the context of the paraxial propagation of optical or charged beams and suggest a possible experiment for measuring the Wigner angle using an electron beam passing through quadrupoles and drift sections. The analogous optical system is also discussed. Author

N95-13928*# George Mason Univ., Fairfax, VA. Dept. of Physics.

PHASE SPACE FLOW OF PARTICLES IN SQUEEZED STATES **c77**

Peter H. Ceperley *In* NASA. Goddard Space Flight Center, Third International Workshop on Squeezed States and Uncertainty Relations May 1994 p 251-256 (For primary document see N95-13896 03-74)

Avail: CASI HC A02/MF A06

The manipulation of noise and uncertainty in squeezed states is governed by the wave nature of the quantum mechanical particles in these states. This paper uses a deterministic model of quantum mechanics in which real guiding waves control the flow of localized particles. This model will be used to examine the phase space flow of particles in typical squeezed states. Author

N95-13929*# European Nuclear Energy Agency, Frascati (Italy). Settore Elettroottica e Laser.

MULTIVARIABLE HERMITE POLYNOMIALS AND PHASE-SPACE DYNAMICS **c77**

G. Dattoli, Amalia Torre, S. Lorenzutta, G. Maino, and C. Chiccoli *In* NASA. Goddard Space Flight Center, Third International Workshop on Squeezed States and Uncertainty Relations May 1994 p 257-268 (For primary document see N95-13896 03-74)

Avail: CASI HC A03/MF A06

The phase-space approach to classical and quantum systems demands for advanced analytical tools. Such an approach characterizes the evolution of a physical system through a set of variables, reducing to the canonically conjugate variables in the classical limit. It often happens that phase-space distributions can be written in terms of quadratic forms involving the above quoted variables. A significant analytical tool to treat these problems may come from the generalized many-variables Hermite polynomials, defined on quadratic forms in R(exp n). They form an orthonormal system in many dimensions and seem the natural tool to treat the harmonic oscillator dynamics in phase-space. In this contribution we discuss the properties of these polynomials and present some applications to physical problems. Author

N95-13930*# Ecole Polytechnique, Montreal (Quebec). Dept. de Genie Physique.

UNDERSTANDING SQUEEZING OF QUANTUM STATES WITH THE WIGNER FUNCTION **c77**

Antoine Royer *In* NASA. Goddard Space Flight Center, Third International Workshop on Squeezed States and Uncertainty Relations May 1994 p 269-274 (For primary document see N95-13896 03-74)

Avail: CASI HC A02/MF A06

The Wigner function is argued to be the only natural phase space function evolving classically under quadratic Hamiltonians with time-dependent bilinear part. This is used to understand graphically how certain quadratic time-dependent Hamiltonians induce squeezing of quantum states. The Wigner representation is also used to generalize Ehrenfest's theorem to the quantum uncertainties. This makes it possible to deduce features of the quantum evolution, such as squeezing, from the classical evolution, whatever the Hamiltonian. Author

N95-13931*# Instituto Politecnico Nacional, Mexico City. Dept. de Fisica.

ON THE POSSIBILITY OF A QUANTUM MECHANICAL PHASE SPACE REPRESENTATION **c77**

Gabino Torres-Vega *In* NASA. Goddard Space Flight Center, Third International Workshop on Squeezed States and Uncertainty Relations May

1994 p 275-280 Sponsored by CONACyT and SNI (For primary document see N95-13896 03-74)
Avail: CASI HC A02/MF A06

Probability densities in phase space containing quantum dynamics information are very useful. However, is there a true phase space representation of Quantum Mechanics? Author

N95-13932*# Martin Marietta Corp., Moorestown, NJ. Government Electronic Systems.
PARTICLE LOCALIZATION, SPINOR TWO-VALUEDNESS, AND FERMI QUANTIZATION OF TENSOR SYSTEMS c72
Frank Reifler and Randall Morris *In* NASA. Goddard Space Flight Center, Third International Workshop on Squeezed States and Uncertainty Relations May 1994 p 281-286 (For primary document see N95-13896 03-74)
Avail: CASI HC A02/MF A06

Recent studies of particle localization shows that square-integrable positive energy bispinor fields in a Minkowski space-time cannot be physically distinguished from constrained tensor fields. In this paper we generalize this result by characterizing all classical tensor systems, which admit Fermi quantization, as those having unitary Lie-Poisson brackets. Examples include Euler's tensor equation for a rigid body and Dirac's equation in tensor form. Author

N95-13933*# Johns Hopkins Univ., Laurel, MD. Applied Physics Lab.
QUANTUM PHASE UNCERTAINTIES IN THE CLASSICAL LIMIT c77
James D. Franson *In* NASA. Goddard Space Flight Center, Third International Workshop on Squeezed States and Uncertainty Relations May 1994 p 289-298 Sponsored by ONR (For primary document see N95-13896 03-74)
Avail: CASI HC A02/MF A06

Several sources of phase noise, including spontaneous emission noise and the loss of coherence due to which-path information, are examined in the classical limit of high field intensities. Although the origin of these effects may appear to be quantum-mechanical in nature, it is found that classical analogies for these effects exist in the form of chaos. Author

N95-13934*# Tel-Aviv Univ., Ramat-Aviv, Tel-Aviv (Israel). School of Physics and Astronomy.
HOW TO DETECT AN EXCITED ATOM WITHOUT DISTURBING IT OR HOW TO LOCATE A SUPER-MINE WITHOUT EXPLODING IT c72
Lev Vaidman *In* NASA. Goddard Space Flight Center, Third International Workshop on Squeezed States and Uncertainty Relations May 1994 p 299-305 Sponsored by Basic Research Foundation and and Israel Academy of Sciences and Humanities (For primary document see N95-13896 03-74)
Avail: CASI HC A02/MF A06

Possible realistic implementations of a method for interaction-free measurements, due to Elitzur and Vaidman, are proposed and discussed. It is argued that the effect can be easily demonstrated in an optical laboratory. Author

N95-13935*# Academy of Sciences (USSR), Moscow (USSR). Physical Inst.
THE STOKES LINE WIDTH AND UNCERTAINTY RELATIONS c67
A. I. Nikishov and V. I. Ritus *In* NASA. Goddard Space Flight Center, Third International Workshop on Squeezed States and Uncertainty Relations May 1994 p 307-314 (For primary document see N95-13896 03-74)
Avail: CASI HC A02/MF A06

For a function given by contour integral the two types (conventions) of asymptotic representations are considered: the usual representation by asymptotic series in inverse powers of large parameters and the special division of contour integral in contributions of high and low saddle points. It is shown that the width of the recessive term formation zone (Stokes strip) in the second convention is determined by uncertainty relation and is much less than the zone width in the first convention. The reasons of such a difference is clarified. The results of the work are useful for understanding of formation region of the exponentially small process arising on the background of the strong one. Author

N95-13936*# Atominstitut der Oesterreichischen Hochschulen, Vienna.
MAXIMUM PREDICTIVE POWER AND THE SUPERPOSITION PRINCIPLE c77
Johann Summhammer *In* NASA. Goddard Space Flight Center, Third International Workshop on Squeezed States and Uncertainty Relations May 1994 p 315-320 (For primary document see N95-13896 03-74)
(FFWF Proj. P-8781)
Avail: CASI HC A02/MF A06

In quantum physics the direct observables are probabilities of events. We ask how observed probabilities must be combined to achieve what we call maximum predictive power. According to this concept the accuracy of a prediction must only depend on the number of runs whose data serve as input for the prediction. We transform each probability to an associated variable whose uncertainty interval depends only on the amount of data and strictly decreases with it. We find that for a probability which is a function of two other probabilities maximum predictive power is achieved when linearly summing their associated variables and transforming back to a probability. This recovers the quantum mechanical superposition principle. Author

N95-13937*# Villanova Univ., PA. Dept. of Physics.
CORRELATED QUADRATURES OF RESONANCE FLUORESCENCE AND THE GENERALIZED UNCERTAINTY RELATION c72
Henk F. Arnoldus, Thomas F. George, and Rolf W. F. Gross *In* NASA. Goddard Space Flight Center, Third International Workshop on Squeezed States and Uncertainty Relations May 1994 p 321-329 (For primary document see N95-13896 03-74)
(Grant NSF CHE-91-96214)
Avail: CASI HC A02/MF A06

Resonance fluorescence from a two-state atom has been predicted to exhibit quadrature squeezing below the Heisenberg uncertainty limit, provided that the optical parameters (Rabi frequency, detuning, laser linewidth, etc.) are chosen carefully. When the correlation between two quadratures of the radiation field does not vanish, however, the Heisenberg limit for quantum fluctuations might be an unrealistic lower bound. A generalized uncertainty relation, due to Schroedinger, takes into account the possible correlation between the quadrature components of the radiation, and it suggests a modified definition of squeezing. We show that the coherence between the two levels of a laser-driven atom is responsible for the correlation between the quadrature components of the emitted fluorescence, and that the Schrodinger uncertainty limit increases monotonically with the coherence. On the other hand, the fluctuations in the quadrature field diminish with an increasing coherence, and can disappear completely when the coherence reaches 1/2, provided that certain phase relations hold. Author

N95-13938*# Salerno Univ. (Italy). Dipt. di Fisica.
MINIMUM UNCERTAINTY AND SQUEEZING IN DIFFUSION PROCESSES AND STOCHASTIC QUANTIZATION c77
S. DeMartino, S. DeSiena, Fabrizo Illuminati, and Giuseppe Vitiello *In* NASA. Goddard Space Flight Center, Third International Workshop on Squeezed States and Uncertainty Relations May 1994 p 331-336 Prepared in cooperation with Istituto Nazionale di Fisica Nucleare, Naples, Italy (For primary document see N95-13896 03-74)
Avail: CASI HC A02/MF A06

We show that uncertainty relations, as well as minimum uncertainty coherent and squeezed states, are structural properties for diffusion processes. Through Nelson stochastic quantization we derive the stochastic image of the quantum mechanical coherent and squeezed states. Author

N95-13939*# Missouri Univ., Columbia, MO. Dept. of Physics and Astronomy.
APPLICATIONS OF SQUEEZED STATES: BOGOLIUBOV TRANSFORMATIONS AND WAVELETS TO THE STATISTICAL MECHANICS OF WATER AND ITS BUBBLES c77
Brian DeFacio, S.-H. Kim, and A. VanNevel *In* NASA. Goddard Space Flight Center, Third International Workshop on Squeezed States and Uncertainty Relations May 1994 p 339-351 (For primary document see N95-13896 03-74)
(Grants AF-AFOSR-0307-90; AF-AFOSR-0203-91)
Avail: CASI HC A03/MF A06

The squeezed states or Bogoliubov transformations and wavelets are applied to two problems in nonrelativistic statistical mechanics: the dielectric

response of liquid water, epsilon(q-vector,w), and the bubble formation in water during insonnification. The wavelets are special phase-space windows which cover the domain and range of L(exp 1) intersection of L(exp 2) of classical causal, finite energy solutions. The multiresolution of discrete wavelets in phase space gives a decomposition into regions of time and scales of frequency thereby allowing the renormalization group to be applied to new systems in addition to the tired 'usual suspects' of the Ising models and lattice gasses. The Bogoliubov transformation: squeeze transformation is applied to the dipolaron collective mode in water and to the gas produced by the explosive cavitation process in bubble formation. Author

N95-13940*# Liverpool Univ. (England). Dept. of Electrical Engineering and Electronics.

COHERENT STATES ON THE m-SHEETED COMPLEX PLANE AS m-PHOTON STATES **c72**

Apostolos Vourdas *In* NASA. Goddard Space Flight Center, Third International Workshop on Squeezed States and Uncertainty Relations May 1994 p 353-364 (For primary document see N95-13896 03-74)

Avail: CASI HC A03/MF A06

Coherent states on the m-sheeted complex plane are introduced and properties like overcompleteness and resolution of the identity are studied. They are eigenstates of the operators a(sub m)(+), a(sub m) which create and annihilate clusters of m-particles. Applications of this formalism in the study of Hamiltonians that describe m-particle clustering are also considered. Author

N95-13941*# Naples Univ. (Italy). Dipt. di Scienze Fisiche.

SOME RULES FOR POLYDIMENSIONAL SQUEEZING

Vladimir I. Manko *In* NASA. Goddard Space Flight Center, Third International Workshop on Squeezed States and Uncertainty Relations May 1994 p 365-371 Prepared in cooperation with Istituto Nazionale di Fisica Nucleare, Naples, Italy and Academy of Sciences (USSR), Moscow (For primary document see N95-13896 03-74)

Avail: CASI HC A02/MF A06

The review of the following results is presented: For mixed state light of N-mode electromagnetic field described by Wigner function which has generic Gaussian form, the photon distribution function is obtained and expressed explicitly in terms of Hermite polynomials of 2N-variables. The momenta of this distribution are calculated and expressed as functions of matrix invariants of the dispersion matrix. The role of new uncertainty relation depending on photon state mixing parameter is elucidated. New sum rules for Hermite polynomials of several variables are found. The photon statistics of polymode even and odd coherent light and squeezed polymode Schroedinger cat light is given explicitly. Photon distribution for polymode squeezed number states expressed in terms of multivariable Hermite polynomials is discussed. Author

N95-13942*# University of Southern California, Los Angeles, CA. Dept. of Physics.

SCHROEDINGER OPERATORS WITH THE q-LADDER SYMMETRY ALGEBRAS **c64**

Sergei Skorik and Vyacheslav Spiridonov *In* NASA. Goddard Space Flight Center, Third International Workshop on Squeezed States and Uncertainty Relations May 1994 p 373-379 Sponsored by Natural Sciences and Engineering Research Council and Fonds FCAR (For primary document see N95-13896 03-74)

Avail: CASI HC A02/MF A06

A class of the one-dimensional Schroedinger operators L with the symmetry algebra LB(+/-) = q(+/-2)B(+/-)L, (B(+),B(-)) = P(sub N)(L), is described. Here B(+/-) are the 'q-ladder' operators and P(sub N)(L) is a polynomial of the order N. Peculiarities of the coherent states of this algebra are briefly discussed. Author

N95-13943*# Chungbuk National Univ. (Republic of Korea). Dept. of Physics.

THE WAVE FUNCTION AND MINIMUM UNCERTAINTY FUNCTION OF THE BOUND QUADRATIC HAMILTONIAN SYSTEM **c77**

Kyu Hwang Yeon, Chung In Um, and T. F. George *In* NASA. Goddard Space Flight Center, Third International Workshop on Squeezed States and Uncertainty Relations May 1994 p 381-386 Sponsored by Ministry of Education (For primary document see N95-13896 03-74)

(Contract KOSEF-3-08-00-05; NSF CHE-91-96214)

Avail: CASI HC A02/MF A06

The bound quadratic Hamiltonian system is analyzed explicitly on the basis of quantum mechanics. We have derived the invariant quantity with an auxiliary equation as the classical equation of motion. With the use of this invariant it can be determined whether or not the system is bound. In bound system we have evaluated the exact eigenfunction and minimum uncertainty function through unitary transformation. Author

N95-13944*# Naples Univ. (Italy). Dipt. di Scienze.

THE THERMAL-WAVE MODEL: A SCHROEDINGER-LIKE EQUATION FOR CHARGED PARTICLE BEAM DYNAMICS **c73**

Renato Fedele and G. Miele *In* NASA. Goddard Space Flight Center, Third International Workshop on Squeezed States and Uncertainty Relations May 1994 p 387-392 Prepared in cooperation with Istituto Nazionale di Fisica Nucleare, Naples, Italy (For primary document see N95-13896 03-74)

Avail: CASI HC A02/MF A06

We review some results on longitudinal beam dynamics obtained in the framework of the Thermal Wave Model (TWM). In this model, which has recently shown the capability to describe both longitudinal and transverse dynamics of charged particle beams, the beam dynamics is ruled by Schroedinger-like equations for the beam wave functions, whose squared modulus is proportional to the beam density profile. Remarkably, the role of the Planck constant is played by a diffractive constant epsilon, the emittance, which has a thermal nature. Author (revised)

N95-13945*# Goettingen Univ. (Germany). Inst. fuer Theoretische Physik.

CAUSALITY PROBLEMS FOR FERMI'S TWO-ATOM SYSTEM **c72**

Gerhard C. Hegerfeldt *In* NASA. Goddard Space Flight Center, Third International Workshop on Squeezed States and Uncertainty Relations May 1994 p 393-399 (For primary document see N95-13896 03-74)

Avail: CASI HC A02/MF A06

Let A and B be two atoms or, more generally, a 'source' and a 'detector' separated by some distance R. At t = 0 A is in an excited state, B in its ground state, and no photons are present. A theorem is proved that in contrast to Einstein causality and finite signal velocity the excitation probability of B is nonzero immediately after t = 0. Implications are discussed. Author

N95-13946*# Alabama A & M Univ., Normal, AL. Dept. of Physics.

PSEUDOMASTER EQUATION FOR THE NO-COUNT PROCESS IN A CONTINUOUS PHOTODETECTION **c77**

Ching-Tsung Lee *In* NASA. Goddard Space Flight Center, Third International Workshop on Squeezed States and Uncertainty Relations May 1994 p 401-406 (For primary document see N95-13896 03-74)

(Contract N00014-89-J-1050)

Avail: CASI HC A02/MF A06

The detection of cavity radiation with the detector placed outside the cavity is studied. Each leaked photon has a certain probability of propagating away without being detected. It is viewed as a continuous quantum measurement in which the density matrix is continuously revised according to the readout of the detector. The concept of pseudomaster equation for the no-count process is introduced; its solution leads to the discovery of the superoperator for the same process. It has the potential to become the key equation for continuous measurement process. Author

N95-13947*# Turin Univ. (Italy). Dipt. di Fisica Teorica.

SQUEEZED STATES AND GRAVITON-ENTROPY PRODUCTION IN THE EARLY UNIVERSE **c90**

Massimo Giovannini *In* NASA. Goddard Space Flight Center, Third International Workshop on Squeezed States and Uncertainty Relations May 1994 p 407-412 Prepared in cooperation with Istituto Nazionale di Fisica Nucleare, Turin, Italy (For primary document see N95-13896 03-74)

Avail: CASI HC A02/MF A06

Squeezed states are a very useful framework for the quantum treatment of tensor perturbations (i.e. gravitons production) in the early universe. In particular, the non equilibrium entropy growth in a cosmological process of pair production is completely determined by the associated squeezing

parameter and is insensitive to the number of particles in the initial state. The total produced entropy may represent a significant fraction of the entropy stored today in the cosmic blackbody radiation, provided pair production originates from a change in the background metric at a curvature scale of the Planck order. Within the formalism of squeezed thermal states it is also possible to discuss the stimulated emission of gravitons from an initial thermal bath, under the action of the cosmic gravitational background field. We find that at low energy the graviton production is enhanced, if compared with spontaneous creation from the vacuum; as a consequence, the inflation scale must be lowered, in order not to exceed the observed CMB quadrupole anisotropy. This effect is important, in particular, for models based on a symmetry-breaking transition which require, as initial condition, a state of thermal equilibrium at temperatures higher than the inflation scale and in which inflation has a minimal duration. Author

N95-13948*# Kochi Univ., Akebono (Japan). Dept. of Physics.

TIME-DEPENDENT VARIATIONAL APPROACH IN TERMS OF SQUEEZED COHERENT STATES: IMPLICATION TO SEMI-CLASSICAL APPROXIMATION **c77**

Yasuhiko Tsue *In* NASA. Goddard Space Flight Center, Third International Workshop on Squeezed States and Uncertainty Relations May 1994 p 413-418 (For primary document see N95-13896 03-74)
Avail: CASI HC A02/MF A06

A general framework for time-dependent variational approach in terms of squeezed coherent states is constructed with the aim of describing quantal systems by means of classical mechanics including higher order quantal effects with the aid of canonicity conditions developed in the time-dependent Hartree-Fock theory. The Maslov phase occurring in a semi-classical quantization rule is investigated in this framework. In the limit of a semi-classical approximation in this approach, it is definitely shown that the Maslov phase has a geometric nature analogous to the Berry phase. It is also indicated that this squeezed coherent state approach is a possible way to go beyond the usual WKB approximation. Author

N95-13949*# Pennsylvania State Univ., Schuylkill Haven, PA. Dept. of Physics.

DECOHERENCE AND DISSIPATION FOR A QUANTUM SYSTEM COUPLED TO A LOCAL ENVIRONMENT **c77**

Michael R. Gallis *In* NASA. Goddard Space Flight Center, Third International Workshop on Squeezed States and Uncertainty Relations May 1994 p 419-424 (For primary document see N95-13896 03-74)
Avail: CASI HC A02/MF A06

Decoherence and dissipation in quantum systems has been studied extensively in the context of Quantum Brownian Motion. Effective decoherence in coarse grained quantum systems has been a central issue in recent efforts by Zurek and by Hartle and Gell-Mann to address the Quantum Measurement Problem. Although these models can yield very general classical phenomenology, they are incapable of reproducing relevant characteristics expected of a local environment on a quantum system, such as the characteristic dependence of decoherence on environment spatial correlations. I discuss the characteristics of Quantum Brownian Motion in a local environment by examining aspects of first principle calculations and by the construction of phenomenological models. Effective quantum Langevin equations and master equations are presented in a variety of representations. Comparisons are made with standard results such as the Caldeira-Leggett master equation. Author

N95-13950*# Universidad Nacional Autonoma de Mexico, Cuernavaca.

GENERAL PROPERTIES OF QUANTUM OPTICAL SYSTEMS IN A STRONG FIELD LIMIT

S. M. Chumakov and Andrei B. Klimov *In* NASA. Goddard Space Flight Center, Third International Workshop on Squeezed States and Uncertainty Relations May 1994 p 425-429 Sponsored by CONACyT (For primary document see N95-13896 03-74)
Avail: CASI HC A01/MF A06

We investigate the dynamics of an arbitrary atomic system (n-level atoms or many n-level atoms) interacting with a resonant quantized mode of an em field. If the initial field state is a coherent state with a large photon number then the system dynamics possesses some general features, independently of the particular structure of the atomic system. Namely, trapping states, factorization of the wave function, collapses and revivals of the atomic energy oscillations are discussed. Author

N95-13951*# Universidade Estadual de Campinas (Brazil). Inst. de Fisica.

PROBING THE ANTIFERROMAGNETIC LONG-RANGE ORDER WITH GLAUBER SPIN STATES **c77**

Guillermo G. Cabrera *In* NASA. Goddard Space Flight Center, Third International Workshop on Squeezed States and Uncertainty Relations May 1994 p 431-436 Sponsored by Fundacao de Amparo a Pesquisa do Estado de Sao Paulo and Fundo de Apoio ao Ensino e Pesquisa (For primary document see N95-13896 03-74)
Avail: CASI HC A02/MF A06

It is well known that the ground state of low-dimensional antiferromagnets deviates from Neel states due to strong quantum fluctuations. Even in the presence of long-range order, those fluctuations produce a substantial reduction of the magnetic moment from its saturation value. Numerical simulations in anisotropic antiferromagnetic chains suggest that quantum fluctuations over Neel order appear in the form of localized reversal of pairs of neighboring spins. In this paper, we propose a coherent state representation for the ground state to describe the above situation. In the one-dimensional case, our wave function corresponds to a two-mode Glauber state, when the Neel state is used as a reference, while the boson fields are associated to coherent flip of spin pairs. The coherence manifests itself through the antiferromagnetic long-range order that survives the action of quantum fluctuations. The present representation is different from the standard zero-point spin wave state, and is asymptotically exact in the limit of strong anisotropy. The fermionic version of the theory, obtained through the Jordan-Wigner transformation, is also investigated. Author

N95-13952*# Academy of Sciences (USSR), Moscow (USSR). Optics Div.

BERRY PHASE IN HEISENBERG REPRESENTATION **c77**

V. A. Andreev, Andrei B. Klimov, and Peter B. Lerner *In* NASA. Goddard Space Flight Center, Third International Workshop on Squeezed States and Uncertainty Relations May 1994 p 437-448 Sponsored by Michigan Univ. and ONR (For primary document see N95-13896 03-74)
Avail: CASI HC A03/MF A06

We define the Berry phase for the Heisenberg operators. This definition is motivated by the calculation of the phase shifts by different techniques. These techniques are: the solution of the Heisenberg equations of motion, the solution of the Schrodinger equation in coherent-state representation, and the direct computation of the evolution operator. Our definition of the Berry phase in the Heisenberg representation is consistent with the underlying supersymmetry of the model in the following sense. The structural blocks of the Hamiltonians of supersymmetrical quantum mechanics ('superpairs') are connected by transformations which conserve the similarity in structure of the energy levels of superpairs. These transformations include transformation of phase of the creation-annihilation operators, which are generated by adiabatic cyclic evolution of the parameters of the system. Author

N95-13953*# Maryland Univ., College Park, MD. Lab. for Physical Sciences.

QUANTUM PROPAGATION IN SINGLE MODE FIBER

Lance G. Joneckis and Jeffrey H. Shapiro *In* NASA. Goddard Space Flight Center, Third International Workshop on Squeezed States and Uncertainty Relations May 1994 p 451-463 (For primary document see N95-13896 03-74)
Avail: CASI HC A03/MF A06

This paper presents a theory for quantum light propagation in a single-mode fiber which includes the effects of the Kerr nonlinearity, group-velocity dispersion, and linear loss. The theory reproduces the results of classical self-phase modulation, quantum four-wave mixing, and classical solution physics, within their respective regions of validity. It demonstrates the crucial role played by the Kerr-effect material time constant, in limiting the quantum phase shifts caused by the broadband zero-point fluctuations that accompany any quantized input field. Operator moment equations - approximated, numerically, via a terminated cumulant expansion - are used to obtain results for homodyne-measurement noise spectra when dispersion is negligible. More complicated forms of these equations can be used to incorporate dispersion into the noise calculations. Author

N95-13954*# Indiana Univ.-Purdue Univ., Indianapolis, IN. Dept. of Physics.

QUANTUM AMPLIFICATION AND QUANTUM OPTICAL TAPPING WITH SQUEEZED STATES AND CORRELATED QUANTUM STATES

Z. Y. Ou, S. F. Pereira, and H. J. Kimble *In* NASA. Goddard Space Flight Center, Third International Workshop on Squeezed States and Uncertainty Relations May 1994 p 465-474 Sponsored by ONR and NSF (For primary document see N95-13896 03-74)

Avail: CASI HC A02/MF A06

Quantum fluctuations in a nondegenerate optical parametric amplifier (NOPA) are investigated experimentally with a squeezed state coupled into the internal idler mode of the NOPA. Reductions of the inherent quantum noise of the amplifier are observed with a minimum noise level 0.7 dB below the usual noise level of the amplifier with its idler mode in a vacuum state. With two correlated quantum fields as the amplifier's inputs and proper adjustment of the gain of the amplifier, it is shown that the amplifier's intrinsic quantum noise can be completely suppressed so that noise-free amplification is achieved. It is also shown that the NOPA, when coupled to either a squeezed state or a nonclassically correlated state, can realize quantum tapping of optical information. Author

N95-13955*# Texas A&M Univ., College Station, TX. Dept. of Physics.

QUANTUM NOISE LIMITS TO MATTER-WAVE INTERFEROMETRY c72

Marlan O. Scully (Max-Planck-Inst. fuer Quantenoptik, Garching, Germany.) and Jonathan P. Dowling (Army Missile Command, Redstone Arsenal, AL.) *In* NASA. Goddard Space Flight Center, Third International Workshop on Squeezed States and Uncertainty Relations May 1994 p 475-484 Sponsored by ONR and NAC-NRC (For primary document see N95-13896 03-74)

Avail: CASI HC A02/MF A06

We derive the quantum limits for an atomic interferometer in which the atoms obey either Bose-Einstein or Fermi-Dirac statistics. It is found that the limiting quantum noise is due to the uncertainty associated with the particle sorting between the two branches of the interferometer. As an example, the quantum-limited sensitivity of a matter-wave gyroscope is calculated and compared with that of laser gyroscopes. Author

N95-13956*# Duke Univ., Durham, NC. Dept. of Physics.

BLOCH VECTOR PROJECTION NOISE

Li-Jun Wang, A. M. Bacon, H.-Z. Zhao, and J. E. Thomas *In* NASA. Goddard Space Flight Center, Third International Workshop on Squeezed States and Uncertainty Relations May 1994 p 485-494 Sponsored by NSF; RADC; and AFOSR (For primary document see N95-13896 03-74)

Avail: CASI HC A02/MF A06

In the optical measurement of the Bloch vector components describing a system of N two-level atoms, the quantum fluctuations in these components are coupled into the measuring optical field. This paper develops the quantum theory of optical measurement of Bloch vector projection noise. The preparation and probing of coherence in an effective two-level system consisting of the two ground states in an atomic three-level lambda-scheme are analyzed. Author

N95-13957*# National Aeronautics and Space Administration. Goddard Space Flight Center, Greenbelt, MD.

NEW QUANTUM PROPERTIES AND THEIR DETECTION c77

Maurizo Artoni and Joseph L. Birman *In its* Third International Workshop on Squeezed States and Uncertainty Relations May 1994 p 495-500 (For primary document see N95-13896 03-74)

Avail: CASI HC A02/MF A06

We present a theoretical investigation on new and interesting properties of the phonon polarization field in solids. In particular, non-classical aspects of the phonon population and an experimental scheme that would enable one to detect them will be discussed. Author

N95-13958*# Bilkent Univ., Ankara (Turkey). Dept. of Physics.

QUANTUM STATISTICS OF RAMAN SCATTERING MODEL WITH STOKES MODE GENERATION c77

Bilal Tanatar and Alexander S. Shumovsky *In* NASA. Goddard Space Flight Center, Third International Workshop on Squeezed States and Uncertainty Relations May 1994 p 501-506 (For primary document see N95-13896 03-74)

Avail: CASI HC A02/MF A06

The model describing three coupled quantum oscillators with decay of Rayleigh mode into the Stokes and vibration (phonon) modes is examined. Due to the Manley-Rowe relations the problem of exact eigenvalues and eigenstates is reduced to the calculation of new orthogonal polynomials defined both by the difference and differential equations. The quantum statistical properties are examined in the case when initially: the Stokes mode is in the vacuum state; the Rayleigh mode is in the number state; and the vibration mode is in the number of or squeezed states. The collapses and revivals are obtained for different initial conditions as well as the change in time the sub-Poisson distribution by the super-Poisson distribution and vice versa. Author

N95-13959*# Brookhaven National Lab., Upton, NY. National Synchrotron Light Source.

EVOLUTION OF WAVE FUNCTION IN A DISSIPATIVE SYSTEM c77

Li-Hua Yu and Chang-Pu Sun *In* NASA. Goddard Space Flight Center, Third International Workshop on Squeezed States and Uncertainty Relations May 1994 p 507-513 Sponsored by State Univ. of New York and National Science Foundation of China (For primary document see N95-13896 03-74)

(Contract DE-AC02-76CH-00016)

Avail: CASI HC A02/MF A06

For a dissipative system with Ohmic friction, we obtain a simple and exact solution for the wave function of the system plus the bath. It is described by the direct product in two independent Hilbert space. One of them is described by an effective Hamiltonian, the other represents the effect of the bath, i.e., the Brownian motion, thus clarifying the structure of the wave function of the system whose energy is dissipated by its interaction with the bath. No path integral technology is needed in this treatment. The derivation of the Weisskopf-Wigner line width theory follows easily.

Author

N95-13960*# Academy of Sciences (USSR), Moscow (USSR). Physics Inst.

NONRESONANT INTERACTION OF ULTRASHORT ELECTROMAGNETIC PULSES WITH MULTILEVEL QUANTUM SYSTEMS c77

E. Belenov, V. Isakov, and A. Nazarkin *In* NASA. Goddard Space Flight Center, Third International Workshop on Squeezed States and Uncertainty Relations May 1994 p 515-520 Sponsored by Russian Basic Research Foundation; Wissenschaftskolleg; Schweizerische National-Versicherungs-Gesellschaft; and Alusuisse-Lonza Holding A.G. (For primary document see N95-13896 03-74)

Avail: CASI HC A02/MF A06

Some features of the excitation of multilevel quantum systems under the action of electromagnetic pulses which are shorter than the inverse frequency of interlevel transitions are considered. It is shown that the interaction is characterized by a specific type of selectivity which is not connected with the resonant absorption of radiation. The simplest three-level model displays the inverse population of upper levels. The effect of an ultrashort laser pulse on a multilevel molecule was regarded as an instant reception of the oscillation velocity by the oscillator and this approach showed an effective excitation and dissociation of the molecule. The estimations testify to the fact that these effects can be observed using modern femtosecond lasers. Author

N95-13961*# Boston Univ., MA. Dept. of Physics.

COMPLEMENTARITY AND PATH DISTINGUISHABILITY: SOME RECENT RESULTS CONCERNING PHOTON PAIRS c72

Abner Shimony and Gregg Jaeger *In* NASA. Goddard Space Flight Center, Third International Workshop on Squeezed States and Uncertainty Relations May 1994 p 523-533 (For primary document see N95-13896 03-74)

(Grant NSF PHY-90-22345)

Avail: CASI HC A03/MF A06

Two results concerning photon pairs, one previously reported and one new, are summarized. It was previously shown that if the two photons are prepared in a quantum state formed from bar-A and bar-A' for photon 1 and bar-B and bar-B' for photon 2, then both one- and two-particle interferometry can be studied. If upsilon(sub i) is the visibility of one-photon interference fringes (i = 1,2) and upsilon(sub 12) is the visibility of two-photon

fringes (a concept which we explicitly define), then upsilon(sub i) squared + upsilon(sub 12) squared is less than or equal to 1. The second result concerns the distinguishability of the paths of photon 2, using the known 2-photon state. A proposed measure E for path distinguishability is based upon finding an optimum strategy for betting on the outcome of a path measurement. Mandel has also proposed a measure of distinguishability P(sub D), defined in terms of the density operator rho of photon 2. We show that E is greater than or equal to P(sub D) and that upsilon(sub 2) = (1 - E(exp 2))exp 1/2. Author (revised)

N95-13962*# City Coll. of the City Univ. of New York, NY. Dept. of Physics.

FURTHER EVIDENCE FOR THE EPNT ASSUMPTION c77

Daniel M. Greenberger, Herbert J. Bernstein, Michael Horne, and Anton Zeilinger *In* NASA. Goddard Space Flight Center, Third International Workshop on Squeezed States and Uncertainty Relations May 1994 p 535-543 (For primary document see N95-13896 03-74)

Avail: CASI HC A02/MF A06

We recently proved a theorem extending the Greenberger-Horne-Zeilinger (GHZ) Theorem from multi-particle systems to two-particle systems. This proof depended upon an auxiliary assumption, the EPNT assumption (Emptiness of Paths Not Taken). According to this assumption, if there exists an Einstein-Rosen-Podolsky (EPR) element of reality that determines that a path is empty, then there can be no entity associated with the wave that travels this path (pilot-waves, empty waves, etc.) and reports information to the amplitude, when the paths recombine. We produce some further evidence in support of this assumption, which is certainly true in quantum theory. The alternative is that such a pilot-wave theory would have to violate EPR locality. Author

N95-13963*# Maryland Univ. Baltimore County, Catonsville, MD. Dept. of Physics.

THE PHOTON: EXPERIMENTAL EMPHASIS ON ITS WAVE-PARTICLE DUALITY c72

Yan-Hua Shih, A. V. Sergienko, Morton H. Rubin, Thomas E. Kiess, and Carroll O. Alley *In* NASA. Goddard Space Flight Center, Third International Workshop on Squeezed States and Uncertainty Relations May 1994 p 545-562 (For primary document see N95-13896 03-74)

(Contract N00014-91-J-1430)

Avail: CASI HC A03/MF A06

Two types of Einstein-Podolsky-Rosen experiments were demonstrated recently in our laboratory. It is interesting to see that in an interference experiment (wave-like experiment) the photon exhibits its particle property, and in a beam-splitting experiment (particle-like experiment) the photon exhibits its wave property. The two-photon states are produced from Type 1 and Type 2 optical spontaneous parametric down conversion, respectively. Author

N95-13964*# Maryland Univ. Baltimore County, Catonsville, MD. Dept. of Physics.

THE GENERATION OF ENTANGLED STATES FROM INDEPENDENT PARTICLE SOURCES c72

Morton H. Rubin and Yan-Hua Shih *In* NASA. Goddard Space Flight Center, Third International Workshop on Squeezed States and Uncertainty Relations May 1994 p 563-568 (For primary document see N95-13896 03-74)

(Contract N00014-91-J-1430)

Avail: CASI HC A02/MF A06

The generation of entangled states of two systems from product states is discussed for the case in which the paths of the two systems do not overlap. A particular method of measuring allows one to project out the nonlocal entangled state. An application to the production of four photon entangled states is outlined. Author

N95-13965*# Universidade Federal do Rio de Janeiro (Brazil). Inst. de Fisica.

NONLOCAL EFFECTS ON THE POLARIZATION STATE OF A PHOTON, INDUCED BY DISTANT ABSORBERS c72

Luis Carlos B. Ryff *In* NASA. Goddard Space Flight Center, Third International Workshop on Squeezed States and Uncertainty Relations May 1994 p 569-573 (For primary document see N95-13896 03-74)

Avail: CASI HC A01/MF A06

A variant of a Franson's two-photon correlation experiment is discussed, in which the linear polarization state of one of the photons depends on the path followed in the interferometer. It is shown that although the path difference is greater than the coherence length, the photon can be found in a polarization state represented by the superposition of the polarization states associated to the paths when there is coincident detection. Since the photons, produced via parametric down-conversion, are fairly well localized in space and time, the situation in which one of the photons is detected before the other can reach the interferometer raises an intriguing point: it seems that in some cases the second photon would have to be described by two wave packets simultaneously. Unlike previous experiments, in which nonlocal effects were induced by means of polarizers of phase shifters, in the proposed experiment nonlocal effects can be induced by means of variable absorbers. Author

N95-13966*# Texas A&M Univ., College Station, TX. Dept. of Physics.

THE STRONG BELL INEQUALITIES: A PROPOSED EXPERIMENTAL TEST c77

Edward S. Fry *In* NASA. Goddard Space Flight Center, Third International Workshop on Squeezed States and Uncertainty Relations May 1994 p 575-580 (For primary document see N95-13896 03-74)

(Grant NSF PHY-92-21038; Proj. A-1218)

Avail: CASI HC A02/MF A06

All previous experimental tests of Bell inequalities have required additional assumptions. The strong Bell inequalities (i.e. those requiring no additional assumptions) have never been tested. An experiment has been designed that can, for the first time, provide a definitive test of the strong Bell inequalities. Not only will the detector efficiency loophole be closed; but the locality condition will also be rigorously enforced. The experiment involves producing two Hg-199 atoms by a resonant Raman dissociation of a mercury dimer ((199)Hg2) that is in an electronic and nuclear spin singlet state. Bell inequalities can be tested by measuring angular momentum correlations between the spin one-half nuclei of the two Hg-199 atoms. The method used to make these latter measurements will be described. Author

N95-13967*# Manchester Univ. (England). Dept. of Mathematics.

ON THE NONLOCAL PREDICTIONS OF QUANTUM OPTICS

Trevor W. Marshall, Emilio Santos, and Antonio Vidiella-Barranco *In* NASA. Goddard Space Flight Center, Third International Workshop on Squeezed States and Uncertainty Relations May 1994 p 581-589 (For primary document see N95-13896 03-74)

(Contract DGICYT-PB-92-0507)

Avail: CASI HC A02/MF A06

We give a definition of locality in quantum optics based upon Bell's work, and show that locality has been violated in no experiment performed up to now. We argue that the interpretation of the Wigner function as a probability density gives a very attractive local realistic picture of quantum optics provided that this function is nonnegative. We conjecture that this is the case for all states which can be realized in the laboratory. In particular, we believe that the usual representation of 'single photon states' by a Fock state of the Hilbert space is not correct and that a more physical, although less simple mathematically, representation involves density matrices. We study in some detail the experiment showing anticorrelation after a beam splitter and prove that it naturally involves a positive Wigner function. Our (quantum) predictions for this experiment disagree with the ones reported in the literature. Author

N95-13968*# California Univ., Berkeley, CA. Dept. of Physics.

A LOOPHOLE-FREE BELL'S INEQUALITY EXPERIMENT c77

Paul G. Kwiat, Aephraim M. Steinberg, Raymond Y. Chiao, and Philippe H. Eberhard *In* NASA. Goddard Space Flight Center, Third International Workshop on Squeezed States and Uncertainty Relations May 1994 p 591-602 (For primary document see N95-13896 03-74)

(Contracts N00014-90-J-1259; DE-AC03-76SF-00098)

Avail: CASI HC A03/MF A06

The proof of Nature's nonlocality through Bell-type experiments is a topic of longstanding interest. Nevertheless, no experiments performed thus far have avoided the so-called 'detection loophole,' arising from low detector efficiencies and angular-correlation difficulties. In fact, most, if not all, of the systems employed to date can never close this loophole, even with perfect detectors. In addition, another loophole involving the non-rapid, non-random switching of various parameter settings exists in all past

experiments. We discuss a proposal for a potentially loophole-free Bell's inequality experiment. The source of the EPR-correlated pairs consists of two simultaneously-pumped type-2 phase-matched nonlinear crystals and a polarizing beam splitter. The feasibility of such a scheme with current detector technology seems high, and will be discussed. We also present a single-crystal version, motivated by other work presented at this conference. In a separate experiment, we have measured the absolute detection efficiency and time response of four single-photon detectors. The highest observed efficiencies were 70.7 plus or minus 1.9 percent (at 633 nm, with a device from Rockwell International) and 76.4 plus or minus 2.3 percent (at 702 nm, with an EG&G counting module). Possible efficiencies as high as 90 percent were implied. The EG&G devices displayed sub-nanosecond time resolution. Author

N95-13969*# Atominstitut der Oesterreichischen Hochschulen, Vienna.
THE PROBABILISTIC ORIGIN OF BELL'S INEQUALITY c77
Guenther Krenn *In* NASA. Goddard Space Flight Center, Third International Workshop on Squeezed States and Uncertainty Relations May 1994 p 603-608 (For primary document see N95-13896 03-74)
(FFWF Proj. P-8781)
Avail: CASI HC A02/MF A06

The concept of local realism entails certain restrictions concerning the possible occurrence of correlated events. Although these restrictions are inherent in classical physics they have never been noticed until Bell showed in 1964 that general correlations in quantum mechanics can not be interpreted in a classical way. We demonstrate how a local realistic way of thinking about measurement results necessarily leads to limitations with regard to the possible appearance of correlated events. These limitations, which are equivalent to Bell's inequality can be easily formulated as an immediate consequence of our discussion. Author

N95-13970*# Maryland Univ., College Park, MD. Dept. of Physics.
EINSTEIN-PODOLSKY-ROSEN-BOHM EXPERIMENT AND BELL INEQUALITY VIOLATION USING TYPE 2 PARAMETRIC DOWN CONVERSION c77
Thomas E. Kiess, Yan-Hua Shih, A. V. Sergienko, and Carroll O. Alley *In* NASA. Goddard Space Flight Center, Third International Workshop on Squeezed States and Uncertainty Relations May 1994 p 609-614 (For primary document see N95-13896 03-74)
(Contract N00014-19-J-1430)
Avail: CASI HC A02/MF A06

We report a new two-photon polarization correlation experiment for realizing the Einstein-Podolsky-Rosen-Bohm (EPRB) state and for testing Bell-type inequalities. We use the pair of orthogonally-polarized light quanta generated in Type 2 parametric down conversion. Using 1 nm interference filters in front of our detectors, we observe from the output of a 0.5mm beta - BaB2O4 (BBO) crystal the EPRB correlations in coincidence counts, and measure an associated Bell inequality violation of 22 standard deviations. The quantum state of the photon pair is a polarization analog of the spin-1/2 singlet state. Author

N95-13986# Pacific Northwest Lab., Richland, WA.
A FEMTOSECOND OPTICAL PARAMETRIC OSCILLATOR NEAR 3 MICRONS
G. R. Holtom, R. A. Crowell, and X. S. Xie May 1994 5 p Presented at the 9th International Conference on Ultrafast Phenomena, Dana Point, CA, 1-5 May 1994
(Contract DE-AC06-76RL-01830)
(DE94-014500; PNL-SA-23656; CONF-940593-12) Avail: CASI HC A01/MF A01

An optical parametric oscillator operating at fundamental molecular vibrational frequencies is demonstrated. The 100 femtosecond pulses make possible coherent measurements in a new spectroscopic region. DOE

N95-13992 Direction des Recherches, Etudes et Techniques, Paris (France). Centre de Documentation de l'Armement.
COMPUTING ILLUMINATION USING EXTENDED SOURCES: OBJECT SPACE AND IMAGE SPACE Ph.D. Thesis [CALCUL DE L'ILLUMINATION PAR DES SOURCES ETENDUES: ESPACE OBJET ET ESPACE IMAGE]
C. Vedel 13 Sep. 1993 144 p In FRENCH
(PB94-201282) Avail: Issuing Activity (National Technical Information Service (NTIS))

This thesis deals with the simulation of lighting by extended light sources using the radiosity method. The problem is approached from two distinct angles: computation in object space using a mesh, and computation in image space pixel by pixel. The first two chapters describe the radiosity method and the existing algorithms that are the starting point of this work. In particular, they review the meshing techniques used to code the light intensity function on the surfaces of a scene. The following three chapters introduce a meshing method that is not limited to polyhedral approximation of the environment, and that employees the derivatives of the illumination function to improve its reconstruction from the samples. The final chapters describe two new acceleration techniques to compute lighting from polygonal sources: approximate contour integration and discontinuity tracing in image space. Both are extensions to curved surfaces of previous methods that were valid only for polyhedra. NTIS

N95-14181* National Aeronautics and Space Administration. Pasadena Office, CA.
WAVELENGTH-DIVISION MULTIPLEXED OPTICAL INTEGRATED CIRCUIT WITH VERTICAL DIFFRACTION GRATING Patent
Robert J. Lang, inventor (NASA) and Siamak Forouhar, inventor (to NASA) 11 Oct. 1994 17 p Filed 17 Mar. 1993 Supersedes N93-29848 (31 - 11, p 3579)
(Contract NAS7-918)
(NASA-Case-NPO-18357-1-CU; US-Patent-5,355,237;
US-Patent-Appl-SN-033512; US-Patent-Class-359-130;
US-Patent-Class-359-128; US-Patent-Class-359-163;
US-Patent-Class-385-14; US-Patent-Class-385-37;
Int-Patent-Class-H02J-14/02; Int-Patent-Class-G02B-6/12) Avail: US Patent and Trademark Office

A semiconductor optical integrated circuit for wave division multiplexing has a semiconductor waveguide layer, a succession of diffraction grating points in the waveguide layer along a predetermined diffraction grating contour, a semiconductor diode array in the waveguide layer having plural optical ports facing the succession of diffraction grating points along a first direction, respective semiconductor diodes in the array corresponding to respective ones of a predetermined succession of wavelengths, an optical fiber having one end thereof terminated at the waveguide layer, the one end of the optical fiber facing the succession of diffraction grating points along a second direction, wherein the diffraction grating points are spatially distributed along the predetermined contour in such a manner that the succession of diffraction grating points diffracts light of respective ones of the succession of wavelengths between the one end of the optical fiber and corresponding ones of the optical ports.
Official Gazette of the U.S. Patent and Trademark Office

N95-14272*# Van der Spiegel (Jan), Philadelphia, PA.
TECHNICAL GUIDANCE FOR THE DEVELOPMENT OF A SOLID STATE IMAGE SENSOR FOR HUMAN LOW VISION IMAGE WARPING Final Report
Jan VanderSpiegel Oct. 1994 43 p
(NASA Order T-2901-T)
(NASA-CR-196997; NAS 1.26:196997) Avail: CASI HC A03/MF A01

This report surveys different technologies and approaches to realize sensors for image warping. The goal is to study the feasibility, technical aspects, and limitations of making an electronic camera with special geometries which implements certain transformations for image warping. This work was inspired by the research done by Dr. Juday at NASA Johnson Space Center on image warping. The study has looked into different solid-state technologies to fabricate image sensors. It is found that among the available technologies, CMOS is preferred over CCD technology. CMOS provides more flexibility to design different functions into the sensor, is more widely available, and is a lower cost solution. By using an architecture with row and column decoders one has the added flexibility of addressing the pixels at random, or read out only part of the image. Derived from text

N95-14353# Physical Optics Corp., Torrance, CA. Research and Development Div.
A NOVEL TECHNIQUE FOR 4-DIMENSIONAL ATMOSPHERE AND OCEANOGRAPHIC IRRADIANCE MEASUREMENTS USING 3-D SPATIAL FILTERING Bi-monthly Report, 1 Jun. - 31 Jul. 1994
Steve Acklesoln Jul. 1994 7 p
(Contract N00014-94-C-0099)
(AD-A283758) Avail: CASI HC A02/MF A01

During the first two months of this project Physical Optics Corporation (POC) analytically evaluated the depth discrimination properties of a pixel filter. Numerical simulation results indicate that pixel filters have fine depth discrimination capability. Following the numerical analysis, we started to design experiments to verify the capability of the pixel filter. We performed two experiments: first, we measured the light intensity as a function of depth; second, we conducted measurements in the frequency domain as a function of depth. In the frequency domain, measurements are insensitive to fluctuations in light intensity; thus, a higher signal/noise ratio can be expected. DTIC

N95-14367# Allied-Signal Aerospace Co., Kansas City, MO.
INTEGRATED OPTICAL MAZE
E. V. Roos and J. L. Hendrix Jun. 1994 24 p
(Contract DE-AC04-76DP-00613)
(DE94-015866; KCP-613-5384) Avail: CASI HC A03/MF A01

Improvements to Nuclear Weapons Surety through the development of new detonation control techniques incorporating electro-optic technology are reviewed and proposed in this report. The results of the Kansas City Division's (KCD's) literature and vendor search, potential system architecture synthesis, and device test results are the basis of this report. This study has revealed several potential reconfigureable optical interconnect architectures that meet Los Alamos National Laboratory's preliminary performance specifications. Several planer and global architectures have the potential for meeting the Department of Energy's applications. Preliminary conclusions on the proposed architectures are discussed. The planer approach of monolithic GaAs amplifier switch arrays is the leading candidate because it meets most of the specifications now. LiNbO3 and LiTaO3 planer tree switch arrays are the second choice because they meet all the specifications except for laser power transmission. Although not a top choice, acousto-optical free space switch arrays have been considered andmeet most of the specifications. Symmetric-Self Electro-Optic Effect Devices (S-SEED) free space switch arrays are being considered and have excellent potential for smart reconfigureable optical interconnects in the future. DOE

N95-14413* National Aeronautics and Space Administration. Pasadena Office, CA.
WIDE FIELD STRIP-IMAGING OPTICAL SYSTEM Patent
Arthur H. Vaughan, inventor (to NASA) (Jet Propulsion Lab., California Inst. of Tech., Pasadena, CA.) 20 Sep. 1994 15 p Filed 21 Jul. 1993 Division of US-Patent-Appl-SN-786618, filed 1 Nov. 1991
(NASA-Case-NPO-18146-2-CU; US-Patent-5,349,180;
US-Patent-Appl-SN-089460; US-Patent-Appl-SN-786618;
US-Patent-Class-250-227.2; US-Patent-Class-359-896;
Int-Patent-Class-H01J-5/16) Avail: US Patent and Trademark Office

A strip imaging wide angle optical system is provided. The optical system is provided with a 'virtual' material stop to avoid aberrational effects inherent in wide angle optical systems. The optical system includes a spherical mirror section for receiving light from a 180-degree strip or arc of a target image. Light received by the spherical mirror section is reflected to a frusto-conical mirror section for subsequent rereflection to a row of optical fibers. Each optical fiber transmits a portion of the received light to a detector. The optical system exploits the narrow cone of acceptance associated with optical fibers to substantially eliminate vignetting effects inherent in wide-angle systems. Further, the optical system exploits the narrow cone of acceptance of the optical fibers to substantially limit spherical aberration. The optical system is ideally suited for any application wherein a 180-degree strip image need be detected, and is particularly well adapted for use in hostile environments such as in planetary exploration.
Official Gazette of the U.S. Patent and Trademark Office

N95-14806*# Washington Univ., Saint Louis, MO.
ULTRAVIOLET-INFRARED MAPPING INTERFEROMETIC SPECTROMETER Final Report, 1 Jan. 1991 - 28 Feb. 1994
28 Feb. 1994 14 p
(Grant NAGw-2423)
(NASA-CR-197099; NAS 1.26:197099) Avail: CASI HC A03/MF A01

Prism and grating spectrometers have been the defacto devices for spectral mapping and imaging (hereafter referred to as hyperspectra). We have developed a new, hybrid instrument with many superior capabilities, the Digital Array Scanned Interferometer, DASI. The DASI performs the hyperspectral data acquisition in the same way as a grating or prism spectrograph, but retains the substantial advantages of the two-beam (Michelson) interferometer with additional capabilities not possessed by either of the other devices. The DASI is capable of hyperspectral studies in virtually any space or surface environment at any wavelength from below 50 nm to beyond 12 microns with available array detectors. By our efforts, we have defined simple, low cost, no-moving parts DASI's capable of carrying out hyperspectral science measurements for solar system exploration missions, e.g. for martian, asteroid, lunar, or cometary surveys. DASI capabilities can be utilized to minimize cost, weight, power, pointing, and other physical requirements while maximizing the science data return for spectral mapping missions. Our success in the development of DASI's has become and continues to be an important influence on the efforts of the best research groups developing remote sensing instruments for space and other applications. Author

N95-14908*# Hawaii Univ., Honolulu, HI. Inst. for Astronomy.
A LYMAN-ALPHA TUNABLE ACOUSTO-OPTIC FILTER FOR DETECTING SUPERTHERMAL FLARE PROTONS Final Technical Report, 1 Nov. 1988 - 31 Oct. 1994
Donald L. Mickey 10 Nov. 1994 6 p
(Grant NAGw-1699)
(NASA-CR-197119; NAS 1.26:197119) Avail: CASI HC A02/MF A01

The goal of this project was to develop and characterize a narrow-band, tunable filter for use near the Lyman-alpha line of hydrogen at 121.6 nm. Such a filter could form the critical component of an instrument to observe asymmetries in the solar Lyman-alpha line, caused by energetic protons accelerated during the impulsive phase of solar flares. Characteristic charge-exchange nonthermal emission at Lyman alpha should be produced when sub-MeV protons are injected into the chromosphere, but no instrument suitable for their detection has been developed. Such an instrument would require a narrow-band (less than 0.01 nm) tunable filter with aperture and throughput consistent with imaging a solar active region at 0.1 second intervals. The development of acousto-optic tunable filters (AOTF) suitable for use as compact, simple tunable filters for astronomical work suggested an investigation into the use of an AOTF at Lyman-alpha.
Derived from text

N95-15312# Pacific Northwest Lab., Richland, WA.
SCINTILLATING GLASS FIBER-OPTIC NEUTRON SENSORS
K. H. Abel, R. J. Arthur, and M. Bliss et al Apr. 1994 7 p Presented at the Spring Meeting of the Materials Research Society, San Francisco, CA, 4-8 Apr. 1994
(Contract DE-AC06-76RL-01830)
(DE94-014562; PNL-SA-23184; CONF-940411-38) Avail: CASI HC A02/MF A01

Pacific Northwest Laboratory (PNL) has fabricated cerium-activated lithium silicate scintillating fibers via a hot-downdraw process. These fibers, which, as produced, typically have a transmission length (e(sup -1) length) of greater than 2 meters, are found to undergo aging when subjected to room air. The aging, which is complete in a few weeks, reduces the transmission length to the order of 0.5 meter. Because of the high alkali content of the glass (on the order of 20-30 mole percent lithia), we have attributed this aging to aqueous corrosion at the polymer cladding/glass interface. Changes in transmission with chemical treatment of the surface support the corrosion model. Fiber transmission performance has been preserved by modifying the hot-downdraw to a double crucible to produce glass-on-glass waveguides. DOE

N95-15314# Pacific Northwest Lab., Richland, WA.
THIN GSO SCINTILLATOR FOR NEUTRON DETECTION
P. L. Reeder May 1994 11 p Presented at the 8th Symposium on

Radiation Measurements and Applications, Ann Arbor, MI, 16-19 May 1994
(Contract DE-AC06-76RL-01830)
(DE94-014566; PNL-SA-24259; CONF-940524-8) Avail: CASI HC A03/MF A01

The new scintillator cerium-doped gadolinium orthosilicate (GSO - Gd2SiO5:Ce) has a light output that is about 20 percent that of NaI(Tl). The enormous cross section of Gd for capture of thermal neutrons makes GSO a candidate for novel types of neutron detectors. The characteristic radiations from neutron capture in Gd can be stopped in about 75 (mu)m of GSO. Data obtained from a GSO detector that was about 0.6-mm thick demonstrated that thermal neutrons could easily be detected and that higher energy gamma rays caused minimal interference. DOE

N95-15414 Physical Optics Corp., Torrance, CA.
OPTICALLY CONTROLLED MMW BEAMSTEERING BEAMFORMING ANTENNA Final Report
Lev Sadovnik 21 Jun. 1994 30 p Limited Reproducibility: More than 20% of this document may be affected by microfiche quality
(Contract N00014-93-C-0116)
(AD-A282831) Avail: CASI HC A03

In this research project, Physical Optics Corporation (POC) has developed theoretical and laboratory models of semiconductor waveguides for MMW antennas. The physical model has been tested experimentally demonstrating attenuation of MMW propagation in the semiconductor waveguide. POC has also investigated coupling between semiconductor and metal waveguides. A new type of evanescent-coupling scanning antenna has been demonstrated and tested. The results of this project form the foundation for the fabrication of a light controlled antenna. DTIC

N95-15464 Optical Society of America, Washington, DC.
INTEGRATED PHOTONICS RESEARCH, 1993 Final Report, 5 Mar. 1993 - 4 Mar. 1994
Yaron Silberberg Jun. 1994 540 p Limited Reproducibility: More than 20% of this document may be affected by microfiche quality
(Contract DAAH04-93-G-0060)
(AD-A281578; ARO-31175.1-EL-CF) Avail: Issuing Activity (Defense Technical Information Center (DTIC))

Summaries of papers from the Integrated Photonics Research Topical Meeting, March 22-24, 1993, in Palm Springs, California are presented. Sessions include Novel Material and Devices, Time Domain Methods, Photonic Circuits and Lightwave Reception, III-V Semiconductor Switches and Modulators, Wavelength Selective Components, Optical Waveguide Simulators, Optical Switching, Silica on Silicon, Nonlinear Wave Propagation, Semiconductor Lasers, LiNbO3 and LiTaO3 Devices, Beam Propagation Methods, Photonic Integrated Circuits and Applications, Semiconductor Device Modeling, Waveguide Frequency Conversion, and Spatial and Temporal Solitons. DTIC

N95-15529# Lawrence Livermore National Lab., Livermore, CA.
WHAT THOSE DEFECTS IN OPTICAL COATINGS REALLY LOOK LIKE
R. J. Tench, R. Chow, and M. R. Kozlowski May 1994 10 p Presented at the 1994 International American Vacuum Society Users Conference, Boston, MA, 2-13 May 1994
(Contract W-7405-eng-48)
(DE94-015324; UCRL-JC-117434; CONF-9405139-3) Avail: CASI HC A02/MF A01

Laser-induced damage in optical coatings is generally associated with micrometer-scale defects. A simple geometric model for nodule-shaped defects is commonly used to describe defects in optical coatings. No systematic study has been done, however, to prove the applicability of that model to standard optical coating deposition. Some defects are known not to have a classic nodule geometry. The present study uses atomic force microscopy (AFM) and scanning electron microscopy to characterize the topography of coating defects in a HfO2/SiO2 multilayer mirror system. Focused ion-beam cross-sectioning is then used to study the underlying defect structure. This work develops a model for defect shape such that the overall geometry of a coating defect, particularly seed size and depth, can be inferred from non-destructive evaluation measurements such as AFM. The relative mechanical stabilities of nodular defects can be deduced based on the nodule's geometry. Auger analysis showed that the seed material that causes nodular defects in HfO2/SiO2 is a hafnia oxide. Such characterization capabilities are needed for understanding the enhanced susceptibility of particular defects to laser damage and for developing improved techniques for depositing low-defect density coatings. DOE

N95-15603* National Aeronautics and Space Administration. Pasadena Office, CA.
OPTICAL DETECTOR HAVING A PLURALITY OF MATRIX LAYERS WITH COBALT DISILICIDE PARTICLES EMBEDDED THEREIN Patent
Robert W. Fathauer, inventor (to NASA) and Leo Schowalter, inventor (to NASA) 15 Nov. 1994 5 p Filed 25 Aug. 1993 Division of US-Patent-Appl-SN-912961, filed 10 Jul. 1992
(NASA-Case-NPO-18625-2-CU; US-Patent-5,365,054;
US-Patent-Appl-SN-115962; US-Patent-Appl-SN-912961;
US-Patent-Class-250-214.1; US-Patent-Class-257-456;
US-Patent-Class-437-5; Int-Patent-Class-H01J-40/14) Avail: US Patent and Trademark Office

Silicon and metal are coevaporated onto a silicon substrate in a molecular beam epitaxy system with a larger than stoichiometric amount of silicon so as to epitaxially grow particles of metal silicide embedded in a matrix of single crystal epitaxially grown silicon. The particles interact with incident photons by resonant optical absorption at the surface plasmon resonance frequency. Controlling the substrate temperature and deposition rate and time allows the aspect ratio of the particles to be tailored to desired wavelength photons and polarizations. The plasmon energy may decay as excited charge carriers of phonons, either of which can be monitored to indicate the amount of incident radiation at the selected frequency and polarization. Author

N95-15707 Department of the Navy, Washington, DC.
METHOD AND APPARATUS FOR POLARIZATION-MAINTAINING FIBER OPTICAL AMPLIFICATION WITH ORTHOGONAL POLARIZATION OUTPUT Patent
Irl N. Duling, III, inventor (to Navy) and Ronald D. Esman, inventor (to Navy) 12 Apr. 1994 15 p Filed 15 Mar. 1993
(AD-D016365; US-Patent-5,303,314; US-Patent-Appl-SN-031251;
US-Patent-Class-385-11) Avail: US Patent and Trademark Office

A single-polarization fiber optical amplifier and corresponding method is provided capable of amplifying an optical input signal by a fiber optic amplifier constructed of fiber which may be non-polarization-maintaining. The single-polarization fiber optical amplifier provides a direction-selective coupler which receives an optical input at a first port and outputs an optical output at a second port. A fiber optic amplifier is operatively connected to the direction-selective coupler at a bidirectional port for amplifying the optical input. A retro-reflecting orthogonal polarization converter is operatively connected to the fiber optic amplifier, reflecting the amplified optical input from the fiber optic amplifier in a return direction through the fiber optic amplifier and in an orthogonal polarization to the amplified optical input. The direction-selective coupler outputs the reflected amplified orthogonal optical input at the second port as the optical output of the direction selective coupler. Further configurations adapting the input and output ports to transmit the optical signal through cavity or other structures may be provided to produce, for example, an ultrashort pulse optical source; a single-wavelength, single-polarization, widely-tunable laser source: or an amplified spontaneous emission source. DTIC

N95-15764 Department of the Navy, Washington, DC.
LOW-DAMAGE MULTILAYER MIRROR FOR THE SOFT X RAY REGION Patent
John F. Seely, inventor (to Navy) and William R. Hunter, inventor (to Navy) 26 Apr. 1994 14 p Filed 30 Sep. 1992
(AD-D016362; US-Patent-5,307,395; US-Patent-Appl-SN-953697;
US-Patent-Class-378-84) Avail: US Patent and Trademark Office

A mirror for reflecting radiation at a desired wavelength in the soft x-ray region, comprises a substrate and a coating on the substrate. The coating contains a first section and a second section. The first section comprises at least one layer made up of at least a spacer sublayer and a nodal sublayer. The optical thickness of each spacer sublayer is selected so that, upon application of the radiation of desired wavelength, the mirror generates a standing wave having a node in the middle of each nodal sublayer. The second section is disposed between the first section and the substrate, and comprises a plurality of optically absorptive layers. DTIC

N95-15765 Department of the Navy, Washington, DC.
APPARATUS FOR IMAGING AN OBJECT IN OR THROUGH A SCATTERING MEDIUM USING COHERENT ANTI-STOKES RAMAN SCATTERING Patent
Mark Bashkansky, inventor (to Navy) and John F. Reintjes, inventor (to Navy) 19 Apr. 1994 10 p Filed 3 Nov. 1992
(AD-D016366; US-Patent-5,303,710; US-Patent-Appl-SN-970886; US-Patent-Class-128-665) Avail: US Patent and Trademark Office

A method and apparatus for imaging an object that is part of, embedded in or viewed through a scattering medium is provided. A first broadband beam generator, such as a broadband pulse laser, provides a first broadband beam. A second broadband beam generator, such as a Raman Stokes generator disposed to receive the first broadband beam, generates a second broadband beam capable of correlation with the first broadband beam. A coherent anti-Stokes Raman scattering material is disposed to receive the second broadband beam after dispersion in the scattering medium. A variable delay path also illuminates the coherent anti-Stokes Raman scattering material with the first broadband beam. The coherent anti-Stokes Raman scattering material produces an anti-Stokes beam which contains an extracted image of an object in the scattering medium, which image is recorded on a photodetector. DTIC

N95-15766 Department of the Navy, Washington, DC.
LOW LOSS GLASS AND OPTICAL FIBERS THEREFROM Patent
Paige L. Higby, inventor (to Navy), Ishwar D. Aggarwal, inventor (to Navy), and Edward J. Friebele, inventor (to Navy) 19 Apr. 1994 5 p Filed 3 Aug. 1992
(AD-D016379; US-Patent-5,305,414; US-Patent-Appl-SN-923450; US-Patent-Class-385-142) Avail: US Patent and Trademark Office

Optical fibers and glass composition comprising a mixture of barium oxide, gallium oxide, germanium oxide, and a modifying agent selected from lanthium oxide, indium oxide, and mixtures thereof; molar ratio of barium oxide to gallium oxide is from about 4:1 to about 1:1, preferably 2:1 to 1, and especially about 1:1; amount of germanium oxide is at least 40 mole percent, preferably 60 to 95 mole percent, and especially 65 to 90 mole percent; about 0.1 to about 5 mole percent, preferably 0.5 to 4, of gallium oxide is replaced with the modifying agent. The optical fibers made from the glass composition defined herein, with or without the modifying agent, have light transmission wavelength band of about 0.3 to 4 microns; lower optical loss than silica-based optical fibers, the minimum optical loss of the novel fibers having the potential of 0.05 db/km at 2 microns. DTIC

N95-15772# Arizona Univ., Tucson, AZ. Optical Sciences Center.
NEW ALGORITHMS FOR THE REDUCTION OF IMAGE DEGRADATION DUE TO ATMOSPHERIC TURBULENCE Final Report, 1 Jun. 1992 - 31 May 1994
B. R. Frieden 22 Jul. 1994 5 p
(Contract DAAL03-92-G-0209)
(AD-A284891; ARO-30411.5-MA-SDI) Avail: CASI HC A01/MF A01

The problem of removing the deleterious effects of clear-air turbulence from images has been formally solved. As a spinoff, the method also allows wind velocity/shear to be measured along the optical line of sight. The overall approach uses two short-exposure images as inputs. These are divided in Fourier space. The division data is independent of the object (since it is the same in both images), and depends upon parameters that specify the two point spread functions. A neural net allows these parameters to be found, with good accuracy. The two images are then inverse-filtered, using the p.s.f. information. The average of the two inverse-filtered outputs is then the final reconstruction. Because of the neural net implementation, the entire algorithm can be emplaced upon a logic chip and used in quasi-real time. Future development would seem to promise real-time operation. DTIC

N95-15849*# Johns Hopkins Univ., Baltimore, MD. Dept. of Electrical and Computer Engineering.
HIGH SPEED QPPM DIRECT DETECTION OPTICAL COMMUNICATION RECEIVERS FOR FSDD INTERSATELLITE LINKS Final Report
Frederic M. Davidson and Xiaoli Sun Aug. 1993 105 p
(Contract NAS5-32029)
(NASA-CR-189331; NAS 1.26:189331) Avail: CASI HC A06/MF A02

This final report consists of four separate reports, one for each project involved in this contract. The first report is entitled '325 Mbps QPPM (quaternary pulse position modulation) Direct Detection Free Space Optical Communication Encoder and Receiver,' which was our primary work. The second report is entitled 'Test Results of the 325 Mbps QPPM High Speed Data Transmission GaAs ASICs,' which describes our work in connection with Galaxy Microsystems, Inc. who produced these ASICs for NASA. The third report, 'Receiver Performance Analysis of BPPM Optical Communication Systems Using 1.3 micron Wavelength Transmitter and InGaAs PIN Photodiodes,' was prepared at the request of the NASA/Photonics Branch for their efforts in upgrading the 1773 optical fiber data bus. The fourth report, 'Photomultiplier Tubes for Use at 1.064 micron Wavelength,' was also prepared at the request of the NASA/Photonics Branch as a research project. Author

N95-15872 Naval Postgraduate School, Monterey, CA.
EXPERIMENTAL HARDWARE DEVELOPMENT FOR A PULSED ULTRASONIC DATA COLLECTION FACILITY M.S. Thesis
Peter A. Gatchell Jun. 1994 65 p Limited Reproducibility: More than 20% of this document may be affected by microfiche quality
(AD-A283331) Avail: CASI HC A04

The work reported in this thesis used readily available components to implement a data acquisition system for a pulsed ultrasonic data collection facility. Use of hardware with controlling software is necessary to collect waveforms of acoustic potential at a given distance from the transmitting source. Precise movement and positioning of an acoustic receiver in the collection plane is accomplished by use of an xy coordinate motor-driven slide assembly. A signal generator and transient digitizer transmit and digitize the signal, respectively. These components are brought together synchronously using LabVIEW instrumentation software. This work provides an efficient means to collect waveform data which can be used to verify computer code written previously for the purpose of modeling pulsed ultrasonic acoustic diffraction patterns. DTIC

N95-14064*# Lockheed Missiles and Space Co., Sunnyvale, CA. Space Systems Div.
PREDICTION OF PARTICULATE CONTAMINATION ON APERTURE WINDOW
Aleck L. Lee and Michael C. Fong *In* NASA. Goddard Space Flight Center, Eighteenth Space Simulation Conference: Space Mission Success Through Testing Nov. 1994 p 25-35 (For primary document see N95-14062 03-18)
Avail: CASI HC A03/MF A04

N95-14065*# Nauchno-Issledovatelskii Inst. Grafit, Moscow (Russia).
EXPERIMENTAL STUDY OF SOLAR SIMULATOR MIRROR CRYOCONTAMINATION Abstract Only
V. L. Galjaev, A. A. Makarov, and N. A. Afanassiev *In* NASA. Goddard Space Flight Center, Eighteenth Space Simulation Conference: Space Mission Success Through Testing Nov. 1994 p 37 (For primary document see N95-14062 03-18)
Avail: CASI HC A01/MF A04

N95-14068*# National Aeronautics and Space Administration. Goddard Space Flight Center, Greenbelt, MD.
HUBBLE SPACE TELESCOPE SERVICING MISSION SCIENTIFIC INSTRUMENT PROTECTIVE ENCLOSURE DESIGN REQUIREMENTS AND CONTAMINATION CONTROLS
Patricia A. Hansen (Swales and Associates, Beltsville, MD.), David W. Hughes (Swales and Associates, Beltsville, MD.), Randy J. Hedgeland, Craig J. Chivatero, Robert J. Studer, and Peter J. Kostos *In its* Eighteenth Space Simulation Conference: Space Mission Success Through Testing Nov. 1994 p 75-85 (For primary document see N95-14062 03-18)
Avail: CASI HC A03/MF A04

N95-14449# Grumman Aerospace Corp., Bethpage, NY.
MISSILE INFRARED RADIATION ANALYSIS
Michel Engelhardt *In* AGARD, Missile Aerodynamics Jun. 1994 27 p (For primary document see N95-14445 03-02)
Copyright Avail: CASI HC A03/MF A03

N95-14622*# New Mexico State Univ., Las Cruces, NM.
THE STARK ANOMALOUS DISPERSION OPTICAL FILTER: THE THEORY

B. Yin and T. M. Shay *In* JPL, The Telecommunications and Data Acquisition Report 15 Aug. 1994 p 14-21 (For primary document see N95-14620 03-32)
(RTOP 310-20-67-92-02)
Avail: CASI HC A02/MF A02

N95-14638# Army Strategic Defense Command, Huntsville, AL. Technology Integration and Matrix Management Office.
AERO-OPTICS SYSTEM INTEGRATION
Troy A. Street *In* Huntsville Association of Technical Societies, TABES 1994: 10th Annual Technical and Business Exhibition and Symposium 1994 4 p Sponsored by Secretary of the Army (For primary document see N95-14633 03-12)
(TABES Paper 94-604) Avail: CASI HC A01/MF A04

75 PLASMA PHYSICS

Includes magnetohydrodynamics and plasma fusion.

For ionospheric plasmas see *46 Geophysics*. For space plasmas see *90 Astrophysics*.

N95-13973# Environmental Protection Agency, Research Triangle Park, NC. Atmospheric Research and Exposure Assessment Lab.
PHOTOCHEMICAL URBAN AIRSHED MODELING USING DIAGNOSTIC AND DYNAMIC METEOROLOGICAL FIELDS
J. M. Godowitch and J. M. Vukovich Jun. 1994 24 p Presented at the 87th Annual Air and Waste Management Association Meeting and Exhibition, Cincinnati, OH, 19-24 Jun. 1994 See also PB91-131243
(PB94-176120; EPA/600/A-94/092) Avail: CASI HC A03/MF A01

Spatial pollutant patterns and peak concentrations are strongly influenced by meteorological parameters. Therefore, accurate hourly, gridded meteorological data sets are crucial inputs for photochemical modeling. An effort has been underway to apply both diagnostic and dynamic meteorological models in order to generate inputs needed in photochemical grid model simulations. The model being employed is a modified version of the Urban Airshed Model (UAM), which was designed to accept input files generated from both meteorological approaches. The diagnostic meteorological model (UAMMET) relies on routine or intensive measurements to generate hourly 3-D gridded fields of winds, temperatures, vertical eddy diffusivities, photolytic rates, and hourly spatially-varying fields of mixing height and deposition velocities. The diagnostic wind model (DWM) is a key module used generate 3-D wind fields. A dynamic mesoscale meteorological model (a numerical hydrostatic code equipped with a four-dimensional data assimilation technique) generates a gridded meteorological output file, which is post-processed through an interface program to create UAM-compatible wind and mixing height files. In this effort, both meteorological models were exercised in two different urban domains situated next to water bodies and with significant terrain features (i.e., greater metropolitan NYC and LA basin). Results of simulations with the modified UAM model were evaluated in order to investigate the impact on modeled ozone patterns and peak concentrations using inputs from these two meteorological approaches. A historical high ozone day in the NYC domain was simulated which exhibited a strong large scale flow pattern conducive to interurban transport along the northeastern coast. The evaluation results revealed absolute errors were comparable (about 22%) among the simulations, however, higher peak ozone was obtained using dynamically generated wind fields. Results from simulations of an ozone episode from the 1987 Southern California Air Quality Study (SCAQS) indicated that the simulations using dynamic model winds with data assimilation displayed less absolute error than simulations using diagnostically or objectively-derived winds. NTIS

N95-13997# Los Alamos National Lab., NM. Materials Science and Technology Div.
HOHLRAUM MANUFACTURE FOR INERTIAL CONFINEMENT FUSION
L. R. Foreman, P. Gobby, and J. Bartos 1994 11 p Presented at the 35th Annual Meeting of the American Nuclear Society, New Orleans, LA, 11-16 Jun. 1994
(Contract W-7405-eng-36)
(DE94-014472; LA-UR-94-2065; CONF-940602-10) Avail: CASI HC A03/MF A01

Hohlraums are an integral part of indirect drive targets for Inertial Confinement Fusion (ICF) research. Hohlraums are made by an electroforming process that combines elements of micromachining and coating technology. The authors describe how these target elements are made and an extension of the method that allows fabrication of other, more complex target components. DOE

N95-13998# Los Alamos National Lab., NM.
LOS ALAMOS CONTRIBUTION TO TARGET DIAGNOSTICS ON THE NATIONAL IGNITION FACILITY
J. M. Mack, D. A. Baker, and S. E. Caldwell et al 1994 10 p Presented at the 11th Topical Meeting on the Technology of Fusion Energy, New Orleans, LA, 19-24 Jun. 1994
(Contract W-7405-eng-36)
(DE94-014474; LA-UR-94-1883; CONF-940630-16) Avail: CASI HC A02/MF A01

The National Ignition Facility (NIF) will have a large suite of sophisticated target diagnostics. This will allow thoroughly diagnosed experiments to be performed both at the ignition and pre-ignition levels. As part of the national effort Los Alamos National Laboratory will design, construct and implement a number of diagnostics for the NIF. This paper describes Los Alamos contributions to the 'phase I diagnostics.' Phase I represents the most fundamental and basic measurement systems that will form the core for most work on the NIF. The Los Alamos effort falls into four categories: moderate to hard X-ray time resolved imaging; neutron spectroscopy - primarily with neutron time of flight devices; burn diagnostics utilizing gamma ray measurements; and testing measurement concepts on the TRIDENT laser system at Los Alamos. Because of the high blast, debris and radiation environment, the design of high resolution X-ray imaging systems present significant challenges. Systems with close target proximity require special protection and methods for such protection is described. The system design specifications based on expected target performance parameters is also described. Diagnosis of nuclear yield and burn will be crucial to the NIF operation. Nuclear reaction diagnosis utilizing both neutron and gamma ray detection is discussed. The Los Alamos TRIDENT laser system will be used extensively for the development of new measurement concepts and diagnostic instrumentation. Some its potential roles in the development of diagnostics for NIF are given. DOE

N95-14006 Argonne National Lab., IL.
MHD FLOW IN RECTANGULAR DUCTS WITH INCLINED NON-UNIFORM TRANSVERSE MAGNETIC FIELD
Thanh Q. Hua and J. S. Walker Jun. 1994 27 p Presented at the 3rd International Symposium on Fusion Nuclear Technology, Los Angeles, CA, 27 Jun. - 1 Jul. 1994 Limited Reproducibility: More than 20% of this document may be affected by microfiche quality
(Contract W-31-109-eng-38)
(DE94-013989; ANL/TD/CP-81662; CONF-940664-14) Avail: CASI HC A03

This paper examines the three-dimensional liquid metal MHD flow in rectangular ducts with thin conducting walls and with an inclined nonuniform transverse magnetic field. The Hartmann number and interaction parameter are assumed to be large and the magnetic Reynolds number is assumed to be small. Under these assumptions, viscous and inertial effects are confined to thin boundary layers adjacent to the walls. Outside these layers, the governing equations are significantly simplified. For validation of the numerical solutions, exact analytical solutions are derived for the case of a rectangular duct of equal wall thickness and with a uniform magnetic field. Comparisons of the exact analytical and numerical solutions give excellent agreement. Variation of the fully developed flow pressure gradient with the wall conductance ratio, aspect ratio, and magnetic angle is discussed. Numerical solutions are presented for flow in the varying field region where the flow is perturbed due to three-dimensional effects. The three-dimensional pressure drop, i.e., in excess of the locally fully developed pressure, is presented and its implication to a fusion blanket is discussed. The velocity distributions are also presented. DOE

N95-14007# Los Alamos National Lab., NM.
ADVANCED STELLARATOR POWER PLANTS
R. L. Miller 1994 5 p Presented at the 11th Topical Meeting on the Technology of Fusion Energy, New Orleans, LA, 19-24 Jun. 1994

(Contract W-7405-eng-36)
(DE94-014442; LA-UR-94-1956; CONF-940630-15) Avail: CASI HC A01/MF A01

The stellarator is a class of helical/toroidal magnetic fusion devices. Recent international progress in stellarator power plant conceptual design is reviewed and comparisons in the areas of physics, engineering, and economics are made with recent tokamak design studies. DOE

N95-14012 Argonne National Lab., IL.
TOKAMAK POWER PLANT BURN CYCLE OPTIONS
D. A. Ehst Jun. 1994 9 p Presented at the 11th Topical Meeting on the Technology of Fusion Energy, New Orleans, LA, 19-24 Jun. 1994 Limited Reproducibility: More than 20% of this document may be affected by microfiche quality
(Contract W-31-109-eng-38)
(DE94-014016; ANL/TD/CP-82066; CONF-940630-11) Avail: CASI HC A02

Experiments show that tokamaks can operate in various fashions. Economic analyses show that steady state is most attractive provided the physics and technology of current drive (CD) can be modestly improved. Even with very conservative CD assumptions a hybrid operating mode seems superior to conventional, simple inductive operation. DOE

N95-14262# Sandia National Labs., Albuquerque, NM.
STUDIES OF THE ABLATED PLASMA FROM EXPERIMENTAL PLASMA GUN DISRUPTION SIMULATIONS
P. D. Rockett, J. A. Hunter, J. T. Bradley, III, J. M. Gahl, A. Zhitlukhin, K. Arkhipov, V. Bakhtin, D. Toporkov, V. N. Litunovsky, and I. B. Ovchinnokov et al 1994 16 p Presented at the 11th International Conference on Plasma Surface Interactions in Controlled Fusion Devices, Mito, Japan, 23-27 May 1994
(Contract DE-AC04-94AL-85000)
(DE94-015017; SAND-94-1874C; CONF-940580-6) Avail: CASI HC A03/MF A01

Extensive simulations of Tokamak disruptions have provided a picture of material erosion that is limited by the transfer of energy from the incident plasma to the armor solid surface through a dense vapor shield. Radiation spectra were recorded in the VUV and in the visible at the Efremov Laboratories on VIKA using graphite targets. The VUV data were recorded with a Sandia Labs transmission grating spectrograph, covering 1--40 nm. Plasma parameters were evaluated with incident plasma energy densities varying from 1--10 kJ/sq cm. A second transmission grating spectrograph was taken to 2MK-200 at TRINITI to study the plasma-material interface in magnetic cusp plasma. Target materials included POCO graphite, ATJ graphite, boron nitride, and plasma-sprayed tungsten. Detailed spectra were recorded with a spatial resolution of approximately 1 mm resolution. Time-resolved data with 40--200 ns resolution was also recorded. The data from both plasma gun facilities demonstrated that the hottest plasma region was sitting several millimeters above the armor tile surface. DOE

N95-14328 General Atomics Technologies Corp., San Diego, CA.
DIVERTOR BIAS EXPERIMENTS
G. M. Staebler Jun. 1994 37 p Presented at the 11th International Conference on Plasma Surface Interactions in Controlled Fusion Devices, Mito, Japan, 23-27 May 1994 Limited Reproducibility: More than 20% of this document may be affected by microfiche quality
(Contract DE-AC03-89ER-51114)
(DE94-015720; GA-A-21679; CONF-940580-8) Avail: CASI HC A03

Electrical biasing of the divertor target plates has recently been implemented on several tokamaks. The results of these experiments to date will be reviewed in this paper. The bias electrode configuration is unique in each experiment. The effects of biasing on the scrape-off layer (SOL) plasma also differ. By comparing results between machines, and using theoretical models, an understanding of the basic physics of biasing begins to emerge. Divertor biasing has been demonstrated to have a strong influence on the particle and energy transport within the SOL. The ability to externally control the SOL plasma with biasing has promising applications to future tokamak reactors. DOE

N95-14368# Los Alamos National Lab., NM.
RADIATION RATES FOR LOW Z IMPURITIES IN EDGE PLASMAS
R. Clark, J. Abdallah, and D. Post 1994 13 p Presented at the 11th International Conference on Plasma Surface Interactions in Controlled Fusion Devices, Mito, Japan, 23-27 May 1994
(Contract W-7405-eng-36)
(DE94-016073; LA-UR-94-2268; CONF-940580-12) Avail: CASI HC A03/MF A01

The potential role of impurity radiation in the reduction of heat loads on divertor plates places a new degree of importance on the accuracy of low Z impurity radiation emission rates for electron temperatures below 300 eV. We have calculated the radiated power loss using a collisional-radiative model for Be, B, C, Ne and Ar using a multiple configuration interaction model which includes density dependent effects, as well as a very detailed treatment of the energy levels and meta-stables. These rates indicate that significant enhancements above steady state collisional-radiative rates due to such effects as rapid recycling and charge exchange recombination will be necessary for impurity radiation to reduce the peak heat loads on divertor plates for high heat flux experiments such as ITER. DOE

N95-14373# Wisconsin Univ., Madison, WI. Plasma Physics Research.
CONSERVATION OF MAGNETIC HELICITY DURING PLASMA RELAXATION
H. Ji, S. C. Prager, and J. S. Sarff Jul. 1994 19 p
(Contract DE-FG02-85ER-53198)
(DE94-016770; DOE/ER-53198/244) Avail: CASI HC A03/MF A01

Decay of the total magnetic helicity during the sawtooth relaxation in the MST Reversed-Field Pinch is much larger than the MHD prediction. However, the helicity decay (3-4%) is smaller than the magnetic energy decay (7-9%), modestly supportive of the helicity conservation hypothesis in Taylor's relaxation theory. Enhanced fluctuation-induced helicity transport during the relaxation is observed. DOE

N95-14397# Los Alamos National Lab., NM.
RADIOACTIVITY MEASUREMENTS OF ITER MATERIALS USING THE TFTR D-T NEUTRON FIELD
A. Kumar (California Univ., Los Angeles, CA.), M. A. Abdou (California Univ., Los Angeles, CA.), C. W. Barnes, and H. W. Kugel 1994 30 p Presented at the ISFNT-3: 3rd International Symposium on Fusion Nuclear Technology, Los Angeles, CA, 27 Jun. - 1 Jul. 1994
(Contracts W-7405-eng-3-6; DE-AC02-76CH-03073; DE-FG03-86ER-52123)
(DE94-016094; LA-UR-94-2563; CONF-940664-22) Avail: CASI HC A03/MF A01

The availability of high D-T fusion neutron yields at TFTR has provided a useful opportunity to directly measure D-T neutron-induced radioactivity in a realistic tokamak fusion reactor environment for materials of vital interest to ITER. These measurements are valuable for characterizing radioactivity in various ITER candidate materials, for validating complex neutron transport calculations, and for meeting fusion reactor licensing requirements. The radioactivity measurements at TFTR involve potential ITER materials including stainless steel 316, vanadium, titanium, chromium, silicon, iron, cobalt, nickel, molybdenum, aluminum, copper, zinc, zirconium, niobium, and tungsten. Small samples of these materials were irradiated close to the plasma and just outside the vacuum vessel wall of TFTR, locations of different neutron energy spectra. Saturation activities for both threshold and capture reactions were measured. Data from dosimetric reactions have been used to obtain preliminary neutron energy spectra. Spectra from the first wall were compared to calculations from ITER and to measurements from accelerator-based tests. DOE

N95-14426# General Atomics Co., San Diego, CA.
ADVANCED TOKAMAK RESEARCH ON THE D3-D TOKAMAK
V. S. Chan Jan. 1994 19 p Presented at the Workshop on Nuclear Fusion and Plasma Physics, Hefei, China, 4-15 Oct. 1993
(Contracts DE-FG03-92ER-54150; DE-AC03-89ER-51114)
(DE94-015860; GA-A-21466; CONF-9310340-1) Avail: CASI HC A03/MF A01

The objective of the planned research in advanced tokamak development on DIII-D at General Atomics, San Diego, USA, is to establish improved tokamak operation through significant improvements in the stability factor, confinement quality, and bootstrap current fraction using localized radio frequency (RF) current profile control, RF and neutral beam heating for pressure profile control, as well as control of plasma rotation and optimization of the plasma boundary conditions. Recent research results in H-mode

confinement, modifications of current profiles to achieve higher confinement and higher beta, a new regime of improved confinement (VH-mode), and RF noninductive current drive are encouraging. In this talk, arguments will be presented supporting the need for improved performance in tokamak reactors. Experimentally observed advanced performance regimes on DIII-D will be discussed. Confinement improvement up to H = 4, where H is the ratio of energy confinement time to the ITER89-P scaling H is equivalent to Tau(sub E)/Tau(sub E-ITER89-P), has been achieved. In other discharges beta(sub N) = beta/(I/aB) (% m Tau/MA) approximately greater than 6 has been obtained. These values have so far been achieved transiently and independently. Techniques, will be described which can extend the high performance to quasi-steady-state and sustain the high H and beta(sub N) values simultaneously. Two high performance regimes, one in first stable regime and the other in second stable regime, have been simulated by self-consistently evolving a magnetohydrodynamic (MHD) equilibrium-transport code. Finally, experimental program plans and outstanding important physics issues will be discussed. DOE

N95-14443# Sandia National Labs., Albuquerque, NM.
US-JAPAN WORKSHOP Q-181 ON HIGH HEAT FLUX COMPONENTS AND PLASMA-SURFACE INTERACTIONS FOR NEXT DEVICES: PROCEEDINGS
R. T. McGrath, ed. Apr. 1994 710 p Workshop held in San Diego, CA, 24-27 Jan. 1994
(Contract DE-AC04-94AL-85000)
(DE94-014939; SAND-94-0753; CONF-940190) Avail: CASI HC A99/MF A06

This report contain viewgraphs of papers from the following sessions: plasma facing components issues for future machines; recent PMI results from several tokamaks; high heat flux technology; plasma facing components design and applications; plasma facing component materials and irradiation damage; boundary layer plasma; plasma disruptions; conditioning and tritium; and erosion/redeposition. DOE

N95-14798*# Iowa Univ., Iowa City, IA. Dept. of Physics and Astronomy.
GEOTAIL MCA PLASMA WAVE DATA ANALYSIS Annual Report, 15 Aug. 1993 - 14 Aug. 1994
Roger R. Anderson 1994 14 p
(Grant NAG5-2346)
(NASA-CR-197022; NAS 1.26:197022) Avail: CASI HC A03/MF A01

NASA Grant NAG 5-2346 supports the data analysis effort at The University of Iowa for the GEOTAIL Multi-Channel Analyzer (MCA) which is a part of the GEOTAIL Plasma Wave Instrument (PWI). At the beginning of this reporting period we had just begun to receive our GEOTAIL Sirius data on CD-ROMs. Much programming effort went into adapting and refining the data analysis programs to include the CD-ROM inputs. Programs were also developed to display the high-frequency-resolution PWI Sweep Frequency Analyzer (SFA) data and to include in all the various plot products the electron cyclotron frequency derived from the magnitude of the magnetic field extracted from the GEOTAIL Magnetic Field (MGF) data included in the GEOTAIL Sirius data. We also developed programs to use the MGF data residing in the Institute of Space and Astronautical Science (ISAS) GEOTAIL Scientific Data Base (SDB). Our programmers also developed programs and provided technical support for the GEOTAIL data analysis efforts of Co-Investigator William W. L. Taylor at Nichols Research Corporation (NRC). At the end of this report we have included brief summaries of the NRC effort and the progress being made.
Derived from text

N95-14955# Rochester Univ., NY. Lab. for Laser Energetics.
LLE REVIEW, JANUARY - MARCH 1994
A. Simon, ed. 1994 46 p
(Contract DE-FC03-92SF-19460)
(DE94-015058; DOE/SF-19460/17) Avail: CASI HC A03/MF A01

This volume of the LLE Review, covering the period Jan - Mar 1994, contains articles on backlighting diagnostics; the effect of electron collisions on ion-acoustic waves and heat flow; using PIC code simulations for analysis of ultrashort laser pulses interacting with solid targets; creating a new instrument for characterizing thick cryogenic layers; and a description of a large-aperture ring amplifier for laser-fusion drivers. Three of these articles - backlighting diagnostics; characterizing thick cryogenic layers; and large-aperture ring amplifier - are directly related to the OMEGA Upgrade, now under construction. Separate abstracts have been prepared for articles from this report. DOE

N95-15373# Mississippi State Univ., Mississippi State, MS.
DIAGNOSTIC DEVELOPMENT AND SUPPORT OF MHD TEST FACILITIES
1994 75 p
(Contract DE-AC02-80ET-15601)
(DE94-015344; DOE/ET-15601/47) Avail: CASI HC A04/MF A01

The Diagnostic Instrumentation and Analysis Laboratory (DIAL) at Mississippi State University (MSU) is developing diagnostic instruments for magnetohydrodynamic (MHD) power train data acquisition and for support of MHD component development test facilities. Microprocessor-controlled optical instruments, initially developed for Heat Recovery/Seed Recovery (HRSR) support, are being refined, and new systems to measure temperatures and gas-seed-slag stream characteristics are being developed. To further data acquisition and analysis capabilities, the diagnostic systems are being interfaced with DIAL's computers. Technical support for the diagnostic needs of the national MHD research effort is being provided. DIAL personnel also cooperate with government agencies and private industries to improve the transformation of research and development results into processes, products and services applicable to their needs. DOE

N95-15374# Mississippi State Univ., Mississippi State, MS. Diagnostic Instrumentation and Analysis Lab.
FARADAY ROTATION SYSTEM
L. E. Bauman and W. Wang 1994 61 p
(Contract DE-AC02-80ET-15601)
(DE94-015345; DOE/ET-15601/T62) Avail: CASI HC A04/MF A01

The Faraday Rotation System (FRS) is one of the advanced laser-based diagnostics developed at DIAL to provide support for the demonstration of prototype-scale coal-fired combustion magnetohydrodynamic (MHD) electrical power generation. Intended for application in the MHD channel, the system directly measures electron density through a measurement of the induced rotation in the polarization of a far infrared laser beam after passing through the MHD flow along the magnetic field lines. A measurement of the induced polarization ellipticity provides a measure of the electron collision frequency which together with the electron density gives the electron conductivity, a crucial parameter for MHD channel performance. The theory of the measurements, a description of the system, its capabilities, laboratory demonstration measurements on seeded flames with comparison to emission absorption measurements, and the current status of the system are presented in this final report. DOE

N95-15540# Wisconsin Univ., Madison, WI. Dept. of Physics.
LOWER-HYBRID POLOIDAL CURRENT DRIVE FOR FLUCTUATION REDUCTION IN A REVERSED FIELD PINCH
E. Uchimoto, M. Cekic, R. W. Harvey, C. Litwin, S. C. Prager, J. S. Sarff, and C. R. Sovinec Jun. 1994 13 p
(Contract DE-FG02-85ER-53212)
(DE94-015534; DOE/ER-53212/241) Avail: CASI HC A03/MF A01

Current drive using the lower-hybrid slow wave is shown to be a promising candidate for improving confinement properties of a reversed field pinch (RFP). Ray-tracing calculations indicate that the wave will make a few poloidal turns while spiraling radially into a target zone inside the reversal layer. The poloidal antenna wavelength of the lower hybrid wave can be chosen so that efficient parallel current drive will occur mostly in the poloidal direction in this outer region. Three-dimensional resistive magnetohydrodynamic (MHD) computation demonstrates that an additive poloidal current in this region will reduce the magnetic fluctuations and magnetic stochasticity. DOE

N95-15632 General Atomics Technologies Corp., San Diego, CA.
THE EFFECT OF THE EDGE CURRENT DENSITY ON CONFINEMENT AND KINK MODE STABILITY IN H-MODE AND VH-MODE DISCHARGES
J. R. Ferron, L. L. Lao, T. H. Osborne, E. J. Strait, T. S. Taylor, S. J. Thompson, A. D. Turnbull, and O. Sauter Jul. 1994 4 p Presented at the 21st European Conference on Controlled Fusion and Plasma Physics, Marseilles, France, 26 Jun. - 1 Jul. 1994 Limited Reproducibility: More than 20% of this document may be affected by microfiche quality

(Contract DE-AC03-89ER-51114)
(DE94-015719; GA-A-21737; CONF-940635-4) Avail: Issuing Activity (Department of Energy (DOE))

The effect of the local current density in the outer portion of a tokamak discharge (J((rho) (approximately) a)) is discussed in three situations. In a H-mode discharge, a strong reduction of J((rho) (approximately) a) results in the loss of the H-mode pressure pedestal. A smaller reduction in J((rho) (approximately) a) can prevent the transition from H-mode to VH-mode. Finally, a sufficiently large value of J((rho) (approximately) a) accompanied by a sufficiently large value of the pressure gradient in the same region of the discharge, can destabilize low-n (e.g., n = 1 to 5) kink-type modes in a VH-mode discharge. DOE

N95-15758*# Lockheed Missiles and Space Co., Palo Alto, CA. Space Sciences Lab.
DYNAMICS EXPLORER 1: ENERGETIC ION COMPOSITION SPECTROMETER (EICS) Final Report, 1 Dec. 1989 - 31 Aug. 1994
E. G. Shelley, W. K. Peterson, and H. L. Collin Jul. 1994 35 p
(Contract NAS5-33032; RTOP 602-00-00)
(NASA-CR-189375; NAS 1.26:189375; LMSC-F-254280) Avail: CASI HC A03/MF A01

The Energetic Ion Composition Spectrometer (EICS) experiment was selected as part of the Dynamics Explorer (DE) Program. One of the primary goals of the DE program was to investigate in detail the plasma physics processes responsible for energizing thermal (approximately 1 eV) ionospheric ions and transporting them to the earth's plasma sheet and distant polar cap. The results of the EICS data analysis (including support of other investigators) and of the archiving efforts supported by this contract are summarized in this document. Also reported are some aspects of our operational support activities. Author

N95-15774# Los Alamos National Lab., NM.
AN ALGORITHM FOR REZONING PARTICLE-IN-CELL CALCULATIONS
G. Lapenta and J. U. Brackbill 1994 5 p Presented at the 15th International Conference on the Numerical Simulation of Plasmas, Valley Forge, PA, 7-9 Sep. 1994
(Contract W-7405-eng-36)
(DE94-016056; LA-UR-94-2335; CONF-9409105-1) Avail: CASI HC A01/MF A01

To give particle-in-cell methods (PIC) the same flexibility as finite-difference methods, one must be able to add and delete particles as needed. This flexibility is needed to model flows with large variations in density, to use variable grid spacing to resolve multiple length scale structures, and to use PIC in cylindrical geometry. The PIC method is applied to both kinetic and fluid problems. In kinetic calculations, the information and the interest lies in the distribution in velocity. In fluid calculations, moments of the velocity distribution, e.g., mass, momentum, and energy, are conserved. Thus, different kinds of information must be preserved in fluid and kinetic calculations when particles are added and deleted. We describe two algorithms for controlling the number of particles in PIC calculations, one for kinetic md one for fluid calculations. These algorithms, which we call 'particle rezoners ', are designed to preserve essential information in each case and to be simple and inexpensive to apply. DOE

N95-14571*# Iowa Univ., Iowa City, IA.
PLASMA DUST CRYSTALLIZATION
John Goree, H. Thomas, and G. Morfill *In* NASA. Lewis Research Center, Second Microgravity Fluid Physics Conference Aug. 1994 p 325-330 (For primary document see N95-14522 03-34)
(Grant NAG8-292)
Avail: CASI HC A02/MF A04; 2 functional color pages

76 SOLID-STATE PHYSICS

Includes superconductivity.

For related information, see also *33 Electronics and Electrical Engineering* and *36 Lasers and Masers.*

N95-13681 Argonne National Lab., IL.
SURFACE CURRENTS AND BULK PINNING IN Bi2Sr2CaCu2O8
D. Majer (Weizmann Inst. of Science, Rehovot, Israel.), E. Zeldov (Weizmann Inst. of Science, Rehovot, Israel.), M. Konczykowski (Ecole Polytechnique, Palaiseau, France.), V. B. Geshkenbein (Academy of Sciences, USSR, Moscow, USSR.), and A. I. Larkin (Academy of Sciences, USSR, Moscow, USSR.) May 1994 2 p Presented at the Meeting on Materials and Mechanisms of Superconductivity: High Temperature Superconductors, Grenoble, France, 4-9 Jul. 1994 Limited Reproducibility: More than 20% of this document may be affected by microfiche quality
(Contract W-31-109-eng-38)
(DE94-013873; ANL/MSD/CP-83112; CONF-940701-4) Avail: CASI HC A01

The mechanisms giving rise to the irreversibility line (IL) in the phase diagram of Bi2Sr2CaCu2O8 and the mechanism behind the second maximum in the magnetization loops were determined using a novel Hall-sensor array. The IL is caused by bulk pinning at lower temperatures and by irreversible shielding currents above 22 K. The second maximum is caused by vortex lattice melting, taking place at the same local magnetic induction B(sub m) throughout the sample. DOE

N95-13691 Puerto Rico Univ., Rio Piedras. Dept. of Physics.
KINETIC THEORY FOR ELECTRODIC PHASE TRANSITIONS: THE VOLTAMMOGRAM
L. Blum, M. Legault, and P. Turq 4 May 1994 25 p Limited Reproducibility: More than 20% of this document may be affected by microfiche quality
(Contract N00014-90-J-1263)
(AD-A283039; TR-29) Avail: CASI HC A03

In previous work we have proposed the sticky site model (SSM) for the chemisorption of adsorbates from fluids onto crystal surfaces. The crystal surface is represented by an array of sticky point adsorption sites. This permits the formal decoupling of the statistical mechanics into the 1-dimensional problem of the smooth electrode near an electrolyte, (the classic double layer problem), and the 2-dimensional lattice gas of the adsorption onto the array of sticky sites. In this model the binding process of individual atom is coupled to the cooperative effects that take place at the surface through mean field parameters, and the adsorption process is treated by studying the two dimensional lattice gas of the adsorbates, with two parameters obtained from the double layer problem. In the present work we extend the equilibrium (zero scanning rate) theory to include the dynamic regime of non-zero scanning rates. DTIC

N95-13698# Air Force Inst. of Tech., Wright-Patterson AFB, OH.
ION IMPLANTATION OF He-3 IN TANTALUM FOR USE IN A LOW ENERGY DEUTERON POLARIZATION ANALYZER
Andrew C. Hird, K. A. Fletcher, E. J. Ludwig, and Z. Ayer 1994 32 p
(AD-A283172; AFIT/CI/CIA-94-102) Avail: CASI HC A03/MF A01

The implantation of tantalum foils with He-3 has been accomplished for implant energies from 7 to 20 keV and doses from 1.5-29.3 Coulombs/sq cm. Implant thicknesses are not consistent with the Zero order implantation theory, but are in agreement with previous experiment. Thickness dependence upon implant energy, dose, and temperature are studied. The foils were bombarded with deuterons to determine target thicknesses, thickness lifetimes, and to study the properties of the tensor analyzing power of the He-3(d,p)He-4 reaction near its 430 keV resonance. Ayy is measured and appears energy independent and isotropic in the energy range 222-322 keV. Author (DTIC)

N95-13821# Oak Ridge National Lab., TN.
IN-SITU TEM CRYSTALLIZATION OF SOL-GEL DERIVED BaTiO3 THIN FILMS
M. L. Mecartney (California Univ., Irvine, CA.), M. C. Gust (California Univ., Irvine, CA.), and N. D. Evans (Oak Ridge Inst. for Science and Education, TN.) 1994 2 p Presented at the Microscopy Society of America and Microbeam Analysis Society Joint Meeting, New Orleans, LA, 31 Jul. - 5 Aug. 1994
(Contract DE-AC05-84OR-21400)
(DE94-013260; CONF-940753-19) Avail: CASI HC A01/MF A01

Plan view and cross sectional view samples of pyrolyzed Ba-Ti methoxypropoxide films on (100)Si were prepared in the amorphous form. In-situ hot stage experiments were conducted in a Philips CM30 to follow the crystallization process. With time at 750 C, large grains nucleated

mostly at the BaTiO3 surface; the regions near the Si did not crystallize. DOE

N95-13822# Argonne National Lab., IL.
IN SITU, REAL-TIME ANALYSIS OF THE GROWTH OF FERROELECTRIC AND CONDUCTIVE OXIDE HETEROSTRUCTURES BY A NEW TIME-OF-FLIGHT PULSED ION BEAM SURFACE ANALYSIS TECHNIQUE
O. Auciello (Microelectronics Center of North Carolina, Research Triangle Park, NC.), A. R. Krauss, D. M. Gruen, and Y. Lin 1994 8 p Presented at the Spring Meeting of the Materials Research Society, San Francisco, CA, 4-8 Apr. 1994
(Contract W-31-109-eng-38)
(DE94-013298; ANL/CHM/CP-81247; CONF-940411-27) Avail: CASI HC A02/MF A01

A new time-of-flight ion scattering and recoil spectroscopy (ISARS) technique has been developed and is now used to perform in situ, real-time analysis of ferroelectric and conductive oxide layers during growth. Initial results presented show various major effects, namely: (1) RuO2 films on MgO substrates appear to be terminated in O atoms on the top layer located in between Ru atoms lying in the layer underneath (This effect may have major implications for the explanation of the elimination of polarization fatigue demonstrated for RuO2/PZT/RuO2 heterostructure capacitors); (2) deposition of a Ru monolayer on top of a Pb monolayer results in surface segregation of Pb until a complete Pb layer develops over the Ru monolayer; and (3) a Pb/Zr/Ti layered structure yields a top Pb layer with first evidence of the existence of Pb vacancies, which also may have major implications in relation to the electrical characteristics of PZT-based capacitors. DOE

N95-13999# Los Alamos National Lab., NM.
HIGH FIELD MAGNETOTRANSPORT AND SPECIFIC HEAT IN YbAgCu4
A. Lacerda, T. Graf, and M. Hundley 1994 8 p Presented at the Strongly Correlated Electron Systems, Amsterdam, Netherlands, Aug. 1993
(Contract W-7405-eng-36)
(DE94-014475; LA-UR-94-1892; CONF-9308237-1) Avail: CASI HC A02/MF A01

The electrical resistivity (rho) and magnetoresistance of polycrystalline YbAgCu4 have been measured at temperatures between 25 mK and 300 K, and at magnetic fields (B) to 18 T. The magnetoresistance ((rho)(B)-(rho)(0))/(rho)(0) is positive at all temperatures below 200 K and reaches its maximum of 60% at 18 T and 25 mK. The field- and temperature-dependent resistivity does not scale in a simple way. The opposite magnetoresistance behaviors at ambient and high pressure can be explained qualitatively by crystal-field effects lifting the degeneracy of the J = 7/2 groundstate. The linear coefficient of specific heat (gamma) measured at fields to 10 T shows a quadratic field dependence. The authors do not find a linear relation between gamma(exp 2) and A, the T(exp 2)-coefficient of the temperature-dependent resistivity, with field as the implicit parameter. DOE

N95-14008 Argonne National Lab., IL.
FLUX PINNING AND FORCED ENTANGLEMENT BY SPLAYED COLUMNAR DEFECTS
T. Hwa (Institute for Advanced Study, Princeton, NJ.), P. L. Doussal (Rutgers Univ., Piscataway, NJ.), D. R. Nelson (Harvard Univ., Cambridge, MA.), and V. M. Vinokur May 1994 2 p Presented at the Meeting on Materials and Mechanisms of Superconductivity: High Temperature Superconductors, Grenoble, France, 4-9 Jul. 1994 Limited Reproducibility: More than 20% of this document may be affected by microfiche quality
(Contract W-31-109-eng-38)
(DE94-013994; ANL/MSD/CP-83111; CONF-940701-7) Avail: CASI HC A01

We propose controlled splay of artificial columnar defects in cuprate superconductors as a strategy to enhance transport properties in a field compared to parallel columns. The theory predicts a new 'splayed glass' phase with a greatly reduced flux creep, an entangled ground state, and very slow response to a transverse field. DOE

N95-14009 Argonne National Lab., IL.
ELECTRON SPIN RESONANCE AND BAND ELECTRONIC STRUCTURE STUDY OF THE METAL-INSULATOR TRANSITION IN (BEDT-TTF)3(HSO4)2
L. C. Porter, M. A. Beno, K. D. Carlson, U. Geiser, M. S. Tomasko, H. H. Wang, J. M. Williams, D. B. Kang, and M. H. Whangbo 1994 10 p Limited Reproducibility: More than 20% of this document may be affected by microfiche quality
(Contract W-31-109-eng-38)
(DE94-014005; ANL/CHM/PP-75225) Avail: CASI HC A02

The crystal structure of a 3:2 salt of bis (ethylenedithio) tetrathiafulvalene (BEDT-TTF or simply ET), (ET)3(HSO4)2, has recently been reported. In this salt, two crystallographically nonequivalent ET molecules exist, but they are essentially identical in structure so that they are each described as possessing an average charge of +2/3. (ET)3(HSO4)2 is isostructural with other 3:2 salts, (ET)3(ClO4)2, (ET)3Br2 center dot 2H2O, and (ET)3(BrO4)2. (ET)3(HSO4)2 undergoes a metal-insulator (MI) transition at 130 K under ambient pressure. This phase transition is suppressed by an applied pressure greater than 0.5 kbar, but no superconductivity is found down to 1.3 K. The pressure dependence of the band gap in (ET)3(HSO4)2 suggests that its MI transition does not result from a Peierls instability and is of second order. In the present work, the authors examine the nature of this MI transition on the basis of electron spin resonance (ESR) measurements and band electronic structure calculations. DOE

N95-14188# Argonne National Lab., IL.
INTERMULTIPLET TRANSITIONS IN OPTICALLY OPAQUE EuBa2Cu3O7: AN INELASTIC NEUTRON SCATTERING STUDY
U. Staub, L. Soderholm, R. Osborn, M. Guillaume, A. Furrer, and V. Trounov 1994 15 p Presented at the 2nd International Conference on F-elements, Helsinki, Finland, 1-6-Aug. 1994
(Contract W-31-109-eng-38)
(DE94-013429; ANL/CHM/CP-83030; CONF-9408111-1) Avail: CASI HC A03/MF A01

We report the results of inelastic neutron scattering (INS) studies of the J=0 to J=1 magnetic transitions in EuBa2Cu3O7. The low J values of these multiplets restrict our crystal field analysis to the second order crystalline electric field (CEF) parameters B0 sq and B2 sq obtained by fitting the splitting of the J=I multiplet, and the spin-orbit coupling parameter, which is used to fit the energy of the J=0 to J=I multiplet splitting. We compare our results to those derived from other INS studies on different rare earths, as well as with B0 sq and B2 sq derived from Moessbauer studies. The J=O to J=I splitting observed here is smaller than previously seen by optical spectroscopic studies on a variety of transparent, ionic compounds, necessitating the inclusion of a free-ion parameter in the fitting procedure. This work represents the first time that a complete excited multiplet has been seen for R in RBa2Cu3O7. These results are particularly germane to crystal field analyses of the light rare earth ions inoptically opague materials, where assumptions about free-ion parameters are essential for a meaningful analysis. DOE

N95-14189# California Univ., Berkeley. Lawrence Berkeley Lab, CA.
ION BEAM SYNTHESIS OF SiGe ALLOY LAYERS Ph.D. Thesis
Seongil Im May 1994 106 p
(Contract DE-AC03-76SF-00098)
(DE94-014958; LBL-35580) Avail: CASI HC A06/MF A02

Procedures required for minimizing structural defects generated during ion beam synthesis of SiGe alloy layers were studied. Synthesis of 200 mm SiGe alloy layers by implantation of 120-keV Ge ions into (100) oriented Si wafers yielded various Ge peak concentrations after the following doses, 2x10(exp 16)cm(exp -2), 3x10(exp 16)cm(exp -2), and 5x10(exp 16)cm(exp -2). Following implantation, solid phase epitaxial (SPE) annealing in ambient N2 at 800 C for 1 hr. resulted in only slight redistribution of the Ge. Two kinds of extended defects were observed in alloy layers over 3x10(exp 16)cm(exp -2) dose at room temperature (RT): end-of-range (EOR) dislocation loops and strain-induced stacking faults. Density of EOR dislocation loops was much lower in alloys produced by 77K implantation than by RT implantation. Decreasing the dose to obtain 5 at percent peak Ge concentration prevents strain relaxation, while those SPE layers with more than 7 at percent Ge peak show high densities of misfit-induced stacking faults. Sequential implantation of C following high dose Ge implantation (12 at percent Ge peak concentration in layer) brought about

a remarkable decrease in density of misfit-induced stacking faults. For peak implanted C greater than 0.55 at percent, stacking fault generation in the epitaxial layer was suppressed, owing to strain compensation by C atoms in the SiGe lattice. A SiGe alloy layer with 0.9 at percent C peak concentration under a 12 at percent Ge peak exhibited the best microstructure. Results indicate that optimum Ge/C ratio for strain compensation is between 11 and 22. The interface between amorphous and regrown phases (a/c interface) had a dramatic morphology change during its migration to the surface. Initial (100) planar interface decomposes into a (111) faceted interface, changing the growth kinetics; this is associated with strain relaxation by stacking fault formation on (111) planes in the a/c interface. DOE

N95-14192# Argonne National Lab., IL.
MECHANICAL PROPERTIES OF HIGH-TEMPERATURE SUPERCONDUCTING WIRES
K. C. Goretta, J. A. Cluff, J. Joo, M. T. Lanagan, J. P. Singh, N. Vasanthamohan, Y. Xin, and K. W. Wong Jun. 1994 7 p Presented at the 4th International Conference and Exhibition of the World Congress on Superconductivity, Orlando, FL, 27 Jun. - 1 Jul. 1994
(Contract W-31-109-eng-38)
(DE94-015089; ANL/ET/CP-82304; CONF-940627-2) Avail: CASI HC A02/MF A01

Bending strength, fracture toughness, and elastic modulus data were acquired for YBa2Cu3O(x), Bi2Sr2CaCu2O(x), (Bi,Pb)2Sr2Ca2Cu3O(x), and Tl2Ba2Ca2Cu3O(x) bars. These data and thermal expansion coefficients strongly suggest that the maximum tensile strain without fracture possible in bulk tapes or wires is approximately 0.2%. In Ag-clad conductors, residual stresses will be of limited benefit, but fractures produced by larger strains can be accommodated by shunting of current through the Ag. DOE

N95-14322# Sandia National Labs., Albuquerque, NM.
MATERIALS ISSUES IN MOLECULAR BEAM EPITAXY
J. Y. Tsao 1993 9 p Presented at the Spring Meeting of the Materials Research Society, San Francisco, CA, 4-8 Apr. 1994
(Contract DE-AC04-94AL-85000)
(DE94-015796; SAND-93-2758C; CONF-940411-46) Avail: CASI HC A02/MF A01

The technology of crystal growth has advanced enormously during the past two decades; among those advances, the development and refinement of molecular beam epitaxy (MBE) has been among the most important. Crystals grown by MBE are more precisely controlled than those grown by any other method, and today form the basis for many of the most advanced device structures in solid-state physics, electronics and optoelectronics. In addition to its numerous device applications, MBE is also an enormously rich and interesting area of materials science in and of itself. This paper, discusses a few examples of some of these materials issues, organized according to whether they involve bulk, thin films, or surfaces. DOE

N95-14323# Sandia National Labs., Albuquerque, NM.
MICROSTRUCTURES OF InAs(1-x)Sb(x) (x = 0.07-0.14) ALLOYS AND STRAINED-LAYER SUPERLATTICES
D. M. Follstaedt, R. M. Biefeld, S. R. Kurtz, and K. C. Baucom 1994 17 p Presented at the Electronic Materials Conference, Boulder, CO, 22-24 Jun. 1994
(Contract DE-AC04-94AL-85000)
(DE94-015801; SAND-94-0506C; CONF-940616-1) Avail: CASI HC A03/MF A01

Growth of InAs(1-x),Sb(x) alloys by MOCVD at 475C results in CuPt ordering even at Sb concentrations as low as x = 0.07-0.14. The two (111)(sub B) variants are present, but each exists separately in 1-2 micron regions. However, the ordering is incomplete: it occurs in platelet domains lying on (111) habit planes within a disordered matrix, and is not continuous at the atomic scale within the domains. This ordering apparently explains the reduction in infrared emission energies relative to the bandgaps of bulk alloys. Similar ordering is found in an InAs(0.91)Sb(0.09)/In(0.87)Ga(0.13)As strained-layer superlattice with lower-than, expected emission energy. High-resolution images indicate that the SLS has planar, sharply defined interfaces. Infrared LED's have been made from such superlattices. DOE

N95-14325# Lawrence Livermore National Lab., Livermore, CA.
RELATIVISTIC CONFIGURATION-INTERACTION CALCULATION OF THE CORRELATION ENERGIES OF HELIUMLIKE IONS
K. T. Cheng, M. H. Chen, and W. R. Johnson Apr. 1994 7 p Presented at the 2nd International Conference on Computational Physics, Beijing, China, 13-17 Sep. 1993
(Contract W-7405-eng-48)
(DE94-015190; UCRL-JC-114326-Rev-1; CONF-9309176-1-Rev-1) Avail: CASI HC A02/MF A01

A new relativistic configuration-interaction (CI) method using B-spline basis functions has been developed to study the correlation energies of two-electron heliumlike ions. Based on the relativistic no-pair Hamiltonian, the CI equation leads to a symmetric eigenvalue problem involving large, dense matrices. Davidson's method is used to obtain the lowest few eigenenergies and eigenfunctions. Results on transition energies and finite structure splittings for heliumlike ions are in very good agreement with experiment throughout the periodic table. DOE

N95-14342# Sandia National Labs., Albuquerque, NM.
MAGNETIC FIELD DEPENDENT PHOTOLUMINESCENCE STUDIES OF InGaAs/GaAs STRAINED-SINGLE-QUANTUM WELLS
E. D. Jones, L. R. Dawson, J. F. Klem, S. K. Lyo, D. Heiman, and X. C. Liu 1994 4 p Presented at the Conference on the Application of High Magnetic Fields, Cambridge, MA, 8-12 Aug. 1994
(Contract DE-AC04-94AL-85000)
(DE94-015774; SAND-94-1888C; CONF-940847-2) Avail: CASI HC A01/MF A01

Magnetoluminescence determined conduction-band and valence-band dispersion curves are presented for n-type InGaAs/GaAs stained-single-quantum well structures. The magnetic field range was 0 to 30 tesla, and the temperature varied between 4.2 and 77.4 K. DOE

N95-14382 Argonne National Lab., IL.
PERFORMANCE OF SPHERICALLY FOCUSING Ge(444) BACKSCATTERING ANALYZERS FOR INELASTIC X-RAY SCATTERING
A. T. Macrander, V. I. Kushnir, and R. C. Blasdell 1994 8 p Presented at the International Meeting on Synchrotron Radiation Instrumentation, Stony Brook, NY, 18-22 Jul. 1994 Limited Reproducibility: More than 20% of this document may be affected by microfiche quality
(Contract W-31-109-eng-38)
(DE94-016349; ANL/XFD/CP-82780; CONF-940714-1) Avail: CASI HC A02

A spectrometer designed to use an undulator source and having targeted resolutions of 0.01 eV in one mode of use and 0.2 eV in another will operate at the APS. We report here on analyzers that we have constructed for use on this spectrometer for 0.2 eV resolution. We have tested them at NSLS beamline X21 using focused wiggler radiation and at CHESS using radiation from the CHESS-ANL undulator. Analyzers were constructed by gluing and pressing 90 mm diameter, (111) oriented Ge wafers into concave glass forms having a radius near 1 m. An overall inelastic scattering resolution of 0.3 eV using the (444) reflection was demonstrated at CHESS. Recent results at X21 revealed a useful diameter of 74 mm at an 870 Bragg angle. DOE

N95-14390# Sandia National Labs., Albuquerque, NM.
POLARIZED PHOTOMODULATED REFLECTIVITY AND PHOTOLUMINESCENCE STUDIES OF ORDERED InGaP2 UNDER PRESSURE
R. J. Thomas, H. R. Chandrasekhar, M. Chandrasekhar, E. D. Jones, and R. P. Schneider, Jr. 1994 11 p Presented at the 6th International Conference on High Pressures in Semiconductor Physics, Vancouver, Ontario, 22-24 Aug. 1994
(Contract DE-AC04-94AL-85000)
(DE94-016556; SAND-94-1002C; CONF-940846-1) Avail: CASI HC A03/MF A01

Spontaneous ordering of ternary alloys grown on misoriented substrates has been of recent interest. Ordering induced band gap reduction, and valence band splittings exhibiting novel polarization properties have been investigated by theory and experiment. This paper discusses polarized photomodulated reflectivity (PR) and photoluminescence (PL) studies of MOCVD grown InGaP2 epilayers lattice-matched to a GaAs substrate. These structures were grown on a (001) face with a niisorientation of two degrees

along (110). The high degree of ordering has enabled us to accurately measure the crystal field splitting and additional structure not reported in the PR spectra. For the electric field E parallel to (110) two features in the PR spectra are seen; for E parallel to (110), however, additional features are observed. Comparison with spectra of disordered samples of the same alloy composition has enabled a determination of the band gap reduction due to ordering. Linewidths of the PR peaks are approximately 5-10 meV which has enabled us to study them in detail as a function of hydrostatic pressure at cryogenic temperatures. The pressure dependence is slightly sublinear with the first order term of 8-9 meV/kbar for pressures well below the Gamma-X crossover. Also observed is the indirect level crossing which occurs under pressure at about 40 kbar. A comparison of PR lineshapes at I-bar is also presented at several commonly used experimental temperatures. Data indicate a substantial change in PR lineshapes, showing that interpretation of reflectivity data for these samples must be handled carefully. DOE

N95-14431# National Renewable Energy Lab., Golden, CO.
IN-SITU CHARACTERIZATION OF GROWTH AND INTERFACES IN A-Si:H DEVICES Final Report, 1 May 1991 - 31 May 1994
R. W. Collins (Pennsylvania State Univ., University Park, PA.), C. R. Wronski (Pennsylvania State Univ., University Park, PA.), I. An (Pennsylvania State Univ., University Park, PA.), Y. Lu (Pennsylvania State Univ., University Park, PA.), and H. V. Nguyen (Pennsylvania State Univ., University Park, PA.) Jul. 1994 100 p
(Contract DE-AC36-83CH-10093)
(DE94-011847; NREL/TP-451-7045) Avail: CASI HC A05/MF A02

This report describes work to identify materials parameters that can quantitatively describe the solar cell performance correctly in the initial and stabilized states and are consistent with a microscopic model of the metastable defect site. The objective is to be accomplished by applying results of in-situ analyses of a-Si:H surfaces and the transparent conducting oxide (TCO)/p/i interfaces to complement the present understanding of the electronic properties of materials and devices. A second objective of the program is to demonstrate, characterize, and understand improved doped and undoped 'wide-gap' materials for use in achieving 15% stabilized photovoltaic modules ('wide-gap' materials are defined as those materials with a band gap of at least 1.9 eV). DOE

N95-14601# Minnesota Univ., Minneapolis, MN. Dept. of Chemical Engineering and Materials Science.
ATOMIC FORCE MICROSCOPY OF THE ELECTROCHEMICAL NUCLEATION AND GROWTH OF MOLECULAR CRYSTALS Technical Report No. 1, 1 May 1993 - 30 Jun. 1994
M. D. Ward and A. C. Hillier 23 Jun. 1994 20 p
(Contract N00014-93-1-0563)
(AD-A280958) Avail: CASI HC A03/MF A01

In situ atomic force microscopy reveals the morphology, surface topology, and growth and dissolution characteristics of microscopic single crystals of the low dimensional organic conductor (tetrathiafulvalene)Br(0.76), which are grown by electrocrystallization on a highly oriented pyrolytic graphite electrode in an atomic force microscope liquid cell. The growth modes, and the distribution and orientation of topographic features (i.e., terraces, ledges, and kinks) on specific crystal faces, as assigned by 'atomic force microscopy goniometry,' can be correlated with the strength and direction of anisotropic solid state intermolecular bonding. The influence of substrate structure was evident during growth on the (011) face of (tetrathiafulvalene)Br(0.76) crystals, which involves the formation of oriented self-similar triangular islands ranging from 200 A to 5000 A along a side. These nuclei eventually transform into rectangular rafts at larger length scales, where bulk intermolecular bonding interactions and surface energies dominate over nuclei-substrate interactions. DTIC

N95-14608# Argonne National Lab., IL.
ANOMALOUS TEMPERATURE DEPENDENCE OF THE LATTICE PARAMETERS IN HoPO4 AND HoVO4: RARE EARTH QUADRUPOLAR EFFECTS
S. Skanthakumar, C. K. Loong, L. Soderholm, J. Nipko, J. W. Richardson, Jr., M. M. Abraham, and L. A. Boatner 1994 11 p Presented at the 2nd International Conference on F-Elements, Helsinki, Finland, 1-6 Aug. 1994
(Contracts W-31-109-eng-38; DE-AC05-84OR-21400)
(DE94-015086; ANL/CHM/CP-83031; CONF-9408111-2) Avail: CASI HC A03/MF A01

The temperature dependence of the lattice parameters in tetragonal HoPO4 and HoVO4 was measured using neutron powder-diffraction techniques. Below about 100K, the lattice parameter a of HoPO4 increases with decreasing temperature while c decreases. In HoVO4, the above behavior is reversed, that is, a decreases with decreasing temperature while c increases. Similar measurements on nonmagnetic LUP04 and LuVO4 do not show any anomaly. This observation indicates that the unusual temperature dependence of the lattice constants is magnetic in origin. It can be explained in terms of a Ho(3+) quadrupole interaction with the crystalline lattice. In particular, the calculated electronically-generated quadrupole moment of the Ho(3+) in HoPO4 and HoVO4 exhibits a temperature dependence similar to that observed in the lattice parameters. DOE

N95-14655# California Inst. of Tech., Pasadena, CA. Div. of Engineering and Applied Science.
SURFACE PROCESSES IN CVD DIAMOND GROWTH Final Report
David G. Goodwin 1993 4 p
(Contract N00014-90-J-1386)
(AD-A280964) Avail: CASI HC A01/MF A01

The work performed under this contract consisted of basic research with the objective of improving our understanding of the fundamental science of diamond chemical vapor deposition. The major areas of work were numerical modeling of CVD diamond growth; theoretical studies of growth mechanisms; in-situ diagnostics of gas-phase species during hot-filament diamond growth; ab initio calculations of surface migration on diamond; theoretical studies of transport issues and scaling law development; and measurement of the open site fraction on a diamond surface H exposure. DTIC

N95-14795 Philips Gloeilampenfabrieken N.V., Eindhoven (Netherlands).
STRAINED-LAYER InGaAs(P)/InP QUANTUM WELL SEMICONDUCTOR LASERS GROWN BY ORGANOMETALLIC VAPOUR PHASE EPITAXY Ph.D. Thesis
P. J. A. Thijs 1 Mar. 1994 243 p Prepared in cooperation with Technische Univ., Delft, Netherlands
(PB94-201399) Copyright Avail: Issuing Activity (National Technical Information Service (NTIS))

This thesis describes work carried out in the field of InP-based quantum well semiconductor lasers for optical fiber communication applications. Lower-Pressure Organometallic Vapor Phase Epitaxy (LP-OMVPE), used as the crystal growth technique, runs through these studies like a continuous thread. Chapter headings are as follows: Introduction; (1) InGaAsP/InP Semiconductor Laser--from Bulk to Strain-Layer Quantum Well; (2) Epitaxial Growth Techniques; Characterization of LP-OMVPE Grown InGaAs(P) /In(GaAs)P Interfaces; (3) Characterization and Performance of lambda=1.5 micrometers (Strained-Layer) InGaAs(P) Quantum Well Lasers; (4) High Performance lambda=1.3 micrometers Strained-Layer InGaAsP/InP Quantum Well Lasers; and (5) Summary. NTIS

N95-15308# Stanford Linear Accelerator Center, CA.
HADRONIC WAVEFUNCTIONS IN LIGHT-CONE QUANTIZATION Ph.D. Thesis
T. Hyer May 1994 202 p
(Contract DE-AC03-76SF-00515)
(DE94-014507; SU-SLAC-441) Avail: CASI HC A10/MF A03

The analysis of light-cone wavefunctions seems the most promising theoretical approach to a detailed understanding of the structure of relativistic bound states, particularly hadrons. However, there are numerous complications in this approach. Most importantly, the light-cone approach sacrifices manifest rotational invariance in exchange for the elimination of negative-energy states. The requirement of rotational invariance of the full theory places important constraints on proposed light-cone wavefunctions, whether they are modelled or extracted from some numerical procedure. A formulation of the consequences of the hidden rotational symmetry has been sought for some time; it is presented in Chapter 2. In lattice gauge theory or heavy-quark effective theory, much of the focus is on the extraction of numerical values of operators which are related to the hadronic wavefunction. These operators are to some extent interdependent, with

relations induced by fundamental constraints on the underlying wavefunction. The consequences of the requirement of unitarity are explored in Chapter 3, and are found to have startling phenomenological relevance. To test model light-cone wavefunctions, experimental predictions must be made. The reliability of perturbative QCD as a tool for making such predictions has been questioned. In Chapter 4, the author presents a computation of the rates for nucleon-antinucleon annihilation, improving the reliability of the perturbative computation by taking into account the Sudakov suppression of exclusive processes at large transverse impact parameter. In Chapter 5, he develops the analysis of semiexclusive production. This work focuses on processes in which a single isolated meson is produced perturbatively and recoils against a wide hadronizing system. At energies above about 10 GeV, semiexclusive processes are shown to be the most sensitive experimental probes of hadronic structure. DOE

N95-15317# California Univ., Irvine, CA.
DAMPING MECHANISMS IN NANOSTRUCTURED MATERIALS Report, 12 Aug. 1993 - 31 Jul. 1994
Enrique J. Lavernia 31 Jul. 1994 9 p
(Contract N00014-93-1-1072)
(AD-A283583) Avail: CASI HC A02/MF A01

The objectives of the present ONR program may be described as follows: (1) Determination of the mechanisms controlling the synthesis of nanocrystalline Fe78B13Si9 from both elemental Fe, B, Si powders and Metglass 2605TCA (Fe78B13Si9) during the process of high energy ball milling; (2) Compaction of the milled powders by hot pressing and HIP; (3) Determination of mechanisms governing the thermal stability of the milled powders using differential scanning calorimetry; and (4) The study of the effects of high volume fraction of grain boundaries or interfaces on the damping behavior of the nanocrystalline bulk material. DTIC

N95-15337 California Univ., Berkeley. Lawrence Berkeley Lab, CA.
LOW-FREQUENCY NOISE IN HIGH-(Tc) SUPERCONDUCTOR JOSEPHSON JUNCTIONS, SQUIDs, AND MAGNETOMETERS Ph.D. Thesis
A. H. Miklich May 1994 122 p Limited Reproducibility: More than 20% of this document may be affected by microfiche quality
(Contract DE-AC03-76SF-00098)
(DE94-016873; LBL-35022) Avail: CASI HC A06

Design and performance of high-T(sub c) dc superconducting quantum interference devices (SQUID's), junctions that comprise them, and magnetometers made from them are described, with attention to sources of 1/f noise. Biepitaxial junctions are found to have large levels of critical current fluctuations which make them unsuitable for low-noise SQUID's; this suggests a poorly connected interface at the grain boundary junction. SQUID's from bicrystal junctions have levels of critical current noise controllable using bias current reversal techniques which leave the noise white down to frequencies of a few Hz. A SQUID with an energy resolution of 1.5 x 10(exp -30) J Hz(exp -1) at 1 Hz is reported. Magnetometers in which a (9 mm)(exp 2) pickup loop is directly coupled to a SQUID body have achieved field resolutions of 93 fT Hz(exp -1/2) down to frequencies below 1 Hz, improving to 39 fT Hz(exp -1/2) at 1 Hz with the addition of a 50mm-diameter single-turn flux transformer. Poor coupling to pickup loop makes it difficult to satisfy competing goals of high field resolution and small detector size necessary for multichannel biomagnetic imaging. Improved coupling is demonstrated by the use of multiturn-input-coil flux transformers, and a resolution of 35 fT Hz(exp -1/2) in the white noise region is reported with a (10 mm)(exp 2) pickup loop. However, additional 1/f noise from processed multilayer structures in the transformer limits the resolution at 1 Hz to 114 fT Hz(exp -1/2). High-T(sub c) SQUID's exhibit additional 1/f noise when cooled in a nonzero static magnetic field because of additional flux vortices trapped in the film, with the noise power at 1 Hz typically increasing by a factor of 10-20 in a field of 0.05mT (0.5 G). Finally, a SQUID-based voltmeter with a resolution of 9.2 pV Hz(exp -1/2) at 10 Hz (24 pV Hz(exp -1/2) at 1 Hz) is described. DOE

N95-15338 California Univ., Berkeley. Lawrence Berkeley Lab, CA.
RESONANT TUNNELING IN SMALL CURRENT-BIASED JOSEPHSON JUNCTIONS Ph.D. Thesis
J. M. Schmidt May 1994 163 p Limited Reproducibility: More than 20% of this document may be affected by microfiche quality
(Contract DE-AC03-76SF-00098)
(DE94-016875; LBL-35671) Avail: CASI HC A08

Effects of resonant tunneling between bound quantum states of a current-biased Josephson tunnel junction is studied both theoretically and experimentally. Several effects are predicted to arise from resonant tunneling, including a series of voltage peaks along the supercurrent branch of the current-voltage characteristic, and enhanced rate of escape from zero voltage state to voltage state at particular values of bias current. A model is developed to estimate magnitude and duration of voltage peaks, and to estimate enhancement of the escape rate, which appears as peaks in the rate as a function of bias current. An experimental investigation was carried out in an attempt to observe these predicted peaks in the escape rate distribution in a current-biased DC SQUID, which is shown to be dynamically equivalent to a Josephson junction with adjustable critical current. Electrical contact to each SQUID (fabricated from aluminium) was made through high resistance thin film leads located on the substrate. These resistors provided a high impedance at the plasma frequency which is for the isolation of the SQUID from its electromagnetic environment. Measurements were carried out on a dilution refrigerator at temperatures as low as 19 mK. No evidence was found for resonant tunneling; this is attributed to effective temperatures of hundreds of millikelvin. The behavior is well explained by a heating model where the high effective temperatures are generated by ohmic heating of the electron gas of the isolation resistors, which decouples from the phonon system (hot electron effect). The prospects for further theoretical and experimental research are discussed. DOE

N95-15339 California Univ., Berkeley. Lawrence Berkeley Lab, CA.
PHOTOLUMINESCENCE SPECTROSCOPY AND RUTHERFORD BACKSCATTERING CHANNELING EVALUATION OF VARIOUS CAPPING TECHNIQUES FOR RAPID THERMAL ANNEALING OF ION-IMPLANTED ZnSe
E. L. Allen (San Jose State Univ., CA.), F. X. Zach, K. M. Yu, and E. D. Bourret May 1994 8 p Presented at the Spring Meeting of the Materials Research Society, San Francisco, CA, 4-8 Apr. 1994 Limited Reproducibility: More than 20% of this document may be affected by microfiche quality
(Contract DE-AC03-76SF-00098)
(DE94-016876; LBL-34810; CONF-940411-48; UC-404) Avail: CASI HC A02

We report on the effectiveness of proximity caps and PECVD Si3N4caps during annealing of implanted ZnSe films. OMVPE ZnSe films were grown using diisopropylselenide (DIPSe) and diethylzinc (DEZn) precursors, then ion-implanted with 1 x 10(exp 14) cm(exp -2) N (33 keV) or Ne (45 keV) at room temperature and liquid nitrogen temperature, and rapid thermal annealed at temperatures between 200C and 850C. Rutherford backscattering spectrometry in the channeling orientation was used to investigate damage recovery, and photoluminescence spectroscopy was used to investigate crystal quality and the formation of point defects. Low temperature implants were found to have better luminescence properties than room temperature implants, and results show that annealing, time and temperature may be more important than capping material in determining the optical properties. Effects of various caps, implant and annealing temperature are discussed in terms of photoluminescence spectra. DOE

N95-15341# Argonne National Lab., IL.
TRANSPORT RESISTIVE BROADENING BY AVALANCHE FLUX MOTION IN HIGH-TEMPERATURE SUPERCONDUCTORS: SOC IN A DRIVEN SYSTEM
Zuning Wang and Donglu Shi Oct. 1993 15 p
(Contract W-31-109-eng-38)
(DE94-016901; ANL/MSD/PP-81187) Avail: CASI HC A03/MF A01

Characteristics of self-organized criticality (SOC) are investigated for a driven system in high-Tc superconductors. By applying a bias current to a single crystal of Bi2Sr2CaCu2O(x), we are able to drive the vortex state to criticality. We establish a magnetic field profile for a type-II superconductor by considering both the magnetic force (caused by the Bean critical current) and the Lorentz force (associated with the bias current). The resistive broadening is interpreted in the framework of SOC. We show that the R vs. T curve is divided into regions of flux flow, thermally activated flux avalanche and thermally activated flux creep. DOE

N95-15378# Technische Univ., Delft (Netherlands).
SURFACE SPECTROSCOPIC STUDIES OF HIGH-TEMPERATURE SUPERCONDUCTORS Ph.D. Thesis
G. Rietveld 13 Sep. 1993 176 p See also AD-A202080 Sponsored by Stichting voor Fundamenteel Onderzoek der Materie and Nederlandse Organisatie voor Wetenschappelijk Onderzoek
(PB94-191228; ISBN-90-6275-903-3) Copyright Avail: CASI HC A09/MF A02

In this thesis the results are described of an experimental study in which surface spectroscopic techniques are used to examine the electronic structure of the high-Tc superconductors. Apart from the work presented here, the project also contained growth and analysis of thin films, and development of devices. The in situ preparation of high-quality thin films was essential for performing useful measurements of the surface properties of the high-Tc materials. The aim of the present study is to contribute to the understanding of the character of the superconducting phase transition and of the electronic structure of these materials. The main thread that connects all chapters is the behavior of the chemical potential, which, as we will show, can give useful information with respect to these points.
NTIS

N95-15385# Argonne National Lab., IL.
MAGNETIC AND STRUCTURAL INSTABILITIES OF ULTRATHIN Fe(100) WEDGES
S. D. Bader, Dong-Qi Li, and Z. Q. Qiu May 1994 22 p Presented at the 6th Joint Conference on Magnetism and Magnetic Materials, Albuquerque, NM, 20-23 Jun. 1994
(Contract W-31-109-eng-38)
(DE94-013864; ANL/MSD/CP-83086; CONF-940629-7) Avail: CASI HC A03/MF A01

An overview is provided of recent efforts to explore magnetic and related structural issues for ultrathin Fe films grown epitaxially as wedge structures onto Ag(100) and Cu(100). Experiments were carried out utilizing the surface magneto-optic Kerr effect (SMOKE). Ordinary bcc Fe is lattice-matched to the primitive unit cell of the Ag(100) surface. Fe wedges on Ag(100) can be fabricated whose thick end has in-plane magnetic easy axes due to the shape anisotropy, and whose thin end has perpendicular easy axes due to the surface magnetic anisotrophy. A spin-reorientation transition can thus be studied in the center of the wedge where the competing anisotropies cancel. The goal is to test the Mermin-Wagner theorem which states that long-range order is lost at finite temperatures in an isotropic two-dimensional Heisenberg system. Fe wedges on Cu(100) can be studied in like manner, but the lattice matching permits fcc and tetragonally-distorted fcc phases to provide structural complexity in addition to the interplay of competing magnetic anisotropies. The results of these studies are new phase identifications that help both to put previous work into perspective and to define issues to pursue in the future. DOE

N95-15421# Oak Ridge National Lab., TN.
HTS WIRE DEVELOPMENT WORKSHOP: PROCEEDINGS
Jul. 1994 507 p Workshop held at St. Petersburg, FL, 16-17 Feb. 1994
(Contract DE-AC05-84OR-21400)
(DE94-015650; CONF-940278) Avail: CASI HC A22/MF A04

The 1994 High-Temperature Superconducting Wire Development Workshop was held on February 16-17 at the St. Petersburg Hilton and Towers in St. Petersburg, Florida. The meeting was hosted by Florida Power Corporation and sponsored by the US Department of Energy's Superconductivity Program for Electric Power Systems. The meeting focused on recent high-temperature superconducting wire development activities in the Department of Energy's Superconductivity Systems program. The meeting opened with a general discussion on the needs and benefits of superconductivity from a utility perspective, the US global competitiveness position, and an outlook on the overall prospects of wire development. The meeting then focused on four important technology areas: (1) Wire characterization: issues and needs; (2) technology for overcoming barriers: weak links and flux pinning; (3) manufacturing issues for long wire lengths; and (4) physical properties of HTS coils. Following in-depth presentations, working groups were formed in each technology area to discuss the most important current research and development issues. The working groups identified research areas that have the potential for greatly enhancing the wire development effort. These areas are discussed in the summary reports from each of the working groups. This document is a compilation of the workshop proceedings including all general session presentations and summary reports from the working groups. DOE

N95-15422# Brookhaven National Lab., Upton, NY.
DEFECT PROFILING IN ELEMENTAL AND MULTILAYER SYSTEMS: CORRELATIONS OF FITTED DEFECT CONCENTRATIONS WITH POSITRON IMPLANTATION PROFILES
V. J. Ghosh, B. Nielsen, K. G. Lynn, and D. O. Welch 1994 15 p Presented at the 6th International Workshop on Slow-Positron Beam Techniques for Solids and Surfaces, Makuhari, Japan, 18-22 May 1994
(Contract DE-AC02-76CH-00016)
(DE94-015844; BNL-60588; CONF-9405198-1) Avail: CASI HC A03/MF A01

The results of several positron annihilation (Doppler broadening) experiments have been analyzed using the BNL Monte Carlo implantation profiles and the program VEPFIT. The program VEPFIT has been modified so that scaled, parameterized multilayer profiles can also be used as the initial condition for the diffusion equation solution. The authors have looked at both elemental (e.g. amorphous silicon) and multilayer (e.g. Pd/Si) system. Strong correlations between the input implantation profile parameters and the fitted values obtained for the diffusion lengths and overlayer thicknesses for the multilayer systems have been found. The effect of uncertainties in the mean depth on the value of the diffusion length and hence the defect concentrations will be discussed. The impact of reimplanting backscattered positrons on both the implantation profiles and the fitted diffusion lengths will also be presented. DOE

N95-15426# National Renewable Energy Lab., Golden, CO.
FOURTH WORKSHOP ON THE ROLE OF POINT DEFECTS AND DEFECT COMPLEXES IN SILICON DEVICE PROCESSING
T. Tan, L. Jastrzebski, and B. Sopori Jul. 1994 13 p Workshop held in Beaver Creek, CO, 27-29 Jun. 1994
(Contract DE-AC36-83CH-10093)
(DE94-011850; NREL/TP-413-7050; CONF-9406203-Summ) Avail: CASI HC A03/MF A01

The 4th Point Defect Workshop was aimed at reviewing recent new understanding of the defect engineering techniques that can improve the performance of solar cells fabricated on low-cost silicon substrates. The theme of the workshop was to identify approaches that can lead to 18 percent commercial silicon solar cells in the near future. These approaches also define the research tasks for the forthcoming new DOE/NREL silicon materials research program. It was a consensus of the workshop attendees that the goal of 18 percent-efficient multicrystalline silicon solar cells is right on target, and the payoff for the investment by DOE will manifest itself in the next few years as reduced costs for high-efficiency cell fabrication. DOE

N95-15430# Argonne National Lab., IL.
PHASE SEPARATION AND DOPED-HOLE SEGREGATION IN La(2)CuO(4+DELTA) AND La(2-x)Sr(x)CuO(4+DELTA)
D. C. Johnston (Iowa State Univ. of Science and Technology, Ames, IA.), W. R. Bayless (Sandia National Labs., Albuquerque, NM.), F. Borsa (Iowa State Univ. of Science and Technology, Ames, IA.), P. C. Canfield (Iowa State Univ. of Science and Technology, Ames, IA.), S.-W. Cheong (Bell Telephone Labs., Inc., Murray Hill, NJ.), J. H. Cho (Iowa State Univ. of Science and Technology, Ames, IA.), F. C. Chou (Iowa State Univ. of Science and Technology, Ames, IA.), Z. Fisk (Los Alamos National Lab., NM.), J. D. Jorgensen, and A. Lascialfari et al May 1994 5 p Presented at the Meeting on Materials and Mechanisms of Superconductivity: High Temperature Superconductors, Grenoble, France, 4-9 Jul. 1994
(Contract W-31-109-eng-38)
(DE94-015070; ANL/MSD/CP-83051; CONF-940701-15) Avail: CASI HC A01/MF A01

This paper reviews the magnetic, superconducting and structural phase diagrams of the title systems, with an emphasis on recent results from magnetic and structural neutron diffraction, magnetic susceptibility and (sup 139)La nuclear quadrupole resonance measurements. Results clarify the miscibility gap in the La(2)CuO(4+delta) system and indicate the occurrence of frustrated phase separation on a nanoscopic length scale in the La(2-x)Sr(x)CuO(4) system with 0 less than x approx. less than 0.05.
DOE

N95-15438# Sandia National Labs., Albuquerque, NM.
SANDIA 1993 SUPERCONDUCTING TECHNOLOGY PROGRAM Annual Report
E. P. Roth May 1994 83 p
(Contract DE-AC04-94AL-85000)
(DE94-015601; SAND-94-1279) Avail: CASI HC A05/MF A01

Sandia's STP program is a four-part high-temperature superconductor (HTS) research and development program consisting of efforts in powder synthesis and process development, thallium-based HTS film development, wire and tape fabrication, and HTS motor design. The objective of this work is to develop high-temperature superconducting conductors (wire and tape) capable of meeting requirements for high-power electrical devices of interest to industry. The four research efforts currently underway are: (1) process research on the material synthesis of high-temperature superconductors; (2) investigation of the synthesis and processing of thallium-based high-temperature superconducting thick films; (3) process development and characterization of high-temperature superconducting wire and tape, and (4) cryogenic design of a high-temperature superconducting motor. This report outlines the research that has been performed during FY93 in each of these four areas. A brief background of each project is included to provide historical context and perspective. Major areas of research are described, although no attempt has been made to exhaustively include all work performed in each of these areas. DOE

N95-15531# General Electric Co., Schenectady, NY.
Ru2Ge3: CRYSTAL GROWTH AND SOME PROPERTIES
A. Borshchevsky and J. P. Fleurial Oct. 1993 14 p Presented at the 9th American Conference on Crystal Growth: Crystal Growth, Characterization and Applications, Baltimore, MD, 1-6 Aug. 1993
(Contract DE-AC12-76SN-00052)
(DE94-015360; KAPL-4777; CONF-930851-3) Avail: CASI HC A03/MF A01

Large samples of Ru2Ge3 were grown from Ge-rich off-stoichiometric melts at a temperature close to 1,460 C by a vertical gradient freeze m ethod in graphite and glassy carbon crucibles. Diffusionless transition from high temperature tetragonal structure to low temperature orthorhombic structure causes twinning and crack formation. Thermal expansion coefficients of both low and high temperature phases were measured. Some electrical transport properties in the 25-1,000 C temperature range in different crystallographic directions are also described for this high temperature semiconductor. Substantial anisotropy is observed. DOE

N95-15574# Rice Univ., Houston, TX.
APPLICATION OF SPIN-SENSITIVE ELECTRON SPECTROSCOPIES TO INVESTIGATIONS OF ELECTRONIC AND MAGNETIC PROPERTIES OF SOLID SURFACES AND EPITAXIAL SYSTEMS
G. K. Walters and F. B. Dunning May 1994 5 p
(Contract DE-FG05-86ER-45233)
(DE94-012981; DOE/ER-45233/9) Avail: CASI HC A01/MF A01

Research during the current grant year has focused on: (1) measurements of the relative contributions of dipole- and impact-scattering to the energy loss spectrum of electrons backscattered from paramagnetic and ferromagnetic metal surfaces, using Spin-Polarized Electron Energy Loss Spectroscopy (SPEELS); (2) Studies of the mechanisms whereby He(2(exp 3)S), He(2(exp 1)S), and He(2(exp 3)P) atoms are deexcited at Ar and Xe films deposited on metallic surfaces, using Spin-Polarized Metastable (Atom) Deexcitation Spectroscopy (SPMDS); (3) Development of a high-efficiency Mott polarimeter for use in Scanning Electron Microscopy with Polarization Analysis (SEMPA); and (4) Development of a low-energy spin-polarized He(+) ion beam for magnetic imaging of surfaces and thin epitaxial films. DOE

N95-15576# Brookhaven National Lab., Upton, NY.
DYNAMICAL IMPURITY PROBLEMS
V. J. Emery and S. A. Kivelson 1993 26 p Presented at the 1993 International Summer School on Fundamental Problems in Statistical Mechanics, Altenberg, Germany, 27 Jun. - 10 Jul. 1993
(Contract DE-AC02-76CH-00016)
(DE94-013025; BNL-60297; CONF-9306338-1) Avail: CASI HC A03/MF A01

In the past few years there has been a resurgence of interest in dynamical impurity problems, as a result of developments in the theory of correlated electron systems. The general dynamical impurity problem is a set of conduction electrons interacting with an impurity which has internal degrees of freedom. The simplest and earliest example, the Kondo problem, has attracted interest since the mid-sixties not only because of its physical importance but also as an example of a model displaying logarithmic divergences order by order in perturbation theory. It provided one of the earliest applications of the renormalization group method, which is designed to deal with just such a situation. As we shall see, the antiferromagnetic Kondo model is controlled by a strong-coupling fixed point, and the essence of the renormalization group solution is to carry out the global renormalization numerically starting from the original (weak-coupling) Hamiltonian. In these lectures, we shall describe an alternative route in which we identify an exactly solvable model which renormalizes to the same fixed point as the original dynamical impurity problem. This approach is akin to determining the critical behavior at a second order phase transition point by solving any model in a given universality class. DOE

N95-15577# California Univ., Berkeley. Lawrence Berkeley Lab, CA.
CHARGE COLLECTION IN a-Si:H/a-Si(1-x)C(x MULTILAYERS PHOTODETECTORS
T. Jing, J. Drewray, W. S. Hong, H. Lee, S. N. Kaplan, A. Mireshghi, V. Perez-Mendez, J. C. Delgado, and J. Bertomeu Apr. 1994 12 p Presented at the 2nd International Conference on Thin Film Physics and Applications, Shanghai, China, 14-17 Apr. 1994
(Contract DE-AC03-76SF-00098)
(DE94-013107; LBL-35474; CONF-9404171-1) Avail: CASI HC A03/MF A01

Amorphous semiconductors have been used as thin film transistors (TFT), solar cells, and phototransistors. In this paper we study the charge collected properties of a-Si:H/a-Si(1-x)C:H(x) multilayer pin photodiode. In a-Si:H pin photodiode, the photogenerated carriers can be totally collected under strong electric field under reverse bias. However, our measurements show that in the a-Si:H/a-Si(1-x)C:H(x) multilayer pin photodiode photogenerated electrons and holes drift toward the electrodes under a certain bias, the total collected charge shows no saturation with bias and exhibits a continuous increase with reverse bias. We classify that the device works at two regions. In Region 1, the device behaves like a photodiode. This charge collection efficiency drop from theoretical value may indicate charge capture or confinement at the interfaces and trapping at the a-Si:H potential wells. These charges trapped or confined can be released at the interface and quantum well at higher electric field. In Region 2, above a critical bias voltage, the device works as a breakdown diode with a series photosensitive resistor which contributes higher collection efficiency, namely optical gain greater than unity. DOE

N95-15602* National Aeronautics and Space Administration. Lewis Research Center, Cleveland, OH.
PROCESS FOR THE CONTROLLED GROWTH OF SINGLE-CRYSTAL FILMS OF SILICON CARBIDE POLYTYPES ON SILICON CARBIDE WAFERS Patent
David J. Larkin, inventor (to NASA) and J. Anthony Powell, inventor (to NASA) 15 Nov. 1994 11 p Filed 9 Nov. 1992 Supersedes N93-17413 (31 - 5, p 1327) Continuation-in-part of abandoned US-Patent-Appl-SN-718315, filed 12 Jun. 1991
(NASA-Cas-LEW-15222-3; US-Patent-5,363,800;
US-Patent-Appl-SN-973505; US-Patent-Appl-SN-718315;
US-Patent-Class-117-95; US-Patent-Class-117-97; US-Patent-Class-117-101;
US-Patent-Class-117-106; US-Patent-Class-117-913;
US-Patent-Class-117-923) Avail: US Patent and Trademark Office

This invention is a method for the controlled growth of single-crystal semiconductor-device-quality films of SiC polytypes of vicinal (0001) SiC wafers with low tilt angles. Both homoepitaxial and heteroepitaxial SiC films can be produced on the same wafer. In particular, 3C-SiC and 6H-SiC films can be produced within selected areas of the same 6H-SiC wafer. Author

N95-15746# Pennsylvania State Univ., University Park, PA. Materials Research Lab.
LOW LOSS SUBSTRATES FOR MICROWAVE APPLICATIONS AND SOL-GEL PROCESSING OF SUPERCONDUCTORS Final Technical Report, 1 Sep. 1990 - 31 Mar. 1994

L. E. Cross, Rustum Roy, and Amar S. Bhalla 31 Mar. 1994 165 p
(Contract N00014-90-J-4140)
(AD-A284868) Avail: CASI HC A08/MF A02

Systematic studies on low Kappa oxide substrate materials suitable for epitaxial deposition of high Tc superconducting (HTSC) yttrium barium cuprate (YBCO) films and their microwave applications have been carried out. Several promising new hosts such SrAl(1/2)Ta(1/2)O3, SrAl(1/2)Nb(1/2)O3, and BaMg(1/3)Ta(2/3)O3 in complex oxide perovskite family have been developed. The crystals of these compositions and their associated solid solutions provide new options for ultra low loss, low permittivity substrates with close structural and thermal properties matching to the YBCO. Studies were extended to the twin free perovskites (e.g., modified complex perovskites) with low congruent melting temperatures and alternative compositions with lower dielectric constants (e.g., in spinel, magnetoplumbite, and fluorite structures). DTIC

N95-15748# Trinity Coll., Dublin (Ireland).
SYNTHESIS AND APPLICATIONS OF LARGE HETEROMETALLIC CLUSTER SYSTEMS Interim Report No. 7
Kathleen Puech Oct. 1993 94 p
(Contract DAJA45-90-C-0034)
(AD-A284874; R/D-6307-PM-01) Avail: CASI HC A05/MF A01

Work has proceeded according to schedule on all research topics. Uniquely well defined clusters of gold are now available for optical measurements. A comprehensive experimental investigation has been carried out to determine the non-linearity of these samples on a femtosecond timescale. These results are presented and prove that: the nonlinear refractive index rises and relaxes on a sub-picosecond timescale; the nonlinearity is predominant positive imaginary originating from a hot electron contribution; and the nonlinearity is independent of the size of the particle. DTIC

N95-15752*# Florida Inst. of Tech., Melbourne, FL. Dept. of Physics and Space Sciences.
ELECTRONIC CHARACTERIZATION OF DEFECTS IN NARROW GAP SEMICONDUCTORS Final Report, 25 Nov. 1992 - 25 Nov. 1994
James D. Patterson 1994 108 p
(Grant NAG8-941)
(NASA-CR-197217; NAS 1.26:197217) Avail: CASI HC A06/MF A02

We use a Green's function technique to calculate the position of deep defects in narrow gap semiconductors. We consider substitutional (including antisite), vacancy, and interstitial (self and foreign) deep defects. We also use perturbation theory to look at the effect of nonparabolic bands on shallow defect energies and find nonparabolicity can increase the binding by 10 percent or so. We consider mercury cadmium telluride (MCT), mercury zinc telluride (MZT), and mercury zinc selenide (MZS). For substitutional and interstitial defects we look at the situation with and without relaxation. For substitutional impurities in MCT, MZT, and MZS, we consider x (the concentration of Cd or Zn) in the range 0.1 less than x less than 0.3 and also consider appropriate x so E(sub g) = 0.1 eV for each of the three compounds. We consider several cation site s-like deep levels and anion site p-like levels. For E(sub g) = 0.1 eV, we also consider the effects of relaxation. Similar comments apply to the interstitial deep levels whereas no relaxation is considered for the ideal vacancy model. Relaxation effects can be greater for the interstitial than the substitutional cases. Specific results are given in figures and tables and comparison to experiment is made in a limited number of cases. We find, for example, that I, Se, S, Rn, and N are possible cation site, s-like deep levels in MCT and Zn and Mg are for anion site, p-like levels (both levels for substitutional cases). The corresponding cation and anion site levels for interstitial deep defects are (Au, Ag, Hg, Cd, Cu, Zn) and (N, Ar, O, F). For the substitutional cases we have some examples of relaxation moving the levels into the band gap, whereas for the interstitial case we have examples where relaxation moves it out of the band gap. Future work involves calculating the effects of charge state interaction and seeing the effect of relaxation on vacancy levels. Author (revised)

N95-15754# Materials Research Society, Pittsburg, PA.
LOW TEMPERATURE GROWN AND HIGHLY NON-STOICHIOMETRIC GaAs AND RELATED MATERIALS Final Report, 1 Apr. 1993 - 30 Mar. 1994
David C. Look and Michael R. Melloch 3 Aug. 1994 151 p Spring meeting held in Pittsburgh, PA, 12-16 Apr. 1993
(Contract F49620-93-1-0236)
(AD-A284898; AFOSR-94-0574TR) Avail: CASI HC A08/MF A02

Forty-one papers were presented in five sessions, as follows: Growth Issues, including growth of As and P-based compounds, annealing effects, and characterization by scanning tunneling microscopy (STM) real-time ellipsometry, and positron annihilation; Processing and Characterization, including point-defect and precipitate formations and their characterization by electrical, optical magnetic resonance, and STM techniques; Optical and Optoelectronic Properties, including the materials GaAs, InGaAs, and InGaP, and their responses to light stimulation, explained by various models; InP and Related Ternary Materials, including the Materials InP, InGaAs, InAlAs, and ordered InGaAs/InAlAs layers, characterized by optically detected magnetic resonance, electrical measurements, tunneling electron microscopy, and photoreflectance; Applications of Nonstoichiometric Materials, including power MESFET design, phase noise measurements, coherent microwave generation, excitonic electro-optic observations, and GaAs on Si device applications. DTIC

N95-15776# Los Alamos National Lab., NM.
CLUSTER STUDIES OF La2CuO4: LOCAL GEOMETRIC DISTORTIONS
R. L. Martin 1 Nov. 1993 6 p Presented at the Electronic Structure of Solids Using Cluster Methods Workshop, East Lansing, MI, 17-19 Jul. 1994
(Contract W-7405-eng-36)
(DE94-016203; LA-UR-94-2450; CONF-9407115-1) Avail: CASI HC A02/MF A01

The techniques of ab initio electronic structure theory are used to study Cu2O7 and Cu2O11 cluster models of La2CuO4. Fair agreement is obtained with the experimentally determined spin exchange constant J (90 meV calculated vs. 125 meV measured) at the expense of quite large Configuration Interaction (CI) expansions. Results for various charge states of the cluster are well described by a 'single-band' Pariser-Parr-Pople (PPP) model. As in earlier LDF based parameter determinations, the present work suggests these materials fall in the strong coupling regime. However, a significant intersite Coulomb repulsion is found in the present research. It is of sufficient strength, V is approximately equal to U/5, toindicate that charge fluctuations may be more important in these materials than generally believed. DOE

N95-15808 Rockwell International Science Center, Thousand Oaks, CA.
FUNDAMENTAL STUDIES OF DIAMOND GROWTH AND SURFACE REACTIONS Final Report, 1 Feb. 1991 - 31 May 1994
Alan B. Harker Jul. 1994 143 p Limited Reproducibility: More than 20% of this document may be affected by microfiche quality
(Contract N00014-91-C-0048)
(AD-A284390; SC71046.FR) Avail: Issuing Activity (Defense Technical Information Center (DTIC))

This report summarizes the research carried out during the period March 1991 through May 1994 at Rockwell Science Center under ONR contract No. N00014-91-C-0048. This contract was part of the ONR directed effort on the development of polycrystalline diamond as an optical material. A primary focus of the research was investigating the relationships between the microstructure of polycrystalline diamond and its optical and mechanical properties. The program also involved a considerable effort in the development of characterization techniques for observing the fundamental properties of thick and thin diamond films. A secondary goal of the research was the investigation of the surface reactions of diamond to evaluate their potential for reactive polishing applications. Polishing is critical not only to the ultimate application of diamond as an optical material, but also to the characterization of its detailed microstructure. Also included in this program was an additional task, funded by the Naval Air Warfare Center Aircraft Division (NAWCAD) at Warminster, PA. The additional task was to devise a methodology for bonding diamond with an integral gradient index antireflective surface (moth-eye) to germanium and zinc sulfide and to provide samples of the bonded composites to NAWCAD for liquid jet impact testing. DTIC

N95-15812 Case Western Reserve Univ., Cleveland, OH.
TRANSPORT AND NUCLEATION PROCESSES DURING THE VAPOR GROWTH OF DIAMOND Final Report, 1 Jul. 1989 - 29 Aug. 1994
John C. Angus 29 Aug. 1994 31 p Limited Reproducibility: More than

20% of this document may be affected by microfiche quality
(Contract N00014-89-J-3167)
(AD-A284411) Avail: Issuing Activity (Defense Technical Information Center (DTIC))

The growth of electronic grade diamond crystals at reasonable cost is limited by several factors: lower quality at high growth rates, secondary nucleation, and morphological instabilities. The research performed under this grant addressed these areas. Significant progress was made including: (1) identification of secondary nucleation mechanism through graphitic, sp(sup 2), precursors and (2) determination of influence of twins on diamond growth rate and quality. Preliminary estimates were made of the parameter range that minimizes morphological instabilities. The results also have relevance for the general question of the relationship of diamond quality to growth rate and to the molecular mechanism of diamond growth. DTIC

N95-15818 Woollam (John A.) Co., Lincoln, NE.
REAL-TIME MONITOR AND CONTROL OF MBE GROWTH OF HgCdTe BY SPECTROSCOPIC ELLIPSOMETRY Monthly Progress Report, 30 Sep. - 30 Oct. 1993
30 Oct. 1993 12 p Limited Reproducibility: More than 20% of this document may be affected by microfiche quality
(Contract DAAB07-93-C-U008)
(AD-A284451; TR-4) Avail: CASI HC A03

The overall goal is compositional control of Hg(1-x)Cd(x)Te (MCT) during MBE growth using a commercially viable spectroscopic ellipsometer system. The run-to-run composition reproducibility, as well as the composition uniformity during growth, should be controlled to within +/-0.001. The main task is to develop a knowledge base which includes a quantitative understanding of MCT growth by MBE from an optical/ellipsometric standpoint, and practical application of this understanding to effect real-time composition control. The knowledge base, which will be developed through extensive and systematic in-situ ellipsometry experiments, will be comprehensive and general enough to facilitate the transfer of this composition control technology to other MCT crystal growers. DTIC

N95-15823*# Maryland Univ., College Park, MD. Dept. of Physics.
PROPERTIES OF NEARLY PERFECT CRYSTALS AT VERY LOW TEMPERATURES Final Technical Report
J. Weber and J. J. Hamilton [1994] 8 p
(Grant NAG2-270)
(NASA-CR-197221; NAS 1.26:197221) Avail: CASI HC A02/MF A01

Data shows that the frequency stability of 5 MHz AT-cut quartz crystal oscillators is improved by lowering the temperature to 4.3 K. The resultant level of stability is apparently not, at this point, sufficient for a clock accurate to 1 part in 10(exp 17). However, many improvements are possible in the scheme presented here. These would involve better temperature regulation, better crystal mounting and vibration isolation, and lower temperatures. Below the lambda-transition at 2.17 K the residual bubbling of the bath would be eliminated. Thus, the prospect of a successful clock built on this scheme is not ruled out. Derived from text

N95-14550*# Ohio State Univ., Columbus.
CRYSTAL GROWTH AND FLUID MECHANICS PROBLEMS IN DIRECTIONAL SOLIDIFICATION
Saleh Tanveer, Gregory R. Baker, and Michael R. Foster *In* NASA. Lewis Research Center, Second Microgravity Fluid Physics Conference Aug. 1994 p 187-192 (For primary document see N95-14522 03-34)
Avail: CASI HC A02/MF A04; 2 functional color pages

N95-15838*# Masaryk Univ., Brno, Jihomoravsky (Czechoslovakia). Lab. of Physics of Plasma.
LABORATORY SPECTRA OF C60 AND RELATED MOLECULAR STRUCTURES
J. Janca, M. Solc, and M. Vetesnik *In* NASA. Ames Research Center, The Diffuse Interstellar Bands: Contributed Papers May 1994 p 53-57 (For primary document see N95-15827 03-89)
Avail: CASI HC A01/MF A02

77 THERMODYNAMICS AND STATISTICAL PHYSICS

Includes quantum mechanics; theoretical physics; and Bose and Fermi statistics.

For related information see also *25 Inorganic and Physical Chemistry* and *34 Fluid Mechanics and Heat Transfer.*

N95-15404 Chicago Univ., Chicago, IL.
TOWARDS THE MOLECULAR DESIGN OF COMPOSITE MATERIALS Annual Progress Report, 1 Apr. 1993 - 28 Feb. 1994
Karl F. Freed 28 Feb. 1994 3 p Limited Reproducibility: More than 20% of this document may be affected by microfiche quality
(Contract N00014-91-J-1442)
(AD-A283422) Avail: Issuing Activity (Defense Technical Information Center (DTIC))

The objective of this project is to develop a theory of the statistical thermodynamics of polymer blends and block copolymer systems in which the theory relates microscopic and macroscopic properties and thereby assists in the molecular design of composite materials with desired macroscopic properties. DTIC

N95-15578# California Univ., Berkeley. Lawrence Berkeley Lab, CA.
STUDIES IN CHAOTIC ADIABATIC DYNAMICS
C. Jarzynski Jan. 1994 113 p
(Contract DE-AC03-76SF-00098)
(DE94-013111; LBL-35497) Avail: CASI HC A06/MF A02

Chaotic adiabatic dynamics refers to the study of systems exhibiting chaotic evolution under slowly time-dependent equations of motion. In this dissertation the author restricts his attention to Hamiltonian chaotic adiabatic systems. The results presented are organized around a central theme, namely, that the energies of such systems evolve diffusively. He begins with a general analysis, in which he motivates and derives a Fokker-Planck equation governing this process of energy diffusion. He applies this equation to study the 'goodness' of an adiabatic invariant associated with chaotic motion. This formalism is then applied to two specific examples. The first is that of a gas of noninteracting point particles inside a hard container that deforms slowly with time. Both the two- and three-dimensional cases are considered. The results are discussed in the context of the Wall Formula for one-body dissipation in nuclear physics, and it is shown that such a gas approaches, asymptotically with time, an exponential velocity distribution. The second example involves the Fermi mechanism for the acceleration of cosmic rays. Explicit evolution equations are obtained for the distribution of cosmic ray energies within this model, and the steady-state energy distribution that arises when this equation is modified to account for the injection and removal of cosmic rays is discussed. Finally, the author re-examines the multiple-time-scale approach as applied to the study of phase space evolution under a chaotic adiabatic Hamiltonian. This leads to a more rigorous derivation of the above-mentioned Fokker-Planck equation, and also to a new term which has relevance to the problem of chaotic adiabatic reaction forces (the forces acting on slow, heavy degrees of freedom due to their coupling to light, fast chaotic degrees). DOE

N95-13906*# Moscow State Univ. (Russia). Astronomical Inst.
PRODUCTION OF SQUEEZED STATES FOR MACROSCOPIC MECHANICAL OSCILLATOR
V. V. Kulagin *In* NASA. Goddard Space Flight Center, Third International Workshop on Squeezed States and Uncertainty Relations May 1994 p 83-86 (For primary document see N95-13896 03-74)
Avail: CASI HC A01/MF A06

N95-13907*# Universidad Nacional Autonoma de Mexico, Mexico City. Inst. de Ciencias Nucleares.
SQUEEZING IN A 2-D GENERALIZED OSCILLATOR
Octavio Castanos, Ramon Lopez-Pena, and Vladimir I. Manko *In* NASA. Goddard Space Flight Center, Third International Workshop on Squeezed States and Uncertainty Relations May 1994 p 87-92 Sponsored in part by DGAPA (For primary document see N95-13896 03-74)
Avail: CASI HC A02/MF A06

N95-13910*# Massachusetts Inst. of Tech., Cambridge. Dept. of Electrical Engineering and Computer Science.
ON THE THEORY OF QUANTUM MEASUREMENT
Hermann A. Haus and Franz X. Kaertner *In* NASA. Goddard Space Flight Center, Third International Workshop on Squeezed States and Uncertainty Relations May 1994 p 107-115 (For primary document see N95-13896 03-74)
(Contract N00014-92-J-1302)
Avail: CASI HC A02/MF A06

N95-13913*# Pavia Univ. (Italy). Dipt. di Fisica.
HOMODYNING AND HETERODYNING THE QUANTUM PHASE
Giacomo M. DAriano, C. Macchiavello, and M. G. A. Paris *In* NASA. Goddard Space Flight Center, Third International Workshop on Squeezed States and Uncertainty Relations May 1994 p 129-147 (For primary document see N95-13896 03-74)
Avail: CASI HC A03/MF A06

N95-13914*# Technische Univ., Eindhoven (Netherlands). Theoretical Physics Group.
JOINT AND ANGLE-COVARIANT SPIN MEASUREMENTS WITH A QUADRUPOLE MAGNETIC FIELD
Hans Martens and Willem M. deMuynck *In* NASA. Goddard Space Flight Center, Third International Workshop on Squeezed States and Uncertainty Relations May 1994 p 149-154 Sponsored by Foundation for Philosophical Research and Netherlands Organization for Applied Scientific Research (For primary document see N95-13896 03-74)
Avail: CASI HC A02/MF A06

N95-13916*# Humboldt Univ., Berlin (German D.R.). Arbeitsgruppe Nichtklassische Strahlung.
MEASUREMENT OF VERY SMALL PHASE FLUCTUATIONS BY MEANS OF THE OPERATIONAL APPROACH
Arno Bandilla *In* NASA. Goddard Space Flight Center, Third International Workshop on Squeezed States and Uncertainty Relations May 1994 p 161-165 (For primary document see N95-13896 03-74)
Avail: CASI HC A01/MF A06

N95-13919*# Ulm Univ. (Germany). Abteilung fuer Quantenphysik.
QUANTUM STATE ENGINEERING
Karl Vogel, V. M. Akulin, and W. P. Schleich *In* NASA. Goddard Space Flight Center, Third International Workshop on Squeezed States and Uncertainty Relations May 1994 p 181-188 Sponsored in part by QED Associates (For primary document see N95-13896 03-74)
Avail: CASI HC A02/MF A06

N95-13928*# George Mason Univ., Fairfax, VA. Dept. of Physics.
PHASE SPACE FLOW OF PARTICLES IN SQUEEZED STATES
Peter H. Ceperley *In* NASA. Goddard Space Flight Center, Third International Workshop on Squeezed States and Uncertainty Relations May 1994 p 251-256 (For primary document see N95-13896 03-74)
Avail: CASI HC A02/MF A06

N95-13929*# European Nuclear Energy Agency, Frascati (Italy). Settore Elettroottica e Laser.
MULTIVARIABLE HERMITE POLYNOMIALS AND PHASE-SPACE DYNAMICS
G. Dattoli, Amalia Torre, S. Lorenzutta, G. Maino, and C. Chiccoli *In* NASA. Goddard Space Flight Center, Third International Workshop on Squeezed States and Uncertainty Relations May 1994 p 257-268 (For primary document see N95-13896 03-74)
Avail: CASI HC A03/MF A06

N95-13930*# Ecole Polytechnique, Montreal (Quebec). Dept. de Genie Physique.
UNDERSTANDING SQUEEZING OF QUANTUM STATES WITH THE WIGNER FUNCTION
Antoine Royer *In* NASA. Goddard Space Flight Center, Third International Workshop on Squeezed States and Uncertainty Relations May 1994 p 269-274 (For primary document see N95-13896 03-74)
Avail: CASI HC A02/MF A06

N95-13931*# Instituto Politecnico Nacional, Mexico City. Dept. de Fisica.
ON THE POSSIBILITY OF A QUANTUM MECHANICAL PHASE SPACE REPRESENTATION
Gabino Torres-Vega *In* NASA. Goddard Space Flight Center, Third International Workshop on Squeezed States and Uncertainty Relations May 1994 p 275-280 Sponsored by CONACyT and SNI (For primary document see N95-13896 03-74)
Avail: CASI HC A02/MF A06

N95-13933*# Johns Hopkins Univ., Laurel, MD. Applied Physics Lab.
QUANTUM PHASE UNCERTAINTIES IN THE CLASSICAL LIMIT
James D. Franson *In* NASA. Goddard Space Flight Center, Third International Workshop on Squeezed States and Uncertainty Relations May 1994 p 289-298 Sponsored by ONR (For primary document see N95-13896 03-74)
Avail: CASI HC A02/MF A06

N95-13936*# Atominstitut der Oesterreichischen Hochschulen, Vienna.
MAXIMUM PREDICTIVE POWER AND THE SUPERPOSITION PRINCIPLE
Johann Summhammer *In* NASA. Goddard Space Flight Center, Third International Workshop on Squeezed States and Uncertainty Relations May 1994 p 315-320 (For primary document see N95-13896 03-74)
(FFWF Proj. P-8781)
Avail: CASI HC A02/MF A06

N95-13938*# Salerno Univ. (Italy). Dipt. di Fisica.
MINIMUM UNCERTAINTY AND SQUEEZING IN DIFFUSION PROCESSES AND STOCHASTIC QUANTIZATION
S. DeMartino, S. DeSiena, Fabrizo Illuminati, and Giuseppe Vitiello *In* NASA. Goddard Space Flight Center, Third International Workshop on Squeezed States and Uncertainty Relations May 1994 p 331-336 Prepared in cooperation with Istituto Nazionale di Fisica Nucleare, Naples, Italy (For primary document see N95-13896 03-74)
Avail: CASI HC A02/MF A06

N95-13939*# Missouri Univ., Columbia, MO. Dept. of Physics and Astronomy.
APPLICATIONS OF SQUEEZED STATES: BOGOLIUBOV TRANSFORMATIONS AND WAVELETS TO THE STATISTICAL MECHANICS OF WATER AND ITS BUBBLES
Brian DeFacio, S.-H. Kim, and A. VanNevel *In* NASA. Goddard Space Flight Center, Third International Workshop on Squeezed States and Uncertainty Relations May 1994 p 339-351 (For primary document see N95-13896 03-74)
(Grants AF-AFOSR-0307-90; AF-AFOSR-0203-91)
Avail: CASI HC A03/MF A06

N95-13943*# Chungbuk National Univ. (Republic of Korea). Dept. of Physics.
THE WAVE FUNCTION AND MINIMUM UNCERTAINTY FUNCTION OF THE BOUND QUADRATIC HAMILTONIAN SYSTEM
Kyu Hwang Yeon, Chung In Um, and T. F. George *In* NASA. Goddard Space Flight Center, Third International Workshop on Squeezed States and Uncertainty Relations May 1994 p 381-386 Sponsored by Ministry of Education (For primary document see N95-13896 03-74)
(Contract KOSEF-3-08-00-05; NSF CHE-91-96214)
Avail: CASI HC A02/MF A06

N95-13946*# Alabama A & M Univ., Normal, AL. Dept. of Physics.
PSEUDOMASTER EQUATION FOR THE NO-COUNT PROCESS IN A CONTINUOUS PHOTODETECTION
Ching-Tsung Lee *In* NASA. Goddard Space Flight Center, Third International Workshop on Squeezed States and Uncertainty Relations May 1994 p 401-406 (For primary document see N95-13896 03-74)
(Contract N00014-89-J-1050)
Avail: CASI HC A02/MF A06

N95-13948*# Kochi Univ., Akebono (Japan). Dept. of Physics.
TIME-DEPENDENT VARIATIONAL APPROACH IN TERMS OF SQUEEZED COHERENT STATES: IMPLICATION TO SEMI-CLASSICAL APPROXIMATION
Yasuhiko Tsue *In* NASA. Goddard Space Flight Center, Third International Workshop on Squeezed States and Uncertainty Relations May 1994 p 413-418 (For primary document see N95-13896 03-74)
Avail: CASI HC A02/MF A06

N95-13949*# Pennsylvania State Univ., Schuylkill Haven, PA. Dept. of Physics.
DECOHERENCE AND DISSIPATION FOR A QUANTUM SYSTEM COUPLED TO A LOCAL ENVIRONMENT
Michael R. Gallis *In* NASA. Goddard Space Flight Center, Third International Workshop on Squeezed States and Uncertainty Relations May 1994 p 419-424 (For primary document see N95-13896 03-74)
Avail: CASI HC A02/MF A06

N95-13951*# Universidade Estadual de Campinas (Brazil). Inst. de Fisica.
PROBING THE ANTIFERROMAGNETIC LONG-RANGE ORDER WITH GLAUBER SPIN STATES
Guillermo G. Cabrera *In* NASA. Goddard Space Flight Center, Third International Workshop on Squeezed States and Uncertainty Relations May 1994 p 431-436 Sponsored by Fundacao de Amparo a Pesquisa do Estado de Sao Paulo and Fundo de Apoio ao Ensino e Pesquisa (For primary document see N95-13896 03-74)
Avail: CASI HC A02/MF A06

N95-13952*# Academy of Sciences (USSR), Moscow (USSR). Optics Div.
BERRY PHASE IN HEISENBERG REPRESENTATION
V. A. Andreev, Andrei B. Klimov, and Peter B. Lerner *In* NASA. Goddard Space Flight Center, Third International Workshop on Squeezed States and Uncertainty Relations May 1994 p 437-448 Sponsored by Michigan Univ. and ONR (For primary document see N95-13896 03-74)
Avail: CASI HC A03/MF A06

N95-13957*# National Aeronautics and Space Administration. Goddard Space Flight Center, Greenbelt, MD.
NEW QUANTUM PROPERTIES OF PHONONS AND THEIR DETECTION
Maurizo Artoni and Joseph L. Birman *In its* Third International Workshop on Squeezed States and Uncertainty Relations May 1994 p 495-500 (For primary document see N95-13896 03-74)
Avail: CASI HC A02/MF A06

N95-13958*# Bilkent Univ., Ankara (Turkey). Dept. of Physics.
QUANTUM STATISTICS OF RAMAN SCATTERING MODEL WITH STOKES MODE GENERATION
Bilal Tanatar and Alexander S. Shumovsky *In* NASA. Goddard Space Flight Center, Third International Workshop on Squeezed States and Uncertainty Relations May 1994 p 501-506 (For primary document see N95-13896 03-74)
Avail: CASI HC A02/MF A06

N95-13959*# Brookhaven National Lab., Upton, NY. National Synchrotron Light Source.
EVOLUTION OF WAVE FUNCTION IN A DISSIPATIVE SYSTEM
Li-Hua Yu and Chang-Pu Sun *In* NASA. Goddard Space Flight Center, Third International Workshop on Squeezed States and Uncertainty Relations May 1994 p 507-513 Sponsored by State Univ. of New York and National Science Foundation of China (For primary document see N95-13896 03-74)
(Contract DE-AC02-76CH-00016)
Avail: CASI HC A02/MF A06

N95-13960*# Academy of Sciences (USSR), Moscow (USSR). Physics Inst.
NONRESONANT INTERACTION OF ULTRASHORT ELECTROMAGNETIC PULSES WITH MULTILEVEL QUANTUM SYSTEMS
E. Belenov, V. Isakov, and A. Nazarkin *In* NASA. Goddard Space Flight Center, Third International Workshop on Squeezed States and Uncertainty Relations May 1994 p 515-520 Sponsored by Russian Basic Research Foundation; Wissenschaftskolleg; Schweizerische National-Versicherungs-Gesellschaft; and Alusuisse-Lonza Holding A.G. (For primary document see N95-13896 03-74)
Avail: CASI HC A02/MF A06

N95-13962*# City Coll. of the City Univ. of New York, NY. Dept. of Physics.
FURTHER EVIDENCE FOR THE EPNT ASSUMPTION
Daniel M. Greenberger, Herbert J. Bernstein, Michael Horne, and Anton Zeilinger *In* NASA. Goddard Space Flight Center, Third International Workshop on Squeezed States and Uncertainty Relations May 1994 p 535-543 (For primary document see N95-13896 03-74)
Avail: CASI HC A02/MF A06

N95-13966*# Texas A&M Univ., College Station, TX. Dept. of Physics.
THE STRONG BELL INEQUALITIES: A PROPOSED EXPERIMENTAL TEST
Edward S. Fry *In* NASA. Goddard Space Flight Center, Third International Workshop on Squeezed States and Uncertainty Relations May 1994 p 575-580 (For primary document see N95-13896 03-74)
(Grant NSF PHY-92-21038; Proj. A-1218)
Avail: CASI HC A02/MF A06

N95-13968*# California Univ., Berkeley, CA. Dept. of Physics.
A LOOPHOLE-FREE BELL'S INEQUALITY EXPERIMENT
Paul G. Kwiat, Aephraim M. Steinberg, Raymond Y. Chiao, and Philippe H. Eberhard *In* NASA. Goddard Space Flight Center, Third International Workshop on Squeezed States and Uncertainty Relations May 1994 p 591-602 (For primary document see N95-13896 03-74)
(Contracts N00014-90-J-1259; DE-AC03-76SF-00098)
Avail: CASI HC A03/MF A06

N95-13969*# Atominstitut der Oesterreichischen Hochschulen, Vienna.
THE PROBABILISTIC ORIGIN OF BELL'S INEQUALITY
Guenther Krenn *In* NASA. Goddard Space Flight Center, Third International Workshop on Squeezed States and Uncertainty Relations May 1994 p 603-608 (For primary document see N95-13896 03-74)
(FFWF Proj. P-8781)
Avail: CASI HC A02/MF A06

N95-13970*# Maryland Univ., College Park, MD. Dept. of Physics.
EINSTEIN-PODOLSKY-ROSEN-BOHM EXPERIMENT AND BELL INEQUALITY VIOLATION USING TYPE 2 PARAMETRIC DOWN CONVERSION
Thomas E. Kiess, Yan-Hua Shih, A. V. Sergienko, and Carroll O. Alley *In* NASA. Goddard Space Flight Center, Third International Workshop on Squeezed States and Uncertainty Relations May 1994 p 609-614 (For primary document see N95-13896 03-74)
(Contract N00014-19-J-1430)
Avail: CASI HC A02/MF A06

N95-14284*# Texas Univ., Austin, TX. Center for Space Research.
THE ROLE OF SLR AND LLR IN RELATIVITY
John C. Ries *In* NASA. Goddard Space Flight Center, Satellite Laser Ranging in the 1990s: Report of the 1994 Belmont Workshop Nov. 1994 p 77-79 (For primary document see N95-14274 03-46)
Avail: CASI HC A01/MF A02

80 SOCIAL SCIENCES (GENERAL)

Includes educational matters.

N95-13650*# National Aeronautics and Space Administration, Washington, DC.
OUR MISSION TO PLANET EARTH: A GUIDE TO TEACHING EARTH SYSTEM SCIENCE
Jun. 1994 42 p
(NASA-EP-292; NAS 1.19:292) Avail: CASI HC A03/MF A01
Volcanic eruptions, hurricanes, floods, and El Nino are naturally occurring events over which humans have no control. But can human activities

cause additional environmental change? Can scientists predict the global impacts of increased levels of pollutants in the atmosphere? Will the planet warm because increased levels of greenhouse gases, produced by the burning of fossil fuels, trap heat and prevent it from being radiated back into space? Will the polar ice cap melt, causing massive coastal flooding? Have humans initiated wholesale climatic change? These are difficult questions, with grave implications. Predicting global change and understanding the relationships among earth's components have increased in priority for the nation. The National Aeronautics and Space Administration (NASA), along with many other government agencies, has initiated long-term studies of earth's atmosphere, oceans, and land masses using observations from satellite, balloon, and aircraft-borne instruments. NASA calls its research program Mission to Planet Earth. Because NASA can place scientific instruments far above earth's surface, the program allows scientists to explore earth's components and their interactions on a global scale.

Derived from text

81 ADMINISTRATION AND MANAGEMENT

Includes management planning and research.

N95-14918*# National Aeronautics and Space Administration. John F. Kennedy Space Center, Cocoa Beach, FL.
JOHN F. KENNEDY SPACE CENTER, SAFETY, RELIABILITY, MAINTAINABILITY AND QUALITY ASSURANCE, SURVEY AND AUDIT PROGRAM Final Report
Nov. 1994 55 p
(NASA-TM-109208; NAS 1.15:109208) Avail: CASI HC A04/MF A01

This document is the product of the KSC Survey and Audit Working Group composed of civil service and contractor Safety, Reliability, and Quality Assurance (SR&QA) personnel. The program described herein provides standardized terminology, uniformity of survey and audit operations, and emphasizes process assessments rather than a program based solely on compliance. The program establishes minimum training requirements, adopts an auditor certification methodology, and includes survey and audit metrics for the audited organizations as well as the auditing organization.

Author

N95-14637# Vanderbilt Univ., Nashville, TN. Center for Intelligent Systems.
INTELLIGENT MANUFACTURING SYSTEMS STATE OF THE ART
Gautam Biswas, Kazuhiko Kawamura, and Ashraf Saad *In* Huntsville Association of Technical Societies, TABES 1994: 10th Annual Technical and Business Exhibition and Symposium 1994 7 p (For primary document see N95-14633 03-12)
(TABES Paper 94-503) Avail: CASI HC A02/MF A04

N95-14640# Itall Corp., Meridianville, AL.
DESIGN IN HUNTSVILLE, MANUFACTURE IN ESTONIA, SELL IN EUROPE
Ilmar Luik *In* Huntsville Association of Technical Societies, TABES 1994: 10th Annual Technical and Business Exhibition and Symposium 1994 4 p (For primary document see N95-14633 03-12)
(TABES Paper 94-607) Avail: CASI HC A01/MF A04

N95-14644# ENSR Consulting and Engineering, Florence, AL.
COMPREHENSIVE FACILITY DECOMMISSIONING THROUGH THE USE OF INNOVATIVE TECHNOLOGY TO REDUCE COST, SCHEDULE, AND ENVIRONMENTAL LIABILITY
Scott S. Huismann, Michael S. Astin, and Terrance M. Fleet *In* Huntsville Association of Technical Societies, TABES 1994: 10th Annual Technical and Business Exhibition and Symposium 1994 7 p (For primary document see N95-14633 03-12)
(TABES Paper 94-615) Avail: CASI HC A02/MF A04

82 DOCUMENTATION AND INFORMATION SCIENCE

Includes information management; information storage and retrieval technology; technical writing; graphic arts; and micrography.

For computer documentation see *61 Computer Programming and Software*.

N95-13673# Westinghouse Hanford Co., Richland, WA.
CASE STUDY: ACCELERATED SCHEDULE FOR MULTI LIMS INSTALLATION
T. G. Ibsen May 1994 7 p Presented at the MULTI LIMS Group Conference, Seattle, WA, 4-6 May 1994
(Contract DE-AC06-87RL-10930)
(DE94-012398; WHC-SA-2451; CONF-9405153-1) Avail: CASI HC A02/MF A01

This presentation focuses on the steps taken by the Westinghouse Hanford Company to meet an accelerated schedule for configuration and implementation of the MULTI LIMS in a multiple laboratory environment. The Westinghouse Hanford Company purchased the MULTI LIMS Laboratory Information Management System in August, 1993. Hardware delivery began in October, 1993. Less than four months later, the initial configuration was released for use in two Westinghouse Hanford Company laboratories. Several major obstacles were overcome during implementation. These include information gathering for base table loading, user training, acceptance of the new system by users of a legacy system, and hardware configuration issues. In summary, steps needed to be taken to meet the accelerated implementation schedule of the MULTI LIMS at the Hanford Site. The obstacles faced were overcome through the in-depth knowledge and help of the vendor and the dedication and drive of the technical staff. DOE

N95-13726# Energy Technology Data Exchange, Oak Ridge, TN.
INTERNATIONAL ENERGY: RESEARCH ORGANIZATIONS, 1988-1992
Oct. 1994 80 p Revised
(DE90-017267; ETDE/PUB-3-Rev-1-Suppl-4) Avail: CASI HC A05/MF A01

This supplement contains the standardized names of energy research organizations used in energy information databases that were added to the 'International Energy: Research Organizations, 1988-1992' cumulative through December 1993. It is arranged in three parts. Part 1 is an alphabetical listing of organization names. Each organization is identified by a unique seven-digit code. Part 2 lists organization names in alphabetical order under the country in which they are located. Part 3 lists report number prefixes.

Author

N95-13996# Los Alamos National Lab., NM.
PREPARING TECHNICAL TEXT FOR TRANSLATION: A COMPARISON BETWEEN INTERNATIONAL ENGLISH AND METHODS FOR SIMPLIFYING LANGUAGE
I. Buican, V. Hriscu, and M. Amador 1994 5 p Presented at the IPCC Conference, Banff, Alberta, Sep. 1994
(Contract W-7405-eng-36)
(DE94-014465; LA-UR-94-1843; CONF-9409164-2) Avail: CASI HC A01/MF A01

For the past four and a half years, the International Communication Committee at Los Alamos National Laboratory has been working to develop a set of guidelines for writing technical and scientific documents in International English, that is, English for those whose native language is not English. Originally designed for documents intended for presentation in English to an international audience of technical experts, the International English guidelines apply equally well to the preparation of English text for translation. This is the second workshop in a series devoted to the topic of translation. The authors focus on the advantages of using International English, rather than various methods of simplifying language, to prepare scientific and technical text for translation. DOE

N95-14321# Nielsen Engineering and Research, Inc., Mountain View, CA.
HYPERTEXT KNOWLEDGE PRESENTATION SYSTEM TO TRANSITION BASIC RESEARCH Final Technical Report, 25 Aug. 1992 - 30 Apr. 1994
Laura C. Rodman, David Nixon, Stanley C. Perkins, Jr., Teresa O. Lesieutre,

and Michael R. Mendenhall 22 Jun. 1994 42 p
(Contract N00014-92-C-0221)
(AD-A280796; NEAR-TR-472) Avail: CASI HC A03/MF A01

Efficient technology transfer from the basic research community to the engineering development community is essential for maintaining technological competitiveness. However, the research and the design communities have different objectives, and they also have different perspectives on relevant technical knowledge. In this work, the communication issues resulting from the differing perspectives of these two communities are addressed with a hypertext knowledge presentation system for technology transfer. The objective of this work is to relate research results to a relevant engineering framework, and to use this framework to present both the research and the design communities with information to facilitate research transition. This knowledge presentation system can be used by the engineering development community to access research knowledge that is relevant to a specific design topic and that has the potential for transition. In addition, this system documents the current status of design technology, which can assist program managers in directing research efforts towards those areas that will lead to improved analysis techniques or increased physical understanding at the design level. DTIC

N95-14327# Defense Information Systems Agency, Arlington, VA. Center for Information Management.
DEPARTMENT OF DEFENSE TECHNICAL ARCHITECTURE FRAMEWORK FOR INFORMATION MANAGEMENT. VOLUME 1: OVERVIEW, VERSION 2.0
30 Jun. 1994 67 p See also AD-A286764
(AD-A283763) Avail: CASI HC A04/MF A01

Only Version 1.1 has been signed out by OSD. The TAFIM provides guidance for the evolution of the DOD technical infrastructure. The TAFIM does not provide a specific system architecture. Rather, it provides the services, standards, design concepts, components, and configurations that can be used to guide the development of technical architectures that meet specific mission requirements. This volume presents an overview of the TAFIM. It relates information technology (IT) and information management (IM) guidance published in the DOD directives, instructions, and manuals to the TAFIM. Legal Restrictions. This asset contains public domain data with unlimited rights for all users. Extraction is permitted to all authorized library users. This asset is provided 'as is' and without any expressed or implied warranties. No warranties as to performance, merchantability or fitness for a particular purpose exists. In no event shall any person or, organization of people be held responsible for any direct, indirect, consequential or inconsequential damages. DTIC

N95-14329# Defense Information Systems Agency, Arlington, VA. Center for Information Management.
DEPARTMENT OF DEFENSE TECHNICAL ARCHITECTURE FRAMEWORK FOR INFORMATION MANAGEMENT. VOLUME 2: TECHNICAL REFERENCE MODEL AND STANDARDS PROFILE SUMMARY
30 Jun. 1994 60 p See also AD-A283765
(AD-A283764) Avail: CASI HC A04/MF A01

Only Version 1.1 has been signed out by OSD. The TAFIM provides guidance for the evolution of the DOD technical infrastructure. The TAFIM does not provide a specific system architecture. Rather, it provides the services, standards, design concepts, components, and configurations that can be used to guide the development of technical architectures that meet specific mission requirements. This volume provides a common conceptual framework, defines a common vocabulary, and specifies a base of standards so that the diverse components within DOD can better coordinate acquisition, development, and support of DOD information systems. It also provides a high-level representation of the information system domain showing major service areas. DTIC

N95-14330# Defense Information Systems Agency, Arlington, VA. Center for Information Management.
DEPARTMENT OF DEFENSE TECHNICAL ARCHITECTURE FRAMEWORK FOR INFORMATION MANAGEMENT. VOLUME 3: ARCHITECTURE CONCEPTS AND DESIGN GUIDANCE, VERSION 2.0
30 Jun. 1994 74 p See also AD-A283766
(AD-A283765) Avail: CASI HC A04/MF A01

Only Version 1.1 has been signed out by OSD. The TAFIM provides guidance for the evolution of the DOD technical infrastructure. The TAFIM does not provide a specific system architecture. Rather, it provides the services, standards, design concepts, components, and configurations that can be used to guide the development of technical architectures that meet specific mission requirements. This volume presents technical architecture concepts and design guidance for information systems in DOD. As part of the TAFIM, this volume provides guidance for the evolution of the DOD's technical infrastructure in support of specific mission requirements. The data and mission-specific software architectures are critical elements in information system development. Guidance on their development and use will be provided in separate documents outside of the TAFIM. DTIC

N95-14331# Defense Information Systems Agency, Arlington, VA. Center for Information Management.
DEPARTMENT OF DEFENSE TECHNICAL ARCHITECTURE FRAMEWORK FOR INFORMATION MANAGEMENT. VOLUME 4: DOD STANDARDS-BASED ARCHITECTURE PLANNING GUIDE, VERSION 2.0
30 Jun. 1994 341 p See also AD-A283767
(AD-A283766) Avail: CASI HC A15/MF A03

Only Version 1.1 has been signed out by OSD. The TAFiM provides guidance for the evolution of the DOD technical infrastructure. The TAFIM does not provide a specific system architecture. Rather, it provides the services, standards, design concepts, components, and configurations that can be used to guide the development of technical architectures that meet specific mission requirements. This volumes defines a common framework and profile of standards for the computing and communications infrastructure. The methodology prescribed in this volume provides a way of mapping the technology architecture, which is the primary focus of Volumes 1, 2, and 3 of the TAFIM, to the three other views of an integrated architecture: work, data or information, and applications. DTIC

N95-14332# Defense Information Systems Agency, Arlington, VA. Center for Information Management.
DEPARTMENT OF DEFENSE TECHNICAL ARCHITECTURE FRAMEWORK FOR INFORMATION MANAGEMENT. VOLUME 6: DEPARTMENT OF DEFENSE (DOD) GOAL SECURITY ARCHITECTURE, VERSION 2.0
30 Jun. 1994 145 p See also AD-A275527
(AD-A283767) Avail: CASI HC A07/MF A02

Only Version 1.1 has been signed out by OSD. The TAFIM provides guidance for the evolution of the DOD technical infrastructure. The TAFIM does not provide a specific system architecture. Rather, it provides the services, standards, design concepts, components, and configurations that can be used to guide the development of technical architectures that meet specific mission requirements. This volume describes the DOD Goal Security Architecture (DGSA), but it does not provide a specification for any particular information system or component. Rather, it specifies security principles and target security capabilities that will guide system security architects in creating specific security architectures that are consistent with the DGSA. Further, there is no particular date by which the DGSA will be completely achieved. The DIS architecture and the DGSA are under constant development and will continue to evolve with time and with technological advances. DTIC

N95-14333# Defense Information Systems Agency, Arlington, VA. Center for Information Management.
DEPARTMENT OF DEFENSE TECHNICAL ARCHITECTURE FRAMEWORK FOR INFORMATION MANAGEMENT. VOLUME 8: DEPARTMENT OF DEFENSE HCI STYLE GUIDE, VERSION 2.0
30 Jun. 1994 358 p See also AD-A261280
(AD-A283768) Avail: CASI HC A16/MF A03

Only Version 1.1 has been signed out by OSD. The TAFIM provides guidance for the evolution of the DOD technical infrastructure. The TAFIM does not provide a specific system architecture. Rather, it provides the services, standards, design concepts, components, and configurations that can be used to guide the development of technical architectures that meet specific mission requirements. This volume provides a common framework for Human-Computer Interface (HCI) design and implementation. Through this framework, the long-term functional goals, objectives, and requirements of the HCI will be defined and documented. Interface implementation options will be standardized, enabling all DOD applications to appear and operate in a reasonably consistent manner. Specifying

appearance, operation, and behavior of DOD software applications will support the following operational objectives: higher productivity, less training time, and reduced development time. DTIC

N95-14619*# National Aeronautics and Space Administration. Langley Research Center, Hampton, VA.
NASA/DOD AEROSPACE KNOWLEDGE DIFFUSION RESEARCH PROJECT. PAPER 43: THE ROLE OF INFORMATION RESOURCE TRAINING IN AEROSPACE EDUCATION. EXPANDED VERSION
Barbara Lawrence (American Inst. of Aeronautics and Astronautics, New York, NY.), Thomas E. Pinelli, Rebecca O. Barclay, John M. Kennedy, and Karen Holloway 1994 12 p Presented at the 45th Congress of the International Astronautical Federation (IAF), Jerusalem, Israel, 9-14 Oct. 1994
(NASA-TM-109981; NAS 1.15:109981; IAF-94-P.1.301) Avail: CASI HC A03/MF A01

Information resource instruction for undergraduate aerospace engineering students has traditionally been limited to an occasional part of the education process--a written paper required in the capstone design course or a library tour. Efforts to encourage the use of aerospace literature and information resources have been made in the past decade, with a recent push from information and, especially, networking technology. This paper presents data from a survey of U.S. aerospace engineering students regarding their instruction in the use of information resources. We find that more than 25 percent of the students surveyed had no instruction in technical communications skills or the use of information resources. We consider the need for instruction in the use of information resources and technical communications skills and the opportunities presented for improvement. Author

N95-14837# Technische Univ., Delft (Netherlands).
DYNAMIC MODELLING TO ASSESS THE VALUE OF ELECTRONIC DATA INTERCHANGE: A STUDY IN THE ROTTERDAM PORT COMMUNITY Ph.D. Thesis
R. A. G. J. Streng 2 Nov. 1993 262 p
(PB94-195542; ISBN-90-9006567-9) Copyright Avail: CASI HC A12/MF A03

This dissertation addresses the issue of assessing the value of Electronic Data Interchange (EDI) for organizations in the transport sector. The EDI dilemma that faces decision makers in these organizations is described and placed in a general problem solving model. We hypothesized that it is possible to develop an inquiry system that will support decision-makers in assessing the value of alternative EDI-projects. The research started with the development of a framework for value assessment and the development of an initial version of the inquiry system. This initial system was enhanced on the basis of the experience gained in three case studies where the Layered Actors, Networks and Entities (LANE) approach was prescribed to support organizational decision makers in their struggle with the EDI dilemma. The case studies were: The transport of beer to the USA; The central gate for a stevedore; and The import of audio and video equipment from the Far East. It was concluded that the LANE-approach gives decision-makers in organizations that are involved in transport the means to assess the value of EDI in a cost-effective way. The final section discusses to what extent the results of our research are applicable outside EDI and the transport sector. NTIS

N95-14870*# National Aeronautics and Space Administration. Langley Research Center, Hampton, VA.
NASA/DOD AEROSPACE KNOWLEDGE DIFFUSION RESEARCH PROJECT. PAPER 44: BECOMING AN AEROSPACE ENGINEER: SOME THOUGHTS ON THE CAREER GOALS AND EDUCATIONAL PREPARATION OF AIAA STUDENT MEMBERS
Thomas E. Pinelli, Rebecca O. Barclay, John M. Kennedy, and Laura M. Hecht 1994 6 p Repr. from AIAA Student Journal, v. 32, no. 3, 1994 p 22-26
(NASA-TM-109980; NAS 1.15:109980) Avail: CASI HC A02/MF A01

Similarities and differences between undergraduate and graduate engineering students in the context of two general aspects of educational experience are described. Considered first is the extent to which students differ regarding the factors that led to the choice of a career in aerospace engineering, their current levels of satisfaction with that choice, and career-related goals and objectives. Second, the importance of certain information-use skills for professional success, and the frequency of use and importance of specific information sources and products to meet students' educational needs, are explored. Derived from text

N95-15366# Sandia National Labs., Albuquerque, NM.
ACRONYMS, INITIALISMS, AND ABBREVIATIONS
B. J. Tolman, comp. Apr. 1994 132 p Revised
(Contract DE-AC04-94AL-85000)
(DE94-016686; SAND-89-0217) Avail: CASI HC A07/MF A02

This document lists acronyms used in technical writing. The immense list is supplemented by an appendix containing chemical elements, classified information access, common abbreviations used for functions, conversion factors for selected SI units, a flowcharting template, greek alphabet, metrix terminology, proofreader's marks, signs and symbols, and state abbreviations. DOE

N95-15419# Westinghouse Savannah River Co., Aiken, SC.
ESSENTIAL ELEMENTS OF AN EFFECTIVE DATA QUALIFICATION
E. W. Jenkins 1994 7 p Presented at the Institute of Nuclear Materials Management Annual Meeting, Naples, FL, 17-20 Jul. 1994
(Contract DE-AC09-89SR-18035)
(DE94-015566; WSRC-MS-94-0112; CONF-940748-21) Avail: CASI HC A02/MF A01

Before data is used in any statistical evaluation, it should be subjected to a thorough data qualification to ensure its integrity. Data Qualification efforts may vary in scope but should all contain certain basic elements. Outliers should be eliminated so that any estimates obtained from the data will not be overly biased. Plots may be generated to uncover potential outliers, and these observations can be confirmed as being anomalous through the use of statistical testing. Non-stationarity of the data (i.e., time trends) may also be initially identified through the use of plots and confirmed by the results of statistical analyses, e.g., the use of the Kendall's tau statistic. When the dataset has been qualified, replicates and duplicates should be averaged to create a pseudo-independence between data points. An algorithm based on the groundwater data from the Savannah River Site has been used by the Applied Statistics Group at Westinghouse Savannah River Company for this. DOE

N95-15423# California Univ., Berkeley, CA. Dept. of Electrical Engineering and Computer Science.
SUMMARY OF ACTIVITIES FOR UNIVERSITY OF CALIFORNIA Report, 1 Jun. 1993 - 31 May 1994
Avideh Zakhor 31 May 1994 2 p
(Contract N00014-93-1-0871)
(AD-A283890) Avail: CASI HC A01/MF A01

During the past year, we continued our efforts in the areas of video compression and storage 1, 2. We have developed three strategies for placement of Constant Bit Rate (CBR) video data on parallel disk arrays. Using a low-level disk model and video data from a scalable subband coding technique, we have derived constraints with which to compare the three strategies. In doing so, we have found one of the strategies, constant frame grouping, to be superior to the other two. In addition, two methods for interleaving multiple videos under the constant frame grouping strategy have been developed: nonperiodic and periodic. Periodic interleaving is shown to have the advantages of a lower access time and limited scan and pause functions. The constant frame grouping strategy was tested on an actual array of 8 disks and shown to have performance that is close to the theoretical prediction. The scalable nature of the compressed data was used to relieve the disk system overload for an overly high request rate. Details of this work was presented at the SPIE Symposium on Electronic Imaging in San Jose last February 1. DTIC

N95-15435# EG and G Energy Measurements, Inc., Idaho Falls, ID.
FFCAat CLEARINGHOUSE, DIRECTORY OF ABSTRACTS
T. Harwood May 1994 64 p
(Contract DE-AC07-76ID-01570)
(DE94-015259; DOE/LLW-201-Rev-1) Avail: CASI HC A04/MF A01

The Federal Facility Compliance Act (FFCAct) Clearinghouse is a card catalog of information about the FFCAct and its requirements for developing Site Treatment Plans (STP). The information available in the clearinghouse includes abstracts describing computer applications, technical reports, and a list of technical experts. Information can be accessed for use in responding

to FFCAct requirements, and the clearinghouse provides search capabilities on particular topics and issues related to STP development. Appendix A includes: contacts from each site, for which contact has been made, who are developing STP's; the FFCAct Clearinghouse Fact Sheet and; additional hard copy forms to be used to populate the database. This report contains 50 abstracts related to the Radioactive Waste Technical Support Program. DOE

N95-15528# Pacific Northwest Lab., Richland, WA.
SYSTEM ADMINISTRATOR'S GUIDE TO CDPS
B. T. Didier and M. H. Portwood May 1994 70 p
(Contract DE-AC06-76RL-01830)
(DE94-015288; PNL-9872) Avail: CASI HC A04/MF A01 (US Sales Only)

The System Administrator's Guide to CDPS is intended for those responsible for setting up and maintaining the hardware and software of a Common Mapping Standard (CMS) Date Production System (CDPS) installation. This guide assists the system administrator in performing typical administrative functions. It is not intended to replace the Ultrix Documentation Set that should be available for a DCPS installation. The Ultrix Documentation Set will be required to provide details on referenced Ultrix commands as well as procedures for performing Ultrix maintenance functions. There are six major sections in this guide. Section 1 introduces the system administrator to CDPS and describes the assumptions that are made by this guide. Section 2 describes the CDPS platform configuration. Section 3 describes the platform preparation that is required to install the CDPS software. Section 4 describes the CPS software and its installation procedures. Section 5 describes the CDS software and its installation procedures. Section 6 describes various operation and maintenance procedures. Four appendices are also provided. Appendix A contains a list of used acronyms. Appendix B provides a terse description of common Ultrix commands that are used in administrative functions. Appendix C provides sample CPS and CDS configuration files. Appendix D provides a required list and a recommended list of Ultrix software subsets for installation on a CDPS platform. DOE

N95-15585*# State Univ. of New York, Utica, NY. School of Arts and Sciences.
NASA/DOD AEROSPACE KNOWLEDGE DIFFUSION RESEARCH PROJECT. REPORT 30: COMPUTER-MEDIATED COMMUNICATION (CMC) AND THE COMMUNICATION OF TECHNICAL INFORMATION IN AEROSPACE Ph.D Thesis - Rensselaer Polytechnic Inst. Final Report
Daniel J. Murphy and Thomas E. Pinelli Dec. 1994 285 p
(NASA Order L-45107; RTOP 505-90-00)
(NASA-CR-194973; NAS 1.26:194973) Avail: CASI HC A13/MF A03

This research used survey research to examine the use of communication media in general and electronic media specifically in the U.S. aerospace industry. The survey population included 1,006 randomly selected U.S. aerospace engineers and scientists who belong to the American Institute of Aeronautics and Astronautics (AIAA). Survey data were compared with qualitative information obtained from 32 AIAA members in telephone and face-to-face conversations. The Information Processing (IP) model developed by Tushman and Nadler and Daft and Lengel constituted the study's theoretical basis. This research analyzed responses regarding communication methods of U.S. aerospace engineers and scientists who create use and disseminate aerospace knowledge and explored selected contextual environmental variables related to media use and effective performance. The results indicate that uncertainty is significantly reduced in environments when levels of analyzability are high. When uncertainty is high there is significantly more use of electronic media. However no relation was found between overall effectiveness and media use in environments stratified by levels by analyzability or equivocality. The results indicate modest support for the influences of uncertainty and analyzability on electronic media use. Although most respondents reported that electronic networks are important for their work the data suggest that there are sharply disparate levels of use. Author

N95-15761# Los Alamos National Lab., NM.
ROOM: A RECURSIVE OBJECT ORIENTED METHOD FOR INFORMATION SYSTEMS DEVELOPMENT
T. Thelliez and S. Donahue Feb. 1994 16 p Presented at the 9th ACM SIGPLAN Conference on Object-Oriented Programming System, Languages and Applications, Portland, OR, 27 Oct. 1994
(Contract W-7405-eng-36)
(DE94-007575; LA-UR-94-575; CONF-941071-1) Avail: CASI HC A03/MF A01

Although complementary for the development of complex systems, top-down structured design and object oriented approach are still opposed and not integrated. As the complexity of the systems are still growing, and the so-called software crisis still not solved, it is urgent to provide a framework mixing the two paradigms. This paper presents an elegant attempt in this direction through our Recursive Object-Oriented Method (ROOM) in which a top-down approach divides the complexity of the system and an object oriented method studies a given level of abstraction. Illustrating this recursive schema with a simple example, we demonstrate that we achieve the goal of creating loosely coupled and reusable components. DOE

N95-15781# Executive Office of the President, Washington, DC. National Performance Review.
REENGINEERING THROUGH INFORMATION TECHNOLOGY. ACCOMPANYING REPORT OF THE NATIONAL PERFORMANCE REVIEW
Al Gore Sep. 1993 85 p
(PB94-170362; ISBN-0-16-042011-3) Avail: CASI HC A05/MF A01; SOD HC

This report describes anticipated and proposed changes in the organization and functional activities of the federal government. It includes actions to be taken by the Executive Branch and the Congress to improve performance by taking advantage of recent advances in information technology. Specific items addressed are: Strengthen leadership in information technology by integrating information technologies into the business of government; Implement integrated electronic access to government information and services; Establish a law enforcement/public safety network; Provide intergovernmental tax filing, reporting, and payment processes; Establish an international trade data system; Create a national environmental data index; Improve the government's electronic infrastructure; Develop privacy and security systems; Provide incentives for innovation; and Provide training and technical assistance in information technologies to federal employees. CASI

N95-15801* Mississippi State Univ., Bay Saint Louis, MS. Center for Air Sea Technology.
DESIGN DOCUMENT FOR THE MOODS DATA MANAGEMENT SYSTEM (MDMS), VERSION 1.0
Aug. 1994 48 p Limited Reproducibility: More than 20% of this document may be affected by microfiche quality
(Contract NAS13-330)
(NASA-CR-197016; NAS 1.26:197016; AD-A284150) Avail: Issuing Activity (Defense Technical Information Center (DTIC))

The MOODS Data Management System (MDMS) provides access to the Master Oceanographic Observation Data Set (MOODS) which is maintained by the Naval Oceanographic Office (NAVOCEANO). The MDMS incorporates database technology in providing seamless access to parameter (temperature, salinity, soundspeed) vs. depth observational profile data. The MDMS is an interactive software application with a graphical user interface (GUI) that supports user control of MDMS functional capabilities. The purpose of this document is to define and describe the structural framework and logical design of the software components/units which are integrated into the major computer software configuration item (CSCI) identified as MDMS, Version 1.0. The preliminary design is based on functional specifications and requirements identified in the governing Statement of Work prepared by the Naval Oceanographic Office (NAVOCEANO) and distributed as a request for proposal by the National Aeronautics and Space Administration (NASA). DTIC

N95-14594*# New Hampshire Univ., Durham. Complex Systems Research Center.
LANDSAT PATHFINDER TROPICAL FOREST INFORMATION MANAGEMENT SYSTEM
W. Salas, W. Chomentowski, J. Harville, D. Skole, and K. Vellekamp *In* NASA. Goddard Space Flight Center, 1994 Science Information Management and Data Compression Workshop Sep. 1994 p 83-93 (For primary document see N95-14585 03-59)
Avail: CASI HC A03/MF A02

N95-14596*# Hughes STX, Inc., Greenbelt, MD.
AN OVERVIEW OF THE EOSDIS V0 INFORMATION MANAGEMENT SYSTEM: LESSONS LEARNED FROM THE IMPLEMENTATION OF A DISTRIBUTED DATA SYSTEM Abstract Only
Patrick M. Ryan *In* NASA. Goddard Space Flight Center, 1994 Science Information Management and Data Compression Workshop Sep. 1994 p 105 (For primary document see N95-14585 03-59)
Avail: CASI HC A01/MF A02

N95-14650# Nichols Research Corp., Huntsville, AL. Tactical Systems Integration Div.
PRODUCT LIFE CYCLE DATA BASE, ANALYSIS AND SIMULATION INTEGRATION METHODOLOGY
Catherine Farless, Van Brewer, and Jim McCullough *In* Huntsville Association of Technical Societies, TABES 1994: 10th Annual Technical and Business Exhibition and Symposium 1994 7 p (For primary document see N95-14633 03-12)
(TABES Paper 94-626) Avail: CASI HC A02/MF A04

N95-15846*# Colorado Univ., Boulder, CO. Center for Astrophysics and Space Astronomy.
A BIBLIOGRAPHY OF PAPERS ON THE DIFFUSE INTERSTELLAR BANDS
Theodore P. Snow, Susan Barnes, and Maribeth Heitzmann *In* NASA. Ames Research Center, The Diffuse Interstellar Bands: Contributed Papers May 1994 p 105-127 (For primary document see N95-15827 03-89)
Avail: CASI HC A03/MF A02

83 ECONOMICS AND COST ANALYSIS

Includes cost effectiveness studies.

No abstracts in this category.

84 LAW, POLITICAL SCIENCE AND SPACE POLICY

Includes NASA appropriation hearings; aviation law; space law and policy; international law; international cooperation; and patent policy.

No abstracts in this category.

85 URBAN TECHNOLOGY AND TRANSPORTATION

Includes applications of space technology to urban problems; technology transfer; technology assessment; and surface and mass transportation.

For related information see also *03 Air Transportation and Safety, 16 Space Transportation,* and *44 Energy Production and Conversion.*

N95-15743*# Allied-Signal Aerospace Co., Phoenix, AZ.
ADVANCED TURBINE TECHNOLOGY APPLICATIONS PROJECT (ATTAP) Annual Report, 1993
Jul. 1994 57 p
(Contract DEN3-335; RTOP 778-32-21)
(NASA-CR-195393; E-9171; Rept-31-12089; NAS 1.26:195393) Avail: CASI HC A04/MF A01

Reports technical effort by AlliedSignal Engines in sixth year of DOE/NASA funded project. Topics include: gas turbine engine design modifications of production APU to incorporate ceramic components; fabrication and processing of silicon nitride blades and nozzles; component and engine testing; and refinement and development of critical ceramics technologies, including: hot corrosion testing and environmental life predictive model; advanced NDE methods for internal flaws in ceramic components; and improved carbon pulverization modeling during impact. ATTAP project is oriented toward developing high-risk technology of ceramic structural component design and fabrication to carry forward to commercial production by 'bridging the gap' between structural ceramics in the laboratory and near-term commercial heat engine application. Current ATTAP project goal is to support accelerated commercialization of advanced, high-temperature engines for hybrid vehicles and other applications. Project objectives are to provide essential and substantial early field experience demonstrating ceramic component reliability and durability in modified, available, gas turbine engine applications; and to scale-up and improve manufacturing processes of ceramic turbine engine components and demonstrate application of these processes in the production environment. Author

N95-14635# Wheeling Coll., WV. National Technology Transfer Center.
HELPING SMALL COMPANIES COMMERCIALIZE PUBLIC-SECTOR TECHNOLOGY
Lee W. Rivers *In* Huntsville Association of Technical Societies, TABES 1994: 10th Annual Technical and Business Exhibition and Symposium 1994 8 p (For primary document see N95-14633 03-12)
(TABES Paper 94-407) Avail: CASI HC A02/MF A04

88 SPACE SCIENCES (GENERAL)

N95-14207*# National Aeronautics and Space Administration. Marshall Space Flight Center, Huntsville, AL.
JOINT LAUNCH + ONE YEAR SCIENCE REVIEW OF USML-1 AND USMP-1 WITH THE MICROGRAVITY MEASUREMENT GROUP
N. Ramachandran, ed. (Universities Space Research Association, Huntsville, AL.), Donald. O. Frazier, ed., Sandor L. Lehoczky, ed., and Charles R. Baugher, ed. Washington May 1994 521 p Meeting held in Huntsville, AL, 22-24 Sep. 1993
(NASA-CP-3272-Vol-1; M-750-Vol-1; NAS 1.55:3272-Vol-1) Avail: CASI HC A22/MF A04

This document summarizes from the various investigations their comprehensive results and highlights, and also serves as a combined mission report for the first United States Microgravity Laboratory (USML-1) amd the United States Microgravity Payload (USMP-1). USML-1 included 31 investigations in fluid dynamics, crystal growth, combustion, biotechnology, and technology demonstrations supported by 11 facilities. On the USMP-1 mission, both the MEPHISTO and Lambda Point experiments exceeded by over 100 percent their planned science objectives. The mission was also the first time that acceleration data were down-linked and analyzed in real time. For individual titles, see N95-14208 through N95-14228.

N95-14208*# Jet Propulsion Lab., California Inst. of Tech., Pasadena, CA.
HEAT CAPACITY AND THERMAL RELAXATION OF BULK HELIUM VERY NEAR THE LAMBDA POINT **c25**
John A. Lipa (Stanford Univ., CA.), D. R. Swanson (Stanford Univ., CA.), J. A. Nissen (Stanford Univ., CA.), and T. C. P. Chui *In* NASA. Marshall Space Flight Center, Joint Launch + One Year Science Review of USML-1 and USMP-1 with the Microgravity Measurement Group May 1994 p 5-25 (For primary document see N95-14207 03-88)
(Contract JPL-957448)
Avail: CASI HC A03/MF A04

N95-14209*# Commissariat a l'Energie Atomique, Grenoble (France). Centre d'Etudes Nucleaires.
MASS TRANSPORT PHENOMENA IN MICROGRAVITY: PRELIMINARY RESULTS OF THE FIRST MEPHISTO FLIGHT EXPERIMENT
Jean Jacques Favier, J. P. Garandet, A. Rouzaud, and D. Camel *In* NASA. Marshall Space Flight Center, Joint Launch + One Year Science Review of USML-1 and USMP-1 with the Microgravity Measurement Group May 1994 p 27-44 (For primary document see N95-14207 03-88)
Avail: CASI HC A03/MF A04

N95-14210*# National Aeronautics and Space Administration. Marshall Space Flight Center, Huntsville, AL.
BASIC FEATURES OF THE STS/SPACELAB VIBRATION ENVIRONMENT **c18**
Charles R. Baugher and N. Ramachandran *In its* Joint Launch + One Year Science Review of USML-1 and USMP-1 with the Microgravity Measurement Group May 1994 p 45-64 (For primary document see N95-14207 03-88)
Avail: CASI HC A03/MF A04

N95-14211*# Deutsche Forschungs- und Versuchsanstalt fuer Luft- und Raumfahrt, Cologne (Germany).
REVIEW OF EUROPEAN MICROGRAVITY MEASUREMENTS **c29**
Hans Hamacher *In* NASA. Marshall Space Flight Center, Joint Launch + One Year Science Review of USML-1 and USMP-1 with the Microgravity Measurement Group May 1994 p 65-81 (For primary document see N95-14207 03-88)
Avail: CASI HC A03/MF A04

N95-14212*# National Aeronautics and Space Administration. Lewis Research Center, Cleveland, OH.
THE SOLID SURFACE COMBUSTION EXPERIMENT ABOARD THE USML-1 MISSION **c29**
Robert A. Altenkirch (Mississippi State Univ., Mississippi State, MS.), Kurt Sacksteder, Subrata Bhattacharjee, Prashant A. Ramachandra, Lin Tang, and M. Katherine Wolverton *In* NASA. Marshall Space Flight Center, Joint Launch + One Year Science Review of USML-1 and USMP-1 with the Microgravity Measurement Group May 1994 p 83-101 (For primary document see N95-14207 03-88)
(Contract NAS3-23901)
Avail: CASI HC A03/MF A04

N95-14213*# National Aeronautics and Space Administration. Marshall Space Flight Center, Huntsville, AL.
ORBITAL PROCESSING OF HIGH-QUALITY CdTe COMPOUND SEMICONDUCTORS **c29**
David J. Larson, Jr. (Grumman Aerospace Corp., Bethpage, NY.), J. I. D. Alexander (Alabama Univ., Huntsville, AL.), D. Gillies, F. M. Carlson, J. Wu, and D. Black *In its* Joint Launch + One Year Science Review of USML-1 and USMP-1 with the Microgravity Measurement Group May 1994 p 129-161 (For primary document see N95-14207 03-88)
(Contract NAS8-38147)
Avail: CASI HC A03/MF A04

N95-14214*# National Aeronautics and Space Administration. Marshall Space Flight Center, Huntsville, AL.
CRYSTAL GROWTH OF SELECTED II-VI SEMICONDUCTING ALLOYS BY DIRECTIONAL SOLIDIFICATION **c29**
Sandor L. Lehoczky, F. R. Szofran, D. C. Gillies, S. D. Cobb, C.-H. Su, Y.-G. Sha, and R. N. Andrews *In its* Joint Launch + One Year Science Review of USML-1 and USMP-1 with the Microgravity Measurement Group May 1994 p 163-222 (For primary document see N95-14207 03-88)
Avail: CASI HC A04/MF A04

N95-14215*# Case Western Reserve Univ., Cleveland, OH. Dept. of Materials Science and Engineering.
THE STUDY OF DOPANT SEGREGATION BEHAVIOR DURING THE GROWTH OF GaAs IN MICROGRAVITY **c29**
David H. Matthiesen and J. A. Majewski *In* NASA. Marshall Space Flight Center, Joint Launch + One Year Science Review of USML-1 and USMP-1 with the Microgravity Measurement Group May 1994 p 223-262 (For primary document see N95-14207 03-88)
(Contract NAS8-39695)
Avail: CASI HC A03/MF A04

N95-14216*# Rensselaer Polytechnic Inst., Troy, NY. Dept. of Chemistry.
VAPOR TRANSPORT CRYSTAL GROWTH OF MERCURY-CADMIUM-TELLURIDE IN MICROGRAVITY Interim Report **c29**
Heribert Wiedemeier *In* NASA. Marshall Space Flight Center, Joint Launch + One Year Science Review of USML-1 and USMP-1 with the Microgravity Measurement Group May 1994 p 263-270 (For primary document see N95-14207 03-88)
Avail: CASI HC A02/MF A04

N95-14217*# National Aeronautics and Space Administration. Lewis Research Center, Cleveland, OH.
SURFACE TENSION DRIVEN CONVECTION EXPERIMENT (STDCE) **c29**
Simon Ostrach (Case Western Reserve Univ., Cleveland, OH.), Y. Kamotani (Case Western Reserve Univ., Cleveland, OH.), and A. Pline *In* NASA. Marshall Space Flight Center, Joint Launch + One Year Science Review of USML-1 and USMP-1 with the Microgravity Measurement Group May 1994 p 271-300 (For primary document see N95-14207 03-88)
(Contract NAS3-25973)
Avail: CASI HC A03/MF A04

N95-14218*# Vanderbilt Univ., Nashville, TN. Center for Microgravity Research and Applications.
CORE-CENTERING OF COMPOUND DROPS IN CAPILLARY OSCILLATIONS: OBSERVATIONS ON USML-1 EXPERIMENTS IN SPACE **c29**
Taylor G. Wang, A. V. Anikumar, C. P. Lee, and K. C. Lin *In* NASA. Marshall Space Flight Center, Joint Launch + One Year Science Review of USML-1 and USMP-1 with the Microgravity Measurement Group May 1994 p 301-320 (For primary document see N95-14207 03-88)
Avail: CASI HC A03/MF A04

N95-14219*# Vanderbilt Univ., Nashville, TN. Center for Microgravity Research and Applications.
BIFURCATION OF ROTATING LIQUID DROPS: RESULTS FROM USML-1 EXPERIMENTS IN SPACE **c29**
Taylor G. Wang, A. V. Anilkumar, C. P. Lee, and K. C. Lin *In* NASA. Marshall Space Flight Center, Joint Launch + One Year Science Review of USML-1 and USMP-1 with the Microgravity Measurement Group May 1994 p 321-337 (For primary document see N95-14207 03-88)
Avail: CASI HC A03/MF A04

N95-14220*# Yale Univ., New Haven, CT. Center for Ultrasonics and Sonics.
SURFACE CHARACTERIZATION THROUGH SHAPE OSCILLATIONS OF DROPS IN MICROGRAVITY AND 1-g **c29**
Robert E. Apfel, R. Glynn Holt, Yuren Tian, Tao Shi, and Xiao-Yu Zheng *In* NASA. Marshall Space Flight Center, Joint Launch + One Year Science Review of USML-1 and USMP-1 with the Microgravity Measurement Group May 1994 p 339-359 (For primary document see N95-14207 03-88)
(Contract JPL-958722)
Avail: CASI HC A03/MF A04

N95-14221*# Arizona Univ., Tucson, AZ. Dept. of Materials Science and Engineering.
MEASUREMENT OF INTERFACIAL TENSION OF IMMISCIBLE LIQUID PAIRS IN MICROGRAVITY **c29**
Michael C. Weinberg, George F. Neilson, Carl Baertlein, R. Shankar Subramanian, and Eugene H. Trinh *In* NASA. Marshall Space Flight Center, Joint Launch + One Year Science Review of USML-1 and USMP-1 with the Microgravity Measurement Group May 1994 p 361-374 (For primary document see N95-14207 03-88)
Avail: CASI HC A03/MF A04

N95-14222*# National Aeronautics and Space Administration. Lyndon B. Johnson Space Center, Houston, TX.
EXTENDED DURATION ORBITER MEDICAL PROJECT MICROBIAL AIR SAMPLER (STS-50/USML-1) **c29**
Duane L. Pierson and Sheila W. Boettcher *In* NASA. Marshall Space Flight Center, Joint Launch + One Year Science Review of USML-1 and USMP-1 with the Microgravity Measurement Group May 1994 p 375-381 (For primary document see N95-14207 03-88)
Avail: CASI HC A02/MF A04

N95-14223*# National Aeronautics and Space Administration. Lyndon B. Johnson Space Center, Houston, TX.
EXTENDED DURATION ORBITER MEDICAL PROJECT VARIABILITY OF BLOOD PRESSURE AND HEART RATE (STS-50/USML-1) **c52**
Janice M. Fritsch-Yelle, John B. Charles, and Sheila W. Boettcher *In* NASA. Marshall Space Flight Center, Joint Launch + One Year Science Review of USML-1 and USMP-1 with the Microgravity Measurement Group May 1994 p 383-389 (For primary document see N95-14207 03-88)
Avail: CASI HC A02/MF A04

N95-14224*# National Aeronautics and Space Administration. Lyndon B. Johnson Space Center, Houston, TX.
EXTENDED DURATION ORBITER MEDICAL PROJECT COUNTERMEASURE TO REDUCE POST SPACE FLIGHT ORTHOSTATIC INTOLERANCE (LBNP) (STS-50/USML-1) **c52**
John B. Charles and Sheila W. Boettcher *In* NASA. Marshall Space Flight Center, Joint Launch + One Year Science Review of USML-1 and USMP-1 with the Microgravity Measurement Group May 1994 p 391-407 (For primary document see N95-14207 03-88)
Avail: CASI HC A03/MF A04

N95-14225*# Alabama Univ., Birmingham, AL. Center for Macromolecular Crystallography.
PROTEIN CRYSTAL GROWTH RESULTS FROM THE UNITED STATES MICROGRAVITY LABORATORY-1 MISSION **c29**
Lawrence J. DeLucas, K. M. Moore, M. vanderWoerd, T. L. Bray, C. Smith, M. Carson, S. V. L. Narayana, W. M. Rosenblum, D. Carter, and A. D Clark, Jr. et al *In* NASA. Marshall Space Flight Center, Joint Launch + One Year Science Review of USML-1 and USMP-1 with the Microgravity Measurement Group May 1994 p 409-445 (For primary document see N95-14207 03-88)
Avail: CASI HC A03/MF A04

N95-14226*# Worcester Polytechnic Inst., MA. Dept. of Chemical Engineering.
THE GROWTH OF ZEOLITES A, X AND MORDENITE IN SPACE **c29**
Albert Sacco, Jr., N. Bac, E. N. Coker, A. G. Dixon, J. Warzywoda, and R. W. Thompson *In* NASA. Marshall Space Flight Center, Joint Launch + One Year Science Review of USML-1 and USMP-1 with the Microgravity Measurement Group May 1994 p 447-472 (For primary document see N95-14207 03-88)
Avail: CASI HC A03/MF A04

N95-14227*# Colorado Univ., Boulder, CO. BioServ Space Technologies.
COMMERCIAL INVESTIGATION RESULTS FOR THE GENERIC BIOPROCESSING APPARATUS FLOWN ON UNITED STATES MICROGRAVITY LABORATORY-1 **c51**
Louis S. Stodieck, M. C. Robinson, and M. W. Luttges *In* NASA. Marshall Space Flight Center, Joint Launch + One Year Science Review of USML-1 and USMP-1 with the Microgravity Measurement Group May 1994 p 473-507 (For primary document see N95-14207 03-88)
Avail: CASI HC A03/MF A04

N95-14228*# Wisconsin Univ., Madison, WI. Center for Space Automation and Robotics.
THE ASTROCULTURE (TM)-1 EXPERIMENT ON THE USML-1 MISSION **c54**
Theodore Tibbitts, R. J. Bula, and R. C. Morrow *In* NASA. Marshall Space Flight Center, Joint Launch + One Year Science Review of USML-1 and USMP-1 with the Microgravity Measurement Group May 1994 p 509-523 (For primary document see N95-14207 03-88)
Avail: CASI HC A03/MF A04

89 ASTRONOMY

Includes radio, gamma-ray, and infrared astronomy, and astrometry.

N95-13634*# Smithsonian Astrophysical Observatory, Cambridge, MA. Advanced X-Ray Astrophysics Facility.
HRMA CALIBRATION HANDBOOK: EKC GRAVITY COMPENSATED XRCF MODELS Performance Report
H. D. Tananbaum, D. Jerius, and J. Hughes 6 Jun. 1994 67 p Revised
(Contract NAS8-36123)
(NASA-CR-195818; NAS 1.26:195818; SAO-AXAF-DR-94-088-Rev; DRD-MA-784-002-Rev) Avail: CASI HC A04/MF A01

This document, consisting of hardcopy printout of explanatory text, figures, and tables, represents one incarnation of the AXAF high resolution mirror assembly (HRMA) Calibration Handbook. However, as we have envisioned it, the handbook also consists of electronic versions of this hardcopy printout (in the form of postscript files), the individual scripts which produced the various figures and the associated input data, the model raytrace files, and all scripts, parameter files, and input data necessary to generate the raytraces. These data are all available electronically as either ASCII or FITS files. The handbook is intended to be a living document and will be updated as new information and/or fabrication data on the HRMA are obtained, or when the need for additional results are indicated. The SAO Mission Support Team (MST) is developing a high fidelity HRMA model, consisting of analytical and numerical calculations, computer software, and databases of fundamental physical constants, laboratory measurements, configuration data, finite element models, AXAF assembly data, and so on. This model serves as the basis for the simulations presented in the handbook. The 'core' of the model is the raytrace package OSAC, which we have substantially modified and now refer to as SAOsac. One major structural modification to the software has been to utilize the UNIX binary pipe data transport mechanism for passing rays between program modules. This change has made it possible to simulate rays which are distributed randomly over the entrance aperture of the telescope. It has also resulted in a highly efficient system for tracing large numbers of rays. In one application to date (the analysis of VETA-I ring focus data) we have employed 2 x 10(exp 7) rays, a substantial improvement over the limit of 1 x 10(exp 4) rays in the original OSAC module. A second major modification is the manner in which SAOsac incorporates low spatial frequency surface errors into the geometric raytrace. The original OSAC included the ability to use Legendre-Fourier polynomials to describe deviations from the basic optical prescription. To this we have added bicubic splines to address a deficiency in the handling of the sharper deformations in the areas of mirror support pads. SAO has developed software (TRANS-FIT) to translate the most common finite element analysis models into these forms for incorporation into the raytrace program. Derived from text

N95-13636*# Smithsonian Astrophysical Observatory, Cambridge, MA. Advanced X-Ray Astrophysics Facility.
AXAF SIM FOCUS MECHANISM STUDY
H. D. Tananbaum and E. Whitbeck 16 Feb. 1994 23 p Revised
Original contains color illustrations
(Contract NAS8-36123)
(NASA-CR-196976; NAS 1.26:196976; SAO-AXAF-DR-94-081-Rev; DRD-MA-784-002-Rev) Avail: CASI HC A03/MF A01; 2 functional color pages

The design requirements and initial design concept for the AXAF-I Science Instrument Module (SIM) were reviewed at Ball on September 29, 1993. The concept design SIM focus mechanism utilizes a planetary gearset, with redundant motors, to drive a large ring (called 'main housing bearing') via a spur gearset. This large drive ring actuates three tangent bar links (called 'push rods'), which in turn actuate three levers (called 'pin levers'). Each of the three pin levers rotates an 'eccentric pin,' which in turn moves the base of a bipod flexure in both the radial (normal to optical axis) and axial (focus along optical axis) directions. Three bipod flexures are employed, equally spaced at 120 degrees apart, the base of each being translated in the two directions as described above. A focus adjustment is made by rotating the drive ring, which drives the push rods and therefore the pin levers, which in turn rotate the eccentric pins, finally imparting the two motions to the base of each of the bipod flexures. The axial translation

(focus adjustment) of the focused structure is the sum of the direct axial motion plus axial motion which comes from uniformly squeezing the three bipod bases radially inward. SAO documented the following concerns regarding the focus mechanism in memo WAP-FY94-001, dated October 7, 1993: (1) The focus adjustment depends, in large part, on the structural properties (stiffnesses and end fixities) of the bipod flexures, push rods, pin levers and eccentric pins. If these properties are not matched very well, then lateral translations as well as unwanted rotations of the focussed structure will accompany focus motion. In addition, the stackup of linkage tolerances and any nonuniform wear in the linkages will result in the same unwanted motions. Thermal gradients will also affect these motions. At the review Ball did not present supporting analyses to support their choice of this design concept. (2) The proposed 'primary' method of measuring focus is by counting motor steps. The 'backup' method is by a pot mounted on the drive ring. Neither method provides for a direct measurement of the quantity desired (focus position). This is of concern because of the long and indirect relationship between focus and the sensed quantity (drive ring rotation). There are three sinusoidal relationships and structural stiffness in the path, and the resulting calibration is likely to be highly nonlinear. These methods would require an accurate ground calibration. (3) Ground calibration (and verification) of focus vs. drive position must be done in 1-g on the ground. This calibration will be complicated by both the structural characteristics of the bipods and the fact that the CG of the translating portion of the SIM is not on the optical axis (thereby causing unwated rotations and changing the focus position vs. motor step and pot readout relationships). The SIM translating weight could be offloaded, but the calibration then becomes sensitive to any errors in offloading (both magnitude and direction). There are concerns as to whether a calibration to the required accuracy can be accomplished on the ground. (4) The choice of a potentiometer as the focus position sensor is questionable in terms of reliability for a five year mission. The results of SAO's study of items 1, 2 and 3 described above are presented in this report. Author

N95-13637*# Smithsonian Astrophysical Observatory, Cambridge, MA. Advanced X-Ray Astrophysics Facility.

AXAF VETA-I MIRROR RING FOCUS MEASUREMENTS Performance Report

H. D. Tananbaum and P. Zhao 1 Feb. 1994 19 p Revised
(Contract NAS8-36123)
(NASA-CR-196145; NAS 1.26:196145; SAO-AXAF-DR-94-083-Rev; DRD-MA-784-002-Rev) Avail: CASI HC A03/MF A01

The AXAF VETA-I mirror ring focus measurements were made with an HRI (microchannel plate) X-ray detector. The ring focus is a sharply focused ring formed by X-rays before they reach the VEAT-I focal plane. It is caused by spherical aberrations due to the finite source distance and the despace in the VETA-I test. The ring focus test reveals some aspects fo the test system distortions and the mirror surface figure which are difficult or impossible to detect at the focal plane. The test results show periodic modulations of the ring radius and width which could be caused by gravity, thermal, and/or epoxy shrinkage distortions. The strongest component of the modulation had a 12-fold symmetry, because these distortions were exerted on the mirror through 12 flexures of the VETA-I mount. Ring focus models were developed to simulate the ring image. The models were compared with the data to understand the test system distortions and the mirror glass imperfection. Further studies will be done to complete this work. The ring focus measurement is a very powerful test. We expect that a similar test for the finally assembled mirror of AXAD-I will be highly valuable. Author

N95-13722*# Arizona State Univ., Tempe, AZ.

A ROSAT DEEP SURVEY OF THE BEST STUDIED HIGH LATITUDE AREAS Final Technical Report, 1 Aug. - 31 Jul. 1994

Rogier A. Windhorst 1994 2 p
(Grant NAG5-2322)
(NASA-CR-196265; NAS 1.26:196265) Avail: CASI HC A01/MF A01

A brief description of the primary objectives and scope of the project are presented. Also, a description of the findings to date is given. CASI

N95-13723*# Texas Univ., Austin, TX. Dept. of Astronomy.

HUBBLE SPACE TELESCOPE GTO PROGRAM Semiannual Progress Report No. 6, 1 Jan. - 30 Jun. 1994

William H. Jefferys Jul. 1994 8 p
(Grant NAG5-1603)
(NASA-CR-196263; NAS 1.26:196263) Avail: CASI HC A02/MF A01

The topics covered include the following: meetings and travel; calibration; GTO Program (Texas); software; subcontractors; and the mini-symposium. Derived from text

N95-13887*# Smithsonian Astrophysical Observatory, Cambridge, MA.

SUMMARY OF AXAF CALIBRATION REQUIREMENTS Interim report

E. Kellogg Nov. 1993 41 p
(Contract NAS8-36123)
(NASA-CR-196985; NAS 1.26:196985; SAO-AXAF-DR-93-058) Avail: CASI HC A03/MF A01

The following summarizes requirements on the High Resolution Mirror Assembly (HRMA) and HRMA/SI calibration. The lists of calibration measurements assume that the HRMA meets the CTT requirement that the XRCF test environment shall have not more than a 10 percent effect on the encircled energy in 1 arcsec and that it can be calibrated to 1 percent. This implies that the offloading scheme has been implemented in the HRMA. It should be remembered that there are additional calibrations needed for: aspect system; tracking; gyros; other parts of the PCAS; spacecraft timing and checks on timing accuracy for all SIs after integration in the spacecraft; ficucial lights and periscope; alignments; optical metrology data: lengths and diameters with errors on mirror elements and optical interferometer data on surface figure; and throughput and imaging stability test: an end-to-end test that can be used after the XRCF to verify that the x-ray throughput and imaging quality have not been degraded. The tables presented give a summary of the integration times for HRMA and HRMA/SI calibration. Derived from text

N95-13982 Helsinki Univ. of Technology, Kylmaelae (Finland).

OBSERVATIONS OF EXTRAGALACTIC SOURCES WITH THE METSAEHOVI RADIO TELESCOPE AT 22-87 GHz Ph.D. Thesis

H. Teraesranta 29 Apr. 1994 114 p See also N83-18619 Limited Reproducibility: More than 20% of this document may be affected by microfiche quality
(PB94-197712; ISBN-951-22-2045-8) Avail: CASI HC A06/MF A02

This thesis presents the quasar monitoring program of the Metsahovi Radio Research Station. The program was started in 1980, and since then over 22000 quasar observations have been done at frequencies 12, 22, 37, 77 and 87 GHz. The data reduction procedure and the observational data from 1985.5 to 1990.5 are presented. The use of the data is demonstrated in 9 papers. Four of them use primarily the Metsahovi data and the remaining five are multifrequency efforts. The Metsahovi Radio Research Station is the only observatory where systematic monitoring of extragalactic sources is performed at frequencies higher than 20 GHz. Currently there are about 80 sources in our observing sample. The time scales in the quasar variability at 22 and 37 GHz are typically from some months to some years. From the time scales of the outbursts, brightness temperatures were calculated. In most cases they were well over the Compton limit 10(exp 12) K, thus requiring relativistic boosting. For different classes of sources different average viewing angles were found. For HPQ's theta less than 20 deg, for LPQ's 20 deg less than theta less than 40 deg and radio galaxies theta less than 30 deg. NTIS

N95-14100*# Smithsonian Astrophysical Observatory, Cambridge, MA. Advanced X-Ray Astrophysics Facility.

PERFORMANCE REPORTS: MIRROR ALIGNMENT SYSTEM PERFORMANCE PREDICTION COMPARISON BETWEEN SAO AND EKC

H. D. Tananbaum and J. P. Zhang 14 Mar. 1994 54 p Revised
(Contract NAS8-36123)
(NASA-CR-196013; NAS 1.26:196013; SAO-AXAF-DR-94-082-Rev; DRD-MA-784-002-Rev) Avail: CASI HC A04/MF A01

The objective of this study is to perform an independent analysis of the residual high resolution mirror assembly (HRMA) mirror distortions caused by force and moment errors in the mirror alignment system (MAS) to statistically predict the HRMA performance. These performance predictions are then compared with those performed by Kodak to verify their analysis results. Derived from text

N95-14101*# Smithsonian Astrophysical Observatory, Cambridge, MA. Advanced X-Ray Astrophysics Facility.

PERFORMANCE REPORT: A TIMELINE FOR THE SYNCHROTRON CALIBRATION OF AXAF

H. D. Tananbaum and D. Graessle Jun. 1994 47 p Revised
(Contract NAS8-36123)
(NASA-CR-196489; NAS 1.26:196489; SAO-AXAF-DR-94-090-Rev; DRD-MA-764-002-Rev) Avail: CASI HC A03/MF A01

Presented herein are the known elements of the timeline for synchrotron reflectance calibrations of HRMA witness samples (Section 2). In Section 3, lists of measurements to be done on each witness flat are developed. The elements are then arranged into timelines for the three beamlines we expect to employ in covering the full 50-12,000 eV energy range (Section 4). Although the required AXAF operational range is only 0.1-10 keV, we must calibrate the extent to which radiation just outside this band may contaminate our in-band response. In Section 5, we describe the working relationships which exist with each of the beamlines, and estimate the time available for AXAF measurements on each. From the timelines and the available time, we calculate the number of flats which could be measured in full detail over the duration of the program for each beamline. A suggestion is made regarding a minimum required baselines of witness flats from each element coating run or qualification run to be used in the calibration. We intend that this suggestion open discussion of the issue of witness flat deployment. Derived from text

N95-14429# Los Alamos National Lab., NM.

THE MOXE X-RAY ALL-SKY MONITOR FOR SPECTRUM-X-GAMMA

J. J. M. IntZand, W. C. Priedhorsky, and C. E. Moss et al 1994 15 p Presented at the Annual Meeting of the Society of Photo-Optical Instrumentation Engineers, San Diego, CA, 24-29 Jul. 1994
(Contract W-7405-eng-36)
(DE94-016064; LA-UR-94-2307; CONF-940723-10) Avail: CASI HC A03/MF A01

MOXE is an X-ray all-sky monitor to be flown on the Russian Spectrum-X-Gamma satellite, to be launched in a few years. It will monitor several hundred X-ray sources on a daily basis, and will be the first instrument to monitor most of the X-ray sky most of the time. MOXE will alert users of more sensitive instruments on Russia's giant high energy astrophysics observatory and of other instruments to transient activity. MOXE consists of an array of 6 X-ray pinhole cameras, sensitive from 3 to 25 keV, which views 4 pi steradians (except for a 20 degree x 80 degree patch which includes the Sun). The pinhole apertures of 0.625 x 2.556 cm(exp 2) imply an angular resolution of 2.4 degree x 9.7 degree (on-axis). The MOXE hardware program includes an engineering model, now delivered, and a flight model. The flight instrument will mass approximately 118 kg and draw 38 Watts. For a non-focusing all-sky instrument that is limited by sky background, the limiting sensitivity is a function only of detector area. MOXE, with 6,000 cm(exp 2) of detector area, will, for a 24 hrs exposure, have a sensitivity of approximately 2 mCrab. MOXE distinguishes itself with respect to other all-sky monitors in its high duty cycle, thus being particularly sensitive to transient phenomena with time scales between minutes and hours. DOE

N95-14511*# National Aeronautics and Space Administration, Washington, DC.

SPACE BASED ASTRONOMY: TEACHER'S GUIDE WITH ACTIVITIES

Carla B. Rosenberg, ed., Edward Weiler, Cherilyn Morrow, Pamela M. Bacon, Muriel Thorne, Paul A. Blanchard, Sethane Howard, Patricia R. Pengra, Deborah A. Brown, and Ralph Winrich et al Aug. 1994 93 p
(NASA-EG-102; NAS 1.19/4:102) Avail: CASI HC A05/MF A01

This curriculum guide uses hands-on activities to help students and teachers understand the significance of space-based astronomy - astronomical observations made from outer space. The guide contains few of the traditional activities found in many astronomy guides such as constellation studies, lunar phases, and planetary orbits. Instead, it tells the story of why it is important to observe celestial objects from outer space and how to study the entire electromagnetic spectrum. The guide begins with a survey of astronomy related NASA spacecraft. This is followed by a collection of activities in four units: (1) the atmospheric filter; (2) the electromagnetic spectrum; (3) collecting electromagnetic radiation; and (4) down to Earth. A curriculum index identifies the curriculum areas each activity addresses. The guide concludes with a glossary, reference list, a NASA Resources list, and an evaluation card. It is designed for students in grades 5 through 8. Derived from text

N95-14597# Phillips Lab., Kirtland AFB, NM.

THE 3.5-METER TELESCOPE ENCLOSURE Final Report, 17 Aug. 1991 - 31 Mar. 1993

Michael H. Brady Apr. 1994 28 p
(AD-A280949; AD-E201990; PL-TR-93-1028) Avail: CASI HC A03/MF A01

The 3.5-m telescope enclosure is designed to perform two functions as part of the U.S. Air Force's 3.5-m telescope system: (1) to provide weather and temperature protection when the telescope is not in use and (2) to permit open-air operation of the telescope while minimizing atmospheric disturbances in the field of view (FOV). The use of a standard rotating dome is impractical because of the large telescope and its high rotational rate and acceleration. The enclosure is a 40-ft tall cylinder with a diameter of 72 ft. This steel and aluminum structure does not rotate but collapses vertically to fully expose the telescope to the open air and to provide it with an unobscured view of the horizon at all azimuthal angles. To lessen wind disturbances in the FOV, the enclosure has a moderately sloped roof and smooth, vertical walls. To minimize thermal flow, the outer surface has a high-reflectivity, low-emissivity coating and ambient air is forced through the double-skinned walls and roof. These measures make it possible to keep the enclosure surface temperature near that of the ambient air during viewing. With these features, the enclosure adds minimal degradation to the seeing. DTIC

N95-14667*# National Aeronautics and Space Administration. Goddard Space Flight Center, Albuquerque, NM.

TWELVE-YEAR PLANETARY EPHEMERIS: 1995-2006

Fred Espenak Oct. 1994 263 p
(RTOP 693-00-00)
(NASA-RP-1349; Rept-94B00141; NAS 1.61:1349) Avail: CASI HC A12/MF A03

Accurate geocentric positions and physical ephemerides are tabulated for the Sun, Moon, Mercury, Venus, Mars, Jupiter, Saturn, Uranus, Neptune, and Pluto for the 12-year period 1995 through 2006. The frequency interval is 2 days for the Sun and classical planets. Uranus, Neptune, and Pluto are tabulated at 4-day intervals. Because of its rapid apparent motion, the Moon's ephemeris is given daily. Author

N95-14804*# Massachusetts Inst. of Tech., Cambridge. Center for Space Research.

DETERMINATION OF THE ATMOSPHERIC STRUCTURE OF THE BO STAR COMPANION OF SMC X-1 BY ANALYSIS OF GINGA OBSERVATIONS Final Technical Report, 29 Jul. - 3 Aug. 1989

George W. Clark 8 Nov. 1994 37 p
(Grant NAG8-185)
(NASA-CR-197100; NAS 1.26:197100) Avail: CASI HC A03/MF A01

The x-ray phenomena of the binary system SMC X-1/Sk 160, observed with the Ginga and ROSAT x-ray observatories, are compared with computed phenomena derived from a three dimensional hydrodynamical model of the stellar wind perturbed by x-ray heating and ionization which is described in the accompanying paper. In the model the BOI primary star has a line-driven stellar wind in the region of the x-ray shadow and a thermal wind in the region heated by x-rays. We find general agreement between the observed and predicted x-ray spectra throughout the binary orbit cycle, including the extended, variable, and asymmetric eclipse transitions and the period of deep eclipse. Author

N95-14911*# National Aeronautics and Space Administration. Goddard Space Flight Center, Greenbelt, MD.

PSPC SOFT X-RAY OBSERVATIONS OF SEYFERT 2 GALAXIES

T. J. Turner, C. M. Urry, and R. F. Mushotzky 1993 38 p
(NASA-TM-109968; NAS 1.15:109968) Avail: CASI HC A03/MF A01

We present the results from ROSAT PSPC soft x-ray (0.1-2.0 keV) observations of six Seyfert 2 galaxies, chosen from the brightest Seyfert 2s detected with the Einstein Imaging Proportional Counter. All of the targets were detected with the ROSAT PSPC. Spatial analysis shows that the source density within a few arcmin of each Seyfert 2 galaxy is a factor of approximately eight higher than in the rest of the inner field of

view of the PSPC images. In NGC1365 it appears that the serendipitous sources may be x-ray binary systems in the host galaxy. The proximity of the serendipitous sources, typically within a few arcmin of the target Seyfert 2, means that previous x-ray observations of the Seyfert 2 galaxies have been significantly contaminated, and that source confusion is important on a spatial scale of approximately 1 arcmin. Some spectra, most notably Mrk3 and NGC1365, indicate the presence of a high equivalent width soft x-ray line blend consistent with unresolved iron L and oxygen K emission. Author

N95-15827*# National Aeronautics and Space Administration. Ames Research Center, Moffett Field, CA.

THE DIFFUSE INTERSTELLAR BANDS: CONTRIBUTED PAPERS

Alexander G. G. M. Tielens, ed. May 1994 142 p Symposium held in Boulder, CO, 16-19 May 1994

(RTOP 352-02-03-06)

(NASA-CP-10144; A-94107; NAS 1.55:10144) Avail: CASI HC A07/MF A02

Drawing a coherent picture of the observational characteristics of the Diffuse Interstellar Bands (DIB's) and the physical and chemical properties of its proposed carriers was the focus of this NASA sponsored conference. Information relating to absoption spectra, diffuse radiation carriers, carbon compounds, stellar composition, and interstellar extinction involving T-Tauri stars, Reflection Nebulae, Red Giants, and accretion discs are discussed from those papers presented at the conference, which are included in this analytic. For individual titles, see N95-15828 through N95-15846.

N95-15828*# Hughes STX, Inc., Greenbelt, MD.

NEUTRAL GAS AND DIFFUSE INTERSTELLAR BANDS IN THE LMC

Anthony C. Danks and Brian Penprase *In* NASA. Ames Research Center, The Diffuse Interstellar Bands: Contributed Papers May 1994 p 1-6 (For primary document see N95-15827 03-89)

Avail: CASI HC A02/MF A02

Tracing the dynamics of the neutral gas and observing diffuse interstellar bands in the LMC (Large Magellanic Cloud) was the focus of this study. The S/N values, a Quartz lamp exposure, a T horium Argon Comparision lamp exposure, and spectral plots for each star observed were taken. The stars observed were selected to sample the 30 Dor vicinty. Nal absorption profiles are included. CASI

N95-15829*# National Aeronautics and Space Administration. Ames Research Center, Moffett Field, CA.

DIBS INDEPENDENT OF ACCRETION IN T TAURI STARS

Louma Ghandour (Massachusetts Univ., Amherst, MA.), Peter Jenniskens, and P. Hartigan *In its* The Diffuse Interstellar Bands: Contributed Papers May 1994 p 7-10 (For primary document see N95-15827 03-89)

Avail: CASI HC A01/MF A02

The examination of high resolution spectra (5200 - 7000 Angstroms) of 36 T Tauri stars ranging in accretion rates was performed. Only the lambda lambda 5780, 5797, and 6613 bands were found detectable to within an equivalent width of 10 micro Angstroms. They are strongest in DG Tau, DR Tau, DI Tau, and AS 353A. DR Tau was monitored over the course of four years; during this time, the accretion rate varied by a factor of five, but the equivalent widths of the DIB's (Diffuse Interstellar Bands) remained constant. The lack of correlation of the strength of the bands with the accretion rates implies that the bands are not directly produced by UV radiation from the accretion process. The bands have line strengths and ratios characteristic of the diffuse interstellar medium, from which we conclude that the diffuse interstellar bands seen in the spectra of T Tauri stars do not originate in the stars' immediate environment. Instead, they are part of a foreground extinction, probably due to the parent molecular cloud. Author (revised)

N95-15830*# Universitaets-Sternwarte, Jena (Germany).

DIFFUSE INTERSTELLAR BANDS IN REFLECTION NEBULAE

O. Fischer, Thomas Henning, Werner Pfau, and R. Stognienko *In* NASA. Ames Research Center, The Diffuse Interstellar Bands: Contributed Papers May 1994 p 11-16 (For primary document see N95-15827 03-89)

Avail: CASI HC A02/MF A02

A Monte Carlo code for radiation transport calculations is used to compare the profiles of the lambda lambda 5780 and 6613 Angstrom diffuse interstellar bands in the transmitted and the reflected light of a star embedded within an optically thin dust cloud. In addition, the behavior of polarization across the bands were calculated. The wavelength dependent complex indices of refraction across the bands were derived from the embedded cavity model. In view of the existence of different families of diffuse interstellar bands the question of other parameters of influence is addressed in short. Author (revised)

N95-15831*# University of Central Lancashire, Preston, Lancashire (England). Centre for Astrophysics.

A SEARCH FOR THE 13175 A INFRARED DIFFUSE BAND IN DENSE ENVIRONMENTS Abstract Only

A. J. Adamson, Tom H. Kerr, D. C. B. Whittet, and Walter W. Duley *In* NASA. Ames Research Center, The Diffuse Interstellar Bands: Contributed Papers May 1994 p 17 (For primary document see N95-15827 03-89)

Avail: CASI HC A01/MF A02

Models of ionized interstellar C60 predict a strong transition in the 1.2 micrometer region, and two candidate bands have recently been detected in reddened stars. We have searched for the stronger of these bands (at 13175 A) in the Taurus dark cloud complex, to determine its response to the dark-cloud environment. None of the three lines of sight studied (two near the cloud surface, one reaching A(sub V) greater than 20(sup m)) give rise to a detectable band; in one case the equivalent width is a factor of order three below that predicted. Since such behaviour is also shown by the optical Diffuse Interstellar Bands, we suggest that the 13175 A band is a genuine DIB, but we caution against an automatic interpretation in terms of an ionic carrier. Author

N95-15832*# Edinburgh Univ. (Scotland). Dept. of Physics and Astronomy.

ON THE AFFINITIES OF LAMBDA 5778 AND OTHER BROAD DIFFUSE INTERSTELLAR BANDS

Alan McIntosh and Adrian Webster *In* NASA. Ames Research Center, The Diffuse Interstellar Bands: Contributed Papers May 1994 p 19-22 (For primary document see N95-15827 03-89)

Avail: CASI HC A01/MF A02

The authors examined the broad band 5778 A because of the quantity and quality of data that exists in literature. To investigate the affinity of that band with the bands of Family 1, the ratio W(sub lambda)(4430)/W(sub lambda)(5797) was formed. If the two band belong to the same family then the ratio should be a constant from star to star and it should not be possible to find an independent variable with which the ratio is correlated. If, however, a variable is found which does produce a statistically significant correlation with the ratio of equivalent widths then the bands cannot be in the same family. To test the affinity of the band at 5778 A with the other families the procedure was repeated using the bands at 5780 and 5787 A as being representative of Families 2 and 3 respectively. The measurement results of this test are shown using 21 stars taken from Herbig. Statistically significant correlations resulted when the band at 5778 A was tested against the bands of Families 1 and 2 but there was no correlation with Family 3. It is concluded that lambda 5778 is unlikely a member of Family 1 and so all the broad bands do not have their origin in a single carrier. Also, lambda 5778 does not appear to be a member of Family 2 either, but may be a member of Family 3. It appears that either a single carrier can be the origin of both broad and narrow bands or that the bands are produced by different carriers which exist in similar interstellar habitats. This latter possibility would require the introduction of a fourth family of bands. Derived from text

N95-15833*# Stazione Astronomica Internazionale di Latitudine, Cagliari (Italy).

THE PECULIAR BEHAVIOUR OF THE 5780 AND 5797 DIBs IN HD25137

Ignazio Porceddu and P. Benvenuti *In* NASA. Ames Research Center, The Diffuse Interstellar Bands: Contributed Papers May 1994 p 23-29 (For primary document see N95-15827 03-89)

Avail: CASI HC A02/MF A02

The interstellar environment close to the high latitude molecular cloud Lynds 1569 (L1569, Lynds 1962), also known as MBM 18 (Magnani, Blitz and Mundy, 1985), has been analyzed by Penrase et al. (1990) and Penrase (1993). Their observations of the CH, CH(sup+), and CN molecular features, are consistent with a region having a high molecular and reduced dust

content. They also observed the background star HD 24263- located 8 degrees far from the center of L1569 - reporting a CH rich line of sight and the presence of two intervening clouds from a sodium lines spectra. The infrared excess which has been revealed by the IRAS survey at 12 microns might suggest the presence of PAH's molecules, the well know candidate far from the Unidentified Infrared Bands and Diffuse Interstellar Bands. This interesting scenario led to the investigation of the behavior of the diffuse interstellar bands toward HD 25137, which is supposed to be a background object for L1569 (Penrase et al., 1990); as well as the field star HD 24263. As part of a wider observational program devoted to study the HLC's special environments, the observations of the diffuse interstellar bands (DIB's) at 5780 and 5797 lambda lambda in the direction of the two above mentioned stars, HD 24263 and HD 25137 are presented here.

Author

N95-15834*# Nottingham Univ. (England). Dept. of Chemistry.

DIFFUSE INTERSTELLAR BANDS BETWEEN 3900 A AND 4200 A

Abstract Only

R. E. Hibbins, Janet R. Miles, P. J. Sarre, and G. H. Herbig *In* NASA. Ames Research Center, The Diffuse Interstellar Bands: Contributed Papers May 1994 p 31 (For primary document see N95-15827 03-89)

Avail: CASI HC A01/MF A02

Presented here are spectra and data on five probable diffuse bands with central wavelengths near 4180, 4070, 4040, 4000, and 3980 A which have full-width-half-maxima lying in the range 10-30 A. No narrow unidentified diffuse bands were found, but atomic and diatomic molecular absorptions, including CH and CH(sup +), were readily detected along some lines of sight. Although broad diffuse bands have now been found at longer wavelengths that appeared at one time to be the case (Herbig and Leka, 1991), it is clear that there are no prominent narrow bands at the shorter wavelength end of the diffuse band spectrum. This high-resolution spectra was reported for a number of reddened O- and B-typed and comparison stars, recorded with the 88 inch University of Hawaii telesecope in June of 1993. The sample included the heavily reddened star HD 183143.

Derived from text

N95-15835*# Calgary Univ. (Alberta). Dept. of Physics and Astronomy.

CORRELATION BETWEEN MOLECULAR LINES AND DIFFUSE INTERSTELLAR BANDS

Richard Szczerba, J. Krelowski, G. A. H. Walker, E. T. Kennelly, C. Sneden, Kevin Volk, and G. Hill *In* NASA. Ames Research Center, The Diffuse Interstellar Bands: Contributed Papers May 1994 p 33-38 (For primary document see N95-15827 03-89)

(Grant PSCSR-681/2/91)

Avail: CASI HC A02/MF A02

Observations are presented of the Diffuse Interstellar Bands (DIB's) at 4726, 4763, and 4789 A and at 5780 and 5797 A together with the ultraviolet lines of CH and CN molecules for stars with different shapes of UV extinction curve. The new results concerning the relationship between different characteristics of the interstellar clouds; molecular lines, blue and yellow DIB's, and UV extinction curves are discussed. Derived from text

N95-15836*# Pedagogical Univ., Bydgoszcz, Bydgoszcz (Poland). Inst. of Mathematics.

DIFFUSE BANDS VERSUS EXTINCTION PARAMETERS

Walter Wegner, Theodore P. Snow, C. Sneden, and Jacek Krelowski *In* NASA. Ames Research Center, The Diffuse Interstellar Bands: Contributed Papers May 1994 p 39-43 (For primary document see N95-15827 03-89)

Avail: CASI HC A01/MF A02

All recent available, high quality measurements of the strong diffuse bands 5780 A and 5797 A have been collected. This includes those measurement derived from the authors's recent observations (February, May, and November 1993, taken with a echelle spectrograph) as well as those from a coude spectrograph and from literature. Equivalent widths of the diffuse interstellar bands (DIB's) at 5780 A and 5797 A have been measured on spectrograms. The measured signal-to-noise ratio (S/N) on their own spectrograms ranged from 250 to 500. The Johnson UBV data were used to estimate the color excesses of our targets.

Derived from text

N95-15837*# California State Univ., Fullerton, CA. Dept. of Physics.

PORPHYRINS IN THE INTERSTELLAR MEDIUM (IN GRAINS)

Fred M. Johnson *In* NASA. Ames Research Center, The Diffuse Interstellar Bands: Contributed Papers May 1994 p 47-52 (For primary document see N95-15827 03-89)

Avail: CASI HC A02/MF A02

Spectral sensitivity of the chromophores to their immediate chemical environment establishes some of the chemical constituents of the grains in which they reside. These are: (1) Paraffins, such as, octane, nonane, decane, and others...(needed for Shpolskii matrices and producing quasilines); and (2) Pyridine. The presence of pyridine is required not only to produce the spectral DIB matching, but also to produce the 36 cm(sup -1) crystal field splitting of the S(sub 1) electronic state. The presence of pyridine in the grains can be confirmed spectroscopically. Pyridine produces a transmission window at 2175 A, matching exactly the well known UV hump. On grain reflection, some of the incoming UV radiation is absorbed into the grain's outer layers. Spikes in the lab and in the astronomical data are due to vibronic transitions in pyridine. The lab spectroscopy reported here clearly establishes the presence of MgTBP, H2TPB, and pyridine in the interstellar grains. The high fluorescence efficiency of MgTBP (being optically pumped in the visible) apparently accounts for all the observed UIR emissions.

Derived from text

N95-15838*# Masaryk Univ., Brno, Jihomoravsky (Czechoslovakia). Lab. of Physics of Plasma.

LABORATORY SPECTRA OF C60 AND RELATED MOLECULAR STRUCTURES **c76**

J. Janca, M. Solc, and M. Vetesnik *In* NASA. Ames Research Center, The Diffuse Interstellar Bands: Contributed Papers May 1994 p 53-57 (For primary document see N95-15827 03-89)

Avail: CASI HC A01/MF A02

The electronic spectra of fullerene structures in high frequency discharge are studied in the plasma chemistry laboratory of the Faculty of Science of Masaryk University in Brno. The ultraviolet and visual spectra are investigated in order to be compared with the diffuse interstellar bands and interpreted within the theory of quantum mechanics. The preliminary results of the study are presented here in the form of a poster.

Derived from text

N95-15839*# National Inst. of Standards and Technology, Boulder, CO. Joint Inst. for Lab. Astrophysics.

INVESTIGATING THE 3.3 MICRON INFRARED FLUORESCENCE FROM NAPHTHALENE FOLLOWING ULTRAVIOLET EXCITATION **c72**

Richard M. Williams (Colorado Univ., Boulder, CO.) and Stephen R. Leone *In* NASA Ames Research Center, The Diffuse Interstellar Bands: Contributed Papers May 1994 p 59-64 (For primary document see N95-15827 03-89)

Avail: CASI HC A02/MF A02

Polycyclic aromatic hydrocarbon (PAH) type molecules are proposed as the carriers of the unidentified infrared (UIR) bands. Detailed studies of the 3.3 micrometer infrared emission features from naphthalene, the simplest PAH, following ultraviolet laser excitation are used in the interpretation of the 3.29 micrometer (3040 cm(sup -1)) UIR band. A time-resolved Fourier transform spectrometer is used to record the infrared emission spectrum of gas-phase naphthalene subsequent to ultraviolet excitation facilitated by an excimer laser operated at either 193 nm or 248 nm. The emission spectra differ significantly from the absorption spectrum in the same spectral region. Following 193 nm excitation the maximum in the emission profile is red-shifted 45 cm(sup -1) relative to the absorption maximum; a 25 cm(sup -1) red-shift is observed after 248 nm excitation. The red-shifting of the emission spectrum is reduced as collisional and radiative relaxation removes energy from the highly vibrationally excited molecules. Coupling between the various vibrational modes is thought to account for the differences between absorption and emission spectra. Strong visible emission is also observed following ultraviolet excitation. Visible emission may play an important role in the rate of radiative relaxation, which according to the interstellar PAH hypothesis occurs only by the slow emission of infrared photons. Studying the visible emission properties of PAH type molecules may be useful in the interpretation of the DIB's observed in absorption.

Author

N95-15840*# Alabama Univ., Birmingham, AL. Astro and Solar System Physics Program.

INVESTIGATION OF A LABORATORY CANDIDATE FOR THE CARRIER OF THE 4430 A DIFFUSE INTERSTELLAR BAND

Thomas J. Wdowiak, Luther W. Beegle, Wei Lee, and Michael S. Robinson *In* NASA. Ames Research Center, The Diffuse Interstellar Bands: Contributed Papers May 1994 p 65-70 (For primary document see N95-15827 03-89)

(Grants NAGw-749; NAGw-3902)

Avail: CASI HC A02/MF A02

The 4430 A diffuse interstellar band (DIB) is unique among DIB's in that as one of the strong bands, it is the bluest strong band with no others observed at shorter wavelengths. This position at the edge of the DIF 'forrest' suggests it may be the easiest to replicate in the laboratory. In earlier experiments (Wdowiak 1980) an interesting candidate using a gas discharge followed by cryogenic matrix isolation was produced, and this report details its further investigation. This absorption feature, produced when 1 part CH4 in 200 parts Ar is discharged and frozen out approximately 10 K, is at a wavelength of 4500 A in the argon matrix. Our recent experiments strongly indicate it is due to a carbon-based reactive species that is stable against mercury vapor UV radiation, and not likely to be from a contaminant. The effect of matrix shift can be estimated by considering the blueward shift between Ar and Ne matrices in the cases of the pyrene and C60 cations. This suggests that a shift from 4500 A for an Af matrix to the vicinity of 4300 A for a Ne matrix and the gas phase is not unreasonable. A liquid He cooled Ne matrix isolation experiment was prepared to determine the wavelength of the feature in that matrix. Replacing CH4 with C2H2 results in an equivalent absorption due to C3, greatly diminished absorptions from C2 and Ch, and no observable feature at 4500 A. To date our experiments indicate CH4 is a favored precursor for production of the reactive carrier of the 4500 A feature. Perhaps C2H2 is not suitable because of its tendency to polymerize easily in the discharge. Author (revised)

N95-15841*# National Aeronautics and Space Administration. Ames Research Center, Moffett Field, CA.

FORMATION OF DUST GRAINS WITH IMPURITIES IN RED GIANT WINDS c90

Carsten Dominik *In its* The Diffuse Interstellar Bands: Contributed Papers May 1994 p 73-77 (For primary document see N95-15827 03-89)

Avail: CASI HC A01/MF A02

Among the several proposed carriers of diffuse interstellar bands (DIB's) are impurities in small dust grains, especially in iron oxide grains (Huffman 1977) and silicate grains (Huffman 1970). Most promising are single ion impurities since they can reproduce the observed band widths (Whittet 1992). These oxygen-rich grains are believed to originate mostly in the mass flows from red giants and in supernovae ejecta (e.g. Gehrz 1989). A question of considerable impact for the origin of DIB's is therefore, whether these grains are produced as mainly clean crystals or as some dirty materials. A formalism has been developed that allows tracking of the heterogeneous growth of a dust grain and its internal structure during the dust formation process. This formalism has been applied to the dust formation in the outflow from a red giant star. Derived from text

N95-15842*# National Aeronautics and Space Administration. Ames Research Center, Moffett Field, CA.

THE FORMATION OF SMALL GRAINS IN SHOCKS IN THE ISM c90

Anthony P. Jones (California Univ., Berkeley, CA.) and Alexander G. G. M. Tielens *In its* The Diffuse Interstellar Bands: Contributed Papers 79-83 (SEE N95-15827 03-89) May 1994 (For primary document see N95-15827 03-89)

(Contract NCA2-637; NGR-399-20-01-30)

Avail: CASI HC A01/MF A02

Carbonaceous and silicate grains swept up, and betatron accelerated, by supernova-generated shock waves in the interstellar medium are exposed to grain destructive processing. The degree of grain destruction is determined by the differential gas-grain and grain-grain velocities, which lead to sputtering of the grain surface and grain core disruption (deformation, vaporization and shattering), respectively. The threshold pressure for grain shattering in grain-grain collisions (100 k bar) is considerably lower than that for vaporization (approximately 5 M bar). Therefore, collisions between grains shatter large grains into smaller fragments (i.e., small grains and PAH's). Using a new algorithms for the destructive processes, it was possible to model the formation fo small grain fragments in grain-grain collisions in the warm phase of the interstellar medium. It was found that in one cycle through the warm medium (approximately 3 x 10(sup 6) years) of order 1-2% of the total grain mass is shattered into particles with radii of less than 50 A. Author (revised)

N95-15843*# National Research Council of Canada, Ottawa (Ontario). Inst. for Molecular Sciences.

THE C4H RADICAL AND THE DIFFUSE INTERSTELLAR BANDS. AN ab initio STUDY

Marcin Kolbuszewski *In* NASA. Ames Research Center, The Diffuse Interstellar Bands: Contributed Papers May 1994 p 85-90 (For primary document see N95-15827 03-89)

Avail: CASI HC A02/MF A02

An ab initio study of the low-lying electronic states of C4H has been presented where the species studied has a chi(2)sigma(+) ground state and two low lying pi states. Based on the vertical and adiabatic excitation energies between those states it is suggested that the 4428 A diffuse interstellar band is not carried by C4H. The application of the particle in a box model shows strong coincidences between the strong DIB's and predicted wavelengths of pi-pi transitions in C(2n)H series. Based on those coincidences, it is suggested the C(2n)H species as good candidates for carriers of diffuse interstellar bands. Derived from text

N95-15844*# Ecole Normale Superieure, Paris (France). Astrochimie Quantique.

QUANTUM CHEMISTRY AND EXCITED STATES: FIRST INVESTIGATIONS ON PYRENE-LIKE MOLECULES c72

Olivier Parisel and Y. Ellinger *In* NASA. Ames Research Center, The Diffuse Interstellar Bands: Contributed Papers May 1994 p 91-97 (For primary document see N95-15827 03-89)

Avail: CASI HC A02/MF A02

Although the calculations are expected to be accurate within 10%, it follows then that there cannot be proposed unquestionable one-to-one attribution due to the density of the DIB's (Diffuse Interstellar Bands). Nevertheless, it has been shown that if one is interested in the experimental study of methyl-pyrene cations, for example, then, the most promising candidate is the 1-methyl isomer: this isomer has been investigated by d'Hendecourt and Leger (1993,1994) and their spectrum shows very striking features in very good agreement with both our calculations and a few DIB's. However, 1-methyl-pyrene cation is not the only product susceptible of being formed in this experiment, and further investigations are in progress to give a complete interpretations of the results. This preliminary report on pyrene-like molecules illustrates the role that theoretical calculations can ply in both the design and the interpretation of experiments.

Derived from text

N95-15845*# IBM Watson Research Center, Yorktown Heights, NY.

L(ALPHA)-INDUCED TWO-PHOTON ABSORPTION OF VISIBLE LIGHT EMITTED FROM AN O-TYPE STAR BY H2(+) IONS LOCATED NEAR THE SURFACE OF THE STROMGREN SPHERE SURROUNDING THE STAR: A POSSIBLE EXPLANATION FOR THE DIFFUSE INTERSTELLAR ABSORPTION BANDS (DIDs)

James H. Glownia and Peter P. Sorokin *In* NASA. Ames Research Center, The Diffuse Interstellar Bands: Contributed Papers May 1994 p 99-104 (For primary document see N95-15827 03-89)

Avail: CASI HC A02/MF A02

In this paper, a new model is proposed to account for the DIB's (Diffuse Interstellar Bands). In this model, the DIB's result from a non-linear effect: resonantly-enhanced two-photon absorption of H(2+) ions located near the surface of the Stromgren sphere that surrounds an O- or B- type star. The strong light that is required to 'drive' the two-photon transition is provided by L(alpha) light emerging from the Stromgren sphere that bounds the H II region surrounding the star. A value of approximately 100 micro W/sq cm is estimated for the L(alpha) flux at the Stromgren radius, R(s), of a strong (O5) star. It is shown that a c.w. L(alpha) flux of this intensity should be sufficient to induce a few percent absorption for visible light radiated by the same star at a frequency (omega2) that completes an allowed two-photon transition, provided (1) the L(alpha) radiation happens to be nearly resonant with the frequency of a fully-allowed absorber transition

that effectively represents the first step in the two-photon transition, and (2) an effective column density approximately 10(sup18)/sq cm of the absorber is present near the Stromgren sphere radius, R(sub s).
Derived from text

N95-15846*# Colorado Univ., Boulder, CO. Center for Astrophysics and Space Astronomy.
A BIBLIOGRAPHY OF PAPERS ON THE DIFFUSE INTERSTELLAR BANDS **c82**
Theodore P. Snow, Susan Barnes, and Maribeth Heitzmann *In* NASA. Ames Research Center, The Diffuse Interstellar Bands: Contributed Papers May 1994 p 105-127 (For primary document see N95-15827 03-89)
Avail: CASI HC A03/MF A02

Presented is a compilation of publications on the diffuse interstellar bands, found in the literature dating back to the first known mention of the bands. It has been attempted to make this list complete, but it must be recognized that some papers may be missing. Judgement was required in some cases where the diffuse bands are mentioned, but are not a central theme of a paper; in most instances we kept such papers in a list, rather than omitting them. Author (revised)

N95-15907*# Sonoma State Univ., Rohnert Park, CA. Dept. of Physics and Astronomy.
ROSAT OBSERVATIONS OF THE BINARY BE-STAR AND RADIO PULSAR PSR1259-63 Final Technical Report, 1 Apr. - 15 Aug. 1994
Lynn R. Cominsky 15 Aug. 1994 17 p
(Grant NAG5-1684)
(NASA-CR-196951; NAS 1.26:196951) Avail: CASI HC A03/MF A01

This report discusses the ROSAT guest investigator program for the project 'ROSAT Observations of the Binary Be-star/Radio Pulsar PSR1259-63'. Work was done on this, and a previous grant entitled ROSAT Observations of MXB 1659-29 and EXO 0748-676 during this reporting period. A theory paper was written which proposes a new model to explain the X-ray emission from PSR 1259-63, in which the effects of accretion onto the magnetosphere of the neutron star, rather than onto the light cylinder which is conventionally assumed, is calculated. This approach works well to explain the apastron observations noted earlier. A statistical analysis of the eclipses from EXO0748-676 is also described. CASI

N95-13828# Indian Space Research Organization, Bangalore. Lab. for Electro-Optics Systems
STAR SENSOR FOR INDIAN REMOTE SENSING SATELLITE (IRS 1C)
Philip Thomas, Goparaju Nagendra Rao, G. Pratap, V. Koteswara Rao, and Y. K. Jain *In* ISRO Satellite Centre, Journal of Spacecraft Technology, Volume 4, No . 2, July 1994 Jul. 1994 p 36-42 (For primary document see N95-13825 03-12)
Avail: CASI HC A02/MF A01

N95-14626*# Jet Propulsion Lab., California Inst. of Tech., Pasadena, CA.
A RADIO TELESCOPE FOR THE CALIBRATION OF RADIO SOURCES AT 32 GIGAHERTZ
M. S. Gatti, S. R. Stewart, J. G. Bowen, and E. B. Paulsen *In its* The Telecommunications and Data Acquisition Report 15 Aug. 1994 p 56-82 (For primary document see N95-14620 03-32)
(RTOP 310-30-69-91-01)
Avail: CASI HC A03/MF A02

90 ASTROPHYSICS

Includes cosmology; celestial mechanics; space plasmas; and interstellar and interplanetary gases and dust.

For related information see also *75 Plasma Physics*.

N95-13658*# National Aeronautics and Space Administration. Goddard Space Flight Center, Greenbelt, MD.
INTERPLANETARY MEDIUM DATA BOOK, SUPPLEMENT 5, 1988-1993
Joseph H. King and Natalia E. Papitashvili Sep. 1994 308 p
(NASA-TM-109957; NSSDC/WDC-A-R/S-94-08-Suppl-5; NAS 1.15:109957)
Avail: CASI HC A14/MF A03

This publication represents an extension of the series of Interplanetary Medium Data Books and supplements that have been issued by the National Space Science Data Center since 1977. This volume contains solar wind magnetic field and plasma data from the IMP 8 spacecraft for 1988 through the end of 1993. The normalization of the MIT plasma density and temperature, which has been discussed at length in previous volumes, is implemented as before, using the same normalization constants for 1988-1993 data as for the earlier data. Owing to a combination of non-continuity of IMP 8 telemetry acquisition and IMP's being out of the solar wind for about 40 percent of its orbit, the annual solar wind coverage for 1988-1993 is 40 plus or minus 5 percent. The plots and listings of this supplement are in essentially the same format as in previous supplements. Days for which neither IMF nor plasma data were available for any hours are omitted from the listings. Author

N95-14266*# TRW Space Technology Labs., Redondo Beach, CA. Applied Technology Div.
ICE/ISEE PLASMA WAVE DATA ANALYSIS Final Report, Jan. 1992 - Sep. 1993
E. W. Greenstadt and S. L. Moses Sep. 1993 9 p Original contains color illustrations
(Contract NAS5-31837)
(NASA-CR-196988; NAS 1.26:196988) Avail: CASI HC A02/MF A01; 1 functional color page

This report is one of the final processing of ICE plasma wave (pw) data and analysis of late ISEE 3, ICE cometary, and ICE cruise trajectory data, where coronal mass ejections (CME's) were the first locus of attention. Interest in CME's inspired an effort to represent our pw data in a condensed spectrogram format that facilitated rapid digestion of interplanetary phenomena on long (greater than 1 day) time scales. The format serendipitously allowed us to also examine earth-orbiting data from a new perspective, invigorating older areas of investigation in Earth's immediate environment. We, therefore, continued to examine with great interest the last year of ISEE 3's precomet phase, when it spent considerable time far downwind from Earth, recording for days on end conditions upstream, downstream, and across the very weak, distant flank bow shock. Among other motivations has been the apparent similarity of some shock and post shock structures to the signatures of the bow wave surrounding comet Giacobini-Zinner, whose ICE-phase data we revisited. Author

N95-14311# Sandia National Labs., Albuquerque, NM.
DYNAMICAL PROPERTIES MEASUREMENTS FOR ASTEROID, COMET AND METEORITE MATERIAL APPLICABLE TO IMPACT MODELING AND MITIGATION CALCULATIONS
M. D. Furnish, M. B. Boslough, G. T. Gray, III, and J. L. Remo 1994 11 p Presented at the 1994 Hypervelocity Impact Symposium, Santa Fe, NM, 16-20 Oct. 1994
(Contract DE-AC04-94AL-85000)
(DE94-014142; SAND-94-0058C; CONF-9410131-2) Avail: CASI HC A03/MF A01

We describe methods for measuring dynamical properties for two material categories of interest in understanding large-scale extraterrestrial impacts: iron-nickel and underdense materials (e.g. snow). Particular material properties measured by the present methods include Hugoniot release paths and constitutive properties (stress vs. strain). The iron-nickel materials lend themselves well to conventional shock and quasi-static experiments. As examples, a suite of experiments is described including six impact tests (wave profile compression/release) over the stress range 2-20 GPa, metallography, quasi-static and split Hopkinson pressure bar (SHPB) mechanical testing, and ultrasonic mapping and sound velocity measurements. Temperature sensitivity of the dynamic behavior was measured at high and low strain rates. Among the iron-nickel materials tested, an octahedrite was found to have behavior close to that of Armco iron under shock and quasi-static conditions, while an ataxite exhibited a significantly larger quasi-static yield strength than did the octahedrite or a hexahedrite. The underdense materials pose three primary experimental difficulties. First, the samples are friable; they can melt or sublimate during storage, preparation and testing. Second, they are brittle and crushable; they cannot withstand such treatment as traditional machining or launch in a gun system. Third, with increasing porosity the calculated Hugoniot density becomes rapidly more sensitive to errors in wave time-of-arrival measurements. Carefully chosen simulants eliminate preservation (friability) difficulties, but the other difficulties remain. A family of 36 impact tests

was conducted on snow and snow simulants at Sandia, yielding reliable Hugoniot and reshock states, but limited release property information. Other methods for characterizing these materials are discussed. DOE

N95-14442# California Univ., Berkeley. Lawrence Berkeley Lab, CA.
HADRONIC MATTER AND RAPIDLY ROTATING COMPACT STARS
F. Weber (Ludwig-Maximilians-Univ., Munich, Germany.), C. Kettner (Ludwig-Maximilians-Univ., Munich, Germany.), and N. K. Glendenning Mar. 1994 15 p Presented at the International Conference on Nuclear Structure in the Late Nineties, Hanoi, Viet Nam, 14-18 Mar. 1994
(Contract DE-AC03-76SF-00098)
(DE94-014928; LBL-35525; CONF-9403131-2) Avail: CASI HC A03/MF A01

In part one of this paper the authors review the present status of neutron star matter calculations, and introduce a representative collection of realistic nuclear equations of state which are derived for different assumptions about the physical behavior of dense matter (baryon populations, pion condensation, possible transition of baryon matter to quark matter). Part two deals with the theoretical determination of the minimum possible rotational periods of neutron stars, performed in the framework of general relativity, whose knowledge serves to distinguish between pulsars that can be understood as rotating neutron stars and those that cannot. Likely candidates for the latter are hypothetical strange stars. Their properties are discussed in the third part of this contribution. DOE

N95-14499*# National Aeronautics and Space Administration. Ames Research Center, Moffett Field, CA.
ASTROPHYSICAL SCIENCE WITH A SPACEBORNE PHOTOMETRIC TELESCOPE
Arno F. Granados, ed. (Search for Extraterrestrial Intelligence Inst., Mountain View, CA.) and William J. Borucki, ed. Aug. 1994 89 p The First FRESIP Astrophysics Workshop was held in Mountain View, CA, 11-12 Nov. 1993
(RTOP 196-41-67-05; Proj. FRESIP)
(NASA-CP-10148; A-94111; NAS 1.55:10148) Avail: CASI HC A05/MF A01

The FRESIP Project (FRequency of Earth-Sized Inner Planets) is currently under study at NASA Ames Research Center. The goal of FRESIP is the measurement of the frequency of Earth-sized extra-solar planets in inner orbits via the photometric signature of a transit event. This will be accomplished with a spaceborne telescope/photometer capable of photometric precision of two parts in 100,000 at a magnitude of m(sub v) = 12.5. To achieve the maximum scientific value from the FRESIP mission, an astrophysical science workshop was held at the SETI Institute in Mountain View, California, November 11-12, 1993. Workshop participants were invited as experts in their field of astrophysical research and discussed the astrophysical science that can be achieved within the context of the FRESIP mission. For individual titles, see N95-14500 through N95-14509.

N95-14500*# Lockheed Missiles and Space Co., Palo Alto, CA. Solar and Astrophysics Lab.
STELLAR ACTIVITY: ASTROPHYSICS RELEVANT TO GLOBAL CHANGE
Bernhard M. Haisch *In* NASA. Ames Research Center, Astrophysical Science with a Spaceborne Photometric Telescope Aug. 1994 p 1-10 (For primary document see N95-14499 03-90)
Avail: CASI HC A02/MF A01

FRESIP will obtain a great deal of data on stellar activity and flares on F, G and K dwarfs. Rotation periods, flare distributions and possibly stellar cycles will emerge. This apparently curiosity-driven research actually has implications for our understanding of global climate change. Significant climate change during the seventeenth-century Maunder Minimum is thought to be related to a change in the solar condition. Recently acquired data from the Greenland Ice-core Project suggest that far greater climate changes on decade time scales may have occurred during the previous interglacial. It is possible that a yet more drastic change in state of the Sun was responsible. We have no relevant solar data, but can begin to explore this possibility by observing an ensemble of solar-like stars. Author

N95-14501*# Space Telescope Science Inst., Baltimore, MD.
PROBING SURFACE STRUCTURE ON LATE-TYPE STARS WITH FRESIP
Robert C. Dempsey *In* NASA. Ames Research Center, Astrophysical Science with a Spaceborne Photometric Telescope Aug. 1994 p 11-1 (For primary document see N95-14499 03-90)
Avail: CASI HC A02/MF A01

We discuss possible secondary scientific results obtainable with the FRESIP satellite in regards to surface features on solar-like stars. Author

N95-14502*# National Center for Atmospheric Research, Boulder, CO. High Altitude Observatory.
ASTEROSEISMOLOGY: THEORY AND PHENOMENOLOGY
Timothy M. Brown *In* NASA. Ames Research Center, Astrophysical Science with a Spaceborne Photometric Telescope Aug. 1994 p 17-2 Sponsored by NSF (For primary document see N95-14499 03-90)
Avail: CASI HC A02/MF A01

Seismic studies of the Sun have succeeded in mapping the variation of sound speed with depth in the Sun, and variation of angular velocity with both depth and latitude. Many stars besides the Sun may also be amenable to asteroseismic analysis. Stars of roughly solar type should of course behave in ways similar to the sun, and stars of this sort form a large fraction of the potential targets for asteroseismology. But several other types of stars (delta scuti stars, roAP stars, and the pulsating white dwarfs) also have the desired pulsation characteristics. Pulsations in some of these stars are, for various reasons, much easier to observe than in the Sun-like stars. Virtually all unambiguous observations of multi-mode pulsators relate to these other categories of stars. Since oscillation mode frequencies are arguably the most precise measurement relating to a star that we can make, a few tens of such frequencies may still be of great importance to our understanding of the stellar structure and evolution. Derived from text

N95-14503*# Space Telescope Science Inst., Baltimore, MD.
ASTEROSEISMOLOGY: GROUND BASED EFFORTS AND THE NEED FOR SPACE OBSERVATIONS
Ronald L. Gilliland (Kitt Peak National Observatory, Tucson, AZ.) *In* NASA. Ames Research Center, Astrophysical Science with a Spaceborne Photometric Telescope Aug. 1994 p 27-3 (For primary document see N95-14499 03-90)
Avail: CASI HC A02/MF A01

Detection of the oscillations expected to be present on solar-like stars is very difficult. Photometric observations from the ground suffer from two problems: (1) an atmospheric scintillation noise that drops only slowly with telescope aperture size, and (2) mode frequency spacings that require nearly continuous observations over at least several days for resolution. I will review the very limited possibilities for asteroseismology of solar-like stars from ground-based photometric observations. FRESIP could provide an excellent opportunity for pursuing asteroseismology observations of a far richer nature than can be contemplated from the ground. Author

N95-14504*# Stanford Univ., CA. Center for Space Science and Astrophysics.
ASTEROSEISMOLOGY WITH FRESIP: A METER CLASS SPACE TELESCOPE
Peter Milford *In* NASA. Ames Research Center, Astrophysical Science with a Spaceborne Photometric Telescope Aug. 1994 p 37-4 (For primary document see N95-14499 03-90)
Avail: CASI HC A02/MF A01

The requirements for asteroseismology and searching for occulting inner planets are similar. The FRESIP mission will be suited to making asteroseismology measurements. Recommendation: Use 30-60 second integrations from one or more CCD's in the FRESIP mosaic, sampled continuously for the entire mission to measure stellar non-radial oscillations with amplitudes of parts per million and frequencies of 0.1 to 10 MHz. These measurements lead to determination of stellar interior helium abundances, rotation rates, depth of convection zones and measuring stellar cycle frequency changes for a variety of stellar types, enabling major advances in stellar structure and evolutionary theories. Author

N95-14505*# McDonald Observatory, Austin, TX.
THE SYMBIOSIS OF PHOTOMETRY AND RADIAL-VELOCITY MEASUREMENTS

William D. Cochran *In* NASA. Ames Research Center, Astrophysical Science with a Spaceborne Photometric Telescope Aug. 1994 p 45-4 (For primary document see N95-14499 03-90)
(Grants NAGw-2302; NAGw-2465)
Avail: CASI HC A01/MF A01

The FRESIP mission is optimized to detect the inner planets of a planetary system. According to the current paradigm of planet formation, these planets will probably be small Earth-sized objects. Ground-based radial-velocity programs now have the sensitivity to detect Jovian-mass planets in orbit around bright solar-type stars. We expect the more massive planets to form in the outer regions of a proto-stellar nebula. These two types of measurements will very nicely complement each other, as they have highest detection probability for very different types of planets. The combination of FRESIP photometry and ground-based spectra will provide independent confirmation of the existence of planetary systems in orbit around other stars. Such detection of both terrestrial and Jovian planets in orbit around the same star is essential to test our understanding of planet formation. Author

N95-14506*# Space Telescope Science Inst., Baltimore, MD.
ROTATION AMONG SOLAR-TYPE STARS
D. Soderblom *In* NASA. Ames Research Center, Astrophysical Science with a Spaceborne Photometric Telescope Aug. 1994 p 51-5 (For primary document see N95-14499 03-90)
Avail: CASI HC A01/MF A01

The net result is that FRESIP will produce high quality rotational data for a large (and essentially volume-limited) sample of solar-type stars. Moreover, the observed slight changes in rotation period will indicate the nature and degree of differential rotation on those stars. Both parameters are central to our understanding of the evolution of the Sun. Author

N95-14507*# Planetary Science Inst., Tucson, AZ.
FRESIP PROJECT OBSERVATIONS OF CATACLYSMIC VARIABLES: A UNIQUE OPPORTUNITY
Steve B. Howell *In* NASA. Ames Research Center, Astrophysical Science with a Spaceborne Photometric Telescope Aug. 1994 p 55-6 (For primary document see N95-14499 03-90)
Avail: CASI HC A02/MF A01

FRESIP Project observations of cataclysmic variables would provide unique data sets. In the study of known cataclysmic variables they would provide extended, well sampled temporal photometric information and in addition, they would provide a large area deep survey; obtaining a complete magnitude limited sample of the galaxy in the volume cone defined by the FRESIP field of view. Author

N95-14508*# Georgia State Univ., Atlanta, GA. Dept. of Physics and Astronomy.
OBSERVATIONS OF HOT STARS AND ECLIPSING BINARIES WITH FRESIP
Douglas R. Gies *In* NASA. Ames Research Center, Astrophysical Science with a Spaceborne Photometric Telescope Aug. 1994 p 63-7 Submitted for publication (For primary document see N95-14499 03-90)
(Grant NSF AST-91-15121)
Avail: CASI HC A02/MF A01

The FRESIP project offers an unprecedented opportunity to study pulsations in hot stars (which vary on time scales of a day) over a several year period. The photometric data will determine what frequencies are present, how or if the amplitudes change with time, and whether there is a connection between pulsation and mass loss episodes. It would initiate a new field of asteroseismology studies of hot star interiors. A search should be made for selected hot stars for inclusion in the list of project targets. Many of the primary solar mass targets will be eclipsing binaries, and I present estimates of their frequency and typical light curves. The photometric data combined with follow up spectroscopy and interferometric observations will provide fundamental data on these stars. The data will provide definitive information on the mass ratio distribution of solar-mass binaries (including the incidence of brown dwarf companions) and on the incidence of planets in binary systems. Author

N95-14509*# Ohio State Univ., Columbus. Dept. of Astronomy.
MONITORING THE VARIABILITY OF ACTIVE GALACTIC NUCLEI FROM A SPACE-BASED PLATFORM
Bradley M. Peterson, Bruce Atwood, and Paul L. Byard *In* NASA. Ames Research Center, Astrophysical Science with a Spaceborne Photometric Telescope Aug. 1994 p 73-8 (For primary document see N95-14499 03-90)
(Grant NSF AST-91-17086)
Avail: CASI HC A03/MF A01

Detailed monitoring of AGN's with FRESIP can provide well-sampled light curves for a large number of AGN's. Such data are completely unprecedented in this field, and will provide powerful new constraints on the origin of the UV/optical continuum in AGN's. The FRESIP baseline design will allow 1 percent photometry on sources brighter than V approximately equals 19.6 mag, and we estimate that over 300 sources can be studied. We point out that digitization effects will have a significant negative impact on the faint limit and the number of detectable sources will decrease dramatically if a fixed gain setting (estimated to be nominally 25 e(-) per ADU) is used for all read-outs. We note that the primary limitation to studying AGN's is background (sky and read-out noise) rather than source/background contrast with a focused telescope and by longer integrations. While we believe that it may be possible to achieve the AGN-monitoring science goals with a more compact and much less expensive telescope, the proposed FRESIP satellite affords an excellent opportunity to attain the required data at essentially zero cost as a secondary goal of a more complex mission. Author

N95-13947*# Turin Univ. (Italy). Dipt. di Fisica Teorica.
SQUEEZED STATES AND GRAVITON-ENTROPY PRODUCTION IN THE EARLY UNIVERSE
Massimo Giovannini *In* NASA. Goddard Space Flight Center, Third International Workshop on Squeezed States and Uncertainty Relations May 1994 p 407-412 Prepared in cooperation with Istituto Nazionale di Fisica Nucleare, Turin, Italy (For primary document see N95-13896 03-74)
Avail: CASI HC A02/MF A06

N95-15841*# National Aeronautics and Space Administration. Ames Research Center, Moffett Field, CA.
FORMATION OF DUST GRAINS WITH IMPURITIES IN RED GIANT WINDS
Carsten Dominik *In its* The Diffuse Interstellar Bands: Contributed Papers May 1994 p 73-77 (For primary document see N95-15827 03-89)
Avail: CASI HC A01/MF A02

N95-15842*# National Aeronautics and Space Administration. Ames Research Center, Moffett Field, CA.
THE FORMATION OF SMALL GRAINS IN SHOCKS IN THE ISM
Anthony P. Jones (California Univ., Berkeley, CA.) and Alexander G. G. M. Tielens *In its* The Diffuse Interstellar Bands: Contributed Papers 79-83 (SEE N95-15827 03-89) May 1994 (For primary document see N95-15827 03-89)
(Contract NCA2-637; NGR-399-20-01-30)
Avail: CASI HC A01/MF A02

91 LUNAR AND PLANETARY EXPLORATION

Includes planetology; and manned and unmanned flights.

For spacecraft design or space stations see *18 Spacecraft Design, Testing and Performance.*

N95-13717*# MCAT Inst., Moffett Field, CA.
PLANETARY ENTRY EXPERIMENTS Final Report
Roger A. Craig San Jose, CA Jul. 1994 128 p
(Contract NCC2-762)
(NASA-CR-194215; NAS 1.26:194215; MCAT-94-005) Avail: CASI HC A07/MF A02

The final report summarizes the results from three research areas: (1) window design for the radiometric measurement of the forebody radiative heating experienced by atmospheric entry spacecraft; (2) survey of the current understanding of chemical species on selected solar system bodies and assess the importance of measurements with regard to vehicle environment and with regard to understanding of planetary atmospheres

with emphasis on Venus, Mars, and Titan; and (3) measure and analyze the radiation (VUV to near-IR) from the shock heated gas cap of a blunt body in an Ames arc Jet wind-tunnel facility. For individual titles, see N95-13718 through N95-13721.

N95-13718*# MCAT Inst., Moffett Field, CA.
SCIENCE OBJECTIVES AND PERFORMANCE OF A RADIOMETER AND WINDOW DESIGN FOR ATMOSPHERIC ENTRY EXPERIMENTS c19
Roger A. Craig, William C. Davy, and Ellis E. Whiting *In its* Planetary Entry Experiments Jul. 1994 41 p (For primary document see N95-13717 03-91)
Avail: CASI HC A03/MF A02

The Radiative Heating Experiment, RHE, aboard the Aeroassist Flight Experiment, AFE, (now cancelled) was to make in-situ measurements of the stagnation region shock layer radiation during an aerobraking maneuver from geosynchronous to low earth orbit. The measurements were to provide a data base to help develop and validate aerothermodynamic computational models. Although cancelled, much work was done to develop the science requirements and to successfully meet RHE technical challenges. This paper discusses the RHE scientific objectives and expected science performance of a small sapphire window for the RHE radiometers. The spectral range required was from 170 to 900 nm. The window size was based on radiometer sensitivity requirements including capability of on-orbit solar calibration. Author

N95-13719*# National Aeronautics and Space Administration. Ames Research Center, Moffett Field, CA.
VUV SHOCK LAYER RADIATION IN AN ARC-JET WIND TUNNEL EXPERIMENT c02
Roger A. Craig (MCAT Inst., Moffett Field, CA.), Giuseppe Palumbo (Eloret Corp., Santa Clara, CA.), and Armando Carrasco *In* MCAT Inst., Planetary Entry Experiments Jul. 1994 27 p (For primary document see N95-13717 03-91)
(Contract NCC2-653)
Avail: CASI HC A03/MF A02

Measurements were made of the radiating gas cap of a blunt body in a NASA-Ames 20 MW arc-jet wind tunnel. The test gas was air. Spectra of the flux incident on a small aperture centered at the stagnation region were obtained. A helium-cooled, magnesium fluoride window transmitted the flux into an evacuated collimating system that focused the aperture onto the entrance slit of a spectrometer. Data were obtained with films and by photomultipliers. The spectral ranges covered were the vacuum ultraviolet, VUV, (120 nm to 200 nm) and the ultraviolet to near infrared (200 nm to 900 nm) with resolutions from 0.05 nm to 0.5 nm. This paper presents the preliminary VUV results from the experiment. Results from the 200 nm to 900 nm spectral range have been presented elsewhere. Representative spectral records from 120 nm to 200 nm are shown. The intense atomic oxygen and nitrogen lines which are of concern to hypersonic flight are measured. Carbon lines are are also seen. These results will be used to help develop and validate aerothermodynamic computational models of arc-jet wind tunnel performance and help to assess the importance of VUV heating to entering spacecraft. Author

N95-13720*# National Aeronautics and Space Administration. Ames Research Center, Moffett Field, CA.
MEASURED AND CALCULATED SPECTRAL RADIATION FROM A BLUNT BODY SHOCK LAYER IN AN ARC-JET WIND TUNNEL c02
Dikran S. Babikian (Eloret Corp., Palo Alto, CA.), Giuseppe Palumbo (Eloret Corp., Palo Alto, CA.), Roger A. Craig (MCAT Inst., Moffett Field, CA.), Chul Park, Grant Palmer, and Surendra P. Sharma *In* MCAT Inst., Planetary Entry Experiments Jul. 1994 11 p Presented at the 32d Aerospace Sciences Meeting, Reno, NV, 10-13 Jan. 1994; sponsored by AIAA (For primary document see N95-13717 03-91)
(Contract NCC2-653)
(AIAA Paper 94-0086) Avail: CASI HC A03/MF A02

Spectra of the shock layer radiation incident on the stagnation point of a blunt body placed in an arc-jet wind tunnel were measured over the wavelength range from 600 nm to 880 nm. The test gas was a mixture of 80 percent air and 20 percent argon by mass, and the run was made in a highly nonequilibrium environment. The observed spectra contained contributions from atomic lines of nitrogen, oxygen, and argon, of bound-free and free-free continua, and band systems of N2 and N2(+). The measured spectra were compared with the synthetic spectra, which were obtained through four steps: the calculation of the arc-heater characteristics, of the nozzle flow, of the blunt-body flow, and the nonequilibrium radiation processes. The results show that the atomic lines are predicted approximately correctly, but all other sources are underpredicted by orders of magnitude. A possible explanation for the discrepancy is presented. Author

N95-13721*# MCAT Inst., Moffett Field, CA.
VENUSIAN ATMOSPHERIC EQUILIBRIUM CHEMISTRY AT THE PIONEER VENUS ANOMALOUS EVENT ALTITUDE
Roger A. Craig *In its* Planetary Entry Experiments Jul. 1994 12 p (For primary document see N95-13717 03-91)
(Contract NCC2-653)
Avail: CASI HC A03/MF A02

No convincing explanation for the anomalous behavior of the Atmospheric Structure Experiment temperature sensors at approximately 13 km altitude has been found. It occurred on all of the widely-spaced probes, in a similar fashion. A preliminary effort has been made to determine atmospheric chemical species which might be present at 13 km. The purpose of this effort is to initiate suggestions of possible chemical interactions and to explore the effects of the presence of possible metal reactants including condensation. Equilibrium fractions of chemical species were calculated at a variety of conditions. Baseline calculations were made for the altitudes near 13 km. For comparison calculations were also made at 13 km but with the introduction of plausible metal atoms. Author

N95-13724*# Brown Univ., Providence, RI. Dept. of Geological Sciences.
EXPERIMENTAL STUDY OF CHEMICAL, PHASE AND TEXTURAL EQUILIBRIUM OF HIGH TiO2 MARE BASALTS AND PERIDOTITE
Summary Report, 1984-1993
Paul C. Hess 1994 11 p
(Grant NAG9-109)
(NASA-CR-196480; NAS 1.26:196480) Avail: CASI HC A03/MF A01

The topics covered include the following: (1) basalt petrogenesis; (2) petrogenesis of highly evolved magmas; and (3) chondrites. CASI

N95-14868*# Texas Univ., Austin, TX. Dept. of Aerospace Engineering and Engineering Mechanics.
AN UNMANNED MISSION TO MARS WITH SAMPLE COLLECTION AND IN-SITU RESOURCE UTILIZATION
6 May 1994 95 p Prepared in cooperation with Universities Space Research Association, Columbia, MD
(Contract NASw-4435; Proj. MARVIN)
(NASA-CR-197202; NAS 1.26:197202) Avail: CASI HC A05/MF A01

The design for the Mars Analysis and Return Vehicle with In-Situ Resource Utilization (MARVIN) project is outlined. The MARVIN mission is designed to collect samples of the Martian environment; to produce fuel from local Martian resources; and to use the fuel produced to return the samples to earth. It uses only existing technologies. Exploratory Technologies' mission-design efforts have focused on methods of orbit determination, sample collection, fuel production, power, communications, control, and structural design. Lambert Targeting provided Delta-V's, launch dates, and travel times. The landing site is the Tharsis Plateau, to the southeast of Olympus Mons, chosen for its substantial scientific value. Samples of soil, dust, and atmosphere are collected with lander-based collection devices: the soil sample, with a robotic arm similar to those used in the Viking missions; the atmospheric sample, from a bleed line to the compressor in the fuel-production facility; a dust sample, from the dust-collection container in the fuel-production facility; and a redundant dust sample, with a with a passive filter system, which relies upon neither a power source nor other collection methods. The sample-return capsule (SRC) houses these samples, which are triply contained to prevent contamination. Proven technology can be used to produce methane and oxygen for fuel with relative ease at the landing site: the Sabatier reactor produces methane and water by combining carbon dioxide and hydrogen (brought from earth); the Reverse Water-Gas Shift unit combines carbon dioxide and hydrogen to form carbon monoxide and water; a water-electrolysis unit splits the water into hydrogen and oxygen. The Mars-lander vehicle (MLV) transports the equipment from earth to Mars. The Mars-ascent vehicle (MAV) contains the SRC and the engine, which is the same for both the MLV and the MAV. All equipment that is unnecessary

for the Mars-Earth trajectory remains on Mars. This report presents detailed sizing information, for which a spreadsheet has been developed. The trends suggest possibilities for expansion, and suggestions for future work in these areas are offered. Author (revised)

N95-14037*# National Aeronautics and Space Administration. Ames Research Center, Moffett Field, CA.
THE EXPLORATION METAPHOR
Michael W. McGreevy *In its* Human Machine Interfaces for Teleoperators and Virtual Environments Jun. 1991 p 81-82 (For primary document see N95-14013 03-54)
Avail: CASI HC A01/MF A02

N95-14076*# Able Engineering Co., Inc., Goleta, CA.
MARTIAN ENVIRONMENTAL SIMULATION FOR A DEPLOYABLE LATTICE MAST
Robert M. Warden *In* NASA. Goddard Space Flight Center, Eighteenth Space Simulation Conference: Space Mission Success Through Testing Nov. 1994 p 187-193 (For primary document see N95-14062 03-18)
Avail: CASI HC A02/MF A04

92 SOLAR PHYSICS

Includes solar activity, solar flares, solar radiation and sunspots.
For related information see *93 Space Radiation.*

N95-14376# Los Alamos National Lab., NM.
EARLY SOLAR MASS LOSS, ELEMENT DIFFUSION, AND SOLAR OSCILLATION FREQUENCIES
J. A. Guzik and A. N. Cox 1994 14 p Presented at the Solar Modeling Workshop, Seattle, WA, 21-24 Mar. 1994
(Contract W-7405-eng-36)
(DE94-014802; LA-UR-94-1587; CONF-9403143-1) Avail: CASI HC A03/MF A01

Swenson and Faulkner, and Boothroyd et al. investigated the possibility that early main-sequence mass loss via a stronger early solar wind could be responsible for the observed solar lithium and beryllium depiction. This depletion requires a total mass loss of approximately 0.1 M(circle dot), nearly independent of the mass loss timescale. We have calculated the evolution and oscillation frequencies of solar models including helium and element diffusion, and such early solar mass loss. We show that extreme mass loss of 1 M(circle dot) is easily ruled out by the low-degree p-modes that probe the solar center and sense the steeper molecular weight gradient produced by the early phase of more rapid hydrogen burning. The effects on central structure are much smaller for models with an initial mass of 1.1 M(circle dot) and exponentially-decreasing mass loss rate with e-folding timescale 0.45 Gyr. While such mass loss slightly worsens the agreement between observed and calculated low-degree modes, the observational uncertainties of several tenths of a microhertz weaken this conclusion. Surprisingly, the intermediate-degree modes with much smaller observational uncertainties that probe the convection zone bottom prove to be the key to discriminating between models: (1) the early mass loss phase decreases the total amount of helium and heavier elements diffused from the convection zone, and (2) the extent of the diffusion produced composition gradient just below the convection zone, deteriorating the agreement with observed frequencies for these modes. Thus it appears that oscillations can also rule out this smaller amount of gradual early main-sequence mass loss in the young Sun. The mass loss phase must be confined to substantially under a billion years, probably 0.5 Gyr or less, to simultaneously solve the solar Li/Be problem and avoid discrepancies with solar oscillation frequencies. DOE

N95-15070*# Alabama Univ., Huntsville, AL. Dept. of Mechanical and Aerospace Engineering.
ON THE PHYSICS OF WAVES IN THE SOLAR ATMOSPHERE: WAVE HEATING AND WIND ACCELERATION Final Report
Z. E. Musielak Sep. 1994 12 p
(Grant NAG8-839)
(NASA-CR-196992; NAS 1.26:196992) Avail: CASI HC A03/MF A01

New calculations of the acoustic wave energy fluxes generated in the solar convective zone have been performed. The treatment of convective turbulence in the sun and solar-like stars, in particular, the precise nature of the turbulent power spectrum has been recognized as one of the most important issues in the wave generation problem. Several different functional forms for spatial and temporal spectra have been considered in the literature and differences between the energy fluxes obtained for different forms often exceed two orders of magnitude. The basic criterion for choosing the appropriate spectrum was the maximal efficiency of the wave generation. We have used a different approach based on physical and empirical arguments as well as on some results from numerical simulation of turbulent convection. Derived from text

N95-15773# National Geophysical Data Center, Boulder, CO.
SOLAR-GEOPHYSICAL DATA NUMBER 598, JUNE 1994. PART 2: (COMPREHENSIVE REPORTS). DATA FOR DECEMBER 1993 AND MISCELLANEOUS
Helen E. Coffey, ed. Jun. 1994 54 p See also PB94-187887 and PB94-208824
(PB94-208832; SGD-598-Pt-2) Avail: CASI HC A04/MF A01

This document contains the following Data (December 1993): Solar Flares; Solar Radio Bursts at Fixed Frequencies; Solar X-Ray Radiation from GOES Satellite Graphs; Mass Ejections from the Sun; Active Prominences and Filaments; and IMP-8 Solar Wind Plot. NTIS

N95-15784 National Geophysical Data Center, Boulder, CO.
SOLAR-GEOPHYSICAL DATA NUMBER 598, JUNE 1994. PART 1: (PROMPT REPORTS). DATA FOR MAY, APRIL 1994 AND LATE DATA
Helen E. Coffey, ed. Jun. 1994 118 p See also PB94-187929 and PB94-208832 Limited Reproducibility: More than 20% of this document may be affected by poor print
(PB94-208824; SGD-598-Pt-1) Avail: Issuing Activity (National Technical Information Service (NTIS))

This document contains the following Data for May 1994: Solar-Terrestrial Environment; IUWDS Alert Periods (Advance and Worldwide); Solar Activity Indices; Solar Flares; Solar Radio Emission; and Stanford Mean Solar Magnetic Field; Data for April 1994: Solar Active Regions; Sudden Ionospheric Disturbances; Solar Radio Spectral Observations; Solar Radioheliograph - 164 MHz - Nancay; Cosmic Ray Measurements by Neutron Monitor; New Data: Moscow Neutron Monitor Data; Geomagnetic Indices; and Principal Magnetic Storms. NTIS

93 SPACE RADIATION

Includes cosmic radiation; and inner and outer earth's radiation belts.

For biological effects of radiation see *52 Aerospace Medicine.* For theory see *73 Nuclear and High-Energy Physics.*

N95-14437# Los Alamos National Lab., NM.
PRODUCTION PROFILES OF NUCLIDES BY GALACTIC-COSMIC-RAY PARTICLES IN SMALL METEOROIDS
R. C. Reedy and J. Masarik 1994 4 p Presented at the Workshop on Meteorites From Cold and Hot Deserts, Noerdlingen, Germany, 20-22 Jul. 1994
(Contract W-7405-eng-36)
(DE94-014801; LA-UR-94-1588; CONF-940796-1) Avail: CASI HC A01/MF A01

Many of the meteorites found in cold and hot deserts are small, and many were small bodies in space. Production of cosmic-ray-produced (cosmogenic) nuclides in small meteoroids is expected to be different than that in the larger meteoroids typically studied, with lower levels of nuclide production by galactic-cosmic-ray (GCR) particles and possibly significant production by solar-cosmic-ray (SCR) protons. Motivated by the cosmogenic-nuclide measurements for the very small Salem meteorite and for cosmic spherules, which show high levels of SCR production, we have reported earlier nuclide production rates by SCR protons in small objects in space. The GCR production rates reported for small meteoroids have not been tested and were expected to be poor for meteoroids with radii less than 40 g/cm(exp 2) because of the very simple nature of that semi-empirical model (only one free parameter) and because the mix of neutrons and protons is different (relatively more protons) than that in the model, which was based on larger objects. Thus we have calculated

produciton rates for nuclides mad by GCR particles in small objects with a physical model that is much better suited for unusual targets.
Derived from text

N95-14438# Los Alamos National Lab., NM.
NUMERICAL SIMULATIONS OF PLANETARY GAMMA-RAY SPECTRA INDUCED BY GALACTIC COSMIC RAYS
J. Masarik and R. C. Reedy 1994 4 p Presented at the International Conference on Nuclear Data for Science and Technology, Gatlinburg, TN, 9-13 May 1994
(Contract W-7405-eng-36)
(DE94-014809; LA-UR-94-1616; CONF-940507-25) Avail: CASI HC A01/MF A01

The fluxes of cosmic-ray-produced gamma rays escaping from Mars were calculated using the LAHET Code System and basic nuclear data for gamma-ray production. Both surface water content and atmospheric thickness strongly affect the fluxes of gamma-ray lines escaping from Mars. DOE

N95-14814*# Massachusetts Inst. of Tech., Cambridge. Center for Space Research.
SEARCH FOR GAMMA-RAY EVENTS IN THE BATSE DATA BASE Final Technical Report
Walter Lewin 5 Nov. 1994 9 p
(Grant NAG5-2030)
(NASA-CR-197044; NAS 1.26:197044) Avail: CASI HC A02/MF A01

We find large location errors and error radii in the locations of channel 1 Cygnus X-1 events. These errors and their associated uncertainties are a result of low signal-to-noise ratios (a few sigma) in the two brightest detectors for each event. The untriggered events suffer from similarly low signal-to-noise ratios, and their location errors are expected to be at least as large as those found for Cygnus X-1 with a given signal-to-noise ratio. The statistical error radii are consistent with those found for Cygnus X-1 and with the published estimates. We therefore expect approximately 20 - 30 deg location errors for the untriggered events. Hence, many of the untriggered events occurring within a few months of the triggered activity from SGR 1900 plus 14 are indeed consistent with the SGR source location, although Cygnus X-1 is also a good candidate. Author

N95-15790*# National Aeronautics and Space Administration. Langley Research Center, Hampton, VA.
EXTENSION OF THE BRYNTRN CODE TO MONOENERGETIC LIGHT ION BEAMS
Francis A. Cucinotta, John W. Wilson, and Francis F. Badavi Nov. 1994 36 p
(RTOP 199-45-16-11)
(NASA-TP-3472; L-17394; NAS 1.60:3472) Avail: CASI HC A03/MF A01

A monoenergetic version of the BRYNTRN transport code is extended to beam transport of light ions (H-2, H-3, He-3, and He-4) in shielding materials (thick targets). The redistribution of energy in nuclear reactions is included in transport solutions that use nuclear fragmentation models. We also consider an equilibrium target-fragment spectrum for nuclei with mass number greater than four to include target fragmentation effects in the linear energy transfer (LET) spectrum. Illustrative results for water and aluminum shielding, including energy and LET spectra, are discussed for high-energy beams of H-2 and He-4. Author

99 GENERAL

N95-13640# Advisory Group for Aerospace Research and Development, Neuilly-Sur-Seine (France).
AGARD HIGHLIGHTS 94/2
1994 46 p
(AGARD-HIGHLIGHTS-94/2) Copyright Avail: CASI HC A03/MF A01

Various aspects of research and development in aerospace sciences are discussed. Specific topics considered include: aircraft engine technology transfer; lessons learned from a historical review of aircraft operations; and pilot vertigo. CASI

N95-13663*# National Aeronautics and Space Administration. Langley Research Center, Hampton, VA.
A REVIEW OF 50 YEARS OF AERODYNAMIC RESEARCH WITH NACA/NASA
M. Leroy Spearman Oct. 1994 12 p
(RTOP 505-69-20-01)
(NASA-TM-109163; NAS 1.15:109163) Avail: CASI HC A03/MF A01

Continuous improvements in flight systems have occurred over the past 50 years due, in part, to continuous improvements in aerodynamic research techniques and capabilities. This paper traces that research from the first-hand perspective of the author who, beginning in 1944, has taken part in the NACA/NASA aerodynamic research effort through studies in low-speed wind tunnels, high-speed subsonic tunnels, transonic tunnels, supersonic tunnels, and hypersonic tunnels. New problems were found as systems advanced from low-speed propeller-driven designs to more sophisticated high-speed jet- and rocket-propelled designs. The paper reviews some of these problems and reflects on some of the solutions that have been developed in the course of various aerodynamic research programs in the past. Some of the factors, both technical and nontechnical, that have influenced the aerodynamic design, research, and development of various flight systems will be mentioned. Author (revised)

N95-15065*# National Aeronautics and Space Administration. Langley Research Center, Hampton, VA.
RESEARCH AND TECHNOLOGY HIGHLIGHTS, 1993
Aug. 1994 264 p Contains NCSA Mosaic window view and access instructions as supplement
(NASA-TM-4575; L-17397; NAS 1.15:4575) Avail: CASI HC A12/MF A03

This report contains highlights of the major accomplishments and applications that have been made by Langley researchers and by our university and industry colleagues during the past year. The highlights illustrate both the broad range of the research and technology activities supported by NASA Langley Research Center and the contributions of this work toward maintaining United States leadership in aeronautics and space research. This report also describes some of the Center's most important research and testing facilities. Author (revised)

SUBJECT INDEX

Typical Subject Index Listing

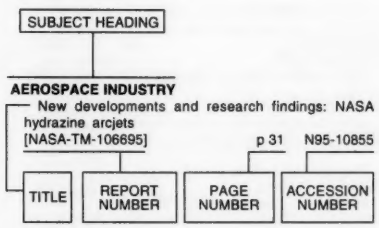

The subject heading is a key to the subject content of the document. Titles, report numbers, and accession numbers of pertinent documents are provided under each subject heading. When the title is insufficiently descriptive of the document content, a title extension is added, separated from the title by three hyphens. The report number helps to indicate the type of document cited (e.g., NASA report, NASA translation, NASA contractor report). The accession number is the number by which the document abstracts are arranged in this journal and by which the document is sold or requested. The page number helps you locate the citation in the abstract section. The titles, with title extensions if present, are arranged under each subject heading in ascending accession number order. The subject headings have been selected from the latest revision of the *NASA Thesaurus*.

A

ABDOMEN
Extended duration orbiter medical project countermeasure to reduce post space flight orthostatic intolerance (LBNP) (STS-50/USML-1)
p 551 N95-14224

ABERRATION
Aberration correction of unstable resonators
[NASA-CASE-NPO-18662-1-CU] p 602 N95-13823

ABLATION
Numerical solution of two-dimensional ablation problems using the finite control volume method with unstructured grids
[DE94-015012] p 428 N95-14664

ABLATIVE MATERIALS
Laser ablation and deposition of alloys
[PB94-191384] p 499 N95-15388

ABSORBENTS
Inelastic neutron scattering and molecular dynamics simulations of water adsorbed in the molecular sieves AlPO4-11, AlPO4-5, AlPO4-8 and VPI-5
[DE94-013337] p 593 N95-13678
Preparation and characterization of composite inorganic zeolite membranes with molecular sieve properties
[PB94-191251] p 450 N95-14151
The growth of zeolites A, X and mordenite in space
p 458 N95-14226
The structure of new synthetic manganese oxide octahedral molecular sieves
[DE94-016348] p 596 N95-15381

ABSORPTION CROSS SECTIONS
Measurements of ultraviolet absorption cross sections of NO2 at various pressures and temperatures
[AD-A283835] p 522 N95-14344

ABSORPTION SPECTRA
Core-level spectroscopy of thin oxides and oxynitrides
[DE94-016598] p 442 N95-15408
The Diffuse Interstellar Bands: Contributed papers
[NASA-CP-10144] p 639 N95-15827
Neutral gas and diffuse interstellar bands in the LMC
p 639 N95-15828
DIBS independent of accretion in T Tauri stars
p 639 N95-15829
Diffuse interstellar bands in reflection nebulae
p 639 N95-15830
Diffuse interstellar bands between 3900 A and 4200 A
p 640 N95-15834
Porphyrins in the interstellar medium (in grains)
p 640 N95-15837
Investigating the 3.3 micron infrared fluorescence from naphthalene following ultraviolet excitation
p 599 N95-15839
Investigation of a laboratory candidate for the carrier of the 4430 A diffuse interstellar band
p 641 N95-15840
Quantum chemistry and excited states: First investigations on pyrene-like molecules
p 599 N95-15844
L(alpha)-induced two-photon absorption of visible light emitted from an O-type star by H2(+) ions located near the surface of the Stromgren sphere surrounding the star: A possible explanation for the diffuse interstellar absorption bands (DIDs) p 641 N95-15845

ABSORPTION SPECTROSCOPY
Infrared absorption spectroscopy and chemical kinetics of free radicals
[DE94-016642] p 438 N95-14392
Core-level spectroscopy of thin oxides and oxynitrides
[DE94-016598] p 442 N95-15408

ABSORPTIVITY
A method of measuring the amplitude-modulated vacuum field near a conducting mirror
p 471 N95-13921

ABSTRACTS
FFCAat Clearinghouse, directory of abstracts
[DE94-015259] p 632 N95-15435

ACCELERATED LIFE TESTS
Hypervelocity Impact Test Facility: A gun for hire
[TABES PAPER 94-605] p 415 N95-14639

ACCELERATION (PHYSICS)
The musculoskeletal and vestibular effects of long term repeated exposure to sustained high-G
[AGARD-AR-317] p 562 N95-14263
Stochastic model of the residual acceleration environment in microgravity p 459 N95-14540

ACCELERATION TOLERANCE
Some genetic aspects of adaptation to hyperdynamic environments p 543 N95-15100
Changing gravity level and the development of animals p 538 N95-15101
Are otoconia dynamic in birds and mammals?
p 538 N95-15103
Vestibular ontogeny: Measuring the influence of the dynamic environment p 544 N95-15105
A mathematical model of the cardiovascular response to +Gz acceleration p 544 N95-15110
Modeling and numerical simulation of the cerebral blood flow under acceleration p 545 N95-15112
The influence of gravity on vestibular nystagmus in humans p 546 N95-15121
Guidelines for a Research and Development (R/D) program for high sustained G p 546 N95-15124
Non-invasive physiological monitoring relevant to G-induced loss of consciousness p 547 N95-15125
Physiological considerations concerning Positive Pressure Breathing (PBG) during +Gz
p 547 N95-15126
Operational requirements for avoidance and eventual elimination of Gz-induced Loss Of Consciousness (G-LOC) in flight p 547 N95-15127
The cardiovascular response to the AGS
p 419 N95-15146
Centrifuges in gravitational physiology research
p 550 N95-15147

ACCELEROMETERS
Results of demonstration test for receiving and processing of flight data from the Space Transportation System
[NASA-CR-194986] p 418 N95-13890
Acceleration recorder and playback module
[NASA-CASE-MSC-22008-1] p 496 N95-14180
Review of European microgravity measurements
p 457 N95-14211
Accelerometer model in APLAC
[PB94-197647] p 497 N95-15413
Test Operation Procedure (TOP): Vibration testing of helicopter equipment
[AD-A284433] p 410 N95-15815

ACCEPTABILITY
High-Speed Research: 1994 Sonic Boom Workshop: Atmospheric Propagation and Acceptability Studies
[NASA-CP-3279] p 401 N95-14878

ACCESS CONTROL
Product life cycle data base, analysis and simulation integration methodology
[TABES PAPER 94-626] p 417 N95-14650

ACCESS TIME
Summary of activities for University of California
[AD-A283890] p 632 N95-15423

ACCRETION DISKS
DIBS independent of accretion in T Tauri stars
p 639 N95-15829

ACETATES
Radical polymerization of vinyl acetate and methyl methacrylate using organochromium initiators complexed with macrocyclic polyamines
[AD-A280828] p 451 N95-14316
Radical polymerization of vinyl acetate in the presence of trialkyl phosphites
[AD-A280829] p 451 N95-14324

ACETYLENE
AEM and HREM evaluation of carbon nanostructures in silica aerogels
[DE94-014913] p 434 N95-14387
Investigation of a laboratory candidate for the carrier of the 4430 A diffuse interstellar band
p 641 N95-15840

ACID RAIN
Oxides of nitrogen: Their formation and control in stationary sources
[AD-A283780] p 522 N95-14337

ACIDITY
Field intercomparison with five automatic ammonia monitors
[PB94-192879] p 523 N95-15389

ACOUSTIC ATTENUATION
Leak detection by acoustic emissions monitoring: An experimental investigation of the acoustic properties of leaks and the attenuation characteristics of soil
[AD-A283250] p 530 N95-15295
Ultrasonic characterization of high T(c) and other unconventional superconductors
[AD-A282835] p 476 N95-15397

ACOUSTIC EMISSION
Leak detection by acoustic emissions monitoring: An experimental investigation of the acoustic properties of leaks and the attenuation characteristics of soil
[AD-A283250] p 530 N95-15295
The modal decomposition of an impedance tube
[AD-A283591] p 591 N95-15320
Leak detection by acoustic emission monitoring. Phase 1: Feasibility study
[AD-A283775] p 493 N95-15332

ACOUSTIC FATIGUE
Simulation of Shuttle launch G forces and acoustic loads using the NASA Ames Research Center 20G centrifuge
p 419 N95-14089

ACOUSTIC FREQUENCIES
Real time system for practical acoustic monitoring of global ocean temperature, volume 3
[AD-A283774] p 535 N95-14335

ACOUSTIC IMPEDANCE
The modal decomposition of an impedance tube
[AD-A283591] p 591 N95-15320

ACOUSTIC LEVITATION
Joint Launch + One Year Science Review of USML-1 and USMP-1 with the Microgravity Measurement Group
[NASA-CP-3272-VOL-1] p 634 N95-14207
Bifurcation of rotating liquid drops: Results from USML-1 experiments in space p 458 N95-14219

Ground based studies of thermocapillary flows in levitated drops p 486 N95-14545

ACOUSTIC MEASUREMENT

Wideband beamforming for a sparse nonuniformly spaced array
[AD-A280833] p 591 N95-14396

ACOUSTIC PROPAGATION

Real time system for practical acoustic monitoring of global ocean temperature, volume 3
[AD-A283774] p 535 N95-14335

On the physics of waves in the solar atmosphere: Wave heating and wind acceleration
[NASA-CR-196992] p 646 N95-15070

ACOUSTIC PROPERTIES

Virtual acoustic displays p 557 N95-14035

Problems in nonlinear acoustics: Surface acoustic waves, diffracting sound beams, and fluid-solid interface effects
[AD-A281714] p 592 N95-15453

ACOUSTIC SCATTERING

The mean acoustic field in layered media with rough interfaces
[AD-A281960] p 590 N95-13683

Atmospheric effects on the risetime and waveshape of sonic booms p 402 N95-14886

ACOUSTIC SIMULATION

NASA LeRC's acoustic fill effect test program and results
[NASA-TM-106688] p 419 N95-13893

ACOUSTIC VELOCITY

Asteroseismology: Theory and phenomenology p 643 N95-14502

Atmospheric propagation at larger lateral distances from the flight track p 402 N95-14885

ACOUSTICS

Modification of the Ames 40- by 80-foot wind tunnel for component acoustic testing for the second generation supersonic transport
[NASA-TM-108850] p 391 N95-13642

The mean acoustic field in layered media with rough interfaces
[AD-A281960] p 590 N95-13683

ACOUSTO-OPTICS

Integrated optical maze
[DE94-015866] p 613 N95-14367

A Lyman-alpha tunable acousto-optic filter for detecting superthermal flare protons
[NASA-CR-197119] p 613 N95-14908

ACQUISITION

Technology access from the FS-X radar program. Lessons for technology transfer and US acquisition policy
[AD-A283773] p 461 N95-14334

ACRYLATES

Radical polymerization of vinyl acetate and methyl methacrylate using organochromium initiators complexed with macrocyclic polyamines
[AD-A280828] p 451 N95-14316

ACTIVATION ENERGY

Electrical characterization of 6H crystalline silicon carbide
[NASA-CR-197047] p 439 N95-14903

Tensile creep strain and activation energy
[AD-A283264] p 513 N95-15620

Chemical kinetics and atmospheric modification
[AD-A283304] p 524 N95-15623

ACTIVE CONTROL

Discrete-layer piezoelectric plate and shell models for active tip-clearance control
[NASA-CR-195383] p 507 N95-14417

Control of unsteady separated flow associated with the dynamic stall of airfoils
[NASA-CR-197024] p 400 N95-14613

Control of selective perception using Bayes nets and decision theory
[TR-468] p 573 N95-15151

ACTIVE GALACTIC NUCLEI

Monitoring the variability of active galactic nuclei from a space-based platform p 644 N95-14509

ACTIVITY (BIOLOGY)

Activity of ornithine decarboxylase in muscle of Japanese quail in hypergravity conditions p 539 N95-15144

ACTIVITY CYCLES (BIOLOGY)

Alterations of body temperature, feeding, drinking and sleep-wake circadian rhythms in Rhesus monkey during a 19 day Spacelab flight simulation p 539 N95-15132

A method for continuous monitoring of the Ground Reaction Force during daily activity p 549 N95-15139

ACTS

Proceedings of the Eighteenth NASA Propagation Experimenters Meeting (NAPEX 18) and the Advanced Communications Technology Satellite (ACTS) Propagation Studies Miniworkshop
[NASA-CR-196959] p 464 N95-14670

ACTS mobile propagation campaign p 465 N95-14677

ACTUATORS

Piezoelectric loudspeaker
[NASA-CASE-LAR-15138-1] p 590 N95-14110

Tactile display device using an electrorheological fluid
[NASA-CASE-LAR-14860-1] p 472 N95-14112

Legged vehicle for underwater mobile operations
[AD-A282891] p 503 N95-15294

High gain GaAs switches for impulse sources: Measurement of the speed of current filaments
[DE94-015281] p 477 N95-15544

Wind-tunnel blockage and actuation systems test of a two-dimensional scramjet inlet unstart model at Mach 6
[NASA-TM-109152] p 495 N95-15898

ADA (PROGRAMMING LANGUAGE)

Ada 9X overview p 570 N95-14166

CIFO 3.0 p 570 N95-14167

ADAPTATION

Psychophysiological aspects of increasing resistance to space motion sickness p 542 N95-15093

Cardiovascular deconditioning effects of long-term simulated weightlessness in rats p 538 N95-15099

Some genetic aspects of adaptation to hyperdynamic environments p 543 N95-15100

Teratogenic effects of delta g: The concept of allometric growth p 538 N95-15102

Behaviour of newly hatched and adult Japanese quail and the feasibility of adaptation to weightlessness p 538 N95-15106

Postural control of fish related to gravity input p 539 N95-15118

Musculoskeletal adaptation to mechanical forces on Earth and in space p 548 N95-15136

Activity of ornithine decarboxylase in muscle of Japanese quail in hypergravity conditions p 539 N95-15144

ADAPTIVE FILTERS

Blocking reduction of Landsat Thematic Mapper JPEG browse images using optimal PSNR estimated spectra adaptive postfiltering p 565 N95-14589

ADAPTIVE OPTICS

Adaptive optics at Lick Observatory: System architecture and operations
[DE94-012387] p 601 N95-13672

Research and development optical deep space antenna sizing study p 463 N95-14628

ADDITIVES

Dynamics of the interface in a model composite system
[AD-A281910] p 433 N95-13655

Development of a moldable, biodegradable polymeric bone repair material
[AD-A283413] p 454 N95-15296

ADHESION

Copolyimides prepared from ODPA, BTDA and 3,4'-ODA
[NASA-CASE-LAR-15109-1] p 449 N95-14109

Poly(arylene ether imidazole) surfacing films for flat and parabolic structures
[NASA-CASE-LAR-14812-1] p 450 N95-14140

ADHESIVE BONDING

Copolyimides prepared from ODPA, BTDA and 3,4'-ODA
[NASA-CASE-LAR-15109-1] p 449 N95-14109

Damage tolerant repair techniques for pressurized aircraft fuselages
[AD-A281982] p 391 N95-14144

Bending effects of unsymmetric adhesively bonded composite repairs on cracked aluminum panels p 507 N95-14456

ADIABATIC EQUATIONS

Studies in chaotic adiabatic dynamics
[DE94-013111] p 627 N95-15578

ADIABATIC FLOW

An application of miniscale experiments on Earth to refine microgravity analysis of adiabatic multiphase flow in space p 459 N95-14567

ADIPOSE TISSUES

20 days bed-rest on insulin action in relation to body fat in young subjects p 549 N95-15145

ADJUSTING

Adjustable bias column end joint assembly
[NASA-CASE-LAR-14899-1] p 459 N95-14111

Adjustable reed for weaving net-shaped tailored fabrics
[NASA-CASE-LAR-15072-1] p 501 N95-14186

ADSORBENTS

Surface Acoustic Wave (SAW) microsensors to monitor multi-component vapor challenges to adsorbents and adsorbent-based air filtration systems
[AD-A284222] p 497 N95-15334

Adsorption and diffusion of fluids in well-characterized adsorbent materials
[DE94-016953] p 454 N95-15344

ADSORPTION

Inelastic neutron scattering and molecular dynamics simulations of water adsorbed in the molecular sieves AlPO4-11, AlPO4-5, AlPO4-8 and VPI-5
[DE94-013337] p 593 N95-13678

Adsorption and diffusion of fluids in well-characterized adsorbent materials
[DE94-016953] p 454 N95-15344

NMR studies of polymers at interfaces
[AD-A281570] p 455 N95-15458

ADVANCED VERY HIGH RESOLUTION RADIOMETER

Compression of regions in the global advanced very high resolution radiometer 1-km data set p 565 N95-14591

Lossless compression of NOAA-AVHRR satellite data p 565 N95-14592

ADVECTION

Point based hydrodynamics applied to shallow water equations
[DE94-016629] p 523 N95-15364

AEROACOUSTICS

NASA LeRC's acoustic fill effect test program and results
[NASA-TM-106688] p 419 N95-13893

Simulation of Shuttle launch G forces and acoustic loads using the NASA Ames Research Center 20G centrifuge p 419 N95-14089

Ultra-high bypass ratio jet noise
[NASA-CR-195394] p 591 N95-14610

Numerical simulation of the SOFIA flowfield
[NASA-CR-197025] p 400 N95-14612

Noise radiation by instability waves in coaxial jets
[NASA-TM-106738] p 591 N95-14618

The aeroacoustics of supersonic coaxial jets
[NASA-TM-106782] p 591 N95-15059

AEROASSIST

Science objectives and performance of a radiometer and window design for atmospheric entry experiments p 429 N95-13718

AERODYNAMIC BALANCE

Free-to-roll tests of X-31 and F-18 subscale models with correlation to flight test results p 394 N95-14237

Static and dynamic force/moment measurements in the Eidetics water tunnel p 395 N95-14238

AERODYNAMIC CHARACTERISTICS

Numerical simulation of the flow about an F-18 aircraft in the high-alpha regime p 394 N95-14232

Fourth High Alpha Conference, volume 2
[NASA-CP-10143-VOL-2] p 395 N95-14239

Building complex simulations rapidly using MATRIX(x): The Space Station redesign
[TABES PAPER 94-632] p 417 N95-14653

Turbulence: Engineering models, aircraft response p 407 N95-14900

Low-speed wind tunnel testing of the NPS and NASA Ames Mach 6 optimized waverider
[AD-A283585] p 404 N95-15319

AERODYNAMIC COEFFICIENTS

Navier-Stokes predictions of missile aerodynamics p 399 N95-14451

Low-speed wind tunnel testing of the NPS and NASA Ames Mach 6 optimized waverider
[AD-A283585] p 404 N95-15319

AERODYNAMIC CONFIGURATIONS

Aerodynamic shape optimization of a HSCT type configuration with improved surface definition
[NASA-CR-197011] p 392 N95-13701

Viper --- Design modification
[NASA-CR-197191] p 408 N95-13703

Fatigue evaluation of empennage, forward wing, and winglets/tip fins on part 23 airplanes
[PB94-196813] p 408 N95-13981

A selection of experimental test cases for the validation of CFD codes, volume 1
[AGARD-AR-303-VOL-1] p 481 N95-14201

Computational aerodynamics based on the Euler equations
[AGARD-AG-325] p 398 N95-14264

AERODYNAMIC DRAG

Scale effects on aircraft and weapon aerodynamics
[AGARD-AG-323] p 393 N95-14103

AERODYNAMIC FORCES

Static and dynamic force/moment measurements in the Eidetics water tunnel p 395 N95-14238

AERODYNAMIC HEATING

Science objectives and performance of a radiometer and window design for atmospheric entry experiments p 429 N95-13718

Thermoacoustic environments to simulate reentry conditions p 426 N95-14096

AERODYNAMIC INTERFERENCE

Lateral jet control for tactical missiles p 399 N95-14448

Propulsion/airframe interference for ducted propfan engines with ground effect
[NASA-CR-197110] p 409 N95-14909

AERODYNAMIC LOADS
Dynamics of the McDonnell-Douglas Large Scale Dynamic Rig and dynamic calibration of the rotor balance
[NASA-TM-108855] p 391 N95-13891
Fatigue evaluation of empennage, forward wing, and winglets/tip fins on part 23 airplanes
[PB94-196813] p 408 N95-13981
Higher harmonic control analysis for vibration reduction of helicopter rotor systems
[NASA-TM-103855] p 391 N95-14419
Extracting a representative loading spectrum from recorded flight data p 410 N95-14469
Pressure measurements on an F/A-18 twin vertical tail in buffeting flow. Volume 2: Steady and unsteady RMS pressure data
[AD-A281581] p 404 N95-15465
Prediction of rotor-blade deformations due to unsteady airloads
[AD-A284467] p 410 N95-15821

AERODYNAMIC STABILITY
Add a dimension to your analysis of the helicopter low airspeed environment
[AD-A283982] p 408 N95-14205
The Aluminum Falcon: A low cost modern commercial transport
[NASA-CR-197180] p 409 N95-15742

AERODYNAMIC STALLING
Control of unsteady separated flow associated with the dynamic stall of airfoils
[NASA-CR-197024] p 400 N95-14613

AERODYNAMICS
A review of 50 years of aerodynamic research with NACA/NASA
[NASA-TM-109163] p 647 N95-13663
Developments in laser-based diagnostics for wind tunnels in the Aeromechanics Division: 1987-1992
[AD-A283011] p 412 N95-13687
VUV shock layer radiation in an arc-jet wind tunnel experiment p 405 N95-13719
Scale effects on aircraft and weapon aerodynamics
[AGARD-AG-323] p 393 N95-14103
Quality assessment for wind tunnel testing
[AGARD-AR-304] p 393 N95-14197
Fourth High Alpha Conference, volume 1
[NASA-CP-10143-VOL-1] p 393 N95-14229
Preparations for flight research to evaluate actuated forebody strakes on the F-18 high-alpha research vehicle p 398 N95-14257
Computational aerodynamics based on the Euler equations
[AGARD-AG-325] p 398 N95-14264
Missile Aerodynamics
[AGARD-R-804] p 399 N95-14445
Aeromechanical design of modern missiles p 399 N95-14446
Engineering Codes for aeroprediction: State-of-the-art and new methods p 399 N95-14447
High angle of attack aerodynamics p 399 N95-14450
Navier-Stokes predictions of missile aerodynamics p 399 N95-14451
Aero-optics system integration
[TABES PAPER 94-604] p 415 N95-14638
The Aluminum Falcon: A low cost modern commercial transport
[NASA-CR-197180] p 409 N95-15742

AEROELASTICITY
User's guide for ENSAERO: A multidisciplinary program for fluid/structural/control interaction studies of aircraft (release 1)
[NASA-TM-108853] p 391 N95-13662
Development and application of structural dynamics analysis capabilities
[NASA-CR-197229] p 513 N95-14922
Linear and nonlinear dynamic analysis of redundant load path bearingless rotor systems
[NASA-CR-197220] p 503 N95-14923
Prediction of rotor-blade deformations due to unsteady airloads
[AD-A284467] p 410 N95-15821

AEROGELS
AEM and HREM evaluation of carbon nanostructures in silica aerogels
[DE94-014913] p 434 N95-14387

AERONAUTICAL ENGINEERING
AGARD highlights 94/2
[AGARD-HIGHLIGHTS-94/2] p 647 N95-13640
Artificial intelligence with applications for aircraft
[DOT/FAA/CT-94/41] p 581 N95-13895
Aeronautical engineering: A continuing bibliography with indexes (supplement 310)
[NASA-SP-7037(310)] p 392 N95-15550

AERONAUTICS
Proceedings of the FAA Inspection Program Area Review
[AD-A283849] p 405 N95-14350
Research and technology highlights, 1993
[NASA-TM-4575] p 647 N95-15065

AEROSOLS
PC-based MIE scattering program for theoretical investigations of the optical properties of atmospheric aerosols as a function of composition and relative humidity
[PB94-192739] p 529 N95-14404
Sensing of radio refractivity and aerosol extinction p 467 N95-14830
Condensation nuclei measurement in the stratosphere for the NASA ACE program
[NASA-CR-197031] p 530 N95-14855
Counting condensation in the Antarctic Ozone Mission
[NASA-CR-197113] p 525 N95-15847

AEROSPACE ENGINEERING
A review of 50 years of aerodynamic research with NACA/NASA
[NASA-TM-109163] p 647 N95-13663
NASA/DOD Aerospace Knowledge Diffusion Research Project. Paper 43: The role of information resource training in aerospace education. Expanded version
[NASA-TM-109981] p 632 N95-14619
NASA/DOD Aerospace Knowledge Diffusion Research Project. Paper 44: Becoming an aerospace engineer: Some thoughts on the career goals and educational preparation of AIAA student members
[NASA-TM-109980] p 632 N95-14870

AEROSPACE ENVIRONMENTS
Selection of solar simulator for solar dynamic ground test
[NASA-TM-106608] p 430 N95-14173
Basic features of the STS/Spacelab vibration environment p 428 N95-14210
The Astroculture (tm)-1 experiment on the USML-1 mission p 564 N95-14228

AEROSPACE INDUSTRY
ASTM E 1559 method for measuring material outgassing/deposition kinetics has applications to aerospace, electronics, and semiconductor industries p 421 N95-14066
Helping small companies commercialize public-sector technology
[TABES PAPER 94-407] p 415 N95-14635
Environmentally sound manufacturing
[TABES PAPER 94-502] p 415 N95-14636
A NASA/industry/university partnership for development of dual-use vibration isolation technology
[TABES PAPER 94-613] p 416 N95-14643
NASA/DOD Aerospace Knowledge Diffusion Research Project. Report 30: Computer-Mediated Communication (CMC) and the communication of technical information in aerospace
[NASA-CR-194973] p 633 N95-15585

AEROSPACE MEDICINE
The effects of autogenic-feedback training on motion sickness severity and heart rate variability in astronauts
[NASA-TM-108840] p 539 N95-13661
Eighteenth Space Simulation Conference: Space Mission Success Through Testing
[NASA-CP-3280] p 420 N95-14062
Development of life sciences equipment for microgravity and hypergravity simulation p 425 N95-14090
Unique life sciences research facilities at NASA Ames Research Center p 426 N95-14091
The applicability of commercial glare test devices in the aeromedical certification of pilot applicants
[DOT/FAA/AM-94/15] p 540 N95-14176
Unreported medications used in incapacitating medical conditions found in fatal civil aviation accidents
[DOT/FAA/AM-94/14] p 540 N95-14177
Joint Launch + One Year Science Review of USML-1 and USMP-1 with the Microgravity Measurement Group
[NASA-CP-3272-VOL-1] p 634 N95-14207
Extended duration orbiter medical project Microbial Air Sampler (STS-50/USML-1) p 458 N95-14222
Extended duration orbiter medical project variability of blood pressure and heart rate (STS-50/USML-1) p 551 N95-14223
Extended duration orbiter medical project countermeasure to reduce post space flight orthostatic intolerance (LBNP) (STS-50/USML-1) p 551 N95-14224
Protein crystal growth results from the United States Microgravity Laboratory-1 mission p 458 N95-14225
Commercial investigation results for the generic bioprocessing apparatus flown on United States Microgravity Laboratory-1 p 538 N95-14227
Naval Aerospace Medical Research Laboratory. 1993 command history
[AD-A284038] p 541 N95-14424
Adaptation of skeletal muscle to spaceflight: Cosmos rhesus project. Cosmos 2044 and 2229
[NASA-CR-197041] p 537 N95-14796
Proposal for an astronaut mass measurement device for the Space Shuttle
[NASA-CR-197198] p 563 N95-14854
The Physiologist, volume 36, number 1, supplement p 541 N95-15089
Gravitational stress and regulation of neuroendocrine elements and fluid volume in humans p 542 N95-15090
Neurohumoral reactions to long-term vestibular stimulation in man p 542 N95-15091
Will man need the vestibular system in generations to come? p 542 N95-15092
Psychophysiological aspects of increasing resistance to space motion sickness p 542 N95-15093
Transesophageal echocardiographic evaluation of baboons during microgravity induced by parabolic flight p 538 N95-15094
Circulatory filling pressures during transient microgravity induced by parabolic flight p 542 N95-15095
Hemodynamic responses to passive body tilts p 542 N95-15096
Cardiovascular response to cold pressor and LBNP tests before and after 20-day-bedrest p 543 N95-15097
Twenty four hours head-down tilt decreases arterial baroreflex function in conscious rat p 538 N95-15098
Cardiovascular deconditioning effects of long-term simulated weightlessness in rats p 538 N95-15099
Some genetic aspects of adaptation to hyperdynamic environments p 543 N95-15100
Changing gravity level and the development of animals p 538 N95-15101
Teratogenic effects of delta g: The concept of allometric growth p 538 N95-15102
Are otoconia dynamic in birds and mammals? p 538 N95-15103
Vestibular ontogeny: Measuring the influence of the dynamic environment p 544 N95-15105
Comparison of hemodynamic and volume responses to different levels of lower body suction and head-up tilt p 544 N95-15107
Body position and volume status as determinants of cardiovascular responses to transition into microgravity in parabolic flight p 544 N95-15108
Cardiovascular and metabolic responses to 6 deg Head-Down Tilt (HDT) and 70 deg Head-Up Tilt (HUT) following exercise p 544 N95-15109
A mathematical model of the cardiovascular response to +Gz acceleration p 544 N95-15110
Effects of 20 days bed-rest on cardio-respiratory functions during sub-maximal exercise in young women p 545 N95-15111
Modeling and numerical simulation of the cerebral blood flow under acceleration p 545 N95-15112
Immune changes in humans concomitant with space flights of up to 10 days duration p 545 N95-15114
Neuronal types in the chicken's statoacoustic ganglion p 539 N95-15116
On-Earth evaluation of the neurovestibular tolerance to centrifuge simulated artificial gravity in humans p 546 N95-15120
The influence of gravity on vestibular nystagmus in humans p 546 N95-15121
The relationship between space sickness and preflight diet p 546 N95-15122
Manipulating the arterial pressure to prevent G-LOC p 546 N95-15123
Guidelines for a Research and Development (R/D) program for high sustained G p 546 N95-15124
Non-invasive physiological monitoring relevant to G-induced loss of consciousness p 547 N95-15125
Physiological considerations concerning Positive Pressure Breathing (PBG) during +Gz p 547 N95-15126
Regional cutaneous microvascular flow responses during gravitational and LBNP stresses p 547 N95-15128
Physiologic mechanisms effecting circulatory and body fluid losses in weightlessness as shown by mathematical modeling p 547 N95-15129
Simulation of the fluid retention effects of a vasopressin analog using the Guyton model of circulation p 547 N95-15130
Transient blood/plasma density and hematocrit effects after passive (sitting) thermoneutral water immersion in men p 548 N95-15131
Alterations of body temperature, feeding, drinking and sleep-wake circadian rhythms in Rhesus monkey during a 19 day Spacelab flight simulation p 539 N95-15132
The regulation of rat activity following exposure to hyperdynamic fields *p 539 N95-15133*
Water intake and urinary volume during 20 days bed-rest in young women p 548 N95-15134

Musculoskeletal adaptation to mechanical forces on Earth and in space p 548 N95-15136
Effects of microgravity on interstitial muscle receptors affecting heart rate and blood pressure during static exercise p 548 N95-15137
Orthostatic stress by lower body negative pressure and its body fluid distribution kinetics under microgravity p 549 N95-15138
A method for continuous monitoring of the Ground Reaction Force during daily activity p 549 N95-15139
Bone geometry, structure and mineral distribution using Dual energy X ray Absorptiometry (DXA) p 549 N95-15140
Influence to organs by ten weeks tail suspension p 539 N95-15142
The cardiovascular response to the AGS p 419 N95-15146
Centrifuges in gravitational physiology research p 550 N95-15147
Enhancement of insulin receptor mediated endocytosis in cultured osteoblastic cells under hypergravity p 539 N95-15148
Isolation of the physiological regulation component of the arterial pressure time variation after postural stresses by a model of the gravitational and arterial kinking effects p 550 N95-15149
A comparison of overall mathematical models of the cardiovascular system for simulating response to orthostatic stresses p 550 N95-15150
Aerospace medicine and biology: A continuing bibliography with indexes (supplement 395)
[NASA-SP-7011(395)] p 550 N95-15304
Collection of real-time, multichannel EEG data from helicopter pilots in flight: A feasibility study
[AD-A284396] p 551 N95-15767

AEROSPACE PLANES
Thermoacoustic environments to simulate reentry conditions p 426 N95-14096
Access to space
[NASA-CR-197153] p 428 N95-14521
Air-breathing aerospace plane development essential: Hypersonic propulsion flight tests
[NASA-TM-108857] p 392 N95-14921

AEROSPACE SCIENCES
Space science in the 1990's and beyond
[TABES PAPER 94-204] p 415 N95-14634

AEROSPACE SYSTEMS
Mechanical system reliability for long life space systems
[NASA-CR-197215] p 505 N95-15584

AEROSPACE TECHNOLOGY TRANSFER
AGARD highlights 94/2
[AGARD-HIGHLIGHTS-94/2] p 647 N95-13640

AEROSPACE VEHICLES
Aerodynamic shape optimization of a HSCT type configuration with improved surface definition
[NASA-CR-197011] p 392 N95-13701
Development and application of structural dynamics analysis capabilities
[NASA-CR-197229] p 513 N95-14922

AEROTHERMOCHEMISTRY
Interaction of chemistry, turbulence, and shock waves in hypervelocity flow
[AD-A282941] p 400 N95-14656

AEROTHERMODYNAMICS
Planetary entry experiments
[NASA-CR-194215] p 644 N95-13717
Science objectives and performance of a radiometer and window design for atmospheric entry experiments p 429 N95-13718
Thermoacoustic environments to simulate reentry conditions p 426 N95-14096
An approximate Riemann solver for thermal and chemical nonequilibrium flows
[NASA-CR-195003] p 492 N95-14912
Laminar and turbulent flow computations of Type 4 shock-shock interference aerothermal loads using unstructured grids
[NASA-CR-195008] p 493 N95-15604

AFFERENT NERVOUS SYSTEMS
Intersensory coordination p 555 N95-14020
Functional participation of the valvula cerebelli on the goldfish dorsal light response p 539 N95-15119

AFRICA
June to September rainfall in the African Sahel: Verification of our 1994 forecasts and an extended range forecast for 1995, 3
[TR-521] p 534 N95-15666

AFTERBURNING
Assessing post-fire combustion of polyurethane
[DE94-011461] p 438 N95-14375

AGGLOMERATION
Powder agglomeration in a microgravity environment
[NASA-CR-197000] p 457 N95-14105

AGING (BIOLOGY)
Age 60 Rule. Part 3: Consolidated database experiments
[DOT/FAA/AM-94/22-PT-3] p 551 N95-13715

AGING (MATERIALS)
Hypervelocity Impact Test Facility: A gun for hire
[TABES PAPER 94-605] p 415 N95-14639

AIR BAG RESTRAINT DEVICES
Bubble dynamics, two-phase flow, and boiling heat transfer in a microgravity environment p 488 N95-14561

AIR BREATHING ENGINES
A graphical user interface for design and analysis of air breathing propulsion systems
[TABES PAPER 94-616] p 411 N95-14645

AIR CONDITIONING EQUIPMENT
Pilot retrofit test of refrigerant R-134a for GDSCC p 456 N95-14629

AIR FILTERS
Surface Acoustic Wave (SAW) microsensors to monitor multi-component vapor challenges to adsorbents and adsorbent-based air filtration systems
[AD-A284222] p 497 N95-15334

AIR FLOW
Transport phenomena in stratified multi-fluid flo w in the presence and absence of gravity p 488 N95-14563

AIR INTAKES
Combustion efficiency in a dual-inlet side-dump ramjet combustor
[AD-A283564] p 411 N95-15329

AIR JETS
Transport phenomena in stratified multi-fluid flo w in the presence and absence of gravity p 488 N95-14563

AIR POLLUTION
Photochemical urban airshed modeling using diagnostic and dynamic meteorological fields
[PB94-176120] p 616 N95-13973
Emerging technology summary: Destruction of organic contaminants in air using advanced ultraviolet flashlamps
[PB94-194479] p 521 N95-14121
Computational modeling issues in next generation air quality models
[PB94-197449] p 521 N95-14122
Study of interferences in ozone UV and chemiluminescence monitors
[PB94-197456] p 521 N95-14123
Oxides of nitrogen: Their formation and control in stationary sources
[AD-A283780] p 522 N95-14337
Test method for the measurement of methanol emissions from stationary sources
[PB94-170297] p 523 N95-15382
Preliminary DIAL model
[DE94-013243] p 469 N95-15583

AIR PURIFICATION
Development and analysis of high-energy corona process for air purification
[DE94-015207] p 524 N95-15432

AIR QUALITY
Photochemical urban airshed modeling using diagnostic and dynamic meteorological fields
[PB94-176120] p 616 N95-13973
Computational modeling issues in next generation air quality models
[PB94-197449] p 521 N95-14122
Field intercomparison with five automatic ammonia monitors
[PB94-192879] p 523 N95-15389

AIR SAMPLING
Extended duration orbiter medical project Microbial Air Sampler (STS-50/USML-1) p 458 N95-14222
Condensation nuclei measurement in the stratosphere for the NASA ACE program
[NASA-CR-197031] p 530 N95-14855
Test method for the measurement of methanol emissions from stationary sources
[PB94-170297] p 523 N95-15382
Results of TSP metals monitoring at McMurdo Station, Antarctica
[DE94-015264] p 524 N95-15455

AIR TRAFFIC CONTROL
Atmospheric and wind modeling for ATC
[NASA-CR-196786] p 532 N95-13725
CTAS data analysis program
[NASA-TM-108842] p 406 N95-14611
Assessment of CTAS ETA prediction capabilities
[NASA-CR-197224] p 497 N95-15728
Groundspeed filtering for CTAS
[NASA-CR-197223] p 497 N95-15785

AIR TRANSPORTATION
Age 60 Rule. Part 3: Consolidated database experiments
[DOT/FAA/AM-94/22-PT-3] p 551 N95-13715

AIR WATER INTERACTIONS
Tidal dynamics and mixing over steep topography
[AD-A283535] p 536 N95-15324
Calculation of movable bed friction factors
[AD-A283529] p 536 N95-15440

AIRBORNE EQUIPMENT
Extracting a representative loading spectrum from recorded flight data p 410 N95-14469

AIRBORNE LASERS
Department of Defense high power laser program guidance
[AD-A282915] p 500 N95-15391

AIRBORNE RADAR
Developments in ground-penetrating radar at LLNL
[DE94-012236] p 554 N95-13671

AIRBORNE/SPACEBORNE COMPUTERS
SODR Memory Control Buffer Control ASIC
[NASA-CR-197001] p 566 N95-14514

AIRCRAFT ACCIDENT INVESTIGATION
Aircraft accident report: Overspeed and loss of power on both engines during descent and power-off emergency, landing Simmons Airlines, Inc., d/b/a, American Eagle Flight 3641, N349SB False River Air Park, New Roads, Lousiana, 1 February 1994
[NTSB/AAR-94/06] p 407 N95-14916

AIRCRAFT ACCIDENTS
AGARD highlights 94/2
[AGARD-HIGHLIGHTS-94/2] p 647 N95-13640
Age 60 Rule. Part 3: Consolidated database experiments
[DOT/FAA/AM-94/22-PT-3] p 551 N95-13715
Unreported medications used in incapacitating medical conditions found in fatal civil aviation accidents
[DOT/FAA/AM-94/14] p 540 N95-14177
Flight in an Adverse Environment
[AGARD-LS-197] p 406 N95-14893
Aircraft accident report: Overspeed and loss of power on both engines during descent and power-off emergency, landing Simmons Airlines, Inc., d/b/a, American Eagle Flight 3641, N349SB False River Air Park, New Roads, Lousiana, 1 February 1994
[NTSB/AAR-94/06] p 407 N95-14916
Annual review of aircraft accident data: US air carrier operations, calendar year 1992
[NTSB/ARC-94/02] p 407 N95-15066

AIRCRAFT ANTENNAS
Spiral microstrip antenna with resistance
[NASA-CASE-LAR-15088-1] p 460 N95-14139

AIRCRAFT COMPARTMENTS
Electromagnetic reverberation characteristics of a large transport aircraft
[AD-A282923] p 411 N95-15392

AIRCRAFT CONFIGURATIONS
Aerodynamic shape optimization of a HSCT type configuration with improved surface definition
[NASA-CR-197011] p 392 N95-13701
Comparison of full-scale, small-scale, and CFD results for F/A-18 forebody slot blowing p 397 N95-14255

AIRCRAFT CONSTRUCTION MATERIALS
High temperature cyclic behaviour of aerospace materials: Room temperature validation tests of Ti-6Al-4V
[AGARD-AR-328] p 506 N95-14198
Thermally stable organic polymers
[AD-A281380] p 451 N95-14363
Residual strength of composites with multiple impact damage
[AD-A284230] p 434 N95-14409
Static strength of riveted joints in Fibre Metal Laminates
[PB94-201472] p 513 N95-15429
The Aluminum Falcon: A low cost modern commercial transport
[NASA-CR-197180] p 409 N95-15742

AIRCRAFT CONTROL
Perceptual and performance consequences of flight in virtual worlds p 558 N95-14043
Fourth High Alpha Conference, volume 1
[NASA-CP-10143-VOL-1] p 393 N95-14229
Comparison of X-31 flight, wind-tunnel, and water-tunnel yawing moment asymmetries at high angles of attack p 394 N95-14234
Parameter identification for X-31A at high angles of attack p 394 N95-14235
Fourth High Alpha Conference, volume 2
[NASA-CP-10143-VOL-2] p 395 N95-14239
X-31 high angle of attack control system performance p 395 N95-14244
Flight test results of the F-16 aircraft modified with the axisymmetric vectoring exhaust nozzle p 396 N95-14245
Flight validation of ground-based assessment for control power requirements at high angles of attack p 396 N95-14246
High angle of attack flying qualities criteria for longitudinal rate command systems p 396 N95-14247

Multi-application controls: Robust nonlinear multivariable aerospace controls applications
p 396 N95-14249
Computing quantitative characteristics of finite-state real-time systems
[AD-A282839] p 412 N95-14343
A SIMULINK environment for flight dynamics and control analysis: Application to the DHC-2 Beaver. Part 1: Implementation of a model library in SIMULINK. Part 2: Nonlinear analysis of the Beaver autopilot
[NONP-NASA-SUPPL-DK-94-2802] p 412 N95-14815

AIRCRAFT DESIGN
Aerodynamic shape optimization of a HSCT type configuration with improved surface definition
[NASA-CR-197011] p 392 N95-13701
Viper --- Design modification
[NASA-CR-197191] p 408 N95-13703
Identification of dynamic systems. Volume 3: Applications to aircraft. Part 2: Nonlinear analysis and manoeuvre design
[AGARD-AG-300-VOL-3-PT-2] p 408 N95-14102
Technology access from the FS-X radar program. Lessons for technology transfer and US acquisition policy
[AD-A283773] p 461 N95-14334
Probabilistic inspection strategies for minimizing service failures p 508 N95-14461
Computational predictive methods for fracture and fatigue p 509 N95-14466
Analysis of small crack behavior for airframe applications p 512 N95-14484
Full-scale testing and analysis of fuselage structure
p 512 N95-14485
Graphical user interface for the NASA FLOPS aircraft performance and sizing code
[NASA-TM-106649] p 408 N95-14604
A SIMULINK environment for flight dynamics and control analysis: Application to the DHC-2 Beaver. Part 1: Implementation of a model library in SIMULINK. Part 2: Nonlinear analysis of the Beaver autopilot
[NONP-NASA-SUPPL-DK-94-2802] p 412 N95-14815
Artificial neural network modeling of damaged aircraft
[AD-A283227] p 409 N95-14849
Research and technology highlights, 1993
[NASA-TM-4575] p 647 N95-15065
More supportable T-38A enhancement study
[AD-A283671] p 392 N95-15331
The F-16 multinational staged improvement program: A case study of risk assessment and risk management
[AD-A281706] p 409 N95-15451
Aeronautical engineering: A continuing bibliography with indexes (supplement 310)
[NASA-SP-7037(310)] p 392 N95-15550
The Aluminum Falcon: A low cost modern commercial transport
[NASA-CR-197180] p 409 N95-15742

AIRCRAFT ENGINES
AGARD highlights 94/2
[AGARD-HIGHLIGHTS-94/2] p 647 N95-13640
Viper --- Design modification
[NASA-CR-197191] p 408 N95-13703
Turbomachinery Design Using CFD
[AGARD-LS-195] p 479 N95-14127
Computational methods for preliminary design and geometry definition in turbomachinery
p 480 N95-14128
Elements of a modern turbomachinery design system
p 480 N95-14129
Designing in three dimensions p 480 N95-14130
The industrial use of CFD in the design of turbomachinery p 480 N95-14133
New methods, new methodology: Advanced CFD in the Snecma turbomachinery design process
p 480 N95-14134
The role of CFD in the design process
p 481 N95-14135
Aero design of turbomachinery components: CFD in complex systems p 481 N95-14136

AIRCRAFT HAZARDS
Flightline aircraft fire incidents and suppression agent effects: Field inquiries and incident analysis
[AD-A284027] p 405 N95-14421
Winter storms research in Canada
p 406 N95-14895
Icing: Accretion, detection, protection
p 406 N95-14897
Heavy rain effects p 407 N95-14899
Aircraft accident report: Overspeed and loss of power on both engines during descent and power-off emergency, landing Simmons Airlines, Inc., d/b/a, American Eagle Flight 3641, N349SB False River Air Park, New Roads, Lousiana, 1 February 1994
[NTSB/AAR-94/06] p 407 N95-14916

AIRCRAFT ICING
Update to the NASA Lewis ice accretion code LEWICE
[NASA-CR-195387] p 481 N95-14295
Winter storms research in Canada
p 406 N95-14895
Icing: Accretion, detection, protection
p 406 N95-14897

AIRCRAFT INDUSTRY
The industrial use of CFD in the design of turbomachinery p 480 N95-14133

AIRCRAFT INSTRUMENTS
Condensation nuclei measurement in the stratosphere for the NASA ACE program
[NASA-CR-197031] p 530 N95-14855

AIRCRAFT LANDING
Perceptual and performance consequences of flight in virtual worlds p 558 N95-14043
Airplane takeoff and landing performance monitoring system
[NASA-CASE-LAR-14745-2-SB] p 412 N95-14415
Assessment of CTAS ETA prediction capabilities
[NASA-CR-197224] p 497 N95-15728

AIRCRAFT MAINTENANCE
Damage tolerant repair techniques for pressurized aircraft fuselages
[AD-A281982] p 391 N95-14144
Proceedings of the FAA Inspection Program Area Review
[AD-A283849] p 405 N95-14350
More supportable T-38A enhancement study
[AD-A283671] p 392 N95-15331

AIRCRAFT MANEUVERS
Comparison of X-31 flight, wind-tunnel, and water-tunnel yawing moment asymmetries at high angles of attack
p 394 N95-14234
X-31 post-stall envelope expansion and tactical utility testing p 395 N95-14242
X-31 high angle of attack control system performance
p 395 N95-14244

AIRCRAFT MODELS
Advanced distributed simulation technology advanced rotary wing aircraft. Study comparing approaches to modeling the ARWA main rotor
[AD-A280824] p 408 N95-14306

AIRCRAFT NOISE
Residents' reactions to long-term sonic boom exposure: Preliminary results p 403 N95-14892

AIRCRAFT PARTS
Advanced method and processing technology for complicated shape airframe part forming
p 410 N95-14486

AIRCRAFT PERFORMANCE
Viper --- Design modification
[NASA-CR-197191] p 408 N95-13703
Scale effects on aircraft and weapon aerodynamics
[AGARD-AG-323] p 393 N95-14103
High Alpha Technology Program (HATP) ground test to flight comparisons p 393 N95-14230
Numerical simulation of the flow about an F-18 aircraft in the high-alpha regime p 394 N95-14232
Comparison of X-31 flight, wind-tunnel, and water-tunnel yawing moment asymmetries at high angles of attack
p 394 N95-14234
Flight validation of ground-based assessment for control power requirements at high angles of attack
p 396 N95-14246
High angle of attack flying qualities criteria for longitudinal rate command systems p 396 N95-14247
Airplane takeoff and landing performance monitoring system
[NASA-CASE-LAR-14745-2-SB] p 412 N95-14415
Aircraft maneuver envelope warning system
[NASA-CASE-ARC-11953-1] p 411 N95-14518
Graphical user interface for the NASA FLOPS aircraft performance and sizing code
[NASA-TM-106649] p 408 N95-14604
Flight in an Adverse Environment
[AGARD-LS-197] p 406 N95-14893
Wind shear and its effects on aircraft
p 407 N95-14898
Heavy rain effects p 407 N95-14899
Turbulence: Engineering models, aircraft response
p 407 N95-14900

AIRCRAFT PILOTS
Age 60 Rule. Part 3: Consolidated database experiments
[DOT/FAA/AM-94/22-PT-3] p 551 N95-13715
Unreported medications used in incapacitating medical conditions found in fatal civil aviation accidents
[DOT/FAA/AM-94/14] p 540 N95-14177
Guidelines for a Research and Development (R/D) program for high sustained G p 546 N95-15124
Collection of real-time, multichannel EEG data from helicopter pilots in flight: A feasibility study
[AD-A284396] p 551 N95-15767
Validation of MMPI scales for personality disorders: A pilot and other aviator study
[AD-A284397] p 553 N95-15768
Aviation Epidemiology Data Register: Gender-specific attrition from the trained US Army aviator cohort of 1988
[AD-A284395] p 551 N95-15810

AIRCRAFT RELIABILITY
A method of calculating the safe fatigue life of compact, highly-stressed components p 509 N95-14464

AIRCRAFT SAFETY
AGARD highlights 94/2
[AGARD-HIGHLIGHTS-94/2] p 647 N95-13640
Risk analysis for the fire safety of airline passengers
[PB94-194065] p 405 N95-14179
The principles of flight test assessment of flight-safety-critical systems in helicopters
[AGARD-AG-300-VOL-12] p 405 N95-14199
Flightline aircraft fire incidents and suppression agent effects: Field inquiries and incident analysis
[AD-A284027] p 405 N95-14421
Flight in an Adverse Environment
[AGARD-LS-197] p 406 N95-14893
Heavy rain effects p 407 N95-14899
Aircraft accident report: Overspeed and loss of power on both engines during descent and power-off emergency, landing Simmons Airlines, Inc., d/b/a, American Eagle Flight 3641, N349SB False River Air Park, New Roads, Lousiana, 1 February 1994
[NTSB/AAR-94/06] p 407 N95-14916
TDWR scan strategy implementation
[AD-A284877] p 534 N95-15749

AIRCRAFT STABILITY
Static and dynamic force/moment measurements in the Eidetics water tunnel p 395 N95-14238

AIRCRAFT STRUCTURES
FAA/NASA International Symposium on Advanced Structural Integrity Methods for Airframe Durability and Damage Tolerance
[NASA-CP-3274-PT-1] p 507 N95-14453
Elastic-plastic models for multi-site damage
p 507 N95-14454
Bending effects of unsymmetric adhesively bonded composite repairs on cracked aluminum panels
p 507 N95-14456
Evaluation of bonded boron/epoxy doublers for commercial aircraft aluminum structures
p 508 N95-14457
Inspecting for widespread fatigue damage: Is partial debonding the key? p 508 N95-14458
Testing and analysis of flat and curved panels with multiple cracks p 508 N95-14460
Probabilistic inspection strategies for minimizing service failures p 508 N95-14461
A method of calculating the safe fatigue life of compact, highly-stressed components p 509 N95-14464
Computational predictive methods for fracture and fatigue p 509 N95-14466
Influence of crack history on the stable tearing behavior of a thin-sheet material with multiple cracks
p 509 N95-14467
Extracting a representative loading spectrum from recorded flight data p 410 N95-14469
The role of fretting corrosion and fretting fatigue in aircraft rivet hole cracking p 510 N95-14470
Fatigue reliability method with in-service inspections
p 505 N95-14475
Nonlinear bulging factor based on R-curve data
p 511 N95-14476
Fracture mechanics validity limits p 511 N95-14480
Challenges for the aircraft structural integrity program
p 410 N95-14481
The effects of pitting on fatigue crack nucleation in 7075-T6 aluminum alloy p 448 N95-14482
Large amplitude nonlinear response of flat aluminum, and carbon fiber plastic beams and plates
[AD-A282440] p 513 N95-15547

AIRCRAFT SURVIVABILITY
Challenge of Future EW System Design
[AGARD-CP-546] p 461 N95-14200
Composite waveform generation for EMP and lightning direct-drive testing
[AD-A284159] p 462 N95-14405
Bibliography of Joint Aircraft Survivability reports and related documents
[AD-A282795] p 409 N95-14840

AIRCRAFT WAKES
Wake turbulence p 405 N95-14894

AIRFOILS
A selection of experimental test cases for the validation of CFD codes, volume 1
[AGARD-AR-303-VOL-1] p 481 N95-14201
Computational aerodynamics based on the Euler equations
[AGARD-AG-325] p 398 N95-14264

Control of unsteady separated flow associated with the dynamic stall of airfoils
[NASA-CR-197024] p 400 N95-14613
Spectral analysis of vortex/free-surface interaction
[AD-A283210] p 492 N95-14658

AIRFRAMES
Evaluation of bonded boron/epoxy doublers for commercial aircraft aluminum structures
p 508 N95-14457
Corrosion and corrosion fatigue of airframe aluminum alloys p 448 N95-14465
Development of the NASA/FLAGRO computer program for analysis of airframe structures p 510 N95-14473
Analysis of small crack behavior for airframe applications p 512 N95-14484
Advanced method and processing technology for complicated shape airframe part forming
p 410 N95-14486

AIRLINE OPERATIONS
Risk analysis for the fire safety of airline passengers
[PB94-194065] p 405 N95-14179

AIRPORT SECURITY
Prototype explosives-detection system based on nuclear-resonance absorption in nitrogen
[DE94-015069] p 442 N95-15387

AIRSPEED
Add a dimension to your analysis of the helicopter low airspeed environment
[AD-A283982] p 408 N95-14205
Groundspeed filtering for CTAS
[NASA-CR-197223] p 497 N95-15785

ALCOHOLS
Low-dose alcohol effects on human behavior and performance: A review of post-1984 research
[DOT/FAA/AM-94/24] p 552 N95-14863
Investigation of syngas interaction in alcohol synthesis catalysts
[DE94-013939] p 442 N95-15386

ALERTNESS
The electrocortical correlates of fluctuating states of attention during vigilance tasks
[NASA-CR-197051] p 552 N95-14864

ALGAE
Design of components for the NASA OCEAN project
[NASA-CR-197207] p 535 N95-14906

ALGEBRA
Schroedinger operators with the q-ladder symmetry algebras p 588 N95-13942
Representation and recognition with algebraic invariants and geometric constraint models
[AD-A282926] p 585 N95-14843

ALGORITHMS
AXAF VETA-I mirror ring focus measurements
[NASA-CR-196145] p 637 N95-13637
An adaptively-refined, Cartesian, cell-based scheme for the Euler and Navier-Stokes equations
[NASA-TM-106754] p 392 N95-13817
Journal of Spacecraft Technology, volume 4, no. 2, July 1994 p 413 N95-13825
Remote programming in INSAT-2A/2B on-board Attitude and Orbit Control Computer (AOCC)
p 413 N95-13827
A vision based attitude and position estimation algorithm for rendezvous and docking p 414 N95-13831
A simulation algorithm for availability computation of a communication satellite constellation
p 414 N95-13832
Efficient bulk-loading of gridfiles
[NASA-CR-194974] p 568 N95-13889
A study of the Invariant Subspace Decomposition Algorithm for banded symmetric matrices
[DE94-013872] p 568 N95-13977
2D regular arrays for a special class of non uniform recurrence equations
[PB94-195633] p 584 N95-13980
Evaluation of sensor placement algorithms for on-orbit identification of space platforms p 425 N95-14088
Performance comparison of token ring protocols for hard-real-time communication p 570 N95-14164
Computational aerodynamics based on the Euler equations
[AGARD-AG-325] p 398 N95-14264
Real time system for practical acoustic monitoring of global ocean temperature, volume 3
[AD-A283774] p 535 N95-14335
The stable and precise motion control for an autonomous mobile robot
[AD-A283776] p 501 N95-14336
Computing quantitative characteristics of finite-state real-time systems
[AD-A282839] p 412 N95-14343
1994 Science Information Management and Data Compression Workshop
[NASA-CP-3277] p 564 N95-14585
Performance of customized DCT quantization tables on scientific data p 564 N95-14586
Radiometric resolution enhancement by lossy compression as compared to truncation followed by lossless compression p 564 N95-14588
Blocking reduction of Landsat Thematic Mapper JPEG browse images using optimal PSNR estimated spectra adaptive postfiltering p 565 N95-14589
Synthetic aperture radar signal data compression using block adaptive quantization p 565 N95-14590
Compression of regions in the global advanced very high resolution radiometer 1-km data set
p 565 N95-14591
The development of lossless data compression technology for remote sensing applications
p 565 N95-14593
Planning/scheduling techniques for VQ-based image compression p 566 N95-14595
The long-term forecast of station view periods
p 419 N95-14621
Convolutional encoding of self-dual block codes (2)
p 462 N95-14623
The Block V Receiver fast acquisition algorithm for the Galileo S-band mission p 463 N95-14627
A trajectory preprocessor for antenna pointing
p 463 N95-14630
Representation and recognition with algebraic invariants and geometric constraint models
[AD-A282926] p 585 N95-14843
On the LU factorization of sequences of identically structured sparse matrices within a distributed memory environment
[AD-A282025] p 578 N95-14953
High performance computational chemistry: Towards fully distributed parallel algorithms
[DE94-014561] p 573 N95-15311
Robust multigrid methods for the steady and unsteady incompressible Navier-Stokes equations in general coordinates
[PB94-195534] p 492 N95-15315
Sequentially t-diagnosable systems
[PB94-205093] p 574 N95-15396
Structured approaches for problems of network design and utilization
[AD-A282925] p 578 N95-15416
A Multiple Divide-and-Conquer (MDC) algorithm for optimal alignments in linear space
[DE94-015457] p 574 N95-15536
Polyhedral approaches for solving 0-1 polynomial programming problems
[AD-A282448] p 575 N95-15549
Vehicle health management using adaptive techniques
[NASA-TM-108472] p 431 N95-15609
Support of Environmental Requirements for Cloud Analysis and Archive (SERCAA): Algorithm descriptions
[AD-A283240] p 534 N95-15614
Fault-tolerance and efficiency in massively parallel algorithms
[AD-A283255] p 579 N95-15617
First results with instance-based state identification for reinforcement learning
[TR-502] p 553 N95-15642
Video transmission for quantized variable bandwidth networks
[AD-A284892] p 470 N95-15750
New algorithms for the reduction of image degradation due to atmospheric turbulence
[AD-A284891] p 615 N95-15772
An algorithm for rezoning particle-in-cell calculations
[DE94-016056] p 619 N95-15774
Density control and on-line labeling problems
[TR-481] p 576 N95-15789
Efficient algorithms for qualitative reasoning about time
[TR-496] p 576 N95-15825
Validation of ERS-1 environmental data products
[NASA-CR-197111] p 517 N95-15848
Learning with incomplete selective perception
[TR-453] p 577 N95-15860

ALIGNMENT
Performance Reports: Mirror alignment system performance prediction comparison between SAO and EKC
[NASA-CR-196013] p 637 N95-14100
A Multiple Divide-and-Conquer (MDC) algorithm for optimal alignments in linear space
[DE94-015457] p 574 N95-15536

ALKALI METALS
Alkali metal Rankine cycle boiler technology challenges and some potential solutions for space nuclear power and propulsion applications
[NASA-TM-106593] p 430 N95-14174
Excimer emission from alkali diatomic and alkaline-earth-noble gas molecules
[AD-A281662] p 596 N95-15446

ALKALIES
Corrosion-resistant coatings for high-temperature high-sulfur-activity applications
[DE94-015155] p 453 N95-14957
Scintillating glass fiber-optic neutron sensors
[DE94-014562] p 613 N95-15312
Excimer emission from alkali diatomic and alkaline-earth-noble gas molecules
[AD-A281662] p 596 N95-15446

ALKALINE EARTH METALS
Excimer emission from alkali diatomic and alkaline-earth-noble gas molecules
[AD-A281662] p 596 N95-15446

ALKANES
Determination of the shear modulus in self-assembled monolayers using quartz resonators
[DE94-013449] p 437 N95-14307

ALKENES
Activity of Ga, In and Cu modified MFI zeolites for amine reactions
[DE94-016532] p 438 N95-14388

ALKYL COMPOUNDS
Laser spectroscopy of combustion intermediates in a supersonic jet expansion
[AD-A283201] p 500 N95-15395

ALL SKY PHOTOGRAPHY
The MOXE x-ray all-sky monitor for Spectrum-X-gamma
[DE94-016064] p 638 N95-14429
Photogrammetric mobile satellite service prediction
p 466 N95-14679

ALLOTROPY
Teratogenic effects of delta g: The concept of allometric growth p 538 N95-15102

ALLOYING
Processing and characterization of mechanically alloyed NiAl-based alloys
[AD-A283959] p 444 N95-14202

ALLOYS
Laser ablation and deposition of alloys
[PB94-191384] p 499 N95-15388

ALPHA PARTICLES
A gate level simulator for alpha-particle-induced transient faults
[AD-A283871] p 474 N95-14355

ALTERNATING CURRENT
Experimental implementation of a robust damped-oscillation control algorithm on a full-sized, two-degree-of-freedom, AC induction motor-driven crane
[DE94-012113] p 501 N95-14005
Fish method: Interaction between AC-machines and switching power converters
[PB94-191210] p 472 N95-14149
Damage analysis of internal faults in flux concentrating permanent magnet motors
[AD-A283883] p 474 N95-14359
Development and analysis of high-energy corona process for air purification
[DE94-015207] p 524 N95-15432

ALTERNATIVES
Tests of a homogeneous Poisson process against clustering and other alternatives
[DE94-015382] p 588 N95-15533

ALTIMETERS
Satellite Laser Ranging in the 1990s: Report of the 1994 Belmont Workshop
[NASA-CP-3283] p 526 N95-14274
Scientific analysis of satellite ranging data
p 517 N95-14275

ALUMINATES
AASERT-93: Electroplating of refractory metals using haloaluminate melts
[AD-A284859] p 447 N95-15744

ALUMINIDES
Processing and characterization of mechanically alloyed NiAl-based alloys
[AD-A283959] p 444 N95-14202
Symposium on Structural Intermetallics: Perspectives on Science and Technology, volume 2
[AD-A283379] p 447 N95-15874
High-temperature corrosion of iron aluminides
[DE94-011505] p 447 N95-15906

ALUMINUM
Direct detection of neutral metal atoms in electron-stimulated desorption: Al from CH3O/Al(111). Velocity distribution and absolute yield
[DE94-014011] p 593 N95-14011
High temperature cyclic behaviour of aerospace materials: Room temperature validation tests of Ti-6Al-4V
[AGARD-AR-328] p 506 N95-14198
Low-speed wind tunnel testing of the NPS and NASA Ames Mach 6 optimized waverider
[AD-A283585] p 404 N95-15319

Large amplitude nonlinear response of flat aluminum, and carbon fiber plastic beams and plates
[AD-A282440] p 513 N95-15547

ALUMINUM ALLOYS
Orientation effects on the measurement and analysis of critical CTOA in an aluminum alloy sheet
[NASA-TM-109153] p 444 N95-13690
New armour materials: Metal matrix composites
[PB94-189131] p 433 N95-14148
High strain rate deformation of NiAl
[DE94-014810] p 445 N95-14439
Microstructurally based model of fatigue initiation and growth p 508 N95-14459
Corrosion and corrosion fatigue of airframe aluminum alloys p 448 N95-14465
Influence of crack history on the stable tearing behavior of a thin-sheet material with multiple cracks p 509 N95-14467
The effects of pitting on fatigue crack nucleation in 7075-T6 aluminum alloy p 448 N95-14482
Modeling time-dependent corrosion fatigue crack propagation in 7000 series aluminum alloys p 448 N95-14483
Coherency strains and coarsening in Ni-Al-Si alloys: An experimental study
[DE94-015020] p 445 N95-14665
X-ray Photoelectron Spectroscopy (XPS), Rutherford Back Scattering (RBS) studies
[NASA-CR-196536] p 439 N95-14867
The effect of specimen geometry on the accuracy of constitutive relations in a superplastic 5083 aluminum alloy
[DE94-014501] p 445 N95-15293
Investigation of dendrite coherency in two commercial Al-Si foundry alloys
[PB94-208238] p 446 N95-15349
Type 304L stainless steel surface microstructure: Performance in hydride storage and acid cleaning
[DE94-014654] p 447 N95-15625

ALUMINUM COATINGS
The realuminizing of the 7-meter-diameter solar simulator collimating mirror p 424 N95-14081

ALUMINUM COMPOUNDS
Adsorption and diffusion of fluids in well-characterized adsorbent materials
[DE94-016953] p 454 N95-15344

ALUMINUM OXIDES
Inelastic neutron scattering and molecular dynamics simulations of water adsorbed in the molecular sieves AlPO4-11, AlPO4-5, AlPO4-8 and VPI-5
[DE94-013337] p 593 N95-13678
Thin composite solid electrolyte film for lithium batteries
[NASA-CASE-NPO-18694-1-CU] p 472 N95-13824

ALUMINUM SILICATES
Relationship between microstructure and efficiency of scintillating glasses
[DE94-014563] p 454 N95-15313

AMBIENCE
Results of TSP metals monitoring at McMurdo Station, Antarctica
[DE94-015264] p 524 N95-15455
Turbulent mixing of the HVOF thermal spray and coating oxidation
[DE94-015414] p 455 N95-15535

AMBIGUITY
Discourse interpretation and the scope of operators
[TR-518] p 586 N95-15595

AMINES
Radical polymerization of vinyl acetate and methyl methacrylate using organochromium initiators complexed with macrocyclic polyamines
[AD-A280826] p 451 N95-14316
Activity of Ga, In and Cu modified MFI zeolites for amine reactions
[DE94-016532] p 438 N95-14388
The transformation of organic amines by transition metal cluster compounds
[DE94-017151] p 441 N95-15346

AMMONIA
Field intercomparison with five automatic ammonia monitors
[PB94-192879] p 523 N95-15389

AMMONIUM COMPOUNDS
Field intercomparison with five automatic ammonia monitors
[PB94-192879] p 523 N95-15389

AMORPHOUS MATERIALS
Nonlinear optical susceptibility of a model guest/host polymeric system as investigated by electro-optics and second harmonic generation
[AD-A283069] p 449 N95-13692
Ion beam synthesis of SiGe alloy layers
[DE94-014958] p 620 N95-14189

AMORPHOUS SEMICONDUCTORS
Small-angle x-ray scattering studies of microvoids in amorphous-silicon-based semiconductors
[DE94-011840] p 520 N95-15406

AMORPHOUS SILICON
Growth mechanisms and characterization of hydrogenated amorphous-silicon-alloy films
[DE94-011842] p 518 N95-14194
In-situ characterization of growth and interfaces in a-Si:H devices
[DE94-011847] p 622 N95-14431
Optimization of transparent and reflecting electrodes for amorphous-silicon solar cells
[DE94-011841] p 520 N95-15355
The effects of spatial location of defect states on the switching characteristics of amorphous and polycrystalline silicon thin film transistors: A numerical simulation using AMPS 2-D
[DE94-013437] p 476 N95-15410
Charge collection in a-Si:H/a-Si(1-x)C(x multilayers photodetectors
[DE94-013107] p 625 N95-15577

AMPLIFICATION
Measurement of very small phase fluctuations by means of the operational approach p 605 N95-13916
Phase properties of multicomponent superposition states in various amplifiers p 605 N95-13923
Quantum amplification and quantum optical tapping with squeezed states and correlated quantum states p 610 N95-13954

AMPLITUDE MODULATION
A method of measuring the amplitude-modulated vacuum field near a conducting mirror p 471 N95-13921

AMPOULES
Cross-effects in microgravity flows p 459 N95-14565

ANALOG CIRCUITS
Theory and implementation of a VLSI stray insensitive switched capacitor composite operational amplifier
[AD-A283536] p 476 N95-15325

ANALOG COMPUTERS
Acceleration recorder and playback module
[NASA-CASE-MSC-22008-1] p 496 N95-14180

ANALOG TO DIGITAL CONVERTERS
Energy and Technology Review, April 1994
[DE94-012133] p 496 N95-13669
A high speed, wide dynamic range digitizer circuit for photomultiplier tubes
[DE94-015187] p 475 N95-15302
Experimental hardware development for a pulsed ultrasonic data collection facility
[AD-A283331] p 615 N95-15872

ANALOGIES
Determination of the similarity theory scaling parameters from the vertical gradients
[AD-A283833] p 533 N95-14340
Comparison of different statistical models of turbulence by similarity methods
[DE94-015326] p 493 N95-15530

ANALYSIS (MATHEMATICS)
Computational analysis of forebody tangential slot blowing p 397 N95-14253
Equilibrium fluid interface behavior under low- and zero-gravity conditions p 484 N95-14534

ANECHOIC CHAMBERS
Modification of the Ames 40- by 80-foot wind tunnel for component acoustic testing for the second generation supersonic transport
[NASA-TM-108850] p 391 N95-13642

ANGLE OF ATTACK
Fourth High Alpha Conference, volume 1
[NASA-CP-10143-VOL-1] p 393 N95-14229
High Alpha Technology Program (HATP) ground test to flight comparisons p 393 N95-14230
Flight and full-scale wind-tunnel comparison of pressure distributions from an F-18 aircraft at high angles of attack --- Conducted in NASA Ames Research Center's 80 by 120 ft wind tunnel p 394 N95-14231
Numerical simulation of the flow about an F-18 aircraft in the high-alpha regime p 394 N95-14232
Hybrid structured/unstructured grid computations for the F/A-18 at high angle of attack p 394 N95-14233
Comparison of X-31 flight, wind-tunnel, and water-tunnel yawing moment asymmetries at high angles of attack p 394 N95-14234
Parameter identification for X-31A at high angles of attack p 394 N95-14235
Validation of the NASA Dryden X-31 simulation and evaluation of mechanization techniques p 394 N95-14236
Fourth High Alpha Conference, volume 2
[NASA-CP-10143-VOL-2] p 395 N95-14239
F-18 high alpha research vehicle: Lessons learned p 395 N95-14240
X-31 high angle of attack control system performance p 395 N95-14244
Flight validation of ground-based assessment for control power requirements at high angles of attack p 396 N95-14246
High angle of attack flying qualities criteria for longitudinal rate command systems p 396 N95-14247
Vista/F-16 Multi-Axis Thrust Vectoring (MATV) control law design and evaluation p 396 N95-14248
Multi-application controls: Robust nonlinear multivariable aerospace controls applications p 396 N95-14249
Combat Agility Management System (CAMS) p 397 N95-14250
Fourth High Alpha Conference, volume 3
[NASA-CP-10143-VOL-3] p 397 N95-14251
Navy and the HARV: High angle of attack tactical utility issues p 397 N95-14252
F/A-18 and F-16 forebody vortex control, static and rotary-balance results p 397 N95-14254
Comparison of full-scale, small-scale, and CFD results for F/A-18 forebody slot blowing p 397 N95-14255
Low-energy pneumatic control of forebody vortices p 398 N95-14256
Preparations for flight research to evaluate actuated forebody strakes on the F-18 high-alpha research vehicle p 398 N95-14257
Integration of a mechanical forebody vortex control system into the F-15 p 398 N95-14258
Engineering Codes for aeroprediction: State-of-the-art and new methods p 399 N95-14447
High angle of attack aerodynamics p 399 N95-14450
Numerical simulation of the flow about the F-18 HARV at high angle of attack
[NASA-CR-197023] p 400 N95-14614

ANGULAR ACCELERATION
Are otoconia dynamic in birds and mammals? p 538 N95-15103

ANGULAR MOMENTUM
Phase-space analysis of charged and optical beam transport: Wigner rotation angle p 606 N95-13927

ANGULAR VELOCITY
Asteroseismology: Theory and phenomenology p 643 N95-14502

ANHYDRIDES
A solvent resistant copolyimide
[NASA-CASE-LAR-15083-1] p 449 N95-14108
Copolyimides prepared from ODPA, BTDA and 3,4'-ODA
[NASA-CASE-LAR-15109-1] p 449 N95-14109

ANIMALS
Blast overpressure studies with animals and man
[AD-A280435] p 540 N95-13971
Some genetic aspects of adaptation to hyperdynamic environments p 543 N95-15100
Changing gravity level and the development of animals p 538 N95-15101

ANIONS
One: Redox chemistry of bimetallic fulvalene complexes. 2: Oligocyclopentadienyl complexes
[DE94-014930] p 443 N95-15667

ANISOTROPIC PLATES
Basic mechanics of laminated composite plates
[NASA-RP-1351] p 436 N95-15763

ANISOTROPY
Convection and morphological stability during directional solidification p 448 N95-14548
Crystal growth and fluid mechanics problems in directional solidification p 486 N95-14550
Carnot-caratheodory spaces seen from within
[PB94-195617] p 586 N95-15412

ANNEALING
Effects of hydrogen annealing, sulfur segregation and diffusion on the cyclic oxidation resistance of superalloys: A review
[NASA-TM-106734] p 444 N95-13667
Study of the long term stability of the effective concentration of ionized space charges (N(sub eff)) of neutron irradiated silicon detectors fabricated by various thermal oxidations
[DE94-013734] p 593 N95-14309
Photoluminescence spectroscopy and Rutherford backscattering channeling evaluation of various capping techniques for rapid thermal annealing of ion-implanted ZnSe
[DE94-016876] p 623 N95-15339
Type 304L stainless steel surface microstructure: Performance in hydride storage and acid cleaning
[DE94-014654] p 447 N95-15625
Low Temperature Grown and Highly Non-Stoichiometric GaAs and Related Materials
[AD-A284898] p 626 N95-15754

ANNIHILATION REACTIONS
Hadronic wavefunctions in light-cone quantization
[DE94-014507] p 622 N95-15308

ANNUAL VARIATIONS
Towards developing an analytical procedure of defining the equatorial electrojet for correcting satellite magnetic anomaly data
[NASA-CR-193621] p 526 N95-14267
The seasonal cycle dependence of temperature fluctuations in the atmosphere
[AD-A283220] p 534 N95-15627
ANNULAR DUCTS
Single-phase heat transfer and pressure drop characteristics of an integral-spine-fin within an annulus
[PB94-194073] p 482 N95-14407
ANNULAR FLOW
Characterization of annular two-phase gas-liquid flows in microgravity p 487 N95-14556
ANNULAR SUSPENSION AND POINTING SYSTEM
Annular Suspension and Pointing System (ASPS) magnetic rotary joint
[NASA-CR-197197] p 502 N95-14907
ANODES
High performance arcjet engines
[NASA-CR-195397] p 430 N95-13697
Practical aspects of corrosion fundamentals
[DE94-015842] p 438 N95-14371
ANOMALIES
Energy flux and hydrogeology of thermal anomalies in the Gulf of Mexico Basin: South Texas example
[DE94-015122] p 530 N95-14956
Meteorological investigation of ozone anomalies during the Arctic Boundary Layer Experiment (ABLE 3A)
[AD-A284494] p 534 N95-15771
ANTARCTIC OCEAN
An analysis of eddy resolving global ocean models in the Southern Ocean
[AD-A283211] p 536 N95-15626
ANTARCTIC REGIONS
From Antarctica to space: Use of telepresence and virtual reality in control of remote vehicles
p 427 N95-14099
Results of TSP metals monitoring at McMurdo Station, Antarctica
[DE94-015264] p 524 N95-15455
An analysis of eddy resolving global ocean models in the Southern Ocean
[AD-A283211] p 536 N95-15626
Counting condensation in the Antarctic Ozone Mission
[NASA-CR-197113] p 525 N95-15847
ANTENNA ARRAYS
Wideband beamforming for a sparse nonuniformly spaced array
[AD-A280833] p 591 N95-14396
Performance comparison AN/FRD-10 versus PUSHER
[AD-A283263] p 469 N95-15619
ANTENNA DESIGN
Measurement and interpretation of crustal deformation rates associated with postglacial rebound
[NASA-CR-196440] p 525 N95-13627
The Telecommunications and Data Acquisition Report
[NASA-CR-196409] p 462 N95-14620
A radio telescope for the calibration of radio sources at 32 gigahertz p 463 N95-14626
Research and development optical deep space antenna sizing study p 463 N95-14628
A trajectory preprocessor for antenna pointing
p 463 N95-14630
Low-Earth-Orbiter resource allocation and capacity planning for the DSN using LEO4CAST
p 419 N95-14632
ANTENNA RADIATION PATTERNS
Earth Observing System (EOS)/Advanced Microwave Sounding Unit-A (AMSU-A) worst-case analysis: Antenna beam pointing
[NASA-CR-197218] p 517 N95-15851
ANTIBODIES
Analysis of electron microscope images: 3-D localization of immuno-markers
[PB94-197977] p 537 N95-13990
ANTIDIURETICS
Simulation of the fluid retention effects of a vasopressin analog using the Guyton model of circulation
p 547 N95-15130
ANTIFERROMAGNETISM
Probing the antiferromagnetic long-range order with Glauber spin states p 609 N95-13951
ANTIREFLECTION COATINGS
What those defects in optical coatings really look like
[DE94-015324] p 614 N95-15529
APERTURES
Laser retroreflector array having cat-eye retroreflectors
[NASA-CASE-GSC-13264-1] p 499 N95-14515
Research and development optical deep space antenna sizing study p 463 N95-14628
Investigation of the coherent synchrotron radiation spectrum as a probe of charge dynamics
[DE94-015340] p 599 N95-15371
APPLICATION SPECIFIC INTEGRATED CIRCUITS
SODR Memory Control Buffer Control ASIC
[NASA-CR-197001] p 566 N95-14514
A high speed, wide dynamic range digitizer circuit for photomultiplier tubes
[DE94-015187] p 475 N95-15302
APPLICATIONS OF MATHEMATICS
Nonlinear and stochastic numerical methods and their applications
[AD-A284863] p 588 N95-14370
APPLICATIONS PROGRAMS (COMPUTERS)
Earth Observing System (EOS)/Advanced Microwave Sounding Unit-A (AMSU-A) software assurance plan
[NASA-CR-196059] p 515 N95-13885
Methodology for the parallel direct solution of finite element systems
[PB94-198009] p 585 N95-13991
Evolutionary Telemetry and Command Processor (TCP) architecture p 420 N95-14162
Formal methods technology transfer: Some lessons learned p 571 N95-14172
Developing molecular dynamics simulation codes using mixed language programming
[DE94-015456] p 571 N95-14190
Thermal structure analyses for CSM testbed (COMET)
[NASA-CR-196998] p 506 N95-14270
Update to the NASA Lewis ice accretion code LEWICE
[NASA-CR-195387] p 481 N95-14295
Analysis of welding-induced residual stresses with the ADINA system
[DE94-015359] p 506 N95-14320
PC-based MIE scattering program for theoretical investigations of the optical properties of atmospheric aerosols as a function of composition and relative humidity
[PB94-192739] p 529 N95-14404
AFOS Terminal Aerodrome Forecast encoding
[PB94-203247] p 533 N95-14410
Development of the NASA/FLAGRO computer program for analysis of airframe structures p 510 N95-14473
Reuseable Objects Software Environment (ROSE): Introduction to Air Force Software Reuse Workshop
[NASA-CR-197017] p 572 N95-14520
Applying CASE technology to the software maintenance life cycle
[TABES PAPER 94-620] p 416 N95-14647
A SIMULINK environment for flight dynamics and control analysis: Application to the DHC-2 Beaver. Part 1: Implementation of a model library in SIMULINK. Part 2: Nonlinear analysis of the Beaver autopilot
[NONP-NASA-SUPPL-DK-94-2802] p 412 N95-14815
Ground wave and diffraction, B p 467 N95-14829
LSENS: A General Chemical Kinetics and Sensitivity Analysis Code for homogeneous gas-phase reactions. Part 1: Theory and numerical solution procedures
[NASA-RP-1328-PT-1] p 440 N95-15056
LSENS: A General Chemical Kinetics and Sensitivity Analysis Code for homogeneous gas-phase reactions. Part 3: Illustrative test problems
[NASA-RP-1330-PT-3] p 440 N95-15057
Using Pro/ENGINEER's (tm) interface module
[DE94-013364] p 574 N95-15384
LSENS, a general chemical kinetics and sensitivity analysis code for homogeneous gas-phase reactions. 2: Code description and usage
[NASA-RP-1329] p 442 N95-15512
The prospects for on-line hybrid coherency protocols on bus-based multiprocessors
[TR-490] p 579 N95-15590
Investigation of Allan variance for determining noise spectral forms with application to microwave radiometry
[NASA-CR-194985] p 516 N95-15727
Assessment of CTAS ETA prediction capabilities
[NASA-CR-197224] p 497 N95-15728
Extension of the BRYNTRN code to monoenergetic light ion beams
[NASA-TP-3472] p 647 N95-15790
Introducing the International Geoid Service
p 516 N95-15792
Enhanced capabilities and updated users manual for axial-flow turbine preliminary sizing code TURBAN
[NASA-CR-195405] p 405 N95-15912
APPROACH CONTROL
Assessment of CTAS ETA prediction capabilities
[NASA-CR-197224] p 497 N95-15728
APPROACH INDICATORS
Spatial awareness comparisons between large-screen, integrated pictorial displays and conventional EFIS displays during simulated landing approaches
[NASA-TP-3467] p 409 N95-14852
APPROXIMATION
CFD methodology and validation for turbomachinery flows p 480 N95-14131
Radiative interactions in multi-dimensional chemically reacting flows using Monte Carlo simulations
[NASA-CR-197012] p 481 N95-14269
Approximate next-to-leading order relation between the low-x F2 scaling violations and the gluon density
[PB94-192283] p 596 N95-15380
Computational methods for PDE's in flow control, superconductivity, fluid flows and other applications
[AD-A282912] p 493 N95-15390
Weighted NP optimization problems: Logical definability and approximation properties
[TR-516] p 587 N95-15596
APTITUDE
The effect of response format on reliability estimates for tacit knowledge scales
[AD-A283547] p 552 N95-15326
AQUEOUS SOLUTIONS
Surfactant-based critical phenomena in microgravity
p 459 N95-14579
ARC DISCHARGES
Conversion of light hydrocarbon gases in metal carbides for production of liquid fuels and chemicals
[DE94-013933] p 439 N95-14435
ARC JET ENGINES
High performance arcjet engines
[NASA-CR-195397] p 430 N95-13697
ARCHITECTURE
Knowledge-based computational approach to architectural precedent analysis
[PB94-191269] p 568 N95-14152
ARCHITECTURE (COMPUTERS)
Advanced distributed simulation technology: Digital Voice Gateway Reference Guide
[AD-A283154] p 460 N95-13696
David Florida Laboratory Thermal Vacuum Data Processing System p 418 N95-14079
Elements of a modern turbomachinery design system
p 480 N95-14129
RICIS Symposium 1992: Mission and Safety Critical Systems Research and Applications
[NASA-CR-196963] p 569 N95-14156
European Workshop Industrical Computer Science Systems approach to design for safety
p 569 N95-14157
MISSION: Mission and Safety Critical Support Environment. Executive overview p 569 N95-14158
Generic architectures for future flight systems
p 567 N95-14159
Architecture for Survivable Systems Processing (ASSP). Technology benefits for Open System Interconnects
p 567 N95-14160
Space Generic Open Avionics Architecture (SGOAA): Overview p 569 N95-14161
Evolutionary Telemetry and Command Processor (TCP) architecture p 420 N95-14162
CAPTIONALS: A computer aided testing environment for the verification and validation of communication protocols p 570 N95-14163
POSIX real-time extensions p 570 N95-14165
Ada 9X overview p 570 N95-14166
DDI, the Data and Dimensions Interface
[DE94-014750] p 522 N95-14317
Department of Defense technical architecture framework for information management. Volume 1: Overview, version 2.0
[AD-A283763] p 631 N95-14327
Department of Defense technical architecture framework for information management. Volume 2: Technical reference model and standards profile summary
[AD-A283764] p 631 N95-14329
Department of Defense technical architecture framework for information management. Volume 3: Architecture concepts and design guidance, version 2.0
[AD-A283765] p 631 N95-14330
Department of Defense technical architecture framework for information management. Volume 4: DOD standards-based architecture planning guide, version 2.0
[AD-A283766] p 631 N95-14331
Department of Defense technical architecture framework for information management. Volume 6: Department of Defense (DOD) goal security architecture, version 2.0
[AD-A283767] p 631 N95-14332
Department of Defense technical architecture framework for information management. Volume 8: Department of Defense HCI style guide, version 2.0
[AD-A283768] p 631 N95-14333
Toward deriving software architectures from quality attributes
[AD-A283827] p 572 N95-14339
Reuseable Objects Software Environment (ROSE): Introduction to Air Force Software Reuse Workshop
[NASA-CR-197017] p 572 N95-14520

An overview of the EOSDIS V0 information management system: Lessons learned from the implementation of a distributed data system p 566 N95-14596
The Network Operations Control Center upgrade task: Lessons learned p 419 N95-14631
Applying CASE technology to the software maintenance life cycle
[TABES PAPER 94-620] p 416 N95-14647
Automated test environment for a real-time control system
[TABES PAPER 94-631] p 417 N95-14652
Structured approaches for problems of network design and utilization
[AD-A282925] p 578 N95-15416
Compiler optimizations for cache locality and coherence
[TR-504] p 586 N95-15589

ARCTIC REGIONS
Meteorological investigation of ozone anomalies during the Arctic Boundary Layer Experiment (ABLE 3A)
[AD-A284494] p 534 N95-15771

ARGON
A theoretical study of 30 to 50 angstrom noble gas heavy ion lithography
[DE94-015262] p 442 N95-15436

ARM (ANATOMY)
Coordination of human upper arm and forearm motion in rapid extensions p 561 N95-14056

ARMATURES
Dual-latching solenoid-actuated valve assembly
[NASA-CASE-MFS-28714-1] p 502 N95-14666

ARMOR
New armour materials: Metal matrix composites
[PB94-189131] p 433 N95-14148
Effect of heat treatment on the microstructure and properties of AerMet (trade name) 100 steel
[AD-A284387] p 447 N95-15807

AROMATIC COMPOUNDS
Poly(arylene ether)s containing pendent ethynyl groups
[NASA-CASE-LAR-15041-1] p 449 N95-13838

ARPA COMPUTER NETWORK
Real time system for practical acoustic monitoring of global ocean temperature, volume 3
[AD-A283774] p 535 N95-14335

ARSENIC
Results of TSP metals monitoring at McMurdo Station, Antarctica
[DE94-015264] p 524 N95-15455

ARTERIES
Extended duration orbiter medical project variability of blood pressure and heart rate (STS-50/USML-1)
p 551 N95-14223
Twenty four hours head-down tilt decreases arterial baroreflex function in conscious rat p 538 N95-15098
Manipulating the arterial pressure to prevent G-LOC
p 546 N95-15123
Operational requirements for avoidance and eventual elimination of Gz-induced Loss Of Consciousness (G-LOC) in flight p 547 N95-15127
Isolation of the physiological regulation component of the arterial pressure time variation after postural stresses by a model of the gravitational and arterial kinking effects p 550 N95-15149

ARTIFICIAL GRAVITY
On-Earth evaluation of the neurovestibular tolerance to centrifuge simulated artificial gravity in humans
p 546 N95-15120
The cardiovascular response to the AGS
p 419 N95-15146

ARTIFICIAL INTELLIGENCE
Remote sensing, processing and transmission of data for an unmanned aerial vehicle
[AD-A283104] p 514 N95-13693
Knowledge-based processing for aircraft flight control
[NASA-CR-194976] p 580 N95-13727
Artificial intelligence with applications for aircraft
[DOT/FAA/CT-94/41] p 581 N95-13895
Knowledge-based computational approach to architectural precedent analysis
[PB94-191269] p 568 N95-14152
Three neural network based sensor systems for environmental monitoring
[DE94-014557] p 522 N95-14195
Artificial neural network modeling of damaged aircraft
[AD-A283227] p 409 N95-14849
Machine intelligence: The key to guidance and control in robotics p 581 N95-14944
Guidance and control for unmanned ground vehicles
p 504 N95-14948
An architecture for intelligent multichip module reliability analysis
[AD-A281574] p 583 N95-15461
On point-based temporal disjointness
[TR-497] p 587 N95-15643
The temporal reasoning systems TimeGraph 1-2
[TR-494-REV] p 584 N95-15786
Intelligence in scientific computing
[AD-A284410] p 584 N95-15811
Efficient algorithms for qualitative reasoning about time
[TR-496] p 576 N95-15825

ARTIFICIAL SATELLITES
Satellite situation report, volume 33, number 2
[NASA-TM-109965] p 428 N95-14510
Optical variability in the equatorial and southeast Pacific
[AD-A283894] p 536 N95-15425

ASCORBIC ACID
Spectrophotometric determination of plutonium-239 based on the spectrum of plutonium 3 chloride
[DE94-015172] p 440 N95-15297

ASPECT RATIO
Field-emitter arrays for RF vacuum microelectronics
[AD-A283549] p 476 N95-15327

ASPHERICITY
Aberration correction of unstable resonators
[NASA-CASE-NPO-18662-1-CU] p 602 N95-13823

ASSAYING
Selection of non-destructive assay methods: Neutron counting or calorimetric assay?
[DE94-016211] p 505 N95-15777

ASSESSMENTS
The F-16 multinational staged improvement program: A case study of risk assessment and risk management
[AD-A281706] p 409 N95-15451

ASTEROIDS
Dynamical properties measurements for asteroid, comet and meteorite material applicable to impact modeling and mitigation calculations
[DE94-014142] p 642 N95-14311

ASTRONAUT TRAINING
The effects of autogenic-feedback training on motion sickness severity and heart rate variability in astronauts
[NASA-TM-108840] p 539 N95-13661

ASTRONAUTS
Extended duration orbiter medical project variability of blood pressure and heart rate (STS-50/USML-1)
p 551 N95-14223
Extended duration orbiter medical project countermeasure to reduce post space flight orthostatic intolerance (LBNP) (STS-50/USML-1)
p 551 N95-14224
Proposal for an astronaut mass measurement device for the Space Shuttle
[NASA-CR-197198] p 563 N95-14854
Gravitational stress and regulation of neuroendocrine elements and fluid volume in humans
p 542 N95-15090
Cardiovascular deconditioning effects of long-term simulated weightlessness in rats p 538 N95-15099
Simulation of the fluid retention effects of a vasopressin analog using the Guyton model of circulation
p 547 N95-15130

ASTRONOMICAL CATALOGS
Twelve-year planetary ephemeris: 1995-2006
[NASA-RP-1349] p 638 N95-14667

ASTRONOMICAL INTERFEROMETRY
Observations of hot stars and eclipsing binaries with FRESIP p 644 N95-14508

ASTRONOMICAL OBSERVATORIES
Adaptive optics at Lick Observatory: System architecture and operations
[DE94-012387] p 601 N95-13672

ASTRONOMICAL PHOTOMETRY
Energy and Technology Review, April 1994
[DE94-012133] p 496 N95-13669
Asteroseismology: Ground based efforts and the need for space observations p 643 N95-14503

ASTRONOMICAL SATELLITES
Space simulation techniques and facilities for SAX STM test campaign p 423 N95-14077
Space based astronomy: Teacher's guide with activities
[NASA-EG-102] p 638 N95-14511

ASTRONOMICAL SPECTROSCOPY
Observations of hot stars and eclipsing binaries with FRESIP p 644 N95-14508
Space based astronomy: Teacher's guide with activities
[NASA-EG-102] p 638 N95-14511

ASTRONOMY
Space based astronomy: Teacher's guide with activities
[NASA-EG-102] p 638 N95-14511
The Bureau Gravimetrique International
p 516 N95-15795
The Diffuse Interstellar Bands: Contributed papers
[NASA-CP-10144] p 639 N95-15827
Diffuse interstellar bands in reflection nebulae
p 639 N95-15830
On the affinities of lambda 5778 and other broad diffuse interstellar bands p 639 N95-15832
Diffuse interstellar bands between 3900 A and 4200 A
p 640 N95-15834
Formation of dust grains with impurities in red giant winds p 641 N95-15841
A bibliography of papers on the diffuse interstellar bands p 634 N95-15846

ASTROPHYSICS
Astrophysical science with a spaceborne photometric telescope
[NASA-CP-10148] p 643 N95-14499
Stellar activity: Astrophysics relevant to global change
p 643 N95-14500
Asteroseismology: Ground based efforts and the need for space observations p 643 N95-14503
Space based astronomy: Teacher's guide with activities
[NASA-EG-102] p 638 N95-14511
A bibliography of papers on the diffuse interstellar bands p 634 N95-15846

ASYMMETRY
Low-energy pneumatic control of forebody vortices
p 398 N95-14256
Variable metric conjugate gradient methods
[DE94-014796] p 585 N95-14381

ASYMPTOTIC METHODS
Nonlinear asymptotic integration algorithms for one-dimensional autonomous dissipative first-order ODEs
[NASA-TM-106780] p 585 N95-14300
Mathematical problems of nonlinear wave propagation and of waves in heterogeneous media
[AD-A282217] p 492 N95-14605

ASYMPTOTIC PROPERTIES
Flow-radiated noise. Study of the propagative spectral range of the wall pressure field
[PB94-201290] p 590 N95-13985
Dynamics on the attractor for the complex Ginzburg-Landau equation
[DE94-016902] p 586 N95-15342

ASYMPTOTIC SERIES
The Stokes line width and uncertainty relations
p 589 N95-13935
Numerical solution of a tunneling equation
[DE94-015514] p 586 N95-15538

ATMOSPHERIC & OCEANOGRAPHIC INFORM SYS
Modern methods in meteorological and oceanographic data acquisition and analyses
[AD-A283038] p 533 N95-14848

ATMOSPHERIC ATTENUATION
PC-based MIE scattering program for theoretical investigations of the optical properties of atmospheric aerosols as a function of composition and relative humidity
[PB94-192739] p 529 N95-14404
Propagation characteristics of 20/30 GHz links with a 40 deg masking angle p 464 N95-14672
Propagation data at 20/40 GHz and the propagation needs of Milstar p 465 N95-14673
Channel characterisation for future Ka-band Mobile Satellite Systems and preliminary results
p 465 N95-14676
Radiometer calibration procedure and beacon attenuation estimation reference level
p 466 N95-14683
Troposcatter at the KU band
[AD-A281575] p 469 N95-15462

ATMOSPHERIC BOUNDARY LAYER
Determination of the similarity theory scaling parameters from the vertical gradients
[AD-A283833] p 533 N95-14340
An experimental and numerical study of the modifications of mixed-layer structure by inhomogeneous surface fluxes and secondary circulations
[DE94-015945] p 529 N95-14428
Meteorological investigation of ozone anomalies during the Arctic Boundary Layer Experiment (ABLE 3A)
[AD-A284494] p 534 N95-15771

ATMOSPHERIC CHEMISTRY
Venusian atmospheric equilibrium chemistry at the Pioneer Venus anomalous event altitude
p 645 N95-13721
Photochemical urban airshed modeling using diagnostic and dynamic meteorological fields
[PB94-176120] p 616 N95-13973
Computational modeling issues in next generation air quality models
[PB94-197449] p 521 N95-14122
Oxides of nitrogen: Their formation and control in stationary sources
[AD-A283780] p 522 N95-14337

ATMOSPHERIC CIRCULATION
Atmospheric and wind modeling for ATC
[NASA-CR-196786] p 532 N95-13725

Short term teleconnections associated with western Pacific tropical cyclones
[AD-A284032] p 533 N95-14423
An experimental and numerical study of the modifications of mixed-layer structure by inhomogeneous surface fluxes and secondary circulations
[DE94-015945] p 529 N95-14428
The seasonal cycle dependence of temperature fluctuations in the atmosphere
[AD-A283220] p 534 N95-15627
Meteorological investigation of ozone anomalies during the Arctic Boundary Layer Experiment (ABLE 3A)
[AD-A284494] p 534 N95-15771

ATMOSPHERIC COMPOSITION
Venusian atmospheric equilibrium chemistry at the Pioneer Venus anomalous event altitude
p 645 N95-13721
A facility to produce an energetic, ground state atomic oxygen beam for the simulation of the Low-Earth Orbit environment p 422 N95-14072
Effects of hydrometeors and atmospheric gases at SHF/EHF p 468 N95-14835
Counting condensation in the Antarctic Ozone Mission
[NASA-CR-197113] p 525 N95-15847

ATMOSPHERIC DIFFUSION
Pilot retrofit test of refrigerant R-134a for GDSCC
p 456 N95-14629

ATMOSPHERIC EFFECTS
Basic features of the STS/Spacelab vibration environment p 428 N95-14210
Engineer's Refractive Effects Prediction System (EREPS), version 3.0
[AD-A283748] p 461 N95-14345
Propagation characteristics of 20/30 GHz links with a 40 deg masking angle p 464 N95-14672
High-Speed Research: 1994 Sonic Boom Workshop: Atmospheric Propagation and Acceptability Studies
[NASA-CP-3279] p 401 N95-14878
Atmospheric effects on the risetime and waveshape of sonic booms p 402 N95-14886
Simple atmospheric perturbation models for sonic-boom-signature distortion studies
p 402 N95-14888
Technical report series on global modeling and data assimilation. Volume 3: An efficient thermal infrared radiation parameterization for use in general circulation models
[NASA-TM-104606-VOL-3] p 531 N95-15745
New algorithms for the reduction of image degradation due to atmospheric turbulence
[AD-A284891] p 615 N95-15772

ATMOSPHERIC ELECTRICITY
Produce documents and media information
[NASA-CR-196521] p 532 N95-14271

ATMOSPHERIC ENTRY
Planetary entry experiments
[NASA-CR-194215] p 644 N95-13717
Science objectives and performance of a radiometer and window design for atmospheric entry experiments
p 429 N95-13718
Measured and calculated spectral radiation from a blunt body shock layer in an arc-jet wind tunnel
[AIAA PAPER 94-0086] p 405 N95-13720

ATMOSPHERIC GENERAL CIRCULATION MODELS
An experimental and numerical study of the modifications of mixed-layer structure by inhomogeneous surface fluxes and secondary circulations
[DE94-015945] p 529 N95-14428
Technical report series on global modeling and data assimilation. Volume 3: An efficient thermal infrared radiation parameterization for use in general circulation models
[NASA-TM-104606-VOL-3] p 531 N95-15745

ATMOSPHERIC MODELS
Atmospheric and wind modeling for ATC
[NASA-CR-196786] p 532 N95-13725
Photochemical urban airshed modeling using diagnostic and dynamic meteorological fields
[PB94-176120] p 616 N95-13973
Analysis of deep convective clouds and their association with non-migrating atmospheric diurnal tides in the tropical troposphere
[PB94-187457] p 526 N95-13974
Computational modeling issues in next generation air quality models
[PB94-197449] p 521 N95-14122
Remote sensing strategy at the first atmospheric radiation measurement field site
[DE94-015091] p 522 N95-14187
DDI, the Data and Dimensions Interface
[DE94-014750] p 522 N95-14317
ADCIRC: An advanced three-dimensional circulation model for shelves, coasts, and estuaries. Report 4: Hurricane storm surge modeling using large domains
[AD-A283868] p 535 N95-14352
Propagation Modelling and Decision Aids for Communications, Radar and Navigation Systems
[AGARD-LS-196] p 466 N95-14825
Propagation in the ionosphere, A p 466 N95-14826
Propagation in the ionosphere, B p 467 N95-14827
Ground wave and diffraction, A p 467 N95-14828
Sensing of radio refractivity and aerosol extinction
p 467 N95-14830
Refractive effects from VHF to EHF. Part B: Propagation models p 467 N95-14832
Electro-optics: Propagation from IR to UV and sensor considerations. Part A: Propagation theory
p 467 N95-14833
Electro-optics: Propagation from IR to UV and sensor considerations. Part B: Tools for exploitation of propagation conditions and system range performance
p 467 N95-14834
Simple atmospheric perturbation models for sonic-boom-signature distortion studies
p 402 N95-14888
Integrated science model for assessment of climate change
[DE94-016363] p 523 N95-15361
Preliminary DIAL model
[DE94-013243] p 469 N95-15583
Support of Environmental Requirements for Cloud Analysis and Archive (SERCAA): Algorithm descriptions
[AD-A283240] p 534 N95-15614
Progress report on terrestrial model development (TERRA and HABITAT): Research in support of the CERES earth system modeling project
[DE94-016362] p 524 N95-15779
The operational forecasting/nowcasting of precipitation type in the southeastern United States type of precipitation: Descriptive and objective guidance
[AD-A284456] p 535 N95-15819
Development and testing of a high-resolution model for tropospheric sulfate driven by observation-derived meteorology
[DE94-014910] p 525 N95-15864

ATMOSPHERIC MOISTURE
Measurements of upper tropospheric moisture with a Raman lidar
[DE94-015748] p 531 N95-15411

ATMOSPHERIC RADIATION
Remote sensing strategy at the first atmospheric radiation measurement field site
[DE94-015091] p 522 N95-14187

ATMOSPHERIC SCATTERING
PC-based MIE scattering program for theoretical investigations of the optical properties of atmospheric aerosols as a function of composition and relative humidity
[PB94-192739] p 529 N95-14404

ATMOSPHERIC SOUNDING
High-spatial-resolution passive microwave sounding systems
[NASA-CR-197131] p 531 N95-15586

ATMOSPHERIC TEMPERATURE
Earth Observing System (EOS)/Advanced Microwave Sounding Unit-A (AMSU-A): Calibration management plan
[NASA-CR-189376] p 515 N95-13704
Simple atmospheric perturbation models for sonic-boom-signature distortion studies
p 402 N95-14888
Water vapor and temperature inversions near the 0 C level over the tropical western Pacific
[AD-A282023] p 533 N95-14952
Ru2Ge3: Crystal growth and some properties
[DE94-015360] p 625 N95-15531
High-spatial-resolution passive microwave sounding systems
[NASA-CR-197131] p 531 N95-15586
Nowcasting convective storm evolution in east-central Florida using satellite and Doppler radar data
[AD-A283260] p 534 N95-15618

ATMOSPHERIC TIDES
Analysis of deep convective clouds and their association with non-migrating atmospheric diurnal tides in the tropical troposphere
[PB94-187457] p 526 N95-13974

ATMOSPHERIC TURBULENCE
Fine structure of transient waves in a random medium: The correlation and spectral density functions
p 401 N95-14882
Numerical model for the weakly nonlinear propagation of sound through turbulence p 401 N95-14883
Sonic boom interaction with turbulence
p 402 N95-14884
Atmospheric effects on the risetime and waveshape of sonic booms p 402 N95-14886
The effect of aircraft speed on the penetration of sonic boom noise into a flat ocean p 402 N95-14887
Simple atmospheric perturbation models for sonic-boom-signature distortion studies
p 402 N95-14888
Turbulence: Engineering models, aircraft response
p 407 N95-14900
New algorithms for the reduction of image degradation due to atmospheric turbulence
[AD-A284891] p 615 N95-15772

ATOMIC BEAMS
Small UHV compatible hyperthermal oxygen atom generator
[NASA-CAS-LAR-14674-1] p 503 N95-15601

ATOMIC EXCITATIONS
How to detect an excited atom without disturbing it or how to locate a super-mine without exploding it
p 598 N95-13934
Causality problems for Fermi's two-atom system
p 598 N95-13945

ATOMIC FORCE MICROSCOPY
Atomic Oxygen (ATOX) simulation of Teflon FEP and Kapton H surfaces using a high intensity, low energy, mass selected, ion beam facility p 422 N95-14073
Atomic force microscopy of the electrochemical nucleation and growth of molecular crystals
[AD-A280958] p 622 N95-14601
What those defects in optical coatings really look like
[DE94-015324] p 614 N95-15529

ATOMIC INTERACTIONS
Excimer emission from alkali diatomic and alkaline-earth-noble gas molecules
[AD-A281662] p 596 N95-15446

ATOMIC PHYSICS
How to detect an excited atom without disturbing it or how to locate a super-mine without exploding it
p 598 N95-13934
Correlated quadratures of resonance fluorescence and the generalized uncertainty relation p 598 N95-13937
Causality problems for Fermi's two-atom system
p 598 N95-13945
The atom-atom potential in pressure-broadened line width calculations for XY2-AB: New expressions in the II(R), II(L), and I(R) representations
[AD-A282011] p 595 N95-14950

ATOMIC SPECTRA
Measured and calculated spectral radiation from a blunt body shock layer in an arc-jet wind tunnel
[AIAA PAPER 94-0086] p 405 N95-13720

ATOMIC STRUCTURE
Electron spin resonance and band electronic structure study of the metal-insulator transition in (BEDT-TTF)3(HSO4)2
[DE94-014005] p 620 N95-14009
Relativistic configuration-interaction calculation of the correlation energies of heliumlike ions
[DE94-015190] p 621 N95-14325
Magnetic field dependent photoluminescence studies of InGaAs/GaAs strained-single-quantum wells
[DE94-015774] p 621 N95-14342
Polarized photomodulated reflectivity and photoluminescence studies of ordered InGaP2 under pressure
[DE94-016556] p 621 N95-14390
Surface spectroscopic studies of high-temperature superconductors
[PB94-191228] p 624 N95-15378
Introduction to muSR: What, how, where
[PB94-192267] p 596 N95-15379
Cluster studies of La2CuO4: Local geometric distortions
[DE94-016203] p 626 N95-15776

ATOMIZERS
Combustion efficiency in a dual-inlet side-dump ramjet combustor
[AD-A283564] p 411 N95-15329

ATOMIZING
The breakup of a liquid jet at microgravity
p 484 N95-14535

ATOMS
Squeezed light from multi-level closed-cycling atomic systems p 598 N95-13920
General properties of quantum optical systems in a strong field limit p 609 N95-13950
Quantum noise limits to matter-wave interferometry
p 598 N95-13955
Bloch vector projection noise p 610 N95-13956
ENDL type formats for the LLNL Evaluated Atomic Data Library, EADL, for the Evaluated Electron Data Library, EEDL, and for the Evaluated Photon Data Library, EPDL
[DE94-016487] p 594 N95-14385

ATROPHY
Adaptation of skeletal muscle to spaceflight: Cosmos rhesus project. Cosmos 2044 and 2229
[NASA-CR-197041] p 537 N95-14796
Influence to organs by ten weeks tail suspension
p 539 N95-15142

Relationship between hind-limb muscle atrophy and serum enzymes in tail suspended rats
p 539 N95-15143

ATTENTION
The electrocortical correlates of fluctuating states of attention during vigilance tasks
[NASA-CR-197051] p 552 N95-14864
Perception of auditory events: Attentional limitations
[AD-A284399] p 553 N95-15770

ATTITUDE (INCLINATION)
Star sensor for Indian Remote Sensing Satellite (IRS 1C)
p 413 N95-13828
A vision based attitude and position estimation algorithm for rendezvous and docking
p 414 N95-13831
Photon statistics of a two-mode squeezed vacuum
p 598 N95-13909
Tilting wind tunnel for fire behavior studies
[PB94-204625] p 413 N95-14513
Building complex simulations rapidly using MATRIX(x): The Space Station redesign
[TABES PAPER 94-632] p 417 N95-14653
Hemodynamic responses to passive body tilts
p 542 N95-15096
Twenty four hours head-down tilt decreases arterial baroreflex function in conscious rat
p 538 N95-15098
Comparison of hemodynamic and volume responses to different levels of lower body suction and head-up tilt
p 544 N95-15107
Cardiovascular and metabolic responses to 6 deg Head-Down Tilt (HDT) and 70 deg Head-Up Tilt (HUT) following exercise
p 544 N95-15109
Regional cutaneous microvascular flow responses during gravitational and LBNP stresses
p 547 N95-15128
A comparison of overall mathematical models of the cardiovascular system for simulating response to orthostatic stresses
p 550 N95-15150

ATTITUDE CONTROL
Three-axis stabilization of spacecraft using parameter-independent nonlinear quaternion feedback
[NASA-TM-109150] p 420 N95-13729
Journal of Spacecraft Technology, volume 4, no. 2, July 1994
p 413 N95-13825
Remote programming in INSAT-2A/2B on-board Attitude and Orbit Control Computer (AOCC)
p 413 N95-13827
A vision based attitude and position estimation algorithm for rendezvous and docking
p 414 N95-13831
Neural networks: Alternatives to conventional techniques for automatic docking
[TABES PAPER 94-627] p 417 N95-14651

ATTITUDE STABILITY
Three-axis stabilization of spacecraft using parameter-independent nonlinear quaternion feedback
[NASA-TM-109150] p 420 N95-13729
Basic features of the STS/Spacelab vibration environment
p 428 N95-14210

AUDIO EQUIPMENT
Virtual acoustic displays
p 557 N95-14035

AUDIO SIGNALS
S-Band propagation measurements
p 466 N95-14682

AUDIOMETRY
Monitoring audiometry in hearing conservation programs
[AD-A282024] p 540 N95-14145

AUDITORY DEFECTS
Monitoring audiometry in hearing conservation programs
[AD-A282024] p 540 N95-14145

AUDITORY PERCEPTION
Auditory interfaces: The human perceiver
p 554 N95-14015
Binaural room simulation
p 561 N95-14053
Improving transient signal synthesis through noise modeling and noise removal
[AD-A281677] p 592 N95-15448
Perception of auditory events: Attentional limitations
[AD-A284399] p 553 N95-15770

AUDITORY STIMULI
Auditory interfaces: The human perceiver
p 554 N95-14015
Perception of auditory events: Attentional limitations
[AD-A284399] p 553 N95-15770

AUGER SPECTROSCOPY
X-ray Photoelectron Spectroscopy (XPS), Rutherford Back Scattering (RBS) studies
[NASA-CR-196536] p 439 N95-14867

AUGMENTATION
The console password feature for DEC workstations
[DE94-015721] p 566 N95-14338
High performance computational chemistry: Towards fully distributed parallel algorithms
[DE94-014561] p 573 N95-15311

AURORAL IONIZATION
Study of auroral dynamics with combined spacecraft and incoherent scatter radar data
[NASA-CR-196974] p 526 N95-13818

AURORAS
Ultrasensitive infrared chemiluminescence detection
[AD-A283531] p 440 N95-14958
Dynamics Explorer 1, retarding ion mass spectrometer summary spectrograms: 82/001 to 82/109 spin-time spectrograms for H(+), He(+), O(+), N(+), O(++), M/Z=2, and molecular ions
[NASA-TM-108468] p 443 N95-15607
Dynamics Explorer 1: Energetic Ion Composition Spectrometer (EICS)
[NASA-CR-189375] p 619 N95-15758

AUTOMATA THEORY
On accessing and hiding information
p 587 N95-15641
Connections among space-bounded and multihead probabilistic automata
[TR-476] p 575 N95-15645
Upward separation for FewP and related classes
[TR-488] p 575 N95-15721

AUTOMATIC CONTROL
Telerobotics in the deep ocean
p 504 N95-14026
Guidance and control for unmanned ground vehicles
p 504 N95-14948
Steering capaciflector sensor
[NASA-CASE-GSC-13489-1] p 583 N95-15598

AUTOMATIC PILOTS
A SIMULINK environment for flight dynamics and control analysis: Application to the DHC-2 Beaver. Part 1: Implementation of a model library in SIMULINK. Part 2: Nonlinear analysis of the Beaver autopilot
[NONP-NASA-SUPPL-DK-94-2802] p 412 N95-14815

AUTOMATION
Automated cleaning of electronic components
[DE94-014122] p 476 N95-15356

AUTOMOBILE FUELS
Addendum: Tenth International Symposium on Alcohol Fuels, The Road to Commercialization
[DE93-018219] p 457 N95-14003

AUTOMOBILES
Minutes of the Third Annual Workshop on Chromate Replacements in Light Metal Finishing
[DE94-015163] p 446 N95-15368

AUTONOMIC NERVOUS SYSTEM
Cardiovascular response to cold pressor and LBNP tests before and after 20-day-bedrest
p 543 N95-15097
Comparison of hemodynamic and volume responses to different levels of lower body suction and head-up tilt
p 544 N95-15107

AUTONOMOUS NAVIGATION
Advanced Guidance and Control Aspects in Robotics
[AGARD-LS-193] p 581 N95-14942
Guidance and control for unmanned ground vehicles
p 504 N95-14948

AUTONOMOUS SPACECRAFT CLOCKS
Properties of nearly perfect crystals at very low temperatures
[NASA-CR-197221] p 627 N95-15823

AUTONOMY
The stable and precise motion control for an autonomous mobile robot
[AD-A283776] p 501 N95-14336

AVALANCHE DIODES
Design of reliable high voltage avalanche transistor pulsers
[DE94-015323] p 473 N95-14261
Receiver design, performance analysis, and evaluation for space-borne laser altimeters and space-to-space laser ranging systems
[NASA-CR-197050] p 499 N95-14901

AVIATION METEOROLOGY
AFOS Terminal Aerodrome Forecast encoding
[PB94-203247] p 533 N95-14410
Flight in an Adverse Environment
[AGARD-LS-197] p 406 N95-14893
Winter storms research in Canada
p 406 N95-14895

AVIATION PSYCHOLOGY
Validation of MMPI scales for personality disorders: A pilot and other aviator study
[AD-A284397] p 553 N95-15768

AVIONICS
Artificial intelligence with applications for aircraft
[DOT/FAA/CT-94/41] p 581 N95-13895
Technical Revue Thomson-CSF, volume 26, no. 1, March 1994. Flat panels for visualisation
[PB94-197969] p 410 N95-13984
Space Generic Open Avionics Architecture (SGOAA): Overview
p 569 N95-14161
Strategic avionics technology definition studies, power voter redundancy management. Power voter applications in new vehicle architectures
[NASA-CR-197049] p 411 N95-14799
Electromagnetic reverberation characteristics of a large transport aircraft
[AD-A282923] p 411 N95-15392

AXIAL COMPRESSION LOADS
Analytical tripping loads for stiffened plates
[AD-A284368] p 514 N95-15805

AXIAL FLOW TURBINES
Wind/hybrid power system test facilities in the United States and Canada
[DE94-006930] p 519 N95-15290
Enhanced capabilities and updated users manual for axial-flow turbine preliminary sizing code TURBAN
[NASA-CR-195405] p 405 N95-15912

AXISYMMETRIC BODIES
Evaluation of energy-sink stability criteria for dual-spin spacecraft
[AD-A283228] p 428 N95-14850

AXISYMMETRIC FLOW
The flow induced by the coalescence of two initially stationary drops
[NASA-TM-106752] p 478 N95-13653
Numerical simulation of shock-induced combustion past blunt bodies using shock-fitting technique
[NASA-CR-197013] p 437 N95-14268

AZIMUTH
Add a dimension to your analysis of the helicopter low airspeed environment
[AD-A283982] p 408 N95-14205

AZOLES
Fluorescent compounds for plastic scintillation applications
[DE94-013235] p 497 N95-15580

B

B STARS
Diffuse interstellar bands between 3900 A and 4200 A
p 640 N95-15834
ROSAT observations of the binary Be-star and radio pulsar PSR1259-63
[NASA-CR-196951] p 642 N95-15907

BABOONS
Transesophageal echocardiographic evaluation of baboons during microgravity induced by parabolic flight
p 538 N95-15094
Circulatory filling pressures during transient microgravity induced by parabolic flight
p 542 N95-15095

BACK INJURIES
The musculoskeletal and vestibular effects of long term repeated exposure to sustained high-G
[AGARD-AR-317] p 562 N95-14263

BACKGROUND NOISE
Research on characterization of the upper atmosphere using lidar
[AD-A283241] p 530 N95-15401

BACKSCATTERING
Microcontamination detection using Heavy Ion Backscattering Spectrometry
[DE94-014182] p 437 N95-14312
High performance YBCO films
[AD-A283870] p 451 N95-14354
Performance of spherically focusing Ge(444) backscattering analyzers for inelastic x-ray scattering
[DE94-016349] p 621 N95-14382
X-ray Photoelectron Spectroscopy (XPS), Rutherford Back Scattering (RBS) studies
[NASA-CR-196536] p 439 N95-14867
Low energy electron and atom elastic scattering cross sections from 0.1 to 30 keV
[AD-A283584] p 595 N95-15318
Photoluminescence spectroscopy and Rutherford backscattering channeling evaluation of various capping techniques for rapid thermal annealing of ion-implanted ZnSe
[DE94-016876] p 623 N95-15339
Defect profiling in elemental and multilayer systems: Correlations of fitted defect concentrations with positron implantation profiles
[DE94-015844] p 624 N95-15422
Time-of-flight detector for heavy ion backscattering spectrometry
[DE94-015600] p 596 N95-15437

BALLISTIC MISSILES
Department of Defense high power laser program guidance
[AD-A282915] p 500 N95-15391

BALLISTICS
New armour materials: Metal matrix composites
[PB94-189131] p 433 N95-14148
Ballistic performance and adiabatic shear behavior of AerMet(tm) 100 steel
[AD-A283266] p 447 N95-15622

BANDPASS FILTERS
A Lyman-alpha tunable acousto-optic filter for detecting superthermal flare protons
[NASA-CR-197119] p 613 N95-14908
BANDWIDTH
SUNMOS for the Intel Paragon, a brief user's guide
[DE94-015277] p 574 N95-15543
BARIUM OXIDES
High performance YBCO films
[AD-A283870] p 451 N95-14354
Sandia 1993 Superconducting Technology Program
[DE94-015601] p 625 N95-15438
Low loss glass and optical fibers therefrom
[AD-D016379] p 615 N95-15766
BARIUM TITANATES
In-situ TEM crystallization of sol-gel derived BaTiO3 thin films
[DE94-013260] p 619 N95-13821
BARORECEPTORS
Extended duration orbiter medical project variability of blood pressure and heart rate (STS-50/USML-1)
p 551 N95-14223
Cardiovascular deconditioning effects of long-term simulated weightlessness in rats p 538 N95-15099
BAROTROPIC FLOW
Comparison of hemodynamic and volume responses to different levels of lower body suction and head-up tilt
p 544 N95-15107
BARRIER LAYERS
Development of large-area monolithically integrated Silicon-Film(tm) photovoltaic modules
[DE94-011830] p 520 N95-15405
BARYONS
Topics in the structure of hadronic systems
[DE94-014924] p 597 N95-15865
BASALT
Experimental study of chemical, phase and textural equilibrium of high TiO2 mare basalts and peridotite
[NASA-CR-196480] p 645 N95-13724
The 226RA and 231PA systematics of axial, MORB, crustal residence ages, and MAGMA chamber characteristics at 9 to 10 degree N East Pacific Rise
[DE94-013084] p 529 N95-14434
BASE FLOW
Base passive porosity for drag reduction
[NASA-CASE-LAR-15246-1] p 501 N95-14183
On the behavior of three-dimensional wave packets in viscously spreading mixing layers
[NASA-TM-106770] p 495 N95-15908
BATHYMETERS
An analysis of eddy resolving global ocean models in the Southern Ocean
[AD-A283211] p 536 N95-15626
BATHYTHERMOGRAPHS
Data processing routines for the Sippican MK-12 XBT system
[AD-A283570] p 536 N95-15330
BAYES THEOREM
A multiscale random field model for Bayesian image segmentation
[AD-A283875] p 515 N95-14358
Control of selective perception using Bayes nets and decision theory
[TR-468] p 573 N95-15151
BEACONS
Test and Evaluation Master Plan (TEMP) for Fixed Ground Antenna Radomes (FGAR)
[AD-A283839] p 461 N95-14346
Radiometer calibration procedure and beacon attenuation estimation reference level
p 466 N95-14683
BEAMFORMING
Wideband beamforming for a sparse nonuniformly spaced array
[AD-A280833] p 591 N95-14396
Optically controlled MMW beamsteering beamforming antenna
[AD-A282831] p 614 N95-15414
BEAMS (SUPPORTS)
Martian environmental simulation for a deployable lattice mast p 423 N95-14076
Joint for a variable geometry truss and method of constructing same
[NASA-CASE-LAR-15136-1] p 506 N95-14138
Bone geometry, structure and mineral distribution using Dual energy X ray Absorptiometry (DXA)
p 549 N95-15140
Large amplitude nonlinear response of flat aluminum, and carbon fiber plastic beams and plates
[AD-A282440] p 513 N95-15547
BEARINGLESS ROTORS
Linear and nonlinear dynamic analysis of redundant load path bearingless rotor systems
[NASA-CR-197220] p 503 N95-14923
BEARINGS
Vehicle health management using adaptive techniques
[NASA-TM-108472] p 431 N95-15609
BED REST
Cardiovascular response to cold pressor and LBNP tests before and after 20-day-bedrest p 543 N95-15097
Effects of 20 days bed-rest on cardio-respiratory functions during sub-maximal exercise in young women
p 545 N95-15111
Water intake and urinary volume during 20 days bed-rest in young women p 548 N95-15134
20 days bed-rest on insulin action in relation to body fat in young subjects p 549 N95-15145
BENARD CELLS
Onset of hexagons in surface-tension-driven Benard convection p 483 N95-14527
Oscillatory/chaotic thermocapillary flow induced by radiant heating p 483 N95-14531
BEND TESTS
Mechanical properties of high-temperature superconducting wires
[DE94-015089] p 621 N95-14192
Size and deformation limits to maintain constraint in K(sub Ic) and J(sub c) testing of bend specimens
[AD-A284363] p 514 N95-15802
BENDING
Bending effects of unsymmetric adhesively bonded composite repairs on cracked aluminum panels
p 507 N95-14456
Buckling of composite beams (CDDF)
[NASA-TP-3512] p 435 N95-14913
Three-dimensional effects of crack closure in laminated composite plates subjected to bending loads
[AD-A283342] p 436 N95-15873
BENDING FATIGUE
Mechanical properties of high-temperature superconducting wires
[DE94-015089] p 621 N95-14192
BENDING MOMENTS
Analytical tripping loads for stiffened plates
[AD-A284368] p 514 N95-15805
BENZENE
Fluorescent compounds for plastic scintillation applications
[DE94-013235] p 497 N95-15580
BERYLLIUM
Boron atom matrix chemistry
[AD-A282840] p 434 N95-14366
Results of TSP metals monitoring at McMurdo Station, Antarctica
[DE94-015264] p 524 N95-15455
BERYLLIUM ISOTOPES
Beta decay data for neutron-rich Li-Cl nuclides
[DE94-014556] p 595 N95-15310
BETA PARTICLES
Searches for massive neutrino emission in C-14 beta and Fe-55 electron-capture decays
[DE94-016863] p 594 N95-14374
Beta decay data for neutron-rich Li-Cl nuclides
[DE94-014556] p 595 N95-15310
BEVERAGES
Low-dose alcohol effects on human behavior and performance: A review of post-1984 research
[DOT/FAA/AM-94/24] p 552 N95-14863
BIAS
Adjustable bias column end joint assembly
[NASA-CASE-LAR-14899-1] p 459 N95-14111
Divertor bias experiments
[DE94-015720] p 617 N95-14328
Essential elements of an effective data qualification
[DE94-015566] p 632 N95-15419
BIBLIOGRAPHIES
International energy: Research organizations, 1988-1992
[DE90-017267] p 630 N95-13726
Medical research publications: A bibliography of Walter Reed Army Medical Center staff, 1986-1992, volume 2
[PB94-177797] p 541 N95-14394
Electronics and Electrical Engineering Laboratory Technical Progress Bulletin covering laboratory programs, January to March 1994 with 1994/1995 EEEL events calendar
[PB94-193810] p 474 N95-14402
Bibliography of Joint Aircraft Survivability reports and related documents
[AD-A282795] p 409 N95-14840
Aerospace medicine and biology: A continuing bibliography with indexes (supplement 395)
[NASA-SP-7011(395)] p 550 N95-15304
Aeronautical engineering: A continuing bibliography with indexes (supplement 310)
[NASA-SP-7037(310)] p 392 N95-15550
Large scale obscuration and related climate effects open literature bibliography
[DE94-012992] p 524 N95-15575
A bibliography of papers on the diffuse interstellar bands p 634 N95-15846
BIMETALS
One: Redox chemistry of bimetallic fulvalene complexes. 2: Oligocyclopentadienyl complexes
[DE94-014930] p 443 N95-15667
BINARY ALLOYS
Convection and morphological stability during directional solidification p 448 N95-14548
Shear stabilization of solidification fronts
p 448 N95-14549
Experiments to examine the contribution of gas atoms to void formation in irradiated metals
[DE94-015209] p 446 N95-15433
BINARY CODES
Spin glasses and error-correcting codes
p 462 N95-14624
BINARY DATA
Hardware implementation of a desktop supercomputer for high performance image processing. Color image processing using cellular neural networks
[AD-A283071] p 571 N95-14178
BINARY FLUIDS
Turbidity of a binary fluid mixture: Determining eta
p 487 N95-14552
A coarse grained approach to thermocapillarity effects in binary systems p 487 N95-14553
Measurement of resistance to solute transport across surfactant-laden interfaces using a Fluorescence Recovery After Photobleaching (FRAP) technique
p 490 N95-14574
BINARY MIXTURES
Solubility, viscosity and density of refrigerant and lubricant mixtures
[DE94-016949] p 454 N95-15343
Interacting fronts in a model for binary-mixture convection
[DE94-013595] p 494 N95-15861
BINARY STARS
ROSAT observations of the binary Be star and radio pulsar PSR1259-63
[NASA-CR-196951] p 642 N95-15907
BINAURAL HEARING
Binaural room simulation p 561 N95-14053
BINDERS (MATERIALS)
Thin composite solid electrolyte film for lithium batteries
[NASA-CASE-NPO-18694-1-CU] p 472 N95-13824
Recycled plastic: A clean and low cost rocket fuel
[TABES PAPER 94-610] p 416 N95-14642
BIOASSAY
Transient blood/plasma density and hematocrit effects after passive (sitting) thermoneutral water immersion in men p 548 N95-15131
BIOASTRONAUTICS
Cosmos 2229 immunology study (Experiment K-8-07)
[NASA-CR-196984] p 537 N95-13638
Joint Launch + One Year Science Review of USML-1 and USMP-1 with the Microgravity Measurement Group
[NASA-CP-3272-VOL-1] p 634 N95-14207
Commercial investigation results for the generic bioprocessing apparatus flown on United States Microgravity Laboratory-1 p 538 N95-14227
The Astroculture (tm)-1 experiment on the USML-1 mission p 564 N95-14228
BIOCHEMISTRY
Measurement and regulation of central noradrenergic receptors
[AD-A284219] p 541 N95-14408
BIODEGRADABILITY
Development of a moldable, biodegradable polymeric bone repair material
[AD-A283413] p 454 N95-15296
BIODYNAMICS
Coordination of human upper arm and forearm motion in rapid extensions p 561 N95-14056
The musculoskeletal and vestibular effects of long term repeated exposure to sustained high-G
[AGARD-AR-317] p 562 N95-14263
BIOENGINEERING
Naval Aerospace Medical Research Laboratory. 1993 command history
[AD-A284038] p 541 N95-14424
BIOGEOCHEMISTRY
Optical variability in the equatorial and southeast Pacific
[AD-A283894] p 536 N95-15425
BIOLOGICAL EFFECTS
Aerospace medicine and biology: A continuing bibliography with indexes (supplement 395)
[NASA-SP-7011(395)] p 550 N95-15304
BIOLOGICAL EVOLUTION
Will man need the vestibular system in generations to come? p 542 N95-15092
Changing gravity level and the development of animals p 538 N95-15101

The avian embryo responding to microgravity of space flight p 538 N95-15104
Behaviour of newly hatched and adult Japanese quail and the feasibility of adaptation to weightlessness p 538 N95-15106

BIOPROCESSING
Commercial investigation results for the generic bioprocessing apparatus flown on United States Microgravity Laboratory-1 p 538 N95-14227
Electrophoretic interactions and aggregation of colloidal biological particles p 444 N95-14578

BIOSATELLITES
Effect of short- and long-term spaceflight on the contractile properties of rat skeletal muscles with different functions p 539 N95-15141

BIOTECHNOLOGY
A decade of telerobotics in rehabilitation: Demonstrated utility blocked by the high cost of manipulation and the complexity of the user interface p 558 N95-14044
Naval Aerospace Medical Research Laboratory. 1993 command history
[AD-A284038] p 541 N95-14424

BIRDS
Are otoconia dynamic in birds and mammals? p 538 N95-15103
Behaviour of newly hatched and adult Japanese quail and the feasibility of adaptation to weightlessness p 538 N95-15106
Activity of ornithine decarboxylase in muscle of Japanese quail in hypergravity conditions p 539 N95-15144

BIREFRINGENCE
Nonlinear optical susceptibility of a model guest/host polymeric system as investigated by electro-optics and second harmonic generation
[AD-A283069] p 449 N95-13692

BISMUTH COMPOUNDS
Ferroelectric oxide memory FET (FEMFET) development
[AD-A283203] p 476 N95-15399

BISMUTH OXIDES
High performance YBCO films
[AD-A283870] p 451 N95-14354
Transport resistive broadening by avalanche flux motion in high-temperature superconductors: SOC in a driven system
[DE94-016901] p 623 N95-15341
Ferroelectric oxide memory FET (FEMFET) development
[AD-A283203] p 476 N95-15399

BISPHENOLS
Poly(arylene ether)s containing pendent ethynyl groups
[NASA-CASE-LAR-15041-1] p 449 N95-13838

BIT ERROR RATE
Spin glasses and error-correcting codes p 462 N95-14624
A simple analytical model for dense WDM/OOK systems
[AD-A283229] p 478 N95-15628

BL LACERTAE OBJECTS
Observations of extragalactic sources with the Metsaehovi radio telescope at 22-87 GHz
[PB94-197712] p 637 N95-13982

BLACK BODY RADIATION
Squeezed states and graviton-entropy production in the early universe p 608 N95-13947

BLACKOUT
The Physiologist, volume 36, number 1, supplement p 541 N95-15089
Guidelines for a Research and Development (R/D) program for high sustained G p 546 N95-15124

BLADE-VORTEX INTERACTION
Prediction of rotor-blade deformations due to unsteady airloads
[AD-A284467] p 410 N95-15821

BLANKETS (FUSION REACTORS)
MHD flow in rectangular ducts with inclined non-uniform transverse magnetic field
[DE94-013989] p 616 N95-14006

BLAST LOADS
Blast overpressure studies with animals and man
[AD-A280435] p 540 N95-13971

BLOCK COPOLYMERS
Preparation of well defined polystyrene-block-poly (methylphenylsilylene) copolymers
[AD-A280799] p 450 N95-14304
Towards the molecular design of composite materials
[AD-A283422] p 627 N95-15404
NMR studies of polymers at interfaces
[AD-A281570] p 455 N95-15458

BLOCK DIAGRAMS
Earth Observing System (EOS)/Advanced Microwave Sounding Unit-A (AMSU-A): Instrument logic diagrams
[NASA-CR-189378] p 567 N95-13633
Experimental hardware development for a pulsed ultrasonic data collection facility
[AD-A283331] p 615 N95-15872

BLOCKING
Blocking reduction of Landsat Thematic Mapper JPEG browse images using optimal PSNR estimated spectra adaptive postfiltering p 565 N95-14589
Synthetic aperture radar signal data compression using block adaptive quantization p 565 N95-14590
Compression of regions in the global advanced very high resolution radiometer 1-km data set p 565 N95-14591
Convolutional encoding of self-dual block codes (2) p 462 N95-14623
Wind-tunnel blockage and actuation systems test of a two-dimensional scramjet inlet unstart model at Mach 6
[NASA-TM-109152] p 495 N95-15898

BLOOD CIRCULATION
Comparison of hemodynamic and volume responses to different levels of lower body suction and head-up tilt p 544 N95-15107
Manipulating the arterial pressure to prevent G-LOC p 546 N95-15123
Non-invasive physiological monitoring relevant to G-induced loss of consciousness p 547 N95-15125
Regional cutaneous microvascular flow responses during gravitational and LBNP stresses p 547 N95-15128
Physiologic mechanisms effecting circulatory and body fluid losses in weightlessness as shown by mathematical modeling p 547 N95-15129

BLOOD FLOW
Circulatory filling pressures during transient microgravity induced by parabolic flight p 542 N95-15095
Modeling and numerical simulation of the cerebral blood flow under acceleration p 545 N95-15112
Physiological considerations concerning Positive Pressure Breathing (PBG) during +Gz p 547 N95-15126

BLOOD PLASMA
Transient blood/plasma density and hematocrit effects after passive (sitting) thermoneutral water immersion in men p 548 N95-15131

BLOOD PRESSURE
Extended duration orbiter medical project variability of blood pressure and heart rate (STS-50/USML-1) p 551 N95-14223
Circulatory filling pressures during transient microgravity induced by parabolic flight p 542 N95-15095
Hemodynamic responses to passive body tilts p 542 N95-15096
Body position and volume status as determinants of cardiovascular responses to transition into microgravity in parabolic flight p 544 N95-15108
Manipulating the arterial pressure to prevent G-LOC p 546 N95-15123
Physiological considerations concerning Positive Pressure Breathing (PBG) during +Gz p 547 N95-15126
Operational requirements for avoidance and eventual elimination of Gz-induced Loss Of Consciousness (G-LOC) in flight p 547 N95-15127
Effects of microgravity on interstitial muscle receptors affecting heart rate and blood pressure during static exercise p 548 N95-15137
Isolation of the physiological regulation component of the arterial pressure time variation after postural stresses by a model of the gravitational and arterial kinking effects p 550 N95-15149

BLOOD VOLUME
Transient blood/plasma density and hematocrit effects after passive (sitting) thermoneutral water immersion in men p 548 N95-15131
20 days bed-rest on insulin action in relation to body fat in young subjects p 549 N95-15145
A comparison of overall mathematical models of the cardiovascular system for simulating response to orthostatic stresses p 550 N95-15150

BLOWERS
Integration of a mechanical forebody vortex control system into the F-15 p 398 N95-14258

BLOWING
Experiments to verify nonparallel stability theory at Virginia Polytechnic Institute and State University, Blacksburg, Virginia
[NASA-CR-196993] p 479 N95-13664
Computational analysis of forebody tangential slot blowing p 397 N95-14253
Comparison of full-scale, small-scale, and CFD results for F/A-18 forebody slot blowing p 397 N95-14255
Low-energy pneumatic control of forebody vortices p 398 N95-14256

BLUNT BODIES
Numerical simulation of shock-induced combustion past blunt bodies using shock-fitting technique
[NASA-CR-197013] p 437 N95-14268

BODY CENTERED CUBIC LATTICES
Magnetic and structural instabilities of ultrathin Fe(100) wedges
[DE94-013864] p 624 N95-15385

BODY FLUIDS
Proposal for an astronaut mass measurement device for the Space Shuttle
[NASA-CR-197198] p 563 N95-14854
Physiologic mechanisms effecting circulatory and body fluid losses in weightlessness as shown by mathematical modeling p 547 N95-15129
Simulation of the fluid retention effects of a vasopressin analog using the Guyton model of circulation p 547 N95-15130
Water intake and urinary volume during 20 days bed-rest in young women p 548 N95-15134
Orthostatic stress by lower body negative pressure and its body fluid distribution kinetics under microgravity p 549 N95-15138

BODY TEMPERATURE
Alterations of body temperature, feeding, drinking and sleep-wake circadian rhythms in Rhesus monkey during a 19 day Spacelab flight simulation p 539 N95-15132
The regulation of rat activity following exposure to hyperdynamic fields p 539 N95-15133

BODY WEIGHT
Proposal for an astronaut mass measurement device for the Space Shuttle
[NASA-CR-197198] p 563 N95-14854
Water intake and urinary volume during 20 days bed-rest in young women p 548 N95-15134
20 days bed-rest on insulin action in relation to body fat in young subjects p 549 N95-15145

BOEING 707 AIRCRAFT
Electromagnetic reverberation characteristics of a large transport aircraft
[AD-A282923] p 411 N95-15392

BOEING 747 AIRCRAFT
Numerical simulation of the SOFIA flowfield
[NASA-CR-197025] p 400 N95-14612

BOILERS
Alkali metal Rankine cycle boiler technology challenges and some potential solutions for space nuclear power and propulsion applications
[NASA-TM-106593] p 430 N95-14174

BOILING
Bubble dynamics, two-phase flow, and boiling heat transfer in a microgravity environment p 488 N95-14561
Pool and flow boiling in variable and microgravity p 459 N95-14562

BOLTED JOINTS
Bolted joint studies in GRP
[AD-A283843] p 434 N95-14348
Experimental analysis of thread movement in bolted connections due to vibrations
[NASA-CR-197065] p 502 N95-14904

BOLTS
Experimental analysis of thread movement in bolted connections due to vibrations
[NASA-CR-197065] p 502 N95-14904
Saddle clamp assembly
[NASA-CASE-MFS-28701-1] p 503 N95-15305

BOLTZMANN TRANSPORT EQUATION
Proceedings of the 3rd International Workshop on Computational Electronics
[AD-A284214] p 475 N95-14444
Extension of the BRYNTRN code to monoenergetic light ion beams
[NASA-TP-3472] p 647 N95-15790

BONDING
Service equipment for use in hostile environments
[NASA-CASE-LEW-14906-2-SB] p 504 N95-15914

BONE MARROW
Cosmos 2229 immunology study (Experiment K-8-07)
[NASA-CR-196984] p 537 N95-13638

BONE MINERAL CONTENT
Bone geometry, structure and mineral distribution using Dual energy X ray Absorptiometry (DXA) p 549 N95-15140

BONES
Teratogenic effects of delta g: The concept of allometric growth p 538 N95-15102
Development of the chick's auditory ossicle, the columella p 539 N95-15115
A method for continuous monitoring of the Ground Reaction Force during daily activity p 549 N95-15139
Bone geometry, structure and mineral distribution using Dual energy X ray Absorptiometry (DXA) p 549 N95-15140
Development of a moldable, biodegradable polymeric bone repair material
[AD-A283413] p 454 N95-15296

BOOLEAN ALGEBRA
Unambiguous computation: Boolean hierarchies an sparse Turing-complete sets
[TR-483] p 575 N95-15597
Lower bounds for perceptrons solving some separation problems and oracle separation of AM from PP
[TR-498] p 588 N95-15855
P-selectivity: Intersections and indices
[TR-482] p 577 N95-15858

BOREHOLES
The crosswell electromagnetic response of layered media
[DE94-014929] p 470 N95-15866

BORON
ASSERT-1992. Fundamental studies of a high energy molecular system: Spectroscopy of boron in hydrogen clusters
[AD-A283181] p 593 N95-14155
Boron atom matrix chemistry
[AD-A282840] p 434 N95-14366

BORON CARBIDES
Solid target boronization of the MST reversed-field pinch during pulsed discharge cleaning
[DE94-015535] p 442 N95-15541

BORON-EPOXY COMPOSITES
Evaluation of bonded boron/epoxy doublers for commercial aircraft aluminum structures
p 508 N95-14457

BOSON FIELDS
Probing the antiferromagnetic long-range order with Glauber spin states p 609 N95-13951

BOSONS
Simultaneous two component squeezing in generalized q-coherent states p 598 N95-13908
Finite boson mappings of fermion systems
[DE94-014476] p 593 N95-14000
From the shell model to the interacting boson model
[DE94-014486] p 593 N95-14001
Production properties of Z bosons with jets in 1.8 TeV (anti p)p collisions
[DE94-015184] p 595 N95-15301
Electroweak boson pair production at CDF
[DE94-015183] p 597 N95-15629
Search for W(prime) (yields) e(nu) in p(anti p) collisions at (radical)s = 1,800 GeV
[DE94-015188] p 597 N95-15630

BOUNDARY CONDITIONS
Static image theory for a sphere with impedance surface
[PB94-189073] p 590 N95-13988
Computational aerodynamics based on the Euler equations
[AGARD-AG-325] p 398 N95-14264
Computations of drop collision and coalescence
p 485 N95-14542
The extensional rheology of non-Newtonian materials
p 489 N95-14569
Dynamics on the attractor for the complex Ginzburg-Landau equation
[DE94-016902] p 586 N95-15342
Numerical solution of a tunneling equation
[DE94-015514] p 586 N95-15538

BOUNDARY LAYER CONTROL
Experiments to verify nonparallel stability theory at Virginia Polytechnic Institute and State University, Blacksburg, Virginia
[NASA-CR-196993] p 479 N95-13664
Control of unsteady separated flow associated with the dynamic stall of airfoils
[NASA-CR-197024] p 400 N95-14613

BOUNDARY LAYER FLOW
Computational analysis in support of the SSTO flowpath test
[NASA-TM-106757] p 479 N95-13665
Eddy viscosity transport equations and their relation to the k-epsilon model
[NASA-TM-108854] p 481 N95-14273
Computations of drop collision and coalescence
p 485 N95-14542
On the evolution of centrifugal instabilities within curved incompressible mixing layers
[NASA-CR-194991] p 495 N95-15917

BOUNDARY LAYER SEPARATION
The breakup of a liquid jet at microgravity
p 484 N95-14535

BOUNDARY LAYER STABILITY
Experiments to verify nonparallel stability theory at Virginia Polytechnic Institute and State University, Blacksburg, Virginia
[NASA-CR-196993] p 479 N95-13664
The breakup of a liquid jet at microgravity
p 484 N95-14535

BOUNDARY LAYER TRANSITION
Experiments to verify nonparallel stability theory at Virginia Polytechnic Institute and State University, Blacksburg, Virginia
[NASA-CR-196993] p 479 N95-13664
Oscillatory thermocapillary convection
p 483 N95-14526

BOUNDARY LAYERS
Flow-radiated noise. Study of the propagative spectral range of the wall pressure field
[PB94-201290] p 590 N95-13985
Experimental investigation of the Marangoni effect on the stability of a double-diffusive layer
p 483 N95-14528
Calculation of movable bed friction factors
[AD-A283529] p 536 N95-15440
Turbulent mixing of the HVOF thermal spray and coating oxidation
[DE94-015414] p 455 N95-15535

BOUNDARY LUBRICATION
Wear mechanism evaluation and measurement in fuel-lubricated components
[AD-A284870] p 504 N95-15747

BOUNDARY VALUE PROBLEMS
An efficient spectral method for ordinary differential equations with rational function coefficients
[NASA-TM-106762] p 585 N95-14296
Mathematical problems of nonlinear wave propagation and of waves in heterogeneous media
[AD-A282217] p 492 N95-14605
Workshop on Advances in Scientific Computation and Differential Equations 1993 (SCADE)
[AD-A283111] p 585 N95-14657
Linear and nonlinear dynamic analysis of redundant load path bearingless rotor systems
[NASA-CR-197220] p 503 N95-14923
Numerical solution of a tunneling equation
[DE94-015514] p 586 N95-15538

BOW WAVES
ICE/ISEE plasma wave data analysis
[NASA-CR-196988] p 642 N95-14266
Numerical simulation of shock-induced combustion past blunt bodies using shock-fitting technique
[NASA-CR-197013] p 437 N95-14268

BRAIN
Measurement and modification of the EEG and related behavior p 557 N95-14038
Measurement and regulation of central noradrenergic receptors
[AD-A284219] p 541 N95-14408
Modeling and numerical simulation of the cerebral blood flow under acceleration p 545 N95-15112
Functional participation of the valvula cerebelli on the goldfish dorsal light response p 539 N95-15119
Operational requirements for avoidance and eventual elimination of Gz-induced Loss Of Consciousness (G-LOC) in flight p 547 N95-15127

BRAIN CIRCULATION
Modeling and numerical simulation of the cerebral blood flow under acceleration p 545 N95-15112
Physiological considerations concerning Positive Pressure Breathing (PBG) during +Gz
p 547 N95-15126

BRAIN DAMAGE
The musculoskeletal and vestibular effects of long term repeated exposure to sustained high-G
[AGARD-AR-317] p 562 N95-14263

BRAKING
Measuring temporal gravitational variations using SLR data p 527 N95-14277

BRANCHING (MATHEMATICS)
Interactions between solidification and compositional convection in mushy layers p 448 N95-14551
Dynamics on the attractor for the complex Ginzburg-Landau equation
[DE94-016902] p 586 N95-15342

BREATHING APPARATUS
Guidelines for a Research and Development (R/D) program for high sustained G p 546 N95-15124

BREMSSTRAHLUNG
Investigation of the coherent synchrotron radiation spectrum as a probe of charge dynamics
[DE94-015340] p 599 N95-15371

BRIDGMAN METHOD
Crystal growth and fluid mechanics problems in directional solidification p 486 N95-14550

BRIGHTNESS
The applicability of commercial glare test devices in the aeromedical certification of pilot applicants
[DOT/FAA/AM-94/15] p 540 N95-14176
Monitoring the variability of active galactic nuclei from a space-based platform p 644 N95-14509

BRIGHTNESS DISTRIBUTION
Diffuse bands versus extinction parameters
p 640 N95-15836

BRIGHTNESS TEMPERATURE
Observations of extragalactic sources with the Metsaehovi radio telescope at 22-87 GHz
[PB94-197712] p 637 N95-13982

BROADBAND
An evaluation of B-ISDN for the communication architecture requirements of Distributed Interactive Simulation (DIS)
[AD-A280783] p 578 N95-14292
Wideband beamforming for a sparse nonuniformly spaced array
[AD-A280833] p 591 N95-14396
Wideband electromagnetic scattering/analysis program. Electromagnetic scattering from the trunks and branches of trees
[AD-A283112] p 469 N95-15394
Apparatus for imaging an object in or through a scattering medium using coherent anti-Stokes Raman scattering
[AD-D016366] p 615 N95-15765
On the affinities of lambda 5778 and other broad diffuse interstellar bands p 639 N95-15832
Diffuse interstellar bands between 3900 A and 4200 A
p 640 N95-15834

BROADCASTING
Satellite communication technology and applications, 1995-2010 p 413 N95-13826
S-Band propagation measurements
p 466 N95-14682

BROKEN SYMMETRY
Nucleation and chiral symmetry breaking under controlled hydrodynamic flows p 489 N95-14570
Topics in the structure of hadronic systems
[DE94-014924] p 597 N95-15865

BROWNIAN MOVEMENTS
Decoherence and dissipation for a quantum system coupled to a local environment p 609 N95-13949
Evolution of wave function in a dissipative system
p 610 N95-13959
Dynamics of hard sphere colloidal dispersions
p 490 N95-14573

BRUSH SEALS
A new tribological test for candidate brush seal materials evaluation
[NASA-TM-106753] p 431 N95-13631

BSCCO SUPERCONDUCTORS
Surface currents and bulk pinning in Bi2Sr2CaCu2O8
[DE94-013873] p 619 N95-13681
Progress in development of tapes and magnets made from Bi-2223 superconductors
[DE94-015067] p 475 N95-14606

BUBBLES
Surface characterization through shape oscillations of drops in microgravity and 1-g p 458 N95-14220
Nonlinear dynamics of drops and bubbles and chaotic phenomena p 485 N95-14541
Thermocapillary migration and interactions of bubbles and drops p 486 N95-14546
Interfacial force field characterization of a constrained vapor bubble thermosyphon using IAI
p 488 N95-14560

BUCKLING
The buckling response of symmetrically laminated composite plates having a trapezoidal planform area
[NASA-CR-196975] p 505 N95-13839
Buckling of composite beams (CDDF)
[NASA-TP-3512] p 435 N95-14913

BUCKMINSTERFULLERENE
Electrodeposition of conductors and semiconductors with controlled stoichiometries and morphologies
[AD-A280743] p 437 N95-14141

BUFFER STORAGE
Data flow manager for DART
[DE94-013236] p 579 N95-15581

BUFFETING
Pressure measurements on an F/A-18 twin vertical tail in buffeting flow. Volume 2: Steady and unsteady RMS pressure data
[AD-A281581] p 404 N95-15465

BULGING
Nonlinear bulging factor based on R-curve data
p 511 N95-14476

BUOYANCY
Oscillatory thermocapillary convection
p 483 N95-14526
Interactions between solidification and compositional convection in mushy layers p 448 N95-14551
Activated buoyancy propulsion = Paradox Power (tm)
[TABES PAPER 94-619] p 405 N95-14646
Postural control of fish related to gravity input
p 539 N95-15118

BURGER EQUATION
Effect of stratification and geometrical spreading on sonic boom rise time p 401 N95-14880

BURNING RATE
Assessing post-fire combustion of polyurethane
[DE94-011461] p 438 N95-14375

Turbulent upward flame spread on a vertical wall under external radiation
[PB94-207388] p 441 N95-15353
Comparison of wall-fire behavior with and without a ceiling
[PB94-207404] p 441 N95-15354
Fire growth models for materials
[PB94-195856] p 443 N95-15810
Gas turbine prediffuser-combustor performance during operation with air-water mixture
[DOT/FAA/CT-93/52] p 411 N95-15683
Burn rates of TiH2/KClO4/Viton and output testing of NASA SKD26100098-301 pressure cartridges
[NASA-CR-188357] p 443 N95-15715

BUTT JOINTS
An inelastic analysis of a welded aluminum joint
[NASA-TP-3508] p 513 N95-15055

BYPASS RATIO
Ultra-high bypass ratio jet noise
[NASA-CR-195394] p 591 N95-14610

C

C (PROGRAMMING LANGUAGE)
Remote sensing, processing and transmission of data for an unmanned aerial vehicle
[AD-A283104] p 514 N95-13693

CABIN ATMOSPHERES
Design of components for the NASA OCEAN project
[NASA-CR-197207] p 535 N95-14906

CADMIUM
Results of TSP metals monitoring at McMurdo Station, Antarctica
[DE94-015264] p 524 N95-15455
Module process optimization and device efficiency improvement for stable, low-cost, large-area, cadmium telluride-based photovoltaic module production
[DE94-011817] p 521 N95-15863

CADMIUM TELLURIDES
Orbital processing of high-quality CdTe compound semiconductors p 458 N95-14213
Role of polycrystallinity in CdTe and CuInSe2 photovoltaic cells
[DE94-011849] p 519 N95-14432
Module process optimization and device efficiency improvement for stable, low-cost, large-area, cadmium telluride-based photovoltaic module production
[DE94-011817] p 521 N95-15863

CALCIUM OXIDES
Transport resistive broadening by avalanche flux motion in high-temperature superconductors: SOC in a driven system
[DE94-016901] p 623 N95-15341
Sandia 1993 Superconducting Technology Program
[DE94-015601] p 625 N95-15438

CALIBRATING
HRMA calibration handbook: EKC gravity compensated XRCF models
[NASA-CR-195818] p 636 N95-13634
AXAF SIM focus mechanism study
[NASA-CR-196976] p 636 N95-13636
Resolution measurement for scanning electron microscopes
[DE94-012747] p 601 N95-13674
Earth Observing System (EOS)/Advanced Microwave Sounding Unit-A (AMSU-A): Calibration management plan
[NASA-CR-189376] p 515 N95-13704
Deployment mechanism calibration system
p 414 N95-13833
Summary of AXAF calibration requirements
[NASA-CR-196985] p 637 N95-13887
Dynamics of the McDonnell-Douglas Large Scale Dynamic Rig and dynamic calibration of the rotor balance
[NASA-TM-108855] p 391 N95-13891
Partial pressure analysis in space testing
p 424 N95-14084
Performance Report: A timeline for the synchrotron calibration of AXAF
[NASA-CR-196489] p 638 N95-14101
Calibration and characterization of wide range hydrogen sensors
[DE94-013765] p 496 N95-14146
Radar altimeter calibration using SLR
p 471 N95-14283
A radio telescope for the calibration of radio sources at 32 gigahertz p 463 N95-14626
Radiometer calibration procedure and beacon attenuation estimation reference level
p 466 N95-14683
High Temperature Calibration Furnace System user's guide
[NASA-CR-196526] p 573 N95-14905
Spectrophotometric determination of plutonium-239 based on the spectrum of plutonium 3 chloride
[DE94-015172] p 440 N95-15297
The modal decomposition of an impedance tube
[AD-A283591] p 591 N95-15320
A proposed framework for computational fluid dynamics code calibration and validation
[DE94-015799] p 493 N95-15351
New five-standard calibration procedures for network analyzers and wafer probes
[PB94-197662] p 478 N95-15611

CALORIMETERS
Heat capacity and thermal relaxation of bulk helium very near the lambda point p 444 N95-14208
A high speed, wide dynamic range digitizer circuit for photomultiplier tubes
[DE94-015187] p 475 N95-15302
Selection of non-destructive assay methods: Neutron counting or calorimetric assay?
[DE94-016211] p 505 N95-15777

CAMERAS
Energy and Technology Review, April 1994
[DE94-012133] p 496 N95-13669
Computer aided techniques for the realisation of the diaphragm of the PSM for the IRS-1C
p 413 N95-13829
Martian environmental simulation for a deployable lattice mast p 423 N95-14076
Technical guidance for the development of a solid state image sensor for human low vision image warping
[NASA-CR-196997] p 612 N95-14272

CANADA
Geodetic survey of Canada: Results on a geoid questionnaire p 516 N95-15793

CANADIAN SPACE PROGRAM
Thermal balance testing of the MSAT spacecraft
p 424 N95-14082

CANARD CONFIGURATIONS
Fatigue evaluation of empennage, forward wing, and winglets/tip fins on part 23 airplanes
[PB94-196813] p 408 N95-13981

CANONICAL FORMS
Phase-space analysis of charged and optical beam transport: Wigner rotation angle p 606 N95-13927

CANOPIES (VEGETATION)
Wideband electromagnetic scattering/analysis program. Electromagnetic scattering from the trunks and branches of trees
[AD-A283112] p 469 N95-15394

CANTILEVER BEAMS
Buckling of composite beams (CDDF)
[NASA-TP-3512] p 435 N95-14913

CAPACITANCE
Capacitance calculations in nanostructure devices via the quantum Liouville equation in the coordinate representation
[AD-A281936] p 589 N95-13656
Accelerometer model in APLAC
[PB94-197647] p 497 N95-15413
Steering capaciflector sensor
[NASA-CASE-GSC-13489-1] p 583 N95-15598

CAPACITANCE-VOLTAGE CHARACTERISTICS
Capacitance calculations in nanostructure devices via the quantum Liouville equation in the coordinate representation
[AD-A281936] p 589 N95-13656

CAPACITORS
In situ, real-time analysis of the growth of ferroelectric and conductive oxide heterostructures by a new time-of-flight pulsed ion beam surface analysis technique
[DE94-013298] p 620 N95-13822
Design of reliable high voltage avalanche transistor pulsers
[DE94-015323] p 473 N95-14261
High performance YBCO films
[AD-A283870] p 451 N95-14354
Hypervelocity Impact Test Facility: A gun for hire
[TABES PAPER 94-605] p 415 N95-14639
Theory and implementation of a VLSI stray insensitive switched capacitor composite operational amplifier
[AD-A283536] p 476 N95-15325

CAPE KENNEDY LAUNCH COMPLEX
John F. Kennedy Space Center, Safety, Reliability, Maintainability and Quality Assurance, Survey and Audit Program
[NASA-TM-109208] p 630 N95-14918

CAPILLARY FLOW
Core-centering of compound drops in capillary oscillations: Observations on USML-1 experiments in space p 458 N95-14218
Stabilization of thermocapillary convection by means of nonplanar flow oscillations p 482 N95-14524
Control of oscillatory thermocapillary convection in microgravity p 483 N95-14525
Oscillatory thermocapillary convection
p 483 N95-14526
Thermocapillary convection in floating zones under simulated reduced-gravity conditions
p 483 N95-14529
The behavior of unsteady thermocapillary flows
p 483 N95-14530
Oscillatory/chaotic thermocapillary flow induced by radiant heating p 483 N95-14531
Phase segregation due to simultaneous migration and coalescence p 484 N95-14537
Thermocapillary motion of deformable drops
p 485 N95-14544
Ground based studies of thermocapillary flows in levitated drops p 486 N95-14545
Thermocapillary migration and interactions of bubbles and drops p 486 N95-14546
Effects of thermocapillarity on an evaporating extended meniscus in microgravity p 488 N95-14559
Regional cutaneous microvascular flow responses during gravitational and LBNP stresses
p 547 N95-15128

CAPILLARY TUBES
Equilibrium fluid interface behavior under low- and zero-gravity conditions p 484 N95-14534
An application of miniscale experiments on Earth to refine microgravity analysis of adiabatic multiphase flow in space p 459 N95-14567
A new procedure for measuring contact angle
[DE94-014971] p 457 N95-14659

CAPSULES
High temperature superconductors with improved current densities
[AD-A282996] p 472 N95-13685

CARBENES
Theoretical studies of hydrocarbon combustion chemistry
[DE94-017155] p 441 N95-15347

CARBIDES
Conversion of light hydrocarbon gases in metal carbides for production of liquid fuels and chemicals
[DE94-013933] p 439 N95-14435

CARBON
Graphite fluoride from iodine intercalated graphitized carbon
[NASA-CASE-LEW-15360-1] p 441 N95-15303
Adsorption and diffusion of fluids in well-characterized adsorbent materials
[DE94-016953] p 454 N95-15344

CARBON COMPOUNDS
Graphite fluoride from iodine intercalated graphitized carbon
[NASA-CASE-LEW-15360-1] p 441 N95-15303
One: Redox chemistry of bimetallic fulvalene complexes. 2: Oligocyclopentadienyl complexes
[DE94-014930] p 443 N95-15667
The Diffuse Interstellar Bands: Contributed papers
[NASA-CP-10144] p 639 N95-15827
Investigation of a laboratory candidate for the carrier of the 4430 A diffuse interstellar band
p 641 N95-15840

CARBON DIOXIDE
Fluid dynamic effects on precision cleaning with supercritical fluids
[DE94-015001] p 439 N95-14663

CARBON DIOXIDE CONCENTRATION
Integrated science model for assessment of climate change
[DE94-016363] p 523 N95-15361

CARBON FIBER REINFORCED PLASTICS
Large amplitude nonlinear response of flat aluminum, and carbon fiber plastic beams and plates
[AD-A282440] p 513 N95-15547

CARBON FIBERS
Monitoring fiber stress during curing of single fiber glass- and graphite-epoxy composites
[NASA-TM-4568] p 432 N95-13641
Processing of thermoset prepreg laminate via exposure to microwave radiation
[DE94-013268] p 432 N95-13643
Electrodeposition of conductors and semiconductors with controlled stoichiometries and morphologies
[AD-A280743] p 437 N95-14141
AEM and HREM evaluation of carbon nanostructures in silica aerogels
[DE94-014913] p 434 N95-14387
Effect of matrix stiffness on wavy fiber behavior in single-carbon-fiber-epoxy composites
[AD-A280970] p 435 N95-15427
Oxidation resistant coating for carbon-carbon composites at ultra-high temperatures
[AD-A283323] p 456 N95-15624

CARBON ISOTOPES
A search for the 13175 A infrared diffuse band in dense environments p 639 N95-15831
Laboratory spectra of C60 and related molecular structures p 627 N95-15838

CARBON MONOXIDE
Engine system assessment study using Martian propellants
[NASA-CR-189188] p 431 N95-14669
CARBON STEELS
Ballistic performance and adiabatic shear behavior of AerMet(tm) 100 steel
[AD-A283266] p 447 N95-15622
CARBON 14
Searches for massive neutrino emission in C-14 beta and Fe-55 electron-capture decays
[DE94-016863] p 594 N95-14374
CARBON-CARBON COMPOSITES
High performance arcjet engines
[NASA-CR-195397] p 430 N95-13697
Mechanical behavior of high temperature composites
[AD-A281582] p 436 N95-15441
Oxidation resistant coating for carbon-carbon composites at ultra-high temperatures
[AD-A283323] p 456 N95-15624
CARBONACEOUS MATERIALS
The formation of small grains in shocks in the ISM
p 641 N95-15842
CARBONATES
MCFC Product Development Test
[DE94-014334] p 518 N95-14143
Development of the fuel cell power generation technology, 2
[DE94-780614] p 520 N95-15376
Development of the fuel cell power generation technology, 1
[DE94-780648] p 520 N95-15377
Thin lithium cobalt dioxide rechargeable cells using polyacrylonitrile-based polymer electrolytes
[AD-A283253] p 455 N95-15615
CARBONIZATION
The oxidative stabilization and carbonization of mesophase pitch
[AD-A282026] p 453 N95-14954
CARBONYL COMPOUNDS
Optically driven surface reactions: Laser probes of surface dynamics
[DE94-015311] p 441 N95-15370
CARDIOVASCULAR SYSTEM
Extended duration orbiter medical project countermeasure to reduce post space flight orthostatic intolerance (LBNP) (STS-50/USML-1)
p 551 N95-14224
The Physiologist, volume 36, number 1, supplement
p 541 N95-15089
Gravitational stress and regulation of neuroendocrine elements and fluid volume in humans
p 542 N95-15090
Transesophageal echocardiographic evaluation of baboons during microgravity induced by parabolic flight
p 538 N95-15094
Hemodynamic responses to passive body tilts
p 542 N95-15096
Cardiovascular response to cold pressor and LBNP tests before and after 20-day-bedrest p 543 N95-15097
Twenty four hours head-down tilt decreases arterial baroreflex function in conscious rat p 538 N95-15098
Cardiovascular deconditioning effects of long-term simulated weightlessness in rats p 538 N95-15099
Comparison of hemodynamic and volume responses to different levels of lower body suction and head-up tilt
p 544 N95-15107
Body position and volume status as determinants of cardiovascular responses to transition into microgravity in parabolic flight p 544 N95-15108
Cardiovascular and metabolic responses to 6 deg Head-Down Tilt (HDT) and 70 deg Head-Up Tilt (HUT) following exercise p 544 N95-15109
A mathematical model of the cardiovascular response to +Gz acceleration p 544 N95-15110
Effects of 20 days bed-rest on cardio-respiratory functions during sub-maximal exercise in young women
p 545 N95-15111
Immune changes in humans concomitant with space flights of up to 10 days duration p 545 N95-15114
The relationship between space sickness and preflight diet p 546 N95-15122
Non-invasive physiological monitoring relevant to G-induced loss of consciousness p 547 N95-15125
Regional cutaneous microvascular flow responses during gravitational and LBNP stresses
p 547 N95-15128
Physiologic mechanisms effecting circulatory and body fluid losses in weightlessness as shown by mathematical modeling p 547 N95-15129
Simulation of the fluid retention effects of a vasopressin analog using the Guyton model of circulation
p 547 N95-15130
Orthostatic stress by lower body negative pressure and its body fluid distribution kinetics under microgravity
p 549 N95-15138
The cardiovascular response to the AGS
p 419 N95-15146
Isolation of the physiological regulation component of the arterial pressure time variation after postural stresses by a model of the gravitational and arterial kinking effects p 550 N95-15149
A comparison of overall mathematical models of the cardiovascular system for simulating response to orthostatic stresses p 550 N95-15150
CARDS
FFCAat Clearinghouse, directory of abstracts
[DE94-015259] p 632 N95-15435
CARRIER DENSITY (SOLID STATE)
Electrical characterization of 6H crystalline silicon carbide
[NASA-CR-197047] p 439 N95-14903
CARRIER FREQUENCIES
L(alpha)-induced two-photon absorption of visible light emitted from an O-type star by H2(+) ions located near the surface of the Stromgren sphere surrounding the star: A possible explanation for the diffuse interstellar absorption bands (DIBs) p 641 N95-15845
CARTESIAN COORDINATES
An adaptively-refined, Cartesian, cell-based scheme for the Euler and Navier-Stokes equations
[NASA-TM-106754] p 392 N95-13817
A Cartesian, cell-based approach for adaptively-refined solutions of the Euler and Navier-Stokes equations
[NASA-TM-106786] p 398 N95-14297
CARTRIDGES
Burn rates of TiH2/KClO4/Viton and output testing of NASA SKD26100098-301 pressure cartridges
[NASA-CR-188357] p 443 N95-15715
CASE HISTORIES
Age 60 Rule. Part 3: Consolidated database experiments
[DOT/FAA/AM-94/22-PT-3] p 551 N95-13715
CAST ALLOYS
Crystal growth of selected II-VI semiconducting alloys by directional solidification p 458 N95-14214
CATACLYSMIC VARIABLES
FRESIP project observations of cataclysmic variables: A unique opportunity p 644 N95-14507
CATALOGS (PUBLICATIONS)
CIFO 3.0 p 570 N95-14167
Satellite situation report, volume 33, number 2
[NASA-TM-109965] p 428 N95-14510
FFCAat Clearinghouse, directory of abstracts
[DE94-015259] p 632 N95-15435
CATALYSIS
Positron studies in catalysis research
[DE94-012793] p 597 N95-15572
CATALYSTS
The growth of zeolites A, X and mordenite in space
p 458 N95-14226
Radical polymerization of vinyl acetate and methyl methacrylate using organochromium initiators complexed with macrocyclic polyamines
[AD-A280828] p 451 N95-14316
Radical polymerization of vinyl acetate in the presence of trialkyl phosphites
[AD-A280829] p 451 N95-14324
Activity of Ga, In and Cu modified MFI zeolites for amine reactions
[DE94-016532] p 438 N95-14388
Ring-opening polymerization of strained cyclotetrasilanes as a new route towards well defined polysilylenes
[AD-A280840] p 452 N95-14399
Study on titanium-silicalite-1 and related systems
[PB94-195500] p 445 N95-14845
The structure of new synthetic manganese oxide octahedral molecular sieves
[DE94-016348] p 596 N95-15381
Investigation of syngas interaction in alcohol synthesis catalysts
[DE94-013939] p 442 N95-15386
CATALYTIC ACTIVITY
Activity of Ga, In and Cu modified MFI zeolites for amine reactions
[DE94-016532] p 438 N95-14388
Positron studies in catalysis research
[DE94-012793] p 597 N95-15572
CATHODES
Pulsed mode cathode
[NASA-CASE-LEW-15753-1] p 475 N95-14516
Field-emitter arrays for RF vacuum microelectronics
[AD-A283549] p 476 N95-15327
CATIONS
Activity of Ga, In and Cu modified MFI zeolites for amine reactions
[DE94-016532] p 438 N95-14388
Defects and transport in mixed oxides
[DE94-015652] p 454 N95-15358
Cation disorder in high dose neutron irradiated spinel
[DE94-013118] p 455 N95-15579
Quantum chemistry and excited states: First investigations on pyrene-like molecules
p 599 N95-15844
CAVITATION FLOW
Applications of squeezed states: Bogoliubov transformations and wavelets to the statistical mechanics of water and its bubbles p 607 N95-13939
CAVITIES
Aberration correction of unstable resonators
[NASA-CASE-NPO-18662-1-CU] p 602 N95-13823
Quantum state engineering p 605 N95-13919
Oscillatory thermocapillary convection
p 483 N95-14526
Eccentricity of the electron beam in a gyrotron cavity
[PB94-197639] p 496 N95-14839
CEILINGS (ARCHITECTURE)
Comparison of wall-fire behavior with and without a ceiling
[PB94-207404] p 441 N95-15354
CELESTIAL BODIES
Space based astronomy: Teacher's guide with activities
[NASA-EG-102] p 638 N95-14511
CELLS (BIOLOGY)
Neuronal types in the chicken's statoacoustic ganglion
p 539 N95-15116
Enhancement of insulin receptor mediated endocytosis in cultured osteoblastic cells under hypergravity
p 539 N95-15148
CEMENTITE
The effect of microstresses on fatigue crack propagation in steel
[AD-A283872] p 506 N95-14356
CENTER OF GRAVITY
Fatigue evaluation of empennage, forward wing, and winglets/tip fins on part 23 airplanes
[PB94-196813] p 408 N95-13981
CENTRAL NERVOUS SYSTEM
Cardiovascular response to cold pressor and LBNP tests before and after 20-day-bedrest p 543 N95-15097
CENTRIFUGAL FORCE
Modeling and numerical simulation of the cerebral blood flow under acceleration p 545 N95-15112
On the evolution of centrifugal instabilities within curved incompressible mixing layers
[NASA-CR-194991] p 495 N95-15917
CENTRIFUGES
Life Sciences Centrifuge Facility review
[NASA-CR-196849] p 537 N95-13702
Eighteenth Space Simulation Conference: Space Mission Success Through Testing
[NASA-CP-3280] p 420 N95-14062
Simulation of Shuttle launch G forces and acoustic loads using the NASA Ames Research Center 20G centrifuge
p 419 N95-14089
Development of life sciences equipment for microgravity and hypergravity simulation p 425 N95-14090
Unique life sciences research facilities at NASA Ames Research Center p 426 N95-14091
The Physiologist, volume 36, number 1, supplement
p 541 N95-15089
On-Earth evaluation of the neurovestibular tolerance to centrifuge simulated artificial gravity in humans
p 546 N95-15120
The influence of gravity on vestibular nystagmus in humans p 546 N95-15121
Manipulating the arterial pressure to prevent G-LOC
p 546 N95-15123
Non-invasive physiological monitoring relevant to G-induced loss of consciousness p 547 N95-15125
Activity of ornithine decarboxylase in muscle of Japanese quail in hypergravity conditions
p 539 N95-15144
The cardiovascular response to the AGS
p 419 N95-15146
Centrifuges in gravitational physiology research
p 550 N95-15147
CENTRIFUGING
The regulation of rat activity following exposure to hyperdynamic fields p 539 N95-15133
CENTRIPETAL FORCE
Centrifuges in gravitational physiology research
p 550 N95-15147
CERAMIC COATINGS
Oxidation resistant coating for carbon-carbon composites at ultra-high temperatures
[AD-A283323] p 456 N95-15624
CERAMIC FIBERS
Effects of in situ fiber strength characteristics on mechanical properties of SiC(f)/SiC composites
[DE94-013965] p 433 N95-13682
CERAMIC MATRIX COMPOSITES
Effects of in situ fiber strength characteristics on mechanical properties of SiC(f)/SiC composites
[DE94-013965] p 433 N95-13682

Effects of thermal cycling on thermal expansion and mechanical properties of SiC fiber-reinforced reaction-bonded Si3N4 composites
[NASA-TM-106665] p 433 N95-14298
Mechanical behavior of high temperature composites
[AD-A281582] p 436 N95-15441

CERAMICS
High temperature superconductors with improved current densities
[AD-A282996] p 472 N95-13685
Nondestructive characterization of structural ceramic components
[DE94-013961] p 449 N95-13978
Powder agglomeration in a microgravity environment
[NASA-CR-197000] p 457 N95-14105
Center for advanced materials of high quality dynamic performance (fellowships)
[AD-A281377] p 434 N95-14360
Dense ceramic membranes for partial oxygenation of methane
[DE94-015021] p 453 N95-14609
Development of large-area monolithically integrated Silicon-Film(tm) photovoltaic modules
[DE94-011830] p 520 N95-15405
The Ceramic Manufacturability Center: A new partnership with US industry
[DE94-015851] p 456 N95-15634
Advanced Turbine Technology Applications Project (ATTAP)
[NASA-CR-195393] p 634 N95-15743
Recent progress and future prospects in the surface engineering and tribology of ceramics
[DE94-016315] p 456 N95-15778

CEREBRUM
Non-invasive physiological monitoring relevant to G-induced loss of consciousness p 547 N95-15125

CERENKOV RADIATION
Investigation of the coherent synchrotron radiation spectrum as a probe of charge dynamics
[DE94-015340] p 599 N95-15371

CHANNELS (DATA TRANSMISSION)
Lossless compression of NOAA-AVHRR satellite data
p 565 N95-14592

CHAOS
Quantum phase uncertainties in the classical limit
p 607 N95-13933
Studies in chaotic adiabatic dynamics
[DE94-013111] p 627 N95-15578

CHARACTERIZATION
Surface characterization through shape oscillations of drops in microgravity and 1-g p 458 N95-14220
Sequentially t-diagnosable systems
[PB94-205093] p 574 N95-15396
First Year PIDDP Report on gamma-ray and x-ray spectroscopy: X-ray remote sensing and in situ spectroscopy for planetary exploration missions and gamma-ray remote sensing and in situ spectroscopy for planetary exploration missions
[NASA-CR-189374] p 517 N95-15916

CHARGE COUPLED DEVICES
Technical guidance for the development of a solid state image sensor for human low vision image warping
[NASA-CR-196997] p 612 N95-14272
SLR 2000 p 471 N95-14288

CHARGE DISTRIBUTION
Charge state distributions from highly charged ions channeled at a metal surface
[DE94-012755] p 592 N95-13675

CHARGED PARTICLES
Manipulation of quantum evolution
p 598 N95-13918
The thermal-wave model: A Schroedinger-like equation for charged particle beam dynamics
p 601 N95-13944
Electrophoretic interactions and aggregation of colloidal biological particles p 444 N95-14578

CHARM (PARTICLE PHYSICS)
Measurement of the B cross section at CDF via B semileptonic decays
[DE94-013842] p 593 N95-13680
Research in high energy physics
[DE94-015519] p 600 N95-15539
Studies of quarkonia production with CDF
[DE94-013220] p 597 N95-15862

CHARRING
Behavior of charring materials in simulated fire environments
[PB94-196045] p 439 N95-14838
Simulation of coal and char nitrogen reactions in combustion
[DE94-013941] p 440 N95-15291

CHECKOUT
CTAS data analysis program
[NASA-TM-108842] p 406 N95-14611

CHELATES
Reactive polymers: Main chain coordination polymers for air separation
[AD-A281614] p 455 N95-15444

CHEMICAL CLEANING
Fluid dynamic effects on precision cleaning with supercritical fluids
[DE94-015001] p 439 N95-14663

CHEMICAL COMPOSITION
Atomic Oxygen (ATOX) simulation of Teflon FEP and Kapton H surfaces using a high intensity, low energy, mass selected, ion beam facility p 422 N95-14073
Real-time monitor and control of MBE growth of HgCdTe by spectroscopic ellipsometry
[AD-A284451] p 627 N95-15818
Porphyrins in the interstellar medium (in grains)
p 640 N95-15837

CHEMICAL PROPERTIES
The Diffuse Interstellar Bands: Contributed papers
[NASA-CP-10144] p 639 N95-15827

CHEMICAL PROPULSION
Engine system assessment study using Martian propellants
[NASA-CR-189188] p 431 N95-14669

CHEMICAL REACTIONS
Venusian atmospheric equilibrium chemistry at the Pioneer Venus anomalous event altitude
p 645 N95-13721
Interaction of chemistry, turbulence, and shock waves in hypervelocity flow
[AD-A282941] p 400 N95-14656
Ultrasensitive infrared chemiluminescence detection
[AD-A283531] p 440 N95-14958
LSENS: A General Chemical Kinetics and Sensitivity Analysis Code for homogeneous gas-phase reactions. Part 1: Theory and numerical solution procedures
[NASA-RP-1328-PT-1] p 440 N95-15056
LSENS: A General Chemical Kinetics and Sensitivity Analysis Code for homogeneous gas-phase reactions. Part 3: Illustrative test problems
[NASA-RP-1330-PT-3] p 440 N95-15057
Theoretical studies of hydrocarbon combustion chemistry
[DE94-017155] p 441 N95-15347
LSENS, a general chemical kinetics and sensitivity analysis code for homogeneous gas-phase reactions. 2: Code description and usage
[NASA-RP-1329] p 442 N95-15512

CHEMICAL REACTORS
Modeling, simulation and engineering scale-up procedures for design of CVD reactors
[AD-A284919] p 494 N95-15760

CHEMILUMINESCENCE
Developments in laser-based diagnostics for wind tunnels in the Aeromechanics Division: 1987-1992
[AD-A283011] p 412 N95-13687
Study of interferences in ozone UV and chemiluminescence monitors
[PB94-197456] p 521 N95-14123
Ultrasensitive infrared chemiluminescence detection
[AD-A283531] p 440 N95-14958

CHEMISORPTION
Kinetic theory for electrodic phase transitions: The voltammogram
[AD-A283039] p 619 N95-13691

CHEST
Transesophageal echocardiographic evaluation of baboons during microgravity induced by parabolic flight
p 538 N95-15094

CHICKENS
The avian embryo responding to microgravity of space flight p 538 N95-15104
Development of the chick's auditory ossicle, the columella p 539 N95-15115
Neuronal types in the chicken's statoacoustic ganglion
p 539 N95-15116
Structure of avian tectorial, otolithic and cupular membranes p 539 N95-15117

CHIPS
Automated hierarchical testable design of digital circuits
[PB94-197936] p 472 N95-13983

CHIPS (ELECTRONICS)
Theory and implementation of a VLSI stray insensitive switched capacitor composite operational amplifier
[AD-A283536] p 476 N95-15325
An architecture for intelligent multichip module reliability analysis
[AD-A281574] p 583 N95-15461
RF vacuum microelectronics
[AD-A283123] p 478 N95-15613

CHIRAL DYNAMICS
Nucleation and chiral symmetry breaking under controlled hydrodynamic flows p 489 N95-14570

CHIRALITY
Polarizability properties of bianisotropic spheres with noncomplete magnetoelectric dyadics
[PB94-189065] p 589 N95-13987
Topics in the structure of hadronic systems
[DE94-014924] p 597 N95-15865

CHLORATES
Nucleation and chiral symmetry breaking under controlled hydrodynamic flows p 489 N95-14570

CHLORIDES
Chemically modified electrodes by nucleophilic substitution of chlorosilylated platinum oxide surfaces
[AD-A281567] p 477 N95-15456

CHLORINATION
Process development of thermal hydrodechlorination
[PB94-195518] p 525 N95-15870

CHLOROFLUOROCARBONS
Thermophysical properties of HCFC alternatives
[DE94-016646] p 438 N95-14372
Pilot retrofit test of refrigerant R-134a for GDSCC
p 456 N95-14629

CHROMATES
Minutes of the Third Annual Workshop on Chromate Replacements in Light Metal Finishing
[DE94-015163] p 446 N95-15368

CHROMIUM
Influence of transmutation on microstructure, density change, and embrittlement of vanadium and vanadium alloys irradiated in HFIR
[DE94-015202] p 446 N95-15431
Results of TSP metals monitoring at McMurdo Station, Antarctica
[DE94-015264] p 524 N95-15455

CHROMIUM ALLOYS
Investigation of syngas interaction in alcohol synthesis catalysts
[DE94-013939] p 442 N95-15386

CHROMOPHORES
Investigation of dipolar reorientation dynamics of pure bulk polymers using second harmonic generation
[AD-A283023] p 448 N95-13688
Relaxation of polar orientational order in nonlinear optical polymers by second harmonic generation
[AD-A283024] p 449 N95-13689
Nonlinear optical susceptibility of a model guest/host polymeric system as investigated by electro-optics and second harmonic generation
[AD-A283069] p 449 N95-13692

CHROMOSPHERE
On the physics of waves in the solar atmosphere: Wave heating and wind acceleration
[NASA-CR-196992] p 646 N95-15070

CIRCADIAN RHYTHMS
The Physiologist, volume 36, number 1, supplement
p 541 N95-15089
Alterations of body temperature, feeding, drinking and sleep-wake circadian rhythms in Rhesus monkey during a 19 day Spacelab flight simulation p 539 N95-15132
The regulation of rat activity following exposure to hyperdynamic fields p 539 N95-15133
New findings regarding light intensity and its effects as a zeitgeber in the Sprague-Dawley rat
p 539 N95-15135

CIRCUIT BOARDS
Assembly feasibility and reliability studies of surface mount circuit boards manufactured with lead-free solders
[DE94-013783] p 472 N95-13975
Design of reliable high voltage avalanche transistor pulsers
[DE94-015323] p 473 N95-14261
Electromagnetic reverberation characteristics of a large transport aircraft
[AD-A282923] p 411 N95-15392

CIRCUIT DIAGRAMS
Earth Observing System (EOS)/Advanced Microwave Sounding Unit-A (AMSU-A): Instrument logic diagrams
[NASA-CR-189378] p 567 N95-13633

CIRCUIT PROTECTION
Strategic avionics technology definition studies, power voter redundancy management. Power voter applications in new vehicle architectures
[NASA-CR-197049] p 411 N95-14799

CIRCUIT RELIABILITY
Assembly feasibility and reliability studies of surface mount circuit boards manufactured with lead-free solders
[DE94-013783] p 472 N95-13975
Design of power electronics for TVC and EMA systems
[NASA-CR-197067] p 475 N95-14866

CIRCULAR ORBITS
The long-term forecast of station view periods
p 419 N95-14621

CIRCULATORY SYSTEM
On-Earth evaluation of the neurovestibular tolerance to centrifuge simulated artificial gravity in humans
p 546 N95-15120

CIRRUS CLOUDS
Support of Environmental Requirements for Cloud Analysis and Archive (SERCAA): Algorithm descriptions [AD-A283240] p 534 N95-15614
CITIES
Photogrammetric mobile satellite service prediction p 466 N95-14679
CIVIL AVIATION
Unreported medications used in incapacitating medical conditions found in fatal civil aviation accidents [DOT/FAA/AM-94/14] p 540 N95-14177
Aircraft accident report: Overspeed and loss of power on both engines during descent and power-off emergency, landing Simmons Airlines, Inc., d/b/a, American Eagle Flight 3641, N349SB False River Air Park, New Roads, Lousiana, 1 February 1994 [NTSB/AAR-94/06] p 407 N95-14916
Research and technology highlights, 1993 [NASA-TM-4575] p 647 N95-15065
CLAMPS
Saddle clamp assembly [NASA-CASE-MFS-28701-1] p 503 N95-15305
Service equipment for use in hostile environments [NASA-CASE-LEW-14906-2-SB] p 504 N95-15914
CLASSICAL MECHANICS
Time-dependent variational approach in terms of squeezed coherent states: Implication to semi-classical approximation p 609 N95-13948
Quantum propagation in single mode fiber p 609 N95-13953
CLASSIFICATIONS
World Reference Center for Arboviruses [AD-A281635] p 550 N95-15445
CLAYS
Adsorption and diffusion of fluids in well-characterized adsorbent materials [DE94-016953] p 454 N95-15344
CLEAN ENERGY
Activated buoyancy propulsion = Paradox Power (tm) [TABES PAPER 94-619] p 405 N95-14646
CLEAN ROOMS
Using a temperature-controlled quartz crystal microbalance in a space equipment cleanroom to monitor molecular contamination p 421 N95-14069
Clean assembly and integration techniques for the Hubble Space Telescope High Fidelity Mechanical Simulator p 418 N95-14070
CLEANERS
Fluid dynamic effects on precision cleaning with supercritical fluids [DE94-015001] p 439 N95-14663
CLEANING
Automated cleaning of electronic components [DE94-014122] p 476 N95-15356
Solid target boronization of the MST reversed-field pinch during pulsed discharge cleaning [DE94-015535] p 442 N95-15541
Type 304L stainless steel surface microstructure: Performance in hydride storage and acid cleaning [DE94-014654] p 447 N95-15625
CLEANLINESS
Hubble Space Telescope servicing mission scientific instrument protective enclosure design requirements and contamination controls p 421 N95-14068
Clean assembly and integration techniques for the Hubble Space Telescope High Fidelity Mechanical Simulator p 418 N95-14070
CLEAR AIR TURBULENCE
New algorithms for the reduction of image degradation due to atmospheric turbulence [AD-A284891] p 615 N95-15772
CLIMATE
Progress report on terrestrial model development (TERRA and HABITAT): Research in support of the CERES earth system modeling project [DE94-016362] p 524 N95-15779
CLIMATE CHANGE
Our Mission to Planet Earth: A guide to teaching Earth system science [NASA-EP-292] p 629 N95-13650
Integrated science model for assessment of climate change [DE94-016363] p 523 N95-15361
Climatological data summary 1993 with historical data [DE94-016624] p 523 N95-15363
Large scale obscuration and related climate effects open literature bibliography [DE94-012992] p 524 N95-15575
The seasonal cycle dependence of temperature fluctuations in the atmosphere [AD-A283220] p 534 N95-15627
CLIMATOLOGY
Statistical aspects of the precipitation regimes at Miami International Airport (MIA) and Palm Beach International Airport (PBI): 1961-1990 [PB94-194289] p 532 N95-14118
Global surface-based cloud observation for ISCCP [NASA-CR-196990] p 532 N95-14265
Introduction to HEFeS (Hierarchical Environmental Feature Simulator) [AD-A283244] p 534 N95-15402
The seasonal cycle dependence of temperature fluctuations in the atmosphere [AD-A283220] p 534 N95-15627
CLOSED CYCLES
Squeezed light from multi-level closed-cycling atomic systems p 598 N95-13920
CLOSED ECOLOGICAL SYSTEMS
Design of components for the NASA OCEAN project [NASA-CR-197207] p 535 N95-14906
Behaviour of newly hatched and adult Japanese quail and the feasibility of adaptation to weightlessness p 538 N95-15106
CLOUD COVER
Remote sensing strategy at the first atmospheric radiation measurement field site [DE94-015091] p 522 N95-14187
Global surface-based cloud observation for ISCCP [NASA-CR-196990] p 532 N95-14265
CLOUD HEIGHT INDICATORS
Global surface-based cloud observation for ISCCP [NASA-CR-196990] p 532 N95-14265
CLOUD PHYSICS
Effects of hydrometeors and atmospheric gases at SHF/EHF p 468 N95-14835
CLOUDS
Nowcasting convective storm evolution in east-central Florida using satellite and Doppler radar data [AD-A283260] p 534 N95-15618
CLOUDS (METEOROLOGY)
Global surface-based cloud observation for ISCCP [NASA-CR-196990] p 532 N95-14265
Support of Environmental Requirements for Cloud Analysis and Archive (SERCAA): Algorithm descriptions [AD-A283240] p 534 N95-15614
CLUSTERS
Coherent states on the m-sheeted complex plane as m-photon states p 598 N95-13940
CLUTTER
Effects of hydrometeors and atmospheric gases at SHF/EHF p 468 N95-14835
CMOS
Technical guidance for the development of a solid state image sensor for human low vision image warping [NASA-CR-196997] p 612 N95-14272
A gate level simulator for alpha-particle-induced transient faults [AD-A283871] p 474 N95-14355
SODR Memory Control Buffer Control ASIC [NASA-CR-197001] p 566 N95-14514
Theory and implementation of a VLSI stray insensitive switched capacitor composite operational amplifier [AD-A283536] p 476 N95-15325
COAGULATION
Flocculation and aggregation in a microgravity environment (FAME) p 459 N95-14572
Electrophoretic interactions and aggregation of colloidal biological particles p 444 N95-14578
COAL
Simulation of coal and char nitrogen reactions in combustion [DE94-013941] p 440 N95-15291
COAL GASIFICATION
High temperature membranes for H2S and SO2 separations [DE94-017125] p 441 N95-15345
High-temperature corrosion of iron aluminides [DE94-011505] p 447 N95-15906
COAL UTILIZATION
High temperature membranes for H2S and SO2 separations [DE94-017125] p 441 N95-15345
COALESCING
The flow induced by the coalescence of two initially stationary drops [NASA-TM-106752] p 478 N95-13653
Phase segregation due to simultaneous migration and coalescence p 484 N95-14537
Computations of drop collision and coalescence p 485 N95-14542
COASTAL CURRENTS
Tidal dynamics and mixing over steep topography [AD-A283535] p 536 N95-15324
COASTAL WATER
Tidal dynamics and mixing over steep topography [AD-A283535] p 536 N95-15324
COASTS
ADCIRC: An advanced three-dimensional circulation model for shelves, coasts, and estuaries. Report 4: Hurricane storm surge modeling using large domains [AD-A283868] p 535 N95-14352
COATING
Gravity-dependent transport in industrial processes p 459 N95-14580
Minutes of the Third Annual Workshop on Chromate Replacements in Light Metal Finishing [DE94-015163] p 446 N95-15368
COATINGS
Surface acoustic wave oxygen pressure sensor [NASA-CASE-LAR-15266-1-CU] p 496 N95-13837
What those defects in optical coatings really look like [DE94-015324] p 614 N95-15529
RF vacuum microelectronics [AD-A283123] p 478 N95-15613
COAXIAL FLOW
Noise radiation by instability waves in coaxial jets [NASA-TM-106738] p 591 N95-14618
The aeroacoustics of supersonic coaxial jets [NASA-TM-106782] p 591 N95-15059
COAXIAL NOZZLES
Noise radiation by instability waves in coaxial jets [NASA-TM-106738] p 591 N95-14618
COBALT
Optical detector having a plurality of matrix layers with cobalt disilicide particles embedded therein [NASA-CASE-NPO-18625-2-CU] p 614 N95-15603
COBALT ALLOYS
Investigation of syngas interaction in alcohol synthesis catalysts [DE94-013939] p 442 N95-15386
COBALT OXIDES
Defects and transport in mixed oxides [DE94-015652] p 454 N95-15358
Thin lithium cobalt dioxide rechargeable cells using polyacrylonitrile-based polymer electrolytes [AD-A283253] p 455 N95-15615
COCHLEA
Are otoconia dynamic in birds and mammals? p 538 N95-15103
Neuronal types in the chicken's statoacoustic ganglion p 539 N95-15116
Structure of avian tectorial, otolithic and cupular membranes p 539 N95-15117
COCKPITS
Objective evaluation of situation awareness for dynamic decision makers in teleoperations p 559 N95-14047
Electromagnetic reverberation characteristics of a large transport aircraft [AD-A282923] p 411 N95-15392
CODING
Convolutional encoding of self-dual block codes (2) p 462 N95-14623
Summary of activities for University of California [AD-A283890] p 632 N95-15423
A promise class at least as hard as the polynomial hierarchy [TR-484] p 576 N95-15788
COEFFICIENT OF FRICTION
Physical and tribological characteristics of ion-implanted diamond films [NASA-TM-106682] p 450 N95-14303
The role of fretting corrosion and fretting fatigue in aircraft rivet hole cracking p 510 N95-14470
COGNITION
EPIC computational models of psychological refractory-period effects in human multiple-task performance [AD-A280924] p 540 N95-14142
COGNITIVE PSYCHOLOGY
Augmentation of research on cognitive control [AD-A280956] p 552 N95-14600
ASPM2: Progress toward the analysis of symbolic parameter models [AD-A284437] p 576 N95-15817
COHERENCE COEFFICIENT
How to characterize the nonlinear amplifier? p 471 N95-13922
COHERENT ELECTROMAGNETIC RADIATION
Q-derivatives, coherent states and squeezing p 589 N95-13901
COHERENT LIGHT
Sum-frequency generation from photon number squeezed light p 603 N95-13902
Spectral, noise and correlation properties of intense squeezed light generated by a coupling in two laser fields p 500 N95-13903
Multimode squeezing, biphotons and uncertainty relations in polarization quantum optics p 603 N95-13904
Squeezing in a 2-D generalized oscillator p 603 N95-13907
Measurement of very small phase fluctuations by means of the operational approach p 605 N95-13916
A method of measuring the amplitude-modulated vacuum field near a conducting mirror p 471 N95-13921

Some rules for polydimensional squeezing
p 608 N95-13941

COHERENT RADIATION
Simultaneous two component squeezing in generalized q-coherent states p 598 N95-13908
On the theory of quantum measurement
p 604 N95-13910
Investigation of the coherent synchrotron radiation spectrum as a probe of charge dynamics
[DE94-015340] p 599 N95-15371

COLD FLOW TESTS
Cold flow simulation of the alternate turbopump development turbine of the Space Shuttle main engine high pressure fuel turbopump
[AD-A281676] p 419 N95-15447

COLLAGENS
Commercial investigation results for the generic bioprocessing apparatus flown on United States Microgravity Laboratory-1 p 538 N95-14227

COLLIMATION
Experimental study of solar simulator mirror cryocontamination p 421 N95-14065
The realuminizing of the 7-meter-diameter solar simulator collimating mirror p 424 N95-14081

COLLISION AVOIDANCE
Investigating and implementing enhancements to the simulation of short-term collision hazards
p 426 N95-14092

COLLISIONS
Applications of a fast and efficient method for simulating orbital mission safety p 426 N95-14093
Production properties of Z bosons with jets in 1.8 TeV (anti p)p collisions
[DE94-015184] p 595 N95-15301
Research accomplishments and future goals in particle physics
[DE94-015483] p 596 N95-15537
Electroweak boson pair production at CDF
[DE94-015183] p 597 N95-15629
Search for W(prime) (yields) e(nu) in p(anti p) collisions at (radical)s = 1,800 GeV
[DE94-015188] p 597 N95-15630
The formation of small grains in shocks in the ISM
p 641 N95-15842

COLLOIDS
Analysis of electron microscope images: 3-D localization of immuno-markers
[PB94-197977] p 537 N95-13990
Dynamics of hard sphere colloidal dispersions
p 490 N95-14573
New techniques for diffusing-wave spectroscopy
p 444 N95-14575
Electrophoretic interactions and aggregation of colloidal biological particles p 444 N95-14578
Electrokinetic transport of heterogeneous particles in suspension p 444 N95-14581

COLOR CODING
Hardware implementation of a desktop supercomputer for high performance image processing. Color image processing using cellular neural networks
[AD-A283071] p 571 N95-14178

COMBAT
Combat Agility Management System (CAMS)
p 397 N95-14250
Aircraft maneuver envelope warning system
[NASA-CASE-ARC-11953-1] p 411 N95-14518

COMBINATORIAL ANALYSIS
Discourse interpretation and the scope of operators
[TR-518] p 586 N95-15595

COMBUSTIBLE FLOW
Numerical simulation of shock-induced combustion past blunt bodies using shock-fitting technique
[NASA-CR-197013] p 437 N95-14268

COMBUSTION
Assessing post-fire combustion of polyurethane
[DE94-011461] p 438 N95-14375
Conceptual design of the Space Station fluids module
p 429 N95-14584
Behavior of charring materials in simulated fire environments
[PB94-196045] p 439 N95-14838
Simulation of coal and char nitrogen reactions in combustion
[DE94-013941] p 440 N95-15291

COMBUSTION CHAMBERS
Combustion efficiency in a dual-inlet side-dump ramjet combustor
[AD-A283564] p 411 N95-15329
Gas turbine prediffuser-combustor performance during operation with air-water mixture
[DOT/FAA/CT-93/52] p 411 N95-15683

COMBUSTION CHEMISTRY
Behavior of charring materials in simulated fire environments
[PB94-196045] p 439 N95-14838
Theoretical studies of hydrocarbon combustion chemistry
[DE94-017155] p 441 N95-15347

COMBUSTION EFFICIENCY
Combustion efficiency in a dual-inlet side-dump ramjet combustor
[AD-A283564] p 411 N95-15329

COMBUSTION PHYSICS
Assessing post-fire combustion of polyurethane
[DE94-011461] p 438 N95-14375
Infrared absorption spectroscopy and chemical kinetics of free radicals
[DE94-016642] p 438 N95-14392

COMBUSTION PRODUCTS
The solid surface combustion experiment aboard the USML-1 mission p 458 N95-14212
Recycled plastic: A clean and low cost rocket fuel
[TABES PAPER 94-610] p 416 N95-14642
High temperature membranes for H2S and SO2 separations
[DE94-017125] p 441 N95-15345
Burn rates of TiH2/KClO4/Viton and output testing of NASA SKD26100098-301 pressure cartridges
[NASA-CR-188357] p 443 N95-15715

COMETARY COLLISIONS
Dynamical properties measurements for asteroid, comet and meteorite material applicable to impact modeling and mitigation calculations
[DE94-014142] p 642 N95-14311

COMETS
Dynamical properties measurements for asteroid, comet and meteorite material applicable to impact modeling and mitigation calculations
[DE94-014142] p 642 N95-14311

COMMAND AND CONTROL
Human factors requirements for telerobotic command and control: The European Space Agency experimental programme p 562 N95-14059
Evolutionary Telemetry and Command Processor (TCP) architecture p 420 N95-14162
Efficient mission control for the 48-satellite Globalstar constellation
[TABES PAPER 94-609] p 415 N95-14641
Wireless technology for command control and communications
[AD-A284367] p 470 N95-15804

COMMERCE
Benefits of CMM-based software process improvement: Initial results
[AD-A283848] p 572 N95-14349
Design in Huntsville, manufacture in Estonia, sell in Europe
[TABES PAPER 94-607] p 415 N95-14640

COMMERCIAL AIRCRAFT
Proceedings of the FAA Inspection Program Area Review
[AD-A283849] p 405 N95-14350
Evaluation of bonded boron/epoxy doublers for commercial aircraft aluminum structures
p 508 N95-14457
Annual review of aircraft accident data: US air carrier operations, calendar year 1992
[NTSB/ARC-94/02] p 407 N95-15066
The Aluminum Falcon: A low cost modern commercial transport
[NASA-CR-197180] p 409 N95-15742

COMMODITIES
Energy review
[DE94-015828] p 518 N95-14326

COMMUNICATION NETWORKS
Models of remote manipulation in space
p 504 N95-14027
From Antarctica to space: Use of telepresence and virtual reality in control of remote vehicles
p 427 N95-14099
CAPTIONALS: A computer aided testing environment for the verification and validation of communication protocols p 570 N95-14163
Performance comparison of token ring protocols for hard-real-time communication p 570 N95-14164
An evaluation of B-ISDN for the communication architecture requirements of Distributed Interactive Simulation (DIS)
[AD-A280783] p 578 N95-14292
Propagation considerations for the Odyssey system design p 466 N95-14680
High-data-rate UHF line-of-sight communication experiment
[AD-A283592] p 468 N95-15321
NASA/DOD Aerospace Knowledge Diffusion Research Project. Report 30: Computer-Mediated Communication (CMC) and the communication of technical information in aerospace
[NASA-CR-194973] p 633 N95-15585
Performance modeling and analysis of parallel processing and Low Earth Orbit satellite communication systems
[AD-A283243] p 470 N95-15652
Wireless technology for command control and communications
[AD-A284367] p 470 N95-15804
Discrete-event-dynamic-system-based approaches for control in integrated voice/data multihop radio networks
[AD-A284413] p 470 N95-15813

COMMUNICATION SATELLITES
Journal of Spacecraft Technology, volume 4, no. 2, July 1994 p 413 N95-13825
Satellite communication technology and applications, 1995-2010 p 413 N95-13826
A simulation algorithm for availability computation of a communication satellite constellation
p 414 N95-13832
Environmental testing to prevent on-orbit TDRS failures p 423 N95-14078
Efficient mission control for the 48-satellite Globalstar constellation
[TABES PAPER 94-609] p 415 N95-14641
Olympus propagation experiments
p 464 N95-14671
The 40 and 50 GHz propagation experiments at the Rutherford Appleton Laboratory, UK, using the ITALSAT beacons p 465 N95-14674

COMMUTER AIRCRAFT
Fatigue evaluation of empennage, forward wing, and winglets/tip fins on part 23 airplanes
[PB94-196813] p 408 N95-13981

COMPARISON
Flight and full-scale wind-tunnel comparison of pressure distributions from an F-18 aircraft at high angles of attack --- Conducted in NASA Ames Research Center's 80 by 120 ft wind tunnel p 394 N95-14231

COMPATIBILITY
Type 304L stainless steel surface microstructure: Performance in hydride storage and acid cleaning
[DE94-014654] p 447 N95-15625

COMPENSATORY TRACKING
Rotational wind indicator enhances control of rotated displays p 559 N95-14048

COMPETITION
The 24th International Physics Olympiad
[AD-A280584] p 589 N95-13972

COMPILERS
Compiler optimizations for cache locality and coherence
[TR-504] p 586 N95-15589
The lambda loop transformation toolkit (user's reference manual)
[TR-511] p 587 N95-15733

COMPLETENESS
Conditional graph completions
[AD-A282914] p 587 N95-15612

COMPLEX NUMBERS
A general method to construct oracles realizing given relationships between complexity classes
[TR-500] p 588 N95-15854

COMPLEX SYSTEMS
Aero design of turbomachinery components: CFD in complex systems p 481 N95-14136
The principles of fault-tolerant and efficient parallel computation
[AD-A283254] p 579 N95-15616
On accessing and hiding information
p 587 N95-15641
On point-based temporal disjointness
[TR-497] p 587 N95-15643
Intelligence in scientific computing
[AD-A284410] p 584 N95-15811

COMPLEX VARIABLES
Coherent states on the m-sheeted complex plane as m-photon states p 598 N95-13940
Study of multiple cracks in airplane fuselage by micromechanics and complex variables
p 509 N95-14468

COMPLEXITY
Upward separation for FewP and related classes
[TR-488] p 575 N95-15721
A general method to construct oracles realizing given relationships between complexity classes
[TR-500] p 588 N95-15854

COMPONENT RELIABILITY
Earth Observing System (EOS) Advanced Microwave Sounding Unit-A (AMSU-A) Spares Program Plan
[NASA-CR-189380] p 567 N95-13632

COMPOSITE MATERIALS
Thin composite solid electrolyte film for lithium batteries
[NASA-CASE-NPO-18694-1-CU] p 472 N95-13824
Improved composite material and method for production of improved composite material
[NASA-CASE-LAR-14892-1] p 433 N95-13836

Analysis of neutron diffraction peak broadening caused by internal stresses in composite materials
[DE94-014453] p 433 N95-13993
Poly(arylene ether imidazole) surfacing films for flat and parabolic structures
[NASA-CASE-LAR-14812-1] p 450 N95-14140
AEM and HREM evaluation of carbon nanostructures in silica aerogels
[DE94-014913] p 434 N95-14387
Development of a composite repair and the associated inspection intervals for the F-111C stiffener runout region p 392 N95-14477
Towards the molecular design of composite materials
[AD-A283422] p 627 N95-15404

COMPOSITE STRUCTURES
Residual strength of composites with multiple impact damage
[AD-A284230] p 434 N95-14409
Discrete-layer piezoelectric plate and shell models for active tip-clearance control
[NASA-CR-195383] p 507 N95-14417
Milestone 4: Thrust structure concepts and IHM screening Graphite Composite Primary Structure (GCPS)
[NASA-CR-197053] p 434 N95-14800
Innovative design of composite structures: Design, manufacturing, and testing of plates utilizing curvilinear fiber trajectories
[NASA-CR-197045] p 435 N95-14865

COMPRESSIBILITY
Interaction of chemistry, turbulence, and shock waves in hypervelocity flow
[AD-A282941] p 400 N95-14656
Composites with improved compressive properties
[AD-A283411] p 435 N95-15417

COMPRESSIBLE BOUNDARY LAYER
Noise radiation by instability waves in coaxial jets
[NASA-TM-106738] p 591 N95-14618

COMPRESSIBLE FLOW
Numerical study of the effects of icing on viscous flow over wings
[NASA-CR-197102] p 400 N95-14803
Polymer-polymer interactions
[AD-A282944] p 453 N95-14844
Embedded function methods for compressible high speed turbulent flow
[NASA-CR-196936] p 492 N95-14932

COMPRESSING
Photon statistics of a two-mode squeezed vacuum p 598 N95-13909
Squeezed light from multi-level closed-cycling atomic systems p 598 N95-13920

COMPRESSION RATIO
1994 Science Information Management and Data Compression Workshop
[NASA-CP-3277] p 564 N95-14585
Blocking reduction of Landsat Thematic Mapper JPEG browse images using optimal PSNR estimated spectra adaptive postfiltering p 565 N95-14589
Compression of regions in the global advanced very high resolution radiometer 1-km data set p 565 N95-14591
Lossless compression of NOAA-AVHRR satellite data p 565 N95-14592
The development of lossless data compression technology for remote sensing applications p 565 N95-14593
Planning/scheduling techniques for VQ-based image compression p 566 N95-14595
Neural networks: Alternatives to conventional techniques for automatic docking
[TABES PAPER 94-627] p 417 N95-14651

COMPRESSION TESTS
Innovative design of composite structures: Design, manufacturing, and testing of plates utilizing curvilinear fiber trajectories
[NASA-CR-197045] p 435 N95-14865

COMPRESSOR BLADES
Elements of a modern turbomachinery design system p 480 N95-14129
Designing in three dimensions p 480 N95-14130
The industrial use of CFD in the design of turbomachinery p 480 N95-14133
New methods, new methodology: Advanced CFD in the Snecma turbomachinery design process p 480 N95-14134
Experimental/analytical approach to understanding mistuning in a transonic wind tunnel compressor
[NASA-TM-108833] p 512 N95-14617

COMPRESSORS
Experimental/analytical approach to understanding mistuning in a transonic wind tunnel compressor
[NASA-TM-108833] p 512 N95-14617
Gas turbine prediffuser-combustor performance during operation with air-water mixture
[DOT/FAA/CT-93/52] p 411 N95-15683

COMPUTATION
Methodology for the parallel direct solution of finite element systems
[PB94-198009] p 585 N95-13991
Relativistic configuration-interaction calculation of the correlation energies of heliumlike ions
[DE94-015190] p 621 N95-14325
Workshop on Advances in Scientific Computation and Differential Equations 1993 (SCADE)
[AD-A283111] p 585 N95-14657
High performance computational chemistry: Towards fully distributed parallel algorithms
[DE94-014561] p 573 N95-15311
Unambiguous computation: Boolean hierarchies an sparse Turing-complete sets
[TR-483] p 575 N95-15597
Universally serializable computation
[TR-520] p 587 N95-15732

COMPUTATIONAL CHEMISTRY
Computational modeling issues in next generation air quality models
[PB94-197449] p 521 N95-14122
LSENS: A General Chemical Kinetics and Sensitivity Analysis Code for homogeneous gas-phase reactions. Part 1: Theory and numerical solution procedures
[NASA-RP-1328-PT-1] p 440 N95-15056
LSENS: A General Chemical Kinetics and Sensitivity Analysis Code for homogeneous gas-phase reactions. Part 3: Illustrative test problems
[NASA-RP-1330-PT-3] p 440 N95-15057
High performance computational chemistry: Towards fully distributed parallel algorithms
[DE94-014561] p 573 N95-15311
Computational chemistry packages on the CRAY Y-MP in trondheim
[PB94-208246] p 595 N95-15350
SAM1 semiempirical parameters
[AD-A284400] p 443 N95-15782

COMPUTATIONAL FLUID DYNAMICS
The flow induced by the coalescence of two initially stationary drops
[NASA-TM-106752] p 478 N95-13653
User's guide for ENSAERO: A multidisciplinary program for fluid/structural/control interaction studies of aircraft (release 1)
[NASA-TM-108853] p 391 N95-13662
Developments in laser-based diagnostics for wind tunnels in the Aeromechanics Division: 1987-1992
[AD-A283011] p 412 N95-13687
An adaptively-refined, Cartesian, cell-based scheme for the Euler and Navier-Stokes equations
[NASA-TM-106754] p 392 N95-13817
Numerical modeling of a cryogenic fluid within a fuel tank
[NASA-TM-4651] p 479 N95-13892
Turbomachinery Design Using CFD
[AGARD-LS-195] p 479 N95-14127
Computational methods for preliminary design and geometry definition in turbomachinery p 480 N95-14128
Designing in three dimensions p 480 N95-14130
CFD methodology and validation for turbomachinery flows p 480 N95-14131
Unsteady flows in turbines: Impact on design procedure p 480 N95-14132
The industrial use of CFD in the design of turbomachinery p 480 N95-14133
New methods, new methodology: Advanced CFD in the Snecma turbomachinery design process p 480 N95-14134
The role of CFD in the design process p 481 N95-14135
Aero design of turbomachinery components: CFD in complex systems p 481 N95-14136
A selection of experimental test cases for the validation of CFD codes, volume 1
[AGARD-AR-303-VOL-1] p 481 N95-14201
Hybrid structured/unstructured grid computations for the F/A-18 at high angle of attack p 394 N95-14233
Computational aerodynamics based on the Euler equations
[AGARD-AG-325] p 398 N95-14264
A Cartesian, cell-based approach for adaptively-refined solutions of the Euler and Navier-Stokes equations
[NASA-TM-106786] p 398 N95-14297
Engineering Codes for aeroprediction: State-of-the-art and new methods p 399 N95-14447
Navier-Stokes predictions of missile aerodynamics p 399 N95-14451
Computation of supersonic air-intakes p 400 N95-14452
A modified mixing length turbulence model for zero and adverse pressure gradients
[NASA-TM-106772] p 492 N95-14607
Numerical simulation of the flow about the F-18 HARV at high angle of attack
[NASA-CR-197023] p 400 N95-14614
Numerical study of the effects of icing on viscous flow over wings
[NASA-CR-197102] p 400 N95-14803
An approximate Riemann solver for thermal and chemical nonequilibrium flows
[NASA-CR-195003] p 492 N95-14912
Development and application of structural dynamics analysis capabilities
[NASA-CR-197229] p 513 N95-14922
Embedded function methods for compressible high speed turbulent flow
[NASA-CR-196936] p 492 N95-14932
Robust multigrid methods for the steady and unsteady incompressible Navier-Stokes equations in general coordinates
[PB94-195534] p 492 N95-15315
A proposed framework for computational fluid dynamics code calibration and validation
[DE94-015799] p 493 N95-15351
Computational methods for PDE's in flow control, superconductivity, fluid flows and other applications
[AD-A282912] p 493 N95-15390
Numerical design of advanced multi-element airfoils
[NASA-CR-197135] p 404 N95-15762
An approach for dynamic grids
[NASA-TM-106774] p 404 N95-15853

COMPUTATIONAL GEOMETRY
Aerodynamic shape optimization of a HSCT type configuration with improved surface definition
[NASA-CR-197011] p 392 N95-13701
Computational methods for preliminary design and geometry definition in turbomachinery p 480 N95-14128

COMPUTATIONAL GRIDS
An adaptively-refined, Cartesian, cell-based scheme for the Euler and Navier-Stokes equations
[NASA-TM-106754] p 392 N95-13817
Turbomachinery Design Using CFD
[AGARD-LS-195] p 479 N95-14127
Aero design of turbomachinery components: CFD in complex systems p 481 N95-14136
Hybrid structured/unstructured grid computations for the F/A-18 at high angle of attack p 394 N95-14233
A Cartesian, cell-based approach for adaptively-refined solutions of the Euler and Navier-Stokes equations
[NASA-TM-106786] p 398 N95-14297
Parallel isosurface generator for huge data sets
[AD-A284030] p 578 N95-14422
Thermocapillary motion of deformable drops p 485 N95-14544
Numerical solution of two-dimensional ablation problems using the finite control volume method with unstructured grids
[DE94-015012] p 428 N95-14664
Xwake 1.0: A new tool for wakefield and impedance calculations
[DE94-015545] p 574 N95-15418
An algorithm for rezoning particle-in-cell calculations
[DE94-016056] p 619 N95-15774
An approach for dynamic grids
[NASA-TM-106774] p 404 N95-15853

COMPUTER AIDED DESIGN
Aerodynamic shape optimization of a HSCT type configuration with improved surface definition
[NASA-CR-197011] p 392 N95-13701
A prototype lisp-based soft real-time object-oriented Graphical User Interface for control system development
[NASA-TM-106743] p 566 N95-13716
Journal of Spacecraft Technology, volume 4, no. 2, July 1994 p 413 N95-13825
Computer aided techniques for the realisation of the diaphragm of the PSM for the IRS-1C p 413 N95-13829
The exploration metaphor p 557 N95-14037
Turbomachinery Design Using CFD
[AGARD-LS-195] p 479 N95-14127
Designing in three dimensions p 480 N95-14130
New methods, new methodology: Advanced CFD in the Snecma turbomachinery design process p 480 N95-14134
Aero design of turbomachinery components: CFD in complex systems p 481 N95-14136
Knowledge-based computational approach to architectural precedent analysis
[PB94-191269] p 568 N95-14152
Computer Aided Engineering (CAE) overview
[AD-A280966] p 572 N95-14616
A SIMULINK environment for flight dynamics and control analysis: Application to the DHC-2 Beaver. Part 1: Implementation of a model library in SIMULINK. Part 2: Nonlinear analysis of the Beaver autopilot
[NONP-NASA-SUPPL-DK-94-2802] p 412 N95-14815

Robust multigrid methods for the steady and unsteady incompressible Navier-Stokes equations in general coordinates
[PB94-195534] p 492 N95-15315
Modelling and investigation of EHD point contacts
[AD-A283571] p 454 N95-15316
Using Pro/ENGINEER's (tm) interface module
[DE94-013364] p 574 N95-15384
Experimental evaluation of cursors for B-2 Synthetic Aperture Radar (SAR) application
[AD-A283025] p 468 N95-15393
Rapid prototyping applications at Sandia National Laboratories
[DE94-006360] p 460 N95-15409

COMPUTER AIDED MANUFACTURING
Intelligent manufacturing systems state of the art
[TABES PAPER 94-503] p 415 N95-14637
Rapid prototyping applications at Sandia National Laboratories
[DE94-006360] p 460 N95-15409

COMPUTER AIDED MAPPING
Hardware implementation of a desktop supercomputer for high performance image processing. Color image processing using cellular neural networks
[AD-A283071] p 571 N95-14178

COMPUTER AIDED TOMOGRAPHY
The advanced development of x-ray computed tomography applications
[AD-A284211] p 434 N95-14411

COMPUTER ANIMATION
Implementation of a three degree of freedom, motor/brake hybrid force output device for virtual environment control tasks p 562 N95-14058
VERDEX: A virtual environment demonstrator for remote driving applications p 562 N95-14060

COMPUTER ASSISTED INSTRUCTION
Summary Proceedings of the Joint Industry-FAA Conference on the Development and use of PC-Based Aviation Training Devices
[DOT/FAA/AM-94/25] p 573 N95-14917

COMPUTER COMPATIBLE TAPES
Two heads are better than two tapes
[TR-493] p 575 N95-15644
Connections among space-bounded and multihead probabilistic automata
[TR-476] p 575 N95-15645

COMPUTER DESIGN
The prospects for on-line hybrid coherency protocols on bus-based multiprocessors
[TR-490] p 579 N95-15590

COMPUTER GRAPHICS
PHOENIX user manual. First version
[PB94-189081] p 568 N95-13989
Virtual reality at work p 556 N95-14033
The Ames Virtual Environment Workstation: Implementation issues and requirements p 557 N95-14034
Development of visual 3D virtual environment for control software p 559 N95-14048
The role of CFD in the design process p 481 N95-14135
Parallel image rendering algorithm and architecture based on ray tracing and radiosity shading
[PB94-191277] p 569 N95-14153
A high performance graphics algorithm
[DE94-015033] p 571 N95-14196
DDI, the Data and Dimensions Interface
[DE94-014750] p 522 N95-14317
Parallel isosurface generator for huge data sets
[AD-A284030] p 578 N95-14422
CTAS data analysis program
[NASA-TM-108842] p 406 N95-14611
Spatial awareness comparisons between large-screen, integrated pictorial displays and conventional EFIS displays during simulated landing approaches
[NASA-TP-3467] p 409 N95-14852
Modelling and investigation of EHD point contacts
[AD-A283571] p 454 N95-15316
The principles of fault-tolerant and efficient parallel computation
[AD-A283254] p 579 N95-15616
Graphical aids for the users of GEMACS (GAUGE): Ray tracing enhancements
[AD-A284903] p 470 N95-15756

COMPUTER INFORMATION SECURITY
An efficient network for interconnecting remote monitoring instruments and computers
[DE94-016213] p 581 N95-14377

COMPUTER NETWORKS
Advanced distributed simulation technology: Digital Voice Gateway Reference Guide
[AD-A283154] p 460 N95-13696
David Florida Laboratory Thermal Vacuum Data Processing System p 418 N95-14079
Three neural network based sensor systems for environmental monitoring
[DE94-014557] p 522 N95-14195
An evaluation of B-ISDN for the communication architecture requirements of Distributed Interactive Simulation (DIS)
[AD-A280783] p 578 N95-14292
Automated network protocol reachability analysis with supertrace algorithm and TESTGEN: Automated generation of test sequence for a formal protocol specification
[AD-A280788] p 461 N95-14293
An efficient network for interconnecting remote monitoring instruments and computers
[DE94-016213] p 581 N95-14377
1994 Science Information Management and Data Compression Workshop
[NASA-CP-3277] p 564 N95-14585
Planning/scheduling techniques for VQ-based image compression p 566 N95-14595
An overview of the EOSDIS V0 information management system: Lessons learned from the implementation of a distributed data system p 566 N95-14596
Structured approaches for problems of network design and utilization
[AD-A282925] p 578 N95-15416
Automatic TLI recognition system, part 2
[DE94-015393] p 579 N95-15534
Robust routing in dynamic networks, part 1
[AD-A282445] p 583 N95-15548
Data flow manager for DART
[DE94-013236] p 579 N95-15581
NASA/DOD Aerospace Knowledge Diffusion Research Project. Report 30: Computer-Mediated Communication (CMC) and the communication of technical information in aerospace
[NASA-CR-194973] p 633 N95-15585

COMPUTER PROGRAM INTEGRITY
Earth Observing System (EOS)/Advanced Microwave Sounding Unit-A (AMSU-A) software assurance plan
[NASA-CR-196059] p 515 N95-13885
Formal methods technology transfer: Some lessons learned p 571 N95-14172
Automated test environment for a real-time control system
[TABES PAPER 94-631] p 417 N95-14652
The principles of fault-tolerant and efficient parallel computation
[AD-A283254] p 579 N95-15616

COMPUTER PROGRAMMING
Remote sensing, processing and transmission of data for an unmanned aerial vehicle
[AD-A283104] p 514 N95-13693
Advanced distributed simulation technology: Digital Voice Gateway Reference Guide
[AD-A283154] p 460 N95-13696
Hybrid verification by exploiting the environment
[NASA-CR-195810] p 568 N95-13699
Knowledge-based processing for aircraft flight control
[NASA-CR-194976] p 580 N95-13727
Earth Observing System (EOS)/Advanced Microwave Sounding Unit-A (AMSU-A) software assurance plan
[NASA-CR-196059] p 515 N95-13885
Elements of a modern turbomachinery design system p 480 N95-14129
New methods, new methodology: Advanced CFD in the Snecma turbomachinery design process p 480 N95-14134
Formal methods technology transfer: Some lessons learned p 571 N95-14172
ADST ARWA visual system module software design document
[AD-A283874] p 572 N95-14357
Data processing routines for the Sippican MK-12 XBT system
[AD-A283570] p 536 N95-15330
Universally serializable computation
[TR-520] p 587 N95-15732
Genetic programming with adaptive representations
[TR-489] p 576 N95-15856

COMPUTER PROGRAMS
Remote programming in INSAT-2A/2B on-board Attitude and Orbit Control Computer (AOCC) p 413 N95-13827
GSOSTATS database: USAF synchronous satellite catalog data conversion software. User's guide and software maintenance manual, version 2.1
[NASA-TM-106760] p 568 N95-13894
The role of CFD in the design process p 481 N95-14135
Aero design of turbomachinery components: CFD in complex systems p 481 N95-14136
ASSERT-1992. Fundamental studies of a high energy molecular system: Spectroscopy of boron in hydrogen clusters
[AD-A283181] p 593 N95-14155

Generic architectures for future flight systems p 567 N95-14159
A high performance graphics algorithm
[DE94-015033] p 571 N95-14196
Radiative interactions in multi-dimensional chemically reacting flows using Monte Carlo simulations
[NASA-CR-197012] p 481 N95-14269
Benefits of CMM-based software process improvement: Initial results
[AD-A283848] p 572 N95-14349
Recent advances in the modelling of crack growth under fatigue loading conditions p 511 N95-14478
Pre-flight POLAR code predictions for the CHAWS space flight experiment
[AD-A280951] p 428 N95-14599
Applying CASE technology to the software maintenance life cycle
[TABES PAPER 94-620] p 416 N95-14647
Artificial neural network modeling of damaged aircraft
[AD-A283227] p 409 N95-14849
USAF single-event sonic boom prediction model: PCBoom3 p 403 N95-14889
Speakeasy software development
[AD-A283816] p 468 N95-15333
A proposed framework for computational fluid dynamics code calibration and validation
[DE94-015799] p 493 N95-15351
Large-scale data envelopment analysis models and related applications
[AD-A283214] p 588 N95-15400
A theoretical study of 30 to 50 angstrom noble gas heavy ion lithography
[DE94-015262] p 442 N95-15436
Connection machine software conversion of the Navy TOPS model
[AD-A281681] p 579 N95-15450
LSENS, a general chemical kinetics and sensitivity analysis code for homogeneous gas-phase reactions. 2: Code description and usage
[NASA-RP-1329] p 442 N95-15512
System administrator's guide to CDPS
[DE94-015288] p 633 N95-15528
The principles of fault-tolerant and efficient parallel computation
[AD-A283254] p 579 N95-15616
Fault-tolerance and efficiency in massively parallel algorithms
[AD-A283255] p 579 N95-15617
Technical report series on global modeling and data assimilation. Volume 3: An efficient thermal infrared radiation parameterization for use in general circulation models
[NASA-TM-104606-VOL-3] p 531 N95-15745
Experimental hardware development for a pulsed ultrasonic data collection facility
[AD-A283331] p 615 N95-15872

COMPUTER STORAGE DEVICES
Acceleration recorder and playback module
[NASA-CASE-MSC-22008-1] p 496 N95-14180
Compiler optimizations for cache locality and coherence
[TR-504] p 586 N95-15589

COMPUTER SYSTEMS DESIGN
Advanced distributed simulation technology: Digital Voice Gateway Reference Guide
[AD-A283154] p 460 N95-13696
A prototype lisp-based soft real-time object-oriented Graphical User Interface for control system development
[NASA-TM-106743] p 566 N95-13716
The exploration metaphor p 557 N95-14037
RICIS Symposium 1992: Mission and Safety Critical Systems Research and Applications
[NASA-CR-196963] p 569 N95-14156
POSIX real-time extensions p 570 N95-14165
Formal methods technology transfer: Some lessons learned p 571 N95-14172
An efficient network for interconnecting remote monitoring instruments and computers
[DE94-016213] p 581 N95-14377
TABES 1994: 10th Annual Technical and Business Exhibition and Symposium p 414 N95-14633
ROOM: A recursive object oriented method for information systems development
[DE94-007575] p 633 N95-15761
Design document for the MOODS Data Management System (MDMS), version 1.0
[NASA-CR-197016] p 633 N95-15801

COMPUTER SYSTEMS PERFORMANCE
Earth Observing System (EOS)/Advanced Microwave Sounding Unit-A (AMSU-A) software assurance plan
[NASA-CR-196059] p 515 N95-13885
David Florida Laboratory Thermal Vacuum Data Processing System p 418 N95-14079
MISSION: Mission and Safety Critical Support Environment. Executive overview p 569 N95-14158

Generic architectures for future flight systems p 567 N95-14159
Architecture for Survivable Systems Processing (ASSP). Technology benefits for Open System Interconnects p 567 N95-14160
Space Generic Open Avionics Architecture (SGOAA): Overview p 569 N95-14161
Evolutionary Telemetry and Command Processor (TCP) architecture p 420 N95-14162
POSIX real-time extensions p 570 N95-14165
Software development for safety-critical medical applications p 571 N95-14171
Computing quantitative characteristics of finite-state real-time systems
[AD-A282839] p 412 N95-14343
Performance measurement and analysis techniques for parallel and distributed programs
[DE94-016429] p 578 N95-14384

COMPUTER SYSTEMS PROGRAMS
Three neural network based sensor systems for environmental monitoring
[DE94-014557] p 522 N95-14195
Toward deriving software architectures from quality attributes
[AD-A283827] p 572 N95-14339
An efficient network for interconnecting remote monitoring instruments and computers
[DE94-016213] p 581 N95-14377
Structured approaches for problems of network design and utilization
[AD-A282925] p 578 N95-15416
Design document for the Surface Currents Data Base (SCDB) Management System (SCDBMS), version 1.0
[NASA-CR-197019] p 537 N95-15751

COMPUTER SYSTEMS SIMULATION
Modeling and simulation of a Fiber Distributed Data Interface Local Area Network (FDDI LAN) using OPNET (tm) for interfacing through the Common Data Link (CDL)
[AD-A283124] p 469 N95-15651

COMPUTER TECHNIQUES
Computer aided techniques for the realisation of the diaphragm of the PSM for the IRS-1C p 413 N95-13829
European Workshop Industrical Computer Science Systems approach to design for safety p 569 N95-14157
CAPTIONALS: A computer aided testing environment for the verification and validation of communication protocols p 570 N95-14163
Software development for safety-critical medical applications p 571 N95-14171
Developing Guided Search 3.0. The next generation of a model visual search
[AD-A283956] p 552 N95-14369
Study of multiple cracks in airplane fuselage by micromechanics and complex variables p 509 N95-14468
Extracting a representative loading spectrum from recorded flight data p 410 N95-14469
A graphical user interface for design and analysis of air breathing propulsion systems
[TABES PAPER 94-616] p 411 N95-14645
Building complex simulations rapidly using MATRIX(x): The Space Station redesign
[TABES PAPER 94-632] p 417 N95-14653
Propagation in the ionosphere, B p 467 N95-14827
Ground wave and diffraction, B p 467 N95-14829
Electro-optics: Propagation from IR to UV and sensor considerations. Part B: Tools for exploitation of propagation conditions and system range performance p 467 N95-14834
Interactive Computer-Enhanced Remote Viewing System (ICERVS): Subsystem design report, phase 2
[DE94-014513] p 563 N95-15309
FFCAst Clearinghouse, directory of abstracts
[DE94-015259] p 632 N95-15435
Research in high energy physics
[DE94-015519] p 600 N95-15539
On accessing and hiding information p 587 N95-15641
Reengineering through information technology. Accompanying report of the National Performance Review
[PB94-170362] p 633 N95-15781
Seeing behind occlusions
[TR-487] p 576 N95-15857
Enhanced capabilities and updated users manual for axial-flow turbine preliminary sizing code TURBAN
[NASA-CR-195405] p 405 N95-15912

COMPUTER VISION
Eye movement control and top-down scanpath vision as a design metaphor for robotic vision and control p 555 N95-14022
Variable window Gabor filters and their use in focus and correspondence
[AD-A282837] p 573 N95-14842
Control of selective perception using Bayes nets and decision theory
[TR-468] p 573 N95-15151
Vision-based navigation and recognition
[AD-A282962] p 583 N95-15398
Gaze selection for visual search
[TR-512] p 587 N95-15775
Vision, learning, and development
[TR-492-REV] p 553 N95-15787
Seeing behind occlusions
[TR-487] p 576 N95-15857

COMPUTERIZED SIMULATION
Measurement and interpretation of crustal deformation rates associated with postglacial rebound
[NASA-CR-196440] p 525 N95-13627
HRMA calibration handbook: EKC gravity compensated XRCF models
[NASA-CR-195818] p 636 N95-13634
A simulation algorithm for availability computation of a communication satellite constellation p 414 N95-13832
An optical simulation of shared memory
[DE94-013824] p 568 N95-13976
Computing illumination using extended sources: Object space and image space
[PB94-201282] p 612 N95-13992
Some criteria for teleoperators and virtual environments from experiences with vehicle/operator simulation p 556 N95-14028
Varieties of virtualization p 557 N95-14036
The exploration metaphor p 557 N95-14037
A two dimensional artificial reality p 560 N95-14052
Active localization of virtual sounds p 561 N95-14054
Implementation of a three degree of freedom, motor/brake hybrid force output device for virtual environment control tasks p 562 N95-14058
Destabilizing effects of visual environment motions simulating eye movements or head movements p 562 N95-14061
Self contamination effects in the TAUVEX UV Telescope: Ground testing and computer simulation p 421 N95-14067
A simulation facility for testing Space Station assembly procedures p 423 N95-14075
HYDRA, a new tool for mechanical testing p 418 N95-14086
Evaluation of sensor placement algorithms for on-orbit identification of space platforms p 425 N95-14088
Unique life sciences research facilities at NASA Ames Research Center p 426 N95-14091
Applications of a fast and efficient method for simulating orbital mission safety p 426 N95-14093
Simulation of a spatial, servo-hydraulic test facility for space structures p 418 N95-14095
The role of CFD in the design process p 481 N95-14135
EPIC computational models of psychological refractory-period effects in human multiple-task performance
[AD-A280924] p 540 N95-14142
Parallel image rendering algorithm and architecture based on ray tracing and radiosity shading
[PB94-191277] p 569 N95-14153
CAPTIONALS: A computer aided testing environment for the verification and validation of communication protocols p 570 N95-14163
Developing molecular dynamics simulation codes using mixed language programming
[DE94-015456] p 571 N95-14190
Radiative interactions in multi-dimensional chemically reacting flows using Monte Carlo simulations
[NASA-CR-197012] p 461 N95-14269
An evaluation of B-ISDN for the communication architecture requirements of Distributed Interactive Simulation (DIS)
[AD-A280783] p 578 N95-14292
DDI, the Data and Dimensions Interface
[DE94-014750] p 522 N95-14317
Analysis of welding-induced residual stresses with the ADINA system
[DE94-015359] p 506 N95-14320
ADST ARWA visual system module software design document
[AD-A283874] p 572 N95-14357
Developing Guided Search 3.0. The next generation of a model visual search
[AD-A283956] p 552 N95-14369
Second International Conference on Computer Simulation of Radiation Effects in Solids
[DE94-016368] p 594 N95-14383
Lithological and rheological constraints on fault rupture scenarios for ground motion hazard prediction
[DE94-014742] p 529 N95-14436
Numerical simulations of planetary gamma-ray spectra induced by galactic cosmic rays
[DE94-014809] p 647 N95-14438
Proceedings of the 3rd International Workshop on Computational Electronics
[AD-A284214] p 475 N95-14444
Fatigue analysis of multiple site damage at a row of holes in a wide panel p 508 N95-14463
Development of the NASA/FLAGRO computer program for analysis of airframe structures p 510 N95-14473
Space Shuttle fatigue loads spectra for prelaunch and liftoff loads p 419 N95-14474
Fatigue reliability method with in-service inspections p 505 N95-14475
Probing surface structure on late-type stars with FRESIP p 643 N95-14501
Thermocapillary convection in floating zones under simulated reduced-gravity conditions p 483 N95-14529
Multilayer fluid dynamics of immiscible liquids p 483 N95-14532
Wetting and spreading at the molecular scale p 484 N95-14539
Pre-flight POLAR code predictions for the CHAWS space flight experiment
[AD-A280951] p 428 N95-14599
Numerical simulation of the SOFIA flowfield
[NASA-CR-197025] p 400 N95-14612
Computer Aided Engineering (CAE) overview
[AD-A280966] p 572 N95-14616
The long-term forecast of station view periods p 419 N95-14621
Spin glasses and error-correcting codes p 462 N95-14624
The Block V Receiver fast acquisition algorithm for the Galileo S-band mission p 463 N95-14627
A trajectory preprocessor for antenna pointing p 463 N95-14630
TABES 1994: 10th Annual Technical and Business Exhibition and Symposium p 414 N95-14633
A graphical user interface for design and analysis of air breathing propulsion systems
[TABES PAPER 94-616] p 411 N95-14645
Product life cycle data base, analysis and simulation integration methodology
[TABES PAPER 94-626] p 417 N95-14650
Automated test environment for a real-time control system
[TABES PAPER 94-631] p 417 N95-14652
Building complex simulations rapidly using MATRIX(x): The Space Station redesign
[TABES PAPER 94-632] p 417 N95-14653
A SIMULINK environment for flight dynamics and control analysis: Application to the DHC-2 Beaver. Part 1: Implementation of a model library in SIMULINK. Part 2: Nonlinear analysis of the Beaver autopilot
[NONP-NASA-SUPPL-DK-94-2802] p 412 N95-14815
Propagation Modelling and Decision Aids for Communications, Radar and Navigation Systems
[AGARD-LS-196] p 466 N95-14825
Electro-optics: Propagation from IR to UV and sensor considerations. Part B: Tools for exploitation of propagation conditions and system range performance p 467 N95-14834
Evaluation of energy-sink stability criteria for dual-spin spacecraft
[AD-A283228] p 428 N95-14850
An in-home study of subjective response to simulated sonic booms p 403 N95-14891
Receiver design, performance analysis, and evaluation for space-borne laser altimeters and space-to-space laser ranging systems
[NASA-CR-197050] p 499 N95-14901
Multi-dimensional modeling of pressurization and expulsion of multi-phase hydrogen propellant
[NASA-CR-195156] p 457 N95-14902
Development and application of structural dynamics analysis capabilities
[NASA-CR-197229] p 513 N95-14922
Physiologic mechanisms effecting circulatory and body fluid losses in weightlessness as shown by mathematical modeling p 547 N95-15129
Simulation of the fluid retention effects of a vasopressin analog using the Guyton model of circulation p 547 N95-15130
Modelling and investigation of EHD point contacts
[AD-A283571] p 454 N95-15316
Computational chemistry packages on the CRAY Y-MP in trondheim
[PB94-208246] p 595 N95-15350
Gouge initiation in high-velocity rocket sled testing
[DE94-014288] p 418 N95-15357

Introduction to HEFeS (Hierarchical Environmental Feature Simulator)
[AD-A283244] p 534 N95-15402
Spatio-temporal neural networks for vision, reasoning and rapid decision making
[AD-A283251] p 583 N95-15403
The effects of spatial location of defect states on the switching characteristics of amorphous and polycrystalline silicon thin film transistors: A numerical simulation using AMPS 2-D
[DE94-013437] p 476 N95-15410
Accelerometer model in APLAC
[PB94-197647] p 497 N95-15413
Electron-molecule collisions and UV signatures in flowfields
[AD-A281569] p 596 N95-15457
LSENS, a general chemical kinetics and sensitivity analysis code for homogeneous gas-phase reactions. 2: Code description and usage
[NASA-RP-1329] p 442 N95-15512
A three-dimensional fast solver for arbitrary vorton distributions
[DE94-012581] p 404 N95-15570
Computational modeling of fiber-reinforced composites
[DE94-012914] p 436 N95-15573
Fault-tolerance and efficiency in massively parallel algorithms
[AD-A283255] p 579 N95-15617
Technical report series on global modeling and data assimilation. Volume 3: An efficient thermal infrared radiation parameterization for use in general circulation models
[NASA-TM-104606-VOL-3] p 531 N95-15745
Graphical aids for the users of GEMACS (GAUGE): Ray tracing enhancements
[AD-A284903] p 470 N95-15756
Modeling, simulation and engineering scale-up procedures for design of CVD reactors
[AD-A284919] p 494 N95-15760
Progress report on terrestrial model development (TERRA and HABITAT): Research in support of the CERES earth system modeling project
[DE94-016362] p 524 N95-15779
Introducing the International Geoid Service
p 516 N95-15792
Computer modeling the fatigue crack growth rate behavior of metals in corrosive environments
[NASA-CR-194982-REV] p 448 N95-15918

COMPUTERS
System administrator's guide to CDPS
[DE94-015288] p 633 N95-15528

CONCENTRATION (COMPOSITION)
Study of the long term stability of the effective concentration of ionized space charges (N(sub eff)) of neutron irradiated silicon detectors fabricated by various thermal oxidations
[DE94-013734] p 593 N95-14309

CONCENTRIC CYLINDERS
Two-layer viscous instability in a rotating couette device p 489 N95-14566

CONCURRENT ENGINEERING
Intelligent manufacturing systems state of the art
[TABES PAPER 94-503] p 415 N95-14637
Efficient mission control for the 48-satellite Globalstar constellation
[TABES PAPER 94-609] p 415 N95-14641
Product life cycle data base, analysis and simulation integration methodology
[TABES PAPER 94-626] p 417 N95-14650

CONCURRENT PROCESSING
Hybrid verification by exploiting the environment
[NASA-CR-195810] p 568 N95-13699
Development of visual 3D virtual environment for control software p 559 N95-14048

CONDENSATION NUCLEI
Condensation nuclei measurement in the stratosphere for the NASA ACE program
[NASA-CR-197031] p 530 N95-14855
Counting condensation in the Antarctic Ozone Mission
[NASA-CR-197113] p 525 N95-15847

CONDUCTING FLUIDS
Role of dielectric constant in electrohydrodynamics of conducting fluids p 478 N95-14577

CONDUCTING POLYMERS
Electrically conducting polyimide film containing tin complexes
[NASA-CASE-LAR-14936-1] p 450 N95-14113
Polysilanes with various architectures
[AD-A280842] p 452 N95-14400

CONDUCTION BANDS
Magnetic field dependent photoluminescence studies of InGaAs/GaAs strained-single-quantum wells
[DE94-015774] p 621 N95-14342

CONDUCTION ELECTRONS
Dynamical impurity problems
[DE94-013025] p 625 N95-15576

CONDUCTIVE HEAT TRANSFER
A realistic model of evaporation for a liquid droplet
p 485 N95-14543
Energy flux and hydrogeology of thermal anomalies in the Gulf of Mexico Basin: South Texas example
[DE94-015122] p 530 N95-14956

CONDUCTIVITY
Conductivity of polyacrylonitrile based lithium polymer electrolytes
[AD-A283965] p 450 N95-14203
Conductive paints
[DE94-014069] p 453 N95-15292

CONFERENCES
Addendum: Tenth International Symposium on Alcohol Fuels, The Road to Commercialization
[DE93-018219] p 457 N95-14003
Eighteenth Space Simulation Conference: Space Mission Success Through Testing
[NASA-CP-3280] p 420 N95-14062
RICIS Symposium 1992: Mission and Safety Critical Systems Research and Applications
[NASA-CR-196963] p 569 N95-14156
Fourth High Alpha Conference, volume 1
[NASA-CP-10143-VOL-1] p 393 N95-14229
Fourth High Alpha Conference, volume 2
[NASA-CP-10143-VOL-2] p 395 N95-14239
Fourth High Alpha Conference, volume 3
[NASA-CP-10143-VOL-3] p 397 N95-14251
Proceedings of the FAA Inspection Program Area Review
[AD-A283849] p 405 N95-14350
Second International Conference on Computer Simulation of Radiation Effects in Solids
[DE94-016368] p 594 N95-14383
US-Japan workshop Q-181 on High Heat Flux Components and Plasma-Surface Interactions for Next Devices: Proceedings
[DE94-014939] p 618 N95-14443
Proceedings of the 3rd International Workshop on Computational Electronics
[AD-A284214] p 475 N95-14444
FAA/NASA International Symposium on Advanced Structural Integrity Methods for Airframe Durability and Damage Tolerance
[NASA-CP-3274-PT-1] p 507 N95-14453
Second Microgravity Fluid Physics Conference
[NASA-CP-3276] p 482 N95-14522
Proceedings of the Eighteenth NASA Propagation Experimenters Meeting (NAPEX 18) and the Advanced Communications Technology Satellite (ACTS) Propagation Studies Miniworkshop
[NASA-CR-196959] p 464 N95-14670
High-Speed Research: 1994 Sonic Boom Workshop: Atmospheric Propagation and Acceptability Studies
[NASA-CP-3279] p 401 N95-14878
HTS Wire Development Workshop: Proceedings
[DE94-015650] p 624 N95-15421
International Semiconductor Device Research Symposium (ISDRS-93)
[AD-A281715] p 477 N95-15454
Low Temperature Grown and Highly Non-Stoichiometric GaAs and Related Materials
[AD-A284898] p 626 N95-15754
Technology and Science at at High-Power Spallation Source: Proceedings
[DE94-009685] p 597 N95-15826
The Diffuse Interstellar Bands: Contributed papers
[NASA-CP-10144] p 639 N95-15827
Symposium on Structural Intermetallics: Perspectives on Science and Technology, volume 2
[AD-A283379] p 447 N95-15874

CONFIGURATION INTERACTION
Relativistic configuration-interaction calculation of the correlation energies of heliumlike ions
[DE94-015190] p 621 N95-14325
Radiation rates for low Z impurities in edge plasmas
[DE94-016073] p 617 N95-14368

CONFIGURATION MANAGEMENT
Product life cycle data base, analysis and simulation integration methodology
[TABES PAPER 94-626] p 417 N95-14650

CONFINEMENT
Advanced tokamak research on the D3-D tokamak
[DE94-015860] p 617 N95-14426
Two-layer viscous instability in a rotating couette device p 489 N95-14566
Comparison of different statistical models of turbulence by similarity methods
[DE94-015326] p 493 N95-15530
Lower-hybrid poloidal current drive for fluctuation reduction in a reversed field pinch
[DE94-015534] p 618 N95-15540

CONFORMAL MAPPING
2D regular arrays for a special class of non uniform recurrence equations
[PB94-195633] p 584 N95-13980
Technical guidance for the development of a solid state image sensor for human low vision image warping
[NASA-CR-196997] p 612 N95-14272

CONICAL FLOW
Low-speed wind tunnel testing of the NPS and NASA Ames Mach 6 optimized waverider
[AD-A283585] p 404 N95-15319

CONJUGATE GRADIENT METHOD
Variable metric conjugate gradient methods
[DE94-014796] p 585 N95-14381

CONJUGATES
Multivariable Hermite polynomials and phase-space dynamics p 606 N95-13929

CONNECTION MACHINE
Connection machine software conversion of the Navy TOPS model
[AD-A281681] p 579 N95-15450

CONNECTORS
Adjustable bias column end joint assembly
[NASA-CASE-LAR-14899-1] p 459 N95-14111

CONSCIOUSNESS
Manipulating the arterial pressure to prevent G-LOC
p 546 N95-15123
Non-invasive physiological monitoring relevant to G-induced loss of consciousness p 547 N95-15125
Physiological considerations concerning Positive Pressure Breathing (PBG) during +Gz
p 547 N95-15126
Operational requirements for avoidance and eventual elimination of Gz-induced Loss Of Consciousness (G-LOC) in flight p 547 N95-15127

CONSISTENCY
The prospects for on-line hybrid coherency protocols on bus-based multiprocessors
[TR-490] p 579 N95-15590
On point-based temporal disjointness
[TR-497] p 587 N95-15843

CONSOLES
The console password feature for DEC workstations
[DE94-015721] p 566 N95-14338

CONSTITUTIVE EQUATIONS
Basic mechanics of laminated composite plates
[NASA-RP-1351] p 436 N95-15763

CONSTRAINTS
Robust multigrid methods for the steady and unsteady incompressible Navier-Stokes equations in general coordinates
[PB94-195534] p 492 N95-15315

CONSTRUCTION
Evaluation of sensor placement algorithms for on-orbit identification of space platforms p 425 N95-14088

CONSUMABLES (SPACECRAFT)
The Astroculture (tm)-1 experiment on the USML-1 mission p 564 N95-14228

CONTAMINANTS
Prediction of particulate contamination on aperture window p 420 N95-14064
Three neural network based sensor systems for environmental monitoring
[DE94-014557] p 522 N95-14195
Oxides of nitrogen: Their formation and control in stationary sources
[AD-A283780] p 522 N95-14337

CONTAMINATION
Prediction of particulate contamination on aperture window p 420 N95-14064
Experimental study of solar simulator mirror cryocontamination p 421 N95-14065
Self contamination effects in the TAUVEX UV Telescope: Ground testing and computer simulation
p 421 N95-14067
Hubble Space Telescope servicing mission scientific instrument protective enclosure design requirements and contamination controls p 421 N95-14068
Using a temperature-controlled quartz crystal microbalance in a space equipment cleanroom to monitor molecular contamination p 421 N95-14069
Clean assembly and integration techniques for the Hubble Space Telescope High Fidelity Mechanical Simulator p 418 N95-14070
Laboratory simulation of Low Earth Orbit (LEO) atomic oxygen effects p 422 N95-14071
Partial pressure analysis in space testing
p 424 N95-14084
Microcontamination detection using Heavy Ion Backscattering Spectrometry
[DE94-014182] p 437 N95-14312
Flightline aircraft fire incidents and suppression agent effects: Field inquiries and incident analysis
[AD-A284027] p 405 N95-14421
Comprehensive facility decommissioning through the use of innovative technology to reduce cost, schedule, and environmental liability
[TABES PAPER 94-615] p 416 N95-14644

Time-of-flight detector for heavy ion backscattering spectrometry
[DE94-015600] p 596 N95-15437
Mass analysis addition to the Differential Ion Flux Probe (DIFP) study
[NASA-CR-196531] p 429 N95-15824

CONTINENTAL SHELVES
ADCIRC: An advanced three-dimensional circulation model for shelves, coasts, and estuaries. Report 4: Hurricane storm surge modeling using large domains
[AD-A283868] p 535 N95-14352
Calculation of movable bed friction factors
[AD-A283529] p 536 N95-15440

CONTINUITY (MATHEMATICS)
On the behavior of three-dimensional wave packets in viscously spreading mixing layers
[NASA-TM-106770] p 495 N95-15908

CONTINUOUS RADIATION
Direct-current proton-beam measurements at Los Alamos
[DE94-016280] p 599 N95-15360

CONTINUUM FLOW
Field intercomparison with five automatic ammonia monitors
[PB94-192879] p 523 N95-15389

CONTINUUM MODELING
Damage tolerant repair techniques for pressurized aircraft fuselages
[AD-A281982] p 391 N95-14144

CONTINUUMS
Monitoring the variability of active galactic nuclei from a space-based platform p 644 N95-14509
Cross-effects in microgravity flows p 459 N95-14565

CONTRACT MANAGEMENT
Model contracts/agreements. Comprehensive Approach to Reusable Defense Software (CARDS)
[AD-A284403] p 575 N95-15783

CONTRACTION
Effect of short- and long-term spaceflight on the contractile properties of rat skeletal muscles with different functions p 539 N95-15141
Legged vehicle for underwater mobile operations
[AD-A282891] p 503 N95-15294

CONTROL
Knowledge-based processing for aircraft flight control
[NASA-CR-194976] p 580 N95-13727
Review of drive symmetry measurement and control experiments on the Nova laser system
[DE94-014455] p 498 N95-13994
Method and apparatus for detection and control of prelasing in a Q-switched laser
[NASA-CASE-LAR-14790-1] p 499 N95-14519

CONTROL EQUIPMENT
Comparison of full-scale, small-scale, and CFD results for F/A-18 forebody slot blowing p 397 N95-14255

CONTROL STABILITY
Analysis of the human operator subsystems p 555 N95-14019
On the role of exchange of power and information signals in control and stability of the human-robot interaction p 560 N95-14051
Multi-application controls: Robust nonlinear multivariable aerospace controls applications p 396 N95-14249
The stable and precise motion control for an autonomous mobile robot
[AD-A283776] p 501 N95-14336

CONTROL STICKS
Implementation issues for a compact 6 degree of freedom force reflecting handcontroller with cueing of modes p 560 N95-14050

CONTROL SURFACES
Free-to-roll tests of X-31 and F-18 subscale models with correlation to flight test results p 394 N95-14237
Multi-application controls: Robust nonlinear multivariable aerospace controls applications p 396 N95-14249

CONTROL SYSTEMS DESIGN
Adaptive optics at Lick Observatory: System architecture and operations
[DE94-012387] p 601 N95-13672
A prototype lisp-based soft real-time object-oriented Graphical User Interface for control system development
[NASA-TM-106743] p 566 N95-13716
Three-axis stabilization of spacecraft using parameter-independent nonlinear quaternion feedback
[NASA-TM-109150] p 420 N95-13729
Deployment mechanism calibration system p 414 N95-13833
Experimental implementation of a robust damped-oscillation control algorithm on a full-sized, two-degree-of-freedom, AC induction motor-driven crane
[DE94-012113] p 501 N95-14005
Eye movement control and top-down scanpath vision as a design metaphor for robotic vision and control p 555 N95-14022
Issues in the design of high dexterity, force reflective teleoperators p 555 N95-14024
Eighteenth Space Simulation Conference: Space Mission Success Through Testing
[NASA-CP-3280] p 420 N95-14062
Thermal design verification testing of the Clementine spacecraft: Quick, cheap, and useful p 424 N95-14083
HYDRA, a new tool for mechanical testing p 418 N95-14086
Simulation of a spatial, servo-hydraulic test facility for space structures p 418 N95-14095
Dextrous gripping in a hazardous environment
[PB94-191244] p 501 N95-14150
Generic architectures for future flight systems p 567 N95-14159
Space Generic Open Avionics Architecture (SGOAA): Overview p 569 N95-14161
Expert systems in the process industries p 571 N95-14169
X-31 high angle of attack control system performance p 395 N95-14244
High angle of attack flying qualities criteria for longitudinal rate command systems p 396 N95-14247
Vista/F-16 Multi-Axis Thrust Vectoring (MATV) control law design and evaluation p 396 N95-14248
Multi-application controls: Robust nonlinear multivariable aerospace controls applications p 396 N95-14249
Integrated optical maze
[DE94-015866] p 613 N95-14367
SODR Memory Control Buffer Control ASIC
[NASA-CR-197001] p 566 N95-14514
The Telecommunications and Data Acquisition Report
[NASA-CR-196409] p 462 N95-14620
Linear quadratic Gaussian and feedforward controllers for the DSS-13 antenna p 463 N95-14625
TABES 1994: 10th Annual Technical and Business Exhibition and Symposium p 414 N95-14633
Efficient mission control for the 48-satellite Globalstar constellation
[TABES PAPER 94-609] p 415 N95-14641
Automated test environment for a real-time control system
[TABES PAPER 94-631] p 417 N95-14652
A SIMULINK environment for flight dynamics and control analysis: Application to the DHC-2 Beaver. Part 1: Implementation of a model library in SIMULINK. Part 2: Nonlinear analysis of the Beaver autopilot
[NONP-NASA-SUPPL-DK-94-2802] p 412 N95-14815
Annular Suspension and Pointing System (ASPS) magnetic rotary joint
[NASA-CR-197197] p 502 N95-14907
Control and operation of space manipulator systems p 582 N95-14946

CONTROL THEORY
Hybrid verification by exploiting the environment
[NASA-CR-195810] p 568 N95-13699
The human operator transfer function: Identification of the limb mechanics subsystem p 558 N95-14040
Simulation of a spatial, servo-hydraulic test facility for space structures p 418 N95-14095
Fourth High Alpha Conference, volume 1
[NASA-CP-10143-VOL-1] p 393 N95-14229
Fourth High Alpha Conference, volume 3
[NASA-CP-10143-VOL-3] p 397 N95-14251

CONTROLLABILITY
Multi-application controls: Robust nonlinear multivariable aerospace controls applications p 396 N95-14249

CONTROLLERS
A physical control interface with proprioceptive feedback and multiple degrees of freedom p 559 N95-14045
Implementation issues for a compact 6 degree of freedom force reflecting handcontroller with cueing of modes p 560 N95-14050
Implementation of a three degree of freedom, motor/brake hybrid force output device for virtual environment control tasks p 562 N95-14058
Linear quadratic Gaussian and feedforward controllers for the DSS-13 antenna p 463 N95-14625
Slave controller for effecting a block transfer of sixteen bit words between a memory and a data transfer bus
[AD-D016463] p 574 N95-15336
Defining a controller architecture for the long-reach manipulator
[DE94-015165] p 583 N95-15369

CONVECTION
Oscillatory thermocapillary convection p 483 N95-14526
Thermocapillary convection in floating zones under simulated reduced-gravity conditions p 483 N95-14529
Thermocapillary motion of deformable drops p 485 N95-14544
Convection and morphological stability during directional solidification p 448 N95-14548
Crystal growth and fluid mechanics problems in directional solidification p 486 N95-14550
Interactions between solidification and compositional convection in mushy layers p 448 N95-14551
Nucleation and chiral symmetry breaking under controlled hydrodynamic flows p 489 N95-14570
Nowcasting convective storm evolution in east-central Florida using satellite and Doppler radar data
[AD-A283260] p 534 N95-15618
Interacting fronts in a model for binary-mixture convection
[DE94-013595] p 494 N95-15861

CONVECTION CLOUDS
Analysis of deep convective clouds and their association with non-migrating atmospheric diurnal tides in the tropical troposphere
[PB94-187457] p 526 N95-13974

CONVECTIVE FLOW
Multilayer fluid dynamics of immiscible liquids p 483 N95-14532
Stochastic model of the residual acceleration environment in microgravity p 459 N95-14540

CONVECTIVE HEAT TRANSFER
A realistic model of evaporation for a liquid droplet p 485 N95-14543
On the physics of waves in the solar atmosphere: Wave heating and wind acceleration
[NASA-CR-196992] p 646 N95-15070

CONVERSATION
Discourse interpretation and the scope of operators
[TR-518] p 586 N95-15595

CONVEXITY
Piezoelectric loudspeaker
[NASA-CASE-LAR-15138-1] p 590 N95-14110

CONVOLUTION INTEGRALS
Convolutional encoding of self-dual block codes (2) p 462 N95-14623
Spin glasses and error-correcting codes p 462 N95-14624

COOLING
Service equipment for use in hostile environments
[NASA-CASE-LEW-14906-2-SB] p 504 N95-15914

COOLING SYSTEMS
Lunar base heat pump
[NASA-CR-188356] p 492 N95-14869

COORDINATION
Intersensory coordination p 555 N95-14020
The Network Operations Control Center upgrade task: Lessons learned p 419 N95-14631

COORDINATION POLYMERS
Reactive polymers: Main chain coordination polymers for air separation
[AD-A281614] p 455 N95-15444

COPOLYMERIZATION
Preparation of well defined polystyrene-block-poly (methylphenylsilylene) copolymers
[AD-A280799] p 450 N95-14304

COPOLYMERS
Poly(arylene ether)s containing pendent ethynyl groups
[NASA-CASE-LAR-15041-1] p 449 N95-13838
Modifications of polysilanes and polysilane copolymers
[AD-A280839] p 452 N95-14398
Polysilanes with various architectures
[AD-A280842] p 452 N95-14400
AASERT 92: Synthesis and properties of complex polyarylene vinylenes
[AD-A284215] p 452 N95-14406
Highly crosslinked silicon polymers for gas chromatography columns
[NASA-CASE-ARC-11960-2-NP] p 452 N95-14602
Self-organization of graft copolymers at surfaces, interfaces and in bulk
[DE94-016884] p 454 N95-15340

COPPER
Activity of Ga, In and Cu modified MFI zeolites for amine reactions
[DE94-016532] p 438 N95-14388

COPPER ALLOYS
Investigation of syngas interaction in alcohol synthesis catalysts
[DE94-013939] p 442 N95-15386
Experiments to examine the contribution of gas atoms to void formation in irradiated metals
[DE94-015209] p 446 N95-15433

COPPER OXIDES
Flux pinning and forced entanglement by splayed columnar defects
[DE94-013994] p 620 N95-14008
High performance YBCO films
[AD-A283870] p 451 N95-14354

Transport resistive broadening by avalanche flux motion in high-temperature superconductors: SOC in a driven system
[DE94-016901] p 623 N95-15341
Phase separation and doped-hole segregation in La(2)CuO(4+delta) and La(2-x)Sr(x)CuO(4+delta)
[DE94-015070] p 624 N95-15430
Cluster studies of La2CuO4: Local geometric distortions
[DE94-016203] p 626 N95-15776

COPPER SELENIDES
Role of polycrystallinity in CdTe and CuInSe2 photovoltaic cells
[DE94-011849] p 519 N95-14432
Alternative fabrication techniques for high-efficiency CuInSe2 and CuInSe2-alloy films and cells
[DE94-011846] p 521 N95-15407

CORE STORAGE
The prospects for on-line hybrid coherency protocols on bus-based multiprocessors
[TR-490] p 579 N95-15590

CORIOLIS EFFECT
Psychophysiological aspects of increasing resistance to space motion sickness p 542 N95-15093

CORNERS
Initiation and propagation of small corner cracks p 510 N95-14471
Upward flame spread along the vertical corner walls (October 1993)
[PB94-206299] p 441 N95-15352

CORONAL HOLES
On the physics of waves in the solar atmosphere: Wave heating and wind acceleration
[NASA-CR-196992] p 646 N95-15070

CORONAS
Development and analysis of high-energy corona process for air purification
[DE94-015207] p 524 N95-15432

CORRECTION
Subsurface object position and image correction for standoff ground penetrating radar
[DE94-015180] p 468 N95-15300
A strategy for geoid repairing p 517 N95-15798

CORRELATION
Sub-Poissonian light and photocurrent shot-noise suppression in closed opto-electronic loop p 606 N95-13924
Decoherence and dissipation for a quantum system coupled to a local environment p 609 N95-13949
Computational methods for preliminary design and geometry definition in turbomachinery p 480 N95-14128
Fine structure of transient waves in a random medium: The correlation and spectral density functions p 401 N95-14882
Relationship between microstructure and efficiency of scintillating glasses
[DE94-014563] p 454 N95-15313
Defect profiling in elemental and multilayer systems: Correlations of fitted defect concentrations with positron implantation profiles
[DE94-015844] p 624 N95-15422
Dynamical impurity problems
[DE94-013025] p 625 N95-15576
On the affinities of lambda 5778 and other broad diffuse interstellar bands p 639 N95-15832
Correlation between molecular lines and diffuse interstellar bands p 640 N95-15835

CORROSION
Effect of surface roughness on local film cooling effectiveness and heat transfer coefficients
[AD-A283854] p 482 N95-14351
Practical aspects of corrosion fundamentals
[DE94-015842] p 438 N95-14371
Corrosion and corrosion fatigue of airframe aluminum alloys p 448 N95-14465
The effects of pitting on fatigue crack nucleation in 7075-T6 aluminum alloy p 448 N95-14482
Modeling time-dependent corrosion fatigue crack propagation in 7000 series aluminum alloys p 448 N95-14483
Mechanical system reliability for long life space systems
[NASA-CR-197215] p 505 N95-15584

CORROSION RESISTANCE
Practical aspects of corrosion fundamentals
[DE94-015842] p 438 N95-14371
Corrosion-resistant coatings for high-temperature high-sulfur-activity applications
[DE94-015155] p 453 N95-14957
Stress corrosion crack tip microstructure in nickel-based alloys
[DE94-015362] p 446 N95-15532
Effect of heat treatment on the microstructure and properties of AerMet (trade name) 100 steel
[AD-A284387] p 447 N95-15807
High-temperature corrosion of iron aluminides
[DE94-011505] p 447 N95-15906

CORROSION TESTS
Advanced Turbine Technology Applications Project (ATTAP)
[NASA-CR-195393] p 634 N95-15743

COSMIC RAYS
Squeezed states and graviton-entropy production in the early universe p 608 N95-13947
Research accomplishments and future goals in particle physics
[DE94-015483] p 596 N95-15537

COSMOLOGY
Squeezed states and graviton-entropy production in the early universe p 608 N95-13947

COST EFFECTIVENESS
David Florida Laboratory Thermal Vacuum Data Processing System p 418 N95-14079
The National Wind Technology Center
[DE94-011853] p 519 N95-14433
Low-Earth-Orbiter resource allocation and capacity planning for the DSN using LEO4CAST p 419 N95-14632
Space science in the 1990's and beyond
[TABES PAPER 94-204] p 415 N95-14634
Reengineering through information technology. Accompanying report of the National Performance Review
[PB94-170362] p 633 N95-15781

COST ESTIMATES
Pilot retrofit test of refrigerant R-134a for GDSCC p 456 N95-14629
Space transfer vehicle concepts and requirements study. Volume 3: Program cost estimates. Book 2: WBS and dictionary
[NASA-CR-192447] p 419 N95-15552

COST REDUCTION
Alpha LAMP Integration Facility p 418 N95-14094
New potentials of NIICHIMMASH's thermal vacuum facilities p 418 N95-14098
Recycled plastic: A clean and low cost rocket fuel
[TABES PAPER 94-610] p 416 N95-14642
Comprehensive facility decommissioning through the use of innovative technology to reduce cost, schedule, and environmental liability
[TABES PAPER 94-615] p 416 N95-14644
More supportable T-38A enhancement study
[AD-A283671] p 392 N95-15331

COSTS
Evaluation of sensor placement algorithms for on-orbit identification of space platforms p 425 N95-14088
Simulation of Shuttle launch G forces and acoustic loads using the NASA Ames Research Center 20G centrifuge p 419 N95-14089
Monitoring solar-thermal systems: An outline of methods and procedures
[DE94-015599] p 521 N95-15420

COUETTE FLOW
Two-layer viscous instability in a rotating couette device p 489 N95-14566

COUNTERMEASURES
A mathematical model of the cardiovascular response to +Gz acceleration p 544 N95-15110
Simulation of the fluid retention effects of a vasopressin analog using the Guyton model of circulation p 547 N95-15130

COUNTERS
Condensation nuclei measurement in the stratosphere for the NASA ACE program
[NASA-CR-197031] p 530 N95-14855

COUPLERS
Induction heating coupler
[NASA-CASE-LAR-14278-1] p 473 N95-14294

COUPLING
Multilayer fluid dynamics of immiscible liquids p 483 N95-14532

COUPLINGS
Electroweak boson pair production at CDF
[DE94-015183] p 597 N95-15629
Search for W(prime) (yields) e(nu) in p(anti p) collisions at (radical)s = 1,800 GeV
[DE94-015188] p 597 N95-15630

COWLINGS
Computational analysis in support of the SSTO flowpath test
[NASA-TM-106757] p 479 N95-13665
Wind-tunnel blockage and actuation systems test of a two-dimensional scramjet inlet unstart model at Mach 6
[NASA-TM-109152] p 495 N95-15898

CRACK ARREST
Development of the NASA/FLAGRO computer program for analysis of airframe structures p 510 N95-14473
Axial crack propagation and arrest in pressurized fuselage p 511 N95-14479
Three-dimensional effects of crack closure in laminated composite plates subjected to bending loads
[AD-A283342] p 436 N95-15873

CRACK CLOSURE
Recent advances in the modelling of crack growth under fatigue loading conditions p 511 N95-14478
Three-dimensional effects of crack closure in laminated composite plates subjected to bending loads
[AD-A283342] p 436 N95-15873

CRACK GEOMETRY
Fatigue analysis of multiple site damage at a row of holes in a wide panel p 508 N95-14463
Corrosion and corrosion fatigue of airframe aluminum alloys p 448 N95-14465
Study of multiple cracks in airplane fuselage by micromechanics and complex variables p 509 N95-14468
The role of fretting corrosion and fretting fatigue in aircraft rivet hole cracking p 510 N95-14470
Fracture mechanics validity limits p 511 N95-14480

CRACK INITIATION
Inspecting for widespread fatigue damage: Is partial debonding the key? p 508 N95-14458
Microstructurally based model of fatigue initiation and growth p 508 N95-14459
Nonlinear fracture mechanics-based analysis of thin wall cylinders p 508 N95-14462
Fatigue analysis of multiple site damage at a row of holes in a wide panel p 508 N95-14463
Initiation and propagation of small corner cracks p 510 N95-14471
Statistical investigation of fatigue crack initiation and growth around chamfered rivet holes in Alclad 2024 T3 as affected by corrosion p 510 N95-14472
The characterization of widespread fatigue damage in fuselage structure
[NASA-TM-109142] p 432 N95-14920
Fatigue in single crystal nickel superalloys
[AD-A282917] p 446 N95-15415
Ru2Ge3: Crystal growth and some properties
[DE94-015360] p 625 N95-15531
Characterization of damage progression in SCS-6/Timetal 21S (0)4 under thermomechanical fatigue loadings
[NASA-CR-195399] p 436 N95-15911
Computer modeling the fatigue crack growth rate behavior of metals in corrosive environments
[NASA-CR-194982-REV] p 448 N95-15918

CRACK OPENING DISPLACEMENT
Orientation effects on the measurement and analysis of critical CTOA in an aluminum alloy sheet
[NASA-TM-109153] p 444 N95-13690

CRACK PROPAGATION
Orientation effects on the measurement and analysis of critical CTOA in an aluminum alloy sheet
[NASA-TM-109153] p 444 N95-13690
High temperature cyclic behaviour of aerospace materials: Room temperature validation tests of Ti-6Al-4V
[AGARD-AR-328] p 506 N95-14198
The effect of microstresses on fatigue crack propagation in steel
[AD-A283872] p 506 N95-14356
FAA/NASA International Symposium on Advanced Structural Integrity Methods for Airframe Durability and Damage Tolerance
[NASA-CP-3274-PT-1] p 507 N95-14453
Elastic-plastic models for multi-site damage p 507 N95-14454
Small crack test program for helicopter materials p 507 N95-14455
Bending effects of unsymmetric adhesively bonded composite repairs on cracked aluminum panels p 507 N95-14456
Evaluation of bonded boron/epoxy doublers for commercial aircraft aluminum structures p 508 N95-14457
Inspecting for widespread fatigue damage: Is partial debonding the key? p 508 N95-14458
Microstructurally based model of fatigue initiation and growth p 508 N95-14459
Testing and analysis of flat and curved panels with multiple cracks p 508 N95-14460
Fatigue analysis of multiple site damage at a row of holes in a wide panel p 508 N95-14463
Corrosion and corrosion fatigue of airframe aluminum alloys p 448 N95-14465
Influence of crack history on the stable tearing behavior of a thin-sheet material with multiple cracks p 509 N95-14467
Study of multiple cracks in airplane fuselage by micromechanics and complex variables p 509 N95-14468
Initiation and propagation of small corner cracks p 510 N95-14471

Statistical investigation of fatigue crack initiation and growth around chamfered rivet holes in Alclad 2024 T3 as affected by corrosion p 510 N95-14472
Development of the NASA/FLAGRO computer program for analysis of airframe structures p 510 N95-14473
Fatigue reliability method with in-service inspections p 505 N95-14475
Nonlinear bulging factor based on R-curve data p 511 N95-14476
Development of a composite repair and the associated inspection intervals for the F-111C stiffener runout region p 392 N95-14477
Recent advances in the modelling of crack growth under fatigue loading conditions p 511 N95-14478
Axial crack propagation and arrest in pressurized fuselage p 511 N95-14479
Fracture mechanics validity limits p 511 N95-14480
Modeling time-dependent corrosion fatigue crack propagation in 7000 series aluminum alloys p 448 N95-14483
Analysis of small crack behavior for airframe applications p 512 N95-14484
Full-scale testing and analysis of fuselage structure p 512 N95-14485
The characterization of widespread fatigue damage in fuselage structure
[NASA-TM-109142] p 432 N95-14920
Fatigue in single crystal nickel superalloys
[AD-A282917] p 446 N95-15415
Theory of nonlinear, distortive phenomena in solids: Martensitic, crack, and multiscale structures-phenomenology and physics
[DE94-015653] p 447 N95-15631
Three-dimensional effects of crack closure in laminated composite plates subjected to bending loads
[AD-A283342] p 436 N95-15873
Characterization of damage progression in SCS-6/Timetal 21S (0)4 under thermomechanical fatigue loadings
[NASA-CR-195399] p 436 N95-15911
Computer modeling the fatigue crack growth rate behavior of metals in corrosive environments
[NASA-CR-194982-REV] p 448 N95-15918

CRACK TIPS
Orientation effects on the measurement and analysis of critical CTOA in an aluminum alloy sheet
[NASA-TM-109153] p 444 N95-13690
Study of multiple cracks in airplane fuselage by micromechanics and complex variables p 509 N95-14468
Initiation and propagation of small corner cracks p 510 N95-14471
Axial crack propagation and arrest in pressurized fuselage p 511 N95-14479
Modeling time-dependent corrosion fatigue crack propagation in 7000 series aluminum alloys p 448 N95-14483
Full-scale testing and analysis of fuselage structure p 512 N95-14485
Stress corrosion crack tip microstructure in nickel-based alloys
[DE94-015362] p 446 N95-15532
Size and deformation limits to maintain constraint in K(sub Ic) and J(sub c) testing of bend specimens
[AD-A284363] p 514 N95-15802
Three-dimensional effects of crack closure in laminated composite plates subjected to bending loads
[AD-A283342] p 436 N95-15873

CRACKING (CHEMICAL ENGINEERING)
The growth of zeolites A, X and mordenite in space p 458 N95-14226

CRACKING (FRACTURING)
Welding irradiated stainless steel
[DE94-013661] p 500 N95-13645
Orientation effects on the measurement and analysis of critical CTOA in an aluminum alloy sheet
[NASA-TM-109153] p 444 N95-13690
Observation of microcrack development in concrete by use of TV-holography and deformation phase gradient calculation
[PB94-207990] p 513 N95-15348
Fatigue in single crystal nickel superalloys
[AD-A282917] p 446 N95-15415
Three-dimensional effects of crack closure in laminated composite plates subjected to bending loads
[AD-A283342] p 436 N95-15873

CRACKS
Testing and analysis of flat and curved panels with multiple cracks p 508 N95-14460
Influence of crack history on the stable tearing behavior of a thin-sheet material with multiple cracks p 509 N95-14467
Challenges for the aircraft structural integrity program p 410 N95-14481
Effect of matrix stiffness on wavy fiber behavior in single-carbon-fiber-epoxy composites
[AD-A280970] p 435 N95-15427
Theory of nonlinear, distortive phenomena in solids: Martensitic, crack, and multiscale structures-phenomenology and physics
[DE94-015653] p 447 N95-15631

CRANES
Experimental implementation of a robust damped-oscillation control algorithm on a full-sized, two-degree-of-freedom, AC induction motor-driven crane
[DE94-012113] p 501 N95-14005

CRASH LANDING
Aircraft accident report: Overspeed and loss of power on both engines during descent and power-off emergency, landing Simmons Airlines, Inc., d/b/a, American Eagle Flight 3641, N349SB False River Air Park, New Roads, Lousiana, 1 February 1994
[NTSB/AAR-94/06] p 407 N95-14916

CRATERING
Cratering and penetration experiments in teflon targets at velocities from 1 to 7 km/s
[NASA-TM-104797] p 432 N95-13646

CRAY COMPUTERS
Computational chemistry packages on the CRAY Y-MP in trondheim
[PB94-208246] p 595 N95-15350

CREEP PROPERTIES
Symposium on Structural Intermetallics: Perspectives on Science and Technology, volume 2
[AD-A283379] p 447 N95-15874

CREEP STRENGTH
Processing and characterization of mechanically alloyed NiAl-based alloys
[AD-A283959] p 444 N95-14202

CREEP TESTS
Loading-strain equivalence between thermomechanical, creep, and tensile tests: High density polyethylene
[AD-A283265] p 513 N95-15621

CRITERIA
Joint and angle-covariant spin measurements with a quadrupole magnetic field p 604 N95-13914

CRITICAL POINT
Turbidity of a binary fluid mixture: Determining eta p 487 N95-14552

CRITICAL TEMPERATURE
High performance YBCO films
[AD-A283870] p 451 N95-14354
Turbidity of a binary fluid mixture: Determining eta p 487 N95-14552

CRITICAL VELOCITY
Helium 2 slosh in low gravity p 487 N95-14554

CROSS SECTIONS
Electroweak boson pair production at CDF
[DE94-015183] p 597 N95-15629

CROSSLINKING
Diamines and polyimides containing pendent ethynyl groups
[NASA-CASE-LAR-14825-1] p 452 N95-14416
Highly crosslinked silicon polymers for gas chromatography columns
[NASA-CASE-ARC-11960-2-NP] p 452 N95-14602

CRUDE OIL
The crosswell electromagnetic response of layered media
[DE94-014929] p 470 N95-15866

CRUSTAL FRACTURES
Measurement and interpretation of crustal deformation rates associated with postglacial rebound
[NASA-CR-196440] p 525 N95-13627

CRYOGENIC EQUIPMENT
Experimental design for the evaluation of high-T(sub c) superconductive thermal bridges in a sensor satellite
[NASA-CR-197003] p 429 N95-14106
Multilayer thin film Hall effect device
[NASA-CASE-MFS-28764-1] p 590 N95-14137

CRYOGENIC FLUIDS
Numerical modeling of a cryogenic fluid within a fuel tank
[NASA-TM-4651] p 479 N95-13892

CRYOGENIC STORAGE
Milestone 5 test report. Task 5, subtask 5.2: Tile to foam strength tests
[NASA-CR-197241] p 514 N95-15913

CRYOGENIC TEMPERATURE
Photoluminescence spectroscopy and Rutherford backscattering channeling evaluation of various capping techniques for rapid thermal annealing of ion-implanted ZnSe
[DE94-016876] p 623 N95-15339
Properties of nearly perfect crystals at very low temperatures
[NASA-CR-197221] p 627 N95-15823

CRYOGENICS
Refurbishment of a 39 foot thermal vacuum chamber p 418 N95-14085
Numerical studies of the surface tension effect of cryogenic liquid helium
[NASA-CR-197014] p 479 N95-14104
Optical analysis methods for material films condensed on cryogenic surfaces of spacecraft
[AD-A284014] p 427 N95-14420
LLE review, January - March 1994
[DE94-015058] p 618 N95-14955
Sandia 1993 Superconducting Technology Program
[DE94-015601] p 625 N95-15438
International Semiconductor Device Research Symposium (ISDRS-93)
[AD-A281715] p 477 N95-15454

CRYSTAL DEFECTS
Flux pinning and forced entanglement by splayed columnar defects
[DE94-013994] p 620 N95-14008
Ion beam synthesis of SiGe alloy layers
[DE94-014958] p 620 N95-14189
Orbital processing of high-quality CdTe compound semiconductors p 458 N95-14213
In-situ characterization of growth and interfaces in a-Si:H devices
[DE94-011847] p 622 N95-14431
The effects of spatial location of defect states on the switching characteristics of amorphous and polycrystalline silicon thin film transistors: A numerical simulation using AMPS 2-D
[DE94-013437] p 476 N95-15410
Defect profiling in elemental and multilayer systems: Correlations of fitted defect concentrations with positron implantation profiles
[DE94-015844] p 624 N95-15422
Cluster studies of La2CuO4: Local geometric distortions
[DE94-016203] p 626 N95-15776

CRYSTAL DISLOCATIONS
Fatigue in single crystal nickel superalloys
[AD-A282917] p 446 N95-15415

CRYSTAL FIELD THEORY
Intermultiplet transitions in optically opaque EuBa2Cu3O7: An inelastic neutron scattering study
[DE94-013429] p 620 N95-14188
Polarized photomodulated reflectivity and photoluminescence studies of ordered InGaP2 under pressure
[DE94-016556] p 621 N95-14390

CRYSTAL GROWTH
Growth mechanisms and characterization of hydrogenated amorphous-silicon-alloy films
[DE94-011842] p 518 N95-14194
Mass transport phenomena in microgravity: Preliminary results of the first MEPHISTO flight experiment p 634 N95-14209
Orbital processing of high-quality CdTe compound semiconductors p 458 N95-14213
Crystal growth of selected II-VI semiconducting alloys by directional solidification p 458 N95-14214
The study of dopant segregation behavior during the growth of GaAs in microgravity p 458 N95-14215
Vapor transport crystal growth of mercury-cadmium-telluride in microgravity p 458 N95-14216
The growth of zeolites A, X and mordenite in space p 458 N95-14226
Role of point defects and defect complexes in silicon device processing: Book of abstracts
[DE94-011828] p 519 N95-14430
In-situ characterization of growth and interfaces in a-Si:H devices
[DE94-011847] p 622 N95-14431
Crystal growth and fluid mechanics problems in directional solidification p 486 N95-14550
Cross-effects in microgravity flows p 459 N95-14565
Dynamics of hard sphere colloidal dispersions p 490 N95-14573
Gravity-dependent transport in industrial processes p 459 N95-14580
Atomic force microscopy of the electrochemical nucleation and growth of molecular crystals
[AD-A280958] p 622 N95-14601
Surface processes in CVD diamond growth
[AD-A280964] p 622 N95-14655
Photoluminescence spectroscopy and Rutherford backscattering channeling evaluation of various capping techniques for rapid thermal annealing of ion-implanted ZnSe
[DE94-016876] p 623 N95-15339
Optimization of transparent and reflecting electrodes for amorphous-silicon solar cells
[DE94-011841] p 520 N95-15355
Alternative fabrication techniques for high-efficiency CuInSe2 and CuInSe2-alloy films and cells
[DE94-011846] p 521 N95-15407

Fourth Workshop on the Role of Point Defects and Defect Complexes in Silicon Device Processing
[DE94-011850] p 624 N95-15426
Ru2Ge3: Crystal growth and some properties
[DE94-015360] p 625 N95-15531
Process for the controlled growth of single-crystal films of silicon carbide polytypes on silicon carbide wafers
[NASA-CAS-LEW-15222-3] p 625 N95-15602
Fundamental studies of diamond growth and surface reactions
[AD-A284390] p 626 N95-15808
Transport and nucleation processes during the vapor growth of diamond
[AD-A284411] p 626 N95-15812

CRYSTAL LATTICES
Plasma dust crystallization p 490 N95-14571

CRYSTAL OSCILLATORS
Shear stabilization of solidification fronts
p 448 N95-14549
Properties of nearly perfect crystals at very low temperatures
[NASA-CR-197221] p 627 N95-15823

CRYSTAL STRUCTURE
Electron spin resonance and band electronic structure study of the metal-insulator transition in (BEDT-TTF)3(HSO4)2
[DE94-014005] p 620 N95-14009
Vapor transport crystal growth of mercury-cadmium-telluride in microgravity
p 458 N95-14216
Protein crystal growth results from the United States Microgravity Laboratory-1 mission p 458 N95-14225
Crystal growth and fluid mechanics problems in directional solidification p 486 N95-14550
Interactions between solidification and compositional convection in mushy layers p 448 N95-14551
Damping mechanisms in nanostructured materials
[AD-A283583] p 623 N95-15317
Cation disorder in high dose neutron irradiated spinel
[DE94-013118] p 455 N95-15579
Optical detector having a plurality of matrix layers with cobalt disilicide particles embedded therein
[NASA-CASE-NPO-18625-2-CU] p 614 N95-15603

CRYSTAL SURFACES
Growth mechanisms and characterization of hydrogenated amorphous-silicon-alloy films
[DE94-011842] p 518 N95-14194
Fatigue in single crystal nickel superalloys
[AD-A282917] p 446 N95-15415

CRYSTALLINITY
Role of polycrystallinity in CdTe and CuInSe2 photovoltaic cells
[DE94-011849] p 519 N95-14432

CRYSTALLITES
Dynamics of hard sphere colloidal dispersions
p 490 N95-14573

CRYSTALLIZATION
In-situ TEM crystallization of sol-gel derived BaTiO3 thin films
[DE94-013260] p 619 N95-13821
Preparation and characterization of composite inorganic zeolite membranes with molecular sieve properties
[PB94-191251] p 450 N95-14151
The 226RA and 231PA systematics of axial, MORB, crustal residence ages, and MAGMA chamber characteristics at 9 to 10 degree N East Pacific Rise
[DE94-013084] p 529 N95-14434
Interactions between solidification and compositional convection in mushy layers p 448 N95-14551
Nucleation and chiral symmetry breaking under controlled hydrodynamic flows p 489 N95-14570
Plasma dust crystallization p 490 N95-14571

CRYSTALS
Materials issues in molecular beam epitaxy
[DE94-015796] p 621 N95-14322

CUBES (MATHEMATICS)
Parallel isosurface generator for huge data sets
[AD-A284030] p 578 N95-14422

CUFFS
Orthostatic stress by lower body negative pressure and its body fluid distribution kinetics under microgravity
p 549 N95-15138

CUMULATIVE DAMAGE
Fatigue analysis of multiple site damage at a row of holes in a wide panel p 508 N95-14463

CURING
Monitoring fiber stress during curing of single fiber glass- and graphite-epoxy composites
[NASA-TM-4568] p 432 N95-13641
Processing of thermoset prepreg laminate via exposure to microwave radiation
[DE94-013268] p 432 N95-13643

CURRENT ALGEBRA
Topics in the structure of hadronic systems
[DE94-014924] p 597 N95-15865

CURRENT DENSITY
Legged vehicle for underwater mobile operations
[AD-A282891] p 503 N95-15294
Field-emitter arrays for RF vacuum microelectronics
[AD-A283549] p 476 N95-15327
The effect of the edge current density on confinement and kink mode stability in H-mode and VH-mode discharges
[DE94-015719] p 618 N95-15632

CURVATURE
Milestone 5 test report. Task 5, subtask 5.2: Tile to foam strength tests
[NASA-CR-197241] p 514 N95-15913
On the evolution of centrifugal instabilities within curved incompressible mixing layers
[NASA-CR-194991] p 495 N95-15917

CURVED PANELS
Testing and analysis of flat and curved panels with multiple cracks p 508 N95-14460
Nonlinear bulging factor based on R-curve data
p 511 N95-14476

CURVES (GEOMETRY)
Carnot-caratheodory spaces seen from within
[PB94-195617] p 586 N95-15412

CYANIDES
The peculiar behaviour of the 5780 and 5797 DIBs in HD25137 p 639 N95-15833
Correlation between molecular lines and diffuse interstellar bands p 640 N95-15835

CYANO COMPOUNDS
Simulation of coal and char nitrogen reactions in combustion
[DE94-013941] p 440 N95-15291

CYBERNETICS
Tele-existence and/or cybernetic interface studies in Japan p 555 N95-14025

CYCLIC LOADS
Characterization of damage progression in SCS-6/Timetal 21S (0)4 under thermomechanical fatigue loadings
[NASA-CR-195399] p 436 N95-15911

CYCLONES
Short term teleconnections associated with western Pacific tropical cyclones
[AD-A284032] p 533 N95-14423
Upgrade of tropical cyclone surface wind field model
[AD-A283530] p 533 N95-15323

CYCLOTRON RESONANCE DEVICES
Eccentricity of the electron beam in a gyrotron cavity
[PB94-197639] p 496 N95-14839

CYGNUS CONSTELLATION
Search for gamma-ray events in the BATSE data base
[NASA-CR-197044] p 647 N95-14814

CYLINDRICAL BODIES
Adjustable bias column end joint assembly
[NASA-CASE-LAR-14899-1] p 459 N95-14111
Surface Tension Driven Convection Experiment (STDCE) p 458 N95-14217
Nonlinear fracture mechanics-based analysis of thin wall cylinders p 508 N95-14462
Flex-gear power transmission system for transmitting EMF between Sun and ring gears
[NASA-CASE-GSC-13540-1] p 502 N95-14517
Oscillatory/chaotic thermocapillary flow induced by radiant heating p 483 N95-14531
Equilibrium fluid interface behavior under low- and zero-gravity conditions p 484 N95-14534
The extensional rheology of non-Newtonian materials
p 489 N95-14569
Saddle clamp assembly
[NASA-CASE-MFS-28701-1] p 503 N95-15305

CYLINDRICAL COORDINATES
Discrete-layer piezoelectric plate and shell models for active tip-clearance control
[NASA-CR-195383] p 507 N95-14417

CYLINDRICAL TANKS
Impulsive response of nonuniform density liquid in a laterally excited tank
[DE94-013722] p 479 N95-13679

CYTOLOGY
Analysis of electron microscope images: 3-D localization of immuno-markers
[PB94-197977] p 537 N95-13990

D

DAMAGE
Flightline aircraft fire incidents and suppression agent effects: Field inquiries and incident analysis
[AD-A284027] p 405 N95-14421
Elastic-plastic models for multi-site damage
p 507 N95-14454
What those defects in optical coatings really look like
[DE94-015324] p 614 N95-15529
Characterization of damage progression in SCS-6/Timetal 21S (0)4 under thermomechanical fatigue loadings
[NASA-CR-195399] p 436 N95-15911

DAMAGE ASSESSMENT
Damage analysis of internal faults in flux concentrating permanent magnet motors
[AD-A283883] p 474 N95-14359
Inspecting for widespread fatigue damage: Is partial debonding the key? p 508 N95-14458
Probabilistic inspection strategies for minimizing service failures p 508 N95-14461
Fatigue analysis of multiple site damage at a row of holes in a wide panel p 508 N95-14463
A method of calculating the safe fatigue life of compact, highly-stressed components p 509 N95-14464
Computational predictive methods for fracture and fatigue p 509 N95-14466
Initiation and propagation of small corner cracks
p 510 N95-14471
Development of the NASA/FLAGRO computer program for analysis of airframe structures p 510 N95-14473
Recent advances in the modelling of crack growth under fatigue loading conditions p 511 N95-14476
Challenges for the aircraft structural integrity program
p 410 N95-14481
Analysis of small crack behavior for airframe applications p 512 N95-14484
Full-scale testing and analysis of fuselage structure
p 512 N95-14485
Space Shuttle Main Engine turbopump bearing assessment program
[TABES PAPER 94-621] p 417 N95-14648
Artificial neural network modeling of damaged aircraft
[AD-A283227] p 409 N95-14849
Analysis of space environment damage to solar cell assemblies from LDEF experiment A0171-GSFC test plate
[NASA-CR-197066] p 519 N95-14853

DAMPERS
Dynamics of the McDonnell-Douglas Large Scale Dynamic Rig and dynamic calibration of the rotor balance
[NASA-TM-108855] p 391 N95-13891

DAMPING
Experimental implementation of a robust damped-oscillation control algorithm on a full-sized, two-degree-of-freedom, AC induction motor-driven crane
[DE94-012113] p 501 N95-14005
Damping mechanisms in nanostructured materials
[AD-A283583] p 623 N95-15317

DARK MATTER
Energy and Technology Review, April 1994
[DE94-012133] p 496 N95-13669

DATA ACQUISITION
Automated hierarchical testable design of digital circuits
[PB94-197936] p 472 N95-13983
Three neural network based sensor systems for environmental monitoring
[DE94-014557] p 522 N95-14195
A multiscale random field model for Bayesian image segmentation
[AD-A283875] p 515 N95-14358
An overview of the EOSDIS V0 information management system: Lessons learned from the implementation of a distributed data system p 566 N95-14596
The Telecommunications and Data Acquisition Report
[NASA-CR-196409] p 462 N95-14620
Modern methods in meteorological and oceanographic data acquisition and analyses
[AD-A283038] p 533 N95-14848
Subsurface object position and image correction for standoff ground penetrating radar
[DE94-015180] p 468 N95-15300
Interactive Computer-Enhanced Remote Viewing System (ICERVS): Subsystem design report, phase 2
[DE94-014513] p 563 N95-15309
Diagnostic development and support of MHD test facilities
[DE94-015344] p 618 N95-15373
Prototype explosives-detection system based on nuclear-resonance absorption in nitrogen
[DE94-015069] p 442 N95-15387
Monitoring solar-thermal systems: An outline of methods and procedures
[DE94-015599] p 521 N95-15420
Nowcasting convective storm evolution in east-central Florida using satellite and Doppler radar data
[AD-A283260] p 534 N95-15618
International Geoid Service Bulletin No. 1
[BULL-1] p 516 N95-15791
Geodetic survey of Canada: Results on a geoid questionnaire p 516 N95-15793
The European Geoid Project p 516 N95-15796

Experimental hardware development for a pulsed ultrasonic data collection facility
[AD-A283331] p 615 N95-15872

DATA BASE MANAGEMENT SYSTEMS
Case study: Accelerated schedule for MULTI LIMS installation
[DE94-012398] p 630 N95-13673
GSOSTATS database: USAF synchronous satellite catalog data conversion software. User's guide and software maintenance manual, version 2.1
[NASA-TM-106760] p 568 N95-13894
Product life cycle data base, analysis and simulation integration methodology
[TABES PAPER 94-626] p 417 N95-14650
Reusable rocket engine turbopump health management system
[NASA-CR-195388] p 431 N95-15058
Design document for the Surface Currents Data Base (SCDB) Management System (SCDBMS), version 1.0
[NASA-CR-197019] p 537 N95-15751
Users manual for the Surface Currents Data Base (SCDB) Management System (SCDBMS), version 1.0
[NASA-CR-197021] p 537 N95-15753
ROOM: A recursive object oriented method for information systems development
[DE94-007575] p 633 N95-15761
Design document for the MOODS Data Management System (MDMS), version 1.0
[NASA-CR-197016] p 633 N95-15801

DATA BASES
Age 60 Rule. Part 3: Consolidated database experiments
[DOT/FAA/AM-94/22-PT-3] p 551 N95-13715
International energy: Research organizations, 1988-1992
[DE90-017267] p 630 N95-13726
Efficient bulk-loading of gridfiles
[NASA-CR-194974] p 568 N95-13889
A selection of experimental test cases for the validation of CFD codes, volume 1
[AGARD-AR-303-VOL-1] p 481 N95-14201
Produce documents and media information
[NASA-CR-196521] p 532 N95-14271
Energy review
[DE94-015828] p 518 N95-14326
A database for propagation models
p 465 N95-14675
Development of a systemic land cover/land use database for the Upper Mississippi River System derived from Landsat Thematic Mapper satellite data. Long term resource monitoring program
[PB94-186889] p 515 N95-14793
Performance information management system (PIMS) communication
[AD-A284851] p 574 N95-15335
FFCAst Clearinghouse, directory of abstracts
[DE94-015259] p 632 N95-15435
Support of Environmental Requirements for Cloud Analysis and Archive (SERCAA): Algorithm descriptions
[AD-A283240] p 534 N95-15614
Design document for the Surface Currents Data Base (SCDB) Management System (SCDBMS), version 1.0
[NASA-CR-197019] p 537 N95-15751
A strategy for geoid repairing p 517 N95-15798

DATA COMPRESSION
1994 Science Information Management and Data Compression Workshop
[NASA-CP-3277] p 564 N95-14585
Comparison of transform coding methods with an optimal predictor for the data compression of digital elevation models p 564 N95-14587
Radiometric resolution enhancement by lossy compression as compared to truncation followed by lossless compression p 564 N95-14588
Blocking reduction of Landsat Thematic Mapper JPEG browse images using optimal PSNR estimated spectra adaptive postfiltering p 565 N95-14589
Synthetic aperture radar signal data compression using block adaptive quantization p 565 N95-14590
Compression of regions in the global advanced very high resolution radiometer 1-km data set
p 565 N95-14591
Lossless compression of NOAA-AVHRR satellite data
p 565 N95-14592
The development of lossless data compression technology for remote sensing applications
p 565 N95-14593
Landsat Pathfinder tropical forest information management system p 565 N95-14594
Planning/scheduling techniques for VQ-based image compression p 566 N95-14595
Neural networks: Alternatives to conventional techniques for automatic docking
[TABES PAPER 94-627] p 417 N95-14651
Summary of activities for University of California
[AD-A283890] p 632 N95-15423

DATA CONVERSION ROUTINES
GSOSTATS database: USAF synchronous satellite catalog data conversion software. User's guide and software maintenance manual, version 2.1
[NASA-TM-106760] p 568 N95-13894
AFOS Terminal Aerodrome Forecast encoding
[PB94-203247] p 533 N95-14410
Connection machine software conversion of the Navy TOPS model
[AD-A281681] p 579 N95-15450

DATA CORRELATION
Nowcasting convective storm evolution in east-central Florida using satellite and Doppler radar data
[AD-A283260] p 534 N95-15618

DATA INTEGRATION
Validation of ERS-1 environmental data products
[NASA-CR-197111] p 517 N95-15848

DATA LINKS
Propagation considerations for the Odyssey system design p 466 N95-14680
Modeling and simulation of a Fiber Distributed Data Interface Local Area Network (FDDI LAN) using OPNET (tm) for interfacing through the Common Data Link (CDL)
[AD-A283124] p 469 N95-15651

DATA MANAGEMENT
A multi-level object store and its application to HEP data analysis
[DE94-014010] p 568 N95-14010
Design document for the MOODS Data Management System (MDMS), version 1.0
[NASA-CR-197016] p 633 N95-15801

DATA PROCESSING
Develop advanced nonlinear signal analysis topographical mapping system
[NASA-CR-194414] p 514 N95-13639
Remote sensing, processing and transmission of data for an unmanned aerial vehicle
[AD-A283104] p 514 N95-13693
Results of demonstration test for receiving and processing of flight data from the Space Transportation System
[NASA-CR-194986] p 418 N95-13890
Analysis of electron microscope images: 3-D localization of immuno-markers
[PB94-197977] p 537 N95-13990
Three neural network based sensor systems for environmental monitoring
[DE94-014557] p 522 N95-14195
Review of European microgravity measurements
p 457 N95-14211
ICE/ISEE plasma wave data analysis
[NASA-CR-196988] p 642 N95-14266
SODR Memory Control Buffer Control ASIC
[NASA-CR-197001] p 566 N95-14514
CTAS data analysis program
[NASA-TM-108842] p 406 N95-14611
The Global Emergency Observation and Warning System
[TABES PAPER 94-622] p 417 N95-14649
Geotail MCA plasma wave data analysis
[NASA-CR-197022] p 618 N95-14798
Data processing routines for the Sippican MK-12 XBT system
[AD-A283570] p 536 N95-15330
Large-scale data envelopment analysis models and related applications
[AD-A283214] p 588 N95-15400
Essential elements of an effective data qualification
[DE94-015566] p 632 N95-15419
Tests of a homogeneous Poisson process against clustering and other alternatives
[DE94-015382] p 588 N95-15533
Support of Environmental Requirements for Cloud Analysis and Archive (SERCAA): Algorithm descriptions
[AD-A283240] p 534 N95-15614
Nowcasting convective storm evolution in east-central Florida using satellite and Doppler radar data
[AD-A283260] p 534 N95-15618
Performance comparison AN/FRD-10 versus PUSHER
[AD-A283263] p 469 N95-15619
Search for W(prime) (yields) e(nu) in p(anti p) collisions at (radical)s = 1,800 GeV
[DE94-015188] p 597 N95-15630

DATA PROCESSING EQUIPMENT
David Florida Laboratory Thermal Vacuum Data Processing System p 418 N95-14079

DATA PROCESSING TERMINALS
Technical Revue Thomson-CSF, volume 26, no. 1, March 1994. Flat panels for visualisation
[PB94-197969] p 410 N95-13984

DATA REDUCTION
Observations of extragalactic sources with the Metsaehovi radio telescope at 22-87 GHz
[PB94-197712] p 637 N95-13982
Performance of customized DCT quantization tables on scientific data p 564 N95-14586
Radiometric resolution enhancement by lossy compression as compared to truncation followed by lossless compression p 564 N95-14588
Geotail MCA plasma wave data analysis
[NASA-CR-197022] p 618 N95-14798
Data processing routines for the Sippican MK-12 XBT system
[AD-A283570] p 536 N95-15330

DATA RETRIEVAL
Efficient bulk-loading of gridfiles
[NASA-CR-194974] p 568 N95-13889
Validation of ERS-1 environmental data products
[NASA-CR-197111] p 517 N95-15848

DATA SMOOTHING
New methods, new methodology: Advanced CFD in the Snecma turbomachinery design process
p 480 N95-14134

DATA STORAGE
Two-dimensional signal processing, optical information storage and processing, and electromagnetic measurements
[AD-A281937] p 460 N95-13657
Efficient bulk-loading of gridfiles
[NASA-CR-194974] p 568 N95-13889
A multi-level object store and its application to HEP data analysis
[DE94-014010] p 568 N95-14010

DATA STRUCTURES
Knowledge-based processing for aircraft flight control
[NASA-CR-194976] p 580 N95-13727
A high performance graphics algorithm
[DE94-015033] p 571 N95-14196
High performance computational chemistry: Towards fully distributed parallel algorithms
[DE94-014561] p 573 N95-15311

DATA TRANSFER (COMPUTERS)
Dynamic modelling to assess the value of Electronic Data Interchange: A study in the Rotterdam port community
[PB94-195542] p 632 N95-14837
Slave controller for effecting a block transfer of sixteen bit words between a memory and a data transfer bus
[AD-D016463] p 574 N95-15336

DATA TRANSMISSION
Project OART: WDM, EDFA's and mixed data rates in a real-world testbed
[DE94-012234] p 601 N95-13670
Remote sensing, processing and transmission of data for an unmanned aerial vehicle
[AD-A283104] p 514 N95-13693
Results of demonstration test for receiving and processing of flight data from the Space Transportation System
[NASA-CR-194986] p 418 N95-13890
Use of 64 kbits/s digital channel for image transmission: Using low scan two-way video
[PB94-189099] p 461 N95-14147
An efficient network for interconnecting remote monitoring instruments and computers
[DE94-016213] p 581 N95-14377
Dynamic modelling to assess the value of Electronic Data Interchange: A study in the Rotterdam port community
[PB94-195542] p 632 N95-14837
Modeling and simulation of a Fiber Distributed Data Interface Local Area Network (FDDI LAN) using OPNET (tm) for interfacing through the Common Data Link (CDL)
[AD-A283124] p 469 N95-15651
Video transmission for quantized variable bandwidth networks
[AD-A284892] p 470 N95-15750
High speed QPPM direct detection optical communication receivers for FSDD intersatellite links
[NASA-CR-189331] p 615 N95-15849

DATUM (ELEVATION)
International Geoid Service Bulletin No. 1
[BULL-1] p 516 N95-15791
The GEOMED Project p 516 N95-15794
The Bureau Gravimetrique International
p 516 N95-15795
The European Geoid Project p 516 N95-15796
Validation of the global digital height model ETOPO5U referring to the Italian model (Italian DEM)
p 517 N95-15797
A strategy for geoid repairing p 517 N95-15798

DEBONDING (MATERIALS)
Nondestructive analysis and development
[NASA-CR-196987] p 505 N95-13886
Inspecting for widespread fatigue damage: Is partial debonding the key? p 508 N95-14458

DECISION MAKING
Objective evaluation of situation awareness for dynamic decision makers in teleoperations p 559 N95-14047

Risk analysis for the fire safety of airline passengers [PB94-194065] p 405 N95-14179
Low-Earth-Orbiter resource allocation and capacity planning for the DSN using LEO4CAST p 419 N95-14632
Environmentally sound manufacturing [TABES PAPER 94-502] p 415 N95-14636
Intelligent manufacturing systems state of the art [TABES PAPER 94-503] p 415 N95-14637
Propagation in the ionosphere, A p 466 N95-14826
Propagation in the ionosphere, B p 467 N95-14827
Large-scale data envelopment analysis models and related applications [AD-A283214] p 588 N95-15400
Spatio-temporal neural networks for vision, reasoning and rapid decision making [AD-A283251] p 583 N95-15403

DECISION THEORY
Intelligent alarming p 570 N95-14168
Control of selective perception using Bayes nets and decision theory [TR-468] p 573 N95-15151
Large-scale data envelopment analysis models and related applications [AD-A283214] p 588 N95-15400

DECODING
Blocking reduction of Landsat Thematic Mapper JPEG browse images using optimal PSNR estimated spectra adaptive postfiltering p 565 N95-14589

DECOMMISSIONING
Comprehensive facility decommissioning through the use of innovative technology to reduce cost, schedule, and environmental liability [TABES PAPER 94-615] p 416 N95-14644

DECOMPOSITION
The modal decomposition of an impedance tube [AD-A283591] p 591 N95-15320
Optically driven surface reactions: Laser probes of surface dynamics [DE94-015311] p 441 N95-15370

DECONDITIONING
Cardiovascular deconditioning effects of long-term simulated weightlessness in rats p 538 N95-15099
Orthostatic stress by lower body negative pressure and its body fluid distribution kinetics under microgravity p 549 N95-15138

DECOUPLING
Kinetic theory for electrodic phase transitions: The voltammogram [AD-A283039] p 619 N95-13691

DEEP SPACE
The Stark anomalous dispersion optical filter: The theory p 462 N95-14622

DEEP SPACE NETWORK
The Telecommunications and Data Acquisition Report [NASA-CR-196409] p 462 N95-14620
The long-term forecast of station view periods p 419 N95-14621
A radio telescope for the calibration of radio sources at 32 gigahertz p 463 N95-14626
The Block V Receiver fast acquisition algorithm for the Galileo S-band mission p 463 N95-14627
Research and development optical deep space antenna sizing study p 463 N95-14628
Pilot retrofit test of refrigerant R-134a for GDSCC p 456 N95-14629
A trajectory preprocessor for antenna pointing p 463 N95-14630
The Network Operations Control Center upgrade task: Lessons learned p 419 N95-14631
Low-Earth-Orbiter resource allocation and capacity planning for the DSN using LEO4CAST p 419 N95-14632

DEFECTS
Influence of defect shape on laser-induced damage in multilayer coatings [DE94-016543] p 451 N95-14389
Defects and transport in mixed oxides [DE94-015652] p 454 N95-15358
What those defects in optical coatings really look like [DE94-015324] p 614 N95-15529

DEFENSE PROGRAM
Department of Defense technical architecture framework for information management. Volume 1: Overview, version 2.0 [AD-A283763] p 631 N95-14327
Department of Defense technical architecture framework for information management. Volume 2: Technical reference model and standards profile summary [AD-A283764] p 631 N95-14329
Department of Defense technical architecture framework for information management. Volume 3: Architecture concepts and design guidance, version 2.0 [AD-A283765] p 631 N95-14330
Department of Defense technical architecture framework for information management. Volume 4: DOD standards-based architecture planning guide, version 2.0 [AD-A283766] p 631 N95-14331
Department of Defense technical architecture framework for information management. Volume 6: Department of Defense (DOD) goal security architecture, version 2.0 [AD-A283767] p 631 N95-14332
Department of Defense technical architecture framework for information management. Volume 8: Department of Defense HCI style guide, version 2.0 [AD-A283768] p 631 N95-14333
Department of Defense high power laser program guidance [AD-A282915] p 500 N95-15391
Model contracts/agreements. Comprehensive Approach to Reusable Defense Software (CARDS) [AD-A284403] p 575 N95-15783
Software Technology for Adaptable, Reliable Systems (STARS) [AD-A284373] p 576 N95-15806

DEFLAGRATION
Effects of two-phase flow on the deflagration of porous energetic materials [DE94-015353] p 442 N95-15375

DEFORESTATION
Landsat Pathfinder tropical forest information management system p 565 N95-14594

DEFORMATION
High temperature superconductors with improved current densities [AD-A282996] p 472 N95-13685
High strain rate deformation of NiAl [DE94-014810] p 445 N95-14439
Thermocapillary motion of deformable drops p 485 N95-14544
Observation of microcrack development in concrete by use of TV-holography and deformation phase gradient calculation [PB94-207990] p 513 N95-15348
Gouge initiation in high-velocity rocket sled testing [DE94-014288] p 418 N95-15357

DEGRADATION
Summary of solar cell data from the Long Duration Exposure Facility (LDEF) [NASA-CR-197069] p 519 N95-14802

DEGREES OF FREEDOM
A high performance two degree-of-freedom kinesthetic interface p 558 N95-14042
A physical control interface with proprioceptive feedback and multiple degrees of freedom p 559 N95-14045
Implementation issues for a compact 6 degree of freedom force reflecting handcontroller with cueing of modes p 560 N95-14050
Implementation of a three degree of freedom, motor/brake hybrid force output device for virtual environment control tasks p 562 N95-14058
HYDRA, a new tool for mechanical testing p 418 N95-14086
Low-speed wind tunnel testing of the NPS and NASA Ames Mach 6 optimized waverider [AD-A283585] p 404 N95-15319

DEICERS
Development of anti-icing technology [PB94-195369] p 407 N95-15439

DEICING
Icing: Accretion, detection, protection p 406 N95-14897

DELPHI METHOD (FORECASTING)
Aero-optics system integration [TABES PAPER 94-604] p 415 N95-14638

DELTA FUNCTION
High-speed fixed and floating point implementation of delta-operator formulated discrete time systems [AD-A283109] p 584 N95-13694

DELTA LAUNCH VEHICLE
Delta, America's space ambassador [NASA-TM-110046] p 419 N95-13700

DELTA WINGS
A selection of experimental test cases for the validation of CFD codes, volume 1 [AGARD-AR-303-VOL-1] p 481 N95-14201

DENDRITIC CRYSTALS
Crystal growth and fluid mechanics problems in directional solidification p 486 N95-14550
Investigation of dendrite coherency in two commercial Al-Si foundry alloys [PB94-208238] p 446 N95-15349

DENSITY (MASS/VOLUME)
Proposal for an astronaut mass measurement device for the Space Shuttle [NASA-CR-197198] p 563 N95-14854
Solid target boronization of the MST reversed-field pinch during pulsed discharge cleaning [DE94-015535] p 442 N95-15541

DENSITY DISTRIBUTION
Impulsive response of nonuniform density liquid in a laterally excited tank [DE94-013722] p 479 N95-13679

DENSITY MEASUREMENT
A radio telescope for the calibration of radio sources at 32 gigahertz p 463 N95-14626
Research on characterization of the upper atmosphere using lidar [AD-A283241] p 530 N95-15401
Influence of transmutation on microstructure, density change, and embrittlement of vanadium and vanadium alloys irradiated in HFIR [DE94-015202] p 446 N95-15431

DEPENDENCE
2D regular arrays for a special class of non uniform recurrence equations [PB94-195633] p 584 N95-13980

DEPENDENT VARIABLES
Dependent random variables in uncertainty analysis [PB94-191293] p 585 N95-14154

DEPLETION
Early solar mass loss, element diffusion, and solar oscillation frequencies [DE94-014802] p 646 N95-14376

DEPLOYMENT
Deployment mechanism calibration system p 414 N95-13833

DEPOSITION
ASTM E 1559 method for measuring material outgassing/deposition kinetics has applications to aerospace, electronics, and semiconductor industries p 421 N95-14066
Growth mechanisms and characterization of hydrogenated amorphous-silicon-alloy films [DE94-011842] p 518 N95-14194
Corrosion-resistant coatings for high-temperature high-sulfur-activity applications [DE94-015155] p 453 N95-14957
Development of large-area monolithically integrated Silicon-Film(tm) photovoltaic modules [DE94-011830] p 520 N95-15405
Small-angle x-ray scattering studies of microvoids in amorphous-silicon-based semiconductors [DE94-011840] p 520 N95-15406
Alternative fabrication techniques for high-efficiency CuInSe2 and CuInSe2-alloy films and cells [DE94-011846] p 521 N95-15407
What those defects in optical coatings really look like [DE94-015324] p 614 N95-15529

DERIVATION
Fluorescent compounds for plastic scintillation applications [DE94-013235] p 497 N95-15580

DESERTS
June to September rainfall in the African Sahel: Verification of our 1994 forecasts and an extended range forecast for 1995, 3 [TR-521] p 534 N95-15666

DESIGN ANALYSIS
Earth Observing System (EOS) Advanced Microwave Sounding Unit-A (AMSU-A): Instrumentation interface control document [NASA-CR-189377] p 567 N95-13651
Computer aided techniques for the realisation of the diaphragm of the PSM for the IRS-1C p 413 N95-13829
Deployment mechanism calibration system p 414 N95-13833
Hubble Space Telescope servicing mission scientific instrument protective enclosure design requirements and contamination controls p 421 N95-14068
Computational methods for preliminary design and geometry definition in turbomachinery p 480 N95-14128
The industrial use of CFD in the design of turbomachinery p 480 N95-14133
The role of CFD in the design process p 481 N95-14135
Aero design of turbomachinery components: CFD in complex systems p 481 N95-14136
European Workshop Industrical Computer Science Systems approach to design for safety p 569 N95-14157
Product life cycle data base, analysis and simulation integration methodology [TABES PAPER 94-626] p 417 N95-14650
Building complex simulations rapidly using MATRIX(x): The Space Station redesign [TABES PAPER 94-632] p 417 N95-14653
Requirements report for SSTO vertical take-off and horizontal landing vehicle [NASA-CR-197029] p 409 N95-14794
Design review and analysis for a Pratt and Whitney fluid-film bearing and seal testing rig [NASA-CR-197035] p 502 N95-14797

Design of power electronics for TVC and EMA systems
[NASA-CR-197067] p 475 N95-14866
Mission, technologies and design of planetary mobile vehicle p 504 N95-14947
An architecture for intelligent multichip module reliability analysis
[AD-A281574] p 583 N95-15461
The Aluminum Falcon: A low cost modern commercial transport
[NASA-CR-197180] p 409 N95-15742
Mass analysis addition to the Differential Ion Flux Probe (DIFP) study
[NASA-CR-196531] p 429 N95-15824

DESORPTION
Direct detection of neutral metal atoms in electron-stimulated desorption: Al from CH3O/Al(111). Velocity distribution and absolute yield
[DE94-014011] p 593 N95-14011
Core-level spectroscopy of thin oxides and oxynitrides
[DE94-016598] p 442 N95-15408

DESTABILIZATION
Stabilization of thermocapillary convection by means of nonplanar flow oscillations p 482 N95-14524

DESTRUCTION
Oxides of nitrogen: Their formation and control in stationary sources
[AD-A283780] p 522 N95-14337
The formation of small grains in shocks in the ISM p 641 N95-15842
Process development of thermal hydrodechlorination
[PB94-195518] p 525 N95-15870

DESULFURIZING
Effects of hydrogen annealing, sulfur segregation and diffusion on the cyclic oxidation resistance of superalloys: A review
[NASA-TM-106734] p 444 N95-13667
High temperature membranes for H2S and SO2 separations
[DE94-017125] p 441 N95-15345

DETECTION
Homodyning and heterodyning the quantum phase p 604 N95-13913
Quantum state engineering p 605 N95-13919
How to detect an excited atom without disturbing it or how to locate a super-mine without exploding it p 598 N95-13934
Microcontamination detection using Heavy Ion Backscattering Spectrometry
[DE94-014182] p 437 N95-14312
Benefits of CMM-based software process improvement: Initial results
[AD-A283848] p 572 N95-14349
The symbiosis of photometry and radial-velocity measurements p 643 N95-14505
Thin GSO scintillator for neutron detection
[DE94-014586] p 613 N95-15314
Leak detection by acoustic emission monitoring. Phase 1: Feasibility study
[AD-A283775] p 493 N95-15332
Prototype explosives-detection system based on nuclear-resonance absorption in nitrogen
[DE94-015069] p 442 N95-15387

DETERMINANTS
Phase space flow of particles in squeezed states p 606 N95-13928

DETONATION WAVES
Blast overpressure studies with animals and man
[AD-A280435] p 540 N95-13971

DETONATORS
Integrated optical maze
[DE94-015866] p 613 N95-14367

DEUTERIUM PLASMA
Radioactivity measurements of ITER materials using the TFTR D-T neutron field
[DE94-016094] p 617 N95-14397

DEUTERON IRRADIATION
Ion implantation of He-3 in tantalum for use in a low energy deuteron polarization analyzer
[AD-A283172] p 619 N95-13698

DHC 2 AIRCRAFT
A SIMULINK environment for flight dynamics and control analysis: Application to the DHC-2 Beaver. Part 1: Implementation of a model library in SIMULINK. Part 2: Nonlinear analysis of the Beaver autopilot
[NONP-NASA-SUPPL-DK-94-2802] p 412 N95-14815

DIAGNOSIS
Developments in laser-based diagnostics for wind tunnels in the Aeromechanics Division: 1987-1992
[AD-A283011] p 412 N95-13687
Expert systems in the process industries p 571 N95-14169
Design of reliable high voltage avalanche transistor pulsers
[DE94-015323] p 473 N95-14261
LLE review, January - March 1994
[DE94-015058] p 618 N95-14955
Faraday rotation system
[DE94-015345] p 618 N95-15374

DIAMINES
A solvent resistant copolyimide
[NASA-CASE-LAR-15083-1] p 449 N95-14108
Thermally stable organic polymers
[AD-A281380] p 451 N95-14363
Diamines and polyimides containing pendent ethynyl groups
[NASA-CASE-LAR-14825-1] p 452 N95-14416

DIAMOND FILMS
Physical and tribological characteristics of ion-implanted diamond films
[NASA-TM-106682] p 450 N95-14303
Surface processes in CVD diamond growth
[AD-A280964] p 622 N95-14655
Fundamental studies of diamond growth and surface reactions
[AD-A284390] p 626 N95-15808

DIAMONDS
Development of chemical-vapor-deposited diamond for infrared optical applications: Summary of properties
[AD-A282999] p 448 N95-13686
Fundamental studies of diamond growth and surface reactions
[AD-A284390] p 626 N95-15808
Transport and nucleation processes during the vapor growth of diamond
[AD-A284411] p 626 N95-15812

DIATOMIC GASES
Excimer emission from alkali diatomic and alkaline-earth-noble gas molecules
[AD-A281662] p 596 N95-15446

DICTIONARIES
Acronyms, initialisms, and abbreviations
[DE94-016686] p 632 N95-15366

DIELECTRIC POLARIZATION
Wideband electromagnetic scattering/analysis program. Electromagnetic scattering from the trunks and branches of trees
[AD-A283112] p 469 N95-15394

DIELECTRIC PROPERTIES
Development of chemical-vapor-deposited diamond for infrared optical applications: Summary of properties
[AD-A282999] p 448 N95-13686
Applications of squeezed states: Bogoliubov transformations and wavelets to the statistical mechanics of water and its bubbles p 607 N95-13939
Wideband electromagnetic scattering/analysis program. Electromagnetic scattering from the trunks and branches of trees
[AD-A283112] p 469 N95-15394
Low loss substrates for microwave applications and sol-gel processing of superconductors
[AD-A284868] p 625 N95-15746

DIELECTRICS
High performance YBCO films
[AD-A283870] p 451 N95-14354
Ferroelectric oxide memory FET (FEMFET) development
[AD-A283203] p 476 N95-15399
Xwake 1.0: A new tool for wakefield and impedance calculations
[DE94-015545] p 574 N95-15418
Development and analysis of high-energy corona process for air purification
[DE94-015207] p 524 N95-15432
Low dielectric polyimide fibers
[NASA-CASE-LAR-14526-1] p 455 N95-15599

DIESEL ENGINES
Preliminary design of a miniature thermoelectric generator
[AD-A283834] p 518 N95-14341
Definition of high-temperature use limits for MIL-L-2104 engine oils
[AD-A282838] p 451 N95-14365
Wear mechanism evaluation and measurement in fuel-lubricated components
[AD-A284870] p 504 N95-15747

DIETS
The relationship between space sickness and preflight diet p 546 N95-15122

DIFFERENCE EQUATIONS
Quantum statistics of Raman scattering model with Stokes mode generation p 610 N95-13958

DIFFERENTIAL EQUATIONS
Quantum statistics of Raman scattering model with Stokes mode generation p 610 N95-13958
Computational aerodynamics based on the Euler equations
[AGARD-AG-325] p 398 N95-14264
An efficient spectral method for ordinary differential equations with rational function coefficients
[NASA-TM-106762] p 585 N95-14296
Nonlinear asymptotic integration algorithms for one-dimensional autonomous dissipative first-order ODEs
[NASA-TM-106780] p 585 N95-14300
Workshop on Advances in Scientific Computation and Differential Equations 1993 (SCADE)
[AD-A283111] p 585 N95-14657
Two methods for the study of vortex patch evolution on locally refined grids
[DE94-014965] p 494 N95-15867
Neutrino oscillations in noisy media
[DE94-014973] p 598 N95-15869

DIFFERENTIAL PRESSURE
High temperature superconductors with improved current densities
[AD-A282996] p 472 N95-13685

DIFFRACTION
Observation of diffraction effects in positron channeling
[DE94-014909] p 594 N95-14441
Theoretical studies in elementary particle physics
[DE94-015343] p 595 N95-15372
Theory of nonlinear, distortive phenomena in solids: Martensitic, crack, and multiscale structures-phenomenology and physics
[DE94-015653] p 447 N95-15631

DIFFRACTION PROPAGATION
Experimental hardware development for a pulsed ultrasonic data collection facility
[AD-A283331] p 615 N95-15872

DIFFUSE RADIATION
The Diffuse Interstellar Bands: Contributed papers
[NASA-CP-10144] p 639 N95-15827
Neutral gas and diffuse interstellar bands in the LMC p 639 N95-15828
Diffuse interstellar bands in reflection nebulae p 639 N95-15830
The peculiar behaviour of the 5780 and 5797 DIBs in HD25137 p 639 N95-15833
Diffuse interstellar bands between 3900 A and 4200 A p 640 N95-15834
Correlation between molecular lines and diffuse interstellar bands p 640 N95-15835
Investigation of a laboratory candidate for the carrier of the 4430 A diffuse interstellar band p 641 N95-15840
The C4H radical and the diffuse interstellar bands. An ab initio study p 641 N95-15843

DIFFUSION
Minimum uncertainty and squeezing in diffusion processes and stochastic quantization p 607 N95-13938
Diffusion of adatoms on face-centered cubic transition metal surfaces
[DE94-014230] p 445 N95-15307
Adsorption and diffusion of fluids in well-characterized adsorbent materials
[DE94-016953] p 454 N95-15344
Burn rates of TiH2/KClO4/Viton and output testing of NASA SKD26100098-301 pressure cartridges
[NASA-CR-188357] p 443 N95-15715

DIFFUSION COEFFICIENT
The seasonal cycle dependence of temperature fluctuations in the atmosphere
[AD-A283220] p 534 N95-15627

DIFFUSION THEORY
Minimum uncertainty and squeezing in diffusion processes and stochastic quantization p 607 N95-13938

DIGITAL COMPUTERS
Remote sensing, processing and transmission of data for an unmanned aerial vehicle
[AD-A283104] p 514 N95-13693
Advanced distributed simulation technology: Digital Voice Gateway Reference Guide
[AD-A283154] p 460 N95-13696
The exploration metaphor p 557 N95-14037
Slave controller for effecting a block transfer of sixteen bit words between a memory and a data transfer bus
[AD-D016463] p 574 N95-15336

DIGITAL DATA
A multiscale random field model for Bayesian image segmentation
[AD-A283875] p 515 N95-14358
Comparison of transform coding methods with an optimal predictor for the data compression of digital elevation models p 564 N95-14587
Satellite imagery and topographic data in verification
[AD-A280950] p 530 N95-14598
Neural networks: Alternatives to conventional techniques for automatic docking
[TABES PAPER 94-627] p 417 N95-14651

DIGITAL ELECTRONICS
Automated hierarchical testable design of digital circuits
[PB94-197936] p 472 N95-13983

A high speed, wide dynamic range digitizer circuit for photomultiplier tubes
[DE94-015187] p 475 N95-15302

DIGITAL SIMULATION
A gate level simulator for alpha-particle-induced transient faults
[AD-A283871] p 474 N95-14355
Damage analysis of internal faults in flux concentrating permanent magnet motors
[AD-A283883] p 474 N95-14359
The principles of fault-tolerant and efficient parallel computation
[AD-A283254] p 579 N95-15616
An algorithm for rezoning particle-in-cell calculations
[DE94-016056] p 619 N95-15774

DIGITAL SYSTEMS
Project OART: WDM, EDFA's and mixed data rates in a real-world testbed
[DE94-012234] p 601 N95-13670
An evaluation of B-ISDN for the communication architecture requirements of Distributed Interactive Simulation (DIS)
[AD-A280783] p 578 N95-14292
Wireless technology for command control and communications
[AD-A284367] p 470 N95-15804

DIGITAL TECHNIQUES
Energy and Technology Review, April 1994
[DE94-012133] p 496 N95-13669
Monitoring the variability of active galactic nuclei from a space-based platform p 644 N95-14509
A high speed, wide dynamic range digitizer circuit for photomultiplier tubes
[DE94-015187] p 475 N95-15302

DILATATIONAL WAVES
Torsional shear wave transducer
[AD-D016347] p 496 N95-14841

DIMENSIONAL ANALYSIS
Nonlinear bulging factor based on R-curve data p 511 N95-14476

DIMENSIONAL MEASUREMENT
Ground penetrating radar surveys to characterize pavement layer thickness variations at GPS sites
[PB94-190170] p 460 N95-14119
A new procedure for measuring contact angle
[DE94-014971] p 457 N95-14659

DIMERS
One: Redox chemistry of bimetallic fulvalene complexes. 2: Oligocyclopentadienyl complexes
[DE94-014930] p 443 N95-15667

DIMETHYL COMPOUNDS
Development and testing of a high-resolution model for tropospheric sulfate driven by observation-derived meteorology
[DE94-014910] p 525 N95-15864

DIODES
High power diode pumped solid state laser development at Lawrence Livermore National Laboratory
[DE94-015899] p 499 N95-14427

DIPOLE MOMENTS
Electrokinetic transport of heterogeneous particles in suspension p 444 N95-14581

DIRECT CURRENT
Direct-current proton-beam measurements at Los Alamos
[DE94-016280] p 599 N95-15360
The Ceramic Manufacturability Center: A new partnership with US industry
[DE94-015851] p 456 N95-15634

DIRECTIONAL CONTROL
X-31 quasi-tailless flight demonstration p 395 N95-14243

DIRECTIONAL COUPLERS
Integrated optical maze
[DE94-015866] p 613 N95-14367

DIRECTIONAL SOLIDIFICATION (CRYSTALS)
Crystal growth of selected II-VI semiconducting alloys by directional solidification p 458 N95-14214
The study of dopant segregation behavior during the growth of GaAs in microgravity p 458 N95-14215
Convection and morphological stability during directional solidification p 448 N95-14548
Shear stabilization of solidification fronts p 448 N95-14549
Crystal growth and fluid mechanics problems in directional solidification p 486 N95-14550

DIRECTIONAL STABILITY
X-31 quasi-tailless flight demonstration p 395 N95-14243

DIRECTORIES
FFCAat Clearinghouse, directory of abstracts
[DE94-015259] p 632 N95-15435

DISASTERS
The Global Emergency Observation and Warning System
[TABES PAPER 94-622] p 417 N95-14649

DISCONTINUITY
Computing illumination using extended sources: Object space and image space
[PB94-201282] p 612 N95-13992

DISCRETE COSINE TRANSFORM
Performance of customized DCT quantization tables on scientific data p 564 N95-14586
Comparison of transform coding methods with an optimal predictor for the data compression of digital elevation models p 564 N95-14587

DISCRETE FUNCTIONS
CFD methodology and validation for turbomachinery flows p 480 N95-14131
Computational aerodynamics based on the Euler equations
[AGARD-AG-325] p 398 N95-14264
Discrete-layer piezoelectric plate and shell models for active tip-clearance control
[NASA-CR-195383] p 507 N95-14417
Density control and on-line labeling problems
[TR-481] p 576 N95-15789

DISILICIDES
Optical detector having a plurality of matrix layers with cobalt disilicide particles embedded therein
[NASA-CASE-NPO-18625-2-CU] p 614 N95-15603
Symposium on Structural Intermetallics: Perspectives on Science and Technology, volume 2
[AD-A283379] p 447 N95-15874

DISORDERS
Validation of MMPI scales for personality disorders: A pilot and other aviator study
[AD-A284397] p 553 N95-15788

DISPLACEMENT
Earth Observing System (EOS)/Advanced Microwave Sounding Unit-A (AMSU-A) worst-case analysis: Antenna beam pointing
[NASA-CR-197218] p 517 N95-15851

DISPLAY DEVICES
Nonresonant interaction of ultrashort electromagnetic pulses with multilevel quantum systems p 610 N95-13960
Technical Revue Thomson-CSF, volume 26, no. 1, March 1994. Flat panels for visualisation
[PB94-197969] p 410 N95-13984
The display of tactile information p 554 N95-14017
The exploration metaphor p 557 N95-14037
Rotational wind indicator enhances control of rotated displays p 559 N95-14046
Human operator tracking performance with a vibrotactile display p 560 N95-14049
Tactile display device using an electrorheological fluid
[NASA-CASE-LAR-14860-1] p 472 N95-14112
Aircraft maneuver envelope warning system
[NASA-CASE-ARC-11953-1] p 411 N95-14518
A graphical user interface for design and analysis of air breathing propulsion systems
[TABES PAPER 94-616] p 411 N95-14645
Spatial awareness comparisons between large-screen, integrated pictorial displays and conventional EFIS displays during simulated landing approaches
[NASA-TP-3467] p 409 N95-14852

DISSIPATION
Decoherence and dissipation for a quantum system coupled to a local environment p 609 N95-13949
Evolution of wave function in a dissipative system p 610 N95-13959
Wake turbulence p 405 N95-14894
Comparison of different statistical models of turbulence by similarity methods
[DE94-015326] p 493 N95-15530
Studies in chaotic adiabatic dynamics
[DE94-013111] p 627 N95-15578

DISSOCIATION
Small UHV compatible hyperthermal oxygen atom generator
[NASA-CAS-LAR-14674-1] p 503 N95-15601

DISTANCE
Atmospheric propagation at larger lateral distances from the flight track p 402 N95-14885

DISTORTION
Diffusion of adatoms on face-centered cubic transition metal surfaces
[DE94-014230] p 445 N95-15307
Cluster studies of La2CuO4: Local geometric distortions
[DE94-016203] p 626 N95-15776

DISTRIBUTED PROCESSING
Paradigms and strategies for scientific computing on distributed memory concurrent computers
[DE94-013305] p 567 N95-13676
Methodology for the parallel direct solution of finite element systems
[PB94-198009] p 585 N95-13991
CIFO 3.0 p 570 N95-14167
An informal introduction to program transformation and parallel processors
[DE94-016343] p 578 N95-14380
Performance measurement and analysis techniques for parallel and distributed programs
[DE94-016429] p 578 N95-14384
Intelligent manufacturing systems state of the art
[TABES PAPER 94-503] p 415 N95-14637
Low latency remote memory access on the Intel Paragon
[DE94-014993] p 566 N95-14662
Checkpointing and rollback recovery in distributed shared memory systems
[AD-A281583] p 579 N95-15442
The principles of fault-tolerant and efficient parallel computation
[AD-A283254] p 579 N95-15616
Distributed heterogeneous visualization, BOP (Bag-O-Polygons) and BOP view
[AD-A284393] p 567 N95-15809

DISTRIBUTION FUNCTIONS
On the possibility of a quantum mechanical phase space representation p 606 N95-13931
Some rules for polydimensional squeezing p 606 N95-13941
The parton distribution functions in the limit chi(sub Bj) approaches 1
[DE94-013799] p 597 N95-15545

DIURETICS
Water intake and urinary volume during 20 days bed-rest in young women p 548 N95-15134

DIURNAL VARIATIONS
Analysis of deep convective clouds and their association with non-migrating atmospheric diurnal tides in the tropical troposphere
[PB94-187457] p 526 N95-13974
Towards developing an analytical procedure of defining the equatorial electrojet for correcting satellite magnetic anomaly data
[NASA-CR-193621] p 526 N95-14267
Tidal dynamics and mixing over steep topography
[AD-A283535] p 536 N95-15324

DIVERTERS
Computational analysis in support of the SSTO flowpath test
[NASA-TM-106757] p 479 N95-13665
US-Japan workshop Q-181 on High Heat Flux Components and Plasma-Surface Interactions for Next Devices: Proceedings
[DE94-014939] p 618 N95-14443

DOCUMENTATION
Bibliography of Joint Aircraft Survivability reports and related documents
[AD-A282795] p 409 N95-14840
LSENS, a general chemical kinetics and sensitivity analysis code for homogeneous gas-phase reactions. 2: Code description and usage
[NASA-RP-1329] p 442 N95-15512
Enhanced capabilities and updated users manual for axial-flow turbine preliminary sizing code TURBAN
[NASA-CR-195405] p 405 N95-15912

DOCUMENTS
Produce documents and media information
[NASA-CR-196521] p 532 N95-14271

DOMES (STRUCTURAL FORMS)
The 3.5-meter telescope enclosure
[AD-A280949] p 638 N95-14597

DOPED CRYSTALS
Nonlinear optical susceptibility of a model guest/host polymeric system as investigated by electro-optics and second harmonic generation
[AD-A283069] p 449 N95-13692
The study of dopant segregation behavior during the growth of GaAs in microgravity p 458 N95-14215
In-situ characterization of growth and interfaces in a-Si:H devices
[DE94-011847] p 622 N95-14431
Electrical characterization of 6H crystalline silicon carbide
[NASA-CR-197047] p 439 N95-14903
Optimization of transparent and reflecting electrodes for amorphous-silicon solar cells
[DE94-011841] p 520 N95-15355

DOPPLER EFFECT
The Stark anomalous dispersion optical filter: The theory p 462 N95-14622
Defect profiling in elemental and multilayer systems: Correlations of fitted defect concentrations with positron implantation profiles
[DE94-015844] p 624 N95-15422
Troposcatter at the KU band
[AD-A281575] p 469 N95-15462
Positron studies in catalysis research
[DE94-012793] p 597 N95-15572

DOPPLER RADAR
Probing surface structure on late-type stars with FRESIP p 643 N95-14501
Nowcasting convective storm evolution in east-central Florida using satellite and Doppler radar data [AD-A283260] p 534 N95-15618
TDWR scan strategy implementation [AD-A284877] p 534 N95-15749
DOSAGE
Ion implantation of He-3 in tantalum for use in a low energy deuteron polarization analyzer [AD-A283172] p 619 N95-13698
DOWN-CONVERTERS
Time-dependent distinguishability: Choosing to be a wave or a particle p 600 N95-13912
DRAG REDUCTION
Base passive porosity for drag reduction [NASA-CASE-LAR-15246-1] p 501 N95-14183
DRAINAGE
Numerical modeling of a cryogenic fluid within a fuel tank [NASA-TM-4651] p 479 N95-13892
Microgravity foam structure and rheology p 459 N95-14568
DRINKING
Low-dose alcohol effects on human behavior and performance: A review of post-1984 research [DOT/FAA/AM-94/24] p 552 N95-14863
Alterations of body temperature, feeding, drinking and sleep-wake circadian rhythms in Rhesus monkey during a 19 day Spacelab flight simulation p 539 N95-15132
New findings regarding light intensity and its effects as a zeitgeber in the Sprague-Dawley rat p 539 N95-15135
DROP SIZE
Phase segregation due to simultaneous migration and coalescence p 484 N95-14537
DROP TOWERS
Bubble dynamics, two-phase flow, and boiling heat transfer in a microgravity environment p 488 N95-14561
DROPS (LIQUIDS)
The flow induced by the coalescence of two initially stationary drops [NASA-TM-106752] p 478 N95-13653
Joint Launch + One Year Science Review of USML-1 and USMP-1 with the Microgravity Measurement Group [NASA-CP-3272-VOL-1] p 634 N95-14207
Core-centering of compound drops in capillary oscillations: Observations on USML-1 experiments in space p 458 N95-14218
Bifurcation of rotating liquid drops: Results from USML-1 experiments in space p 458 N95-14219
Surface characterization through shape oscillations of drops in microgravity and 1-g p 458 N95-14220
Measurement of interfacial tension of immiscible liquid pairs in microgravity p 458 N95-14221
Wetting and spreading at the molecular scale p 484 N95-14539
Nonlinear dynamics of drops and bubbles and chaotic phenomena p 485 N95-14541
Computations of drop collision and coalescence p 485 N95-14542
A realistic model of evaporation for a liquid droplet p 485 N95-14543
Thermocapillary motion of deformable drops p 485 N95-14544
Ground based studies of thermocapillary flows in levitated drops p 486 N95-14545
Thermocapillary migration and interactions of bubbles and drops p 486 N95-14546
Electrohydrodynamic deformation and interaction of a pair of emulsion drops p 490 N95-14576
Role of dielectric constant in electrohydrodynamics of conducting fluids p 478 N95-14577
DRUGS
Unreported medications used in incapacitating medical conditions found in fatal civil aviation accidents [DOT/FAA/AM-94/14] p 540 N95-14177
DRUMS (CONTAINERS)
Acoustic resonance spectroscopy intrinsic seals [DE94-016207] p 591 N95-15359
DUAL SPIN SPACECRAFT
Evaluation of energy-sink stability criteria for dual-spin spacecraft [AD-A283228] p 428 N95-14850
DUALITY THEOREM
Duality theorem in the multivariable Iwasawa theory of local fields [PB94-192325] p 589 N95-13979
DUCTED FANS
Propulsion/airframe interference for ducted propfan engines with ground effect [NASA-CR-197110] p 409 N95-14909
DUCTED FLOW
MHD flow in rectangular ducts with inclined non-uniform transverse magnetic field [DE94-013989] p 616 N95-14006
DUCTILE-BRITTLE TRANSITION
Transient failure behavior of HT9 [DE94-016320] p 445 N95-14378
Impact fracture behavior of HT9 duct [DE94-016328] p 445 N95-14379
DUCTILITY
Processing and characterization of mechanically alloyed NiAl-based alloys [AD-A283959] p 444 N95-14202
DUCTS
Refractive effects from VHF to EHF. Part A: Propagation Mechanisms p 467 N95-14831
Refractive effects from VHF to EHF. Part B: Propagation models p 467 N95-14832
DUPLEXERS
Advanced distributed simulation technology: Digital Voice Gateway Reference Guide [AD-A283154] p 460 N95-13696
DURABILITY
Environmental durability issues for solar power systems in low Earth orbit [NASA-TM-106775] p 431 N95-15769
DUST
Formation of dust grains with impurities in red giant winds p 641 N95-15841
DWARF STARS
Stellar activity: Astrophysics relevant to global change p 643 N95-14500
Probing surface structure on late-type stars with FRESIP p 643 N95-14501
Asteroseismology: Theory and phenomenology p 643 N95-14502
DYADICS
Polarizability properties of bianisotropic spheres with noncomplete magnetoelectric dyadics [PB94-189065] p 589 N95-13987
DYNAMIC CHARACTERISTICS
Effect of dispersion forces on squeezing with Rydberg atoms p 456 N95-13899
Dynamical properties measurements for asteroid, comet and meteorite material applicable to impact modeling and mitigation calculations [DE94-014142] p 642 N95-14311
Modelling of eddy currents related to large angle magnetic suspension test fixture [NASA-CR-197028] p 475 N95-14851
DYNAMIC CONTROL
Modelling of eddy currents related to large angle magnetic suspension test fixture [NASA-CR-197028] p 475 N95-14851
DYNAMIC LOADS
Selecting wave gauge sites for monitoring harbor oscillations: A case study for Kahului Harbor, Hawaii [AD-A281707] p 536 N95-15452
Computational modeling of fiber-reinforced composites [DE94-012914] p 436 N95-15573
DYNAMIC MODELS
Photochemical urban airshed modeling using diagnostic and dynamic meteorological fields [PB94-176120] p 616 N95-13973
Evaluation of sensor placement algorithms for on-orbit identification of space platforms p 425 N95-14088
DYNAMIC PRESSURE
Low-speed wind tunnel testing of the NPS and NASA Ames Mach 6 optimized waverider [AD-A283585] p 404 N95-15319
Pressure measurements on an F/A-18 twin vertical tail in buffeting flow. Volume 2: Steady and unsteady RMS pressure data [AD-A281581] p 404 N95-15465
DYNAMIC PROGRAMMING
2D regular arrays for a special class of non uniform recurrence equations [PB94-195633] p 584 N95-13980
A Multiple Divide-and-Conquer (MDC) algorithm for optimal alignments in linear space [DE94-015457] p 574 N95-15536
DYNAMIC RANGE
A high speed, wide dynamic range digitizer circuit for photomultiplier tubes [DE94-015187] p 475 N95-15302
DYNAMIC RESPONSE
Impulsive response of nonuniform density liquid in a laterally excited tank [DE94-013722] p 479 N95-13679
Turbulence: Engineering models, aircraft response p 407 N95-14900
Dynamic response of rigid tanks with inhomogeneous liquids [DE94-012619] p 493 N95-15571
Computational modeling of fiber-reinforced composites [DE94-012914] p 436 N95-15573
Studies in chaotic adiabatic dynamics [DE94-013111] p 627 N95-15578
Individual variability in the transmission of vertical vibration from seat to head [ISVR-TR-236] p 563 N95-15850
DYNAMIC STRUCTURAL ANALYSIS
User's guide for ENSAERO: A multidisciplinary program for fluid/structural/control interaction studies of aircraft (release 1) [NASA-TM-108853] p 391 N95-13662
Impulsive response of nonuniform density liquid in a laterally excited tank [DE94-013722] p 479 N95-13679
Development and application of structural dynamics analysis capabilities [NASA-CR-197229] p 513 N95-14922
Linear and nonlinear dynamic analysis of redundant load path bearingless rotor systems [NASA-CR-197220] p 503 N95-14923
Prediction of rotor-blade deformations due to unsteady airloads [AD-A284467] p 410 N95-15821
DYNAMIC TESTS
Selection of solar simulator for solar dynamic ground test [NASA-TM-106608] p 430 N95-14173
Design review and analysis for a Pratt and Whitney fluid-film bearing and seal testing rig [NASA-CR-197035] p 502 N95-14797
Large amplitude nonlinear response of flat aluminum, and carbon fiber plastic beams and plates [AD-A282440] p 513 N95-15547
DYNAMICAL SYSTEMS
Identification of dynamic systems. Volume 3: Applications to aircraft. Part 2: Nonlinear analysis and manoeuvre design [AGARD-AG-300-VOL-3-PT-2] p 408 N95-14102
Dynamic modelling to assess the value of Electronic Data Interchange: A study in the Rotterdam port community [PB94-195542] p 632 N95-14837

E

EARTH ATMOSPHERE
Remote sensing strategy at the first atmospheric radiation measurement field site [DE94-015091] p 522 N95-14187
An experimental and numerical study of the modifications of mixed-layer structure by inhomogeneous surface fluxes and secondary circulations [DE94-015945] p 529 N95-14428
EARTH CRUST
The 226RA and 231PA systematics of axial, MORB, crustal residence ages, and MAGMA chamber characteristics at 9 to 10 degree N East Pacific Rise [DE94-013084] p 529 N95-14434
EARTH GRAVITATION
Development of life sciences equipment for microgravity and hypergravity simulation p 425 N95-14090
EARTH IONOSPHERE
Propagation in the ionosphere, A p 466 N95-14826
EARTH MAGNETOSPHERE
An observational test of magnetospheric field models at geosynchronous orbit [DE94-014462] p 526 N95-13995
EARTH MANTLE
Measurement and interpretation of crustal deformation rates associated with postglacial rebound [NASA-CR-196440] p 525 N95-13627
EARTH MOVEMENTS
Lithological and rheological constraints on fault rupture scenarios for ground motion hazard prediction [DE94-014742] p 529 N95-14436
EARTH OBSERVATIONS (FROM SPACE)
Our Mission to Planet Earth: A guide to teaching Earth system science [NASA-EP-292] p 629 N95-13650
Satellite Laser Ranging in the 1990s: Report of the 1994 Belmont Workshop [NASA-CP-3283] p 526 N95-14274
Earth orientation parameters p 527 N95-14281
1994 Science Information Management and Data Compression Workshop [NASA-CP-3277] p 564 N95-14585
The Global Emergency Observation and Warning System [TABES PAPER 94-622] p 417 N95-14649
US space-based remote sensing: Challenges and prospects [AD-A282439] p 515 N95-15546
EARTH OBSERVING SYSTEM (EOS)
Earth Observing System (EOS) Advanced Microwave Sounding Unit-A (AMSU-A) Spares Program Plan [NASA-CR-189380] p 567 N95-13632

Earth Observing System (EOS)/Advanced Microwave Sounding Unit-A (AMSU-A): Instrument logic diagrams [NASA-CR-189378] p 567 N95-13633
Earth Observing System (EOS) Advanced Microwave Sounding Unit-A (AMSU-A): Instrumentation interface control document [NASA-CR-189377] p 567 N95-13651
Earth Observing System (EOS)/Advanced Microwave Sounding Unit-A (AMSU-A): Calibration management plan [NASA-CR-189376] p 515 N95-13704
Earth Observing System (EOS)/Advanced Microwave Sounding Unit-A (AMSU-A) software assurance plan [NASA-CR-196059] p 515 N95-13885
An overview of the EOSDIS V0 information management system: Lessons learned from the implementation of a distributed data system p 566 N95-14596
Earth Observing System (EOS)/Advanced Microwave Sounding Unit-A (AMSU-A) worst-case analysis: Antenna beam pointing [NASA-CR-197218] p 517 N95-15851

EARTH ORBITAL ENVIRONMENTS
Investigation of the effects of long duration space exposure on active optical system components [NASA-CR-4632] p 601 N95-13660
Modelling the low Earth space debris environment p 414 N95-13830
A facility to produce an energetic, ground state atomic oxygen beam for the simulation of the Low-Earth Orbit environment p 422 N95-14072
The effect of Low Earth Orbit exposure on some experimental fluorine and silicon-containing polymers p 422 N95-14074
Space simulation techniques and facilities for SAX STM test campaign p 423 N95-14077
Environmental testing to prevent on-orbit TDRS failures p 423 N95-14078
Joint Launch + One Year Science Review of USML-1 and USMP-1 with the Microgravity Measurement Group [NASA-CP-3272-VOL-1] p 634 N95-14207
The growth of zeolites A, X and mordenite in space p 458 N95-14226
The Astroculture (tm)-1 experiment on the USML-1 mission p 564 N95-14228
Satellite situation report, volume 33, number 2 [NASA-TM-109965] p 428 N95-14510
Results of the examination of LDEF polyurethane thermal control coatings [NASA-CR-4617] p 432 N95-14603
Summary of solar cell data from the Long Duration Exposure Facility (LDEF) [NASA-CR-197069] p 519 N95-14802
Environmental durability issues for solar power systems in low Earth orbit [NASA-TM-106775] p 431 N95-15769

EARTH ORBITS
Laboratory simulation of Low Earth Orbit (LEO) atomic oxygen effects p 422 N95-14071
Investigating and implementing enhancements to the simulation of short-term collision hazards p 426 N95-14092
Satellite situation report, volume 33, number 2 [NASA-TM-109965] p 428 N95-14510
Efficient mission control for the 48-satellite Globalstar constellation [TABES PAPER 94-609] p 415 N95-14641
Analysis of space environment damage to solar cell assemblies from LDEF experiment A0171-GSFC test plate [NASA-CR-197066] p 519 N95-14853

EARTH ORIENTATION
Earth orientation parameters p 527 N95-14281

EARTH RESOURCES
EMAP Information Management Strategic Plan, 1993-1997 [PB94-176823] p 522 N95-14124
A multiscale random field model for Bayesian image segmentation [AD-A283875] p 515 N95-14358

EARTH ROTATION
The role of SLR and LLR in relativity p 528 N95-14284
Satellite Laser Ranging operations p 500 N95-14287

EARTH SCIENCES
Our Mission to Planet Earth: A guide to teaching Earth system science [NASA-EP-292] p 629 N95-13650

EARTH TIDES
Satellite Laser Ranging operations p 500 N95-14287

EARTHQUAKES
Impulsive response of nonuniform density liquid in a laterally excited tank [DE94-013722] p 479 N95-13679

ECCENTRICITY
Global reference frame: Intercomparison of results (SLR, VLBI and GPS) p 527 N95-14276
Eccentricity of the electron beam in a gyrotron cavity [PB94-197639] p 496 N95-14839

ECHOCARDIOGRAPHY
Transesophageal echocardiographic evaluation of baboons during microgravity induced by parabolic flight p 538 N95-15094

ECLIPSING BINARY STARS
Observations of hot stars and eclipsing binaries with FRESIP p 644 N95-14508
Determination of the atmospheric structure of the BO star companion of SMC X-1 by analysis of Ginga observations [NASA-CR-197100] p 638 N95-14804

ECONOMIC ANALYSIS
Tokamak power plant burn cycle options [DE94-014016] p 617 N95-14012

ECONOMIC FACTORS
The integration of renewable energy sources into electric power distribution systems. Volume 1: National assessment [DE94-015935] p 519 N95-14393
The advanced development of x-ray computed tomography applications [AD-A284211] p 434 N95-14411
Space science in the 1990's and beyond [TABES PAPER 94-204] p 415 N95-14634

ECONOMICS
Energy review [DE94-015828] p 518 N95-14326

ECOSYSTEMS
Progress report on terrestrial model development (TERRA and HABITAT): Research in support of the CERES earth system modeling project [DE94-016362] p 524 N95-15779
Development of techniques for the evaluation of toxicant impacts to multispecies systems [AD-A284426] p 524 N95-15814

EDDY CURRENTS
Modelling of eddy currents related to large angle magnetic suspension test fixture [NASA-CR-197028] p 475 N95-14851
Applied Computational Electromagnetics Society Journal, volume 9, number 2 [AD-A281576] p 469 N95-15463

EDDY VISCOSITY
Eddy viscosity transport equations and their relation to the k-epsilon model [NASA-TM-108854] p 481 N95-14273

EDGE DETECTION
Neural networks: Alternatives to conventional techniques for automatic docking [TABES PAPER 94-627] p 417 N95-14651
The design and development of Histogram-based Morphological Edge Detector (HMED) [AD-A284458] p 470 N95-15820

EDITING ROUTINES (COMPUTERS)
NLEdit: A generic graphical user interface for Fortran programs [NASA-TM-4543] p 572 N95-14206

EDUCATION
Our Mission to Planet Earth: A guide to teaching Earth system science [NASA-EP-292] p 629 N95-13650
Suited for spacewalking: Teacher's guide with activities for physical and life science [NASA-EG-101] p 554 N95-13888
Formal methods technology transfer: Some lessons learned p 571 N95-14172
Space based astronomy: Teacher's guide with activities [NASA-EG-102] p 638 N95-14511
NASA/DOD Aerospace Knowledge Diffusion Research Project. Paper 43: The role of information resource training in aerospace education. Expanded version [NASA-TM-109981] p 632 N95-14619
Space science in the 1990's and beyond [TABES PAPER 94-204] p 415 N95-14634
Helping small companies commercialize public-sector technology [TABES PAPER 94-407] p 415 N95-14635
A graphical user interface for design and analysis of air breathing propulsion systems [TABES PAPER 94-616] p 411 N95-14645
Modern methods in meteorological and oceanographic data acquisition and analyses [AD-A283038] p 533 N95-14848
NASA/DOD Aerospace Knowledge Diffusion Research Project. Paper 44: Becoming an aerospace engineer: Some thoughts on the career goals and educational preparation of AIAA student members [NASA-TM-109980] p 632 N95-14870
The Bureau Gravimetrique International p 516 N95-15795

EFFERENT NERVOUS SYSTEMS
Intersensory coordination p 555 N95-14020

EFFICIENCY
Results of demonstration test for receiving and processing of flight data from the Space Transportation System [NASA-CR-194986] p 418 N95-13890
Computing quantitative characteristics of finite-state real-time systems [AD-A282839] p 412 N95-14343
Large-scale data envelopment analysis models and related applications [AD-A283214] p 588 N95-15400

EIGENVALUES
Parallel performance of a symmetric eigensolver based on the Invariant Subspace Decomposition approach [DE94-013314] p 577 N95-13677
Quantum statistics of Raman scattering model with Stokes mode generation p 610 N95-13958
A study of the Invariant Subspace Decomposition Algorithm for banded symmetric matrices [DE94-013872] p 568 N95-13977
Relativistic configuration-interaction calculation of the correlation energies of heliumlike ions [DE94-015190] p 621 N95-14325

EIGENVECTORS
Parallel performance of a symmetric eigensolver based on the Invariant Subspace Decomposition approach [DE94-013314] p 577 N95-13677
Quantum statistics of Raman scattering model with Stokes mode generation p 610 N95-13958
A study of the Invariant Subspace Decomposition Algorithm for banded symmetric matrices [DE94-013872] p 568 N95-13977
Relativistic configuration-interaction calculation of the correlation energies of heliumlike ions [DE94-015190] p 621 N95-14325

ELASTIC BUCKLING
Analytical tripping loads for stiffened plates [AD-A284368] p 514 N95-15805

ELASTIC DEFORMATION
Deformation, strength, and failure modes of laminated conventional and hybrid polymer-matrix composites loaded in the thickness direction [AD-A281587] p 436 N95-15443
Size and deformation limits to maintain constraint in K(sub Ic) and J(sub c) testing of bend specimens [AD-A284363] p 514 N95-15802
Prediction of rotor-blade deformations due to unsteady airloads [AD-A284467] p 410 N95-15821

ELASTIC PROPERTIES
Orientation effects on the measurement and analysis of critical CTOA in an aluminum alloy sheet [NASA-TM-109153] p 444 N95-13690
Elastic-plastic models for multi-aite damage p 507 N95-14454
Modelling and investigation of EHD point contacts [AD-A283571] p 454 N95-15316
Basic mechanics of laminated composite plates [NASA-RP-1351] p 436 N95-15763

ELASTIC SCATTERING
Low energy electron and atom elastic scattering cross sections from 0.1 to 30 keV [AD-A283584] p 595 N95-15318

ELASTIC WAVES
Mathematical problems of nonlinear wave propagation and of waves in heterogeneous media [AD-A282217] p 492 N95-14605

ELASTOHYDRODYNAMICS
Modelling and investigation of EHD point contacts [AD-A283571] p 454 N95-15316

ELASTOMERS
Self-organization of graft copolymers at surfaces, interfaces and in bulk [DE94-016884] p 454 N95-15340
Surface epoxidation of elastomers [AD-D016352] p 456 N95-15800

ELASTOPLASTICITY
Effects of tensile loading on upper shelf fracture toughness [AD-A284364] p 514 N95-15803

ELBOW (ANATOMY)
The human operator transfer function: Identification of the limb mechanics subsystem p 558 N95-14040

ELECTRIC ARCS
Plasma arc welding torch having means for vortexing plasma gas exiting the welding torch [NASA-CASE-MFS-28828-1] p 503 N95-15670

ELECTRIC BATTERIES
Thin composite solid electrolyte film for lithium batteries [NASA-CASE-NPO-18694-1-CU] p 472 N95-13824
Corrosion-resistant coatings for high-temperature high-sulfur-activity applications [DE94-015155] p 453 N95-14957

Thin lithium cobalt dioxide rechargeable cells using polyacrylonitrile-based polymer electrolytes
[AD-A283253] p 455 N95-15615

ELECTRIC CHARGE

Quartz resonator state-of-charge monitor for lead-acid batteries
[DE94-013823] p 473 N95-14310

ELECTRIC CONNECTORS

Experimental design for the evaluation of high-T(sub c) superconductive thermal bridges in a sensor satellite
[NASA-CR-197003] p 429 N95-14106
Service equipment for use in hostile environments
[NASA-CASE-LEW-14906-2-SB] p 504 N95-15914

ELECTRIC CONTACTS

Modelling and investigation of EHD point contacts
[AD-A283571] p 454 N95-15316

ELECTRIC CURRENT

Sub-Poissonian light and photocurrent shot-noise suppression in closed opto-electronic loop
p 606 N95-13924

ELECTRIC DISCHARGES

ESD and lightning interactions on aircraft
p 406 N95-14896

ELECTRIC EQUIPMENT

Electronics and Electrical Engineering Laboratory Technical Progress Bulletin covering laboratory programs, January to March 1994 with 1994/1995 EEEL events calendar
[PB94-193810] p 474 N95-14402

ELECTRIC FIELDS

Nonlinear optical susceptibility of a model guest/host polymeric system as investigated by electro-optics and second harmonic generation
[AD-A283069] p 449 N95-13692
Study of auroral dynamics with combined spacecraft and incoherent scatter radar data
[NASA-CR-196974] p 526 N95-13818
Electrohydrodynamic deformation and interaction of a pair of emulsion drops p 490 N95-14576
Development and analysis of high-energy corona process for air purification
[DE94-015207] p 524 N95-15432

ELECTRIC FURNACES

High Temperature Calibration Furnace System user's guide
[NASA-CR-196526] p 573 N95-14905

ELECTRIC GENERATORS

The integration of renewable energy sources into electric power distribution systems. Volume 1: National assessment
[DE94-015935] p 519 N95-14393

ELECTRIC MOTOR VEHICLES

Materials and mechanisms of high temperature lithium sulfide batteries
[DE94-012634] p 471 N95-13684

ELECTRIC MOTORS

Fuzzy logic motor control for pollution prevention and improved energy efficiency
[PB94-190865] p 523 N95-14403
Design of power electronics for TVC and EMA systems
[NASA-CR-197067] p 475 N95-14866

ELECTRIC POTENTIAL

Piezoelectric loudspeaker
[NASA-CASE-LAR-15138-1] p 590 N95-14110
Tactile display device using an electrorheological fluid
[NASA-CASE-LAR-14860-1] p 472 N95-14112
Design of reliable high voltage avalanche transistor pulsers
[DE94-015323] p 473 N95-14261
Quartz resonator state-of-charge monitor for lead-acid batteries
[DE94-013823] p 473 N95-14310
Divertor bias experiments
[DE94-015720] p 617 N95-14328
Design of power electronics for TVC and EMA systems
[NASA-CR-197067] p 475 N95-14866
Resonant tunneling in small current-biased Josephson junctions
[DE94-016875] p 623 N95-15338
High gain GaAs switches for impulse sources: Measurement of the speed of current filaments
[DE94-015281] p 477 N95-15544

ELECTRIC POWER SUPPLIES

Materials and mechanisms of high temperature lithium sulfide batteries
[DE94-012634] p 471 N95-13684
HTS Wire Development Workshop: Proceedings
[DE94-015650] p 624 N95-15421
Programmable high voltage power supply with regulation confined to the high voltage section
[NASA-CASE-GSC-13289-1] p 478 N95-15681

ELECTRIC POWER TRANSMISSION

The integration of renewable energy sources into electric power distribution systems. Volume 1: National assessment
[DE94-015935] p 519 N95-14393

ELECTRIC PROPULSION

High performance arcjet engines
[NASA-CR-195397] p 430 N95-13697
Damage analysis of internal faults in flux concentrating permanent magnet motors
[AD-A283883] p 474 N95-14359

ELECTRIC SWITCHES

Fish method: Interaction between AC-machines and switching power converters
[PB94-191210] p 472 N95-14149
Strategic avionics technology definition studies, power voter redundancy management. Power voter applications in new vehicle architectures
[NASA-CR-197049] p 411 N95-14799

ELECTRICAL ENGINEERING

Electronics and Electrical Engineering Laboratory Technical Progress Bulletin covering laboratory programs, January to March 1994 with 1994/1995 EEEL events calendar
[PB94-193810] p 474 N95-14402

ELECTRICAL FAULTS

Method of locating ground faults
[NASA-CASE-LEW-15407-1] p 478 N95-15669

ELECTRICAL GROUNDING

Space experiments aboard rockets: SPEAR 3
[AD-A280778] p 414 N95-14290

ELECTRICAL IMPEDANCE

Static image theory for a sphere with impedance surface
[PB94-189073] p 590 N95-13988
Determination of the shear modulus in self-assembled monolayers using quartz resonators
[DE94-013449] p 437 N95-14307

ELECTRICAL PROPERTIES

Semiconductor measurement technology: Improved characterization and evaluation measurments for HgCdTe detector materials, processes, and devices used on the GOES and TIROS satellites
[PB94-188810] p 474 N95-14401
Screening of charged electrodes in aqueous electrolytes
[AD-A284065] p 474 N95-14425
Modelling of eddy currents related to large angle magnetic suspension test fixture
[NASA-CR-197028] p 475 N95-14851

ELECTRICAL RESISTIVITY

High field magnetotransport and specific heat in YbAgCu4
[DE94-014475] p 620 N95-13999
Electrical characterization of 6H crystalline silicon carbide
[NASA-CR-197047] p 439 N95-14903
Defects and transport in mixed oxides
[DE94-015652] p 454 N95-15358
The crosswell electromagnetic response of layered media
[DE94-014929] p 470 N95-15866

ELECTRICITY

Energy review
[DE94-015828] p 518 N95-14326

ELECTRO-OPTICS

Investigation of the effects of long duration space exposure on active optical system components
[NASA-CR-4632] p 601 N95-13660
Nonlinear optical susceptibility of a model guest/host polymeric system as investigated by electro-optics and second harmonic generation
[AD-A283069] p 449 N95-13692
Integrated optical maze
[DE94-015866] p 613 N95-14367
Electro-optics: Propagation from IR to UV and sensor considerations. Part A: Propagation theory
p 467 N95-14833
Electro-optics: Propagation from IR to UV and sensor considerations. Part B: Tools for exploitation of propagation conditions and system range performance
p 467 N95-14834
International Semiconductor Device Research Symposium (ISDRS-93)
[AD-A281715] p 477 N95-15454
Asymmetric coupled quantum wells for high speed optical modulators at communication wavelengths
[AD-A281572] p 477 N95-15459
High-efficiency electro-optic grating on PLZT ceramic wafer for optical switching
[AD-A281573] p 477 N95-15460
Integrated photonics research, 1993
[AD-A281578] p 614 N95-15464

ELECTROCARDIOGRAPHY

Hemodynamic responses to passive body tilts
p 542 N95-15096

ELECTROCATALYSTS

One: Redox chemistry of bimetallic fulvalene complexes. 2: Oligocyclopentadienyl complexes
[DE94-014930] p 443 N95-15667

ELECTROCHEMISTRY

Electrodeposition of conductors and semiconductors with controlled stoichiometries and morphologies
[AD-A280743] p 437 N95-14141
Atomic force microscopy of the electrochemical nucleation and growth of molecular crystals
[AD-A280958] p 622 N95-14601

ELECTRODE MATERIALS

Materials and mechanisms of high temperature lithium sulfide batteries
[DE94-012634] p 471 N95-13684
High performance arcjet engines
[NASA-CR-195397] p 430 N95-13697

ELECTRODEPOSITION

Kinetic theory for electrodic phase transitions: The voltammogram
[AD-A283039] p 619 N95-13691
Electrodeposition of conductors and semiconductors with controlled stoichiometries and morphologies
[AD-A280743] p 437 N95-14141
Corrosion-resistant coatings for high-temperature high-sulfur-activity applications
[DE94-015155] p 453 N95-14957

ELECTRODES

Tactile display device using an electrorheological fluid
[NASA-CASE-LAR-14860-1] p 472 N95-14112
Divertor bias experiments
[DE94-015720] p 617 N95-14328
Screening of charged electrodes in aqueous electrolytes
[AD-A284065] p 474 N95-14425
Chemically modified electrodes by nucleophilic substitution of chlorosilylated platinum oxide surfaces
[AD-A281567] p 477 N95-15456
High-efficiency electro-optic grating on PLZT ceramic wafer for optical switching
[AD-A281573] p 477 N95-15460
Charge collection in a-Si:H/a-Si(1-x)C(x multilayers photodetectors
[DE94-013107] p 625 N95-15577

ELECTROENCEPHALOGRAPHY

Measurement and modification of the EEG and related behavior p 557 N95-14038
The electrocortical correlates of fluctuating states of attention during vigilance tasks
[NASA-CR-197051] p 552 N95-14864
Collection of real-time, multichannel EEG data from helicopter pilots in flight: A feasibility study
[AD-A284396] p 551 N95-15767

ELECTROFORMING

Hohlraum manufacture for inertial confinement fusion
[DE94-014472] p 616 N95-13997

ELECTROHYDRODYNAMICS

Electrohydrodynamic deformation and interaction of a pair of emulsion drops p 490 N95-14576
Role of dielectric constant in electrohydrodynamics of conducting fluids p 478 N95-14577
Electrophoretic interactions and aggregation of colloidal biological particles p 444 N95-14578

ELECTROKINETICS

Electrokinetic transport of heterogeneous particles in suspension p 444 N95-14581

ELECTROLESS DEPOSITION

The realuminizing of the 7-meter-diameter solar simulator collimating mirror p 424 N95-14081

ELECTROLYTES

Screening of charged electrodes in aqueous electrolytes
[AD-A284065] p 474 N95-14425

ELECTROLYTIC CELLS

Development of the fuel cell power generation technology, 2
[DE94-780614] p 520 N95-15376
Development of the fuel cell power generation technology, 1
[DE94-780648] p 520 N95-15377

ELECTROMAGNETIC ABSORPTION

Field intercomparison with five automatic ammonia monitors
[PB94-192879] p 523 N95-15389
Optical detector having a plurality of matrix layers with cobalt disilicide particles embedded therein
[NASA-CASE-NPO-18625-2-CU] p 614 N95-15603

ELECTROMAGNETIC COMPATIBILITY

Electromagnetic reverberation characteristics of a large transport aircraft
[AD-A282923] p 411 N95-15392
Research in high energy physics
[DE94-015519] p 600 N95-15539

ELECTROMAGNETIC COUPLING
Intermultiplet transitions in optically opaque EuBa2Cu3O7: An inelastic neutron scattering study
[DE94-013429] p 620 N95-14188
ELECTROMAGNETIC FIELDS
Advanced laser source research
[AD-A283110] p 498 N95-13695
High-order squeezing of the quantum electromagnetic field and the generalized uncertainty relations in two-mode squeezed states p 471 N95-13900
Homodyning and heterodyning the quantum phase p 604 N95-13913
A method of measuring the amplitude-modulated vacuum field near a conducting mirror p 471 N95-13921
Modes in light wave propagating in semiconductor laser p 500 N95-13925
Applied Computational Electromagnetics Society Journal, volume 9, number 2
[AD-A281576] p 469 N95-15463
RF vacuum microelectronics
[AD-A283123] p 478 N95-15613
ELECTROMAGNETIC INTERACTIONS
Effect of dispersion forces on squeezing with Rydberg atoms p 456 N95-13899
ELECTROMAGNETIC INTERFERENCE
Propagation Modelling and Decision Aids for Communications, Radar and Navigation Systems
[AGARD-LS-196] p 466 N95-14825
Propagation in the ionosphere, A p 466 N95-14826
Ground wave and diffraction, A p 467 N95-14828
Ground wave and diffraction, B p 467 N95-14829
Refractive effects from VHF to EHF. Part A: Propagation Mechanisms p 467 N95-14831
Refractive effects from VHF to EHF. Part B: Propagation models p 467 N95-14832
Effects of hydrometeors and atmospheric gases at SHF/EHF p 468 N95-14835
Radiation and EMI effects in the NIF environment
[DE94-016635] p 468 N95-15365
ELECTROMAGNETIC MEASUREMENT
Two-dimensional signal processing, optical information storage and processing, and electromagnetic measurements
[AD-A281937] p 460 N95-13657
Direct-current proton-beam measurements at Los Alamos
[DE94-016280] p 599 N95-15360
The crosswell electromagnetic response of layered media
[DE94-014929] p 470 N95-15866
ELECTROMAGNETIC NOISE MEASUREMENT
Electromagnetic reverberation characteristics of a large transport aircraft
[AD-A282923] p 411 N95-15392
ELECTROMAGNETIC PULSES
Advanced laser source research
[AD-A283110] p 498 N95-13695
Nonresonant interaction of ultrashort electromagnetic pulses with multilevel quantum systems p 610 N95-13960
Composite waveform generation for EMP and lightning direct-drive testing
[AD-A284159] p 462 N95-14405
ELECTROMAGNETIC RADIATION
Space based astronomy: Teacher's guide with activities
[NASA-EG-102] p 638 N95-14511
Radiation and EMI effects in the NIF environment
[DE94-016635] p 468 N95-15365
Graphical aids for the users of GEMACS (GAUGE): Ray tracing enhancements
[AD-A284903] p 470 N95-15756
ELECTROMAGNETIC SCATTERING
Wideband electromagnetic scattering/analysis program. Electromagnetic scattering from the trunks and branches of trees
[AD-A283112] p 469 N95-15394
ELECTROMAGNETIC SPECTRA
The electromagnetic spectrum. Research investigation directed toward extending the useful range of the electromagnetic spectrum
[AD-A281378] p 461 N95-14361
ELECTROMAGNETIC WAVE TRANSMISSION
Engineer's Refractive Effects Prediction System (EREPS), version 3.0
[AD-A283748] p 461 N95-14345
ELECTROMAGNETISM
Polarizability properties of bianisotropic spheres with noncomplete magnetoelectric dyadics
[PB94-189065] p 589 N95-13987
Applied Computational Electromagnetics Society Journal, volume 9, number 2
[AD-A281576] p 469 N95-15463
ELECTROMECHANICAL DEVICES
Flex-gear power transmission system for transmitting EMF between Sun and ring gears
[NASA-CASE-GSC-13540-1] p 502 N95-14517
ELECTROMYOGRAPHY
Coordination of human upper arm and forearm motion in rapid extensions p 561 N95-14056
Robotic control using muscular and neural electrical signals
[AD-A284908] p 551 N95-15757
ELECTRON ATTACHMENT
Chemical kinetics and atmospheric modification
[AD-A283304] p 524 N95-15623
ELECTRON BEAMS
Phase-space analysis of charged and optical beam transport: Wigner rotation angle p 606 N95-13927
Eccentricity of the electron beam in a gyrotron cavity
[PB94-197639] p 496 N95-14839
Investigation of the coherent synchrotron radiation spectrum as a probe of charge dynamics
[DE94-015340] p 599 N95-15371
ELECTRON BOMBARDMENT
Direct detection of neutral metal atoms in electron-stimulated desorption: Al from CH3O/Al(111). Velocity distribution and absolute yield
[DE94-014011] p 593 N95-14011
ELECTRON CAPTURE
Searches for massive neutrino emission in C-14 beta and Fe-55 electron-capture decays
[DE94-016863] p 594 N95-14374
Charge collection in a-Si:H/a-Si(1-x)C(x multilayers photodetectors
[DE94-013107] p 625 N95-15577
ELECTRON DENSITY (CONCENTRATION)
Faraday rotation system
[DE94-015345] p 618 N95-15374
ELECTRON ENERGY
Low energy electron and atom elastic scattering cross sections from 0.1 to 30 keV
[AD-A283584] p 595 N95-15318
Application of spin-sensitive electron spectroscopies to investigations of electronic and magnetic properties of solid surfaces and epitaxial systems
[DE94-012981] p 625 N95-15574
ELECTRON GUNS
The realuminizing of the 7-meter-diameter solar simulator collimating mirror p 424 N95-14081
ELECTRON IMPACT
Development and analysis of high-energy corona process for air purification
[DE94-015207] p 524 N95-15432
ELECTRON IRRADIATION
Experiments to examine the contribution of gas atoms to void formation in irradiated metals
[DE94-015209] p 446 N95-15433
ELECTRON MICROSCOPES
Resolution measurement for scanning electron microscopes
[DE94-012747] p 601 N95-13674
Analysis of electron microscope images: 3-D localization of immuno-markers
[PB94-197977] p 537 N95-13990
ELECTRON MICROSCOPY
Stress corrosion crack tip microstructure in nickel-based alloys
[DE94-015362] p 446 N95-15532
ELECTRON MOBILITY
Proceedings of the 3rd International Workshop on Computational Electronics
[AD-A284214] p 475 N95-14444
ELECTRON PARAMAGNETIC RESONANCE
Electron spin resonance and band electronic structure study of the metal-insulator transition in (BEDT-TTF)3(HSO4)2
[DE94-014005] p 620 N95-14009
ELECTRON PRECIPITATION
Study of auroral dynamics with combined spacecraft and incoherent scatter radar data
[NASA-CR-196974] p 526 N95-13818
ELECTRON SCATTERING
LLE review, January - March 1994
[DE94-015058] p 618 N95-14955
Low energy electron and atom elastic scattering cross sections from 0.1 to 30 keV
[AD-A283584] p 595 N95-15318
Electron-molecule collisions and UV signatures in flowfields
[AD-A281569] p 596 N95-15457
ELECTRON SPECTROSCOPY
Application of spin-sensitive electron spectroscopies to investigations of electronic and magnetic properties of solid surfaces and epitaxial systems
[DE94-012981] p 625 N95-15574
ELECTRON SPIN
Application of spin-sensitive electron spectroscopies to investigations of electronic and magnetic properties of solid surfaces and epitaxial systems
[DE94-012981] p 625 N95-15574
ELECTRON STATES
Ultrasensitive infrared chemiluminescence detection
[AD-A283531] p 440 N95-14958
Quantum chemistry and excited states: First investigations on pyrene-like molecules p 599 N95-15844
ELECTRON TRANSFER
Proceedings of the 3rd International Workshop on Computational Electronics
[AD-A284214] p 475 N95-14444
ELECTRON TRANSITIONS
Intermultiplet transitions in optically opaque EuBa2Cu3O7: An inelastic neutron scattering study
[DE94-013429] p 620 N95-14188
X-ray Photoelectron Spectroscopy (XPS), Rutherford Back Scattering (RBS) studies
[NASA-CR-196536] p 439 N95-14867
The C4H radical and the diffuse interstellar bands. An ab initio study p 641 N95-15843
Quantum chemistry and excited states: First investigations on pyrene-like molecules p 599 N95-15844
ELECTRON TUNNELING
The effect of Low Earth Orbit exposure on some experimental fluorine and silicon-containing polymers p 422 N95-14074
ELECTRONIC CONTROL
Fuzzy logic motor control for pollution prevention and improved energy efficiency
[PB94-190865] p 523 N95-14403
ELECTRONIC COUNTERMEASURES
Challenge of Future EW System Design
[AGARD-CP-546] p 461 N95-14200
ELECTRONIC EQUIPMENT
Electronics and Electrical Engineering Laboratory Technical Progress Bulletin covering laboratory programs, January to March 1994 with 1994/1995 EEEL events calendar
[PB94-193810] p 474 N95-14402
Automated cleaning of electronic components
[DE94-014122] p 476 N95-15356
Radiation and EMI effects in the NIF environment
[DE94-016635] p 468 N95-15365
ELECTRONIC EQUIPMENT TESTS
I(sub DDQ) testing for ultimate low power design verification and defect detection
[DE94-014281] p 473 N95-14314
Semiconductor measurement technology: Improved characterization and evaluation measurments for HgCdTe detector materials, processes, and devices used on the GOES and TIROS satellites
[PB94-188810] p 474 N95-14401
ELECTRONIC MAIL
Dynamic modelling to assess the value of Electronic Data Interchange: A study in the Rotterdam port community
[PB94-195542] p 632 N95-14837
ELECTRONIC SPECTRA
Laboratory spectra of C60 and related molecular structures p 627 N95-15838
Quantum chemistry and excited states: First investigations on pyrene-like molecules p 599 N95-15844
ELECTRONIC WARFARE
Challenge of Future EW System Design
[AGARD-CP-546] p 461 N95-14200
Engineer's Refractive Effects Prediction System (EREPS), version 3.0
[AD-A283748] p 461 N95-14345
ELECTRONS
ENDL type formats for the LLNL Evaluated Atomic Data Library, EADL, for the Evaluated Electron Data Library, EEDL, and for the Evaluated Photon Data Library, EPDL
[DE94-016487] p 594 N95-14385
ELECTROPHORESIS
Role of dielectric constant in electrohydrodynamics of conducting fluids p 478 N95-14577
Electrophoretic interactions and aggregation of colloidal biological particles p 444 N95-14578
Electrokinetic transport of heterogeneous particles in suspension p 444 N95-14581
ELECTROPHYSIOLOGY
Measurement and modification of the EEG and related behavior p 557 N95-14038
Tactile discrimination and representations of texture, shape, and softness p 558 N95-14041
ELECTROPLATING
AASERT-93: Electroplating of refractory metals using haloaluminate melts
[AD-A284859] p 447 N95-15744

ELECTRORHEOLOGICAL FLUIDS
Tactile display device using an electrorheological fluid
[NASA-CASE-LAR-14860-1] p 472 N95-14112
ELECTROSTATIC CHARGE
ESD and lightning interactions on aircraft
p 406 N95-14896
ELECTROSTATIC PROBES
Space experiments aboard rockets: SPEAR 3
[AD-A280778] p 414 N95-14290
ELECTROSTATICS
Static image theory for a sphere with impedance surface
[PB94-189073] p 590 N95-13988
Nonlinear dynamics of drops and bubbles and chaotic phenomena p 485 N95-14541
ELECTROWEAK INTERACTIONS (FIELD THEORY)
Electroweak and b-physics at the Tevatron collider
[DE94-013239] p 600 N95-15582
Electroweak boson pair production at CDF
[DE94-015183] p 597 N95-15629
ELEMENTARY PARTICLE INTERACTIONS
Recent QCD results from the Tevatron (-p)p collider at the square root of s = 1.8 TeV
[DE94-014986] p 594 N95-14661
ELEVATION ANGLE
Measurement and interpretation of crustal deformation rates associated with postglacial rebound
[NASA-CR-196440] p 525 N95-13627
Photogrammetric mobile satellite service prediction
p 466 N95-14679
ELLIPSOMETRY
Real-time monitor and control of MBE growth of HgCdTe by spectroscopic ellipsometry
[AD-A284451] p 627 N95-15818
ELLIPTIC DIFFERENTIAL EQUATIONS
Radiative interactions in multi-dimensional chemically reacting flows using Monte Carlo simulations
[NASA-CR-197012] p 481 N95-14269
EMBEDDING
Preparation and characterization of composite inorganic zeolite membranes with molecular sieve properties
[PB94-191251] p 450 N95-14151
Discrete-layer piezoelectric plate and shell models for active tip-clearance control
[NASA-CR-195383] p 507 N95-14417
Apparatus for imaging an object in or through a scattering medium using coherent anti-Stokes Raman scattering
[AD-D016366] p 615 N95-15765
EMBRITTLEMENT
Welding irradiated stainless steel
[DE94-013661] p 500 N95-13645
Influence of transmutation on microstructure, density change, and embrittlement of vanadium and vanadium alloys irradiated in HFIR
[DE94-015202] p 446 N95-15431
EMBRYOS
The avian embryo responding to microgravity of space flight p 538 N95-15104
EMERGENCIES
The Global Emergency Observation and Warning System
[TABES PAPER 94-622] p 417 N95-14649
EMISSION SPECTRA
Laser spectroscopy of combustion intermediates in a supersonic jet expansion
[AD-A283201] p 500 N95-15395
ROSAT observations of the binary Be-star and radio pulsar PSR1259-63
[NASA-CR-196951] p 642 N95-15907
EMITTANCE
Small UHV compatible hyperthermal oxygen atom generator
[NASA-CAS-LAR-14674-1] p 503 N95-15601
EMULSIONS
New techniques for diffusing-wave spectroscopy
p 444 N95-14575
Electrohydrodynamic deformation and interaction of a pair of emulsion drops p 490 N95-14576
ENCEPHALITIS
World Reference Center for Arboviruses
[AD-A281635] p 550 N95-15445
Selective RF pulses in NMR and their effect on coupled and uncoupled spin systems
[PB94-195526] p 471 N95-15871
ENCLOSURE
Test and Evaluation Master Plan (TEMP) for Fixed Ground Antenna Radomes (FGAR)
[AD-A283839] p 461 N95-14346
The 3.5-meter telescope enclosure
[AD-A280949] p 638 N95-14597
END EFFECTORS
Dextrous gripping in a hazardous environment
[PB94-191244] p 501 N95-14150
Sample Acquisition and Instrument Deployment (SAID)
[NASA-CR-197104] p 502 N95-14910
END PLATES
High temperature superconductors with improved current densities
[AD-A282996] p 472 N95-13685
ENDOCRINE SECRETIONS
Gravitational stress and regulation of neuroendocrine elements and fluid volume in humans
p 542 N95-15090
Neurohumoral reactions to long-term vestibular stimulation in man p 542 N95-15091
ENDOCRINOLOGY
Gravitational stress and regulation of neuroendocrine elements and fluid volume in humans
p 542 N95-15090
ENERGY ABSORPTION
Landing gear energy absorption system
[NASA-CASE-MSC-22277-1] p 503 N95-15306
ENERGY CONSERVATION
Fuzzy logic motor control for pollution prevention and improved energy efficiency
[PB94-190865] p 523 N95-14403
The Ceramic Manufacturability Center: A new partnership with US industry
[DE94-015851] p 456 N95-15634
ENERGY CONSUMPTION
Research and development optical deep space antenna sizing study p 463 N95-14628
ENERGY CONVERSION EFFICIENCY
Fuzzy logic motor control for pollution prevention and improved energy efficiency
[PB94-190865] p 523 N95-14403
Alternative fabrication techniques for high-efficiency CuInSe2 and CuInSe2-alloy films and cells
[DE94-011846] p 521 N95-15407
Module process optimization and device efficiency improvement for stable, low-cost, large-area, cadmium telluride-based photovoltaic module production
[DE94-011817] p 521 N95-15863
ENERGY DISSIPATION
Sqeezing generated by a nonlinear master equation and by amplifying-dissipative Hamiltonians
p 588 N95-13926
Evaluation of energy-sink stability criteria for dual-spin spacecraft
[AD-A283228] p 428 N95-14850
Application of spin-sensitive electron spectroscopies to investigations of electronic and magnetic properties of solid surfaces and epitaxial systems
[DE94-012981] p 625 N95-15574
ENERGY GAPS (SOLID STATE)
International Semiconductor Device Research Symposium (ISDRS-93)
[AD-A281715] p 477 N95-15454
ENERGY SOURCES
The integration of renewable energy sources into electric power distribution systems. Volume 1: National assessment
[DE94-015935] p 519 N95-14393
ENERGY STORAGE
Design of reliable high voltage avalanche transistor pulsers
[DE94-015323] p 473 N95-14261
The transformation of organic amines by transition metal cluster compounds
[DE94-017151] p 441 N95-15346
ENERGY TECHNOLOGY
International energy: Research organizations, 1988-1992
[DE90-017267] p 630 N95-13726
Wind-electric ice making for villages in the developing world
[DE94-011854] p 518 N95-14191
The integration of renewable energy sources into electric power distribution systems. Volume 1: National assessment
[DE94-015935] p 519 N95-14393
The National Wind Technology Center
[DE94-011853] p 519 N95-14433
The Ceramic Manufacturability Center: A new partnership with US industry
[DE94-015851] p 456 N95-15634
ENERGY TRANSFER
Divertor bias experiments
[DE94-015720] p 617 N95-14328
Infrared/submillimeter wave studies of molecular collision kinetics
[AD-A281379] p 594 N95-14362
ENGINE AIRFRAME INTEGRATION
Propulsion/airframe interference for ducted propfan engines with ground effect
[NASA-CR-197110] p 409 N95-14909
ENGINE DESIGN
Turbomachinery Design Using CFD
[AGARD-LS-195] p 479 N95-14127
Computational methods for preliminary design and geometry definition in turbomachinery
p 480 N95-14128
Elements of a modern turbomachinery design system
p 480 N95-14129
Designing in three dimensions p 480 N95-14130
Unsteady flows in turbines: Impact on design procedure p 480 N95-14132
New methods, new methodology: Advanced CFD in the Snecma turbomachinery design process
p 480 N95-14134
Aero design of turbomachinery components: CFD in complex systems p 481 N95-14136
Computational predictive methods for fracture and fatigue p 509 N95-14466
The Aluminum Falcon: A low cost modern commercial transport
[NASA-CR-197180] p 409 N95-15742
Advanced Turbine Technology Applications Project (ATTAP)
[NASA-CR-195393] p 634 N95-15743
ENGINE INLETS
Computational analysis in support of the SSTO flowpath test
[NASA-TM-106757] p 479 N95-13665
Computation of supersonic air-intakes
p 400 N95-14452
Wind-tunnel blockage and actuation systems test of a two-dimensional scramjet inlet unstart model at Mach 6
[NASA-TM-109152] p 495 N95-15898
Two-dimensional scramjet inlet unstart model: Wind-tunnel blockage and actuation systems test
[NASA-TM-109984] p 495 N95-15899
ENGINE MONITORING INSTRUMENTS
Reusable rocket engine turbopump health management system
[NASA-CR-195388] p 431 N95-15058
ENGINE PARTS
A new tribological test for candidate brush seal materials evaluation
[NASA-TM-106753] p 431 N95-13631
ENGINE TESTS
Develop advanced nonlinear signal analysis topographical mapping system
[NASA-CR-194414] p 514 N95-13639
Development status of the NASA 30-cm ion thruster and power processor
[NASA-TM-106740] p 430 N95-14301
Definition of high-temperature use limits for MIL-L-2104 engine oils
[AD-A282838] p 451 N95-14365
Advanced Turbine Technology Applications Project (ATTAP)
[NASA-CR-195393] p 634 N95-15743
ENGINEERING MANAGEMENT
Engineering, technical, and management support services
[NASA-CR-196977] p 505 N95-13840
ENGINEERS
Engineer's Refractive Effects Prediction System (EREPS), version 3.0
[AD-A283748] p 461 N95-14345
NASA/DOD Aerospace Knowledge Diffusion Research Project. Paper 44: Becoming an aerospace engineer: Some thoughts on the career goals and educational preparation of AIAA student members
[NASA-TM-109980] p 632 N95-14870
ENGLISH LANGUAGE
Preparing technical text for translation: A comparison between International English and methods for simplifying language
[DE94-014465] p 630 N95-13996
ENTRAINMENT
Turbulent mixing of the HVOF thermal spray and coating oxidation
[DE94-015414] p 455 N95-15535
ENVIRONMENT EFFECTS
Analysis of space environment damage to solar cell assemblies from LDEF experiment A0171-GSFC test plate
[NASA-CR-197066] p 519 N95-14853
The effect of aircraft speed on the penetration of sonic boom noise into a flat ocean p 402 N95-14887
The avian embryo responding to microgravity of space flight p 538 N95-15104
Integrated science model for assessment of climate change
[DE94-016363] p 523 N95-15361
Large scale obscuration and related climate effects open literature bibliography
[DE94-012992] p 524 N95-15575
Progress report on terrestrial model development (TERRA and HABITAT): Research in support of the CERES earth system modeling project
[DE94-016362] p 524 N95-15779

Development of techniques for the evaluation of toxicant impacts to multispecies systems
[AD-A284426] p 524 N95-15814

ENVIRONMENT MODELS
Hybrid verification by exploiting the environment
[NASA-CR-195810] p 568 N95-13699
Thermal design verification testing of the Clementine spacecraft: Quick, cheap, and useful
p 424 N95-14083
Computational modeling issues in next generation air quality models
[PB94-197449] p 521 N95-14122
Progress report on terrestrial model development (TERRA and HABITAT): Research in support of the CERES earth system modeling project
[DE94-016362] p 524 N95-15779

ENVIRONMENT POLLUTION
TABES 1994: 10th Annual Technical and Business Exhibition and Symposium p 414 N95-14633

ENVIRONMENT PROTECTION
Environmentally sound manufacturing
[TABES PAPER 94-502] p 415 N95-14636
Intelligent manufacturing systems state of the art
[TABES PAPER 94-503] p 415 N95-14637
Recycled plastic: A clean and low cost rocket fuel
[TABES PAPER 94-610] p 416 N95-14642
Comprehensive facility decommissioning through the use of innovative technology to reduce cost, schedule, and environmental liability
[TABES PAPER 94-615] p 416 N95-14644

ENVIRONMENT SIMULATION
A two dimensional artificial reality p 560 N95-14052
Binaural room simulation p 561 N95-14053
Active localization of virtual sounds
p 561 N95-14054
Destabilizing effects of visual environment motions simulating eye movements or head movements
p 562 N95-14061
Martian environmental simulation for a deployable lattice mast p 423 N95-14076

ENVIRONMENT SIMULATORS
Tele-existence and/or cybernetic interface studies in Japan p 555 N95-14025
Introduction to HEFeS (Hierarchical Environmental Feature Simulator)
[AD-A283244] p 534 N95-15402

ENVIRONMENTAL CONTROL
Development of visual 3D virtual environment for control software p 559 N95-14048
Implementation of a three degree of freedom, motor/brake hybrid force output device for virtual environment control tasks p 562 N95-14058
Design of components for the NASA OCEAN project
[NASA-CR-197207] p 535 N95-14906

ENVIRONMENTAL MONITORING
EMAP Information Management Strategic Plan, 1993-1997
[PB94-176823] p 522 N95-14124
Three neural network based sensor systems for environmental monitoring
[DE94-014557] p 522 N95-14195
Satellite situation report, volume 33, number 2
[NASA-TM-109965] p 428 N95-14510
Results of TSP metals monitoring at McMurdo Station, Antarctica
[DE94-015264] p 524 N95-15455

ENVIRONMENTAL SURVEYS
Martian environmental simulation for a deployable lattice mast p 423 N95-14076
The Global Emergency Observation and Warning System
[TABES PAPER 94-622] p 417 N95-14649
The effect of aircraft speed on the penetration of sonic boom noise into a flat ocean p 402 N95-14887

ENVIRONMENTAL TESTS
HYDRA, a new tool for mechanical testing
p 418 N95-14086
Vestibular ontogeny: Measuring the influence of the dynamic environment p 544 N95-15105

ENZYMES
Relationship between hind-limb muscle atrophy and serum enzymes in tail suspended rats
p 539 N95-15143
Activity of ornithine decarboxylase in muscle of Japanese quail in hypergravity conditions
p 539 N95-15144

EPIDEMIOLOGY
Aviation Epidemiology Data Register: Gender-specific attrition from the trained US Army aviator cohort of 1988
[AD-A284395] p 551 N95-15810

EPITAXY
Ion beam synthesis of SiGe alloy layers
[DE94-014958] p 620 N95-14189
Positron studies in catalysis research
[DE94-012793] p 597 N95-15572
Application of spin-sensitive electron spectroscopies to investigations of electronic and magnetic properties of solid surfaces and epitaxial systems
[DE94-012981] p 625 N95-15574
Low loss substrates for microwave applications and sol-gel processing of superconductors
[AD-A284868] p 625 N95-15746
Low Temperature Grown and Highly Non-Stoichiometric GaAs and Related Materials
[AD-A284898] p 626 N95-15754

EPOXIDATION
Surface epoxidation of elastomers
[AD-D016352] p 456 N95-15800

EPOXY MATRIX COMPOSITES
Monitoring fiber stress during curing of single fiber glass- and graphite-epoxy composites
[NASA-TM-4568] p 432 N95-13641
Dynamics of the interface in a model composite system
[AD-A281910] p 433 N95-13655
Effect of matrix stiffness on wavy fiber behavior in single-carbon-fiber-epoxy composites
[AD-A280970] p 435 N95-15427

EPOXY RESINS
Monitoring fiber stress during curing of single fiber glass- and graphite-epoxy composites
[NASA-TM-4568] p 432 N95-13641
Processing of thermoset prepreg laminate via exposure to microwave radiation
[DE94-013268] p 432 N95-13643

EQUATIONS OF MOTION
Berry phase in Heisenberg representation
p 609 N95-13952
Proposal for an astronaut mass measurement device for the Space Shuttle
[NASA-CR-197198] p 563 N95-14854
Dynamic response of rigid tanks with inhomogeneous liquids
[DE94-012619] p 493 N95-15571

EQUATORIAL ELECTROJET
Towards developing an analytical procedure of defining the equatorial electrojet for correcting satellite magnetic anomaly data
[NASA-CR-193621] p 526 N95-14267

EQUILIBRIUM EQUATIONS
Kinetic theory for electrodic phase transitions: The voltammogram
[AD-A283039] p 619 N95-13691

EQUIPMENT SPECIFICATIONS
A compact high voltage pulse generator
[DE94-015282] p 474 N95-14319

EQUIVALENT CIRCUITS
Design of power electronics for TVC and EMA systems
[NASA-CR-197067] p 475 N95-14866
Accelerometer model in APLAC
[PB94-197647] p 497 N95-15413

EROSION
Laboratory simulation of Low Earth Orbit (LEO) atomic oxygen effects p 422 N95-14071

ERROR ANALYSIS
Errors induced in triaxial stress tensor calculations using incorrect lattice parameters
[DE94-013256] p 444 N95-13820
Performance Reports: Mirror alignment system performance prediction comparison between SAO and EKC
[NASA-CR-196013] p 637 N95-14100
Fault detection and diagnosis using neural network approaches p 571 N95-14170
Quality assessment for wind tunnel testing
[AGARD-AR-304] p 393 N95-14197
Sequentially t-diagnosable systems
[PB94-205093] p 574 N95-15396
Earth Observing System (EOS)/Advanced Microwave Sounding Unit-A (AMSU-A) worst-case analysis: Antenna beam pointing
[NASA-CR-197218] p 517 N95-15851

ERROR CORRECTING CODES
Spin glasses and error-correcting codes
p 462 N95-14624
Linear quadratic Gaussian and feedforward controllers for the DSS-13 antenna p 463 N95-14625

ERROR DETECTION CODES
1994 Science Information Management and Data Compression Workshop
[NASA-CP-3277] p 564 N95-14585
Comparison of transform coding methods with an optimal predictor for the data compression of digital elevation models p 564 N95-14587
Lossless compression of NOAA-AVHRR satellite data
p 565 N95-14592
The development of lossless data compression technology for remote sensing applications
p 565 N95-14593
A strategy for geoid repairing p 517 N95-15798

ERRORS
Errors induced in triaxial stress tensor calculations using incorrect lattice parameters
[DE94-013256] p 444 N95-13820

ESOPHAGUS
Transesophageal echocardiographic evaluation of baboons during microgravity induced by parabolic flight
p 538 N95-15094

ESTIMATES
Fatigue reliability method with in-service inspections
p 505 N95-14475
The effect of response format on reliability estimates for tacit knowledge scales
[AD-A283547] p 552 N95-15326
Automatic TLI recognition system, part 1
[DE94-015253] p 578 N95-15434

ESTIMATING
Two new kinds of uncertainty relations
p 588 N95-13915

ESTONIA
TABES 1994: 10th Annual Technical and Business Exhibition and Symposium p 414 N95-14633
Design in Huntsville, manufacture in Estonia, sell in Europe
[TABES PAPER 94-607] p 415 N95-14640

ESTUARIES
ADCIRC: An advanced three-dimensional circulation model for shelves, coasts, and estuaries. Report 4: Hurricane storm surge modeling using large domains
[AD-A283868] p 535 N95-14352

ETCHING
A theoretical study of 30 to 50 angstrom noble gas heavy ion lithography
[DE94-015262] p 442 N95-15436

ETHERS
Poly(arylene ether)s containing pendent ethynyl groups
[NASA-CASE-LAR-15041-1] p 449 N95-13838

ETHYL ALCOHOL
Addendum: Tenth International Symposium on Alcohol Fuels, The Road to Commercialization
[DE93-018219] p 457 N95-14003

ETHYL COMPOUNDS
Theoretical studies of hydrocarbon combustion chemistry
[DE94-017155] p 441 N95-15347

ETHYLENE
Single-phase heat transfer and pressure drop characteristics of an integral-spine-fin within an annulus
[PB94-194073] p 482 N95-14407

ETHYLENE COMPOUNDS
Electron spin resonance and band electronic structure study of the metal-insulator transition in (BEDT-TTF)3(HSO4)2
[DE94-014005] p 620 N95-14009
Thin lithium cobalt dioxide rechargeable cells using polyacrylonitrile-based polymer electrolytes
[AD-A283253] p 455 N95-15615

EULER EQUATIONS OF MOTION
User's guide for ENSAERO: A multidisciplinary program for fluid/structural/control interaction studies of aircraft (release 1)
[NASA-TM-108853] p 391 N95-13662
An adaptively-refined, Cartesian, cell-based scheme for the Euler and Navier-Stokes equations
[NASA-TM-106754] p 392 N95-13817
The role of CFD in the design process
p 481 N95-14135
Computational aerodynamics based on the Euler equations
[AGARD-AG-325] p 398 N95-14264
A Cartesian, cell-based approach for adaptively-refined solutions of the Euler and Navier-Stokes equations
[NASA-TM-106786] p 398 N95-14297
Development and testing of a high-resolution model for tropospheric sulfate driven by observation-derived meteorology
[DE94-014910] p 525 N95-15864
Two methods for the study of vortex patch evolution on locally refined grids
[DE94-014965] p 494 N95-15867

EULER-LAGRANGE EQUATION
An approach for dynamic grids
[NASA-TM-106774] p 404 N95-15853

EUROPE
The European Geoid Project p 516 N95-15796

EUROPEAN SPACE PROGRAMS
Review of European microgravity measurements
p 457 N95-14211

EUTECTICS
Investigation of dendrite coherency in two commercial Al-Si foundry alloys
[PB94-208238] p 446 N95-15349
AASERT-93: Electroplating of refractory metals using haloaluminate melts
[AD-A284859] p 447 N95-15744

EVAPORATION
A realistic model of evaporation for a liquid droplet p 485 N95-14543
Effects of thermocapillarity on an evaporating extended meniscus in microgravity p 488 N95-14559
EVOLUTION (DEVELOPMENT)
Vision, learning, and development [TR-492-REV] p 553 N95-15787
EXCIMERS
Excimer emission from alkali diatomic and alkaline-earth-noble gas molecules [AD-A281662] p 596 N95-15446
EXCITATION
Nonresonant interaction of ultrashort electromagnetic pulses with multilevel quantum systems p 610 N95-13960
EXERCISE PHYSIOLOGY
Unique life sciences research facilities at NASA Ames Research Center p 426 N95-14091
EXHAUST EMISSION
Recycled plastic: A clean and low cost rocket fuel [TABES PAPER 94-610] p 416 N95-14642
Development and testing of a high-resolution model for tropospheric sulfate driven by observation-derived meteorology [DE94-014910] p 525 N95-15864
Process development of thermal hydrodechlorination [PB94-195518] p 525 N95-15870
EXHAUST GASES
Optical analysis methods for material films condensed on cryogenic surfaces of spacecraft [AD-A284014] p 427 N95-14420
EXHAUST NOZZLES
Ultra-high bypass ratio jet noise [NASA-CR-195394] p 591 N95-14610
EXOTHERMIC REACTIONS
Effects of two-phase flow on the deflagration of porous energetic materials [DE94-015353] p 442 N95-15375
EXPERIMENT DESIGN
Cratering and penetration experiments in teflon targets at velocities from 1 to 7 km/s [NASA-TM-104797] p 432 N95-13646
A loophole-free Bell's inequality experiment p 611 N95-13968
Laboratory simulation of Low Earth Orbit (LEO) atomic oxygen effects p 422 N95-14071
Thermal design verification testing of the Clementine spacecraft: Quick, cheap, and useful p 424 N95-14083
Simulation of Shuttle launch G forces and acoustic loads using the NASA Ames Research Center 20G centrifuge p 419 N95-14089
Experimental design for the evaluation of high-T(sub c) superconductive thermal bridges in a sensor satellite [NASA-CR-197003] p 429 N95-14106
ASSERT-1992. Fundamental studies of a high energy molecular system: Spectroscopy of boron in hydrogen clusters [AD-A283181] p 593 N95-14155
Joint Launch + One Year Science Review of USML-1 and USMP-1 with the Microgravity Measurement Group [NASA-CP-3272-VOL-1] p 634 N95-14207
Heat capacity and thermal relaxation of bulk helium very near the lambda point p 444 N95-14208
Review of European microgravity measurements p 457 N95-14211
The solid surface combustion experiment aboard the USML-1 mission p 458 N95-14212
Bifurcation of rotating liquid drops: Results from USML-1 experiments in space p 458 N95-14219
Measurement of interfacial tension of immiscible liquid pairs in microgravity p 458 N95-14221
Protein crystal growth results from the United States Microgravity Laboratory-1 mission p 458 N95-14225
Flocculation and aggregation in a microgravity environment (FAME) p 459 N95-14572
Dynamics of hard sphere colloidal dispersions p 490 N95-14573
The path to an experiment in space (from concept to flight) p 417 N95-14582
Fluids flight hardware p 491 N95-14583
Conceptual design of the Space Station fluids module p 429 N95-14584
EXPERT SYSTEMS
Knowledge-based processing for aircraft flight control [NASA-CR-194976] p 580 N95-13727
Artificial intelligence with applications for aircraft [DOT/FAA/CT-94/41] p 581 N95-13895
Automated hierarchical testable design of digital circuits [PB94-197936] p 472 N95-13983
Knowledge-based computational approach to architectural precedent analysis [PB94-191269] p 568 N95-14152
RICIS Symposium 1992: Mission and Safety Critical Systems Research and Applications [NASA-CR-196963] p 569 N95-14156
Intelligent alarming p 570 N95-14168
Expert systems in the process industries p 571 N95-14169
Fault detection and diagnosis using neural network approaches p 571 N95-14170
Reusable rocket engine turbopump health management system [NASA-CR-195388] p 431 N95-15058
EXPLORER 1 SATELLITE
Dynamics Explorer 1, retarding ion mass spectrometer summary spectrograms: 82/001 to 82/109 spin-time spectrograms for H(+), He(+), O(+), N(+), O(++), M/Z=2, and molecular ions [NASA-TM-108468] p 443 N95-15607
EXPLOSIVES
Prototype explosives-detection system based on nuclear-resonance absorption in nitrogen [DE94-015069] p 442 N95-15387
EXPOSURE
Extended duration orbiter medical project Microbial Air Sampler (STS-50/USML-1) p 458 N95-14222
Residents' reactions to long-term sonic boom exposure: Preliminary results p 403 N95-14892
The relationship between space sickness and preflight diet p 546 N95-15122
EXPULSION
Multi-dimensional modeling of pressurization and expulsion of multi-phase hydrogen propellant [NASA-CR-195156] p 457 N95-14902
EXTINCTION
Sensing of radio refractivity and aerosol extinction p 467 N95-14830
Electro-optics: Propagation from IR to UV and sensor considerations. Part A: Propagation theory p 467 N95-14833
Electro-optics: Propagation from IR to UV and sensor considerations. Part B: Tools for exploitation of propagation conditions and system range performance p 467 N95-14834
EXTINGUISHING
Flightline aircraft fire incidents and suppression agent effects: Field inquiries and incident analysis [AD-A284027] p 405 N95-14421
EXTRAGALACTIC RADIO SOURCES
Observations of extragalactic sources with the Metsaehovi radio telescope at 22-87 GHz [PB94-197712] p 637 N95-13982
EXTRAPOLATION
An evaluation of rise time characterization and prediction methods p 401 N95-14881
EXTRAVEHICULAR ACTIVITY
Suited for spacewalking: Teacher's guide with activities for physical and life science [NASA-EG-101] p 554 N95-13888
EXTRAVEHICULAR MOBILITY UNITS
Suited for spacewalking: Teacher's guide with activities for physical and life science [NASA-EG-101] p 554 N95-13888
EXTREMELY HIGH FREQUENCIES
A radio telescope for the calibration of radio sources at 32 gigahertz p 463 N95-14626
Propagation characteristics of 20/30 GHz links with a 40 deg masking angle p 464 N95-14672
Propagation data at 20/40 GHz and the propagation needs of Milstar p 465 N95-14673
The 40 and 50 GHz propagation experiments at the Rutherford Appleton Laboratory, UK, using the ITALSAT beacons p 465 N95-14674
Channel characterisation for future Ka-band Mobile Satellite Systems and preliminary results p 465 N95-14676
Propagation considerations for the Odyssey system design p 466 N95-14680
Refractive effects from VHF to EHF. Part A: Propagation Mechanisms p 467 N95-14831
Refractive effects from VHF to EHF. Part B: Propagation models p 467 N95-14832
Effects of hydrometeors and atmospheric gases at SHF/EHF p 468 N95-14835
EXTRUDING
Processing and characterization of mechanically alloyed NiAl-based alloys [AD-A283959] p 444 N95-14202
EYE MOVEMENTS
Intersensory coordination p 555 N95-14020
Eye movement control and top-down scanpath vision as a design metaphor for robotic vision and control p 555 N95-14022
Destabilizing effects of visual environment motions simulating eye movements or head movements p 562 N95-14061

F

F-111 AIRCRAFT
Development of a composite repair and the associated inspection intervals for the F-111C stiffener runout region p 392 N95-14477
F-15 AIRCRAFT
Integration of a mechanical forebody vortex control system into the F-15 p 398 N95-14258
Flight evaluation of pneumatic forebody vortex control in post-stall flight p 398 N95-14259
F-16 AIRCRAFT
Flight test results of the F-16 aircraft modified with the axisymmetric vectoring exhaust nozzle p 396 N95-14245
Vista/F-16 Multi-Axis Thrust Vectoring (MATV) control law design and evaluation p 396 N95-14248
F/A-18 and F-16 forebody vortex control, static and rotary-balance results p 397 N95-14254
The F-16 multinational staged improvement program: A case study of risk assessment and risk management [AD-A281706] p 409 N95-15451
F-18 AIRCRAFT
Flight and full-scale wind-tunnel comparison of pressure distributions from an F-18 aircraft at high angles of attack --- Conducted in NASA Ames Research Center's 80 by 120 ft wind tunnel p 394 N95-14231
Numerical simulation of the flow about an F-18 aircraft in the high-alpha regime p 394 N95-14232
Hybrid structured/unstructured grid computations for the F/A-18 at high angle of attack p 394 N95-14233
Free-to-roll tests of X-31 and F-18 subscale models with correlation to flight test results p 394 N95-14237
F-18 high alpha research vehicle: Lessons learned p 395 N95-14240
Design and development of an F/A-18 inlet distortion rake: A cost and time saving solution p 395 N95-14241
Flight validation of ground-based assessment for control power requirements at high angles of attack p 396 N95-14246
Navy and the HARV: High angle of attack tactical utility issues p 397 N95-14252
Preparations for flight research to evaluate actuated forebody strakes on the F-18 high-alpha research vehicle p 398 N95-14257
Numerical simulation of the flow about the F-18 HARV at high angle of attack [NASA-CR-197023] p 400 N95-14614
Pressure measurements on an F/A-18 twin vertical tail in buffeting flow. Volume 2: Steady and unsteady RMS pressure data [AD-A281581] p 404 N95-15465
FABRICATION
Investigations into mirror fabrication metrology analysis [NASA-CR-196522] p 602 N95-13841
Hohlraum manufacture for inertial confinement fusion [DE94-014472] p 616 N95-13997
Synthesis, processing and properties of materials for SOFCs [DE94-014491] p 517 N95-14002
Clean assembly and integration techniques for the Hubble Space Telescope High Fidelity Mechanical Simulator p 418 N95-14070
Scintillating glass fiber-optic neutron sensors [DE94-014562] p 613 N95-15312
Alternative fabrication techniques for high-efficiency CuInSe2 and CuInSe2-alloy films and cells [DE94-011846] p 521 N95-15407
Advanced Turbine Technology Applications Project (ATTAP) [NASA-CR-195393] p 634 N95-15743
Transducers and methods for making same [AD-D016349] p 497 N95-15799
FABRICS
Adjustable reed for weaving net-shaped tailored fabrics [NASA-CASE-LAR-15072-1] p 501 N95-14186
Development of large-area monolithically integrated Silicon-Film(tm) photovoltaic modules [DE94-011830] p 520 N95-15405
FACE CENTERED CUBIC LATTICES
Diffusion of adatoms on face-centered cubic transition metal surfaces [DE94-014230] p 445 N95-15307
Magnetic and structural instabilities of ultrathin Fe(100) wedges [DE94-013864] p 624 N95-15385
FACTORIZATION
On the LU factorization of sequences of identically structured sparse matrices within a distributed memory environment [AD-A282025] p 578 N95-14953

FAIL-SAFE SYSTEMS
European Workshop Industrical Computer Science Systems approach to design for safety p 569 N95-14157
FAILURE ANALYSIS
Environmental testing to prevent on-orbit TDRS failures p 423 N95-14078
The advanced development of x-ray computed tomography applications [AD-A284211] p 434 N95-14411
Nonlinear fracture mechanics-based analysis of thin wall cylinders p 508 N95-14462
Influence of crack history on the stable tearing behavior of a thin-sheet material with multiple cracks p 509 N95-14467
Statistical investigation of fatigue crack initiation and growth around chamfered rivet holes in Alclad 2024 T3 as affected by corrosion p 510 N95-14472
Mechanical behavior of high temperature composites [AD-A281582] p 436 N95-15441
Computational modeling of fiber-reinforced composites [DE94-012914] p 436 N95-15573
Vehicle health management using adaptive techniques [NASA-TM-108472] p 431 N95-15609
Milestone 5 test report. Task 5, subtask 5.2: Tile to foam strength tests [NASA-CR-197241] p 514 N95-15913
FAILURE MODES
Develop advanced nonlinear signal analysis topographical mapping system [NASA-CR-194414] p 514 N95-13639
Refurbishment of a 39 foot thermal vacuum chamber p 418 N95-14085
Fault detection and diagnosis using neural network approaches p 571 N95-14170
FAA/NASA International Symposium on Advanced Structural Integrity Methods for Airframe Durability and Damage Tolerance [NASA-CP-3274-PT-1] p 507 N95-14453
Probabilistic inspection strategies for minimizing service failures p 508 N95-14461
Deformation, strength, and failure modes of laminated conventional and hybrid polymer-matrix composites loaded in the thickness direction [AD-A281587] p 436 N95-15443
Computational modeling of fiber-reinforced composites [DE94-012914] p 436 N95-15573
Mechanical system reliability for long life space systems [NASA-CR-197215] p 505 N95-15584
FAIRINGS
NASA LeRC's acoustic fill effect test program and results [NASA-TM-106688] p 419 N95-13893
FAR INFRARED RADIATION
Infrared/submillimeter wave studies of molecular collision kinetics [AD-A281379] p 594 N95-14362
Faraday rotation system [DE94-015345] p 618 N95-15374
FAR ULTRAVIOLET RADIATION
Planetary entry experiments [NASA-CR-194215] p 644 N95-13717
VUV shock layer radiation in an arc-jet wind tunnel experiment p 405 N95-13719
Studies of the ablated plasma from experimental plasma gun disruption simulations [DE94-015017] p 617 N95-14262
FARADAY EFFECT
Faraday rotation system [DE94-015345] p 618 N95-15374
Method of locating ground faults [NASA-CASE-LEW-15407-1] p 478 N95-15669
FAST FOURIER TRANSFORMATIONS
The Block V Receiver fast acquisition algorithm for the Galileo S-band mission p 463 N95-14627
FATIGUE (MATERIALS)
Orientation effects on the measurement and analysis of critical CTOA in an aluminum alloy sheet [NASA-TM-109153] p 444 N95-13690
The effect of microstresses on fatigue crack propagation in steel [AD-A283872] p 506 N95-14356
FAA/NASA International Symposium on Advanced Structural Integrity Methods for Airframe Durability and Damage Tolerance [NASA-CP-3274-PT-1] p 507 N95-14453
Inspecting for widespread fatigue damage: Is partial debonding the key? p 508 N95-14458
Study of multiple cracks in airplane fuselage by micromechanics and complex variables p 509 N95-14468
Statistical investigation of fatigue crack initiation and growth around chamfered rivet holes in Alclad 2024 T3 as affected by corrosion p 510 N95-14472
Recent advances in the modelling of crack growth under fatigue loading conditions p 511 N95-14478
The effects of pitting on fatigue crack nucleation in 7075-T6 aluminum alloy p 448 N95-14482
Modeling time-dependent corrosion fatigue crack propagation in 7000 series aluminum alloys p 448 N95-14483
Analysis of small crack behavior for airframe applications p 512 N95-14484
The characterization of widespread fatigue damage in fuselage structure [NASA-TM-109142] p 432 N95-14920
Mechanical system reliability for long life space systems [NASA-CR-197215] p 505 N95-15584
Computer modeling the fatigue crack growth rate behavior of metals in corrosive environments [NASA-CR-194982-REV] p 448 N95-15918
FATIGUE LIFE
Inspecting for widespread fatigue damage: Is partial debonding the key? p 508 N95-14458
Microstructurally based model of fatigue initiation and growth p 508 N95-14459
Probabilistic inspection strategies for minimizing service failures p 508 N95-14461
A method of calculating the safe fatigue life of compact, highly-stressed components p 509 N95-14464
Corrosion and corrosion fatigue of airframe aluminum alloys p 448 N95-14465
Computational predictive methods for fracture and fatigue p 509 N95-14466
Influence of crack history on the stable tearing behavior of a thin-sheet material with multiple cracks p 509 N95-14467
Extracting a representative loading spectrum from recorded flight data p 410 N95-14469
The role of fretting corrosion and fretting fatigue in aircraft rivet hole cracking p 510 N95-14470
Statistical investigation of fatigue crack initiation and growth around chamfered rivet holes in Alclad 2024 T3 as affected by corrosion p 510 N95-14472
Space Shuttle fatigue loads spectra for prelaunch and liftoff loads p 419 N95-14474
Fatigue reliability method with in-service inspections p 505 N95-14475
The effects of pitting on fatigue crack nucleation in 7075-T6 aluminum alloy p 448 N95-14482
Analysis of small crack behavior for airframe applications p 512 N95-14484
Full-scale testing and analysis of fuselage structure p 512 N95-14485
Advanced method and processing technology for complicated shape airframe part forming p 410 N95-14486
FATIGUE TESTS
High temperature cyclic behaviour of aerospace materials: Room temperature validation tests of Ti-6Al-4V [AGARD-AR-328] p 506 N95-14198
Fatigue analysis of multiple site damage at a row of holes in a wide panel p 508 N95-14463
Modeling time-dependent corrosion fatigue crack propagation in 7000 series aluminum alloys p 448 N95-14483
Milestone 4: Test plan for Reusable Hydrogen Composite Tank System (RHCTS). Task 3: Composite tank materials [NASA-CR-197036] p 435 N95-14801
The characterization of widespread fatigue damage in fuselage structure [NASA-TM-109142] p 432 N95-14920
Fatigue in single crystal nickel superalloys [AD-A282917] p 446 N95-15415
FAULT DETECTION
Intelligent alarming p 570 N95-14168
Fault detection and diagnosis using neural network approaches p 571 N95-14170
I(sub DDQ) testing for ultimate low power design verification and defect detection [DE94-014281] p 473 N95-14314
Observation of microcrack development in concrete by use of TV-holography and deformation phase gradient calculation [PB94-207990] p 513 N95-15348
Method of locating ground faults [NASA-CASE-LEW-15407-1] p 478 N95-15669
FAULT TOLERANCE
Challenges for the aircraft structural integrity program p 410 N95-14481
Strategic avionics technology definition studies, power voter redundancy management. Power voter applications in new vehicle architectures [NASA-CR-197049] p 411 N95-14799
The principles of fault-tolerant and efficient parallel computation [AD-A283254] p 579 N95-15616
Fault-tolerance and efficiency in massively parallel algorithms [AD-A283255] p 579 N95-15617
FEASIBILITY
Assembly feasibility and reliability studies of surface mount circuit boards manufactured with lead-free solders [DE94-013783] p 472 N95-13975
Leak detection by acoustic emission monitoring. Phase 1: Feasibility study [AD-A283775] p 493 N95-15332
A theoretical study of 30 to 50 angstrom noble gas heavy ion lithography [DE94-015262] p 442 N95-15436
FEEDBACK
Navy and the HARV: High angle of attack tactical utility issues p 397 N95-14252
FEEDBACK CONTROL
Three-axis stabilization of spacecraft using parameter-independent nonlinear quaternion feedback [NASA-TM-109150] p 420 N95-13729
Some criteria for teleoperators and virtual environments from experiences with vehicle/operator simulation p 556 N95-14028
Implementation of a three degree of freedom, motor/brake hybrid force output device for virtual environment control tasks p 562 N95-14058
Computational methods for PDE's in flow control, superconductivity, fluid flows and other applications [AD-A282912] p 493 N95-15390
i-speech: Experiments with a single level feedback paradigm [TR-509] p 575 N95-15640
FEEDFORWARD CONTROL
Implementation of a three degree of freedom, motor/brake hybrid force output device for virtual environment control tasks p 562 N95-14058
Linear quadratic Gaussian and feedforward controllers for the DSS-13 antenna p 463 N95-14625
A trajectory preprocessor for antenna pointing p 463 N95-14630
FEMALES
Effects of 20 days bed-rest on cardio-respiratory functions during sub-maximal exercise in young women p 545 N95-15111
Water intake and urinary volume during 20 days bed-rest in young women p 548 N95-15134
Aviation Epidemiology Data Register: Gender-specific attrition from the trained US Army aviator cohort of 1988 [AD-A284395] p 551 N95-15810
FERMI-DIRAC STATISTICS
Particle localization, spinor two-valuedness, and Fermi quantization of tensor systems p 598 N95-13932
Causality problems for Fermi's two-atom system p 598 N95-13945
Quantum noise limits to matter-wave interferometry p 598 N95-13955
FERMIONS
Finite boson mappings of fermion systems [DE94-014478] p 593 N95-14000
From the shell model to the interacting boson model [DE94-014486] p 593 N95-14001
Search for W(prime) (yields) e(nu) in p(anti p) collisions at (radical)s = 1,800 GeV [DE94-015188] p 597 N95-15630
Topics in the structure of hadronic systems [DE94-014924] p 597 N95-15865
FERRITIC STAINLESS STEELS
Transient failure behavior of HT9 [DE94-016320] p 445 N95-14378
Impact fracture behavior of HT9 duct [DE94-016328] p 445 N95-14379
FERROCENES
AEM and HREM evaluation of carbon nanostructures in silica aerogels [DE94-014913] p 434 N95-14387
FERROELECTRICITY
Ferroelectric oxide memory FET (FEMFET) development [AD-A283203] p 476 N95-15399
FERROMAGNETIC MATERIALS
Ferromagnetic grain boundary signature in die-upset RE-Fe-B magnets [DE94-014904] p 590 N95-14440
FETUSES
Passive fetal heart rate monitoring apparatus and method with enhanced fetal heart beat discrimination [NASA-CASE-LAR-15129-1] p 541 N95-14184
Teratogenic effects of delta g: The concept of allometric growth p 538 N95-15102
The avian embryo responding to microgravity of space flight p 538 N95-15104
FIBER COMPOSITES
Effects of in situ fiber strength characteristics on mechanical properties of SiC(f)/SiC composites [DE94-013965] p 433 N95-13682

Nondestructive characterization of structural ceramic components
[DE94-013961] p 449 N95-13978
Effects of thermal cycling on thermal expansion and mechanical properties of SiC fiber-reinforced reaction-bonded Si3N4 composites
[NASA-TM-106665] p 433 N95-14298
Innovative design of composite structures: Design, manufacturing, and testing of plates utilizing curvilinear fiber trajectories
[NASA-CR-197045] p 435 N95-14865
Composites with improved compressive properties
[AD-A283411] p 435 N95-15417
Effect of matrix stiffness on wavy fiber behavior in single-carbon-fiber-epoxy composites
[AD-A280970] p 435 N95-15427
Static strength of riveted joints in Fibre Metal Laminates
[PB94-201472] p 513 N95-15429
Computational modeling of fiber-reinforced composites
[DE94-012914] p 436 N95-15573
Apparatus for performing high-temperature fiber push-out testing
[NASA-CASE-LEW-15470-1] p 497 N95-15915

FIBER OPTICS
The 24th International Physics Olympiad
[AD-A280584] p 589 N95-13972
Wavelength-division multiplexed optical integrated circuit with vertical diffraction grating
[NASA-CASE-NPO-18357-1-CU] p 612 N95-14181
Flocculation and aggregation in a microgravity environment (FAME) p 459 N95-14572
Scintillating glass fiber-optic neutron sensors
[DE94-014562] p 613 N95-15312
Asymmetric coupled quantum wells for high speed optical modulators at communication wavelengths
[AD-A281572] p 477 N95-15459
Modeling and simulation of a Fiber Distributed Data Interface Local Area Network (FDDI LAN) using OPNET (tm) for interfacing through the Common Data Link (CDL)
[AD-A283124] p 469 N95-15651
Method and apparatus for polarization-maintaining fiber optical amplification with orthogonal polarization output
[AD-D016365] p 614 N95-15707

FIBER ORIENTATION
Innovative design of composite structures: Design, manufacturing, and testing of plates utilizing curvilinear fiber trajectories
[NASA-CR-197045] p 435 N95-14865

FIBER PULLOUT
Effects of in situ fiber strength characteristics on mechanical properties of SiC(f)/SiC composites
[DE94-013965] p 433 N95-13682
Apparatus for performing high-temperature fiber push-out testing
[NASA-CASE-LEW-15470-1] p 497 N95-15915

FIBER STRENGTH
Effects of in situ fiber strength characteristics on mechanical properties of SiC(f)/SiC composites
[DE94-013965] p 433 N95-13682

FIBER-MATRIX INTERFACES
Dynamics of the interface in a model composite system
[AD-A281910] p 433 N95-13655
Composites with improved compressive properties
[AD-A283411] p 435 N95-15417

FIBERS
Low dielectric polyimide fibers
[NASA-CASE-LAR-14526-1] p 455 N95-15599

FIELD EFFECT TRANSISTORS
Ferroelectric oxide memory FET (FEMFET) development
[AD-A283203] p 476 N95-15399
The effects of spatial location of defect states on the switching characteristics of amorphous and polycrystalline silicon thin film transistors: A numerical simulation using AMPS 2-D
[DE94-013437] p 476 N95-15410
International Semiconductor Device Research Symposium (ISDRS-93)
[AD-A281715] p 477 N95-15454

FIELD EMISSION
RF vacuum microelectronics
[AD-A283123] p 478 N95-15613

FIELD OF VIEW
Star sensor for Indian Remote Sensing Satellite (IRS 1C) p 413 N95-13828
Wide field strip-imaging optical system
[NASA-CASE-NPO-18146-2-CU] p 613 N95-14413
FRESIP project observations of cataclysmic variables: A unique opportunity p 644 N95-14507
Laser retroreflector array having cat-eye retroreflectors
[NASA-CASE-GSC-13264-1] p 499 N95-14515
Gaze selection for visual search
[TR-512] p 587 N95-15775

FIELD STRENGTH
Development and analysis of high-energy corona process for air purification
[DE94-015207] p 524 N95-15432

FIELD THEORY (ALGEBRA)
Duality theorem in the multivariable Iwasawa theory of local fields
[PB94-192325] p 589 N95-13979

FIELD THEORY (PHYSICS)
Interfacial force field characterization of a constrained vapor bubble thermosyphon using IAI p 488 N95-14560
Hadronization of QCD and effective interactions
[DE94-014975] p 594 N95-14660

FIGHTER AIRCRAFT
High angle of attack flying qualities criteria for longitudinal rate command systems p 396 N95-14247
Combat Agility Management System (CAMS) p 397 N95-14250
Comparison of full-scale, small-scale, and CFD results for F/A-18 forebody slot blowing p 397 N95-14255
Modeling and numerical simulation of the cerebral blood flow under acceleration p 545 N95-15112
Operational requirements for avoidance and eventual elimination of Gz-induced Loss Of Consciousness (G-LOC) in flight p 547 N95-15127

FILE MAINTENANCE (COMPUTERS)
Software Technology for Adaptable, Reliable Systems (STARS)
[AD-A284373] p 576 N95-15806

FILM BOILING
Pool and flow boiling in variable and microgravity p 459 N95-14562

FILM COOLING
Effect of surface roughness on local film cooling effectiveness and heat transfer coefficients
[AD-A283854] p 482 N95-14351

FILM THICKNESS
Characterization of annular two-phase gas-liquid flows in microgravity p 487 N95-14556

FINGERS
Neural mechanisms of kinesthesia p 555 N95-14018
Body position and volume status as determinants of cardiovascular responses to transition into microgravity in parabolic flight p 544 N95-15108

FINITE DIFFERENCE THEORY
The flow induced by the coalescence of two initially stationary drops
[NASA-TM-106752] p 478 N95-13653
Numerical modeling of a cryogenic fluid within a fuel tank
[NASA-TM-4651] p 479 N95-13892
Nonlinear and stochastic numerical methods and their applications
[AD-A284863] p 588 N95-14370
Point based hydrodynamics applied to shallow water equations
[DE94-016629] p 523 N95-15364
Xwake 1.0: A new tool for wakefield and impedance calculations
[DE94-015545] p 574 N95-15418
Applied Computational Electromagnetics Society Journal, volume 9, number 2
[AD-A281576] p 469 N95-15463
An approach for dynamic grids
[NASA-TM-106774] p 404 N95-15853

FINITE ELEMENT METHOD
The buckling response of symmetrically laminated composite plates having a trapezoidal planform area
[NASA-CR-196975] p 505 N95-13839
Nondestructive analysis and development
[NASA-CR-196987] p 505 N95-13886
Methodology for the parallel direct solution of finite element systems
[PB94-198009] p 585 N95-13991
Evaluation of sensor placement algorithms for on-orbit identification of space platforms p 425 N95-14088
Thermal structure analyses for CSM testbed (COMET)
[NASA-CR-196998] p 506 N95-14270
ADCIRC: An advanced three-dimensional circulation model for shelves, coasts, and estuaries. Report 4: Hurricane storm surge modeling using large domains
[AD-A283868] p 535 N95-14352
Discrete-layer piezoelectric plate and shell models for active tip-clearance control
[NASA-CR-195383] p 507 N95-14417
Higher harmonic control analysis for vibration reduction of helicopter rotor systems
[NASA-TM-103855] p 391 N95-14419
Elastic-plastic models for multi-site damage p 507 N95-14454
Bending effects of unsymmetric adhesively bonded composite repairs on cracked aluminum panels p 507 N95-14456
Influence of crack history on the stable tearing behavior of a thin-sheet material with multiple cracks p 509 N95-14467
Full-scale testing and analysis of fuselage structure p 512 N95-14485
Mathematical problems of nonlinear wave propagation and of waves in heterogeneous media
[AD-A282217] p 492 N95-14605
Computational methods for PDE's in flow control, superconductivity, fluid flows and other applications
[AD-A282912] p 493 N95-15390
An architecture for intelligent multichip module reliability analysis
[AD-A281574] p 583 N95-15461
Applied Computational Electromagnetics Society Journal, volume 9, number 2
[AD-A281576] p 469 N95-15463

FINITE VOLUME METHOD
An adaptively-refined, Cartesian, cell-based scheme for the Euler and Navier-Stokes equations
[NASA-TM-106754] p 392 N95-13817
Radiative interactions in multi-dimensional chemically reacting flows using Monte Carlo simulations
[NASA-CR-197012] p 481 N95-14269
Numerical solution of two-dimensional ablation problems using the finite control volume method with unstructured grids
[DE94-015012] p 428 N95-14664
Robust multigrid methods for the steady and unsteady incompressible Navier-Stokes equations in general coordinates
[PB94-195534] p 492 N95-15315

FINS
Fatigue evaluation of empennage, forward wing, and winglets/tip fins on part 23 airplanes
[PB94-196813] p 408 N95-13981

FIRE EXTINGUISHERS
Flightline aircraft fire incidents and suppression agent effects: Field inquiries and incident analysis
[AD-A284027] p 405 N95-14421

FIRE PREVENTION
Risk analysis for the fire safety of airline passengers
[PB94-194065] p 405 N95-14179

FIRES
Flightline aircraft fire incidents and suppression agent effects: Field inquiries and incident analysis
[AD-A284027] p 405 N95-14421
Turbulent upward flame spread on a vertical wall under external radiation
[PB94-207388] p 441 N95-15353
Comparison of wall-fire behavior with and without a ceiling
[PB94-207404] p 441 N95-15354
Fire growth models for materials
[PB94-195856] p 443 N95-15610

FIRING (IGNITING)
Assessing post-fire combustion of polyurethane
[DE94-011461] p 438 N95-14375

FISHES
Postural control of fish related to gravity input p 539 N95-15118
Functional participation of the valvula cerebelli on the goldfish dorsal light response p 539 N95-15119

FIXED POINT ARITHMETIC
High-speed fixed and floating point implementation of delta-operator formulated discrete time systems
[AD-A283109] p 584 N95-13694

FIXTURES
Modelling of eddy currents related to large angle magnetic suspension test fixture
[NASA-CR-197028] p 475 N95-14851

FLAME PROPAGATION
The solid surface combustion experiment aboard the USML-1 mission p 458 N95-14212
Modeling turbulent flame propagation
[DE94-016618] p 438 N95-14391
Upward flame spread along the vertical corner walls (October 1993)
[PB94-206299] p 441 N95-15352
Turbulent upward flame spread on a vertical wall under external radiation
[PB94-207388] p 441 N95-15353
Comparison of wall-fire behavior with and without a ceiling
[PB94-207404] p 441 N95-15354
Fire growth models for materials
[PB94-195856] p 443 N95-15610

FLAMEOUT
Assessing post-fire combustion of polyurethane
[DE94-011461] p 438 N95-14375
Gas turbine prediffuser-combustor performance during operation with air-water mixture
[DOT/FAA/CT-93/52] p 411 N95-15683

FLAMES
Modeling turbulent flame propagation
[DE94-016618] p 438 N95-14391
Upward flame spread along the vertical corner walls (October 1993)
[PB94-206299] p 441 N95-15352
Burn rates of TiH2/KClO4/Viton and output testing of NASA SKD26100098-301 pressure cartridges
[NASA-CR-188357] p 443 N95-15715
FLANGES
Saddle clamp assembly
[NASA-CASE-MFS-28701-1] p 503 N95-15305
FLASH LAMPS
Emerging technology summary: Destruction of organic contaminants in air using advanced ultraviolet flashlamps
[PB94-194479] p 521 N95-14121
FLAT PLATES
Experimental and theoretical studies of rewetting of unheated/heated grooved plates p 487 N95-14558
Innovative design of composite structures: Design, manufacturing, and testing of plates utilizing curvilinear fiber trajectories
[NASA-CR-197045] p 435 N95-14865
FLICKER
Investigation of Allan variance for determining noise spectral forms with application to microwave radiometry
[NASA-CR-194985] p 516 N95-15727
FLIGHT CHARACTERISTICS
Parameter identification for X-31A at high angles of attack p 394 N95-14235
Validation of the NASA Dryden X-31 simulation and evaluation of mechanization techniques
p 394 N95-14236
Free-to-roll tests of X-31 and F-18 subscale models with correlation to flight test results p 394 N95-14237
High angle of attack flying qualities criteria for longitudinal rate command systems p 396 N95-14247
Fourth High Alpha Conference, volume 3
[NASA-CP-10143-VOL-3] p 397 N95-14251
Flight in an Adverse Environment
[AGARD-LS-197] p 406 N95-14893
Turbulence: Engineering models, aircraft response
p 407 N95-14900
FLIGHT CONDITIONS
Flight in an Adverse Environment
[AGARD-LS-197] p 406 N95-14893
Winter storms research in Canada
p 406 N95-14895
ESD and lightning interactions on aircraft
p 406 N95-14896
Icing: Accretion, detection, protection
p 406 N95-14897
Wind shear and its effects on aircraft
p 407 N95-14898
FLIGHT CONTROL
Perceptual and performance consequences of flight in virtual worlds p 558 N95-14043
Evolutionary Telemetry and Command Processor (TCP) architecture p 420 N95-14162
The principles of flight test assessment of flight-safety-critical systems in helicopters
[AGARD-AG-300-VOL-12] p 405 N95-14199
Add a dimension to your analysis of the helicopter low airspeed environment
[AD-A283982] p 408 N95-14205
Combat Agility Management System (CAMS)
p 397 N95-14250
FLIGHT CREWS
Preliminary analysis of Army aircrew requirements for Joint Surveillance Target Attack Radar System (JSTARS): Human performance requirements and job demands
[AD-A284917] p 563 N95-15759
FLIGHT ENVELOPES
X-31 post-stall envelope expansion and tactical utility testing p 395 N95-14242
Flight test results of the F-16 aircraft modified with the axisymmetric vectoring exhaust nozzle
p 396 N95-14245
Composite waveform generation for EMP and lightning direct-drive testing
[AD-A284159] p 462 N95-14405
FLIGHT FATIGUE
Crew factors in flight operations 2: Psychophysiological responses to short-haul air transport operations
[NASA-TM-108856] p 550 N95-15649
FLIGHT HAZARDS
Produce documents and media information
[NASA-CR-196521] p 532 N95-14271
Aircraft maneuver envelope warning system
[NASA-CASE-ARC-11953-1] p 411 N95-14518
Flight in an Adverse Environment
[AGARD-LS-197] p 406 N95-14893
Wake turbulence p 405 N95-14894
Winter storms research in Canada
p 406 N95-14895
ESD and lightning interactions on aircraft
p 406 N95-14896
Icing: Accretion, detection, protection
p 406 N95-14897
Heavy rain effects p 407 N95-14899
Operational requirements for avoidance and eventual elimination of Gz-induced Loss Of Consciousness (G-LOC) in flight p 547 N95-15127
FLIGHT MANAGEMENT SYSTEMS
The principles of flight test assessment of flight-safety-critical systems in helicopters
[AGARD-AG-300-VOL-12] p 405 N95-14199
Combat Agility Management System (CAMS)
p 397 N95-14250
Airplane takeoff and landing performance monitoring system
[NASA-CASE-LAR-14745-2-SB] p 412 N95-14415
FLIGHT PATHS
Identification of dynamic systems. Volume 3: Applications to aircraft. Part 2: Nonlinear analysis and manoeuvre design
[AGARD-AG-300-VOL-3-PT-2] p 408 N95-14102
Atmospheric propagation at larger lateral distances from the flight track p 402 N95-14885
Assessment of CTAS ETA prediction capabilities
[NASA-CR-197224] p 497 N95-15728
FLIGHT SAFETY
Age 60 Rule. Part 3: Consolidated database experiments
[DOT/FAA/AM-94/22-PT-3] p 551 N95-13715
The principles of flight test assessment of flight-safety-critical systems in helicopters
[AGARD-AG-300-VOL-12] p 405 N95-14199
Flight in an Adverse Environment
[AGARD-LS-197] p 406 N95-14893
Winter storms research in Canada
p 406 N95-14895
Wind shear and its effects on aircraft
p 407 N95-14898
Annual review of aircraft accident data: US air carrier operations, calendar year 1992
[NTSB/ARC-94/02] p 407 N95-15066
TDWR scan strategy implementation
[AD-A284877] p 534 N95-15749
FLIGHT SIMULATION
Validation of the NASA Dryden X-31 simulation and evaluation of mechanization techniques
p 394 N95-14236
High angle of attack flying qualities criteria for longitudinal rate command systems p 396 N95-14247
Vista/F-16 Multi-Axis Thrust Vectoring (MATV) control law design and evaluation p 396 N95-14248
Advanced distributed simulation technology advanced rotary wing aircraft. Study comparing approaches to modeling the ARWA main rotor
[AD-A280824] p 408 N95-14306
Hypervelocity Impact Test Facility: A gun for hire
[TABES PAPER 94-605] p 415 N95-14639
Turbulence: Engineering models, aircraft response
p 407 N95-14900
FLIGHT SIMULATORS
Summary Proceedings of the Joint Industry-FAA Conference on the Development and use of PC-Based Aviation Training Devices
[DOT/FAA/AM-94/25] p 573 N95-14917
Vertical flight terminal operational procedures. A summary of FAA research and development
[AD-A283550] p 413 N95-15328
FLIGHT TEST INSTRUMENTS
Identification of dynamic systems. Volume 3: Applications to aircraft. Part 2: Nonlinear analysis and manoeuvre design
[AGARD-AG-300-VOL-3-PT-2] p 408 N95-14102
FLIGHT TESTS
Identification of dynamic systems. Volume 3: Applications to aircraft. Part 2: Nonlinear analysis and manoeuvre design
[AGARD-AG-300-VOL-3-PT-2] p 408 N95-14102
Civil use of night vision devices: Evaluation pilot's guide, part 2
[DOT/FAA/RD-94/19] p 410 N95-14175
The principles of flight test assessment of flight-safety-critical systems in helicopters
[AGARD-AG-300-VOL-12] p 405 N95-14199
Commercial investigation results for the generic bioprocessing apparatus flown on United States Microgravity Laboratory-1 p 538 N95-14227
Flight and full-scale wind-tunnel comparison of pressure distributions from an F-18 aircraft at high angles of attack --- Conducted in NASA Ames Research Center's 80 by 120 ft wind tunnel p 394 N95-14231
Comparison of X-31 flight, wind-tunnel, and water-tunnel yawing moment asymmetries at high angles of attack
p 394 N95-14234
Parameter identification for X-31A at high angles of attack p 394 N95-14235
Free-to-roll tests of X-31 and F-18 subscale models with correlation to flight test results p 394 N95-14237
Fourth High Alpha Conference, volume 2
[NASA-CP-10143-VOL-2] p 395 N95-14239
F-18 high alpha research vehicle: Lessons learned
p 395 N95-14240
X-31 post-stall envelope expansion and tactical utility testing p 395 N95-14242
X-31 quasi-tailless flight demonstration
p 395 N95-14243
Flight test results of the F-16 aircraft modified with the axisymmetric vectoring exhaust nozzle
p 396 N95-14245
Flight validation of ground-based assessment for control power requirements at high angles of attack
p 396 N95-14246
Vista/F-16 Multi-Axis Thrust Vectoring (MATV) control law design and evaluation p 396 N95-14248
Preparations for flight research to evaluate actuated forebody strakes on the F-18 high-alpha research vehicle p 398 N95-14257
Flight evaluation of pneumatic forebody vortex control in post-stall flight p 398 N95-14259
An optical technique for examining aircraft shock wave structures in flight p 401 N95-14879
Flight in an Adverse Environment
[AGARD-LS-197] p 406 N95-14893
Air-breathing aerospace plane development essential: Hypersonic propulsion flight tests
[NASA-TM-108857] p 392 N95-14921
Circulatory filling pressures during transient microgravity induced by parabolic flight p 542 N95-15095
Test Operation Procedure (TOP): Vibration testing of helicopter equipment
[AD-A284433] p 410 N95-15815
FLIGHT TIME
Crew factors in flight operations 2: Psychophysiological responses to short-haul air transport operations
[NASA-TM-108856] p 550 N95-15649
FLIGHT TRAINING
Summary Proceedings of the Joint Industry-FAA Conference on the Development and use of PC-Based Aviation Training Devices
[DOT/FAA/AM-94/25] p 573 N95-14917
FLOAT ZONES
Thermocapillary convection in floating zones under simulated reduced-gravity conditions
p 483 N95-14529
FLOATING POINT ARITHMETIC
High-speed fixed and floating point implementation of delta-operator formulated discrete time systems
[AD-A283109] p 584 N95-13694
A high speed, wide dynamic range digitizer circuit for photomultiplier tubes
[DE94-015187] p 475 N95-15302
FLOCCULATING
Flocculation and aggregation in a microgravity environment (FAME) p 459 N95-14572
FLORIDA
Statistical aspects of the precipitation regimes at Miami International Airport (MIA) and Palm Beach International Airport (PBI): 1961-1990
[PB94-194289] p 532 N95-14118
Florida hurricanes and tropical storms 1871-1993: An historical survey
[PB94-198017] p 532 N95-14120
Florida's propagation report p 466 N95-14684
FLOW CHARACTERISTICS
CFD methodology and validation for turbomachinery flows p 480 N95-14131
Unsteady flows in turbines: Impact on design procedure p 480 N95-14132
The industrial use of CFD in the design of turbomachinery p 480 N95-14133
FLOW COEFFICIENTS
Comparison of full-scale, small-scale, and CFD results for F/A-18 forebody slot blowing p 397 N95-14255
FLOW DISTRIBUTION
The industrial use of CFD in the design of turbomachinery p 480 N95-14133
Numerical simulation of the flow about an F-18 aircraft in the high-alpha regime p 394 N95-14232
Hybrid structured/unstructured grid computations for the F/A-18 at high angle of attack p 394 N95-14233
Axis switching and spreading of an asymmetric jet: Role of vorticity dynamics
[NASA-TM-106385] p 398 N95-14418
Computation of supersonic air-intakes
p 400 N95-14452
Thermocapillary motion of deformable drops
p 485 N95-14544
Ground based studies of thermocapillary flows in levitated drops p 486 N95-14545
Effects of thermocapillarity on an evaporating extended meniscus in microgravity p 488 N95-14559

Numerical simulation of the SOFIA flowfield
[NASA-CR-197025] p 400 N95-14612
An optical technique for examining aircraft shock wave structures in flight p 401 N95-14879
Propulsion/airframe interference for ducted propfan engines with ground effect
[NASA-CR-197110] p 409 N95-14909
Cold flow simulation of the alternate turbopump development turbine of the Space Shuttle main engine high pressure fuel turbopump
[AD-A281676] p 419 N95-15447
Electron-molecule collisions and UV signatures in flowfields
[AD-A281569] p 596 N95-15457
A three-dimensional fast solver for arbitrary vorton distributions
[DE94-012581] p 404 N95-15570
Gas turbine prediffuser-combustor performance during operation with air-water mixture
[DOT/FAA/CT-93/52] p 411 N95-15683
Two-dimensional scramjet inlet unstart model: Wind-tunnel blockage and actuation systems test
[NASA-TM-109984] p 495 N95-15899

FLOW GEOMETRY
Elements of a modern turbomachinery design system p 480 N95-14129
The behavior of unsteady thermocapillary flows p 483 N95-14530
Dynamics and statics of nonaxisymmetric and symmetric liquid bridges p 484 N95-14533
Microscale hydrodynamics near moving contact lines p 484 N95-14536
Influence of flow on interface shape stability in low gravity p 484 N95-14538
Calculation of movable bed friction factors
[AD-A283529] p 536 N95-15440

FLOW MEASUREMENT
Quality assessment for wind tunnel testing
[AGARD-AR-304] p 393 N95-14197
Design and development of an F/A-18 inlet distortion rake: A cost and time saving solution p 395 N95-14241
Active thermal isolation for temperature responsive sensors
[NASA-CASE-LAR-14612-2] p 496 N95-14414
Cold flow simulation of the alternate turbopump development turbine of the Space Shuttle main engine high pressure fuel turbopump
[AD-A281676] p 419 N95-15447

FLOW STABILITY
Oscillatory thermocapillary convection p 483 N95-14526
Experimental investigation of the Marangoni effect on the stability of a double-diffusive layer p 483 N95-14528
The behavior of unsteady thermocapillary flows p 483 N95-14530
The breakup of a liquid jet at microgravity p 484 N95-14535
Noise radiation by instability waves in coaxial jets
[NASA-TM-106738] p 591 N95-14618

FLOW VELOCITY
High-temperature corrosion of iron aluminides
[DE94-011505] p 447 N95-15906

FLOW VISUALIZATION
Surface Tension Driven Convection Experiment (STDCE) p 458 N95-14217
Numerical simulation of the flow about an F-18 aircraft in the high-alpha regime p 394 N95-14232
Free-to-roll tests of X-31 and F-18 subscale models with correlation to flight test results p 394 N95-14237
Thermocapillary convection in floating zones under simulated reduced-gravity conditions p 483 N95-14529
Multilayer fluid dynamics of immiscible liquids p 483 N95-14532
Thermocapillary motion of deformable drops p 485 N95-14544
Ground based studies of thermocapillary flows in levitated drops p 486 N95-14545
An optical technique for examining aircraft shock wave structures in flight p 401 N95-14879
Cold flow simulation of the alternate turbopump development turbine of the Space Shuttle main engine high pressure fuel turbopump
[AD-A281676] p 419 N95-15447
A three-dimensional fast solver for arbitrary vorton distributions
[DE94-012581] p 404 N95-15570
Gas turbine prediffuser-combustor performance during operation with air-water mixture
[DOT/FAA/CT-93/52] p 411 N95-15683
Two-dimensional scramjet inlet unstart model: Wind-tunnel blockage and actuation systems test
[NASA-TM-109984] p 495 N95-15899

FLUCTUATION THEORY
Sum-frequency generation from photon number squeezed light p 603 N95-13902

FLUID BOUNDARIES
Equilibrium fluid interface behavior under low- and zero-gravity conditions p 484 N95-14534

FLUID DYNAMICS
Second Microgravity Fluid Physics Conference
[NASA-CP-3276] p 482 N95-14522
Future directions in two-phase flow and heat transfer in space p 482 N95-14523
Stabilization of thermocapillary convection by means of nonplanar flow oscillations p 482 N95-14524
Control of oscillatory thermocapillary convection in microgravity p 483 N95-14525
Oscillatory thermocapillary convection p 483 N95-14526
Onset of hexagons in surface-tension-driven Benard convection p 483 N95-14527
Experimental investigation of the Marangoni effect on the stability of a double-diffusive layer p 483 N95-14528
Thermocapillary convection in floating zones under simulated reduced-gravity conditions p 483 N95-14529
The behavior of unsteady thermocapillary flows p 483 N95-14530
Oscillatory/chaotic thermocapillary flow induced by radiant heating p 483 N95-14531
Multilayer fluid dynamics of immiscible liquids p 483 N95-14532
Dynamics and statics of nonaxisymmetric and symmetric liquid bridges p 484 N95-14533
The breakup of a liquid jet at microgravity p 484 N95-14535
Microscale hydrodynamics near moving contact lines p 484 N95-14536
Phase segregation due to simultaneous migration and coalescence p 484 N95-14537
Influence of flow on interface shape stability in low gravity p 484 N95-14538
Crystal growth and fluid mechanics problems in directional solidification p 486 N95-14550
Isolation of the physiological regulation component of the arterial pressure time variation after postural stresses by a model of the gravitational and arterial kinking effects p 550 N95-15149

FLUID FILMS
Characterization of annular two-phase gas-liquid flows in microgravity p 487 N95-14556
Experimental and theoretical studies of rewetting of unheated/heated grooved plates p 487 N95-14558
Design review and analysis for a Pratt and Whitney fluid-film bearing and seal testing rig
[NASA-CR-197035] p 502 N95-14797

FLUID FLOW
The flow induced by the coalescence of two initially stationary drops
[NASA-TM-106752] p 478 N95-13653
Tactile display device using an electrorheological fluid
[NASA-CASE-LAR-14860-1] p 472 N95-14112
Computational methods for PDE's in flow control, superconductivity, fluid flows and other applications
[AD-A282912] p 493 N95-15390

FLUID MANAGEMENT
An application of miniscale experiments on Earth to refine microgravity analysis of adiabatic multiphase flow in space p 459 N95-14567

FLUID MECHANICS
Computations of drop collision and coalescence p 485 N95-14542
Conceptual design of the Space Station fluids module p 429 N95-14584

FLUORESCENCE
Ultrasensitive infrared chemiluminescence detection
[AD-A283531] p 440 N95-14958
Research on characterization of the upper atmosphere using lidar
[AD-A283241] p 530 N95-15401
Core-level spectroscopy of thin oxides and oxynitrides
[DE94-016598] p 442 N95-15408
Fluorescent compounds for plastic scintillation applications
[DE94-013235] p 497 N95-15580
Porphyrins in the interstellar medium (in grains) p 640 N95-15837
Investigating the 3.3 micron infrared fluorescence from naphthalene following ultraviolet excitation p 599 N95-15839

FLUORIDES
Graphite fluoride from iodine intercalated graphitized carbon
[NASA-CASE-LEW-15360-1] p 441 N95-15303

FLUORINE ORGANIC COMPOUNDS
Infrared/submillimeter wave studies of molecular collision kinetics
[AD-A281379] p 594 N95-14362

FLUOROHYDROCARBONS
Low dielectric polyimide fibers
[NASA-CASE-LAR-14526-1] p 455 N95-15599

FLUX (RATE)
Mass analysis addition to the Differential Ion Flux Probe (DIFP) study
[NASA-CR-196531] p 429 N95-15824
Neutrino oscillations in noisy media
[DE94-014973] p 598 N95-15869

FLUX DENSITY
Specifying the surface finish of x ray mirrors
[DE94-013537] p 601 N95-13644
A radio telescope for the calibration of radio sources at 32 gigahertz p 463 N95-14626
Behavior of charring materials in simulated fire environments
[PB94-196045] p 439 N95-14838
Energy flux and hydrogeology of thermal anomalies in the Gulf of Mexico Basin: South Texas example
[DE94-015122] p 530 N95-14956
Macroturbulence in superconductors
[DE94-016371] p 595 N95-15362
Ultrasonic characterization of high T(c) and other unconventional superconductors
[AD-A282835] p 476 N95-15397

FLUX PINNING
Flux pinning and forced entanglement by splayed columnar defects
[DE94-013994] p 620 N95-14008
HTS Wire Development Workshop: Proceedings
[DE94-015650] p 624 N95-15421

FLUX TRANSFER EVENTS
On the physics of waves in the solar atmosphere: Wave heating and wind acceleration
[NASA-CR-196992] p 646 N95-15070

FOAMS
Microgravity foam structure and rheology p 459 N95-14568
Milestone 5 test report. Task 5, subtask 5.2: Tile to foam strength tests
[NASA-CR-197241] p 514 N95-15913

FOCUSING
AXAF SIM focus mechanism study
[NASA-CR-196976] p 636 N95-13636
Performance of spherically focusing Ge(444) backscattering analyzers for inelastic x-ray scattering
[DE94-016349] p 621 N95-14382

FOLDS (GEOLOGY)
The crosswell electromagnetic response of layered media
[DE94-014929] p 470 N95-15866

FOLIAGE
ACTS mobile propagation campaign p 465 N95-14677

FOOD INTAKE
The relationship between space sickness and preflight diet p 546 N95-15122
Alterations of body temperature, feeding, drinking and sleep-wake circadian rhythms in Rhesus monkey during a 19 day Spacelab flight simulation p 539 N95-15132
New findings regarding light intensity and its effects as a zeitgeber in the Sprague-Dawley rat p 539 N95-15135
20 days bed-rest on insulin action in relation to body fat in young subjects p 549 N95-15145

FOOD PRODUCTION (IN SPACE)
The Astroculture (tm)-1 experiment on the USML-1 mission p 564 N95-14228

FORCE
Manual discrimination of force p 561 N95-14057

FORCE DISTRIBUTION
Free-to-roll tests of X-31 and F-18 subscale models with correlation to flight test results p 394 N95-14237

FORCED CONVECTION
Pool and flow boiling in variable and microgravity p 459 N95-14562

FORCED VIBRATION
Dynamic response of rigid tanks with inhomogeneous liquids
[DE94-012619] p 493 N95-15571

FOREBODIES
High Alpha Technology Program (HATP) ground test to flight comparisons p 393 N95-14230
Fourth High Alpha Conference, volume 3
[NASA-CP-10143-VOL-3] p 397 N95-14251
Computational analysis of forebody tangential slot blowing p 397 N95-14253
F/A-18 and F-16 forebody vortex control, static and rotary-balance results p 397 N95-14254
Comparison of full-scale, small-scale, and CFD results for F/A-18 forebody slot blowing p 397 N95-14255

Low-energy pneumatic control of forebody vortices p 398 N95-14256
Preparations for flight research to evaluate actuated forebody strakes on the F-18 high-alpha research vehicle p 398 N95-14257
Integration of a mechanical forebody vortex control system into the F-15 p 398 N95-14258
Flight evaluation of pneumatic forebody vortex control in post-stall flight p 398 N95-14259

FORECASTING
Propagation in the ionosphere, B p 467 N95-14827

FOREST FIRES
Tilting wind tunnel for fire behavior studies [PB94-204625] p 413 N95-14513

FOREST MANAGEMENT
Forest cover from Landsat Thematic Mapper data for use in the Catahoula Ranger District Geographic Information System [PB94-203056] p 515 N95-14125
Landsat Pathfinder tropical forest information management system p 565 N95-14594

FORESTS
Forest cover from Landsat Thematic Mapper data for use in the Catahoula Ranger District Geographic Information System [PB94-203056] p 515 N95-14125

FORGING
High temperature superconductors with improved current densities [AD-A282996] p 472 N95-13685

FORM FACTORS
Nonlinear bulging factor based on R-curve data p 511 N95-14476
Investigation of the coherent synchrotron radiation spectrum as a probe of charge dynamics [DE94-015340] p 599 N95-15371

FORMALISM
Simultaneous two component squeezing in generalized q-coherent states p 598 N95-13908

FORMAT
DDI, the Data and Dimensions Interface [DE94-014750] p 522 N95-14317

FORMING TECHNIQUES
Advanced method and processing technology for complicated shape airframe part forming p 410 N95-14486

FORTRAN
Paradigms and strategies for scientific computing on distributed memory concurrent computers [DE94-013305] p 567 N95-13676
NLEdit: A generic graphical user interface for Fortran programs [NASA-TM-4543] p 572 N95-14206

FOSSIL FUELS
Energy review [DE94-015828] p 518 N95-14326

FOUR-WAVE MIXING
Spectral, noise and correlation properties of intense squeezed light generated by a coupling in two laser fields p 500 N95-13903
Quantum propagation in single mode fiber p 609 N95-13953

FOURIER TRANSFORMATION
Multi-velocity component LDV [NASA-CASE-ARC-11925-1] p 499 N95-14668

FRACTALS
Specifying the surface finish of x ray mirrors [DE94-013537] p 601 N95-13644

FRACTURE MECHANICS
Impact fracture behavior of HT9 duct [DE94-016328] p 445 N95-14379
Nonlinear fracture mechanics-based analysis of thin wall cylinders p 508 N95-14462
Fatigue analysis of multiple site damage at a row of holes in a wide panel p 508 N95-14463
Computational predictive methods for fracture and fatigue p 509 N95-14466
Influence of crack history on the stable tearing behavior of a thin-sheet material with multiple cracks p 509 N95-14467
Development of the NASA/FLAGRO computer program for analysis of airframe structures p 510 N95-14473
Fracture mechanics validity limits p 511 N95-14480
Challenges for the aircraft structural integrity program p 410 N95-14481
Damping mechanisms in nanostructured materials [AD-A283583] p 623 N95-15317
Observation of microcrack development in concrete by use of TV-holography and deformation phase gradient calculation [PB94-207990] p 513 N95-15348
Fatigue in single crystal nickel superalloys [AD-A282917] p 446 N95-15415
Size and deformation limits to maintain constraint in K(sub Ic) and J(sub c) testing of bend specimens [AD-A284363] p 514 N95-15802
Effects of tensile loading on upper shelf fracture toughness [AD-A284364] p 514 N95-15803

FRACTURE STRENGTH
Effects of in situ fiber strength characteristics on mechanical properties of SiC(f)/SiC composites [DE94-013965] p 433 N95-13682
Mechanical properties of high-temperature superconducting wires [DE94-015089] p 621 N95-14192
Transient failure behavior of HT9 [DE94-016320] p 445 N95-14378
Impact fracture behavior of HT9 duct [DE94-016328] p 445 N95-14379
Ballistic performance and adiabatic shear behavior of AerMet(tm) 100 steel [AD-A283266] p 447 N95-15622
Size and deformation limits to maintain constraint in K(sub Ic) and J(sub c) testing of bend specimens [AD-A284363] p 514 N95-15802
Effects of tensile loading on upper shelf fracture toughness [AD-A284364] p 514 N95-15803

FRACTURING
Stress corrosion crack tip microstructure in nickel-based alloys [DE94-015362] p 446 N95-15532

FRAGMENTATION
Modelling the low Earth space debris environment p 414 N95-13830
Studies of quarkonia production with CDF [DE94-013220] p 597 N95-15862

FRANCK-CONDON PRINCIPLE
Modes in light wave propagating in semiconductor laser p 500 N95-13925

FREE BOUNDARIES
Thermocapillary motion of deformable drops p 485 N95-14544

FREE ELECTRON LASERS
Simulations of the high average power SELENE free electron laser prototype [AD-A280780] p 498 N95-14291

FREE FLOW
Two-dimensional scramjet inlet unstart model: Wind-tunnel blockage and actuation systems test [NASA-TM-109984] p 495 N95-15899

FREE JETS
Axis switching and spreading of an asymmetric jet: Role of vorticity dynamics [NASA-TM-106385] p 398 N95-14418

FREE RADICALS
Infrared absorption spectroscopy and chemical kinetics of free radicals [DE94-016642] p 438 N95-14392
Laser spectroscopy of combustion intermediates in a supersonic jet expansion [AD-A283201] p 500 N95-15395

FREE VIBRATION
Dynamic response of rigid tanks with inhomogeneous liquids [DE94-012619] p 493 N95-15571

FREEZING
Update to the NASA Lewis ice accretion code LEWICE [NASA-CR-195387] p 481 N95-14295
Dependence of segregation potential on the thermal and hydraulic conditions predicted by model M1 [AD-A280969] p 530 N95-14862
Water vapor and temperature inversions near the 0 C level over the tropical western Pacific [AD-A282023] p 533 N95-14952
Traveling wave solutions to the problem of quasi-steady freezing of soils [AD-A280971] p 531 N95-15428
Ru2Ge3: Crystal growth and some properties [DE94-015360] p 625 N95-15531

FRENCH SPACE PROGRAM
Mass transport phenomena in microgravity: Preliminary results of the first MEPHISTO flight experiment p 634 N95-14209

FREQUENCIES
A novel technique for 4-dimensional atmosphere and oceanographic irradiance measurements using 3-D spatial filtering [AD-A283758] p 613 N95-14353
Asteroseismology: Ground based efforts and the need for space observations p 643 N95-14503
Observations of hot stars and eclipsing binaries with FRESIP p 644 N95-14508
Multi-velocity component LDV [NASA-CASE-ARC-11925-1] p 499 N95-14668
A simple analytical model for dense WDM/OOK systems [AD-A283229] p 478 N95-15628

FREQUENCY CONTROL
Burst-by-burst laser frequency monitor [NASA-CASE-NPO-18596-1-CU] p 498 N95-13629

FREQUENCY MEASUREMENT
Astrophysical science with a spaceborne photometric telescope [NASA-CP-10148] p 643 N95-14499
Asteroseismology with FRESIP: A meter class space telescope p 643 N95-14504
Modelling of eddy currents related to large angle magnetic suspension test fixture [NASA-CR-197028] p 475 N95-14851

FREQUENCY RANGES
Flow-radiated noise. Study of the propagative spectral range of the wall pressure field [PB94-201290] p 590 N95-13985

FREQUENCY RESPONSE
Acoustic resonance spectroscopy intrinsic seals [DE94-016207] p 591 N95-15359

FREQUENCY SHIFT
Troposcatter at the KU band [AD-A281575] p 469 N95-15462

FREQUENCY STABILITY
Variable window Gabor filters and their use in focus and correspondence [AD-A282837] p 573 N95-14842
Properties of nearly perfect crystals at very low temperatures [NASA-CR-197221] p 627 N95-15823

FRETTING
The role of fretting corrosion and fretting fatigue in aircraft rivet hole cracking p 510 N95-14470

FRETTING CORROSION
The role of fretting corrosion and fretting fatigue in aircraft rivet hole cracking p 510 N95-14470

FRICTION
Calculation of movable bed friction factors [AD-A283529] p 536 N95-15440

FRICTION FACTOR
Deployment mechanism calibration system p 414 N95-13833
Single-phase heat transfer and pressure drop characteristics of an integral-spine-fin within an annulus [PB94-194073] p 482 N95-14407
Calculation of movable bed friction factors [AD-A283529] p 536 N95-15440

FUEL CELL POWER PLANTS
MCFC Product Development Test [DE94-014334] p 518 N95-14143

FUEL CELLS
Synthesis, processing and properties of materials for SOFCs [DE94-014491] p 517 N95-14002
MCFC Product Development Test [DE94-014334] p 518 N95-14143
Development of the fuel cell power generation technology, 2 [DE94-780614] p 520 N95-15376
Development of the fuel cell power generation technology, 1 [DE94-780648] p 520 N95-15377

FUEL COMBUSTION
High-temperature corrosion of iron aluminides [DE94-011505] p 447 N95-15906

FUEL INJECTION
Investigation of ramp injectors for supersonic mixing enhancement [NASA-CR-4634] p 494 N95-15605
Wear mechanism evaluation and measurement in fuel-lubricated components [AD-A284870] p 504 N95-15747

FUEL PRODUCTION
Dense ceramic membranes for partial oxygenation of methane [DE94-015021] p 453 N95-14609
Engine system assessment study using Martian propellants [NASA-CR-189188] p 431 N95-14669
An unmanned mission to Mars with sample collection and in-situ resource utilization [NASA-CR-197202] p 645 N95-14868

FUEL TANKS
Numerical modeling of a cryogenic fluid within a fuel tank [NASA-TM-4651] p 479 N95-13892

FUEL TESTS
Recycled plastic: A clean and low cost rocket fuel [TABES PAPER 94-610] p 416 N95-14642

FULL SCALE TESTS
Computational analysis of forebody tangential slot blowing p 397 N95-14253
Testing and analysis of flat and curved panels with multiple cracks p 508 N95-14460

FULLERENES
Laboratory spectra of C60 and related molecular structures p 627 N95-15838

FUNCTION SPACE
Carnot-caratheodory spaces seen from within
[PB94-195617] p 586 N95-15412
FUNCTIONAL DESIGN SPECIFICATIONS
A decade of telerobotics in rehabilitation: Demonstrated utility blocked by the high cost of manipulation and the complexity of the user interface p 558 N95-14044
European Workshop Industrical Computer Science Systems approach to design for safety p 569 N95-14157
Department of Defense technical architecture framework for information management. Volume 8: Department of Defense HCI style guide, version 2.0
[AD-A283768] p 631 N95-14333
Integrated optical maze
[DE94-015866] p 613 N95-14367
The Global Emergency Observation and Warning System
[TABES PAPER 94-622] p 417 N95-14649
FURNACES
Mass transport phenomena in microgravity: Preliminary results of the first MEPHISTO flight experiment p 634 N95-14209
Orbital processing of high-quality CdTe compound semiconductors p 458 N95-14213
Crystal growth of selected II-VI semiconducting alloys by directional solidification p 458 N95-14214
The study of dopant segregation behavior during the growth of GaAs in microgravity p 458 N95-14215
FUSELAGES
Damage tolerant repair techniques for pressurized aircraft fuselages
[AD-A281982] p 391 N95-14144
Study of multiple cracks in airplane fuselage by micromechanics and complex variables p 509 N95-14468
Axial crack propagation and arrest in pressurized fuselage p 511 N95-14479
Full-scale testing and analysis of fuselage structure p 512 N95-14485
The characterization of widespread fatigue damage in fuselage structure
[NASA-TM-109142] p 432 N95-14920
FUSION REACTORS
Radioactivity measurements of ITER materials using the TFTR D-T neutron field
[DE94-016094] p 617 N95-14397
Radiation and EMI effects in the NIF environment
[DE94-016635] p 468 N95-15365
FUZZY SETS
Vehicle health management using adaptive techniques
[NASA-TM-108472] p 431 N95-15609
FUZZY SYSTEMS
Artificial intelligence with applications for aircraft
[DOT/FAA/CT-94/41] p 581 N95-13895
Fuzzy logic motor control for pollution prevention and improved energy efficiency
[PB94-190865] p 523 N95-14403

G

G STARS
The symbiosis of photometry and radial-velocity measurements p 643 N95-14505
Rotation among solar-type stars p 644 N95-14506
GALACTIC COSMIC RAYS
Production profiles of nuclides by galactic-cosmic-ray particles in small meteoroids
[DE94-014801] p 646 N95-14437
Numerical simulations of planetary gamma-ray spectra induced by galactic cosmic rays
[DE94-014809] p 647 N95-14438
Multiple-scattering model for inclusive proton production in heavy ion collisions
[NASA-TP-3470] p 600 N95-15606
GALAXIES
FRESIP project observations of cataclysmic variables: A unique opportunity p 644 N95-14507
GALILEO PROJECT
The Block V Receiver fast acquisition algorithm for the Galileo S-band mission p 463 N95-14627
GALLIUM
Activity of Ga, In and Cu modified MFI zeolites for amine reactions
[DE94-016532] p 438 N95-14388
Surface passivation for 3-5 semiconductor processing: Stable gallium sulphide films by MOCVD
[NASA-TM-106761] p 477 N95-15587
GALLIUM ARSENIDES
Growth mechanisms and characterization of hydrogenated amorphous-silicon-alloy films
[DE94-011842] p 518 N95-14194
The study of dopant segregation behavior during the growth of GaAs in microgravity p 458 N95-14215
Magnetic field dependent photoluminescence studies of InGaAs/GaAs strained-single-quantum wells
[DE94-015774] p 621 N95-14342
High gain GaAs switches for impulse sources: Measurement of the speed of current filaments
[DE94-015281] p 477 N95-15544
Surface passivation for 3-5 semiconductor processing: Stable gallium sulphide films by MOCVD
[NASA-TM-106761] p 477 N95-15587
Low Temperature Grown and Highly Non-Stoichiometric GaAs and Related Materials
[AD-A284898] p 626 N95-15754
GALLIUM OXIDES
Low loss glass and optical fibers therefrom
[AD-D016379] p 615 N95-15766
GALLIUM PHOSPHIDES
Polarized photomodulated reflectivity and photoluminescence studies of ordered InGaP2 under pressure
[DE94-016556] p 621 N95-14390
GAMMA RAY ASTRONOMY
Search for gamma-ray events in the BATSE data base
[NASA-CR-197044] p 647 N95-14814
GAMMA RAY BURSTS
Search for gamma-ray events in the BATSE data base
[NASA-CR-197044] p 647 N95-14814
GAMMA RAY SPECTRA
Los Alamos contribution to target diagnostics on the National Ignition Facility
[DE94-014474] p 616 N95-13998
Numerical simulations of planetary gamma-ray spectra induced by galactic cosmic rays
[DE94-014809] p 647 N95-14438
GAMMA RAY SPECTROMETERS
Selection of non-destructive assay methods: Neutron counting or calorimetric assay?
[DE94-016211] p 505 N95-15777
First Year PIDDP Report on gamma-ray and x-ray spectroscopy: X-ray remote sensing and in situ spectroscopy for planetary exploration missions and gamma-ray remote sensing and in situ spectroscopy for planetary exploration missions
[NASA-CR-189374] p 517 N95-15916
GAMMA RAYS
Thin GSO scintillator for neutron detection
[DE94-014566] p 613 N95-15314
GAS ANALYSIS
Test method for the measurement of methanol emissions from stationary sources
[PB94-170297] p 523 N95-15382
GAS CHROMATOGRAPHY
Highly crosslinked silicon polymers for gas chromatography columns
[NASA-CASE-ARC-11960-2-NP] p 452 N95-14602
GAS DENSITY
Ultrasensitive infrared chemiluminescence detection
[AD-A283531] p 440 N95-14958
Turbulent mixing of the HVOF thermal spray and coating oxidation
[DE94-015414] p 455 N95-15535
GAS DETECTORS
Calibration and characterization of wide range hydrogen sensors
[DE94-013765] p 496 N95-14146
GAS DYNAMICS
Polymer-polymer interactions
[AD-A282944] p 453 N95-14844
LSENS: A General Chemical Kinetics and Sensitivity Analysis Code for homogeneous gas-phase reactions. Part 1: Theory and numerical solution procedures
[NASA-RP-1328-PT-1] p 440 N95-15056
LSENS: A General Chemical Kinetics and Sensitivity Analysis Code for homogeneous gas-phase reactions. Part 3: Illustrative test problems
[NASA-RP-1330-PT-3] p 440 N95-15057
GAS EXPANSION
Laser spectroscopy of combustion intermediates in a supersonic jet expansion
[AD-A283201] p 500 N95-15395
GAS FLOW
An approximate Riemann solver for thermal and chemical nonequilibrium flows
[NASA-CR-195003] p 492 N95-14912
Effects of two-phase flow on the deflagration of porous energetic materials
[DE94-015353] p 442 N95-15375
GAS IONIZATION
Development and analysis of high-energy corona process for air purification
[DE94-015207] p 524 N95-15432
GAS JETS
The aeroacoustics of supersonic coaxial jets
[NASA-TM-106782] p 591 N95-15059
Resonant interaction of a linear array of supersonic rectangular jets: An experimental study
[NASA-CR-195398] p 404 N95-15852
GAS MIXTURES
Numerical simulation of shock-induced combustion past blunt bodies using shock-fitting technique
[NASA-CR-197013] p 437 N95-14268
Surface Acoustic Wave (SAW) microsensors to monitor multi-component vapor challenges to adsorbents and adsorbent-based air filtration systems
[AD-A284222] p 497 N95-15334
GAS PRESSURE
Surface acoustic wave oxygen pressure sensor
[NASA-CASE-LAR-15266-1-CU] p 496 N95-13837
Partial pressure analysis in space testing p 424 N95-14084
GAS STREAMS
Development and analysis of high-energy corona process for air purification
[DE94-015207] p 524 N95-15432
GAS TEMPERATURE
High-temperature corrosion of iron aluminides
[DE94-011505] p 447 N95-15906
GAS TRANSPORT
Reactive polymers: Main chain coordination polymers for air separation
[AD-A281614] p 455 N95-15444
GAS TUNGSTEN ARC WELDING
Welding irradiated stainless steel
[DE94-013661] p 500 N95-13645
GAS TURBINE ENGINES
Effect of surface roughness on local film cooling effectiveness and heat transfer coefficients
[AD-A283854] p 482 N95-14351
Gas turbine prediffuser-combustor performance during operation with air-water mixture
[DOT/FAA/CT-93/52] p 411 N95-15683
Advanced Turbine Technology Applications Project (ATTAP)
[NASA-CR-195393] p 634 N95-15743
GAS TURBINES
Turbomachinery Design Using CFD
[AGARD-LS-195] p 479 N95-14127
GAS-LIQUID INTERACTIONS
Characterization of annular two-phase gas-liquid flows in microgravity p 487 N95-14556
GAS-METAL INTERACTIONS
Welding irradiated stainless steel
[DE94-013661] p 500 N95-13645
GAS-SOLID INTERACTIONS
Hydrogen transport and trapping in graphite
[UTIAS-347] p 437 N95-13652
GAS-SOLID INTERFACES
Hydrogen transport and trapping in graphite
[UTIAS-347] p 437 N95-13652
Strained-layer InGaAs(P)/InP quantum well semiconductor lasers grown by organometallic vapour phase epitaxy
[PB94-201399] p 622 N95-14795
NMR studies of polymers at interfaces
[AD-A281570] p 455 N95-15458
GASEOUS DIFFUSION
Hydrogen transport and trapping in graphite
[UTIAS-347] p 437 N95-13652
GASEOUS FUELS
Simulation of coal and char nitrogen reactions in combustion
[DE94-013941] p 440 N95-15291
GASOLINE
Preliminary design of a miniature thermoelectric generator
[AD-A283834] p 518 N95-14341
GATES (CIRCUITS)
Ferroelectric oxide memory FET (FEMFET) development
[AD-A283203] p 476 N95-15399
RF vacuum microelectronics
[AD-A283123] p 478 N95-15613
GEAR TEETH
Flex-gear power transmission system for transmitting EMF between Sun and ring gears
[NASA-CASE-GSC-13540-1] p 502 N95-14517
GEARS
Flex-gear power transmission system for transmitting EMF between Sun and ring gears
[NASA-CASE-GSC-13540-1] p 502 N95-14517
GENERAL OVERVIEWS
A review of 50 years of aerodynamic research with NACA/NASA
[NASA-TM-109163] p 647 N95-13663
Effects of hydrogen annealing, sulfur segregation and diffusion on the cyclic oxidation resistance of superalloys: A review
[NASA-TM-106734] p 444 N95-13667
Computer Aided Engineering (CAE) overview
[AD-A280966] p 572 N95-14616
Low-dose alcohol effects on human behavior and performance: A review of post-1984 research
[DOT/FAA/AM-94/24] p 552 N95-14863

GENETIC ALGORITHMS
Genetic programming with adaptive representations
[TR-489] p 576 N95-15856
GENETICS
Some genetic aspects of adaptation to hyperdynamic environments p 543 N95-15100
Structure of avian tectorial, otolithic and cupular membranes p 539 N95-15117
GEOCENTRIC COORDINATES
Twelve-year planetary ephemeris: 1995-2006
[NASA-RP-1349] p 638 N95-14667
GEOCHRONOLOGY
The 226RA and 231PA systematics of axial, MORB, crustal residence ages, and MAGMA chamber characteristics at 9 to 10 degree N East Pacific Rise
[DE94-013084] p 529 N95-14434
GEODESY
Satellite Laser Ranging in the 1990s: Report of the 1994 Belmont Workshop
[NASA-CP-3283] p 526 N95-14274
Global and regional kinematics with GPS p 527 N95-14279
Introducing the International Geoid Service p 516 N95-15792
The GEOMED Project p 516 N95-15794
The Bureau Gravimetrique International p 516 N95-15795
The European Geoid Project p 516 N95-15796
A strategy for geoid repairing p 517 N95-15798
GEODETIC ACCURACY
Introducing the International Geoid Service p 516 N95-15792
GEODETIC SATELLITES
Measuring temporal gravitational variations using SLR data p 527 N95-14277
The role of SLR and LLR in relativity p 528 N95-14284
GEODETIC SURVEYS
Earth orientation parameters p 527 N95-14281
Geodetic survey of Canada: Results on a geoid questionnaire p 516 N95-15793
GEODYNAMICS
Global and regional kinematics from SLR stations p 527 N95-14278
Global and regional kinematics with VLBI p 527 N95-14280
GEOIDS
International Geoid Service Bulletin No. 1
[BULL-1] p 516 N95-15791
Introducing the International Geoid Service p 516 N95-15792
Geodetic survey of Canada: Results on a geoid questionnaire p 516 N95-15793
The GEOMED Project p 516 N95-15794
The Bureau Gravimetrique International p 516 N95-15795
The European Geoid Project p 516 N95-15796
Validation of the global digital height model ETOPO5U referring to the Italian model (Italian DEM) p 517 N95-15797
A strategy for geoid repairing p 517 N95-15798
GEOLOGICAL FAULTS
Lithological and rheological constraints on fault rupture scenarios for ground motion hazard prediction
[DE94-014742] p 529 N95-14436
GEOLOGICAL SURVEYS
Compression of regions in the global advanced very high resolution radiometer 1-km data set p 565 N95-14591
Survey of the 1991 geothermal exploration promotion
[DE94-780690] p 530 N95-14836
GEOMAGNETIC TAIL
Geotail MCA plasma wave data analysis
[NASA-CR-197022] p 618 N95-14798
GEOMAGNETISM
An observational test of magnetospheric field models at geosynchronous orbit
[DE94-014462] p 526 N95-13995
Towards developing an analytical procedure of defining the equatorial electrojet for correcting satellite magnetic anomaly data
[NASA-CR-193621] p 526 N95-14267
Geotail MCA plasma wave data analysis
[NASA-CR-197022] p 618 N95-14798
Propagation in the ionosphere, B p 467 N95-14827
GEOMETRIC RECTIFICATION (IMAGERY)
Development of a systemic land cover/land use database for the Upper Mississippi River System derived from Landsat Thematic Mapper satellite data. Long term resource monitoring program
[PB94-186889] p 515 N95-14793
GEOMETRICAL THEORY OF DIFFRACTION
Wideband electromagnetic scattering/analysis program. Electromagnetic scattering from the trunks and branches of trees
[AD-A283112] p 469 N95-15394
GEOPHYSICAL OBSERVATORIES
SLR 2000 p 471 N95-14288
GEOPOTENTIAL
Introducing the International Geoid Service p 516 N95-15792
GEOSYNCHRONOUS ORBITS
Journal of Spacecraft Technology, volume 4, no. 2, July 1994 p 413 N95-13825
Remote programming in INSAT-2A/2B on-board Attitude and Orbit Control Computer (AOCC) p 413 N95-13827
An observational test of magnetospheric field models at geosynchronous orbit
[DE94-014462] p 526 N95-13995
Satellite Laser Ranging in the 1990s: Report of the 1994 Belmont Workshop
[NASA-CP-3283] p 526 N95-14274
GEOTHERMAL RESOURCES
Survey of the 1991 geothermal exploration promotion
[DE94-780690] p 530 N95-14836
GEOTHERMAL TECHNOLOGY
Survey of the 1991 geothermal exploration promotion
[DE94-780690] p 530 N95-14836
GERMANIUM
Performance of spherically focusing Ge(444) backscattering analyzers for inelastic x-ray scattering
[DE94-016349] p 621 N95-14382
GERMANIUM ALLOYS
Ion beam synthesis of SiGe alloy layers
[DE94-014958] p 620 N95-14189
GERMANIUM OXIDES
Low loss glass and optical fibers therefrom
[AD-D016379] p 615 N95-15766
GERMANY
Electro-optics: Propagation from IR to UV and sensor considerations. Part A: Propagation theory p 467 N95-14833
GET AWAY SPECIALS (STS)
Pool and flow boiling in variable and microgravity p 459 N95-14562
GLARE
The applicability of commercial glare test devices in the aeromedical certification of pilot applicants
[DOT/FAA/AM-94/15] p 540 N95-14176
GLASS
Scintillating glass fiber-optic neutron sensors
[DE94-014562] p 613 N95-15312
Relationship between microstructure and efficiency of scintillating glasses
[DE94-014563] p 454 N95-15313
Low loss glass and optical fibers therefrom
[AD-D016379] p 615 N95-15766
GLASS FIBER REINFORCED PLASTICS
Monitoring fiber stress during curing of single fiber glass- and graphite-epoxy composites
[NASA-TM-4568] p 432 N95-13641
Dynamics of the interface in a model composite system
[AD-A281910] p 433 N95-13655
Bolted joint studies in GRP
[AD-A283843] p 434 N95-14348
GLASS FIBERS
Monitoring fiber stress during curing of single fiber glass- and graphite-epoxy composites
[NASA-TM-4568] p 432 N95-13641
Processing of thermoset prepreg laminate via exposure to microwave radiation
[DE94-013268] p 432 N95-13643
GLASSY CARBON
Ru2Ge3: Crystal growth and some properties
[DE94-015360] p 625 N95-15531
GLAUBER THEORY
Probing the antiferromagnetic long-range order with Glauber spin states p 609 N95-13951
Multiple-scattering model for inclusive proton production in heavy ion collisions
[NASA-TP-3470] p 600 N95-15606
GLOBAL ATMOSPHERIC RESEARCH PROGRAM
Earth Observing System (EOS)/Advanced Microwave Sounding Unit-A (AMSU-A): Calibration management plan
[NASA-CR-189376] p 515 N95-13704
GLOBAL POSITIONING SYSTEM
Measurement and interpretation of crustal deformation rates associated with postglacial rebound
[NASA-CR-196440] p 525 N95-13627
Satellite Laser Ranging in the 1990s: Report of the 1994 Belmont Workshop
[NASA-CP-3283] p 526 N95-14274
Global reference frame: Intercomparison of results (SLR, VLBI and GPS) p 527 N95-14276
Global and regional kinematics with GPS p 527 N95-14279
Earth orientation parameters p 527 N95-14281
SLR tracking of GPS-35 p 471 N95-14285
Synergism of SLR and GPS p 471 N95-14286
A strawman SLR program plan for the 1990s p 471 N95-14289
International Geoid Service Bulletin No. 1
[BULL-1] p 516 N95-15791
The European Geoid Project p 516 N95-15796
GLOBAL TRACKING NETWORK
Global and regional kinematics from SLR stations p 527 N95-14278
GLOBAL WARMING
Integrated science model for assessment of climate change
[DE94-016363] p 523 N95-15361
GLUONS
Approximate next-to-leading order relation between the low-x F2 scaling violations and the gluon density
[PB94-192283] p 596 N95-15380
Studies of quarkonia production with CDF
[DE94-013220] p 597 N95-15862
GLYCOLS
Single-phase heat transfer and pressure drop characteristics of an integral-spine-fin within an annulus
[PB94-194073] p 482 N95-14407
Development of a moldable, biodegradable polymeric bone repair material
[AD-A283413] p 454 N95-15296
GOES SATELLITES
Semiconductor measurement technology: Improved characterization and evaluation measurments for HgCdTe detector materials, processes, and devices used on the GOES and TIROS satellites
[PB94-188810] p 474 N95-14401
GOGGLES
Civil use of night vision devices: Evaluation pilot's guide, part 2
[DOT/FAA/RD-94/19] p 410 N95-14175
Distance estimation training with night vision goggles: A preliminary study
[AD-A284900] p 563 N95-15755
GOLD
Synthesis and applications of large heterometallic cluster systems
[AD-A284874] p 626 N95-15748
GONIOMETERS
Time-of-flight detector for heavy ion backscattering spectrometry
[DE94-015600] p 596 N95-15437
GOVERNMENT/INDUSTRY RELATIONS
TABES 1994: 10th Annual Technical and Business Exhibition and Symposium p 414 N95-14633
Space science in the 1990's and beyond
[TABES PAPER 94-204] p 415 N95-14634
Helping small companies commercialize public-sector technology
[TABES PAPER 94-407] p 415 N95-14635
A NASA/industry/university partnership for development of dual-use vibration isolation technology
[TABES PAPER 94-613] p 416 N95-14643
Research and technology highlights, 1993
[NASA-TM-4575] p 647 N95-15065
Reengineering through information technology. Accompanying report of the National Performance Review
[PB94-170362] p 633 N95-15781
GOVERNMENTS
Reengineering through information technology. Accompanying report of the National Performance Review
[PB94-170362] p 633 N95-15781
GRADIENTS
Ru2Ge3: Crystal growth and some properties
[DE94-015360] p 625 N95-15531
GRAIN BOUNDARIES
Ferromagnetic grain boundary signature in die-upset RE-Fe-B magnets
[DE94-014904] p 590 N95-14440
Damping mechanisms in nanostructured materials
[AD-A283583] p 623 N95-15317
GRAIN SIZE
Investigation of dendrite coherency in two commercial Al-Si foundry alloys
[PB94-208238] p 446 N95-15349
The formation of small grains in shocks in the ISM p 641 N95-15842
GRAPH THEORY
Conditional graph completions
[AD-A282914] p 587 N95-15612
GRAPHICAL USER INTERFACE
A prototype lisp-based soft real-time object-oriented Graphical User Interface for control system development
[NASA-TM-106743] p 566 N95-13716
Integration/evaluation of a HCI prototyping environment
[NASA-CR-196996] p 566 N95-14107
NLEdit: A generic graphical user interface for Fortran programs
[NASA-TM-4543] p 572 N95-14206

Graphical user interface for the NASA FLOPS aircraft performance and sizing code
[NASA-TM-106649] p 408 N95-14604
A graphical user interface for design and analysis of air breathing propulsion systems
[TABES PAPER 94-616] p 411 N95-14645
Users manual for the Surface Currents Data Base (SCDB) Management System (SCDBMS), version 1.0
[NASA-CR-197021] p 537 N95-15753

GRAPHITE
Hydrogen transport and trapping in graphite
[UTIAS-347] p 437 N95-13652
AEM and HREM evaluation of carbon nanostructures in silica aerogels
[DE94-014913] p 434 N95-14387
Graphite fluoride from iodine intercalated graphitized carbon
[NASA-CASE-LEW-15360-1] p 441 N95-15303
Ru2Ge3: Crystal growth and some properties
[DE94-015360] p 625 N95-15531

GRAPHITE-EPOXY COMPOSITES
Monitoring fiber stress during curing of single fiber glass- and graphite-epoxy composites
[NASA-TM-4568] p 432 N95-13641
The buckling response of symmetrically laminated composite plates having a trapezoidal planform area
[NASA-CR-196975] p 505 N95-13839
Residual strength of composites with multiple impact damage
[AD-A284230] p 434 N95-14409
Milestone 4: Thrust structure concepts and IHM screening Graphite Composite Primary Structure (GCPS)
[NASA-CR-197053] p 434 N95-14800
Deformation, strength, and failure modes of laminated conventional and hybrid polymer-matrix composites loaded in the thickness direction
[AD-A281587] p 436 N95-15443
Milestone 5 test report. Task 5, subtask 5.2: Tile to foam strength tests
[NASA-CR-197241] p 514 N95-15913

GRAPHITIZATION
Graphite fluoride from iodine intercalated graphitized carbon
[NASA-CASE-LEW-15360-1] p 441 N95-15303

GRAPHS (CHARTS)
2D regular arrays for a special class of non uniform recurrence equations
[PB94-195633] p 584 N95-13980
Conditional graph completions
[AD-A282914] p 587 N95-15612
The temporal reasoning systems TimeGraph 1-2
[TR-494-REV] p 584 N95-15786
Efficient algorithms for qualitative reasoning about time
[TR-496] p 576 N95-15825

GRASHOF NUMBER
Oscillatory thermocapillary convection p 483 N95-14526

GRASSLANDS
Essential elements of an effective data qualification
[DE94-015566] p 632 N95-15419

GRATINGS (SPECTRA)
Wavelength-division multiplexed optical integrated circuit with vertical diffraction grating
[NASA-CASE-NPO-18357-1-CU] p 612 N95-14181
High-efficiency electro-optic grating on PLZT ceramic wafer for optical switching
[AD-A281573] p 477 N95-15460

GRAVITATION
Transport phenomena in stratified multi-fluid flo w in the presence and absence of gravity p 488 N95-14563
Teratogenic effects of delta g: The concept of allometric growth p 538 N95-15102

GRAVITATIONAL EFFECTS
AXAF VETA-I mirror ring focus measurements
[NASA-CR-196145] p 637 N95-13637
Heat capacity and thermal relaxation of bulk helium very near the lambda point p 444 N95-14208
Basic features of the STS/Spacelab vibration environment p 428 N95-14210
Orbital processing of high-quality CdTe compound semiconductors p 458 N95-14213
Vapor transport crystal growth of mercury-cadmium-telluride in microgravity p 458 N95-14216
Measurement of interfacial tension of immiscible liquid pairs in microgravity p 458 N95-14221
Protein crystal growth results from the United States Microgravity Laboratory-1 mission p 458 N95-14225
Scientific analysis of satellite ranging data p 517 N95-14275
Stochastic model of the residual acceleration environment in microgravity p 459 N95-14540
Nonlinear dynamics of drops and bubbles and chaotic phenomena p 485 N95-14541
Bubble dynamics, two-phase flow, and boiling heat transfer in a microgravity environment p 488 N95-14561
Particle experiments in thermal and velocity gradients p 489 N95-14564
Gravity-dependent transport in industrial processes p 459 N95-14580
Proposal for an astronaut mass measurement device for the Space Shuttle
[NASA-CR-197198] p 563 N95-14854
Gravitational stress and regulation of neuroendocrine elements and fluid volume in humans p 542 N95-15090
Hemodynamic responses to passive body tilts p 542 N95-15096
The influence of gravity on vestibular nystagmus in humans p 546 N95-15121
Centrifuges in gravitational physiology research p 550 N95-15147
Isolation of the physiological regulation component of the arterial pressure time variation after postural stresses by a model of the gravitational and arterial kinking effects p 550 N95-15149

GRAVITATIONAL FIELDS
Squeezed states and graviton-entropy production in the early universe p 608 N95-13947
Satellite Laser Ranging in the 1990s: Report of the 1994 Belmont Workshop
[NASA-CP-3283] p 526 N95-14274
Measuring temporal gravitational variations using SLR data p 527 N95-14277
Interfacial force field characterization of a constrained vapor bubble thermosyphon using IAI p 488 N95-14560
The extensional rheology of non-Newtonian materials p 489 N95-14569
Some genetic aspects of adaptation to hyperdynamic environments p 543 N95-15100
Are otoconia dynamic in birds and mammals? p 538 N95-15103
Vestibular ontogeny: Measuring the influence of the dynamic environment p 544 N95-15105
On-Earth evaluation of the neurovestibular tolerance to centrifuge simulated artificial gravity in humans p 546 N95-15120
The GEOMED Project p 516 N95-15794
The Bureau Gravimetrique International p 516 N95-15795
The European Geoid Project p 516 N95-15796
A strategy for geoid repairing p 517 N95-15798

GRAVITATIONAL PHYSIOLOGY
Development of life sciences equipment for microgravity and hypergravity simulation p 425 N95-14090
Unique life sciences research facilities at NASA Ames Research Center p 426 N95-14091
Adaptation of skeletal muscle to spaceflight: Cosmos rhesus project. Cosmos 2044 and 2229
[NASA-CR-197041] p 537 N95-14796
The Physiologist, volume 36, number 1, supplement p 541 N95-15089
Neurohumoral reactions to long-term vestibular stimulation in man p 542 N95-15091
Will man need the vestibular system in generations to come? p 542 N95-15092
Psychophysiological aspects of increasing resistance to space motion sickness p 542 N95-15093
Circulatory filling pressures during transient microgravity induced by parabolic flight p 542 N95-15095
Cardiovascular response to cold pressor and LBNP tests before and after 20-day-bedrest p 543 N95-15097
Twenty four hours head-down tilt decreases arterial baroreflex function in conscious rat p 538 N95-15098
Some genetic aspects of adaptation to hyperdynamic environments p 543 N95-15100
Changing gravity level and the development of animals p 538 N95-15101
Teratogenic effects of delta g: The concept of allometric growth p 538 N95-15102
Are otoconia dynamic in birds and mammals? p 538 N95-15103
The avian embryo responding to microgravity of space flight p 538 N95-15104
Vestibular ontogeny: Measuring the influence of the dynamic environment p 544 N95-15105
Behaviour of newly hatched and adult Japanese quail and the feasibility of adaptation to weightlessness p 538 N95-15106
Comparison of hemodynamic and volume responses to different levels of lower body suction and head-up tilt p 544 N95-15107
Body position and volume status as determinants of cardiovascular responses to transition into microgravity in parabolic flight p 544 N95-15108
Cardiovascular and metabolic responses to 6 deg Head-Down Tilt (HDT) and 70 deg Head-Up Tilt (HUT) following exercise p 544 N95-15109
A mathematical model of the cardiovascular response to +Gz acceleration p 544 N95-15110
Effects of 20 days bed-rest on cardio-respiratory functions during sub-maximal exercise in young women p 545 N95-15111
Modeling and numerical simulation of the cerebral blood flow under acceleration p 545 N95-15112
Space flight and humoral and cellular immunity of animals p 538 N95-15113
Immune changes in humans concomitant with space flights of up to 10 days duration p 545 N95-15114
Postural control of fish related to gravity input p 539 N95-15118
Functional participation of the valvula cerebelli on the goldfish dorsal light response p 539 N95-15119
The influence of gravity on vestibular nystagmus in humans p 546 N95-15121
The relationship between space sickness and preflight diet p 546 N95-15122
Manipulating the arterial pressure to prevent G-LOC p 546 N95-15123
Guidelines for a Research and Development (R/D) program for high sustained G p 546 N95-15124
Non-invasive physiological monitoring relevant to G-induced loss of consciousness p 547 N95-15125
Physiological considerations concerning Positive Pressure Breathing (PBG) during +Gz p 547 N95-15126
Operational requirements for avoidance and eventual elimination of Gz-induced Loss Of Consciousness (G-LOC) in flight p 547 N95-15127
Regional cutaneous microvascular flow responses during gravitational and LBNP stresses p 547 N95-15128
Physiologic mechanisms effecting circulatory and body fluid losses in weightlessness as shown by mathematical modeling p 547 N95-15129
Simulation of the fluid retention effects of a vasopressin analog using the Guyton model of circulation p 547 N95-15130
Transient blood/plasma density and hematocrit effects after passive (sitting) thermoneutral water immersion in men p 548 N95-15131
Alterations of body temperature, feeding, drinking and sleep-wake circadian rhythms in Rhesus monkey during a 19 day Spacelab flight simulation p 539 N95-15132
The regulation of rat activity following exposure to hyperdynamic fields p 539 N95-15133
Musculoskeletal adaptation to mechanical forces on Earth and in space p 548 N95-15136
Effects of microgravity on interstitial muscle receptors affecting heart rate and blood pressure during static exercise p 548 N95-15137
Orthostatic stress by lower body negative pressure and its body fluid distribution kinetics under microgravity p 549 N95-15138
Effect of short- and long-term spaceflight on the contractile properties of rat skeletal muscles with different functions p 539 N95-15141
Influence to organs by ten weeks tail suspension p 539 N95-15142
Relationship between hind-limb muscle atrophy and serum enzymes in tail suspended rats p 539 N95-15143
Activity of ornithine decarboxylase in muscle of Japanese quail in hypergravity conditions p 539 N95-15144
The cardiovascular response to the AGS p 419 N95-15146
Centrifuges in gravitational physiology research p 550 N95-15147
Enhancement of insulin receptor mediated endocytosis in cultured osteoblastic cells under hypergravity p 539 N95-15148
Isolation of the physiological regulation component of the arterial pressure time variation after postural stresses by a model of the gravitational and arterial kinking effects p 550 N95-15149
A comparison of overall mathematical models of the cardiovascular system for simulating response to orthostatic stresses p 550 N95-15150

GRAVITONS
Squeezed states and graviton-entropy production in the early universe p 608 N95-13947

GRAVITY PROBE B
Numerical studies of the surface tension effect of cryogenic liquid helium
[NASA-CR-197014] p 479 N95-14104

GRAVITY WAVES
Meso-beta scale numerical simulation studies of terrain-induced jet streak mass/momentum perturbations
[NASA-CR-197226] p 531 N95-15684

GREEN'S FUNCTIONS
Lithological and rheological constraints on fault rupture scenarios for ground motion hazard prediction
[DE94-014742] p 529 N95-14436

GREENHOUSE EFFECT
Oxides of nitrogen: Their formation and control in stationary sources
[AD-A283780] p 522 N95-14337
Simulation of coal and char nitrogen reactions in combustion
[DE94-013941] p 440 N95-15291
Integrated science model for assessment of climate change
[DE94-016363] p 523 N95-15361
Progress report on terrestrial model development (TERRA and HABITAT): Research in support of the CERES earth system modeling project
[DE94-016362] p 524 N95-15779
GRID GENERATION (MATHEMATICS)
Aerodynamic shape optimization of a HSCT type configuration with improved surface definition
[NASA-CR-197011] p 392 N95-13701
An adaptively-refined, Cartesian, cell-based scheme for the Euler and Navier-Stokes equations
[NASA-TM-106754] p 392 N95-13817
The role of CFD in the design process
p 481 N95-14135
Computational aerodynamics based on the Euler equations
[AGARD-AG-325] p 398 N95-14264
Radiative interactions in multi-dimensional chemically reacting flows using Monte Carlo simulations
[NASA-CR-197012] p 481 N95-14269
A Cartesian, cell-based approach for adaptively-refined solutions of the Euler and Navier-Stokes equations
[NASA-TM-106786] p 398 N95-14297
Parallel isosurface generator for huge data sets
[AD-A284030] p 578 N95-14422
An approach for dynamic grids
[NASA-TM-106774] p 404 N95-15853
Two methods for the study of vortex patch evolution on locally refined grids
[DE94-014965] p 494 N95-15867
GROUND EFFECT (AERODYNAMICS)
Propulsion/airframe interference for ducted propfan engines with ground effect
[NASA-CR-197110] p 409 N95-14909
GROUND OPERATIONAL SUPPORT SYSTEM
Architecture for Survivable Systems Processing (ASSP). Technology benefits for Open System Interconnects
p 567 N95-14160
GROUND SPEED
Groundspeed filtering for CTAS
[NASA-CR-197223] p 497 N95-15785
GROUND STATE
Quantum state engineering p 605 N95-13919
Causality problems for Fermi's two-atom system
p 598 N95-13945
Probing the antiferromagnetic long-range order with Glauber spin states p 609 N95-13951
Bloch vector projection noise p 610 N95-13956
A facility to produce an energetic, ground state atomic oxygen beam for the simulation of the Low-Earth Orbit environment p 422 N95-14072
The C4H radical and the diffuse interstellar bands. An ab initio study p 641 N95-15843
GROUND STATIONS
The long-term forecast of station view periods
p 419 N95-14621
GROUND SUPPORT SYSTEMS
SLR 2000 p 471 N95-14288
GROUND TESTS
Self contamination effects in the TAUVEX UV Telescope: Ground testing and computer simulation
p 421 N95-14067
Simulation of Shuttle launch G forces and acoustic loads using the NASA Ames Research Center 20G centrifuge
p 419 N95-14089
Development of life sciences equipment for microgravity and hypergravity simulation p 425 N95-14090
Alpha LAMP Integration Facility p 418 N95-14094
The AEDC aerospace chamber 7V: An advanced test capability for infrared surveillance and seeker sensors
p 418 N95-14097
New potentials of NIICHIMMASH's thermal vacuum facilities p 418 N95-14098
Selection of solar simulator for solar dynamic ground test
[NASA-TM-106608] p 430 N95-14173
High Alpha Technology Program (HATP) ground test to flight comparisons p 393 N95-14230
Test and Evaluation Master Plan (TEMP) for Fixed Ground Antenna Radomes (FGAR)
[AD-A283839] p 481 N95-14346
A multiscale random field model for Bayesian image segmentation
[AD-A283875] p 515 N95-14358
Pool and flow boiling in variable and microgravity
p 459 N95-14562
Lunar base heat pump
[NASA-CR-188356] p 492 N95-14869
Centrifuges in gravitational physiology research
p 550 N95-15147
GROUND TRUTH
Remote sensing, processing and transmission of data for an unmanned aerial vehicle
[AD-A283104] p 514 N95-13693
Development of a systemic land cover/land use database for the Upper Mississippi River System derived from Landsat Thematic Mapper satellite data. Long term resource monitoring program
[PB94-186889] p 515 N95-14793
GROUND WATER
Essential elements of an effective data qualification
[DE94-015566] p 632 N95-15419
The crosswell electromagnetic response of layered media
[DE94-014929] p 470 N95-15866
GROUND WIND
Upgrade of tropical cyclone surface wind field model
[AD-A283530] p 533 N95-15323
GROUP VELOCITY
Quantum propagation in single mode fiber
p 609 N95-13953
Interacting fronts in a model for binary-mixture convection
[DE94-013595] p 494 N95-15861
GROWTH
Electrodeposition of conductors and semiconductors with controlled stoichiometries and morphologies
[AD-A280743] p 437 N95-14141
Teratogenic effects of delta g: The concept of allometric growth p 538 N95-15102
Formation of dust grains with impurities in red giant winds p 641 N95-15841
GUIDANCE (MOTION)
Advanced Guidance and Control Aspects in Robotics
[AGARD-LS-193] p 581 N95-14942
Machine intelligence: The key to guidance and control in robotics p 581 N95-14944
Guidance and control for unmanned ground vehicles
p 504 N95-14948
GUIDANCE SENSORS
Aero-optics system integration
[TABES PAPER 94-604] p 415 N95-14638
GULF OF MEXICO
Energy flux and hydrogeology of thermal anomalies in the Gulf of Mexico Basin: South Texas example
[DE94-015122] p 530 N95-14956
GYROSCOPIC STABILITY
Evaluation of energy-sink stability criteria for dual-spin spacecraft
[AD-A283228] p 428 N95-14850

H

HADRONS
Hadronic matter and rapidly rotating compact stars
[DE94-014928] p 643 N95-14442
Hadronization of QCD and effective interactions
[DE94-014975] p 594 N95-14660
Hadronic wavefunctions in light-cone quantization
[DE94-014507] p 622 N95-15308
Research in high energy physics
[DE94-015519] p 600 N95-15539
A relativistic cascade for heavy ion collisions
[DE94-015846] p 600 N95-15633
HAFNIUM OXIDES
Influence of defect shape on laser-induced damage in multilayer coatings
[DE94-016543] p 451 N95-14389
HAIL
The operational forecasting/nowcasting of precipitation type in the southeastern United States type of precipitation: Descriptive and objective guidance
[AD-A284456] p 535 N95-15819
HAIR
Are otoconia dynamic in birds and mammals?
p 538 N95-15103
Neuronal types in the chicken's statoacoustic ganglion
p 539 N95-15116
HALF LIFE
Beta decay data for neutron-rich Li-Cl nuclides
[DE94-014556] p 595 N95-15310
HALL EFFECT
Multilayer thin film Hall effect device
[NASA-CASE-MFS-28764-1] p 590 N95-14137
Electrical characterization of 6H crystalline silicon carbide
[NASA-CR-197047] p 439 N95-14903
HALOCARBONS
Chemical kinetics and atmospheric modification
[AD-A283304] p 524 N95-15623
HALOGEN COMPOUNDS
Process development of thermal hydrodechlorination
[PB94-195518] p 525 N95-15870
HALOGENS
AASERT-93: Electroplating of refractory metals using haloaluminate melts
[AD-A284859] p 447 N95-15744
HAMILTONIAN FUNCTIONS
Joint and angle-covariant spin measurements with a quadrupole magnetic field p 604 N95-13914
Sqeezing generated by a nonlinear master equation and by amplifying-dissipative Hamiltonians
p 588 N95-13926
Understanding squeezing of quantum states with the Wigner function p 606 N95-13930
The wave function and minimum uncertainty function of the bound quadratic Hamiltonian system
p 608 N95-13943
Berry phase in Heisenberg representation
p 609 N95-13952
Evolution of wave function in a dissipative system
p 610 N95-13959
Finite boson mappings of fermion systems
[DE94-014478] p 593 N95-14000
From the shell model to the interacting boson model
[DE94-014486] p 593 N95-14001
Relativistic configuration-interaction calculation of the correlation energies of heliumlike ions
[DE94-015190] p 621 N95-14325
Studies in chaotic adiabatic dynamics
[DE94-013111] p 627 N95-15578
Neutrino oscillations in noisy media
[DE94-014973] p 598 N95-15869
HAND (ANATOMY)
Manual discrimination of force p 561 N95-14057
HANDBOOKS
HRMA calibration handbook: EKC gravity compensated XRCF models
[NASA-CR-195818] p 636 N95-13634
A NASA/industry/university partnership for development of dual-use vibration isolation technology
[TABES PAPER 94-613] p 416 N95-14643
HARBORS
Selecting wave gauge sites for monitoring harbor oscillations: A case study for Kahului Harbor, Hawaii
[AD-A281707] p 536 N95-15452
HARDNESS
Ballistic performance and adiabatic shear behavior of AerMet(tm) 100 steel
[AD-A283266] p 447 N95-15622
Effect of heat treatment on the microstructure and properties of AerMet (trade name) 100 steel
[AD-A284387] p 447 N95-15807
HARDWARE
Experimental hardware development for a pulsed ultrasonic data collection facility
[AD-A283331] p 615 N95-15872
HARMONIC CONTROL
Higher harmonic control analysis for vibration reduction of helicopter rotor systems
[NASA-TM-103855] p 391 N95-14419
HARMONIC GENERATIONS
Investigation of dipolar reorientation dynamics of pure bulk polymers using second harmonic generation
[AD-A283023] p 448 N95-13688
Relaxation of polar orientational order in nonlinear optical polymers by second harmonic generation
[AD-A283024] p 449 N95-13689
Nonlinear optical susceptibility of a model guest/host polymeric system as investigated by electro-optics and second harmonic generation
[AD-A283069] p 449 N95-13692
HARMONIC OSCILLATORS
Squeezing in a 2-D generalized oscillator
p 603 N95-13907
Sqeezing generated by a nonlinear master equation and by amplifying-dissipative Hamiltonians
p 588 N95-13926
Multivariable Hermite polynomials and phase-space dynamics p 606 N95-13929
High power diode pumped solid state laser development at Lawrence Livermore National Laboratory
[DE94-015899] p 499 N95-14427
HARTREE APPROXIMATION
High performance computational chemistry: Towards fully distributed parallel algorithms
[DE94-014561] p 573 N95-15311
HAWAII
Selecting wave gauge sites for monitoring harbor oscillations: A case study for Kahului Harbor, Hawaii
[AD-A281707] p 536 N95-15452
HAZARDS
Blast overpressure studies with animals and man
[AD-A280435] p 540 N95-13971

Eighteenth Space Simulation Conference: Space Mission Success Through Testing
[NASA-CP-3280] p 420 N95-14062
Investigating and implementing enhancements to the simulation of short-term collision hazards
p 426 N95-14092
Applications of a fast and efficient method for simulating orbital mission safety p 426 N95-14093
The Global Emergency Observation and Warning System
[TABES PAPER 94-622] p 417 N95-14649

HEAD DOWN TILT
Cardiovascular and metabolic responses to 6 deg Head-Down Tilt (HDT) and 70 deg Head-Up Tilt (HUT) following exercise p 544 N95-15109
Effects of 20 days bed-rest on cardio-respiratory functions during sub-maximal exercise in young women
p 545 N95-15111

HEAD MOVEMENT
Destabilizing effects of visual environment motions simulating eye movements or head movements
p 562 N95-14061

HEAD-UP DISPLAYS
Airplane takeoff and landing performance monitoring system
[NASA-CASE-LAR-14745-2-SB] p 412 N95-14415

HEALTH
Telerobotics in rehabilitation: Barriers to a virtual existence p 556 N95-14030
Extended duration orbiter medical project Microbial Air Sampler (STS-50/USML-1) p 458 N95-14222
Oxides of nitrogen: Their formation and control in stationary sources
[AD-A283780] p 522 N95-14337

HEARING
Auditory interfaces: The human perceiver
p 554 N95-14015
Monitoring audiometry in hearing conservation programs
[AD-A282024] p 540 N95-14145

HEART
Cardiovascular deconditioning effects of long-term simulated weightlessness in rats p 538 N95-15099

HEART FUNCTION
Cardiovascular response to cold pressor and LBNP tests before and after 20-day-bedrest p 543 N95-15097
Body position and volume status as determinants of cardiovascular responses to transition into microgravity in parabolic flight p 544 N95-15108
Cardiovascular and metabolic responses to 6 deg Head-Down Tilt (HDT) and 70 deg Head-Up Tilt (HUT) following exercise p 544 N95-15109
A mathematical model of the cardiovascular response to +Gz acceleration p 544 N95-15110
The cardiovascular response to the AGS
p 419 N95-15146

HEART RATE
The effects of autogenic-feedback training on motion sickness severity and heart rate variability in astronauts
[NASA-TM-108840] p 539 N95-13661
Passive fetal heart rate monitoring apparatus and method with enhanced fetal heart beat discrimination
[NASA-CASE-LAR-15129-1] p 541 N95-14184
Extended duration orbiter medical project variability of blood pressure and heart rate (STS-50/USML-1)
p 551 N95-14223
Comparison of hemodynamic and volume responses to different levels of lower body suction and head-up tilt
p 544 N95-15107
Body position and volume status as determinants of cardiovascular responses to transition into microgravity in parabolic flight p 544 N95-15108
Effects of 20 days bed-rest on cardio-respiratory functions during sub-maximal exercise in young women
p 545 N95-15111
Effects of microgravity on interstitial muscle receptors affecting heart rate and blood pressure during static exercise p 548 N95-15137

HEAT ENGINES
Nondestructive characterization of structural ceramic components
[DE94-013961] p 449 N95-13978
Advanced Turbine Technology Applications Project (ATTAP)
[NASA-CR-195393] p 634 N95-15743

HEAT FLUX
Hypersonic engine leading edge experiments in a high heat flux, supersonic flow environment
[NASA-TM-106742] p 482 N95-14299
Determination of the similarity theory scaling parameters from the vertical gradients
[AD-A283833] p 533 N95-14340
Radiation rates for low Z impurities in edge plasmas
[DE94-016073] p 617 N95-14368
An experimental and numerical study of the modifications of mixed-layer structure by inhomogeneous surface fluxes and secondary circulations
[DE94-015945] p 529 N95-14428
US-Japan workshop Q-181 on High Heat Flux Components and Plasma-Surface Interactions for Next Devices: Proceedings
[DE94-014939] p 618 N95-14443
Study of two-phase flow and heat transfer in reduced gravities p 487 N95-14555
Pool and flow boiling in variable and microgravity
p 459 N95-14562
Behavior of charring materials in simulated fire environments
[PB94-196045] p 439 N95-14838

HEAT MEASUREMENT
Fire growth models for materials
[PB94-195856] p 443 N95-15610

HEAT OF COMBUSTION
Behavior of charring materials in simulated fire environments
[PB94-196045] p 439 N95-14838

HEAT OF VAPORIZATION
Fire growth models for materials
[PB94-195856] p 443 N95-15610

HEAT PUMPS
Lunar base heat pump
[NASA-CR-188356] p 492 N95-14869

HEAT RESISTANT ALLOYS
Effects of hydrogen annealing, sulfur segregation and diffusion on the cyclic oxidation resistance of superalloys: A review
[NASA-TM-106734] p 444 N95-13667
High temperature cyclic behaviour of aerospace materials: Room temperature validation tests of Ti-6Al-4V
[AGARD-AR-328] p 506 N95-14198
Fatigue in single crystal nickel superalloys
[AD-A282917] p 446 N95-15415

HEAT TRANSFER
Experimental design for the evaluation of high-T(sub c) superconductive thermal bridges in a sensor satellite
[NASA-CR-197003] p 429 N95-14106
Second Microgravity Fluid Physics Conference
[NASA-CP-3276] p 482 N95-14522
Future directions in two-phase flow and heat transfer in space p 482 N95-14523
Control of oscillatory thermocapillary convection in microgravity p 483 N95-14525
Onset of hexagons in surface-tension-driven Benard convection p 483 N95-14527
Experimental investigation of the Marangoni effect on the stability of a double-diffusive layer
p 483 N95-14528
Thermocapillary convection in floating zones under simulated reduced-gravity conditions
p 483 N95-14529
Oscillatory/chaotic thermocapillary flow induced by radiant heating p 483 N95-14531
Study of two-phase flow and heat transfer in reduced gravities p 487 N95-14555
Effects of thermocapillarity on an evaporating extended meniscus in microgravity p 488 N95-14559
Bubble dynamics, two-phase flow, and boiling heat transfer in a microgravity environment
p 488 N95-14561
Pool and flow boiling in variable and microgravity
p 459 N95-14562
An analysis of eddy resolving global ocean models in the Southern Ocean
[AD-A283211] p 536 N95-15626

HEAT TRANSFER COEFFICIENTS
Effect of surface roughness on local film cooling effectiveness and heat transfer coefficients
[AD-A283854] p 482 N95-14351
Single-phase heat transfer and pressure drop characteristics of an integral-spine-fin within an annulus
[PB94-194073] p 482 N95-14407

HEAT TRANSMISSION
LLE review, January - March 1994
[DE94-015058] p 618 N95-14955

HEAT TREATMENT
The effect of microstresses on fatigue crack propagation in steel
[AD-A283872] p 506 N95-14356
Ballistic performance and adiabatic shear behavior of AerMet(tm) 100 steel
[AD-A283266] p 447 N95-15622
Effect of heat treatment on the microstructure and properties of AerMet (trade name) 100 steel
[AD-A284387] p 447 N95-15807
Process development of thermal hydrodechlorination
[PB94-195518] p 525 N95-15870
Milestone 5 test report. Task 5, subtask 5.2: Tile to foam strength tests
[NASA-CR-197241] p 514 N95-15913

HEATERS
Pulsed mode cathode
[NASA-CASE-LEW-15753-1] p 475 N95-14516

HEATING
Ground based studies of thermocapillary flows in levitated drops p 486 N95-14545

HEATING EQUIPMENT
Induction heating coupler
[NASA-CASE-LAR-14278-1] p 473 N95-14294

HEAVY IONS
Microcontamination detection using Heavy Ion Backscattering Spectrometry
[DE94-014182] p 437 N95-14312
A theoretical study of 30 to 50 angstrom noble gas heavy ion lithography
[DE94-015262] p 442 N95-15436
Time-of-flight detector for heavy ion backscattering spectrometry
[DE94-015600] p 596 N95-15437
Multiple-scattering model for inclusive proton production in heavy ion collisions
[NASA-TP-3470] p 600 N95-15606
A comparison of driver concepts for heavy-ion fusion
[DE94-016451] p 600 N95-15780

HEISENBERG THEORY
Q-derivatives, coherent states and squeezing
p 589 N95-13901
Uncertainty relations as Hilbert space geometry
p 588 N95-13911
Phase space flow of particles in squeezed states
p 606 N95-13928
Berry phase in Heisenberg representation
p 609 N95-13952
Further evidence for the EPNT assumption
p 611 N95-13962

HELICAL FLOW
Conservation of magnetic helicity during plasma relaxation
[DE94-016770] p 617 N95-14373

HELICOPTER PERFORMANCE
Add a dimension to your analysis of the helicopter low airspeed environment
[AD-A283982] p 408 N95-14205

HELICOPTERS
Civil use of night vision devices: Evaluation pilot's guide, part 2
[DOT/FAA/RD-94/19] p 410 N95-14175
The principles of flight test assessment of flight-safety-critical systems in helicopters
[AGARD-AG-300-VOL-12] p 405 N95-14199
Higher harmonic control analysis for vibration reduction of helicopter rotor systems
[NASA-TM-103855] p 391 N95-14419
Small crack test program for helicopter materials
p 507 N95-14455
A method of calculating the safe fatigue life of compact, highly-stressed components p 509 N95-14464
Vertical flight terminal operational procedures. A summary of FAA research and development
[AD-A283550] p 413 N95-15328
Collection of real-time, multichannel EEG data from helicopter pilots in flight: A feasibility study
[AD-A284396] p 551 N95-15767
Test Operation Procedure (TOP): Vibration testing of helicopter equipment
[AD-A284433] p 410 N95-15815

HELIUM
Welding irradiated stainless steel
[DE94-013661] p 500 N95-13645
Heat capacity and thermal relaxation of bulk helium very near the lambda point p 444 N95-14208
Asteroseismology with FRESIP: A meter class space telescope p 643 N95-14504
Influence of transmutation on microstructure, density change, and embrittlement of vanadium and vanadium alloys irradiated in HFIR
[DE94-015202] p 446 N95-15431

HELIUM IONS
Relativistic configuration-interaction calculation of the correlation energies of heliumlike ions
[DE94-015190] p 621 N95-14325

HELIUM ISOTOPES
Ion implantation of He-3 in tantalum for use in a low energy deuteron polarization analyzer
[AD-A283172] p 619 N95-13698
Extension of the BRYNTRN code to monoenergetic light ion beams
[NASA-TP-3472] p 647 N95-15790

HELIUM PLASMA
Solid target boronization of the MST reversed-field pinch during pulsed discharge cleaning
[DE94-015535] p 442 N95-15541

HELMET MOUNTED DISPLAYS
Virtual reality at work p 556 N95-14033
Perceptual and performance consequences of flight in virtual worlds p 558 N95-14043

VERDEX: A virtual environment demonstrator for remote driving applications p 562 N95-14060

HEMATOCRIT

Transient blood/plasma density and hematocrit effects after passive (sitting) thermoneutral water immersion in men p 548 N95-15131

HEMODYNAMIC RESPONSES

Hemodynamic responses to passive body tilts p 542 N95-15096

Comparison of hemodynamic and volume responses to different levels of lower body suction and head-up tilt p 544 N95-15107

Manipulating the arterial pressure to prevent G-LOC p 546 N95-15123

HEPTANES

Interfacial force field characterization of a constrained vapor bubble thermosyphon using IAI p 488 N95-14560

HERBIG-HARO OBJECTS

On the affinities of lambda 5778 and other broad diffuse interstellar bands p 639 N95-15832

HERMETIC SEALS

A High Temperature Hermetic Primer and a Variable Spring Tester
[DE94-012073] p 457 N95-14004

HERMITIAN POLYNOMIAL

Squeezing in a 2-D generalized oscillator p 603 N95-13907

Multivariable Hermite polynomials and phase-space dynamics p 606 N95-13929

Some rules for polydimensional squeezing p 608 N95-13941

Variable metric conjugate gradient methods
[DE94-014796] p 585 N95-14381

HETERODYNING

Homodyning and heterodyning the quantum phase p 604 N95-13913

HETEROGENEITY

An overview of the EOSDIS V0 information management system: Lessons learned from the implementation of a distributed data system p 566 N95-14596

Mathematical problems of nonlinear wave propagation and of waves in heterogeneous media
[AD-A282217] p 492 N95-14605

Simulation of coal and char nitrogen reactions in combustion
[DE94-013941] p 440 N95-15291

Formation of dust grains with impurities in red giant winds p 641 N95-15841

HETEROJUNCTION DEVICES

The electromagnetic spectrum. Research investigation directed toward extending the useful range of the electromagnetic spectrum
[AD-A281378] p 461 N95-14361

HEXAGONS

Onset of hexagons in surface-tension-driven Benard convection p 483 N95-14527

HIERARCHIES

Unambiguous computation: Boolean hierarchies an sparse Turing-complete sets
[TR-483] p 575 N95-15597

A promise class at least as hard as the polynomial hierarchy
[TR-484] p 576 N95-15788

HIGH ENERGY INTERACTIONS

A multi-level object store and its application to HEP data analysis
[DE94-014010] p 568 N95-14010

A high speed, wide dynamic range digitizer circuit for photomultiplier tubes
[DE94-015187] p 475 N95-15302

Research accomplishments and future goals in particle physics
[DE94-015483] p 596 N95-15537

Research in high energy physics
[DE94-015519] p 600 N95-15539

HIGH FLUX ISOTOPE REACTORS

Influence of transmutation on microstructure, density change, and embrittlement of vanadium and vanadium alloys irradiated in HFIR
[DE94-015202] p 446 N95-15431

HIGH FREQUENCIES

RF vacuum microelectronics
[AD-A283123] p 478 N95-15613

HIGH GAIN

High gain GaAs switches for impulse sources: Measurement of the speed of current filaments
[DE94-015281] p 477 N95-15544

HIGH GRAVITY ENVIRONMENTS

Development of life sciences equipment for microgravity and hypergravity simulation p 425 N95-14090

The Physiologist, volume 36, number 1, supplement p 541 N95-15089

Changing gravity level and the development of animals p 538 N95-15101

A mathematical model of the cardiovascular response to +Gz acceleration p 544 N95-15110

Physiological considerations concerning Positive Pressure Breathing (PBG) during +Gz p 547 N95-15126

Activity of ornithine decarboxylase in muscle of Japanese quail in hypergravity conditions p 539 N95-15144

Enhancement of insulin receptor mediated endocytosis in cultured osteoblastic cells under hypergravity p 539 N95-15148

HIGH IMPULSE

High gain GaAs switches for impulse sources: Measurement of the speed of current filaments
[DE94-015281] p 477 N95-15544

HIGH POWER LASERS

Department of Defense high power laser program guidance
[AD-A282915] p 500 N95-15391

HIGH PRESSURE

Effect of surface roughness on local film cooling effectiveness and heat transfer coefficients
[AD-A283854] p 482 N95-14351

Space Shuttle Main Engine turbopump bearing assessment program
[TABES PAPER 94-621] p 417 N95-14648

Meso-beta scale numerical simulation studies of terrain-induced jet streak mass/momentum perturbations
[NASA-CR-197226] p 531 N95-15684

HIGH RESOLUTION

Self contamination effects in the TAUVEX UV Telescope: Ground testing and computer simulation p 421 N95-14067

Measurements of ultraviolet absorption cross sections of NO2 at various pressures and temperatures
[AD-A283835] p 522 N95-14344

Support of Environmental Requirements for Cloud Analysis and Archive (SERCAA): Algorithm descriptions
[AD-A283240] p 534 N95-15614

Development and testing of a high-resolution model for tropospheric sulfate driven by observation-derived meteorology
[DE94-014910] p 525 N95-15864

HIGH REYNOLDS NUMBER

Numerical simulation of the flow about an F-18 aircraft in the high-alpha regime p 394 N95-14232

Numerical simulation of the flow about the F-18 HARV at high angle of attack
[NASA-CR-197023] p 400 N95-14614

HIGH SPEED

High-speed fixed and floating point implementation of delta-operator formulated discrete time systems
[AD-A283109] p 584 N95-13694

High-Speed Research: 1994 Sonic Boom Workshop: Atmospheric Propagation and Acceptability Studies
[NASA-CP-3279] p 401 N95-14878

A high speed, wide dynamic range digitizer circuit for photomultiplier tubes
[DE94-015187] p 475 N95-15302

HIGH STRENGTH

Ballistic performance and adiabatic shear behavior of AerMet(tm) 100 steel
[AD-A283266] p 447 N95-15622

HIGH STRENGTH STEELS

Effect of heat treatment on the microstructure and properties of AerMet (trade name) 100 steel
[AD-A284387] p 447 N95-15807

HIGH TEMPERATURE

A High Temperature Hermetic Primer and a Variable Spring Tester
[DE94-012073] p 457 N95-14004

Definition of high-temperature use limits for MIL-L-2104 engine oils
[AD-A282838] p 451 N95-14365

High Temperature Calibration Furnace System user's guide
[NASA-CR-196526] p 573 N95-14905

Corrosion-resistant coatings for high-temperature high-sulfur-activity applications
[DE94-015155] p 453 N95-14957

High temperature membranes for H2S and SO2 separations
[DE94-017125] p 441 N95-15345

Surface spectroscopic studies of high-temperature superconductors
[PB94-191228] p 624 N95-15378

Ru2Ge3: Crystal growth and some properties
[DE94-015360] p 625 N95-15531

Small UHV compatible hyperthermal oxygen atom generator
[NASA-CAS-LAR-14674-1] p 503 N95-15601

Apparatus for performing high-temperature fiber push-out testing
[NASA-CASE-LEW-15470-1] p 497 N95-15915

HIGH TEMPERATURE ENVIRONMENTS

Hypersonic engine leading edge experiments in a high heat flux, supersonic flow environment
[NASA-TM-106742] p 482 N95-14299

Lunar base heat pump
[NASA-CR-188356] p 492 N95-14869

Stress corrosion crack tip microstructure in nickel-based alloys
[DE94-015362] p 446 N95-15532

HIGH TEMPERATURE SUPERCONDUCTORS

High temperature superconductors with improved current densities
[AD-A282996] p 472 N95-13685

Flux pinning and forced entanglement by splayed columnar defects
[DE94-013994] p 620 N95-14008

Experimental design for the evaluation of high-T(sub c) superconductive thermal bridges in a sensor satellite
[NASA-CR-197003] p 429 N95-14106

Mechanical properties of high-temperature superconducting wires
[DE94-015089] p 621 N95-14192

Low-frequency noise in high-(Tc) superconductor Josephson junctions, SQUIDs, and magnetometers
[DE94-016873] p 623 N95-15337

Transport resistive broadening by avalanche flux motion in high-temperature superconductors: SOC in a driven system
[DE94-016901] p 623 N95-15341

Surface spectroscopic studies of high-temperature superconductors
[PB94-191228] p 624 N95-15378

HTS Wire Development Workshop: Proceedings
[DE94-015650] p 624 N95-15421

Sandia 1993 Superconducting Technology Program
[DE94-015601] p 625 N95-15438

Dynamical impurity problems
[DE94-013025] p 625 N95-15576

HIGH TEMPERATURE TESTS

Compact simultaneous-beam optical strain measurement system, phase 5
[NASA-CR-195396] p 601 N95-13666

HIGH VACUUM ORBITAL SIMULATOR

ASTM E 1559 method for measuring material outgassing/deposition kinetics has applications to aerospace, electronics, and semiconductor industries p 421 N95-14066

HIGH VOLTAGES

Design of reliable high voltage avalanche transistor pulsers
[DE94-015323] p 473 N95-14261

Development and analysis of high-energy corona process for air purification
[DE94-015207] p 524 N95-15432

Programmable high voltage power supply with regulation confined to the high voltage section
[NASA-CASE-GSC-13289-1] p 478 N95-15681

Mass analysis addition to the Differential Ion Flux Probe (DIFP) study
[NASA-CR-196531] p 429 N95-15824

HILBERT SPACE

Uncertainty relations as Hilbert space geometry p 588 N95-13911

Coherent states on the m-sheeted complex plane as m-photon states p 598 N95-13940

Evolution of wave function in a dissipative system p 610 N95-13959

HISTOGRAMS

The design and development of Histogram-based Morphological Edge Detector (HMED)
[AD-A284458] p 470 N95-15820

HISTORIES

A review of 50 years of aerodynamic research with NACA/NASA
[NASA-TM-109163] p 647 N95-13663

Florida hurricanes and tropical storms 1871-1993: An historical survey
[PB94-198017] p 532 N95-14120

Energy review
[DE94-015828] p 518 N95-14326

HOHLRAUMS

Hohlraum manufacture for inertial confinement fusion
[DE94-014472] p 616 N95-13997

HOLE DISTRIBUTION (MECHANICS)

Fatigue analysis of multiple site damage at a row of holes in a wide panel p 508 N95-14463

HOLES (MECHANICS)

Statistical investigation of fatigue crack initiation and growth around chamfered rivet holes in Alclad 2024 T3 as affected by corrosion p 510 N95-14472

Innovative design of composite structures: Design, manufacturing, and testing of plates utilizing curvilinear fiber trajectories
[NASA-CR-197045] p 435 N95-14865

HOLMIUM
Anomalous temperature dependence of the lattice parameters in HoPO4 and HoVO4: Rare earth quadrupolar effects
[DE94-015086] p 622 N95-14608

HOLOGRAPHIC INTERFEROMETRY
Developments in laser-based diagnostics for wind tunnels in the Aeromechanics Division: 1987-1992
[AD-A283011] p 412 N95-13687

HOLOGRAPHY
Observation of microcrack development in concrete by use of TV-holography and deformation phase gradient calculation
[PB94-207990] p 513 N95-15348

HOMODYNE RECEPTION
A method of measuring the amplitude-modulated vacuum field near a conducting mirror
p 471 N95-13921

HOT CORROSION
High-temperature corrosion of iron aluminides
[DE94-011505] p 447 N95-15906

HOT ISOSTATIC PRESSING
High temperature superconductors with improved current densities
[AD-A282996] p 472 N95-13685

HOT PRESSING
Damping mechanisms in nanostructured materials
[AD-A283583] p 623 N95-15317

HOT STARS
Observations of hot stars and eclipsing binaries with FRESIP p 644 N95-14508

HUBBLE SPACE TELESCOPE
Hubble Space Telescope GTO program
[NASA-CR-196263] p 637 N95-13723
Hubble Space Telescope servicing mission scientific instrument protective enclosure design requirements and contamination controls p 421 N95-14068
Using a temperature-controlled quartz crystal microbalance in a space equipment cleanroom to monitor molecular contamination p 421 N95-14069
Clean assembly and integration techniques for the Hubble Space Telescope High Fidelity Mechanical Simulator p 418 N95-14070
Asteroseismology with FRESIP: A meter class space telescope p 643 N95-14504

HUBS
Dynamics of the McDonnell-Douglas Large Scale Dynamic Rig and dynamic calibration of the rotor balance
[NASA-TM-108855] p 391 N95-13891

HUMAN BEHAVIOR
Low-dose alcohol effects on human behavior and performance: A review of post-1984 research
[DOT/FAA/AM-94/24] p 552 N95-14863
The relationship between space sickness and preflight diet p 546 N95-15122

HUMAN BEINGS
Will man need the vestibular system in generations to come? p 542 N95-15092
Space flight and humoral and cellular immunity of animals p 538 N95-15113
The cardiovascular response to the AGS p 419 N95-15146

HUMAN BODY
Gravitational stress and regulation of neuroendocrine elements and fluid volume in humans p 542 N95-15090
On-Earth evaluation of the neurovestibular tolerance to centrifuge simulated artificial gravity in humans p 546 N95-15120
Robotic control using muscular and neural electrical signals
[AD-A284906] p 551 N95-15757

HUMAN CENTRIFUGES
Operational requirements for avoidance and eventual elimination of Gz-induced Loss Of Consciousness (G-LOC) in flight p 547 N95-15127

HUMAN FACTORS ENGINEERING
Tactual interfaces: The human perceiver p 554 N95-14016
The Ames Virtual Environment Workstation: Implementation issues and requirements p 557 N95-14034
Human factors requirements for telerobotic command and control: The European Space Agency experimental programme p 562 N95-14059
VERDEX: A virtual environment demonstrator for remote driving applications p 562 N95-14060
Use of 64 kbits/s digital channel for image transmission: Using low scan two-way video
[PB94-189099] p 461 N95-14147
Aircraft maneuver envelope warning system
[NASA-CASE-ARC-11953-1] p 411 N95-14518
A graphical user interface for design and analysis of air breathing propulsion systems
[TABES PAPER 94-616] p 411 N95-14645
Proposal for an astronaut mass measurement device for the Space Shuttle
[NASA-CR-197198] p 563 N95-14854
Human factors considerations for remote manipulation p 564 N95-14949
Experimental evaluation of cursors for B-2 Synthetic Aperture Radar (SAR) application
[AD-A283025] p 468 N95-15393

HUMAN PERFORMANCE
Measurement and modification of the EEG and related behavior p 557 N95-14038
EPIC computational models of psychological refractory-period effects in human multiple-task performance
[AD-A280924] p 540 N95-14142
Low-dose alcohol effects on human behavior and performance: A review of post-1984 research
[DOT/FAA/AM-94/24] p 552 N95-14863
The electrocortical correlates of fluctuating states of attention during vigilance tasks
[NASA-CR-197051] p 552 N95-14864
Preliminary analysis of Army aircrew requirements for Joint Surveillance Target Attack Radar System (JSTARS): Human performance requirements and job demands
[AD-A284917] p 563 N95-15759
Target acquisition: Human observer performance studies and TARGAC model validation
[AD-A284436] p 553 N95-15816

HUMAN REACTIONS
Residents' reactions to long-term sonic boom exposure: Preliminary results p 403 N95-14892

HUMAN TOLERANCES
Deriving a dosage-response relationship for community response to high-energy impulsive noise p 403 N95-14890
An in-home study of subjective response to simulated sonic booms p 403 N95-14891
A mathematical model of the cardiovascular response to +Gz acceleration p 544 N95-15110

HUMAN-COMPUTER INTERFACE
Human Machine Interfaces for Teleoperators and Virtual Environments
[NASA-CP-10071] p 554 N95-14013
Watch what you say, your computer might be listening: A review of automated speech recognition p 555 N95-14021
Creating better virtual worlds p 556 N95-14031
Virtual reality at work p 556 N95-14033
The Ames Virtual Environment Workstation: Implementation issues and requirements p 557 N95-14034
Varieties of virtualization p 557 N95-14036
A two dimensional artificial reality p 560 N95-14052
Integration/evaluation of a HCI prototyping environment
[NASA-CR-196996] p 566 N95-14107
Department of Defense technical architecture framework for information management. Volume 8: Department of Defense HCI style guide, version 2.0
[AD-A283768] p 631 N95-14333
A graphical user interface for design and analysis of air breathing propulsion systems
[TABES PAPER 94-616] p 411 N95-14645
Experimental evaluation of cursors for B-2 Synthetic Aperture Radar (SAR) application
[AD-A283025] p 468 N95-15393
Use of the user action notation at the Naval Research Laboratory Human-Computer Interaction Laboratory
[AD-A281680] p 563 N95-15449
Intelligence in scientific computing
[AD-A284410] p 584 N95-15811

HUMIDITY
Study of interferences in ozone UV and chemiluminescence monitors
[PB94-197456] p 521 N95-14123
Remote sensing strategy at the first atmospheric radiation measurement field site
[DE94-015091] p 522 N95-14187
Determination of the similarity theory scaling parameters from the vertical gradients
[AD-A283833] p 533 N95-14340
Effect of stratification and geometrical spreading on sonic boom rise time p 401 N95-14880
Water vapor and temperature inversions near the 0 C level over the tropical western Pacific
[AD-A282023] p 533 N95-14952

HUMIDITY MEASUREMENT
Overview of PAMS meteorological monitoring requirements
[PB94-176658] p 534 N95-15383
High-spatial-resolution passive microwave sounding systems
[NASA-CR-197131] p 531 N95-15586

HURRICANES
Florida hurricanes and tropical storms 1871-1993: An historical survey
[PB94-198017] p 532 N95-14120
ADCIRC: An advanced three-dimensional circulation model for shelves, coasts, and estuaries. Report 4: Hurricane storm surge modeling using large domains
[AD-A283868] p 535 N95-14352

HYBRID COMPOSITES
Deformation, strength, and failure modes of laminated conventional and hybrid polymer-matrix composites loaded in the thickness direction
[AD-A281587] p 436 N95-15443

HYBRID COMPUTERS
Hybrid verification by exploiting the environment
[NASA-CR-195810] p 568 N95-13699

HYBRID PROPELLANTS
Recycled plastic: A clean and low cost rocket fuel
[TABES PAPER 94-610] p 416 N95-14642

HYBRID PROPULSION
TABES 1994: 10th Annual Technical and Business Exhibition and Symposium p 414 N95-14633

HYDRAULIC EQUIPMENT
Simulation of a spatial, servo-hydraulic test facility for space structures p 418 N95-14095
The industrial use of CFD in the design of turbomachinery p 480 N95-14133

HYDROCARBON COMBUSTION
Theoretical studies of hydrocarbon combustion chemistry
[DE94-017155] p 441 N95-15347

HYDROCARBON FUELS
Addendum: Tenth International Symposium on Alcohol Fuels, The Road to Commercialization
[DE93-018219] p 457 N95-14003

HYDROCARBONS
Conversion of light hydrocarbon gases in metal carbides for production of liquid fuels and chemicals
[DE94-013933] p 439 N95-14435
Correlation between molecular lines and diffuse interstellar bands p 640 N95-15835
The C4H radical and the diffuse interstellar bands. An ab initio study p 641 N95-15843

HYDROCHLORIC ACID
Department of Defense technical architecture framework for information management. Volume 8: Department of Defense HCI style guide, version 2.0
[AD-A283768] p 631 N95-14333
High-temperature corrosion of iron aluminides
[DE94-011505] p 447 N95-15906

HYDRODYNAMICS
ADCIRC: An advanced three-dimensional circulation model for shelves, coasts, and estuaries. Report 4: Hurricane storm surge modeling using large domains
[AD-A283868] p 535 N95-14352
Microscale hydrodynamics near moving contact lines p 484 N95-14536
Nucleation and chiral symmetry breaking under controlled hydrodynamic flows p 489 N95-14570
Point based hydrodynamics applied to shallow water equations
[DE94-016629] p 523 N95-15364
Comparison of different statistical models of turbulence by similarity methods
[DE94-015326] p 493 N95-15530

HYDROGEN
Effects of hydrogen annealing, sulfur segregation and diffusion on the cyclic oxidation resistance of superalloys: A review
[NASA-TM-106734] p 444 N95-13667
Calibration and characterization of wide range hydrogen sensors
[DE94-013765] p 496 N95-14146
ASSERT-1992. Fundamental studies of a high energy molecular system: Spectroscopy of boron in hydrogen clusters
[AD-A283181] p 593 N95-14155
Numerical simulation of shock-induced combustion past blunt bodies using shock-fitting technique
[NASA-CR-197013] p 437 N95-14268
Boron atom matrix chemistry
[AD-A282840] p 434 N95-14366
Experiments to examine the contribution of gas atoms to void formation in irradiated metals
[DE94-015209] p 446 N95-15433
Solid target boronization of the MST reversed-field pinch during pulsed discharge cleaning
[DE94-015535] p 442 N95-15541
Type 304L stainless steel surface microstructure: Performance in hydride storage and acid cleaning
[DE94-014654] p 447 N95-15625

HYDROGEN FUELS
Uniform hydrogen fuel layers for inertial fusion targets by microgravity p 459 N95-14547

HYDROGEN IONS
Hydrogen transport and trapping in graphite
[UTIAS-347] p 437 N95-13652
L(alpha)-induced two-photon absorption of visible light emitted from an O-type star by H2(+) ions located near the surface of the Stromgren sphere surrounding the star: A possible explanation for the diffuse interstellar absorption bands (DIDs) p 641 N95-15845
HYDROGEN ISOTOPES
Extension of the BRYNTRN code to monoenergetic light ion beams
[NASA-TP-3472] p 647 N95-15790
HYDROGEN PEROXIDE
Study on titanium-silicalite-1 and related systems
[PB94-195500] p 445 N95-14845
HYDROGEN PLASMA
Solid target boronization of the MST reversed-field pinch during pulsed discharge cleaning
[DE94-015535] p 442 N95-15541
HYDROGEN SULFIDE
High temperature membranes for H2S and SO2 separations
[DE94-017125] p 441 N95-15345
High-temperature corrosion of iron aluminides
[DE94-011505] p 447 N95-15906
HYDROGENATION
Growth mechanisms and characterization of hydrogenated amorphous-silicon-alloy films
[DE94-011842] p 518 N95-14194
Small-angle x-ray scattering studies of microvoids in amorphous-silicon-based semiconductors
[DE94-011840] p 520 N95-15406
HYDROGEOLOGY
Energy flux and hydrogeology of thermal anomalies in the Gulf of Mexico Basin: South Texas example
[DE94-015122] p 530 N95-14956
HYDROGRAPHY
Optical variability in the equatorial and southeast Pacific
[AD-A283894] p 536 N95-15425
An analysis of eddy resolving global ocean models in the Southern Ocean
[AD-A283211] p 536 N95-15626
HYDROPONICS
Design of components for the NASA OCEAN project
[NASA-CR-197207] p 535 N95-14906
HYDROSTATIC PRESSURE
Hybrid bearings for turbopumps and the like
[NASA-CASE-MFS-28491-1] p 500 N95-13819
Modeling and numerical simulation of the cerebral blood flow under acceleration p 545 N95-15112
Manipulating the arterial pressure to prevent G-LOC p 546 N95-15123
HYPERBOLAS
Carnot-caratheodory spaces seen from within
[PB94-195617] p 586 N95-15412
HYPERSONIC AIRCRAFT
Numerical modeling of a cryogenic fluid within a fuel tank
[NASA-TM-4651] p 479 N95-13892
HYPERSONIC COMBUSTION
Numerical simulation of shock-induced combustion past blunt bodies using shock-fitting technique
[NASA-CR-197013] p 437 N95-14268
HYPERSONIC FLIGHT
Hypersonic engine leading edge experiments in a high heat flux, supersonic flow environment
[NASA-TM-106742] p 482 N95-14299
Air-breathing aerospace plane development essential: Hypersonic propulsion flight tests
[NASA-TM-108857] p 392 N95-14921
HYPERSONIC FLOW
Thermoacoustic environments to simulate reentry conditions p 426 N95-14096
Laminar and turbulent flow computations of Type 4 shock-shock interference aerothermal loads using unstructured grids
[NASA-CR-195008] p 493 N95-15604
HYPERSONIC HEAT TRANSFER
Hypersonic engine leading edge experiments in a high heat flux, supersonic flow environment
[NASA-TM-106742] p 482 N95-14299
HYPERSONIC INLETS
Computational analysis in support of the SSTO flowpath test
[NASA-TM-106757] p 479 N95-13665
Wind-tunnel blockage and actuation systems test of a two-dimensional scramjet inlet unstart model at Mach 6
[NASA-TM-109152] p 495 N95-15898
Two-dimensional scramjet inlet unstart model: Wind-tunnel blockage and actuation systems test
[NASA-TM-109984] p 495 N95-15899
HYPERSONIC SPEED
Low-speed wind tunnel testing of the NPS and NASA Ames Mach 6 optimized waverider
[AD-A283585] p 404 N95-15319
HYPERSONIC WIND TUNNELS
Wind-tunnel blockage and actuation systems test of a two-dimensional scramjet inlet unstart model at Mach 6
[NASA-TM-109152] p 495 N95-15898
Two-dimensional scramjet inlet unstart model: Wind-tunnel blockage and actuation systems test
[NASA-TM-109984] p 495 N95-15899
HYPERSONICS
An approximate Riemann solver for thermal and chemical nonequilibrium flows
[NASA-CR-195003] p 492 N95-14912
HYPERVELOCITY FLOW
Interaction of chemistry, turbulence, and shock waves in hypervelocity flow
[AD-A282941] p 400 N95-14656
HYPERVELOCITY IMPACT
Cratering and penetration experiments in teflon targets at velocities from 1 to 7 km/s
[NASA-TM-104797] p 432 N95-13646
Dynamical properties measurements for asteroid, comet and meteorite material applicable to impact modeling and mitigation calculations
[DE94-014142] p 642 N95-14311
TABES 1994: 10th Annual Technical and Business Exhibition and Symposium p 414 N95-14633
Hypervelocity Impact Test Facility: A gun for hire
[TABES PAPER 94-605] p 415 N95-14639
Analysis of space environment damage to solar cell assemblies from LDEF experiment A0171-GSFC test plate
[NASA-CR-197066] p 519 N95-14853
Gouge initiation in high-velocity rocket sled testing
[DE94-014288] p 418 N95-15357
HYPERVOLEMIA
Body position and volume status as determinants of cardiovascular responses to transition into microgravity in parabolic flight p 544 N95-15108
HYPOKINESIA
Twenty four hours head-down tilt decreases arterial baroreflex function in conscious rat p 538 N95-15098
HYPOTHESES
Tests of a homogeneous Poisson process against clustering and other alternatives
[DE94-015382] p 588 N95-15533
HYPOVOLEMIA
Comparison of hemodynamic and volume responses to different levels of lower body suction and head-up tilt p 544 N95-15107
HYPOXIA
Modeling and numerical simulation of the cerebral blood flow under acceleration p 545 N95-15112
HYSTERESIS
Interacting fronts in a model for binary-mixture convection
[DE94-013595] p 494 N95-15861

I

ICE
Wind-electric ice making for villages in the developing world
[DE94-011854] p 518 N95-14191
Dependence of segregation potential on the thermal and hydraulic conditions predicted by model M1
[AD-A280969] p 530 N95-14862
Traveling wave solutions to the problem of quasi-steady freezing of soils
[AD-A280971] p 531 N95-15428
ICE PREVENTION
Icing: Accretion, detection, protection p 406 N95-14897
Development of anti-icing technology
[PB94-195369] p 407 N95-15439
IDENTIFYING
Time-dependent distinguishability: Choosing to be a wave or a particle p 600 N95-13912
Toward deriving software architectures from quality attributes
[AD-A283827] p 572 N95-14339
Analysis of phase distribution phenomena in microgravity environments p 459 N95-14557
IGNITION
A High Temperature Hermetic Primer and a Variable Spring Tester
[DE94-012073] p 457 N95-14004
Fire growth models for materials
[PB94-195856] p 443 N95-15610
IGNITION TEMPERATURE
Fire growth models for materials
[PB94-195856] p 443 N95-15610
ILLUMINANCE
Global surface-based cloud observation for ISCCP
[NASA-CR-196990] p 532 N95-14265
ILLUMINATING
Computing illumination using extended sources: Object space and image space
[PB94-201282] p 612 N95-13992
ILMENITE
Experimental study of chemical, phase and textural equilibrium of high TiO2 mare basalts and peridotite
[NASA-CR-196480] p 645 N95-13724
IMAGE ANALYSIS
Satellite imagery and topographic data in verification
[AD-A280950] p 530 N95-14593
Variable window Gabor filters and their use in focus and correspondence
[AD-A282837] p 573 N95-14842
Space debris detection and analysis
[AD-A282012] p 428 N95-14951
Sequentially t-diagnosable systems
[PB94-205093] p 574 N95-15396
The design and development of Histogram-based Morphological Edge Detector (HMED)
[AD-A284458] p 470 N95-15820
Seeing behind occlusions
[TR-487] p 576 N95-15857
IMAGE CLASSIFICATION
Forest cover from Landsat Thematic Mapper data for use in the Catahoula Ranger District Geographic Information System
[PB94-203056] p 515 N95-14125
Development of a systemic land cover/land use database for the Upper Mississippi River System derived from Landsat Thematic Mapper satellite data. Long term resource monitoring program
[PB94-186889] p 515 N95-14793
IMAGE CONTRAST
The applicability of commercial glare test devices in the aeromedical certification of pilot applicants
[DOT/FAA/AM-94/15] p 540 N95-14176
IMAGE CONVERTERS
Hypervelocity Impact Test Facility: A gun for hire
[TABES PAPER 94-605] p 415 N95-14639
IMAGE ENHANCEMENT
Performance of customized DCT quantization tables on scientific data p 564 N95-14586
IMAGE PROCESSING
A vision based attitude and position estimation algorithm for rendezvous and docking p 414 N95-13831
PHOENIX user manual. First version
[PB94-189081] p 568 N95-13989
Analysis of electron microscope images: 3-D localization of immuno-markers
[PB94-197977] p 537 N95-13990
Parallel image rendering algorithm and architecture based on ray tracing and radiosity shading
[PB94-191277] p 569 N95-14153
Hardware implementation of a desktop supercomputer for high performance image processing. Color image processing using cellular neural networks
[AD-A283071] p 571 N95-14178
A high performance graphics algorithm
[DE94-015033] p 571 N95-14196
1994 Science Information Management and Data Compression Workshop
[NASA-CP-3277] p 564 N95-14585
Performance of customized DCT quantization tables on scientific data p 564 N95-14586
Comparison of transform coding methods with an optimal predictor for the data compression of digital elevation models p 564 N95-14587
Blocking reduction of Landsat Thematic Mapper JPEG browse images using optimal PSNR estimated spectra adaptive postfiltering p 565 N95-14589
Synthetic aperture radar signal data compression using block adaptive quantization p 565 N95-14590
Compression of regions in the global advanced very high resolution radiometer 1-km data set p 565 N95-14591
Lossless compression of NOAA-AVHRR satellite data p 565 N95-14592
The development of lossless data compression technology for remote sensing applications p 565 N95-14593
Landsat Pathfinder tropical forest information management system p 565 N95-14594
Planning/scheduling techniques for VQ-based image compression p 566 N95-14595
An overview of the EOSDIS V0 information management system: Lessons learned from the implementation of a distributed data system p 566 N95-14596
Neural networks: Alternatives to conventional techniques for automatic docking
[TABES PAPER 94-627] p 417 N95-14651
Variable window Gabor filters and their use in focus and correspondence
[AD-A282837] p 573 N95-14842
Vision-based navigation and recognition
[AD-A282962] p 583 N95-15398

Linear estimation of hyperspectral mixed pixel components
[AD-A283893] p 586 N95-15424
Automatic TLI recognition system, part 1
[DE94-015253] p 578 N95-15434
Automatic TLI recognition system, part 2
[DE94-015393] p 579 N95-15534
New algorithms for the reduction of image degradation due to atmospheric turbulence
[AD-A284891] p 615 N95-15772
Seeing behind occlusions
[TR-487] p 576 N95-15857

IMAGE RECONSTRUCTION
New algorithms for the reduction of image degradation due to atmospheric turbulence
[AD-A284891] p 615 N95-15772

IMAGE RESOLUTION
Resolution measurement for scanning electron microscopes
[DE94-012747] p 601 N95-13674
Variable window Gabor filters and their use in focus and correspondence
[AD-A282837] p 573 N95-14842

IMAGING RADAR
Experimental evaluation of cursors for B-2 Synthetic Aperture Radar (SAR) application
[AD-A283025] p 468 N95-15393

IMAGING SPECTROMETERS
Ultraviolet-Infrared Mapping Interferometic Spectrometer
[NASA-CR-197099] p 613 N95-14806

IMAGING TECHNIQUES
Specifying the surface finish of x ray mirrors
[DE94-013537] p 601 N95-13644
Static image theory for a sphere with impedance surface
[PB94-189073] p 590 N95-13988
Produce documents and media information
[NASA-CR-196521] p 532 N95-14271
Technical guidance for the development of a solid state image sensor for human low vision image warping
[NASA-CR-196997] p 612 N95-14272
Interferometric synthetic aperture radar terrain elevation mapping from multiple observations
[DE94-014185] p 515 N95-14313
A multiscale random field model for Bayesian image segmentation
[AD-A283875] p 515 N95-14358
Wide field strip-imaging optical system
[NASA-CASE-NPO-18146-2-CU] p 613 N95-14413
Radiometric resolution enhancement by lossy compression as compared to truncation followed by lossless compression p 564 N95-14588
Transesophageal echocardiographic evaluation of baboons during microgravity induced by parabolic flight p 538 N95-15094
Prototype explosives-detection system based on nuclear-resonance absorption in nitrogen
[DE94-015069] p 442 N95-15387
Distance estimation training with night vision goggles: A preliminary study
[AD-A284900] p 563 N95-15755
Apparatus for imaging an object in or through a scattering medium using coherent anti-Stokes Raman scattering
[AD-D016366] p 615 N95-15765

IMMUNE SYSTEMS
Cosmos 2229 immunology study (Experiment K-8-07)
[NASA-CR-196984] p 537 N95-13638

IMMUNOLOGY
Cosmos 2229 immunology study (Experiment K-8-07)
[NASA-CR-196984] p 537 N95-13638
The Physiologist, volume 36, number 1, supplement p 541 N95-15089
Space flight and humoral and cellular immunity of animals p 538 N95-15113
Immune changes in humans concomitant with space flights of up to 10 days duration p 545 N95-15114

IMP
Interplanetary medium data book, supplement 5, 1988-1993
[NASA-TM-109957] p 642 N95-13658

IMPACT DAMAGE
Development of chemical-vapor-deposited diamond for infrared optical applications: Summary of properties
[AD-A282999] p 448 N95-13686
Impact fracture behavior of HT9 duct
[DE94-016328] p 445 N95-14379
Residual strength of composites with multiple impact damage
[AD-A284230] p 434 N95-14409
Analysis of space environment damage to solar cell assemblies from LDEF experiment A0171-GSFC test plate
[NASA-CR-197066] p 519 N95-14853
Environmental durability issues for solar power systems in low Earth orbit
[NASA-TM-106775] p 431 N95-15769

IMPACT FUSION
A comparison of driver concepts for heavy-ion fusion
[DE94-016451] p 600 N95-15780

IMPACT MELTS
Gouge initiation in high-velocity rocket sled testing
[DE94-014288] p 418 N95-15357

IMPACT TESTS
Dynamical properties measurements for asteroid, comet and meteorite material applicable to impact modeling and mitigation calculations
[DE94-014142] p 642 N95-14311
Impact fracture behavior of HT9 duct
[DE94-016328] p 445 N95-14379
Hypervelocity Impact Test Facility: A gun for hire
[TABES PAPER 94-605] p 415 N95-14639
Milestone 4: Test plan for Reusable Hydrogen Composite Tank System (RHCTS). Task 3: Composite tank materials
[NASA-CR-197036] p 435 N95-14801

IMPACT TOLERANCES
Effect of heat treatment on the microstructure and properties of AerMet (trade name) 100 steel
[AD-A284387] p 447 N95-15807

IMPEDANCE
Xwake 1.0: A new tool for wakefield and impedance calculations
[DE94-015545] p 574 N95-15418

IMPINGEMENT
Turbulent mixing of the HVOF thermal spray and coating oxidation
[DE94-015414] p 455 N95-15535

IMPLANTATION
Hydrogen transport and trapping in graphite
[UTIAS-347] p 437 N95-13652
Introduction to muSR: What, how, where
[PB94-192267] p 596 N95-15379
Defect profiling in elemental and multilayer systems: Correlations of fitted defect concentrations with positron implantation profiles
[DE94-015844] p 624 N95-15422

IMPLOSIONS
Review of drive symmetry measurement and control experiments on the Nova laser system
[DE94-014455] p 498 N95-13994
Comparison of different statistical models of turbulence by similarity methods
[DE94-015326] p 493 N95-15530

IMPULSES
High gain GaAs switches for impulse sources: Measurement of the speed of current filaments
[DE94-015281] p 477 N95-15544

IMPURITIES
Radiation rates for low Z impurities in edge plasmas
[DE94-016073] p 617 N95-14368
Role of point defects and defect complexes in silicon device processing: Book of abstracts
[DE94-011828] p 519 N95-14430
Fourth Workshop on the Role of Point Defects and Defect Complexes in Silicon Device Processing
[DE94-011850] p 624 N95-15426
Time-of-flight detector for heavy ion backscattering spectrometry
[DE94-015600] p 596 N95-15437
Dynamical impurity problems
[DE94-013025] p 625 N95-15576
Electronic characterization of defects in narrow gap semiconductors
[NASA-CR-197217] p 626 N95-15752
Formation of dust grains with impurities in red giant winds p 641 N95-15841

IN SITU MEASUREMENT
Science objectives and performance of a radiometer and window design for atmospheric entry experiments p 429 N95-13718
In situ, real-time analysis of the growth of ferroelectric and conductive oxide heterostructures by a new time-of-flight pulsed ion beam surface analysis technique
[DE94-013298] p 620 N95-13822
Quartz resonator state-of-charge monitor for lead-acid batteries
[DE94-013823] p 473 N95-14310

IN-FLIGHT MONITORING
Design and development of an F/A-18 inlet distortion rake: A cost and time saving solution p 395 N95-14241
Airplane takeoff and landing performance monitoring system
[NASA-CASE-LAR-14745-2-SB] p 412 N95-14415
Collection of real-time, multichannel EEG data from helicopter pilots in flight: A feasibility study
[AD-A284396] p 551 N95-15767
Test Operation Procedure (TOP): Vibration testing of helicopter equipment
[AD-A284433] p 410 N95-15815

INCENTIVES
Design in Huntsville, manufacture in Estonia, sell in Europe
[TABES PAPER 94-607] p 415 N95-14640
Reengineering through information technology. Accompanying report of the National Performance Review
[PB94-170362] p 633 N95-15781

INCOHERENT SCATTER RADAR
Study of auroral dynamics with combined spacecraft and incoherent scatter radar data
[NASA-CR-196974] p 526 N95-13818

INCOMPRESSIBLE FLOW
Flow-radiated noise. Study of the propagative spectral range of the wall pressure field
[PB94-201290] p 590 N95-13985
Robust multigrid methods for the steady and unsteady incompressible Navier-Stokes equations in general coordinates
[PB94-195534] p 492 N95-15315
Two methods for the study of vortex patch evolution on locally refined grids
[DE94-014965] p 494 N95-15867
On the evolution of centrifugal instabilities within curved incompressible mixing layers
[NASA-CR-194991] p 495 N95-15917

INDEXES
Aerospace medicine and biology: A continuing bibliography with indexes (supplement 395)
[NASA-SP-7011(395)] p 550 N95-15304

INDEXES (DOCUMENTATION)
Aeronautical engineering: A continuing bibliography with indexes (supplement 310)
[NASA-SP-7037(310)] p 392 N95-15550

INDIAN SPACECRAFT
Journal of Spacecraft Technology, volume 4, no. 2, July 1994 p 413 N95-13825
Remote programming in INSAT-2A/2B on-board Attitude and Orbit Control Computer (AOCC) p 413 N95-13827
Star sensor for Indian Remote Sensing Satellite (IRS 1C) p 413 N95-13828
Computer aided techniques for the realisation of the diaphragm of the PSM for the IRS-1C p 413 N95-13829
Modelling the low Earth space debris environment p 414 N95-13830
Deployment mechanism calibration system p 414 N95-13833

INDICATING INSTRUMENTS
Study of interferences in ozone UV and chemiluminescence monitors
[PB94-197456] p 521 N95-14123

INDIUM
Activity of Ga, In and Cu modified MFI zeolites for amine reactions
[DE94-016532] p 438 N95-14388

INDIUM ANTIMONIDES
Microstructures of InAs(1-x)Sb(x) (x = 0.07-0.14) alloys and strained-layer superlattices
[DE94-015801] p 621 N95-14323

INDIUM ARSENIDES
Microstructures of InAs(1-x)Sb(x) (x = 0.07-0.14) alloys and strained-layer superlattices
[DE94-015801] p 621 N95-14323
Magnetic field dependent photoluminescence studies of InGaAs/GaAs strained-single-quantum wells
[DE94-015774] p 621 N95-14342

INDIUM COMPOUNDS
Alternative fabrication techniques for high-efficiency CuInSe2 and CuInSe2-alloy films and cells
[DE94-011846] p 521 N95-15407
Low loss glass and optical fibers therefrom
[AD-D016379] p 615 N95-15766

INDIUM GALLIUM ARSENIDES
Strained-layer InGaAs(P)/InP quantum well semiconductor lasers grown by organometallic vapour phase epitaxy
[PB94-201399] p 622 N95-14795

INDIUM PHOSPHIDES
Polarized photomodulated reflectivity and photoluminescence studies of ordered InGaP2 under pressure
[DE94-016556] p 621 N95-14390
Strained-layer InGaAs(P)/InP quantum well semiconductor lasers grown by organometallic vapour phase epitaxy
[PB94-201399] p 622 N95-14795

INDUCTION HEATING
Induction heating coupler
[NASA-CASE-LAR-14278-1] p 473 N95-14294

INDUCTION MOTORS
Experimental implementation of a robust damped-oscillation control algorithm on a full-sized, two-degree-of-freedom, AC induction motor-driven crane
[DE94-012113] p 501 N95-14005
INDUCTORS
Solid target boronization of the MST reversed-field pinch during pulsed discharge cleaning
[DE94-015535] p 442 N95-15541
INDUSTRIAL MANAGEMENT
Helping small companies commercialize public-sector technology
[TABES PAPER 94-407] p 415 N95-14635
INDUSTRIAL PLANTS
Comprehensive facility decommissioning through the use of innovative technology to reduce cost, schedule, and environmental liability
[TABES PAPER 94-615] p 416 N95-14644
Test method for the measurement of methanol emissions from stationary sources
[PB94-170297] p 523 N95-15382
Research in high energy physics
[DE94-015519] p 600 N95-15539
INDUSTRIAL SAFETY
Monitoring audiometry in hearing conservation programs
[AD-A282024] p 540 N95-14145
INDUSTRIES
Technology access from the FS-X radar program. Lessons for technology transfer and US acquisition policy
[AD-A283773] p 461 N95-14334
Minutes of the Third Annual Workshop on Chromate Replacements in Light Metal Finishing
[DE94-015163] p 446 N95-15368
INELASTIC SCATTERING
Intermultiplet transitions in optically opaque EuBa2Cu3O7: An inelastic neutron scattering study
[DE94-013429] p 620 N95-14188
Performance of spherically focusing Ge(444) backscattering analyzers for inelastic x-ray scattering
[DE94-016349] p 621 N95-14382
Theoretical studies in elementary particle physics
[DE94-015343] p 595 N95-15372
INEQUALITIES
The strong Bell inequalities: A proposed experimental test p 611 N95-13966
A loophole-free Bell's inequality experiment p 611 N95-13968
The probabilistic origin of Bell's inequality p 612 N95-13969
Einstein-Podolsky-Rosen-Bohm experiment and Bell inequality violation using Type 2 parametric down conversion p 612 N95-13970
INERTIA
The behavior of unsteady thermocapillary flows p 483 N95-14530
INERTIAL CONFINEMENT FUSION
Hohlraum manufacture for inertial confinement fusion
[DE94-014472] p 616 N95-13997
Uniform hydrogen fuel layers for inertial fusion targets by microgravity p 459 N95-14547
INERTIAL FUSION (REACTOR)
A comparison of driver concepts for heavy-ion fusion
[DE94-016451] p 600 N95-15780
INFECTIOUS DISEASES
Immune changes in humans concomitant with space flights of up to 10 days duration p 545 N95-15114
INFORMATION
NASA/DOD Aerospace Knowledge Diffusion Research Project. Paper 43: The role of information resource training in aerospace education. Expanded version
[NASA-TM-109981] p 632 N95-14619
INFORMATION DISSEMINATION
International energy: Research organizations, 1988-1992
[DE90-017267] p 630 N95-13726
Preparing technical text for translation: A comparison between International English and methods for simplifying language
[DE94-014465] p 630 N95-13996
NASA/DOD Aerospace Knowledge Diffusion Research Project. Paper 43: The role of information resource training in aerospace education. Expanded version
[NASA-TM-109981] p 632 N95-14619
Variable window Gabor filters and their use in focus and correspondence
[AD-A282837] p 573 N95-14842
NASA/DOD Aerospace Knowledge Diffusion Research Project. Paper 44: Becoming an aerospace engineer: Some thoughts on the career goals and educational preparation of AIAA student members
[NASA-TM-109980] p 632 N95-14870
NASA/DOD Aerospace Knowledge Diffusion Research Project. Report 30: Computer-Mediated Communication (CMC) and the communication of technical information in aerospace
[NASA-CR-194973] p 633 N95-15585
INFORMATION FLOW
Methodology for the parallel direct solution of finite element systems
[PB94-198009] p 585 N95-13991
Bubble dynamics, two-phase flow, and boiling heat transfer in a microgravity environment p 488 N95-14561
Data flow manager for DART
[DE94-013236] p 579 N95-15581
INFORMATION MANAGEMENT
Case study: Accelerated schedule for MULTI LIMS installation
[DE94-012398] p 630 N95-13673
EMAP Information Management Strategic Plan, 1993-1997
[PB94-176823] p 522 N95-14124
Department of Defense technical architecture framework for information management. Volume 1: Overview, version 2.0
[AD-A283763] p 631 N95-14327
Department of Defense technical architecture framework for information management. Volume 2: Technical reference model and standards profile summary
[AD-A283764] p 631 N95-14329
Department of Defense technical architecture framework for information management. Volume 3: Architecture concepts and design guidance, version 2.0
[AD-A283765] p 631 N95-14330
Department of Defense technical architecture framework for information management. Volume 4: DOD standards-based architecture planning guide, version 2.0
[AD-A283766] p 631 N95-14331
Department of Defense technical architecture framework for information management. Volume 6: Department of Defense (DOD) goal security architecture, version 2.0
[AD-A283767] p 631 N95-14332
Department of Defense technical architecture framework for information management. Volume 8: Department of Defense HCI style guide, version 2.0
[AD-A283768] p 631 N95-14333
Landsat Pathfinder tropical forest information management system p 565 N95-14594
An overview of the EOSDIS V0 information management system: Lessons learned from the implementation of a distributed data system p 566 N95-14596
Dynamic modelling to assess the value of Electronic Data Interchange: A study in the Rotterdam port community
[PB94-195542] p 632 N95-14837
Performance information management system (PIMS) communication
[AD-A284851] p 574 N95-15335
INFORMATION PROCESSING (BIOLOGY)
Neural mechanisms of kinesthesia p 555 N95-14018
Intersensory coordination p 555 N95-14020
EPIC computational models of psychological refractory-period effects in human multiple-task performance
[AD-A280924] p 540 N95-14142
Augmentation of research on cognitive control
[AD-A280956] p 552 N95-14600
Visual motion perception and visual information processing
[AD-A282928] p 581 N95-14847
INFORMATION RETRIEVAL
DDI, the Data and Dimensions Interface
[DE94-014750] p 522 N95-14317
Introduction to HEFeS (Hierarchical Environmental Feature Simulator)
[AD-A283244] p 534 N95-15402
INFORMATION SYSTEMS
EMAP Information Management Strategic Plan, 1993-1997
[PB94-176823] p 522 N95-14124
The applicability of commercial glare test devices in the aeromedical certification of pilot applicants
[DOT/FAA/AM-94/15] p 540 N95-14176
1994 Science Information Management and Data Compression Workshop
[NASA-CP-3277] p 564 N95-14585
Planning/scheduling techniques for VQ-based image compression p 566 N95-14595
An overview of the EOSDIS V0 information management system: Lessons learned from the implementation of a distributed data system p 566 N95-14596
Dynamic modelling to assess the value of Electronic Data Interchange: A study in the Rotterdam port community
[PB94-195542] p 632 N95-14837
Use of the user action notation at the Naval Research Laboratory Human-Computer Interaction Laboratory
[AD-A281680] p 563 N95-15449
NASA/DOD Aerospace Knowledge Diffusion Research Project. Report 30: Computer-Mediated Communication (CMC) and the communication of technical information in aerospace
[NASA-CR-194973] p 633 N95-15585
ROOM: A recursive object oriented method for information systems development
[DE94-007575] p 633 N95-15761
Reengineering through information technology. Accompanying report of the National Performance Review
[PB94-170362] p 633 N95-15781
Design document for the MOODS Data Management System (MDMS), version 1.0
[NASA-CR-197016] p 633 N95-15801
INFORMATION TRANSFER
On the role of exchange of power and information signals in control and stability of the human-robot interaction p 560 N95-14051
Produce documents and media information
[NASA-CR-196521] p 532 N95-14271
Performance of customized DCT quantization tables on scientific data p 564 N95-14586
Landsat Pathfinder tropical forest information management system p 565 N95-14594
An overview of the EOSDIS V0 information management system: Lessons learned from the implementation of a distributed data system p 566 N95-14596
Helping small companies commercialize public-sector technology
[TABES PAPER 94-407] p 415 N95-14635
The Global Emergency Observation and Warning System
[TABES PAPER 94-622] p 417 N95-14649
NASA/DOD Aerospace Knowledge Diffusion Research Project. Report 30: Computer-Mediated Communication (CMC) and the communication of technical information in aerospace
[NASA-CR-194973] p 633 N95-15585
Discourse interpretation and the scope of operators
[TR-518] p 586 N95-15595
On accessing and hiding information p 587 N95-15641
INFRARED ABSORPTION
Infrared absorption spectroscopy and chemical kinetics of free radicals
[DE94-016642] p 438 N95-14392
INFRARED ASTRONOMY
A search for the 13175 A infrared diffuse band in dense environments p 639 N95-15831
The peculiar behaviour of the 5780 and 5797 DIBs in HD25137 p 639 N95-15833
Diffuse bands versus extinction parameters p 640 N95-15836
INFRARED DETECTORS
The AEDC aerospace chamber 7V: An advanced test capability for infrared surveillance and seeker sensors p 418 N95-14097
Experimental design for the evaluation of high-T(sub c) superconductive thermal bridges in a sensor satellite
[NASA-CR-197003] p 429 N95-14106
Semiconductor measurement technology: Improved characterization and evaluation measurments for HgCdTe detector materials, processes, and devices used on the GOES and TIROS satellites
[PB94-188810] p 474 N95-14401
Ultrasensitive infrared chemiluminescence detection
[AD-A283531] p 440 N95-14958
INFRARED IMAGERY
The study of dopant segregation behavior during the growth of GaAs in microgravity p 458 N95-14215
Target acquisition: Human observer performance studies and TARGAC model validation
[AD-A284436] p 553 N95-15816
The design and development of Histogram-based Morphological Edge Detector (HMED)
[AD-A284458] p 470 N95-15820
INFRARED INSTRUMENTS
Aero-optics system integration
[TABES PAPER 94-604] p 415 N95-14636
INFRARED LASERS
Faraday rotation system
[DE94-015345] p 618 N95-15374
INFRARED RADIATION
A femtosecond optical parametric oscillator near 3 microns
[DE94-014500] p 612 N95-13986
Thermal balance testing of MSAT 2 spacecraft p 424 N95-14080

Orbital processing of high-quality CdTe compound semiconductors p 458 N95-14213
Missile infrared radiation analysis p 399 N95-14449
Ultrasensitive infrared chemiluminescence detection [AD-A283531] p 440 N95-14958
Technical report series on global modeling and data assimilation. Volume 3: An efficient thermal infrared radiation parameterization for use in general circulation models [NASA-TM-104606-VOL-3] p 531 N95-15745
A search for the 13175 A infrared diffuse band in dense environments p 639 N95-15831
The peculiar behaviour of the 5780 and 5797 DIBs in HD25137 p 639 N95-15833
Investigating the 3.3 micron infrared fluorescence from naphthalene following ultraviolet excitation p 599 N95-15839

INFRARED SIGNATURES
Missile infrared radiation analysis p 399 N95-14449

INFRARED SPECTRA
Prediction of particulate contamination on aperture window p 420 N95-14064
Self contamination effects in the TAUVEX UV Telescope: Ground testing and computer simulation p 421 N95-14067
Boron atom matrix chemistry [AD-A282840] p 434 N95-14366
A search for the 13175 A infrared diffuse band in dense environments p 639 N95-15831
Investigating the 3.3 micron infrared fluorescence from naphthalene following ultraviolet excitation p 599 N95-15839

INFRARED SPECTROMETERS
Ultraviolet-Infrared Mapping Interferometic Spectrometer [NASA-CR-197099] p 613 N95-14806

INFRARED SPECTROSCOPY
Non-invasive physiological monitoring relevant to G-induced loss of consciousness p 547 N95-15125

INHOMOGENEITY
Modes in light wave propagating in semiconductor laser p 500 N95-13925

INJECTION
Combustion efficiency in a dual-inlet side-dump ramjet combustor [AD-A283564] p 411 N95-15329

INJECTION LOCKING
Research on characterization of the upper atmosphere using lidar [AD-A283241] p 530 N95-15401

INJECTORS
Investigation of ramp injectors for supersonic mixing enhancement [NASA-CR-4634] p 494 N95-15605

INLET FLOW
Computational analysis in support of the SSTO flowpath test [NASA-TM-108757] p 479 N95-13665
Design and development of an F/A-18 inlet distortion rake: A cost and time saving solution p 395 N95-14241
Wind-tunnel blockage and actuation systems test of a two-dimensional scramjet inlet unstart model at Mach 6 [NASA-TM-109152] p 495 N95-15898
Two-dimensional scramjet inlet unstart model: Wind-tunnel blockage and actuation systems test [NASA-TM-109984] p 495 N95-15899

INPUT/OUTPUT ROUTINES
How to characterize the nonlinear amplifier? p 471 N95-13922
Receiver design, performance analysis, and evaluation for space-borne laser altimeters and space-to-space laser ranging systems [NASA-CR-197050] p 499 N95-14901

INSPECTION
Proceedings of the FAA Inspection Program Area Review [AD-A283849] p 405 N95-14350
Probabilistic inspection strategies for minimizing service failures p 508 N95-14461
A method of calculating the safe fatigue life of compact, highly-stressed components p 509 N95-14464
Computational predictive methods for fracture and fatigue p 509 N95-14466
Fatigue reliability method with in-service inspections p 505 N95-14475
Development of a composite repair and the associated inspection intervals for the F-111C stiffener runout region p 392 N95-14477
Full-scale testing and analysis of fuselage structure p 512 N95-14485

INSTALLING
System administrator's guide to CDPS [DE94-015288] p 633 N95-15528

INSTRUCTORS
Space based astronomy: Teacher's guide with activities [NASA-EG-102] p 638 N95-14511

INSTRUMENT COMPENSATION
Earth Observing System (EOS) Advanced Microwave Sounding Unit-A (AMSU-A): Instrumentation interface control document [NASA-CR-189377] p 567 N95-13651

INSTRUMENT ERRORS
Specifying the surface finish of x ray mirrors [DE94-013537] p 601 N95-13644
Partial pressure analysis in space testing p 424 N95-14084
Study of interferences in ozone UV and chemiluminescence monitors [PB94-197456] p 521 N95-14123
Global and regional kinematics with GPS p 527 N95-14279
Earth Observing System (EOS)/Advanced Microwave Sounding Unit-A (AMSU-A) worst-case analysis: Antenna beam pointing [NASA-CR-197218] p 517 N95-15851

INSTRUMENT ORIENTATION
Star sensor for Indian Remote Sensing Satellite (IRS 1C) p 413 N95-13828

INSULATION
Evaluation of reformulated thermal control coatings in a simulated space environment. Part 1: YB-71 p 420 N95-14063
Milestone 5 test report. Task 5, subtask 5.2: Tile to foam strength tests [NASA-CR-197241] p 514 N95-15913

INSULIN
20 days bed-rest on insulin action in relation to body fat in young subjects p 549 N95-15145
Enhancement of insulin receptor mediated endocytosis in cultured osteoblastic cells under hypergravity p 539 N95-15148

INTEGRALS
The Stokes line width and uncertainty relations p 589 N95-13935

INTEGRATED CIRCUITS
Wavelength-division multiplexed optical integrated circuit with vertical diffraction grating [NASA-CASE-NPO-18357-1-CU] p 612 N95-14181
Ion beam synthesis of SiGe alloy layers [DE94-014958] p 620 N95-14189
I(sub DDQ) testing for ultimate low power design verification and defect detection [DE94-014281] p 473 N95-14314
Cut-off-mesa isolated rib optical waveguide for 3-5 heterostructure PICs [DE94-014661] p 474 N95-14315
A gate level simulator for alpha-particle-induced transient faults [AD-A283871] p 474 N95-14355
In situ grown quantum-wire lasers [AD-A281381] p 499 N95-14364
Computer Aided Engineering (CAE) overview [AD-A280966] p 572 N95-14616
Integrated photonics research, 1993 [AD-A281578] p 614 N95-15464
New five-standard calibration procedures for network analyzers and wafer probes [PB94-197662] p 478 N95-15611
High speed QPPM direct detection optical communication receivers for FSDD intersatellite links [NASA-CR-189331] p 615 N95-15849

INTEGRATED ENERGY SYSTEMS
The integration of renewable energy sources into electric power distribution systems. Volume 1: National assessment [DE94-015935] p 519 N95-14393

INTEGRATED OPTICS
Wavelength-division multiplexed optical integrated circuit with vertical diffraction grating [NASA-CASE-NPO-18357-1-CU] p 612 N95-14181
In situ grown quantum-wire lasers [AD-A281381] p 499 N95-14364

INTEGRATORS
Nonlinear asymptotic integration algorithms for one-dimensional autonomous dissipative first-order ODEs [NASA-TM-106780] p 585 N95-14300

INTELLIGENCE
The effect of response format on reliability estimates for tacit knowledge scales [AD-A283547] p 552 N95-15326

INTERATOMIC FORCES
The atom-atom potential in pressure-broadened line width calculations for XY2-AB: New expressions in the II(R), II(L), and I(R) representations [AD-A282011] p 595 N95-14950

INTERFACE STABILITY
Influence of flow on interface shape stability in low gravity p 484 N95-14538
Convection and morphological stability during directional solidification p 448 N95-14548
Shear stabilization of solidification fronts p 448 N95-14549

INTERFACES
Future directions in two-phase flow and heat transfer in space p 482 N95-14523
Phase segregation due to simultaneous migration and coalescence p 484 N95-14537
Technology and Science at at High-Power Spallation Source: Proceedings [DE94-009685] p 597 N95-15826

INTERFACIAL ENERGY
Improved composite material and method for production of improved composite material [NASA-CASE-LAR-14892-1] p 433 N95-13836

INTERFACIAL TENSION
The flow induced by the coalescence of two initially stationary drops [NASA-TM-106752] p 478 N95-13653
Numerical studies of the surface tension effect of cryogenic liquid helium [NASA-CR-197014] p 479 N95-14104
Surface Tension Driven Convection Experiment (STDCE) p 458 N95-14217
Core-centering of compound drops in capillary oscillations: Observations on USML-1 experiments in space p 458 N95-14218
Measurement of interfacial tension of immiscible liquid pairs in microgravity p 458 N95-14221
Onset of hexagons in surface-tension-driven Benard convection p 483 N95-14527
Influence of flow on interface shape stability in low gravity p 484 N95-14538
Thermocapillary migration and interactions of bubbles and drops p 486 N95-14546
Crystal growth and fluid mechanics problems in directional solidification p 486 N95-14550
New techniques for diffusing-wave spectroscopy p 444 N95-14575

INTERFEROMETERS
Time-dependent distinguishability: Choosing to be a wave or a particle p 600 N95-13912
How to detect an excited atom without disturbing it or how to locate a super-mine without exploding it p 598 N95-13934
Quantum noise limits to matter-wave interferometry p 598 N95-13955
Interfacial force field characterization of a constrained vapor bubble thermosyphon using IAI p 488 N95-14560
Ultraviolet-Infrared Mapping Interferometic Spectrometer [NASA-CR-197099] p 613 N95-14806
Investigation of the coherent synchrotron radiation spectrum as a probe of charge dynamics [DE94-015340] p 599 N95-15371

INTERFEROMETRY
Quantum noise limits to matter-wave interferometry p 598 N95-13955
Complementarity and path distinguishability: Some recent results concerning photon pairs p 598 N95-13961
The photon: Experimental emphasis on its wave-particle duality p 599 N95-13963
Nonlocal effects on the polarization state of a photon, induced by distant absorbers p 599 N95-13965
Interferometric synthetic aperture radar terrain elevation mapping from multiple observations [DE94-014185] p 515 N95-14313

INTERMETALLICS
High field magnetotransport and specific heat in YbAgCu4 [DE94-014475] p 620 N95-13999
Processing and characterization of mechanically alloyed NiAl-based alloys [AD-A283959] p 444 N95-14202
High strain rate deformation of NiAl [DE94-014810] p 445 N95-14439
Investigation of syngas interaction in alcohol synthesis catalysts [DE94-013939] p 442 N95-15386
Symposium on Structural Intermetallics: Perspectives on Science and Technology, volume 2 [AD-A283379] p 447 N95-15874

INTERMOLECULAR FORCES
Wetting and spreading at the molecular scale p 484 N95-14539
The atom-atom potential in pressure-broadened line width calculations for XY2-AB: New expressions in the II(R), II(L), and I(R) representations [AD-A282011] p 595 N95-14950

INTERNAL COMBUSTION ENGINES
Direct observation of oil consumption mechanisms in a production spark ignition engine using fluorescence techniques
[AD-A283842] p 501 N95-14347
INTERNAL WAVES
Tidal dynamics and mixing over steep topography
[AD-A283535] p 536 N95-15324
Meso-beta scale numerical simulation studies of terrain-induced jet streak mass/momentum perturbations
[NASA-CR-197226] p 531 N95-15684
INTERNATIONAL COOPERATION
Review of European microgravity measurements
p 457 N95-14211
SLR tracking of GPS-35 p 471 N95-14285
A strawman SLR program plan for the 1990s
p 471 N95-14289
TABES 1994: 10th Annual Technical and Business Exhibition and Symposium p 414 N95-14633
Space science in the 1990's and beyond
[TABES PAPER 94-204] p 415 N95-14634
The Global Emergency Observation and Warning System
[TABES PAPER 94-622] p 417 N95-14649
International Geoid Service Bulletin No. 1
[BULL-1] p 516 N95-15791
Introducing the International Geoid Service
p 516 N95-15792
The Bureau Gravimetrique International
p 516 N95-15795
The European Geoid Project p 516 N95-15796
INTERNATIONAL SUN EARTH EXPLORER 3
ICE/ISEE plasma wave data analysis
[NASA-CR-196988] p 642 N95-14266
INTERNATIONAL SYSTEM OF UNITS
Metric path to global markets and new jobs: A question-and-answer and thematic discussion
[PB94-206307] p 459 N95-14512
Metrication in a global environment
[NASA-TM-108469] p 459 N95-14919
A metric for success
[PB94-187630] p 459 N95-15322
INTERNATIONAL TRADE
Metric path to global markets and new jobs: A question-and-answer and thematic discussion
[PB94-206307] p 459 N95-14512
TABES 1994: 10th Annual Technical and Business Exhibition and Symposium p 414 N95-14633
Design in Huntsville, manufacture in Estonia, sell in Europe
[TABES PAPER 94-607] p 415 N95-14640
Dynamic modelling to assess the value of Electronic Data Interchange: A study in the Rotterdam port community
[PB94-195542] p 632 N95-14837
Reengineering through information technology. Accompanying report of the National Performance Review
[PB94-170362] p 633 N95-15781
INTERPLANETARY DUST
Hypervelocity Impact Test Facility: A gun for hire
[TABES PAPER 94-605] p 415 N95-14639
Diffuse interstellar bands in reflection nebulae
p 639 N95-15830
The formation of small grains in shocks in the ISM
p 641 N95-15842
INTERPLANETARY MEDIUM
Interplanetary medium data book, supplement 5, 1988-1993
[NASA-TM-109957] p 642 N95-13658
INTERPLANETARY SPACE
Alkali metal Rankine cycle boiler technology challenges and some potential solutions for space nuclear power and propulsion applications
[NASA-TM-106593] p 430 N95-14174
INTERPOLATION
Computer modeling the fatigue crack growth rate behavior of metals in corrosive environments
[NASA-CR-194982-REV] p 448 N95-15918
INTERPROCESSOR COMMUNICATION
CAPTIONALS: A computer aided testing environment for the verification and validation of communication protocols p 570 N95-14163
Automated network protocol reachability analysis with supertrace algorithm and TESTGEN: Automated generation of test sequence for a formal protocol specification
[AD-A280788] p 461 N95-14293
Dynamic modelling to assess the value of Electronic Data Interchange: A study in the Rotterdam port community
[PB94-195542] p 632 N95-14837
Modeling and simulation of a Fiber Distributed Data Interface Local Area Network (FDDI LAN) using OPNET (tm) for interfacing through the Common Data Link (CDL)
[AD-A283124] p 469 N95-15651
INTERSTELLAR EXTINCTION
The Diffuse Interstellar Bands: Contributed papers
[NASA-CP-10144] p 639 N95-15827
DIBS independent of accretion in T Tauri stars
p 639 N95-15829
Diffuse bands versus extinction parameters
p 640 N95-15836
INTERSTELLAR MATTER
Porphyrins in the interstellar medium (in grains)
p 640 N95-15837
Investigation of a laboratory candidate for the carrier of the 4430 A diffuse interstellar band
p 641 N95-15840
The formation of small grains in shocks in the ISM
p 641 N95-15842
The C4H radical and the diffuse interstellar bands. An ab initio study p 641 N95-15843
A bibliography of papers on the diffuse interstellar bands p 634 N95-15846
INTERSTELLAR RADIATION
On the affinities of lambda 5778 and other broad diffuse interstellar bands p 639 N95-15832
The peculiar behaviour of the 5780 and 5797 DIBs in HD25137 p 639 N95-15833
Diffuse interstellar bands between 3900 A and 4200 A
p 640 N95-15834
Correlation between molecular lines and diffuse interstellar bands p 640 N95-15835
Investigation of a laboratory candidate for the carrier of the 4430 A diffuse interstellar band
p 641 N95-15840
The C4H radical and the diffuse interstellar bands. An ab initio study p 641 N95-15843
A bibliography of papers on the diffuse interstellar bands p 634 N95-15846
INTERSTITIALS
Effects of microgravity on interstitial muscle receptors affecting heart rate and blood pressure during static exercise p 548 N95-15137
Orthostatic stress by lower body negative pressure and its body fluid distribution kinetics under microgravity
p 549 N95-15138
Electronic characterization of defects in narrow gap semiconductors
[NASA-CR-197217] p 626 N95-15752
INTOXICATION
Low-dose alcohol effects on human behavior and performance: A review of post-1984 research
[DOT/FAA/AM-94/24] p 552 N95-14863
INVARIANCE
Representation and recognition with algebraic invariants and geometric constraint models
[AD-A282926] p 585 N95-14843
INVENTIONS
Burst-by-burst laser frequency monitor
[NASA-CASE-NPO-18596-1-CU] p 498 N95-13629
INVENTORY CONTROLS
Earth Observing System (EOS) Advanced Microwave Sounding Unit-A (AMSU-A) Spares Program Plan
[NASA-CR-189380] p 567 N95-13632
INVERSIONS
Polarizability properties of bianisotropic spheres with noncomplete magnetoelectric dyadics
[PB94-189065] p 589 N95-13987
INVERTERS
Theory and implementation of a VLSI stray insensitive switched capacitor composite operational amplifier
[AD-A283536] p 476 N95-15325
INVESTMENT
Design in Huntsville, manufacture in Estonia, sell in Europe
[TABES PAPER 94-607] p 415 N95-14640
INVISCID FLOW
An approximate Riemann solver for thermal and chemical nonequilibrium flows
[NASA-CR-195003] p 492 N95-14912
Dynamic response of rigid tanks with inhomogeneous liquids
[DE94-012619] p 493 N95-15571
IODINE
Graphite fluoride from iodine intercalated graphitized carbon
[NASA-CASE-LEW-15360-1] p 441 N95-15303
ION ACCELERATORS
A comparison of driver concepts for heavy-ion fusion
[DE94-016451] p 600 N95-15760
ION ACOUSTIC WAVES
LLE review, January - March 1994
[DE94-015058] p 618 N95-14955
ION BEAMS
Atomic Oxygen (ATOX) simulation of Teflon FEP and Kapton H surfaces using a high intensity, low energy, mass selected, ion beam facility p 422 N95-14073
Ion beam synthesis of SiGe alloy layers
[DE94-014958] p 620 N95-14189
Microcontamination detection using Heavy Ion Backscattering Spectrometry
[DE94-014182] p 437 N95-14312
Accelerator and Fusion Research Division: 1993 Summary of activities
[DE94-015157] p 599 N95-15367
Extension of the BRYNTRN code to monoenergetic light ion beams
[NASA-TP-3472] p 647 N95-15790
ION CHARGE
Charge state distributions from highly charged ions channeled at a metal surface
[DE94-012755] p 592 N95-13675
ION CURRENTS
Conductivity of polyacrylonitrile based lithium polymer electrolytes
[AD-A283965] p 450 N95-14203
Pre-flight POLAR code predictions for the CHAWS space flight experiment
[AD-A280951] p 428 N95-14599
Thin lithium cobalt dioxide rechargeable cells using polyacrylonitrile-based polymer electrolytes
[AD-A283253] p 455 N95-15615
ION ENGINES
Development status of the NASA 30-cm ion thruster and power processor
[NASA-TM-106740] p 430 N95-14301
Pulsed mode cathode
[NASA-CASE-LEW-15753-1] p 475 N95-14516
ION EXCHANGE RESINS
Preparation and characterization of composite inorganic zeolite membranes with molecular sieve properties
[PB94-191251] p 450 N95-14151
Study on titanium-silicalite-1 and related systems
[PB94-195500] p 445 N95-14845
ION IMPLANTATION
Ion implantation of He-3 in tantalum for use in a low energy deuteron polarization analyzer
[AD-A283172] p 619 N95-13698
Ion beam synthesis of SiGe alloy layers
[DE94-014958] p 620 N95-14189
Physical and tribological characteristics of ion-implanted diamond films
[NASA-TM-106682] p 450 N95-14303
ION IRRADIATION
Hydrogen transport and trapping in graphite
[UTIAS-347] p 437 N95-13652
ION PROPULSION
Development status of the NASA 30-cm ion thruster and power processor
[NASA-TM-106740] p 430 N95-14301
Pulsed mode cathode
[NASA-CASE-LEW-15753-1] p 475 N95-14516
ION SCATTERING
Charge state distributions from highly charged ions channeled at a metal surface
[DE94-012755] p 592 N95-13675
IONIC COLLISIONS
Multiple-scattering model for inclusive proton production in heavy ion collisions
[NASA-TP-3470] p 600 N95-15606
A relativistic cascade for heavy ion collisions
[DE94-015846] p 600 N95-15633
IONIC DIFFUSION
Defects and transport in mixed oxides
[DE94-015652] p 454 N95-15358
IONIC REACTIONS
Field-emitter arrays for RF vacuum microelectronics
[AD-A283549] p 476 N95-15327
IONIZED GASES
Neutral gas and diffuse interstellar bands in the LMC
p 639 N95-15828
IONOSPHERIC ELECTRON DENSITY
Propagation in the ionosphere, B p 467 N95-14827
IONOSPHERIC PROPAGATION
Propagation Modelling and Decision Aids for Communications, Radar and Navigation Systems
[AGARD-LS-196] p 466 N95-14825
Propagation in the ionosphere, A p 466 N95-14826
Propagation in the ionosphere, B p 467 N95-14827
Ground wave and diffraction, A p 467 N95-14828
Ground wave and diffraction, B p 467 N95-14829
Sensing of radio refractivity and aerosol extinction
p 467 N95-14830
Refractive effects from VHF to EHF. Part A: Propagation Mechanisms p 467 N95-14831
Refractive effects from VHF to EHF. Part B: Propagation models p 467 N95-14832

IONOSPHERIC SOUNDING
Sensing of radio refractivity and aerosol extinction
p 467 N95-14830
IONS
Charge state distributions from highly charged ions channeled at a metal surface
[DE94-012755] p 592 N95-13675
Relativistic configuration-interaction calculation of the correlation energies of heliumlike ions
[DE94-015190] p 621 N95-14325
IRIDIUM
Oxidation resistant coating for carbon-carbon composites at ultra-high temperatures
[AD-A283323] p 456 N95-15624
IRON
Ferromagnetic grain boundary signature in die-upset RE-Fe-B magnets
[DE94-014904] p 590 N95-14440
Magnetic and structural instabilities of ultrathin Fe(100) wedges
[DE94-013864] p 624 N95-15385
SAM1 semiempirical parameters
[AD-A284400] p 443 N95-15782
IRON ALLOYS
Symposium on Structural Intermetallics: Perspectives on Science and Technology, volume 2
[AD-A283379] p 447 N95-15874
High-temperature corrosion of iron aluminides
[DE94-011505] p 447 N95-15906
IRON COMPOUNDS
One: Redox chemistry of bimetallic fulvalene complexes. 2: Oligocyclopentadienyl complexes
[DE94-014930] p 443 N95-15667
IRON ISOTOPES
Searches for massive neutrino emission in C-14 beta and Fe-55 electron-capture decays
[DE94-016863] p 594 N95-14374
IRON OXIDES
Defects and transport in mixed oxides
[DE94-015652] p 454 N95-15358
Formation of dust grains with impurities in red giant winds p 641 N95-15841
IRRADIANCE
A novel technique for 4-dimensional atmosphere and oceanographic irradiance measurements using 3-D spatial filtering
[AD-A283758] p 613 N95-14353
IRRADIATION
Welding irradiated stainless steel
[DE94-013661] p 500 N95-13645
ISENTROPE
Meteorological investigation of ozone anomalies during the Arctic Boundary Layer Experiment (ABLE 3A)
[AD-A284494] p 534 N95-15771
ISOLATORS
Active thermal isolation for temperature responsive sensors
[NASA-CASE-LAR-14612-2] p 496 N95-14414
ISOMERS
Quantum chemistry and excited states: First investigations on pyrene-like molecules
p 599 N95-15844
ISOTONICITY
Simulation of the fluid retention effects of a vasopressin analog using the Guyton model of circulation
p 547 N95-15130
ISOTOPES
Beta decay data for neutron-rich Li-Cl nuclides
[DE94-014556] p 595 N95-15310
ITALY
Validation of the global digital height model ETOPO5U referring to the Italian model (Italian DEM)
p 517 N95-15797
ITERATIVE SOLUTION
Parallel performance of a symmetric eigensolver based on the Invariant Subspace Decomposition approach
[DE94-013314] p 577 N95-13677
Variable metric conjugate gradient methods
[DE94-014796] p 585 N95-14381
Aero-optics system integration
[TABES PAPER 94-604] p 415 N95-14638

J

J INTEGRAL
Elastic-plastic models for multi-site damage
p 507 N95-14454
Size and deformation limits to maintain constraint in K(sub Ic) and J(sub c) testing of bend specimens
[AD-A284363] p 514 N95-15802
Effects of tensile loading on upper shelf fracture toughness
[AD-A284364] p 514 N95-15803
JET AIRCRAFT
The Aluminum Falcon: A low cost modern commercial transport
[NASA-CR-197180] p 409 N95-15742
JET AIRCRAFT NOISE
Ultra-high bypass ratio jet noise
[NASA-CR-195394] p 591 N95-14610
Noise radiation by instability waves in coaxial jets
[NASA-TM-106738] p 591 N95-14618
The aeroacoustics of supersonic coaxial jets
[NASA-TM-106782] p 591 N95-15059
JET CONTROL
Lateral jet control for tactical missiles
p 399 N95-14448
JET ENGINE FUELS
Leak detection by acoustic emissions monitoring: An experimental investigation of the acoustic properties of leaks and the attenuation characteristics of soil
[AD-A283250] p 530 N95-15295
JET FLOW
Lateral jet control for tactical missiles
p 399 N95-14448
The breakup of a liquid jet at microgravity
p 484 N95-14535
JET MIXING FLOW
Axis switching and spreading of an asymmetric jet: Role of vorticity dynamics
[NASA-TM-106385] p 398 N95-14418
Noise radiation by instability waves in coaxial jets
[NASA-TM-106738] p 591 N95-14618
JET STREAMS (METEOROLOGY)
Meso-beta scale numerical simulation studies of terrain-induced jet streak mass/momentum perturbations
[NASA-CR-197226] p 531 N95-15684
JOINTS (JUNCTIONS)
Joint for a variable geometry truss and method of constructing same
[NASA-CASE-LAR-15136-1] p 506 N95-14138
The role of fretting corrosion and fretting fatigue in aircraft rivet hole cracking p 510 N95-14470
Bone geometry, structure and mineral distribution using Dual energy X ray Absorptiometry (DXA)
p 549 N95-15140
JOSEPHSON JUNCTIONS
Low-frequency noise in high-(Tc) superconductor Josephson junctions, SQUIDs, and magnetometers
[DE94-016873] p 623 N95-15337
Resonant tunneling in small current-biased Josephson junctions
[DE94-016875] p 623 N95-15338
JOURNAL BEARINGS
Hybrid bearings for turbopumps and the like
[NASA-CASE-MFS-28491-1] p 500 N95-13819
JP-4 JET FUEL
Development of techniques for the evaluation of toxicant impacts to multispecies systems
[AD-A284426] p 524 N95-15814
JP-8 JET FUEL
Development of techniques for the evaluation of toxicant impacts to multispecies systems
[AD-A284426] p 524 N95-15814

K

K STARS
Stellar activity: Astrophysics relevant to global change
p 643 N95-14500
K-EPSILON TURBULENCE MODEL
Eddy viscosity transport equations and their relation to the k-epsilon model
[NASA-TM-108854] p 481 N95-14273
KALMAN FILTERS
Groundspeed filtering for CTAS
[NASA-CR-197223] p 497 N95-15785
KELVIN-HELMHOLTZ INSTABILITY
Comparison of different statistical models of turbulence by similarity methods
[DE94-015326] p 493 N95-15530
KERR MAGNETOOPTICAL EFFECT
Magnetic and structural instabilities of ultrathin Fe(100) wedges
[DE94-013864] p 624 N95-15385
KETONES
Study on titanium-silicalite-1 and related systems
[PB94-195500] p 445 N95-14845
KINEMATICS
Coordination of human upper arm and forearm motion in rapid extensions p 561 N95-14056
Introduction to HEFeS (Hierarchical Environmental Feature Simulator)
[AD-A283244] p 534 N95-15402
KINESTHESIA
Neural mechanisms of kinesthesia
p 555 N95-14018
Models of remote manipulation in space
p 504 N95-14027
KINETIC ENERGY
Thermocapillary motion of deformable drops
p 485 N95-14544
Activated buoyancy propulsion = Paradox Power (tm)
[TABES PAPER 94-619] p 405 N95-14646
Spectral analysis of vortex/free-surface interaction
[AD-A283210] p 492 N95-14658
Laser ablation and deposition of alloys
[PB94-191384] p 499 N95-15388
KINETIC THEORY
Kinetic theory for electrodic phase transitions: The voltammogram
[AD-A283039] p 619 N95-13691
KLYSTRONS
Simulations of the high average power SELENE free electron laser prototype
[AD-A280780] p 498 N95-14291
KNOWLEDGE BASED SYSTEMS
Hypertext knowledge presentation system to transition basic research
[AD-A280796] p 630 N95-14321
Intelligent manufacturing systems state of the art
[TABES PAPER 94-503] p 415 N95-14637
Spatio-temporal neural networks for vision, reasoning and rapid decision making
[AD-A283251] p 583 N95-15403
KNOWLEDGE BASES (ARTIFICIAL INTELLIGENCE)
Knowledge-based processing for aircraft flight control
[NASA-CR-194976] p 580 N95-13727
Automated hierarchical testable design of digital circuits
[PB94-197936] p 472 N95-13983
Knowledge-based computational approach to architectural precedent analysis
[PB94-191269] p 568 N95-14152
Three neural network based sensor systems for environmental monitoring
[DE94-014557] p 522 N95-14195
Real-time monitor and control of MBE growth of HgCdTe by spectroscopic ellipsometry
[AD-A284451] p 627 N95-15818
KNOWLEDGE REPRESENTATION
Automated hierarchical testable design of digital circuits
[PB94-197936] p 472 N95-13983
Knowledge-based computational approach to architectural precedent analysis
[PB94-191269] p 568 N95-14152
RICIS Symposium 1992: Mission and Safety Critical Systems Research and Applications
[NASA-CR-196963] p 569 N95-14156
Expert systems in the process industries
p 571 N95-14169
Fault detection and diagnosis using neural network approaches p 571 N95-14170
The temporal reasoning systems TimeGraph 1-2
[TR-494-REV] p 584 N95-15786
Efficient algorithms for qualitative reasoning about time
[TR-496] p 576 N95-15825
KONDO EFFECT
Dynamical impurity problems
[DE94-013025] p 625 N95-15576
KRYPTON
A theoretical study of 30 to 50 angstrom noble gas heavy ion lithography
[DE94-015262] p 442 N95-15436

L

LABORATORIES
Case study: Accelerated schedule for MULTI LIMS installation
[DE94-012398] p 630 N95-13673
Eighteenth Space Simulation Conference: Space Mission Success Through Testing
[NASA-CP-3280] p 420 N95-14062
LABORATORY EQUIPMENT
Life Sciences Centrifuge Facility review
[NASA-CR-196849] p 537 N95-13702
LAGRANGE MULTIPLIERS
Comparison of transform coding methods with an optimal predictor for the data compression of digital elevation models p 564 N95-14587
LAGRANGIAN FUNCTION
Sqeezing generated by a nonlinear master equation and by amplifying-dissipative Hamiltonians
p 588 N95-13926
Discrete-layer piezoelectric plate and shell models for active tip-clearance control
[NASA-CR-195383] p 507 N95-14417

LAMINAR BOUNDARY LAYER
Experiments to verify nonparallel stability theory at Virginia Polytechnic Institute and State University, Blacksburg, Virginia
[NASA-CR-196993] p 479 N95-13664
LAMINAR FLOW
Transport phenomena in stratified multi-fluid flo w in the presence and absence of gravity p 488 N95-14563
Laminar and turbulent flow computations of Type 4 shock-shock interference aerothermal loads using unstructured grids
[NASA-CR-195008] p 493 N95-15604
LAMINAR FLOW AIRFOILS
Viper --- Design modification
[NASA-CR-197191] p 408 N95-13703
LAMINAR HEAT TRANSFER
Single-phase heat transfer and pressure drop characteristics of an integral-spine-fin within an annulus
[PB94-194073] p 482 N95-14407
LAMINATES
Processing of thermoset prepreg laminate via exposure to microwave radiation
[DE94-013268] p 432 N95-13643
Improved composite material and method for production of improved composite material
[NASA-CASE-LAR-14892-1] p 433 N95-13836
The buckling response of symmetrically laminated composite plates having a trapezoidal planform area
[NASA-CR-196975] p 505 N95-13839
Damage tolerant repair techniques for pressurized aircraft fuselages
[AD-A281982] p 391 N95-14144
Discrete-layer piezoelectric plate and shell models for active tip-clearance control
[NASA-CR-195383] p 507 N95-14417
Milestone 4: Test plan for Reusable Hydrogen Composite Tank System (RHCTS). Task 3: Composite tank materials
[NASA-CR-197036] p 435 N95-14801
Buckling of composite beams (CDDF)
[NASA-TP-3512] p 435 N95-14913
Static strength of riveted joints in Fibre Metal Laminates
[PB94-201472] p 513 N95-15429
Deformation, strength, and failure modes of laminated conventional and hybrid polymer-matrix composites loaded in the thickness direction
[AD-A281587] p 436 N95-15443
Basic mechanics of laminated composite plates
[NASA-RP-1351] p 436 N95-15763
Three-dimensional effects of crack closure in laminated composite plates subjected to bending loads
[AD-A283342] p 436 N95-15873
LAND SURFACE TEMPERATURE
The seasonal cycle dependence of temperature fluctuations in the atmosphere
[AD-A283220] p 534 N95-15627
LAND USE
Development of a systemic land cover/land use database for the Upper Mississippi River System derived from Landsat Thematic Mapper satellite data. Long term resource monitoring program
[PB94-186889] p 515 N95-14793
LANDAU-GINZBURG EQUATIONS
Dynamics on the attractor for the complex Ginzburg-Landau equation
[DE94-016902] p 586 N95-15342
Interacting fronts in a model for binary-mixture convection
[DE94-013595] p 494 N95-15861
LANDING AIDS
Assessment of CTAS ETA prediction capabilities
[NASA-CR-197224] p 497 N95-15728
LANDING GEAR
Landing gear energy absorption system
[NASA-CASE-MSC-22277-1] p 503 N95-15306
The Aluminum Falcon: A low cost modern commercial transport
[NASA-CR-197180] p 409 N95-15742
LANDING LOADS
Landing gear energy absorption system
[NASA-CASE-MSC-22277-1] p 503 N95-15306
LANDING SIMULATION
Spatial awareness comparisons between large-screen, integrated pictorial displays and conventional EFIS displays during simulated landing approaches
[NASA-TP-3467] p 409 N95-14852
LANDSAT SATELLITES
Landsat Pathfinder tropical forest information management system p 565 N95-14594
LANGEVIN FORMULA
Decoherence and dissipation for a quantum system coupled to a local environment p 609 N95-13949
LANGUAGE PROGRAMMING
Developing molecular dynamics simulation codes using mixed language programming
[DE94-015456] p 571 N95-14190
LANTHANUM
Oxidation resistant coating for carbon-carbon composites at ultra-high temperatures
[AD-A283323] p 456 N95-15624
LANTHANUM COMPOUNDS
High-efficiency electro-optic grating on PLZT ceramic wafer for optical switching
[AD-A281573] p 477 N95-15460
Cluster studies of La2CuO4: Local geometric distortions
[DE94-016203] p 626 N95-15776
LANTHANUM OXIDES
Phase separation and doped-hole segregation in La(2)CuO(4 + delta) and La(2-x)Sr(x)CuO(4 + delta)
[DE94-015070] p 624 N95-15430
Low loss glass and optical fibers therefrom
[AD-D016379] p 615 N95-15766
LAP JOINTS
Full-scale testing and analysis of fuselage structure p 512 N95-14485
The characterization of widespread fatigue damage in fuselage structure
[NASA-TM-109142] p 432 N95-14920
Static strength of riveted joints in Fibre Metal Laminates
[PB94-201472] p 513 N95-15429
LARGE SCALE INTEGRATION
Large-scale data envelopment analysis models and related applications
[AD-A283214] p 588 N95-15400
LARGE SPACE STRUCTURES
Evaluation of sensor placement algorithms for on-orbit identification of space platforms p 425 N95-14088
Simulation of a spatial, servo-hydraulic test facility for space structures p 418 N95-14095
LASER ABLATION
Laser ablation and deposition of alloys
[PB94-191384] p 499 N95-15388
LASER APPLICATIONS
Compact simultaneous-beam optical strain measurement system, phase 5
[NASA-CR-195396] p 601 N95-13666
Man-machine interfaces in health care p 556 N95-14029
Alpha LAMP Integration Facility p 418 N95-14094
Method and apparatus for detection and control of prelasing in a Q-switched laser
[NASA-CASE-LAR-14790-1] p 499 N95-14519
Excimer emission from alkali diatomic and alkaline-earth-noble gas molecules
[AD-A281662] p 596 N95-15446
LASER ARRAYS
Laser retroreflector array having cat-eye retroreflectors
[NASA-CASE-GSC-13264-1] p 499 N95-14515
LASER BEAMS
Double ionization in gases driven by optical field ionization using ultrashort laser pulses
[DE94-015137] p 498 N95-14318
Laser retroreflector array having cat-eye retroreflectors
[NASA-CASE-GSC-13264-1] p 499 N95-14515
Multi-velocity component LDV
[NASA-CASE-ARC-11925-1] p 499 N95-14668
Propagation Modelling and Decision Aids for Communications, Radar and Navigation Systems
[AGARD-LS-196] p 466 N95-14825
Electro-optics: Propagation from IR to UV and sensor considerations. Part A: Propagation theory p 467 N95-14833
Electro-optics: Propagation from IR to UV and sensor considerations. Part B: Tools for exploitation of propagation conditions and system range performance p 467 N95-14834
Faraday rotation system
[DE94-015345] p 618 N95-15374
LASER DAMAGE
Influence of defect shape on laser-induced damage in multilayer coatings
[DE94-016543] p 451 N95-14389
LASER DEPOSITION
Influence of defect shape on laser-induced damage in multilayer coatings
[DE94-016543] p 451 N95-14389
Laser ablation and deposition of alloys
[PB94-191384] p 499 N95-15388
LASER DOPPLER VELOCIMETERS
Developments in laser-based diagnostics for wind tunnels in the Aeromechanics Division: 1987-1992
[AD-A283011] p 412 N95-13687
Multi-velocity component LDV
[NASA-CASE-ARC-11925-1] p 499 N95-14668
LASER FUSION
Los Alamos contribution to target diagnostics on the National Ignition Facility
[DE94-014474] p 616 N95-13998
Radiation and EMI effects in the NIF environment
[DE94-016635] p 468 N95-15365
LASER GUIDANCE
Department of Defense high power laser program guidance
[AD-A282915] p 500 N95-15391
LASER GYROSCOPES
Quantum noise limits to matter-wave interferometry p 598 N95-13955
LASER INDUCED FLUORESCENCE
Developments in laser-based diagnostics for wind tunnels in the Aeromechanics Division: 1987-1992
[AD-A283011] p 412 N95-13687
Correlated quadratures of resonance fluorescence and the generalized uncertainty relation p 598 N95-13937
ASSERT-1992. Fundamental studies of a high energy molecular system: Spectroscopy of boron in hydrogen clusters
[AD-A283181] p 593 N95-14155
Direct observation of oil consumption mechanisms in a production spark ignition engine using fluorescence techniques
[AD-A283842] p 501 N95-14347
Measurement of resistance to solute transport across surfactant-laden interfaces using a Fluorescence Recovery After Photobleaching (FRAP) technique p 490 N95-14574
Laser spectroscopy of combustion intermediates in a supersonic jet expansion
[AD-A283201] p 500 N95-15395
Preliminary DIAL model
[DE94-013243] p 469 N95-15583
LASER MODES
Advanced laser source research
[AD-A283110] p 498 N95-13695
Aberration correction of unstable resonators
[NASA-CASE-NPO-18662-1-CU] p 602 N95-13823
LASER OUTPUTS
Burst-by-burst laser frequency monitor
[NASA-CASE-NPO-18596-1-CU] p 498 N95-13629
Review of drive symmetry measurement and control experiments on the Nova laser system
[DE94-014455] p 498 N95-13994
ASSERT-1992. Fundamental studies of a high energy molecular system: Spectroscopy of boron in hydrogen clusters
[AD-A283181] p 593 N95-14155
Simulations of the high average power SELENE free electron laser prototype
[AD-A280780] p 498 N95-14291
The Stark anomalous dispersion optical filter: The theory p 462 N95-14622
Research and development optical deep space antenna sizing study p 463 N95-14628
Receiver design, performance analysis, and evaluation for space-borne laser altimeters and space-to-space laser ranging systems
[NASA-CR-197050] p 499 N95-14901
LASER POWER BEAMING
Simulations of the high average power SELENE free electron laser prototype
[AD-A280780] p 498 N95-14291
LASER RANGE FINDERS
Satellite Laser Ranging in the 1990s: Report of the 1994 Belmont Workshop
[NASA-CP-3283] p 526 N95-14274
Scientific analysis of satellite ranging data p 517 N95-14275
Global reference frame: Intercomparison of results (SLR, VLBI and GPS) p 527 N95-14276
Measuring temporal gravitational variations using SLR data p 527 N95-14277
Global and regional kinematics from SLR stations p 527 N95-14278
Global and regional kinematics with GPS p 527 N95-14279
Earth orientation parameters p 527 N95-14281
Precision orbit determination of altimetric satellites p 418 N95-14282
Radar altimeter calibration using SLR p 471 N95-14283
The role of SLR and LLR in relativity p 528 N95-14284
SLR tracking of GPS-35 p 471 N95-14285
Synergism of SLR and GPS p 471 N95-14286
Satellite Laser Ranging operations p 500 N95-14287
SLR 2000 p 471 N95-14288
A strawman SLR program plan for the 1990s p 471 N95-14289

LASER SPECTROSCOPY
Laser spectroscopy of combustion intermediates in a supersonic jet expansion
[AD-A283201] p 500 N95-15395
LASER TARGET INTERACTIONS
Laser ablation and deposition of alloys
[PB94-191384] p 499 N95-15388
LASER TARGETS
Hohlraum manufacture for inertial confinement fusion
[DE94-014472] p 616 N95-13997
Los Alamos contribution to target diagnostics on the National Ignition Facility
[DE94-014474] p 616 N95-13998
LASER WEAPONS
Department of Defense high power laser program guidance
[AD-A282915] p 500 N95-15391
LASERS
Developments in laser-based diagnostics for wind tunnels in the Aeromechanics Division: 1987-1992
[AD-A283011] p 412 N95-13687
Optically driven surface reactions: Laser probes of surface dynamics
[DE94-015311] p 441 N95-15370
High gain GaAs switches for impulse sources: Measurement of the speed of current filaments
[DE94-015281] p 477 N95-15544
LASING
Squeezed light from multi-level closed-cycling atomic systems p 598 N95-13920
Method and apparatus for detection and control of prelasing in a Q-switched laser
[NASA-CASE-LAR-14790-1] p 499 N95-14519
LATE STARS
Probing surface structure on late-type stars with FRESIP p 643 N95-14501
LATERAL CONTROL
Flight evaluation of pneumatic forebody vortex control in post-stall flight p 398 N95-14259
Lateral jet control for tactical missiles p 399 N95-14448
LATERAL STABILITY
Perceptual and performance consequences of flight in virtual worlds p 558 N95-14043
LATTICE PARAMETERS
Errors induced in triaxial stress tensor calculations using incorrect lattice parameters
[DE94-013256] p 444 N95-13820
Anomalous temperature dependence of the lattice parameters in HoPO4 and HoVO4: Rare earth quadrupolar effects
[DE94-015086] p 622 N95-14608
LATTICES (MATHEMATICS)
Phase transitions and connectivity in three-dimensional vortex equilibria
[DE94-014967] p 494 N95-15868
LAUNCH DATES
Space Shuttle fatigue loads spectra for prelaunch and liftoff loads p 419 N95-14474
LAUNCH VEHICLE CONFIGURATIONS
Access to space
[NASA-CR-197153] p 428 N95-14521
Requirements report for SSTO vertical take-off and horizontal landing vehicle
[NASA-CR-197029] p 409 N95-14794
LAUNCH VEHICLES
Architecture for Survivable Systems Processing (ASSP). Technology benefits for Open System Interconnects p 567 N95-14160
LAW (JURISPRUDENCE)
Model contracts/agreements. Comprehensive Approach to Reusable Defense Software (CARDS)
[AD-A284403] p 575 N95-15783
LAY-UP
Buckling of composite beams (CDDF)
[NASA-TP-3512] p 435 N95-14913
LAYERS
Hardware implementation of a desktop supercomputer for high performance image processing. Color image processing using cellular neural networks
[AD-A283071] p 571 N95-14178
LEAD (METAL)
Results of TSP metals monitoring at McMurdo Station, Antarctica
[DE94-015264] p 524 N95-15455
LEAD ACID BATTERIES
Quartz resonator state-of-charge monitor for lead-acid batteries
[DE94-013823] p 473 N95-14310
LEAD ZIRCONATE TITANATES
In situ, real-time analysis of the growth of ferroelectric and conductive oxide heterostructures by a new time-of-flight pulsed ion beam surface analysis technique
[DE94-013298] p 620 N95-13822
Ferroelectric oxide memory FET (FEMFET) development
[AD-A283203] p 476 N95-15399
High-efficiency electro-optic grating on PLZT ceramic wafer for optical switching
[AD-A281573] p 477 N95-15460
LEADERSHIP
Reengineering through information technology. Accompanying report of the National Performance Review
[PB94-170362] p 633 N95-15781
LEADING EDGE FLAPS
Hybrid structured/unstructured grid computations for the F/A-18 at high angle of attack p 394 N95-14233
LEADING EDGES
Hypersonic engine leading edge experiments in a high heat flux, supersonic flow environment
[NASA-TM-106742] p 482 N95-14299
Control of unsteady separated flow associated with the dynamic stall of airfoils
[NASA-CR-197024] p 400 N95-14613
LEAKAGE
Leak detection by acoustic emissions monitoring: An experimental investigation of the acoustic properties of leaks and the attenuation characteristics of soil
[AD-A283250] p 530 N95-15295
Leak detection by acoustic emission monitoring. Phase 1: Feasibility study
[AD-A283775] p 493 N95-15332
LEAR JET AIRCRAFT
Characterization of annular two-phase gas-liquid flows in microgravity p 487 N95-14556
LEARNING THEORY
Vision, learning, and development
[TR-492-REV] p 553 N95-15787
Learning with incomplete selective perception
[TR-453] p 577 N95-15860
LEAST SQUARES METHOD
Interferometric synthetic aperture radar terrain elevation mapping from multiple observations
[DE94-014185] p 515 N95-14313
Computational methods for PDE's in flow control, superconductivity, fluid flows and other applications
[AD-A282912] p 493 N95-15390
Linear estimation of hyperspectral mixed pixel components
[AD-A283893] p 586 N95-15424
LENNARD-JONES POTENTIAL
Wetting and spreading at the molecular scale p 484 N95-14539
LEPTONS
Measurement of the B cross section at CDF via B semileptonic decays
[DE94-013842] p 593 N95-13680
LEVITATION
Nonlinear dynamics of drops and bubbles and chaotic phenomena p 485 N95-14541
LIABILITIES
Comprehensive facility decommissioning through the use of innovative technology to reduce cost, schedule, and environmental liability
[TABES PAPER 94-615] p 416 N95-14644
LIE GROUPS
Carnot-caratheodory spaces seen from within
[PB94-195617] p 586 N95-15412
LIFE (DURABILITY)
Effect of surface roughness on local film cooling effectiveness and heat transfer coefficients
[AD-A283854] p 482 N95-14351
First Year PIDDP Report on gamma-ray and x-ray spectroscopy: X-ray remote sensing and in situ spectroscopy for planetary exploration missions and gamma-ray remote sensing and in situ spectroscopy for planetary exploration missions
[NASA-CR-189374] p 517 N95-15916
LIFE CYCLE COSTS
Generic architectures for future flight systems p 567 N95-14159
Reuseable Objects Software Environment (ROSE): Introduction to Air Force Software Reuse Workshop
[NASA-CR-197017] p 572 N95-14520
Access to space
[NASA-CR-197153] p 428 N95-14521
Applying CASE technology to the software maintenance life cycle
[TABES PAPER 94-620] p 416 N95-14647
Product life cycle data base, analysis and simulation integration methodology
[TABES PAPER 94-626] p 417 N95-14650
LIFE SCIENCES
Life Sciences Centrifuge Facility review
[NASA-CR-196849] p 537 N95-13702
Development of life sciences equipment for microgravity and hypergravity simulation p 425 N95-14090
Unique life sciences research facilities at NASA Ames Research Center p 426 N95-14091
Aerospace medicine and biology: A continuing bibliography with indexes (supplement 395)
[NASA-SP-7011(395)] p 550 N95-15304
LIFE SUPPORT SYSTEMS
MISSION: Mission and Safety Critical Support Environment. Executive overview p 569 N95-14158
The Astroculture (tm)-1 experiment on the USML-1 mission p 564 N95-14228
Lunar base heat pump
[NASA-CR-188356] p 492 N95-14869
Aerospace medicine and biology: A continuing bibliography with indexes (supplement 395)
[NASA-SP-7011(395)] p 550 N95-15304
LIFT
Scale effects on aircraft and weapon aerodynamics
[AGARD-AG-323] p 393 N95-14103
Numerical design of advanced multi-element airfoils
[NASA-CR-197135] p 404 N95-15762
LIGANDS
Enhancement of insulin receptor mediated endocytosis in cultured osteoblastic cells under hypergravity p 539 N95-15148
LIGHT (VISIBLE RADIATION)
Studies of the ablated plasma from experimental plasma gun disruption simulations
[DE94-015017] p 617 N95-14262
Automatic TLI recognition system, part 1
[DE94-015253] p 578 N95-15434
L(alpha)-induced two-photon absorption of visible light emitted from an O-type star by H2(+) ions located near the surface of the Stromgren sphere surrounding the star: A possible explanation for the diffuse interstellar absorption bands (DIDs) p 641 N95-15845
LIGHT AMPLIFIERS
Quantum amplification and quantum optical tapping with squeezed states and correlated quantum states p 610 N95-13954
A simple analytical model for dense WDM/OOK systems
[AD-A283229] p 478 N95-15628
Method and apparatus for polarization-maintaining fiber optical amplification with orthogonal polarization output
[AD-D016365] p 614 N95-15707
LIGHT BEAMS
Phase-space analysis of charged and optical beam transport: Wigner rotation angle p 606 N95-13927
LIGHT EMISSION
AASERT 92: Synthesis and properties of complex polyarylene vinylenes
[AD-A284215] p 452 N95-14406
LIGHT GAS GUNS
Cratering and penetration experiments in teflon targets at velocities from 1 to 7 km/s
[NASA-TM-104797] p 432 N95-13646
LIGHT IONS
Extension of the BRYNTRN code to monoenergetic light ion beams
[NASA-TP-3472] p 647 N95-15790
LIGHT MODULATION
Asymmetric coupled quantum wells for high speed optical modulators at communication wavelengths
[AD-A281572] p 477 N95-15459
LIGHT SCATTERING
Prediction of particulate contamination on aperture window p 420 N95-14064
PC-based MIE scattering program for theoretical investigations of the optical properties of atmospheric aerosols as a function of composition and relative humidity
[PB94-192739] p 529 N95-14404
Flocculation and aggregation in a microgravity environment (FAME) p 459 N95-14572
New techniques for diffusing-wave spectroscopy p 444 N95-14575
LIGHT SOURCES
Computing illumination using extended sources: Object space and image space
[PB94-201282] p 612 N95-13992
Functional participation of the valvula cerebelli on the goldfish dorsal light response p 539 N95-15119
LIGHT TRANSMISSION
Field intercomparison with five automatic ammonia monitors
[PB94-192879] p 523 N95-15389
Method of locating ground faults
[NASA-CASE-LEW-15407-1] p 478 N95-15669
LIGHT-CONE EXPANSION
Hadronic wavefunctions in light-cone quantization
[DE94-014507] p 622 N95-15308
LIGHTNING
Produce documents and media information
[NASA-CR-196521] p 532 N95-14271
Composite waveform generation for EMP and lightning direct-drive testing
[AD-A284159] p 462 N95-14405

ESD and lightning interactions on aircraft
p 406 N95-14896

LIMBS (ANATOMY)
A physical control interface with proprioceptive feedback and multiple degrees of freedom p 559 N95-14045

LIMITERS (FUSION REACTORS)
US-Japan workshop Q-181 on High Heat Flux Components and Plasma-Surface Interactions for Next Devices: Proceedings
[DE94-014939] p 618 N95-14443

LINE OF SIGHT
A search for the 13175 A infrared diffuse band in dense environments p 639 N95-15831
Diffuse interstellar bands between 3900 A and 4200 A
p 640 N95-15834

LINE OF SIGHT COMMUNICATION
High-data-rate UHF line-of-sight communication experiment
[AD-A283592] p 468 N95-15321

LINE SPECTRA
VUV shock layer radiation in an arc-jet wind tunnel experiment p 405 N95-13719
The Stokes line width and uncertainty relations
p 589 N95-13935
The atom-atom pctential in pressure-broadened line width calculations for XY2-AB: New expressions in the II(R), II(L), and I(R) representations
[AD-A282011] p 595 N95-14950
The peculiar behaviour of the 5780 and 5797 DIBs in HD25137 p 639 N95-15833
Correlation between molecular lines and diffuse interstellar bands p 640 N95-15835
Diffuse bands versus extinction parameters
p 640 N95-15836

LINEAR ACCELERATORS
Proposal for an astronaut mass measurement device for the Space Shuttle
[NASA-CR-197198] p 563 N95-14854

LINEAR AMPLIFIERS
How to characterize the nonlinear amplifier?
p 471 N95-13922

LINEAR ARRAYS
Resonant interaction of a linear array of supersonic rectangular jets: An experimental study
[NASA-CR-195398] p 404 N95-15852

LINEAR EQUATIONS
Discrete-layer piezoelectric plate and shell models for active tip-clearance control
[NASA-CR-195383] p 507 N95-14417

LINEAR POLARIZATION
Nonlocal effects on the polarization state of a photon, induced by distant absorbers p 599 N95-13965

LINEAR PROGRAMMING
Polyhedral approaches for solving 0-1 polynomial programming problems
[AD-A282448] p 575 N95-15549

LINEAR QUADRATIC GAUSSIAN CONTROL
Linear quadratic Gaussian and feedforward controllers for the DSS-13 antenna p 463 N95-14625

LINEAR SYSTEMS
High-speed fixed and floating point implementation of delta-operator formulated discrete time systems
[AD-A283109] p 584 N95-13694
Variable metric conjugate gradient methods
[DE94-014796] p 585 N95-14381

LINEAR TRANSFORMATIONS
Phase-space analysis of charged and optical beam transport: Wigner rotation angle p 606 N95-13927
The lambda loop transformation toolkit (user's reference manual)
[TR-511] p 587 N95-15733

LIOUVILLE EQUATIONS
Capacitance calculations in nanostructure devices via the quantum Liouville equation in the coordinate representation
[AD-A281936] p 589 N95-13656

LIQUID BEARINGS
Design review and analysis for a Pratt and Whitney fluid-film bearing and seal testing rig
[NASA-CR-197035] p 502 N95-14797

LIQUID BRIDGES
Dynamics and statics of nonaxisymmetric and symmetric liquid bridges p 484 N95-14533
The extensional rheology of non-Newtonian materials
p 489 N95-14569

LIQUID CRYSTALS
Technical Revue Thomson-CSF, volume 26, no. 1, March 1994. Flat panels for visualisation
[PB94-197969] p 410 N95-13984

LIQUID FUELS
Preliminary design of a miniature thermoelectric generator
[AD-A283834] p 518 N95-14341
Conversion of light hydrocarbon gases in metal carbides for production of liquid fuels and chemicals
[DE94-013933] p 439 N95-14435

LIQUID HELIUM 2
Numerical studies of the surface tension effect of cryogenic liquid helium
[NASA-CR-197014] p 479 N95-14104
Helium 2 slosh in low gravity p 487 N95-14554

LIQUID HYDROGEN
Engine system assessment study using Martian propellants
[NASA-CR-189188] p 431 N95-14669
Milestone 4: Test plan for Reusable Hydrogen Composite Tank System (RHCTS). Task 3: Composite tank materials
[NASA-CR-197036] p 435 N95-14801
Multi-dimensional modeling of pressurization and expulsion of multi-phase hydrogen propellant
[NASA-CR-195156] p 457 N95-14902

LIQUID METALS
MHD flow in rectangular ducts with inclined non-uniform transverse magnetic field
[DE94-013989] p 616 N95-14006

LIQUID OXYGEN
Engine system assessment study using Martian propellants
[NASA-CR-189188] p 431 N95-14669

LIQUID PHASES
Surfactant-based critical phenomena in microgravity
p 459 N95-14579
Effects of two-phase flow on the deflagration of porous energetic materials
[DE94-015353] p 442 N95-15375

LIQUID ROCKET PROPELLANTS
Engine system assessment study using Martian propellants
[NASA-CR-189188] p 431 N95-14669

LIQUID SLOSHING
Impulsive response of nonuniform density liquid in a laterally excited tank
[DE94-013722] p 479 N95-13679
Numerical studies of the surface tension effect of cryogenic liquid helium
[NASA-CR-197014] p 479 N95-14104
Helium 2 slosh in low gravity p 487 N95-14554
Dynamic response of rigid tanks with inhomogeneous liquids
[DE94-012619] p 493 N95-15571

LIQUID SURFACES
Surface Tension Driven Convection Experiment (STDCE) p 458 N95-14217

LIQUID-GAS MIXTURES
Characterization of annular two-phase gas-liquid flows in microgravity p 487 N95-14556

LIQUID-LIQUID INTERFACES
The flow induced by the coalescence of two initially stationary drops
[NASA-TM-106752] p 478 N95-13653
Multilayer fluid dynamics of immiscible liquids
p 483 N95-14532
Thermocapillary migration and interactions of bubbles and drops p 486 N95-14546
Measurement of resistance to solute transport across surfactant-laden interfaces using a Fluorescence Recovery After Photobleaching (FRAP) technique
p 490 N95-14574

LIQUID-SOLID INTERFACES
Problems in nonlinear acoustics: Surface acoustic waves, diffracting sound beams, and fluid-solid interface effects
[AD-A281714] p 592 N95-15453

LIQUID-VAPOR INTERFACES
Numerical modeling of a cryogenic fluid within a fuel tank
[NASA-TM-4651] p 479 N95-13892
Numerical studies of the surface tension effect of cryogenic liquid helium
[NASA-CR-197014] p 479 N95-14104
Influence of flow on interface shape stability in low gravity p 484 N95-14538
Characterization of annular two-phase gas-liquid flows in microgravity p 487 N95-14556
Effects of thermocapillarity on an evaporating extended meniscus in microgravity p 488 N95-14559

LISP (PROGRAMMING LANGUAGE)
An informal introduction to program transformation and parallel processors
[DE94-016343] p 578 N95-14380

LITHIUM
Thin composite solid electrolyte film for lithium batteries
[NASA-CASE-NPO-18694-1-CU] p 472 N95-13824
Conductivity of polyacrylonitrile based lithium polymer electrolytes
[AD-A283965] p 450 N95-14203
Scintillating glass fiber-optic neutron sensors
[DE94-014562] p 613 N95-15312

LITHIUM COMPOUNDS
Thin lithium cobalt dioxide rechargeable cells using polyacrylonitrile-based polymer electrolytes
[AD-A283253] p 455 N95-15615

LITHIUM ISOTOPES
Beta decay data for neutron-rich Li-Cl nuclides
[DE94-014556] p 595 N95-15310

LITHIUM OXIDES
Thin lithium cobalt dioxide rechargeable cells using polyacrylonitrile-based polymer electrolytes
[AD-A283253] p 455 N95-15615

LITHIUM SULFUR BATTERIES
Materials and mechanisms of high temperature lithium sulfide batteries
[DE94-012634] p 471 N95-13684

LITHOGRAPHY
Rapid prototyping applications at Sandia National Laboratories
[DE94-006360] p 460 N95-15409
A theoretical study of 30 to 50 angstrom noble gas heavy ion lithography
[DE94-015262] p 442 N95-15436

LOADING RATE
Loading-strain equivalence between thermomechanical, creep, and tensile tests: High density polyethylene
[AD-A283265] p 513 N95-15621

LOADS (FORCES)
Fatigue evaluation of empennage, forward wing, and winglets/tip fins on part 23 airplanes
[PB94-196813] p 408 N95-13981
System level mechanical testing of the Clementine spacecraft p 425 N95-14087
Simulation of Shuttle launch G forces and acoustic loads using the NASA Ames Research Center 20G centrifuge
p 419 N95-14089
Piezoelectric loudspeaker
[NASA-CASE-LAR-15138-1] p 590 N95-14110
Space Shuttle fatigue loads spectra for prelaunch and liftoff loads p 419 N95-14474
Musculoskeletal adaptation to mechanical forces on Earth and in space p 548 N95-15136
A method for continuous monitoring of the Ground Reaction Force during daily activity p 549 N95-15139
High gain GaAs switches for impulse sources: Measurement of the speed of current filaments
[DE94-015281] p 477 N95-15544

LOCAL AREA NETWORKS
Modern methods in meteorological and oceanographic data acquisition and analyses
[AD-A283038] p 533 N95-14848
Modeling and simulation of a Fiber Distributed Data Interface Local Area Network (FDDI LAN) using OPNET (tm) for interfacing through the Common Data Link (CDL)
[AD-A283124] p 469 N95-15651

LOCKING
Experimental analysis of thread movement in bolted connections due to vibrations
[NASA-CR-197065] p 502 N95-14904

LOCOMOTION
New findings regarding light intensity and its effects as a zeitgeber in the Sprague-Dawley rat
p 539 N95-15135

LOGIC CIRCUITS
Automated hierarchical testable design of digital circuits
[PB94-197936] p 472 N95-13983

LOGISTICS
More supportable T-38A enhancement study
[AD-A283671] p 392 N95-15331

LONG DURATION EXPOSURE FACILITY
Cratering and penetration experiments in teflon targets at velocities from 1 to 7 km/s
[NASA-TM-104797] p 432 N95-13646
Investigation of the effects of long duration space exposure on active optical system components
[NASA-CR-4632] p 601 N95-13660
Results of the examination of LDEF polyurethane thermal control coatings
[NASA-CR-4617] p 432 N95-14603
Summary of solar cell data from the Long Duration Exposure Facility (LDEF)
[NASA-CR-197069] p 519 N95-14802
Analysis of space environment damage to solar cell assemblies from LDEF experiment A0171-GSFC test plate
[NASA-CR-197066] p 519 N95-14853

LONG DURATION SPACE FLIGHT
Extended duration orbiter medical project Microbial Air Sampler (STS-50/USML-1) p 458 N95-14222
Extended duration orbiter medical project variability of blood pressure and heart rate (STS-50/USML-1)
p 551 N95-14223

Extended duration orbiter medical project countermeasure to reduce post space flight orthostatic intolerance (LBNP) (STS-50/USML-1)
p 551 N95-14224
Cardiovascular deconditioning effects of long-term simulated weightlessness in rats p 538 N95-15099
Musculoskeletal adaptation to mechanical forces on Earth and in space p 548 N95-15136

LONG RANGE WEATHER FORECASTING
Short term teleconnections associated with western Pacific tropical cyclones
[AD-A284032] p 533 N95-14423
June to September rainfall in the African Sahel: Verification of our 1994 forecasts and an extended range forecast for 1995, 3
[TR-521] p 534 N95-15666

LONGITUDINAL CONTROL
Comparison of X-31 flight, wind-tunnel, and water-tunnel yawing moment asymmetries at high angles of attack
p 394 N95-14234
High angle of attack flying qualities criteria for longitudinal rate command systems p 396 N95-14247

LOOP TRANSFER FUNCTIONS
Phase transitions and connectivity in three-dimensional vortex equilibria
[DE94-014967] p 494 N95-15868

LORENTZ FORCE
Transport resistive broadening by avalanche flux motion in high-temperature superconductors: SOC in a driven system
[DE94-016901] p 623 N95-15341

LORENTZ TRANSFORMATIONS
A new approach to the photon localization problem
p 603 N95-13905

LOSSY MEDIA
Radiometric resolution enhancement by lossy compression as compared to truncation followed by lossless compression p 564 N95-14588
Compression of regions in the global advanced very high resolution radiometer 1-km data set
p 565 N95-14591

LOUDNESS
An evaluation of rise time characterization and prediction methods p 401 N95-14881
Deriving a dosage-response relationship for community response to high-energy impulsive noise
p 403 N95-14890

LOUDSPEAKERS
Piezoelectric loudspeaker
[NASA-CASE-LAR-15138-1] p 590 N95-14110

LOW COST
Thermal design verification testing of the Clementine spacecraft: Quick, cheap, and useful
p 424 N95-14083
Automatic TLI recognition system, part 1
[DE94-015253] p 578 N95-15434

LOW CURRENTS
I(sub DDQ) testing for ultimate low power design verification and defect detection
[DE94-014281] p 473 N95-14314

LOW FREQUENCIES
Specifying the surface finish of x ray mirrors
[DE94-013537] p 601 N95-13644
Torsional shear wave transducer
[AD-D016347] p 496 N95-14841
Investigation of the coherent synchrotron radiation spectrum as a probe of charge dynamics
[DE94-015340] p 599 N95-15371

LOW MOLECULAR WEIGHTS
Development of a moldable, biodegradable polymeric bone repair material
[AD-A283413] p 454 N95-15296

LOW NOISE
A radio telescope for the calibration of radio sources at 32 gigahertz p 463 N95-14626

LOW PASS FILTERS
A simple analytical model for dense WDM/OOK systems
[AD-A283229] p 478 N95-15628

LOW PRESSURE
A facility to produce an energetic, ground state atomic oxygen beam for the simulation of the Low-Earth Orbit environment p 422 N95-14072

LOW SPEED
Low-speed wind tunnel testing of the NPS and NASA Ames Mach 6 optimized waverider
[AD-A283585] p 404 N95-15319

LOW SPEED WIND TUNNELS
Tilting wind tunnel for fire behavior studies
[PB94-204625] p 413 N95-14513

LOW TEMPERATURE
Technical Revue Thomson-CSF, volume 26, no. 1, March 1994. Flat panels for visualisation
[PB94-197969] p 410 N95-13984
Heat capacity and thermal relaxation of bulk helium very near the lambda point p 444 N95-14208
Effect of matrix stiffness on wavy fiber behavior in single-carbon-fiber-epoxy composites
[AD-A280970] p 435 N95-15427
Ru2Ge3: Crystal growth and some properties
[DE94-015360] p 625 N95-15531
Low Temperature Grown and Highly Non-Stoichiometric GaAs and Related Materials
[AD-A284898] p 626 N95-15754

LOW VOLTAGE
Programmable high voltage power supply with regulation confined to the high voltage section
[NASA-CASE-GSC-13289-1] p 478 N95-15681

LOWER ATMOSPHERE
Engineer's Refractive Effects Prediction System (EREPS), version 3.0
[AD-A283748] p 461 N95-14345

LOWER BODY NEGATIVE PRESSURE
Extended duration orbiter medical project countermeasure to reduce post space flight orthostatic intolerance (LBNP) (STS-50/USML-1)
p 551 N95-14224
Cardiovascular response to cold pressor and LBNP tests before and after 20-day-bedrest p 543 N95-15097
Comparison of hemodynamic and volume responses to different levels of lower body suction and head-up tilt
p 544 N95-15107
Guidelines for a Research and Development (R/D) program for high sustained G p 546 N95-15124
Regional cutaneous microvascular flow responses during gravitational and LBNP stresses
p 547 N95-15128
Transient blood/plasma density and hematocrit effects after passive (sitting) thermoneutral water immersion in men p 548 N95-15131
Musculoskeletal adaptation to mechanical forces on Earth and in space p 548 N95-15136
Orthostatic stress by lower body negative pressure and its body fluid distribution kinetics under microgravity
p 549 N95-15138
A comparison of overall mathematical models of the cardiovascular system for simulating response to orthostatic stresses p 550 N95-15150

LOWER IONOSPHERE
Space experiments aboard rockets: SPEAR 3
[AD-A280778] p 414 N95-14290

LUBRICANT TESTS
Wear mechanism evaluation and measurement in fuel-lubricated components
[AD-A284870] p 504 N95-15747

LUBRICANTS
Solubility, viscosity and density of refrigerant and lubricant mixtures
[DE94-016949] p 454 N95-15343

LUBRICATING OILS
Definition of high-temperature use limits for MIL-L-2104 engine oils
[AD-A282838] p 451 N95-14365

LUBRICATION
Hybrid bearings for turbopumps and the like
[NASA-CASE-MFS-28491-1] p 500 N95-13819
Definition of high-temperature use limits for MIL-L-2104 engine oils
[AD-A282838] p 451 N95-14365
Modelling and investigation of EHD point contacts
[AD-A283571] p 454 N95-15316
Recent progress and future prospects in the surface engineering and tribology of ceramics
[DE94-016315] p 456 N95-15778

LUMBAR REGION
The musculoskeletal and vestibular effects of long term repeated exposure to sustained high-G
[AGARD-AR-317] p 562 N95-14263

LUMINAIRES
The realuminizing of the 7-meter-diameter solar simulator collimating mirror p 424 N95-14081

LUMINOSITY
Production properties of Z bosons with jets in 1.8 TeV (anti p)p collisions
[DE94-015184] p 595 N95-15301

LUMINOUS INTENSITY
Computing illumination using extended sources: Object space and image space
[PB94-201282] p 612 N95-13992
New findings regarding light intensity and its effects as a zeitgeber in the Sprague-Dawley rat
p 539 N95-15135

LUNAR BASED EQUIPMENT
Lunar base heat pump
[NASA-CR-188356] p 492 N95-14869

LUNAR BASES
The rationale/benefits of nuclear thermal rocket propulsion for NASA's lunar space transportation system
[NASA-TM-106739] p 431 N95-15682

LUNAR ENVIRONMENT
Lunar base heat pump
[NASA-CR-188356] p 492 N95-14869

LUNAR EXPLORATION
Fast track NTR systems assessment for NASA's first lunar outpost scenario
[NASA-TM-106748] p 429 N95-13668
Space transfer vehicle concepts and requirements study. Volume 3: Program cost estimates. Book 2: WBS and dictionary
[NASA-CR-192447] p 419 N95-15552

LUNAR GRAVITATIONAL EFFECTS
The role of SLR and LLR in relativity
p 528 N95-14284

LUNAR ORBITAL RENDEZVOUS
The rationale/benefits of nuclear thermal rocket propulsion for NASA's lunar space transportation system
[NASA-TM-106739] p 431 N95-15682

LUNAR ORBITS
Measuring temporal gravitational variations using SLR data p 527 N95-14277

LUNAR RESOURCES
Engine system assessment study using Martian propellants
[NASA-CR-189188] p 431 N95-14669

LUNAR SPACECRAFT
Fast track NTR systems assessment for NASA's first lunar outpost scenario
[NASA-TM-106748] p 429 N95-13668

LUTETIUM COMPOUNDS
Anomalous temperature dependence of the lattice parameters in HoPO4 and HoVO4: Rare earth quadrupolar effects
[DE94-015086] p 622 N95-14608

LYMAN ALPHA RADIATION
A Lyman-alpha tunable acousto-optic filter for detecting superthermal flare protons
[NASA-CR-197119] p 613 N95-14908
L(alpha)-induced two-photon absorption of visible light emitted from an O-type star by H2(+) ions located near the surface of the Stromgren sphere surrounding the star: A possible explanation for the diffuse interstellar absorption bands (DIDs) p 641 N95-15845

LYMPHOCYTES
Enhancement of insulin receptor mediated endocytosis in cultured osteoblastic cells under hypergravity
p 539 N95-15148

M

MACHINE LEARNING
Supervised learning without output labels
[TR-510-REV] p 552 N95-15588
First results with instance-based state identification for reinforcement learning
[TR-502] p 553 N95-15642
Vision, learning, and development
[TR-492-REV] p 553 N95-15787
Genetic programming with adaptive representations
[TR-489] p 576 N95-15856
Learning with incomplete selective perception
[TR-453] p 577 N95-15860

MACHINE TOOLS
Adjustable reed for weaving net-shaped tailored fabrics
[NASA-CASE-LAR-15072-1] p 501 N95-14186
The Ceramic Manufacturability Center: A new partnership with US industry
[DE94-015851] p 456 N95-15634

MACHINE-INDEPENDENT PROGRAMS
The stable and precise motion control for an autonomous mobile robot
[AD-A283776] p 501 N95-14336

MACHINERY
Fluid dynamic effects on precision cleaning with supercritical fluids
[DE94-015001] p 439 N95-14663

MAGELLANIC CLOUDS
Neutral gas and diffuse interstellar bands in the LMC
p 639 N95-15828
Diffuse interstellar bands in reflection nebulae
p 639 N95-15830

MAGMA
Experimental study of chemical, phase and textural equilibrium of high TiO2 mare basalts and peridotite
[NASA-CR-196480] p 645 N95-13724
The 226RA and 231PA systematics of axial, MORB, crustal residence ages, and MAGMA chamber characteristics at 9 to 10 degree N East Pacific Rise
[DE94-013084] p 529 N95-14434

MAGNESIUM
Boron atom matrix chemistry
[AD-A282840] p 434 N95-14366

MAGNESIUM ALLOYS
Investigation of dendrite coherency in two commercial Al-Si foundry alloys
[PB94-208238] p 446 N95-15349

MAGNESIUM FLUORIDES
High performance YBCO films
[AD-A283870] p 451 N95-14354
MAGNESIUM OXIDES
Formation of dust grains with impurities in red giant winds p 641 N95-15841
MAGNET COILS
Modelling of eddy currents related to large angle magnetic suspension test fixture
[NASA-CR-197028] p 475 N95-14851
MAGNETIC ANOMALIES
Towards developing an analytical procedure of defining the equatorial electrojet for correcting satellite magnetic anomaly data
[NASA-CR-193621] p 526 N95-14267
Research accomplishments and future goals in particle physics
[DE94-015483] p 596 N95-15537
MAGNETIC BEARINGS
Annular Suspension and Pointing System (ASPS) magnetic rotary joint
[NASA-CR-197197] p 502 N95-14907
MAGNETIC CLOUDS
Interplanetary medium data book, supplement 5, 1988-1993
[NASA-TM-109957] p 642 N95-13658
MAGNETIC COILS
Induction heating coupler
[NASA-CASE-LAR-14278-1] p 473 N95-14294
MAGNETIC DIPOLES
Uniform hydrogen fuel layers for inertial fusion targets by microgravity p 459 N95-14547
The crosswell electromagnetic response of layered media
[DE94-014929] p 470 N95-15866
MAGNETIC DISPERSION
Effect of dispersion forces on squeezing with Rydberg atoms p 456 N95-13899
MAGNETIC FIELDS
Joint and angle-covariant spin measurements with a quadrupole magnetic field p 604 N95-13914
Manipulation of quantum evolution p 598 N95-13918
Magnetic field dependent photoluminescence studies of InGaAs/GaAs strained-single-quantum wells
[DE94-015774] p 621 N95-14342
Faraday rotation system
[DE94-015345] p 618 N95-15374
Ultrasonic characterization of high T(c) and other unconventional superconductors
[AD-A282835] p 476 N95-15397
Applied Computational Electromagnetics Society Journal, volume 9, number 2
[AD-A281576] p 469 N95-15463
The crosswell electromagnetic response of layered media
[DE94-014929] p 470 N95-15866
MAGNETIC FILMS
Magnetic and structural instabilities of ultrathin Fe(100) wedges
[DE94-013864] p 624 N95-15385
MAGNETIC FLUX
Flux pinning and forced entanglement by splayed columnar defects
[DE94-013994] p 620 N95-14008
Towards developing an analytical procedure of defining the equatorial electrojet for correcting satellite magnetic anomaly data
[NASA-CR-193621] p 526 N95-14267
Transport resistive broadening by avalanche flux motion in high-temperature superconductors: SOC in a driven system
[DE94-016901] p 623 N95-15341
Macroturbulence in superconductors
[DE94-016371] p 595 N95-15362
HTS Wire Development Workshop: Proceedings
[DE94-015650] p 624 N95-15421
MAGNETIC INDUCTION
Advanced laser source research
[AD-A283110] p 498 N95-13695
MAGNETIC MEASUREMENT
Multilayer thin film Hall effect device
[NASA-CASE-MFS-28764-1] p 590 N95-14137
MAGNETIC MIRRORS
A method of measuring the amplitude-modulated vacuum field near a conducting mirror p 471 N95-13921
MAGNETIC MOMENTS
Probing the antiferromagnetic long-range order with Glauber spin states p 609 N95-13951
Neutrino oscillations in noisy media
[DE94-014973] p 598 N95-15869
MAGNETIC MONOPOLES
Research accomplishments and future goals in particle physics
[DE94-015483] p 596 N95-15537
MAGNETIC PROPERTIES
Intermultiplet transitions in optically opaque EuBa2Cu3O7: An inelastic neutron scattering study
[DE94-013429] p 620 N95-14188
Magnetic and structural instabilities of ultrathin Fe(100) wedges
[DE94-013864] p 624 N95-15385
Investigation of syngas interaction in alcohol synthesis catalysts
[DE94-013939] p 442 N95-15386
Application of spin-sensitive electron spectroscopies to investigations of electronic and magnetic properties of solid surfaces and epitaxial systems
[DE94-012981] p 625 N95-15574
MAGNETIC SIGNATURES
Ferromagnetic grain boundary signature in die-upset RE-Fe-B magnets
[DE94-014904] p 590 N95-14440
MAGNETIC SUSPENSION
Modelling of eddy currents related to large angle magnetic suspension test fixture
[NASA-CR-197028] p 475 N95-14851
Annular Suspension and Pointing System (ASPS) magnetic rotary joint
[NASA-CR-197197] p 502 N95-14907
MAGNETIC VARIATIONS
Neutrino oscillations in noisy media
[DE94-014973] p 598 N95-15869
MAGNETIZATION
Surface currents and bulk pinning in Bi2Sr2CaCu2O8
[DE94-013873] p 619 N95-13681
Macroturbulence in superconductors
[DE94-016371] p 595 N95-15362
MAGNETOHYDRODYNAMIC FLOW
MHD flow in rectangular ducts with inclined non-uniform transverse magnetic field
[DE94-013989] p 616 N95-14006
Faraday rotation system
[DE94-015345] p 618 N95-15374
MAGNETOHYDRODYNAMIC GENERATORS
Faraday rotation system
[DE94-015345] p 618 N95-15374
MAGNETOHYDRODYNAMIC STABILITY
Conservation of magnetic helicity during plasma relaxation
[DE94-016770] p 617 N95-14373
Advanced tokamak research on the D3-D tokamak
[DE94-015860] p 617 N95-14426
MAGNETOHYDRODYNAMICS
Diagnostic development and support of MHD test facilities
[DE94-015344] p 618 N95-15373
Faraday rotation system
[DE94-015345] p 618 N95-15374
Lower-hybrid poloidal current drive for fluctuation reduction in a reversed field pinch
[DE94-015534] p 618 N95-15540
MAGNETOMETERS
Low-frequency noise in high-(Tc) superconductor Josephson junctions, SQUIDs, and magnetometers
[DE94-016873] p 623 N95-15337
MAGNETOPLASMADYNAMICS
Pulsed mode cathode
[NASA-CASE-LEW-15753-1] p 475 N95-14516
MAGNETORESISTIVITY
High field magnetotransport and specific heat in YbAgCu4
[DE94-014475] p 620 N95-13999
MAGNETOSHEATH
ICE/ISEE plasma wave data analysis
[NASA-CR-196988] p 642 N95-14266
Geotail MCA plasma wave data analysis
[NASA-CR-197022] p 618 N95-14798
MAGNETOSPHERE-IONOSPHERE COUPLING
Study of auroral dynamics with combined spacecraft and incoherent scatter radar data
[NASA-CR-196974] p 526 N95-13818
MAGNETOSPHERES
Dynamics Explorer 1, retarding ion mass spectrometer summary spectrograms: 82/001 to 82/109 spin-time spectrograms for H(+), He(+), O(+), N(+), O(++), M/Z=2, and molecular ions
[NASA-TM-108468] p 443 N95-15607
MAGNETS
Ferromagnetic grain boundary signature in die-upset RE-Fe-B magnets
[DE94-014904] p 590 N95-14440
MAIN SEQUENCE STARS
The symbiosis of photometry and radial-velocity measurements p 643 N95-14505
Rotation among solar-type stars p 644 N95-14506
MAINTAINABILITY
Engineering, technical, and management support services
[NASA-CR-196977] p 505 N95-13840
John F. Kennedy Space Center, Safety, Reliability, Maintainability and Quality Assurance, Survey and Audit Program
[NASA-TM-109208] p 630 N95-14918
MAINTENANCE
Applying CASE technology to the software maintenance life cycle
[TABES PAPER 94-620] p 416 N95-14647
System administrator's guide to CDPS
[DE94-015288] p 633 N95-15528
MALFUNCTIONS
Develop advanced nonlinear signal analysis topographical mapping system
[NASA-CR-194414] p 514 N95-13639
MAMMALS
Unique life sciences research facilities at NASA Ames Research Center p 426 N95-14091
Are otoconia dynamic in birds and mammals? p 538 N95-15103
Neuronal types in the chicken's statoacoustic ganglion p 539 N95-15116
MAMMARY GLANDS
Activity of ornithine decarboxylase in muscle of Japanese quail in hypergravity conditions p 539 N95-15144
MAN MACHINE SYSTEMS
Human Machine Interfaces for Teleoperators and Virtual Environments
[NASA-CP-10071] p 554 N95-14013
Tactual interfaces: The human perceiver p 554 N95-14016
The display of tactile information p 554 N95-14017
Analysis of the human operator subsystems p 555 N95-14019
Watch what you say, your computer might be listening: A review of automated speech recognition p 555 N95-14021
Telerobotic remote presence: Achievements and challenges p 504 N95-14023
Tele-existence and/or cybernetic interface studies in Japan p 555 N95-14025
Man-machine interfaces in health care p 556 N95-14029
Telerobotics in rehabilitation: Barriers to a virtual existence p 556 N95-14030
Creating better virtual worlds p 556 N95-14031
Interacting with virtual worlds p 556 N95-14032
Virtual reality at work p 556 N95-14033
Virtual acoustic displays p 557 N95-14035
The exploration metaphor p 557 N95-14037
The Teleprasenz Consortium: Structure and intentions p 558 N95-14039
A high performance two degree-of-freedom kinesthetic interface p 558 N95-14042
A decade of telerobotics in rehabilitation: Demonstrated utility blocked by the high cost of manipulation and the complexity of the user interface p 558 N95-14044
A physical control interface with proprioceptive feedback and multiple degrees of freedom p 559 N95-14045
Rotational wind indicator enhances control of rotated displays p 559 N95-14046
Objective evaluation of situation awareness for dynamic decision makers in teleoperations p 559 N95-14047
Human operator tracking performance with a vibrotactile display p 560 N95-14049
Implementation issues for a compact 6 degree of freedom force reflecting handcontroller with cueing of modes p 560 N95-14050
On the role of exchange of power and information signals in control and stability of the human-robot interaction p 560 N95-14051
Human-machine interface hardware: The next decade p 561 N95-14055
Manual discrimination of force p 561 N95-14057
VERDEX: A virtual environment demonstrator for remote driving applications p 562 N95-14060
Destabilizing effects of visual environment motions simulating eye movements or head movements p 562 N95-14061
From Antarctica to space: Use of telepresence and virtual reality in control of remote vehicles p 427 N95-14099
The console password feature for DEC workstations
[DE94-015721] p 566 N95-14338
Human factors considerations for remote manipulation p 564 N95-14949
Aerospace medicine and biology: A continuing bibliography with indexes (supplement 395)
[NASA-SP-7011(395)] p 550 N95-15304
Interactive Computer-Enhanced Remote Viewing System (ICERVS): Subsystem design report, phase 2
[DE94-014513] p 563 N95-15309
MANAGEMENT
Energy review
[DE94-015828] p 518 N95-14326

MANAGEMENT INFORMATION SYSTEMS
Case study: Accelerated schedule for MULTI LIMS installation
[DE94-012398] p 630 N95-13673
Performance information management system (PIMS) communication
[AD-A284851] p 574 N95-15335
MANAGEMENT METHODS
Large-scale data envelopment analysis models and related applications
[AD-A283214] p 588 N95-15400
Reengineering through information technology. Accompanying report of the National Performance Review
[PB94-170362] p 633 N95-15781
MANAGEMENT PLANNING
Work Breakdown Structure (WBS) and WBS dictionary --- advanced x ray astrophysics facility (AXAF)
[NASA-CR-196448] p 567 N95-13835
Earth Observing System (EOS)/Advanced Microwave Sounding Unit-A (AMSU-A): Calibration management plan
[NASA-CR-189376] p 515 N95-13704
EMAP Information Management Strategic Plan, 1993-1997
[PB94-176823] p 522 N95-14124
Design in Huntaville, manufacture in Estonia, sell in Europe
[TABES PAPER 94-607] p 415 N95-14640
The F-16 multinational staged improvement program: A case study of risk assessment and risk management
[AD-A281706] p 409 N95-15451
Space transfer vehicle concepts and requirements study. Volume 3: Program cost estimates. Book 2: WBS and dictionary
[NASA-CR-192447] p 419 N95-15552
MANAGEMENT SYSTEMS
An application of miniscale experiments on Earth to refine microgravity analysis of adiabatic multiphase flow in space p 459 N95-14567
MANEUVERABILITY
Parameter identification for X-31A at high angles of attack p 394 N95-14235
Vista/F-16 Multi-Axis Thrust Vectoring (MATV) control law design and evaluation p 396 N95-14248
Combat Agility Management System (CAMS) p 397 N95-14250
MANEUVERS
Aircraft maneuver envelope warning system
[NASA-CASE-ARC-11953-1] p 411 N95-14518
Neural networks: Alternatives to conventional techniques for automatic docking
[TABES PAPER 94-627] p 417 N95-14651
Physiological considerations concerning Positive Pressure Breathing (PBG) during +Gz p 547 N95-15126
MANGANESE OXIDES
Defects and transport in mixed oxides
[DE94-015652] p 454 N95-15358
The structure of new synthetic manganese oxide octahedral molecular sieves
[DE94-016348] p 596 N95-15381
MANIPULATORS
Welding nozzle position manipulator
[NASA-CASE-MFS-29837-1] p 500 N95-13654
Issues in the design of high dexterity, force reflective teleoperators p 555 N95-14024
Models of remote manipulation in space p 504 N95-14027
A high performance two degree-of-freedom kinesthetic interface p 558 N95-14042
A decade of telerobotics in rehabilitation: Demonstrated utility blocked by the high cost of manipulation and the complexity of the user interface p 558 N95-14044
On the role of exchange of power and information signals in control and stability of the human-robot interaction p 560 N95-14051
Human factors requirements for telerobotic command and control: The European Space Agency experimental programme p 562 N95-14059
Dextrous gripping in a hazardous environment
[PB94-191244] p 501 N95-14150
Sample Acquisition and Instrument Deployment (SAID)
[NASA-CR-197104] p 502 N95-14910
Advanced Guidance and Control Aspects in Robotics
[AGARD-LS-193] p 581 N95-14942
Robotics technology developments in the United States space telerobotics program p 581 N95-14943
Control of remotely operated manipulation systems p 582 N95-14945
Human factors considerations for remote manipulation p 564 N95-14949
Defining a controller architecture for the long-reach manipulator
[DE94-015165] p 583 N95-15369
MANNED MARS MISSIONS
Alkali metal Rankine cycle boiler technology challenges and some potential solutions for space nuclear power and propulsion applications
[NASA-TM-106593] p 430 N95-14174
MANUAL CONTROL
A high performance two degree-of-freedom kinesthetic interface p 558 N95-14042
MANUALS
Department of Defense technical architecture framework for information management. Volume 1: Overview, version 2.0
[AD-A283763] p 631 N95-14327
Enhanced capabilities and updated users manual for axial-flow turbine preliminary sizing code TURBAN
[NASA-CR-195405] p 405 N95-15912
MANUFACTURING
Assembly feasibility and reliability studies of surface mount circuit boards manufactured with lead-free solders
[DE94-013783] p 472 N95-13975
TABES 1994: 10th Annual Technical and Business Exhibition and Symposium p 414 N95-14633
Environmentally sound manufacturing
[TABES PAPER 94-502] p 415 N95-14636
Design in Huntaville, manufacture in Estonia, sell in Europe
[TABES PAPER 94-607] p 415 N95-14640
Recycled plastic: A clean and low cost rocket fuel
[TABES PAPER 94-610] p 416 N95-14642
The Ceramic Manufacturability Center: A new partnership with US industry
[DE94-015851] p 456 N95-15634
MAPPING
Validation of the global digital height model ETOPO5U referring to the Italian model (Italian DEM) p 517 N95-15797
MARANGONI CONVECTION
Stabilization of thermocapillary convection by means of nonplanar flow oscillations p 482 N95-14524
Control of oscillatory thermocapillary convection in microgravity p 483 N95-14525
Onset of hexagons in surface-tension-driven Benard convection p 483 N95-14527
Experimental investigation of the Marangoni effect on the stability of a double-diffusive layer p 483 N95-14528
Oscillatory/chaotic thermocapillary flow induced by radiant heating p 483 N95-14531
A realistic model of evaporation for a liquid droplet p 485 N95-14543
Ground based studies of thermocapillary flows in levitated drops p 486 N95-14545
MARIA
Experimental study of chemical, phase and textural equilibrium of high TiO2 mare basalts and peridotite
[NASA-CR-196480] p 645 N95-13724
MARINE ENVIRONMENTS
The effect of aircraft speed on the penetration of sonic boom noise into a flat ocean p 402 N95-14887
Improving transient signal synthesis through noise modeling and noise removal
[AD-A281677] p 592 N95-15448
Development of techniques for the evaluation of toxicant impacts to multispecies systems
[AD-A284426] p 524 N95-15814
MARINE TRANSPORTATION
Dynamic modelling to assess the value of Electronic Data Interchange: A study in the Rotterdam port community
[PB94-195542] p 632 N95-14837
MARKET RESEARCH
A NASA/industry/university partnership for development of dual-use vibration isolation technology
[TABES PAPER 94-613] p 416 N95-14643
MARS (PLANET)
Martian environmental simulation for a deployable lattice mast p 423 N95-14076
Numerical simulations of planetary gamma-ray spectra induced by galactic cosmic rays
[DE94-014809] p 647 N95-14438
MARS EXPLORATION
Martian environmental simulation for a deployable lattice mast p 423 N95-14076
Engine system assessment study using Martian propellants
[NASA-CR-189188] p 431 N95-14669
Mission, technologies and design of planetary mobile vehicle p 504 N95-14947
MARS LANDING
An unmanned mission to Mars with sample collection and in-situ resource utilization
[NASA-CR-197202] p 645 N95-14868
MARS SAMPLE RETURN MISSIONS
An unmanned mission to Mars with sample collection and in-situ resource utilization
[NASA-CR-197202] p 645 N95-14868
MARS SURFACE
Martian environmental simulation for a deployable lattice mast p 423 N95-14076
Sample Acquisition and Instrument Deployment (SAID)
[NASA-CR-197104] p 502 N95-14910
Mission, technologies and design of planetary mobile vehicle p 504 N95-14947
MARTENSITE
Theory of nonlinear, distortive phenomena in solids: Martensitic, crack, and multiscale structures-phenomenology and physics
[DE94-015653] p 447 N95-15631
MARTENSITIC TRANSFORMATION
Theory of nonlinear, distortive phenomena in solids: Martensitic, crack, and multiscale structures-phenomenology and physics
[DE94-015653] p 447 N95-15631
MASKS
Compression of regions in the global advanced very high resolution radiometer 1-km data set p 585 N95-14591
MASS DISTRIBUTION
Measuring temporal gravitational variations using SLR data p 527 N95-14277
Mass analysis addition to the Differential Ion Flux Probe (DIFP) study
[NASA-CR-196531] p 429 N95-15824
MASS DRIVERS
A comparison of driver concepts for heavy-ion fusion
[DE94-016451] p 600 N95-15780
MASS FLOW
A facility to produce an energetic, ground state atomic oxygen beam for the simulation of the Low-Earth Orbit environment p 422 N95-14072
Comparison of full-scale, small-scale, and CFD results for F/A-18 forebody slot blowing p 397 N95-14255
MASS FLOW RATE
Experimental and theoretical studies of rewetting of unheated/heated grooved plates p 487 N95-14558
MASS SPECTRA
Studies of quarkonia production with CDF
[DE94-013220] p 597 N95-15862
MASS SPECTROMETERS
Microcontamination detection using Heavy Ion Backscattering Spectrometry
[DE94-014182] p 437 N95-14312
Dynamics Explorer 1, retarding ion mass spectrometer summary spectrograms: 82/001 to 82/109 spin-time spectrograms for H(+), He(+), O(+), N(+), O(++), M/Z=2, and molecular ions
[NASA-TM-108468] p 443 N95-15607
Dynamics Explorer 1: Energetic Ion Composition Spectrometer (EICS)
[NASA-CR-189375] p 619 N95-15758
MASS SPECTROSCOPY
The 226RA and 231PA systematics of axial, MORB, crustal residence ages, and MAGMA chamber characteristics at 9 to 10 degree N East Pacific Rise
[DE94-013084] p 529 N95-14434
MASS TRANSFER
Mass transport phenomena in microgravity: Preliminary results of the first MEPHISTO flight experiment p 634 N95-14209
Early solar mass loss, element diffusion, and solar oscillation frequencies
[DE94-014802] p 646 N95-14376
Behavior of charring materials in simulated fire environments
[PB94-196045] p 439 N95-14838
MASSIVELY PARALLEL PROCESSORS
High performance computational chemistry: Towards fully distributed parallel algorithms
[DE94-014561] p 573 N95-15311
Fault-tolerance and efficiency in massively parallel algorithms
[AD-A283255] p 579 N95-15617
MATERIALS HANDLING
Experimental implementation of a robust damped-oscillation control algorithm on a full-sized, two-degree-of-freedom, AC induction motor-driven crane
[DE94-012113] p 501 N95-14005
MATERIALS TESTS
Laboratory simulation of Low Earth Orbit (LEO) atomic oxygen effects p 422 N95-14071
Atomic Oxygen (ATOX) simulation of Teflon FEP and Kapton H surfaces using a high intensity, low energy, mass selected, ion beam facility p 422 N95-14073
The effect of Low Earth Orbit exposure on some experimental fluorine and silicon-containing polymers p 422 N95-14074
Studies of the ablated plasma from experimental plasma gun disruption simulations
[DE94-015017] p 617 N95-14262

MATHEMATICAL LOGIC
Weighted NP optimization problems: Logical definability and approximation properties
[TR-516] p 587 N95-15596
Connections among space-bounded and multihead probabilistic automata
[TR-476] p 575 N95-15645
MATHEMATICAL MODELS
Modelling the low Earth space debris environment p 414 N95-13830
A simulation algorithm for availability computation of a communication satellite constellation p 414 N95-13832
Numerical modeling of a cryogenic fluid within a fuel tank
[NASA-TM-4651] p 479 N95-13892
The thermal-wave model: A Schroedinger-like equation for charged particle beam dynamics p 601 N95-13944
Pseudomaster equation for the no-count process in a continuous photodetection p 608 N95-13946
Flow-radiated noise. Study of the propagative spectral range of the wall pressure field
[PB94-201290] p 590 N95-13985
Computing illumination using extended sources: Object space and image space
[PB94-201282] p 612 N95-13992
An observational test of magnetospheric field models at geosynchronous orbit
[DE94-014462] p 526 N95-13995
Space simulation techniques and facilities for SAX STM test campaign p 423 N95-14077
Thermal design verification testing of the Clementine spacecraft: Quick, cheap, and useful p 424 N95-14083
Unsteady flows in turbines: Impact on design procedure p 480 N95-14132
Fish method: Interaction between AC-machines and switching power converters
[PB94-191210] p 472 N95-14149
Parallel image rendering algorithm and architecture based on ray tracing and radiosity shading
[PB94-191277] p 569 N95-14153
Dependent random variables in uncertainty analysis
[PB94-191293] p 585 N95-14154
Add a dimension to your analysis of the helicopter low airspeed environment
[AD-A283982] p 408 N95-14205
Surface Tension Driven Convection Experiment (STDCE) p 458 N95-14217
Numerical simulation of the flow about an F-18 aircraft in the high-alpha regime p 394 N95-14232
Validation of the NASA Dryden X-31 simulation and evaluation of mechanization techniques p 394 N95-14236
Higher harmonic control analysis for vibration reduction of helicopter rotor systems
[NASA-TM-103855] p 391 N95-14419
FAA/NASA International Symposium on Advanced Structural Integrity Methods for Airframe Durability and Damage Tolerance
[NASA-CP-3274-PT-1] p 507 N95-14453
Elastic-plastic models for multi-site damage p 507 N95-14454
Bending effects of unsymmetric adhesively bonded composite repairs on cracked aluminum panels p 507 N95-14456
Microstructurally based model of fatigue initiation and growth p 508 N95-14459
Nonlinear fracture mechanics-based analysis of thin wall cylinders p 508 N95-14462
The role of fretting corrosion and fretting fatigue in aircraft rivet hole cracking p 510 N95-14470
Development of a composite repair and the associated inspection intervals for the F-111C stiffener runout region p 392 N95-14477
Recent advances in the modelling of crack growth under fatigue loading conditions p 511 N95-14478
Axial crack propagation and arrest in pressurized fuselage p 511 N95-14479
Fracture mechanics validity limits p 511 N95-14480
Stochastic model of the residual acceleration environment in microgravity p 459 N95-14540
Role of dielectric constant in electrohydrodynamics of conducting fluids p 478 N95-14577
Comparison of transform coding methods with an optimal predictor for the data compression of digital elevation models p 564 N95-14587
Noise radiation by instability waves in coaxial jets
[NASA-TM-106738] p 591 N95-14618
The long-term forecast of station view periods p 419 N95-14621
The Stark anomalous dispersion optical filter: The theory p 462 N95-14622
A NASA/industry/university partnership for development of dual-use vibration isolation technology
[TABES PAPER 94-613] p 416 N95-14643
Surface processes in CVD diamond growth
[AD-A280964] p 622 N95-14655
Propagation in the ionosphere, A p 466 N95-14826
Ground wave and diffraction, A p 467 N95-14828
Refractive effects from VHF to EHF. Part B: Propagation models p 467 N95-14832
Dependence of segregation potential on the thermal and hydraulic conditions predicted by model M1
[AD-A280969] p 530 N95-14862
Numerical model for the weakly nonlinear propagation of sound through turbulence p 401 N95-14883
USAF single-event sonic boom prediction model: PCBoom3 p 403 N95-14889
Multi-dimensional modeling of pressurization and expulsion of multi-phase hydrogen propellant
[NASA-CR-195156] p 457 N95-14902
A mathematical model of the cardiovascular response to +Gz acceleration p 544 N95-15110
Physiologic mechanisms effecting circulatory and body fluid losses in weightlessness as shown by mathematical modeling p 547 N95-15129
Musculoskeletal adaptation to mechanical forces on Earth and in space p 548 N95-15136
A method for continuous monitoring of the Ground Reaction Force during daily activity p 549 N95-15139
Isolation of the physiological regulation component of the arterial pressure time variation after postural stresses by a model of the gravitational and arterial kinking effects p 550 N95-15149
A comparison of overall mathematical models of the cardiovascular system for simulating response to orthostatic stresses p 550 N95-15150
Subsurface object position and image correction for standoff ground penetrating radar
[DE94-015180] p 468 N95-15300
Upward flame spread along the vertical corner walls (October 1993)
[PB94-206299] p 441 N95-15352
Turbulent upward flame spread on a vertical wall under external radiation
[PB94-207388] p 441 N95-15353
Gouge initiation in high-velocity rocket sled testing
[DE94-014288] p 418 N95-15357
Accelerometer model in APLAC
[PB94-197647] p 497 N95-15413
Traveling wave solutions to the problem of quasi-steady freezing of soils
[AD-A280971] p 531 N95-15428
Comparison of different statistical models of turbulence by similarity methods
[DE94-015326] p 493 N95-15530
Preliminary DIAL model
[DE94-013243] p 469 N95-15583
Fire growth models for materials
[PB94-195856] p 443 N95-15610
A simple analytical model for dense WDM/OOK systems
[AD-A283229] p 478 N95-15628
Meso-beta scale numerical simulation studies of terrain-induced jet streak mass/momentum perturbations
[NASA-CR-197226] p 531 N95-15684
A strategy for geoid repairing p 517 N95-15798
ASPM2: Progress toward the analysis of symbolic parameter models
[AD-A284437] p 576 N95-15817
Development and testing of a high-resolution model for tropospheric sulfate driven by observation-derived meteorology
[DE94-014910] p 525 N95-15864
On the behavior of three-dimensional wave packets in viscously spreading mixing layers
[NASA-TM-106770] p 495 N95-15908
Milestone 5 test report. Task 5, subtask 5.2: Tile to foam strength tests
[NASA-CR-197241] p 514 N95-15913
MATHEMATICAL PROGRAMMING
Developing molecular dynamics simulation codes using mixed language programming
[DE94-015456] p 571 N95-14190
Large-scale data envelopment analysis models and related applications
[AD-A283214] p 588 N95-15400
Technical report series on global modeling and data assimilation. Volume 3: An efficient thermal infrared radiation parameterization for use in general circulation models
[NASA-TM-104606-VOL-3] p 531 N95-15745
MATRICES (MATHEMATICS)
Methodology for the parallel direct solution of finite element systems
[PB94-198009] p 585 N95-13991
Higher harmonic control analysis for vibration reduction of helicopter rotor systems
[NASA-TM-103855] p 391 N95-14419
On the LU factorization of sequences of identically structured sparse matrices within a distributed memory environment
[AD-A282025] p 578 N95-14953
Linear estimation of hyperspectral mixed pixel components
[AD-A283893] p 586 N95-15424
Conditional graph completions
[AD-A282914] p 587 N95-15612
The lambda loop transformation toolkit (user's reference manual)
[TR-511] p 587 N95-15733
Lower bounds for perceptrons solving some separation problems and oracle separation of AM from PP
[TR-498] p 588 N95-15855
Neutrino oscillations in noisy media
[DE94-014973] p 598 N95-15869
MATRIX MATERIALS
Technical Revue Thomson-CSF, volume 26, no. 1, March 1994. Flat panels for visualisation
[PB94-197969] p 410 N95-13984
Thermally stable organic polymers
[AD-A281380] p 451 N95-14363
Effect of matrix stiffness on wavy fiber behavior in single-carbon-fiber-epoxy composites
[AD-A280970] p 435 N95-15427
Apparatus for performing high-temperature fiber push-out testing
[NASA-CASE-LEW-15470-1] p 497 N95-15915
MATRIX METHODS
Linear and nonlinear dynamic analysis of redundant load path bearingless rotor systems
[NASA-CR-197220] p 503 N95-14923
Development of the fuel cell power generation technology, 2
[DE94-780614] p 520 N95-15376
MATRIX THEORY
A study of the Invariant Subspace Decomposition Algorithm for banded symmetric matrices
[DE94-013872] p 568 N95-13977
MATTER (PHYSICS)
Hadronic matter and rapidly rotating compact stars
[DE94-014928] p 643 N95-14442
A relativistic cascade for heavy ion collisions
[DE94-015846] p 600 N95-15633
MAXIMUM LIKELIHOOD ESTIMATES
Interferometric synthetic aperture radar terrain elevation mapping from multiple observations
[DE94-014185] p 515 N95-14313
MCMURDO SOUND
Results of TSP metals monitoring at McMurdo Station, Antarctica
[DE94-015264] p 524 N95-15455
MEAN SQUARE VALUES
How to characterize the nonlinear amplifier? p 471 N95-13922
MEASUREMENT
A loophole-free Bell's inequality experiment p 611 N95-13988
The probabilistic origin of Bell's inequality p 612 N95-13989
MEASURING INSTRUMENTS
Partial pressure analysis in space testing p 424 N95-14084
The effect of specimen geometry on the accuracy of constitutive relations in a superplastic 5083 aluminum alloy
[DE94-014501] p 445 N95-15293
Selecting wave gauge sites for monitoring harbor oscillations: A case study for Kahului Harbor, Hawaii
[AD-A281707] p 536 N95-15452
MECHANICAL OSCILLATORS
Production of squeezed states for macroscopic mechanical oscillator p 603 N95-13906
MECHANICAL PROPERTIES
Development of chemical-vapor-deposited diamond for infrared optical applications: Summary of properties
[AD-A282999] p 448 N95-13688
HYDRA, a new tool for mechanical testing p 418 N95-14086
Bolted joint studies in GRP
[AD-A283843] p 434 N95-14348
Results of the examination of LDEF polyurethane thermal control coatings
[NASA-CR-4617] p 432 N95-14603
Damping mechanisms in nanostructured materials
[AD-A283583] p 623 N95-15317
Influence of transmutation on microstructure, density change, and embrittlement of vanadium and vanadium alloys irradiated in HFIR
[DE94-015202] p 446 N95-15431

MECHANORECEPTORS
Tactile discrimination and representations of texture, shape, and softness p 558 N95-14041
MEDICAL ELECTRONICS
Measurement and modification of the EEG and related behavior p 557 N95-14038
MEDICAL EQUIPMENT
Man-machine interfaces in health care p 556 N95-14029
Software development for safety-critical medical applications p 571 N95-14171
MEDICAL SCIENCE
Medical research publications: A bibliography of Walter Reed Army Medical Center staff, 1986-1992, volume 2 [PB94-177797] p 541 N95-14394
Naval Aerospace Medical Research Laboratory, 1993 command history [AD-A284038] p 541 N95-14424
MEDICAL SERVICES
Man-machine interfaces in health care p 556 N95-14029
Telerobotics in rehabilitation: Barriers to a virtual existence p 556 N95-14030
MEDITERRANEAN SEA
The GEOMED Project p 516 N95-15794
MELTING POINTS
Mass transport phenomena in microgravity: Preliminary results of the first MEPHISTO flight experiment p 634 N95-14209
Low loss substrates for microwave applications and sol-gel processing of superconductors [AD-A284868] p 625 N95-15746
MELTS (CRYSTAL GROWTH)
Joint Launch + One Year Science Review of USML-1 and USMP-1 with the Microgravity Measurement Group [NASA-CP-3272-VOL-1] p 634 N95-14207
Crystal growth of selected II-VI semiconducting alloys by directional solidification p 458 N95-14214
The study of dopant segregation behavior during the growth of GaAs in microgravity p 458 N95-14215
The growth of zeolites A, X and mordenite in space p 458 N95-14226
Ultrasonic characterization of high T(c) and other unconventional superconductors [AD-A282835] p 476 N95-15397
MEMBRANES
Preparation and characterization of composite inorganic zeolite membranes with molecular sieve properties [PB94-191251] p 450 N95-14151
Dense ceramic membranes for partial oxygenation of methane [DE94-015021] p 453 N95-14609
Development of the chick's auditory ossicle, the columella p 539 N95-15115
Structure of avian tectorial, otolithic and cupular membranes p 539 N95-15117
Enhancement of insulin receptor mediated endocytosis in cultured osteoblastic cells under hypergravity p 539 N95-15148
High temperature membranes for H2S and SO2 separations [DE94-017125] p 441 N95-15345
MEMORY
Augmentation of research on cognitive control [AD-A280956] p 552 N95-14600
MEMORY (COMPUTERS)
An optical simulation of shared memory [DE94-013824] p 568 N95-13976
SODR Memory Control Buffer Control ASIC [NASA-CR-197001] p 566 N95-14514
Low latency remote memory access on the Intel Paragon [DE94-014993] p 566 N95-14662
High performance computational chemistry: Towards fully distributed parallel algorithms [DE94-014561] p 573 N95-15311
Slave controller for effecting a block transfer of sixteen bit words between a memory and a data transfer bus [AD-D016463] p 574 N95-15336
Checkpointing and rollback recovery in distributed shared memory systems [AD-A281583] p 579 N95-15442
Compiler optimizations for cache locality and coherence [TR-504] p 586 N95-15589
The prospects for on-line hybrid coherency protocols on bus-based multiprocessors [TR-490] p 579 N95-15590
The principles of fault-tolerant and efficient parallel computation [AD-A283254] p 579 N95-15616
Two heads are better than two tapes [TR-493] p 575 N95-15644
MENISCI
Microscale hydrodynamics near moving contact lines p 484 N95-14536
Effects of thermocapillarity on an evaporating extended meniscus in microgravity p 488 N95-14559
Interfacial force field characterization of a constrained vapor bubble thermosyphon using IAI p 488 N95-14560
MENTAL PERFORMANCE
The electrocortical correlates of fluctuating states of attention during vigilance tasks [NASA-CR-197051] p 552 N95-14864
MERCURY (METAL)
Results of TSP metals monitoring at McMurdo Station, Antarctica [DE94-015264] p 524 N95-15455
MERCURY CADMIUM TELLURIDES
Vapor transport crystal growth of mercury-cadmium-telluride in microgravity p 458 N95-14216
Semiconductor measurement technology: Improved characterization and evaluation measurments for HgCdTe detector materials, processes, and devices used on the GOES and TIROS satellites [PB94-188810] p 474 N95-14401
Electronic characterization of defects in narrow gap semiconductors [NASA-CR-197217] p 626 N95-15752
Real-time monitor and control of MBE growth of HgCdTe by spectroscopic ellipsometry [AD-A284451] p 627 N95-15818
MERCURY TELLURIDES
Electronic characterization of defects in narrow gap semiconductors [NASA-CR-197217] p 626 N95-15752
MESOMETEOROLOGY
Photochemical urban airshed modeling using diagnostic and dynamic meteorological fields [PB94-176120] p 616 N95-13973
MESONS
Measurement of the B cross section at CDF via B semileptonic decays [DE94-013842] p 593 N95-13680
Hadronic wavefunctions in light-cone quantization [DE94-014507] p 622 N95-15308
Research in high energy physics [DE94-015519] p 600 N95-15539
Electroweak and b-physics at the Tevatron collider [DE94-013239] p 600 N95-15582
Studies of quarkonia production with CDF [DE94-013220] p 597 N95-15862
Topics in the structure of hadronic systems [DE94-014924] p 597 N95-15865
MESOSCALE PHENOMENA
An experimental and numerical study of the modifications of mixed-layer structure by inhomogeneous surface fluxes and secondary circulations [DE94-015945] p 529 N95-14428
MESSAGE PROCESSING
Performance comparison of token ring protocols for hard-real-time communication p 570 N95-14164
Checkpointing and rollback recovery in distributed shared memory systems [AD-A281583] p 579 N95-15442
MESSAGES
PHOENIX user manual. First version [PB94-189081] p 568 N95-13989
Nexus: An interoperability layer for parallel and distributed computer systems [DE94-015816] p 578 N95-14116
Checkpointing and rollback recovery in distributed shared memory systems [AD-A281583] p 579 N95-15442
METABOLISM
The Physiologist, volume 36, number 1, supplement p 541 N95-15089
Cardiovascular and metabolic responses to 6 deg Head-Down Tilt (HDT) and 70 deg Head-Up Tilt (HUT) following exercise p 544 N95-15109
METAL BONDING
Diffusion of adatoms on face-centered cubic transition metal surfaces [DE94-014230] p 445 N95-15307
METAL CLUSTERS
The transformation of organic amines by transition metal cluster compounds [DE94-017151] p 441 N95-15346
Synthesis and applications of large heterometallic cluster systems [AD-A284874] p 626 N95-15748
METAL COATINGS
Laser ablation and deposition of alloys [PB94-191384] p 499 N95-15388
METAL CRYSTALS
Magnetic and structural instabilities of ultrathin Fe(100) wedges [DE94-013864] p 624 N95-15385
METAL FATIGUE
Welding irradiated stainless steel [DE94-013661] p 500 N95-13645
Mechanical properties of high-temperature superconducting wires [DE94-015089] p 621 N95-14192
High temperature cyclic behaviour of aerospace materials: Room temperature validation tests of Ti-6Al-4V [AGARD-AR-328] p 506 N95-14198
Fatigue in single crystal nickel superalloys [AD-A282917] p 446 N95-15415
Static strength of riveted joints in Fibre Metal Laminates [PB94-201472] p 513 N95-15429
Ballistic performance and adiabatic shear behavior of AerMet(tm) 100 steel [AD-A283266] p 447 N95-15622
Characterization of damage progression in SCS-6/Timetal 21S (0)4 under thermomechanical fatigue loadings [NASA-CR-195399] p 436 N95-15911
Computer modeling the fatigue crack growth rate behavior of metals in corrosive environments [NASA-CR-194982-REV] p 448 N95-15918
METAL FIBERS
Damage tolerant repair techniques for pressurized aircraft fuselages [AD-A281982] p 391 N95-14144
METAL FINISHING
Minutes of the Third Annual Workshop on Chromate Replacements in Light Metal Finishing [DE94-015163] p 446 N95-15368
METAL FOILS
Ion implantation of He-3 in tantalum for use in a low energy deuteron polarization analyzer [AD-A283172] p 619 N95-13698
METAL HYDRIDES
Boron atom matrix chemistry [AD-A282840] p 434 N95-14366
METAL MATRIX COMPOSITES
New armour materials: Metal matrix composites [PB94-189131] p 433 N95-14148
Center for advanced materials of high quality dynamic performance (fellowships) [AD-A281377] p 434 N95-14360
Static strength of riveted joints in Fibre Metal Laminates [PB94-201472] p 513 N95-15429
Computational modeling of fiber-reinforced composites [DE94-012914] p 436 N95-15573
Characterization of damage progression in SCS-6/Timetal 21S (0)4 under thermomechanical fatigue loadings [NASA-CR-195399] p 436 N95-15911
METAL OXIDE SEMICONDUCTORS
International Semiconductor Device Research Symposium (ISDRS-93) [AD-A281715] p 477 N95-15454
METAL SHEETS
Orientation effects on the measurement and analysis of critical CTOA in an aluminum alloy sheet [NASA-TM-109153] p 444 N95-13690
Influence of crack history on the stable tearing behavior of a thin-sheet material with multiple cracks p 509 N95-14467
METAL SURFACES
Charge state distributions from highly charged ions channeled at a metal surface [DE94-012755] p 592 N95-13675
Diffusion of adatoms on face-centered cubic transition metal surfaces [DE94-014230] p 445 N95-15307
Chemically modified electrodes by nucleophilic substitution of chlorosilylated platinum oxide surfaces [AD-A281567] p 477 N95-15456
Application of spin-sensitive electron spectroscopies to investigations of electronic and magnetic properties of solid surfaces and epitaxial systems [DE94-012981] p 625 N95-15574
Type 304L stainless steel surface microstructure: Performance in hydride storage and acid cleaning [DE94-014654] p 447 N95-15625
METAL VAPOR LASERS
Advanced laser source research [AD-A283110] p 498 N95-13695
METAL VAPORS
Venusian atmospheric equilibrium chemistry at the Pioneer Venus anomalous event altitude p 645 N95-13721
METALLOGRAPHY
The effects of pitting on fatigue crack nucleation in 7075-T6 aluminum alloy p 448 N95-14482

METALORGANIC CHEMICAL VAPOR DEPOSITION
Microstructures of InAs(1-x)Sb(x) (x = 0.07-0.14) alloys and strained-layer superlattices
[DE94-015801] p 621 N95-14323
Surface passivation for 3-5 semiconductor processing: Stable gallium sulphide films by MOCVD
[NASA-TM-106761] p 477 N95-15587
METALS
Practical aspects of corrosion fundamentals
[DE94-015842] p 438 N95-14371
Results of TSP metals monitoring at McMurdo Station, Antarctica
[DE94-015264] p 524 N95-15455
METASTABLE STATE
Surfactant-based critical phenomena in microgravity p 459 N95-14579
Ultrasensitive infrared chemiluminescence detection
[AD-A283531] p 440 N95-14958
METEORITE COLLISIONS
Dynamical properties measurements for asteroid, comet and meteorite material applicable to impact modeling and mitigation calculations
[DE94-014142] p 642 N95-14311
METEORITIC COMPOSITION
Production profiles of nuclides by galactic-cosmic-ray particles in small meteoroids
[DE94-014801] p 646 N95-14437
METEOROID SHOWERS
Propagation in the ionosphere, B p 467 N95-14827
METEOROIDS
Production profiles of nuclides by galactic-cosmic-ray particles in small meteoroids
[DE94-014801] p 646 N95-14437
METEOROLOGICAL INSTRUMENTS
Overview of PAMS meteorological monitoring requirements
[PB94-176658] p 534 N95-15383
METEOROLOGICAL PARAMETERS
Florida's propagation report p 466 N95-14684
Modern methods in meteorological and oceanographic data acquisition and analyses
[AD-A283038] p 533 N95-14848
Climatological data summary 1993 with historical data
[DE94-016624] p 523 N95-15363
Meso-beta scale numerical simulation studies of terrain-induced jet streak mass/momentum perturbations
[NASA-CR-197226] p 531 N95-15684
METEOROLOGICAL RADAR
TDWR scan strategy implementation
[AD-A284877] p 534 N95-15749
METEOROLOGY
Climatological data summary 1993 with historical data
[DE94-016624] p 523 N95-15363
Meteorological investigation of ozone anomalies during the Arctic Boundary Layer Experiment (ABLE 3A)
[AD-A284494] p 534 N95-15771
METHANE
Dense ceramic membranes for partial oxygenation of methane
[DE94-015021] p 453 N95-14609
Engine system assessment study using Martian propellants
[NASA-CR-189188] p 431 N95-14669
Investigation of a laboratory candidate for the carrier of the 4430 A diffuse interstellar band p 641 N95-15840
METHYL ALCOHOL
Addendum: Tenth International Symposium on Alcohol Fuels, The Road to Commercialization
[DE93-018219] p 457 N95-14003
Test method for the measurement of methanol emissions from stationary sources
[PB94-170297] p 523 N95-15382
METHYL CHLORIDE
Infrared/submillimeter wave studies of molecular collision kinetics
[AD-A281379] p 594 N95-14362
METHYL COMPOUNDS
Radical polymerization of vinyl acetate and methyl methacrylate using organochromium initiators complexed with macrocyclic polyamines
[AD-A280828] p 451 N95-14316
Polymer-polymer interactions
[AD-A282944] p 453 N95-14844
Chemical kinetics and atmospheric modification
[AD-A283304] p 524 N95-15623
Quantum chemistry and excited states: First investigations on pyrene-like molecules p 599 N95-15844
METRICATION
Metrication in a global environment
[NASA-TM-108469] p 459 N95-14919
A metric for success
[PB94-187630] p 459 N95-15322
METROLOGY
Investigations into mirror fabrication metrology analysis
[NASA-CR-196522] p 602 N95-13841
Metric path to global markets and new jobs: A question-and-answer and thematic discussion
[PB94-206307] p 459 N95-14512
Metrication in a global environment
[NASA-TM-108469] p 459 N95-14919
MICE
Teratogenic effects of delta g: The concept of allometric growth p 538 N95-15102
MICROANALYSIS
AEM and HREM evaluation of carbon nanostructures in silica aerogels
[DE94-014913] p 434 N95-14387
MICROBALANCES
Using a temperature-controlled quartz crystal microbalance in a space equipment cleanroom to monitor molecular contamination p 421 N95-14069
Atomic Oxygen (ATOX) simulation of Teflon FEP and Kapton H surfaces using a high intensity, low energy, mass selected, ion beam facility p 422 N95-14073
MICROCRACKS
Observation of microcrack development in concrete by use of TV-holography and deformation phase gradient calculation
[PB94-207990] p 513 N95-15348
Recent progress and future prospects in the surface engineering and tribology of ceramics
[DE94-016315] p 456 N95-15778
MICROELECTRONICS
The electromagnetic spectrum. Research investigation directed toward extending the useful range of the electromagnetic spectrum
[AD-A281378] p 461 N95-14361
Fuzzy logic motor control for pollution prevention and improved energy efficiency
[PB94-190865] p 523 N95-14403
Field-emitter arrays for RF vacuum microelectronics
[AD-A283549] p 476 N95-15327
Time-of-flight detector for heavy ion backscattering spectrometry
[DE94-015600] p 596 N95-15437
MICROGRAVITY
Powder agglomeration in a microgravity environment
[NASA-CR-197000] p 457 N95-14105
Joint Launch + One Year Science Review of USML-1 and USMP-1 with the Microgravity Measurement Group
[NASA-CP-3272-VOL-1] p 634 N95-14207
Heat capacity and thermal relaxation of bulk helium very near the lambda point p 444 N95-14208
Mass transport phenomena in microgravity: Preliminary results of the first MEPHISTO flight experiment p 634 N95-14209
Basic features of the STS/Spacelab vibration environment p 428 N95-14210
Review of European microgravity measurements p 457 N95-14211
The solid surface combustion experiment aboard the USML-1 mission p 458 N95-14212
Orbital processing of high-quality CdTe compound semiconductors p 458 N95-14213
Crystal growth of selected II-VI semiconducting alloys by directional solidification p 458 N95-14214
The study of dopant segregation behavior during the growth of GaAs in microgravity p 458 N95-14215
Vapor transport crystal growth of mercury-cadmium-telluride in microgravity p 458 N95-14216
Core-centering of compound drops in capillary oscillations: Observations on USML-1 experiments in space p 458 N95-14218
Bifurcation of rotating liquid drops: Results from USML-1 experiments in space p 458 N95-14219
Surface characterization through shape oscillations of drops in microgravity and 1-g p 458 N95-14220
Measurement of interfacial tension of immiscible liquid pairs in microgravity p 458 N95-14221
Extended duration orbiter medical project Microbial Air Sampler (STS-50/USML-1) p 458 N95-14222
Protein crystal growth results from the United States Microgravity Laboratory-1 mission p 458 N95-14225
The growth of zeolites A, X and mordenite in space p 458 N95-14226
Commercial investigation results for the generic bioprocessing apparatus flown on United States Microgravity Laboratory-1 p 538 N95-14227
The Astroculture (tm)-1 experiment on the USML-1 mission p 564 N95-14228
Second Microgravity Fluid Physics Conference
[NASA-CP-3276] p 482 N95-14522
Future directions in two-phase flow and heat transfer in space p 482 N95-14523
Control of oscillatory thermocapillary convection in microgravity p 483 N95-14525
Oscillatory thermocapillary convection p 483 N95-14526
Onset of hexagons in surface-tension-driven Benard convection p 483 N95-14527
Experimental investigation of the Marangoni effect on the stability of a double-diffusive layer p 483 N95-14528
Thermocapillary convection in floating zones under simulated reduced-gravity conditions p 483 N95-14529
Dynamics and statics of nonaxisymmetric and symmetric liquid bridges p 484 N95-14533
Equilibrium fluid interface behavior under low- and zero-gravity conditions p 484 N95-14534
The breakup of a liquid jet at microgravity p 484 N95-14535
Influence of flow on interface shape stability in low gravity p 484 N95-14538
Stochastic model of the residual acceleration environment in microgravity p 459 N95-14540
Nonlinear dynamics of drops and bubbles and chaotic phenomena p 485 N95-14541
Helium 2 slosh in low gravity p 487 N95-14554
Study of two-phase flow and heat transfer in reduced gravities p 487 N95-14555
Characterization of annular two-phase gas-liquid flows in microgravity p 487 N95-14556
Analysis of phase distribution phenomena in microgravity environments p 459 N95-14557
Effects of thermocapillarity on an evaporating extended meniscus in microgravity p 488 N95-14559
Bubble dynamics, two-phase flow, and boiling heat transfer in a microgravity environment p 488 N95-14561
Pool and flow boiling in variable and microgravity p 459 N95-14562
Cross-effects in microgravity flows p 459 N95-14565
An application of miniscale experiments on Earth to refine microgravity analysis of adiabatic multiphase flow in space p 459 N95-14567
Microgravity foam structure and rheology p 459 N95-14568
The extensional rheology of non-Newtonian materials p 489 N95-14569
Plasma dust crystallization p 490 N95-14571
Flocculation and aggregation in a microgravity environment (FAME) p 459 N95-14572
Dynamics of hard sphere colloidal dispersions p 490 N95-14573
New techniques for diffusing-wave spectroscopy p 444 N95-14575
Surfactant-based critical phenomena in microgravity p 459 N95-14579
Gravity-dependent transport in industrial processes p 459 N95-14580
The path to an experiment in space (from concept to flight) p 417 N95-14582
A new procedure for measuring contact angle
[DE94-014971] p 457 N95-14659
Transesophageal echocardiographic evaluation of baboons during microgravity induced by parabolic flight p 538 N95-15094
Circulatory filling pressures during transient microgravity induced by parabolic flight p 542 N95-15095
Twenty four hours head-down tilt decreases arterial baroreflex function in conscious rat p 538 N95-15098
Cardiovascular deconditioning effects of long-term simulated weightlessness in rats p 538 N95-15099
Changing gravity level and the development of animals p 538 N95-15101
Teratogenic effects of delta g: The concept of allometric growth p 538 N95-15102
The avian embryo responding to microgravity of space flight p 538 N95-15104
Vestibular ontogeny: Measuring the influence of the dynamic environment p 544 N95-15105
Body position and volume status as determinants of cardiovascular responses to transition into microgravity in parabolic flight p 544 N95-15108
Immune changes in humans concomitant with space flights of up to 10 days duration p 545 N95-15114
On-Earth evaluation of the neurovestibular tolerance to centrifuge simulated artificial gravity in humans p 546 N95-15120
Alterations of body temperature, feeding, drinking and sleep-wake circadian rhythms in Rhesus monkey during a 19 day Spacelab flight simulation p 539 N95-15132
The regulation of rat activity following exposure to hyperdynamic fields p 539 N95-15133
Effects of microgravity on interstitial muscle receptors affecting heart rate and blood pressure during static exercise p 548 N95-15137
Orthostatic stress by lower body negative pressure and its body fluid distribution kinetics under microgravity p 549 N95-15138

Influence to organs by ten weeks tail suspension p 539 N95-15142
Relationship between hind-limb muscle atrophy and serum enzymes in tail suspended rats p 539 N95-15143

MICROGRAVITY APPLICATIONS
Oscillatory thermocapillary convection p 483 N95-14526
Stochastic model of the residual acceleration environment in microgravity p 459 N95-14540
Ground based studies of thermocapillary flows in levitated drops p 486 N95-14545
Uniform hydrogen fuel layers for inertial fusion targets by microgravity p 459 N95-14547

MICROMECHANICS
Study of multiple cracks in airplane fuselage by micromechanics and complex variables p 509 N95-14468
Structure of avian tectorial, otolithic and cupular membranes p 539 N95-15117

MICROORGANISMS
Extended duration orbiter medical project Microbial Air Sampler (STS-50/USML-1) p 458 N95-14222
Immune changes in humans concomitant with space flights of up to 10 days duration p 545 N95-15114

MICROPARTICLES
Plasma dust crystallization p 490 N95-14571
Activated buoyancy propulsion = Paradox Power (tm) [TABES PAPER 94-619] p 405 N95-14646

MICROPHONES
The modal decomposition of an impedance tube [AD-A283591] p 591 N95-15320

MICROPROCESSORS
Diagnostic development and support of MHD test facilities [DE94-015344] p 618 N95-15373

MICROSCOPES
Positron studies in catalysis research [DE94-012793] p 597 N95-15572

MICROSCOPY
Interfacial force field characterization of a constrained vapor bubble thermosyphon using IAI p 488 N95-14560

MICROSTRIP ANTENNAS
Spiral microstrip antenna with resistance [NASA-CASE-LAR-15088-1] p 460 N95-14139

MICROSTRUCTURE
Ion beam synthesis of SiGe alloy layers [DE94-014958] p 620 N95-14189
Microstructures of InAs(1-x)Sb(x) (x = 0.07-0.14) alloys and strained-layer superlattices [DE94-015801] p 621 N95-14323
Microstructurally based model of fatigue initiation and growth p 508 N95-14459
Analysis of small crack behavior for airframe applications p 512 N95-14484
Microgravity foam structure and rheology p 459 N95-14568
Progress in development of tapes and magnets made from Bi-2223 superconductors [DE94-015067] p 475 N95-14606
Relationship between microstructure and efficiency of scintillating glasses [DE94-014563] p 454 N95-15313
Small-angle x-ray scattering studies of microvoids in amorphous-silicon-based semiconductors [DE94-011840] p 520 N95-15406
Influence of transmutation on microstructure, density change, and embrittlement of vanadium and vanadium alloys irradiated in HFIR [DE94-015202] p 446 N95-15431
Stress corrosion crack tip microstructure in nickel-based alloys [DE94-015362] p 446 N95-15532
Type 304L stainless steel surface microstructure: Performance in hydride storage and acid cleaning [DE94-014654] p 447 N95-15625
Effect of heat treatment on the microstructure and properties of AerMet (trade name) 100 steel [AD-A284387] p 447 N95-15807
Fundamental studies of diamond growth and surface reactions [AD-A284390] p 626 N95-15808
Symposium on Structural Intermetallics: Perspectives on Science and Technology, volume 2 [AD-A283379] p 447 N95-15874

MICROWAVE AMPLIFIERS
Eccentricity of the electron beam in a gyrotron cavity [PB94-197639] p 496 N95-14839

MICROWAVE ANTENNAS
Optically controlled MMW beamsteering beamforming antenna [AD-A282831] p 614 N95-15414

MICROWAVE CIRCUITS
New five-standard calibration procedures for network analyzers and wafer probes [PB94-197662] p 478 N95-15611

MICROWAVE FREQUENCIES
Impulse response measurements in the 1850-1990 MHz band in large outdoor cells [PB94-204906] p 462 N95-14412
Wideband electromagnetic scattering/analysis program. Electromagnetic scattering from the trunks and branches of trees [AD-A283112] p 469 N95-15394

MICROWAVE LANDING SYSTEMS
Spatial awareness comparisons between large-screen, integrated pictorial displays and conventional EFIS displays during simulated landing approaches [NASA-TP-3467] p 409 N95-14852

MICROWAVE RADIOMETERS
Earth Observing System (EOS) Advanced Microwave Sounding Unit-A (AMSU-A) Spares Program Plan [NASA-CR-189380] p 567 N95-13632
Earth Observing System (EOS)/Advanced Microwave Sounding Unit-A (AMSU-A): Instrument logic diagrams [NASA-CR-189378] p 567 N95-13633
Earth Observing System (EOS) Advanced Microwave Sounding Unit-A (AMSU-A): Instrumentation interface control document [NASA-CR-189377] p 567 N95-13651
Earth Observing System (EOS)/Advanced Microwave Sounding Unit-A (AMSU-A): Calibration management plan [NASA-CR-189376] p 515 N95-13704
Investigation of Allan variance for determining noise spectral forms with application to microwave radiometry [NASA-CR-194985] p 516 N95-15727

MICROWAVE SOUNDING
Earth Observing System (EOS) Advanced Microwave Sounding Unit-A (AMSU-A): Instrumentation interface control document [NASA-CR-189377] p 567 N95-13651
Earth Observing System (EOS)/Advanced Microwave Sounding Unit-A (AMSU-A): Calibration management plan [NASA-CR-189376] p 515 N95-13704
High-spatial-resolution passive microwave sounding systems [NASA-CR-197131] p 531 N95-15586
Earth Observing System (EOS)/Advanced Microwave Sounding Unit-A (AMSU-A) worst-case analysis: Antenna beam pointing [NASA-CR-197218] p 517 N95-15851

MICROWAVE TRANSMISSION
Measurement and interpretation of crustal deformation rates associated with postglacial rebound [NASA-CR-196440] p 525 N95-13627
Impulse response measurements in the 1850-1990 MHz band in large outdoor cells [PB94-204906] p 462 N95-14412
Olympus propagation experiments p 464 N95-14671
ACTS mobile propagation campaign p 465 N95-14677
Propagation considerations for the Odyssey system design p 466 N95-14680

MICROWAVE TUBES
RF vacuum microelectronics [AD-A283123] p 478 N95-15613

MICROWAVES
Processing of thermoset prepreg laminate via exposure to microwave radiation [DE94-013268] p 432 N95-13643
Low loss substrates for microwave applications and sol-gel processing of superconductors [AD-A284868] p 625 N95-15746

MIDDLE EAR
Development of the chick's auditory ossicle, the columella p 539 N95-15115

MIE SCATTERING
PC-based MIE scattering program for theoretical investigations of the optical properties of atmospheric aerosols as a function of composition and relative humidity [PB94-192739] p 529 N95-14404

MILITARY AIRCRAFT
Proceedings of the FAA Inspection Program Area Review [AD-A283849] p 405 N95-14350
Research and technology highlights, 1993 [NASA-TM-4575] p 647 N95-15065

MILITARY HELICOPTERS
Advanced distributed simulation technology advanced rotary wing aircraft. Study comparing approaches to modeling the ARWA main rotor [AD-A280824] p 408 N95-14306

MILITARY OPERATIONS
Preliminary analysis of Army aircrew requirements for Joint Surveillance Target Attack Radar System (JSTARS): Human performance requirements and job demands [AD-A284917] p 563 N95-15759

MILITARY TECHNOLOGY
Challenge of Future EW System Design [AGARD-CP-546] p 461 N95-14200

MILLIMETER WAVES
Optically controlled MMW beamsteering beamforming antenna [AD-A282831] p 614 N95-15414
High-spatial-resolution passive microwave sounding systems [NASA-CR-197131] p 531 N95-15586

MIMD (COMPUTERS)
SUNMOS for the Intel Paragon, a brief user's guide [DE94-015277] p 574 N95-15543

MINE DETECTORS
Developments in ground-penetrating radar at LLNL [DE94-012236] p 554 N95-13671

MINERALS
Are otoconia dynamic in birds and mammals? p 538 N95-15103

MINES (ORDNANCE)
Developments in ground-penetrating radar at LLNL [DE94-012236] p 554 N95-13671

MINIATURIZATION
Preliminary design of a miniature thermoelectric generator [AD-A283834] p 518 N95-14341

MIRRORS
HRMA calibration handbook: EKC gravity compensated XRCF models [NASA-CR-195818] p 636 N95-13634
AXAF VETA-I mirror ring focus measurements [NASA-CR-196145] p 637 N95-13637
Specifying the surface finish of x ray mirrors [DE94-013537] p 601 N95-13644
Investigations into mirror fabrication metrology analysis [NASA-CR-196522] p 602 N95-13841
Summary of AXAF calibration requirements [NASA-CR-196985] p 637 N95-13887
Experimental study of solar simulator mirror cryocontamination p 421 N95-14065
Hubble Space Telescope servicing mission scientific instrument protective enclosure design requirements and contamination controls p 421 N95-14068
Using a temperature-controlled quartz crystal microbalance in a space equipment cleanroom to monitor molecular contamination p 421 N95-14069
The realuminizing of the 7-meter-diameter solar simulator collimating mirror p 424 N95-14081
Alpha LAMP Integration Facility p 418 N95-14094
Performance Reports: Mirror alignment system performance prediction comparison between SAO and EKC [NASA-CR-196013] p 637 N95-14100
Wide field strip-imaging optical system [NASA-CASE-NPO-18146-2-CU] p 613 N95-14413
Low-damage multilayer mirror for the soft x ray region [AD-D016362] p 614 N95-15764

MIS (SEMICONDUCTORS)
Surface passivation for 3-5 semiconductor processing: Stable gallium sulphide films by MOCVD [NASA-TM-106761] p 477 N95-15587

MISSILE CONFIGURATIONS
A selection of experimental test cases for the validation of CFD codes, volume 1 [AGARD-AR-303-VOL-1] p 481 N95-14201
Missile Aerodynamics [AGARD-R-804] p 399 N95-14445
Engineering Codes for aeroprediction: State-of-the-art and new methods p 399 N95-14447
Navier-Stokes predictions of missile aerodynamics p 399 N95-14451

MISSILE CONTROL
Lateral jet control for tactical missiles p 399 N95-14448

MISSILE DEFENSE
Department of Defense high power laser program guidance [AD-A282915] p 500 N95-15391

MISSILE DESIGN
Aeromechanical design of modern missiles p 399 N95-14446

MISSILE DETECTION
Missile infrared radiation analysis p 399 N95-14449

MISSILE SIGNATURES
Missile infrared radiation analysis p 399 N95-14449

MISSILES
Missile Aerodynamics [AGARD-R-804] p 399 N95-14445
Aeromechanical design of modern missiles p 399 N95-14446

Engineering Codes for aeroprediction: State-of-the-art and new methods p 399 N95-14447
Missile infrared radiation analysis p 399 N95-14449
High angle of attack aerodynamics p 399 N95-14450
Navier-Stokes predictions of missile aerodynamics p 399 N95-14451

MISSION PLANNING
Applications of a fast and efficient method for simulating orbital mission safety p 426 N95-14093
RICIS Symposium 1992: Mission and Safety Critical Systems Research and Applications [NASA-CR-196963] p 569 N95-14156
MISSION: Mission and Safety Critical Support Environment. Executive overview p 569 N95-14158
Generic architectures for future flight systems p 567 N95-14159
Architecture for Survivable Systems Processing (ASSP). Technology benefits for Open System Interconnects p 567 N95-14160
Space Generic Open Avionics Architecture (SGOAA): Overview p 569 N95-14161
Evolutionary Telemetry and Command Processor (TCP) architecture p 420 N95-14162
CAPTIONALS: A computer aided testing environment for the verification and validation of communication protocols p 570 N95-14163
Department of Defense technical architecture framework for information management. Volume 1: Overview, version 2.0 [AD-A283763] p 631 N95-14327
Department of Defense technical architecture framework for information management. Volume 2: Technical reference model and standards profile summary [AD-A283764] p 631 N95-14329
Department of Defense technical architecture framework for information management. Volume 3: Architecture concepts and design guidance, version 2.0 [AD-A283765] p 631 N95-14330
Department of Defense technical architecture framework for information management. Volume 4: DOD standards-based architecture planning guide, version 2.0 [AD-A283766] p 631 N95-14331
Department of Defense technical architecture framework for information management. Volume 6: Department of Defense (DOD) goal security architecture, version 2.0 [AD-A283767] p 631 N95-14332
Department of Defense technical architecture framework for information management. Volume 8: Department of Defense HCI style guide, version 2.0 [AD-A283768] p 631 N95-14333
The long-term forecast of station view periods p 419 N95-14621
Efficient mission control for the 48-satellite Globalstar constellation [TABES PAPER 94-609] p 415 N95-14641
An unmanned mission to Mars with sample collection and in-situ resource utilization [NASA-CR-197202] p 645 N95-14868
Mission, technologies and design of planetary mobile vehicle p 504 N95-14947
The rationale/benefits of nuclear thermal rocket propulsion for NASA's lunar space transportation system [NASA-TM-106739] p 431 N95-15682

MISSISSIPPI RIVER (US)
Development of a systemic land cover/land use database for the Upper Mississippi River System derived from Landsat Thematic Mapper satellite data. Long term resource monitoring program [PB94-186889] p 515 N95-14793

MIXING LAYERS (FLUIDS)
Resonant interaction of a linear array of supersonic rectangular jets: An experimental study [NASA-CR-195398] p 404 N95-15852
On the behavior of three-dimensional wave packets in viscously spreading mixing layers [NASA-TM-106770] p 495 N95-15908
On the evolution of centrifugal instabilities within curved incompressible mixing layers [NASA-CR-194991] p 495 N95-15917

MIXING LENGTH FLOW THEORY
A modified mixing length turbulence model for zero and adverse pressure gradients [NASA-TM-106772] p 492 N95-14607

MOBILE COMMUNICATION SYSTEMS
Thermal balance testing of MSAT 2 spacecraft p 424 N95-14080
Thermal balance testing of the MSAT spacecraft p 424 N95-14082
Efficient mission control for the 48-satellite Globalstar constellation [TABES PAPER 94-609] p 415 N95-14641
Channel characterisation for future Ka-band Mobile Satellite Systems and preliminary results p 465 N95-14676
ACTS mobile propagation campaign p 465 N95-14677
Photogrammetric mobile satellite service prediction p 466 N95-14679
Propagation considerations for the Odyssey system design p 466 N95-14680
Communications availability: Estimation studies at AMSC p 466 N95-14681
Wireless technology for command control and communications [AD-A284367] p 470 N95-15804

MODAL RESPONSE
Nondestructive analysis and development [NASA-CR-196987] p 505 N95-13886
Dynamics of the McDonnell-Douglas Large Scale Dynamic Rig and dynamic calibration of the rotor balance [NASA-TM-108855] p 391 N95-13891

MODES
The breakup of a liquid jet at microgravity p 484 N95-14535
Experimental/analytical approach to understanding mistuning in a transonic wind tunnel compressor [NASA-TM-108833] p 512 N95-14617

MODULATION
Field-emitter arrays for RF vacuum microelectronics [AD-A283549] p 476 N95-15327

MODULATION DOPING
Asymmetric coupled quantum wells for high speed optical modulators at communication wavelengths [AD-A281572] p 477 N95-15459

MODULATORS
Asymmetric coupled quantum wells for high speed optical modulators at communication wavelengths [AD-A281572] p 477 N95-15459
A simple analytical model for dense WDM/OOK systems [AD-A283229] p 478 N95-15628

MODULES
Module process optimization and device efficiency improvement for stable, low-cost, large-area, cadmium telluride-based photovoltaic module production [DE94-011817] p 521 N95-15863

MODULUS OF ELASTICITY
Mechanical properties of high-temperature superconducting wires [DE94-015089] p 621 N95-14192
New techniques for diffusing-wave spectroscopy p 444 N95-14575

MOIRE EFFECTS
Radiographic Moire [NASA-CASE-LAR-15104-1] p 505 N95-13835

MOLECULAR BEAM EPITAXY
Materials issues in molecular beam epitaxy [DE94-015796] p 621 N95-14322
Optical detector having a plurality of matrix layers with cobalt disilicide particles embedded therein [NASA-CASE-NPO-18625-2-CU] p 614 N95-15603
Real-time monitor and control of MBE growth of HgCdTe by spectroscopic ellipsometry [AD-A284451] p 627 N95-15818

MOLECULAR CHAINS
Investigation of dipolar reorientation dynamics of pure bulk polymers using second harmonic generation [AD-A283023] p 448 N95-13688
Relaxation of polar orientational order in nonlinear optical polymers by second harmonic generation [AD-A283024] p 449 N95-13689
Nonlinear optical susceptibility of a model guest/host polymeric system as investigated by electro-optics and second harmonic generation [AD-A283069] p 449 N95-13692

MOLECULAR CLOUDS
A search for the 13175 A infrared diffuse band in dense environments p 639 N95-15831
The peculiar behaviour of the 5780 and 5797 DIBs in HD25137 p 639 N95-15833
Diffuse bands versus extinction parameters p 640 N95-15836

MOLECULAR CLUSTERS
ASSERT-1992. Fundamental studies of a high energy molecular system: Spectroscopy of boron in hydrogen clusters [AD-A283181] p 593 N95-14155
Laboratory spectra of C60 and related molecular structures p 627 N95-15838

MOLECULAR COLLISIONS
Infrared/submillimeter wave studies of molecular collision kinetics [AD-A281379] p 594 N95-14362
Electron-molecule collisions and UV signatures in flowfields [AD-A281569] p 596 N95-15457

MOLECULAR DYNAMICS
Inelastic neutron scattering and molecular dynamics simulations of water adsorbed in the molecular sieves AlPO4-11, AlPO4-5, AlPO4-8 and VPI-5 [DE94-013337] p 593 N95-13678
Developing molecular dynamics simulation codes using mixed language programming [DE94-015456] p 571 N95-14190
Screening of charged electrodes in aqueous electrolytes [AD-A284065] p 474 N95-14425
High performance computational chemistry: Towards fully distributed parallel algorithms [DE94-014561] p 573 N95-15311

MOLECULAR ENERGY LEVELS
The 24th International Physics Olympiad [AD-A280584] p 589 N95-13972

MOLECULAR EXCITATION
Laser spectroscopy of combustion intermediates in a supersonic jet expansion [AD-A283201] p 500 N95-15395
Investigating the 3.3 micron infrared fluorescence from naphthalene following ultraviolet excitation p 599 N95-15839
The C4H radical and the diffuse interstellar bands. An ab initio study p 641 N95-15843
Quantum chemistry and excited states: First investigations on pyrene-like molecules p 599 N95-15844

MOLECULAR GASES
Ultrasensitive infrared chemiluminescence detection [AD-A283531] p 440 N95-14958
Adsorption and diffusion of fluids in well-characterized adsorbent materials [DE94-016953] p 454 N95-15344

MOLECULAR INTERACTIONS
Excimer emission from alkali diatomic and alkaline-earth-noble gas molecules [AD-A281662] p 596 N95-15446
Chemical kinetics and atmospheric modification [AD-A283304] p 524 N95-15623

MOLECULAR IONS
Dynamics Explorer 1, retarding ion mass spectrometer summary spectrograms: 82/001 to 82/109 spin-time spectrograms for H(+), He(+), O(+), N(+), O(++), M/Z=2, and molecular ions [NASA-TM-108468] p 443 N95-15607

MOLECULAR OSCILLATIONS
Activated buoyancy propulsion = Paradox Power (tm) [TABES PAPER 94-619] p 405 N95-14646
Neutrino oscillations in noisy media [DE94-014973] p 598 N95-15869

MOLECULAR RELAXATION
Investigation of dipolar reorientation dynamics of pure bulk polymers using second harmonic generation [AD-A283023] p 448 N95-13688
Relaxation of polar orientational order in nonlinear optical polymers by second harmonic generation [AD-A283024] p 449 N95-13689
Conservation of magnetic helicity during plasma relaxation [DE94-016770] p 617 N95-14373

MOLECULAR SPECTRA
The C4H radical and the diffuse interstellar bands. An ab initio study p 641 N95-15843

MOLECULAR SPECTROSCOPY
ASSERT-1992. Fundamental studies of a high energy molecular system: Spectroscopy of boron in hydrogen clusters [AD-A283181] p 593 N95-14155

MOLECULAR STRUCTURE
Screening of charged electrodes in aqueous electrolytes [AD-A284065] p 474 N95-14425
The structure of new synthetic manganese oxide octahedral molecular sieves [DE94-016348] p 596 N95-15381
Towards the molecular design of composite materials [AD-A283422] p 627 N95-15404
Chemical kinetics and atmospheric modification [AD-A283304] p 524 N95-15623
Cluster studies of La2CuO4: Local geometric distortions [DE94-016203] p 626 N95-15776
Laboratory spectra of C60 and related molecular structures p 627 N95-15838

MOLECULAR WEIGHT
Synthesis of well defined polymers by radical polymerization [AD-A280830] p 452 N95-14395

MOLTEN SALT ELECTROLYTES
Materials and mechanisms of high temperature lithium sulfide batteries [DE94-012634] p 471 N95-13684

MOLYBDATES
Corrosion-resistant coatings for high-temperature high-sulfur-activity applications
[DE94-015155] p 453 N95-14957
MOLYBDENUM ALLOYS
Symposium on Structural Intermetallics: Perspectives on Science and Technology, volume 2
[AD-A283379] p 447 N95-15874
MOLYBDENUM CARBIDES
Corrosion-resistant coatings for high-temperature high-sulfur-activity applications
[DE94-015155] p 453 N95-14957
MOLYBDENUM COMPOUNDS
Optically driven surface reactions: Laser probes of surface dynamics
[DE94-015311] p 441 N95-15370
Symposium on Structural Intermetallics: Perspectives on Science and Technology, volume 2
[AD-A283379] p 447 N95-15874
MOMENTS OF INERTIA
Centrifuges in gravitational physiology research
p 550 N95-15147
MOMENTUM TRANSFER
Activated buoyancy propulsion = Paradox Power (tm)
[TABES PAPER 94-619] p 405 N95-14646
Meso-beta scale numerical simulation studies of terrain-induced jet streak mass/momentum perturbations
[NASA-CR-197226] p 531 N95-15684
MONITORS
Passive fetal heart rate monitoring apparatus and method with enhanced fetal heart beat discrimination
[NASA-CASE-LAR-15129-1] p 541 N95-14184
Quartz resonator state-of-charge monitor for lead-acid batteries
[DE94-013823] p 473 N95-14310
Field intercomparison with five automatic ammonia monitors
[PB94-192879] p 523 N95-15389
MONKEYS
Cosmos 2229 immunology study (Experiment K-8-07)
[NASA-CR-196984] p 537 N95-13638
Adaptation of skeletal muscle to spaceflight: Cosmos rhesus project. Cosmos 2044 and 2229
[NASA-CR-197041] p 537 N95-14796
Space flight and humoral and cellular immunity of animals p 538 N95-15113
Alterations of body temperature, feeding, drinking and sleep-wake circadian rhythms in Rhesus monkey during a 19 day Spacelab flight simulation p 539 N95-15132
MONOCULAR VISION
Visual motion perception and visual information processing
[AD-A282928] p 581 N95-14847
MONOMERS
Synthesis of well defined polymers by radical polymerization
[AD-A280830] p 452 N95-14395
Modifications of polysilanes and polysilane copolymers
[AD-A280839] p 452 N95-14398
Ring-opening polymerization of strained cyclotetrasilanes as a new route towards well defined polysilylenes
[AD-A280840] p 452 N95-14399
The synthesis of monomers with pendent ethynyl groups for modified high performance thermoplastics
[NASA-CR-196935] p 453 N95-14931
MONTE CARLO METHOD
A simulation algorithm for availability computation of a communication satellite constellation
p 414 N95-13832
Dependent random variables in uncertainty analysis
[PB94-191293] p 585 N95-14154
Radiative interactions in multi-dimensional chemically reacting flows using Monte Carlo simulations
[NASA-CR-197012] p 481 N95-14269
Fatigue reliability method with in-service inspections
p 505 N95-14475
Production properties of Z bosons with jets in 1.8 TeV (anti p)p collisions
[DE94-015184] p 595 N95-15301
Low energy electron and atom elastic scattering cross sections from 0.1 to 30 keV
[AD-A283584] p 595 N95-15318
Defect profiling in elemental and multilayer systems: Correlations of fitted defect concentrations with positron implantation profiles
[DE94-015844] p 624 N95-15422
Diffuse interstellar bands in reflection nebulae
p 639 N95-15830
Phase transitions and connectivity in three-dimensional vortex equilibria
[DE94-014967] p 494 N95-15868
MORPHOLOGY
Atomic Oxygen (ATOX) simulation of Teflon FEP and Kapton H surfaces using a high intensity, low energy, mass selected, ion beam facility p 422 N95-14073
Electrodeposition of conductors and semiconductors with controlled stoichiometries and morphologies
[AD-A280743] p 437 N95-14141
Adaptation of skeletal muscle to spaceflight: Cosmos rhesus project. Cosmos 2044 and 2229
[NASA-CR-197041] p 537 N95-14796
Self-organization of graft copolymers at surfaces, interfaces and in bulk
[DE94-016884] p 454 N95-15340
MOSAICS
Asteroseismology with FRESIP: A meter class space telescope p 643 N95-14504
Development of a systemic land cover/land use database for the Upper Mississippi River System derived from Landsat Thematic Mapper satellite data. Long term resource monitoring program
[PB94-186889] p 515 N95-14793
MOTION PERCEPTION
Remote sensing, processing and transmission of data for an unmanned aerial vehicle
[AD-A283104] p 514 N95-13693
Visual motion perception and visual information processing
[AD-A282928] p 581 N95-14847
Vision-based navigation and recognition
[AD-A282962] p 583 N95-15398
MOTION SICKNESS
The effects of autogenic-feedback training on motion sickness severity and heart rate variability in astronauts
[NASA-TM-108840] p 539 N95-13661
Neurohumoral reactions to long-term vestibular stimulation in man p 542 N95-15091
Psychophysiological aspects of increasing resistance to space motion sickness p 542 N95-15093
The relationship between space sickness and preflight diet p 546 N95-15122
MOUNTAINS
Meso-beta scale numerical simulation studies of terrain-induced jet streak mass/momentum perturbations
[NASA-CR-197226] p 531 N95-15684
MOUNTING
Service equipment for use in hostile environments
[NASA-CASE-LEW-14906-2-SB] p 504 N95-15914
MSAT
Thermal balance testing of MSAT 2 spacecraft
p 424 N95-14080
Thermal balance testing of the MSAT spacecraft
p 424 N95-14082
MTBF
Preliminary design of a miniature thermoelectric generator
[AD-A283834] p 518 N95-14341
MULTIGRID METHODS
CFD methodology and validation for turbomachinery flows p 480 N95-14131
Robust multigrid methods for the steady and unsteady incompressible Navier-Stokes equations in general coordinates
[PB94-195534] p 492 N95-15315
MULTIMEDIA
Hypertext knowledge presentation system to transition basic research
[AD-A280796] p 630 N95-14321
MULTIPATH TRANSMISSION
Measurement and interpretation of crustal deformation rates associated with postglacial rebound
[NASA-CR-196440] p 525 N95-13627
Multipath noise reduction spread spectrum signals
[NASA-CASE-NPO-18970-1-CU] p 460 N95-13628
Impulse response measurements in the 1850-1990 MHz band in large outdoor cells
[PB94-204906] p 462 N95-14412
Ground wave and diffraction, B p 467 N95-14829
High-data-rate UHF line-of-sight communication experiment
[AD-A283592] p 468 N95-15321
Troposcatter at the KU band
[AD-A281575] p 469 N95-15462
MULTIPHASE FLOW
Second Microgravity Fluid Physics Conference
[NASA-CP-3276] p 482 N95-14522
Microscale hydrodynamics near moving contact lines
p 484 N95-14536
Analysis of phase distribution phenomena in microgravity environments p 459 N95-14557
Particle experiments in thermal and velocity gradients
p 489 N95-14564
An application of miniscale experiments on Earth to refine microgravity analysis of adiabatic multiphase flow in space p 459 N95-14567
Multi-dimensional modeling of pressurization and expulsion of multi-phase hydrogen propellant
[NASA-CR-195156] p 457 N95-14902
MULTIPLEXING
Acceleration recorder and playback module
[NASA-CASE-MSC-22008-1] p 496 N95-14180
MULTIPLIERS
Programmable high voltage power supply with regulation confined to the high voltage section
[NASA-CASE-GSC-13289-1] p 478 N95-15681
MULTIPROCESSING (COMPUTERS)
Low latency remote memory access on the Intel Paragon
[DE94-014993] p 566 N95-14662
Compiler optimizations for cache locality and coherence
[TR-504] p 586 N95-15589
The prospects for on-line hybrid coherency protocols on bus-based multiprocessors
[TR-490] p 579 N95-15590
MULTISENSOR APPLICATIONS
Automatic TLI recognition system, part 1
[DE94-015253] p 578 N95-15434
Automatic TLI recognition system, part 2
[DE94-015393] p 579 N95-15534
MULTISENSOR FUSION
Automatic TLI recognition system, part 1
[DE94-015253] p 578 N95-15434
Automatic TLI recognition system, part 2
[DE94-015393] p 579 N95-15534
MUON SPIN ROTATION
Introduction to muSR: What, how, where
[PB94-192267] p 596 N95-15379
MUONS
Introduction to muSR: What, how, where
[PB94-192267] p 596 N95-15379
Research accomplishments and future goals in particle physics
[DE94-015483] p 596 N95-15537
MUSCLES
Neural mechanisms of kinesthesia
p 555 N95-14018
Adaptation of skeletal muscle to spaceflight: Cosmos rhesus project. Cosmos 2044 and 2229
[NASA-CR-197041] p 537 N95-14796
Effects of microgravity on interstitial muscle receptors affecting heart rate and blood pressure during static exercise p 548 N95-15137
Activity of ornithine decarboxylase in muscle of Japanese quail in hypergravity conditions
p 539 N95-15144
20 days bed-rest on insulin action in relation to body fat in young subjects p 549 N95-15145
Legged vehicle for underwater mobile operations
[AD-A282891] p 503 N95-15294
MUSCULAR FUNCTION
The human operator transfer function: Identification of the limb mechanics subsystem p 558 N95-14040
Activity of ornithine decarboxylase in muscle of Japanese quail in hypergravity conditions
p 539 N95-15144
Robotic control using muscular and neural electrical signals
[AD-A284908] p 551 N95-15757
MUSCULAR STRENGTH
On the role of exchange of power and information signals in control and stability of the human-robot interaction
p 560 N95-14051
Musculoskeletal adaptation to mechanical forces on Earth and in space p 548 N95-15136
A method for continuous monitoring of the Ground Reaction Force during daily activity p 549 N95-15139
MUSCULAR TONUS
Effect of short- and long-term spaceflight on the contractile properties of rat skeletal muscles with different functions p 539 N95-15141
Influence to organs by ten weeks tail suspension
p 539 N95-15142
MUSCULOSKELETAL SYSTEM
The musculoskeletal and vestibular effects of long term repeated exposure to sustained high-G
[AGARD-AR-317] p 562 N95-14263
The Physiologist, volume 36, number 1, supplement
p 541 N95-15089
Musculoskeletal adaptation to mechanical forces on Earth and in space p 548 N95-15136
Effect of short- and long-term spaceflight on the contractile properties of rat skeletal muscles with different functions p 539 N95-15141
Influence to organs by ten weeks tail suspension
p 539 N95-15142
Relationship between hind-limb muscle atrophy and serum enzymes in tail suspended rats
p 539 N95-15143
MYOCARDIAL INFARCTION
Cardiovascular deconditioning effects of long-term simulated weightlessness in rats p 538 N95-15099

N

N-TYPE SEMICONDUCTORS
Electrical characterization of 6H crystalline silicon carbide
[NASA-CR-197047] p 439 N95-14903

NAPHTHALENE
The Diffuse Interstellar Bands: Contributed papers
[NASA-CP-10144] p 639 N95-15827
Investigating the 3.3 micron infrared fluorescence from naphthalene following ultraviolet excitation
p 599 N95-15839

NASA PROGRAMS
A review of 50 years of aerodynamic research with NACA/NASA
[NASA-TM-109163] p 647 N95-13663
Engineering, technical, and management support services
[NASA-CR-196977] p 505 N95-13840
A strawman SLR program plan for the 1990s
p 471 N95-14289
The development of lossless data compression technology for remote sensing applications
p 565 N95-14593
Space science in the 1990's and beyond
[TABES PAPER 94-204] p 415 N95-14634
A NASA/industry/university partnership for development of dual-use vibration isolation technology
[TABES PAPER 94-613] p 416 N95-14643
Research and technology highlights, 1993
[NASA-TM-4575] p 647 N95-15065

NASA SPACE PROGRAMS
Our Mission to Planet Earth: A guide to teaching Earth system science
[NASA-EP-292] p 629 N95-13650
Design for reliability: NASA reliability preferred practices for design and test
[NASA-TM-106313] p 420 N95-13728
Space Generic Open Avionics Architecture (SGOAA): Overview p 569 N95-14161
Robotics technology developments in the United States space telerobotics program p 581 N95-14943

NATIONAL AIRSPACE SYSTEM
Vertical flight terminal operational procedures. A summary of FAA research and development
[AD-A283550] p 413 N95-15328

NATURAL LANGUAGE (COMPUTERS)
Discourse interpretation and the scope of operators
[TR-518] p 586 N95-15595

NATURAL LANGUAGE PROCESSING
Discourse interpretation and the scope of operators
[TR-518] p 586 N95-15595

NAUSEA
The effects of autogenic-feedback training on motion sickness severity and heart rate variability in astronauts
[NASA-TM-108840] p 539 N95-13661

NAVIER-STOKES EQUATION
The flow induced by the coalescence of two initially stationary drops
[NASA-TM-106752] p 478 N95-13653
User's guide for ENSAERO: A multidisciplinary program for fluid/structural/control interaction studies of aircraft (release 1)
[NASA-TM-108853] p 391 N95-13662
An adaptively-refined, Cartesian, cell-based scheme for the Euler and Navier-Stokes equations
[NASA-TM-106754] p 392 N95-13817
Numerical modeling of a cryogenic fluid within a fuel tank
[NASA-TM-4651] p 479 N95-13892
CFD methodology and validation for turbomachinery flows p 480 N95-14131
The role of CFD in the design process
p 481 N95-14135
Hybrid structured/unstructured grid computations for the F/A-18 at high angle of attack p 394 N95-14233
Radiative interactions in multi-dimensional chemically reacting flows using Monte Carlo simulations
[NASA-CR-197012] p 481 N95-14269
Eddy viscosity transport equations and their relation to the k-epsilon model
[NASA-TM-108854] p 481 N95-14273
A Cartesian, cell-based approach for adaptively-refined solutions of the Euler and Navier-Stokes equations
[NASA-TM-106786] p 398 N95-14297
Navier-Stokes predictions of missile aerodynamics
p 399 N95-14451
Two-layer viscous instability in a rotating couette device p 489 N95-14566
Numerical study of the effects of icing on viscous flow over wings
[NASA-CR-197102] p 400 N95-14803
Robust multigrid methods for the steady and unsteady incompressible Navier-Stokes equations in general coordinates
[PB94-195534] p 492 N95-15315
Computational methods for PDE's in flow control, superconductivity, fluid flows and other applications
[AD-A282912] p 493 N95-15390

NAVIGATION
Vision-based navigation and recognition
[AD-A282962] p 583 N95-15398

NAVIGATION AIDS
Spatial awareness comparisons between large-screen, integrated pictorial displays and conventional EFIS displays during simulated landing approaches
[NASA-TP-3467] p 409 N95-14852

NAVIGATION SATELLITES
Synergism of SLR and GPS p 471 N95-14286

NAVIGATION TECHNOLOGY SATELLITES
Journal of Spacecraft Technology, volume 4, no. 2, July 1994 p 413 N95-13825
Satellite communication technology and applications, 1995-2010 p 413 N95-13826

NAVY
Navy and the HARV: High angle of attack tactical utility issues p 397 N95-14252

NEAR INFRARED RADIATION
VUV shock layer radiation in an arc-jet wind tunnel experiment p 405 N95-13719

NEBULAE
The symbiosis of photometry and radial-velocity measurements p 643 N95-14505

NEEDS (DATA SYSTEM)
Geodetic survey of Canada: Results on a geoid questionnaire p 516 N95-15793

NEON
A theoretical study of 30 to 50 angstrom noble gas heavy ion lithography
[DE94-015262] p 442 N95-15436

NERVES
Tactile discrimination and representations of texture, shape, and softness p 558 N95-14041

NETWORK ANALYSIS
Automated network protocol reachability analysis with supertrace algorithm and TESTGEN: Automated generation of test sequence for a formal protocol specification
[AD-A280788] p 461 N95-14293
Robust routing in dynamic networks, part 1
[AD-A282445] p 583 N95-15548
New five-standard calibration procedures for network analyzers and wafer probes
[PB94-197662] p 478 N95-15611

NETWORK CONTROL
The Network Operations Control Center upgrade task: Lessons learned p 419 N95-14631
Robust routing in dynamic networks, part 1
[AD-A282445] p 583 N95-15548
Discrete-event-dynamic-system-based approaches for control in integrated voice/data multihop radio networks
[AD-A284413] p 470 N95-15813

NEURAL NETS
Artificial intelligence with applications for aircraft
[DOT/FAA/CT-94/41] p 581 N95-13895
Watch what you say, your computer might be listening: A review of automated speech recognition
p 555 N95-14021
Fault detection and diagnosis using neural network approaches p 571 N95-14170
Hardware implementation of a desktop supercomputer for high performance image processing. Color image processing using cellular neural networks
[AD-A283071] p 571 N95-14178
Three neural network based sensor systems for environmental monitoring
[DE94-014557] p 522 N95-14195
Neural networks: Alternatives to conventional techniques for automatic docking
[TABES PAPER 94-627] p 417 N95-14651
Artificial neural network modeling of damaged aircraft
[AD-A283227] p 409 N95-14849
Spatio-temporal neural networks for vision, reasoning and rapid decision making
[AD-A283251] p 583 N95-15403
Improving transient signal synthesis through noise modeling and noise removal
[AD-A281677] p 592 N95-15448
Supervised learning without output labels
[TR-510-REV] p 552 N95-15588
Vehicle health management using adaptive techniques
[NASA-TM-108472] p 431 N95-15609
First results with instance-based state identification for reinforcement learning
[TR-502] p 553 N95-15642

NEUROLOGY
Neural mechanisms of kinesthesia
p 555 N95-14018

NEURONS
Neuronal types in the chicken's statoacoustic ganglion
p 539 N95-15116

NEUROPHYSIOLOGY
Neuronal types in the chicken's statoacoustic ganglion
p 539 N95-15116

NEUROTRANSMITTERS
Measurement and regulation of central noradrenergic receptors
[AD-A284219] p 541 N95-14408
Neurohumoral reactions to long-term vestibular stimulation in man p 542 N95-15091

NEUTRAL ATOMS
Direct detection of neutral metal atoms in electron-stimulated desorption: Al from CH3O/Al(111). Velocity distribution and absolute yield
[DE94-014011] p 593 N95-14011

NEUTRAL GASES
Plasma dust crystallization p 490 N95-14571

NEUTRAL PARTICLES
Joint and angle-covariant spin measurements with a quadrupole magnetic field p 604 N95-13914

NEUTRINOS
Searches for massive neutrino emission in C-14 beta and Fe-55 electron-capture decays
[DE94-016863] p 594 N95-14374
Research accomplishments and future goals in particle physics
[DE94-015483] p 596 N95-15537
Search for W(prime) (yields) e(nu) in p(anti p) collisions at (radical)s = 1,800 GeV
[DE94-015188] p 597 N95-15630

NEUTRON BEAMS
Radioactivity measurements of ITER materials using the TFTR D-T neutron field
[DE94-016094] p 617 N95-14397

NEUTRON COUNTERS
Selection of non-destructive assay methods: Neutron counting or calorimetric assay?
[DE94-016211] p 505 N95-15777

NEUTRON DIFFRACTION
Analysis of neutron diffraction peak broadening caused by internal stresses in composite materials
[DE94-014453] p 433 N95-13993
The effect of microstresses on fatigue crack propagation in steel
[AD-A283872] p 506 N95-14356

NEUTRON EMISSION
Beta decay data for neutron-rich Li-Cl nuclides
[DE94-014556] p 595 N95-15310

NEUTRON IRRADIATION
Study of the long term stability of the effective concentration of ionized space charges (N(sub eff)) of neutron irradiated silicon detectors fabricated by various thermal oxidations
[DE94-013734] p 593 N95-14309
Radioactivity measurements of ITER materials using the TFTR D-T neutron field
[DE94-016094] p 617 N95-14397
Experiments to examine the contribution of gas atoms to void formation in irradiated metals
[DE94-015209] p 446 N95-15433
Cation disorder in high dose neutron irradiated spinel
[DE94-013118] p 455 N95-15579

NEUTRON SCATTERING
Inelastic neutron scattering and molecular dynamics simulations of water adsorbed in the molecular sieves AlPO4-11, AlPO4-5, AlPO4-8 and VPI-5
[DE94-013337] p 593 N95-13678
Intermultiplet transitions in optically opaque EuBa2Cu3O7: An inelastic neutron scattering study
[DE94-013429] p 620 N95-14188

NEUTRON STARS
Hadronic matter and rapidly rotating compact stars
[DE94-014928] p 643 N95-14442
ROSAT observations of the binary Be-star and radio pulsar PSR1259-63
[NASA-CR-196951] p 642 N95-15907

NEUTRONS
Scintillating glass fiber-optic neutron sensors
[DE94-014562] p 613 N95-15312

NEWTON METHODS
Higher harmonic control analysis for vibration reduction of helicopter rotor systems
[NASA-TM-103855] p 391 N95-14419

NICKEL
Influence of transmutation on microstructure, density change, and embrittlement of vanadium and vanadium alloys irradiated in HFIR
[DE94-015202] p 446 N95-15431
Stress corrosion crack tip microstructure in nickel-based alloys
[DE94-015362] p 446 N95-15532

NICKEL ALLOYS
Effects of hydrogen annealing, sulfur segregation and diffusion on the cyclic oxidation resistance of superalloys: A review
[NASA-TM-106734] p 444 N95-13667
Processing and characterization of mechanically alloyed NiAl-based alloys
[AD-A283959] p 444 N95-14202
High strain rate deformation of NiAl
[DE94-014810] p 445 N95-14439
Coherency strains and coarsening in Ni-Al-Si alloys: An experimental study
[DE94-015020] p 445 N95-14665
Fatigue in single crystal nickel superalloys
[AD-A282917] p 446 N95-15415
Stress corrosion crack tip microstructure in nickel-based alloys
[DE94-015362] p 446 N95-15532
Type 304L stainless steel surface microstructure: Performance in hydride storage and acid cleaning
[DE94-014654] p 447 N95-15625
Symposium on Structural Intermetallics: Perspectives on Science and Technology, volume 2
[AD-A283379] p 447 N95-15874

NIGHT VISION
Civil use of night vision devices: Evaluation pilot's guide, part 2
[DOT/FAA/RD-94/19] p 410 N95-14175
Distance estimation training with night vision goggles: A preliminary study
[AD-A284900] p 563 N95-15755

NITINOL ALLOYS
Legged vehicle for underwater mobile operations
[AD-A282891] p 503 N95-15294

NITRAMINE PROPELLANTS
Effects of two-phase flow on the deflagration of porous energetic materials
[DE94-015353] p 442 N95-15375

NITRIC OXIDE
Oxides of nitrogen: Their formation and control in stationary sources
[AD-A283780] p 522 N95-14337

NITROGEN
Ultrasensitive infrared chemiluminescence detection
[AD-A283531] p 440 N95-14958
Simulation of coal and char nitrogen reactions in combustion
[DE94-013941] p 440 N95-15291
Prototype explosives-detection system based on nuclear-resonance absorption in nitrogen
[DE94-015069] p 442 N95-15387

NITROGEN DIOXIDE
Oxides of nitrogen: Their formation and control in stationary sources
[AD-A283780] p 522 N95-14337

NITROGEN ISOTOPES
Beta decay data for neutron-rich Li-Cl nuclides
[DE94-014556] p 595 N95-15310

NITROGEN OXIDES
Oxides of nitrogen: Their formation and control in stationary sources
[AD-A283780] p 522 N95-14337
Simulation of coal and char nitrogen reactions in combustion
[DE94-013941] p 440 N95-15291

NITROUS OXIDES
Simulation of coal and char nitrogen reactions in combustion
[DE94-013941] p 440 N95-15291

NODULES
What those defects in optical coatings really look like
[DE94-015324] p 614 N95-15529

NOISE (SOUND)
Improving transient signal synthesis through noise modeling and noise removal
[AD-A281677] p 592 N95-15448

NOISE GENERATORS
Noise radiation by instability waves in coaxial jets
[NASA-TM-106738] p 591 N95-14618
Resonant interaction of a linear array of supersonic rectangular jets: An experimental study
[NASA-CR-195398] p 404 N95-15852

NOISE INTENSITY
Quantum amplification and quantum optical tapping with squeezed states and correlated quantum states
p 610 N95-13954
Ultra-high bypass ratio jet noise
[NASA-CR-195394] p 591 N95-14610
An in-home study of subjective response to simulated sonic booms p 403 N95-14891

NOISE PREDICTION
Noise radiation by instability waves in coaxial jets
[NASA-TM-106738] p 591 N95-14618
Investigation of Allan variance for determining noise spectral forms with application to microwave radiometry
[NASA-CR-194985] p 516 N95-15727

NOISE PREDICTION (AIRCRAFT)
Ultra-high bypass ratio jet noise
[NASA-CR-195394] p 591 N95-14610
The aeroacoustics of supersonic coaxial jets
[NASA-TM-106782] p 591 N95-15059

NOISE REDUCTION
Multipath noise reduction spread spectrum signals
[NASA-CASE-NPO-18970-1-CU] p 460 N95-13628
Modification of the Ames 40- by 80-foot wind tunnel for component acoustic testing for the second generation supersonic transport
[NASA-TM-108850] p 391 N95-13642
Simultaneous two component squeezing in generalized q-coherent states p 598 N95-13908
How to characterize the nonlinear amplifier?
p 471 N95-13922
Sub-Poissonian light and photocurrent shot-noise suppression in closed opto-electronic loop
p 606 N95-13924
Ultra-high bypass ratio jet noise
[NASA-CR-195394] p 591 N95-14610
The aeroacoustics of supersonic coaxial jets
[NASA-TM-106782] p 591 N95-15059
Resonant interaction of a linear array of supersonic rectangular jets: An experimental study
[NASA-CR-195398] p 404 N95-15852

NOISE SPECTRA
Investigation of Allan variance for determining noise spectral forms with application to microwave radiometry
[NASA-CR-194985] p 516 N95-15727

NOISE THRESHOLD
How to characterize the nonlinear amplifier?
p 471 N95-13922
Performance comparison AN/FRD-10 versus PUSHER
[AD-A283263] p 469 N95-15619

NOISE TOLERANCE
Deriving a dosage-response relationship for community response to high-energy impulsive noise
p 403 N95-14890
An in-home study of subjective response to simulated sonic booms p 403 N95-14891
Residents' reactions to long-term sonic boom exposure: Preliminary results p 403 N95-14892

NOMENCLATURES
Acronyms, initialisms, and abbreviations
[DE94-016686] p 632 N95-15366

NONANES
Porphyrins in the interstellar medium (in grains)
p 640 N95-15837

NONDESTRUCTIVE TESTS
Nondestructive analysis and development
[NASA-CR-196987] p 505 N95-13886
Nondestructive characterization of structural ceramic components
[DE94-013961] p 449 N95-13978
Ground penetrating radar surveys to characterize pavement layer thickness variations at GPS sites
[PB94-190170] p 460 N95-14119
The advanced development of x-ray computed tomography applications
[AD-A284211] p 434 N95-14411
Analysis of small crack behavior for airframe applications p 512 N95-14484
Space Shuttle Main Engine turbopump bearing assessment program
[TABES PAPER 94-621] p 417 N95-14648
Milestone 4: Thrust structure concepts and IHM screening Graphite Composite Primary Structure (GCPS)
[NASA-CR-197053] p 434 N95-14800
Advanced Turbine Technology Applications Project (ATTAP)
[NASA-CR-195393] p 634 N95-15743

NONEQUILIBRIUM FLOW
An approximate Riemann solver for thermal and chemical nonequilibrium flows
[NASA-CR-195003] p 492 N95-14912

NONEQUILIBRIUM PLASMAS
Development and analysis of high-energy corona process for air purification
[DE94-015207] p 524 N95-15432

NONEQUILIBRIUM RADIATION
Measured and calculated spectral radiation from a blunt body shock layer in an arc-jet wind tunnel
[AIAA PAPER 94-0086] p 405 N95-13720

NONGRAY GAS
Radiative interactions in multi-dimensional chemically reacting flows using Monte Carlo simulations
[NASA-CR-197012] p 481 N95-14269

NONINTRUSIVE MEASUREMENT
Compact simultaneous-beam optical strain measurement system, phase 5
[NASA-CR-195396] p 601 N95-13666
Measurement of resistance to solute transport across surfactant-laden interfaces using a Fluorescence Recovery After Photobleaching (FRAP) technique
p 490 N95-14574

NONLINEAR EQUATIONS
Sqeezing generated by a nonlinear master equation and by amplifying-dissipative Hamiltonians
p 588 N95-13926
Nonlinear asymptotic integration algorithms for one-dimensional autonomous dissipative first-order ODEs
[NASA-TM-106780] p 585 N95-14300
Linear and nonlinear dynamic analysis of redundant load path bearingless rotor systems
[NASA-CR-197220] p 503 N95-14923

NONLINEAR FEEDBACK
Three-axis stabilization of spacecraft using parameter-independent nonlinear quaternion feedback
[NASA-TM-109150] p 420 N95-13729

NONLINEAR FILTERS
Passive fetal heart rate monitoring apparatus and method with enhanced fetal heart beat discrimination
[NASA-CASE-LAR-15129-1] p 541 N95-14184

NONLINEAR OPTICS
Investigation of dipolar reorientation dynamics of pure bulk polymers using second harmonic generation
[AD-A283023] p 448 N95-13688
Relaxation of polar orientational order in nonlinear optical polymers by second harmonic generation
[AD-A283024] p 449 N95-13689
On the theory of quantum measurement
p 604 N95-13910

NONLINEAR SYSTEMS
Identification of dynamic systems. Volume 3: Applications to aircraft. Part 2: Nonlinear analysis and manoeuvre design
[AGARD-AG-300-VOL-3-PT-2] p 408 N95-14102
A Workshop on New Directions in Extremal Stochastic Analysis of Nonlinear Ocean Systems
[AD-A283969] p 535 N95-14204
Mathematical problems of nonlinear wave propagation and of waves in heterogeneous media
[AD-A282217] p 492 N95-14605
Linear quadratic Gaussian and feedforward controllers for the DSS-13 antenna p 463 N95-14625

NONLINEARITY
Chaotic time series. Part 2: System identification and prediction
[PB94-207115] p 589 N95-13630
A vision based attitude and position estimation algorithm for rendezvous and docking p 414 N95-13831
On the theory of quantum measurement
p 604 N95-13910
How to characterize the nonlinear amplifier?
p 471 N95-13922
Quantum propagation in single mode fiber
p 609 N95-13953
Nonlinear and stochastic numerical methods and their applications
[AD-A284863] p 588 N95-14370
Nonlinear fracture mechanics-based analysis of thin wall cylinders p 508 N95-14462
Fracture mechanics validity limits p 511 N95-14480
Nonlinear dynamics of drops and bubbles and chaotic phenomena p 485 N95-14541
Two-layer viscous instability in a rotating couette device p 489 N95-14566
Lossless compression of NOAA-AVHRR satellite data
p 565 N95-14592
Linear quadratic Gaussian and feedforward controllers for the DSS-13 antenna p 463 N95-14625
Numerical model for the weakly nonlinear propagation of sound through turbulence p 401 N95-14883
Sonic boom interaction with turbulence
p 402 N95-14884
Computational methods for PDE's in flow control, superconductivity, fluid flows and other applications
[AD-A282912] p 493 N95-15390
Problems in nonlinear acoustics: Surface acoustic waves, diffracting sound beams, and fluid-solid interface effects
[AD-A281714] p 592 N95-15453
Theory of nonlinear, distortive phenomena in solids: Martensitic, crack, and multiscale structures-phenomenology and physics
[DE94-015653] p 447 N95-15631

NONNEWTONIAN FLUIDS
Resonator response to non-Newtonian fluids
[DE94-013450] p 473 N95-14308

NONUNIFORM MAGNETIC FIELDS
MHD flow in rectangular ducts with inclined non-uniform transverse magnetic field
[DE94-013989] p 616 N95-14006

NONUNIFORMITY
Bone geometry, structure and mineral distribution using Dual energy X ray Absorptiometry (DXA)
p 549 N95-15140

NORADRENALINE
Measurement and regulation of central noradrenergic receptors
[AD-A284219] p 541 N95-14408
NOREPINEPHRINE
Measurement and regulation of central noradrenergic receptors
[AD-A284219] p 541 N95-14408
NORMAL DENSITY FUNCTIONS
Modes in light wave propagating in semiconductor laser p 500 N95-13925
Some rules for polydimensional squeezing p 608 N95-13941
NOVA LASER SYSTEM
Review of drive symmetry measurement and control experiments on the Nova laser system
[DE94-014455] p 498 N95-13994
NOWCASTING
Nowcasting convective storm evolution in east-central Florida using satellite and Doppler radar data
[AD-A283260] p 534 N95-15618
The operational forecasting/nowcasting of precipitation type in the southeastern United States type of precipitation: Descriptive and objective guidance
[AD-A284456] p 535 N95-15819
NOZZLE GEOMETRY
Ultra-high bypass ratio jet noise
[NASA-CR-195394] p 591 N95-14610
Investigation of ramp injectors for supersonic mixing enhancement
[NASA-CR-4634] p 494 N95-15605
NOZZLE INSERTS
Investigation of ramp injectors for supersonic mixing enhancement
[NASA-CR-4634] p 494 N95-15605
NOZZLES
Welding nozzle position manipulator
[NASA-CASE-MFS-29837-1] p 500 N95-13654
NUCLEAR ELECTRIC POWER GENERATION
General properties of quantum optical systems in a strong field limit p 609 N95-13950
NUCLEAR ELECTRIC PROPULSION
Alkali metal Rankine cycle boiler technology challenges and some potential solutions for space nuclear power and propulsion applications
[NASA-TM-106593] p 430 N95-14174
NUCLEAR ENGINE FOR ROCKET VEHICLES
The rationale/benefits of nuclear thermal rocket propulsion for NASA's lunar space transportation system
[NASA-TM-106739] p 431 N95-15682
NUCLEAR EXPLOSIONS
Large scale obscuration and related climate effects open literature bibliography
[DE94-012992] p 524 N95-15575
NUCLEAR FUSION
Tokamak power plant burn cycle options
[DE94-014016] p 617 N95-14012
Accelerator and Fusion Research Division: 1993 Summary of activities
[DE94-015157] p 599 N95-15367
NUCLEAR MAGNETIC RESONANCE
NMR studies of polymers at interfaces
[AD-A281570] p 455 N95-15458
Selective RF pulses in NMR and their effect on coupled and uncoupled spin systems
[PB94-195526] p 471 N95-15871
NUCLEAR MODELS
Finite boson mappings of fermion systems
[DE94-014478] p 593 N95-14000
From the shell model to the interacting boson model
[DE94-014486] p 593 N95-14001
NUCLEAR PHYSICS
Accelerator and Fusion Research Division: 1993 Summary of activities
[DE94-015157] p 599 N95-15367
NUCLEAR POWER PLANTS
Advanced stellarator power plants
[DE94-014442] p 616 N95-14007
Tokamak power plant burn cycle options
[DE94-014016] p 617 N95-14012
NUCLEAR PROPULSION
Fast track NTR systems assessment for NASA's first lunar outpost scenario
[NASA-TM-106748] p 429 N95-13668
The rationale/benefits of nuclear thermal rocket propulsion for NASA's lunar space transportation system
[NASA-TM-106739] p 431 N95-15682
NUCLEAR ROCKET ENGINES
Fast track NTR systems assessment for NASA's first lunar outpost scenario
[NASA-TM-106748] p 429 N95-13668
NUCLEAR SPIN
The strong Bell inequalities: A proposed experimental test p 611 N95-13986
NUCLEAR WEAPONS
Integrated optical maze
[DE94-015866] p 613 N95-14367
NUCLEATE BOILING
Pool and flow boiling in variable and microgravity p 459 N95-14562
NUCLEATION
Nucleation and chiral symmetry breaking under controlled hydrodynamic flows p 489 N95-14570
Dynamics of hard sphere colloidal dispersions p 490 N95-14573
Atomic force microscopy of the electrochemical nucleation and growth of molecular crystals
[AD-A280958] p 622 N95-14601
Experiments to examine the contribution of gas atoms to void formation in irradiated metals
[DE94-015209] p 446 N95-15433
Transport and nucleation processes during the vapor growth of diamond
[AD-A284411] p 626 N95-15812
NUCLEONS
Research accomplishments and future goals in particle physics
[DE94-015483] p 596 N95-15537
Research in high energy physics
[DE94-015519] p 600 N95-15539
NUCLEOPHILES
Chemically modified electrodes by nucleophilic substitution of chlorosilylated platinum oxide surfaces
[AD-A281567] p 477 N95-15456
NUCLIDES
Production profiles of nuclides by galactic-cosmic-ray particles in small meteoroids
[DE94-014801] p 646 N95-14437
Beta decay data for neutron-rich Li-Cl nuclides
[DE94-014556] p 595 N95-15310
NUMERICAL ANALYSIS
The solid surface combustion experiment aboard the USML-1 mission p 458 N95-14212
Bifurcation of rotating liquid drops: Results from USML-1 experiments in space p 458 N95-14219
A novel technique for 4-dimensional atmosphere and oceanographic irradiance measurements using 3-D spatial filtering
[AD-A283758] p 613 N95-14353
Nonlinear and stochastic numerical methods and their applications
[AD-A284863] p 588 N95-14370
Workshop on Advances in Scientific Computation and Differential Equations 1993 (SCADE)
[AD-A283111] p 585 N95-14657
Eccentricity of the electron beam in a gyrotron cavity
[PB94-197639] p 496 N95-14839
Modelling and investigation of EHD point contacts
[AD-A283571] p 454 N95-15316
Data processing routines for the Sippican MK-12 XBT system
[AD-A283570] p 536 N95-15330
A strategy for geoid repairing p 517 N95-15798
Two methods for the study of vortex patch evolution on locally refined grids
[DE94-014965] p 494 N95-15867
NUMERICAL CONTROL
Adaptive optics at Lick Observatory: System architecture and operations
[DE94-012387] p 601 N95-13672
Diagnostic development and support of MHD test facilities
[DE94-015344] p 618 N95-15373
NUMERICAL INTEGRATION
Nonlinear asymptotic integration algorithms for one-dimensional autonomous dissipative first-order ODEs
[NASA-TM-106780] p 585 N95-14300
NUMERICAL STABILITY
Nonlinear asymptotic integration algorithms for one-dimensional autonomous dissipative first-order ODEs
[NASA-TM-106780] p 585 N95-14300
NUMERICAL WEATHER FORECASTING
The operational forecasting/nowcasting of precipitation type in the southeastern United States type of precipitation: Descriptive and objective guidance
[AD-A284456] p 535 N95-15819
NUTRITION
The relationship between space sickness and preflight diet p 546 N95-15122
20 days bed-rest on insulin action in relation to body fat in young subjects p 549 N95-15145
NUTS (FASTENERS)
Experimental analysis of thread movement in bolted connections due to vibrations
[NASA-CR-197065] p 502 N95-14904

O

O RING SEALS
Burn rates of TiH2/KClO4/Viton and output testing of NASA SKD26100098-301 pressure cartridges
[NASA-CR-188357] p 443 N95-15715
O STARS
Diffuse interstellar bands between 3900 A and 4200 A p 640 N95-15834
L(alpha)-induced two-photon absorption of visible light emitted from an O-type star by H2(+) ions located near the surface of the Stromgren sphere surrounding the star: A possible explanation for the diffuse interstellar absorption bands (DIBs) p 641 N95-15845
OBJECT-ORIENTED PROGRAMMING
A prototype lisp-based soft real-time object-oriented Graphical User Interface for control system development
[NASA-TM-106743] p 566 N95-13716
Knowledge-based processing for aircraft flight control
[NASA-CR-194976] p 580 N95-13727
A multi-level object store and its application to HEP data analysis
[DE94-014010] p 568 N95-14010
RICIS Symposium 1992: Mission and Safety Critical Systems Research and Applications
[NASA-CR-196963] p 569 N95-14156
Ada 9X overview p 570 N95-14166
CIFO 3.0 p 570 N95-14167
Expert systems in the process industries p 571 N95-14169
Reuseable Objects Software Environment (ROSE): Introduction to Air Force Software Reuse Workshop
[NASA-CR-197017] p 572 N95-14520
Product life cycle data base, analysis and simulation integration methodology
[TABES PAPER 94-626] p 417 N95-14650
Introduction to HEFeS (Hierarchical Environmental Feature Simulator)
[AD-A283244] p 534 N95-15402
ROOM: A recursive object oriented method for information systems development
[DE94-007575] p 633 N95-15761
OBSERVATION
Direct observation of oil consumption mechanisms in a production spark ignition engine using fluorescence techniques
[AD-A283842] p 501 N95-14347
Learning with incomplete selective perception
[TR-453] p 577 N95-15860
OBSERVATORIES
Observations of extragalactic sources with the Metsaehovi radio telescope at 22-87 GHz
[PB94-197712] p 637 N95-13982
OCCULTATION
Prediction of particulate contamination on aperture window p 420 N95-14064
OCEAN BOTTOM
From Antarctica to space: Use of telepresence and virtual reality in control of remote vehicles p 427 N95-14099
OCEAN CURRENTS
Design document for the Surface Currents Data Base (SCDB) Management System (SCDBMS), version 1.0
[NASA-CR-197019] p 537 N95-15751
Users manual for the Surface Currents Data Base (SCDB) Management System (SCDBMS), version 1.0
[NASA-CR-197021] p 537 N95-15753
OCEAN DYNAMICS
Selecting wave gauge sites for monitoring harbor oscillations: A case study for Kahului Harbor, Hawaii
[AD-A281707] p 536 N95-15452
OCEAN MODELS
Connection machine software conversion of the Navy TOPS model
[AD-A281681] p 579 N95-15450
Selecting wave gauge sites for monitoring harbor oscillations: A case study for Kahului Harbor, Hawaii
[AD-A281707] p 536 N95-15452
An analysis of eddy resolving global ocean models in the Southern Ocean
[AD-A283211] p 536 N95-15626
OCEAN SURFACE
Precision orbit determination of altimetric satellites p 418 N95-14262
International Geoid Service Bulletin No. 1
[BULL-1] p 516 N95-15791
The GEOMED Project p 516 N95-15794
The Bureau Gravimetrique International p 516 N95-15795
Validation of ERS-1 environmental data products
[NASA-CR-197111] p 517 N95-15848
OCEAN TEMPERATURE
Real time system for practical acoustic monitoring of global ocean temperature, volume 3
[AD-A283774] p 535 N95-14335

OCEANOGRAPHIC PARAMETERS
A Workshop on New Directions in Extremal Stochastic Analysis of Nonlinear Ocean Systems
[AD-A283969] p 535 N95-14204
Modern methods in meteorological and oceanographic data acquisition and analyses
[AD-A283038] p 533 N95-14848
Users manual for the Surface Currents Data Base (SCDB) Management System (SCDBMS), version 1.0
[NASA-CR-197021] p 537 N95-15753
Design document for the MOODS Data Management System (MDMS), version 1.0
[NASA-CR-197016] p 633 N95-15801
OCEANOGRAPHY
A novel technique for 4-dimensional atmosphere and oceanographic irradiance measurements using 3-D spatial filtering
[AD-A283758] p 613 N95-14353
OCEANS
Calculation of movable bed friction factors
[AD-A283529] p 536 N95-15440
Validation of ERS-1 environmental data products
[NASA-CR-197111] p 517 N95-15848
OFF-ON CONTROL
A simple analytical model for dense WDM/OOK systems
[AD-A283229] p 478 N95-15628
OILS
Direct observation of oil consumption mechanisms in a production spark ignition engine using fluorescence techniques
[AD-A283842] p 501 N95-14347
OLIGOMERS
Phenylethynyl terminated imide oligomers
[NASA-CASE-LAR-15175-1] p 450 N95-14185
AASERT 92: Synthesis and properties of complex polyarylene vinylenes
[AD-A284215] p 452 N95-14406
ON-LINE SYSTEMS
The prospects for on-line hybrid coherency protocols on bus-based multiprocessors
[TR-490] p 579 N95-15590
Density control and on-line labeling problems
[TR-481] p 576 N95-15789
ONTOGENY
Vestibular ontogeny: Measuring the influence of the dynamic environment p 544 N95-15105
OPERATING SYSTEMS (COMPUTERS)
POSIX real-time extensions p 570 N95-14165
System administrator's guide to CDPS
[DE94-015288] p 633 N95-15528
OPERATING TEMPERATURE
Pulsed mode cathode
[NASA-CASE-LEW-15753-1] p 475 N95-14516
High Temperature Calibration Furnace System user's guide
[NASA-CR-196526] p 573 N95-14905
OPERATIONAL AMPLIFIERS
Theory and implementation of a VLSI stray insensitive switched capacitor composite operational amplifier
[AD-A283536] p 476 N95-15325
OPERATOR PERFORMANCE
Human operator tracking performance with a vibrotactile display p 560 N95-14049
Human factors requirements for telerobotic command and control: The European Space Agency experimental programme p 562 N95-14059
OPERATORS (MATHEMATICS)
High-speed fixed and floating point implementation of delta-operator formulated discrete time systems
[AD-A283109] p 584 N95-13694
Phase properties of multicomponent superposition states in various amplifiers p 605 N95-13923
Schroedinger operators with the q-ladder symmetry algebras p 588 N95-13942
Two methods for the study of vortex patch evolution on locally refined grids
[DE94-014965] p 494 N95-15867
OPHTHALMOLOGY
Technical guidance for the development of a solid state image sensor for human low vision image warping
[NASA-CR-196997] p 612 N95-14272
OPTICAL COMMUNICATION
An optical simulation of shared memory
[DE94-013824] p 568 N95-13976
The Telecommunications and Data Acquisition Report
[NASA-CR-196409] p 462 N95-14620
The Stark anomalous dispersion optical filter: The theory p 462 N95-14622
Research and development optical deep space antenna sizing study p 463 N95-14628
Asymmetric coupled quantum wells for high speed optical modulators at communication wavelengths
[AD-A281572] p 477 N95-15459
A simple analytical model for dense WDM/OOK systems
[AD-A283229] p 478 N95-15628
High speed QPPM direct detection optical communication receivers for FSDD intersatellite links
[NASA-CR-189331] p 615 N95-15849
OPTICAL COMPUTERS
An optical simulation of shared memory
[DE94-013824] p 568 N95-13976
OPTICAL COUPLING
Aberration correction of unstable resonators
[NASA-CASE-NPO-18662-1-CU] p 602 N95-13823
Spectral, noise and correlation properties of intense squeezed light generated by a coupling in two laser fields p 500 N95-13903
OPTICAL DATA PROCESSING
Two-dimensional signal processing, optical information storage and processing, and electromagnetic measurements
[AD-A281937] p 460 N95-13657
OPTICAL DISKS
SODR Memory Control Buffer Control ASIC
[NASA-CR-197001] p 566 N95-14514
OPTICAL EQUIPMENT
Investigation of the effects of long duration space exposure on active optical system components
[NASA-CR-4632] p 601 N95-13660
A femtosecond optical parametric oscillator near 3 microns
[DE94-014500] p 612 N95-13986
Self contamination effects in the TAUVEX UV Telescope: Ground testing and computer simulation p 421 N95-14067
Alpha LAMP Integration Facility p 418 N95-14094
Cut-off-mesa isolated rib optical waveguide for 3-5 heterostructure PICs
[DE94-014661] p 474 N95-14315
Wide field strip-imaging optical system
[NASA-CASE-NPO-18146-2-CU] p 613 N95-14413
Diagnostic development and support of MHD test facilities
[DE94-015344] p 618 N95-15373
Integrated photonics research, 1993
[AD-A281578] p 614 N95-15464
OPTICAL FIBERS
Project OART: WDM, EDFA's and mixed data rates in a real-world testbed
[DE94-012234] p 601 N95-13670
Quantum propagation in single mode fiber p 609 N95-13953
Wide field strip-imaging optical system
[NASA-CASE-NPO-18146-2-CU] p 613 N95-14413
Scintillating glass fiber-optic neutron sensors
[DE94-014562] p 613 N95-15312
Low loss glass and optical fibers therefrom
[AD-D016379] p 615 N95-15766
OPTICAL FILTERS
The Stark anomalous dispersion optical filter: The theory p 462 N95-14622
Variable window Gabor filters and their use in focus and correspondence
[AD-A282837] p 573 N95-14842
A simple analytical model for dense WDM/OOK systems
[AD-A283229] p 478 N95-15628
OPTICAL MATERIALS
The electromagnetic spectrum. Research investigation directed toward extending the useful range of the electromagnetic spectrum
[AD-A281378] p 461 N95-14361
Aero-optics system integration
[TABES PAPER 94-604] p 415 N95-14638
What those defects in optical coatings really look like
[DE94-015324] p 614 N95-15529
Low-damage multilayer mirror for the soft x ray region
[AD-D016362] p 614 N95-15764
Fundamental studies of diamond growth and surface reactions
[AD-A284390] p 626 N95-15808
OPTICAL MEASUREMENT
On the theory of quantum measurement p 604 N95-13910
Bloch vector projection noise p 610 N95-13956
OPTICAL MEASURING INSTRUMENTS
Compact simultaneous-beam optical strain measurement system, phase 5
[NASA-CR-195396] p 601 N95-13666
OPTICAL MEMORY (DATA STORAGE)
Two-dimensional signal processing, optical information storage and processing, and electromagnetic measurements
[AD-A281937] p 460 N95-13657
SODR Memory Control Buffer Control ASIC
[NASA-CR-197001] p 566 N95-14514
OPTICAL MICROSCOPES
Analysis of electron microscope images: 3-D localization of immuno-markers
[PB94-197977] p 537 N95-13990
OPTICAL PATHS
Method of locating ground faults
[NASA-CASE-LEW-15407-1] p 478 N95-15669
OPTICAL PROPERTIES
Development of chemical-vapor-deposited diamond for infrared optical applications: Summary of properties
[AD-A282999] p 448 N95-13686
PC-based MIE scattering program for theoretical investigations of the optical properties of atmospheric aerosols as a function of composition and relative humidity
[PB94-192739] p 529 N95-14404
Optical analysis methods for material films condensed on cryogenic surfaces of spacecraft
[AD-A284014] p 427 N95-14420
Results of the examination of LDEF polyurethane thermal control coatings
[NASA-CR-4617] p 432 N95-14603
Relationship between microstructure and efficiency of scintillating glasses
[DE94-014563] p 454 N95-15313
Synthesis and applications of large heterometallic cluster systems
[AD-A284874] p 626 N95-15748
Low Temperature Grown and Highly Non-Stoichiometric GaAs and Related Materials
[AD-A284898] p 626 N95-15754
Low loss glass and optical fibers therefrom
[AD-D016379] p 615 N95-15766
OPTICAL PUMPING
Double ionization in gases driven by optical field ionization using ultrashort laser pulses
[DE94-015137] p 498 N95-14318
High power diode pumped solid state laser development at Lawrence Livermore National Laboratory
[DE94-015899] p 499 N95-14427
OPTICAL RADAR
Burst-by-burst laser frequency monitor
[NASA-CASE-NPO-18596-1-CU] p 498 N95-13629
Propagation Modelling and Decision Aids for Communications, Radar and Navigation Systems
[AGARD-LS-196] p 466 N95-14825
Sensing of radio refractivity and aerosol extinction p 467 N95-14830
Receiver design, performance analysis, and evaluation for space-borne laser altimeters and space-to-space laser ranging systems
[NASA-CR-197050] p 499 N95-14901
Research on characterization of the upper atmosphere using lidar
[AD-A283241] p 530 N95-15401
Measurements of upper tropospheric moisture with a Raman lidar
[DE94-015748] p 531 N95-15411
Preliminary DIAL model
[DE94-013243] p 469 N95-15583
OPTICAL RESONATORS
Aberration correction of unstable resonators
[NASA-CASE-NPO-18662-1-CU] p 602 N95-13823
Production of squeezed states for macroscopic mechanical oscillator p 603 N95-13906
OPTICAL SCANNERS
The effect of Low Earth Orbit exposure on some experimental fluorine and silicon-containing polymers p 422 N95-14074
OPTICAL SWITCHING
Integrated optical maze
[DE94-015866] p 613 N95-14367
High power diode pumped solid state laser development at Lawrence Livermore National Laboratory
[DE94-015899] p 499 N95-14427
Asymmetric coupled quantum wells for high speed optical modulators at communication wavelengths
[AD-A281572] p 477 N95-15459
High-efficiency electro-optic grating on PLZT ceramic wafer for optical switching
[AD-A281573] p 477 N95-15460
Integrated photonics research, 1993
[AD-A281578] p 614 N95-15464
OPTICAL THICKNESS
Low-damage multilayer mirror for the soft x ray region
[AD-D016362] p 614 N95-15764
OPTICAL TRACKING
Human operator tracking performance with a vibrotactile display p 560 N95-14049
Global and regional kinematics from SLR stations p 527 N95-14278
SLR tracking of GPS-35 p 471 N95-14285
SLR 2000 p 471 N95-14288
Space debris detection and analysis
[AD-A282012] p 428 N95-14951

OPTICAL WAVEGUIDES
Modes in light wave propagating in semiconductor laser p 500 N95-13925
Cut-off-mesa isolated rib optical waveguide for 3-5 heterostructure PICs
[DE94-014661] p 474 N95-14315
Optically controlled MMW beamsteering beamforming antenna
[AD-A282831] p 614 N95-15414
Integrated photonics research, 1993
[AD-A281578] p 614 N95-15464
OPTIMAL CONTROL
Computational methods for PDE's in flow control, superconductivity, fluid flows and other applications
[AD-A282912] p 493 N95-15390
OPTIMIZATION
Computer aided techniques for the realisation of the diaphragm of the PSM for the IRS-1C
p 413 N95-13829
Turbomachinery Design Using CFD
[AGARD-LS-195] p 479 N95-14127
Computational methods for preliminary design and geometry definition in turbomachinery
p 480 N95-14128
Elements of a modern turbomachinery design system
p 480 N95-14129
Comparison of transform coding methods with an optimal predictor for the data compression of digital elevation models p 564 N95-14587
A Multiple Divide-and-Conquer (MDC) algorithm for optimal alignments in linear space
[DE94-015457] p 574 N95-15536
Weighted NP optimization problems: Logical definability and approximation properties
[TR-516] p 587 N95-15596
Module process optimization and device efficiency improvement for stable, low-cost, large-area, cadmium telluride-based photovoltaic module production
[DE94-011817] p 521 N95-15863
OPTOELECTRONIC DEVICES
Sub-Poissonian light and photocurrent shot-noise suppression in closed opto-electronic loop
p 606 N95-13924
Cut-off-mesa isolated rib optical waveguide for 3-5 heterostructure PICs
[DE94-014661] p 474 N95-14315
In situ grown quantum-wire lasers
[AD-A281381] p 499 N95-14364
ORBIT CALCULATION
Precision orbit determination of altimetric satellites
p 418 N95-14282
Synergism of SLR and GPS p 471 N95-14286
Satellite Laser Ranging operations
p 500 N95-14287
An unmanned mission to Mars with sample collection and in-situ resource utilization
[NASA-CR-197202] p 645 N95-14868
ORBIT TRANSFER VEHICLES
Fast track NTR systems assessment for NASA's first lunar outpost scenario
[NASA-TM-106748] p 429 N95-13668
Space transfer vehicle concepts and requirements study. Volume 3: Program cost estimates. Book 2: WBS and dictionary
[NASA-CR-192447] p 419 N95-15552
ORBITAL ASSEMBLY
A simulation facility for testing Space Station assembly procedures p 423 N95-14075
ORBITAL LIFETIME
A simulation algorithm for availability computation of a communication satellite constellation
p 414 N95-13832
ORBITAL POSITION ESTIMATION
The long-term forecast of station view periods
p 419 N95-14621
ORBITAL RENDEZVOUS
A vision based attitude and position estimation algorithm for rendezvous and docking p 414 N95-13831
Neural networks: Alternatives to conventional techniques for automatic docking
[TABES PAPER 94-627] p 417 N95-14651
ORBITAL SERVICING
Hubble Space Telescope servicing mission scientific instrument protective enclosure design requirements and contamination controls p 421 N95-14068
ORDER-DISORDER TRANSFORMATIONS
Polarized photomodulated reflectivity and photoluminescence studies of ordered InGaP2 under pressure
[DE94-016556] p 621 N95-14390
ORDNANCE
Subsurface object position and image correction for standoff ground penetrating radar
[DE94-015180] p 468 N95-15300
ORGANIC COMPOUNDS
Emerging technology summary: Destruction of organic contaminants in air using advanced ultraviolet flashlamps
[PB94-194479] p 521 N95-14121
ORGANISMS
The avian embryo responding to microgravity of space flight p 538 N95-15104
ORGANIZATIONS
International energy: Research organizations, 1988-1992
[DE90-017267] p 630 N95-13726
The Teleprasenz Consortium: Structure and intentions
p 558 N95-14039
Benefits of CMM-based software process improvement: Initial results
[AD-A283848] p 572 N95-14349
ORGANOMETALLIC COMPOUNDS
Radical polymerization of vinyl acetate and methyl methacrylate using organochromium initiators complexed with macrocyclic polyamines
[AD-A280828] p 451 N95-14316
The transformation of organic amines by transition metal cluster compounds
[DE94-017151] p 441 N95-15346
ORIENTATION
Neural networks: Alternatives to conventional techniques for automatic docking
[TABES PAPER 94-627] p 417 N95-14651
ORTHOSTATIC TOLERANCE
Extended duration orbiter medical project countermeasure to reduce post space flight orthostatic intolerance (LBNP) (STS-50/USML-1)
p 551 N95-14224
Simulation of the fluid retention effects of a vasopressin analog using the Guyton model of circulation
p 547 N95-15130
Orthostatic stress by lower body negative pressure and its body fluid distribution kinetics under microgravity
p 549 N95-15138
OSCILLATING FLOW
Oscillatory/chaotic thermocapillary flow induced by radiant heating p 483 N95-14531
Nonlinear dynamics of drops and bubbles and chaotic phenomena p 485 N95-14541
OSCILLATIONS
Nonresonant interaction of ultrashort electromagnetic pulses with multilevel quantum systems
p 610 N95-13960
Experimental implementation of a robust damped-oscillation control algorithm on a full-sized, two-degree-of-freedom, AC induction motor-driven crane
[DE94-012113] p 501 N95-14005
Core-centering of compound drops in capillary oscillations: Observations on USML-1 experiments in space p 458 N95-14218
Surface characterization through shape oscillations of drops in microgravity and 1-g p 458 N95-14220
Asteroseismology: Theory and phenomenology
p 643 N95-14502
Stabilization of thermocapillary convection by means of nonplanar flow oscillations p 482 N95-14524
Control of oscillatory thermocapillary convection in microgravity p 483 N95-14525
Oscillatory thermocapillary convection
p 483 N95-14526
Dynamics and statics of nonaxisymmetric and symmetric liquid bridges p 484 N95-14533
OSCILLATORS
Advanced laser source research
[AD-A283110] p 498 N95-13695
Homodyning and heterodyning the quantum phase
p 604 N95-13913
Measurement of very small phase fluctuations by means of the operational approach p 605 N95-13916
Quantum statistics of Raman scattering model with Stokes mode generation p 610 N95-13958
Selecting wave,gauge sites for monitoring harbor oscillations: A case study for Kahului Harbor, Hawaii
[AD-A281707] p 536 N95-15452
OSMIUM COMPOUNDS
The transformation of organic amines by transition metal cluster compounds
[DE94-017151] p 441 N95-15346
OSTWALD RIPENING
Coherency strains and coarsening in Ni-Al-Si alloys: An experimental study
[DE94-015020] p 445 N95-14665
OTOLITH ORGANS
The musculoskeletal and vestibular effects of long term repeated exposure to sustained high-G
[AGARD-AR-317] p 562 N95-14263
Are otoconia dynamic in birds and mammals?
p 538 N95-15103
OUTGASSING
ASTM E 1559 method for measuring material outgassing/deposition kinetics has applications to aerospace, electronics, and semiconductor industries
p 421 N95-14066
Hubble Space Telescope servicing mission scientific instrument protective enclosure design requirements and contamination controls p 421 N95-14068
Optical analysis methods for material films condensed on cryogenic surfaces of spacecraft
[AD-A284014] p 427 N95-14420
Mass analysis addition to the Differential Ion Flux Probe (DIFP) study
[NASA-CR-196531] p 429 N95-15824
OVERPRESSURE
Blast overpressure studies with animals and man
[AD-A280435] p 540 N95-13971
OXIDATION
Effects of thermal cycling on thermal expansion and mechanical properties of SiC fiber-reinforced reaction-bonded Si3N4 composites
[NASA-TM-106665] p 433 N95-14298
Study of the long term stability of the effective concentration of ionized space charges (N(sub eff)) of neutron irradiated silicon detectors fabricated by various thermal oxidations
[DE94-013734] p 593 N95-14309
Effect of surface roughness on local film cooling effectiveness and heat transfer coefficients
[AD-A283854] p 482 N95-14351
The oxidative stabilization and carbonization of mesophase pitch
[AD-A282026] p 453 N95-14954
Stress corrosion crack tip microstructure in nickel-based alloys
[DE94-015362] p 446 N95-15532
Turbulent mixing of the HVOF thermal spray and coating oxidation
[DE94-015414] p 455 N95-15535
OXIDATION RESISTANCE
Effects of hydrogen annealing, sulfur segregation and diffusion on the cyclic oxidation resistance of superalloys: A review
[NASA-TM-106734] p 444 N95-13667
Mechanical behavior of high temperature composites
[AD-A281582] p 436 N95-15441
Oxidation resistant coating for carbon-carbon composites at ultra-high temperatures
[AD-A283323] p 456 N95-15624
OXIDATION-REDUCTION REACTIONS
One: Redox chemistry of bimetallic fulvalene complexes. 2: Oligocyclopentadienyl complexes
[DE94-014930] p 443 N95-15667
OXIDE FILMS
In situ, real-time analysis of the growth of ferroelectric and conductive oxide heterostructures by a new time-of-flight pulsed ion beam surface analysis technique
[DE94-013298] p 620 N95-13822
Ferroelectric oxide memory FET (FEMFET) development
[AD-A283203] p 476 N95-15399
Core-level spectroscopy of thin oxides and oxynitrides
[DE94-016598] p 442 N95-15408
OXIDES
Polymer-polymer interactions
[AD-A282944] p 453 N95-14844
Core-level spectroscopy of thin oxides and oxynitrides
[DE94-016598] p 442 N95-15408
OXIDIZERS
Recycled plastic: A clean and low cost rocket fuel
[TABES PAPER 94-610] p 416 N95-14642
OXYGEN
Piezoelectric loudspeaker
[NASA-CASE-LAR-15138-1] p 590 N95-14110
Reactive polymers: Main chain coordination polymers for air separation
[AD-A281614] p 455 N95-15444
Small UHV compatible hyperthermal oxygen atom generator
[NASA-CAS-LAR-14674-1] p 503 N95-15601
Formation of dust grains with impurities in red giant winds p 641 N95-15841
OXYGEN ATOMS
Laboratory simulation of Low Earth Orbit (LEO) atomic oxygen effects p 422 N95-14071
A facility to produce an energetic, ground state atomic oxygen beam for the simulation of the Low-Earth Orbit environment p 422 N95-14072
Atomic Oxygen (ATOX) simulation of Teflon FEP and Kapton H surfaces using a high intensity, low energy, mass selected, ion beam facility p 422 N95-14073
The effect of Low Earth Orbit exposure on some experimental fluorine and silicon-containing polymers
p 422 N95-14074

Environmental durability issues for solar power systems in low Earth orbit
[NASA-TM-106775] p 431 N95-15769

OXYGENATION
Dense ceramic membranes for partial oxygenation of methane
[DE94-015021] p 453 N95-14609

OXYNITRIDES
Core-level spectroscopy of thin oxides and oxynitrides
[DE94-016598] p 442 N95-15408

OZONE
Photochemical urban airshed modeling using diagnostic and dynamic meteorological fields
[PB94-176120] p 616 N95-13973
Meteorological investigation of ozone anomalies during the Arctic Boundary Layer Experiment (ABLE 3A)
[AD-A284494] p 534 N95-15771

OZONE DEPLETION
Oxides of nitrogen: Their formation and control in stationary sources
[AD-A283780] p 522 N95-14337
The Telecommunications and Data Acquisition Report
[NASA-CR-196409] p 462 N95-14620
Pilot retrofit test of refrigerant R-134a for GDSCC
p 456 N95-14629
Environmentally sound manufacturing
[TABES PAPER 94-502] p 415 N95-14636
Counting condensation in the Antarctic Ozone Mission
[NASA-CR-197113] p 525 N95-15847

OZONOMETRY
Study of interferences in ozone UV and chemiluminescence monitors
[PB94-197456] p 521 N95-14123
Overview of PAMS meteorological monitoring requirements
[PB94-176658] p 534 N95-15383

OZONOSPHERE
Simulation of coal and char nitrogen reactions in combustion
[DE94-013941] p 440 N95-15291

P

P-I-N JUNCTIONS
High speed QPPM direct detection optical communication receivers for FSDD intersatellite links
[NASA-CR-189331] p 615 N95-15849

P-TYPE SEMICONDUCTORS
Electrical characterization of 6H crystalline silicon carbide
[NASA-CR-197047] p 439 N95-14903

PACIFIC OCEAN
Water vapor and temperature inversions near the 0 C level over the tropical western Pacific
[AD-A282023] p 533 N95-14952

PACKAGING
Minutes of the Third Annual Workshop on Chromate Replacements in Light Metal Finishing
[DE94-015163] p 446 N95-15368

PACKET TRANSMISSION
Performance modeling and analysis of parallel processing and Low Earth Orbit satellite communication systems
[AD-A283243] p 470 N95-15652
Discrete-event-dynamic-system-based approaches for control in integrated voice/data multihop radio networks
[AD-A284413] p 470 N95-15813

PAINTS
Conductive paints
[DE94-014069] p 453 N95-15292

PAIR PRODUCTION
Squeezed states and graviton-entropy production in the early universe p 608 N95-13947
Electroweak boson pair production at CDF
[DE94-015183] p 597 N95-15629

PALLADIUM
Type 304L stainless steel surface microstructure: Performance in hydride storage and acid cleaning
[DE94-014654] p 447 N95-15625

PANELS
Bending effects of unsymmetric adhesively bonded composite repairs on cracked aluminum panels
p 507 N95-14456
Full-scale testing and analysis of fuselage structure
p 512 N95-14485
Advanced method and processing technology for complicated shape airframe part forming
p 410 N95-14486

PARABOLIC FLIGHT
Transesophageal echocardiographic evaluation of baboons during microgravity induced by parabolic flight
p 538 N95-15094
Circulatory filling pressures during transient microgravity induced by parabolic flight p 542 N95-15095
Behaviour of newly hatched and adult Japanese quail and the feasibility of adaptation to weightlessness
p 538 N95-15106
Body position and volume status as determinants of cardiovascular responses to transition into microgravity in parabolic flight p 544 N95-15108

PARACHUTES
Parachute having improved vent line stacking
[NASA-CASE-MFS-28508-1] p 393 N95-14182

PARADOXES
On the theory of quantum measurement
p 604 N95-13910
The photon: Experimental emphasis on its wave-particle duality p 599 N95-13963
The probabilistic origin of Bell's inequality
p 612 N95-13969
Einstein-Podolsky-Rosen-Bohm experiment and Bell inequality violation using Type 2 parametric down conversion p 612 N95-13970
Discourse interpretation and the scope of operators
[TR-518] p 586 N95-15595

PARAFFINS
Porphyrins in the interstellar medium (in grains)
p 640 N95-15837

PARALLEL COMPUTERS
An optical simulation of shared memory
[DE94-013824] p 568 N95-13976
Nexus: An interoperability layer for parallel and distributed computer systems
[DE94-015816] p 578 N95-14116
Robust multigrid methods for the steady and unsteady incompressible Navier-Stokes equations in general coordinates
[PB94-195534] p 492 N95-15315

PARALLEL PROCESSING (COMPUTERS)
Parallel performance of a symmetric eigensolver based on the Invariant Subspace Decomposition approach
[DE94-013314] p 577 N95-13677
An optical simulation of shared memory
[DE94-013824] p 568 N95-13976
A study of the Invariant Subspace Decomposition Algorithm for banded symmetric matrices
[DE94-013872] p 568 N95-13977
Methodology for the parallel direct solution of finite element systems
[PB94-198009] p 585 N95-13991
Nexus: An interoperability layer for parallel and distributed computer systems
[DE94-015816] p 578 N95-14116
Parallel image rendering algorithm and architecture based on ray tracing and radiosity shading
[PB94-191277] p 569 N95-14153
Hardware implementation of a desktop supercomputer for high performance image processing. Color image processing using cellular neural networks
[AD-A283071] p 571 N95-14178
Developing molecular dynamics simulation codes using mixed language programming
[DE94-015456] p 571 N95-14190
Relativistic configuration-interaction calculation of the correlation energies of heliumlike ions
[DE94-015190] p 621 N95-14325
An informal introduction to program transformation and parallel processors
[DE94-016343] p 578 N95-14380
Performance measurement and analysis techniques for parallel and distributed programs
[DE94-016429] p 578 N95-14384
Parallel isosurface generator for huge data sets
[AD-A284030] p 578 N95-14422
Workshop on Advances in Scientific Computation and Differential Equations 1993 (SCADE)
[AD-A283111] p 585 N95-14657
Artificial neural network modeling of damaged aircraft
[AD-A283227] p 409 N95-14849
On the LU factorization of sequences of identically structured sparse matrices within a distributed memory environment
[AD-A282025] p 578 N95-14953
Vision-based navigation and recognition
[AD-A282962] p 583 N95-15398
Large-scale data envelopment analysis models and related applications
[AD-A283214] p 588 N95-15400
Structured approaches for problems of network design and utilization
[AD-A282925] p 578 N95-15416
Automatic TLI recognition system, part 1
[DE94-015253] p 578 N95-15434
Connection machine software conversion of the Navy TOPS model
[AD-A281681] p 579 N95-15450
Electron-molecule collisions and UV signatures in flowfields
[AD-A281569] p 596 N95-15457
Automatic TLI recognition system, part 2
[DE94-015393] p 579 N95-15534
The principles of fault-tolerant and efficient parallel computation
[AD-A283254] p 579 N95-15616
Fault-tolerance and efficiency in massively parallel algorithms
[AD-A283255] p 579 N95-15617
Performance modeling and analysis of parallel processing and Low Earth Orbit satellite communication systems
[AD-A283243] p 470 N95-15652

PARALLEL PROGRAMMING
Paradigms and strategies for scientific computing on distributed memory concurrent computers
[DE94-013305] p 567 N95-13676
Hybrid verification by exploiting the environment
[NASA-CR-195810] p 568 N95-13699
Nexus: An interoperability layer for parallel and distributed computer systems
[DE94-015816] p 578 N95-14116
The lambda loop transformation toolkit (user's reference manual)
[TR-511] p 587 N95-15733

PARAMETER IDENTIFICATION
Identification of dynamic systems. Volume 3: Applications to aircraft. Part 2: Nonlinear analysis and manoeuvre design
[AGARD-AG-300-VOL-3-PT-2] p 408 N95-14102
Parameter identification for X-31A at high angles of attack p 394 N95-14235
Integrated optical maze
[DE94-015866] p 613 N95-14367
Technical report series on global modeling and data assimilation. Volume 3: An efficient thermal infrared radiation parameterization for use in general circulation models
[NASA-TM-104606-VOL-3] p 531 N95-15745

PARAMETERIZATION
ASPM2: Progress toward the analysis of symbolic parameter models
[AD-A284437] p 576 N95-15817

PARAMETRIC AMPLIFIERS
Photon statistics of a two-mode squeezed vacuum
p 598 N95-13909
How to characterize the nonlinear amplifier?
p 471 N95-13922
Sqeezing generated by a nonlinear master equation and by amplifying-dissipative Hamiltonians
p 588 N95-13926
Quantum amplification and quantum optical tapping with squeezed states and correlated quantum states
p 610 N95-13954
A femtosecond optical parametric oscillator near 3 microns
[DE94-014500] p 612 N95-13986

PARTIAL PRESSURE
Partial pressure analysis in space testing
p 424 N95-14084

PARTICLE ACCELERATOR TARGETS
Prototype explosives-detection system based on nuclear-resonance absorption in nitrogen
[DE94-015069] p 442 N95-15387

PARTICLE ACCELERATORS
Direct-current proton-beam measurements at Los Alamos
[DE94-016280] p 599 N95-15360
Data flow manager for DART
[DE94-013236] p 579 N95-15581
Electroweak and b-physics at the Tevatron collider
[DE94-013239] p 600 N95-15582

PARTICLE BEAMS
The thermal-wave model: A Schroedinger-like equation for charged particle beam dynamics
p 601 N95-13944

PARTICLE COLLISIONS
Computations of drop collision and coalescence
p 485 N95-14542

PARTICLE DECAY
Measurement of the B cross section at CDF via B semileptonic decays
[DE94-013842] p 593 N95-13680
Relaxation of polar orientational order in nonlinear optical polymers by second harmonic generation
[AD-A283024] p 449 N95-13689
Research accomplishments and future goals in particle physics
[DE94-015483] p 596 N95-15537
Electroweak and b-physics at the Tevatron collider
[DE94-013239] p 600 N95-15582
Studies of quarkonia production with CDF
[DE94-013220] p 597 N95-15862

PARTICLE DIFFUSION
Interacting fronts in a model for binary-mixture convection
[DE94-013595] p 494 N95-15861

PARTICLE ENERGY
Divertor bias experiments
[DE94-015720] p 617 N95-14328
ENDL type formats for the LLNL Evaluated Atomic Data Library, EADL, for the Evaluated Electron Data Library, EEDL, and for the Evaluated Photon Data Library, EPDL
[DE94-016487] p 594 N95-14385
PARTICLE IN CELL TECHNIQUE
Paradigms and strategies for scientific computing on distributed memory concurrent computers
[DE94-013305] p 567 N95-13676
An algorithm for rezoning particle-in-cell calculations
[DE94-016056] p 619 N95-15774
PARTICLE INTERACTIONS
ENDL type formats for the LLNL Evaluated Atomic Data Library, EADL, for the Evaluated Electron Data Library, EEDL, and for the Evaluated Photon Data Library, EPDL
[DE94-016487] p 594 N95-14385
PARTICLE MOTION
Phase space flow of particles in squeezed states
p 606 N95-13928
Electrophoretic interactions and aggregation of colloidal biological particles p 444 N95-14578
Electrokinetic transport of heterogeneous particles in suspension p 444 N95-14581
PARTICLE PRODUCTION
Multiple-scattering model for inclusive proton production in heavy ion collisions
[NASA-TP-3470] p 600 N95-15606
Studies of quarkonia production with CDF
[DE94-013220] p 597 N95-15862
PARTICLE SPIN
Probing the antiferromagnetic long-range order with Glauber spin states p 609 N95-13951
Selective RF pulses in NMR and their effect on coupled and uncoupled spin systems
[PB94-195526] p 471 N95-15871
PARTICLE THEORY
Research accomplishments and future goals in particle physics
[DE94-015483] p 596 N95-15537
PARTICULATE SAMPLING
Condensation nuclei measurement in the stratosphere for the NASA ACE program
[NASA-CR-197031] p 530 N95-14855
PARTICULATES
Prediction of particulate contamination on aperture window p 420 N95-14064
Hypervelocity Impact Test Facility: A gun for hire
[TABES PAPER 94-605] p 415 N95-14639
Results of TSP metals monitoring at McMurdo Station, Antarctica
[DE94-015264] p 524 N95-15455
PARTONS
The parton distribution functions in the limit chi(sub Bj) approaches 1
[DE94-013799] p 597 N95-15545
PASSENGER AIRCRAFT
The Aluminum Falcon: A low cost modern commercial transport
[NASA-CR-197180] p 409 N95-15742
PASSIVITY
Fourth Workshop on the Role of Point Defects and Defect Complexes in Silicon Device Processing
[DE94-011850] p 624 N95-15426
Surface passivation for 3-5 semiconductor processing: Stable gallium sulphide films by MOCVD
[NASA-TM-106761] p 477 N95-15587
PATHOGENS
Extended duration orbiter medical project Microbial Air Sampler (STS-50/USML-1) p 458 N95-14222
PATTERN RECOGNITION
Neural networks: Alternatives to conventional techniques for automatic docking
[TABES PAPER 94-627] p 417 N95-14651
Spatio-temporal neural networks for vision, reasoning and rapid decision making
[AD-A283251] p 583 N95-15403
Supervised learning without output labels
[TR-510-REV] p 552 N95-15588
Seeing behind occlusions
[TR-487] p 576 N95-15857
PAVEMENTS
Ground penetrating radar surveys to characterize pavement layer thickness variations at GPS sites
[PB94-190170] p 460 N95-14119
Development of anti-icing technology
[PB94-195369] p 407 N95-15439
PAYLOADS
NASA LeRC's acoustic fill effect test program and results
[NASA-TM-106688] p 419 N95-13893
PENETRATION
Processing of thermoset prepreg laminate via exposure to microwave radiation
[DE94-013268] p 432 N95-13643
Welding irradiated stainless steel
[DE94-013661] p 500 N95-13645
Cratering and penetration experiments in teflon targets at velocities from 1 to 7 km/s
[NASA-TM-104797] p 432 N95-13646
The flow induced by the coalescence of two initially stationary drops
[NASA-TM-106752] p 478 N95-13653
The crosswell electromagnetic response of layered media
[DE94-014929] p 470 N95-15866
PENTANES
Interfacial force field characterization of a constrained vapor bubble thermosyphon using IAI
p 488 N95-14560
PERCEPTION
EPIC computational models of psychological refractory-period effects in human multiple-task performance
[AD-A280924] p 540 N95-14142
First results with instance-based state identification for reinforcement learning
[TR-502] p 553 N95-15642
On point-based temporal disjointness
[TR-497] p 587 N95-15643
Learning with incomplete selective perception
[TR-453] p 577 N95-15860
PERFORATED PLATES
Experiments to verify nonparallel stability theory at Virginia Polytechnic Institute and State University, Blacksburg, Virginia
[NASA-CR-196993] p 479 N95-13664
PERFORMANCE
Monitoring solar-thermal systems: An outline of methods and procedures
[DE94-015599] p 521 N95-15420
PERFORMANCE PREDICTION
Performance Reports: Mirror alignment system performance prediction comparison between SAO and EKC
[NASA-CR-196013] p 637 N95-14100
The industrial use of CFD in the design of turbomachinery p 480 N95-14133
EPIC computational models of psychological refractory-period effects in human multiple-task performance
[AD-A280924] p 540 N95-14142
Airplane takeoff and landing performance monitoring system
[NASA-CASE-LAR-14745-2-SB] p 412 N95-14415
Software reliability studies
[NASA-CR-197027] p 572 N95-14615
Communications availability: Estimation studies at AMSC p 466 N95-14681
Electro-optics: Propagation from IR to UV and sensor considerations. Part B: Tools for exploitation of propagation conditions and system range performance
p 467 N95-14834
Performance comparison AN/FRD-10 versus PUSHER
[AD-A283263] p 469 N95-15619
Performance modeling and analysis of parallel processing and Low Earth Orbit satellite communication systems
[AD-A283243] p 470 N95-15652
PERFORMANCE TESTS
Developments in ground-penetrating radar at LLNL
[DE94-012236] p 554 N95-13671
Summary of AXAF calibration requirements
[NASA-CR-196985] p 637 N95-13887
A femtosecond optical parametric oscillator near 3 microns
[DE94-014500] p 612 N95-13986
A High Temperature Hermetic Primer and a Variable Spring Tester
[DE94-012073] p 457 N95-14004
Ground penetrating radar surveys to characterize pavement layer thickness variations at GPS sites
[PB94-190170] p 460 N95-14119
Milestone 4: Test plan for Reusable Hydrogen Composite Tank System (RHCTS). Task 3: Composite tank materials
[NASA-CR-197036] p 435 N95-14801
Legged vehicle for underwater mobile operations
[AD-A282891] p 503 N95-15294
Subsurface object position and image correction for standoff ground penetrating radar
[DE94-015180] p 468 N95-15300
Computational chemistry packages on the CRAY Y-MP in trondheim
[PB94-208246] p 595 N95-15350
Time-of-flight detector for heavy ion backscattering spectrometry
[DE94-015600] p 596 N95-15437
Preliminary DIAL model
[DE94-013243] p 469 N95-15583
Performance comparison AN/FRD-10 versus PUSHER
[AD-A283263] p 469 N95-15619
PERIDOTITE
Experimental study of chemical, phase and textural equilibrium of high TiO2 mare basalts and peridotite
[NASA-CR-196480] p 645 N95-13724
PERIODICALS
Low Temperature Grown and Highly Non-Stoichiometric GaAs and Related Materials
[AD-A284898] p 626 N95-15754
PERMAFROST
Dependence of segregation potential on the thermal and hydraulic conditions predicted by model M1
[AD-A280969] p 530 N95-14862
Traveling wave solutions to the problem of quasi-steady freezing of soils
[AD-A280971] p 531 N95-15428
PERMANENT MAGNETS
Damage analysis of internal faults in flux concentrating permanent magnet motors
[AD-A283883] p 474 N95-14359
Dual-latching solenoid-actuated valve assembly
[NASA-CASE-MFS-28714-1] p 502 N95-14666
PERMITTIVITY
Role of dielectric constant in electrohydrodynamics of conducting fluids p 478 N95-14577
PERSONAL COMPUTERS
Summary Proceedings of the Joint Industry-FAA Conference on the Development and use of PC-Based Aviation Training Devices
[DOT/FAA/AM-94/25] p 573 N95-14917
PERSONALITY TESTS
Validation of MMPI scales for personality disorders: A pilot and other aviator study
[AD-A284397] p 553 N95-15768
PERSONNEL DEVELOPMENT
Aviation Epidemiology Data Register: Gender-specific attrition from the trained US Army aviator cohort of 1988
[AD-A284395] p 551 N95-15810
PERSONNEL MANAGEMENT
Reengineering through information technology. Accompanying report of the National Performance Review
[PB94-170362] p 633 N95-15781
PERTURBATION
Squeezed states and graviton-entropy production in the early universe p 608 N95-13947
The behavior of unsteady thermocapillary flows
p 483 N95-14530
Simple atmospheric perturbation models for sonic-boom-signature distortion studies
p 402 N95-14888
On the behavior of three-dimensional wave packets in viscously spreading mixing layers
[NASA-TM-106770] p 495 N95-15908
PETROGRAPHY
Energy flux and hydrogeology of thermal anomalies in the Gulf of Mexico Basin: South Texas example
[DE94-015122] p 530 N95-14956
PETROLOGY
Experimental study of chemical, phase and textural equilibrium of high TiO2 mare basalts and peridotite
[NASA-CR-196480] p 645 N95-13724
PHASE DIAGRAMS
Surface currents and bulk pinning in Bi2Sr2CaCu2O8
[DE94-013873] p 619 N95-13681
Phase separation and doped-hole segregation in La(2)CuO(4+delta) and La(2-x)Sr(x)CuO(4+delta)
[DE94-015070] p 624 N95-15430
Theory of nonlinear, distortive phenomena in solids: Martensitic, crack, and multiscale structures-phenomenology and physics
[DE94-015653] p 447 N95-15631
PHASE SEPARATION (MATERIALS)
Phase segregation due to simultaneous migration and coalescence p 484 N95-14537
A coarse grained approach to thermocapillarity effects in binary systems p 487 N95-14553
Surfactant-based critical phenomena in microgravity
p 459 N95-14579
PHASE SHIFT
Developments in laser-based diagnostics for wind tunnels in the Aeromechanics Division: 1987-1992
[AD-A283011] p 412 N95-13687
PHASE STABILITY (MATERIALS)
Convection and morphological stability during directional solidification p 448 N95-14548
Shear stabilization of solidification fronts
p 448 N95-14549
Interactions between solidification and compositional convection in mushy layers p 448 N95-14551
PHASE TRANSFORMATIONS
Kinetic theory for electrodic phase transitions: The voltammogram
[AD-A283039] p 619 N95-13691

Berry phase in Heisenberg representation
p 609 N95-13952
Electron spin resonance and band electronic structure study of the metal-insulator transition in (BEDT-TTF)3(HSO4)2
[DE94-014005] p 620 N95-14009
Interactions between solidification and compositional convection in mushy layers p 448 N95-14551
Theory of nonlinear, distortive phenomena in solids: Martensitic, crack, and multiscale structures-phenomenology and physics
[DE94-015653] p 447 N95-15631
Phase transitions and connectivity in three-dimensional vortex equilibria
[DE94-014967] p 494 N95-15868

PHASE-SPACE INTEGRAL
Multivariable Hermite polynomials and phase-space dynamics p 606 N95-13929
On the possibility of a quantum mechanical phase space representation p 606 N95-13931

PHASED ARRAYS
Technology access from the FS-X radar program. Lessons for technology transfer and US acquisition policy
[AD-A283773] p 461 N95-14334

PHENOLS
Study on titanium-silicalite-1 and related systems
[PB94-195500] p 445 N95-14845

PHENOMENOLOGY
Decoherence and dissipation for a quantum system coupled to a local environment p 609 N95-13949
Asteroseismology: Theory and phenomenology
p 643 N95-14502
Hadronic wavefunctions in light-cone quantization
[DE94-014507] p 622 N95-15308

PHENYLS
Polymer-polymer interactions
[AD-A282944] p 453 N95-14844

PHONONS
New quantum properties of phonons and their detection p 610 N95-13957
Quantum statistics of Raman scattering model with Stokes mode generation p 610 N95-13958

PHOSPHATES
Anomalous temperature dependence of the lattice parameters in HoPO4 and HoVO4: Rare earth quadrupolar effects
[DE94-015086] p 622 N95-14608
Adsorption and diffusion of fluids in well-characterized adsorbent materials
[DE94-016953] p 454 N95-15344
Porphyrins in the interstellar medium (in grains)
p 640 N95-15837

PHOSPHORIC ACID FUEL CELLS
Development of the fuel cell power generation technology, 2
[DE94-780614] p 520 N95-15376
Development of the fuel cell power generation technology, 1
[DE94-780648] p 520 N95-15377

PHOSPHORUS
SAM1 semiempirical parameters
[AD-A284400] p 443 N95-15782

PHOSPHORUS COMPOUNDS
Inelastic neutron scattering and molecular dynamics simulations of water adsorbed in the molecular sieves AlPO4-11, AlPO4-5, AlPO4-8 and VPI-5
[DE94-013337] p 593 N95-13678
Radical polymerization of vinyl acetate in the presence of trialkyl phosphites
[AD-A280829] p 451 N95-14324

PHOTOCHEMICAL REACTIONS
Photochemical urban airshed modeling using diagnostic and dynamic meteorological fields
[PB94-176120] p 616 N95-13973
Computational modeling issues in next generation air quality models
[PB94-197449] p 521 N95-14122
Optically driven surface reactions: Laser probes of surface dynamics
[DE94-015311] p 441 N95-15370

PHOTOCONDUCTIVE CELLS
Semiconductor measurement technology: Improved characterization and evaluation measurments for HgCdTe detector materials, processes, and devices used on the GOES and TIROS satellites
[PB94-188810] p 474 N95-14401

PHOTOCONDUCTIVITY
High gain GaAs switches for impulse sources: Measurement of the speed of current filaments
[DE94-015281] p 477 N95-15544

PHOTODECOMPOSITION
Optically driven surface reactions: Laser probes of surface dynamics
[DE94-015311] p 441 N95-15370

PHOTODIODES
Receiver design, performance analysis, and evaluation for space-borne laser altimeters and space-to-space laser ranging systems
[NASA-CR-197050] p 499 N95-14901
Charge collection in a-Si:H/a-Si(1-x)C(x multilayers photodetectors
[DE94-013107] p 625 N95-15577
High speed QPPM direct detection optical communication receivers for FSDD intersatellite links
[NASA-CR-189331] p 615 N95-15849

PHOTOELECTRIC EFFECT
The 24th International Physics Olympiad
[AD-A280584] p 589 N95-13972

PHOTOELECTRON SPECTROSCOPY
X-ray Photoelectron Spectroscopy (XPS), Rutherford Back Scattering (RBS) studies
[NASA-CR-196536] p 439 N95-14867
Core-level spectroscopy of thin oxides and oxynitrides
[DE94-016598] p 442 N95-15408

PHOTOELECTRONS
Core-level spectroscopy of thin oxides and oxynitrides
[DE94-016598] p 442 N95-15408

PHOTOGRAMMETRY
Photogrammetric mobile satellite service prediction
p 466 N95-14679

PHOTOIONIZATION
Direct detection of neutral metal atoms in electron-stimulated desorption: Al from CH3O/Al(111). Velocity distribution and absolute yield
[DE94-014011] p 593 N95-14011
Double ionization in gases driven by optical field ionization using ultrashort laser pulses
[DE94-015137] p 498 N95-14318

PHOTOLUMINESCENCE
Magnetic field dependent photoluminescence studies of InGaAs/GaAs strained-single-quantum wells
[DE94-015774] p 621 N95-14342
Polarized photomodulated reflectivity and photoluminescence studies of ordered InGaP2 under pressure
[DE94-016556] p 621 N95-14390
Photoluminescence spectroscopy and Rutherford backscattering channeling evaluation of various capping techniques for rapid thermal annealing of ion-implanted ZnSe
[DE94-016876] p 623 N95-15339

PHOTOMETERS
Pseudomaster equation for the no-count process in a continuous photodetection p 608 N95-13946
Apparatus for imaging an object in or through a scattering medium using coherent anti-Stokes Raman scattering
[AD-D016366] p 615 N95-15765

PHOTOMETRY
Astrophysical science with a spaceborne photometric telescope
[NASA-CP-10148] p 643 N95-14499
The symbiosis of photometry and radial-velocity measurements p 643 N95-14505
FRESIP project observations of cataclysmic variables: A unique opportunity p 644 N95-14507
Observations of hot stars and eclipsing binaries with FRESIP p 644 N95-14508
Monitoring the variability of active galactic nuclei from a space-based platform p 644 N95-14509

PHOTOMULTIPLIER TUBES
A high speed, wide dynamic range digitizer circuit for photomultiplier tubes
[DE94-015187] p 475 N95-15302
Mass analysis addition to the Differential Ion Flux Probe (DIFP) study
[NASA-CR-196531] p 429 N95-15824

PHOTON DENSITY
Research on characterization of the upper atmosphere using lidar
[AD-A283241] p 530 N95-15401

PHOTONICS
Integrated photonics research, 1993
[AD-A281578] p 614 N95-15464

PHOTONS
A new approach to the photon localization problem
p 603 N95-13905
Photon statistics of a two-mode squeezed vacuum
p 598 N95-13909
On the theory of quantum measurement
p 604 N95-13910
Time-dependent distinguishability: Choosing to be a wave or a particle p 600 N95-13912
Measurement of very small phase fluctuations by means of the operational approach p 605 N95-13916
How to characterize the nonlinear amplifier?
p 471 N95-13922
Coherent states on the m-sheeted complex plane as m-photon states p 598 N95-13940
Some rules for polydimensional squeezing
p 608 N95-13941
Causality problems for Fermi's two-atom system
p 598 N95-13945
General properties of quantum optical systems in a strong field limit p 609 N95-13950
Complementarity and path distinguishability: Some recent results concerning photon pairs
p 598 N95-13961
The photon: Experimental emphasis on its wave-particle duality p 599 N95-13963
The generation of entangled states from independent particle sources p 599 N95-13964
Nonlocal effects on the polarization state of a photon, induced by distant absorbers p 599 N95-13965
On the nonlocal predictions of quantum optics
p 611 N95-13967
A loophole-free Bell's inequality experiment
p 611 N95-13968
Einstein-Podolsky-Rosen-Bohm experiment and Bell inequality violation using Type 2 parametric down conversion p 612 N95-13970
ENDL type formats for the LLNL Evaluated Atomic Data Library, EADL, for the Evaluated Electron Data Library, EEDL, and for the Evaluated Photon Data Library, EPDL
[DE94-016487] p 594 N95-14385
L(alpha)-induced two-photon absorption of visible light emitted from an O-type star by H2(+) ions located near the surface of the Stromgren sphere surrounding the star: A possible explanation for the diffuse interstellar absorption bands (DIDs) p 641 N95-15845

PHOTOOXIDATION
Emerging technology summary: Destruction of organic contaminants in air using advanced ultraviolet flashlamps
[PB94-194479] p 521 N95-14121

PHOTOPRODUCTION
Research in high energy physics
[DE94-015519] p 600 N95-15539

PHOTOSYNTHESIS
The Astroculture (tm)-1 experiment on the USML-1 mission p 564 N95-14228

PHOTOVOLTAIC CONVERSION
The integration of renewable energy sources into electric power distribution systems. Volume 1: National assessment
[DE94-015935] p 519 N95-14393

PHYSICAL EXAMINATIONS
Unreported medications used in incapacitating medical conditions found in fatal civil aviation accidents
[DOT/FAA/AM-94/14] p 540 N95-14177

PHYSICAL EXERCISE
Cardiovascular response to cold pressor and LBNP tests before and after 20-day-bedrest p 543 N95-15097
Cardiovascular and metabolic responses to 6 deg Head-Down Tilt (HDT) and 70 deg Head-Up Tilt (HUT) following exercise p 544 N95-15109
Effects of 20 days bed-rest on cardio-respiratory functions during sub-maximal exercise in young women
p 545 N95-15111
On-Earth evaluation of the neurovestibular tolerance to centrifuge simulated artificial gravity in humans
p 546 N95-15120
Musculoskeletal adaptation to mechanical forces on Earth and in space p 548 N95-15136
Effects of microgravity on interstitial muscle receptors affecting heart rate and blood pressure during static exercise p 548 N95-15137
A method for continuous monitoring of the Ground Reaction Force during daily activity p 549 N95-15139
20 days bed-rest on insulin action in relation to body fat in young subjects p 549 N95-15145

PHYSICAL OPTICS
A novel technique for 4-dimensional atmosphere and oceanographic irradiance measurements using 3-D spatial filtering
[AD-A283758] p 613 N95-14353

PHYSICAL PROPERTIES
HTS Wire Development Workshop: Proceedings
[DE94-015650] p 624 N95-15421

PHYSICAL WORK
Legged vehicle for underwater mobile operations
[AD-A282891] p 503 N95-15294
Influence of transmutation on microstructure, density change, and embrittlement of vanadium and vanadium alloys irradiated in HFIR
[DE94-015202] p 446 N95-15431

PHYSIOCHEMISTRY
Adaptation of skeletal muscle to spaceflight: Cosmos rhesus project. Cosmos 2044 and 2229
[NASA-CR-197041] p 537 N95-14796

PHYSIOLOGICAL EFFECTS
The musculoskeletal and vestibular effects of long term repeated exposure to sustained high-G
[AGARD-AR-317] p 562 N95-14263
Naval Aerospace Medical Research Laboratory, 1993 command history
[AD-A284038] p 541 N95-14424

Adaptation of skeletal muscle to spaceflight: Cosmos rhesus project. Cosmos 2044 and 2229
[NASA-CR-197041] p 537 N95-14796
Proposal for an astronaut mass measurement device for the Space Shuttle
[NASA-CR-197198] p 563 N95-14854

PHYSIOLOGICAL FACTORS
Aerospace medicine and biology: A continuing bibliography with indexes (supplement 395)
[NASA-SP-7011(395)] p 550 N95-15304

PHYSIOLOGICAL RESPONSES
The effects of autogenic-feedback training on motion sickness severity and heart rate variability in astronauts
[NASA-TM-108840] p 539 N95-13661
EPIC computational models of psychological refractory-period effects in human multiple-task performance
[AD-A280924] p 540 N95-14142
The musculoskeletal and vestibular effects of long term repeated exposure to sustained high-G
[AGARD-AR-317] p 562 N95-14263
Cardiovascular response to cold pressor and LBNP tests before and after 20-day-bedrest p 543 N95-15097
Twenty four hours head-down tilt decreases arterial baroreflex function in conscious rat p 538 N95-15098
Body position and volume status as determinants of cardiovascular responses to transition into microgravity in parabolic flight p 544 N95-15108
Cardiovascular and metabolic responses to 6 deg Head-Down Tilt (HDT) and 70 deg Head-Up Tilt (HUT) following exercise p 544 N95-15109
A mathematical model of the cardiovascular response to +Gz acceleration p 544 N95-15110
Space flight and humoral and cellular immunity of animals p 538 N95-15113
The regulation of rat activity following exposure to hyperdynamic fields p 539 N95-15133
Effects of microgravity on interstitial muscle receptors affecting heart rate and blood pressure during static exercise p 548 N95-15137
The cardiovascular response to the AGS p 419 N95-15146
Crew factors in flight operations 2: Psychophysiological responses to short-haul air transport operations
[NASA-TM-108856] p 550 N95-15649

PHYSIOLOGICAL TESTS
The electrocortical correlates of fluctuating states of attention during vigilance tasks
[NASA-CR-197051] p 552 N95-14864
Gravitational stress and regulation of neuroendocrine elements and fluid volume in humans p 542 N95-15090
Neurohumoral reactions to long-term vestibular stimulation in man p 542 N95-15091

PHYSIOLOGY
A physical control interface with proprioceptive feedback and multiple degrees of freedom p 559 N95-14045
The applicability of commercial glare test devices in the aeromedical certification of pilot applicants
[DOT/FAA/AM-94/15] p 540 N95-14176

PIEZOELECTRIC TRANSDUCERS
Torsional shear wave transducer
[AD-D016347] p 496 N95-14841
Transducers and methods for making same
[AD-D016349] p 497 N95-15799
Test Operation Procedure (TOP): Vibration testing of helicopter equipment
[AD-A284433] p 410 N95-15815

PIEZOELECTRICITY
Piezoelectric loudspeaker
[NASA-CASE-LAR-15138-1] p 590 N95-14110
Discrete-layer piezoelectric plate and shell models for active tip-clearance control
[NASA-CR-195383] p 507 N95-14417
Torsional shear wave transducer
[AD-D016347] p 496 N95-14841

PILOT PERFORMANCE
Age 60 Rule. Part 3: Consolidated database experiments
[DOT/FAA/AM-94/22-PT-3] p 551 N95-13715
Unreported medications used in incapacitating medical conditions found in fatal civil aviation accidents
[DOT/FAA/AM-94/14] p 540 N95-14177
Crew factors in flight operations 2: Psychophysiological responses to short-haul air transport operations
[NASA-TM-108856] p 550 N95-15649
Collection of real-time, multichannel EEG data from helicopter pilots in flight: A feasibility study
[AD-A284396] p 551 N95-15767

PILOT PLANTS
MCFC Product Development Test
[DE94-014334] p 518 N95-14143
Process development of thermal hydrodechlorination
[PB94-195518] p 525 N95-15870

PILOT SELECTION
Preliminary analysis of Army aircrew requirements for Joint Surveillance Target Attack Radar System (JSTARS): Human performance requirements and job demands
[AD-A284917] p 563 N95-15759

PILOT TRAINING
Operational requirements for avoidance and eventual elimination of Gz-induced Loss Of Consciousness (G-LOC) in flight p 547 N95-15127
Vertical flight terminal operational procedures. A summary of FAA research and development
[AD-A283550] p 413 N95-15328
Distance estimation training with night vision goggles: A preliminary study
[AD-A284900] p 563 N95-15755

PILOTS (PERSONNEL)
Civil use of night vision devices: Evaluation pilot's guide, part 2
[DOT/FAA/RD-94/19] p 410 N95-14175

PINNING
Surface currents and bulk pinning in Bi2Sr2CaCu2O8
[DE94-013873] p 619 N95-13681

PINS
Service equipment for use in hostile environments
[NASA-CASE-LEW-14906-2-SB] p 504 N95-15914

PIPELINES
Leak detection by acoustic emission monitoring. Phase 1: Feasibility study
[AD-A283775] p 493 N95-15332

PIPES (TUBES)
Single-phase heat transfer and pressure drop characteristics of an integral-spine-fin within an annulus
[PB94-194073] p 482 N95-14407

PISTONS
Direct observation of oil consumption mechanisms in a production spark ignition engine using fluorescence techniques
[AD-A283842] p 501 N95-14347
Burn rates of TiH2/KClO4/Viton and output testing of NASA SKD26100098-301 pressure cartridges
[NASA-CR-188357] p 443 N95-15715

PITCH (MATERIAL)
The oxidative stabilization and carbonization of mesophase pitch
[AD-A282026] p 453 N95-14954

PITCHING MOMENTS
Static and dynamic force/moment measurements in the Eidetics water tunnel p 395 N95-14238
Flight evaluation of pneumatic forebody vortex control in post-stall flight p 398 N95-14259

PITTING
The effects of pitting on fatigue crack nucleation in 7075-T6 aluminum alloy p 448 N95-14482

PIXELS
Computing illumination using extended sources: Object space and image space
[PB94-201282] p 612 N95-13992
Radiometric resolution enhancement by lossy compression as compared to truncation followed by lossless compression p 564 N95-14588
Linear estimation of hyperspectral mixed pixel components
[AD-A283893] p 586 N95-15424

PLAINS
Meso-beta scale numerical simulation studies of terrain-induced jet streak mass/momentum perturbations
[NASA-CR-197226] p 531 N95-15684

PLANET EPHEMERIDES
Twelve-year planetary ephemeris: 1995-2006
[NASA-RP-1349] p 638 N95-14667

PLANETARY ATMOSPHERES
Planetary entry experiments
[NASA-CR-194215] p 644 N95-13717
First Year PIDDP Report on gamma-ray and x-ray spectroscopy: X-ray remote sensing and in situ spectroscopy for planetary exploration missions and gamma-ray remote sensing and in situ spectroscopy for planetary exploration missions
[NASA-CR-189374] p 517 N95-15916

PLANETARY BOUNDARY LAYER
ADCIRC: An advanced three-dimensional circulation model for shelves, coasts, and estuaries. Report 4: Hurricane storm surge modeling using large domains
[AD-A283868] p 535 N95-14352

PLANETARY EVOLUTION
The symbiosis of photometry and radial-velocity measurements p 643 N95-14505
Rotation among solar-type stars p 644 N95-14506

PLANETARY GEOLOGY
Experimental study of chemical, phase and textural equilibrium of high TiO2 mare basalts and peridotite
[NASA-CR-196480] p 645 N95-13724

PLANETARY MANTLES
Experimental study of chemical, phase and textural equilibrium of high TiO2 mare basalts and peridotite
[NASA-CR-196480] p 645 N95-13724

PLANETARY SYSTEMS
The symbiosis of photometry and radial-velocity measurements p 643 N95-14505

PLANETS
Asteroseismology with FRESIP: A meter class space telescope p 643 N95-14504

PLANNING
Low-Earth-Orbiter resource allocation and capacity planning for the DSN using LEO4CAST p 419 N95-14632

PLANT DESIGN
Advanced stellarator power plants
[DE94-014442] p 616 N95-14007

PLASMA ARC WELDING
Plasma arc welding torch having means for vortexing plasma gas exiting the welding torch
[NASA-CASE-MFS-28828-1] p 503 N95-15670

PLASMA CHEMISTRY
Laboratory spectra of C60 and related molecular structures p 627 N95-15838

PLASMA CLOUDS
Interplanetary medium data book, supplement 5, 1988-1993
[NASA-TM-109957] p 642 N95-13658

PLASMA COMPOSITION
Radiation rates for low Z impurities in edge plasmas
[DE94-016073] p 617 N95-14368

PLASMA CONTROL
Advanced tokamak research on the D3-D tokamak
[DE94-015860] p 617 N95-14426
The effect of the edge current density on confinement and kink mode stability in H-mode and VH-mode discharges
[DE94-015719] p 618 N95-15632

PLASMA CURRENTS
Advanced tokamak research on the D3-D tokamak
[DE94-015860] p 617 N95-14426

PLASMA DECAY
Conservation of magnetic helicity during plasma relaxation
[DE94-016770] p 617 N95-14373

PLASMA DENSITY
Interplanetary medium data book, supplement 5, 1988-1993
[NASA-TM-109957] p 642 N95-13658
Transient blood/plasma density and hematocrit effects after passive (sitting) thermoneutral water immersion in men p 548 N95-15131

PLASMA DIAGNOSTICS
Los Alamos contribution to target diagnostics on the National Ignition Facility
[DE94-014474] p 616 N95-13998
Studies of the ablated plasma from experimental plasma gun disruption simulations
[DE94-015017] p 617 N95-14262

PLASMA GUNS
Studies of the ablated plasma from experimental plasma gun disruption simulations
[DE94-015017] p 617 N95-14262
Conversion of light hydrocarbon gases in metal carbides for production of liquid fuels and chemicals
[DE94-013933] p 439 N95-14435

PLASMA HEATING
Advanced tokamak research on the D3-D tokamak
[DE94-015860] p 617 N95-14426

PLASMA INTERACTIONS
Hydrogen transport and trapping in graphite
[UTIAS-347] p 437 N95-13652
US-Japan workshop Q-181 on High Heat Flux Components and Plasma-Surface Interactions for Next Devices: Proceedings
[DE94-014939] p 618 N95-14443

PLASMA LAYERS
Dynamics Explorer 1: Energetic Ion Composition Spectrometer (EICS)
[NASA-CR-189375] p 619 N95-15758

PLASMA PHYSICS
Hydrogen transport and trapping in graphite
[UTIAS-347] p 437 N95-13652
Plasma dust crystallization p 490 N95-14571
Dynamics Explorer 1: Energetic Ion Composition Spectrometer (EICS)
[NASA-CR-189375] p 619 N95-15758

PLASMA SHEATHS
Space experiments aboard rockets: SPEAR 3
[AD-A280778] p 414 N95-14290
Pre-flight POLAR code predictions for the CHAWS space flight experiment
[AD-A280951] p 428 N95-14599

PLASMA SPRAYING
Oxidation resistant coating for carbon-carbon composites at ultra-high temperatures
[AD-A283323] p 456 N95-15624

PLASMA TEMPERATURE
Interplanetary medium data book, supplement 5, 1988-1993
[NASA-TM-109957] p 642 N95-13658
PLASMA TORCHES
Plasma arc welding torch having means for vortexing plasma gas exiting the welding torch
[NASA-CASE-MFS-28828-1] p 503 N95-15670
PLASMA WAVES
ICE/ISEE plasma wave data analysis
[NASA-CR-196988] p 642 N95-14266
Geotail MCA plasma wave data analysis
[NASA-CR-197022] p 618 N95-14798
PLASMAS (PHYSICS)
Technical Revue Thomson-CSF, volume 26, no. 1, March 1994. Flat panels for visualisation
[PB94-197969] p 410 N95-13984
Studies of the ablated plasma from experimental plasma gun disruption simulations
[DE94-015017] p 617 N95-14262
Divertor bias experiments
[DE94-015720] p 617 N95-14328
Plasma dust crystallization p 490 N95-14571
Laser ablation and deposition of alloys
[PB94-191384] p 499 N95-15388
Numerical solution of a tunneling equation
[DE94-015514] p 586 N95-15538
A relativistic cascade for heavy ion collisions
[DE94-015846] p 600 N95-15633
Plasma arc welding torch having means for vortexing plasma gas exiting the welding torch
[NASA-CASE-MFS-28828-1] p 503 N95-15670
An algorithm for rezoning particle-in-cell calculations
[DE94-016056] p 619 N95-15774
PLASTIC BODIES
Large amplitude nonlinear response of flat aluminum, and carbon fiber plastic beams and plates
[AD-A282440] p 513 N95-15547
PLASTIC DEFORMATION
The effect of microstresses on fatigue crack propagation in steel
[AD-A283872] p 506 N95-14356
An inelastic analysis of a welded aluminum joint
[NASA-TP-3508] p 513 N95-15055
PLASTIC FLOW
Center for advanced materials of high quality dynamic performance (fellowships)
[AD-A281377] p 434 N95-14360
Recent advances in the modelling of crack growth under fatigue loading conditions p 511 N95-14478
PLASTIC PLATES
Large amplitude nonlinear response of flat aluminum, and carbon fiber plastic beams and plates
[AD-A282440] p 513 N95-15547
PLASTIC PROPERTIES
Orientation effects on the measurement and analysis of critical CTOA in an aluminum alloy sheet
[NASA-TM-109153] p 444 N95-13690
Elastic-plastic models for multi-site damage p 507 N95-14454
PLATE THEORY
Discrete-layer piezoelectric plate and shell models for active tip-clearance control
[NASA-CR-195383] p 507 N95-14417
PLATES (STRUCTURAL MEMBERS)
The buckling response of symmetrically laminated composite plates having a trapezoidal planform area
[NASA-CR-196975] p 505 N95-13839
Three-dimensional effects of crack closure in laminated composite plates subjected to bending loads
[AD-A283342] p 436 N95-15873
PLATINUM OXIDES
Chemically modified electrodes by nucleophilic substitution of chlorosilylated platinum oxide surfaces
[AD-A281567] p 477 N95-15456
PLUTONIUM
Spectrophotometric determination of plutonium-239 based on the spectrum of plutonium 3 chloride
[DE94-015172] p 440 N95-15297
PLUTONIUM OXIDES
Spectrophotometric determination of plutonium-239 based on the spectrum of plutonium 3 chloride
[DE94-015172] p 440 N95-15297
PLUTONIUM 239
Spectrophotometric determination of plutonium-239 based on the spectrum of plutonium 3 chloride
[DE94-015172] p 440 N95-15297
PNEUMATIC CONTROL
A physical control interface with proprioceptive feedback and multiple degrees of freedom p 559 N95-14045
F/A-18 and F-16 forebody vortex control, static and rotary-balance results p 397 N95-14254
Low-energy pneumatic control of forebody vortices p 398 N95-14256
Flight evaluation of pneumatic forebody vortex control in post-stall flight p 398 N95-14259
PNEUMATICS
F/A-18 and F-16 forebody vortex control, static and rotary-balance results p 397 N95-14254
Low-energy pneumatic control of forebody vortices p 398 N95-14256
Integration of a mechanical forebody vortex control system into the F-15 p 398 N95-14258
POINT DEFECTS
Role of point defects and defect complexes in silicon device processing: Book of abstracts
[DE94-011828] p 519 N95-14430
POINT SOURCES
A theoretical study of 30 to 50 angstrom noble gas heavy ion lithography
[DE94-015262] p 442 N95-15436
POINTING CONTROL SYSTEMS
The Telecommunications and Data Acquisition Report
[NASA-CR-196409] p 462 N95-14620
A trajectory preprocessor for antenna pointing p 463 N95-14630
POINTS (MATHEMATICS)
On point-based temporal disjointness
[TR-497] p 587 N95-15643
Density control and on-line labeling problems
[TR-481] p 576 N95-15789
POISSON DENSITY FUNCTIONS
Tests of a homogeneous Poisson process against clustering and other alternatives
[DE94-015382] p 588 N95-15533
POISSON EQUATION
Sub-Poissonian light and photocurrent shot-noise suppression in closed opto-electronic loop p 606 N95-13924
POISSON RATIO
An inelastic analysis of a welded aluminum joint
[NASA-TP-3508] p 513 N95-15055
POLAR ORBITS
Dynamics Explorer 1, retarding ion mass spectrometer summary spectrograms: 82/001 to 82/109 spin-time spectrograms for H(+), He(+), O(+), N(+), O(++), M/Z=2, and molecular ions
[NASA-TM-108468] p 443 N95-15607
POLAR WANDERING (GEOLOGY)
Satellite Laser Ranging in the 1990s: Report of the 1994 Belmont Workshop
[NASA-CP-3283] p 526 N95-14274
Global and regional kinematics from SLR stations p 527 N95-14278
Earth orientation parameters p 527 N95-14281
POLARITONS
New quantum properties of phonons and their detection p 610 N95-13957
POLARIZATION
Investigation of dipolar reorientation dynamics of pure bulk polymers using second harmonic generation
[AD-A283023] p 448 N95-13688
Relaxation of polar orientational order in nonlinear optical polymers by second harmonic generation
[AD-A283024] p 449 N95-13689
POLARIZATION (SPIN ALIGNMENT)
Nonlinear optical susceptibility of a model guest/host polymeric system as investigated by electro-optics and second harmonic generation
[AD-A283069] p 449 N95-13692
POLARIZATION CHARACTERISTICS
Polarizability properties of bianisotropic spheres with noncomplete magnetoelectric dyadics
[PB94-189065] p 589 N95-13987
Polarized photomodulated reflectivity and photoluminescence studies of ordered InGaP2 under pressure
[DE94-016556] p 621 N95-14390
Wideband electromagnetic scattering/analysis program. Electromagnetic scattering from the trunks and branches of trees
[AD-A283112] p 469 N95-15394
POLARIZED LIGHT
Multimode squeezing, biphotons and uncertainty relations in polarization quantum optics p 603 N95-13904
Method and apparatus for polarization-maintaining fiber optical amplification with orthogonal polarization output
[AD-D016365] p 614 N95-15707
POLARIZED RADIATION
The Stark anomalous dispersion optical filter: The theory p 462 N95-14622
Ground wave and diffraction, A p 467 N95-14828
POLICIES
Technology access from the FS-X radar program. Lessons for technology transfer and US acquisition policy
[AD-A283773] p 461 N95-14334
The Network Operations Control Center upgrade task: Lessons learned p 419 N95-14631
US space-based remote sensing: Challenges and prospects
[AD-A282439] p 515 N95-15546
POLISHING
Specifying the surface finish of x ray mirrors
[DE94-013537] p 601 N95-13644
Fundamental studies of diamond growth and surface reactions
[AD-A284390] p 626 N95-15808
POLLUTION CONTROL
Emerging technology summary: Destruction of organic contaminants in air using advanced ultraviolet flashlamps
[PB94-194479] p 521 N95-14121
Fuzzy logic motor control for pollution prevention and improved energy efficiency
[PB94-190865] p 523 N95-14403
Environmentally sound manufacturing
[TABES PAPER 94-502] p 415 N95-14636
Comprehensive facility decommissioning through the use of innovative technology to reduce cost, schedule, and environmental liability
[TABES PAPER 94-615] p 416 N95-14644
POLLUTION MONITORING
Test method for the measurement of methanol emissions from stationary sources
[PB94-170297] p 523 N95-15382
POLYACRYLONITRILE
Conductivity of polyacrylonitrile based lithium polymer electrolytes
[AD-A283965] p 450 N95-14203
Thin lithium cobalt dioxide rechargeable cells using polyacrylonitrile-based polymer electrolytes
[AD-A283253] p 455 N95-15615
POLYCRYSTALS
Role of polycrystallinity in CdTe and CuInSe2 photovoltaic cells
[DE94-011849] p 519 N95-14432
The effects of spatial location of defect states on the switching characteristics of amorphous and polycrystalline silicon thin film transistors: A numerical simulation using AMPS 2-D
[DE94-013437] p 476 N95-15410
Fundamental studies of diamond growth and surface reactions
[AD-A284390] p 626 N95-15808
POLYCYCLIC AROMATIC HYDROCARBONS
The peculiar behaviour of the 5780 and 5797 DIBs in HD25137 p 639 N95-15833
The formation of small grains in shocks in the ISM p 641 N95-15842
POLYETHYLENES
Thin composite solid electrolyte film for lithium batteries
[NASA-CASE-NPO-18694-1-CU] p 472 N95-13824
Recycled plastic: A clean and low cost rocket fuel
[TABES PAPER 94-610] p 416 N95-14642
Loading-strain equivalence between thermomechanical, creep, and tensile tests: High density polyethylene
[AD-A283265] p 513 N95-15621
POLYGONS
Distributed heterogeneous visualization, BOP (Bag-O-Polygons) and BOP view
[AD-A284393] p 567 N95-15809
POLYHEDRONS
Laboratory spectra of C60 and related molecular structures p 627 N95-15838
POLYIMIDE RESINS
Phenylethynyl terminated imide oligomers
[NASA-CASE-LAR-15175-1] p 450 N95-14185
Diamines and polyimides containing pendent ethynyl groups
[NASA-CASE-LAR-14825-1] p 452 N95-14416
Low dielectric polyimide fibers
[NASA-CASE-LAR-14526-1] p 455 N95-15599
POLYIMIDES
A solvent resistant copolyimide
[NASA-CASE-LAR-15083-1] p 449 N95-14108
Copolyimides prepared from ODPA, BTDA and 3,4'-ODA
[NASA-CASE-LAR-15109-1] p 449 N95-14109
Electrically conducting polyimide film containing tin complexes
[NASA-CASE-LAR-14936-1] p 450 N95-14113
Phenylethynyl terminated imide oligomers
[NASA-CASE-LAR-15175-1] p 450 N95-14185
Thermally stable organic polymers
[AD-A281380] p 451 N95-14363
Diamines and polyimides containing pendent ethynyl groups
[NASA-CASE-LAR-14825-1] p 452 N95-14416
Low dielectric polyimide fibers
[NASA-CASE-LAR-14526-1] p 455 N95-15599
POLYMER BLENDS
Thermally stable organic polymers
[AD-A281380] p 451 N95-14363

Microscale hydrodynamics near moving contact lines
p 484 N95-14536
Towards the molecular design of composite materials
[AD-A283422] p 627 N95-15404

POLYMER CHEMISTRY
Preparation of well defined polystyrene-block-poly (methylphenylsilylene) copolymers
[AD-A280799] p 450 N95-14304
Introduction of living polymerization. Living and/or controlled polymerization
[AD-A280800] p 451 N95-14305
Radical polymerization of vinyl acetate in the presence of trialkyl phosphites
[AD-A280829] p 451 N95-14324
Synthesis of well defined polymers by radical polymerization
[AD-A280830] p 452 N95-14395
Modifications of polysilanes and polysilane copolymers
[AD-A280839] p 452 N95-14398
Ring-opening polymerization of strained cyclotetrasilanes as a new route towards well defined polysilylenes
[AD-A280840] p 452 N95-14399
Polysilanes with various architectures
[AD-A280842] p 452 N95-14400
AASERT 92: Synthesis and properties of complex polyarylene vinylenes
[AD-A284215] p 452 N95-14406
The synthesis of monomers with pendent ethynyl groups for modified high performance thermoplastics
[NASA-CR-196935] p 453 N95-14931
NMR studies of polymers at interfaces
[AD-A281570] p 455 N95-15458

POLYMER MATRIX COMPOSITES
Processing of thermoset prepreg laminate via exposure to microwave radiation
[DE94-013268] p 432 N95-13643
Technical Revue Thomson-CSF, volume 26, no. 1, March 1994. Flat panels for visualisation
[PB94-197969] p 410 N95-13984
Thermally stable organic polymers
[AD-A281380] p 451 N95-14363
Composites with improved compressive properties
[AD-A283411] p 435 N95-15417
Deformation, strength, and failure modes of laminated conventional and hybrid polymer-matrix composites loaded in the thickness direction
[AD-A281587] p 436 N95-15443

POLYMERIC FILMS
Electrically conducting polyimide film containing tin complexes
[NASA-CASE-LAR-14936-1] p 450 N95-14113
Poly(arylene ether imidazole) surfacing films for flat and parabolic structures
[NASA-CASE-LAR-14812-1] p 450 N95-14140
Self-organization of graft copolymers at surfaces, interfaces and in bulk
[DE94-016884] p 454 N95-15340

POLYMERIZATION
Introduction of living polymerization. Living and/or controlled polymerization
[AD-A280800] p 451 N95-14305
Radical polymerization of vinyl acetate and methyl methacrylate using organochromium initiators complexed with macrocyclic polyamines
[AD-A280828] p 451 N95-14316
Radical polymerization of vinyl acetate in the presence of trialkyl phosphites
[AD-A280829] p 451 N95-14324
Synthesis of well defined polymers by radical polymerization
[AD-A280830] p 452 N95-14395
Modifications of polysilanes and polysilane copolymers
[AD-A280839] p 452 N95-14398
Ring-opening polymerization of strained cyclotetrasilanes as a new route towards well defined polysilylenes
[AD-A280840] p 452 N95-14399
Polysilanes with various architectures
[AD-A280842] p 452 N95-14400
Highly crosslinked silicon polymers for gas chromatography columns
[NASA-CASE-ARC-11960-2-NP] p 452 N95-14602

POLYMERS
Investigation of dipolar reorientation dynamics of pure bulk polymers using second harmonic generation
[AD-A283023] p 448 N95-13688
Relaxation of polar orientational order in nonlinear optical polymers by second harmonic generation
[AD-A283024] p 449 N95-13689
Nonlinear optical susceptibility of a model guest/host polymeric system as investigated by electro-optics and second harmonic generation
[AD-A283089] p 449 N95-13692
Behavior of charring materials in simulated fire environments
[PB94-196045] p 439 N95-14838

POLYMETHYL METHACRYLATE
A theoretical study of 30 to 50 angstrom noble gas heavy ion lithography
[DE94-015262] p 442 N95-15436
Fire growth models for materials
[PB94-195856] p 443 N95-15610
Tensile creep strain and activation energy
[AD-A283264] p 513 N95-15620

POLYNOMIALS
Chaotic time series. Part 2: System identification and prediction
[PB94-207115] p 589 N95-13630
An efficient spectral method for ordinary differential equations with rational function coefficients
[NASA-TM-106762] p 585 N95-14296
Polyhedral approaches for solving 0-1 polynomial programming problems
[AD-A282448] p 575 N95-15549
Pseudorandom generators and the frequency of simplicity
[UR-DCS-TR-94-507] p 586 N95-15594
Weighted NP optimization problems: Logical definability and approximation properties
[TR-516] p 587 N95-15596
Unambiguous computation: Boolean hierarchies an sparse Turing-complete sets
[TR-483] p 575 N95-15597
Upward separation for FewP and related classes
[TR-488] p 575 N95-15721
A promise class at least as hard as the polynomial hierarchy
[TR-484] p 576 N95-15788
Density control and on-line labeling problems
[TR-481] p 576 N95-15789
P-selectivity: Intersections and indices
[TR-482] p 577 N95-15858
Seeking stronger separations: Probability one balanced- and bi-immunity
[TR-480] p 589 N95-15859

POLYSILANES
Modifications of polysilanes and polysilane copolymers
[AD-A280839] p 452 N95-14398
Ring-opening polymerization of strained cyclotetrasilanes as a new route towards well defined polysilylenes
[AD-A280840] p 452 N95-14399
Polysilanes with various architectures
[AD-A280842] p 452 N95-14400

POLYSTYRENE
Preparation of well defined polystyrene-block-poly (methylphenylsilylene) copolymers
[AD-A280799] p 450 N95-14304
Polymer-polymer interactions
[AD-A282944] p 453 N95-14844
Self-organization of graft copolymers at surfaces, interfaces and in bulk
[DE94-016884] p 454 N95-15340

POLYURETHANE RESINS
Assessing post-fire combustion of polyurethane
[DE94-011461] p 438 N95-14375
Results of the examination of LDEF polyurethane thermal control coatings
[NASA-CR-4617] p 432 N95-14603

POMERONS
Theoretical studies in elementary particle physics
[DE94-015343] p 595 N95-15372

POPULATION INVERSION
Squeezed light from multi-level closed-cycling atomic systems p 598 N95-13920

POPULATIONS
New quantum properties of phonons and their detection p 610 N95-13957

POROSITY
Base passive porosity for drag reduction
[NASA-CASE-LAR-15246-1] p 501 N95-14183
Effects of two-phase flow on the deflagration of porous energetic materials
[DE94-015353] p 442 N95-15375

POROUS MATERIALS
Highly crosslinked silicon polymers for gas chromatography columns
[NASA-CASE-ARC-11960-2-NP] p 452 N95-14602
Effects of two-phase flow on the deflagration of porous energetic materials
[DE94-015353] p 442 N95-15375

PORPHYRINS
The Diffuse Interstellar Bands: Contributed papers
[NASA-CP-10144] p 639 N95-15827
Porphyrins in the interstellar medium (in grains)
p 640 N95-15837

POSITION (LOCATION)
Active localization of virtual sounds
p 561 N95-14054
Low-energy pneumatic control of forebody vortices
p 398 N95-14256
Scientific analysis of satellite ranging data
p 517 N95-14275
The long-term forecast of station view periods
p 419 N95-14621
Twelve-year planetary ephemeris: 1995-2006
[NASA-RP-1349] p 638 N95-14667
Search for gamma-ray events in the BATSE data base
[NASA-CR-197044] p 647 N95-14814
Subsurface object position and image correction for standoff ground penetrating radar
[DE94-015180] p 468 N95-15300
Method of locating ground faults
[NASA-CASE-LEW-15407-1] p 478 N95-15669
International Geoid Service Bulletin No. 1
[BULL-1] p 516 N95-15791
Selective RF pulses in NMR and their effect on coupled and uncoupled spin systems
[PB94-195526] p 471 N95-15871

POSITION ERRORS
Global reference frame: Intercomparison of results (SLR, VLBI and GPS) p 527 N95-14276
Global and regional kinematics with GPS
p 527 N95-14279
Global and regional kinematics with VLBI
p 527 N95-14280
Precision orbit determination of altimetric satellites
p 418 N95-14282
Radar altimeter calibration using SLR
p 471 N95-14283
SLR tracking of GPS-35 p 471 N95-14285

POSITION INDICATORS
Spatial awareness comparisons between large-screen, integrated pictorial displays and conventional EFIS displays during simulated landing approaches
[NASA-TP-3467] p 409 N95-14852
Experimental evaluation of cursors for B-2 Synthetic Aperture Radar (SAR) application
[AD-A283025] p 468 N95-15393

POSITIONING DEVICES (MACHINERY)
Welding nozzle position manipulator
[NASA-CASE-MFS-29837-1] p 500 N95-13654

POSITRON ANNIHILATION
Defect profiling in elemental and multilayer systems: Correlations of fitted defect concentrations with positron implantation profiles
[DE94-015844] p 624 N95-15422

POSITRONS
Observation of diffraction effects in positron channeling
[DE94-014909] p 594 N95-14441
Defect profiling in elemental and multilayer systems: Correlations of fitted defect concentrations with positron implantation profiles
[DE94-015844] p 624 N95-15422
Positron studies in catalysis research
[DE94-012793] p 597 N95-15572

POSTLAUNCH REPORTS
STS-66 post flight presentation
[NASA-TM-110077] p 419 N95-15900

POSTURE
Functional participation of the valvula cerebelli on the goldfish dorsal light response p 539 N95-15119
Centrifuges in gravitational physiology research
p 550 N95-15147
Isolation of the physiological regulation component of the arterial pressure time variation after postural stresses by a model of the gravitational and arterial kinking effects p 550 N95-15149

POTENTIAL ENERGY
The atom-atom potential in pressure-broadened line width calculations for XY2-AB: New expressions in the li(R), li(L), and i(R) representations
[AD-A282011] p 595 N95-14950

POTENTIOMETERS (RESISTORS)
Design of reliable high voltage avalanche transistor pulsers
[DE94-015323] p 473 N95-14261

POWDER (PARTICLES)
Powder agglomeration in a microgravity environment
[NASA-CR-197000] p 457 N95-14105
Sandia 1993 Superconducting Technology Program
[DE94-015601] p 625 N95-15438

POWER CONVERTERS
Fish method: Interaction between AC-machines and switching power converters
[PB94-191210] p 472 N95-14149

POWER LOSS
Aircraft accident report: Overspeed and loss of power on both engines during descent and power-off emergency, landing Simmons Airlines, Inc., d/b/a, American Eagle Flight 3641, N349SB False River Air Park, New Roads, Louisiana, 1 February 1994
[NTSB/AAR-94/06] p 407 N95-14916

POWER SPECTRA
Specifying the surface finish of x ray mirrors
[DE94-013537] p 601 N95-13644
POWER SUPPLY CIRCUITS
Development status of the NASA 30-cm ion thruster and power processor
[NASA-TM-106740] p 430 N95-14301
Design of power electronics for TVC and EMA systems
[NASA-CR-197067] p 475 N95-14866
PREAMPLIFIERS
Receiver design, performance analysis, and evaluation for space-borne laser altimeters and space-to-space laser ranging systems
[NASA-CR-197050] p 499 N95-14901
PRECESSION
Neutrino oscillations in noisy media
[DE94-014973] p 598 N95-15869
PRECIPITATION PARTICLE MEASUREMENT
High-spatial-resolution passive microwave sounding systems
[NASA-CR-197131] p 531 N95-15586
PRECISION
Uncertainty relations as Hilbert space geometry
p 588 N95-13911
Astrophysical science with a spaceborne photometric telescope
[NASA-CP-10148] p 643 N95-14499
PREDICTION ANALYSIS TECHNIQUES
Engineer's Refractive Effects Prediction System (EREPS), version 3.0
[AD-A283748] p 461 N95-14345
Computational predictive methods for fracture and fatigue p 509 N95-14466
Comparison of transform coding methods with an optimal predictor for the data compression of digital elevation models p 564 N95-14587
The long-term forecast of station view periods
p 419 N95-14621
Propagation Modelling and Decision Aids for Communications, Radar and Navigation Systems
[AGARD-LS-196] p 466 N95-14825
Propagation in the ionosphere, B p 467 N95-14827
An evaluation of rise time characterization and prediction methods p 401 N95-14881
USAF single-event sonic boom prediction model: PCBoom3 p 403 N95-14889
Milestone 5 test report. Task 5, subtask 5.2: Tile to foam strength tests
[NASA-CR-197241] p 514 N95-15913
PREDICTIONS
Chaotic time series. Part 2: System identification and prediction
[PB94-207115] p 589 N95-13630
Maximum predictive power and the superposition principle p 607 N95-13936
Engineer's Refractive Effects Prediction System (EREPS), version 3.0
[AD-A283748] p 461 N95-14345
Lithological and rheological constraints on fault rupture scenarios for ground motion hazard prediction
[DE94-014742] p 529 N95-14436
Fracture mechanics validity limits p 511 N95-14480
Aero-optics system integration
[TABES PAPER 94-604] p 415 N95-14638
Wind shear and its effects on aircraft
p 407 N95-14898
Calculation of movable bed friction factors
[AD-A283529] p 536 N95-15440
PREFORMS
Transducers and methods for making same
[AD-D016349] p 497 N95-15799
PREPREGS
Processing of thermoset prepreg laminate via exposure to microwave radiation
[DE94-013268] p 432 N95-13643
Improved composite material and method for production of improved composite material
[NASA-CASE-LAR-14892-1] p 433 N95-13836
PRESSURE BREATHING
Guidelines for a Research and Development (R/D) program for high sustained G p 546 N95-15124
Physiological considerations concerning Positive Pressure Breathing (PBG) during +Gz
p 547 N95-15126
PRESSURE BROADENING
The atom-atom potential in pressure-broadened line width calculations for XY2-AB: New expressions in the II(R), II(L), and I(R) representations
[AD-A282011] p 595 N95-14950
PRESSURE DISTRIBUTION
Impulsive response of nonuniform density liquid in a laterally excited tank
[DE94-013722] p 479 N95-13679
Flow-radiated noise. Study of the propagative spectral range of the wall pressure field
[PB94-201290] p 590 N95-13985
Base passive porosity for drag reduction
[NASA-CASE-LAR-15246-1] p 501 N95-14183
Flight and full-scale wind-tunnel comparison of pressure distributions from an F-18 aircraft at high angles of attack --- Conducted in NASA Ames Research Center's 80 by 120 ft wind tunnel p 394 N95-14231
Numerical simulation of the SOFIA flowfield
[NASA-CR-197025] p 400 N95-14612
Activated buoyancy propulsion = Paradox Power (tm)
[TABES PAPER 94-619] p 405 N95-14646
Upgrade of tropical cyclone surface wind field model
[AD-A283530] p 533 N95-15323
Pressure measurements on an F/A-18 twin vertical tail in buffeting flow. Volume 2: Steady and unsteady RMS pressure data
[AD-A281581] p 404 N95-15465
PRESSURE EFFECTS
Hybrid bearings for turbopumps and the like
[NASA-CASE-MFS-28491-1] p 500 N95-13819
Nonlinear dynamics of drops and bubbles and chaotic phenomena p 485 N95-14541
Physiological considerations concerning Positive Pressure Breathing (PBG) during +Gz
p 547 N95-15126
Effects of two-phase flow on the deflagration of porous energetic materials
[DE94-015353] p 442 N95-15375
PRESSURE GRADIENTS
A modified mixing length turbulence model for zero and adverse pressure gradients
[NASA-TM-106772] p 492 N95-14607
Leak detection by acoustic emissions monitoring: An experimental investigation of the acoustic properties of leaks and the attenuation characteristics of soil
[AD-A283250] p 530 N95-15295
The effect of the edge current density on confinement and kink mode stability in H-mode and VH-mode discharges
[DE94-015719] p 618 N95-15632
PRESSURE MEASUREMENT
Design and development of an F/A-18 inlet distortion rake: A cost and time saving solution
p 395 N95-14241
Body position and volume status as determinants of cardiovascular responses to transition into microgravity in parabolic flight p 544 N95-15108
The modal decomposition of an impedance tube
[AD-A283591] p 591 N95-15320
Overview of PAMS meteorological monitoring requirements
[PB94-176658] p 534 N95-15383
Pressure measurements on an F/A-18 twin vertical tail in buffeting flow. Volume 2: Steady and unsteady RMS pressure data
[AD-A281581] p 404 N95-15465
PRESSURE OSCILLATIONS
Flow-radiated noise. Study of the propagative spectral range of the wall pressure field
[PB94-201290] p 590 N95-13985
PRESSURE REDUCTION
Extended duration orbiter medical project countermeasure to reduce post space flight orthostatic intolerance (LBNP) (STS-50/USML-1)
p 551 N95-14224
PRESSURE SENSORS
Surface acoustic wave oxygen pressure sensor
[NASA-CASE-LAR-15266-1-CU] p 496 N95-13837
Design and development of an F/A-18 inlet distortion rake: A cost and time saving solution
p 395 N95-14241
PRESSURE SUITS
Manipulating the arterial pressure to prevent G-LOC
p 546 N95-15123
Guidelines for a Research and Development (R/D) program for high sustained G p 546 N95-15124
Operational requirements for avoidance and eventual elimination of Gz-induced Loss Of Consciousness (G-LOC) in flight p 547 N95-15127
PRESSURIZING
Multi-dimensional modeling of pressurization and expulsion of multi-phase hydrogen propellant
[NASA-CR-195156] p 457 N95-14902
PRESTRESSING
Adjustable bias column end joint assembly
[NASA-CASE-LAR-14899-1] p 459 N95-14111
PRIMERS (EXPLOSIVES)
A High Temperature Hermetic Primer and a Variable Spring Tester
[DE94-012073] p 457 N95-14004
PRINTED CIRCUITS
Tactile display device using an electrorheological fluid
[NASA-CASE-LAR-14860-1] p 472 N95-14112
PROBABILITY DENSITY FUNCTIONS
Two new kinds of uncertainty relations
p 588 N95-13915
Fine structure of transient waves in a random medium: The correlation and spectral density functions
p 401 N95-14882
PROBABILITY DISTRIBUTION FUNCTIONS
Phase properties of multicomponent superposition states in various amplifiers p 605 N95-13923
Density control and on-line labeling problems
[TR-481] p 576 N95-15789
PROBABILITY THEORY
Homodyning and heterodyning the quantum phase
p 604 N95-13913
Maximum predictive power and the superposition principle p 607 N95-13936
Causality problems for Fermi's two-atom system
p 598 N95-13945
The probabilistic origin of Bell's inequality
p 612 N95-13969
Applications of a fast and efficient method for simulating orbital mission safety p 426 N95-14093
Microstructurally based model of fatigue initiation and growth p 508 N95-14459
Probabilistic inspection strategies for minimizing service failures p 508 N95-14461
Statistical investigation of fatigue crack initiation and growth around chamfered rivet holes in Alclad 2024 T3 as affected by corrosion p 510 N95-14472
Comparison of transform coding methods with an optimal predictor for the data compression of digital elevation models p 564 N95-14587
Seeking stronger separations: Probability one balanced- and bi-immunity
[TR-480] p 589 N95-15859
PROBLEM SOLVING
Environmentally sound manufacturing
[TABES PAPER 94-502] p 415 N95-14636
On accessing and hiding information
p 587 N95-15641
First results with instance-based state identification for reinforcement learning
[TR-502] p 553 N95-15642
Genetic programming with adaptive representations
[TR-489] p 576 N95-15856
PROCESS CONTROL (INDUSTRY)
RICIS Symposium 1992: Mission and Safety Critical Systems Research and Applications
[NASA-CR-196963] p 569 N95-14156
Intelligent alarming p 570 N95-14168
Expert systems in the process industries
p 571 N95-14169
Fault detection and diagnosis using neural network approaches p 571 N95-14170
Intelligent manufacturing systems state of the art
[TABES PAPER 94-503] p 415 N95-14637
Real-time monitor and control of MBE growth of HgCdTe by spectroscopic ellipsometry
[AD-A284451] p 627 N95-15818
PROCUREMENT
A metric for success
[PB94-187630] p 459 N95-15322
Defining a controller architecture for the long-reach manipulator
[DE94-015165] p 583 N95-15369
PROCUREMENT MANAGEMENT
Space science in the 1990's and beyond
[TABES PAPER 94-204] p 415 N95-14634
PRODUCT DEVELOPMENT
The AEDC aerospace chamber 7V: An advanced test capability for infrared surveillance and seeker sensors
p 418 N95-14097
MCFC Product Development Test
[DE94-014334] p 518 N95-14143
Intelligent manufacturing systems state of the art
[TABES PAPER 94-503] p 415 N95-14637
Design in Huntsville, manufacture in Estonia, sell in Europe
[TABES PAPER 94-607] p 415 N95-14640
A NASA/industry/university partnership for development of dual-use vibration isolation technology
[TABES PAPER 94-613] p 416 N95-14643
Product life cycle data base, analysis and simulation integration methodology
[TABES PAPER 94-626] p 417 N95-14650
Rapid prototyping applications at Sandia National Laboratories
[DE94-006360] p 460 N95-15409
PRODUCTION COSTS
Design in Huntsville, manufacture in Estonia, sell in Europe
[TABES PAPER 94-607] p 415 N95-14640
Product life cycle data base, analysis and simulation integration methodology
[TABES PAPER 94-626] p 417 N95-14650

PRODUCTIVITY
Reengineering through information technology. Accompanying report of the National Performance Review
[PB94-170362] p 633 N95-15781
PROGRAM VERIFICATION (COMPUTERS)
Hybrid verification by exploiting the environment
[NASA-CR-195810] p 568 N95-13699
Remote programming in INSAT-2A/2B on-board Attitude and Orbit Control Computer (AOCC)
p 413 N95-13827
CAPTIONALS: A computer aided testing environment for the verification and validation of communication protocols p 570 N95-14163
Software reliability studies
[NASA-CR-197027] p 572 N95-14615
Automated test environment for a real-time control system
[TABES PAPER 94-631] p 417 N95-14652
Speakeasy software development
[AD-A283816] p 468 N95-15333
PROGRAMMABLE LOGIC DEVICES
Slave controller for effecting a block transfer of sixteen bit words between a memory and a data transfer bus
[AD-D016463] p 574 N95-15336
PROGRAMMING ENVIRONMENTS
Development of visual 3D virtual environment for control software p 559 N95-14048
Integration/evaluation of a HCI prototyping environment
[NASA-CR-196996] p 566 N95-14107
PROGRAMMING LANGUAGES
The stable and precise motion control for an autonomous mobile robot
[AD-A283776] p 501 N95-14336
SUNMOS for the Intel Paragon, a brief user's guide
[DE94-015277] p 574 N95-15543
Pseudorandom generators and the frequency of simplicity
[UR-DCS-TR-94-507] p 586 N95-15594
Universally serializable computation
[TR-520] p 587 N95-15732
PROJECT MANAGEMENT
Work Breakdown Structure (WBS) and WBS dictionary --- advanced x ray astrophysics facility (AXAF)
[NASA-CR-196448] p 567 N95-13635
Hubble Space Telescope GTO program
[NASA-CR-196263] p 637 N95-13723
Engineering, technical, and management support services
[NASA-CR-196977] p 505 N95-13840
The path to an experiment in space (from concept to flight) p 417 N95-14582
The Telecommunications and Data Acquisition Report
[NASA-CR-196409] p 462 N95-14620
The Network Operations Control Center upgrade task: Lessons learned p 419 N95-14631
Low-Earth-Orbiter resource allocation and capacity planning for the DSN using LEO4CAST
p 419 N95-14632
Space science in the 1990's and beyond
[TABES PAPER 94-204] p 415 N95-14634
Environmentally sound manufacturing
[TABES PAPER 94-502] p 415 N95-14636
Comprehensive facility decommissioning through the use of innovative technology to reduce cost, schedule, and environmental liability
[TABES PAPER 94-615] p 416 N95-14644
Space transfer vehicle concepts and requirements study. Volume 3: Program cost estimates. Book 2: WBS and dictionary
[NASA-CR-192447] p 419 N95-15552
PROJECT PLANNING
Earth Observing System (EOS) Advanced Microwave Sounding Unit-A (AMSU-A) Spares Program Plan
[NASA-CR-189380] p 567 N95-13632
A strawman SLR program plan for the 1990s
p 471 N95-14289
PROJECT SETI
Astrophysical science with a spaceborne photometric telescope
[NASA-CP-10148] p 643 N95-14499
PROJECTILES
Numerical simulation of shock-induced combustion past blunt bodies using shock-fitting technique
[NASA-CR-197013] p 437 N95-14268
PROJECTORS
Use of 64 kbits/s digital channel for image transmission: Using low scan two-way video
[PB94-189099] p 461 N95-14147
PROP-FAN TECHNOLOGY
Propulsion/airframe interference for ducted propfan engines with ground effect
[NASA-CR-197110] p 409 N95-14909
PROPAGATION MODES
Quantum propagation in single mode fiber
p 609 N95-13953
PROPELLANT TANKS
Milestone 4: Test plan for Reusable Hydrogen Composite Tank System (RHCTS). Task 3: Composite tank materials
[NASA-CR-197036] p 435 N95-14801
Multi-dimensional modeling of pressurization and expulsion of multi-phase hydrogen propellant
[NASA-CR-195156] p 457 N95-14902
PROPELLER FANS
Propulsion/airframe interference for ducted propfan engines with ground effect
[NASA-CR-197110] p 409 N95-14909
PROPELLERS
Aircraft accident report: Overspeed and loss of power on both engines during descent and power-off emergency, landing Simmons Airlines, Inc., d/b/a, American Eagle Flight 3641, N349SB False River Air Park, New Roads, Lousiana, 1 February 1994
[NTSB/AAR-94/06] p 407 N95-14916
PROPRIOCEPTION
A physical control interface with proprioceptive feedback and multiple degrees of freedom p 559 N95-14045
PROPULSION
Activated buoyancy propulsion = Paradox Power (tm)
[TABES PAPER 94-619] p 405 N95-14646
PROPULSION SYSTEM CONFIGURATIONS
Computational aerodynamics based on the Euler equations
[AGARD-AG-325] p 398 N95-14264
Development status of the NASA 30-cm ion thruster and power processor
[NASA-TM-106740] p 430 N95-14301
Damage analysis of internal faults in flux concentrating permanent magnet motors
[AD-A283883] p 474 N95-14359
Access to space
[NASA-CR-197153] p 428 N95-14521
The rationale/benefits of nuclear thermal rocket propulsion for NASA's lunar space transportation system
[NASA-TM-106739] p 431 N95-15682
PROPULSION SYSTEM PERFORMANCE
Fourth High Alpha Conference, volume 1
[NASA-CP-10143-VOL-1] p 393 N95-14229
Development status of the NASA 30-cm ion thruster and power processor
[NASA-TM-106740] p 430 N95-14301
Damage analysis of internal faults in flux concentrating permanent magnet motors
[AD-A283883] p 474 N95-14359
A graphical user interface for design and analysis of air breathing propulsion systems
[TABES PAPER 94-616] p 411 N95-14645
Gas turbine prediffuser-combustor performance during operation with air-water mixture
[DOT/FAA/CT-93/52] p 411 N95-15683
PROPYLENE
Thin lithium cobalt dioxide rechargeable cells using polyacrylonitrile-based polymer electrolytes
[AD-A283253] p 455 N95-15615
PROSTHETIC DEVICES
A physical control interface with proprioceptive feedback and multiple degrees of freedom p 559 N95-14045
PROTACTINIUM ISOTOPES
The 226RA and 231PA systematics of axial, MORB, crustal residence ages, and MAGMA chamber characteristics at 9 to 10 degree N East Pacific Rise
[DE94-013084] p 529 N95-14434
PROTECTION
New armour materials: Metal matrix composites
[PB94-189131] p 433 N95-14148
PROTECTIVE COATINGS
Influence of defect shape on laser-induced damage in multilayer coatings
[DE94-016543] p 451 N95-14389
PROTEIN CRYSTAL GROWTH
Protein crystal growth results from the United States Microgravity Laboratory-1 mission p 458 N95-14225
PROTEINS
Measurement and regulation of central noradrenergic receptors
[AD-A284219] p 541 N95-14408
Are otoconia dynamic in birds and mammals?
p 538 N95-15103
PROTOCOL (COMPUTERS)
RICIS Symposium 1992: Mission and Safety Critical Systems Research and Applications
[NASA-CR-196963] p 569 N95-14156
Generic architectures for future flight systems
p 567 N95-14159
Space Generic Open Avionics Architecture (SGOAA): Overview p 569 N95-14161
Evolutionary Telemetry and Command Processor (TCP) architecture p 420 N95-14162
CAPTIONALS: A computer aided testing environment for the verification and validation of communication protocols p 570 N95-14163
Performance comparison of token ring protocols for hard-real-time communication p 570 N95-14164
POSIX real-time extensions p 570 N95-14165
CIFO 3.0 p 570 N95-14167
An evaluation of B-ISDN for the communication architecture requirements of Distributed Interactive Simulation (DIS)
[AD-A280783] p 578 N95-14292
Automated network protocol reachability analysis with supertrace algorithm and TESTGEN: Automated generation of test sequence for a formal protocol specification
[AD-A280788] p 461 N95-14293
Landsat Pathfinder tropical forest information management system p 565 N95-14594
The Network Operations Control Center upgrade task: Lessons learned p 419 N95-14631
Compiler optimizations for cache locality and coherence
[TR-504] p 586 N95-15589
The prospects for on-line hybrid coherency protocols on bus-based multiprocessors
[TR-490] p 579 N95-15590
Modeling and simulation of a Fiber Distributed Data Interface Local Area Network (FDDI LAN) using OPNET (tm) for interfacing through the Common Data Link (CDL)
[AD-A283124] p 469 N95-15651
PROTON BEAMS
Direct-current proton-beam measurements at Los Alamos
[DE94-016280] p 599 N95-15360
Prototype explosives-detection system based on nuclear-resonance absorption in nitrogen
[DE94-015069] p 442 N95-15387
PROTON IRRADIATION
Receiver design, performance analysis, and evaluation for space-borne laser altimeters and space-to-space laser ranging systems
[NASA-CR-197050] p 499 N95-14901
PROTON SCATTERING
Multiple-scattering model for inclusive proton production in heavy ion collisions
[NASA-TP-3470] p 600 N95-15606
PROTONS
Recent QCD results from the Tevatron (-p)p collider at the square root of s = 1.8 TeV
[DE94-014986] p 594 N95-14661
Introduction to muSR: What, how, where
[PB94-192267] p 596 N95-15379
Research accomplishments and future goals in particle physics
[DE94-015483] p 596 N95-15537
PROTOSTARS
The symbiosis of photometry and radial-velocity measurements p 643 N95-14505
PROTOTYPES
SLR 2000 p 471 N95-14288
Microcontamination detection using Heavy Ion Backscattering Spectrometry
[DE94-014182] p 437 N95-14312
Design of power electronics for TVC and EMA systems
[NASA-CR-197067] p 475 N95-14866
Automated cleaning of electronic components
[DE94-014122] p 476 N95-15356
Investigation of the coherent synchrotron radiation spectrum as a probe of charge dynamics
[DE94-015340] p 599 N95-15371
Rapid prototyping applications at Sandia National Laboratories
[DE94-006360] p 460 N95-15409
PROVING
Clean assembly and integration techniques for the Hubble Space Telescope High Fidelity Mechanical Simulator p 418 N95-14070
CFD methodology and validation for turbomachinery flows p 480 N95-14131
CAPTIONALS: A computer aided testing environment for the verification and validation of communication protocols p 570 N95-14163
Software development for safety-critical medical applications p 571 N95-14171
The symbiosis of photometry and radial-velocity measurements p 643 N95-14505
Validation of ERS-1 environmental data products
[NASA-CR-197111] p 517 N95-15848
PROXIMITY
Steering capacifiector sensor
[NASA-CASE-GSC-13489-1] p 583 N95-15598
PSYCHOACOUSTICS
Perception of auditory events: Attentional limitations
[AD-A284399] p 553 N95-15770

PSYCHOLOGICAL TESTS
Validation of MMPI scales for personality disorders: A pilot and other aviator study
[AD-A284397] p 553 N95-15768
PSYCHOMETRICS
Validation of MMPI scales for personality disorders: A pilot and other aviator study
[AD-A284397] p 553 N95-15768
PSYCHOPHYSIOLOGY
Crew factors in flight operations 2: Psychophysiological responses to short-haul air transport operations
[NASA-TM-108856] p 550 N95-15649
PSYCHOSES
Validation of MMPI scales for personality disorders: A pilot and other aviator study
[AD-A284397] p 553 N95-15768
PUBLIC HEALTH
Man-machine interfaces in health care
p 556 N95-14029
PULSARS
ROSAT observations of the binary Be-star and radio pulsar PSR1259-63
[NASA-CR-196951] p 642 N95-15907
PULSE COMMUNICATION
High-data-rate UHF line-of-sight communication experiment
[AD-A283592] p 468 N95-15321
PULSE DURATION
High gain GaAs switches for impulse sources: Measurement of the speed of current filaments
[DE94-015281] p 477 N95-15544
PULSE GENERATORS
Design of reliable high voltage avalanche transistor pulsers
[DE94-015323] p 473 N95-14261
A compact high voltage pulse generator
[DE94-015282] p 474 N95-14319
High gain GaAs switches for impulse sources: Measurement of the speed of current filaments
[DE94-015281] p 477 N95-15544
PULSE MODULATION
High speed QPPM direct detection optical communication receivers for FSDD intersatellite links
[NASA-CR-189331] p 615 N95-15849
PULSED LASERS
Advanced laser source research
[AD-A283110] p 498 N95-13695
Nonresonant interaction of ultrashort electromagnetic pulses with multilevel quantum systems
p 610 N95-13960
Review of drive symmetry measurement and control experiments on the Nova laser system
[DE94-014455] p 498 N95-13994
Double ionization in gases driven by optical field ionization using ultrashort laser pulses
[DE94-015137] p 498 N95-14318
LLE review, January - March 1994
[DE94-015058] p 618 N95-14955
Laser ablation and deposition of alloys
[PB94-191384] p 499 N95-15388
Apparatus for imaging an object in or through a scattering medium using coherent anti-Stokes Raman scattering
[AD-D016366] p 615 N95-15765
PYRENES
Investigation of a laboratory candidate for the carrier of the 4430 A diffuse interstellar band
p 641 N95-15840
Quantum chemistry and excited states: First investigations on pyrene-like molecules
p 599 N95-15844
PYRIDINES
Porphyrins in the interstellar medium (in grains)
p 640 N95-15837
PYROLYSIS
Upward flame spread along the vertical corner walls (October 1993)
[PB94-206299] p 441 N95-15352
PYROTECHNICS
Burn rates of TiH2/KClO4/Viton and output testing of NASA SKD26100098-301 pressure cartridges
[NASA-CR-188357] p 443 N95-15715

Q

Q SWITCHED LASERS
Method and apparatus for detection and control of prelasing in a Q-switched laser
[NASA-CASE-LAR-14790-1] p 499 N95-14519
QUADRATIC EQUATIONS
Multivariable Hermite polynomials and phase-space dynamics p 606 N95-13929
Convolutional encoding of self-dual block codes (2)
p 462 N95-14623
QUADRATURES
Correlated quadratures of resonance fluorescence and the generalized uncertainty relation p 598 N95-13937
QUADRUPOLES
Joint and angle-covariant spin measurements with a quadrupole magnetic field p 604 N95-13914
Anomalous temperature dependence of the lattice parameters in HoPO4 and HoVO4: Rare earth quadrupolar effects
[DE94-015086] p 622 N95-14608
QUALIFICATIONS
Essential elements of an effective data qualification
[DE94-015566] p 632 N95-15419
QUALITATIVE ANALYSIS
Selection of non-destructive assay methods: Neutron counting or calorimetric assay?
[DE94-016211] p 505 N95-15777
QUALITY
Toward deriving software architectures from quality attributes
[AD-A283827] p 572 N95-14339
QUALITY CONTROL
Engineering, technical, and management support services
[NASA-CR-196977] p 505 N95-13840
Earth Observing System (EOS)/Advanced Microwave Sounding Unit-A (AMSU-A) software assurance plan
[NASA-CR-196059] p 515 N95-13885
I(sub DDQ) testing for ultimate low power design verification and defect detection
[DE94-014281] p 473 N95-14314
John F. Kennedy Space Center, Safety, Reliability, Maintainability and Quality Assurance, Survey and Audit Program
[NASA-TM-109208] p 630 N95-14918
Development of a moldable, biodegradable polymeric bone repair material
[AD-A283413] p 454 N95-15296
Time-of-flight detector for heavy ion backscattering spectrometry
[DE94-015600] p 596 N95-15437
QUANTITATIVE ANALYSIS
Enhancement of insulin receptor mediated endocytosis in cultured osteoblastic cells under hypergravity
p 539 N95-15148
QUANTUM AMPLIFIERS
How to characterize the nonlinear amplifier?
p 471 N95-13922
Quantum amplification and quantum optical tapping with squeezed states and correlated quantum states
p 610 N95-13954
QUANTUM CHEMISTRY
Computational chemistry packages on the CRAY Y-MP in trondheim
[PB94-208246] p 595 N95-15350
Quantum chemistry and excited states: First investigations on pyrene-like molecules
p 599 N95-15844
L(alpha)-induced two-photon absorption of visible light emitted from an O-type star by H2(+) ions located near the surface of the Stromgren sphere surrounding the star: A possible explanation for the diffuse interstellar absorption bands (DIDs) p 641 N95-15845
QUANTUM CHROMODYNAMICS
Hadronization of QCD and effective interactions
[DE94-014975] p 594 N95-14660
Recent QCD results from the Tevatron (-p)p collider at the square root of s = 1.8 TeV
[DE94-014986] p 594 N95-14661
Production properties of Z bosons with jets in 1.8 TeV (anti p)p collisions
[DE94-015184] p 595 N95-15301
Hadronic wavefunctions in light-cone quantization
[DE94-014507] p 622 N95-15308
Theoretical studies in elementary particle physics
[DE94-015343] p 595 N95-15372
QUANTUM ELECTRODYNAMICS
Relativistic configuration-interaction calculation of the correlation energies of heliumlike ions
[DE94-015190] p 621 N95-14325
QUANTUM ELECTRONICS
Capacitance calculations in nanostructure devices via the quantum Liouville equation in the coordinate representation
[AD-A281936] p 589 N95-13656
The electromagnetic spectrum. Research investigation directed toward extending the useful range of the electromagnetic spectrum
[AD-A281378] p 461 N95-14361
In situ grown quantum-wire lasers
[AD-A281381] p 499 N95-14364
QUANTUM MECHANICS
Third International Workshop on Squeezed States and Uncertainty Relations
[NASA-CP-3270] p 602 N95-13896
High-order squeezing of the quantum electromagnetic field and the generalized uncertainty relations in two-mode squeezed states p 471 N95-13900
Multimode squeezing, biphotons and uncertainty relations in polarization quantum optics
p 603 N95-13904
On the theory of quantum measurement
p 604 N95-13910
Uncertainty relations as Hilbert space geometry
p 588 N95-13911
Two new kinds of uncertainty relations
p 588 N95-13915
The quantum measurement of time
p 590 N95-13917
Quantum state engineering p 605 N95-13919
Understanding squeezing of quantum states with the Wigner function p 606 N95-13930
On the possibility of a quantum mechanical phase space representation p 606 N95-13931
Particle localization, spinor two-valuedness, and Fermi quantization of tensor systems p 598 N95-13932
Quantum phase uncertainties in the classical limit
p 607 N95-13933
How to detect an excited atom without disturbing it or how to locate a super-mine without exploding it
p 598 N95-13934
Maximum predictive power and the superposition principle p 607 N95-13936
Minimum uncertainty and squeezing in diffusion processes and stochastic quantization
p 607 N95-13938
Schroedinger operators with the q-ladder symmetry algebras p 588 N95-13942
The wave function and minimum uncertainty function of the bound quadratic Hamiltonian system
p 608 N95-13943
Berry phase in Heisenberg representation
p 609 N95-13952
Complementarity and path distinguishability: Some recent results concerning photon pairs
p 598 N95-13961
Further evidence for the EPNT assumption
p 611 N95-13962
The photon: Experimental emphasis on its wave-particle duality p 599 N95-13963
The generation of entangled states from independent particle sources p 599 N95-13964
Nonlocal effects on the polarization state of a photon, induced by distant absorbers p 599 N95-13965
The strong Bell inequalities: A proposed experimental test p 611 N95-13966
On the nonlocal predictions of quantum optics
p 611 N95-13967
A loophole-free Bell's inequality experiment
p 611 N95-13968
The probabilistic origin of Bell's inequality
p 612 N95-13969
Einstein-Podolsky-Rosen-Bohm experiment and Bell inequality violation using Type 2 parametric down conversion p 612 N95-13970
QUANTUM NUMBERS
Probing the antiferromagnetic long-range order with Glauber spin states p 609 N95-13951
QUANTUM OPTICS
Third International Workshop on Squeezed States and Uncertainty Relations
[NASA-CP-3270] p 602 N95-13896
Properties of two-mode squeezed number states
p 602 N95-13897
Sum-frequency generation from photon number squeezed light p 603 N95-13902
Spectral, noise and correlation properties of intense squeezed light generated by a coupling in two laser fields p 500 N95-13903
Multimode squeezing, biphotons and uncertainty relations in polarization quantum optics
p 603 N95-13904
A new approach to the photon localization problem
p 603 N95-13905
Production of squeezed states for macroscopic mechanical oscillator p 603 N95-13906
On the theory of quantum measurement
p 604 N95-13910
General properties of quantum optical systems in a strong field limit p 609 N95-13950
New quantum properties of phonons and their detection p 610 N95-13957
On the nonlocal predictions of quantum optics
p 611 N95-13967
QUANTUM STATISTICS
Quantum noise limits to matter-wave interferometry
p 598 N95-13955
Quantum statistics of Raman scattering model with Stokes mode generation p 610 N95-13958

QUANTUM THEORY
Third International Workshop on Squeezed States and Uncertainty Relations
[NASA-CP-3270] p 602 N95-13896
Homodyning and heterodyning the quantum phase p 604 N95-13913
Two new kinds of uncertainty relations p 588 N95-13915
The quantum measurement of time p 590 N95-13917
Correlated quadratures of resonance fluorescence and the generalized uncertainty relation p 598 N95-13937
Pseudomaster equation for the no-count process in a continuous photodetection p 608 N95-13946
Quantum propagation in single mode fiber p 609 N95-13953
Bloch vector projection noise p 610 N95-13956

QUANTUM WELL LASERS
Strained-layer InGaAs(P)/InP quantum well semiconductor lasers grown by organometallic vapour phase epitaxy
[PB94-201399] p 622 N95-14795

QUANTUM WELLS
Asymmetric coupled quantum wells for high speed optical modulators at communication wavelengths
[AD-A281572] p 477 N95-15459

QUARK PARTON MODEL
The parton distribution functions in the limit chi(sub Bj) approaches 1
[DE94-013799] p 597 N95-15545

QUARKS
Theoretical studies in elementary particle physics
[DE94-015343] p 595 N95-15372
Research in high energy physics
[DE94-015519] p 600 N95-15539
The parton distribution functions in the limit chi(sub Bj) approaches 1
[DE94-013799] p 597 N95-15545
A relativistic cascade for heavy ion collisions
[DE94-015846] p 600 N95-15633
Studies of quarkonia production with CDF
[DE94-013220] p 597 N95-15862
Topics in the structure of hadronic systems
[DE94-014924] p 597 N95-15865

QUARTZ CRYSTALS
Using a temperature-controlled quartz crystal microbalance in a space equipment cleanroom to monitor molecular contamination p 421 N95-14069
Quartz resonator state-of-charge monitor for lead-acid batteries
[DE94-013823] p 473 N95-14310
Properties of nearly perfect crystals at very low temperatures
[NASA-CR-197221] p 627 N95-15823

QUASARS
Observations of extragalactic sources with the Metsaehovi radio telescope at 22-87 GHz
[PB94-197712] p 637 N95-13982

QUATERNIONS
Three-axis stabilization of spacecraft using parameter-independent nonlinear quaternion feedback
[NASA-TM-109150] p 420 N95-13729

QUEUEING THEORY
Performance modeling and analysis of parallel processing and Low Earth Orbit satellite communication systems
[AD-A283243] p 470 N95-15652

R

RADAR CLUTTER MAPS
Effects of hydrometeors and atmospheric gases at SHF/EHF p 468 N95-14835

RADAR DATA
Synthetic aperture radar signal data compression using block adaptive quantization p 565 N95-14590
CTAS data analysis program
[NASA-TM-108842] p 406 N95-14611
Nowcasting convective storm evolution in east-central Florida using satellite and Doppler radar data
[AD-A283260] p 534 N95-15618

RADAR FILTERS
Groundspeed filtering for CTAS
[NASA-CR-197223] p 497 N95-15785

RADAR IMAGERY
Developments in ground-penetrating radar at LLNL
[DE94-012236] p 554 N95-13671
Interferometric synthetic aperture radar terrain elevation mapping from multiple observations
[DE94-014185] p 515 N95-14313
Synthetic aperture radar signal data compression using block adaptive quantization p 565 N95-14590

RADAR MAPS
Interferometric synthetic aperture radar terrain elevation mapping from multiple observations
[DE94-014185] p 515 N95-14313

RADAR MEASUREMENT
Ground penetrating radar surveys to characterize pavement layer thickness variations at GPS sites
[PB94-190170] p 460 N95-14119
Measurements of upper tropospheric moisture with a Raman lidar
[DE94-015748] p 531 N95-15411

RADAR NAVIGATION
Experimental evaluation of cursors for B-2 Synthetic Aperture Radar (SAR) application
[AD-A283025] p 468 N95-15393

RADAR SCATTERING
Study of auroral dynamics with combined spacecraft and incoherent scatter radar data
[NASA-CR-196974] p 526 N95-13818

RADAR TARGETS
Experimental evaluation of cursors for B-2 Synthetic Aperture Radar (SAR) application
[AD-A283025] p 468 N95-15393

RADAR TRACKING
Study of auroral dynamics with combined spacecraft and incoherent scatter radar data
[NASA-CR-196974] p 526 N95-13818

RADIAL VELOCITY
The symbiosis of photometry and radial-velocity measurements p 643 N95-14505

RADIANT HEATING
Science objectives and performance of a radiometer and window design for atmospheric entry experiments p 429 N95-13718
VUV shock layer radiation in an arc-jet wind tunnel experiment p 405 N95-13719
Remote sensing strategy at the first atmospheric radiation measurement field site
[DE94-015091] p 522 N95-14187
Oscillatory/chaotic thermocapillary flow induced by radiant heating p 483 N95-14531

RADIATION ABSORPTION
Nonresonant interaction of ultrashort electromagnetic pulses with multilevel quantum systems p 610 N95-13960

RADIATION DAMAGE
Receiver design, performance analysis, and evaluation for space-borne laser altimeters and space-to-space laser ranging systems
[NASA-CR-197050] p 499 N95-14901
Fluorescent compounds for plastic scintillation applications
[DE94-013235] p 497 N95-15580

RADIATION DETECTORS
Study of the long term stability of the effective concentration of ionized space charges (N(sub eff)) of neutron irradiated silicon detectors fabricated by various thermal oxidations
[DE94-013734] p 593 N95-14309

RADIATION EFFECTS
Advanced solar cells for satellite power systems
[NASA-TM-106777] p 473 N95-14302
Study of the long term stability of the effective concentration of ionized space charges (N(sub eff)) of neutron irradiated silicon detectors fabricated by various thermal oxidations
[DE94-013734] p 593 N95-14309
Radiation rates for low Z impurities in edge plasmas
[DE94-016073] p 617 N95-14368
Transient failure behavior of HT9
[DE94-016320] p 445 N95-14378
Second International Conference on Computer Simulation of Radiation Effects in Solids
[DE94-016368] p 594 N95-14383
Radioactivity measurements of ITER materials using the TFTR D-T neutron field
[DE94-016094] p 617 N95-14397
US-Japan workshop Q-181 on High Heat Flux Components and Plasma-Surface Interactions for Next Devices: Proceedings
[DE94-014939] p 618 N95-14443
Analysis of space environment damage to solar cell assemblies from LDEF experiment A0171-GSFC test plate
[NASA-CR-197066] p 519 N95-14853
Immune changes in humans concomitant with space flights of up to 10 days duration p 545 N95-15114
Turbulent upward flame spread on a vertical wall under external radiation
[PB94-207388] p 441 N95-15353
Radiation and EMI effects in the NIF environment
[DE94-016635] p 468 N95-15365
Cation disorder in high dose neutron irradiated spinel
[DE94-013118] p 455 N95-15579
Technology and Science at at High-Power Spallation Source: Proceedings
[DE94-009685] p 597 N95-15826

RADIATION MEASUREMENT
Remote sensing strategy at the first atmospheric radiation measurement field site
[DE94-015091] p 522 N95-14187
Radioactivity measurements of ITER materials using the TFTR D-T neutron field
[DE94-016094] p 617 N95-14397

RADIATION MEASURING INSTRUMENTS
An efficient network for interconnecting remote monitoring instruments and computers
[DE94-016213] p 581 N95-14377

RADIATION SHIELDING
Extension of the BRYNTRN code to monoenergetic light ion beams
[NASA-TP-3472] p 647 N95-15790

RADIATION SOURCES
Accelerator and Fusion Research Division: 1993 Summary of activities
[DE94-015157] p 599 N95-15367

RADIATION SPECTRA
Science objectives and performance of a radiometer and window design for atmospheric entry experiments p 429 N95-13718
Studies of the ablated plasma from experimental plasma gun disruption simulations
[DE94-015017] p 617 N95-14262

RADIATION TOLERANCE
Dextrous gripping in a hazardous environment
[PB94-191244] p 501 N95-14150

RADIATION TRANSPORT
Extension of the BRYNTRN code to monoenergetic light ion beams
[NASA-TP-3472] p 647 N95-15790
Diffuse interstellar bands in reflection nebulae p 639 N95-15830

RADIATIVE HEAT TRANSFER
Radiative interactions in multi-dimensional chemically reacting flows using Monte Carlo simulations
[NASA-CR-197012] p 481 N95-14269
Missile infrared radiation analysis p 399 N95-14449
Behavior of charring materials in simulated fire environments
[PB94-196045] p 439 N95-14838
Technical report series on global modeling and data assimilation. Volume 3: An efficient thermal infrared radiation parameterization for use in general circulation models
[NASA-TM-104606-VOL-3] p 531 N95-15745

RADIATIVE TRANSFER
Computing illumination using extended sources: Object space and image space
[PB94-201282] p 612 N95-13992
Parallel image rendering algorithm and architecture based on ray tracing and radiosity shading
[PB94-191277] p 569 N95-14153
Excimer emission from alkali diatomic and alkaline-earth-noble gas molecules
[AD-A281662] p 596 N95-15446

RADICALS
Theoretical studies of hydrocarbon combustion chemistry
[DE94-017155] p 441 N95-15347
The C4H radical and the diffuse interstellar bands. An ab initio study p 641 N95-15843

RADII
AXAF VETA-I mirror ring focus measurements
[NASA-CR-196145] p 637 N95-13637

RADIO ALTIMETERS
Precision orbit determination of altimetric satellites p 418 N95-14282
Radar altimeter calibration using SLR p 471 N95-14283

RADIO ASTRONOMY
The formation of small grains in shocks in the ISM p 641 N95-15842
The C4H radical and the diffuse interstellar bands. An ab initio study p 641 N95-15843

RADIO ATTENUATION
Ground wave and diffraction, A p 467 N95-14828

RADIO COMMUNICATION
Impulse response measurements in the 1850-1990 MHz band in large outdoor cells
[PB94-204906] p 462 N95-14412
Proceedings of the Eighteenth NASA Propagation Experimenters Meeting (NAPEX 18) and the Advanced Communications Technology Satellite (ACTS) Propagation Studies Miniworkshop
[NASA-CR-196959] p 464 N95-14670
Olympus propagation experiments p 464 N95-14671
Propagation data at 20/40 GHz and the propagation needs of Milstar p 465 N95-14673

The 40 and 50 GHz propagation experiments at the Rutherford Appleton Laboratory, UK, using the ITALSAT beacons p 465 N95-14674
A database for propagation models p 465 N95-14675
Channel characterisation for future Ka-band Mobile Satellite Systems and preliminary results p 465 N95-14676
ACTS mobile propagation campaign p 465 N95-14677
Slant path L- and S-Band tree shadowing measurements p 465 N95-14678
Propagation considerations for the Odyssey system design p 466 N95-14680
Communications availability: Estimation studies at AMSC p 466 N95-14681
S-Band propagation measurements p 466 N95-14682
Wireless technology for command control and communications
[AD-A284367] p 470 N95-15804
Discrete-event-dynamic-system-based approaches for control in integrated voice/data multihop radio networks
[AD-A284413] p 470 N95-15813

RADIO FREQUENCIES
Burst-by-burst laser frequency monitor
[NASA-CASE-NPO-18596-1-CU] p 498 N95-13629
Propagation Modelling and Decision Aids for Communications, Radar and Navigation Systems
[AGARD-LS-196] p 466 N95-14825
Propagation in the ionosphere, A p 466 N95-14826
Propagation in the ionosphere, B p 467 N95-14827
Ground wave and diffraction, B p 467 N95-14829
Sensing of radio refractivity and aerosol extinction p 467 N95-14830
Field-emitter arrays for RF vacuum microelectronics
[AD-A283549] p 476 N95-15327
Numerical solution of a tunneling equation
[DE94-015514] p 586 N95-15538
RF vacuum microelectronics
[AD-A283123] p 478 N95-15613
Performance comparison AN/FRD-10 versus PUSHER
[AD-A283263] p 469 N95-15619
Selective RF pulses in NMR and their effect on coupled and uncoupled spin systems
[PB94-195526] p 471 N95-15871

RADIO GALAXIES
Observations of extragalactic sources with the Metsaehovi radio telescope at 22-87 GHz
[PB94-197712] p 637 N95-13982

RADIO RECEIVERS
The 40 and 50 GHz propagation experiments at the Rutherford Appleton Laboratory, UK, using the ITALSAT beacons p 465 N95-14674

RADIO SIGNALS
Florida's propagation report p 466 N95-14684
Ground wave and diffraction, A p 467 N95-14828

RADIO SOURCES (ASTRONOMY)
A radio telescope for the calibration of radio sources at 32 gigahertz p 463 N95-14626

RADIO SPECTRA
Selective RF pulses in NMR and their effect on coupled and uncoupled spin systems
[PB94-195526] p 471 N95-15871

RADIO TELEMETRY
Collection of real-time, multichannel EEG data from helicopter pilots in flight: A feasibility study
[AD-A284396] p 551 N95-15767

RADIO TELESCOPES
Observations of extragalactic sources with the Metsaehovi radio telescope at 22-87 GHz
[PB94-197712] p 637 N95-13982
A radio telescope for the calibration of radio sources at 32 gigahertz p 463 N95-14626

RADIO TRANSMISSION
Proceedings of the Eighteenth NASA Propagation Experimenters Meeting (NAPEX 18) and the Advanced Communications Technology Satellite (ACTS) Propagation Studies Miniworkshop
[NASA-CR-196959] p 464 N95-14670
Propagation characteristics of 20/30 GHz links with a 40 deg masking angle p 464 N95-14672
A database for propagation models p 465 N95-14675
Channel characterisation for future Ka-band Mobile Satellite Systems and preliminary results p 465 N95-14676
Slant path L- and S-Band tree shadowing measurements p 465 N95-14678
S-Band propagation measurements p 466 N95-14682
Florida's propagation report p 466 N95-14684
Sensing of radio refractivity and aerosol extinction p 467 N95-14830
Refractive effects from VHF to EHF. Part B: Propagation models p 467 N95-14832
Discrete-event-dynamic-system-based approaches for control in integrated voice/data multihop radio networks
[AD-A284413] p 470 N95-15813

RADIO WAVES
A database for propagation models p 465 N95-14675
Refractive effects from VHF to EHF. Part A: Propagation Mechanisms p 467 N95-14831

RADIOACTIVE DECAY
Searches for massive neutrino emission in C-14 beta and Fe-55 electron-capture decays
[DE94-016863] p 594 N95-14374
Beta decay data for neutron-rich Li-Cl nuclides
[DE94-014556] p 595 N95-15310
Introduction to muSR: What, how, where
[PB94-192267] p 596 N95-15379

RADIOACTIVE WASTES
FFCAat Clearinghouse, directory of abstracts
[DE94-015259] p 632 N95-15435

RADIOGENIC MATERIALS
Energy flux and hydrogeology of thermal anomalies in the Gulf of Mexico Basin: South Texas example
[DE94-015122] p 530 N95-14956

RADIOGRAPHY
Radiographic Moire
[NASA-CASE-LAR-15104-1] p 505 N95-13835

RADIOMETERS
Planetary entry experiments
[NASA-CR-194215] p 644 N95-13717
Science objectives and performance of a radiometer and window design for atmospheric entry experiments p 429 N95-13718
Radiometric resolution enhancement by lossy compression as compared to truncation followed by lossless compression p 564 N95-14588
Radiometer calibration procedure and beacon attenuation estimation reference level p 466 N95-14683

RADIOMETRIC RESOLUTION
1994 Science Information Management and Data Compression Workshop
[NASA-CP-3277] p 564 N95-14585
Radiometric resolution enhancement by lossy compression as compared to truncation followed by lossless compression p 564 N95-14588
Synthetic aperture radar signal data compression using block adaptive quantization p 565 N95-14590
Lossless compression of NOAA-AVHRR satellite data p 565 N95-14592

RADIUM ISOTOPES
The 226RA and 231PA systematics of axial, MORB, crustal residence ages, and MAGMA chamber characteristics at 9 to 10 degree N East Pacific Rise
[DE94-013084] p 529 N95-14434

RADOMES
Test and Evaluation Master Plan (TEMP) for Fixed Ground Antenna Radomes (FGAR)
[AD-A283839] p 461 N95-14346

RAILS
Gouge initiation in high-velocity rocket sled testing
[DE94-014288] p 418 N95-15357

RAIN
Statistical aspects of the precipitation regimes at Miami International Airport (MIA) and Palm Beach International Airport (PBI): 1961-1990
[PB94-194289] p 532 N95-14118
Propagation data at 20/40 GHz and the propagation needs of Milstar p 465 N95-14673
Effects of hydrometeors and atmospheric gases at SHF/EHF p 468 N95-14835
Heavy rain effects p 407 N95-14899
June to September rainfall in the African Sahel: Verification of our 1994 forecasts and an extended range forecast for 1995, 3
[TR-521] p 534 N95-15666

RAMAN SPECTRA
Quantum statistics of Raman scattering model with Stokes mode generation p 610 N95-13958
Apparatus for imaging an object in or through a scattering medium using coherent anti-Stokes Raman scattering
[AD-D016366] p 615 N95-15765

RAMAN SPECTROSCOPY
Relationship between microstructure and efficiency of scintillating glasses
[DE94-014563] p 454 N95-15313

RAMJET ENGINES
Combustion efficiency in a dual-inlet side-dump ramjet combustor
[AD-A283564] p 411 N95-15329

RAMJET MISSILES
Computation of supersonic air-intakes p 400 N95-14452

RANDOM ACCESS MEMORY
In situ, real-time analysis of the growth of ferroelectric and conductive oxide heterostructures by a new time-of-flight pulsed ion beam surface analysis technique
[DE94-013298] p 620 N95-13822
Ferroelectric oxide memory FET (FEMFET) development
[AD-A283203] p 476 N95-15399

RANDOM NOISE
Investigation of Allan variance for determining noise spectral forms with application to microwave radiometry
[NASA-CR-194985] p 516 N95-15727
Neutrino oscillations in noisy media
[DE94-014973] p 598 N95-15869

RANDOM VARIABLES
Dependent random variables in uncertainty analysis
[PB94-191293] p 585 N95-14154
Pseudorandom generators and the frequency of simplicity
[UR-DCS-TR-94-507] p 586 N95-15594

RANGE (EXTREMES)
Flow-radiated noise. Study of the propagative spectral range of the wall pressure field
[PB94-201290] p 590 N95-13985

RANKINE CYCLE
Alkali metal Rankine cycle boiler technology challenges and some potential solutions for space nuclear power and propulsion applications
[NASA-TM-106593] p 430 N95-14174

RANKING
Large-scale data envelopment analysis models and related applications
[AD-A283214] p 588 N95-15400

RAPID QUENCHING (METALLURGY)
The study of dopant segregation behavior during the growth of GaAs in microgravity p 458 N95-14215

RARE EARTH COMPOUNDS
Anomalous temperature dependence of the lattice parameters in HoPO4 and HoVO4: Rare earth quadrupolar effects
[DE94-015086] p 622 N95-14608

RARE GASES
A theoretical study of 30 to 50 angstrom noble gas heavy ion lithography
[DE94-015262] p 442 N95-15436

RATIONAL FUNCTIONS
An efficient spectral method for ordinary differential equations with rational function coefficients
[NASA-TM-106762] p 585 N95-14296

RATS
Simulation of Shuttle launch G forces and acoustic loads using the NASA Ames Research Center 20G centrifuge p 419 N95-14089
Twenty four hours head-down tilt decreases arterial baroreflex function in conscious rat p 538 N95-15098
Cardiovascular deconditioning effects of long-term simulated weightlessness in rats p 538 N95-15099
Space flight and humoral and cellular immunity of animals p 538 N95-15113
The regulation of rat activity following exposure to hyperdynamic fields p 539 N95-15133
New findings regarding light intensity and its effects as a zeitgeber in the Sprague-Dawley rat p 539 N95-15135
Effect of short- and long-term spaceflight on the contractile properties of rat skeletal muscles with different functions p 539 N95-15141
Influence to organs by ten weeks tail suspension p 539 N95-15142
Relationship between hind-limb muscle atrophy and serum enzymes in tail suspended rats p 539 N95-15143

RAY TRACING
HRMA calibration handbook: EKC gravity compensated XRCF models
[NASA-CR-195818] p 636 N95-13634
Parallel image rendering algorithm and architecture based on ray tracing and radiosity shading
[PB94-191277] p 569 N95-14153
Real time system for practical acoustic monitoring of global ocean temperature, volume 3
[AD-A283774] p 535 N95-14335
Propagation in the ionosphere, A p 466 N95-14826
Tidal dynamics and mixing over steep topography
[AD-A283535] p 536 N95-15324
Lower-hybrid poloidal current drive for fluctuation reduction in a reversed field pinch
[DE94-015534] p 618 N95-15540
Graphical aids for the users of GEMACS (GAUGE): Ray tracing enhancements
[AD-A284903] p 470 N95-15756

RAYLEIGH EQUATIONS
The breakup of a liquid jet at microgravity p 484 N95-14535

RAYLEIGH SCATTERING
Developments in laser-based diagnostics for wind tunnels in the Aeromechanics Division: 1987-1992
[AD-A283011] p 412 N95-13687
RAYLEIGH WAVES
Problems in nonlinear acoustics: Surface acoustic waves, diffracting sound beams, and fluid-solid interface effects
[AD-A281714] p 592 N95-15453
RAYLEIGH-RITZ METHOD
The buckling response of symmetrically laminated composite plates having a trapezoidal planform area
[NASA-CR-196975] p 505 N95-13839
REACTING FLOW
Radiative interactions in multi-dimensional chemically reacting flows using Monte Carlo simulations
[NASA-CR-197012] p 481 N95-14269
REACTION KINETICS
Practical aspects of corrosion fundamentals
[DE94-015842] p 438 N95-14371
Determination of solvation kinetics in supercritical fluids
[DE94-016491] p 438 N95-14386
Infrared absorption spectroscopy and chemical kinetics of free radicals
[DE94-016642] p 438 N95-14392
LSENS: A General Chemical Kinetics and Sensitivity Analysis Code for homogeneous gas-phase reactions. Part 1: Theory and numerical solution procedures
[NASA-RP-1328-PT-1] p 440 N95-15056
LSENS: A General Chemical Kinetics and Sensitivity Analysis Code for homogeneous gas-phase reactions. Part 3: Illustrative test problems
[NASA-RP-1330-PT-3] p 440 N95-15057
Development and analysis of high-energy corona process for air purification
[DE94-015207] p 524 N95-15432
LSENS, a general chemical kinetics and sensitivity analysis code for homogeneous gas-phase reactions. 2: Code description and usage
[NASA-RP-1329] p 442 N95-15512
Tensile creep strain and activation energy
[AD-A283264] p 513 N95-15620
Chemical kinetics and atmospheric modification
[AD-A283304] p 524 N95-15623
Process development of thermal hydrodechlorination
[PB94-195518] p 525 N95-15870
REACTIVITY
Boron atom matrix chemistry
[AD-A282840] p 434 N95-14366
Determination of solvation kinetics in supercritical fluids
[DE94-016491] p 438 N95-14386
The transformation of organic amines by transition metal cluster compounds
[DE94-017151] p 441 N95-15346
Reactive polymers: Main chain coordination polymers for air separation
[AD-A281614] p 455 N95-15444
REACTOR MATERIALS
Transient failure behavior of HT9
[DE94-016320] p 445 N95-14378
Impact fracture behavior of HT9 duct
[DE94-016328] p 445 N95-14379
Radioactivity measurements of ITER materials using the TFTR D-T neutron field
[DE94-016094] p 617 N95-14397
Experiments to examine the contribution of gas atoms to void formation in irradiated metals
[DE94-015209] p 446 N95-15433
READING
Augmentation of research on cognitive control
[AD-A280956] p 552 N95-14600
REAGENTS
Space flight and humoral and cellular immunity of animals p 538 N95-15113
World Reference Center for Arboviruses
[AD-A281635] p 550 N95-15445
REAL TIME OPERATION
Burst-by-burst laser frequency monitor
[NASA-CASE-NPO-18596-1-CU] p 498 N95-13629
A prototype lisp-based soft real-time object-oriented Graphical User Interface for control system development
[NASA-TM-106743] p 566 N95-13716
Results of demonstration test for receiving and processing of flight data from the Space Transportation System
[NASA-CR-194986] p 418 N95-13890
Tele-existence and/or cybernetic interface studies in Japan p 555 N95-14025
Virtual acoustic displays p 557 N95-14035
MISSION: Mission and Safety Critical Support Environment. Executive overview p 569 N95-14158
Performance comparison of token ring protocols for hard-real-time communication p 570 N95-14164
POSIX real-time extensions p 570 N95-14165
CIFO 3.0 p 570 N95-14167
Intelligent alarming p 570 N95-14168
Expert systems in the process industries p 571 N95-14169
Fault detection and diagnosis using neural network approaches p 571 N95-14170
Review of European microgravity measurements p 457 N95-14211
Real time system for practical acoustic monitoring of global ocean temperature, volume 3
[AD-A283774] p 535 N95-14335
Computing quantitative characteristics of finite-state real-time systems
[AD-A282839] p 412 N95-14343
Airplane takeoff and landing performance monitoring system
[NASA-CASE-LAR-14745-2-SB] p 412 N95-14415
A graphical user interface for design and analysis of air breathing propulsion systems
[TABES PAPER 94-616] p 411 N95-14645
Automated test environment for a real-time control system
[TABES PAPER 94-631] p 417 N95-14652
Support of Environmental Requirements for Cloud Analysis and Archive (SERCAA): Algorithm descriptions
[AD-A283240] p 534 N95-15614
RECEIVERS
Real time system for practical acoustic monitoring of global ocean temperature, volume 3
[AD-A283774] p 535 N95-14335
The Block V Receiver fast acquisition algorithm for the Galileo S-band mission p 463 N95-14627
Research and development optical deep space antenna sizing study p 463 N95-14628
Experimental hardware development for a pulsed ultrasonic data collection facility
[AD-A283331] p 615 N95-15872
RECEPTORS (PHYSIOLOGY)
Neural mechanisms of kinesthesia p 555 N95-14018
Intersensory coordination p 555 N95-14020
RECESSION
Numerical solution of two-dimensional ablation problems using the finite control volume method with unstructured grids
[DE94-015012] p 428 N95-14664
RECOGNITION
Vision-based navigation and recognition
[AD-A282962] p 583 N95-15398
RECONNAISSANCE
FRESIP project observations of cataclysmic variables: A unique opportunity p 644 N95-14507
RECORDING INSTRUMENTS
Acceleration recorder and playback module
[NASA-CASE-MSC-22008-1] p 496 N95-14180
RECTANGULAR PLATES
Analytical tripping loads for stiffened plates
[AD-A284368] p 514 N95-15805
RECTIFICATION
Intelligent alarming p 570 N95-14168
REDUNDANCY
Checkpointing and rollback recovery in distributed shared memory systems
[AD-A281583] p 579 N95-15442
REDUNDANCY ENCODING
Representation and recognition with algebraic invariants and geometric constraint models
[AD-A282926] p 585 N95-14843
REENTRY EFFECTS
Science objectives and performance of a radiometer and window design for atmospheric entry experiments p 429 N95-13718
VUV shock layer radiation in an arc-jet wind tunnel experiment p 405 N95-13719
REENTRY SHIELDING
Thermoacoustic environments to simulate reentry conditions p 426 N95-14096
REFINING
An application of miniscale experiments on Earth to refine microgravity analysis of adiabatic multiphase flow in space p 459 N95-14567
Investigation of dendrite coherency in two commercial Al-Si foundry alloys
[PB94-208238] p 446 N95-15349
REFLECTANCE
Performance Report: A timeline for the synchrotron calibration of AXAF
[NASA-CR-196489] p 638 N95-14101
Polarized photomodulated reflectivity and photoluminescence studies of ordered InGaP2 under pressure
[DE94-016556] p 621 N95-14390
Nowcasting convective storm evolution in east-central Florida using satellite and Doppler radar data
[AD-A283260] p 534 N95-15618
REFLECTION
Optimization of transparent and reflecting electrodes for amorphous-silicon solar cells
[DE94-011841] p 520 N95-15355
REFLECTION NEBULAE
Diffuse interstellar bands in reflection nebulae p 639 N95-15830
REFLECTORS
Earth Observing System (EOS)/Advanced Microwave Sounding Unit-A (AMSU-A) worst-case analysis: Antenna beam pointing
[NASA-CR-197218] p 517 N95-15851
REFRACTION
Refractive effects from VHF to EHF. Part A: Propagation Mechanisms p 467 N95-14831
REFRACTIVITY
Engineer's Refractive Effects Prediction System (EREPS), version 3.0
[AD-A283748] p 461 N95-14345
Propagation Modelling and Decision Aids for Communications, Radar and Navigation Systems
[AGARD-LS-196] p 466 N95-14825
Sensing of radio refractivity and aerosol extinction p 467 N95-14830
Refractive effects from VHF to EHF. Part A: Propagation Mechanisms p 467 N95-14831
Refractive effects from VHF to EHF. Part B: Propagation models p 467 N95-14832
Investigation of the coherent synchrotron radiation spectrum as a probe of charge dynamics
[DE94-015340] p 599 N95-15371
REFRACTORY MATERIALS
Thermally stable organic polymers
[AD-A281380] p 451 N95-14363
Mechanical behavior of high temperature composites
[AD-A281582] p 436 N95-15441
REFRACTORY METALS
AASERT-93: Electroplating of refractory metals using haloaluminate melts
[AD-A284859] p 447 N95-15744
REFRACTORY PERIOD
EPIC computational models of psychological refractory-period effects in human multiple-task performance
[AD-A280924] p 540 N95-14142
REFRIGERANTS
Thermophysical properties of HCFC alternatives
[DE94-016646] p 438 N95-14372
Pilot retrofit test of refrigerant R-134a for GDSCC p 456 N95-14629
Solubility, viscosity and density of refrigerant and lubricant mixtures
[DE94-016949] p 454 N95-15343
REFRIGERATING
Wind-electric ice making for villages in the developing world
[DE94-011854] p 518 N95-14191
REFRIGERATORS
Wind-electric ice making for villages in the developing world
[DE94-011854] p 518 N95-14191
REGENERATION (PHYSIOLOGY)
The Astroculture (tm)-1 experiment on the USML-1 mission p 564 N95-14228
REGULATIONS
Fatigue evaluation of empennage, forward wing, and winglets/tip fins on part 23 airplanes
[PB94-196813] p 408 N95-13981
Civil use of night vision devices: Evaluation pilot's guide, part 2
[DOT/FAA/RD-94/19] p 410 N95-14175
REINFORCED PLATES
Analytical tripping loads for stiffened plates
[AD-A284368] p 514 N95-15805
REINFORCEMENT
First results with instance-based state identification for reinforcement learning
[TR-502] p 553 N95-15642
REINFORCING FIBERS
Effects of in situ fiber strength characteristics on mechanical properties of SiC(f)/SiC composites
[DE94-013965] p 433 N95-13682
REINFORCING MATERIALS
Composites with improved compressive properties
[AD-A283411] p 435 N95-15417
RELATIVISTIC PARTICLES
The thermal-wave model: A Schroedinger-like equation for charged particle beam dynamics p 601 N95-13944
RELATIVITY
The 24th International Physics Olympiad
[AD-A280584] p 589 N95-13972
The role of SLR and LLR in relativity p 528 N95-14284

RELAXATION TIME
Tensile creep strain and activation energy
[AD-A283264] p 513 N95-15620
RELIABILITY
Engineering, technical, and management support services
[NASA-CR-196977] p 505 N95-13840
Fatigue reliability method with in-service inspections
p 505 N95-14475
John F. Kennedy Space Center, Safety, Reliability, Maintainability and Quality Assurance, Survey and Audit Program
[NASA-TM-109208] p 630 N95-14918
The effect of response format on reliability estimates for tacit knowledge scales
[AD-A283547] p 552 N95-15326
Monitoring solar-thermal systems: An outline of methods and procedures
[DE94-015599] p 521 N95-15420
RELIABILITY ANALYSIS
Environmental testing to prevent on-orbit TDRS failures p 423 N95-14078
Software reliability studies
[NASA-CR-197027] p 572 N95-14615
An architecture for intelligent multichip module reliability analysis
[AD-A281574] p 583 N95-15461
Mechanical system reliability for long life space systems
[NASA-CR-197215] p 505 N95-15584
RELIABILITY ENGINEERING
AXAF VETA-I mirror ring focus measurements
[NASA-CR-196145] p 637 N95-13637
Design for reliability: NASA reliability preferred practices for design and test
[NASA-TM-106313] p 420 N95-13728
Remote programming in INSAT-2A/2B on-board Attitude and Orbit Control Computer (AOCC)
p 413 N95-13827
MISSION: Mission and Safety Critical Support Environment. Executive overview p 569 N95-14158
The principles of flight test assessment of flight-safety-critical systems in helicopters
[AGARD-AG-300-VOL-12] p 405 N95-14199
The Network Operations Control Center upgrade task: Lessons learned p 419 N95-14631
RELIEF MAPS
Interferometric synthetic aperture radar terrain elevation mapping from multiple observations
[DE94-014185] p 515 N95-14313
Satellite imagery and topographic data in verification
[AD-A280950] p 530 N95-14598
REMANENCE
Ferromagnetic grain boundary signature in die-upset RE-Fe-B magnets
[DE94-014904] p 590 N95-14440
REMOTE CONTROL
Remote programming in INSAT-2A/2B on-board Attitude and Orbit Control Computer (AOCC)
p 413 N95-13827
Analysis of the human operator subsystems
p 555 N95-14019
Tele-existence and/or cybernetic interface studies in Japan p 555 N95-14025
Models of remote manipulation in space
p 504 N95-14027
Dextrous gripping in a hazardous environment
[PB94-191244] p 501 N95-14150
Control of remotely-operated manipulation systems
p 582 N95-14945
Human factors considerations for remote manipulation
p 564 N95-14949
Interactive Computer-Enhanced Remote Viewing System (ICERVS): Subsystem design report, phase 2
[DE94-014513] p 563 N95-15309
Performance information management system (PIMS) communication
[AD-A284851] p 574 N95-15335
REMOTE HANDLING
Dextrous gripping in a hazardous environment
[PB94-191244] p 501 N95-14150
REMOTE MANIPULATOR SYSTEM
Control and operation of space manipulator systems
p 582 N95-14946
REMOTE SENSING
Earth Observing System (EOS)/Advanced Microwave Sounding Unit-A (AMSU-A): Instrument logic diagrams
[NASA-CR-189378] p 567 N95-13633
Remote sensing, processing and transmission of data for an unmanned aerial vehicle
[AD-A283104] p 514 N95-13693
Earth Observing System (EOS)/Advanced Microwave Sounding Unit-A (AMSU-A): Calibration management plan
[NASA-CR-189376] p 515 N95-13704
Star sensor for Indian Remote Sensing Satellite (IRS 1C) p 413 N95-13828
Computer aided techniques for the realisation of the diaphragm of the PSM for the IRS-1C
p 413 N95-13829
Remote sensing strategy at the first atmospheric radiation measurement field site
[DE94-015091] p 522 N95-14187
Satellite Laser Ranging in the 1990s: Report of the 1994 Belmont Workshop
[NASA-CP-3283] p 526 N95-14274
A multiscale random field model for Bayesian image segmentation
[AD-A283875] p 515 N95-14358
Radiometric resolution enhancement by lossy compression as compared to truncation followed by lossless compression p 564 N95-14588
The development of lossless data compression technology for remote sensing applications
p 565 N95-14593
The Global Emergency Observation and Warning System
[TABES PAPER 94-622] p 417 N95-14649
Development of a systemic land cover/land use database for the Upper Mississippi River System derived from Landsat Thematic Mapper satellite data. Long term resource monitoring program
[PB94-186889] p 515 N95-14793
Sensing of radio refractivity and aerosol extinction
p 467 N95-14830
Space debris detection and analysis
[AD-A282012] p 428 N95-14951
US space-based remote sensing: Challenges and prospects
[AD-A282439] p 515 N95-15546
Steering capaciflector sensor
[NASA-CASE-GSC-13489-1] p 583 N95-15598
Support of Environmental Requirements for Cloud Analysis and Archive (SERCAA): Algorithm descriptions
[AD-A283240] p 534 N95-15614
International Geoid Service Bulletin No. 1
[BULL-1] p 516 N95-15791
Geodetic survey of Canada: Results on a geoid questionnaire p 516 N95-15793
The GEOMED Project p 516 N95-15794
Validation of ERS-1 environmental data products
[NASA-CR-197111] p 517 N95-15848
First Year PIDDP Report on gamma-ray and x-ray spectroscopy: X-ray remote sensing and in situ spectroscopy for planetary exploration missions and gamma-ray remote sensing and in situ spectroscopy for planetary exploration missions
[NASA-CR-189374] p 517 N95-15916
REMOTELY PILOTED VEHICLES
Telerobotics in the deep ocean p 504 N95-14026
RENAL FUNCTION
Gravitational stress and regulation of neuroendocrine elements and fluid volume in humans
p 542 N95-15090
RENDEZVOUS GUIDANCE
A vision based attitude and position estimation algorithm for rendezvous and docking p 414 N95-13831
Neural networks: Alternatives to conventional techniques for automatic docking
[TABES PAPER 94-627] p 417 N95-14651
RENORMALIZATION GROUP METHODS
Dynamical impurity problems
[DE94-013025] p 625 N95-15576
Topics in the structure of hadronic systems
[DE94-014924] p 597 N95-15865
REQUIREMENTS
David Florida Laboratory Thermal Vacuum Data Processing System p 418 N95-14079
Geodetic survey of Canada: Results on a geoid questionnaire p 516 N95-15793
RESCUE OPERATIONS
Satellite communication technology and applications, 1995-2010 p 413 N95-13826
RESEARCH
Medical research publications: A bibliography of Walter Reed Army Medical Center staff, 1986-1992, volume 2
[PB94-177797] p 541 N95-14394
RESEARCH AIRCRAFT
Fourth High Alpha Conference, volume 2
[NASA-CP-10143-VOL-2] p 395 N95-14239
F-18 high alpha research vehicle: Lessons learned
p 395 N95-14240
Design and development of an F/A-18 inlet distortion rake: A cost and time saving solution
p 395 N95-14241
Flight test results of the F-16 aircraft modified with the axisymmetric vectoring exhaust nozzle
p 396 N95-14245
Flight validation of ground-based assessment for control power requirements at high angles of attack
p 396 N95-14246
Numerical simulation of the flow about the F-18 HARV at high angle of attack
[NASA-CR-197023] p 400 N95-14614
RESEARCH AND DEVELOPMENT
A review of 50 years of aerodynamic research with NACA/NASA
[NASA-TM-109163] p 647 N95-13663
Energy and Technology Review, April 1994
[DE94-012133] p 496 N95-13689
Hypertext knowledge presentation system to transition basic research
[AD-A280796] p 630 N95-14321
Helping small companies commercialize public-sector technology
[TABES PAPER 94-407] p 415 N95-14635
Research and technology highlights, 1993
[NASA-TM-4575] p 647 N95-15065
Guidelines for a Research and Development (R/D) program for high sustained G p 548 N95-15124
Vertical flight terminal operational procedures. A summary of FAA research and development
[AD-A283550] p 413 N95-15328
Sandia 1993 Superconducting Technology Program
[DE94-015601] p 625 N95-15438
RESEARCH FACILITIES
Eighteenth Space Simulation Conference: Space Mission Success Through Testing
[NASA-CP-3280] p 420 N95-14062
Evaluation of reformulated thermal control coatings in a simulated space environment. Part 1: YB-71
p 420 N95-14063
A facility to produce an energetic, ground state atomic oxygen beam for the simulation of the Low-Earth Orbit environment p 422 N95-14072
A simulation facility for testing Space Station assembly procedures p 423 N95-14075
David Florida Laboratory Thermal Vacuum Data Processing System p 418 N95-14079
Thermal balance testing of MSAT 2 spacecraft
p 424 N95-14080
Thermal balance testing of the MSAT spacecraft
p 424 N95-14082
Refurbishment of a 39 foot thermal vacuum chamber
p 418 N95-14085
System level mechanical testing of the Clementine spacecraft p 425 N95-14087
Simulation of Shuttle launch G forces and acoustic loads using the NASA Ames Research Center 20G centrifuge
p 419 N95-14089
Unique life sciences research facilities at NASA Ames Research Center p 426 N95-14091
Thermoacoustic environments to simulate reentry conditions p 426 N95-14096
The AEDC aerospace chamber 7V: An advanced test capability for infrared surveillance and seeker sensors
p 418 N95-14097
Review of European microgravity measurements
p 457 N95-14211
Helping small companies commercialize public-sector technology
[TABES PAPER 94-407] p 415 N95-14635
Research and technology highlights, 1993
[NASA-TM-4575] p 647 N95-15065
International Geoid Service Bulletin No. 1
[BULL-1] p 516 N95-15791
Introducing the International Geoid Service
p 516 N95-15792
RESEARCH VEHICLES
Preparations for flight research to evaluate actuated forebody strakes on the F-18 high-alpha research vehicle p 398 N95-14257
RESERVOIRS
Survey of the 1991 geothermal exploration promotion
[DE94-780690] p 530 N95-14836
RESIDENTIAL AREAS
Residents' reactions to long-term sonic boom exposure: Preliminary results p 403 N95-14892
RESIDUAL STRENGTH
Residual strength of composites with multiple impact damage
[AD-A284230] p 434 N95-14409
Testing and analysis of flat and curved panels with multiple cracks p 508 N95-14460
Characterization of damage progression in SCS-6/Timetal 21S (0)4 under thermomechanical fatigue loadings
[NASA-CR-195399] p 436 N95-15911
RESIDUAL STRESS
Monitoring fiber stress during curing of single fiber glass- and graphite-epoxy composites
[NASA-TM-4568] p 432 N95-13641
Analysis of neutron diffraction peak broadening caused by internal stresses in composite materials
[DE94-014453] p 433 N95-13993

Mechanical properties of high-temperature superconducting wires
[DE94-015089] p 621 N95-14192
Analysis of welding-induced residual stresses with the ADINA system
[DE94-015359] p 506 N95-14320
Residual strength of composites with multiple impact damage
[AD-A284230] p 434 N95-14409
Advanced method and processing technology for complicated shape airframe part forming
p 410 N95-14486

RESIN MATRIX COMPOSITES
Thermally stable organic polymers
[AD-A281380] p 451 N95-14363
Composites with improved compressive properties
[AD-A283411] p 435 N95-15417

RESISTORS
Spiral microstrip antenna with resistance
[NASA-CASE-LAR-15088-1] p 460 N95-14139
Calibration and characterization of wide range hydrogen sensors
[DE94-013765] p 496 N95-14146
Theory and implementation of a VLSI stray insensitive switched capacitor composite operational amplifier
[AD-A283536] p 476 N95-15325

RESONANCE
Resonator response to non-Newtonian fluids
[DE94-013450] p 473 N95-14308
Effects of hydrometeors and atmospheric gases at SHF/EHF p 468 N95-14835
Introduction to muSR: What, how, where
[PB94-192267] p 596 N95-15379

RESONANCE CHARGE EXCHANGE
Ion implantation of He-3 in tantalum for use in a low energy deuteron polarization analyzer
[AD-A283172] p 619 N95-13698

RESONANCE FLUORESCENCE
Correlated quadratures of resonance fluorescence and the generalized uncertainty relation p 598 N95-13937

RESONANT FREQUENCIES
Aberration correction of unstable resonators
[NASA-CASE-NPO-18662-1-CU] p 602 N95-13823
Resonator response to non-Newtonian fluids
[DE94-013450] p 473 N95-14308
Experimental/analytical approach to understanding mistuning in a transonic wind tunnel compressor
[NASA-TM-108833] p 512 N95-14617

RESONANT TUNNELING
Resonant tunneling in small current-biased Josephson junctions
[DE94-016875] p 623 N95-15338

RESONANT VIBRATION
Quartz resonator state-of-charge monitor for lead-acid batteries
[DE94-013823] p 473 N95-14310
Stochastic model of the residual acceleration environment in microgravity p 459 N95-14540
Acoustic resonance spectroscopy intrinsic seals
[DE94-016207] p 591 N95-15359

RESONATORS
Determination of the shear modulus in self-assembled monolayers using quartz resonators
[DE94-013449] p 437 N95-14307
Resonator response to non-Newtonian fluids
[DE94-013450] p 473 N95-14308
Quartz resonator state-of-charge monitor for lead-acid batteries
[DE94-013823] p 473 N95-14310

RESOURCE ALLOCATION
The Telecommunications and Data Acquisition Report
[NASA-CR-196409] p 462 N95-14620
Low-Earth-Orbiter resource allocation and capacity planning for the DSN using LEO4CAST
p 419 N95-14632
Space science in the 1990's and beyond
[TABES PAPER 94-204] p 415 N95-14634
Intelligent manufacturing systems state of the art
[TABES PAPER 94-503] p 415 N95-14637
On accessing and hiding information
p 587 N95-15641

RESPIRATION
Effects of 20 days bed-rest on cardio-respiratory functions during sub-maximal exercise in young women
p 545 N95-15111

RESPONSE TIME (COMPUTERS)
Computing quantitative characteristics of finite-state real-time systems
[AD-A282839] p 412 N95-14343

RESTORATION
New algorithms for the reduction of image degradation due to atmospheric turbulence
[AD-A284891] p 615 N95-15772

RETINA
New findings regarding light intensity and its effects as a zeitgeber in the Sprague-Dawley rat
p 539 N95-15135

RETRACTABLE EQUIPMENT
The 3.5-meter telescope enclosure
[AD-A280949] p 638 N95-14597

RETRAINING
Investigation of dipolar reorientation dynamics of pure bulk polymers using second harmonic generation
[AD-A283023] p 448 N95-13688

RETROFITTING
Pilot retrofit test of refrigerant R-134a for GDSCC
p 456 N95-14629

RETROREFLECTORS
Radar altimeter calibration using SLR
p 471 N95-14283
SLR tracking of GPS-35 p 471 N95-14285
Synergism of SLR and GPS p 471 N95-14286
Laser retroreflector array having cat-eye retroreflectors
[NASA-CASE-GSC-13264-1] p 499 N95-14515

REUSABLE LAUNCH VEHICLES
The rationale/benefits of nuclear thermal rocket propulsion for NASA's lunar space transportation system
[NASA-TM-106739] p 431 N95-15682

REUSABLE ROCKET ENGINES
Reusable rocket engine turbopump health management system
[NASA-CR-195388] p 431 N95-15058

REVERBERATION
Electromagnetic reverberation characteristics of a large transport aircraft
[AD-A282923] p 411 N95-15392

REVERSE ENGINEERING
Reuseable Objects Software Environment (ROSE): Introduction to Air Force Software Reuse Workshop
[NASA-CR-197017] p 572 N95-14520
Applying CASE technology to the software maintenance life cycle
[TABES PAPER 94-620] p 416 N95-14647

REVERSE FIELD PINCH
Conservation of magnetic helicity during plasma relaxation
[DE94-016770] p 617 N95-14373
Lower-hybrid poloidal current drive for fluctuation reduction in a reversed field pinch
[DE94-015534] p 618 N95-15540
Solid target boronization of the MST reversed-field pinch during pulsed discharge cleaning
[DE94-015535] p 442 N95-15541

REYNOLDS NUMBER
Experiments to verify nonparallel stability theory at Virginia Polytechnic Institute and State University, Blacksburg, Virginia
[NASA-CR-196993] p 479 N95-13664
Scale effects on aircraft and weapon aerodynamics
[AGARD-AG-323] p 393 N95-14103
High Alpha Technology Program (HATP) ground test to flight comparisons p 393 N95-14230
Modelling and investigation of EHD point contacts
[AD-A283571] p 454 N95-15316
Dynamics on the attractor for the complex Ginzburg-Landau equation
[DE94-016902] p 586 N95-15342

RHENIUM COMPOUNDS
The transformation of organic amines by transition metal cluster compounds
[DE94-017151] p 441 N95-15346

RHEOLOGY
Surface characterization through shape oscillations of drops in microgravity and 1-g p 458 N95-14220
Microgravity foam structure and rheology
p 459 N95-14568
The extensional rheology of non-Newtonian materials
p 489 N95-14569

RHEOMETERS
Microgravity foam structure and rheology
p 459 N95-14568

RHODIUM
Oxidation resistant coating for carbon-carbon composites at ultra-high temperatures
[AD-A283323] p 456 N95-15624

RIEMANN MANIFOLD
Coherent states on the m-sheeted complex plane as m-photon states p 598 N95-13940
Carnot-caratheodory spaces seen from within
[PB94-195617] p 586 N95-15412

RIEMANN WAVES
Computational aerodynamics based on the Euler equations
[AGARD-AG-325] p 398 N95-14264

RIGID ROTORS
Higher harmonic control analysis for vibration reduction of helicopter rotor systems
[NASA-TM-103855] p 391 N95-14419

RIMS
Dynamics Explorer 1, retarding ion mass spectrometer summary spectrograms: 82/001 to 82/109 spin-time spectrograms for H(+), He(+), O(+), N(+), O(++), M/Z=2, and molecular ions
[NASA-TM-108468] p 443 N95-15607

RING LASERS
Advanced laser source research
[AD-A283110] p 498 N95-13695

RISK
Modelling the low Earth space debris environment
p 414 N95-13830
Risk analysis for the fire safety of airline passengers
[PB94-194065] p 405 N95-14179
Extended duration orbiter medical project Microbial Air Sampler (STS-50/USML-1) p 458 N95-14222
Operational requirements for avoidance and eventual elimination of Gz-Induced Loss Of Consciousness (G-LOC) in flight p 547 N95-15127
The F-16 multinational staged improvement program: A case study of risk assessment and risk management
[AD-A281706] p 409 N95-15451

RIVETED JOINTS
The characterization of widespread fatigue damage in fuselage structure
[NASA-TM-109142] p 432 N95-14920
Static strength of riveted joints in Fibre Metal Laminates
[PB94-201472] p 513 N95-15429

RIVETING
Damage tolerant repair techniques for pressurized aircraft fuselages
[AD-A281982] p 391 N95-14144

RIVETS
The role of fretting corrosion and fretting fatigue in aircraft rivet hole cracking p 510 N95-14470
Statistical investigation of fatigue crack initiation and growth around chamfered rivet holes in Alclad 2024 T3 as affected by corrosion p 510 N95-14472

ROASTING
Preparation and characterization of composite inorganic zeolite membranes with molecular sieve properties
[PB94-191251] p 450 N95-14151

ROBOT ARMS
A simulation facility for testing Space Station assembly procedures p 423 N95-14075
Dextrous gripping in a hazardous environment
[PB94-191244] p 501 N95-14150
Sample Acquisition and Instrument Deployment (SAID)
[NASA-CR-197104] p 502 N95-14910
Robotic control using muscular and neural electrical signals
[AD-A284908] p 551 N95-15757

ROBOT CONTROL
Analysis of the human operator subsystems
p 555 N95-14019
Eye movement control and top-down scanpath vision as a design metaphor for robotic vision and control
p 555 N95-14022
Telerobotic remote presence: Achievements and challenges p 504 N95-14023
Tele-existence and/or cybernetic interface studies in Japan p 555 N95-14025
Telerobotics in the deep ocean p 504 N95-14026
Models of remote manipulation in space
p 504 N95-14027
Interacting with virtual worlds p 556 N95-14032
The stable and precise motion control for an autonomous mobile robot
[AD-A283776] p 501 N95-14336
Advanced Guidance and Control Aspects in Robotics
[AGARD-LS-193] p 581 N95-14942
Machine intelligence: The key to guidance and control in robotics p 581 N95-14944
Control of remotely operated manipulation systems
p 582 N95-14945
Control and operation of space manipulator systems
p 582 N95-14946
Guidance and control for unmanned ground vehicles
p 504 N95-14948
Robotic control using muscular and neural electrical signals
[AD-A284908] p 551 N95-15757

ROBOT DYNAMICS
Automated cleaning of electronic components
[DE94-014122] p 476 N95-15356

ROBOTICS
VERDEX: A virtual environment demonstrator for remote driving applications p 562 N95-14060
A simulation facility for testing Space Station assembly procedures p 423 N95-14075
Flex-gear power transmission system for transmitting EMF between Sun and ring gears
[NASA-CASE-GSC-13540-1] p 502 N95-14517
Sample Acquisition and Instrument Deployment (SAID)
[NASA-CR-197104] p 502 N95-14910

Advanced Guidance and Control Aspects in Robotics [AGARD-LS-193] p 581 N95-14942
Robotics technology developments in the United States space telerobotics program p 581 N95-14943
Machine intelligence: The key to guidance and control in robotics p 581 N95-14944
Control and operation of space manipulator systems p 582 N95-14946
Legged vehicle for underwater mobile operations [AD-A282891] p 503 N95-15294
Interactive Computer-Enhanced Remote Viewing System (ICERVS): Subsystem design report, phase 2 [DE94-014513] p 563 N95-15309
Defining a controller architecture for the long-reach manipulator [DE94-015165] p 583 N95-15369
First results with instance-based state identification for reinforcement learning [TR-502] p 553 N95-15642
Robotic control using muscular and neural electrical signals [AD-A284908] p 551 N95-15757

ROBOTS
Auditory interfaces: The human perceiver p 554 N95-14015
Analysis of the human operator subsystems p 555 N95-14019
Issues in the design of high dexterity, force reflective teleoperators p 555 N95-14024
Tele-existence and/or cybernetic interface studies in Japan p 555 N95-14025
Models of remote manipulation in space p 504 N95-14027
Some criteria for teleoperators and virtual environments from experiences with vehicle/operator simulation p 556 N95-14028
On the role of exchange of power and information signals in control and stability of the human-robot interaction p 560 N95-14051
Robotics technology developments in the United States space telerobotics program p 581 N95-14943
Control and operation of space manipulator systems p 582 N95-14946
Mission, technologies and design of planetary mobile vehicle p 504 N95-14947
Automated cleaning of electronic components [DE94-014122] p 476 N95-15356

ROBUSTNESS (MATHEMATICS)
Multi-application controls: Robust nonlinear multivariable aerospace controls applications p 396 N95-14249

ROCKET ENGINE DESIGN
Fast track NTR systems assessment for NASA's first lunar outpost scenario [NASA-TM-106748] p 429 N95-13668
Engine system assessment study using Martian propellants [NASA-CR-189188] p 431 N95-14669

ROCKET ENGINES
Hybrid bearings for turbopumps and the like [NASA-CASE-MFS-28491-1] p 500 N95-13819

ROCKET EXHAUST
Optical analysis methods for material films condensed on cryogenic surfaces of spacecraft [AD-A284014] p 427 N95-14420

ROCKET PROPELLANTS
Recycled plastic: A clean and low cost rocket fuel [TABES PAPER 94-610] p 416 N95-14642

ROCKET PROPELLED SLEDS
Gouge initiation in high-velocity rocket sled testing [DE94-014288] p 418 N95-15357

ROCKET-BORNE INSTRUMENTS
Space experiments aboard rockets: SPEAR 3 [AD-A280778] p 414 N95-14290

RODS
Improved composite material and method for production of improved composite material [NASA-CASE-LAR-14892-1] p 433 N95-13836

ROLLER BEARINGS
Hybrid bearings for turbopumps and the like [NASA-CASE-MFS-28491-1] p 500 N95-13819

ROLLING MOMENTS
Static and dynamic force/moment measurements in the Eidetics water tunnel p 395 N95-14238

ROOM TEMPERATURE
High temperature cyclic behaviour of aerospace materials: Room temperature validation tests of Ti-6Al-4V [AGARD-AR-328] p 506 N95-14198
Experimental and theoretical studies of rewetting of unheated/heated grooved plates p 487 N95-14558

ROSAT MISSION
A ROSAT deep survey of the best studied high latitude areas [NASA-CR-196265] p 637 N95-13722
ROSAT observations of the binary Be-star and radio pulsar PSR1259-63 [NASA-CR-196951] p 642 N95-15907

ROSSBY REGIMES
Short term teleconnections associated with western Pacific tropical cyclones [AD-A284032] p 533 N95-14423

ROTARY STABILITY
F/A-18 and F-16 forebody vortex control, static and rotary-balance results p 397 N95-14254

ROTARY WING AIRCRAFT
ADST ARWA visual system module software design document [AD-A283874] p 572 N95-14357
Vertical flight terminal operational procedures. A summary of FAA research and development [AD-A283550] p 413 N95-15328

ROTARY WINGS
Advanced distributed simulation technology advanced rotary wing aircraft. Study comparing approaches to modeling the ARWA main rotor [AD-A280824] p 408 N95-14306
Higher harmonic control analysis for vibration reduction of helicopter rotor systems [NASA-TM-103855] p 391 N95-14419
Prediction of rotor-blade deformations due to unsteady airloads [AD-A284467] p 410 N95-15821

ROTATING BODIES
Building complex simulations rapidly using MATRIX(x): The Space Station redesign [TABES PAPER 94-632] p 417 N95-14653

ROTATING LIQUIDS
Bifurcation of rotating liquid drops: Results from USML-1 experiments in space p 458 N95-14219
Surface characterization through shape oscillations of drops in microgravity and 1-g p 458 N95-14220
Measurement of interfacial tension of immiscible liquid pairs in microgravity p 458 N95-14221

ROTATION
Rotational wind indicator enhances control of rotated displays p 559 N95-14046
Stellar activity: Astrophysics relevant to global change p 643 N95-14500
Probing surface structure on late-type stars with FRESIP p 643 N95-14501
Asteroseismology with FRESIP: A meter class space telescope p 643 N95-14504
Rotation among solar-type stars p 644 N95-14506
Two-layer viscous instability in a rotating couette device p 489 N95-14566
Electrokinetic transport of heterogeneous particles in suspension p 444 N95-14581
Experimental/analytical approach to understanding mistuning in a transonic wind tunnel compressor [NASA-TM-108833] p 512 N95-14617
Neurohumoral reactions to long-term vestibular stimulation in man p 542 N95-15091

ROTATIONAL STATES
Infrared/submillimeter wave studies of molecular collision kinetics [AD-A281379] p 594 N95-14362

ROTOR AERODYNAMICS
Dynamics of the McDonnell-Douglas Large Scale Dynamic Rig and dynamic calibration of the rotor balance [NASA-TM-108855] p 391 N95-13891

ROTOR BLADES (TURBOMACHINERY)
Unsteady flows in turbines: Impact on design procedure p 480 N95-14132

ROTOR DYNAMICS
Advanced distributed simulation technology advanced rotary wing aircraft. Study comparing approaches to modeling the ARWA main rotor [AD-A280824] p 408 N95-14306
Linear and nonlinear dynamic analysis of redundant load path bearingless rotor systems [NASA-CR-197220] p 503 N95-14923

ROTOR SPEED
Experimental/analytical approach to understanding mistuning in a transonic wind tunnel compressor [NASA-TM-108833] p 512 N95-14617

ROTORS
Evaluation of energy-sink stability criteria for dual-spin spacecraft [AD-A283228] p 428 N95-14850

ROVING VEHICLES
Mission, technologies and design of planetary mobile vehicle p 504 N95-14947
Guidance and control for unmanned ground vehicles p 504 N95-14948

RUNGE-KUTTA METHOD
The role of CFD in the design process p 481 N95-14135
Workshop on Advances in Scientific Computation and Differential Equations 1993 (SCADE) [AD-A283111] p 585 N95-14657

RURAL AREAS
Photogrammetric mobile satellite service prediction p 466 N95-14679

RUTHENIUM COMPOUNDS
One: Redox chemistry of bimetallic fulvalene complexes. 2: Oligocyclopentadienyl complexes [DE94-014930] p 443 N95-15667

S

S WAVES
Torsional shear wave transducer [AD-D016347] p 496 N95-14841
Ultrasonic characterization of high T(c) and other unconventional superconductors [AD-A282835] p 476 N95-15397

SAFETY
Engineering, technical, and management support services [NASA-CR-196977] p 505 N95-13840
Design of components for the NASA OCEAN project [NASA-CR-197207] p 535 N95-14906
John F. Kennedy Space Center, Safety, Reliability, Maintainability and Quality Assurance, Survey and Audit Program [NASA-TM-109208] p 630 N95-14918

SAFETY DEVICES
Risk analysis for the fire safety of airline passengers [PB94-194065] p 405 N95-14179

SAFETY FACTORS
Applications of a fast and efficient method for simulating orbital mission safety p 426 N95-14093
RICIS Symposium 1992: Mission and Safety Critical Systems Research and Applications [NASA-CR-196963] p 569 N95-14156
European Workshop Industrial Computer Science Systems approach to design for safety p 569 N95-14157
MISSION: Mission and Safety Critical Support Environment. Executive overview p 569 N95-14158
Generic architectures for future flight systems p 567 N95-14159
CAPTIONALS: A computer aided testing environment for the verification and validation of communication protocols p 570 N95-14163
Software development for safety-critical medical applications p 571 N95-14171
Recycled plastic: A clean and low cost rocket fuel [TABES PAPER 94-610] p 416 N95-14642
Wake turbulence p 405 N95-14894

SALINITY
An analysis of eddy resolving global ocean models in the Southern Ocean [AD-A283211] p 536 N95-15626

SALT SPRAY TESTS
Statistical investigation of fatigue crack initiation and growth around chamfered rivet holes in Alclad 2024 T3 as affected by corrosion p 510 N95-14472
The effects of pitting on fatigue crack nucleation in 7075-T6 aluminum alloy p 448 N95-14482
Modeling time-dependent corrosion fatigue crack propagation in 7000 series aluminum alloys p 448 N95-14483

SAMPLED DATA SYSTEMS
Chaotic time series. Part 2: System identification and prediction [PB94-207115] p 589 N95-13630

SAMPLING
Sample Acquisition and Instrument Deployment (SAID) [NASA-CR-197104] p 502 N95-14910

SANDS
Leak detection by acoustic emissions monitoring: An experimental investigation of the acoustic properties of leaks and the attenuation characteristics of soil [AD-A283250] p 530 N95-15295

SATELLITE ALTIMETRY
Measuring temporal gravitational variations using SLR data p 527 N95-14277
Global and regional kinematics from SLR stations p 527 N95-14278
Earth orientation parameters p 527 N95-14281
Precision orbit determination of altimetric satellites p 418 N95-14282
Radar altimeter calibration using SLR p 471 N95-14283
The role of SLR and LLR in relativity p 528 N95-14284
SLR tracking of GPS-35 p 471 N95-14285
Synergism of SLR and GPS p 471 N95-14286
Satellite Laser Ranging operations p 500 N95-14287

A strawman SLR program plan for the 1990s p 471 N95-14289

SATELLITE COMMUNICATION
Satellite communication technology and applications, 1995-2010 p 413 N95-13826
From Antarctica to space: Use of telepresence and virtual reality in control of remote vehicles p 427 N95-14099
Architecture for Survivable Systems Processing (ASSP). Technology benefits for Open System Interconnects p 567 N95-14160
Space Generic Open Avionics Architecture (SGOAA): Overview p 569 N95-14161
Proceedings of the Eighteenth NASA Propagation Experimenters Meeting (NAPEX 18) and the Advanced Communications Technology Satellite (ACTS) Propagation Studies Miniworkshop [NASA-CR-196959] p 464 N95-14670
Olympus propagation experiments p 464 N95-14671
Propagation characteristics of 20/30 GHz links with a 40 deg masking angle p 464 N95-14672
Propagation data at 20/40 GHz and the propagation needs of Milstar p 465 N95-14673
The 40 and 50 GHz propagation experiments at the Rutherford Appleton Laboratory, UK, using the ITALSAT beacons p 465 N95-14674
Channel characterisation for future Ka-band Mobile Satellite Systems and preliminary results p 465 N95-14676
ACTS mobile propagation campaign p 465 N95-14677
Slant path L- and S-Band tree shadowing measurements p 465 N95-14678
Photogrammetric mobile satellite service prediction p 466 N95-14679
Propagation considerations for the Odyssey system design p 466 N95-14680
Communications availability: Estimation studies at AMSC p 466 N95-14681
S-Band propagation measurements p 466 N95-14682
Performance modeling and analysis of parallel processing and Low Earth Orbit satellite communication systems [AD-A283243] p 470 N95-15652
High speed QPPM direct detection optical communication receivers for FSDD intersatellite links [NASA-CR-189331] p 615 N95-15849

SATELLITE CONSTELLATIONS
Journal of Spacecraft Technology, volume 4, no. 2, July 1994 p 413 N95-13825
A simulation algorithm for availability computation of a communication satellite constellation p 414 N95-13832
Environmental testing to prevent on-orbit TDRS failures p 423 N95-14078
Investigating and implementing enhancements to the simulation of short-term collision hazards p 426 N95-14092
Global and regional kinematics with GPS p 527 N95-14279
Global and regional kinematics with VLBI p 527 N95-14280
A strawman SLR program plan for the 1990s p 471 N95-14289
Efficient mission control for the 48-satellite Globalstar constellation [TABES PAPER 94-609] p 415 N95-14641

SATELLITE DESIGN
HYDRA, a new tool for mechanical testing p 418 N95-14086
System level mechanical testing of the Clementine spacecraft p 425 N95-14087

SATELLITE IMAGERY
Forest cover from Landsat Thematic Mapper data for use in the Catahoula Ranger District Geographic Information System [PB94-203056] p 515 N95-14125
Produce documents and media information [NASA-CR-196521] p 532 N95-14271
1994 Science Information Management and Data Compression Workshop [NASA-CP-3277] p 564 N95-14585
Landsat Pathfinder tropical forest information management system p 565 N95-14594
Satellite imagery and topographic data in verification [AD-A280950] p 530 N95-14598
Development of a systemic land cover/land use database for the Upper Mississippi River System derived from Landsat Thematic Mapper satellite data. Long term resource monitoring program [PB94-186889] p 515 N95-14793
Nowcasting convective storm evolution in east-central Florida using satellite and Doppler radar data [AD-A283260] p 534 N95-15618

SATELLITE INSTRUMENTS
AXAF SIM focus mechanism study [NASA-CR-196976] p 636 N95-13636
Satellite Laser Ranging in the 1990s: Report of the 1994 Belmont Workshop [NASA-CP-3283] p 526 N95-14274
Scientific analysis of satellite ranging data p 517 N95-14275
Global reference frame: Intercomparison of results (SLR, VLBI and GPS) p 527 N95-14276
Global and regional kinematics from SLR stations p 527 N95-14278
Earth orientation parameters p 527 N95-14281
The role of SLR and LLR in relativity p 528 N95-14284
Satellite Laser Ranging operations p 500 N95-14287
A strawman SLR program plan for the 1990s p 471 N95-14289

SATELLITE NAVIGATION SYSTEMS
Generic architectures for future flight systems p 567 N95-14159

SATELLITE OBSERVATION
Study of auroral dynamics with combined spacecraft and incoherent scatter radar data [NASA-CR-196974] p 526 N95-13818
Star sensor for Indian Remote Sensing Satellite (IRS 1C) p 413 N95-13828
Computer aided techniques for the realisation of the diaphragm of the PSM for the IRS-1C p 413 N95-13829
Global surface-based cloud observation for ISCCP [NASA-CR-196990] p 532 N95-14265
Satellite Laser Ranging in the 1990s: Report of the 1994 Belmont Workshop [NASA-CP-3283] p 526 N95-14274
Global and regional kinematics from SLR stations p 527 N95-14278
Radiometric resolution enhancement by lossy compression as compared to truncation followed by lossless compression p 564 N95-14588
Geotail MCA plasma wave data analysis [NASA-CR-197022] p 618 N95-14798
Support of Environmental Requirements for Cloud Analysis and Archive (SERCAA): Algorithm descriptions [AD-A283240] p 534 N95-15614
Validation of ERS-1 environmental data products [NASA-CR-197111] p 517 N95-15848

SATELLITE ORBITS
Scientific analysis of satellite ranging data p 517 N95-14275
Precision orbit determination of altimetric satellites p 418 N95-14282
Satellite situation report, volume 33, number 2 [NASA-TM-109965] p 428 N95-14510
The Bureau Gravimetrique International p 516 N95-15795

SATELLITE POWER TRANSMISSION
Simulations of the high average power SELENE free electron laser prototype [AD-A280780] p 498 N95-14291

SATELLITE ROTATION
Numerical studies of the surface tension effect of cryogenic liquid helium [NASA-CR-197014] p 479 N95-14104

SATELLITE SOLAR ENERGY CONVERSION
Alkali metal Rankine cycle boiler technology challenges and some potential solutions for space nuclear power and propulsion applications [NASA-TM-106593] p 430 N95-14174

SATELLITE TEMPERATURE
Evaluation of reformulated thermal control coatings in a simulated space environment. Part 1: YB-71 p 420 N95-14063

SATELLITE TRACKING
GSOSTATS database: USAF synchronous satellite catalog data conversion software. User's guide and software maintenance manual, version 2.1 [NASA-TM-106760] p 568 N95-13894
Scientific analysis of satellite ranging data p 517 N95-14275
Global and regional kinematics with GPS p 527 N95-14279
Global and regional kinematics with VLBI p 527 N95-14280
Radar altimeter calibration using SLR p 471 N95-14283
Synergism of SLR and GPS p 471 N95-14286
Satellite Laser Ranging operations p 500 N95-14287
SLR 2000 p 471 N95-14288
A strawman SLR program plan for the 1990s p 471 N95-14289
Linear quadratic Gaussian and feedforward controllers for the DSS-13 antenna p 463 N95-14625
A radio telescope for the calibration of radio sources at 32 gigahertz p 463 N95-14626
Research and development optical deep space antenna sizing study p 463 N95-14628
A trajectory preprocessor for antenna pointing p 463 N95-14630
Low-Earth-Orbiter resource allocation and capacity planning for the DSN using LEO4CAST p 419 N95-14632
Efficient mission control for the 48-satellite Globalstar constellation [TABES PAPER 94-609] p 415 N95-14641

SCALE EFFECT
Scale effects on aircraft and weapon aerodynamics [AGARD-AG-323] p 393 N95-14103

SCANNERS
Summary of activities for University of California [AD-A283890] p 632 N95-15423
TDWR scan strategy implementation [AD-A284877] p 534 N95-15749

SCANNING ELECTRON MICROSCOPY
Resolution measurement for scanning electron microscopes [DE94-012747] p 601 N95-13674
The effect of Low Earth Orbit exposure on some experimental fluorine and silicon-containing polymers p 422 N95-14074
What those defects in optical coatings really look like [DE94-015324] p 614 N95-15529
Type 304L stainless steel surface microstructure: Performance in hydride storage and acid cleaning [DE94-014654] p 447 N95-15625

SCATTER PROPAGATION
Propagation Modelling and Decision Aids for Communications, Radar and Navigation Systems [AGARD-LS-196] p 466 N95-14825

SCATTERING
Graphical aids for the users of GEMACS (GAUGE): Ray tracing enhancements [AD-A284903] p 470 N95-15756
Apparatus for imaging an object in or through a scattering medium using coherent anti-Stokes Raman scattering [AD-D016366] p 615 N95-15765

SCATTERING COEFFICIENTS
Propagation Modelling and Decision Aids for Communications, Radar and Navigation Systems [AGARD-LS-196] p 466 N95-14825
Electro-optics: Propagation from IR to UV and sensor considerations. Part B: Tools for exploitation of propagation conditions and system range performance p 467 N95-14834
Effects of hydrometeors and atmospheric gases at SHF/EHF p 468 N95-14835

SCATTERING CROSS SECTIONS
Low energy electron and atom elastic scattering cross sections from 0.1 to 30 keV [AD-A283584] p 595 N95-15318

SCATTERING FUNCTIONS
Prediction of particulate contamination on aperture window p 420 N95-14064
Electro-optics: Propagation from IR to UV and sensor considerations. Part A: Propagation theory p 467 N95-14833

SCENE ANALYSIS
Control of selective perception using Bayes nets and decision theory [TR-468] p 573 N95-15151
Sequentially t-diagnosable systems [PB94-205093] p 574 N95-15396

SCHEDULES
Real time system for practical acoustic monitoring of global ocean temperature, volume 3 [AD-A283774] p 535 N95-14335
Comprehensive facility decommissioning through the use of innovative technology to reduce cost, schedule, and environmental liability [TABES PAPER 94-615] p 416 N95-14644

SCHEDULING
Planning/scheduling techniques for VQ-based image compression p 566 N95-14595
Data flow manager for DART [DE94-013236] p 579 N95-15581
Universally serializable computation [TR-520] p 587 N95-15732

SCHLIEREN PHOTOGRAPHY
An optical technique for examining aircraft shock wave structures in flight p 401 N95-14879
Two-dimensional scramjet inlet unstart model: Wind-tunnel blockage and actuation systems test [NASA-TM-109984] p 495 N95-15899

SCHOOLS
Space based astronomy: Teacher's guide with activities [NASA-EG-102] p 638 N95-14511

SCHROEDINGER EQUATION
On the possibility of a quantum mechanical phase space representation p 606 N95-13931
Schroedinger operators with the q-ladder symmetry algebras p 588 N95-13942
SCIENTIFIC VISUALIZATION
Virtual reality at work p 556 N95-14033
1994 Science Information Management and Data Compression Workshop
[NASA-CP-3277] p 564 N95-14585
Performance of customized DCT quantization tables on scientific data p 564 N95-14586
Compression of regions in the global advanced very high resolution radiometer 1-km data set p 565 N95-14591
Landsat Pathfinder tropical forest information management system p 565 N95-14594
Planning/scheduling techniques for VQ-based image compression p 566 N95-14595
Interactive Computer-Enhanced Remote Viewing System (ICERVS): Subsystem design report, phase 2
[DE94-014513] p 563 N95-15309
Distributed heterogeneous visualization, BOP (Bag-O-Polygons) and BOP view
[AD-A284393] p 567 N95-15809
SCINTILLATING FIBERS
Scintillating glass fiber-optic neutron sensors
[DE94-014562] p 613 N95-15312
SCINTILLATION
Scintillating glass fiber-optic neutron sensors
[DE94-014562] p 613 N95-15312
Relationship between microstructure and efficiency of scintillating glasses
[DE94-014563] p 454 N95-15313
Fluorescent compounds for plastic scintillation applications
[DE94-013235] p 497 N95-15580
SCINTILLATION COUNTERS
Thin GSO scintillator for neutron detection
[DE94-014566] p 613 N95-15314
SCORING
The effect of response format on reliability estimates for tacit knowledge scales
[AD-A283547] p 552 N95-15326
SCUTUM CONSTELLATION
Asteroseismology: Theory and phenomenology p 643 N95-14502
SEA ICE
From Antarctica to space: Use of telepresence and virtual reality in control of remote vehicles p 427 N95-14099
SEA LEVEL
Precision orbit determination of altimetric satellites p 418 N95-14282
Satellite Laser Ranging operations p 500 N95-14287
SEA SURFACE TEMPERATURE
The seasonal cycle dependence of temperature fluctuations in the atmosphere
[AD-A283220] p 534 N95-15627
SEALS (STOPPERS)
Design review and analysis for a Pratt and Whitney fluid-film bearing and seal testing rig
[NASA-CR-197035] p 502 N95-14797
Acoustic resonance spectroscopy intrinsic seals
[DE94-016207] p 591 N95-15359
SEARCHING
Gaze selection for visual search
[TR-512] p 587 N95-15775
SEATS
Individual variability in the transmission of vertical vibration from seat to head
[ISVR-TR-236] p 563 N95-15850
SECONDARY FLOW
Elements of a modern turbomachinery design system p 480 N95-14129
SECULAR VARIATIONS
Measuring temporal gravitational variations using SLR data p 527 N95-14277
SECURITY
Department of Defense technical architecture framework for information management. Volume 6: Department of Defense (DOD) goal security architecture, version 2.0
[AD-A283767] p 631 N95-14332
The console password feature for DEC workstations
[DE94-015721] p 566 N95-14338
SEISMOGRAMS
Lithological and rheological constraints on fault rupture scenarios for ground motion hazard prediction
[DE94-014742] p 529 N95-14436
SEISMOLOGY
Astrophysical science with a spaceborne photometric telescope
[NASA-CP-10148] p 643 N95-14499
Asteroseismology: Theory and phenomenology p 643 N95-14502
Asteroseismology: Ground based efforts and the need for space observations p 643 N95-14503
SEIZURES
Measurement and modification of the EEG and related behavior p 557 N95-14038
SELENIUM
The study of dopant segregation behavior during the growth of GaAs in microgravity p 458 N95-14215
SELF ADAPTIVE CONTROL SYSTEMS
First results with instance-based state identification for reinforcement learning
[TR-502] p 553 N95-15642
SELF ORGANIZING SYSTEMS
Chaotic time series. Part 2: System identification and prediction
[PB94-207115] p 589 N95-13630
Supervised learning without output labels
[TR-510-REV] p 552 N95-15588
SEMANTICS
Discourse interpretation and the scope of operators
[TR-518] p 586 N95-15595
SEMICONDUCTING FILMS
Growth mechanisms and characterization of hydrogenated amorphous-silicon-alloy films
[DE94-011842] p 518 N95-14194
SEMICONDUCTOR DEVICES
Capacitance calculations in nanostructure devices via the quantum Liouville equation in the coordinate representation
[AD-A281936] p 589 N95-13656
Multilayer thin film Hall effect device
[NASA-CASE-MFS-28764-1] p 590 N95-14137
International Semiconductor Device Research Symposium (ISDRS-93)
[AD-A281715] p 477 N95-15454
Integrated photonics research, 1993
[AD-A281578] p 614 N95-15464
Process for the controlled growth of single-crystal films of silicon carbide polytypes on silicon carbide wafers
[NASA-CAS-LEW-15222-3] p 625 N95-15602
SEMICONDUCTOR LASERS
Modes in light wave propagating in semiconductor laser p 500 N95-13925
In situ grown quantum-wire lasers
[AD-A281381] p 499 N95-14364
High power diode pumped solid state laser development at Lawrence Livermore National Laboratory
[DE94-015899] p 499 N95-14427
Integrated photonics research, 1993
[AD-A281578] p 614 N95-15464
High gain GaAs switches for impulse sources: Measurement of the speed of current filaments
[DE94-015281] p 477 N95-15544
SEMICONDUCTORS (MATERIALS)
ASTM E 1559 method for measuring material outgassing/deposition kinetics has applications to aerospace, electronics, and semiconductor industries p 421 N95-14066
Electrically conducting polyimide film containing tin complexes
[NASA-CASE-LAR-14936-1] p 450 N95-14113
Wavelength-division multiplexed optical integrated circuit with vertical diffraction grating
[NASA-CASE-NPO-18357-1-CU] p 612 N95-14181
Joint Launch + One Year Science Review of USML-1 and USMP-1 with the Microgravity Measurement Group
[NASA-CP-3272-VOL-1] p 634 N95-14207
Orbital processing of high-quality CdTe compound semiconductors p 458 N95-14213
Crystal growth of selected II-VI semiconducting alloys by directional solidification p 458 N95-14214
Materials issues in molecular beam epitaxy
[DE94-015796] p 621 N95-14322
Semiconductor measurement technology: Improved characterization and evaluation measurments for HgCdTe detector materials, processes, and devices used on the GOES and TIROS satellites
[PB94-188810] p 474 N95-14401
Design of power electronics for TVC and EMA systems
[NASA-CR-197067] p 475 N95-14866
Optically controlled MMW beamsteering beamforming antenna
[AD-A282831] p 614 N95-15414
High gain GaAs switches for impulse sources: Measurement of the speed of current filaments
[DE94-015281] p 477 N95-15544
Surface passivation for 3-5 semiconductor processing: Stable gallium sulphide films by MOCVD
[NASA-TM-106761] p 477 N95-15587
Electronic characterization of defects in narrow gap semiconductors
[NASA-CR-197217] p 626 N95-15752
SENSE ORGANS
Vestibular ontogeny: Measuring the influence of the dynamic environment p 544 N95-15105
Neuronal types in the chicken's statoacoustic ganglion p 539 N95-15116
Functional participation of the valvula cerebelli on the goldfish dorsal light response p 539 N95-15119
SENSITIVITY
Computer aided techniques for the realisation of the diaphragm of the PSM for the IRS-1C p 413 N95-13829
LSENS, a general chemical kinetics and sensitivity analysis code for homogeneous gas-phase reactions. 2: Code description and usage
[NASA-RP-1329] p 442 N95-15512
Compiler optimizations for cache locality and coherence
[TR-504] p 586 N95-15589
SENSORY FEEDBACK
Tele-existence and/or cybernetic interface studies in Japan p 555 N95-14025
Postural control of fish related to gravity input p 539 N95-15118
SENSORY PERCEPTION
Neural mechanisms of kinesthesia p 555 N95-14018
Intersensory coordination p 555 N95-14020
Manual discrimination of force p 561 N95-14057
Vestibular ontogeny: Measuring the influence of the dynamic environment p 544 N95-15105
SENSORY STIMULATION
Postural control of fish related to gravity input p 539 N95-15118
SEPARATED FLOW
Multilayer fluid dynamics of immiscible liquids p 483 N95-14532
Control of unsteady separated flow associated with the dynamic stall of airfoils
[NASA-CR-197024] p 400 N95-14613
SEPARATION
Upward separation for FewP and related classes
[TR-488] p 575 N95-15721
SEPARATORS
Reactive polymers: Main chain coordination polymers for air separation
[AD-A281614] p 455 N95-15444
SEQUENCING
A Multiple Divide-and-Conquer (MDC) algorithm for optimal alignments in linear space
[DE94-015457] p 574 N95-15536
SERUMS
Relationship between hind-limb muscle atrophy and serum enzymes in tail suspended rats p 539 N95-15143
SERVICE LIFE
FAA/NASA International Symposium on Advanced Structural Integrity Methods for Airframe Durability and Damage Tolerance
[NASA-CP-3274-PT-1] p 507 N95-14453
Probabilistic inspection strategies for minimizing service failures p 508 N95-14461
Development of the NASA/FLAGRO computer program for analysis of airframe structures p 510 N95-14473
Challenges for the aircraft structural integrity program p 410 N95-14481
Module process optimization and device efficiency improvement for stable, low-cost, large-area, cadmium telluride-based photovoltaic module production
[DE94-011817] p 521 N95-15863
SERVOCONTROL
Issues in the design of high dexterity, force reflective teleoperators p 555 N95-14024
SERVOMECHANISMS
Simulation of a spatial, servo-hydraulic test facility for space structures p 418 N95-14095
SET THEORY
Carnot-caratheodory spaces seen from within
[PB94-195617] p 586 N95-15412
On accessing and hiding information p 587 N95-15641
Upward separation for FewP and related classes
[TR-488] p 575 N95-15721
A general method to construct oracles realizing given relationships between complexity classes
[TR-500] p 588 N95-15854
Lower bounds for perceptrons solving some separation problems and oracle separation of AM from PP
[TR-498] p 588 N95-15855
P-selectivity: Intersections and indices
[TR-482] p 577 N95-15858
Seeking stronger separations: Probability one balanced- and bi-immunity
[TR-480] p 589 N95-15859
SEWING
Parachute having improved vent line stacking
[NASA-CASE-MFS-28508-1] p 393 N95-14182

SEYFERT GALAXIES
PSPC soft x-ray observations of Seyfert 2 galaxies
[NASA-TM-109968] p 638 N95-14911
SHAFTS (MACHINE ELEMENTS)
Damage analysis of internal faults in flux concentrating permanent magnet motors
[AD-A283883] p 474 N95-14359
Space Shuttle Main Engine turbopump bearing assessment program
[TABES PAPER 94-621] p 417 N95-14648
SHALLOW WATER
Point based hydrodynamics applied to shallow water equations
[DE94-016629] p 523 N95-15364
SHAPE CONTROL
Computational methods for PDE's in flow control, superconductivity, fluid flows and other applications
[AD-A282912] p 493 N95-15390
SHAPERS
Selective RF pulses in NMR and their effect on coupled and uncoupled spin systems
[PB94-195526] p 471 N95-15871
SHAPES
Manipulation of quantum evolution
p 598 N95-13918
Surface characterization through shape oscillations of drops in microgravity and 1-g p 458 N95-14220
Advanced method and processing technology for complicated shape airframe part forming
p 410 N95-14486
SHEAR FLOW
On the behavior of three-dimensional wave packets in viscously spreading mixing layers
[NASA-TM-106770] p 495 N95-15908
SHEAR PROPERTIES
Determination of the shear modulus in self-assembled monolayers using quartz resonators
[DE94-013449] p 437 N95-14307
Resonator response to non-Newtonian fluids
[DE94-013450] p 473 N95-14308
SHEAR STRENGTH
Static strength of riveted joints in Fibre Metal Laminates
[PB94-201472] p 513 N95-15429
SHEAR STRESS
ADCIRC: An advanced three-dimensional circulation model for shelves, coasts, and estuaries. Report 4: Hurricane storm surge modeling using large domains
[AD-A283868] p 535 N95-14352
Initiation and propagation of small corner cracks
p 510 N95-14471
Calculation of movable bed friction factors
[AD-A283529] p 536 N95-15440
SHELL THEORY
Discrete-layer piezoelectric plate and shell models for active tip-clearance control
[NASA-CR-195383] p 507 N95-14417
SHIELDING
Analysis of space environment damage to solar cell assemblies from LDEF experiment A0171-GSFC test plate
[NASA-CR-197066] p 519 N95-14853
SHIP HULLS
Bolted joint studies in GRP
[AD-A283843] p 434 N95-14348
SHIPS
Bolted joint studies in GRP
[AD-A283843] p 434 N95-14348
SHOCK ABSORBERS
Landing gear energy absorption system
[NASA-CASE-MSC-22277-1] p 503 N95-15306
SHOCK FRONTS
ICE/ISEE plasma wave data analysis
[NASA-CR-196988] p 642 N95-14266
Atmospheric propagation at larger lateral distances from the flight track p 402 N95-14885
SHOCK LAYERS
Science objectives and performance of a radiometer and window design for atmospheric entry experiments
p 429 N95-13718
VUV shock layer radiation in an arc-jet wind tunnel experiment p 405 N95-13719
Measured and calculated spectral radiation from a blunt body shock layer in an arc-jet wind tunnel
[AIAA PAPER 94-0086] p 405 N95-13720
Numerical simulation of shock-induced combustion past blunt bodies using shock-fitting technique
[NASA-CR-197013] p 437 N95-14268
Laminar and turbulent flow computations of Type 4 shock-shock interference aerothermal loads using unstructured grids
[NASA-CR-195008] p 493 N95-15604
SHOCK WAVE INTERACTION
Numerical model for the weakly nonlinear propagation of sound through turbulence p 401 N95-14883
Sonic boom interaction with turbulence
p 402 N95-14884
Atmospheric effects on the risetime and waveshape of sonic booms p 402 N95-14886
The effect of aircraft speed on the penetration of sonic boom noise into a flat ocean p 402 N95-14887
Laminar and turbulent flow computations of Type 4 shock-shock interference aerothermal loads using unstructured grids
[NASA-CR-195008] p 493 N95-15604
Wind-tunnel blockage and actuation systems test of a two-dimensional scramjet inlet unstart model at Mach 6
[NASA-TM-109152] p 495 N95-15898
SHOCK WAVE PROPAGATION
An evaluation of rise time characterization and prediction methods p 401 N95-14881
Numerical model for the weakly nonlinear propagation of sound through turbulence p 401 N95-14883
Atmospheric propagation at larger lateral distances from the flight track p 402 N95-14885
Simple atmospheric perturbation models for sonic-boom-signature distortion studies
p 402 N95-14888
USAF single-event sonic boom prediction model: PCBoom3 p 403 N95-14889
SHOCK WAVES
ICE/ISEE plasma wave data analysis
[NASA-CR-196988] p 642 N95-14266
Numerical simulation of shock-induced combustion past blunt bodies using shock-fitting technique
[NASA-CR-197013] p 437 N95-14268
An optical technique for examining aircraft shock wave structures in flight p 401 N95-14879
The formation of small grains in shocks in the ISM
p 641 N95-15842
SHOT NOISE
Sub-Poissonian light and photocurrent shot-noise suppression in closed opto-electronic loop
p 606 N95-13924
SHROUDS
Clean assembly and integration techniques for the Hubble Space Telescope High Fidelity Mechanical Simulator p 418 N95-14070
Refurbishment of a 39 foot thermal vacuum chamber
p 418 N95-14085
SHUTDOWNS
Hybrid bearings for turbopumps and the like
[NASA-CASE-MFS-28491-1] p 500 N95-13819
SIDE-LOOKING RADAR
Developments in ground-penetrating radar at LLNL
[DE94-012236] p 554 N95-13671
SIDESLIP
Flight evaluation of pneumatic forebody vortex control in post-stall flight p 398 N95-14259
SIGNAL ANALYSIS
Develop advanced nonlinear signal analysis topographical mapping system
[NASA-CR-194414] p 514 N95-13639
SIGNAL ANALYZERS
Speakeasy software development
[AD-A283816] p 468 N95-15333
SIGNAL DETECTION
Passive fetal heart rate monitoring apparatus and method with enhanced fetal heart beat discrimination
[NASA-CASE-LAR-15129-1] p 541 N95-14184
SIGNAL DETECTORS
Surface acoustic wave oxygen pressure sensor
[NASA-CASE-LAR-15266-1-CU] p 496 N95-13837
Passive fetal heart rate monitoring apparatus and method with enhanced fetal heart beat discrimination
[NASA-CASE-LAR-15129-1] p 541 N95-14184
SIGNAL FADING
ACTS mobile propagation campaign
p 465 N95-14677
Slant path L- and S-Band tree shadowing measurements p 465 N95-14678
Florida's propagation report p 466 N95-14684
SIGNAL GENERATORS
Experimental hardware development for a pulsed ultrasonic data collection facility
[AD-A283331] p 615 N95-15872
SIGNAL PROCESSING
Earth Observing System (EOS)/Advanced Microwave Sounding Unit-A (AMSU-A): Instrument logic diagrams
[NASA-CR-189378] p 567 N95-13633
Two-dimensional signal processing, optical information storage and processing, and electromagnetic measurements
[AD-A281937] p 460 N95-13657
Virtual acoustic displays p 557 N95-14035
Acceleration recorder and playback module
[NASA-CASE-MSC-22008-1] p 496 N95-14180
Passive fetal heart rate monitoring apparatus and method with enhanced fetal heart beat discrimination
[NASA-CASE-LAR-15129-1] p 541 N95-14184
Wideband beamforming for a sparse nonuniformly spaced array
[AD-A280833] p 591 N95-14396
The Telecommunications and Data Acquisition Report
[NASA-CR-196409] p 462 N95-14620
Convolutional encoding of self-dual block codes (2)
p 462 N95-14623
Spin glasses and error-correcting codes
p 462 N95-14624
Linear quadratic Gaussian and feedforward controllers for the DSS-13 antenna p 463 N95-14625
A radio telescope for the calibration of radio sources at 32 gigahertz p 463 N95-14626
The Block V Receiver fast acquisition algorithm for the Galileo S-band mission p 463 N95-14627
Electro-optics: Propagation from IR to UV and sensor considerations. Part A: Propagation theory
p 467 N95-14833
Speakeasy software development
[AD-A283816] p 468 N95-15333
SIGNAL RECEPTION
SLR 2000 p 471 N95-14288
SIGNAL TO NOISE RATIOS
Lossless compression of NOAA-AVHRR satellite data
p 565 N95-14592
The development of lossless data compression technology for remote sensing applications
p 565 N95-14593
The Block V Receiver fast acquisition algorithm for the Galileo S-band mission p 463 N95-14627
Performance comparison AN/FRD-10 versus PUSHER
[AD-A283263] p 469 N95-15619
Diffuse bands versus extinction parameters
p 640 N95-15836
SIGNATURES
Review of drive symmetry measurement and control experiments on the Nova laser system
[DE94-014455] p 498 N95-13994
An in-home study of subjective response to simulated sonic booms p 403 N95-14891
Search for W(prime) (yields) e(nu) in p(anti p) collisions at (radical)s = 1,800 GeV
[DE94-015188] p 597 N95-15630
SIGNS AND SYMPTOMS
Modeling and numerical simulation of the cerebral blood flow under acceleration p 545 N95-15112
SILANES
Dynamics of the interface in a model composite system
[AD-A281910] p 433 N95-13655
Growth mechanisms and characterization of hydrogenated amorphous-silicon-alloy films
[DE94-011842] p 518 N95-14194
SILICA GEL
AEM and HREM evaluation of carbon nanostructures in silica aerogels
[DE94-014913] p 434 N95-14387
SILICATES
Formation of dust grains with impurities in red giant winds p 641 N95-15841
The formation of small grains in shocks in the ISM
p 641 N95-15842
SILICON
Role of point defects and defect complexes in silicon device processing: Book of abstracts
[DE94-011828] p 519 N95-14430
Observation of diffraction effects in positron channeling
[DE94-014909] p 594 N95-14441
Proceedings of the 3rd International Workshop on Computational Electronics
[AD-A284214] p 475 N95-14444
The effects of spatial location of defect states on the switching characteristics of amorphous and polycrystalline silicon thin film transistors: A numerical simulation using AMPS 2-D
[DE94-013437] p 476 N95-15410
Fourth Workshop on the Role of Point Defects and Defect Complexes in Silicon Device Processing
[DE94-011850] p 624 N95-15426
A theoretical study of 30 to 50 angstrom noble gas heavy ion lithography
[DE94-015262] p 442 N95-15436
Optical detector having a plurality of matrix layers with cobalt disilicide particles embedded therein
[NASA-CASE-NPO-18625-2-CU] p 614 N95-15603
SAM1 semiempirical parameters
[AD-A284400] p 443 N95-15782
SILICON ALLOYS
Growth mechanisms and characterization of hydrogenated amorphous-silicon-alloy films
[DE94-011842] p 518 N95-14194
Coherency strains and coarsening in Ni-Al-Si alloys: An experimental study
[DE94-015020] p 445 N95-14665

Investigation of dendrite coherency in two commercial Al-Si foundry alloys
[PB94-208238] p 446 N95-15349

SILICON CARBIDES
Effects of in situ fiber strength characteristics on mechanical properties of SiC(f)/SiC composites
[DE94-013965] p 433 N95-13682
Effects of thermal cycling on thermal expansion and mechanical properties of SiC fiber-reinforced reaction-bonded Si3N4 composites
[NASA-TM-106665] p 433 N95-14298
Electrical characterization of 6H crystalline silicon carbide
[NASA-CR-197047] p 439 N95-14903
Process for the controlled growth of single-crystal films of silicon carbide polytypes on silicon carbide wafers
[NASA-CAS-LEW-15222-3] p 625 N95-15602

SILICON COMPOUNDS
Small-angle x-ray scattering studies of microvoids in amorphous-silicon-based semiconductors
[DE94-011840] p 520 N95-15406
Chemically modified electrodes by nucleophilic substitution of chlorosilylated platinum oxide surfaces
[AD-A281567] p 477 N95-15456

SILICON DIOXIDE
Preparation and characterization of composite inorganic zeolite membranes with molecular sieve properties
[PB94-191251] p 450 N95-14151
Influence of defect shape on laser-induced damage in multilayer coatings
[DE94-016543] p 451 N95-14389
Ferroelectric oxide memory FET (FEMFET) development
[AD-A283203] p 476 N95-15399
Type 304L stainless steel surface microstructure: Performance in hydride storage and acid cleaning
[DE94-014654] p 447 N95-15625

SILICON FILMS
Growth mechanisms and characterization of hydrogenated amorphous-silicon-alloy films
[DE94-011842] p 518 N95-14194
Development of large-area monolithically integrated Silicon-Film(tm) photovoltaic modules
[DE94-011830] p 520 N95-15405
Process for the controlled growth of single-crystal films of silicon carbide polytypes on silicon carbide wafers
[NASA-CAS-LEW-15222-3] p 625 N95-15602

SILICON NITRIDES
Effects of thermal cycling on thermal expansion and mechanical properties of SiC fiber-reinforced reaction-bonded Si3N4 composites
[NASA-TM-106665] p 433 N95-14298
Photoluminescence spectroscopy and Rutherford backscattering channeling evaluation of various capping techniques for rapid thermal annealing of ion-implanted ZnSe
[DE94-016876] p 623 N95-15339
Advanced Turbine Technology Applications Project (ATTAP)
[NASA-CR-195393] p 634 N95-15743

SILICON OXIDES
Study on titanium-silicalite-1 and related systems
[PB94-195500] p 445 N95-14845
Formation of dust grains with impurities in red giant winds p 641 N95-15841

SILICON POLYMERS
Technical Revue Thomson-CSF, volume 26, no. 1, March 1994. Flat panels for visualisation
[PB94-197969] p 410 N95-13984

SILICONES
Surface Tension Driven Convection Experiment (STDCE) p 458 N95-14217
Highly crosslinked silicon polymers for gas chromatography columns
[NASA-CASE-ARC-11960-2-NP] p 452 N95-14602

SIM
AXAF SIM focus mechanism study
[NASA-CR-196976] p 636 N95-13636

SIMULATION
Cross-effects in microgravity flows p 459 N95-14565
Simulation of coal and char nitrogen reactions in combustion
[DE94-013941] p 440 N95-15291
Subsurface object position and image correction for standoff ground penetrating radar
[DE94-015180] p 468 N95-15300
Xwake 1.0: A new tool for wakefield and impedance calculations
[DE94-015545] p 574 N95-15418
Cold flow simulation of the alternate turbopump development turbine of the Space Shuttle main engine high pressure fuel turbopump
[AD-A281676] p 419 N95-15447
Theory of nonlinear, distortive phenomena in solids: Martensitic, crack, and multiscale structures-phenomenology and physics
[DE94-015653] p 447 N95-15631

SIMULATORS
Some criteria for teleoperators and virtual environments from experiences with vehicle/operator simulation p 556 N95-14028
The exploration metaphor p 557 N95-14037
Clean assembly and integration techniques for the Hubble Space Telescope High Fidelity Mechanical Simulator p 418 N95-14070
A gate level simulator for alpha-particle-induced transient faults
[AD-A283871] p 474 N95-14355
Survey of the 1991 geothermal exploration promotion
[DE94-780690] p 530 N95-14836
The cardiovascular response to the AGS p 419 N95-15146

SINE WAVES
A method of measuring the amplitude-modulated vacuum field near a conducting mirror p 471 N95-13921

SINGLE CRYSTALS
High performance arcjet engines
[NASA-CR-195397] p 430 N95-13697
Advanced solar cells for satellite power systems
[NASA-TM-106777] p 473 N95-14302
Center for advanced materials of high quality dynamic performance (fellowships)
[AD-A281377] p 434 N95-14360
Observation of diffraction effects in positron channeling
[DE94-014909] p 594 N95-14441
Atomic force microscopy of the electrochemical nucleation and growth of molecular crystals
[AD-A280958] p 622 N95-14601
Ultrasonic characterization of high T(c) and other unconventional superconductors
[AD-A282835] p 476 N95-15397
Fatigue in single crystal nickel superalloys
[AD-A282917] p 446 N95-15415
Process for the controlled growth of single-crystal films of silicon carbide polytypes on silicon carbide wafers
[NASA-CAS-LEW-15222-3] p 625 N95-15602
Optical detector having a plurality of matrix layers with cobalt disilicide particles embedded therein
[NASA-CASE-NPO-18625-2-CU] p 614 N95-15603

SINGLE EVENT UPSETS
A gate level simulator for alpha-particle-induced transient faults
[AD-A283871] p 474 N95-14355

SINGLE STAGE TO ORBIT VEHICLES
Access to space
[NASA-CR-197153] p 428 N95-14521
Requirements report for SSTO vertical take-off and horizontal landing vehicle
[NASA-CR-197029] p 409 N95-14794
Milestone 4: Thrust structure concepts and IHM screening Graphite Composite Primary Structure (GCPS)
[NASA-CR-197053] p 434 N95-14800
Milestone 4: Test plan for Reusable Hydrogen Composite Tank System (RHCTS). Task 3: Composite tank materials
[NASA-CR-197036] p 435 N95-14801

SINGULARITY (MATHEMATICS)
Mathematical problems of nonlinear wave propagation and of waves in heterogeneous media
[AD-A282217] p 492 N95-14605

SINTERING
Synthesis, processing and properties of materials for SOFCs
[DE94-014491] p 517 N95-14002
Center for advanced materials of high quality dynamic performance (fellowships)
[AD-A281377] p 434 N95-14360

SITE SELECTION
Selecting wave gauge sites for monitoring harbor oscillations: A case study for Kahului Harbor, Hawaii
[AD-A281707] p 536 N95-15452

SITTING POSITION
Transient blood/plasma density and hematocrit effects after passive (sitting) thermoneutral water immersion in men p 548 N95-15131
Individual variability in the transmission of vertical vibration from seat to head
[ISVR-TR-236] p 563 N95-15850

SIZE DISTRIBUTION
Combustion efficiency in a dual-inlet side-dump ramjet combustor
[AD-A283564] p 411 N95-15329
Counting condensation in the Antarctic Ozone Mission
[NASA-CR-197113] p 525 N95-15847

SKY SURVEYS (ASTRONOMY)
A ROSAT deep survey of the best studied high latitude areas
[NASA-CR-196265] p 637 N95-13722
Space simulation techniques and facilities for SAX STM test campaign p 423 N95-14077
Space based astronomy: Teacher's guide with activities
[NASA-EG-102] p 638 N95-14511

SLEEP
Extended duration orbiter medical project variability of blood pressure and heart rate (STS-50/USML-1) p 551 N95-14223
Crew factors in flight operations 2: Psychophysiological responses to short-haul air transport operations
[NASA-TM-108856] p 550 N95-15649

SLENDER BODIES
A selection of experimental test cases for the validation of CFD codes, volume 1
[AGARD-AR-303-VOL-1] p 481 N95-14201

SLIDING CONTACT
Gouge initiation in high-velocity rocket sled testing
[DE94-014288] p 418 N95-15357

SLIDING FRICTION
A new tribological test for candidate brush seal materials evaluation
[NASA-TM-106753] p 431 N95-13631
Physical and tribological characteristics of ion-implanted diamond films
[NASA-TM-106682] p 450 N95-14303

SLITS
On the theory of quantum measurement p 604 N95-13910
Laser retroreflector array having cat-eye retroreflectors
[NASA-CASE-GSC-13264-1] p 499 N95-14515

SLOPES
Tilting wind tunnel for fire behavior studies
[PB94-204625] p 413 N95-14513

SLOTS
Computational analysis of forebody tangential slot blowing p 397 N95-14253
Comparison of full-scale, small-scale, and CFD results for F/A-18 forebody slot blowing p 397 N95-14255

SLUSH HYDROGEN
Multi-dimensional modeling of pressurization and expulsion of multi-phase hydrogen propellant
[NASA-CR-195156] p 457 N95-14902

SMART STRUCTURES
Representation and recognition with algebraic invariants and geometric constraint models
[AD-A282926] p 585 N95-14843

SNELLS LAW
Refractive effects from VHF to EHF. Part A: Propagation Mechanisms p 467 N95-14831

SNOW
The operational forecasting/nowcasting of precipitation type in the southeastern United States type of precipitation: Descriptive and objective guidance
[AD-A284456] p 535 N95-15819

SODIUM
Research on characterization of the upper atmosphere using lidar
[AD-A283241] p 530 N95-15401
The peculiar behaviour of the 5780 and 5797 DIBs in HD25137 p 639 N95-15833

SODIUM COMPOUNDS
Nucleation and chiral symmetry breaking under controlled hydrodynamic flows p 489 N95-14570

SOFIA (AIRBORNE OBSERVATORY)
Numerical simulation of the SOFIA flowfield
[NASA-CR-197025] p 400 N95-14612

SOFTWARE ENGINEERING
Advanced distributed simulation technology: Digital Voice Gateway Reference Guide
[AD-A283154] p 460 N95-13696
Knowledge-based processing for aircraft flight control
[NASA-CR-194976] p 580 N95-13727
Earth Observing System (EOS)/Advanced Microwave Sounding Unit-A (AMSU-A) software assurance plan
[NASA-CR-196059] p 515 N95-13885
Development of visual 3D virtual environment for control software p 559 N95-14048
RICIS Symposium 1992: Mission and Safety Critical Systems Research and Applications
[NASA-CR-196963] p 569 N95-14156
Generic architectures for future flight systems p 567 N95-14159
Ada 9X overview p 570 N95-14166
Software development for safety-critical medical applications p 571 N95-14171
Formal methods technology transfer: Some lessons learned p 571 N95-14172
Toward deriving software architectures from quality attributes
[AD-A283827] p 572 N95-14339

Benefits of CMM-based software process improvement: Initial results
[AD-A283848] p 572 N95-14349
ADST ARWA visual system module software design document
[AD-A283874] p 572 N95-14357
Reuseable Objects Software Environment (ROSE): Introduction to Air Force Software Reuse Workshop
[NASA-CR-197017] p 572 N95-14520
The Network Operations Control Center upgrade task: Lessons learned p 419 N95-14631
Applying CASE technology to the software maintenance life cycle
[TABES PAPER 94-620] p 416 N95-14647
Automated test environment for a real-time control system
[TABES PAPER 94-631] p 417 N95-14652
Machine intelligence: The key to guidance and control in robotics p 581 N95-14944
Interactive Computer-Enhanced Remote Viewing System (ICERVS): Subsystem design report, phase 2
[DE94-014513] p 563 N95-15309
Model contracts/agreements. Comprehensive Approach to Reusable Defense Software (CARDS)
[AD-A284403] p 575 N95-15783
Software Technology for Adaptable, Reliable Systems (STARS)
[AD-A284373] p 576 N95-15806

SOFTWARE RELIABILITY

Remote programming in INSAT-2A/2B on-board Attitude and Orbit Control Computer (AOCC) p 413 N95-13827
European Workshop Industrical Computer Science Systems approach to design for safety p 569 N95-14157
MISSION: Mission and Safety Critical Support Environment. Executive overview p 569 N95-14158
Architecture for Survivable Systems Processing (ASSP). Technology benefits for Open System Interconnects p 567 N95-14160
Space Generic Open Avionics Architecture (SGOAA): Overview p 569 N95-14161
Evolutionary Telemetry and Command Processor (TCP) architecture p 420 N95-14162
Software development for safety-critical medical applications p 571 N95-14171
Software reliability studies
[NASA-CR-197027] p 572 N95-14615

SOFTWARE REUSE

Reuseable Objects Software Environment (ROSE): Introduction to Air Force Software Reuse Workshop
[NASA-CR-197017] p 572 N95-14520
Model contracts/agreements. Comprehensive Approach to Reusable Defense Software (CARDS)
[AD-A284403] p 575 N95-15783
Software Technology for Adaptable, Reliable Systems (STARS)
[AD-A284373] p 576 N95-15806

SOFTWARE TOOLS

PHOENIX user manual. First version
[PB94-189081] p 568 N95-13989
Investigating and implementing enhancements to the simulation of short-term collision hazards p 426 N95-14092
Integration/evaluation of a HCI prototyping environment
[NASA-CR-196996] p 566 N95-14107
Parallel isosurface generator for huge data sets
[AD-A284030] p 578 N95-14422
Computer Aided Engineering (CAE) overview
[AD-A280966] p 572 N95-14616
Applying CASE technology to the software maintenance life cycle
[TABES PAPER 94-620] p 416 N95-14647
Product life cycle data base, analysis and simulation integration methodology
[TABES PAPER 94-626] p 417 N95-14650
Automated test environment for a real-time control system
[TABES PAPER 94-631] p 417 N95-14652
Propagation Modelling and Decision Aids for Communications, Radar and Navigation Systems
[AGARD-LS-196] p 466 N95-14825
Ground wave and diffraction, B p 467 N95-14829
Using Pro/ENGINEER's (tm) interface module
[DE94-013364] p 574 N95-15384
An architecture for intelligent multichip module reliability analysis
[AD-A281574] p 583 N95-15461
The lambda loop transformation toolkit (user's reference manual)
[TR-511] p 587 N95-15733
Intelligence in scientific computing
[AD-A284410] p 584 N95-15811
ASPM2: Progress toward the analysis of symbolic parameter models
[AD-A284437] p 576 N95-15817

SOIL SCIENCE

Dependence of segregation potential on the thermal and hydraulic conditions predicted by model M1
[AD-A280969] p 530 N95-14862
Traveling wave solutions to the problem of quasi-steady freezing of soils
[AD-A280971] p 531 N95-15428

SOL-GEL PROCESSES

In-situ TEM crystallization of sol-gel derived BaTiO3 thin films
[DE94-013260] p 619 N95-13821
Low loss substrates for microwave applications and sol-gel processing of superconductors
[AD-A284868] p 625 N95-15746

SOLAR ACTIVITY

Solar-geophysical data number 598, June 1994. Part 2: (Comprehensive reports). Data for December 1993 and miscellaneous
[PB94-208832] p 646 N95-15773
Solar-geophysical data number 598, June 1994. Part 1: (Prompt reports). Data for May, April 1994 and late data
[PB94-208824] p 646 N95-15784

SOLAR ACTIVITY EFFECTS

Early solar mass loss, element diffusion, and solar oscillation frequencies
[DE94-014802] p 646 N95-14376

SOLAR ARRAYS

Advanced solar cells for satellite power systems
[NASA-TM-106777] p 473 N95-14302
Building complex simulations rapidly using MATRIX(x): The Space Station redesign
[TABES PAPER 94-632] p 417 N95-14653
Summary of solar cell data from the Long Duration Exposure Facility (LDEF)
[NASA-CR-197069] p 519 N95-14802
Analysis of space environment damage to solar cell assemblies from LDEF experiment A0171-GSFC test plate
[NASA-CR-197066] p 519 N95-14853

SOLAR ATMOSPHERE

On the physics of waves in the solar atmosphere: Wave heating and wind acceleration
[NASA-CR-196992] p 646 N95-15070

SOLAR CELLS

Alkali metal Rankine cycle boiler technology challenges and some potential solutions for space nuclear power and propulsion applications
[NASA-TM-106593] p 430 N95-14174
Advanced solar cells for satellite power systems
[NASA-TM-106777] p 473 N95-14302
Role of point defects and defect complexes in silicon device processing: Book of abstracts
[DE94-011828] p 519 N95-14430
In-situ characterization of growth and interfaces in a-Si:H devices
[DE94-011847] p 622 N95-14431
Role of polycrystallinity in CdTe and CuInSe2 photovoltaic cells
[DE94-011849] p 519 N95-14432
Summary of solar cell data from the Long Duration Exposure Facility (LDEF)
[NASA-CR-197069] p 519 N95-14802
Analysis of space environment damage to solar cell assemblies from LDEF experiment A0171-GSFC test plate
[NASA-CR-197066] p 519 N95-14853
Optimization of transparent and reflecting electrodes for amorphous-silicon solar cells
[DE94-011841] p 520 N95-15355
Development of large-area monolithically integrated Silicon-Film(tm) photovoltaic modules
[DE94-011830] p 520 N95-15405
Small-angle x-ray scattering studies of microvoids in amorphous-silicon-based semiconductors
[DE94-011840] p 520 N95-15406
Alternative fabrication techniques for high-efficiency CuInSe2 and CuInSe2-alloy films and cells
[DE94-011846] p 521 N95-15407
Fourth Workshop on the Role of Point Defects and Defect Complexes in Silicon Device Processing
[DE94-011850] p 624 N95-15426
Module process optimization and device efficiency improvement for stable, low-cost, large-area, cadmium telluride-based photovoltaic module production
[DE94-011817] p 521 N95-15863

SOLAR CONVECTION (ASTRONOMY)

Early solar mass loss, element diffusion, and solar oscillation frequencies
[DE94-014802] p 646 N95-14376

SOLAR ENERGY

Monitoring solar-thermal systems: An outline of methods and procedures
[DE94-015599] p 521 N95-15420

SOLAR FLARES

A Lyman-alpha tunable acousto-optic filter for detecting superthermal flare protons
[NASA-CR-197119] p 613 N95-14908
Solar-geophysical data number 598, June 1994. Part 2: (Comprehensive reports). Data for December 1993 and miscellaneous
[PB94-208832] p 646 N95-15773
Solar-geophysical data number 598, June 1994. Part 1: (Prompt reports). Data for May, April 1994 and late data
[PB94-208824] p 646 N95-15784

SOLAR FLUX

Neutrino oscillations in noisy media
[DE94-014973] p 598 N95-15869

SOLAR GENERATORS

Environmental durability issues for solar power systems in low Earth orbit
[NASA-TM-106775] p 431 N95-15769

SOLAR INSTRUMENTS

A Lyman-alpha tunable acousto-optic filter for detecting superthermal flare protons
[NASA-CR-197119] p 613 N95-14908

SOLAR MAGNETIC FIELD

Solar-geophysical data number 598, June 1994. Part 1: (Prompt reports). Data for May, April 1994 and late data
[PB94-208824] p 646 N95-15784
Neutrino oscillations in noisy media
[DE94-014973] p 598 N95-15869

SOLAR NEUTRINOS

Neutrino oscillations in noisy media
[DE94-014973] p 598 N95-15869

SOLAR OSCILLATIONS

Early solar mass loss, element diffusion, and solar oscillation frequencies
[DE94-014802] p 646 N95-14376

SOLAR PROTONS

A Lyman-alpha tunable acousto-optic filter for detecting superthermal flare protons
[NASA-CR-197119] p 613 N95-14908

SOLAR RADIATION

Evaluation of reformulated thermal control coatings in a simulated space environment. Part 1: YB-71 p 420 N95-14063

SOLAR RADIO EMISSION

Solar-geophysical data number 598, June 1994. Part 2: (Comprehensive reports). Data for December 1993 and miscellaneous
[PB94-208832] p 646 N95-15773
Solar-geophysical data number 598, June 1994. Part 1: (Prompt reports). Data for May, April 1994 and late data
[PB94-208824] p 646 N95-15784

SOLAR SIMULATORS

Experimental study of solar simulator mirror cryocontamination p 421 N95-14065
The realuminizing of the 7-meter-diameter solar simulator collimating mirror p 424 N95-14081
Selection of solar simulator for solar dynamic ground test
[NASA-TM-106608] p 430 N95-14173

SOLAR TERRESTRIAL INTERACTIONS

Geotail MCA plasma wave data analysis
[NASA-CR-197022] p 618 N95-14798

SOLAR WIND

Interplanetary medium data book, supplement 5, 1988-1993
[NASA-TM-109957] p 642 N95-13658
Study of auroral dynamics with combined spacecraft and incoherent scatter radar data
[NASA-CR-196974] p 526 N95-13818
ICE/ISEE plasma wave data analysis
[NASA-CR-196988] p 642 N95-14266
Geotail MCA plasma wave data analysis
[NASA-CR-197022] p 618 N95-14798
On the physics of waves in the solar atmosphere: Wave heating and wind acceleration
[NASA-CR-196992] p 646 N95-15070

SOLDERS

Assembly feasibility and reliability studies of surface mount circuit boards manufactured with lead-free solders
[DE94-013783] p 472 N95-13975

SOLENOID VALVES

Dual-latching solenoid-actuated valve assembly
[NASA-CASE-MFS-28714-1] p 502 N95-14666

SOLID ELECTROLYTES

Thin composite solid electrolyte film for lithium batteries
[NASA-CASE-NPO-18694-1-CU] p 472 N95-13824

Synthesis, processing and properties of materials for SOFCs
[DE94-014491] p 517 N95-14002
Conductivity of polyacrylonitrile based lithium polymer electrolytes
[AD-A283965] p 450 N95-14203
Development of the fuel cell power generation technology, 1
[DE94-780648] p 520 N95-15377
Thin lithium cobalt dioxide rechargeable cells using polyacrylonitrile-based polymer electrolytes
[AD-A283253] p 455 N95-15615

SOLID LUBRICANTS
Recent progress and future prospects in the surface engineering and tribology of ceramics
[DE94-016315] p 456 N95-15778

SOLID MECHANICS
Basic mechanics of laminated composite plates
[NASA-RP-1351] p 436 N95-15763

SOLID PHASES
Ion beam synthesis of SiGe alloy layers
[DE94-014958] p 620 N95-14189

SOLID PROPELLANT ROCKET ENGINES
Recycled plastic: A clean and low cost rocket fuel
[TABES PAPER 94-610] p 416 N95-14642

SOLID SOLUTIONS
Defects and transport in mixed oxides
[DE94-015652] p 454 N95-15358
NMR studies of polymers at interfaces
[AD-A281570] p 455 N95-15458

SOLID STATE LASERS
High power diode pumped solid state laser development at Lawrence Livermore National Laboratory
[DE94-015899] p 499 N95-14427

SOLID STATE PHYSICS
Technology and Science at at High-Power Spallation Source: Proceedings
[DE94-009685] p 597 N95-15826

SOLID SURFACES
The solid surface combustion experiment aboard the USML-1 mission p 458 N95-14212

SOLID-SOLID INTERFACES
NMR studies of polymers at interfaces
[AD-A281570] p 455 N95-15458

SOLIDIFICATION
Interactions between solidification and compositional convection in mushy layers p 448 N95-14551

SOLIDS
New quantum properties of phonons and their detection p 610 N95-13957
Second International Conference on Computer Simulation of Radiation Effects in Solids
[DE94-016368] p 594 N95-14383
Theory of nonlinear, distortive phenomena in solids: Martensitic, crack, and multiscale structures-phenomenology and physics
[DE94-015653] p 447 N95-15631

SOLITARY WAVES
Interacting fronts in a model for binary-mixture convection
[DE94-013595] p 494 N95-15861

SOLUBILITY
Polymer-polymer interactions
[AD-A282944] p 453 N95-14844
Solubility, viscosity and density of refrigerant and lubricant mixtures
[DE94-016949] p 454 N95-15343

SOLUTES
Determination of solvation kinetics in supercritical fluids
[DE94-016491] p 438 N95-14386
Measurement of resistance to solute transport across surfactant-laden interfaces using a Fluorescence Recovery After Photobleaching (FRAP) technique p 490 N95-14574

SOLVATION
Determination of solvation kinetics in supercritical fluids
[DE94-016491] p 438 N95-14386

SOLVENTS
A solvent resistant copolyimide
[NASA-CASE-LAR-15083-1] p 449 N95-14108

SONAR
The stable and precise motion control for an autonomous mobile robot
[AD-A283776] p 501 N95-14336

SONIC BOOMS
High-Speed Research: 1994 Sonic Boom Workshop: Atmospheric Propagation and Acceptability Studies
[NASA-CP-3279] p 401 N95-14878
Effect of stratification and geometrical spreading on sonic boom rise time p 401 N95-14880
An evaluation of rise time characterization and prediction methods p 401 N95-14881
Fine structure of transient waves in a random medium: The correlation and spectral density functions p 401 N95-14882
Numerical model for the weakly nonlinear propagation of sound through turbulence p 401 N95-14883
Sonic boom interaction with turbulence p 402 N95-14884
Atmospheric propagation at larger lateral distances from the flight track p 402 N95-14885
Atmospheric effects on the risetime and waveshape of sonic booms p 402 N95-14886
The effect of aircraft speed on the penetration of sonic boom noise into a flat ocean p 402 N95-14887
Simple atmospheric perturbation models for sonic-boom-signature distortion studies p 402 N95-14888
USAF single-event sonic boom prediction model: PCBoom3 p 403 N95-14889
Deriving a dosage-response relationship for community response to high-energy impulsive noise p 403 N95-14890
An in-home study of subjective response to simulated sonic booms p 403 N95-14891
Residents' reactions to long-term sonic boom exposure: Preliminary results p 403 N95-14892

SOOT
The solid surface combustion experiment aboard the USML-1 mission p 458 N95-14212

SORTING ALGORITHMS
A high performance graphics algorithm
[DE94-015033] p 571 N95-14196

SOUND DETECTING AND RANGING
Leak detection by acoustic emissions monitoring: An experimental investigation of the acoustic properties of leaks and the attenuation characteristics of soil
[AD-A283250] p 530 N95-15295

SOUND FIELDS
The mean acoustic field in layered media with rough interfaces
[AD-A281960] p 590 N95-13683
Binaural room simulation p 561 N95-14053

SOUND INTENSITY
NASA LeRC's acoustic fill effect test program and results
[NASA-TM-106688] p 419 N95-13893

SOUND LOCALIZATION
Active localization of virtual sounds p 561 N95-14054

SOUND PRESSURE
NASA LeRC's acoustic fill effect test program and results
[NASA-TM-106688] p 419 N95-13893
Numerical simulation of the SOFIA flowfield
[NASA-CR-197025] p 400 N95-14612

SOUND WAVES
The mean acoustic field in layered media with rough interfaces
[AD-A281960] p 590 N95-13683
Surface acoustic wave oxygen pressure sensor
[NASA-CASE-LAR-15266-1-CU] p 496 N95-13837
Real time system for practical acoustic monitoring of global ocean temperature, volume 3
[AD-A283774] p 535 N95-14335
The modal decomposition of an impedance tube
[AD-A283591] p 591 N95-15320
Surface Acoustic Wave (SAW) microsensors to monitor multi-component vapor challenges to adsorbents and adsorbent-based air filtration systems
[AD-A284222] p 497 N95-15334
Acoustic resonance spectroscopy intrinsic seals
[DE94-016207] p 591 N95-15359
Ultrasonic characterization of high T(c) and other unconventional superconductors
[AD-A282835] p 476 N95-15397
Problems in nonlinear acoustics: Surface acoustic waves, diffracting sound beams, and fluid-solid interface effects
[AD-A281714] p 592 N95-15453

SOUNDING ROCKETS
Enhancement of insulin receptor mediated endocytosis in cultured osteoblastic cells under hypergravity p 539 N95-15148

SPACE
Suited for spacewalking: Teacher's guide with activities for physical and life science
[NASA-EG-101] p 554 N95-13888

SPACE ADAPTATION SYNDROME
Adaptation of skeletal muscle to spaceflight: Cosmos rhesus project. Cosmos 2044 and 2229
[NASA-CR-197041] p 537 N95-14796
The relationship between space sickness and preflight diet p 546 N95-15122
Physiologic mechanisms effecting circulatory and body fluid losses in weightlessness as shown by mathematical modeling p 547 N95-15129

SPACE CHARGE
Study of the long term stability of the effective concentration of ionized space charges (N(sub eff)) of neutron irradiated silicon detectors fabricated by various thermal oxidations
[DE94-013734] p 593 N95-14309

SPACE COMMERCIALIZATION
Commercial investigation results for the generic bioprocessing apparatus flown on United States Microgravity Laboratory-1 p 538 N95-14227
Access to space
[NASA-CR-197153] p 428 N95-14521
TABES 1994: 10th Annual Technical and Business Exhibition and Symposium p 414 N95-14633

SPACE COMMUNICATION
Research and development optical deep space antenna sizing study p 463 N95-14628

SPACE DEBRIS
Journal of Spacecraft Technology, volume 4, no. 2, July 1994 p 413 N95-13825
Modelling the low Earth space debris environment p 414 N95-13830
Investigating and implementing enhancements to the simulation of short-term collision hazards p 426 N95-14092
Applications of a fast and efficient method for simulating orbital mission safety p 426 N95-14093
Satellite situation report, volume 33, number 2
[NASA-TM-109965] p 428 N95-14510
Hypervelocity Impact Test Facility: A gun for hire
[TABES PAPER 94-605] p 415 N95-14639
Analysis of space environment damage to solar cell assemblies from LDEF experiment A0171-GSFC test plate
[NASA-CR-197066] p 519 N95-14853
Space debris detection and analysis
[AD-A282012] p 428 N95-14951

SPACE ENVIRONMENT SIMULATION
Modelling the low Earth space debris environment p 414 N95-13830
Eighteenth Space Simulation Conference: Space Mission Success Through Testing
[NASA-CP-3280] p 420 N95-14062
Evaluation of reformulated thermal control coatings in a simulated space environment. Part 1: YB-71 p 420 N95-14063
Experimental study of solar simulator mirror cryocontamination p 421 N95-14065
ASTM E 1559 method for measuring material outgassing/deposition kinetics has applications to aerospace, electronics, and semiconductor industries p 421 N95-14066
Self contamination effects in the TAUVEX UV Telescope: Ground testing and computer simulation p 421 N95-14067
Using a temperature-controlled quartz crystal microbalance in a space equipment cleanroom to monitor molecular contamination p 421 N95-14069
Laboratory simulation of Low Earth Orbit (LEO) atomic oxygen effects p 422 N95-14071
A facility to produce an energetic, ground state atomic oxygen beam for the simulation of the Low-Earth Orbit environment p 422 N95-14072
Atomic Oxygen (ATOX) simulation of Teflon FEP and Kapton H surfaces using a high intensity, low energy, mass selected, ion beam facility p 422 N95-14073
The effect of Low Earth Orbit exposure on some experimental fluorine and silicon-containing polymers p 422 N95-14074
A simulation facility for testing Space Station assembly procedures p 423 N95-14075
Space simulation techniques and facilities for SAX STM test campaign p 423 N95-14077
Environmental testing to prevent on-orbit TDRS failures p 423 N95-14078
David Florida Laboratory Thermal Vacuum Data Processing System p 418 N95-14079
Thermal balance testing of MSAT 2 spacecraft p 424 N95-14080
The realuminizing of the 7-meter-diameter solar simulator collimating mirror p 424 N95-14081
Thermal balance testing of the MSAT spacecraft p 424 N95-14082
Thermal design verification testing of the Clementine spacecraft: Quick, cheap, and useful p 424 N95-14083
Partial pressure analysis in space testing p 424 N95-14084
Refurbishment of a 39 foot thermal vacuum chamber p 418 N95-14085
HYDRA, a new tool for mechanical testing p 418 N95-14086
System level mechanical testing of the Clementine spacecraft p 425 N95-14087

Simulation of Shuttle launch G forces and acoustic loads using the NASA Ames Research Center 20G centrifuge p 419 N95-14089
Development of life sciences equipment for microgravity and hypergravity simulation p 425 N95-14090
Unique life sciences research facilities at NASA Ames Research Center p 426 N95-14091
Investigating and implementing enhancements to the simulation of short-term collision hazards p 426 N95-14092
Applications of a fast and efficient method for simulating orbital mission safety p 426 N95-14093
Alpha LAMP Integration Facility p 418 N95-14094
Simulation of a spatial, servo-hydraulic test facility for space structures p 418 N95-14095
Thermoacoustic environments to simulate reentry conditions p 426 N95-14096
The AEDC aerospace chamber 7V: An advanced test capability for infrared surveillance and seeker sensors p 418 N95-14097
New potentials of NIICHIMMASH's thermal vacuum facilities p 418 N95-14098
From Antarctica to space: Use of telepresence and virtual reality in control of remote vehicles p 427 N95-14099
Hypervelocity Impact Test Facility: A gun for hire [TABES PAPER 94-605] p 415 N95-14639
Space flight and humoral and cellular immunity of animals p 538 N95-15113
On-Earth evaluation of the neurovestibular tolerance to centrifuge simulated artificial gravity in humans p 546 N95-15120
The influence of gravity on vestibular nystagmus in humans p 546 N95-15121
Alterations of body temperature, feeding, drinking and sleep-wake circadian rhythms in Rhesus monkey during a 19 day Spacelab flight simulation p 539 N95-15132
Relationship between hind-limb muscle atrophy and serum enzymes in tail suspended rats p 539 N95-15143

SPACE ERECTABLE STRUCTURES
Joint for a variable geometry truss and method of constructing same [NASA-CASE-LAR-15136-1] p 506 N95-14138

SPACE EXPLORATION
From Antarctica to space: Use of telepresence and virtual reality in control of remote vehicles p 427 N95-14099
First Year PIDDP Report on gamma-ray and x-ray spectroscopy: X-ray remote sensing and in -situ spectroscopy for planetary exploration missions and gamma-ray remote sensing and in situ spectroscopy for planetary exploration missions [NASA-CR-189374] p 517 N95-15916

SPACE FLIGHT
Cosmos 2229 immunology study (Experiment K-8-07) [NASA-CR-196984] p 537 N95-13638
Immune changes in humans concomitant with space flights of up to 10 days duration p 545 N95-15114
On-Earth evaluation of the neurovestibular tolerance to centrifuge simulated artificial gravity in humans p 546 N95-15120
Effect of short- and long-term spaceflight on the contractile properties of rat skeletal muscles with different functions p 539 N95-15141

SPACE FLIGHT FEEDING
The relationship between space sickness and preflight diet p 546 N95-15122

SPACE FLIGHT STRESS
Development of life sciences equipment for microgravity and hypergravity simulation p 425 N95-14090

SPACE FLIGHT TRAINING
The effects of autogenic-feedback training on motion sickness severity and heart rate variability in astronauts [NASA-TM-108840] p 539 N95-13661

SPACE LABORATORIES
Life Sciences Centrifuge Facility review [NASA-CR-196849] p 537 N95-13702
Thermal balance testing of the MSAT spacecraft p 424 N95-14082

SPACE MAINTENANCE
Hubble Space Telescope servicing mission scientific instrument protective enclosure design requirements and contamination controls p 421 N95-14068

SPACE MISSIONS
Eighteenth Space Simulation Conference: Space Mission Success Through Testing [NASA-CP-3280] p 420 N95-14062
Advanced solar cells for satellite power systems [NASA-TM-106777] p 473 N95-14302
Bubble dynamics, two-phase flow, and boiling heat transfer in a microgravity environment p 488 N95-14561
Circulatory filling pressures during transient microgravity induced by parabolic flight p 542 N95-15095

SPACE PERCEPTION
Spatial awareness comparisons between large-screen, integrated pictorial displays and conventional EFIS displays during simulated landing approaches [NASA-TP-3467] p 409 N95-14852
Distance estimation training with night vision goggles: A preliminary study [AD-A284900] p 563 N95-15755

SPACE PLASMAS
Geotail MCA plasma wave data analysis [NASA-CR-197022] p 618 N95-14798
Dynamics Explorer 1: Energetic Ion Composition Spectrometer (EICS) [NASA-CR-189375] p 619 N95-15758
Mass analysis addition to the Differential Ion Flux Probe (DIFP) study [NASA-CR-196531] p 429 N95-15824

SPACE PLATFORMS
Evaluation of sensor placement algorithms for on-orbit identification of space platforms p 425 N95-14088

SPACE PROCESSING
Powder agglomeration in a microgravity environment [NASA-CR-197000] p 457 N95-14105
Joint Launch + One Year Science Review of USML-1 and USMP-1 with the Microgravity Measurement Group [NASA-CP-3272-VOL-1] p 634 N95-14207
Mass transport phenomena in microgravity: Preliminary results of the first MEPHISTO flight experiment p 634 N95-14209
Orbital processing of high-quality CdTe compound semiconductors p 458 N95-14213
Crystal growth of selected II-VI semiconducting alloys by directional solidification p 458 N95-14214
Vapor transport crystal growth of mercury-cadmium-telluride in microgravity p 458 N95-14216
Core-centering of compound drops in capillary oscillations: Observations on USML-1 experiments in space p 458 N95-14218
Bifurcation of rotating liquid drops: Results from USML-1 experiments in space p 458 N95-14219
Measurement of interfacial tension of immiscible liquid pairs in microgravity p 458 N95-14221
Protein crystal growth results from the United States Microgravity Laboratory-1 mission p 458 N95-14225
The growth of zeolites A, X and mordenite in space p 458 N95-14226
Commercial investigation results for the generic bioprocessing apparatus flown on United States Microgravity Laboratory-1 p 538 N95-14227
Surfactant-based critical phenomena in microgravity p 459 N95-14579
Gravity-dependent transport in industrial processes p 459 N95-14580

SPACE PROGRAMS
Delta, America's space ambassador [NASA-TM-110046] p 419 N95-13700
Space science in the 1990's and beyond [TABES PAPER 94-204] p 415 N95-14634
Musculoskeletal adaptation to mechanical forces on Earth and in space p 548 N95-15136

SPACE RENDEZVOUS
Journal of Spacecraft Technology, volume 4, no. 2, July 1994 p 413 N95-13825

SPACE SHUTTLE MAIN ENGINE
Develop advanced nonlinear signal analysis topographical mapping system [NASA-CR-194414] p 514 N95-13639
Space Shuttle Main Engine turbopump bearing assessment program [TABES PAPER 94-621] p 417 N95-14648
Automated test environment for a real-time control system [TABES PAPER 94-631] p 417 N95-14652
Cold flow simulation of the alternate turbopump development turbine of the Space Shuttle main engine high pressure fuel turbopump [AD-A281676] p 419 N95-15447
Vehicle health management using adaptive techniques [NASA-TM-108472] p 431 N95-15609

SPACE SHUTTLE MISSIONS
Basic features of the STS/Spacelab vibration environment p 428 N95-14210
Extended duration orbiter medical project variability of blood pressure and heart rate (STS-50/USML-1) p 551 N95-14223

SPACE SHUTTLE ORBITERS
Nondestructive analysis and development [NASA-CR-196987] p 505 N95-13886
The solid surface combustion experiment aboard the USML-1 mission p 458 N95-14212

SPACE SHUTTLE PAYLOADS
Fluids flight hardware p 491 N95-14583

SPACE SHUTTLES
The effect of Low Earth Orbit exposure on some experimental fluorine and silicon-containing polymers p 422 N95-14074
Space Shuttle fatigue loads spectra for prelaunch and liftoff loads p 419 N95-14474

SPACE SIMULATORS
Selection of solar simulator for solar dynamic ground test [NASA-TM-106608] p 430 N95-14173

SPACE STATION FREEDOM
A simulation facility for testing Space Station assembly procedures p 423 N95-14075

SPACE STATION PAYLOADS
Conceptual design of the Space Station fluids module p 429 N95-14584

SPACE STATION STRUCTURES
A simulation facility for testing Space Station assembly procedures p 423 N95-14075

SPACE STATIONS
Evaluation of sensor placement algorithms for on-orbit identification of space platforms p 425 N95-14088
TABES 1994: 10th Annual Technical and Business Exhibition and Symposium p 414 N95-14633
Building complex simulations rapidly using MATRIX(x): The Space Station redesign [TABES PAPER 94-632] p 417 N95-14653
Control and operation of space manipulator systems p 582 N95-14946

SPACE SURVEILLANCE (SPACEBORNE)
US space-based remote sensing: Challenges and prospects [AD-A282439] p 515 N95-15546

SPACE TOOLS
Control of remotely operated manipulation systems p 582 N95-14945

SPACE TRANSPORTATION
Fast track NTR systems assessment for NASA's first lunar outpost scenario [NASA-TM-106748] p 429 N95-13668
Access to space [NASA-CR-197153] p 428 N95-14521
Design of power electronics for TVC and EMA systems [NASA-CR-197067] p 475 N95-14866
Air-breathing aerospace plane development essential: Hypersonic propulsion flight tests [NASA-TM-108857] p 392 N95-14921
Space transfer vehicle concepts and requirements study. Volume 3: Program cost estimates. Book 2: WBS and dictionary [NASA-CR-192447] p 419 N95-15552

SPACE TRANSPORTATION SYSTEM
Results of demonstration test for receiving and processing of flight data from the Space Transportation System [NASA-CR-194986] p 418 N95-13890
The rationale/benefits of nuclear thermal rocket propulsion for NASA's lunar space transportation system [NASA-TM-106739] p 431 N95-15682

SPACE TRANSPORTATION SYSTEM FLIGHTS
The effects of autogenic-feedback training on motion sickness severity and heart rate variability in astronauts [NASA-TM-108840] p 539 N95-13661
The effect of Low Earth Orbit exposure on some experimental fluorine and silicon-containing polymers p 422 N95-14074
Core-centering of compound drops in capillary oscillations: Observations on USML-1 experiments in space p 458 N95-14218
Extended duration orbiter medical project countermeasure to reduce post space flight orthostatic intolerance (LBNP) (STS-50/USML-1) p 551 N95-14224
STS-66 post flight presentation [NASA-TM-110077] p 419 N95-15900

SPACE-TIME FUNCTIONS
CFD methodology and validation for turbomachinery flows p 480 N95-14131
Two methods for the study of vortex patch evolution on locally refined grids [DE94-014965] p 494 N95-15867

SPACEBORNE ASTRONOMY
ICE/ISEE plasma wave data analysis [NASA-CR-196988] p 642 N95-14266

SPACEBORNE EXPERIMENTS
Cosmos 2229 immunology study (Experiment K-8-07) [NASA-CR-196984] p 537 N95-13638
Experimental design for the evaluation of high-T(sub c) superconductive thermal bridges in a sensor satellite [NASA-CR-197003] p 429 N95-14106
Joint Launch + One Year Science Review of USML-1 and USMP-1 with the Microgravity Measurement Group [NASA-CP-3272-VOL-1] p 634 N95-14207
Review of European microgravity measurements p 457 N95-14211

The solid surface combustion experiment aboard the USML-1 mission p 458 N95-14212
Crystal growth of selected II-VI semiconducting alloys by directional solidification p 458 N95-14214
Bifurcation of rotating liquid drops: Results from USML-1 experiments in space p 458 N95-14219
Surface characterization through shape oscillations of drops in microgravity and 1-g p 458 N95-14220
Protein crystal growth results from the United States Microgravity Laboratory-1 mission p 458 N95-14225
Commercial investigation results for the generic bioprocessing apparatus flown on United States Microgravity Laboratory-1 p 538 N95-14227
Space experiments aboard rockets: SPEAR 3 [AD-A280778] p 414 N95-14290
Flocculation and aggregation in a microgravity environment (FAME) p 459 N95-14572
The path to an experiment in space (from concept to flight) p 417 N95-14582
Fluids flight hardware p 491 N95-14583
Conceptual design of the Space Station fluids module p 429 N95-14584
Pre-flight POLAR code predictions for the CHAWS space flight experiment [AD-A280951] p 428 N95-14599
Olympus propagation experiments p 464 N95-14671
The 40 and 50 GHz propagation experiments at the Rutherford Appleton Laboratory, UK, using the ITALSAT beacons p 465 N95-14674
The avian embryo responding to microgravity of space flight p 538 N95-15104
Behaviour of newly hatched and adult Japanese quail and the feasibility of adaptation to weightlessness p 538 N95-15106
Space flight and humoral and cellular immunity of animals p 538 N95-15113
Postural control of fish related to gravity input p 539 N95-15118
Alterations of body temperature, feeding, drinking and sleep-wake circadian rhythms in Rhesus monkey during a 19 day Spacelab flight simulation p 539 N95-15132
Effect of short- and long-term spaceflight on the contractile properties of rat skeletal muscles with different functions p 539 N95-15141
Centrifuges in gravitational physiology research p 550 N95-15147
STS-66 post flight presentation [NASA-TM-110077] p 419 N95-15900

SPACEBORNE TELESCOPES
Astrophysical science with a spaceborne photometric telescope [NASA-CP-10148] p 643 N95-14499

SPACECRAFT CHARGING
Space experiments aboard rockets: SPEAR 3 [AD-A280778] p 414 N95-14290
Pre-flight POLAR code predictions for the CHAWS space flight experiment [AD-A280951] p 428 N95-14599

SPACECRAFT CONTAMINATION
Optical analysis methods for material films condensed on cryogenic surfaces of spacecraft [AD-A284014] p 427 N95-14420
Environmental durability issues for solar power systems in low Earth orbit [NASA-TM-106775] p 431 N95-15769

SPACECRAFT CONTROL
Three-axis stabilization of spacecraft using parameter-independent nonlinear quaternion feedback [NASA-TM-109150] p 420 N95-13729

SPACECRAFT DESIGN
AXAF SIM focus mechanism study [NASA-CR-196976] p 636 N95-13636
Eighteenth Space Simulation Conference: Space Mission Success Through Testing [NASA-CP-3280] p 420 N95-14062
New potentials of NIICHIMMASH's thermal vacuum facilities p 418 N95-14098
Access to space [NASA-CR-197153] p 428 N95-14521
Bubble dynamics, two-phase flow, and boiling heat transfer in a microgravity environment p 488 N95-14561
Building complex simulations rapidly using MATRIX(x): The Space Station redesign [TABES PAPER 94-632] p 417 N95-14653
Requirements report for SSTO vertical take-off and horizontal landing vehicle [NASA-CR-197029] p 409 N95-14794
An unmanned mission to Mars with sample collection and in-situ resource utilization [NASA-CR-197202] p 645 N95-14868

SPACECRAFT DOCKING
A vision based attitude and position estimation algorithm for rendezvous and docking p 414 N95-13831
TABES 1994: 10th Annual Technical and Business Exhibition and Symposium p 414 N95-14633
Neural networks: Alternatives to conventional techniques for automatic docking [TABES PAPER 94-627] p 417 N95-14651

SPACECRAFT ENVIRONMENTS
Evaluation of reformulated thermal control coatings in a simulated space environment. Part 1: YB-71 p 420 N95-14063

SPACECRAFT EQUIPMENT
Investigation of the effects of long duration space exposure on active optical system components [NASA-CR-4632] p 601 N95-13660

SPACECRAFT INSTRUMENTS
Results of demonstration test for receiving and processing of flight data from the Space Transportation System [NASA-CR-194986] p 418 N95-13890
Ultraviolet-Infrared Mapping Interferometic Spectrometer [NASA-CR-197099] p 613 N95-14806

SPACECRAFT LANDING
Landing gear energy absorption system [NASA-CASE-MSC-22277-1] p 503 N95-15306

SPACECRAFT LAUNCHING
Simulation of Shuttle launch G forces and acoustic loads using the NASA Ames Research Center 20G centrifuge p 419 N95-14089
STS-66 post flight presentation [NASA-TM-110077] p 419 N95-15900

SPACECRAFT MODELS
Analysis of phase distribution phenomena in microgravity environments p 459 N95-14557

SPACECRAFT ORBITS
Heat capacity and thermal relaxation of bulk helium very near the lambda point p 444 N95-14208
The Block V Receiver fast acquisition algorithm for the Galileo S-band mission p 463 N95-14627

SPACECRAFT POWER SUPPLIES
Advanced solar cells for satellite power systems [NASA-TM-106777] p 473 N95-14302
Environmental durability issues for solar power systems in low Earth orbit [NASA-TM-106775] p 431 N95-15769

SPACECRAFT PROPULSION
Fast track NTR systems assessment for NASA's first lunar outpost scenario [NASA-TM-106748] p 429 N95-13668

SPACECRAFT RELIABILITY
Design for reliability: NASA reliability preferred practices for design and test [NASA-TM-106313] p 420 N95-13728
Mechanical system reliability for long life space systems [NASA-CR-197215] p 505 N95-15584

SPACECRAFT STABILITY
Evaluation of energy-sink stability criteria for dual-spin spacecraft [AD-A283228] p 428 N95-14850

SPACECRAFT STRUCTURES
Simulation of a spatial, servo-hydraulic test facility for space structures p 418 N95-14095
Milestone 4: Thrust structure concepts and IHM screening Graphite Composite Primary Structure (GCPS) [NASA-CR-197053] p 434 N95-14800

SPACECRAFT TEMPERATURE
Thermal design verification testing of the Clementine spacecraft: Quick, cheap, and useful p 424 N95-14083

SPACECRAFT TRACKING
SLR tracking of GPS-35 p 471 N95-14285

SPACECRAFT TRAJECTORIES
ICE/ISEE plasma wave data analysis [NASA-CR-196988] p 642 N95-14266

SPACECREWS
Joint Launch + One Year Science Review of USML-1 and USMP-1 with the Microgravity Measurement Group [NASA-CP-3272-VOL-1] p 634 N95-14207
Psychophysiological aspects of increasing resistance to space motion sickness p 542 N95-15093
Circulatory filling pressures during transient microgravity induced by parabolic flight p 542 N95-15095
Immune changes in humans concomitant with space flights of up to 10 days duration p 545 N95-15114

SPACELAB
Joint Launch + One Year Science Review of USML-1 and USMP-1 with the Microgravity Measurement Group [NASA-CP-3272-VOL-1] p 634 N95-14207
Basic features of the STS/Spacelab vibration environment p 428 N95-14210
Extended duration orbiter medical project Microbial Air Sampler (STS-50/USML-1) p 458 N95-14222

SPALLATION
Cratering and penetration experiments in teflon targets at velocities from 1 to 7 km/s [NASA-TM-104797] p 432 N95-13646
Technology and Science at at High-Power Spallation Source: Proceedings [DE94-009685] p 597 N95-15826

SPARE PARTS
Earth Observing System (EOS) Advanced Microwave Sounding Unit-A (AMSU-A) Spares Program Plan [NASA-CR-189380] p 567 N95-13632

SPARK IGNITION
Direct observation of oil consumption mechanisms in a production spark ignition engine using fluorescence techniques [AD-A283842] p 501 N95-14347

SPATIAL DISTRIBUTION
Modelling the low Earth space debris environment p 414 N95-13830
Investigating and implementing enhancements to the simulation of short-term collision hazards p 426 N95-14092
Spatio-temporal neural networks for vision, reasoning and rapid decision making [AD-A283251] p 583 N95-15403
The effects of spatial location of defect states on the switching characteristics of amorphous and polycrystalline silicon thin film transistors: A numerical simulation using AMPS 2-D [DE94-013437] p 476 N95-15410
Optical variability in the equatorial and southeast Pacific [AD-A283894] p 536 N95-15425

SPATIAL FILTERING
A novel technique for 4-dimensional atmosphere and oceanographic irradiance measurements using 3-D spatial filtering [AD-A283758] p 613 N95-14353
Variable window Gabor filters and their use in focus and correspondence [AD-A282837] p 573 N95-14842

SPECIFIC HEAT
High field magnetotransport and specific heat in YbAgCu4 [DE94-014475] p 620 N95-13999
Heat capacity and thermal relaxation of bulk helium very near the lambda point p 444 N95-14208
Behavior of charring materials in simulated fire environments [PB94-196045] p 439 N95-14838

SPECIFICATIONS
Earth Observing System (EOS) Advanced Microwave Sounding Unit-A (AMSU-A): Instrumentation interface control document [NASA-CR-189377] p 567 N95-13651
Architecture for Survivable Systems Processing (ASSP). Technology benefits for Open System Interconnects p 567 N95-14160
POSIX real-time extensions p 570 N95-14165
Computational predictive methods for fracture and fatigue p 509 N95-14466
Upgrade of tropical cyclone surface wind field model [AD-A283530] p 533 N95-15323

SPECIMEN GEOMETRY
The effect of specimen geometry on the accuracy of constitutive relations in a superplastic 5083 aluminum alloy [DE94-014501] p 445 N95-15293
Size and deformation limits to maintain constraint in K(sub Ic) and J(sub c) testing of bend specimens [AD-A284363] p 514 N95-15802

SPECKLE PATTERNS
Compact simultaneous-beam optical strain measurement system, phase 5 [NASA-CR-195396] p 601 N95-13666

SPECTRA
Measured and calculated spectral radiation from a blunt body shock layer in an arc-jet wind tunnel [AIAA PAPER 94-0086] p 405 N95-13720

SPECTRAL BANDS
A bibliography of papers on the diffuse interstellar bands p 634 N95-15846

SPECTRAL CORRELATION
Spectral, noise and correlation properties of intense squeezed light generated by a coupling in two laser fields p 500 N95-13903
Radiative interactions in multi-dimensional chemically reacting flows using Monte Carlo simulations [NASA-CR-197012] p 481 N95-14269

SPECTRAL EMISSION
L(alpha)-induced two-photon absorption of visible light emitted from an O-type star by H2(+) ions located near the surface of the Stromgren sphere surrounding the star: A possible explanation for the diffuse interstellar absorption bands (DIDs) p 641 N95-15845

SPECTRAL LINE WIDTH
A method of measuring the amplitude-modulated vacuum field near a conducting mirror p 471 N95-13921

The Stokes line width and uncertainty relations
p 589 N95-13935
The atom-atom potential in pressure-broadened line width calculations for XY2-AB: New expressions in the II(R), II(L), and I(R) representations
[AD-A282011] p 595 N95-14950

SPECTRAL METHODS
An efficient spectral method for ordinary differential equations with rational function coefficients
[NASA-TM-106762] p 585 N95-14296

SPECTRAL SIGNATURES
Electron-molecule collisions and UV signatures in flowfields
[AD-A281569] p 596 N95-15457

SPECTROGRAMS
Dynamics Explorer 1, retarding ion mass spectrometer summary spectrograms: 82/001 to 82/109 spin-time spectrograms for H(+), He(+), O(+), N(+), O(++), M/Z=2, and molecular ions
[NASA-TM-108468] p 443 N95-15607

SPECTROGRAPHS
Measurements of ultraviolet absorption cross sections of NO2 at various pressures and temperatures
[AD-A283835] p 522 N95-14344

SPECTROMETERS
Performance of spherically focusing Ge(444) backscattering analyzers for inelastic x-ray scattering
[DE94-016349] p 621 N95-14382
Field intercomparison with five automatic ammonia monitors
[PB94-192879] p 523 N95-15389
Time-of-flight detector for heavy ion backscattering spectrometry
[DE94-015600] p 596 N95-15437
Positron studies in catalysis research
[DE94-012793] p 597 N95-15572
Counting condensation in the Antarctic Ozone Mission
[NASA-CR-197113] p 525 N95-15847

SPECTROPHOTOMETRY
Spectrophotometric determination of plutonium-239 based on the spectrum of plutonium 3 chloride
[DE94-015172] p 440 N95-15297

SPECTROSCOPIC ANALYSIS
Studies of the ablated plasma from experimental plasma gun disruption simulations
[DE94-015017] p 617 N95-14262
Infrared absorption spectroscopy and chemical kinetics of free radicals
[DE94-016642] p 438 N95-14392
Real-time monitor and control of MBE growth of HgCdTe by spectroscopic ellipsometry
[AD-A284451] p 627 N95-15818

SPECTROSCOPY
In situ, real-time analysis of the growth of ferroelectric and conductive oxide heterostructures by a new time-of-flight pulsed ion beam surface analysis technique
[DE94-013298] p 620 N95-13822
New techniques for diffusing-wave spectroscopy
p 444 N95-14575
Photoluminescence spectroscopy and Rutherford backscattering channeling evaluation of various capping techniques for rapid thermal annealing of ion-implanted ZnSe
[DE94-016876] p 623 N95-15339
Acoustic resonance spectroscopy intrinsic seals
[DE94-016207] p 591 N95-15359
Surface spectroscopic studies of high-temperature superconductors
[PB94-191228] p 624 N95-15378
Introduction to muSR: What, how, where
[PB94-192267] p 596 N95-15379

SPECTRUM ANALYSIS
Develop advanced nonlinear signal analysis topographical mapping system
[NASA-CR-194414] p 514 N95-13639
Spectral analysis of vortex/free-surface interaction
[AD-A283210] p 492 N95-14658
Laboratory spectra of C60 and related molecular structures p 627 N95-15838

SPEECH
Watch what you say, your computer might be listening: A review of automated speech recognition
p 555 N95-14021

SPEECH RECOGNITION
Watch what you say, your computer might be listening: A review of automated speech recognition
p 555 N95-14021
i-speech: Experiments with a single level feedback paradigm
[TR-509] p 575 N95-15640

SPEED CONTROL
Fuzzy logic motor control for pollution prevention and improved energy efficiency
[PB94-190865] p 523 N95-14403

SPHERICAL COORDINATES
Discrete-layer piezoelectric plate and shell models for active tip-clearance control
[NASA-CR-195383] p 507 N95-14417

SPIN DECOUPLING
Selective RF pulses in NMR and their effect on coupled and uncoupled spin systems
[PB94-195526] p 471 N95-15871

SPIN GLASS
Spin glasses and error-correcting codes
p 462 N95-14624
Theory of nonlinear, distortive phenomena in solids: Martensitic, crack, and multiscale structures-phenomenology and physics
[DE94-015653] p 447 N95-15631

SPIN RESONANCE
Selective RF pulses in NMR and their effect on coupled and uncoupled spin systems
[PB94-195526] p 471 N95-15871

SPIN STABILIZATION
System level mechanical testing of the Clementine spacecraft p 425 N95-14087

SPINAL CORD
The musculoskeletal and vestibular effects of long term repeated exposure to sustained high-G
[AGARD-AR-317] p 562 N95-14263

SPINEL
Defects and transport in mixed oxides
[DE94-015652] p 454 N95-15358
Cation disorder in high dose neutron irradiated spinel
[DE94-013118] p 455 N95-15579

SPINOR GROUPS
Particle localization, spinor two-valuedness, and Fermi quantization of tensor systems p 598 N95-13932

SPIRAL ANTENNAS
Spiral microstrip antenna with resistance
[NASA-CASE-LAR-15088-1] p 460 N95-14139

SPLEEN
Cosmos 2229 immunology study (Experiment K-8-07)
[NASA-CR-196984] p 537 N95-13638

SPONTANEOUS EMISSION
Quantum phase uncertainties in the classical limit
p 607 N95-13933

SPRAY NOZZLES
Investigation of ramp injectors for supersonic mixing enhancement
[NASA-CR-4634] p 494 N95-15605

SPRAYERS
Turbulent mixing of the HVOF thermal spray and coating oxidation
[DE94-015414] p 455 N95-15535

SPREAD SPECTRUM TRANSMISSION
Multipath noise reduction spread spectrum signals
[NASA-CASE-NPO-18970-1-CU] p 460 N95-13628

SPREADING
Wetting and spreading at the molecular scale
p 484 N95-14539
Effect of stratification and geometrical spreading on sonic boom rise time p 401 N95-14880

SQUEEZE FILMS
Accelerometer model in APLAC
[PB94-197647] p 497 N95-15413

SQUEEZED STATES (QUANTUM THEORY)
Third International Workshop on Squeezed States and Uncertainty Relations
[NASA-CP-3270] p 602 N95-13896
Properties of two-mode squeezed number states
p 602 N95-13897
Supersymmetry and radial squeezed states for Rydberg wave packets p 598 N95-13898
Effect of dispersion forces on squeezing with Rydberg atoms p 456 N95-13899
High-order squeezing of the quantum electromagnetic field and the generalized uncertainty relations in two-mode squeezed states p 471 N95-13900
Q-derivatives, coherent states and squeezing
p 589 N95-13901
Sum-frequency generation from photon number squeezed light p 603 N95-13902
Spectral, noise and correlation properties of intense squeezed light generated by a coupling in two laser fields p 500 N95-13903
Multimode squeezing, biphotons and uncertainty relations in polarization quantum optics
p 603 N95-13904
Production of squeezed states for macroscopic mechanical oscillator p 603 N95-13906
Squeezing in a 2-D generalized oscillator
p 603 N95-13907
Simultaneous two component squeezing in generalized q-coherent states p 598 N95-13908
Photon statistics of a two-mode squeezed vacuum
p 598 N95-13909
Homodyning and heterodyning the quantum phase
p 604 N95-13913
Phase properties of multicomponent superposition states in various amplifiers p 605 N95-13923
Modes in light wave propagating in semiconductor laser p 500 N95-13925
Sqeezing generated by a nonlinear master equation and by amplifying-dissipative Hamiltonians
p 588 N95-13926
Phase-space analysis of charged and optical beam transport: Wigner rotation angle p 606 N95-13927
Phase space flow of particles in squeezed states
p 606 N95-13928
Understanding squeezing of quantum states with the Wigner function p 606 N95-13930
Minimum uncertainty and squeezing in diffusion processes and stochastic quantization
p 607 N95-13938
Applications of squeezed states: Bogoliubov transformations and wavelets to the statistical mechanics of water and its bubbles p 607 N95-13939
Some rules for polydimensional squeezing
p 608 N95-13941
Squeezed states and graviton-entropy production in the early universe p 608 N95-13947
Time-dependent variational approach in terms of squeezed coherent states: Implication to semi-classical approximation p 609 N95-13948
New quantum properties of phonons and their detection p 610 N95-13957
Quantum statistics of Raman scattering model with Stokes mode generation p 610 N95-13958

SQUID (DETECTORS)
Low-frequency noise in high-(Tc) superconductor Josephson junctions, SQUIDs, and magnetometers
[DE94-016873] p 623 N95-15337

STABILITY
Study of the long term stability of the effective concentration of ionized space charges (N(sub eff)) of neutron irradiated silicon detectors fabricated by various thermal oxidations
[DE94-013734] p 593 N95-14309
The stable and precise motion control for an autonomous mobile robot
[AD-A283776] p 501 N95-14336
Influence of crack history on the stable tearing behavior of a thin-sheet material with multiple cracks
p 509 N95-14467
Control of oscillatory thermocapillary convection in microgravity p 483 N95-14525
Dynamics and statics of nonaxisymmetric and symmetric liquid bridges p 484 N95-14533
Search for W(prime) (yields) e(nu) in p(anti p) collisions at (radical)s = 1,800 GeV
[DE94-015188] p 597 N95-15630
The effect of the edge current density on confinement and kink mode stability in H-mode and VH-mode discharges
[DE94-015719] p 618 N95-15632
Symposium on Structural Intermetallics: Perspectives on Science and Technology, volume 2
[AD-A283379] p 447 N95-15874
On the evolution of centrifugal instabilities within curved incompressible mixing layers
[NASA-CR-194991] p 495 N95-15917

STABILITY AUGMENTATION
Processing of thermoset prepreg laminate via exposure to microwave radiation
[DE94-013268] p 432 N95-13643

STABILITY TESTS
Two-layer viscous instability in a rotating couette device p 489 N95-14566

STABILIZATION
Stabilization of thermocapillary convection by means of nonplanar flow oscillations p 482 N95-14524
Equilibrium fluid interface behavior under low- and zero-gravity conditions p 484 N95-14534
Shear stabilization of solidification fronts
p 448 N95-14549
The oxidative stabilization and carbonization of mesophase pitch
[AD-A282026] p 453 N95-14954

STABILIZED PLATFORMS
Star sensor for Indian Remote Sensing Satellite (IRS 1C) p 413 N95-13828

STABILIZERS (FLUID DYNAMICS)
X-31 quasi-tailless flight demonstration
p 395 N95-14243
Pressure measurements on an F/A-18 twin vertical tail in buffeting flow. Volume 2: Steady and unsteady RMS pressure data
[AD-A281581] p 404 N95-15465

STAINLESS STEELS
Welding irradiated stainless steel
[DE94-013661] p 500 N95-13645
Type 304L stainless steel surface microstructure: Performance in hydride storage and acid cleaning
[DE94-014654] p 447 N95-15625

STANDARD DEVIATION
Two new kinds of uncertainty relations p 588 N95-13915
STANDARDIZATION
Preparing technical text for translation: A comparison between International English and methods for simplifying language
[DE94-014465] p 630 N95-13996
ASTM E 1559 method for measuring material outgassing/deposition kinetics has applications to aerospace, electronics, and semiconductor industries p 421 N95-14066
Evolutionary Telemetry and Command Processor (TCP) architecture p 420 N95-14162
STANDARDS
RICIS Symposium 1992: Mission and Safety Critical Systems Research and Applications
[NASA-CR-196963] p 569 N95-14156
Architecture for Survivable Systems Processing (ASSP). Technology benefits for Open System Interconnects p 567 N95-14160
Ada 9X overview p 570 N95-14166
CIFO 3.0 p 570 N95-14167
New five-standard calibration procedures for network analyzers and wafer probes
[PB94-197662] p 478 N95-15611
STANDING WAVES
Low-damage multilayer mirror for the soft x ray region
[AD-D016362] p 614 N95-15764
STAR TRACKERS
Journal of Spacecraft Technology, volume 4, no. 2, July 1994 p 413 N95-13825
Star sensor for Indian Remote Sensing Satellite (IRS 1C) p 413 N95-13828
Space simulation techniques and facilities for SAX STM test campaign p 423 N95-14077
STARK EFFECT
The Stark anomalous dispersion optical filter: The theory p 462 N95-14622
STATIC AERODYNAMIC CHARACTERISTICS
Engineering Codes for aeroprediction: State-of-the-art and new methods p 399 N95-14447
STATIC PRESSURE
Flight and full-scale wind-tunnel comparison of pressure distributions from an F-18 aircraft at high angles of attack --- Conducted in NASA Ames Research Center's 80 by 120 ft wind tunnel p 394 N95-14231
STATIC TESTS
Development of a composite repair and the associated inspection intervals for the F-111C stiffener runout region p 392 N95-14477
STATICS
Dynamics and statics of nonaxisymmetric and symmetric liquid bridges p 484 N95-14533
STATIONARY ORBITS
Environmental testing to prevent on-orbit TDRS failures p 423 N95-14078
STATIONKEEPING
Building complex simulations rapidly using MATRIX(x): The Space Station redesign
[TABES PAPER 94-632] p 417 N95-14653
STATISTICAL ANALYSIS
Applications of a fast and efficient method for simulating orbital mission safety p 426 N95-14093
A multiscale random field model for Bayesian image segmentation
[AD-A283875] p 515 N95-14358
Electro-optics: Propagation from IR to UV and sensor considerations. Part A: Propagation theory p 467 N95-14833
Sequentially t-diagnosable systems
[PB94-205093] p 574 N95-15396
Essential elements of an effective data qualification
[DE94-015566] p 632 N95-15419
STATISTICAL CORRELATION
Radiative interactions in multi-dimensional chemically reacting flows using Monte Carlo simulations
[NASA-CR-197012] p 481 N95-14269
The seasonal cycle dependence of temperature fluctuations in the atmosphere
[AD-A283220] p 534 N95-15627
STATISTICAL DISTRIBUTIONS
Fault detection and diagnosis using neural network approaches p 571 N95-14170
STATISTICAL MECHANICS
Two new kinds of uncertainty relations p 588 N95-13915
Applications of squeezed states: Bogoliubov transformations and wavelets to the statistical mechanics of water and its bubbles p 607 N95-13939
STATISTICAL WEATHER FORECASTING
June to September rainfall in the African Sahel: Verification of our 1994 forecasts and an extended range forecast for 1995, 3
[TR-521] p 534 N95-15666
The operational forecasting/nowcasting of precipitation type in the southeastern United States type of precipitation: Descriptive and objective guidance
[AD-A284456] p 535 N95-15819
STATORS
Fish method: Interaction between AC-machines and switching power converters
[PB94-191210] p 472 N95-14149
Effect of surface roughness on local film cooling effectiveness and heat transfer coefficients
[AD-A283854] p 482 N95-14351
STDN (NETWORK)
Evolutionary Telemetry and Command Processor (TCP) architecture p 420 N95-14162
STEADY FLOW
Control of oscillatory thermocapillary convection in microgravity p 483 N95-14525
STEADY STATE
Experimental/analytical approach to understanding mistuning in a transonic wind tunnel compressor
[NASA-TM-108833] p 512 N95-14617
STEAM
The crosswell electromagnetic response of layered media
[DE94-014929] p 470 N95-15866
STEEL STRUCTURES
The 3.5-meter telescope enclosure
[AD-A280949] p 638 N95-14597
STEELS
The effect of microstresses on fatigue crack propagation in steel
[AD-A283872] p 506 N95-14356
Type 304L stainless steel surface microstructure: Performance in hydride storage and acid cleaning
[DE94-014654] p 447 N95-15625
Effects of tensile loading on upper shelf fracture toughness
[AD-A284364] p 514 N95-15803
STEERING
Optically controlled MMW beamsteering beamforming antenna
[AD-A282831] p 614 N95-15414
STELLAR ACTIVITY
Stellar activity: Astrophysics relevant to global change p 643 N95-14500
STELLAR COMPOSITION
The Diffuse Interstellar Bands: Contributed papers
[NASA-CP-10144] p 639 N95-15827
STELLAR CORONAS
ICE/ISEE plasma wave data analysis
[NASA-CR-196988] p 642 N95-14266
STELLAR ENVELOPES
Determination of the atmospheric structure of the BO star companion of SMC X-1 by analysis of Ginga observations
[NASA-CR-197100] p 638 N95-14804
STELLAR EVOLUTION
Early solar mass loss, element diffusion, and solar oscillation frequencies
[DE94-014802] p 646 N95-14376
STELLAR FLARES
Stellar activity: Astrophysics relevant to global change p 643 N95-14500
STELLAR INTERIORS
Asteroseismology with FRESIP: A meter class space telescope p 643 N95-14504
STELLAR MASS
Early solar mass loss, element diffusion, and solar oscillation frequencies
[DE94-014802] p 646 N95-14376
Observations of hot stars and eclipsing binaries with FRESIP p 644 N95-14508
STELLAR MASS EJECTION
ICE/ISEE plasma wave data analysis
[NASA-CR-196988] p 642 N95-14266
STELLAR MODELS
Early solar mass loss, element diffusion, and solar oscillation frequencies
[DE94-014802] p 646 N95-14376
Determination of the atmospheric structure of the BO star companion of SMC X-1 by analysis of Ginga observations
[NASA-CR-197100] p 638 N95-14804
STELLAR OSCILLATIONS
Asteroseismology: Ground based efforts and the need for space observations p 643 N95-14503
Asteroseismology with FRESIP: A meter class space telescope p 643 N95-14504
STELLAR RADIATION
Neutral gas and diffuse interstellar bands in the LMC p 639 N95-15828
STELLAR ROTATION
Hadronic matter and rapidly rotating compact stars
[DE94-014928] p 643 N95-14442
STELLAR SPECTRA
DIBS independent of accretion in T Tauri stars p 639 N95-15829
Diffuse interstellar bands in reflection nebulae p 639 N95-15830
Diffuse bands versus extinction parameters p 640 N95-15836
STELLAR STRUCTURE
Probing surface structure on late-type stars with FRESIP p 643 N95-14501
Determination of the atmospheric structure of the BO star companion of SMC X-1 by analysis of Ginga observations
[NASA-CR-197100] p 638 N95-14804
STELLAR WINDS
Determination of the atmospheric structure of the BO star companion of SMC X-1 by analysis of Ginga observations
[NASA-CR-197100] p 638 N95-14804
Formation of dust grains with impurities in red giant winds p 641 N95-15841
STELLARATORS
Advanced stellarator power plants
[DE94-014442] p 616 N95-14007
STEPPING MOTORS
Deployment mechanism calibration system p 414 N95-13833
STIFFENING
Analytical tripping loads for stiffened plates
[AD-A284368] p 514 N95-15805
STIFFNESS
The human operator transfer function: Identification of the limb mechanics subsystem p 558 N95-14040
Development of a composite repair and the associated inspection intervals for the F-111C stiffener runout region p 392 N95-14477
Effect of matrix stiffness on wavy fiber behavior in single-carbon-fiber-epoxy composites
[AD-A280970] p 435 N95-15427
Characterization of damage progression in SCS-6/Timetal 21S (0)4 under thermomechanical fatigue loadings
[NASA-CR-195399] p 436 N95-15911
STIMULATED EMISSION
Squeezed states and graviton-entropy production in the early universe p 608 N95-13947
STIMULATION
Neurohumoral reactions to long-term vestibular stimulation in man p 542 N95-15091
STOCHASTIC PROCESSES
Chaotic time series. Part 2: System identification and prediction
[PB94-207115] p 589 N95-13630
Minimum uncertainty and squeezing in diffusion processes and stochastic quantization p 607 N95-13938
A Workshop on New Directions in Extremal Stochastic Analysis of Nonlinear Ocean Systems
[AD-A283969] p 535 N95-14204
Nonlinear and stochastic numerical methods and their applications
[AD-A284863] p 588 N95-14370
Stochastic model of the residual acceleration environment in microgravity p 459 N95-14540
Introduction to HEFeS (Hierarchical Environmental Feature Simulator)
[AD-A283244] p 534 N95-15402
Tests of a homogeneous Poisson process against clustering and other alternatives
[DE94-015382] p 588 N95-15533
Lower-hybrid poloidal current drive for fluctuation reduction in a reversed field pinch
[DE94-015534] p 618 N95-15540
STOICHIOMETRY
Copolyimides prepared from ODPA, BTDA and 3,4'-ODA
[NASA-CASE-LAR-15109-1] p 449 N95-14109
Low Temperature Grown and Highly Non-Stoichiometric GaAs and Related Materials
[AD-A284898] p 626 N95-15754
STOKES LAW OF RADIATION
The Stokes line width and uncertainty relations p 589 N95-13935
STORAGE RINGS (PARTICLE ACCELERATORS)
Approximate next-to-leading order relation between the low-x F2 scaling violations and the gluon density
[PB94-192283] p 596 N95-15380
STORAGE TANKS
Leak detection by acoustic emissions monitoring: An experimental investigation of the acoustic properties of leaks and the attenuation characteristics of soil
[AD-A283250] p 530 N95-15295
Leak detection by acoustic emission monitoring. Phase 1: Feasibility study
[AD-A283775] p 493 N95-15332

STORM SURGES
ADCIRC: An advanced three-dimensional circulation model for shelves, coasts, and estuaries. Report 4: Hurricane storm surge modeling using large domains
[AD-A283868] p 535 N95-14352
STORMS
Winter storms research in Canada
p 406 N95-14895
STRAIN DISTRIBUTION
Fatigue analysis of multiple site damage at a row of holes in a wide panel p 508 N95-14463
STRAIN ENERGY METHODS
Nonlinear bulging factor based on R-curve data
p 511 N95-14476
STRAIN ENERGY RELEASE RATE
Bending effects of unsymmetric adhesively bonded composite repairs on cracked aluminum panels
p 507 N95-14456
STRAIN GAGE BALANCES
Static and dynamic force/moment measurements in the Eidetics water tunnel p 395 N95-14238
STRAIN GAGES
Static and dynamic force/moment measurements in the Eidetics water tunnel p 395 N95-14238
Extracting a representative loading spectrum from recorded flight data p 410 N95-14469
Initiation and propagation of small corner cracks
p 510 N95-14471
STRAIN HARDENING
High strain rate deformation of NiAl
[DE94-014810] p 445 N95-14439
STRAIN MEASUREMENT
Compact simultaneous-beam optical strain measurement system, phase 5
[NASA-CR-195396] p 601 N95-13666
Errors induced in triaxial stress tensor calculations using incorrect lattice parameters
[DE94-013256] p 444 N95-13820
Static and dynamic force/moment measurements in the Eidetics water tunnel p 395 N95-14238
STRAIN RATE
High strain rate deformation of NiAl
[DE94-014810] p 445 N95-14439
A method for continuous monitoring of the Ground Reaction Force during daily activity p 549 N95-15139
STRAKES
Preparations for flight research to evaluate actuated forebody strakes on the F-18 high-alpha research vehicle p 398 N95-14257
Integration of a mechanical forebody vortex control system into the F-15 p 398 N95-14258
STRANGE ATTRACTORS
Dynamics on the attractor for the complex Ginzburg-Landau equation
[DE94-016902] p 586 N95-15342
STRAPS
Axial crack propagation and arrest in pressurized fuselage p 511 N95-14479
STRATIFICATION
Effect of stratification and geometrical spreading on sonic boom rise time p 401 N95-14880
STRATOSPHERE
Condensation nuclei measurement in the stratosphere for the NASA ACE program
[NASA-CR-197031] p 530 N95-14855
Counting condensation in the Antarctic Ozone Mission
[NASA-CR-197113] p 525 N95-15847
STREAMLINING
Aero design of turbomachinery components: CFD in complex systems p 481 N95-14136
STRESS (PHYSIOLOGY)
Extended duration orbiter medical project countermeasure to reduce post space flight orthostatic intolerance (LBNP) (STS-50/USML-1)
p 551 N95-14224
The musculoskeletal and vestibular effects of long term repeated exposure to sustained high-G
[AGARD-AR-317] p 562 N95-14263
Measurement and regulation of central noradrenergic receptors
[AD-A284219] p 541 N95-14408
STRESS ANALYSIS
Errors induced in triaxial stress tensor calculations using incorrect lattice parameters
[DE94-013256] p 444 N95-13820
Fatigue evaluation of empennage, forward wing, and winglets/tip fins on part 23 airplanes
[PB94-196813] p 408 N95-13981
Analysis of neutron diffraction peak broadening caused by internal stresses in composite materials
[DE94-014453] p 433 N95-13993
Analysis of welding-induced residual stresses with the ADINA system
[DE94-015359] p 506 N95-14320
Composite waveform generation for EMP and lightning direct-drive testing
[AD-A284159] p 462 N95-14405
A method of calculating the safe fatigue life of compact, highly-stressed components p 509 N95-14464
Development of a composite repair and the associated inspection intervals for the F-111C stiffener runout region p 392 N95-14477
An inelastic analysis of a welded aluminum joint
[NASA-TP-3508] p 513 N95-15055
Basic mechanics of laminated composite plates
[NASA-RP-1351] p 436 N95-15763
STRESS CORROSION
Stress corrosion crack tip microstructure in nickel-based alloys
[DE94-015362] p 446 N95-15532
STRESS CORROSION CRACKING
Modeling time-dependent corrosion fatigue crack propagation in 7000 series aluminum alloys
p 448 N95-14483
Stress corrosion crack tip microstructure in nickel-based alloys
[DE94-015362] p 446 N95-15532
Effect of heat treatment on the microstructure and properties of AerMet (trade name) 100 steel
[AD-A284387] p 447 N95-15807
Computer modeling the fatigue crack growth rate behavior of metals in corrosive environments
[NASA-CR-194982-REV] p 448 N95-15918
STRESS DISTRIBUTION
Development of the NASA/FLAGRO computer program for analysis of airframe structures p 510 N95-14473
STRESS INTENSITY FACTORS
FAA/NASA International Symposium on Advanced Structural Integrity Methods for Airframe Durability and Damage Tolerance
[NASA-CP-3274-PT-1] p 507 N95-14453
Elastic-plastic models for multi-site damage
p 507 N95-14454
Bending effects of unsymmetric adhesively bonded composite repairs on cracked aluminum panels
p 507 N95-14456
Inspecting for widespread fatigue damage: Is partial debonding the key? p 508 N95-14458
Recent advances in the modelling of crack growth under fatigue loading conditions p 511 N95-14478
Fracture mechanics validity limits p 511 N95-14480
Challenges for the aircraft structural integrity program
p 410 N95-14481
The effects of pitting on fatigue crack nucleation in 7075-T6 aluminum alloy p 448 N95-14482
STRESS MEASUREMENT
Radiographic Moire
[NASA-CASE-LAR-15104-1] p 505 N95-13835
STRESS TENSORS
Errors induced in triaxial stress tensor calculations using incorrect lattice parameters
[DE94-013256] p 444 N95-13820
STRESS-STRAIN RELATIONSHIPS
Elastic-plastic models for multi-site damage
p 507 N95-14454
Small crack test program for helicopter materials
p 507 N95-14455
Evaluation of bonded boron/epoxy doublers for commercial aircraft aluminum structures
p 508 N95-14457
Inspecting for widespread fatigue damage: Is partial debonding the key? p 508 N95-14458
Corrosion and corrosion fatigue of airframe aluminum alloys p 448 N95-14465
An inelastic analysis of a welded aluminum joint
[NASA-TP-3508] p 513 N95-15055
The effect of specimen geometry on the accuracy of constitutive relations in a superplastic 5083 aluminum alloy
[DE94-014501] p 445 N95-15293
Computational modeling of fiber-reinforced composites
[DE94-012914] p 436 N95-15573
STRONTIUM OXIDES
Transport resistive broadening by avalanche flux motion in high-temperature superconductors: SOC in a driven system
[DE94-016901] p 623 N95-15341
Phase separation and doped-hole segregation in La(2)CuO(4+delta) and La(2-x)Sr(x)CuO(4+delta)
[DE94-015070] p 624 N95-15430
STRUCTURAL ANALYSIS
Methodology for the parallel direct solution of finite element systems
[PB94-198009] p 585 N95-13991
Thermal structure analyses for CSM testbed (COMET)
[NASA-CR-196998] p 506 N95-14270
FAA/NASA International Symposium on Advanced Structural Integrity Methods for Airframe Durability and Damage Tolerance
[NASA-CP-3274-PT-1] p 507 N95-14453
Elastic-plastic models for multi-site damage
p 507 N95-14454
Small crack test program for helicopter materials
p 507 N95-14455
Bending effects of unsymmetric adhesively bonded composite repairs on cracked aluminum panels
p 507 N95-14456
Evaluation of bonded boron/epoxy doublers for commercial aircraft aluminum structures
p 508 N95-14457
Inspecting for widespread fatigue damage: Is partial debonding the key? p 508 N95-14458
Microstructurally based model of fatigue initiation and growth p 508 N95-14459
Testing and analysis of flat and curved panels with multiple cracks p 508 N95-14460
Probabilistic inspection strategies for minimizing service failures p 508 N95-14461
Nonlinear fracture mechanics-based analysis of thin wall cylinders p 508 N95-14462
Fatigue analysis of multiple site damage at a row of holes in a wide panel p 508 N95-14463
A method of calculating the safe fatigue life of compact, highly-stressed components p 509 N95-14464
Corrosion and corrosion fatigue of airframe aluminum alloys p 448 N95-14465
Computational predictive methods for fracture and fatigue p 509 N95-14466
Influence of crack history on the stable tearing behavior of a thin-sheet material with multiple cracks
p 509 N95-14467
Study of multiple cracks in airplane fuselage by micromechanics and complex variables
p 509 N95-14468
Extracting a representative loading spectrum from recorded flight data p 410 N95-14469
Initiation and propagation of small corner cracks
p 510 N95-14471
Statistical investigation of fatigue crack initiation and growth around chamfered rivet holes in Alclad 2024 T3 as affected by corrosion p 510 N95-14472
Development of the NASA/FLAGRO computer program for analysis of airframe structures p 510 N95-14473
Space Shuttle fatigue loads spectra for prelaunch and liftoff loads p 419 N95-14474
Fatigue reliability method with in-service inspections
p 505 N95-14475
Nonlinear bulging factor based on R-curve data
p 511 N95-14476
Development of a composite repair and the associated inspection intervals for the F-111C stiffener runout region p 392 N95-14477
Recent advances in the modelling of crack growth under fatigue loading conditions p 511 N95-14478
Axial crack propagation and arrest in pressurized fuselage p 511 N95-14479
Fracture mechanics validity limits p 511 N95-14480
Challenges for the aircraft structural integrity program
p 410 N95-14481
The effects of pitting on fatigue crack nucleation in 7075-T6 aluminum alloy p 448 N95-14482
Modeling time-dependent corrosion fatigue crack propagation in 7000 series aluminum alloys
p 448 N95-14483
Analysis of small crack behavior for airframe applications p 512 N95-14484
Full-scale testing and analysis of fuselage structure
p 512 N95-14485
Advanced method and processing technology for complicated shape airframe part forming
p 410 N95-14486
Static strength of riveted joints in Fibre Metal Laminates
[PB94-201472] p 513 N95-15429
Surface passivation for 3-5 semiconductor processing: Stable gallium sulphide films by MOCVD
[NASA-TM-106761] p 477 N95-15587
Analytical tripping loads for stiffened plates
[AD-A284368] p 514 N95-15805
STRUCTURAL DESIGN
Eighteenth Space Simulation Conference: Space Mission Success Through Testing
[NASA-CP-3280] p 420 N95-14062
Hubble Space Telescope servicing mission scientific instrument protective enclosure design requirements and contamination controls p 421 N95-14068
Martian environmental simulation for a deployable lattice mast p 423 N95-14076
Environmental testing to prevent on-orbit TDRS failures p 423 N95-14078
System level mechanical testing of the Clementine spacecraft p 425 N95-14087
Integrated optical maze
[DE94-015866] p 613 N95-14367

FAA/NASA International Symposium on Advanced Structural Integrity Methods for Airframe Durability and Damage Tolerance
[NASA-CP-3274-PT-1] p 507 N95-14453
Access to space
[NASA-CR-197153] p 428 N95-14521
The 3.5-meter telescope enclosure
[AD-A280949] p 638 N95-14597
Requirements report for SSTO vertical take-off and horizontal landing vehicle
[NASA-CR-197029] p 409 N95-14794
Design review and analysis for a Pratt and Whitney fluid-film bearing and seal testing rig
[NASA-CR-197035] p 502 N95-14797
Milestone 4: Thrust structure concepts and IHM screening Graphite Composite Primary Structure (GCPS)
[NASA-CR-197053] p 434 N95-14800
An unmanned mission to Mars with sample collection and in-situ resource utilization
[NASA-CR-197202] p 645 N95-14868

STRUCTURAL DESIGN CRITERIA
Higher harmonic control analysis for vibration reduction of helicopter rotor systems
[NASA-TM-103855] p 391 N95-14419

STRUCTURAL FAILURE
Damage tolerant repair techniques for pressurized aircraft fuselages
[AD-A281982] p 391 N95-14144
FAA/NASA International Symposium on Advanced Structural Integrity Methods for Airframe Durability and Damage Tolerance
[NASA-CP-3274-PT-1] p 507 N95-14453
Challenges for the aircraft structural integrity program
p 410 N95-14481

STRUCTURAL STABILITY
Module process optimization and device efficiency improvement for stable, low-cost, large-area, cadmium telluride-based photovoltaic module production
[DE94-011817] p 521 N95-15863

STRUCTURAL STRAIN
Loading-strain equivalence between thermomechanical, creep, and tensile tests: High density polyethylene
[AD-A283265] p 513 N95-15621

STRUCTURAL VIBRATION
Large amplitude nonlinear response of flat aluminum, and carbon fiber plastic beams and plates
[AD-A282440] p 513 N95-15547

STUDENTS
Space based astronomy: Teacher's guide with activities
[NASA-EG-102] p 638 N95-14511
NASA/DOD Aerospace Knowledge Diffusion Research Project. Paper 44: Becoming an aerospace engineer: Some thoughts on the career goals and educational preparation of AIAA student members
[NASA-TM-109960] p 632 N95-14870

STYRENES
NMR studies of polymers at interfaces
[AD-A281570] p 455 N95-15458

SUBGIANT STARS
Asteroseismology: Ground based efforts and the need for space observations p 643 N95-14503

SUBMERGING
Surface epoxidation of elastomers
[AD-D016352] p 456 N95-15800

SUBMILLIMETER WAVES
Quantum noise limits to matter-wave interferometry
p 598 N95-13955
Infrared/submillimeter wave studies of molecular collision kinetics
[AD-A281379] p 594 N95-14362

SUBROUTINE LIBRARIES (COMPUTERS)
Distributed heterogeneous visualization, BOP (Bag-O-Polygons) and BOP view
[AD-A284393] p 567 N95-15809

SUBSIDIARIES
Design in Huntsville, manufacture in Estonia, sell in Europe
[TABES PAPER 94-607] p 415 N95-14640

SUBSONIC FLOW
Axis switching and spreading of an asymmetric jet: Role of vorticity dynamics
[NASA-TM-106385] p 398 N95-14418

SUBSONIC SPEED
Ultra-high bypass ratio jet noise
[NASA-CR-195394] p 591 N95-14610

SUBSONIC WIND TUNNELS
Modification of the Ames 40- by 80-foot wind tunnel for component acoustic testing for the second generation supersonic transport
[NASA-TM-108850] p 391 N95-13642

SUBSTITUTES
Thermophysical properties of HCFC alternatives
[DE94-016646] p 438 N95-14372

SUBSTRATES
Electrodeposition of conductors and semiconductors with controlled stoichiometries and morphologies
[AD-A280743] p 437 N95-14141
Development of large-area monolithically integrated Silicon-Film(tm) photovoltaic modules
[DE94-011830] p 520 N95-15405
Turbulent mixing of the HVOF thermal spray and coating oxidation
[DE94-015414] p 455 N95-15535
Low loss substrates for microwave applications and sol-gel processing of superconductors
[AD-A284868] p 625 N95-15746

SUBURBAN AREAS
Photogrammetric mobile satellite service prediction
p 466 N95-14679

SUCTION
Experiments to verify nonparallel stability theory at Virginia Polytechnic Institute and State University, Blacksburg, Virginia
[NASA-CR-196993] p 479 N95-13664

SULFATES
Development and testing of a high-resolution model for tropospheric sulfate driven by observation-derived meteorology
[DE94-014910] p 525 N95-15864

SULFIDES
Corrosion-resistant coatings for high-temperature high-sulfur-activity applications
[DE94-015155] p 453 N95-14957
Surface passivation for 3-5 semiconductor processing: Stable gallium sulphide films by MOCVD
[NASA-TM-106761] p 477 N95-15587

SULFUR
SAM1 semiempirical parameters
[AD-A284400] p 443 N95-15782
Development and testing of a high-resolution model for tropospheric sulfate driven by observation-derived meteorology
[DE94-014910] p 525 N95-15864

SULFUR DIOXIDES
Development and testing of a high-resolution model for tropospheric sulfate driven by observation-derived meteorology
[DE94-014910] p 525 N95-15864

SULFUR OXIDES
High temperature membranes for H2S and SO2 separations
[DE94-017125] p 441 N95-15345

SUN
Asteroseismology: Theory and phenomenology
p 643 N95-14502
Rotation among solar-type stars p 644 N95-14506

SUNSPOTS
Probing surface structure on late-type stars with FRESIP p 643 N95-14501

SUPERCOMPUTERS
Hardware implementation of a desktop supercomputer for high performance image processing. Color image processing using cellular neural networks
[AD-A283071] p 571 N95-14178
High performance computational chemistry: Towards fully distributed parallel algorithms
[DE94-014561] p 573 N95-15311
SUNMOS for the Intel Paragon, a brief user's guide
[DE94-015277] p 574 N95-15543

SUPERCONDUCTING FILMS
High performance YBCO films
[AD-A283870] p 451 N95-14354
Sandia 1993 Superconducting Technology Program
[DE94-015601] p 625 N95-15438
Low loss substrates for microwave applications and sol-gel processing of superconductors
[AD-A284868] p 625 N95-15746

SUPERCONDUCTING MAGNETS
Progress in development of tapes and magnets made from Bi-2223 superconductors
[DE94-015067] p 475 N95-14606
Accelerator and Fusion Research Division: 1993 Summary of activities
[DE94-015157] p 599 N95-15367

SUPERCONDUCTIVITY
Surface spectroscopic studies of high-temperature superconductors
[PB94-191228] p 624 N95-15378
Sandia 1993 Superconducting Technology Program
[DE94-015601] p 625 N95-15438

SUPERCONDUCTORS (MATERIALS)
Mechanical properties of high-temperature superconducting wires
[DE94-015089] p 621 N95-14192
Phase separation and doped-hole segregation in La(2)CuO(4+delta) and La(2-x)Sr(x)CuO(4+delta)
[DE94-015070] p 624 N95-15430

SUPERCRITICAL FLOW
Polymer-polymer interactions
[AD-A282944] p 453 N95-14844

SUPERCRITICAL FLUIDS
Determination of solvation kinetics in supercritical fluids
[DE94-016491] p 438 N95-14386
Fluid dynamic effects on precision cleaning with supercritical fluids
[DE94-015001] p 439 N95-14663
Polymer-polymer interactions
[AD-A282944] p 453 N95-14844

SUPERFLUIDITY
Numerical studies of the surface tension effect of cryogenic liquid helium
[NASA-CR-197014] p 479 N95-14104
Helium 2 slosh in low gravity p 487 N95-14554
Phase transitions and connectivity in three-dimensional vortex equilibria
[DE94-014967] p 494 N95-15868

SUPERHIGH FREQUENCIES
ACTS mobile propagation campaign
p 465 N95-14677
S-Band propagation measurements
p 466 N95-14682
Effects of hydrometeors and atmospheric gases at SHF/EHF p 468 N95-14835
Troposcatter at the KU band
[AD-A281575] p 469 N95-15462

SUPERLATTICES
Microstructures of InAs(1-x)Sb(x) (x = 0.07-0.14) alloys and strained-layer superlattices
[DE94-015801] p 621 N95-14323
Strained-layer InGaAs(P)/InP quantum well semiconductor lasers grown by organometallic vapour phase epitaxy
[PB94-201399] p 622 N95-14795

SUPERNOVAE
The formation of small grains in shocks in the ISM
p 641 N95-15842

SUPERPOSITION (MATHEMATICS)
Phase properties of multicomponent superposition states in various amplifiers p 605 N95-13923
Maximum predictive power and the superposition principle p 607 N95-13936

SUPERSONIC BOUNDARY LAYERS
Embedded function methods for compressible high speed turbulent flow
[NASA-CR-196936] p 492 N95-14932

SUPERSONIC COMBUSTION
Laser spectroscopy of combustion intermediates in a supersonic jet expansion
[AD-A283201] p 500 N95-15395

SUPERSONIC COMBUSTION RAMJET ENGINES
Air-breathing aerospace plane development essential: Hypersonic propulsion flight tests
[NASA-TM-108857] p 392 N95-14921
Investigation of ramp injectors for supersonic mixing enhancement
[NASA-CR-4634] p 494 N95-15605
Wind-tunnel blockage and actuation systems test of a two-dimensional scramjet inlet unstart model at Mach 6
[NASA-TM-109152] p 495 N95-15898
Two-dimensional scramjet inlet unstart model: Wind-tunnel blockage and actuation systems test
[NASA-TM-109984] p 495 N95-15899

SUPERSONIC FLIGHT
The effect of aircraft speed on the penetration of sonic boom noise into a flat ocean p 402 N95-14887

SUPERSONIC FLOW
Embedded function methods for compressible high speed turbulent flow
[NASA-CR-196936] p 492 N95-14932
Investigation of ramp injectors for supersonic mixing enhancement
[NASA-CR-4634] p 494 N95-15605

SUPERSONIC INLETS
Computation of supersonic air-intakes
p 400 N95-14452

SUPERSONIC JET FLOW
Noise radiation by instability waves in coaxial jets
[NASA-TM-106738] p 591 N95-14618
The aeroacoustics of supersonic coaxial jets
[NASA-TM-106782] p 591 N95-15059
Laser spectroscopy of combustion intermediates in a supersonic jet expansion
[AD-A283201] p 500 N95-15395
Resonant interaction of a linear array of supersonic rectangular jets: An experimental study
[NASA-CR-195398] p 404 N95-15852

SUPERSONIC NOZZLES
Resonant interaction of a linear array of supersonic rectangular jets: An experimental study
[NASA-CR-195398] p 404 N95-15852

SUPERSONIC TRANSPORTS
Modification of the Ames 40- by 80-foot wind tunnel for component acoustic testing for the second generation supersonic transport
[NASA-TM-108850] p 391 N95-13642
Aerodynamic shape optimization of a HSCT type configuration with improved surface definition
[NASA-CR-197011] p 392 N95-13701
SUPERSYMMETRY
Supersymmetry and radial squeezed states for Rydberg wave packets p 598 N95-13898
Berry phase in Heisenberg representation p 609 N95-13952
SUPINE POSITION
Hemodynamic responses to passive body tilts p 542 N95-15096
Effects of 20 days bed-rest on cardio-respiratory functions during sub-maximal exercise in young women p 545 N95-15111
Operational requirements for avoidance and eventual elimination of Gz-induced Loss Of Consciousness (G-LOC) in flight p 547 N95-15127
Transient blood/plasma density and hematocrit effects after passive (sitting) thermoneutral water immersion in men p 548 N95-15131
Water intake and urinary volume during 20 days bed-rest in young women p 548 N95-15134
20 days bed-rest on insulin action in relation to body fat in young subjects p 549 N95-15145
SUPPORT SYSTEMS
Development of the fuel cell power generation technology, 2
[DE94-780614] p 520 N95-15376
SURFACE ACOUSTIC WAVE DEVICES
Surface acoustic wave oxygen pressure sensor
[NASA-CASE-LAR-15266-1-CU] p 496 N95-13837
Surface Acoustic Wave (SAW) microsensors to monitor multi-component vapor challenges to adsorbents and adsorbent-based air filtration systems
[AD-A284222] p 497 N95-15334
SURFACE CRACKS
Welding irradiated stainless steel
[DE94-013661] p 500 N95-13645
Orientation effects on the measurement and analysis of critical CTOA in an aluminum alloy sheet
[NASA-TM-109153] p 444 N95-13690
Small crack test program for helicopter materials p 507 N95-14455
Nonlinear fracture mechanics-based analysis of thin wall cylinders p 508 N95-14462
Observation of microcrack development in concrete by use of TV-holography and deformation phase gradient calculation
[PB94-207990] p 513 N95-15348
Three-dimensional effects of crack closure in laminated composite plates subjected to bending loads
[AD-A283342] p 436 N95-15873
SURFACE EMITTING LASERS
In situ grown quantum-wire lasers
[AD-A281381] p 499 N95-14364
SURFACE FINISHING
Specifying the surface finish of x ray mirrors
[DE94-013537] p 601 N95-13644
Investigations into mirror fabrication metrology analysis
[NASA-CR-196522] p 602 N95-13841
Poly(arylene ether imidazole) surfacing films for flat and parabolic structures
[NASA-CASE-LAR-14812-1] p 450 N95-14140
SURFACE LAYERS
Determination of the similarity theory scaling parameters from the vertical gradients
[AD-A283833] p 533 N95-14340
Diffusion of adatoms on face-centered cubic transition metal surfaces
[DE94-014230] p 445 N95-15307
SURFACE NAVIGATION
Guidance and control for unmanned ground vehicles p 504 N95-14948
SURFACE PROPERTIES
Experimental and theoretical studies of rewetting of unheated/heated grooved plates p 487 N95-14558
Surface processes in CVD diamond growth
[AD-A280964] p 622 N95-14655
Time-of-flight detector for heavy ion backscattering spectrometry
[DE94-015600] p 596 N95-15437
Technology and Science at at High-Power Spallation Source: Proceedings
[DE94-009685] p 597 N95-15826
SURFACE REACTIONS
Hydrogen transport and trapping in graphite
[UTIAS-347] p 437 N95-13652
Studies of the ablated plasma from experimental plasma gun disruption simulations
[DE94-015017] p 617 N95-14262
Optically driven surface reactions: Laser probes of surface dynamics
[DE94-015311] p 441 N95-15370
Chemically modified electrodes by nucleophilic substitution of chlorosilylated platinum oxide surfaces
[AD-A281567] p 477 N95-15456
Surface epoxidation of elastomers
[AD-D016352] p 456 N95-15800
Fundamental studies of diamond growth and surface reactions
[AD-A284390] p 626 N95-15808
SURFACE ROUGHNESS
Uniform hydrogen fuel layers for inertial fusion targets by microgravity p 459 N95-14547
SURFACE ROUGHNESS EFFECTS
The mean acoustic field in layered media with rough interfaces
[AD-A281960] p 590 N95-13683
Effect of surface roughness on local film cooling effectiveness and heat transfer coefficients
[AD-A283854] p 482 N95-14351
SURFACE TEMPERATURE
Behavior of charring materials in simulated fire environments
[PB94-196045] p 439 N95-14838
SURFACE TREATMENT
Chemically modified electrodes by nucleophilic substitution of chlorosilylated platinum oxide surfaces
[AD-A281567] p 477 N95-15456
SURFACE VEHICLES
Base passive porosity for drag reduction
[NASA-CASE-LAR-15246-1] p 501 N95-14183
SURFACTANTS
Measurement of resistance to solute transport across surfactant-laden interfaces using a Fluorescence Recovery After Photobleaching (FRAP) technique p 490 N95-14574
Surfactant-based critical phenomena in microgravity p 459 N95-14579
SURGEONS
Man-machine interfaces in health care p 556 N95-14029
SURVEILLANCE
The AEDC aerospace chamber 7V: An advanced test capability for infrared surveillance and seeker sensors p 418 N95-14097
SURVEILLANCE RADAR
Test and Evaluation Master Plan (TEMP) for Fixed Ground Antenna Radomes (FGAR)
[AD-A283839] p 461 N95-14346
CTAS data analysis program
[NASA-TM-108842] p 406 N95-14611
SURVEYS
Global reference frame: Intercomparison of results (SLR, VLBI and GPS) p 527 N95-14276
John F. Kennedy Space Center, Safety, Reliability, Maintainability and Quality Assurance, Survey and Audit Program
[NASA-TM-109208] p 630 N95-14918
Software Technology for Adaptable, Reliable Systems (STARS)
[AD-A284373] p 576 N95-15806
SURVIVAL
Will man need the vestibular system in generations to come? p 542 N95-15092
SWEPT FORWARD WINGS
The Aluminum Falcon: A low cost modern commercial transport
[NASA-CR-197180] p 409 N95-15742
SWIMMING
Postural control of fish related to gravity input p 539 N95-15118
SWITCHES
High gain GaAs switches for impulse sources: Measurement of the speed of current filaments
[DE94-015281] p 477 N95-15544
SWITCHING
The effects of spatial location of defect states on the switching characteristics of amorphous and polycrystalline silicon thin film transistors: A numerical simulation using AMPS 2-D
[DE94-013437] p 476 N95-15410
High gain GaAs switches for impulse sources: Measurement of the speed of current filaments
[DE94-015281] p 477 N95-15544
SWITCHING CIRCUITS
Fish method: Interaction between AC-machines and switching power converters
[PB94-191210] p 472 N95-14149
Integrated optical maze
[DE94-015866] p 613 N95-14367
Strategic avionics technology definition studies, power voter redundancy management. Power voter applications in new vehicle architectures
[NASA-CR-197049] p 411 N95-14799
SYMBIOSIS
The symbiosis of photometry and radial-velocity measurements p 643 N95-14505
SYMBOLS
Comparison of transform coding methods with an optimal predictor for the data compression of digital elevation models p 564 N95-14587
SYMMETRY
Schroedinger operators with the q-ladder symmetry algebras p 588 N95-13942
Uniform hydrogen fuel layers for inertial fusion targets by microgravity p 459 N95-14547
SYNCHRONOUS MOTORS
Damage analysis of internal faults in flux concentrating permanent magnet motors
[AD-A283883] p 474 N95-14359
SYNCHRONOUS SATELLITES
A simulation algorithm for availability computation of a communication satellite constellation p 414 N95-13832
GSOSTATS database: USAF synchronous satellite catalog data conversion software. User's guide and software maintenance manual, version 2.1
[NASA-TM-106760] p 568 N95-13894
SYNCHROTRON RADIATION
Accelerator and Fusion Research Division: 1993 Summary of activities
[DE94-015157] p 599 N95-15367
Investigation of the coherent synchrotron radiation spectrum as a probe of charge dynamics
[DE94-015340] p 599 N95-15371
SYNCHROTRONS
Performance Report: A timeline for the synchrotron calibration of AXAF
[NASA-CR-196489] p 638 N95-14101
SYNOPTIC METEOROLOGY
Overview of PAMS meteorological monitoring requirements
[PB94-176658] p 534 N95-15383
SYNTHESIS
Ion beam synthesis of SiGe alloy layers
[DE94-014958] p 620 N95-14189
SYNTHESIS (CHEMISTRY)
Poly(arylene ether)s containing pendent ethynyl groups
[NASA-CASE-LAR-15041-1] p 449 N95-13838
Synthesis, processing and properties of materials for SOFCs
[DE94-014491] p 517 N95-14002
AASERT 92: Synthesis and properties of complex polyarylene vinylenes
[AD-A284215] p 452 N95-14406
Diamines and polyimides containing pendent ethynyl groups
[NASA-CASE-LAR-14825-1] p 452 N95-14416
Study on titanium-silicalite-1 and related systems
[PB94-195500] p 445 N95-14845
The synthesis of monomers with pendent ethynyl groups for modified high performance thermoplastics
[NASA-CR-196935] p 453 N95-14931
Graphite fluoride from iodine intercalated graphitized carbon
[NASA-CASE-LEW-15360-1] p 441 N95-15303
Synthesis and applications of large heterometallic cluster systems
[AD-A284874] p 626 N95-15748
SYNTHETIC APERTURE RADAR
Interferometric synthetic aperture radar terrain elevation mapping from multiple observations
[DE94-014185] p 515 N95-14313
Synthetic aperture radar signal data compression using block adaptive quantization p 565 N95-14590
Subsurface object position and image correction for standoff ground penetrating radar
[DE94-015180] p 468 N95-15300
Experimental evaluation of cursors for B-2 Synthetic Aperture Radar (SAR) application
[AD-A283025] p 468 N95-15393
SYNTHETIC FUELS
Dense ceramic membranes for partial oxygenation of methane
[DE94-015021] p 453 N95-14609
Investigation of syngas interaction in alcohol synthesis catalysts
[DE94-013939] p 442 N95-15386
SYSTEM EFFECTIVENESS
Bibliography of Joint Aircraft Survivability reports and related documents
[AD-A282795] p 409 N95-14840
SYSTEM FAILURES
The principles of flight test assessment of flight-safety-critical systems in helicopters
[AGARD-AG-300-VOL-12] p 405 N95-14199

SYSTEM IDENTIFICATION
Chaotic time series. Part 2: System identification and prediction
[PB94-207115] p 589 N95-13630
SYSTEMS ANALYSIS
Analysis of the human operator subsystems p 555 N95-14019
System level mechanical testing of the Clementine spacecraft p 425 N95-14087
Software development for safety-critical medical applications p 571 N95-14171
Review of European microgravity measurements p 457 N95-14211
Performance comparison AN/FRD-10 versus PUSHER
[AD-A283263] p 469 N95-15619
SYSTEMS ENGINEERING
Design for reliability: NASA reliability preferred practices for design and test
[NASA-TM-106313] p 420 N95-13728
Refurbishment of a 39 foot thermal vacuum chamber p 418 N95-14085
Alpha LAMP Integration Facility p 418 N95-14094
European Workshop Industrial Computer Science Systems approach to design for safety p 569 N95-14157
Challenge of Future EW System Design
[AGARD-CP-546] p 461 N95-14200
Department of Defense technical architecture framework for information management. Volume 3: Architecture concepts and design guidance, version 2.0
[AD-A283765] p 631 N95-14330
ADST ARWA visual system module software design document
[AD-A283874] p 572 N95-14357
Aeromechanical design of modern missiles p 399 N95-14446
The Network Operations Control Center upgrade task: Lessons learned p 419 N95-14631
Efficient mission control for the 48-satellite Globalstar constellation
[TABES PAPER 94-609] p 415 N95-14641
Automated test environment for a real-time control system
[TABES PAPER 94-631] p 417 N95-14652
Propagation Modelling and Decision Aids for Communications, Radar and Navigation Systems
[AGARD-LS-196] p 466 N95-14825
Electro-optics: Propagation from IR to UV and sensor considerations. Part A: Propagation theory p 467 N95-14833
SYSTEMS INTEGRATION
Aero-optics system integration
[TABES PAPER 94-604] p 415 N95-14638
Defining a controller architecture for the long-reach manipulator
[DE94-015165] p 583 N95-15369
SYSTEMS MANAGEMENT
Preliminary analysis of Army aircrew requirements for Joint Surveillance Target Attack Radar System (JSTARS): Human performance requirements and job demands
[AD-A284917] p 563 N95-15759
SYSTEMS SIMULATION
Advanced distributed simulation technology: Digital Voice Gateway Reference Guide
[AD-A283154] p 460 N95-13696
Eighteenth Space Simulation Conference: Space Mission Success Through Testing
[NASA-CP-3280] p 420 N95-14062
Simulations of the high average power SELENE free electron laser prototype
[AD-A280780] p 498 N95-14291
SYSTOLIC ARRAYS
2D regular arrays for a special class of non uniform recurrence equations
[PB94-195633] p 584 N95-13980

T

T TAURI STARS
DIBS independent of accretion in T Tauri stars p 639 N95-15829
T-38 AIRCRAFT
More supportable T-38A enhancement study
[AD-A283671] p 392 N95-15331
TABLES (DATA)
Satellite situation report, volume 33, number 2
[NASA-TM-109965] p 428 N95-14510
Performance of customized DCT quantization tables on scientific data p 564 N95-14586
Twelve-year planetary ephemeris: 1995-2006
[NASA-RP-1349] p 638 N95-14867
TABS (CONTROL SURFACES)
Axis switching and spreading of an asymmetric jet: Role of vorticity dynamics
[NASA-TM-106385] p 398 N95-14418
TACTICS
Challenge of Future EW System Design
[AGARD-CP-546] p 461 N95-14200
TACTILE DISCRIMINATION
Tactile discrimination and representations of texture, shape, and softness p 558 N95-14041
Manuel discrimination of force p 561 N95-14057
TACTILE SENSORS (ROBOTICS)
Tactile discrimination and representations of texture, shape, and softness p 558 N95-14041
TAIL ASSEMBLIES
Fatigue evaluation of empennage, forward wing, and winglets/tip fins on part 23 airplanes
[PB94-196813] p 408 N95-13981
Pressure measurements on an F/A-18 twin vertical tail in buffeting flow. Volume 2: Steady and unsteady RMS pressure data
[AD-A281581] p 404 N95-15465
TAIL SURFACES
Pressure measurements on an F/A-18 twin vertical tail in buffeting flow. Volume 2: Steady and unsteady RMS pressure data
[AD-A281581] p 404 N95-15465
TAILLESS AIRCRAFT
X-31 quasi-tailless flight demonstration p 395 N95-14243
TAKEOFF
Airplane takeoff and landing performance monitoring system
[NASA-CASE-LAR-14745-2-SB] p 412 N95-14415
TANTALUM
Ion implantation of He-3 in tantalum for use in a low energy deuteron polarization analyzer
[AD-A283172] p 619 N95-13898
TAPE RECORDERS
Tactile display device using an electrorheological fluid
[NASA-CASE-LAR-14860-1] p 472 N95-14112
TAPES
Progress in development of tapes and magnets made from Bi-2223 superconductors
[DE94-015067] p 475 N95-14606
TARGET ACQUISITION
Developing Guided Search 3.0. The next generation of a model visual search
[AD-A283956] p 552 N95-14369
Gaze selection for visual search
[TR-512] p 587 N95-15775
Target acquisition: Human observer performance studies and TARGAC model validation
[AD-A284436] p 553 N95-15816
TARGET RECOGNITION
The AEDC aerospace chamber 7V: An advanced test capability for infrared surveillance and seeker sensors p 418 N95-14097
Neural networks: Alternatives to conventional techniques for automatic docking
[TABES PAPER 94-627] p 417 N95-14651
Automatic TLI recognition system, part 1
[DE94-015253] p 578 N95-15434
Automatic TLI recognition system, part 2
[DE94-015393] p 579 N95-15534
TARGET THICKNESS
Ion implantation of He-3 in tantalum for use in a low energy deuteron polarization analyzer
[AD-A283172] p 619 N95-13898
TARGETS
Observations of hot stars and eclipsing binaries with FRESIP p 644 N95-14508
Uniform hydrogen fuel layers for inertial fusion targets by microgravity p 459 N95-14547
Lower-hybrid poloidal current drive for fluctuation reduction in a reversed field pinch
[DE94-015534] p 618 N95-15540
Solid target boronization of the MST reversed-field pinch during pulsed discharge cleaning
[DE94-015535] p 442 N95-15541
TDR SATELLITES
Environmental testing to prevent on-orbit TDRS failures p 423 N95-14078
TECHNICAL WRITING
NASA/DOD Aerospace Knowledge Diffusion Research Project. Paper 43: The role of information resource training in aerospace education. Expanded version
[NASA-TM-109981] p 632 N95-14619
TECHNOLOGY ASSESSMENT
Addendum: Tenth International Symposium on Alcohol Fuels, The Road to Commercialization
[DE93-018219] p 457 N95-14003
Challenge of Future EW System Design
[AGARD-CP-546] p 461 N95-14200
An evaluation of B-ISDN for the communication architecture requirements of Distributed Interactive Simulation (DIS)
[AD-A280783] p 578 N95-14292
Robotics technology developments in the United States space telerobotics program p 581 N95-14943
TECHNOLOGY TRANSFER
Formal methods technology transfer: Some lessons learned p 571 N95-14172
Hypertext knowledge presentation system to transition basic research
[AD-A280796] p 630 N95-14321
Technology access from the FS-X radar program. Lessons for technology transfer and US acquisition policy
[AD-A283773] p 461 N95-14334
Helping small companies commercialize public-sector technology
[TABES PAPER 94-407] p 415 N95-14635
Intelligent manufacturing systems state of the art
[TABES PAPER 94-503] p 415 N95-14637
Research and technology highlights, 1993
[NASA-TM-4575] p 647 N95-15065
TECHNOLOGY UTILIZATION
Journal of Spacecraft Technology, volume 4, no. 2, July 1994 p 413 N95-13825
Satellite communication technology and applications, 1995-2010 p 413 N95-13826
A decade of telerobotics in rehabilitation: Demonstrated utility blocked by the high cost of manipulation and the complexity of the user interface p 558 N95-14044
Atomic Oxygen (ATOX) simulation of Teflon FEP and Kapton H surfaces using a high intensity, low energy, mass selected, ion beam facility p 422 N95-14073
The advanced development of x-ray computed tomography applications
[AD-A284211] p 434 N95-14411
TABES 1994: 10th Annual Technical and Business Exhibition and Symposium p 414 N95-14633
Space science in the 1990's and beyond
[TABES PAPER 94-204] p 415 N95-14634
Reengineering through information technology. Accompanying report of the National Performance Review
[PB94-170362] p 633 N95-15781
TECTONICS
Measurement and interpretation of crustal deformation rates associated with postglacial rebound
[NASA-CR-196440] p 525 N95-13627
Global and regional kinematics with VLBI p 527 N95-14280
Satellite Laser Ranging operations p 500 N95-14287
TEFLON (TRADEMARK)
Cratering and penetration experiments in teflon targets at velocities from 1 to 7 km/s
[NASA-TM-104797] p 432 N95-13646
TELECOMMUNICATION
Use of 64 kbits/s digital channel for image transmission: Using low scan two-way video
[PB94-189099] p 461 N95-14147
The Telecommunications and Data Acquisition Report
[NASA-CR-196409] p 462 N95-14620
Low-Earth-Orbiter resource allocation and capacity planning for the DSN using LEO4CAST p 419 N95-14632
Efficient mission control for the 48-satellite Globalstar constellation
[TABES PAPER 94-609] p 415 N95-14641
The Global Emergency Observation and Warning System
[TABES PAPER 94-622] p 417 N95-14649
Speakeasy software development
[AD-A283816] p 468 N95-15333
Performance information management system (PIMS) communication
[AD-A284851] p 574 N95-15335
TELECONFERENCING
Virtual acoustic displays p 557 N95-14035
TELECONNECTIONS (METEOROLOGY)
Short term teleconnections associated with western Pacific tropical cyclones
[AD-A284032] p 533 N95-14423
TELEMETRY
Evolutionary Telemetry and Command Processor (TCP) architecture p 420 N95-14162
TELEOPERATORS
Human Machine Interfaces for Teleoperators and Virtual Environments
[NASA-CP-10071] p 554 N95-14013
Visual interfaces: The human perceiver p 554 N95-14014
Tactual interfaces: The human perceiver p 554 N95-14016
Analysis of the human operator subsystems p 555 N95-14019
Telerobotic remote presence: Achievements and challenges p 504 N95-14023
Issues in the design of high dexterity, force reflective teleoperators p 555 N95-14024
Tele-existence and/or cybernetic interface studies in Japan p 555 N95-14025

Models of remote manipulation in space p 504 N95-14027
Some criteria for teleoperators and virtual environments from experiences with vehicle/operator simulation p 556 N95-14028
Man-machine interfaces in health care p 556 N95-14029
Telerobotics in rehabilitation: Barriers to a virtual existence p 556 N95-14030
Interacting with virtual worlds p 556 N95-14032
Virtual reality at work p 556 N95-14033
The Ames Virtual Environment Workstation: Implementation issues and requirements p 557 N95-14034
Virtual acoustic displays p 557 N95-14035
Varieties of virtualization p 557 N95-14036
The exploration metaphor p 557 N95-14037
The Teleprasenz Consortium: Structure and intentions p 558 N95-14039
Perceptual and performance consequences of flight in virtual worlds p 558 N95-14043
Objective evaluation of situation awareness for dynamic decision makers in teleoperations p 559 N95-14047
Implementation issues for a compact 6 degree of freedom force reflecting handcontroller with cueing of modes p 560 N95-14050
Human-machine interface hardware: The next decade p 561 N95-14055
Manual discrimination of force p 561 N95-14057
Human factors requirements for telerobotic command and control: The European Space Agency experimental programme p 562 N95-14059
VERDEX: A virtual environment demonstrator for remote driving applications p 562 N95-14060
A simulation facility for testing Space Station assembly procedures p 423 N95-14075
From Antarctica to space: Use of telepresence and virtual reality in control of remote vehicles p 427 N95-14099
Human factors considerations for remote manipulation p 564 N95-14949

TELEROBOTICS
Human Machine Interfaces for Teleoperators and Virtual Environments [NASA-CP-10071] p 554 N95-14013
Analysis of the human operator subsystems p 555 N95-14019
Eye movement control and top-down scanpath vision as a design metaphor for robotic vision and control p 555 N95-14022
Telerobotic remote presence: Achievements and challenges p 504 N95-14023
Issues in the design of high dexterity, force reflective teleoperators p 555 N95-14024
Telerobotics in the deep ocean p 504 N95-14026
Models of remote manipulation in space p 504 N95-14027
Man-machine interfaces in health care p 556 N95-14029
Telerobotics in rehabilitation: Barriers to a virtual existence p 556 N95-14030
Interacting with virtual worlds p 556 N95-14032
The Ames Virtual Environment Workstation: Implementation issues and requirements p 557 N95-14034
Virtual acoustic displays p 557 N95-14035
Varieties of virtualization p 557 N95-14036
A decade of telerobotics in rehabilitation: Demonstrated utility blocked by the high cost of manipulation and the complexity of the user interface p 558 N95-14044
Human factors requirements for telerobotic command and control: The European Space Agency experimental programme p 562 N95-14059
Control of remotely operated manipulation systems p 582 N95-14945
Guidance and control for unmanned ground vehicles p 504 N95-14948
Human factors considerations for remote manipulation p 564 N95-14949

TELESCOPES
Adaptive optics at Lick Observatory: System architecture and operations [DE94-012387] p 601 N95-13672
The 3.5-meter telescope enclosure [AD-A280949] p 638 N95-14597
Space debris detection and analysis [AD-A282012] p 428 N95-14951

TELEVISION SYSTEMS
Satellite communication technology and applications, 1995-2010 p 413 N95-13826
Technical Revue Thomson-CSF, volume 26, no. 1, March 1994. Flat panels for visualisation [PB94-197969] p 410 N95-13984
Thermal balance testing of MSAT 2 spacecraft p 424 N95-14080

TEMPERATURE CONTROL
Heat capacity and thermal relaxation of bulk helium very near the lambda point p 444 N95-14208
Active thermal isolation for temperature responsive sensors [NASA-CASE-LAR-14612-2] p 496 N95-14414
Study of two-phase flow and heat transfer in reduced gravities p 487 N95-14555
Transport phenomena in stratified multi-fluid flo w in the presence and absence of gravity p 488 N95-14563
An application of miniscale experiments on Earth to refine microgravity analysis of adiabatic multiphase flow in space p 459 N95-14567
High Temperature Calibration Furnace System user's guide [NASA-CR-196526] p 573 N95-14905

TEMPERATURE DEPENDENCE
Effects of in situ fiber strength characteristics on mechanical properties of SiC(f)/SiC composites [DE94-013965] p 433 N95-13682
ASTM E 1559 method for measuring material outgassing/deposition kinetics has applications to aerospace, electronics, and semiconductor industries p 421 N95-14066
Laboratory simulation of Low Earth Orbit (LEO) atomic oxygen effects p 422 N95-14071
US-Japan workshop Q-181 on High Heat Flux Components and Plasma-Surface Interactions for Next Devices: Proceedings [DE94-014939] p 618 N95-14443
Anomalous temperature dependence of the lattice parameters in HoPO4 and HoVO4: Rare earth quadrupolar effects [DE94-015086] p 622 N95-14608
Electrical characterization of 6H crystalline silicon carbide [NASA-CR-197047] p 439 N95-14903
Conductive paints [DE94-014069] p 453 N95-15292
Chemical kinetics and atmospheric modification [AD-A283304] p 524 N95-15623

TEMPERATURE DISTRIBUTION
Surface Tension Driven Convection Experiment (STDCE) p 458 N95-14217
Determination of the similarity theory scaling parameters from the vertical gradients [AD-A283833] p 533 N95-14340
Effect of surface roughness on local film cooling effectiveness and heat transfer coefficients [AD-A283854] p 482 N95-14351
Numerical solution of two-dimensional ablation problems using the finite control volume method with unstructured grids [DE94-015012] p 428 N95-14664

TEMPERATURE EFFECTS
Using a temperature-controlled quartz crystal microbalance in a space equipment cleanroom to monitor molecular contamination p 421 N95-14069
Study of the long term stability of the effective concentration of ionized space charges (N(sub eff)) of neutron irradiated silicon detectors fabricated by various thermal oxidations [DE94-013734] p 593 N95-14309
Transient failure behavior of HT9 [DE94-016320] p 445 N95-14378
Thermocapillary migration and interactions of bubbles and drops p 486 N95-14546
Turbidity of a binary fluid mixture: Determining eta p 487 N95-14552
Simple atmospheric perturbation models for sonic-boom-signature distortion studies p 402 N95-14888
Fire growth models for materials [PB94-195856] p 443 N95-15610
Advanced Turbine Technology Applications Project (ATTAP) [NASA-CR-195393] p 634 N95-15743
Effect of heat treatment on the microstructure and properties of AerMet (trade name) 100 steel [AD-A284387] p 447 N95-15807
Earth Observing System (EOS)/Advanced Microwave Sounding Unit-A (AMSU-A) worst-case analysis: Antenna beam pointing [NASA-CR-197218] p 517 N95-15851

TEMPERATURE GRADIENTS
Thermocapillary migration and interactions of bubbles and drops p 486 N95-14546
A coarse grained approach to thermocapillarity effects in binary systems p 487 N95-14553
Effects of thermocapillarity on an evaporating extended meniscus in microgravity p 488 N95-14559
Pool and flow boiling in variable and microgravity p 459 N95-14562
Particle experiments in thermal and velocity gradients p 489 N95-14564
Simple atmospheric perturbation models for sonic-boom-signature distortion studies p 402 N95-14888
High-temperature corrosion of iron aluminides [DE94-011505] p 447 N95-15906

TEMPERATURE INVERSIONS
Water vapor and temperature inversions near the 0 C level over the tropical western Pacific [AD-A282023] p 533 N95-14952

TEMPERATURE MEASUREMENT
Wind-electric ice making for villages in the developing world [DE94-011854] p 518 N95-14191
Active thermal isolation for temperature responsive sensors [NASA-CASE-LAR-14612-2] p 496 N95-14414
Radiometer calibration procedure and beacon attenuation estimation reference level p 486 N95-14683
Overview of PAMS meteorological monitoring requirements [PB94-176658] p 534 N95-15383
Research on characterization of the upper atmosphere using lidar [AD-A283241] p 530 N95-15401
High-spatial-resolution passive microwave sounding systems [NASA-CR-197131] p 531 N95-15586

TEMPERATURE PROFILES
Assessing post-fire combustion of polyurethane [DE94-011461] p 438 N95-14375
Transport phenomena in stratified multi-fluid flo w in the presence and absence of gravity p 488 N95-14563
Behavior of charring materials in simulated fire environments [PB94-196045] p 439 N95-14838
Chemical kinetics and atmospheric modification [AD-A283304] p 524 N95-15623
Oxidation resistant coating for carbon-carbon composites at ultra-high temperatures [AD-A283323] p 456 N95-15624

TEMPERATURE SENSORS
Active thermal isolation for temperature responsive sensors [NASA-CASE-LAR-14612-2] p 496 N95-14414

TEMPORAL DISTRIBUTION
Measuring temporal gravitational variations using SLR data p 527 N95-14277
Spatio-temporal neural networks for vision, reasoning and rapid decision making [AD-A283251] p 583 N95-15403
The temporal reasoning systems TimeGraph 1-2 [TR-494-REV] p 584 N95-15786
Efficient algorithms for qualitative reasoning about time [TR-496] p 576 N95-15825

TEMPORAL LOGIC
On point-based temporal disjointness [TR-497] p 587 N95-15643

TEMPORAL RESOLUTION
An analysis of eddy resolving global ocean models in the Southern Ocean [AD-A283211] p 536 N95-15626

TENSILE CREEP
Tensile creep strain and activation energy [AD-A283264] p 513 N95-15620

TENSILE DEFORMATION
Three-dimensional effects of crack closure in laminated composite plates subjected to bending loads [AD-A283342] p 436 N95-15873

TENSILE PROPERTIES
Effects of thermal cycling on thermal expansion and mechanical properties of SiC fiber-reinforced reaction-bonded Si3N4 composites [NASA-TM-106665] p 433 N95-14298

TENSILE STRENGTH
Effect of matrix stiffness on wavy fiber behavior in single-carbon-fiber-epoxy composites [AD-A280970] p 435 N95-15427
Static strength of riveted joints in Fibre Metal Laminates [PB94-201472] p 513 N95-15429
Tensile creep strain and activation energy [AD-A283264] p 513 N95-15620

TENSILE STRESS
Mechanical properties of high-temperature superconducting wires [DE94-015089] p 621 N95-14192
Effects of tensile loading on upper shelf fracture toughness [AD-A284364] p 514 N95-15803

TENSILE TESTS
Innovative design of composite structures: Design, manufacturing, and testing of plates utilizing curvilinear fiber trajectories [NASA-CR-197045] p 435 N95-14885

The effect of specimen geometry on the accuracy of constitutive relations in a superplastic 5083 aluminum alloy
[DE94-014501] p 445 N95-15293
Effect of matrix stiffness on wavy fiber behavior in single-carbon-fiber-epoxy composites
[AD-A280970] p 435 N95-15427
Loading-strain equivalence between thermomechanical, creep, and tensile tests: High density polyethylene
[AD-A283265] p 513 N95-15621
Effects of tensile loading on upper shelf fracture toughness
[AD-A284364] p 514 N95-15803

TENSOR ANALYSIS
Ion implantation of He-3 in tantalum for use in a low energy deuteron polarization analyzer
[AD-A283172] p 619 N95-13698
Particle localization, spinor two-valuedness, and Fermi quantization of tensor systems p 598 N95-13932

TENSORS
Particle localization, spinor two-valuedness, and Fermi quantization of tensor systems p 598 N95-13932
Squeezed states and graviton-entropy production in the early universe p 608 N95-13947

TERMINAL BALLISTICS
New armour materials: Metal matrix composites
[PB94-189131] p 433 N95-14148

TERMINAL FACILITIES
TDWR scan strategy implementation
[AD-A284877] p 534 N95-15749

TERMINOLOGY
Preparing technical text for translation: A comparison between International English and methods for simplifying language
[DE94-014465] p 630 N95-13996
A proposed framework for computational fluid dynamics code calibration and validation
[DE94-015799] p 493 N95-15351

TERNARY ALLOYS
Coherency strains and coarsening in Ni-Al-Si alloys: An experimental study
[DE94-015020] p 445 N95-14665

TERNARY SYSTEMS
Defects and transport in mixed oxides
[DE94-015652] p 454 N95-15358

TERRAIN ANALYSIS
Interferometric synthetic aperture radar terrain elevation mapping from multiple observations
[DE94-014185] p 515 N95-14313
Propagation Modelling and Decision Aids for Communications, Radar and Navigation Systems
[AGARD-LS-196] p 466 N95-14825
Validation of the global digital height model ETOPO5U referring to the Italian model (Italian DEM) p 517 N95-15797

TERRESTRIAL RADIATION
Technical report series on global modeling and data assimilation. Volume 3: An efficient thermal infrared radiation parameterization for use in general circulation models
[NASA-TM-104606-VOL-3] p 531 N95-15745

TEST CHAMBERS
Characterization of annular two-phase gas-liquid flows in microgravity p 487 N95-14556

TEST EQUIPMENT
Small crack test program for helicopter materials p 507 N95-14455

TEST FACILITIES
A new tribological test for candidate brush seal materials evaluation
[NASA-TM-106753] p 431 N95-13631
AXAF VETA-I mirror ring focus measurements
[NASA-CR-196145] p 637 N95-13637
HYDRA, a new tool for mechanical testing p 418 N95-14086
Simulation of a spatial, servo-hydraulic test facility for space structures p 418 N95-14095
New potentials of NIICHIMMASH's thermal vacuum facilities p 418 N95-14098
The National Wind Technology Center
[DE94-011853] p 519 N95-14433
Hypervelocity Impact Test Facility: A gun for hire
[TABES PAPER 94-605] p 415 N95-14639
Comprehensive facility decommissioning through the use of innovative technology to reduce cost, schedule, and environmental liability
[TABES PAPER 94-615] p 416 N95-14644
Design review and analysis for a Pratt and Whitney fluid-film bearing and seal testing rig
[NASA-CR-197035] p 502 N95-14797
Wind/hybrid power system test facilities in the United States and Canada
[DE94-006930] p 519 N95-15290
Diagnostic development and support of MHD test facilities
[DE94-015344] p 618 N95-15373

TEST FIRING
Studies of the ablated plasma from experimental plasma gun disruption simulations
[DE94-015017] p 617 N95-14262

TETHERING
A facility to produce an energetic, ground state atomic oxygen beam for the simulation of the Low-Earth Orbit environment p 422 N95-14072

TEXTS
Augmentation of research on cognitive control
[AD-A280956] p 552 N95-14600

THEMATIC MAPPERS (LANDSAT)
Blocking reduction of Landsat Thematic Mapper JPEG browse images using optimal PSNR estimated spectra adaptive postfiltering p 565 N95-14589
Development of a systemic land cover/land use database for the Upper Mississippi River System derived from Landsat Thematic Mapper satellite data. Long term resource monitoring program
[PB94-186889] p 515 N95-14793

THEMATIC MAPPING
Forest cover from Landsat Thematic Mapper data for use in the Catahoula Ranger District Geographic Information System
[PB94-203056] p 515 N95-14125

THEOREM PROVING
Lower bounds for perceptrons solving some separation problems and oracle separation of AM from PP
[TR-498] p 588 N95-15855
Seeking stronger separations: Probability one balanced- and bi-immunity
[TR-480] p 589 N95-15859

THEOREMS
Density control and on-line labeling problems
[TR-481] p 576 N95-15789
A general method to construct oracles realizing given relationships between complexity classes
[TR-500] p 588 N95-15854

THEORETICAL PHYSICS
Research accomplishments and future goals in particle physics
[DE94-015483] p 596 N95-15537
Research in high energy physics
[DE94-015519] p 600 N95-15539

THERAPY
Telerobotics in rehabilitation: Barriers to a virtual existence p 556 N95-14030
Measurement and modification of the EEG and related behavior p 557 N95-14038

THERMAL ANALYSIS
Thermal balance testing of MSAT 2 spacecraft p 424 N95-14080
Thermal balance testing of the MSAT spacecraft p 424 N95-14082
Thermal design verification testing of the Clementine spacecraft: Quick, cheap, and useful p 424 N95-14083
Missile infrared radiation analysis p 399 N95-14449
Development of a composite repair and the associated inspection intervals for the F-111C stiffener runout region p 392 N95-14477
An architecture for intelligent multichip module reliability analysis
[AD-A281574] p 583 N95-15461

THERMAL CONDUCTIVITY
Heat capacity and thermal relaxation of bulk helium very near the lambda point p 444 N95-14208
Energy flux and hydrogeology of thermal anomalies in the Gulf of Mexico Basin: South Texas example
[DE94-015122] p 530 N95-14956
Conductive paints
[DE94-014069] p 453 N95-15292

THERMAL CONTROL COATINGS
Evaluation of reformulated thermal control coatings in a simulated space environment. Part 1: YB-71 p 420 N95-14063
Results of the examination of LDEF polyurethane thermal control coatings
[NASA-CR-4617] p 432 N95-14603

THERMAL CYCLING TESTS
Assembly feasibility and reliability studies of surface mount circuit boards manufactured with lead-free solders
[DE94-013783] p 472 N95-13975
Effects of thermal cycling on thermal expansion and mechanical properties of SiC fiber-reinforced reaction-bonded Si3N4 composites
[NASA-TM-106665] p 433 N95-14298
Milestone 4: Test plan for Reusable Hydrogen Composite Tank System (RHCTS). Task 3: Composite tank materials
[NASA-CR-197036] p 435 N95-14801

THERMAL DEGRADATION
Definition of high-temperature use limits for MIL-L-2104 engine oils
[AD-A282838] p 451 N95-14365
Mechanical system reliability for long life space systems
[NASA-CR-197215] p 505 N95-15584
Characterization of damage progression in SCS-6/Timetal 21S (0)4 under thermomechanical fatigue loadings
[NASA-CR-195399] p 436 N95-15911

THERMAL DISSOCIATION
Chemical kinetics and atmospheric modification
[AD-A283304] p 524 N95-15623

THERMAL EXPANSION
Monitoring fiber stress during curing of single fiber glass- and graphite-epoxy composites
[NASA-TM-4568] p 432 N95-13641
Effects of thermal cycling on thermal expansion and mechanical properties of SiC fiber-reinforced reaction-bonded Si3N4 composites
[NASA-TM-106665] p 433 N95-14298
Ru2Ge3: Crystal growth and some properties
[DE94-015360] p 625 N95-15531
Low loss substrates for microwave applications and sol-gel processing of superconductors
[AD-A284868] p 625 N95-15746

THERMAL FATIGUE
Environmental durability issues for solar power systems in low Earth orbit
[NASA-TM-106775] p 431 N95-15769
Characterization of damage progression in SCS-6/Timetal 21S (0)4 under thermomechanical fatigue loadings
[NASA-CR-195399] p 436 N95-15911

THERMAL INSULATION
Cratering and penetration experiments in teflon targets at velocities from 1 to 7 km/s
[NASA-TM-104797] p 432 N95-13646

THERMAL NEUTRONS
Thin GSO scintillator for neutron detection
[DE94-014566] p 613 N95-15314

THERMAL PLASMAS
Conversion of light hydrocarbon gases in metal carbides for production of liquid fuels and chemicals
[DE94-013933] p 439 N95-14435

THERMAL PROTECTION
Nondestructive analysis and development
[NASA-CR-196987] p 505 N95-13886
Evaluation of reformulated thermal control coatings in a simulated space environment. Part 1: YB-71 p 420 N95-14063
Thermoacoustic environments to simulate reentry conditions p 426 N95-14096
Requirements report for SSTO vertical take-off and horizontal landing vehicle
[NASA-CR-197029] p 409 N95-14794

THERMAL STABILITY
A solvent resistant copolyimide
[NASA-CASE-LAR-15083-1] p 449 N95-14108
Thermally stable organic polymers
[AD-A281380] p 451 N95-14363
Practical aspects of corrosion fundamentals
[DE94-015842] p 438 N95-14371
Damping mechanisms in nanostructured materials
[AD-A283583] p 623 N95-15317

THERMAL STRESSES
Thermal structure analyses for CSM testbed (COMET)
[NASA-CR-196998] p 506 N95-14270
Hypersonic engine leading edge experiments in a high heat flux, supersonic flow environment
[NASA-TM-106742] p 482 N95-14299
Laminar and turbulent flow computations of Type 4 shock-shock interference aerothermal loads using unstructured grids
[NASA-CR-195008] p 493 N95-15604

THERMAL VACUUM TESTS
Eighteenth Space Simulation Conference: Space Mission Success Through Testing
[NASA-CP-3280] p 420 N95-14062
Experimental study of solar simulator mirror cryocontamination p 421 N95-14065
David Florida Laboratory Thermal Vacuum Data Processing System p 418 N95-14079
Thermal balance testing of MSAT 2 spacecraft p 424 N95-14080
Thermal balance testing of the MSAT spacecraft p 424 N95-14082
Thermal design verification testing of the Clementine spacecraft: Quick, cheap, and useful p 424 N95-14083
Refurbishment of a 39 foot thermal vacuum chamber p 418 N95-14085
Thermoacoustic environments to simulate reentry conditions p 426 N95-14096
New potentials of NIICHIMMASH's thermal vacuum facilities p 418 N95-14098
Apparatus for performing high-temperature fiber push-out testing
[NASA-CASE-LEW-15470-1] p 497 N95-15915

THERMIONIC EMISSION
Hydrogen transport and trapping in graphite
[UTIAS-347] p 437 N95-13652
THERMISTORS
Surface Tension Driven Convection Experiment (STDCE) p 458 N95-14217
THERMOCLINES
Tidal dynamics and mixing over steep topography
[AD-A283535] p 536 N95-15324
THERMOCOUPLES
High Temperature Calibration Furnace System user's guide
[NASA-CR-196526] p 573 N95-14905
THERMODYNAMIC EQUILIBRIUM
Squeezed states and graviton-entropy production in the early universe p 608 N95-13947
THERMODYNAMIC PROPERTIES
Development of chemical-vapor-deposited diamond for infrared optical applications: Summary of properties
[AD-A282999] p 448 N95-13686
Particle experiments in thermal and velocity gradients p 489 N95-14564
Modelling and investigation of EHD point contacts
[AD-A283571] p 454 N95-15316
Towards the molecular design of composite materials
[AD-A283422] p 627 N95-15404
Process development of thermal hydrodechlorination
[PB94-195518] p 525 N95-15870
THERMODYNAMICS
Update to the NASA Lewis ice accretion code LEWICE
[NASA-CR-195387] p 481 N95-14295
Polymer-polymer interactions
[AD-A282944] p 453 N95-14844
THERMOELECTRIC GENERATORS
Preliminary design of a miniature thermoelectric generator
[AD-A283834] p 518 N95-14341
THERMOLUMINESCENCE
Relationship between microstructure and efficiency of scintillating glasses
[DE94-014563] p 454 N95-15313
THERMOMECHANICAL TREATMENT
Loading-strain equivalence between thermomechanical, creep, and tensile tests: High density polyethylene
[AD-A283265] p 513 N95-15621
THERMOMETERS
Heat capacity and thermal relaxation of bulk helium very near the lambda point p 444 N95-14208
THERMONUCLEAR REACTIONS
Studies of the ablated plasma from experimental plasma gun disruption simulations
[DE94-015017] p 617 N95-14262
Radioactivity measurements of ITER materials using the TFTR D-T neutron field
[DE94-016094] p 617 N95-14397
THERMOPHYSICAL PROPERTIES
Thermophysical properties of HCFC alternatives
[DE94-016646] p 438 N95-14372
THERMOPLASTIC RESINS
Copolyimides prepared from ODPA, BTDA and 3,4'-ODA
[NASA-CASE-LAR-15109-1] p 449 N95-14109
The synthesis of monomers with pendent ethynyl groups for modified high performance thermoplastics
[NASA-CR-196935] p 453 N95-14931
THERMOPLASTICITY
Self-organization of graft copolymers at surfaces, interfaces and in bulk
[DE94-016884] p 454 N95-15340
THERMOSETTING RESINS
Phenylethynyl terminated imide oligomers
[NASA-CASE-LAR-15175-1] p 450 N95-14185
THERMOSIPHONS
Interfacial force field characterization of a constrained vapor bubble thermosyphon using IAI p 488 N95-14560
THICKNESS
Ground penetrating radar surveys to characterize pavement layer thickness variations at GPS sites
[PB94-190170] p 460 N95-14119
Deformation, strength, and failure modes of laminated conventional and hybrid polymer-matrix composites loaded in the thickness direction
[AD-A281587] p 436 N95-15443
On the evolution of centrifugal instabilities within curved incompressible mixing layers
[NASA-CR-194991] p 495 N95-15917
THIGH
Orthostatic stress by lower body negative pressure and its body fluid distribution kinetics under microgravity p 549 N95-15138
THIN FILMS
In-situ TEM crystallization of sol-gel derived BaTiO3 thin films
[DE94-013260] p 619 N95-13821
Thin composite solid electrolyte film for lithium batteries
[NASA-CASE-NPO-18694-1-CU] p 472 N95-13824
Technical Revue Thomson-CSF, volume 26, no. 1, March 1994. Flat panels for visualisation
[PB94-197969] p 410 N95-13984
Multilayer thin film Hall effect device
[NASA-CASE-MFS-28764-1] p 590 N95-14137
Advanced solar cells for satellite power systems
[NASA-TM-106777] p 473 N95-14302
The electromagnetic spectrum. Research investigation directed toward extending the useful range of the electromagnetic spectrum
[AD-A281378] p 461 N95-14361
Experimental and theoretical studies of rewetting of unheated/heated grooved plates p 487 N95-14558
Surface spectroscopic studies of high-temperature superconductors
[PB94-191228] p 624 N95-15378
Magnetic and structural instabilities of ultrathin Fe(100) wedges
[DE94-013864] p 624 N95-15385
Laser ablation and deposition of alloys
[PB94-191384] p 499 N95-15388
Ferroelectric oxide memory FET (FEMFET) development
[AD-A283203] p 476 N95-15399
Alternative fabrication techniques for high-efficiency CuInSe2 and CuInSe2-alloy films and cells
[DE94-011846] p 521 N95-15407
Core-level spectroscopy of thin oxides and oxynitrides
[DE94-016598] p 442 N95-15408
The effects of spatial location of defect states on the switching characteristics of amorphous and polycrystalline silicon thin film transistors: A numerical simulation using AMPS 2-D
[DE94-013437] p 476 N95-15410
Fourth Workshop on the Role of Point Defects and Defect Complexes in Silicon Device Processing
[DE94-011850] p 624 N95-15426
THIN WALLS
Nonlinear fracture mechanics-based analysis of thin wall cylinders p 508 N95-14482
THIOLS
Determination of the shear modulus in self-assembled monolayers using quartz resonators
[DE94-013449] p 437 N95-14307
THREADS
Nexus: An interoperability layer for parallel and distributed computer systems
[DE94-015816] p 578 N95-14116
THREE DIMENSIONAL FLOW
MHD flow in rectangular ducts with inclined non-uniform transverse magnetic field
[DE94-013989] p 616 N95-14006
Designing in three dimensions p 480 N95-14130
Unsteady flows in turbines: Impact on design procedure p 480 N95-14132
Aero design of turbomachinery components: CFD in complex systems p 481 N95-14136
The behavior of unsteady thermocapillary flows p 483 N95-14530
Cold flow simulation of the alternate turbopump development turbine of the Space Shuttle main engine high pressure fuel turbopump
[AD-A281676] p 419 N95-15447
A three-dimensional fast solver for arbitrary vorton distributions
[DE94-012581] p 404 N95-15570
Numerical design of advanced multi-element airfoils
[NASA-CR-197135] p 404 N95-15762
THREE DIMENSIONAL MODELS
Photochemical urban airshed modeling using diagnostic and dynamic meteorological fields
[PB94-176120] p 616 N95-13973
Development of visual 3D virtual environment for control software p 559 N95-14048
Turbomachinery Design Using CFD
[AGARD-LS-195] p 479 N95-14127
Designing in three dimensions p 480 N95-14130
Unsteady flows in turbines: Impact on design procedure p 480 N95-14132
The role of CFD in the design process p 481 N95-14135
Add a dimension to your analysis of the helicopter low airspeed environment
[AD-A283982] p 408 N95-14205
ADCIRC: An advanced three-dimensional circulation model for shelves, coasts, and estuaries. Report 4: Hurricane storm surge modeling using large domains
[AD-A283868] p 535 N95-14352
Multi-dimensional modeling of pressurization and expulsion of multi-phase hydrogen propellant
[NASA-CR-195156] p 457 N95-14902
Robust multigrid methods for the steady and unsteady incompressible Navier-Stokes equations in general coordinates
[PB94-195534] p 492 N95-15315
Using Pro/ENGINEER's (tm) interface module
[DE94-013364] p 574 N95-15384
Development and testing of a high-resolution model for tropospheric sulfate driven by observation-derived meteorology
[DE94-014910] p 525 N95-15864
Phase transitions and connectivity in three-dimensional vortex equilibria
[DE94-014967] p 494 N95-15868
Three-dimensional effects of crack closure in laminated composite plates subjected to bending loads
[AD-A283342] p 436 N95-15873
THRUST VECTOR CONTROL
Fourth High Alpha Conference, volume 1
[NASA-CP-10143-VOL-1] p 393 N95-14229
Parameter identification for X-31A at high angles of attack p 394 N95-14235
Fourth High Alpha Conference, volume 2
[NASA-CP-10143-VOL-2] p 395 N95-14239
F-18 high alpha research vehicle: Lessons learned p 395 N95-14240
X-31 post-stall envelope expansion and tactical utility testing p 395 N95-14242
X-31 quasi-tailless flight demonstration p 395 N95-14243
X-31 high angle of attack control system performance p 395 N95-14244
Flight test results of the F-16 aircraft modified with the axisymmetric vectoring exhaust nozzle p 396 N95-14245
Vista/F-16 Multi-Axis Thrust Vectoring (MATV) control law design and evaluation p 396 N95-14248
Multi-application controls: Robust nonlinear multivariable aerospace controls applications p 396 N95-14249
Navy and the HARV: High angle of attack tactical utility issues p 397 N95-14252
Preparations for flight research to evaluate actuated forebody strakes on the F-18 high-alpha research vehicle p 398 N95-14257
Design of power electronics for TVC and EMA systems
[NASA-CR-197067] p 475 N95-14866
THRUST-WEIGHT RATIO
The rationale/benefits of nuclear thermal rocket propulsion for NASA's lunar space transportation system
[NASA-TM-106739] p 431 N95-15682
THUNDERSTORMS
Verification of severe local storms forecasts issued by the National Severe Storms Forecast Center: 1993
[PB94-195898] p 532 N95-14117
Nowcasting convective storm evolution in east-central Florida using satellite and Doppler radar data
[AD-A283260] p 534 N95-15618
TIDES
Tidal dynamics and mixing over steep topography
[AD-A283535] p 536 N95-15324
TILES
Nondestructive analysis and development
[NASA-CR-196987] p 505 N95-13886
Milestone 5 test report. Task 5, subtask 5.2: Tile to foam strength tests
[NASA-CR-197241] p 514 N95-15913
TIMBER IDENTIFICATION
Forest cover from Landsat Thematic Mapper data for use in the Catahoula Ranger District Geographic Information System
[PB94-203056] p 515 N95-14125
TIME
The quantum measurement of time p 590 N95-13917
TIME CONSTANT
Quantum propagation in single mode fiber p 609 N95-13953
Loading-strain equivalence between thermomechanical, creep, and tensile tests: High density polyethylene
[AD-A283265] p 513 N95-15621
TIME DEPENDENCE
Time-dependent distinguishability: Choosing to be a wave or a particle p 600 N95-13912
Manipulation of quantum evolution p 598 N95-13918
Understanding squeezing of quantum states with the Wigner function p 606 N95-13930
Time-dependent variational approach in terms of squeezed coherent states: Implication to semi-classical approximation p 609 N95-13948
Modeling time-dependent corrosion fatigue crack propagation in 7000 series aluminum alloys p 448 N95-14483
Sensing of radio refractivity and aerosol extinction p 467 N95-14830

Studies in chaotic adiabatic dynamics
[DE94-013111] p 627 N95-15578
An approach for dynamic grids
[NASA-TM-106774] p 404 N95-15853

TIME LAG
Human factors requirements for telerobotic command and control: The European Space Agency experimental programme p 562 N95-14059
F/A-18 and F-16 forebody vortex control, static and rotary-balance results p 397 N95-14254

TIME MEASUREMENT
The quantum measurement of time
p 590 N95-13917

TIME OF FLIGHT SPECTROMETERS
Los Alamos contribution to target diagnostics on the National Ignition Facility
[DE94-014474] p 616 N95-13998
Beta decay data for neutron-rich Li-Cl nuclides
[DE94-014556] p 595 N95-15310
Time-of-flight detector for heavy ion backscattering spectrometry
[DE94-015600] p 596 N95-15437
Mass analysis addition to the Differential Ion Flux Probe (DIFP) study
[NASA-CR-196531] p 429 N95-15824

TIME SERIES ANALYSIS
Chaotic time series. Part 2: System identification and prediction
[PB94-207115] p 589 N95-13630
High-speed fixed and floating point implementation of delta-operator formulated discrete time systems
[AD-A283109] p 584 N95-13694
Statistical aspects of the precipitation regimes at Miami International Airport (MIA) and Palm Beach International Airport (PBI): 1961-1990
[PB94-194289] p 532 N95-14118
Satellite imagery and topographic data in verification
[AD-A280950] p 530 N95-14598

TIME TEMPERATURE PARAMETER
ASTM E 1559 method for measuring material outgassing/deposition kinetics has applications to aerospace, electronics, and semiconductor industries
p 421 N95-14066
Tensile creep strain and activation energy
[AD-A283264] p 513 N95-15620
Ballistic performance and adiabatic shear behavior of AerMet(tm) 100 steel
[AD-A283266] p 447 N95-15622

TIN OXIDES
Electrically conducting polyimide film containing tin complexes
[NASA-CASE-LAR-14936-1] p 450 N95-14113

TIROS SATELLITES
Semiconductor measurement technology: Improved characterization and evaluation measurments for HgCdTe detector materials, processes, and devices used on the GOES and TIROS satellites
[PB94-188810] p 474 N95-14401

TITANIUM
Study on titanium-silicalite-1 and related systems
[PB94-195500] p 445 N95-14845
Characterization of damage progression in SCS-6/Timetal 21S (0)4 under thermomechanical fatigue loadings
[NASA-CR-195399] p 436 N95-15911

TITANIUM ALLOYS
High temperature cyclic behaviour of aerospace materials: Room temperature validation tests of Ti-6Al-4V
[AGARD-AR-328] p 506 N95-14198
Symposium on Structural Intermetallics: Perspectives on Science and Technology, volume 2
[AD-A283379] p 447 N95-15874

TITANIUM COMPOUNDS
Study on titanium-silicalite-1 and related systems
[PB94-195500] p 445 N95-14845

TITANIUM OXIDES
Burn rates of TiH2/KClO4/Viton and output testing of NASA SKD26100098-301 pressure cartridges
[NASA-CR-188357] p 443 N95-15715

TOKAMAK DEVICES
Advanced stellarator power plants
[DE94-014442] p 616 N95-14007
Tokamak power plant burn cycle options
[DE94-014016] p 617 N95-14012
Studies of the ablated plasma from experimental plasma gun disruption simulations
[DE94-015017] p 617 N95-14262
Divertor bias experiments
[DE94-015720] p 617 N95-14328
Radioactivity measurements of ITER materials using the TFTR D-T neutron field
[DE94-016094] p 617 N95-14397
Advanced tokamak research on the D3-D tokamak
[DE94-015860] p 617 N95-14426
US-Japan workshop Q-181 on High Heat Flux Components and Plasma-Surface Interactions for Next Devices: Proceedings
[DE94-014939] p 618 N95-14443
The effect of the edge current density on confinement and kink mode stability in H-mode and VH-mode discharges
[DE94-015719] p 618 N95-15632

TOLERANCES (MECHANICS)
FAA/NASA International Symposium on Advanced Structural Integrity Methods for Airframe Durability and Damage Tolerance
[NASA-CP-3274-PT-1] p 507 N95-14453
Development of the NASA/FLAGRO computer program for analysis of airframe structures p 510 N95-14473
Recent advances in the modelling of crack growth under fatigue loading conditions p 511 N95-14478

TOPOGRAPHY
Satellite imagery and topographic data in verification
[AD-A280950] p 530 N95-14598
Tidal dynamics and mixing over steep topography
[AD-A283535] p 536 N95-15324
What those defects in optical coatings really look like
[DE94-015324] p 614 N95-15529
An analysis of eddy resolving global ocean models in the Southern Ocean
[AD-A283211] p 536 N95-15626
The GEOMED Project p 516 N95-15794
Validation of the global digital height model ETOPO5U referring to the Italian model (Italian DEM)
p 517 N95-15797

TORNADOES
Verification of severe local storms forecasts issued by the National Severe Storms Forecast Center: 1993
[PB94-195898] p 532 N95-14117

TORQUE
Deployment mechanism calibration system
p 414 N95-13833

TORSION
Buckling of composite beams (CDDF)
[NASA-TP-3512] p 435 N95-14913

TORSIONAL VIBRATION
Torsional shear wave transducer
[AD-D016347] p 496 N95-14841

TOTAL OZONE MAPPING SPECTROMETER
Meteorological investigation of ozone anomalies during the Arctic Boundary Layer Experiment (ABLE 3A)
[AD-A284494] p 534 N95-15771

TOUCH
Tactual interfaces: The human perceiver
p 554 N95-14016
The display of tactile information p 554 N95-14017

TOUGHNESS
Ballistic performance and adiabatic shear behavior of AerMet(tm) 100 steel
[AD-A283266] p 447 N95-15622

TOXICITY
Development of techniques for the evaluation of toxicant impacts to multispecies systems
[AD-A284426] p 524 N95-15814

TOXICITY AND SAFETY HAZARD
Dextrous gripping in a hazardous environment
[PB94-191244] p 501 N95-14150
Environmentally sound manufacturing
[TABES PAPER 94-502] p 415 N95-14636
Recycled plastic: A clean and low cost rocket fuel
[TABES PAPER 94-610] p 416 N95-14642
Comprehensive facility decommissioning through the use of innovative technology to reduce cost, schedule, and environmental liability
[TABES PAPER 94-615] p 416 N95-14644

TOXICOLOGY
Unreported medications used in incapacitating medical conditions found in fatal civil aviation accidents
[DOT/FAA/AM-94/14] p 540 N95-14177
Development of techniques for the evaluation of toxicant impacts to multispecies systems
[AD-A284426] p 524 N95-15814

TRACE ELEMENTS
Time-of-flight detector for heavy ion backscattering spectrometry
[DE94-015600] p 596 N95-15437

TRACKING (POSITION)
Remote sensing, processing and transmission of data for an unmanned aerial vehicle
[AD-A283104] p 514 N95-13693

TRACKING NETWORKS
Produce documents and media information
[NASA-CR-196521] p 532 N95-14271
Global reference frame: Intercomparison of results (SLR, VLBI and GPS) p 527 N95-14276
Global and regional kinematics with GPS
p 527 N95-14279
Global and regional kinematics with VLBI
p 527 N95-14280
SLR tracking of GPS-35 p 471 N95-14285
Synergism of SLR and GPS p 471 N95-14286
Satellite Laser Ranging operations
p 500 N95-14287
SLR 2000 p 471 N95-14288
A strawman SLR program plan for the 1990s
p 471 N95-14289

TRADEOFFS
A gate level simulator for alpha-particle-induced transient faults
[AD-A283871] p 474 N95-14355

TRAINING AIRCRAFT
Viper --- Design modification
[NASA-CR-197191] p 408 N95-13703

TRAINING DEVICES
Summary Proceedings of the Joint Industry-FAA Conference on the Development and use of PC-Based Aviation Training Devices
[DOT/FAA/AM-94/25] p 573 N95-14917
Psychophysiological aspects of increasing resistance to space motion sickness p 542 N95-15093

TRAJECTORY ANALYSIS
Investigating and implementing enhancements to the simulation of short-term collision hazards
p 426 N95-14092

TRAJECTORY MEASUREMENT
Linear quadratic Gaussian and feedforward controllers for the DSS-13 antenna p 463 N95-14625
A trajectory preprocessor for antenna pointing
p 463 N95-14630

TRANSATMOSPHERIC VEHICLES
Access to space
[NASA-CR-197153] p 428 N95-14521

TRANSCONTINENTAL SYSTEMS
Global and regional kinematics with VLBI
p 527 N95-14280

TRANSDUCERS
Surface acoustic wave oxygen pressure sensor
[NASA-CASE-LAR-15266-1-CU] p 496 N95-13837
Leak detection by acoustic emissions monitoring: An experimental investigation of the acoustic properties of leaks and the attenuation characteristics of soil
[AD-A283250] p 530 N95-15295

TRANSFER FUNCTIONS
The human operator transfer function: Identification of the limb mechanics subsystem p 558 N95-14040

TRANSFORMATIONS (MATHEMATICS)
Eddy viscosity transport equations and their relation to the k-epsilon model
[NASA-TM-108854] p 481 N95-14273
Carnot-caratheodory spaces seen from within
[PB94-195617] p 586 N95-15412

TRANSFORMERS
Low-frequency noise in high-(Tc) superconductor Josephson junctions, SQUIDs, and magnetometers
[DE94-016873] p 623 N95-15337
Solid target boronization of the MST reversed-field pinch during pulsed discharge cleaning
[DE94-015535] p 442 N95-15541

TRANSIENT OSCILLATIONS
Experimental/analytical approach to understanding mistuning in a transonic wind tunnel compressor
[NASA-TM-108833] p 512 N95-14617

TRANSIENT RESPONSE
Fine structure of transient waves in a random medium: The correlation and spectral density functions
p 401 N95-14882

TRANSISTOR AMPLIFIERS
A radio telescope for the calibration of radio sources at 32 gigahertz p 463 N95-14626

TRANSISTOR CIRCUITS
Design of reliable high voltage avalanche transistor pulsers
[DE94-015323] p 473 N95-14261

TRANSISTORS
Calibration and characterization of wide range hydrogen sensors
[DE94-013765] p 496 N95-14146
Ion beam synthesis of SiGe alloy layers
[DE94-014958] p 620 N95-14189

TRANSITION FLOW
CFD methodology and validation for turbomachinery flows p 480 N95-14131

TRANSITION METALS
Diffusion of adatoms on face-centered cubic transition metal surfaces
[DE94-014230] p 445 N95-15307
The transformation of organic amines by transition metal cluster compounds
[DE94-017151] p 441 N95-15346
AASERT-93: Electroplating of refractory metals using haloaluminate melts
[AD-A284859] p 447 N95-15744

TRANSITION TEMPERATURE
Ru2Ge3: Crystal growth and some properties
[DE94-015360] p 625 N95-15531

TRANSLATING
Preparing technical text for translation: A comparison between International English and methods for simplifying language
[DE94-014465] p 630 N95-13996
TRANSMISSION EFFICIENCY
Performance comparison of token ring protocols for hard-real-time communication p 570 N95-14164
TRANSMISSION ELECTRON MICROSCOPY
In-situ TEM crystallization of sol-gel derived BaTiO3 thin films
[DE94-013260] p 619 N95-13821
TRANSMISSION LOSS
Propagation characteristics of 20/30 GHz links with a 40 deg masking angle p 464 N95-14672
Slant path L- and S-Band tree shadowing measurements p 465 N95-14678
TRANSMISSION RATE (COMMUNICATIONS)
Project OART: WDM, EDFA's and mixed data rates in a real-world testbed
[DE94-012234] p 601 N95-13670
TRANSMISSIVITY
Prototype explosives-detection system based on nuclear-resonance absorption in nitrogen
[DE94-015069] p 442 N95-15387
TRANSMITTERS
Research and development optical deep space antenna sizing study p 463 N95-14628
TRANSMUTATION
Direct-current proton-beam measurements at Los Alamos
[DE94-016280] p 599 N95-15360
Influence of transmutation on microstructure, density change, and embrittlement of vanadium and vanadium alloys irradiated in HFIR
[DE94-015202] p 446 N95-15431
TRANSONIC SPEED
Scale effects on aircraft and weapon aerodynamics
[AGARD-AG-323] p 393 N95-14103
TRANSONIC WIND TUNNELS
Experimental/analytical approach to understanding mistuning in a transonic wind tunnel compressor
[NASA-TM-108833] p 512 N95-14617
TRANSPARENCE
Development of chemical-vapor-deposited diamond for infrared optical applications: Summary of properties
[AD-A282999] p 448 N95-13686
Advanced laser source research
[AD-A283110] p 498 N95-13695
Optimization of transparent and reflecting electrodes for amorphous-silicon solar cells
[DE94-011841] p 520 N95-15355
TRANSPONDERS
Satellite communication technology and applications, 1995-2010 p 413 N95-13826
Evolutionary Telemetry and Command Processor (TCP) architecture p 420 N95-14162
SLR 2000 p 471 N95-14288
TRANSPORT AIRCRAFT
Numerical design of advanced multi-element airfoils
[NASA-CR-197135] p 404 N95-15762
TRANSPORT PROPERTIES
Flux pinning and forced entanglement by splayed columnar defects
[DE94-013994] p 620 N95-14008
Eddy viscosity transport equations and their relation to the k-epsilon model
[NASA-TM-108854] p 481 N95-14273
ENDL type formats for the LLNL Evaluated Atomic Data Library, EADL, for the Evaluated Electron Data Library, EEDL, and for the Evaluated Photon Data Library, EPDL
[DE94-016487] p 594 N95-14385
Transport phenomena in stratified multi-fluid flo w in the presence and absence of gravity p 488 N95-14563
Measurement of resistance to solute transport across surfactant-laden interfaces using a Fluorescence Recovery After Photobleaching (FRAP) technique p 490 N95-14574
Gravity-dependent transport in industrial processes p 459 N95-14580
Transport and nucleation processes during the vapor growth of diamond
[AD-A284411] p 626 N95-15812
TRANSPORT THEORY
Electrokinetic transport of heterogeneous particles in suspension p 444 N95-14581
Extension of the BRYNTRN code to monoenergetic light ion beams
[NASA-TP-3472] p 647 N95-15790
TRANSPORTATION NETWORKS
Dynamic modelling to assess the value of Electronic Data Interchange: A study in the Rotterdam port community
[PB94-195542] p 632 N95-14837
TRAPEZOIDS
The buckling response of symmetrically laminated composite plates having a trapezoidal planform area
[NASA-CR-196975] p 505 N95-13839
TRAPPED PARTICLES
Hydrogen transport and trapping in graphite
[UTIAS-347] p 437 N95-13652
TRAPPING
General properties of quantum optical systems in a strong field limit p 609 N95-13950
TREES (MATHEMATICS)
Intelligent alarming p 570 N95-14168
TREES (PLANTS)
Slant path L- and S-Band tree shadowing measurements p 465 N95-14678
Wideband electromagnetic scattering/analysis program. Electromagnetic scattering from the trunks and branches of trees
[AD-A283112] p 469 N95-15394
TREND ANALYSIS
A multiscale random field model for Bayesian image segmentation
[AD-A283875] p 515 N95-14358
The long-term forecast of station view periods p 419 N95-14621
TRENDS
Satellite communication technology and applications, 1995-2010 p 413 N95-13826
Radar altimeter calibration using SLR p 471 N95-14283
Low energy electron and atom elastic scattering cross sections from 0.1 to 30 keV
[AD-A283584] p 595 N95-15318
TRIAXIAL STRESSES
Errors induced in triaxial stress tensor calculations using incorrect lattice parameters
[DE94-013256] p 444 N95-13820
TRIBOLOGY
A new tribological test for candidate brush seal materials evaluation
[NASA-TM-106753] p 431 N95-13631
Physical and tribological characteristics of ion-implanted diamond films
[NASA-TM-106682] p 450 N95-14303
Recent progress and future prospects in the surface engineering and tribology of ceramics
[DE94-016315] p 456 N95-15778
TRIGGER CIRCUITS
Design of reliable high voltage avalanche transistor pulsers
[DE94-015323] p 473 N95-14261
TRIODES
RF vacuum microelectronics
[AD-A283123] p 478 N95-15613
TRITIUM
Welding irradiated stainless steel
[DE94-013661] p 500 N95-13645
TROPICAL METEOROLOGY
Water vapor and temperature inversions near the 0 C level over the tropical western Pacific
[AD-A282023] p 533 N95-14952
TROPICAL REGIONS
Analysis of deep convective clouds and their association with non-migrating atmospheric diurnal tides in the tropical troposphere
[PB94-187457] p 526 N95-13974
Landsat Pathfinder tropical forest information management system p 565 N95-14594
TROPICAL STORMS
Florida hurricanes and tropical storms 1871-1993: An historical survey
[PB94-198017] p 532 N95-14120
Short term teleconnections associated with western Pacific tropical cyclones
[AD-A284032] p 533 N95-14423
Upgrade of tropical cyclone surface wind field model
[AD-A283530] p 533 N95-15323
TROPOPAUSE
Meteorological investigation of ozone anomalies during the Arctic Boundary Layer Experiment (ABLE 3A)
[AD-A284494] p 534 N95-15771
TROPOSPHERE
Analysis of deep convective clouds and their association with non-migrating atmospheric diurnal tides in the tropical troposphere
[PB94-187457] p 526 N95-13974
Measurements of upper tropospheric moisture with a Raman lidar
[DE94-015748] p 531 N95-15411
Development and testing of a high-resolution model for tropospheric sulfate driven by observation-derived meteorology
[DE94-014910] p 525 N95-15864
TROPOSPHERIC SCATTERING
Troposcatter at the KU band
[AD-A281575] p 469 N95-15462
TRUSSES
Joint for a variable geometry truss and method of constructing same
[NASA-CASE-LAR-15136-1] p 506 N95-14138
TUBE CATHODES
RF vacuum microelectronics
[AD-A283123] p 478 N95-15613
TUMBLING MOTION
Surface characterization through shape oscillations of drops in microgravity and 1-g p 458 N95-14220
TUNGSTEN ALLOYS
High performance arcjet engines
[NASA-CR-195397] p 430 N95-13697
TUNGSTEN COMPOUNDS
One: Redox chemistry of bimetallic fulvalene complexes. 2: Oligocyclopentadienyl complexes
[DE94-014930] p 443 N95-15667
TUNING
Experimental/analytical approach to understanding mistuning in a transonic wind tunnel compressor
[NASA-TM-108833] p 512 N95-14617
A Lyman-alpha tunable acousto-optic filter for detecting superthermal flare protons
[NASA-CR-197119] p 613 N95-14908
TUNNEL JUNCTIONS
Resonant tunneling in small current-biased Josephson junctions
[DE94-016875] p 623 N95-15338
TURBIDITY
Turbidity of a binary fluid mixture: Determining eta p 487 N95-14552
TURBINE BLADES
The industrial use of CFD in the design of turbomachinery p 480 N95-14133
New methods, new methodology: Advanced CFD in the Snecma turbomachinery design process p 480 N95-14134
TURBINE ENGINES
Effect of surface roughness on local film cooling effectiveness and heat transfer coefficients
[AD-A283854] p 482 N95-14351
TURBINE PUMPS
Hybrid bearings for turbopumps and the like
[NASA-CASE-MFS-28491-1] p 500 N95-13819
Space Shuttle Main Engine turbopump bearing assessment program
[TABES PAPER 94-621] p 417 N95-14648
Reusable rocket engine turbopump health management system
[NASA-CR-195388] p 431 N95-15058
Cold flow simulation of the alternate turbopump development turbine of the Space Shuttle main engine high pressure fuel turbopump
[AD-A281676] p 419 N95-15447
Vehicle health management using adaptive techniques
[NASA-TM-108472] p 431 N95-15609
TURBINES
Effect of surface roughness on local film cooling effectiveness and heat transfer coefficients
[AD-A283854] p 482 N95-14351
TURBOCOMPRESSORS
Computational methods for preliminary design and geometry definition in turbomachinery p 480 N95-14128
Elements of a modern turbomachinery design system p 480 N95-14129
TURBOFAN ENGINES
Gas turbine prediffuser-combustor performance during operation with air-water mixture
[DOT/FAA/CT-93/52] p 411 N95-15683
TURBOGENERATORS
Development of the fuel cell power generation technology, 2
[DE94-780614] p 520 N95-15376
TURBOMACHINERY
Turbomachinery Design Using CFD
[AGARD-LS-195] p 479 N95-14127
Designing in three dimensions p 480 N95-14130
CFD methodology and validation for turbomachinery flows p 480 N95-14131
The industrial use of CFD in the design of turbomachinery p 480 N95-14133
New methods, new methodology: Advanced CFD in the Snecma turbomachinery design process p 480 N95-14134
The role of CFD in the design process p 481 N95-14135
Aero design of turbomachinery components: CFD in complex systems p 481 N95-14136
TURBULENCE
Flow-radiated noise. Study of the propagative spectral range of the wall pressure field
[PB94-201290] p 590 N95-13985
Determination of the similarity theory scaling parameters from the vertical gradients
[AD-A283833] p 533 N95-14340

Spectral analysis of vortex/free-surface interaction
[AD-A283210] p 492 N95-14658
Electro-optics: Propagation from IR to UV and sensor considerations. Part A: Propagation theory
p 467 N95-14833
On the physics of waves in the solar atmosphere: Wave heating and wind acceleration
[NASA-CR-196992] p 646 N95-15070
Turbulent upward flame spread on a vertical wall under external radiation
[PB94-207388] p 441 N95-15353

TURBULENCE EFFECTS
Numerical model for the weakly nonlinear propagation of sound through turbulence p 401 N95-14883
Atmospheric effects on the risetime and waveshape of sonic booms p 402 N95-14886
The effect of aircraft speed on the penetration of sonic boom noise into a flat ocean p 402 N95-14887
Wake turbulence p 405 N95-14894
New algorithms for the reduction of image degradation due to atmospheric turbulence.
[AD-A284891] p 615 N95-15772

TURBULENCE MODELS
Modeling turbulent flame propagation
[DE94-016618] p 438 N95-14391
A modified mixing length turbulence model for zero and adverse pressure gradients
[NASA-TM-106772] p 492 N95-14607
Turbulence: Engineering models, aircraft response
p 407 N95-14900
Comparison of different statistical models of turbulence by similarity methods
[DE94-015326] p 493 N95-15530
Laminar and turbulent flow computations of Type 4 shock-shock interference aerothermal loads using unstructured grids
[NASA-CR-195008] p 493 N95-15604
Phase transitions and connectivity in three-dimensional vortex equilibria
[DE94-014967] p 494 N95-15868

TURBULENT BOUNDARY LAYER
A modified mixing length turbulence model for zero and adverse pressure gradients
[NASA-TM-106772] p 492 N95-14607
Atmospheric effects on the risetime and waveshape of sonic booms p 402 N95-14886
Embedded function methods for compressible high speed turbulent flow
[NASA-CR-196936] p 492 N95-14932

TURBULENT FLOW
CFD methodology and validation for turbomachinery flows p 480 N95-14131
Modeling turbulent flame propagation
[DE94-016618] p 438 N95-14391
Transport phenomena in stratified multi-fluid flo w in the presence and absence of gravity p 488 N95-14563
A modified mixing length turbulence model for zero and adverse pressure gradients
[NASA-TM-106772] p 492 N95-14607
Interaction of chemistry, turbulence, and shock waves in hypervelocity flow
[AD-A282941] p 400 N95-14656
Embedded function methods for compressible high speed turbulent flow
[NASA-CR-196936] p 492 N95-14932
On the physics of waves in the solar atmosphere: Wave heating and wind acceleration
[NASA-CR-196992] p 646 N95-15070
Leak detection by acoustic emissions monitoring: An experimental investigation of the acoustic properties of leaks and the attenuation characteristics of soil
[AD-A283250] p 530 N95-15295
Comparison of different statistical models of turbulence by similarity methods
[DE94-015326] p 493 N95-15530
Laminar and turbulent flow computations of Type 4 shock-shock interference aerothermal loads using unstructured grids
[NASA-CR-195008] p 493 N95-15604

TURBULENT MIXING
Turbulent mixing of the HVOF thermal spray and coating oxidation
[DE94-015414] p 455 N95-15535
Investigation of ramp injectors for supersonic mixing enhancement
[NASA-CR-4634] p 494 N95-15605

TURING MACHINES
Unambiguous computation: Boolean hierarchies an sparse Turing-complete sets
[TR-483] p 575 N95-15597
On accessing and hiding information
p 587 N95-15641
Two heads are better than two tapes
[TR-493] p 575 N95-15644
Connections among space-bounded and multihead probabilistic automata
[TR-476] p 575 N95-15645

TWINNING
Ru2Ge3: Crystal growth and some properties
[DE94-015360] p 625 N95-15531

TWO BODY PROBLEM
Causality problems for Fermi's two-atom system
p 598 N95-13945

TWO DIMENSIONAL FLOW
An adaptively-refined, Cartesian, cell-based scheme for the Euler and Navier-Stokes equations
[NASA-TM-106754] p 392 N95-13817
The behavior of unsteady thermocapillary flows
p 483 N95-14530
Two methods for the study of vortex patch evolution on locally refined grids
[DE94-014965] p 494 N95-15867

TWO DIMENSIONAL MODELS
High-speed fixed and floating point implementation of delta-operator formulated discrete time systems
[AD-A283109] p 584 N95-13694
A two dimensional artificial reality p 560 N95-14052
Numerical solution of two-dimensional ablation problems using the finite control volume method with unstructured grids
[DE94-015012] p 428 N95-14664

TWO FLUID MODELS
Helium 2 slosh in low gravity p 487 N95-14554
Analysis of phase distribution phenomena in microgravity environments p 459 N95-14557

TWO PHASE FLOW
Future directions in two-phase flow and heat transfer in space p 482 N95-14523
Experimental investigation of the Marangoni effect on the stability of a double-diffusive layer
p 483 N95-14528
Thermocapillary convection in floating zones under simulated reduced-gravity conditions
p 483 N95-14529
The behavior of unsteady thermocapillary flows
p 483 N95-14530
Phase segregation due to simultaneous migration and coalescence p 484 N95-14537
Influence of flow on interface shape stability in low gravity p 484 N95-14538
Study of two-phase flow and heat transfer in reduced gravities p 487 N95-14555
Characterization of annular two-phase gas-liquid flows in microgravity p 487 N95-14556
Analysis of phase distribution phenomena in microgravity environments p 459 N95-14557
Bubble dynamics, two-phase flow, and boiling heat transfer in a microgravity environment
p 488 N95-14561
An application of miniscale experiments on Earth to refine microgravity analysis of adiabatic multiphase flow in space p 459 N95-14567
Survey of the 1991 geothermal exploration promotion
[DE94-780690] p 530 N95-14836
Effects of two-phase flow on the deflagration of porous energetic materials
[DE94-015353] p 442 N95-15375
Gas turbine prediffuser-combustor performance during operation with air-water mixture
[DOT/FAA/CT-93/52] p 411 N95-15683

U

U-2 AIRCRAFT
Counting condensation in the Antarctic Ozone Mission
[NASA-CR-197113] p 525 N95-15847

UBV SPECTRA
Diffuse bands versus extinction parameters
p 640 N95-15836

ULLAGE
Multi-dimensional modeling of pressurization and expulsion of multi-phase hydrogen propellant
[NASA-CR-195156] p 457 N95-14902

ULTRAHIGH FREQUENCIES
Slant path L- and S-Band tree shadowing measurements p 465 N95-14678
Communications availability: Estimation studies at AMSC p 466 N95-14681
S-Band propagation measurements
p 466 N95-14682
High-data-rate UHF line-of-sight communication experiment
[AD-A283592] p 468 N95-15321

ULTRAHIGH VACUUM
Physical and tribological characteristics of ion-implanted diamond films
[NASA-TM-106682] p 450 N95-14303
RF vacuum microelectronics
[AD-A283123] p 478 N95-15613

ULTRASONIC TESTS
Experimental hardware development for a pulsed ultrasonic data collection facility
[AD-A283331] p 615 N95-15872

ULTRASONICS
Nonlinear dynamics of drops and bubbles and chaotic phenomena p 485 N95-14541
Ultrasonic characterization of high T(c) and other unconventional superconductors
[AD-A282835] p 476 N95-15397

ULTRAVIOLET ABSORPTION
Study of interferences in ozone UV and chemiluminescence monitors
[PB94-197456] p 521 N95-14123
Measurements of ultraviolet absorption cross sections of NO2 at various pressures and temperatures
[AD-A283835] p 522 N95-14344

ULTRAVIOLET ASTRONOMY
Correlation between molecular lines and diffuse interstellar bands p 640 N95-15835
Porphyrins in the interstellar medium (in grains)
p 640 N95-15837

ULTRAVIOLET FILTERS
A Lyman-alpha tunable acousto-optic filter for detecting superthermal flare protons
[NASA-CR-197119] p 613 N95-14908

ULTRAVIOLET RADIATION
The effect of Low Earth Orbit exposure on some experimental fluorine and silicon-containing polymers
p 422 N95-14074
Emerging technology summary: Destruction of organic contaminants in air using advanced ultraviolet flashlamps
[PB94-194479] p 521 N95-14121
Environmental durability issues for solar power systems in low Earth orbit
[NASA-TM-106775] p 431 N95-15769
DIBS independent of accretion in T Tauri stars
p 639 N95-15829

ULTRAVIOLET SPECTRA
Electron-molecule collisions and UV signatures in flowfields
[AD-A281569] p 596 N95-15457
Correlation between molecular lines and diffuse interstellar bands p 640 N95-15835
Porphyrins in the interstellar medium (in grains)
p 640 N95-15837
Laboratory spectra of C60 and related molecular structures p 627 N95-15838

ULTRAVIOLET SPECTROMETERS
Ultraviolet-Infrared Mapping Interferometic Spectrometer
[NASA-CR-197099] p 613 N95-14806

ULTRAVIOLET TELESCOPES
Self contamination effects in the TAUVEX UV Telescope: Ground testing and computer simulation
p 421 N95-14067

UNDERGROUND STORAGE
Leak detection by acoustic emissions monitoring: An experimental investigation of the acoustic properties of leaks and the attenuation characteristics of soil
[AD-A283250] p 530 N95-15295
Leak detection by acoustic emission monitoring. Phase 1: Feasibility study
[AD-A283775] p 493 N95-15332

UNDERWATER ACOUSTICS
Flow-radiated noise. Study of the propagative spectral range of the wall pressure field
[PB94-201290] p 590 N95-13985
Improving transient signal synthesis through noise modeling and noise removal
[AD-A281677] p 592 N95-15448

UNDERWATER RESEARCH LABORATORIES
Design of components for the NASA OCEAN project
[NASA-CR-197207] p 535 N95-14906

UNDERWATER VEHICLES
Telerobotics in the deep ocean p 504 N95-14026
From Antarctica to space: Use of telepresence and virtual reality in control of remote vehicles
p 427 N95-14099

UNITED NATIONS
The Bureau Gravimetrique International
p 516 N95-15795

UNITED STATES
Helping small companies commercialize public-sector technology
[TABES PAPER 94-407] p 415 N95-14635
Annual review of aircraft accident data: US air carrier operations, calendar year 1992
[NTSB/ARC-94/02] p 407 N95-15066

UNIVERSITIES
A NASA/industry/university partnership for development of dual-use vibration isolation technology
[TABES PAPER 94-613] p 416 N95-14643

UNIX (OPERATING SYSTEM)
Xwake 1.0: A new tool for wakefield and impedance calculations
[DE94-015545] p 574 N95-15418
UNSTEADY AERODYNAMICS
User's guide for ENSAERO: A multidisciplinary program for fluid/structural/control interaction studies of aircraft (release 1)
[NASA-TM-108853] p 391 N95-13662
Higher harmonic control analysis for vibration reduction of helicopter rotor systems
[NASA-TM-103855] p 391 N95-14419
Sonic boom interaction with turbulence
p 402 N95-14884
UNSTEADY FLOW
The flow induced by the coalescence of two initially stationary drops
[NASA-TM-106752] p 478 N95-13653
Unsteady flows in turbines: Impact on design procedure p 480 N95-14132
Aero design of turbomachinery components: CFD in complex systems p 481 N95-14136
Observations of hot stars and eclipsing binaries with FRESIP p 644 N95-14508
The behavior of unsteady thermocapillary flows
p 483 N95-14530
Control of unsteady separated flow associated with the dynamic stall of airfoils
[NASA-CR-197024] p 400 N95-14613
Spectral analysis of vortex/free-surface interaction
[AD-A283210] p 492 N95-14658
Numerical study of the effects of icing on viscous flow over wings
[NASA-CR-197102] p 400 N95-14803
Prediction of rotor-blade deformations due to unsteady airloads
[AD-A284467] p 410 N95-15821
UNSWEPT WINGS
Numerical design of advanced multi-element airfoils
[NASA-CR-197135] p 404 N95-15762
UPPER ATMOSPHERE
Ultrasensitive infrared chemiluminescence detection
[AD-A283531] p 440 N95-14958
Overview of PAMS meteorological monitoring requirements
[PB94-176658] p 534 N95-15383
Research on characterization of the upper atmosphere using lidar
[AD-A283241] p 530 N95-15401
UPWELLING WATER
An analysis of eddy resolving global ocean models in the Southern Ocean
[AD-A283211] p 536 N95-15626
UPWIND SCHEMES (MATHEMATICS)
CFD methodology and validation for turbomachinery flows p 480 N95-14131
Computational aerodynamics based on the Euler equations
[AGARD-AG-325] p 398 N95-14264
URANIUM
A theoretical study of 30 to 50 angstrom noble gas heavy ion lithography
[DE94-015262] p 442 N95-15436
UROLOGY
Water intake and urinary volume during 20 days bed-rest in young women p 548 N95-15134
USER MANUALS (COMPUTER PROGRAMS)
User's guide for ENSAERO: A multidisciplinary program for fluid/structural/control interaction studies of aircraft (release 1)
[NASA-TM-108853] p 391 N95-13662
GSOSTATS database: USAF synchronous satellite catalog data conversion software. User's guide and software maintenance manual, version 2.1
[NASA-TM-106760] p 568 N95-13894
PHOENIX user manual. First version
[PB94-189081] p 568 N95-13989
NLEdit: A generic graphical user interface for Fortran programs
[NASA-TM-4543] p 572 N95-14206
Update to the NASA Lewis ice accretion code LEWICE
[NASA-CR-195387] p 481 N95-14295
Graphical user interface for the NASA FLOPS aircraft performance and sizing code
[NASA-TM-106649] p 408 N95-14604
CTAS data analysis program
[NASA-TM-108842] p 406 N95-14611
LSENS, a general chemical kinetics and sensitivity analysis code for homogeneous gas-phase reactions. 2: Code description and usage
[NASA-RP-1329] p 442 N95-15512
Automatic TLI recognition system, part 2
[DE94-015393] p 579 N95-15534
The lambda loop transformation toolkit (user's reference manual)
[TR-511] p 587 N95-15733
Users manual for the Surface Currents Data Base (SCDB) Management System (SCDBMS), version 1.0
[NASA-CR-197021] p 537 N95-15753
Enhanced capabilities and updated users manual for axial-flow turbine preliminary sizing code TURBAN
[NASA-CR-195405] p 405 N95-15912
USER REQUIREMENTS
Human-machine interface hardware: The next decade
p 561 N95-14055
Use of the user action notation at the Naval Research Laboratory Human-Computer Interaction Laboratory
[AD-A281680] p 563 N95-15449

V

VACANCIES (CRYSTAL DEFECTS)
Small-angle x-ray scattering studies of microvoids in amorphous-silicon-based semiconductors
[DE94-011840] p 520 N95-15406
Fourth Workshop on the Role of Point Defects and Defect Complexes in Silicon Device Processing
[DE94-011850] p 624 N95-15426
Electronic characterization of defects in narrow gap semiconductors
[NASA-CR-197217] p 626 N95-15752
VACCINES
World Reference Center for Arboviruses
[AD-A281635] p 550 N95-15445
VACUUM
Photon statistics of a two-mode squeezed vacuum
p 598 N95-13909
Field-emitter arrays for RF vacuum microelectronics
[AD-A283549] p 476 N95-15327
VACUUM CHAMBERS
Eighteenth Space Simulation Conference: Space Mission Success Through Testing
[NASA-CP-3280] p 420 N95-14062
Refurbishment of a 39 foot thermal vacuum chamber
p 418 N95-14085
Alpha LAMP Integration Facility p 418 N95-14094
The AEDC aerospace chamber 7V: An advanced test capability for infrared surveillance and seeker sensors
p 418 N95-14097
New potentials of NIICHIMMASH's thermal vacuum facilities p 418 N95-14098
VACUUM EFFECTS
A method of measuring the amplitude-modulated vacuum field near a conducting mirror
p 471 N95-13921
VACUUM SYSTEMS
Experimental study of solar simulator mirror cryocontamination p 421 N95-14065
David Florida Laboratory Thermal Vacuum Data Processing System p 418 N95-14079
The realuminizing of the 7-meter-diameter solar simulator collimating mirror p 424 N95-14081
Partial pressure analysis in space testing
p 424 N95-14084
Measurements of ultraviolet absorption cross sections of NO2 at various pressures and temperatures
[AD-A283835] p 522 N95-14344
VALENCE
The structure of new synthetic manganese oxide octahedral molecular sieves
[DE94-016348] p 596 N95-15381
VALIDITY
Fracture mechanics validity limits p 511 N95-14480
A proposed framework for computational fluid dynamics code calibration and validation
[DE94-015799] p 493 N95-15351
VANADATES
Anomalous temperature dependence of the lattice parameters in HoPO4 and HoVO4: Rare earth quadrupolar effects
[DE94-015086] p 622 N95-14608
VANADIUM
High temperature cyclic behaviour of aerospace materials: Room temperature validation tests of Ti-6Al-4V
[AGARD-AR-328] p 506 N95-14198
Influence of transmutation on microstructure, density change, and embrittlement of vanadium and vanadium alloys irradiated in HFIR
[DE94-015202] p 446 N95-15431
VANADIUM ALLOYS
Influence of transmutation on microstructure, density change, and embrittlement of vanadium and vanadium alloys irradiated in HFIR
[DE94-015202] p 446 N95-15431
VANADIUM COMPOUNDS
Inelastic neutron scattering and molecular dynamics simulations of water adsorbed in the molecular sieves AlPO4-11, AlPO4-5, AlPO4-8 and VPI-5
[DE94-013337] p 593 N95-13678
VANES
Effect of surface roughness on local film cooling effectiveness and heat transfer coefficients
[AD-A283854] p 482 N95-14351
VAPOR DEPOSITION
Development of chemical-vapor-deposited diamond for infrared optical applications: Summary of properties
[AD-A282999] p 448 N95-13686
Vapor transport crystal growth of mercury-cadmium-telluride in microgravity
p 458 N95-14216
Cross-effects in microgravity flows
p 459 N95-14565
Surface processes in CVD diamond growth
[AD-A280964] p 622 N95-14655
Optimization of transparent and reflecting electrodes for amorphous-silicon solar cells
[DE94-011841] p 520 N95-15355
Surface passivation for 3-5 semiconductor processing: Stable gallium sulphide films by MOCVD
[NASA-TM-106761] p 477 N95-15587
Modeling, simulation and engineering scale-up procedures for design of CVD reactors
[AD-A284919] p 494 N95-15760
Transport and nucleation processes during the vapor growth of diamond
[AD-A284411] p 626 N95-15812
VAPOR PHASE EPITAXY
Vapor transport crystal growth of mercury-cadmium-telluride in microgravity
p 458 N95-14216
Protein crystal growth results from the United States Microgravity Laboratory-1 mission p 458 N95-14225
Strained-layer InGaAs(P)/InP quantum well semiconductor lasers grown by organometallic vapour phase epitaxy
[PB94-201399] p 622 N95-14795
VAPOR PHASES
Simulation of coal and char nitrogen reactions in combustion
[DE94-013941] p 440 N95-15291
LSENS, a general chemical kinetics and sensitivity analysis code for homogeneous gas-phase reactions. 2: Code description and usage
[NASA-RP-1329] p 442 N95-15512
Investigating the 3.3 micron infrared fluorescence from naphthalene following ultraviolet excitation
p 599 N95-15839
Investigation of a laboratory candidate for the carrier of the 4430 A diffuse interstellar band
p 641 N95-15840
VAPOR PRESSURE
Solubility, viscosity and density of refrigerant and lubricant mixtures
[DE94-016949] p 454 N95-15343
VAPORIZING
ASSERT-1992. Fundamental studies of a high energy molecular system: Spectroscopy of boron in hydrogen clusters
[AD-A283181] p 593 N95-14155
VAPORS
Effects of thermocapillarity on an evaporating extended meniscus in microgravity p 488 N95-14559
Interfacial force field characterization of a constrained vapor bubble thermosyphon using IAI
p 488 N95-14560
Cross-effects in microgravity flows
p 459 N95-14565
Surface Acoustic Wave (SAW) microsensors to monitor multi-component vapor challenges to adsorbents and adsorbent-based air filtration systems
[AD-A284222] p 497 N95-15334
Excimer emission from alkali diatomic and alkaline-earth-noble gas molecules
[AD-A281662] p 596 N95-15446
VARIABILITY
Observations of extragalactic sources with the Metsaehovi radio telescope at 22-87 GHz
[PB94-197712] p 637 N95-13982
Towards developing an analytical procedure of defining the equatorial electrojet for correcting satellite magnetic anomaly data
[NASA-CR-193621] p 526 N95-14267
Monitoring the variability of active galactic nuclei from a space-based platform p 644 N95-14509
Regional cutaneous microvascular flow responses during gravitational and LBNP stresses
p 547 N95-15128
Optical variability in the equatorial and southeast Pacific
[AD-A283894] p 536 N95-15425

Individual variability in the transmission of vertical vibration from seat to head
[ISVR-TR-236] p 563 N95-15850

VARIABLE STARS
Asteroseismology: Theory and phenomenology
p 643 N95-14502

VARIANCE (STATISTICS)
Investigation of Allan variance for determining noise spectral forms with application to microwave radiometry
[NASA-CR-194985] p 516 N95-15727

VECTOR ANALYSIS
On the possibility of a quantum mechanical phase space representation p 606 N95-13931

VECTOR PROCESSING (COMPUTERS)
Methodology for the parallel direct solution of finite element systems
[PB94-198009] p 585 N95-13991

VECTOR QUANTIZATION
1994 Science Information Management and Data Compression Workshop
[NASA-CP-3277] p 564 N95-14585
Radiometric resolution enhancement by lossy compression as compared to truncation followed by lossless compression p 564 N95-14588
Synthetic aperture radar signal data compression using block adaptive quantization p 565 N95-14590
Planning/scheduling techniques for VQ-based image compression p 566 N95-14595

VEGETATION GROWTH
Design of components for the NASA OCEAN project
[NASA-CR-197207] p 535 N95-14906

VELOCITY DISTRIBUTION
Interplanetary medium data book, supplement 5, 1988-1993
[NASA-TM-109957] p 642 N95-13658
Photochemical urban airshed modeling using diagnostic and dynamic meteorological fields
[PB94-176120] p 616 N95-13973
Transport phenomena in stratified multi-fluid flo w in the presence and absence of gravity p 488 N95-14563
Particle experiments in thermal and velocity gradients
p 489 N95-14564
Upgrade of tropical cyclone surface wind field model
[AD-A283530] p 533 N95-15323
A three-dimensional fast solver for arbitrary vorton distributions
[DE94-012581] p 404 N95-15570
An algorithm for rezoning particle-in-cell calculations
[DE94-016056] p 619 N95-15774
Validation of ERS-1 environmental data products
[NASA-CR-197111] p 517 N95-15848
On the behavior of three-dimensional wave packets in viscously spreading mixing layers
[NASA-TM-106770] p 495 N95-15908

VELOCITY MEASUREMENT
Multi-velocity component LDV
[NASA-CASE-ARC-11925-1] p 499 N95-14668
Ultrasonic characterization of high T(c) and other unconventional superconductors
[AD-A282835] p 476 N95-15397
Groundspeed filtering for CTAS
[NASA-CR-197223] p 497 N95-15785

VENTS
Parachute having improved vent line stacking
[NASA-CASE-MFS-28508-1] p 393 N95-14182

VENUS (PLANET)
A radio telescope for the calibration of radio sources at 32 gigahertz p 463 N95-14626

VENUS ATMOSPHERE
Venusian atmospheric equilibrium chemistry at the Pioneer Venus anomalous event altitude
p 645 N95-13721

VERBAL COMMUNICATION
NASA/DOD Aerospace Knowledge Diffusion Research Project. Paper 43: The role of information resource training in aerospace education. Expanded version
[NASA-TM-109961] p 632 N95-14619

VERTEBRATES
Neuronal types in the chicken's statoacoustic ganglion
p 539 N95-15116

VERTICAL AIR CURRENTS
Simple atmospheric perturbation models for sonic-boom-signature distortion studies
p 402 N95-14888

VERTICAL FLIGHT
Vertical flight terminal operational procedures. A summary of FAA research and development
[AD-A283550] p 413 N95-15328

VERTICAL LANDING
Vertical flight terminal operational procedures. A summary of FAA research and development
[AD-A283550] p 413 N95-15328

VERY HIGH FREQUENCIES
Refractive effects from VHF to EHF. Part A: Propagation Mechanisms p 467 N95-14831
Refractive effects from VHF to EHF. Part B: Propagation models p 467 N95-14832

VERY LARGE SCALE INTEGRATION
A gate level simulator for alpha-particle-induced transient faults
[AD-A283871] p 474 N95-14355
The development of lossless data compression technology for remote sensing applications
p 565 N95-14593
Theory and implementation of a VLSI stray insensitive switched capacitor composite operational amplifier
[AD-A283536] p 476 N95-15325

VERY LONG BASE INTERFEROMETRY
Global reference frame: Intercomparison of results (SLR, VLBI and GPS) p 527 N95-14276
Global and regional kinematics with GPS
p 527 N95-14279
Global and regional kinematics with VLBI
p 527 N95-14280
Earth orientation parameters p 527 N95-14281
Low-Earth-Orbiter resource allocation and capacity planning for the DSN using LEO4CAST
p 419 N95-14632

VESTIBULAR NYSTAGMUS
The influence of gravity on vestibular nystagmus in humans p 546 N95-15121

VESTIBULAR TESTS
Neurohumoral reactions to long-term vestibular stimulation in man p 542 N95-15091
Will man need the vestibular system in generations to come? p 542 N95-15092
Psychophysiological aspects of increasing resistance to space motion sickness p 542 N95-15093
Vestibular ontogeny: Measuring the influence of the dynamic environment p 544 N95-15105
The influence of gravity on vestibular nystagmus in humans p 546 N95-15121

VESTIBULES
The musculoskeletal and vestibular effects of long term repeated exposure to sustained high-G
[AGARD-AR-317] p 562 N95-14263
Will man need the vestibular system in generations to come? p 542 N95-15092
Structure of avian tectorial, otolithic and cupular membranes p 539 N95-15117
Functional participation of the valvula cerebelli on the goldfish dorsal light response p 539 N95-15119

VIBRATION
Nondestructive analysis and development
[NASA-CR-196987] p 505 N95-13886
Adjustable bias column end joint assembly
[NASA-CASE-LAR-14899-1] p 459 N95-14111
Dynamics and statics of nonaxisymmetric and symmetric liquid bridges p 484 N95-14533
Individual variability in the transmission of vertical vibration from seat to head
[ISVR-TR-236] p 563 N95-15850

VIBRATION DAMPING
Higher harmonic control analysis for vibration reduction of helicopter rotor systems
[NASA-TM-103855] p 391 N95-14419

VIBRATION EFFECTS
Stochastic model of the residual acceleration environment in microgravity p 459 N95-14540
Experimental analysis of thread movement in bolted connections due to vibrations
[NASA-CR-197065] p 502 N95-14904

VIBRATION ISOLATORS
Basic features of the STS/Spacelab vibration environment p 428 N95-14210
A NASA/industry/university partnership for development of dual-use vibration isolation technology
[TABES PAPER 94-613] p 416 N95-14643

VIBRATION MEASUREMENT
Acceleration recorder and playback module
[NASA-CASE-MSC-22008-1] p 496 N95-14180
Acoustic resonance spectroscopy intrinsic seals
[DE94-016207] p 591 N95-15359
Test Operation Procedure (TOP): Vibration testing of helicopter equipment
[AD-A284433] p 410 N95-15815

VIBRATION MODE
Quantum statistics of Raman scattering model with Stokes mode generation p 610 N95-13958

VIBRATION TESTS
Dynamics of the McDonnell-Douglas Large Scale Dynamic Rig and dynamic calibration of the rotor balance
[NASA-TM-108855] p 391 N95-13891
System level mechanical testing of the Clementine spacecraft p 425 N95-14087
Evaluation of sensor placement algorithms for on-orbit identification of space platforms p 425 N95-14088
Space Shuttle Main Engine turbopump bearing assessment program
[TABES PAPER 94-621] p 417 N95-14648
Experimental analysis of thread movement in bolted connections due to vibrations
[NASA-CR-197065] p 502 N95-14904
Vestibular ontogeny: Measuring the influence of the dynamic environment p 544 N95-15105
Vehicle health management using adaptive techniques
[NASA-TM-108472] p 431 N95-15609
Advanced Turbine Technology Applications Project (ATTAP)
[NASA-CR-195393] p 634 N95-15743
Test Operation Procedure (TOP): Vibration testing of helicopter equipment
[AD-A284433] p 410 N95-15815

VIBRATIONAL SPECTRA
Basic features of the STS/Spacelab vibration environment p 428 N95-14210

VIBRATIONAL STATES
Infrared/submillimeter wave studies of molecular collision kinetics
[AD-A281379] p 594 N95-14362

VIBRATORY LOADS
Higher harmonic control analysis for vibration reduction of helicopter rotor systems
[NASA-TM-103855] p 391 N95-14419
Experimental analysis of thread movement in bolted connections due to vibrations
[NASA-CR-197065] p 502 N95-14904

VIDEO COMMUNICATION
Project OART: WDM, EDFA's and mixed data rates in a real-world testbed
[DE94-012234] p 601 N95-13670
Use of 64 kbits/s digital channel for image transmission: Using low scan two-way video
[PB94-189099] p 461 N95-14147

VIDEO COMPRESSION
Performance of customized DCT quantization tables on scientific data p 564 N95-14586
Summary of activities for University of California
[AD-A283890] p 632 N95-15423
Video transmission for quantized variable bandwidth networks
[AD-A284892] p 470 N95-15750

VIDEO DATA
Summary of activities for University of California
[AD-A283890] p 632 N95-15423

VIEWING
Interactive Computer-Enhanced Remote Viewing System (ICERVS): Subsystem design report, phase 2
[DE94-014513] p 563 N95-15309

VIKING LANDER SPACECRAFT
Martian environmental simulation for a deployable lattice mast p 423 N95-14076

VINYL POLYMERS
Radical polymerization of vinyl acetate and methyl methacrylate using organochromium initiators complexed with macrocyclic polyamines
[AD-A280828] p 451 N95-14316
Radical polymerization of vinyl acetate in the presence of trialkyl phosphites
[AD-A280829] p 451 N95-14324

VINYL RADICAL
NMR studies of polymers at interfaces
[AD-A281570] p 455 N95-15458

VIRTUAL MEMORY SYSTEMS
Performance measurement and analysis techniques for parallel and distributed programs
[DE94-016429] p 578 N95-14384

VIRTUAL REALITY
Human Machine Interfaces for Teleoperators and Virtual Environments
[NASA-CP-10071] p 554 N95-14013
Visual interfaces: The human perceiver
p 554 N95-14014
Tactual interfaces: The human perceiver
p 554 N95-14016
The display of tactile information p 554 N95-14017
Telerobotic remote presence: Achievements and challenges p 504 N95-14023
Issues in the design of high dexterity, force reflective teleoperators p 555 N95-14024
Tele-existence and/or cybernetic interface studies in Japan p 555 N95-14025
Some criteria for teleoperators and virtual environments from experiences with vehicle/operator simulation
p 556 N95-14026
Man-machine interfaces in health care
p 556 N95-14029
Telérobotics in rehabilitation: Barriers to a virtual existence p 556 N95-14030
Creating better virtual worlds p 556 N95-14031
Interacting with virtual worlds p 556 N95-14032
Virtual reality at work p 556 N95-14033
The Ames Virtual Environment Workstation: Implementation issues and requirements
p 557 N95-14034
Virtual acoustic displays p 557 N95-14035

Varieties of virtualization p 557 N95-14036
The exploration metaphor p 557 N95-14037
The Teleprasenz Consortium: Structure and intentions p 558 N95-14039
A high performance two degree-of-freedom kinesthetic interface p 558 N95-14042
Perceptual and performance consequences of flight in virtual worlds p 558 N95-14043
Development of visual 3D virtual environment for control software p 559 N95-14048
A two dimensional artificial reality p 560 N95-14052
Binaural room simulation p 561 N95-14053
Active localization of virtual sounds p 561 N95-14054
Human-machine interface hardware: The next decade p 561 N95-14055
Manual discrimination of force p 561 N95-14057
Implementation of a three degree of freedom, motor/brake hybrid force output device for virtual environment control tasks p 562 N95-14058
VERDEX: A virtual environment demonstrator for remote driving applications p 562 N95-14060
Destabilizing effects of visual environment motions simulating eye movements or head movements p 562 N95-14061
From Antarctica to space: Use of telepresence and virtual reality in control of remote vehicles p 427 N95-14099

VIRUSES
World Reference Center for Arboviruses
[AD-A281635] p 550 N95-15445

VISCOELASTICITY
Dynamics of hard sphere colloidal dispersions p 490 N95-14573
New techniques for diffusing-wave spectroscopy p 444 N95-14575

VISCOSITY
The flow induced by the coalescence of two initially stationary drops
[NASA-TM-106752] p 478 N95-13653
Resonator response to non-Newtonian fluids
[DE94-013450] p 473 N95-14308
Two-layer viscous instability in a rotating couette device p 489 N95-14566
The extensional rheology of non-Newtonian materials p 489 N95-14569
Solubility, viscosity and density of refrigerant and lubricant mixtures
[DE94-016949] p 454 N95-15343

VISCOUS FLOW
CFD methodology and validation for turbomachinery flows p 480 N95-14131
Aero design of turbomachinery components: CFD in complex systems p 481 N95-14136
Numerical simulation of shock-induced combustion past blunt bodies using shock-fitting technique
[NASA-CR-197013] p 437 N95-14268
The breakup of a liquid jet at microgravity p 484 N95-14535
Numerical study of the effects of icing on viscous flow over wings
[NASA-CR-197102] p 400 N95-14803
Computational methods for PDE's in flow control, superconductivity, fluid flows and other applications
[AD-A282912] p 493 N95-15390
Cold flow simulation of the alternate turbopump development turbine of the Space Shuttle main engine high pressure fuel turbopump
[AD-A281676] p 419 N95-15447

VISCOUS FLUIDS
Tactile display device using an electrorheological fluid
[NASA-CASE-LAR-14860-1] p 472 N95-14112
Resonator response to non-Newtonian fluids
[DE94-013450] p 473 N95-14308

VISIBLE SPECTRUM
Laboratory spectra of C60 and related molecular structures p 627 N95-15838

VISION
Vision, learning, and development
[TR-492-REV] p 553 N95-15787

VISUAL ACUITY
The applicability of commercial glare test devices in the aeromedical certification of pilot applicants
[DOT/FAA/AM-94/15] p 540 N95-14176
Developing Guided Search 3.0. The next generation of a model visual search
[AD-A283956] p 552 N95-14369

VISUAL DISCRIMINATION
A vision based attitude and position estimation algorithm for rendezvous and docking p 414 N95-13831

VISUAL OBSERVATION
Global surface-based cloud observation for ISCCP
[NASA-CR-198990] p 532 N95-14265

VISUAL PERCEPTION
Visual interfaces: The human perceiver p 554 N95-14014
The applicability of commercial glare test devices in the aeromedical certification of pilot applicants
[DOT/FAA/AM-94/15] p 540 N95-14176
Developing Guided Search 3.0. The next generation of a model visual search
[AD-A283956] p 552 N95-14369
Visual motion perception and visual information processing
[AD-A282928] p 581 N95-14847
Control of selective perception using Bayes nets and decision theory
[TR-468] p 573 N95-15151

VISUAL STIMULI
Visual motion perception and visual information processing
[AD-A282928] p 581 N95-14847

VISUAL TASKS
Developing Guided Search 3.0. The next generation of a model visual search
[AD-A283956] p 552 N95-14369
The electrocortical correlates of fluctuating states of attention during vigilance tasks
[NASA-CR-197051] p 552 N95-14864
Target acquisition: Human observer performance studies and TARGAC model validation
[AD-A284436] p 553 N95-15816

VITERBI DECODERS
Convolutional encoding of self-dual block codes (2) p 462 N95-14623

VOICE COMMUNICATION
Advanced distributed simulation technology: Digital Voice Gateway Reference Guide
[AD-A283154] p 460 N95-13696
Communications availability: Estimation studies at AMSC p 466 N95-14681
Discrete-event-dynamic-system-based approaches for control in integrated voice/data multihop radio networks
[AD-A284413] p 470 N95-15813

VOICE CONTROL
Watch what you say, your computer might be listening: A review of automated speech recognition p 555 N95-14021

VOICE DATA PROCESSING
i-speech: Experiments with a single level feedback paradigm
[TR-509] p 575 N95-15640

VOIDS
Experiments to examine the contribution of gas atoms to void formation in irradiated metals
[DE94-015209] p 446 N95-15433

VOLT-AMPERE CHARACTERISTICS
Kinetic theory for electrodic phase transitions: The voltammogram
[AD-A283039] p 619 N95-13691
Pre-flight POLAR code predictions for the CHAWS space flight experiment
[AD-A280951] p 428 N95-14599

VOLTAGE CONTROLLED OSCILLATORS
Programmable high voltage power supply with regulation confined to the high voltage section
[NASA-CASE-GSC-13289-1] p 478 N95-15681

VOLTAGE CONVERTERS (DC TO DC)
Programmable high voltage power supply with regulation confined to the high voltage section
[NASA-CASE-GSC-13289-1] p 478 N95-15681

VOLTAGE REGULATORS
Programmable high voltage power supply with regulation confined to the high voltage section
[NASA-CASE-GSC-13289-1] p 478 N95-15681

VORTEX GENERATORS
Axis switching and spreading of an asymmetric jet: Role of vorticity dynamics
[NASA-TM-106385] p 398 N95-14418

VORTEX LATTICE METHOD
Phase transitions and connectivity in three-dimensional vortex equilibria
[DE94-014967] p 494 N95-15868

VORTEX SHEDDING
High angle of attack aerodynamics p 399 N95-14450
Computational methods for PDE's in flow control, superconductivity, fluid flows and other applications
[AD-A282912] p 493 N95-15390

VORTICES
Hybrid structured/unstructured grid computations for the F/A-18 at high angle of attack p 394 N95-14233
F/A-18 and F-16 forebody vortex control, static and rotary-balance results p 397 N95-14254
Low-energy pneumatic control of forebody vortices p 398 N95-14256
Integration of a mechanical forebody vortex control system into the F-15 p 398 N95-14258
Flight evaluation of pneumatic forebody vortex control in post-stall flight p 398 N95-14259
Computational aerodynamics based on the Euler equations
[AGARD-AG-325] p 398 N95-14264
Axis switching and spreading of an asymmetric jet: Role of vorticity dynamics
[NASA-TM-106385] p 398 N95-14418
High angle of attack aerodynamics p 399 N95-14450
Spectral analysis of vortex/free-surface interaction
[AD-A283210] p 492 N95-14658
Wake turbulence p 405 N95-14894
Turbulent mixing of the HVOF thermal spray and coating oxidation
[DE94-015414] p 455 N95-15535
A three-dimensional fast solver for arbitrary vorton distributions
[DE94-012581] p 404 N95-15570
An analysis of eddy resolving global ocean models in the Southern Ocean
[AD-A283211] p 536 N95-15626
Plasma arc welding torch having means for vortexing plasma gas exiting the welding torch
[NASA-CASE-MFS-28828-1] p 503 N95-15670
Two methods for the study of vortex patch evolution on locally refined grids
[DE94-014965] p 494 N95-15867
Phase transitions and connectivity in three-dimensional vortex equilibria
[DE94-014967] p 494 N95-15868

VORTICITY
Axis switching and spreading of an asymmetric jet: Role of vorticity dynamics
[NASA-TM-106385] p 398 N95-14418
Interaction of chemistry, turbulence, and shock waves in hypervelocity flow
[AD-A282941] p 400 N95-14656
Meteorological investigation of ozone anomalies during the Arctic Boundary Layer Experiment (ABLE 3A)
[AD-A284494] p 534 N95-15771
Two methods for the study of vortex patch evolution on locally refined grids
[DE94-014965] p 494 N95-15867
Phase transitions and connectivity in three-dimensional vortex equilibria
[DE94-014967] p 494 N95-15868

W

WAFERS
Piezoelectric loudspeaker
[NASA-CASE-LAR-15138-1] p 590 N95-14110

WALL PRESSURE
Flow-radiated noise. Study of the propagative spectral range of the wall pressure field
[PB94-201290] p 590 N95-13985

WALLS
Upward flame spread along the vertical corner walls (October 1993)
[PB94-206299] p 441 N95-15352
Turbulent upward flame spread on a vertical wall under external radiation
[PB94-207388] p 441 N95-15353
Comparison of wall-fire behavior with and without a ceiling
[PB94-207404] p 441 N95-15354

WARNING SYSTEMS
Verification of severe local storms forecasts issued by the National Severe Storms Forecast Center: 1993
[PB94-195898] p 532 N95-14117
Intelligent alarming p 570 N95-14168
Aircraft maneuver envelope warning system
[NASA-CASE-ARC-11953-1] p 411 N95-14518
The Global Emergency Observation and Warning System
[TABES PAPER 94-622] p 417 N95-14649

WASTE TREATMENT
Process development of thermal hydrodechlorination
[PB94-195518] p 525 N95-15870

WATER
Inelastic neutron scattering and molecular dynamics simulations of water adsorbed in the molecular sieves AlPO4-11, AlPO4-5, AlPO4-8 and VPI-5
[DE94-013337] p 593 N95-13678
Applications of squeezed states: Bogoliubov transformations and wavelets to the statistical mechanics of water and its bubbles p 607 N95-13939
Single-phase heat transfer and pressure drop characteristics of an integral-spine-fin within an annulus
[PB94-194073] p 482 N95-14407
Adsorption and diffusion of fluids in well-characterized adsorbent materials
[DE94-016953] p 454 N95-15344

WATER DEPTH
Calculation of movable bed friction factors
[AD-A283529] p 536 N95-15440

WATER IMMERSION
Transient blood/plasma density and hematocrit effects after passive (sitting) thermoneutral water immersion in men p 548 N95-15131
WATER LOSS
Water intake and urinary volume during 20 days bed-rest in young women p 548 N95-15134
WATER POLLUTION
Process development of thermal hydrodechlorination [PB94-195518] p 525 N95-15870
WATER TREATMENT
Process development of thermal hydrodechlorination [PB94-195518] p 525 N95-15870
WATER TUNNEL TESTS
Comparison of X-31 flight, wind-tunnel, and water-tunnel yawing moment asymmetries at high angles of attack p 394 N95-14234
Static and dynamic force/moment measurements in the Eidetics water tunnel p 395 N95-14238
Spectral analysis of vortex/free-surface interaction [AD-A283210] p 492 N95-14658
WATER VAPOR
Determination of the similarity theory scaling parameters from the vertical gradients [AD-A283833] p 533 N95-14340
Water vapor and temperature inversions near the 0 C level over the tropical western Pacific [AD-A282023] p 533 N95-14952
Measurements of upper tropospheric moisture with a Raman lidar [DE94-015748] p 531 N95-15411
Gas turbine prediffuser-combustor performance during operation with air-water mixture [DOT/FAA/CT-93/52] p 411 N95-15683
WATER WAVES
Calculation of movable bed friction factors [AD-A283529] p 536 N95-15440
Selecting wave gauge sites for monitoring harbor oscillations: A case study for Kahului Harbor, Hawaii [AD-A281707] p 536 N95-15452
WAVE AMPLIFICATION
Sqeezing generated by a nonlinear master equation and by amplifying-dissipative Hamiltonians p 588 N95-13926
WAVE DIFFRACTION
Ground wave and diffraction, A p 467 N95-14828
Ground wave and diffraction, B p 467 N95-14829
Sonic boom interaction with turbulence p 402 N95-14884
Atmospheric propagation at larger lateral distances from the flight track p 402 N95-14885
Simple atmospheric perturbation models for sonic-boom-signature distortion studies p 402 N95-14888
Problems in nonlinear acoustics: Surface acoustic waves, diffracting sound beams, and fluid-solid interface effects [AD-A281714] p 592 N95-15453
WAVE EQUATIONS
Real time system for practical acoustic monitoring of global ocean temperature, volume 3 [AD-A283774] p 535 N95-14335
Applied Computational Electromagnetics Society Journal, volume 9, number 2 [AD-A281576] p 469 N95-15463
WAVE FRONT DEFORMATION
Adaptive optics at Lick Observatory: System architecture and operations [DE94-012387] p 601 N95-13672
WAVE FRONTS
Interacting fronts in a model for binary-mixture convection [DE94-013595] p 494 N95-15861
WAVE FUNCTIONS
Squeezing in a 2-D generalized oscillator p 603 N95-13907
Quantum phase uncertainties in the classical limit p 607 N95-13933
The wave function and minimum uncertainty function of the bound quadratic Hamiltonian system p 608 N95-13943
The thermal-wave model: A Schroedinger-like equation for charged particle beam dynamics p 601 N95-13944
General properties of quantum optical systems in a strong field limit p 609 N95-13950
Probing the antiferromagnetic long-range order with Glauber spin states p 609 N95-13951
Evolution of wave function in a dissipative system p 610 N95-13959
Hadronic wavefunctions in light-cone quantization [DE94-014507] p 622 N95-15308
WAVE GENERATION
On the physics of waves in the solar atmosphere: Wave heating and wind acceleration [NASA-CR-196992] p 646 N95-15070
Meso-beta scale numerical simulation studies of terrain-induced jet streak mass/momentum perturbations [NASA-CR-197226] p 531 N95-15684
WAVE PACKETS
Supersymmetry and radial squeezed states for Rydberg wave packets p 598 N95-13898
Manipulation of quantum evolution p 598 N95-13918
On the behavior of three-dimensional wave packets in viscously spreading mixing layers [NASA-TM-106770] p 495 N95-15908
WAVE PROPAGATION
Modes in light wave propagating in semiconductor laser p 500 N95-13925
Flow-radiated noise. Study of the propagative spectral range of the wall pressure field [PB94-201290] p 590 N95-13985
Mathematical problems of nonlinear wave propagation and of waves in heterogeneous media [AD-A282217] p 492 N95-14605
Proceedings of the Eighteenth NASA Propagation Experimenters Meeting (NAPEX 18) and the Advanced Communications Technology Satellite (ACTS) Propagation Studies Miniworkshop [NASA-CR-196959] p 464 N95-14670
Propagation characteristics of 20/30 GHz links with a 40 deg masking angle p 464 N95-14672
Propagation data at 20/40 GHz and the propagation needs of Milstar p 465 N95-14673
A database for propagation models p 465 N95-14675
Channel characterisation for future Ka-band Mobile Satellite Systems and preliminary results p 465 N95-14676
Electro-optics: Propagation from IR to UV and sensor considerations. Part A: Propagation theory p 467 N95-14833
Electro-optics: Propagation from IR to UV and sensor considerations. Part B: Tools for exploitation of propagation conditions and system range performance p 467 N95-14834
Effects of hydrometeors and atmospheric gases at SHF/EHF p 468 N95-14835
Torsional shear wave transducer [AD-D016347] p 496 N95-14841
Fine structure of transient waves in a random medium: The correlation and spectral density functions p 401 N95-14882
Tidal dynamics and mixing over steep topography [AD-A283535] p 536 N95-15324
Applied Computational Electromagnetics Society Journal, volume 9, number 2 [AD-A281576] p 469 N95-15463
Integrated photonics research, 1993 [AD-A281578] p 614 N95-15464
Experimental hardware development for a pulsed ultrasonic data collection facility [AD-A283331] p 615 N95-15872
WAVE REFLECTION
The 24th International Physics Olympiad [AD-A280584] p 589 N95-13972
WAVEFORMS
Composite waveform generation for EMP and lightning direct-drive testing [AD-A284159] p 462 N95-14405
Design of power electronics for TVC and EMA systems [NASA-CR-197067] p 475 N95-14866
Effect of stratification and geometrical spreading on sonic boom rise time p 401 N95-14880
An evaluation of rise time characterization and prediction methods p 401 N95-14881
Fine structure of transient waves in a random medium: The correlation and spectral density functions p 401 N95-14882
Atmospheric propagation at larger lateral distances from the flight track p 402 N95-14885
Atmospheric effects on the risetime and waveshape of sonic booms p 402 N95-14886
Experimental hardware development for a pulsed ultrasonic data collection facility [AD-A283331] p 615 N95-15872
WAVEGUIDE ANTENNAS
The Telecommunications and Data Acquisition Report [NASA-CR-196409] p 462 N95-14620
Linear quadratic Gaussian and feedforward controllers for the DSS-13 antenna p 463 N95-14625
WAVEGUIDES
Wavelength-division multiplexed optical integrated circuit with vertical diffraction grating [NASA-CASE-NPO-18357-1-CU] p 612 N95-14181
WAVELENGTH DIVISION MULTIPLEXING
Project OART: WDM, EDFA's and mixed data rates in a real-world testbed [DE94-012234] p 601 N95-13670
Wavelength-division multiplexed optical integrated circuit with vertical diffraction grating [NASA-CASE-NPO-18357-1-CU] p 612 N95-14181
A simple analytical model for dense WDM/OOK systems [AD-A283229] p 478 N95-15628
WAVELET ANALYSIS
A new approach to the photon localization problem p 603 N95-13905
Applications of squeezed states: Bogoliubov transformations and wavelets to the statistical mechanics of water and its bubbles p 607 N95-13939
WAVERIDERS
Low-speed wind tunnel testing of the NPS and NASA Ames Mach 6 optimized waverider [AD-A283585] p 404 N95-15319
WAVES
Noise radiation by instability waves in coaxial jets [NASA-TM-106738] p 591 N95-14618
WAXES
Development of a moldable, biodegradable polymeric bone repair material [AD-A283413] p 454 N95-15296
WEAPONS
Scale effects on aircraft and weapon aerodynamics [AGARD-AG-323] p 393 N95-14103
WEAR
Hybrid bearings for turbopumps and the like [NASA-CASE-MFS-28491-1] p 500 N95-13819
Physical and tribological characteristics of ion-implanted diamond films [NASA-TM-106682] p 450 N95-14303
Space Shuttle Main Engine turbopump bearing assessment program [TABES PAPER 94-621] p 417 N95-14648
Mechanical system reliability for long life space systems [NASA-CR-197215] p 505 N95-15584
Wear mechanism evaluation and measurement in fuel-lubricated components [AD-A284870] p 504 N95-15747
Recent progress and future prospects in the surface engineering and tribology of ceramics [DE94-016315] p 456 N95-15778
WEAR RESISTANCE
Wear mechanism evaluation and measurement in fuel-lubricated components [AD-A284870] p 504 N95-15747
WEAR TESTS
A new tribological test for candidate brush seal materials evaluation [NASA-TM-106753] p 431 N95-13631
Vehicle health management using adaptive techniques [NASA-TM-108472] p 431 N95-15609
Wear mechanism evaluation and measurement in fuel-lubricated components [AD-A284870] p 504 N95-15747
WEATHER
Florida's propagation report p 466 N95-14684
WEATHER FORECASTING
Verification of severe local storms forecasts issued by the National Severe Storms Forecast Center: 1993 [PB94-195898] p 532 N95-14117
AFOS Terminal Aerodrome Forecast encoding [PB94-203247] p 533 N95-14410
Winter storms research in Canada p 406 N95-14895
WEAVING
Adjustable reed for weaving net-shaped tailored fabrics [NASA-CASE-LAR-15072-1] p 501 N95-14186
WEDGES
Magnetic and structural instabilities of ultrathin Fe(100) wedges [DE94-013864] p 624 N95-15385
WEIGHTLESSNESS
Development of life sciences equipment for microgravity and hypergravity simulation p 425 N95-14090
Extended duration orbiter medical project countermeasure to reduce post space flight orthostatic intolerance (LBNP) (STS-50/USML-1) p 551 N95-14224
A new procedure for measuring contact angle [DE94-014971] p 457 N95-14659
Proposal for an astronaut mass measurement device for the Space Shuttle [NASA-CR-197198] p 563 N95-14854
Gravitational stress and regulation of neuroendocrine elements and fluid volume in humans p 542 N95-15090
Neurohumoral reactions to long-term vestibular stimulation in man p 542 N95-15091
Transesophageal echocardiographic evaluation of baboons during microgravity induced by parabolic flight p 538 N95-15094

Changing gravity level and the development of animals p 538 N95-15101
Behaviour of newly hatched and adult Japanese quail and the feasibility of adaptation to weightlessness p 538 N95-15106
Cardiovascular and metabolic responses to 6 deg Head-Down Tilt (HDT) and 70 deg Head-Up Tilt (HUT) following exercise p 544 N95-15109
Postural control of fish related to gravity input p 539 N95-15118
Physiologic mechanisms effecting circulatory and body fluid losses in weightlessness as shown by mathematical modeling p 547 N95-15129
Effects of microgravity on interstitial muscle receptors affecting heart rate and blood pressure during static exercise p 548 N95-15137
Effect of short- and long-term spaceflight on the contractile properties of rat skeletal muscles with different functions p 539 N95-15141

WEIGHTLESSNESS SIMULATION
Twenty four hours head-down tilt decreases arterial baroreflex function in conscious rat p 538 N95-15098
Cardiovascular deconditioning effects of long-term simulated weightlessness in rats p 538 N95-15099

WELD STRENGTH
Analysis of welding-induced residual stresses with the ADINA system
[DE94-015359] p 506 N95-14320

WELD TESTS
Welding irradiated stainless steel
[DE94-013661] p 500 N95-13645

WELDED JOINTS
Analysis of welding-induced residual stresses with the ADINA system
[DE94-015359] p 506 N95-14320
An inelastic analysis of a welded aluminum joint
[NASA-TP-3508] p 513 N95-15055

WELDING MACHINES
Welding nozzle position manipulator
[NASA-CASE-MFS-29837-1] p 500 N95-13654

WELLS
Magnetic field dependent photoluminescence studies of InGaAs/GaAs strained-single-quantum wells
[DE94-015774] p 621 N95-14342
Survey of the 1991 geothermal exploration promotion
[DE94-780690] p 530 N95-14836

WENTZEL-KRAMER-BRILLOUIN METHOD
Time-dependent variational approach in terms of squeezed coherent states: Implication to semi-classical approximation p 609 N95-13948

WETTING
Microscale hydrodynamics near moving contact lines p 484 N95-14536
Wetting and spreading at the molecular scale p 484 N95-14539

WHITE NOISE
Spectral, noise and correlation properties of intense squeezed light generated by a coupling in two laser fields p 500 N95-13903
Low-frequency noise in high-(Tc) superconductor Josephson junctions, SQUIDs, and magnetometers
[DE94-016873] p 623 N95-15337
Investigation of Allan variance for determining noise spectral forms with application to microwave radiometry
[NASA-CR-194985] p 516 N95-15727

WIDEBAND COMMUNICATION
Troposcatter at the KU band
[AD-A281575] p 469 N95-15462

WIGNER COEFFICIENT
Phase-space analysis of charged and optical beam transport: Wigner rotation angle p 606 N95-13927
Understanding squeezing of quantum states with the Wigner function p 606 N95-13930

WIND (METEOROLOGY)
Atmospheric and wind modeling for ATC
[NASA-CR-196786] p 532 N95-13725
Rotational wind indicator enhances control of rotated displays p 559 N95-14046

WIND DIRECTION
Space Shuttle fatigue loads spectra for prelaunch and liftoff loads p 419 N95-14474
Meso-beta scale numerical simulation studies of terrain-induced jet streak mass/momentum perturbations
[NASA-CR-197226] p 531 N95-15684

WIND EFFECTS
Tilting wind tunnel for fire behavior studies
[PB94-204625] p 413 N95-14513
Calculation of movable bed friction factors
[AD-A283529] p 536 N95-15440

WIND MEASUREMENT
Overview of PAMS meteorological monitoring requirements
[PB94-176658] p 534 N95-15383

WIND PRESSURE
ADCIRC: An advanced three-dimensional circulation model for shelves, coasts, and estuaries. Report 4: Hurricane storm surge modeling using large domains
[AD-A283868] p 535 N95-14352

WIND PROFILES
Atmospheric and wind modeling for ATC
[NASA-CR-196786] p 532 N95-13725
Upgrade of tropical cyclone surface wind field model
[AD-A283530] p 533 N95-15323

WIND SHEAR
ADCIRC: An advanced three-dimensional circulation model for shelves, coasts, and estuaries. Report 4: Hurricane storm surge modeling using large domains
[AD-A283868] p 535 N95-14352
Simple atmospheric perturbation models for sonic-boom-signature distortion studies p 402 N95-14888
Wind shear and its effects on aircraft p 407 N95-14898
Heavy rain effects p 407 N95-14899
TDWR scan strategy implementation
[AD-A284877] p 534 N95-15749

WIND TUNNEL MODELS
Access to space
[NASA-CR-197153] p 428 N95-14521

WIND TUNNEL TESTS
Experiments to verify nonparallel stability theory at Virginia Polytechnic Institute and State University, Blacksburg, Virginia
[NASA-CR-196993] p 479 N95-13664
VUV shock layer radiation in an arc-jet wind tunnel experiment p 405 N95-13719
Measured and calculated spectral radiation from a blunt body shock layer in an arc-jet wind tunnel
[AIAA PAPER 94-0086] p 405 N95-13720
Dynamics of the McDonnell-Douglas Large Scale Dynamic Rig and dynamic calibration of the rotor balance
[NASA-TM-108855] p 391 N95-13891
Scale effects on aircraft and weapon aerodynamics
[AGARD-AG-323] p 393 N95-14103
Quality assessment for wind tunnel testing
[AGARD-AR-304] p 393 N95-14197
A selection of experimental test cases for the validation of CFD codes, volume 1
[AGARD-AR-303-VOL-1] p 481 N95-14201
High Alpha Technology Program (HATP) ground test to flight comparisons p 393 N95-14230
Flight and full-scale wind-tunnel comparison of pressure distributions from an F-18 aircraft at high angles of attack --- Conducted in NASA Ames Research Center's 80 by 120 ft wind tunnel p 394 N95-14231
Comparison of X-31 flight, wind-tunnel, and water-tunnel yawing moment asymmetries at high angles of attack p 394 N95-14234
Free-to-roll tests of X-31 and F-18 subscale models with correlation to flight test results p 394 N95-14237
Computational analysis of forebody tangential slot blowing p 397 N95-14253
F/A-18 and F-16 forebody vortex control, static and rotary-balance results p 397 N95-14254
Tilting wind tunnel for fire behavior studies
[PB94-204625] p 413 N95-14513
Ultra-high bypass ratio jet noise
[NASA-CR-195394] p 591 N95-14610
Control of unsteady separated flow associated with the dynamic stall of airfoils
[NASA-CR-197024] p 400 N95-14613
Low-speed wind tunnel testing of the NPS and NASA Ames Mach 6 optimized waverider
[AD-A283585] p 404 N95-15319
Pressure measurements on an F/A-18 twin vertical tail in buffeting flow. Volume 2: Steady and unsteady RMS pressure data
[AD-A281581] p 404 N95-15465
Investigation of ramp injectors for supersonic mixing enhancement
[NASA-CR-4634] p 494 N95-15605
Wind-tunnel blockage and actuation systems test of a two-dimensional scramjet inlet unstart model at Mach 6
[NASA-TM-109152] p 495 N95-15898
Two-dimensional scramjet inlet unstart model: Wind-tunnel blockage and actuation systems test
[NASA-TM-109984] p 495 N95-15899

WIND TUNNELS
Developments in laser-based diagnostics for wind tunnels in the Aeromechanics Division: 1987-1992
[AD-A283011] p 412 N95-13687
Quality assessment for wind tunnel testing
[AGARD-AR-304] p 393 N95-14197
Computational analysis of forebody tangential slot blowing p 397 N95-14253
F/A-18 and F-16 forebody vortex control, static and rotary-balance results p 397 N95-14254
Flight evaluation of pneumatic forebody vortex control in post-stall flight p 398 N95-14259
Research and technology highlights, 1993
[NASA-TM-4575] p 647 N95-15065
Low-speed wind tunnel testing of the NPS and NASA Ames Mach 6 optimized waverider
[AD-A283585] p 404 N95-15319

WIND TURBINES
Wind-electric ice making for villages in the developing world
[DE94-011854] p 518 N95-14191
The National Wind Technology Center
[DE94-011853] p 519 N95-14433
Wind/hybrid power system test facilities in the United States and Canada
[DE94-006930] p 519 N95-15290

WIND VELOCITY
Photochemical urban airshed modeling using diagnostic and dynamic meteorological fields
[PB94-176120] p 616 N95-13973
Space Shuttle fatigue loads spectra for prelaunch and liftoff loads p 419 N95-14474
Upgrade of tropical cyclone surface wind field model
[AD-A283530] p 533 N95-15323
Groundspeed filtering for CTAS
[NASA-CR-197223] p 497 N95-15785
Validation of ERS-1 environmental data products
[NASA-CR-197111] p 517 N95-15848

WINDOWS (APERTURES)
Development of chemical-vapor-deposited diamond for infrared optical applications: Summary of properties
[AD-A282999] p 448 N95-13686
Science objectives and performance of a radiometer and window design for atmospheric entry experiments p 429 N95-13718
Prediction of particulate contamination on aperture window p 420 N95-14064

WINDOWS (COMPUTER PROGRAMS)
Variable window Gabor filters and their use in focus and correspondence
[AD-A282837] p 573 N95-14842

WINDPOWER UTILIZATION
Wind-electric ice making for villages in the developing world
[DE94-011854] p 518 N95-14191
The integration of renewable energy sources into electric power distribution systems. Volume 1: National assessment
[DE94-015935] p 519 N95-14393
The National Wind Technology Center
[DE94-011853] p 519 N95-14433
Wind/hybrid power system test facilities in the United States and Canada
[DE94-006930] p 519 N95-15290

WING FLAPS
Numerical design of advanced multi-element airfoils
[NASA-CR-197135] p 404 N95-15762

WING ROOTS
The Aluminum Falcon: A low cost modern commercial transport
[NASA-CR-197180] p 409 N95-15742

WINGLETS
Fatigue evaluation of empennage, forward wing, and winglets/tip fins on part 23 airplanes
[PB94-196813] p 408 N95-13981

WINGS
Computational aerodynamics based on the Euler equations
[AGARD-AG-325] p 398 N95-14264
Development of a composite repair and the associated inspection intervals for the F-111C stiffener runout region p 392 N95-14477
Numerical study of the effects of icing on viscous flow over wings
[NASA-CR-197102] p 400 N95-14803

WIRE
Mechanical properties of high-temperature superconducting wires
[DE94-015089] p 621 N95-14192
A NASA/industry/university partnership for development of dual-use vibration isolation technology
[TABES PAPER 94-613] p 416 N95-14643
HTS Wire Development Workshop: Proceedings
[DE94-015650] p 624 N95-15421
Sandia 1993 Superconducting Technology Program
[DE94-015601] p 625 N95-15438

WIRELESS COMMUNICATION
Wireless technology for command control and communications
[AD-A284367] p 470 N95-15804

WORKING FLUIDS
Solubility, viscosity and density of refrigerant and lubricant mixtures
[DE94-016949] p 454 N95-15343

WORKLOADS (PSYCHOPHYSIOLOGY)
EPIC computational models of psychological refractory-period effects in human multiple-task performance
[AD-A280924] p 540 N95-14142
Civil use of night vision devices: Evaluation pilot's guide, part 2
[DOT/FAA/RD-94/19] p 410 N95-14175
WORKSTATIONS
The Ames Virtual Environment Workstation: Implementation issues and requirements
p 557 N95-14034
The exploration metaphor p 557 N95-14037
The console password feature for DEC workstations
[DE94-015721] p 566 N95-14338
Compiler optimizations for cache locality and coherence
[TR-504] p 586 N95-15589
WOVEN COMPOSITES
Oxidation resistant coating for carbon-carbon composites at ultra-high temperatures
[AD-A283323] p 456 N95-15624

X

X RAY ANALYSIS
The advanced development of x-ray computed tomography applications
[AD-A284211] p 434 N95-14411
X RAY ASTRONOMY
Space simulation techniques and facilities for SAX STM test campaign p 423 N95-14077
The MOXE x-ray all-sky monitor for Spectrum-X-gamma
[DE94-016064] p 638 N95-14429
Determination of the atmospheric structure of the BO star companion of SMC X-1 by analysis of Ginga observations
[NASA-CR-197100] p 638 N95-14804
PSPC soft x-ray observations of Seyfert 2 galaxies
[NASA-TM-109968] p 638 N95-14911
ROSAT observations of the binary Be-star and radio pulsar PSR1259-63
[NASA-CR-196951] p 642 N95-15907
X RAY ASTROPHYSICS FACILITY
HRMA calibration handbook: EKC gravity compensated XRCF models
[NASA-CR-195818] p 636 N95-13634
Work Breakdown Structure (WBS) and WBS dictionary --- advanced x ray astrophysics facility (AXAF)
[NASA-CR-196448] p 567 N95-13635
AXAF SIM focus mechanism study
[NASA-CR-196976] p 636 N95-13636
AXAF VETA-I mirror ring focus measurements
[NASA-CR-196145] p 637 N95-13637
Investigations into mirror fabrication metrology analysis
[NASA-CR-196522] p 602 N95-13841
Summary of AXAF calibration requirements
[NASA-CR-196985] p 637 N95-13867
Performance Reports: Mirror alignment system performance prediction comparison between SAO and EKC
[NASA-CR-196013] p 637 N95-14100
Performance Report: A timeline for the synchrotron calibration of AXAF
[NASA-CR-196489] p 638 N95-14101
X RAY BINARIES
Determination of the atmospheric structure of the BO star companion of SMC X-1 by analysis of Ginga observations
[NASA-CR-197100] p 638 N95-14804
PSPC soft x-ray observations of Seyfert 2 galaxies
[NASA-TM-109968] p 638 N95-14911
X RAY DETECTORS
AXAF VETA-I mirror ring focus measurements
[NASA-CR-196145] p 637 N95-13637
The MOXE x-ray all-sky monitor for Spectrum-X-gamma
[DE94-016064] p 638 N95-14429
First Year PIDDP Report on gamma-ray and x-ray spectroscopy: X-ray remote sensing and in situ spectroscopy for planetary exploration missions and gamma-ray remote sensing and in situ spectroscopy for planetary exploration missions
[NASA-CR-189374] p 517 N95-15916
X RAY IMAGERY
Los Alamos contribution to target diagnostics on the National Ignition Facility
[DE94-014474] p 616 N95-13998
X RAY INSPECTION
Radiographic Moire
[NASA-CASE-LAR-15104-1] p 505 N95-13835
The advanced development of x-ray computed tomography applications
[AD-A284211] p 434 N95-14411
X RAY OPTICS
Specifying the surface finish of x ray mirrors
[DE94-013537] p 601 N95-13644
X RAY SCATTERING
Performance of spherically focusing Ge(444) backscattering analyzers for inelastic x-ray scattering
[DE94-016349] p 621 N95-14382
Small-angle x-ray scattering studies of microvoids in amorphous-silicon-based semiconductors
[DE94-011840] p 520 N95-15406
X RAY SOURCES
A ROSAT deep survey of the best studied high latitude areas
[NASA-CR-196265] p 637 N95-13722
Space simulation techniques and facilities for SAX STM test campaign p 423 N95-14077
The MOXE x-ray all-sky monitor for Spectrum-X-gamma
[DE94-016064] p 638 N95-14429
Search for gamma-ray events in the BATSE data base
[NASA-CR-197044] p 647 N95-14814
ROSAT observations of the binary Be-star and radio pulsar PSR1259-63
[NASA-CR-196951] p 642 N95-15907
X RAY SPECTRA
Specifying the surface finish of x ray mirrors
[DE94-013537] p 601 N95-13644
Determination of the atmospheric structure of the BO star companion of SMC X-1 by analysis of Ginga observations
[NASA-CR-197100] p 638 N95-14804
PSPC soft x-ray observations of Seyfert 2 galaxies
[NASA-TM-109968] p 638 N95-14911
X RAY SPECTROSCOPY
Performance of spherically focusing Ge(444) backscattering analyzers for inelastic x-ray scattering
[DE94-016349] p 621 N95-14382
X-ray Photoelectron Spectroscopy (XPS), Rutherford Back Scattering (RBS) studies
[NASA-CR-196536] p 439 N95-14867
First Year PIDDP Report on gamma-ray and x-ray spectroscopy: X-ray remote sensing and in situ spectroscopy for planetary exploration missions and gamma-ray remote sensing and in situ spectroscopy for planetary exploration missions
[NASA-CR-189374] p 517 N95-15916
X RAY STARS
Neutral gas and diffuse interstellar bands in the LMC
p 639 N95-15828
X RAYS
Bone geometry, structure and mineral distribution using Dual energy X ray Absorptiometry (DXA)
p 549 N95-15140
Low-damage multilayer mirror for the soft x ray region
[AD-D016362] p 614 N95-15764
X-29 AIRCRAFT
Integration of a mechanical forebody vortex control system into the F-15 p 398 N95-14258
Flight evaluation of pneumatic forebody vortex control in post-stall flight p 398 N95-14259
X-31 AIRCRAFT
Comparison of X-31 flight, wind-tunnel, and water-tunnel yawing moment asymmetries at high angles of attack
p 394 N95-14234
Parameter identification for X-31A at high angles of attack p 394 N95-14235
Validation of the NASA Dryden X-31 simulation and evaluation of mechanization techniques
p 394 N95-14236
Free-to-roll tests of X-31 and F-18 subscale models with correlation to flight test results p 394 N95-14237
X-31 post-stall envelope expansion and tactical utility testing p 395 N95-14242
X-31 quasi-tailless flight demonstration
p 395 N95-14243
X-31 high angle of attack control system performance
p 395 N95-14244
XENON
Development status of the NASA 30-cm ion thruster and power processor
[NASA-TM-106740] p 430 N95-14301
A theoretical study of 30 to 50 angstrom noble gas heavy ion lithography
[DE94-015262] p 442 N95-15436
XENON LAMPS
Emerging technology summary: Destruction of organic contaminants in air using advanced ultraviolet flashlamps
[PB94-194479] p 521 N95-14121

Y

YAW
Comparison of full-scale, small-scale, and CFD results for F/A-18 forebody slot blowing p 397 N95-14255
Preparations for flight research to evaluate actuated forebody strakes on the F-18 high-alpha research vehicle p 398 N95-14257
YAWING MOMENTS
Comparison of X-31 flight, wind-tunnel, and water-tunnel yawing moment asymmetries at high angles of attack
p 394 N95-14234
Validation of the NASA Dryden X-31 simulation and evaluation of mechanization techniques
p 394 N95-14236
Static and dynamic force/moment measurements in the Eidetics water tunnel p 395 N95-14238
Computational analysis of forebody tangential slot blowing p 397 N95-14253
Comparison of full-scale, small-scale, and CFD results for F/A-18 forebody slot blowing p 397 N95-14255
Flight evaluation of pneumatic forebody vortex control in post-stall flight p 398 N95-14259
YBCO SUPERCONDUCTORS
High performance YBCO films
[AD-A283870] p 451 N95-14354
Macroturbulence in superconductors
[DE94-016371] p 595 N95-15362
Ultrasonic characterization of high T(c) and other unconventional superconductors
[AD-A282835] p 476 N95-15397
Low loss substrates for microwave applications and sol-gel processing of superconductors
[AD-A284868] p 625 N95-15746
YIELD POINT
Loading-strain equivalence between thermomechanical, creep, and tensile tests: High density polyethylene
[AD-A283265] p 513 N95-15621
YIELD STRENGTH
Static strength of riveted joints in Fibre Metal Laminates
[PB94-201472] p 513 N95-15429
YTTRIUM OXIDES
High performance YBCO films
[AD-A283870] p 451 N95-14354

Z

ZEOLITES
Preparation and characterization of composite inorganic zeolite membranes with molecular sieve properties
[PB94-191251] p 450 N95-14151
The growth of zeolites A, X and mordenite in space
p 458 N95-14226
Activity of Ga, In and Cu modified MFI zeolites for amine reactions
[DE94-016532] p 438 N95-14388
Study on titanium-silicalite-1 and related systems
[PB94-195500] p 445 N95-14845
Adsorption and diffusion of fluids in well-characterized adsorbent materials
[DE94-016953] p 454 N95-15344
ZINC OXIDES
Optimization of transparent and reflecting electrodes for amorphous-silicon solar cells
[DE94-011841] p 520 N95-15355
ZINC SELENIDES
Photoluminescence spectroscopy and Rutherford backscattering channeling evaluation of various capping techniques for rapid thermal annealing of ion-implanted ZnSe
[DE94-016876] p 623 N95-15339
Electronic characterization of defects in narrow gap semiconductors
[NASA-CR-197217] p 626 N95-15752
ZINC TELLURIDES
Electronic characterization of defects in narrow gap semiconductors
[NASA-CR-197217] p 626 N95-15752
ZIRCONIUM
Spectrophotometric determination of plutonium-239 based on the spectrum of plutonium 3 chloride
[DE94-015172] p 440 N95-15297

Typical Personal Author Index Listing

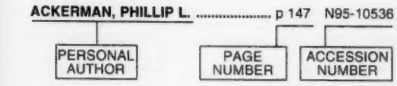

Listings in this index are arranged alphabetically by personal author. The page number helps you locate the citation in the abstract section. The accession number denotes the number by which the citation is identified.

A

ABBOTT, TROY D. ..... p 396 N95-14246
ABDALLAH, J. ..... p 617 N95-14366
ABDOLLAHIAN, DAVOOD ..... p 487 N95-14555
ABDOU, M. A. ..... p 617 N95-14397
ABEL, K. H. ..... p 613 N95-15312
ABELSON, HAL ..... p 584 N95-15811
ABERG, J. ..... p 459 N95-14919
ABRAHAM, M. M. ..... p 622 N95-14608
ACKLESOLN, STEVE ..... p 613 N95-14353
ACTIS, RICARDO L. ..... p 507 N95-14454
ADAMS, D. A. ..... p 476 N95-15399
ADAMS, R. D. ..... p 441 N95-15346
ADAMS, W. P. ..... p 575 N95-15549
ADAMSON, A. J. ..... p 639 N95-15831
ADDESSIO, F. L. ..... p 436 N95-15573
ADELSTEIN, BERNARD D. ..... p 558 N95-14042
ADLER, RICHARD W. ..... p 469 N95-15619
AFANASSIEV, N. A. ..... p 421 N95-14065
p 418 N95-14098
AGGARWAL, ISHWAR D. ..... p 615 N95-15766
AGOSTA-GREENMAN, ROXANA M. ..... p 397 N95-14253
AGRAWAL, V. K. ..... p 413 N95-13827
AGRAWALA, ASHOK K. ..... p 583 N95-15548
AHUJA, J. K. ..... p 437 N95-14268
AIDUN, J. B. ..... p 436 N95-15573
AKAO, J. H. ..... p 494 N95-15868
AKATSU, H. ..... p 442 N95-15408
AKTURAN, RIZA ..... p 466 N95-14679
AKULIN, V. M. ..... p 598 N95-13909
p 605 N95-13919
ALBRECHT, G. ..... p 499 N95-14427
ALBRIGHT, S. P. ..... p 521 N95-15863
ALBUS, J. ..... p 456 N95-14629
ALEKSANDROV, V. N. ..... p 584 N95-13980
ALEXANDER, J. I. D. ..... p 458 N95-14213
ALEXANDER, J. IWAN D. ..... p 484 N95-14533
ALEXANDER, STEPHEN W. ..... p 429 N95-13668
ALLEN, E. L. ..... p 623 N95-15339
ALLEY, CARROLL O. ..... p 599 N95-13963
p 612 N95-13970
ALLMEN, J. R. ..... p 391 N95-13642
ALTENKIRCH, ROBERT A. ..... p 458 N95-14212
ALZMANN, MELANIE A. ..... p 532 N95-14271
AMADOR, M. ..... p 630 N95-13996
AMARI, HARUO ..... p 559 N95-14048
AMSTUTZ, B. E. ..... p 509 N95-14467
AMTHOR, J. S. ..... p 524 N95-15779
AN, I. ..... p 622 N95-14431
AN, J. ..... p 601 N95-13672
ANANTHARAJ, VALENTINE ..... p 537 N95-15753
ANDERSEN, DALE ..... p 427 N95-14099
ANDERSON, C. L. ..... p 522 N95-14317
ANDERSON, J. C. ..... p 438 N95-14375
ANDERSON, JOHN L. ..... p 444 N95-14581
ANDERSON, PAUL B. ..... p 579 N95-15450
ANDERSON, ROGER R. ..... p 618 N95-14798
ANDREEV, V. A. ..... p 609 N95-13952
ANDREWS, LESTER ..... p 434 N95-14366
ANDREWS, R. N. ..... p 458 N95-14214
ANESTIS, RAPHAEL ..... p 476 N95-15325
ANGUS, JOHN C. ..... p 626 N95-15812
ANIKUMAR, A. V. ..... p 458 N95-14218
ANILKUMAR, A. V. ..... p 458 N95-14219
ANNA, PAUL D. ..... p 396 N95-14245
ANNIGERI, BAL ..... p 507 N95-14455
ANNIS, CHARLES ..... p 446 N95-15415
ANSARI, RAFAT R. ..... p 459 N95-14572
ANSCHUETZ, ROBERT ..... p 572 N95-14357
ANSONG, OMARI ..... p 453 N95-14931
ANTHONY, R. W. ..... p 532 N95-14117
ANTOINE, MIQUEL D. ..... p 453 N95-14931
ANTONIEWICZ, BOB ..... p 396 N95-14249
ANTONUTTO, G. ..... p 546 N95-15120
APFEL, ROBERT E. ..... p 458 N95-14220
APRA, E. ..... p 573 N95-15311
ARABSHAHI, ABDOLLAH ..... p 409 N95-14909
ARBESSER-RASTBURG, BERTRAM ..... p 464 N95-14671
p 465 N95-14676
ARCE, R. ..... p 601 N95-13670
ARENDT, CORY ..... p 507 N95-14456
ARIAS, CHRISTOPHER V. ..... p 578 N95-14292
ARKHIPOV, K. ..... p 617 N95-14262
ARMSTRONG, T. A. ..... p 517 N95-14002
ARNBERG, L. ..... p 446 N95-15349
ARNOLDUS, HENK F. ..... p 598 N95-13937
ARNONE, G. ..... p 442 N95-15387
ARPACI, V. S. ..... p 485 N95-14543
ARTAKI, I. ..... p 472 N95-13975
ARTHUR, R. J. ..... p 613 N95-15312
ARTONI, MAURIZO ..... p 610 N95-13957
ASHURST, W. T. ..... p 438 N95-14391
ASTIN, MICHAEL S. ..... p 416 N95-14644
ATKINSON, COLIN ..... p 569 N95-14158
ATTIA, ALAN I. ..... p 472 N95-13824
ATWOOD, BRUCE ..... p 644 N95-14509
ATWOOD, C. L. ..... p 460 N95-15409
p 588 N95-15533
AUCIELLO, O. ..... p 620 N95-13822
AUNG, M. ..... p 463 N95-14627
AVICOLA, K. ..... p 601 N95-13672
AVILES, WALTER A. ..... p 504 N95-14023
AXELROD, M. C. ..... p 524 N95-15779
AXFORD, R. A. ..... p 468 N95-15321
AYER, Z. ..... p 619 N95-13698
AYERS, JOSEPH ..... p 503 N95-15294
AYOTTE, P. ..... p 465 N95-14673

B

BABCOCK, S. R. ..... p 474 N95-14319
BABIC, SLAVOLJUB ..... p 568 N95-13894
BABIKIAN, DIKRAN S. ..... p 405 N95-13720
BAC, N. ..... p 458 N95-14226
BACA, A. G. ..... p 477 N95-15544
BACKMAN, D. K. ..... p 555 N95-14024
BACON, A. M. ..... p 610 N95-13956
BACON, PAMELA M. ..... p 638 N95-14511
BADAVI, FRANCIS F. ..... p 647 N95-15790
BADER, S. D. ..... p 624 N95-15385
BAERTLEIN, CARL ..... p 458 N95-14221
BAGLEY, CALVIN F. ..... p 515 N95-14358
BAISCH, F. J. ..... p 549 N95-15138
BAKER, D. A. ..... p 616 N95-13998
BAKER, GREGORY R. ..... p 486 N95-14550
BAKER, LEONARD H. ..... p 461 N95-14346
BAKHTIN, V. ..... p 617 N95-14262
BALACHANDRAN, U. ..... p 475 N95-14606
p 453 N95-14609
BALANTEKIN, A. B. ..... p 598 N95-15869
BALASUBRAMANIAM, R. ..... p 486 N95-14546
BALLARD, DANA H. ..... p 575 N95-15640
p 576 N95-15856
p 576 N95-15857
BALLARD, RICHARD E. ..... p 547 N95-15128
BALLARD, RODNEY W. ..... p 550 N95-15147
BALLMANN, J. ..... p 410 N95-15821
BALMINO, G. ..... p 516 N95-15795
BALSA, THOMAS F. ..... p 495 N95-15908
BALZAMO, EMMANUEL ..... p 539 N95-15132
BANAVAR, JAYANTH R. ..... p 484 N95-14539
BANDA, E. ..... p 521 N95-15407
BANDILLA, ARNO ..... p 605 N95-13916
BANDYOPADHYAY, K. ..... p 493 N95-15571
BANERJEE, SUBIR ..... p 414 N95-13830
BANFORD, MICHAEL ..... p 404 N95-15465
BANKOFF, S. GEORGE ..... p 482 N95-14523
BANKS, BRUCE A. ..... p 431 N95-15769
BANKS, D. W. ..... p 393 N95-14230
BANKS, J. C. ..... p 437 N95-14312
p 596 N95-15437
BARCH, DON ..... p 427 N95-14099
BARCLAY, REBECCA O. ..... p 632 N95-14619
p 632 N95-14870
BAREZ, FRED ..... p 487 N95-14555
BARKENAES, J. E. ..... p 513 N95-15348
BARKER, LINDA ..... p 416 N95-14647
BARLOW, DOUGLAS N. ..... p 482 N95-14351
BARLOW, S. E. ..... p 524 N95-15432
BARNES, C. W. ..... p 617 N95-14397
BARNES, P. N. ..... p 450 N95-14303
BARNES, P. R. ..... p 519 N95-14393
BARNES, SUSAN ..... p 634 N95-15846
BARNETT, A. M. ..... p 520 N95-15405
BARNETT, TERRY R. ..... p 436 N95-15441
BARRON, ANDREW R. ..... p 477 N95-15587
BARTH, T. ..... p 585 N95-14381
BARTOS, J. ..... p 616 N95-13997
BARZAGHI, R. ..... p 517 N95-15798
BASARAN, CUNEYT ..... p 461 N95-14293
BASHKANSKY, MARK ..... p 615 N95-15765
BASKAYA, MEHMET ..... p 436 N95-15873
BASKINGER, PATRICIA J. ..... p 468 N95-15333
BASS, HENRY E. ..... p 402 N95-14886
BASS, JOHN C. ..... p 518 N95-14341
BASS, LEN ..... p 572 N95-14339
BATCHELOR, D. B. ..... p 586 N95-15538
BATEMAN, PETER J. ..... p 504 N95-14948
BATES, J. L. ..... p 517 N95-14002
BATIZA, R. ..... p 529 N95-14434
BATY, R. S. ..... p 404 N95-15570
BAUCOM, K. C. ..... p 621 N95-14323
BAUER, PETER H. ..... p 584 N95-13694
BAUER, STEVEN X. S. ..... p 501 N95-14183
BAUGHER, CHARLES R. ..... p 634 N95-14207
p 428 N95-14210
BAUM, K. ..... p 548 N95-15137
BAUMAN, L. E. ..... p 618 N95-15374
BAUMGARTNER, ROBERT M. ..... p 403 N95-14892
BAYERDOERFER, GERHARD ..... p 426 N95-14096
BAYGENTS, JAMES C. ..... p 490 N95-14576
BAYLESS, W. R. ..... p 624 N95-15430
BEATTY, JOHN H. ..... p 447 N95-15622
BEEGLE, LUTHER W. ..... p 641 N95-15840
BEGEAL, D. R. ..... p 457 N95-14004
BEHAL, S. K. ..... p 454 N95-15340
BEHL, Y. K. ..... p 524 N95-15575
BELASON, BRUCE ..... p 508 N95-14457
BELENOV, E. ..... p 610 N95-13960
BELL, J. BRETT ..... p 475 N95-14866
BELONGIE, M. L. ..... p 462 N95-14624
BELROSE, CHARLES R. ..... p 503 N95-15305
BELYTSCHKO, T. ..... p 505 N95-14475
BENARROUS, E. ..... p 590 N95-13985
BENKOVITZ, C. M. ..... p 525 N95-15864
BENNETT, C. THOMAS ..... p 558 N95-14043
BENO, M. A. ..... p 620 N95-14009
BENTLEY, J. ..... p 601 N95-13674
BENVENUTI, P. ..... p 639 N95-15833
BEREZHNOV, E. S. ..... p 542 N95-15093
BERG, D. ..... p 579 N95-15581
BERGEY, M. ..... p 518 N95-14191
BERGSMAN, T. M. ..... p 524 N95-15432
BERMAN, DAVID H. ..... p 590 N95-13683
BERNER, J. B. ..... p 463 N95-14627
BERNHARD, RONALD P. ..... p 432 N95-13646
BERNHOLDT, D. E. ..... p 573 N95-15311
BERNSTEIN, HERBERT J. ..... p 611 N95-13962
BERRY, CASSIE ..... p 408 N95-13703
BERRY, K. J. ..... p 534 N95-15666

BERTOMEU, J. p 625 N95-15577
BERTRAND, W. T. p 427 N95-14420
BESICH, WILLIAM J. p 553 N95-15768
BEST, S. p 415 N95-14639
BEYER, NEIL p 563 N95-14854
BHALLA, AMAR S. p 625 N95-15746
BHATT, R. T. p 433 N95-14298
BHATTACHARJEE, SUBRATA p 458 N95-14212
BIBBER, J. p 446 N95-15368
BIEDRON, ROBERT T. p 394 N95-14233
BIEFELD, R. M. p 621 N95-14323
BIGGERS, K. B. p 555 N95-14024
BIJI, P. p 553 N95-15816
BILCIK, B. p 538 N95-15106
BING, GUOYING p 541 N95-14408
BIRMAN, JOSEPH L. p 610 N95-13957
BISCHOF, C. p 577 N95-13677
p 568 N95-13977
BISHOP, MICHAEL p 416 N95-14647
BISSON, S. E. p 531 N95-15411
BISWAS, GAUTAM p 415 N95-14637
BITTKER, DAVID A. p 440 N95-15057
p 442 N95-15512
BIVENS, COURTLAND C. p 411 N95-14518
BJURSTEDT, HILDING p 541 N95-15089
p 546 N95-15123
BLACK, D. p 458 N95-14213
p 579 N95-15581
BLACKBURN, R. R. p 407 N95-15439
BLACKSTOCK, DAVID T. p 401 N95-14880
BLACKWELL, B. F. p 428 N95-14664
BLAIN, C. A. p 535 N95-14352
BLANC-BENON, PHILIPPE p 401 N95-14883
BLANCHARD, PAUL A. p 638 N95-14511
BLASBERGER, A. p 421 N95-14067
BLASDELL, R. C. p 621 N95-14382
BLAUERT, JENS p 558 N95-14039
p 561 N95-14053
BLISS, M. p 613 N95-15312
p 454 N95-15313
BLOCK, MARTIN p 600 N95-15539
BLUE, M. D. p 601 N95-13660
BLUHM, ROBERT p 598 N95-13898
BLUM, FRANK D. p 433 N95-13655
p 455 N95-15458
BLUM, L. p 619 N95-13691
BOALBEY, RICHARD E. p 398 N95-14258
BOATNER, L. A. p 622 N95-14608
BODA, K. p 538 N95-15106
BODA, KOLOMAN p 539 N95-15144
BODINE-FOWLER, SUE p 537 N95-14796
BOEHM, ALBERT R. p 534 N95-15402
BOETTCHER, SHEILA W. p 458 N95-14222
p 551 N95-14223
p 551 N95-14224
BOLAS, M. p 557 N95-14034
BOLENDER, MICHAEL A. p 497 N95-15728
BOLTON, P. R. p 498 N95-14318
BONETTO, FABIAN p 459 N95-14557
BOOTH, R. p 473 N95-14261
BORDEN, C. p 419 N95-14632
BORHAN, ALI p 485 N95-14544
BOROWSKI, STANLEY K. p 429 N95-13668
p 431 N95-15682
BORSA, C. p 433 N95-13993
BORSA, F. p 624 N95-15430
BORSHCHEVSKY, A. p 625 N95-15531
BORUCKI, WILLIAM J. p 643 N95-14499
BOSCHAN, R. H. p 451 N95-14363
BOSE, B. K. p 523 N95-14403
BOSLOUGH, M. B. p 642 N95-14311
BOSSI, RICHARD H. p 434 N95-14411
BOULANGER, PATRICE p 402 N95-14886
BOULAY, JEAN LOUIS p 406 N95-14896
BOUMAN, CHARLES p 515 N95-14358
BOURKE, M. A. M. p 433 N95-13993
BOURRET, E. D. p 623 N95-15339
BOUSMAN, W. SCOTT p 487 N95-14556
BOWEN, B. ARCHIE p 581 N95-14944
BOWEN, DAVID G. p 581 N95-14944
BOWEN, J. G. p 463 N95-14626
BOWERS, ALBION H. p 395 N95-14240
BOWLES, KENNETH J. p 432 N95-13641
BOWMAN, ROSS p 415 N95-14636
BOYD, ROBERT C. p 502 N95-14910
BOZAK, M. J. p 439 N95-14867
BOZEMAN, RICHARD J., JR. p 496 N95-14180
BRAATEN, ERIC p 600 N95-15539
BRACKBILL, J. U. p 619 N95-15774
BRADEN, W. B. p 570 N95-14168
BRADLEY, J. T., III p 617 N95-14262
BRADT, R. C. p 455 N95-15579
BRADY, MICHAEL H. p 638 N95-14597
BRANDEMUEHL, M. p 518 N95-14191
BRANNING, D. p 600 N95-13912
BRANSON, ROGER p 408 N95-14306
BRASE, J. M. p 601 N95-13672
BRAUNSTEIN, SAMUEL L. p 588 N95-13911
BRAY, T. L. p 458 N95-14225
BREEMAN, J. H. p 408 N95-14102
BREHOB, E. p 441 N95-15353
BREIT, G. A. p 419 N95-14089
BREIT, GREGORY A. p 547 N95-15128
BREITHAUPT, BARBARA SPIEGEL p 417 N95-14648
BRETT, T. p 448 N95-13688
BREWER, JOHN p 508 N95-14458
BREWER, VAN p 417 N95-14650
BRIGHT, F. V. p 438 N95-14386
BRINKMANN, P. W. p 418 N95-14086
BRISKMAN, ROBERT D. p 466 N95-14682
BRITCHER, COLIN P. p 475 N95-14851
BROCKENBROUGH, J. R. p 508 N95-14459
BROEK, DAVID p 508 N95-14460
BROICHHAUSEN, KLAUS p 481 N95-14136
BROOKS, FREDERICK P., JR. p 556 N95-14033
BROSS, A. D. p 497 N95-15580
BROT, ABRAHAM p 508 N95-14461
BROTHERS, C. p 519 N95-15290
BROVELLI, M. A. p 516 N95-15794
p 517 N95-15798
BROWN, B. p 456 N95-14629
BROWN, CHRISTOPHER M. p 553 N95-15787
BROWN, D. S. p 443 N95-15667
BROWN, DANSEN p 404 N95-15465
BROWN, DEBORAH A. p 638 N95-14511
BROWN, SHERILYN A. p 403 N95-14891
BROWN, TIMOTHY M. p 643 N95-14502
BROWNE, EDWARD P. p 490 N95-14574
BROWNING, R. p 595 N95-15318
BRUDNICKI, MYRON J. p 502 N95-14666
BRUNGER, CLIFFORD A. p 409 N95-14849
BRUST, FREDERICK W. p 508 N95-14462
BRYAN, D. p 468 N95-15321
BRYANT, MARK p 409 N95-15742
BRYANT, ROBERT G. p 450 N95-14185
BRYCE, E. A. p 460 N95-15409
BRYSON, S. p 557 N95-14034
BUCCI, R. J. p 508 N95-14459
BUCHHEIT, R. G. p 446 N95-15368
BUCHHOLZ, DAVID p 600 N95-15539
BUCKLEY, JOHN D. p 473 N95-14294
BUCKNER, JAMES A. p 409 N95-14840
BUDDE, B. A. p 427 N95-14420
BUDNICK, E. K. p 405 N95-14421
BUGAJSKI, DANIEL J. p 396 N95-14249
BUHAY, H. p 476 N95-15399
BUHLER, KIMBERLEY p 508 N95-14463
BUICAN, I. p 630 N95-13996
BUKLEY, ANGELIA P. p 417 N95-14649
BULA, R. J. p 564 N95-14228
BUONOMO, SERGIO p 465 N95-14676
BURK, K. W. p 523 N95-15363
BURKA, MICHAEL p 530 N95-15401
BURKE, KATHY A. p 578 N95-14422
BURLEY, RICHARD R. p 395 N95-14241
BURR, T. p 591 N95-15359
BURTON, RUSSELL R. p 546 N95-15124
BUSH, HAROLD G. p 459 N95-14111
BUSQUETS, ANTHONY M. p 409 N95-14852
BUU, C. M. p 463 N95-14627
BYARD, PAUL L. p 644 N95-14509
BYUN, D. W. p 521 N95-14122

C

CABERA, DAVID JOSE FERNANDEZ p 598 N95-13918
CABRERA, GUILLERMO G. p 609 N95-13951
CADDY, LARRY A. p 415 N95-14636
CADOGON, J. B. p 519 N95-14433
CAFFEY, H. p 571 N95-14190
CAFLISCH, RUSSEL E. p 588 N95-14370
CAIN, DARYL p 416 N95-14647
CALDWELL, JOHN A. p 551 N95-15767
CALDWELL, S. E. p 616 N95-13998
CALDWELL, W. F. p 426 N95-14091
CALEDONIA, GEORGE E. p 422 N95-14071
CALLAHAN, P. X. p 539 N95-15135
CAMEL, D. p 634 N95-14209
CAMM, FRANK p 409 N95-15451
CAMPOS, S. p 412 N95-14343
CANADA, J. p 496 N95-13669
CANDLER, G. V. p 400 N95-14656
CANFIELD, DENNIS V. p 540 N95-14177
CANFIELD, P. C. p 624 N95-15430
CANNON, PAUL S. p 466 N95-14826
p 467 N95-14827
CANTER, DAVE p 395 N95-14242
CAO, H. p 596 N95-15381
CAO, W. p 434 N95-14387
CAPPIELLO, C. C. p 442 N95-15387
CARDENAS, FRANK p 432 N95-13646
CARDICK, ARTHUR W. p 509 N95-14464
CARDONE, VINCENT J. p 533 N95-15323
CARDUS, DAVID p 419 N95-15146
CARLETON, ANITA p 572 N95-14349
CARLIN, PATRICK S. p 420 N95-14063
CARLISLE, J. A. p 442 N95-15408
CARLSON, F. M. p 458 N95-14213
CARLSON, K. D. p 620 N95-14009
CARLSON, L. p 446 N95-15368
CARRADO, K. A. p 596 N95-15381
CARRASCO, ARMANDO p 405 N95-13719
CARRAWAY, DEBRA L. p 496 N95-14414
CARRINGTON, C. K. p 417 N95-14653
CARSON, M. p 458 N95-14225
CARTER, D. p 458 N95-14225
CARTER, JOHN p 396 N95-14249
CARTER, M. D. p 586 N95-15538
CARVER, G. P. p 459 N95-14512
CARVER, GARY P. p 459 N95-15322
CASEY, M. V. p 480 N95-14128
p 480 N95-14133
CASSANDRAS, CHRISTOS G. p 470 N95-15813
CASTANOS, OCTAVIO p 603 N95-13907
CASTELL, KAREN D. p 478 N95-15681
CASTELLI, MICHAEL G. p 436 N95-15911
CAVANAGH, R. R. p 441 N95-15370
CAWLEY, JAMES D. p 457 N95-14105
CEDRUN, MARK E. p 404 N95-15319
CEKIC, M. p 618 N95-15540
CELEGHINI, E. p 589 N95-13901
CEPERLEY, PETER H. p 606 N95-13928
CERBUS, CLIFFORD A. p 420 N95-14063
CERNOSEK, R. W. p 473 N95-14308
p 473 N95-14310
CESARIO, CHERYL p 537 N95-15751
p 537 N95-15753
CHA, HUNGSE p 474 N95-14355
CHAE, E. U. p 542 N95-15096
CHAI, AN-TI p 485 N95-14543
CHAIKIN, PAUL M. p 490 N95-14573
CHALMER, P. p 446 N95-15368
CHALOUPKA, T. p 415 N95-14639
CHAMBERS, J. Q. p 524 N95-15779
CHAMPEROUX, P. p 538 N95-15098
CHAMPIGNY, P. p 399 N95-14448
p 399 N95-14450
CHAN, K. S. p 512 N95-14484
CHAN, SHIH H. p 487 N95-14558
CHAN, V. S. p 617 N95-14426
CHANDLER, G. T. p 500 N95-13645
CHANDRASEKHAR, H. R. p 621 N95-14390
CHANDRASEKHAR, M. p 621 N95-14390
CHANG, A. T. p 509 N95-14466
CHANG, ALICE C. p 422 N95-14074
p 449 N95-14108
p 449 N95-14109
CHANG, IKE Y., JR. p 461 N95-14334
CHANG, JOON-SUNG p 471 N95-13921
CHANG, Y. W. p 479 N95-13679
CHAPMAN, WELDON p 567 N95-13632
CHAPPELL, P. J. p 523 N95-14403
CHAPPELOW, C. C. p 407 N95-15439
CHARGIN, MLADEN K. p 512 N95-14617
CHARLES, JOHN B. p 551 N95-14223
p 551 N95-14224
p 546 N95-15122
p 547 N95-15129
p 547 N95-15130
p 550 N95-15150
CHARLES, STEVE p 556 N95-14029
CHASE, JOE p 563 N95-15449
CHEN, CHUAN F. p 483 N95-14528
CHEN, CHUN-HSIEN p 477 N95-15456
CHEN, G. S. p 448 N95-14465
CHEN, H. p 445 N95-14665
CHEN, JIE p 538 N95-15099
CHEN, M. H. p 621 N95-14325
CHEN, Q. p 484 N95-14536
CHEN, W. p 593 N95-14309
CHEN, Y. p 520 N95-15406
CHENG, K. T. p 621 N95-14325
CHEONG, S.-W. p 624 N95-15430
CHERFILS, C. p 493 N95-15530
CHERNOV, A. A. p 448 N95-14548
CHEW, J. p 599 N95-15367
CHIAO, RAYMOND Y. p 611 N95-13968
CHICCOLI, C. p 606 N95-13929
CHIGIER, NORMAN p 488 N95-14563
CHILDS, DARA W. p 502 N95-14797
CHIU, S. p 437 N95-13652
CHIU, W. K. p 392 N95-14477
CHIVATERO, CRAIG J. p 421 N95-14068
CHIZHOV, ALEXEI V. p 602 N95-13897
CHO, J. H. p 624 N95-15430

CHO, W. D. ..... p 447 N95-15906
CHOMENTOWSKI, W. ..... p 565 N95-14594
CHOU, F. C. ..... p 624 N95-15430
CHOU, MING-DAH ..... p 531 N95-15745
CHOU, TSO-CHUAN ..... p 478 N95-15628
CHOUEIRY, ELIE ..... p 418 N95-14079
p 424 N95-14080
CHOW, R. ..... p 424 N95-14082
p 451 N95-14389
p 614 N95-15529
CHRISTOPHERSEN, N. ..... p 589 N95-13630
CHRUSCICKI, MARY C. ..... p 468 N95-15333
CHRUSCIEL, J. ..... p 452 N95-14399
p 452 N95-14400
CHUI, B. ..... p 595 N95-15318
CHUI, T. C. P. ..... p 444 N95-14208
CHUMAKOV, S. M. ..... p 609 N95-13950
CHUNG, JACOB N. ..... p 488 N95-14561
CHURCH, E. L. ..... p 601 N95-13644
CICINELLI, J. G. ..... p 561 N95-14054
CINTALA, MARK ..... p 432 N95-13646
CITURS, KEVIN D. ..... p 396 N95-14247
p 398 N95-14258
CLARK, A. D, JR. ..... p 458 N95-14225
CLARK, E. A. ..... p 447 N95-15625
CLARK, FRANCIS J. ..... p 555 N95-14018
CLARK, GEORGE W. ..... p 638 N95-14804
CLARK, IVAN O. ..... p 489 N95-14564
CLARK, R. ..... p 617 N95-14368
CLARK, R. N. ..... p 519 N95-15290
CLARKE, E. ..... p 412 N95-14343
CLARKE, JERRY A. ..... p 567 N95-15809
CLEEK, TAMMY ..... p 549 N95-15140
CLELAND, J. G. ..... p 523 N95-14403
CLERE, J. M. ..... p 547 N95-15126
CLERE, JEAN-MICHEL ..... p 544 N95-15110
CLEVELAND, ROBIN O. ..... p 401 N95-14880
CLIFT, JAMES ..... p 535 N95-14906
CLUFF, J. A. ..... p 621 N95-14192
COATS, C. J. ..... p 521 N95-14122
COBB, S. D. ..... p 458 N95-14214
COBLEIGH, BRENT R. ..... p 394 N95-14234
COCHRAN, R. J. ..... p 428 N95-14664
COCHRAN, WILLIAM D. ..... p 643 N95-14505
COCUZZO, F. ..... p 567 N95-13635
COELHO, EMANUEL F. ..... p 536 N95-15324
COFFEY, EDGAR L. ..... p 470 N95-15756
COFFEY, HELEN E. ..... p 646 N95-15773
p 646 N95-15784
COHEN, GLENN M. ..... p 539 N95-15115
p 539 N95-15116
p 539 N95-15117
COIRIER, WILLIAM J. ..... p 398 N95-14297
COIRIER, WILLIAM JOHN ..... p 392 N95-13817
COKER, E. N. ..... p 458 N95-14226
COLBERG, FRANCIS R. ..... p 474 N95-14359
COLBURN, H. STEVEN ..... p 554 N95-14015
COLDREN, L. A. ..... p 499 N95-14364
COLER, C. ..... p 557 N95-14034
COLLIN, H. L. ..... p 619 N95-15758
COLLINS, J. ..... p 595 N95-15372
COLLINS, JOHN ..... p 431 N95-14669
COLLINS, R. W. ..... p 622 N95-14431
COMINSKY, LYNN R. ..... p 642 N95-15907
CONCUS, P. ..... p 457 N95-14659
CONCUS, PAUL ..... p 484 N95-14534
CONLEY, JULIANNE M. ..... p 492 N95-14607
CONNELL, JOHN W. ..... p 422 N95-14074
p 450 N95-14140
CONNELL, LINDA J. ..... p 550 N95-15649
COOKE, DAVID L. ..... p 428 N95-14599
COOKE, RICHARD ..... p 456 N95-15624
COPELAND, CARL E. ..... p 473 N95-14294
CORDES, J. ..... p 509 N95-14466
CORIELL, SAM R. ..... p 448 N95-14548
CORKILL, DANIEL D. ..... p 583 N95-15461
CORLISS, J. M. ..... p 419 N95-14089
CORZINE, S. W. ..... p 499 N95-14364
COTERA, CARLOS FLORES ..... p 471 N95-13922
COTTER, J. E. ..... p 520 N95-15405
COTTRELL, WILLIAM L. ..... p 572 N95-14520
COULTRIP, ROBERT H. ..... p 473 N95-14294
COUTSIAS, EVANGELOS A. ..... p 585 N95-14296
COWINGS, PATRICIA S. ..... p 539 N95-13661
COX, A. N. ..... p 646 N95-14376
COX, ANDREW T. ..... p 533 N95-15323
COX, S. F. J. ..... p 596 N95-15379
CRABTREE, G. W. ..... p 595 N95-15362
CRAIG, DAVID F. ..... p 510 N95-14471
CRAIG, KEN H. ..... p 468 N95-14835
CRAIG, R. A. ..... p 454 N95-15313
CRAIG, ROGER A. ..... p 644 N95-13717
p 429 N95-13718
p 405 N95-13719
p 405 N95-13720
p 645 N95-13721
CRANE, ROBERT K. ..... p 466 N95-14683
p 469 N95-15462
CRAWFORD, G. ..... p 415 N95-14639
CREASEY, G. H. ..... p 559 N95-14045
CREMERS, T. L. ..... p 505 N95-15777
CRESCENTI, G. H. ..... p 534 N95-15383
CRISMAN, R. P. ..... p 542 N95-15095
CROOM, MARK A. ..... p 394 N95-14234
CROSS, L. E. ..... p 625 N95-15746
CROWELL, R. A. ..... p 612 N95-13986
CRUMPLER, M. ..... p 415 N95-14639
CUCHE, J. L. ..... p 538 N95-15098
CUCINOTTA, FRANCIS A. ..... p 600 N95-15606
p 647 N95-15790
CULL, RONALD C. ..... p 478 N95-15669
CULLEN, D. E. ..... p 594 N95-14385
CUMMING, IAN ..... p 565 N95-14590
CUMMINGS, RUSSELL M. ..... p 397 N95-14253
p 404 N95-15762
CUNNINGHAM, H. A. ..... p 559 N95-14046
CUNNINGHAM, STEPHEN G. ..... p 552 N95-14864
CURETON, K. L. ..... p 411 N95-14799
CURL, R. F. ..... p 438 N95-14392
CURLETT, BRIAN P. ..... p 572 N95-14206
p 408 N95-14604
CUTLER, ROBERT M. ..... p 423 N95-14078
CYPRYK, M. ..... p 452 N95-14399

D

DAANE, ELIZABETH ..... p 538 N95-15102
DAHL, MILO D. ..... p 591 N95-14618
p 591 N95-15059
DAHLE, A. K. ..... p 446 N95-15349
DANIELSON, D. A. ..... p 514 N95-15805
DANKS, ANTHONY C. ..... p 639 N95-15828
DARIANO, GIACOMO M. ..... p 604 N95-13913
DARLING, STEPHEN R. ..... p 551 N95-15767
DAROLIA, R. ..... p 445 N95-14439
DAS, VISHNUMOHAN ..... p 537 N95-15751
DASARO, D. ..... p 557 N95-14034
DASGUPTA, SUNANDO ..... p 488 N95-14560
DATTOLI, G. ..... p 606 N95-13927
p 606 N95-13929
DAVARIAN, FARAMAZ ..... p 464 N95-14670
p 464 N95-14672
DAVIDSON, D. L. ..... p 512 N95-14484
DAVIDSON, FREDERIC M. ..... p 499 N95-14901
p 615 N95-15849
DAVIDSON, J. R. ..... p 578 N95-15434
p 579 N95-15534
DAVIDSON, JOHN B. ..... p 396 N95-14247
DAVIDSON, WILLIAM ..... p 432 N95-13646
DAVIES, P. G. ..... p 485 N95-14674
DAVIES, PHIL ..... p 550 N95-15147
DAVIS, C. C. ..... p 555 N95-14024
DAVIS, H. ..... p 518 N95-14191
DAVIS, JAMES L. ..... p 525 N95-13627
DAVIS, M. E. ..... p 593 N95-13678
DAVIS, ROBERT H. ..... p 484 N95-14537
p 444 N95-14578
DAVIS, STEPHEN H. ..... p 448 N95-14549
DAVISON, MARK R. ..... p 503 N95-15601
DAVY, WILLIAM C. ..... p 429 N95-13718
DAWICKE, D. S. ..... p 444 N95-13690
p 509 N95-14467
DAWSON, L. R. ..... p 621 N95-14342
DEBONI, T. ..... p 571 N95-14190
DEFACIO, BRIAN ..... p 607 N95-13939
DEGENNARO, STEPHEN V. ..... p 555 N95-14021
DEGNAN, JOHN J. ..... p 526 N95-14274
p 471 N95-14288
p 471 N95-14289
DEGROH, KIM K. ..... p 431 N95-15769
DEGYVEZ, JOSE P. ..... p 571 N95-14178
DEIMLER, JIM D. ..... p 551 N95-13715
DEKONING, A. U. ..... p 511 N95-14478
DELABEAUJARDIERE, ODILE ..... p 526 N95-13818
DELAMATER, N. D. ..... p 498 N95-13994
DELARUBIA, T. D. ..... p 594 N95-14383
DELGADO, J. C. ..... p 625 N95-15577
DELGENIO, A. D. ..... p 531 N95-15411
DELLACORTE, CHRISTOPHER ..... p 431 N95-13631
DELUCA, D. P. ..... p 446 N95-15415
DELUCAS, LAWRENCE J. ..... p 458 N95-14225
DEMARIA-PESCE, VICTOR H. ..... p 539 N95-15132
DEMARTINO, S. ..... p 589 N95-13901
p 607 N95-13938
DEMPSEY, ROBERT C. ..... p 643 N95-14501
DEMUYNCK, WILLEM M. ..... p 604 N95-13914
DENDA, MITSUNORI ..... p 509 N95-14468
DENHARTOG, D. J. ..... p 442 N95-15541
DENKER, HEINER ..... p 516 N95-15796
DENLINGER, EDGAR J. ..... p 451 N95-14354
DENNIS, R. L. ..... p 521 N95-14122
DENTON, J. D. ..... p 480 N95-14130
DENTREMONT, R. P. ..... p 534 N95-15614
DENYER, ANTHONY G. ..... p 410 N95-14469
DEPLACHETT, CHARLES P. ..... p 411 N95-14645
DEPPE, MARTIN W. ..... p 411 N95-15329
DERBY, B. ..... p 433 N95-13993
DEROSHIA, C. W. ..... p 539 N95-15135
DESIENA, S. ..... p 589 N95-13901
p 607 N95-13938
DESZCZ-PAN, M. ..... p 470 N95-15866
DEV, D. SAM DAYALA ..... p 413 N95-13829
DEVORE, L. ..... p 496 N95-13669
DEVRIES, SHERRI M. ..... p 544 N95-15105
DEWITT, KENNETH ..... p 483 N95-14531
DHADWAL, HARBANS S. ..... p 459 N95-14572
DIAZ, A. F. ..... p 439 N95-14435
DICARLO, DANIEL J. ..... p 398 N95-14257
DICKES, EDWARD ..... p 394 N95-14236
DIDIER, B. T. ..... p 633 N95-15528
DIEBOLD, A. C. ..... p 437 N95-14312
DIECKMANN, R. ..... p 454 N95-15358
DILLARD, ROBERT M. ..... p 551 N95-15767
DIMMOCK, JOHN O. ..... p 602 N95-13841
DIMOTAKIS, P. E. ..... p 400 N95-14656
DING, ZHAO-PING ..... p 538 N95-15099
DINKINS, JAMES R. ..... p 473 N95-14294
DIPRAMPERO, P. E. ..... p 546 N95-15120
DISKO, M. ..... p 454 N95-15340
DIXON, A. G. ..... p 458 N95-14226
DODDS, ROBERT H., JR. ..... p 514 N95-15802
DODONOV, V. V. ..... p 588 N95-13926
DOEHRING, F ..... p 532 N95-14120
DOLCE, JAMES L. ..... p 504 N95-15914
DOLLAR, MAREK ..... p 444 N95-14202
DOMINIK, CARSTEN ..... p 641 N95-15841
DONAHUE, S. ..... p 633 N95-15761
DONG, Y. F. ..... p 509 N95-14468
DORAN, J. C. ..... p 529 N95-14428
DOROGY, WILLIAM E., JR. ..... p 455 N95-15599
DOUSSAL, P. L. ..... p 620 N95-14008
DOWLING, JONATHAN P. ..... p 598 N95-13955
DOWNING, JULIE ..... p 459 N95-14567
DOWNING, MICAH ..... p 403 N95-14889
DOYAL, JEFFREY A. ..... p 468 N95-15393
DOYAL, ROY ..... p 540 N95-13971
DOYLE, B. L. ..... p 596 N95-15437
DOZIER, W. D. ..... p 454 N95-15340
DRACH, R. ..... p 522 N95-14317
DRBOHLAV, JOSEPH, III ..... p 453 N95-14954
DREWRAY, J. ..... p 625 N95-15577
DROTNING, W. ..... p 476 N95-15356
DROUILHET, S. ..... p 518 N95-14191
DU, CONG-SHI ..... p 603 N95-13902
DUBOIS, LINDA M. ..... p 544 N95-15105
DUEDALL, I. W. ..... p 532 N95-14120
DUKE, P. JACKIE ..... p 538 N95-15102
DULEY, WALTER W. ..... p 639 N95-15831
DULING, IRL N., III ..... p 614 N95-15707
DUMAIS, BRYAN ..... p 535 N95-14906
DUMBRAJS, O. ..... p 496 N95-14839
DUNCAN, BEVERLY S. ..... p 479 N95-13665
DUNGAO, M. ..... p 456 N95-14629
DUNHAM, R. EARL, JR. ..... p 407 N95-14899
DUNN, PETER J. ..... p 527 N95-14278
DUNN, RICHARD L. ..... p 454 N95-15296
DUNNING, F. B. ..... p 625 N95-15574
DURCHHOLZ, MATTHEW L. ..... p 588 N95-15400
DURIAN, DOUGLAS J. ..... p 459 N95-14568
DURLACH, NATHANIEL I. ..... p 554 N95-14013
p 561 N95-14057
DUSEK, J. T. ..... p 453 N95-14609
DUTKIEWICZ, MELANIE ..... p 565 N95-14590
DUTTA, PIYUSH K. ..... p 435 N95-15427
DYMEK, STANISLAW ..... p 444 N95-14202
DZIMIANSKI, J. W. ..... p 476 N95-15399

E

EANES, RICHARD J. ..... p 527 N95-14281
EATHER, ROBERT H. ..... p 428 N95-14951
EBERHARD, PHILIPPE H. ..... p 611 N95-13968
EBIHARA, BEN T. ..... p 497 N95-15915
ECONOMIDES, GREGORY ..... p 580 N95-13727
ECONOMY, JAMES ..... p 435 N95-15417
EDWARDS, ARTHUR A. ..... p 418 N95-14085
EHERNBERGER, L. J. ..... p 402 N95-14888
EHST, D. A. ..... p 617 N95-14012
ELDRIDGE, JEFFREY I. ..... p 497 N95-15915
ELLER, B. G. ..... p 396 N95-14248
ELLINGER, Y. ..... p 599 N95-15844
ELLINGSON, W. A. ..... p 449 N95-13978
ELLIOTT, CHARLES B., III ..... p 510 N95-14470
ELLIS, STEPHEN R. ..... p 554 N95-14013
p 557 N95-14036
ELLYIN, FERDNAND ..... p 510 N95-14471

ELTGROTH, P. ..... p 523 N95-15364
ELY, WAYNE ..... p 517 N95-15851
ELY, WAYNE L. ..... p 398 N95-14258
EMERY, JEFF ..... p 549 N95-15139
EMERY, V. J. ..... p 625 N95-15576
ENDSLEY, MICA R. ..... p 559 N95-14047
ENGELFRIED, J. ..... p 579 N95-15581
ENGELHARDT, MICHEL ..... p 399 N95-14449
ENGLISH, J. H. ..... p 499 N95-14364
ENNS, DALE F. ..... p 396 N95-14249
EPPERSON, J. E. ..... p 445 N95-14665
ERDEMIR, A. ..... p 456 N95-15778
EREMIN, V. ..... p 593 N95-14309
ERNST, HUGO A. ..... p 511 N95-14480
ERZBERGER, HEINZ ..... p 406 N95-14611
ESMAN, RONALD D. ..... p 614 N95-15707
ESPENAK, FRED ..... p 638 N95-14667
ESPROLES, CARLOS ..... p 498 N95-13629
ESSFELD, D. ..... p 548 N95-15137
EVANS, D. L. ..... p 515 N95-14125
EVANS, J. ..... p 425 N95-14090
EVANS, JEFFREY A. ..... p 470 N95-15756
EVANS, N. D. ..... p 601 N95-13674
p 619 N95-13821
EZZELL, STEPHEN A. ..... p 450 N95-14113

F

FADRAGAS, M. I. ..... p 510 N95-14472
FAGALY, ROBERT L. ..... p 459 N95-14547
FAHMY, A. A. ..... p 436 N95-15443
FANG, N. ..... p 568 N95-14152
FANTON, JOHN W. ..... p 538 N95-15094
p 542 N95-15095
FARLESS, CATHERINE ..... p 417 N95-14650
FARLEY, GARY L. ..... p 433 N95-13836
p 501 N95-14186
FARTHING, CHARLES L. ..... p 411 N95-15392
FATHAUER, ROBERT W. ..... p 614 N95-15603
FATHY, ALY ..... p 451 N95-14354
FAVIER, JEAN JACQUES ..... p 634 N95-14209
FEDELE, RENATO ..... p 601 N95-13944
FEELEY, T. JENS ..... p 415 N95-14634
FEEN, A. ..... p 521 N95-15407
FELLENSTEIN, JAMES A. ..... p 431 N95-13631
FENG, C. ..... p 570 N95-14163
FENG, Z. C. ..... p 485 N95-14541
FEO, J. T. ..... p 571 N95-14190
FERRON, J. R. ..... p 618 N95-15632
FETTER, M. ..... p 546 N95-15121
FIDANOVA, S. ..... p 584 N95-13980
FIDELL, SANFORD ..... p 403 N95-14890
FIELD, CHRISTOPHER T. ..... p 499 N95-14901
FIELDS, JAMES M. ..... p 403 N95-14892
FINE, M. E. ..... p 510 N95-14472
FINN, R. ..... p 457 N95-14659
FINN, ROBERT ..... p 484 N95-14534
FISCHBACH, D. ..... p 492 N95-14869
FISCHER, D. ..... p 546 N95-15121
FISCHER, O. ..... p 639 N95-15830
FISHER, ALVAN, JR. ..... p 536 N95-15330
FISHER, DAVID F. ..... p 393 N95-14230
p 394 N95-14231
p 394 N95-14237
FISHER, SCOTT S. ..... p 557 N95-14034
FISK, Z. ..... p 624 N95-15430
FITTINGHOFF, D. N. ..... p 498 N95-14318
FIX, LIMOR ..... p 568 N95-13699
FLEEGE, E. J. ..... p 407 N95-15439
FLEET, TERRANCE M. ..... p 416 N95-14644
FLEMIG, JO ..... p 540 N95-14177
FLEMING, M. ..... p 505 N95-14475
FLETCHER, K. A. ..... p 619 N95-13698
FLEURIAL, J. P. ..... p 625 N95-15531
FLICK, BRADLEY C. ..... p 395 N95-14240
FLOOD, DENNIS J. ..... p 473 N95-14302
FLOWERS, L. ..... p 518 N95-14191
FLOWERS, WOODIE ..... p 562 N95-14058
FLYNN, GEORGE ..... p 461 N95-14361
FOLKERTS, L. ..... p 592 N95-13675
FOLLSTAEDT, D. M. ..... p 621 N95-14323
FONASH, S. ..... p 476 N95-15410
FONG, MICHAEL C. ..... p 420 N95-14064
FONG, TERRENCE W. ..... p 427 N95-14099
FORD, W. E. ..... p 583 N95-15369
FOREMAN, L. R. ..... p 616 N95-13997
FORMAN, R. G. ..... p 510 N95-14473
FORNARI, D. J. ..... p 529 N95-14434
FOROUHAR, SIAMAK ..... p 612 N95-14181
FORTE, THOMAS P. ..... p 508 N95-14462
FORTNEY, S. M. ..... p 547 N95-15130
FOSSUM, E. ..... p 452 N95-14399
FOSSUM, ERIC ..... p 450 N95-14304
FOSTER, G. W. ..... p 475 N95-15302
FOSTER, I. ..... p 578 N95-14116
FOSTER, I. T. ..... p 567 N95-13676
FOSTER, JOHN V. ..... p 396 N95-14246
FOSTER, LUCAS E. ..... p 475 N95-14851
FOSTER, M. S. ..... p 537 N95-15751
p 537 N95-15753
FOSTER, MICHAEL R. ..... p 486 N95-14550
FOUSHEE, H. CLAYTON ..... p 550 N95-15649
FOWLER, ROBERT J. ..... p 579 N95-15590
FOX, DAVID M. ..... p 434 N95-14348
FOX, G. ..... p 419 N95-14632
FOX, ROBERT L. ..... p 473 N95-14294
FOXALL, W. ..... p 529 N95-14436
FRACK, KENNETH L., JR. ..... p 592 N95-15448
FRAME, EDWIN A. ..... p 451 N95-14365
FRANCO-FERREIRA, E. A. ..... p 500 N95-13645
FRANCOMBE, M. H. ..... p 476 N95-15399
FRANK, M. R. ..... p 594 N95-14660
FRANSON, JAMES D. ..... p 607 N95-13933
FRASER, M. E. ..... p 440 N95-14958
FRAZIER, DONALD. O. ..... p 634 N95-14207
FRAZIER, S. J. ..... p 462 N95-14405
FREDELL, ROBERT S. ..... p 391 N95-14144
FREED, ALAN D. ..... p 585 N95-14300
FREED, KARL F. ..... p 627 N95-15404
FREEMAN, BENNY D. ..... p 455 N95-15444
FREEMAN, FREDERICK ..... p 552 N95-14864
FREYER, GUSTAV J. ..... p 411 N95-15392
FRIEBELE, EDWARD J. ..... p 615 N95-15766
FRIEDEN, B. R. ..... p 615 N95-15772
FRITSCH-YELLE, JANICE M. ..... p 551 N95-14223
FRY, EDWARD S. ..... p 611 N95-13966
FRYE, DANIEL E. ..... p 535 N95-14335
FRYE, G. C. ..... p 437 N95-14307
p 473 N95-14308
FUCHS, W. K. ..... p 579 N95-15442
FULKERSON, E. S. ..... p 473 N95-14261
FULLER, CHARLES A. ..... p 539 N95-15133
p 550 N95-15147
FURNESS, THOMAS A., III ..... p 556 N95-14031
FURNISH, M. D. ..... p 642 N95-14311
FURRER, A. ..... p 620 N95-14188

G

GADOLIN, R. E. ..... p 541 N95-14424
GAFFIE, D. ..... p 545 N95-15112
GAHL, J. M. ..... p 617 N95-14262
GAIBLE, F. ..... p 400 N95-14452
GAINER, K. E. ..... p 581 N95-14377
GALEA, S. C. ..... p 434 N95-14409
GALJAEV, V. L. ..... p 421 N95-14065
p 418 N95-14098
GALLAGHER, A. ..... p 518 N95-14194
GALLAGHER, CHRISTOPHER ..... p 489 N95-14566
GALLEGOS, R. R. ..... p 477 N95-15544
GALLIS, MICHAEL R. ..... p 609 N95-13949
GALLOWAY, HOYT W. ..... p 541 N95-14394
GAMACHE, R. R. ..... p 595 N95-14950
GAMBHIR, R. D. ..... p 414 N95-13832
GANDER, PHILIPPA H. ..... p 550 N95-15649
GANESHAN, A. S. ..... p 414 N95-13830
GANG, HU ..... p 444 N95-14575
GANGLOFF, RICHARD P. ..... p 448 N95-14483
p 448 N95-15918
GAO, M. ..... p 448 N95-14465
GARANDET, J. P. ..... p 634 N95-14209
GARDNER, S. D. ..... p 442 N95-15387
GARDNER, SHANNON ..... p 535 N95-14906
GARDNER, WILFORD D. ..... p 536 N95-15425
GARGIULO, JOE ..... p 418 N95-14094
GARNER, F. A. ..... p 446 N95-15431
p 446 N95-15433
GARNER, H. DOUGLAS ..... p 455 N95-15579
GARNERO, P. ..... p 472 N95-14112
GAROFF, STEPHEN ..... p 400 N95-14452
p 484 N95-14536
GARRETT, J. W. ..... p 444 N95-14581
GARSCADDEN, A. ..... p 421 N95-14066
GARTENBERG, E. ..... p 450 N95-14303
GATCHELL, PETER A. ..... p 494 N95-15605
GATTI, M. S. ..... p 615 N95-15872
GAUDET, SAMUEL ..... p 463 N95-14626
GAWRONSKI, W. K. ..... p 489 N95-14569
GAYNOR, SCOTT ..... p 463 N95-14625
p 451 N95-14316
p 452 N95-14395
GEE, KEN ..... p 397 N95-14253
GEFFNEY, F. ANDREW ..... p 538 N95-15094
GEISER, U. ..... p 620 N95-14009
GEITGEY, J. ..... p 524 N95-15575
GELLES, D. S. ..... p 445 N95-14379
GENKIN, L. ..... p 421 N95-14067
GENTRY, S. ..... p 469 N95-15583
GEORGE, T. F. ..... p 608 N95-13943
GEORGE, THOMAS F. ..... p 598 N95-13937
GERARD, PAUL L. ..... p 550 N95-15149
GEREVINI, ALFONSO ..... p 587 N95-15643
p 584 N95-15786
p 576 N95-15825
GESHKENBEIN, V. B. ..... p 619 N95-13681
GEUS, E. R. ..... p 450 N95-14151
GEVARGIZ, J. M. ..... p 463 N95-14627
GHAFFARI, F. ..... p 393 N95-14230
GHANDOUR, LOUMA ..... p 639 N95-15829
GHIGLIA, D. C. ..... p 515 N95-14313
GHOSH, V. J. ..... p 624 N95-15422
GIBONI, K. L. ..... p 517 N95-15916
GIDDINGS, THOMAS E. ..... p 402 N95-14884
GIES, DOUGLAS R. ..... p 644 N95-14508
GILBERT, JEFFREY L. ..... p 500 N95-13654
GILBERT, L. E. PAUL ..... p 408 N95-13703
GILLIES, D. ..... p 458 N95-14213
GILLIES, D. C. ..... p 458 N95-14214
GILLILAND, RONALD L. ..... p 643 N95-14503
GILMER, G. H. ..... p 594 N95-14383
GINOCCHIO, J. N. ..... p 593 N95-14000
p 593 N95-14001
GIORDANO, PIETRO ..... p 423 N95-14077
GIOVANNINI, MASSIMO ..... p 608 N95-13947
GLADDEN, HERBERT J. ..... p 482 N95-14299
GLAISTER, DAVID H. ..... p 547 N95-15125
GLASS, EMILY ..... p 580 N95-13727
GLASS, G. P. ..... p 438 N95-14392
GLASSBURN, ROBIN S. ..... p 425 N95-14088
GLASSFORD, A. P. M. ..... p 421 N95-14066
GLASSMAN, ARTHUR J. ..... p 405 N95-15912
GLEASON, K. ..... p 496 N95-13669
GLENDENNING, N. K. ..... p 643 N95-14442
GLOSLI, JAMES N. ..... p 474 N95-14425
GLOWNIA, JAMES H. ..... p 641 N95-15845
GOBBI, BRUNO ..... p 600 N95-15539
GOBBY, P. ..... p 616 N95-13997
GODOWITCH, J. M. ..... p 616 N95-13973
GOLDBERG, L. A. ..... p 568 N95-13976
GOLDEN, JOHNNY L. ..... p 432 N95-14603
GOLDHIRSH, JULIUS ..... p 465 N95-14677
GOLDISH, JUDITH ..... p 419 N95-14474
GOLDMAN, JEFFREY H. ..... p 492 N95-14869
GOLDSMITH, J. E. M. ..... p 531 N95-15411
GOLDSTEIN, S. J. ..... p 529 N95-14434
GOLUB, GENE H. ..... p 585 N95-14657
GONG, S. S. ..... p 449 N95-13692
GONZALEZ, ELISA ..... p 586 N95-15424
GOODBERLET, MARK A. ..... p 517 N95-15848
GOODSON, T., III ..... p 449 N95-13692
GOODWIN, DAVID G. ..... p 622 N95-14655
GOPAL, ANTHONY D. ..... p 459 N95-14568
GORDON, ANDREW L. ..... p 504 N95-15914
GORDON, R. G. ..... p 520 N95-15355
GORE, AL ..... p 633 N95-15781
GOREE, JOHN ..... p 490 N95-14571
GORETTA, K. C. ..... p 621 N95-14192
GOSSARD, A. C. ..... p 499 N95-14364
GOSTELOW, C. R. ..... p 506 N95-14198
GOTO, S. ..... p 549 N95-15145
GOTT, J. ..... p 539 N95-15135
GOTTEN, WILLIAM M., JR. ..... p 551 N95-15757
GOVINDAN, T. R. ..... p 589 N95-13656
GOW, D. ..... p 559 N95-14045
GRAEBER, R. CURTIS ..... p 550 N95-15649
GRAESSLE, D. ..... p 638 N95-14101
GRAF, T. ..... p 620 N95-13999
GRANADOS, ARNO F. ..... p 643 N95-14499
GRANDT, ALTEN F., JR. ..... p 508 N95-14463
GRAVES, C. M., JR. ..... p 462 N95-14405
GRAVES, JOHN H. ..... p 447 N95-15622
p 447 N95-15807
GRAY, DAVID L. ..... p 496 N95-14414
GRAY, G. T., III ..... p 642 N95-14311
p 445 N95-14439
GRAY, W. M. ..... p 534 N95-15666
GRAYSON, T. P. ..... p 600 N95-13912
GREEN, DAVID L. ..... p 410 N95-14175
GREEN, H. J. ..... p 519 N95-15290
GREENBERG, H. S. ..... p 409 N95-14794
p 434 N95-14800
p 435 N95-14801
p 514 N95-15913
GREENBERGER, DANIEL M. ..... p 611 N95-13962
GREENSTADT, E. W. ..... p 642 N95-14266
GREENWOOD, J. A. ..... p 533 N95-15323
GREER, DONALD S. ..... p 479 N95-13892
GREGORY, J. D. L. ..... p 405 N95-14199
GRESZTA, DOROTA ..... p 451 N95-14324
p 452 N95-14395
GRIFFIN, J. W. ..... p 522 N95-14187
GRIFFIN, MICHAEL J. ..... p 563 N95-15850
GRIFFITH, J. B. ..... p 419 N95-14089
p 425 N95-14090
GRIGORIEV, ANATOLY I. ..... p 542 N95-15091
GROMOV, M. ..... p 586 N95-15412

GROSS, ROLF W. F. p 598 N95-13937
GROSSMAN, E. p 421 N95-14067
p 422 N95-14073
GROSSMAN, R. L. p 568 N95-14010
GRUBER, M. L. p 512 N95-14485
GRUBIN, HAROLD L. p 589 N95-13656
GRUEN, D. M. p 620 N95-13822
p 593 N95-14011
GU, S. H. p 449 N95-13689
GUAN, H. W. p 448 N95-13688
p 449 N95-13689
GUAN, X. p 574 N95-15536
GUBBINS, K. E. p 454 N95-15344
GUEST, M. F. p 573 N95-15311
GUILINGER, T. R. p 446 N95-15368
GUILLAUME, A. p 545 N95-15112
GUILLAUME, M. p 620 N95-14188
GUIST, ROY p 512 N95-14617
GUNDO, D. P. p 419 N95-14089
p 425 N95-14090
GUNGA, HANNS-CHRISTIAN p 548 N95-15131
GUNJI, A. p 549 N95-15145
GUNJI, ATSUAKI p 543 N95-15097
GUNZBURGER, MAX D. p 493 N95-15390
GURJEVA, T. S. p 538 N95-15106
GURUSWAMY, GURU P. p 391 N95-13662
GUST, M. C. p 619 N95-13821
GUSTAFSON, G. B. p 534 N95-15614
GUTOW, DAVID A. p 500 N95-13654
GUZA, R. T. p 536 N95-15452
GUZIK, J. A. p 646 N95-14376

H

HAAG, THOMAS W. p 430 N95-14301
HAASZ, A. A. p 437 N95-13652
HACKEL, L. p 499 N95-14427
HACKETT, C. M. p 455 N95-15535
HADFIELD, STEVEN M. p 578 N95-14953
HAGSTROM, THOMAS p 585 N95-14296
HAHN, H. p 418 N95-14095
HAIMOVITCH, Y. p 494 N95-15605
HAINES, A. BARRY p 393 N95-14103
HAISCH, BERNHARD M. p 643 N95-14500
HAJ-HARIRI, HOSSEIN p 485 N95-14544
HAJARE, ANKUR R. p 423 N95-14075
HALBIG, J. K. p 581 N95-14377
HALDAR, P. p 475 N95-14606
HALL, R. B. p 520 N95-15405
HALL, R. M. p 393 N95-14230
HALL, RONALD O. p 417 N95-14652
HALLINAN, KEVIN P. p 488 N95-14559
HALPERT, GERALD p 472 N95-13824
HAMACHER, HANS p 457 N95-14211
HAMILL, T. M. p 534 N95-15614
HAMILTON, C. H. p 445 N95-15293
HAMILTON, DAVID p 571 N95-14172
HAMILTON, J. J. p 627 N95-15823
HAMILTON, MARK F. p 401 N95-14880
p 592 N95-15453
HAMLEY, JOHN A. p 430 N95-14301
HAMM, KEN p 512 N95-14617
HAMPTON, ROY W. p 512 N95-14617
HAN, D. p 602 N95-13896
p 603 N95-13905
HAN, YENJO p 586 N95-15594
p 587 N95-15641
HANNAFORD, BLAKE p 504 N95-14027
HANSEN, CHRISTOPHER P. p 503 N95-15306
HANSEN, E. A. p 513 N95-15348
HANSEN, FRANK V. p 533 N95-14340
HANSEN, PATRICIA A. p 421 N95-14068
HANSEN, REED S. p 512 N95-14617
HARA, K. p 600 N95-15582
HARBAUGH, STEPHEN P. p 398 N95-14258
HARFOUSH, F. A. p 574 N95-15418
HARGENS, ALAN R. p 547 N95-15128
HARKER, ALAN B. p 626 N95-15808
HARKNESS, H. H. p 505 N95-14475
HARLOW, D. G. p 448 N95-14465
HARMAN, GEORGE G. p 474 N95-14401
HARPER, J. p 425 N95-14090
HARPER, JENNIFER P. p 551 N95-15810
HARRIS, CHARLES E. p 507 N95-14453
HARRIS, DANIEL C. p 448 N95-13686
HARRIS, REGINA M. p 551 N95-13715
HARRIS, STEPHEN E. p 498 N95-13695
HARRISON, A. K. p 493 N95-15530
HARRISON, L. p 581 N95-13895
HART, KENNETH A. p 533 N95-14952
HARTIGAN, P. p 639 N95-15829
HARTMAN, JUDITH O. p 541 N95-14394
HARUNA, YUICHIRO p 543 N95-15097
HARVEY, R. W. p 618 N95-15540
HARVILLE, J. p 565 N95-14594
HARWOOD, D. W. p 407 N95-15439
HARWOOD, T. p 632 N95-15435
HASH, M. C. p 471 N95-13684
HASLACH, HENRY W., JR. p 585 N95-14300
HATFIELD, MICHAEL O. p 411 N95-15392
HATTAN, C. P. p 461 N95-14345
HATTON, T. ALAN p 490 N95-14574
HAUER, A. A. p 498 N95-13994
HAUGHTON, JAMES p 425 N95-14087
HAUS, HERMANN A. p 604 N95-13910
HAUSER, JOSEPH p 425 N95-14087
HAUSHEER, F. p 571 N95-14190
HAVENS, STEPHEN J. p 450 N95-14185
HAWKER, DEBRA p 484 N95-14537
HAWKINS, C. F. p 473 N95-14314
HAYARD, MICHEL p 504 N95-14947
HAYDUK, MICHAEL J. p 477 N95-15459
HAYES, E. D. p 405 N95-14421
HAYNES, GERALD p 432 N95-13646
HAYNES, W. M. p 438 N95-14372
HE, Q. p 488 N95-14559
HEATH, W. O. p 524 N95-15432
HEBERT, C. p 561 N95-14054
HECHT, LAURA M. p 632 N95-14870
HEDGELAND, RANDY J. p 421 N95-14068
p 418 N95-14070
HEFLIN, M. p 527 N95-14276
HEGERFELDT, GERHARD C. p 598 N95-13945
HEIDGER, S. p 450 N95-14303
HEIMAN, D. p 621 N95-14342
HEINEMANN, KLAUS W. p 513 N95-14922
HEITZMANN, MARIBETH p 634 N95-15846
HELD, RICHARD M. p 554 N95-14014
HELGESON, W. D. p 477 N95-15544
HELLBAUM, RICHARD F. p 590 N95-14110
HELMKEN, HENRY p 466 N95-14684
HEMASPAANDRA, LANE A. p 586 N95-15594
p 575 N95-15597
p 587 N95-15732
p 577 N95-15858
p 589 N95-15859
HENDERSON, D. R. p 454 N95-15343
HENDRIX, J. L. p 613 N95-14367
HENGEL, JOHN E. p 393 N95-14182
HENNIG, P. p 399 N95-14446
HENNING, RUDOLF p 466 N95-14684
HENNING, THOMAS p 639 N95-15830
HENRIKSEN, G. L. p 471 N95-13684
HENRIKSEN, T. K. p 511 N95-14478
HENSLEY, W. K. p 595 N95-15310
HEPP, ALOYSIUS F. p 477 N95-15587
HERBIG, G. H. p 640 N95-15834
HERBSLEB, JAMES p 572 N95-14349
HERGENROTHER, PAUL M. p 449 N95-13838
p 450 N95-14185
p 452 N95-14416
HERNANDEZ, ESTELA p 409 N95-15742
HERNANDEZ, JUAN CARLOS p 535 N95-14906
HERRERA-FIERRO, P. p 450 N95-14303
HERRERO, H. p 494 N95-15861
HERRICK, ROBERT D., II p 437 N95-14141
HERSING, WALTER p 539 N95-15115
HESS, PAUL C. p 645 N95-13724
HEWLETT, F. W. p 473 N95-14314
HEYLIGER, P. R. p 507 N95-14417
HIBBINS, R. E. p 640 N95-15834
HICKS, WILLIAM p 540 N95-13971
HIGBY, PAIGE L. p 615 N95-15766
HILL, D. C. p 415 N95-14639
HILL, DAVID C. p 519 N95-14802
p 519 N95-14853
HILL, G. p 640 N95-15835
HILLIARD, R. DAVID p 403 N95-14891
HILLIER, A. C. p 622 N95-14601
HILLMAN, DONALD J. p 551 N95-13715
HIMPSEL, F. J. p 442 N95-15408
HINDMAN, RICHARD G. p 404 N95-15853
HINDMAN, WARD p 533 N95-14848
HINE, BUTLER P., III p 427 N95-14099
HINGHOFER-SZALKAY, HELMUT p 544 N95-15107
p 548 N95-15131
HINKLE, A. J. p 508 N95-14459
HINZE, WILLIAM J. p 526 N95-14267
HIRD, ANDREW C. p 619 N95-13698
HIROSE, MICHITAKA p 559 N95-14048
HIRSCH, CH. p 480 N95-14131
HISHINUMA, A. p 446 N95-15431
HITNEY, H. V. p 461 N95-14345
HITNEY, HERBERT V. p 467 N95-14831
p 467 N95-14832
HIX, DEBORAH p 563 N95-15449
HJALMARSON, H. P. p 477 N95-15544
HLAVACEK, VLADIMIR p 494 N95-15780
HO, HAU H. p 466 N95-14680
HOCK, S. M. p 519 N95-14433
HODSON, ROBERT F. p 566 N95-14514
HOECK, E. p 517 N95-15797
HOEHN, J. G., JR. p 475 N95-14806
HOEPPNER, DAVID W. p 510 N95-14470
p 448 N95-14482
HOFERT, GLENN D. p 492 N95-14658
HOFFMAN, J. R. p 462 N95-14412
HOFFMANN, U. p 548 N95-15137
HOGAN, M. O. p 439 N95-14663
HOGAN, R. E. p 428 N95-14664
HOITINK, D. J. p 523 N95-15363
HOLDER, ANDREW J. p 443 N95-15782
HOLLAND, SCOTT D. p 495 N95-15898
p 495 N95-15899
HOLLAS, C. L. p 442 N95-15387
HOLLENBERG, G. W. p 455 N95-15579
HOLLEY, D. C. p 539 N95-15135
HOLLINGSWORTH, WILLIAM B. p 398 N95-14258
HOLLOWAY, FRANK A. p 552 N95-14863
HOLLOWAY, KAREN p 632 N95-14619
HOLT, R. G. p 485 N95-14541
HOLT, R. GLYNN p 458 N95-14220
HOLTOM, G. R. p 612 N95-13986
HOLTZCLAW, K. W. p 440 N95-14958
HOLY, JOHN A. p 443 N95-15715
HOLY, X. p 539 N95-15148
HONG, W. S. p 625 N95-15577
HONGYAN, L. p 461 N95-14147
HONOHAN, ANDREW p 484 N95-14535
HONTALAS, PHIL p 427 N95-14099
HOPKINS, K. W. p 578 N95-14380
HOPPA, MARY ANN p 572 N95-14615
HORDINSKY, JERRY p 540 N95-14177
HORNE, MICHAEL p 611 N95-13962
HORNER, GARNETT C. p 506 N95-14138
HORNUNG, H. G. p 400 N95-14656
HORZ, FRIEDRICH p 432 N95-13646
HOWARD, DONALD B. p 514 N95-13693
HOWARD, J. B. p 439 N95-14435
HOWARD, SETHANE p 638 N95-14511
HOWARTH, THOMAS R. p 496 N95-14841
HOWELL, STEVE B. p 644 N95-14507
HOZAKI, SHIG p 513 N95-14922
HRISCU, V. p 630 N95-13996
HRKACH, J. p 452 N95-14398
HSIEH, KWANG-CHUNG p 483 N95-14531
HU, F. Q. p 495 N95-15917
HU, J. p 520 N95-15355
HUA, THANH Q. p 616 N95-14006
HUANG, F. H. p 445 N95-14378
p 445 N95-14379
HUBER, PETER p 395 N95-14243
p 395 N95-14244
HUDAK, S. J., JR. p 512 N95-14484
HUDGENS, E. E. p 521 N95-14123
HUENNEKENS, JOHN p 596 N95-15446
HUFFER, WILLIAM E. p 454 N95-15296
HUGENBERG, K. p 601 N95-13670
HUGHES, DAVID W. p 421 N95-14068
p 418 N95-14070
HUGHES, J. p 636 N95-13634
HUGHES, K. L. p 496 N95-14146
HUGHES, WILLIAM O. p 419 N95-13893
HUISMANN, SCOTT S. p 416 N95-14644
HULL, ANDREW J. p 591 N95-15320
HULLINGER, RONALD L. p 538 N95-15104
HUNDLEY, M. p 620 N95-13999
HUNG, CHING-CHEH p 441 N95-15303
HUNG, R. J. p 479 N95-14104
HUNT, A. J. p 434 N95-14387
HUNTER, D. G. p 582 N95-14946
HUNTER, IAN W. p 555 N95-14019
p 558 N95-14040
HUNTER, J. A. p 617 N95-14262
HUNTER, WILLIAM R. p 614 N95-15764
HUNTRESS, WESLEY T., JR. p 415 N95-14634
HURD, W. J. p 463 N95-14627
HUSS-LEDERMAN, S. p 577 N95-13677
HUTCHINGS, L. p 529 N95-14436
HUTCHISON, JAMES H. p 477 N95-15456
HUTH, JEFFREY p 426 N95-14093
HUTH, JEFFREY S. p 426 N95-14092
HWA, T. p 620 N95-14008
HWANG, D. p 521 N95-14122
HWANG, SEUNG-JOON p 444 N95-14202
HWANG, Y. p 476 N95-15356
HYER, M. W. p 505 N95-13839
p 435 N95-14865
HYER, T. p 622 N95-15308
HYLAND, DIANE T. p 551 N95-13715
HYMAN, NELSON L. p 424 N05-14083
HYNEK, DANIEL P. p 534 N95-15749

I

IANNO, N. J. p 453 N95-15292

IBSEN, T. G. p 630 N95-13673
ILLUMINATI, FABRIZO p 607 N95-13938
IM, SEONGIL p 620 N95-14189
INAMURA, KOHEI p 559 N95-14048
INBAR, GIDEON F. p 560 N95-14049
INGRAM, A. E. p 520 N95-15405
INTZAND, J. J. M. p 638 N95-14429
IRVIN, JANET G. p 468 N95-15393
ISAAC, GEORGE A. p 406 N95-14895
ISAACS, H. S. p 438 N95-14371
ISAACS, R. G. p 534 N95-15614
ISAKOV, V. p 610 N95-13960
ISHIDA, H. p 441 N95-15352
ISHIHAMA, LINDA M. p 539 N95-15133
ITO, KATSUKO p 548 N95-15134
ITOH, K. p 545 N95-15111
ITON, L. E. p 593 N95-13678
IVANOV, ALEXEY NIKOLAYEVICH
p 430 N95-13697
IVERSEN, E. K. p 555 N95-14024
IYENGAR, SITHARAMA p 470 N95-15820
IYER, A. N. p 475 N95-14606

J

JACKSON, A. M. p 472 N95-13975
JACKSON, T. L. p 495 N95-15917
JACKSON, WILLIAM G. p 553 N95-15768
JACOBS, DONALD T. p 487 N95-14552
JACOBS, MARK p 431 N95-14669
JACOBSEN, STEPHEN C. p 555 N95-14024
JACOBUS, CHARLES p 560 N95-14050
JACOBUS, HEIDI p 560 N95-14050
JACOBY, R. p 557 N95-14034
JAEGER, E. F. p 586 N95-15538
JAEGER, GREGG p 598 N95-13961
JAIN, A. K. p 523 N95-15361
JAIN, Y. K. p 413 N95-13828
JALBERT, JIM p 503 N95-15294
JALINK, ANTONY, JR. p 590 N95-14110
JAMES, KEVIN D. p 397 N95-14255
JANCA, J. p 627 N95-15838
JANKELA, JAN p 539 N95-15144
JANOWITZ, J. p 581 N95-13895
JANSEN, A. N. p 471 N95-13684
JANSEN, J. F. p 501 N95-14005
JANSSENS, BOB p 579 N95-15442
JARVIS, N. L. p 497 N95-15334
JARZYNSKI, C. p 627 N95-15578
JASNOW, DAVID p 487 N95-14553
JASTRZEBSKI, L. p 624 N95-15426
JAYANTY, M. p 523 N95-15382
JAYANTY, R. K. M. p 523 N95-15382
JAYNE, D. T. p 444 N95-13667
p 450 N95-14303
JEFFERYS, WILLIAM H. p 637 N95-13723
JENKINS, E. W. p 632 N95-15419
JENKINS, PHILLIP P. p 477 N95-15587
JENKINS, ROBERT C. p 502 N95-14904
JENNIONS, IAN K. p 480 N95-14129
p 481 N95-14135
JENNISKENS, PETER p 639 N95-15829
JENSEN, BRIAN J. p 449 N95-13838
p 450 N95-14185
p 452 N95-14416
JENSTROM, DEL T. p 583 N95-15598
JEONG, DAVID Y. p 508 N95-14460
p 511 N95-14476
JERIUS, D. p 636 N95-13634
JEX, HENRY R. p 556 N95-14028
JI, H. p 617 N95-14373
JIANG, TAO p 575 N95-15644
JIANG, ZHIGEN p 577 N95-15858
JIN, Y. p 462 N95-14623
JING, T. p 625 N95-15577
JOHNSON, C. W. p 593 N95-14000
p 593 N95-14001
JOHNSON, CALVIN R. p 415 N95-14639
JOHNSON, D. M. p 411 N95-15392
JOHNSON, DANA J. p 515 N95-15546
JOHNSON, DANIEL L. p 540 N95-13971
JOHNSON, DENNIS A. p 499 N95-14668
JOHNSON, EDWARD J. p 489 N95-14564
JOHNSON, FRED M. p 640 N95-15837
JOHNSON, K. I. p 445 N95-15293
JOHNSON, PARLEY P. p 551 N95-15767
JOHNSON, S. X. p 521 N95-15863
JOHNSON, SAMUEL D. p 473 N95-14294
JOHNSON, W. R. p 621 N95-14325
JOHNSTON, D. C. p 624 N95-15430
JOHNSTON, DAVID F. p 473 N95-14294
JOLLEY, RICHARD p 429 N95-15824
JONE, S. J. p 520 N95-15406
JONECKIS, LANCE G. p 609 N95-13953
JONES, ANTHONY P. p 641 N95-15842
JONES, E. D. p 621 N95-14342
p 621 N95-14390
JONES, LYNETTE A. p 555 N95-14019
p 558 N95-14040
JONES, P. L. p 593 N95-14011
JONES, R. p 434 N95-14409
p 392 N95-14477
JONES, TIMOTHY A. p 544 N95-15105
JONG, JEN-YI p 514 N95-13639
JONGKIND, W. p 501 N95-14150
JOO, J. p 621 N95-14192
JORGENSEN, J. D. p 624 N95-15430
JOSHI, SURESH M. p 420 N95-13729
JOYCE, J. A. p 514 N95-15803
JULKA, VIBHOR p 470 N95-15813
JURANI, M. p 538 N95-15106
JURANI, MARIAN p 539 N95-15144
JURANIOVA, ERIKA p 539 N95-15144
JURGENS, T. G. p 574 N95-15418
JURIC, DAMIR p 485 N95-14542
JUSTAK, JOHN F. p 500 N95-13819

K

KAERTNER, FRANZ X. p 604 N95-13910
KAHANA, S. H. p 600 N95-15633
KAHN, MANFRED p 497 N95-15799
KAISER, TERI p 512 N95-14617
KALER, ERIC W. p 459 N95-14579
KALIL, CAROL G. p 422 N95-14074
KALKAN, A. p 476 N95-15410
KALLISTRATOVA, DMITRI KOUZNETSOV
p 471 N95-13922
KALOKITIS, DAVID p 451 N95-14354
KALP, DIRK p 576 N95-15817
KALRA, P. p 518 N95-14194
KAMAT, SANJAY p 570 N95-14164
KAMENSKY, SERGEI p 426 N95-14093
KAMOTANI, Y. p 458 N95-14217
KAMOTANI, YASUHIRO p 459 N95-14580
KANAZIREV, V. p 438 N95-14388
KANE, R. J. p 468 N95-15300
KANELLAKIS, PARIS O. p 579 N95-15616
p 579 N95-15617
KANG, D. B. p 620 N95-14009
KANG, SOON p 477 N95-15587
KANGAS, L. J. p 522 N95-14195
KANNE, W. R., JR. p 500 N95-13645
KANTAK, ANIL V. p 464 N95-14672
p 465 N95-14675
KAPLAN, AUDREY S. p 437 N95-14141
KAPLAN, MICHAEL L. p 531 N95-15684
KAPLAN, S. N. p 625 N95-15577
KARAM, E. H. p 550 N95-15150
KARASSIOV, V. P. p 603 N95-13904
KARASZ, FRANK E. p 452 N95-14406
KAREMAKER, JOHN M. p 544 N95-15108
KAUKLER, WILLIAM F. p 484 N95-14533
KAUN, T. D. p 471 N95-13684
KAWAKUBO, K. p 549 N95-15145
KAWAKUBO, KIYOSHI p 543 N95-15097
KAWAMURA, KAZUHIKO p 415 N95-14637
KAY, EDWIN J. p 551 N95-13715
KAY, JACOB p 394 N95-14236
KAZEROONI, H. p 560 N95-14051
KAZMAN, RICK p 572 N95-14339
KEDZIERSKI, M. A. p 482 N95-14407
KELKAR, ATUL G. p 420 N95-13729
KELLER, JOSEPH p 492 N95-14605
KELLER, P. E. p 522 N95-14195
KELLOGG, E. p 637 N95-13887
KELLY, M. J. p 446 N95-15368
KELLY, ROBERT E. p 482 N95-14524
KENDIG, M. p 446 N95-15368
KENDRICK, R. D. p 442 N95-15541
KENIK, E. A. p 601 N95-13674
KENNEDY, JOHN M. p 632 N95-14619
p 632 N95-14870
KENNEL, ELLIOT B. p 430 N95-13697
KENNELLY, E. T. p 640 N95-15835
KENNY, JOHN M. p 535 N95-14335
KENSHOLE, G. p 521 N95-15407
KERCHER, J. R. p 524 N95-15779
KERR, D. p 557 N95-14034
KERR, TOM H. p 639 N95-15831
KESS, BARBARA L. p 565 N95-14591
KESSELMAN, C. p 578 N95-14116
KETSDEVER, ANDREW D. p 422 N95-14072
KETTNER, C. p 643 N95-14442
KHALEEL, M. A. p 445 N95-15293
KHERUNTSYAN, KAREN V. p 500 N95-13903
KHESHGI, H. S. p 523 N95-15361
KHUTOROVSKY, ZACHARI p 426 N95-14093
KICZA, MARY E. p 415 N95-14634
KIDMAN, DAVID S. p 396 N95-14245
KIERAS, DAVID E. p 540 N95-14142
KIESS, THOMAS E. p 599 N95-13963
p 612 N95-13970
KILPATRICK, JAMES F. p 530 N95-15295
KILPATRICK, WILLIAM T. p 392 N95-15331
KIM, CHULHO p 497 N95-15799
KIM, H. K. p 452 N95-14400
KIM, J. H. p 431 N95-15609
KIM, JEONG H. p 424 N95-14083
KIM, KYUNG-HOON p 454 N95-15316
KIM, M. S. p 605 N95-13923
p 482 N95-14407
KIM, S.-H. p 607 N95-13939
KIM, Y. p 509 N95-14466
p 595 N95-15310
KIM, Y. S. p 602 N95-13896
p 603 N95-13905
p 465 N95-14673
KIMBLE, H. J. p 610 N95-13954
KING, D. S. p 441 N95-15370
KING, GREGORY p 409 N95-15742
KING, JOSEPH H. p 642 N95-13658
KING, RAYMOND E. p 553 N95-15768
KING, ROBERT W. p 527 N95-14279
KINGSLEY, J. J. p 517 N95-14002
KIRITANI, M. p 446 N95-15433
KIRK, MARK T. p 514 N95-15802
KIRVEL, R. D p 496 N95-13669
KISSEL, R. p 431 N95-15609
KIVELSON, S. A. p 625 N95-15576
KLEEFISCH, M. S. p 453 N95-14609
KLEINDIENST, T. E. p 521 N95-14123
KLEM, J. F. p 621 N95-14342
KLEY, M. p 461 N95-14147
KLIMOV, ANDREI B. p 609 N95-13950
p 609 N95-13952
KLOSKO, STEVEN M. p 471 N95-14283
KLOSTERBUER, S. F. p 581 N95-14377
KLOTZ, STEPHEN P. p 400 N95-14612
KNAPP, BEVERLY G. p 563 N95-15759
KNAPP, J. A. p 437 N95-14312
p 596 N95-15437
KNICKERBOCKER, K. p 475 N95-15302
KNIGHT, JEFFREY p 432 N95-13646
KNIGHT, JOHN C. p 571 N95-14171
KNIGHT, STEPHEN M. p 454 N95-15296
KNUTSON, BENJAMIN W. p 434 N95-14411
KOBAYASHI, A. S. p 511 N95-14479
KOBYLINSKI, T. P. p 453 N95-14609
KOENIG, E. p 546 N95-15121
KOENIG, EVA MARIA p 544 N95-15107
KOENIG, EVA MARIE p 548 N95-15131
KOENIG, L. p 476 N95-15356
KOENIG, S. C. p 542 N95-15095
KOHL, RANDALL L. p 546 N95-15122
KOHNLE, ANTON p 467 N95-14833
p 467 N95-14834
KOJIMA, S. p 446 N95-15433
KOLBUSZEWSKI, MARCIN p 641 N95-15843
KOLWEY, HERMAN p 408 N95-14205
KONCZYKOWSKI, M. p 619 N95-13681
KONRAD, A. p 469 N95-15463
KOOYMAN, P. J. p 445 N95-14845
KOPANSKI, JOSEPH J. p 474 N95-14401
KOPLIK, JOEL p 484 N95-14539
KOPPENHOEFER, KYLE C. p 514 N95-15802
KORENYI-BOTH, A. L. p 450 N95-14303
KOSAI, M. p 511 N95-14479
KOSSEL, HORST p 405 N95-14646
KOSTAL, L. p 538 N95-15106
KOSTELECKY, V. ALAN p 598 N95-13898
KOSTER, JEAN N. p 483 N95-14532
KOSTOS, PETER J. p 421 N95-14068
KOSUGI, KAZUO p 539 N95-15142
p 539 N95-15143
KOSURI, RANGA P. p 432 N95-13641
KOU, SINDO p 483 N95-14529
KOUZES, R. T. p 522 N95-14195
KOWAL, MICHAEL T. p 505 N95-15584
KOZACZEK, K. J. p 444 N95-13820
KOZLOWSKI, M. R. p 451 N95-14389
p 614 N95-15529
KRAAK, M. p 472 N95-13983
KRALL, A. H. p 444 N95-14575
KRAMER, BRIAN p 397 N95-14254
KRAMER, MARK A. p 571 N95-14170
KRANER, H. W. p 593 N95-14309
KRANTZ, J. H. p 562 N95-14061
KRAUSS, A. R. p 620 N95-13822
KRAUSS, R. A. p 442 N95-15387
KRECH, ROBERT H. p 422 N95-14071
KRELOWSKI, J. p 640 N95-15835
KRELOWSKI, JACEK p 640 N95-15836
KRENN, GUENTHER p 612 N95-13969
KRESS, R. L. p 501 N95-14005
KRISNNAMAGARU, RAMESH p 537 N95-15751
p 537 N95-15753

KROL, MARK F. p 477 N95-15459
KROLIK, JEFF p 591 N95-14396
KROOPNICK, H. p 496 N95-13669
KROPNEWICKI, TOM p 489 N95-14566
KRUEGER, MYRON W. p 560 N95-14052
KRUMHANSL, J. A. p 447 N95-15631
KRYUCHKYAN, GAGIK YU. p 500 N95-13903
KUDUVALLI, GOPINATH p 565 N95-14590
KUGEL, H. W. p 617 N95-14397
KUGIUMTZIS, D. p 589 N95-13630
KUITTINEN, P. p 568 N95-13989
KUJAWSKI, DANIEL p 510 N95-14471
KULAGIN, V. V. p 603 N95-13906
KULKARNI, A. K. p 441 N95-15353
KUMAR, A. p 617 N95-14397
KUMPATY, S. K. p 440 N95-15291
KUNTZ, L. A. p 562 N95-14061
KURTZ, S. R. p 621 N95-14323
KUSHNIR, V. I. p 621 N95-14382
KUSSMAUL, MICHAEL T. p 430 N95-14301
KWIAT, PAUL G. p 611 N95-13968

L

LACAU, P. G. p 399 N95-14446
LACAU, R. G. p 399 N95-14448
p 400 N95-14452
LACERDA, A. p 620 N95-13999
LACEY, PAUL I. p 504 N95-15747
LACKEY, JAMES B. p 396 N95-14246
p 397 N95-14252
LACKNER, JAMES R. p 555 N95-14020
LACKS, D. p 520 N95-15355
LACOLLEY, P. p 538 N95-15098
LADD, D. N. p 465 N95-14674
LAHEY, RICHARD, JR. p 459 N95-14557
LAING, P. p 411 N95-15683
LALLI, VINCENT R. p 420 N95-13728
LAMBERT, DENNIS M. p 511 N95-14480
LAMBORN, DANA p 408 N95-13703
LAMOTTE, R. H. p 558 N95-14041
LAMPE, DONALD R. p 476 N95-15399
LANAGAN, M. T. p 621 N95-14192
LANDIS, WAYNE G. p 524 N95-15814
LANDSEA, C. W. p 534 N95-15666
LANG, ROBERT J. p 602 N95-13823
p 612 N95-14181
LANGSTON, MICHAEL A. p 578 N95-15416
LANSER, WENDY R. p 393 N95-14230
p 394 N95-14231
p 397 N95-14255
LANT, CHRISTIAN T. p 601 N95-13666
LAO, L. L. p 618 N95-15632
LAPAEV, E. V. p 542 N95-15093
LAPENTA, G. p 619 N95-15774
LAQUER, H. L. p 472 N95-13685
LARACUENTE, A. p 518 N95-14194
LARKIN, A. I. p 619 N95-13681
LARKIN, DAVID J. p 625 N95-15602
LARSON, A. C. p 455 N95-15579
LARSON, DAVID J., JR. p 458 N95-14213
LARUS, J. R. p 578 N95-14384
LASALVIA, JAMES M. p 468 N95-15393
LASCIALFARI, A. p 624 N95-15430
LASSAHN, G. D. p 578 N95-15434
p 579 N95-15534
LATHAM, RICK D. p 544 N95-15108
LATHAM, RICKY D. p 538 N95-15094
p 542 N95-15095
LAU, BENTON p 391 N95-13891
LAU, NELSON D. p 574 N95-15336
LAUBER, JOHN K. p 550 N95-15649
LAUSTRUP, M. S. p 515 N95-14793
LAVELLE, THOMAS M. p 408 N95-14604
LAVENDER, C. A. p 445 N95-15293
LAVERNIA, ENRIQUE J. p 623 N95-15317
LAVERS, J. D. p 469 N95-15463
LAVERY, DAVID p 581 N95-14943
LAWRENCE, BARBARA p 632 N95-14619
LE, CHOUNG p 464 N95-14672
p 465 N95-14675
LEAL, L. G. p 485 N95-14541
LEBED, R. F. p 597 N95-15865
LECHTENBERG, LEON p 395 N95-14241
LEE, ALECK L. p 420 N95-14064
LEE, BURNETT p 411 N95-14518
LEE, C. H. p 470 N95-15804
LEE, C. P. p 458 N95-14218
p 458 N95-14219
LEE, CHING-TSUNG p 608 N95-13946
LEE, H. p 625 N95-15577
LEE, JAI-HYUNG p 471 N95-13921
LEE, KANG-SOO p 605 N95-13923
LEE, KASEY M. p 429 N95-14106
LEE, S. p 419 N95-14631
LEE, TEN-MIN p 501 N95-14336
LEE, WEI p 641 N95-15840
LEGAULT, M. p 619 N95-13691
LEGREE, PETER J. p 552 N95-15326
LEHNERT, H. p 561 N95-14053
LEHOCZKY, SANDOR L. p 634 N95-14207
p 458 N95-14214
LEIFER, LARRY p 556 N95-14030
p 558 N95-14044
LEIGHTON, DAVID T. p 489 N95-14566
LEIGHTY, BRADLEY D. p 496 N95-13837
LEIMBACH, K.-D. p 418 N95-14095
LEIS, BRIAN N. p 508 N95-14462
LEKANG, DAWNE E. p 426 N95-14092
LEMPERT, G. D. p 422 N95-14073
LEMPERT, ROBERT J. p 515 N95-15546
LEMPNER, STEPHEN E. p 439 N95-14903
LEONARD, A. p 400 N95-14656
LEONARD, B. P. p 492 N95-14607
LEONARD, J. T. p 405 N95-14421
LEONE, STEPHEN R. p 599 N95-15839
LERNER-LAM, ARTHUR p 530 N95-14598
LERNER, PETER B. p 609 N95-13952
LESIEUTRE, TERESA O. p 630 N95-14321
LESSOR, D. L. p 524 N95-15432
LEUTENEGGER, SCOTT T. p 568 N95-13889
LEVY, MOISES p 476 N95-15397
LEWIN, WALTER p 647 N95-14814
LEWIS, JAMES A. p 551 N95-15767
LEWIS, L. HENDERSON p 590 N95-14440
LEWIS, MICHAEL p 564 N95-14587
LI, DONG-QI p 624 N95-15385
LI, SHI-QUN p 603 N95-13902
LI, T. Z. p 595 N95-15318
LI, WEI p 586 N95-15589
p 587 N95-15733
LI, X. p 595 N95-15350
LI, XI-ZENG p 471 N95-13900
LI, Z. p 593 N95-14309
LIANG, H. p 520 N95-15355
LICHTENSTEIN, BERNARD p 493 N95-15332
LIFKA, D. p 568 N95-14010
LIFSHITZ, Y. p 421 N95-14067
p 422 N95-14073
LILLEKJENDLIE, B. p 589 N95-13630
LILLY, W. D. p 439 N95-14838
LIN, H. X. p 585 N95-13991
LIN, K. C. p 458 N95-14218
p 458 N95-14219
LIN, M. Y. p 454 N95-15340
LIN, SUNG P. p 484 N95-14535
LIN, Y. p 620 N95-13822
LIN, YUH-LANG p 531 N95-15684
LINARES, IRVING p 565 N95-14589
LINCOLN, JOHN W. p 410 N95-14481
LINDELL, I. V. p 590 N95-13988
LINDEM, G. E. p 461 N95-14345
LINDGREN, M. p 475 N95-15302
LINDSTROEM, G. p 593 N95-14309
LING, J.-R. p 449 N95-13978
LINK, R. E. p 514 N95-15803
LINNARSSON, D. p 546 N95-15120
LIOU, MENG-SING p 404 N95-15853
LIPA, JOHN A. p 444 N95-14208
LIPKENS, BART p 401 N95-14883
LITCHFIELD, JOHN K. p 456 N95-15624
LITT, JONATHAN p 566 N95-13716
LITUNOVSKY, V. N. p 617 N95-14262
LITWIN, C. p 618 N95-15540
LIU, JIWEN p 481 N95-14269
LIU, X. C. p 621 N95-14342
LIVINGSTON, DAVID L. p 541 N95-14184
LIVNY, MIRON p 564 N95-14586
LLAMBIAS, JORGE p 487 N95-14553
LO, M. W. p 419 N95-14621
LOCKARD, GEORGE E. p 499 N95-14519
LOEW, L. H. p 462 N95-14412
LOEWENBERG, MICHAEL p 444 N95-14578
LOMBARDI, FABRIZIO p 570 N95-14163
LOMME, JON p 563 N95-14854
LOOK, DAVID C. p 626 N95-15754
LOOMIS, JACK M. p 561 N95-14054
LOONG, C. K. p 622 N95-14608
LOOSE, R. R. p 519 N95-14433
LOPEZ-PENA, RAMON p 603 N95-13907
LOR, ALEX CHOUA p 409 N95-15742
LORENZUTTA, S. p 606 N95-13929
LORETI, F. N. p 598 N95-15869
LOUBRIEL, G. M. p 477 N95-15544
LOVE, JOHN E. p 539 N95-15116
LOW, JOHN K. C. p 591 N95-14610
LOWENBERG, C. D. p 515 N95-14793
LOWNEY, JEREMIAH R. p 474 N95-14401
LOYALKA, SUDARSHAN K. p 459 N95-14565
LU, Y. p 622 N95-14431
LUDWIG, E. J. p 619 N95-13698
LUETTICH, R. A., JR. p 535 N95-14352
LUGAR, R. M. p 524 N95-15455
LUIK, ILMAR p 415 N95-14640
LUSTED, RODERICK M. p 501 N95-14347
LUTTGES, M. W. p 538 N95-14227
LYNN, K. G. p 594 N95-14441
p 624 N95-15422
LYNN, PETER p 425 N95-14087
LYO, S. K. p 621 N95-14342

M

MA, CHOPO p 527 N95-14276
p 527 N95-14280
MA, JIN p 538 N95-15099
MA, LI p 448 N95-14482
MACARIE, IOAN I. p 575 N95-15645
MACCABE, A. B. p 574 N95-15543
MACCHIAVELLO, C. p 604 N95-13913
MACINNES, ANDREW N. p 477 N95-15587
MACK, J. M. p 498 N95-13994
p 616 N95-13998
MACPHERSON, J. IAN p 406 N95-14895
MACRANDER, A. T. p 621 N95-14382
MADARAS, ERIC IRVINE p 505 N95-13835
MADHUKAR, MADHU S. p 432 N95-13641
p 435 N95-15427
MADSEN, OLE S. p 536 N95-15440
MAGNUSEN, P. E. p 508 N95-14459
MAHDAVI, M. p 517 N95-15916
MAINO, G. p 606 N95-13929
MAINVILLE, ANDRE p 516 N95-15793
MAIYA, P. S. p 453 N95-14609
MAJER, D. p 619 N95-13681
MAJEWSKI, J. A. p 458 N95-14215
MAKAROV, A. A. p 421 N95-14065
p 418 N95-14098
MAKITA, Y. p 549 N95-15145
MAKOWITZ, H. p 442 N95-15436
MALCOLM, GERALD N. p 395 N95-14238
MALIK, N. K. p 413 N95-13827
MALLASCH, PAUL G. p 568 N95-13894
MALLAT, H. p 568 N95-13989
MALON, D. p 568 N95-14010
MALOUVIER, A. p 539 N95-15148
MALOY, S. A. p 445 N95-14439
MAMANTOV, GLEB p 447 N95-15744
MANDEL, LEONARD p 600 N95-13912
MANJUNATHA, R. S. p 413 N95-13827
MANKO, MARGARITA A. p 500 N95-13925
MANKO, VLADIMIR I. p 603 N95-13907
p 598 N95-13909
p 608 N95-13941
MANNING, CHERYL A. p 554 N95-13888
MANNING, JEROME E. p 419 N95-13893
MANOHAR, MAREBOYANA p 564 N95-14588
p 566 N95-14595
MANOHAR, S. p 441 N95-15353
MANSFELD, F. p 446 N95-15368
MANTENIEKS, MARIS A. p 430 N95-14301
MANTEUFFEL, T. p 585 N95-14381
MANZELLA, DAVID H. p 430 N95-14301
MARCH, PATRICK A. p 530 N95-15295
MARCHIOLLI, M. A. p 588 N95-13926
MARCUS, ELIZABETH A. p 561 N95-14055
MARDARE, DANIELA p 451 N95-14316
p 451 N95-14324
p 452 N95-14395
MARGOLIS, S. B. p 442 N95-15375
MARHEFKA, R. J. p 469 N95-15394
MARIE, P. J. p 539 N95-15148
MARINELLI, W. J. p 440 N95-14958
MARRERO, W. p 412 N95-14343
MARROCCO, MATTHEW p 451 N95-14363
MARSHALL, TREVOR W. p 611 N95-13967
MARTEL, E. p 538 N95-15098
MARTENS, HANS p 604 N95-13914
MARTIN, BRIAN p 489 N95-14570
MARTIN, CHRISTINE p 459 N95-14567
MARTIN, ELIZABETH L. p 563 N95-15755
MARTIN, R. L. p 626 N95-15776
MARTIN, S. J. p 437 N95-14307
p 473 N95-14308
p 473 N95-14310
MARTINSON, SCOTT D. p 496 N95-14414
MARUR, P. R. p 414 N95-13833
MASALOV, A. V. p 606 N95-13924
MASARIK, J. p 646 N95-14437
p 647 N95-14438
MASER, K. R. p 460 N95-14119
MASON, KEVIN T. p 551 N95-15810
MASON, MARK E. p 448 N95-14483
MASON, T. G. p 444 N95-14575
MATHIAS, DONOVAN L. p 404 N95-15762
MATIAS, Y. p 568 N95-13976

MATTHEWS, RAYMOND H. ..... p 413 N95-15328
MATTHIESEN, DAVID H. ..... p 458 N95-14215
MATYJASZEWSKI, K. ..... p 452 N95-14399
MATYJASZEWSKI, KRZYSZTOF .. p 450 N95-14304
p 451 N95-14305
p 451 N95-14316
p 451 N95-14324
p 452 N95-14395
p 452 N95-14398
p 452 N95-14400
MAURICE, MARK S. ..... p 412 N95-13687
MAXKA, J. ..... p 452 N95-14400
MAXWELL, M. A. ..... p 523 N95-14403
MAY, E. ..... p 568 N95-14010
MAYER, K. S. ..... p 541 N95-14424
MCCALLUM, R. ANDREW ..... p 553 N95-15642
p 577 N95-15860
MCCALLUM, W. G. ..... p 589 N95-13979
MCCARTY, G. D. ..... p 460 N95-15409
MCCLUNG, R. C. ..... p 512 N95-14484
MCCOLLOUGH, HOLLY ..... p 563 N95-14854
MCCOMAS, D. J. ..... p 526 N95-13995
MCCONNELL, ROBERT L. ..... p 583 N95-15598
MCCORMICK, BARNES W. ..... p 405 N95-14894
MCCORMICK, WILLIAM D. ..... p 483 N95-14527
MCCREADY, MARK J. ..... p 489 N95-14566
MCCULLOUGH, JIM ..... p 417 N95-14650
MCCURDY, DAVID A. ..... p 401 N95-14878
p 403 N95-14891
MCCURLEY, K. S. ..... p 574 N95-15543
MCDERMOTT, ROGER J. ..... p 598 N95-13908
MCDOWALL, I. ..... p 557 N95-14034
MCELROY, F. F. ..... p 521 N95-14123
MCELROY, L. ..... p 496 N95-13669
MCFADDEN, DAVID L. ..... p 524 N95-15623
MCFADDEN, G. B. ..... p 448 N95-14548
MCGAHEY, MARK ..... p 418 N95-14094
MCGEE, WILLIAM F. ..... p 503 N95-15670
MCGINNIS, B. P. ..... p 477 N95-15459
MCGRANE, E. J. ..... p 407 N95-15439
MCGRATH, JAMES ..... p 451 N95-14363
MCGRATH, R. T. ..... p 618 N95-14443
MCGREEVY, MICHAEL W. ..... p 557 N95-14037
MCINTOSH, ALAN ..... p 639 N95-15832
MCKAY, CHARLES ..... p 569 N95-14158
MCKINLEY, GARETH H. ..... p 489 N95-14569
MCKINNEY, J. A. ..... p 411 N95-14799
MCKNIGHT, DARREN ..... p 426 N95-14093
MCKNIGHT, DARREN S. ..... p 426 N95-14092
MCKOY, VINCENT ..... p 596 N95-15457
MCNELIS, MARK E. ..... p 419 N95-13893
MCQUILLEN, JOHN B. ..... p 487 N95-14556
MCTAGGART, WESLEY G. ..... p 419 N95-15146
MCWHORTER, P. J. ..... p 496 N95-14146
MEADOWS, B. ..... p 559 N95-14045
MECARTNEY, M. L. ..... p 619 N95-13821
MEEHAN, THOMAS K. ..... p 460 N95-13628
MEEK, T. T. ..... p 432 N95-13643
MEEUWISSEN, A. M. H. ..... p 585 N95-14154
MEHTA, UNMEEL B. ..... p 392 N95-14921
MEI, CHUH ..... p 506 N95-14270
MEIRANS, L. ..... p 476 N95-15356
MEIRON, D. I. ..... p 400 N95-14656
MELCHIOR, F. ..... p 547 N95-15126
MELCHIOR, FRANCOIS M. ..... p 544 N95-15110
MELE, G. ..... p 539 N95-15135
MELIS, MATTHEW E. ..... p 482 N95-14299
MELLOCH, MICHAEL R. ..... p 626 N95-15754
MELLSTROM, J. A. ..... p 463 N95-14625
MENDENHALL, MICHAEL R. ..... p 630 N95-14321
MENNEN, M. G. ..... p 523 N95-15389
MENTER, F. R. ..... p 481 N95-14273
MERSEREAU, RUSSELL M. ..... p 565 N95-14589
MERTE, HERMAN, JR. ..... p 459 N95-14562
MESSIDORO, PIERO ..... p 423 N95-14077
MEYER, DAVID E. ..... p 540 N95-14142
MEYER, F. W. ..... p 592 N95-13675
MEYN, LARRY A. ..... p 397 N95-14255
MICHALOWSKI, STEFAN ..... p 556 N95-14030
p 558 N95-14044
MICKEY, DONALD L. ..... p 613 N95-14908
MIDDLETON, DAVID B. ..... p 412 N95-14415
MIELE, G. ..... p 601 N95-13944
MIELKE, P. W., JR. ..... p 534 N95-15666
MIELNIK, BOGDAN ..... p 598 N95-13918
MIEVILLE, R. L. ..... p 453 N95-14609
MIGLIACCIO, F. ..... p 516 N95-15792
MIKLICH, A. H. ..... p 623 N95-15337
MILES, ERIC ..... p 427 N95-14099
MILES, JANET R. ..... p 640 N95-15834
MILEY, H. S. ..... p 595 N95-15310
MILFORD, PETER ..... p 643 N95-14504
MILLER, B. P. ..... p 578 N95-14384
MILLER, DONALD ..... p 600 N95-15539
MILLER, EDWIN S. ..... p 538 N95-15113
MILLER, G.A. ..... p 532 N95-14271
MILLER, M. ..... p 512 N95-14485
MILLER, MATTHEW ..... p 508 N95-14457
p 432 N95-14920
MILLER, R. L. ..... p 616 N95-14007
MILLER, S. L. ..... p 496 N95-14146
MILLER, WARNER H. ..... p 565 N95-14593
MILOSAVLJEVIC, I. ..... p 439 N95-14838
MINEA, M. ..... p 412 N95-14343
MINION, M. L. ..... p 494 N95-15867
MINOTT, PETER O. ..... p 499 N95-14515
MIODUSHEVSKY, P. V. ..... p 410 N95-14486
MIRESHGHI, A. ..... p 625 N95-15577
MISRA, PRABHAKAR ..... p 500 N95-15395
MISSLISCH, H. ..... p 546 N95-15121
MITCHELL, WILLIAM J. ..... p 421 N95-14069
MITLER, H. E. ..... p 441 N95-15354
MIYOSHI, K. ..... p 450 N95-14303
MIZRAHI, SOLOMON S. ..... p 588 N95-13926
MODESTINO, A. J. ..... p 439 N95-14435
MOESSER, MARK ..... p 510 N95-14470
MOLDWIN, M. B. ..... p 526 N95-13995
MOLENT, L. ..... p 392 N95-14477
MONTGOMERY, RONALD W. ..... p 540 N95-14176
MONTUFAR-SOLIS, DINA ..... p 538 N95-15102
MOORE, FRANK G. ..... p 399 N95-14447
MOORE, K. M. ..... p 458 N95-14225
MOORE, LORETTA A. ..... p 566 N95-14107
MORAN, B. ..... p 510 N95-14472
p 505 N95-14475
MORFILL, G. ..... p 490 N95-14571
MORGADO, R. E. ..... p 442 N95-15387
MORILAK, DANIEL P. ..... p 429 N95-14584
MORRIS, JAMES H. ..... p 414 N95-14290
MORRIS, PHILIP J. ..... p 591 N95-14618
MORRIS, RANDALL ..... p 598 N95-13932
MORRIS, T. O. ..... p 456 N95-15634
MORROW, CHERILYN ..... p 638 N95-14511
MORROW, R. C. ..... p 564 N95-14228
MOSES, S. L. ..... p 642 N95-14266
MOSLEHY, FAISSAL A. ..... p 505 N95-13886
MOSS, C. E. ..... p 638 N95-14429
MOTOWIDLO, L. R. ..... p 475 N95-14606
MOUKAWSHER, E. J. ..... p 508 N95-14463
MOULTON, CAREY ..... p 403 N95-14892
MOUSSA, M. H. Y. ..... p 588 N95-13926
MUCHNIK, ANDREI A. ..... p 588 N95-15854
MUELLER, D. ..... p 597 N95-15545
MUHAMAD, M. R. ..... p 456 N95-13899
MUI, D. ..... p 499 N95-14364
MUKODA, I. ..... p 446 N95-15433
MUKUNDAN, R. ..... p 414 N95-13831
MULDER, J. A. ..... p 408 N95-14102
MULENBURG, G. M. ..... p 419 N95-14089
p 425 N95-14090
p 426 N95-14091
MULLER, CLIFFORD H. ..... p 500 N95-15391
MULQUEEN, JOHN A. ..... p 417 N95-14649
MUNDRANE, MICHAEL R. ..... p 483 N95-14526
MUNDY, JOSEPH L. ..... p 585 N95-14843
MUNTZ, E. P. ..... p 422 N95-14072
MURAKAMI, DEAN M. ..... p 539 N95-15133
MURALIDHARAN, G. ..... p 445 N95-14665
MURAT, M. ..... p 421 N95-14067
MURMAN, SCOTT M. ..... p 394 N95-14232
p 400 N95-14614
MURPHREE, G. ..... p 446 N95-15368
MURPHY, DANIEL J. ..... p 633 N95-15585
MURPHY, H. C. ..... p 440 N95-14958
MURPHY, JACK ..... p 408 N95-13703
MURPHY, W. H. ..... p 444 N95-13667
MURRAY, BRUCE T. ..... p 448 N95-14548
MURRAY, R. W. ..... p 477 N95-15456
MURRELL, M. T. ..... p 529 N95-14434
MURRI, D. G. ..... p 393 N95-14230
MURRI, DANIEL G. ..... p 398 N95-14257
MURTHY, GITA ..... p 547 N95-15128
MURTHY, S. N. B. ..... p 411 N95-15683
MURTHY, V. R. ..... p 503 N95-14923
MURZAKHMETOV, B. K. ..... p 602 N95-13897
MUSHER, J. ..... p 520 N95-15355
MUSHOTZKY, R. F. ..... p 638 N95-14911
MUSIELAK, Z. E. ..... p 646 N95-15070
MUSSER, JANA ..... p 409 N95-15742
MUZZIO, DOUG ..... p 512 N95-14617
MYERS, ROGER M. ..... p 430 N95-14301
p 475 N95-14516
MYOI, TAKESHI ..... p 559 N95-14048

N

NAGANO, J. ..... p 545 N95-15111
NAGANO, JUNKO ..... p 548 N95-15134
NAGASUBRAMANIAN, GANESAN ..... p 472 N95-13824
NAHVI, MAHMOOD ..... p 561 N95-14056
NAIR, R. ..... p 441 N95-15353
NAKAGAWARA, VAN B. ..... p 540 N95-14176
NAKANO, YOSHISUKE ..... p 530 N95-14862
p 531 N95-15428
NAKAYA, MASAYUKI ..... p 539 N95-15142
p 539 N95-15143
NARAYANA, S. V. L. ..... p 458 N95-14225
NARAYANAN, R. V. RAGHU ..... p 414 N95-13831
NAS, SELMAN ..... p 485 N95-14542
NASH, JON ..... p 483 N95-14531
NASH, PHILIP ..... p 444 N95-14202
NASTASI, M. ..... p 455 N95-15579
NATESAN, K. ..... p 447 N95-15906
NAYAK, M. MAHENDRA ..... p 413 N95-13827
NAZARKIN, A. ..... p 610 N95-13960
NEELY, W. C. ..... p 439 N95-14867
NEILSON, GEORGE F. ..... p 458 N95-14221
NEIRA, HEGEL G. ..... p 572 N95-14616
NEITZEL, G. PAUL ..... p 483 N95-14525
NELMS, R. MARK ..... p 475 N95-14866
NELSON, C. B. ..... p 442 N95-15436
NELSON, D. R. ..... p 620 N95-14008
NELSON, D. Z. ..... p 500 N95-13645
NELSON, MAX ..... p 515 N95-15546
NELSON, N. ..... p 509 N95-14466
NELSON, RICK C. ..... p 544 N95-15105
NELSON, ROBERT C. ..... p 394 N95-14237
NEMAT-NASSER, SIAVOUCHE ..... p 434 N95-14360
NEMETH, M. P. ..... p 505 N95-13839
NEREM, ROBERT S. ..... p 527 N95-14277
NESHYBA, S. P. ..... p 595 N95-14950
NETTLES, ALAN T. ..... p 436 N95-15763
NEUMAN, FRANK ..... p 406 N95-14611
NEWMAN, J. C., JR. ..... p 444 N95-13690
p 509 N95-14467
p 510 N95-14473
NG, S. K. ..... p 456 N95-13899
NGUYEN, H. V. ..... p 622 N95-14431
NGUYEN, KHANH ..... p 391 N95-13891
NGUYEN, KHANH Q. ..... p 391 N95-14419
NGUYEN, NHAN ..... p 512 N95-14617
NI, R. H. ..... p 480 N95-14132
NICHIPORUK, IGOR A. ..... p 542 N95-15091
NICHOLS, SCOTT C. ..... p 444 N95-14578
NICOL, DAVID M. ..... p 568 N95-13889
NIELSEN, B. ..... p 624 N95-15422
NIKISHOV, A. I. ..... p 589 N95-13935
NIKITENKO, V. I. ..... p 595 N95-15362
NIKOLAYEV, YURI VYACHESLAVOVICH
p 430 N95-13697
NIPKO, J. ..... p 622 N95-14608
NISSEN, J. A. ..... p 444 N95-14208
NIVAGGIOLI, THIERRY ..... p 490 N95-14574
NIX, ERNEST E., JR. ..... p 469 N95-15651
NIXON, DAVID ..... p 630 N95-14321
NOAKES, M. W. ..... p 501 N95-14005
NOBARI, M. R. ..... p 478 N95-13653
NOBARI, MOHAMMED H. R. ..... p 485 N95-14542
NOLAN, LAURA ..... p 535 N95-14906
NOLD, DEAN E. ..... p 409 N95-14852
NOLLER, E. W. ..... p 424 N95-14081
NORBURY, JOHN R. ..... p 465 N95-14674
NORSK, PETER ..... p 542 N95-15090
NORTH, M. J. ..... p 571 N95-14196
NORTH, R. C. ..... p 468 N95-15321
NORTON, RICHARD L. ..... p 454 N95-15296
NOTER, Y. ..... p 421 N95-14067
NOWOTARSKI, A. A. ..... p 469 N95-15394
NOZ, MARILYN E. ..... p 603 N95-13905
NWOKOGU, GODSON C. ..... p 453 N95-14931

O

OAKES, DAVID B. ..... p 422 N95-14071
OAKES, ROBERT ..... p 600 N95-15539
OBERKAMPF, W. L. ..... p 493 N95-15351
OCARROLL, ROSEMARIE ..... p 536 N95-15626
ODELL, V. ..... p 579 N95-15581
ODMAN, M. T. ..... p 521 N95-14122
OGANOV, V. S. ..... p 539 N95-15141
OGBURN, MARILYN E. ..... p 396 N95-14246
OGIHARA, MITSUNORI ..... p 587 N95-15732
OGLESBY, DONALD M. ..... p 496 N95-13837
OHNUKI, S. ..... p 446 N95-15431
OKELLY, CHRIS ..... p 408 N95-13703
OKIHIRO, MICHELE ..... p 536 N95-15452
OKUMURA, MITCHIO ..... p 593 N95-14155
OLINGER, C. T. ..... p 591 N95-15359
OLLISON, W. M. ..... p 521 N95-14123
OLSON, R. ..... p 578 N95-14116
OMALIEY, M. W. ..... p 477 N95-15544
OOSTERLEE, C. W. ..... p 492 N95-15315
OR, ARTHUR ..... p 482 N95-14524
OREILLY, W. C. ..... p 536 N95-15452
ORLANDO, T. M. ..... p 524 N95-15432
ORLOV, OLEG I. ..... p 542 N95-15091

ORTASSE, RAPHAEL ..... p 419 N95-14474
ORTIZ, JOE ..... p 454 N95-15316
ORTIZ, VINCENT M. ..... p 428 N95-14850
OSBORN, R. ..... p 620 N95-14188
OSBORNE, T. H. ..... p 618 N95-15632
OSHIRO, RICHARD ..... p 418 N95-14094
OSSARD, G. ..... p 547 N95-15126
OSSARD, GERARD ..... p 544 N95-15110
OSTRACH, SIMON ..... p 458 N95-14217
p 459 N95-14580
OTJES, R. P. ..... p 523 N95-15389
OTTO, S. R. ..... p 495 N95-15917
OU, Z. Y. ..... p 610 N95-13954
OUTLAW, RONALD A. ..... p 503 N95-15601
OVCHINNOKOV, I. B. ..... p 617 N95-14262
OWENS, GREGG R. ..... p 500 N95-13819
OZAROW, LARRY ..... p 468 N95-15333

P

PADDAN, GURMAIL S. ..... p 563 N95-15850
PAGE, JULIET A. ..... p 403 N95-14889
PAHLE, JOSEPH W. ..... p 396 N95-14246
PAINTER, JOHN H. ..... p 580 N95-13727
PALATHINGAL, J. C. ..... p 594 N95-14441
PALCZER, A. R. ..... p 433 N95-14298
PALEVSKY, ALAN ..... p 478 N95-15613
PALMER, GRANT ..... p 405 N95-13720
PALMER, K. F. ..... p 427 N95-14420
PALUMBO, GIUSEPPE ..... p 405 N95-13719
p 405 N95-13720
PANG, KENNETH ..... p 424 N95-14082
PANG, XIAO-DONG ..... p 561 N95-14057
PANG, Y. ..... p 600 N95-15633
PANKAJAKSHAN, RAMESH ..... p 409 N95-14909
PANT, N. ..... p 413 N95-13826
PAPADIMITRIOU, V. ..... p 597 N95-15862
PAPITASHVILI, NATALIA E. ..... p 642 N95-13658
PARDO, B. T. ..... p 460 N95-15409
PARIS, M. G. A. ..... p 604 N95-13913
PARISEL, OLIVIER ..... p 599 N95-15844
PARK, CHUL ..... p 405 N95-13720
PARK, MIA ..... p 535 N95-14906
PARKINSON, W. H. ..... p 522 N95-14344
PARKS, P. B. ..... p 459 N95-14547
PARRISH, RUSSELL V. ..... p 409 N95-14852
PARTIN, J. K. ..... p 578 N95-15434
p 579 N95-15534
PASTORE, RICHARD E. ..... p 553 N95-15770
PATE, B. A. ..... p 523 N95-15382
PATTERSON, JAMES D. ..... p 626 N95-15752
PATTERSON, JOHN C. ..... p 553 N95-15768
PATTERSON, MICHAEL J. ..... p 430 N95-14301
PATTERSON, RICHARD L. ..... p 478 N95-15669
PATTERSON, W. L. ..... p 461 N95-14345
PAUL, DONALD R. ..... p 453 N95-14844
PAUL, J. ..... p 392 N95-14477
PAUL, J. J. ..... p 434 N95-14409
PAULAITIS, MICHAEL E. ..... p 459 N95-14579
PAULAUSKAS, F. L. ..... p 432 N95-13643
PAULEY, M. A. ..... p 448 N95-13688
PAULSEN, E. B. ..... p 463 N95-14626
PAULUS, R. A. ..... p 461 N95-14345
PAVEL, MISHA ..... p 559 N95-14046
PAVLIS, ERRICOS C. ..... p 471 N95-14285
PAWEL, J. ..... p 446 N95-15431
PEARLMAN, MICHAEL R. ..... p 500 N95-14287
PEARSONS, KARL S. ..... p 403 N95-14890
PEASE, R. F. ..... p 595 N95-15318
PEDERSON, L. R. ..... p 517 N95-14002
PEDROZO, SONJA P. ..... p 522 N95-14337
PEFFLEY, A. F. ..... p 419 N95-15552
PEI, K. C. ..... p 507 N95-14417
PEI, S. ..... p 453 N95-14609
PEIFFER, D. G. ..... p 454 N95-15340
PELACCIO, DENNIS ..... p 431 N95-14669
PELED, EMMANUEL ..... p 472 N95-13824
PELLIN, M. J. ..... p 593 N95-14011
PEMSLER, J. P. ..... p 456 N95-15624
PENDLETON, ED ..... p 404 N95-15465
PENDRICK, VALERIE ..... p 451 N95-14354
PENG, J. P. ..... p 594 N95-14441
PENGRA, PATRICIA R. ..... p 638 N95-14511
PENPRASE, BRIAN ..... p 639 N95-15828
PEOPLES, DON ..... p 535 N95-14906
PEREIRA, S. F. ..... p 610 N95-13954
PEREZ-MENDEZ, V. ..... p 625 N95-15577
PERFIT, M. R. ..... p 529 N95-14434
PERKINS, L. ..... p 445 N95-15307
PERKINS, S. T. ..... p 594 N95-14385
PERKINS, STANLEY C., JR. ..... p 630 N95-14321
PERRAULT, D. J. ..... p 405 N95-14421
PERSON, LEE H., JR. ..... p 412 N95-14415
PETERS, PALMER N. ..... p 590 N95-14137
PETERS, W. A. ..... p 439 N95-14435
PETERSON, BRADLEY M. ..... p 644 N95-14509
PETERSON, M. R. ..... p 523 N95-15382
PETERSON, TODD T. ..... p 429 N95-14584
PETERSON, W. K. ..... p 619 N95-15758
PETOT, BERTRAND ..... p 480 N95-14134
PETRI, M. ..... p 445 N95-14665
PETTERSON, B. ..... p 476 N95-15356
PETTIT, CHRIS ..... p 404 N95-15465
PEUHKURI, M. ..... p 461 N95-14147
PEURRUNG, A. J. ..... p 524 N95-15432
PEYGHAMBERIAN, N. ..... p 477 N95-15459
PFAU, WERNER ..... p 639 N95-15830
PHAN, S.-E. ..... p 490 N95-14573
PHELPS, M. R. ..... p 439 N95-14663
PHILIP, N. K. ..... p 414 N95-13831
PHILLIPS, ELIZABETH ..... p 535 N95-14906
PHILLIPS, RONALD L. ..... p 398 N95-14258
PHILLIPS, W. MORRIS ..... p 473 N95-14294
PHILPOTT, MICHAEL R. ..... p 474 N95-14425
PIASCIK, ROBERT S. ..... p 432 N95-14920
PIERCE, ALLAN D. ..... p 402 N95-14885
PIERCE, P. ..... p 566 N95-14662
PIERSON, DUANE L. ..... p 458 N95-14222
PIKE, VERA J. ..... p 509 N95-14464
PINELLI, THOMAS E. ..... p 632 N95-14619
p 632 N95-14870
p 633 N95-15585
PINERO, LUIS R. ..... p 430 N95-14301
PINGALI, KESHAV ..... p 587 N95-15733
PIROTTON, MICHEL J. ..... p 550 N95-15149
PITMAN, S. G. ..... p 445 N95-15293
PLA-DALMAU, A. ..... p 497 N95-15580
PLAETSCHKE, ERMIN ..... p 394 N95-14235
PLAWSKY, JOEL L. ..... p 488 N95-14560
PLINE, A. ..... p 458 N95-14217
PLOTKIN, KENNETH J. ..... p 403 N95-14889
PLUT, T. A. ..... p 477 N95-15544
POCHET, THIERRY F. ..... p 550 N95-15149
POESIO, MASSIMO ..... p 586 N95-15595
POLK, THAD A. ..... p 576 N95-15817
POLYANSKII, A. A. ..... p 595 N95-15362
POMPETZKI, W. ..... p 561 N95-14053
POPE, JONATHAN M. ..... p 448 N95-15918
PORADA, WILLIAM ..... p 397 N95-14250
PORANSKI, CHESTER F., JR. ..... p 456 N95-15800
PORCEDDU, IGNAZIO ..... p 639 N95-15833
PORTER, L. C. ..... p 620 N95-14009
PORTWOOD, M. H. ..... p 633 N95-15528
POST, D. ..... p 617 N95-14368
POSTLETHWAITE, TIMOTHY A. ..... p 477 N95-15456
POTE, KENNETH G. ..... p 538 N95-15103
POWELL, J. ANTHONY ..... p 625 N95-15602
POWELL, KENNETH G. ..... p 398 N95-14297
POWER, MICHAEL B. ..... p 477 N95-15587
PRABHU, RAMADAS K. ..... p 492 N95-14912
PRAGER, S. C. ..... p 617 N95-14373
p 618 N95-15540
PRATAP, G. ..... p 413 N95-13828
PRETLOW, ROBERT A., III ..... p 541 N95-14184
PRICE, BRADFORD ..... p 563 N95-14854
PRICE, G. L. ..... p 438 N95-14388
PRIEDHORSKY, W. C. ..... p 638 N95-14429
PRYTZ, K. ..... p 596 N95-15380
PUECH, KATHLEEN ..... p 626 N95-15748
PUROHIT, V. N. ..... p 414 N95-13832
PUTILIN, A. A. ..... p 606 N95-13924

Q

QIAN, C. ..... p 441 N95-15352
QIN, X. ..... p 568 N95-14010
QIU, Z. Q. ..... p 624 N95-15385
QUACH, W. ..... p 502 N95-14907
QUANDIEU, P. ..... p 545 N95-15112
QUICK, DENNIS D. ..... p 498 N95-14291
QUINTANA, JASON ..... p 549 N95-15139
QUINTIERE, J. G. ..... p 443 N95-15610
QUIRK, W. J. ..... p 496 N95-13669

R

RABEONY, M. ..... p 454 N95-15340
RACHELE, HENRY ..... p 533 N95-14340
RACHO, C. S. ..... p 463 N95-14625
RADHAKRISHNAN, KRISHNAN ..... p 440 N95-15056
p 440 N95-15057
p 442 N95-15512
RADLOFF, H. D., II ..... p 505 N95-13839
RAGHAVAN, S. G. ..... p 414 N95-13833
RAHKO, K. ..... p 461 N95-14147
RAHKO, M. ..... p 461 N95-14147
RAIMONDO, GIACOMO ..... p 423 N95-14077
RAINES, RICHARD A. ..... p 470 N95-15652
RAJ, SHREERAM ..... p 508 N95-14457
RAJESHWARI, P. S. ..... p 414 N95-13832
RAJEVSKAYA, G. A. ..... p 410 N95-14486
RALSTON, JOHN ..... p 394 N95-14236
RAMACHANDRA, PRASHANT A. ..... p 458 N95-14212
RAMACHANDRAN, N. ..... p 634 N95-14207
p 428 N95-14210
RAMAN, GANESH ..... p 404 N95-15852
RAMANI, N. ..... p 414 N95-13832
RAME, ENRIQUE ..... p 484 N95-14536
RAMEY, G. ED ..... p 502 N95-14904
RAMIREZ, G. ..... p 507 N95-14417
RAND, J. A. ..... p 520 N95-15405
RAO, GOPARAJU NAGENDRA ..... p 413 N95-13828
RAO, RAJESH P. N. ..... p 575 N95-15721
p 576 N95-15857
RAO, S. ..... p 568 N95-13976
RAO, V. KOTESWARA ..... p 413 N95-13828
RAPCSAK, M. ..... p 539 N95-15141
RAPOTKOV, ALEXANDER N. ..... p 542 N95-15091
RASETTI, M. ..... p 589 N95-13901
RASHIDNIA, NASSER ..... p 488 N95-14563
RASMUSSEN, CRAIG W. ..... p 587 N95-15612
RASMUSSEN, DARYL ..... p 427 N95-14099
RASPET, RICHARD ..... p 402 N95-14886
RATHNAKARA, S. C. ..... p 414 N95-13830
RATNAKAR, VIRESH ..... p 564 N95-14586
RAUW, MARC O. ..... p 412 N95-14815
RAVAT, DHANANJAY ..... p 526 N95-14267
RAWLIN, VINCENT K. ..... p 430 N95-14301
RAWLIN, VINVENT K. ..... p 475 N95-14516
RAWLINS, W. T. ..... p 440 N95-14958
RAY, RONALD J. ..... p 395 N95-14241
RAYNOR, WILLIAM ..... p 425 N95-14087
REDA, DANIEL C. ..... p 496 N95-14414
REEDER, P. L. ..... p 595 N95-15310
p 454 N95-15313
p 613 N95-15314
REEDY, R. C. ..... p 646 N95-14437
p 647 N95-14438
REEVES, G. D. ..... p 526 N95-13995
REGAN, CURTIS RANDALL ..... p 590 N95-14110
REGENIE, VICTORIA A. ..... p 395 N95-14240
REICHENBACH, STEPHEN E. ..... p 565 N95-14591
REIFLER, FRANK ..... p 598 N95-13932
REINMANN, JOHN J. ..... p 406 N95-14897
REINTJES, JOHN F. ..... p 615 N95-15765
REISING, JACK D. ..... p 563 N95-15755
REIST, PARKER C. ..... p 529 N95-14404
REMO, J. L. ..... p 642 N95-14311
RESNICK, ANDREW H. ..... p 484 N95-14533
RHATIGAN, JENNIFER L. ..... p 429 N95-14584
RHODES, B. ..... p 443 N95-15610
RHODES, PERCY H. ..... p 478 N95-14577
RICHARDS, REX A. ..... p 415 N95-14636
RICHARDSON, J. W., JR. ..... p 622 N95-14608
RICHARDSON, JOHN N. ..... p 477 N95-15456
RICHARDSON, MARY J. ..... p 536 N95-15425
RICHEY, EDWARD, III ..... p 448 N95-15918
RICHTER, JUERGEN H. ..... p 467 N95-14830
RIECKE, H. ..... p 494 N95-15861
RIES, JOHN C. ..... p 418 N95-14282
p 528 N95-14284
RIESEN, R. ..... p 574 N95-15543
RIETVELD, G. ..... p 624 N95-15378
RIGGS, ALAN J. ..... p 560 N95-14050
RIMEY, RAYMOND D. ..... p 573 N95-15151
RITUS, V. I. ..... p 589 N95-13935
RIVERS, LEE W. ..... p 415 N95-14635
RIZK, YEHIA M. ..... p 394 N95-14232
p 397 N95-14253
ROBBINS, HENRY H. ..... p 570 N95-14165
ROBERTS, A. S., JR. ..... p 494 N95-15605
ROBERTS, GLYN O. ..... p 478 N95-14577
ROBINSON, LEICK D. ..... p 401 N95-14881
ROBINSON, M. C. ..... p 538 N95-14227
ROBINSON, MICHAEL S. ..... p 641 N95-15840
ROCKETT, A. ..... p 521 N95-15407
ROCKETT, P. D. ..... p 617 N95-14262
RODMAN, LAURA C. ..... p 630 N95-14321
RODRIGUEZ, J. L. ..... p 496 N95-14146
ROGERS, PAT ..... p 570 N95-14167
ROHLF, D. ..... p 394 N95-14235
ROHN, DENNIS W. ..... p 429 N95-14584
ROHRBACH, WAYNE W. ..... p 590 N95-14110
ROHRBAUGH, J. M. ..... p 474 N95-14402
ROHWEIN, G. J. ..... p 474 N95-14319
ROLAND, CHARLES M. ..... p 456 N95-15800
ROOS, E. V. ..... p 613 N95-14367
ROOS, FREDERICK W. ..... p 398 N95-14256
ROSADO, JOEL M. ..... p 411 N95-14518
ROSCA, JUSTINIAN P. ..... p 576 N95-15856
ROSE, ALLEN H. ..... p 478 N95-15669
ROSE, M. F. ..... p 415 N95-14639
ROSE, M. FRANK ..... p 519 N95-14802
p 519 N95-14853
ROSEN, JEROME ..... p 600 N95-15539

ROSEN, MICHAEL J. p 558 N95-14042
ROSENBAUM, E. R. p 405 N95-14421
ROSENBERG, CARLA B. p 554 N95-13888
p 638 N95-14511
ROSENBLUM, W. M. p 458 N95-14225
ROSENFELD, AZRIEL p 583 N95-15398
ROSENKRANZ, P. W. p 531 N95-15586
ROSENTHAL, A. p 521 N95-15420
ROSENTHAL, S. L. p 532 N95-14118
ROSING, M. p 566 N95-14662
ROSS, GRAHAM O. p 487 N95-14554
ROSS, HOLLY M. p 396 N95-14246
ROSS, J. C. p 393 N95-14230
ROTH, E. P. p 625 N95-15438
ROTHE, JOERG p 575 N95-15721
p 576 N95-15788
ROTHE, JORG p 575 N95-15597
ROTHE, PAUL H. p 459 N95-14567
ROUZAUD, A. p 634 N95-14209
ROY, RUSTUM p 625 N95-15746
ROYER, ANTOINE p 606 N95-13930
ROZUM, JAMES p 572 N95-14349
RUBIN, MORTON H. p 602 N95-13896
p 599 N95-13963
p 599 N95-13964
RUFFINS, T. R. p 520 N95-15405
RUITBERG, ARTHUR P. p 478 N95-15681
RUMPF, A. N. p 473 N95-14310
RUSAK, ZVI p 402 N95-14884
RUSSEL, W. B. p 490 N95-14573
RUSSELL, JAMES W. p 418 N95-13890
RUSSELL, N. A. p 524 N95-15575
RUSSELL, PAUL p 580 N95-13727
RUSSO, MASSIMO p 562 N95-14058
RUST, R. J. p 435 N95-14865
RUTHERFORD, PAUL p 508 N95-14457
RUTKOWSKI, RICHARD J. p 419 N95-15447
RUUD, C. O. p 444 N95-13820
RYAN, PATRICK M. p 566 N95-14596
RYBICKI, DANIEL J. p 503 N95-15670
RYFF, LUIS CARLOS B. p 599 N95-13965

S

SAAD, ASHRAF p 415 N95-14637
SAAR, N. p 421 N95-14067
SABO, V. p 538 N95-15106
SABO, VLADIMIR p 539 N95-15144
SACCO, ALBERT, JR. p 458 N95-14226
SACKSTEDER, KURT p 458 N95-14212
SADEGHI, FARSHID p 454 N95-15316
SADHAL, SATWINDAR SINGH p 486 N95-14545
SADOVNIK, LEV p 614 N95-15414
SAEWERT, G. W. p 574 N95-15418
SAFAR, M. E. p 538 N95-15098
SAHU, JUBARAJ p 399 N95-14451
SAILOR, MICHAEL J. p 437 N95-14141
SAITO, K. p 441 N95-15352
SALAS, W. p 565 N95-14594
SALZMAN, JACK A. p 417 N95-14582
SAMPALA, J. H. p 472 N95-13975
SAMSON, SERGE p 424 N95-14080
p 424 N95-14082
SANCHEZ, ISSAC C. p 453 N95-14844
SANKAR, L. N. p 400 N95-14803
SANSO, FERNANDO p 516 N95-15792
SANTOS, EMILIO p 611 N95-13967
SARFF, J. S. p 617 N95-14373
p 618 N95-15540
SARGIS, P. D. p 554 N95-13671
SARIC, WILLIAM S. p 479 N95-13664
SARRAJ, M. p 475 N95-15302
SARRE, P. J. p 640 N95-15834
SARUKKAI, RAMESH R. p 552 N95-15588
p 575 N95-15640
SAULNIER, BERNARD p 519 N95-15290
SAUNDERS, P. p 581 N95-13895
SAUNDERS, T. p 392 N95-14477
SAUSENG-FELLEGGER, GABRIELE
p 544 N95-15107
SAUTER, O. p 618 N95-15632
SAVAGE, S. J. p 433 N95-14148
SCHAEFER, H. F., III p 441 N95-15347
SCHAEFFER, J. C. p 444 N95-13667
SCHAEFFER, STEPHANIE p 584 N95-15786
SCHAFER, RONALD W. p 460 N95-13657
SCHARLER, H. p 517 N95-15797
SCHATZ, MICHAEL F. p 483 N95-14527
SCHAWLOW, ARTHUR L. p 498 N95-13695
SCHEIL, CHRISTINE p 431 N95-14669
SCHELLENGER, HARVEY G. p 395 N95-14243
SCHELLMAN, HEIDI p 600 N95-15539
p 600 N95-15539
SCHEMPF, HAGEN p 504 N95-14026
SCHIFF, LEWIS B. p 397 N95-14253
SCHIPPERS, S. p 592 N95-13675
SCHLAGEL, T. J. p 600 N95-15633
SCHLECHTRIEM, S. p 410 N95-15821
SCHLEICH, W. P. p 598 N95-13909
p 605 N95-13919
SCHMIDT, J. M. p 623 N95-15338
SCHMIDT, W. p 398 N95-14264
SCHMISSEUR, JOHN D. p 412 N95-13687
SCHMITT, D. A. p 539 N95-15148
SCHMITZ, F. H. p 391 N95-13642
SCHNEIDER, FRED B. p 568 N95-13699
SCHNEIDER, GEORGE p 507 N95-14455
SCHNEIDER, J. D. p 599 N95-15360
SCHNEIDER, JOHN R. p 420 N95-14162
SCHNEIDER, R. P., JR. p 621 N95-14390
SCHNEIDER, T. W. p 437 N95-14307
p 473 N95-14308
SCHOFIELD, GARY L. p 553 N95-15768
SCHOWALTER, LEO p 614 N95-15603
SCHRADE, GUENTER p 598 N95-13909
SCHUBERT, LENHART p 587 N95-15643
p 584 N95-15786
p 576 N95-15825
SCHUELLER, MICHAEL S. p 406 N95-14611
SCHULTZ, P. J. p 594 N95-14441
SCHULZ, THEREAS Y. p 540 N95-14145
SCHULZE, J. p 574 N95-15384
SCHULZE, KENNETH W. p 416 N95-14642
SCHULZE, T. P. p 448 N95-14549
SCHUTZ, BOB E. p 471 N95-14286
SCHWANTJE, ROBERT p 515 N95-13885
SCHWEITZER, J. S. p 517 N95-15916
SCHWIRZKE, MARTIN p 558 N95-14043
SCOTT, ELAINE P. p 429 N95-14106
SCULLY, MARLAN O. p 598 N95-13955
SEAMOUNT, PATRICIA p 395 N95-14244
SEE, THOMAS H. p 432 N95-13646
SEEDHOUSE, ERIK L. O. p 544 N95-15109
SEELY, JOHN F. p 614 N95-15764
SEIBERT, GEORGE L. p 412 N95-13687
SEIFERAS, JOEL I. p 575 N95-15644
SEIFERT, H. L. p 595 N95-15310
SEILER, DAVID G. p 474 N95-14401
SELMAN, J. R. p 453 N95-14957
SENTURIA, S. D. p 473 N95-14308
SEPELEV, E. JA. p 538 N95-15106
SERGIENKO, A. V. p 599 N95-13963
p 612 N95-13970
SEROVA, LYUBOV V. p 538 N95-15101
SETHNA, J. P. p 447 N95-15631
SETTLES, G. S. p 455 N95-15535
SFORZA, MARIO p 465 N95-14676
SHA, Y.-G. p 458 N95-14214
SHAFER, STEVEN A. p 573 N95-14842
SHAH, GAUTAM H. p 398 N95-14257
SHAH, R. R. p 524 N95-15432
SHANNON, SAMUEL G. p 551 N95-15810
SHAPIRO, JEFFREY H. p 609 N95-13953
SHAPIRO, MICHAEL p 515 N95-14358
SHAPOW, ERIC p 450 N95-14203
SHARMA, O. P. p 480 N95-14132
SHARMA, SURENDRA P. p 405 N95-13720
SHARMAN, ROBERT D. p 402 N95-14888
SHARP, EARL D. p 468 N95-15393
SHARP, J. M., JR. p 530 N95-14956
SHARP, W. M. p 600 N95-15780
SHASTRI, LOKENDRA p 583 N95-15403
SHATTUCK, PAUL L. p 582 N95-14945
SHAW, GRAEME p 428 N95-14599
SHAW, NANCY p 491 N95-14583
SHAW, T. L. p 419 N95-14089
SHAY, T. M. p 462 N95-14622
SHEEHAN, L. p 451 N95-14389
SHEHAD, NAGY M. p 423 N95-14075
SHEI, S. A. p 446 N95-15532
SHELLEY, E. G. p 619 N95-15758
SHEN, L. S. p 569 N95-14153
SHEN, THOMAS C. p 452 N95-14602
SHEN, Y. F. p 596 N95-15381
SHEN, Y. N. p 570 N95-14163
SHEPANEK, R. F. p 522 N95-14124
SHEPARD, SCOTT R. p 590 N95-13917
SHEPHERD, MICHAEL T. p 475 N95-14866
SHERIDAN, THOMAS B. p 554 N95-14013
p 564 N95-14949
SHERIF, J. S. p 419 N95-14631
SHERMAN, J. p 599 N95-15360
SHERRICK, CARL E. p 554 N95-14017
SHI, DONGLU p 623 N95-15341
SHI, QINGPING p 485 N95-14544
SHI, TAO p 458 N95-14220
SHIBA, K. p 446 N95-15431
SHIGEMOTO, TAKEO p 452 N95-14395
SHIH, YAN-HUA p 602 N95-13896
p 599 N95-13963
p 599 N95-13964
p 612 N95-13970
SHIMABUKURO, FRED I. p 465 N95-14673
SHIMAMOTO, A. p 511 N95-14479
SHIMOMURA, Y. p 446 N95-15433
SHIMONY, ABNER p 598 N95-13961
SHINOZAKI, ARITOMO p 487 N95-14553
SHIVAKUMAR, P. p 493 N95-15571
SHIVAKUMAR, V. p 510 N95-14473
SHIVELY, DAVID G. p 460 N95-14139
SHOGRIN, B. p 450 N95-14303
SHOPE, ROBERT E. p 550 N95-15445
SHORT, NICHOLAS M., JR. p 566 N95-14595
SHROYER, CYNTHIA A. p 513 N95-15547
SHULTZ, LOUIS A. p 503 N95-14923
SHUM, C. K. p 418 N95-14282
SHUMAN, D. p 562 N95-14061
SHUMOVSKY, ALEXANDER S. p 610 N95-13958
SHUR, MICHAEL p 477 N95-15454
SHVARTSMAN, ALEX A. p 579 N95-15617
SICKAFUS, K. E. p 455 N95-15579
SIEGEL, JANE p 572 N95-14349
SIEVERS, A. J. p 599 N95-15371
SIEWERT, RONALD p 428 N95-14951
SIGLER, C. EDWARD, JR. p 466 N95-14681
SIHVOLA, A. H. p 589 N95-13987
SILBERBERG, YARON p 614 N95-15464
SILVA, L. J. p 439 N95-14663
SILVONEN, K. p 478 N95-15611
SIMANONOK, KARL E. p 546 N95-15122
p 547 N95-15129
p 547 N95-15130
SIMENTAL, EDMUNDO p 586 N95-15424
SIMON, A. p 618 N95-14955
SIMON, DONALD L. p 566 N95-13716
SIMPSON, DAVID p 530 N95-14598
SIMPSON, W. R. p 418 N95-14097
SIMS, MICHAEL p 427 N95-14099
SINGH, D. p 433 N95-13682
SINGH, D. J. p 437 N95-14268
SINGH, J. P. p 433 N95-13682
p 621 N95-14192
SIOCHI, EMILIE J. p 422 N95-14074
SISK, R. CHARLES p 590 N95-14137
SITES, J. R. p 519 N95-14432
SIVASUBRAMANIAN, N. p 413 N95-13829
SIVERS, E. A. p 449 N95-13978
SKANTHAKUMAR, S. p 622 N95-14608
SKATRUD, DAVID D. p 594 N95-14362
SKOLE, D. p 565 N95-14594
SKORIK, SERGEI p 588 N95-13942
SKOW, ANDREW p 397 N95-14250
SKUNDBERG, T. p 425 N95-14090
SLAGTER, W. J. p 513 N95-15429
SLANE, STEVE p 450 N95-14203
p 455 N95-15615
SLATER, GARY L. p 532 N95-13725
p 497 N95-15785
SLATER, JOHN W. p 404 N95-15853
SLIMMER, D. p 579 N95-15581
SLOAN, Y. p 559 N95-14045
SLOOFF, J. W. p 398 N95-14264
SLOTBOOM, J. p 471 N95-15871
SMARSH, DAVID A. p 534 N95-15771
SMEPLASS, S. p 513 N95-15348
SMIALEK, J. L. p 444 N95-13667
SMITH, ARTHUR H. p 543 N95-15100
SMITH, BROOKE p 397 N95-14254
SMITH, C. p 458 N95-14225
SMITH, CHRISTOPHER p 405 N95-14350
SMITH, CLAUDE p 515 N95-13885
SMITH, D. A. p 563 N95-15309
SMITH, DAN p 415 N95-14641
SMITH, DANIELA C. p 431 N95-15769
SMITH, DAVID E. p 517 N95-14275
SMITH, J. p 476 N95-15410
SMITH, J. T. p 445 N95-15293
SMITH, LINDA G. p 412 N95-13687
SMITH, M. T. p 445 N95-15293
SMITH, MARC K. p 483 N95-14530
SMITH, MARK p 456 N95-15624
SMITH, MARK J. T. p 565 N95-14589
SMITH, R. E. p 474 N95-14315
SMITH, R. L. p 405 N95-14179
SMITH, SUZANNE WEAVER p 425 N95-14088
SMITH, W. E. p 502 N95-14907
SNEDEN, C. p 640 N95-15835
p 640 N95-15836
SNOW, J. L. p 506 N95-14320
SNOW, THEODORE P. p 640 N95-15836
p 634 N95-15846
SNYDER, ROBERT S. p 478 N95-14577
SODEN, J. M. p 473 N95-14314
SODERBLOM, D. p 644 N95-14506
SODERHOLM, L. p 620 N95-14188
p 622 N95-14608
SODERMAN, P. T. p 391 N95-13642
SOLARZ, R. p 499 N95-14427

SOLC, M. p 627 N95-15838
SOLCOVA, I. p 538 N95-15106
SOLOMON, ALLAN I. p 598 N95-13908
SOLOMON, G. p 462 N95-14623
SONG, Q. W. p 477 N95-15460
SONG, X. Y. p 434 N95-14387
SONNENFELD, GERALD p 537 N95-13638
p 538 N95-15113
SOPORI, B. p 624 N95-15426
SOROKIN, PETER P. p 641 N95-15845
SOUKUP, R. J. p 453 N95-15292
SOUZA, CRAIG A. p 535 N95-15819
SOVEY, JAMES S. p 430 N95-14301
SOVINEC, C. R. p 618 N95-15540
SOWERS, DENNIS p 418 N95-14094
SPARROW, J. M. p 534 N95-15614
SPARROW, VICTOR W. p 402 N95-14887
SPEARMAN, M. LEROY p 647 N95-13663
SPENCER, G. p 456 N95-14629
SPERLING, GEORGE p 581 N95-14847
SPIEGEL, RONALD J. p 523 N95-14403
SPIEGELBERG, STEPHEN H. p 489 N95-14569
SPIESBERGER, JOHN L. p 535 N95-14335
SPINDT, C. A. p 476 N95-15327
SPIRIDONOV, VYACHESLAV p 588 N95-13942
SPRINGER, CORY A. p 533 N95-14423
SQUARER, DAVID p 488 N95-14563
SRIDHAR, J. K. p 408 N95-14102
SRINIVASAN, M. A. p 554 N95-14016
p 558 N95-14041
SRINIVASAN, R. SRINI p 544 N95-15110
p 547 N95-15129
p 550 N95-15150
SRINVASAN, R. SRINI p 547 N95-15130
SRIVATSAN, RAGHAVACHARI p 412 N95-14415
ST.CLAIR, ANNE K. p 450 N95-14113
p 455 N95-15599
ST.CLAIR, TERRY L. p 449 N95-14108
p 449 N95-14109
STADLER, ED p 460 N95-13696
STAEBLER, G. M. p 617 N95-14328
STAELIN, D. H. p 531 N95-15586
STANLEY, G. M. p 571 N95-14169
STANLEY, WILLIAM D. p 516 N95-15727
STARINK, J. P. P. p 537 N95-13990
STARK, LAWRENCE p 559 N95-14048
STARK, LAWRENCE W. p 555 N95-14022
STARRETT, H. S. p 436 N95-15441
STATHIS, P. p 468 N95-15365
STAUB, U. p 620 N95-14188
STEAKLEY, J. M. p 421 N95-14066
STECHER, JOSEPH L., III p 420 N95-14062
STECKENRIDER, J. S. p 449 N95-13978
STECKLER, K. D. p 441 N95-15354
STEELE, JAY p 427 N95-14099
STEEN, PAUL H. p 484 N95-14538
STEENKEN, WILLIAM G. p 395 N95-14241
STEGEMANN, J. p 548 N95-15137
STEINBERG, AEPHRAIM M. p 611 N95-13968
STEINBERG, RICHARD K. p 411 N95-14645
STEINWAND, DANIEL R. p 565 N95-14591
STEPHENS, B. p 415 N95-14639
STEPHENS, S. A. p 463 N95-14627
STEPHENSON, D. p 469 N95-15583
STERMAN, M. B. p 557 N95-14038
STERNBERG, CHARLES A. p 396 N95-14246
p 397 N95-14252
STEVENS, R. R. p 599 N95-15360
STEWART, S. R. p 463 N95-14626
STIEBER, M. E. p 582 N95-14946
STODIECK, LOUIS S. p 538 N95-14227
STOGNIENKO, R. p 639 N95-15830
STOK, WIM J. p 544 N95-15108
STOKER, CAROL p 427 N95-14099
STONE, ERIC A. p 541 N95-14408
STONE, JAMES R. p 430 N95-14174
STONE, P. p 557 N95-14034
STONE, ROBERT J. p 562 N95-14059
p 562 N95-14060
STOVALL, JOHN R. p 569 N95-14161
STRAIT, E. J. p 618 N95-15632
STREET, TROY A. p 415 N95-14638
STRENG, R. A. G. J. p 632 N95-14837
STRICKLAND, J. H. p 404 N95-15570
STUDER, ROBERT J. p 421 N95-14068
SU, BAO-XIA p 471 N95-13900
SU, C.-H. p 458 N95-14214
SUAREX, MAX J. p 531 N95-15745
SUAREZ, CARLOS J. p 395 N95-14238
SUBRAMANIAN, R. SHANKAR p 458 N95-14221
p 486 N95-14546
SUH, KWANG I. p 459 N95-14572
SUH, SUNG-JAE p 444 N95-14202
SUH, Y. S. p 542 N95-15096
SUIB, S. L. p 596 N95-15381
SUMMHAMMER, JOHANN p 607 N95-13936
SUN, C. T. p 507 N95-14456
SUN, CHANG-PU p 610 N95-13959
SUN, X. p 577 N95-13677
p 568 N95-13977
p 570 N95-14163
SUN, XIAOLI p 499 N95-14901
p 615 N95-15849
SUNBERG, D. S. p 454 N95-15313
SURKO, PAMELA p 431 N95-15058
SUSSMAN, GERALD J. p 584 N95-15811
SUTTON, M. A. p 444 N95-13690
p 509 N95-14467
SUUBERG, E. M. p 439 N95-14838
SUWITRA, KRISJANI p 465 N95-14675
SUZUKI, Y. p 545 N95-15111
p 549 N95-15145
SUZUKI, YOJI p 543 N95-15097
p 548 N95-15134
SWAIM, ROBERT J. p 473 N95-14294
SWANSON, D. R. p 444 N95-14208
SWEENEY, S. M. p 453 N95-14609
SWEIDER, D. p 601 N95-13670
SWIFT, CALVIN T. p 517 N95-15848
SWIFT, JOHN B. p 483 N95-14527
SWINNEY, HARRY L. p 483 N95-14527
SWOLINSKY, MANFRED p 407 N95-14900
SYKORA, J. p 538 N95-15106
SZABO, BARNA A. p 507 N95-14454
SZCZERBA, RICHARD p 640 N95-15835
SZILAGYI, T. p 539 N95-15141
SZOFRAN, F. R. p 458 N95-14214
SZOOR, A. p 539 N95-15141

T

TABIB-AZAR, MASSOOD p 477 N95-15587
TACHAU, R. D. M. p 418 N95-15357
TACHI, SUSUMU p 555 N95-14025
TADROS, ALFRED p 562 N95-14058
TAGHAVI, RAY p 404 N95-15852
TAKABAYASHI, AKIRA p 539 N95-15118
TAKAC, P. p 586 N95-15342
TAKACS, P. Z. p 601 N95-13644
TAKAGI, MIKIO p 565 N95-14592
TAKAGI, SADAHARU p 539 N95-15118
p 539 N95-15119
TAKAHASHI, H. p 446 N95-15431
TAKAMURA, SEISHI p 565 N95-14592
TAKEUCHI, SHUJI p 539 N95-15142
p 539 N95-15143
TALBOT, JOHN p 428 N95-14599
TAMRAT, B. F. p 394 N95-14234
TAN, HONG-Z. p 561 N95-14057
TAN, P. p 511 N95-14479
TAN, T. p 624 N95-15426
TANANBAUM, H. D. p 636 N95-13634
p 636 N95-13636
p 637 N95-13637
p 637 N95-14100
p 638 N95-14101
TANATAR, BILAL p 610 N95-13958
TANENBAUM, D. p 518 N95-14194
TANG, LIN p 458 N95-14212
TANG, Y. p 479 N95-13679
TANNY, JOSEF p 483 N95-14526
TANRIKUT, S. p 480 N95-14132
TANVEER, SALEH p 486 N95-14550
TAO, Y. p 483 N95-14529
TAPLEY, BYRON D. p 418 N95-14282
TATE, DAVID p 563 N95-15449
TAYLOR, GERALD R. p 545 N95-15114
TAYLOR, J. p 469 N95-15583
TAYLOR, T. S. p 618 N95-15632
TEMER, D. J. p 440 N95-15297
TEMPLEMAN, JAMES p 563 N95-15449
TEN, SERGEY p 477 N95-15459
TENCH, R. J. p 451 N95-14389
p 614 N95-15529
TENHOEVE, H. J. p 511 N95-14478
TENKATE, A. J. B. p 525 N95-15870
TENNERY, V. J. p 456 N95-15634
TERAESRANTA, H. p 637 N95-13982
TESCHE, F. M. p 519 N95-14393
TESTER, J. W. p 439 N95-14435
TETREAULT, R. p 492 N95-14869
THALER, BARRY p 451 N95-14354
THARRINGTON, ARNOLD p 489 N95-14570
THAYER, JEFFREY P. p 526 N95-13818
THELLIEZ, T. p 633 N95-15761
THIJS, P. J. A. p 622 N95-14795
THIYAGARAJAN, P. p 454 N95-15340
THOMAS, ALMUTTIL M. p 392 N95-13701
THOMAS, C. J. p 520 N95-15405
THOMAS, H. p 490 N95-14571
THOMAS, J. E. p 610 N95-13956
THOMAS, JEFF p 403 N95-14892
THOMAS, PHILIP p 413 N95-13828
THOMAS, R. J. p 621 N95-14390
THOMAS, W. p 502 N95-14907
THOMBLEY, L. p 601 N95-13670
THOMPSON, EDWARD F. p 533 N95-15323
THOMPSON, P. p 435 N95-14913
THOMPSON, R. W. p 458 N95-14226
THOMPSON, ROBERT L. p 483 N95-14531
THOMPSON, S. J. p 618 N95-15632
THOMSEN, M. F. p 526 N95-13995
THOMSON, DOUGLAS p 508 N95-14460
THORNE, MURIEL p 638 N95-14511
THORNTON, DON p 395 N95-14241
THORNTON, J. p 520 N95-15355
THRESHER, R. W. p 519 N95-14433
THURBER, W. ROBERT p 474 N95-14401
TIAN, YUREN p 458 N95-14220
TIBBITTS, THEODORE p 564 N95-14228
TIELENS, ALEXANDER G. G. M. p 639 N95-15827
p 641 N95-15842
TIGNER, M. p 599 N95-15371
TILFORD, CHARLES R. p 424 N95-14084
TILLMAN, MARK p 535 N95-14906
TILTON, JAMES C. p 564 N95-14585
p 564 N95-14588
p 566 N95-14595
TINKER, MICHAEL L. p 416 N95-14643
TISCHLER, A. C. p 539 N95-15135
TITTLE, JAMES S. p 558 N95-14043
TIWARI, S. N. p 437 N95-14268
TIWARI, SURENDRA N. p 392 N95-13701
p 481 N95-14269
TOBIN, BRIDGET F. p 534 N95-15827
TODD, PAUL p 444 N95-14578
TODD, R. I. p 433 N95-13993
TOERMAENEN, V. p 568 N95-13989
TOLBERT, CAROL M. p 430 N95-14173
TOLMAN, B. J. p 632 N95-15366
TOMASKO, M. S. p 620 N95-14009
TONG, PIN p 511 N95-14476
TOPORKOV, D. p 617 N95-14262
TORGE, WOLFGANG p 516 N95-15796
TORGERSON, J. R. p 600 N95-13912
TORIKOSHI, S. p 545 N95-15111
TORIKOSHI, SHIGEYO p 548 N95-15134
TORRE, AMALIA p 606 N95-13927
p 606 N95-13929
TORRENCE, GEOFFREY W. p 465 N95-14677
p 465 N95-14678
TORRES-VEGA, GABINO p 606 N95-13931
TORRES, DAVID p 585 N95-14296
TOSCANO, WILLIAM B. p 539 N95-13661
TOWELL, TIMOTHY W. p 450 N95-14140
TRAN, T.-L. p 419 N95-14631
TRAVEN, RICARDO p 396 N95-14246
p 397 N95-14252
TREFNY, CHARLES J. p 479 N95-13665
TREU, MARVIN H. p 534 N95-15618
TRIGS, DEANNE p 409 N95-15742
TRINH, EUGENE H. p 458 N95-14221
p 485 N95-14541
p 486 N95-14545
TROUNOV, V. p 620 N95-14188
TROUW, F. p 593 N95-13678
TRUAX, J. A. p 517 N95-15916
TRUCANO, T. G. p 418 N95-15357
TRUDEL, CAMERON P. p 582 N95-14946
TRYGGVASON, G. p 478 N95-13653
TRYGGVASON, GRETAR p 485 N95-14542
TSAO, A. p 577 N95-13677
p 568 N95-13977
TSAO, J. Y. p 621 N95-14322
TSCHIRHART, R. p 475 N95-15302
TSUE, YASUHIKO p 609 N95-13948
TUCKER, J. p 426 N95-14091
TUECKE, S. p 578 N95-14116
TUNICK, ARNOLD p 533 N95-14340
TURNBULL, A. D. p 618 N95-15632
TURNBULL, T. p 577 N95-13677
p 568 N95-13977
TURNER, T. J. p 638 N95-14911
TURQ, P. p 619 N95-13691
TWEED, D. p 546 N95-15121
TYLER, CHARLES p 412 N95-13687
TYLER, S. R. p 463 N95-14630

U

UBERBACHER, E. C. p 574 N95-15536
UCHIMOTO, E. p 618 N95-15540
UFFINK, JOS p 588 N95-13915
UM, CHUNG IN p 608 N95-13943
UPCHURCH, BILLY T. p 496 N95-13837
URRY, C. M. p 638 N95-14911

USSERY, L. E. ..... p 442 N95-15387

V

VAIDMAN, LEV ..... p 598 N95-13934
VAJDA, S. ..... p 517 N95-15916
VALETON, J. M. ..... p 553 N95-15816
VALSAMIS, D. ..... p 568 N95-14010
VANDERLOOS, MACHIEL ..... p 556 N95-14030
p 558 N95-14044
VANDERSPIEGEL, JAN ..... p 612 N95-14272
VANDERWOERD, M. ..... p 458 N95-14225
VANDYKE, J. W. ..... p 519 N95-14393
VANELZAKKER, B. G. ..... p 523 N95-15389
VANHELLEMOND, J. ..... p 523 N95-15389
VANHOOK, DAN ..... p 460 N95-13696
VANHOOK, STEPHEN J. ..... p 483 N95-14527
VANINGEN, R. P. ..... p 499 N95-15388
VANLEHN, A. L. ..... p 566 N95-14338
VANLEHN, KURT ..... p 576 N95-15817
VANNEVEL, A. ..... p 607 N95-13939
VANZANDT, DAVID ..... p 483 N95-14531
VASANTHAMOHAN, N. ..... p 621 N95-14192
VASILYEV, MICHAEL V. ..... p 606 N95-13924
VASQUES, M. ..... p 425 N95-14090
p 426 N95-14091
VAUGHAN, ARTHUR H. ..... p 613 N95-14413
VAUGHAN, R. E. ..... p 513 N95-15055
VAWTER, G. A. ..... p 474 N95-14315
VEAL, B. W. ..... p 595 N95-15362
VEDEL, C. ..... p 612 N95-13992
VEENSTRA, JACK E. ..... p 579 N95-15590
VEIJOLA, T. ..... p 497 N95-15413
VELEGOL, D. ..... p 444 N95-14581
VELETSOS, A. ..... p 493 N95-15571
VELLEKAMP, K. ..... p 565 N95-14594
VELTMAN, A. ..... p 472 N95-14149
VEMAGANTI, GURURAJA R. ..... p 493 N95-15604
VERED, R. ..... p 422 N95-14073
VERESHCHAGIN, NIKOLAI K. ..... p 588 N95-15854
p 588 N95-15855
VERNALIS, MARIANA N. ..... p 542 N95-15095
VERNALIS, MARINA N. ..... p 538 N95-15094
VERONNEAU, STEPHEN ..... p 540 N95-14177
VETESNIK, M. ..... p 627 N95-15838
VIANCO, P. T. ..... p 472 N95-13975
VIDIELLA-BARRANCO, ANTONIO ..... p 611 N95-13967
VIEIRA, D. J. ..... p 595 N95-15310
VIKHAGEN, E. ..... p 513 N95-15348
VINALS, JORGE ..... p 459 N95-14540
VINCENT, WILBUR R. ..... p 469 N95-15619
VINOKUR, V. M. ..... p 620 N95-14008
VINZ, BRADLEY L. ..... p 417 N95-14651
VISSERS, D. R. ..... p 471 N95-13684
VITANYI, PAUL M. B. ..... p 575 N95-15644
VITIELLO, G. ..... p 589 N95-13901
VITIELLO, GIUSEPPE ..... p 607 N95-13938
VLASKO-VLASOV, V. K. ..... p 595 N95-15362
VNUK, D. R. ..... p 591 N95-15359
VOGEL, KARL ..... p 605 N95-13919
VOGEL, WOLFHARD J. ..... p 465 N95-14677
p 465 N95-14678
p 466 N95-14679
VOGT, GREGORY L. ..... p 554 N95-13888
VOLK, KEVIN ..... p 640 N95-15835
VOROBJEV, O. A. ..... p 542 N95-15093
VOROS, ROBERT S. ..... p 551 N95-13715
VOURDAS, APOSTOLOS ..... p 598 N95-13940
VRANE, DAVID R. ..... p 483 N95-14530
VRANISH, JOHN M. ..... p 502 N95-14517
VUILLEZ, CHRISTOPHE ..... p 480 N95-14134
VUKOVICH, J. M. ..... p 616 N95-13973

W

WACHTER, J. R. ..... p 505 N95-15777
WAHIDDIN, M. R. B. ..... p 456 N95-13899
WAHL, D. E. ..... p 515 N95-14313
WALCHLI, LAWRENCE A. ..... p 398 N95-14259
WALDEN, ALAN K. ..... p 496 N95-14841
WALKER, D. ..... p 492 N95-14869
WALKER, D. W. ..... p 567 N95-13676
WALKER, G. A. H. ..... p 640 N95-15835
WALKER, J. D. A. ..... p 492 N95-14932
WALKER, J. S. ..... p 616 N95-14006
WALKER, KEVIN P. ..... p 585 N95-14300
WALKER, L. F. ..... p 440 N95-15297
WALKER, LEN ..... p 512 N95-14617
WALKER, S. I. ..... p 511 N95-14479
WALLSOM, RICHARD E. ..... p 459 N95-14111
WALTERS, G. K. ..... p 625 N95-15574
WANG, C. H. ..... p 448 N95-13686
p 449 N95-13689
p 449 N95-13692
WANG, C. Y. ..... p 586 N95-15538
WANG, H. H. ..... p 620 N95-14009
WANG, HUA ..... p 484 N95-14537
WANG, LI-JUN ..... p 610 N95-13956
WANG, TAYLOR G. ..... p 458 N95-14218
p 458 N95-14219
WANG, W. ..... p 618 N95-15374
WANG, ZUNING ..... p 623 N95-15341
WANTZ, J. F. ..... p 533 N95-14410
WAPMAN, W. ..... p 476 N95-15356
WARD, M. D. ..... p 622 N95-14601
WARDEN, ROBERT M. ..... p 423 N95-14076
WARNAS, ALBERT A. ..... p 513 N95-15620
p 513 N95-15621
WARNER, R. A. ..... p 595 N95-15310
WARZYWODA, J. ..... p 458 N95-14226
WASSERMAN, S. R. ..... p 596 N95-15381
WATANABE, OSAMU ..... p 575 N95-15721
WATANABE, SATORU ..... p 539 N95-15118
p 539 N95-15119
WATENPAUGH, DONALD E. ..... p 547 N95-15128
WATERMANN, JURGEN ..... p 526 N95-13818
WATERS, W. A., JR. ..... p 435 N95-14865
WATKINS, MICHAEL M. ..... p 527 N95-14276
WAYNER, PETER C., JR. ..... p 488 N95-14560
WDOWIAK, THOMAS J. ..... p 641 N95-15840
WEAVER, DAVID P. ..... p 422 N95-14072
WEBER, F. ..... p 643 N95-14442
WEBER, HEIDI ..... p 563 N95-14854
WEBER, J. ..... p 627 N95-15823
WEBER, M. J. ..... p 454 N95-15313
WEBSTER, ADRIAN ..... p 639 N95-15832
WEGNER, WALTER ..... p 640 N95-15836
WEI, R. P. ..... p 448 N95-14465
WEILER, EDWARD ..... p 638 N95-14511
WEINACHT, PAUL ..... p 399 N95-14451
WEINBERG, IRVING ..... p 473 N95-14302
WEINBERG, MICHAEL C. ..... p 458 N95-14221
WEINSTEIN, LEONARD M. ..... p 401 N95-14879
WEINSTEIN, YECHIEL ..... p 560 N95-14050
WEISE, D. R. ..... p 413 N95-14513
WEISS, L. A. ..... p 526 N95-13995
WEISS, MEL ..... p 411 N95-14799
WEISS, S. ..... p 394 N95-14235
WEITZ, DAVID A. ..... p 444 N95-14575
WELCH, D. O. ..... p 590 N95-14440
p 624 N95-15422
WELLER, DAVID G. ..... p 570 N95-14166
WELP, U. ..... p 595 N95-15362
WENNEMYR, MAGNUS ..... p 469 N95-15462
WENZEL, ALAN R. ..... p 401 N95-14882
WENZEL, ELIZABETH M. ..... p 557 N95-14034
p 557 N95-14035
WEPMAN, J. A. ..... p 462 N95-14412
WESELY, M. L. ..... p 522 N95-14187
WESSENDORF, K. O. ..... p 473 N95-14310
WESTERINK, J. J. ..... p 535 N95-14352
WETZIG, JOACHIM ..... p 542 N95-15092
WHALEN, ROBERT ..... p 548 N95-15136
p 549 N95-15139
p 549 N95-15140
WHANGBO, M. H. ..... p 620 N95-14009
WHEAT, S. R. ..... p 574 N95-15543
WHEELER, M. J. ..... p 433 N95-13682
WHITAKER, DAVID L. ..... p 394 N95-14233
WHITBECK, E. ..... p 636 N95-13636
WHITE, C. D. ..... p 542 N95-15095
WHITE, J. M. ..... p 442 N95-15387
WHITE, KEITH D. ..... p 562 N95-14061
WHITING, ELLIS E. ..... p 429 N95-13718
WHITMORE, J. ..... p 475 N95-15302
WHITNEY, PAUL ..... p 552 N95-14600
WHITTEKER, JIM H. ..... p 467 N95-14828
p 467 N95-14829
WHITTEN, J. E. ..... p 593 N95-14011
WHITTET, D. C. B. ..... p 639 N95-15831
WICK, DANIEL T. ..... p 423 N95-14075
WIEDEMEIER, HERIBERT ..... p 458 N95-14216
WIETFELDT, F. E. ..... p 594 N95-14374
WIKRAMANAYAKE, PALITHA N. ..... p 536 N95-15440
WILBUR, P. J. ..... p 450 N95-14303
WILDER, M. C. ..... p 400 N95-14613
WILKENING, W. W. ..... p 506 N95-14320
WILKERSON, JOHN C. ..... p 517 N95-15848
WILKINS, K. E. ..... p 512 N95-14485
WILKINSON, C. ..... p 506 N95-14198
WILLARD, SCOTT A. ..... p 432 N95-14920
WILLIAMS, C. R. ..... p 526 N95-13974
WILLIAMS, D. N. ..... p 522 N95-14317
WILLIAMS, DAVID L., II ..... p 394 N95-14237
WILLIAMS, F. A. ..... p 442 N95-15375
WILLIAMS, J. M. ..... p 620 N95-14009
p 532 N95-14120
WILLIAMS, J. R. ..... p 439 N95-14867
WILLIAMS, KEVIN W. ..... p 573 N95-14917
WILLIAMS, M. Z. ..... p 427 N95-14420
WILLIAMS, RICHARD M. ..... p 599 N95-15839
WILLIAMS, ROY E. ..... p 556 N95-14029
WILLIAMS, STEVEN P. ..... p 409 N95-14852
WILLIAMS, W. R. ..... p 438 N95-14375
WILLIAMSON, D. L. ..... p 520 N95-15406
WILLSON, K. R. ..... p 484 N95-14536
WILSON, ALLEN W. ..... p 448 N95-15918
WILSON, DAVID J. ..... p 396 N95-14247
WILSON, JAMES CHARLES ..... p 530 N95-14855
p 525 N95-15847
WILSON, JOHN W. ..... p 647 N95-15790
WILSON, LARRY W. ..... p 572 N95-14615
WILSON, WILLIAM E. ..... p 529 N95-14404
WINDER, A. A. ..... p 493 N95-15332
WINDHORST, ROGIER A. ..... p 637 N95-13722
WINGET, C. M. ..... p 539 N95-15135
WINHOLTZ, R. A. ..... p 506 N95-14356
WINKLER, JERRY ..... p 432 N95-13646
WINNICK, J. ..... p 441 N95-15345
WINRICH, RALPH ..... p 638 N95-14511
WINTER, KATHRYN P. ..... p 574 N95-15335
WIXSON, LAMBERT ERNEST ..... p 587 N95-15775
WOLFE, HOWARD F. ..... p 513 N95-15547
WOLFE, JEREMY M. ..... p 552 N95-14389
WOLVERTON, M. KATHERINE ..... p 458 N95-14212
WONG, EDMOND ..... p 566 N95-13716
WONG, K. W. ..... p 621 N95-14192
WONICA, D. ..... p 463 N95-14628
WOOD, EARL ..... p 547 N95-15127
WOOD, KATHRYN J. ..... p 540 N95-14176
WOOD, RICHARD J. ..... p 567 N95-14159
p 567 N95-14160
WOOD, RICHARD M. ..... p 501 N95-14183
WOODFIELD, ALAN A. ..... p 407 N95-14898
WOODROFFE, J. M. ..... p 465 N95-14674
WOODS, C. B. ..... p 562 N95-14061
WORDEN, R. E. ..... p 512 N95-14485
WORSTER, M. GRAE ..... p 448 N95-14551
WOUTERS, J. M. ..... p 595 N95-15310
WRAY, RICHARD B. ..... p 569 N95-14161
WRIGHT, JENNA ..... p 535 N95-14906
WRIGHT, K. H., JR. ..... p 429 N95-15824
WRIGHT, WILLIAM B. ..... p 481 N95-14295
WRONSKI, C. R. ..... p 622 N95-14431
WU, J. ..... p 458 N95-14213
WU, LING-AN ..... p 603 N95-13902
WU, MEI-JUAN ..... p 603 N95-13902
WU, R. L. C. ..... p 450 N95-14303
WU, X. Y. ..... p 594 N95-14441
WU, XIAO-LUN ..... p 489 N95-14570
WUEBBLES, D. J. ..... p 523 N95-15361
WURTELE, MORTON G. ..... p 402 N95-14888
WYERS, G. P. ..... p 523 N95-15389

X

XIAO, MIN ..... p 598 N95-13920
XIE, X. S. ..... p 612 N95-13986
XIN, Y. ..... p 621 N95-14192
XIONG, B. ..... p 483 N95-14529
XIONG, YALIN ..... p 573 N95-14842
XU, J. ..... p 574 N95-15396
XU, MIN ..... p 488 N95-14563
XU, W. ..... p 568 N95-14010
XUE, DAVID Y. ..... p 506 N95-14270

Y

YAMASHITA, HIROSHI ..... p 539 N95-15142
YANAGIHARA, DAI ..... p 539 N95-15119
YANG, JEFF ..... p 502 N95-14666
YANG, L. C. ..... p 521 N95-15407
YANG, W. J. ..... p 446 N95-15532
YAREMA, R. J. ..... p 475 N95-15302
YE, JUN ..... p 595 N95-15318
YEE, SUSAN ..... p 409 N95-15742
YEH, PEN-SHU ..... p 565 N95-14593
YELVERTON, JOHN T. ..... p 540 N95-13971
YEON, KYU HWANG ..... p 608 N95-13943
YEW, C. H. ..... p 418 N95-15357
YIM, SOLOMON C. ..... p 535 N95-14204
YIN, B. ..... p 462 N95-14622
YOERGER, DANA R. ..... p 504 N95-14026
YOKOZAWA, K. ..... p 545 N95-15111
YOKOZAWA, KIKUKO ..... p 548 N95-15134
YOSHINO, KOUICHI ..... p 522 N95-14344
YOUN, SUN-HYUN ..... p 471 N95-13921
YOUNG, A. D. ..... p 393 N95-14103
YOUNG, C. E. ..... p 593 N95-14011
YOUNG, LAURENCE R. ..... p 537 N95-13702
YOUNG, MICHAEL A. ..... p 579 N95-15450
YOUNG, PHILIP R. ..... p 422 N95-14074
YU, C.-T. ..... p 511 N95-14479
YU, CHRISTOPHER C. ..... p 470 N95-15750

YU, JAEHOON ..... p 594 N95-14661
YU, K. M. ..... p 623 N95-15339
YU, LI-HUA ..... p 610 N95-13959
YU, N. ..... p 455 N95-15579
YUCHS, S. E. ..... p 596 N95-15381
YUEN, JOSEPH H. ..... p 462 N95-14620
YUHAS, ANDREW J. ..... p 395 N95-14241

Z

ZACH, F. X. ..... p 623 N95-15339
ZACHARY, WOODFORD W. ..... p 602 N95-13896
ZAHORIAN, STEPHEN A. ..... p 541 N95-14184
ZAHRT, J. D. ..... p 442 N95-15387
ZAININGER, H. W. ..... p 519 N95-14393
ZAK, B. D. ..... p 524 N95-15575
ZAKHOR, AVIDEH ..... p 632 N95-15423
ZALEWSKI, JANUSZ ..... p 569 N95-14157
ZAMAN, K. B. M. Q. ..... p 398 N95-14418
ZARE, RICHARD N. ..... p 498 N95-13695
ZAUGG, T. ..... p 599 N95-15360
ZAVADIL, K. R. ..... p 446 N95-15368
ZEBIB, ABDELFATTAH ..... p 483 N95-14526
ZEILINGER, ANTON ..... p 611 N95-13962
ZELDOV, E. ..... p 619 N95-13681
ZELTZER, DAVID ..... p 556 N95-14032
p 562 N95-14058
ZEMEL, IRINA ..... p 456 N95-15800
ZERATH, E. ..... p 539 N95-15148
ZHANG, J. P. ..... p 637 N95-14100
ZHANG, JU ..... p 576 N95-15789
ZHANG, LI-FAN ..... p 538 N95-15099
ZHANG, YI ..... p 541 N95-14408
ZHANG, YIQIANG ..... p 484 N95-14533
ZHAO, H.-Z. ..... p 610 N95-13956
ZHAO, P. ..... p 637 N95-13637
ZHAO, S. ..... p 571 N95-14196
ZHAO, WEI ..... p 570 N95-14164
ZHENG, XIAO-YU ..... p 458 N95-14220
ZHITLUKHIN, A. ..... p 617 N95-14262
ZHONG, S. ..... p 529 N95-14428
ZHOU, Z. Y. ..... p 595 N95-15310
ZHU, J. X. ..... p 490 N95-14573
ZHU, YI-FU ..... p 598 N95-13920
ZHU, YIMEI ..... p 590 N95-14440
ZIMAND, MARIUS ..... p 587 N95-15596
p 589 N95-15859
ZIMMERMAN, T. ..... p 475 N95-15302
ZOU, X.-Y. ..... p 600 N95-13912
ZUBROW, DAVID ..... p 572 N95-14349
ZUTAVERN, F. J. ..... p 477 N95-15544
ZWERNEMAN, W. D. ..... p 396 N95-14248

CORPORATE SOURCE INDEX

Typical Corporate Source Index Listing

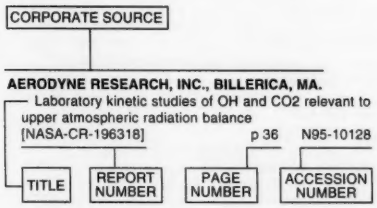

Listings in this index are arranged alphabetically by corporate source. The title of the document provides the user with a brief description of the subject matter. The report number helps to indicate the type of document cited (e.g., NASA report, translation, NASA contractor report). The accession number denotes the number by which the citation is identified. The page number helps you locate the citation in the abstract section. The titles are arranged under each corporate source in ascending accession number order.

A

ABLE ENGINEERING CO., INC., GOLETA, CA.
Martian environmental simulation for a deployable lattice mast p 423 N95-14076
ACADEMIA SINICA, BEIJING (CHINA).
Sum-frequency generation from photon number squeezed light p 603 N95-13902
ACADEMY OF SCIENCES OF THE ARMENIAN SSR, ERIVAN.
Spectral, noise and correlation properties of intense squeezed light generated by a coupling in two laser fields p 500 N95-13903
ACADEMY OF SCIENCES (USSR), MOSCOW (USSR).
Multimode squeezing, biphotons and uncertainty relations in polarization quantum optics p 603 N95-13904
Sub-Poissonian light and photocurrent shot-noise suppression in closed opto-electronic loop p 606 N95-13924
Modes in light wave propagating in semiconductor laser p 500 N95-13925
The Stokes line width and uncertainty relations p 589 N95-13935
Some rules for polydimensional squeezing p 608 N95-13941
Berry phase in Heisenberg representation p 609 N95-13952
Nonresonant interaction of ultrashort electromagnetic pulses with multilevel quantum systems p 610 N95-13960
Advanced method and processing technology for complicated shape airframe part forming p 410 N95-14486
Psychophysiological aspects of increasing resistance to space motion sickness p 542 N95-15093
ADVISORY GROUP FOR AEROSPACE RESEARCH AND DEVELOPMENT, NEUILLY-SUR-SEINE (FRANCE).
AGARD highlights 94/2 [AGARD-HIGHLIGHTS-94/2] p 647 N95-13640
Identification of dynamic systems. Volume 3: Applications to aircraft. Part 2: Nonlinear analysis and manoeuvre design [AGARD-AG-300-VOL-3-PT-2] p 408 N95-14102
Scale effects on aircraft and weapon aerodynamics [AGARD-AG-323] p 393 N95-14103
Turbomachinery Design Using CFD [AGARD-LS-195] p 479 N95-14127
Quality assessment for wind tunnel testing [AGARD-AR-304] p 393 N95-14197
High temperature cyclic behaviour of aerospace materials: Room temperature validation tests of Ti-6Al-4V [AGARD-AR-328] p 506 N95-14198
The principles of flight test assessment of flight-safety-critical systems in helicopters [AGARD-AG-300-VOL-12] p 405 N95-14199
Challenge of Future EW System Design [AGARD-CP-546] p 461 N95-14200
A selection of experimental test cases for the validation of CFD codes, volume 1 [AGARD-AR-303-VOL-1] p 481 N95-14201
The musculoskeletal and vestibular effects of long term repeated exposure to sustained high-G [AGARD-AR-317] p 562 N95-14263
Computational aerodynamics based on the Euler equations [AGARD-AG-325] p 398 N95-14264
Missile Aerodynamics [AGARD-R-804] p 399 N95-14445
Propagation Modelling and Decision Aids for Communications, Radar and Navigation Systems [AGARD-LS-196] p 466 N95-14825
Flight in an Adverse Environment [AGARD-LS-197] p 406 N95-14893
Advanced Guidance and Control Aspects in Robotics [AGARD-LS-193] p 581 N95-14942
AEROJET-GENERAL CORP., AZUSA, CA.
Earth Observing System (EOS) Advanced Microwave Sounding Unit-A (AMSU-A) Spares Program Plan [NASA-CR-189380] p 567 N95-13632
Earth Observing System (EOS)/Advanced Microwave Sounding Unit-A (AMSU-A): Instrument logic diagrams [NASA-CR-189378] p 567 N95-13633
Earth Observing System (EOS) Advanced Microwave Sounding Unit-A (AMSU-A): Instrumentation interface control document [NASA-CR-189377] p 567 N95-13651
Earth Observing System (EOS)/Advanced Microwave Sounding Unit-A (AMSU-A): Calibration management plan [NASA-CR-189376] p 515 N95-13704
Earth Observing System (EOS)/Advanced Microwave Sounding Unit-A (AMSU-A) software assurance plan [NASA-CR-196059] p 515 N95-13885
Earth Observing System (EOS)/Advanced Microwave Sounding Unit-A (AMSU-A) worst-case analysis: Antenna beam pointing [NASA-CR-197218] p 517 N95-15851
AERONAUTICAL RESEARCH LABS., MELBOURNE (AUSTRALIA).
Residual strength of composites with multiple impact damage [AD-A284230] p 434 N95-14409
AERONAUTICAL SYSTEMS DIV., WRIGHT-PATTERSON AFB, OH.
Challenges for the aircraft structural integrity program p 410 N95-14481
AEROSPACE CORP., EL SEGUNDO, CA.
Propagation data at 20/40 GHz and the propagation needs of Milstar p 465 N95-14673
AEROSPACE MEDICAL RESEARCH LABS., BROOKS AFB, TX.
Transesophageal echocardiographic evaluation of baboons during microgravity induced by parabolic flight p 538 N95-15094
Circulatory filling pressures during transient microgravity induced by parabolic flight p 542 N95-15095
Guidelines for a Research and Development (R/D) program for high sustained G p 546 N95-15124
Validation of MMPI scales for personality disorders: A pilot and other aviator study [AD-A284397] p 553 N95-15768
AEROSPATIALE, VERRIERES-L-BUISSON (FRANCE).
Computation of supersonic air-intakes p 400 N95-14452
AI SIGNAL RESEARCH, INC., HUNTSVILLE, AL.
Develop advanced nonlinear signal analysis topographical mapping system [NASA-CR-194414] p 514 N95-13639
AIR FORCE INST. OF TECH., WRIGHT-PATTERSON AFB, OH.
Ion implantation of He-3 in tantalum for use in a low energy deuteron polarization analyzer [AD-A283172] p 619 N95-13698
Damage tolerant repair techniques for pressurized aircraft fuselages [AD-A281982] p 391 N95-14144
Monitoring audiometry in hearing conservation programs [AD-A282024] p 540 N95-14145
Effect of surface roughness on local film cooling effectiveness and heat transfer coefficients [AD-A283854] p 482 N95-14351
Water vapor and temperature inversions near the 0 C level over the tropical western Pacific [AD-A282023] p 533 N95-14952
On the LU factorization of sequences of identically structured sparse matrices within a distributed memory environment [AD-A282025] p 578 N95-14953
The oxidative stabilization and carbonization of mesophase pitch [AD-A282026] p 453 N95-14954
Large-scale data envelopment analysis models and related applications [AD-A283214] p 588 N95-15400
Nowcasting convective storm evolution in east-central Florida using satellite and Doppler radar data [AD-A283260] p 534 N95-15618
The seasonal cycle dependence of temperature fluctuations in the atmosphere [AD-A283220] p 534 N95-15627
Performance modeling and analysis of parallel processing and Low Earth Orbit satellite communication systems [AD-A283243] p 470 N95-15652
ALABAMA A & M UNIV., NORMAL, AL.
Pseudomaster equation for the no-count process in a continuous photodetection p 608 N95-13946
ALABAMA UNIV., BIRMINGHAM, AL.
Protein crystal growth results from the United States Microgravity Laboratory-1 mission p 458 N95-14225
Investigation of a laboratory candidate for the carrier of the 4430 A diffuse interstellar band p 641 N95-15840
ALABAMA UNIV., HUNTSVILLE, AL.
Investigations into mirror fabrication metrology analysis [NASA-CR-196522] p 602 N95-13841
Numerical studies of the surface tension effect of cryogenic liquid helium [NASA-CR-197014] p 479 N95-14104
Produce documents and media information [NASA-CR-196521] p 532 N95-14271
Dynamics and statics of nonaxisymmetric and symmetric liquid bridges p 484 N95-14533
Neural networks: Alternatives to conventional techniques for automatic docking [TABES PAPER 94-627] p 417 N95-14651
On the physics of waves in the solar atmosphere: Wave heating and wind acceleration [NASA-CR-196992] p 646 N95-15070
Mass analysis addition to the Differential Ion Flux Probe (DIFP) study [NASA-CR-196531] p 429 N95-15824
ALBERTA UNIV., EDMONTON.
Initiation and propagation of small corner cracks p 510 N95-14471
ALCATEL ESPACE, TOULOUSE (FRANCE).
Mission, technologies and design of planetary mobile vehicle p 504 N95-14947

ALENIA SPAZIO S.P.A., TURIN (ITALY).
Space simulation techniques and facilities for SAX STM test campaign p 423 N95-14077
ALLIED-SIGNAL AEROSPACE CO., KANSAS CITY, MO.
Integrated optical maze
[DE94-015866] p 613 N95-14367
ALLIED-SIGNAL AEROSPACE CO., PHOENIX, AZ.
Advanced Turbine Technology Applications Project (ATTAP)
[NASA-CR-195393] p 634 N95-15743
ALUMINUM CO. OF AMERICA, ALCOA CENTER, PA.
Microstructurally based model of fatigue initiation and growth p 508 N95-14459
AMERICAN ASSOCIATION OF PHYSICS TEACHERS, COLLEGE PARK, MD.
The 24th International Physics Olympiad
[AD-A280584] p 589 N95-13972
AMERICAN MOBILE SATELLITE CORP., RESTON, VA.
Communications availability: Estimation studies at AMSC p 466 N95-14681
AMES LAB., IA.
Diffusion of adatoms on face-centered cubic transition metal surfaces
[DE94-014230] p 445 N95-15307
AMSTERDAM UNIV. (NETHERLANDS).
Body position and volume status as determinants of cardiovascular responses to transition into microgravity in parabolic flight p 544 N95-15108
ANALYTIC SCIENCES CORP., NEW HARTFORD, NY.
Speakeasy software development
[AD-A283816] p 468 N95-15333
ANALYTICAL SERVICES AND MATERIALS, INC., HAMPTON, VA.
Hybrid structured/unstructured grid computations for the F/A-18 at high angle of attack p 394 N95-14233
ARGONNE NATIONAL LAB., IL.
Paradigms and strategies for scientific computing on distributed memory concurrent computers
[DE94-013305] p 567 N95-13676
Parallel performance of a symmetric eigensolver based on the Invariant Subspace Decomposition approach
[DE94-013314] p 577 N95-13677
Inelastic neutron scattering and molecular dynamics simulations of water adsorbed in the molecular sieves AlPO4-11, AlPO4-5, AlPO4-8 and VPI-5
[DE94-013337] p 593 N95-13678
Impulsive response of nonuniform density liquid in a laterally excited tank
[DE94-013722] p 479 N95-13679
Surface currents and bulk pinning in Bi2Sr2CaCu2O8
[DE94-013873] p 619 N95-13681
Effects of in situ fiber strength characteristics on mechanical properties of SiC(f)/SiC composites
[DE94-013965] p 433 N95-13682
Materials and mechanisms of high temperature lithium sulfide batteries
[DE94-012634] p 471 N95-13684
In situ, real-time analysis of the growth of ferroelectric and conductive oxide heterostructures by a new time-of-flight pulsed ion beam surface analysis technique
[DE94-013298] p 620 N95-13822
A study of the Invariant Subspace Decomposition Algorithm for banded symmetric matrices
[DE94-013872] p 568 N95-13977
Nondestructive characterization of structural ceramic components
[DE94-013961] p 449 N95-13978
MHD flow in rectangular ducts with inclined non-uniform transverse magnetic field
[DE94-013989] p 616 N95-14006
Flux pinning and forced entanglement by splayed columnar defects
[DE94-013994] p 620 N95-14008
Electron spin resonance and band electronic structure study of the metal-insulator transition in (BEDT-TTF)3(HSO4)2
[DE94-014005] p 620 N95-14009
A multi-level object store and its application to HEP data analysis
[DE94-014010] p 568 N95-14010
Direct detection of neutral metal atoms in electron-stimulated desorption: Al from CH3O/Al(111). Velocity distribution and absolute yield
[DE94-014011] p 593 N95-14011
Tokamak power plant burn cycle options
[DE94-014016] p 617 N95-14012
Nexus: An interoperability layer for parallel and distributed computer systems
[DE94-015816] p 578 N95-14116
Remote sensing strategy at the first atmospheric radiation measurement field site
[DE94-015091] p 522 N95-14187
Intermultiplet transitions in optically opaque EuBa2Cu3O7: An inelastic neutron scattering study
[DE94-013429] p 620 N95-14188
Mechanical properties of high-temperature superconducting wires
[DE94-015089] p 621 N95-14192
A high performance graphics algorithm
[DE94-015033] p 571 N95-14196
An informal introduction to program transformation and parallel processors
[DE94-016343] p 578 N95-14380
Performance of spherically focusing Ge(444) backscattering analyzers for inelastic x-ray scattering
[DE94-016349] p 621 N95-14382
Progress in development of tapes and magnets made from Bi-2223 superconductors
[DE94-015067] p 475 N95-14606
Anomalous temperature dependence of the lattice parameters in HoPO4 and HoVO4: Rare earth quadrupolar effects
[DE94-015086] p 622 N95-14608
Dense ceramic membranes for partial oxygenation of methane
[DE94-015021] p 453 N95-14609
Coherency strains and coarsening in Ni-Al-Si alloys: An experimental study
[DE94-015020] p 445 N95-14665
Self-organization of graft copolymers at surfaces, interfaces and in bulk
[DE94-016884] p 454 N95-15340
Transport resistive broadening by avalanche flux motion in high-temperature superconductors: SOC in a driven system
[DE94-016901] p 623 N95-15341
Dynamics on the attractor for the complex Ginzburg-Landau equation
[DE94-016902] p 586 N95-15342
Macroturbulence in superconductors
[DE94-016371] p 595 N95-15362
The structure of new synthetic manganese oxide octahedral molecular sieves
[DE94-016348] p 596 N95-15381
Magnetic and structural instabilities of ultrathin Fe(100) wedges
[DE94-013864] p 624 N95-15385
Phase separation and doped-hole segregation in La(2)CuO(4+delta) and La(2-x)Sr(x)CuO(4+delta)
[DE94-015070] p 624 N95-15430
Recent progress and future prospects in the surface engineering and tribology of ceramics
[DE94-016315] p 456 N95-15778
Technology and Science at at High-Power Spallation Source: Proceedings
[DE94-009685] p 597 N95-15826
High-temperature corrosion of iron aluminides
[DE94-011505] p 447 N95-15906
ARIZONA STATE UNIV., TEMPE, AZ.
Experiments to verify nonparallel stability theory at Virginia Polytechnic Institute and State University, Blacksburg, Virginia
[NASA-CR-196993] p 479 N95-13664
A ROSAT deep survey of the best studied high latitude areas
[NASA-CR-196265] p 637 N95-13722
ARIZONA UNIV., PHOENIX, AZ.
Experimental investigation of the Marangoni effect on the stability of a double-diffusive layer p 483 N95-14528
ARIZONA UNIV., TUCSON, AZ.
Measurement of interfacial tension of immiscible liquid pairs in microgravity p 458 N95-14221
Electrohydrodynamic deformation and interaction of a pair of emulsion drops p 490 N95-14576
Asymmetric coupled quantum wells for high speed optical modulators at communication wavelengths
[AD-A281572] p 477 N95-15459
New algorithms for the reduction of image degradation due to atmospheric turbulence
[AD-A284891] p 615 N95-15772
On the behavior of three-dimensional wave packets in viscously spreading mixing layers
[NASA-TM-106770] p 495 N95-15908
ARKANSAS UNIV., FAYETTEVILLE, AR.
Squeezed light from multi-level closed-cycling atomic systems p 598 N95-13920
ARMY AEROMEDICAL RESEARCH LAB., FORT RUCKER, AL.
Body position and volume status as determinants of cardiovascular responses to transition into microgravity in parabolic flight p 544 N95-15108
Collection of real-time, multichannel EEG data from helicopter pilots in flight: A feasibility study
[AD-A284396] p 551 N95-15767
Aviation Epidemiology Data Register: Gender-specific attrition from the trained US Army aviator cohort of 1988
[AD-A284395] p 551 N95-15810
ARMY ARMAMENT RESEARCH, DEVELOPMENT AND ENGINEERING CENTER, PICATINNY ARSENAL, NJ.
Computer Aided Engineering (CAE) overview
[AD-A280966] p 572 N95-14616
ARMY COLD REGIONS RESEARCH AND ENGINEERING LAB., HANOVER, NH.
Dependence of segregation potential on the thermal and hydraulic conditions predicted by model M1
[AD-A280969] p 530 N95-14862
Effect of matrix stiffness on wavy fiber behavior in single-carbon-fiber-epoxy composites
[AD-A280970] p 435 N95-15427
Traveling wave solutions to the problem of quasi-steady freezing of soils
[AD-A280971] p 531 N95-15428
ARMY COMMUNICATIONS-ELECTRONICS COMMAND, FORT MONMOUTH, NJ.
Spatial awareness comparisons between large-screen, integrated pictorial displays and conventional EFIS displays during simulated landing approaches
[NASA-TP-3467] p 409 N95-14852
ARMY CONSTRUCTION ENGINEERING RESEARCH LAB., CHAMPAIGN, IL.
A multiscale random field model for Bayesian image segmentation
[AD-A283875] p 515 N95-14358
ARMY ENGINEER WATERWAYS EXPERIMENT STATION, VICKSBURG, MS.
ADCIRC: An advanced three-dimensional circulation model for shelves, coasts, and estuaries. Report 4: Hurricane storm surge modeling using large domains
[AD-A283868] p 535 N95-14352
ARMY RESEARCH INST. FOR THE BEHAVIORAL AND SOCIAL SCIENCES, ALEXANDRIA, VA.
The effect of response format on reliability estimates for tacit knowledge scales
[AD-A283547] p 552 N95-15326
ARMY RESEARCH LAB., ABERDEEN PROVING GROUND, MD.
Navier-Stokes predictions of missile aerodynamics p 399 N95-14451
Preliminary analysis of Army aircrew requirements for Joint Surveillance Target Attack Radar System (JSTARS): Human performance requirements and job demands
[AD-A284917] p 563 N95-15759
ARMY RESEARCH LAB., ADELPHI, MD.
A prototype lisp-based soft real-time object-oriented Graphical User Interface for control system development
[NASA-TM-106743] p 566 N95-13716
ARMY RESEARCH LAB., CLEVELAND, OH.
Effects of thermal cycling on thermal expansion and mechanical properties of SiC fiber-reinforced reaction-bonded Si3N4 composites
[NASA-TM-106665] p 433 N95-14298
ARMY RESEARCH LAB., FORT MONMOUTH, NJ.
Conductivity of polyacrylonitrile based lithium polymer electrolytes
[AD-A283965] p 450 N95-14203
Thin lithium cobalt dioxide rechargeable cells using polyacrylonitrile-based polymer electrolytes
[AD-A283253] p 455 N95-15615
ARMY RESEARCH LAB., WATERTOWN, MA.
Tensile creep strain and activation energy
[AD-A283264] p 513 N95-15620
Loading-strain equivalence between thermomechanical, creep, and tensile tests: High density polyethylene
[AD-A283265] p 513 N95-15621
Ballistic performance and adiabatic shear behavior of AerMet(tm) 100 steel
[AD-A283266] p 447 N95-15622
Effect of heat treatment on the microstructure and properties of AerMet (trade name) 100 steel
[AD-A284387] p 447 N95-15807
ARMY RESEARCH LAB., WHITE SANDS MISSLE RANGE, NM.
Determination of the similarity theory scaling parameters from the vertical gradients
[AD-A283833] p 533 N95-14340
ARMY STRATEGIC DEFENSE COMMAND, HUNTSVILLE, AL.
Aero-optics system integration
[TABES PAPER 94-604] p 415 N95-14638
ARMY TEST AND EVALUATION COMMAND, ABERDEEN PROVING GROUND, MD.
Test Operation Procedure (TOP): Vibration testing of helicopter equipment
[AD-A284433] p 410 N95-15815
ARMY TOPOGRAPHIC ENGINEERING CENTER, FORT BELVOIR, VA.
Linear estimation of hyperspectral mixed pixel components
[AD-A283893] p 586 N95-15424

ARNOLD ENGINEERING DEVELOPMENT CENTER, ARNOLD AFS, TN.
Optical analysis methods for material films condensed on cryogenic surfaces of spacecraft
[AD-A284014] p 427 N95-14420
ARTIFICIAL REALITY CORP., VERNON, CT.
A two dimensional artificial reality p 560 N95-14052
ATMOSPHERIC AND ENVIRONMENTAL RESEARCH, INC., CAMBRIDGE, MA.
Support of Environmental Requirements for Cloud Analysis and Archive (SERCAA): Algorithm descriptions
[AD-A283240] p 534 N95-15614
ATOMINSTITUT DER OESTERREICHISCHEN HOCHSCHULEN, VIENNA.
Maximum predictive power and the superposition principle p 607 N95-13936
The probabilistic origin of Bell's inequality
p 612 N95-13969
ATRIX LABS., INC., FORT COLLINS, CO.
Development of a moldable, biodegradable polymeric bone repair material
[AD-A283413] p 454 N95-15296
AUBURN UNIV., AL.
Integration/evaluation of a HCI prototyping environment
[NASA-CR-196996] p 566 N95-14107
Hypervelocity Impact Test Facility: A gun for hire
[TABES PAPER 94-605] p 415 N95-14639
Summary of solar cell data from the Long Duration Exposure Facility (LDEF)
[NASA-CR-197069] p 519 N95-14802
Analysis of space environment damage to solar cell assemblies from LDEF experiment A0171-GSFC test plate
[NASA-CR-197066] p 519 N95-14853
Design of power electronics for TVC and EMA systems
[NASA-CR-197067] p 475 N95-14866
X-ray Photoelectron Spectroscopy (XPS), Rutherford Back Scattering (RBS) studies
[NASA-CR-196536] p 439 N95-14867
Experimental analysis of thread movement in bolted connections due to vibrations
[NASA-CR-197065] p 502 N95-14904

B

BATEMAN (PETER J.), CAMBERLY (ENGLAND).
Guidance and control for unmanned ground vehicles
p 504 N95-14948
BATTELLE MEMORIAL INST., COLUMBUS, OH.
Nonlinear fracture mechanics-based analysis of thin wall cylinders p 508 N95-14462
BAYLOR COLL. OF MEDICINE, HOUSTON, TX.
The cardiovascular response to the AGS
p 419 N95-15146
BAYLOR UNIV., WACO, TX.
The quantum measurement of time
p 590 N95-13917
BBN SYSTEMS AND TECHNOLOGIES CORP., CANOGA PARK, CA.
Deriving a dosage-response relationship for community response to high-energy impulsive noise
p 403 N95-14890
BIHRLE APPLIED RESEARCH, INC., JERICHO, NY.
Validation of the NASA Dryden X-31 simulation and evaluation of mechanization techniques
p 394 N95-14236
BILKENT UNIV., ANKARA (TURKEY).
Quantum statistics of Raman scattering model with Stokes mode generation p 610 N95-13958
BOEING AEROSPACE AND ELECTRONICS CO., SEATTLE, WA.
Space transfer vehicle concepts and requirements study. Volume 3: Program cost estimates. Book 2: WBS and dictionary
[NASA-CR-192447] p 419 N95-15552
BOEING CO., SEATTLE, WA.
Full-scale testing and analysis of fuselage structure
p 512 N95-14485
BOEING DEFENSE AND SPACE GROUP, SEATTLE, WA.
The advanced development of x-ray computed tomography applications
[AD-A284211] p 434 N95-14411
Results of the examination of LDEF polyurethane thermal control coatings
[NASA-CR-4617] p 432 N95-14603
BOSTON COLL., CHESTNUT HILL, MA.
Chemical kinetics and atmospheric modification
[AD-A283304] p 524 N95-15623
BOSTON UNIV., MA.
Complementarity and path distinguishability: Some recent results concerning photon pairs
p 598 N95-13961
Auditory interfaces: The human perceiver
p 554 N95-14015
Atmospheric propagation at larger lateral distances from the flight track p 402 N95-14885
Research accomplishments and future goals in particle physics
[DE94-015483] p 596 N95-15537
BRANDEIS UNIV., WALTHAM, MA.
Intersensory coordination p 555 N95-14020
BRIGHAM AND WOMEN'S HOSPITAL, BOSTON, MA.
Developing Guided Search 3.0. The next generation of a model visual search
[AD-A283956] p 552 N95-14369
BROOKHAVEN NATIONAL LAB., UPTON, NY.
Specifying the surface finish of x ray mirrors
[DE94-013537] p 601 N95-13644
Evolution of wave function in a dissipative system
p 610 N95-13959
Study of the long term stability of the effective concentration of ionized space charges (N(sub eff)) of neutron irradiated silicon detectors fabricated by various thermal oxidations
[DE94-013734] p 593 N95-14309
Practical aspects of corrosion fundamentals
[DE94-015842] p 438 N95-14371
Ferromagnetic grain boundary signature in die-upset RE-Fe-B magnets
[DE94-014904] p 590 N95-14440
Observation of diffraction effects in positron channeling
[DE94-014909] p 594 N95-14441
Defect profiling in elemental and multilayer systems: Correlations of fitted defect concentrations with positron implantation profiles
[DE94-015844] p 624 N95-15422
Dynamic response of rigid tanks with inhomogeneous liquids
[DE94-012619] p 493 N95-15571
Dynamical impurity problems
[DE94-013025] p 625 N95-15576
A relativistic cascade for heavy ion collisions
[DE94-015846] p 600 N95-15633
Development and testing of a high-resolution model for tropospheric sulfate driven by observation-derived meteorology
[DE94-014910] p 525 N95-15864
BROWN UNIV., PROVIDENCE, RI.
Experimental study of chemical, phase and textural equilibrium of high TiO2 mare basalts and peridotite
[NASA-CR-196480] p 645 N95-13724
Behavior of charring materials in simulated fire environments
[PB94-196045] p 439 N95-14838
The principles of fault-tolerant and efficient parallel computation
[AD-A283254] p 579 N95-15616
Fault-tolerance and efficiency in massively parallel algorithms
[AD-A283255] p 579 N95-15617
BUNKA WOMEN'S UNIV. (JAPAN).
Effects of 20 days bed-rest on cardio-respiratory functions during sub-maximal exercise in young women
p 545 N95-15111
BUREAU GRAVIMETRIQUE INTERNATIONAL, TOULOUSE (FRANCE).
The Bureau Gravimetrique International
p 516 N95-15795

C

CAE-LINK CORP., HOUSTON, TX.
Ada 9X overview p 570 N95-14166
CALGARY UNIV. (ALBERTA).
Correlation between molecular lines and diffuse interstellar bands p 640 N95-15835
CALIFORNIA INST. OF TECH., PASADENA, CA.
ASSERT-1992. Fundamental studies of a high energy molecular system: Spectroscopy of boron in hydrogen clusters
[AD-A283181] p 593 N95-14155
Surface processes in CVD diamond growth
[AD-A280964] p 622 N95-14655
Interaction of chemistry, turbulence, and shock waves in hypervelocity flow
[AD-A282941] p 400 N95-14656
Electron-molecule collisions and UV signatures in flowfields
[AD-A281569] p 596 N95-15457
CALIFORNIA POLYTECHNIC STATE UNIV., SAN LUIS OBISPO, CA.
Coordination of human upper arm and forearm motion in rapid extensions p 561 N95-14056
Numerical design of advanced multi-element airfoils
[NASA-CR-197135] p 404 N95-15762
CALIFORNIA STATE UNIV., FULLERTON, CA.
Porphyrins in the interstellar medium (in grains)
p 640 N95-15837
CALIFORNIA UNIV., BERKELEY, CA.
A loophole-free Bell's inequality experiment
p 611 N95-13988
Eye movement control and top-down scanpath vision as a design metaphor for robotic vision and control
p 555 N95-14022
Varieties of virtualization p 557 N95-14036
Development of visual 3D virtual environment for control software p 559 N95-14048
Summary of activities for University of California
[AD-A283890] p 632 N95-15423
CALIFORNIA UNIV., BERKELEY. LAWRENCE BERKELEY LAB, CA.
Ion beam synthesis of SiGe alloy layers
[DE94-014958] p 620 N95-14189
Searches for massive neutrino emission in C-14 beta and Fe-55 electron-capture decays
[DE94-016863] p 594 N95-14374
AEM and HREM evaluation of carbon nanostructures in silica aerogels
[DE94-014913] p 434 N95-14387
Hadronic matter and rapidly rotating compact stars
[DE94-014928] p 643 N95-14442
Equilibrium fluid interface behavior under low- and zero-gravity conditions p 484 N95-14534
A new procedure for measuring contact angle
[DE94-014971] p 457 N95-14659
Low-frequency noise in high-(Tc) superconductor Josephson junctions, SQUIDs, and magnetometers
[DE94-016873] p 623 N95-15337
Resonant tunneling in small current-biased Josephson junctions
[DE94-016875] p 623 N95-15338
Photoluminescence spectroscopy and Rutherford backscattering channeling evaluation of various capping techniques for rapid thermal annealing of ion-implanted ZnSe
[DE94-016876] p 623 N95-15339
Accelerator and Fusion Research Division: 1993 Summary of activities
[DE94-015157] p 599 N95-15367
Charge collection in a-Si:H/a-Si(1-x)C(x multilayers photodetectors
[DE94-013107] p 625 N95-15577
Studies in chaotic adiabatic dynamics
[DE94-013111] p 627 N95-15578
One: Redox chemistry of bimetallic fulvalene complexes. 2: Oligocyclopentadienyl complexes
[DE94-014930] p 443 N95-15667
Topics in the structure of hadronic systems
[DE94-014924] p 597 N95-15865
The crosswell electromagnetic response of layered media
[DE94-014929] p 470 N95-15866
Two methods for the study of vortex patch evolution on locally refined grids
[DE94-014965] p 494 N95-15867
Phase transitions and connectivity in three-dimensional vortex equilibria
[DE94-014967] p 494 N95-15868
CALIFORNIA UNIV., DAVIS, CA.
Some genetic aspects of adaptation to hyperdynamic environments p 543 N95-15100
The regulation of rat activity following exposure to hyperdynamic fields p 539 N95-15133
CALIFORNIA UNIV., IRVINE, CA.
Visual motion perception and visual information processing
[AD-A282928] p 581 N95-14847
Damping mechanisms in nanostructured materials
[AD-A283583] p 623 N95-15317
CALIFORNIA UNIV., LA JOLLA, CA.
Adaptation of skeletal muscle to spaceflight: Cosmos rhesus project. Cosmos 2044 and 2229
[NASA-CR-197041] p 537 N95-14796
CALIFORNIA UNIV., LOS ANGELES, CA.
Measurement and modification of the EEG and related behavior p 557 N95-14038
Nonlinear and stochastic numerical methods and their applications
[AD-A284863] p 588 N95-14370
Stabilization of thermocapillary convection by means of nonplanar flow oscillations p 482 N95-14524
Ground based studies of thermocapillary flows in levitated drops p 486 N95-14545
Microgravity foam structure and rheology
p 459 N95-14568
CALIFORNIA UNIV., SAN DIEGO, LA JOLLA, CA.
Electrodeposition of conductors and semiconductors with controlled stoichiometries and morphologies
[AD-A280743] p 437 N95-14141

Center for advanced materials of high quality dynamic performance (fellowships)
[AD-A281377] p 434 N95-14360

CALIFORNIA UNIV., SANTA BARBARA, CA.
Active localization of virtual sounds p 561 N95-14054
In situ grown quantum-wire lasers
[AD-A281381] p 499 N95-14364

CALSPAN CORP., ARNOLD AFS, TN.
The AEDC aerospace chamber 7V: An advanced test capability for infrared surveillance and seeker sensors p 418 N95-14097

CAMBRIDGE UNIV., CAMBRIDGE (ENGLAND).
Designing in three dimensions p 480 N95-14130

CANADIAN SPACE AGENCY, OTTAWA (ONTARIO).
David Florida Laboratory Thermal Vacuum Data Processing System p 418 N95-14079

CANADIAN SPACE AGENCY, SAINT HUBERT (QUEBEC).
Control and operation of space manipulator systems p 582 N95-14946

CARNEGIE-MELLON UNIV., PITTSBURGH, PA.
Preparation of well defined polystyrene-block-poly (methylphenylsilylene) copolymers
[AD-A280799] p 450 N95-14304
Introduction of living polymerization. Living and/or controlled polymerization
[AD-A280800] p 451 N95-14305
Radical polymerization of vinyl acetate and methyl methacrylate using organochromium initiators complexed with macrocyclic polyamines
[AD-A280828] p 451 N95-14316
Radical polymerization of vinyl acetate in the presence of trialkyl phosphites
[AD-A280829] p 451 N95-14324
Toward deriving software architectures from quality attributes
[AD-A283827] p 572 N95-14339
Computing quantitative characteristics of finite-state real-time systems
[AD-A282839] p 412 N95-14343
Benefits of CMM-based software process improvement: Initial results
[AD-A283848] p 572 N95-14349
Synthesis of well defined polymers by radical polymerization
[AD-A280830] p 452 N95-14395
Modifications of polysilanes and polysilane copolymers
[AD-A280839] p 452 N95-14398
Ring-opening polymerization of strained cyclotetrasilanes as a new route towards well defined polysilylenes
[AD-A280840] p 452 N95-14399
Polysilanes with various architectures
[AD-A280842] p 452 N95-14400
Microscale hydrodynamics near moving contact lines p 484 N95-14536
Transport phenomena in stratified multi-fluid flo w in the presence and absence of gravity p 488 N95-14563
Electrokinetic transport of heterogeneous particles in suspension p 444 N95-14581
Variable window Gabor filters and their use in focus and correspondence
[AD-A282837] p 573 N95-14842

CASE WESTERN RESERVE UNIV., CLEVELAND, OH.
The study of dopant segregation behavior during the growth of GaAs in microgravity p 458 N95-14215
Gravity-dependent transport in industrial processes p 459 N95-14580
Transport and nucleation processes during the vapor growth of diamond
[AD-A284411] p 626 N95-15812

CASTLE TECHNOLOGY CORP., WOBURN, MA.
Oxidation resistant coating for carbon-carbon composites at ultra-high temperatures
[AD-A283323] p 456 N95-15624

CD RADIO, INC., WASHINGTON, DC.
S-Band propagation measurements p 466 N95-14682

CENTER FOR ENGINEERING APPLICATIONS, MEMPHIS, TN.
Man-machine interfaces in health care p 556 N95-14029

CENTRE D'ENSEIGNEMENT ET DE RECHERCHES DE MEDECINE AERONAUTIQUE, BRETIGNY (FRANCE).
Modeling and numerical simulation of the cerebral blood flow under acceleration p 545 N95-15112
Enhancement of insulin receptor mediated endocytosis in cultured osteoblastic cells under hypergravity p 539 N95-15148

CENTRE NATIONAL DE LA RECHERCHE SCIENTIFIQUE, ECULLY (FRANCE).
Numerical model for the weakly nonlinear propagation of sound through turbulence p 401 N95-14883

CENTRE NATIONAL DE LA RECHERCHE SCIENTIFIQUE, PARIS (FRANCE).
Alterations of body temperature, feeding, drinking and sleep-wake circadian rhythms in Rhesus monkey during a 19 day Spacelab flight simulation p 539 N95-15132

CERB, BAUGY (FRANCE).
Twenty four hours head-down tilt decreases arterial baroreflex function in conscious rat p 538 N95-15098

CHICAGO UNIV., CHICAGO, IL.
Towards the molecular design of composite materials
[AD-A283422] p 627 N95-15404

CHRISTOPHER NEWPORT COLL., NEWPORT NEWS, VA.
SODR Memory Control Buffer Control ASIC
[NASA-CR-197001] p 566 N95-14514

CHUNGBUK NATIONAL UNIV. (REPUBLIC OF KOREA).
The wave function and minimum uncertainty function of the bound quadratic Hamiltonian system p 608 N95-13943

CINCINNATI UNIV., OH.
Atmospheric and wind modeling for ATC
[NASA-CR-196786] p 532 N95-13725
Assessment of CTAS ETA prediction capabilities
[NASA-CR-197224] p 497 N95-15728
Groundspeed filtering for CTAS
[NASA-CR-197223] p 497 N95-15785

CITY COLL. OF THE CITY UNIV. OF NEW YORK, NY.
Further evidence for the EPNT assumption p 611 N95-13962
Wetting and spreading at the molecular scale p 484 N95-14539
Modern methods in meteorological and oceanographic data acquisition and analyses
[AD-A283038] p 533 N95-14848

CIVIL AEROMEDICAL INST., OKLAHOMA CITY, OK.
Age 60 Rule. Part 3: Consolidated database experiments
[DOT/FAA/AM-94/22-PT-3] p 551 N95-13715

CLARKSON UNIV., POTSDAM, NY.
The breakup of a liquid jet at microgravity p 484 N95-14535

CLEMSON UNIV., SC.
Polyhedral approaches for solving 0-1 polynomial programming problems
[AD-A282448] p 575 N95-15549

CLEVELAND STATE UNIV., OH.
Electrical characterization of 6H crystalline silicon carbide
[NASA-CR-197047] p 439 N95-14903

COASTAL ENGINEERING RESEARCH CENTER, VICKSBURG, MS.
Selecting wave gauge sites for monitoring harbor oscillations: A case study for Kahului Harbor, Hawaii
[AD-A281707] p 536 N95-15452

COLBY COLL., WATERVILLE, ME.
Supersymmetry and radial squeezed states for Rydberg wave packets p 598 N95-13898

COLORADO STATE UNIV., FORT COLLINS, CO.
Discrete-layer piezoelectric plate and shell models for active tip-clearance control
[NASA-CR-195383] p 507 N95-14417
June to September rainfall in the African Sahel: Verification of cur 1994 forecasts and an extended range forecast for 1995, 3
[TR-521] p 534 N95-15666

COLORADO UNIV., BOULDER, CO.
Commercial investigation results for the generic bioprocessing apparatus flown on United States Microgravity Laboratory-1 p 538 N95-14227
Global surface-based cloud observation for ISCCP
[NASA-CR-196990] p 532 N95-14265
Multilayer fluid dynamics of immiscible liquids p 483 N95-14532
Phase segregation due to simultaneous migration and coalescence p 484 N95-14537
Electrophoretic interactions and aggregation of colloidal biological particles p 444 N95-14578
A bibliography of papers on the diffuse interstellar bands p 634 N95-15846

COLUMBIA UNIV., NEW YORK, NY.
The electromagnetic spectrum. Research investigation directed toward extending the useful range of the electromagnetic spectrum
[AD-A281378] p 461 N95-14361

COMMISSARIAT A L'ENERGIE ATOMIQUE, GRENOBLE (FRANCE).
Mass transport phenomena in microgravity: Preliminary results of the first MEPHISTO flight experiment p 634 N95-14209

COMMUNICATIONS RESEARCH CENTRE, OTTAWA (ONTARIO).
Ground wave and diffraction, A p 467 N95-14828
Ground wave and diffraction, B p 467 N95-14829

COMPENGSERV LTD., OTTAWA (ONTARIO).
Machine intelligence: The key to guidance and control in robotics p 581 N95-14944

COMPUTER SCIENCES CORP., FALLS CHURCH, VA.
Parallel isosurface generator for huge data sets
[AD-A284030] p 578 N95-14422
Distributed heterogeneous visualization, BOP (Bag-O-Polygons) and BOP view
[AD-A284393] p 567 N95-15809

CORNELL UNIV., ITHACA, NY.
Hybrid verification by exploiting the environment
[NASA-CR-195810] p 568 N95-13699
Influence of flow on interface shape stability in low gravity p 484 N95-14538
Adsorption and diffusion of fluids in well-characterized adsorbent materials
[DE94-016953] p 454 N95-15344
Defects and transport in mixed oxides
[DE94-015652] p 454 N95-15358
Investigation of the coherent synchrotron radiation spectrum as a probe of charge dynamics
[DE94-015340] p 599 N95-15371
Theory of nonlinear, distortive phenomena in solids: Martensitic, crack, and multiscale structures-phenomenology and physics
[DE94-015653] p 447 N95-15631

CREARE, INC., HANOVER, NH.
An application of miniscale experiments on Earth to refine microgravity analysis of adiabatic multiphase flow in space p 459 N95-14567

CRYOPOWER ASSOCIATES, LOS ALAMOS, NM.
High temperature superconductors with improved current densities
[AD-A282996] p 472 N95-13685

CYBERNET SYSTEMS CORP., ANN ARBOR, MI.
Implementation issues for a compact 6 degree of freedom force reflecting handcontroller with cueing of modes p 560 N95-14050

D

DANISH AEROSPACE MEDICAL CENTER OF RESEARCH, COPENHAGEN (DENMARK).
Gravitational stress and regulation of neuroendocrine elements and fluid volume in humans p 542 N95-15090

DARTMOUTH COLL., HANOVER, NH.
Troposcatter at the KU band
[AD-A281575] p 469 N95-15462

DAVID SARNOFF RESEARCH CENTER, PRINCETON, NJ.
High performance YBCO films
[AD-A283870] p 451 N95-14354

DAYTON UNIV., OH.
Effects of thermocapillarity on an evaporating extended meniscus in microgravity p 488 N95-14559
Distance estimation training with night vision goggles: A preliminary study
[AD-A284900] p 563 N95-15755

DAYTON UNIV. RESEARCH INST., OH.
Evaluation of reformulated thermal control coatings in a simulated space environment. Part 1: YB-71 p 420 N95-14063

DECISION-SCIENCE APPLICATIONS, INC., ARLINGTON, VA.
Graphical aids for the users of GEMACS (GAUGE): Ray tracing enhancements
[AD-A284903] p 470 N95-15756

DEFENCE METALLURGICAL RESEARCH LAB., HYDERABAD (INDIA).
Symposium on Structural Intermetallics: Perspectives on Science and Technology, volume 2
[AD-A283379] p 447 N95-15874

DEFENCE RESEARCH AGENCY, FARNBOROUGH, HAMPSHIRE (ENGLAND).
A method of calculating the safe fatigue life of compact, highly-stressed components p 509 N95-14464

DEFENCE RESEARCH AGENCY, MALVERN (ENGLAND).
Propagation in the ionosphere, A p 466 N95-14826
Propagation in the ionosphere, B p 467 N95-14827

DEFENSE INFORMATION SYSTEMS AGENCY, ARLINGTON, VA.
Department of Defense technical architecture framework for information management. Volume 1: Overview, version 2.0
[AD-A283763] p 631 N95-14327
Department of Defense technical architecture framework for information management. Volume 2: Technical reference model and standards profile summary
[AD-A283764] p 631 N95-14329
Department of Defense technical architecture framework for information management. Volume 3: Architecture concepts and design guidance, version 2.0
[AD-A283765] p 631 N95-14330

Department of Defense technical architecture framework for information management. Volume 4: DOD standards-based architecture planning guide, version 2.0
[AD-A283766] p 631 N95-14331
Department of Defense technical architecture framework for information management. Volume 6: Department of Defense (DOD) goal security architecture, version 2.0
[AD-A283767] p 631 N95-14332
Department of Defense technical architecture framework for information management. Volume 8: Department of Defense HCI style guide, version 2.0
[AD-A283768] p 631 N95-14333

DELAWARE UNIV., NEWARK, DE.
Surfactant-based critical phenomena in microgravity
p 459 N95-14579

DENVER UNIV., DENVER, CO.
Condensation nuclei measurement in the stratosphere for the NASA ACE program
[NASA-CR-197031] p 530 N95-14855
Counting condensation in the Antarctic Ozone Mission
[NASA-CR-197113] p 525 N95-15847

DEPARTMENT OF ENERGY, WASHINGTON, DC.
Energy review
[DE94-015828] p 518 N95-14326

DEPARTMENT OF THE NAVY, WASHINGTON, DC.
Torsional shear wave transducer
[AD-D016347] p 496 N95-14841
Slave controller for effecting a block transfer of sixteen bit words between a memory and a data transfer bus
[AD-D016463] p 574 N95-15336
Method and apparatus for polarization-maintaining fiber optical amplification with orthogonal polarization output
[AD-D016365] p 614 N95-15707
Low-damage multilayer mirror for the soft x ray region
[AD-D016362] p 614 N95-15764
Apparatus for imaging an object in or through a scattering medium using coherent anti-Stokes Raman scattering
[AD-D016366] p 615 N95-15765
Low loss glass and optical fibers therefrom
[AD-D016379] p 615 N95-15766
Transducers and methods for making same
[AD-D016349] p 497 N95-15799
Surface epoxidation of elastomers
[AD-D016352] p 456 N95-15800

DEUTSCHE AEROSPACE A.G., MUNICH (GERMANY).
X-31 quasi-tailless flight demonstration
p 395 N95-14243
Aeromechanical design of modern missiles
p 399 N95-14446

DEUTSCHE FORSCHUNGS- UND VERSUCHSANSTALT FUER LUFT- UND RAUMFAHRT, BRUNSWICK (GERMANY).
Parameter identification for X-31A at high angles of attack p 394 N95-14235

DEUTSCHE FORSCHUNGS- UND VERSUCHSANSTALT FUER LUFT- UND RAUMFAHRT, COLOGNE (GERMANY).
Review of European microgravity measurements
p 457 N95-14211

DEUTSCHE GESELLSCHAFT FUER LUFT- UND RAUMFAHRT, COLOGNE (GERMANY).
Orthostatic stress by lower body negative pressure and its body fluid distribution kinetics under microgravity
p 549 N95-15138

DEUTSCHE SPORTHOCHSCHULE, COLOGNE (GERMANY).
Effects of microgravity on interstitial muscle receptors affecting heart rate and blood pressure during static exercise p 548 N95-15137

DIRECTION DES RECHERCHES, ETUDES ET TECHNIQUES, PARIS (FRANCE).
Computing illumination using extended sources: Object space and image space
[PB94-201282] p 612 N95-13992

DUKE UNIV., DURHAM, NC.
Bloch vector projection noise p 610 N95-13956
Infrared/submillimeter wave studies of molecular collision kinetics
[AD-A281379] p 594 N95-14362

E

ECLECTIC, INC., OAK RIDGE, TN.
Leak detection by acoustic emissions monitoring: An experimental investigation of the acoustic properties of leaks and the attenuation characteristics of soil
[AD-A283250] p 530 N95-15295

ECOLE NORMALE SUPERIEURE, PARIS (FRANCE).
Quantum chemistry and excited states: First investigations on pyrene-like molecules
p 599 N95-15844

ECOLE POLYTECHNIQUE, MONTREAL (QUEBEC).
Understanding squeezing of quantum states with the Wigner function p 606 N95-13930

EDGERTON, GERMESHAUSEN AND GRIER, INC., ALBUQUERQUE, NM.
Blast overpressure studies with animals and man
[AD-A280435] p 540 N95-13971

EDINBURGH UNIV. (SCOTLAND).
A physical control interface with proprioceptive feedback and multiple degrees of freedom p 559 N95-14045
On the affinities of lambda 5778 and other broad diffuse interstellar bands p 639 N95-15832

EG AND G ENERGY MEASUREMENTS, INC., IDAHO FALLS, ID.
Automatic TLI recognition system, part 1
[DE94-015253] p 578 N95-15434
FFCAat Clearinghouse, directory of abstracts
[DE94-015259] p 632 N95-15435
A theoretical study of 30 to 50 angstrom noble gas heavy ion lithography
[DE94-015262] p 442 N95-15436
Results of TSP metals monitoring at McMurdo Station, Antarctica
[DE94-015264] p 524 N95-15455
Tests of a homogeneous Poisson process against clustering and other alternatives
[DE94-015382] p 588 N95-15533
Automatic TLI recognition system, part 2
[DE94-015393] p 579 N95-15534

EG AND G MOUND APPLIED TECHNOLOGIES, MIAMISBURG, OH.
Burn rates of TiH2/KClO4/Viton and output testing of NASA SKD26100098-301 pressure cartridges
[NASA-CR-188357] p 443 N95-15715

EIDETICS AIRCRAFT, INC., TORRANCE, CA.
Static and dynamic force/moment measurements in the Eidetics water tunnel p 395 N95-14238
Combat Agility Management System (CAMS)
p 397 N95-14250
F/A-18 and F-16 forebody vortex control, static and rotary-balance results p 397 N95-14254

ELORET CORP., PALO ALTO, CA.
Development and application of structural dynamics analysis capabilities
[NASA-CR-197229] p 513 N95-14922

EMR-PHOTOELECTRIC, PRINCETON, NJ.
First Year PIDDP Report on gamma-ray and x-ray spectroscopy: X-ray remote sensing and in situ spectroscopy for planetary exploration missions and gamma-ray remote sensing and in situ spectroscopy for planetary exploration missions
[NASA-CR-189374] p 517 N95-15916

ENERGY, MINES AND RESOURCES CANADA, OTTAWA (ONTARIO).
Geodetic survey of Canada: Results on a geoid questionnaire p 516 N95-15793

ENERGY TECHNOLOGY DATA EXCHANGE, OAK RIDGE, TN.
International energy: Research organizations, 1988-1992
[DE90-017267] p 630 N95-13726

ENGINEERING SOFTWARE RESEARCH AND DEVELOPMENT, INC., SAINT LOUIS, MO.
Elastic-plastic models for multi-site damage
p 507 N95-14454

ENHANCED TECHNOLOGIES, HOUSTON, TX.
A simulation facility for testing Space Station assembly procedures p 423 N95-14075

ENSR CONSULTING AND ENGINEERING, FLORENCE, AL.
Recycled plastic: A clean and low cost rocket fuel
[TABES PAPER 94-610] p 416 N95-14642
Comprehensive facility decommissioning through the use of innovative technology to reduce cost, schedule, and environmental liability
[TABES PAPER 94-615] p 416 N95-14644

ENVIRONMENTAL PROTECTION AGENCY, CINCINNATI, OH.
Emerging technology summary: Destruction of organic contaminants in air using advanced ultraviolet flashlamps
[PB94-194479] p 521 N95-14121

ENVIRONMENTAL PROTECTION AGENCY, RESEARCH TRIANGLE PARK, NC.
Photochemical urban airshed modeling using diagnostic and dynamic meteorological fields
[PB94-176120] p 616 N95-13973
Fuzzy logic motor control for pollution prevention and improved energy efficiency
[PB94-190865] p 523 N95-14403
PC-based MIE scattering program for theoretical investigations of the optical properties of atmospheric aerosols as a function of composition and relative humidity
[PB94-192739] p 529 N95-14404

ENVIRONMENTAL PROTECTION AGENCY, WASHINGTON, DC.
EMAP Information Management Strategic Plan, 1993-1997
[PB94-176823] p 522 N95-14124

EUROPEAN NUCLEAR AGENCY, ROME (ITALY).
Phase-space analysis of charged and optical beam transport: Wigner rotation angle p 606 N95-13927

EUROPEAN NUCLEAR ENERGY AGENCY, FRASCATI (ITALY).
Multivariable Hermite polynomials and phase-space dynamics p 606 N95-13929

EUROPEAN SPACE AGENCY. EUROPEAN SPACE RESEARCH AND TECHNOLOGY CENTER, ESTEC, NOORDWIJK (NETHERLANDS).
HYDRA, a new tool for mechanical testing
p 418 N95-14086
Olympus propagation experiments
p 464 N95-14671
Channel characterisation for future Ka-band Mobile Satellite Systems and preliminary results
p 465 N95-14676

EXECUTIVE OFFICE OF THE PRESIDENT, WASHINGTON, DC.
Reengineering through information technology. Accompanying report of the National Performance Review
[PB94-170362] p 633 N95-15781

EXOS, INC., LEXINGTON, MA.
Human-machine interface hardware: The next decade
p 561 N95-14055

F

FAIRCHILD SPACE CO., GERMANTOWN, MD.
Evolutionary Telemetry and Command Processor (TCP) architecture p 420 N95-14162

FEDERAL AVIATION ADMINISTRATION, ATLANTA, GA.
Test and Evaluation Master Plan (TEMP) for Fixed Ground Antenna Radomes (FGAR)
[AD-A283839] p 461 N95-14346

FEDERAL AVIATION ADMINISTRATION, ATLANTIC CITY, NJ.
Proceedings of the FAA Inspection Program Area Review
[AD-A283849] p 405 N95-14350

FEDERAL AVIATION ADMINISTRATION, CAMBRIDGE, MA.
Inspecting for widespread fatigue damage: Is partial debonding the key? p 508 N95-14458
Nonlinear bulging factor based on R-curve data
p 511 N95-14476

FEDERAL AVIATION ADMINISTRATION, KANSAS CITY, MO.
Fatigue evaluation of empennage, forward wing, and winglets/tip fins on part 23 airplanes
[PB94-196813] p 408 N95-13981

FEDERAL AVIATION ADMINISTRATION, OKLAHOMA CITY, OK.
The applicability of commercial glare test devices in the aeromedical certification of pilot applicants
[DOT/FAA/AM-94/15] p 540 N95-14176
Unreported medications used in incapacitating medical conditions found in fatal civil aviation accidents
[DOT/FAA/AM-94/14] p 540 N95-14177
Summary Proceedings of the Joint Industry-FAA Conference on the Development and use of PC-Based Aviation Training Devices
[DOT/FAA/AM-94/25] p 573 N95-14917

FERMI NATIONAL ACCELERATOR LAB., BATAVIA, IL.
Measurement of the B cross section at CDF via B semileptonic decays
[DE94-013842] p 593 N95-13680
Recent QCD results from the Tevatron (-p)p collider at the square root of s = 1.8 TeV
[DE94-014986] p 594 N95-14661
Production properties of Z bosons with jets in 1.8 TeV (anti p)p collisions
[DE94-015184] p 595 N95-15301
A high speed, wide dynamic range digitizer circuit for photomultiplier tubes
[DE94-015187] p 475 N95-15302
Xwake 1.0: A new tool for wakefield and impedance calculations
[DE94-015545] p 574 N95-15418
Fluorescent compounds for plastic scintillation applications
[DE94-013235] p 497 N95-15580
Data flow manager for DART
[DE94-013236] p 579 N95-15581
Electroweak and b-physics at the Tevatron collider
[DE94-013239] p 600 N95-15582
Electroweak boson pair production at CDF
[DE94-015183] p 597 N95-15629

Search for W(prime) (yields) e(nu) in p(anti p) collisions at (radical)s = 1,800 GeV
[DE94-015188] p 597 N95-15630
Studies of quarkonia production with CDF
[DE94-013220] p 597 N95-15862

FIELDS (JAMES M.), SILVER SPRING, MD.
Residents' reactions to long-term sonic boom exposure: Preliminary results p 403 N95-14892

FISH AND WILDLIFE SERVICE, ONALASKA, WI.
Development of a systemic land cover/land use database for the Upper Mississippi River System derived from Landsat Thematic Mapper satellite data. Long term resource monitoring program
[PB94-186889] p 515 N95-14793

FLORENCE UNIV. (ITALY).
Q-derivatives, coherent states and squeezing p 589 N95-13901

FLORIDA ATLANTIC UNIV., BOCA RATON, FL.
Florida's propagation report p 466 N95-14684

FLORIDA INST. OF TECH., MELBOURNE, FL.
Florida hurricanes and tropical storms 1871-1993: An historical survey
[PB94-198017] p 532 N95-14120
Development of the chick's auditory ossicle, the columella p 539 N95-15115
Neuronal types in the chicken's statoacoustic ganglion p 539 N95-15116
Structure of avian tectorial, otolithic and cupular membranes p 539 N95-15117
Electronic characterization of defects in narrow gap semiconductors
[NASA-CR-197217] p 626 N95-15752

FLORIDA SEA GRANT COLL., GAINESVILLE, FL.
Florida hurricanes and tropical storms 1871-1993: An historical survey
[PB94-198017] p 532 N95-14120

FLORIDA STATE UNIV., TALLAHASSEE, FL.
Stochastic model of the residual acceleration environment in microgravity p 459 N95-14540

FLORIDA UNIV., GAINESVILLE, FL.
Destabilizing effects of visual environment motions simulating eye movements or head movements p 562 N95-14061
Design of components for the NASA OCEAN project
[NASA-CR-197207] p 535 N95-14906

FOREST SERVICE, NEW ORLEANS, LA.
Forest cover from Landsat Thematic Mapper data for use in the Catahoula Ranger District Geographic Information System
[PB94-203056] p 515 N95-14125

FORSCHUNGSINSTITUT FUER OPTIK, TUEBINGEN (GERMANY).
Electro-optics: Propagation from IR to UV and sensor considerations. Part A: Propagation theory p 467 N95-14833
Electro-optics: Propagation from IR to UV and sensor considerations. Part B: Tools for exploitation of propagation conditions and system range performance p 467 N95-14834

FOSTER-MILLER ASSOCIATES, INC., WALTHAM, MA.
Lunar base heat pump
[NASA-CR-188356] p 492 N95-14869

FRACTURESEARCH, INC., GALENA, OH.
Testing and analysis of flat and curved panels with multiple cracks p 508 N95-14460

FUEL CELL ENGINEERING CORP., DANBURY, CT.
MCFC Product Development Test
[DE94-014334] p 518 N95-14143

FUJITA HEALTH UNIV., TOYOHASHI (JAPAN).
Postural control of fish related to gravity input p 539 N95-15118

G

GALAXY SCIENTIFIC CORP., PLEASANTVILLE, NJ.
Artificial intelligence with applications for aircraft
[DOT/FAA/CT-94/41] p 581 N95-13895

GENERAL ATOMICS CO., SAN DIEGO, CA.
Advanced tokamak research on the D3-D tokamak
[DE94-015860] p 617 N95-14428

GENERAL ATOMICS TECHNOLOGIES CORP., SAN DIEGO, CA.
Divertor bias experiments
[DE94-015720] p 617 N95-14328
Uniform hydrogen fuel layers for inertial fusion targets by microgravity p 459 N95-14547
The effect of the edge current density on confinement and kink mode stability in H-mode and VH-mode discharges
[DE94-015719] p 618 N95-15632

GENERAL ELECTRIC CO., CINCINNATI, OH.
Elements of a modern turbomachinery design system p 480 N95-14129
The role of CFD in the design process p 481 N95-14135

GENERAL ELECTRIC CO., SCHENECTADY, NY.
Analysis of welding-induced residual stresses with the ADINA system
[DE94-015359] p 506 N95-14320
Representation and recognition with algebraic invariants and geometric constraint models
[AD-A282926] p 585 N95-14843
Ru2Ge3: Crystal growth and some properties
[DE94-015360] p 625 N95-15531
Stress corrosion crack tip microstructure in nickel-based alloys
[DE94-015362] p 446 N95-15532

GENSYM CORP., THE WOODLANDS, TX.
Expert systems in the process industries p 571 N95-14169

GEORGE MASON UNIV., FAIRFAX, VA.
Phase space flow of particles in squeezed states p 606 N95-13928

GEORGIA INST. OF TECH., ATLANTA, GA.
Two-dimensional signal processing, optical information storage and processing, and electromagnetic measurements
[AD-A281937] p 460 N95-13657
Investigation of the effects of long duration space exposure on active optical system components
[NASA-CR-4632] p 601 N95-13660
Fracture mechanics validity limits p 511 N95-14480
Control of oscillatory thermocapillary convection in microgravity p 483 N95-14525
The behavior of unsteady thermocapillary flows p 483 N95-14530
Blocking reduction of Landsat Thematic Mapper JPEG browse images using optimal PSNR estimated spectra adaptive postfiltering p 565 N95-14589
Numerical study of the effects of icing on viscous flow over wings
[NASA-CR-197102] p 400 N95-14803
High temperature membranes for H2S and SO2 separations
[DE94-017125] p 441 N95-15345
Meteorological investigation of ozone anomalies during the Arctic Boundary Layer Experiment (ABLE 3A)
[AD-A284494] p 534 N95-15771

GEORGIA STATE UNIV., ATLANTA, GA.
Observations of hot stars and eclipsing binaries with FRESIP p 644 N95-14508

GEORGIA UNIV., ATHENS.
Theoretical studies of hydrocarbon combustion chemistry
[DE94-017155] p 441 N95-15347

GLAMORGAN UNIV., PONTYPRIDD, GLAMORGAN (WALES).
Comparison of transform coding methods with an optimal predictor for the data compression of digital elevation models p 564 N95-14587

GOETTINGEN UNIV. (GERMANY).
Causality problems for Fermi's two-atom system p 598 N95-13945

GOLDEN PHOTON, INC., GOLDEN, CO.
Module process optimization and device efficiency improvement for stable, low-cost, large-area, cadmium telluride-based photovoltaic module production
[DE94-011817] p 521 N95-15863

GRAZ UNIV. (AUSTRIA).
Comparison of hemodynamic and volume responses to different levels of lower body suction and head-up tilt p 544 N95-15107
Transient blood/plasma density and hematocrit effects after passive (sitting) thermoneutral water immersion in men p 548 N95-15131
Validation of the global digital height model ETOPO5U referring to the Italian model (Italian DEM) p 517 N95-15797

GRUMMAN AEROSPACE CORP., BETHPAGE, NY.
Missile infrared radiation analysis p 399 N95-14449

H

HAMPTON UNIV., VA.
The synthesis of monomers with pendent ethynyl groups for modified high performance thermoplastics
[NASA-CR-196935] p 453 N95-14931

HARVARD COLL. OBSERVATORY, CAMBRIDGE, MA.
Measurements of ultraviolet absorption cross sections of NO2 at various pressures and temperatures
[AD-A283635] p 522 N95-14344

HARVARD MEDICAL SCHOOL, BOSTON, MA.
Are otoconia dynamic in birds and mammals? p 538 N95-15103

HARVARD UNIV., CAMBRIDGE, MA.
The extensional rheology of non-Newtonian materials p 489 N95-14569
Optimization of transparent and reflecting electrodes for amorphous-silicon solar cells
[DE94-011841] p 520 N95-15355

HAWAII UNIV., HONOLULU, HI.
A Lyman-alpha tunable acousto-optic filter for detecting superthermal flare protons
[NASA-CR-197119] p 613 N95-14908

HELSINKI UNIV. OF TECHNOLOGY, ESPOO (FINLAND).
Polarizability properties of bianisotropic spheres with noncomplete magnetoelectric dyadics
[PB94-189065] p 589 N95-13987
Static image theory for a sphere with impedance surface
[PB94-189073] p 590 N95-13988
PHOENIX user manual. First version
[PB94-189081] p 568 N95-13989
Use of 64 kbits/s digital channel for image transmission: Using low scan two-way video
[PB94-189099] p 461 N95-14147
Accelerometer model in APLAC
[PB94-197647] p 497 N95-15413
New five-standard calibration procedures for network analyzers and wafer probes
[PB94-197662] p 478 N95-15611

HELSINKI UNIV. OF TECHNOLOGY, KYLMAELAE (FINLAND).
Observations of extragalactic sources with the Metsaehovi radio telescope at 22-87 GHz
[PB94-197712] p 637 N95-13982

HELSINKI UNIV. OF TECHNOLOGY, OTANIEMI (FINLAND).
Eccentricity of the electron beam in a gyrotron cavity
[PB94-197639] p 496 N95-14839

HERCULES, INC., WILMINGTON, DE.
Milestone 5 test report. Task 5, subtask 5.2: Tile to foam strength tests
[NASA-CR-197241] p 514 N95-15913

HI-Z TECHNOLOGY, INC., LA JOLLA, CA.
Preliminary design of a miniature thermoelectric generator
[AD-A283834] p 518 N95-14341

HOUSTON UNIV., TX.
Laser spectroscopy of combustion intermediates in a supersonic jet expansion
[AD-A283201] p 500 N95-15395

HUGHES STX, INC., GREENBELT, MD.
Global and regional kinematics from SLR stations p 527 N95-14278
Radar altimeter calibration using SLR p 471 N95-14283
Compression of regions in the global advanced very high resolution radiometer 1-km data set p 565 N95-14591
An overview of the EOSDIS V0 information management system: Lessons learned from the implementation of a distributed data system p 566 N95-14596
Neutral gas and diffuse interstellar bands in the LMC p 639 N95-15828

HUGHES STX, INC., LEXINGTON, MA.
Introduction to HEFeS (Hierarchical Environmental Feature Simulator)
[AD-A283244] p 534 N95-15402

HUMBOLDT UNIV., BERLIN (GERMAN D.R.).
Measurement of very small phase fluctuations by means of the operational approach p 605 N95-13916

HUNTSVILLE ASSOCIATION OF TECHNICAL SOCIETIES, AL.
TABES 1994: 10th Annual Technical and Business Exhibition and Symposium p 414 N95-14633

I

IBM FEDERAL SYSTEMS DIV., HOUSTON, TX.
POSIX real-time extensions p 570 N95-14165
Formal methods technology transfer: Some lessons learned p 571 N95-14172

IBM WATSON RESEARCH CENTER, YORKTOWN HEIGHTS, NY.
L(alpha)-induced two-photon absorption of visible light emitted from an O-type star by H2(+) ions located near the surface of the Stromgren sphere surrounding the star: A possible explanation for the diffuse interstellar absorption bands (DIBs) p 641 N95-15845

ILLINOIS INST. OF TECH., CHICAGO, IL.
Processing and characterization of mechanically alloyed NiAl-based alloys
[AD-A283959] p 444 N95-14202
Corrosion-resistant coatings for high-temperature high-sulfur-activity applications
[DE94-015155] p 453 N95-14957

ILLINOIS UNIV., CHAMPAIGN, IL.
Composites with improved compressive properties
[AD-A283411] p 435 N95-15417

ILLINOIS UNIV., URBANA, IL.
A gate level simulator for alpha-particle-induced transient faults
[AD-A283871] p 474 N95-14355

Checkpointing and rollback recovery in distributed shared memory systems
[AD-A281583] p 579 N95-15442
Size and deformation limits to maintain constraint in K(sub Ic) and J(sub c) testing of bend specimens
[AD-A284363] p 514 N95-15802

INDIAN SPACE RESEARCH ORGANIZATION, AHMEDABAD.
Satellite communication technology and applications, 1995-2010 p 413 N95-13826

INDIAN SPACE RESEARCH ORGANIZATION, BANGALORE.
Star sensor for Indian Remote Sensing Satellite (IRS 1C) p 413 N95-13828
Modelling the low Earth space debris environment p 414 N95-13830

INDIAN SPACE RESEARCH ORGANIZATION, TRIVANDRUM.
Computer aided techniques for the realisation of the diaphragm of the PSM for the IRS-1C p 413 N95-13829

INDIANA UNIV.-PURDUE UNIV., INDIANAPOLIS, IN.
Quantum amplification and quantum optical tapping with squeezed states and correlated quantum states p 610 N95-13954

INDUSTRIEANLAGEN-BETRIEBSGESELLSCHAFT M.B.H., OTTOBRUNN (GERMANY).
Thermoacoustic environments to simulate reentry conditions p 426 N95-14096

INFRASENSE, INC., CAMBRIDGE, MA.
Ground penetrating radar surveys to characterize pavement layer thickness variations at GPS sites
[PB94-190170] p 460 N95-14119

INSTITUT DES HAUTES ETUDES SCIENTIFIQUES, BURES-SUR-YVETTE (FRANCE).
Duality theorem in the multivariable Iwasawa theory of local fields
[PB94-192325] p 589 N95-13979
Carnot-caratheodory spaces seen from within
[PB94-195617] p 586 N95-15412

INSTITUTE FOR AEROSPACE RESEARCH, OTTAWA (ONTARIO).
Winter storms research in Canada p 406 N95-14895

INSTITUTE FOR COMPUTER APPLICATIONS IN SCIENCE AND ENGINEERING, HAMPTON, VA.
Efficient bulk-loading of gridfiles
[NASA-CR-194974] p 568 N95-13889
On the evolution of centrifugal instabilities within curved incompressible mixing layers
[NASA-CR-194991] p 495 N95-15917

INSTITUTE FOR PERCEPTION RVO-TNO, SOESTERBERG (NETHERLANDS).
Target acquisition: Human observer performance studies and TARGAC model validation
[AD-A284436] p 553 N95-15816

INSTITUTE OF BIOMEDICAL PROBLEMS, MOSCOW (USSR).
Neurohumoral reactions to long-term vestibular stimulation in man p 542 N95-15091
Changing gravity level and the development of animals p 538 N95-15101
Effect of short- and long-term spaceflight on the contractile properties of rat skeletal muscles with different functions p 539 N95-15141

INSTITUTE OF SOUND AND VIBRATION RESEARCH, SOUTHAMPTON (ENGLAND).
Individual variability in the transmission of vertical vibration from seat to head
[ISVR-TR-236] p 563 N95-15850

INSTITUTE OF THEORETICAL ASTRONOMY, CAMBRIDGE (ENGLAND).
Interactions between solidification and compositional convection in mushy layers p 448 N95-14551

INSTITUTO POLITECNICO NACIONAL, MEXICO CITY.
Manipulation of quantum evolution p 598 N95-13918
On the possibility of a quantum mechanical phase space representation p 606 N95-13931

INTERNATIONAL BUSINESS MACHINES CORP., SAN JOSE, CA.
Screening of charged electrodes in aqueous electrolytes
[AD-A284065] p 474 N95-14425

INTERNATIONAL BUSINESS MACHINES CORP., YORKTOWN HEIGHTS, NY.
Watch what you say, your computer might be listening: A review of automated speech recognition p 555 N95-14021

INTERNATIONAL COMPUTER SCIENCE INST., BERKELEY, CA.
Spatio-temporal neural networks for vision, reasoning and rapid decision making
[AD-A283251] p 583 N95-15403

INTERNATIONAL UNION OF PHYSIOLOGICAL SCIENCES.
The Physiologist, volume 36, number 1, supplement p 541 N95-15089

IOWA UNIV., IOWA CITY, IA.
The mean acoustic field in layered media with rough interfaces
[AD-A281960] p 590 N95-13683
Plasma dust crystallization p 490 N95-14571
Geotail MCA plasma wave data analysis
[NASA-CR-197022] p 618 N95-14798

ISRAEL AIRCRAFT INDUSTRIES LTD., TASHAN (ISRAEL).
Probabilistic inspection strategies for minimizing service failures p 508 N95-14461

ISRAEL INST. OF TECH., HAIFA (ISRAEL).
Uncertainty relations as Hilbert space geometry p 588 N95-13911

ISRO SATELLITE CENTRE, PEENYA, BANGALORE (INDIA).
Journal of Spacecraft Technology, volume 4, no. 2, July 1994 p 413 N95-13825
Remote programming in INSAT-2A/2B on-board Attitude and Orbit Control Computer (AOCC) p 413 N95-13827
A vision based attitude and position estimation algorithm for rendezvous and docking p 414 N95-13831
A simulation algorithm for availability computation of a communication satellite constellation p 414 N95-13832
Deployment mechanism calibration system p 414 N95-13833

ISTITUTO NAZIONALE DI FISICA NUCLEARE, NAPLES (ITALY).
Minimum uncertainty and squeezing in diffusion processes and stochastic quantization p 607 N95-13938
Some rules for polydimensional squeezing p 608 N95-13941
The thermal-wave model: A Schroedinger-like equation for charged particle beam dynamics p 601 N95-13944

ISTITUTO NAZIONALE DI FISICA NUCLEARE, TURIN (ITALY).
Squeezed states and graviton-entropy production in the early universe p 608 N95-13947

ITALL CORP., MERIDIANVILLE, AL.
Design in Huntsville, manufacture in Estonia, sell in Europe
[TABES PAPER 94-607] p 415 N95-14640

J

JET PROPULSION LAB., CALIFORNIA INST. OF TECH., PASADENA, CA.
Multipath noise reduction spread spectrum signals
[NASA-CASE-NPO-18970-1-CU] p 460 N95-13628
Aberration correction of unstable resonators
[NASA-CASE-NPO-18662-1-CU] p 602 N95-13823
Thin composite solid electrolyte film for lithium batteries
[NASA-CASE-NPO-18694-1-CU] p 472 N95-13824
The realuminizing of the 7-meter-diameter solar simulator collimating mirror p 424 N95-14081
Wavelength-division multiplexed optical integrated circuit with vertical diffraction grating
[NASA-CASE-NPO-18357-1-CU] p 612 N95-14181
Heat capacity and thermal relaxation of bulk helium very near the lambda point p 444 N95-14208
Wide field strip-imaging optical system
[NASA-CASE-NPO-18146-2-CU] p 613 N95-14413
Nonlinear dynamics of drops and bubbles and chaotic phenomena p 485 N95-14541
The Telecommunications and Data Acquisition Report
[NASA-CR-196409] p 462 N95-14620
The long-term forecast of station view periods p 419 N95-14621
Spin glasses and error-correcting codes p 462 N95-14624
Linear quadratic Gaussian and feedforward controllers for the DSS-13 antenna p 463 N95-14625
A radio telescope for the calibration of radio sources at 32 gigahertz p 463 N95-14626
The Block V Receiver fast acquisition algorithm for the Galileo S-band mission p 463 N95-14627
Research and development optical deep space antenna sizing study p 463 N95-14628
Pilot retrofit test of refrigerant R-134a for GDSCC p 456 N95-14629
A trajectory preprocessor for antenna pointing p 463 N95-14630
The Network Operations Control Center upgrade task: Lessons learned p 419 N95-14631

LAB. DE MEDECINE AEROSPATIALE
Low-Earth-Orbiter resource allocation and capacity planning for the DSN using LEO4CAST p 419 N95-14632
Proceedings of the Eighteenth NASA Propagation Experimenters Meeting (NAPEX 18) and the Advanced Communications Technology Satellite (ACTS) Propagation Studies Miniworkshop
[NASA-CR-196959] p 464 N95-14670
Propagation characteristics of 20/30 GHz links with a 40 deg masking angle p 464 N95-14672
A database for propagation models p 465 N95-14675

JIKEI UNIV., TOKYO (JAPAN).
Influence to organs by ten weeks tail suspension p 539 N95-15142
Relationship between hind-limb muscle atrophy and serum enzymes in tail suspended rats p 539 N95-15143

JOHNS HOPKINS UNIV., BALTIMORE, MD.
Receiver design, performance analysis, and evaluation for space-borne laser altimeters and space-to-space laser ranging systems
[NASA-CR-197050] p 499 N95-14901
High speed QPPM direct detection optical communication receivers for FSDD intersatellite links
[NASA-CR-189331] p 615 N95-15849

JOHNS HOPKINS UNIV., LAUREL, MD.
Quantum phase uncertainties in the classical limit p 607 N95-13933
ACTS mobile propagation campaign p 465 N95-14677

JOINT INST. FOR NUCLEAR RESEARCH, MOSCOW (USSR).
Properties of two-mode squeezed number states p 602 N95-13897

JOINT TECHNICAL COORDINATING GROUP FOR AIRCRAFT SURVIVABILITY, WRIGHT-PATTERSON AFB, OH.
Bibliography of Joint Aircraft Survivability reports and related documents
[AD-A282795] p 409 N95-14840

K

KAMAN SCIENCES CORP., ALEXANDRIA, VA.
Investigating and implementing enhancements to the simulation of short-term collision hazards p 426 N95-14092
Applications of a fast and efficient method for simulating orbital mission safety p 426 N95-14093

KAROLINSKA INST., STOCKHOLM (SWEDEN).
Manipulating the arterial pressure to prevent G-LOC p 546 N95-15123

KASSEL UNIV. (GERMANY).
Simulation of a spatial, servo-hydraulic test facility for space structures p 418 N95-14095

KEIMYUNG UNIV., TAEGU (REPUBLIC OF KOREA).
Hemodynamic responses to passive body tilts p 542 N95-15096

KENTUCKY UNIV., LEXINGTON, KY.
Evaluation of sensor placement algorithms for on-orbit identification of space platforms p 425 N95-14088
Upward flame spread along the vertical corner walls (October 1993)
[PB94-206299] p 441 N95-15352

KEO CONSULTANTS, BROOKLINE, MA.
Space debris detection and analysis
[AD-A282012] p 428 N95-14951

KINETIC RESEARCH CORP., ANNAPOLIS, MD.
System level mechanical testing of the Clementine spacecraft p 425 N95-14087

KOCHI UNIV., AKEBONO (JAPAN).
Time-dependent variational approach in terms of squeezed coherent states: Implication to semi-classical approximation p 609 N95-13948

KOSSEL (HORST), SHREWSBURY, MA.
Activated buoyancy propulsion = Paradox Power (tm)
[TABES PAPER 94-619] p 405 N95-14646

KRUG LIFE SCIENCES, INC., HOUSTON, TX.
Simulation of the fluid retention effects of a vasopressin analog using the Guyton model of circulation p 547 N95-15130

L

LABORATOIRE DE MEDECINE AEROSPATIALE, BRETIGNY-SUR-ORGE (FRANCE).
A mathematical model of the cardiovascular response to +Gz acceleration p 544 N95-15110
Physiological considerations concerning Positive Pressure Breathing (PBG) during +Gz p 547 N95-15126

LAMONT-DOHERTY GEOLOGICAL OBSERVATORY, PALISADES, NY.
Satellite imagery and topographic data in verification
[AD-A280950] p 530 N95-14598
LAWRENCE LIVERMORE NATIONAL LAB., LIVERMORE, CA.
Energy and Technology Review, April 1994
[DE94-012133] p 496 N95-13669
Project OART: WDM, EDFA's and mixed data rates in a real-world testbed
[DE94-012234] p 601 N95-13670
Developments in ground-penetrating radar at LLNL
[DE94-012236] p 554 N95-13671
Adaptive optics at Lick Observatory: System architecture and operations
[DE94-012387] p 601 N95-13672
Developing molecular dynamics simulation codes using mixed language programming
[DE94-015456] p 571 N95-14190
Design of reliable high voltage avalanche transistor pulsers
[DE94-015323] p 473 N95-14261
DDI, the Data and Dimensions Interface
[DE94-014750] p 522 N95-14317
Double ionization in gases driven by optical field ionization using ultrashort laser pulses
[DE94-015137] p 498 N95-14318
Relativistic configuration-interaction calculation of the correlation energies of heliumlike ions
[DE94-015190] p 621 N95-14325
The console password feature for DEC workstations
[DE94-015721] p 566 N95-14338
Second International Conference on Computer Simulation of Radiation Effects in Solids
[DE94-016368] p 594 N95-14383
ENDL type formats for the LLNL Evaluated Atomic Data Library, EADL, for the Evaluated Electron Data Library, EEDL, and for the Evaluated Photon Data Library, EPDL
[DE94-016487] p 594 N95-14385
Influence of defect shape on laser-induced damage in multilayer coatings
[DE94-016543] p 451 N95-14389
High power diode pumped solid state laser development at Lawrence Livermore National Laboratory
[DE94-015899] p 499 N95-14427
Lithological and rheological constraints on fault rupture scenarios for ground motion hazard prediction
[DE94-014742] p 529 N95-14436
Subsurface object position and image correction for standoff ground penetrating radar
[DE94-015180] p 468 N95-15300
Integrated science model for assessment of climate change
[DE94-016363] p 523 N95-15361
Point based hydrodynamics applied to shallow water equations
[DE94-016629] p 523 N95-15364
Radiation and EMI effects in the NIF environment
[DE94-016635] p 468 N95-15365
Core-level spectroscopy of thin oxides and oxynitrides
[DE94-016598] p 442 N95-15408
What those defects in optical coatings really look like
[DE94-015324] p 614 N95-15529
Comparison of different statistical models of turbulence by similarity methods
[DE94-015326] p 493 N95-15530
Progress report on terrestrial model development (TERRA and HABITAT): Research in support of the CERES earth system modeling project
[DE94-016362] p 524 N95-15779
A comparison of driver concepts for heavy-ion fusion
[DE94-016451] p 600 N95-15780
LEHIGH UNIV., BETHLEHEM, PA.
Corrosion and corrosion fatigue of airframe aluminum alloys p 448 N95-14465
Embedded function methods for compressible high speed turbulent flow
[NASA-CR-196936] p 492 N95-14932
Excimer emission from alkali diatomic and alkaline-earth-noble gas molecules
[AD-A281662] p 596 N95-15446
LEVY (SALOMON), INC., CAMPBELL, CA.
Study of two-phase flow and heat transfer in reduced gravities p 487 N95-14555
LIEGE UNIV. (BELGIUM).
Isolation of the physiological regulation component of the arterial pressure time variation after postural stresses by a model of the gravitational and arterial kinking effects p 550 N95-15149
LIVERPOOL UNIV. (ENGLAND).
Coherent states on the m-sheeted complex plane as m-photon states p 598 N95-13940
LOCKHEED AERONAUTICAL SYSTEMS CO., MARIETTA, GA.
Thermally stable organic polymers
[AD-A281380] p 451 N95-14363
LOCKHEED CORP., FORT WORTH, TX.
Flight test results of the F-16 aircraft modified with the axisymmetric vectoring exhaust nozzle p 396 N95-14245
Vista/F-16 Multi-Axis Thrust Vectoring (MATV) control law design and evaluation p 396 N95-14248
LOCKHEED ENGINEERING AND SCIENCES CO., HAMPTON, VA.
Results of demonstration test for receiving and processing of flight data from the Space Transportation System
[NASA-CR-194986] p 418 N95-13890
An approximate Riemann solver for thermal and chemical nonequilibrium flows
[NASA-CR-195003] p 492 N95-14912
Laminar and turbulent flow computations of Type 4 shock-shock interference aerothermal loads using unstructured grids
[NASA-CR-195008] p 493 N95-15604
LOCKHEED ENGINEERING AND SCIENCES CO., HOUSTON, TX.
Space Generic Open Avionics Architecture (SGOAA): Overview p 569 N95-14161
LOCKHEED MISSILES AND SPACE CO., PALO ALTO, CA.
Stellar activity: Astrophysics relevant to global change p 643 N95-14500
Helium 2 slosh in low gravity p 487 N95-14554
Dynamics Explorer 1: Energetic Ion Composition Spectrometer (EICS)
[NASA-CR-189375] p 619 N95-15758
LOCKHEED MISSILES AND SPACE CO., SUNNYVALE, CA.
Prediction of particulate contamination on aperture window p 420 N95-14064
ASTM E 1559 method for measuring material outgassing/deposition kinetics has applications to aerospace, electronics, and semiconductor industries p 421 N95-14066
LORAL AEROSYS, SEABROOK, MD.
Efficient mission control for the 48-satellite Globalstar constellation
[TABES PAPER 94-609] p 415 N95-14641
LORAL SYSTEMS, INC., ORLANDO, FL.
Advanced distributed simulation technology: Digital Voice Gateway Reference Guide
[AD-A283154] p 460 N95-13696
Advanced distributed simulation technology advanced rotary wing aircraft. Study comparing approaches to modeling the ARWA main rotor
[AD-A280824] p 408 N95-14306
ADST ARWA visual system module software design document
[AD-A283874] p 572 N95-14357
LOS ALAMOS NATIONAL LAB., NM.
Analysis of neutron diffraction peak broadening caused by internal stresses in composite materials
[DE94-014453] p 433 N95-13993
Review of drive symmetry measurement and control experiments on the Nova laser system
[DE94-014455] p 498 N95-13994
An observational test of magnetospheric field models at geosynchronous orbit
[DE94-014462] p 526 N95-13995
Preparing technical text for translation: A comparison between International English and methods for simplifying language
[DE94-014465] p 630 N95-13996
Hohlraum manufacture for inertial confinement fusion
[DE94-014472] p 616 N95-13997
Los Alamos contribution to target diagnostics on the National Ignition Facility
[DE94-014474] p 616 N95-13998
High field magnetotransport and specific heat in YbAgCu4
[DE94-014475] p 620 N95-13999
Finite boson mappings of fermion systems
[DE94-014478] p 593 N95-14000
From the shell model to the interacting boson model
[DE94-014486] p 593 N95-14001
Advanced stellarator power plants
[DE94-014442] p 616 N95-14007
Radiation rates for low Z impurities in edge plasmas
[DE94-016073] p 617 N95-14368
Early solar mass loss, element diffusion, and solar oscillation frequencies
[DE94-014802] p 646 N95-14376
An efficient network for interconnecting remote monitoring instruments and computers
[DE94-016213] p 581 N95-14377
Variable metric conjugate gradient methods
[DE94-014796] p 585 N95-14381
Radioactivity measurements of ITER materials using the TFTR D-T neutron field
[DE94-016094] p 617 N95-14397
The MOXE x-ray all-sky monitor for Spectrum-X-gamma
[DE94-016064] p 638 N95-14429
The 226RA and 231PA systematics of axial, MORB, crustal residence ages, and MAGMA chamber characteristics at 9 to 10 degree N East Pacific Rise
[DE94-013084] p 529 N95-14434
Production profiles of nuclides by galactic-cosmic-ray particles in small meteoroids
[DE94-014801] p 646 N95-14437
Numerical simulations of planetary gamma-ray spectra induced by galactic cosmic rays
[DE94-014809] p 647 N95-14438
High strain rate deformation of NiAl
[DE94-014810] p 445 N95-14439
Spectrophotometric determination of plutonium-239 based on the spectrum of plutonium 3 chloride
[DE94-015172] p 440 N95-15297
Acoustic resonance spectroscopy intrinsic seals
[DE94-016207] p 591 N95-15359
Direct-current proton-beam measurements at Los Alamos
[DE94-016280] p 599 N95-15360
Prototype explosives-detection system based on nuclear-resonance absorption in nitrogen
[DE94-015069] p 442 N95-15387
Computational modeling of fiber-reinforced composites
[DE94-012914] p 436 N95-15573
Cation disorder in high dose neutron irradiated spinel
[DE94-013118] p 455 N95-15579
ROOM: A recursive object oriented method for information systems development
[DE94-007575] p 633 N95-15761
An algorithm for rezoning particle-in-cell calculations
[DE94-016056] p 619 N95-15774
Cluster studies of La2CuO4: Local geometric distortions
[DE94-016203] p 626 N95-15776
Selection of non-destructive assay methods: Neutron counting or calorimetric assay?
[DE94-016211] p 505 N95-15777
LOUISIANA STATE UNIV., BATON ROUGE, LA.
Activity of Ga, In and Cu modified MFI zeolites for amine reactions
[DE94-016532] p 438 N95-14388
The design and development of Histogram-based Morphological Edge Detector (HMED)
[AD-A284458] p 470 N95-15820
LOUISVILLE UNIV., KY.
Cosmos 2229 immunology study (Experiment K-8-07)
[NASA-CR-196984] p 537 N95-13638
Space flight and humoral and cellular immunity of animals p 538 N95-15113

M

MACDONALD, DETTWILER AND ASSOCIATES LTD., RICHMOND (BRITISH COLUMBIA).
Synthetic aperture radar signal data compression using block adaptive quantization p 565 N95-14590
MAINZ UNIV. (GERMANY).
Will man need the vestibular system in generations to come? p 542 N95-15092
MALAYA UNIV., KUALA-LUMPUR.
Effect of dispersion forces on squeezing with Rydberg atoms p 456 N95-13899
MANCHESTER UNIV. (ENGLAND).
On the nonlocal predictions of quantum optics p 611 N95-13967
MANTECH ENVIRONMENTAL TECHNOLOGY, INC., RESEARCH TRIANGLE PARK, NC.
Study of interferences in ozone UV and chemiluminescence monitors
[PB94-197456] p 521 N95-14123
MARTIN MARIETTA CORP., DENVER, CO.
Sample Acquisition and Instrument Deployment (SAID)
[NASA-CR-197104] p 502 N95-14910
Control of remotely operated manipulation systems p 582 N95-14945
MARTIN MARIETTA CORP., MOORESTOWN, NJ.
Particle localization, spinor two-valuedness, and Fermi quantization of tensor systems p 598 N95-13932
MARYLAND UNIV., COLLEGE PARK, MD.
Quantum propagation in single mode fiber p 609 N95-13953
Einstein-Podolsky-Rosen-Bohm experiment and Bell inequality violation using Type 2 parametric down conversion p 612 N95-13970
SLR tracking of GPS-35 p 471 N95-14285
Vision-based navigation and recognition
[AD-A282962] p 583 N95-15398
Robust routing in dynamic networks, part 1
[AD-A282445] p 583 N95-15548
Fire growth models for materials
[PB94-195856] p 443 N95-15610

Properties of nearly perfect crystals at very low temperatures
[NASA-CR-197221] p 627 N95-15823

MARYLAND UNIV. BALTIMORE COUNTY, CATONSVILLE, MD.
The photon: Experimental emphasis on its wave-particle duality p 599 N95-13963
The generation of entangled states from independent particle sources p 599 N95-13964

MASARYK UNIV., BRNO, JIHOMORAVSKY (CZECHOSLOVAKIA).
Laboratory spectra of C60 and related molecular structures p 627 N95-15838

MASSA PRODUCTS CORP., HINGHAM, MA.
Legged vehicle for underwater mobile operations
[AD-A282891] p 503 N95-15294

MASSACHUSETTS INST. OF TECH., CAMBRIDGE.
On the theory of quantum measurement p 604 N95-13910
Visual interfaces: The human perceiver p 554 N95-14014
Tactual interfaces: The human perceiver p 554 N95-14016
Interacting with virtual worlds p 556 N95-14032
Tactile discrimination and representations of texture, shape, and softness p 558 N95-14041
A high performance two degree-of-freedom kinesthetic interface p 558 N95-14042
Manual discrimination of force p 561 N95-14057
Implementation of a three degree of freedom, motor/brake hybrid force output device for virtual environment control tasks p 562 N95-14058
Fault detection and diagnosis using neural network approaches p 571 N95-14170
Global and regional kinematics with GPS p 527 N95-14279
Direct observation of oil consumption mechanisms in a production spark ignition engine using fluorescence techniques
[AD-A283842] p 501 N95-14347
Bolted joint studies in GRP
[AD-A283843] p 434 N95-14348
Damage analysis of internal faults in flux concentrating permanent magnet motors
[AD-A283883] p 474 N95-14359
Conversion of light hydrocarbon gases in metal carbides for production of liquid fuels and chemicals
[DE94-013933] p 439 N95-14435
Measurement of resistance to solute transport across surfactant-laden interfaces using a Fluorescence Recovery After Photobleaching (FRAP) technique p 490 N95-14574
Determination of the atmospheric structure of the BO star companion of SMC X-1 by analysis of Ginga observations
[NASA-CR-197100] p 638 N95-14804
Search for gamma-ray events in the BATSE data base
[NASA-CR-197044] p 647 N95-14814
Human factors considerations for remote manipulation p 564 N95-14949
Calculation of movable bed friction factors
[AD-A283529] p 536 N95-15440
High-spatial-resolution passive microwave sounding systems
[NASA-CR-197131] p 531 N95-15586
TDWR scan strategy implementation
[AD-A284877] p 534 N95-15749
Intelligence in scientific computing
[AD-A284410] p 584 N95-15811

MASSACHUSETTS UNIV., AMHERST, MA.
AASERT 92: Synthesis and properties of complex polyarylene vinylenes
[AD-A284215] p 452 N95-14406
An architecture for intelligent multichip module reliability analysis
[AD-A281574] p 583 N95-15461
Discrete-event-dynamic-system-based approaches for control in integrated voice/data multihop radio networks
[AD-A284413] p 470 N95-15813
Validation of ERS-1 environmental data products
[NASA-CR-197111] p 517 N95-15848

MASSACHUSETTS UNIV., LOWELL, MA.
The atom-atom potential in pressure-broadened line width calculations for XY2-AB: New expressions in the II(R), II(L), and I(R) representations
[AD-A282011] p 595 N95-14950

MATERIALS RESEARCH SOCIETY, PITTSBURG, PA.
Low Temperature Grown and Highly Non-Stoichiometric GaAs and Related Materials
[AD-A284898] p 626 N95-15754

MAYO CLINIC, ROCHESTER, MN.
Operational requirements for avoidance and eventual elimination of Gz-induced Loss Of Consciousness (G-LOC) in flight p 547 N95-15127

MCAT INST., MOFFETT FIELD, CA.
Planetary entry experiments
[NASA-CR-194215] p 644 N95-13717
Science objectives and performance of a radiometer and window design for atmospheric entry experiments p 429 N95-13718
Venusian atmospheric equilibrium chemistry at the Pioneer Venus anomalous event altitude p 645 N95-13721

MCAT INST., SAN JOSE, CA.
Numerical simulation of the SOFIA flowfield
[NASA-CR-197025] p 400 N95-14612
Control of unsteady separated flow associated with the dynamic stall of airfoils
[NASA-CR-197024] p 400 N95-14613
Numerical simulation of the flow about the F-18 HARV at high angle of attack
[NASA-CR-197023] p 400 N95-14614

MCDONALD OBSERVATORY, AUSTIN, TX.
The symbiosis of photometry and radial-velocity measurements p 643 N95-14505

MCDONNELL-DOUGLAS CORP., SAINT LOUIS, MO.
Integration of a mechanical forebody vortex control system into the F-15 p 398 N95-14258

MCDONNELL-DOUGLAS RESEARCH LABS., SAINT LOUIS, MO.
Low-energy pneumatic control of forebody vortices p 398 N95-14256

MCDONNELL-DOUGLAS SPACE SYSTEMS CO., ROCKVILLE, MD.
Using a temperature-controlled quartz crystal microbalance in a space equipment cleanroom to monitor molecular contamination p 421 N95-14069

MCGILL UNIV., MONTREAL (QUEBEC).
Analysis of the human operator subsystems p 555 N95-14019
The human operator transfer function: Identification of the limb mechanics subsystem p 558 N95-14040

MECHANICAL TECHNOLOGY, INC., LATHAM, NY.
Interactive Computer-Enhanced Remote Viewing System (ICERVS): Subsystem design report, phase 2
[DE94-014513] p 563 N95-15309

MEMPHIS STATE UNIV., TN.
Multi-dimensional modeling of pressurization and expulsion of multi-phase hydrogen propellant
[NASA-CR-195156] p 457 N95-14902

METRAFLU, ECULLY (FRANCE).
Flow-radiated noise. Study of the propagative spectral range of the wall pressure field
[PB94-201290] p 590 N95-13985

MIAMI UNIV., FL.
Statistical aspects of the precipitation regimes at Miami International Airport (MIA) and Palm Beach International Airport (PBI): 1961-1990
[PB94-194289] p 532 N95-14118

MICHIGAN UNIV., ANN ARBOR, MI.
EPIC computational models of psychological refractory-period effects in human multiple-task performance
[AD-A280924] p 540 N95-14142
Computations of drop collision and coalescence p 485 N95-14542
Pool and flow boiling in variable and microgravity p 459 N95-14562
Positron studies in catalysis research
[DE94-012793] p 597 N95-15572

MICROSENSOR SYSTEMS, INC., SPRINGFIELD, VA.
Surface Acoustic Wave (SAW) microsensors to monitor multi-component vapor challenges to adsorbents and adsorbent-based air filtration systems
[AD-A284222] p 497 N95-15334

MIDWEST RESEARCH INST., GOLDEN, CO.
Addendum: Tenth International Symposium on Alcohol Fuels, The Road to Commercialization
[DE93-018219] p 457 N95-14003
Module process optimization and device efficiency improvement for stable, low-cost, large-area, cadmium telluride-based photovoltaic module production
[DE94-011817] p 521 N95-15863

MIDWEST RESEARCH INST., KANSAS CITY, MO.
Development of anti-icing technology
[PB94-195369] p 407 N95-15439

MINISTRY OF INTERNATIONAL TRADE AND INDUSTRY, TSUKUBA (JAPAN).
Tele-existence and/or cybernetic interface studies in Japan p 555 N95-14025

MINNESOTA DEPT. OF TRANSPORTATION, DULUTH, MN.
Development of anti-icing technology
[PB94-195369] p 407 N95-15439

MINNESOTA UNIV., MINNEAPOLIS, MN.
On the role of exchange of power and information signals in control and stability of the human-robot interaction p 560 N95-14051
Parallel isosurface generator for huge data sets
[AD-A284030] p 578 N95-14422
Access to space
[NASA-CR-197153] p 428 N95-14521
Atomic force microscopy of the electrochemical nucleation and growth of molecular crystals
[AD-A280958] p 622 N95-14601
Distributed heterogeneous visualization, BOP (Bag-O-Polygons) and BOP view
[AD-A284393] p 567 N95-15809

MISSISSIPPI STATE UNIV., BAY SAINT LOUIS, MS.
Design document for the Surface Currents Data Base (SCDB) Management System (SCDBMS), version 1.0
[NASA-CR-197019] p 537 N95-15751
Users manual for the Surface Currents Data Base (SCDB) Management System (SCDBMS), version 1.0
[NASA-CR-197021] p 537 N95-15753
Design document for the MOODS Data Management System (MDMS), version 1.0
[NASA-CR-197016] p 633 N95-15801

MISSISSIPPI STATE UNIV., MISSISSIPPI STATE, MS.
Diagnostic development and support of MHD test facilities
[DE94-015344] p 618 N95-15373
Faraday rotation system
[DE94-015345] p 618 N95-15374

MISSISSIPPI STATE UNIV., STATE COLLEGE, MS.
Propulsion/airframe interference for ducted propfan engines with ground effect
[NASA-CR-197110] p 409 N95-14909

MISSISSIPPI UNIV., UNIVERSITY, MS.
Atmospheric effects on the risetime and waveshape of sonic booms p 402 N95-14886

MISSOURI UNIV., COLUMBIA, MO.
Applications of squeezed states: Bogoliubov transformations and wavelets to the statistical mechanics of water and its bubbles p 607 N95-13939
The effect of microstresses on fatigue crack propagation in steel
[AD-A283872] p 506 N95-14356
Cross-effects in microgravity flows p 459 N95-14565

MISSOURI UNIV., KANSAS CITY.
SAM1 semiempirical parameters
[AD-A284400] p 443 N95-15782

MISSOURI UNIV., ROLLA, MO.
Dynamics of the interface in a model composite system
[AD-A281910] p 433 N95-13655
NMR studies of polymers at interfaces
[AD-A281570] p 455 N95-15458

MITRE CORP., GREENBELT, MD.
Environmental testing to prevent on-orbit TDRS failures p 423 N95-14078

MONASH UNIV., CLAYTON (AUSTRALIA).
Development of a composite repair and the associated inspection intervals for the F-111C stiffener runout region p 392 N95-14477

MOSCOW PHYSICAL-TECHNICAL INST. (RUSSIA).
Sqeezing generated by a nonlinear master equation and by amplifying-dissipative Hamiltonians p 588 N95-13926

MOSCOW STATE UNIV. (RUSSIA).
Production of squeezed states for macroscopic mechanical oscillator p 603 N95-13906

MSB SYSTEMS, INC., NORWALK, CT.
Leak detection by acoustic emission monitoring. Phase 1: Feasibility study
[AD-A283775] p 493 N95-15332

N

NAPLES UNIV. (ITALY).
Some rules for polydimensional squeezing p 608 N95-13941
The thermal-wave model: A Schroedinger-like equation for charged particle beam dynamics p 601 N95-13944

NATIONAL ADVANCED ROBOTICS RESEARCH CENTRE, SALFORD, LANCASHIRE (ENGLAND).
Human factors requirements for telerobotic command and control: The European Space Agency experimental programme p 562 N95-14059
VERDEX: A virtual environment demonstrator for remote driving applications p 562 N95-14060

NATIONAL AERONAUTICS AND SPACE ADMINISTRATION, WASHINGTON, DC.
Our Mission to Planet Earth: A guide to teaching Earth system science
[NASA-EP-292] p 629 N95-13650
Suited for spacewalking: Teacher's guide with activities for physical and life science
[NASA-EG-101] p 554 N95-13888
Space based astronomy: Teacher's guide with activities
[NASA-EG-102] p 638 N95-14511

Space science in the 1990's and beyond
[TABES PAPER 94-204] p 415 N95-14634
Robotics technology developments in the United States space telerobotics program p 581 N95-14943
Aerospace medicine and biology: A continuing bibliography with indexes (supplement 395)
[NASA-SP-7011(395)] p 550 N95-15304
Aeronautical engineering: A continuing bibliography with indexes (supplement 310)
[NASA-SP-7037(310)] p 392 N95-15550

NATIONAL AERONAUTICS AND SPACE ADMINISTRATION. AMES RESEARCH CENTER, MOFFETT FIELD, CA.

Modification of the Ames 40- by 80-foot wind tunnel for component acoustic testing for the second generation supersonic transport
[NASA-TM-108850] p 391 N95-13642
The effects of autogenic-feedback training on motion sickness severity and heart rate variability in astronauts
[NASA-TM-108840] p 539 N95-13661
User's guide for ENSAERO: A multidisciplinary program for fluid/structural/control interaction studies of aircraft (release 1)
[NASA-TM-108853] p 391 N95-13662
VUV shock layer radiation in an arc-jet wind tunnel experiment p 405 N95-13719
Measured and calculated spectral radiation from a blunt body shock layer in an arc-jet wind tunnel
[AIAA PAPER 94-0086] p 405 N95-13720
Dynamics of the McDonnell-Douglas Large Scale Dynamic Rig and dynamic calibration of the rotor balance
[NASA-TM-108855] p 391 N95-13891
Human Machine Interfaces for Teleoperators and Virtual Environments
[NASA-CP-10071] p 554 N95-14013
The Ames Virtual Environment Workstation: Implementation issues and requirements p 557 N95-14034
Virtual acoustic displays p 557 N95-14035
Varieties of virtualization p 557 N95-14036
The exploration metaphor p 557 N95-14037
Perceptual and performance consequences of flight in virtual worlds p 558 N95-14043
Rotational wind indicator enhances control of rotated displays p 559 N95-14046
Simulation of Shuttle launch G forces and acoustic loads using the NASA Ames Research Center 20G centrifuge p 419 N95-14089
Development of life sciences equipment for microgravity and hypergravity simulation p 425 N95-14090
Unique life sciences research facilities at NASA Ames Research Center p 426 N95-14091
From Antarctica to space: Use of telepresence and virtual reality in control of remote vehicles p 427 N95-14099
Numerical simulation of the flow about an F-18 aircraft in the high-alpha regime p 394 N95-14232
Free-to-roll tests of X-31 and F-18 subscale models with correlation to flight test results p 394 N95-14237
Computational analysis of forebody tangential slot blowing p 397 N95-14253
Comparison of full-scale, small-scale, and CFD results for F/A-18 forebody slot blowing p 397 N95-14255
Eddy viscosity transport equations and their relation to the k-epsilon model
[NASA-TM-108854] p 481 N95-14273
Higher harmonic control analysis for vibration reduction of helicopter rotor systems
[NASA-TM-103855] p 391 N95-14419
Astrophysical science with a spaceborne photometric telescope
[NASA-CP-10148] p 643 N95-14499
Aircraft maneuver envelope warning system
[NASA-CASE-ARC-11953-1] p 411 N95-14518
Highly crosslinked silicon polymers for gas chromatography columns
[NASA-CASE-ARC-11960-2-NP] p 452 N95-14602
CTAS data analysis program
[NASA-TM-108842] p 406 N95-14611
Experimental/analytical approach to understanding mistuning in a transonic wind tunnel compressor
[NASA-TM-108833] p 512 N95-14617
Multi-velocity component LDV
[NASA-CASE-ARC-11925-1] p 499 N95-14668
Air-breathing aerospace plane development essential: Hypersonic propulsion flight tests
[NASA-TM-108857] p 392 N95-14921
Regional cutaneous microvascular flow responses during gravitational and LBNP stresses p 547 N95-15128
New findings regarding light intensity and its effects as a zeitgeber in the Sprague-Dawley rat p 539 N95-15135
Musculoskeletal adaptation to mechanical forces on Earth and in space p 548 N95-15136
A method for continuous monitoring of the Ground Reaction Force during daily activity p 549 N95-15139
Bone geometry, structure and mineral distribution using Dual energy X ray Absorptiometry (DXA) p 549 N95-15140
Centrifuges in gravitational physiology research p 550 N95-15147
Crew factors in flight operations 2: Psychophysiological responses to short-haul air transport operations
[NASA-TM-108856] p 550 N95-15649
The Diffuse Interstellar Bands: Contributed papers
[NASA-CP-10144] p 639 N95-15827
DIBS independent of accretion in T Tauri stars p 639 N95-15829
Formation of dust grains with impurities in red giant winds p 641 N95-15841
The formation of small grains in shocks in the ISM p 641 N95-15842

NATIONAL AERONAUTICS AND SPACE ADMINISTRATION. GODDARD SPACE FLIGHT CENTER, ALBUQUERQUE, NM.

Twelve-year planetary ephemeris: 1995-2006
[NASA-RP-1349] p 638 N95-14667

NATIONAL AERONAUTICS AND SPACE ADMINISTRATION. GODDARD SPACE FLIGHT CENTER, GREENBELT, MD.

Interplanetary medium data book, supplement 5, 1988-1993
[NASA-TM-109957] p 642 N95-13658
Delta, America's space ambassador
[NASA-TM-110046] p 419 N95-13700
Third International Workshop on Squeezed States and Uncertainty Relations
[NASA-CP-3270] p 602 N95-13896
A new approach to the photon localization problem p 603 N95-13905
New quantum properties of phonons and their detection p 610 N95-13957
Eighteenth Space Simulation Conference: Space Mission Success Through Testing
[NASA-CP-3280] p 420 N95-14062
Hubble Space Telescope servicing mission scientific instrument protective enclosure design requirements and contamination controls p 421 N95-14068
Clean assembly and integration techniques for the Hubble Space Telescope High Fidelity Mechanical Simulator p 418 N95-14070
Satellite Laser Ranging in the 1990s: Report of the 1994 Belmont Workshop
[NASA-CP-3283] p 526 N95-14274
Scientific analysis of satellite ranging data p 517 N95-14275
Global reference frame: Intercomparison of results (SLR, VLBI and GPS) p 527 N95-14276
Measuring temporal gravitational variations using SLR data p 527 N95-14277
Global and regional kinematics with VLBI p 527 N95-14280
SLR 2000 p 471 N95-14288
A strawman SLR program plan for the 1990s p 471 N95-14289
Satellite situation report, volume 33, number 2
[NASA-TM-109965] p 428 N95-14510
Laser retroreflector array having cat-eye retroreflectors
[NASA-CASE-GSC-13264-1] p 499 N95-14515
Flex-gear power transmission system for transmitting EMF between Sun and ring gears
[NASA-CASE-GSC-13540-1] p 502 N95-14517
1994 Science Information Management and Data Compression Workshop
[NASA-CP-3277] p 564 N95-14585
Radiometric resolution enhancement by lossy compression as compared to truncation followed by lossless compression p 564 N95-14588
The development of lossless data compression technology for remote sensing applications p 565 N95-14593
Planning/scheduling techniques for VQ-based image compression p 566 N95-14595
PSPC soft x-ray observations of Seyfert 2 galaxies
[NASA-TM-109968] p 638 N95-14911
Steering capaciflector sensor
[NASA-CASE-GSC-13489-1] p 583 N95-15598
Programmable high voltage power supply with regulation confined to the high voltage section
[NASA-CASE-GSC-13289-1] p 478 N95-15681
Technical report series on global modeling and data assimilation. Volume 3: An efficient thermal infrared radiation parameterization for use in general circulation models
[NASA-TM-104606-VOL-3] p 531 N95-15745

NATIONAL AERONAUTICS AND SPACE ADMINISTRATION. HUGH L. DRYDEN FLIGHT RESEARCH CENTER, EDWARDS, CA.

Fourth High Alpha Conference, volume 1
[NASA-CP-10143-VOL-1] p 393 N95-14229
Flight and full-scale wind-tunnel comparison of pressure distributions from an F-18 aircraft at high angles of attack p 394 N95-14231
Fourth High Alpha Conference, volume 2
[NASA-CP-10143-VOL-2] p 395 N95-14239
F-18 high alpha research vehicle: Lessons learned p 395 N95-14240
Design and development of an F/A-18 inlet distortion rake: A cost and time saving solution p 395 N95-14241
X-31 high angle of attack control system performance p 395 N95-14244
Multi-application controls: Robust nonlinear multivariable aerospace controls applications p 396 N95-14249
Fourth High Alpha Conference, volume 3
[NASA-CP-10143-VOL-3] p 397 N95-14251
Simple atmospheric perturbation models for sonic-boom-signature distortion studies p 402 N95-14888

NATIONAL AERONAUTICS AND SPACE ADMINISTRATION. HUGH L. DRYDEN FLIGHT RESEARCH FACILITY, EDWARDS, CA.

Numerical modeling of a cryogenic fluid within a fuel tank
[NASA-TM-4651] p 479 N95-13892

NATIONAL AERONAUTICS AND SPACE ADMINISTRATION. JOHN F. KENNEDY SPACE CENTER, COCOA BEACH, FL.

John F. Kennedy Space Center, Safety, Reliability, Maintainability and Quality Assurance, Survey and Audit Program
[NASA-TM-109208] p 630 N95-14918

NATIONAL AERONAUTICS AND SPACE ADMINISTRATION. LYNDON B. JOHNSON SPACE CENTER, HOUSTON, TX.

Cratering and penetration experiments in teflon targets at velocities from 1 to 7 km/s
[NASA-TM-104797] p 432 N95-13646
Acceleration recorder and playback module
[NASA-CASE-MSC-22008-1] p 496 N95-14180
Extended duration orbiter medical project Microbial Air Sampler (STS-50/USML-1) p 458 N95-14222
Extended duration orbiter medical project variability of blood pressure and heart rate (STS-50/USML-1) p 551 N95-14223
Extended duration orbiter medical project countermeasure to reduce post space flight orthostatic intolerance (LBNP) (STS-50/USML-1) p 551 N95-14224
Development of the NASA/FLAGRO computer program for analysis of airframe structures p 510 N95-14473
Immune changes in humans concomitant with space flights of up to 10 days duration p 545 N95-15114
Landing gear energy absorption system
[NASA-CASE-MSC-22277-1] p 503 N95-15306
STS-66 post flight presentation
[NASA-TM-110077] p 419 N95-15900

NATIONAL AERONAUTICS AND SPACE ADMINISTRATION. LANGLEY RESEARCH CENTER, HAMPTON, VA.

A review of 50 years of aerodynamic research with NACA/NASA
[NASA-TM-109163] p 647 N95-13663
Orientation effects on the measurement and analysis of critical CTOA in an aluminum alloy sheet
[NASA-TM-109153] p 444 N95-13690
Three-axis stabilization of spacecraft using parameter-independent nonlinear quaternion feedback
[NASA-TM-109150] p 420 N95-13729
Radiographic Moire
[NASA-CASE-LAR-15104-1] p 505 N95-13835
Improved composite material and method for production of improved composite material
[NASA-CASE-LAR-14892-1] p 433 N95-13836
Surface acoustic wave oxygen pressure sensor
[NASA-CASE-LAR-15266-1-CU] p 496 N95-13837
Poly(arylene ether)s containing pendent ethynyl groups
[NASA-CASE-LAR-15041-1] p 449 N95-13838
The effect of Low Earth Orbit exposure on some experimental fluorine and silicon-containing polymers p 422 N95-14074
A solvent resistant copolyimide
[NASA-CASE-LAR-15083-1] p 449 N95-14108
Copolyimides prepared from ODPA, BTDA and 3,4'-ODA
[NASA-CASE-LAR-15109-1] p 449 N95-14109
Piezoelectric loudspeaker
[NASA-CASE-LAR-15138-1] p 590 N95-14110

Adjustable bias column end joint assembly
[NASA-CASE-LAR-14899-1] p 459 N95-14111
Tactile display device using an electrorheological fluid
[NASA-CASE-LAR-14860-1] p 472 N95-14112
Electrically conducting polyimide film containing tin complexes
[NASA-CASE-LAR-14936-1] p 450 N95-14113
Joint for a variable geometry truss and method of constructing same
[NASA-CASE-LAR-15136-1] p 506 N95-14138
Spiral microstrip antenna with resistance
[NASA-CASE-LAR-15088-1] p 460 N95-14139
Poly(arylene ether imidazole) surfacing films for flat and parabolic structures
[NASA-CASE-LAR-14812-1] p 450 N95-14140
Base passive porosity for drag reduction
[NASA-CASE-LAR-15246-1] p 501 N95-14183
Passive fetal heart rate monitoring apparatus and method with enhanced fetal heart beat discrimination
[NASA-CASE-LAR-15129-1] p 541 N95-14184
Phenylethynyl terminated imide oligomers
[NASA-CASE-LAR-15175-1] p 450 N95-14185
Adjustable reed for weaving net-shaped tailored fabrics
[NASA-CASE-LAR-15072-1] p 501 N95-14186
High Alpha Technology Program (HATP) ground test to flight comparisons p 393 N95-14230
Comparison of X-31 flight, wind-tunnel, and water-tunnel yawing moment asymmetries at high angles of attack p 394 N95-14234
Flight validation of ground-based assessment for control power requirements at high angles of attack p 396 N95-14246
High angle of attack flying qualities criteria for longitudinal rate command systems p 396 N95-14247
Preparations for flight research to evaluate actuated forebody strakes on the F-18 high-alpha research vehicle p 398 N95-14257
Induction heating coupler
[NASA-CASE-LAR-14278-1] p 473 N95-14294
Active thermal isolation for temperature responsive sensors
[NASA-CASE-LAR-14612-2] p 496 N95-14414
Airplane takeoff and landing performance monitoring system
[NASA-CASE-LAR-14745-2-SB] p 412 N95-14415
Diamines and polyimides containing pendent ethynyl groups
[NASA-CASE-LAR-14825-1] p 452 N95-14416
FAA/NASA International Symposium on Advanced Structural Integrity Methods for Airframe Durability and Damage Tolerance
[NASA-CP-3274-PT-1] p 507 N95-14453
Influence of crack history on the stable tearing behavior of a thin-sheet material with multiple cracks p 509 N95-14467
Method and apparatus for detection and control of prelasing in a Q-switched laser
[NASA-CASE-LAR-14790-1] p 499 N95-14519
Particle experiments in thermal and velocity gradients p 489 N95-14564
NASA/DOD Aerospace Knowledge Diffusion Research Project. Paper 43: The role of information resource training in aerospace education. Expanded version
[NASA-TM-109981] p 632 N95-14619
Spatial awareness comparisons between large-screen, integrated pictorial displays and conventional EFIS displays during simulated landing approaches
[NASA-TP-3467] p 409 N95-14852
NASA/DOD Aerospace Knowledge Diffusion Research Project. Paper 44: Becoming an aerospace engineer: Some thoughts on the career goals and educational preparation of AIAA student members
[NASA-TM-109980] p 632 N95-14870
High-Speed Research: 1994 Sonic Boom Workshop: Atmospheric Propagation and Acceptability Studies
[NASA-CP-3279] p 401 N95-14878
An optical technique for examining aircraft shock wave structures in flight p 401 N95-14879
An in-home study of subjective response to simulated sonic booms p 403 N95-14891
Heavy rain effects p 407 N95-14899
The characterization of widespread fatigue damage in fuselage structure
[NASA-TM-109142] p 432 N95-14920
Research and technology highlights, 1993
[NASA-TM-4575] p 647 N95-15065
Low dielectric polyimide fibers
[NASA-CASE-LAR-14526-1] p 455 N95-15599
Small UHV compatible hyperthermal oxygen atom generator
[NASA-CAS-LAR-14674-1] p 503 N95-15601
Multiple-scattering model for inclusive proton production in heavy ion collisions
[NASA-TP-3470] p 600 N95-15606
Extension of the BRYNTRN code to monoenergetic light ion beams
[NASA-TP-3472] p 647 N95-15790
Wind-tunnel blockage and actuation systems test of a two-dimensional scramjet inlet unstart model at Mach 6
[NASA-TM-109152] p 495 N95-15898
Two-dimensional scramjet inlet unstart model: Wind-tunnel blockage and actuation systems test
[NASA-TM-109984] p 495 N95-15899

NATIONAL AERONAUTICS AND SPACE ADMINISTRATION. LEWIS RESEARCH CENTER, CLEVELAND, OH.

A new tribological test for candidate brush seal materials evaluation
[NASA-TM-106753] p 431 N95-13631
Monitoring fiber stress during curing of single fiber glass- and graphite-epoxy composites
[NASA-TM-4568] p 432 N95-13641
The flow induced by the coalescence of two initially stationary drops
[NASA-TM-106752] p 478 N95-13653
Computational analysis in support of the SSTO flowpath test
[NASA-TM-106757] p 479 N95-13665
Effects of hydrogen annealing, sulfur segregation and diffusion on the cyclic oxidation resistance of superalloys: A review
[NASA-TM-106734] p 444 N95-13667
Fast track NTR systems assessment for NASA's first lunar outpost scenario
[NASA-TM-106748] p 429 N95-13668
A prototype lisp-based soft real-time object-oriented Graphical User Interface for control system development
[NASA-TM-106743] p 566 N95-13716
Design for reliability: NASA reliability preferred practices for design and test
[NASA-TM-106313] p 420 N95-13728
An adaptively-refined, Cartesian, cell-based scheme for the Euler and Navier-Stokes equations
[NASA-TM-106754] p 392 N95-13817
NASA LeRC's acoustic fill effect test program and results
[NASA-TM-106688] p 419 N95-13893
GSOSTATS database: USAF synchronous satellite catalog data conversion software. User's guide and software maintenance manual, version 2.1
[NASA-TM-106760] p 568 N95-13894
Selection of solar simulator for solar dynamic ground test
[NASA-TM-106608] p 430 N95-14173
Alkali metal Rankine cycle boiler technology challenges and some potential solutions for space nuclear power and propulsion applications
[NASA-TM-106593] p 430 N95-14174
NLEdit: A generic graphical user interface for Fortran programs
[NASA-TM-4543] p 572 N95-14206
The solid surface combustion experiment aboard the USML-1 mission p 458 N95-14212
Surface Tension Driven Convection Experiment (STDCE) p 458 N95-14217
An efficient spectral method for ordinary differential equations with rational function coefficients
[NASA-TM-106762] p 585 N95-14296
A Cartesian, cell-based approach for adaptively-refined solutions of the Euler and Navier-Stokes equations
[NASA-TM-106786] p 398 N95-14297
Effects of thermal cycling on thermal expansion and mechanical properties of SiC fiber-reinforced reaction-bonded Si3N4 composites
[NASA-TM-106665] p 433 N95-14298
Hypersonic engine leading edge experiments in a high heat flux, supersonic flow environment
[NASA-TM-106742] p 482 N95-14299
Nonlinear asymptotic integration algorithms for one-dimensional autonomous dissipative first-order ODEs
[NASA-TM-106780] p 585 N95-14300
Development status of the NASA 30-cm ion thruster and power processor
[NASA-TM-106740] p 430 N95-14301
Advanced solar cells for satellite power systems
[NASA-TM-106777] p 473 N95-14302
Physical and tribological characteristics of ion-implanted diamond films
[NASA-TM-106682] p 450 N95-14303
Axis switching and spreading of an asymmetric jet: Role of vorticity dynamics
[NASA-TM-106385] p 398 N95-14418
Pulsed mode cathode
[NASA-CASE-LEW-15753-1] p 475 N95-14516
Second Microgravity Fluid Physics Conference
[NASA-CP-3276] p 482 N95-14522
Oscillatory/chaotic thermocapillary flow induced by radiant heating p 483 N95-14531
A realistic model of evaporation for a liquid droplet p 485 N95-14543
Thermocapillary migration and interactions of bubbles and drops p 486 N95-14546
Characterization of annular two-phase gas-liquid flows in microgravity p 487 N95-14556
Flocculation and aggregation in a microgravity environment (FAME) p 459 N95-14572
The path to an experiment in space (from concept to flight) p 417 N95-14582
Fluids flight hardware p 491 N95-14583
Conceptual design of the Space Station fluids module p 429 N95-14584
Graphical user interface for the NASA FLOPS aircraft performance and sizing code
[NASA-TM-106649] p 408 N95-14604
A modified mixing length turbulence model for zero and adverse pressure gradients
[NASA-TM-106772] p 492 N95-14607
Noise radiation by instability waves in coaxial jets
[NASA-TM-106738] p 591 N95-14618
Icing: Accretion, detection, protection p 406 N95-14897
LSENS: A General Chemical Kinetics and Sensitivity Analysis Code for homogeneous gas-phase reactions. Part 1: Theory and numerical solution procedures
[NASA-RP-1328-PT-1] p 440 N95-15056
LSENS: A General Chemical Kinetics and Sensitivity Analysis Code for homogeneous gas-phase reactions. Part 3: Illustrative test problems
[NASA-RP-1330-PT-3] p 440 N95-15057
The aeroacoustics of supersonic coaxial jets
[NASA-TM-106782] p 591 N95-15059
Graphite fluoride from iodine intercalated graphitized carbon
[NASA-CASE-LEW-15360-1] p 441 N95-15303
LSENS, a general chemical kinetics and sensitivity analysis code for homogeneous gas-phase reactions. 2: Code description and usage
[NASA-RP-1329] p 442 N95-15512
Surface passivation for 3-5 semiconductor processing: Stable gallium sulphide films by MOCVD
[NASA-TM-106761] p 477 N95-15587
Process for the controlled growth of single-crystal films of silicon carbide polytypes on silicon carbide wafers
[NASA-CAS-LEW-15222-3] p 625 N95-15602
Method of locating ground faults
[NASA-CASE-LEW-15407-1] p 478 N95-15669
The rationale/benefits of nuclear thermal rocket propulsion for NASA's lunar space transportation system
[NASA-TM-106739] p 431 N95-15682
Environmental durability issues for solar power systems in low Earth orbit
[NASA-TM-106775] p 431 N95-15769
An approach for dynamic grids
[NASA-TM-106774] p 404 N95-15853
On the behavior of three-dimensional wave packets in viscously spreading mixing layers
[NASA-TM-106770] p 495 N95-15908
Service equipment for use in hostile environments
[NASA-CASE-LEW-14906-2-SB] p 504 N95-15914
Apparatus for performing high-temperature fiber push-out testing
[NASA-CASE-LEW-15470-1] p 497 N95-15915

NATIONAL AERONAUTICS AND SPACE ADMINISTRATION. MARSHALL SPACE FLIGHT CENTER, HUNTSVILLE, AL.

Welding nozzle position manipulator
[NASA-CASE-MFS-29837-1] p 500 N95-13654
Hybrid bearings for turbopumps and the like
[NASA-CASE-MFS-28491-1] p 500 N95-13819
Multilayer thin film Hall effect device
[NASA-CASE-MFS-28764-1] p 590 N95-14137
Parachute having improved vent line stacking
[NASA-CASE-MFS-28508-1] p 393 N95-14182
Joint Launch + One Year Science Review of USML-1 and USMP-1 with the Microgravity Measurement Group
[NASA-CP-3272-VOL-1] p 634 N95-14207
Basic features of the STS/Spacelab vibration environment p 428 N95-14210
Orbital processing of high-quality CdTe compound semiconductors p 458 N95-14213
Crystal growth of selected II-VI semiconducting alloys by directional solidification p 458 N95-14214
Role of dielectric constant in electrohydrodynamics of conducting fluids p 478 N95-14577
Environmentally sound manufacturing
[TABES PAPER 94-502] p 415 N95-14636
A NASA/industry/university partnership for development of dual-use vibration isolation technology
[TABES PAPER 94-613] p 416 N95-14643
Space Shuttle Main Engine turbopump bearing assessment program
[TABES PAPER 94-621] p 417 N95-14648

The Global Emergency Observation and Warning System
[TABES PAPER 94-622] p 417 N95-14649
Building complex simulations rapidly using MATRIX(x): The Space Station redesign
[TABES PAPER 94-632] p 417 N95-14653
Dual-latching solenoid-actuated valve assembly
[NASA-CASE-MFS-28714-1] p 502 N95-14666
Buckling of composite beams (CDDF)
[NASA-TP-3512] p 435 N95-14913
Metrication in a global environment
[NASA-TM-108469] p 459 N95-14919
An inelastic analysis of a welded aluminum joint
[NASA-TP-3508] p 513 N95-15055
Saddle clamp assembly
[NASA-CASE-MFS-28701-1] p 503 N95-15305
Dynamics Explorer 1, retarding ion mass spectrometer summary spectrograms: 82/001 to 82/109 spin-time spectrograms for H(+), He(+), O(+), N(+), O(++), M/Z=2, and molecular ions
[NASA-TM-108468] p 443 N95-15607
Vehicle health management using adaptive techniques
[NASA-TM-108472] p 431 N95-15609
Plasma arc welding torch having means for vortexing plasma gas exiting the welding torch
[NASA-CASE-MFS-28828-1] p 503 N95-15670
Basic mechanics of laminated composite plates
[NASA-RP-1351] p 436 N95-15763

NATIONAL AERONAUTICS AND SPACE ADMINISTRATION. PASADENA OFFICE, CA.
Multipath noise reduction spread spectrum signals
[NASA-CASE-NPO-18970-1-CU] p 460 N95-13628
Burst-by-burst laser frequency monitor
[NASA-CASE-NPO-18596-1-CU] p 498 N95-13629
Aberration correction of unstable resonators
[NASA-CASE-NPO-18662-1-CU] p 602 N95-13823
Thin composite solid electrolyte film for lithium batteries
[NASA-CASE-NPO-18694-1-CU] p 472 N95-13824
Wavelength-division multiplexed optical integrated circuit with vertical diffraction grating
[NASA-CASE-NPO-18357-1-CU] p 612 N95-14181
Wide field strip-imaging optical system
[NASA-CASE-NPO-18146-2-CU] p 613 N95-14413
Optical detector having a plurality of matrix layers with cobalt disilicide particles embedded therein
[NASA-CASE-NPO-18625-2-CU] p 614 N95-15603

NATIONAL AEROSPACE LAB., AMSTERDAM (NETHERLANDS).
Recent advances in the modelling of crack growth under fatigue loading conditions p 511 N95-14478

NATIONAL CENTER FOR ATMOSPHERIC RESEARCH, BOULDER, CO.
Asteroseismology: Theory and phenomenology p 643 N95-14502

NATIONAL DEFENCE RESEARCH ESTABLISHMENT, STOCKHOLM (SWEDEN).
New armour materials: Metal matrix composites
[PB94-189131] p 433 N95-14148

NATIONAL GEOPHYSICAL DATA CENTER, BOULDER, CO.
Solar-geophysical data number 598, June 1994. Part 2: (Comprehensive reports). Data for December 1993 and miscellaneous
[PB94-208832] p 646 N95-15773
Solar-geophysical data number 598, June 1994. Part 1: (Prompt reports). Data for May, April 1994 and late data
[PB94-208824] p 646 N95-15784

NATIONAL INST. OF STANDARDS AND TECHNOLOGY, BOULDER, CO.
Growth mechanisms and characterization of hydrogenated amorphous-silicon-alloy films
[DE94-011842] p 518 N95-14194
Thermophysical properties of HCFC alternatives
[DE94-016846] p 438 N95-14372
Investigating the 3.3 micron infrared fluorescence from naphthalene following ultraviolet excitation p 599 N95-15839

NATIONAL INST. OF STANDARDS AND TECHNOLOGY, GAITHERSBURG, MD.
Partial pressure analysis in space testing p 424 N95-14084
Risk analysis for the fire safety of airline passengers
[PB94-194065] p 405 N95-14179
Semiconductor measurement technology: Improved characterization and evaluation measurments for HgCdTe detector materials, processes, and devices used on the GOES and TIROS satellites
[PB94-188810] p 474 N95-14401
Electronics and Electrical Engineering Laboratory Technical Progress Bulletin covering laboratory programs, January to March 1994 with 1994/1995 EEEL events calendar
[PB94-193810] p 474 N95-14402
Single-phase heat transfer and pressure drop characteristics of an integral-spine-fin within an annulus
[PB94-194073] p 482 N95-14407
Metric path to global markets and new jobs: A question-and-answer and thematic discussion
[PB94-206307] p 459 N95-14512
Convection and morphological stability during directional solidification p 448 N95-14548
Behavior of charring materials in simulated fire environments
[PB94-196045] p 439 N95-14838
A metric for success
[PB94-187630] p 459 N95-15322
Comparison of wall-fire behavior with and without a ceiling
[PB94-207404] p 441 N95-15354
Optically driven surface reactions: Laser probes of surface dynamics
[DE94-015311] p 441 N95-15370
Fire growth models for materials
[PB94-195856] p 443 N95-15610

NATIONAL OCEANIC AND ATMOSPHERIC ADMINISTRATION, BOULDER, CO.
Analysis of deep convective clouds and their association with non-migrating atmospheric diurnal tides in the tropical troposphere
[PB94-187457] p 526 N95-13974

NATIONAL OCEANIC AND ATMOSPHERIC ADMINISTRATION, RESEARCH TRIANGLE PARK, NC.
Computational modeling issues in next generation air quality models
[PB94-197449] p 521 N95-14122

NATIONAL OCEANIC AND ATMOSPHERIC ADMINISTRATION, SILVER SPRING, MD.
Overview of PAMS meteorological monitoring requirements
[PB94-176658] p 534 N95-15383

NATIONAL RENEWABLE ENERGY LAB., GOLDEN, CO.
Wind-electric ice making for villages in the developing world
[DE94-011854] p 518 N95-14191
Growth mechanisms and characterization of hydrogenated amorphous-silicon-alloy films
[DE94-011842] p 518 N95-14194
Role of point defects and defect complexes in silicon device processing: Book of abstracts
[DE94-011828] p 519 N95-14430
In-situ characterization of growth and interfaces in a-Si:H devices
[DE94-011847] p 622 N95-14431
Role of polycrystallinity in CdTe and CuInSe2 photovoltaic cells
[DE94-011849] p 519 N95-14432
The National Wind Technology Center
[DE94-011853] p 519 N95-14433
Wind/hybrid power system test facilities in the United States and Canada
[DE94-006930] p 519 N95-15290
Optimization of transparent and reflecting electrodes for amorphous-silicon solar cells
[DE94-011841] p 520 N95-15355
Development of large-area monolithically integrated Silicon-Film(tm) photovoltaic modules
[DE94-011830] p 520 N95-15405
Small-angle x-ray scattering studies of microvoids in amorphous-silicon-based semiconductors
[DE94-011840] p 520 N95-15406
Alternative fabrication techniques for high-efficiency CuInSe2 and CuInSe2-alloy films and cells
[DE94-011846] p 521 N95-15407
Fourth Workshop on the Role of Point Defects and Defect Complexes in Silicon Device Processing
[DE94-011850] p 624 N95-15426

NATIONAL RESEARCH COUNCIL OF CANADA, OTTAWA (ONTARIO).
The C4H radical and the diffuse interstellar bands. An ab initio study p 641 N95-15843

NATIONAL SCIENCE FOUNDATION, ARLINGTON, VA.
Duality theorem in the multivariable Iwasawa theory of local fields
[PB94-192325] p 589 N95-13979

NATIONAL SCIENCE FOUNDATION, WASHINGTON, DC.
Proceedings of the 3rd International Workshop on Computational Electronics
[AD-A284214] p 475 N95-14444
Propulsion/airframe interference for ducted propfan engines with ground effect
[NASA-CR-197110] p 409 N95-14909

NATIONAL SEVERE STORMS FORECAST CENTER, KANSAS CITY, MO.
Verification of severe local storms forecasts issued by the National Severe Storms Forecast Center: 1993
[PB94-195898] p 532 N95-14117

NATIONAL TELECOMMUNICATIONS AND INFORMATION ADMINISTRATION, BOULDER, CO.
Impulse response measurements in the 1850-1990 MHz band in large outdoor cells
[PB94-204906] p 462 N95-14412

NATIONAL TRANSPORTATION SAFETY BOARD, WASHINGTON, DC.
Aircraft accident report: Overspeed and loss of power on both engines during descent and power-off emergency, landing Simmons Airlines, Inc., d/b/a, American Eagle Flight 3641, N349SB False River Air Park, New Roads, Lousiana, 1 February 1994
[NTSB/AAR-94/06] p 407 N95-14916
Annual review of aircraft accident data: US air carrier operations, calendar year 1992
[NTSB/ARC-94/02] p 407 N95-15066

NATIONAL WEATHER SERVICE, SILVER SPRING, MD.
AFOS Terminal Aerodrome Forecast encoding
[PB94-203247] p 533 N95-14410

NAUCHNO-ISSLEDOVATELSKII INST. GRAFIT, MOSCOW (RUSSIA).
Experimental study of solar simulator mirror cryocontamination p 421 N95-14065
New potentials of NIICHIMMASH's thermal vacuum facilities p 418 N95-14098

NAVAL ACADEMY, ANNAPOLIS, MD.
Robotic control using muscular and neural electrical signals
[AD-A284908] p 551 N95-15757

NAVAL AEROSPACE MEDICAL RESEARCH LAB., PENSACOLA, FL.
Naval Aerospace Medical Research Laboratory. 1993 command history
[AD-A284038] p 541 N95-14424

NAVAL AIR WARFARE CENTER, CHINA LAKE, CA.
Development of chemical-vapor-deposited diamond for infrared optical applications: Summary of properties
[AD-A282999] p 448 N95-13686

NAVAL AIR WARFARE CENTER, PATUXENT RIVER, MD.
Add a dimension to your analysis of the helicopter low airspeed environment
[AD-A283982] p 408 N95-14205
X-31 post-stall envelope expansion and tactical utility testing p 395 N95-14242
Navy and the HARV: High angle of attack tactical utility issues p 397 N95-14252
Composite waveform generation for EMP and lightning direct-drive testing
[AD-A284159] p 462 N95-14405

NAVAL COMMAND, CONTROL AND OCEAN SURVEILLANCE CENTER, SAN DIEGO, CA.
Engineer's Refractive Effects Prediction System (EREPS), version 3.0
[AD-A283748] p 461 N95-14345
Sensing of radio refractivity and aerosol extinction p 467 N95-14830
Refractive effects from VHF to EHF. Part A: Propagation Mechanisms p 467 N95-14831
Refractive effects from VHF to EHF. Part B: Propagation models p 467 N95-14832
High-data-rate UHF line-of-sight communication experiment
[AD-A283592] p 468 N95-15321
Data processing routines for the Sippican MK-12 XBT system
[AD-A283570] p 536 N95-15330

NAVAL OCEAN SYSTEMS CENTER, KAILUA, HI.
Telerobotic remote presence: Achievements and challenges p 504 N95-14023

NAVAL POSTGRADUATE SCHOOL, MONTEREY, CA.
Remote sensing, processing and transmission of data for an unmanned aerial vehicle
[AD-A283104] p 514 N95-13693
Space experiments aboard rockets: SPEAR 3
[AD-A280778] p 414 N95-14290
Simulations of the high average power SELENE free electron laser prototype
[AD-A280780] p 498 N95-14291
An evaluation of B-ISDN for the communication architecture requirements of Distributed Interactive Simulation (DIS)
[AD-A280783] p 578 N95-14292
Automated network protocol reachability analysis with supertrace algorithm and TESTGEN: Automated generation of test sequence for a formal protocol specification
[AD-A280788] p 461 N95-14293
The stable and precise motion control for an autonomous mobile robot
[AD-A283776] p 501 N95-14336
Oxides of nitrogen: Their formation and control in stationary sources
[AD-A283780] p 522 N95-14337

Short term teleconnections associated with western Pacific tropical cyclones
[AD-A284032] p 533 N95-14423
Spectral analysis of vortex/free-surface interaction
[AD-A283210] p 492 N95-14658
Artificial neural network modeling of damaged aircraft
[AD-A283227] p 409 N95-14849
Evaluation of energy-sink stability criteria for dual-spin spacecraft
[AD-A283228] p 428 N95-14850
Low-speed wind tunnel testing of the NPS and NASA Ames Mach 6 optimized waverider
[AD-A283585] p 404 N95-15319
Tidal dynamics and mixing over steep topography
[AD-A283535] p 536 N95-15324
Theory and implementation of a VLSI stray insensitive switched capacitor composite operational amplifier
[AD-A283536] p 476 N95-15325
Combustion efficiency in a dual-inlet side-dump ramjet combustor
[AD-A283564] p 411 N95-15329
Cold flow simulation of the alternate turbopump development turbine of the Space Shuttle main engine high pressure fuel turbopump
[AD-A281676] p 419 N95-15447
Improving transient signal synthesis through noise modeling and noise removal
[AD-A281677] p 592 N95-15448
Applied Computational Electromagnetics Society Journal, volume 9, number 2
[AD-A281576] p 469 N95-15463
Conditional graph completions
[AD-A282914] p 587 N95-15612
Performance comparison AN/FRD-10 versus PUSHER
[AD-A283263] p 469 N95-15619
An analysis of eddy resolving global ocean models in the Southern Ocean
[AD-A283211] p 536 N95-15626
A simple analytical model for dense WDM/OOK systems
[AD-A283229] p 478 N95-15628
Modeling and simulation of a Fiber Distributed Data Interface Local Area Network (FDDI LAN) using OPNET (tm) for interfacing through the Common Data Link (CDL)
[AD-A283124] p 469 N95-15651
Wireless technology for command control and communications
[AD-A284367] p 470 N95-15804
Analytical tripping loads for stiffened plates
[AD-A284368] p 514 N95-15805
Experimental hardware development for a pulsed ultrasonic data collection facility
[AD-A283331] p 615 N95-15872
Three-dimensional effects of crack closure in laminated composite plates subjected to bending loads
[AD-A283342] p 436 N95-15873

NAVAL RESEARCH LAB., WASHINGTON, DC.
Thermal design verification testing of the Clementine spacecraft: Quick, cheap, and useful
p 424 N95-14083
Flightline aircraft fire incidents and suppression agent effects: Field inquiries and incident analysis
[AD-A284027] p 405 N95-14421
Use of the user action notation at the Naval Research Laboratory Human-Computer Interaction Laboratory
[AD-A281680] p 563 N95-15449
Connection machine software conversion of the Navy TOPS model
[AD-A281681] p 579 N95-15450
Video transmission for quantized variable bandwidth networks
[AD-A284892] p 470 N95-15750

NAVAL SURFACE WARFARE CENTER, BETHESDA, MD.
Effects of tensile loading on upper shelf fracture toughness
[AD-A284364] p 514 N95-15803

NAVAL SURFACE WARFARE CENTER, DAHLGREN, VA.
Engineering Codes for aeroprediction: State-of-the-art and new methods p 399 N95-14447
Electromagnetic reverberation characteristics of a large transport aircraft
[AD-A282923] p 411 N95-15392

NAVAL UNDERSEA WARFARE CENTER, NEWPORT, RI.
The modal decomposition of an impedance tube
[AD-A283591] p 591 N95-15320

NAVY COMPUTER AND TELECOMMUNICATIONS STATION, PENSACOLA, FL.
Performance information management system (PIMS) communication
[AD-A284851] p 574 N95-15335

NEBRASKA UNIV., LINCOLN, NE.
Investigation of dipolar reorientation dynamics of pure bulk polymers using second harmonic generation
[AD-A283023] p 448 N95-13688
Relaxation of polar orientational order in nonlinear optical polymers by second harmonic generation
[AD-A283024] p 449 N95-13689
Nonlinear optical susceptibility of a model guest/host polymeric system as investigated by electro-optics and second harmonic generation
[AD-A283069] p 449 N95-13692
Compression of regions in the global advanced very high resolution radiometer 1-km data set
p 565 N95-14591
Vestibular ontogeny: Measuring the influence of the dynamic environment p 544 N95-15105

NEBRASKA UNIV., OMAHA, NE.
Neural mechanisms of kinesthesia
p 555 N95-14018
Conductive paints
[DE94-014069] p 453 N95-15292

NEW ENERGY AND INDUSTRIAL TECHNOLOGY DEVELOPMENT ORGANIZATION, TOKYO (JAPAN).
Survey of the 1991 geothermal exploration promotion
[DE94-780690] p 530 N95-14836
Development of the fuel cell power generation technology, 2
[DE94-780614] p 520 N95-15376
Development of the fuel cell power generation technology, 1
[DE94-780648] p 520 N95-15377

NEW HAMPSHIRE UNIV., DURHAM.
Landsat Pathfinder tropical forest information management system p 565 N95-14594

NEW MEXICO STATE UNIV., LAS CRUCES, NM.
The Stark anomalous dispersion optical filter: The theory p 462 N95-14622

NEW YORK UNIV. MEDICAL CENTER, NEW YORK, NY.
Measurement and regulation of central noradrenergic receptors
[AD-A284219] p 541 N95-14408

NEWCASTLE-UPON-TYNE UNIV., NEWCASTLE (ENGLAND).
2D regular arrays for a special class of non uniform recurrence equations
[PB94-195633] p 584 N95-13980
Sequentially t-diagnosable systems
[PB94-205093] p 574 N95-15396

NICHOLS RESEARCH CORP., HUNTSVILLE, AL.
Product life cycle data base, analysis and simulation integration methodology
[TABES PAPER 94-626] p 417 N95-14650

NIELSEN ENGINEERING AND RESEARCH, INC., MOUNTAIN VIEW, CA.
Hypertext knowledge presentation system to transition basic research
[AD-A280796] p 630 N95-14321

NORTH CAROLINA STATE UNIV., RALEIGH, NC.
Deformation, strength, and failure modes of laminated conventional and hybrid polymer-matrix composites loaded in the thickness direction
[AD-A281587] p 436 N95-15443
Reactive polymers: Main chain coordination polymers for air separation
[AD-A281614] p 455 N95-15444
Meso-beta scale numerical simulation studies of terrain-induced jet streak mass/momentum perturbations
[NASA-CR-197226] p 531 N95-15684

NORTH CAROLINA UNIV., CHAPEL HILL, NC.
Virtual reality at work p 556 N95-14033
Chemically modified electrodes by nucleophilic substitution of chlorosilylated platinum oxide surfaces
[AD-A281567] p 477 N95-15456

NORTH CAROLINA UNIV., RALEIGH, NC.
The operational forecasting/nowcasting of precipitation type in the southeastern United States type of precipitation: Descriptive and objective guidance
[AD-A284456] p 535 N95-15819

NORTHROP CORP., LOMITA, CA.
Objective evaluation of situation awareness for dynamic decision makers in teleoperations p 559 N95-14047

NORTHWESTERN POLYTECHNICAL UNIV., XIAN (CHINA).
Cardiovascular deconditioning effects of long-term simulated weightlessness in rats p 538 N95-15099

NORTHWESTERN UNIV., EVANSTON, IL.
Statistical investigation of fatigue crack initiation and growth around chamfered rivet holes in Alclad 2024 T3 as affected by corrosion p 510 N95-14472
Fatigue reliability method with in-service inspections
p 505 N95-14475
Future directions in two-phase flow and heat transfer in space p 482 N95-14523
Shear stabilization of solidification fronts
p 448 N95-14549
Research in high energy physics
[DE94-015519] p 600 N95-15539
Interacting fronts in a model for binary-mixture convection
[DE94-013595] p 494 N95-15861

NOTRE DAME UNIV., IN.
High-speed fixed and floating point implementation of delta-operator formulated discrete time systems
[AD-A283109] p 584 N95-13694
Two-layer viscous instability in a rotating couette device p 489 N95-14566

NOTTINGHAM UNIV. (ENGLAND).
Diffuse interstellar bands between 3900 A and 4200 A
p 640 N95-15834

NYMA, INC., BROOK PARK, OH.
Update to the NASA Lewis ice accretion code LEWICE
[NASA-CR-195387] p 481 N95-14295
Resonant interaction of a linear array of supersonic rectangular jets: An experimental study
[NASA-CR-195398] p 404 N95-15852
Characterization of damage progression in SCS-6/Timetal 21S (0)4 under thermomechanical fatigue loadings
[NASA-CR-195399] p 436 N95-15911

O

OAK RIDGE NATIONAL LAB., TN.
Processing of thermoset prepreg laminate via exposure to microwave radiation
[DE94-013268] p 432 N95-13643
Resolution measurement for scanning electron microscopes
[DE94-012747] p 601 N95-13674
Charge state distributions from highly charged ions channeled at a metal surface
[DE94-012755] p 592 N95-13675
Errors induced in triaxial stress tensor calculations using incorrect lattice parameters
[DE94-013256] p 444 N95-13820
In-situ TEM crystallization of sol-gel derived BaTiO3 thin films
[DE94-013260] p 619 N95-13821
Experimental implementation of a robust damped-oscillation control algorithm on a full-sized, two-degree-of-freedom, AC induction motor-driven crane
[DE94-012113] p 501 N95-14005
Assessing post-fire combustion of polyurethane
[DE94-011461] p 438 N95-14375
The integration of renewable energy sources into electric power distribution systems. Volume 1: National assessment
[DE94-015935] p 519 N95-14393
HTS Wire Development Workshop: Proceedings
[DE94-015650] p 624 N95-15421
A Multiple Divide-and-Conquer (MDC) algorithm for optimal alignments in linear space
[DE94-015457] p 574 N95-15536
Numerical solution of a tunneling equation
[DE94-015514] p 586 N95-15538
The Ceramic Manufacturability Center: A new partnership with US industry
[DE94-015851] p 456 N95-15634

OAK RIDGE Y-12 PLANT, TN.
The Ceramic Manufacturability Center: A new partnership with US industry
[DE94-015851] p 456 N95-15634

OCEANWEATHER, INC., COS COB, CT.
Upgrade of tropical cyclone surface wind field model
[AD-A283530] p 533 N95-15323

OFFICE NATIONAL D'ETUDES ET DE RECHERCHES AEROSPATIALES, PARIS (FRANCE).
Lateral jet control for tactical missiles
p 399 N95-14448
High angle of attack aerodynamics
p 399 N95-14450
ESD and lightning interactions on aircraft
p 406 N95-14896
Modeling and numerical simulation of the cerebral blood flow under acceleration p 545 N95-15112

OHIO STATE UNIV., COLUMBUS.
Powder agglomeration in a microgravity environment
[NASA-CR-197000] p 457 N95-14105
Monitoring the variability of active galactic nuclei from a space-based platform p 644 N95-14509
Crystal growth and fluid mechanics problems in directional solidification p 486 N95-14550
Wideband electromagnetic scattering/analysis program. Electromagnetic scattering from the trunks and branches of trees
[AD-A283112] p 469 N95-15394

OKLAHOMA UNIV., NORMAN, OK.
Radiometer calibration procedure and beacon attenuation estimation reference level
p 466 N95-14683
OKLAHOMA UNIV. HEALTH SCIENCES CENTER, NORMAN, OK.
Low-dose alcohol effects on human behavior and performance: A review of post-1984 research
[DOT/FAA/AM-94/24] p 552 N95-14863
OLD DOMINION UNIV., NORFOLK, VA.
Aerodynamic shape optimization of a HSCT type configuration with improved surface definition
[NASA-CR-197011] p 392 N95-13701
Numerical simulation of shock-induced combustion past blunt bodies using shock-fitting technique
[NASA-CR-197013] p 437 N95-14268
Radiative interactions in multi-dimensional chemically reacting flows using Monte Carlo simulations
[NASA-CR-197012] p 481 N95-14269
Thermal structure analyses for CSM testbed (COMET)
[NASA-CR-196998] p 506 N95-14270
Software reliability studies
[NASA-CR-197027] p 572 N95-14615
Modelling of eddy currents related to large angle magnetic suspension test fixture
[NASA-CR-197028] p 475 N95-14851
The electrocortical correlates of fluctuating states of attention during vigilance tasks
[NASA-CR-197051] p 552 N95-14864
Annular Suspension and Pointing System (ASPS) magnetic rotary joint
[NASA-CR-197197] p 502 N95-14907
Investigation of ramp injectors for supersonic mixing enhancement
[NASA-CR-4634] p 494 N95-15605
Investigation of Allan variance for determining noise spectral forms with application to microwave radiometry
[NASA-CR-194985] p 516 N95-15727
OPEN UNIV., MILTON KEYNES (ENGLAND).
Simultaneous two component squeezing in generalized q-coherent states p 598 N95-13908
OPTICAL SOCIETY OF AMERICA, WASHINGTON, DC.
Integrated photonics research, 1993
[AD-A281578] p 614 N95-15464
OREGON STATE UNIV., CORVALLIS, OR.
A Workshop on New Directions in Extremal Stochastic Analysis of Nonlinear Ocean Systems
[AD-A283969] p 535 N95-14204
OSAKA UNIV., TOYONAKA (JAPAN).
Functional participation of the valvula cerebelli on the goldfish dorsal light response p 539 N95-15119
OSLO UNIV. (NORWAY).
Chaotic time series. Part 2: System identification and prediction
[PB94-207115] p 589 N95-13630

P

PACIFIC NORTHWEST LAB., RICHLAND, WA.
A femtosecond optical parametric oscillator near 3 microns
[DE94-014500] p 612 N95-13986
Synthesis, processing and properties of materials for SOFCs
[DE94-014491] p 517 N95-14002
Three neural network based sensor systems for environmental monitoring
[DE94-014557] p 522 N95-14195
An experimental and numerical study of the modifications of mixed-layer structure by inhomogeneous surface fluxes and secondary circulations
[DE94-015945] p 529 N95-14428
Low latency remote memory access on the Intel Paragon
[DE94-014993] p 566 N95-14662
Fluid dynamic effects on precision cleaning with supercritical fluids
[DE94-015001] p 439 N95-14663
The effect of specimen geometry on the accuracy of constitutive relations in a superplastic 5083 aluminum alloy
[DE94-014501] p 445 N95-15293
Beta decay data for neutron-rich Li-Cl nuclides
[DE94-014556] p 595 N95-15310
High performance computational chemistry: Towards fully distributed parallel algorithms
[DE94-014561] p 573 N95-15311
Scintillating glass fiber-optic neutron sensors
[DE94-014562] p 613 N95-15312
Relationship between microstructure and efficiency of scintillating glasses
[DE94-014563] p 454 N95-15313
Thin GSO scintillator for neutron detection
[DE94-014566] p 613 N95-15314
Climatological data summary 1993 with historical data
[DE94-016624] p 523 N95-15363
Influence of transmutation on microstructure, density change, and embrittlement of vanadium and vanadium alloys irradiated in HFIR
[DE94-015202] p 446 N95-15431
Development and analysis of high-energy corona process for air purification
[DE94-015207] p 524 N95-15432
Experiments to examine the contribution of gas atoms to void formation in irradiated metals
[DE94-015209] p 446 N95-15433
System administrator's guide to CDPS
[DE94-015288] p 633 N95-15528
PACIFIC SOUTHWEST FOREST AND RANGE EXPERIMENT STATION, BERKELEY, CA.
Tilting wind tunnel for fire behavior studies
[PB94-204625] p 413 N95-14513
PAVIA UNIV. (ITALY).
Homodyning and heterodyning the quantum phase
p 604 N95-13913
PEDAGOGICAL UNIV., BYDGOSZCZ, BYDGOSZCZ (POLAND).
Diffuse bands versus extinction parameters
p 640 N95-15836
PENNSYLVANIA STATE UNIV., SCHUYLKILL HAVEN, PA.
Decoherence and dissipation for a quantum system coupled to a local environment p 609 N95-13949
PENNSYLVANIA STATE UNIV., UNIVERSITY PARK, PA.
The effect of aircraft speed on the penetration of sonic boom noise into a flat ocean p 402 N95-14887
Wake turbulence p 405 N95-14894
Turbulent upward flame spread on a vertical wall under external radiation
[PB94-207388] p 441 N95-15353
Theoretical studies in elementary particle physics
[DE94-015343] p 595 N95-15372
Turbulent mixing of the HVOF thermal spray and coating oxidation
[DE94-015414] p 455 N95-15535
Low loss substrates for microwave applications and sol-gel processing of superconductors
[AD-A284868] p 625 N95-15746
PHILIPS GLOEILAMPENFABRIEKEN N.V., EINDHOVEN (NETHERLANDS).
Strained-layer InGaAs(P)/InP quantum well semiconductor lasers grown by organometallic vapour phase epitaxy
[PB94-201399] p 622 N95-14795
Laser ablation and deposition of alloys
[PB94-191384] p 499 N95-15388
PHILLIPS LAB., EDWARDS AFB, CA.
A facility to produce an energetic, ground state atomic oxygen beam for the simulation of the Low-Earth Orbit environment p 422 N95-14072
PHILLIPS LAB., HANSCOM AFB, MA.
Pre-flight POLAR code predictions for the CHAWS space flight experiment
[AD-A280951] p 428 N95-14599
PHILLIPS LAB., KIRTLAND AFB, NM.
The 3.5-meter telescope enclosure
[AD-A280949] p 638 N95-14597
Department of Defense high power laser program guidance
[AD-A282915] p 500 N95-15391
PHOTOMETRICS, INC., WOBURN, MA.
Research on characterization of the upper atmosphere using lidar
[AD-A283241] p 530 N95-15401
PHYSICAL OPTICS CORP., TORRANCE, CA.
A novel technique for 4-dimensional atmosphere and oceanographic irradiance measurements using 3-D spatial filtering
[AD-A283758] p 613 N95-14353
Optically controlled MMW beamsteering beamforming antenna
[AD-A282831] p 614 N95-15414
PHYSICAL SCIENCES, INC., ANDOVER, MA.
Laboratory simulation of Low Earth Orbit (LEO) atomic oxygen effects p 422 N95-14071
Ultrasensitive infrared chemiluminescence detection
[AD-A283531] p 440 N95-14958
PITTSBURGH UNIV., PITTSBURGH, PA.
A coarse grained approach to thermocapillarity effects in binary systems p 487 N95-14553
Nucleation and chiral symmetry breaking under controlled hydrodynamic flows p 489 N95-14570
ASPM2: Progress toward the analysis of symbolic parameter models
[AD-A284437] p 576 N95-15817
PLANETARY SCIENCE INST., TUCSON, AZ.
FRESIP project observations of cataclysmic variables: A unique opportunity p 644 N95-14507
POLITECNICO DI MILANO, MILAN (ITALY).
International Geoid Service Bulletin No. 1
[BULL-1] p 516 N95-15791
Introducing the International Geoid Service
p 516 N95-15792
The GEOMED Project p 516 N95-15794
PRATT AND WHITNEY AIRCRAFT, EAST HARTFORD, CT.
Unsteady flows in turbines: Impact on design procedure p 480 N95-14132
Ultra-high bypass ratio jet noise
[NASA-CR-195394] p 591 N95-14610
PRATT AND WHITNEY AIRCRAFT, WEST PALM BEACH, FL.
Fatigue in single crystal nickel superalloys
[AD-A282917] p 446 N95-15415
PRINCESS MARGARET ROSE ORTHOPAEDIC HOSPITAL, EDINBURGH, LOTHIAN (SCOTLAND).
A physical control interface with proprioceptive feedback and multiple degrees of freedom p 559 N95-14045
PRINCETON UNIV., NJ.
The display of tactile information p 554 N95-14017
Dynamics of hard sphere colloidal dispersions
p 490 N95-14573
New techniques for diffusing-wave spectroscopy
p 444 N95-14575
PUERTO RICO UNIV., RIO PIEDRAS.
Kinetic theory for electrodic phase transitions: The voltammogram
[AD-A283039] p 619 N95-13691
PURDUE UNIV., WEST LAFAYETTE, IN.
Towards developing an analytical procedure of defining the equatorial electrojet for correcting satellite magnetic anomaly data
[NASA-CR-193621] p 526 N95-14267
Bending effects of unsymmetric adhesively bonded composite repairs on cracked aluminum panels
p 507 N95-14456
Fatigue analysis of multiple site damage at a row of holes in a wide panel p 508 N95-14463
The avian embryo responding to microgravity of space flight p 538 N95-15104
Gas turbine prediffuser-combustor performance during operation with air-water mixture
[DOT/FAA/CT-93/52] p 411 N95-15683

R

RAND CORP., SANTA MONICA, CA.
Technology access from the FS-X radar program. Lessons for technology transfer and US acquisition policy
[AD-A283773] p 461 N95-14334
The F-16 multinational staged improvement program: A case study of risk assessment and risk management
[AD-A281706] p 409 N95-15451
US space-based remote sensing: Challenges and prospects
[AD-A282439] p 515 N95-15546
RAYTHEON CO., LEXINGTON, MA.
RF vacuum microelectronics
[AD-A283123] p 478 N95-15613
REGGIO CALABRIA UNIV., REGGIO CALABRIA, REGGIO CALABRIA (ITALY).
A strategy for geoid repairing p 517 N95-15798
RENSSELAER POLYTECHNIC INST., TROY, NY.
Vapor transport crystal growth of mercury-cadmium-telluride in microgravity
p 458 N95-14216
Analysis of phase distribution phenomena in microgravity environments p 459 N95-14557
Interfacial force field characterization of a constrained vapor bubble thermosyphon using IAI
p 488 N95-14560
Sonic boom interaction with turbulence
p 402 N95-14884
RESEARCH INST. FOR COMPUTING AND INFORMATION SYSTEMS, HOUSTON, TX.
RICIS Symposium 1992: Mission and Safety Critical Systems Research and Applications
[NASA-CR-196963] p 569 N95-14156
MISSION: Mission and Safety Critical Support Environment. Executive overview p 569 N95-14158
RESEARCH TRIANGLE INST., RESEARCH TRIANGLE PARK, NC.
Test method for the measurement of methanol emissions from stationary sources
[PB94-170297] p 523 N95-15382
RICE UNIV., HOUSTON, TX.
Infrared absorption spectroscopy and chemical kinetics of free radicals
[DE94-016642] p 438 N95-14392

Application of spin-sensitive electron spectroscopies to investigations of electronic and magnetic properties of solid surfaces and epitaxial systems
[DE94-012981] p 625 N95-15574

RIJKSINSTITUUT VOOR VOLKSGEZONDHEID EN MILIEUHYGIEENE, BILTHOVEN (NETHERLANDS).
Field intercomparison with five automatic ammonia monitors
[PB94-192879] p 523 N95-15389

ROCHESTER UNIV., NY.
Time-dependent distinguishability: Choosing to be a wave or a particle p 600 N95-13912
LLE review, January - March 1994
[DE94-015058] p 618 N95-14955
Control of selective perception using Bayes nets and decision theory
[TR-468] p 573 N95-15151
Supervised learning without output labels
[TR-510-REV] p 552 N95-15588
Compiler optimizations for cache locality and coherence
[TR-504] p 586 N95-15589
The prospects for on-line hybrid coherency protocols on bus-based multiprocessors
[TR-490] p 579 N95-15590
Pseudorandom generators and the frequency of simplicity
[UR-DCS-TR-94-507] p 586 N95-15594
Discourse interpretation and the scope of operators
[TR-518] p 586 N95-15595
Weighted NP optimization problems: Logical definability and approximation properties
[TR-516] p 587 N95-15596
Unambiguous computation: Boolean hierarchies an sparse Turing-complete sets
[TR-483] p 575 N95-15597
i-speech: Experiments with a single level feedback paradigm
[TR-509] p 575 N95-15640
On accessing and hiding information
p 587 N95-15641
First results with instance-based state identification for reinforcement learning
[TR-502] p 553 N95-15642
On point-based temporal disjointness
[TR-497] p 587 N95-15643
Two heads are better than two tapes
[TR-493] p 575 N95-15644
Connections among space-bounded and multihead probabilistic automata
[TR-476] p 575 N95-15645
Upward separation for FewP and related classes
[TR-488] p 575 N95-15721
Universally serializable computation
[TR-520] p 587 N95-15732
The lambda loop transformation toolkit (user's reference manual)
[TR-511] p 587 N95-15733
Gaze selection for visual search
[TR-512] p 587 N95-15775
The temporal reasoning systems TimeGraph 1-2
[TR-494-REV] p 584 N95-15786
Vision, learning, and development
[TR-492-REV] p 553 N95-15787
A promise class at least as hard as the polynomial hierarchy
[TR-484] p 576 N95-15788
Density control and on-line labeling problems
[TR-481] p 576 N95-15789
Efficient algorithms for qualitative reasoning about time
[TR-496] p 576 N95-15825
A general method to construct oracles realizing given relationships between complexity classes
[TR-500] p 588 N95-15854
Lower bounds for perceptrons solving some separation problems and oracle separation of AM from PP
[TR-498] p 586 N95-15855
Genetic programming with adaptive representations
[TR-489] p 576 N95-15856
Seeing behind occlusions
[TR-487] p 576 N95-15857
P-selectivity: Intersections and indices
[TR-482] p 577 N95-15858
Seeking stronger separations: Probability one balanced- and bi-immunity
[TR-480] p 589 N95-15859
Learning with incomplete selective perception
[TR-453] p 577 N95-15860

ROCKWELL INTERNATIONAL CORP., DOWNEY, CA.
Space Shuttle fatigue loads spectra for prelaunch and liftoff loads p 419 N95-14474
Requirements report for SSTO vertical take-off and horizontal landing vehicle
[NASA-CR-197029] p 409 N95-14794
Strategic avionics technology definition studies, power voter redundancy management. Power voter applications in new vehicle architectures
[NASA-CR-197049] p 411 N95-14799
Milestone 4: Thrust structure concepts and IHM screening Graphite Composite Primary Structure (GCPS)
[NASA-CR-197053] p 434 N95-14800
Milestone 4: Test plan for Reusable Hydrogen Composite Tank System (RHCTS). Task 3: Composite tank materials
[NASA-CR-197036] p 435 N95-14801
Milestone 5 test report. Task 5, subtask 5.2: Tile to foam strength tests
[NASA-CR-197241] p 514 N95-15913

ROCKWELL INTERNATIONAL CORP., EL SEGUNDO, CA.
Extracting a representative loading spectrum from recorded flight data p 410 N95-14469

ROCKWELL INTERNATIONAL CORP., HUNTSVILLE, AL.
Automated test environment for a real-time control system
[TABES PAPER 94-631] p 417 N95-14652

ROCKWELL INTERNATIONAL SCIENCE CENTER, THOUSAND OAKS, CA.
Fundamental studies of diamond growth and surface reactions
[AD-A284390] p 626 N95-15808

ROCKWELL SPACE OPERATIONS CO., HOUSTON, TX.
Reuseable Objects Software Environment (ROSE): Introduction to Air Force Software Reuse Workshop
[NASA-CR-197017] p 572 N95-14520

ROME LAB., GRIFFISS AFB, NY.
Generic architectures for future flight systems
p 567 N95-14159
Architecture for Survivable Systems Processing (ASSP). Technology benefits for Open System Interconnects
p 567 N95-14160

ROYAL AIR FORCE INST. OF AVIATION MEDICINE, FARNBOROUGH (ENGLAND).
Non-invasive physiological monitoring relevant to G-induced loss of consciousness p 547 N95-15125

RUHR UNIV., BOCHUM (GERMANY).
The Teleprasenz Consortium: Structure and intentions
p 558 N95-14039
Binaural room simulation p 561 N95-14053

RUST COLL., HOLLY SPRINGS, MS.
Simulation of coal and char nitrogen reactions in combustion
[DE94-013941] p 440 N95-15291

RUTGERS UNIV., PISCATAWAY, NJ.
Study of multiple cracks in airplane fuselage by micromechanics and complex variables
p 509 N95-14468
Oscillatory thermocapillary convection
p 483 N95-14526

RUTHERFORD APPLETON LAB., CHILTON (ENGLAND).
The 40 and 50 GHz propagation experiments at the Rutherford Appleton Laboratory, UK, using the ITALSAT beacons p 465 N95-14674
Effects of hydrometeors and atmospheric gases at SHF/EHF p 468 N95-14835
Introduction to muSR: What, how, where
[PB94-192267] p 596 N95-15379
Approximate next-to-leading order relation between the low-x F2 scaling violations and the gluon density
[PB94-192283] p 596 N95-15380

S

SALERNO UNIV. (ITALY).
Minimum uncertainty and squeezing in diffusion processes and stochastic quantization
p 607 N95-13938

SAN JOSE STATE UNIV., CA.
New findings regarding light intensity and its effects as a zeitgeber in the Sprague-Dawley rat
p 539 N95-15135

SANDIA NATIONAL LABS., ALBUQUERQUE, NM.
Assembly feasibility and reliability studies of surface mount circuit boards manufactured with lead-free solders
[DE94-013783] p 472 N95-13975
An optical simulation of shared memory
[DE94-013824] p 568 N95-13976
A High Temperature Hermetic Primer and a Variable Spring Tester
[DE94-012073] p 457 N95-14004
Calibration and characterization of wide range hydrogen sensors
[DE94-013765] p 496 N95-14146
Studies of the ablated plasma from experimental plasma gun disruption simulations
[DE94-015017] p 617 N95-14262
Determination of the shear modulus in self-assembled monolayers using quartz resonators
[DE94-013449] p 437 N95-14307
Resonator response to non-Newtonian fluids
[DE94-013450] p 473 N95-14308
Quartz resonator state-of-charge monitor for lead-acid batteries
[DE94-013823] p 473 N95-14310
Dynamical properties measurements for asteroid, comet and meteorite material applicable to impact modeling and mitigation calculations
[DE94-014142] p 642 N95-14311
Microcontamination detection using Heavy Ion Backscattering Spectrometry
[DE94-014182] p 437 N95-14312
Interferometric synthetic aperture radar terrain elevation mapping from multiple observations
[DE94-014185] p 515 N95-14313
I(sub DDQ) testing for ultimate low power design verification and defect detection
[DE94-014281] p 473 N95-14314
Cut-off-mesa isolated rib optical waveguide for 3-5 heterostructure PICs
[DE94-014661] p 474 N95-14315
A compact high voltage pulse generator
[DE94-015282] p 474 N95-14319
Materials issues in molecular beam epitaxy
[DE94-015796] p 621 N95-14322
Microstructures of InAs(1-x)Sb(x) (x = 0.07-0.14) alloys and strained-layer superlattices
[DE94-015801] p 621 N95-14323
Magnetic field dependent photoluminescence studies of InGaAs/GaAs strained-single-quantum wells
[DE94-015774] p 621 N95-14342
Polarized photomodulated reflectivity and photoluminescence studies of ordered InGaP2 under pressure
[DE94-016556] p 621 N95-14390
Modeling turbulent flame propagation
[DE94-016618] p 438 N95-14391
US-Japan workshop Q-181 on High Heat Flux Components and Plasma-Surface Interactions for Next Devices: Proceedings
[DE94-014939] p 618 N95-14443
Numerical solution of two-dimensional ablation problems using the finite control volume method with unstructured grids
[DE94-015012] p 428 N95-14664
A proposed framework for computational fluid dynamics code calibration and validation
[DE94-015799] p 493 N95-15351
Automated cleaning of electronic components
[DE94-014122] p 476 N95-15356
Gouge initiation in high-velocity rocket sled testing
[DE94-014288] p 418 N95-15357
Acronyms, initialisms, and abbreviations
[DE94-016686] p 632 N95-15366
Minutes of the Third Annual Workshop on Chromate Replacements in Light Metal Finishing
[DE94-015163] p 446 N95-15368
Defining a controller architecture for the long-reach manipulator
[DE94-015165] p 583 N95-15369
Effects of two-phase flow on the deflagration of porous energetic materials
[DE94-015353] p 442 N95-15375
Using Pro/ENGINEER's (tm) interface module
[DE94-013364] p 574 N95-15384
Rapid prototyping applications at Sandia National Laboratories
[DE94-006360] p 460 N95-15409
The effects of spatial location of defect states on the switching characteristics of amorphous and polycrystalline silicon thin film transistors: A numerical simulation using AMPS 2-D
[DE94-013437] p 476 N95-15410
Measurements of upper tropospheric moisture with a Raman lidar
[DE94-015748] p 531 N95-15411
Monitoring solar-thermal systems: An outline of methods and procedures
[DE94-015599] p 521 N95-15420
Time-of-flight detector for heavy ion backscattering spectrometry
[DE94-015600] p 596 N95-15437
Sandia 1993 Superconducting Technology Program
[DE94-015601] p 625 N95-15438
SUNMOS for the Intel Paragon, a brief user's guide
[DE94-015277] p 574 N95-15543
High gain GaAs switches for impulse sources: Measurement of the speed of current filaments
[DE94-015281] p 477 N95-15544
A three-dimensional fast solver for arbitrary vorton distributions
[DE94-012581] p 404 N95-15570

Large scale obscuration and related climate effects open literature bibliography
[DE94-012992] p 524 N95-15575
Preliminary DIAL model
[DE94-013243] p 469 N95-15583

SAYLES ENTERPRISES, INC., OMAHA, NE.
Conductive paints
[DE94-014069] p 453 N95-15292

SBS ENGINEERING, INC., HOUSTON, TX.
CIFO 3.0 p 570 N95-14167

SCIENCE APPLICATIONS, INC., MCLEAN, VA.
Experimental evaluation of cursors for B-2 Synthetic Aperture Radar (SAR) application
[AD-A283025] p 468 N95-15393

SCIENCE APPLICATIONS INTERNATIONAL CORP., ARLINGTON, VA.
Civil use of night vision devices: Evaluation pilot's guide, part 2
[DOT/FAA/RD-94/19] p 410 N95-14175

SCIENCE APPLICATIONS INTERNATIONAL CORP., AUSTIN, TX.
An evaluation of rise time characterization and prediction methods p 401 N95-14881

SCIENCE APPLICATIONS INTERNATIONAL CORP., SAN DIEGO, CA.
Reusable rocket engine turbopump health management system
[NASA-CR-195388] p 431 N95-15058

SCIENCE APPLICATIONS INTERNATIONAL CORP., TORRANCE, CA.
Engine system assessment study using Martian propellants
[NASA-CR-189188] p 431 N95-14869

SCIENTIFIC RESEARCH ASSOCIATES, INC., GLASTONBURY, CT.
Capacitance calculations in nanostructure devices via the quantum Liouville equation in the coordinate representation
[AD-A281936] p 589 N95-13656

SCRIPPS INSTITUTION OF OCEANOGRAPHY, LA JOLLA, CA.
Wideband beamforming for a sparse nonuniformly spaced array
[AD-A280833] p 591 N95-14396

SELSKAPET FOR INDUSTRIELL OG TEKNISK FORSKNING, OSLO (NORWAY).
Chaotic time series. Part 2: System identification and prediction
[PB94-207115] p 589 N95-13630

SELSKAPET FOR INDUSTRIELL OG TEKNISK FORSKNING, TRONDHEIM (NORWAY).
Observation of microcrack development in concrete by use of TV-holography and deformation phase gradient calculation
[PB94-207990] p 513 N95-15348
Investigation of dendrite coherency in two commercial Al-Si foundry alloys
[PB94-208238] p 446 N95-15349
Computational chemistry packages on the CRAY Y-MP in trondheim
[PB94-208246] p 595 N95-15350

SEOUL NATIONAL UNIV. (REPUBLIC OF KOREA).
A method of measuring the amplitude-modulated vacuum field near a conducting mirror p 471 N95-13921

SHEFFIELD UNIV. (ENGLAND).
Cardiovascular and metabolic responses to 6 deg Head-Down Tilt (HDT) and 70 deg Head-Up Tilt (HUT) following exercise p 544 N95-15109

SLOVAK ACADEMY OF SCIENCES, BRATISLAVA (CZECHOSLOVAKIA).
Behaviour of newly hatched and adult Japanese quail and the feasibility of adaptation to weightlessness p 538 N95-15106
Activity of ornithine decarboxylase in muscle of Japanese quail in hypergravity conditions p 539 N95-15144

SMITHSONIAN ASTROPHYSICAL OBSERVATORY, CAMBRIDGE, MA.
Measurement and interpretation of crustal deformation rates associated with postglacial rebound
[NASA-CR-196440] p 525 N95-13627
HRMA calibration handbook: EKC gravity compensated XRCF models
[NASA-CR-195818] p 636 N95-13634
Work Breakdown Structure (WBS) and WBS dictionary
[NASA-CR-196448] p 567 N95-13635
AXAF SIM focus mechanism study
[NASA-CR-196976] p 636 N95-13636
AXAF VETA-I mirror ring focus measurements
[NASA-CR-196145] p 637 N95-13637
Summary of AXAF calibration requirements
[NASA-CR-196985] p 637 N95-13887
Performance Reports: Mirror alignment system performance prediction comparison between SAO and EKC
[NASA-CR-196013] p 637 N95-14100
Performance Report: A timeline for the synchrotron calibration of AXAF
[NASA-CR-196489] p 638 N95-14101
Satellite Laser Ranging operations p 500 N95-14287

SOCIETE NATIONALE D'ETUDE ET DE CONSTRUCTION DE MOTEURS D'AVIATION, MOISSY-CRAMAYEL (FRANCE).
New methods, new methodology: Advanced CFD in the Snecma turbomachinery design process p 480 N95-14134

SOGANG UNIV., SEOUL (REPUBLIC OF KOREA).
Phase properties of multicomponent superposition states in various amplifiers p 605 N95-13923

SOLOMON (G.), PASADENA, CA.
Convolutional encoding of self-dual block codes (2) p 462 N95-14623

SONOMA STATE UNIV., ROHNERT PARK, CA.
ROSAT observations of the binary Be-star and radio pulsar PSR1259-63
[NASA-CR-196951] p 642 N95-15907

SOREQ RESEARCH ESTABLISHMENT, ISRAEL ATOMIC ENERGY COMMISSION, YAVNEH (ISRAEL).
Self contamination effects in the TAUVEX UV Telescope: Ground testing and computer simulation p 421 N95-14067
Atomic Oxygen (ATOX) simulation of Teflon FEP and Kapton H surfaces using a high intensity, low energy, mass selected, ion beam facility p 422 N95-14073

SOUTH CAROLINA UNIV., COLUMBIA, SC.
The transformation of organic amines by transition metal cluster compounds
[DE94-017151] p 441 N95-15346

SOUTHERN RESEARCH INST., BIRMINGHAM, AL.
Mechanical behavior of high temperature composites
[AD-A281582] p 436 N95-15441

SOUTHWEST RESEARCH INST., SAN ANTONIO, TX.
Definition of high-temperature use limits for MIL-L-2104 engine oils
[AD-A282838] p 451 N95-14365
Analysis of small crack behavior for airframe applications p 512 N95-14484
Wear mechanism evaluation and measurement in fuel-lubricated components
[AD-A284870] p 504 N95-15747

SOUTHWEST TEXAS STATE UNIV., SAN MARCOS, TX.
European Workshop Industrical Computer Science Systems approach to design for safety p 569 N95-14157

SPACE BIOMEDICAL RESEARCH INST., HOUSTON, TX.
A comparison of overall mathematical models of the cardiovascular system for simulating response to orthostatic stresses p 550 N95-15150

SPACE EXPLORATION ASSOCIATION, CEDARVILLE, OH.
High performance arcjet engines
[NASA-CR-195397] p 430 N95-13697

SPACE SYSTEMS/LORAL, PALO ALTO, CA.
Refurbishment of a 39 foot thermal vacuum chamber p 418 N95-14085

SPACE TELESCOPE SCIENCE INST., BALTIMORE, MD.
Probing surface structure on late-type stars with FRESIP p 643 N95-14501
Asteroseismology: Ground based efforts and the need for space observations p 643 N95-14503
Rotation among solar-type stars p 644 N95-14506

SPAR AEROSPACE LTD., SAINTE-ANNE-DE-BELLEVUE (QUEBEC).
Thermal balance testing of MSAT 2 spacecraft p 424 N95-14080
Thermal balance testing of the MSAT spacecraft p 424 N95-14082

SPAUSCHUS ASSOCIATES, INC., STOCKBRIDGE, GA.
Solubility, viscosity and density of refrigerant and lubricant mixtures
[DE94-016949] p 454 N95-15343

SPECTRA RESEARCH SYSTEMS, INC., HUNTSVILLE, AL.
A graphical user interface for design and analysis of air breathing propulsion systems
[TABES PAPER 94-616] p 411 N95-14645

SRI INTERNATIONAL CORP., MENLO PARK, CA.
Study of auroral dynamics with combined spacecraft and incoherent scatter radar data
[NASA-CR-196974] p 526 N95-13818
Field-emitter arrays for RF vacuum microelectronics
[AD-A283549] p 476 N95-15327

STANFORD LINEAR ACCELERATOR CENTER, CA.
Hadronic wavefunctions in light-cone quantization
[DE94-014507] p 622 N95-15308
The parton distribution functions in the limit chi(sub Bj) approaches 1
[DE94-013799] p 597 N95-15545

STANFORD UNIV., CA.
Advanced laser source research
[AD-A283110] p 498 N95-13695
Telerobotics in rehabilitation: Barriers to a virtual existence p 556 N95-14030
A decade of telerobotics in rehabilitation: Demonstrated utility blocked by the high cost of manipulation and the complexity of the user interface p 558 N95-14044
Rotational wind indicator enhances control of rotated displays p 559 N95-14046
Asteroseismology with FRESIP: A meter class space telescope p 643 N95-14504
Mathematical problems of nonlinear wave propagation and of waves in heterogeneous media
[AD-A282217] p 492 N95-14605
Workshop on Advances in Scientific Computation and Differential Equations 1993 (SCADE)
[AD-A283111] p 585 N95-14657
Low energy electron and atom elastic scattering cross sections from 0.1 to 30 keV
[AD-A283584] p 595 N95-15318

STARMARK CORP., ARLINGTON, VA.
Civil use of night vision devices: Evaluation pilot's guide, part 2
[DOT/FAA/RD-94/19] p 410 N95-14175

STATE UNIV. OF NEW YORK, BINGHAMTON, NY.
Perception of auditory events: Attentional limitations
[AD-A284399] p 553 N95-15770

STATE UNIV. OF NEW YORK, BUFFALO, NY.
Determination of solvation kinetics in supercritical fluids
[DE94-016491] p 438 N95-14386
Modeling, simulation and engineering scale-up procedures for design of CVD reactors
[AD-A284919] p 494 N95-15760

STATE UNIV. OF NEW YORK, UTICA, NY.
NASA/DOD Aerospace Knowledge Diffusion Research Project. Report 30: Computer-Mediated Communication (CMC) and the communication of technical information in aerospace
[NASA-CR-194973] p 633 N95-15585

STAZIONE ASTRONOMICA INTERNAZIONALE DI LATITUDINE, CAGLIARI (ITALY).
The peculiar behaviour of the 5780 and 5797 DIBs in HD25137 p 639 N95-15833

STEVENS INST. OF TECH., HOBOKEN, NJ.
Computational predictive methods for fracture and fatigue p 509 N95-14466

SULZER INNOTEC A.G., WINTERTHUR (SWITZERLAND).
Computational methods for preliminary design and geometry definition in turbomachinery p 480 N95-14128
The industrial use of CFD in the design of turbomachinery p 480 N95-14133

SUMMITEC CORP., OAK RIDGE, TN.
High Temperature Calibration Furnace System user's guide
[NASA-CR-196526] p 573 N95-14905

SVERDRUP TECHNOLOGY, INC., BROOK PARK, OH.
Compact simultaneous-beam optical strain measurement system, phase 5
[NASA-CR-195396] p 601 N95-13666

SYRACUSE UNIV., NY.
Linear and nonlinear dynamic analysis of redundant load path bearingless rotor systems
[NASA-CR-197220] p 503 N95-14923
High-efficiency electro-optic grating on PLZT ceramic wafer for optical switching
[AD-A281573] p 477 N95-15460

SYSTEMS CONTROL TECHNOLOGY, INC., ARLINGTON, VA.
Vertical flight terminal operational procedures. A summary of FAA research and development
[AD-A283550] p 413 N95-15328

SYSTEMS TECHNOLOGY, INC., HAWTHORNE, CA.
Some criteria for teleoperators and virtual environments from experiences with vehicle/operator simulation p 556 N95-14028

SYTRONICS, INC., DAYTON, OH.
More supportable T-38A enhancement study
[AD-A283671] p 392 N95-15331

T

TECHNICAL UNIV. OF NORWAY, TRONDHEIM.
Observation of microcrack development in concrete by use of TV-holography and deformation phase gradient calculation
[PB94-207990] p 513 N95-15348

TECHNION - ISRAEL INST. OF TECH., HAIFA (ISRAEL).
Human operator tracking performance with a vibrotactile display p 560 N95-14049
TECHNISCHE HOCHSCHULE, AACHEN (GERMANY).
Prediction of rotor-blade deformations due to unsteady airloads
[AD-A284467] p 410 N95-15821
TECHNISCHE UNIV., BRUNSWICK (GERMANY).
Turbulence: Engineering models, aircraft response p 407 N95-14900
TECHNISCHE UNIV., DELFT (NETHERLANDS).
Automated hierarchical testable design of digital circuits
[PB94-197936] p 472 N95-13983
Analysis of electron microscope images: 3-D localization of immuno-markers
[PB94-197977] p 537 N95-13990
Methodology for the parallel direct solution of finite element systems
[PB94-198009] p 585 N95-13991
Fish method: Interaction between AC-machines and switching power converters
[PB94-191210] p 472 N95-14149
Dextrous gripping in a hazardous environment
[PB94-191244] p 501 N95-14150
Preparation and characterization of composite inorganic zeolite membranes with molecular sieve properties
[PB94-191251] p 450 N95-14151
Knowledge-based computational approach to architectural precedent analysis
[PB94-191269] p 568 N95-14152
Parallel image rendering algorithm and architecture based on ray tracing and radiosity shading
[PB94-191277] p 569 N95-14153
Dependent random variables in uncertainty analysis
[PB94-191293] p 585 N95-14154
Strained-layer InGaAs(P)/InP quantum well semiconductor lasers grown by organometallic vapour phase epitaxy
[PB94-201399] p 622 N95-14795
A SIMULINK environment for flight dynamics and control analysis: Application to the DHC-2 Beaver. Part 1: Implementation of a model library in SIMULINK. Part 2: Nonlinear analysis of the Beaver autopilot
[NONP-NASA-SUPPL-DK-94-2802] p 412 N95-14815
Dynamic modelling to assess the value of Electronic Data Interchange: A study in the Rotterdam port community
[PB94-195542] p 632 N95-14837
Study on titanium-silicalite-1 and related systems
[PB94-195500] p 445 N95-14845
Robust multigrid methods for the steady and unsteady incompressible Navier-Stokes equations in general coordinates
[PB94-195534] p 492 N95-15315
Surface spectroscopic studies of high-temperature superconductors
[PB94-191228] p 624 N95-15378
Laser ablation and deposition of alloys
[PB94-191384] p 499 N95-15388
Static strength of riveted joints in Fibre Metal Laminates
[PB94-201472] p 513 N95-15429
Process development of thermal hydrodechlorination
[PB94-195518] p 525 N95-15870
Selective RF pulses in NMR and their effect on coupled and uncoupled spin systems
[PB94-195526] p 471 N95-15871
TECHNISCHE UNIV., EINDHOVEN (NETHERLANDS).
Joint and angle-covariant spin measurements with a quadrupole magnetic field p 604 N95-13914
TECHNISCHE UNIV., HANOVER (GERMANY).
The European Geoid Project p 516 N95-15796
TECHNISCHE UNIV., MUNICH (GERMANY).
Aero design of turbomachinery components: CFD in complex systems p 481 N95-14136
TEL-AVIV UNIV., RAMAT-AVIV, TEL-AVIV (ISRAEL).
How to detect an excited atom without disturbing it or how to locate a super-mine without exploding it p 598 N95-13934
TENNESSEE UNIV., KNOXVILLE, TN.
Structured approaches for problems of network design and utilization
[AD-A282925] p 578 N95-15416
AASERT-93: Electroplating of refractory metals using haloaluminate melts
[AD-A284859] p 447 N95-15744
TEXACO, INC., HOUSTON, TX.
Intelligent alarming p 570 N95-14168
TEXAS A&M UNIV., COLLEGE STATION, TX.
Knowledge-based processing for aircraft flight control
[NASA-CR-194976] p 580 N95-13727
Quantum noise limits to matter-wave interferometry p 598 N95-13955
The strong Bell inequalities: A proposed experimental test p 611 N95-13966
CAPTIONALS: A computer aided testing environment for the verification and validation of communication protocols p 570 N95-14163
Performance comparison of token ring protocols for hard-real-time communication p 570 N95-14164
Hardware implementation of a desktop supercomputer for high performance image processing. Color image processing using cellular neural networks
[AD-A283071] p 571 N95-14178
Design review and analysis for a Pratt and Whitney fluid-film bearing and seal testing rig
[NASA-CR-197035] p 502 N95-14797
Optical variability in the equatorial and southeast Pacific
[AD-A283894] p 536 N95-15425
TEXAS UNIV., AUSTIN, TX.
Hubble Space Telescope GTO program
[NASA-CR-196263] p 637 N95-13723
Earth orientation parameters p 527 N95-14281
Precision orbit determination of altimetric satellites p 418 N95-14282
The role of SLR and LLR in relativity p 528 N95-14284
Synergism of SLR and GPS p 471 N95-14286
Onset of hexagons in surface-tension-driven Benard convection p 483 N95-14527
Slant path L- and S-Band tree shadowing measurements p 465 N95-14678
Photogrammetric mobile satellite service prediction p 466 N95-14679
Polymer-polymer interactions
[AD-A282944] p 453 N95-14844
An unmanned mission to Mars with sample collection and in-situ resource utilization
[NASA-CR-197202] p 645 N95-14868
Effect of stratification and geometrical spreading on sonic boom rise time p 401 N95-14880
Energy flux and hydrogeology of thermal anomalies in the Gulf of Mexico Basin: South Texas example
[DE94-015122] p 530 N95-14956
Problems in nonlinear acoustics: Surface acoustic waves, diffracting sound beams, and fluid-solid interface effects
[AD-A281714] p 592 N95-15453
TEXAS UNIV. HEALTH SCIENCE CENTER, HOUSTON, TX.
Teratogenic effects of delta g: The concept of allometric growth p 538 N95-15102
TEXTRON SPECIALTY MATERIALS, LOWELL, MA.
Evaluation of bonded boron/epoxy doublers for commercial aircraft aluminum structures p 508 N95-14457
THOMSON-CSF, PARIS (FRANCE).
Technical Revue Thomson-CSF, volume 26, no. 1, March 1994. Flat panels for visualisation
[PB94-197969] p 410 N95-13984
TIANJIN UNIV. (CHINA).
High-order squeezing of the quantum electromagnetic field and the generalized uncertainty relations in two-mode squeezed states p 471 N95-13900
TOKYO ELECTRIC POWER CO., INC. (JAPAN).
Development of visual 3D virtual environment for control software p 559 N95-14048
TOKYO UNIV. (JAPAN).
Development of visual 3D virtual environment for control software p 559 N95-14048
Lossless compression of NOAA-AVHRR satellite data p 565 N95-14592
Cardiovascular response to cold pressor and LBNP tests before and after 20-day-bedrest p 543 N95-15097
20 days bed-rest on insulin action in relation to body fat in young subjects p 549 N95-15145
TOKYO WOMAN'S CHRISTIAN UNIV. (JAPAN).
Water intake and urinary volume during 20 days bed-rest in young women p 548 N95-15134
TOLEDO UNIV., OH.
Enhanced capabilities and updated users manual for axial-flow turbine preliminary sizing code TURBAN
[NASA-CR-195405] p 405 N95-15912
TORONTO UNIV. (ONTARIO).
Hydrogen transport and trapping in graphite
[UTIAS-347] p 437 N95-13652
TRINITY COLL., DUBLIN (IRELAND).
Synthesis and applications of large heterometallic cluster systems
[AD-A284874] p 626 N95-15748
TRW, INC., REDONDO BEACH, CA.
Alpha LAMP Integration Facility p 418 N95-14094
Propagation considerations for the Odyssey system design p 466 N95-14680
TRW SPACE TECHNOLOGY LABS., REDONDO BEACH, CA.
ICE/ISEE plasma wave data analysis
[NASA-CR-196988] p 642 N95-14266
TUEBINGEN UNIV. (GERMANY).
The influence of gravity on vestibular nystagmus in humans p 546 N95-15121
TURIN UNIV. (ITALY).
Squeezed states and graviton-entropy production in the early universe p 608 N95-13947

U

UDINE UNIV. (ITALY).
On-Earth evaluation of the neurovestibular tolerance to centrifuge simulated artificial gravity in humans p 546 N95-15120
ULM UNIV. (GERMANY).
Photon statistics of a two-mode squeezed vacuum p 598 N95-13909
Quantum state engineering p 605 N95-13919
UNISYS CORP., HOUSTON, TX.
Applying CASE technology to the software maintenance life cycle
[TABES PAPER 94-620] p 416 N95-14647
UNISYS CORP., RESTON, VA.
Model contracts/agreements. Comprehensive Approach to Reusable Defense Software (CARDS)
[AD-A284403] p 575 N95-15783
Software Technology for Adaptable, Reliable Systems (STARS)
[AD-A284373] p 576 N95-15806
UNITED TECHNOLOGIES RESEARCH CENTER, EAST HARTFORD, CT.
Small crack test program for helicopter materials p 507 N95-14455
UNIVERSAL ENERGY SYSTEMS, INC., DAYTON, OH.
Modelling and investigation of EHD point contacts
[AD-A283571] p 454 N95-15316
UNIVERSIDAD NACIONAL AUTONOMA DE MEXICO, CUERNAVACA.
General properties of quantum optical systems in a strong field limit p 609 N95-13950
UNIVERSIDAD NACIONAL AUTONOMA DE MEXICO, MEXICO CITY.
Squeezing in a 2-D generalized oscillator p 603 N95-13907
How to characterize the nonlinear amplifier? p 471 N95-13922
UNIVERSIDADE ESTADUAL DE CAMPINAS (BRAZIL).
Probing the antiferromagnetic long-range order with Glauber spin states p 609 N95-13951
UNIVERSIDADE FEDERAL DO RIO DE JANEIRO (BRAZIL).
Nonlocal effects on the polarization state of a photon, induced by distant absorbers p 599 N95-13965
UNIVERSITAETS-STERNWARTE, JENA (GERMANY).
Diffuse interstellar bands in reflection nebulae p 639 N95-15830
UNIVERSITIES SPACE RESEARCH ASSOCIATION, COLUMBIA, MD.
Viper
[NASA-CR-197191] p 408 N95-13703
Proposal for an astronaut mass measurement device for the Space Shuttle
[NASA-CR-197198] p 563 N95-14854
An unmanned mission to Mars with sample collection and in-situ resource utilization
[NASA-CR-197202] p 645 N95-14868
Design of components for the NASA OCEAN project
[NASA-CR-197207] p 535 N95-14906
Annular Suspension and Pointing System (ASPS) magnetic rotary joint
[NASA-CR-197197] p 502 N95-14907
The Aluminum Falcon: A low cost modern commercial transport
[NASA-CR-197180] p 409 N95-15742
UNIVERSITIES SPACE RESEARCH ASSOCIATION, HOUSTON, TX.
The relationship between space sickness and preflight diet p 546 N95-15122
Physiologic mechanisms effecting circulatory and body fluid losses in weightlessness as shown by mathematical modeling p 547 N95-15129
UNIVERSITY MEDICAL SCHOOL OF DEBRECEN, DEBRECEN (HUNGARY).
Effect of short- and long-term spaceflight on the contractile properties of rat skeletal muscles with different functions p 539 N95-15141
UNIVERSITY OF CENTRAL FLORIDA, ORLANDO, FL.
Nondestructive analysis and development
[NASA-CR-196987] p 505 N95-13886
UNIVERSITY OF CENTRAL LANCASHIRE, PRESTON, LANCASHIRE (ENGLAND).
A search for the 13175 A infrared diffuse band in dense environments p 639 N95-15831

UNIVERSITY OF SOUTHERN CALIFORNIA, LOS ANGELES, CA.
Schroedinger operators with the q-ladder symmetry algebras p 588 N95-13942
A facility to produce an energetic, ground state atomic oxygen beam for the simulation of the Low-Earth Orbit environment p 422 N95-14072

UNIVERSITY OF WESTERN WASHINGTON, BELLINGHAM, WA.
Development of techniques for the evaluation of toxicant impacts to multispecies systems
[AD-A284426] p 524 N95-15814

UTAH UNIV., SALT LAKE CITY, UT.
Issues in the design of high dexterity, force reflective teleoperators p 555 N95-14024
The role of fretting corrosion and fretting fatigue in aircraft rivet hole cracking p 510 N95-14470
The effects of pitting on fatigue crack nucleation in 7075-T6 aluminum alloy p 448 N95-14482

UTRECHT STATE UNIV. (NETHERLANDS).
Two new kinds of uncertainty relations p 588 N95-13915

V

VAN DER SPIEGEL (JAN), PHILADELPHIA, PA.
Technical guidance for the development of a solid state image sensor for human low vision image warping
[NASA-CR-196997] p 612 N95-14272

VANDERBILT UNIV., NASHVILLE, TN.
Core-centering of compound drops in capillary oscillations: Observations on USML-1 experiments in space p 458 N95-14218
Bifurcation of rotating liquid drops: Results from USML-1 experiments in space p 458 N95-14219
Intelligent manufacturing systems state of the art
[TABES PAPER 94-503] p 415 N95-14637
Mechanical system reliability for long life space systems
[NASA-CR-197215] p 505 N95-15584

VETERANS ADMINISTRATION HOSPITAL, SEPULVEDA, CA.
Measurement and modification of the EEG and related behavior p 557 N95-14038

VILLANOVA UNIV., PA.
Correlated quadratures of resonance fluorescence and the generalized uncertainty relation p 598 N95-13937

VIRGINIA POLYTECHNIC INST. AND STATE UNIV., BLACKSBURG, VA.
The buckling response of symmetrically laminated composite plates having a trapezoidal planform area
[NASA-CR-196975] p 505 N95-13839
Experimental design for the evaluation of high-T(sub c) superconductive thermal bridges in a sensor satellite
[NASA-CR-197003] p 429 N95-14106
Innovative design of composite structures: Design, manufacturing, and testing of plates utilizing curvilinear fiber trajectories
[NASA-CR-197045] p 435 N95-14865
Fine structure of transient waves in a random medium: The correlation and spectral density functions p 401 N95-14882
Computational methods for PDE's in flow control, superconductivity, fluid flows and other applications
[AD-A282912] p 493 N95-15390

VIRGINIA UNIV., CHARLOTTESVILLE, VA.
Software development for safety-critical medical applications p 571 N95-14171
Boron atom matrix chemistry
[AD-A282840] p 434 N95-14366
Modeling time-dependent corrosion fatigue crack propagation in 7000 series aluminum alloys p 448 N95-14483
Thermocapillary motion of deformable drops p 485 N95-14544
International Semiconductor Device Research Symposium (ISDRS-93)
[AD-A281715] p 477 N95-15454
Computer modeling the fatigue crack growth rate behavior of metals in corrosive environments
[NASA-CR-194982-REV] p 448 N95-15918

VITRO CORP., SILVER SPRING, MD.
Engineering, technical, and management support services
[NASA-CR-196977] p 505 N95-13840

VRIJE UNIV., BRUSSELS (BELGIUM).
CFD methodology and validation for turbomachinery flows p 480 N95-14131

W

WALTER REED ARMY MEDICAL CENTER, WASHINGTON, DC.
Medical research publications: A bibliography of Walter Reed Army Medical Center staff, 1986-1992, volume 2
[PB94-177797] p 541 N95-14394

WASHINGTON STATE UNIV., PULLMAN, WA.
Bubble dynamics, two-phase flow, and boiling heat transfer in a microgravity environment p 488 N95-14561
Augmentation of research on cognitive control
[AD-A280956] p 552 N95-14600

WASHINGTON UNIV., SAINT LOUIS, MO.
Ultraviolet-Infrared Mapping Interferometic Spectrometer
[NASA-CR-197099] p 613 N95-14806

WASHINGTON UNIV., SEATTLE, WA.
Models of remote manipulation in space p 504 N95-14027
Creating better virtual worlds p 556 N95-14031
Axial crack propagation and arrest in pressurized fuselage p 511 N95-14479
Hadronization of QCD and effective interactions
[DE94-014975] p 594 N95-14660

WESTINGHOUSE ELECTRIC CORP., BALTIMORE, MD.
Ferroelectric oxide memory FET (FEMFET) development
[AD-A283203] p 476 N95-15399

WESTINGHOUSE HANFORD CO., RICHLAND, WA.
Case study: Accelerated schedule for MULTI LIMS installation
[DE94-012398] p 630 N95-13673
Transient failure behavior of HT9
[DE94-016320] p 445 N95-14378
Impact fracture behavior of HT9 duct
[DE94-016328] p 445 N95-14379

WESTINGHOUSE SAVANNAH RIVER CO., AIKEN, SC.
Welding irradiated stainless steel
[DE94-013661] p 500 N95-13645
Essential elements of an effective data qualification
[DE94-015566] p 632 N95-15419
Type 304L stainless steel surface microstructure: Performance in hydride storage and acid cleaning
[DE94-014654] p 447 N95-15625

WHEELING COLL., WV.
Helping small companies commercialize public-sector technology
[TABES PAPER 94-407] p 415 N95-14635

WISCONSIN UNIV., MADISON, WI.
The Astroculture (tm)-1 experiment on the USML-1 mission p 564 N95-14228
Conservation of magnetic helicity during plasma relaxation
[DE94-016770] p 617 N95-14373
Performance measurement and analysis techniques for parallel and distributed programs
[DE94-016429] p 578 N95-14384
Thermocapillary convection in floating zones under simulated reduced-gravity conditions p 483 N95-14529
Performance of customized DCT quantization tables on scientific data p 564 N95-14586
Lower-hybrid poloidal current drive for fluctuation reduction in a reversed field pinch
[DE94-015534] p 618 N95-15540
Solid target boronization of the MST reversed-field pinch during pulsed discharge cleaning
[DE94-015535] p 442 N95-15541
Neutrino oscillations in noisy media
[DE94-014973] p 598 N95-15869

WISCONSIN UNIV., MILWAUKEE, WI.
Experimental and theoretical studies of rewetting of unheated/heated grooved plates p 487 N95-14558
Ultrasonic characterization of high T(c) and other unconventional superconductors
[AD-A282835] p 476 N95-15397

WOODFIELD (ALAN A.), BEDFORD (ENGLAND).
Wind shear and its effects on aircraft p 407 N95-14898

WOODS HOLE OCEANOGRAPHIC INST., MA.
Telerobotics in the deep ocean p 504 N95-14026
Real time system for practical acoustic monitoring of global ocean temperature, volume 3
[AD-A283774] p 535 N95-14335

WOOLLAM (JOHN A.) CO., LINCOLN, NE.
Real-time monitor and control of MBE growth of HgCdTe by spectroscopic ellipsometry
[AD-A284451] p 627 N95-15818

WOOSTER COLL., OH.
Turbidity of a binary fluid mixture: Determining eta p 487 N95-14552

WORCESTER POLYTECHNIC INST., MA.
The growth of zeolites A, X and mordenite in space p 458 N95-14226

WRIGHT LAB., WRIGHT-PATTERSON AFB, OH.
Developments in laser-based diagnostics for wind tunnels in the Aeromechanics Division: 1987-1992
[AD-A283011] p 412 N95-13687
Flight evaluation of pneumatic forebody vortex control in post-stall flight p 398 N95-14259
Pressure measurements on an F/A-18 twin vertical tail in buffeting flow. Volume 2: Steady and unsteady RMS pressure data
[AD-A281581] p 404 N95-15465
Large amplitude nonlinear response of flat aluminum, and carbon fiber plastic beams and plates
[AD-A282440] p 513 N95-15547

WYLE LABS., INC., ARLINGTON, VA.
USAF single-event sonic boom prediction model: PCBoom3 p 403 N95-14889

X

XAVIER UNIV. OF LOUISIANA, NEW ORLEANS, LA.
Investigation of syngas interaction in alcohol synthesis catalysts
[DE94-013939] p 442 N95-15386

Y

YALE UNIV., NEW HAVEN, CT.
Surface characterization through shape oscillations of drops in microgravity and 1-g p 458 N95-14220
World Reference Center for Arboviruses
[AD-A281635] p 550 N95-15445

YOUNG (LAURENCE R.), RUMNEY, NH.
Life Sciences Centrifuge Facility review
[NASA-CR-196849] p 537 N95-13702

Typical Contract Number Index Listing

AF- AFOSR-0090-93 ..... p 173 N95-10812

CONTRACT NUMBER | PAGE NUMBER | ACCESSION NUMBER

Listings in this index are arranged alphanumerically by contract number. Under each contract number the accession numbers denoting documents that have been produced as a result of research done under that contract are arranged in ascending order. The page number helps to locate the citation in the abstract section. The accession number denotes the number by which the citation is identified.

AF PROJ. 0107 ..... p 427 N95-14420
AF PROJ. 1397 ..... p 507 N95-14456
AF PROJ. 2312 ..... p 541 N95-14408
p 538 N95-15094
p 542 N95-15095
AF PROJ. 2401 ..... p 513 N95-15547
AF PROJ. 2404 ..... p 412 N95-13687
AF PROJ. 3153 ..... p 434 N95-14411
AF PROJ. 3484 ..... p 452 N95-14406
AF PROJ. 7755 ..... p 553 N95-15768
AF-AFOSR-0061-91 ..... p 492 N95-14605
AF-AFOSR-0152B-90 ..... p 444 N95-14202
AF-AFOSR-0191-90 ..... p 575 N95-15549
AF-AFOSR-0203-91 ..... p 607 N95-13939
AF-AFOSR-0291-91 ..... p 524 N95-15814
AF-AFOSR-0307-90 ..... p 607 N95-13939
AF-AFOSR-0479-89 ..... p 453 N95-14844
AF-AFOSR-10407-93 ..... p 552 N95-14369
ARPA ORDER 7597 ..... p 573 N95-14842
ARPA ORDER 8162 ..... p 476 N95-15327
CNES-90/0295 ..... p 539 N95-15132
CNES-90/0313 ..... p 539 N95-15132
DA PROJ. 1L1-61102-AH-45 ..... p 566 N95-13716
DA PROJ. 1L1-62211-A-47-A ..... p 433 N95-14298
p 409 N95-14852
DA PROJ. 1L1-62716-AH-70 ..... p 563 N95-15759
DA PROJ. 3M1-62787-A-878 ..... p 540 N95-13971
DA PROJ. 3M1-62787-A-879 ..... p 551 N95-15767
DA PROJ. 301-62787-A-878 ..... p 551 N95-15810
DA PROJ. 4A1-62720-A-896 ..... p 515 N95-14358
DAAA15-90-C-1028 ..... p 497 N95-15334
DAAB07-93-C-U008 ..... p 627 N95-15818
DAAG29-85-K-0195 ..... p 436 N95-15443
DAAH04-93-G-0060 ..... p 614 N95-15464
DAAH04-93-G-0063 ..... p 596 N95-15446
DAAH04-93-G-0384 ..... p 477 N95-15454
DAAK70-85-C-0007 ..... p 451 N95-14365
DAAK70-87-C-0043 ..... p 451 N95-14365
p 504 N95-15747
DAAK70-92-C-0059 ..... p 451 N95-14365
p 451 N95-14365
p 504 N95-15747
DAAK70-93-C-0062 ..... p 518 N95-14341
DAAL03-86-G-0196 ..... p 434 N95-14360
DAAL03-86-K-0140 ..... p 596 N95-15457
DAAL03-89-C-0038 ..... p 578 N95-14422
DAAL03-89-C-0088 ..... p 567 N95-15809
DAAL03-89-D-0002 ..... p 594 N95-14362
DAAL03-89-D-0003 ..... p 455 N95-15444
DAAL03-89-K-0179 ..... p 484 N95-14535
DAAL03-90-C-0004 ..... p 460 N95-13657
DAAL03-91-C-0016 ..... p 461 N95-14361
DAAL03-91-C-0035 ..... p 589 N95-13656
DAAL03-91-G-0134 ..... p 499 N95-14364
DAAL03-91-G-0162 ..... p 588 N95-14370
DAAL03-92-C-0021 ..... p 451 N95-14363
DAAL03-92-G-0209 ..... p 615 N95-15772
DACA76-92-C-0009 ..... p 583 N95-15398
DACW39-93-C-0022 ..... p 533 N95-15323
DAJA45-90-C-0034 ..... p 626 N95-15748
DAJA45-91-C-0013 ..... p 553 N95-15816
DAMD17-88-C-8141 ..... p 540 N95-13971
DAMD17-90-C-0017 ..... p 454 N95-15296
DAMD17-90-Z-0020 ..... p 550 N95-15445
DARA-10-QV-9050 ..... p 542 N95-15092
DARA-50-WB-9113 ..... p 548 N95-15137
DARPA ORDER 7503 ..... p 476 N95-15399
DARPA ORDER 8228 ..... p 585 N95-14843
DE-AC02-76CH-00016 ..... p 601 N95-13644
p 610 N95-13959
p 593 N95-14309
p 438 N95-14371
p 590 N95-14440
p 594 N95-14441
p 624 N95-15422
p 493 N95-15571
p 625 N95-15576
p 600 N95-15633
p 525 N95-15864
DE-AC02-76CH-03000 ..... p 593 N95-13680
p 594 N95-14661
p 595 N95-15301
p 475 N95-15302
p 574 N95-15418
p 497 N95-15580
p 579 N95-15581
p 600 N95-15582
p 597 N95-15629
p 597 N95-15630
p 597 N95-15862
DE-AC02-76CH-03073 ..... p 617 N95-14397
DE-AC02-80ET-15601 ..... p 618 N95-15373
p 618 N95-15374
DE-AC02-83CH-10093 ..... p 457 N95-14003
p 519 N95-15290
DE-AC02-89ER-40509 ..... p 596 N95-15537
DE-AC03-76SF-00098 ..... p 611 N95-13968
p 620 N95-14189
p 594 N95-14374
p 434 N95-14387
p 643 N95-14442
p 484 N95-14534
p 457 N95-14659
p 453 N95-14957
p 623 N95-15337
p 623 N95-15338
p 623 N95-15339
p 599 N95-15367
p 625 N95-15577
p 627 N95-15578
p 443 N95-15667
p 597 N95-15865
p 470 N95-15866
p 494 N95-15867
p 494 N95-15868
DE-AC03-76SF-00515 ..... p 622 N95-15308
p 597 N95-15545
DE-AC03-89ER-51114 ..... p 617 N95-14328
p 617 N95-14426
p 618 N95-15632
DE-AC04-76DP-00613 ..... p 613 N95-14367
DE-AC04-76DP-00789 ..... p 476 N95-15356
DE-AC04-76DR-00789 ..... p 438 N95-14391
DE-AC04-94AL-85000 ..... p 472 N95-13975
p 457 N95-14004
p 496 N95-14146
p 617 N95-14262
p 437 N95-14307
p 473 N95-14308
p 642 N95-14311
p 437 N95-14312
p 515 N95-14313
p 473 N95-14314
p 474 N95-14315
p 474 N95-14319
p 621 N95-14322
p 621 N95-14323
p 621 N95-14342
p 621 N95-14390
p 618 N95-14443
p 428 N95-14664
p 493 N95-15351
p 476 N95-15356
p 418 N95-15357
p 632 N95-15366
p 446 N95-15368
p 583 N95-15369
p 442 N95-15375
p 574 N95-15384
p 460 N95-15409
p 476 N95-15410
p 531 N95-15411
p 521 N95-15420
p 596 N95-15437
p 625 N95-15438
p 574 N95-15543
p 477 N95-15544
p 404 N95-15570
p 524 N95-15575
p 469 N95-15583
DE-AC05-84OR-21400 ..... p 432 N95-13643
p 601 N95-13674
p 592 N95-13675
p 444 N95-13820
p 619 N95-13821
p 568 N95-13976
p 501 N95-14005
p 473 N95-14310
p 438 N95-14375
p 519 N95-14393
p 622 N95-14608
p 624 N95-15421
p 446 N95-15431
p 574 N95-15536
p 586 N95-15538
p 456 N95-15634
DE-AC06-76RL-01830 ..... p 612 N95-13986
p 517 N95-14002
p 522 N95-14187
p 522 N95-14195
p 529 N95-14428
p 566 N95-14662
p 439 N95-14663
p 445 N95-15293
p 595 N95-15310
p 573 N95-15311
p 613 N95-15312
p 454 N95-15313
p 613 N95-15314
p 523 N95-15383
p 446 N95-15431
p 524 N95-15432
p 446 N95-15433
p 633 N95-15528
DE-AC06-87RL-10930 ..... p 630 N95-13673
p 445 N95-14378
p 445 N95-14379
DE-AC07-76ID-01570 ..... p 578 N95-15434
p 632 N95-15435
p 442 N95-15436
p 524 N95-15455
p 588 N95-15533
p 579 N95-15534
DE-AC09-89SR-18035 ..... p 500 N95-13645
p 632 N95-15419
p 447 N95-15625
DE-AC12-76SN-00052 ..... p 506 N95-14320
p 625 N95-15531
p 446 N95-15532
DE-AC21-92MC-29113 ..... p 563 N95-15309
DE-AC22-92PC-92111 ..... p 439 N95-14435
DE-AC36-83CH-10093 ..... p 518 N95-14191
p 518 N95-14194
p 519 N95-14430
p 622 N95-14431
p 519 N95-14432
p 519 N95-14433
p 520 N95-15355
p 520 N95-15405
p 520 N95-15406
p 521 N95-15407
p 624 N95-15426
p 521 N95-15863
DE-AI01-91CE-50306 ..... p 431 N95-13631
DE-AI05-84ER-13150 ..... p 441 N95-15370
DE-FC03-92SF-19460 ..... p 618 N95-14955
DE-FC05-85ER-25000 ..... p 459 N95-14540

DE-FC21-92MC-29237 p 518 N95-14143
DE-FG01-92CE-15974 p 453 N95-15292
DE-FG02-85ER-53198 p 617 N95-14373
p 442 N95-15541
DE-FG02-85ER-53212 p 618 N95-15540
DE-FG02-88ER-13974 p 454 N95-15344
DE-FG02-88ER-45357 p 454 N95-15358
DE-FG02-88ER-45364 p 447 N95-15631
DE-FG02-90ER-12103 p 597 N95-15572
DE-FG02-90ER-14143 p 438 N95-14386
DE-FG02-90ER-40577 p 595 N95-15372
DE-FG02-91CE-23810 p 438 N95-14372
p 454 N95-15343
DE-FG02-91ER-40684 p 600 N95-15539
DE-FG02-92ER-14302 p 455 N95-15535
DE-FG02-92ER-14303 p 494 N95-15861
DE-FG02-92ER-40734 p 599 N95-15371
DE-FG02-93ER-25176 p 578 N95-14384
DE-FG02-93ER-40768 p 600 N95-15633
DE-FG03-86ER-52123 p 617 N95-14397
DE-FG03-92ER-25128 p 585 N95-14296
DE-FG03-92ER-54150 p 617 N95-14426
DE-FG05-85ER-13439 p 438 N95-14392
DE-FG05-86ER-45233 p 625 N95-15574
DE-FG05-92ER-14278 p 530 N95-14956
DE-FG05-92ER-14291 p 438 N95-14388
DE-FG06-89ER-75522 p 522 N95-14195
DE-FG06-90ER-40561 p 594 N95-14660
p 598 N95-15869
DE-FG09-84ER-13296 p 441 N95-15346
DE-FG09-87ER-13811 p 441 N95-15347
DE-FG22-90PC-90293 p 441 N95-15345
DE-FG22-92MT-92022 p 440 N95-15291
DE-FG22-93MT-93010 p 442 N95-15386
DEN3-335 p 634 N95-15743
DGICYT-PB-92-0507 p 611 N95-13967
DNA001-90-C-0127 p 415 N95-14639
DOT-SHRP-H-208A p 407 N95-15439
DRET-90-1053J p 544 N95-15110
DTFAO3-89-C-00043 p 581 N95-13895
DTFA01-87-C-00014 p 413 N95-15328
DTFA01-93-Z-02012 p 534 N95-15749
DTFA02-90-C-90125 p 551 N95-13715
DTFA03-92-Z-00018 p 405 N95-14179
EPA-R-818282-02 p 523 N95-14403
EPA-68-D0-0106 p 521 N95-14123
EPA-68-D1-0009 p 523 N95-15382
FAA TASK AM-A-91-HRR-138 p 551 N95-13715
FAA-92-G-0004 p 510 N95-14470
FAA-92-G-0005 p 511 N95-14479
FAA-92-G-0006 p 448 N95-14465
FAA-92-G-002 p 411 N95-15683
FAA-93-G-0068 p 510 N95-14470
FFWF PROJ. P-8781 p 607 N95-13936
p 612 N95-13969
F08635-87-C-0366 p 493 N95-15332
F08635-87-C-0377 p 530 N95-15295
F09603-89-G-0096 p 507 N95-14455
F19628-88-C-0173 p 440 N95-14958
F19628-89-K-0007 p 530 N95-14598
F19628-89-K-0043 p 524 N95-15623
F19628-90-C-0002 p 534 N95-15749
F19628-90-C-0003 p 572 N95-14349
F19628-90-C-003 p 572 N95-14339
F19628-90-C-0175 p 530 N95-15401
F19628-92-C-0070 p 428 N95-14951
F19628-92-C-0149 p 534 N95-15614
F19628-92-K-0018 p 595 N95-14950
F19628-93-C-0051 p 534 N95-15402
F19628-93-C-0130 p 575 N95-15783
p 576 N95-15806
F30602-88-D-0025 p 469 N95-15462
F30602-89-D-0050 p 468 N95-15333
F30602-90-C-0010 p 583 N95-15548
F30602-91-C-0010 p 586 N95-15595
p 587 N95-15643
p 576 N95-15825
F30602-93-C-0005 p 477 N95-15459
F30602-93-C-0022 p 470 N95-15756
F30602-93-C-0036 p 477 N95-15460
p 583 N95-15461
F33615-88-C-5055 p 436 N95-15441
F33615-88-C-5404 p 434 N95-14411
F33615-90-C-0005 p 563 N95-15755
F33615-90-C-1465 p 573 N95-14842
F33615-90-C-2038 p 500 N95-15395
F33615-90-C-2086 p 454 N95-15316
F33615-91-C-1729 p 469 N95-15394
F33615-92-D-2293 p 468 N95-15393
F33657-93-C-2440 p 392 N95-15331
F49620-91-C-0003 p 461 N95-14334
p 409 N95-15451
F49620-91-C-0065 p 472 N95-13685
F49620-92-J-0084 p 541 N95-14408
F49620-92-J-0243 p 552 N95-14600
F49620-93-1-0061 p 493 N95-15390
F49620-93-1-0142 p 443 N95-15782
F49620-93-1-0236 p 626 N95-15754
F49620-93-1-0326 p 593 N95-14155
F49620-93-1-0327 p 553 N95-15770
F49620-93-1-0331 p 434 N95-14366
F49620-93-1-0338 p 400 N95-14656
F49620-93-1-0396 p 452 N95-14406
F49620-93-1-0463 p 447 N95-15744
F49620-94-1-0073 p 581 N95-14847
F49620-94-1-0198 p 568 N95-13699
GIT PROJ. E-25-X77-S1 p 483 N95-14532
JPL-956520 p 465 N95-14678
JPL-957448 p 444 N95-14206
JPL-958722 p 458 N95-14220
JSPS ENGR-207 p 586 N95-15594
p 575 N95-15597
p 575 N95-15721
p 587 N95-15732
p 577 N95-15858
KOSEF-3-08-00-05 p 608 N95-13943
MDA972-90-C-0035 p 412 N95-14343
MDA972-91-C-0029 p 476 N95-15327
MDA972-91-C-0032 p 478 N95-15613
MDA972-91-C-0053 p 585 N95-14843
MDA972-92-J-1012 p 573 N95-15151
MDA972-93-1-0004 p 535 N95-14335
NA-36RG-0070 p 532 N95-14120
NAGW-1275 p 544 N95-15105
NAGW-1691 p 419 N95-15146
NAGW-1699 p 613 N95-14908
NAGW-1819 p 526 N95-14267
NAGW-2195 p 539 N95-15133
NAGW-2302 p 643 N95-14505
NAGW-2423 p 613 N95-14806
NAGW-2465 p 643 N95-14505
NAGW-2581 p 517 N95-15848
NAGW-3902 p 641 N95-15840
NAGW-3914 p 564 N95-14586
NAGW-749 p 641 N95-15840
NAG1-1056 p 475 N95-14851
NAG1-1066 p 580 N95-13727
NAG1-1132 p 568 N95-13889
NAG1-1329 p 415 N95-14639
NAG1-1362 p 402 N95-14884
NAG1-1431 p 506 N95-14270
NAG1-1439 p 566 N95-14514
NAG1-1500 p 429 N95-14106
NAG1-226 p 409 N95-14909
NAG1-343 p 505 N95-13839
NAG1-363 p 437 N95-14268
p 481 N95-14269
NAG1-423 p 437 N95-14268
p 481 N95-14269
NAG1-6131-J-1283 p 579 N95-15442
NAG1-745 p 448 N95-14483
p 448 N95-15918
NAG1-750 p 572 N95-14615
NAG1-832 p 492 N95-14932
NAG1-901 p 435 N95-14865
NAG1-905 p 453 N95-14931
NAG1-998 p 532 N95-14265
NAG10-0058 p 505 N95-13886
NAG2-175 p 532 N95-13725
NAG2-270 p 627 N95-15823
NAG2-306 p 503 N95-14923
NAG2-31 p 530 N95-14855
p 525 N95-15847
NAG2-458 p 525 N95-15847
NAG2-614 p 538 N95-15113
NAG2-624 p 538 N95-15113
NAG2-653 p 537 N95-14796
NAG2-707 p 537 N95-13638
p 538 N95-15113
NAG2-893 p 568 N95-13699
NAG3-1094 p 483 N95-14532
NAG3-1122 p 486 N95-14546
NAG3-1158 p 490 N95-14573
NAG3-1165 p 405 N95-15912
NAG3-1284 p 459 N95-14540
NAG3-1292 p 457 N95-14902
NAG3-1317 p 478 N95-13653
p 485 N95-14542
NAG3-1321 p 585 N95-14300
NAG3-1352 p 505 N95-15584
NAG3-1381 p 487 N95-14558
NAG3-1382 p 483 N95-14527
NAG3-1386 p 483 N95-14528
NAG3-1389 p 484 N95-14537
NAG3-1390 p 485 N95-14544
NAG3-1391 p 488 N95-14559
NAG3-1398 p 489 N95-14566
NAG3-1399 p 488 N95-14560
NAG3-1402 p 484 N95-14535
NAG3-1403 p 487 N95-14553
NAG3-1453 p 483 N95-14526
NAG3-1455 p 483 N95-14530
NAG3-1470 p 486 N95-14546
NAG3-1520 p 507 N95-14417
NAG3-510 p 487 N95-14556
NAG3-755 p 457 N95-14105
NAG3-768 p 400 N95-14803
NAG5-10 p 531 N95-15586
NAG5-1603 p 637 N95-13723
NAG5-1684 p 642 N95-15907
NAG5-1790 p 531 N95-15684
NAG5-1930 p 525 N95-13627
NAG5-2030 p 647 N95-14814
NAG5-2232 p 499 N95-14901
NAG5-2322 p 637 N95-13722
NAG5-2346 p 618 N95-14798
NAG5-538 p 525 N95-13627
NAG8-1384 p 484 N95-14533
NAG8-185 p 638 N95-14804
NAG8-292 p 490 N95-14571
NAG8-294 p 502 N95-14797
NAG8-839 p 646 N95-15070
NAG8-938 p 479 N95-14104
NAG8-941 p 626 N95-15752
NAG8-945 p 444 N95-14578
NAG8-964 p 444 N95-14581
NAG9-109 p 645 N95-13724
NAG9-181 p 538 N95-15113
NAG9-234 p 538 N95-15113
NAG9-622 p 507 N95-14454
NASA ORDER A-2401-D p 538 N95-15094
p 542 N95-15095
NASA ORDER H-22785-D p 537 N95-13702
NASA ORDER L-45107 p 633 N95-15585
NASA ORDER T-2901-T p 612 N95-14272
NASA ORDER T-3816-S p 443 N95-15715
NASW-4063 p 526 N95-13818
NASW-4311 p 505 N95-13840
NASW-4435 p 408 N95-13703
p 428 N95-14521
p 563 N95-14854
p 645 N95-14868
p 535 N95-14900
p 502 N95-14907
p 409 N95-15742
NASW-4803 p 487 N95-14554
NASW-4818 p 502 N95-14910
NAS1-14654 p 601 N95-13660
NAS1-18224 p 432 N95-14603
NAS1-19000 p 418 N95-13890
p 492 N95-14912
p 493 N95-15604
NAS1-19247 p 432 N95-14603
NAS1-19480 p 568 N95-13689
p 495 N95-15917
NAS1-19858 p 494 N95-15605
p 516 N95-15727
NAS13-330 p 537 N95-15751
p 537 N95-15753
p 633 N95-15801
NAS2-13571 p 395 N95-14238
NAS3-23901 p 458 N95-14212
NAS3-24105 p 601 N95-13666
NAS3-25685 p 450 N95-14303
NAS3-25776 p 568 N95-13894
p 430 N95-14301
NAS3-25809 p 431 N95-14669
NAS3-25882 p 431 N95-15058
NAS3-25972 p 419 N95-13893
NAS3-25973 p 458 N95-14217
NAS3-26403 p 465 N95-14677
NAS3-26618 p 591 N95-14610
NAS3-27023 p 430 N95-13697
NAS3-27186 p 479 N95-13665
p 481 N95-14295
p 430 N95-14301
p 404 N95-15852
p 436 N95-15911
NAS5-30376 p 602 N95-13896
NAS5-31837 p 642 N95-14266
NAS5-32029 p 615 N95-15849
NAS5-32314 p 567 N95-13632
p 567 N95-13633
p 567 N95-13651
p 515 N95-13704
p 515 N95-13885
p 517 N95-15851
NAS5-32332 p 531 N95-15745
NAS5-32486 p 517 N95-15916
NAS5-32607 p 423 N95-14078
NAS5-33032 p 619 N95-15758
NAS7-918 p 460 N95-13628
p 498 N95-13629
p 602 N95-13823
p 472 N95-13824
p 612 N95-14181
NAS8-36123 p 636 N95-13634
p 567 N95-13635

	p 636	N95-13636
	p 637	N95-13637
	p 637	N95-13887
	p 637	N95-14100
	p 638	N95-14101
NAS8-37855	p 419	N95-15552
NAS8-38147	p 458	N95-14213
NAS8-38609	p 602	N95-13841
	p 532	N95-14271
	p 429	N95-15824
NAS8-39131	p 566	N95-14107
	p 519	N95-14802
	p 519	N95-14853
	p 475	N95-14866
	p 439	N95-14867
	p 502	N95-14904
NAS8-39351	p 573	N95-14905
NAS8-39393	p 514	N95-13639
NAS8-39695	p 458	N95-14215
NAS9-18000	p 572	N95-14520
NAS9-18094	p 560	N95-14050
NAS9-18500	p 419	N95-14474
NAS9-18819	p 492	N95-14869
NAS9-18880	p 411	N95-14799
NATO-CRG-921122	p 483	N95-14532
NCA2-637	p 641	N95-15842
NCC1-176	p 552	N95-14864
NCC1-193	p 409	N95-14794
	p 434	N95-14800
NCC1-68	p 392	N95-13701
NCC2-115	p 539	N95-13661
NCC2-213	p 538	N95-15113
NCC2-307	p 559	N95-14046
NCC2-518	p 513	N95-14922
NCC2-593	p 539	N95-15135
NCC2-636	p 400	N95-14612
NCC2-637	p 400	N95-14613
NCC2-653	p 405	N95-13719
	p 405	N95-13720
	p 645	N95-13721
NCC2-669	p 497	N95-15728
	p 497	N95-15785
NCC2-729	p 400	N95-14614
NCC2-762	p 644	N95-13717
NCC2-813	p 404	N95-15762
NCC2-86	p 555	N95-14022
NCC2-9003	p 409	N95-14794
NCC3-121	p 439	N95-14903
NCC3-210	p 483	N95-14532
NCC3-233	p 478	N95-13653
	p 585	N95-14296
NCC3-329	p 484	N95-14534
NCC8-39	p 409	N95-14794
	p 435	N95-14801
	p 514	N95-15913
NCC9-16	p 569	N95-14156
NF-62-376	p 575	N95-15644
NFI PROJ. ALADDIN	p 575	N95-15644
NGR-399-20-01-30	p 641	N95-15842
NGT-S1113	p 402	N95-14884
NGT-50441	p 404	N95-15853
NGT-50679	p 417	N95-14651
NGT-51070	p 485	N95-14542
NGT-51179	p 483	N95-14532
NIH-RR-09032-1	p 539	N95-15115
NIH-1R24RRO6853	p 553	N95-15642
	p 577	N95-15860
NIH-1R24RR06853	p 575	N95-15640
	p 576	N95-15856
NIST-60NANB0D1042	p 439	N95-14838
NIST-60NANB2D1266	p 443	N95-15610
NIST-60NANB2D1295	p 441	N95-15352
NIST-60NANB8D0849	p 441	N95-15353
NIVR-1823	p 511	N95-14478
NIVR-9691	p 511	N95-14478
NNSF-39170795	p 538	N95-15099
NSERC-OGP-0046613	p 575	N95-15644
NSF AST-91-15121	p 644	N95-14508
NSF AST-91-17086	p 644	N95-14509
NSF CCR-89-57604	p 586	N95-15594
	p 587	N95-15596
	p 575	N95-15597
	p 587	N95-15641
	p 575	N95-15721
	p 587	N95-15732
	p 576	N95-15788
	p 588	N95-15854
	p 588	N95-15855
	p 577	N95-15858
	p 589	N95-15859
NSF CCR-90-03440	p 568	N95-13699
NSF CCR-90-14363	p 568	N95-13699
NSF CCR-92-10372	p 568	N95-13889
NSF CDA-88-22724	p 579	N95-15590
	p 586	N95-15595
	p 575	N95-15645
	p 575	N95-15721
	p 553	N95-15787
	p 576	N95-15857
NSF CHE-91-96214	p 598	N95-13937
	p 608	N95-13943
NSF CTS-89-06846	p 483	N95-14532
NSF CTS-91-14775	p 483	N95-14532
NSF DMR-91-22444	p 459	N95-14579
NSF DMS-89-02831	p 484	N95-14534
NSF DMS-90-02095	p 589	N95-13979
NSF DMS-91-08072	p 585	N95-14296
NSF DMS-93-02976	p 589	N95-13979
NSF DMS-93-04406	p 585	N95-14296
NSF EAR-91-05502	p 525	N95-13627
NSF GER-92-55698	p 483	N95-14532
NSF INT-91-16781	p 586	N95-15594
	p 575	N95-15597
	p 587	N95-15641
	p 575	N95-15721
	p 587	N95-15732
	p 577	N95-15858
NSF IRI-89-03582	p 573	N95-15151
	p 552	N95-15588
	p 575	N95-15640
	p 553	N95-15642
	p 587	N95-15775
	p 576	N95-15856
	p 577	N95-15860
NSF IRI-89-20771	p 573	N95-15151
NSF IRI-92-02816	p 553	N95-15787
NSF IRI-92-24741	p 564	N95-14586
NSF PHY-90-22345	p 598	N95-13961
NSF PHY-92-21038	p 611	N95-13966
NSG-1608	p 479	N95-13664
N00014-19-J-1430	p 612	N95-13970
N00014-88-K-0343	p 578	N95-15416
N00014-89-D-0142	p 591	N95-14396
N00014-89-J-1003	p 592	N95-15453
N00014-89-J-1050	p 608	N95-13946
N00014-89-J-1478	p 536	N95-15425
N00014-89-J-3167	p 626	N95-15812
N00014-89-J-3202	p 584	N95-15811
N00014-89-J-3203	p 494	N95-15760
N00014-90-C-0159	p 476	N95-15399
N00014-90-J-1230	p 477	N95-15456
N00014-90-J-1259	p 611	N95-13968
N00014-90-J-1263	p 619	N95-13691
N00014-90-J-1270	p 474	N95-14355
N00014-90-J-1386	p 622	N95-14655
N00014-90-J-4140	p 625	N95-15746
N00014-91-C-0048	p 626	N95-15808
N00014-91-C-0124	p 446	N95-15415
N00014-91-C-0216	p 451	N95-14354
N00014-91-J-1023	p 498	N95-13695
N00014-91-J-1044	p 435	N95-15417
N00014-91-J-1211	p 476	N95-15397
N00014-91-J-1219	p 568	N95-13699
N00014-91-J-1274	p 433	N95-13655
	p 455	N95-15458
N00014-91-J-1283	p 579	N95-15442
N00014-91-J-1430	p 599	N95-13963
	p 599	N95-13964
N00014-91-J-1442	p 627	N95-15404
N00014-91-J-1529	p 576	N95-15817
N00014-91-J-1613	p 579	N95-15616
	p 579	N95-15617
N00014-92-C-0049	p 456	N95-15624
N00014-92-C-0173	p 474	N95-14425
N00014-92-C-0221	p 630	N95-14321
N00014-92-J-1173	p 540	N95-14142
N00014-92-J-1302	p 604	N95-13910
N00014-92-J-1512	p 586	N95-15595
N00014-92-J-1810	p 437	N95-14141
N00014-92-J-1934	p 585	N95-14657
N00014-92-J-1996	p 595	N95-15318
N00014-92-J-2017	p 470	N95-15813
N00014-92-J-6003	p 470	N95-15820
N00014-93-C-0116	p 614	N95-15414
N00014-93-J-1135	p 592	N95-15453
N00014-93-1-G037	p 522	N95-14344
N00014-93-1-0480	p 535	N95-14204
N00014-93-1-0486	p 533	N95-14848
N00014-93-1-0563	p 622	N95-14601
N00014-93-1-0871	p 632	N95-15423
N00014-93-1-1049	p 506	N95-14356
N00014-93-1-1072	p 623	N95-15317
N00014-93-1-1149	p 583	N95-15403
N00014-94-C-0078	p 503	N95-15294
N00014-94-C-0099	p 613	N95-14353
N00014-94-I-0101	p 452	N95-14395
	p 452	N95-14398
	p 452	N95-14399
	p 452	N95-14400
N00014-94-1-0101	p 450	N95-14304
	p 451	N95-14305
	p 451	N95-14316
	p 451	N95-14324
N00014-94-1-0387	p 584	N95-13694
N00014-94-1-0516	p 571	N95-14178
N00039-91-C-0001	p 465	N95-14677
N00123-89-G-0380	p 474	N95-14359
N00123-89-G-0580	p 501	N95-14347
	p 434	N95-14348
N00123-91-G-0586	p 522	N95-14337
N00167-92-K-0038	p 514	N95-15802
N61339-91-D-0001	p 460	N95-13696
	p 408	N95-14306
	p 572	N95-14357
N61533-90-K-0059	p 514	N95-15802
N68171-94-C-9068	p 410	N95-15821
OSURF PROJ. 718986	p 457	N95-14105
PROJ. A-1218	p 611	N95-13966
PROJ. FRESIP	p 643	N95-14499
PROJ. MARVIN	p 645	N95-14868
PROJ. 52MP02P	p 450	N95-14203
PROJ. 91-20	p 435	N95-14913
PSCSR-681/2/91	p 640	N95-15835
RTOP 140-20-0A	p 430	N95-13697
RTOP 196-41-67-05	p 643	N95-14499
RTOP 199-14-12-04	p 547	N95-15128
RTOP 199-45-16-11	p 600	N95-15606
	p 647	N95-15790
RTOP 199-70-12-14	p 539	N95-13661
RTOP 232-01-04-06	p 492	N95-14912
	p 493	N95-15604
RTOP 232-01-06	p 429	N95-13668
	p 431	N95-15682
RTOP 232-02-02	p 430	N95-14301
RTOP 233-01-OE	p 431	N95-15789
RTOP 233-01-0A	p 473	N95-14302
	p 477	N95-15587
RTOP 233-01-01-05	p 420	N95-13729
RTOP 233-01-03-22	p 516	N95-15727
RTOP 233-03-0B	p 430	N95-14173
RTOP 233-03-02-04	p 432	N95-14603
RTOP 235-01-02	p 568	N95-13894
RTOP 237-01-02-01	p 418	N95-13890
RTOP 310-10-63-50	p 419	N95-14621
RTOP 310-20-65-92-02	p 463	N95-14625
RTOP 310-20-67-92-02	p 462	N95-14622
	p 463	N95-14628
RTOP 310-30-69-91-01	p 463	N95-14626
RTOP 310-30-71-83-02	p 462	N95-14623
RTOP 314-30-43-09-01	p 419	N95-14631
RTOP 314-30-63-01-01	p 463	N95-14627
RTOP 314-40-32-10-23	p 456	N95-14629
RTOP 314-40-42-01-03	p 463	N95-14630
RTOP 315-90-71-10-08	p 419	N95-14632
RTOP 315-91-40-20-36	p 462	N95-14624
RTOP 323-44-19	p 420	N95-13728
RTOP 352-02-03-06	p 639	N95-15827
RTOP 422-00-00	p 567	N95-13632
	p 567	N95-13633
	p 567	N95-13651
	p 515	N95-13704
RTOP 468-01-11	p 566	N95-13716
RTOP 501-01-10	p 433	N95-14298
RTOP 505-38-13	p 391	N95-13642
RTOP 505-52-52	p 591	N95-15059
RTOP 505-59-36	p 391	N95-13891
RTOP 505-59-53	p 392	N95-14921
RTOP 505-59-59	p 481	N95-14273
RTOP 505-61-51	p 391	N95-14419
RTOP 505-62-00	p 450	N95-14303
RTOP 505-62-52	p 392	N95-13817
	p 398	N95-14297
	p 482	N95-14299
	p 398	N95-14418
	p 492	N95-14607
	p 591	N95-14618
	p 440	N95-15056
	p 440	N95-15057
	p 442	N95-15512
	p 404	N95-15853
RTOP 505-63-12	p 432	N95-13641
RTOP 505-63-5A	p 444	N95-13667
	p 585	N95-14300
	p 450	N95-14303
RTOP 505-63-5B	p 507	N95-14417
RTOP 505-64-13	p 406	N95-14611
RTOP 505-64-52-01	p 580	N95-13727
RTOP 505-64-53-03	p 409	N95-14852
RTOP 505-64-53	p 550	N95-15649
RTOP 505-68-10	p 481	N95-14295
RTOP 505-68-30	p 393	N95-14229
RTOP 505-69-20-01	p 647	N95-13663
RTOP 505-69-50	p 572	N95-14206
	p 408	N95-14604
	p 405	N95-15912
RTOP 505-70-59	p 479	N95-13665
RTOP 505-70-62-12	p 494	N95-15605
RTOP 505-70-63	p 479	N95-13892

RTOP 505-90-00 ..... p 633 N95-15585
RTOP 505-90-5K ..... p 585 N95-14296
p 495 N95-15908
RTOP 505-90-52-01 ..... p 568 N95-13889
p 495 N95-15917
RTOP 506-42-72 ..... p 431 N95-14669
RTOP 506-43-61-02 ..... p 432 N95-14603
RTOP 506-43-61-07 ..... p 601 N95-13660
RTOP 506-47-00 ..... p 554 N95-14013
RTOP 509-10-11 ..... p 391 N95-13662
RTOP 537-02-22 ..... p 404 N95-15852
RTOP 537-03-21-03 ..... p 401 N95-14878
RTOP 538-02-10-01 ..... p 444 N95-13690
p 507 N95-14453
p 432 N95-14920
p 448 N95-15918
RTOP 538-03-11 ..... p 591 N95-14610
RTOP 584-03-11 ..... p 601 N95-13666
p 431 N95-15058
RTOP 584-04-21 ..... p 430 N95-14174
RTOP 602-00-00 ..... p 619 N95-15758
RTOP 691-00-00 ..... p 517 N95-15916
RTOP 693-00-00 ..... p 638 N95-14667
RTOP 750-00-00 ..... p 420 N95-14062
RTOP 763-22-41 ..... p 436 N95-15911
RTOP 763-23-35-08 ..... p 495 N95-15898
p 495 N95-15899
RTOP 778-32-21 ..... p 634 N95-15743
RTOP 778-34-28 ..... p 431 N95-13631
RTOP 910-00-00 ..... p 531 N95-15745
RTOP 920-00-00 ..... p 526 N95-14274
RTOP 921-43-00-1A ..... p 492 N95-14869
RTOP 930-00-00 ..... p 564 N95-14585
RTOP 962-24-00 ..... p 482 N95-14522
RTOP-505-68-30 ..... p 395 N95-14239
p 397 N95-14251
SDIO84-C-0003 ..... p 418 N95-14094
SHRP-ID-034 ..... p 460 N95-14119
SRI PROJ. 2781 ..... p 526 N95-13818
USGS-14-34-92-C-40004 ..... p 565 N95-14591
W-31-109-ENG-38 ..... p 567 N95-13676
p 577 N95-13677
p 593 N95-13678
p 479 N95-13679
p 619 N95-13681
p 433 N95-13682
p 471 N95-13684
p 620 N95-13822
p 568 N95-13977
p 449 N95-13978
p 616 N95-14006
p 620 N95-14008
p 620 N95-14009
p 568 N95-14010
p 593 N95-14011
p 617 N95-14012
p 578 N95-14116
p 522 N95-14187
p 620 N95-14188
p 621 N95-14192
p 571 N95-14196
p 578 N95-14380
p 621 N95-14382
p 475 N95-14606
p 622 N95-14608
p 453 N95-14609
p 445 N95-14665
p 454 N95-15340
p 623 N95-15341
p 586 N95-15342
p 595 N95-15362
p 596 N95-15381
p 624 N95-15385
p 624 N95-15430
p 456 N95-15778
p 597 N95-15826
p 447 N95-15906
W-7405-ENG-3-6 ..... p 617 N95-14397
W-7405-ENG-36 ..... p 433 N95-13993
p 498 N95-13994
p 526 N95-13995
p 630 N95-13996
p 616 N95-13997
p 616 N95-13998
p 620 N95-13999
p 593 N95-14000
p 593 N95-14001
p 616 N95-14007
p 617 N95-14368
p 646 N95-14376
p 581 N95-14377
p 585 N95-14381
p 638 N95-14429
p 529 N95-14434
p 646 N95-14437
p 647 N95-14438
p 445 N95-14439
p 440 N95-15297
p 591 N95-15359
p 599 N95-15360
p 442 N95-15387
p 436 N95-15573
p 455 N95-15579
p 633 N95-15761
p 619 N95-15774
p 626 N95-15776
p 505 N95-15777
W-7405-ENG-48 ..... p 496 N95-13669
p 601 N95-13670
p 554 N95-13671
p 601 N95-13672
p 571 N95-14190
p 473 N95-14261
p 522 N95-14317
p 498 N95-14318
p 621 N95-14325
p 566 N95-14338
p 594 N95-14383
p 594 N95-14385
p 451 N95-14389
p 499 N95-14427
p 529 N95-14436
p 468 N95-15300
p 523 N95-15361
p 523 N95-15364
p 468 N95-15365
p 442 N95-15408
p 614 N95-15529
p 493 N95-15530
p 524 N95-15779
p 600 N95-15780
W-7405-ENG-82 ..... p 445 N95-15307

Typical Report Number Index Listing

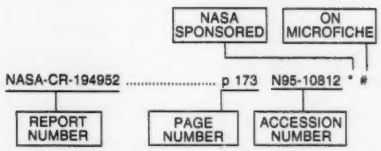

Listings in this index are arranged alphanumerically by report number. The accession number denotes the number by which the citation is identified. The page number helps to locate the citation in the abstract section. An asterisk (*) indicates that the item is a NASA report. A pound sign (#) indicates that the item is available on microfiche.

A-91035 ..... p 554 N95-14013 * #
A-91113 ..... p 391 N95-14419 * #
A-94007 ..... p 391 N95-13891 * #
A-94104 ..... p 512 N95-14617 * #
A-94107 ..... p 639 N95-15827 * #
A-94111 ..... p 643 N95-14499 * #
A-94116 ..... p 539 N95-13661 * #
A-94121 ..... p 406 N95-14611 * #
A-94143 ..... p 391 N95-13642 * #
A-94148 ..... p 391 N95-13662 * #
A-95006 ..... p 481 N95-14273 * #
A-95012 ..... p 550 N95-15649 * #
A-95017 ..... p 392 N95-14921 * #

AD-A279317 ..... p 541 N95-14394 #
AD-A280435 ..... p 540 N95-13971
AD-A280584 ..... p 589 N95-13972 #
AD-A280743 ..... p 437 N95-14141 #
AD-A280778 ..... p 414 N95-14290 #
AD-A280780 ..... p 498 N95-14291 #
AD-A280783 ..... p 578 N95-14292 #
AD-A280788 ..... p 461 N95-14293 #
AD-A280796 ..... p 630 N95-14321 #
AD-A280799 ..... p 450 N95-14304 #
AD-A280800 ..... p 451 N95-14305 #
AD-A280824 ..... p 408 N95-14306 #
AD-A280828 ..... p 451 N95-14316 #
AD-A280829 ..... p 451 N95-14324 #
AD-A280830 ..... p 452 N95-14395 #
AD-A280833 ..... p 591 N95-14396 #
AD-A280839 ..... p 452 N95-14398 #
AD-A280840 ..... p 452 N95-14399 #
AD-A280842 ..... p 452 N95-14400 #
AD-A280924 ..... p 540 N95-14142 #
AD-A280949 ..... p 638 N95-14597 #
AD-A280950 ..... p 530 N95-14598 #
AD-A280951 ..... p 428 N95-14599 #
AD-A280956 ..... p 552 N95-14600 #
AD-A280958 ..... p 622 N95-14601 #
AD-A280964 ..... p 622 N95-14655 #
AD-A280966 ..... p 572 N95-14616 #
AD-A280969 ..... p 530 N95-14862 #
AD-A280970 ..... p 435 N95-15427 #
AD-A280971 ..... p 531 N95-15428 #
AD-A281377 ..... p 434 N95-14360 #
AD-A281378 ..... p 461 N95-14361
AD-A281379 ..... p 594 N95-14362 #
AD-A281380 ..... p 451 N95-14363 #
AD-A281381 ..... p 499 N95-14364 #
AD-A281567 ..... p 477 N95-15456
AD-A281569 ..... p 596 N95-15457
AD-A281570 ..... p 455 N95-15458
AD-A281572 ..... p 477 N95-15459
AD-A281573 ..... p 477 N95-15460
AD-A281574 ..... p 583 N95-15461
AD-A281575 ..... p 469 N95-15462
AD-A281576 ..... p 469 N95-15463
AD-A281578 ..... p 614 N95-15464
AD-A281581 ..... p 404 N95-15465
AD-A281582 ..... p 436 N95-15441
AD-A281583 ..... p 579 N95-15442 *
AD-A281587 ..... p 436 N95-15443
AD-A281614 ..... p 455 N95-15444
AD-A281635 ..... p 550 N95-15445
AD-A281662 ..... p 596 N95-15446
AD-A281676 ..... p 419 N95-15447 #
AD-A281677 ..... p 592 N95-15448
AD-A281680 ..... p 563 N95-15449
AD-A281681 ..... p 579 N95-15450
AD-A281706 ..... p 409 N95-15451
AD-A281707 ..... p 536 N95-15452
AD-A281714 ..... p 592 N95-15453
AD-A281715 ..... p 477 N95-15454
AD-A281910 ..... p 433 N95-13655 #
AD-A281936 ..... p 589 N95-13656 #
AD-A281937 ..... p 460 N95-13657 #
AD-A281960 ..... p 590 N95-13683 #
AD-A281982 ..... p 391 N95-14144 #
AD-A282011 ..... p 595 N95-14950
AD-A282012 ..... p 428 N95-14951
AD-A282023 ..... p 533 N95-14952
AD-A282024 ..... p 540 N95-14145 #
AD-A282025 ..... p 578 N95-14953
AD-A282026 ..... p 453 N95-14954
AD-A282217 ..... p 492 N95-14605 #
AD-A282439 ..... p 515 N95-15546
AD-A282440 ..... p 513 N95-15547
AD-A282445 ..... p 583 N95-15548
AD-A282446 ..... p 575 N95-15549
AD-A282795 ..... p 409 N95-14840 #
AD-A282831 ..... p 614 N95-15414
AD-A282835 ..... p 476 N95-15397
AD-A282837 ..... p 573 N95-14842
AD-A282838 ..... p 451 N95-14365
AD-A282839 ..... p 412 N95-14343
AD-A282840 ..... p 434 N95-14366
AD-A282891 ..... p 503 N95-15294
AD-A282912 ..... p 493 N95-15390
AD-A282914 ..... p 587 N95-15612
AD-A282915 ..... p 500 N95-15391
AD-A282917 ..... p 446 N95-15415
AD-A282923 ..... p 411 N95-15392
AD-A282925 ..... p 578 N95-15416
AD-A282926 ..... p 585 N95-14843
AD-A282928 ..... p 581 N95-14847
AD-A282941 ..... p 400 N95-14656
AD-A282944 ..... p 453 N95-14844
AD-A282962 ..... p 583 N95-15398
AD-A282996 ..... p 472 N95-13685 #
AD-A282999 ..... p 448 N95-13686 #
AD-A283011 ..... p 412 N95-13687 #
AD-A283023 ..... p 448 N95-13688 #
AD-A283024 ..... p 449 N95-13689 #
AD-A283025 ..... p 468 N95-15393
AD-A283038 ..... p 533 N95-14848
AD-A283039 ..... p 619 N95-13691
AD-A283069 ..... p 449 N95-13692 #
AD-A283071 ..... p 571 N95-14178 #
AD-A283104 ..... p 514 N95-13693
AD-A283109 ..... p 584 N95-13694
AD-A283110 ..... p 498 N95-13695
AD-A283111 ..... p 585 N95-14657
AD-A283112 ..... p 469 N95-15394
AD-A283123 ..... p 478 N95-15613
AD-A283124 ..... p 469 N95-15651
AD-A283154 ..... p 460 N95-13696 #
AD-A283172 ..... p 619 N95-13698 #
AD-A283181 ..... p 593 N95-14155 #
AD-A283182 ..... p 568 N95-13699 * #
AD-A283201 ..... p 500 N95-15395
AD-A283203 ..... p 476 N95-15399
AD-A283210 ..... p 492 N95-14658
AD-A283211 ..... p 536 N95-15626
AD-A283214 ..... p 588 N95-15400
AD-A283220 ..... p 534 N95-15627
AD-A283227 ..... p 409 N95-14849 #
AD-A283228 ..... p 428 N95-14850
AD-A283229 ..... p 478 N95-15628 #
AD-A283240 ..... p 534 N95-15614 #
AD-A283241 ..... p 530 N95-15401 #
AD-A283243 ..... p 470 N95-15652
AD-A283244 ..... p 534 N95-15402
AD-A283250 ..... p 530 N95-15295 #
AD-A283251 ..... p 583 N95-15403
AD-A283253 ..... p 455 N95-15615
AD-A283254 ..... p 579 N95-15616
AD-A283255 ..... p 579 N95-15617
AD-A283260 ..... p 534 N95-15618 #
AD-A283263 ..... p 469 N95-15619
AD-A283264 ..... p 513 N95-15620
AD-A283265 ..... p 513 N95-15621
AD-A283266 ..... p 447 N95-15622
AD-A283304 ..... p 524 N95-15623
AD-A283323 ..... p 456 N95-15624
AD-A283331 ..... p 615 N95-15872
AD-A283342 ..... p 436 N95-15873
AD-A283379 ..... p 447 N95-15874
AD-A283411 ..... p 435 N95-15417
AD-A283413 ..... p 454 N95-15296 #
AD-A283422 ..... p 627 N95-15404
AD-A283529 ..... p 536 N95-15440 #
AD-A283530 ..... p 533 N95-15323 #
AD-A283531 ..... p 440 N95-14958 #
AD-A283535 ..... p 536 N95-15324
AD-A283536 ..... p 476 N95-15325 #
AD-A283547 ..... p 552 N95-15326 #
AD-A283549 ..... p 476 N95-15327 #
AD-A283550 ..... p 413 N95-15328 #
AD-A283564 ..... p 411 N95-15329 #
AD-A283570 ..... p 536 N95-15330 #
AD-A283571 ..... p 454 N95-15316 #
AD-A283583 ..... p 623 N95-15317 #
AD-A283584 ..... p 595 N95-15318 #
AD-A283585 ..... p 404 N95-15319 #
AD-A283591 ..... p 591 N95-15320 #
AD-A283592 ..... p 468 N95-15321 #
AD-A283671 ..... p 392 N95-15331 #
AD-A283748 ..... p 461 N95-14345 #
AD-A283758 ..... p 613 N95-14353 #
AD-A283763 ..... p 631 N95-14327 #
AD-A283764 ..... p 631 N95-14329 #
AD-A283765 ..... p 631 N95-14330 #
AD-A283766 ..... p 631 N95-14331 #
AD-A283767 ..... p 631 N95-14332 #
AD-A283768 ..... p 631 N95-14333 #
AD-A283773 ..... p 461 N95-14334 #
AD-A283774 ..... p 535 N95-14335 #
AD-A283775 ..... p 493 N95-15332 #
AD-A283776 ..... p 501 N95-14336 #
AD-A283780 ..... p 522 N95-14337 #
AD-A283816 ..... p 468 N95-15333 #
AD-A283827 ..... p 572 N95-14339 #
AD-A283833 ..... p 533 N95-14340 #
AD-A283834 ..... p 518 N95-14341 #
AD-A283835 ..... p 522 N95-14344 #
AD-A283839 ..... p 461 N95-14346 #
AD-A283842 ..... p 501 N95-14347 #
AD-A283843 ..... p 434 N95-14348 #
AD-A283848 ..... p 572 N95-14349 #
AD-A283849 ..... p 405 N95-14350 #
AD-A283854 ..... p 482 N95-14351 #
AD-A283868 ..... p 535 N95-14352 #
AD-A283870 ..... p 451 N95-14354 #
AD-A283871 ..... p 474 N95-14355 #
AD-A283872 ..... p 506 N95-14356 #
AD-A283874 ..... p 572 N95-14357 #
AD-A283875 ..... p 515 N95-14358 #
AD-A283883 ..... p 474 N95-14359 #
AD-A283890 ..... p 632 N95-15423 #
AD-A283893 ..... p 586 N95-15424 #
AD-A283894 ..... p 536 N95-15425 #
AD-A283956 ..... p 552 N95-14369 #
AD-A283959 ..... p 444 N95-14202 #
AD-A283965 ..... p 450 N95-14203 #
AD-A283969 ..... p 535 N95-14204 #
AD-A283982 ..... p 408 N95-14205 #
AD-A284014 ..... p 427 N95-14420 #
AD-A284027 ..... p 405 N95-14421 #
AD-A284030 ..... p 578 N95-14422 #
AD-A284032 ..... p 533 N95-14423 #
AD-A284038 ..... p 541 N95-14424 #

AD-A284065 ..... p 474 N95-14425 #
AD-A284150 ..... p 633 N95-15801 *
AD-A284159 ..... p 462 N95-14405
AD-A284211 ..... p 434 N95-14411 #
AD-A284214 ..... p 475 N95-14444 #
AD-A284215 ..... p 452 N95-14406 #
AD-A284219 ..... p 541 N95-14408 #
AD-A284222 ..... p 497 N95-15334
AD-A284230 ..... p 434 N95-14409 #
AD-A284363 ..... p 514 N95-15802
AD-A284364 ..... p 514 N95-15803
AD-A284367 ..... p 470 N95-15804
AD-A284368 ..... p 514 N95-15805
AD-A284373 ..... p 576 N95-15806
AD-A284387 ..... p 447 N95-15807
AD-A284390 ..... p 626 N95-15808
AD-A284393 ..... p 567 N95-15809
AD-A284395 ..... p 551 N95-15810
AD-A284396 ..... p 551 N95-15767
AD-A284397 ..... p 553 N95-15768
AD-A284399 ..... p 553 N95-15770
AD-A284400 ..... p 443 N95-15782
AD-A284403 ..... p 575 N95-15783
AD-A284410 ..... p 584 N95-15811
AD-A284411 ..... p 626 N95-15812
AD-A284413 ..... p 470 N95-15813
AD-A284426 ..... p 524 N95-15814
AD-A284433 ..... p 410 N95-15815 #
AD-A284436 ..... p 553 N95-15816
AD-A284437 ..... p 576 N95-15817
AD-A284451 ..... p 627 N95-15818
AD-A284456 ..... p 535 N95-15819 #
AD-A284458 ..... p 470 N95-15820
AD-A284467 ..... p 410 N95-15821
AD-A284494 ..... p 534 N95-15771 #
AD-A284851 ..... p 574 N95-15335
AD-A284859 ..... p 447 N95-15744 #
AD-A284863 ..... p 588 N95-14370 #
AD-A284868 ..... p 625 N95-15746 #
AD-A284870 ..... p 504 N95-15747 #
AD-A284874 ..... p 626 N95-15748 #
AD-A284877 ..... p 534 N95-15749 #
AD-A284891 ..... p 615 N95-15772 #
AD-A284892 ..... p 470 N95-15750 #
AD-A284894 ..... p 537 N95-15751 * #
AD-A284895 ..... p 537 N95-15753 * #
AD-A284898 ..... p 626 N95-15754 #
AD-A284900 ..... p 563 N95-15755 #
AD-A284903 ..... p 470 N95-15756 #
AD-A284908 ..... p 551 N95-15757 #
AD-A284917 ..... p 563 N95-15759 #
AD-A284919 ..... p 494 N95-15760 #

AD-D016347 ..... p 496 N95-14841 #
AD-D016349 ..... p 497 N95-15799
AD-D016352 ..... p 456 N95-15800
AD-D016362 ..... p 614 N95-15764
AD-D016365 ..... p 614 N95-15707
AD-D016366 ..... p 615 N95-15765
AD-D016379 ..... p 615 N95-15766
AD-D016463 ..... p 574 N95-15336

AD-E201980 ..... p 530 N95-14598 #
AD-E201983 ..... p 428 N95-14599 #
AD-E201990 ..... p 638 N95-14597 #
AD-E202063 ..... p 428 N95-14951
AD-E202068 ..... p 534 N95-15614 #
AD-E202069 ..... p 530 N95-15401 #
AD-E202112 ..... p 534 N95-15402
AD-E202153 ..... p 524 N95-15623

ADST/TR-94-003280 ..... p 408 N95-14306 #

ADST/WDL/TR-93-003260 ..... p 460 N95-13696 #
ADST/WDL/TR-94-00325 ..... p 572 N95-14357 #

AEDC-TR-94-3 ..... p 427 N95-14420 #

AEROJET-10340 ..... p 567 N95-13632 * #
AEROJET-10356 ..... p 515 N95-13704 * #
AEROJET-10357 ..... p 517 N95-15851 * #
AEROJET-10448 ..... p 567 N95-13633 * #
AEROJET-10506 ..... p 567 N95-13651 * #

AFIT-CI-94-027D ..... p 470 N95-15652

AFIT-CI/CIA94-034D ..... p 534 N95-15771 #
AFIT-CI/CIA94-126 ..... p 535 N95-15819 #

AFIT/CI-94-026D ..... p 588 N95-15400
AFIT/CI-94-109 ..... p 534 N95-15618 #

AFIT/CI/CIA-94-005D ..... p 578 N95-14953
AFIT/CI/CIA-94-006D ..... p 540 N95-14145 #
AFIT/CI/CIA-94-032 ..... p 533 N95-14952
AFIT/CI/CIA-94-033D ..... p 482 N95-14351 #

AFIT/CI/CIA-94-055 ..... p 453 N95-14954
AFIT/CI/CIA-94-095 ..... p 391 N95-14144 #
AFIT/CI/CIA-94-102 ..... p 619 N95-13698 #
AFIT/CI/CIA-94-103 ..... p 534 N95-15627

AFOSR-94-0328TR ..... p 492 N95-14605 #
AFOSR-94-0370TR ..... p 552 N95-14600 #
AFOSR-94-0423TR ..... p 575 N95-15549
AFOSR-94-0424TR ..... p 453 N95-14844
AFOSR-94-0429TR ..... p 493 N95-15390
AFOSR-94-0445TR ..... p 593 N95-14155 #
AFOSR-94-0448 ..... p 400 N95-14656
AFOSR-94-0452TR ..... p 434 N95-14366
AFOSR-94-0467TR ..... p 472 N95-13685 #
AFOSR-94-0470TR ..... p 581 N95-14847
AFOSR-94-0505TR ..... p 541 N95-14408 #
AFOSR-94-0512TR ..... p 452 N95-14406 #
AFOSR-94-0524TR ..... p 524 N95-15814
AFOSR-94-0541TR ..... p 552 N95-14369 #
AFOSR-94-0545TR ..... p 444 N95-14202 #
AFOSR-94-0546TR ..... p 443 N95-15782
AFOSR-94-0547TR ..... p 553 N95-15770
AFOSR-94-0574TR ..... p 626 N95-15754 #
AFOSR-94-0580TR ..... p 447 N95-15744 #

AGARD-AG-300-VOL-12 ..... p 405 N95-14199 #
AGARD-AG-300-VOL-3-PT-2 ..... p 408 N95-14102 #
AGARD-AG-323 ..... p 393 N95-14103 #
AGARD-AG-325 ..... p 398 N95-14264 #

AGARD-AR-303-VOL-1 ..... p 481 N95-14201 #
AGARD-AR-304 ..... p 393 N95-14197 #
AGARD-AR-317 ..... p 562 N95-14263 #
AGARD-AR-328 ..... p 506 N95-14198 #

AGARD-CP-546 ..... p 461 N95-14200 #

AGARD-HIGHLIGHTS-94/2 ..... p 647 N95-13640 #

AGARD-LS-193 ..... p 581 N95-14942 #
AGARD-LS-195 ..... p 479 N95-14127 #
AGARD-LS-196 ..... p 466 N95-14825 #
AGARD-LS-197 ..... p 406 N95-14893 #

AGARD-R-804 ..... p 399 N95-14445 #

AIAA PAPER 91-2052 ..... p 431 N95-15682 * #
AIAA PAPER 92-3812 ..... p 429 N95-13668 * #
AIAA PAPER 94-0086 ..... p 405 N95-13720 * #
AIAA PAPER 94-0319 ..... p 404 N95-15853 * #
AIAA PAPER 94-2085 ..... p 428 N95-14664 #
AIAA PAPER 94-2190 ..... p 591 N95-14618 * #
AIAA PAPER 94-3981 ..... p 430 N95-14301 * #
AIAA PAPER 95-0566 ..... p 398 N95-14297 * #
AIAA PAPER 95-0889 ..... p 398 N95-14418 * #

AISR-TR-4002-93-09 ..... p 514 N95-13639 * #

AL/AO-TR-1994-0030 ..... p 553 N95-15768

AL/CF-TR-1994-0020 ..... p 468 N95-15393

AL/EQ-TR-1994-0031 ..... p 493 N95-15332 #
AL/EQ-TR-1994-0032 ..... p 530 N95-15295 #

AL/HR-TR-1994-0090 ..... p 563 N95-15755 #

ANL-HEP-CP-94-29 ..... p 568 N95-14010

ANL/CHM/CP-81247 ..... p 620 N95-13822 #
ANL/CHM/CP-82279 ..... p 596 N95-15381 #
ANL/CHM/CP-83030 ..... p 620 N95-14188 #
ANL/CHM/CP-83031 ..... p 622 N95-14608 #

ANL/CHM/PP-73572 ..... p 593 N95-14011
ANL/CHM/PP-75225 ..... p 620 N95-14009

ANL/CMT/CP-82954 ..... p 471 N95-13684 #

ANL/DIS/CP-82284 ..... p 571 N95-14196 #

ANL/ER/CP-83276 ..... p 522 N95-14187 #

ANL/ET/CP-81069 ..... p 453 N95-14609 #
ANL/ET/CP-81654 ..... p 433 N95-13682
ANL/ET/CP-82282 ..... p 447 N95-15906 #
ANL/ET/CP-82304 ..... p 621 N95-14192 #
ANL/ET/CP-82348 ..... p 475 N95-14606 #
ANL/ET/CP-82351 ..... p 449 N95-13978 #
ANL/ET/CP-83508 ..... p 456 N95-15778 #

ANL/IPNS/CP-80966 ..... p 593 N95-13678
ANL/IPNS/CP-83316 ..... p 445 N95-14665 #

ANL/IPNS/PROC-81937 ..... p 597 N95-15826 #

ANL/MCS-TM-189 ..... p 578 N95-14116 #

ANL/MCS/CP-82959 ..... p 577 N95-13677 #
ANL/MCS/CP-82972 ..... p 567 N95-13676 #
ANL/MCS/CP-83197 ..... p 568 N95-13977 #

ANL/MCS/PP-75712 ..... p 586 N95-15342
ANL/MCS/PP-77111 ..... p 578 N95-14380

ANL/MSD/CP-83051 ..... p 624 N95-15430 #
ANL/MSD/CP-83086 ..... p 624 N95-15385 #
ANL/MSD/CP-83111 ..... p 620 N95-14008
ANL/MSD/CP-83112 ..... p 619 N95-13681
ANL/MSD/CP-83617 ..... p 595 N95-15362 #
ANL/MSD/CP-83658 ..... p 454 N95-15340

ANL/MSD/PP-81187 ..... p 623 N95-15341 #

ANL/RE-94/1 ..... p 479 N95-13679

ANL/TD/CP-81662 ..... p 616 N95-14006
ANL/TD/CP-82066 ..... p 617 N95-14012

ANL/XFD/CP-82780 ..... p 621 N95-14382

ARFSD-TR-93045 ..... p 572 N95-14616 #

ARI-RN-94-25 ..... p 552 N95-15326 #

ARL-CR-171 ..... p 578 N95-14422 #
ARL-CR-172 ..... p 567 N95-15809

ARL-MR-156 ..... p 433 N95-14298 * #
ARL-MR-178 ..... p 563 N95-15759 #

ARL-RR-13 ..... p 434 N95-14409 #

ARL-TR-286 ..... p 533 N95-14340 #
ARL-TR-359 ..... p 455 N95-15615
ARL-TR-361 ..... p 450 N95-14203 #
ARL-TR-454 ..... p 447 N95-15622
ARL-TR-455 ..... p 513 N95-15620
ARL-TR-456 ..... p 513 N95-15621
ARL-TR-507 ..... p 447 N95-15807
ARL-TR-571 ..... p 566 N95-13716 * #

ARO-22339.3-MS ..... p 436 N95-15443
ARO-24487.2-EG-SDI ..... p 596 N95-15457
ARO-24619.1-MS-UIF ..... p 434 N95-14360 #
ARO-27554.31-EL-JSE ..... p 460 N95-13657 #
ARO-27888.3-PH ..... p 594 N95-14362 #
ARO-28373.1-CH ..... p 455 N95-15444
ARO-28453.24-EL-JSE ..... p 461 N95-14361
ARO-28646.4-EL ..... p 589 N95-13656 #
ARO-28922.14-EL-SDI ..... p 499 N95-14364 #
ARO-30357.1-MS ..... p 451 N95-14363 #
ARO-30411.5-MA-SDI ..... p 615 N95-15772 #
ARO-30440.4-PH ..... p 596 N95-15446
ARO-31175.1-EL-CF ..... p 614 N95-15464

ASR-6 ..... p 592 N95-15453

ATC-222 ..... p 534 N95-15749 #

A2-1852 ..... p 477 N95-15460

BFLRF-286 ..... p 504 N95-15747 #
BFLRF-295 ..... p 451 N95-14365

BNL-49792 ..... p 438 N95-14371 #
BNL-52420 ..... p 493 N95-15571 #
BNL-60294 ..... p 593 N95-14309 #
BNL-60297 ..... p 625 N95-15576 #
BNL-60378 ..... p 601 N95-13644 #
BNL-60437 ..... p 590 N95-14440 #
BNL-60535 ..... p 525 N95-15864 #
BNL-60538 ..... p 594 N95-14441 #
BNL-60588 ..... p 624 N95-15422 #
BNL-60633 ..... p 600 N95-15633 #

BULL-1 ..... p 516 N95-15791 #

CARDIVNSWC-SSM-61-93/23 ..... p 514 N95-15803

CARDIVNSWC-TR-61-CR-94/01 . p 514 N95-15802

CAST-TN-7-94 ..... p 537 N95-15753 * #
CAST-TN-8-94 ..... p 537 N95-15751 * #

CCMS-94-10 ..... p 505 N95-13839 * #

CECOM-TR-94-E-1 ..... p 409 N95-14852 * #

CERC-MP-94-10 ..... p 536 N95-15452
CERC-MP-94-14 ..... p 533 N95-15323 #

CERL-TR-EC-94/21 ..... p 515 N95-14358 #

CMU-CS-94-147 ..... p 412 N95-14343

CMU-RI-TR-94-06 ..... p 573 N95-14842

CMU/SEI-94-TR-10 ..... p 572 N95-14339 #
CMU/SEI-94-TR-13 ..... p 572 N95-14349 #

CONF-9305159-10 ..... p 601 N95-13644 #
CONF-9305339 ..... p 597 N95-15826 #
CONF-9306176-23 ..... p 597 N95-15862 #
CONF-9306338-1 ..... p 625 N95-15576 #
CONF-9306354-1 ..... p 506 N95-14320 #
CONF-9308237-1 ..... p 620 N95-13999 #
CONF-930851-3 ..... p 625 N95-15531 #
CONF-9309176-1-REV-1 ..... p 621 N95-14325 #
CONF-9309386-2 ..... p 597 N95-15545 #
CONF-9309388-SUMM ..... p 446 N95-15368 #
CONF-9310340-1 ..... p 617 N95-14426 #
CONF-931048-9-REV-1 ..... p 600 N95-15780 #
CONF-9311211-ADD ..... p 457 N95-14003 #
CONF-940190 ..... p 618 N95-14443 #
CONF-940222-17 ..... p 446 N95-15532 #
CONF-940278 ..... p 624 N95-15421 #
CONF-9403122-1 ..... p 600 N95-15582 #
CONF-9403122-2 ..... p 594 N95-14661 #
CONF-9403123-2 ..... p 592 N95-13675 #
CONF-9403131-2 ..... p 643 N95-14442 #
CONF-9403135-1 ..... p 593 N95-14001 #
CONF-9403136-1 ..... p 517 N95-14002 #
CONF-9403142-1 ..... p 585 N95-14381 #
CONF-9403143-1 ..... p 646 N95-14376 #
CONF-940391-8 ..... p 601 N95-13672 #
CONF-940411-25 ..... p 497 N95-15580 #
CONF-940411-27 ..... p 620 N95-13822 #
CONF-940411-29 ..... p 432 N95-13643 #
CONF-940411-36 ..... p 454 N95-15313 #
CONF-940411-38 ..... p 613 N95-15312 #
CONF-940411-41 ..... p 434 N95-14387 #
CONF-940411-46 ..... p 621 N95-14322 #
CONF-940411-48 ..... p 623 N95-15339
CONF-9404137-3 ..... p 494 N95-15861 #
CONF-940416-10 ..... p 455 N95-15579 #
CONF-940416-13 ..... p 433 N95-13682
CONF-9404162-7 ..... p 469 N95-15583 #
CONF-9404171-1 ..... p 625 N95-15577 #
CONF-9404181-1 ..... p 433 N95-13993
CONF-940428-3 ..... p 567 N95-13676 #
CONF-940456-21 ..... p 573 N95-15311 #
CONF-940492-5 ..... p 579 N95-15581 #
CONF-940492-7 ..... p 568 N95-14010
CONF-940507-23 ..... p 595 N95-15310 #
CONF-940507-25 ..... p 647 N95-14438 #
CONF-9405100-8 ..... p 577 N95-13677 #
CONF-9405109-6 ..... p 438 N95-14375 #
CONF-9405130-3 ..... p 471 N95-13684 #
CONF-9405132-6 ..... p 594 N95-14660 #
CONF-9405139-3 ..... p 614 N95-15529 #
CONF-9405143-1 ..... p 600 N95-15633 #
CONF-9405153-1 ..... p 447 N95-15906 #
CONF-9405159-1 ..... p 630 N95-13673 #
CONF-9405159-3 ..... p 554 N95-13671 #
CONF-9405168-3 ..... p 468 N95-15300 #
CONF-9405170-6 ..... p 475 N95-15302 #
CONF-9405178-1 ..... p 594 N95-14441 #
CONF-9405187-1 ..... p 496 N95-14146 #
CONF-9405193-1 ..... p 449 N95-13978 #
CONF-9405197-1 ..... p 445 N95-15293 #
CONF-9405198-1 ..... p 522 N95-14195 #
CONF-9405200-1 ..... p 624 N95-15422 #
CONF-940524-8 ..... p 571 N95-14190 #
CONF-940529-18 ..... p 613 N95-15314 #
CONF-940529-20 ..... p 438 N95-14371 #
CONF-940548-2 ..... p 442 N95-15408
CONF-940548-5 ..... p 519 N95-15290 #
CONF-940548-6 ..... p 519 N95-14433 #
CONF-940554-1 ..... p 518 N95-14191 #
CONF-940580-12 ..... p 499 N95-14427 #
CONF-940580-6 ..... p 617 N95-14368 #
CONF-940580-7 ..... p 617 N95-14262 #
CONF-940580-8 ..... p 442 N95-15541
CONF-940593-12 ..... p 617 N95-14328
CONF-940602-10 ..... p 612 N95-13986 #
CONF-9406127-2 ..... p 616 N95-13997 #
CONF-9406143-1 ..... p 444 N95-13820 #
CONF-9406168-2 ..... p 524 N95-15432 #
CONF-940616-1 ..... p 621 N95-14323 #
CONF-9406169-1 ..... p 451 N95-14389
CONF-9406181-3 ..... p 601 N95-13670 #
CONF-9406184-1 ..... p 439 N95-14663 #
CONF-9406186-1 ..... p 568 N95-13977 #
CONF-9406188-3 ..... p 568 N95-13976 #
CONF-9406192-1 ..... p 493 N95-15351 #
CONF-9406203-SUMM ..... p 526 N95-13995 #
CONF-9406203 ..... p 624 N95-15426 #
CONF-9406204-1 ..... p 519 N95-14430 #
CONF-9406205-1 ..... p 590 N95-14440 #
CONF-9406205-2 ..... p 566 N95-14662 #
CONF-9406206-1 ..... p 574 N95-15543 #
CONF-940625-8 ..... p 445 N95-14439 #
CONF-940627-2 ..... p 428 N95-14664 #
CONF-940627-3 ..... p 621 N95-14192 #
CONF-940629-7 ..... p 475 N95-14606 #
CONF-940630-11 ..... p 624 N95-15385 #
CONF-940630-15 ..... p 617 N95-14012
CONF-940630-16 ..... p 616 N95-14007 #
CONF-940630-22 ..... p 616 N95-13998 #
CONF-940632-10-REV-1 ..... p 498 N95-13994 #
CONF-940635-4 ..... p 523 N95-15361 #
CONF-940657-1 ..... p 618 N95-15632
CONF-940657-4 ..... p 500 N95-13645 #
CONF-940659-9 ..... p 446 N95-15431 #
CONF-940664-14 ..... p 493 N95-15530 #
CONF-940664-22 ..... p 616 N95-14006
CONF-940678-4 ..... p 617 N95-14397 #
CONF-940678-5 ..... p 477 N95-15544 #
CONF-940684-4 ..... p 473 N95-14261 #
CONF-940697-1 ..... p 455 N95-15535 #
CONF-940701-15 ..... p 593 N95-14000 #
CONF-940701-17 ..... p 624 N95-15430 #
CONF-940701-4 ..... p 595 N95-15362 #
CONF-940701-7 ..... p 619 N95-13681
CONF-940704-1 ..... p 620 N95-14008
CONF-9407102-1 ..... p 445 N95-14665 #
CONF-9407103-15 ..... p 474 N95-14319 #
CONF-9407106-1 ..... p 599 N95-15360 #
CONF-9407109-1 ..... p 531 N95-15411 #
CONF-9407115-1 ..... p 456 N95-15778 #
CONF-940713-1 ..... p 626 N95-15776 #
CONF-940714-1 ..... p 453 N95-14609 #
CONF-940719-3 ..... p 621 N95-14382
CONF-940722-11 ..... p 436 N95-15573 #
CONF-940722-12 ..... p 597 N95-15629 #
CONF-940722-13 ..... p 597 N95-15630 #
CONF-940722-2 ..... p 595 N95-15301 #
CONF-940723-10 ..... p 593 N95-13680
CONF-940731-ABSTS ..... p 638 N95-14429 #
CONF-940744-3 ..... p 594 N95-14383
CONF-940744-5 ..... p 593 N95-13678
CONF-940748-21 ..... p 438 N95-14388 #
CONF-940748-39 ..... p 632 N95-15419 #
CONF-940748-40 ..... p 505 N95-15777 #
CONF-940748-67 ..... p 591 N95-15359 #
CONF-940753-19 ..... p 581 N95-14377 #
CONF-940766-5 ..... p 619 N95-13821 #
CONF-940769-6 ..... p 601 N95-13674 #
CONF-940776-1 ..... p 529 N95-14428 #
CONF-940793-1 ..... p 457 N95-14004 #
CONF-940796-1 ..... p 447 N95-15625 #
CONF-940799-1 ..... p 646 N95-14437 #
CONF-9408102-1 ..... p 457 N95-14659 #
CONF-9408109-2 ..... p 529 N95-14434 #
CONF-9408111-1 ..... p 472 N95-13975 #
CONF-9408111-2 ..... p 620 N95-14188 #
CONF-9408118-1 ..... p 622 N95-14608 #
CONF-9408120-1 ..... p 522 N95-14187 #
CONF-9408121-1 ..... p 571 N95-14196 #
CONF-9408131-1 ..... p 498 N95-14318 #
CONF-940838-7 ..... p 596 N95-15381 #
CONF-940846-1 ..... p 438 N95-14391 #
CONF-940847-2 ..... p 621 N95-14390 #
CONF-940859-19 ..... p 621 N95-14342 #
CONF-9409105-1 ..... p 501 N95-14005 #
CONF-9409163-1 ..... p 619 N95-15774 #
CONF-9409164-2 ..... p 476 N95-15356 #
CONF-9409167-1 ..... p 630 N95-13996 #
CONF-9409176-1 ..... p 529 N95-14436 #
CONF-941006-1 ..... p 446 N95-15433 #
CONF-9410116-1 ..... p 474 N95-14315 #
CONF-9410131-2 ..... p 476 N95-15410 #
CONF-9410131-3 ..... p 642 N95-14311 #
CONF-9410132-1 ..... p 418 N95-15357 #
CONF-941055-1 ..... p 437 N95-14312 #
CONF-941061-4 ..... p 460 N95-15409 #
CONF-941063-3 ..... p 593 N95-14309 #
CONF-941063-4 ..... p 473 N95-14308 #
CONF-941063-5 ..... p 437 N95-14307 #
CONF-941071-1 ..... p 473 N95-14310 #
CONF-941085-4 ..... p 633 N95-15761 #
CONF-941087-1 ..... p 522 N95-14317 #
CONF-941090-2 ..... p 473 N95-14314 #
p 515 N95-14313 #

CRDL-309 ..... p 515 N95-13885 * #

CRHC-94-13 ..... p 474 N95-14355 #

CRREL-SR-94-10 ..... p 435 N95-15427 #

CRREL-94-3 ..... p 531 N95-15428 #
CRREL-94-4 ..... p 530 N95-14862 #

CSE-94-16 ..... p 566 N95-14107 * #

DCN 1-4-EA-00896 ..... p 537 N95-13702 * #

DE90-017267 ..... p 630 N95-13726 #
DE93-018219 ..... p 457 N95-14003 #
DE94-006360 ..... p 460 N95-15409 #
DE94-006930 ..... p 519 N95-15290 #
DE94-007575 ..... p 633 N95-15761 #
DE94-009685 ..... p 597 N95-15826 #
DE94-011461 ..... p 438 N95-14375 #
DE94-011505 ..... p 447 N95-15906 #
DE94-011817 ..... p 521 N95-15863 #
DE94-011828 ..... p 519 N95-14430 #
DE94-011830 ..... p 520 N95-15405 #
DE94-011840 ..... p 520 N95-15406 #
DE94-011841 ..... p 520 N95-15355 #
DE94-011842 ..... p 518 N95-14194 #
DE94-011846 ..... p 521 N95-15407 #
DE94-011847 ..... p 622 N95-14431 #
DE94-011849 ..... p 519 N95-14432 #
DE94-011850 ..... p 624 N95-15426 #
DE94-011853 ..... p 519 N95-14433 #
DE94-011854 ..... p 518 N95-14191 #
DE94-012073 ..... p 457 N95-14004 #
DE94-012113 ..... p 501 N95-14005 #
DE94-012133 ..... p 496 N95-13669 #
DE94-012234 ..... p 601 N95-13670 #
DE94-012236 ..... p 554 N95-13671 #
DE94-012387 ..... p 601 N95-13672 #
DE94-012398 ..... p 630 N95-13673 #
DE94-012581 ..... p 404 N95-15570 #
DE94-012619 ..... p 493 N95-15571 #
DE94-012634 ..... p 471 N95-13684 #
DE94-012747 ..... p 601 N95-13674 #
DE94-012755 ..... p 592 N95-13675 #
DE94-012793 ..... p 597 N95-15572 #
DE94-012914 ..... p 436 N95-15573 #
DE94-012981 ..... p 625 N95-15574 #
DE94-012992 ..... p 524 N95-15575 #
DE94-013025 ..... p 625 N95-15576 #
DE94-013084 ..... p 529 N95-14434 #
DE94-013107 ..... p 625 N95-15577 #
DE94-013111 ..... p 627 N95-15578 #
DE94-013118 ..... p 455 N95-15579 #
DE94-013220 ..... p 597 N95-15862 #
DE94-013235 ..... p 497 N95-15580 #
DE94-013236 ..... p 579 N95-15581 #
DE94-013239 ..... p 600 N95-15582 #
DE94-013243 ..... p 469 N95-15583 #
DE94-013256 ..... p 444 N95-13820 #
DE94-013260 ..... p 619 N95-13821 #
DE94-013268 ..... p 432 N95-13643 #
DE94-013298 ..... p 620 N95-13822 #
DE94-013305 ..... p 567 N95-13676 #
DE94-013314 ..... p 577 N95-13677 #
DE94-013337 ..... p 593 N95-13678
DE94-013364 ..... p 574 N95-15384 #
DE94-013429 ..... p 620 N95-14188 #
DE94-013437 ..... p 476 N95-15410 #
DE94-013449 ..... p 437 N95-14307 #
DE94-013450 ..... p 473 N95-14308 #
DE94-013537 ..... p 601 N95-13644 #
DE94-013595 ..... p 494 N95-15861 #
DE94-013661 ..... p 500 N95-13645 #
DE94-013722 ..... p 479 N95-13679
DE94-013734 ..... p 593 N95-14309 #
DE94-013765 ..... p 496 N95-14146 #
DE94-013783 ..... p 472 N95-13975 #
DE94-013799 ..... p 597 N95-15545 #
DE94-013823 ..... p 473 N95-14310 #
DE94-013824 ..... p 568 N95-13976 #
DE94-013842 ..... p 593 N95-13680
DE94-013864 ..... p 624 N95-15385 #
DE94-013872 ..... p 568 N95-13977 #
DE94-013873 ..... p 619 N95-13681
DE94-013933 ..... p 439 N95-14435 #
DE94-013939 ..... p 442 N95-15386 #
DE94-013941 ..... p 440 N95-15291 #
DE94-013961 ..... p 449 N95-13978 #
DE94-013965 ..... p 433 N95-13682
DE94-013989 ..... p 616 N95-14006
DE94-013994 ..... p 620 N95-14008
DE94-014005 ..... p 620 N95-14009
DE94-014010 ..... p 568 N95-14010
DE94-014011 ..... p 593 N95-14011
DE94-014016 ..... p 617 N95-14012
DE94-014069 ..... p 453 N95-15292 #
DE94-014122 ..... p 476 N95-15356 #
DE94-014142 ..... p 642 N95-14311 #
DE94-014182 ..... p 437 N95-14312 #
DE94-014185 ..... p 515 N95-14313 #
DE94-014230 ..... p 445 N95-15307 #
DE94-014281 ..... p 473 N95-14314 #

DE94-014288 ..... p 418 N95-15357 #
DE94-014334 ..... p 518 N95-14143
DE94-014442 ..... p 616 N95-14007 #
DE94-014453 ..... p 433 N95-13993
DE94-014455 ..... p 498 N95-13994 #
DE94-014462 ..... p 526 N95-13995 #
DE94-014465 ..... p 630 N95-13996 #
DE94-014472 ..... p 616 N95-13997 #
DE94-014474 ..... p 616 N95-13998 #
DE94-014475 ..... p 620 N95-13999 #
DE94-014478 ..... p 593 N95-14000 #
DE94-014486 ..... p 593 N95-14001 #
DE94-014491 ..... p 517 N95-14002 #
DE94-014500 ..... p 612 N95-13986 #
DE94-014501 ..... p 445 N95-15293 #
DE94-014507 ..... p 622 N95-15308 #
DE94-014513 ..... p 563 N95-15309 #
DE94-014556 ..... p 595 N95-15310 #
DE94-014557 ..... p 522 N95-14195 #
DE94-014561 ..... p 573 N95-15311 #
DE94-014562 ..... p 613 N95-15312 #
DE94-014563 ..... p 454 N95-15313 #
DE94-014566 ..... p 613 N95-15314 #
DE94-014654 ..... p 447 N95-15625 #
DE94-014661 ..... p 474 N95-14315 #
DE94-014742 ..... p 529 N95-14436 #
DE94-014750 ..... p 522 N95-14317 #
DE94-014796 ..... p 585 N95-14381 #
DE94-014801 ..... p 646 N95-14437 #
DE94-014802 ..... p 646 N95-14376 #
DE94-014809 ..... p 647 N95-14438 #
DE94-014810 ..... p 445 N95-14439 #
DE94-014904 ..... p 590 N95-14440 #
DE94-014909 ..... p 594 N95-14441 #
DE94-014910 ..... p 525 N95-15864 #
DE94-014913 ..... p 434 N95-14387 #
DE94-014924 ..... p 597 N95-15865 #
DE94-014928 ..... p 643 N95-14442 #
DE94-014929 ..... p 470 N95-15866 #
DE94-014930 ..... p 443 N95-15667 #
DE94-014939 ..... p 618 N95-14443 #
DE94-014958 ..... p 620 N95-14189 #
DE94-014965 ..... p 494 N95-15867 #
DE94-014967 ..... p 494 N95-15868 #
DE94-014971 ..... p 457 N95-14659 #
DE94-014973 ..... p 598 N95-15869 #
DE94-014975 ..... p 594 N95-14660 #
DE94-014986 ..... p 594 N95-14661 #
DE94-014993 ..... p 566 N95-14662 #
DE94-015001 ..... p 439 N95-14663 #
DE94-015012 ..... p 428 N95-14664 #
DE94-015017 ..... p 617 N95-14262 #
DE94-015020 ..... p 445 N95-14665 #
DE94-015021 ..... p 453 N95-14609 #
DE94-015033 ..... p 571 N95-14196 #
DE94-015058 ..... p 618 N95-14955 #
DE94-015067 ..... p 475 N95-14606 #
DE94-015069 ..... p 442 N95-15387 #
DE94-015070 ..... p 624 N95-15430 #
DE94-015086 ..... p 622 N95-14608 #
DE94-015089 ..... p 621 N95-14192 #
DE94-015091 ..... p 522 N95-14187 #
DE94-015122 ..... p 530 N95-14956 #
DE94-015137 ..... p 498 N95-14318 #
DE94-015155 ..... p 453 N95-14957 #
DE94-015157 ..... p 599 N95-15367 #
DE94-015163 ..... p 446 N95-15368 #
DE94-015165 ..... p 583 N95-15369 #
DE94-015172 ..... p 440 N95-15297 #
DE94-015180 ..... p 468 N95-15300 #
DE94-015183 ..... p 597 N95-15629 #
DE94-015184 ..... p 595 N95-15301 #
DE94-015187 ..... p 475 N95-15302 #
DE94-015188 ..... p 597 N95-15630 #
DE94-015190 ..... p 621 N95-14325 #
DE94-015202 ..... p 446 N95-15431 #
DE94-015207 ..... p 524 N95-15432 #
DE94-015209 ..... p 446 N95-15433 #
DE94-015253 ..... p 578 N95-15434 #
DE94-015259 ..... p 632 N95-15435 #
DE94-015262 ..... p 442 N95-15436 #
DE94-015264 ..... p 524 N95-15455 #
DE94-015277 ..... p 574 N95-15543 #
DE94-015281 ..... p 477 N95-15544 #
DE94-015282 ..... p 474 N95-14319 #
DE94-015288 ..... p 633 N95-15528 #
DE94-015311 ..... p 441 N95-15370 #
DE94-015323 ..... p 473 N95-14261 #
DE94-015324 ..... p 614 N95-15529 #
DE94-015326 ..... p 493 N95-15530 #
DE94-015340 ..... p 599 N95-15371 #
DE94-015343 ..... p 595 N95-15372 #
DE94-015344 ..... p 618 N95-15373 #
DE94-015345 ..... p 618 N95-15374 #
DE94-015353 ..... p 442 N95-15375 #
DE94-015359 ..... p 506 N95-14320 #
DE94-015360 ..... p 625 N95-15531 #
DE94-015362 ..... p 446 N95-15532 #
DE94-015382 ..... p 588 N95-15533 #
DE94-015393 ..... p 579 N95-15534 #
DE94-015414 ..... p 455 N95-15535 #
DE94-015456 ..... p 571 N95-14190 #
DE94-015457 ..... p 574 N95-15536 #
DE94-015483 ..... p 596 N95-15537 #
DE94-015514 ..... p 586 N95-15538 #
DE94-015519 ..... p 600 N95-15539 #
DE94-015534 ..... p 618 N95-15540 #
DE94-015535 ..... p 442 N95-15541
DE94-015545 ..... p 574 N95-15418 #
DE94-015566 ..... p 632 N95-15419 #
DE94-015599 ..... p 521 N95-15420 #
DE94-015600 ..... p 596 N95-15437 #
DE94-015601 ..... p 625 N95-15438 #
DE94-015650 ..... p 624 N95-15421 #
DE94-015652 ..... p 454 N95-15358 #
DE94-015653 ..... p 447 N95-15631 #
DE94-015719 ..... p 618 N95-15632
DE94-015720 ..... p 617 N95-14328
DE94-015721 ..... p 566 N95-14338 #
DE94-015748 ..... p 531 N95-15411 #
DE94-015774 ..... p 621 N95-14342 #
DE94-015796 ..... p 621 N95-14322 #
DE94-015799 ..... p 493 N95-15351 #
DE94-015801 ..... p 621 N95-14323 #
DE94-015816 ..... p 578 N95-14116 #
DE94-015828 ..... p 518 N95-14326 #
DE94-015842 ..... p 438 N95-14371 #
DE94-015844 ..... p 624 N95-15422 #
DE94-015846 ..... p 600 N95-15633 #
DE94-015851 ..... p 456 N95-15634 #
DE94-015860 ..... p 617 N95-14426 #
DE94-015866 ..... p 613 N95-14967 #
DE94-015899 ..... p 499 N95-14427 #
DE94-015935 ..... p 519 N95-14393 #
DE94-015945 ..... p 529 N95-14428 #
DE94-016056 ..... p 619 N95-15774 #
DE94-016064 ..... p 638 N95-14429 #
DE94-016073 ..... p 617 N95-14368 #
DE94-016094 ..... p 617 N95-14397 #
DE94-016203 ..... p 626 N95-15776 #
DE94-016207 ..... p 591 N95-15359 #
DE94-016211 ..... p 505 N95-15777 #
DE94-016213 ..... p 581 N95-14377 #
DE94-016280 ..... p 599 N95-15360 #
DE94-016315 ..... p 456 N95-15778 #
DE94-016320 ..... p 445 N95-14378 #
DE94-016328 ..... p 445 N95-14379 #
DE94-016343 ..... p 578 N95-14380
DE94-016348 ..... p 596 N95-15381 #
DE94-016349 ..... p 621 N95-14382
DE94-016362 ..... p 524 N95-15779 #
DE94-016363 ..... p 523 N95-15361 #
DE94-016368 ..... p 594 N95-14383
DE94-016371 ..... p 595 N95-15362 #
DE94-016429 ..... p 578 N95-14384 #
DE94-016451 ..... p 600 N95-15780 #
DE94-016487 ..... p 594 N95-14385 #
DE94-016491 ..... p 438 N95-14386 #
DE94-016532 ..... p 438 N95-14388 #
DE94-016543 ..... p 451 N95-14389
DE94-016556 ..... p 621 N95-14390 #
DE94-016598 ..... p 442 N95-15408
DE94-016618 ..... p 438 N95-14391 #
DE94-016624 ..... p 523 N95-15363 #
DE94-016629 ..... p 523 N95-15364 #
DE94-016635 ..... p 468 N95-15365 #
DE94-016642 ..... p 438 N95-14392 #
DE94-016646 ..... p 438 N95-14372 #
DE94-016686 ..... p 632 N95-15366 #
DE94-016770 ..... p 617 N95-14373 #
DE94-016863 ..... p 594 N95-14374 #
DE94-016873 ..... p 623 N95-15337
DE94-016875 ..... p 623 N95-15338
DE94-016876 ..... p 623 N95-15339
DE94-016884 ..... p 454 N95-15340
DE94-016901 ..... p 623 N95-15341 #
DE94-016902 ..... p 586 N95-15342
DE94-016949 ..... p 454 N95-15343
DE94-016953 ..... p 454 N95-15344
DE94-017125 ..... p 441 N95-15345
DE94-017151 ..... p 441 N95-15346
DE94-017155 ..... p 441 N95-15347
DE94-780614 ..... p 520 N95-15376 #
DE94-780648 ..... p 520 N95-15377 #
DE94-780690 ..... p 530 N95-14836
DOC-0710-001 ..... p 392 N95-15331 #
DODA-AR-008-383 ..... p 434 N95-14409 #
DOE/CE-15974/T8 ..... p 453 N95-15292 #
DOE/CE-23810/34 ..... p 454 N95-15343
DOE/CE-23810/42A ..... p 438 N95-14372 #
DOE/CH-10093/245-ADD ..... p 457 N95-14003 #
DOE/EIA-0384(93) ..... p 518 N95-14326 #
DOE/ER-12103/3 ..... p 597 N95-15572 #
DOE/ER-13150/T5 ..... p 441 N95-15370 #
DOE/ER-13296/10 ..... p 441 N95-15346
DOE/ER-13439/T4 ..... p 438 N95-14392 #
DOE/ER-13811/6 ..... p 441 N95-15347
DOE/ER-13974/T2 ..... p 454 N95-15344
DOE/ER-14143/3 ..... p 438 N95-14386 #
DOE/ER-14278/T2 ..... p 530 N95-14956 #
DOE/ER-14303/3 ..... p 494 N95-15861 #
DOE/ER-25176/1 ..... p 578 N95-14384 #
DOE/ER-40509/4 ..... p 596 N95-15537 #
DOE/ER-40561/143 ..... p 598 N95-15869 #
DOE/ER-40561/147 ..... p 594 N95-14660 #
DOE/ER-40577/4 ..... p 595 N95-15372 #
DOE/ER-40684/4 ..... p 600 N95-15539 #
DOE/ER-40734/2 ..... p 599 N95-15371 #
DOE/ER-45233/9 ..... p 625 N95-15574 #
DOE/ER-45357/7 ..... p 454 N95-15358 #
DOE/ER-45364/T4 ..... p 447 N95-15631 #
DOE/ER-53198/242 ..... p 442 N95-15541
DOE/ER-53198/244 ..... p 617 N95-14373 #
DOE/ER-53212/241 ..... p 618 N95-15540 #
DOE/ET-15601/T62 ..... p 618 N95-15374 #
DOE/ET-15601/47 ..... p 618 N95-15373 #
DOE/LLW-201-REV-1 ..... p 632 N95-15435 #
DOE/MC-29113/3766-PHASE-2 .. p 563 N95-15309 #
DOE/MC-29237/3798 ..... p 518 N95-14143
DOE/MT-92022/1 ..... p 440 N95-15291 #
DOE/MT-93010/1 ..... p 442 N95-15386 #
DOE/NASA/50306-6 ..... p 431 N95-13631 * #
DOE/PC-90293/T13 ..... p 441 N95-15345
DOE/PC-92111/5 ..... p 439 N95-14435 #
DOE/SF-19460/17 ..... p 618 N95-14955 #
DOT/FAA/AM-94/14 ..... p 540 N95-14177 #
DOT/FAA/AM-94/15 ..... p 540 N95-14176 #
DOT/FAA/AM-94/22-PT-3 ..... p 551 N95-13715 #
DOT/FAA/AM-94/24 ..... p 552 N95-14863 #
DOT/FAA/AM-94/25 ..... p 573 N95-14917 #
DOT/FAA/CT-TN93/17 ..... p 461 N95-14346 #
DOT/FAA/CT-93/52 ..... p 411 N95-15683 #
DOT/FAA/CT-94/41 ..... p 581 N95-13895 #
DOT/FAA/CT-94/64 ..... p 405 N95-14350 #
DOT/FAA/RD-94/19 ..... p 410 N95-14175 #
DOT/FAA/RD-94/24 ..... p 413 N95-15328 #
DRD-MA-784-002-REV ..... p 636 N95-13634 * #
DRD-MA-784-002-REV ..... p 636 N95-13636 * #
DRD-MA-784-002-REV ..... p 637 N95-13637 * #
DRD-MA-784-002-REV ..... p 637 N95-14100 * #
DRD-MA-784-002-REV ..... p 638 N95-14101 * #
DRD-MA-784-004-REV ..... p 567 N95-13635 * #
DSA-105/1460 ..... p 470 N95-15756 #
D180-32040-3-VOL-3-BK-2 ..... p 419 N95-15552 * #
E-0265-079 ..... p 431 N95-14669 * #
E-5140-1-PT-1 ..... p 440 N95-15056 * #
E-5140-2 ..... p 442 N95-15512 * #
E-5140-3-PT-3 ..... p 440 N95-15057 * #
E-8049 ..... p 572 N95-14206 * #
E-8053 ..... p 420 N95-13728 * #
E-8522 ..... p 432 N95-13641 * #
E-8863 ..... p 430 N95-14174 * #
E-8889 ..... p 430 N95-14173 * #
E-8957 ..... p 408 N95-14604 * #
E-8983 ..... p 433 N95-14298 * #
E-9044 ..... p 419 N95-13893 * #
E-9046 ..... p 482 N95-14522 * #
E-9112 ..... p 444 N95-13667 * #
E-9124-1 ..... p 404 N95-15853 * #
E-9128 ..... p 404 N95-15852 * #
E-9133 ..... p 507 N95-14417 * #
E-9139 ..... p 431 N95-13631 * #
E-9141 ..... p 591 N95-14618 * #
E-9142 ..... p 431 N95-15682 * #
E-9146 ..... p 450 N95-14303 * #
E-9147 ..... p 430 N95-14301 * #
E-9150 ..... p 481 N95-14295 * #

E-9152 ..... p 482 N95-14299 * #
E-9153 ..... p 431 N95-15058 * #
E-9155 ..... p 566 N95-13716 * #
E-9164 ..... p 429 N95-13666 * #
E-9168 ..... p 478 N95-13653 * #
E-9171 ..... p 634 N95-15743 * #
E-9172 ..... p 591 N95-14610 * #
E-9174 ..... p 392 N95-13817 * #
E-9179 ..... p 479 N95-13665 * #
E-9195 ..... p 568 N95-13894 * #
E-9197 ..... p 601 N95-13666 * #
E-9199 ..... p 430 N95-13697 * #
E-9201 ..... p 477 N95-15587 * #
E-9205 ..... p 585 N95-14296 * #
E-9218 ..... p 495 N95-15908 * #
E-9220 ..... p 492 N95-14607 * #
E-9221 ..... p 436 N95-15911 * #
E-9226 ..... p 431 N95-15769 * #
E-9229 ..... p 473 N95-14302 * #
E-9230 ..... p 398 N95-14418 * #
E-9233 ..... p 585 N95-14300 * #
E-9235 ..... p 591 N95-15059 * #
E-9241 ..... p 398 N95-14297 * #
E-9252 ..... p 405 N95-15912 * #

ECE-TR-94-09 ..... p 499 N95-14364 #

EGG-CIET-11270 ..... p 524 N95-15455 #

EGG-EE-11298-PT-1 ..... p 578 N95-15434 #
EGG-EE-11298-PT-2 ..... p 579 N95-15534 #

EGG-MS-11063 ..... p 442 N95-15436 #

EGG-RAAM-11182 ..... p 588 N95-15533 #

EPA/540/SR-93/516 ..... p 521 N95-14121 #
EPA/600/A-94/092 ..... p 616 N95-13973 #
EPA/600/A-94/099 ..... p 534 N95-15383 #
EPA/600/A-94/118 ..... p 523 N95-14403 #
EPA/600/A-94/148 ..... p 521 N95-14122 #
EPA/600/A-94/149 ..... p 521 N95-14123 #
EPA/600/J-94/306 ..... p 529 N95-14404
EPA/600/R-94/080 ..... p 523 N95-15382 #
EPA/620/R-94-017 ..... p 522 N95-14124 #

ERDEC-CR-133 ..... p 497 N95-15334

ERP-1147 ..... p 428 N95-14599 #

ESC-TR-94-010 ..... p 572 N95-14339 #
ESC-TR-94-013 ..... p 572 N95-14349 #

ESL-724733-3 ..... p 469 N95-15394

ETDE/JP-MF-94780614 ..... p 520 N95-15376 #
ETDE/JP-MF-94780648 ..... p 520 N95-15377 #
ETDE/JP-MF-94780690 ..... p 530 N95-14836

ETDE/PUB-3-REV-1-SUPPL-4 ..... p 630 N95-13726 #

FAA-AAM-A-HRR-126 ..... p 552 N95-14863 #

FAA/ACE-100-01 ..... p 408 N95-13981

FE-MIT-92111-5 ..... p 439 N95-14435 #

FNAL-TM-1895 ..... p 475 N95-15302 #

FNAL/C-93/291-E ..... p 597 N95-15862 #
FNAL/C-94-167 ..... p 594 N95-14661 #
FNAL/C-94/088-E ..... p 600 N95-15582 #
FNAL/C-94/100 ..... p 497 N95-15580 #
FNAL/C-94/104 ..... p 579 N95-15581 #
FNAL/C-94/134-E ..... p 593 N95-13680
FNAL/C-94/154-E ..... p 595 N95-15301 #
FNAL/C-94/155-E ..... p 597 N95-15630 #
FNAL/C-94/158-E ..... p 597 N95-15629 #
FNAL/C-94/191 ..... p 574 N95-15418 #

FOA-C-20961-2.4 ..... p 433 N95-14148 #

FR2198-20 ..... p 446 N95-15415

FSGTR-SO-99 ..... p 515 N95-14125 #

FSRN-PSW-417 ..... p 413 N95-14513 #

FTR-528226 ..... p 583 N95-15461

F93-2B-0R15 ..... p 408 N95-13703 * #

GA-A-21466 ..... p 617 N95-14426 #
GA-A-21679 ..... p 617 N95-14328
GA-A-21737 ..... p 618 N95-15632

GALCIT-FM-94-2 ..... p 400 N95-14656

H-2007-VOL-1 ..... p 393 N95-14229 * #
H-2007-VOL-2 ..... p 395 N95-14239 * #
H-2007-VOL-3 ..... p 397 N95-14251 * #
H-2029 ..... p 479 N95-13892 * #

HZ-08084-1 ..... p 518 N95-14341 #

IAF-94-P.1.301 ..... p 632 N95-14619 * #

ICASE-94-74 ..... p 568 N95-13889 * #
ICASE-94-83 ..... p 495 N95-15917 * #

ICOMP-94-24 ..... p 478 N95-13653 * #
ICOMP-94-25 ..... p 585 N95-14296 * #
ICOMP-94-26 ..... p 495 N95-15908 * #

IHES/M/94/11 ..... p 589 N95-13979 #
IHES/M/94/6 ..... p 586 N95-15412 #

INT-PATENT-CLASS-B23K-10/00 p 503 N95-15670 *
INT-PATENT-CLASS-B23K-37/02 p 500 N95-13654 *
INT-PATENT-CLASS-B23K-9/00 . p 503 N95-15670 *
INT-PATENT-CLASS-B25B-5/00 . p 504 N95-15914 *
INT-PATENT-CLASS-B64C-25/58 p 503 N95-15306 *
INT-PATENT-CLASS-B64D-17/02 p 393 N95-14182 *

INT-PATENT-CLASS-C01B-31/04 p 441 N95-15303 *
INT-PATENT-CLASS-C07C-211/54 p 452 N95-14416 *
INT-PATENT-CLASS-C07C-211/56 p 452 N95-14416 *

INT-PATENT-CLASS-F16C-21/00 p 500 N95-13819 *
INT-PATENT-CLASS-F16H-57/00 p 502 N95-14517 *
INT-PATENT-CLASS-F16L-3/10 .. p 503 N95-15305 *

INT-PATENT-CLASS-G01C-21/00 p 411 N95-14518 *
INT-PATENT-CLASS-G01F-1/88 . p 496 N95-14414 *
INT-PATENT-CLASS-G01M-9/00 p 496 N95-14414 *
INT-PATENT-CLASS-G01N-3/42 . p 497 N95-15915 *
INT-PATENT-CLASS-G01R-23/02 p 498 N95-13629 *
INT-PATENT-CLASS-G01R-27/26 p 583 N95-15598 *
INT-PATENT-CLASS-G01R-31/08 p 478 N95-15669 *
INT-PATENT-CLASS-G02B-5/126 p 499 N95-14515 *
INT-PATENT-CLASS-G02B-6/12 . p 612 N95-14181 *
INT-PATENT-CLASS-G06F-15/74 p 496 N95-14180 *
INT-PATENT-CLASS-G08B-21/00 p 412 N95-14415 *
INT-PATENT-CLASS-G08C-19/10 p 583 N95-15598 *

INT-PATENT-CLASS-H01H-47/12 p 583 N95-15598 *
INT-PATENT-CLASS-H01J-1/14 .. p 475 N95-14516 *
INT-PATENT-CLASS-H01J-1/15 .. p 475 N95-14516 *
INT-PATENT-CLASS-H01J-40/14 p 614 N95-15603 *
INT-PATENT-CLASS-H01J-5/16 .. p 613 N95-14413 *
INT-PATENT-CLASS-H01M-6/18 p 472 N95-13824 *
INT-PATENT-CLASS-H01R-13/639 p 504 N95-15914 *
INT-PATENT-CLASS-H01S-3/00 . p 499 N95-14519 *
INT-PATENT-CLASS-H01S-3/08 . p 602 N95-13823 *
INT-PATENT-CLASS-H02J-14/02 p 612 N95-14181 *
INT-PATENT-CLASS-H02M-3/335 p 478 N95-15681 *
INT-PATENT-CLASS-H05B-6/14 . p 473 N95-14294 *
INT-PATENT-CLASS-H05H-3/00 . p 503 N95-15601 *

IS-T-1675 ..... p 445 N95-15307 #

ISBN-0-16-042011-3 ..... p 633 N95-15781 #
ISBN-0-309-05761-2 ..... p 407 N95-15439
ISBN-0-912747-08-0 ..... p 532 N95-14120 #
ISBN-90-5269-133-9 ..... p 568 N95-14152 #
ISBN-90-6275-903-3 ..... p 624 N95-15378 #
ISBN-90-6275-907-6 ..... p 471 N95-15871 #
ISBN-90-6275-911-4 ..... p 525 N95-15870 #
ISBN-90-9005806-0 ..... p 501 N95-14150
ISBN-90-9005917-2 ..... p 537 N95-13990
ISBN-90-9006471-0 ..... p 585 N95-14154
ISBN-90-9006567-9 ..... p 632 N95-14837 #
ISBN-90-9006763-9 ..... p 472 N95-14149 #
ISBN-90-9007089-3 ..... p 513 N95-15429
ISBN-92-835-0716-9 ..... p 506 N95-14198 #
ISBN-92-835-0744-4 ..... p 461 N95-14200 #
ISBN-92-835-0745-2 ..... p 562 N95-14263 #
ISBN-92-835-0748-7 ..... p 408 N95-14102 #
ISBN-92-835-0749-5 ..... p 479 N95-14127 #
ISBN-92-835-0751-7 ..... p 581 N95-14942 #
ISBN-92-835-0752-5 ..... p 399 N95-14445 #
ISBN-92-835-0753-3 ..... p 393 N95-14197 #
ISBN-92-835-0754-1 ..... p 393 N95-14103 #
ISBN-92-836-1001-6 ..... p 405 N95-14199 #
ISBN-92-836-1002-4 ..... p 481 N95-14201 #
ISBN-92-836-1004-0 ..... p 466 N95-14825 #
ISBN-92-836-1005-9 ..... p 398 N95-14264 #
ISBN-92-836-1006-7 ..... p 406 N95-14893 #
ISBN-951-22-1988-3 ..... p 497 N95-15413 #
ISBN-951-22-1989-1 ..... p 478 N95-15611 #
ISBN-951-22-2004-0 ..... p 589 N95-13987 #
ISBN-951-22-2033-4 ..... p 590 N95-13988 #

ISBN-951-22-2045-8 ..... p 637 N95-13982

ISVR-TR-236 ..... p 563 N95-15850

JPL-PUBL-94-19 ..... p 464 N95-14670 * #

JPL-TDA-PR-42-118 ..... p 462 N95-14620 * #

JTCG/AS-94-D-004 ..... p 409 N95-14840 #

KAPL-4763 ..... p 446 N95-15532 #
KAPL-4777 ..... p 625 N95-15531 #
KAPL-4782 ..... p 506 N95-14320 #

KCP-613-5384 ..... p 613 N95-14367 #

L-17356 ..... p 409 N95-14852 * #
L-17387 ..... p 600 N95-15606 * #
L-17394 ..... p 647 N95-15790 * #
L-17397 ..... p 647 N95-15065 * #
L-17432-PT-1 ..... p 507 N95-14453 * #
L-17434 ..... p 401 N95-14878 * #

LA-UR-94-1520 ..... p 436 N95-15573 #
LA-UR-94-1587 ..... p 646 N95-14376 #
LA-UR-94-1588 ..... p 646 N95-14437 #
LA-UR-94-1602 ..... p 585 N95-14381 #
LA-UR-94-1616 ..... p 647 N95-14438 #
LA-UR-94-1668 ..... p 529 N95-14434 #
LA-UR-94-1697 ..... p 445 N95-14439 #
LA-UR-94-1729 ..... p 455 N95-15579 #
LA-UR-94-1843 ..... p 630 N95-13996 #
LA-UR-94-1883 ..... p 616 N95-13998 #
LA-UR-94-1887 ..... p 498 N95-13994 #
LA-UR-94-1891 ..... p 433 N95-13993
LA-UR-94-1892 ..... p 620 N95-13999 #
LA-UR-94-1956 ..... p 616 N95-14007 #
LA-UR-94-2065 ..... p 616 N95-13997 #
LA-UR-94-2100 ..... p 593 N95-14000 #
LA-UR-94-2130 ..... p 526 N95-13995 #
LA-UR-94-2228 ..... p 593 N95-14001 #
LA-UR-94-2268 ..... p 617 N95-14368 #
LA-UR-94-2307 ..... p 638 N95-14429 #
LA-UR-94-2335 ..... p 619 N95-15774 #
LA-UR-94-2377 ..... p 505 N95-15777 #
LA-UR-94-2445 ..... p 591 N95-15359 #
LA-UR-94-2450 ..... p 626 N95-15776 #
LA-UR-94-2531 ..... p 581 N95-14377 #
LA-UR-94-2553 ..... p 599 N95-15360 #
LA-UR-94-2563 ..... p 617 N95-14397 #
LA-UR-94-575 ..... p 633 N95-15761 #

LA-12765 ..... p 440 N95-15297 #
LA-12776-MS ..... p 442 N95-15387 #

LBL-34810 ..... p 623 N95-15339
LBL-35022 ..... p 623 N95-15337
LBL-35127 ..... p 443 N95-15667 #
LBL-35339 ..... p 453 N95-14957 #
LBL-35371 ..... p 597 N95-15865 #
LBL-35474 ..... p 625 N95-15577 #
LBL-35476 ..... p 599 N95-15367 #
LBL-35487 ..... p 470 N95-15866 #
LBL-35497 ..... p 627 N95-15578 #
LBL-35525 ..... p 643 N95-14442 #
LBL-35568 ..... p 594 N95-14374 #
LBL-35580 ..... p 620 N95-14189 #
LBL-35626 ..... p 434 N95-14387 #
LBL-35630 ..... p 494 N95-15868 #
LBL-35669 ..... p 457 N95-14659 #
LBL-35671 ..... p 623 N95-15338
LBL-35719 ..... p 494 N95-15867 #

LG94ER0099 ..... p 451 N95-14383 #

LMSC-F-254280 ..... p 619 N95-15758 * #

LTRMP-94-T001 ..... p 515 N95-14793

M-750-VOL-1 ..... p 634 N95-14207 * #
M-760 ..... p 513 N95-15055 * #
M-764 ..... p 436 N95-15763 * #
M-765 ..... p 435 N95-14913 * #

M/FAA/002-93-1 ..... p 411 N95-15683 #

MCAT-94-005 ..... p 644 N95-13717 * #
MCAT-94-11 ..... p 400 N95-14614 * #
MCAT-94-20 ..... p 400 N95-14613 * #

MCR-94-1328 ..... p 502 N95-14910 * #

MIT-OSP-89029 ..... p 531 N95-15586 * #

MPL-U-9/94 ..... p 591 N95-14396 #

MSB-228 ..... p 493 N95-15332 #

NAS 1.15:103855 ..... p 391 N95-14419 * #
NAS 1.15:104606-VOL-3 ..... p 531 N95-15745 * #
NAS 1.15:104797 ..... p 432 N95-13646 * #
NAS 1.15:106313 ..... p 420 N95-13728 * #
NAS 1.15:106385 ..... p 398 N95-14418 * #
NAS 1.15:106593 ..... p 430 N95-14174 * #
NAS 1.15:106608 ..... p 430 N95-14173 * #
NAS 1.15:106649 ..... p 408 N95-14604 * #
NAS 1.15:10665 ..... p 433 N95-14298 * #
NAS 1.15:106682 ..... p 450 N95-14303 * #
NAS 1.15:106688 ..... p 419 N95-13893 * #
NAS 1.15:106734 ..... p 444 N95-13667 * #
NAS 1.15:106738 ..... p 591 N95-14618 * #
NAS 1.15:106739 ..... p 431 N95-15682 * #
NAS 1.15:106740 ..... p 430 N95-14301 * #
NAS 1.15:106742 ..... p 482 N95-14299 * #
NAS 1.15:106743 ..... p 566 N95-13716 * #
NAS 1.15:106748 ..... p 429 N95-13668 * #
NAS 1.15:106752 ..... p 478 N95-13653 * #
NAS 1.15:106753 ..... p 431 N95-13631 * #
NAS 1.15:106754 ..... p 392 N95-13817 * #
NAS 1.15:106757 ..... p 479 N95-13665 * #
NAS 1.15:106760 ..... p 568 N95-13894 * #
NAS 1.15:106761 ..... p 477 N95-15587 * #
NAS 1.15:106762 ..... p 585 N95-14296 * #
NAS 1.15:106770 ..... p 495 N95-15908 * #
NAS 1.15:106772 ..... p 492 N95-14607 * #
NAS 1.15:106774 ..... p 404 N95-15853 * #
NAS 1.15:106775 ..... p 431 N95-15769 * #
NAS 1.15:106777 ..... p 473 N95-14302 * #
NAS 1.15:106780 ..... p 585 N95-14300 * #
NAS 1.15:106782 ..... p 591 N95-15059 * #
NAS 1.15:106786 ..... p 398 N95-14297 * #
NAS 1.15:108468 ..... p 443 N95-15607 * #
NAS 1.15:108469 ..... p 459 N95-14919 * #
NAS 1.15:108472 ..... p 431 N95-15609 * #
NAS 1.15:108833 ..... p 512 N95-14617 * #
NAS 1.15:108840 ..... p 539 N95-13661 * #
NAS 1.15:108842 ..... p 406 N95-14611 * #
NAS 1.15:108850 ..... p 391 N95-13642 * #
NAS 1.15:108853 ..... p 391 N95-13662 * #
NAS 1.15:108854 ..... p 481 N95-14273 * #
NAS 1.15:108855 ..... p 391 N95-13891 * #
NAS 1.15:108856 ..... p 550 N95-15649 * #
NAS 1.15:108857 ..... p 392 N95-14921 * #
NAS 1.15:109142 ..... p 432 N95-14920 * #
NAS 1.15:109150 ..... p 420 N95-13729 * #
NAS 1.15:109152 ..... p 495 N95-15898 * #
NAS 1.15:109153 ..... p 444 N95-13690 * #
NAS 1.15:109163 ..... p 647 N95-13663 * #
NAS 1.15:109208 ..... p 630 N95-14918 * #
NAS 1.15:109957 ..... p 642 N95-13658 * #
NAS 1.15:109965 ..... p 428 N95-14510 * #
NAS 1.15:109968 ..... p 638 N95-14911 * #
NAS 1.15:109980 ..... p 632 N95-14870 * #
NAS 1.15:109981 ..... p 632 N95-14619 * #
NAS 1.15:4543 ..... p 572 N95-14206 * #
NAS 1.15:4568 ..... p 432 N95-13641 * #
NAS 1.15:4575 ..... p 647 N95-15065 * #
NAS 1.15:4651 ..... p 479 N95-13892 * #
NAS 1.19/4:101 ..... p 554 N95-13888 * #
NAS 1.19/4:102 ..... p 638 N95-14511 * #
NAS 1.19:292 ..... p 629 N95-13650 * #
NAS 1.21:7011(395) ..... p 550 N95-15304 *
NAS 1.21:7037(310) ..... p 392 N95-15550 *
NAS 1.26:188356 ..... p 492 N95-14869 * #
NAS 1.26:188357 ..... p 443 N95-15715 * #
NAS 1.26:189188 ..... p 431 N95-14669 * #
NAS 1.26:189331 ..... p 615 N95-15849 * #
NAS 1.26:189374 ..... p 517 N95-15916 * #
NAS 1.26:189375 ..... p 619 N95-15758 * #
NAS 1.26:189376 ..... p 515 N95-13704 * #
NAS 1.26:189377 ..... p 567 N95-13651 * #
NAS 1.26:189378 ..... p 567 N95-13633 * #
NAS 1.26:189380 ..... p 567 N95-13632 * #
NAS 1.26:192447 ..... p 419 N95-15552 * #
NAS 1.26:193621 ..... p 526 N95-14267 * #
NAS 1.26:194215 ..... p 644 N95-13717 * #
NAS 1.26:194414 ..... p 514 N95-13639 * #
NAS 1.26:194973 ..... p 633 N95-15585 * #
NAS 1.26:194974 ..... p 568 N95-13889 * #
NAS 1.26:194976 ..... p 580 N95-13727 * #
NAS 1.26:194982-REV ..... p 448 N95-15918 * #
NAS 1.26:194985 ..... p 516 N95-15727 * #
NAS 1.26:194986 ..... p 418 N95-13890 * #
NAS 1.26:194991 ..... p 495 N95-15917 * #
NAS 1.26:195003 ..... p 492 N95-14912 * #
NAS 1.26:195008 ..... p 493 N95-15604 * #
NAS 1.26:195156 ..... p 457 N95-14902 * #
NAS 1.26:195383 ..... p 507 N95-14417 * #
NAS 1.26:195387 ..... p 481 N95-14295 * #
NAS 1.26:195388 ..... p 431 N95-15058 * #
NAS 1.26:195393 ..... p 634 N95-15743 * #
NAS 1.26:195394 ..... p 591 N95-14610 * #
NAS 1.26:195396 ..... p 601 N95-13666 * #
NAS 1.26:195397 ..... p 430 N95-13697 * #
NAS 1.26:195398 ..... p 404 N95-15852 * #
NAS 1.26:195399 ..... p 436 N95-15911 * #
NAS 1.26:195405 ..... p 405 N95-15912 * #
NAS 1.26:195810 ..... p 568 N95-13699 * #
NAS 1.26:195818 ..... p 636 N95-13634 * #
NAS 1.26:196013 ..... p 637 N95-14100 * #
NAS 1.26:196059 ..... p 515 N95-13885 * #
NAS 1.26:196145 ..... p 637 N95-13637 * #
NAS 1.26:196263 ..... p 637 N95-13723 * #
NAS 1.26:196265 ..... p 637 N95-13722 * #
NAS 1.26:196409 ..... p 462 N95-14620 * #
NAS 1.26:196440 ..... p 525 N95-13627 * #
NAS 1.26:196448 ..... p 567 N95-13635 * #
NAS 1.26:196480 ..... p 645 N95-13724 * #
NAS 1.26:196489 ..... p 638 N95-14101 * #
NAS 1.26:196521 ..... p 532 N95-14271 * #
NAS 1.26:196522 ..... p 602 N95-13841 * #
NAS 1.26:196526 ..... p 573 N95-14905 * #
NAS 1.26:196531 ..... p 429 N95-15824 * #
NAS 1.26:196536 ..... p 439 N95-14867 * #
NAS 1.26:196786 ..... p 532 N95-13725 * #
NAS 1.26:196849 ..... p 537 N95-13702 * #
NAS 1.26:196886 ..... p 579 N95-15442 *
NAS 1.26:196935 ..... p 453 N95-14931 * #
NAS 1.26:196936 ..... p 492 N95-14932 * #
NAS 1.26:196951 ..... p 642 N95-15907 * #
NAS 1.26:196959 ..... p 464 N95-14670 * #
NAS 1.26:196963 ..... p 569 N95-14156 * #
NAS 1.26:196974 ..... p 526 N95-13818 * #
NAS 1.26:196975 ..... p 505 N95-13839 * #
NAS 1.26:196976 ..... p 636 N95-13636 * #
NAS 1.26:196977 ..... p 505 N95-13840 * #
NAS 1.26:196984 ..... p 537 N95-13638 * #
NAS 1.26:196985 ..... p 637 N95-13887 * #
NAS 1.26:196987 ..... p 505 N95-13886 * #
NAS 1.26:196988 ..... p 642 N95-14266 * #
NAS 1.26:196990 ..... p 532 N95-14265 * #
NAS 1.26:196992 ..... p 646 N95-15070 * #
NAS 1.26:196993 ..... p 479 N95-13664 * #
NAS 1.26:196996 ..... p 566 N95-14107 * #
NAS 1.26:196997 ..... p 612 N95-14272 * #
NAS 1.26:196998 ..... p 506 N95-14270 * #
NAS 1.26:197000 ..... p 457 N95-14105 * #
NAS 1.26:197001 ..... p 566 N95-14514 * #
NAS 1.26:197003 ..... p 429 N95-14106 * #
NAS 1.26:197011 ..... p 392 N95-13701 * #
NAS 1.26:197012 ..... p 481 N95-14269 * #
NAS 1.26:197013 ..... p 437 N95-14268 * #
NAS 1.26:197014 ..... p 479 N95-14104 * #
NAS 1.26:197016 ..... p 633 N95-15801 *
NAS 1.26:197017 ..... p 572 N95-14520 * #
NAS 1.26:197019 ..... p 537 N95-15751 * #
NAS 1.26:197021 ..... p 537 N95-15753 * #
NAS 1.26:197022 ..... p 618 N95-14798 * #
NAS 1.26:197023 ..... p 400 N95-14814 * #
NAS 1.26:197024 ..... p 400 N95-14613 * #
NAS 1.26:197025 ..... p 400 N95-14612 * #
NAS 1.26:197027 ..... p 572 N95-14615 * #
NAS 1.26:197028 ..... p 475 N95-14851 * #
NAS 1.26:197029 ..... p 409 N95-14794 * #
NAS 1.26:197031 ..... p 530 N95-14855 * #
NAS 1.26:197035 ..... p 502 N95-14797 * #
NAS 1.26:197036 ..... p 435 N95-14801 * #
NAS 1.26:197041 ..... p 537 N95-14796 * #
NAS 1.26:197044 ..... p 647 N95-14814 * #
NAS 1.26:197045 ..... p 435 N95-14865 * #
NAS 1.26:197047 ..... p 439 N95-14903 * #
NAS 1.26:197049 ..... p 411 N95-14799 * #
NAS 1.26:197050 ..... p 499 N95-14901 * #
NAS 1.26:197051 ..... p 552 N95-14864 * #
NAS 1.26:197053 ..... p 434 N95-14800 * #
NAS 1.26:197065 ..... p 502 N95-14904 * #
NAS 1.26:197066 ..... p 519 N95-14853 * #
NAS 1.26:197067 ..... p 475 N95-14868 * #
NAS 1.26:197069 ..... p 519 N95-14802 * #
NAS 1.26:197099 ..... p 613 N95-14806 * #
NAS 1.26:197100 ..... p 638 N95-14804 * #
NAS 1.26:197102 ..... p 400 N95-14803 * #
NAS 1.26:197104 ..... p 502 N95-14910 * #
NAS 1.26:197110 ..... p 409 N95-14909 * #
NAS 1.26:197111 ..... p 517 N95-15848 * #
NAS 1.26:197113 ..... p 525 N95-15847 * #
NAS 1.26:197119 ..... p 613 N95-14908 * #
NAS 1.26:197131 ..... p 531 N95-15586 * #
NAS 1.26:197135 ..... p 404 N95-15762 * #
NAS 1.26:197153 ..... p 428 N95-14521 * #
NAS 1.26:197180 ..... p 409 N95-15742 * #
NAS 1.26:197191 ..... p 408 N95-13703 * #
NAS 1.26:197197 ..... p 502 N95-14907 * #
NAS 1.26:197198 ..... p 563 N95-14854 * #
NAS 1.26:197202 ..... p 645 N95-14868 * #
NAS 1.26:197207 ..... p 535 N95-14906 * #
NAS 1.26:197215 ..... p 505 N95-15584 * #
NAS 1.26:197217 ..... p 626 N95-15752 * #
NAS 1.26:197218 ..... p 517 N95-15851 * #
NAS 1.26:197220 ..... p 503 N95-14923 * #
NAS 1.26:197221 ..... p 627 N95-15823 * #
NAS 1.26:197223 ..... p 497 N95-15785 * #
NAS 1.26:197224 ..... p 497 N95-15728 * #
NAS 1.26:197226 ..... p 531 N95-15684 * #
NAS 1.26:197229 ..... p 513 N95-14922 * #
NAS 1.26:197241 ..... p 514 N95-15913 * #
NAS 1.26:4617 ..... p 432 N95-14603 * #
NAS 1.26:4632 ..... p 601 N95-13660 * #
NAS 1.26:4634 ..... p 494 N95-15605 * #
NAS 1.55:10071 ..... p 554 N95-14013 * #
NAS 1.55:10143-VOL-1 ..... p 393 N95-14229 * #
NAS 1.55:10143-VOL-2 ..... p 395 N95-14239 * #
NAS 1.55:10143-VOL-3 ..... p 397 N95-14251 * #
NAS 1.55:10144 ..... p 639 N95-15827 * #
NAS 1.55:10148 ..... p 643 N95-14499 * #
NAS 1.55:3270 ..... p 602 N95-13896 * #
NAS 1.55:3272-VOL-1 ..... p 634 N95-14207 * #
NAS 1.55:3274-PT-1 ..... p 507 N95-14453 * #
NAS 1.55:3276 ..... p 482 N95-14522 * #
NAS 1.55:3277 ..... p 564 N95-14585 * #
NAS 1.55:3279 ..... p 401 N95-14878 * #
NAS 1.55:3280 ..... p 420 N95-14062 * #
NAS 1.55:3283 ..... p 526 N95-14274 * #
NAS 1.60:3467 ..... p 409 N95-14852 * #
NAS 1.60:3470 ..... p 600 N95-15606 * #
NAS 1.60:3472 ..... p 647 N95-15790 * #
NAS 1.60:3508 ..... p 513 N95-15055 * #
NAS 1.60:3512 ..... p 435 N95-14913 * #
NAS 1.61:1328-PT-1 ..... p 440 N95-15056 * #
NAS 1.61:1329 ..... p 442 N95-15512 * #
NAS 1.61:1330-PT-3 ..... p 440 N95-15057 * #
NAS 1.61:1349 ..... p 638 N95-14667 * #
NAS 1.61:1351 ..... p 436 N95-15763 * #
NAS 1.71:ARC-11925-1 ..... p 499 N95-14668 * #
NAS 1.71:LAR-14812-1 ..... p 450 N95-14140 * #
NAS 1.71:LAR-14860-1 ..... p 472 N95-14112 * #
NAS 1.71:LAR-14892-1 ..... p 433 N95-13836 * #
NAS 1.71:LAR-14899-1 ..... p 459 N95-14111 * #
NAS 1.71:LAR-14936-1 ..... p 450 N95-14113 * #
NAS 1.71:LAR-15041-1 ..... p 449 N95-13838 * #
NAS 1.71:LAR-15072-1 ..... p 501 N95-14186 * #
NAS 1.71:LAR-15083-1 ..... p 449 N95-14108 * #
NAS 1.71:LAR-15088-1 ..... p 460 N95-14139 * #
NAS 1.71:LAR-15104-1 ..... p 505 N95-13835 * #
NAS 1.71:LAR-15109-1 ..... p 449 N95-14109 * #
NAS 1.71:LAR-15129-1 ..... p 541 N95-14184 * #
NAS 1.71:LAR-15136-1 ..... p 506 N95-14138 * #
NAS 1.71:LAR-15138-1 ..... p 590 N95-14110 * #
NAS 1.71:LAR-15175-1 ..... p 450 N95-14185 * #
NAS 1.71:LAR-15246-1 ..... p 501 N95-14183 * #
NAS 1.71:LAR-15266-1-CU ..... p 496 N95-13837 * #
NAS 1.71:MFS-28714-1 ..... p 502 N95-14666 * #
NAS 1.71:MFS-28764-1 ..... p 590 N95-14137 * #

NAS-8819-FM-9614-856 ..... p 492 N95-14869 * #

NASA-CAS-LAR-14674-1 ..... p 503 N95-15601 *

NASA-CAS-LEW-15222-3 ..... p 625 N95-15602 *

NASA-CASE-ARC-11925-1 ..... p 499 N95-14668 * #
NASA-CASE-ARC-11953-1 ..... p 411 N95-14518 *
NASA-CASE-ARC-11960-2-NP .... p 452 N95-14602 *

NASA-CASE-GSC-13264-1 ..... p 499 N95-14515 *
NASA-CASE-GSC-13289-1 ..... p 478 N95-15681 *
NASA-CASE-GSC-13489-1 ..... p 583 N95-15598 *
NASA-CASE-GSC-13540-1 ..... p 502 N95-14517 *

NASA-CASE-LAR-14278-1 ..... p 473 N95-14294 *
NASA-CASE-LAR-14526-1 ..... p 455 N95-15599 *
NASA-CASE-LAR-14612-2 ..... p 496 N95-14414 *
NASA-CASE-LAR-14745-2-SB .... p 412 N95-14415 *
NASA-CASE-LAR-14790-1 ..... p 499 N95-14519 *
NASA-CASE-LAR-14812-1 ..... p 450 N95-14140 * #
NASA-CASE-LAR-14825-1 ..... p 452 N95-14416 *
NASA-CASE-LAR-14860-1 ..... p 472 N95-14112 * #
NASA-CASE-LAR-14892-1 ..... p 433 N95-13836 * #
NASA-CASE-LAR-14899-1 ..... p 459 N95-14111 * #
NASA-CASE-LAR-14936-1 ..... p 450 N95-14113 * #
NASA-CASE-LAR-15041-1 ..... p 449 N95-13838 * #
NASA-CASE-LAR-15072-1 ..... p 501 N95-14186 * #
NASA-CASE-LAR-15083-1 ..... p 449 N95-14108 * #
NASA-CASE-LAR-15088-1 ..... p 460 N95-14139 * #
NASA-CASE-LAR-15104-1 ..... p 505 N95-13835 * #
NASA-CASE-LAR-15109-1 ..... p 449 N95-14109 * #
NASA-CASE-LAR-15129-1 ..... p 541 N95-14184 * #
NASA-CASE-LAR-15136-1 ..... p 506 N95-14138 * #
NASA-CASE-LAR-15138-1 ..... p 590 N95-14110 * #
NASA-CASE-LAR-15175-1 ..... p 450 N95-14185 * #
NASA-CASE-LAR-15246-1 ..... p 501 N95-14183 * #
NASA-CASE-LAR-15266-1-CU .... p 496 N95-13837 * #

NASA-CASE-LEW-14906-2-SB .... p 504 N95-15914 *

NASA-CASE-LEW-15360-1 ..... p 441 N95-15303 *
NASA-CASE-LEW-15407-1 ..... p 478 N95-15669 *
NASA-CASE-LEW-15470-1 ..... p 497 N95-15915 *
NASA-CASE-LEW-15753-1 ..... p 475 N95-14516 *

NASA-CASE-MFS-28491-1 ..... p 500 N95-13819 *
NASA-CASE-MFS-28508-1 ..... p 393 N95-14182 *
NASA-CASE-MFS-28701-1 ..... p 503 N95-15305 *
NASA-CASE-MFS-28714-1 ..... p 502 N95-14666 * #
NASA-CASE-MFS-28764-1 ..... p 590 N95-14137 * #
NASA-CASE-MFS-28828-1 ..... p 503 N95-15670 *
NASA-CASE-MFS-29837-1 ..... p 500 N95-13654 *

NASA-CASE-MSC-22008-1 ..... p 496 N95-14180 *
NASA-CASE-MSC-22277-1 ..... p 503 N95-15306 *

NASA-CASE-NPO-18146-2-CU .... p 613 N95-14413 *
NASA-CASE-NPO-18357-1-CU .... p 612 N95-14181 *
NASA-CASE-NPO-18596-1-CU .... p 498 N95-13629 *
NASA-CASE-NPO-18625-2-CU .... p 614 N95-15603 *
NASA-CASE-NPO-18662-1-CU .... p 602 N95-13823 *
NASA-CASE-NPO-18694-1-CU .... p 472 N95-13824 *
NASA-CASE-NPO-18970-1-CU .... p 460 N95-13628 *

NASA-CP-10071 ..... p 554 N95-14013 * #
NASA-CP-10143-VOL-1 ..... p 393 N95-14229 * #
NASA-CP-10143-VOL-2 ..... p 395 N95-14239 * #
NASA-CP-10143-VOL-3 ..... p 397 N95-14251 * #
NASA-CP-10144 ..... p 639 N95-15827 * #
NASA-CP-10148 ..... p 643 N95-14499 * #
NASA-CP-3270 ..... p 602 N95-13896 * #
NASA-CP-3272-VOL-1 ..... p 634 N95-14207 * #
NASA-CP-3274-PT-1 ..... p 507 N95-14453 * #
NASA-CP-3276 ..... p 482 N95-14522 * #
NASA-CP-3277 ..... p 564 N95-14585 * #
NASA-CP-3279 ..... p 401 N95-14878 * #
NASA-CP-3280 ..... p 420 N95-14062 * #
NASA-CP-3283 ..... p 526 N95-14274 * #

NASA-CR-188356 ..... p 492 N95-14869 * #
NASA-CR-188357 ..... p 443 N95-15715 * #
NASA-CR-189188 ..... p 431 N95-14669 * #
NASA-CR-189331 ..... p 615 N95-15849 * #
NASA-CR-189374 ..... p 517 N95-15916 * #
NASA-CR-189375 ..... p 619 N95-15758 * #
NASA-CR-189376 ..... p 515 N95-13704 * #
NASA-CR-189377 ..... p 567 N95-13651 * #
NASA-CR-189378 ..... p 567 N95-13633 * #
NASA-CR-189380 ..... p 567 N95-13632 * #
NASA-CR-192447 ..... p 419 N95-15552 * #
NASA-CR-193621 ..... p 526 N95-14267 * #
NASA-CR-194215 ..... p 644 N95-13717 * #
NASA-CR-194414 ..... p 514 N95-13639 * #
NASA-CR-194973 ..... p 633 N95-15585 * #
NASA-CR-194974 ..... p 568 N95-13889 * #
NASA-CR-194976 ..... p 580 N95-13727 * #
NASA-CR-194982-REV ..... p 448 N95-15918 * #
NASA-CR-194985 ..... p 516 N95-15727 * #
NASA-CR-194986 ..... p 418 N95-13890 * #
NASA-CR-194991 ..... p 495 N95-15917 * #
NASA-CR-195003 ..... p 492 N95-14912 * #
NASA-CR-195008 ..... p 493 N95-15604 * #
NASA-CR-195156 ..... p 457 N95-14902 * #
NASA-CR-195383 ..... p 507 N95-14417 * #
NASA-CR-195387 ..... p 481 N95-14295 * #
NASA-CR-195388 ..... p 431 N95-15058 * #
NASA-CR-195393 ..... p 634 N95-15743 * #
NASA-CR-195394 ..... p 591 N95-14610 * #
NASA-CR-195396 ..... p 601 N95-13666 * #
NASA-CR-195397 ..... p 430 N95-13697 * #
NASA-CR-195398 ..... p 404 N95-15852 * #
NASA-CR-195399 ..... p 436 N95-15911 * #
NASA-CR-195405 ..... p 405 N95-15912 * #
NASA-CR-195810 ..... p 568 N95-13699 * #
NASA-CR-195818 ..... p 636 N95-13634 * #
NASA-CR-196013 ..... p 637 N95-14100 * #
NASA-CR-196059 ..... p 515 N95-13885 * #
NASA-CR-196145 ..... p 637 N95-13637 * #
NASA-CR-196263 ..... p 637 N95-13723 * #
NASA-CR-196265 ..... p 637 N95-13722 * #
NASA-CR-196409 ..... p 462 N95-14620 * #
NASA-CR-196440 ..... p 525 N95-13627 * #
NASA-CR-196448 ..... p 567 N95-13635 * #
NASA-CR-196480 ..... p 645 N95-13724 * #
NASA-CR-196489 ..... p 638 N95-14101 * #
NASA-CR-196521 ..... p 532 N95-14271 * #
NASA-CR-196522 ..... p 602 N95-13841 * #
NASA-CR-196526 ..... p 573 N95-14905 * #
NASA-CR-196531 ..... p 429 N95-15824 * #
NASA-CR-196536 ..... p 439 N95-14867 * #
NASA-CR-196786 ..... p 532 N95-13725 * #
NASA-CR-196849 ..... p 537 N95-13702 * #
NASA-CR-196886 ..... p 579 N95-15442 *
NASA-CR-196935 ..... p 453 N95-14931 * #
NASA-CR-196936 ..... p 492 N95-14932 * #
NASA-CR-196951 ..... p 642 N95-15907 * #
NASA-CR-196959 ..... p 464 N95-14670 * #
NASA-CR-196963 ..... p 569 N95-14156 * #
NASA-CR-196974 ..... p 526 N95-13818 * #
NASA-CR-196975 ..... p 505 N95-13839 * #
NASA-CR-196976 ..... p 636 N95-13636 * #
NASA-CR-196977 ..... p 505 N95-13840 * #
NASA-CR-196984 ..... p 537 N95-13638 * #
NASA-CR-196985 ..... p 637 N95-13887 * #
NASA-CR-196987 ..... p 505 N95-13886 * #
NASA-CR-196988 ..... p 642 N95-14266 * #
NASA-CR-196990 ..... p 532 N95-14265 * #
NASA-CR-196992 ..... p 646 N95-15070 * #
NASA-CR-196993 ..... p 479 N95-13664 * #
NASA-CR-196996 ..... p 566 N95-14107 * #
NASA-CR-196997 ..... p 612 N95-14272 * #
NASA-CR-196998 ..... p 506 N95-14270 * #
NASA-CR-197000 ..... p 457 N95-14105 * #
NASA-CR-197001 ..... p 566 N95-14514 * #
NASA-CR-197003 ..... p 429 N95-14106 * #
NASA-CR-197011 ..... p 392 N95-13701 * #
NASA-CR-197012 ..... p 481 N95-14269 * #
NASA-CR-197013 ..... p 437 N95-14268 * #
NASA-CR-197014 ..... p 479 N95-14104 * #
NASA-CR-197016 ..... p 633 N95-15801 *
NASA-CR-197017 ..... p 572 N95-14520 * #
NASA-CR-197019 ..... p 537 N95-15751 * #
NASA-CR-197021 ..... p 537 N95-15753 * #
NASA-CR-197022 ..... p 618 N95-14798 * #
NASA-CR-197023 ..... p 400 N95-14614 * #
NASA-CR-197024 ..... p 400 N95-14613 * #
NASA-CR-197025 ..... p 400 N95-14612 * #
NASA-CR-197027 ..... p 572 N95-14615 * #
NASA-CR-197028 ..... p 475 N95-14851 * #
NASA-CR-197029 ..... p 409 N95-14794 * #
NASA-CR-197031 ..... p 530 N95-14855 * #
NASA-CR-197035 ..... p 502 N95-14797 * #
NASA-CR-197036 ..... p 435 N95-14801 * #
NASA-CR-197041 ..... p 537 N95-14796 * #
NASA-CR-197044 ..... p 647 N95-14814 * #
NASA-CR-197045 ..... p 435 N95-14865 * #
NASA-CR-197047 ..... p 439 N95-14903 * #
NASA-CR-197049 ..... p 411 N95-14799 * #
NASA-CR-197050 ..... p 499 N95-14901 * #
NASA-CR-197051 ..... p 552 N95-14864 * #
NASA-CR-197053 ..... p 434 N95-14800 * #
NASA-CR-197065 ..... p 502 N95-14904 * #
NASA-CR-197066 ..... p 519 N95-14853 * #
NASA-CR-197067 ..... p 475 N95-14866 * #
NASA-CR-197069 ..... p 519 N95-14802 * #
NASA-CR-197099 ..... p 613 N95-14806 * #
NASA-CR-197100 ..... p 638 N95-14804 * #
NASA-CR-197102 ..... p 400 N95-14803 * #
NASA-CR-197104 ..... p 502 N95-14910 * #
NASA-CR-197110 ..... p 409 N95-14909 * #
NASA-CR-197111 ..... p 517 N95-15848 * #
NASA-CR-197113 ..... p 525 N95-15847 * #
NASA-CR-197119 ..... p 613 N95-14908 * #
NASA-CR-197131 ..... p 531 N95-15586 * #
NASA-CR-197135 ..... p 404 N95-15762 * #
NASA-CR-197153 ..... p 428 N95-14521 * #
NASA-CR-197180 ..... p 409 N95-15742 * #
NASA-CR-197191 ..... p 408 N95-13703 * #
NASA-CR-197197 ..... p 502 N95-14907 * #
NASA-CR-197198 ..... p 563 N95-14854 * #
NASA-CR-197202 ..... p 645 N95-14868 * #
NASA-CR-197207 ..... p 535 N95-14906 * #
NASA-CR-197215 ..... p 505 N95-15584 * #
NASA-CR-197217 ..... p 626 N95-15752 * #
NASA-CR-197218 ..... p 517 N95-15851 * #
NASA-CR-197220 ..... p 503 N95-14923 * #
NASA-CR-197221 ..... p 627 N95-15823 * #
NASA-CR-197223 ..... p 497 N95-15785 * #
NASA-CR-197224 ..... p 497 N95-15728 * #
NASA-CR-197226 ..... p 531 N95-15684 * #
NASA-CR-197229 ..... p 513 N95-14922 * #
NASA-CR-197241 ..... p 514 N95-15913 * #
NASA-CR-4617 ..... p 432 N95-14603 * #
NASA-CR-4632 ..... p 601 N95-13660 * #
NASA-CR-4634 ..... p 494 N95-15605 * #

NASA-EG-101 ..... p 554 N95-13888 * #
NASA-EG-102 ..... p 638 N95-14511 * #

NASA-EP-292 ..... p 629 N95-13650 * #

NASA-RP-1328-PT-1 ..... p 440 N95-15056 * #
NASA-RP-1329 ..... p 442 N95-15512 * #
NASA-RP-1330-PT-3 ..... p 440 N95-15057 * #
NASA-RP-1349 ..... p 638 N95-14667 * #
NASA-RP-1351 ..... p 436 N95-15763 * #

NASA-SP-7011(395) ..... p 550 N95-15304 *
NASA-SP-7037(310) ..... p 392 N95-15550 *

NASA-TM-103855 ..... p 391 N95-14419 * #
NASA-TM-104606-VOL-3 ..... p 531 N95-15745 * #
NASA-TM-104797 ..... p 432 N95-13646 * #
NASA-TM-106313 ..... p 420 N95-13728 * #
NASA-TM-106385 ..... p 398 N95-14418 * #
NASA-TM-106593 ..... p 430 N95-14174 * #
NASA-TM-106608 ..... p 430 N95-14173 * #
NASA-TM-106649 ..... p 408 N95-14604 * #
NASA-TM-106665 ..... p 433 N95-14298 * #
NASA-TM-106682 ..... p 450 N95-14303 * #
NASA-TM-106688 ..... p 419 N95-13893 * #
NASA-TM-106734 ..... p 444 N95-13667 * #
NASA-TM-106738 ..... p 591 N95-14618 * #
NASA-TM-106739 ..... p 431 N95-15682 * #
NASA-TM-106740 ..... p 430 N95-14301 * #
NASA-TM-106742 ..... p 482 N95-14299 * #
NASA-TM-106743 ..... p 566 N95-13716 * #
NASA-TM-106748 ..... p 429 N95-13668 * #
NASA-TM-106752 ..... p 478 N95-13653 * #
NASA-TM-106753 ..... p 431 N95-13631 * #
NASA-TM-106754 ..... p 392 N95-13817 * #
NASA-TM-106757 ..... p 479 N95-13685 * #
NASA-TM-106760 ..... p 568 N95-13894 * #
NASA-TM-106761 ..... p 477 N95-15587 * #
NASA-TM-106762 ..... p 585 N95-14296 * #
NASA-TM-106770 ..... p 495 N95-15908 * #
NASA-TM-106772 ..... p 492 N95-14607 * #
NASA-TM-106774 ..... p 404 N95-15853 * #
NASA-TM-106775 ..... p 431 N95-15769 * #
NASA-TM-106777 ..... p 473 N95-14302 * #
NASA-TM-106780 ..... p 585 N95-14300 * #
NASA-TM-106782 ..... p 591 N95-15059 * #
NASA-TM-106786 ..... p 398 N95-14297 * #
NASA-TM-108468 ..... p 443 N95-15607 * #
NASA-TM-108469 ..... p 459 N95-14919 * #
NASA-TM-108472 ..... p 431 N95-15609 * #
NASA-TM-108833 ..... p 512 N95-14617 * #
NASA-TM-108840 ..... p 539 N95-13661 * #
NASA-TM-108842 ..... p 406 N95-14611 * #
NASA-TM-108850 ..... p 391 N95-13642 * #
NASA-TM-108853 ..... p 391 N95-13662 * #
NASA-TM-108854 ..... p 481 N95-14273 * #
NASA-TM-108855 ..... p 391 N95-13891 * #
NASA-TM-108856 ..... p 550 N95-15649 * #
NASA-TM-108857 ..... p 392 N95-14921 * #
NASA-TM-109142 ..... p 432 N95-14920 * #
NASA-TM-109150 ..... p 420 N95-13729 * #
NASA-TM-109152 ..... p 495 N95-15898 * #
NASA-TM-109153 ..... p 444 N95-13690 * #
NASA-TM-109163 ..... p 647 N95-13663 * #
NASA-TM-109208 ..... p 630 N95-14918 * #
NASA-TM-109957 ..... p 642 N95-13658 * #
NASA-TM-109965 ..... p 428 N95-14510 * #
NASA-TM-109968 ..... p 638 N95-14911 * #
NASA-TM-109980 ..... p 632 N95-14870 * #
NASA-TM-109981 ..... p 632 N95-14619 * #
NASA-TM-109984 ..... p 495 N95-15899 *
NASA-TM-110046 ..... p 419 N95-13700 *
NASA-TM-110077 ..... p 419 N95-15900
NASA-TM-4543 ..... p 572 N95-14206 * #
NASA-TM-4568 ..... p 432 N95-13641 * #
NASA-TM-4575 ..... p 647 N95-15065 * #
NASA-TM-4651 ..... p 479 N95-13892 * #

NASA-TP-3467 ..... p 409 N95-14852 * #
NASA-TP-3470 ..... p 600 N95-15606 * #
NASA-TP-3472 ..... p 647 N95-15790 * #
NASA-TP-3508 ..... p 513 N95-15055 * #
NASA-TP-3512 ..... p 435 N95-14913 * #

NAWC-WPNS-TP-8210 ..... p 448 N95-13686 #

NEAR-TR-472 ..... p 630 N95-14321 #

NIST/GCR-94/638 ..... p 441 N95-15353 #
NIST/GCR-94/645 ..... p 439 N95-14838 #
NIST/GCR-94/647 ..... p 443 N95-15610 #
NIST/GCR-94/648 ..... p 441 N95-15352 #

NIST/SP-400-94 ..... p 474 N95-14401 #

NISTIR-5380 ..... p 441 N95-15354 #
NISTIR-5425 ..... p 459 N95-15322 #
NISTIR-5434 ..... p 474 N95-14402 #
NISTIR-5441 ..... p 405 N95-14179 #
NISTIR-5454 ..... p 482 N95-14407 #
NISTIR-5463 ..... p 459 N95-14512 #

NOAA-NWS-TDL-CP-94-3 ..... p 533 N95-14410 #

NOAA-TM-ERL-AL-13 ..... p 526 N95-13974

NOAA-TM-ERL-AOML-80 ..... p 532 N95-14118 #

NOAA-TM-NWS-NSSFC-38 ..... p 532 N95-14117 #

NONP-NASA-SUPPL-DK-94-28027 p 412 N95-14815 #

NONP-NASA-SUPPL-VT-94-32020 p 495 N95-15899 *

NONP-NASA-VT-94-29668 p 419 N95-13700 *
NONP-NASA-VT-94-33203 p 419 N95-15900

NPS-EC-94-002 p 469 N95-15619
NPS-EC-94-007 p 470 N95-15804

NPS-MA-94-005 p 587 N95-15612
NPS-MA-94-006 p 514 N95-15805

NRAD-TD-2648 p 461 N95-14345 #
NRAD-TD-2658 p 468 N95-15321 #

NREL/CP-413-7033 p 519 N95-14430 #

NREL/TP-411-6855 p 520 N95-15406 #
NREL/TP-411-6856 p 520 N95-15355 #
NREL/TP-411-6864 p 518 N95-14194 #
NREL/TP-413-6633 p 521 N95-15863 #
NREL/TP-413-6853 p 520 N95-15405 #
NREL/TP-413-7050 p 624 N95-15426 #
NREL/TP-440-6628 p 519 N95-14433 #
NREL/TP-441-6626 p 519 N95-15290 #
NREL/TP-441-7044 p 518 N95-14191 #
NREL/TP-451-6862 p 521 N95-15407 #
NREL/TP-451-7045 p 622 N95-14431 #
NREL/TP-451-7047 p 519 N95-14432 #

NRL/MR/5530-94-7488 p 563 N95-15449
NRL/MR/5590-94-7494 p 579 N95-15450
NRL/MR/6120-94-7610 p 470 N95-15750 #

NSSDC/WDC-A-R/S-94-08-SUPPL-5 p 642 N95-13658 * #

NSWCDD/TR-93/339 p 411 N95-15392

NTIA-94-309 p 462 N95-14412 #

NTSB/AAR-94/06 p 407 N95-14916 #

NTSB/ARC-94/02 p 407 N95-15066 #

NUWC-NPT-TR-10675 p 591 N95-15320 #

ODURF-124453 p 506 N95-14270 * #
ODURF-144029 p 437 N95-14268 * #
ODURF-144029 p 481 N95-14269 * #

ORNL-6775-VOL-1 p 519 N95-14393 #

ORNL/TM-12646 p 456 N95-15634 #
ORNL/TM-12721 p 586 N95-15538 #
ORNL/TM-12764 p 574 N95-15536 #

PB94-170297 p 523 N95-15382 #
PB94-170362 p 633 N95-15781 #
PB94-176120 p 616 N95-13973 #
PB94-176658 p 534 N95-15383 #
PB94-176823 p 522 N95-14124 #
PB94-177797 p 541 N95-14394 #
PB94-186889 p 515 N95-14793
PB94-187457 p 526 N95-13974
PB94-187630 p 459 N95-15322 #
PB94-188810 p 474 N95-14401 #
PB94-189065 p 589 N95-13987 #
PB94-189073 p 590 N95-13988 #
PB94-189081 p 566 N95-13989 #
PB94-189099 p 461 N95-14147 #
PB94-189131 p 433 N95-14148 #
PB94-190170 p 460 N95-14119
PB94-190665 p 523 N95-14403 #
PB94-191210 p 472 N95-14149 #
PB94-191228 p 624 N95-15378 #
PB94-191244 p 501 N95-14150
PB94 191251 p 450 N95-14151 #
PB94-191269 p 568 N95-14152 #
PB94-191277 p 569 N95-14153 #
PB94-191293 p 585 N95-14154
PB94-191384 p 499 N95-15388 #
PB94-192267 p 596 N95-15379
PB94-192283 p 596 N95-15380
PB94-192325 p 589 N95-13979 #
PB94-192739 p 529 N95-14404
PB94-192879 p 523 N95-15389 #
PB94-193810 p 474 N95-14402 #
PB94-194065 p 405 N95-14179 #
PB94-194073 p 482 N95-14407 #
PB94-194289 p 532 N95-14118 #
PB94-194479 p 521 N95-14121 #
PB94-195369 p 407 N95-15439
PB94-195500 p 445 N95-14845 #
PB94-195518 p 525 N95-15870 #
PB94-195526 p 471 N95-15871 #
PB94-195534 p 492 N95-15315 #

PB94-195542 p 632 N95-14837 #
PB94-195617 p 586 N95-15412 #
PB94-195633 p 584 N95-13960
PB94-195856 p 443 N95-15610 #
PB94-195898 p 532 N95-14117 #
PB94-196045 p 439 N95-14838 #
PB94-196813 p 408 N95-13981
PB94-197449 p 521 N95-14122 #
PB94-197456 p 521 N95-14123 #
PB94-197639 p 496 N95-14839
PB94-197647 p 497 N95-15413 #
PB94-197662 p 478 N95-15611 #
PB94-197712 p 637 N95-13982
PB94-197936 p 472 N95-13983
PB94-197969 p 410 N95-13984
PB94-197977 p 537 N95-13990
PB94-198009 p 585 N95-13991
PB94-198017 p 532 N95-14120 #
PB94-201282 p 612 N95-13992
PB94-201290 p 590 N95-13985
PB94-201399 p 622 N95-14795
PB94-201472 p 513 N95-15429
PB94-203056 p 515 N95-14125 #
PB94-203247 p 533 N95-14410 #
PB94-204625 p 413 N95-14513 #
PB94-204906 p 462 N95-14412 #
PB94-205093 p 574 N95-15396
PB94-206299 p 441 N95-15352 #
PB94-206307 p 459 N95-14512 #
PB94-207115 p 589 N95-13630
PB94-207388 p 441 N95-15353 #
PB94-207404 p 441 N95-15354 #
PB94-207990 p 513 N95-15348
PB94-208238 p 446 N95-15349
PB94-208246 p 595 N95-15350
PB94-208824 p 646 N95-15784
PB94-208832 p 646 N95-15773 #
PB94-910408 p 407 N95-14916 #
PB95-100319 p 407 N95-15066 #

PL-TR-93-1028 p 638 N95-14597 #
PL-TR-93-2170 p 595 N95-14950
PL-TR-93-2211 p 530 N95-14598 #
PL-TR-93-2266 p 440 N95-14958 #
PL-TR-94-2013 p 534 N95-15402
PL-TR-94-2056 p 428 N95-14599 #
PL-TR-94-2067 p 428 N95-14951
PL-TR-94-2114 p 534 N95-15614 #
PL-TR-94-2136 p 530 N95-15401 #
PL-TR-94-2164 p 524 N95-15623

PNL-SA-23027 p 445 N95-15293 #
PNL-SA-23097 p 595 N95-15310 #
PNL-SA-23184 p 613 N95-15312 #
PNL-SA-23185 p 454 N95-15313 #
PNL-SA-23559 p 529 N95-14428 #
PNL-SA-23656 p 612 N95-13986 #
PNL-SA-23936 p 517 N95-14002 #
PNL-SA-24162 p 573 N95-15311 #
PNL-SA-24175 p 522 N95-14195 #
PNL-SA-24206 p 446 N95-15433 #
PNL-SA-24224 p 446 N95-15431 #
PNL-SA-24259 p 613 N95-15314 #
PNL-SA-24365 p 439 N95-14663 #
PNL-SA-24432 p 524 N95-15432 #
PNL-SA-24486 p 566 N95-14662 #

PNL-9809 p 523 N95-15363 #
PNL-9872 p 633 N95-15528 #

PSI-1059/TR-1277 p 440 N95-14958 #

R/D-6307-PM-01 p 626 N95-15748 #
R/D-6720-EN-01 p 553 N95-15816
R/D-7213-AN-01 p 410 N95-15821

RAL-94-033 p 596 N95-15379
RAL-94-036 p 596 N95-15380

RAND/MR-432-AF p 461 N95-14334 #

RAND/N-3589-AF/A/OSD p 515 N95-15546
RAND/N-3619-AF p 409 N95-15451

RAY/RD/S-5005 p 478 N95-15613

REPT-10428A p 515 N95-13885 * #
REPT-1 p 506 N95-14356 #
REPT-31-12089 p 634 N95-15743 * #
REPT-5-54718-1 p 444 N95-14202 #
REPT-8025-3C-PT-3 p 551 N95-13715 #
REPT-91RR-44-PT-2 p 410 N95-14175 #
REPT-93-549/2 p 571 N95-14178 #
REPT-94B00074 p 602 N95-13896 * #
REPT-94B00116 p 564 N95-14585 * #
REPT-94B00132 p 420 N95-14062 * #

REPT-94B00141 p 638 N95-14667 * #
REPT-95B00003 p 526 N95-14274 * #
REPT-95B00011-VOL-3 p 531 N95-15745 * #

RIVM-223107002 p 523 N95-15389 #

RL-NP-93-2 p 468 N95-15333 #

RL-TR-88-316 p 470 N95-15756 #
RL-TR-94-37-PT-2 p 583 N95-15548
RL-TR-94-68 p 477 N95-15460
RL-TR-94-69 p 477 N95-15459
RL-TR-94-70 p 469 N95-15462
RL-TR-94-71 p 583 N95-15461

S-771 p 432 N95-13646 * #

SAND-89-0217 p 632 N95-15366 #
SAND-92-2244 p 524 N95-15575 #
SAND-93-1641 p 404 N95-15570 #
SAND-93-2018C p 476 N95-15356 #
SAND-93-2243C p 477 N95-15544 #
SAND-93-2525C p 493 N95-15351 #
SAND-93-2563 p 446 N95-15368 #
SAND-93-2758C p 621 N95-14322 #
SAND-94-0007 p 521 N95-15420 #
SAND-94-0058C p 642 N95-14311 #
SAND-94-0140C p 472 N95-13975 #
SAND-94-0179C p 460 N95-15409 #
SAND-94-0192C p 457 N95-14004 #
SAND-94-0391 p 596 N95-15437 #
SAND-94-0506C p 621 N95-14323 #
SAND-94-0512C p 568 N95-13976 #
SAND-94-0514 p 583 N95-15369 #
SAND-94-0624C p 515 N95-14313 #
SAND-94-0721C p 496 N95-14146 #
SAND-94-0753 p 618 N95-14443 #
SAND-94-1002C p 621 N95-14390 #
SAND-94-1244C p 473 N95-14310 #
SAND-94-1279 p 625 N95-15438 #
SAND-94-1308C p 473 N95-14308 #
SAND-94-1309C p 437 N95-14307 #
SAND-94-1316C p 473 N95-14314 #
SAND-94-1333C p 418 N95-15357 #
SAND-94-1381C p 476 N95-15410 #
SAND-94-1388 p 574 N95-15384 #
SAND-94-1501C p 469 N95-15583 #
SAND-94-1503C p 474 N95-14315 #
SAND-94-1583C p 574 N95-15543 #
SAND-94-1619C p 437 N95-14312 #
SAND-94-1644C p 428 N95-14664 #
SAND-94-1782C p 474 N95-14319 #
SAND-94-1874C p 617 N95-14262 #
SAND-94-1888C p 621 N95-14342 #
SAND-94-8649 p 442 N95-15375 #
SAND-94-8701C p 438 N95-14391 #
SAND-94-8716C p 531 N95-15411 #

SAO-AXAF-DR-93-058 p 637 N95-13887 * #
SAO-AXAF-DR-94-067-REV p 567 N95-13635 * #
SAO-AXAF-DR-94-081-REV p 636 N95-13636 * #
SAO-AXAF-DR-94-082-REV p 637 N95-14100 * #
SAO-AXAF-DR-94-083-REV p 637 N95-13637 * #
SAO-AXAF-DR-94-088-REV p 636 N95-13634 * #
SAO-AXAF-DR-94-090-REV p 638 N95-14101 * #

SCT-92-RR-9 p 413 N95-15328 #

SC71046.FR p 626 N95-15808

SD94D0329 p 435 N95-14801 * #

SGD-598-PT-1 p 646 N95-15784
SGD-598-PT-2 p 646 N95-15773 #

SHRP-H-385 p 407 N95-15439

SHRP-P-397 p 460 N95-14119

SR-1 p 595 N95-14950
SR-1 p 428 N95-14951
SR-2 p 534 N95-15402
SR-2 p 534 N95-15614 #

SRS-586 p 514 N95-15802

SSD94D0217B p 409 N95-14794 * #
SSD94D0298 p 514 N95-15913 * #
SSD94D0328 p 434 N95-14800 * #
SSD94D0343 p 411 N95-14799 * #

STARS-VC-B014/001/00 p 575 N95-15783

STF10-A94002 p 595 N95-15350
STF19-A93015 p 513 N95-15348
STF31-A93046-PT-2 p 589 N95-13630

STF34-A93248 ..... p 446 N95-15349

SU-SLAC-PUB-6496 ..... p 597 N95-15545 #

SU-SLAC-441 ..... p 622 N95-15308 #

TABES PAPER 94-204 ..... p 415 N95-14634 * #
TABES PAPER 94-407 ..... p 415 N95-14635 #
TABES PAPER 94-502 ..... p 415 N95-14636 * #
TABES PAPER 94-503 ..... p 415 N95-14637 #
TABES PAPER 94-604 ..... p 415 N95-14638 #
TABES PAPER 94-605 ..... p 415 N95-14639 * #
TABES PAPER 94-607 ..... p 415 N95-14640 #
TABES PAPER 94-609 ..... p 415 N95-14641 #
TABES PAPER 94-610 ..... p 416 N95-14642 #
TABES PAPER 94-613 ..... p 416 N95-14643 * #
TABES PAPER 94-615 ..... p 416 N95-14644 #
TABES PAPER 94-616 ..... p 411 N95-14645 #
TABES PAPER 94-619 ..... p 405 N95-14646 #
TABES PAPER 94-620 ..... p 416 N95-14647 #
TABES PAPER 94-621 ..... p 417 N95-14648 * #
TABES PAPER 94-622 ..... p 417 N95-14649 * #
TABES PAPER 94-626 ..... p 417 N95-14650 #
TABES PAPER 94-627 ..... p 417 N95-14651 * #
TABES PAPER 94-631 ..... p 417 N95-14652 #
TABES PAPER 94-632 ..... p 417 N95-14653 * #

TASC-STR-6005-2 ..... p 468 N95-15333 #

TEC-R-235 ..... p 586 N95-15424 #

TEC-0047 ..... p 583 N95-15398

TKK-F-C162 ..... p 496 N95-14839

TKO-C66 ..... p 568 N95-13989 #

TOP-7-3-531 ..... p 410 N95-15815 #

TP-71 ..... p 532 N95-14120 #

TR-10 ..... p 451 N95-14305 #
TR-10 ..... p 474 N95-14425 #
TR-12 ..... p 452 N95-14398 #
TR-13 ..... p 452 N95-14399 #
TR-15 ..... p 452 N95-14400 #
TR-21 ..... p 451 N95-14316 #
TR-22 ..... p 451 N95-14324 #
TR-29 ..... p 619 N95-13691
TR-30-ONR ..... p 449 N95-13692 #
TR-453 ..... p 577 N95-15860 #
TR-468 ..... p 573 N95-15151 #
TR-476 ..... p 575 N95-15645 #
TR-480 ..... p 589 N95-15859 #
TR-481 ..... p 576 N95-15789 #
TR-482 ..... p 577 N95-15858 #
TR-483 ..... p 575 N95-15597 #
TR-484 ..... p 576 N95-15788 #
TR-487 ..... p 576 N95-15857 #
TR-488 ..... p 575 N95-15721 #
TR-489 ..... p 576 N95-15856 #
TR-490 ..... p 579 N95-15590 #
TR-492-REV ..... p 553 N95-15787 #
TR-493 ..... p 575 N95-15644 #
TR-494-REV ..... p 584 N95-15786 #
TR-496 ..... p 576 N95-15825 #
TR-497 ..... p 587 N95-15643 #
TR-498 ..... p 588 N95-15855 #
TR-4 ..... p 627 N95-15818
TR-500 ..... p 588 N95-15854 #
TR-502 ..... p 553 N95-15642 #
TR-504 ..... p 586 N95-15589 #
TR-509 ..... p 575 N95-15640 #
TR-510-REV ..... p 552 N95-15588 #
TR-511 ..... p 587 N95-15733 #
TR-512 ..... p 587 N95-15775 #
TR-516 ..... p 587 N95-15596 #
TR-518 ..... p 586 N95-15595 #
TR-520 ..... p 587 N95-15732 #
TR-521 ..... p 534 N95-15666 #
TR-58 ..... p 477 N95-15456
TR-6 ..... p 452 N95-14395 #
TR-8-ONR ..... p 437 N95-14141 #
TR-94-1436 ..... p 568 N95-13699 * #
TR-94/ONR-EPIC-2 ..... p 540 N95-14142 #
TR-9 ..... p 450 N95-14304 #

TRS-462 ..... p 584 N95-13980
TRS-481 ..... p 574 N95-15396

UAH-5-33359/60 ..... p 602 N95-13841 * #
UAH-5-33407 ..... p 532 N95-14271 * #

UC-404 ..... p 623 N95-15339

UCRL-ID-116677 ..... p 524 N95-15779 #

UCRL-ID-117420 ..... p 523 N95-15364 #
UCRL-ID-117796 ..... p 594 N95-14385 #
UCRL-ID-118202 ..... p 488 N95-15365 #

UCRL-JC-114326-REV-1 ..... p 621 N95-14325 #
UCRL-JC-114969-REV-1 ..... p 600 N95-15780 #
UCRL-JC-115106 ..... p 601 N95-13672 #
UCRL-JC-115161 ..... p 451 N95-14389
UCRL-JC-116074 ..... p 554 N95-13671 #
UCRL-JC-116238 ..... p 522 N95-14317 #
UCRL-JC-116309 ..... p 473 N95-14261 #
UCRL-JC-116437 ..... p 529 N95-14436 #
UCRL-JC-116526-REV-1 ..... p 523 N95-15361 #
UCRL-JC-116641 ..... p 571 N95-14190 #
UCRL-JC-116823 ..... p 499 N95-14427 #
UCRL-JC-117191 ..... p 468 N95-15300 #
UCRL-JC-117400 ..... p 601 N95-13670 #
UCRL-JC-117404 ..... p 493 N95-15530 #
UCRL-JC-117434 ..... p 614 N95-15529 #
UCRL-JC-117504 ..... p 442 N95-15408
UCRL-JC-117523 ..... p 498 N95-14318 #

UCRL-MA-115604 ..... p 566 N95-14338 #

UCRL-52000-94-4 ..... p 496 N95-13669 #

UILU-ENG-94-2002 ..... p 514 N95-15802
UILU-ENG-94-2228 ..... p 474 N95-14355 #

UMR-FDB-40 ..... p 433 N95-13655 #

UMR-FDR-41 ..... p 455 N95-15458

UR-DCS-TR-94-507 ..... p 586 N95-15594 #

US-PATENT-APPL-SN-006413 ..... p 478 N95-15669 *
US-PATENT-APPL-SN-008424 ..... p 502 N95-14517 *
US-PATENT-APPL-SN-010030 ..... p 500 N95-13819 *
US-PATENT-APPL-SN-020813 ..... p 602 N95-13823 *
US-PATENT-APPL-SN-023252 ..... p 498 N95-13629 *
US-PATENT-APPL-SN-031251 ..... p 614 N95-15707
US-PATENT-APPL-SN-032067 ..... p 411 N95-14518 *
US-PATENT-APPL-SN-033512 ..... p 612 N95-14181 *
US-PATENT-APPL-SN-037877 ..... p 393 N95-14182 *
US-PATENT-APPL-SN-039783 ..... p 460 N95-13628 *
US-PATENT-APPL-SN-041373 ..... p 478 N95-15681 *
US-PATENT-APPL-SN-045337 ..... p 412 N95-14415 *
US-PATENT-APPL-SN-045345 ..... p 452 N95-14416 *
US-PATENT-APPL-SN-060940 ..... p 473 N95-14294 *
US-PATENT-APPL-SN-076135 ..... p 497 N95-15799
US-PATENT-APPL-SN-081893 ..... p 475 N95-14516 *
US-PATENT-APPL-SN-082766 ..... p 412 N95-14415 *
US-PATENT-APPL-SN-088963 ..... p 503 N95-15601 *
US-PATENT-APPL-SN-089460 ..... p 613 N95-14413 *
US-PATENT-APPL-SN-104951 ..... p 504 N95-15914 *
US-PATENT-APPL-SN-106183 ..... p 452 N95-14602 *
US-PATENT-APPL-SN-112483 ..... p 472 N95-13824 *
US-PATENT-APPL-SN-114043 ..... p 500 N95-13654 *
US-PATENT-APPL-SN-115962 ..... p 614 N95-15603 *
US-PATENT-APPL-SN-158327 ..... p 503 N95-15670 *
US-PATENT-APPL-SN-159606 ..... p 503 N95-15306 *
US-PATENT-APPL-SN-181938 ..... p 496 N95-14414 *
US-PATENT-APPL-SN-192562 ..... p 412 N95-14415 *
US-PATENT-APPL-SN-209504 ..... p 449 N95-13838 * #
US-PATENT-APPL-SN-209512 ..... p 450 N95-14185 * #
US-PATENT-APPL-SN-238040 ..... p 496 N95-13837 * #
US-PATENT-APPL-SN-238102 ..... p 450 N95-14140 * #
US-PATENT-APPL-SN-251434 ..... p 505 N95-13835 * #
US-PATENT-APPL-SN-260162 ..... p 501 N95-14186 * #
US-PATENT-APPL-SN-265361 ..... p 433 N95-13836 * #
US-PATENT-APPL-SN-269268 ..... p 460 N95-14139 * #
US-PATENT-APPL-SN-282849 ..... p 450 N95-14113 * #
US-PATENT-APPL-SN-286031 ..... p 472 N95-14112 * #
US-PATENT-APPL-SN-296551 ..... p 502 N95-14666 * #
US-PATENT-APPL-SN-297343 ..... p 459 N95-14111 * #
US-PATENT-APPL-SN-299172 ..... p 449 N95-14109 * #
US-PATENT-APPL-SN-299384 ..... p 449 N95-14108 * #
US-PATENT-APPL-SN-317071 ..... p 590 N95-14137 * #
US-PATENT-APPL-SN-323943 ..... p 541 N95-14184 * #
US-PATENT-APPL-SN-325723 ..... p 506 N95-14138 * #
US-PATENT-APPL-SN-326804 ..... p 590 N95-14110 * #
US-PATENT-APPL-SN-327061 ..... p 501 N95-14183 * #
US-PATENT-APPL-SN-43641 ..... p 496 N95-14841 #
US-PATENT-APPL-SN-718315 ..... p 625 N95-15602 *
US-PATENT-APPL-SN-727263 ..... p 499 N95-14668 * #
US-PATENT-APPL-SN-755248 ..... p 412 N95-14415 *
US-PATENT-APPL-SN-786618 ..... p 613 N95-14413 *
US-PATENT-APPL-SN-820431 ..... p 496 N95-14414 *
US-PATENT-APPL-SN-851380 ..... p 452 N95-14602 *
US-PATENT-APPL-SN-870003 ..... p 455 N95-15599 *
US-PATENT-APPL-SN-884097 ..... p 441 N95-15303 *
US-PATENT-APPL-SN-889572 ..... p 504 N95-15914 *
US-PATENT-APPL-SN-902749 ..... p 456 N95-15800
US-PATENT-APPL-SN-912961 ..... p 614 N95-15603 *
US-PATENT-APPL-SN-923450 ..... p 615 N95-15766
US-PATENT-APPL-SN-937624 ..... p 574 N95-15336

US-PATENT-APPL-SN-940420 ..... p 496 N95-14180 *
US-PATENT-APPL-SN-949199 ..... p 499 N95-14515 *
US-PATENT-APPL-SN-953697 ..... p 614 N95-15764
US-PATENT-APPL-SN-968087 ..... p 497 N95-15915 *
US-PATENT-APPL-SN-970886 ..... p 615 N95-15765
US-PATENT-APPL-SN-973505 ..... p 625 N95-15602 *
US-PATENT-APPL-SN-977466 ..... p 503 N95-15305 *
US-PATENT-APPL-SN-979987 ..... p 583 N95-15598 *
US-PATENT-APPL-SN-988082 ..... p 499 N95-14519 *

US-PATENT-CLASS-117-101 ..... p 625 N95-15602 *
US-PATENT-CLASS-117-106 ..... p 625 N95-15602 *
US-PATENT-CLASS-117-913 ..... p 625 N95-15602 *
US-PATENT-CLASS-117-923 ..... p 625 N95-15602 *
US-PATENT-CLASS-117-95 ..... p 625 N95-15602 *
US-PATENT-CLASS-117-97 ..... p 625 N95-15602 *
US-PATENT-CLASS-128-665 ..... p 615 N95-15765
US-PATENT-CLASS-156-380.2 .... p 473 N95-14294 *
US-PATENT-CLASS-188-381 ..... p 503 N95-15306 *
US-PATENT-CLASS-219-121.45 .. p 503 N95-15670 *
US-PATENT-CLASS-219-121.48 .. p 503 N95-15670 *
US-PATENT-CLASS-219-121.49 .. p 503 N95-15670 *
US-PATENT-CLASS-219-121.51 .. p 503 N95-15670 *
US-PATENT-CLASS-219-633 ..... p 473 N95-14294 *
US-PATENT-CLASS-219-635 ..... p 473 N95-14294 *
US-PATENT-CLASS-219-659 ..... p 473 N95-14294 *
US-PATENT-CLASS-219-670 ..... p 473 N95-14294 *
US-PATENT-CLASS-228-02 ..... p 500 N95-13654 *
US-PATENT-CLASS-228-45 ..... p 500 N95-13654 *
US-PATENT-CLASS-244-100R .... p 503 N95-15306 *
US-PATENT-CLASS-244-104R .... p 503 N95-15306 *
US-PATENT-CLASS-244-142 ..... p 393 N95-14182 *
US-PATENT-CLASS-244-145 ..... p 393 N95-14182 *
US-PATENT-CLASS-248-74.4 ..... p 503 N95-15305 *
US-PATENT-CLASS-250-214.1 .... p 614 N95-15603 *
US-PATENT-CLASS-250-227.2 .... p 613 N95-14413 *
US-PATENT-CLASS-250-251 ..... p 503 N95-15601 *
US-PATENT-CLASS-257-456 ..... p 614 N95-15603 *
US-PATENT-CLASS-264-178F .... p 455 N95-15599 *
US-PATENT-CLASS-264-183 ..... p 455 N95-15599 *
US-PATENT-CLASS-310-333 ..... p 496 N95-14841 #
US-PATENT-CLASS-310-358 ..... p 497 N95-15799
US-PATENT-CLASS-313-231.51 .. p 503 N95-15670 *
US-PATENT-CLASS-313-341 ..... p 475 N95-14516 *
US-PATENT-CLASS-313-346DC .. p 475 N95-14516 *
US-PATENT-CLASS-313-346R .... p 475 N95-14516 *
US-PATENT-CLASS-315-111.81 .. p 475 N95-14516 *
US-PATENT-CLASS-324-501 ..... p 478 N95-15669 *
US-PATENT-CLASS-324-509 ..... p 478 N95-15669 *
US-PATENT-CLASS-324-512 ..... p 478 N95-15669 *
US-PATENT-CLASS-324-539 ..... p 478 N95-15669 *
US-PATENT-CLASS-324-661 ..... p 583 N95-15598 *
US-PATENT-CLASS-324-688 ..... p 583 N95-15598 *
US-PATENT-CLASS-324-76.48 .... p 496 N95-13629 *
US-PATENT-CLASS-324-76.62 .... p 496 N95-13629 *
US-PATENT-CLASS-324-96 ..... p 478 N95-15669 *
US-PATENT-CLASS-340-870.37 .. p 583 N95-15598 *
US-PATENT-CLASS-340-945 ..... p 411 N95-14518 *
US-PATENT-CLASS-340-959 ..... p 412 N95-14415 *
US-PATENT-CLASS-340-971 ..... p 411 N95-14518 *
US-PATENT-CLASS-340-978 ..... p 411 N95-14518 *
US-PATENT-CLASS-359-128 ..... p 612 N95-14181 *
US-PATENT-CLASS-359-130 ..... p 612 N95-14181 *
US-PATENT-CLASS-359-163 ..... p 612 N95-14181 *
US-PATENT-CLASS-359-534 ..... p 499 N95-14515 *
US-PATENT-CLASS-359-546 ..... p 499 N95-14515 *
US-PATENT-CLASS-359-731 ..... p 499 N95-14515 *
US-PATENT-CLASS-359-896 ..... p 613 N95-14413 *
US-PATENT-CLASS-361-181 ..... p 583 N95-15598 *
US-PATENT-CLASS-363-21 ..... p 478 N95-15681 *
US-PATENT-CLASS-364-427 ..... p 412 N95-14415 *
US-PATENT-CLASS-372-12 ..... p 499 N95-14519 *
US-PATENT-CLASS-372-38 ..... p 499 N95-14519 *
US-PATENT-CLASS-372-95 ..... p 602 N95-13823 *
US-PATENT-CLASS-372-99 ..... p 602 N95-13823 *
US-PATENT-CLASS-375-10 ..... p 460 N95-13628 *
US-PATENT-CLASS-375-1 ..... p 460 N95-13628 *
US-PATENT-CLASS-375-34 ..... p 460 N95-13628 *
US-PATENT-CLASS-375-58 ..... p 460 N95-13628 *
US-PATENT-CLASS-375-99 ..... p 460 N95-13628 *
US-PATENT-CLASS-377-42 ..... p 498 N95-13629 *
US-PATENT-CLASS-378-84 ..... p 614 N95-15764
US-PATENT-CLASS-380-2 ..... p 460 N95-13628 *
US-PATENT-CLASS-380-34 ..... p 460 N95-13628 *
US-PATENT-CLASS-384-101 ..... p 500 N95-13819 *
US-PATENT-CLASS-385-11 ..... p 614 N95-15707
US-PATENT-CLASS-385-142 ..... p 615 N95-15766
US-PATENT-CLASS-385-14 ..... p 612 N95-14181 *
US-PATENT-CLASS-385-37 ..... p 612 N95-14181 *
US-PATENT-CLASS-395-425 ..... p 574 N95-15336
US-PATENT-CLASS-403-12 ..... p 503 N95-15305 *
US-PATENT-CLASS-403-21 ..... p 503 N95-15305 *
US-PATENT-CLASS-403-234 ..... p 503 N95-15305 *
US-PATENT-CLASS-423-448 ..... p 441 N95-15303 *
US-PATENT-CLASS-423-460 ..... p 441 N95-15303 *
US-PATENT-CLASS-428-364 ..... p 455 N95-15599 *

US-PATENT-CLASS-428-364 ..... p 455 N95-15599 *
US-PATENT-CLASS-428-394 ..... p 455 N95-15599 *
US-PATENT-CLASS-428-395 ..... p 455 N95-15599 *
US-PATENT-CLASS-429-191 ..... p 472 N95-13824 *
US-PATENT-CLASS-429-192 ..... p 472 N95-13824 *
US-PATENT-CLASS-437-5 ..... p 614 N95-15603 *
US-PATENT-CLASS-439-196 ..... p 504 N95-15914 *
US-PATENT-CLASS-439-372 ..... p 504 N95-15914 *
US-PATENT-CLASS-439-374 ..... p 504 N95-15914 *
US-PATENT-CLASS-475-149 ..... p 502 N95-14517 *
US-PATENT-CLASS-475-344 ..... p 502 N95-14517 *
US-PATENT-CLASS-475-345 ..... p 502 N95-14517 *
US-PATENT-CLASS-522-99 ..... p 452 N95-14602 *
US-PATENT-CLASS-525-385 ..... p 456 N95-15800
US-PATENT-CLASS-525-477 ..... p 452 N95-14602 *
US-PATENT-CLASS-528-10 ..... p 452 N95-14602 *
US-PATENT-CLASS-528-14 ..... p 452 N95-14602 *
US-PATENT-CLASS-528-24 ..... p 452 N95-14602 *
US-PATENT-CLASS-528-32 ..... p 452 N95-14602 *
US-PATENT-CLASS-528-353 ..... p 452 N95-14416 *
US-PATENT-CLASS-528-353 ..... p 455 N95-15599 *
US-PATENT-CLASS-564-330 ..... p 452 N95-14416 *
US-PATENT-CLASS-564-335 ..... p 452 N95-14416 *
US-PATENT-CLASS-60-203.1 ..... p 475 N95-14516 *
US-PATENT-CLASS-73-147 ..... p 496 N95-14414 *
US-PATENT-CLASS-73-178T ..... p 412 N95-14415 *
US-PATENT-CLASS-73-204.18 .... p 496 N95-14414 *
US-PATENT-CLASS-73-590 ..... p 496 N95-14180 *
US-PATENT-CLASS-73-593 ..... p 496 N95-14180 *
US-PATENT-CLASS-73-842 ..... p 497 N95-15915 *
US-PATENT-CLASS-74-411 ..... p 502 N95-14517 *

US-PATENT-5,281,042 ..... p 503 N95-15305 *
US-PATENT-5,286,471 ..... p 441 N95-15303 *
US-PATENT-5,303,314 ..... p 614 N95-15707
US-PATENT-5,303,710 ..... p 615 N95-15765
US-PATENT-5,305,414 ..... p 615 N95-15766
US-PATENT-5,307,395 ..... p 614 N95-15764
US-PATENT-5,310,819 ..... p 456 N95-15800
US-PATENT-5,319,767 ..... p 574 N95-15336
US-PATENT-5,321,333 ..... p 496 N95-14841 #
US-PATENT-5,325,011 ..... p 497 N95-15799
US-PATENT-5,344,982 ..... p 452 N95-14416 *
US-PATENT-5,345,168 ..... p 498 N95-13629 *
US-PATENT-5,347,536 ..... p 460 N95-13628 *
US-PATENT-5,348,401 ..... p 500 N95-13819 *
US-PATENT-5,349,180 ..... p 613 N95-14413 *
US-PATENT-5,349,851 ..... p 496 N95-14414 *
US-PATENT-5,350,902 ..... p 473 N95-14294 *
US-PATENT-5,353,022 ..... p 412 N95-14415 *
US-PATENT-5,355,237 ..... p 612 N95-14181 *
US-PATENT-5,355,383 ..... p 499 N95-14519 *
US-PATENT-5,355,388 ..... p 602 N95-13823 *
US-PATENT-5,357,371 ..... p 499 N95-14515 *
US-PATENT-5,357,747 ..... p 475 N95-14516 *
US-PATENT-5,358,460 ..... p 502 N95-14517 *
US-PATENT-5,359,326 ..... p 411 N95-14518 *
US-PATENT-5,359,896 ..... p 496 N95-14180 *
US-PATENT-5,360,157 ..... p 500 N95-13654 *
US-PATENT-5,360,187 ..... p 393 N95-14182 *
US-PATENT-5,360,686 ..... p 472 N95-13824 *
US-PATENT-5,360,878 ..... p 452 N95-14602 *
US-PATENT-5,361,641 ..... p 497 N95-15915 *
US-PATENT-5,362,938 ..... p 503 N95-15670 *
US-PATENT-5,363,051 ..... p 583 N95-15598 *
US-PATENT-5,363,288 ..... p 478 N95-15681 *
US-PATENT-5,363,800 ..... p 625 N95-15602 *
US-PATENT-5,365,054 ..... p 614 N95-15603 *
US-PATENT-5,365,175 ..... p 478 N95-15669 *
US-PATENT-5,366,181 ..... p 503 N95-15306 *
US-PATENT-5,366,384 ..... p 504 N95-15914 *
US-PATENT-5,367,046 ..... p 455 N95-15599 *
US-PATENT-5,367,161 ..... p 503 N95-15601 *

US-PATERNT-CLASS-372-10 ..... p 499 N95-14519 *

USAARL-94-26 ..... p 551 N95-15767
USAARL-94-36 ..... p 551 N95-15810

USNA-TSPR-216 ..... p 551 N95-15757 #

UTIAS-347 ..... p 437 N95-13652

UVA/525025/EE94/101 ..... p 477 N95-15454

VPI-E-94-07 ..... p 505 N95-13839 * #
VPI-E-94-06 ..... p 435 N95-14865 * #

WES/CR/DRP-94-5 ..... p 536 N95-15440 #

WES/TR/DRP-92-6 ..... p 535 N95-14352 #

WHC-SA-2451 ..... p 630 N95-13673 #
WHC-SA-2512 ..... p 445 N95-14379 #
WHC-SA-2513 ..... p 445 N95-14378 #

WL-TM-94-3065-VOL-2 ..... p 404 N95-15465
WL-TM-94-3077 ..... p 513 N95-15547

WL-TR-93-1172 ..... p 469 N95-15394
WL-TR-93-3519 ..... p 405 N95-14421 #
WL-TR-93-4016 ..... p 434 N95-14411 #
WL-TR-94-2013 ..... p 454 N95-15316 #
WL-TR-94-2034 ..... p 500 N95-15395
WL-TR-94-3054 ..... p 412 N95-13687 #
WL-TR-94-4060 ..... p 436 N95-15441

WSRC-MS-93-619 ..... p 500 N95-13645 #
WSRC-MS-94-0108 ..... p 447 N95-15625 #
WSRC-MS-94-0112 ..... p 632 N95-15419 #

APPENDIX

NASA SCIENTIFIC AND TECHNICAL INFORMATION OFFICE PRODUCTS AND SERVICES

The NASA Scientific and Technical Information (STI) Office provides for the collection and announcement of aerospace-related reports and literature obtained worldwide through agreements and exchanges. The result of the collection is the comprehensive NASA STI Database that covers aeronautics, space, and supporting disciplines.

The STI Database, documents generated or obtained by NASA, and products and services derived from or supporting the database are made available to the NASA research community and to the public. Descriptions and sources of these items are presented in the following pages.

Scientific and Technical Aerospace Reports (STAR) is an abstract journal, listing citations with abstracts for aerospace-related reports obtained from worldwide sources. *STAR* is issued on the first of each month, and announces current documents that have been entered into the NASA STI Database during the previous month. The reports are of the following types:

- NASA, NASA contractor, and NASA grantee reports;
- Reports issued by other U.S. Government agencies, domestic and foreign institutions, universities, and private firms;
- Translations in report form;
- NASA-owned patents and patent applications
- Other U.S. Government agency and foreign patents and patent applications
- Domestic and foreign dissertations and theses.

Journal, book, and conference literature, journal translations, and certain foreign dissertations having the same subject scope as *STAR* are announced in a companion journal, *NASA Open Volumes on Aerospace (NOVA). NOVA* is issued on the 15th of each month and is available from the NASA Center for AeroSpace Information, at the address below.

ELIGIBILITY AND REGISTRATION FOR NASA STI PRODUCTS AND SERVICES

Organizations of the type listed below that have registered with NASA can receive products and services.

- NASA offices and installations, contractors, subcontractors, grantees, and consultants;
- Other U.S. Government agencies and their contractors;
- Libraries in the United States that have arrangements with NASA to maintain collections of NASA documents for public reference;
- Other organizations in the United States having a need for NASA documents in work related to aeronautics and space research;
- Organizations abroad that have established reciprocal documents exchange arrangements with NASA.

The central service points—central points of document acquisition and control within qualified organizations—or individuals are eligible to register for NASA STI products and services. Domestic organizations or individuals may be eligible to receive various classes of NASA publications and services and should address their requests for registration or further information to:

ATTN: Registration Services
NASA Center for AeroSpace Information
800 Elkridge Landing Road
Linthicum Heights, MD 21090-2934
301-621-0390

Organizations abroad should direct requests to:

National Aeronautics and Space Administration
Scientific and Technical Information Office (JTT)
International STI Office
Washington, DC 20546-0001
USA
703-271-5640

SUBJECT SCOPE

The subject scope of *STAR* and *NOVA* includes all aspects of aeronautics and space research and development, supporting basic and applied research, and applications. Aerospace aspects of Earth resources, energy development, conservation, oceanography, environmental protection, urban transportation, and other topics of high national priority are also covered.

HOW TO USE *STAR* SUBJECT CATEGORIES

Abstracts in *STAR* are categorized by 10 major subject divisions that are divided further into 76 specific subject categories. The subject divisions and categories are listed in the Table of Contents together with a note for each that defines its scope and provides any cross-references. For example:

> **16 SPACE TRANSPORTATION**
>
> Includes passenger and cargo space transportation, e.g., shuttle operations; and space rescue techniques. For related information see also *03 Air Transportation and Safety* and *18 Spacecraft Design, Testing and Performance*. For space suits see *54 Man/System Technology and Life Support*.

CROSS-REFERENCES

Individual *STAR* abstracts are not ordinarily cross-referenced, except for certain conference reports or book translations that have had separate abstracts written for their component papers or chapters. Citations and abstracts of the components follow immediately after those of the parent document. When the subject content of a component differs sufficiently from the general content of the parent, a cross-reference citation also is printed at the end of the category to which it normally would have been assigned if it were independent.

DOCUMENTS ON MICROFICHE

Documents available on microfiche are designated by a pound sign (#) following the accession number.

LIMITED REPRODUCIBILITY

A note of limited reproducibility appears in the citation, if there are factors affecting the reproducibility of more than 20% of the document. These factors include faint or broken type, color photographs, black and white photographs, foldouts, dot matrix print, or some other factor that limits the reproducibility of the document. This notation also appears on the microfiche header.

NASA PATENTS AND PATENT APPLICATIONS

Patents and patent applications owned by NASA are announced in *STAR* under appropriate subject categories and are referenced in the *STAR* indexes. In the Report Number Index, patents are indexed by the NASA Case Number, and the U.S. Patent Class. Patent applications are indexed by the NASA Case Number and the U.S. Patent Application Serial Number.

Printed copies of patents (which are not microfiched) are available for purchase from the U.S. Patent and Trademark Office.

When ordering patents, the U.S. Patent Number should be used, and payment must be remitted in advance, by money order or check payable to the Commissioner of Patents and Trademarks. Prepaid purchase coupons for ordering are also available from the U.S. Patent and Trademark Office.

NASA patent application specifications are sold in both paper copy and microfiche by the NASA Center for AeroSpace Information (CASI). The N accession number should be used in ordering either paper copy or microfiche from CASI.

The patents and patent applications announced in *STAR* are owned by NASA and are available for royalty-free licensing. Requests for licensing terms and further information should be addressed to:

National Aeronautics and Space Administration
Associate General Counsel for Intellectual Property
Code GP
Washington, DC 20546-0001

SOURCES FOR DOCUMENTS

One or more sources from which a document announced in *STAR* is available to the public is ordinarily given on the last line of the citation. The most commonly indicated sources and their acronyms or abbreviations are listed below, and their addresses are listed on page A-6. If the publication is available from a source other than those listed, the publisher and his address will be displayed on the availability line or in combination with the corporate source line.

Avail: CASI. Sold by the NASA Center for AeroSpace Information. Prices for hard copy (HC) and microfiche (MF) are indicated by a price code following the letters HC or MF in the *STAR* citation. Current values for the price codes are given in the tables on page A-7.

NOTE ON ORDERING DOCUMENTS: When ordering publications from NASA CASI, use the N accession number or other report number. It is also advisable to cite the title and other bibliographic identification.

Avail: SOD (or GPO). Sold by the Superintendent of Documents, U.S. Government Printing Office, in hard copy.

Avail: BLL (formerly NLL): British Library Lending Division, Boston Spa, Wetherby, Yorkshire, England. Photocopies available from this organization at the price shown. (If none is given, inquiry should be addressed to the BLL.)

Avail: DOE Depository Libraries. Organizations in U.S. cities and abroad that maintain collections of Department of Energy reports, usually in microfiche form, are listed in *Energy Research Abstracts*. Services available from the DOE and its depositories are described in a booklet, *DOE Technical Information Center - Its Functions and Services* (TID-4660), which may be obtained without charge from the DOE Technical Information Center.

Avail: ESDU. Pricing information on specific data, computer programs, and details on Engineering Sciences Data Unit (ESDU) topic categories can be obtained from ESDU International Ltd. Requesters in North America should use the Virginia address while all other requesters should use the London address, both of which are on page A-6.

Avail: Fachinformationszentrum Karlsruhe. Gesellschaft für wissenschaftlich-technische Information mbH 76344 Eggenstein-Leopoldshafen, Germany.

Avail: HMSO. Publications of Her Majesty's Stationery Office are sold in the U.S. by Pendragon House, Inc. (PHI), Redwood City, CA. The U.S. price (including a service and mailing charge) is given, or a conversion table may be obtained from PHI.

Avail: Issuing Activity, or Corporate Author, or no indication of availability. Inquiries as to the availability of these documents should be addressed to the organization shown in the citation as the corporate author of the document.

Avail: NASA Public Document Rooms. Documents so indicated may be examined at or purchased from the National Aeronautics and Space Administration (JBD-4), Public Documents Room (Room 1H23), Washington, DC 20546-0001, or public document rooms located at NASA installations, and the NASA Pasadena Office at the Jet Propulsion Laboratory.

Avail: NTIS. Sold by the National Technical Information Service. Igitially distributed microfiche under the NTIS SRIM (Selected Research in Microfiche) are available. For information concerning this service, consult the NTIS Subscription Section, Springfield, VA 22161.

Avail: Univ. Microfilms. Documents so indicated are dissertations selected from *Dissertation Abstracts* and are sold by University Microfilms as xerographic copy (HC) and microfilm. All requests should cite the author and the Order Number as they appear in the citation.

Avail: US Patent and Trademark Office. Sold by Commissioner of Patents and Trademarks, U.S. Patent and Trademark Office, at the standard price of $1.50 each, postage free. (See discussion of NASA patents and patent applications on page A-3.)

Avail: (US Sales Only). These foreign documents are available to users within the United States from the National Technical Information Service (NTIS). They are available to users outside the United States through the International Nuclear Information Service (INIS) representative in their country, or by applying directly to the issuing organization.

Avail: USGS. Originals of many reports from the U.S. Geological Survey, which may contain color illustrations, or otherwise may not have the quality of illustrations preserved in the microfiche or facsimile reproduction, may be examined by the public at the libraries of the USGS field offices whose addresses are listed on page A-6. The libraries may be queried concerning the availability of specific documents and the possible utilization of local copying services, such as color reproduction.

FEDERAL DEPOSITORY LIBRARY PROGRAM

In order to provide the general public with greater access to U.S. Government publications, Congress established the Federal Depository Library Program under the Government Printing Office (GPO), with 53 regional depositories responsible for permanent retention of material, inter-library loan, and reference services. At least one copy of nearly every NASA and NASA-sponsored publication, either in printed or microfiche format, is received and retained by the 53 regional depositories. A list of the regional GPO libraries, arranged alphabetically by state, appears on page A-8. These libraries are *not* sales outlets. A local library can contact a regional depository to help locate specific reports, or direct contact may be made by an individual.

PUBLIC COLLECTION OF NASA DOCUMENTS

An extensive collection of NASA and NASA-sponsored publications is maintained by the British Library Lending Division, Boston Spa, Wetherby, Yorkshire, England for public access. The British Library Lending Division also has available many of the non-NASA publications cited in *STAR*. European requesters may purchase facsimile copy or microfiche of NASA and NASA-sponsored documents, those identified by both the symbols # and * from ESA — Information Retrieval Service European Space Agency, 8-10 rue Mario-Nikis, 75738 CEDEX 15, France.

SUBMITTING DOCUMENTS

All users of this abstract service are urged to forward reports to be considered for announcement in *STAR*. This will aid NASA in its efforts to provide the fullest possible coverage of all scientific and technical publications that might support aeronautics and space research and development. If you have prepared relevant reports (other than those you will transmit to NASA, DOD, or DOE through the

usual contract- or grant-reporting channels), please send them for consideration to the NASA Center for AeroSpace Information, 800 Elkridge Landing Road, Linthicum Heights, MD 21090-2934.

Reprints of journal articles, book chapters, and conference papers are also welcome. These will be considered for announcement in *STAR's* companion journal, *NOVA*.

You may specify a particular source to be included in a report announcement if you wish; otherwise the report will be placed on a public sale at the NASA Center for AeroSpace Information. Copyrighted publications will be announced but not distributed or sold.

PURCHASE OF *STAR*

STAR is publicly available on annual subscription from the NASA Center for AeroSpace Information (CASI). 1995 *STAR* subscription prices are $100.00/domestic and $125.00/foreign. Single copy prices: $33.00/domestic, $41.00/foreign.

An annual, cumulative *STAR Index* is also available at $70.00/domestic and foreign.

STAR is available to registered users on annual subscription from the NASA Center for AeroSpace Information, ATTN: Registration Services, 800 Elkridge Landing Road, Linthicum Heights, MD 21090-2934.

ADDRESSES OF ORGANIZATIONS

British Library Lending Division
Boston Spa, Wetherby, Yorkshire
England

Commissioner of Patents and Trademarks
U.S. Patent and Trademark Office
Washington, DC 20231

Department of Energy
Technical Information Center
P.O. Box 62
Oak Ridge, TN 37830

European Space Agency-
Information Retrieval Service ESRIN
Via Galileo Galilei
00044 Frascati (Rome) Italy

Engineering Sciences Data Unit International
P.O. Box 1633
Manassas, VA 22110

Engineering Sciences Data Unit
International, Ltd.
251-259 Regent Street
London, W1R 7AD, England

Fachinformationszentrum Karlsruhe
Gesellschaft für wissenschaftlich-technische
Information mbH
76344 Eggenstein-Leopoldshafen, Germany

Her Majesty's Stationery Office
P.O. Box 569, S.E. 1
London, England

NASA Center for AeroSpace Information
800 Elkridge Landing Road
Linthicum Heights, MD 21090-2934

National Aeronautics and Space Administration
Scientific and Technical Information Office
(JTT)
Washington, DC 20546-0001

National Technical Information Service
5285 Port Royal Road
Springfield, VA 22161

Pendragon House, Inc.
899 Broadway Avenue
Redwood City, CA 94063

Superintendent of Documents
U.S. Government Printing Office
Washington, DC 20402

University Microfilms
A Xerox Company
300 North Zeeb Road
Ann Arbor, MI 48106

University Microfilms, Ltd.
Tylers Green
London, England

U.S. Geological Survey Library National Center
MS 950
12201 Sunrise Valley Drive
Reston, VA 22092

U.S. Geological Survey Library
2255 North Gemini Drive
Flagstaff, AZ 86001

U.S. Geological Survey
345 Middlefield Road
Menlo Park, CA 94025

U.S. Geological Survey Library
Box 25046
Denver Federal Center, MS914
Denver, CO 80225

NASA CASI PRICE CODE TABLE

(Effective January 1, 1995)

CASI PRICE CODE	NORTH AMERICAN PRICE	FOREIGN PRICE
A01	$ 6.00	$ 12.00
A02	9.00	18.00
A03	17.50	35.00
A04-A05	19.50	39.00
A06-A09	27.00	54.00
A10-A13	36.50	73.00
A14-A17	44.50	89.00
A18-A21	52.00	104.00
A22-A25	61.00	122.00
A99	Call For Price	Call For Price

IMPORTANT NOTICE

For users not registered at the NASA CASI, prepayment is required. Additionally, a shipping and handling fee of $1.00 per document for delivery within the United States and $9.00 per document for delivery outside the United States is charged.

For users registered at the NASA CASI, document orders may be invoiced at the end of the month, charged against a deposit account, or paid by check or credit card. NASA CASI accepts American Express, Diners' Club, MasterCard, and VISA credit cards. There are no shipping and handling charges. To register at the NASA CASI, please request a registration form through the NASA Access Help Desk at the address or numbers below.

NASA Center for AeroSpace Information
800 Elkridge Landing Road
Linthicum Heights, MD 21090-2934
Telephone: (301) 621-0390
E-mail: help@sti.nasa.gov
Fax: (301) 621-0134

FEDERAL REGIONAL DEPOSITORY LIBRARIES

ALABAMA

AUBURN UNIV. AT MONTGOMERY LIBRARY
Documents Dept.
7300 University Dr.
Montgomery, AL 36117-3596
(205) 244-3650 Fax: (205) 244-0678

UNIV. OF ALABAMA
Amelia Gayle Gorgas Library
Govt. Documents
P.O. Box 870266
Tuscaloosa, AL 35487-0266
(205) 348-6046 Fax: (205) 348-0760

ARIZONA

DEPT. OF LIBRARY, ARCHIVES, AND PUBLIC RECORDS
Research Division
Third Floor, State Capitol
1700 West Washington
Phoenix, AZ 85007
(602) 542-3701 Fax: (602) 542-4400

ARKANSAS

ARKANSAS STATE LIBRARY
State Library Service Section
Documents Service Section
One Capitol Mall
Little Rock, AR 72201-1014
(501) 682-2053 Fax: (501) 682-1529

CALIFORNIA

CALIFORNIA STATE LIBRARY
Govt. Publications Section
P.O. Box 942837 - 914 Capitol Mall
Sacramento, CA 94337-0091
(916) 654-0069 Fax: (916) 654-0241

COLORADO

UNIV. OF COLORADO - BOULDER
Libraries - Govt. Publications
Campus Box 184
Boulder, CO 80309-0184
(303) 492-8834 Fax: (303) 492-1881

DENVER PUBLIC LIBRARY
Govt. Publications Dept. BSG
1357 Broadway
Denver, CO 80203-2165
(303) 640-8846 Fax: (303) 640-8817

CONNECTICUT

CONNECTICUT STATE LIBRARY
231 Capitol Avenue
Hartford, CT 06106
(203) 566-4971 Fax: (203) 566-3322

FLORIDA

UNIV. OF FLORIDA LIBRARIES
Documents Dept.
240 Library West
Gainesville, FL 32611-2048
(904) 392-0366 Fax: (904) 392-7251

GEORGIA

UNIV. OF GEORGIA LIBRARIES
Govt. Documents Dept.
Jackson Street
Athens, GA 30602-1645
(706) 542-8949 Fax: (706) 542-4144

HAWAII

UNIV. OF HAWAII
Hamilton Library
Govt. Documents Collection
2550 The Mall
Honolulu, HI 96822
(808) 948-8230 Fax: (808) 956-5968

IDAHO

UNIV. OF IDAHO LIBRARY
Documents Section
Rayburn Street
Moscow, ID 83844-2353
(208) 885-6344 Fax: (208) 885-6817

ILLINOIS

ILLINOIS STATE LIBRARY
Federal Documents Dept.
300 South Second Street
Springfield, IL 62701-1796
(217) 782-7596 Fax: (217) 782-6437

INDIANA

INDIANA STATE LIBRARY
Serials/Documents Section
140 North Senate Avenue
Indianapolis, IN 46204-2296
(317) 232-3679 Fax: (317) 232-3728

IOWA

UNIV. OF IOWA LIBRARIES
Govt. Publications
Washington & Madison Streets
Iowa City, IA 52242-1166
(319) 335-5926 Fax: (319) 335-5900

KANSAS

UNIV. OF KANSAS
Govt. Documents & Maps Library
6001 Malott Hall
Lawrence, KS 66045-2800
(913) 864-4660 Fax: (913) 864-3855

KENTUCKY

UNIV. OF KENTUCKY
King Library South
Govt. Publications/Maps Dept.
Patterson Drive
Lexington, KY 40506-0039
(606) 257-3139 Fax: (606) 257-3139

LOUISIANA

LOUISIANA STATE UNIV.
Middleton Library
Govt. Documents Dept.
Baton Rouge, LA 70803-3312
(504) 388-2570 Fax: (504) 388-6992

LOUISIANA TECHNICAL UNIV.
Prescott Memorial Library
Govt. Documents Dept.
Ruston, LA 71272-0046
(318) 257-4962 Fax: (318) 257-2447

MAINE

UNIV. OF MAINE
Raymond H. Fogler Library
Govt. Documents Dept.
Orono, ME 04469-5729
(207) 581-1673 Fax: (207) 581-1653

MARYLAND

UNIV. OF MARYLAND - COLLEGE PARK
McKeldin Library
Govt. Documents/Maps Unit
College Park, MD 20742
(301) 405-9165 Fax: (301) 314-9416

MASSACHUSETTS

BOSTON PUBLIC LIBRARY
Govt. Documents
666 Boylston Street
Boston, MA 02117-0286
(617) 536-5400, ext. 226
Fax: (617) 536-7758

MICHIGAN

DETROIT PUBLIC LIBRARY
5201 Woodward Avenue
Detroit, MI 48202-4093
(313) 833-1025 Fax: (313) 833-0156

LIBRARY OF MICHIGAN
Govt. Documents Unit
P.O. Box 30007
717 West Allegan Street
Lansing, MI 48909
(517) 373-1300 Fax: (517) 373-3381

MINNESOTA

UNIV. OF MINNESOTA
Govt. Publications
409 Wilson Library
309 19th Avenue South
Minneapolis, MN 55455
(612) 624-5073 Fax: (612) 626-9353

MISSISSIPPI

UNIV. OF MISSISSIPPI
J.D. Williams Library
106 Old Gym Bldg.
University, MS 38677
(601) 232-5857 Fax: (601) 232-7465

MISSOURI

UNIV. OF MISSOURI - COLUMBIA
106B Ellis Library
Govt. Documents Sect.
Columbia, MO 65201-5149
(314) 882-6733 Fax: (314) 882-8044

MONTANA

UNIV. OF MONTANA
Mansfield Library
Documents Division
Missoula, MT 59812-1195
(406) 243-6700 Fax: (406) 243-2060

NEBRASKA

UNIV. OF NEBRASKA - LINCOLN
D.L. Love Memorial Library
Lincoln, NE 68588-0410
(402) 472-2562 Fax: (402) 472-5131

NEVADA

THE UNIV. OF NEVADA LIBRARIES
Business and Govt. Information Center
Reno, NV 89557-0044
(702) 784-6579 Fax: (702) 784-1751

NEW JERSEY

NEWARK PUBLIC LIBRARY
Science Div. - Public Access
P.O. Box 630
Five Washington Street
Newark, NJ 07101-7812
(201) 733-7782 Fax: (201) 733-5648

NEW MEXICO

UNIV. OF NEW MEXICO
General Library
Govt. Information Dept.
Albuquerque, NM 87131-1466
(505) 277-5441 Fax: (505) 277-6019

NEW MEXICO STATE LIBRARY
325 Don Gaspar Avenue
Santa Fe, NM 87503
(505) 827-3824 Fax: (505) 827-3888

NEW YORK

NEW YORK STATE LIBRARY
Cultural Education Center
Documents/Gift & Exchange Section
Empire State Plaza
Albany, NY 12230-0001
(518) 474-5355 Fax: (518) 474-5786

NORTH CAROLINA

UNIV. OF NORTH CAROLINA - CHAPEL HILL
Walter Royal Davis Library
CB 3912, Reference Dept.
Chapel Hill, NC 27514-8890
(919) 962-1151 Fax: (919) 962-4451

NORTH DAKOTA

NORTH DAKOTA STATE UNIV. LIB.
Documents
P.O. Box 5599
Fargo, ND 58105-5599
(701) 237-8886 Fax: (701) 237-7138

UNIV. OF NORTH DAKOTA
Chester Fritz Library
University Station
P.O. Box 9000 - Centennial and University Avenue
Grand Forks, ND 58202-9000
(701) 777-4632 Fax: (701) 777-3319

OHIO

STATE LIBRARY OF OHIO
Documents Dept.
65 South Front Street
Columbus, OH 43215-4163
(614) 644-7051 Fax: (614) 752-9178

OKLAHOMA

OKLAHOMA DEPT. OF LIBRARIES
U.S. Govt. Information Division
200 Northeast 18th Street
Oklahoma City, OK 73105-3298
(405) 521-2502, ext. 253
Fax: (405) 525-7804

OKLAHOMA STATE UNIV.
Edmon Low Library
Stillwater, OK 74078-0375
(405) 744-6546 Fax: (405) 744-5183

OREGON

PORTLAND STATE UNIV.
Branford P. Millar Library
934 Southwest Harrison
Portland, OR 97207-1151
(503) 725-4123 Fax: (503) 725-4524

PENNSYLVANIA

STATE LIBRARY OF PENN.
Govt. Publications Section
116 Walnut & Commonwealth Ave.
Harrisburg, PA 17105-1601
(717) 787-3752 Fax: (717) 783-2070

SOUTH CAROLINA

CLEMSON UNIV.
Robert Muldrow Cooper Library
Public Documents Unit
P.O. Box 343001
Clemson, SC 29634-3001
(803) 656-5174 Fax: (803) 656-3025

UNIV. OF SOUTH CAROLINA
Thomas Cooper Library
Green and Sumter Streets
Columbia, SC 29208
(803) 777-4841 Fax: (803) 777-9503

TENNESSEE

UNIV. OF MEMPHIS LIBRARIES
Govt. Publications Dept.
Memphis, TN 38152-0001
(901) 678-2206 Fax: (901) 678-2511

TEXAS

TEXAS STATE LIBRARY
United States Documents
P.O. Box 12927 - 1201 Brazos
Austin, TX 78701-0001
(512) 463-5455 Fax: (512) 463-5436

TEXAS TECH. UNIV. LIBRARIES
Documents Dept.
Lubbock, TX 79409-0002
(806) 742-2282 Fax: (806) 742-1920

UTAH

UTAH STATE UNIV.
Merrill Library Documents Dept.
Logan, UT 84322-3000
(801) 797-2678 Fax: (801) 797-2677

VIRGINIA

UNIV. OF VIRGINIA
Alderman Library
Govt. Documents
University Ave. & McCormick Rd.
Charlottesville, VA 22903-2498
(804) 824-3133 Fax: (804) 924-4337

WASHINGTON

WASHINGTON STATE LIBRARY
Govt. Publications
P.O. Box 42478
16th and Water Streets
Olympia, WA 98504-2478
(206) 753-4027 Fax: (206) 586-7575

WEST VIRGINIA

WEST VIRGINIA UNIV. LIBRARY
Govt. Documents Section
P.O. Box 6069 - 1549 University Ave.
Morgantown, WV 26506-6069
(304) 293-3051 Fax: (304) 293-6638

WISCONSIN

ST. HIST. SOC. OF WISCONSIN LIBRARY
Govt. Publication Section
816 State Street
Madison, WI 53706
(608) 264-6525 Fax: (608) 264-6520

MILWAUKEE PUBLIC LIBRARY
Documents Division
814 West Wisconsin Avenue
Milwaukee, WI 53233
(414) 286-3073 Fax: (414) 286-8074

•U.S. GOVERNMENT PRINTING OFFICE:1995-387-253/20001

National Aeronautics and
Space Administration
Code JTT
Washington, DC 20546-0001